Deepak N. Bhatia
Gregory I. Bain
Gary G. Poehling
Benjamin R. Graves
Editors

Arthroscopy and Endoscopy of the Elbow, Wrist and Hand

Surgical Anatomy and Techniques

ISAKOS
International Society of Arthroscopy, Knee Surgery and Orthopaedic Sports Medicine

Springer

Arthroscopy and Endoscopy of the Elbow, Wrist and Hand

Deepak N. Bhatia • Gregory I. Bain
Gary G. Poehling • Benjamin R. Graves
Editors

Arthroscopy and Endoscopy of the Elbow, Wrist and Hand

Surgical Anatomy and Techniques

ISAKOS
International Society of Arthroscopy, Knee Surgery and Orthopaedic Sports Medicine

Springer

Editors
Deepak N. Bhatia
Department of Orthopaedic Surgery
Sir HN Reliance Foundation Hospital
and Research Center
Mumbai
India

Gary G. Poehling
Department of Orthopaedic Surgery
Wake Forest School of Medicine
Winston-Salem, NC
USA

Gregory I. Bain
Department of Orthopaedic Surgery
Flinders University
Adelaide, SA
Australia

Benjamin R. Graves
Department of Orthopaedic Surgery
Wake Forest School of Medicine
Winston-Salem, NC
USA

ISBN 978-3-030-79422-4 ISBN 978-3-030-79423-1 (eBook)
https://doi.org/10.1007/978-3-030-79423-1

© ISAKOS 2022
This work is subject to copyright. All rights are reserved by the Publisher, whether the whole or part of the material is concerned, specifically the rights of translation, reprinting, reuse of illustrations, recitation, broadcasting, reproduction on microfilms or in any other physical way, and transmission or information storage and retrieval, electronic adaptation, computer software, or by similar or dissimilar methodology now known or hereafter developed.
The use of general descriptive names, registered names, trademarks, service marks, etc. in this publication does not imply, even in the absence of a specific statement, that such names are exempt from the relevant protective laws and regulations and therefore free for general use.
The publisher, the authors, and the editors are safe to assume that the advice and information in this book are believed to be true and accurate at the date of publication. Neither the publisher nor the authors or the editors give a warranty, expressed or implied, with respect to the material contained herein or for any errors or omissions that may have been made. The publisher remains neutral with regard to jurisdictional claims in published maps and institutional affiliations.

This Springer imprint is published by the registered company Springer Nature Switzerland AG
The registered company address is: Gewerbestrasse 11, 6330 Cham, Switzerland

I dedicate this book to my teachers and mentors: The surgeon-scientists who believed in and taught an evidence based approach to innovation.

To my parents, Naveen and Rajkumari, and my family, Shilpa and Shraayan: Gratitude, for the love and encouragement all along.

Deepak N. Bhatia
Chairman, Elbow, Wrist, and Hand Committee, ISAKOS

I dedicate this book to the aspiring young who……dream to make a difference, develop a discipline to learn, and devote themselves to discovering the new dawn. We trust that you will be dedicated to and inspired by the next generation, just as our teachers were.

Gregory I. Bain

In loving memory of my wife Sandy, whose support and encouragement will be cherished always.

Gary G. Poehling

To my wife Jennifer and daughter Lily - your love, support, and friendship mean everything to me.

Benjamin R. Graves

Foreword

Minimally invasive surgery has become the current standard of care for many, if not most, surgical procedures. From cataracts to coronary arteries, from gall bladders to gynecology, minimally invasive surgery has supplanted Arnold K. Henry's Extensile Exposure [1] for surgical access to internal anatomic structures. In orthopedics, arthroscopy is expanding minimally invasive surgical techniques from major joints to smaller joints and even to potential spaces between tissue planes. Standards of care are an evolutionary concept. Surgical arthroscopy and a touch of bravado helped grow the broad shoulders of pioneering giants on which we stand today to advance the field of upper extremity joint surgery.

This work you are holding is a comprehensive textbook of today's approaches to elbow, wrist, and hand joint procedures. It contains, in addition, some trailblazing initiatives that may become tomorrow's conventional wisdom in upper extremity joint surgery. The contributing chapter authors represent global leaders in joint surgery, selected for their expertise and their support of ISAKOS. While journal articles are giving way to online "how-to" videos in surgical education, they are no substitute for personal medical libraries of classic, published articles and comprehensive textbooks for reference citation and review. This book traces upper extremity minimally invasive joint surgery from its historical origins to its present techniques to its potential future. It describes the insightful understanding of joint pathology and pathomechanics and the creative imagination that have brought newer surgical potentials to reality. The many chapter authors collectively have created both a timely and timeless reference text for upper extremity surgeons.

The scriptural Book of Proverbs, written principally by Solomon who arguably was one of the wisest of men and philosophers, entreats us to seek wisdom and, with wisdom, understanding (Proverbs 4:5-8). This textbook offers both—wisdom and understanding—with respect to the spectrum of joint pathology in the elbow, the wrist, and the hand. The surgical techniques are complemented with excellent, illustrative graphics and anatomic dissections. Moreover, the surgical technique discussions include the all-sanguine "why" to elucidate the advantages of newer surgical approaches to orthopedic treatments, whether they be diagnostic, reparative, or reconstructive.

While some of the procedures described are perhaps not yet standards of care, they are sufficiently detailed to serve as instructive reference for the next stage of advancement in surgical treatments. Thus, this book is wonderfully instructive, more than a primer in upper extremity arthroscopy but also a

stimulus for those inclined to read tomorrow's crystal ball and devise new and even greater surgical innovations.

I commend all the authors' courage in compiling this elegant textbook on upper extremity, minimally invasive joint surgery. It can be read with enjoyment, for deep wisdom and understanding.

Terry L. Whipple
Lifetime Honourary President
International Wrist Arthroscopy Society
Paris, France

Reference

1. Henry, AK, Extensile Exposure. E & S Livingstone Ltd, Edinburgh. 1945 and 1957

Preface

ISAKOS Elbow Wrist and Hand Committee

The EWH committee is a relatively new subspecialist committee in ISAKOS. The EWH committee was formed in 2015 and the aim was to foster growth of EWH surgery and arthroscopy. Subspecialist member surgeons were selected from the global ISAKOS membership with Prof Gregory I. Bain as the chair. The EWH committee has since conducted ICLs at the ISAKOS biannual congress, facilitated lectures, JISAKOS publications and provided ISAKOS books. In 2017, ISAKOS and the EWH committee initiated the Gary G. Poehling Award for the best EWH research paper presented at an ISAKOS conference. The current committee (2019–2021) took charge at the ISAKOS conference at Cancun, Mexico, and proposed the book titled *Arthroscopy and Endoscopy of the Elbow, Wrist, and Hand* that would encompass the most progressive and modern techniques, ranging from basic to advanced.

Aim of the Book

Arthroscopic surgery of the EWH has undergone a paradigm shift in the last decade and several procedures which were considered "experimental" are now routinely performed. Arthroscopy has advanced beyond the confines of the joint, with soft-tissue endoscopy emerging as a minimally invasive solution to extraarticular pathology. This book brings together basic and advanced techniques that would be useful to surgeons and trainees at all levels of expertise. Surgical anatomy is the foundation for safe reproducibility of any new surgical technique, and this aspect has been emphasized using cadaveric dissections, arthroscopic images, and illustrations. Many of the techniques have been written by the innovator surgeons and those who have extensive experience with these procedures. The book also features some previously unpublished techniques that will appear here for the first time.

Organization and Content

The book begins with an interesting description of historical aspects of arthroscopy and especially wrist arthroscopy.

The technical content is segregated into three parts: elbow, wrist, and hand. Each part has subsections beginning with the basic science that forms the foundation of these techniques. The procedures are subdivided according to the pathology (instability, fractures, etc.) or grouped by the region within the anatomical area (distal biceps, ulnar nerve, TFCC, carpometacarpal joint, etc.). Arthroscopic and endoscopic procedures for specific pathological conditions are described under each of these sections. Each chapter includes a brief background and key surgical anatomy pertaining to the technique. The surgical technique is simplified into a "step-by-step" approach with technical tips, pitfalls, and rehabilitations guidelines. A few open surgical techniques have been included specifically due to their "gold-standard" position in current treatment algorithms and also to highlight regional anatomical details. Evolving endoscopic techniques have been grouped as a separate subsection in each part.

The book concludes with chapters on guidelines for incorporating newer techniques into practice, and the editors' perspective on the future of elbow, wrist, hand arthroscopy, and endoscopy.

Acknowledgments

This book was written at a time of a global healthcare crisis and many contributors to this book are involved in the battle against the pandemic. We are thankful to every contributor for the remarkable dedication to their academic and educational commitments.

Massimiliano Crespi from Italy was the illustrator for the book. Max has provided 184 anatomical and surgical illustrations. The illustrations were supported by a generous grant from ISAKOS.

Mumbai, India — Deepak N. Bhatia
Adelaide, Australia — Gregory I. Bain
Winston-Salem, USA — Gary G. Poehling
Winston-Salem, USA — Benjamin R. Graves

Contents

Part I History

1 The Early Development of Arthroscopy 3
Andrew Baker, Terry L. Whipple, Gary G. Poehling, and Gregory I. Bain

2 History of Wrist Arthroscopy 15
Andrew Baker, Terry L. Whipple, Gary G. Poehling, and Gregory I. Bain

Part II Elbow: Basic Science

3 Clinical Anatomy of the Elbow 47
Gregory I. Bain, Benjamin Seah Renyi, and Janak A. Mehta

4 Elbow Anatomy: A Layered Approach 63
Deepak N. Bhatia

5 Surgical Anatomy of the Nerves Around the Elbow 79
Celli Andrea, Serafini Fabio, Peruzzi Marco, and Pederzini Luigi Adriano

6 Arthroscopic Equipment and Set-Up for Elbow Arthroscopy . . . 89
Richard S. Page, Janina Henze, and Kevin Eng

7 Portals and Technique for Diagnostic Elbow Arthroscopy 97
Benjamin R. Graves, Michael T. Freehill, Gary G. Poehling, and Gregory I. Bain

8 Transarticular Posterolateral Portal for Elbow Arthroscopy . . . 109
Minoo Patel

9 Dry Elbow Arthroscopy 113
Benjamin Seah Renyi, Joideep Phadnis, and Gregory I. Bain

Part III Elbow: Instability

10 Classification of Elbow Instability 119
Alessandro Marinelli, Enrico Guerra, Marco Cavallo, Alice Ritali, and Roberto Rotini

11 Arthroscopic Evaluation of Elbow Instability 127
Melanie Amarasooriya, Benjamin Seah Renyi, Gregory I. Bain, and Joideep Phadnis

12 Ten-Point Arthroscopic Assessment of Chronic Elbow Instability 133
Deepak N. Bhatia

13 Arthroscopic Evaluation of Elbow Instability: An Alternative Technique 143
Sebastian Lappen, Nadine Ott, Lars P. Müller, and Kilian Wegmann

14 Arthroscopic Repair of Lateral Ulnar Collateral Ligament Injuries 149
Felix H. Savoie, Zachary J. Finley, and Michael O'Brien

15 Arthroscopic Lateral Collateral Ligament Imbrication 159
Christina J. Lorenz and Roger P. van Riet

16 Arthroscopic Plication in Medial and Lateral Elbow Instability 167
Francesco Luceri, Davide Cucchi, Joseph Martin Nikhil, Pietro Simone Randelli, and Paolo Arrigoni

17 The Posterolateral Ligament of the Elbow: Surgical Anatomy, Assessment and Repair Technique 171
Adam C. Watts and Chen G. Tu

18 Lateral and Medial Elbow Instability: Graft Reconstruction Techniques 179
Shay Ribenzaft, Yoav Rosenthal, and Mark I. Loebenberg

19 Arthroscopic Management of Posterior Elbow Impingement in Athletes 187
Deepak N. Bhatia

20 Valgus Extension Overload 195
T. David Luo and Michael T. Freehill

Part IV Elbow: Fractures

21 Arthroscopic Approaches to Radial Head Fracture Fixation . . . 207
Davide Cucchi, Francesco Luceri, Paolo Arrigoni, Roslind Karolina Hackenberg, Alfonso Vaquero-Picado, and Raul Barco

22 Arthroscopic Reduction and Internal Fixation of Elbow Fractures 213
Enrico Guerra, Alessandro Marinelli, Marco Cavallo, Alice Ritali, Andrea Sessa, and Roberto Rotini

23 Arthroscopic Fixation of Elbow Fractures: How I Do It 225
T. Leschinger, Lars P. Müller, and K. Wegmann

24 Arthroscopic Fixation of Radial Neck Fractures in Children 233
Deepak N. Bhatia

25 Arthroscopic Radial Head Resection Using the "Radial Head Portal" 239
Deepak N. Bhatia

26 Arthroscopic Fixation of Coronoid Fractures: Retrograde Wire Technique 249
Jan Debeij and Roger P. van Riet

27 Arthroscopic Fixation of Coronoid Fractures: Antegrade Wire Technique 255
Francesco Luceri, Davide Cucchi, Rahul Sinha, Paolo Arrigoni, and Pietro Simone Randelli

28 Arthroscopic-Assisted Fixation of Capitello-Trochlear Fractures 261
Yiyang Zhang and Graham J. W. King

29 Arthroscopic Capitellum Excision and Capitelloplasty 269
Deepak N. Bhatia

Part V Elbow: Osteochondritis Dessicans

30 Osteochondritis Dissecans of the Elbow: Concepts of Etiology 281
Simon MacLean and Gregory I. Bain

31 Arthroscopic Treatment of Osteochondritis Dissecans of the Elbow 287
Myrthe Nagel, Rens Bexkens, Bertram The, and Denise Eygendaal

32 Arthroscopic Evaluation and Management of Osteochondritis Dissecans 293
L. A. Pederzini, A. F. Cheli, M. Bartoli, G. Stelitano, and A. Celli

33 Elbow Osteochondritis Dissecans: Arthroscopy and Reconstructive Procedures 299
Kozo Shimada, Ko Temporin, and Keiichiro Oura

Part VI Elbow: Epicondylitis

34 Arthroscopic Anatomic Insertional Release (AAIR) Procedure for Refractory Lateral Epicondilitis 315
Deepak N. Bhatia

35 Posterior Interosseous Nerve Release in Lateral Epicondylitis 323
Gregory Hoy and Richard P. Jamieson

36 Lateral Epicondylitis and Symptomatic Minor Instability of the Lateral Elbow (SMILE) 329
Francesco Luceri, Davide Cucchi, Paul Muriithi Miano, Paolo Arrigoni, and Pietro Simone Randelli

Part VII Elbow: Arthritis and Contractures

37 Classification of Elbow Stiffness 337
Alessandro Marinelli, Enrico Guerra, Gregory I. Bain, and Roberto Rotini

38 Arthroscopic Adhesiolysis in a Stiff Elbow 343
L. A. Pederzini, F. Serafini, F. Nicoletta, and A. Celli

39 All-Endoscopic Sub-brachialis Capsulectomy for Severe Elbow Contractures 349
Deepak N. Bhatia

40 Arthroscopic Management of Elbow Osteoarthritis 359
Luigi Adriano Pederzini, Vito Duca, Matteo Bartoli, and Andrea Celli

41 Arthroscopic Transhumeral Ulnohumeral Arthroplasty 365
Richard S. Page, Janina Henze, and Kevin Eng

42 Arthroscopic Ulnohumeral Arthroplasty 375
Ilse Degreef

43 Arthroscopic Partial Radial Head Resection for Rheumatoid Arthritis 381
Kozo Shimada, Ko Temporin, Keiichiro Oura, and Satoshi Miyamura

44 Arthroscopic Releases of the Proximal Radioulnar Joint 387
Eugene T. Ek and Kemble K. Wang

Part VIII Elbow Tumour-Like Lesions

45 Arthroscopic Transarticular Excision of Elbow Ganglion Cyst 395
Deepak N. Bhatia

46 Arthroscopic Management of Intra-articular Benign Tumours of the Elbow 403
Deepak N. Bhatia

Part IX Biceps Tendon

47 Distal Biceps Anatomy: Structural Morphometry and Dynamic Relationships 413
Deepak N. Bhatia

48 The "All-Endoscopic" Approach to Distal Biceps: Overview, Portals, and Anatomy-at-Risk 419
Deepak N. Bhatia

49 All-Endoscopic Management of Partial Tears of Distal Biceps Tendon 425
Deepak N. Bhatia

50 All-Endoscopic Repair of Complete Retracted Distal Biceps Ruptures 431
Deepak N. Bhatia

51 All-Endoscopic Autograft Augmentation and Reconstruction of Chronic Retracted Distal Biceps Tendon Tears. 439
Deepak N. Bhatia

52 Endoscopic-Assisted Onlay Repair for Distal Biceps Tears . . . 447
Deepak N. Bhatia

53 Endoscopic-Assisted Footprint Repair of Distal Biceps Tendon Ruptures 453
Mina Derias, Gregory I. Bain, and Joideep Phadnis

54 Minimally Invasive Acute Distal Biceps Repair 459
Gregory Hoy and Simon Hoy

Part X Triceps Tendon

55 Surgical Anatomy of the Distal Triceps Tendon 467
Raul Barco

56 Endoscopic Distal Triceps Repair 473
Donovan Johnson, Michael Esantsi, Michael O'Brien, and Felix H. Savoie

57 Acute and Chronic Triceps Tendon Tears: Transosseous Repair Technique. 481
Deepak N. Bhatia

Part XI Elbow: Ulnar Nerve

58 Endoscopic Ulnar Nerve Decompression 491
Raul Barco

59 Endoscopic Ulnar Nerve Release and Transposition: Two Portal Technique 497
Margaret Woon Man Fok and Gregory I. Bain

60 Endoscopic Ulnar Nerve Release and Transposition: Single Portal Technique 505
Paul Max Jarrett and Allan Wang

61 Endoscopic Robotic Decompression of the Ulnar Nerve 515
Jose Carlos Garcia Jr. and Matheus Ribeiro Barcelos

Part XII Elbow Endoscopy: Evolving Techniques

62 Endoscopic Olecranon Bursectomy and Spur Resection 521
Vikas Singh and Gregory I. Bain

63 Endoscopic Four Compartment Decompression for Chronic Exertional Compartment Syndrome 527
Paul Max Jarrett

64 Endoscopic Forearm Fasciotomy: How I Do it 533
Jessica Cobb and Tyson Cobb

65 Arthroscopic Management of the Painful Elbow Arthroplasty 539
Timothy Eves, Gregory I. Bain, and Joideep Phadnis

66 Endoscopic Pronator Release (Proximal Forearm Median Nerve Decompression) 547
Michael J. Fitzmaurice

Part XIII Wrist: Basic Science

67 Functional Anatomy of the Wrist 553
Simon MacLean, Melanie Amarasooriya, and Gregory I. Bain

68 Clinical Biomechanics of the Wrist 563
Melanie Amarasooriya, Simon MacLean, and Gregory I. Bain

69 Arthroscopic Equipment and Set Up for Wrist Arthroscopy 579
Richard S. Page, Janina Henze, and Kevin Eng

70 Diagnostic Arthroscopy of the Wrist: Anatomy and Portals 585
Benjamin R. Graves, Eric J. Sarkissian, and Gary G. Poehling

71 Wrist Portals and Arthroscopic Anatomy 601
F. Corella, M. Ocampos, M. C. Manzanares-Céspedes, and M. Dalmau-Pastor

Part XIV Wrist: Scapholunate Arthroscopy

72 Anatomy and Biomechanics of Scapholunate Ligament 633
Nicholas Chang and Nina Suh

73 Surgical Anatomy and Classification of Scapholunate Tears . . 641
Lorenzo Merlini and Christophe Mathoulin

74 Arthroscopic Scapholunate Ligament Thermal Shrinkage . . . 647
Eugene T. Ek and Rachel M. Blackshaw

75 Arthroscopic Treatment of Scapholunate Instability 655
Ahlam Arnaout and Christophe Mathoulin

76 Modified Brunelli Technique for Scapholunate Reconstruction 665
Gregory Hoy and Gayan Padmasekera

77 Arthroscopic Ligamentoplasty for Scapholunate Instability 669
F. Corella, M. Ocampos, and R. Larrainzar Garijo

78 Arthroscopic-Assisted Combined Dorsal and Volar Scapholunate Ligament Reconstruction with Tendon Graft for Chronic SL Instability 691
Siu-cheong Jeffrey Justin Koo and Pak-cheong Ho

79 Arthroscopic Interposition Tendon Arthroplasty for Stage-Two Scapholunate Advanced Collapse 707
C. Mathoulin and Margareta Arianni

80 Arthroscopic Resection Arthroplasty for Scapholunate Advanced Collapse (SLAC Wrist) 715
Jessica Cobb and Tyson Cobb

Part XV Wrist: Scaphotrapeziotrapezoid Arthroscopy

81 Arthroscopic Resection Arthroplasty for Scaphotrapeziotrapezoid Arthritis 725
Akio Iida and Shohei Omokawa

82 Arthroscopic-Assisted Pyrocarbon Interposition Arthroplasty for Scapho-Trapezium-Trapezoid Joint Arthritis 733
Christophe Mathoulin and Margareta Arianni

Part XVI Wrist: Pisotriquetral Arthroscopy

83 Arthroscopy of the Pisotriquetral Joint: An Overview 741
Eugene T. Ek and Richard P. Jamieson

84 Pisotriquetral Arthroscopy: Access, Evaluation, and Resection 747
Deepak N. Bhatia

Part XVII Wrist: Distal Radioulnar Joint

85 Surgical Anatomy of the Distal Radioulnar Joint 757
Parham Daneshvar and Ruby Grewal

86 DRUJ Arthroscopy: Portals and Arthroscopic Anatomy 767
M. Esplugas, A. Scott-Tennent, A. Lluch, and M. Llusá-Pérez

87 Arthroscopic Technique of Wafer Resection 779
Riccardo Luchetti, Marcovici Lucian Lior, and Roberto Cozzolino

Part XVIII Wrist: Triangular Fibrocartilage Complex

88 Arthroscopic Evaluation, Classification and Techniques for TFCC Tears 801
Richard S. Page, Janina Henze, and Kevin Eng

89 Arthroscopic Debridement of Triangular Fibrocartilage Complex Tears 811
Richard S. Page, Janina Henze, and Kevin Eng

90 Arthroscopic TFCC Repair: Inside out Technique 817
Margaret Woon Man Fok, Chris Yuk Kwan Tang, and Boris Kwok Keung Fung

91 Ligament-Specific Transosseous Foveal Repair of TFCC 823
Bo Liu and Margareta Arianni

92 Arthroscopic-Assisted TFCC Reconstruction with Tendon Graft for Chronic DRUJ Instability 829
Michael Chu-kay Mak, Wing-lim Tse, and Pak-cheong Ho

Part XIX Wrist: Fractures and Dislocations

93 Vascular Anatomy of the Scaphoid and Implications in Surgery 845
Mohamed Morsy and Steven L. Moran

94 Arthroscopic Fixation of Scaphoid Fractures Using a "Scaphoid Portal" 855
Deepak N. Bhatia

95 Arthroscopic Management of Scaphoid Fractures and Nonunions 865
Clara Wong and Pak-cheong Ho

96 Arthroscopic Replacement of Proximal Pole Scaphoid Fracture 887
Mathilde Gras and Christophe Mathoulin

97 Minimally Invasive Fixation of Ultra-Small Proximal Pole Scaphoid Fractures 891
Eugene T. Ek and Kemble K. Wang

98 Proximal Hamate Autograft for Scaphoid Fractures: Surgical Anatomy and Technique 899
Spencer B. Chambers and Nina Suh

99 Arthroscopic Management of Acute Perilunate Dislocations . . . 907
Bo Liu and Feiran Wu

100 Arthroscopic Management of Chronic Perilunate Dislocations 917
Deepak N. Bhatia

101 Arthroscopic Management of Irreducible Volar Dislocation of the Distal Radioulnar Joint 925
Deepak N. Bhatia

102 Arthroscopic Management of Distal Radius Fractures 935
Margaret Woon Man Fok, Christian Xinshuo Fang, and Frankie Ka Li Leung

103 Minimally Invasive Plate Fixation for Distal Radius Fractures . . . 943
Paul Max Jarrett

Part XX Wrist: The Stiff Wrist

104 Arthroscopic Arthrolysis of the Wrist 953
Gregory I. Bain, Karthikraj Kuberakani, Riccardo Luchetti, and Andrea Atzei

105 Arthroscopic Management of Kienbock's Disease 963
Simon MacLean and Gregory I. Bain

106 Arthroscopic Limited Wrist Fusion 975
Michael Chu-kay Mak and Pak-cheong Ho

107 Arthroscopic Transplantation of Osteochondral Autograft for Treatment of Cartilage Defects in the Wrist 989
Pak-cheong Ho

108 Arthroscopic Full Wrist Fusion 1005
Tendai Mwaturura and Gregory I. Bain

Part XXI Wrist: Miscellaneous

109 Surgical Anatomy and Management of Intersection Syndrome . . 1015
Gregory Hoy and Simon Hoy

110 Arthroscopic Decompression of Intraosseous Cysts of the Lunate 1019
Deepak N. Bhatia and Gregory I. Bain

111 Arthroscopic Bone Graft for Lunate Ganglion 1025
Lorenzo Merlini and Christophe Mathoulin

112 Arthroscopic Excision of Dorsal and Volar Ganglion Cysts . . . 1031
Mireia Esplugas, Alex Lluch, Fabiana Necci, and Manuel Llusa Pérez

113 Ulnar Styloid Enthesopathy and Extensor Carpi Ulnaris Instability: Styloidectomy and Groove-Plasty 1041
Gregory Hoy and Timothy Wood

114 Arthrosopic Ulnar Styloidectomy for Ulnar Styloid Impaction Syndrome 1047
Gregory I. Bain and Kevin Eng

Part XXII Hand Arthroscopy: Basic Science

115 Portals in Hand Arthroscopy 1055
Deepak N. Bhatia

Part XXIII Carpometacarpal Arthroscopy

116 Arthroscopic Partial Trapeziectomy for Trapeziometacarpal Arthritis 1063
Deepak N. Bhatia

117 Arthroscopic Complete Trapeziectomy and Suspension Arthroplasty: "Three-Steps Arthroscopic Trapeziectomy Technique" 1073
F. Corella, M. Ocampos, R. Laredo, J. Tabuenca, M. Carnicer, and R. Larrainzar-Garijo

118 Arthroscopic Treatment of Basal Joint Fractures 1093
Didier Fontès

119 Arthroscopic Debridement and Metacarpal Base Osteotomy for Trapeziometacarpal Joint Osteoarthritis 1101
Allan Wang

Part XXIV Metacarpophalangeal (MCP), Proximal Interphalangeal (PIP), and Distal Interphalangeal (DIP) Joint Arthroscopy

120 Metacarpophalangeal Joint Arthroscopy: Portals, Anatomy, and Technique 1109
Deepak N. Bhatia

121 Arthroscopic Management of Metacarpophalangeal Articular Fractures 1117
Alejandro Badia

122 Arthroscopic Fixation of Metacarpal Head Fractures 1127
Deepak N. Bhatia

123 Arthroscopy of Proximal and Distal Interphalangeal Joints . . 1135
Isato Sekiya, Hideki Okamoto, and Masaaki Kobayashi

Part XXV Wrist and Hand Endoscopy

124 Endoscopic Release of De Quervain's Tenosynovitis 1145
Michael J. Fitzmaurice

125 Endoscopic Superficial Radial Nerve Decompression 1149
Paul Max Jarrett

126 Endoscopic Carpal Tunnel Release (Supraretinacular Technique) 1155
Michael J. Fitzmaurice

127 Endoscopic-Assisted Tendon Transfer for Extensor Pollicis Longus Rupture 1159
Paul Max Jarrett

128 Endoscopic Trigger Finger Release 1165
Michael J. Fitzmaurice

129 Thenar Endoscopy: Endoscopic Excision of a Thenar Ganglion Cyst 1169
Deepak N. Bhatia

130 Osteoscopy for Benign Tumour Surgery in the Hand 1175
Paul Max Jarrett

Part XXVI The Future

131 Developing and Innovating Newer Techniques in Elbow Surgery 1185
Deepak N. Bhatia, Gregory I. Bain, and Felix H. Savoie

132 The Future of Elbow, Wrist, and Hand Arthroscopy 1189
Benjamin R. Graves, Deepak N. Bhatia, Gregory I. Bain, and Gary G. Poehling

Part I

History

1 The Early Development of Arthroscopy

Andrew Baker, Terry L. Whipple, Gary G. Poehling, and Gregory I. Bain

1.1 Introduction

Arthroscopy as a technique has existed for a little over 100 years, initially attempted by many doctors around the world including Severin Nordentoft (Denmark), Kenji Takagi (Japan), Eugen Bircher (Switzerland), and Philip Kreuscher (USA). These early proponents of arthroscopy used scopes designed for other body cavities such as cystoscopes. It was Takagi and his protégé Masaki Watanabe (Japan) who developed the first scopes specifically designed for arthroscopy. They progressively improved their designs over the first half of the twentieth century, resulting in small, robust scopes that could be utilized for therapeutic purposes across joints of all sizes.

1.2 The Primitive Phase

The origins of modern endoscopy lie at the start of the nineteenth century in Germany. Philipp Bozzini developed a device he termed the Lichtleiter (Fig. 1.1) in 1806 [2]. It utilized a beeswax candle as a light source, and he used it to examine the nasopharynx, rectum, and vagina. Other illumination methods included the use of glowworms in 1826 by Pierre Salomon Ségalas, and alcohol and turpentine spirit lamps in 1853 by Desormeaux [1]. The candles and lamps were dangerous and uncomfortably hot and the fumes engulfed the patient. The development of the "Bruck diaphanoscope" utilizing an electric incandescent globe was clearly a significant advance (Fig. 1.2). The initial versions were battery powered and water cooled; however their naming as "fire and water contraptions" hints at the dangers of their design.

Arthroscopy was a relatively late application of endoscopic technology given its emergence in the early twentieth century. By this stage, proctoscopes, laparoscopes, and cystoscopes were all in clinical use [3].

A. Baker
Faculty of Health and Medical Sciences, The University of Adelaide, Adelaide, SA, Australia
e-mail: andrew@andrewmbaker.com

T. L. Whipple
Hillelson-Whipple Clinic, Richmond, VA, USA

University of Virginia, Charlottesville, VA, USA

Virginia Commonwealth University, Richmond, VA, USA

Orthopaedic Research of Virginia, Richmond, VA, USA

G. G. Poehling
Department of Orthopaedic Surgery, Wake Forest School of Medicine, Winston-Salem, NC, USA
e-mail: poehling@wakehealth.edu

G. I. Bain (✉)
Department of Orthopaedics and Trauma Surgery, Flinders University and Flinders Medical Centre, Adelaide, SA, Australia
e-mail: admin@gregbain.com.au; greg@gregbain.com.au

© ISAKOS 2022
D. N. Bhatia et al. (eds.), *Arthroscopy and Endoscopy of the Elbow, Wrist and Hand*,
https://doi.org/10.1007/978-3-030-79423-1_1

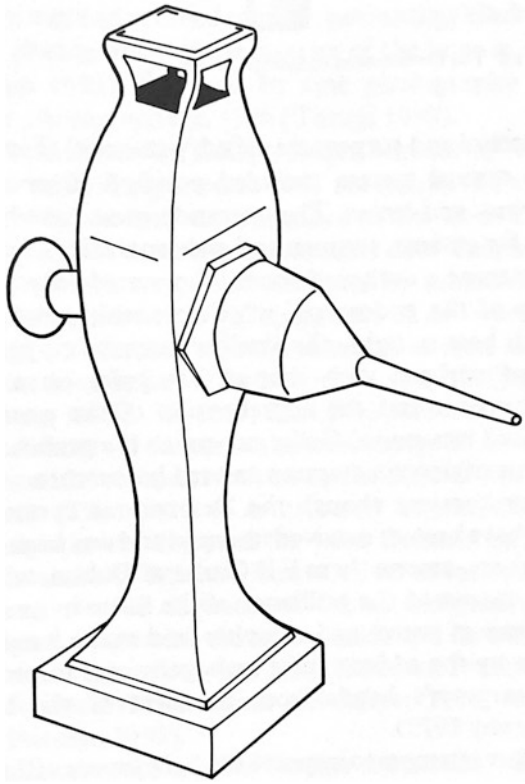

Fig. 1.1 Bozzini's original schematics for his primitive endoscope from 1806, lit by beeswax candle. (Reprinted from Arthroscopic surgery of the knee, 2nd Edition, Dandy DJ, Development of arthroscopy and arthroscopic surgery, p. 1, Copyright 1981, with permissions from Elsevier [1])

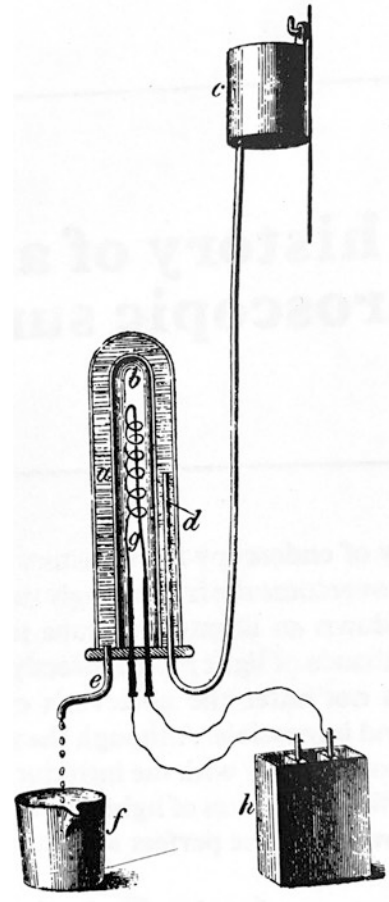

Fig. 1.2 The Bruck diaphanoscope, also termed the "fire and water contraption," utilized a water-cooled incandescent globe for illumination. (Reprinted from Arthroscopic surgery of the knee, 2nd Edition, Dandy DJ, Development of arthroscopy and arthroscopic surgery, p. 2, Copyright 1981, with permissions from Elsevier [1])

1.3 Early Development

Japan was the epicenter of arthroscopy technological advancement in the first half of the twentieth century. Takagi (Fig. 1.3) performed his first arthroscopy on a cadaveric knee joint in 1918, using a 7.3 mm Charrier No. 22 cystoscope [5]. Clinical use came within 2 years, as Takagi made use of a cystoscope to diagnose tuberculosis of the knee in patients (Fig. 1.4) [4]. Others followed shortly after. Eugen Bircher (Switzerland) (Fig. 1.5) published the first clinical arthroscopy report in 1921 [6], describing a procedure that utilized a Jacobaeus laparoscope and oxygen dilatation (Fig. 1.6). Philip Kreuscher (USA) described an early diagnostic application of arthroscopy in 1925 when he described arthroscopic meniscal injury assessment [7].

Takagi's work was predated by that of a Danish surgeon, Severin Nordentoft. In 1912, Nordentoft delivered a presentation at a meeting in Germany outlining the use of a 5 mm device to examine the knee joint [8]. He called this device an arthroscope, and thus the field of arthroscopy was born!

Robert Jackson (USA) was instrumental in bringing arthroscopy to North America [9]. In 1964, he undertook a fellowship in Japan and sought out Watanabe to learn more about the new

Fig. 1.3 Kenji Takagi (Japan), a pioneer of arthroscopy. (Reprinted from Atlas of Arthroscopy, 3rd edition, Watanabe M, Takeda S, Ikeuchi H, Preface, Copyright 1979, with permission from Springer [4])

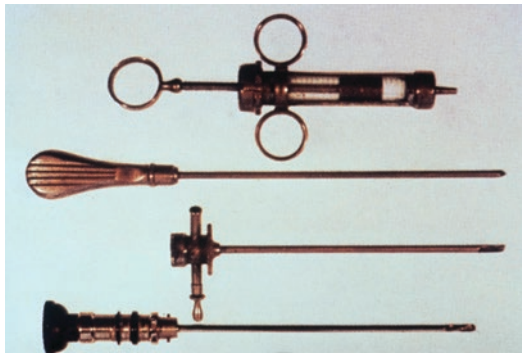

Fig. 1.4 Kenji Takagi's No. 1 Arthroscope from 1931, 3.5 mm diameter. (Reprinted from Atlas of Arthroscopy, 3rd edition, Watanabe M, Takeda S, Ikeuchi H, History of Arthroscopy, p. 2, Copyright 1979, with permission from Springer [4])

Fig. 1.5 Eugen Bircher (Switzerland) published the first clinical arthroscopy report in 1921, performing the procedure with a laparoscope. (Reprinted from Atlas of Arthroscopy, 3rd edition, Watanabe et al., History of Arthroscopy, p. 3, Copyright 1979, with permission from Springer [4])

Fig. 1.6 Eugen Bircher performing knee arthroscopy in the 1920s. (Reprinted from The Journal of Arthroscopic & Related Surgery, Vol 19, no. 7, Kieser CW, Jackson RW, Eugen Bircher (1882–1956) the first knee surgeon to use diagnostic arthroscopy, p. 773, Copyright 2003, with permission from Elsevier)

technique of arthroscopy. Ikeuchi, one of Watanabe's assistants, had spent time in the USA, and became a translator for Jackson and Watanabe. After the completion of his fellowship in 1965, Jackson took a Watanabe No. 21 arthroscope back to Toronto General Hospital. Jackson noted that he was a skeptic at first, but he soon realized the "tremendous value of the technique and became a convert" [9] (Fig. 1.7).

The knee joint was the primary focus of early proponents of arthroscopy. However, Michael Burman (USA) (Fig. 1.8) published his attempts at arthroscopy of other joints in 1931 [10]. Burman examined more than 90 joints, including knees (40), hips (20), shoulders (25), wrists (4), and 2 or 3 ankle or elbow joints. This early period was marked by experiments to determine the most effective methods of joint distention. Combinations of various gases, boric acid solutions, distilled water, and saline were trialed. Traction was also utilized, and Burman noted that this was of particular benefit in the wrist, increasing the joint space by "as much as one-eighth to one-quarter of an inch."

1.4 The Beginnings of Therapeutic Arthroscopy

The early exponents of arthroscopy were limited to diagnostic uses owing to the poor ergonomics of the viewing ports, their fragile incandescent bulbs, and the large diameter of the scopes. The light bulbs in particular were a real liability on early models because their offset position at the tip of the scope left them vulnerable to separation from the rest of the scope [11]. Despite the frustrations of damaged scopes, this actually prompted the advent of therapeutic arthroscopy! Ikeuchi reported this problem to his mentor Watanabe (Fig. 1.9), who suggested the use of a second arthroscope to find the light bulb within

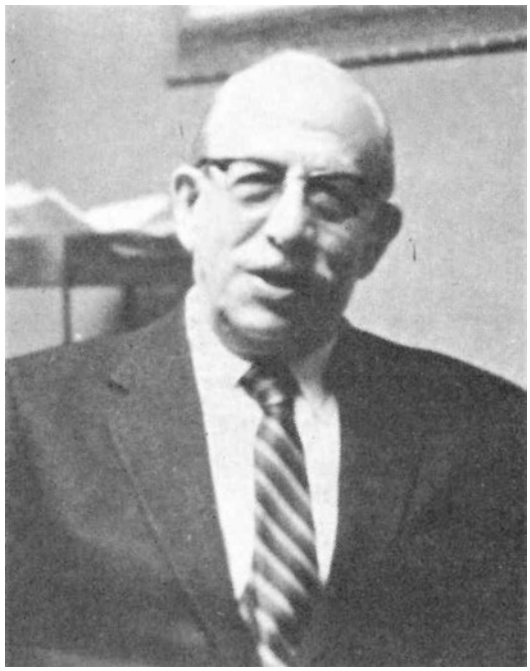

Fig. 1.7 Michael Burman (USA) was one of the first surgeons to experiment with the use of arthroscopy in joints other than the knee, examining hips, shoulders, wrists, ankles, and elbows in the early 1930s. (Reprinted from Atlas of Arthroscopy, 3rd edition, Watanabe et al., History of Arthroscopy, p. 3, Copyright 1979, with permission from Springer [4])

Fig. 1.8 Masaki Watanabe made many contributions to the technical development of the arthroscope. He was the first to develop standardized methods of arthroscopy and published the first Atlas of Arthroscopy [5]. (Courtesy Gary G. Poehling)

the joint, and then use of a second portal to fetch the bulb using a pair of forceps. The next time a bulb broke, this technique was used, and thus therapeutic arthroscopy was born!

Ikeuchi and Watanabe were inspired to consider therapeutic possibilities for arthroscopy, and began to experiment with a number of new procedures. Watanabe undertook a punch biopsy in 1950, excised a giant cell tumor 5 years later, and removed a loose body in 1961 [11]. These procedures were overshadowed by his next step forward, an arthroscopic partial meniscectomy Watanabe performed on a young basketball player in 1962 [12].

Watanabe continued Takagi's early work, developing a number of prototypes before No. 21 (Fig. 1.10) became the first production arthroscope in 1959. This design offered both side- and direct-viewing telescopes, with a 6 mm sheath around the scope and the tungsten bulb carrier which was offset from the tip of the scope [13, 14]. The optics of this scope were a significant step forward, providing a wide field of vision (100° in air and 88° in water), and a focal length from 1 mm to infinity. Watanabe described the view as like "a human eye has been placed there."

At this stage, it was principally rheumatologists that used arthroscopy. In the mid-1960s, a number of rheumatologists in England and Mexico were the only known doctors performing arthroscopy outside Japan [9]. However even in Japan, orthopedic surgeons did not have a high regard for arthroscopy and it was certainly not in routine use. Into the 1970s, arthroscopy was developed more widely but continued to be largely restricted to the knee. By the 1980s, arthroscopy in other joints was becoming more widespread, and included the wrist [15].

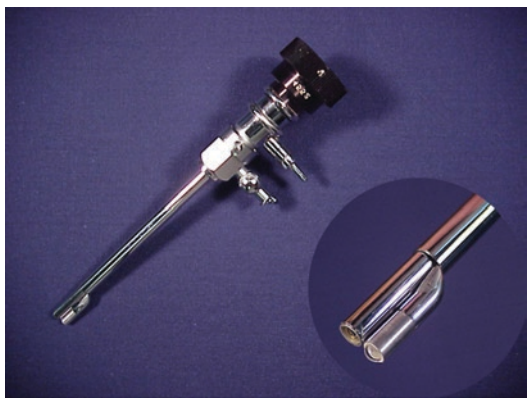

Fig. 1.9 The Watanabe No. 21 was the first production arthroscope, and had optics that brought its field of view close to that of the human eye. (Courtesy Gary G. Poehling)

1.5 A Period of Refinement

Early scopes precluded the use of arthroscopy in small joints, because they were large in diameter and prone to breakage. A number of advances in the early 1970s were instrumental in allowing the development of smaller diameter arthroscopes [13]. The rod lens was a significant development by Hopkins (Fig. 1.11), which replaced the telescope-based lens design of early endoscopes [1]. The early scopes had glass lenses separated by air, while the rod lens was thicker and more robust. The rod lens was able to transmit more light at a smaller diameter, crucial for the miniaturization of arthroscopes. The first of these small arthroscopes to be developed by Watanabe was the 2.7 mm No. 11, which was small enough for joints such as the wrist; however it did not focus particularly well. Watanabe also made use of a Japanese innovation from the Nippon Sheet Glass Company who produced a fiber-optic lighting system called Selfoc. This system enabled clear focus and a wide-viewing angle for these smaller scopes [16].

The Selfoc lighting system was included in the 1970 1.7 mm No. 24 arthroscope, resulting in a scope with clear focus and a wide-viewing angle of 55–70° despite its small diameter. This scope was small enough for use in the wrist, as Watanabe reported the examination of 21 wrists with the No. 24 by 1972. Through the rest of the 1970s, the No. 24 arthroscope was developed further with fore-oblique and direct-viewing designs (Fig. 1.12) and four diameters from 3.2 mm down to 1.7 mm [13]. The No. 24 scope was marketed as the Selfoc scope in deference to the underlying technological breakthrough, while in the USA Dyonics used the name Needlescope.

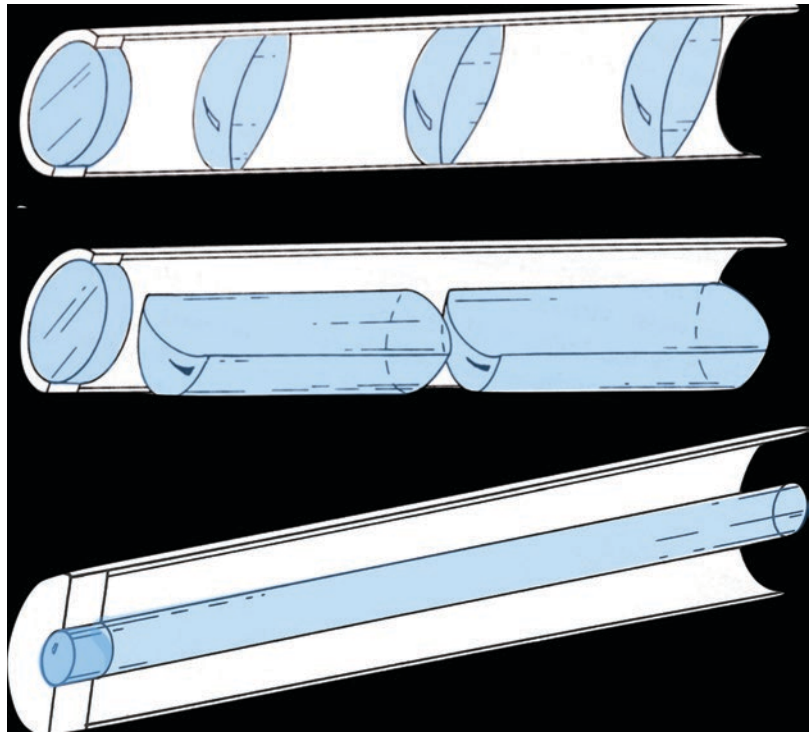

Fig. 1.10 Early lenses were based on telescopes, with convex lens separated by air. The development of the rod lens allowed more light to be transmitted through a thinner diameter, enabling miniaturization of scopes for use in small joints. (Adapted from Arthroscopic surgery: Principles and practice, 3rd edition, Johnson LL, p. 1481, Copyright 1986, with permission from The C.V. Mosby Company)

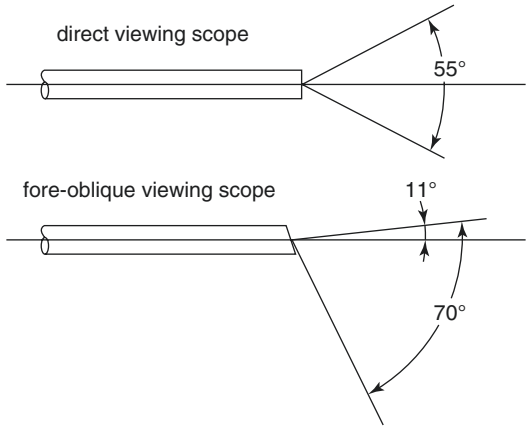

Fig. 1.11 A diagram from the third edition of the Atlas of Arthroscopy showing the viewing arc of the direct and fore-oblique options of the No. 24 arthroscope. (Reprinted from Atlas of Arthroscopy, 3rd edition, Watanabe M, Takeda S, Ikeuchi H, Present State of Arthroscopy, p. 29, Copyright 1979, with permission from Springer [4])

The No. 24 scope had a rod lens, which was remarkably only 1 mm thick despite being 134 mm long. While these rod lenses allowed excellent light transmission, there were two issues. Such a small example of the rod lens was very fragile and thus frequently broke, and further, the image relayed to the user was inverted. A second technological innovation was required: the Amici prism. The Amici prism is two prisms in series which corrects the inverted image (Fig. 1.13) [1].

It was not only the scopes that needed to be miniaturized to enable small joint arthroscopy. The early camera systems were large and in combination with the small, fragile scopes only made failure all the more frequent (Fig. 1.14). Camera technology rapidly improved, allowing them to shrink from the size of a bread box to the size of a fist. These smaller chip cameras made complex

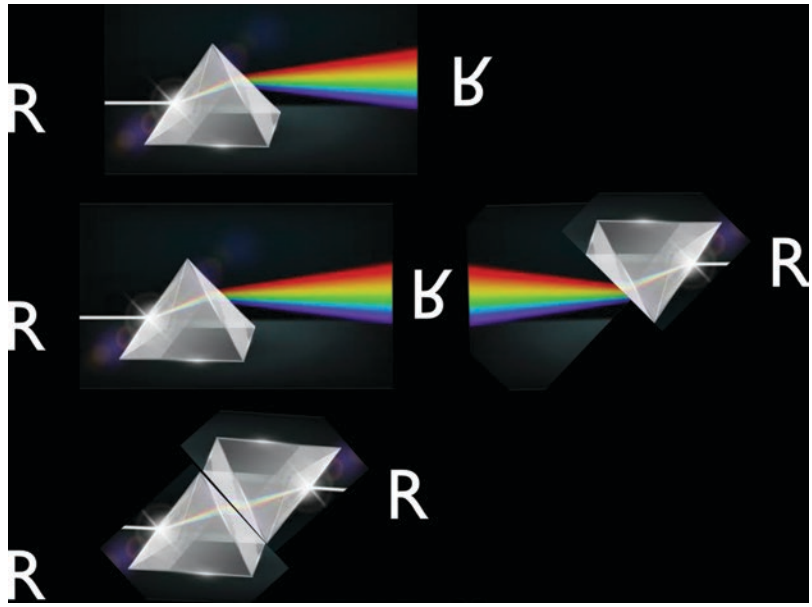

Fig. 1.12 The Amici prism was a key development, as it allowed the image transmitted by the lens to be oriented correctly. The two prisms in series flipped the image and corrected the inverted image from early scopes. (Copyright Gregory I. Bain)

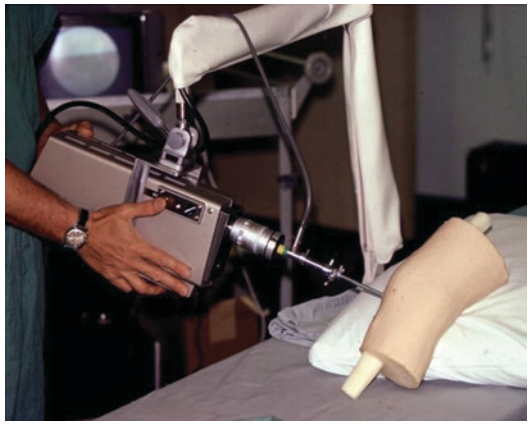

Fig. 1.13 An early camera, shown in use with a knee arthroscopy teaching model (1975). (Courtesy Gary G. Poehling)

therapeutic procedures possible in small joints as they allowed unencumbered manipulation of the arthroscope within the joint (Fig. 1.15) [18]. John McGinty (USA) placed a video camera onto the arthroscope and connected it to the television. This allowed the surgeon, assistant, and theatre staff to observe the procedure. The most recent arthroscope designs such as the Arthrex Nanoscope place the camera within the tip of the scope, further improving the maneuverability of the scope and reducing the risk of damage.

One final but particularly important area of development was the sterilization of scopes. The early scopes were soaked in a chemical sterilizer; however this became troublesome as electronic lighting and camera systems became embedded in the scopes. Sterilized plastic sleeves were developed to protect the camera/lighting systems. Another sterilization technique described was formalin gas chambers, which Yung-Cheng Chen (Japan) used to sterilize his scopes [19]. Modern scopes are capable of withstanding the pressure and heat associated with autoclave sterilization, and single-use arthroscopes are even in production.

These incremental improvements to the underlying technology brought arthroscopy to a point at which small joint arthroscopy was not just technically feasible, but practical and clinically useful. Without Takagi and Watanabe's decades-long dedication to perfecting the arthroscope, it is unlikely that arthroscopy as a clinical tool would be in the same place it is now.

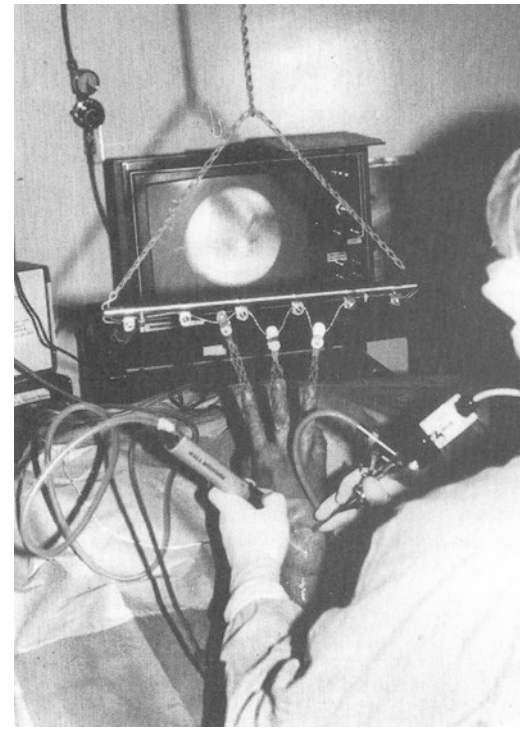

Fig. 1.14 A smaller "chip" camera demonstrated by James Roth. (Copyright James Roth. Reprinted from The Wrist and its Disorders, 3rd edition, Roth JH, Whipple TL. Wrist arthroscopy, p. 108–28, Copyright 1988, with permission from W. B. Saunders Company)

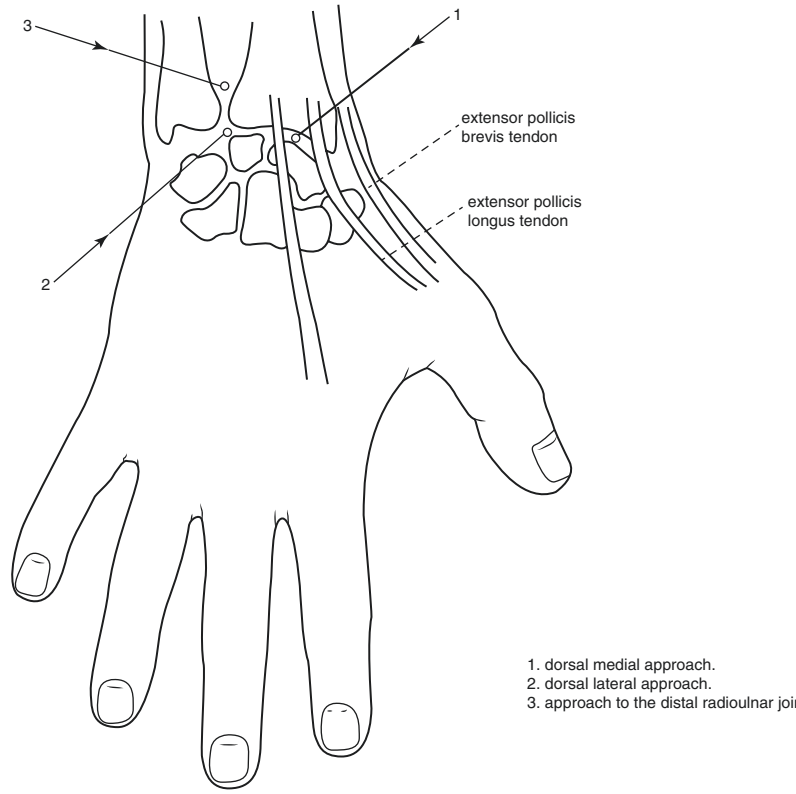

Fig. 1.15 The first edition of Watanabe's Atlas of Arthroscopy featured hand-painted depictions of the view down the arthroscope, as Watanabe believed that the photos were not of adequate quality [17]. In later editions, Watanabe included photos taken through the arthroscope. (Copyright Masaki Watanabe)

1.6 Timeline

1912 Severin Nordentoft (Denmark) reports arthroscopic examination of the knee joint [8].

1918 Kenji Takagi (Japan) performs arthroscopy on a TB knee using a 7.3 mm cystoscope [5].

1921 Eugen Bircher (Switzerland) publishes the first clinical arthroscopy report [6].

1931 Michael Burman (USA) publishes the first report of wrist arthroscopy [10] (Fig. 1.7).

1932 Takagi takes first black-and-white photos via arthroscopy [4].

1936 Takagi takes first color photographs and cinematographs (16 mm black and white) [4].

1955 Masaki Watanabe develops the concept of triangulation [3].

1957 Masaki Watanabe publishes Atlas of Arthroscopy (first Edition) (Fig. 1.16) [17].

1959 Masaki Watanabe (Japan) releases No. 21, the first production model arthroscope [13].

1962 Masaki Watanabe (Japan) performs first arthroscopic meniscectomy on a 17-year-old male [12].

1965 Robert Jackson (Canada) introduces arthroscopy to Toronto General Hospital [9].

1968 Robert Jackson presents the first instructional course on arthroscopy for AAOS.

1970 Masaki Watanabe (Japan) releases 1.9 mm No. 24 arthroscope, for small joints [13].

Acknowledgements Kimberley Bryant for assistance in preparation of manuscript.

- Christophe Mathoulin
- Max Haerle
- Riccardo Luchetti
- PC Ho
- Jan-Ragnar Haugstvedt
- Guillaume Herzberg
- Graham King
- Dan Nagle
- Toshi Nakamura
- Lee Osterman
- David Slutsky
- Steven Viegas
- Buddy Savoie
- Luigi Pederzini

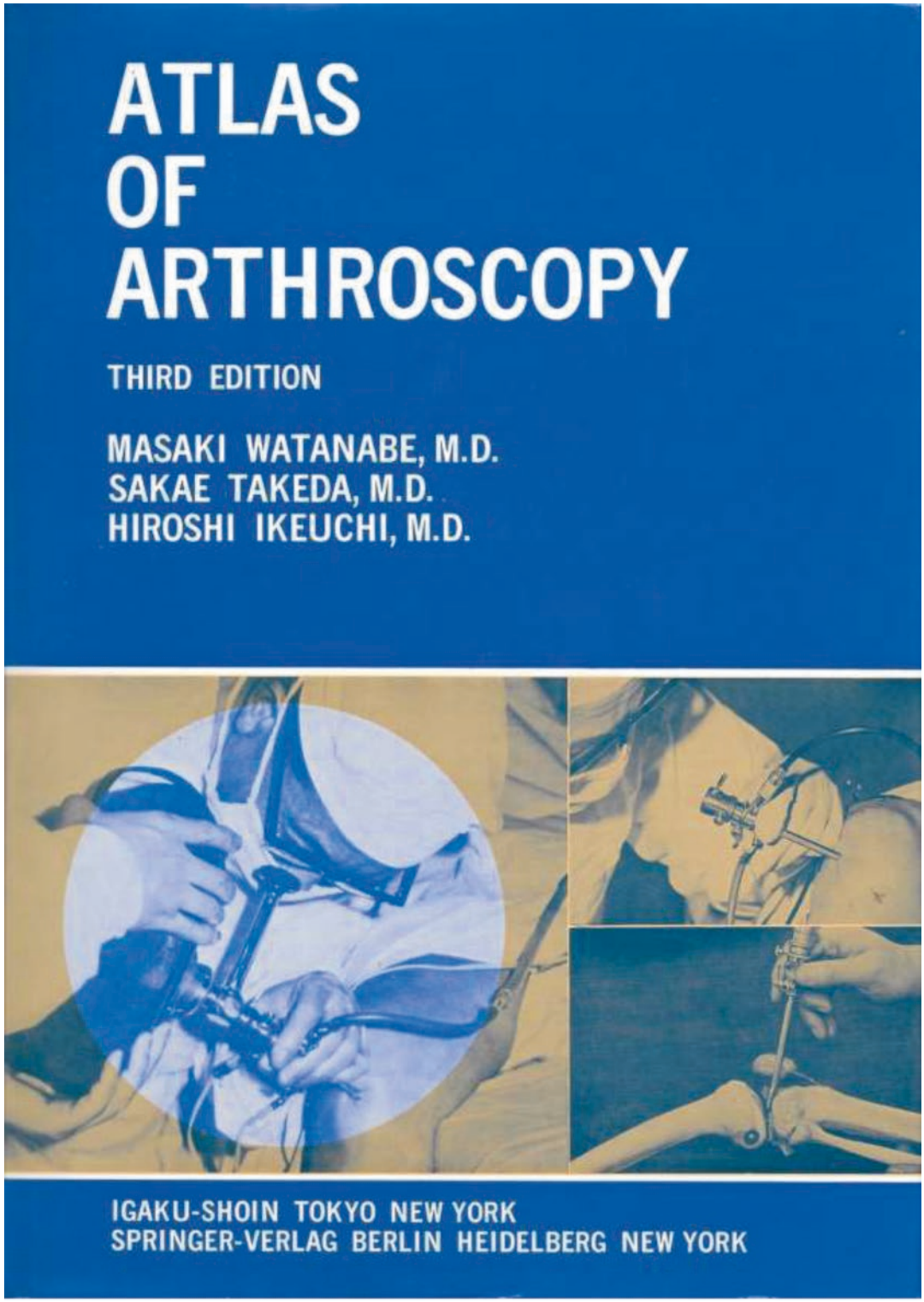

Fig. 1.16 The "Atlas of Arthroscopy" was the first text book of arthroscopy. The image is of the front cover of the 3rd edition

References

1. Dandy DJ. Arthroscopic surgery of the knee. 2nd ed. New York: Churchill Livingstone; 1981.
2. Bush RB, Leonhardt H, Bush IM, Landes RR. Dr. Bozzini's lichtleiter: a translation of his original article (1806). Urology. 1974;3(1):119–23.
3. Goebel L, Madry H. History of arthroscopy. In: Randelli P, Dejour D, van Dijk CN, Denti M, Seil R, editors. Arthroscopy: basic to advanced. Berlin Heidelberg: Springer; 2016. p. 3–12.
4. Watanabe M, Takeda S, Ikeuchi H. Atlas of arthroscopy. 3rd ed. Tokyo: Igaku-Shoin; 1979. p. 1–11.
5. Watanabe M. Memories of the early days of arthroscopy. Arthroscopy. 1986;2(4):209–14.
6. Bircher E. Die arthroendoskopie [Arthroendoscopy]. Zentralbl Chir 1921;48:1460–1.
7. Kreuscher PH. Semilunar cartilage disease: a plea for the early recognition by means of the arthroscope. Illinois Med J. 1925;47:290–2.
8. Kieser CW, Jackson RW. Severin Nordentoft: the first arthroscopist. Arthroscopy. 2001;17(5):532–5.
9. Jackson RW. Memories of the early days of arthroscopy: 1965-1975. The formative years. Arthroscopy. 1987;3(1):1–3.
10. Burman MS. Arthroscopy or the direct visualization of joints: an experimental cadaver study. J Bone Joint Surg. 1931;13(4):669–95.
11. DeMaio M. Giants of orthopaedic surgery: Masaki Watanabe MD. Clin Orthop Relat Res. 2013;471(8):2443–8.
12. Ikeuchi H. The early days of arthroscopic surgery in Japan. Arthroscopy. 1988;4(3):222–5.
13. Watanabe M. Present state of arthroscopy. Int Orthop. 1978;2(2):101–8.
14. Jackson RW. Diagnostic uses of arthroscopy. In: McKibbin B. Recent advances in orthopaedics. No. 2. Edinburgh: Churchill Livingstone. 1975. p. 218–234.
15. McGinty JB, Caspari RB, Jackson RW, Poehling GG. Operative arthroscopy. Philadelphia: Lippincott-Raven Publishers; 1996.
16. Whipple TL. The basics of wrist arthroscopy. In: Whipple TL, editor. Arthroscopic surgery—the wrist. Philadelphia: J.B. Lippincott; 1992. p. 7–9.
17. Watanabe M. Atlas of arthroscopy. 1st ed. Igaku-Shoin: Tokyo; 1957.
18. Poehling GG. Instrumentation for small joints: the arthroscope. Arthroscopy. 1988;4(1):45–6.
19. Chen YC. Arthroscopy of the wrist and finger joints. Orthop Clin North Am. 1979;10:505–15.

History of Wrist Arthroscopy

2

Andrew Baker, Terry L. Whipple, Gary G. Poehling, and Gregory I. Bain

2.1 Introduction

The history of wrist arthroscopy is built on the foundations laid by the Japanese surgeons Kenji Takagi and Masaki Watanabe in the first half of the twentieth century, but truly began as improving technology allowed the miniaturization of lens and camera technology to fit into the wrist joint. Individuals such as Terry Whipple (USA), Gary G. Poehling (USA), and James Roth (Canada) took these new scopes and developed the basis for our modern practice of wrist arthroscopy.

A. Baker
Faculty of Health and Medical Sciences, The University of Adelaide, Adelaide, SA, Australia
e-mail: andrew@andrewmbaker.com

T. L. Whipple
Hillelson-Whipple Clinic, Richmond, VA, USA

University of Virginia, Charlottesville, VA, USA

Virginia Commonwealth University, Richmond, VA, USA

Orthopaedic Research of Virginia, Richmond, VA, USA

G. G. Poehling
Department of Orthopaedic Surgery, Wake Forest School of Medicine, Winston-Salem, NC, USA
e-mail: poehling@wakehealth.edu

G. I. Bain (✉)
Department of Orthopaedics and Trauma Surgery, Flinders University and Flinders Medical Centre, Adelaide, SA, Australia
e-mail: admin@gregbain.com.au

In the 1980s, the core principles of wrist arthroscopy including access portals and joint distraction were developed, before the therapeutic applications flourished in the 1990s and 2000s. The European Wrist Arthroscopy Society (EWAS), International Wrist Arthroscopy Society (IWAS), and the Asia Pacific Wrist Association (APWA) provided the professional networks for surgeons around the world to rapidly increase the scope of practice for wrist arthroscopy. They also supported workshops around the world, ensuring that more and more patients have benefited from these new techniques.

This chapter is based on the recollections and publications of influential surgeons from around the world including Takagi, Watanabe, Hiroshi Ikeuchi (Japan), Robert Jackson (Canada), and Christophe Mathoulin (France), and an interview Gregory I. Bain (Australia) conducted with Whipple and Poehling in October 2019. These sources provide an in-depth exploration of the global history of wrist arthroscopy's development from the early experiments to its modern role as a highly effective therapeutic tool.

2.2 Early Wrist Arthroscopy

The most detailed early descriptions of wrist arthroscopy came from Japan, with Watanabe and Yung-Cheng Chen (Japan) both publishing their early cases [1, 2]. Both surgeons used the

© ISAKOS 2022

D. N. Bhatia et al. (eds.), *Arthroscopy and Endoscopy of the Elbow, Wrist and Hand*,
https://doi.org/10.1007/978-3-030-79423-1_2

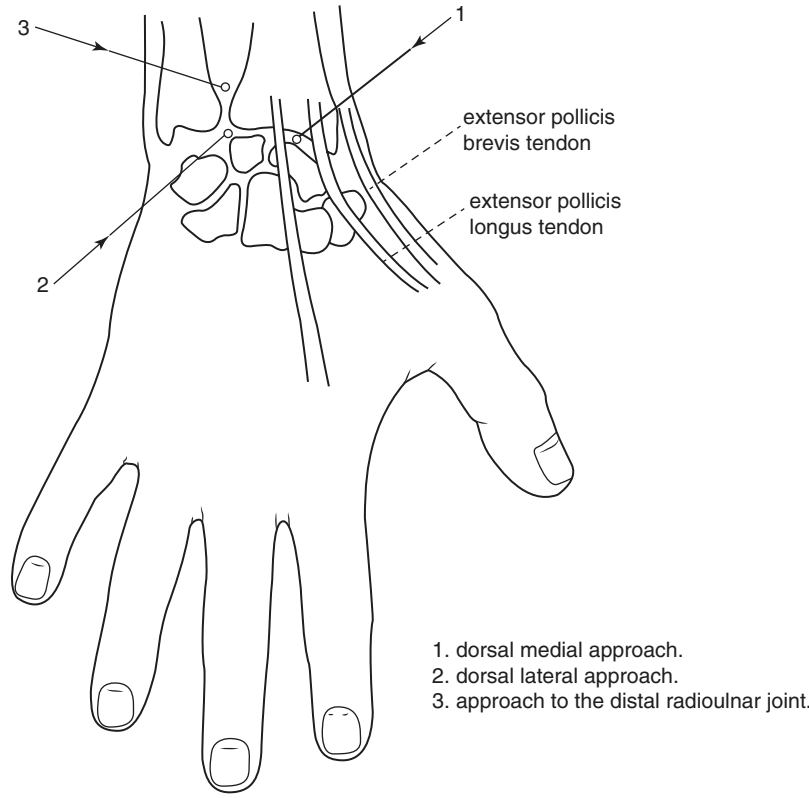

Fig. 2.1 Image of Watanabe's wrist arthroscopy portals from the third edition of Masaki Watanabe's book Atlas of Arthroscopy (1979). Copyright Masaki Watanabe. (Reprinted from Atlas of Arthroscopy, third edition, Watanabe M, Takeda S, Ikeuchi H, Arthroscopy of Joints other than Knee, p. 140, Copyright 1979, with permission from Springer [1])

No. 24 arthroscope, and similar portals. Watanabe's portals were on the dorsal aspect of the wrist on the ulnar side of the EPL tendon for access to the radiocarpal joint (Fig. 2.1). Chen used portals between the EPL and EDC and between EDC and EDM (Fig. 2.2), terming these the dorsoradial and dorsoulnar portals. Watanabe reported on 67 wrist arthroscopies including distal radioulnar joint visualization, as well as interphalangeal joint, thumb metacarpophalangeal joint, and carpometacarpal joint arthroscopies [1]. Chen performed over 90 small joint arthroscopies of various joints of the hand and acknowledged Watanabe's assistance [2].

Lanny Johnson (USA) was another surgeon who made early attempts at wrist arthroscopy. In 1981, he published a textbook covering arthroscopic techniques for a number of joints and included a chapter on wrist arthroscopy using a Needlescope arthroscope [3]. He attempted to access the wrist via the anatomic snuffbox (Fig. 2.3); however it is unclear how successful this was. This highlights the lack of standardization in technique during this early period of experimentation with wrist arthroscopy. Johnson also included the results of a 1978 survey of the American Academy of Orthopaedic Surgeons members which reported on the use of arthroscopy in various joints. While 50% of surveyed members had performed knee arthroscopy, only 6% had attempted arthroscopy in any other joints.

2.3 A Match Was Struck

The recollections of Terry Whipple and Gary G. Poehling provide a unique insight into the early development of wrist arthroscopy in the United States. Captain Poehling was posted to Japan as a military medical officer in 1972 (Fig. 2.4). Before his departure, his department director Leonard Goldner (Fig. 2.5) asked for "a Watanabe No. 26, please," which Poehling obliging purchased from Watanabe (Fig. 2.6). Upon his return from Japan,

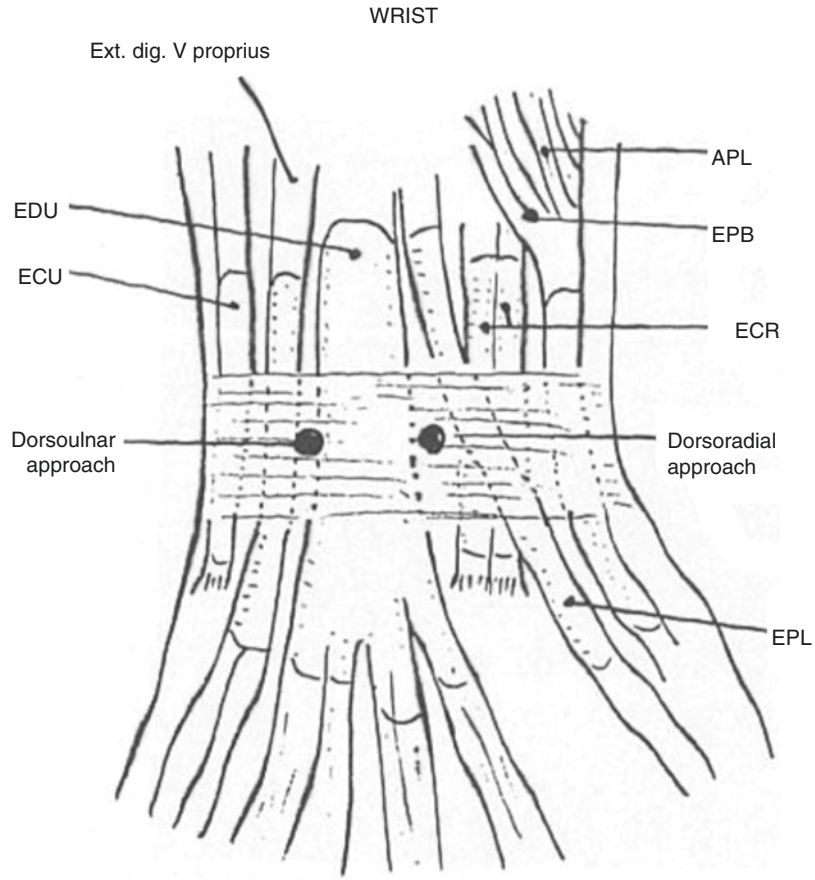

Fig. 2.2 Chen (Japan) published a series of clinical and cadaveric small joint arthroscopy in 1979, utilizing similar portals to Watanabe [2]. He acknowledged learning the techniques from Watanabe. *APL* abductor pollicis longus, *ECR* extensor carpi radialis longus and brevis, *ECU* extensor carpi ulnaris, *EDC* extensor digitorum communis, *EPB* extensor pollicis brevis, *EPL* extensor pollicis longus. (Reprinted from Arthroscopy of the Wrist and Finger Joints, Vol 10, Chen YC, Orthopedics Clinic of North America, p. 723–33, Copyright 1979 with permission from W. B. Saunders Company)

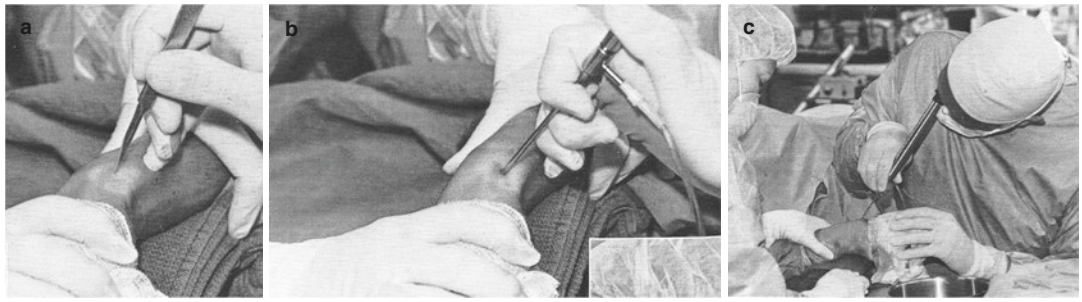

Fig. 2.3 (**a**) Lanny Johnson published major textbooks on arthroscopy. He used a "laceration of the skin only, avoiding superficial branch of the radial nerve" to enter the radioulnar joint through the snuff box to assess the wrist. (**b**) Another image from Lanny Johnson's arthroscopy textbook, showing his technique to insert a Needlescope into the radioulnar joint. (Reproduced from Lanny Johnson). (**c**) Lanny Johnson using a Needlescope to view the distal radioulnar joint. (Reproduced from Lanny Johnson. Copyright Lanny Johnson. Reprinted from Arthroscopic surgery: Principles and practice, third edition, Johnson LL, p. 1481, Copyright 1986, with permission from The C.V. Mosby Company)

Fig. 2.4 Captain Gary G. Poehling during his Air Force service in Japan in 1970–1972. (Courtesy Gary G. Poehling)

Fig. 2.5 Leonard Goldner (USA) was an important mentor to Gary G. Poehling and Terry Whipple. On his return from service in Japan, Goldner appointed Poehling to be the Director of Arthroscopy. When Poehling left, Whipple was appointed to this position. (Courtesy Gary G. Poehling)

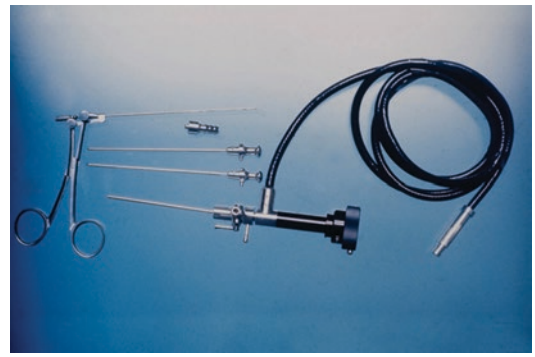

Fig. 2.6 A Watanabe No. 26 arthroscope, the same model Gary G. Poehling purchased and brought back to the United States in 1972. (Courtesy Gary G. Poehling)

Goldner appointed him Head of Arthroscopy despite only being a junior resident! Poehling only succeeded in completing half of his first case with the fragile new 1.9 mm scope, before it broke. Poehling passed on the arthroscopy role to Whipple in 1975, as he moved to Winston-Salem. Whipple was a first-year resident at the time.

Whipple had the good fortune to work for Frank Bassett (USA) (Fig. 2.7), a leading sports orthopedic surgeon, in 1976–1977 who gave him the opportunity to do arthroscopy on knees prior to open meniscectomy. On top of this clinical experience, Whipple also spent time further developing his arthroscopic techniques and anatomic knowledge on cadaveric knees, including triangulation [4]. While Bassett was accommodating, the broader acceptance of arthroscopy as a viable clinical tool faced significant opposition.

In 1985, Jack Powell (USA), a sports medicine fellow, was enlisted by Whipple to assist his research into safe techniques for wrist arthroscopy. The wrist is a particularly challenging and potentially dangerous joint to access arthroscopically owing to the close proximity of numerous nerves, tendons, and vessels. Through a series of cadaveric studies, Powell and Whipple were able to define safe wrist arthroscopy portals, including the radiocarpal, midcarpal, and distal radioulnar joints [5]. They named the portals based on the

Fig. 2.7 Frank Bassett (USA) was a sports orthopedic surgeon who allowed Terry Whipple to practice arthroscopic techniques in the knee prior to open procedures in 1976–1977. (Image courtesy of Dukes Athletics)

extensor compartments of the wrist (Fig. 2.8). Access to the joint also required a distraction technique, so Whipple developed the use of Chinese finger traps and the traction tower. The terminology and techniques they developed allow safe and reliable wrist arthroscopy, and are still in use today!

A chance meeting in May 1985 was key to the success of wrist arthroscopy in North America. Whipple (Fig. 2.9), Poehling, and James Roth (Fig. 2.10) had dinner together at the Winkler Hotel at the International Society of the Knee meeting in Salzburg, Austria (Fig. 2.11). Despite being a knee meeting, they realized that they were all interested in hand surgery and arthroscopy. Over dinner they formulated a plan to bring wrist arthroscopy to the surgeons of North America. They returned home with a three-part plan: Whipple developed an improved arthroscope and miniaturized surgical instruments and a teaching model (Fig. 2.12); Poehling organized a cadaveric laboratory course for North American hand surgeons; and Roth wrote a paper introducing the technique of wrist arthroscopy.

Poehling's course took place in 1986, in Winston-Salem, North Carolina, USA (Fig. 2.13). A central goal of Whipple, Poehling, and Roth's approach was to avoid the skepticism and obstruction that had impeded the introduction of knee arthroscopy to North America (Video 4). They brought their mentor James Urbaniak (USA) (Fig. 2.14) (President of the American Society for Surgery of the Hand (ASSH)) on board, who helped put together a list of eminent wrist surgeons. It was decided that active involvement of the most accomplished hand surgeons would ensure that they understood and accepted this new technique. Urbaniak personally invited 57 surgeons, of whom 47 attended. Ten were former presidents of the ASSH.

Whipple led the demonstrations during this first course, which included assessment of the triangular fibrocartilage. Bill Bowers (USA), a leader in anatomy and surgical techniques [6], was in attendance and asked "How do you know that the TFC is intact?" Whipple suggested that arthroscopy of the distal radioulnar joint could be used and proceeded to just that, not mentioning that he had in fact never attempted such a procedure before (Video 5)! Luckily for Whipple, it worked and the internal anatomy was clearly visible. Bowers told Whipple that he had learnt more about the anatomy of the wrist joint from one arthroscopic demonstration than he had from many years of cadaveric dissections.

As an adjunct to the workshop, Whipple produced a video presentation of arthroscopic techniques for the wrist. This video used cadaveric dissections to describe the portals, traction tower and finger traps, and diagnostic arthroscopy. Whipple also demonstrated a series of therapeutic procedures including TFC debridement, loose body removal, and synovectomy. These basic techniques would have been impressive on their own at the time, but Whipple then proceeded to describe fixation of scaphoid fractures with the Herbert-Whipple cannulated headless screw; reduction and fixation of distal radius fractures; and stabilization of scapholunate instability with

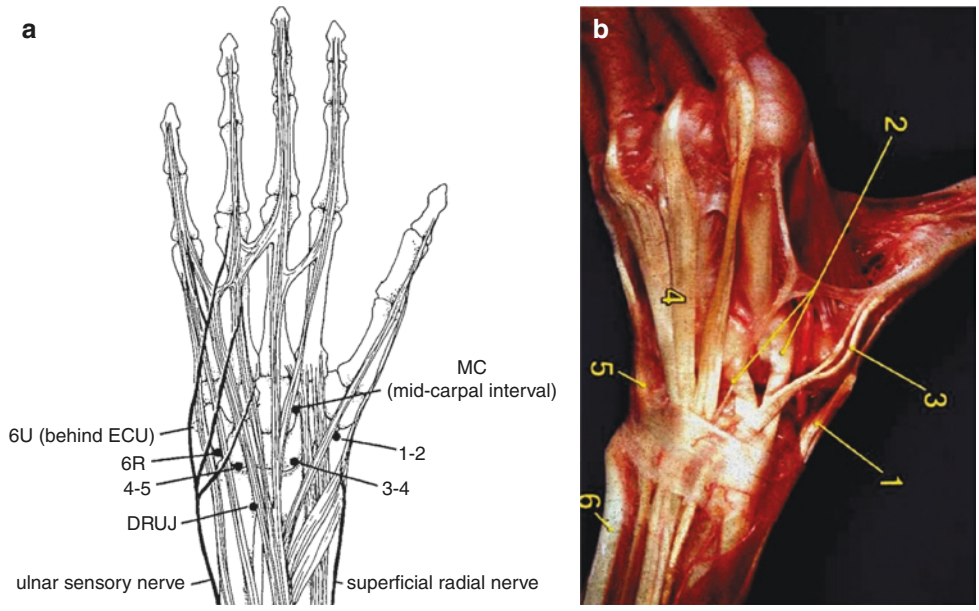

Fig. 2.8 (**a**) This diagram is from Whipple's 1986 paper on wrist arthroscopy techniques, showing the portals which are still utilized today [5]. (Courtesy Terry Whipple). (**b**) This dissection of the dorsal aspect of the wrist visualizes Whipple and Powell's wrist arthroscopy portals as they relate to the extensor compartments of the wrist. (Courtesy Terry Whipple). Each extensor compartment is numbered (1–6). *DRUJ* distal radioulnar joint, *ECU* extensor carpi ulnaris, *MC* midcarpal

Fig. 2.9 Terry Whipple performed cadaveric dissections to create the named extensor compartment portals we use today. He developed the traction tower and finger traps. These aspects allowed wrist arthroscopy to become safe and standardized. (Courtesy Terry Whipple)

Fig. 2.10 James Roth (Canada) operating with sports orthopedic surgeon Peter Fowler (right), who became Foundation President of ISAKOS. (Courtesy Graham King)

Kirschner wires (the arthrofibrosis technique)—all advanced techniques, in 1986! It could only be described as a master class, and is still relevant today.

Not all of the surgeons in attendance took up wrist arthroscopy, but more importantly they allowed and encouraged their junior colleagues to utilize new technique in their prac-

Fig. 2.11 Terry Whipple, Gary G. Poehling, and James Roth at the Winkler Hotel in Salzburg, Austria, during the 1985 International Knee Association meeting. All three were interested in hand and wrist surgery. They agreed upon a strategy to introduce wrist arthroscopy to the United States: Whipple would develop a teaching model, Poehling organized a course, and Roth wrote a paper. (Courtesy Gary G. Poehling)

tices (Fig. 2.15). The younger surgeons in attendance were inspired to join the rapidly expanding wrist arthroscopy community, and made their own contributions to the literature, including William Cooney (USA) [7], Lee Osterman (USA) (Fig. 2.16) [8–11], Andrew Palmer (USA) [12, 13], Steven Viegas (USA) [14–17] (Fig. 2.17), and Daniel Nagle (USA) (Fig. 2.18) [18, 19].

2.4 Broadening the Possibilities

While smaller scopes enabled wrist arthroscopy, it was initially limited to a diagnostic role, similarly to the early days of knee arthroscopy. Increasing experience with the technique and the production of smaller, stronger scopes allowed surgeons to utilize wrist arthroscopy for therapeutic purposes. Without miniaturization, therapeutic wrist arthroscopy would not have been possible [20]. Many surgeons have contributed new arthroscopic therapeutic techniques that have been utilized by surgeons around the world.

As wrist arthroscopy blossomed, it became clear that its efficacy should be compared to the gold standard for diagnosis at the time, arthrography. In 1986, Roth and Richard Haddad compared the two modalities for the diagnosis of ulnar wrist pain in an award-winning paper [21]. They found that arthroscopy was superior for the identification of triangular fibrocartilage (TFC) tears. Their paper helped wrist arthroscopy become the "gold standard for diagnosis" of ulnar sided wrist pain [22].

Roth continued to contribute to the field of wrist arthroscopy. In 1988, he wrote on his interest in further developing wrist arthroscopy to reduce the rate of arthrotomy, which was associated with poor prognosis for patients [23]. He believed that arthroscopy of the wrist could be similarly successful to knee, shoulder, and ankle arthroscopy. Roth also described a series of therapeutic wrist arthroscopy procedures in 1988 including central excision of unstable TFC tears, synovectomy, and loose body removal [24]. These advances were part of an exciting time for wrist arthroscopy, as complex problems such as ulnar wrist pain could now be readily diagnosed and treated with handheld instruments. Arthroscopic excision "-ectomy" procedures of the wrist including proximal row carpectomy were another of Roth's contributions to wrist arthroscopy [25].

Fig. 2.12 Whipple's teaching model allowed him to demonstrate techniques for wrist arthroscopy in a controlled and repeatable environment. It was also hugely beneficial in planning procedures, as the maneuvers required could be rehearsed until perfected prior to undertaking the procedure. (Courtesy Terry Whipple)

Roth's new techniques were not the only significant contribution to wrist arthroscopy in 1988. Whipple outlined the use of powered instruments for wrist arthroscopy [26], which followed on from the well-described techniques for their use in the knee and shoulder. Powered instruments conferred significant benefits for arthroscopy, particularly faster tissue resection and built-in suction-aspiration systems. Whipple had tried numerous different designs for these miniaturized instruments based on the existing knee and shoulder instruments. However due to the limitations posed by the smaller diameter, not all were suitable for wrist arthroscopy.

The first textbook dedicated to wrist arthroscopy followed 4 years later in 1992. Whipple published his seminal text, "Arthroscopic Surgery: The Wrist" (Fig. 2.19). This textbook combined concise descriptions, imaging, and photos to provide a clear and in-depth review of the technique of wrist arthroscopy. Diagnostic and therapeutic roles of wrist arthroscopy were described including arthroscopic assisted reduction and fixation of distal radius fractures and intra-articular synovectomy among many others [27]. It sold out!

Viegas [14–17] and Richard (Dick) Berger (USA) [28–30] (Fig. 2.20) made advances in the understanding of wrist anatomy, allowing safe and effective use of wrist arthroscopy in many joints including the midcarpal, radiocarpal, and DRUJ. By 1995, surgeons were starting to use arthroscopes to evaluate and treat more conditions, and even expanding its use to other areas including the soft-tissue compartments of the forearm [31]. Randall Culp (USA) (Fig. 2.21) was the one to push the boundaries of arthroscopic surgery, describing a technique for arthroscopic proximal row carpectomy [33]. He was aware of the risks of the increased range of arthroscopic procedures, publishing important work on the complications of wrist arthroscopy [32].

Throughout the 1990s, Osterman made frequent additions to the catalogue of arthroscopic techniques. In 1990, he described a technique for triangular fibrocartilage injury debridement [8]. During 1993, Osterman published an approach to evaluation and treatment of carpal instability [10]. In 1995, he described the arthroscopic reduction and internal fixation of distal radius fractures [9] and also developed a technique for dorsal wrist ganglion resection, and in 1997 he helped Culp form a technique for proximal row carpectomy [33]. In 2002, Osterman published further research on techniques for dorsal wrist ganglion resection [34].

Guillaume Herzberg (France) (Fig. 2.22) has contributed to the literature on perilunate injuries over a number of decades. In 1993, he published a defining review of 157 perilunate dislocations [35], and some 20 years later described the concept of perilunate injury, not dislocated (PLIND) [36]. He demonstrated that accurate early diagnosis of these injuries was best done using wrist arthroscopy.

Another French surgeon, Christophe Mathoulin (Fig. 2.23), made many contributions, first describing the arthroscopic reduction and fixation of intra-articular distal radius fractures [37], before expanding our knowledge of scapholunate injuries. First improving understanding of the anatomy of the scapholunate interval, Mathoulin then developed the EWAS classification of scapholunate instability as well as techniques for arthroscopic scapholunate capsulodesis [38–41]. Perhaps more significant than this work was his work to establish and grow EWAS into

b

1 Scolt Bowen, M.D. *Winston-Salem, NC*
2 Kenny Caldwell, M.D. *Winston-Salem, NC*
3 Paul Rush, M.D. *Winston-Salem, NC*
4 C. Berwyn Rush, M.D. *Bounettsagille, SC*
5 Victoria Masear, M.D. *Bimingham, AL*
6 David P, Green *San Antorio, TX*
7 Steven Viegas *Gatveston, TX*
8 J. Olbe Edmunds, Jr. M.D. *New Orleans, LA*
9 Jarres R. Urbaniak, M.D. *Daham, NC*
10 John S. Gould, M.D. *Binmingham, AL*
11 Michael Vender, M.D. *Harsford, CT*
12 James R. Boatright, M.D. Charlotte, NC
13 David Black, M.D. *Hastford, CT*
14 John P. Buddery, M.D *Tiocaloosa, AL*
15 Richard D. Meyer, M.D. *Birnighamn, AL*
16 William H, Bowers, M.D. *Asheulle, NC*
17 Dean S. Louis, M.D. *Ann Arbor, MI*
18 Clinton McAliser, M.D. *Bossier City, LA*
19 Franeis M. Watson, Jr. M.D. *Atlanta, GA*
20 Robert S. Adelaar, M.D. *Rsehmord. VA*
21 Wallace F. Andrew, M.D. *Raleigh, NC*
22. Wlliam P. Cooney, M.D. *Rochester, NY*
23 Julio Takisnik, M.D. *Orange, CA*
24 James H, Roth, M.D. *London Ontario, Canada*
25 James E. Culver, M.D. *Clerland, Oliso*
26 James H. Dobyns, M.D. *Rochster, MN*
27 Joscph D. Defiore, Jr., M.D. *Krosxville, TN*
28 John W. Packer, M.D. *Raleigh, NC*
29 H. Kirk WAtson, M.D. *Hartford CT*
30 Ladislas Laro, III, M.D. *Oxlousas, LA*
31 Richard T, Harick, M.D. *Oyelka, AL*
32 Eugene J, Dabezies, M.D. *New Orieas, LA*
33 James S. Thompson, M.D. *Baltinore, M.D.*
34 J. Russell Moore, M.D. *Baltunore, M.D.*
35 Glen Barden, M.D. *Lakeland, FL*
36 Stevan Z, Glxkd, M.D. *New York, NY*
37 David N. Paker, M.D. *Conxs Christi, TX*
38 Andrew Palmer, M.D. *Syracuse, NY*
39 A. Lee Oxterman, M.D. *Pholadalvelala, PA*
40 John P. Evans, M.D. *Greeville, SC*
41 Lamar Pleming, M.D. *Alanta, GA*
42 Donald K, Bynum, M.D. *Chaxl Hill, NC*
43 Terry Whipple, M.D. *Richanond, VA*
44 Harold M, Stokes, M.D. *New Orkars, LA*
45 Gary G, Poetting M.D. *Winston-Salem, NC*
46 L. Andrew Koman, M.D. *Winston-Salem, NC*
47 Jams A. Nunley, M.D. *Duhan, NC*

Fig. 2.13 Attendees at the first wrist arthroscopy workshop at the Bowman Gray School of Medicine, Winston-Salem, USA, 1986. This was the start of the new era, which enabled wrist arthroscopy to be promoted and developed in an organized way. (**a**) Photograph, (**b**) diagram of names of attendees, (**c**) the faculty. (Courtesy Gary G. Poehling)

Fig. 2.13 (continued)

Fig. 2.14 James Urbaniak (USA) assisted in the smooth introduction of wrist arthroscopy in the USA. He invited 57 senior surgeons, including 10 Presidents of the American Society of Surgery of the Hand. Of these 47 surgeons attended. (Courtesy Gary G. Poehling)

the global platform of education and professional networking it has become [42, 43].

Arthroscopic management of scaphoid fractures was described in 2001 by Joe Slade (USA) (Fig. 2.24), who demonstrated a dorsal approach [44, 45]. PC Ho (Hong Kong) (Fig. 2.25) also outlined a procedure for scaphoid fractures in the early 2000s [46], before going on to describe limited wrist fusion [47] and volar ganglion resection [48]. Riccardo Luchetti (Italy) (Fig. 2.26) also published his approach to arthroscopic wrist arthrolysis for postsurgical and post-traumatic wrist stiffness in 2001 [49].

Gregory I. Bain (Fig. 2.27) has made several important contributions relating to wrist arthroscopy. In 2006, he described the arthroscopic assessment and management of Kienbock's disease, which while divergent to Lichtman's radiological classification (Fig. 2.28) was complementary in clinical practice [50]. His other contributions include the inside-out volar portal and management of ulnar styloid impaction and intraosseous ganglions [51–57].

For many years, fluid distention was considered essential for wrist arthroscopy, despite the success of other forms of endoscopic and arthroscopic surgery without fluid distention. In 2007, Francisco (Paco) del Piñal (Spain) (Fig. 2.29) described a technique for dry wrist arthroscopy [58]. Piñal also published papers on the management of distal radius fractures and malunions [59]. Later, he expanded his research on arthroscopic distal radius fracture management to publish an EWAS textbook on the topic, before releasing a second textbook covering ulnar sided pain, and redefining how chronic regional pain syndrome (CRPS) is understood [60–62].

The arthroscopic diagnosis and treatment of TFC tears have been aided by contributions from around the world. Palmer published a classification of TFC tears [12] as did Andrea Atzei (Italy) (Fig. 2.30) and Luchetti [63], and Toshi Nakamura (Japan) (Fig. 2.31) contributed important anatomical and clinical studies [64]. Poehling described the inside-out suture technique, and

Fig. 2.15 Leonard Goldner (USA, center bottom) performs his first wrist arthroscopy at the first Wrist Course in 1986. A young Bill Cooney (center top) and Andy Koman (right) look on. Both later made significant contributions to the development of wrist arthroscopy. (Courtesy Gary G. Poehling)

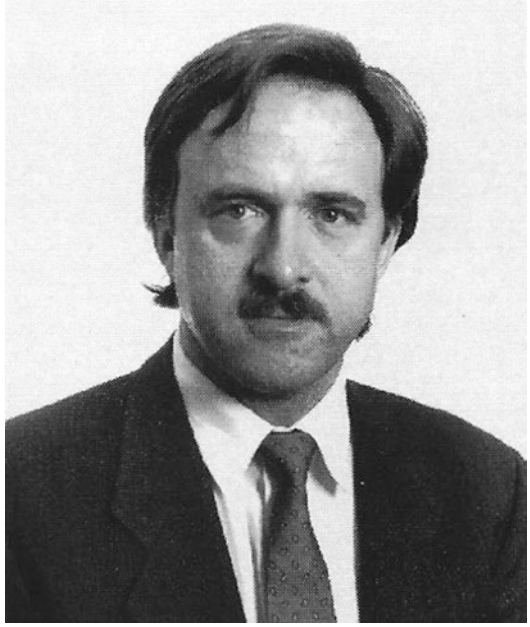

Fig. 2.16 Lee Osterman (USA) made many contributions to wrist arthroscopy. He developed techniques for dorsal wrist ganglion excision, triangular fibrocartilage injuries, distal radius fractures, and carpal instability. He has also been one of the great teachers. (Reprinted from Atlas of the Hand Clinics, Vol 11, Osterman L, Foreward, p. ii–iv, Copyright 2006 with permission from W. B. Saunders Company)

Jan-Ragnar Haugstvedt (Norway) developed techniques for both TFC tears and lunotriquetral tears [65–67] (Fig. 2.32).

Another clinical entity with global collaboration is scapholunate instability. The foundation of modern understanding and management of the condition is based on the arthrofibrosis technique described by Whipple [68], William Geissler's (USA) (Fig. 2.33) arthroscopic classification [69], and Tommy Lindau's (Sweden) (Fig. 2.34) study of the natural history of scapholunate ligament and TFC tears with distal radius fractures [70]. More recent studies including Mathoulin scapholunate tenodesis technique [38], as well as additions from Marc Garcia-Elias (Spain) (Fig. 2.35) [71, 72] and Giorgio Brunello (Italy) [73], have further advanced the treatment of scapholunate instability.

Arthroscopic techniques quickly expanded beyond the wrist joint. Endoscopic carpal tunnel release is one of the most popular, and was independently described by both Ichiro Okutsu (Japan) and James Chow (USA) in 1989 [74, 75]. John Agee (USA) described a single portal technique in 1992, which used a pistol-grip device with a retractable blade [76]. Also popular is Reiner Hoffmann's (Germany) endoscopic cubital tunnel release [77].

Fig. 2.17 Steve Viegas (USA) has been a leader in the advancement of the understanding of wrist arthroscopy, anatomy, and biomechanics [14–17]. He has also been involved in the development of the treatment of scapholunate ligament lesions. (Courtesy PC Ho)

Fig. 2.18 Daniel Nagle (USA) was involved in the development of the clinical application of lasers in wrist arthroscopy. (Courtesy Daniel Nagle)

A number of other nerve compression syndromes have been treated by endoscopic means including pronator teres syndrome and radial tunnel syndrome, and Guyon's canal release [78]. Endoscopic surgical releases have been described for compartment syndrome, first extensor compartment, and intersection syndrome. Tendon, nerve, vessel, and bone grafts; tendon transfers; pisiform excision; bursectomy; and fasciotomy have also been performed using arthroscopic techniques [54].

Other surgeons who have made significant contributions include Lars Adolfsson (Sweden) (Fig. 2.36) [79], Alejandro Badia (USA) [80, 81], Tyson Cobb (USA) (Fig. 2.37) [82], Max Haerle (Fig. 2.38) [83], Peter Jorgsholm (Denmark) [84], Daniel Nagle (Fig. 2.18) [18, 19, 85], Buddy Savoie (USA) (Fig. 2.39) [69], David Slutsky (USA) (Fig. 2.40) [85, 87–89], John Stanley (England) [90], and Arnold-Peter Weiss (USA) (Fig. 2.41) [91].

2.5 Organizations

In 1974 the International Arthroscopy Association was founded with Watanabe as its inaugural president [92]. Its main focus was clearly on the knee.

The Wrist Group of the Italian Society for the Surgery of the Hand (SICM) was founded by Luchetti and Atzei in 1999. At the third course in 2001, Mathoulin was the invited guest (Fig. 2.42). The course consisted of presentations and live surgery in Verona for 2 days, and then a flight to Barcelona, for a cadaveric lab with Marc Garcia-Elias and Manel Llusa.

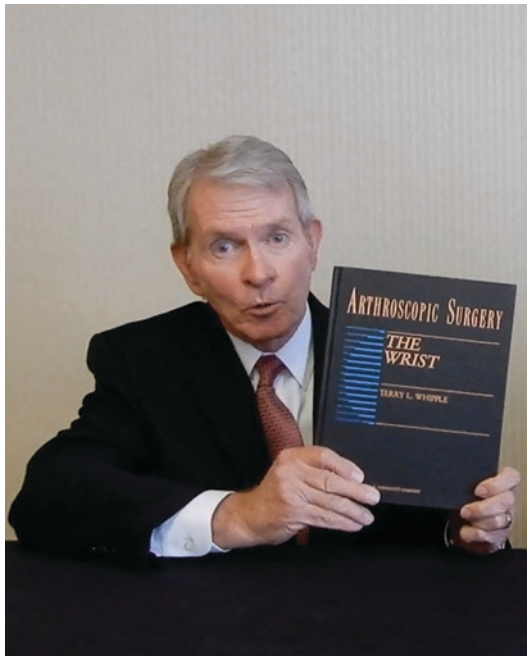

Fig. 2.19 Terry Whipple and his 1992 textbook, "Arthroscopic Surgery: The Wrist." It was the first textbook on wrist arthroscopy. It sold out! [27]. (Courtesy Gregory I. Bain)

Fig. 2.20 Richard (Dick) Berger (USA) has been a leader in the advancement of the understanding of wrist anatomy and biomechanics [28–30]. (Courtesy PC Ho)

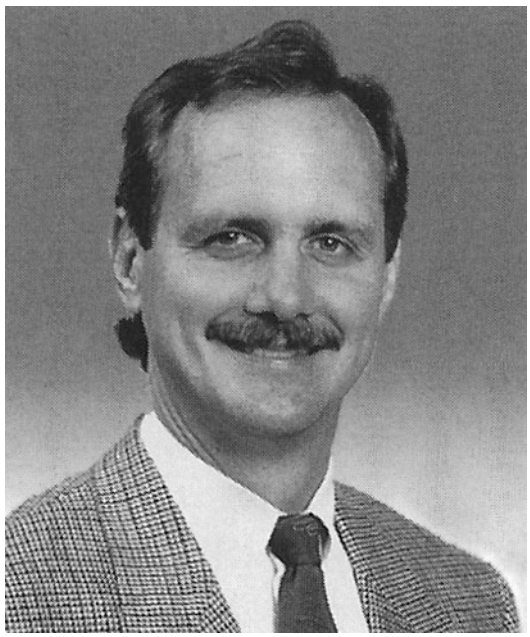

Fig. 2.21 Randall Culp "Randy" (USA) worked with Lee Osterman, and developed many new techniques. He also contributed to our knowledge of complications [32]. (Reproduced from Hand Clinics of North America, Vol 15, Culp R, Preface, p. xi, Copyright 1999 with permission from Elsevier.)

Fig. 2.22 Guillaume Herzberg (France) has made contributions to the perilunate injuries and their arthroscopic management [35, 36]. (Courtesy PC Ho)

Fig. 2.23 Christophe Mathoulin (France) as a guest speaker at the third Italian Wrist Course, 2003. He has played a significant role in creating the European Wrist Arthroscopy Society, which has run courses all over the world. EWAS evolved into the International Wrist Arthroscopy Society in 2019. (Courtesy Riccardo Luchetti)

Fig. 2.24 Joe Slade (USA) was a dynamic personality who was actively involved in the advancements of arthroscopic management of scaphoid fractures [44, 45]. (Courtesy PC Ho)

In 2005, Mathoulin formed the European Wrist Arthroscopy Society (EWAS) (www.wristarthroscopy.eu) (Fig. 2.43). EWAS was instrumental in the European and subsequently global education of wrist arthroscopy. This included multiple cadaveric workshops all over the world, EWAS symposia at all of the major meetings, publication of many quality well-illustrated books, research into the basic science of wrist arthroscopy, and a website to share their information. Christophe has built a strong team around him, such that the organization has been a platform, which enabled many surgeons to be able to develop and advance wrist arthroscopy, and take international leadership roles. This clearly shifted the epicenter of wrist arthroscopy across the Atlantic to Europe.

In 2015, PC Ho established the Asia Pacific Wrist Association (APWA) (www.apwa.asia). With the support of Bain, Nakamura, Wendong Xu (China), and Jeff Ecker (Australia), this vibrant group is focused on disorders of the wrist, and provides an annual congress with a high-quality interactive program (Fig. 2.44). It also supports cadaveric wrist open and arthroscopic workshops throughout the Asian region. The APWA congress and workshops have provided opportunities for a new generation of surgeons.

In 2019, recognizing the global role this organization had taken on, EWAS became the International Wrist Arthroscopy Society (IWAS). Whipple and Mathoulin were made lifetime Presidents of IWAS. IWAS continues to play a vital role in education and professional networking for wrist arthroscopy around the world. Each year, more than 30 courses on wrist arthroscopy take place under the auspices of IWAS.

This global community was scarcely believable to Whipple, who exclaimed in a speech in 2019 that “I struck a match and started a fire. I had no concept of how hot it would burn, and how widely it would spread” (Fig. 2.45). We all owe Terry, and many others, so much for leaving us this legacy, a tool which is so useful to assess and manage our patients with disorders of the wrist.

Fig. 2.25 PC Ho visited Terry Whipple in 1996 to learn more about wrist arthroscopy. A couple of years later, PC Ho started the Hong Kong wrist arthroscopy course. (Courtesy Terry Whipple)

Fig. 2.26 Riccardo Luchetti was important in the evolution of wrist arthroscopy in Italy and Europe. (Courtesy Riccardo Luchetti)

2.6 Journals and Books

Takagi would scarcely be able to believe the current landscape of arthroscopy, having suggested to Watanabe in 1937 that "I am sure that a chapter on arthroscopy will appear in the orthopaedic textbook of the future" [93]. Arthroscopy has certainly surpassed Takagi's expectations!

In 1957, Watanabe published the first edition of the textbook "Atlas of Arthroscopy." Watanabe stated that he wanted to create a "complete atlas of arthroscopy" but due to a lack of finances he created a "little atlas," which was made up of 68 hand-painted images chosen from several hundred intra-articular pictures (Fig. 2.46). Two further editions of Watanabe's Atlas of Arthroscopy have been published, widening the scope of conditions described, and replacing the hand-painted images with color photographs.

Watanabe was not the only surgeon who had worked on an atlas of arthroscopy, as he discovered in 1957. In that year, he visited another of the early proponents of arthroscopy, Burman, and brought with him a copy of the first edition of his atlas as a gift. Burman told Watanabe that he had written his own atlas of arthroscopy, but "no publisher would accept publication" of it. Burman thought that Watanabe's atlas was "what I should have written," and he gave Watanabe his manuscript as he no longer had a use for it [93].

More than just color photographs, the third edition (Fig. 2.47) of Watanabe's atlas also included a chapter on arthroscopy of small joints which included detailed descriptions of wrist arthroscopy (Fig. 2.1). This edition, published in 1979, marks one of the earliest descriptions of a technique for wrist arthroscopy, predating the published works of Whipple, Poehling, and Roth

Fig. 2.27 Gregory I. Bain (Australia) and PC Ho at the Hong Kong Hand Society meeting in 1995. (Courtesy PC Ho)

Fig. 2.28 David Lichtman (USA) has contributed significantly to many conditions of the wrist, including Kienbock's disease and carpal mechanics. (Courtesy PC Ho)

by half a decade. Johnson had also described wrist arthroscopy in 1981; however this was only a short review of his limited clinical experience with the technique [96].

With further research on arthroscopic surgery, the need for a dedicated journal heightened. In 1985, the Arthroscopy Association of North America and the International Arthroscopy Association launched the journal *Arthroscopy: The Journal of Arthroscopic and Related Surgery* [97]. Dr. Robert Metcalf (Fig. 2.48) was primarily responsible for establishing the journal, but then handed over the reins to Ward Casscells, who became the founding editor in chief. In 1989, Gary G. Poehling became the editor in chief until he retired in 2014.

The late 1980s and early 1990s saw a number of important works published on wrist arthroscopy. In 1988, David Lichtman's book "The Wrist and Its Disorders" included chapters on wrist arthroscopy by Whipple and Roth, which described the technique and the clinical applications for it [23]. In the early 1990s, Lippincott Company published a series of books on arthroscopic surgery of the shoulder, foot, and ankle, edited by Whipple, including Whipple's 1992 book focusing on the wrist (Fig. 2.19) [27].

In the years that followed, a number of books on general arthroscopy and wrist arthroscopy were published. Stanley and Philippe Saffar (France) (Fig. 2.49) published "Wrist Arthroscopy" in 1994 [20], in 1995 Hand Clinics published an edition dedicated to wrist arthroscopy [98], and in 1996, the Operative Arthroscopy included a chapter on wrist arthroscopy [99].

In 2012, the Journal of Wrist Surgery was founded by David Slutsky [86]. Slutsky, the inaugural editor in chief, noted: "the advent of wrist arthroscopy has led to a better understanding of

Fig. 2.29 Francisco (Paco) del Piñal (Spain) has played an important role in the development of dry arthroscopy [58, 59], management of distal radius fractures, and malunions. Recently he has changed our understanding of CRPS [60–62]. He has also contributed with quality EWAS arthroscopic texts. (Courtesy Dr. Paco del Piñal)

Fig. 2.30 Andrea Atzei (Italy) has worked alongside Ricardo Luchetti in Italy to create the Wrist Group of the Italian Society for Surgery of the Hand. He has also contributed to our knowledge of triangular fibrocartilage injuries and wrist arthrolysis. (Courtesy Ricardo Luchetti)

the pathological conditions affecting the wrist and their treatment, which has set the stage for a journal solely dedicated to the wrist joint." Wrist arthroscopy has become an integral part of diagnosis and management of wrist conditions. Slutsky made many contributions, including editing textbooks [85, 87] and writing academic papers [88, 89].

EWAS has played an important role in the publication of educational texts relating to wrist arthroscopy. Piñal's two books [60, 61] as well as others by Mathoulin [100], etc. have furthered the understanding of wrist arthroscopy's role in diagnosis and management, and ensured that emerging techniques are accessible to surgeons around the world.

2.7 Timeline

1931 Michael Burman (USA) publishes the first report of wrist arthroscopy [101].

1970 Masaki Watanabe (Japan) releases the 1.9 mm No. 24 arthroscope, for small joints [95].

1972 Gary G. Poehling (USA) purchases No. 26 arthroscope for Leonard Goldner (USA).

1979 Yung-Cheng Chen (Japan) reports 90 wrist and finger joint arthroscopies, with No. 24 arthroscope [2].

1979 Stryker Chondrotome developed to mechanically resect soft tissue [102].

1984 Terry Whipple and Jack Powell (USA) Cadaver dissections and development of named

Fig. 2.31 Toshi Nakamura (Japan) has contributed to our knowledge of triangular fibrocartilage injuries. He was President of EWAS in 2011–2012, and is the current editor of the Journal of Wrist Surgery. (Courtesy PC Ho)

Fig. 2.32 Jan-Ragnar Haugstvedt (Norway) developed techniques for the management of ulnar sided wrist disorders including TFC tears and lunotriquetral instability [65–67]. He has also been actively involved in the leadership of EWAS and IWAS. (Courtesy PC Ho)

safe wrist arthroscopy portals, traction towers, and finger traps [5].

1986 Gary G. Poehling, Terry Whipple (USA), and James Roth (Canada) organize the first wrist arthroscopy course in Winston-Salem, USA.

1986 Terry Whipple publishes paper on Techniques of Wrist Arthroscopy [5].

1990 Luigi Pederzini and Riccardo Luchetti (Italy) organize first Italian upper limb arthroscopy course, with guest speaker James Roth (Fig. 2.50).

1992 Terry Whipple publishes first textbook on wrist arthroscopy: "Arthroscopic Surgery—The Wrist" (Lippincott) [27].

1997 PC Ho (Hong Kong) organizes first Hong Kong Wrist Arthroscopy Course.

1997 International Arthroscopy Association and International Society of the Knee amalgamate to form the International Society of Arthroscopy, Knee Surgery and Orthopaedic Sports Medicine (ISAKOS).

1999 Riccardo Luchetti and Andrea Atzei (Italy) create the Wrist Group of the Italian Society for Surgery of the Hand. First meeting in Verona.

2005 Christophe Mathoulin (France) founded the European Wrist Arthroscopy Society (EWAS). First EWAS cadaveric arthroscopy workshop in Strasbourg (Fig. 2.51).

2012 David Slutsky (USA) inaugural editor in chief, Journal of Wrist Surgery [86]. Toshi Nakamura (Japan) is the current editor.

2015 PC Ho (Hong Kong), Foundation President of Asia Pacific Wrist Association.

2019 EWAS evolves into the International Wrist Arthroscopy Society (IWAS). Terry

Fig. 2.33 William Geissler (USA) was involved with the development of the scapholunate classification and arthroscopic management of sports injuries [69]. (Courtesy William Geissler)

Fig. 2.35 Marc Garcia-Elias (Spain) has made many contributions to the understanding of anatomy, pathoanatomy, and treatment of wrist injuries [71, 72]. (Courtesy Marc Garcia-Elias)

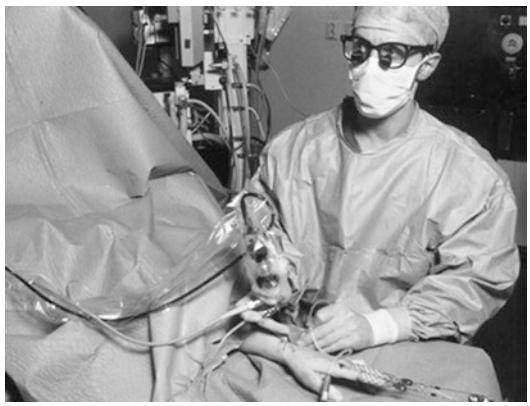

Fig. 2.34 Tommy Lindau (Sweden) provided quality long-term prospective studies of ligamentous injuries associated with distal radius fractures [70]. (Courtesy PC Ho)

Whipple and Christophe Mathoulin both made Honorary Lifetime Presidents [42].

Acknowledgements Kimberley Bryant for assistance in preparation of manuscript. We thank the following surgeons who provided information, support or images:

- Christophe Mathoulin, Max Haerle, Riccardo Luchetti, PC Ho, Jan-Ragnar Haugstvedt, Guillaume Herzberg, Graham King, Dan Nagle, Toshi Nakamura, Lee Osterman, David Slutsky, Steven Viegas, Buddy Savoie, Luigi Pederzini

Fig. 2.36 Lars Adolffsson (Sweden) was an early leader of wrist arthroscopy in the Nordic countries. He developed the concepts of arthroscopic management of synovitis of the wrist [79]. (Courtesy PC Ho)

Fig. 2.37 Tyson Cobb (USA) has been involved with the development of resection arthroplasty for the SLAC wrist and endoscopic procedures. (Courtesy Tyson Cobb)

Fig. 2.38 Max Haerle (Germany) has been involved with the development of the vascularized bone grafts and scapholunate instability [83]. He has also been actively involved in the leadership of FESSH, EWAS, and IWAS. (Courtesy Max Haerle)

Fig. 2.39 Felix "Buddy" Savoie (USA, left, with Dr. Dick Caspari) has contributed to the understanding of injuries associated with distal radius fractures. (Courtesy Buddy Savoie)

Fig. 2.40 David Slutsky (USA) established the Journal of Wrist Surgery in 2012 [86]. He also published many other papers and texts [85, 87–89]. (Courtesy Dr. Gregory I. Bain)

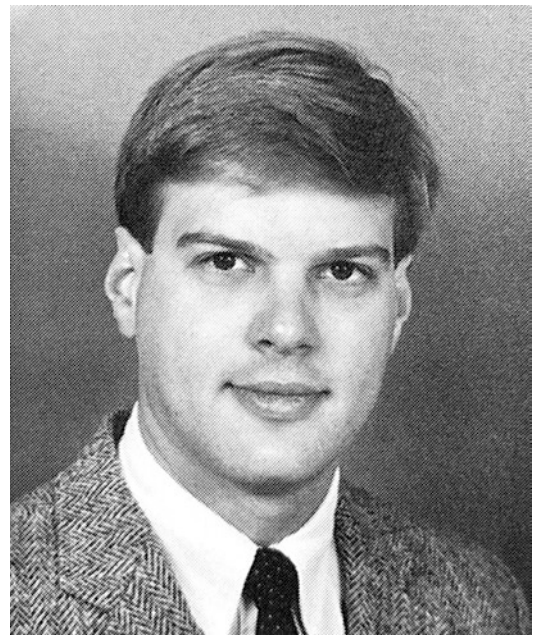

Fig. 2.41 Arnold-Peter Weiss (USA) has contributed to our knowledge of intracarpal ligament injuries [74]. (Courtesy Arnold-Peter Weiss)

Fig. 2.42 Riccardo Luchetti, Christophe Mathoulin (Guest), Andrea Atzei, Paulo, and Del Croix Luca at the third Meeting of the Wrist Group of the Italian Society for Surgery of the Hand (2001). (Courtesy Riccardo Luchetti)

Fig. 2.43 In 2004, Groupe Européan pour l'Arthroscopie du Poignet (GEAP) was formed in France to bring together interests in wrist arthroscopy. In 2005, this evolved into the European Wrist Arthroscopy Society (EWAS). In 2019 it further evolved into the International Wrist Arthroscopy Society. (Courtesy Max Haerle)

Fig. 2.44 Attendees at APWA's inaugural congress in Hong Kong in 2015. (Copyright Asia Pacific Wrist Association)

Fig. 2.45 Terry Whipple receiving the "Lifetime Honorary President of IWAS" at the Inaugural Annual General Meeting of the International Wrist Arthroscopy Society, in Berlin 2019. (Courtesy Gregory I. Bain)

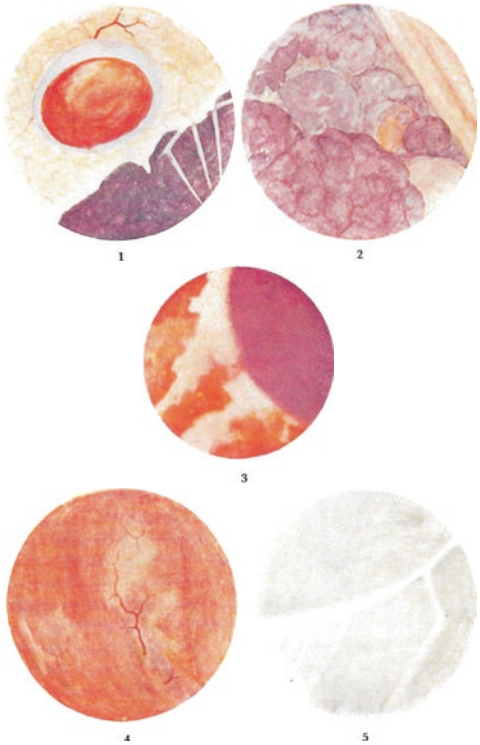

Fig. 2.46 The first edition of Watanabe's Atlas of Arthroscopy featured hand-painted depictions of the view down the arthroscope, as Watanabe believed that the photos were not of adequate quality [94]. In later editions, Watanabe included photos taken through the arthroscope. Copyright Masaki Watanabe. (Reprinted from Atlas of Arthroscopy, third edition, Watanabe M, Takeda S, Ikeuchi H, History of Arthroscopy, p. 10, Copyright 1979, with permission from Springer [1])

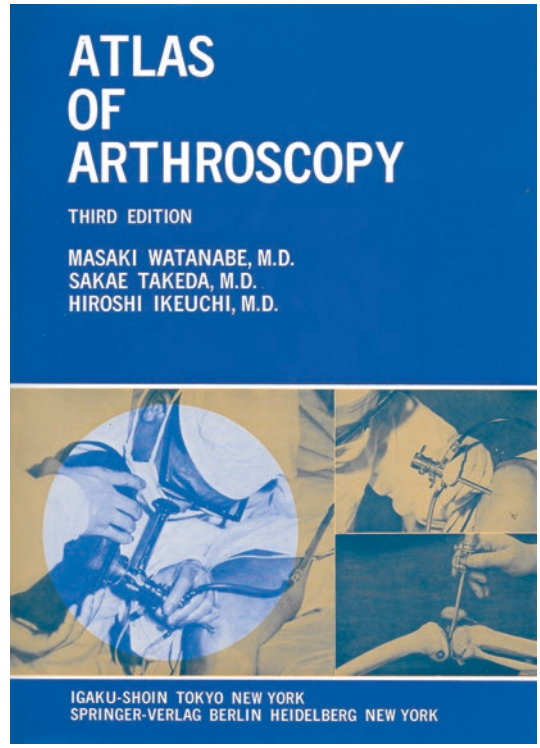

Fig. 2.47 Front cover of Masaki Watanabe's Atlas of Arthroscopy, published in 1979. This was one of the earliest books to describe arthroscopy techniques and pathology [1]. (Reprinted from Atlas of Arthroscopy, first edition, Watanabe M, Takeda S, Ikeuchi H, Cover, Copyright 1957, with permission from Springer [95])

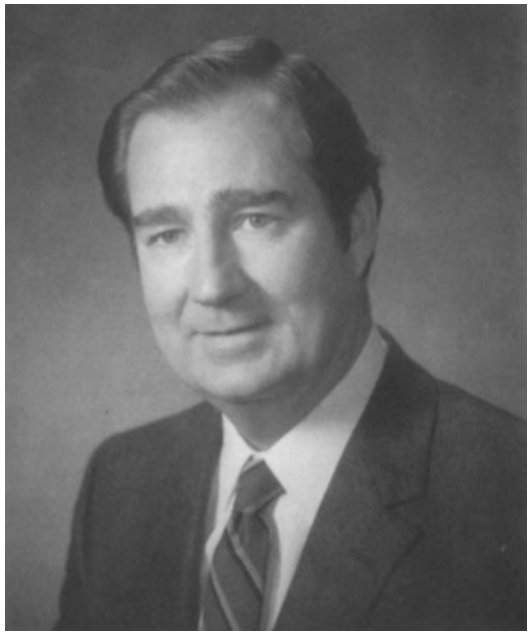

Fig. 2.48 Robert Metcalf (USA) was responsible for establishing Arthroscopy: The Journal of Arthroscopic and Related Surgery and organizing 26 national seminars between 1978 and 1991. (Reprinted from Arthroscopy: The Journal of Arthroscopic and Related Surgery, Vol 7, McGinty JB, In memoriam, p. 340–41, Copyright 1991 with permission from Wolters Kluwer Health, Inc.)

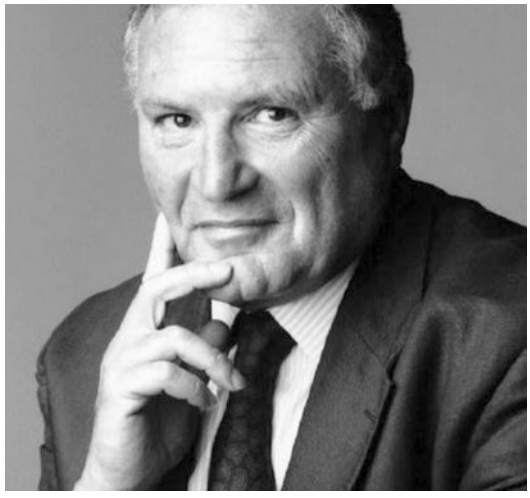

Fig. 2.49 Phillippe Saffar (France) was an important pioneer in reconstruction wrist surgery and edited one of the first books on wrist arthroscopy [20]. (Courtesy Michèle Saffar)

Fig. 2.50 James Roth and Luigi Pederzini together at an Italian upper limb arthroscopy course in 1990. (Courtesy Luigi Pederzini)

Fig. 2.51 Terry Whipple (front and center), a pioneer of wrist arthroscopy, is surrounded by past and future presidents of the EWAS in 2013, at the IRCAD-EITS center in Strasbourg, France. From left to right standing: past presidents: Didier Fontes (France), Riccardo Luchetti (Italy), Francesco de Piñal (Spain), Terry Whipple, Tommy Lindau (Sweden/UK), Toshiyasu Nakamura (Japan), Max Haerle (Germany), and David Slutsky (USA), with upcoming presidents Andrea Atzei (Italy) and Pak-Cheong Ho (Hong Kong). Front row (kneeling): founder of the EWAS, Christophe Mathoulin (France), and secretary general, Jan-Ragnar Haugstvedt (Norway) [43]

References

1. Watanabe M, Takeda S, Ikeuchi H. Atlas of arthroscopy. 3rd ed. Tokyo: Igaku-Shoin; 1979. p. 1–11.
2. Chen YC. Arthroscopy of the wrist and finger joints. Orthop Clin North Am. 1979;10:505–15.
3. Johnson LL. Arthroscopic surgery: principles and practice. 3rd ed. St. Louis: The C.V. Mosby Company; 1986.
4. Whipple TL, Bassett FH III. Arthroscopic examination of the knee—polypuncture technique with percutaneous intra-articular manipulation. J Bone Joint Surg Am. 1978;80(4):444–58.
5. Whipple TL, Marotta JJ, Powell JH. Techniques of wrist arthroscopy. Arthroscopy. 1986;2(4):244–52.
6. Bowers WH. Distal radioulnar joint arthroplasty: the hemiresection-interposition technique. J Hand Surg Am. 1985;10(2):169–78.
7. Cooney WP, Dobyns JH, Linscheid RL. Arthroscopy of the wrist: anatomy and classification of carpal instability. Arthroscopy. 1990;6:133–40.
8. Osterman AL. Arthroscopic debridement of triangular fibrocartilage complex tears. Arthroscopy. 1990;6(2):120–4.
9. Culp RW, Osterman AL. Arthroscopic reduction and internal fixation of distal radius fractures. Orthop Clin North Am. 1995;26:739–48.
10. Bednar JM, Osterman AL. Carpal instability: evaluation and treatment. J Am Acad Orthop Surg. 1993;1:10–7.
11. Osterman AL, Raphael J. Arthroscopic resection of dorsal ganglion of the wrist. Hand Clin. 1995;11(1):7–12.
12. Palmer AK. Triangular fibrocartilage complex lesions: a classification. J Hand Surg. 1989;14:594–606.

13. Wnorowski DC, Palmer AK, Werner FW. Anatomic and biomechanical analysis of the arthroscopic wafer procedure. Arthroscopy. 1992;8:204–12.
14. Viegas SF, Ballantyne G. Attritional lesions of the wrist joint. J Hand Surg. 1987;12:1025–9.
15. Viegas SF. Intraarticular ganglion of the dorsal interosseous scapholunate ligament: a case for arthroscopy. Arthroscopy. 1986;2(2):93–5.
16. Viegas SF, Patterson RM, Hobanson JA, Davis J. Wrist anatomy: incidence distribution and correlation of anatomic variations tears and arthrosis. J Hand Surg Am. 1993;18(a):463–75.
17. Viegas SF. The lunatohamate articulation of the midcarpal joint. Arthroscopy. 1990;6(1):5–10.
18. Nagle DJ. Arthroscopic treatment of degenerative tears of the triangular fibrocartilage. Hand Clin. 1994;10:615–24.
19. Nagle DJ. Laser-assisted wrist arthroscopy. Hand Clin. 1999;15(3):495–9.
20. Stanley J, Saffar P. Wrist arthroscopy. London: Martin Dunitz; 1994. p. 111–4.
21. Roth JH, Haddad RG. Radiocarpal arthroscopy and arthrography in the diagnosis of ulnar wrist pain. Arthroscopy. 1986;2(4):234–43.
22. Pederzini L, Luchetti R, Soragni O, Alfarano M, Montagna G, Cerofolini E, Colombini R, Roth JH. Evaluation of the triangular fibrocartilage complex tears by arthroscopy, arthrography, and magnetic resonance imaging. Arthroscopy. 1992;8(2):191–7.
23. Roth JH, Whipple TL. Wrist arthroscopy. In: Lichtman DM, editor. The wrist and its disorders. Philadelphia: W. B. Saunders Company; 1988. p. 108–28.
24. Roth JH, Poehling GG, Whipple TL. Hand instrumentation for small joint arthroscopy. Arthroscopy. 1988;4(2):126–8.
25. Roth JH, Poehling GG. Arthroscopic "-ectomy" surgery of the wrist. Arthroscopy. 1990;6(2):141–7.
26. Whipple TL. Powered instruments for wrist arthroscopy. Arthroscopy. 1988;4(4):290–4.
27. Whipple TL. The basics of wrist arthroscopy. In: Whipple TL, editor. Arthroscopic surgery—the wrist. Philadelphia: J.B. Lippincott; 1992. p. 7–9.
28. Berger RA. The anatomy of the ligaments of the wrist and distal radioulnar joints. Clin Orthop Relat Res. 2001;38(3):32–40.
29. Cooney WP, Berger RA. Treatment of complex fractures of the distal radius. Combined use of internal and external fixation and arthroscopic reduction. Hand Clin. 1993;9(4):603–12.
30. Berger RA. Arthroscopic anatomy of the wrist and distal radioulnar joint. Hand Clin. 1999;15(3):393–413.
31. Cooney WP. The future of arthroscopic surgery in the hand and wrist. In: Osterman AL, editor. Hand clinics: advanced wrist arthroscopy and endoscopy. Philadelphia: W.B. Saunders Company; 1995;11(1): p. 97–99.
32. Culp RW. Complications of wrist arthroscopy. Hand Clin North Am. 1993;15(3):529–35.
33. Culp RW, Lee Osterman A, Talsania JS. Arthroscopic proximal row carpectomy. Tech Hand Upper Extrem Surg. 1997;1(2):116–9.
34. Wiedrich T, Osterman AL. Arthroscopic excision of dorsal carpal ganglion cysts. Oper Tech Plast Reconstr Surg. 2002;9(4):118–23.
35. Herzberg G, Comtet JJ, Linscheid RL, Amadio PC, Cooney WP, Stalder J. Perilunate dislocations and fracture-dislocations: a multicenter study. J Hand Surg Am. 1993;18(5):768–79.
36. Herzberg G. Perilunate injuries, not dislocated (PLIND). J Wrist Surg. 2013;2(4):337–45.
37. Mathoulin C, Sbihi A, Panciera P. Intérêt de l'arthroscopie du poignet dans le traitement des fractures articulaires du 1/4 inférieur du radius: à propos de 27 cas [Interest in wrist arthroscopy for treatment of articular fractures of the distal radius: report of 27 cases]. Chir Main. 2001;20(5):342–50.
38. Papadogeorgou E, Mathoulin C. Extensor carpi radialis brevis ligamentoplasty and dorsal capsulodesis for the treatment of chronic post-traumatic scapholunate instability. Chir Main. 2010;29(3):172–9.
39. Messina JC, Van Overstraeten L, Luchetti R, Fairplay T, Mathoulin CL. The EWAS classification of scapholunate tears: an anatomical arthroscopic study. J Wrist Surg. 2013;2(2):105–9.
40. Mathoulin CL, Dauphin N, Wahegaonkar AL. Arthroscopic dorsal capsuloligamentous repair in chronic scapholunate ligament tears. Hand Clin. 2011;27(4):563–72.
41. Mathoulin C, Lando M, Reuda-Villegas C, Pagliei A, Valenti PH. Lésion du ligament scapho-lunaire: intérêt de l'arthroscopie, propositions thérapeutiques à propos d'une série de 62 patients [Scapholunate ligament injury: value of arthroscopy, therapeutic proposals for a series of 62 patients]. Mémoires de l'Academie Nationale de Chirurgie. 2004;3(1):62–72.
42. Mathoulin C. Farewell message. J Wrist Surg. 2020;9(01):90–2.
43. Mathoulin C. Letter to the editor, EWAS milestone achieved in Strasbourg. J Wrist Surg. 2014;3(1): 64–5.
44. Slade JF, Grauer JN, Mahoney JD. Arthroscopic reduction and percutaneous fixation of scaphoid fractures with a novel dorsal technique. Orthop Clin North Am. 2001;32(2):247–61.
45. Slade JF III, Geissler WB, Gutow AP, Merrell GA. Percutaneous internal fixation of selected scaphoid nonunions with an arthroscopically assisted dorsal approach. J Bone Joint Surg Am. 2003;85(Suppl 4):20–32.
46. Wong WY, Ho PC. Minimal invasive management of scaphoid fractures: from fresh to nonunion. Hand Clin. 2011;27(3):291–307.
47. Ho PC. Arthroscopic partial wrist fusion. Tech Hand Up Extrem Surg. 2008;12(4):242–65.
48. Ho PC, Lo WN, Hung LK. Arthroscopic resection of volar ganglion of the wrist: a new technique. Arthroscopy. 2003;19(2):218–21.

49. Luchetti R, Atzei A, Mustapha B. Arthroscopic wrist arthrolysis. Atlas Hand Clinics. 2001;6: 371–87.
50. Bain GI, Begg M. Arthroscopic assessment and classification of Kienbock's disease. Tech Hand Upper Extrem Surg. 2006;10(1):8–13.
51. Ashwood N, Bain GI, Fogg Q. Results of arthroscopic debridement for isolated scaphotrapeziotrapezoid arthritis. J Hand Surg. 2003;28(5):729–32.
52. Bain GI, Bidwell TA. Arthroscopic excision of ulnar styloid in stylocarpal impaction. Arthroscopy. 2006;22:677.e1–3.
53. Verhellen R, Bain GI. Arthroscopic capsular release for contracture of the wrist: a new technique. Arthroscopy. 2000;16:106–10.
54. Bain GI, Jadav B. The future: endoscopic surgery of the wrist and forearm. In: Savoie FH III, Field LD, Steinmann SP, editors. The elbow and wrist: AANA advanced arthroscopic surgical techniques. Slack Incorporated; 2016. p. 417–424.
55. Mehta JA, Bain GI, Heptinstall RJ. Anatomical reduction of intra-articular fractures of the distal radius. An arthroscopically-assisted approach. J Bone Joint Surg. 2000;82(1):79–86.
56. Bain GI, Munt J, Turner PC. New advances in wrist arthroscopy. Arthroscopy. 2008;24(3):355–67.
57. Pathak G, Bain G. Arthroscopic capsular shrinkage for midcarpal instability of the wrist. J Bone Joint Surg Br. 2003;85B:177.
58. del Piñal F, García-Bernal FJ, Pisani D, Regalado J, Ayala H, Studer A. Dry arthroscopy of the wrist: surgical technique. J Hand Surg Am. 2007;32(1):119–23.
59. del Piñal F. Dry arthroscopy of the wrist: its role in the management of articular distal radius fractures. Scand J Surg. 2008;97:298–304.
60. del Piñal F, Mathoulin C, Luchetti R. Arthroscopic management of distal radius fractures. Berlin: Springer; 2010. 264 p.
61. del Piñal F, Mathoulin C, Nakamura T. Arthroscopic management of ulnar pain. Berlin: Springer; 2012. 374 p.
62. del Piñal F, Herrero F, Cruz-Camara A, San JJ. Complete avulsion of the distal posterior interosseous nerve during wrist arthroscopy: a possible cause of persistent pain after arthroscopy. J Hand Surg Am. 1999;24(2):240–2.
63. Atzei A, Luchetti R, Garcia-Elias M. Lesioni capsulelegamentose della radio-ulnare distale e fibrocartilagine triangolare [Capsule ligament injuries of the distal radioulnar and triangular fibrocartilage]. In: Landi A, Catalano F, Luchetti R, editors. Trattato di chirurgia della mano. Italy: Verduci Editore Roma; 2006. p. 159–87.
64. Nakamura T, Takayama S, Horiuchi Y, Yabe Y. Origins and insertions of the triangular fibrocartilage complex: a histological study. J Hand Surg Br. 2001;26(5):446–54.
65. Haugstvedt JR, Husby T. Results of repair of peripheral tears in the triangular fibrocartilage complex using an arthroscopic suture technique. Scand J Plast Reconstr Surg Hand Surg. 1999;33(4):439–47.
66. Haugstvedt JR. LT tears and arthroscopic repair. In: del Piñal F, editor. Arthroscopic management of ulnar pain. Berlin: Springer; 2012.
67. Husby T, Haugstvedt JR. Long term results after arthroscopic resection of lesions of the triangular fibrocartilage complex. Scand J Plast Reconstr Surg Hand Surg. 2001;35:1,79–83.
68. Whipple TL. The role of arthroscopy in the treatment of scapholunate instability. Hand Clin. 1995;11(1):37–40.
69. Geissler WB, Freeland AE, Savoie FH, McIntyre LW, Whipple TL. Intracarpal soft-tissue lesions associated with an intra-articular fracture of the distal end of the radius. J Bone Joint Surg Am. 1996;78(3):357–65.
70. Lindau T, Adlercreutz C, Aspenberg P. Peripheral tears of the triangular fibrocartilage complex cause distal radioulnar joint instability after distal radial fractures. J Hand Surg Am. 2000;25(3):464–8.
71. Andersson JK, Garcia-Elias M. Dorsal scapholunate ligament injury: a classification of clinical forms. J Hand Surg Eur Vol. 2013;38(2):165–9.
72. Garcia-Elias M, Lluch AL, Stanley JK. Three-ligament tenodesis for the treatment of scapholunate dissociation: indications and surgical technique. J Hand Surg Am. 2006;31(1):125–34.
73. Brunelli GA, Brunelli GR. A new surgical technique for carpal instability with scapholunate dissociation. Surg Technol Int. 1996;5:370–4.
74. Okutsu I, Ninomiya S, Takatori Y, Ugawa Y. Endoscopic management of carpal tunnel syndrome. Arthroscopy. 1989;5(1):11–8.
75. Chow JCY. Endoscopic release of the carpal ligament: a new technique for carpal tunnel syndrome. Arthroscopy. 1989;5(1):19–24.
76. Agee JM, McCarroll HR, Tortosa RD, Berry DA, Szabo RM, Peimer CA. Endoscopic release of the carpal tunnel: a randomized prospective multicenter study. J Hand Surg Am. 1992;17(6):987–95.
77. Hoffmann R, Siemionow M. The endoscopic management of cubital tunnel syndrome. J Hand Surg Br. 2006;31(1):23–9.
78. Leclère FMP, Bignion D, Franz T, Mathys L, Vögelin E. Endoscopically assisted nerve decompression of rare nerve compression syndromes at the upper extremity. Arch Orthop Trauma Surg. 2013;133(4):575–82.
79. Adolfsson L, Nylander G. Arthroscopic synovectomy of the rheumatoid wrist. J Hand Surg Br. 1993;18(1):92–6.
80. Badia A, Khanchandani P. Suture welding for arthroscopic repair of peripheral triangular fibrocartilage complex tears. Tech Hand Upper Extrem Surg. 2007;11:45–50.
81. Badia A, Khanchandani P. The floating lunate: arthroscopic treatment of simultaneous complete tears of the scapholunate and lunotriquetral ligaments. Hand (New York, N.Y.). 2009;4(3):250–5.

82. Cobb TK, Walden AL, Wilt JM. Arthroscopic resection arthroplasty of the radial column for SLAC wrist. J Wrist Surg. 2014;3:114–22.
83. Del Gaudio T, Haerle M. [Arthroscopic partial resection of the ulnar head for ulnocarpal decompression]. Operative Orthopadie und Traumatologie. 2016.
84. Buijze GA, Jørgsholm P, Thomsen NO, Björkman A, Besjakov J, Ring D. Factors associated with arthroscopically determined scaphoid fracture displacement and instability. J Hand Surg Am. 2012;37(7):1405–10.
85. Slutsky DJ, Nagle DJ, editors. Techniques in wrist and hand arthroscopy. Philadelphia: Elsevier; 2007.
86. Slutsky DJ. Editorial. J Wrist Surg. 2012;1(1):1–2.
87. Slutsky DJ, editor. Principles and practice of wrist surgery. Philadelphia: Elsevier; 2010.
88. Slutsky DJ. Volar portals in wrist arthroscopy. J Am Soc Surg Hand. 2002;2(4):225–32.
89. Slutsky DJ. The management of dorsal radiocarpal ligament tears. J Am Soc Surg Hand. 2005;5(3):167–74.
90. Thurston AJ, Stanley JK. Hamato-lunate impingement: an uncommon cause of ulnar-sided wrist pain. Arthroscopy. 2000;16(5):540–4.
91. Weiss AP, Sachar K, Glowacki KA. Arthroscopic debridement alone for intercarpal ligament tears. J Hand Surg Am. 1997;22(2):344–9.
92. Jackson RW. Memories of the early days of arthroscopy: 1965-1975. The formative years. Arthroscopy. 1987;3(1):1–3.
93. Watanabe M. Memories of the early days of arthroscopy. Arthroscopy. 1986;2(4):209–14.
94. Watanabe M. Atlas of arthroscopy. 1st ed. Igaku-Shoin: Tokyo; 1957.
95. Watanabe M. Present state of arthroscopy. Int Orthop. 1978;2(2):101–8.
96. Johnson LL. Diagnostic and surgical arthroscopy: the knee and other joints. 2nd ed. St. Louis: The C.V. Mosby Company; 1981. p. 400–3.
97. Ward CS. A new journal: arthroscopy. Arthroscopy. 1985;1(1):1.
98. Osterman AL. Hand clinics: advanced wrist arthroscopy and endoscopy. Philadelphia: W. B. Saunders Company; 1995;11(1):p. 97–9.
99. McGinty JB, Caspari RB, Jackson RW, Poehling GG. Operative arthroscopy. Philadelphia: Lippincott-Raven Publishers; 1996.
100. Mathoulin C. Wrist arthroscopy techniques. 2nd ed. New York: Thieme; 2019.
101. Burman MS. Arthroscopy or the direct visualization of joints: an experimental cadaver study. J Bone Joint Surg. 1931;13(4):669–95.
102. United States Patent and Trademark Office. Official gazette of the United States patent and trademark office: patents. Vol. 1007(1). U.S. Department of Commerce, Patent and Trademark Office; 1981. p. 127.

Part II

Elbow: Basic Science

Clinical Anatomy of the Elbow

3

Gregory I. Bain, Benjamin Seah Renyi, and Janak A. Mehta

3.1 Clinical Anatomy of the Elbow

The upper limb is a cylinder consisting of a skeleton on which muscles and its accompanying neurovascular structures lie (Fig. 3.1a). The investing layer of deep fascia encircles the muscles and divides it into flexor and extensor compartments with the assistance of the medial and lateral intermuscular septa. Superficial to the deep fascia is the subcutaneous tissue consisting of superficial veins, lymphatic vessels and cutaneous nerves (Fig. 3.1b). Lastly, the skin encases the entire arm.

3.1.1 Osseous Anatomy

The elbow is a complex joint, sometimes also called a trochleo-ginglymoid joint, due to the movements it performs. Its three main articulations consist of the radiohumeral, ulnohumeral and proximal radioulnar joints. A fourth articulation is present between the lateral trochlear ridge and radial head, called the zona conoidea. A theory exists that significant contact between the radial head and the zona conoidea in supination, the position in which the radial head is most congruent with the lesser sigmoid notch, is associated with the initiation of osteoarthritis of the elbow in this area.

The condyles show a 30° anterior flexion in relation to the humeral axis, a 6–8° valgus tilt and a 5° internal rotation in relation to the epicondylar axis. The radial neck has a 15° angle with the long axis; the greater sigmoid notch angulates 30° with the ulna shaft. The centre of rotation of the elbow runs from the inferior edge of the medial epicondyle to the small tubercle of the lateral epicondyle (Fig. 3.2).

The proximal ulna has a dorsal (PUDA), varus and torsional angulation. These angles should be considered when performing osteosynthesis for proximal ulna fractures. In the proximal ulna of most patients, a transverse segment of less or no articular cartilage coverage (bare area) divides the sigmoid notch into two parts: an anterior section consisting of the coronoid, and the olecranon. As variations exist in the hyaline cartilage distribution in the proximal ulna, deficiencies in hyaline cartilage are often misinterpreted as osteochondral injury. When an olecranon

G. I. Bain (✉)
Department of Orthopaedics and Trauma Surgery, Flinders Medical Centre and Flinders University, Adelaide, SA, Australia
e-mail: admin@gregbain.com.au

B. S. Renyi
Department of Orthopaedic Surgery, Sengkang General Hospital, Singhealth, Singapore, Singapore

J. A. Mehta
Department of Orthopaedic and Trauma Surgery, Royal Darwin Hospital, Darwin, Northern Territory, Australia

© ISAKOS 2022

D. N. Bhatia et al. (eds.), *Arthroscopy and Endoscopy of the Elbow, Wrist and Hand*,
https://doi.org/10.1007/978-3-030-79423-1_3

osteotomy needs to be performed, we recommend that it should cross the articular surface at this bare area (incisura trochlearis) to minimize cartilage injury. The cortical bone below the bare area is very thick and bridges the two facets. This cortical bone is supported by trabeculae that span the dorsal cortex.

Approximately 12 cm above the lateral ridge is a sulcus in which the radial nerve passes over the humeral shaft. This is an important anatomical landmark when plating humeral shaft fractures, when applying the distal lock of a humeral nail or when applying an external fixator.

At the base of the coronoid, the ulnar collateral ligament is attached at the sublime tubercle. The lateral ligament originates from the inferior part of the lateral epicondyle and is attached to the supinator crest where part of the supinator muscle originates.

The distal humeral diaphysis has minimal internal bone and is supplied by a single nutrient artery. The trochlea, olecranon fossa and coronoid fossa are watershed areas. The lateral column is supplied predominantly by posterior segmental vessels, whereas the medial column is supplied by both anterior and posterior segmental vessels (Fig. 3.3). This solitary posterior blood supply of the capitellum is one of the reasons that the capitellum is prone to subchondral stress fractures. This also results in the lateral trochlea being more prone to fracture non-union or malunion. The radial shaft has a nutrient artery within

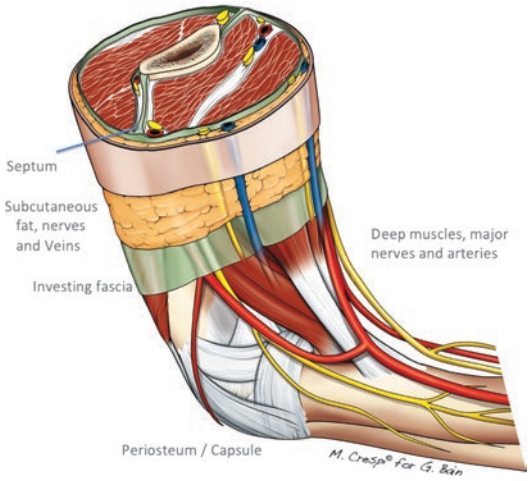

Fig. 3.1 The cylinder of the arm, with the skin, subcutaneous tissues with the cutaneous nerves and veins. The deep fascia encircles the muscular compartment with the major nerves and vessels, which are separated by the medial and lateral intermuscular septa into the extensor and flexor compartments (copyright Dr. Gregory I. Bain and Max Crespi)

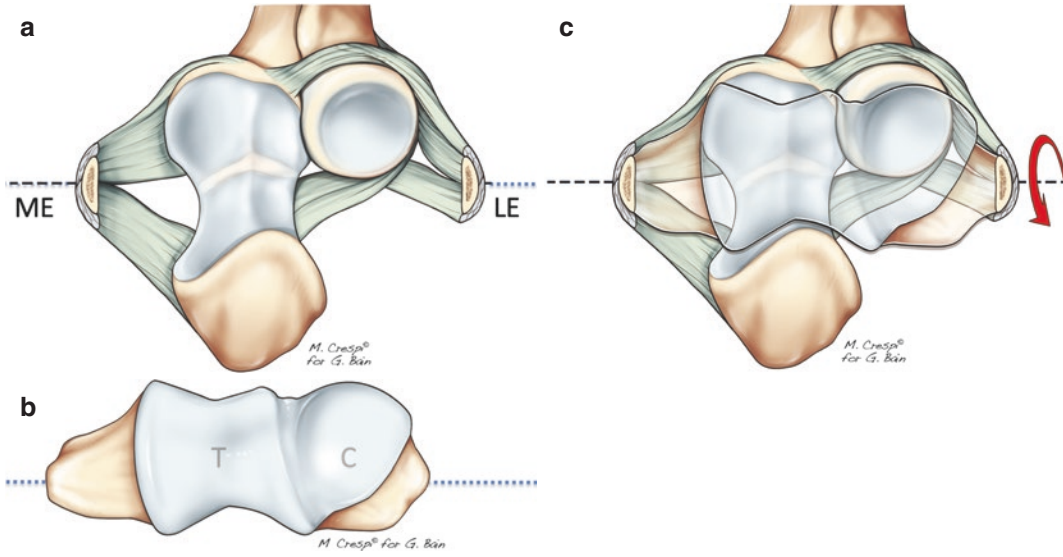

Fig. 3.2 The centre of rotation of the elbow joint. (**a**) Axis of rotation passes through the inferior edge of the medial epicondyle to the small tubercle of the lateral epicondyle. (**b**) This coincides with the centre of rotation of the capitellum and trochlear. (**c**) Humerus and ulnar seen together (copyright Dr. Gregory I. Bain and Max Crespi)

the intramedullary canal, with vessels supplying the radial head (Fig. 3.4).

Elbow ossification during childhood occurs at six elbow ossification centres in a reproducible order. Its order of appearance is the capitellum, radial head, internal epicondyle, trochlea, olecranon and external epicondyle (CRITOE). Being familiar with this order of ossification of the elbow is important in distinguishing pathology from a normal ossification centre.

3.1.2 Subcutaneous Plane

The subcutaneous plane includes the subcutaneous fat, which is abundant except over the epicondyles and the subcutaneous border of the olecranon and the ulnar shaft. The superficial veins are located predominantly in the anterior aspect and drain into the cephalic and basilic veins proximally. The cutaneous nerves are located in the very depths of the subcutaneous fat, just superficial to the investing layer. If the surgeon elevates the subcutaneous tissues at the level of the deep fascia, the cutaneous nerves will be protected.

The lateral cutaneous nerve of the forearm runs adjacent to the cephalic vein over the lateral forearm and just lateral from the distal biceps tendon at the elbow. The medial cutaneous nerve of the forearm and the superficial lymphatics follows the superficial veins. This includes some of the lymphatics from the hand, which accompany the basilica vein to the supratrochlear node just proximal to the medial epicondyle. Consequently, disorders of the hand can present with a swollen supratrochlear node.

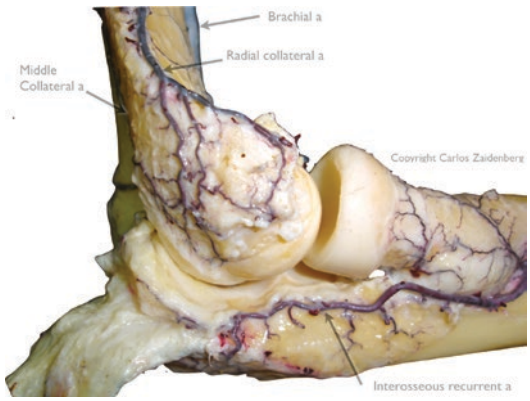

Fig. 3.3 Lateral view of blood supply of distal humerus, with vessels to the epicondyle (copyright Carlos Zaidenberg, Argentina)

3.1.3 Deep Investing Fascia of the Upper Limb

The deep investing layer of fascia encircles the muscular compartments and inserts into the medial and lateral intermuscular septum. These intermuscular septa separate the arm into anterior and posterior compartments and stabilize the fascia to the distal humerus, namely the medial and lateral supracondylar ridges.

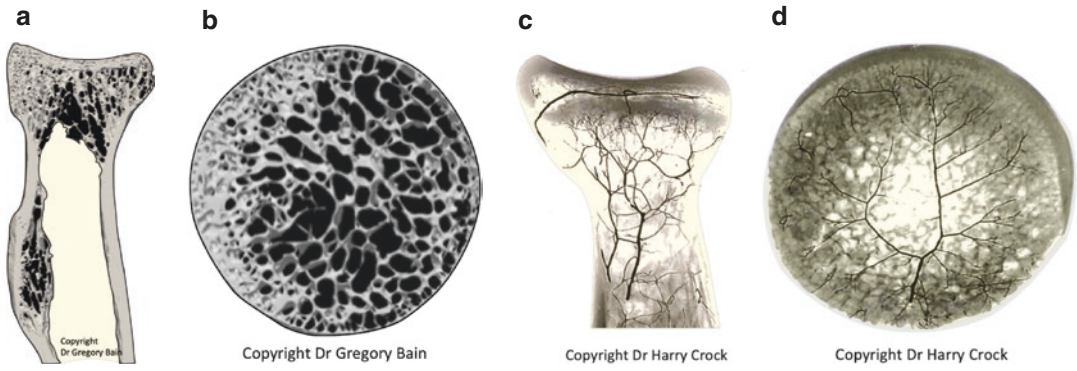

Fig. 3.4 Radial head anatomy. Radial head micro-CT scan image coronal (**a**) and axial (**b**) planes. Vascularity of the radial head. (**c**) End vessels that supply the radial head (13-year-old boy). (**d**) Arterial grid within the radial head (55-year-old man). (From Crock HV. An atlas of vascular anatomy of the skeleton & spinal cord. first ed. London: Martin Dunitz; 1996. Figures copyright HV Crock AO)

The lateral intermuscular septum (LIMS) is perforated by the radial nerve and anterior descending branch of the profunda brachii artery, approximately 10 cm proximal to the lateral epicondyle. On the medial aspect, the medial intermuscular septum (MIMS) is perforated by the ulna nerve and ulnar collateral artery, about 8 cm above the medial epicondyle.

3.2 Muscular Layer

3.2.1 Biceps Brachii Muscle

The biceps brachii muscle is composed of two heads and tends to merge at the level of the deltoid tuberosity. It is innervated by a branch of the musculocutaneous nerve, commonly entering the muscle belly 134 mm from the edge of the acromion (Fig. 3.5a). Occasionally, a second branch enters the muscle 24 mm distal to the initial innervation. Variants with the presence of three or more heads have been reported but are uncommon.

The proximal tendon of the long head is attached to the supraglenoid tubercle, posterior to the labrum in most cases, and is extra-synovial within the glenohumeral joint. The proximal tendon of the short head is attached to the coracoid process. The biceps muscle and tendon rotate 90° externally from origin to its insertion onto the biceps tuberosity distally and act on three joints: the glenohumeral, ulnohumeral and proximal radioulnar joints. A completely bifurcated distal tendon insertion is not uncommon. The short head of the distal biceps tendon inserts more distally, while the long head insertion is more eccentric, medial and proximal. The moment arm of the long head is greater in supination, while the short head is greater in pronation and neutral position. These findings may allow functional independence and isolated rupture of each portion and have consequences for restoring the native anatomy during a surgical repair. Several

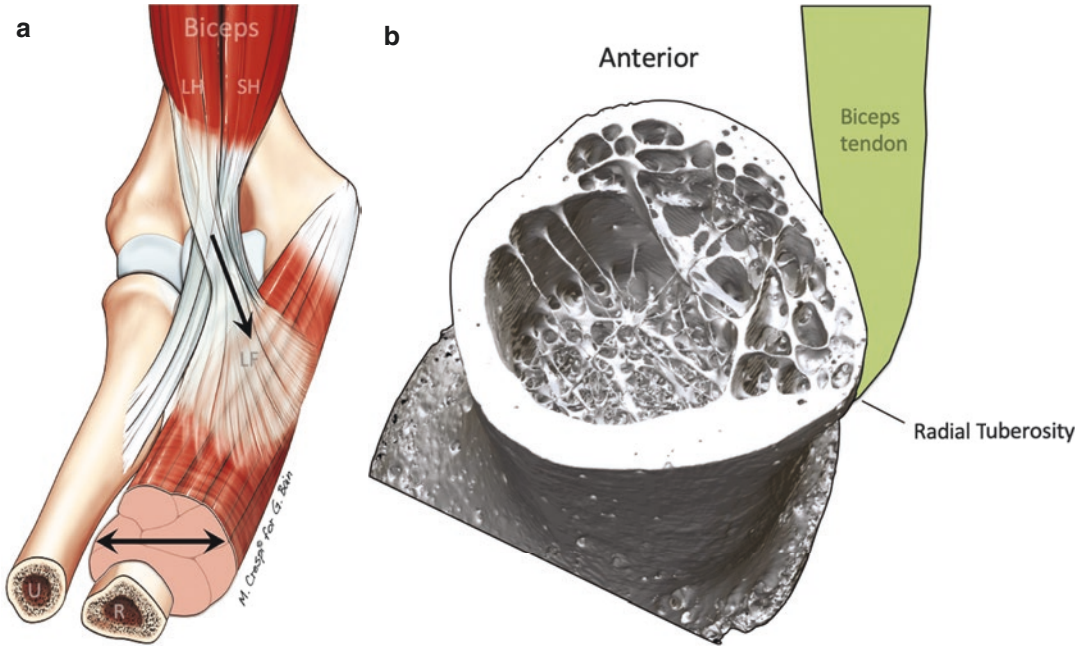

Fig. 3.5 Biceps tendon, with the long (LH) and short heads (SH). (**a**) The lacertus fibrosus is connected to the long head, and surrounds the short head, and then coalesces with the deep fascia of the forearm. Contraction of the forearm muscles tightens the fascia and the lacertus, pulling the biceps medially, and passively increasing the tension (copyright Dr. Gregory I. Bain and Max Crespi). (**b**) Insertion of the biceps tendon into the radial

authors reported an isolated rupture of one of the two tendons in cases of bifurcated distal biceps tendons.

The bicipital aponeurosis (lacertus fibrosus) is a thickening of the deep fascia that spans from the distal biceps tendon to the subcutaneous border of the ulna. It encases the forearm flexor muscles and stabilizes the distal biceps tendon, mainly the short head. It contributes to ulna flexion and provides a coordinated elbow flexion and forearm rotational movement. As the forearm flexors contract, the lacertus becomes tense, resulting in a medial pull on the biceps tendon, thereby increasing its force. This may increase its risk of rupture. In low-demand patients with a distal biceps tear, an intact lacertus fibrosus may help lessen the overall functional deficit and thus the need for surgical reconstruction of the distal biceps. If distal biceps surgical reconstruction or repair is chosen, the lacertus can be released and subsequently repaired post-procedure but must not be repaired tight as this can result in impingement of the median nerve and/or brachial artery. A surgical technique using the lacertus fibrosus as a local graft source for chronic distal biceps tendon ruptures to avoid harvest-site morbidity has been described. Next to the lacertus fibrosus (Fig. 3.1), the muscular layer is divided into the flexor extensor compartments by the medial and lateral intermuscular septum [1].

The bicipito-radial bursa drapes over the two biceps brachii tendons near their insertion, lying between the brachialis muscle and the distal tendons when the elbow is extended and between the proximal radius and biceps tendon in pronation. This structure is of clinical importance during endoscopic evaluation of the distal biceps tendon after injury. Injection of the bursa under ultrasound control can be part of the conservative treatment regime. The biceps tendon inserts into the radial tuberosity, with its two components, the long head inserting proximally and the short head distally. The internal structure of the radial tuberosity consists of internal braces, which accommodate the considerable rotatory torque from the biceps tendon (Fig. 3.5b).

As described by Seiler et al. [2], the distal biceps tendon is a paratenon-covered extrasynovial tendon with three zones of vascularity. The proximal zone receives blood supply from branches of the brachial artery while the distal zone receives its supply from the posterior interosseous recurrent artery. The middle zone obtains its blood supply from both sources but as its supply is tenuous, it has been proposed to be an area of transition and is more prone to attrition, rupture and reduced healing capabilities.

3.2.2 Triceps Brachii Muscle

The primary and only extensor of the elbow is the triceps brachii muscle that occupies the entire posterior aspect of the arm (Fig. 3.6). The radial nerve (C6–C8) provides muscular branches to the long and medial head proximal to the spiral groove, and to the medial and lateral heads within the spiral groove. The anconeus is supplied by the second branch to the medial head and is therefore at risk during any surgical approach proximal to the anconeus.

The triceps brachii originates from three proximal heads (long, lateral and medial) that insert on the tip of the olecranon. The long head arises from the infraglenoid tuberosity of the scapula and has a dual effect on both the shoulder and elbow. The lateral head is the strongest of the three, due to its extensive humeral origin proximal to the spiral groove. The medial head arises distal to the spiral groove, deep to the above two heads, and is also appropriately named “the deep head”. The long and lateral heads coalesce in the midline to form a common superficial tendon, which inserts into the proximal olecranon and adjacent deep fascia. The deep medial head is muscular and inserts mainly into the olecranon and joint capsule. At the lateral side, the triceps expands beyond the olecranon and continues with the anconeus muscle and the antebrachial fascia and finally inserts on the ulna. The subtendinous olecranon bursa protects the triceps from the top of the olecranon.

A partial rupture of the medial head has been described. The long and lateral heads have minimal activity except in resisted extension. In contrast, the medial head is active in all aspects of

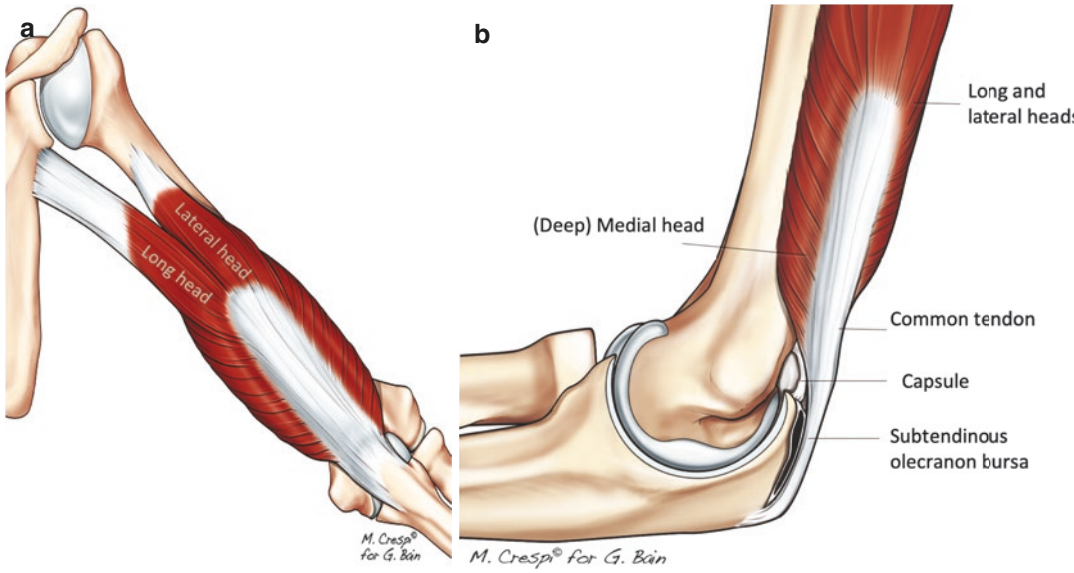

Fig. 3.6 Triceps anatomy. (**a**) Posterior view of the triceps long and lateral heads, which coalesce to create a conjoined superficial tendon. The medial head is deep, takes origin from the distal humerus and both intermuscular septa. (**b**) Medial view of the triceps tendon insertion into proximal olecranon (copyright Dr. Gregory I. Bain and Max Crespi)

extension. This may explain the common scenario of avulsion of the conjoined superficial head (long and lateral) with an intact deep medial head. The triceps has its greatest lever arm when the elbow is fully flexed but has its greatest power when the elbow is near full extension. It can also assist with fine movements of the hand and forearm by stabilizing the elbow joint in a fixed position.

Rarely, a prominent medial head can dislocate over the medial epicondyle. In addition to pain symptoms, it can cause tendon and nerve pathology. Known as snapping triceps syndrome, it is usually due to an anomalous slip of the triceps muscle that passes behind the medial epicondyle on elbow extension and snaps anteriorly with flexion. In this scenario, a bursa will exist between the snapping tendon and the epicondyle.

3.2.3 Anconeus Muscle

The anconeus arises from a small depression on the posterior aspect of the lateral epicondyle and inserts into the proximal ulna (Fig. 3.7a). Innervation is via the radial nerve, namely the second motor branch of the medial head of the triceps, that inserts into the proximal aspect of the muscle (Fig. 3.7b, c). The anconeus muscle has a joint-stabilizing function. It has been used as a local transposition flap for skin coverage, interposition between the radius and ulna and between the radial neck and capitellum. It provides an important landmark for surgical approaches on the lateral side of the elbow.

3.2.4 Supinator Muscle

The supinator is important because of its close proximity to the posterior interosseous nerve (PIN). It consists of two heads proximally: (1) the deep ulnar head takes origins from the supinator fossa and crest of the ulna and (2) the superficial head arises from the distal aspect of the lateral epicondyle, just anterior from the anconeus, and the radial collateral ligament and proximal ulna, just behind the supinator crest. The arcade of Frohse is the fibrous arch of the proximal aspect

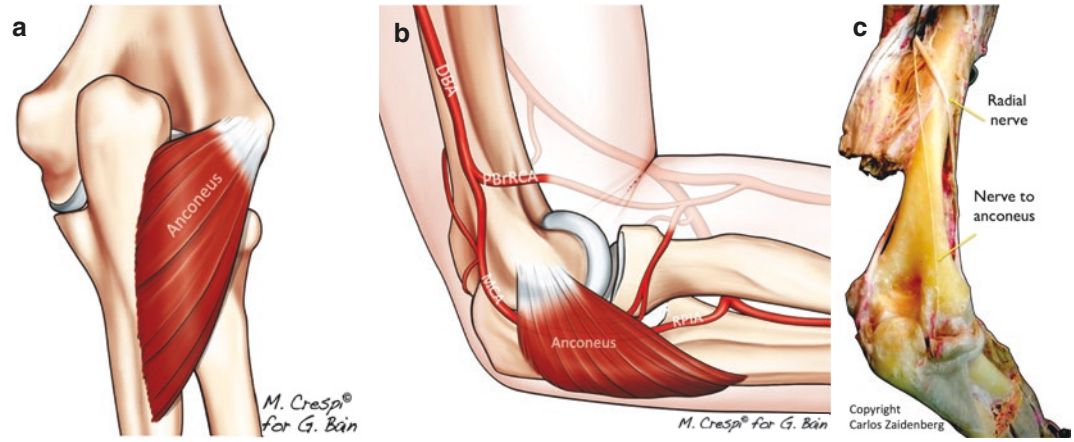

Fig. 3.7 Anconeus muscle. (**a**) Extends from the lateral condyle to the subcutaneous border of the proximal ulna. (**b**) The vessels that supply the anconeus muscles. Olecranon (copyright Dr. Gregory I. Bain and Max Crespi). The nerve to anconeus passes from proximal radial nerve to the interval between the epicondyle and olecranon (copyright Dr. Carlos Zaidenberg, Argentina)

of the superficial head of the supinator muscle. It is a common site of compression of the PIN. The supinator wraps around the radius, inserting into the proximal radius distally between the posterior and anterior oblique lines [3].

The PIN supplies both heads, then passes between the heads and exits 2 cm from the distal edge of the supinator muscle, to supply the remaining extensor muscles of the wrist and fingers. Hilton's law states that "a nerve supplying a joint also supplies both the muscles that move the joint and the skin covering the articular insertion of these muscles" [4].

3.2.5 Cubital Fossa

The cubital fossa is a triangular space bordered **proximally** by a line between the lateral and medial epicondyles, **laterally** by the brachii radialis and **medially** by the pronator teres muscles. The contents of the cubital fossa, from medial to lateral, include the median nerve, brachial artery, biceps tendon, radial nerve and PIN. The floor is formed by the brachialis and supinator muscles. The roof is formed by the deep fascia of the forearm and the bicipital aponeurosis (lacertus fibrosus) (Fig. 3.8). It is a convenient site for both

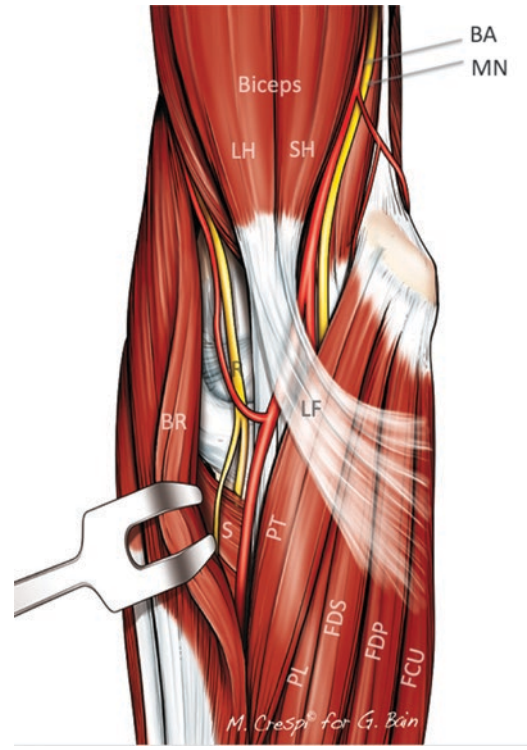

Fig. 3.8 Cubital fossa. The cubital fossa is the triangular space formed by a line joining the medial and lateral epicondyles and the borders of the brachioradialis and pronator teres. The contents from the medial aspect are the median nerve, brachial artery, biceps tendon and radial nerve (copyright Dr. Gregory I. Bain and Max Crespi)

venous and arterial access and anaesthetic blocks of the forearm and hand.

3.2.6 Pronator Teres Muscle

The pronator teres muscle is the most anterior, proximal and medial muscle of the flexor pronator group. It has two heads: a large humeral head, originating from the medial supracondylar ridge and anterior superior medial epicondyle, and a smaller ulnar head that originates from the coronoid process. The median nerve passes between and supplies both heads. A fibrous arch exists between both heads of the pronator teres and can cause impingement of the median nerve along its path. The pronator teres has a common insertion onto the most radial border of the radius in its middle third. Its main function is to pronate the forearm. A small secondary function would be to assist in elbow flexion.

A well-known anatomical variant is the **anteromedial supracondylar spur**, 5–7 cm above the medial epicondyle. The **ligament of Struthers** spans from this spur to the medial epicondyle and is the origin of an accessory pronator teres muscle. This ligament can entrap the median nerve and/or the brachial artery.

Fig. 3.9 The two heads of the brachialis muscle; superficial head of the brachialis (SH) has a long humeral origin, and a long tendon so that it looks similar to the biceps tendon. The deep head (DH) is the "anterior anconeus", which with the true anconeus provides dynamic rotatory stability of the elbow (copyright Dr. Gregory I. Bain and Max Crespi)

3.2.7 Brachialis Muscle

The brachialis muscle originates from the anterior part of the distal half of the humerus near the insertion of the deltoid muscle. There are two heads, a superficial and a deep head (Fig. 3.9) [5]. The **superficial** head has a long proximal origin with a cordlike tendon that attaches to the anterior proximal humerus. The thick superficial tendon can be transferred into the distal stump of the biceps tendon, to create a new active supinator, if the biceps brachialis tendon is disrupted. The superficial brachialis tendon can also become entrapped between the radial neck and the proximal ulnar, so that it obstructs reduction of the radial head [6]. The **deep** head is a short fleshy muscle that takes origin from the anterior distal humerus and medial intermuscular septum, and inserts obliquely into the proximal ulnar, as if it were the "anterior anconeus". This "anterior anconeus" and the true anconeus provide a dynamic sling between the humerus and ulna, to stabilize the elbow against rotatory instability. Use of the brachialis for tendon transfer has also ever been described in brachial plexus injuries.

The deep head is more important for initiation of flexion from full extension, and the superficial head provides greater power once the elbow is flexed. The brachialis is the strongest flexor of the elbow joint. This muscle has the largest cross-sectional area of all flexors but suffers from a

poor mechanical advantage because it crosses closer to the axis of rotation.

The brachialis muscle is innervated by the musculocutaneous nerve (C5–C7), which runs on its superficial surface. It is often considered that the lateral aspect of the brachialis is supplied by the radial nerve. However, it is more likely that the radial nerve supplies the superficial head of the brachialis.

3.2.8 Brachioradialis Muscle

The brachioradialis muscle runs exclusively across the elbow. It originates from the lateral intermuscular septum and the proximal aspect of the distal humerus lateral supracondylar ridge and inserts into the distal styloid process of the radius. It has the greatest mechanical advantage of any elbow flexor. It assists in elbow flexion when the forearm is pronated as the biceps brachii is mechanically disadvantaged in pronation. It will also produce forearm rotation back to the neutral position (i.e. supinates the pronated forearm and vice versa).

3.2.9 Extensor Muscles

The forearm extensor muscles originate from the lateral distal humerus and is innervated by the radial nerve. The extensor carpi radialis longus originates from the distal aspect of the supracondylar ridge just below the origin of the brachioradialis muscle and inserts into the base of the second metacarpal. The common extensor origin, at the lateral epicondyle, includes the extensor carpi radialis brevis, extensor digitorum communis, extensor digiti minimi and extensor carpi ulnaris.

3.2.10 Neural Tubes About the Elbow

The three major nerves all pass through fibrous tunnels as they traverse the elbow. The sites of common entrapment are listed in Table 3.1.

Table 3.1 Sites of nerve entrapment about the elbow

Ulnar nerve	Median nerve	Radial nerve and PIN
Arcade of Struthers	Ligament of Struthers	ECRB edge
Anconeus epitrochlearis	**Lacertus fibrosus**	**Arcade of Frohse**
Osborne's fascia	**Pronator teres**	Recurrent leash of Henry
Flexor pronator aponeurosis	FDS arch proximal free edge	Distal edge of supinator

Causes from proximal to distal. Most common sites in **bold**

3.2.11 Ulnar Nerve

The ulnar nerve arises from the medial cord of the brachial plexus (C8–T1). It traverses the MIMS 8 cm proximal to the medial epicondyle with the superior ulnar collateral artery along the medial aspect of the triceps. The ulnar nerve provides no branches within the arm. The ulnar nerve passes deep to the proximal fibrous arch of the flexor carpi ulnaris muscle, commonly referred to as Osborne's fascia (Fig. 3.10). Two small articular branches supply the elbow joint. The ulnar nerve provides motor branches to both heads of the flexor carpi ulnaris before passing between the heads to innervate the ulnar half of the flexor digitorum profundus tendons as it advances distally into the forearm. Sites of entrapment around the elbow include the **arcade of Struthers** proximally, which is a band of fascia between the medial intermuscular septum and the fascia over the triceps brachii. It should be released following anterior transposition of the ulnar nerve. The **cubital tunnel** is a fibro-osseous tunnel through which the ulnar nerve passes at the elbow. Its borders include Osborne's fascia (roof), posterior and transverse bands of the medial collateral ligament (floor), medial epicondyle (medial) and proximal ulna (lateral). During elbow flexion, the cubital retinaculum is stretched, potentially compressing the ulnar nerve. This places the motor fibres of the FDP and FCU at greater risk of entrapment as they are superficial. Another possible cause of ulnar

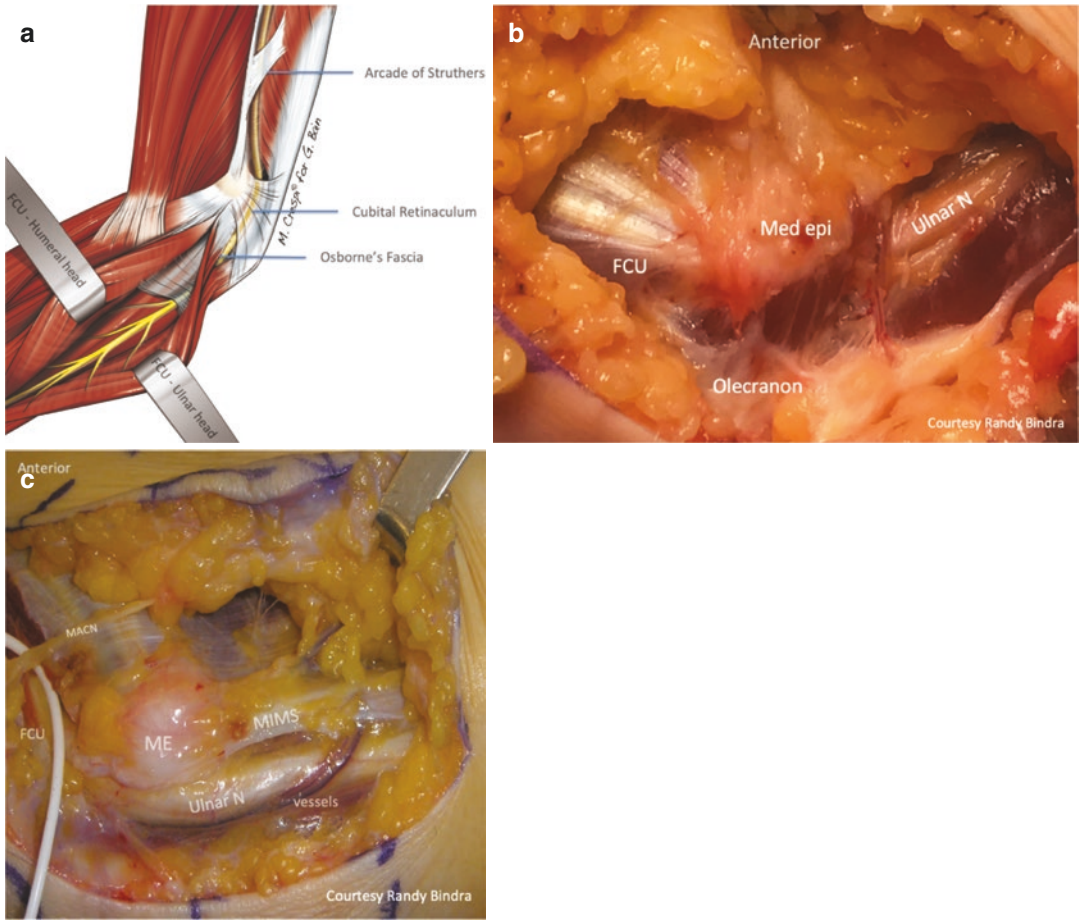

Fig. 3.10 Ulnar nerve. (**a**) The ulnar nerve passes through the arcade of Struthers (fibrous tissue that spans from the triceps fascia to the MIMS), the cubital tunnel and the arcade of Osborne (fascia between the two heads of FCU) (copyright Dr. Gregory I. Bain and Max Crespi). (**b**) The anconeus epitrochlearis muscle extends from the medial epicondyle to the olecranon (courtesy Randy Bindra). (**c**) There is a vessel 2 cm proximal to the medial epicondyle that is identified at the time of ulnar nerve release. When excising the medial intermuscular septum (MIMS) it can be identified (copyright Dr. Randi Bindra)

nerve entrapment is the **anconeus epitrochlearis** (Fig. 3.10b), a small anomalous muscle that extends from the medial olecranon to the medial epicondyle. It is present in approximately 2% of cases. We believe that traction on the muscle leads to a thickening of the cubital retinaculum and then indirectly, to ulnar nerve entrapment. There is a vessel 2 cm proximal to the medial epicondyle, which is at risk during dissection in this area.

3.2.12 Radial Nerve

The radial nerve is a terminal branch of the posterior cord of the brachial plexus (C5–T1). It innervates the long and medial heads of the triceps before entering the spiral groove where it provides branches to the medial and lateral heads. It perforates the LIMS 10 cm proximal to the lateral epicondyle, with the anterior descending branch of the profunda brachii artery, as it enters the ante-

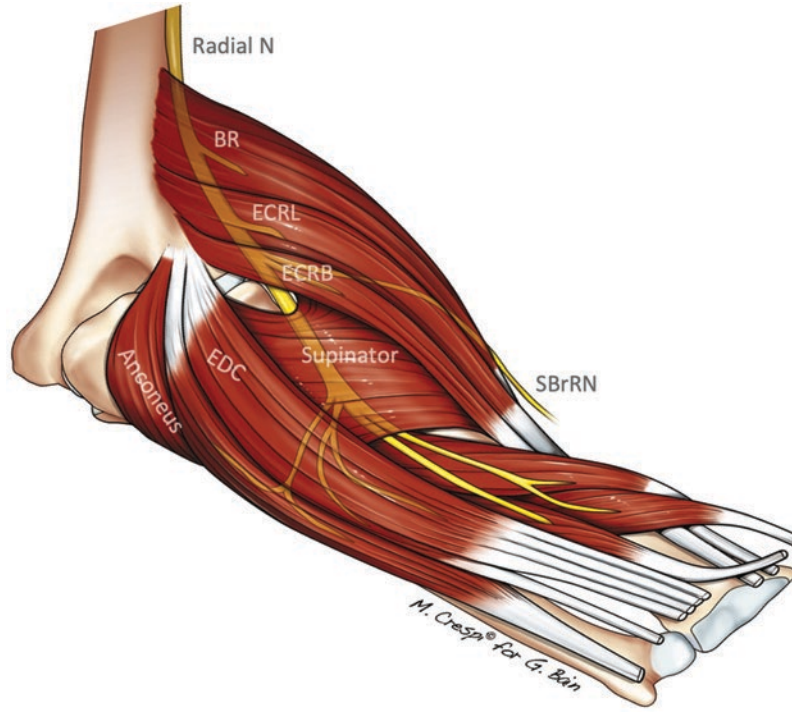

Fig. 3.11 The radial nerve passes through the spiral groove, and then between the brachialis and brachioradialis. It supplies both wrist extensors, and then at the level of the elbow, it passes over the anterior elbow capsule. It bifurcates into the PIN and the superficial branch of the radial nerve. The PIN courses between the two heads of supinator, and supplies the ECU and the extensors of all the digits (copyright Dr. Gregory I. Bain and Max Crespi)

rior compartment of the arm and lies between the brachialis and brachioradialis muscles. It provides innervation to both muscles (Fig. 3.11).

The radial tunnel extends 5 cm from the radiocapitellar joint to a level just distal to the proximal aspect of the superficial head of the supinator muscle. The lateral wall is formed by the brachioradialis and extensor carpi radialis longus and brevis. Medially it is bounded by the distal biceps brachii tendon and the brachialis. The roof of the tunnel is formed by the brachioradialis, which spirals over the radial nerve from lateral to anterior. The floor of the radial tunnel is the anterior capsule proximally and the deep head of the supinator distally. The radial nerve provides a branch to the ECRL, and then bifurcates into the superficial branch of the radial nerve (SBRN) and the PIN. The PIN supplies the two heads of the supinator, and then passes between the two heads before supplying the remaining extensors of the hand and wrist. The commonest site of compression of the PIN is beneath the arcade of Frohse, which is the fibrous proximal edge of the superficial head of the supinator.

The SBRN passes superficial to the supinator muscle as it advances distally into the forearm. It supplies the cutaneous innervation to the dorsal aspect of the base of the thumb and first webspace, and deep sensation and proprioception to the wrist and interosseous membrane [3, 7].

3.2.13 Median Nerve

The median nerve comprises both the lateral (C6–7 roots) and medial cords (C8–T1 roots) of the brachial plexus. It lies in the cubital fossa, anterior to brachioradialis, and medial to the brachial artery and biceps tendon (Fig. 3.12). At the elbow, from proximal to distal, the nerve can be entrapped by the ligament of Struthers, lacertus fibrosus, fibrous bands between the two heads of pronator teres and fibrous arch of FDS.

The bicipital aponeurosis is now recognized to be an important cause of median nerve entrapment. In a patient who fails to respond to carpal tunnel surgical release, compression proximally at its two more common sites, the bicipital

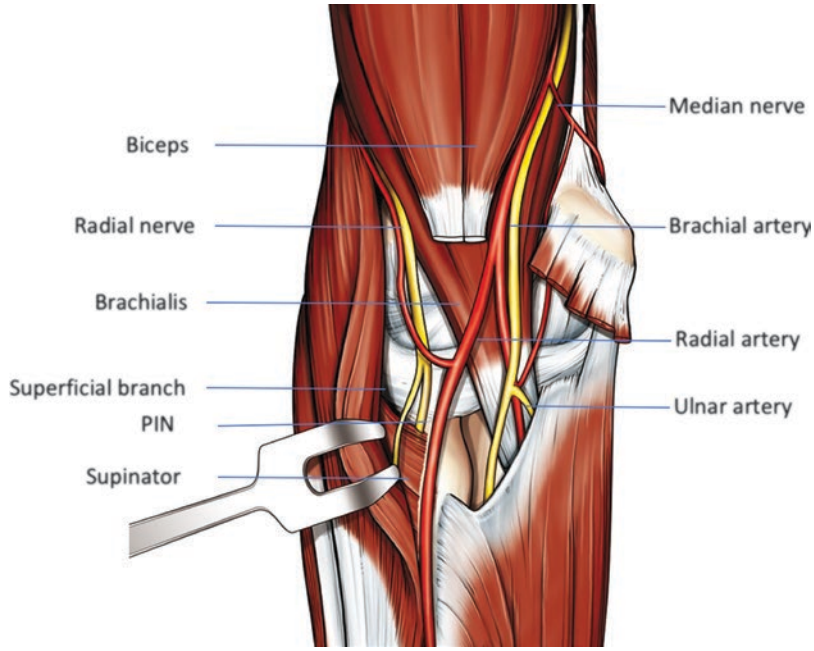

Fig. 3.12 The median nerve passes below the lacertus fibrosus, between the two heads of the pronator teres, and beneath the FDS arch (copyright Dr. Gregory I. Bain and Max Crespi)

aponeurosis or fibrous arch between the two heads of the pronator teres, should be considered.

3.2.14 Capsular Anatomy

The joint capsule encases the three elbow joints and the olecranon, coronoid and radial fossae. At the level of the radial head, distal from the radial annular ligament, the joint capsule forms a recess to preserve good rotation of the radius. The joint capsule is thickened on the medial and lateral aspects to form the collateral ligaments, which provide stability against varus, valgus and rotational stresses. The capsule is loose anteriorly and especially the posterior aspects to allow flexion and extension of the elbow (Fig. 3.13). The mean capsular capacity in the normal elbow joint is 23 mL. The capsule is most lax at 70° flexion and patients with capsular pathology prefer this position. This is the position in which elbow arthroscopy is commonly performed. The articularis cubiti (muscle) prevents the capsule from being entrapped in the joint.

3.2.15 Ulnar Collateral Ligament

The medial collateral ligament is a triangular ligamentous complex consisting of three separate components: anterior ligament, a posterior ligament of Bardinet and a transverse ligament of Cooper (Fig. 3.14). The humeral origin is eccentric with respect to the rotational axis of the joint. The anterior ligament consists of parallel fibres running from its origin on the antero-inferior aspect of the medial epicondyle, and inserts onto the medial coronoid process (mean length 27.1 mm, width 4.7 mm), also known as the sublime tubercle. It is the strongest of the three ligaments and protects against excessive valgus stresses. This anterior ligament can be divided into an anterior and a posterior band, which have slightly different functions in resisting a valgus stress. The anterior band of the anterior ligament is the primary restraint to valgus stress up to 90° flexion and becomes less important with more flexion. The posterior band of the anterior ligament is more important between 60° and maximum flexion.

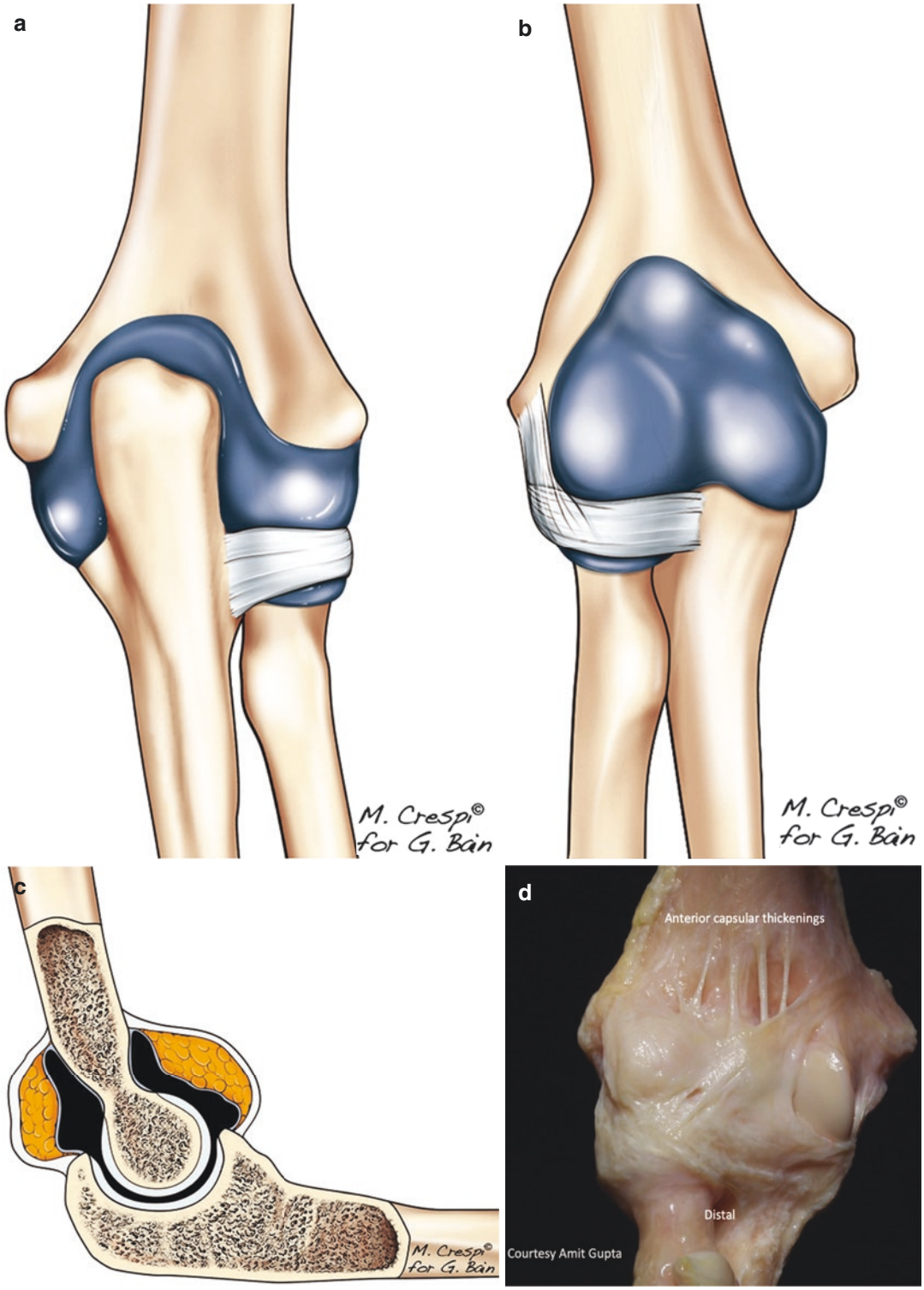

Fig. 3.13 Elbow capsule and synovial reflections. (**a**) Anterior view. (**b**) Posterior view. (**c**) Lateral view of capsule with the Haversian fat pad that is displaced with a hem-arthrosis, and is responsible for the fat pad sign (copyright Dr. Gregory I. Bain and Max Crespi). (**d**) Anterior capsule thickening that restrains hyperextension. Post-traumatic contracture creates a fixed flexion deformity (courtesy Dr Amit Gupta)

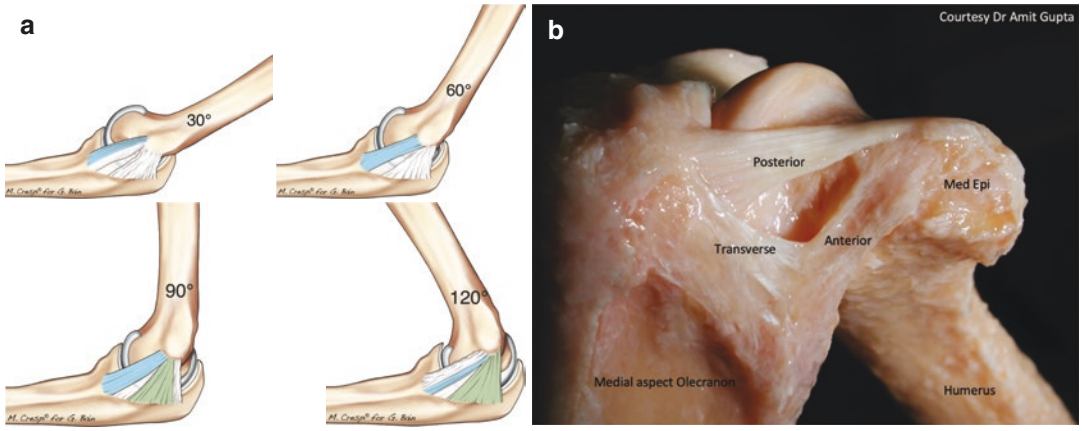

Fig. 3.14 (**a**) Anterior and posterior parts of ulnar collateral ligament in different flexion angles. The coloured aspect demonstrates taut part of ligament (copyright Dr. Gregory I. Bain and Max Crespi). (**b**) Cadaveric dissection with the three parts of the ligament (courtesy Dr. Amit Gupta)

The posterior ligament is a fan-shaped thickening of the capsule that originates from the inferior aspect of the medial epicondyle and inserts onto the medial margin of the semilunar notch of the olecranon (mean length 24.2 mm, width 5.3 mm). The posterior ligament forms the floor of the cubital tunnel. It is an important stabilizer to pronation, and if thickened can restrict flexion. It is a secondary restraint to valgus, as it is loaded when the anterior bundle is ruptured [8, 9].

As the normal elbow moves from flexion to extension, the point of loading changes from the coronoid to the olecranon process. Between the processes is the bare area. The transverse ligament connects the medial coronoid and olecranon processes, which resists the tensile forces which occur with co-contraction of the triceps and the brachialis. Therefore, this ligament is a restraint to the central dislocation (disruption) [10].

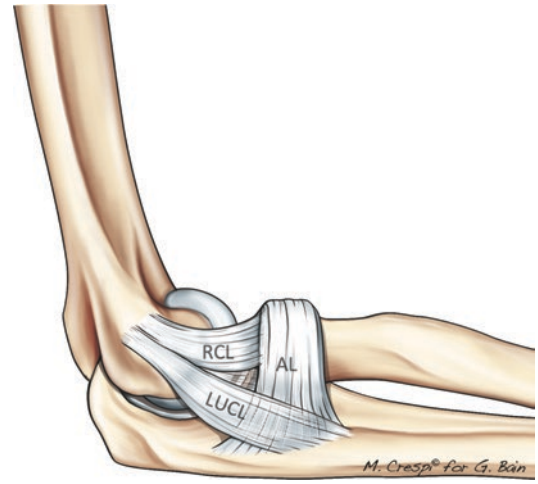

Fig. 3.15 Lateral ligament complex; with the lateral ulnar collateral ligament (LUCL), accessory lateral ulnar ligament, radial collateral ligament (RCL) and annular ligament (AL) (copyright Dr. Gregory I. Bain and Max Crespi)

3.2.16 Lateral Ligament Complex

The lateral collateral ligament complex consists of four distinct bundles: lateral ulnar collateral ligament (LUCL), accessory lateral ulnar ligament, radial collateral ligament (RCL) and annular ligament (AL) (Fig. 3.15). These ligaments form a complex, but it can be difficult to distinguish the separate structures. The anterior and posterior parts of the radial collateral ligament are tight in extension and flexion, respectively, while the middle part is tight between extension and flexion. The RCL extends to the annular ligament, and together, they become a varus restraint. The quadrate ligament spans from the radius to the ulna, and also attaches to the distal edge of the annular ligament. The accessory lateral ulnar ligament runs from the lateral epicondyle to the

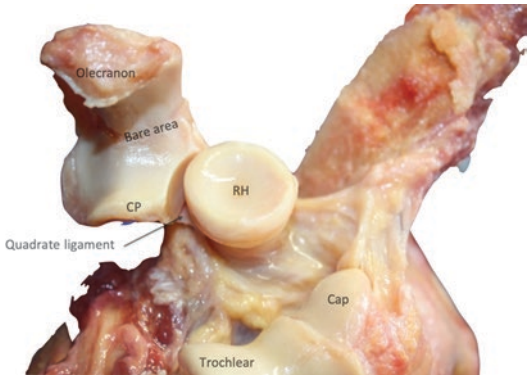

Fig. 3.16 Proximal radioulnar joint with the quadrate ligament spanning from the radius to the ulna (copyright Dr. Gregory I. Bain)

supinator crest of the ulna and the inferior margin of the AL. The LUCL attaches to the supinator crest of the ulna in three various ways [11]:

- Type 1: Bilobed LUCL insertion (27%)
- Type II: LUCL coalesces with the AL insertion (23%)
- Type III: LUCL and AL insert with a conjoined broad base at the supinator crest (50%)

The annular ligament encircles the radial head and attaches to the margins of the sigmoid notch. It acts to stabilize the proximal radioulnar joint and the radiocapitellar joint.

The quadrate ligament of Denucé is the most proximal aspect of the interosseous membrane, and is located just distal to the annular ligament (Fig. 3.16). This quadrate ligament reinforces the inferior aspect of the elbow capsule and contributes to stability by securing the proximal radius to the radial notch. For the patient who has a restricted supination, it can be a restraint that may require release.

The interosseous membrane transmits the load from the hand to the radius, and then onto the ulna (Fig. 3.17). It prevents radius proximal migration (Essex-Lopresti lesion or longitudinal radioulnar dissociation) and divergence.

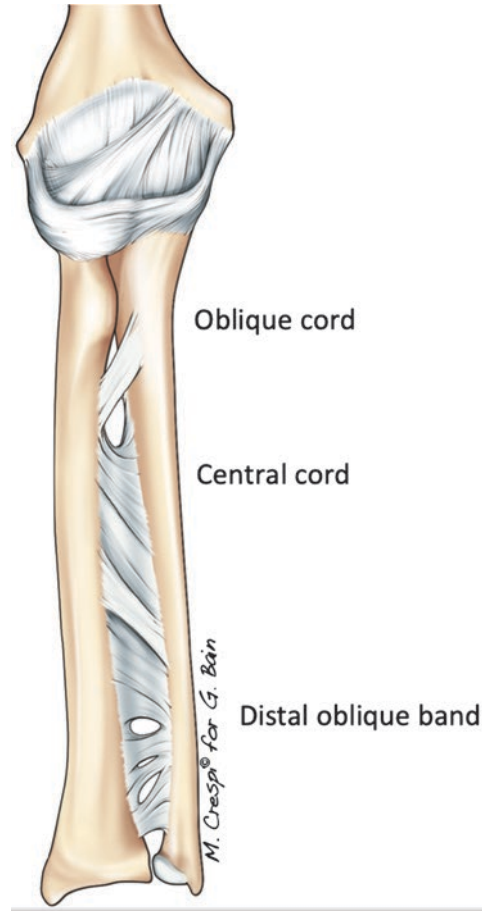

Fig. 3.17 Interosseous membrane, with the oblique cord, central cord and distal oblique band (copyright Dr. Gregory I. Bain and Max Crespi)

References

1. Basmajian JV. Muscles alive. 2nd ed. Baltimore: Williams & Wilkins; 1967.
2. Seiler JG III, Parker LM, Patricia D, Chamberland C, Sherbourne GM, Carpenter WA. The distal biceps tendon. J Shoulder Elbow Surg. 1995;4:149–56.
3. Spinner M. The arcade of Frohse and its relationship to posterior interosseous nerve paralysis. J Bone Joint Surg. 1968;50B:809–12.
4. Bateman JE. Denervation of the elbow joint for the relief of pain. A preliminary report. J Bone Joint Surg Br. 1948;30B:635–41.
5. Leonello DT, Galley IJ, Bain GI, Carter CD. Brachialis muscle anatomy; a study in cadavers. J Bone Joint Surg Am. 2007;89:1293–7.

6. Camp CL, O'Driscoll SW. Transbrachialis buttonholing of the radial head as a cause for irreducible radiocapitellar dislocation: a case report. J Pediatr Orthop. 2015;35(7):e67–71.
7. Lister GD, Belsole RB, Kleinert HE. The radial tunnel syndrome. J Hand Surg. 1979;4A:52–9.
8. Fuss FK. The ulnar collateral ligament of the human elbow joint. Anatomy, function and biomechanics. J Anat. 1991;175:203–12.
9. O'Driscoll SW, Jaloszynski R, Morrey BF, An KN. Origin of the medial ulnar collateral ligament. J Hand Surg. 1992;17(1):164–8.
10. Ring D, Jupiter JB. Fracture-dislocation of the elbow. J Bone Joint Surg Am. 1998;80(4):566–80.
11. Cohen MS, Hastings H 2nd. Rotatory instability of the elbow. The anatomy and role of the lateral stabilizers. J Bone Joint Surg Am. 1997;79(2):225–33.

4 Elbow Anatomy: A Layered Approach

Deepak N. Bhatia

4.1 Background

The elbow is a complex anatomical region formed by a multilayered soft-tissue sleeve of muscles, ligaments, and neurovascular structures. The anatomical locations of these structures are unpredictable due to paucity of anatomical landmarks and frequent variations; to add to this variability, dynamic movement at the joint further changes the surface markings for most structures. Safety during arthroscopic and endoscopic surgery around the elbow necessitates an in-depth knowledge of the reliable anatomic landmarks and their interrelationship with surrounding vital structures.

Elbow soft-tissue anatomy can be conceptualized as a set of layers formed by muscles and ligaments. Different neurovascular structures course through or in between these layers from proximal to distal. The layered approach to elbow anatomy is useful during minimally invasive open, endoscopic assisted, and all-endoscopic procedures around the elbow. The anatomical planes between layers can be utilized for safe passage of the endoscope and instruments during lower arm and cubital fossa endoscopy for access to extra-articular structures. Familiarity with the course of neurovascular structures through and between the layers helps identify safe and unsafe zones across the elbow.

4.2 Anatomical Layers of the Elbow

Anatomical structures that span the distal arm and upper forearm can be segregated into four layers formed by muscles and capsuloligamentous structures. Each layer has associated neurovascular structures and it is necessary to identify and protect these during surgical dissection (Fig. 4.1a, b).

Layer 1: The first layer is formed by the biceps brachii muscle along with distal biceps tendon and the lacertus fibrosus. The lateral and medial antebrachial cutaneous nerves of the arm are vital structures of the first layer and are closely associated with the cephalic and basilic veins.

- Biceps Brachii

  The biceps brachii is an important flexor and supinator of the elbow and forearm, and gives shape to the arm contour. The proximal long and short heads of the biceps form muscular bellies that further continue into the long and short components of the distal biceps tendon (DBT) (Fig. 4.2). Supernumerary heads at the origin and insertion have been described [1, 2]. The biceps muscular fibers merge into the DBT approximately 2–3 cm proximal to

D. N. Bhatia (✉)
SPORTSMED Mumbai, and Sir HN Reliance Foundation Hospital, Mumbai, India
e-mail: shoulderclinic@gmail.com

© ISAKOS 2022

D. N. Bhatia et al. (eds.), *Arthroscopy and Endoscopy of the Elbow, Wrist and Hand*,
https://doi.org/10.1007/978-3-030-79423-1_4

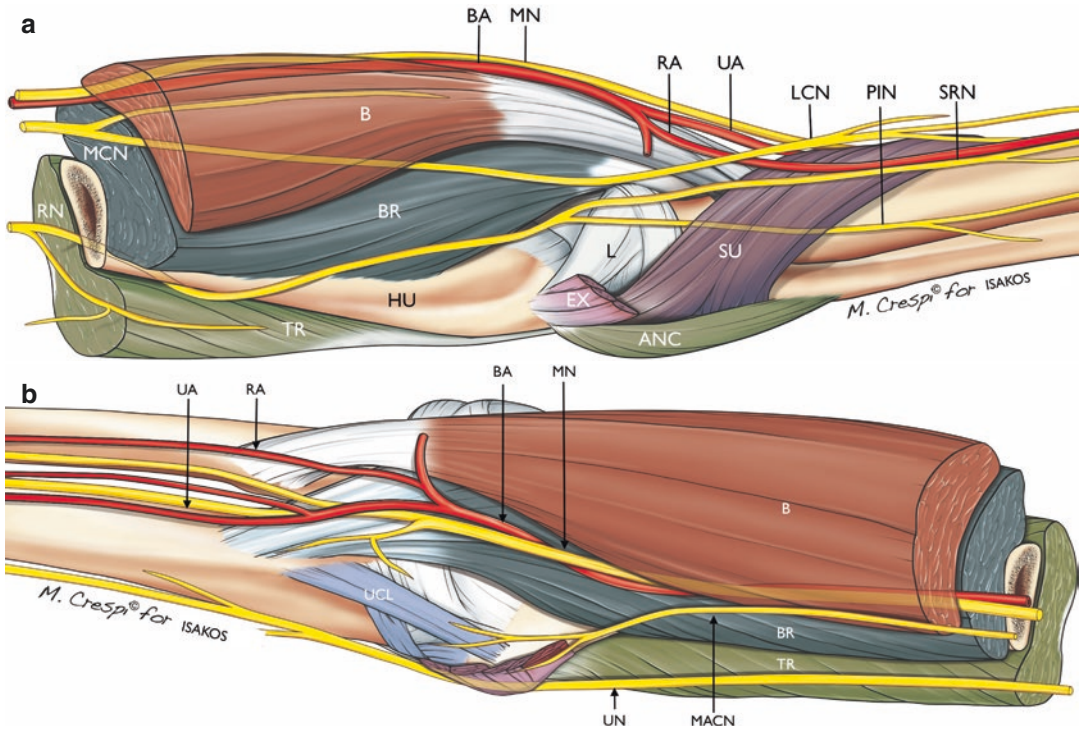

Fig. 4.1 The layered approach to elbow anatomy demonstrates anatomical planes and their associated neurovascular structures. (**a**) Lateral view. (**b**) Medial view. Layer 1: Biceps (B), medial and lateral antebrachial cutaneous nerves (MACN, LCN), and superficial veins (not shown). Layer 2: Brachialis (BR), musculocutaneous nerve (MCN), brachial artery (BA), radial and ulnar arteries (RA, UA), median nerve (MN), and radial nerve (RN). Layer 3: Distal humerus (HU), elbow capsule and ligaments (L, UCL), common extensor origin (EX), supinator (SU), superficial radial nerve (SRN), and posterior interosseous nerve (PIN). Layer 4: Triceps (TR), anconeus (ANC), radial nerve (RN, posterior compartment), ulnar nerve (UN). Note that the distal biceps tendon (DBT) traverses the lower arm and cubital fossa across all layers and connects the first and fourth layers (M. Crespi © for ISAKOS)

the AEC; the DBT then courses obliquely in the sagittal plane across the arm and cubital fossa for 7–12 cm and inserts into a distinct footprint at the bicipital tuberosity [1]. The lacertus fibrosus LF is an aponeurosis on the medial aspect of the DBT that merges distally with the deep fascia over the forearm and envelopes the muscles. The LF possibly stabilizes the DBT and facilitates the flexion force during biceps contraction. During surgical dissection, the DBT and LF can be used as anatomical landmarks to locate and protect the medial neurovascular structures that course deep to the LF in the cubital fossa. The "parabiceps space" is a region on the deep lateral aspect of the DBT that communicates with the bicipitoradial bursa in the forearm [3] (Fig. 4.3). The DBT insertion on the bicipital tuberosity has been described as a unique intraoperative reference point and is useful in dynamic rotation for predicting the position of five major neurovascular (NV) structures in the cubital fossa [4]. The biceps is innervated by the musculocutaneous nerve (C567). The detailed surgical anatomy of the DBT is described in another chapter in this book.

- Nerves
  - The lateral antebrachial cutaneous nerve (LCN) is a continuation of the musculocutaneous nerve and exits the biceps undersurface and fascia approximately at or distal to the musculotendinous junction. The nerve can be identified in the region approximately 1–3 cm proximal to the

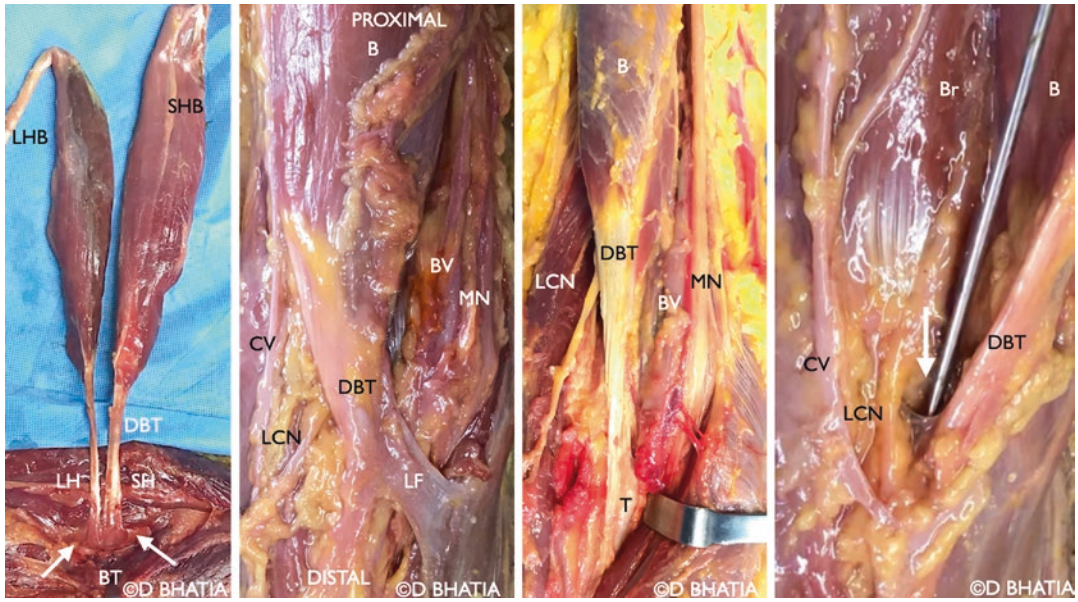

Fig. 4.2 The first anatomical layer is shown (left to right). The long and short proximal biceps tendons (LHB, SHB) continue distally to form the long and short heads (LH, SH) of distal biceps tendon (DBT) and insert on the biceps tuberosity (arrows, BT, left image). The DBT is superficial in lower arm and passes deep across the cubital fossa to insert on the tuberosity T (middle images). The "parabiceps space" communicates with bicipitoradial bursa and tuberosity (arrow, right image). *Br* brachialis, *B* biceps muscle, *LF* lacertus fibrosus, *CV* cephalic vein, *LCN* lateral cutaneous nerve, *BV* brachial vessels, *MN* median nerve (© D. Bhatia)

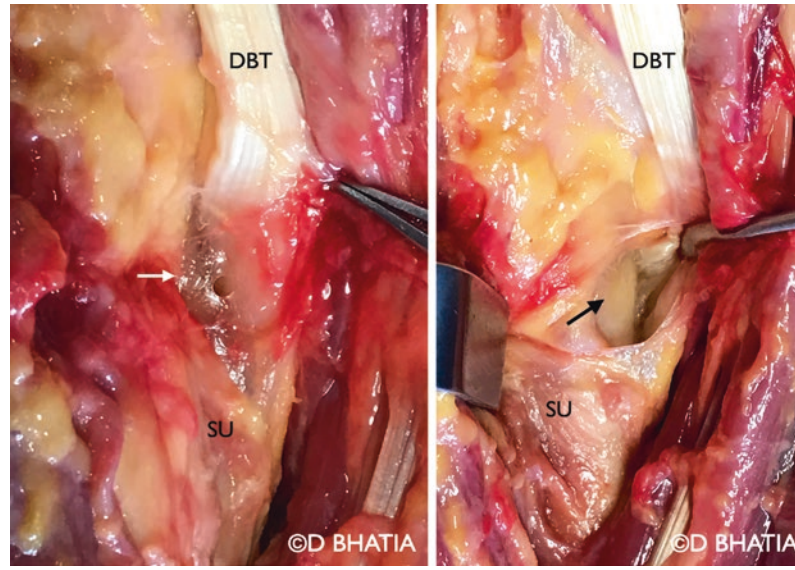

Fig. 4.3 The bicipitoradial bursa (arrow, left image) encloses a consistent bare area on the tuberosity (arrow, right) along with the supinator (SU) and distal biceps tendon (DBT) (© D. Bhatia)

AEC, and 3–4 cm from the lateral epicondyle (Figs. 4.1a and 4.2). The LCN is closely associated with the cephalic vein at the AEC and in upper forearm [5]. At the elbow joint, the LCN divides into volar and dorsal sensory branches that course distally up to the wrist and supply cutaneous innervation along the radial forearm.The medial antebrachial cutaneous nerve (MACN) pierces the deep fascia with the basilic

vein, in the mid-arm, and divides into a volar (anterior) branch (anterior to basilic vein, descends into ulnar forearm) and an ulnar (posterior) branch (medial to basilic vein, anterior aspect of medial epicondyle) (Fig. 4.1b). The anterior branch runs through the distal arm with the basilic vein, passes anterior to the elbow between the biceps tendon and medial humeral epicondyle, and courses superficial to the flexor carpi ulnaris muscle. The anterior branch provides cutaneous innervation to the distal anterior arm, antecubital fossa, and anteroulnar forearm. The posterior branch crosses anterior to the elbow and then courses posteriorly over the common flexor tendons; however, the nerve may variably cross posteriorly either proximal or distal to the medial humeral epicondyle. The posterior branch provides cutaneous innervation over the posterior olecranon and proximal half of the posteroulnar forearm [6, 7].

Surgical Significance

- The DBT is the "lighthouse" of the elbow and is a reference landmark during elbow endoscopy. The DBT begins at the first layer and courses obliquely from proximal-anterior to distal posterior across all layers to attach at the tuberosity. In the lower arm, the region lateral to the DBT is the "safe zone," and the medial aspect is "unsafe zone" with major neurovascular structures. Distal to the AEC, the insertional region can be used as a dynamic intraoperative landmark to assess neurovascular relations in this region [4].
- The "parabiceps space" provides a safe zone for placement of the "parabiceps portal" and this is the main visualization portal for the all-endoscopic approach for distal biceps repairs and reconstructions [3].
- The bicipitoradial bursa and bare tuberosity area are consistent anatomical landmarks for biceps endoscopy [3].
- The LF is often torn or stretched in retracted DBT tears. When intact, the LF prevents severe retraction of the ruptured DBT and may need to be released in chronic tears for adequate retrieval.
- The LCN must be protected during placement of the parabiceps portal for biceps endoscopy. LCN entrapment and compression neuropathy have been described and may be treated with a surgical decompression [8].
- The posterior (ulnar) branch(es) of MCN may cross the surgical incision during medial elbow procedures and must be identified and protected during procedures for medial epicondylitis, ulnar collateral ligament reconstructions, and cubital tunnel release.

Layer 2: The second layer is formed by the brachialis muscle that spans across the lower arm and elbow joint. The musculocutaneous nerve (MCN) and LCN, radial nerve, brachial vessels, and median nerve are closely related to the brachialis within this layer.

- Brachialis (BR): The brachialis is the strongest and largest (cross-sectional) flexor of the elbow. The brachialis muscle originates from the anterior surface of the distal half of the humerus, and is attached to the intermuscular septa of the arm on either side, with a more extensive attachment to the medial intermuscular septum (Fig. 4.4a). The BR has been described recently to have two heads: The larger, superficial head originates from the middle third of the anterolateral humerus and the lateral intermuscular septum (deltoid tuberosity to the origin of the brachioradialis), and partially encircles the deltoid muscle insertion proximally [9]. The smaller, deep head has been described as an oblique fan-shaped muscle that originates from the distal third of the anterior humerus and the medial intermuscular septum. The radial nerve courses on the lateral aspect of the brachialis muscle in a groove between its two heads. Distally, the superficial head merges into a thick circular tendon that inserts on the ulnar tuberosity. The deep head fibers converge onto an aponeurosis, which inserts obliquely (sagittal) into the proximal ulna, medial to the inser-

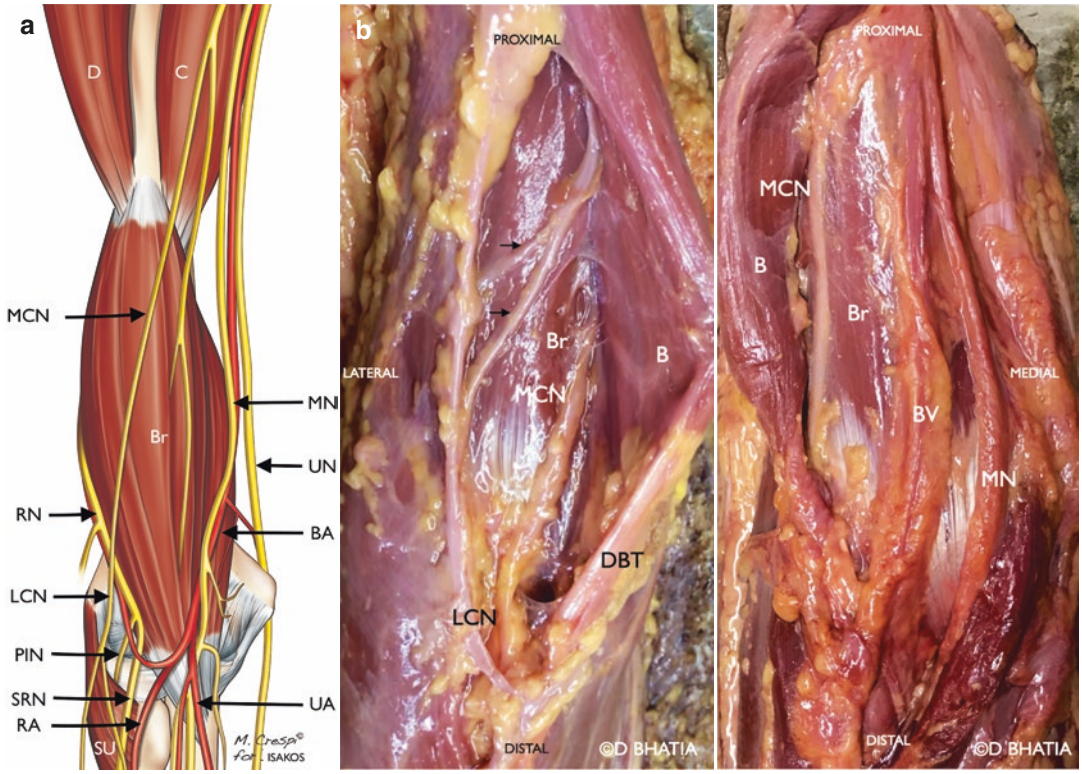

Fig. 4.4 (**a**) The brachialis muscle and associated neurovascular structures are illustrated (*Br* brachialis, *D* deltoid, *C* coracobrachialis, *SU* supinator, *MCN* musculocutaneous nerve, *LCN* lateral cutaneous nerve, *BA* brachial artery, *RA* radial artery, *UA* ulnar artery, *RN* radial nerve, *PIN* posterior interosseous nerve, *SRN* superficial radial nerve, *MN* median nerve, *UN* ulnar nerve) (M. Crespi © for ISAKOS). (**b**) Cadaveric demonstration of brachialis and related structures viewed with the biceps reflected along lateral (left) and medial (right) aspects. Arrows show the motor branches of MCN to BR (*Br* brachialis, *MCN* musculocutaneous nerve, *LCN* lateral cutaneous nerve, *BV* brachial vessels, *MN* median nerve) (© D. Bhatia)

tion of the tendon of the superficial head. Fibers from the deep aspect of the deep head may directly attach to the anterior elbow joint capsule (*articularis cubitus*). Tubbs et al. have described variable connective tissue attachments between the BR and capsule with the greatest concentration on anteromedial one-third of the capsule [10]. The ulnar insertional footprint measures approximately 2–4 cm in length and has been classified by Kameneni et al. into three types (proximally wide, distally wide, and irregular shape) [11]. The brachialis muscle is innervated by the musculocutaneous nerve and may have a dual or even a triple innervation (median and radial nerves).

- Musculocutaneous nerve (MCN) and LCN: The MCN traverses the coracobrachialis and courses along diagonally the superficial surface of brachialis. Motor branches arise from the nerve in this plane. The nerve exits at the lateral border of the biceps in the lower arm and continues as the lateral cutaneous nerve of the forearm (LCN) (Fig. 4.4b). The MCN provides motor innervation to all muscles in the anterior compartment of arm, and supplies sensory innervation to radial aspect of forearm via LCN.
- Radial nerve (RN): The RN crosses from posterior to anterior compartment 8–10 cm proximal to lateral epicondyle and lies between the BR and brachioradialis (BRD) (Fig. 4.5a).

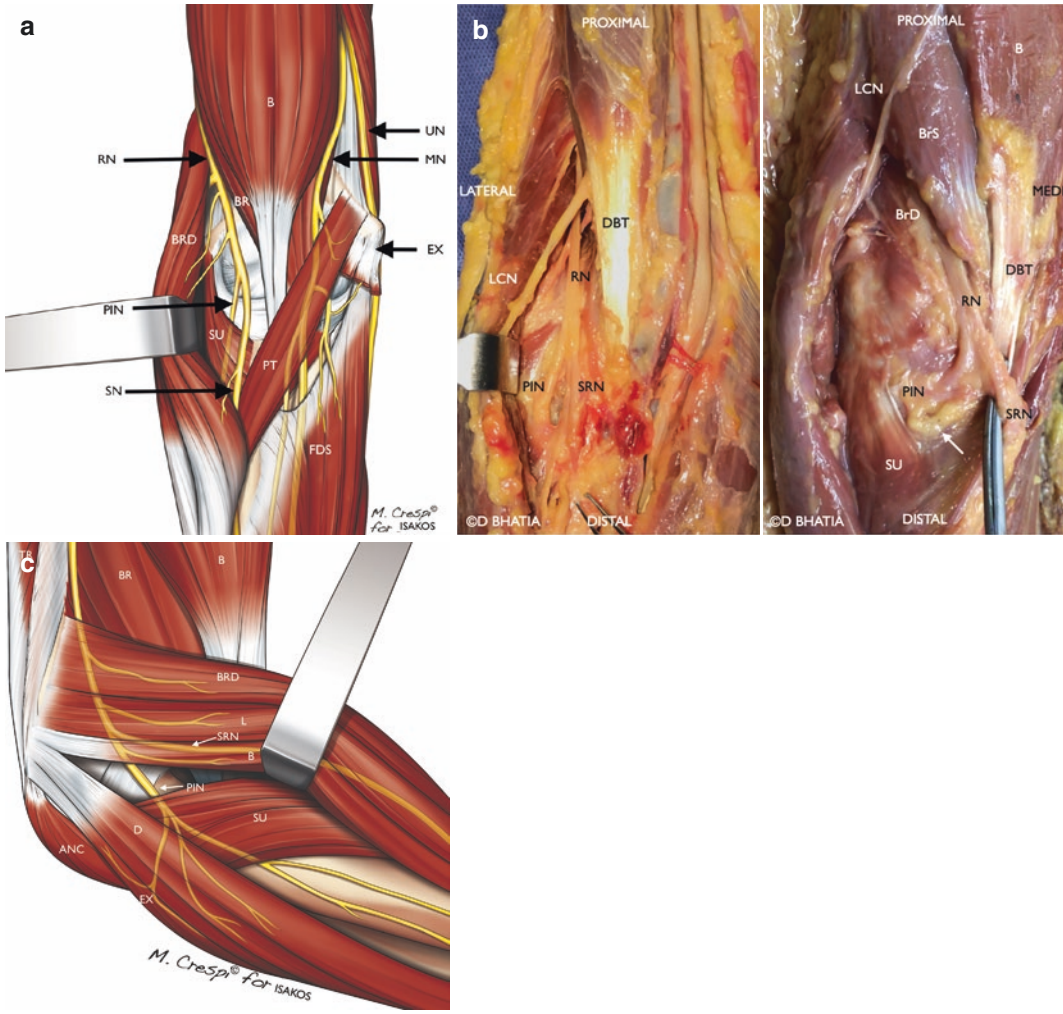

Fig. 4.5 (**a**) The course of radial nerve in lower arm and cubital fossa is illustrated (*B* biceps, *Br* brachialis, *SU* supinator, *BRD* brachioradialis, *PT* pronator teres, *FDS* flexor digitorum superficialis, *Ex* common extensors, *MCN* musculocutaneous nerve, *LCN* lateral cutaneous nerve, *RN* radial nerve, *PIN* posterior interosseous nerve, *SRN* superficial radial nerve, *MN* median nerve, *UN* ulnar nerve) (M. Crespi © for ISAKOS). (**b**) Cadaveric demonstration of superficial and deep relations of the radial nerve and its branches in lower arm and cubital fossa (*B* biceps, *BrS* superficial head of brachialis, *BrD* deep head of brachialis, *SU* supinator, *LCN* lateral cutaneous nerve, *RN* radial nerve, *PIN* posterior interosseous nerve, *SRN* superficial radial nerve, *DBT* distal biceps tendon, arrow: arcade of Frohse) (© D. Bhatia). (**c**) Branches of radial nerve in the upper forearm arm are illustrated (*B* biceps, *Br* brachialis, *TR* triceps, *SU* supinator, *BRD* brachioradialis, *PT* pronator teres, *L* ECRL, *B* ECRB, *D* EDC, *Ex* other extensors, *Anc* anconeus, *FDS* flexor digitorum superficialis, *Ex* common extensors, *MCN* musculocutaneous nerve, *LCN* lateral cutaneous nerve, *PIN* posterior interosseous nerve, *SRN* superficial radial nerve) (M. Crespi © for ISAKOS)

The nerve courses distally in the groove between the superficial and deep heads of brachialis [8] and passes anterior to the lateral epicondyle and capitellum to enter the forearm. Here, the RN divides into two branches: The superficial radial nerve (SRN) passes superficial to the supinator on the deep surface of the BRD. The posterior interosseous nerve (PIN) passes under a fibrous arch of the supinator muscle (arcade of Frohse) and passes

between the heads of the supinator muscle into the posterior forearm (Fig. 4.5b). In the lower arm, the RN gives branches to the lateral BR, BRD, and extensor carpi radialis longus (ECRL), and may supply the ECRB (Fig. 4.5c). At the radiocapitellar joint, it provides articular branches to lateral ligaments and capsule.

- Median nerve (MN): The MN crosses the brachial artery (BA) and courses medial to it in the mid and lower arm. The neurovascular bundle is superficial to the brachialis throughout the lower arm (Fig. 4.6a, b). The nerve passes under the LF and then courses between the humeral and ulnar heads of pronator teres. Thereafter, it passes deep to the flexor digitorum superficialis (FDS) and courses linearly in the forearm between the humeroulnar and radial heads of FDS along with the ulnar artery. The MN does not give branches to any muscle in the arm. Articular branches arise under the LF and it supplies the PT as it enters between the two heads. The anterior interosseous nerve (AIN) arises from the MN as it passes between the PT heads, and courses deep to FDS along with anterior interosseous artery.
- Brachial artery (BA) and bifurcation (BB): The BA courses along the anterior surface of brachialis, passes under the LF, and bifurcates into radial (RA) and ulnar (UA) arteries. The BA is medial to the DBT in the lower arm, and lies anterior to it at the bifurcation. The RA runs in a superficial plane between the FDS and BRD, and gives rise to a leash of vessels that enter the BRD. The ulnar artery is closely related to the DBT and is closest to it in neutral forearm position (Fig. 4.6c).

Surgical Significance

- The broad brachialis is an intervening structure between the anterior capsule and several vital neurovascular structures. The muscle

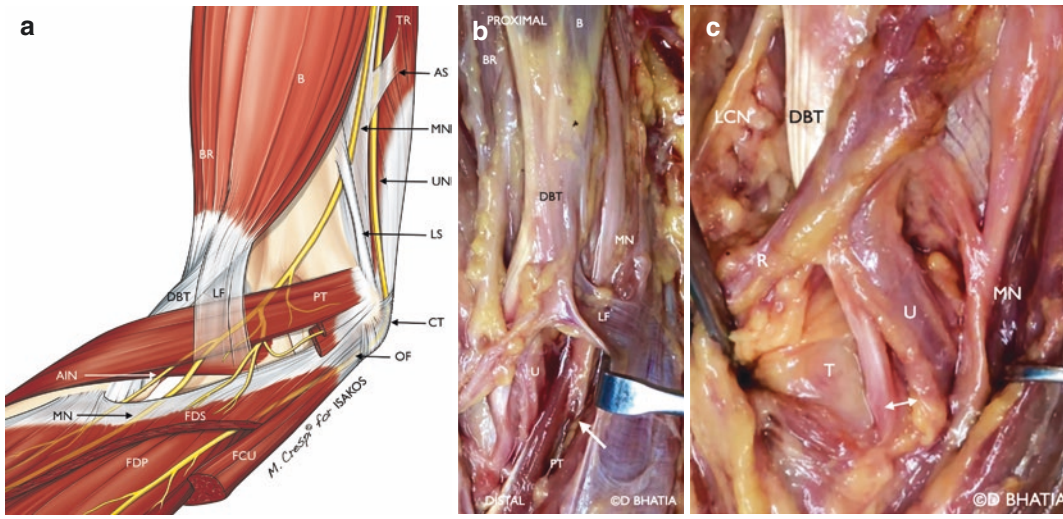

Fig. 4.6 (**a**) The course of median nerve (MN), anterior interosseous nerve (AIN), and ulnar nerve (UN) and possible compression sites are illustrated. Note that the deep medial aspect of brachialis is not shown here (*B* biceps, *Br* brachialis, *LF* lacertus fibrosus, *DBT* distal biceps tendon, *PT* pronator teres, *FDS* flexor digitorum superficialis, *FDP* flexor digitorum profundus, *FCU* flexor carpi ulnaris, *Tr* triceps, *AS* arcade of Struthers, *LS* ligament of Struthers, *CT* cubital tunnel, *OF* Osborne's fascia) (M. Crespi © for ISAKOS). (**b**) Cadaveric demonstration of median nerve (MN) in lower arm and cubital fossa. The nerve is seen passing under the lacertus fibrosus (LF) and courses between the heads of pronator teres (PT) (*B* biceps, *Br* brachialis, *U* ulnar artery) (© D. Bhatia). (**c**) Cadaveric demonstration of close proximity of ulnar artery (U) and median nerve (MN) to the DBT insertion (arrows) at tuberosity (T) superficial and deep relations of the radial nerve and its branches in lower arm and cubital fossa (*LCN* lateral cutaneous nerve, *R* radial artery) (© D. Bhatia)

fibers can be used as an anatomical landmark for safe capsular resection in this region.
- The "sub-brachialis space" is a region between the brachialis and the anterior capsule that may be utilized during endoscopic extra-articular capsular resection. The detailed anatomy of this region is described in another chapter in this book.
- The MSN and LCN should be protected during endoscopic or open mobilization of chronic retracted DBT ruptures. The midbiceps portal (MBP) for arm endoscopy is placed along the anterior surface of brachialis and the MCN or its branches can be identified and protected.
- The radial nerve is in close contact with the anterior elbow capsule distal to the radiocapitellar joint, and is at risk of iatrogenic injury during capsulectomy. The arcade of Frohse is a site of potential entrapment of the PIN.
- The MN passes through several regions that may potentially compress it. The ligament of Struthers, LF, heads of PT, and FDS arch are the regions of potential entrapment.
- The UA should be protected during procedures on the DBT. The UA transversely crosses the DBT on its medial side and is at risk of injury during passage of tendon through the proximal radioulnar space (two-incision approach) [4].

Layer 3: The third layer is formed by the elbow joint capsule and ligaments. The common extensor origin, supinator muscle, and deep branch of radial nerve (PIN) are closely associated and surgically significant structures in this layer.

- *Common extensor origin (CEO)*: The tendons of extensor carpi radialis brevis (ECRB), extensor digitorum communis (EDC), extensor carpi ulnaris (ECU), and extensor digiti minimi (EDM) collectively form the common extensor tendon and attach at the lateral epicondylar area. The ECRB and EDC have distinct footprints in the proximal half of the lateral epicondyle (Fig. 4.7a). The ECRB footprint is centered at the proximal articular margin of the capitellum, and just posterior to the capsular attachment. The EDC footprint is further posterior to the ECRB. The ECU and EDM attach along the posterior aspect of this region (Fig. 4.7b).
- *Supinator muscle (SU)*: The SU is a posterior forearm compartment muscle that assists in supination with the biceps. The muscle has two heads in layers that form a plane for passage of PIN (Fig. 4.8a, b). The superficial humeral head attaches to the lateral epicondyle, annular ligament, and lateral collateral ligament complex (LCL). The footprints of the SU and LCL overlap at the origin in part. The deep head originates at the supinator crest of posterolateral ulna. The two heads wrap around the radial neck, bicipital tuberosity, and proximal radial shaft and insert on the lateral radius proximal to PT insertion. The SU encloses a bare area on the tuberosity lateral to the DBT footprint and this forms a consistent anatomical landmark for biceps endoscopy (Fig. 4.2).
- *Anterior and posterior capsule*: The elbow capsule encloses the radiocapitellar (RC), ulnotrochlear (UT), and proximal radioulnar (RU) joints, and consists of an outer fibrous capsule (CP) and a distinct inner synovial membrane (SM) layer (Fig. 4.9a). The anterior capsule attaches at the lateral and medial peripheral nonarticular margins of the trochlea and capitellum. Proximally, the capsule attaches beyond the articular margins on the anterior supracondylar surface of distal humerus. The proximal attachment has been described as a "wave shape" or "double-arch" insertion, and is proximal to the coronoid (CF) and radial (RF) fossae [12, 13]. The proximal insertion has been measured to be approximately 9 mm proximal to cartilage bone junction on the medial aspect, and approximately 12 mm proximal at the coronoid fossa. On the lateral aspect and proximal to radial fossa, this insertion may be further proximal, and the lowest point (nadir) of the "wave" attaches between the fossae. The lateral capsule is thickened and constitutes the lateral collateral ligamentous complex. The anterior border of this ligamentous zone is at the mid radiocapi-

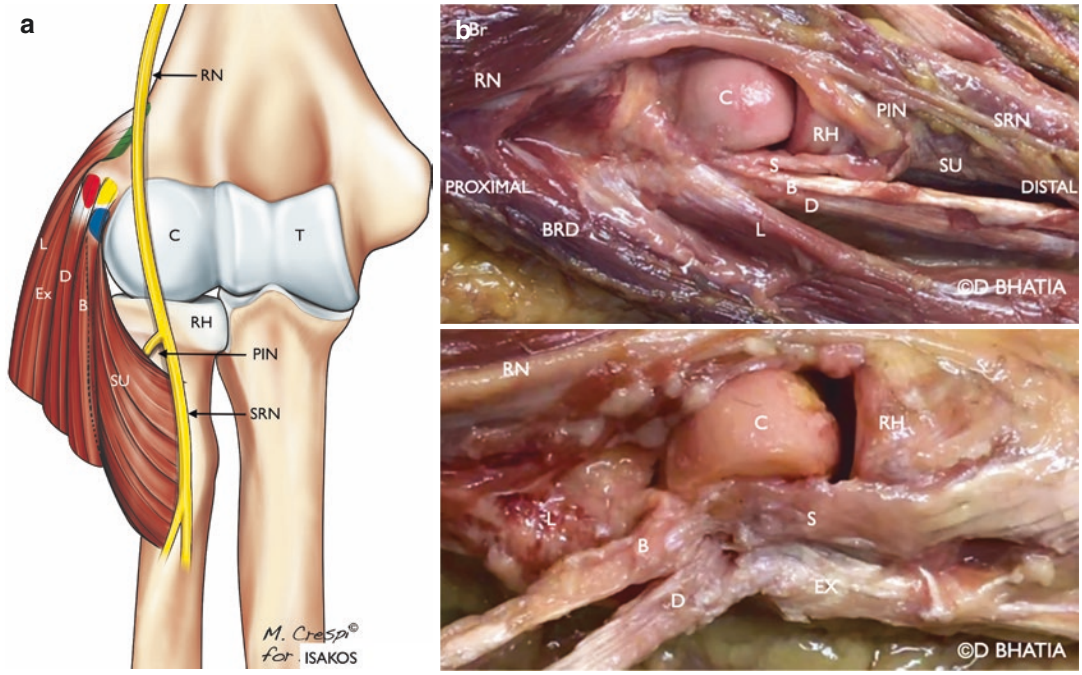

Fig. 4.7 (**a**) The interrelationship between tendon insertional footprints of supinator (SU), ECRB (B), EDC (D), and ECRL (L) at the lateral epicondyle and distal humerus is illustrated. The radial nerve is shown for reference (*RN* radial nerve, *PIN* posterior interosseous nerve, *SRN* superficial radial nerve, *C* capitellum, *T* trochlea, *RH* radial head, *Ex* other extensors) (M. Crespi © for ISAKOS). (**b**) Cadaveric demonstration of the origin of common extensor tendons at the lateral epicondyle and their relationship to the radial nerve and its branches. The ECRB and EDC are reflected proximally to show the attachments of supinator and other extensors. Note that the humeral attachment of supinator overlaps the attachments of lateral ligaments on the lateral epicondyle (*C* capitellum, *RH* radial head, *Br* brachialis, *SU* supinator, *S* humeral head of supinator, *B* ECRB, *D* EDC, *L* ECRL, *BRD* brachioradialis, *Ex* other common extensors, *RN* radial nerve, *PIN* posterior interosseous nerve, *SRN* superficial radial nerve) (© D. Bhatia)

tellar aspect and should be protected during surgery. Similarly, the medial capsule demonstrates a thickening that constitutes the medial collateral ligamentous complex (MCL), and the anterior band (aMCL) attaches to the sublime tubercle on the medial coronoid process. The distal aspect of the capsule attaches to the radial neck distal to the annular ligament, and approximately 6 mm distal to the coronoid tip. The coronoid footprint of the capsule is twice as broad on the radial aspect of the brachialis insertion (12 mm) as compared to the ulnar aspect (6 mm) [14]. Posteriorly, the capsule follows the periphery of the trochlea and capitellum, and extends proximally to enclose the olecranon fossa (Fig. 4.9b). The capsular attachment to the olecranon is deep to the muscular head of triceps and encloses a bare area at the olecranon process apex. In a recent cadaveric study, three distinct bands have been identified in the anterior capsule (anterior lateral band, anterior medial oblique band, and anterior transverse) and posterior capsule (posterior transverse, posterior medial, and posterior lateral) and these are postulated to function as secondary stabilizers and checkreins to elbow hyperextension (anterior bands) and hyperflexion (posterior bands) [15].

The inner synovial membrane insertion follows the double-arch insertion pattern and inserts 11–13 mm proximal to the transepicondylar line (TL). The nadir of the synovial membrane inserts just above the lateral end of the trochlea between the coronoid and radial fossae and can be visualized arthroscopically. The arches demonstrate a valgus orientation

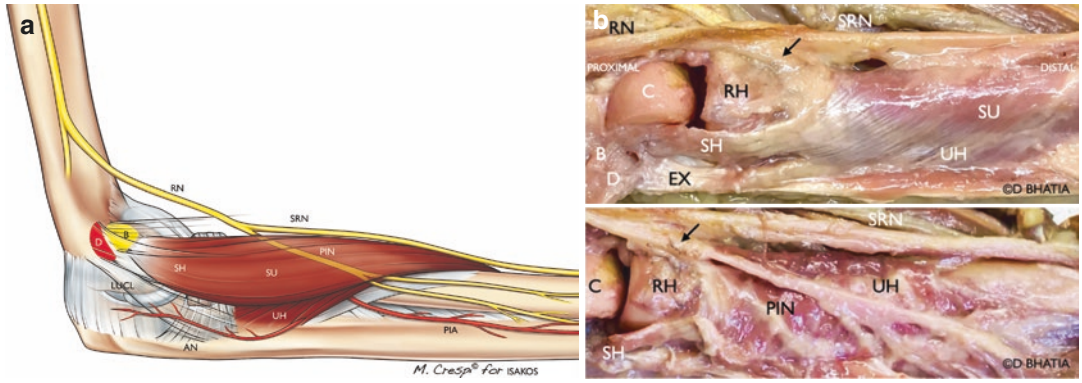

Fig. 4.8 (**a**) The structure and relations of supinator muscle are illustrated. Note the close association of the humeral origin with ECRB and EDC footprints, and with the lateral ligaments. The PIN passes between the two heads, and SRN courses superficially (*SH* humeral head of supinator, *UH* ulnar head of supinator, *B* ECRB, *D* EDC, *RN* radial nerve, *PIN* posterior interosseous nerve, *SRN* superficial radial nerve, *LUCL* lateral ulnar collateral ligament, *AN* annular ligament, *PIA* posterior interosseous artery) (M. Crespi © for ISAKOS). (**b**) The supinator muscle (SU) and its relationship with radial nerve branches are shown on a cadaveric specimen. The superficial head of supinator is reflected (lower image) to show the passage of PIN from anterior to posterior compartment. Arrow shows the close proximity of PIN to the radial neck prior to its entry into supinator (*C* capitellum, *RH* radial head, *SH* humeral head of supinator, *UH* ulnar head of supinator, *B* ECRB, *D* EDC, *EX* other extensors, *RN* radial nerve, *PIN* posterior interosseous nerve, *SRN* superficial radial nerve) (© D. Bhatia)

relative to the axis perpendicular to the TL, and a thickened infolded extension of the SM is often observed overlying the medial aspect of the trochlea. Distally, the SM attaches to the annular ligament and anterior aspect of the coronoid process [12].

The anterior capsule is closely related to several vital neurovascular structures. In general, the distance of these structures from the capsule is greater on the proximal and medial aspect in a ratio of 2 to 1 (proximal to distal and medial to lateral) [13]. The radial nerve is the closest structure to the capsule, and is at risk of iatrogenic injury during lateral capsulectomy [16]. The brachialis muscle is superficial to the anterior capsule and deep to vital neurovascular structures.

- *Ulnar collateral ligament (UCL)*: The UCL is the primary static stabilizer to valgus stress on the medial elbow, and resists valgus and extension stress from 70 to 120° of elbow flexion. The UCL consists of three bundles: anterior (aUCL), posterior (pUCL), and oblique fibers (oUCL) (Fig. 4.10). The proximal attachment of the aUCL has been shown to be approximately 8 mm distal and lateral (anterior) to the medial epicondyle (ME), and centered approximately 15 mm from the joint line [17]. The distal insertion on the ulna is broad and is centered approximately 1.5 mm distal to the sublime tubercle along the ulnar ridge, and is closer to the joint line (7 mm) as compared to the humeral attachment. The pUCL has a proximal attachment approximately 7–9 mm distal and lateral (posterior) to the ME. The distal attachment (ulnar) footprint of pUCL is approximately 1–2 mm distal and 10 mm anterior to the olecranon tip and 4–5 mm posterior to the joint line. The FDS, FCU, and PT tendons are closely associated with the UCL. In one study, the FDS tendon was found to attach along approximately half of the distal length of aUCL, and the FCU tendon overlapped with approximately one-fourth of the distal (ulnar) footprint of the aUCL. Additionally, the PT was shown to be attached along the distal lateral border of the anterior bundle and medial to the brachialis insertion.
- Lateral collateral ligament complex (LCLC): The lateral ligaments are comprised of the lateral ulnar collateral ligament (LUCL),

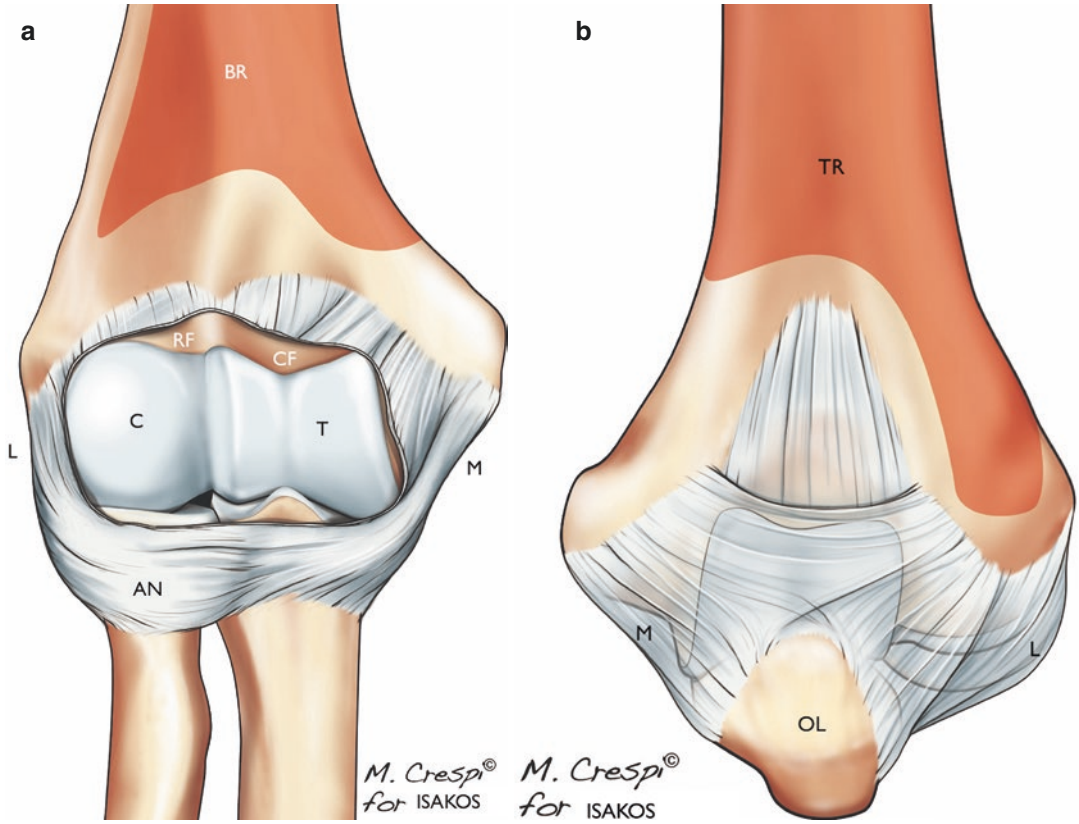

Fig. 4.9 (**a**) Anterior elbow capsular attachments and boundaries for capsulectomy are illustrated. The radial and coronoid fossae (RF, CF) are anatomic landmarks and the capsule is attached proximal to them (*C* capitellum, *T* trochlea, *M* medial collateral ligaments, *L* lateral collateral ligaments, *AN* annular ligament, *BR* origin of brachialis) (M. Crespi © for ISAKOS). (**b**) Posterior elbow capsular attachments are illustrated. Note the oblique and transversely oriented bands of capsular fibers and the close relation of collateral ligaments (*OL* olecranon, *M* medial collateral ligaments, *L* lateral collateral ligaments, *TR* origin of triceps) (M. Crespi © for ISAKOS)

radial collateral ligament (RCL), and annular ligament (AN) (Fig. 4.11a, b). The LUCL is the primary restraint to posterolateral rotatory instability (PLRI) [18]. The humeral attachments of LUCL and RCL are centered approximately 10 mm and 7 mm, respectively, from the apex of the lateral epicondyle, 7–8 mm proximal to the articular margin of the capitellum, and at a distance of 5 mm from each other. The LUCL fibers blend with the AN and insert further distally as a distinct broad footprint centered approximately 3–4 mm distal to the apex of the supinator crest. The humeral attachment of supinator muscle is closely associated with the LUCL and RCL attachments.

Surgical Significance

- The ECRB can be identified and released arthroscopically during the arthroscopic anatomic insertional release procedure (AAIR). The EDC tendon is visible only after the ECRB is released. The release should be restricted to the proximal half of the CEO attachment area to prevent iatrogenic injury to SU and LCL.
- The radial and coronoid fossae are intra-articular anatomic landmarks and can be visualized by excising the inner synovial membrane.
- The sublime tubercle is a consistent anatomic landmark and can be used as a reference for anatomic aUCL reconstruction. The joint line

is an additional reference and is useful in revision surgery where the bony anatomy may be altered. Insertional attachments of the FDS, FCU, and PT must be preserved during UCL surgery.

Layer 4: The fourth layer is the posterior aspect of the elbow and consists of the triceps muscle and tendon, and anconeus muscle, and is closely associated with the radial and ulnar nerves.

- Triceps surae (Tr): The Tr is a broad muscle along the posterior arm and is a powerful elbow extensor. The muscle consists of three heads with different origins. The *long head* originates from the infraglenoid tubercle of scapula, and the lateral and medial (deep) heads originate from the proximal and distal posterior humerus and the lateral and medial intermuscular septa, respectively (Fig. 4.12a, b). The long and lateral heads merge into a superficial tendon with a distinct footprint on the posterior olecranon, and the medial (deep) head forms a muscular insertion anterior to this. The elbow capsule is the anteriormost attachment on the olecranon followed by a bare area [18] (Fig. 4.12c, d). The detailed anatomy of this region is presented in a separate chapter.
- Anconeus muscle (ANC): This is a triangular muscle variably blended with the triceps and

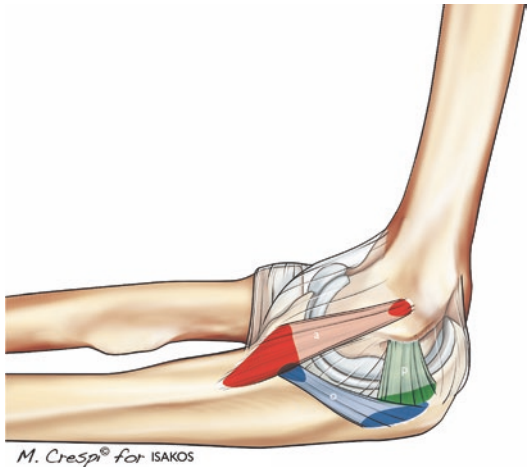

Fig. 4.10 The structure and footprints of ulnar collateral ligaments are illustrated. Note the broad ulnar attachment of the anterior band (a) and its close proximity to the joint line (p: posterior band, o: oblique band) (M. Crespi © for ISAKOS)

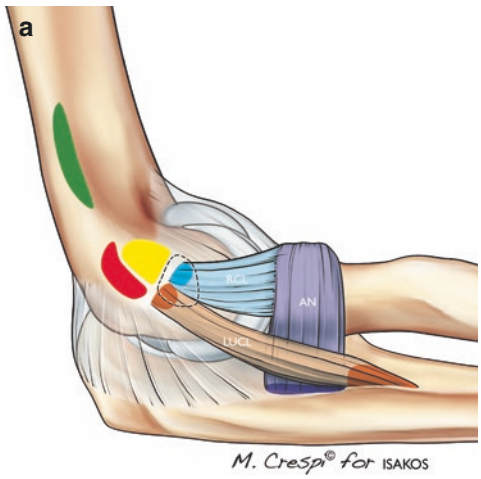

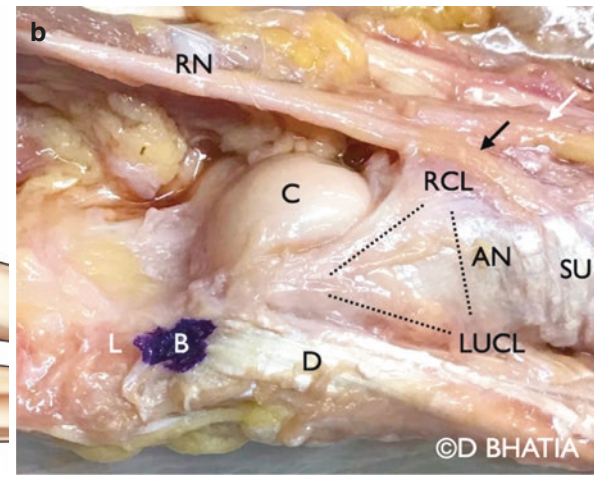

Fig. 4.11 (**a**) The structure and footprints of lateral collateral ligaments are illustrated. Note the broad ulnar attachment of the lateral ulnar collateral ligament (LUCL) beyond the annular ligament (AN). The footprints of ECRB (yellow), EDC (red), and ECRL (green) are shown for reference. The dotted area shows the supinator footprint overlapping the LUCL and radial collateral ligament (RCL) attachments on the lateral epicondyle (M. Crespi © for ISAKOS). (**b**) The lateral collateral ligaments (dotted lines) are shown in a cadaveric specimen (*C* capitellum, *SU* supinator, *B* ECRB, *D* EDC, *L* ECRL, *RN* radial nerve, *black arrow* posterior interosseous nerve, *white arrow* superficial radial nerve, *RCL* radial collateral ligament, *LUCL* lateral ulnar collateral ligament, *AN* annular ligament) (© D. Bhatia)

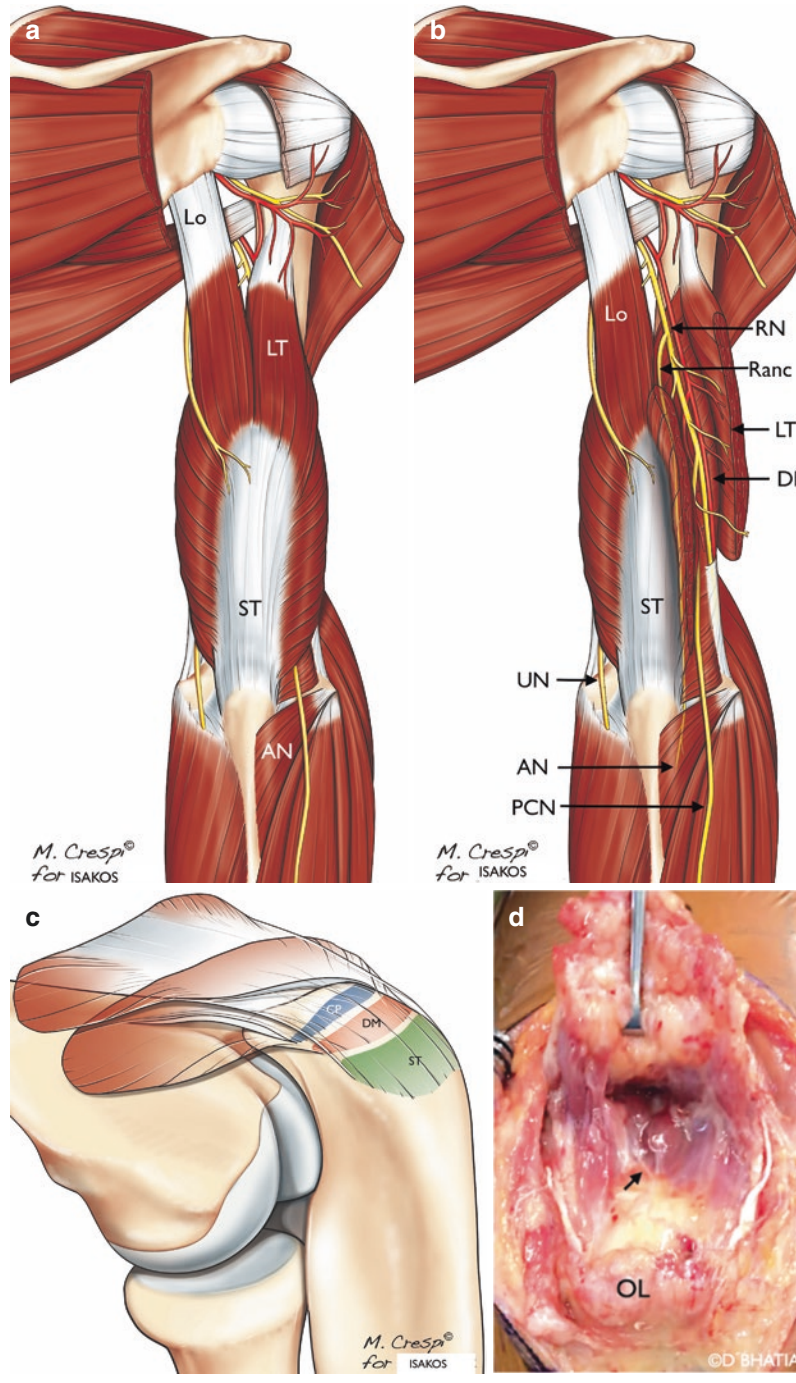

Fig. 4.12 (**a**, **b**) The origin and insertion of the three heads of triceps and the radial nerve (RN) are illustrated. The long (Lo) and lateral (LT) heads combine to form a superficial tendon (ST). The medial head forms the deep muscular head (DM). Note the course of the branch to anconeus (AN) muscle (Ranc) (*UN* ulnar nerve, *PCN* posterior cutaneous nerve) (M. Crespi © for ISAKOS). (**c**) The insertional footprint of the superficial tendon (ST) and deep muscular head (DM) on the olecranon process is shown. Note that the capsule attaches anterior to DM and encloses a bare area of olecranon tip (M. Crespi © for ISAKOS). (**d**) Intraoperative view of a triceps tear shows an avulsion of the superficial tendon (reflected) and an intact part of the deep muscular head (arrow) (*OL* olecranon) (© D. Bhatia)

assists in elbow extension and possible ulnar abduction in pronation. The muscle has a separate tendon that attaches to the posterior aspect of lateral epicondyle. The fibers diverge medially and cross the annular ligament towards the ulna. The muscle inserts on the olecranon and proximal ulna. The ANC is supplied by the medial head branch of radial nerve, as described below (Fig. 4.12a, b).

- Radial nerve (RN): The RN crosses the triangular space and courses through the radial groove along with the profunda brachii artery

between the long and lateral heads of triceps. Thereafter, approximately 5 cm below the deltoid tuberosity, it pierces the lateral intermuscular septum and enters the anterior arm (Figs. 4.12a, b). The nerve gives motor branches to each head of triceps before and during passage through the groove, and cutaneous innervation to posterior arm and forearm. The branch to medial head and anconeus rises from the main trunk and passes medial to lateral over the medial (deep) head. This branch supplies the medial head and enters the anconeus lateral to the olecranon [19]. The posterior antebrachial cutaneous nerve (PCN) traverses the spiral groove and descends along the posterior intermuscular septum. It pierces the fascial approximately 8 mm proximal to lateral epicondyle and gives branches to the lateral epicondyle and skin over posterolateral forearm.

- Ulnar nerve (UN): The UN pierces the medial intermuscular septum (MIS) in the midarm accompanied by the superior ulnar collateral vessels, and courses along the anterior surface of the medial head of triceps (Fig. 4.1b). It passes under the arcade of Struthers (8–10 cm proximal to medial epicondyle), formed by a fascial band between the medial head and MIS, and descends to the dorsal aspect of the medial epicondyle. Here, the UN passes through the cubital tunnel to enter the forearm under the Osborne's ligament (fascial condensation) and courses between the humeral and ulnar heads of FCU (Fig. 4.6a). In the upper forearm, the UN descends over the anterior surface of flexor digitorum profundus and is covered by FDS. The ulnar artery crosses over to lie lateral to the nerve. The UN gives an articular branch in the cubital tunnel, and supplies the FCU and ulnar FDS in the forearm. Palmar and dorsal branches arise in the mid and lower forearm and provide cutaneous innervation to the hypothenar eminence and ulnar 1.5 fingers.

Surgical Significance

- Isolated head ruptures of triceps tendon have been described; superficial tendon ruptures are common and are ideal for endoscopic repairs.
- Radial nerve branches to anconeus and PCN may be at risk during posterolateral and soft-spot portal placement [20].

In summary, the layered approach to elbow anatomy is useful during minimally invasive arthroscopic or endoscopic procedures around the elbow. The distal biceps tendon traverses the layers from superficial to deep planes, and even extends to the posterior aspect in full pronation. The "parabiceps space" is therefore a useful and safe passage across anatomic planes in the lower arm and cubital fossa for elbow endoscopy. Neurovascular structures in each layer should be protected during surgery and consistent anatomic landmarks described above are useful intraoperative indicators of their location. Lastly, the major nerves are at risk of entrapment during their course, and anatomical structures that predispose to compression must be evaluated and released during surgery.

Conflict of Interest The author certifies that he has no commercial associations (e.g., consultancies, stock ownership, equity interest) that might pose a conflict of interest in connection with the submitted article. The author retains the copyright to the images, videos, and content in this chapter.

References

1. Bhatia DN, Kandhari V, DasGupta B. Cadaveric study of insertional anatomy of distal biceps tendon and its relationship to the dynamic proximal radioulnar space. J Hand Surg Am. 2017;42(1):e15–23.
2. Bhatia DN. Distal biceps tendon insertional trifurcation and a new footprint configuration: case report of an anatomical variant. Eur J Anat. 24(3):235–8.
3. Bhatia DN. Endoscopic distal biceps repair: endoscopic anatomy and dual-anchor repair using a proximal anterolateral "parabiceps portal". Arthrosc Tech. 2015;4:e785–93. https://doi.org/10.1016/j.eats.2015.07.031.

4. Bhatia D, Naskar R, DeNiese P. Dynamic rotational alteration in positional relationship of neurovascular structures and distal biceps tendon insertion: a cadaveric study. J ISAKOS. 2019;4:296–301.
5. Im HS, Im JY, Kim KH, Kim DH, Park BK. Ultrasonographic study of the anatomical relationship between the lateral antebrachial cutaneous nerve and the cephalic vein. Ann Rehabil Med. 2017;41(3):421–5. https://doi.org/10.5535/arm.2017.41.3.421.
6. Masear VR, Meyer RD, Pichora DR. Surgical anatomy of the medial antebrachial cutaneous nerve. J Hand Surg Am. 1989;14:267–71.
7. Benedikt S, Parvizi D, Feigl G, Koch H. Anatomy of the medial antebrachial cutaneous nerve and its significance in ulnar nerve surgery: an anatomical study. J Plast Reconstr Aesthet Surg. 2017;70(11):1582–8. https://doi.org/10.1016/j.bjps.2017.06.025.
8. Gillingham BL, Mack GR. Compression of the lateral antebrachial cutaneous nerve by the biceps tendon. J Shoulder Elbow Surg. 1996;5(4):330–2. https://doi.org/10.1016/s1058-2746(96)80062-0.
9. Leonello DT, Galley IJ, Bain GI, Carter CD. Brachialis muscle anatomy. A study in cadavers. J Bone Joint Surg Am. 2007;89(6):1293–7. https://doi.org/10.2106/JBJS.F.00343.
10. Tubbs RS, Yablick MW, Loukas M, et al. Capsular attachment of the brachialis muscle (Portal's muscle): an anatomical and functional study. Surg Radiol Anat. 2008;30:229–32. https://doi.org/10.1007/s00276-008-0312-y.
11. Kamineni S, Bachoura A, Behrens W, Kamineni E, Deane A. Distal insertional footprint of the brachialis muscle: 3D morphometric study. Anat Res Int. 2015;2015:786508. https://doi.org/10.1155/2015/786508.
12. Kamineni S, Bachoura A, Sasaki K, et al. Inner synovial membrane footprint of the anterior elbow capsule: an arthroscopic boundary. Anat Res Int. 2015;2015:426974. https://doi.org/10.1155/2015/426974.
13. Thoreux P, Blondeau C, Durand S, Masquelet AC. Anatomical basis of arthroscopic capsulotomy for elbow stiffness. Surg Radiol Anat. 2006;28(4):409–15.
14. Shimura H, Nimura A, Nasu H, et al. Joint capsule attachment to the coronoid process of the ulna: an anatomic study with implications regarding the type 1 fractures of the coronoid process of the O'Driscoll classification. J Shoulder Elbow Surg. 2016;25(9):1517–22. https://doi.org/10.1016/j.jse.2016.01.024.
15. Reichel LM, Morales OA. Gross anatomy of the elbow capsule: a cadaveric study. J Hand Surg Am. 2013;38(1):110–6. https://doi.org/10.1016/j.jhsa.2012.09.031.
16. Omid R, Hamid N, Keener JD, Galatz LM, Yamaguchi K. Relation of the radial nerve to the anterior capsule of the elbow: anatomy with correlation to arthroscopy. Arthroscopy. 2012;28(12):1800–4.
17. Frangiamore SJ, Moatshe G, Kruckeberg BM, et al. Qualitative and quantitative analyses of the dynamic and static stabilizers of the medial elbow: an anatomic study. Am J Sports Med. 2018;46(3):687–94. https://doi.org/10.1177/0363546517743749.
18. Barco R, Sánchez P, Morrey ME, Morrey BF, Sánchez-Sotelo J. The distal triceps tendon insertional anatomy-implications for surgery. JSES Open Access. 2017;1(2):98–103.
19. Ozer H, Açar HI, Cömert A, Tekdemir I, Elhan A, Turanli S. Course of the innervation supply of medial head of triceps muscle and anconeus muscle at the posterior aspect of humerus (anatomical study). Arch Orthop Trauma Surg. 2006;126(8):549–53. https://doi.org/10.1007/s00402-006-0183-9.
20. Adolfsson L. Arthroscopy of the elbow joint: a cadaveric study of portal placement. J Shoulder Elbow Surg. 1994;3(2):53–61. https://doi.org/10.1016/S1058-2746(09)80110-9.

Surgical Anatomy of the Nerves Around the Elbow

5

Celli Andrea, Serafini Fabio, Peruzzi Marco, and Pederzini Luigi Adriano

5.1 Background

The elbow joint is a complex structure that provides important functions and forms the mechanical link in the upper extremity between the hand, the wrist and the shoulder. Its primary functions include the positioning of the hand in space, and loss of this can cause significant impairment in carrying out daily-life activities. The elbow joint is crossed by various nerve structures which may be put at risk during both arthroscopic and open surgery. The nerve structures are also subject to changes of position and traction during range of motion of the elbow. This is a very important aspect to be considered in the post-operative period when the patient regains their pre-existing functions. It follows that it is important to know both the anatomical course of the nerves around the elbow and the points of possible compression.

C. Andrea (✉)
Department of Orthopaedic and Traumatology Surgery, Shoulder and Elbow Unit, Hesperia Hospital, Modena, Italy

S. Fabio · P. Marco · P. L. Adriano
Department of Orthopaedic, Traumatology and Arthroscopic Surgeries, Nuovo Ospedale di Sassuolo, Modena, Italy

5.2 Cutaneous Nerves of the Upper Limb

All approaches to the distal humerus, the elbow and the proximal forearm involve the risk of injuring the branches of the superficial cutaneous nerves (CN).

The nerve supply of the skin of the arm is as follows [1]:

- **Laterally:**
  - *Superior lateral CN of the arm:* It arises from the axillary nerve and it innervates the skin of the lateral aspect of the shoulder.
  - *Inferior lateral CN of the arm:* It arises from the radial nerve and it provides three cutaneous branches, two of which supply the skin of the lateral arm and forearm while the third supplies the skin of the posterior aspect of the arm.
- **Medially:**
  - *Intercostobrachial nerve and medial CN of the arm:* It arises from the medial cord of the brachial plexus as one or two branches that frequently communicate with the intercostobrachial CN. It innervates the skin of the medial arm, except for a small portion of the upper medial arm which is supplied by the intercostobrachial nerve arising from the second intercostal nerve.

© ISAKOS 2022

D. N. Bhatia et al. (eds.), *Arthroscopy and Endoscopy of the Elbow, Wrist and Hand*,
https://doi.org/10.1007/978-3-030-79423-1_5

- **Posteriorly:**
  - *Posterior CN of the arm*: It is the first branch arising from the RN in the axilla supplying the skin of the medial back.

The nerve supply of the skin of the forearm is as follows [1]:

- **Anterolaterally:**
  - *Lateral CN of the forearm*: The terminal branch of the musculocutaneous nerve emerges as the lateral CN of the forearm. The anterior branch supplies the anterolateral margin of the radius. The posterior branch descends posteriorly and supplies the skin of the lateral surface of the radius, ending on the dorsal aspect of the wrist joint.
- **Anteromedially:**
  - *Medial CN of the forearm*: It arises from the medial cord of the brachial plexus. The two terminal branches provide several smaller branches, supplying the skin of the anterior aspect of the arm and the anteromedial aspect of the forearm.
- **Posteriorly:**
  - *Posterior CN of the forearm:* It arises from the inferior lateral CN of the arm and it supplies branches to the skin of the posterior and lateral forearm regions.

5.3 Radial Nerve

- The radial nerve (RN) derives from the posterior cord of the brachial plexus, behind the third portion of the axillary artery. In the axilla, it descends behind the brachial artery, anteriorly to the subscapularis muscle and to the insertion of the teres major (TM) and the latissimus dorsi tendon. It crosses the posterior aspect of the humerus close to the bone, without interposed muscle fibres, and it passes in front of the long head of the triceps to reach the spiral groove, along with the deep brachial artery and veins.
- On the lateral border of the medial head of the triceps, the RN pierces the intermuscular septum (10–12 cm from the lateral epicondyle); it leaves the extensor compartment and enters the flexor compartment of the arm, running distally in the interval between the brachialis and brachioradialis muscle. Anteriorly it is covered by the lateral portion of the brachialis muscle. At this level further branches run from the main trunk to (a) lateral portion of the brachialis muscle, 5–6 cm from the tip of the epicondyle; (b) brachioradialis; and (c) extensor carpi radialis longus muscle (Fig. 5.1).
- Articular fibres arise in the RN as it passes in front of the radiocapitellar joint and supply the lateral epicondyle, the annular ligament and the lateral ulnar collateral ligament.
- Anterior to the lateral epicondyle and under the brachioradialis and wrist extensor muscles, the RN divides into two terminal branches, a superficial sensory and a deep motor branch (Fig. 5.1) that pass 1 cm distal to the biceps tendon.
  - The superficial RN passes superficial to the supinator muscle and continues distally along the deep surface of the brachioradialis muscle; it pierces the fascia on the ulnar side of the brachioradialis tendon, approximately 7 cm above the wrist; it divides into terminal fibres and descends along the dorsoradial side of the wrist, ending in the hand.
  - The posterior interosseous nerve (PIN) (Figs. 5.1 and 5.2) runs obliquely through the supinator muscle and it crosses the proximal radius to enter the extensor compartment of the forearm. The motor branches to the extensor carpi radialis brevis have a very variable origin: they may arise from the superficial or the deep terminal branch of the RN, but they often originate before their bifurcation into terminal branches [2]. The PIN is separated from the radius by the deep head of the supinator muscle (Figs. 5.1 and 5.2). As the PIN leaves the supinator muscle and its inferior border, it divides into three terminal branches: (a) a posterior branch for extensor carpi ulnaris, the extensor digitorum communis and the extensor digiti minimi; (b) an anterior branch for the long abductor and the short and long extensor of the

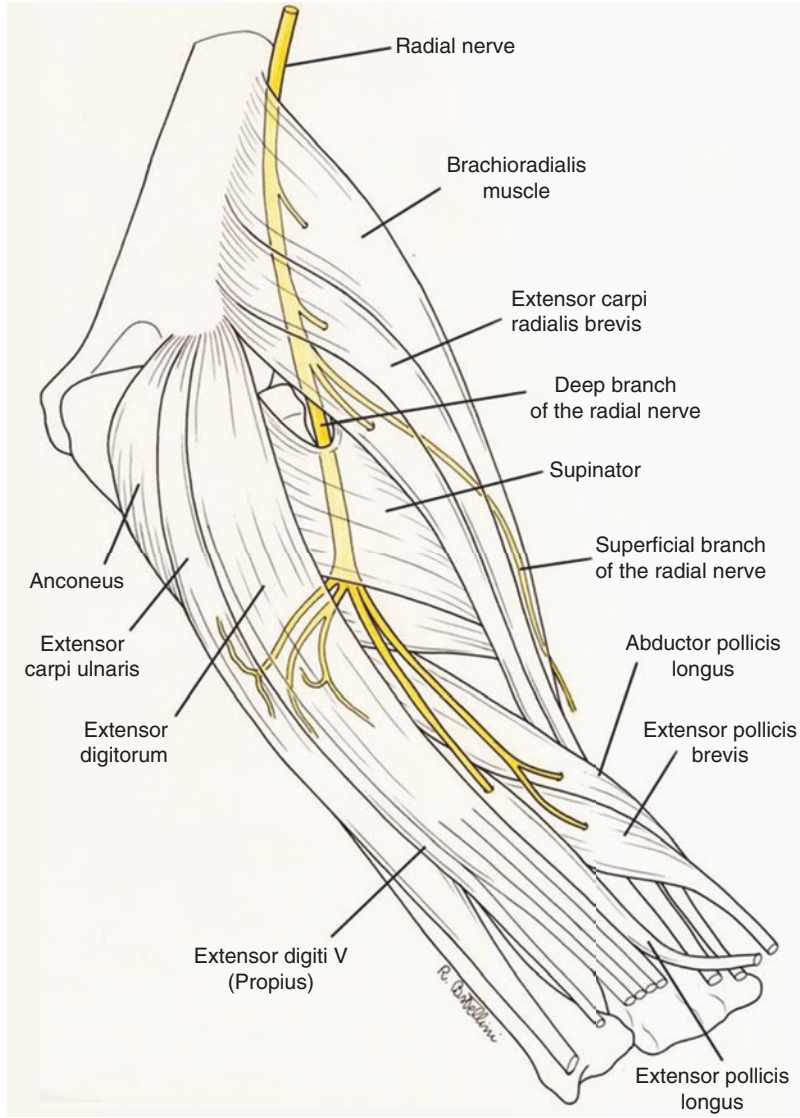

Fig. 5.1 Anatomical course of the radial nerve around the elbow and its terminal branches are illustrated

thumb and the extensor of the index finger; and (c) the third branch providing sensory innervation to the wrist.

5.3.1 Radial Tunnel and Posterior Interosseous Nerve

The radial tunnel is defined as the space that begins proximally near the external bicipital groove and ends distally at the level of the motor branch of the radial nerve from the supinator muscle. The radial tunnel can be divided into three levels: upper, middle and lower [3, 4].

- In the upper portion (tunnel entrance) the nerve is located medially at the brachialis muscle and lies on the bottom of the lateral bicipital groove. Thereafter, the nerve splits into its sensory (SRN) and motor (PIN) branches; the PIN heads posteriorly towards the capitellum and the joint capsule. In this area the nerve runs in a wide space and it is unsheathed by loose connective tissue which binds it to the nearby muscles, the joint capsule and the radial collateral ligament (anterior bundle) [3, 4].
- In the middle portion, the posterior interosseous nerve is engaged below the extensor carpi

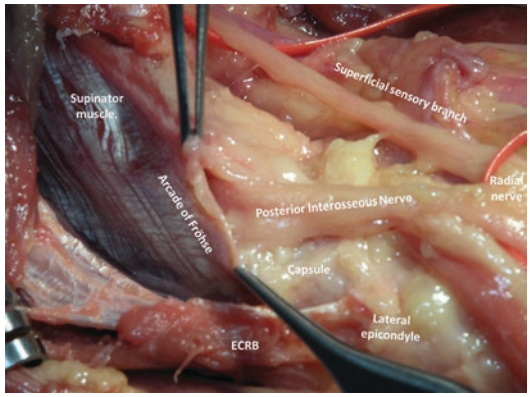

Fig. 5.2 Superficial radial nerve and posterior interosseous nerves are shown. The fibrous arcade of the supinator brevis muscle has been called Frohse arcade

brevis, whose arched free edge (spanning from the lateral epicondyle to the deep antibrachialis bundle and the aponeurosis of the flexor digitorum muscles) can be thicker and fibrotic.

- In the lower portion, the motor branch overtakes the arcade of the extensor carpi radialis brevis and it then penetrates between the bundles of the superficial and deep heads of the supinator brevis muscle [3, 4]. The fibrous arcade of the supinator brevis muscle has been called Frohse arcade [3, 4] (Fig. 5.2).

5.4 Median Nerve

- The median nerve (MN) is formed by the medial and lateral cord of the brachial plexus and it carries fibres from all the spinal nerves into the plexus. The MN courses down the arm posterior to the pectoralis major muscle and lateral to the brachial artery and it runs distally medial to the brachialis and the biceps muscle.
- At mid-arm level, at the insertion of the coracobrachialis muscle, the MN crosses over the front of the brachial artery to lie on its medial side. The MN does not supply any muscle in the arm. It runs down into the forearm, along the medial aspect of the brachialis muscle, beneath the bicipital aponeurosis and medial to the brachial artery and vein.
- Articular branches supply the elbow joint and the proximal radioulnar joint. Beneath the bicipital aponeurosis, some MN branches arise from the medial MN tract and supply the pronator teres (PT) as the MN penetrates it.
- The anterior interosseous nerve (ION) arises from the posterolateral MN tract, just distal to the proximal margin of the superficial head of the PT and 5–8 cm distal to the medial epicondyle (Figs. 5.3 and 5.4).
- After emerging from the PT, the MN courses beneath the fascial arcade of the proximal margin of the flexor digitorum superficialis (FDS) along with the anterior ION and it descends into the forearm between the FDS and the flexor digitorum profundus (FDP). It becomes superficial 5 cm above the wrist, where it emerges between the FDS and the flexor carpi radialis.
- The MN reaches the hand through the carpal tunnel, where it provides terminal branches.

5.4.1 The Supracondylar Process and Ligament of Struthers

Some patients have a bone spur in the form of a supracondylar process that arises from the medial aspect of the humerus, approximately 3–5 cm above the medial epicondyle. The ligament of Struthers extends from the spur and inserts distally onto the medial epicondyle [5, 6].

5.4.2 Lacertus Fibrosus and the Pronator Teres

The pronator syndrome is an entrapment neuropathy of the median nerve in the anatomic area of the distal humerus and proximal forearm, below the lacertus fibrosus or between the two heads of the pronator teres muscle and the fibrous arch of the sublimis muscle (flexor digitorum superficialis) [5–7] (Fig. 5.5).

5.5 Ulnar Nerve

- The ulnar nerve (UN) arises as an extension of the medial cord of the brachial plexus and descends medial to the brachial artery as far as

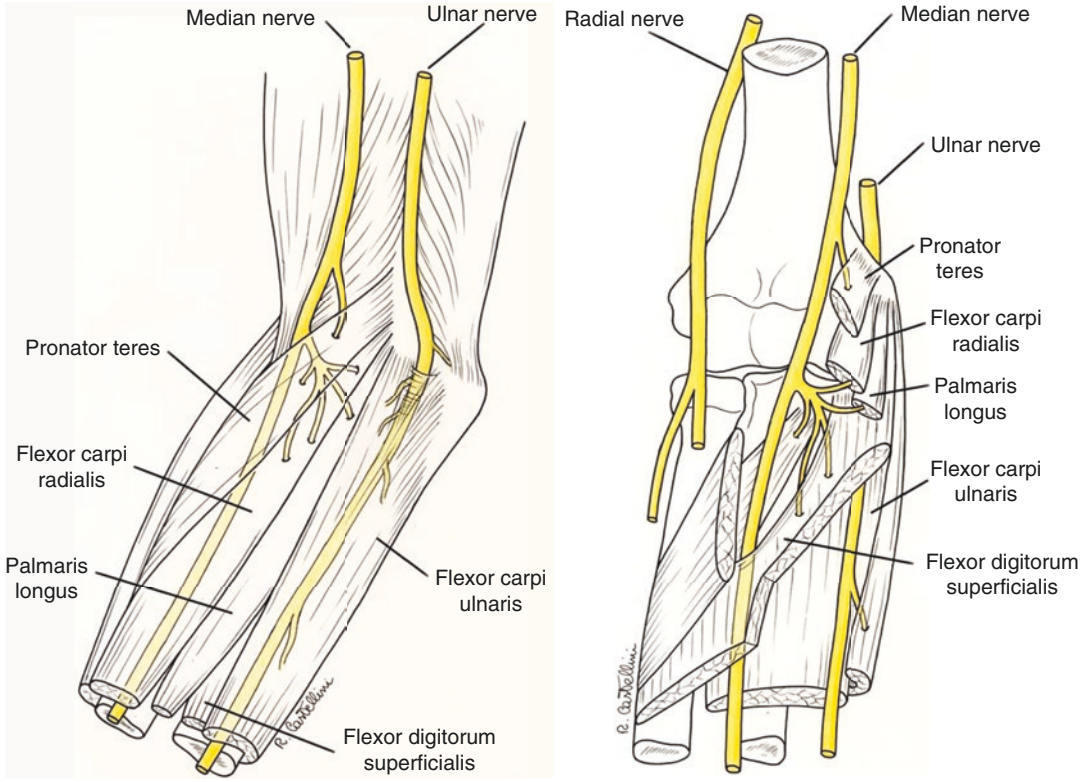

Fig. 5.3 Anatomical course of the **median and ulnar nerves** around the elbow and its terminal branches are illustrated

the middle third of the arm. It then pierces the medial intermuscular septum approximately 10 cm above the medial epicondyle to lie on the medial side of the triceps muscle beneath the fascia.

- The superior ulnar collateral artery, a branch of the brachial artery, and the UN pierce the intermuscular septum; they then descend distally together to the ulnar groove on the anterior surface of the medial head of the triceps muscle and lie on the dorsal aspect of the medial epicondyle (cubital tunnel) (Fig. 5.3). Although the UN does not innervate any muscle of the arm, in the second part of the cubital tunnel, it provides a branch to the elbow joint.
- In the forearm, the UN proximally supplies the flexor carpi ulnaris (FCU) muscle. After coursing through the cubital tunnel, the UN remains between the humeral and ulnar heads of the FCU and descends distally between the FCU and the FDP, to lie on the palmar surface.
- This relationship is maintained in the proximal third of the forearm, whereas in the middle third, the UN runs parallel to the ulnar artery remaining medial to it.
- In the distal third of the forearm, the UN becomes superficial, lying just radial to the FCU muscle.
- Once it reaches the wrist, it divides into a deep and a superficial branch. The deep motor branch supplies the hypothenar muscles, the third and fourth lumbrical and all the interosseous muscles, and it ends in the adductor pollicis muscle and the small deep head of the flexor pollicis brevis. The superficial branch provides two small motor branches to the palmaris brevis muscle; it then becomes purely sensory for the fifth finger and for the ulnar side of the fourth finger.

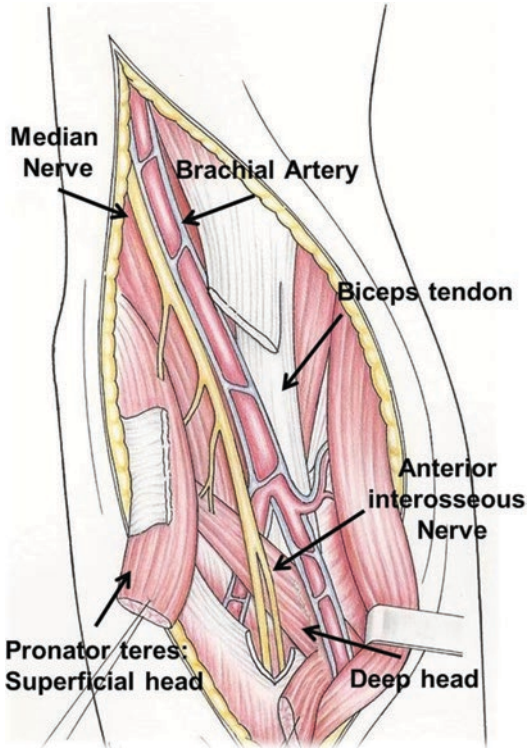

Fig. 5.4 Median nerve and anterior interosseous nerve at the elbow are illustrated

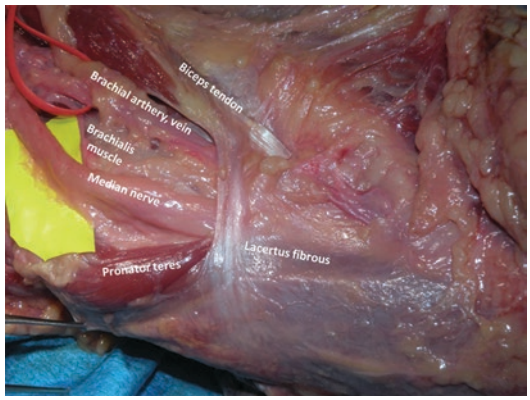

Fig. 5.5 The anatomical relationship of median nerve to the lacertus fibrosus and the pronator teres is demonstrated

5.5.1 Arcade of Struthers

The arcade of Struthers is a thickening of the deep fascia of the arm which is found 8–10 cm proximal to the medial epicondyle (it is present in 70% of anatomical specimens) [4]. It originates from the posterior aspect of the medial intermuscular septum, in the distal third of the humerus, passing superficial to the UN to enter the deep fascia of the medial head of the triceps (Fig. 5.6).

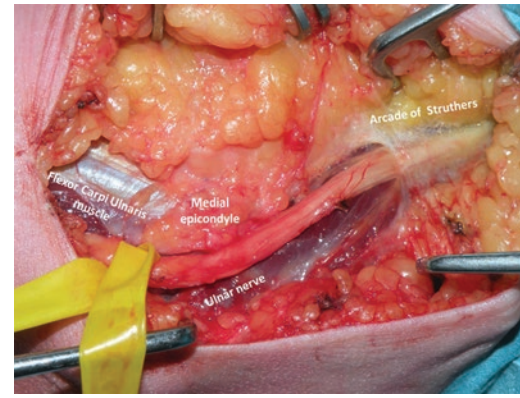

Fig. 5.6 The ulnar nerve and the arcade of Struthers are demonstrated

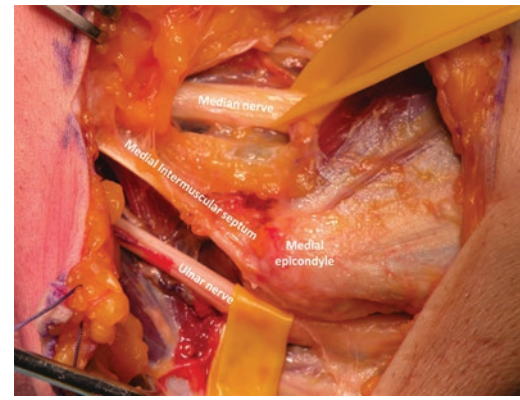

Fig. 5.7 The ulnar nerve and medial intermuscular septum are demonstrated

5.5.2 Medial Intermuscular Septum

At the epicondyle site the septum is attached to the width of the epicondyle, forming a sharp surface. Its inferior portion is thick and distinct at the site where it attaches to the medial epicondyle and the supracondylar ridge, whereas its superior portion is thinner and the attachment less distinct (Fig. 5.7).

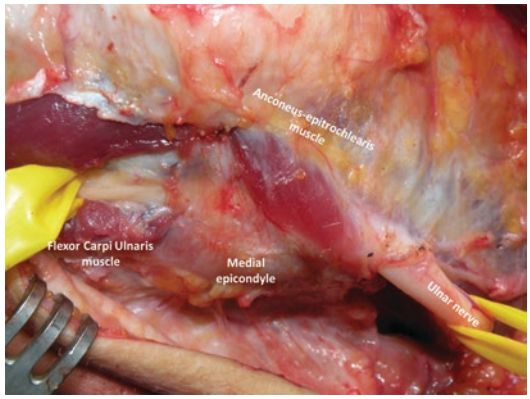

Fig. 5.8 The ulnar nerve and anconeus epitrochlearis muscle are shown

5.5.3 Anconeus Epitrochlearis Muscle

An abnormal anconeus epitrochlearis muscle extends across the proximal entrance of the cubital tunnel in 4–34% of the individuals [8–10]. The muscle arises from the medial border of the olecranon; as it enters the medial epicondyle it crosses posterior to the UN just proximal to the aponeurosis, joining the humeral and the ulnar head of the FCU [17] (Fig. 5.8).

5.5.4 Cubital Tunnel

The fibro-osseous cubital tunnel lies posterior to the medial epicondyle. Its floor is formed by the posterior MCL portion and the medial aspect of the humeroulnar capsule. Its roof is formed by a thick fibrous sheet stretching between the epicondyle and the olecranon and fusing distally with the FCU muscle fascia [11]. Osborne described it as a band of thick fibrous tissue spanning between the humeral and the ulnar head of the FCU and forming the distal part of the cubital tunnel [12].

5.5.5 Deep Flexor-Pronator Aponeurosis

The common flexor aponeurosis (CFA) lies between the origin of the flexor-pronator and the flexor digitorum superficialis (FDS) muscle. The UN crosses over the CFA approximately 5 cm distal to the medial epicondyle and 2–3 cm distal to the cubital tunnel [1].

5.6 Lateral Cutaneous Nerve of the Forearm

The lateral cutaneous nerve of the forearm (LCNF) is the terminal branch of the MCN. It is a purely sensory nerve that lies subcutaneously at the level of the antecubital fossa. After supplying the coracobrachialis, biceps and brachialis muscle, it extends distally in the intermuscular plane between the biceps and brachialis muscle, supplying the skin over the anterolateral aspect of the forearm. Its terminal branch emerges laterally beneath the biceps tendon and penetrates into the brachial fascia as LCNF (Fig. 5.9).

5.6.1 Lateral Free Edge of the Biceps Tendon

The flat, sharp border of the biceps tendon tightens when the elbow is extended and it becomes even tauter if the tendon contracts against resisted flexion and pronation, whereas if the forearm is passively pronated with the elbow extended, the nerve gets stretched and it may be compressed against the biceps tendon [13, 14].

5.7 Arthroscopic Portals and Neurovascular Structures

The relationship between elbow arthroscopy portals and neurovascular structures is of surgical significance. The relationships of medial, lateral and posterior elbow portals with adjacent neurovascular structures are detailed in Tables 5.1, 5.2, and 5.3.

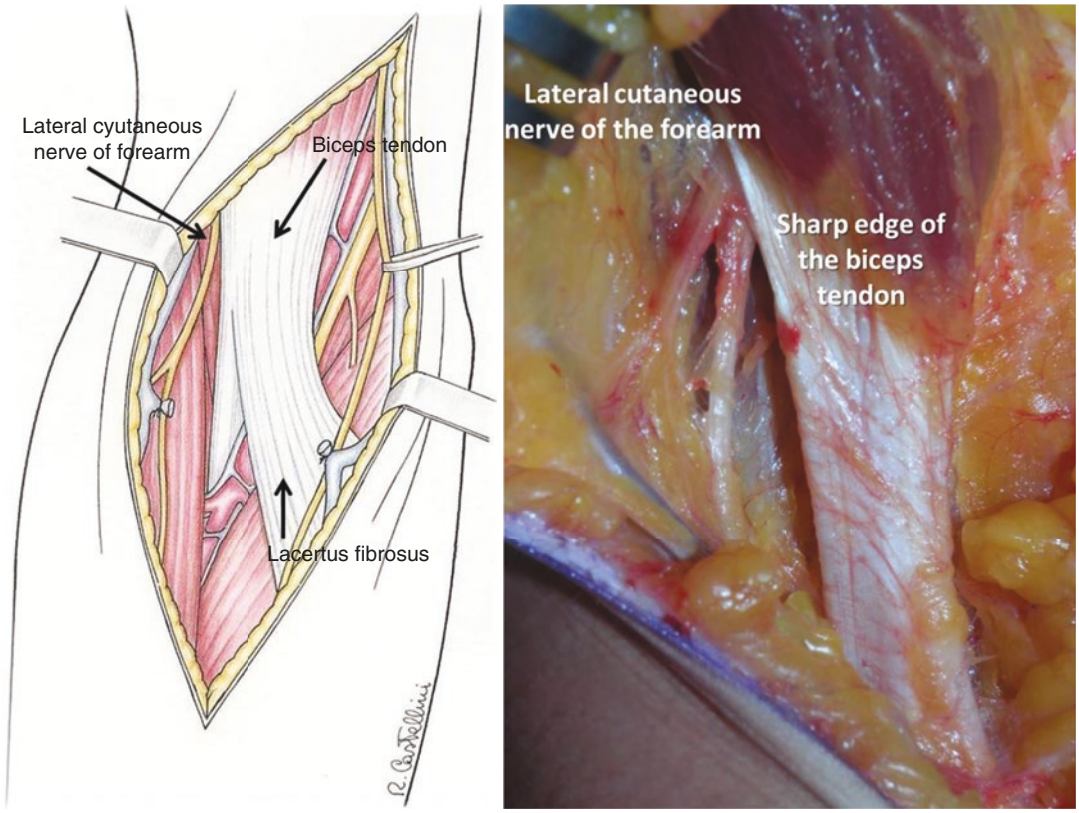

Fig. 5.9 The lateral cutaneous nerve of the forearm is demonstrated

Table 5.1 Medial arthroscopic portals and the neurovascular structures

Portals	Location	Neurovascular structures
Proximal medial	2 cm proximal to medial epicondyle. Slightly anterior to the intermuscular septum	- **Median nerve** ≈ 12.4 mm extended / ≈ 7.6 mm flexed, [15-20] - **Ulner nerve** ≈ 12 mm [20] - **Medial antebrachialcutaneous nerve** (≈ 6 mm at 90° flexion) [20] - **Brachial artery** ≈ 18 mm [18]
Mid-anteromedial	1 cm proximal and 1 cm anterior to the medial epicondyle	- **Medial antebrachial cutaneous nerve** ≈ 7 mm [18] - **Median nerve** ≈ 13 mm - 14 mm [19,20] - **Brachial artery** ≈ 17.6 mm [19,20]
Anteromedial	2 cm anterior and 2 cm distal to the medial epicondyle	- **Medial antebrachial cutaneous nerve** 1 mm - 8.9 mm [16,17] - **Median nerve** 7 mm - 2 mm with the elbow extended or flexed [15-18]. Unlu et al found the mean distance as high as 12.0 mm. [19] - **Brachial artery:** 15.2 to 16.6 mm [16,17, 19,20]

Table 5.2 Lateral arthroscopic portals and the neurovascular structures

Portals	Location	Neurovascular structures
Distal Anterolateral	3 cm distal and 1 cm anterior to the lateral epicondyle just anterior to the radial neck and head.	- **Radial nerve** 4.0 to 7.2 mm mm [15-19,21] - **Posterior antebrachial cutaneous nerve** 7.6 to 12.6 mm [16-18] Many surgeons moves this portal more proximal. to avoid the risk of radial nerve injury [19]
Mid Anterolateral	1 cm distal and 1 cm anterior to lateral epicondyle. In a sulcus between radial head and capitellum	- **Radial nerve** 3 mm - 9.2 mm [18-21] - **Posterior antebrachial cutaneous nerve** ≈ 2 mm at 90° flexion [20] More distal this portal is placed, the closer it becomes to the radial nerve
Proximal Anterolateral	2 cm proximal and 1 cm anterior to the lateral epicondyle	- **Radial nerve** 9.9 to 13.7 mm [18-21] 9.9 mm at 90° / 4.9 mm in extension [20] - **Lateral antebrachial cutaneous nerve** ≈ 6.1 mm [21]

Table 5.3 Posterior arthroscopic portals and the neurovascular structures

Portals	Location	Neurovascular structures
Direct posterior «straight posterior»	3 cm proximal to the tip of olecranon and pierces through the tendinous portion of the triceps	- **Posterior antebrachial cutaneous nerve** ≈ 23 mm [18 - 20] - **Ulnar nerve** ≈ 25 mm [18 - 21] it is relatively safe from neurovascular structures [15,16,18,20]
Direct lateral	In the soft spot of the elbow at the center of a triangle connecting the olecranon tip, lateral epicondyle and radial head.	- **Posterior antebrachial cutaneous nerve** ≈ 9.6 mm [18,19]
Postero lateral	3 cm proximal to olecranon, superior and 1 cm anterior to the midpoint of a line connecting the olecranon and the posterior lateral epicondyle,	- **Medial and posterior antebrachial cutaneous nerves** ≈ 25 mm [19] This portal is relatively safe [20]
Distal ulnar	3 to 4 cm distal to the radiocapitellar joint along the lateral border of the ulna [22]	There is little risk for the neurovascular structures [19,22]

References

1. Testut L. Trattato d'anatomia umana Sistema nervoso periferico. 3a Ed. Italiana Unione Tipografica Torinese; 1923. pp. 191–194.
2. Gelberman RH, editor. Operative nerve repair and reconstruction. Philadelphia: J.B. Lippincott; 1991. p. 393–407.
3. Celli A, Rovesta C, Marongiu MC. Elbow nerve tunnel syndromes I. In: Morrey CC, editor. Treatment of elbow lesions. Springer; 2008. pp. 281–297.
4. Spinner M. Management of nerve compression lesions of the upper extremity. In: Omer GE, Spinner M, editors. Management of peripheral nerve problems. Philadelphia: WB Saunders; 1980. p. 569–87.
5. Spinner M. The anterior interosseous nerve syndrome with special attention to its variations. J Bone Joint Surg Am. 1970;52:84–94.
6. Fearn CBD, Goodfellow JW. Anterior interosseous nerve palsy. J Bone Joint Surg Br. 1965;47:91–3.
7. Spinner RJ. Nerve entrapment syndromes. In: Morrey BF, Sanchez-Sotelo, editors. The elbow and its disorders. Philadelphia: W.B. Saunders; 2009. p. 1090–118.
8. Van Clemens HJ. Zur Morphologie des ligamentum epitrochleo anconeum. Anat Anz. 1957;104:343–344.
9. Dahners LE, Wood FM. Anconeous epitrochlearis, a rare cause of cubital tunnel syndrome: a case report. J Hand Surg (Am). 1984;9:579–80.
10. Wachsmuth W, Wilhelm A. Der musculus epitrochleoanconeous und seine klinishe bedeuntung. Mschr Unfallheilk 1968;71:1–22.
11. Apfeldeberg DB, Larson SJ. Dynamic anatomy of the ulnar nerve at the elbow. Plast Reconstr Surg. 1973;51:76–81.
12. Osborne G. The surgical treatment of Tardy ulnar neuritis. J Bone Joint Surg Br. 1957;39:782.
13. Braddom RL, Wolfe C. Musculocutaneous nerve injury after heavy exercise. Arch Phys Med Rehabil. 1978;59:290–1.
14. Basset FH, Nunley JA. Compression of the musculocutaneous nerve at the elbow. J Bone Joint Surg Am. 1982;64(A):1050–2.
15. Marshall PD, Fairclough JA, Johnson SR, Evans EJ. Avoiding nerve damage during elbow arthroscopy. J Bone Joint Surg Br. 1993;75:129–31.
16. Stothers K, Day B, Regan WR. Arthroscopy of the elbow: anatomy, portal sites, and a description of the proximal lateral portal. Arthroscopy. 1995;11:449–57.
17. Lynch GJ, Meyers JF, Whipple TL, Caspari RB. Neurovascular anatomy and elbow arthroscopy: inherent risks. Arthroscopy. 1986;2:190–7.
18. Unlu MC, Kesmezacar H, Akgun I, Ogut T, Uzun I. Anatomic relationship between elbow arthroscopy portals and neurovascular structures in different elbow and forearm positions. J Shoulder Elb Surg. 2006;15:457–62.
19. Camp CL, Degen RM, Sanchez-Sotelo J, Altchek DW, Dines JS. Basics of elbow arthroscopy part I: surface anatomy, portals, and structures at risk. Arthrosc Tech. 2016;5(6):e1339–43.
20. Malageladaa F, Dalmau-Pastorb M, Vegac J, Golanób P. Elbow anatomy. In: Nedim DM, Jon K, editors. Sports injuries. Berlin Heidelberg: Springer; 2014. p. 1–30.
21. Field LD, Altchek DW, Warren RF, O'Brien SJ, Skyhar MJ, Wickiewicz TL. Arthroscopic anatomy of the lateral elbow: a comparison of three portals. Arthroscopy. 1994;10:602–7.
22. van den Ende K, McIntosh AL, Adams JE, Steinmann SP. Osteochondritis dissecans of the capitellum: a review of the literature and a distal ulnar portal. Arthroscopy. 2011;27:122–8.

6 Arthroscopic Equipment and Set-Up for Elbow Arthroscopy

Richard S. Page, Janina Henze, and Kevin Eng

6.1 Background

Elbow arthroscopy has established itself as an effective surgical procedure, for the management of intra-articular elbow pathology. It brings technical challenges due to the limited space in the joint and the proximity of the neurovascular structures. The procedure requires surgeon experience and the preparation plays a major role in determining the outcome.

Elbow arthroscopy was first described by Burman in 1931 who used the Jacobaeus laparoscope in a joint filled with oxygen or nitrogen gas [1]. In his first publication he stated that the elbow was not a suitable joint for arthroscopy due to the limited space in the anterior compartment. However, after cadaveric studies performed in Dresden, Germany, 1932, Burman revised his opinion. Burman's studies were performed on cadavers and even though he acknowledged the method was still in its infancy. He believed that arthroscopy could become a useful procedure in the treatment of elbow pathology.

After the first description of elbow arthroscopy, only a small number of cases were reported in Germany and Japan [2, 3]. Subsequently, the development of the 1.7 mm endoscope by Watanabe in 1971 made the procedure suitable for small joints [3].

In the 1985, Andrew and Carson continued to undertake further studies and established the additional portals [2]. Following these investigations elbow arthroscopy underwent rapid development, which in turn led to improvements in instrumentation and surgical utilisation.

Elbow arthroscopy has advanced sufficiently for the procedure to be considered safe. The complication rates are described in a number of studies with a range of 1–14%, which is regarded as high in comparison to the knee arthroscopy, with a 1–2% complication rate. However, most of the complications are described as minor with an incidence under 1% [4–6]. A key factor of note for more serious complications is the proximity

R. S. Page (✉)
Department of Orthopaedics, School of Medicine, Deakin University, Geelong, VIC, Australia

Barwon Centre for Orthopaedic Research and Education (B-CORE), Barwon Health and St John of God Hospital, Geelong, VIC, Australia

Geelong Orthopaedics, SJOG Specialist Centre, Geelong, VIC, Australia
e-mail: richardpage@geelongortho.com.au

J. Henze
Barwon Centre for Orthopaedic Research and Education (B-CORE), Barwon Health and St John of God Hospital, Geelong, VIC, Australia

K. Eng
Barwon Centre for Orthopaedic Research and Education (B-CORE), Barwon Health and St John of God Hospital, Geelong, VIC, Australia

Geelong Orthopaedics, SJOG Specialist Centre, Geelong, VIC, Australia

© ISAKOS 2022

D. N. Bhatia et al. (eds.), *Arthroscopy and Endoscopy of the Elbow, Wrist and Hand*,
https://doi.org/10.1007/978-3-030-79423-1_6

of the surrounding neurovascular structures, making portal placement critical.

6.2 Planning and Layout

Before the commencement of surgery, a documented clinical history and examination, which includes the range of motion and stability in comparison with the other elbow, is essential. Imaging should be undertaken to clearly define the anatomy and pathology of the patient. As a minimum, basic diagnostic radiographs should be available and for pathologies involving the soft-tissue/ligamentous anatomy, an MRI or occasionally an ultrasound can be helpful. CT scans with 3D reconstruction are preferable to assess the bony pathology with associated loose bodies and osteoarthritis (OA) or following trauma to plan the approach and assist with fixation. In cases of advanced OA with impingement, CT scans in flexion and/or extension can detect further relevant pathology.

The surgeon should stand on the side of the elbow that will be operated on and the monitor should be on the opposite side of the operating table in direct view, visible to the surgical team (Fig. 6.1).

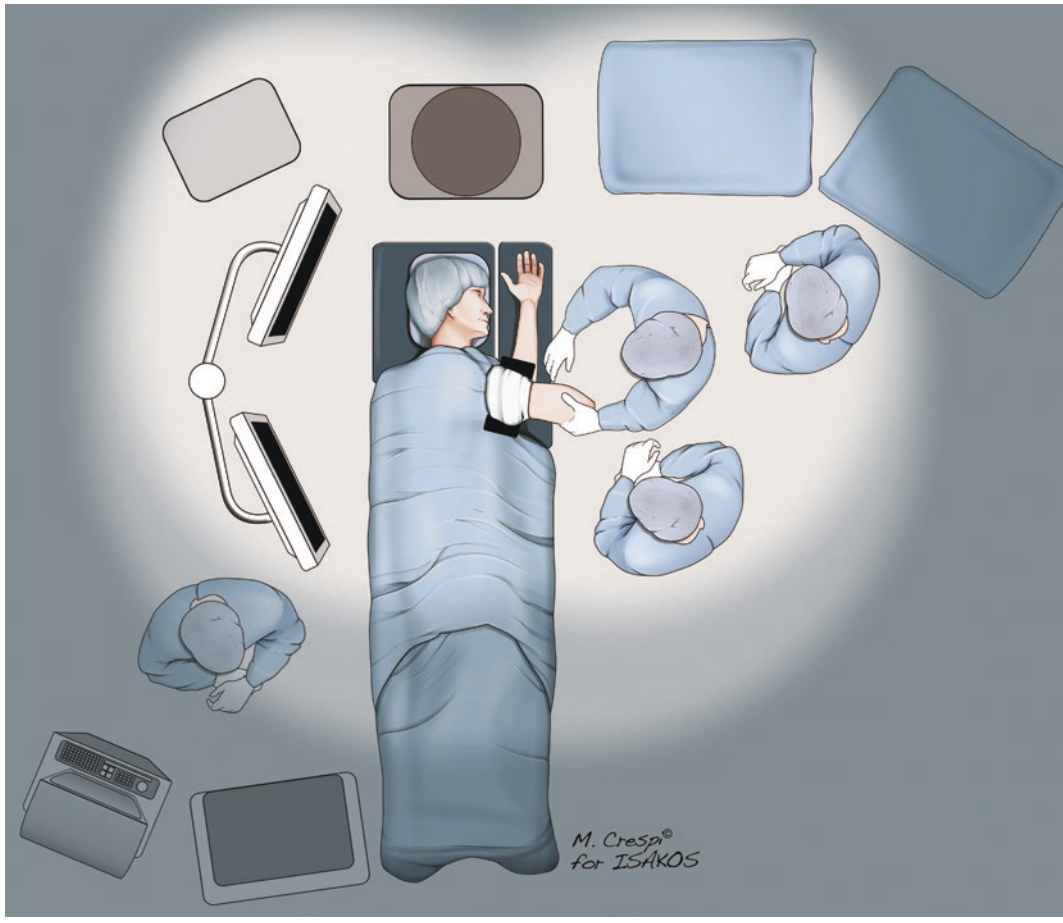

Fig. 6.1 Map of theatre layout for elbow arthroscopy. The surgeon stands on the side of the elbow and the monitors are on the opposite side. The instrument table, suction pump and arthroscopy tower (right to left) are at the head end of the operation table. The anaesthetist and ventilator are at the foot end on the table (M. Crespi © for ISAKOS) from drawings by Dr J Henze

6.3 Anaesthesia

Elbow arthroscopy can be performed under general or regional anaesthesia. Each has their supportive reasons. The patient's position on the table and equipment set-up are crucial factors that must be considered prior to anaesthesia.

- General anaesthesia is more comfortable for the patient whilst covered by the surgical drapes and muscular relaxation can be achieved. General anaesthesia can be combined with local or regional anaesthesia.
- Regional anaesthesia, such as an axillary block, can reduce the risks associated with a general anaesthesia but has two major downsides. Patients must be compliant for the procedure. Secondly it can cloud post-operative neurological evaluation.
- At the end of every procedure, local anaesthesia (e.g. ropivacaine 0.75%) can be injected to the joint and the portal sites to minimise post-operative pain.

6.4 Positioning

There are three main positions that are predominately used for elbow arthroscopy, which are detailed below. The first position employed and popularised by Andrews et al. was the supine position, until Poehling et al. established the prone position [2, 7]. In 1993, O'Driscoll and Morrey developed the lateral decubitus position, the most common in current use [7, 8]. Whichever position is utilised, adequate padding and support for the patient's trunk needs to be used to avoid unwanted movement during surgery and to protect pressure areas and nerves from compression injury [9].

- *Supine position*: The patient is placed horizontally with the face and torso up on the table, whilst the elbow is flexed to 90° fixed to an extension boom or any other limb positioner. This position has some advantages; first the anatomy is set in a natural familiar direction for the surgeon, which assists with intra-articular orientation. No assistance is needed for movement of the elbow held with a limb positioner, the arm can be placed freely in space, it is easier for the anaesthetist to control the airway and positioning is simpler for obese patients (in comparison to lateral or prone positioning). Disadvantages are the requirement for an (potentially) expensive traction device. Some surgeons also describe a feeling of instability in this position [2, 7].
- *Prone position*: The patient is prone whilst the shoulder is abducted 90° from the side of the body, whilst the elbow is hanging freely with a 90° flection. This creates unlimited access to all compartments and provides free movement and manipulation of the arm. The disadvantage is the poor airway access and pressure management particularly of the face. It is also difficult to switch into an open procedure during the surgery [8].
- *Lateral decubitus position*: The lateral decubitus position has evolved from the prone position. This position offers similar advantages to the prone position with improved access to the airway. The patient is placed on the bean bag and is then turned on their side with the operative elbow facing up. The body is held by two body/pelvis supporters, one on each side of the table. The arm is positioned on a padded arm holder or preferably on a short T-bar, to allow elbow flexion and extension. An axillary bolster can be placed under the axilla if desired. It is important that the anaesthetist has access to the airway and IV lines. It may be difficult when switching to an open procedure to access the anterior compartment [7, 8, 10]. However, the majority of the elbow can be accessed via a universal posterior or lateral approaches (Fig. 6.2).

6.5 Equipment

- An example arthroscopy tower and equipment are shown in Fig. 6.3.
- A 4.0 mm arthroscope with a 30° viewing angle is used by most surgeons. In some cases, such as small females and children the smaller 2.7 mm arthroscope may be more suitable (Fig. 6.4).

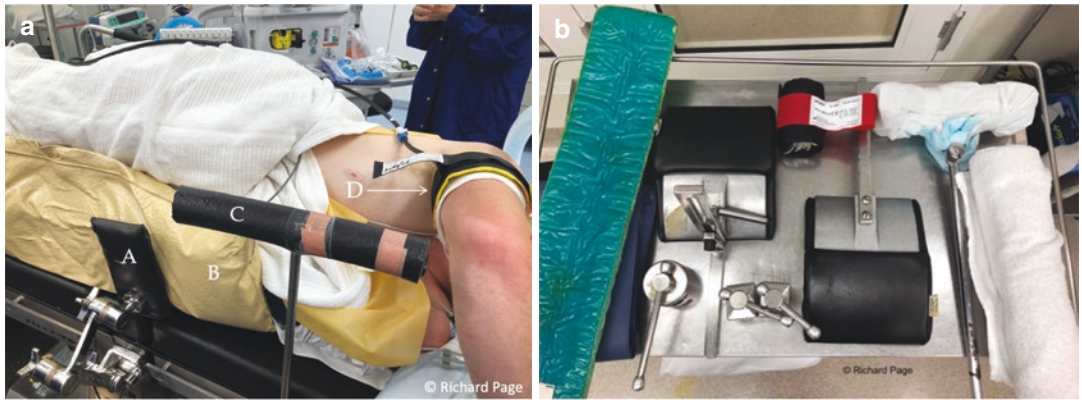

Fig. 6.2 Patient set-up in the lateral decubitus position with the required elements (image **a**), the supporting equipment is laid out on a trolley (image **b**). (A) Side support, (B) bean bag moulded and air vacuum extracted, (C) short T-bar that will support the elbow during arthroscopy, (D) tourniquet placed high up the arm to allow unrestricted portal or open access if required (© Richard Page)

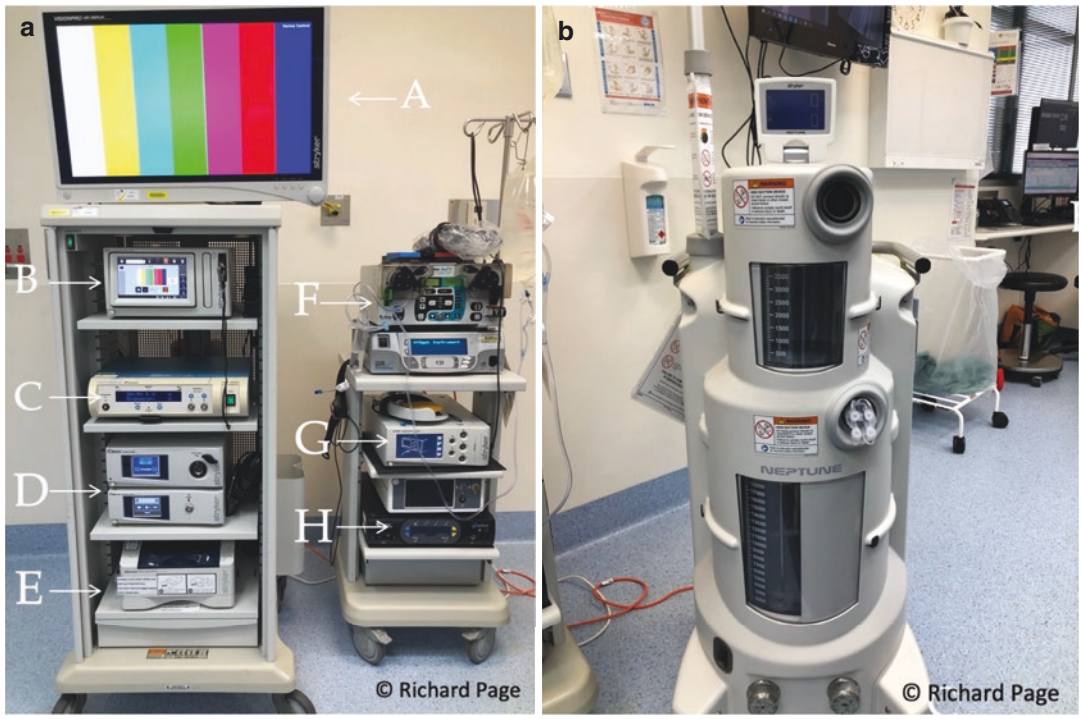

Fig. 6.3 (**a**) Arthroscopic tower with (A) video screen, (B) arthroscopic camera and image management system, (C) small joint shaver system, (D) arthroscopic light source, (E) arthroscopic image printer, (F) fluid management system, (G) power shaver console, (H) radiofrequency ablation device. (**b**) Large-capacity suction device (Neptune fluid suction system) (© Richard Page)

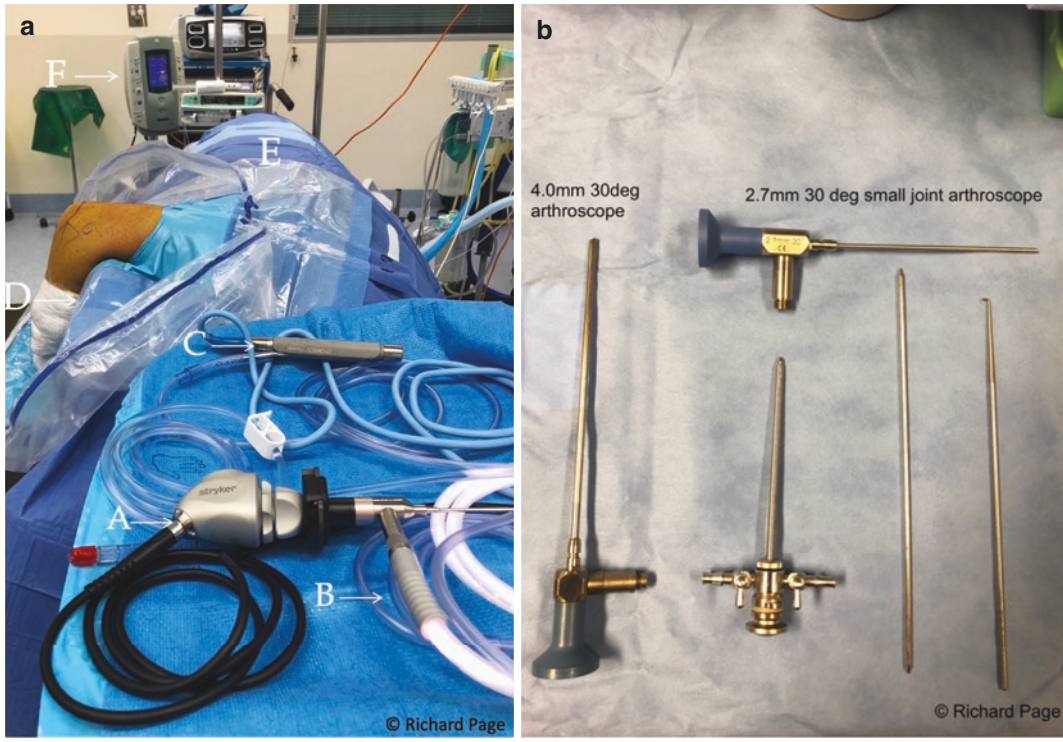

Fig. 6.4 (**a**) Set-up during surgery; the equipment is placed at the head end of the patient on a Mayo stand covered in a sterile drape. The cords are coiled and secured to the drape to minimise tangling. (A) Camera, (B) light source lead, (C) shaver motor and (D) arm draped with elbow over a support. (**b**) Arthroscopes, probe and equipment required for elbow arthroscopy (© Richard Page)

- The rest of the equipment is similar to other large joint arthroscopy sets. Cannulae may be utilised to switch the working and viewing portals in order to minimise trauma to the capsule. They should be compatible with the 4.0 and 2.7 mm arthroscopes, particularly in length.
- A fluid management pump or gravity feed may be used to maintain the intra-articular pressure and guarantee adequate visibility during the procedure. A hand pump that uses a gravity flow, however, has the risk of wide swings in pressure. A fluid management system can produce a more consistent flow and the pressure should aim to be ~35–40 mm Hg. It is advisable to familiarise with the specific pump system in use in advance, as the scale is inconsistent between company devices, and the pump should be regularly calibrated.

6.6 Getting Started

- Once positioned, the medial and lateral epicondyles, the capitulum of the humerus, the olecranon, the radius head and the ulnar nerve are identified and marked. The ulnar nerve is palpated in flexion and extension to ensure that the nerve does not subluxate anteriorly, to a position that would place it at risk during entry via the medial portal. Furthermore, the utilised portals should be identified and marked (Fig. 6.5). The range of motion and stability of the elbow are recorded.
- Prior to the commencement of surgery, the patient identification and operative side are checked as part of the 'Time Out' process as per WHO guidelines [11].
- The first step of the surgery is to inflate the elbow joint with 20–30 mL of sterile saline,

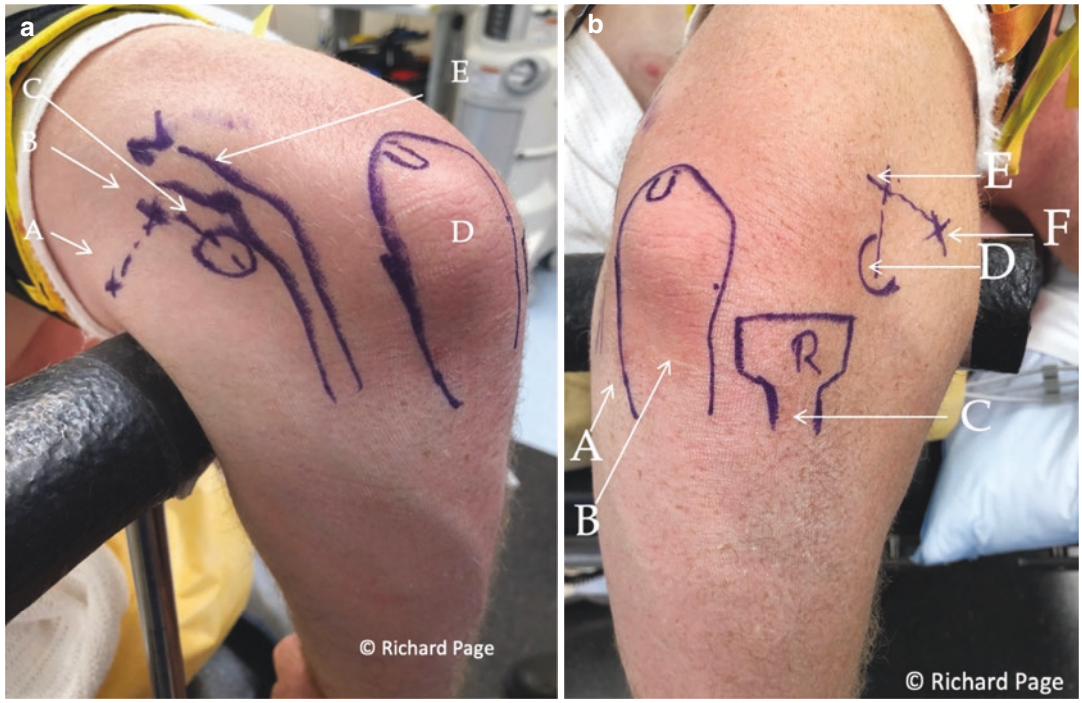

Fig. 6.5 Landmarks of the elbow are demonstrated. (**a**) Medial view of a right elbow is shown in lateral decubitus position: (A) Proximal anteromedial portal (PAMP), (B) medial intermuscular septum (MIMS), (C) medial epicondyle, (D) olecranon, (E) ulnar nerve (N). (**b**) Dorsal view of a right elbow is shown in lateral decubitus position: (A) Medial epicondyle, (B) olecranon, (C) radial head (R), (D) lateral epicondyle, (E) lateral intermuscular septum (LIMS), (F) proximal anterolateral portal (PALP) (© Richard Page)

which is injected through the posterior soft spot in the mid-lateral portal (Fig. 6.6). The fluid increases the joint space and therefore more distance is created between the neurovascular structures, capsule and instruments. Then the surgery can begin with the introduction of the arthroscope into the joint, usually through the medial portal. If a trocar is utilised to assist with arthroscopic entry, the conical not sharp tip should be used to minimise iatrogenic injury (Fig. 6.4 (b)) as shown.

6.7 Tips and Tricks

- The position of the patient and the elbow is important for surgery, especially the flexion of the elbow, which should be tested prior to the draping. Furthermore, for the set-up we recommend a short T-bar that allows rotation and reduces the interference from drapes or edges of the T-bar. This improves the mobility of the arm and access to the different articular compartments.
- Exsanguination of the limb prior to tourniquet inflation reduces intra-articular bleeding and improves visualisation.
- A range of arthroscope sizes and shavers/burrs should be available in theatre (2.7–4.0 mm) for different sized patients and various pathologies encountered.
- Start the arthroscopy with the anterior compartment, to have an overview over the joint first. When switching the portals, a 3 mm switching rod can be helpful.

Fig. 6.6 Inflation of the elbow joint with sterile saline via the posterior soft-spot portal to aid arthroscope entry with minimal trauma. (A) Sterile saline, (B) sterile draping, (C) compression bandage on the forearm, (D) radius head, (F) lateral epicondyle, (E) olecranon (© Richard Page)

Table 6.1 Elbow arthroscopy equipment checklist for the basic set-up

Arthroscope	**To establish portals**
– 4.0 mm arthroscope 30° – Small joint arthroscope 2.7 mm (if needed) 30°	– Forceps mosquito straight – Forceps mosquito curved – Forceps artery curved – Mayo scissor – Scalpel – Dissector Gillies forceps – Elevator Hohmann—small
Special arthroscopy equipment: – Grasper alligator— small joint – Instrument pins – Trocar blunt – Trocar 4.0 round – Trocar 4.0 bullnose – Nibbler bone medium – Cannula – Attachment cannula tap – Cannula nut – Switching rod 3.0 mm x 23 cm – Cage 40 mm × 40 mm – O-ring (arthroscopic seal) – Osteotome small and medium – Shaver blades and burrs (3.5 and 4.5 mm) – Radiofrequency ablation device (small)	**Other:** Suture material Sterile tapes/draping Mallet small

- If difficulty is encountered accessing the anterior compartment (e.g. capsular thickened OA males) then the arthroscope can be introduced initially into the posterior 'soft-spot' portal. Then with traction, space can be created to pass a narrow-diameter scope via the trochlea-capitellar interval to visualise the anterior compartment, whilst a 3.0 mm switching rod is introduced from the antero-superolateral portal into the anterior compartment. This can then be used to introduce the scope cannula anteriorly.
- Utilising additional 'accessory' portals, particularly posteriorly, can assist in accessing loose material, chondral lesions or osteophytes along the joint margins of the posterior compartment.
- A list of basic set up equipment with optional instruments for more advanced elbow arthroscopy is given at Table 6.1.

References

1. Burman MS. Arthroscopy or the direct visualization of joints: an experimental cadaveric study. J Bone Joint Surg. 1931;13:669–95.
2. Andrews JR, Carson WG. Arthroscopy of the elbow. Arthroscopy. 1985;1:97–107.
3. Baker CL Jr, Jones GL, Poehling GG, Whipple TL, Sisco L, Goldman B. Arthroscopy of the elbow. Am J Sports Med. 1999;27(2):251–64.
4. Nelson GN, Wu T, Galatz LM, Yamaguchi K, Keener JD. Elbow arthroscopy: early complications and associated risk factors. J Shoulder Elbow Surg. 2014;23(2):273–8.
5. Elfeddali R, Schreuder MH, Eygendaal D. Arthroscopic elbow surgery, is it safe? J Shoulder Elbow Surg. 2013;22(5):647–52.
6. Kelly EW, Morrey BF, O'Driscoll SW. Complications of elbow arthroscopy. J Bone Joint Surg Am. 2001;83(1):25–34.
7. Camp CL, Degen RM, Dines JS, Sanchez-Sotelo J, Altchek DW. Basics of elbow arthroscopy part II: positioning and diagnostic arthroscopy in the supine position. Arthrosc Tech. 2016;5(6):e1345–9.
8. O'Driscoll SW, Morrey BF. Arthroscopy of the elbow. Diagnostic and therapeutic benefits and hazards. J Bone Joint Surg Am. 1992;74(1):84–94.
9. Ng AK, Page RS. Greater auricular nerve neuropraxia with beach chair positioning during shoulder surgery. Int J Shoulder Surg. 2010;4(2):48–50.
10. Steinmann SP. Elbow arthroscopy: where are we now? Arthroscopy. 2007;23(11):1231–6.
11. World alliance for patient safety. implementation manual who surgical safety checklist (first edition) safe surgery saves lives. WHO/IER/PSP/2008.05

7 Portals and Technique for Diagnostic Elbow Arthroscopy

Benjamin R. Graves, Michael T. Freehill, Gary G. Poehling, and Gregory I. Bain

7.1 Introduction

Arthroscopy of the elbow is a useful operative technique that allows safe and effective access to difficult regions of the joint in a minimally invasive manner. In their initial description of setup and portal placement, Andrews and Carson [1] preferred supine patient positioning with the creation of an anterolateral portal first. Poehling and Whipple subsequently described the prone position, and preferred starting with the proximal medial portal, as this portal provides a safe, reliable, and reproducible entrance into the joint [2]. Anesthesia access was improved with the transition from prone to lateral decubitus positioning, but the arthroscopic approach was unchanged.

The goal of the diagnostic arthroscopy of the elbow is to evaluate all intra-articular structures of both the anterior and posterior compartments. This includes assessment of articular surfaces of the humerus, ulna, and radial head, as well as soft tissues such as ligaments and capsule. Advanced arthroscopic surgical techniques have been developed to address particular pathologic lesions in the elbow, and will be discussed within dedicated chapters in this book. The following is our technique for arthroscopic diagnostic evaluation of the elbow joint in its entirety.

7.2 Indications

- Localized osteophytes (posteromedial impingement in the throwing athlete)
- Loose body extraction
- Septic joint
- Inflammatory arthritis and hemophilia
- Cartilage lesions or osteochondral defects
- Contracture
- Fractures or instability
- Lateral epicondylitis
- Plica

7.3 Contraindications

- Extra-articular pathology: extensive heterotopic ossification, malunion, or destructive arthritis.
- Distorted anatomy, inability to create safe portals, need for extracapsular release.

B. R. Graves · G. G. Poehling (✉)
Department of Orthopaedic Surgery,
Wake Forest School of Medicine,
Winston-Salem, NC, USA
e-mail: poehling@wakehealth.edu

M. T. Freehill
Department of Orthopaedic Surgery, Stanford University, Stanford, CA, USA

G. I. Bain
Department of Orthopaedics and Trauma Surgery,
Flinders Medical Centre and Flinders University,
Adelaide, SA, Australia
e-mail: greg@gregbain.com.au

© ISAKOS 2022

D. N. Bhatia et al. (eds.), *Arthroscopy and Endoscopy of the Elbow, Wrist and Hand*,
https://doi.org/10.1007/978-3-030-79423-1_7

- Prior ulnar nerve surgery (e.g., transposition, subcutaneous, or submuscular).
  - In some cases, this may be safely performed with technique modification, starting with a proximal lateral portal. If a medial portal is needed, the ulnar nerve must be identified first through a small open incision.

7.4 Equipment

- Standard **30° arthroscope**.
- **Trocar** with **no fenestrations**, as they can lead to extracapsular fluid extravasation.
- **Probe, graspers,** and **basket forceps**.
- Arthroscopic **shaver**, **burr,** and **electrocautery wand**.
- **Wissinger rod** (switching stick) allows safe and quick exchange between visualization and working portals, and can be used as retractors when soft tissues obstruct visualization.

7.5 Position

Numerous positions have been described including supine (arm free), supine (arm suspended), prone, and lateral decubitus. Each has its advantages and disadvantages. The authors' preference is the lateral position, as it allows improved access to the posterior compartment and benefits for anesthesia and airway maintenance (Fig. 7.1a, b). If open access to the anterior compartment is anticipated, the patient can be positioned in a supine position with the arm placed across the chest. The arm can be straightened onto a hand table during the open portion of the procedure.

Preferred Lateral Technique: Setup and Position

- We *recommend to not use* preoperative nerve blocks. This allows immediate and accurate assessment of postoperative nerve function.
- General anesthesia in supine position.

Fig. 7.1 (**a**, **b**) Lateral decubitus positioning. Tourniquet at the level of padded arm holder, arm elevated above horizontal to aid in elbow flexion and extension ROM. Anesthesia positioned to the back of the patient at the head of the bed (© B. R. Graves)

- Roll into lateral position, operative extremity up, axillary role in nonoperative arm, ensure that all bony prominences are padded.
- Bean bag vacuum aspiration, table strap placed.
- A **tourniquet** is placed high above the elbow. Use a sterile tourniquet for patients with shorter arms, and for complex cases that may require conversion to an open procedure.
- Modified padded arm holder.
- Shoulder 90° abduction, elbow 90° flexion. Elevating the patient's arm by raising the arm holder can help facilitate greater intraoperative elbow flexion.
- Stockinette and Coban wrap helps prevent extravasation into the forearm.

7.6 The Elbow "Joint Box" Concept

The elbow's complex anatomy and multiplanar range of motion can make arthroscopy of this joint challenging early in one's practice. One helpful technique is to think of the elbow joint as a "box" (Fig. 7.2). The sides of this "box" provide multiple access points for visualization and instrumentation of the medial and lateral aspects of the anterior and posterior compartments of the elbow.

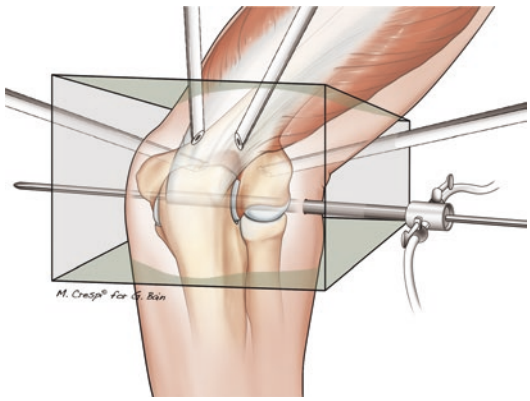

Fig. 7.2 The "joint box" concept. The elbow joint can be thought of as a box, where the arthroscope and working instruments can be inserted from various positions throughout to enable optimal visualization and instrumentation in the anterior and posterior compartments of the elbow (M. Crespi © for Gregory I. Bain)

7.7 Surface Anatomy

Marking the skin aids in spatial understanding of the deeper anatomy, which helps prevent injury to neurovascular structures:

- Medial epicondyle, medial intermuscular septum, and ulnar nerve.
- Olecranon process.
- Lateral epicondyle, radial head, and "soft spot." One useful technique to help with spatial orientation during a case is to remember that the radial head always points toward the patient's head.

7.8 Joint Distension

Distending the joint with fluid increases the distance of neurovascular structures from the cartilage surfaces, which improves visualization and creates space to work. The normal joint accommodates 20–30 mL of fluid at 70° of flexion. Intra-articular fluid insufflation distends the joint capsule, increasing the distance from the articular surface to the nerves, but does not change the distance between the capsule and neurovascular structures (Figs. 7.3 and 7.4).

Caution must be taken following fluid insufflation when working around the capsule itself. The distance between the capsule and the neurovascular structures may, in effect, ***decrease*** with joint distension as the anterior structures become increasingly compressed by the expanding capsule.

Technique

- 18G needle into the "soft spot" of the elbow (space between lateral epicondyle, radial head, and olecranon process).
- 20–30 cc of normal saline injected.
- Return of fluid should be noted when pressure is removed from the syringe's stylus. If fluid backflow is not seen, the injection may not be intra-articular.
- Alternatively, with the elbow flexed to 90° the needle can be placed directly posterior into the olecranon fossa through a postero-

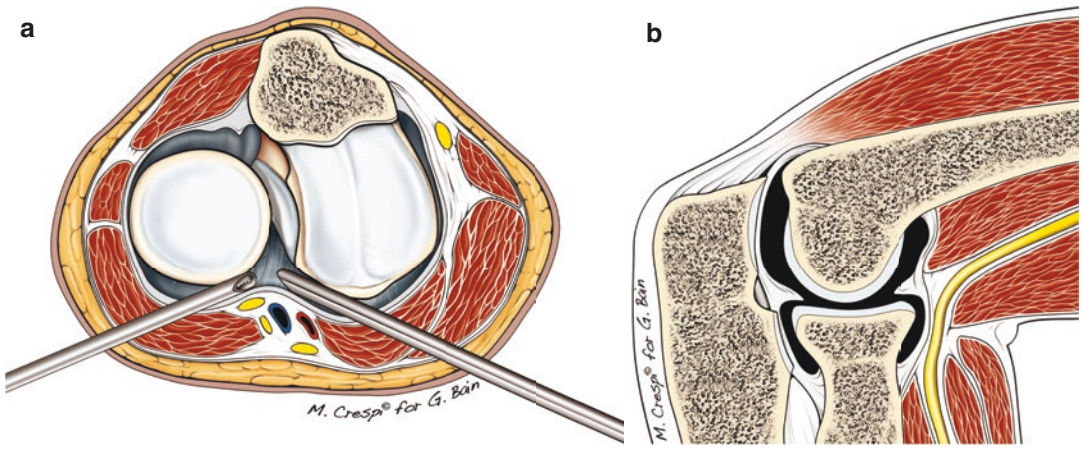

Fig. 7.3 Before fluid insufflation. Elbow joint cross section (**a**) and sagittal plane (**b**) representations during arthroscopy. Note the relationships between (1) the articular surfaces and the anterior capsule, and (2) the anterior capsule and neurovascular structures (M. Crespi © for Gregory I. Bain)

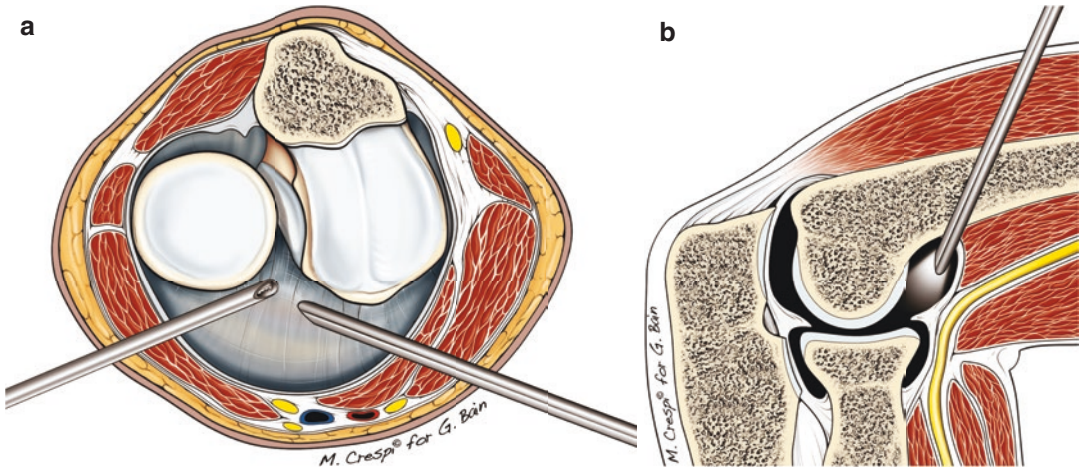

Fig. 7.4 After fluid insufflation. Elbow joint cross section (**a**) and sagittal plane (**b**) representations during arthroscopy. Note the expanded distance between the articular surfaces and the anterior capsule, and the decreased distance between the anterior capsule and neurovascular structures (M. Crespi © for Gregory I. Bain)

central portal approach. Palpate approximately one finger breadth proximal to the tip of the olecranon. The needle is inserted directly posterior and distal at this location until the bone of the humeral olecranon fossa is reached. The needle is slightly withdrawn while the saline is delivered intra-articularly.

7.9 Portals

The authors prefer to start in the anterior compartment and create a medial-sided portal initially. The medial side is safer and more predictable for anterior portal creation with regard to the neurovascular structures and their position in comparison to the lateral side of the

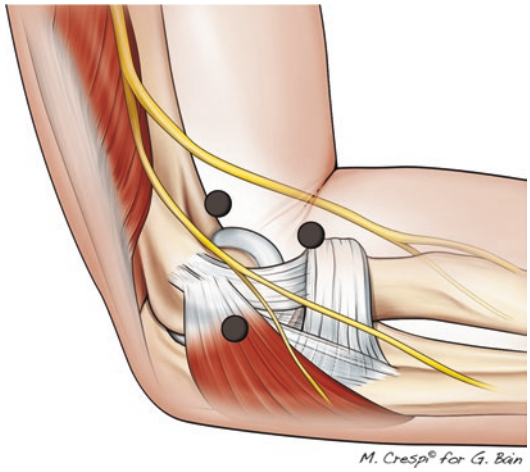

Fig. 7.6 (Right) Lateral: Proximal anterolateral, anterolateral, and "soft-spot" portals (M. Crespi © for Gregory I. Bain)

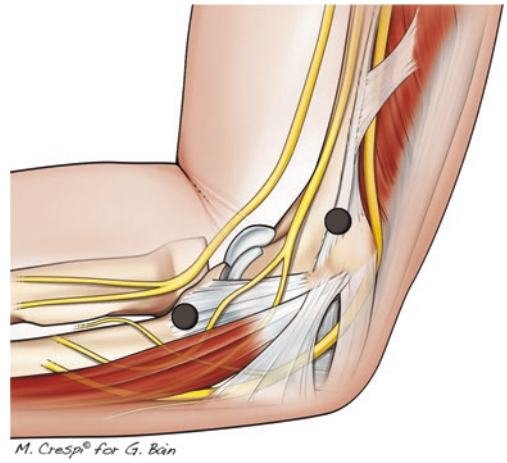

Fig. 7.5 (Left) Medial: Proximal anteromedial and anteromedial portals (M. Crespi © for Gregory I. Bain)

elbow. The "knick-and-spread" technique for creating portals involves a superficial skin incision with a scalpel through the dermis, and then a blunt hemostat is used to spread the subcutaneous tissues to minimize the risk to cutaneous sensory nerves. Using this technique, a number of portals can be safely created on both the medial and lateral sides of the elbow (Figs. 7.5 and 7.6).

7.10 The "2 cm Rule"

The main *working portals* are 2 cm proximal to their bony prominences. The anterior compartment working portals are the **proximal anterolateral** and **proximal anteromedial portals**. These portals are 2 cm proximal to the lateral and medial epicondyles, respectively.

The posterior compartment working portals are the **posterolateral** and **posterocentral portals**, which are located 2 cm proximal to the olecranon. We ***advise against*** posteromedial portals as they place the ulnar nerve at high risk of injury (Table 7.1).

The *accessory portals* help complement the working portals for work and visualization, and include the **anteromedial**, **anterolateral**, and **"soft-spot"** portals. These portals are 2 cm distal to their respective epicondyles (Table 7.2).

7.10.1 Anterior Compartment

Establishing two portals, one for visualization and one for working, allows a thorough evaluation of the anterior compartment. Medially, the surgeon must identify the ulnar nerve before performing any skin incision. The ulnar nerve is at risk when performing the proximal medial portal, but is also at risk with any medial portal, particularly if there has been an ulnar nerve transposition. When the nerve cannot be clearly identified, such as with previous ulnar nerve surgery, then an open medial incision must be performed to safely utilize the medial portal.

Technique: Anterior Portals

- **Proximal anteromedial (superomedial) portal** [2]
- 2 cm above the medial epicondyle.
- Stay just anterior to the intermuscular septum. This allows a plane between the anterior humeral cortex and the brachialis muscle, protecting the median nerve and the brachial artery.
- The ulnar nerve needs to be safely managed [3]. The ulnar nerve is posterior to the intermuscular septum just proximal to the lateral epicondyle (Fig. 7.7a). Examine for subluxation of the nerve (Fig. 7.7b). If the ulnar nerve is unstable, then hold it reduced with the surgeon's thumb, and then introduce the scope

Table 7.1 Working portals: Located 2 cm proximal to bony prominences. These portals provide visualization of the majority of joint surfaces, and are the safest portals to use

Portal	Location	Visualization	At risk
Proximal anteromedial	2 cm proximal to medial epicondyle Anterior to MIMS	Anterolateral joint	Ulnar nerve
Proximal anterolateral	2 cm proximal to lateral epicondyle	Anteromedial joint	Radial nerve
Posterocentral	2 cm proximal to olecranon	Posterior joint	Ulnar nerve
Posterolateral	2 cm proximal to lateral olecranon	Posterior joint and lateral gutter	None

MIMS medial intermuscular septum

Table 7.2 Accessory portals: The 2 cm rule also applies to these portals

Portal	Location	Visualization	At risk
Anteromedial	2 cm distal and 2 cm anterior to medial epicondyle	Anterolateral joint	Median nerve
Anterolateral	2 cm distal and 2 cm anterior to lateral epicondyle	Anteromedial joint	Radial nerve, PIN
"Soft-spot" portal	Soft spot between radial head, capitellum, and olecranon	Radiocapitellar joint	Radial nerve

PIN posterior interosseous nerve

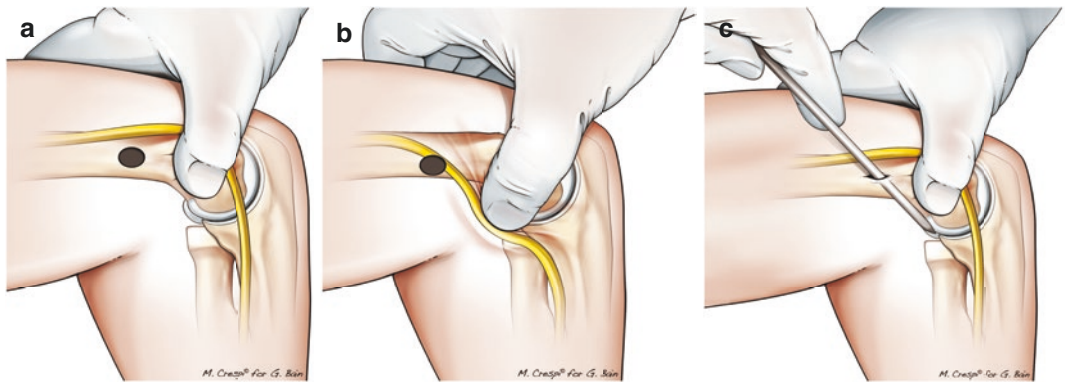

Fig. 7.7 Ulnar nerve: (**a**) The ulnar nerve typically lies posterior to the olecranon; (**b**) palpate the ulnar nerve. If subluxation is present, (**c**) hold the ulnar nerve posterior to safely create the proximal anteromedial portal (M. Crespi © for Gregory I. Bain)

anterior to the thumb (Fig. 7.7c). If the ulnar nerve cannot be identified an open medial incision must be performed.

- **At risk**: Ulnar nerve, palpate nerve.
- **Helpful tips**: Skin incision *should not* penetrate the subcutaneous tissues, and use conical, blunt-tipped trocars only. Additionally, care must be taken when instruments are removed and reinserted.
- **Proximal anterolateral portal**
  - 2 cm proximal to the lateral epicondyle.
  - Just anterior to the humerus and the intermuscular septum.
  - "Inside-out" technique with blunt-tipped switching stick allows a predictable path into the joint on initial pass, thus minimizing injury to the radial nerve and preserving capsule integrity.
  - The trocar is aimed toward the coronoid process and slid on the anterior humerus. It pierces the brachioradialis and lateral capsule.
  - **At risk:** Radial nerve.
  - **Helpful tip**: During times of challenging visualization this portal can be utilized as an accessory portal for placement of a blunt-tipped switching stick, which is used

for capsular retraction while working through alternative lateral portals.

- **Anterolateral portal**
  - 2 cm anterior and 2 cm distal to the lateral epicondyle.
  - The scope is directed toward the coronoid process, perforating the ECRB and supinator.
  - The portal provides visualization of the medial and lateral anterior joint.
  - The arthroscope enters the joint between the radial head and capitellum.
  - **At risk**: Radial nerve, PIN, and posterior antebrachial cutaneous nerve.
  - **Helpful tip**: An "outside-in" technique can be used with a needle and visualized inside the joint. This enables the position and direction of the portal to be created before the skin is incised helping to avoid damage to the lateral structures of the joint and helps the surgeon find the optimal working angle.
- **Anteromedial (accessory medial portal)**
  - Not frequently used.
  - Can have value as a second medial portal providing good visualization of the lateral joint, coronoid fossa, and proximal capsular insertion.
  - 2 cm anterior and 2 cm distal to medial epicondyle.
  - To establish this portal, introduce a switching stick from the lateral side of the joint and pass across to the medial side using an inside-out technique (Fig. 7.8).
  - **At risk**: Medial antebrachial cutaneous nerve.
  - **Helpful tip**: The portal is safer with elbow flexion, as the median nerve can lie in contact with the scope with the elbow fully extended.
- **Mid-lateral accessory portal**
  - "Soft-spot" portal is created within the triangular space between lateral epicondyle, radial head, and olecranon.
  - Visualization of the inferior and posterior capitellum and the radioulnar joint (Fig. 7.9).

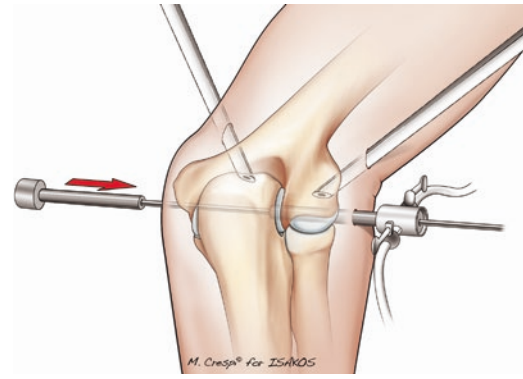

Fig. 7.8 Inside-out technique used to create the accessory anteromedial portal

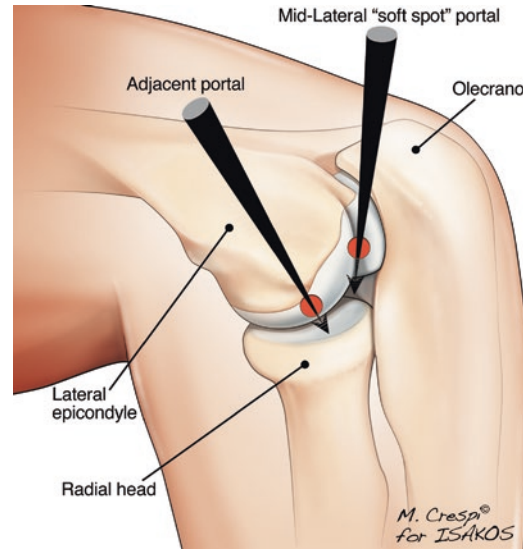

Fig. 7.9 Illustration of the lateral elbow. The posterior and inferior capitellum, as well as inferior radioulnar joint, can be readily visualized from the mid-lateral "soft-spot" portal (orange circle). A lateral "adjacent portal" can be used to address posterior and inferior pathology (orange circle)

  - Can visualize the olecranon-humeral articulation. At its base is the normal bare area devoid of articular cartilage.
  - With gradual extension of the elbow one can pass the scope up into the olecranon fossa. This may serve as the viewing portal for the olecranon fossa.
  - **At risk**: Articular surfaces, so a "wrist" scope is often preferred.

– **Helpful tip**: Spinal needle can be used to find the most "adjacent" position for addressing pathology posterior and inferior of the radio-capitellar joint (Fig. 7.9).

Technique: Diagnostic Arthroscopy of the Anterior Compartment

- Arthroscope inserted via proximal anteromedial portal and aimed toward the radiocapitellar joint for evaluation of anterior compartment.
  – Capitellum and radial head articular surfaces should be identified first (Fig. 7.10a).
  – Rotation of the forearm allows the entirety of the radial head and its cartilage surfaces to be seen. Assess the proximal radioulnar joint (PRUJ, Fig. 7.10b) and radial gutter for loose bodies.
  – Slowly withdrawing the arthroscope while rotating the camera angle enhances visualization of the anterior and lateral capsule. This enables viewing of the capsular region which is just inside the tendinous insertion of the extensor tendons.
  – Further rotation of the camera angle enables viewing of the coronoid, the coronoid fossa, and the trochlea (Fig. 7.10c). The medial gutter is also viewed from this portal. Thorough visualization of the gutters is imperative as this is a common hiding place for loose bodies.

7.10.2 Posterior Compartment

A thorough evaluation of the posterior compartment can be performed through two portals. However, we routinely create the mid-lateral "soft-spot" portal to adequately see the posterior and inferior radiocapitellar joint and the inferior aspect of the radioulnar articulation.

- **Posterocentral (straight posterior)**
  – 2 cm proximal to olecranon tip, usually piercing the triceps musculotendinous junction.
  – The intra-articular fat pad is debrided with a shaver to improve visualization.
  – Visualization of the entire olecranon fossa and medial and lateral gutters is possible (Fig. 7.11).
- **Proximal posterolateral**
  – 2 cm proximal to the lateral border of the proximal olecranon.
  – Aim trocar toward olecranon fossa.
  – Visualization of the olecranon tip and fossa and the posterior trochlea possible.
  – The inferior and posterior capitellum is not seen well from this portal.

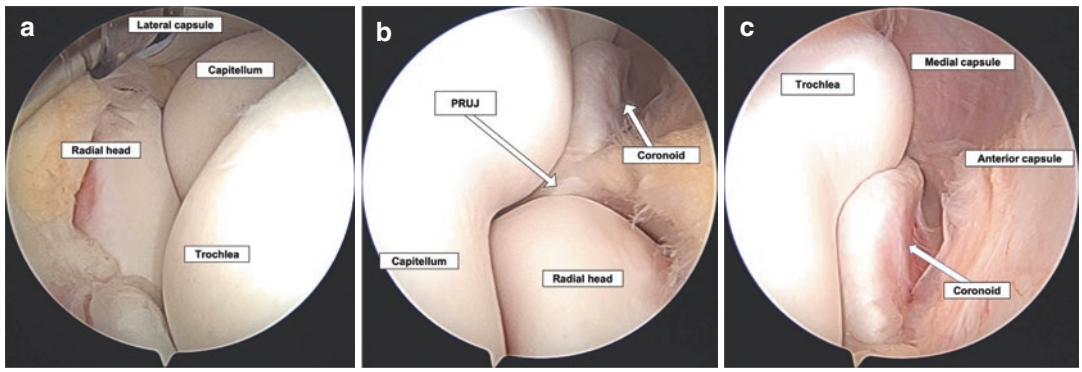

Fig. 7.10 (**a**) Anterior compartment as viewed from proximal anteromedial portal. Radiocapitellar joint and lateral capsule are well visualized (© B. R. Graves). (**b**) View from anterolateral portal reveals proximal radioulnar joint (© B. R. Graves). (**c**) Trochlea, coronoid, and anterior and medial capsule (© B. R. Graves)

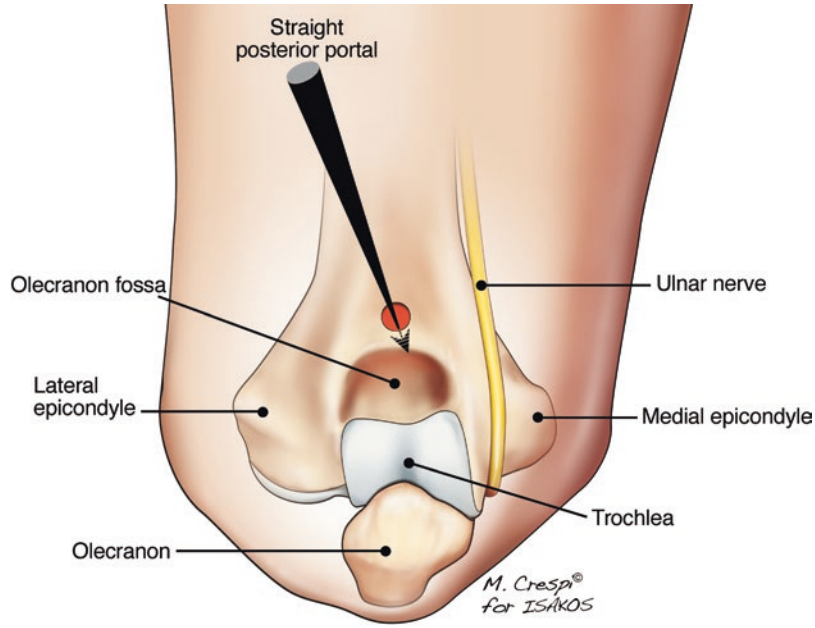

Fig. 7.11 Illustration of the posterior elbow. The straight posterior portal is 2 cm from the tip of the olecranon (orange circle). Midline and lateral placement is safe. The ulnar nerve is at risk if the portal is made medially

7.11 Tips and Tricks

- Ensure that the patient is as close as safely possible to the edge of the table to allow more motion of the elbow in the modified arm holder. The surgeon should be able to bring arm from full extension to 110° flexion. This will allow ease of work in joint with less struggle and obstruction.
- Routine distention of the joint through the "soft-spot" or posterocentral approach of up to 30 mL prior to incision can help prevent injury to the neurovascular structures and aids in the ability to enter the joint.
- Use only conical shaped, blunt trocars.
- Keep the elbow flexed 90° to increase the distance between the nerves and the capsule.
- The *2 cm rule*: The working portals are 2 cm proximal to the bony prominences of the elbow.
- Start with the proximal anteromedial portal (superomedial). This is the safest and most predictable portal to avoid neurovascular injury and successfully enter the joint.
- *Nick-and-spread* technique to minimize injury to cutaneous nerves during portal creation.
- An inside-out technique for anterolateral portal placement is safe and effective and helps minimize injury to lateral nerves.
- The more distal the lateral portal, the greater the risk to the radial nerve.
- Use of retractors in select procedures (e.g., capsular release and fractures) allows for greater visualization and exposure aiding in prevention of nerve injury.
- Dry arthroscopy at the start allows a clear diagnostic arthroscopy and ensures that the soft tissues are not filled with fluid [4].

7.12 Pitfalls

- Preoperative nerve blocks and local anesthetics around the portal sites can result in neural deficits, which can confuse the postoperative evaluation.
- For poor visualization, a tourniquet and increased pump pressures can be beneficial; however, both should be used for short durations.
- Avoid utilizing strong suction on the shaver, as this will pull the capsule into the blades and increase the risk of nerve injury.

- Extreme caution in cases requiring arthroscopic identification of nerves.

7.13 Postoperative Management and Rehabilitation

This is dependent on the pathology addressed. For general elbow arthroscopy procedures such as debridement or loose body removal, we recommend the following postoperative protocol:

- Sling for comfort only.
- Start passive range of motion post-op day 1.
- Progress to active range of motion as tolerated.
- Begin strengthening after recovered range of motion.
- Sport-specific activity within 2–3 weeks.

7.14 Complications

The complication rate in elbow arthroscopy is reported to be up to 14%, with the major complication rate ranging from 0.5 to 4.8% [5]. However, a survey of the American Society for Surgery of the Hand members reported a total of 222 major nerve injuries over a 5-year period and concluded that these injuries are likely underreported in the literature [6].

Though usually transient, nerve injury remains a feared complication of elbow arthroscopy [7]. A report of 473 cases identified that all major and cutaneous nerves about the elbow were at risk. The ulnar nerve is the most at risk [7]. The cause can be secondary to direct injury when making the portals or during intra-articular work with shavers/electrocautery, compression of nerves with instrumentation, or aggressive joint distention with fluid extravasation. Injuries to the median and anterior interosseous nerves are associated with creation of the anteromedial portal.

Injuries to the radial nerve, its superficial branch, and the posterior interosseous nerve have been associated with creation of the anterolateral portal. Lastly, injury to the superficial cutaneous nerves around the elbow can result in neuroma formation. A recent retrospective review of 253 elbow arthroscopies performed during a 10-year period at a single institution reported a 4.4% minor and 0.9% major nerve complication rate and found no correlation between nerve injury and the surgeon's experience level or training, patient BMI, tourniquet time, type of anesthesia, or diagnosis at the time of surgery [8].

Other complications include infection, heterotopic ossification, and joint contracture. Nelson et al. noted increased infection rates with intraoperative steroid injections. Lastly, increased complication rates have been reported with rheumatoid arthritis and in posttraumatic cases [5, 7].

7.15 Results

There is clinical evidence that supports elbow arthroscopy in a wide variety of conditions in which it is currently being used. However, the quality of this evidence is generally fair to poor [9]. In cases of osteoarthritis of the elbow, significant improvement in range of motion, pain, and Mayo performance index scores has been reported [10].

References

1. Andrews JR, Carson WG. Arthroscopy of the elbow. Arthroscopy. 1985;1(2):97–107.
2. Poehling GG, Whipple TI, Sisco L, Goldman B. Elbow arthroscopy: a new technique. Arthroscopy. 1989;5:222–4.
3. Sahajpal DT, Blonna D, O'Driscoll SW. Anteromedial elbow arthroscopy portals in patients with prior ulnar nerve transposition or subluxation. Arthroscopy. 2010;26(8):1045–52.
4. Phadnis J, Bain G. Dry arthroscopy of the elbow. Arthrosc Tech. 2015;4(4):e335–9.
5. Nelson GN, Wu T, Galatz LM, Yamaguchi K, Keener JD. Elbow arthroscopy: early complications and associated risk factors. J Shoulder Elbow Surg. 2014;23(2):273–8.
6. Desai MJ, Mithani SK, Lodha SJ, Richard MJ, Leversedge FJ, Ruch DS. Major peripheral nerve injuries after elbow arthroscopy. Arthroscopy. 2016;32(6):999–1002.

7. Kelly EW, Morrey BF, O'Driscoll SW. Complications of elbow arthroscopy. J Bone Joint Surg Am. 2001;83(1):25–34.
8. Jinnah AH, Luo TD, Wiesler ER, Li Z, Poehling GG, Tuohy CJ, Graves BR, Freehill MT, Papadonikolakis A. Peripheral nerve injury after elbow arthroscopy: an analysis of risk factors. Arthroscopy. 2018;34(5):1447–52.
9. Yeoh KM, King GJ, Faber KJ, Glazebrook MA, Athwal GS. Evidence-based indications for elbow arthroscopy. Arthroscopy. 2012;28(2):272–82.
10. Adams JE, Wolff LH 3rd, Merten SM, Steinmann SP. Osteoarthritis of the elbow: results of arthroscopic osteophyte resection and capsulectomy. J Shoulder Elbow Surg. 2008;17(1):126–31.

8 Transarticular Posterolateral Portal for Elbow Arthroscopy

Minoo Patel

8.1 Background

The transarticular posterolateral (TPL) portal is a novel versatile portal that allows access to the anterior part of the elbow joint from the posterior aspect. The TPL view is useful for the assessment of the radiocapitellar and humeroulnar joints and superior aspect of the proximal radioulnar joint. In an otherwise very congruent joint the lateral compartment of the elbow is relatively unconstrained and spacious. The anconeus muscle wraps around the posterolateral aspect of the elbow, over the posterior soft spot of the elbow [1, 2]. With the elbow flexed 90° there is an articular "soft spot" and this corresponds to a diamond-shaped space. The boundaries of this space are the medial aspect of the capitellum, lateral aspect of the trochlea, lateral aspect of the coronoid, and medial aspect of the radial head. This region permits the passage of a small-diameter arthroscope from posterior to anterior and forms the transarticular posterolateral portal (TPL) (Fig. 8.1).

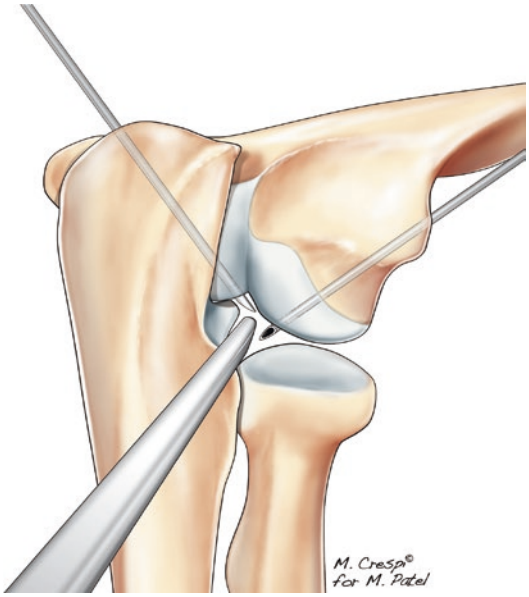

Fig. 8.1 The arthroscope is placed in the transarticular posterolateral portal and visualizes the anterior compartment. Needles show the position of proximal anteromedial and anterolateral portals (M. Crespi © for M. Patel)

8.2 Indications and Contraindications

- The posterolateral portal can be used for the assessment and procedures on the radial head, capitellum, and trochlea (radial head debridement and fracture fixation, capitellum/trochlear cartilage lesions).

M. Patel (✉)
The Epworth Centre, Richmond, VIC, Australia

© ISAKOS 2022

D. N. Bhatia et al. (eds.), *Arthroscopy and Endoscopy of the Elbow, Wrist and Hand*,
https://doi.org/10.1007/978-3-030-79423-1_8

- The TPL portal can be used during arthroscopy of the unlinked prosthetic elbow joint including distal humerus elbow hemiarthroplasty and radial head arthroplasty.
- Posteriorly the portal is useful for lateral olecranon pathology such as seen in valgus extension overload syndrome seen in throwing athletes.
- The TPL portal can be used to access the anterior compartment. This is particularly useful in joint contractures, given the small anterior joint space. This allows accurate placement of anterior portals, which can be localized with a spinal needle. This is also useful in teenagers and adolescents with smaller joint space.
- Transarticular arthroscopy is also a good teaching tool for residents, since it avoids the left-right parallax seen in elbow arthroscopy.
- The TPL portal also allows both the anteromedial and anterolateral portals to be used as instrument portals avoiding instrument crowding.

8.3 Surgical Technique

The patient is positioned in the lateral decubitus position with an arm holder. A 2.7 mm 30-degree arthroscope is used, and a 70-degree scope may be used as necessary.

- The joint is inflated with saline via the posterior soft spot. The PL portal starts 5–7 mm lateral to the edge of the olecranon and 3 mm superior to the radial head, and the needle is directed slightly antero-supero-medial. An obturator is used to establish the portal and a 2.7 mm arthroscope is inserted to visualize the radiocapitellar and humeroulnar joints (Figs. 8.2 and 8.3).
- The scope is then advanced between the capitellum and trochlea to lie just lateral to the coronoid process. The scope lies parallel to the articular surface of radial head and is directed slightly medially to exit the articular space.
- Under direct visualization, standard anteromedial (AM) and anterolateral (AL) portals are established and are used for instrumentation in different pathologies (Figs. 8.4 and 8.5).

8.4 Tips and Tricks

Care must be taken to avoid scraping the distal humerus articular cartilage. This can be done by advancing the scope under direct visualization using a rotatory oscillating movement. Alternately, a switching stick may be used to enter the articular soft spot and the sheath is gently advanced over it.

8.5 Pitfalls

Flexion or extension of the elbow while viewing from the TPL portal may damage the chondral surfaces or arthroscope. One of the most important limitations of transarticular portal is the inability to flex or extend the elbow with the scope in situ.

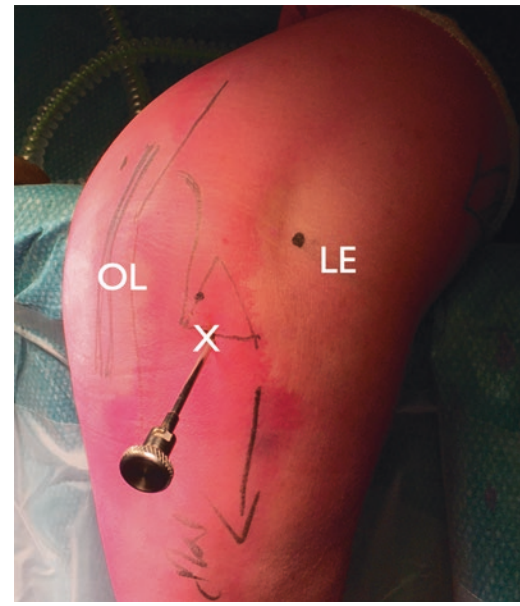

Fig. 8.2 Anatomical landmarks with the patient in the lateral decubitus position. A blunt obturator is used to confirm the trajectory of the scope

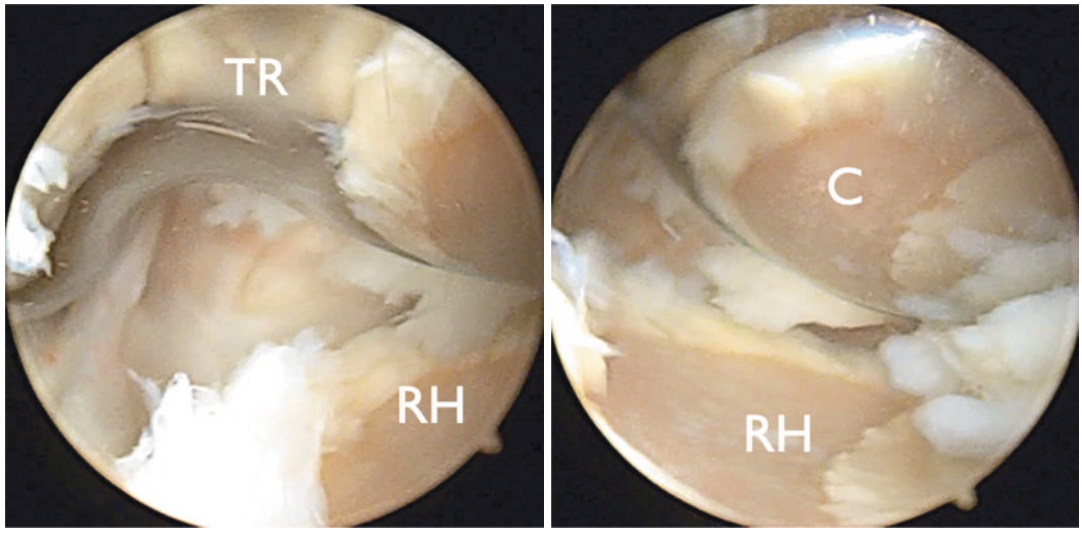

Fig. 8.3 TPL portal view of the radiocapitellar joint showing radial head chondral loss secondary to elbow hemiarthroplasty [*TR* trochlea, *C* capitellum, *RH* radial head]

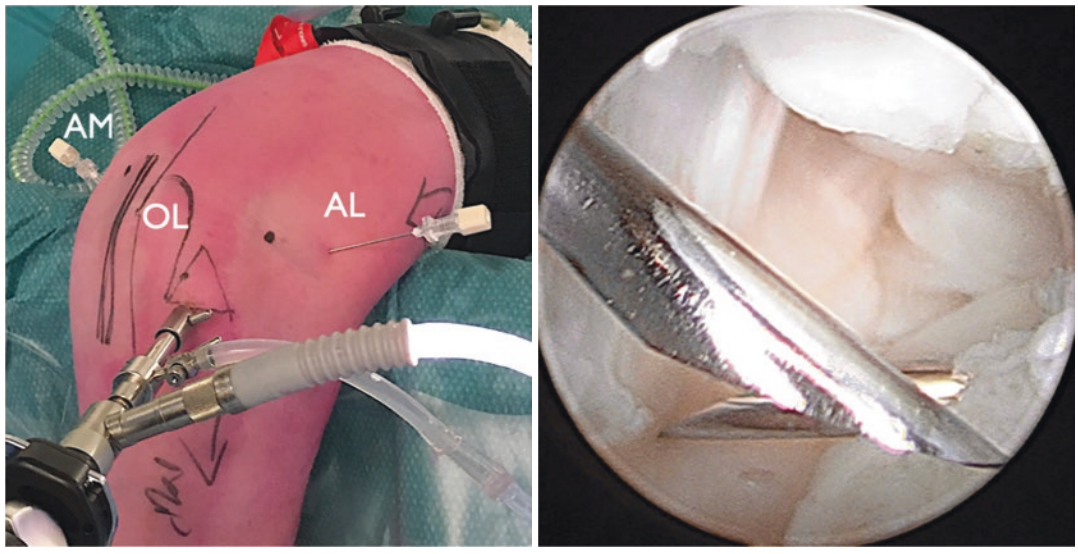

Fig. 8.4 A 2.7 mm scope is in the transarticular posterolateral portal (TPL), and spinal needles mark the anterolateral (AL) and anteromedial (AL) portals. Note the absence of left-right parallax

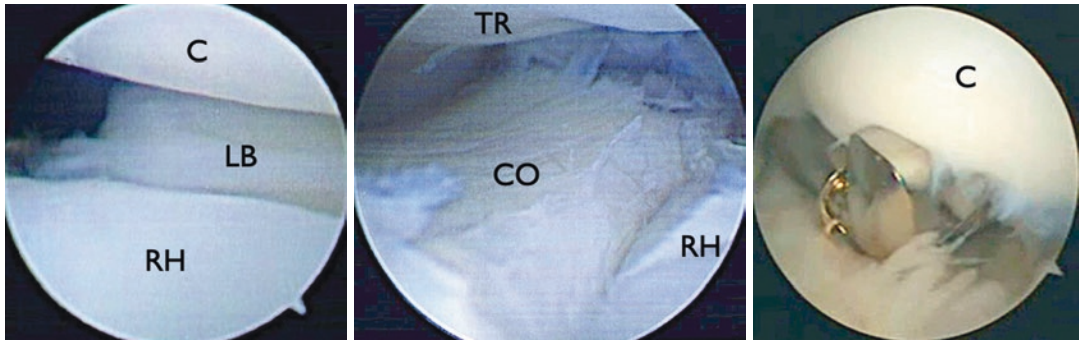

Fig. 8.5 The TPL portal shows a large locked loose body (LB, left image) in the anterior compartment. Arthroscopic view via the TPL portal looking medially into the humeroulnar joint (middle image). Articular surface damage is clearly seen over the anteromedial facet of the coronoid (CO). TPL view shows debridement of an OCD lesion in the capitellum (C) (right image). An anterior portal is used for instrumentation [*C* capitellum, *RH* radial head, *TR* trochlea]

8.6 Complications

The most important complication is inadvertent articular surface damage during the passage of arthroscope.

References

1. Poehling GG, Whipple TL, Sisco L, Goldman B. Elbow arthroscopy: a new technique. Arthroscopy. 1989;5:222–4.
2. Camp CL, Degen RM, Sanchez-Sotelo J, Altchek DW, Dines JS. Basics of elbow arthroscopy part I: surface anatomy, portals, and structures at risk. Arthrosc Tech. 2016;5(6):e1339–43.

Dry Elbow Arthroscopy

9

Benjamin Seah Renyi, Joideep Phadnis, and Gregory I. Bain

9.1 Background

Elbow arthroscopy is a useful tool for the investigation and management of elbow pathology. Traditionally, this has been performed as a wet procedure. However, following advantages noted during dry arthroscopy of both the wrist and shoulder joints [1–3], the dry technique was extended to the elbow with good effect. De Pinal has highlighted the use of this technique in wrist arthroscopy and especially in complex cases [2, 4]. The senior author (GB) routinely performs all elbow arthroscopic procedures with this dry technique [5, 6].

Dry elbow arthroscopy is advantageous (Table 9.1): (a) Visualization and image quality are superior to standard wet arthroscopy. The presence of an air-fluid interface on articular cartilage and synovium allows the reflection of light, and subtle chondral and synovial changes are better seen with superior definition and depth perception. This interface is absent in wet arthroscopy and the image quality deteriorates further because of debris and synovium suspended in water (Figs. 9.1, 9.2, and 9.3). (b) With dry arthroscopy at atmospheric pressure, small blood vessels are clearly seen and maintain their natural color. This is lost in wet arthroscopy as the fluid pressure results in collapse of these vessels in soft tissues. This clear visualization potentially aids in a more thorough debridement in patients with synovitis as the extent of inflammation is better defined. (c) Complications associated with fluid extravasation (swelling, portal track distortion, pain, and compartment syndrome) are avoided and this results in less discomfort, easier rehabilitation,

Table 9.1 Advantages of dry and wet elbow arthroscopy

Dry arthroscopy
Better definition and depth perception (chondral surfaces, synovium, vasculature)
Less fluid extravasation, swelling, post-op discomfort, and compartment pressure
Obtain microbiology and histology specimens without fluid contamination
Retention of surface landmarks
Easier dissection on conversion to open surgery
Less expensive
Wet arthroscopy
Familiar technique
Sustained joint distension
Irrigation and cooling of joint
Suspension of loose bodies

B. S. Renyi
Department of Orthopaedic Surgery, Sengkang General Hospital, Singhealth, Singapore, Singapore

J. Phadnis
Department of Trauma and Orthopedics, Brighton and Sussex University Hospitals, NHS Trust, East Sussex, UK
e-mail: joideep@doctors.org.uk

G. I. Bain (✉)
Department of Orthopaedics and Trauma Surgery, Flinders Medical Centre and Flinders University, North Adelaide, SA, Australia
e-mail: admin@gregbain.com.au

© ISAKOS 2022

D. N. Bhatia et al. (eds.), *Arthroscopy and Endoscopy of the Elbow, Wrist and Hand*,
https://doi.org/10.1007/978-3-030-79423-1_9

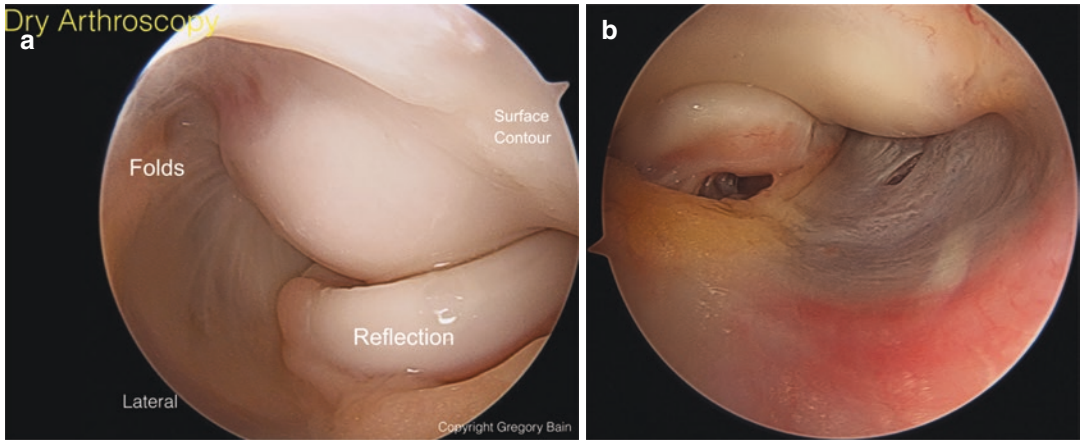

Fig. 9.1 Diagnostic dry arthroscopy of the anterior compartment. (**a**) Reflection of light from air-synovial fluid interface results in greater clarity of the radiocapitellar joint cartilage. (**b**) The capsular and perichondral vessels are easily identified due to the absence of fluid pressure making them collapse (© Dr. Gregory I. Bain)

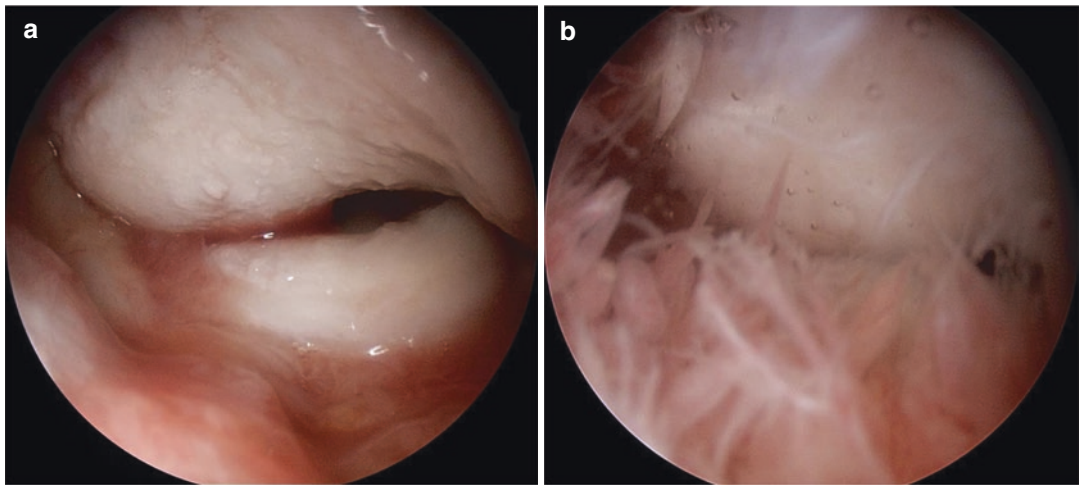

Fig. 9.2 Arthroscopy of an arthritic elbow with synovitis. (**a**) Dry arthroscopy: the synovium coalesces at the bottom due to gravity, allowing a clear view of the irregular and worn articular cartilage. (**b**) Wet arthroscopy: the synovium floats, obscuring the view of the cartilage, potentially concealing the arthritic changes (© Dr. Gregory I. Bain)

and faster recovery. (d) Conversion to pen surgery is easier due to minimal swelling and distortion of soft-tissue planes.

9.2 Indications

Both dry and wet arthroscopies have similar indications and contraindications. Relative contraindications include distorted local anatomy, local pedicle flaps, and previous ulnar nerve transposition [3].

9.3 Surgical Technique

- The setup for dry arthroscopy is similar to that of wet technique.
- An arm tourniquet is used during the procedure.

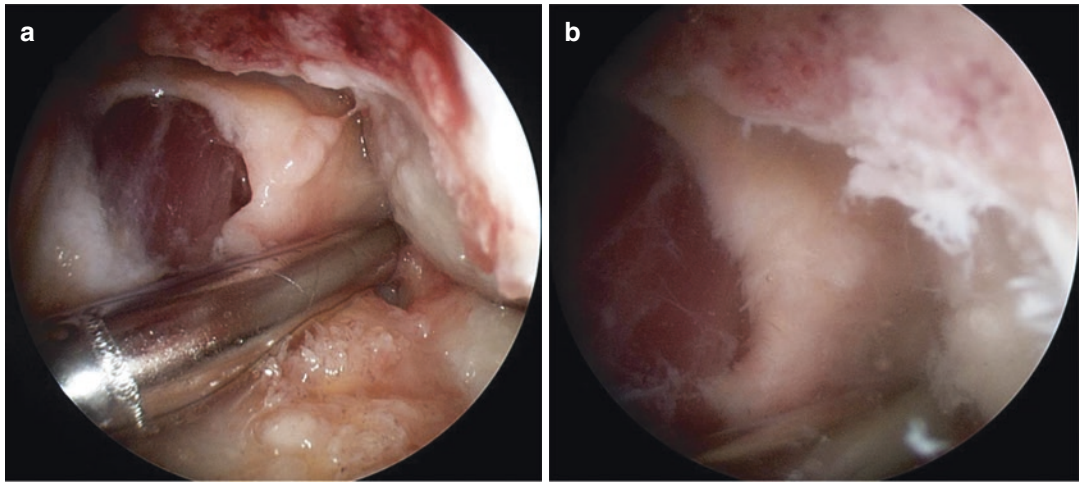

Fig. 9.3 Arthroscopic images after release of anterior capsule and excision of osteophyte. (**a**) Dry arthroscopy with clear image. (**b**) Wet arthroscopy with a blurred image due to particles suspended in the fluid (© Dr. Gregory I. Bain)

- Dry and wet arthroscopies are performed interchangeably in the same patient, utilizing the advantages of both techniques. Saline aids in clearing debris from the joint and shaver tip, and prevents rise in temperature if a cautery is used.
- If bleeding occurs, fluid inflow can clear the blood. Suction is then applied to remove the fluid and dry arthroscopy is continued.

9.4 Tips and Tricks

- Do not use a pump to introduce air into the joint. The minimum volume of air required to potentially cause an asymptomatic air embolus is 50 ml. Therefore, if air is to be used for joint insufflation, the volume is limited to 20 ml. Air insufflation should not be used in fractures.
- Do not breach the capsule with the hemostat when initially making the portal and only use the trocar/cannula. A hemostat is larger in size and this could potentially permit air or saline to escape.
- Fogging of the lens can be minimized by placing the lens in warm saline prior to its introduction into the joint. During surgery, the tip of the arthroscope can be gently pushed onto the synovium or fat to clear the fogging. If this is insufficient, the arthroscope can be removed from the joint and the lens wiped with an alcohol swab.
- To remove blood that accumulates in the joint during surgery, short bursts of low-pressure suction can be used. This may require the addition and aspiration of a small amount of saline to aid in the process. Keep the cannula valve open during suctioning to prevent collapse of the capsule.
- When a shaver is used, ensure that its direction of rotation is pointing away from the arthroscope to minimize the splash of blood and debris onto the tip of the arthroscope. It is useful to have 20 ml syringe of 0.9% saline on standby or pre-assembled to the cannula valve for joint irrigation as needed without compromising the dry scope.
- A radiofrequency probe works better in a saline environment. If used in dry arthroscopy, activate the probe in short bursts and with a low setting as this minimizes the risk of thermal injury to the surrounding cartilage. To remove intra-articular smoke, the valve on the arthroscopic sheath is opened and the soft tissues balloted, acting as bellows. Alternatively,

saline can be introduced and aspirated or low-pressure intermittent suction can be applied.
- Retractors placed through accessory portals can help maintain the field of view.

9.5 Pitfalls

- Multiple passes into joint should be avoided as this allows air to escape from the joint.
- Aggressive suction is avoided as it can collapse the working space and may draw neurovascular structures toward blade.

References

1. Rupenian P. Dry arthroscopy of the shoulder. Arthrosc Tech. 2013;2(4):e437–40.
2. Del Pinal F. Dry arthroscopy and its applications. Hand Clin. 2011;27(3):335–45.
3. Netto HBP, et al. Wrist arthroscopy: basic tips for dry arthroscopic exploration. Acta Ortop Bras. 2017;25(6):291–4.
4. Del Pinal F, et al. Dry arthroscopy of the wrist: surgical technique. J Hand Surg Am. 2007;32(1):119–23.
5. Phadnis J, Bain G. Dry arthroscopy of the elbow. Arthrosc Tech. 2015;4(4):e335–9.
6. Bain GI, et al. Dry elbow arthroscopy. In: Bain G, Eygendaal D, van Riet RP, editors. Surgical techniques for trauma and sports related injuries of the elbow. Springer Nature; 2019.

Part III

Elbow: Instability

Classification of Elbow Instability

10

Alessandro Marinelli, Enrico Guerra,
Marco Cavallo, Alice Ritali, and Roberto Rotini

10.1 Background

Elbow instability includes a wide spectrum of different forms [1]. Instability patterns can be acute, chronic recurrent, or chronic persistent. The affected stabilizers and their combined involvement can vary, based on the different dislocation mechanisms and diverse etiologies. Moreover, the instability can involve the ulnohumeral or the radio-humeral joint, with different degrees of severity (partial subluxation to complete dislocation). Because of this great variety of clinical symptoms and anatomical presentations, it is not easy to summarize all the different instability patterns in a single and simple classification.

In the past several authors have proposed useful classifications for elbow instability, focusing their attention mostly on the more common acute and traumatic types [2–4]. Until recently, the chronic forms were not extensively investigated, and typically, the term "chronic" was used to indicate both recurrent and persistent dislocation. Moreover, differently from acute forms, in chronic instability cases no distinction was considered between instability caused by soft-tissue lesions (simple forms) and association between bony and soft-tissue lesions (complex forms). This distinction is important for the prognosis and the treatment strategy, and it has been reported that not differentiating between simple and complex forms in chronic instability patterns leads to a greater rate of treatment failure [5].

With increasing experience and complexity of the cases treated, the Italian Society of Shoulder and Elbow Surgery (SICSeG) felt the need for an exhaustive classification and a shared language to decrease possible misunderstandings and to improve the comparison among case series [6].

10.2 Classification

The fundamental of the new classification is that for an accurate characterization of elbow instability, six parameters should be considered (Table 10.1):

Timing

- Acute forms: fractures or fracture-dislocations.
- Chronic recurrent forms (dynamic forms): The elbow, basically reduced, depending on the applied stress, can have a partial or complete dislocation.
- Chronic persistent forms (static forms): The elbow is statically dislocated and it is not

A. Marinelli (✉) · E. Guerra · M. Cavallo · A. Ritali
R. Rotini
Shoulder and Elbow Unit, Istituto Ortopedico Rizzoli
IRCCS, Bologna, Italy
e-mail: alessandro.marinelli@ior.it;
enrico.guerra@ior.it; marco.cavallo@ior.it;
alice.ritali@ior.it; roberto.rotini@ior.it

© ISAKOS 2022

D. N. Bhatia et al. (eds.), *Arthroscopy and Endoscopy of the Elbow, Wrist and Hand*,
https://doi.org/10.1007/978-3-030-79423-1_10

Table 10.1 Within this table the elbow instability patterns are schematically described. Elbow instability is characterized by six different parameters, each representing different subtypes. From the combination of the subtypes of each parameter, all the possible instability forms can be described

1 TIMING	2 STABILIZERS	3 ETIOLOGY	4 JOINTS	5 GRAVITY	6 DIRECTION
ACUTE	SIMPLE	TRAUMA	HUMERO-ULNAR	SUBLUXATION	PLRI
		OVER-USE			PMRI
		CONGENITAL			
RECURRENT	COMPLEX	INFLAM-MATORY	HUMERO-RADIAL	DISLOCATION	DIRECT AXIAL
PERSISTENT		INFECTION			VARUS
		IATROGENIC			VALGUS

possible to reduce it without an extensive surgical release.

Involved stabilizers

- Simple forms if only soft tissues are involved
- Complex forms if bony structures are also involved

Etiology

Instability can be caused by traumatic, overuse or congenital, inflammatory, iatrogenic, post-infective disorders.

Involved joint

Dislocation can occur at the ulno-humeral joint or at the radio-humeral joint.

Gravity of the instability

The dislocation can be partial or complete.

Mechanism of dislocation

The post-traumatic conditions can recognize a posterolateral (PLRI) or posteromedial (PMRI) rotatory instability, direct axial load, or a prevalent valgus or varus stress.

Based on the first two parameters (involved stabilizers and timing), it is possible to classify the instability forms into six patterns: simple acute, simple recurrent, simple persistent, complex acute, complex recurrent, and complex persistent (Table 10.2). Since 2015, the SICSeG (Italian Society of Shoulder and Elbow Surgery) adopted this classification for elbow instability, the use of which has been experienced to be practical and effective in including all the instability patterns encountered in the clinical practice.

10.2.1 SICSeG Elbow Instability Classification

10.2.1.1 Simple Acute

This group includes simple elbow instability cases: acute and traumatic dislocation or subluxation caused by isolated soft-tissue lesion. Simple acute forms can be posterior, anterior, or divergent. Mostly in adults the direction is nearly always posterior. The most commonly described mechanism of simple elbow dislocation is the PLRI [7, 8]: by falling on the hand with the elbow extended, axial force, combined

Table 10.2 SICSeG Elbow Instability Classification identifies six patterns of instability, based on the timing and involved stabilizers [6]

ELBOW INSTABILITY CLASSIFICATION SICSeG	ACUTE	CHRONIC RECURRENT (dynamic condition)	CHRONIC PERSISTENT (static condition)
SIMPLE SOFT TISSUE ONLY	SIMPLE ACUTE	SIMPLE RECURRENT	SIMPLE PERSISTENT
COMPLEX BONY FRACTURE + SOFT TISSUE	COMPLEX ACUTE	COMPLEX RECURRENT	COMPLEX PERSISTENT

with valgus and supination stress, produces a circular lesion of the stabilizers. The lesion starts in the lateral collateral ligament and, through three successive stages, progressively involves the anterior and posterior capsule, until it involves the medial collateral ligament (Horii circle) [1, 9]. Several authors have postulated that in some cases the posterior dislocation mechanism might occur in the opposite direction from medial to lateral, by axial compression and valgus stress [10–13]. Regardless of the mechanism by which it occurs, the treatment of a simple elbow dislocation is the same: after reduction, most of the cases (about 90%) can be treated conservatively, and only the most severe cases should be treated surgically.

10.2.1.2 Simple Recurrent

In this group the articular surfaces are intact, but ligament incompetence causes a recurring instability: depending on the applied stress, the elbow goes from a reduced position to a dislocation or subluxation.

This group includes forms with different etiologies:

- Post-traumatic: Most forms of evident recurrent instability occur by the PLRI mechanism as the sequela of failed healing of a lateral collateral ligament (LCL) injury. Recurrent valgus instability due to an acute MCL lesion is rarer.
- Overuse: The most common cause of symptomatic instability due to overuse is the MCL lesion caused by progressive stretching (chronic attenuation) which occurs in professional athletes who play overhead sport, especially baseball. Rare cases of varus instability can be due to overuse of the LCL in people walking with crutches [4].
- Some rare congenital forms, e.g., Ehlers-Danlos syndrome, may cause simple recurrent elbow instability due to the laxity of the capsulo-ligamentous structures and symptomatic subluxation in hyperextension [14].
- Rheumatic disease: Initial forms of rheumatoid arthritis, mainly involving the soft tissues

(grades 1–2 of Larsen classification), might produce recurrent instability.

Repair or reconstruction is indicated in post-traumatic and overuse type of instability, and braces are usually used for congenital and rheumatic forms. Replacement can be considered in symptomatic rheumatic etiology.

10.2.1.3 Simple Persistent

Persistent soft-tissue dislocations are static forms that cannot be reduced without an extensive surgical arthrolysis. The articular surfaces are intact. This group can be subclassified into "neglected forms" (rare in developed countries) and "failed treatment" forms (not so uncommon) caused by an inappropriate or failed treatment. In the latter cases, a re-dislocation occurs in a plaster cast or in a brace, and the diagnosis can be delayed if a strict clinical and/or radiographic follow-up is not performed. When the joint has been dislocated for longer than 2–3 weeks, it can no longer be reduced conservatively. Treatment requires extended arthrolysis and repair/reconstruction of the collateral ligaments, and may require the use of an external fixator. Reconstruction of ligaments with autologous or homologous grafts is usually always required after 3 months or more of dislocation.

10.2.1.4 Complex Acute

The complex acute instabilities, also known as acute fracture-dislocations, include a heterogenous group of acute and traumatic lesions that are characterized by elbow joint dislocation caused by an associated lesion of bony (radial head, coronoid, olecranon, rarely distal humerus) and soft-tissue stabilizers. The three main groups of fractures are the so-called complex elbow instability described by Morrey [2, 15].

- **Olecranon fracture-dislocation**: They are fractures of the greater sigmoid notch in which the olecranon (always affected) is usually multi-fragmented, and the coronoid process (often involved) is usually fractured at its base. The ulno-humeral joint is consistently disrupted, with a dislocation or a fracture/dislocation of the radio-capitellar joint. The proximal radioulnar joint is intact, and this characteristic distinguishes the olecranon fracture-dislocations from the Monteggia injuries. Based on the level of comminution of the greater sigmoid notch, of the anteromedial coronoid facet, and of the proximal ulna metaphysis, the olecranon fracture-dislocations can be divided into simple and complex [16]. Based on the position of the radial head with respect to the capitellum, the trans-olecranon fracture-dislocations can be divided into anterior and posterior [17, 18]. Posterior olecranon fracture-dislocations can be considered the most proximal injury type among the spectrum of posterior (Bado type 2) Monteggia lesion, because the principle and pitfalls of treatment are similar [17, 19, 20]. Anterior trans-olecranon fracture-dislocations are often associated with larger coronoid fractures and radial head fractures, but typically intact collateral ligaments [16]. For this reason, in anterior olecranon fracture-dislocations, once the alignment of the olecranon and coronoid is restored, elbow stability and forearm function are usually recovered [16]. In contrast, in case of posterior olecranon fracture-dislocation, elbow stability and forearm function are usually involved [17]. The surgical treatment is performed with a posterior midline skin incision approach, preserving the triceps insertion. Coronoid exposure can be carried out usually through the olecranon fracture or, in case of basal or anteromedial coronoid fracture, through a medial window, by elevating the FCU from the medial proximal ulna. The fixation is usually performed with screws passing through the anatomical olecranon plate or, depending on the size, comminution, and location of the fracture with free screws, K-wires, or rarely a specific coronoid plate [17, 21]. The radial head injury can be treated through the fractured olecranon and the injured anconeus muscle; otherwise a separate lateral approach can be used. A radial head osteotomy is usually contraindicated. When it is possible, radial head fixation is the preferred choice;

otherwise a radial head replacement is performed. Finally, the greater sigmoid notch can be fixed with a pre-contoured proximal ulna plate: tension-band wiring presents a high failure rate and should be reserved for different patterns of fractures: simple, noncomminuted transverse, or short oblique fractures of the olecranon [15, 17].

- **Terrible triad**: This lesion is characterized by dislocation or subluxation of the elbow which occurs by fracture of the radial head and of coronoid process and lesion of the lateral collateral ligament. The most common mechanism by which the terrible triad occurs is the PLRI. Terrible triads include a wide spectrum of lesions; although select terrible triad injuries can be managed non-operatively [22, 23], most injuries are treated with stable surgical repair to allow early elbow motion [24–26]. In terrible triad lesions, there is agreement:
  - To avoid radial head osteotomy, considering fixation, when it is possible, or replacement using a lateral or posterior skin approach [24–28]
  - To fix with screws all the significant coronoid fragments, using the window created by the osteotomy of the radial head in preparation of the subsequent replacement [21]
  - To repair the lateral collateral ligament [25]

The necessity to fix smaller coronoid fragments and the threshold of instability to consider repair of the medial collateral ligament or to use an external fixator is debatable [29, 30].

- **Fracture of the anteromedial portion of the coronoid process and LCL injury**: The anteromedial coronoid fractures can be sometimes associated with radial head fractures and occur by a PMRI mechanism [17]. They usually cause an ulno-humeral incongruity rather than a complete joint dislocation [17]. Anteromedial coronoid fractures may appear benign on X-ray views but, if not treated, they can cause an ulno-humeral subluxation during physiological varus stress with an early arthritis evolution. The surgical indication is considered on the CT scan evaluation of the coronoid fracture pattern (sublime tubercle involvement, fragment size, and dislocation), ulno-humeral joint reduction, and associated lesions [31–33]. Often, an evaluation under anesthesia allows the surgeon to appreciate the real amount of instability conceived on CT scan, confirming the choice of surgical indication [31, 32]. Depending on the case, the anteromedial coronoid fractures can be fixed with free screws or dedicated plates [17, 21]; in this second case a more extensive medial approach is required. If a valgus instability persists, the LCL repair should be performed [31, 32].

10.2.1.5 Complex Recurrent

This group includes clinical cases of recurrent instability where the bone deficit is combined with a ligamentous lesion. These include:

- Iatrogenic cases: Excision of the radial head combined with untreated (or unsuccessfully treated) injuries of the collateral ligaments and/or coronoid process.
- Rheumatic disease: Advanced stages (grades 3–4 of Larsen classification).
- Post-traumatic deformity (more common) or congenital deformity: The bone deformity of the medial condyle (cubitus varus) or coronoid process over time causes abnormal varus stresses, producing a chronic attenuation of the LCL, and a progressive instability can occur by the PLRI mechanism [34–36].

In complex recurrent forms it is important to recognize and treat the bone injury along with the repair of collateral ligaments: repairing or reconstructing only the LCL would result in failure, if not combined with the treatment of the bone injury, which consists of valgus osteotomy for cubitus varus and bone graft for the coronoid deficit [35, 36]. In low-demand and rheumatic patients a total elbow replacement may be a good option.

10.2.1.6 Complex Persistent

Chronic persistent forms are a challenge even for the most skilled elbow surgeon. As before, we can divide this group into "neglected forms" (very rare in developed countries) and "failed treatment" forms (not uncommon even in developed countries). The most common type found in our experience is the terrible triad not treated or treated by simply removing the radial head, without fixing the coronoid process or repairing the lateral collateral ligament. Other possible cases are caused by the failure to repair a large fragment of the coronoid process in trans-olecranon fracture-dislocations.

In this type of injury stiffness and instability coexist and treating one may risk aggravating the other. Surgery of these lesions consists of extensive arthrolysis, replacing the radial head bone defect with a prosthesis, reconstructing the coronoid process with grafts, reconstructing the collateral ligaments (generally with grafts), and possibly protecting the joint with an external fixator. In some cases osteotomy of the radial neck and proximal ulna has been described [36] to address appropriately the joint surfaces. In case of severe and debilitating joint damage, a total elbow procedure can be considered a surgical option, especially in old and low-demand patients.

10.3 Summary

Based on the timing and involved stabilizers, six patterns of elbow instability can be identified: simple acute, simple recurrent, simple persistent, complex acute, complex recurrent, and complex persistent. Each of the six groups includes instability with variable severity, requiring different treatment options, and therefore a straightforward treatment algorithm cannot be proposed using this classification. Clearly differentiating between recurrent and persistent instability, and considering the role of the bony stabilizers in recurrent and persistent forms, is fundamental for a correct classification and an adequate treatment of elbow instability.

References

1. O'Driscoll SW, Morrey BF, Korinek S, An KN. Elbow subluxation and dislocation. A spectrum of instability. Clin Orthop Relat Res. 1992;(280):186–197.
2. Morrey BF. Complex instability of the elbow. J Bone Joint Surg Am. 1997;79(3):460–9.
3. Hildebrand KA, Patterson SD, King GJ. Acute elbow dislocations: simple and complex. Orthop Clin North Am. 1999;30(1):63–79.
4. O'Driscoll SW. Classification and evaluation of recurrent instability of the elbow. Clin Orthop Relat Res. 2000;370:34–43.
5. Sanchez-Sotelo J, Morrey BF, O'Driscoll SW. Ligamentous repair and reconstruction for posterolateral rotatory instability of the elbow. J Bone Joint Surg Br. 2005;87(1):54–61. PubMed PMID: 15686238.
6. Marinelli A, Guerra E, Rotini R. Elbow instability: are we able to classify it? Review of the literature and proposal of an all-inclusive classification system. Musculoskelet Surg. 2016;100(Suppl 1):61–71.
7. O'Driscoll SW, Bell DF, Morrey BF. Posterolateral rotatory instability of the elbow. J Bone Joint Surg Am. 1991;73(3):440–6.
8. Mehta JA, Bain GI. Posterolateral rotatory instability of the elbow. J Am Acad Orthop Surg. 2004;12(6):405–15. Review. PubMed PMID: 15615506.
9. O'Driscoll SW, Jupiter JB, King GJ, Hotchkiss RN, Morrey BF. The unstable elbow. Instr Course Lect. 2001;50:89–102. Review. PubMed PMID: 11372363.
10. Søjbjerg JO, Helmig P, Kjaersgaard-Andersen P. Dislocation of the elbow: an experimental study of the ligamentous injuries. Orthopedics. 1989;12(3):461–3.
11. Josefsson PO, Johnell O, Wendeberg B. Ligamentous injuries in dislocations of the elbow joint. Clin Orthop Relat Res. 1987;221:221–5.
12. Schreiber JJ, Potter HG, Warren RF, Hotchkiss RN, Daluiski A. Magnetic resonance imaging findings in acute elbow dislocation: insight into mechanism. J Hand Surg Am. 2014;39(2):199–205.
13. Robinson PM, Griffiths E, Watts AC. Simple elbow dislocation. Shoulder Elbow. 2017;9(3):195–204. https://doi.org/10.1177/1758573217694163. Epub 2017 Jan 1. Review. PubMed PMID: 28588660; PubMed Central PMCID: PMC5444606.
14. Cole AS, Hill GA, Abela M, Carr AJ. Recurrent instability of the elbow in the Ehlers-Danlos syndrome. A report of three cases and a new technique of surgical stabilisation. J Bone Joint Surg Br. 2000;82(5):702–4.
15. Chan K, King GJ, Faber KJ. Treatment of complex elbow fracture-dislocations. Curr Rev Musculoskelet Med. 2016;9:185–9.
16. Ring D, Jupiter JB, Sanders RW, Mast J, Simpson NS. Transolecranon fracture-dislocation of the elbow. J Orthop Trauma. 1997;11(8):545–50. https://doi.org/10.1097/00005131-199711000-00001.

17. O'Driscoll SW, Jupiter JB, Cohen MS, Ring D, McKee MD. Difficult elbow fractures: pearls and pitfalls. Instr Course Lect. 2003;52:113–34. Review. PubMed PMID: 12690844.
18. Manidakis N, Sperelakis I, Hackney R, Kontakis G. Fractures of the ulnar coronoid process. Injury. 2012;43(7):989–98. https://doi.org/10.1016/j.injury.2011.08.030. Epub 2011 Sep 29. Review. PubMed PMID: 21963158.
19. Ring D, Jupiter JB, Simpson NS. Monteggia fractures in adults. J Bone Joint Surg Am. 1998;80(12):1733–44. PubMed PMID: 9875931.
20. Jupiter JB, Leibovic SJ, Ribbans W, Wilk RM. The posterior Monteggia lesion. J Orthop Trauma. 1991;5(4):395–402. PubMed PMID: 1761999.
21. Steinmann SP. Coronoid process fracture. J Am Acad Orthop Surg. 2008;16(9):519–29. Review. PubMed PMID: 18768709.
22. Guitton TG, Ring D. Nonsurgically treated terrible triad injuries of the elbow: report of four cases. J Hand Surg Am. 2010;35(3):464–7. https://doi.org/10.1016/j.jhsa.2009.12.015. PubMed PMID: 20193862.
23. Chan K, MacDermid JC, Faber KJ, King GJ, Athwal GS. Can we treat select terrible triad injuries nonoperatively? Clin Orthop Relat Res. 2014;472(7):2092–9. https://doi.org/10.1007/s11999-014-3518-9. PubMed PMID: 24549776; PubMed Central PMCID: PMC4048392.
24. Ring D, Jupiter JB, Zilberfarb J. Posterior dislocation of the elbow with fractures of the radial head and coronoid. J Bone Joint Surg Am. 2002;84(4):547–51. PubMed PMID: 11940613.
25. Pugh DM, Wild LM, Schemitsch EH, King GJ, McKee MD. Standard surgical protocol to treat elbow dislocations with radial head and coronoid fractures. J Bone Joint Surg Am. 2004;86(6):1122–30. PubMed PMID: 15173283.
26. Gupta A, Barei D, Khwaja A, Beingessner D. Single-staged treatment using a standardized protocol results in functional motion in the majority of patients with a terrible triad elbow injury. Clin Orthop Relat Res. 2014;472(7):2075–83. https://doi.org/10.1007/s11999-014-3475-3. PubMed PMID: 24474324; PubMed Central PMCID: PMC4048418.
27. Antuña SA, Sánchez-Márquez JM, Barco R. Long-term results of radial head resection following isolated radial head fractures in patients younger than forty years old. J Bone Joint Surg Am. 2010;92(3):558–66. https://doi.org/10.2106/JBJS.I.00332.
28. Schneeberger AG, Sadowski MM, Jacob HA. Coronoid process and radial head as posterolateral rotatory stabilizers of the elbow. J Bone Joint Surg Am. 2004;86(5):975–82.
29. Papatheodorou LK, Rubright JH, Heim KA, Weiser RW, Sotereanos DG. Terrible triad injuries of the elbow: does the coronoid always need to be fixed? Clin Orthop Relat Res. 2014;472(7):2084–91. https://doi.org/10.1007/s11999-014-3471-7. PubMed PMID: 24474322; PubMed Central PMCID: PMC4048399.
30. Hartzler RU, Llusa-Perez M, Steinmann SP, Morrey BF, Sanchez-Sotelo J. Transverse coronoid fracture: when does it have to be fixed? Clin Orthop Relat Res. 2014;472(7):2068–74. https://doi.org/10.1007/s11999-014-3477-1.
31. Rhyou IH, Kim KC, Lee JH, Kim SY. Strategic approach to O'Driscoll type 2 anteromedial coronoid facet fracture. J Shoulder Elbow Surg. 2014;23(7):924–32. https://doi.org/10.1016/j.jse.2014.02.016. Epub 2014 May 6. PubMed PMID:24810081.
32. Park SM, Lee JS, Jung JY, Kim JY, Song KS. How should anteromedial coronoid facet fracture be managed? A surgical strategy based on O'Driscoll classification and ligament injury. J Shoulder Elbow Surg. 2015;24(1):74–82. https://doi.org/10.1016/j.jse.2014.07.010. Epub 2014 Oct 7. PubMed PMID: 25304044.
33. Foruria AM, Gutiérrez B, Cobos J, Haeni DL, Valencia M, Calvo E. Most coronoid fractures and fracture-dislocations with no radial head involvement can be treated nonsurgically with elbow immobilization. J Shoulder Elbow Surg. 2019;28(7):1395–405. https://doi.org/10.1016/j.jse.2019.01.005. Epub 2019 Apr 5. PubMed PMID: 30956143.
34. O'Driscoll SW, Spinner RJ, McKee MD, Kibler WB, Hastings H 2nd, Morrey BF, Kato H, Takayama S, Imatani J, Toh S, Graham HK. Tardy posterolateral rotatory instability of the elbow due to cubitus varus. J Bone Joint Surg Am. 2001;83-A(9):1358–69.
35. Okazaki M, Takayama S, Seki A, Ikegami H, Nakamura T. Posterolateral rotatory instability of the elbow with insufficient coronoid process of the ulna: a report of 3 patients. J Hand Surg Am. 2007;32(2):236–9.
36. Bellato E, Rotini R, Marinelli A, Guerra E, O'Driscoll SW. Coronoid reconstruction with an osteochondral radial head graft. J Shoulder Elbow Surg. 2016;25(12):2071–7. https://doi.org/10.1016/j.jse.2016.09.003. Epub 2016 Oct 14. PubMed PMID: 27751721.

11 Arthroscopic Evaluation of Elbow Instability

Melanie Amarasooriya, Benjamin Seah Renyi, Gregory I. Bain, and Joideep Phadnis

11.1 Background

Elbow instability commonly results from an acute dislocation, mainly affecting men in their second and third decades. Dislocations occur mostly during athletic activities. Ongoing instability is uncommon; however, once occurred, it imposes a significant functional limitation upon young athletic population. Arthroscopy is a useful adjunct in elbow instability, although some controversy exists with regard to its use in an acute setting. Arthroscopy allows (a) direct joint visualization and assessment and grading of concomitant intra-articular pathology and arthritis, (b) accurate clinical staging of instability that is systematic and reproducible and (c) immediate appropriate corrective surgery in the same setting. This chapter presents the arthroscopic evaluation of elbow instability, focussing on the appropriate diagnostic manoeuvres and its associated signs.

11.2 Surgical Anatomy

Elbow stability is conferred by both static (osseous and soft tissue) and dynamic stabilizers. Function of the elbow stabilizers is influenced by elbow flexion angle [1]. Osseous stability is maximum at <20° and >120° of flexion. Static medial and lateral collateral ligament complexes provide soft-tissue stability with the support of dynamic stabilizers, i.e. common flexor and extensor origins, biceps brachii and triceps brachii. The amount of support provided by the medial and lateral soft-tissue structures depends on the position of elbow flexion. In flexion, most of the valgus stability is provided by the anterior bundle of the medial collateral ligament (aMCL). It is the primary stabilizer against valgus strain at 30°–110° of flexion. In flexion, varus stability is provided mainly by the lateral collateral ligament (LCL) complex, which comprises the lateral ulnar collateral ligament (LUCL), annular ligament, radial collateral ligament (RCL) and accessory lateral collateral ligament. While the RCL stabilizes the elbow against varus forces, the LUCL prevents the ulna supinating around the trochlea.

M. Amarasooriya (✉)
Flinders University, South Australia, Adelaide, Australia

University of Colombo, Colombo, Sri Lanka
e-mail: amar0041@flinders.edu.au

B. S. Renyi
Department of Orthopaedic Surgery, Sengkang General Hospital, Singhealth, Singapore, Singapore
e-mail: benjamin.seah.r.y@singhealth.com.sg

G. I. Bain
Department of Orthopaedic and Trauma Surgery, Flinders University and Flinders Medical Centre, Adelaide, SA, Australia
e-mail: admin@gregbain.com.au

J. Phadnis
Brighton and Sussex University Hospitals, Brighton, UK
e-mail: joideep@doctors.org.uk

© ISAKOS 2022

D. N. Bhatia et al. (eds.), *Arthroscopy and Endoscopy of the Elbow, Wrist and Hand*,
https://doi.org/10.1007/978-3-030-79423-1_11

In a systematic review by Goodwin et al., it was concluded that arthroscopy is a valuable adjunct for evaluation of elbow instability [2]. They concluded that arthroscopy offers an exceptional view of the joint and has the ability to address intra-articular pathology without the adverse clinical consequences of open surgery. Arrigoni et al. noted that intra-articular pathology diagnosed arthroscopically may suggest minor lateral elbow instability in patients with recalcitrant lateral elbow pain initially diagnosed as lateral epicondylitis (SMILE—symptomatic minor instability of the lateral elbow) [3]. In addition, arthroscopy can be used as a post-procedure assessment tool. Holt et al. used arthroscopic 'drive-through sign' to decide the adequacy of plication for posterolateral rotatory instability (PLRI) [4]. If post-procedure drive-through sign is negative, the procedure can be decided to be satisfactory. Spahn et al. used arthroscopy to assess the completeness of thermal shrinkage and this predicted good outcome after a follow-up of 30 months [5].

11.3 Surgical Technique

Arthroscopy in elbow instability can be performed in both acute and chronic settings, although its use in acute dislocations is controversial. Most patients are asymptomatic after a conservatively managed simple elbow dislocation, with only up to 8% of patients reporting persistent instability. If arthroscopy is to be performed in an acute setting, the surgeon has to be aware that the procedure is technically challenging due to soft-tissue swelling and presence of an intra-articular haematoma. With an extensive soft-tissue injury and a capsular rent, there will likely be extravasation of fluid with wet arthroscopy, resulting in an increased risk of compartment syndrome. Therefore, we recommend that dry arthroscopy be considered in an acute setting, with occasional use of saline to evacuate the joint haematoma.

Patient Positioning and Equipment: The patient is placed in the lateral decubitus position with an arm holder. Immediately post-induction, an examination under anaesthesia (EUA) is performed. The elbow is brought through its full range of movement before subjecting it to stability testing (varus/valgus stress, pivot shift test and posterior drawer test). Fluoroscopy aids in detecting subtle instability. A sterile tourniquet is applied. Superficial landmarks are identified. The joint is marked as per arthroscopy and a standard 4 mm 30° arthroscope is preferred. Dry arthroscopy is subsequently performed.

Anterior compartment evaluation: The author prefers to start with an examination of the anterior compartment.

1. From the anterior medial (AM) portal, the anterior compartment is examined for the presence of synovitis, osteophytes and chondropathy of both the radial head and capitellum. A 70° arthroscope is useful when viewing the LCL footprint from the AM portal.
2. Signs of lateral laxity or PLRI include [3]:
   (a) Loose collar sign: Sagging of the annular ligament to the radial neck (below cartilaginous portion of the radial head). This is usually more evident with the elbow in 90° flexion (Fig. 11.1).
   (b) Torn or loose lateral collateral ligament (LCL) complex, with the torn tissue occasionally flipped into the RC joint.
   (c) Positive LCL pull-up sign: The ability to pull up the LCL 1 cm vertically to the lateral side of the capitellum from its displaced position.
   (d) Application of a valgus force with supination may lead to posterolateral radial head subluxation with respect to the capitellum. As this subluxation appears to close the radiocapitellar joint in most patients, unless a high index of suspicion is maintained, it can occasionally be falsely interpreted as a stable joint. A varus force is finally applied with or without longitudinal traction and an opening (>1 mm) of the radiocapitellar joint can be seen in lateral complex insufficiency. Radiocapitellar joint gapping with longitudinal traction is shown in Fig. 11.2.

(e) The anterior compartment examination is continued via the anterolateral (AL) portal. The ulnohumeral joint is examined for anterior synovitis, osteophytes and osteochondral injury. A valgus stress is applied. Widening of the ulnohumeral joint medially by >1 mm is positive for an ulnar collateral ligament (UCL) injury [6].

Posterior compartment evaluation: The posterior compartment is now examined through the posterior portals. Some surgeons prefer a posterolateral portal in athletes to minimize potential scarring of the triceps tendon.

1. The medial gutter is first examined. Osteophytes and posterior band ± anterior band of the UCL may be seen. The elbow is positioned in full pronation, 70° of flexion, and a valgus force is applied [7]. In a partial UCL injury (anterior bundle), the ulnohumeral joint opens 1–4 mm. A complete UCL disruption results in 4–10 mm joint widening [6]. A tearing of the capsule near the posterior aspect of the medial epicondyle may be seen in medial sided instability (Fig. 11.3).
2. Moving to the lateral gutter, the origin of the LCL complex on the posterolateral aspect of the lateral epicondyle is examined (Fig. 11.4). In lateral sided instability, it may be stripped off with the common extensor origin and displaced to a level just above the centre of the olecranon fossa. An Osborne and Cotterill lesion may also be seen on the posterior aspect of the capitellum [8]. Signs of rotatory instability viewed posteriorly from the lateral gutter include the following:
   (a) Drive-through sign (Fig. 11.5) is the ability to pass the arthroscope from the posterolateral gutter through the UH joint to the medial gutter [4]. Occasionally, bone fragments can be seen in the UH joint. It is important to be aware that the drive-through sign can be positive in both UCL insufficiency and PLRI.
   (b) Positive arthroscopic rotatory instability (ARI) test: Full supination of the forearm and application of a varus stress reveal widening of the RC joint and a posterior translation of the radial head. Application of a longitudinal traction on the forearm

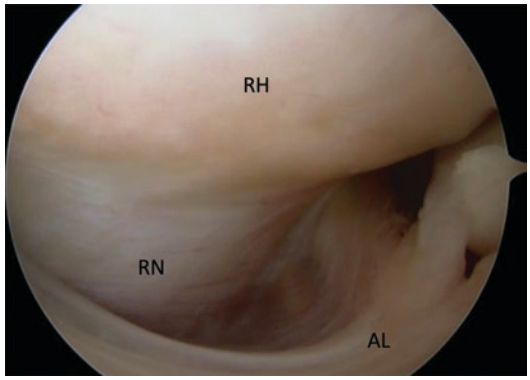

Fig. 11.1 Loose collar sign is shown and the exposed radial neck is visualized (Courtesy of Prof. R P Van Riet, University Hospital Antwerp, Edegem, Belgium)

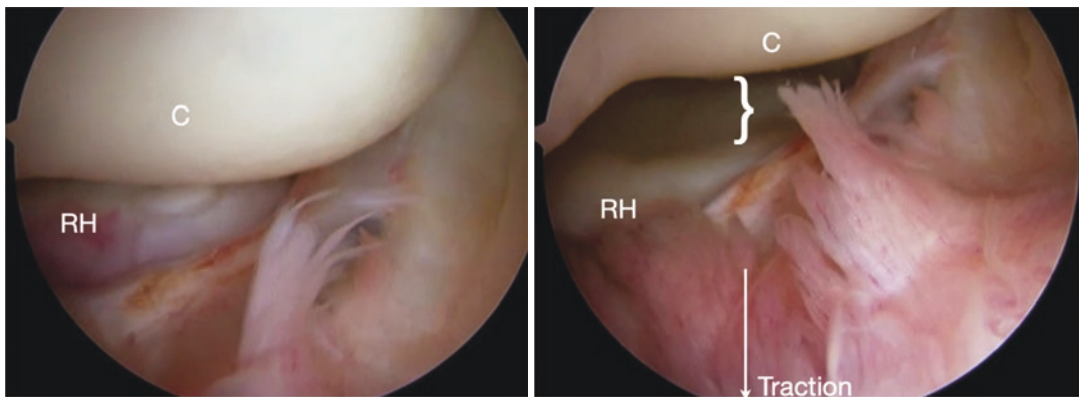

Fig. 11.2 Traction view identifies the opening of capitellar-radial head space with traction (Courtesy of Prof. R P Van Riet, University Hospital Antwerp, Edegem, Belgium)

may accentuate RC joint widening (Fig. 11.6).

(c) Positive annular drive-through (ADT): The ability to pass a 4.2 mm arthroscopic shaver between the radial head and annular ligament with minimal resistance [3].

(d) Arrigoni et al. concluded that subtle lateral sided instability can be a cause of persistent lateral sided elbow pain. The authors coined the condition SMILE—symptomatic minor instability of the lateral elbow [3]. This is considered positive and a radial LCL plication is indicated if there are two lateral patho-laxity signs or one lateral patho-laxity sign and one pathological intra-articular sign.

The lateral patho-laxity signs are (1) positive annular drive through (ADT) (Fig. 11.7), (2) positive loose collar sign and (3) positive R-LCL pull-up sign. Pathological intra-articular signs are (1) anterior or anteromedial synovitis, (2) chondropathy of the radial head, (3) chondropathy of the lateral aspect of the capitellum and (4) anterolateral capsular insufficiency or tear.

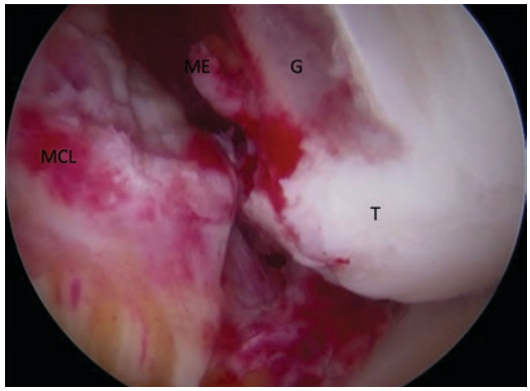

Fig. 11.3 Acute elbow instability—posteromedial view: Avulsion of the MCL from the medial epicondyle is seen. Note the groove (G) in the posterior trochlea (T) (Courtesy of Prof. R P Van Riet, University Hospital Antwerp, Edegem, Belgium)

11.4 Pitfalls

1. Elbow arthroscopy is technically challenging, especially in the evaluation of an unstable joint or in an acute dislocation. Intra-articular

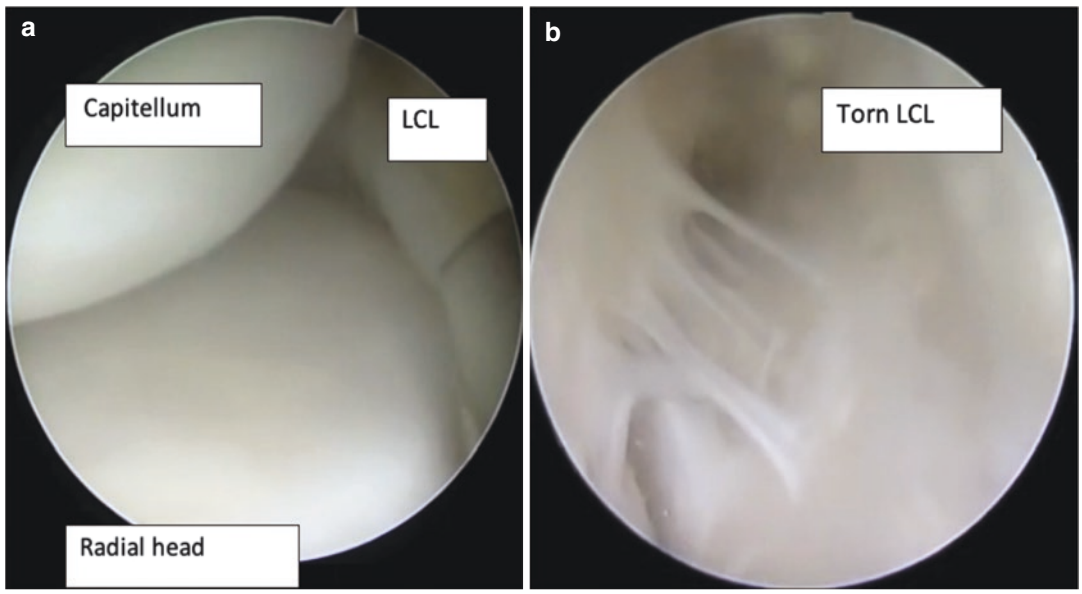

Fig. 11.4 Visualization of LCL insertion via posterolateral compartment is shown. With the arthroscope in the posterolateral portal the scope is directed to view the humeral origin of the LCL at the lateral-most aspect of the radiocapitellar joint. (**a**) Intact LCL. (**b**) Torn LCL in chronic PLRI

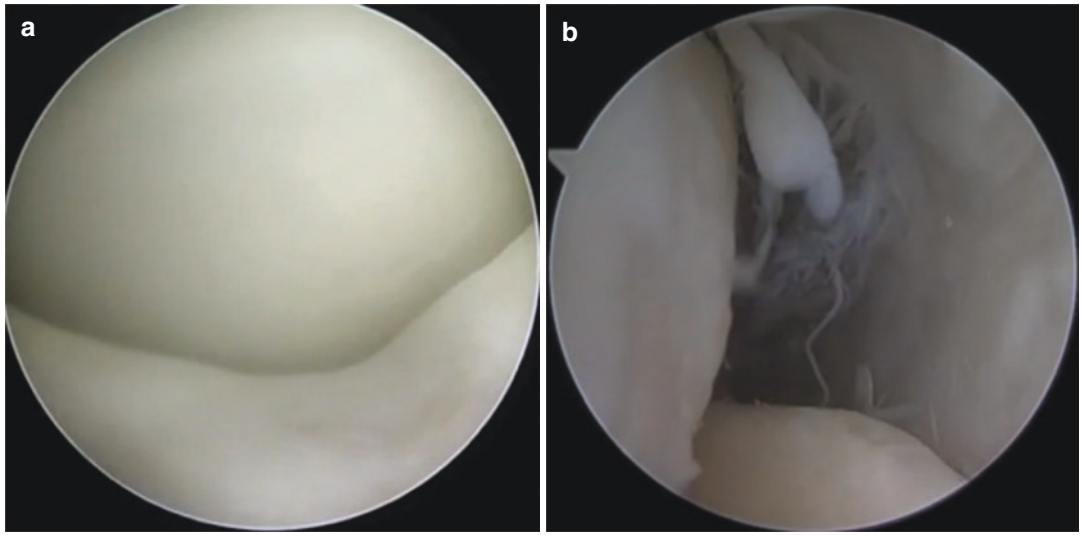

Fig. 11.5 Drive-through sign via posterolateral compartment is demonstrated. With the arthroscope in the posterolateral portal viewing the posterolateral compartment, the scope is directed to view the posterolateral ulnohumeral joint immediately adjacent to the radiocapitellar joint. In a normal elbow the cartilage of the greater sigmoid notch of the ulna (olecranon) is visible distal to the bare area of the olecranon. In PLRI, the scope can be driven into the anterior compartment or the medial ulnohumeral gutter depending on the instability. (**a**) Negative drive-through test. (**b**) Positive drive-through test

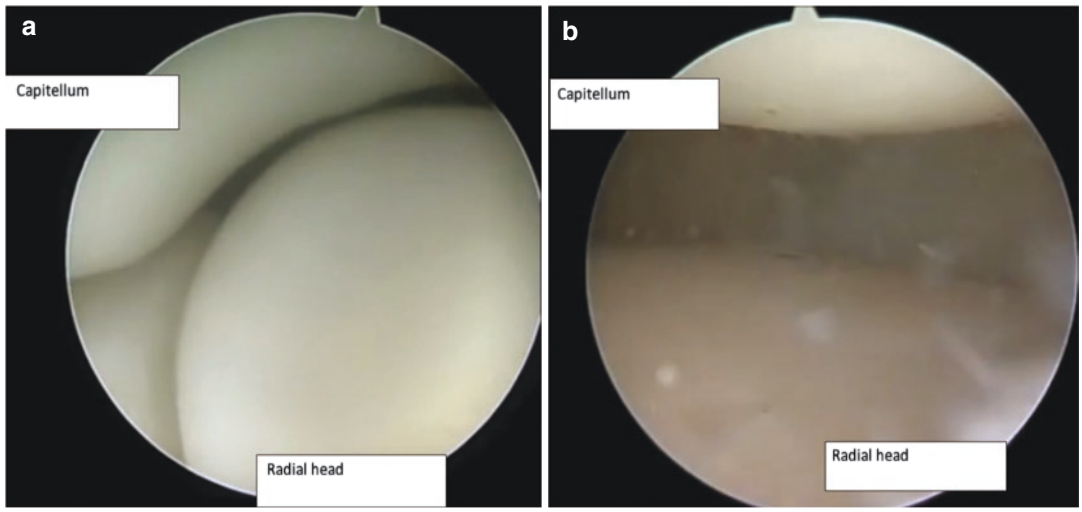

Fig. 11.6 Posterolateral compartment. With the scope in the posterolateral compartment through the posterolateral portal, the radiocapitellar joint is visualized. With supination of the forearm tilting open of the radiocapitellar joint can be seen and described as 'arthroscopic rotatory instability test'. With axial traction, pathologic gapping of the radiocapitellar joint can be demonstrated. (**a**) Normal radiocapitellar congruency. (**b**) Widening of radiocapitellar joint with anterior rim of radial head visible in PLRI

Fig. 11.7 Annular drive-through sign. In this position, it is possible to easily introduce a 4.2 mm shaver between the radial head and the annular ligament through the mid-lateral portal (Courtesy of Prof. R P Van Riet, University Antwerp, Edegem, Belgium)

landmarks can be distorted, and the positions of the neurovascular structures displaced.

2. In addition, direct visualization of the ligament can be technically difficult. Field and colleagues found that in ten cadaveric specimens subjected to elbow arthroscopy they could visualize the anterior bundle of the UCL in only one specimen [6]. Timmerman et al. suggested that only 20–30% of the anterior bundle and 40–50% of the posterior bundle can be seen during arthroscopy [9].

References

1. Morrey BF, An KN. Articular and ligamentous contributions to the stability of the elbow joint. Am J Sports Med. 1983;11:315–9.
2. Goodwin D, Dynin M, Macdonnell JR, Kessler MW. The role of arthroscopy in chronic elbow instability. Arthroscopy. 2013;29(12):2029–36. https://doi.org/10.1016/j.arthro.2013.08.016.
3. Arrigoni P, Cucchi D, D'Ambrosi R, Butt U, Safran MR, Denard P, et al. Intra-articular findings in symptomatic minor instability of the lateral elbow (SMILE). Knee Surg Sport Traumatol Arthrosc. 2017;25:2255–63.
4. Holt MS, Savoie FH, Field LD, Ramsey JR. Arthroscopic management of elbow trauma. Hand Clin. 2004;20:485–95.
5. Spahn G, Kirschbaum S, Klinger HM, Wittig R. Arthroscopic electrothermal shrinkage of chronic posterolateral elbow instability: Good or moderate outcome in 21 patients followed for an average of 2.5 years. Acta Orthop. 2006;77:285–9.
6. Field LD, Callaway GH, O'brien SJ, Altchek DW. Arthroscopic assessment of the medial collateral ligament complex of the elbow. Am J Sports Med. 1995;23:396–400.
7. Field LD, Altchek DW. Evaluation of the arthroscopic valgus instability test of the elbow. Am J Sports Med. 1996;24:177–81.
8. Osborne G, Cotterill P. Recurrent dislocation of the elbow. J Bone Joint Surg Br. 1966;48:340–6.
9. Timmerman LA, Andrews JR, Laura A. The American journal of sports medicine and arthroscopic anatomy of the ulnar collateral ligament of the elbow. Histology. 1994:667–73.

12 Ten-Point Arthroscopic Assessment of Chronic Elbow Instability

Deepak N. Bhatia

12.1 Background

Chronic elbow instability is a spectrum of disorders that may result from traumatic elbow dislocation (contact sports) or repetitive microtrauma (throwing sports). The diagnosis of instability is based on clinical tests and radiological imaging. However, interpretation of several clinical tests requires experience and skills, and is subjective. Moreover, clinical signs may not be apparent in less severe forms of instability and radiological findings must be interpreted with clinical correlation. Arthroscopy is a valuable adjunct in the diagnosis and management of chronic elbow instability [1]. Visualization of the radiocapitellar (RC) and ulnotrochlear (UT) joints is possible from the anterior and posterior compartments, and alteration in RC and UT relations after external manipulation (similar to clinical testing) can be quantified.

This chapter presents a ten-point arthroscopic assessment that is useful in the diagnosis and possibly grading of medial and lateral elbow instability. Systematic evaluation of anterior and posterior compartments is performed and six anterior and four posterior compartment signs are described.

D. N. Bhatia (✉)
SPORTSMED Mumbai, and Sir HN Reliance Foundation Hospital, Mumbai, India
e-mail: shoulderclinic@gmail.com

12.2 Indications and Contraindications

Arthroscopic assessment is indicated for diagnostic evaluation and staging of chronic elbow instability.

Arthroscopy using fluid inflow is best avoided in the acute setting due to the risk of fluid extravasation through capsular rents and presence of hematoma.

12.3 Surgical Technique

The surgery is performed with the patient in lateral decubitus position, and a tourniquet is used during the procedure. A 2.9 mm arthroscope (30 and 70-degree lens) and sheath (ConMed, Linvatec, Largo) are used, and gravity inflow is used to minimize fluid extravasation into the arm and forearm.

Portals: Four standard portals are used in the procedure:

- Proximal anteromedial portal (AM) is used for radiocapitellar and lateral ulnotrochlear visualization. The humeral attachment of lateral capsular structures can be visualized using a 70-degree arthroscope.
- Proximal anterolateral portal (AL) is used for medial ulnotrochlear visualization. The humeral attachment of medial capsular

© ISAKOS 2022

D. N. Bhatia et al. (eds.), *Arthroscopy and Endoscopy of the Elbow, Wrist and Hand*,
https://doi.org/10.1007/978-3-030-79423-1_12

structures can be visualized using a 70-degree arthroscope.
- Posterior central portal (PC) is used for initial evaluation of posterior compartment and permits visualization of medial and lateral gutters and UT articulation.
- Posterior lateral portal (PL) is used for instability evaluation and permits access to the radial head, semilunar notch of olecranon, and posterior trochlea.

The ten-point instability assessment: Elbow instability assessment involves evaluation of six arthroscopic tests/signs in the anterior compartment and four arthroscopic tests/signs in the posterior compartment.

12.3.1 Anterior Compartment Signs

AM and AL portals are used to assess lateral and medial instability: Instability signs in the anterior compartment are described below:

12.3.1.1 Traction Test: RC Distraction and Telescoping Signs

The RC joint is visualized via AM portal and any chondral wear/defects are noted. The static RC joint space is observed with the forearm in neutral position. Next, the forearm is grasped and longitudinal traction is applied while visualizing the RC joint. In a stable elbow, the RC joint surfaces are in apposition with and without traction (Fig. 12.1a). Lateral or multiligamentous instability results in a static gravity-induced distraction and gapping at RC joint; the static gap reduces with elimination of gravity forces and increases to >4 mm with traction (telescoping) (Fig. 12.1b). The distraction at RC joint surfaces can be quantified using a probe or a 4 mm shaver.

12.3.1.2 Anterior Radiocapitellar Drive-through Sign

The RC joint is visualized via AM portal and the arthroscope is gradually advanced between the radial head and capitellum. In a stable elbow, it is not possible to advance a 2.9 mm or 4 mm arthroscope through this space. In lateral or multiligamentous instability, the arthroscope can be advanced to the posterior aspect of the RC space with ease, and the posterior capsule and posterior radial rim are visualized (positive drive-through sign). In severe instability, the arthroscope can be driven across medially through the RC space and into the lateral ulnotrochlear space (Fig. 12.2).

12.3.1.3 Radiocapitellar Posterior Drawer Test

The forearm is placed in neutral position and a posteriorly directed force is applied on the proximal radius and radial head. In a stable elbow, the radial head shows minimal posterior translation. In the presence of lateral, posterolateral, or multiligamentous insufficiency, the posterior translation is significant and the radial head subluxates and disappears from view (AM portal) (Fig. 12.3).

12.3.1.4 Varus Stress Test

The elbow is held in 70 degrees of flexion and supination and a varus force is applied. Distraction at the RC joint ± lateral UT joint space widening indicates lateral ligamentous insufficiency (Fig. 12.4) [2].

12.3.1.5 Valgus Stress Test

The elbow is held in 60–70 degrees of flexion and pronation and a valgus force is applied. Distraction and medial UT joint space widening indicates medial ligamentous insufficiency (Fig. 12.5). Complete disruption of the anterior band of medial collateral ligament (MCL) results in 1–2 mm of medial UT joint space widening. Rupture of the entire MCL results in 4–10 mm UT space opening [3, 4].

12.3.1.6 Accessory Signs of Instability/Laxity

1. *Capsule tears and chondral lesions:* Disruption of capsular attachment or flap tears are often associated with elbow instability; however, these have also been observed in stable elbows. Chondral lesions and osteochondral fragments may be visualized and are related to a dislocation episode (Fig. 12.6a) [5].
2. *Laxity signs:* The annular ligament wraps around the radial head and attaches to the

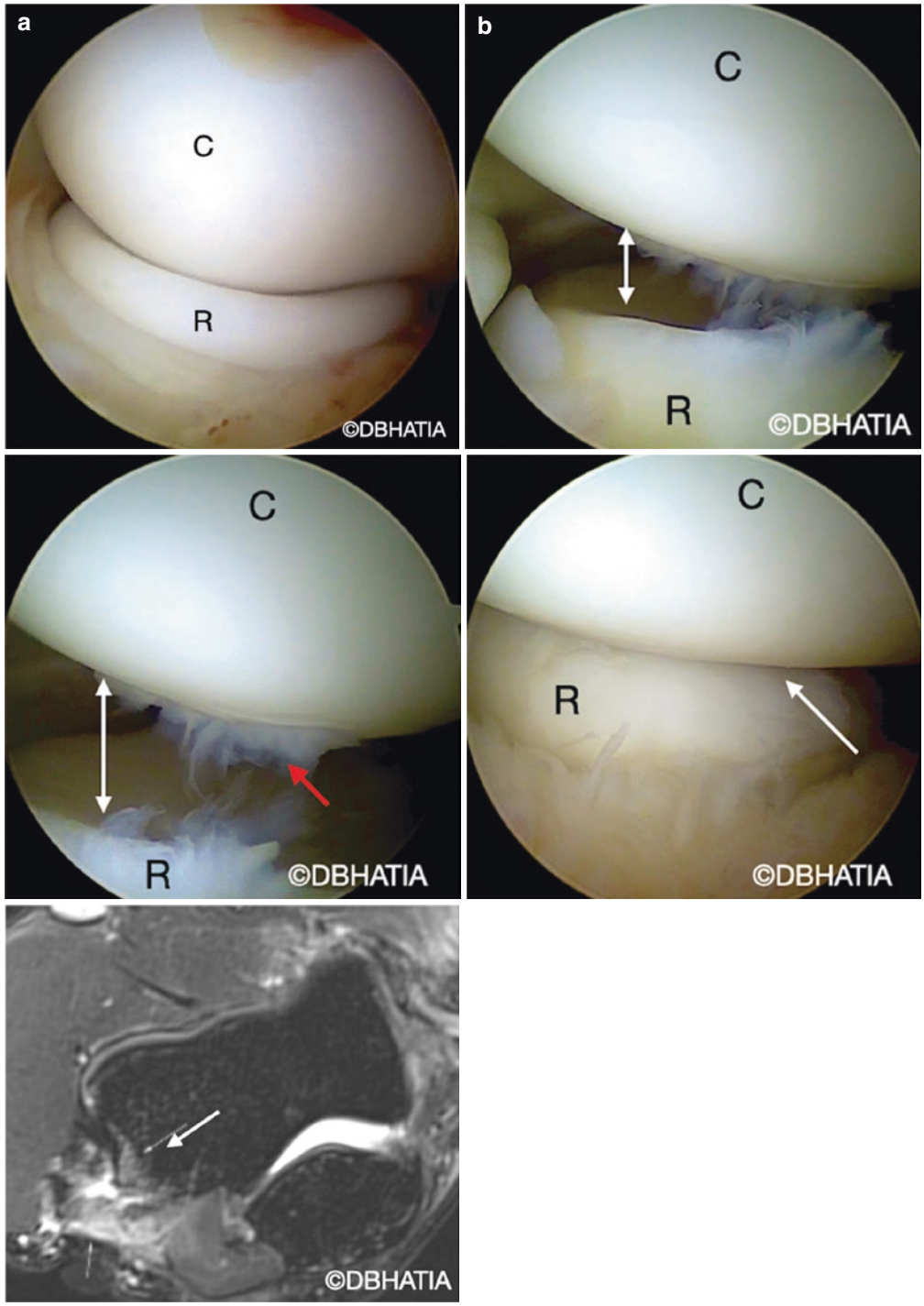

Fig. 12.1 The traction test is demonstrated and visualized via AM portal. (**a**) A normal radiocapitellar (RC) joint shows congruous surfaces in close apposition (top left). (**b**) Radiocapitellar (RC) joint surfaces show a widening (arrows) under gravity (top right) and this is further accentuated (arrows) when longitudinal traction is applied (middle left). The RC surface is in apposition (arrow) when gravity is eliminated (middle right). MRI shows disruption of the lateral ligaments (arrow, bottom image). Chondral injury to C (red arrow) and R can be seen [© DN Bhatia]

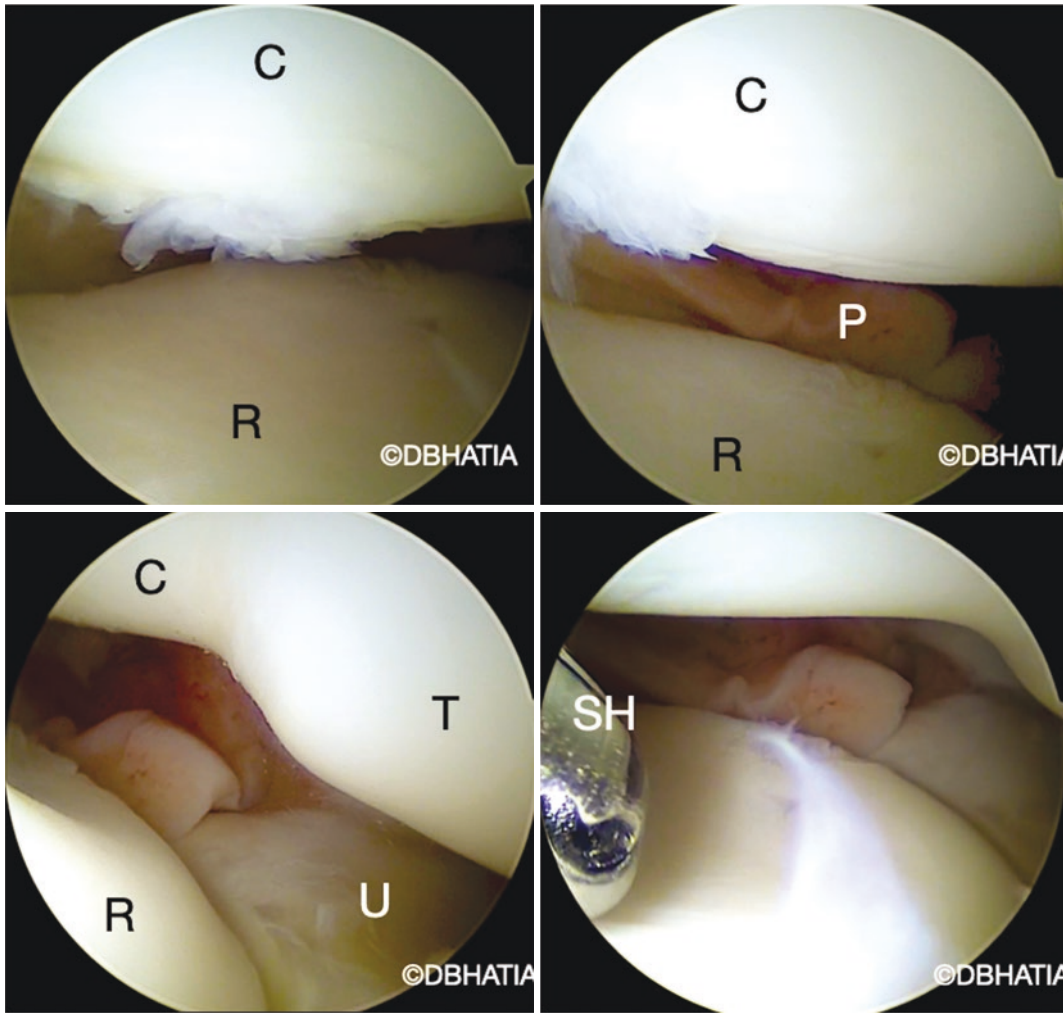

Fig. 12.2 Anterior drive-through sign is demonstrated. The posterior radial head rim and posterior capsule (P) can be visualized (top images) and the scope can be driven across into the ulnotrochlear joint (UT, bottom left image) [SH: 4 mm shaver] [© DN Bhatia]

sigmoid notch of the ulna. A lax annular ligament may sag below the cartilaginous radial head at the level of the neck (annular sag/loose collar sign) (Fig. 12.6b) [6, 7]. The arthroscope and sheath (4 mm) can be passed between the radial head and annular ligament with ease and the inferior aspect of the proximal radioulnar joint is visualized (anterior annular drive-through sign). The sagging annular ligament can be pulled proximally to completely cover the radial head (>1 cm, annular pull-up sign) [7]. The "looseness" of the annular ligament may be considered as an indirect sign of ligament laxity; however, this may be a normal anatomical finding and should be correlated with clinical findings.

12.3.2 Posterior Compartment Evaluation and Signs

Posterior compartment assessment is performed using PC and PL portals. Instability signs in the posterior compartment are described below:

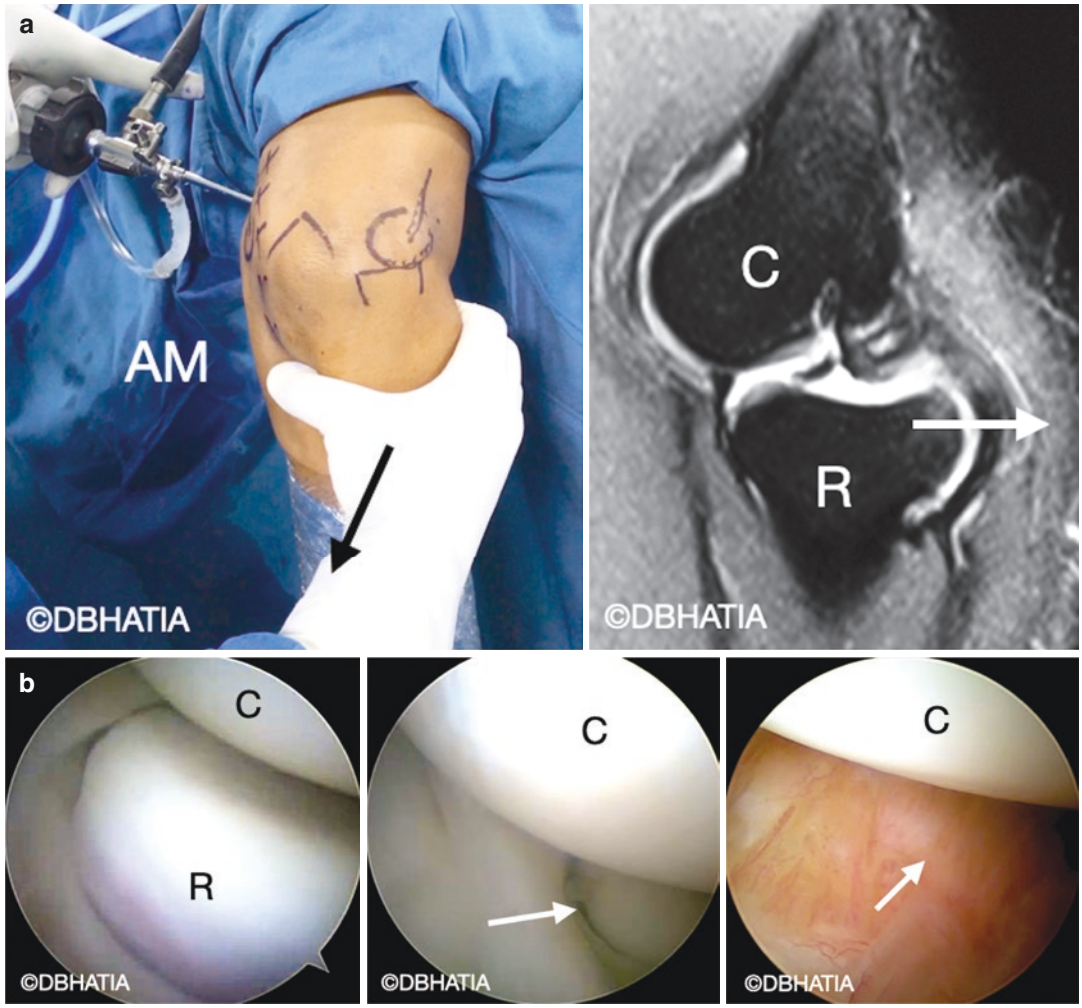

Fig. 12.3 Radiocapitellar posterior drawer test is demonstrated. (**a**) A posteriorly directed force is applied on the radial head (R) and the translation is viewed from anteromedial portal (AM) [© DN Bhatia]. (**b**) Posterior subluxation of RC joint is visualized (arrow, left and middle images) and R may disappear from AM view (arrow, right) [© DN Bhatia]

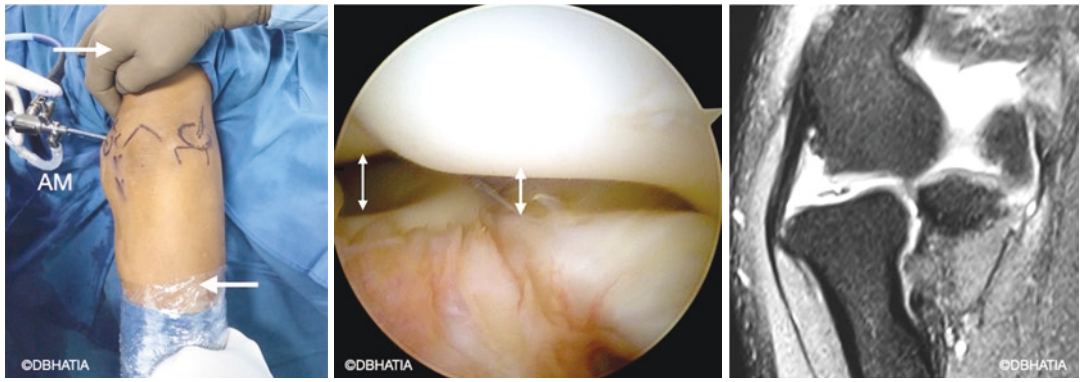

Fig. 12.4 Varus stress test is demonstrated (left). Lateral opening of radiocapitellar and ulnotrochlear joints (arrows, middle and right images) is seen [© DN Bhatia]

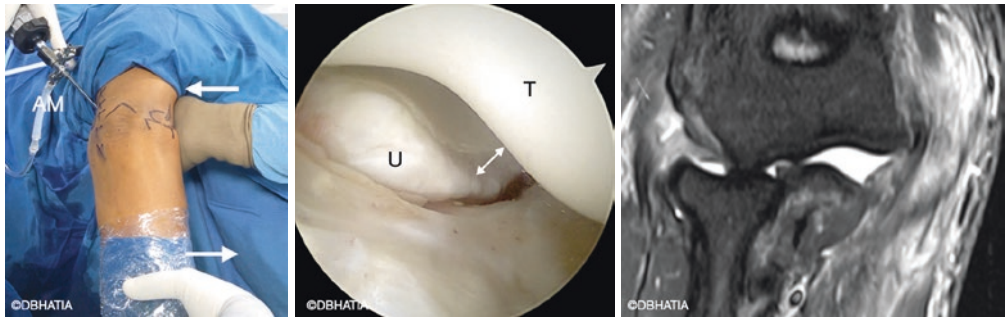

Fig. 12.5 Valgus stress test is demonstrated (left). Medial opening of ulnotrochlear (UT) joint (arrows, middle image) is seen. MRI shows multiligamentous injury with disruption of medial collateral ligament and flexor-pronator mass [© DN Bhatia]

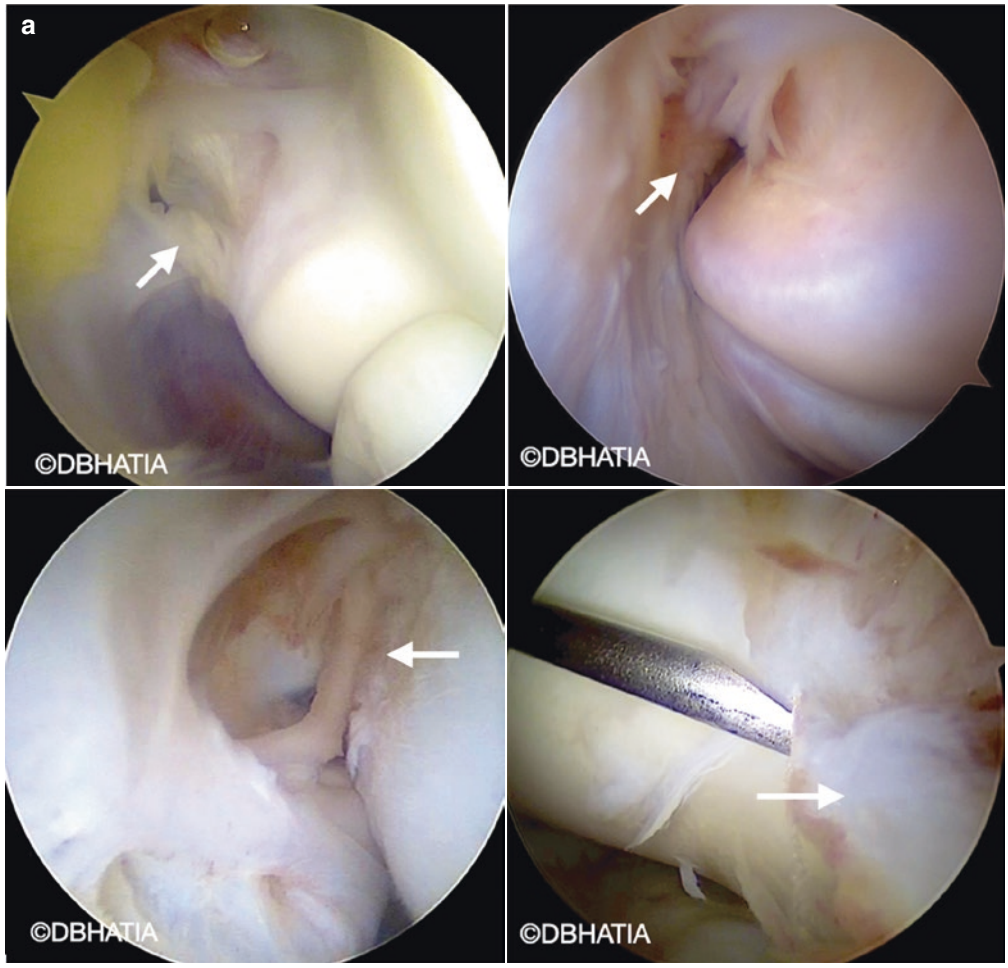

Fig. 12.6 Accessory signs of elbow instability are shown. (**a**) Medial capsular tear and disruption of humeral attachment of MCL (arrow, top images) are visualized via anterolateral portal. In chronic instability, a 70-degree view demonstrates the chronic medial capsule and possible MCL disruption (arrow, bottom left). An osteochondral flap is avulsed off from the medial trochlea (arrow, bottom right) [© DN Bhatia]. (**b**) Laxity of annular ligament is demonstrated by annular sagging (arrow, top left) and anterior annular drive-through (top right, RU: radioulnar joint). The annular ligament can be pulled up laterally using a grasper in anterolateral portal (arrow, bottom images) [© DN Bhatia]

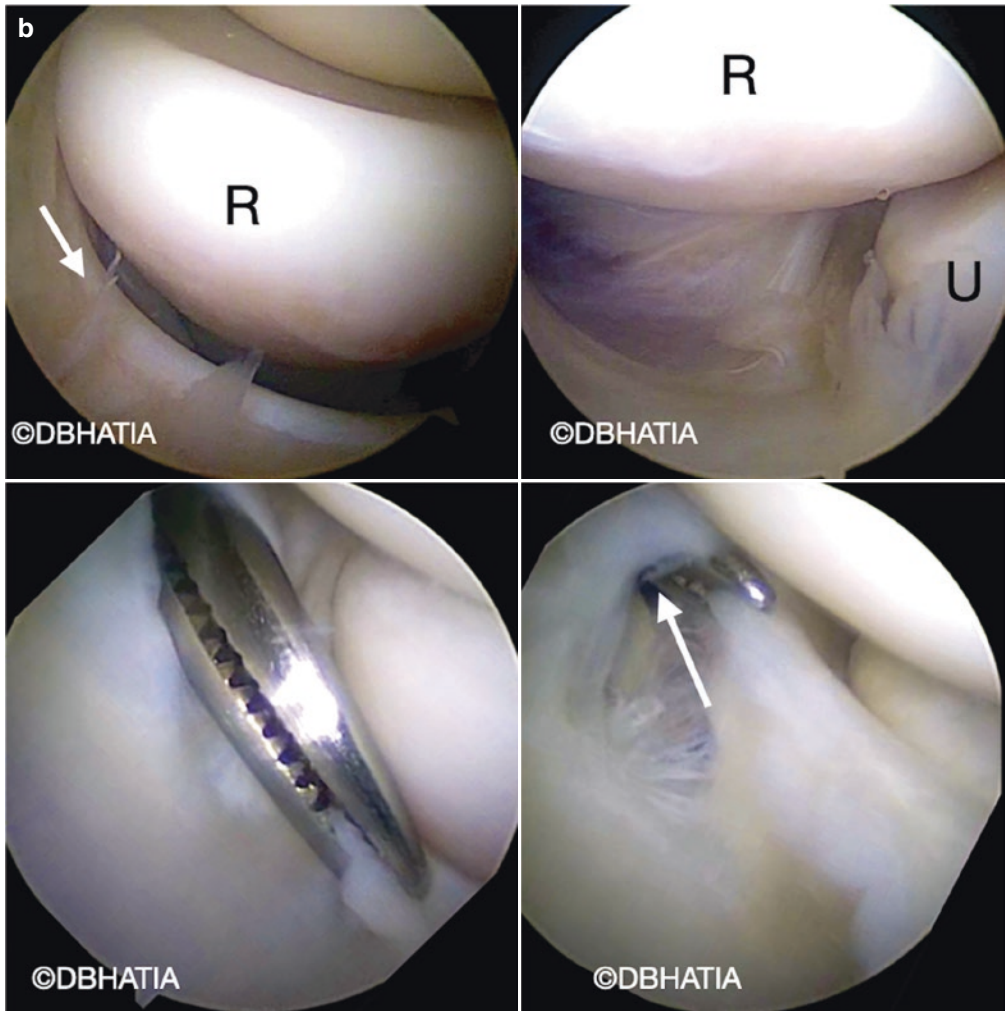

Fig. 12.6 (continued)

12.3.2.1 Ulnotrochlear Widening

The arthroscope is placed in the posterocentral or posterolateral portal and the ulnotrochlear (UT) articulation is visualized. The forearm is placed in full supination and the lateral UT space is observed for widening. In a stable elbow, 1–2 mm UT gap may be observed. In an unstable elbow, the gap is larger and a 4 mm arthroscope can be advanced between the joint surfaces (Fig. 12.7). Similarly, medial UT joint space widening may be observed with full pronation in severe instability.

12.3.2.2 Arthroscopic Rotatory Instability Test (Pull and Rotate)

The arthroscope is placed in the posterolateral portal and is advanced into the lateral gutter to visualize the RC joint. The forearm is held in full supinated position, and the radial head is observed for posterior translation (Fig. 12.8). Varus force and longitudinal traction on the forearm result in RC joint widening, and this can be quantified using a 4 mm shaver or probe passed through an accessory portal [8].

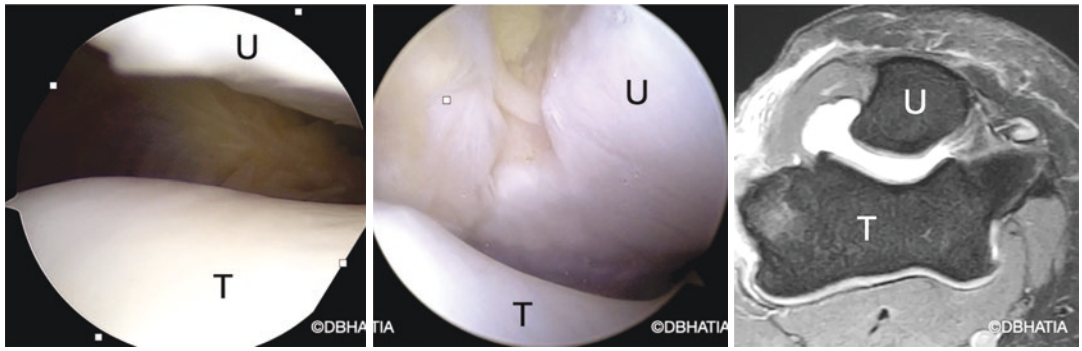

Fig. 12.7 Posterior ulnotrochlear (UT) joint widening is demonstrated with forearm supination [© DN Bhatia]

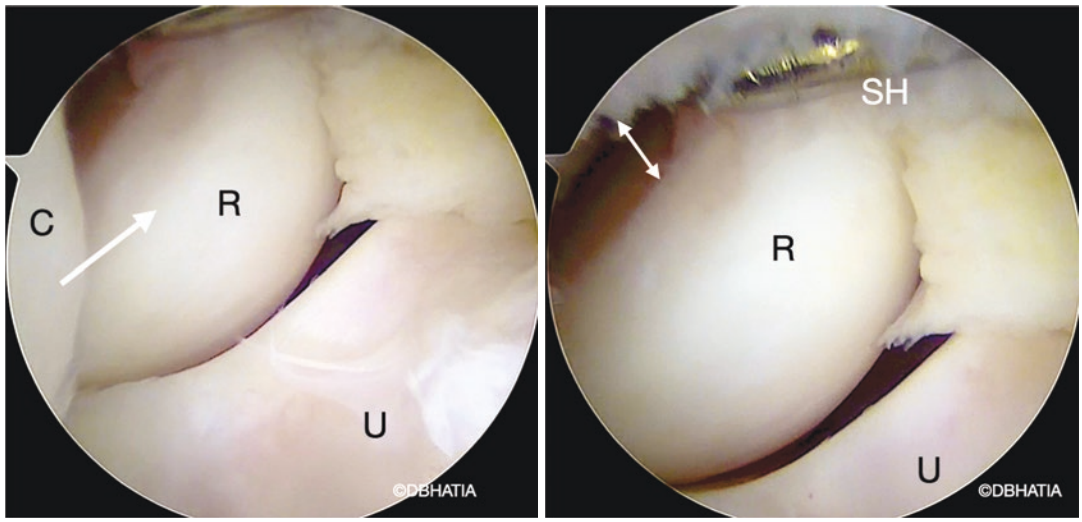

Fig. 12.8 Arthroscopic rotatory instability test is demonstrated. Posterior radial head translation (left image) and radiocapitellar (RC) widening are seen when varus stress and traction are applied on a fully supinated forearm. A 4 mm shaver (SH) is used to quantify the RC distraction [© DN Bhatia]

12.3.2.3 Posterior Drive-Through Sign

The arthroscope is placed in the posterolateral portal and is advanced into the lateral gutter to visualize the RC joint. The scope is then directed medially to visualize the proximal RU joint and UT joint. In a positive drive-through test, the semilunar notch of the ulna is visualized far beyond the bare area and the arthroscope can be sufficiently advanced to visualize the medial gutter (Fig. 12.9). The test is positive in posterolateral, medial, or multiligamentous insufficiency [6].

12.3.2.4 Posterior Capitellar Defect (Osborne and Cotterill Lesion)

A 70-degree arthroscope is placed in the posterolateral portal and is advanced into the lateral gutter to visualize the RC joint. The lens is turned towards the lateral aspect to visualize the posteroinferior capitellum. An osteochondral defect in the posterolateral capitellum is strongly suggestive of a past subluxation episode and instability (Fig. 12.10) [9].

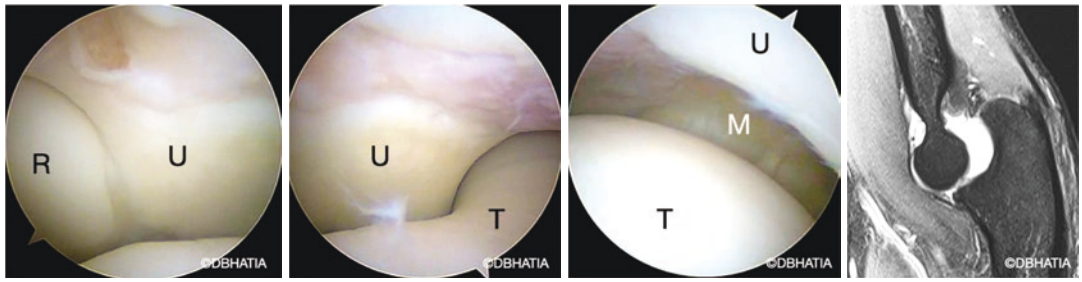

Fig. 12.9 Posterior drive-through sign is demonstrated. The arthroscope is placed in posterolateral gutter and can be gently advanced medially in the ulnotrochlear (UT) joint. The radioulnar (RU) and UT joints and medial gutter (M) are sequentially visualized. The semilunar notch of ulna can be visualized on either side of the bare area [© DN Bhatia]

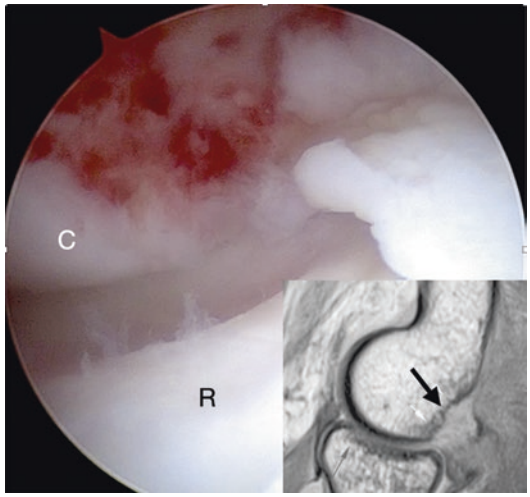

Fig. 12.10 A posterolateral capitellar osteochondral defect (Osborne and Cotterill lesion) is visualized [© DN Bhatia]

In summary, the ten-point assessment provides greater insight into the diagnosis of medial and lateral instability, and is recommended prior to any surgical intervention.

Conflict of Interest The author certifies that he has no commercial associations (e.g., consultancies, stock ownership, equity interest) that might pose a conflict of interest in connection with the submitted chapter. The author retains the copyright to the images, videos, and content in this chapter.

References

1. Goodwin D, Dynin M, Macdonnell JR, Kessler MW. The role of arthroscopy in chronic elbow instability. Arthroscopy. 2013;29(12):2029–36. https://doi.org/10.1016/j.arthro.2013.08.016.
2. McAdams TR, Masters GW, Srivastava S. The effect of arthroscopic sectioning of the lateral ligament complex of the elbow on posterolateral rotatory stability. J Shoulder Elbow Surg. 2005;14(3):298–301. https://doi.org/10.1016/j.jse.2004.08.003.
3. Timmerman LA, Andrews JR. Histology and arthroscopic anatomy of the ulnar collateral ligament of the elbow. Am J Sports Med. 1994;22:667–73.
4. Field LD, Altchek DW. Evaluation of the arthroscopic valgus instability test of the elbow. Am J Sports Med. 1996;24:177–81.
5. Field LD, Callaway GH, O'Brien SJ, Altchek DW. Arthroscopic assessment of the medial collateral ligament complex of the elbow. Am J Sports Med. 1995;23:396–400.
6. O'Brien MJ, Savoie FH 3rd. Arthroscopic and open management of posterolateral rotatory instability of the elbow. Sports Med Arthrosc Rev. 2014;22(3):194–200. https://doi.org/10.1097/JSA.0000000000000029.
7. Arrigoni P, Cucchi D, D'Ambrosi R, et al. Intra-articular findings in symptomatic minor instability of the lateral elbow (SMILE). Knee Surg Sports Traumatol Arthrosc. 2017;25(7):2255–63. https://doi.org/10.1007/s00167-017-4530-x.
8. van Riet RP. Arthroscopic assessment and Management of Instability: when and how to do surgery in simple dislocations. In: Bain G, Eygendaal D, van Riet R, editors. Surgical techniques for trauma and sports related injuries of the elbow. Berlin, Heidelberg: Springer; 2020.
9. Osborne G, Cotterill P. Recurrent dislocation of the elbow. J Bone Joint Surg Br. 1966;48:340–6.

13 Arthroscopic Evaluation of Elbow Instability: An Alternative Technique

Sebastian Lappen, Nadine Ott, Lars P. Müller, and Kilian Wegmann

13.1 Background

The stability of the elbow joint depends on the bony, ligamentous, and musculoskeletal structures of the elbow [1]. Arthroscopic instability tests are an add-on to patient's history, clinical examination, and standard imaging studies for diagnosing both mild and complex forms of instability. Arthroscopic examination is therefore an option in clinically and radiologically suspected cases of elbow instability. This chapter presents the author's technique of using a switching stick for assessment of elbow instability.

13.1.1 Surgical Anatomy

The stability of the elbow joint depends on a complex interplay of bony articulations, capsuloligamentous components, and musculotendinous structures.

- The bony structures particularly stabilize the elbow when the joint is flexed less than 30° or more than 100° [2]. The ulnohumeral joint contributes most to the stability, and the radial head the least.
- The ligaments around the elbow consist mainly of the medial and lateral collateral ligament complex. The lateral collateral ligament (LCL) consists of four components:
  - The lateral ulnar collateral ligament (LUCL) originates from the lateral epicondyle and extends in a slight arc to its insertion point, the supinator crest. As the structure mainly responsible for the stability of the lateral elbow joint, it plays an important role in preventing posterolateral rotatory instability (PLRI).
  - The radial collateral ligament (RCL) also originates from the lateral epicondyle, where it cannot be distinguished from the LUCL. From here it runs distally and eventually merges with the annular ligament. The two structures insert as one on the anterior and posterior margins of the radial notch. Although the RCL is mainly responsible for the lateral stability of the elbow joint, only the combined insufficiency of the LUCL and the RCL leads to PLRI [3].
  - The annular ligament encircles the radial head and holds it in position against the

S. Lappen
Department of Orthopaedic Sports Medicine, Klinikum rechts der Isar, Technical University of Münich, Münich, Germany

N. Ott · L. P. Müller · K. Wegmann (✉)
Center for Orthopedic and Trauma Surgery, University Medical Center of Cologne, Cologne, Germany
e-mail: kilian.wegmann@uk-koeln.de

© ISAKOS 2022

D. N. Bhatia et al. (eds.), *Arthroscopy and Endoscopy of the Elbow, Wrist and Hand*,
https://doi.org/10.1007/978-3-030-79423-1_13

radial notch of the ulna. It originates and inserts at the incisura radialis ulnae.
  - The accessory lateral collateral ligament runs from the inferior margin of the annular ligament to the supinator crest of the ulna.
- The medial collateral ligament (MCL) is made up of three bundles:
  - The anterior oblique ligament (AOL) runs from the anterior inferior aspect of the medial epicondyle to the sublime tubercle of the ulna. Histologically, it consists of a deep layer within the medial capsule and a superficial layer on the surface of the capsule. It is mainly responsible for the stability of the medial elbow joint and contributes significantly to valgus stability [2].
  - The posterior oblique ligament (POL) is a fan-shaped capsule thickening that originates posterior to the AOL on the medial epicondyle and inserts with a wide insertion point on the medial edge of the olecranon.
  - The transverse ligament is a variable structure spanning over the insertion sites of the AOL and POL.
- The muscular structures serve as further important dynamic stabilizers. The extensor muscles stabilize the lateral side while the flexor muscles stabilize the medial side of the elbow joint.
- The stabilizing effects of the bony, ligamentous, and muscular structures change depending on the elbow positioning:
  - In full extension, the valgus stability is provided in equal parts by the MCL, the anterior elbow capsule, and the bony articulation [2]. Varus stability is determined mostly by the bony articulation (55%), with the anterior capsule contributing 32% and the radial collateral ligament 14% [2].
  - In 90° flexion, valgus stability is mainly provided by the MCL (55%), with the bony structures and the anterior capsule making lower contributions with 33% and 13%, respectively [2]. Varus stability is provided by the bony articulation (75%), anterior capsule (13%), and radial collateral ligament (9%) [2].

13.2 Indications and Contraindications

Arthroscopic instability testing is a sensitive adjunct to the classical methods of taking patient's history, clinical examination, and imaging analysis to detect and quantify both mild and complex forms of instability. An arthroscopic examination is therefore potentially indicated to strengthen or support suspicion of instability of the elbow [4].

The general contraindications of elbow arthroscopy apply.

13.3 Surgical Technique

The preparation for surgery corresponds to that of diagnostic elbow arthroscopy. The use of a tourniquet with a pressure of 250 mm Hg is recommended but not essential for the procedure. Important anatomical landmarks and standard portals should be marked.

Instability tests are performed using a 4 mm switching stick as a reference value. The stick is used to palpate and evaluate joint gapping to gain an impression of joint stability. Additionally, the end point is as important as the joint gap width, and a firm or soft-end feeling is documented. During arthroscopic evaluation, one has to consider influence of altered muscle tone in general anesthesia, potential pressure by the water pump, pull of gravity on the arm in lateral decubitus position, and further individual patient factors like hyperlaxity. A relevant drawback of arthroscopic stability testing is that the contralateral side cannot be involved in the evaluation.

13.3.1 Posterior Compartment

The camera is placed in the proximal posterolateral portal to examine the posterior structures (Fig. 13.1).

- To test for instability, a switching stick is inserted into the joint via the trans-triceps portal and advanced between the distal humerus

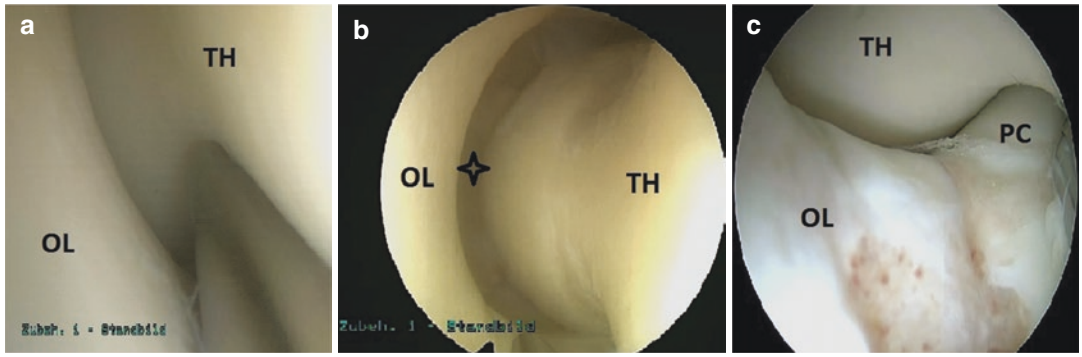

Fig. 13.1 Arthroscopic view of the humeroulnar joint via the posterolateral portal; the switching stick is shown attempting a subluxation of the joint. (**a**) In stage 0 PLRI, the stick cannot be placed between the trochlea (TH) and the olecranon (OL), and the joint is stable. (**b**) In stage I PLRI, the stick can be placed between the trochlea and the olecranon until the bare area (*). (**c**) In PRLI stage II, subluxation of the coronoid process (PC) is demonstrated

and the olecranon tip medially. The humeroulnar compartment is now expanded from medial to lateral, thereby testing the MCL and LCL (Table 13.1). If the MCL is intact, the switching stick usually cannot displace the ulna off the humerus in the ulnar third of the joint. The LCL is evaluated by trying to expand the joint in its radial third. It is important to know that even with an intact LCL, the joint can often be physiologically expanded to the full width of the switching stick, on the radial side of the joint.

- The camera optics are now moved radially and then distally, so that a dorsal view of all three partial joints (radio-humeral joint, proximal radioulnar joint, lateral aspect of ulno-humeral joint) of the posterolateral corner of the elbow is obtained. Physiologically, a congruent joint position should be seen for all joint sections. A switching stick is inserted via the direct lateral portal for stability testing (Table 13.2).
- The annular ligament is tested by inserting the switching stick between the radius and ulna. The insertion usually is not possible with an intact annular ligament.
- To test the LCL, the switching stick is inserted between the humerus and the radius. Here we see some variability in individual stability conditions. However, marked gapping between the humerus and ulna, which can be increased by careful levering with the stick to a point, at which the coronoid base is visible, is documented as posterolateral rotatory instability. With increments of instability, by using the switching stick the coronoid tip can be visualized.
- To evaluate the MCL, the switching stick is used to open up the medial aspect of the ulnohumeral joint space. Usually this is not possible. In case of a defect in medial collateral ligament complex, gapping of the medial joint space will give sight on the articular surface of the medial capsule, beyond the trochlea.
- PLRI is also determined by the dorsal translation of the radial head to the capitulum. The radial head is pulled posterolaterally with the distal humerus fixed in position. Hypersupination may also result in visible posterior subluxation of the radial head in relation to the capitulum and can be used during arthroscopy. However, it should be noted that due to the physiological elasticity of the ligament structures, a stable joint can also be opened to some degree. PLRI can be classified based on the criteria of O'Driscoll [5, 6]. The details are shown in Table 13.3.

Table 13.1 Expansion of the humeroulnar joint

	Structure	Physiological opening	First-degree opening	Second-degree opening
Medial third	MCL	0–2 mm (resilient resistance)	2–4 mm (insertion of the tip possible)	≥4 mm (full insertion possible)
Central third	MCL + LCL	0–2 mm (resilient resistance)	2–4 mm (insertion of the tip possible)	≥4 mm (full insertion possible)
Lateral third	LCL	0–4 mm (up to 1× switching stick)	4–8 mm (up to 2× switching stick)	≥8 mm (>2× switching stick)

Table 13.2 Expansion of the radioulnar, humeroradial, and humeroulnar joint

	Structure	Physiological opening	First-degree opening	Second-degree opening	Third-degree opening
Radioulnar	Annular ligament	0–2 mm (resilient resistance)	2–4 mm (insertion of the tip)	≥4 mm (full insertion possible)	–
Humeroradial	LCL	0–2 mm (resilient resistance)	2–4 mm (insertion of the tip)	≥4 mm (full insertion possible)	–
Humeroulnar (ventral)	MCL	0–4 mm (up to 1× switching stick)	4–6 mm (up to 2× switching stick)	6–8 mm (up to 2× switching stick)	≥8 mm (>2× switching stick)

Table 13.3 Stages of PLRI (adapted from O'Driscoll [5, 6])

	Stage 0	Stage 1	Stage 2	Stage 3
Description		Posterolateral subluxation of the radial head; the humeroulnar joint remains centered	Posterolateral subluxation of the radial head; the humeroulnar joint is decentered	Complete posterolateral dislocation
Affected anatomic structures		Disruption of the LUCL, possibly the RCL and posterolateral capsule	Disruption of the LCL complex and the anterior and posterior capsule	Disruption of the MCL
Humeroulnar width	No relative opening	Can be opened up to 5 mm Fixed-band stop	Subluxation >5 mm Soft-band stop	Complete luxation
Radial head shift	None	<25%	25–50%	>50%
Opening of the proximal radioulnar joint	None	2–3 mm	3–5 mm	>5 mm
Medial humeroulnar joint	Joint line cannot be opened	Joint line can be opened via switching stick		

13.3.2 Anterior Compartment

To complete the instability test, we switch to an anterior portal. The congruence of the joint between the coronoid process and the trochlea is of particular interest for anterior instability diagnosis (Fig. 13.2a).

- The optimal joint position for checking the medial stability is about 70° flexion. An additional pronation movement can increase the opening of the humeroulnar compartment in the presence of ligament insufficiency or respective injury. With an intact MCL (Fig. 13.2b), the joint gap cannot be widened or may open only slightly (<1 mm) [7]. An opening of more than 4 mm under valgus stress is considered pathognomonic for valgus instability. The anterior humeroradial joint is evaluated in a similar manner.
- In some cases the arthroscope can be driven through the lateral gutter into the lateral aspect of the ulnohumeral joint. This is called the "elbow drive-through sign" and can be seen

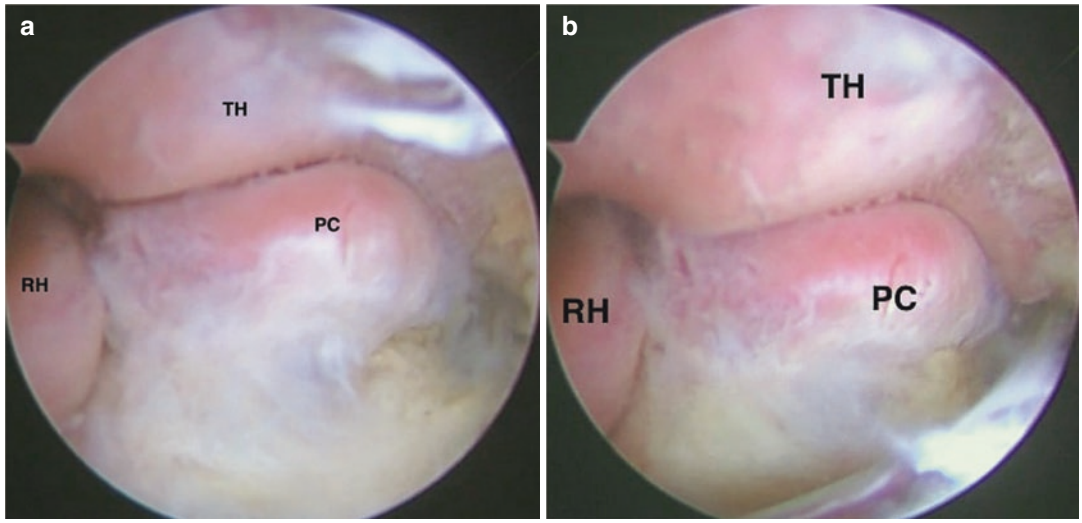

Fig. 13.2 Arthroscopic view of the anterior compartment via the anteromedial portal; congruence of the joint between coronoid process (PC) and trochlea (TH) in 90° flexion (**a**) and 70° flexion and pronation (**b**) of the elbow is seen (RH radial head)

particularly in cases with PLRI stages 2–3 and in combined multidirectional instabilities [8]. Also, a pivot-shift maneuver can show the radial head rotating and translating posteriorly in cases of PLRI [9].

13.4 Technical Tips

Before the surgical intervention begins, stability tests should be performed under anesthesia in different degrees of flexion; this helps to differentiate between pain-related signs and structural signs of instability.

13.5 Pitfalls

Stability testing is carried out without force as iatrogenic cartilage damage must be avoided.

PLRI testing cannot be objectified and requires an experienced surgeon.

It is often difficult to arthroscopically determine the exact severity of PLRI, and clinical correlation is necessary.

13.6 Post-op Management and Rehabilitation

Stitches are removed 12–14 days after the procedure. Early functional exercises with accompanying physiotherapy and lymphatic drainage are initiated to prevent stiffness. Heavy lifting should be avoided for about 6 weeks. If further operative procedures have been performed, the rehabilitation should be adjusted accordingly.

13.7 Complications

Iatrogenic nerve injury, paresthesia, and stiffness are possible complications [10] (Fig. 13.3).

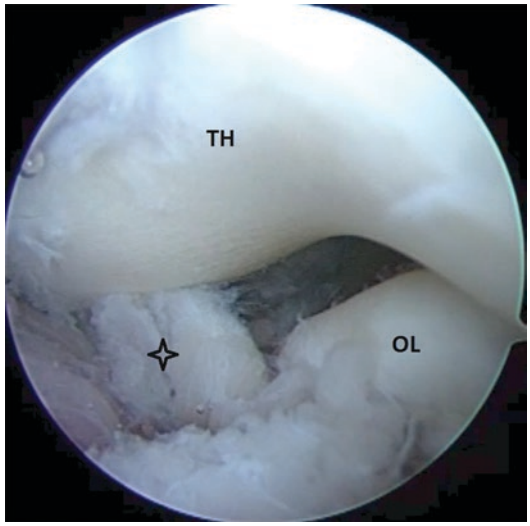

Fig. 13.3 Valgus instability is demonstrated via the anteromedial portal, and incongruence of the joint between coronoid process (OL) and trochlea (TH) in valgus stress is seen (*STAR = MCL) (The Authors)

References

1. Morrey BF. Anatomy of the elbow joint. In: Morrey B, editor. The elbow and its disorders. Philadelphia: Saunders; 2000. p. 13–42.
2. Morrey BF, An KN. Articular and ligamentous contributions to the stability of the elbow joint. Am J Sports Med. 1983;11:315–9.
3. Cheung EV. Chronic lateral elbow instability. Orthop Clin North Am. 2008;39(2):221–8. https://doi.org/10.1016/j.ocl.2007.12.007.
4. Goodwin D, Dynin M, Macdonnell JR, Kessler MW. The role of arthroscopy in chronic elbow instability. Arthroscopy. 2013;29(12):2029–36. https://doi.org/10.1016/j.arthro.2013.08.016.
5. O'Driscoll SW, Morrey BF, et al. Elbow subluxation and dislocation. A spectrum of instability. Clin Orthop Relat Res. 1992;280:186–97.
6. O'Driscoll SW. Classification and evaluation of recurrent instability of the elbow. Clin Orthop. 2000;510:34–43.
7. Field LD, Altchek DW. Evaluation of the arthroscopic valgus instability test of the elbow. Am J Sports Med. 1996;24(2):177–81. https://doi.org/10.1177/036354659602400210.
8. O'Brien MJ, Savoie FH 3rd. Arthroscopic and open management of posterolateral rotatory instability of the elbow. Sports Med Arthrosc Rev. 2014;22(3):194–200. https://doi.org/10.1097/JSA.0000000000000029.
9. O'Driscoll SW, Bell DF, Morrey BF. Posterolateral rotatory instability of the elbow. J Bone Joint Surg Am. 1991;73:440–6.
10. Kelly EW, Morrey BF, O'Driscoll SW. Complications of elbow arthroscopy. J Bone Joint Surg Am. 2001;83(1):25–34. https://doi.org/10.2106/00004623-200101000-00004.

14 Arthroscopic Repair of Lateral Ulnar Collateral Ligament Injuries

Felix H. Savoie, Zachary J. Finley, and Michael O'Brien

14.1 Background

Injuries to the lateral ulnar collateral ligament (LUCL) of the elbow can be caused by simple elbow dislocations as well as complex trauma or iatrogenic injury. Simple dislocations account for 10–30% of all injuries to the elbow, and occur in the United States at 5.21 per 100,000 person-years with nearly half of those dislocations associated with athletic activities [1, 2]. In athletes and nonathletes alike, a simple elbow dislocation can often be treated successfully with bracing and rehabilitation. However, failure of the LUCL to heal can lead to varus and posterolateral rotatory instability of the elbow (PLRI). Simple activities of daily living, such as pushing up from a chair or lifting objects with the elbow extended, become painful and difficult, not to mention the more demanding forces exerted across the elbow in sports such as wrestling, gymnastics, and football [1–12].

14.1.1 Surgical Anatomy

PLRI was first described by O'Driscoll et al. in 1991 and is the most common instability pattern in the elbow [3, 4]. PLRI represents a transient external rotatory subluxation of the ulna on the humerus, with posterior and valgus displacement. This in turn can lead to subluxation or dislocation of the radial head from the radiocapitellar joint [5]. The anatomical structure injured in PLRI is the lateral ligament complex, including the radial ulnohumeral ligament (RUHL), the lateral collateral or radial collateral ligament (LCL or RCL), and the annular ligament. If the RUHL does not heal properly after injury and becomes nonfunctional, the radial head rolls off of the capitellum during forearm supination. As the radial head subluxates posterolaterally, the ulnohumeral joint begins to gap, and as the pattern of instability continues the entire elbow joint may dislocate [3, 6]. Most injuries occur proximally, with the RUHL and LCL avulsed off the humerus, often with a small fragment of bone. Surgically, therefore this can often be repaired back to the humerus by either open or arthroscopic techniques. In some cases, especially in those with prior surgery there may be multiple areas of injury requiring reconstruction using autograft or allograft to restore stability.

F. H. Savoie (✉) · Z. J. Finley · M. O'Brien
Department of Orthopaedic Surgery, Tulane University School of Medicine, New Orleans, LA, USA
e-mail: fsavoie@tulane.edu; zfinley@tulane.edu; mobrien@tulane.edu

© ISAKOS 2022

D. N. Bhatia et al. (eds.), *Arthroscopy and Endoscopy of the Elbow, Wrist and Hand*,
https://doi.org/10.1007/978-3-030-79423-1_14

14.2 Indications/ Contraindications

Surgical management of PLRI is indicated for functional impairment. In most instances this follows an instability episode, but can occur after chronic overuse or surgery for lateral epicondylitis. In those individuals involved in sports requiring high level of elbow function (gymnastics, wrestling, racquet sports), early surgical intervention may allow a more rapid return of function.

These patients may complain of lateral sided elbow pain and discomfort with activities. Frequently mechanical symptoms are reported with subjective locking, catching, clicking, snapping, or slipping [5, 6]. These are most noted when the elbow is at the mid-flexion arc as the elbow goes into extension with the forearm supinated. Activities such as opening doors or pushing up from a seated position can exacerbate these symptoms because the combination of supination, valgus force, and axial load can allow the radial head to subluxate posterolaterally in an unstable elbow. The patient may notice a prominence on the lateral elbow during these activities as the forearm dissociates from the humerus with apparent radial head subluxation.

In addition to the history of trauma including simple or complex elbow dislocation, a thorough history is important to obtain. Generalized ligamentous laxity or chronic cubitus varus can contribute to an incompetent LCL complex. Surgical history as well as history of injections are also important as iatrogenic causes can damage the LUCL. These include steroid injections for lateral epicondylitis or connective tissue disease, open or arthroscopic procedures to the lateral side of the elbow, radial head resection, or coronoid insufficiency [5, 8–13].

Physical exam of the elbow can help elucidate the etiology of the condition in addition to making the diagnosis. The elbow should be examined superficially, noticing possible scars as a sign of previous surgical procedures or signs of past trauma. On examination, there are multiple tests that have been cited to help diagnose PLRI and an incompetent LUCL. The first and best of these is the lateral pivot-shift test of the elbow. This test, first described by O'Driscoll et al., can be performed in the supine, sitting, or prone position and will elicit gross instability or simply pain and apprehension [3]. The senior author's preferred method for performing this test is to examine the elbow with the patient in the prone position and use the table as a base to stabilize the humerus. Begin by manually rotating the forearm with the elbow in 90 degrees of flexion, palpating the radiocapitellar joint and using the wrist to supinate the forearm. This movement reproduces the radial column subluxation as the forearm rotates away from the humerus. The radial head movement on the capitellum is more easily seen and felt in this position, and the elbow can be flexed and extended while maintaining the subluxation force.

Two additional clinical tests have been described by Regan and Lapner, and are also useful in the diagnosis of PLRI [14]. The chair push-up test is performed with the patient pushing up from an armchair with the palms facing inward and forearms supinated. The table-top relocation test requires the patient to push up from a prone or wall-leaning position first with the forearms maximally pronated and then repeating the test with the forearms maximally supinated. The tests are considered positive when they reproduce the patient's pain, instability, or both.

Lastly, in more subtle instability patients flexing the elbow to 100–110° and then applying a gentle valgus force while supinating the forearm may reproduce a palpable shift of the radial head on the capitellum that can be palpated by the examiner's thumb that is positioned on the posterior aspect of the radiocapitellar joint.

Imaging studies for PLRI can help to confirm the diagnosis. Radiographs are often normal, but, in acute cases, may reveal an avulsion fragment from the posterior aspect of the lateral epicondyle of the humerus (Fig. 14.1). A stress radiograph or fluoroscopy while performing the pivot-shift test may show the radial head and proximal ulna moving together in a subluxated and posterolaterally rotated position. Magnetic resonance imaging (MRI) of the elbow has been described to identify a lesion in the lateral ulnar collateral ligament (LUCL) [15]. MRI arthrogra-

phy is the best modality to identify lesions to the medial and lateral collateral ligaments (Fig. 14.2).

Contraindications may include prior radial head resection, infection, or lack of understanding of the surgical anatomy of the ligamentous structure of the lateral elbow.

Fig. 14.1 Bone avulsion (arrow) of the humeral attachment of the radial ulnohumeral ligament with the fragment displaced into the elbow joint

14.3 Surgical Technique

The equipment needed includes suture anchors as well as standard arthroscopy equipment including a 4.0 mm 30-degree arthroscope. Additional equipment needed for surgical repair or reconstruction are outlined in Table 14.1, but may include suture retrievers and suture shuttles.

Table 14.1 Equipment for arthroscopic technique

• Sterile tourniquet
• 18-gauge spinal needle
• Motorized shaver
• Rasp
• Hewson suture passer
• No. 2 braided, nonabsorbable suture
• Implants (tendon allograft if not using autograft)
• Double- or triple-loaded suture anchors
• 4 mm 30-degree arthroscope
• Interchangeable arthroscopic cannulas
• Retrograde suture retriever
• Suture grasper
• Arthroscopic knot pusher
• Suture for skin closure (surgeon preference)
• Dressing and splint material

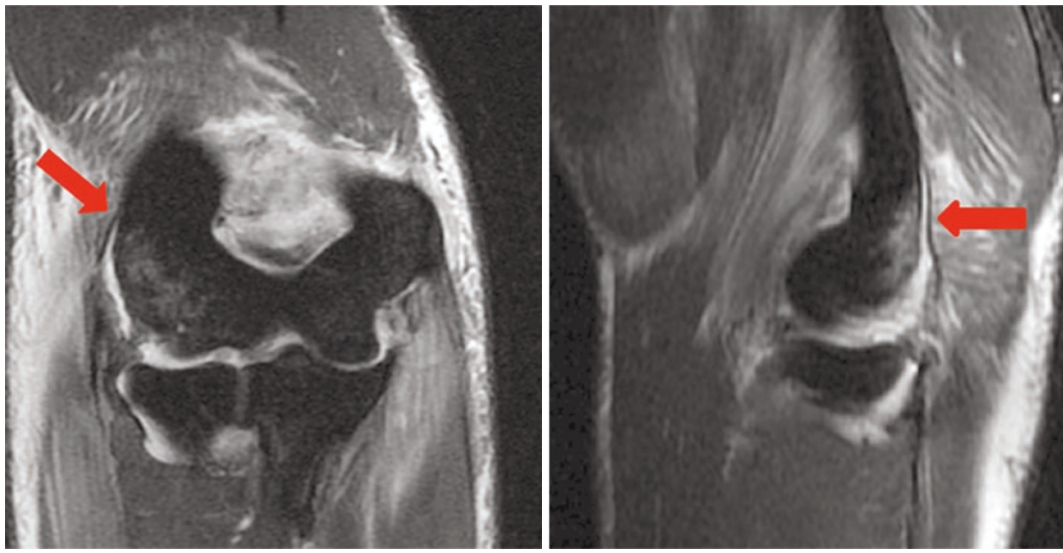

Fig. 14.2 Magnetic resonance imaging showing a complete tear of the lateral ligament complex

14.3.1 Arthroscopic LUCL Repair

Arthroscopic repair can be performed in the lateral decubitus or prone position (author's preferred position).

- The procedure begins with the establishment of a proximal anterior medial portal and a diagnostic arthroscopy of the anterior compartment. Fractures of the radial head or coronoid can be identified. In the acute setting, one may encounter an abundant hematoma and tearing of the anterior capsule. One can often see the damage to the brachialis muscle through the torn capsule (Fig. 14.3). A proximal anterior lateral portal can be positioned to clean out the associated hematoma.
- On the lateral side, laxity of the annular ligament and LCL complex will be evident in every case (Fig. 14.4). Occasionally, the entire LCL complex will be flipped into the radiocapitellar joint. It is important to view the annular ligament for damage and place a suture in it if necessary.
- Valgus load and forearm supination demonstrate PLRI with the radial head subluxating off the capitellum, indicative of injury to the LUCL. On the medial side, an arthroscopic valgus stress test can be performed to evaluate the incompetence of the medial ulnar collateral ligament [16].

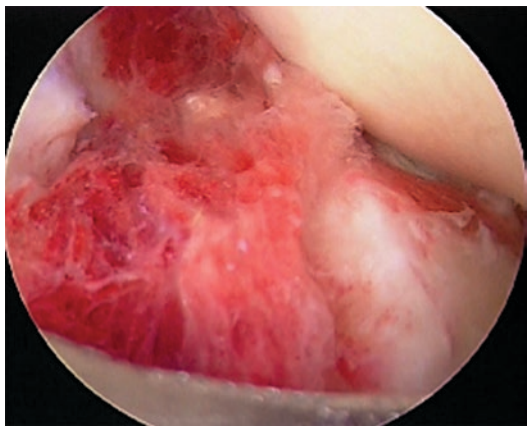

Fig. 14.3 A traumatic tear of the anterior elbow capsule as part of an acute elbow dislocation, revealing the damaged brachialis muscle

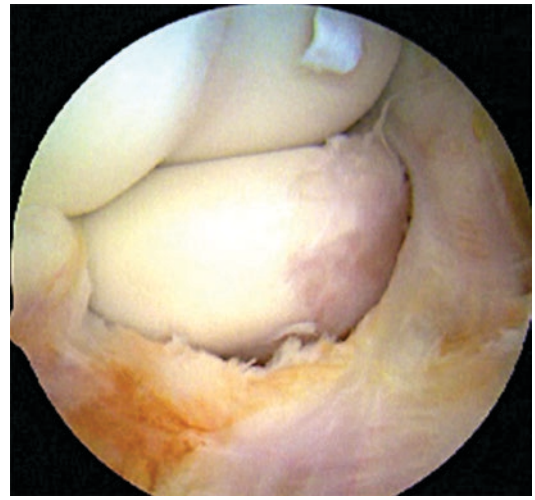

Fig. 14.4 In the initial view of the anterior compartment, the laxity of the annular ligament and associated chondral damage to radial head from chronic instability is seen

- The arthroscope is then moved into the posterior compartment via a posterocentral portal, and the inflow is via the proximal anteromedial portal so that the flow circulates through the radiocapitellar joint and out the arthroscope. A proximal posterolateral portal is established 2–3 cm proximal to the tip of the ulna to allow a superior view and instrumentation. Both of these portals need to be relatively proximal to allow for the later repair of the ligament, usually at least 3 cm above the olecranon tip.
- In PLRI, one common finding is the ability to move an arthroscope placed down the posterolateral gutter from the posterior central portal straight across the ulnohumeral articulation into the medial gutter. This maneuver is not possible in a stable elbow and is termed the "drive-through sign of the elbow" (Fig. 14.5). The elimination of the laxity that allows this maneuver is one of the key aspects of confirming an adequate arthroscopic reconstruction in patients with PLRI.
- The lateral gutter and capsule are evaluated next. The arthroscope is easily advanced down the lateral gutter, owing to incompetence of the LCL complex. It is important to stay close to the ulna as the lateral gutter is evaluated and

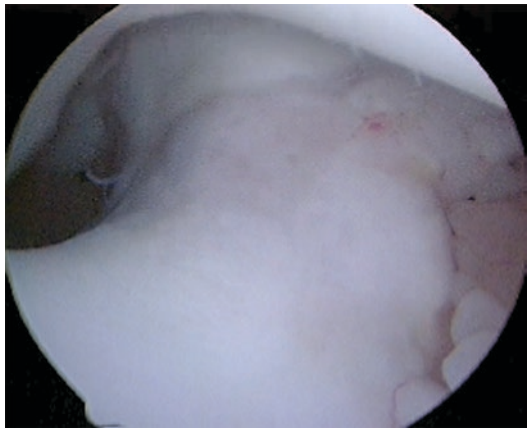

Fig. 14.5 In instability cases, the arthroscope can be shifted from the lateral gutter to the medial gutter ("drive-through" sign). Here the distal humerus is superior and the entire ulnohumeral articulation can be visualized. The medial gutter is seen to the left and the lateral gutter to the right

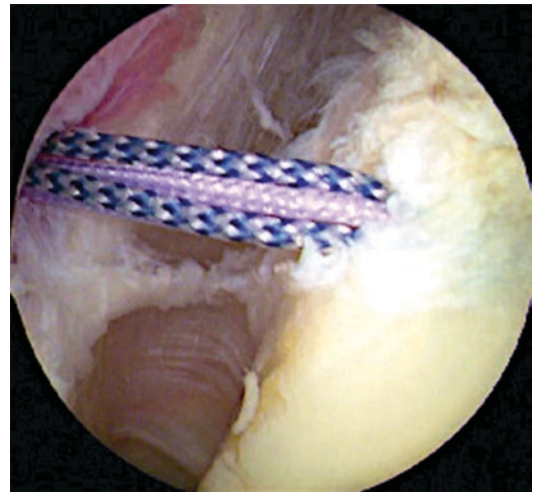

Fig. 14.7 The point of ligament avulsion is easily seen arthroscopically in instability cases. The edge of the proximal RUHL is seen just below the sutures and the humerus is to the right

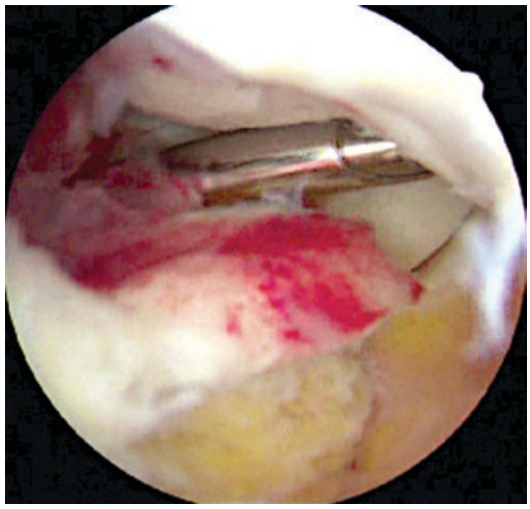

Fig. 14.6 Arthroscopic view from the posterior central portal shows the bone fragment with attached RUHL interposed within the posterior elbow joint. This is the fragment seen on the radiograph in Fig. 14.2

the hematoma debrided, as the avulsed ligament and bone fragments are displaced distally, often into the joint, and may inadvertently be removed by the shaver (Fig. 14.6).

- The origin of the LCL complex on the posterior aspect of the lateral epicondyle can be visualized as a bare area where the ligament has avulsed off of the humerus. It is usually directly lateral and slightly inferior to the center of the olecranon fossa. This area on the posterior humerus should be lightly debrided with a motorized shaver. Once the area of damage has been defined, an arthroscopic anchor may be placed into the humerus at the site of origin of the LUCL (Fig. 14.7).
- A percutaneous suture passer is placed through a "soft-spot" portal to retrieve the sutures. The limbs of the suture are retrieved to place two horizontal mattress sutures through the non-injured part of the ligament (Fig. 14.8a, b). In the case of a bony avulsion, one set of sutures is placed around the bone fragment and the other distal to the fragment.
- The sutures are tensioned while viewing with the arthroscope down the lateral gutter, which should have the effect of pushing the arthroscope out of the lateral gutter as tension is restored to the LCL complex. The elbow is extended to approximately 30° and the sutures are tied beneath the anconeus muscle, tightening the ligament. Motion and stability are evaluated with the arthroscope back in the anterior compartment, confirming that tension has been restored to the annular ligament (Fig. 14.9).

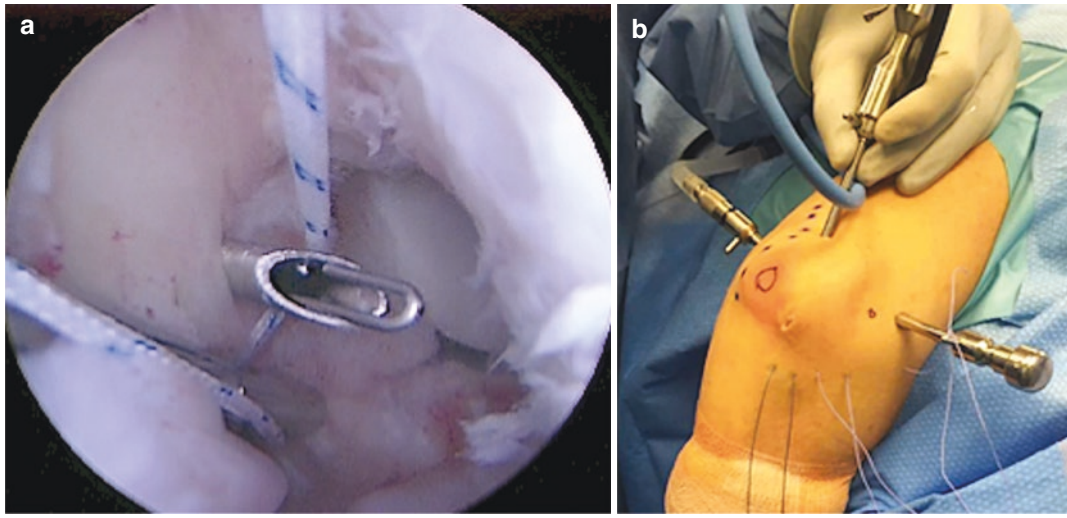

Fig. 14.8 (**a**) A retrograde suture retriever can be seen coming in through the ligament and preparing to retrieve the suture. (**b**) External view of multiple sutures after retrieval through the ligament and capsule and before retrieval under the skin

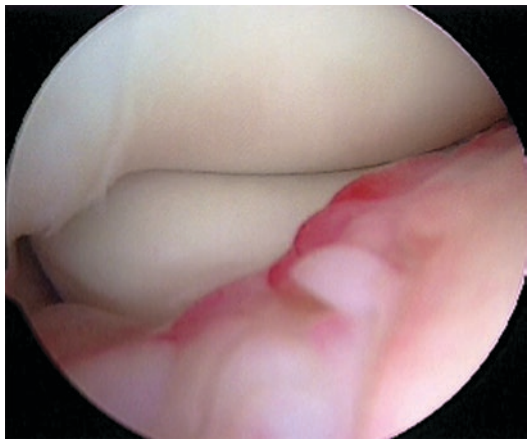

Fig. 14.9 In this view from proximal anterior medial portal, the restored annular ligament is visualized, indicating a satisfactory restoration of the entire lateral ligament complex

14.3.2 Arthroscopic Plication

The development of an arthroscopic technique for the treatment of chronic PLRI was described by Smith et al. in 2001 [17]. Chronic posterolateral instability is more readily seen during examination under anesthesia and during arthroscopic evaluation. While viewing from the proximal anterior medial portal, the ulna and radial head can be seen to subluxate posterolaterally during the performance of a pivot-shift test. In most cases, the annular ligament is intact as the entire proximal radioulnar joint shifts on the humerus.

The arthroscopic technique for chronic instability has two key features: plication of the two major components of the complex and repair of the complex to the humerus [18]. Both components can be managed by arthroscopic techniques if there is enough ligamentous and capsular tissue. This assessment is, in part, determined by the preoperative evaluation, including palpation of the structures in the area to be reconstructed, the amount of prior surgery, and the tissue present on MRI arthrography.

- If adequate lateral tissue is present, the tissue in the posterolateral gutter is assessed arthroscopically and prepared with a shaver or rasp.
- Four to seven absorbable sutures are then placed in oblique manner beginning at the most distal extent of the LUCL complex attached to the ulna.
- The sutures are placed into the lateral gutter using an 18-gauge spinal needle that slides along the radial border of the ulna. The first suture is delivered into the joint through the midportion of the annular ligament.

Subsequent sutures are brought into the joint in a progressively more proximal position.

- Each suture is immediately retrieved with a retrograde suture retriever that passes into the joint from the posterior lateral aspect of the lateral epicondyle (Fig. 14.10a and b). It is important that the retrograde retriever comes under the entire LUCL near its proximal attachment to the humerus.
- Once all the sutures have been placed, they are retrieved one at a time percutaneously through the existing skin portals and pulled to tension the sutures and evaluate the plication. If the repair has been properly performed and the tissue is adequate for plication, the arthroscope is driven out of the lateral gutter as this tensioning occurs (Fig. 14.11a).

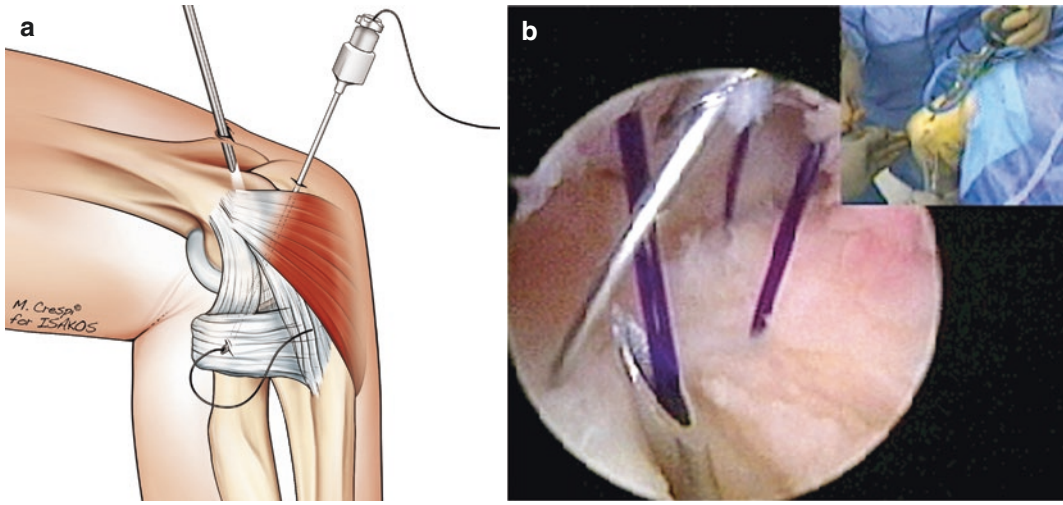

Fig. 14.10 (**a**) Suture passage for arthroscopic plication is illustrated. (**b**) In this view of the lateral gutter in chronic PLRI patient the multiple plication stitches can be seen traversing the lateral capsule and ligaments (M. Crespi © for ISAKOS)

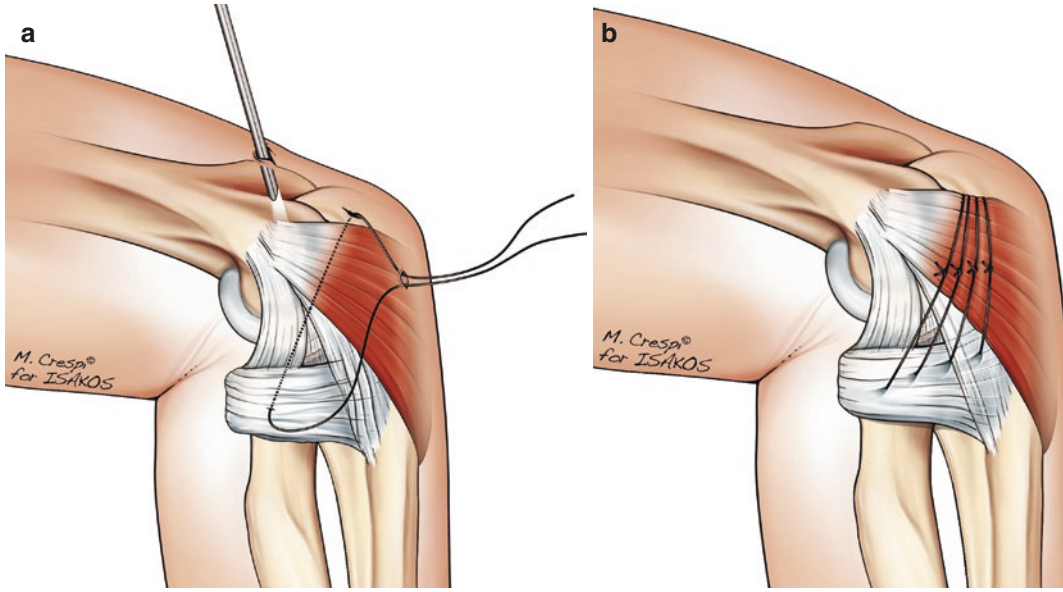

Fig. 14.11 (**a**) Sutures are seen retrieved percutaneously through the soft-spot portal. (**b**) Sutures are tied to retention in the lateral ligaments (M. Crespi © for ISAKOS)

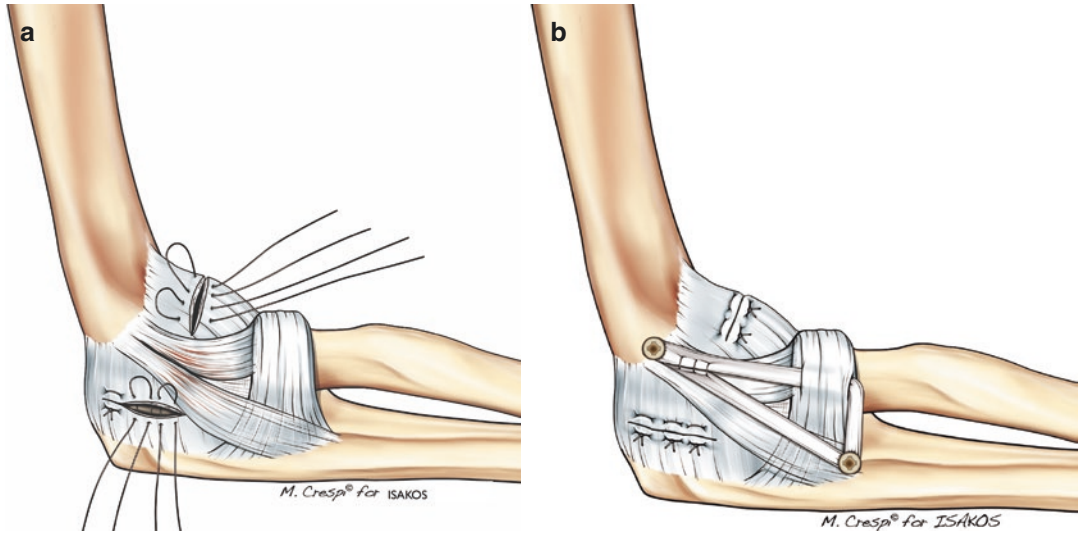

Fig. 14.12 (**a**) Surgical technique of open repair when tissue is adequate. (**b**) Surgical technique of open graft reconstruction when tissue is inadequate (M. Crespi © for ISAKOS)

- The arthroscope is removed, the elbow extended, and the sutures are tied individually from distal to proximal (Fig. 14.11b).
- Arthroscopic examination of the radiocapitellar joint is repeated with the arthroscope placed first in the posterior central portal and then in the proximal anterior medial portal, using the pivot-shift test to evaluate the adequacy of the repair. If there is laxity or subluxation still present after the sutures are pretensioned, an anchor can be placed at the isometric point of the lateral epicondyle to further tension the LCL complex to the humerus.
- An anchor is placed in the acute repairs, and one limb of suture is passed under all of the loops of the plication sutures to a retriever and then retrieved back over the plicated sutures to pull the entire plicated complex back to the humerus. This is usually noted as part of the preoperative planning and is accomplished before the plication sutures are tied.

14.3.3 Open Technique

The open technique for plication and repair is similar to that described by O'Driscoll et al. [3].

- A diagnostic arthroscopy may be performed to confirm the presence of instability and the absence of associated pathology, such as loose osteochondral fragments. A posterolateral approach is used and the anconeus muscle is split and retracted to access the LUCL complex. If adequate tissue is found to allow repair, the ligaments are plicated and repaired back to the humerus as described in the above section on arthroscopic repair (Fig. 14.12a).
- In revision surgery, or in patients with inadequate tissue for repair, a palmaris autograft or gracilis allograft may be used to reconstruct the lateral ligament complex. The supinator crest of the ulna, just posterior to the radial neck, is dissected free and the insertion site identified. A 4 mm bone tunnel is created at the supinator crest, at the ulnar attachment of the LUCL, and the midportion of the graft is secured into the ulna using an interference screw technique. Alternatively, a double-loaded suture anchor may be placed into the insertion site and the midportion of the graft sewn into the ulna. The two free graft limbs are then brought proximally, pulling one under the annular ligament and one over the ligament, and attached to the isometric point on the posterior aspect of the lateral epicondyle

(Fig. 14.12b). Bringing one limb of the graft under the annular ligament creates a more anatomic reconstruction, with the added benefit of increasing stability of the proximal radioulnar joint. The graft should be slightly lax in extension and should tighten with flexion.

14.4 Tips and Tricks

- Portal placement for the arthroscopic techniques is one key, as is having the flow from anterior rather than via the arthroscope.
- Anterior flow allows easy visualization of the pathology, while flow via the arthroscope will displace the ligaments away from the field and prevent accurate assessment of the anatomical structures.

14.5 Pitfalls

Surgical efficiency, to obtain the repair, is also critical. As with any ligament repair, isometry is critical. Nonanatomical placement can result in loss of motion.

14.6 Postoperative Management and Rehabilitation

Following both acute repair and chronic reconstruction, patients are immediately placed into a splint or hinged brace with the elbow in approximately 30 degrees of extension to relax tension on the repair. Fluoroscopy or radiographs should be obtained to check the reduction after the splint or brace is applied, as additional flexion may be necessary to tighten the reconstruction and keep the joint reduced. The first postoperative visit usually takes place within 3–5 days of the surgery, and the patient is placed into a hinged elbow brace that allows comfortable movement, usually 0–45°. Shoulder, periscapular, wrist, and hand exercises are allowed as long as they do not produce pain in the elbow.

The patient is seen at 2-week intervals postoperatively and motion is slowly increased 10–20° per week as pain and swelling allow. Physical therapy is initiated at 6–8 weeks postoperatively to include upper extremity and core-strengthening exercises with the elbow brace in place. Full range of motion of the elbow should be obtained by 8 weeks, if not sooner. Depending on individual progression, patients are allowed to start strengthening exercises out of the brace at 10–12 weeks. They must be able to perform all strengthening exercises pain-free in the brace, before progression out of the brace.

In the acute repair we allow a return to sport in 2–3 weeks in the elbow brace and rapidly allow full motion by 4–6 weeks postoperatively, moving through rehabilitation stages much more rapidly.

14.7 Results

Savoie and colleagues reported a retrospective review on 54 patients with PLRI who underwent surgical repair [18, 19]. Forty-one patients (20 arthroscopic and 21 open) had a combined plication and repair; 10 patients (6 open, 4 arthroscopic) had acute or subacute repairs for recurrent elbow instability, and 3 patients (all open) were reconstructed with a free tendon graft. The average follow-up was 41 months (range 12–103 months). Overall, Andrews-Carson scores for all repairs improved from 145 to 180 ($P < 0.0001$). Subdividing the technique revealed that arthroscopic repairs improved from 146 to 176 ($P = 0.0001$) and open repairs 144 to 182 ($P < 0.001$). Acute repairs performed the best, with 9 of 10 returning to normal activities. There was no statistically significant difference between the results of open versus arthroscopic repair.

References

1. Mehlhoff TL, Noble PC, Bennett JB, Tullos HS. Simple dislocation of the elbow in the adult. Results after closed treatment. J Bone Joint Surg Am.

1988;70(2):244–9. https://www.ncbi.nlm.nih.gov/pubmed/3343270. Accessed 1 Feb 1988.
2. Stoneback JW, Owens BD, Sykes J, Athwal GS, Pointer L, Wolf JM. Incidence of elbow dislocations in the United States population. J Bone Joint Surg Am. 2012;94(3):240–5. https://doi.org/10.2106/JBJS.J.01663.
3. O'Driscoll SW, Bell DF, Morrey BF. Posterolateral rotatory instability of the elbow. J Bone Joint Surg Am. 1991;73(3):440–6. https://www.ncbi.nlm.nih.gov/pubmed/2002081. Accessed 1 Mar 1991.
4. O'Driscoll SW. Classification and evaluation of recurrent instability of the elbow. Clin Orthop Relat Res. 2000;370:34–43. https://doi.org/10.1097/00003086-200001000-00005.
5. Anakwenze OA, Kancherla VK, Iyengar J, Ahmad CS, Levine WN. Posterolateral rotatory instability of the elbow. Am J Sports Med. 2014;42(2):485–91. https://doi.org/10.1177/0363546513494579.
6. O'Brien MJ, Savoie FH. Arthroscopic and open management of posterolateral rotatory instability of the elbow. Sports Med Arthrosc Rev. 2014;22(3):194–200. https://doi.org/10.1097/JSA.0000000000000029.
7. Epidemiology of elbow dislocations in high school athletes. https://www.ncbi.nlm.nih.gov/pubmed/26546303.
8. Charalambous CP, Stanley JK. Posterolateral rotatory instability of the elbow. J Bone Joint Surg Br. 2008;90(3):272–9. https://doi.org/10.1302/0301-620X.90B3.19868.
9. Cohen MS, Hastings H. Rotatory instability of the elbow. The anatomy and role of the lateral stabilizers. J Bone Joint Surg Am. 1997;79(2):225–33. https://www.ncbi.nlm.nih.gov/pubmed/9052544. Accessed 1 Feb 1997.
10. Dzugan SS, Savoie FH, Field LD, O'Brien MJ, You Z. Acute radial ulno-humeral ligament injury in patients with chronic lateral epicondylitis: an observational report. J Shoulder Elbow Surg. 2012;21(12):1651–5. https://doi.org/10.1016/j.jse.2012.04.008.
11. Hall JA, McKee MD. Posterolateral rotatory instability of the elbow following radial head resection. J Bone Joint Surg Am. 2005;87(7):1571–9. https://doi.org/10.2106/JBJS.D.02829.
12. Kalainov DM, Cohen MS. Posterolateral rotatory instability of the elbow in association with lateral epicondylitis. A report of three cases. J Bone Joint Surg Am. 2005;87(5):1120–5. https://doi.org/10.2106/JBJS.D.02293.
13. Okazaki M, Takayama S, Seki A, Ikegami H, Nakamura T. Posterolateral rotatory instability of the elbow with insufficient coronoid process of the ulna: a report of 3 patients. J Hand Surg. 2007;32(2):236–9. https://doi.org/10.1016/j.jhsa.2006.11.001.
14. Regan W, Lapner PC. Prospective evaluation of two diagnostic apprehension signs for posterolateral instability of the elbow. J Shoulder Elbow Surg. 2006;15(3):344–6. https://doi.org/10.1016/j.jse.2005.03.009.
15. Potter HG, Weiland AJ, Schatz JA, Paletta GA, Hotchkiss RN. Posterolateral rotatory instability of the elbow: usefulness of MR imaging in diagnosis. Radiology. 1997;204(1):185–9. https://doi.org/10.1148/radiology.204.1.9205244.
16. O'Driscoll SWM, Lawton RL, Smith AM. The "moving valgus stress test" for medial collateral ligament tears of the elbow. Am J Sports Med. 2005;33(2):231–9.
17. Smith JP, Savoie FH, Field LD. Posterolateral rotatory instability of the elbow. Clin Sports Med. 2001;20(1):47–58. https://www.ncbi.nlm.nih.gov/pubmed/11227708. Accessed 1 Jan 2001.
18. Savoie FH, Field LD, Gurley DJ. Arthroscopic and open radial ulnohumeral ligament reconstruction for posterolateral rotatory instability of the elbow. Hand Clin. 2009;25(3):323–9. https://doi.org/10.1016/j.hcl.2009.05.010.
19. Savoie FH, O'Brien MJ, Field LD, Gurley DJ. Arthroscopic and open radial ulnohumeral ligament reconstruction for posterolateral rotatory instability of the elbow. Clin Sports Med. 2010;29(4):611–8. https://doi.org/10.1016/j.csm.2010.06.008.

Arthroscopic Lateral Collateral Ligament Imbrication

15

Christina J. Lorenz and Roger P. van Riet

15.1 Introduction

The most frequent cause of injury or deficiency of the lateral collateral ligament complex (LCLC) is a simple dislocation of the elbow. Other mechanisms include repeated cortisone injections for lateral epicondylitis and iatrogenic damage during surgery in this area.

Posterolateral rotatory instability (PLRI) of the elbow was first described in 1991 by O'Driscoll et al. [1] and is the result of a disruption of the lateral ulnar collateral ligament (LUCL). Symptomatic PLRI occurs, when both the radial collateral ligament (RCL) and LUCL are disrupted.

Patients usually present with a feeling of instability, snapping, or clicking during movement, as well as lateral elbow pain. A variety of clinical tests have been described. It is important to combine these tests as none have a 100% sensitivity or specificity. MRI scans may show a ruptured ligament or scarring on the lateral side of the elbow, as well as cartilage injury.

A simple dislocation can usually be treated conservatively with good clinical results. However, in some patients the lateral structures may not heal and these patients can develop chronic PLRI. In this chapter we present our arthroscopic technique for imbrication of the LUCL.

15.2 Surgical Anatomy

The lateral collateral ligament complex (LCLC) is comprised of three parts. The annular ligament (AL) attaches to the anterior and posterior aspects of the lesser sigmoid notch of ulna. The AL is intact in patients with PLRI but sagging of AL can often be found. The radial collateral ligament (RCL) inserts on the lateral epicondyle and its fibers coalesce with fibers of the AL distally. Sagging of AL is caused by rupture or avulsion of the combined insertion of RCL and LUCL. Together with the trochlea and coronoid process, RCL is responsible for varus stability of the elbow. LUCL shares its insertion at the lateral epicondyle with the RCL, runs over and into the AL, and inserts at the supinator crest of the ulna. The anconeus is a small muscle overlying the LCLC and the posterolateral capsule. It may play a small role in lateral stability, but its specific purpose remains unclear at the moment. In the

C. J. Lorenz
AZ Monica, Antwerp, Belgium

Department of Trauma-, Hand-, Plastic- and Reconstructive Surgery (Surgery II), University Hospital Wuerzburg, Wuerzburg, Germany

R. P. van Riet (✉)
AZ Monica, Antwerp, Belgium

University Hospital Antwerp, Edegem, Belgium
e-mail: drrogervanriet@azmonica.be

© ISAKOS 2022

D. N. Bhatia et al. (eds.), *Arthroscopy and Endoscopy of the Elbow, Wrist and Hand*,
https://doi.org/10.1007/978-3-030-79423-1_15

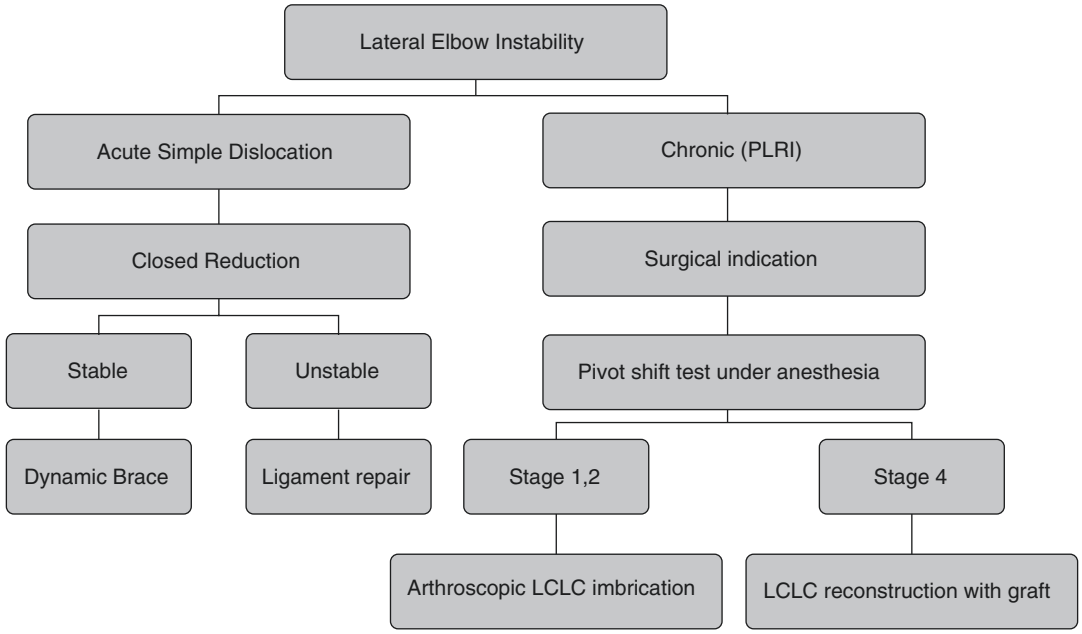

Fig. 15.1 Algorithm for the treatment of lateral elbow instability. *PLRI* Posterolateral rotatory instability, *LCLC* lateral collateral ligament complex (Courtesy of MoRe Foundation)

surgical procedure presented in this chapter, an imbrication of LUCL, together with the lateral capsule, and anconeus is performed.

15.3 Indications and Contraindications

The management algorithm for lateral instability is shown in Fig. 15.1 [2].

Chronic symptomatic PLRI (stages 1–2) that is refractory to conservative treatment can be treated with arthroscopic LCLC imbrication.

The procedure is contraindicated in severe posterolateral rotatory instability and bony instability, and these should be managed with more conventional stabilization procedures.

15.4 Surgical Technique

Under general anesthesia, range of motion (ROM) and stability are tested and documented. The patient is placed in a lateral decubitus position with the arm over a support, making sure that there is no compression on the antecubital space. The elbow joint is then insufflated with about 30 mL of saline. As the capsule is usually loose, a relatively high volume of saline is needed to achieve optimal insufflation.

- An anteromedial viewing portal is made, and the anterior compartment of the elbow is inspected. If necessary, an anterolateral working portal is made under direct view. A needle is used to position this portal.
- A standard diagnostic elbow arthroscopy is performed and associated pathologies are addressed. Axial traction with and without varus stress will show an opening of the radiocapitellar joint. An indirect sign of laxity is a noticeable sagging of the annular ligament.
- A posterolateral portal is made, and the arthroscope is brought into the posterior compartment. The arthroscope is directed to the ulnar gutter and valgus stress is applied to test the integrity of the medial collateral ligament (MCL). A drive-through sign may be present. The tip of the olecranon and the olecranon fossa are inspected before directing the scope into the

lateral gutter. A needle is used to verify the position of the soft-spot portal. The arthroscopic rotatory instability (ARI) test is performed: the forearm is supinated and varus stress together with axial traction is applied. This will then open the radiohumeral joint and the radial head will subluxate posterior to the capitellum [3].

- A 14G needle is loaded with a no. 2 PDS suture. The needle is then inserted into the center of the lateral epicondyle and directed towards the radiohumeral gutter (Fig. 15.2a). The suture is shuttled into the radiohumeral gutter and pulled out of the soft-spot portal with a grasper (Fig. 15.2b).

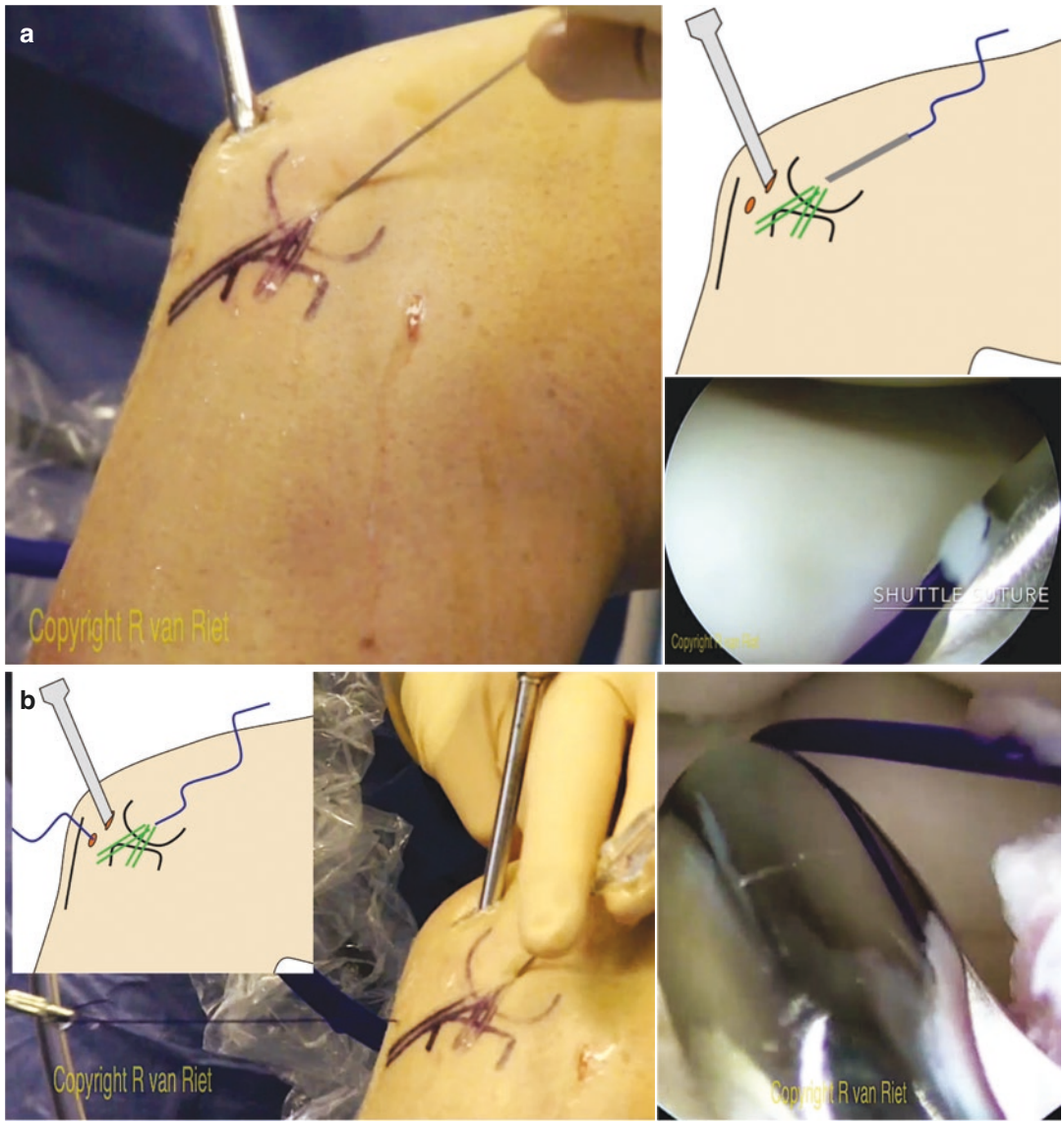

Fig. 15.2 (**a**) A 14G needle is used to shuttle a PDS suture from the origin of the LUCL into the radial gutter (Courtesy of MoRe Foundation). (**b**) The distal end of the suture exits the joint through the soft-spot portal (Courtesy of MoRe Foundation)

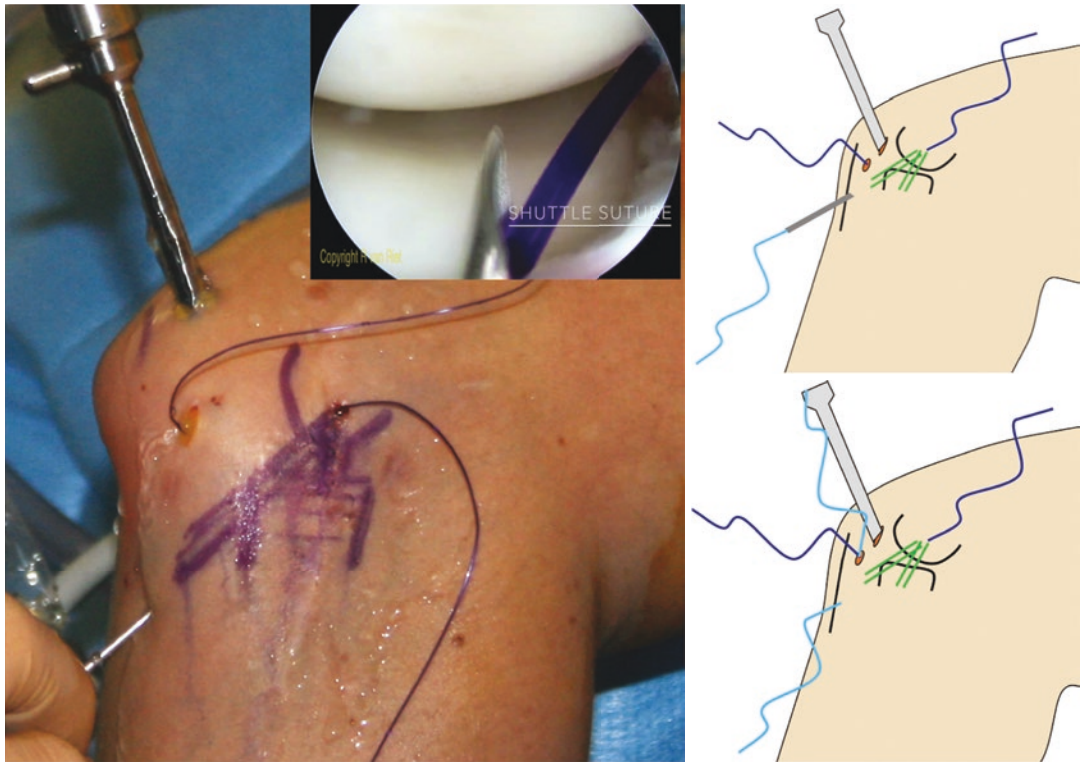

Fig. 15.3 A second suture is brought into the radial gutter from the subcutaneous border of the ulna, through the insertion of the LUCL, and is retrieved through the soft-spot portal. The ends of both sutures exit the joint through the soft-spot portal (Courtesy of MoRe Foundation)

- The needle is removed and reloaded with a second PDS suture. This is now inserted into the skin at the subcutaneous border of the ulna just distal to the radial head and aimed towards the radial gutter, passing through the insertion of the LUCL. It is important to stay close to the bone while inserting the needle. This will strengthen the imbrication, and will keep the needle and suture away from the neuromuscular structures. This suture is also pulled out by a grasper through the soft-spot portal (Fig. 15.3).
- There are now two PDS sutures in place. One enters the skin from the insertion of the LUCL on the lateral epicondyle, runs through the capsule and the LCLC into the radial gutter, and exits the joint through the soft-spot portal. The second suture enters just distal to the insertion of the LUCL, deep to the anconeus muscle; pierces the capsule and LUCL insertion, into the radial gutter; and also exits the joint through the soft-spot portal. The next step is to tie the suture ends that exit the soft spot together, and when pulled proximally the knot will exit the skin (Fig. 15.4a).
- This suture can now be used as a shuttle to pass a double-PDS suture. For this, a loop is tied into the proximal end of the first PDS, and a new strand is doubled through this loop which can be pulled distally. Now, two strands of PDS run intra-articularly, from the origin to the insertion of the LUCL. The two ends at each side are shuttled subcutaneously out of the soft-spot portal (Fig. 15.4b).
- The sutures are tightened, and stability testing is repeated under direct arthroscopic view. If stability if restored, the arthroscope is removed and the sutures are tied separately with the correct tension. The knots are buried and moved away from the portal. The applied suture now tightens the lateral capsule, the LCL complex, and the anconeus (Fig. 15.5).

Fig. 15.4 (**a**) One suture is shuttled out through the proximal portal (Courtesy of MoRe Foundation). (**b**) A double-PDS suture is shuttled through the proximal and distal needle entry points (Courtesy of MoRe Foundation)

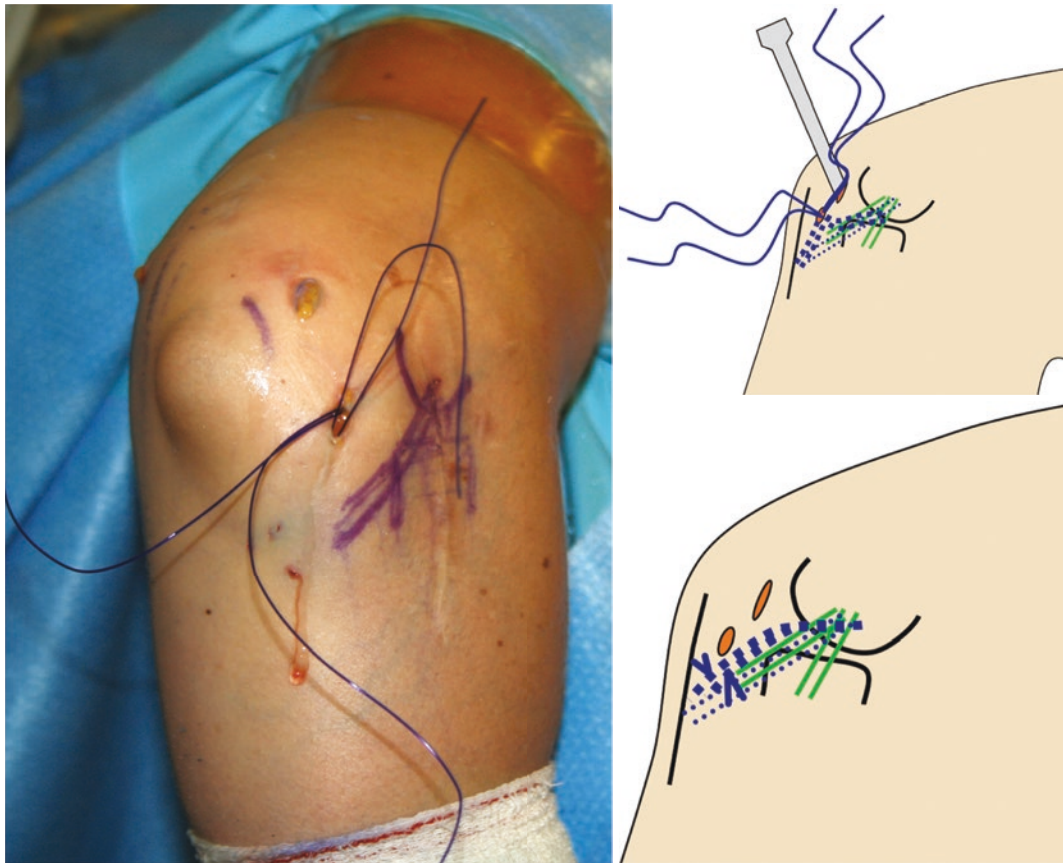

Fig. 15.5 The double-PDS sutures are retrieved subcutaneously through the soft-spot portal and knotted to each other (Courtesy of MoRe Foundation)

15.5 Tips and Tricks

- Address concomitant pathologies during arthroscopy which contributes to instability.
- Use the ARI test to test stability under direct view.
- To gain complete reduction, remove the scope before tightening the sutures.
- To prevent knot irritation, tie the sutures separately and bury them away from the portal.

15.6 Pitfalls

- The PDS suture may break when overtightened.
- For severe instability this method has not been proven to be useful.

15.7 Postoperative Management and Rehabilitation

Starting with the first postoperative day, a dynamic brace is used for a total period of 6 weeks. For the first 2 weeks, extension is allowed up to 60°, followed by 30° for another 2 weeks. Full range of motion is allowed from week 4.

15.8 Complications

- Specific complications related to this type of surgery and trauma include persistent instability, stiffness, and post-traumatic osteoarthritis.

- Patients frequently complain of irritation of the knots. This resolves within 3–6 months, as the suture resorbs.

15.9 Results

In 2001, Smith et al. were the first to report on an arthroscopic technique to treat symptomatic PLRI [4]. Good outcomes of the technique were published in 2009 in a mixed group of 20 patients, and no significant difference was found between open or arthroscopic repair and imbrication [5]. In the first 20 patients treated with the technique presented in this chapter, we found a resolution of instability in 95%, with an average Mayo Elbow Performance Score of 90 [3].

Conflict of Interest Roger P. van Riet has a teaching and speaking agreement with Acumed. The author retains the copyright to images and videos.

References

1. O'Driscoll SW, Bell DF, Morrey BF. Posterolateral rotatory instability of the elbow. J Bone Joint Surg Am. 1991;73(3):440–6.
2. Conti Mica M, Caekebeke P, van Riet R. Lateral collateral ligament injuries of the elbow—chronic posterolateral rotatory instability (PLRI). EFORT Open Rev. 2017;1(12):461–8.
3. Vandenberghe M, van Riet R. Chapter 7–The unstable elbow: from open ligamentoplasty to arthroscopic techniques. In: Antuna S, Barco Laakso, editors. Essential techniques in elbow surgery.
4. Smith JP 3rd, Savoie FH 3rd, Field LD. Posterolateral rotatory instability of the elbow. Clin Sports Med. 2001;20(1):47–58.
5. Savoie FH 3rd, Field LD, Gurley DJ. Arthroscopic and open radial ulnohumeral ligament reconstruction for posterolateral rotatory instability of the elbow. Hand Clin. 2009;25(3):323–9.

Arthroscopic Plication in Medial and Lateral Elbow Instability

16

Francesco Luceri, Davide Cucchi, Joseph Martin Nikhil, Pietro Simone Randelli, and Paolo Arrigoni

16.1 Background

Elbow instability can occur as post-traumatic sequelae or due to chronic overuse syndromes. Patients with chronic instability classically present with pain, apprehension, or mechanical symptoms after movements that result in joint subluxation. Arthroscopic plication of R-LCL and aMCL is an innovative surgical technique that enables an anatomic and minimally invasive ligament retensioning. Several arthroscopic signs of minor elbow instability should be assessed during the procedure and their negativization at the end of the procedure corresponds to a restored stability of the elbow.

Francesco Luceri and Davide Cucchi contributed equally to this work.

Pietro Simone Randelli and Paolo Arrigoni equally contributed to this chapter as Senior Authors.

F. Luceri (✉)
U.O.C. Clinica Ortopedica e Traumatologica Universitaria CTO, Azienda Socio Sanitaria Territoriale Centro Specialistico Ortopedico Traumatologico Gaetano Pini-CTO, Milan, Italy

D. Cucchi
Department of Orthopaedics and Trauma Surgery, Universitätsklinikum Bonn, Bonn, Germany

J. M. Nikhil
Cochin, India

P. S. Randelli · P. Arrigoni
U.O.C. Clinica Ortopedica e Traumatologica Universitaria CTO, Azienda Socio Sanitaria Territoriale Centro Specialistico Ortopedico Traumatologico Gaetano Pini-CTO, Milan, Italy

Research Center for Adult and Pediatric Rheumatic Diseases (RECAP-RD), Department of Biomedical Sciences for Health, Università degli Studi di Milano, Milan, Italy

16.2 Indications and Contraindications

- Arthroscopic assisted MCL plication is indicated in medial elbow pain with valgus instability. This procedure is usually performed after 6 months of failed conservative management. Commonly, the patients report either trauma to the medial side of the elbow or repetitive stretching activity. The surgery may be advised for low-demand patients with instability and with a desire to return to physical activity [1].
- Arthroscopic plication of radial component of LCL is indicated in:
  - Lateral elbow pain recalcitrant to at least 6 months of conservative treatment
  - Arthroscopic confirmation of at least two lateral patholaxity signs or copresence of one lateral patholaxity sign and one pathologic intra-articular finding (see below)

© ISAKOS 2022

D. N. Bhatia et al. (eds.), *Arthroscopy and Endoscopy of the Elbow, Wrist and Hand*,
https://doi.org/10.1007/978-3-030-79423-1_16

16.3 Surgical Techniques

The procedures are generally performed under general anesthesia. Patient is placed in the lateral decubitus position with the involved upper limb flexed over a padded arm support and the forearm hanging free to gravity. Standard arthroscopic portals are established.

16.3.1 Arthroscopically Assisted Plication of Medial Collateral Ligament

- A limited ulnar nerve release is routinely performed through a posteromedial approach. The nerve is isolated for approximately 7 cm proximal and distal to the epicondyle without being displaced or transposed.
- The anterior compartment is addressed first by arthroscopy. Proximal anteromedial and anterolateral portals are created in order to evaluate the anterior joint. The anterior chamber includes the anterior joint capsule with MCL, the distal humerus, the radial head with the annular ligament, and the proximal radioulnar joint.
- Posterior compartment is evaluated via the posterior central portal. A 70° arthroscope is used to visualize the medial gutter and identify the aMCL (identified as capsular thickening) (Fig. 16.1). The ligament usually appears lax and partially degenerated at its proximal insertion, with an increased space between the capsule and the medial epicondyle than in normal situation. A possible sign is the asymmetrical coronoid process, lateralized into the trochlea.
- After this arthroscopic assessment, a medial open approach is performed. A 3–5 cm curved incision centered over the medial epicondyle is performed. A proper ulnar de-roofing is performed in order to identify the nerve and to prevent nerve damage. Care is taken not to destabilize the nerve.
- The common flexor tendon on the medial epicondyle is exposed and is split in its middle third. The flexor muscle mass is separated in the deep portion of the surgical incision to identify lax capsule/aMCL.
- A standard bioabsorbable double-loaded anchor (Lupine, DePuy Synthes, Warsaw, IN) with high-resistance sutures is inserted into the anteroinferior surface of the medial epicondyle with an approximatively inferior-to-superior 45° angle relatively to the intercondylar line (Fig. 16.2). After adequate restraint and preparation of the proximal aMCL, two bioabsorbable sutures are passed through the ligament for plication of 1–1.5 cm of tissue.
- Stability of the aMCL in valgus stress is tested at the end of the plication. The flexor pronator fascia is sutured with simple bioabsorbable sutures. A final arthroscopic reassessment of the medial part of the elbow for any residual

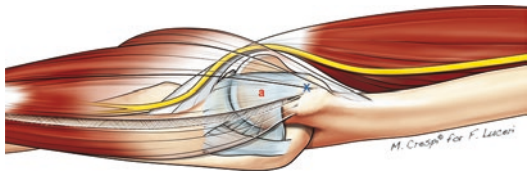

Fig. 16.1 Medial collateral ligament; **a:** anterior bundle of medial collateral ligament; **X:** the standard bioabsorbable double-loaded anchor insertion site into the anteroinferior surface of the medial epicondyle (M. Crespi © for F. Luceri)

Fig. 16.2 Mini-open medial collateral ligament plication: suture anchor positioning

sign of laxity is performed. Tensioning of the plicated aMCL is reassessed and once the articular space between the capsule and the medial epicondyle is successfully restored at the end of the procedure, the coronoid process is re-evaluated to verify whether it is displaced to a more centered position into the trochlea compared with the initial evaluation.

16.3.2 Arthroscopic R-LCL Plication

- The presence of the following three signs of laxity are evaluated at elbow arthroscopy: the annular drive through (ADT), the loose collar sign (LCS), and the R-LCL pull-up sign (RPS). The annular drive through (ADT) is performed by pushing the radial head anteriorly with the surgeon's thumb from posteriorly, while looking with the scope in the posterolateral portal. If this maneuver allows enough space for a 4.2 mm shaver to slide between the radial head and the annular ligament with no or minimal resistance through the soft-spot portal, the ADT is considered positive [2, 3]. A positive loose collar sign (LCS) indicates a characteristic annular ligament that at 90° of flexion lies low on the radial head, so that the radial neck is clearly exposed under the cartilaginous portion when observed from the anteromedial portal. The R-LCL pull-up sign (RPS) is performed while looking from the anteromedial portal, introducing a grasper via the anterolateral portal and pulling the R-LCL to the lateral side of the capitellum. If a vertical (distal to proximal) translation of 1 linear centimeter is possible, the sign is considered positive. Other pathologic findings should also be considered, including synovitis anterior to the radial head, anterolateral capsular tears, and chondropathy of either the radial head or the lateral portion of the capitellum. Patients, who present at least one of the previous signs of minor instability in addition to one or more intra-articular associated lesions, are considered eligible for R-LCL plication (Fig. 16.3).
- To perform arthroscopic R-LCL plication, a dedicated spade drill is introduced via the proximal anterolateral portal under direct visual control from the anteromedial portal; after drilling, a bioabsorbable suture anchor is inserted high and lateral in the anterolateral aspect of the capitellum at the capsular insertion (Fig. 16.4).
- Sutures are then passed into the R-LCL, either using an outside-in shuttling technique with a percutaneous needle or using a suture retriever via the anterolateral portal (Fig. 16.5). Care is taken to pass the sutures beyond a level anterior to the midpoint of the radial head and approximately 0.5 cm proximal to the radiocapitellar joint line.
- Sutures are then retrieved from the anterolateral portal and a standard sliding knot is performed, ensuring that it lies extra-articularly (Fig. 16.6).

Fig. 16.3 Arthroscopic evaluation of the patholaxity of lateral collateral ligament

16.4 Postoperative Rehabilitation and Management

After medial plication, an elbow brace locked at 90° of flexion is placed for just 10 days to allow soft tissues to heal. From days 10 to 20, ROM is limited to a maximum of 30° of extension and free flexion. From day 20, ROM is left free. And patients are encouraged to obtain full passive ROM with physiotherapist assistance. Active wrist, elbow, and shoulder range-of-motion exercises are progressively initiated. After 4 weeks, strengthening exercises are begun. Valgus stress is not allowed until 4 months after surgery. The rehabilitation protocol after R-LCL plication includes the use of a brace in 90° of flexion in the first 2 weeks. During the following weeks, the

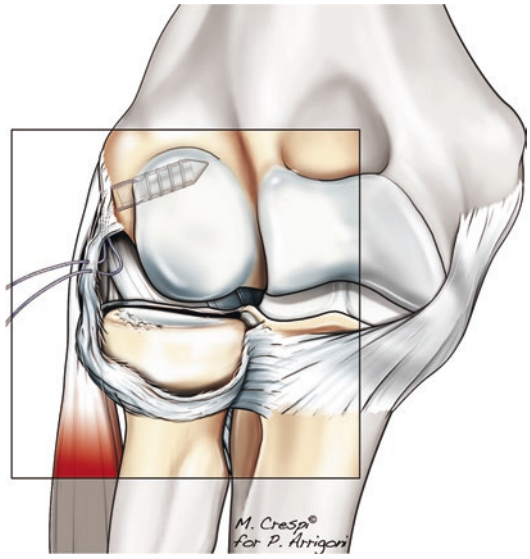

Fig. 16.4 The bioabsorbable suture anchor is inserted high and lateral in the anterolateral aspect of the capitellum at the capsular insertion (M. Crespi © for Arrigoni) (reprinted with permission from Springer Nature Customer Service Centre GmbH: Springer Nature; Surgical Techniques for Trauma and Sports Related Injuries of the Elbow 2020; Arthroscopic Plication of the Radial Component of the Lateral Collateral Ligament (R-LCL) Arrigoni et al. Copyright © 2020, ISAKOS)

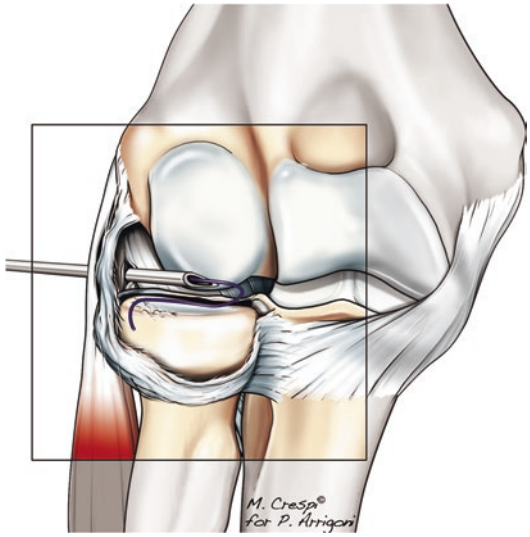

Fig. 16.5 Outside-in shuttling technique with a percutaneous needle via the anterolateral portal (M. Crespi © for Arrigoni) (reprinted with permission from Springer Nature Customer Service Centre GmbH: Springer Nature; Arrigoni et al. [7], in Surgical Techniques for Trauma and Sports Related Injuries of the Elbow; Copyright © 2020, ISAKOS)

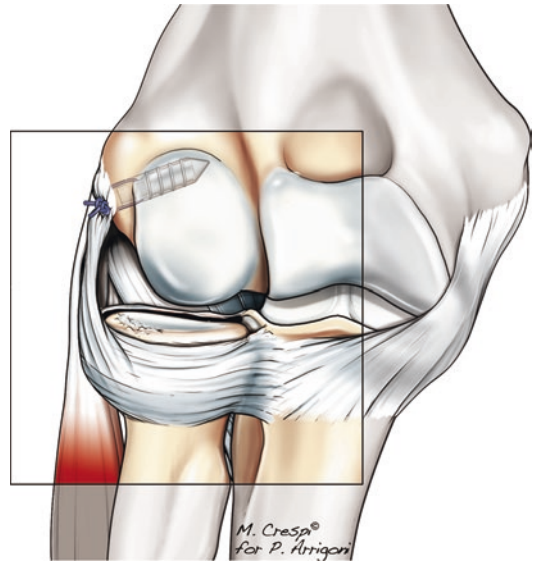

Fig. 16.6 Standard sliding knot for arthroscopic R-LCL plication (M. Crespi © for Arrigoni) (reprinted with permission from Springer Nature Customer Service Centre GmbH: Springer Nature; Arrigoni et al. [7], in Surgical Techniques for Trauma and Sports Related Injuries of the Elbow; Copyright © 2020, ISAKOS)

range of motion (ROM) and strengthening are progressively increased to achieve maximum extension at the sixth week.

References

1. Arrigoni P, Luceri F, Cucchi D, Tamini J, Randelli PS. Reliability of anterior medial collateral ligament plication of the elbow. Musculoskelet Surg. 2018;102:85–91.
2. Cucchi D, Guerra E, Luceri F, Lenich A, Nicoletti S, Randelli P, Wirtz DC, Eygendaal D, Arrigoni P; ESSKA Elbow and Wrist Committee 2016–2018. A combination of an anteromedial, anterolateral and midlateral portals is sufficient for 360° exposure of the radial head for arthroscopic fracture fixation. Knee Surg Sports Traumatol Arthrosc. 2019;27(1):319–25. https://doi.org/10.1007/s00167-018-5077-1. Epub 2018 Aug 1. PMID: 30069651.
3. Arrigoni P, Cucchi D, Luceri F, Menon A, Zaolino C, Zagarella A, Catapano M, Radici M, Migliaccio N, Polli D, Randelli PS. Lateral elbow laxity is affected by the integrity of the radial band of the lateral collateral ligament complex: a cadaveric model with sequential releases and varus stress simulating everyday activities. Am J Sports Med. 2021;49(9):2332–40. https://doi.org/10.1177/03635465211018208. Epub 2021 Jun 11. PMID: 34115528.

17 The Posterolateral Ligament of the Elbow: Surgical Anatomy, Assessment and Repair Technique

Adam C. Watts and Chen G. Tu

17.1 Background

In 1966, Osborne and Cotterill described a case series of 8 patients with recurrent elbow dislocation ascribed to a failure of the posterolateral ligamentous and capsular structures [1]. They identified "an osteochondral fracture in the posterolateral margin of the capitellum" as a key component of this condition. Jeon et al. later termed this abnormality an Osborne-Cotterill lesion (OCL) and described a shear or avulsion fracture of the posterolateral capsular component from the capitellum and lateral condyle readily seen on radiographs [2]. The senior author has observed in his own practice that this posterolateral capsular avulsion injury can occur with very small flakes of bone as with other ligament avulsions around the elbow, or as an isolated soft-tissue avulsion injury. Surgical repair may be necessary in symptomatic patients with signs of posterior radial head instability.

17.1.1 Surgical Anatomy

Historical representations of the elbow identify the lateral and posterior capsule of the elbow as ligamentous structures. Contemporary representations of lateral soft-tissue stabilisers identify four key elements to the lateral ligament complex (radial collateral ligament, annular ligament, lateral ulnar collateral ligament and accessory ulnar collateral ligament) and no stabilising role is attributed to the posterolateral capsule. Observation of posterior capitellar flake avulsion injuries in elbow trauma led to the investigation of the role of the posterolateral joint capsule. Biomechanical studies undertaken have shown that in the otherwise intact elbow, sectioning of the posterolateral ligament alone can cause increase in radial head translation on posterior drawer, in particular in 30–60° of elbow flexion (Fig. 17.1) [3]. The posterolateral capsular component is therefore thought to be an important ligamentous structure, and is termed the "posterolateral ligament (PLL) of the elbow" or Osborne-Cotterill ligament (Fig. 17.2).

The PLL has a triangular origin with a base arising from the posterior and inferior aspect of the lateral epicondyle, a small bony protuberance on the lateral condyle of the humerus and narrowing as it extends posteriorly on to the posterior capitellum. Posteriorly the articular cartilage extends up to the origin of the ligament; therefore, bare bone found in this area indicates an avulsion injury. The ligament travels in a posterior or dorsal direction in a fan shape to insert to the medial border of the greater sigmoid notch. Distally the ligament blends with the posterior fibres of the lateral ulnar collateral ligament (Figs. 17.3 and 17.4).

A. C. Watts (✉) · C. G. Tu
Wrightington Hospital Upper Limb Unit, Wigan, UK

© ISAKOS 2022

D. N. Bhatia et al. (eds.), *Arthroscopy and Endoscopy of the Elbow, Wrist and Hand*,
https://doi.org/10.1007/978-3-030-79423-1_17

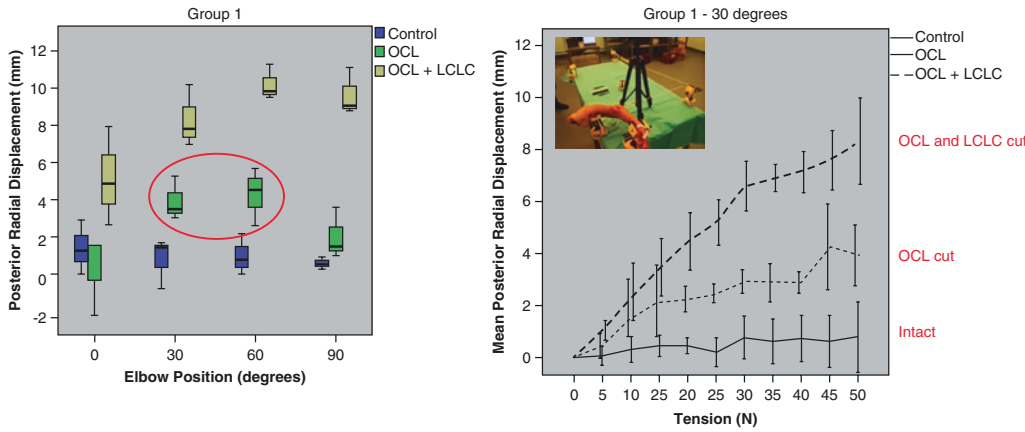

Fig. 17.1 Biomechanical study demonstrating increased posterior draw of the radial head with isolated sectioning of the posterolateral ligament (© Adam Watts)

Fig. 17.2 The significance of posterolateral ligament (PLL) on posterior translation of the radial head is shown in the setting of intact lateral collateral ligament complex (left image: PLL intact, right image: PLL sectioned) (© Adam Watts)

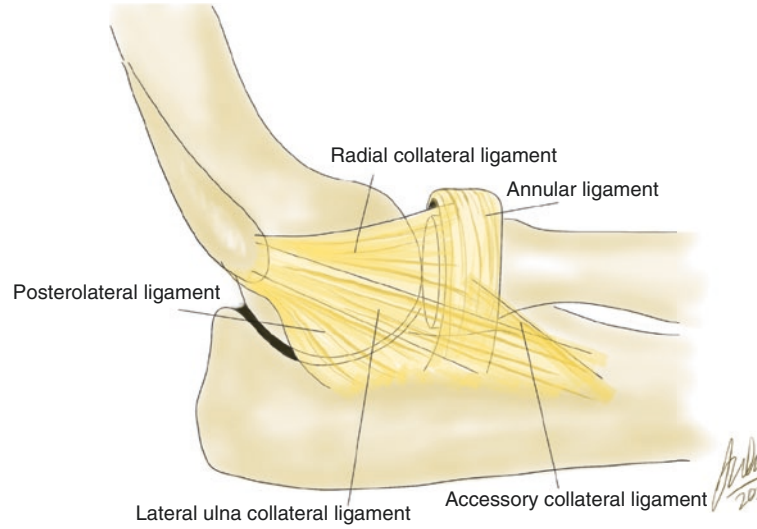

Fig. 17.3 Anatomical drawing showing the lateral ligament complex and posterolateral ligament (© Adam Watts)

17.2 Indications and Contraindications

Avulsion of the posterolateral ligament can affect the stability of the elbow as an isolated injury, as part of a more extensive injury to the lateral collateral ligament complex (LCLC) or as part of an osseoligamentous injury. Acutely the injury may be identified from plain radiographs as a bony avulsion from the posterior capitellum, but many will be missed, and these and more subtle flake avulsion injuries will be identified on computed tomography scans (Fig. 17.4). Magnetic resonance imaging (MRI) is useful to assess soft-tissue injuries, and addition of injected contrast (MRA) can aid diagnosis in later presentations.

A high index of suspicion is required to identify the acute injury. The patient will usually present with a clear history of trauma, either falling on to the outstretched hand or directly on to the elbow. Mechanical symptoms may not be apparent acutely due to swelling and guarding but the patient may report a feeling of instability.

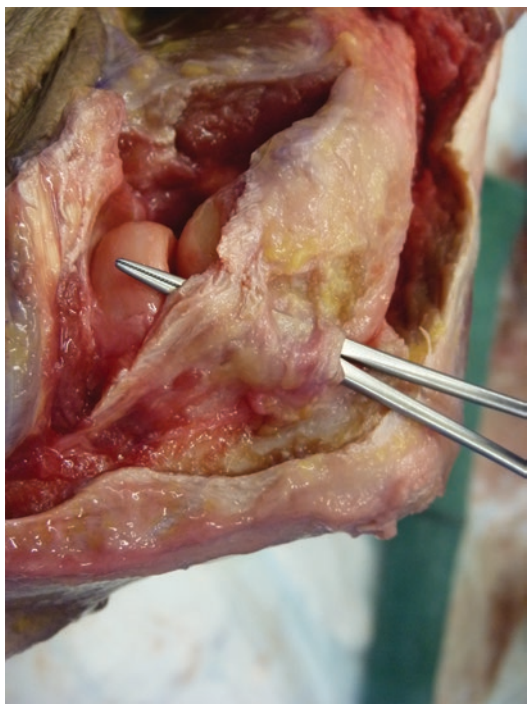

Fig. 17.4 Cadaveric anatomy of the posterolateral ligament (© Adam Watts)

Table 17.1 Two types of PLRI

Type 1	Positive posterior draw	Negative pivot shift	Avulsion posterolateral ligament LUCL intact
Type II	Positive posterior draw	Positive pivot shift	LUCL avulsion ± PLL

Bruising or haematoma on the lateral aspect of the elbow often suggests a high-grade soft-tissue injury as usually the tough lateral fascia will contain haematoma beneath it. The elbow is likely to have a restricted range of flexion and extension. In many cases the injury may be found incidentally during investigation of other injuries. Particular attention should be paid in patients with a history of dislocation, those with radial head fractures and those with terrible triad injuries.

In isolated posterolateral ligament injuries the pivot-shift test is usually negative but posterior drawer test is positive (type 1 PLRI) [4, 5]. A positive pivot shift would suggest a more extensive soft-tissue lesion involving the lateral ligament complex (type 2 PLRI) (Table 17.1). Examination of the acutely injured elbow is challenging; a false-negative pivot-shift test is frequent because of guarding, but it may be possible to elicit a positive posterior drawer by asking the patient to be seated with their injured forearm resting on their lap [6]. The radial head can be gripped between the examiner's thumb and index finger and a posterior force applied. This should be compared to the contralateral side. A positive test is where the dorsal translation of the radial head is increased. Other instability tests such as the push-up test or table-top test are unlikely to be performed successfully in the acute setting but may assist in the diagnosis in delayed presentation [6].

In combined lateral ligament complex (LLC) and posterolateral ligament avulsion, as seen in valgus external rotation injuries, it may be sufficient to repair only the LLC. On occasion, however, it has been noted that increased posterior draw of the radial head is still apparent on the operating table. Repair of the PLL will address this persistent instability.

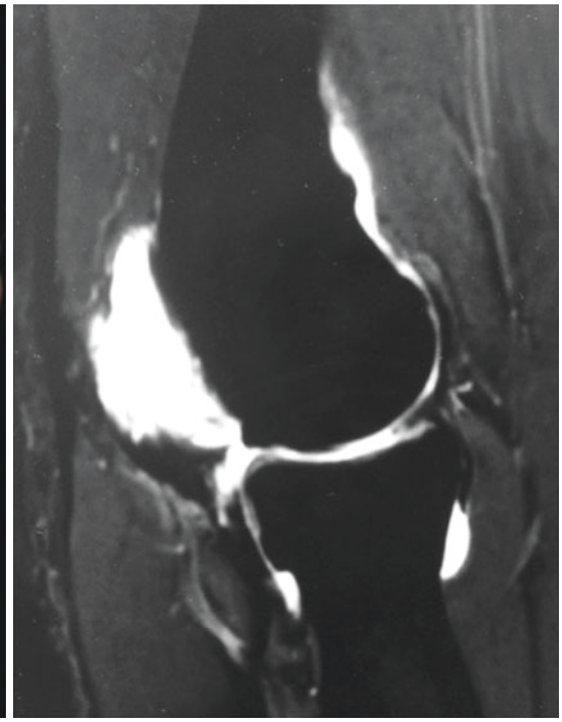

Fig. 17.5 CT scan showing bone fragments from the posterior capitellum, the Osborne-Cotterill lesion, indicating avulsion of the posterolateral ligament (left image). MR arthrogram showing intact bone but soft-tissue stripping of the posterolateral ligament from the posterior capitellum (right image) (© Adam Watts)

Posterolateral ligament and lateral ligament complex injuries are often identified late. The patient may report symptoms of ongoing lateral elbow pain, mechanical symptoms (such as "catching" or "locking") or elbow stiffness. An index of suspicion should be maintained in the patient with an apparently innocuous partial articular radial head fracture who is failing to progress with rehabilitation as expected. Posterior drawer test, table-top test, push-up test and relocation test can all help in the diagnosis [7]. The pivot-shift test is most useful in the anaesthetised patient. An MRA can aid in the diagnosis with the appearance of the "peel-back sign" of the capsule from the posterior capitellum with or without bone avulsion (Fig. 17.5).

PLL injuries may remain undiagnosed. A high proportion of patients with radial head fractures have been found to have lateral ligament complex injuries when subject to an MRI scan but most are not clinically relevant [8, 9]. The authors are not encouraging over-investigation of elbow injuries to look for posterior ligament avulsion, as this will surely lead to overtreatment, but in symptomatic patients with signs of posterior radial head instability it should be considered in the differential diagnosis.

Surgery is not indicated if the patient has stable pain-free movement through a functional range.

17.3 Surgical Technique

Acute PLL injuries can be treated with open or arthroscopic repair.

17.3.1 Open PLL Repair

The injury is usually an avulsion of the humeral origin. The open approach is performed through a Boyd interval [10], which is an internervous plane between anconeus and subcutaneous bor-

Fig. 17.6 Right elbow posterolateral ligament visualised through open surgery. Scissors mark the footprint of the posterolateral ligament, and the posterolateral ligament is held by forceps (left image). The posterolateral ligament of the elbow held in anatomical position at the insertion (right image) (© Adam Watts)

der of ulna. The patient is placed in the lateral decubitus position, under general anaesthesia with a high arm tourniquet, and the arm is placed over a lateral support. Prophylactic antibiotics are administered prior to inflation of the tourniquet.

- A straight 5 cm longitudinal incision is placed over the radial aspect of the olecranon approximately 1 cm from the palpable subcutaneous ulnar ridge.
- The dissection is continued through the investing fascia of the anconeus muscle 1 cm from the ulna, which is then elevated from the muscle towards the ulna bone.
- The Boyd interval between ulna and anconaeus is developed, being careful not to detach the ulna insertion of the LCLC or PLL. A periosteal elevator can be used to gently separate the anconeus from the ligaments.
- The posterolateral ligament defect is usually identifiable but a linear capsulotomy in line with the dissection may be required to enter the joint.
- A bare avulsion footprint will be visible proximal to the articular cartilage on the posterior capitellum (Fig. 17.6a, b). The Osborne-Cotterill lesion is debrided, small loose osteochondral fragments are removed and the joint is irrigated.
- An anchor or transosseous sutures are placed at the footprint of the ligamentous attachment (Fig. 17.7). The suture ends are passed through the posterolateral ligament of the elbow and secured to restore the ligamentous insertion. Large osseous Osborne-Cotterill lesions can

Fig. 17.7 Repair of the ligament with bone anchor into the footprint of the posterolateral ligament is shown (© Adam Watts)

be excised and a ligament repair performed to the floor of the defect or the bone fragment can be secured with a screw and offloaded with sutures passed through the PLL to an anchor placed more proximally in the posterior humerus.

17.3.2 Arthroscopic PLL Repair

For arthroscopic repair patient preparation and positioning are the same as those for open repair.

- After diagnostic anterior arthroscopy and posterior arthroscopy, the lateral compartment is viewed through a proximal lateral portal created just proximal to the midpoint of a line connecting the lateral epicondyle and olecranon process (Fig. 17.8). A direct lateral working portal is made 2 cm distal to this. The two portals can be used interchangeably as viewing and working portals.
- Arthroscopically the footprint is debrided if necessary, and any loose fragments are removed. A loaded anchor can be passed arthroscopically into the footprint of the posterolateral ligament just superior to the capitellum through the direct lateral portal.
- A suture shuttle device is passed through direct lateral portal to the avulsed PLL and one tail of the anchor is delivered through the PLL from deep to superficial. The second suture is grasped in the same manner at a different point in the ligament. The two tails are then tied using a knot pusher and the ligament is secured. These steps are similar to the technique for arthroscopic lateral ligament plication described earlier in this book.
- Elbow stability is finally reassessed after repair.
- In patients presenting late with persistent symptoms of instability, it may be possible to undertake a direct repair as detailed above. If this is not possible, then a reefing procedure can be undertaken as described by Van Riet in a previous chapter (Fig. 17.9) [11].

Fig. 17.8 Arthroscopy portals for the lateral compartment. The proximal lateral portal is made just proximal to the midpoint (green dot) of the line joining the lateral epicondyle and olecranon (blue dots). The direct lateral portal is 2 cm distal to this. These portals can be connected to perform an arthrotomy if required (© Adam Watts)

17.4 Tips and Tricks

- Ensure that the patient is relaxed and comfortable before attempting the posterior drawer test. Muscular guarding will limit the findings.
- A mechanical suture passer can be used to grasp the posterolateral ligament when undertaking an arthroscopic repair.
- If the bone lesion is very large it can produce instability in the same way an engaging Hill-Sachs lesion does in the shoulder. As the elbow is extended the radial head can "drop" into the defect. Lateral ligament reconstruction alone may not address this issue. The senior author has found that imbrication of the posterolateral joint capsule into the floor of the defect can satisfactorily address persistent instability.

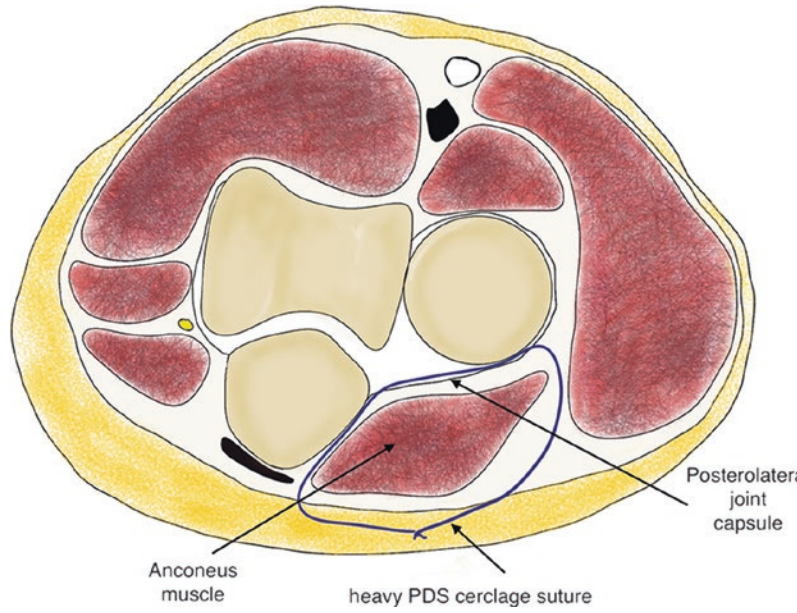

Fig. 17.9 Schematic of the arthroscopic posterolateral capsular reefing procedure (© Adam Watts)

17.5 Pitfalls

- Do not overtighten the PLL repair as it will usually fail when the elbow is flexed. Check the repair tension through a full range of elbow flexion before securing the knot.
- Make sure that the bone quality is adequate to hold an anchor. In osteopenic patients it may be necessary to create bone tunnels to perform a transosseous repair.
- Choose a short anchor so that the tip of the anchor does not penetrate the joint anteriorly.

17.6 Postoperative Management and Rehabilitation

After acute repair or reefing, the patient is placed in a sling and given advise on immediate protected active range-of-movement exercises. The patient is asked to lie on their back with the shoulder flexed to 90° and the forearm in neutral rotation. In this position they can do elbow flexion and extension exercises [12]. Active pronosupination exercises are performed in the seated position with the elbow flexed to 90°. The patient is asked to perform the exercises hourly and to rest in the sling between exercises. When muscle hypertonia is reduced active open- and closed-chain exercises can commence. These can then progress to in-line loading, varus/valgus loading and plyometric exercises guided by a physiotherapist.

17.7 Complications

Specific complications that may occur include repair failure, elbow stiffness, heterotopic ossification and recurrent instability.

References

1. Osborne G, Cotterill P. Recurrent dislocation of the elbow. J Bone Joint Surg Br. 1966;48(2):340–6.
2. Jeon IH, Micic ID, Yamamoto N, Morrey BF. Osborne-cotterill lesion: an osseous defect of the capitellum associated with instability of the elbow. Am J Roentgenol. 2008;191(3):727–9.
3. Edwards DS, Arshad MS, Luokkala T, Kedgley AE, Watts AC. The contribution of the posterolateral capsule to elbow joint stability: a cadaveric biomechanical investigation. J Shoulder Elbow Surg. 2018;27(7):1178–84.
4. O'Driscoll SW, Bell DF, Morrey BF. Posterolateral rotatory instability of the elbow. J Bone Joint Surg Am. 1991;73(3):440–6.

5. O'Driscoll SW, Jupiter JB, King GJ, Hotchkiss RN, Morrey BF. The unstable elbow. Instr Course Lect. 2001;50:89–102.
6. Regan W, Lapner PC. Prospective evaluation of two diagnostic apprehension signs for posterolateral instability of the elbow. J Shoulder Elbow Surg. 2006;15(3):344–6.
7. Arvind CHV, Hargreaves DG. Table top relocation test—new clinical test for posterolateral rotatory instability of the elbow. J Shoulder Elbow Surg. 2006;15(4):500–1.
8. Kaas L, Turkenburg JL, van Riet RP, Vroemen JPAM, Eygendaal D. Magnetic resonance imaging findings in 46 elbows with a radial head fracture. Acta Orthop. 2010;81(3):373–6.
9. Kaas L, van Riet RP, Turkenburg JL, Vroemen JPAM, van Dijk CN, Eygendaal D. Magnetic resonance imaging in radial head fractures: most associated injuries are not clinically relevant. J Shoulder Elbow Surg. 2011;20(8):1282–8.
10. Boyd H. Surgical exposure of the ulna and proximal third of the radius through one incision. Surg Gynecol Obstet. 1940;71:87–8.
11. van Riet RP. Arthroscopic lateral collateral ligament imbrication. In: Bain G, Eygendaal D, van Riet RP, editors. Surgical techniques for trauma and sports related injuries of the elbow [Internet]. Berlin: Springer Berlin Heidelberg; 2020 [cited 2020 Apr 12]. p. 263–7. http://link.springer.com/10.1007/978-3-662-58931-1_35.
12. Schreiber JJ, Paul S, Hotchkiss RN, Daluiski A. Conservative management of elbow dislocations with an overhead motion protocol. J Hand Surg. 2015;40(3):515–9.

18 Lateral and Medial Elbow Instability: Graft Reconstruction Techniques

Shay Ribenzaft, Yoav Rosenthal, and Mark I. Loebenberg

18.1 Background

Medial ulnar collateral ligament (MUCL) injuries of the elbow commonly occur among overhead throwing athletes (baseball pitchers, javelin throwers) due to significant repetitive valgus stress on their elbows. The incidence of MUCL injuries and reconstructions has increased in recent years [1]. UCL reconstruction, commonly known as "Tommy John surgery," was first published by Jobe et al. in 1986 and has become the preferred treatment modality over ligamentous repair over the years [2–4]. The technique for MUCL reconstruction has been modified with various techniques including the docking technique and the modified Jobe technique [5]. A relatively new modification to current techniques includes a synthetic graft augmentation with cross-linked suture tape meant to achieve a stronger construct and to decrease the chance of graft failure [6].

Lateral ulnar collateral ligament (LUCL) tear may cause clinically symptomatic posterolateral rotatory instability (PLRI), as first described by O'Driscoll et al. [7]. Several techniques and modifications of LUCL reconstruction have been described, and include docking via bone tunnels, direct suturing, suture anchors, interference screws, tension-slide technique using a button, sutures over a bone bridge, and interference knot fixation.

This chapter describes the author's double-docking graft reconstruction techniques for medial and lateral instability. The MUCL reconstruction is done in a hybrid fashion (docking the humeral side and tension slide on the ulnar side) using two buttons. An autograft (usually gracilis or palmaris longus) is used and is augmented with a cross-linked suture tape for added strength. The LUCL reconstruction is performed using the double-docking technique with an autograft or a synthetic allograft.

18.2 Indications and Contraindications

- UCL reconstruction is indicated in significant dysfunction and persistent medial elbow pain that is nonresponsive to conservative management and is coupled with a desire to return to competition at the same or higher level. UCL reconstruction is mostly performed for partial UCL tears in high-level throwers and in other sports that involve the upper extremity.

Neither of the authors mentioned has received anything of value from or has stock or stock options held in a commercial company or institution related directly or indirectly to the subject of this chapter.

S. Ribenzaft · Y. Rosenthal · M. I. Loebenberg (✉)
Department of Orthopedic Surgery, Rabin Medical Center, Beilinson Campus, Tel Aviv, Israel

© ISAKOS 2022

D. N. Bhatia et al. (eds.), *Arthroscopy and Endoscopy of the Elbow, Wrist and Hand*,
https://doi.org/10.1007/978-3-030-79423-1_18

- LUCL reconstruction is performed for an irreparable LUCL tear in the setting of an acute complex elbow dislocation, and in symptomatic chronic posterolateral rotatory instability.

Contraindications for ligament reconstructions include:

- Inability or unwillingness to complete the rigorous postoperative rehabilitation program.
- Significant ulnotrochlear or radiocapitellar arthritis.
- Athletes with asymptomatic tears.
- Acute or chronic infection at the surgical site.
- If foreign body sensitivity is suspected, sensitivity ruled out with appropriate tests prior to implantation of a synthetic ligament.

18.3 Surgical Technique

18.3.1 UCL Reconstruction

The patient is placed supine with the upper extremity on an arm board, and shoulder in abduction and external rotation. A tourniquet is applied. Before incision, several folded sterile towels are placed under the elbow for easier exposure of the medial elbow.

- A longitudinal incision is made on the medial aspect of the elbow, angled at the medial condyle, approximately 10 cm in length. The incision is made posterior to the medial epicondyle extending proximally 5 cm. Distally, the incision is extended another 5 cm along the flexor carpi ulnaris (FCU) muscle. After initial incision, a dissection of the medial muscular fascia is performed while identifying and protecting the medial antebrachial cutaneous nerve and its branches.
- The ulnar nerve is identified near the cubital tunnel proximal to the medial epicondyle, and is dissected and protected during the surgery. A vessel loop is used to mark the nerve and help with dissection.
- Dissection continues through the intermuscular plane between FCU and flexor mass, and proximally towards the medial epicondyle. The fascia on the anterosuperior medial epicondyle is incised to expose the location where the anterior hole will be drilled in the epicondyle.
- Distally, the muscle is elevated from the sublime tubercle and 2 cm further distally, to identify the tubercle and the remnant of the MUCL.
- A blunt Hohmann retractor or small right-angle retractor is placed over the anterior edge of the ulna. The native MUCL is incised in line with its fibers to identify the joint.
- *Ulnar bone tunnel*: A 3.2 mm guide drill is used to create a bicortical distal tunnel in the location of the sublime tubercle. This tunnel should be oblique to the surface of the ulna, passing from proximal medial to distal lateral. This will allow for a direct line of pull during the later tension slide. Then, after measuring the graft's diameter, an enlarged unicortical tunnel is created by overdrilling the 3.2 mm guide pin with a cannulated headed reamer to accommodate the graft. This is usually about 4–5 mm (Fig. 18.1a).
- *Humeral bone tunnel*: The humeral sided tunnel is drilled at the medial epicondyle at the anatomic insertion of the MUCL directed superiorly and laterally to create a blind tunnel, which stays within the medial column of the distal humerus. A 2.5 mm guide drill is used to create a unicortical distal tunnel aiming slightly laterally and proximally while making sure not to perforate the posterior humeral cortex. Ideally the socket length should be 15–20 mm. Next, an enlarged unicortical tunnel is reamed over the guide pin in the same fashion that was done in the ulnar tunnel. This is usually about 4–5 mm in diameter. Thereafter, a 2.5 mm drill is used to create a drill hole in the blind socket, starting on the posterior aspect of the medial epicondyle, exiting into the socket that was drilled previously while protecting the ulnar nerve.
- *Graft preparation*: Gracilis tendon autograft is harvested from ipsilateral or contralateral leg

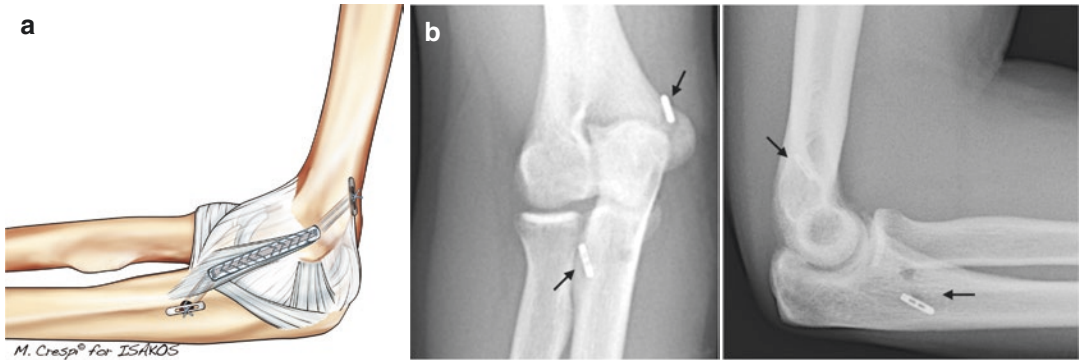

Fig. 18.1 (**a**) Tunnel positions and graft orientation for reconstruction of the UCL are illustrated. (**b**) Lateral and anteroposterior postoperative radiographs demonstrating the placement of the humeral and ulnar buttons for UCL reconstruction (M. Crespi © for ISAKOS)

as described by Dugas et al. [8]. The length of the graft is determined by measuring the distance from ulnar hole to humeral distal hole and adding 1 cm length on each side. A FiberTape® (Arthrex™, Naples, FL) suture augmentation is incorporated into the graft using a #2 fiberwire fiberloop (Arthrex™, Naples, FL) in a whipstitch fashion, starting from the middle and continuing distally on one limb. The combined gracilis-FiberTape® graft is now ready to use with fiberloop attached to one side of it.

- *Humeral side graft passage*: Using a suture shuttle, the two free suture limbs are passed with a suture shuttle through the distal blind tunnel and out the smaller proximal drill hole while protecting the ulnar nerve. The BicepsButton™ is secured to the sutures; tension is placed on each suture limb simultaneously to dock the graft into the humeral bone tunnel, and the button sits flush against the posterior humeral hole. Once the graft is fully docked in the humeral reamed hole, a knot is placed on top of the humeral button to secure it in place.
- *Ulnar side graft passage*: Once the graft is docked through the humeral hole, it is measured again with tension towards the ulnar medial hole to make sure that the graft is long enough to be docked in the ulna but not too long to prevent the needed tensioning. Excess graft is cut (to allow for about 1 cm of graft to fully enter the tunnel). Another #2 fiberwire fiberloop (Arthrex™, Naples, FL) is whipstitched from the center of the graft towards the ulnar end, through the fibertape augmentation. The BicepsButton™ is threaded in the same fashion as on the humeral side. The graft is docked on the ulnar hole using a tension slide technique. Once the BicepsButton™ has been secured, tension is placed on each suture limb simultaneously to dock the graft into the ulnar bone tunnel. Tension slide continues through the ulnar hole until adequate tension is achieved. This should be done while the elbow is held in 30–40 degrees of flexion and while making sure that there is no valgus force applied to the elbow. A free needle is used to pass one limb through the graft and a knot is tied to set and maintain the tension. Cortical interference screws can then be placed if there is room for them next to the graft (Fig. 18.1b).
- *Final assessment*: It is important to examine the range of motion, stability, and tension of the graft. If the ulnar nerve is unstable, it may be transposed anteriorly.

A 2-0 Vicryl suture is passed along the edges of the graft to secure it to the surrounding soft tissue, preventing it from folding on itself.

18.3.2 LUCL Reconstruction

The patient is placed supine with the upper extremity on an arm board and a tourniquet is applied.

- A modified Kocher approach between the anconeus and the extensor carpi ulnaris is performed in order to achieve exposure from supinator crest distally to lateral epicondyle proximally. A small portion of the extensor mass origin needs to be slightly elevated anteriorly to allow for access to the center of the lateral epicondyle. A remnant or absent lateral collateral ligament is found and may be used later for augmentation. The visible capsule of the elbow joint is usually left intact as the reconstruction is extra-articular.
- *Proximal docking site*: Two converging bone tunnels are created through the distal humerus. A 2.5 mm guide drill is drilled laterally at the center of rotation of the capitellum, which is best correlated with the point of isometry for the lateral collateral complex. This point may be found using fluoroscopy, or simply by estimation. The drill guide pin should aim obliquely in a medial diagonal direction up the lateral column and be roughly 2 cm in length. As previously described, the tunnel should be enlarged over the drill guide by cannulated reamers to accommodate the graft. This is usually about 6 mm but can be as large as 8 mm depending on the size of the patient and the graft size. In order to dock the capitellar sutures, a 2.5 mm posterior tunnel is drilled from the posterior aspect of the capitellum aiming anteriorly towards the distal end of the docking tunnel to create a proximal passage for the graft sutures (Fig. 18.2).
- *Distal docking site*: A 3.2 mm guide drill is used to create a bicortical distal tunnel just posterior to the tubercle of the supinator crest. This tunnel should be oblique to the surface of the ulna, drilled from proximal lateral to distal medial. This will allow for a direct line of pull during the later tension-slide portion of the procedure. An enlarged unicortical tunnel is created by drilling over the 3.2 mm guide pin with a cannulated headed reamer as performed in the humerus (Fig. 18.3).
- *Preparation and humeral placement of graft*: The proximal end of the graft is whipstitched with locking sutures. If an autograft or allograft tendon is utilized, the graft is usually double stranded to provide added strength to the reconstruction and the folded ended of the tendon is placed proximally. The synthetic ligament is placed single ply only. The two suture limbs are then passed through the docking tunnel and out of the more proximal posterior tunnel, using a suture shuttle. The sutures are threaded through the button and tied. This will fix the graft statically in the proximal tunnel. Alternatively, after the limbs of the suture have been passed through the button, these limbs can be returned through the posterior tunnel and out the proximal tunnel. This additional step will allow for later further tensioning of the graft on the humeral side if so desired (Fig. 18.4).
- *Ulnar placement of graft*: Once the graft has been placed and secured in the humeral tunnel, the tendon is then tensioned and temporarily placed into the ulnar tunnel. The graft is then measured and trimmed to allow for approximately a centimeter and a half of the tip of the graft to enter the ulnar tunnel. The distal end of the graft is whipstitched and

Fig. 18.2 The proximal humeral tunnel for LUCL reconstruction is drilled laterally at the center of rotation of the capitellum (left image). A 2.5 mm posterior tunnel is drilled from the posterior aspect of the capitellum aiming anteriorly towards the distal end of the docking tunnel to create a passage for the sutures (right image)

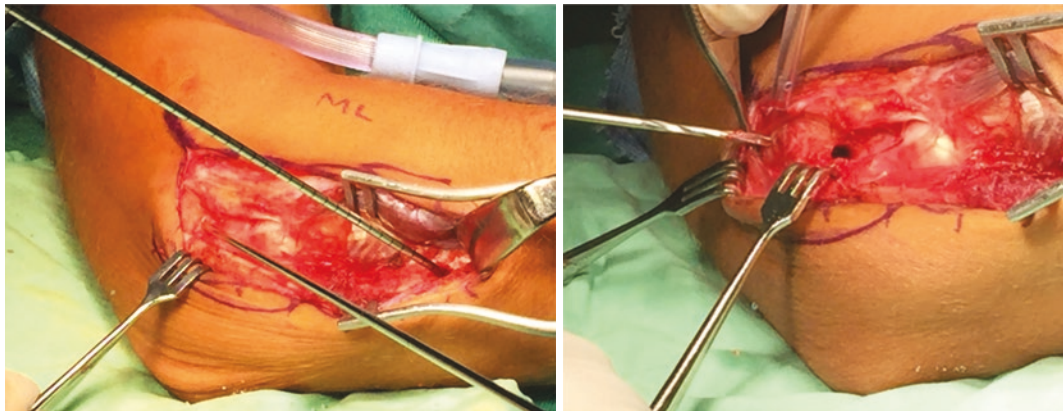

Fig. 18.3 The distal ulnar bicortical tunnel for LUCL reconstruction is drilled in an oblique direction to the surface of the ulna, from proximal lateral to distal medial (black arrowhead)

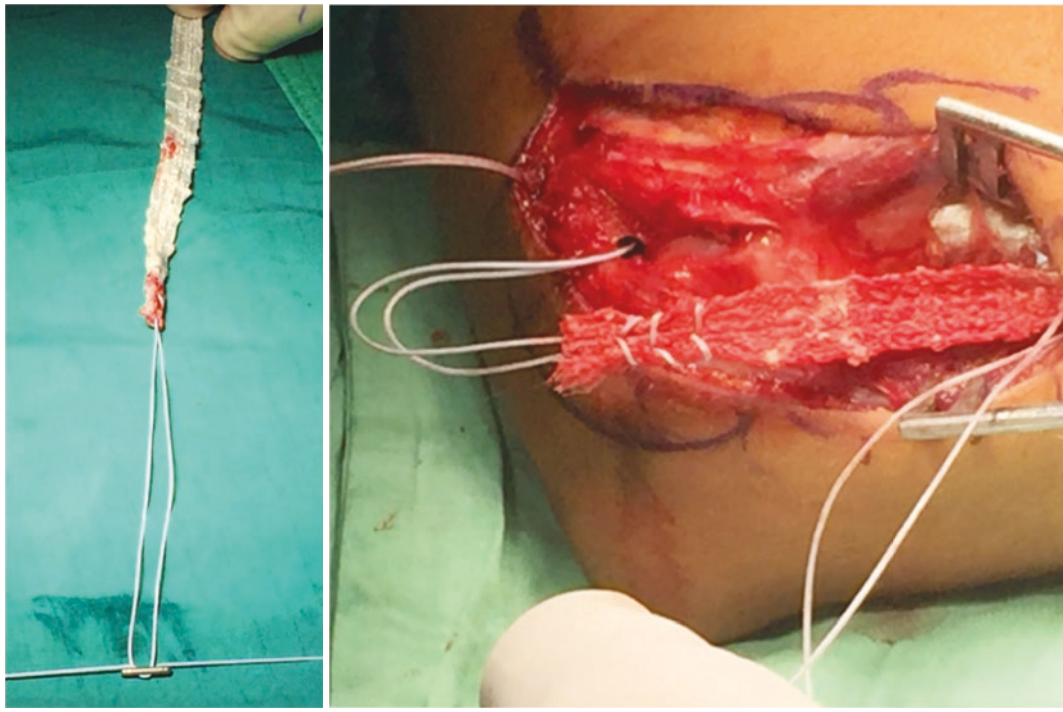

Fig. 18.4 Preparation of the graft is done by whipstitching on one side only (left image). The sutures are shuttled through the humeral holes in order to dock the graft in the humeral tunnel (right image)

threaded through the button. While holding tension for both limbs the button is inserted through both cortices of the distal ulna, using an inserter. Once the button has been secured, tension is placed on each suture limb simultaneously to dock the graft into the ulnar bone tunnel. This should be done while the elbow is held in 30–40 degrees of flexion and the forearm in full pronation. If the graft on the humeral side has been placed with tension slide technique, it can be likewise tensioned. After achieving the desired tension on both sides of the graft, a free needle is used to pass one limb through the graft and a knot is tied to

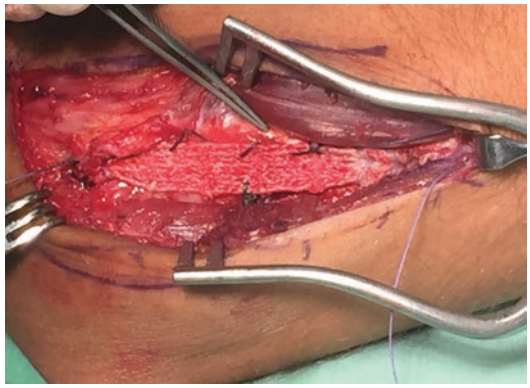

Fig. 18.5 After the graft is tensioned using the buttons, Vicryl sutures are passed along the edges of the graft, securing it to the surrounding soft tissue, preventing it from folding on itself

set and maintain the tension. Cortical interference screws can then be placed if there is room for them to be accommodated in the docking tunnels next to the graft.

Finally, a 2-0 Vicryl suture is passed along the edges of the graft to secure it to the surrounding soft tissue, preventing it from folding on itself (Fig. 18.5).

18.4 Tips and Tricks

- A nerve block should be avoided to examine ulnar nerve function postoperatively.
- While dissecting the medial intermuscular septum, a septal bridge should be left intact to avoid anterior subluxation of the ulnar nerve.
- To determine the correct position of the docking tunnels, the elbow should be flexed at 90° and the ulna should be pressed to the humerus to eliminate varus and valgus angulation.
- Drill the holes obliquely to match the graft's trajectory and smoothen the bony border of the tunnels to avoid sharp edges that might compromise the integrity of the graft.
- Ensure that both sides of the graft and tape augmentation are docked properly into the bone tunnels to allow correct bone-tendon interface.
- Tensioning of the graft requires enough space in the docking tunnel. The graft needs to have at least 0.5–1 cm of room at the end of the tunnels for advancement.
- The graft is tensioned using a slight varus force to ensure adequate tensioning. Additional tensioning after graft fixation can be accomplished if needed with either simple posterior suturing of the graft to the capsule or with the placement of a small suture anchor just posterior to the graft trajectory to add another point of fixation to add tension to the graft.
- It has been demonstrated that the radial collateral ligament is essentially isometric, but the lateral ulnar collateral ligament is not. The LUCL is loose in elbow extension and tight with elbow flexion. The most isometric point for the LUCL graft origin is approximately 2 mm proximal to the center of the capitellum [9].

18.5 Pitfalls

- The docking tunnels should be adequately wide to allow the graft to slide within the tunnel to obtain the tension needed. If the tunnels seem too wide, cortical interference screws can be added to increase the rigidity of the graft within the tunnel. A wider tunnel is much less problematic than a tunnel that is too tight.
- Care should be taken to ensure that the button is placed just posterior to the medial edge to ensure minimal postoperative irritation.

18.6 Postoperative Management and Rehabilitation

Postoperatively, the patient is placed in a long splint with the elbow at 90 degrees of flexion. A week post-surgery, at the first follow-up visit, the splint is removed, passive range of motion is assessed, and anteroposterior and lateral films

are taken. If based on physical examination and elbow films the elbow appears to be stable, and then physical therapy is initiated. For 3 weeks, gentle active and active assistive ROM for the elbow and wrist are performed while avoiding valgus force to the elbow. At 4–8 weeks post-surgery, the goal is to gain gradual increase in elbow ROM. Passive range of motion (PROM) should be initiated in a very controlled and gentle fashion. At 9–12 weeks, the goal is to increase overall strength and endurance as well as achieve full elbow ROM. Exercises include isotonics for shoulder and eccentric elbow flexion strengthening. In weeks 13–20, the patient should have full ROM. The emphasis is on stabilization drills for the elbow and shoulder in protected positions and beginning throwing mechanics education.

18.7 Complications

The most common complication of UCL reconstruction is ulnar neurapraxia. Other surgical complications include medial antebrachial cutaneous (MABC) nerve iatrogenic injury/neuropraxia and fracture of ulna or medial epicondyle. Postoperative complications include elbow stiffness and inability to regain preinjury-level throwing ability.

References

1. Mahure S, Mollon B, Shamah S, Kwon Y, Rokito A. Disproportionate trends in ulnar collateral ligament reconstruction: projections through 2025 and a literature review. J Shoulder Elbow Surg. 2016;25:1005–12.
2. Jobe F, Stark H, Lombardo S. Reconstruction of the ulnar collateral ligament in athletes. J Bone Joint Surg Am. 1986;68:1158–63.
3. Hurwit D, Garcia G, Liu J, Altchek D, Romeo A, Dines J. Management of ulnar collateral ligament injury in throwing athletes: a survey of the American shoulder and elbow surgeons. J Shoulder Elbow Surg. 2017;26:2023–8.
4. Erickson B, Harris J, Fillingham Y, Cvetanovich G, Bush-Joseph C, Bach B, Romeo A, Verma N. Treatment of ulnar collateral ligament injuries and superior labral tears by Major League Baseball Team Physicians. Arthroscopy. 2016;32:1271–6.
5. Chang E, Dodson C, Ciccotti M. Comparison of surgical techniques for ulnar collateral ligament reconstruction in overhead athletes. J Am Acad Orthop Surg. 2016;24:135–49.
6. McGee R, Eudy A, Hoang V, Gupta S, Jacks A, Bruhn S. Ulnar collateral ligament reconstruction technique utilizing suture tape augmentation. Arthrosc Tech. 2020;9:e71–8.
7. O'Driscoll S, Bell D, Morrey B. Posterolateral rotatory instability of the elbow. J Bone Joint Surg Br. 1991;73:440–6.
8. Dugas J, Bilotta J, Watts C, Crum J, Fleisig G, McMichael C, Cain E, Andrews J. Ulnar collateral ligament reconstruction with Gracilis tendon in athletes with intraligamentous bony excision. Am J Sports Med. 2012;40:1578–82.
9. Moritomo H, Murase T, Arimitsu S, Oka K, Yoshikawa H, Sugamoto K. The in vivo isometric point of the lateral ligament of the elbow. J Bone Joint Surg Am. 2007;89:2011–7.

19 Arthroscopic Management of Posterior Elbow Impingement in Athletes

Deepak N. Bhatia

19.1 Background

Posterior elbow impingement is usually an overuse injury in sports that involve a repetitive forced extension and valgus at the elbow (cricket, racquet sports, javelin throw, baseball, swimming, boxing, golf). Medial ligamentous laxity or ulnar collateral ligament (UCL) insufficiency accentuates the valgus-extension overload and results in osteophytic overgrowth in the posterior elbow articulation. Posterior impingement also occurs in middle-aged and recreational athletes and is associated with early degenerative changes. Symptomatic posterior impingement presents with pain in the late phase of throwing action and elbow extension and may progress to locking or terminal extension loss [1]. Arthroscopy is useful for evaluation, and arthroscopic dynamic tracking permits identification of impinging regions. Arthroscopic resection results in predictable symptomatic relief and early return to competitive sports.

19.1.1 Surgical Anatomy

Impingement pathology is variable and includes osteophytic overgrowth and fracture, synovial hypertrophy, and olecranon stress fractures. Osteophytic overgrowth occurs at three levels: the olecranon tip, posterior trochlear junction with the distal olecranon fossa, and proximal olecranon fossa in the distal humerus (Fig. 19.1a). Eventually, this results in progressive cartilage injury (capitellar osteochondritis dissecans) and loose bodies (Fig. 19.1b). Arthroscopic evaluation of the three possible impingement levels is crucial for complete resection of impinging tissues and for complete resolution of symptoms. Repair or reconstruction of UCL is necessary for medial ligamentous insufficiency in addition to the posterior resection.

19.2 Indications/ Contraindications

- Persistent or progressive symptoms of posteromedial impingement refractory to conservative treatment with rest, physical therapy, and sonography-guided corticosteroid injections.
- Loss of terminal extension at elbow is a performance-limiting factor for sports that require complete elbow extension for optimal force generation and is an indication for surgery.

Posteromedial impingement that is associated with elbow instability (UCL insufficiency) is a

D. N. Bhatia (✉)
SPORTSMED Mumbai, and Sir HN Reliance Foundation Hospital, Mumbai, India
e-mail: shoulderclinic@gmail.com

© ISAKOS 2022

D. N. Bhatia et al. (eds.), *Arthroscopy and Endoscopy of the Elbow, Wrist and Hand*,
https://doi.org/10.1007/978-3-030-79423-1_19

Fig. 19.1 (**a**) Pathoanatomy of posterior elbow impingement is illustrated and three levels of impinging osteophytic overgrowth (olecranon tip, posterior trochlear margin, and olecranon fossa) are shown. (M. Crespi © for ISAKOS) (**b**) Magnetic resonance imaging (MRI) shows radiological features of athletic posteromedial impingement. Sagittal and coronal images demonstrate an ununited fracture of an olecranon tip osteophyte (arrow, top left and right images). Sagittal MRI image shows cystic changes in the medial olecranon tip (bottom left) and a loose body in olecranon fossa (bottom right) (© D. Bhatia)

relative contraindication and needs meticulous assessment and possibly UCL reconstruction.

19.3 Surgical Technique

Elbow arthroscopy for posteromedial impingement is performed with the patient in the lateral decubitus position. Both 30- and 70-degree arthroscopes (2.9 mm, Conmed Linvatec, Largo) are used, and a 50 mL syringe is used for initial air arthroscopy. Subsequently, gravity inflow is used to minimize fluid extravasation into the arm and forearm.

Portals: Standard proximal anteromedial (AM) and anterolateral (AL) portals are used for evaluation of anterior elbow. Direct posterior-central (PC, two fingerbreadths proximal to olec-

ranon tip) and posterolateral (PL, lateral to olecranon tip) portals are used to visualize and work in the posterior recess (Fig. 19.2).

Diagnostic Endoscopy and Posterior Bursectomy

- The anterior elbow is evaluated via the AM and AL portals. Medial and lateral elbow recesses are visualized, and the capsular recesses adjacent to radial head and coronoid process are probed for loose bodies. Cartilage is assessed to identify any defects or chondromalacia. Elbow instability is evaluated by arthroscopic tests for medial and lateral instability.
- The posterior elbow is then evaluated via PC portal. Bursectomy and synovectomy may be necessary to better visualize this region. The olecranon fossa and tip are identified and probed to locate impinging osteophytes. Medial and lateral recesses are inspected for loose bodies or impinging osteophytes (Figs. 19.3 and 19.4).

Dynamic olecranon tracking: Dynamic tracking is assessed by bringing the elbow into terminal extension while visualizing the olecranon tip

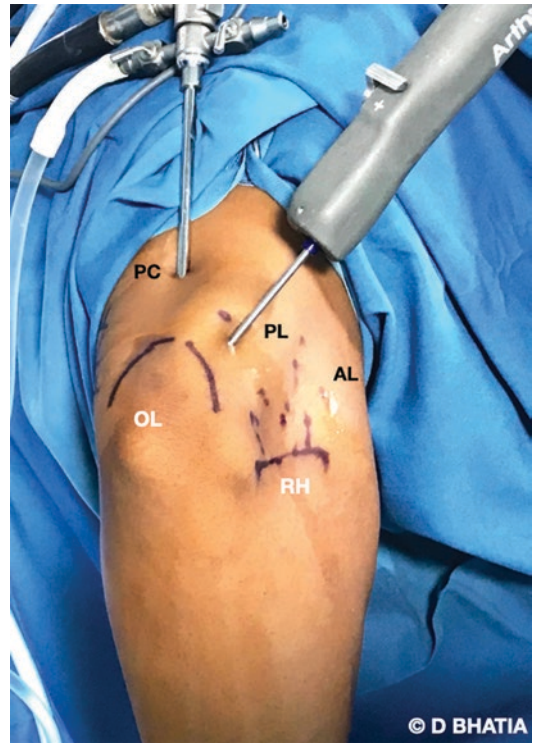

Fig. 19.2 Portals for posterior elbow arthroscopy are shown in lateral decubitus position (*AL* anterolateral portal, *PL* posterolateral portal, *PC* posterocentral portal, *RH* radial head, *C* capitellum) (© D. Bhatia)

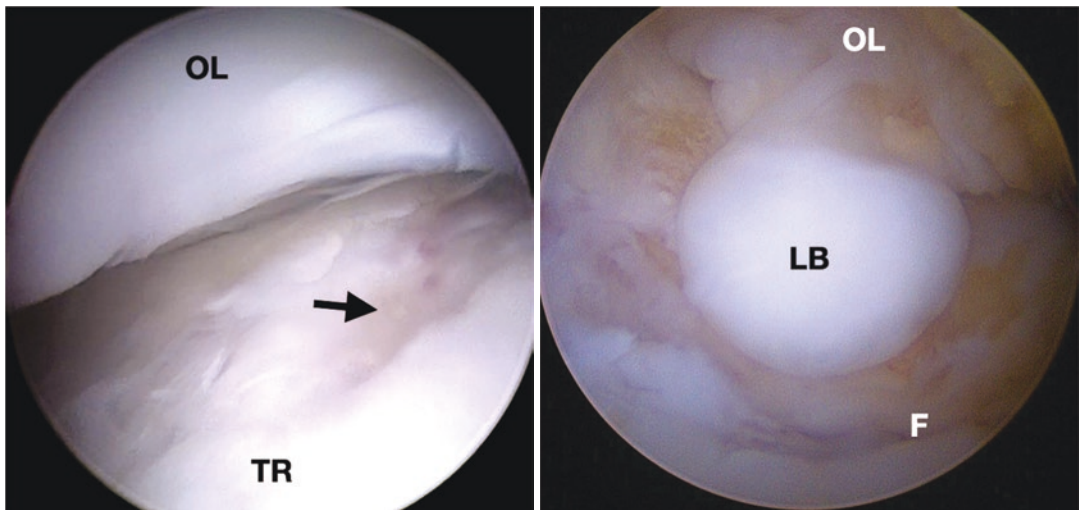

Fig. 19.3 Posterior elbow arthroscopy (viewing through PC portal) shows a cartilage defect (arrow) in the posteromedial trochlea (TR) adjacent to the olecranon (OL) osteophyte (left image). A loose body (LB) is seen at the tip of the olecranon impinging in the fossa (F) (right image) (© D. Bhatia)

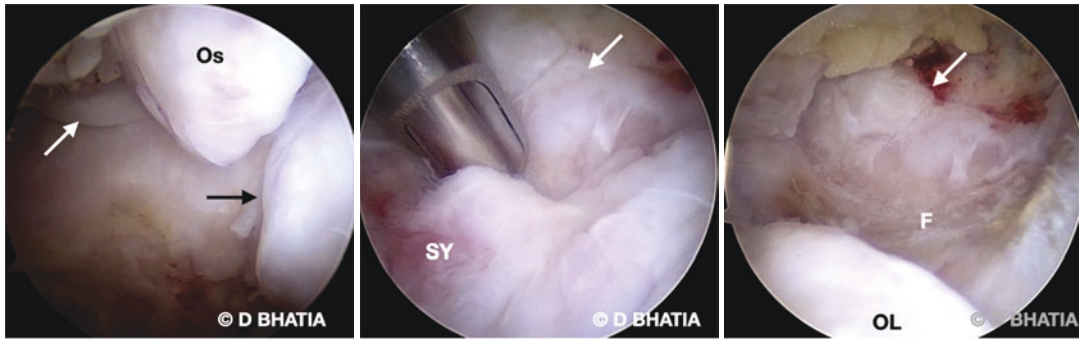

Fig. 19.4 Posterior elbow arthroscopy (viewing through PC portal) shows the prominent osteophyte (Os) on the olecranon (white arrow) and an impinging trochlea osteophyte (black arrow, left image). In a different case, synovial proliferation (SY) is seen in the olecranon fossa and osteophytes are seen at the proximal end of the fossa (arrow, middle and right images, viewing from PL portal) (© D. Bhatia)

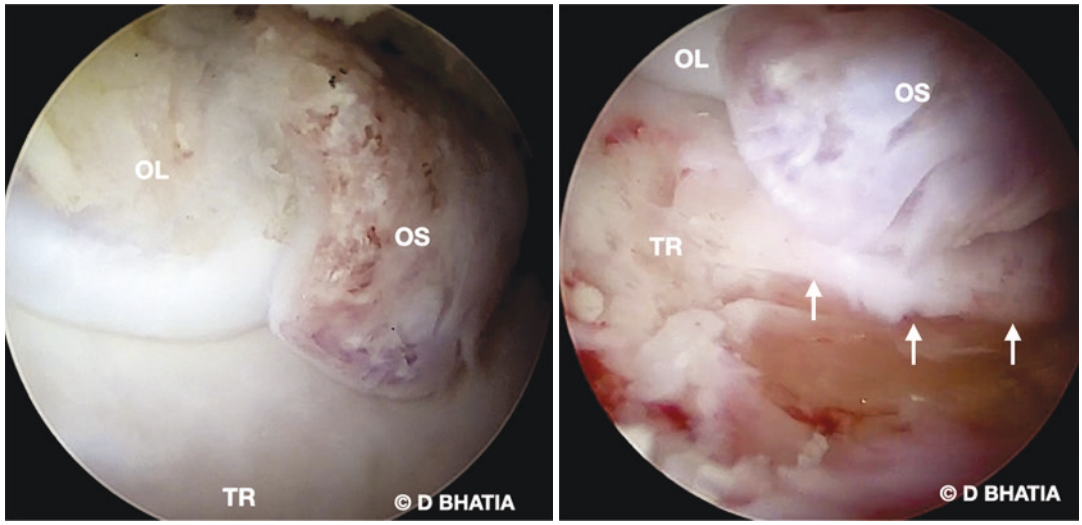

Fig. 19.5 Dynamic olecranon tracking is demonstrated. Posterior elbow arthroscopy (70-degree viewing through PC portal) shows the olecranon osteophyte (Os) articulating with the trochlea (TR) in 90 degrees of elbow flexion (left image). Impingement is demonstrated (right image) as the elbow is extended and an impinging trochlear osteophyte (arrows) restricts further extension (© D. Bhatia)

and fossa using a 70-degree arthroscope. The impinging osteophytes prevent the olecranon tip from engaging the fossa and region of bony impingement is identified. Dynamic tracking is also useful at the end of the procedure to assess complete excision of all impinging tissue. This ensures adequate debridement without excessive resection (Fig. 19.5).

Olecranon osteophyte excision: A small joint shaver (3 mm) is introduced via PL portal and the soft tissue around the olecranon tip osteophyte is debrided. A small joint radiofrequency probe is then used to delineate the osteophyte and its junction with the olecranon is defined. A fractured ununited osteophyte is gently dissected off from the olecranon tip using a shaver. A grasper is then used to excise the osteophyte piecemeal. Soft-tissue remnants and spurs in the medial or lateral recesses are then debrided (Fig. 19.6).

Olecranon fossa debridement: Olecranon fossa osteophytes are identified by dynamic testing. A shaver is used to excise impinging hyper-

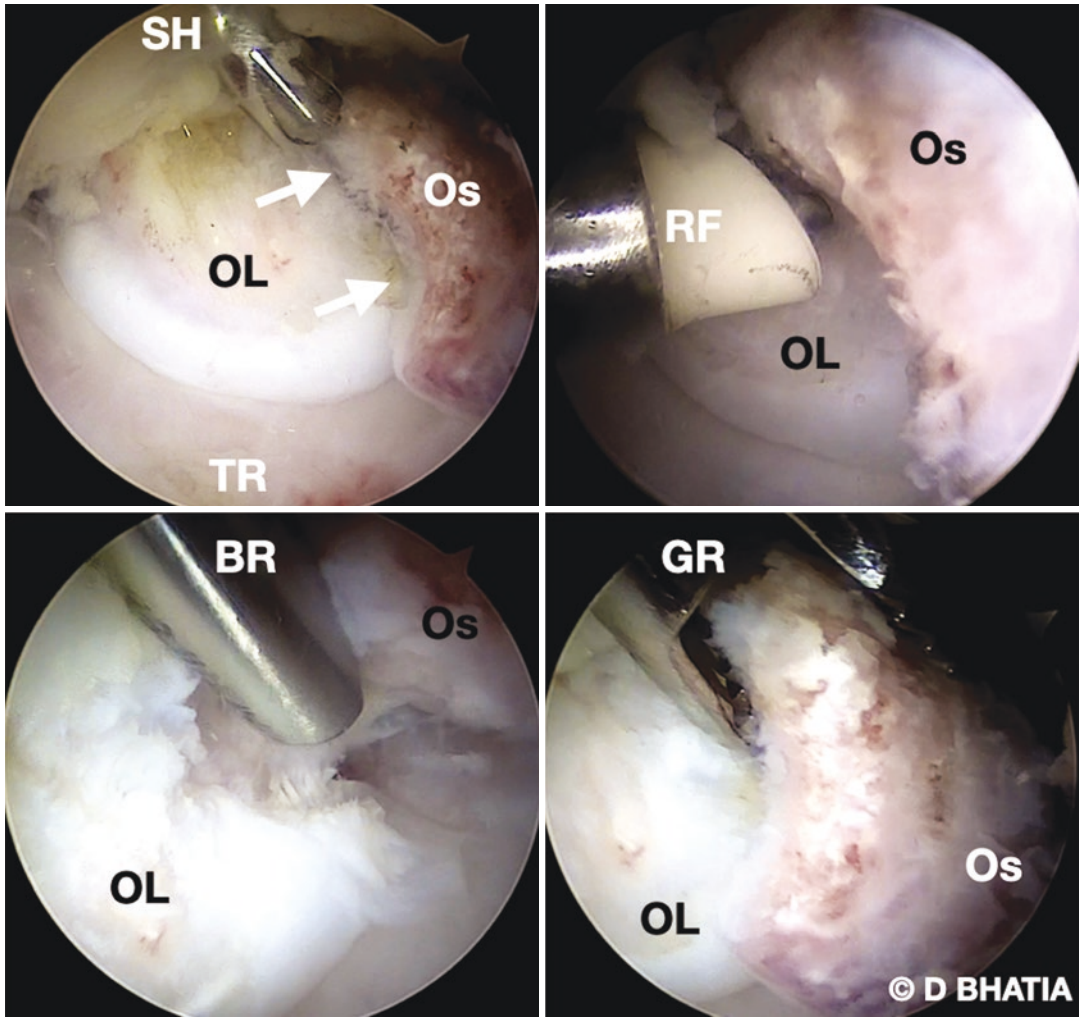

Fig. 19.6 Osteophyte (OS) delineation and dissection (arrows) from the underlying olecranon (OL) are demonstrated using a shaver (SH, top left image), radiofrequency device (RF, top right image), and burr (BR, bottom left image). The dissected fragment is then removed with a grasper (GR, bottom right) (*TR* trochlea) (© D. Bhatia)

trophic synovial tissue and osteophytes at the distal and proximal regions on the fossa are delineated. A small joint burr (3 mm) is used via PL portal and the osteophytes are gently burred and resected (Fig. 19.7a, b).

Final assessment: Dynamic testing of the elbow is finally performed to confirm removal of all impinging tissue. A thorough lavage is necessary in both anterior and posterior recesses of elbow joint to remove all debris (Fig. 19.8).

19.4 Tips and Tricks

- A 70-degree arthroscope and small joint instruments (3 mm) permit better visualization and maneuverability in the posterior elbow and the procedure can be performed without having to shift the viewing and working portals.
- The osteophyte-olecranon junction can be clearly defined and often the fractured osteophyte can be separated from the underlying

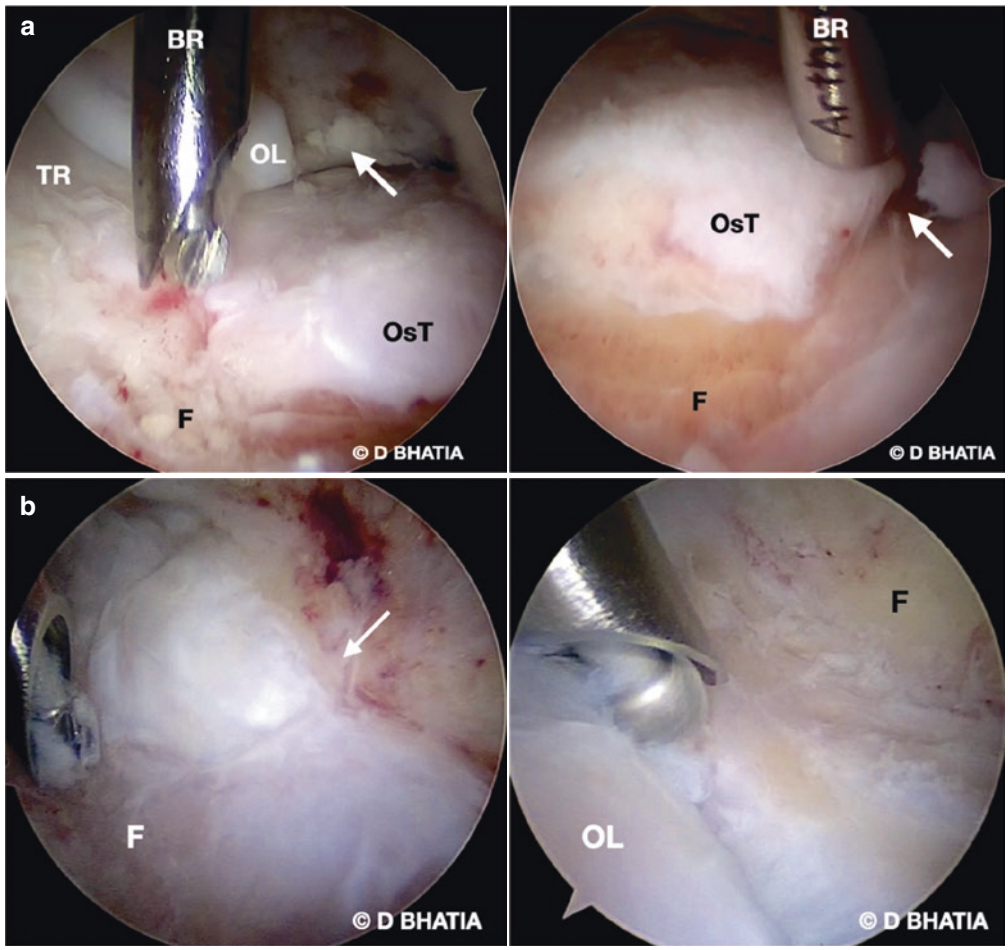

Fig. 19.7 (**a**) Trochlear osteophyte (Ost) is resected using a burr (BR) placed in the posterolateral portal (left image). The resected olecranon border is debrided (arrow). The resection is extended to the spurs on the medial aspect of the trochlea (arrow, right image) (*F* fossa, *TR* trochlea). (**b**) Olecranon fossa proximal osteophyte (arrow) is resected using a burr placed in the posterocentral portal (left image viewing through posterolateral portal). The olecranon tip (OL) is excised (arrow, right image) (*F* fossa) (© D. Bhatia)

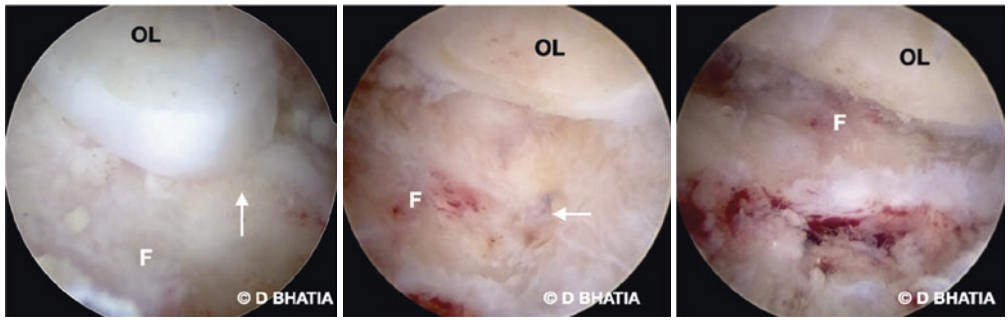

Fig. 19.8 Adequacy of resection is assessed using the dynamic olecranon tracking. The olecranon tip (OL) smoothly glides (arrows) into the fossa (F) without impingement at the site of resected trochlear osteophyte (arrow, left image). The olecranon fossa proximal osteophyte resection site is demonstrated (arrow). The resected olecranon tip can smoothly complete the tracking as shown (right image) (© D. Bhatia)

bone. An angled small joint radiofrequency probe is useful for this dissection.
- The dynamic test is useful to ensure completion of debridement. Complete elbow extension and smooth olecranon tracking must be the goal.

19.5 Pitfalls

- Failure to identify associated instability may result in persistence or worsening of symptoms. Arthroscopic evaluation for signs of medial and lateral instability is useful and the procedure may be combined with ligament reconstruction.
- Excessive resection may worsen any preexisting UCL insufficiency [2]. The dynamic olecranon tracking test is useful to assess the adequacy of resection and ensures quantified removal of impinging tissue.

19.6 Postoperative Management and Rehabilitation

A bulky soft-tissue dressing is used in the immediate postoperative period, and this is changed to portal dressing on the fourth postoperative day. A sling is used for comfort and is discarded within a week. The rehabilitation protocol involves progressive range, strengthening, and sports-specific conditioning over the next 8–12 weeks. Return to throwing and competitive sports is at 6 months.

19.7 Complications

The ulnar nerve is at risk of injury during resection of posteromedial osteophytes in medial recess. The nerve is superficial to the posteromedial capsule, and resection in this region should be performed with caution.

Conflict of Interest The author certifies that he has no commercial associations (e.g., consultancies, stock ownership, equity interest) that might pose a conflict of interest in connection with the submitted chapter. The author retains the copyright to the images, videos, and content in this chapter.

References

1. Dugas JR. Valgus extension overload: diagnosis and treatment. Clin Sports Med. 2010;29(4):645–54.
2. Ahmad CS, Park MC, Elattrache NS. Elbow medial ulnar collateral ligament insufficiency alters posteromedial olecranon contact. Am J Sports Med. 2004;32:1607–12.

Valgus Extension Overload

20

T. David Luo and Michael T. Freehill

20.1 Background

Valgus extension overload (VEO), also referred to as pitcher's elbow, is a constellation of symptoms and pathologic changes to the elbow common to throwing athletes. The condition is caused by repetitive throwing leading to supraphysiologic stresses on the elbow joint. Valgus torque on the elbow and forearm angular velocity may reach 65 Nm and 5000 degrees per second, respectively, during the late cocking and early acceleration phases of throwing. Three massive forces are simultaneously placed on the elbow: (1) tension over the medial aspect of the elbow reaching 300 N of force, (2) compression of the lateral aspect of the elbow reaching 900 N, and (3) shear forces occurring in the posterior compartment (Fig. 20.1) [1]. Over time, repetitive medial tensile stresses may lead to injury or rupture of the ulnar collateral ligament (UCL) and/or flexor pronator muscle mass. In the skeletally immature athlete, an avulsion fracture of the medial epicondyle may also occur [2]. Lateral compression can lead to radiocapitellar joint dysfunction, stress overload, and osteochondral lesions. In the skele-

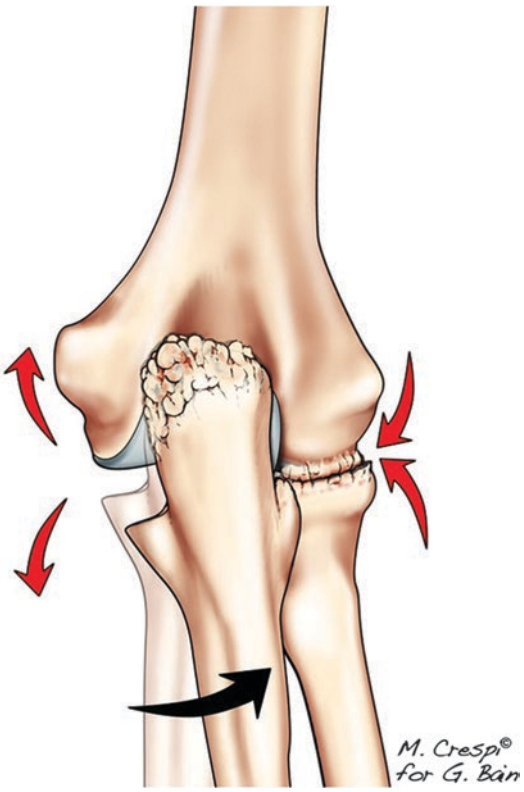

Fig. 20.1 The tensile forces to the medial elbow, compressive forces in the radiocapitellar joint, and posteromedial shear forces seen in valgus extension overload. (Reprinted with permission from Springer Books (Hilgersom et al., Valgus Extension Overload, Surgical Techniques for Trauma and Sports Related Injuries of the Elbow). The authors would like to acknowledge ISAKOS gives permission for reuse of this figure from a previous ISAKOS book

T. D. Luo
Department of Orthopaedic Surgery, Wake Forest School of Medicine, Winston-Salem, NC, USA
e-mail: tluo@wakehealth.edu

M. T. Freehill (✉)
Department of Orthopaedic Surgery, Stanford University School of Medicine, Stanford, CA, USA

© ISAKOS 2022

D. N. Bhatia et al. (eds.), *Arthroscopy and Endoscopy of the Elbow, Wrist and Hand*,
https://doi.org/10.1007/978-3-030-79423-1_20

tally immature athlete, osteochondritis dissecans may result. Excessive compressive forces of the articulation between the posteromedial olecranon and the olecranon fossa lead to reactive bone formation. Osteophytes at the posteromedial tip of the olecranon or loose bodies in the olecranon fossa may subsequently cause catching, locking, and posteromedial impingement.

Athletes with VEO complain of pain during various phases of the throwing cycle associated with where pathologic change may be present and experience decreased throwing velocity. The initial goal of conservative treatment in patients diagnosed with VEO involves relieving pain and inflammation. In the setting of first-time injuries, the patient should rest for a period of 2 weeks, and then initiate specific physical therapy, followed by an interval throwing program. Athletes who present with isolated VEO with an intact UCL should refrain from throwing and other potentially aggravating activities to the elbow. The primary aims of physical therapy are to relieve symptoms and to improve functional flexor-pronator strength [3]. It is essential that the whole body is assessed for weaknesses or deficiencies as this "weak link" in the kinetic chain could manifest as dysfunction at the elbow. In recalcitrant cases, further assessment of the throwing mechanics to improve biomechanical efficiency and decrease symptoms may be beneficial. Physical therapy may not always be curative of VEO, but remains the frontline treatment modality to the athlete's overall rehabilitation. Surgical intervention is reserved for patients who fail the initial course of conservative treatment and continue to experience persistent pain and impingement with an inability to return to competitive throwing or sporting activity. Surgical treatment of VEO has demonstrated effective outcomes as advances in elbow arthroscopy instrumentation and technique have continued to evolve.

20.2 Surgical Anatomy

The elbow is a hinge joint involving articulations of the radiocapitellar, ulnohumeral, and proximal radioulnar joints [4]. They are encapsulated within common fibrous soft tissues that are thickened medially and laterally as the collateral ligaments. The bony anatomy of the elbow contributes to 50% of its stability. Musculotendinous and ligamentous complexes provide the other 50% of elbow stability, especially between 20 and 120 degrees of flexion. The key ligamentous restraints include the aforementioned UCL, the lateral ulnar collateral ligament (LUCL), and the radial collateral ligament (RCL).

The UCL, also known as the medial collateral ligament, consists of three components: (1) anterior oblique ligament (AOL), (2) posterior oblique ligament (POL), and (3) transverse oblique ligament (TOL). Of these, the AOL is the primary medial stabilizer against valgus stress. The AOL is further divided into anterior and posterior bands. The anterior band is the primary medial stabilizer against valgus stress up to 90 degrees of flexion. The posterior band of the AOL is isometric and provides medial stability from 60° to full flexion [5]. The proximal attachment of the UCL is located at the anterior aspect of the medial epicondyle. A cadaveric analysis demonstrated that the mean length of the UCL is 53.9 mm. The distal attachment of the UCL begins proximal to the sublime tubercle and narrows distally along an osseous ridge. This soft-tissue footprint on the ulna averages 29.2 mm, while the mean length of the osseous ridge measures 24.5 mm. The POL is fan shaped, inserts on the posteromedial aspect of the olecranon, and provides secondary stability in flexion beyond 60°. Unlike the AOL and POL, the TOL does not cross the elbow joint and provides minimal function in stabilization.

20.3 Indications and Contraindications

Surgical treatment is indicated in patients with persistent pain and who wish to return to previous level of performance despite a concerted effort with conservative management involving rest, therapeutic modalities, strengthening, and conditioning. The presence of osteophytes alone is not an absolute indication for surgery, as they are commonly seen in throwing athletes and are often

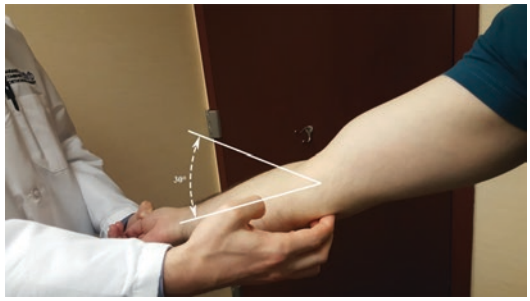

Fig. 20.2 Valgus extension overload syndrome test or valgus extension snap maneuver is performed with moderate valgus stress applied to the elbow, simultaneously palpating the posteromedial olecranon, and then extending the elbow from 20 to 30° of flexion to full extension with the hand in supination. Tenderness over the posteromedial olecranon tip or crepitus secondary to osteophyte or loose body indicates a positive test. (Reprinted with permission from Springer Books (Hilgersom et al., Valgus Extension Overload, Surgical Techniques for Trauma and Sports Related Injuries of the Elbow). The authors would like to acknowledge ISAKOS gives permission for reuse of this figure from a previous ISAKOS book

asymptomatic. Osteophyte on the posteromedial olecranon is the most common finding in professional baseball players undergoing open or arthroscopic elbow surgery. A thorough physical examination, including provocative maneuvers with valgus stress and elbow extension, is necessary when deciding whether to proceed with surgery. Surgery could be indicated when posteromedial impingement or elbow pain secondary to osteophytes is elicited by placing valgus stress at 20–30° of elbow flexion and bringing the elbow into terminal extension with the hand in supination (Fig. 20.2). On the other hand, varus stress to the elbow may bring about pain relief.

Similar to osteophytes, the presence of loose bodies in the posterior elbow joint may become symptomatic, leading to catching, locking, and reduced range of motion to the elbow. Additionally, repetitive microtrauma with persistent throwing and overhead activities may result in chondral flaps and osteochondral lesions within the medial olecranon fossa. Radiographic evaluation may further help to identify these lesions that are pathognomonic for VEO, as well as soft-tissue and ligamentous calcifications. Plain elbow radiographs should include anteroposterior (AP), lateral, and oblique views. Advanced imaging, such as a CT, will further characterize the changes in bony morphology (Figs. 20.3a–d). An MRI is the modality of choice to evaluate the integrity of the UCL and to look for bony edema, osteochondral defects, stress fractures, and synovial plicae (Fig. 20.4) [1].

Contraindications to surgical treatment of VEO include negative impingement of the posteromedial elbow with provocative maneuvers. Insufficiency of the UCL is on the spectrum of instability in VEO and is considered a contraindication to surgery only addressing the posterior compartment. Osteophytes on the posteromedial tip of the olecranon have been postulated to form as a compensatory response to provide elbow stability. Therefore, care must be taken as surgical debridement and excessive resection of these osteophytes could exacerbate asymptomatic UCL injuries and further destabilize the medial elbow [1]. Repair or reconstruction of the UCL should be considered at the time of posteromedial decompression to avoid these complications. Other general considerations that may preclude arthroscopic treatment include previous ulnar nerve transposition (although isolation to the posterior compartment is safe in this setting), other post-traumatic pathologies that prevent safe arthroscopic portal entry, local soft-tissue infection, and joint ankylosis that prevents adequate fluid distention.

20.4 Surgical Technique

Patient position (supine, prone, or lateral decubitus on a bean bag) during arthroscopic treatment of VEO is often surgeon dependent. It is important that both the anterior and posterior elbow compartments can be easily accessed by adjusting the forearm position in space. After induction of anesthesia, preoperative evaluation of the ulnar nerve should be performed to check for subluxation. The operative extremity is then prepared and draped in the usual sterile fashion. Key anatomic landmarks (medial epicondyle and its relationship to the ulnar nerve, olecranon tip, lateral epicondyle, radial head) should be marked for safe portal placement as previously described.

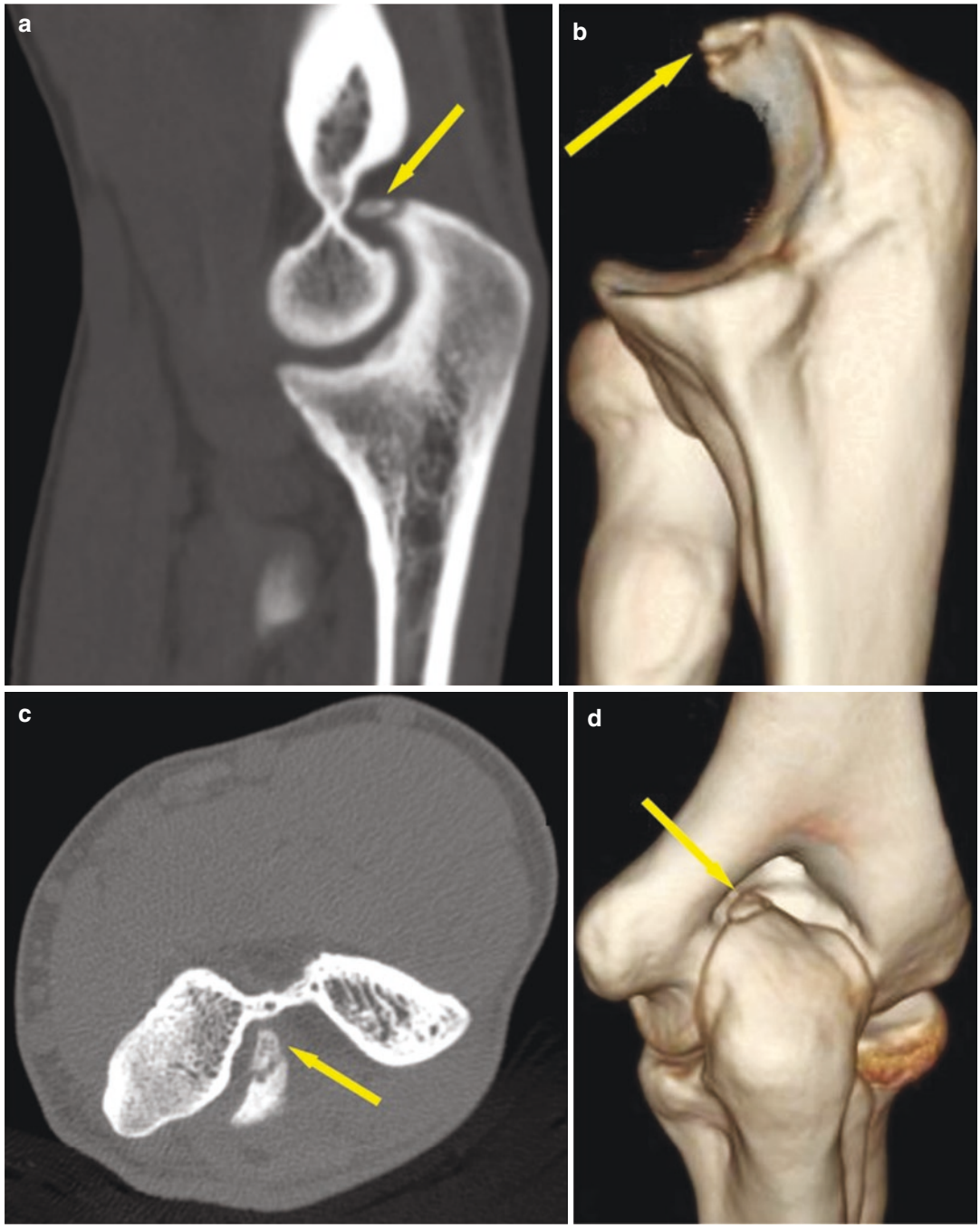

Fig. 20.3 (**a**–**d**) Elbow CT in a 20-year-old male baseball player who presented with several weeks of elbow pain and decreased throwing velocity. (**a**) Sagittal view demonstrating a fractured olecranon osteophyte (yellow arrow). (**b**) 3D reconstruction of the CT demonstrating the same osteophyte fracture. (**c**) Axial view demonstrating the osteophyte within the olecranon fossa. (**d**) Posterior view of the 3D reconstruction. (Reprinted with permission from Springer Books (Hilgersom et al., Valgus Extension Overload, Surgical Techniques for Trauma and Sports Related Injuries of the Elbow). The authors would like to acknowledge ISAKOS gives permission for reuse of this figure from a previous ISAKOS book

Fig. 20.4 Coronal T2 MRI of the same patient from Fig. 20.3 demonstrates an intact UCL and the presence of osteophytic change in the medial olecranon fossa. (Reprinted with permission from Springer Books (Hilgersom et al., Valgus Extension Overload, Surgical Techniques for Trauma and Sports Related Injuries of the Elbow). The authors would like to acknowledge ISAKOS gives permission for reuse of this figure from a previous ISAKOS book

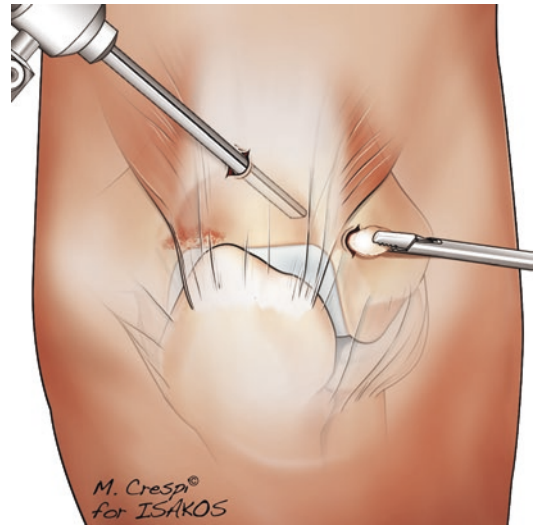

Fig. 20.5 View from outside the elbow of arthroscopic loose body removal. The arthroscope is placed through the direct posterior portal. The osteophyte has been debrided from the posteromedial olecranon and the olecranon fossa through a posterolateral portal. Arthroscopic removal of the loose body was performed using a grasper

The elbow joint is first distended by loading up to 40 mL of sterile saline via an 18-gauge needle through the lateral soft spot.

20.4.1 Posterior Compartment

The primary viewing portal may be either the posterolateral or the direct posterior portal, which is typically placed 2 cm proximal to the olecranon tip through the triceps tendon. The other portal created can be utilized as the working portal for instrumentation, including graspers, motorized shavers, or radiofrequency ablation devices (Fig. 20.5). An initial proximal posterolateral portal 2–3 cm proximal to the tip of the olecranon on the lateral border of the triceps tendon is created with a skin incision with an 11-blade knife. A blunt trocar is aimed towards the olecranon fossa. The posterior brachial cutaneous and posterior antebrachial cutaneous nerves are located approximately 25 mm from this portal, giving this area a large safe zone with which to establish the portal. A standard 4.0 mm, 30-degree arthroscope is placed to provide visualization of the entire posterior elbow compartment, including the olecranon tip and fossa. The posterocentral (straight posterior) portal is then created 2–3 cm proximal to olecranon tip. This generally pierces the musculotendinous junction and allows visualization of the entire olecranon fossa and medial and lateral gutters.

Osteophyte and chondromalacia at the posteromedial olecranon can be visualized and treated accordingly (Fig. 20.6a–d). The posterior radiocapitellar joint can also be visualized for pathology, such as loose bodies. Care must be taken when using instrumentation in the posteromedial gutter as the ulnar nerve lies superficial to the joint capsule in this location. One should refrain from suction when shaving in this area. Using a curved articulating retractor via an accessory posterolateral portal may help to retract the capsule and protect the ulnar nerve [1]. The olec-

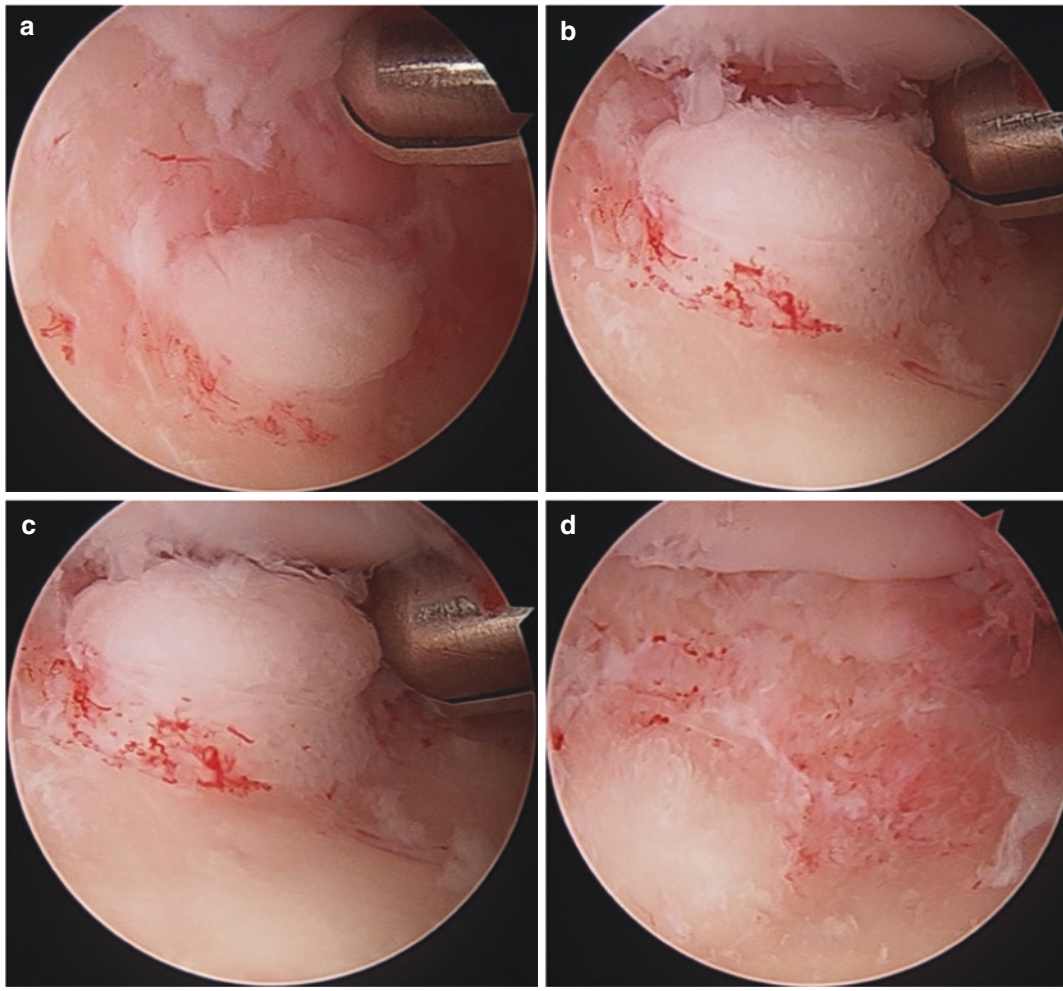

Fig. 20.6 (**a**–**d**) The same patient from Fig. 20.3 underwent arthroscopic debridement. (**a**) The posterolateral portal was used for arthroscopic viewing, while the direct posterior portal was used for instrumentation. The osteophyte within the medial olecranon fossa is identified at the tip of the shaver. (**b**–**c**) The elbow is ranged into terminal extension, which demonstrated impingement of the osteophyte with the olecranon. (**d**) The medial olecranon fossa is visualized immediately after debridement of the osteophyte. (Reprinted with permission from Springer Books (Hilgersom et al., Valgus Extension Overload, Surgical Techniques for Trauma and Sports Related Injuries of the Elbow). The authors would like to acknowledge ISAKOS gives permission for reuse of this figure from a previous ISAKOS book

ranon osteophyte may be encased in soft tissue, which can be seen as irregularly shaped protuberances and may require a combination of shaving and ablation to expose. Debridement should be restricted to the pathologic osteophytes and not into native olecranon, as over-resection of more than 3 mm of the native olecranon may cause further strain to the UCL during valgus loading. In non-throwing athletes, the risk of further strain and injury to UCL is less significant, and more aggressive debridement may be acceptable.

Bony debris are then carefully extracted, and the synovium should be carefully inspected for additional loose bodies. Intraoperative fluoroscopy may be used for confirmation. If impingement persists, the presence of olecranon fossa osteophytes should be evaluated and debrided accordingly. After the osteophyte debridement,

careful inspection of the trochlear chondral surface is performed to look for loose bodies, kissing lesions, or osteochondral defects. Additional procedures such as osteochondral debridement and microfracture are performed as indicated to address the articular cartilage pathology [3]. Arthrofibrosis is commonly seen in overhead athletes and may present in the setting of VEO. This should be evaluated during diagnostic arthroscopy and treated accordingly with capsular release, as residual flexion contracture is a devastating complication in the early postoperative period.

20.4.2 Anterior Compartment

If a diagnostic arthroscopy of the anterior compartment is indicated based on preoperative physical examination, symptoms, and imaging, entry via the proximal anteromedial portal can be accessed 2 cm proximal to the medial epicondyle, just anterior to the intermuscular septum. This portal allows for the assessment of loose bodies and osteochondral defects in the radiocapitellar joint, osteophytes of the coronoid tip and fossa, in addition to chondral lesions of the trochlea [1]. Further evaluation within the medial compartment involves dynamic stress test on the UCL. With the elbow in 70 degrees of flexion, valgus stress is applied to assess for UCL pathology, which is indicated by >3 mm medial trochlea gapping. If needed, a proximal anterolateral working portal would be created.

20.5 Tips and Tricks

- The ulnar nerve is at risk when working near the medial gutter of the elbow, as the nerve lies just superficial to the joint capsule. A curved articulating retractor can be placed via an accessory posterolateral portal to elevate the capsule and protect the adjacent nerve [1].
- Suction should also be extremely limited or disconnected when working with shavers and burrs in the medial gutter. The use of a hooded shaver may provide additional protection of the soft tissues.
- Careful demarcation of osteophyte and native olecranon is necessary to ensure accurate resection. A blunt instrument, such as a freer elevator, introduced from the direct posterior portal can be used to probe for the area of demarcation and to dislodge encased loose bodies.
- Avoid detaching the fragment to facilitate shaving or burring in a rather fixed position. Fragment retrieval is relatively easier through the posterolateral portal as opposed to the direct posterior portal due to fewer layers of soft tissue. Retrieval through the direct posterior portal requires traversing the triceps tendon.
- Osteophytes may form on both the ulnar (olecranon) and humeral sides (olecranon fossa). Simulation of elbow movement should be performed following resection to confirm adequate resection and therefore motion. Residual cause of impingement may be attributed to loose bodies in the posterior radiocapitellar joint.
- Lastly, the UCL and medial laxity should be carefully evaluated intraoperatively for insufficiency. This can be done with valgus stress with the elbow in 70 degrees of flexion.

20.6 Pitfalls

- One of the primary pitfalls occurs prior to surgery, as failure to differentiate VEO from other potential diagnoses of posterior elbow ailments may render the surgical outcomes less successful. A detailed history and physical examination are necessary to pinpoint the cause of pain and impingement in the throwing athlete. For example, medial elbow pain during the late cocking and early arm acceleration phases of throwing is indicative of UCL pathology, whereas posteromedial pain at terminal elbow extension and ball release during the deceleration phase is a more typical presentation of VEO. The athlete's

symptoms may be reproducible outside of throwing activities; however, posteromedial pain with resisted extension may point to tendonitis of the distal triceps.

- During surgery, if possible, one should avoid using a posteromedial portal to prevent iatrogenic injury to the ulnar nerve. All work can be performed through the direct posterior, posterolateral, direct lateral "soft-spot," and proximal lateral portals. While working in the posteromedial gutter, one should always be cognizant of the posterior ligament of the UCL complex and the ulnar nerve. Overexcision of the olecranon osteophyte increases strain on the UCL, potentially transforming a previously asymptomatic insufficient UCL to a symptomatically lax UCL, which will have significant consequences in the throwing athlete.

20.7 Postoperative Management and Rehabilitation

Postoperatively, the elbow is placed in soft, compressive dressing. For the first week, a simple sling may be used for comfort to minimize immobilization. A multiphasic rehabilitation protocol has been advocated and individualized to the sport-specific activities of the athlete.

Phase one: The initial postoperative goals are to restore joint motion, minimize edema and inflammation, and diminish muscle atrophy. The patient may begin passive and active-assisted range of motion (ROM) of the elbow and initiate physical therapy immediately after surgery. ROM exercises should focus not only on flexion/extension but also on forearm pronosupination to prevent joint contracture, which may significantly delay the rehabilitation process. Gradually, typically within the first week, the athlete may advance to active ROM and isometric strength exercises. Early strengthening in flexion/extension of the wrist and elbow, as well as pronosupination of the forearm, helps to minimize muscle atrophy from the injury. Strengthening of the flexor pronator mass further helps to stabilize the medial elbow. The criteria for advancing to the next phase include full, painless elbow ROM and at minimum 4/5 muscle strength.

Phase two: At usually 2 weeks, one may expect elbow motion to return to normal. During this phase, the physical therapy program may progress to include isotonic and resistance exercises to improve functional strength and flexibility of the entire throwing arm with a specific focus on proximal stability and proprioception. Weight-based and elastic band resistance training is performed to target rotator cuff and periscapular muscle function. Loss of glenohumeral ROM, especially internal rotation deficits, should be addressed. The criteria for advancement to the next phase include full painless ROM, no pain at the elbow, and less than 30% deficit in isokinetic strength testing compared to the contralateral arm.

Phase three: This phase typically commences at 3 or 4 weeks and aims to progressively increase the workload to prepare the athlete for return to sport. Plyometric exercises are initiated to continue to improve strength and endurance. An interval throwing program begins at 3–6 weeks after surgery and is gradually advanced to full throwing activities by 3–4 months after surgery, provided that the athlete no longer experiences pain with valgus stress or range of motion. During this rehabilitation period, prevention of future injury requires careful analysis and improvement in proper throwing mechanics. The rehabilitation program is tailored to the throwing athlete's competition level and individual ability and can therefore take 3–6 months before full clearance for sport [3]. Successful return to competitive overhead throwing is contingent upon painless range of motion and satisfactory isokinetic strength and clinical examination.

20.8 Complications

- Iatrogenic neurovascular injury is one of the most common complications of elbow arthroscopy. Nerve injury can occur secondary to knife laceration or blunt trocar penetration. Other described injury mechanisms include compression by an arthroscopic cannula,

swelling from fluid extravasation, or administration of local anesthetics. Utilization of suction should be minimized with the shaver to avoid risk to neurovascular structures, particularly the ulnar nerve when working around the medial aspect of the elbow. In the majority of cases, nerve injury from elbow arthroscopy is transient. A clear understanding of portal placement and potential neurovascular structures at risk is necessary prior to undertaking this technically demanding procedure.

- Debate continues to exist with respect to the optimal amount of osteophyte to remove. The consensus remains that it is only necessary to remove the pathologic lesion without debriding into the native, normal bone, because this adds strain to the UCL and poses a potential for further valgus instability.

20.9 Results

Park et al. [6] reported the first series specific to adolescent baseball players with VEO. The 13 players (seven pitchers) had a mean age of 15.4 years. Four of the players underwent a staged UCL reconstruction 2 weeks after arthroscopic olecranon tip resection. The other nine players had isolated olecranon osteophytes and demonstrated similar ROM but less pain at postoperative evaluation compared to players who required staged surgery. More importantly, the arthroscopic group demonstrated higher rate of return to pre-injury level of performance compared to the staged surgery group. These outcomes likely reflect the more serious nature of the associated UCL insufficiency injuries. Another subsequent series in adolescent baseball players evaluated 15 players with a mean age of 15.7 years [7]. Matsuura et al. [7] reported excellent postoperative elbow ROM and high rate of return to previous level of performance at a mean of 3.4 months after arthroscopic osteophyte excision.

Declaration of Conflict of Interest T. David Luo, M.D.
None declared.
Michael T. Freehill, M.D., F.A.O.A.
AOSSM: Medical Publishing Board of Trustees.
AAOS: Board or committee member.
AOSSM: Board or committee member.
AANA: Board or committee member.
ISAKOS: Board or committee member.
National Institutes of Health (NIH): Research funding.
Regeneration Technologies, Inc.: Research support.
Smith & Nephew: Paid consultant; Research support.
Integra: Paid consultant.

References

1. Paulino FE, Villacis DC, Ahmad CS. Valgus extension overload in baseball players. Am J Orthop (Belle Mead NJ). 2016;45(3):144–51. Epub 2016/03/19.
2. Ahmad CS, Park MC, Elattrache NS. Elbow medial ulnar collateral ligament insufficiency alters posteromedial olecranon contact. Am J Sports Med. 2004;32(7):1607–12. Epub 2004/10/21.
3. Byram IR, Kim HM, Levine WN, Ahmad CS. Elbow arthroscopic surgery update for sports medicine conditions. Am J Sports Med. 2013;41(9):2191–202. Epub 2013/04/11.
4. Miller CD, Savoie FH 3rd. Valgus extension injuries of the elbow in the throwing athlete. J Am Acad Orthop Surg. 1994;2(5):261–9. Epub 1994/10/01.
5. Chen FS, Rokito AS, Jobe FW. Medial elbow problems in the overhead-throwing athlete. J Am Acad Orthop Surg. 2001;9(2):99–113. Epub 2001/04/03.
6. Park JY, Yoo HY, Chung SW, Lee SJ, Kim NR, Ki SY, et al. Valgus extension overload syndrome in adolescent baseball players: clinical characteristics and surgical outcomes. J Shoulder Elbow Surg. 2016;25(12):2048–56. Epub 2016/10/22.
7. Matsuura T, Iwame T, Suzue N, Iwase J, Tamaki S, Yokoyama K, et al. Clinical outcome of arthroscopic treatment for posteromedial elbow impingement in adolescent baseball players. Arthroscopy. 2018;34(1):105–10. Epub 2017/09/04.

Part IV

Elbow: Fractures

Arthroscopic Approaches to Radial Head Fracture Fixation

21

Davide Cucchi, Francesco Luceri, Paolo Arrigoni, Roslind Karolina Hackenberg, Alfonso Vaquero-Picado, and Raul Barco

21.1 Background

In specific fracture types, arthroscopic fixation of radial head (RH) fractures can be a valid alternative to the classic open reduction and internal fixation. Arthroscopy allows direct visualization of the articular surface of the RH, improving the understanding of the fracture's morphology and anatomical reduction. Furthermore, it allows assessment and treatment of concomitant intra-articular pathology, including cartilage defects, ligament injuries, and loose bodies. Arthroscopy also has the advantage of producing minimal damage to the soft tissues and maintains an intact blood supply, possibly improving healing, and decreasing analgesic requirement and hospital stay.

Arthroscopic fixation of RH fractures is currently accepted for type II fractures and less comminuted type III fractures, according to the Mason classification, with indications steadily evolving as surgeons' skills increase. Although current literature is still scarce, especially in studies comparing open and arthroscopic fixation techniques, the results of the available case series are encouraging.

Arthroscopic RH fixation is technically demanding and potentially time consuming, with specific risks and complications [1, 2]. Two aspects are particularly relevant and challenging: appropriate choice of the surgical approach and strategic placement of Kirschner wires for temporary fixation, which will subsequently guide cannulated screws for definitive fixation.

This chapter describes anatomical and functional information relevant to portal placement and outlines arthroscopic approaches that can be used to address RH fractures efficiently.

Davide Cucchi and Francesco Luceri contributed equally with all other contributors.

D. Cucchi · R. K. Hackenberg
Department of Orthopaedics and Trauma Surgery, Universitätsklinikum Bonn, Bonn, Germany
e-mail: roslind.hackenberg@ukbonn.de

F. Luceri
IRCCS Istituto Ortopedico Galeazzi, Milan, Italy

P. Arrigoni
Laboratory of Applied Biomechanics, Department of Biomedical Sciences for Health, Università degli Studi di Milano, Milan, Italy

U.O.C. 1° Clinica Ortopedica, ASST Centro Specialistico Ortopedico Traumatologico Gaetano Pini-CTO, Milan, Italy

REsearch Center for Adult and Pediatric Rheumatic Diseases (RECAP-RD), Department of Biomedical Sciences for Health, Università degli Studi di Milano, Milan, Italy

A. Vaquero-Picado · R. Barco (✉)
Shoulder and Elbow Unit, Hospital Universitario La Paz, Madrid, Spain

© ISAKOS 2022

D. N. Bhatia et al. (eds.), *Arthroscopy and Endoscopy of the Elbow, Wrist and Hand*,
https://doi.org/10.1007/978-3-030-79423-1_21

21.2 General Considerations

During open reduction and internal fixation, the surgical approach permits screw placement in the desired position relatively easily. On the contrary, in arthroscopically assisted procedures, screw trajectory is restricted by portal placement. In fact, once a portal has been established, only minimal deviations in the course between this portal and the RH surface are allowed due to limited soft-tissue displacement and interference of the annular ligament, the radiocapitellar plica, and the overlying muscles. The resistance of all these structures, especially of the annular ligament, can be enough to sidetrack the thin Kirschner wires, which are used to guide cannulated screw placement. Careful selection of the surgical approach is, therefore, of importance for a swift and successful procedure.

Another issue that can influence proper screw placement is the fact that the arthroscopic view is 2-dimensional (screen). Thus, malpositioning of the guide wires is possible, since the RH is a 3-dimensional structure; in addition, the surgeon usually only sees approximately half of it through the arthroscope. To minimize malpositioning due to a limited view, it is critical to obtain an ample and safe working volume and visualize the RH properly. Whenever working intra-articularly on the lateral aspect of the elbow, adequate joint distension, elbow flexion, and forearm supination are recommended, since this position can increase the distance between the most anterior part of the RH and the anterolateral elbow capsule where the posterior interosseous nerve (PIN) lies [3–5].

Most fractures of the RH involve the anterolateral quadrant, which makes the anterior portals the most versatile; however a minority of fractures involve also the posterior quadrants, which are amenable to fixation from a posterior portal. In surgical planning and execution, selecting the appropriate viewing and working portals is a relevant factor for a successful surgery. It is worth reminding that, as a general biomechanical principle, for bones not subject to axial loads as the proximal radius, superior primary stability of screw osteosynthesis is obtained by a screw inserted perpendicular to the fracture line.

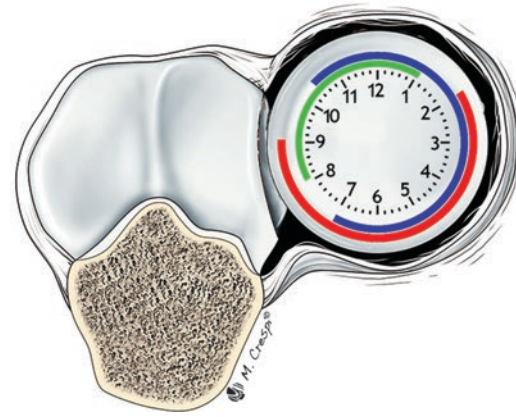

Fig. 21.1 Diagram of the radial head (RH) with superimposed clock reference demonstrating the average arc of the RH, which can be contacted from the anteromedial portal (green), anterolateral portal (blue), and midlateral portal (red). (Reprinted with permission from Springer Nature Customer Service Centre GmbH: Springer Nature; Knee Surgery, Sports Traumatology, Arthroscopy; Cucchi et al. [6], Copyright © 2018, Springer Nature)

Therefore, specific knowledge of the possibilities and limits of each arthroscopic portal is of importance to plan and successfully perform surgery. Recent studies demonstrated that the whole RH circumference can be effectively addressed for fixation of RH fractures with appropriate use of anterolateral (AL), anteromedial (AM), and midlateral (ML) portals and adequate pronation and supination maneuvers of the forearm, which can help in achieving the desired screw trajectory. Advantages and disadvantages of each portal will be discussed in detail in the following sections (Fig. 21.1).

21.3 Lateral Portals

The AL portal provides a wider arc of access to the RH when compared to the AM and ML portals, permitting to reach over the half of the RH circumference (Fig. 21.1), due to its close relation to the RH and the fact that the annular ligament is most mobile in its anterolateral part [6].

When performing any lateral approach to the elbow, special attention must be paid not to endanger the PIN, although this has been reported as an extremely rare adverse event after an

arthroscopic procedure [1, 2]. The PIN, in its proximal course, is separated from the joint capsule by the brachialis muscle, whereas at the level of the RH, no muscle bellies divide the joint from this delicate structure, which lies just extracapsular surrounded by a thin layer of adipose tissue [4]. Injury to the PIN may, therefore, occur, especially when placing a very distal AL portal [1, 4, 7]. Pearls and pitfalls regarding the safety of the PIN have been described in several studies: these must be considered especially during portal placement and during intra-articular procedures, which may accidentally damage the anterior joint capsule [1, 7]. Experience gained in open surgery showed that in full pronation of the forearm, the nerve displaces anteromedially, increasing its distance from the lateral midline as compared to a neutral position and full supination. This behavior has also been confirmed in an arthroscopic cadaveric setting (Fig. 21.2), thus extending the recommendation "protection with pronation" to all situations in which extra-articular procedures with sharp instruments are to be performed on the lateral side of the elbow. This includes establishing any AL portal, inserting Kirschner wires or screws for fracture fixation, or removing bony fragments or loose bodies through lateral portals. Uninterrupted prolonged periods of hyperpronation should be avoided, since this may increase excessively the pressure on the PIN beneath the arcade of Frohse. As an alternative or adjunct to forearm pronation, a retractor can be inserted through an additional proximal AL portal located approximately 3 cm proximal and 1 cm anterior to the lateral epicondyle and directed to the radiocapitellar joint, through which the anterior cap-

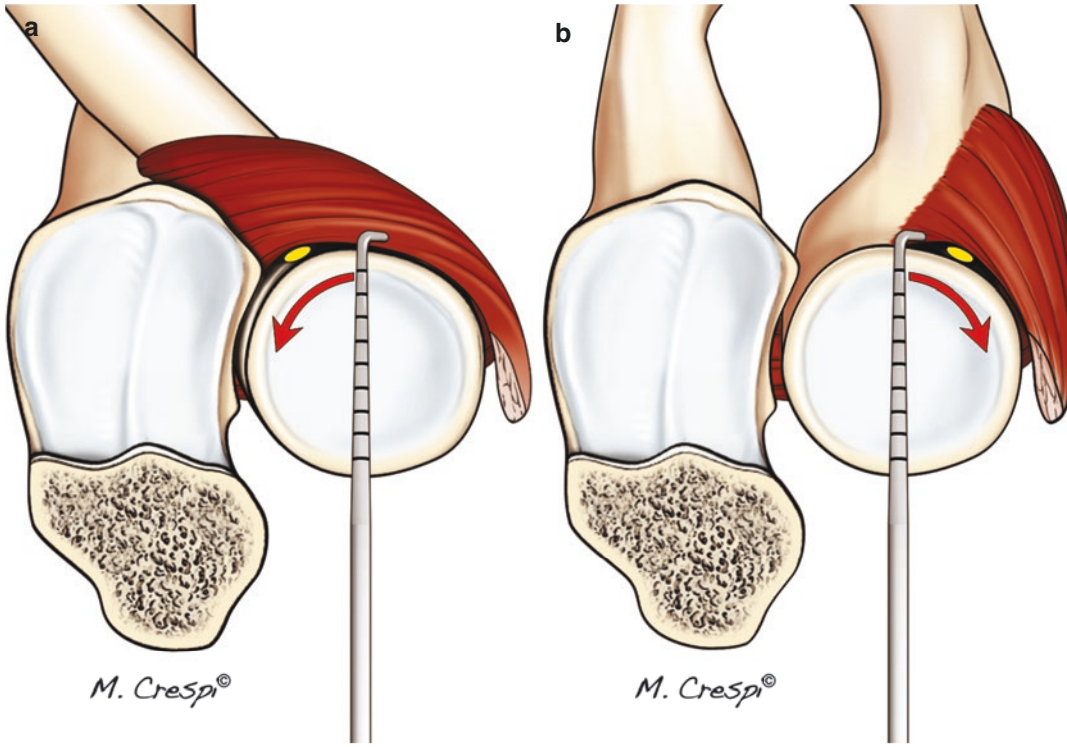

Fig. 21.2 Illustration of the relative position of the posterior interosseous nerve with respect to the anterior aspect of the radial head, as seen intra-articularly. The posterior interosseous nerve (in *yellow*) moves from a medial position with the forearm in full pronation (**a**) to a lateral position with the forearm in full supination (**b**). (Reprinted with permission from Elsevier Inc.: Journal of Shoulder and Elbow Surgery; Arrigoni et al. [3], Copyright © 2018 Journal of Shoulder and Elbow Surgery Board of Trustees)

sule can be displaced anteromedially. This maneuver improves the intra-articular space but does not change the close relationship between the capsule and the PIN.

Several variations of the extremely versatile AL portal have been proposed. In particular, establishing the AL portal in a more distal position (1 cm proximal and 1 cm anterior to the lateral epicondyle) permits to place guide wires for cannulated screws in a "flatter" trajectory, very close to the plane of the RH articular surface (Fig. 21.3), direction in which the commonly used lag screws achieve their highest primary stability, enhancing biomechanical performance of fixation. A distal AL portal appeared reproducible and precise in a cadaveric setting, suggesting potential for a better intraoperative handling of fracture fragments [8] (Fig. 21.4). Especially when placing a distal AL portal, care should be taken not to endanger the PIN, achieving a compromise between ideal biomechanical fixation and safety of the procedure.

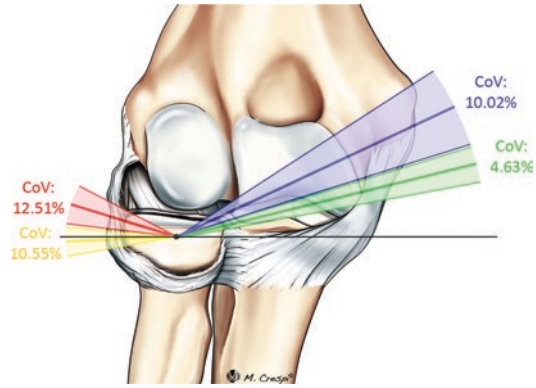

Fig. 21.4 Diagram illustrating the RH with superimposed angles for possible Kirschner wire placement form different portals (thick solid lines) and their 95% confidence interval (colored area) for the standard (red) and distal (yellow) anterolateral portals and standard (blue) and distal (green) anteromedial portals. The width of each colored area is related to the coefficient of variation (CoV) among different observers. (Reprinted with permission from Springer Nature Customer Service Centre GmbH: Springer Nature; Knee Surgery, Sports Traumatology, Arthroscopy; Cucchi et al. [8], Copyright © 2019, Springer Nature)

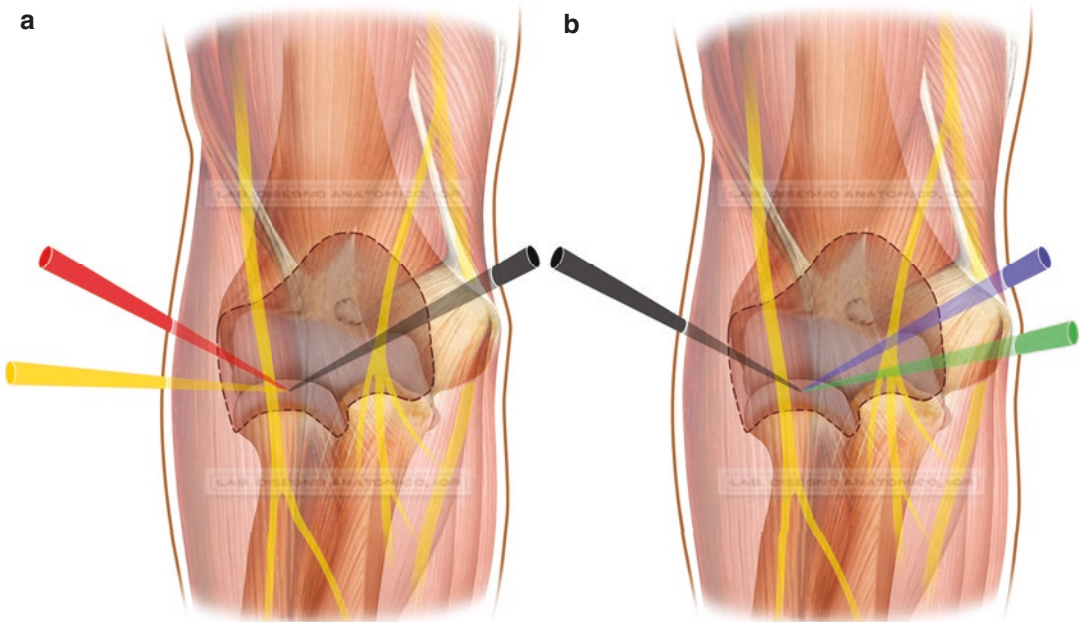

Fig. 21.3 Graphic illustration of a simulated arthroscopic setting with standard and distal arthroscopic portals, illustrating arthroscope and Kirschner wire positions to address the RH from (**a**) standard (red) and distal (yellow) anterolateral portals and (**b**) standard (blue) and distal (green) anteromedial portals. The arthroscope's position is represented in black. (Reprinted with permission from Springer Nature Customer Service Centre GmbH: Springer Nature; Knee Surgery, Sports Traumatology, Arthroscopy; Cucchi et al. [8], Copyright © 2019, Springer Nature)

21.4 Medial Portals

The AM portal permits access to approximately 150° of the RH circumference when rotating the forearm from full pronation to full supination, covering the entire anteromedial quadrant (Fig. 21.1). As compared to the standard AL and the ML portal, it appears to be the most reproducible among different observers. Furthermore, the very distensible capsule in the anteromedial aspect of the elbow allows to obtain a wide safe working volume, superior to that from the AL and ML portals [6]. A retractor inserted through an accessory AM portal can further increase the working volume displacing the anterior capsule anteriorly.

Similarly as in the AL portal, a distalization of the standard AM portal also permits the surgeon to place Kirschner wires in a "flatter" trajectory, facilitating a more parallel placement of the screws with respect to the RH articular surface (Fig. 21.3). As opposed to a distal AL portal, the presence of the coronoid process prevents placement of the guide wires perfectly parallel to the RH articular surface, maintaining a minimal inclination; nevertheless, placement through this portal appears even more precise and reproducible as compared to AL portals (Fig. 21.4) [8]. A distalization of the AM portal can be conducted rather safely, with only a moderate risk of endangering the brachial artery and the median nerve, which lie more superficially, between the muscle bellies of the biceps brachii and the brachialis, and follow the medial border of the biceps brachii in an anterolateral direction. Nevertheless, elbow flexion and fluid joint distension are recommended to increase the distance of the median nerve to the anterior tip of the coronoid and to the anterior border of the trochlea, reducing the risk for neurovascular injuries during placement of medial portals [5, 9, 10]. Regarding the role of forearm rotation, conflicting results have been published, and no clear evidence exists to recommend a specific position (Fig. 21.5).

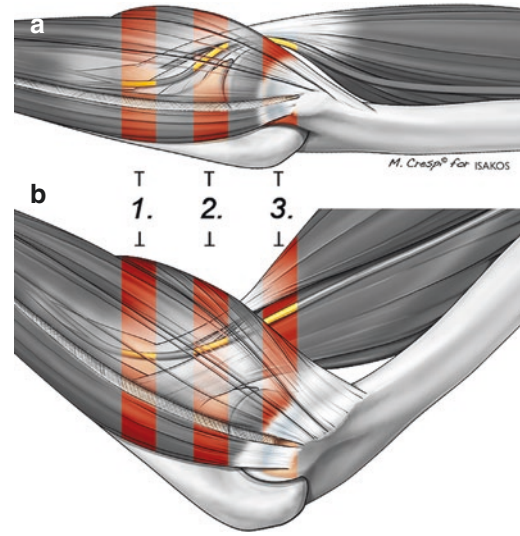

Fig. 21.5 Illustration of the relative position of the median nerve (in *yellow*) with respect to the anteromedial aspect of the elbow. The distance of the median nerve to osseous landmarks increases with elbow flexion (**b**), as compared to full extension (**a**): this is highly relevant for surgical procedures performed at the level of the distal (1) and proximal (2) insertion of the brachialis muscle on the ulnar shaft, at the level of the coronoid tip (2a) and at the level of the medial edge of the humeral trochlea (3) (M. Crespi © for D. Cucchi)

21.5 Posterior Portals

Alternatively to anterior portals, screw fixation via a posterior portal can also be considered. For this purpose, a midlateral portal can be created using external anatomical landmarks (in the middle of a virtual triangle formed by the olecranon's tip, lateral epicondyle, and radial head) or under direct visual control from the AL portal by introducing a needle at the desired level immediately above the superior margin of the RH. This portal allows to contact a relatively wide arc of the RH, covering both posterior quadrants (Fig. 21.1) [6]. However, since most fracture lines enter the posterolateral quadrant and exit the RH through the anterior quadrants, posterior portals frequently allow only a demanding indirect fixation, thus making anterior portals a more versatile option.

A wider variability among surgeons is observed when working from a midlateral portal as compared with anterior portals, showing divergence among operators and thus suggesting caution in the clinical practice, especially for less experienced surgeons. A technical difficulty, which can be encountered when attempting fixation from a posterior portal, is the fact that the annular ligament is less mobile close to the ulnar insertion and this may interfere with screw trajectory; as opposed to this, in the anterolateral aspect of the elbow this ligament is more mobile and more distal with respect to the RH articular plane, allowing more distal screw placement without interference. Nevertheless no relevant neurovascular structures run on the posterolateral aspect of the elbow, making the creation of a midlateral portal extremely safe.

21.6 Conclusion

This chapter reviewed the arthroscopic approaches to achieve an arthroscopic radial head fixation. Although specific portals can be recommended for specific radial head fracture patterns, it is not infrequent to find the need to address these fractures from different portals to adequately assess the fracture lines and find the best angle of approach while minimizing the risk to the neurovascular structures. As with other arthroscopic procedures, experience improves the procedural steps so that cadaver surgical skill labs are strongly recommended to practice these approaches.

References

1. Kelly EW, Morrey BF, O'Driscoll SW. Complications of elbow arthroscopy. J Bone Joint Surg Am. 2001;83-A:25–34.
2. Desai MJ, Mithani SK, Lodha SJ, Richard MJ, Leversedge FJ, Ruch DS. Major peripheral nerve injuries after elbow arthroscopy. Arthroscopy. 2016;32:999–1002.e8.
3. Arrigoni P, Cucchi D, Menon A, Guerra E, Nicoletti S, Colozza A, Luceri F, Pederzini LA, Randelli PS. The posterior interosseous nerve crosses the radial head midline and increases its distance from bony structures with supination of the forearm. J Shoulder Elbow Surg. 2019;28(2):365–70. https://doi.org/10.1016/j.jse.2018.08.019.
4. Arrigoni P, Cucchi D, Guerra E, Marinelli A, Menon A, Randelli PS, Pederzini LA, SIGASCOT Upper Limb Committee. Distance of the posterior interosseous nerve from the radial head during elbow arthroscopy: an anatomical study. Joints. 2017;5:147–51.
5. Hackl M, Lappen S, Burkhart KJ, Leschinger T, Scaal M, Müller LP, Wegmann K. Elbow positioning and joint insufflation substantially influence median and radial nerve locations. Clin Orthop Relat Res. 2015;473:3627–34.
6. Cucchi D, Guerra E, Luceri F, Lenich A, Nicoletti S, Randelli P, Wirtz DC, Eygendaal D, Arrigoni P, ESSKA Elbow and Wrist Committee 2016–2018. A combination of an anteromedial, anterolateral and midlateral portals is sufficient for 360° exposure of the radial head for arthroscopic fracture fixation. Knee Surg Sports Traumatol Arthrosc. 2019;27(1):319–25. https://doi.org/10.1007/s00167-018-5077-1.
7. Lawton JN, Cameron-Donaldson M, Blazar PE, Moore JR. Anatomic considerations regarding the posterior interosseous nerve at the elbow. J Shoulder Elbow Surg. 2007;16:502–7.
8. Cucchi D, Arrigoni P, Luceri F, et al. Modified anteromedial and anterolateral elbow arthroscopy portals show superiority to standard portals in guiding arthroscopic radial head screw fixation. Knee Surg Sport Traumatol Arthrosc. 2019;27(10):3276–83. https://doi.org/10.1007/s00167-019-05411-8.
9. Cushing T, Finley Z, O'Brien MJ, Savoie FH, Myers L, Medvedev G. Safety of anteromedial portals in elbow arthroscopy: a systematic review of cadaveric studies. Arthroscopy. 2019;35:2164–72.
10. Arrigoni P, Cucchi D, Guerra E, Luceri F, Nicoletti S, Menon A, Randelli P. No neurovascular damage after creation of an accessory anteromedial portal for arthroscopic reduction and fixation of coronoid fractures. Knee Surg Sports Traumatol Arthrosc. 2019;27:314–8.

22 Arthroscopic Reduction and Internal Fixation of Elbow Fractures

Enrico Guerra, Alessandro Marinelli, Marco Cavallo, Alice Ritali, Andrea Sessa, and Roberto Rotini

22.1 Background

Arthroscopic reduction and internal fixation (ARIF) procedures in elbow surgery have evolved over the last 15 years [1–4]. In specific types of radial head, capitellum, and coronoid fractures the possibility to reduce small fractured fragments and to fix them with a minimal soft-tissue damage is an appealing option for surgeons skilled in elbow arthroscopy. In addition to the fracture fixation, the arthroscopic technique allows hematoma removal, assessment of intra-articular damage, and excision of small osteochondral fragments. Additionally, elbow stability can be evaluated and associated bony and soft-tissue lesions can be treated. Arthroscopic techniques involve minimal surgical trauma, and may prevent heterotopic ossification. Encouraging results have been reported by few authors; however there is no evidence to suggest faster recovery and better outcomes with less morbidity in comparison with open surgery [5].

Although specific risks and complications have been described, the indications are steadily being defined and surgical techniques are improving. Dedicated instrumentation including specific target guides and cannulas, long cannulated drill, and screwdrivers is currently under development.

The purpose of this chapter is to present the indications, advantages, and surgical techniques of ARIF for intra-articular elbow fractures, and it is based on the authors' personal experience and literature review. The techniques are segregated into four sections for radial head fractures, capitellum and trochlear fractures, coronoid fractures, and combined fractures (terrible triads).

22.2 Radial Head Fractures

ARIF of radial head fractures has advantages over the open approaches. The arthroscopic technique is minimally invasive and preserves the capsular/ligament complex and annular ligament. Occasionally, patients with apparent benign and stable radial head fractures present with more than usual pain and stiffness, especially in forearm rotation. Arthroscopy in these cases may reveal a capitellum cartilaginous lesion (not detectable by the CT scan), with the fragment trapped within the radial head fracture. In these cases, the arthroscopic treatment, consisting of identification of the lesion, removal of the interposed fragment, and, if necessary, stabilization of the radial head fracture, can be a convincing

E. Guerra (✉) · A. Marinelli · M. Cavallo · A. Ritali
A. Sessa · R. Rotini
Shoulder and Elbow Unit, IRCCS Rizzoli Orthopedic Institute, Bologna, Italy
e-mail: enrico.guerra@ior.it; alessandro.marinelli@ior.it; marco.cavallo@ior.it; alice.ritali@ior.it; andrea.sessa@ior.it; roberto.rotini@ior.it

© ISAKOS 2022

D. N. Bhatia et al. (eds.), *Arthroscopy and Endoscopy of the Elbow, Wrist and Hand*,
https://doi.org/10.1007/978-3-030-79423-1_22

treatment option, compared to open surgery. However, arthroscopic radial head fixation is a technically demanding and potentially time-consuming procedure, with specific risks and complications.

22.2.1 Indications and Contraindications

Arthroscopic reduction and internal fixation (ARIF) of radial head fractures is indicated in relatively simple patterns:

- Mason type 1 (if the conservative treatment is considered suboptimal) and some Mason type 2 fractures.
- Specifically, ARIF can be considered for fractures not involving the entire radial head (segmental fractures of the neck), with a maximum of two displaced fragments, both still partially attached to the steady fragment of the radial head.
- Low-grade collateral ligament lesions, with no or mild instability (joint space opening <4 mm under stress), are not a contraindication for the arthroscopic technique.

Contraindications for ARIF technique include Mason type 3 fractures with comminution and fragmentation (fractures with more than three main fragments), complete involvement of the radial neck, and displacement (>5 mm). Other contraindications are fractures associated with significant collateral ligament injuries and/or epicondylar tendon avulsion, or other associated lesions, requiring an open (posterior or lateral) approach.

22.2.2 Surgical Technique

Surgical setup: The patient is positioned in lateral decubitus, with the affected arm supported by a dedicated holder. Anatomical landmarks are drawn and tourniquet is inflated. A spinal needle is inserted through the "soft spot" posterolaterally, to inject sterile saline solution and drain the intra-articular hematoma. This maneuver can be performed also posteriorly through the triceps muscle, but the correct identification of the soft spot is useful to confirm the proper placement of the bony landmarks that are not always easy to be palpated in swollen joints. Pump pressure is kept close to 30–40 mm Hg.

22.2.2.1 Portals

Standard anterior portals:

- Anterolateral (A-L)
- Anteromedial (A-M)
- Proximal anterolateral (pA-L)

The arthroscope is introduced through the A-M portal. The A-L portal is initially used for working instruments and the pA-L for intra-articular retractor.

Standard posterior portals:

- Postero-central (PC)
- Posterolateral (P-L)
- Mid-lateral (M-L)

These are useful to explore the posterior compartment, and for draining the posterior hematoma and removing possible loose bodies.

Specific portals for radial head fractures: With the three standard portals (A-M, A-L, and pA-L), with the help of the forearm rotation, the whole radial head circumference can be effectively exposed. However, to fix the fracture, based on its position, different accessory portals are needed [6, 7]:

- Mid-lateral (M-L) portal is useful for reduction or temporary K-wire fixation.
- Accessory A-L (aA-L) portal is placed slightly distal to the standard A-L portal to optimize the direction of the screw fixation [8].
- Posterolateral (P-L) portal.

22.2.2.2 Reduction

With the scope in the A-M portal, two probes are inserted through the A-L and pA-L portals. Using forearm rotation to assist the maneuver, the fractured fragments are mobilized and then reduced. If necessary, to achieve and maintain the reduction, a third probe can be inserted through the

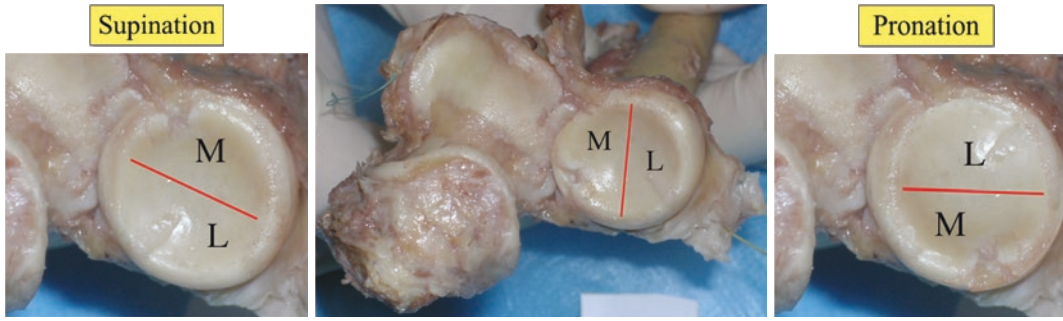

Fig. 22.1 Cadaver specimen showing the medial (M) and the lateral (L) halves of the radial head in different positions of forearm rotation

M-L portal (soft spot). When in doubt, a further confirmation of the reduction can be obtained through visualization via the A-L portal. Once the fragment reduction is achieved, fixation can be performed as described below.

22.2.2.3 Fixation

The working position for screw fixation should be based on the location of the fracture and the safe zone (the part of the radial head that does not come in contact with the lesser sigmoid notch during forearm rotation). Keeping the forearm in neutral rotation, the radial head can be divided into two zones: the medial half includes majority of the articular part of radial head, and the lateral half includes the safe zone (Figs. 22.1 and 22.2).

- Fractures of the ***lateral half*** can be fixed from the anterior aspect (*AL working position*) for reduction, and keeping the forearm in pronation (Figs. 22.2b and 22.3f–j). A 5 mm cannula is inserted through the aA-L portal to protect soft tissues from the rotating tools (K-wire, drills, screwdriver) as well as to prevent bending or breaking of the thin guide wires used to insert the small cannulated screws.
- For the more unstable fractures, fragments can be stabilized with provisional 1.2 mm K-wires inserted from posterior (M-L portal) or lateral (A-L or aA-L) portal. Once the fracture is stable, the guide wire is inserted through the cannula in the aA-L portal and the fixation procedure is performed with drilling and screw insertion.
- The fractures of the lateral half of the radial head could be alternatively fixed working posteriorly (*PL working position*), as described by Rolla et al. [9] (Figs. 22.2c and 22.3a–e). Two accessory portals are necessary: P-L and M-L. A shaver and probe are used to create the space to visualize the fragment. The fixation technique is the same as described. The aA-L portal is necessary to let the cannula and guide wires/screws to enter.
- In the ***medial half fractures***, it is really helpful to use the A-M working position. Looking from the A-L portal, the cannula is inserted through the A-M portal (Figs. 22.2a and 22.3k–r). The fixation technique is the same, and is technically less demanding (especially if more than one screw is necessary) and without requiring accessory portals.
- Because of the difficulty in measurement of screw length over the guide wire, screws from 14 to 18 mm in length are generally used. Radiographs in different positions of forearm rotation are performed after all temporary K-wires are removed.

22.3 Fractures of the Capitellum and Trochlea

The ARIF technique can be used to perform fixation with minimal soft-tissue dissection and associated intra-articular lesions can be addressed simultaneously. The technique is demanding and requires specific skills in elbow arthroscopy. With the arthroscopic technique the screw insertion direction is from posterior

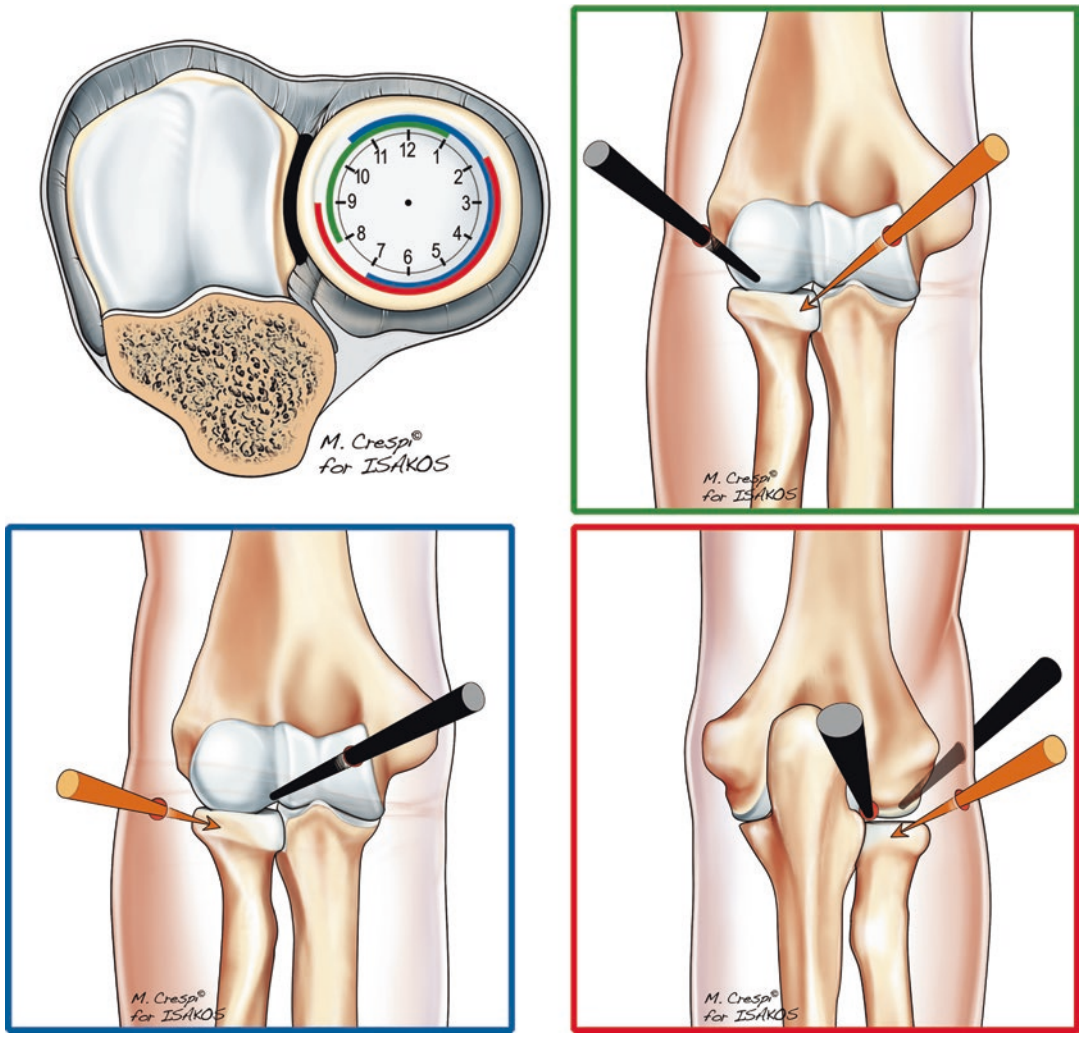

Fig. 22.2 Different working positions to fix radial head fractures arthroscopically are illustrated. The radial head, conventionally shown in neutral forearm rotation, is represented with a superimposed clock reference. The arthroscope position is outlined with a black rod, and the working portal with an orange rod. Based on the radial fracture position, three different arthroscopic working settings can be selected. (**a**) Fractures involving the anteromedial part of the radial head (green arc on the clock) can be fixed through an A-M working portal. (**b**) Fractures involving the anterior and lateral part of the radial head (blue arc) can be fixed with an accessory A-L working portal. (**c**) Fractures involving the posterior part of the radial head can be fixed through an accessory A-L working portal, while looking through the mid-lateral or posterolateral portal (M. Crespi © for ISAKOS)

to anterior to avoid the risk of radial nerve injury. Lateral collateral ligament lesion is reported to be present in up to 40% of the cases, and in these cases, an open technique is recommended. An unrecognized posterior impaction may impede the fragment reduction with arthroscopic technique.

22.3.1 Indications and Contraindications

ARIF of capitellum and trochlear fractures is indicated in relatively simple patterns: a single fragment involving primarily the capitellum, with or without involvement of the lateral troch-

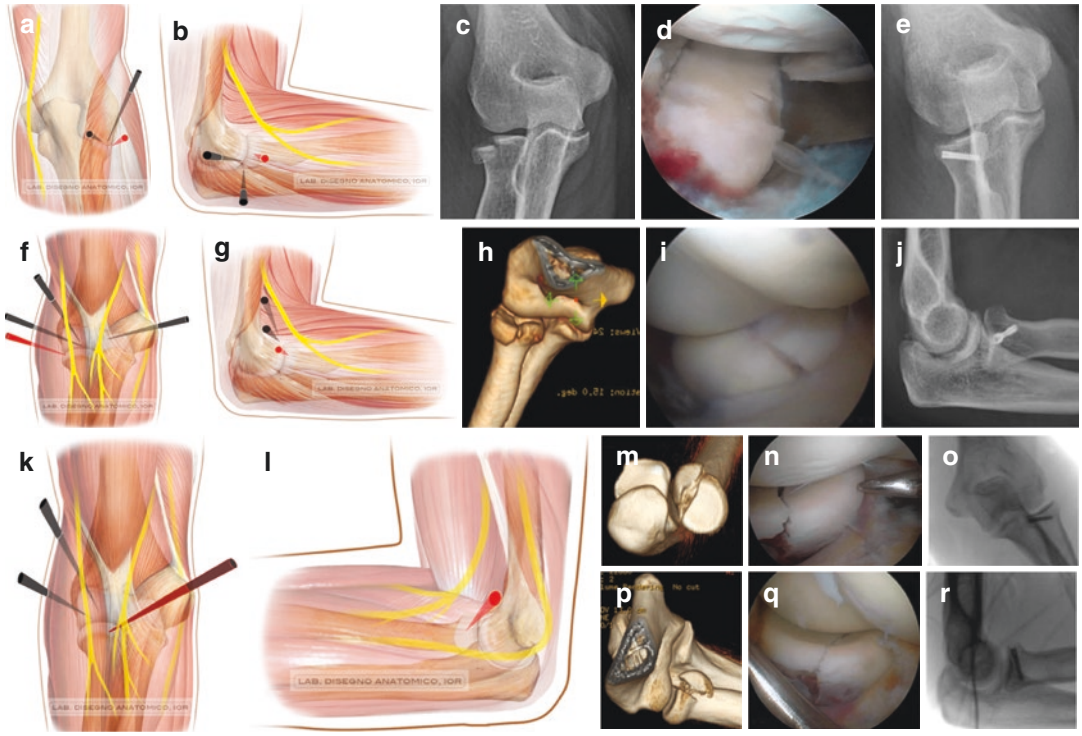

Fig. 22.3 Clinical cases showing the three possible working positions. The red rods represent the portal used to fix the fracture. The black rods represent portals used for the arthroscope and retractors. (**a**, **b**) Posterolateral working position. (**c**) Fracture involving the posterior part of the radial head. (**d**) Arthroscopic view of the fracture reduction. (**e**) Postoperative X-ray showing screw fixation. (**f**, **g**) Anterolateral working position. (**h**) Fracture involving the lateral part of the radial head. (**i**) Arthroscopic view of the fracture reduction. (**j**) Postoperative X-ray showing screw fixation. (**k**, **l**) Anteromedial working position. (**m**, **p**) Fracture involving the medial part of the radial head. (**n**, **q**) Arthroscopic view of fracture reduction. (**o**, **r**) Postoperative X-ray showing screw fixation (Courtesy of Lab Anatomico IOR)

lear ridge, and without involvement of the posterior condyle (Dubberley classification type 1A).

Contraindications include:

- Comminuted fractures of the articular surface (Bryan-Morrey classification type 3), or fractures of both the capitellum and the trochlea as separate fragments (Dubberley classification types 2 and 3)
  - Fractures involving the lateral epicondyle, posterior aspect of the lateral column, posterior aspect of the trochlea, medial epicondyle (Ring classification types 2–5, or Dubberley classification types 1B, 2B, and 3B)
  - Associated lateral collateral ligament (LCL) lesion

22.3.2 Surgical Technique

Surgical setup and portals: These are the same as described for the radial head fractures.

Reduction: The arthroscope is initially placed in the A-M portal and the fragment reduction is performed through the two lateral portals (A-L and pA-L) (Fig. 22.4a–d). The reduction may be facilitated by placing the elbow in extension; however, in the authors' experience, extension reduces the anterior joint space and the elbow should be flexed at 90°.

Fixation: Viewing through the A-M portal and working with two anterolateral portals (A-L and pA-L), percutaneous fixation is performed

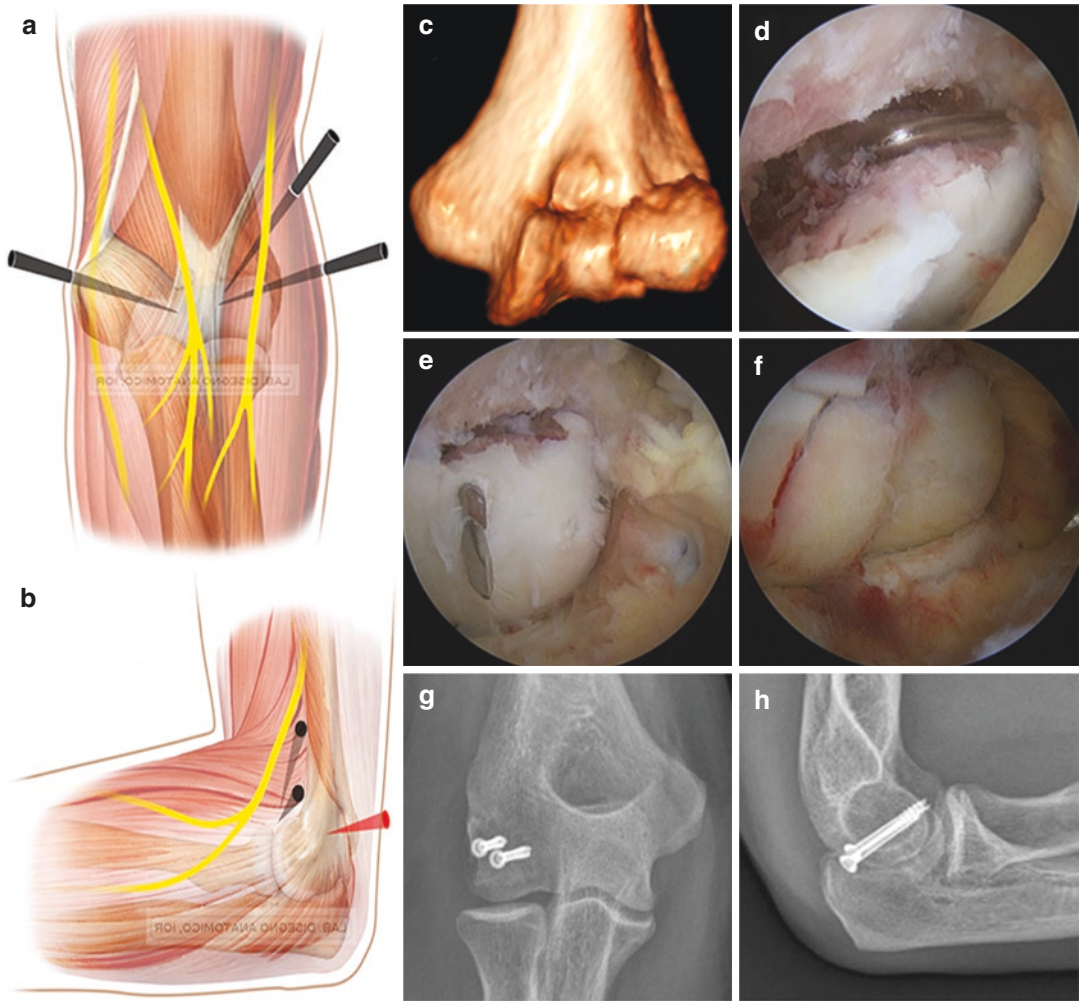

Fig. 22.4 ARIF technique of a capitellar fracture. (**a**, **b**) Arthroscopic portals. The red rod represents the direction in which the percutaneous screws are inserted. (**c**) CT scan shows a relatively simple fracture of the capitellum: a single fragment involving a small part of the lateral trochlear ridge (Dubberley classification type 1A). (**d**) The fracture is reduced with a probe. (**e**) Temporary fixation is performed with K-wires. (**f**) Final intra-articular view of the fracture. (**g**, **h**) Postoperative radiographs (Courtesy of Lab Anatomico IOR)

with temporary K-wires (Fig. 22.4e, f) and cannulated screws (Fig. 22.4g, h). These are inserted from posterior to anterior under fluoroscopic control. If the fractured osteochondral fragment is thin, and an anteroposterior screw direction is preferred, a small incision joining the A-L portal to M-L one (following the incision of the Kocher approach) can be performed to avoid the risk of harming the radial nerve.

22.4 Fractures of the Coronoid Process

ARIF of coronoid fractures avoids extensive soft-tissue dissection that is performed during open surgery in the medial compartment. The fixation can be performed with K-wires, cannulated screws, or sutures. Contrary to the open technique, the ulnar nerve release is not usually required.

22.4.1 Indications and Contraindications

ARIF technique for coronoid fractures is indicated in relatively simple patterns:

- Isolated coronoid tip or anteromedial fractures, not involving the sublime tubercle and without severe displacement or significant joint instability.
- Low-grade collateral ligament lesions, with no or mild instability (joint space opening <4 mm under stress), are not a contraindication for the arthroscopic technique. At the end of the procedure, in less severe LCL lesions, a posterolateral capsule-ligament plication can be performed [10].

Contraindications include:

- Preoperative elbow incongruency (subluxation) on the CT scan
- Clinical instability with complete dislocation, severe fracture displacement, or sublime tubercle involvement
- Associated lesions, requiring an open approach: radial head fractures requiring open fixation or a radial head replacement, associated fractures of the proximal ulna, substantial lesion of lateral collateral ligaments, and/or epicondylar tendon avulsion.

22.4.2 Surgical Technique

Surgical setup and portals: These are the same as described for the radial head fractures. Three standard portals are used (A-M, A-L, and pA-L).

Reduction: The arthroscope is initially placed in the A-M portal and the articular hematoma is removed through the two lateral portals (A-L and pA-L). Then the arthroscope is inserted into the A-L portal to assess the fracture, and the retractor is maintained in the pA-L portal to keep the joint space open. Motorized instruments, thermal ablator, and probe are used from the A-M portal to expose and mobilize the fracture and to achieve reduction.

Fixation: The fractured fragment, with its capsular insertion, is fixed through the dorsal surface of the ulna that is exposed with a small incision. According to the size of the fragments, two different fixation techniques can be used [4, 11, 12]:

- **Cannulated screws and/or K-wires** (Fig. 22.5a–n): The arthroscope is placed in the A-L portal and the fractured coronoid fragment is kept displaced with a lever from the pA-L portal (Fig. 22.5a, b). Two or three K-wires are drilled from the posterior cortex of the ulna into their exit point at the base of the fractured coronoid. Intraoperative fluoroscopic images are useful, especially if the K-wires are inserted with the freehand technique. The target guide commonly used for cruciate ligament surgery is bulky and difficult to use. At least two K-wires are inserted up to the base of the coronoid (Fig. 22.5h). Next, the fracture is reduced with a lever from the pA-L portal, with an arthroscopic grasper from the A-M portal. While maintaining reduction, the K-wires are advanced and passed into the fractured fragment (Fig. 22.5i). When the size of the fractured coronoid is large, a cannulated screw (3.5 mm) can be inserted over one of the K-wires (Fig. 22.5l, m).
- **Osteosuture** (Fig. 22.6): This technique is useful when the fracture is comminuted and the fragments cannot be fixed with screws or K-wires. This fixation will not be as stable as the previous one, but it enables to restore the correct tension of the anteromedial joint capsule and allows a possible consolidation of small coronoid fragments in continuity with it. A shuttle suture (single filament, 1 mm) is passed through the joint capsule attached to the fragments of the coronoid tip. This is performed using a suture passer commonly used for rotator cuff repairs (Fig. 22.6d, Spectrum System, Linvatec Corp, Largo, FL). The shuttle suture is

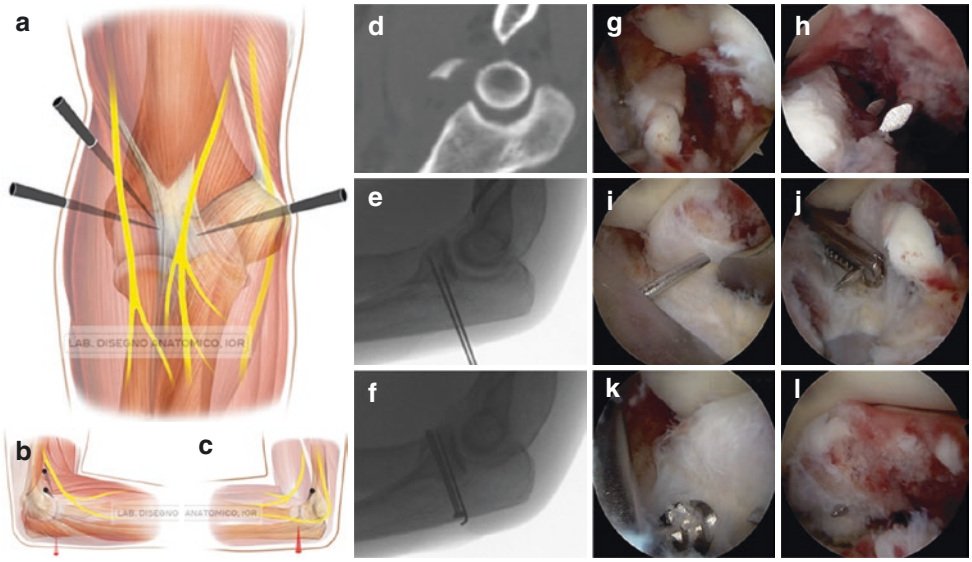

Fig. 22.5 ARIF of coronoid fracture using cannulated screws and K-wires. (**a–c**) Drawing of arthroscopic working position. The red rod represents the direction used to insert K-wires and screws. Coronoid fracture: sagittal CT scan. (**d**) and fluoroscopy images. (**e**, **f**) Two K-wires are pushed forward to the base of the coronoid. (**g**, **h**): The fractured fragment is reduced and the K-wires are further advanced. (**i–l**): A cannulated screw (3.5 mm) replaces one of the two K-wires. Final arthroscopic and radiologic views are shown (Courtesy of Lab Anatomico IOR)

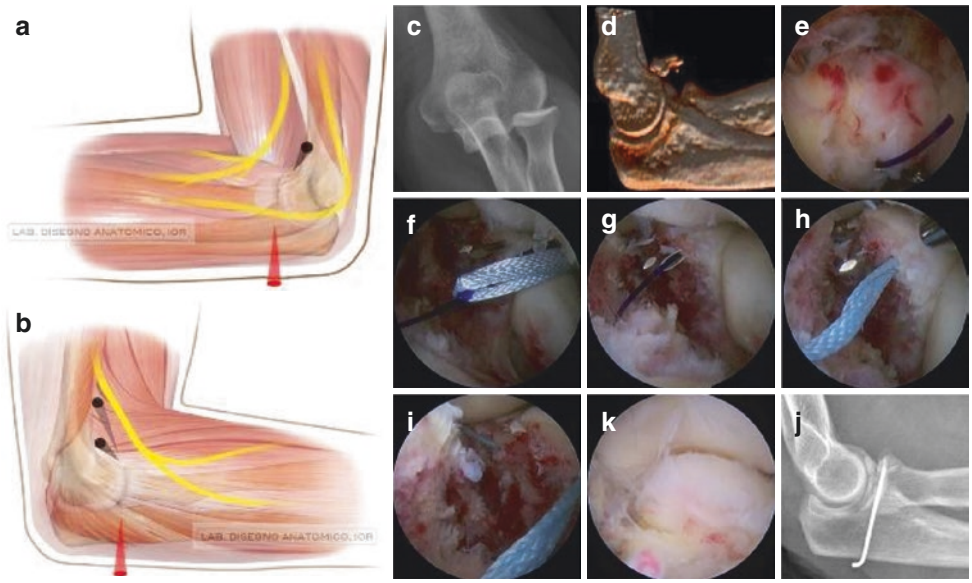

Fig. 22.6 ARIF coronoid fixation using osteosuture and K-wire. (**a**, **b**) Drawing of arthroscopic working position to reduce and fix the coronoid fracture. The red rod represents the direction used to insert sutures and K-wires. (**c**, **d**) Preoperative images showing complete dislocation of the ulno-humeral joint with a small coronoid fracture. (**e**) A shuttle is passed through the capsule, just behind the coronoid fragment. (**f**) An Ultra-Tape suture is carried through the capsule, around the coronoid tip. (**g**) A spinal needle is inserted in two different ulnar bone tunnels to deliver a shuttle suture. (**h**, **i**) Both ends of the Ultra-Tape suture are pulled inside the bone tunnels. A K-wire is positioned at the base of the coronoid for subsequent fixation. (**k**) Final arthroscopic view after having tied the suture and the K-wire has been pushed forward. (**j**) Postoperative X-ray showing the coronoid fixation (Courtesy of Lab Anatomico IOR)

replaced by a high-strength suture. Both ends of the suture are passed through bony ulnar tunnels that are created using a 1.6 mm K-wire. A suture shuttle is passed through the bony tunnels using a spinal needle (Fig. 22.6f). The shuttle suture is retrieved from the A-M portal (Fig. 22.6g) together with one of the ends of the reinforced suture previously passed through the capsule and they are knotted one to the other. The suture shuttle, pulled from its free end, carries the suture through the ulnar bone tunnel (Fig. 22.6h). Using the same technique, the second limb of the suture is passed and knotted on the posterior cortex; reduction is maintained with the probe as the sutures are tensioned. For added stability, the authors supplement the osteosuture with K-wires (Fig. 22.6k, l).

Regardless of the ARIF technique chosen, the fixation must be stable upon palpation and flexion-extension tests of the elbow, to reduce the period of postoperative immobilization to a minimum. At the end of the surgery, the joint stability must be tested and the ligaments may be repaired if necessary.

22.5 Combined Radial Head and Coronoid Fractures

In these cases, ARIF technique helps to avoid a big single incision or two separate incisions. The ARIF technique is particularly demanding and a careful selection of the cases is mandatory. Many times, when an elbow dislocation occurs, small bony fragments from the radial head and coronoid mean a severe lesion of soft tissue, with complete capsular and ligamentous injuries and often tendon avulsions. These injuries are challenging and may require open surgery, and sometimes even an external fixator can be recommended.

22.5.1 Indications and Contraindications

Selected terrible triad lesions can be treated conservatively [13]. However, there are relatively simple terrible triad patterns where conservative treatment is not the best solution and open surgery, requiring extensive approaches to fix very small fragments, or to remove some of them if they are not fixable, could be considered too aggressive. In these cases, arthroscopic technique allows removal of crushed osteochondral fragments, and fixation of small radial head and coronoid fractures may be performed [14]. Stability can be evaluated arthroscopically and the LCL may be reinforced if necessary.

Only a minority (10%) of terrible triad cases can be treated with ARIF. Contraindications are represented by evident joint instability, fragment displacement, need to use plates or radial head prosthesis, and associated lesions requiring open surgery.

22.5.2 Surgical Technique

The ARIF technique combines the surgical steps presented in radial head and coronoid fractures (Fig. 22.7). In case of difficulties or doubts, a low threshold to convert the technique in open surgery is suggested.

22.6 Postoperative Management and Rehabilitation

The rehabilitation program after ARIF of elbow fractures is based on the stability of the fixation and associated lesions. Generally, it begins the day after surgery, with gentle self-assisted active movements. A removable elbow brace is used for 3–4 weeks and strengthening exercises are initiated after 6 weeks.

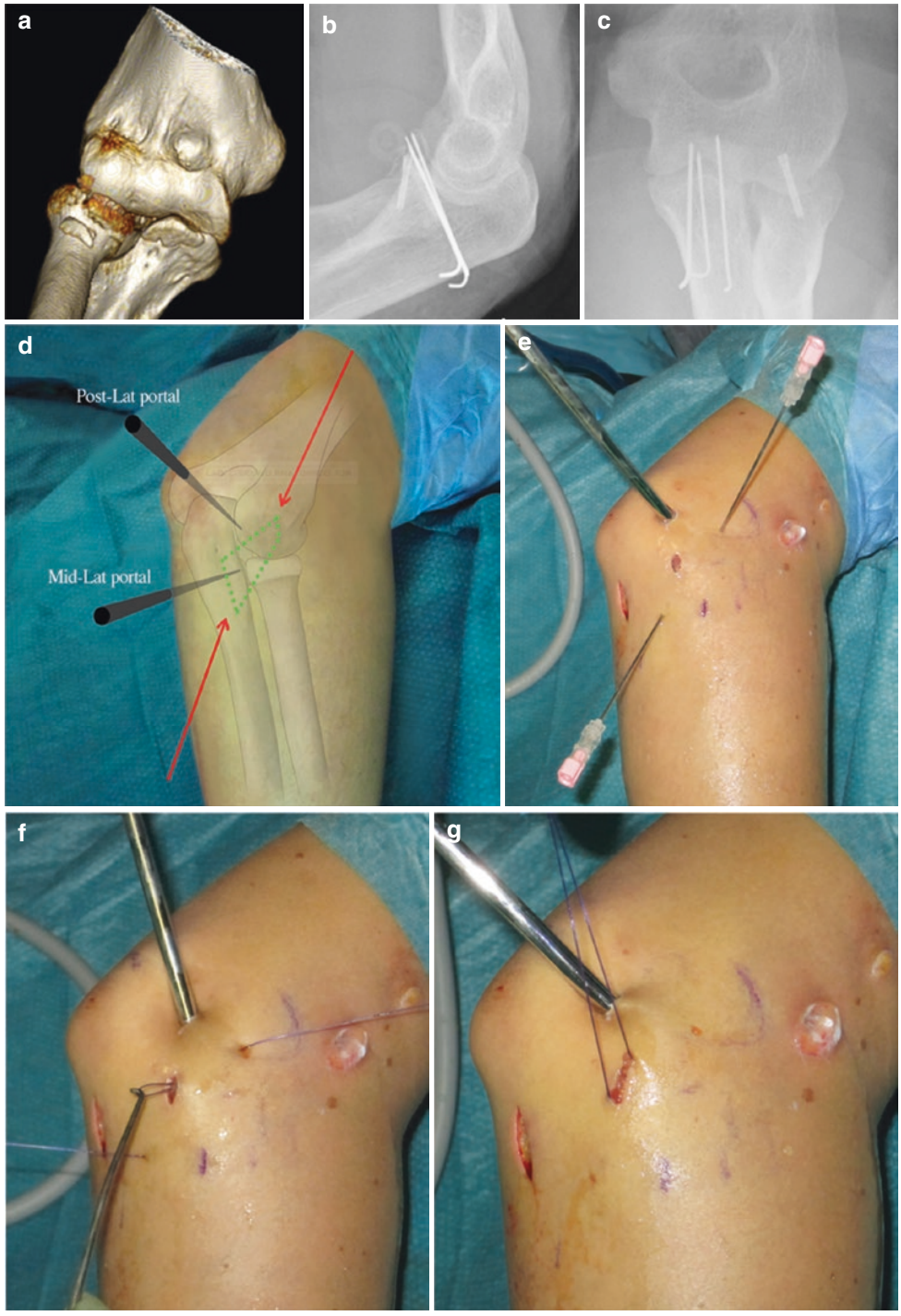

Fig. 22.7 ARIF of terrible triad lesion. (**a**) CT scan, performed after elbow reduction, showing two small radial head and coronoid fractures. (**b**, **c**) Postoperative X-rays showing the screw fixation of the radial head, and the fixation with three K-wires for the coronoid. (**d**–**g**) Posterolateral plication: The scope is through the posterolateral portal while the mid-lateral portal is needed to retrieve the sutures. The sutures are passed percutaneously using two spinal needles inserted in the direction of the fibers of the lateral ulnar collateral ligament

References

1. Holt MS, Savoie FH 3rd, Field LD, Ramsey JR. Arthroscopic management of elbow trauma. Hand Clin. 2004;20(4):485–95. https://doi.org/10.1016/j.hcl.2004.07.003.
2. Van Tongel A, Macdonald P, Van Riet R, Dubberley J. Elbow arthroscopy in acute injuries. Knee Surg Sports Traumatol Arthrosc. 2012;20(12):2542–8. https://doi.org/10.1007/s00167-012-1904-y.
3. Adams JE, King GJ, Steinmann SP, Cohen MS. Elbow arthroscopy: indications, techniques, outcomes, and complications. Instr Course Lect. 2015;64:215–24.
4. Fink Barnes LA, Parsons BO, Hausman M. Arthroscopic management of elbow fractures. Hand Clin. 2015;31(4):651–61. https://doi.org/10.1016/j.hcl.2015.06.011.
5. Yeoh KM, King GJ, Faber KJ, Glazebrook MA, Athwal GS. Evidence-based indications for elbow arthroscopy. Arthroscopy. 2012;28(2):272–82. https://doi.org/10.1016/j.arthro.2011.10.007.
6. Cucchi D, Guerra E, Luceri F, et al. A combination of an anteromedial, anterolateral and midlateral portals is sufficient for 360° exposure of the radial head for arthroscopic fracture fixation. Knee Surg Sports Traumatol Arthrosc. 2019;27(1):319–25.
7. Ballesteros-Betancourt JR, Lázaro-Amorós A, García-Tarriño R, Sastre-Solsona S, Combalia-Aleu A, Llusá-Pérez M. Classification of the transverse pattern of Mason II radial head fractures and its usefulness in arthroscopic osteosynthesis. Anatomo-surgical study. Rev Esp Cir Ortop Traumatol. 2019;63(1):12–9. https://doi.org/10.1016/j.recot.2018.07.003.
8. Cucchi D, Arrigoni P, Luceri F, et al. Modified anteromedial and anterolateral elbow arthroscopy portals show superiority to standard portals in guiding arthroscopic radial head screw fixation. Knee Surg Sports Traumatol Arthrosc. 2019;27(10):3276–83. https://doi.org/10.1007/s00167-019-05411-8.
9. Rolla PR, Surace MF, Bini A, Pilato G. Arthroscopic treatment of fractures of the radial head. Arthroscopy. 2006;22(2):233.e1–6. https://doi.org/10.1016/j.arthro.2005.10.003.
10. van Riet RP. Arthroscopic lateral collateral ligament imbrication. In: Bain G, Eygendaal D, van Riet R, editors. Surgical techniques for trauma and sports related injuries of the elbow. Berlin: Springer; 2020.
11. Lee JM, Yi Y, Kim JW. Arthroscopically assisted surgery for coronoid fractures. Orthopedics. 2015;38(12):742–6. https://doi.org/10.3928/01477447-20151119-04.
12. Arrigoni P, D'Ambrosi R, Cucchi D, Nicoletti S, Guerra E. Arthroscopic fixation of coronoid process fractures through coronoid tunnelling and capsular plication. Joints. 2016;4(3):153–8. https://doi.org/10.11138/jts/2016.4.3.153.
13. Chan K, MacDermid JC, Faber KJ, King GJ, Athwal GS. Can we treat select terrible triad injuries nonoperatively? Clin Orthop Relat Res. 2014;472(7):2092–9. https://doi.org/10.1007/s11999-014-3518-9.
14. Lee SH, Lim KH, Kim JW. Case series of all-arthroscopic treatment for terrible triad of the elbow: indications and clinical outcomes. Arthroscopy. 2020;36(2):431–40. https://doi.org/10.1016/j.arthro.2019.09.014.

Arthroscopic Fixation of Elbow Fractures: How I Do It

23

T. Leschinger, Lars P. Müller, and K. Wegmann

23.1 Background

Arthroscopic fracture fixation in the elbow is a technically demanding procedure. The dangers due to the proximity of neurovascular structures and the potential for intraoperative complications correspond on the one hand to those of elbow arthroscopy in general and, in addition, to the repositioning and fixation of the fracture. A challenging step of these procedures is adequate placement of Kirschner wires for temporary fixation of the fragments as well as drilling for the cannulated screws or lasso techniques. Because screw insertion perpendicular to the fracture line achieves superior primary stability in osteosynthesis, appropriate portals for the steps of drilling and screw or lasso insertion are therefore relevant factors for successful surgery.

23.1.1 Surgical Anatomy

The portals and their proximity to the neurovascular structures correspond to those most commonly used in elbow arthroscopy: anteriorly, the standard anteromedial (2 cm anterior and 2 cm distal to the medial epicondyle) and anterolateral (3 cm distal and 1 cm anterior to the lateral epicondyle) or proximal anterolateral (1–2 cm proximal to the lateral epicondyle) portals. To access the posterior elbow, the direct posterior portal ("transtriceps portal"; 3–4 cm proximal to the tip of the olecranon), the posterolateral portal (lateral border of the triceps tendon), and the direct lateral portal ("soft-spot") are used at the center of a triangle connecting the tip of the olecranon, lateral epicondyle, and radial head.

Modifications to the standard portals, including the distal anteromedial (1 cm proximal and 1 cm anterior to the medial epicondyle) and distal anterolateral portal (1 cm proximal and 1 cm anterior to the lateral epicondyle), permit obtaining a flatter trajectory of the Kirschner wires/cannulated screws and a potential superior biomechanical performance of fixation in radial head fractures [4]. In the case of percutaneous indirect reduction and internal fixation of coronoid fractures from the dorsal ulnar cortex, the shape of the coronoid process implies drilling from dorsal-distal to ventral-proximal and can be estimated based on preoperative radiologic plans.

In the case of a necessary anteromedial approach to the coronoid for a retrograde screw, a corridor between the brachialis muscle, the median intermuscular septum, and the pronator teres was identified through an accessory anteromedial portal, located 2 cm proximal to the standard anteromedial portal, without endangering neurovascular structures in an anatomic study [2].

T. Leschinger · L. P. Müller · K. Wegmann (✉)
Center for Orthopedic and Trauma Surgery, University Medical Center, Cologne, Germany
e-mail: kilian.wegmann@uk-koeln.de

© ISAKOS 2022

D. N. Bhatia et al. (eds.), *Arthroscopy and Endoscopy of the Elbow, Wrist and Hand*,
https://doi.org/10.1007/978-3-030-79423-1_23

23.2 Indications and Contraindications

Noncomminuted two-part fractures are suitable for arthroscopic fixation, including (unstable) Mason type 2 fractures of the radial head (Fig. 23.1a–c), transverse coronoid fractures and Dubberley type 1/2 A fractures of the capitulum and the trochlea (Fig. 23.1a–c).

Contraindications include comminuted fractures, severe ligamentous injuries, and other lesions necessitating open surgery.

23.3 Surgical Technique

The procedure is performed in the lateral decubitus position.

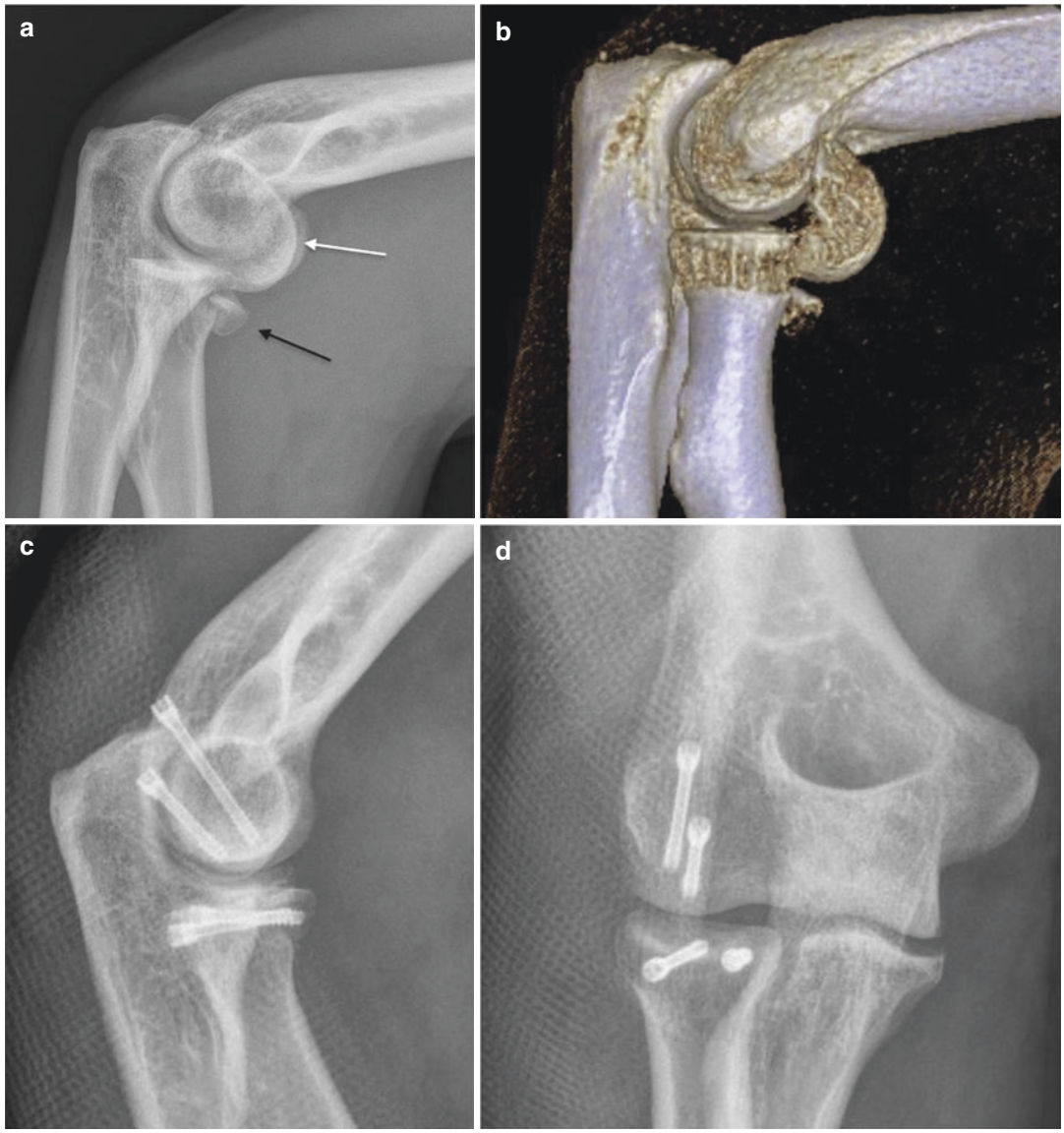

Fig. 23.1 (**a**, **b**) Preoperative X-ray and 3D-CT-Scan of a noncomminuted two-part fracture of the radial head (black arrow) and a distal humerus fracture of the capitulum and the trochlea (Dubberley type 2 A). Postoperative radiographs after arthroscopically assisted reduction and internal fixation (**c**, **d**) (© Bhatia)

- An anterolateral portal is first created with an inflow cannula, and arthroscopy in the posterior compartment is started. The posterolateral portal serves as the camera portal, whereas the direct posterior portal is used as the working portal.
- Next, the anterior compartment can be addressed by creating an anteromedial portal through the already existing anterolateral portal using an "inside-out" technique. Retractors are used to hold the capsule anteriorly to protect neurovascular structures. The rest of the procedure is specific to the fracture. As a component of systematic diagnostic arthroscopy, the fracture pattern is assessed, and existing concomitant injuries are recorded and addressed.

23.3.1 Radial Head Fractures

- After completing diagnostic arthroscopy, the fracture can be visualized through the posterolateral or anteromedial portal and the working instruments are placed in the direct lateral or anterolateral portal (Fig. 23.2a–c).
- Modifications to the anteromedial (1 cm proximal and 1 cm anterior to the medial epicondyle) and anterolateral portals (1 cm proximal and 1 cm anterior to the lateral epicondyle) permit obtaining a flatter trajectory of the Kirschner wires/cannulated screws to the surface of the radial head [4].
- The fragment can usually, after sufficient debridement of the fracture hematoma, be repositioned with an elevator, and the reduction can be held either with the same elevator or alternatively with a hook. An essential and challenging step is the correct placement of two to three 0.8 mm or 1.1 mm Kirschner wires into the radial head to facilitate temporary fixation of the fracture fragments and to serve as a guide wire for cannulated screws for definitive fixation. The screws should be inserted perpendicular to the fracture line parallel to the joint surface or descending towards the radial neck, resulting in superior primary stability of the osteosynthesis (Fig. 23.1c).
- The wires travel up to the opposite predrilled cortex, and via a protrusion measurement, the required screw length can be determined. The screw length should also be estimated preoperatively using a CT scan.
- The Kirschner wires are then drilled, and headless, cannulated screws (2.2 or 3.0 mm) for definitive osteosynthesis are introduced over the Kirschner wires. It is important to take into account that a screw length approximately 4 mm shorter than the protrusion measurement should be chosen to place the screws on both sides of the fracture below the cartilage level.

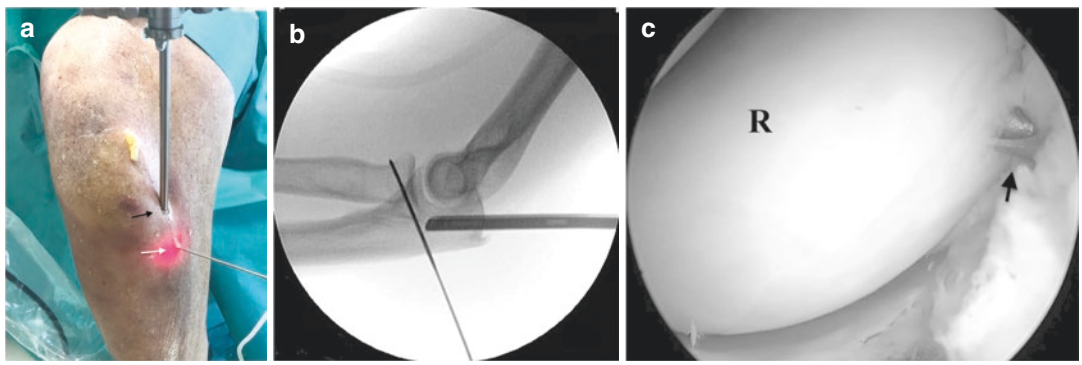

Fig. 23.2 Arthroscopic fixation of radial head fracture is shown. (**a**) Arthroscope (posterolateral portal, black arrow) and K-wire (direct lateral portal, white arrow) are shown. (**b**) Fluoroscopy showing the position of K-wire and radial head reduction. (**c**) Arthroscopic view from the posterolateral portal towards the radial head (R) demonstrates fracture fixation using a K-wire (black arrow) through the direct lateral portal (© Bhatia)

23.3.2 Coronoid Fractures

- After completing diagnostic arthroscopy, the fracture is visualized through the anterolateral portal (Fig. 23.3a).
- The fracture hematoma is removed via the anteromedial portal.
- In Regan/Morrey type 1 fractures, indirect osteosynthesis can usually be performed with the use of a percutaneous "suture lasso technique" from the dorsal ulnar cortex to the fracture bed. To avoid incorrect drilling, it is possible to use targeted instruments or tip-to-tip navigation. The anterior capsule that inserts at the tip of the coronoid process is punctured at ulnar and radial aspects of the fragment to place a nonabsorbable suture, in a horizontal mattress suture configuration around the coronoid fragment. The thread ends are then shuttled over the previously drilled holes through the ulna and exit dorsally. By pulling the sutures, the fragment is successively repositioned. The anatomical reduction can be temporarily held by hooks when the thread is knotted dorsally.
- For larger transverse fractures of the coronoid, compression screw osteosynthesis is performed. Depending on the fragment size, one to two 1.1-mm Kirschner wires are drilled from dorsal to the fracture bed. The direction of the course of the Kirschner wires should be from dorsal-distally to ventral-proximally, thus avoiding intra-articular placement (Fig. 23.3b). After successfully predrilling the Kirschner wires up to the fracture bed and overdrilling the dorsal cortex with a cannulated drill, the elbow can be flexed to relax the adherent soft tissues and to anatomically reduce the fragment. The reduction can be temporarily held with an elevator or a probe hook, and the Kirschner wire can be drilled over the fracture line (Fig. 23.3b). The proximal radioulnar joint must be carefully inspected to rule out that one of the Kirschner wires is placed too far radially, causing impingement. Headless partial thread screws for definitive osteosynthesis are passed and sunk below the dorsal cortex level to avoid soft tissue irritation.

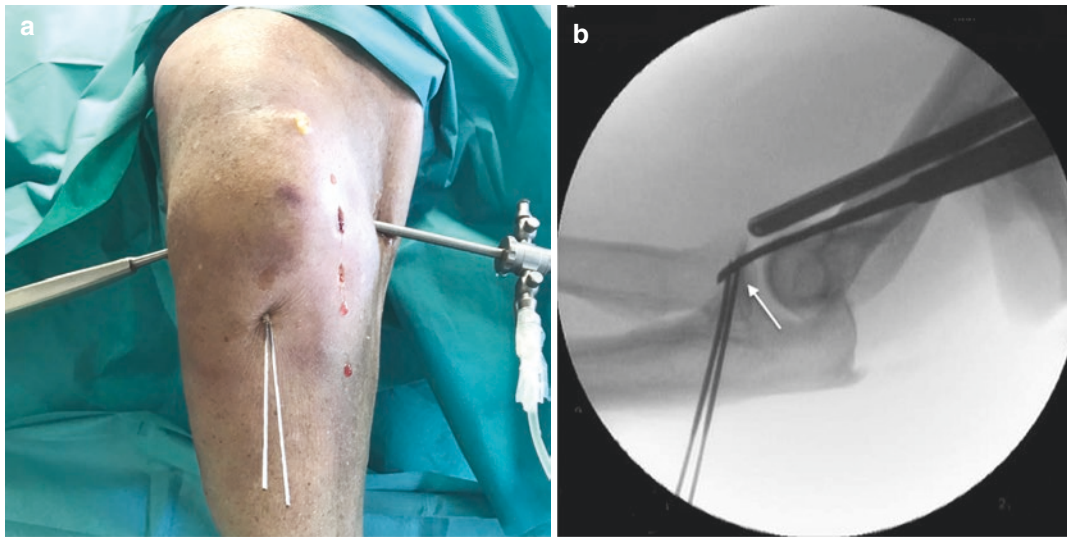

Fig. 23.3 Arthroscopic coronoid fracture fixation is shown. (**a**) Arthroscope (anterolateral portal) and elevator (anteromedial portal) are seen. Kirschner wires are passed percutaneous from the dorsal ulnar cortex. (**b**) Fluoroscopy view: The reduction can be temporarily held with the elevator and the K-wire is drilled to the coronoid tip (white arrow) (© Bhatia)

23.3.3 Capitellum Fractures

- In most cases, the fracture can be visualized through the posterolateral or anterolateral portals with the shaver through the direct lateral portal ("soft-spot"). If the fracture reduction cannot adequately be assessed from the posterolateral direction, the arthroscope can be switched to the anteromedial portal to address the fracture from the anterolateral portal (Fig. 23.4a).
- If the fracture cannot be closed through extension, supination, and varus stress, the fragment must also be manually repositioned with an elevator and be held temporarily. Thereafter, depending on the fragment size, two to three Kirschner wires are inserted directly antegrade into the fracture over the joint surface. The direction of the wires is typically slightly oblique from dorsal-proximal to ventral-distal (Fig. 23.4b).
- After determining the length and over-drilling the Kirschner wires, cannulated partial thread screws are passed from a dorsal direction, and osteosynthesis is completed. Due to the oblique course of the screws, the screw heads usually do not come into contact dorsally with the radial head.

23.4 Postop Management and Rehabilitation

- The application of an immobilizing plaster splint or fixed elbow orthosis can be useful for a short time (3–7 days).
- In particular, assisted movement should be the aim as early as possible to prevent postoperative stiffness with movement and atrophy of muscles due to inactivity. This can be supplemented by lymphatic drainage and occupational therapy. Early change to the elbow movement orthosis for 6 weeks is recommended.
- In the case of capitellum fractures, active movement is initially limited to 90° flexion and full range of movement is started from the third week.
- If an additive collateral ligament reconstruction has been performed, extension in the

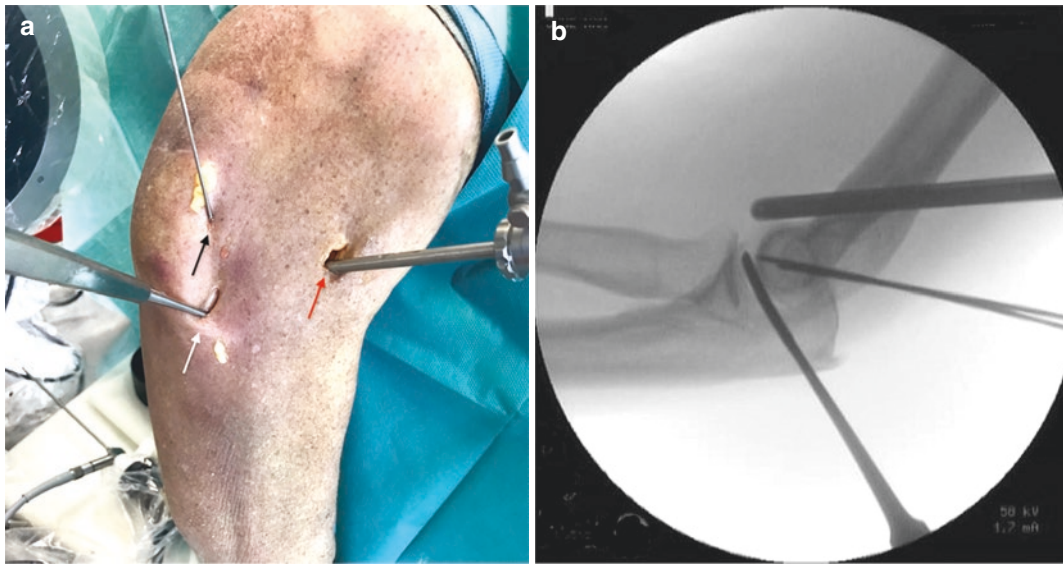

Fig. 23.4 Arthroscopic capitellum fracture fixation is demonstrated. (**a**) Arthroscope (anterolateral portal, red arrow) and elevator (direct lateral portal, white arrow) are seen. The K-wire is passed percutaneous antegrade over the joint surface (black arrow). (**b**) Fluoroscopy view: The K-wire is passed percutaneously antegrade over the joint surface into the fracture (© Bhatia)

orthosis can be limited initially to ensure that the ligaments heal safely (for example, 2 weeks at 40° and 2 weeks at 20°). Forearm rotation should only be performed in 90° flexion and with the elbow approximated to the body for 4–6 weeks.
- Careful loading can take place after 6 weeks. Full loading should only be reached after 10–12 weeks.
- Full loading is permitted after 3 months after radiological bony consolidation.

23.5 Complications

- Implant-associated (soft tissue-irritation or loosening, misalignment or breakage of the implants).
- Intraoperative (neurovascular damage depending on the portals).
- Postoperative (heterotopic ossification, wound healing disorders, nonunion, secondary loss of reduction, posttraumatic arthrosis, persistent instability, pain, and restricted movement).

23.6 Results

Currently published case reports and case series concerning arthroscopically assisted fixation of elbow fractures report promising results; however, clinical data are limited thus far.

Favorable results without relevant complications have been reported after arthroscopic-assisted treatment of radial head after an average follow-up of approximately 5 years [10, 14].

Case series after arthroscopic treatment of coronoid fractures have also shown excellent results in terms of the functional scores [1, 3, 7, 9, 13]. However, complications of ulnar neuropathy and heterotopic ossification have been reported [1]. The data available for arthroscopic-assisted osteosynthesis of B3 fractures of the distal humerus are still limited to case reports with very good to excellent postoperative results [6, 8, 12].

References

1. Adams JE, Merten SM, Steinmann SP. Arthroscopic-assisted treatment of coronoid fractures. Arthroscopy. 2007;23(10):1060–5.
2. Arrigoni P, Cucchi D, Guerra E, Luceri F, Nicoletti S, Menon A, Randelli P. No neurovascular damage after creation of an accessory anteromedial portal for arthroscopic reduction and fixation of coronoid fractures. Knee Surg Sports Traumatol Arthrosc. 2019;27(1):314–8.
3. Arrigoni P, D'Ambrosi R, Cucchi D, Nicoletti S, Guerra E. Arthroscopic fixation of coronoid process fractures through coronoid tunnelling and capsular plication. Joints. 2016;4(3):153–8.
4. Cucchi D, Arrigoni P, Luceri F, Menon A, Guerra E, Muller LP, Burger C, Eygendaal D, Wegmann K, Elbow E, et al. Modified anteromedial and anterolateral elbow arthroscopy portals show superiority to standard portals in guiding arthroscopic radial head screw fixation. Knee Surg Sports Traumatol Arthrosc. 2019;27(10):3276–83.
5. Hackl M, Lappen S, Burkhart KJ, Leschinger T, Scaal M, Muller LP, Wegmann K. Elbow positioning and joint insufflation substantially influence median and radial nerve locations. Clin Orthop Relat Res. 2015;473(11):3627–34.
6. Hardy P, Menguy F, Guillot S. Arthroscopic treatment of capitellum fracture of the humerus. Arthroscopy. 2002;18(4):422–6.
7. Hausman MR, Klug RA, Qureshi S, Goldstein R, Parsons BO. Arthroscopically assisted coronoid fracture fixation: a preliminary report. Clin Orthop Relat Res. 2008;466(12):3147–52.
8. Kuriyama K, Kawanishi Y, Yamamoto K. Arthroscopic-assisted reduction and percutaneous fixation for coronal shear fractures of the distal humerus: report of two cases. J Hand Surg Am. 2010;35(9):1506–9.
9. Lee JM, Yi Y, Kim JW. Arthroscopically assisted surgery for coronoid fractures. Orthopedics. 2015;38(12):742–6.
10. Michels F, Pouliart N, Handelberg F. Arthroscopic management of Mason type 2 radial head fractures. Knee Surg Sports Traumatol Arthrosc. 2007;15(10):1244–50.
11. Miller CD, Jobe CM, Wright MH. Neuroanatomy in elbow arthroscopy. J Shoulder Elbow Surg. 1995;4(3):168–74.
12. Mitani M, Nabeshima Y, Ozaki A, Mori H, Issei N, Fujii H, Fujioka H, Doita M. Arthroscopic reduction and percutaneous cannulated screw fixation of a capitellar fracture of the humerus: a case report. J Shoulder Elbow Surg. 2009;18(2):e6–9.
13. Ouyang K, Wang D, Lu W, Xiong J, Xu J, Peng L, Liu H, Li H, Feng W. Arthroscopic reduction and fixa-

tion of coronoid fractures with an exchange rod-a new technique. J Orthop Surg Res. 2017;12(1):9.
14. Rolla PR, Surace MF, Bini A, Pilato G. Arthroscopic treatment of fractures of the radial head. Arthroscopy. 2006;22(2):233.e231–6.
15. Unlu MC, Kesmezacar H, Akgun I, Ogut T, Uzun I. Anatomic relationship between elbow arthroscopy portals and neurovascular structures in different elbow and forearm positions. J Shoulder Elbow Surg. 2006;15(4):457–62.

24 Arthroscopic Fixation of Radial Neck Fractures in Children

Deepak N. Bhatia

24.1 Background

Radial neck fractures are common in children between 9 and 13 years of age and are usually treated with closed reduction and immobilization. Open reduction is necessary for displaced and angulated fractures, if closed reduction is unsuccessful, to avoid complications like premature physeal closure, stiffness, and cubitus valgus. However, excessive dissection during open reduction may compromise the vascularity of the developing proximal epiphysis and involves a risk of subsequent growth disturbance and heterotopic ossification.

Arthroscopic fixation of radial neck fractures is a minimally invasive technique for repositioning the radial head in correct alignment. Reduction of the radial head is performed under direct visualization to restore the congruency of proximal radioulnar and radiocapitellar joints and K-wires can be passed under visualization via safe portals for fixation.

24.1.1 Surgical Anatomy

The ossification center of the proximal radial epiphysis usually appears around 4–5 years of age and physeal closure is at 14–17 years. Epiphysis of the radial head is completely covered with cartilage and the blood supply enters through the metaphysis. Avascular necrosis of the radial head is rare, as the injury site is distal to the entry of the vessels [1].

Radial neck fractures in children result in cortical buckling at anterolateral aspect of radial neck and subsequent angulation of the radial head. Based on the severity of angulation, the Judet classification has segregated these fractures into four types (Type I, nondisplaced; Type II, <30°; Type III, <30°–60°; Type IVa, 60°–80°; and Type IVb, >80°) [2]. Closed reduction may not optimally align the fracture due to the soft tissue interposition between the radial head and capitellum. Precise reduction of an unossified radial head is often difficult to visualize fluoroscopically and multiple percutaneous attempts at levering the radial head cause iatrogenic disruption of the periosteum and disorganized callus forming synostosis [3]. Arthroscopic experience suggests that the cortical buckling associated with moderate angulation (>30°) can result in failure to maintain the reduction without additional fixation (Fig. 24.1).

D. N. Bhatia (✉)
SPORTSMED Mumbai, and Sir HN Reliance Foundation Hospital, Mumbai, India
e-mail: shoulderclinic@gmail.com

© ISAKOS 2022

D. N. Bhatia et al. (eds.), *Arthroscopy and Endoscopy of the Elbow, Wrist and Hand*,
https://doi.org/10.1007/978-3-030-79423-1_24

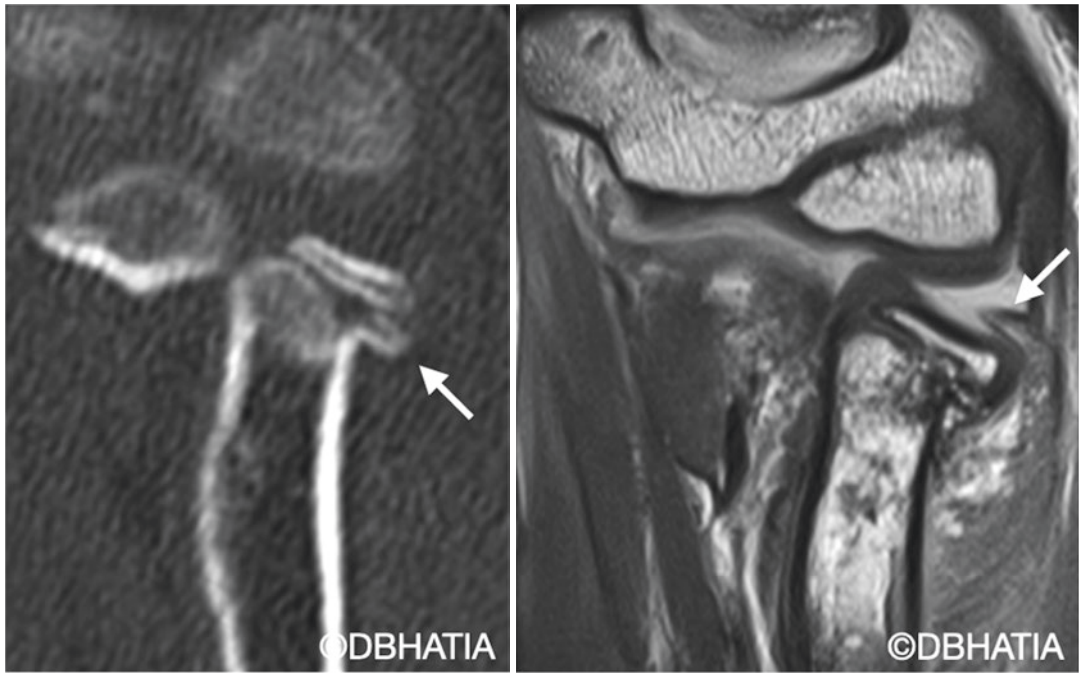

Fig. 24.1 A displaced radial neck fracture is shown on a CT scan (left) and MRI (right). Cortical buckling (arrow, left image) and interposed annular ligament (arrow, right) prevent a stable closed reduction (© Bhatia)

24.2 Indications and Contraindications

Arthroscopic reduction and fixation of radial neck fractures is indicated in moderate to severely displaced fractures (Judet types 3 and 4). Arthroscopy is useful if closed reduction is unsuccessful, and when the radial head is not clearly visualized on fluoroscopy.

There are no absolute contraindications to the procedure. Surgeon inexperience with arthroscopy in pediatric fractures is a relative contraindication.

24.3 Surgical Technique

The surgery is performed with the patient in lateral decubitus position, and a tourniquet is used during the procedure. A 2.9-mm arthroscope and sheath (ConMed, Linvatec, Largo) are used, and gravity inflow is used to minimize fluid extravasation into the arm and forearm.

Portals: Three standard portals are used in the procedure:

- Proximal anteromedial portal (AM) is the viewing portal throughout the procedure.
- Proximal anterolateral portal (AL) is the working portal and is placed slightly anterior to the usual portal site to permit access for reduction.
- The "Radial head portal" (RH) is used for reduction and passage of K-wire(s) [4]. The portal is created using a 6–8 mm incision and a 5 mm capsulotomy is performed for instrumentation (See Chap. 25).

Diagnostic arthroscopy: The AM viewing portal is used to assess the fracture displacement and angulation (Fig. 24.2). The radiocapitellar (RC) and proximal radioulnar (RU) joints are visualized and degree of incongruency noted. A 3.5 mm shaver is introduced via the AL portal and the hematoma is evacuated. A synovectomy is performed if necessary.

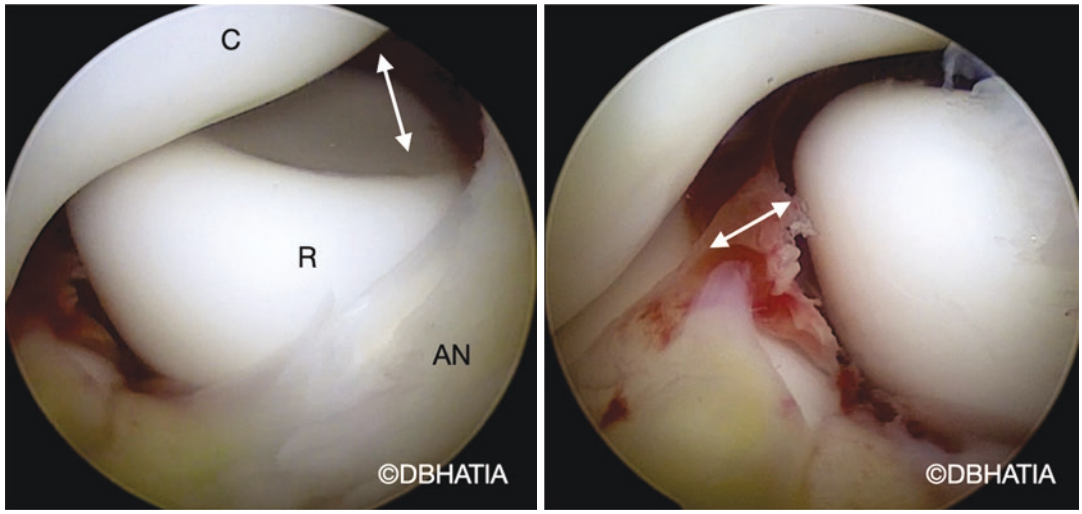

Fig. 24.2 Arthroscopic view shows the angulated radial head and the interposed annular ligament (An, left image). Incongruency of the radiocapitellar (arrows, left) and proximal radioulnar (arrow, right) joints can be assessed, and these are used as a guide to anatomical reduction. (*R* radial head, *C* capitellum) (© Bhatia)

Fracture reduction: The shaver blade is introduced between the annular ligament (AN) and radial head and the interposed soft tissues are retracted. The shaver blade is then used to lever the radial head proximally towards the capitellum (Fig. 24.3). The RC and RU joints are visualized to assess congruency for adequacy of reduction. If reduction is inadequate, an RH portal is created as described above, and a 3.5 mm shaver blade or switching stick is used to apply a distally directed force simultaneously on the medial aspect of radial head (Fig. 24.3b). Release of levering forces usually results in loss of reduction due to lack of cortical stability anterolaterally.

Radial head fixation: The outer sheath of a 3.5 or 4 mm shaver blade is introduced between the radial head and capitellum via the RH portal. The open broad end of the sheath is used as an elevator to stabilize the reduction at the posterior radial neck. A 2 mm K-wire is now passed through the sheath and is drilled across the peripheral cartilaginous radial head into the radial shaft cortex. In the author's experience, use of a sheath via the RH portal, as described here, results in accurate passage of the wire and multiple attempts at wire passage are avoided (Fig. 24.4).

Adequacy of reduction: Anatomical reduction is confirmed arthroscopically by visualization of congruent RC and RU joints. Fluoroscopy is used to measure the radial head-shaft angle to confirm correct alignment (Fig. 24.5).

Finally, the k-wire is cut short and the wire end is exteriorized through another skin tract proximally, or is bent and buried under skin. The portals are closed and sterile dressing is applied.

24.4 Tips and Tricks

- The RC and RU joints should be cleared of any soft tissue prior to reduction.
- A 2 mm shaver is useful via the RH portal for RU joint clearance.
- A blunt probe is wedged between the radial head and annular ligament to maintain reduction and the posterior sheath can be used to further stabilize it while an assistant drills the wire.

24.5 Pitfalls

- Repetitive and forceful leverage anteriorly and posteriorly may result in periosteal damage and subsequent ossification and synostosis is possible.

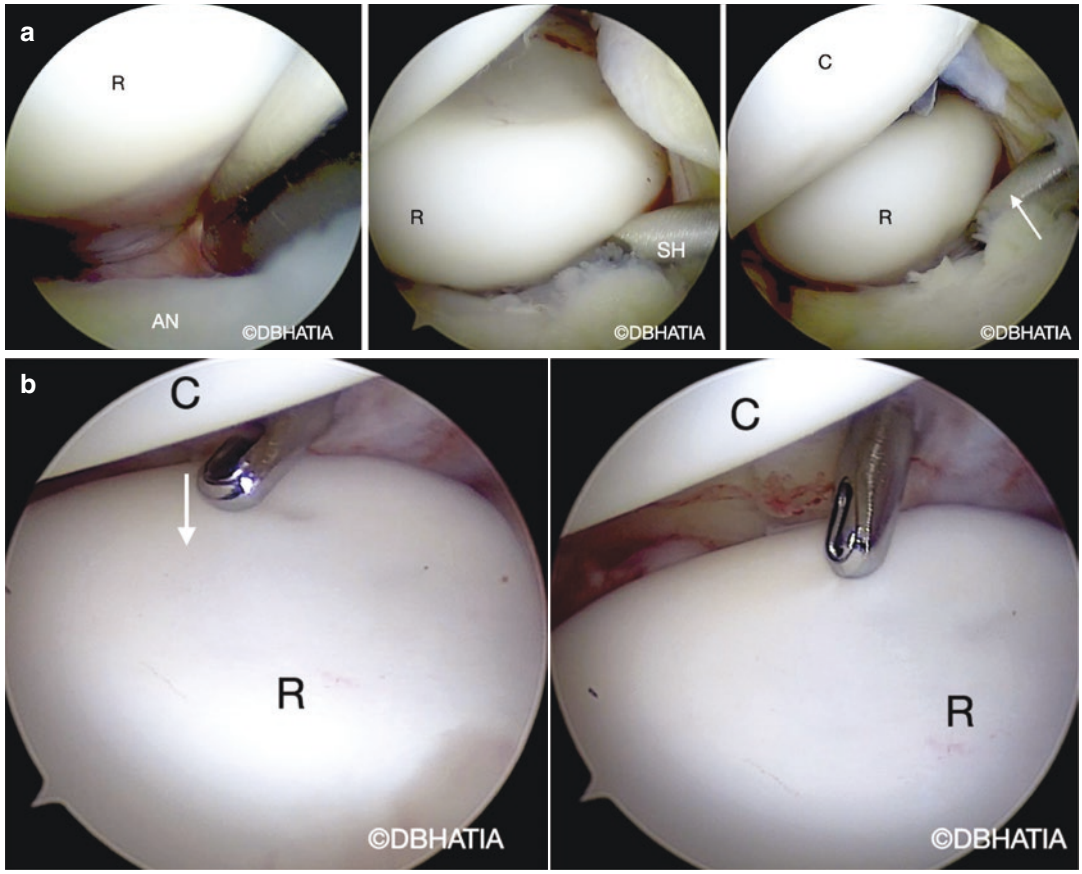

Fig. 24.3 (**a**) Arthroscopic visualization of fracture reduction is demonstrated. A 3.5 mm shaver blade (SH) is passed between the radial head and annular ligament (left image) and the head is levered to reduce angulation (middle image). Anatomical reduction is achieved when the radiocapitellar and proximal radioulnar joints are congruent with rotation (right image). (*AN* annular ligament, *R* radial head, *C* capitellum, arrow: direction of leverage). (© Bhatia). (**b**) A shaver is introduced via the radial head portal and a distally directed pressure (arrow) is applied over the medial aspect of the displaced radial head (left image). This maneuver is useful to achieve further correction of the radial head angulation (right image) (*C* capitellum, *R* radial head) (© Bhatia)

- Multiple passage of K-wires through the physis should be avoided to prevent physeal damage.
- Loss of reduction is possible if a thin K-wire (<2 mm) is used to maintain reduction.
- Both RC and RU joint congruence are important to prevent postoperative loss of rotational movement.

24.6 Postoperative Management and Rehabilitation

An above elbow plaster slab is used for 3–4 weeks. Sutures are removed in 10 days. Radiographs are obtained at 4 weeks to confirm alignment and union, and the percutaneous wire is removed. Thereafter, physiotherapy is initiated. Elbow

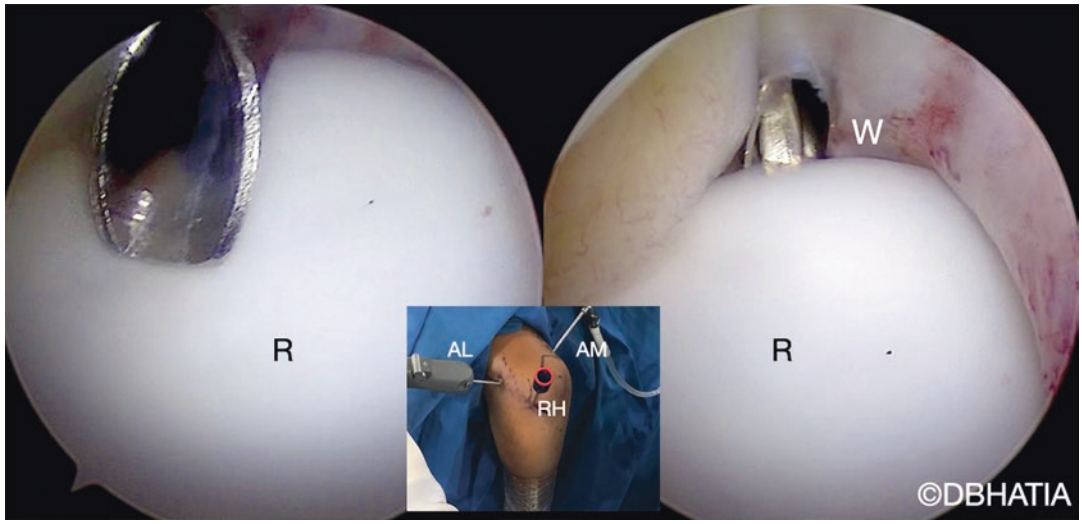

Fig. 24.4 The outer sheath of a shaver blade is used via RH portal to maintain fracture reduction. A 2 mm K-wire is passed through the sheath into the cartilaginous part of the reduced radial head and advanced into the radial shaft cortex. (*AL* anterolateral portal, *AM* anteromedial portal, *RH* radial head portal, *R* radial head, *W* wire) (© Bhatia)

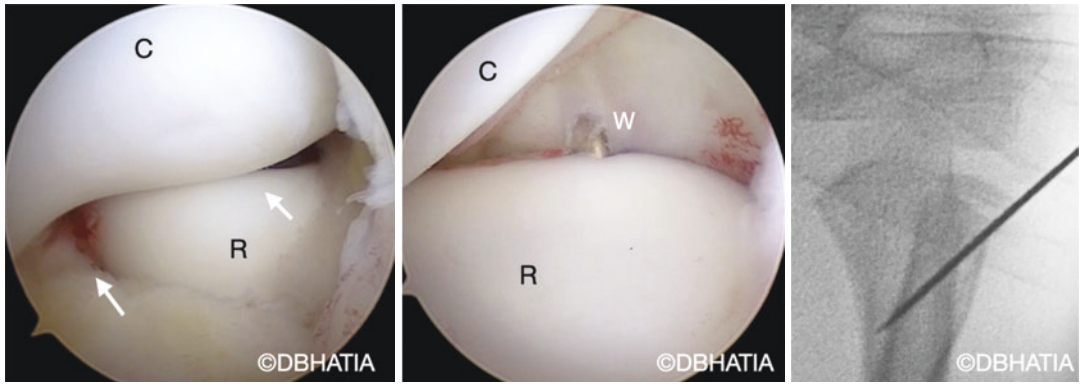

Fig. 24.5 Reduction is assessed by visualizing the congruency of radiocapitellar (right arrow, RC) and radioulnar (left arrow) joints (left image). The K-wire (W) is seen passing through the radial head periphery (middle image). Fluoroscopy is used to measure the radial head-shaft angle to confirm alignment (right image) (© Bhatia)

movements and forearm rotations are permitted without any restrictions. Elbow strengthening progresses simultaneously as range improves, and unrestricted activity is permitted after 6–8 weeks of physiotherapy.

24.7 Complications

Arthroscopic reduction and fixation preserves soft tissues and vascularity, and the usual complications of open surgery are not seen. Loss of

reduction is possible in the immediate postoperative period and use of 2 mm or 2.5 mm K-wire(s) is necessary to avoid this.

Conflict of Interest The author certifies that he has no commercial associations (e.g., consultancies, stock ownership, equity interest) that might pose a conflict of interest in connection with the submitted article. The author retains the copyright to the images, videos, and content in this chapter.

References

1. Rockwood CA, Wilkins KE, King RE. Fractures in children. Philadelphia: Lippincott; 1991. p. 728–51.
2. Judet H, Judet J. Fractures and orthope´dique de l'enfant. Paris: Maloine; 1974. p. 31–9.
3. Young S, Letts M, Jarvis J. Avascular necrosis of the radial head in children. J Pediatr Orthop. 2000;20:15–8.
4. Bhatia DN. Arthroscopic resection of the radial head. In: Bain G, Eygendaal D, van Riet R, editors. Surgical techniques for trauma and sports related injuries of the elbow. Berlin: Springer; 2020.

25 Arthroscopic Radial Head Resection Using the "Radial Head Portal"

Deepak N. Bhatia

25.1 Background

Radial head excision is usually performed for an acute comminuted radial head fracture that precludes surgical fixation. Similarly, a malunited and incongruous radial head surface in chronic radiocapitellar pathology may be treated with partial or complete excision. Arthroscopic resection provides a minimally invasive alternative to open surgery and permits evaluation and concurrent treatment of any associated intra-articular pathology [1]. The "Radial head portal" devised by the author is a safe portal for access to the radial head articular surface and provides access to areas that are difficult to reach via standard portals [2]. Use of this portal permits rapid and measured resection of the radial head and even excision of large fragments in acute fractures.

25.2 Surgical Anatomy

The radiocapitellar (RC) articulation is difficult to access using standard arthroscopy portals and instruments. The standard anterolateral portal is proximal to the RC joint, and the RC articulation space itself is not wide enough to permit use of regular 4 mm shaver and burr blades for resection. The mid-lateral region of the RC joint marks the extent of the lateral ligamentous complex of the elbow, and any capsular resection or instrumentation is restricted anterior to this region. The posterolateral aspect of the RC joint is covered by the extensors and the anconeus, and the Kocher's interval between the anconeus and extensor carpi ulnaris provides safe arthroscopic access for the RC joint space. The posterior interosseous nerve may occasionally be in direct contact with the periosteum of the radial neck; arthroscopic resection must therefore be restricted to the radial head-neck junction [3, 4].

25.3 Indications and Contraindications

- Isolated radial head fracture fragments that involve 25–30% of the head circumference can be removed arthroscopically. Similarly, comminuted fracture fragments may be excised arthroscopically in the acute setting (Fig. 25.1a).
- Chronic neglected radio-capitellar fractures are commonly seen in developing countries and rural regions. Arthroscopic management of these injuries involves excision of malunited radial head and concurrent release of capsular contractures (Fig. 25.1a).
- Open reduction and internal fixation of radiocapitellar fractures may result in prominent

D. N. Bhatia (✉)
SPORTSMED Mumbai, and Sir HN Reliance Hospital, Mumbai, India
e-mail: shoulderclinic@gmail.com

© ISAKOS 2022

D. N. Bhatia et al. (eds.), *Arthroscopy and Endoscopy of the Elbow, Wrist and Hand*,
https://doi.org/10.1007/978-3-030-79423-1_25

Fig. 25.1 (**a**) Acute partial radial head fracture (top left) and a comminuted fracture (arrows, top right) are shown. Radiological images of a chronic neglected radial head fracture demonstrate a malunited radial head (bottom left) and an incongruent radiocapitellar joint (bottom right) (© Bhatia). (**b**) Postoperative radiographs and CT scan image (right inset) demonstrate malpositioned and "proud" radial head screws (arrows) (© Bhatia). (**c**) Radiocapitellar arthritis is seen on lateral radiograph (left) and MRI scan (right) (© Bhatia)

Fig. 25.1 (continued)

fixation implants. Arthroscopic removal of radiocapitellar screws can be performed along with resection of malunited radial head fragments (Fig. 25.1b).

- Radiocapitellar arthritis can be treated with arthroscopic debridement, capsular release, and radial head excision (Fig. 25.1c).

Arthroscopic radial head excision is contraindicated in acute fractures associated with ligamentous injury and associated coronoid fractures. Chronic displaced radial head fragments may be extracapsular and adherent to neurovascular structures, and meticulous open dissection is necessary for excision.

25.4 Surgical Technique

Elbow arthroscopy is performed with the patient in the lateral decubitus position.

Portals: Four portals are used in this procedure:

- **Proximal anteromedial portal (AM)** is the viewing portal throughout the procedure; it is placed 1–2 cm proximal and anterior to the medial epicondyle and is located anterior to the medial intermuscular septum.
- **Proximal anterolateral portal (AL)** is main working portal; it is placed 1–2 cm proximal and anterior to the lateral epicondyle and is located anterior to the lateral intermuscular septum.
- **Direct anterolateral portal (DL)** may be used for additional debridement, or when retraction of soft tissues is necessary. The DL portal is placed anterior to the radial head (R) at the level of the radiocapitellar joint, and its precise position is ascertained using an outside-in technique.
- **Radial head portal (RH)** is a useful working portal for access to the entire radial head [2]. The portal is placed in the interval between the anconeus and extensor carpi ulnaris at the level of the radial head using a 5–10 mm incision and open dissection of the interval. The exact location is determined using an outside-in technique; a needle is passed through the interval and parallel to radial head articular surface. The RH portal is different from the "soft-spot portal" which is placed more proximal and usually passes through the anconeus; the oblique trajectory of the soft-spot portal does not permit easy access to the mid and anterior radial head [2, 5] (Fig. 25.2b).

25.4.1 Arthroscopic Excision of an Intact Radial Head

An intact radial head is usually seen in chronic neglected radial head fractures, failed internal fixation of fractures, and arthritis. These conditions are associated with intra-articular and capsular fibrosis, narrow spaces, and presence of chondral and osseous debris or metallic implants [6]. The steps to perform arthroscopic radial head excision in such cases are detailed below:

Diagnostic arthroscopy and adhesiolysis: The AM portal is used to evaluate the ulnotrochlear and radiocapitellar articulations. Loose bodies are identified and removed, and synovectomy is performed via the proximal AL portal. A 3 mm small joint shaver blade is then introduced sequentially via the three portals (AL, DL, RH) and circumferential adhesiolysis is performed around the radial head.

Surface resection: The RC space is widened by resection of the chondral remnants on the radial head articular surface using a 3 mm shaver blade, and progressively with a 3.5 mm and 4 mm shaver blade. Surface resection is complete when a minimum of 5 mm space is created between the radial head and capitellum (Fig. 25.3).

Radial head resection: A 4 mm arthroscopic burr is introduced via the three portals sequentially and is used to progressively resect the osseous radial head. The AL and DL portals permit resection of the anterolateral radial head, and rotational movements are necessary to provide access to anterior region. The RH portal permits access to the entire radial head and especially the posterior and medial region, and resection can be rapidly completed through the RH portal (Fig. 25.3b). Radial head screws, if present, are loosened by burring around the screws and using angled chisels to dislodge them, and are then grasped and removed via a cannula (Fig. 25.3c).

Peripheral rim resection: Osseous resection leaves behind a peripheral rim of cartilage, and this rim is difficult to resect using shavers. A combination of punches and graspers is used to excise the peripheral rim, and small joint shavers are used for completing the excision. Any persistent loose pieces are meticulous removed, and a thorough wash is given (Fig. 25.4).

Confirmation of Adequacy of Resection

- A radiocapitellar space of 8–10 mm should be achieved and this space can be measured by using 2 breadths of a 4 mm or 5 mm burr.

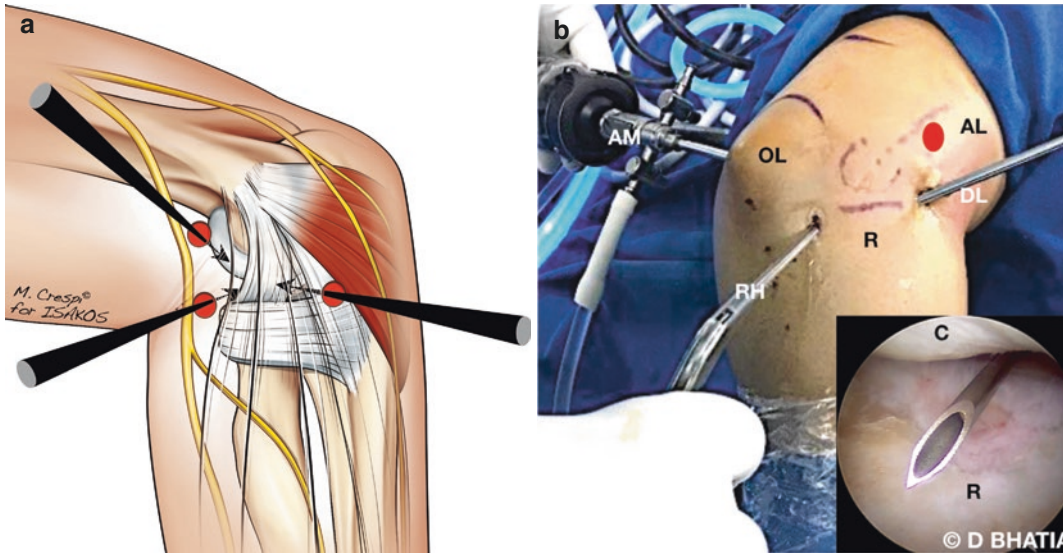

Fig. 25.2 (**a**) Trajectories of three lateral working portals for radial head excision are illustrated. The proximal anterolateral portal (top left) provides oblique access to most lateral and anterior aspect of radial head. The direct lateral portal (lower left) is closer to the radial nerve and provides linear access to approximately half of lateral and anterior aspects of radial head. The radial head portal (right) provides linear access to posterior, medial, and anterolateral aspects of radial head (M. Crespi © for ISAKOS. (**b**) Portals used in arthroscopic radial head excision are demonstrated in a right elbow in the lateral decubitus position. The proximal anterolateral portal (AL) and direct lateral portal (DL) permit access to the anterolateral aspects of the radial head (R). The radial head portal (RH) is positioned at the level of the radial head and is distal to the soft-spot portal. Inset mage shows the outside-in needle for RH portal placement (*OL* olecranon, *C* capitellum, *AM* anteromedial viewing portal) (© Bhatia)

- The radial head ends in the cortical bone of radius shaft; this is visible arthroscopically and has a different feel while using a burr, as compared to the more cancellous radial head.
- Radiographic or fluoroscopic visualization of a 8–10 mm radiocapitellar space (Fig. 25.5).

25.4.2 Arthroscopic Excision of a Fractured Radial Head

An acutely fractured radial head presents a different set of difficulties for arthroscopic removal. Hemorrhage and organized clots, and synovitis, make visualization difficult. The radial head fragments are often large, and inaccessible to burring due to lack of a stable attachment. Moreover, the large size of the fragments precludes removal via cannulae. The steps to perform arthroscopic radial head excision in such cases are detailed below:

Arthroscopic lavage, synovectomy, and fragment removal: The proximal AL portal is used to wash out the clots, and an arthroscopic shaver is used to perform a synovectomy. Care is taken to ensure that the fragments are not displaced into an extra-articular position via preexisting capsular rents. Smaller fragments may be directly removed via the DL portal, and a lateral remnant may be excised using a burr (Figs. 25.6 and 25.7).

Radial head portal placement: A radial head portal is the main working portal for removal of entire fragments of radial head. The portal is placed as described earlier, and can be enlarged to 10 mm if necessary. A 6 mm or 8 mm cannula may be placed via this portal.

Large fragment removal: A large grasper is used to grasp and remove radial head fragments via the RH portal. Fragments larger than 8–10 mm may be held by the grasper, and a burr is used via the DL portal to reduce the size of the fragment for removal (Fig. 25.7).

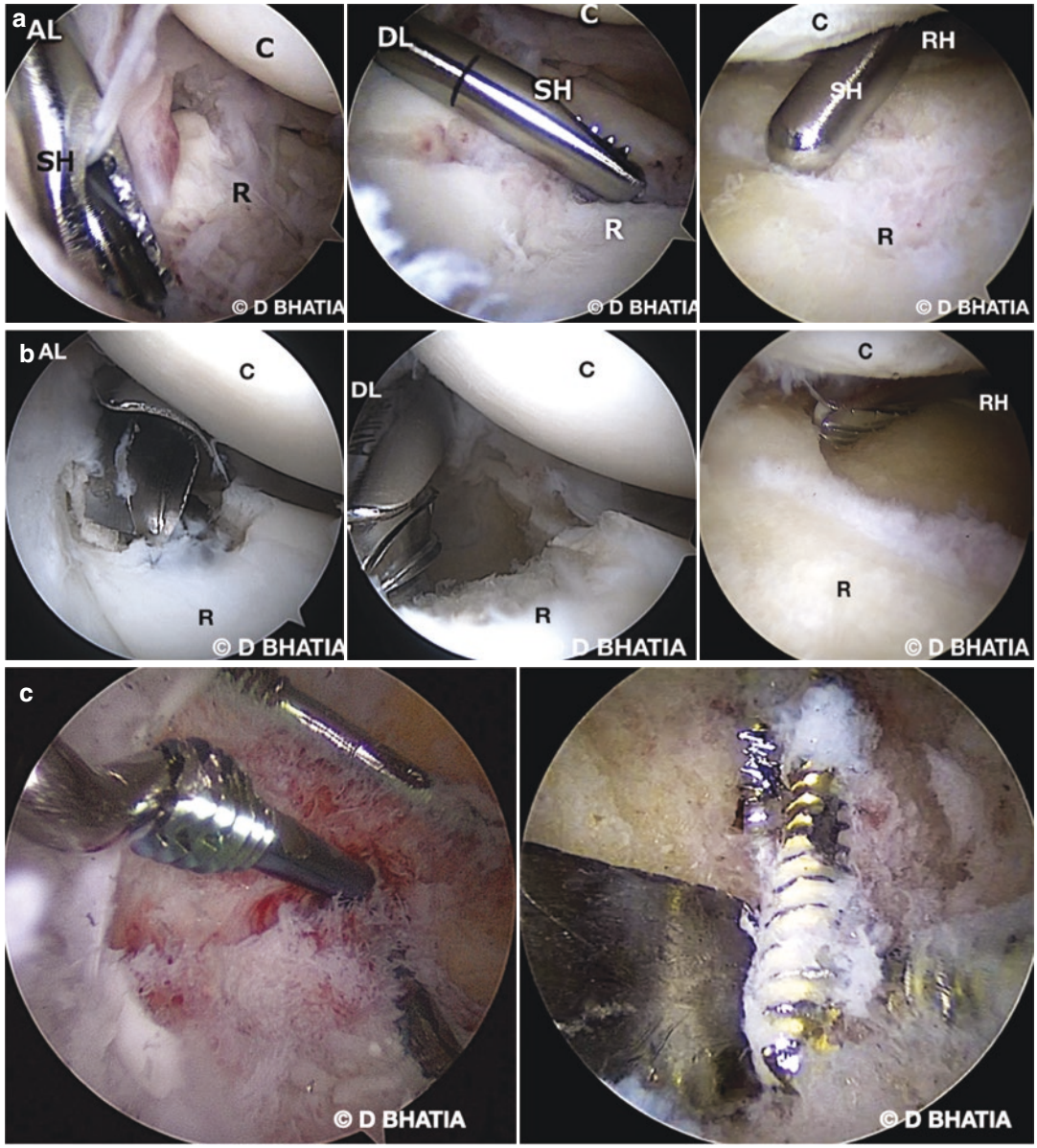

Fig. 25.3 (**a**) Trajectory of the shaver blade (SH) and surface area accessible via the AL portal (left image), DL portal (middle image), and RH portal (right image) is demonstrated in a chronic malunited radial head fracture with severe chondral damage (© Bhatia). (**b**) Bony resection is performed via three portals. The AL and DL portals (left and middle images) are used for resection of anterolateral radial head (R). The RH portal (right image) provides access to posterior and medial aspect of radial head. (*C* capitellum) (© Bhatia). (**c**) Removal of radial head compression screws (left) and mini fragment screws (right) is demonstrated (© Bhatia)

Radial head coplaning: After removing the loose fragments of the radial head, the residual intact remnant of the head is excised using shavers and burrs passed via the RH portal. Cartilage rim remnants are also grasped and excised via the RH portal. Finally, a shaver is used to debride any remaining tissue until adequate resection is achieved (Fig. 25.8).

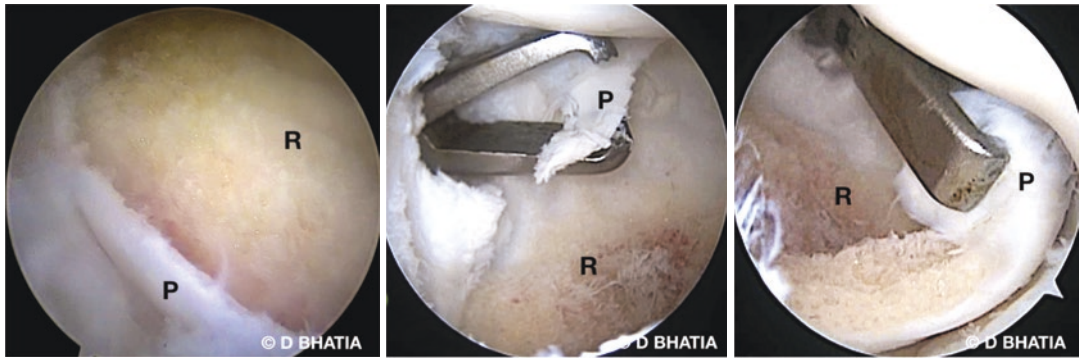

Fig. 25.4 Peripheral rim of radial head cartilage is excised using a grasper in DL and RH portals. (*R* radial head, *C* capitellum) (© Bhatia)

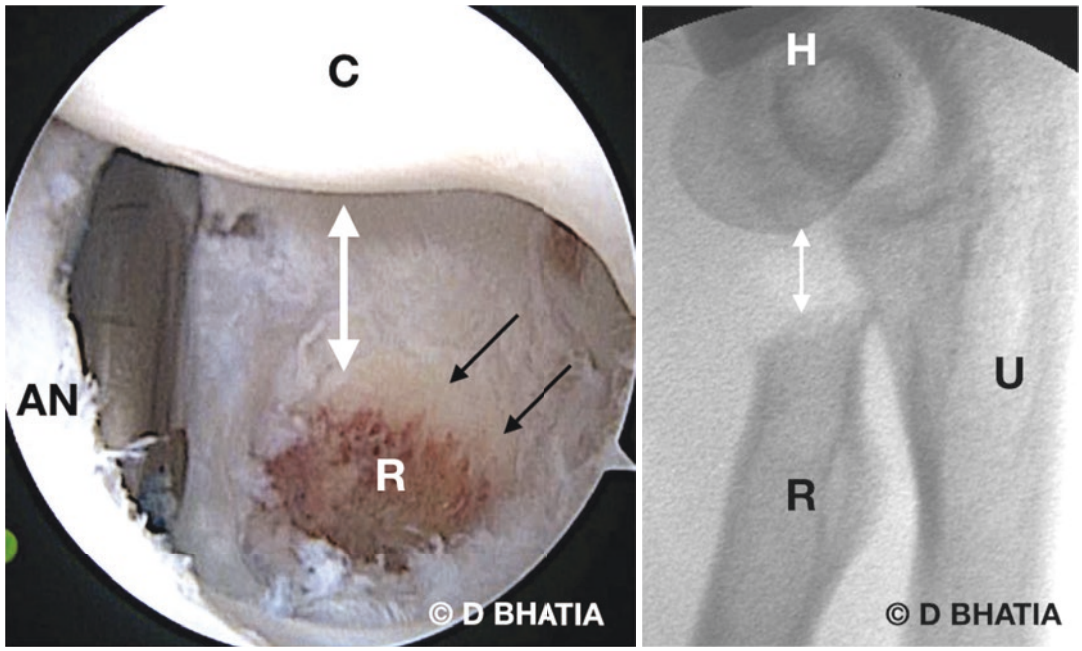

Fig. 25.5 Final arthroscopic view (left image) shows adequate excision and space (arrows) between the radial head (R) and capitellum (C). The cortical rim of the radial neck (black arrows) and intact annular ligament AN is demonstrated. Fluoroscopy (right image) is used to confirm complete resection (arrows) (© Bhatia)

25.5 Tips and Tricks

- The RH portal may be created using a mini-open dissection technique using a 1 cm incision. This ensures safe passage of large instruments and fragments via the portal. In chronic cases, small joint instruments (3 mm) are used via RH portal to create a working space for larger instruments, and incremental increase in size of shavers and burrs (3.5–5 mm) is useful for rapid excision.
- A grasper with broad and large jaws is useful for en-masse excision of large fragments via the RH portal (Fig. 25.7).

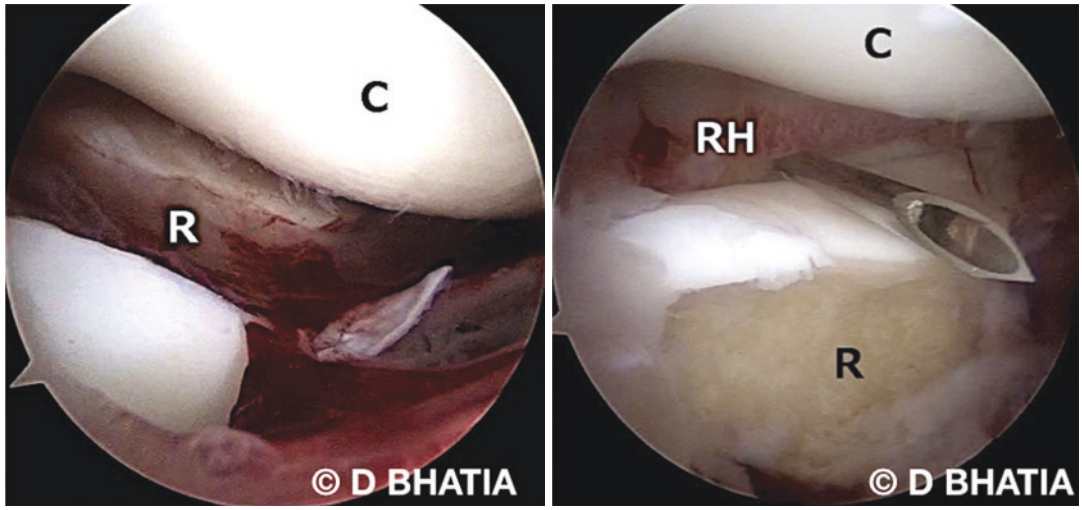

Fig. 25.6 Arthroscopic image of acute radial head fracture (R) shows fragments and organized clots within the elbow joint (left image). A radial head portal (RH) is placed for access to larger fragments. (*C* capitellum) (© Bhatia)

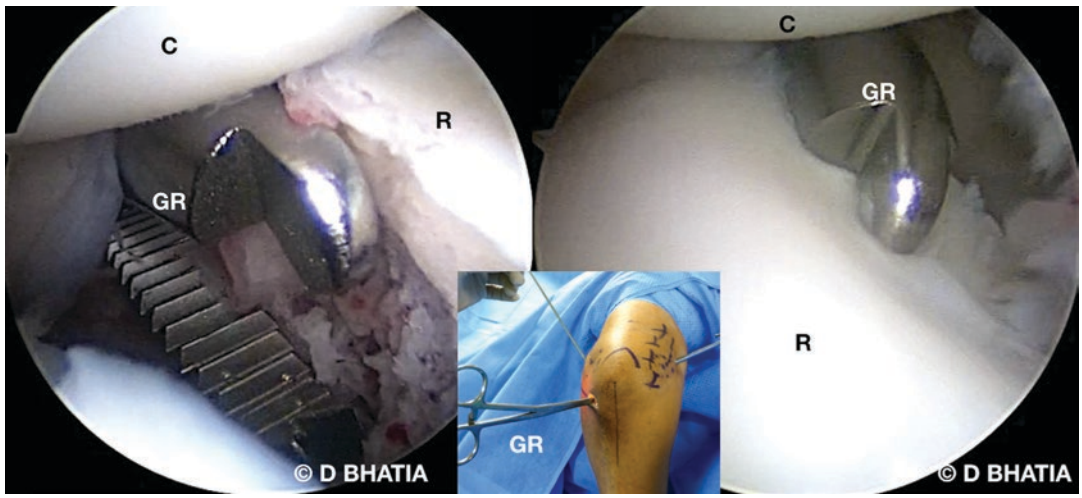

Fig. 25.7 Arthroscopic image shows a grasper (GR) passed via the RH portal (left image) for removal of large radial head fragments (Right image). Inset image shows the passage of the grasper. (*R* radial head, *C* capitellum) (© Bhatia)

- The annular ligament is protected and preserved, and this acts as an interposition tissue between the radial neck and the capitellum.

25.6 Pitfalls

Neurovascular damage: The DL portal is close to the radial nerve, and the RH portal is a safer alternative. Care should be taken to limit the resection to the radial neck, as described earlier.

Iatrogenic lateral ligament injury: The lateral ligamentous complex of the elbow may be injured during passage of instruments via RH portal. This may be minimized by placing a 4–5 mm sheath for shavers and burrs to avoid repetitive soft tissue trauma. When using the RH portal for large fragment excision at the end of the procedure, the capsule should be repaired using strong absorbable sutures.

Inadequate and excessive resection: Overzealous resection of the radial head can result in longitudi-

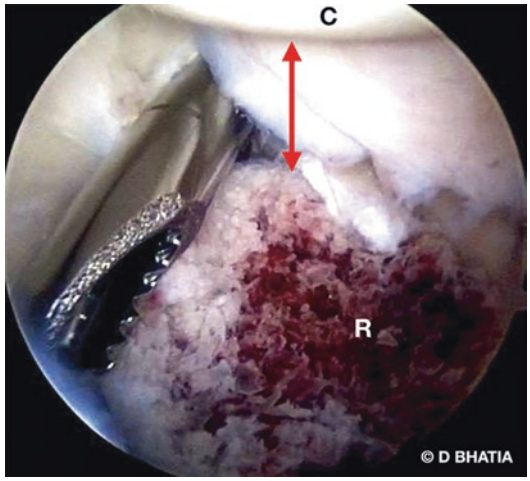

Fig. 25.8 Final arthroscopic view (left image) shows complete excision and adequate space (double arrow) between the radial head (R) and capitellum (C) (© Bhatia)

nal forearm instability, and resultant forearm and wrist pain. Similarly, inadequate resection may result in radiocapitellar contact and progressive capitellar wear.

25.7 Postoperative Management and Rehabilitation

A bulky soft tissue dressing is used in the immediate postoperative period, and this is changed to portal dressing on the fourth postoperative day. A sling is used for comfort. Elbow movements and forearm rotations are permitted without any restrictions. The rehabilitation protocol involves early passive and active range-of- motion exercises (weeks 1 through 6) and simultaneous gradual strengthening. Achievement of full range is dependent on the initial severity of the problem and usually 3–6 months of rehabilitation are necessary in chronic pathology. Light work is permitted after 6 weeks, and a return to heavy work is permitted only after 3 months.

Conflict of Interest The author certifies that he has no commercial associations (e.g., consultancies, stock ownership, equity interest) that might pose a conflict of interest in connection with the submitted article. The author retains the copyright to the images, videos, and content in this chapter.

References

1. Bhatia DN. Arthroscopic radial head implant removal and resection. Arthrosc Tech. 2016;5(4):e705–11.
2. Bhatia DN. Arthroscopic resection of the radial head. In: Bain G, Eygendaal D, van Riet R, editors. Surgical techniques for trauma and sports related injuries of the elbow. Berlin: Springer; 2020. p. 581–8.
3. Tornetta P 3rd, Hochwald N, Bono C, Grossman M. Anatomy of the posterior interosseous nerve in relation to fixation of the radial head. Clin Orthop Relat Res. 1997;(345):215–8.
4. Calfee RP, Wilson JM, Wong AH. Variations in the anatomic relations of the posterior interosseous nerve associated with proximal forearm trauma. J Bone Joint Surg Am. 2011;93(1):81–90.
5. Freehill MT, Poehling GG, Bain G. Portals and diagnostic elbow arthroscopy. In: Bain G, Eygendaal D, van Riet R, editors. Surgical techniques for trauma and sports related injuries of the elbow. Berlin: Springer; 2020.
6. Lapner PC, Leith JM, Regan WD. Arthroscopic debridement of the elbow for arthrofibrosis resulting from nondisplaced fracture of the radial head. Arthroscopy. 2005;21:1492.

26 Arthroscopic Fixation of Coronoid Fractures: Retrograde Wire Technique

Jan Debeij and Roger P. van Riet

26.1 Background

Isolated coronoid fractures are rare, with an incidence of 7.5 per 100,000 persons per year [1]. They are often part of an extensive proximal ulna fracture or a so-called terrible triad injury. Coronoid fractures are classified according to the Regan-Morrey classification or the more comprehensive classification described by O'Driscoll. Surgical treatment of coronoid fractures has historically been reserved for larger fragments. However, it has since been shown that persistent elbow instability and early onset osteoarthritis can also occur following coronoid fractures with relatively small fragments and a more aggressive approach is now advocated [2]. The decision to perform surgery is based less on fragment size and more on its impact on elbow joint stability. However, fixation of a coronoid fracture can be challenging and often requires a second incision and a large surgical approach, and this is associated with increased operating time and complication risk.

J. Debeij
Haga Hospital, Den Haag, The Netherlands

Xpert Clinic, Rotterdam, The Netherlands

AZ Monica, Antwerp, Belgium

R. P. van Riet (✉)
AZ Monica, Antwerp, Belgium

University Hospital Antwerp, Edegem, Belgium
e-mail: drrogervanriet@azmonica.be

There are several potential advantages to an arthroscopic approach to coronoid fractures [3–6]. Arthroscopic fixation avoids an extensile approach and the fracture can be better visualized. Associated chondral injury to articular surfaces and any soft tissue injuries can be evaluated and treated simultaneously. However, reduction and fixation can be challenging, and some fracture types may not be amendable for arthroscopic fixation. Experience in elbow arthroscopy is necessary to avoid iatrogenic injury and complications.

26.2 Indications and Contraindications

Arthroscopic coronoid repair can be performed in almost all types of coronoid fractures, unless comminution of the fragments requires plate fixation. Depending on the size of the fragment, a choice has to be made whether to perform an osteosynthesis with a headless compression screw using retrograde (or antegrade) K-wires or to perform a suture fixation with the anterior capsule (Fig. 26.1).

Contraindications for arthroscopic fixation are similar to any arthroscopic procedure and are not specific to coronoid fixation. A relative contraindication would be the need for an open procedure such as a radial head replacement and arthroscopy could potentially complicate the open part

© ISAKOS 2022

D. N. Bhatia et al. (eds.), *Arthroscopy and Endoscopy of the Elbow, Wrist and Hand*,
https://doi.org/10.1007/978-3-030-79423-1_26

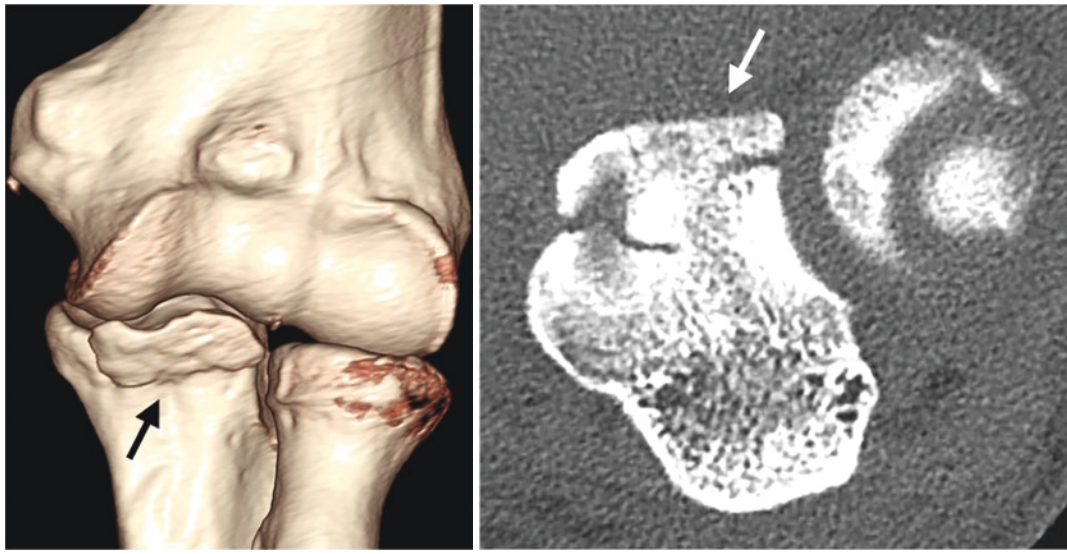

Fig. 26.1 Computed tomography image of a coronoid process fracture. (Courtesy of MoRe Foundation)

of the procedure due to swelling of the soft tissues.

26.3 Surgical Technique

The patient is placed in a lateral decubitus position with the arm over a support after making sure that there is no compression on the antecubital space. A tourniquet is applied after exsanguination. The elbow is in approximately 70°–90° of flexion.

- The hemarthrosis is aspirated through the soft spot and the elbow is rinsed with saline. The elbow joint is then insufflated with about 20 ml of saline. As the capsule is usually torn, it is recommended not to inject too much saline to prevent soft tissue swelling.
- A standard proximal anteromedial (AM) viewing portal and an anterolateral (AL) working portal are created. A needle is used to position the AL portal. It is important that the tip of the needle can reach the coronoid without any manipulation. Typically, this means that the portal is somewhat more anterior to the standard anterolateral portal. This increases the risk to the radial nerve, so extra care must be taken not to injure the nerve.
- A shaver is used to further remove the hemarthrosis and to improve the view. The joint is inspected, and the medial and lateral ligaments, fractures, cartilage, and stability are assessed. Loose osteochondral fragments may need to be removed. The fracture site is debrided, and the fragment is reduced (Fig. 26.2).
- *Suture fixation of small fragment*: If the fragment is too small or too comminuted for a screw fixation, but the elbow is unstable, we prefer to perform a suture fixation of the fragments and the anterior capsule. Under direct arthroscopic view, the open mouth of a shaver is used to reduce the fracture and hold the fragment in place. A 1.5- or 2-mm K-wire is drilled from the posterolateral aspect of the olecranon to the medial edge of the fracture site. A second drill hole is made entering the ulna 5 mm distal to the previous hole, creating a small bone bridge (Fig. 26.3a, b). A 5 mm skin incision is made. This K-wire should enter the fracture site on the lateral edge of the fracture. We prefer to perform this step under arthroscopic view, but an ACL guide or fluoroscopy may be used to

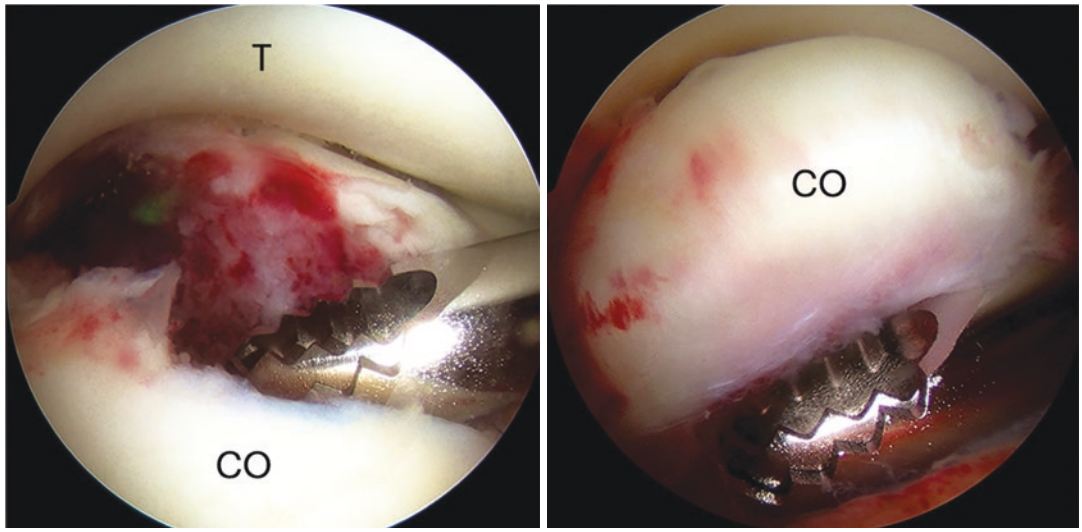

Fig. 26.2 Arthroscopic view from the anteromedial viewing portal demonstrates a coronoid process (CO) fracture. The fracture site is debrided with a shaver. (Left image). The open mouth of a shaver is used to reduce the fracture and keep the fragment in place (right image). (Courtesy of MoRe Foundation)

guide wire placement. From the lateral portal, a suture is passed through the anterior capsule. This can be done with a variety of instruments used in arthroscopic surgery, or by selecting a suture with a needle that is brought into the joint, similar to what would be done during open surgery. If the fragments are large enough, the suture can be passed through the fragments to improve the strength of fixation. A suture retriever is then used to pass both limbs of the suture through the previous drill holes, out of the previously made posterior incision. The fracture is reduced under arthroscopic view and the suture is tied over the bone bridge. Care is taken to bury the knot under the anconeus muscle (Fig. 26.4). We then routinely complete the arthroscopy by inspecting the posterior part of the joint. If present loose bodies are removed, cartilage lesions may need to be debrided and an arthroscopic fixation of the lateral collateral ligament can be performed at this time.

- *Screw fixation of large fragment*: If the fragment is deemed large enough for a screw fixation, the fragment is reduced from the lateral portal. The open mouth of a shaver is used to hold the fragment in place. If the fragment is large enough for two screws, the guide wire is drilled from the posterolateral border of the ulna lateral or medial to the center of the fragment to allow for two screws to be inserted. The second guide wire is then drilled in the fragment and the desired length is determined. If only one screw is used, the guide wire is drilled into the center of the fragment. A second wire is often used to provide rotational stability when screwing the fragment in place. The guide wire is then overdrilled with a cannulated drill bit (Fig. 26.5). The guide wire is securely held in place to avoid advancement of the wire while drilling. A cannulated screw is used to fix the fragment (Fig. 26.6). The second wire shoulder not be overdrilled before the first screw is in place as it will otherwise lose stability. The steps are repeated if a second screw is used (Fig. 26.7).

26.4 Tips and Tricks

- A subcutaneous knot may cause irritation in suture fixation. The drill holes should therefore be made lateral to the subcutaneous border, so the knot can be buried under the anconeus (Fig. 26.4).

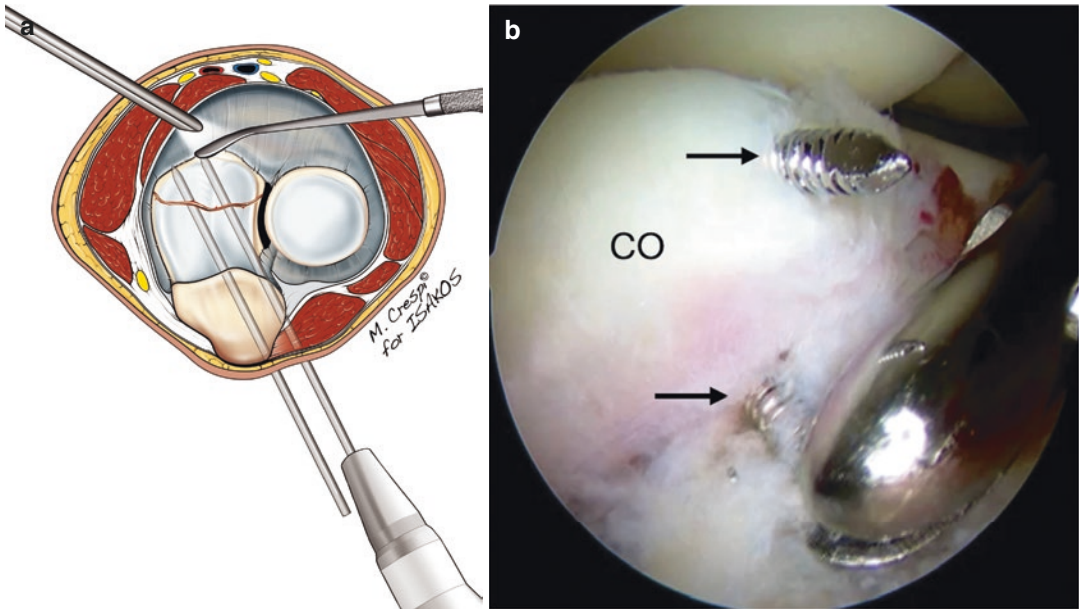

Fig. 26.3 (**a**) Two K-wires are drilled from the posterolateral aspect of the olecranon across the fracture site and into the coronoid fragment. (**b**) Arthroscopic view of the two K-wires (arrows) passed through the coronoid fragment (CO) is shown. (Courtesy of MoRe Foundation; M. Crespi © for ISAKOS)

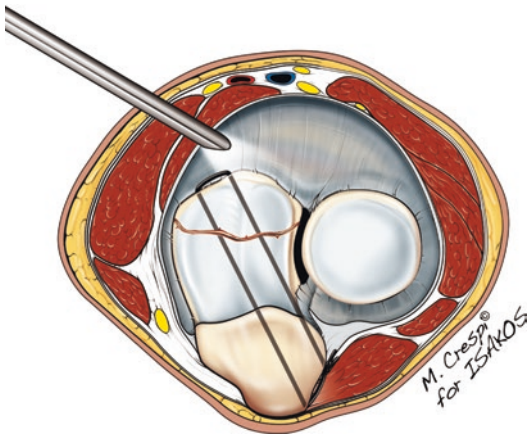

Fig. 26.4 The fracture is reduced under arthroscopic view and the suture is tied over the bone bridge. Care is taken to bury the knot under the anconeus muscle

- Screws should not protrude into the joint and should preferably be covered by the bone of the posterior ulna to avoid hardware irritation (Fig. 26.6).

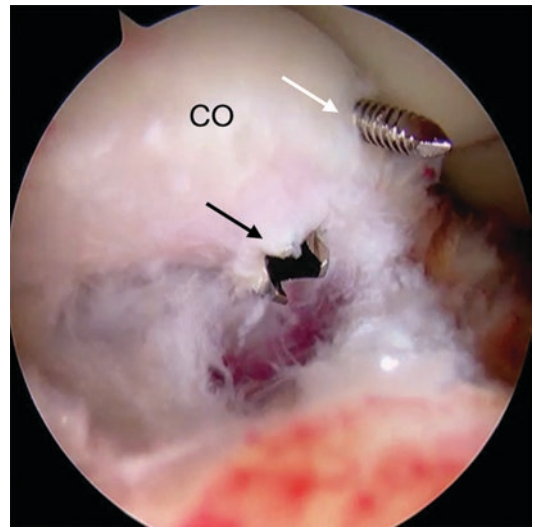

Fig. 26.5 Two K-wires (white arrow) are drilled from the posterior aspect of the olecranon to the tip of the coronoid (CO). The guide wires are overdrilled with a cannulated drill bit (black arrow). (Courtesy of MoRe Foundation; M. Crespi © for ISAKOS)

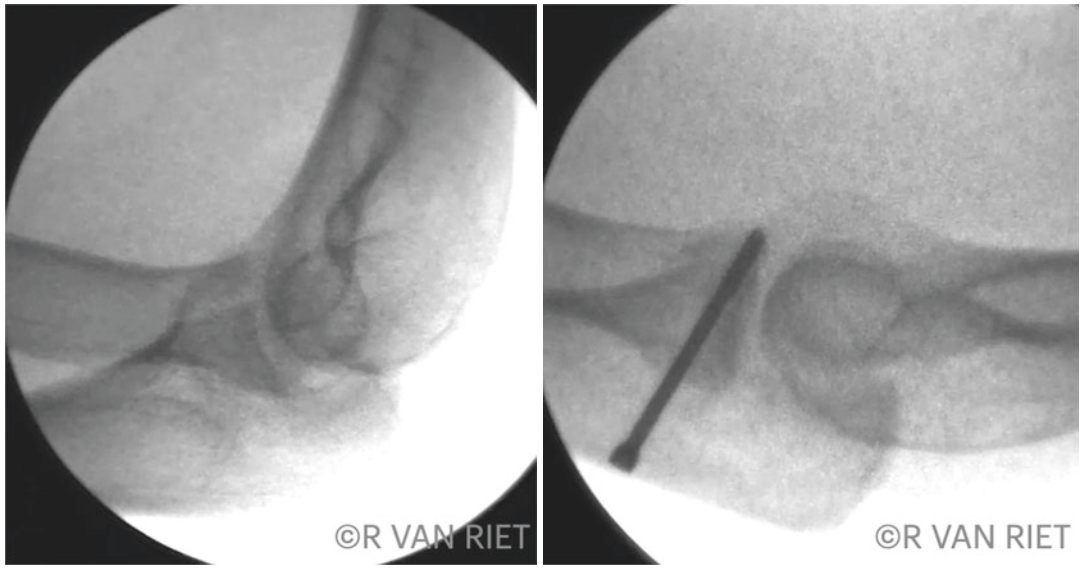

Fig. 26.6 Pre- and post-fixation fluoroscopic views demonstrate the fracture fixation with a cannulated screw. (Courtesy of MoRe Foundation; ©Van Riet)

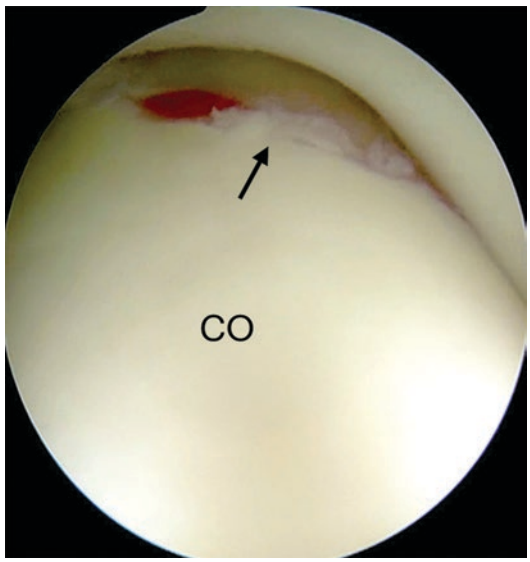

Fig. 26.7 Arthroscopic image demonstrates congruent reduction (arrow) of coronoid fragment (CO). (Courtesy of MoRe Foundation)

26.5 Pitfalls

- Soft tissue swelling can quickly become a problem with higher saline pressure and flow, as the anterior capsule is often torn.
- The indication for arthroscopy should preferably be made prior to surgery as conversion to an open procedure may be difficult due to swelling.
- Hardware irritation is common if the knot is not placed correctly or screws are protruding out of the bone.
- Do not forget the posterior part of the joint as loose bodies and ligamentous avulsions are common.

26.6 Postoperative Rehabilitation

In a patient with an isolated coronoid fracture with stable fixation, the arm is placed in a posterior plaster splint with the elbow extended to decrease swelling. A physiotherapist will instruct the patient on both passive and active motion exercises and the patient is discharged on the same day. The splint is removed after 24 h and the patient will start mobilizing the elbow. Ligamentous injuries or other fractures may change this protocol, depending on the injury.

26.7 Complications

Specific complications related to this surgery and trauma include persistent instability, stiffness,

post-traumatic osteoarthritis, nonunion, and failure or irritation of hardware.

Conflict of Interest Roger P. van Riet has a teaching and speaking agreement with Acumed.

The author (RVR) retains the copyright to images, videos, and content in the chapter.

References

1. Sheps DM, Kemp KA, Hildebrand KA. Population-based incidence of proximal radial and ulnar fractures among adults in a Canadian metropolitan area. Curr Orthopaed Pract. 2012;23:364.
2. Doornberg JN, Ring DC. Fracture of the anteromedial facet of the coronoid process. J Bone Joint Surg. 2006;88A:2216.
3. Hausman MR, Klug RA, Qureshi S, Goldstein R, Parsons BO. Arthroscopically assisted coronoid fracture fixation: a preliminary report. Clin Orthop Relat Res. 2008;466(12):3147–52. https://doi.org/10.1007/s11999-008-0502-2.
4. Adams JE, Merton SM, Steinmann SP. Arthroscopic-assisted treatment of coronoid fractures. Arthroscopy. 2007;23:1060.
5. Arrigoni P, D'Ambrosi R, Cucchi D, Nicoletti S, Guerra E. Arthroscopic fixation of coronoid process fractures through coronoid tunnelling and capsular plication. Joints. 2016;04(03):153–8.
6. Rashid A, Copas D, Granville-Chapman J, Watts A. Arthroscopically-assisted fixation of anteromedial coronoid facet fracture and lateral ulnar collateral ligament repair for acute posteromedial rotatory fracture dislocation of the elbow. Shoulder Elbow. 2019;11(5):378–83.

27 Arthroscopic Fixation of Coronoid Fractures: Antegrade Wire Technique

Francesco Luceri, Davide Cucchi, Rahul Sinha, Paolo Arrigoni, and Pietro Simone Randelli

27.1 Background

Coronoid process (CP) fractures are relatively uncommon, yet critical injuries to recognize and treat. CP fractures commonly occur with elbow dislocations and are usually associated with elbow instability. Historically, recommendations have been to fix all Morrey type II and III fractures and current consensus suggests fixation in every case of CP fracture associated with elbow instability [1]. Classical open techniques are technically challenging and may endanger neurovascular structures and residual elbow capsule. Arthroscopic reduction and fixation of CP has been proposed to overcome these limitations of open approaches.

Arthroscopic techniques for CP fixation involve insertion of retrograde guide wire and passage of a retrograde cannulated screw. This method is widely used; however, the step of directing the guide wire from dorsal aspect of ulna towards the tip of the CP is technically challenging. Guide systems used for knee ligament reconstructions are difficult to position accurately and peri-articular swelling can impede advancement of the retrograde K-wire in the correct position. The authors use a new surgical procedure of arthroscopic-assisted CP fracture reduction and insertion of an antegrade guide wire for internal fixation of CP fractures. A new accessory anteromedial portal allows the surgeon to obtain a better working angle for reduction of these fractures without requiring a cruciate ligament guide. This portal permits fixation of the CP fracture using a more perpendicular angulation to the fracture line as compared to a standard anteromedial portal.

Francesco Luceri and Davide Cucchi contributed equally to this work. Paolo Arrigoni and Pietro Simone Randelli equally contributed to this paper as Senior Authors.

F. Luceri
U.O.C. Clinica Ortopedica e Traumatologica Universitaria CTO, Azienda Socio Sanitaria Territoriale Centro Specialistico Ortopedico Traumatologico Gaetano Pini-CTO, Milan, Italy

D. Cucchi
Department of Orthopaedics and Trauma Surgery, Universitätsklinikum Bonn, Bonn, Germany

Department of Biomedical Sciences for Health, Università degli Studi di Milano, Milan, Italy

R. Sinha
Medica Institute of Orthopaedic Sciences, Bhagwan Mahavir Medica Superspeciality Hospital, Ranchi, Jharkhand, India

P. Arrigoni (✉) · P. S. Randelli
Department of Biomedical Sciences for Health, Università degli Studi di Milano, Milan, Italy

U.O.C. Clinica Ortopedica e Traumatologica Universitaria CTO, Azienda Socio Sanitaria Territoriale Centro Specialistico Ortopedico Traumatologico Gaetano Pini-CTO, Milan, Italy

Research Center for Adult and Pediatric Rheumatic Diseases (RECAP-RD), Department of Biomedical Sciences for Health, Università degli Studi di Milano, Milan, Italy

© ISAKOS 2022

D. N. Bhatia et al. (eds.), *Arthroscopy and Endoscopy of the Elbow, Wrist and Hand*,
https://doi.org/10.1007/978-3-030-79423-1_27

27.1.1 Surgical Anatomy

The medial and lateral collateral ligaments are primary elbow stabilizers along with the ulnohumeral articulation. The radial head, capsule, flexor, and the extensor muscles are structures that play a relevant role especially in case of insufficiency of one or more primary stabilizers [2]. The coronoid process (CP) is therefore an important stabilizer of the elbow joint, which, together with the radial head, prevents posterior ulnar translation. The CP functions as a bony buttress to posterior ulnar displacement. Three important soft tissue structures insert on this bony process: anterior joint capsule, brachialis muscle and the medial ulnar collateral ligament (UCL) [3, 4]. The anterior capsule attaches very close to its tip and the brachialis inserts anteriorly and distal to the capsule. The UCL inserts distally and medially on the sublime tubercle.

The most common pattern of instability is posterolateral rotatory instability; disruption of lateral collateral ligament (LCL) and external rotation of the forearm over the humerus result in posterolateral elbow dislocation. This type of elbow instability may be accompanied by a combined radial head and CP fracture (terrible triad). Another mechanism of injury that can cause a CP fracture is posteromedial rotatory instability; this injury is associated with a large CP fracture (anteromedial facet), LCL rupture, and partial UCL rupture without radial head fracture and elbow dislocation.

27.2 Indications and Contraindications

Coronoid process fractures associated with elbow instability should be reduced and fixed anatomically using arthroscopic techniques.

Contraindication to arthroscopic technique would be associated acute partial articular fractures that are difficult to reconstruct, and these are treated with distal humeral hemiarthroplasty [5].

27.3 Surgical Technique

Arthroscopy is performed using an axillary block and general anaesthesia. The patient is placed in a modified lateral decubitus position with the operative arm placed in 100° flexion and 90° internal rotation of shoulder and supported by an arm holder. The elbow is positioned in 90° flexion, with forearm hanging free under gravity. A pneumatic tourniquet is placed high in axilla and the elbow joint is distended by injecting 20 cc sterile saline through an 18 G needle via proximal posterior portal.

- A *proximal accessory anteromedial portal* is located 2 cm proximal to the standard anteromedial (AM) portal that is marked at approximately 2 cm proximal and 1 cm anterior to medial epicondyle. In case of isolated CP fracture, this portal is created first and a 30° scope can be inserted for intra-articular diagnostic evaluation, before making the anterolateral portal. In the presence of associated lesions like radial head fracture, standard anterolateral and anteromedial portals are created first and diagnostic workup is done [6]. A midlateral portal can be created to assist reduction and fixation depending upon the fracture pattern.
- After diagnostic evaluation of the CP fracture is performed through the accessory anteromedial portal, a blunt Wissinger rod is now inserted in this portal to maintain access to the joint and the scope is passed in the anterolateral portal, which is used as viewing portal for the CP osteosynthesis. A standard anteromedial portal (2 cm proximal and 1 cm anterior to medial epicondyle) can be created as secondary working portal to assist reduction with a blunt trocar.
- An arthroscopic cannula is introduced through the accessory anteromedial portal. A 0.9 mm K-wire is passed down the cannula and pointed on the fractured ulna. The K-wire is drilled through the CP base to the dorsolateral ulna, without entering the fragment (Fig. 27.1). The K-wire is pulled from the dorsolateral ulna

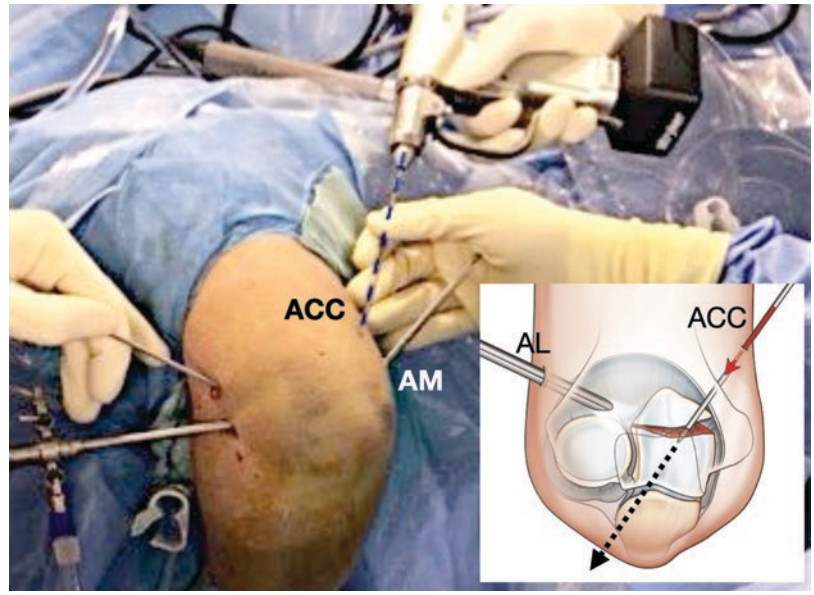

Fig. 27.1 Antegrade wire passage through the accessory anteromedial portal (ACC) is demonstrated. Note that the ACC portal is placed 2 cm proximal to the standard anteromedial portal (AM) (*AL* anterolateral portal). (M. Crespi © for Arrigoni)

until it disappears in the CP bone (Fig. 27.2). The CP is reduced using a blunt trocar inserted via the accessory anteromedial portal and the K-wire is advanced in the fracture fragment. Intraoperative radiographic control can be useful to confirm correct positioning of the wire (Fig. 27.3).

- A stab incision is given on the dorsolateral forearm and retrograde drilling is performed over the wire. Thereafter, a retrograde cannulated screw (Synthes 3.0 mm Cannulated Screw) is introduced from the dorsolateral ulna to the tip of CP, checking under arthroscopy that the reduction is maintained throughout the whole procedure (Fig. 27.4).
- At the end of the procedure, the complete range of motion (ROM) of the elbow is tested under visual control and CP stability is tested. Intraoperative radiographs are used to confirm correct reduction and fixation.

27.4 Tips and Tricks

- *Accessory anteromedial portal*: To avoid damage to brachial artery and median nerve, incise only the skin and then use a cannulated needle system to establish the portal. The cannulated needle system is directed perpendicular to the long axis of the arm until contact with the anterior humeral cortex is achieved. The cannulated needle system is then advanced obliquely towards the joint, always maintaining constant contact with the anterior humeral cortex until the elbow capsule is reached [6].
- *Anterolateral portal*: Pronation of the forearm is recommended when establishing the portal, since pronation displaces the posterior interosseous nerve (PIN) anteromedially, protecting it from iatrogenic injuries [7]. If an outside-in technique is used, it is advisable to check the needle entry point from the anteromedial portal, and to carefully incise the skin and subcutaneous tissue before inserting the arthroscope sheath and trocar; alternatively, this portal can be established through an inside-out technique. However, uninterrupted prolonged periods of hyperpronation are not recommended, since this may increase excessively the pressure on the PIN beneath the arcade of Frohse.

27.5 Pitfalls

The medial neurovascular structures are potentially at risk of injury with the new portal. To protect neurovascular structures, it is necessary

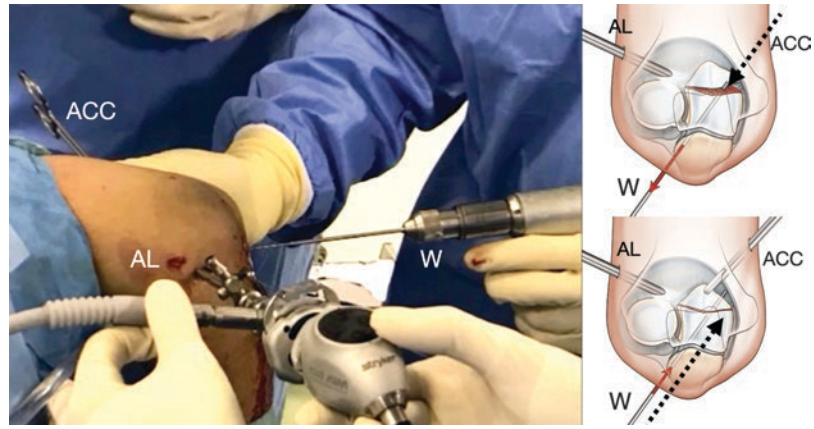

Fig. 27.2 The antegrade wire (W) passage through the posterior ulna is demonstrated (left and top right images). The wire is drilled through the fracture fragments after reduction (bottom right image) (*AL* anterolateral portal)

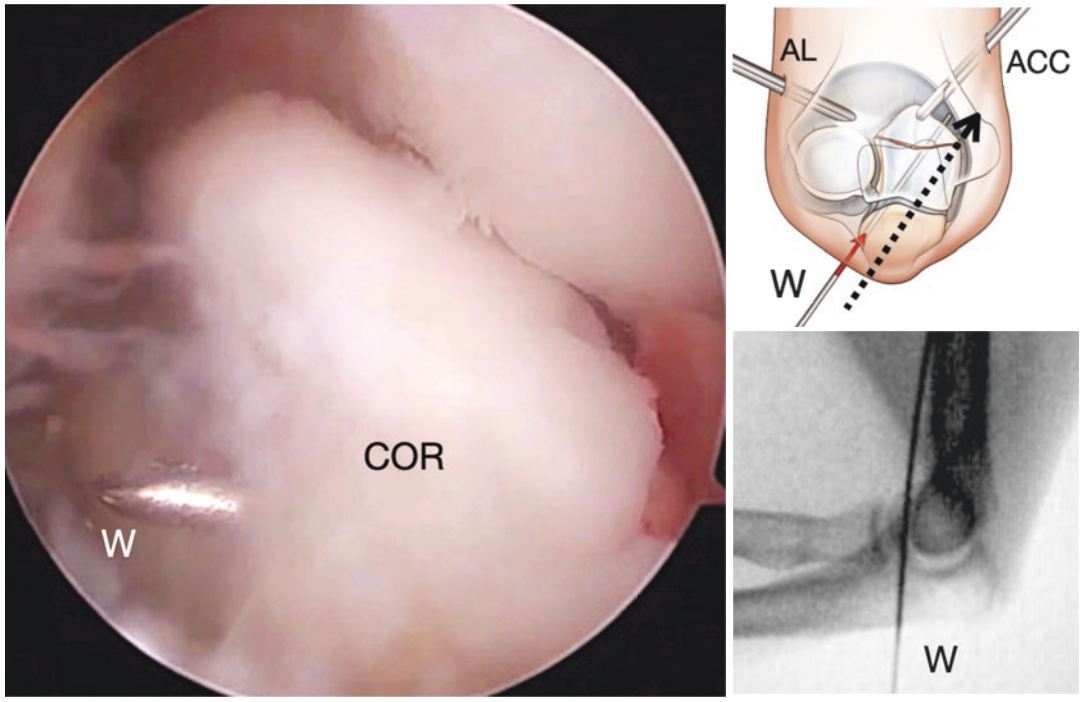

Fig. 27.3 Retrograde K-wire (W) drilling into the coronoid fragment (COR) is demonstrated (*ACC* accessory anteromedial portal, *AL* anterolateral portal). (M. Crespi © for Arrigoni)

to create the accessory anteromedial portal far away from the midline. Also, the K-wire should be directed posteriorly towards the humerus and perpendicularly to its long axis until contact with the anterior cortex is felt. At the bend of the elbow, the brachial artery sinks deeply into the antecubital fossa, where it divides in the radial and the ulnar arteries above the CP. At the level of the accessory anteromedial portal creation, the brachial artery and the median nerve lie superficial in a groove between the biceps brachii and the brachialis bellies. All lateral structures are considered safe with anteromedial approaches.

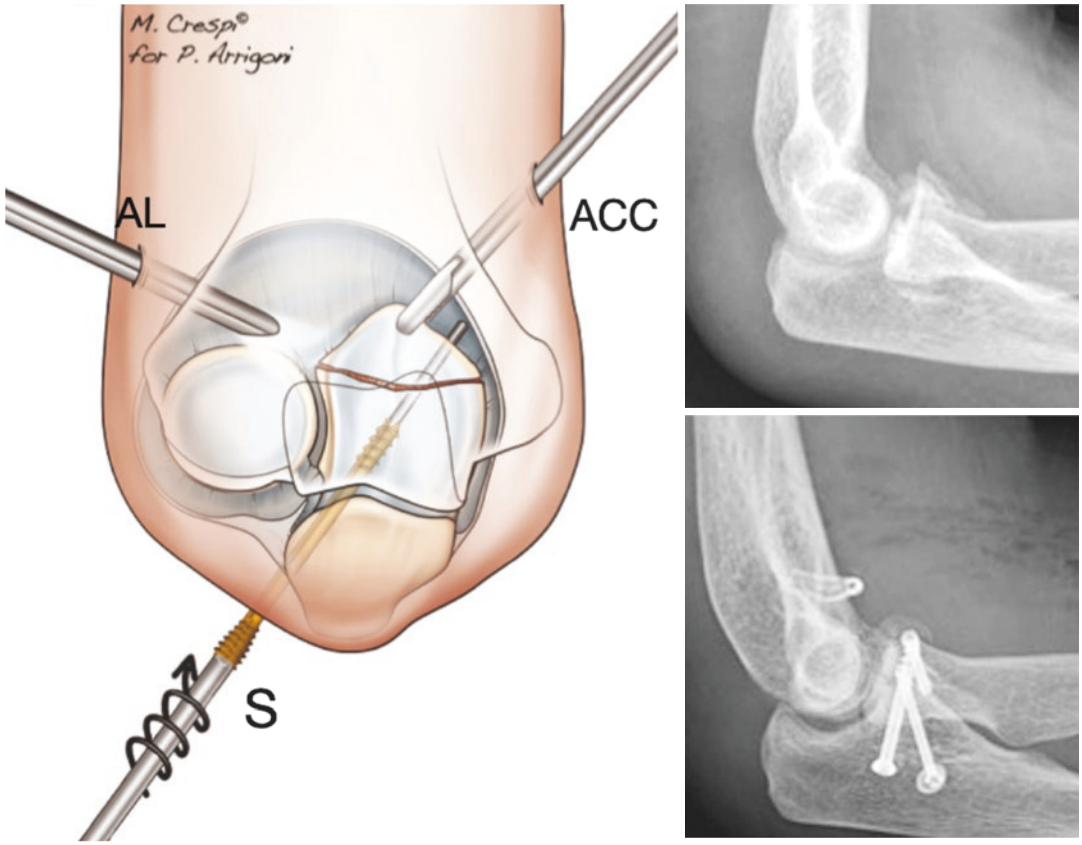

Fig. 27.4 Coronoid fracture fixation is performed using a screw (S) passed over the wire. Pre- and postoperative radiographs demonstrate coronoid fracture fixation. (M. Crespi © for Arrigoni)

27.6 Rehabilitation Protocol

After surgery, the elbow joint is immobilized in a brace with the forearm in neutral rotation and the elbow at 90° of flexion. A 30° to 60° active ROM is allowed after the first 15 days. Active wrist and shoulder ROM exercises are progressively initiated. In the next few weeks, active ROM is slowly increased, with the help of a physiotherapist, until the functional arc of motion is recovered. At 6 weeks, the brace can be removed for activities without risk of trauma and complete brace removal occurs at 8 weeks. Approximately 10 weeks after surgery, the patient is encouraged to obtain full passive ROM assisted by a physiotherapist and to start muscle-strengthening exercises.

27.7 Complications

- Medial neurovascular structures (brachial artery, median nerve, and ulnar nerve injuries) are potentially at risk of iatrogenic injury. Brachial artery and median nerve are at risk over anteromedial aspect and posterior interosseous nerve (PIN) over anterolateral aspect. PIN injury may occur during portal placement and after accidental damage to the anterior joint capsule, which is separated from the nerve just by a thin layer of muscle and adipose tissue [7]. The ulnar nerve damage can occur during portal placement or by using motorized instruments inside the joint in close proximity to the medial capsule.

- The K-wire drilling is another delicate surgical step and should be performed carefully to avoid fragment commination.

References

1. Regan W, Morrey B. Fractures of the coronoid process of the ulna. J Bone Joint Surg Am. 1989;71(9):1348–54.
2. Luceri F, Lesman JJ, Cucchi D, Domzalski M, Randelli PS, Arrigoni P. Antegrade reduction and fixation of coronoid fractures: a new arthroscopic technique. Tech Shoulder Elb Surg. 2020;21(1):1–5.
3. Arrigoni P, Luceri F, Cucchi D, Tamini J, Randelli PS. Reliability of anterior medial collateral ligament plication of the elbow. Musculoskelet Surg. 2018;102:85–91.
4. Lesman J, Luceri F, Domzalski M, Randelli PS, Arrigoni P. The mini-open plication of medial collateral ligament of the elbow: a new arthroscopically assisted technique. Tech Shoulder Elb Surg. 2019;20(4):121–4.
5. Arrigoni P, Luceri F, Brioschi M, D'Ambrosi R, Pulici L, Randelli P. Distal humeral hemiarthroplasty: indications and expected results. Elb Arthroplast. 2020:217–20.
6. Arrigoni P, Cucchi D, Guerra E, Luceri F, Nicoletti S, Menon A, Randelli P. No neurovascular damage after creation of an accessory anteromedial portal for arthroscopic reduction and fixation of coronoid fractures. Knee Surg Sport Traumatol Arthrosc. 2019;27(1):314–8.
7. Arrigoni P, Cucchi D, Menon A, Guerra E, Nicoletti S, Colozza A, Luceri F, Pederzini LA, Randelli PS. The posterior interosseous nerve crosses the radial head midline and increases its distance from bony structures with supination of the forearm. J Shoulder Elb Surg. 2019;28:365–70.

Arthroscopic-Assisted Fixation of Capitello-Trochlear Fractures

28

Yiyang Zhang and Graham J. W. King

28.1 Background

Treatment options for the management of capitellum/trochlea fractures include closed reduction and casting, open reduction and internal fixation, arthroscopic-assisted reduction and internal fixation, fragment excision, and arthroplasty. Open surgical fixation is the most common procedure for these injuries. Arthroscopic-assisted reduction and internal fixation (AARIF) of capitellum/trochlea fractures is a minimally invasive alternative and offers an excellent visualization of the fracture reduction while minimizing soft tissue dissection. This chapter describes the authors' technique of AARIF for capitello-trochlear fractures.

28.2 Surgical Anatomy

The blood supply to the capitellum comes primarily from the radial recurrent and interosseous recurrent arteries [1, 2]. These vessels are anastomoses from the radial and medial collateral arteries with both being branches of the profunda brachii. Theoretically, limited posterolateral dissection is recommended in operative management to avoid disruption of the lateral arcade potentially leading to avascular necrosis [1].

Arthroscopic visualization of the elbow is divided into three compartments. The anterior compartment comprises the capitellum, radial head, radial fossa, anterior trochlea, coronoid, coronoid fossa, and medial and lateral condyles. The posterior compartment includes the olecranon, olecranon fossa, and medial and lateral gutters. Finally, the posterolateral compartment contains the radial head, olecranon, lateral gutter, and capitellum. With AARIF, typically only an anterior compartment arthroscopy needs to be performed in order to reduce and assess the capitellum fracture. In some cases, with posterior comminution a posterolateral arthroscopy is required to remove fragments interfering with reduction and to ensure the quality of the reduction.

Knowledge of elbow anatomy is essential in establishing portals and avoiding neurovascular complications. There are a standard set of portals available in elbow arthroscopy with each varying in distance to neurovascular structures (Fig. 28.1). The proximal anteromedial portal is 2 cm proximal and 1 cm anterior to the medial epicondyle. The median nerve and brachial artery are approximately 12 mm and 18 mm away from this portal,

Y. Zhang
Roth|McFarlane Hand and Upper Limb Centre, St Joseph's Health Care, London, ON, Canada

G. J. W. King (✉)
Roth|McFarlane Hand and Upper Limb Centre, St Joseph's Health Care, London, ON, Canada

Department of Surgery, Western University, London, ON, Canada
e-mail: Graham.King@sjhc.london.on.ca

© ISAKOS 2022

D. N. Bhatia et al. (eds.), *Arthroscopy and Endoscopy of the Elbow, Wrist and Hand*,
https://doi.org/10.1007/978-3-030-79423-1_28

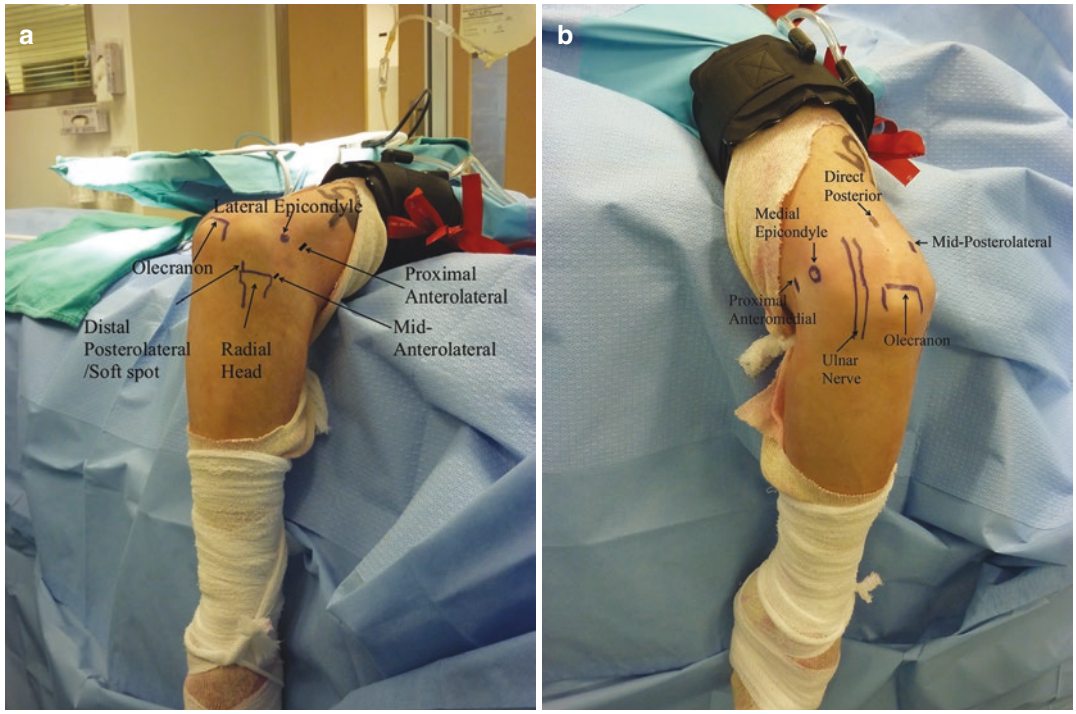

Fig. 28.1 Right elbow with surface anatomy drawn and portals marked. Lateral side (**a**). Medial side (**b**). Courtesy of GJW King with patient permission

respectively [3]. The proximal anterolateral portal is 2 cm proximal and slightly anterior to the lateral epicondyle. This is one of the safest anterolateral portals averaging from 10 to 14 mm away from the radial nerve. Both the proximal anteromedial and proximal anterolateral portals are used to assess the anterior compartment of the joint. In some patients, a mid-anterolateral portal can be useful to allow placement of instruments to facilitate fracture reduction while using the proximal anterolateral portal for a retractor. The mid-anterolateral portal is located directly anterior to the radiocapitellar joint. The radial nerve is approximately 10 mm away from this portal and becomes closer with more distal portal placement. This portal can be made in an inside-out fashion in order to minimize the neurovascular risk.

In viewing the posterior compartment, if required, the direct posterior and mid-posterolateral portals are used. The direct posterior portal is located 3 cm proximal to the tip of the olecranon. It is created by splitting the triceps. The posterolateral portal is just lateral to the triceps, at the level of the olecranon tip. Both portals are relatively safe with respect to the distance from any neurovascular structures. It is important to palpate and routinely draw the ulnar nerve on the skin when performing elbow arthroscopy so there can be no confusion as to its location throughout surgery.

The posterolateral compartment can be visualized with the mid-posterolateral portal and additional "soft spot" or distal posterolateral portal. The soft spot portal is located in the center of a triangle created by the lateral epicondyle, olecranon, and radial head. The lateral antebrachial cutaneous nerve lies approximately 10 mm away. Accessory portals can be made anywhere along the line between the mid-posterolateral portal and the soft spot portal for use of retractors and for the placement of cannulated screws for capitellar fixation.

28.3 Indications and Contraindications

Arthroscopically assisted reduction and internal fixation of capitellum fractures is best suited for Dubberley 1A and 2A fracture types. Fractures with posterior comminution (Type B) are more challenging to manage with arthroscopy as the reduction is harder to achieve and fixation may require the use of a plate which requires an open rather than a percutaneous approach. AARIF can be performed in the setting of lateral collateral ligament injury; however, in those cases the authors prefer recommend an open approach for the visualization and fixation of the capitellum/trochlea fractures and subsequent repair of the ligament injury through the same incision. Arthroscopic lateral collateral ligament repair has been reported and is an option for those with advanced arthroscopic experience [4, 5]. Concomitant medial collateral ligament injuries are typically managed nonoperatively, so they are not a contraindication to an arthroscopic approach for the capitellum fracture.

Surgeons should be wary of a subluxating ulnar nerve or prior ulnar nerve surgery. In the setting of a prior subcutaneous transposition, a larger portal will have to be made to identify the nerve or ensure that it is protected during portal insertion. A prior submuscular transposition is a contraindication to elbow arthroscopy.

28.4 Surgical Technique

Patient is positioned in lateral decubitus position with arm supported by an arm holder while all bony prominences are padded. A sterile tourniquet is used. Initially, elbow stability is assessed with varus and valgus force to ensure that there is no concomitant ligament injury. A closed reduction is then attempted by extending and placing a varus force on the elbow while the capitellar fragment is pushed inferiorly. The elbow is then flexed to maintain the reduction which is confirmed with fluoroscopy. If the reduction is unsuccessful, an AARIF is performed.

- Elbow arthroscopy is started by marking out the location of ulnar nerve. The ulnar nerve is examined through flexion and extension to see if it subluxates. A small incision should be made to identify the nerve in the setting of previous ulnar nerve transposition. The proximal anteromedial and proximal anterolateral portals are marked. Then, the capsule is insufflated with 20 cc of normal saline injected into the joint through the direct posterior portal.
- In the setting of capitellar fractures, the proximal anteromedial portal is established first and the joint is visualized through this portal with a standard 4.0 mm 30° arthroscope (Fig. 28.2).
- The proximal anterolateral portal is then established with the assistance of direct visualization from within the joint. A needle can be used to assist with localization. The hematoma is then cleared from the joint by using a shaver through this portal.
- The fracture reduction is then assessed to confirm if the initial closed reduction was successful. A probe or blunt instrument can be inserted into the proximal anterolateral portal to make fine adjustments to the articular reduction (Fig. 28.3a–e).
- If visualization is suboptimal, a mid-anterolateral portal can be established using an inside-out technique to allow placement of an elevator to retract the anterior capsule and

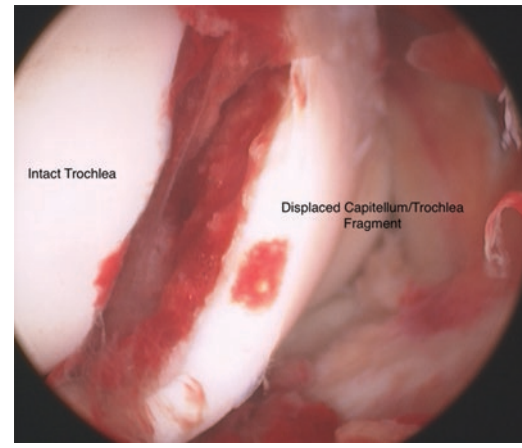

Fig. 28.2 View of fracture from proximal anteromedial portal after debridement of hematoma

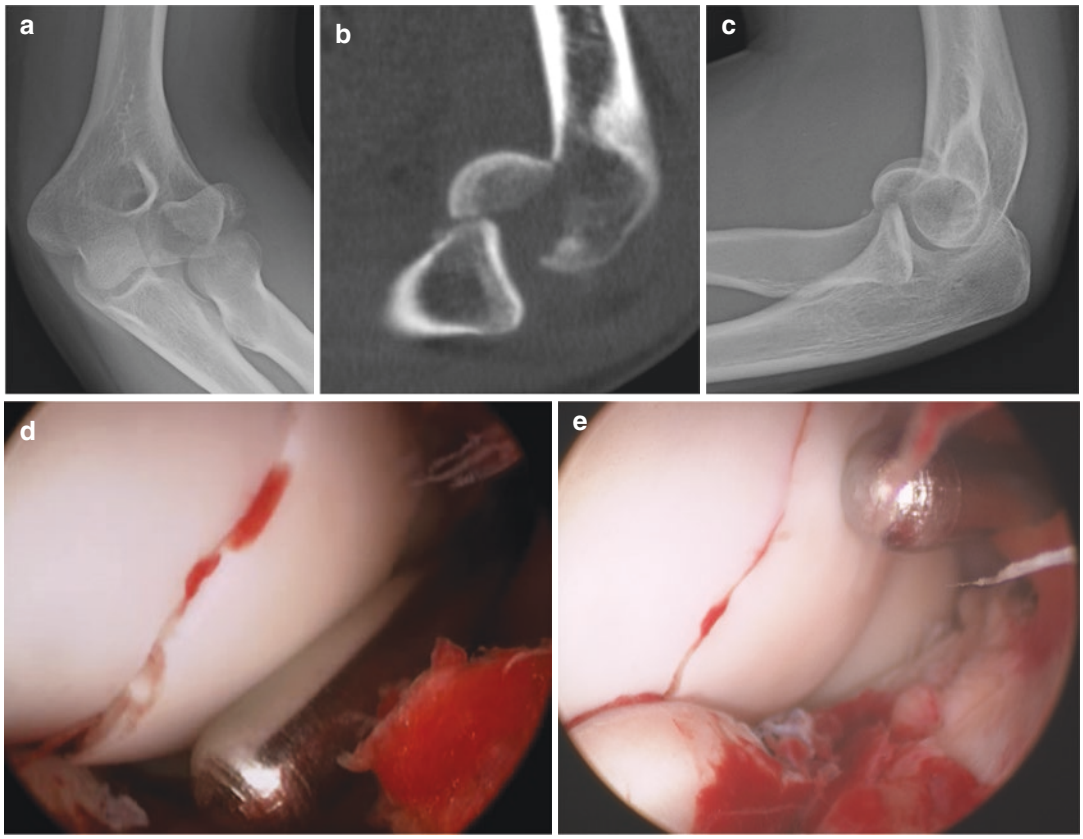

Fig. 28.3 (**a**, **b**) Radiographs show isolated capitellum/trochlea fracture in a 24-year-old female who fell on her outstretched hand. (**c**) Absence of posterior comminution was verified on CT scan. (**d**) A closed reduction was performed successfully in the OR prior to arthroscopy. Fine tuning of the reduction was performed with a switching stick. (**e**) Flexion of the elbow maintains the reduction as the coronoid and radial head capture the fragment

underlying posterior interosseous nerve. Mid and distal posterolateral portals can also be established to assess the reduction posteriorly. These portals are particularly useful if there is posterior comminution blocking an anatomic reduction.

- If the fracture was not reduced closed initially, a Howarth elevator or switching stick can then be introduced to push the superiorly displaced capitellar fragment inferiorly and into place. If the fracture is reduced, but the capitellar fragment slides as the elbow is flexed, then the Howarth is used to help guide the radial head over the capitellum as the elbow is moved from extension to flexion, in essence, shoehorning the capitellum fragment in place.
- Once a satisfactory reduction of the fracture is obtained, guide wires from a cannulated screw system are placed 90° to the fracture orientation from a posterior to anterior direction through the lateral triceps to capture the capitellar fragment. The fracture reduction is held by a blunt instrument as the guide wires are passed through the articular surface to ensure optimal positioning and length. The placement of the guide wires is then assessed by fluoroscopy and by arthroscopy to ensure that they are backed up so they are just underneath the articular surface.
- After confirmation of wire positioning, small stab incisions are made over the K-wires down onto bone (Fig. 28.4a, b). The K-wire lengths are then measured, and appropriately sized cannulated headed or headless screws are inserted for definitive fixation.
- Depending on the size of the capitellar fragment, usually the fragment is captured with at least three screws. If satisfied with the fixation

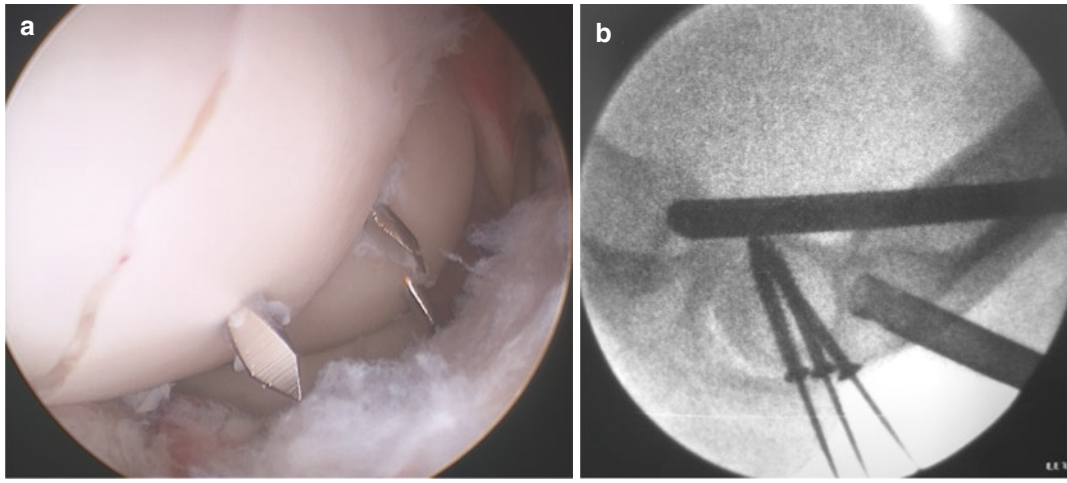

Fig. 28.4 Arthroscopic assessment of guide wire placement (**a**), and insertion of partially threaded cannulated screws (**b**)

and articular congruity, the arthroscopy is then terminated, and the portal sites are sutured. A sterile dressing and a backslab with the elbow at 90° is applied.

28.5 Tips and Tricks

- Do an examination under anesthesia with fluoroscopy to check collateral ligament integrity.
- Perform an initial closed reduction to make AARIF technically easier.
- Fine tune the articular reduction using a switching stick or Howarth elevator.
- Wait 3–5 days after the fracture has occurred before proceeding with AARIF to reduce intraoperative bleeding which can obscure visualization.
- View the fracture from proximal anteromedial portal and reduce from anterolateral portals.
- If visualization is poor, use a retractor.
- If reduction cannot be achieved using anterior portals, consider posterolateral arthroscopy to check for a block to reduction.
- Convert to open procedure if unable to reduce the fracture.
- Drive cannulated guide wires through articular surface to check positioning. Back up until under articular surface before measuring length.
- Check reduction and screw placement with fluoroscopy.

28.6 Pitfalls

- Attempting AARIF of comminuted capitellum/trochlear fractures is not recommended.
- Setting pump pressure too high results in swelling which increases risk of neurovascular injury during portal placement and overall difficulty of arthroscopy.
- Proceeding with AARIF less than 3 days after fracture results in bleeding, obscuring visualization.
- Proceeding with AARIF more than 7 days after fracture makes closed and arthroscopic reduction more difficult.

28.7 Postoperative Management and Rehabilitation

- Due to the minimally invasive surgery, patients with AARIF of capitellum/trochlea fractures can typically be managed as outpatients. If satisfied with intraoperative fixation and in the setting of no ligament injury, the rehabilitation process is initiated a few days after surgery. The patient is transitioned to a 90° resting thermoplastic splint and gentle active range of motion exercise can then be commenced.
- If there is concomitant lateral ligament injury or repair, the forearm is splinted in 90° and pronation. Patients perform gentle flexion and

extension with the forearm pronated [6]. With the elbow flexed to more than 90°, patients perform forearm rotation exercises.

- Conversely, if there is a concomitant medial ligament injury, a thermoplastic splint is provided with the forearm in supination. Active flexion and extension are performed with the forearm in supination [7]. Forearm rotation exercises are performed with the elbow flexed to more than 90°.
- If at any point in radiographic follow-up a drop sign occurs [8], isometric exercises of the biceps and triceps are initiated with the elbow remaining in the splint. In addition, flexion, extension, and forearm rotation exercises are transitioned to overhead protocol with the patients in supine position [9]. This aims to take advantage of gravity and muscle activation to reduce ulnohumeral gapping.
- Typically, the patients are reassessed 2 weeks after surgery for suture removal and 6 weeks for fracture healing. More frequent follow-up is recommended if concomitant ligament injuries are present to ensure a congruous reduction is maintained. Serial radiographs are obtained to ensure maintenance of reduction and bony healing. Patients should be followed up for up to 2 years clinically and radiographically to monitor for the development of avascular necrosis (Fig. 28.5).

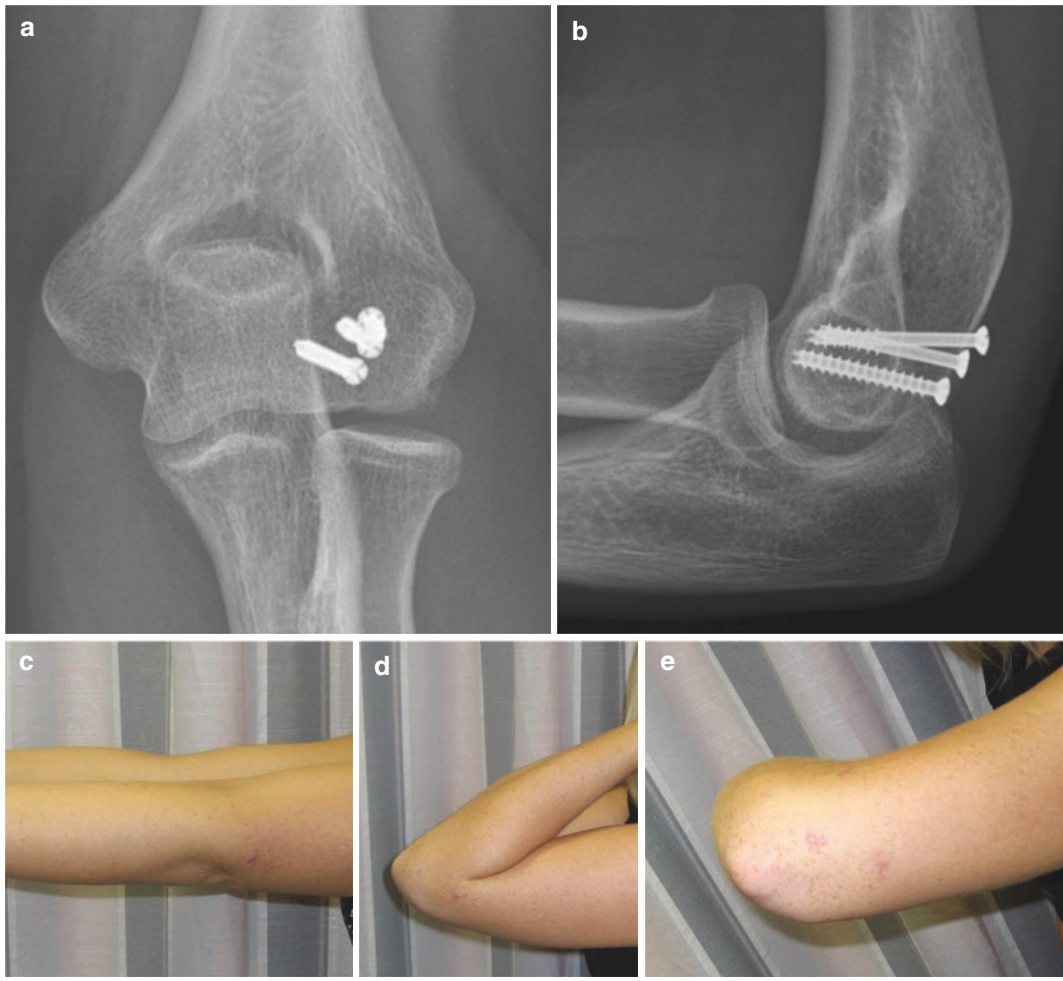

Fig. 28.5 AP (**a**) and lateral (**b**) X-ray of patient 3 months postoperatively with union at fracture site, no evidence of avascular necrosis, full range of motion (**c**, **d**), and healed incisions (**e**)

28.8 Complications

With regard to capitellum fractures, most concerning complications are nonunion and avascular necrosis (AVN). The nonunion rate for capitellum fractures is quoted to be 0–27% in open series. There have been no reports of nonunion or AVN for arthroscopically assisted reduction and internal fixation of capitellum/trochlea fractures; however the literature is currently very limited. Theoretically, the blood supply to the capitellum should be preserved with the minimal posterior dissection in AARIF. However, the soft tissue attachment to the fragment(s) is typically limited to a small portion of anterolateral capsule so it would be expected that AVN will also be seen with AARIF when larger case series are reported.

One of the more common complications is stiffness. In one study of patients with open reduction and internal fixation of capitellar-trochlear fractures, function-limiting stiffness requiring a secondary operation was as high as 29% [10]. Most patients, however, achieve functional range of motion through nonoperative means. Other potential complications can include infection and hardware irritation. Given the rarity of this fracture, these complications are not well reported.

28.9 Results

There have been three case series, totalling four patients, reporting the outcome of AARIF of capitellum/trochlea fractures. Hardy et al. was the first to report their case study [11]. They achieved reduction through three laterally based arthroscopic portals and inserted anterior to posterior screws for fixation. They ensured that the screws were buried deep to the cartilage. Subsequently, Kuriyama et al. and Mitani et al. individually reported three patients in total that had their capitellum/trochlea fractures managed with AARIF [12, 13]. Similar to Hardy, Kuriyama also used laterally based portals while Mitani established a proximal anteromedial and a proximal anterolateral portal. Kuriyama and Mitani both used headless screws inserted from a posterior to anterior direction. In all three case studies, all patients healed, attained functional range of motion, and returned to normal activities without any signs of avascular necrosis.

The authors prefer to insert screws in from a posterior to anterior direction. The advantages are avoiding large holes in the articular surface, less risk of neurovascular damage during placement, and having a large surface area to insert screws perpendicular to the fracture. Biomechanically, there is evidence to suggest as well that posterior to anterior screws are stronger than anterior to posterior screws [14].

28.10 Summary

Isolated capitellum/trochlea fractures are uncommon. Arthroscopically assisted reduction and internal fixation of capitellum/trochlea fractures is a useful technique for surgeons experienced with elbow arthroscopy. Arthroscopy allows for accurate assessment of intraarticular reduction while minimizing soft tissue dissection.

References

1. Yamaguchi K, Sweet FA, Bindra R, Morrey BF, Gelberman RH. The extraosseous and intraosseous arterial anatomy of the adult elbow. J Bone Joint Surg Am. 1997;79(11):1653–62.
2. Kimball JP, Glowczewskie F, Wright TW. Intraosseous blood supply to the distal humerus. J Hand Surg. 2007;32(5):642–6.
3. Unlu MC, Kesmezacar H, Akgun I, Ogut T, Uzun I. Anatomic relationship between elbow arthroscopy portals and neurovascular structures in different elbow and forearm positions. J Shoulder Elb Surg. 2006;15(4):457–62.
4. Smith JP, Savoie FH, Field LD. Posterolateral rotatory instability of the elbow. Clin Sports Med. 2001;20(1):47–58.
5. Savoie FH III, O'Brien MJ, Field LD, Gurley DJ. Arthroscopic and open radial ulnohumeral ligament reconstruction for posterolateral rotatory instability of the elbow. Clin Sports Med. 2010;29(4):611–8.
6. Dunning CE, Duck TR, King GJW, Johnson JA. Simulated active control produces repeatable

motion pathways of the elbow in an in vitro testing system. J Biomech. 2001;34(8):1039–48.
7. Armstrong AD, Dunning CE, Faber KJ, Duck TR, Johnson JA, King GJW. Rehabilitation of the medial collateral ligament-deficient elbow: an in vitro biomechanical study. J Hand Surg. 2000;25(6):1051–7.
8. Coonrad RW, Roush TF, Major NM, Basamania CJ. The drop sign, a radiographic warning sign of elbow instability. J Shoulder Elb Surg. 2005;14(3):312–7.
9. Wolff AL, Hotchkiss RN. Lateral elbow instability: nonoperative, operative, and postoperative management. J Hand Ther. 2006;19(2):238–44.
10. Ring D, Jupiter JB, Gulotta L. Articular fractures of the distal part of the humerus. JBJS. 2003;85(2):232–8.
11. Hardy P, Menguy F, Guillot S. Arthroscopic treatment of capitellum fracture of the humerus. Arthrosc J Arthrosc Relat Surg. 2002;18(4):422–6.
12. Kuriyama K, Kawanishi Y, Yamamoto K. Arthroscopic-assisted reduction and percutaneous fixation for coronal shear fractures of the distal humerus: report of two cases. J Hand Surg. 2010;35(9):1506–9.
13. Mitani M, Nabeshima Y, Ozaki A, Mori H, Issei N, Fujii H, et al. Arthroscopic reduction and percutaneous cannulated screw fixation of a capitellar fracture of the humerus: a case report. J Shoulder Elb Surg. 2009;18(2):e6–9.
14. Elkowitz S, Polatsch D, Egol K, Kummer F, Koval K. Capitellum fractures: a biomechanical evaluation of three fixation methods. J Orthop Trauma. 2002;16(7):503–6.

Arthroscopic Capitellum Excision and Capitelloplasty

29

Deepak N. Bhatia

29.1 Background

Capitellum fracture is an uncommon elbow injury and surgical intervention is necessary. Surgical fixation is recommended for type 1 fractures (large osseous fragment), and excision of capitellum and fragments is indicated in type 2 (minimal subchondral bone) and type 3 (comminuted) fractures [1, 2]. Rarely, capitellum fractures are neglected or left untreated and the resultant malunion or nonunion is associated with disabling pain and range restriction. Arthroscopy is useful in the acute setting for excision of fragments (Bryan and Morrey types 2 and 3 capitellum fractures) with minimal soft tissue trauma, and early return to activities and work is possible. Arthroscopic capitellar excision and capsular release can be performed to treat chronic nonunions of capitellum fractures with good outcomes. Arthroscopic capitelloplasty involves partial or complete capitellar resection and reshaping of the capitellum and is useful in chronic malunions in untreated capitellum fractures.

29.1.1 Surgical Anatomy

The radiocapitellar articulation is important for normal elbow kinematics and excision of capitellum has been reported to result in elbow instability [3]. However, several biomechanical studies have shown that excision of the capitellum in the setting of intact ligamentous structures does not result in significant instability in either the adducted varus-loaded or valgus-loaded positions of the elbow [4–6]. Others have shown only a mild increase in the varus-valgus laxity of up to 3° in active elbow flexion, with the forearm in pronation but not in supination [7]. Instability after capitellar excision may however occur if the lateral ulnar collateral ligament (LUCL) is damaged and the torn LUCL should be repaired. Similarly, capitellar fractures with significant trochlear involvement are likely to result in instability after excision [3, 4].

29.2 Indications and Contraindications

- Acute displaced type 2 and type 3 capitellum fractures (Bryan and Morrey classification), especially in elderly and sedentary patients and in those with comorbidities, can be treated with arthroscopic excision (Fig. 29.1a).
- Symptomatic nonunions of untreated capitellar fractures with partial resorption of bone

D. N. Bhatia (✉)
SPORTSMED Mumbai, Mumbai, India

Sir HN Reliance Foundation Hospital, Mumbai, India
e-mail: shoulderclinic@gmail.com

© ISAKOS 2022

D. N. Bhatia et al. (eds.), *Arthroscopy and Endoscopy of the Elbow, Wrist and Hand*,
https://doi.org/10.1007/978-3-030-79423-1_29

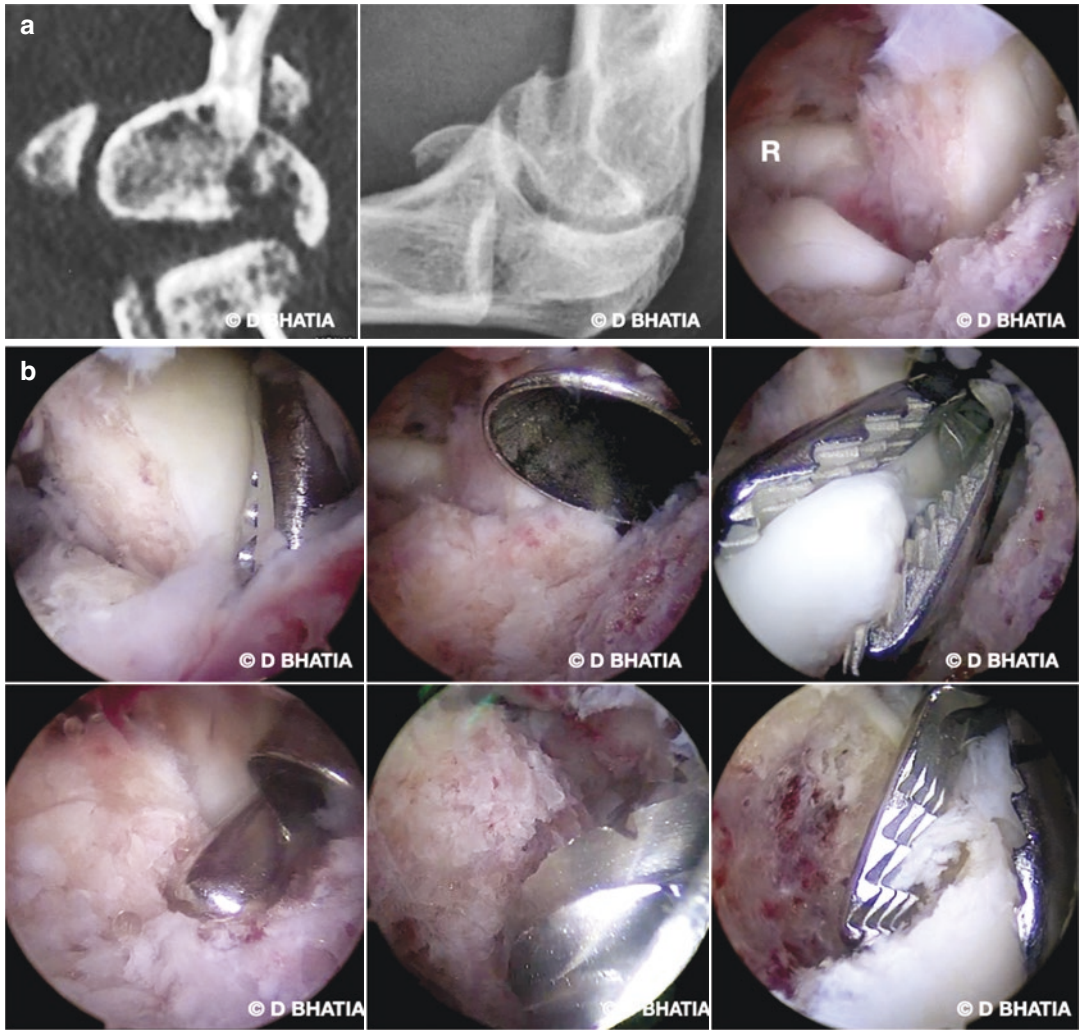

Fig. 29.1 (**a**) A capitellum fracture with comminution is shown on CT scan (left image) and radiograph (middle image). Arthroscopy demonstrates the comminuted fragments anterior to the radial head (R). (**b**) Technical steps for arthroscopic excision of the capitellar fragments are demonstrated. A plane is dissected anterior to fragments (top left) and a cannula is placed via lateral portal (top middle). Smaller fragments are excised first (top right) and large fragments are removed piecemeal (bottom left) and with burrs (bottom middle and right). (**c**) Arthroscopic (left image) and radiographic appearance (right images) after completion of capitellar excision. (© Bhatia)

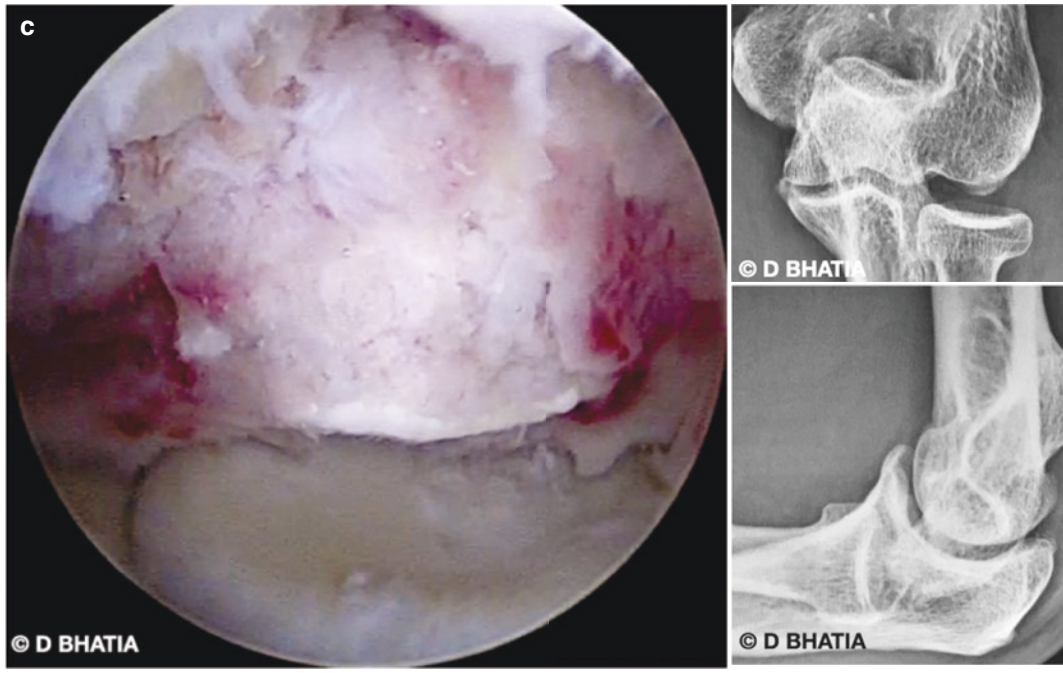

Fig. 29.1 (continued)

can be treated with arthroscopic excision of the fragment and is usually combined with capsular release and adhesiolysis.
- Capitellar malunions that result in a mechanical block to elbow flexion-extension can be treated with arthroscopic capitelloplasty.
- Prominent capitellar fixation screws with avascular necrosis of the capitellum can be treated with arthroscopic screw removal and debridement or capitelloplasty.

Osteosynthesis of the capitellum should be performed if the fragments retain sufficient subchondral bone to achieve stable fixation and excision is contraindicated. An intact LUCL is necessary for excision and should be repaired if excision is performed. Involvement of trochlear articular surface is a relative contraindication and excision is contraindicated in younger and active patients.

29.3 Surgical Technique

Elbow arthroscopy is performed with the patient in the lateral decubitus position.

Portals: The portals used in this procedure are as follows:

- **Proximal anteromedial portal (AM)** is the viewing portal throughout the procedure; it is placed 1 cm proximal and anterior to the medial epicondyle and is located anterior to the medial intermuscular septum.
- **Proximal anterolateral portal (AL)** is the main working portal; it is placed 1 cm proximal and anterior to the lateral epicondyle and is located anterior to the lateral intermuscular septum.
- **Direct anterolateral portal (DL)** may be used for additional debridement, or when retraction of soft tissues is necessary. The direct lateral portal (DL) is placed anterior to the radial head (R) at the level of the radiocapitellar joint, and its precise position is ascertained using an outside-in technique.
- **Radial head portal (RH)**, devised by the author, is a useful portal for manipulating large fragments and for fractures that involve the posterior capitellum [8]. The portal is created in the interval between the anconeus and extensor carpi ulnaris at the level of the radial head, and its exact location is determined

using an outside-in technique. The fractured capitellum provides adequate space for using this as a working portal.
- **Posterocentral (PC) and posterolateral (PL) portals** are used for posterior capitellar fractures and osteochondral lesions.

29.3.1 Arthroscopic Excision of a Comminuted Capitellum Fracture

- The AM portal is used to evaluate the anterior elbow joint. A shaver is introduced via the AL and organized clots or adhesions are excised. A DL portal is used for retracting the capsule anterior to the fragments for better visualization.
- Smaller fragments are first removed using a grasper. Larger fragments are broken into smaller fragments using graspers and punches and removed piecemeal.
- Large fragments may also be grasped via the RH or DL portals and a burr is used for excision.
- The distal humeral fracture surface is debrided lightly to smoothen any sharp edges and to remove fragments than may be loosely adherent.
- A thorough lavage is given and assessment of stability is performed (Fig. 29.1a–c).

29.3.2 Arthroscopic Capitellar Screw Removal and Capitellar Debridement

- Avascular necrosis and collapse of capitellum fragment is a complication that may occur after capitellum osteosynthesis. This results in screw tip prominence and eventual radiocapitellar arthritis is a possibility. These patients often present with refractory elbow pain and stiffness and surgical intervention is necessary.
- Arthroscopic evaluation is performed via standard portals. The cartilage is probed and screw tip is identified. Loose cartilage flaps and intra-articular adhesions are debrided and synovectomy is performed.
- Compression screws that have been passed from the posterior aspect are easier to remove arthroscopically. The posterior screw tip is identified using fluoroscopy and a small incision is made for passage of a cannula up to the posterior screw site. A guide wire is passed through the cannulated screw from the posterior aspect and is seen exiting the screw tip anteriorly. A cannulated screwdriver is then passed over the wire to engage the screw head and the compression screw is removed.
- The capitellum is then debrided to remove unhealthy bone fragments and the cartilage debris. A capsular release is then performed for restoration of range of motion (Fig. 29.2a, b).

29.3.3 Arthroscopic Excision of a Capitellum Fracture Nonunion

- A long-standing nonunion of a capitellum fracture results in partial bone resorption and these fractures are not suitable for osteosynthesis. Capitellum nonunions present with restricted range of motion, usually terminal flexion and extension and pain at end-range. Intra-articular adhesions are mild, and access to the joint is not difficult.
- The AM portal is used to evaluate the anterior elbow joint. A shaver is introduced via the AL or DL portals and retraction may not be necessary.
- The nonunion site is debrided and the fragment is burred on the subchondral aspect.
- A grasper is used to excise the shell-like fragment through the AL portal. A thorough lavage is given and synovectomy is performed. Capsular release is not necessary (Fig. 29.3).

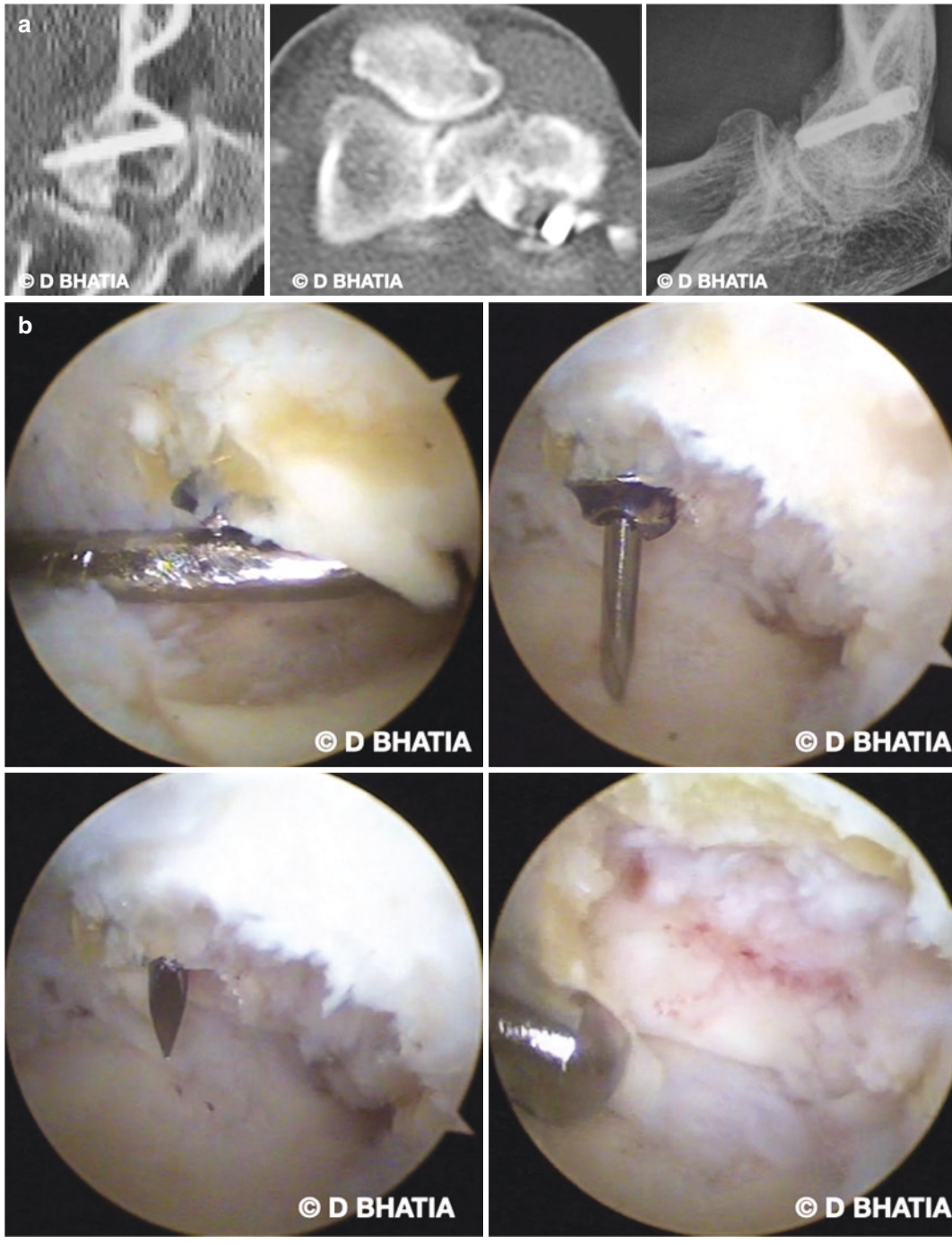

Fig. 29.2 (**a**) Collapse of capitellar fragment and prominence of compression screw are shown. (**b**) Technical steps for arthroscopic screw removal and capitellum debridement are shown. A probe demonstrates loose cartilage flaps and prominent screw (top left). A guide wire is inserted from the posterior screw tip and is seen exiting anteriorly (top right image). The screw is removed over the wire and the capitellum is debrided to stable bone (bottom images). (© Bhatia)

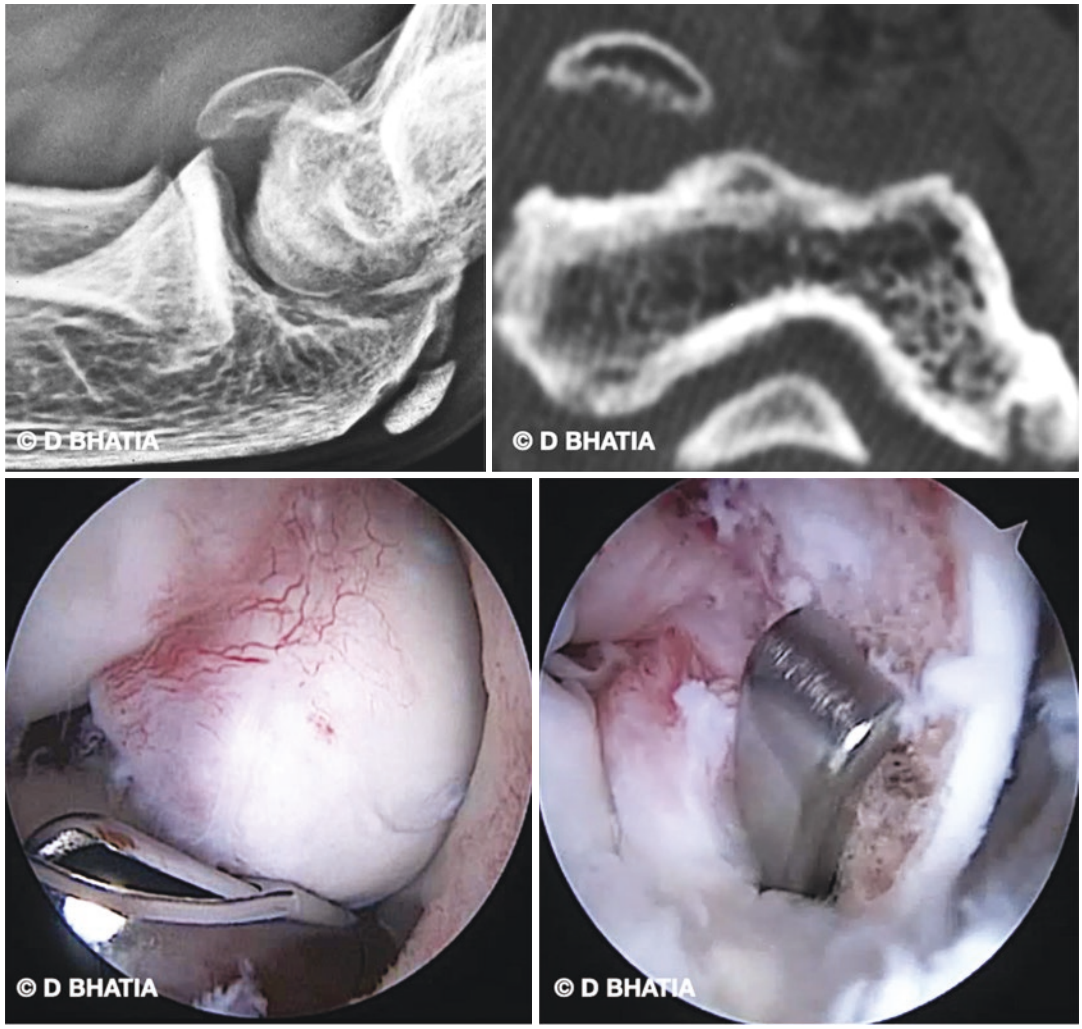

Fig. 29.3 Nonunion of a capitellum fracture is demonstrated on radiological imaging (top images). Arthroscopic appearance and excision of the fragment is shown (bottom images). (© Bhatia)

29.3.4 Arthroscopic Excision of a Malunited Capitellum Fracture

- Untreated and neglected capitellum fractures may malunite at the anterior intra-articular supracondylar aspect of the distal humerus. The malunion results in a mechanical block to range of motion and both flexion and extension are severely affected due to development of secondary adhesions.
- Arthroscopic access to the anterior elbow is difficult from the lateral aspect due to the large fragment and surrounding adhesions. A small joint arthroscope (2.5 mm) is useful for initial access and visualization. The AM portal is used for visualization and RH portal is used for initial working access for clearance of lateral adhesions.
- Next, the AL portal is used to dissect a plane between the malunited fragment and anterior capsule and a burr is used for excision of the fragment.
- The entire malunited fragment need not be excised and the malunited bone is burred sufficiently to eliminate the mechanical block (capitelloplasty).

- A capsular release is performed after capitelloplasty for further gain in range. Posterior elbow adhesions are released thereafter (Fig. 29.4).

29.3.5 Arthroscopic Excision of a Posterior Capitellum Fracture

- Posterior capitellar fractures are rare and may occur with traumatic elbow dislocations. An untreated fracture can result in nonunion of the fragment in the posterior radiocapitellar region and is associated with a painful elbow extension block and fixed flexion deformity (Fig. 29.5a).
- Posterior capitellar region is visualized using a PC or PL portal and a 70° arthroscope is necessary. The PL portal sheath can be passed deep into the posterolateral gutter and posterior radiocapitellar joint is visible.
- A RH portal is used as a working portal for direct access to the posterior capitellum.

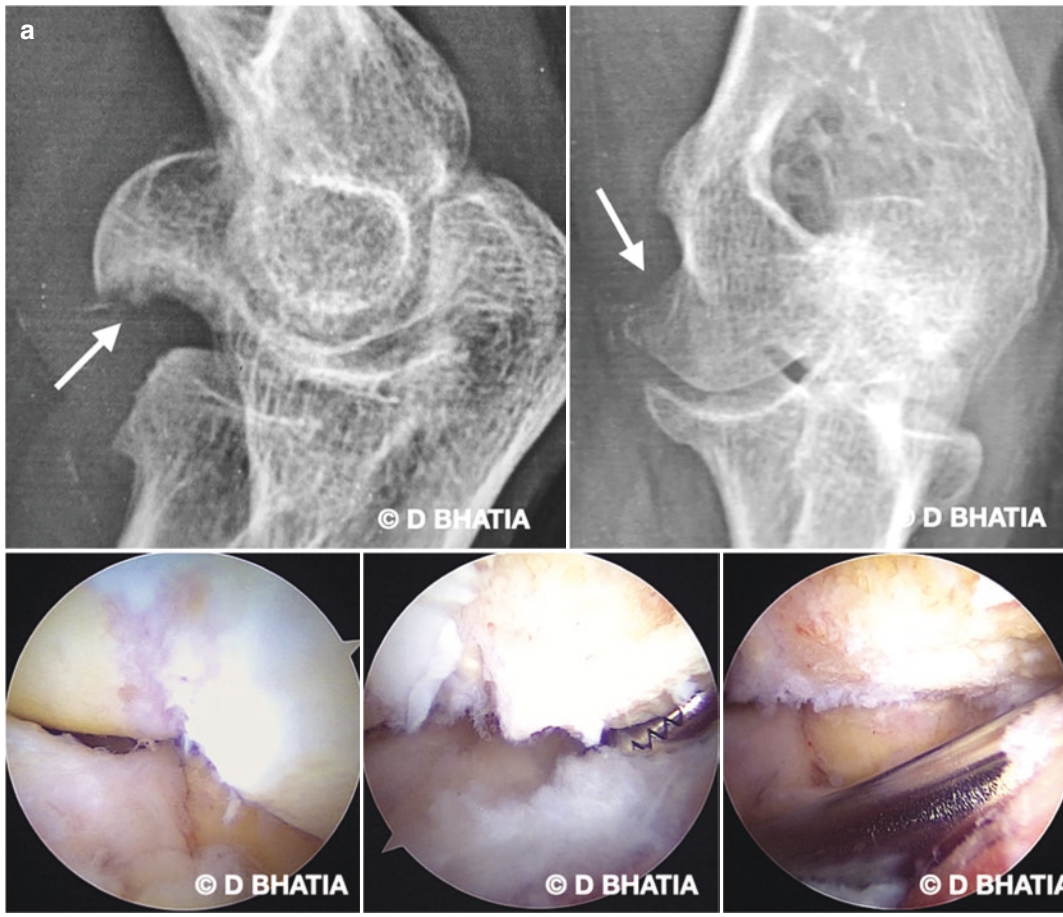

Fig. 29.4 (**a**) A malunited capitellum creates a mechanical block for the radial head in flexion (arrow, top images). Arthroscopic appearance of the fragment (bottom left) showing a large fragment in the anterior elbow recess extending into the superior recess. The anterior capsule is separated from the fragment (bottom middle image) and a capitelloplasty is performed (bottom right image). (**b**) Malunion of a capitellum fracture in the supratrochlear region is shown (arrows, top images). A plane is dissected between the fragment and distal humerus (bottom left), and the fragment is excised (bottom right). Arrows demonstrate the original fracture site (white arrow) and malunion region (black arrow). (© Bhatia)

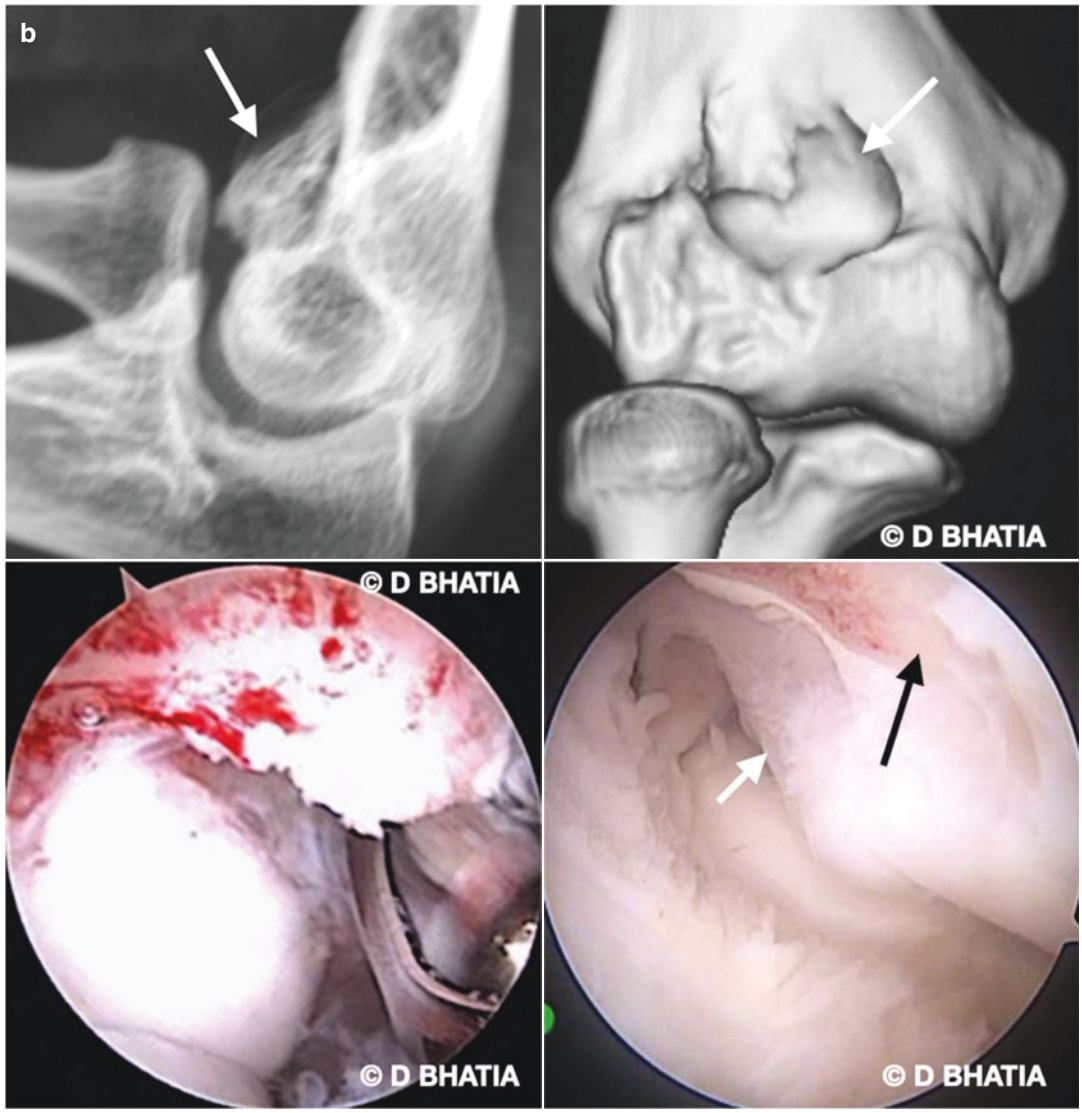

Fig. 29.4 (continued)

- A shaver via RH portal is used to excise fibrosis around the fragment and a probe is used to locate the bony fragment.
- The fragment is grasped via RH portal and excised piecemeal. A part of the fragment may be adherent to the capsule and is gently dissected and excised.
- The defect in the capitellum is debrided and microfractured. The capsular defect can be sutured via the RH portal (Fig. 29.5b).

29.4 Tips and Tricks

- Removal of all smaller fragments first creates more space for instruments for excision of large fragments.
- Fluid inflow should be restricted as capsular tears in acute cases will result in fluid extravasation and swelling.
- A small joint arthroscope (2.5 mm) is useful in stiff joints and malunions and can be changed to a larger arthroscope (4 mm).

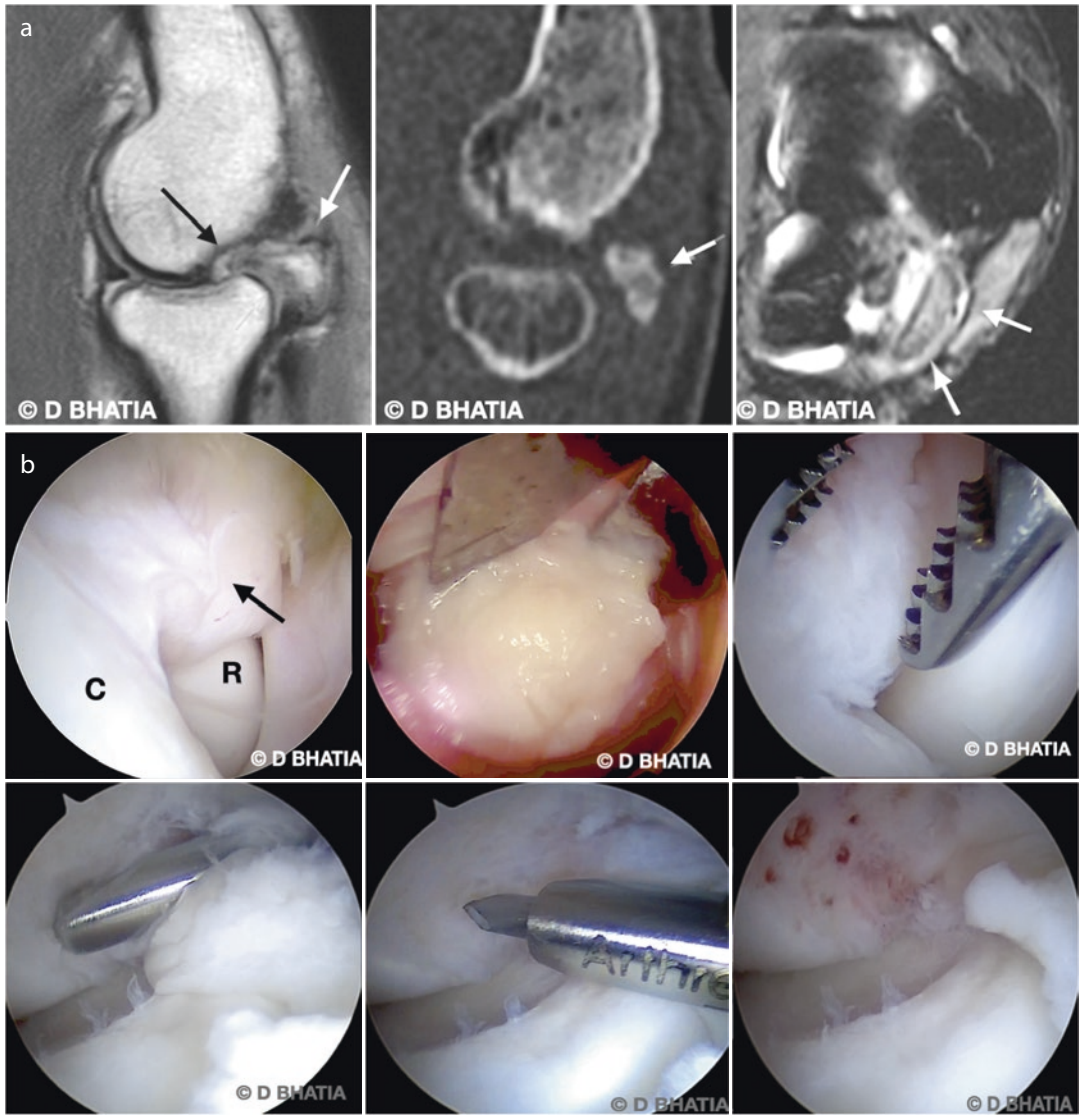

Fig. 29.5 (**a**) Radiological appearance of nonunion of a posterior capitellum fracture (arrows); posterior radiocapitellar impingement is demonstrated. (**b**) Technical steps for excision of a posterior capitellum fracture fragment are shown. Posterolateral portal view showing fibrosis around the fractured fragment (arrow, left). The fragment is dissected via the radial head portal (top middle image) and excised piecemeal (top right). The capitellum fracture surface is debrided and microfractured (bottom images). (© Bhatia)

29.5 Pitfalls

- Vital structures adjacent to the anterior capsule are at risk and must be protected when working around malunited fragments.
- The lateral ligamentous complex of the elbow may be injured during passage of instruments via RH portal. This may be minimized by placing a 4–5 mm sheath for shavers and burrs to avoid repetitive soft tissue trauma. For large fragment excision at the end of the procedure, the capsule should be repaired using strong absorbable sutures.
- Capitelloplasty for a malunited capitellum involves resection of sufficient bone for elimination of mechanical block. Intraoperative

assessment of range and fluoroscopic examination is useful to determine adequacy of resection.

29.6 Postoperative Management and Rehabilitation

A bulky soft tissue dressing is used in the immediate postoperative period, and this is changed to portal dressing on the fourth postoperative day. A sling is used for comfort. Elbow movements and forearm rotations are permitted without any restrictions. The rehabilitation protocol involves early passive and active range-of-motion exercises (weeks 1–6) and simultaneous gradual strengthening. Achievement of full range is dependent on the initial severity of the problem and usually 3–6 months of rehabilitation are necessary in chronic pathology. Light work is permitted after 6 weeks, and a return to heavy work is permitted after 3 months.

Conflict of Interest The author certifies that he has no commercial associations (e.g., consultancies, stock ownership, equity interest) that might pose a conflict of interest in connection with the submitted article. The author retains the copyright to the images, videos, and content in this chapter.

References

1. Bryan RS, Morrey BF. Fractures of the distal humerus. In: Morrey BF, editor. The elbow and its disorders. Philadelphia: WB Saunders; 1985. p. 302–9.
2. Feldman MD. Arthroscopic excision of type II capitellar fractures. Arthroscopy. 1997;13:743–8.
3. Grantham SA, Norris TR, Bush DC. Isolated fracture of the humeral capitellum. Clin Orthop Relat Res. 1981;161:262–9.
4. Root CG, Meyers K, Wright T, Hotchkiss R. Capitellum excision: mechanical implications and clinical consequences. J Orthop Res. 2014;32(2):346–50.
5. Sabo MT, Fay K, McDonald CP, et al. Effect of coronal shear fractures of the distal humerus on elbow kinematics and stability. J Shoulder Elb Surg. 2010;19:670–80.
6. Dushuttle RP, Coyle MP, Zawadsky JP, et al. Fractures of the capitellum. J Trauma. 1985;25:317–21.
7. Sabo MT, Shannon HL, Deluce S, et al. Capitellar excision and hemiarthroplasty affects elbow kinematics and stability. J Shoulder Elb Surg. 2012;21:1024–31.
8. Bhatia DN. Arthroscopic resection of the radial head. In: Bain G, Eygendaal D, van Riet R, editors. Surgical techniques for trauma and sports related injuries of the elbow. Berlin: Springer; 2020. p. 581–8.

Part V

Elbow: Osteochondritis Dessicans

30 Osteochondritis Dissecans of the Elbow: Concepts of Etiology

Simon MacLean and Gregory I. Bain

30.1 Background

Osteochondritis of the capitellum (OCD) is a condition found in the adolescent or young adult, and is often seen in the dominant arm of pitching athletes (Fig. 30.1). It may involve focal areas or the entire capitellum in the younger child (Panner's Disease) or may occur as "Osteochondritis Dissecans" (OCD) typically in a child over 12 years. Like avascular necrosis (AVN) in other locations, such as Perthes' and Kienbock's disease, the exact etiology is poorly understood; however, in clinical practice we identify the "at-risk patient" at the "at-risk location." Factors postulated in the etiology of the disease in the literature include patient genetics, anatomical location, morphology, trauma, vascular, metabolic, nutritional and inflammatory factors [1–5]. A better understanding of the etiology and pathogenesis will help dictate treatment strategies in the future. We present our current theories on the etiology of the disease.

S. MacLean (✉)
Department of Orthopaedic Surgery, Tauranga Hospital, Tauranga, New Zealand

G. I. Bain
Department of Orthopaedics and Trauma Surgery, Flinders University and Flinders Medical Centre, Adelaide, SA, Australia
e-mail: admin@gregbain.com.au

30.1.1 At-Risk Factors

AVN has traditionally been thought of as pathology caused by disruption to arterial flow, affecting either large or small vessels. This was previously thought to be due to a number of causes; traumatic disruption of vessels, embolism from clot, fat, or air, and local or systemic disease affecting the patency of these vessels. AVN secondary to traumatic arterial disruption in the elbow is rare. Therefore, other mechanical and biological factors must be responsible for AVN of the capitellum.

30.1.2 The At-Risk Individual

The "at-risk" individual is the young overhead athlete or pitcher. Six distinct phases of throwing have been previously described [6]. Repetitive cycling through these phases has the following effects:

- During the late cocking phase of throwing, there is significant valgus force at the elbow and there is maximal stress at the medial collateral ligament complex.
- The acceleration phase then follows with sustained valgus strain and high activity of ECRB and ECRL.
- Repetition of this activity causes impaction and overload through the lateral column.

© ISAKOS 2022

D. N. Bhatia et al. (eds.), *Arthroscopy and Endoscopy of the Elbow, Wrist and Hand*,
https://doi.org/10.1007/978-3-030-79423-1_30

Fig. 30.1 OCD of the capitellum in a 13-year-old boy. Plain radiographs (**a**) and (**b**) show focal subchondral lucency within the capitellum, and some flattening with linear calcification overlying the joint space seen on the lateral. There is an associated joint effusion. MRI proton-density, fat-saturated images (**c**) and (**d**) show a completely detached osteochondral fragment arising from the anterior aspect of the capitellum measuring 8 mm AP with the displaced osteochondral fragment lying in the posterior recess. (Copyright of Mr. Simon McLean)

- The MCL becomes attenuated or ruptures and fails to act as a checkrein to valgus force. Thus, a cycle develops where compression through the lateral column increases further.
- Repetitive axial and shearing forces cause point-loading of the capitellum with the medially placed ulnohumeral joint acting as a fulcrum.
- During the remaining four phases of throwing, there is less loading through the lateral column of the elbow and flexor forces through the medial side of the elbow predominate.

Anatomical variants may predispose to AVN of the capitellum. It has been found to be more common in patients with a relatively varus carrying angle compared to the normal population. A more valgus carrying angle may be protective to OCD as more force is directed as shear rather than axial load through the cap-

itellum [7]. It has been shown to occur in patients who begin playing baseball at an earlier age [7]. Younger patients may be predisposed to damage due to differences to cartilaginous blood supply, constituents, or anchorage points to the underlying subchondral bone.

30.1.3 Osseous Factors: Microarchitecture

The capitellum subchondral bone plate has been shown to be only a single trabecular layer and 0.1 mm thick on micro-CT scan (Fig. 30.2). This makes it susceptible to stress fracture, particularly when the load-absorbing properties of the overlying subchondral bone have been compromised. The remainder of the distal humerus subchondral bone plate has secondary trabecular layers that provide additional support to the subchondral plate.

30.1.4 Vascular Factors and the Compartment Syndrome Model

We have hypothesized a "compartment syndrome model" in the etiology of Kienbock's disease based on basic science and intricate anatomical studies by Crock [3, 5]. We postulate a similar role in the etiology of OCD of the capitellum. When considering the capitellum as a "compartment," factors that will change the pressure within it include the inflow (arterial flow or emboli), the contents (predominantly bone marrow), and outflow (venous system).

Intraosseous pressures have been shown to be raised higher than that of systolic blood pressure in AVN of the femoral head and lunate [1, 4, 8]. This may be position dependent; in the lunate, pressures have been found to be increased in wrist extension. Similarly, in the capitellum, valgus force during throwing may increase intraosseous pressures although this has not been proven.

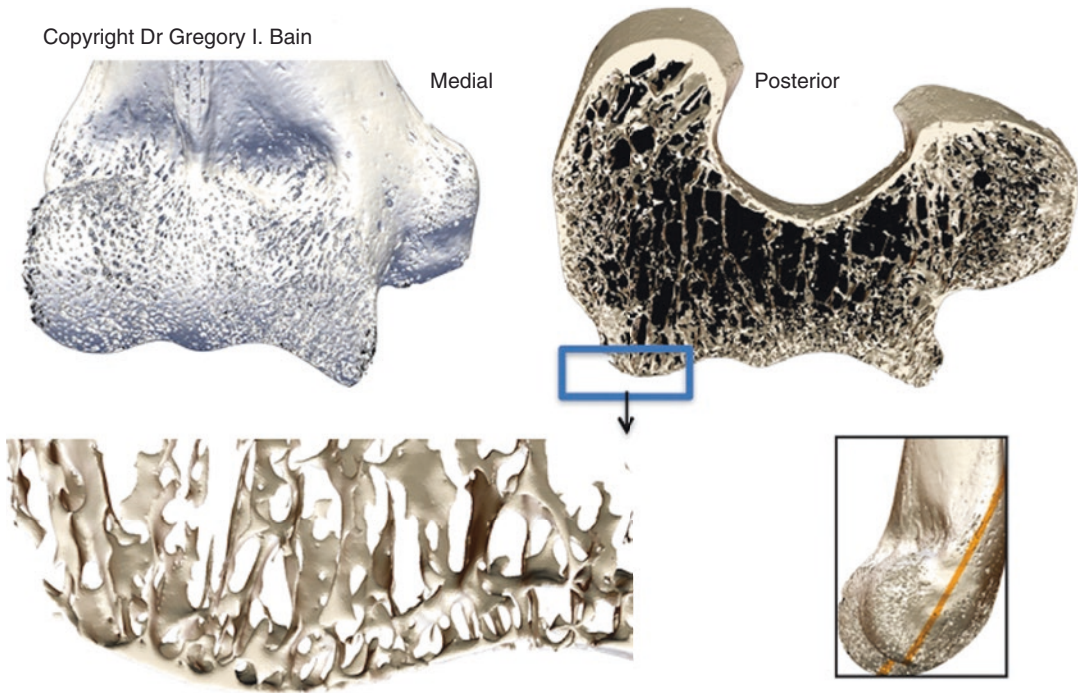

Fig. 30.2 3D Micro-CT of the distal humerus in the oblique coronal plane. Note the single trabecular layer of the capitellar subchondral bone plate, which is 0.1 mm thick. (Copyright of Gregory I. Bain)

30.1.4.1 Arterial Factors

Arterial supply is mainly from vessels from the lateral epicondyle that enter the capitellum posteriorly. There is no supply from anterior or medial. It is rare for this supply to be disrupted but it can occur in cases of complex injury of the lateral condyle. Embolization to these vessels is also extremely uncommon (Figs. 30.3 and 30.4).

30.1.4.2 Venous Factors

Vascular anatomy described by Dr. Harry Crock [3] identified the subarticular venous plexus (Fig. 30.5). This is a series of wavy parallel venules, just deep to the subchondral bone plate. These venules converge to the lateral epicondyle. Being directly adjacent to the subchondral bone plate, this makes this area vulnerable to even a stress fracture.

30.1.4.3 Intraosseous Factors

The majority of the compartment contents of the capitellum consist of intraosseous fat. As fat is sensitive to ischemia, once necrosis occurs, an inflammatory response and edema increases the compartment pressure and compartment syndrome occurs.

30.1.4.4 The Compartment Syndrome Model

Venous hypertension and venous ischemia is a recognized cause of failure of tissue flaps and in the lower limb can lead to fibrosis and gangrene. Altered perfusion due to repetitive loading and stress fracture leads to damage to the subarticular venous plexus. Venous hypertension results and edema and necrosis of the fat cells occur resulting in a compartment syndrome of bone (Fig. 30.6). The fracture propagates through dead trabecular bone. Repetitive loading on an incongruent capitellum furthers the vascular insult. The stress fracture progresses to involve a larger segment of capitellar condyle with characteristic findings on MRI (Fig. 30.1).

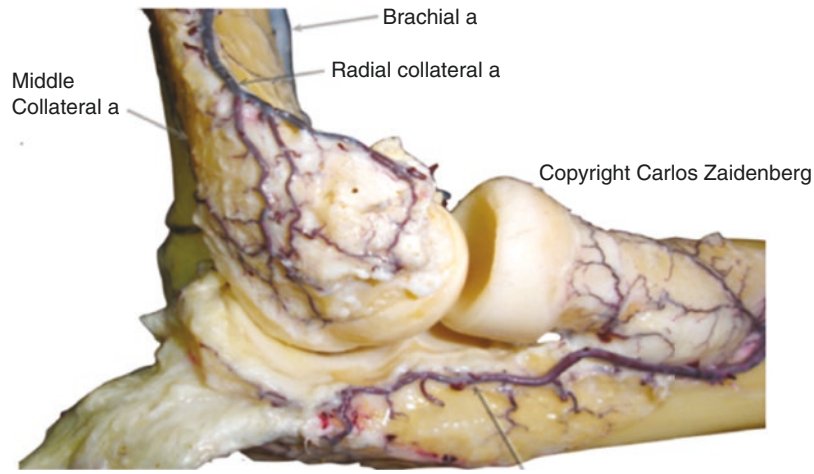

Fig. 30.3 Distal humerus vascularity (lateral aspect). Vessels perforate the posterior and lateral aspects of the lateral condyle and capitellum. (Copyright Carlos Zaidenberg)

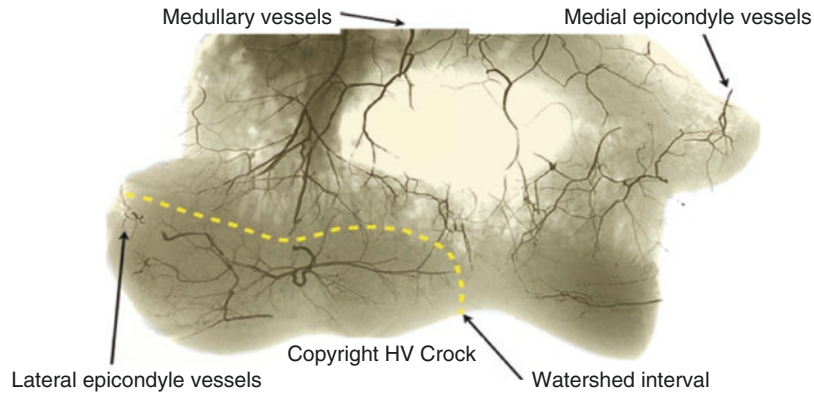

Fig. 30.4 Arterial supply of the distal humerus. The medullary vessels supply the diaphysis and part of the metaphysis, but do not supply the lateral condyle. Note the watershed interval between the two vascular inputs. (Modified and reproduced by Dr. Gregory I. Bain with permission and copyright of HV Crock AO)

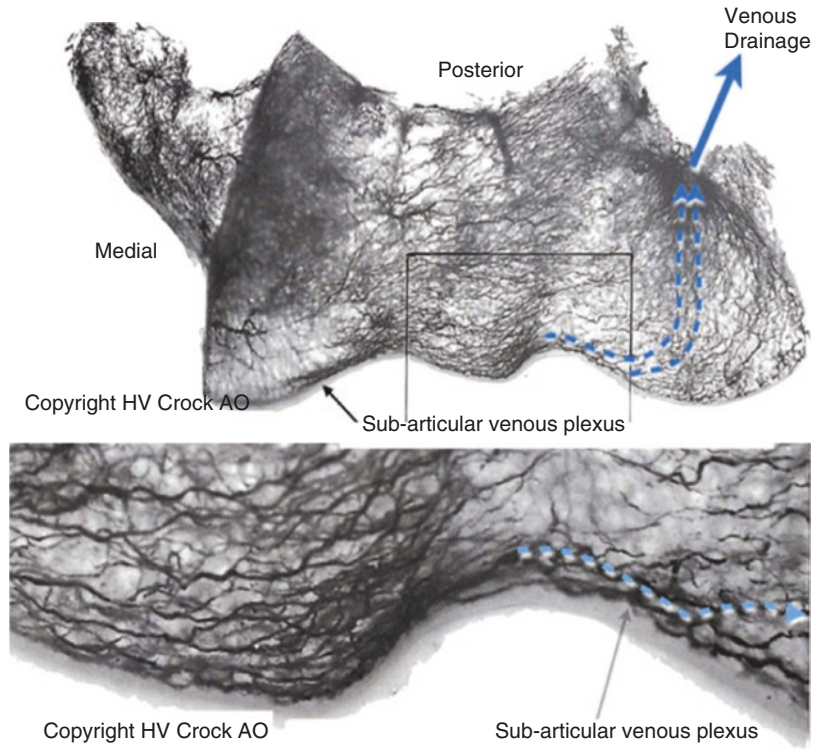

Fig. 30.5 Venous drainage of the distal humerus. (**a**) The subarticular plexus has parallel venules just deep into the subchondral bone plate. The veins converge to the lateral epicondyle. (**b**) Magnified view. (Modified and reproduced by Dr Gregory I. Bain with permission and copyright of HV Crock AO)

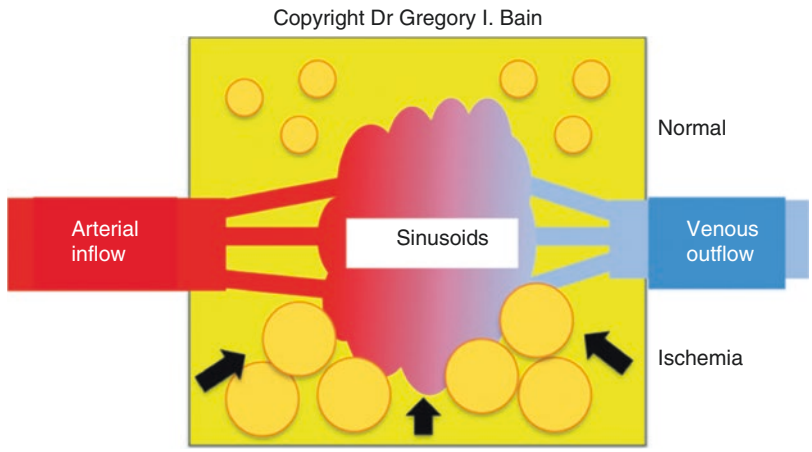

Fig. 30.6 Compartment syndrome of the bone. Upper half has normal bone, fat cells, and venous drainage. The lower half has ischemia with interstitial edema, swollen marrow fat cells, and local venous obstruction. This causes tamponade of the sinuses, decreases the venous drainage, which further increases the intraosseous pressure, reducing arterial inflow leading to necrosis. (Copyright of Gregory I. Bain)

30.2 Conclusions

AVN of the capitellum occurs in an "at-risk individual" and an "at risk location." Further research is needed to dictate the best treatment for the individual.

References

1. Hungerford DS. Pathogenetic considerations in ischemic necrosis of bone. Can J Surg. 1981;24(6):583–587, 590.
2. Solomon L. Idiopathic necrosis of the femoral head: pathogenesis and treatment. Can J Surg. 1981;24(6):573–8.

3. Crock HV. An atlas of vascular anatomy of the skeleton & spinal cord. 1st ed. London: Martin Dunitz; 1996.
4. Schiltenwolf M, Martini AK, Mau HC, Eversheim S, Brocai DR, Jensen CH. Further investigations of the intraosseous pressure characteristics in necrotic lunates (Kienböck's disease). J Hand Surg Am. 1996;21(5):754–8. https://doi.org/10.1016/S0363-5023(96)80187-0.
5. Bain G, MacLean S, Yeo C, Perilli E, Lichtman D. The etiology and pathogenesis of Kienböck disease. J Wrist Surg. 2016;05(04):248–54. https://doi.org/10.1055/s-0036-1583755.
6. Weber AE, Kontaxis A, O'Brien SJ, Bedi A. The biomechanics of throwing. Sports Med Arthrosc. 2014;22(2):72–9. https://doi.org/10.1097/JSA.0000000000000019.
7. Kida Y, Morihara T, Kotoura Y, et al. Prevalence and clinical characteristics of osteochondritis dissecans of the humeral capitellum among adolescent baseball players. Am J Sports Med. 2014;42(8):1963–71. https://doi.org/10.1177/0363546514536843.
8. Jensen CH. Intraosseous pressure in Kienböck's disease. J Hand Surg Am. 1993;18(2):355–9. https://doi.org/10.1016/0363-5023(93)90375-D.

31 Arthroscopic Treatment of Osteochondritis Dissecans of the Elbow

Myrthe Nagel, Rens Bexkens, Bertram The, and Denise Eygendaal

31.1 Background

Osteochondritis dissecans (OCD) of the elbow is an idiopathic disease of the cartilage and subchondral bone in adolescent athletes in sports that involve repetitive stress to the elbow joint, such as gymnastics, baseball and tennis. This results in separation, devascularization and fragmentation of the subchondral bone and its overlying cartilage in the immature skeleton. OCD is commonly localized in the capitellum, but can also occur in the olecranon, radial head and the trochlea. The vast majority is located in the dominant arm and bilateral OCD is reported in approximately 20%.

M. Nagel
University of Amsterdam,
Amsterdam, The Netherlands

Department of Orthopedic Surgery, Amphia Hospital,
Breda, The Netherlands

R. Bexkens · D. Eygendaal (✉)
Department of Orthopedic Surgery, Amphia Hospital,
Breda, The Netherlands

Dept. of orthopedic surgery, Erasmus University
Medical Centre, Rotterdam,
Rotterdam, The Netherlands
e-mail: deygendaal@amphia.nl; denise@eygendaal.nl

B. The
Department of Orthopedic Surgery, Amphia Hospital,
Breda, The Netherlands
e-mail: bthe@amphia.nl

Surgical treatment is indicated for patients with an unstable lesion or failure of appropriate nonoperative treatment of a stable lesion. A lesion is classified as stable when the cartilage is intact.

Various surgical techniques have been described such as antegrade/retrograde drilling, arthroscopic debridement, fragment fixation, microfracture and osteochondral autologous transplantation. The appropriate treatment depends on the size of the OCD lesion, involvement of the lateral wall, state of the growth plates and the presence of a stable cartilage cap. These are assessed with standard radiographs, MRI or CT imaging (Fig. 31.1a, b). The individual performance level is another important factor in the treatment rationale. Arthroscopic debridement with loose body removal is the first choice of treatment of an unstable OCD, without the involvement of the lateral wall and limited to less than 50% of the capitellum [1–4].

The minimal invasiveness of the arthroscopy and the possibility for direct visualization of the defect reduces the risk of operative complications and allows for early rehabilitation.

The goal of arthroscopic debridement of the OCD is to remove identified loose bodies, necrotic bone and unstable cartilage to achieve a stable cartilage rim. This creates an optimal environment for the cartilage to regenerate by improving the nutrient supply. To improve the formation of fibrocartilaginous tissue, micro-

© ISAKOS 2022

D. N. Bhatia et al. (eds.), *Arthroscopy and Endoscopy of the Elbow, Wrist and Hand*,
https://doi.org/10.1007/978-3-030-79423-1_31

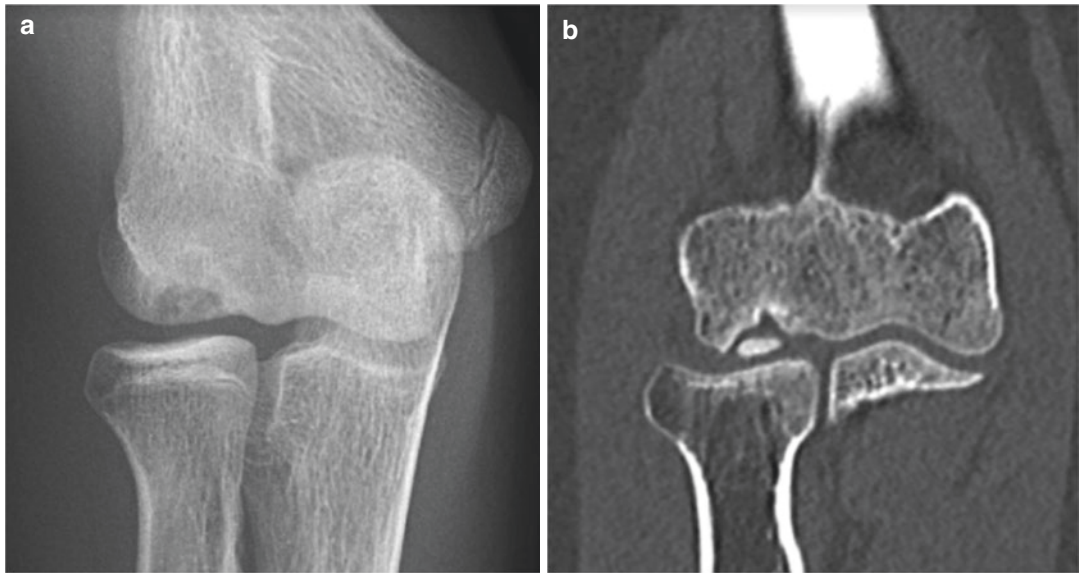

Fig. 31.1 (**a**) Anteroposterior radiographic image shows OCD lesion with flattening of the capitellum and a centrolateral, radiolucent defect. (**b**) CT imaging, coronal view shows OCD lesion with a loose body in situ

fracturing can be added [5]. In order to prevent injury to the neurovascular structures by instruments and portal placement, it is important to have a profound knowledge of the local anatomy of the elbow to perform elbow arthroscopy safely [2].

31.2 Surgical Anatomy

Several mechanisms have been shown to play a role in the development of OCD although the exact aetiology remains unclear. The high prevalence of OCD in overhead throwing athletes and in arm weight-bearing sports suggests that microtrauma to the elbow plays a role due to compression and shear forces, leading to overuse injury of the vulnerable and relatively hypovascular epiphyseal cartilage. The capitellum is primarily vascularized by posterior end arteries traversing the epiphyseal article cartilage; there is no metaphyseal collateral supply which makes the vascularization of the capitellum meagre and easily damaged by microtrauma. Furthermore, the subchondral bone plate on the convex capitellar surface is 0.1 mm thick, which is thin in contrast to the rest of the articular surface of the distal humerus.

The factors mentioned above explain why the capitellum is susceptible to damage by microtrauma which can lead to avascular necrosis and loss of subchondral support for the overlying cartilage. Continued repetitive stress on the lesion leads to fragmentation and separation of the articular surface [6].

OCD lesions are classified as stable or unstable. A stable OCD lesion has a near-normal range of motion, an open capitellar physis and absence of fragmentation of the subchondral bone. Unstable lesions have at least one of the following traits: a restriction of elbow extension, fragmentation, and a closed capitellar physis [7]. Unstable lesions are preferably treated with arthroscopic debridement.

Besides assessing stability and physeal state, the added value of grading capitellar OCD seems limited. However, the golden standard is the intra-operative classification introduced by the International Cartilage Repair Society (ICRS). The ICRS system divides OCD lesions into four categories [6, 8]:

- Grade I: Stable lesion with a continuous but softened area covered by intact cartilage.
- Grade II: Lesion with partial discontinuity that is stable when probed.

- Grade III: Lesion with a complete discontinuity that is not yet dislocated but is unstable when probed.
- Grade IV: Empty defects and defects with a dislocated fragment or a loose fragment within the bed.

31.3 Indications and Contraindications

Indications for arthroscopy in patients with OCD:

- Symptomatic unstable lesion.
- Failure of conservative treatment.
- Locking symptoms after long-standing painless OCD.

Contraindications include:

- Previous transposition of the ulnar nerve (submuscular or subcutaneous).
- Extensive heterotopic ossification or multiple surgery or arthritis (distorted anatomy, inability to create safe portals, need for extracapsular release).

31.4 Surgical Technique

Preoperative examination under anaesthesia is performed and the patient is positioned in lateral decubitus with the arm supported by an arm holder leaving the area around the elbow free.

- Portals: For arthroscopic debridement of the elbow, the elbow is divided into three compartments. To visualize all three compartments, use at least five portals (Fig. 31.2a, b).
  - Anterior compartment: The working portals are the proximal anterolateral and proximal anteromedial portals. These portals are located 2 cm proximal to the lateral and medial epicondyles. The ulnar nerve must be identified before performing any skin incision and is usually palpable behind the medial epicondyle. To avoid ulnar nerve injury, stay anterior of the medial intermuscular septum to keep the ulnar nerve posterior to the portal when placing the proximal medial portal [2] (Fig. 31.2a).
  - Posterior compartment: The working portals are the posterolateral and posterocentral portal. These portals are located 2 cm proximal to the olecranon (Fig. 31.2b).
  - Posterolateral compartment: A single working portal for access to the capitellar joint surface is used to perform the debridement of the OCD lesion, as well as the microfracture procedure. In selected cases, an additional viewing portal can be used for better visualization of the affected area during this procedure.
- The anterior compartment is first inspected via proximal anteromedial portal. Placing of the lateral portal should be done with an outside-in technique under direct arthroscope view using guidance by first introducing a needle at the level or just proximal to the radiocapitellar joint line. Synovitis is debrided, and loose bodies which are frequently found at the coronoid fossa or on the medial side of the coronoid process are removed. A full inspection of the joint including cartilage layers is performed. Capitellar OCD lesions are located anteriorly, but are covered by the radial head with the elbow in 90° of flexion when assessing the joint from the anterior compartment; therefore the capitellum may look intact.
- The posterior compartment is also inspected for loose bodies, including the olecranon fossa and medial and lateral gutters. Care is taken not to injure the ulnar nerve which is in close contact with the tissue in the medial gutter.
- The posterolateral compartment is accessed with the camera using the posterolateral portal. A soft spot portal can then be used to introduce tools to assess and treat the OCD lesion. During this part of the procedure, the ulnohumeral joint is also inspected. Loose bodies can be seen entrapped in the joint and are removed. Slight gapping of the ulnohumeral joint from the lateral side is easily achieved in this patient population allowing for assessment of the quality of the cartilage

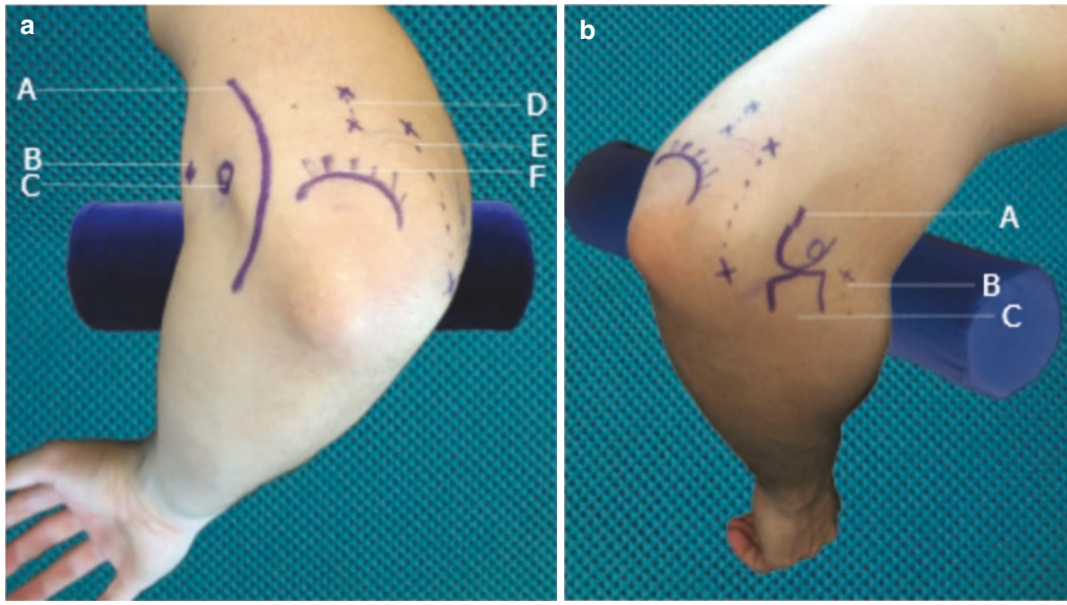

Fig. 31.2 (**a**) Medial side view: Anatomical structures and portals. A: Ulnar nerve; B: Proximal medial portal; C: Medial epicondyle; D: Transtricipetal portals; E: Posterolateral portals; F: Olecranon [2]. (**b**) Lateral side view: Anatomical structures and portals. A: Lateral epicondyle; B: Anterolateral portal; C: Radial head [2]

layers using a hooked probe. Easy introduction of a blunt trocart up to the trochlear groove is normal, but easy introduction past this ridge or a drive-through sign indicate hyperlaxity which may contribute to abnormal loading of the joint and potentially contributing to the problem.

- When visualization is insufficient, a second lateral viewing portal is created in addition to the direct lateral working portal. This is performed with the lateral ligamentous complex in mind, preventing iatrogenic posterolateral instability.
- The OCD lesion is assessed for stability. After removing the unstable tissue, the area is debrided until only healthy tissue remains (Fig. 31.3a, b). The exposed subchondral bone is debrided. A microfracture procedure may be added, especially when the subchondral bone is (partially) devoid of healthy bleeding.
- Debridement is not advised for stable lesions with an intact cartilage cap and a bit soft when probing (ICRS grade 1). These lesions can be treated using retrograde drilling.
- After removing the debris of the debridement procedure, the wounds are closed with non-resorbable sutures and a compressive dressing is applied.

31.5 Tips and Tricks

- Use small shaver blades (3 or 4 mm).
- Always inspect 3 compartments.
- To avoid ulnar nerve injury, stay anterior of the medial intermuscular septum to keep the ulnar nerve posterior to the portal when placing the proximal medial portal.
- Create an accessory portal in the posterolateral compartment for better visualization of the affected area.
- Use the posterolateral and midposterior portal to assess the posterior compartment and avoid using the posteromedial portal as it brings risk for ulnar nerve injury [2].

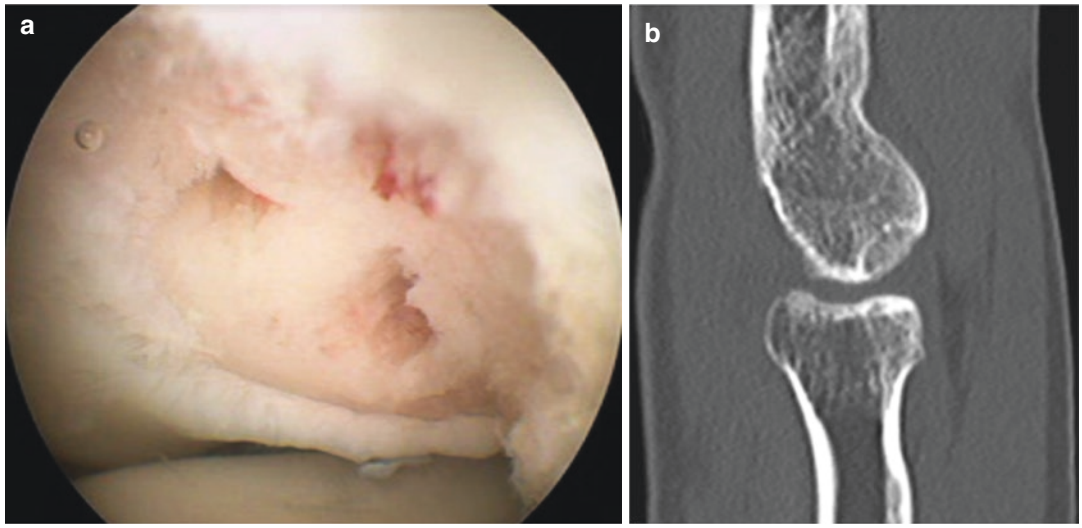

Fig. 31.3 (**a**) Arthroscopic view shows OCD lesion of the capitellum after debridement and microfracture. (**b**) CT imaging shows OCD lesion of the capitellum 6 months after debridement and microfracturing

31.6 Pitfalls

- Loose bodies can be missed when performing arthroscopy and in particular in the anterior compartment. To detect loose bodies, a CT has to be done preoperatively, because loose bodies are not always visible on X-ray or MRI [9].
- In patients with bigger OCD lesions with involvement of the lateral wall, arthroscopy shows suboptimal results. A preoperative CT should be done to assess the OCD lesion. If the OCD lesion is >10 mm, arthroscopy is not recommended and an osteochondral autograft transplant is indicated.
- When nerve injuries occur, the ulnar nerve is affected most often. Therefore, palpation of the ulnar nerve is crucial to locate its position. If the patient has a subluxing or transposed ulnar nerve, an immediate open approach is used to identify and protect the ulnar nerve during the surgical procedure [2].

31.7 Postop Management and Rehab

Postoperative management is essential to determine the outcome after arthroscopy. Rehabilitation under supervision of a physiotherapist is advised after surgery and gravity-assisted exercises will reduce swelling and pain and will help restore range of motion. Within a couple of days, unrestricted range of motion exercises can be started. As pain tolerates, unrestricted range of motion exercises can be started within a couple of days, resistive strength exercises are started 8 weeks after surgery, and axial loading is prohibited until 4 months postoperatively. Once the athlete is painfree and has gained full range of motion, a sports specific throwing program is started before returning to sports [6].

31.8 Complications

General complications of elbow arthroscopy occur in 7–14% of patients and depend on the experience of the surgeon and type of pathology [10]. Most complications are minor and do not affect clinical outcome. Major complications are seen in 0.5–5% of patients [6].

31.9 Results

Return to pre-injury level of play is variable and sport type related. The highest return to play is 80–87% and the lowest 25–40% [1, 11]. However,

improved range of motion and pain relief can be expected. The combination of arthroscopic debridement and marrow stimulation has a return to pre-injury level of sport of 67–85%. Arthroscopic debridement with microfracture has a return to sport rate of 62% of whom 7% return to a lower level [4]. Matsuura et al. evaluated the long-term clinical outcomes in 23 adolescent baseball players who underwent arthroscopic debridement with or without drilling. 87% returned to their pre-injury level of play and the mean follow-up was 11.5 years [11]. Younger patients with open physes, smaller lesions, and shorter duration of symptoms are associated with improved outcomes after arthroscopic debridement. Lesions greater than 50% of the capitellar surface or with involvement of the lateral wall are associated with worse outcomes [1].

References

1. Hilgersom NFJ, Bexkens R, Van den Bekerom MPJ, Eygendaal D. Osteochondritis dissecans of the elbow: arthroscopic debridement. Berlin: Springer; 2019.
2. Hilgersom NFJ, Oh LS, Flipsen M, Eygendaal D, Van den Bekerom MPJ. Tips to avoid nerve injury in elbow arthroscopy. World J Orthop. 2017;8(2):99–106.
3. Van Bergen CJA, van den Ende KIM, ten Brinke B, Eygendaal D. Osteochondritis dissecans of the capitellum in adolescents. World J Orthop. 2016;7(2):102–8.
4. Bexkens R, van den Ende KIM, Ogink PT, van Bergen CJA, van den Bekerom MPJ, Eygendaal D. Clinical outcome after arthroscopic debridement and microfracture for osteochondritis dissecans of the capitellum. Am J Sports Med. 2017;45(10):2312–8.
5. Bexkens R, van Bergen CJA, van den Bekerom MPJ, Kerkhoffs GMMJ, Eygendaal D. Decreased defect size and partial restoration of subchondral bone on computed tomography after arthroscopic debridement and microfracture for osteochondritis dissecans of the capitellum. Am J Sports Med. 2018;46(12):2954–9.
6. Eygendaal D, Bain G, Pederzini L, Poehling G. Osteochondritis dissecans of the elbow: state of the art. J ISAKOS Jt Disord Orthop Sport Med. 2017;2(1):47–57.
7. Takahara M, Mura N, Sasaki J, Harada M, Ogino T. Classification, treatment, and outcome of osteochondritis dissecans of the humeral capitellum. J Bone Jt Surg. 2007;89(6):1205–14.
8. van Steenkiste RL, Opperman J, Kox LS, Maas M. Imaging of the elbow in overhead athletes. Elb Sport:33–59.
9. van den Ende KIM, Renée Keijsers R, van den Bekerom MPJ, Eygendaal D. Imaging and classification of osteochondritis dissecans of the capitellum: X-ray, magnetic resonance imaging or computed tomography? Shoulder Elb. 2019;11(2):129–36.
10. Freehill MT, Poehling GC, Bain G. Portals and diagnostic elbow arthroscopy. In: Bain G, Eygendaal D, van Riet R, editors. Surgical techniques for trauma and sports related injuries of the elbow. Berlin: Springer; 2020.
11. Matsuura T, Iwame T, Suzue N, Kashiwaguchi S, Iwase T, Hamada D, Sairyo K. Long-term outcomes of arthroscopic debridement with or without drilling for osteochondritis dissecans of the capitellum in adolescent baseball players: a ≥10-year follow-up study. Arthroscopy. 2020;36(5):1273–80.

32 Arthroscopic Evaluation and Management of Osteochondritis Dissecans

L. A. Pederzini, A. F. Cheli, M. Bartoli, G. Stelitano, and A. Celli

32.1 Background

Osteochondritis dissecans (OCD) was first described by Konig in 1888 [1]. OCD of the elbow capitellum was first described by Panner in 1929. True OCD must be distinguished from Panner's disease; this is a self-limited osteochondrosis affecting younger individuals (<10 years old) and involving the entire ossification center similar to the Legg-Calvé-Perthes of the hip [2].

Elbow OCD is a condition affecting adolescents (13–17 years old), especially baseball players and gymnasts, and also other throwing athletes and weight lifters. Apart from the capitellum, OCD has also been reported in the trochlea, radial head, and olecranon [3].

32.1.1 Surgical Anatomy

The term chondrosis is more appropriate, because the histopathology is more consistent with necrosis than inflammation. The process starts in subchondral bone and evolves into cartilage breakdown and loose bodies formation [4, 5]. The lateral capitellum has softer cartilage than that of the radial head [6]. Valgus torque increases contact pressures in the radiocapitellar joint and leads to progression of the OCD from stable to unstable [7]. OCD in gymnasts is usually observed 30° more posterior on the capitellum than in baseball players [8]. Osteoarthritis is found in nearly half of the affected elbows when left untreated [5].

Diagnosis and classification: Early diagnosis affects prognosis as the untreated lesion tends to progress. OCD lesion must be defined as stable or unstable to guide the correct treatment [9]. Stability can be predicted from clinical findings and imaging studies. When OCD is suspected on physical examination, radiographs can be sufficient, but early stages could be missed [5]. Anteroposterior radiographic view with the elbow flexed 45° and externally rotated 30°, with forearm supination is helpful. According to Minami, OCD can be classified on X-ray as follows: grade I, local flattening/radiolucency; grade II, nondisplaced fragment; and grade III, displaced fragment [10]. MRI allows for earlier diagnosis compared to radiographs and has shown good correlation with intraoperative findings [11, 12]. However the diameter of the lesions can be overestimated due to bone edema [13]. CT scan allows for a precise evaluation of size and location of the OCD and loose bodies [4].

The following parameters define an unstable OCD: Minami grade III, capitellum epiphyseal

L. A. Pederzini (✉) · A. F. Cheli · M. Bartoli
G. Stelitano
Orthopaedic Unit, New Civil Sassuolo Hospital, Modena, Italy

A. Celli
Orthopaedic Unit, Hesperia Hospital, Modena, Italy

© ISAKOS 2022

D. N. Bhatia et al. (eds.), *Arthroscopy and Endoscopy of the Elbow, Wrist and Hand*,
https://doi.org/10.1007/978-3-030-79423-1_32

closure or a lateral epicondyle visible on X-ray; displaced fragment on CT; a high signal interface on T2 MRI between the fragment and bed; restriction of elbow motion >20°. Nonoperative treatment may be suggested if none of the previous is present [12].

Final evaluation of stability can be made with arthroscopic probing. An arthroscopic classification by Baumgarten and International Cartilage Repair Society (ICRS) is proposed. Grade I: softened but intact cartilage. Grade II: partial cartilage discontinuity. Grade III: complete discontinuity but not dislocated ("dead in situ"). Grade IV: empty defect or dislocated fragment [14]. Thus, fragments that can be displaced by probing are considered unstable (ICRS III and IV).

32.2 Indications and Contraindications

- Surgery must be considered if:
  - There is no radiographic improvement within 3 months.
  - There is pain during daily activities.
  - Locking episodes.
  - Imaging suggests obvious unstable OCD.
- Treatment can be divided into:
  - Reparative techniques (debridement with or without microfracture/drilling; fragment excision/fixation).
  - Reconstruction techniques (autograft, allograft, autologous chondrocyte implantation). OCD lesion greater than 10–12 mm or 50% of the capitellum are better addressed with reconstruction techniques rather than reparative ones [4, 9].
- Surgical procedure can be determined according to the size and location of the OCD [4].
  - Decision can be confirmed intraoperatively according to the ICRS arthroscopic classification.
  - In general, small size lesions can be debrided, medium size lesion can be fixed, and large size lesion can be grafted.
  - Lesions located laterally to a line bisecting the radial head tend to require reconstruction [15].
  - Large lesions, lateral location, open proximal radial physes and radiocapitellar arthritis have a worst prognosis, regardless of treatment. Various authors advocate for osteochondral autograft transplant (OAT) in such cases.
- Stable OCD lesions can be treated conservatively, and surgery is not necessary in most cases. Radiocapitellar arthritis is a relative contraindication to surgery.

32.3 Surgical Techniques

- *Arthroscopic debridement ± drilling*: Simple debridement ± subchondral drilling/microfracture may be an option for ICRS stage 1 lesions after nonoperative treatment failure. Microfracture/drilling is indicated for ICRS II or III lesions less than 10–12 mm (<50% of the capitellum) with intact lateral buttress. Radiocapitellar arthritis is a relative contraindication to surgery and limits treatment for lesions of any stage to debridement [16].
- Arthroscopic loose bodies removal ± drilling/microfracture shows good to excellent results in the short to medium term, especially in small lesions. Drilling can be performed if the lesion bed is sclerotic after debridement. Arthritis has been associated in the long term, but according to a recent paper [11] clinical outcomes were excellent regardless of lesion size at 10 years. Bexkens et al. [17] showed that arthroscopic debridement + microfractures reduced the defect size in width and in depth at CT. Subchondral bone healing was rated good or fair in 85%; however, there was no correlation with the clinical outcomes. This is consistent with another report showing complete defect filling on MRI in 80% of OCD treated with microfracture [18]. Unfortunately, there are no studies comparing microfracture and drilling.
- *Arthroscopic fragment fixation*: Acute, unstable, medium-sized, and unfragmented lesion with sufficient subchondral bone attached to the fragment and non-sclerotic bed may be

Fig. 32.1 Intraoperative position is demonstrated. The affected elbow and ipsilateral knee are draped

amenable to fixation. Even detached loose bodies can be fixed; however healing rate and clinical outcomes are variable and inconsistent. Lesions thicker than 9 mm tend to heal less frequently after fixation [19]. Fixation can be achieved open or arthroscopically using sutures or different devices (pins, darts, small anchors, Kirschner wires, cancellous screws, metal or absorbable Herbert screws) [4, 9]. With correct indication the healing rate has been reported up to 94%. There is a tendency toward a higher and faster union rate and a lower complication rate in patients treated arthroscopically [20].

- *Osteochondral autograft transplant (OAT)*: For larger lesions, reconstruction of the articular surface is recommended (Figs. 32.1, 32.2, 32.3, 32.4, and 32.5). Treatment of large size lesion with reparative techniques has not shown good healing rate and there is a risk of subsequent arthritis [4, 9]. When lateral column involvement is more than 6 mm, OAT is strongly suggested [4, 9]. OAT is the only technique that can address at the same time the articular cartilage and the subchondral bone pathology [21–23]. The plug can be customized to match the recipient site in shape, but not in cartilage thickness. The inferior medial trochlear ridge of the knee has proven to be an optimal donor site, with matched cartilage thickness from MRI mapping [21].

Fig. 32.2 The elbow is hyperflexed and a needle is used to check if the OCD can be perpendicularly addressed from posterior portal

Autograft rib plugs can be a good source for larger plugs (>15 mm) and less donor site morbidity [9, 22]. Even small lesions may benefit from OAT, especially those with insufficient/necrotic subchondral bone, large cysts, or extending to the lateral capitellum. In such cases reparative techniques may be insufficient [24, 25].

32.4 Results

According to a recent review and meta-analysis, surgical management of elbow OCD leads to significant improvements in ROM and patient-reported outcomes, regardless of the technique.

Nevertheless, patients were more likely to return to their level of preoperative sport after OAT autograft (94%) compared with debridement ± marrow stimulation (71%) or fixation (64%); this was regardless of the size of the lesion, that was similar between the groups (about 13 mm).

Medical insurance programs only cover debridement/microfracture treatments for elbow OCD in the US. The OAT procedure can provide lateral column stability and addresses both the subchondral bone and the articular cartilage, and this facilitates return to high-level athletics. Conversely, microfractures rely on the production of fibrocartilage, which may fail to restore subchondral bone and a congruent articular surface. Use of a single large plug, rather than mosaicplasty, has been related to a quicker return to previous level sports. A single large graft may provide more stability and faster osseous union. In larger lesions, reconstruction of half of the defect may be sufficient, decreasing the defect size to less than 10 mm [26, 27]. In a recent review, the mean plug size used for OAT was 7.7 mm, and the mean number of plugs used was 2.1. To date, there is no comparative study between OAT from the knee and rib, but harvesting from the rib has been advocated to fill big defect (>15 mm) with one single graft. A recent meta-analysis showed that harvesting from the knee may lead to donor site morbidity (7.8%).

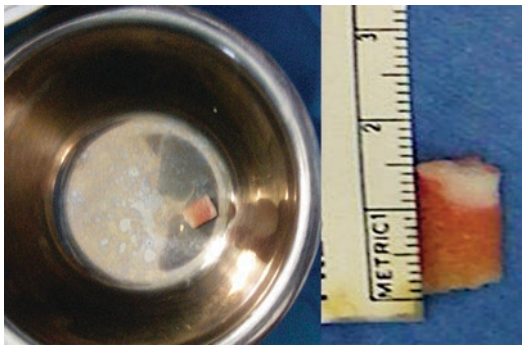

Fig. 32.3 The autograft is harvested from ipsilateral knee (trochlea)

32.5 Conclusions and Future Directions

The application of OAT to the elbow is still at an early stage, but results are promising. In a recent cadaveric study, the nonarticulating part of the radial head and of the lateral side of the olecranon tip have been investigated as alternative donor sites. These two grafts seem to have a proper match in cartilage curvature and thickness [28]. The effect of autologous chondrocyte implantation (ACI) for capitellar OCD remains unclear. ACI is an expensive, two-stage process

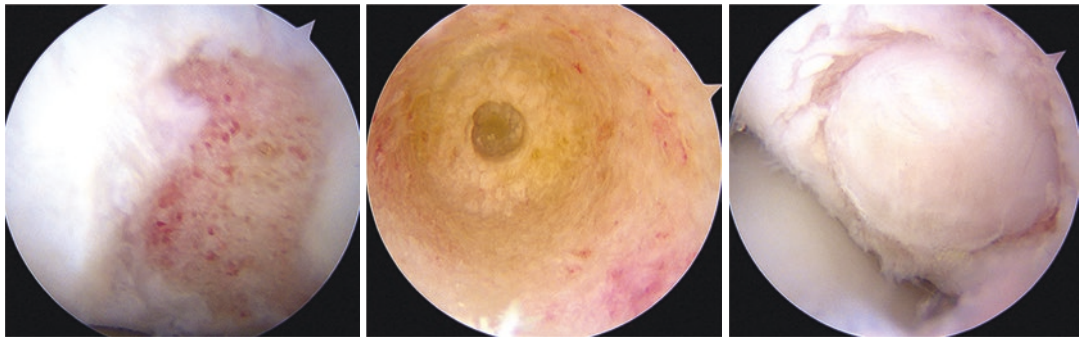

Fig. 32.4 Arthroscopic view of OCD lesion is shown (left image). The lesion is prepared (middle image) and the autograft is used to reconstruct the articular surface (right image)

Fig. 32.5 MRI at 6 months shows graft incorporation

and it does not address the pathology of the subchondral bone [5]. Cartilage tissue engineering techniques and scaffolds such as ultrapurified alginate (UPAL) gel [29] and platelet-rich fibrin (PRF) may provide future directions for management of elbow OCD [30].

References

1. Konig F. The classic: on loose bodies in the joint. 1887. Clin Orthop Relat Res. 2013;471(4):1107–15.
2. Claessen F, Louwerens J, Doornberg JN, van Dijk N, Eygendaal D, van den Bekerom MPJ. Panner's disease: literature review and treatment recommendations. J Child Orthop. 2015;9:9–17.
3. Adams IE. Injury to the throwing arm: a study of traumatic changes in the elbow joints of boy baseball players. Calif Med. 1965;102:102–32.
4. Maruyama M, Takahara M, Satake H. Diagnosis and treatment of osteochondritis dissecans of the humeral capitellum. J Orthop Sci. 2018;23(2):213–9. https://doi.org/10.1016/j.jos.2017.11.013.
5. Bradley JP, Petrie RS. Osteochondritis dissecans of the humeral capitellum. Diagnosis and treatment. Clin Sports Med. 2001;20(3):565–90. https://doi.org/10.1016/s0278-5919(05)70270-2.
6. Schenck RC Jr, Athanasiou KA, Constantinides G, Gomez E. A biomechanical analysis of articular cartilage of the human elbow and a potential relationship to osteochondritis dissecans. Clin Orthop Relat Res. 1994;299:305–12.
7. Kirsch JM, Thomas J, Bedi A, Lawton JN. Current concepts: osteochondritis dissecans of the capitellum and the role of osteochondral autograft transplantation. Hand (N Y). 2016;11(4):396–402.
8. Kajiyama S, Muroi S, Sugaya H, Takahashi N, Matsuki K, Kawai N, et al. Osteochondritis dissecans of the humeral capitellum in young athletes: comparison between baseball players and gymnasts. Orthop J Sports Med. 2017;5(3):2325967117692513.
9. Logli AL, Bernard CD, O'Driscoll SW, et al. Osteochondritis dissecans lesions of the capitellum in overhead athletes: a review of current evidence and proposed treatment algorithm. Curr Rev Musculoskelet Med. 2019;12(1):1–12. https://doi.org/10.1007/s12178-019-09528-8.
10. Minami M, Ishii S, Usui M, Muramatsu I, Ogino T, Fukuda K, Sugawara M. Twenty-five cases of osteochondritis dissecans of the elbow (Japanese). Rinsho Seikei Geka. 1979;14(8):805–10.
11. Matsuura T, Iwame T, Suzue N, et al. Long-term outcomes of arthroscopic debridement with or without drilling for osteochondritis dissecans of the capitellum in adolescent baseball players: a ≥10-year follow-up study. Arthroscopy. 2020;36(5):1273–80. https://doi.org/10.1016/j.arthro.2020.01.020.
12. Satake H, Takahara M, Harada M, Maruyama M. Preoperative imaging criteria for unstable osteochondritis dissecans of the capitellum. Clin Orthop Relat Res. 2013;471(4):1137–43. https://doi.org/10.1007/s11999-012-2462-9.
13. Claessen FM, van den Ende KI, Doornberg JN, et al. Osteochondritis dissecans of the humeral capitellum: reliability of four classification systems using radiographs and computed tomography. J Shoulder Elb Surg. 2015;24(10):1613–8. https://doi.org/10.1016/j.jse.2015.03.029.
14. Ruchelsman DE, Hall MP, Youm T. Osteochondritis dissecans of the capitellum: current concepts. J Am Acad Orthop Surg. 2010;18:557–67.
15. Kolmodin J, Saluan P. Osteochondritis dissecans of the humeral capitellum: the significance of lesion location. Orthop J Sports Med. 2014;2(4):2325967114530840.
16. Ahmad CS, Vitale MA, ElAttrache NS. Elbow arthroscopy: capitellar osteochondritis dissecans and radiocapitellar plica. Instr Course Lect. 2011;60:181–90.
17. Bexkens R, van Bergen CJA, van den Bekerom MPJ, et al. Decreased defect size and partial restoration of subchondral bone on computed tomography after arthroscopic debridement and microfracture for osteochondritis dissecans of the capitellum. Am J Sports Med. 2018;46:2954–9.
18. Wulf CA, Stone RM, Giveans MR, Lervick GN. Magnetic resonance imaging after arthroscopic microfracture of capitellar osteochondritis dissecans. Am J Sports Med. 2012;40(11):2549–56.
19. Nobuta S, Ogawa K, Sato K, Nakagawa T, Hatori M, Itoi E. Clinical outcome of fragment fixation for osteochondritis dissecans of the elbow. Ups J Med Sci. 2009;113:201–8.
20. Lu Y, Li YJ, Guo SY, Zhang HL. Is there any difference between open and arthroscopic treatment for osteochondritis dissecans (OCD) of the humeral

capitellum: a systematic review and meta-analysis. Int Orthop. 2018;42(3):601–7. https://doi.org/10.1007/s00264-018-3768-3.
21. Vezeridis AM, Bae DS. Evaluation of knee donor and elbow recipient sites for osteochondral autologous transplantation surgery in capitellar osteochondritis dissecans. Am J Sports Med. 2016;44(2):511–20.
22. Oka Y, Ikeda M. Treatment of severe osteochondritis dissecans of the elbow using osteochondral grafts from a rib. Bone Joint J. 2001;83(5):738–9.
23. Pederzini LA, Bartoli M, Cheli A, Nicoletta F, Severini G. Encouraging mid-term outcomes for arthroscopic autologous osteochondral transplant (OAT) in capitellum osteochondritis dissecans (OCD). Knee Surg Sports Traumatol Arthrosc. 2019;27(10):3291–6. https://doi.org/10.1007/s00167-019-05568-2.
24. Mihata T, Quigley R, Robicheaux G, McGarry MH, Neo M, Lee TQ. Biomechanical characteristics of osteochondral defects of the humeral capitellum. Am J Sports Med. 2013;41(8):1909–14.
25. Shimada K, Tanaka H, Matsumoto T, et al. Cylindrical costal osteochondral autograft for reconstruction of large defects of the capitellum due to osteochondritis dissecans. J Bone Joint Surg Am. 2012;94:992–1002.
26. Lyons ML, Werner BC, Gluck JS, Freilich AM, Dacus AR, Diduch DR, et al. Osteochondral autograft plug transfer for treatment of osteochondritis dissecans of the capitellum in adolescent athletes. J Shoulder Elb Surg. 2015;24(7):1098–105.
27. Maruyama M, Takahara M, Harada M, Satake H, Takagi M. Outcomes of an open autologous osteochondral plug graft for capitellar osteochondritis dissecans: time to return to sports. Am J Sports Med. 2014;42:2122–7.
28. Bexkens R, Hilgersom NFJ, Britstra R, et al. Histologic analysis of 2 alternative donor sites of the ipsilateral elbow in the treatment of capitellar osteochondritis dissecans. Arthroscopy. 2019;35(11):3025–32. https://doi.org/10.1016/j.arthro.2019.06.027.
29. Iwasaki N. Development of cartilage tissue engineering techniques based on biomedical research. J Orthop Sci. 2014;19(5):699–706.
30. Maruyama M, Satake H, Suzuki T, Honma R, Naganuma Y, Takakubo Y, Takagi M. Comparison of the effects of osteochondral autograft transplantation with platelet-rich plasma or platelet-rich fibrin on osteochondral defects in a rabbit model. Am J Sports Med. 2017;45(14):3280–8.

33 Elbow Osteochondritis Dissecans: Arthroscopy and Reconstructive Procedures

Kozo Shimada, Ko Temporin, and Keiichiro Oura

33.1 Introduction

Osteochondritis dissecans (OCD) of the elbow is sports-related disorders frequently involving young athletes such as baseball players and gymnasts. A goal of treatment is high-level return to sports activity and less-invasive procedure is preferable. Arthroscopic surgery is reasonable approach for this pathology because of its less-invasiveness; however open reconstructive surgery is necessary in selected cases. This chapter describes the arthroscopic procedures and open reconstruction options in OCD of the elbow and the author's treatment algorithm is presented.

33.2 Surgical Anatomy

Elbow joint has 10°–15° valgus carrying angle and distal end of the humerus has 30°–40° tilting angle. The mechanical compression forces load the anterior aspect of the capitellum and therefore the anterior capitellum is frequently involved in elbow OCD. Vascular anatomy is important for reparative process of OCD and arthroscopic approach is useful because of less-invasiveness to the local circulation.

K. Shimada (✉) · K. Temporin · K. Oura
Department of Orthopaedic Surgery, JCHO Osaka Hospital, Osaka, Osaka, Japan
e-mail: k-shimada1960@nifty.com

33.3 Indications and Contraindications

Indications of arthroscopy in elbow OCD include [1]:

- Arthroscopic identification of the lesion including staging diagnosis and sizing of the lesion.
- Arthroscopic fixation of the lesion mainly for the non-advanced lesions (ICRS OCD-II). Fixation can be performed with bony pegs autograft or biodegradable pins such as PLLA.
- Arthroscopic resection of loose bodies and debridement of the lesion for progressed lesions (ICRS OCD-III and -IV). This is recommended for the lesions smaller than 10 mm in diameter.

Fixation procedures are contraindicated in advanced lesions such as ICRS OCD-III and -IV associated with a high failure rate. Similarly, debridement for large aspherical lesions (>15 mm) is associated with a high risk of progression to osteoarthritis. These lesions necessitate reconstructive procedures using an osteochondral autograft; this procedure may be performed arthroscopically but is technically challenging, and an open approach is recommended.

© ISAKOS 2022

D. N. Bhatia et al. (eds.), *Arthroscopy and Endoscopy of the Elbow, Wrist and Hand*,
https://doi.org/10.1007/978-3-030-79423-1_33

33.4 Surgical Techniques

The patient is usually placed prone (or lateral decubitus) with an arm-suspended position.

- For fixation procedures in stable lesions, the elbow is placed in full flexion position ("salute position") and the instruments are introduced through low-direct lateral portals (Fig. 33.1).
- In moderate-sized lesion, we recommend a surgical option of anconeus-pedicled bone graft with periosteal coverage (ABGP) which can be done either in supine or in prone position.
- In large and advanced lesions, open reconstruction such as osteochondral autograft from the knee joint or from the costal rib should be performed, and supine position is recommended.

Portals: Elbow joint is divided into three areas as "anterior", "posterior," and "posterolateral." Two portals in each area are needed for visualization and instrumentation (Fig. 33.2):

- Anteromedial and anterolateral portals for anterior space.
- Posterior and posterolateral portals for posterior space.
- Direct lateral and accessory (low) direct lateral portals for posterolateral space.

Sometimes low posterolateral portal can be used as an alternative to the posterolateral and direct lateral portals. The usual capitellar OCD lesion is located in lower and anterior surface and therefore the location of the low-direct lateral portal is important especially for debridement or fixation of the OCD lesion.

Arthroscopic evaluation and debridement: Arthroscopic inspection is performed initially from the anteromedial portal and the lesion is probed from the anterolateral portal. Synovectomy and resection of the free bodies

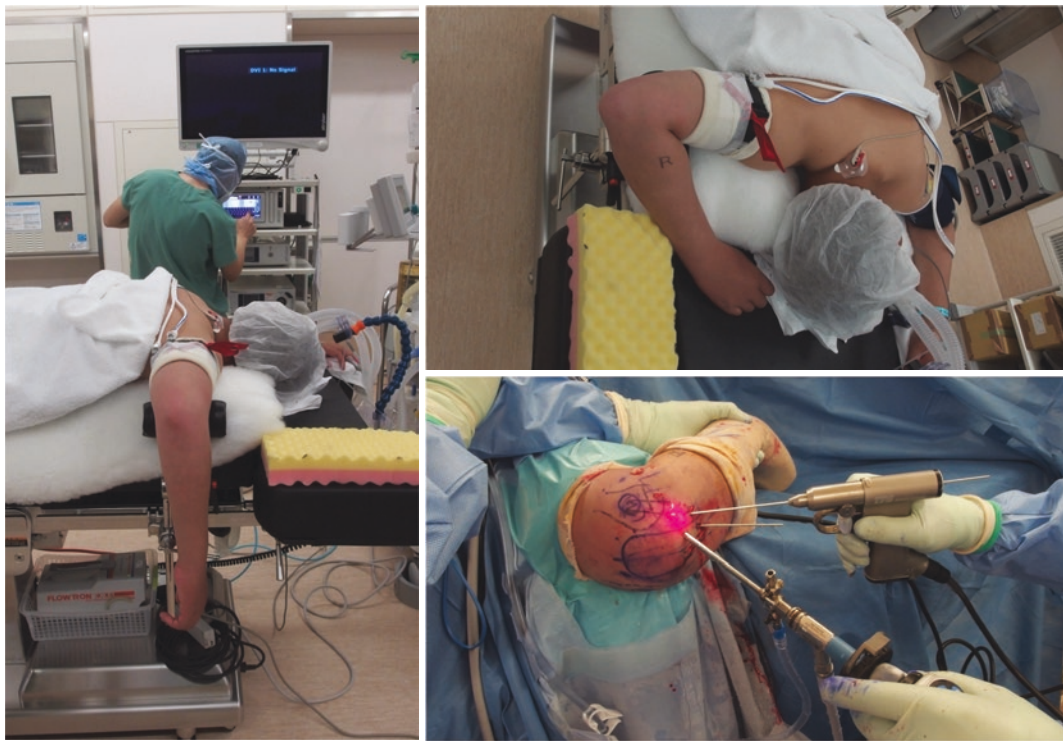

Fig. 33.1 Positioning for OCD procedures is demonstrated. [Left image: Prone position, top right image: Full flexion ("salute position"), bottom right: K-wire insertion in "salute position"]

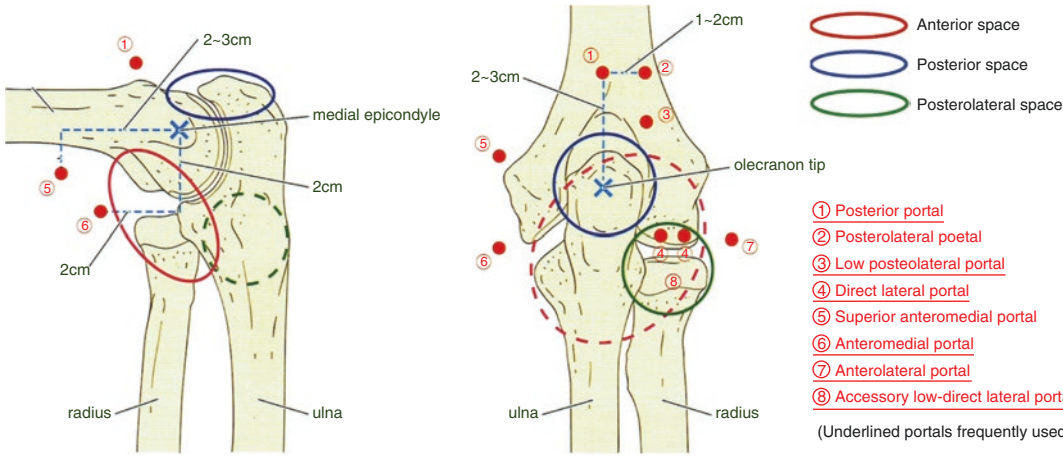

Fig. 33.2 Portals used in arthroscopic procedures for elbow arthroscopy are illustrated. (Copyright permission from the book entitled "OS NEXUS volume 20" Medical view Co Ltd Tokyo, Japan)

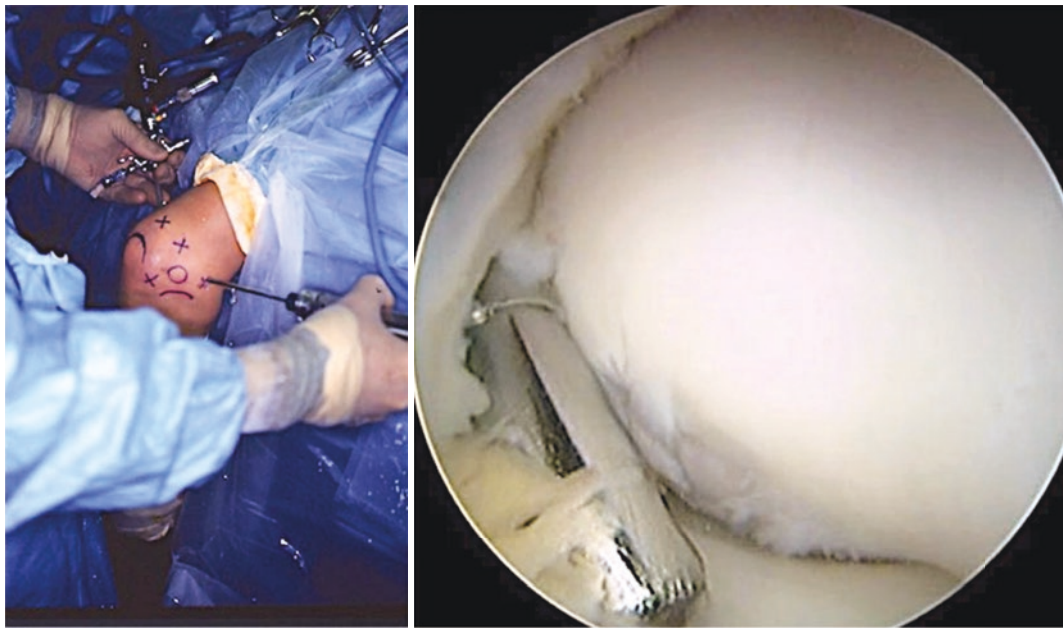

Fig. 33.3 Portals (left) and debridement of a capitellar OCD lesion (right) in the anterior space are demonstrated

are performed (Fig. 33.3). Next, debridement and loose body removal is performed in the posterior part of the joint (Fig. 33.4). This step can be avoided if no free body is identified by preoperative CT and MR images. The direct lateral portal is useful for arthroscopic evaluation and the lesion is probed through the accessory portal (Fig. 33.5).

If the lesion is stable, it is evaluated as ICRS OCD-II and fixation procedures are performed. In case the lesion is unstable or completely free (ICRS OCD-III or -IV), the unstable osteochondral fragments are resected. After debridement, the lesion is measured by a probe and divided in three categories: small (≤10 mm in diameter), moderate (11–14 mm), or large (≥15 mm).

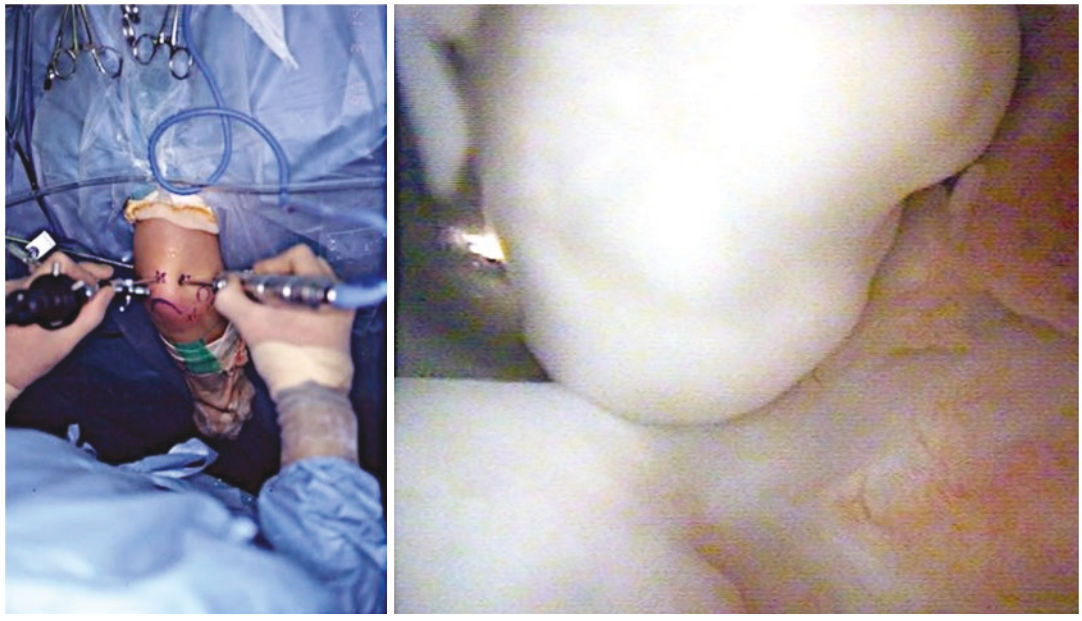

Fig. 33.4 Portals (left) and loose body removal (right) in the posterior space are demonstrated

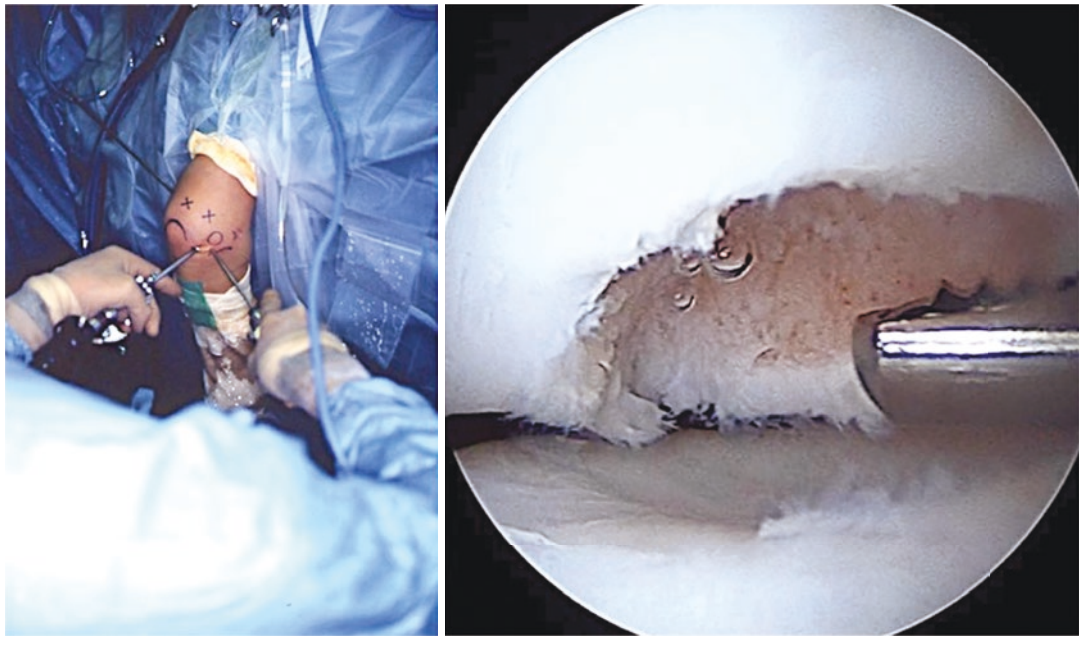

Fig. 33.5 Portals (left) and debridement of a capitellar OCD lesion (right) in the posterolateral space are shown

33.4.1 Surgical Procedures

1. For stable (ICRS OCD-II) lesions: open or arthroscopic bone peg fixation procedure
   (a) **Open fixation by bone pegs**: The lesion is identified and its stability is evaluated using an anconeus-splitting approach. A 3 cm longitudinal incision on the posterior olecranon is used to harvest a 5 mm × 30 mm cortical strut bone and this is cut into three or four bone pegs of 2.5 mm×15 mm. The lesion is drilled using a 2.0 mm or 2.4 mm Kirschner wire and fixation is performed using the bony pegs (Fig. 33.6).
   (b) **Arthroscopic fixation by bone pegs**: Arthroscopic drilling of the lesion is performed using two 2 mm or 2.4 mm Kirschner wires. The lesion is fixed by one K-wire and drilled by another K-wire through a transparent cannula. After removal of the second K-wire, a prepared bone peg is introduced through a transparent cannula and pushed into the lesion by a bone tamp. This procedure is repeated three or four times and the last bone peg is introduced into the hole after removal of the first fixation K-wire. PLLA pins may be used as an alternative to bone pegs. The head of the bone pegs are debrided arthroscopically if they are protruding or show irregular surface (Fig. 33.7).
2. For unstable (ICRS OCD-III or -IV) lesions:
   (a) **Small lesion size (<10 mm): Arthroscopic debridement**

   If preoperative diagnostic images suspect small lesion, the operation should be

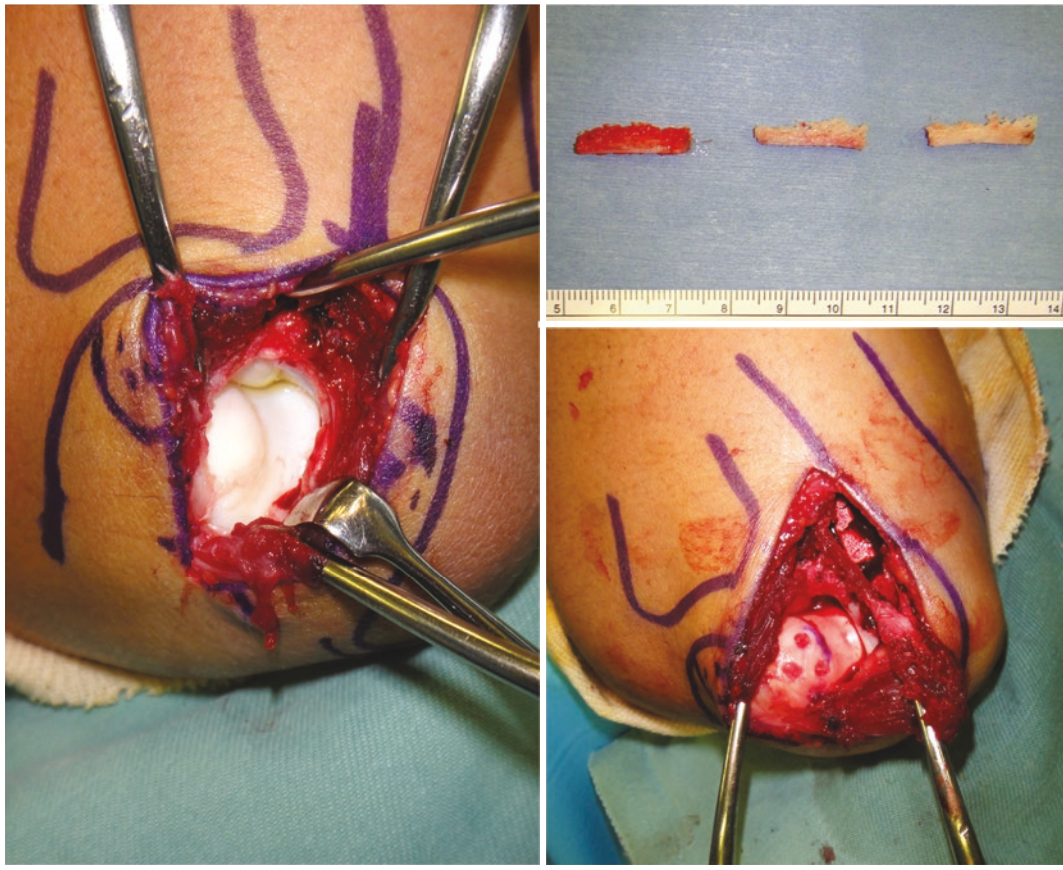

Fig. 33.6 Open bone peg fixation procedure is demonstrated. [Left: Anconeus splitting approach, top right: Bone pegs are harvested from the olecranon, bottom right: Bone pegs fixation "in situ"]

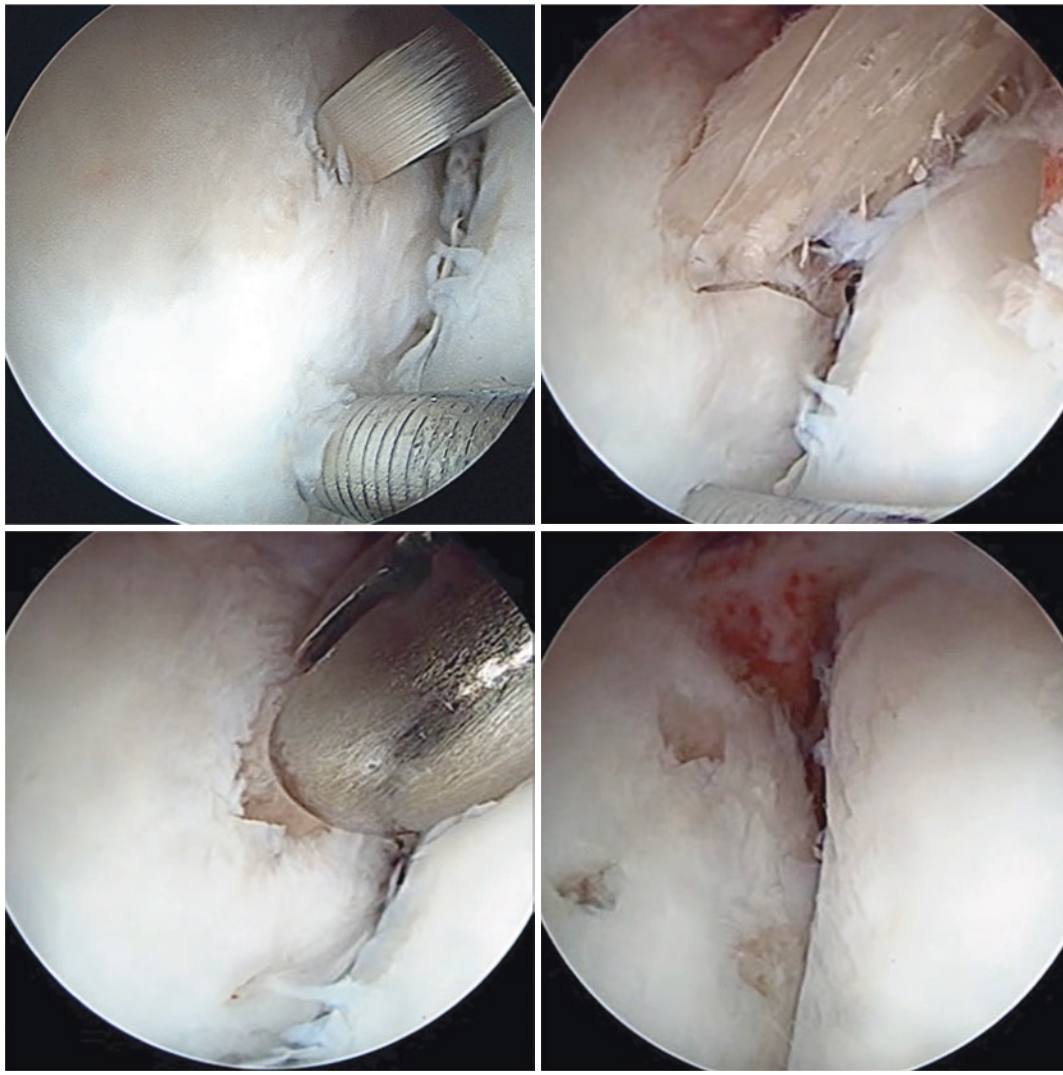

Fig. 33.7 Arthroscopic bone peg fixation procedure is demonstrated. Top left: K-wire fixation (with depth measure, lower) and another K-wire for drilling (upper). Top right: Bone peg insertion through a transparent cannula. Bottom left: Trimming of the top of the bone peg. Bottom right: Insertion of three bone pegs

planned in prone (or lateral decubitus) position. The lesion is identified and debrided, and the final size is measured. Thereafter, the air tourniquet is deflated and the bleeding from the lesion is documented (Fig. 33.8).

(b) **Moderate lesion size (10–15 mm): Open anconeus muscle-pedicled bone graft with periosteal coverage (ABGP) procedure**

ABGP is indicated if the lesion is advanced (ICRS OCD-III or -IV) and categorized as moderate size. This can be performed either in prone or in supine position. After debridement of the lesion, the direct lateral portal incision is enlarged to 5 cm above the joint line. A rectangular strut bone of 15–20 mm length and 7–10 mm width is harvested from posterior part of the lateral condyle with exces-

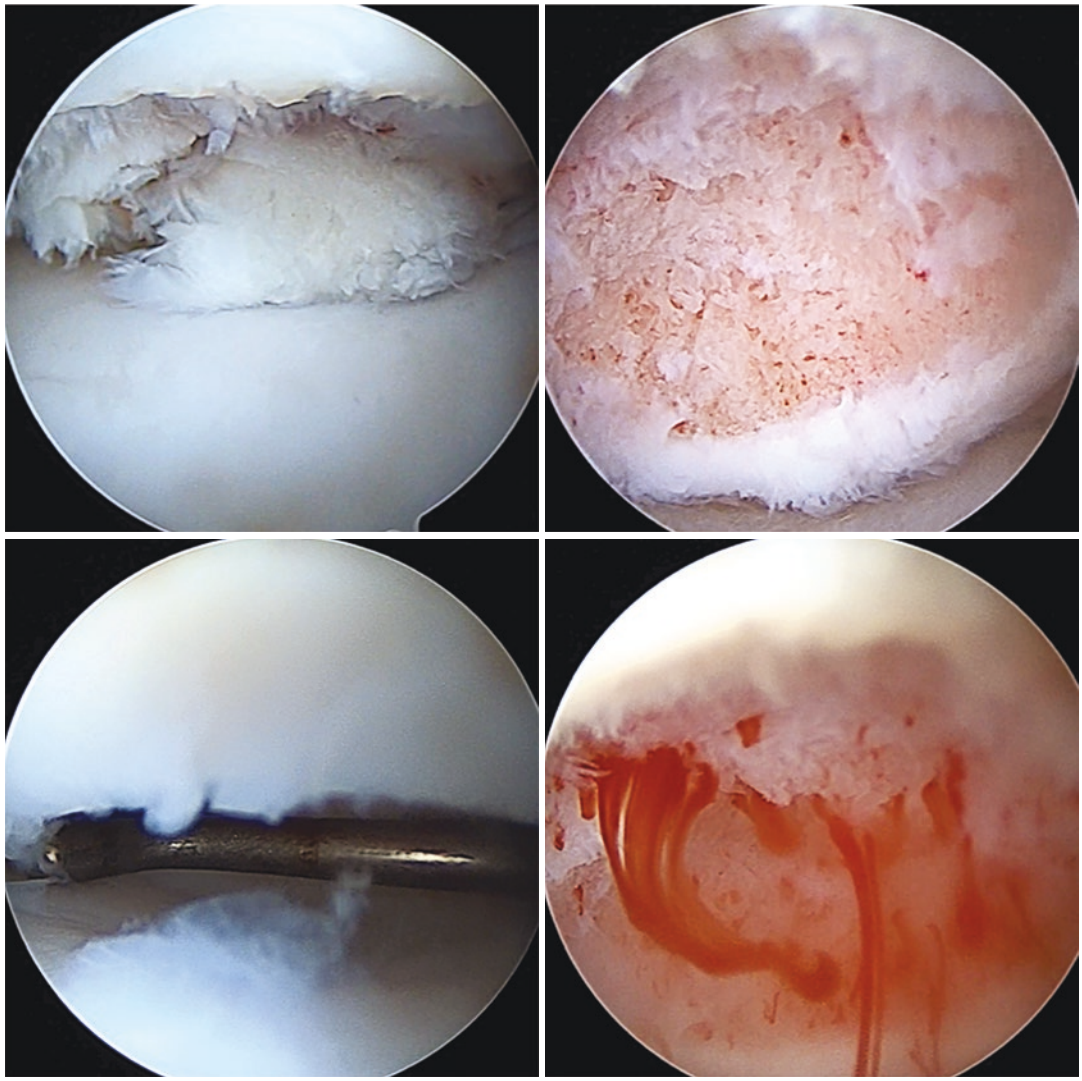

Fig. 33.8 Arthroscopic debridement of OCD lesion is shown. Top left: Unstable lesion (free body in situ). Top right: After removal of the free body and debridement of the lesion. Bottom left: Measurement of the lesion diameter by measuring probe. Bottom right: Bleeding after deflation of the tourniquet

sive periosteum proximally. Anconeus muscle attachment to the graft is preserved to maintain vascular supply. After graft harvest, the bony defect is deepened to the anterior to penetrate to the anterior OCD lesion. The bony tunnel is then widened and the periosteum-covered graft is pulled from posterior to anterior to the lesion to resurface the articular defect (Fig. 33.9).

(c) **Large lesion size (>15 mm): Open osteochondral autograft (knee or rib)**

If the lesion diameter is larger than 15 mm, the articular defect should be resurfaced by mosaicplasty (knee, multiple cylindrical osteochondral autografts transfer) or by cylindrical costal osteochondral autograft (rib, CCOA). As these procedures are performed in supine position, operation should be planned in supine

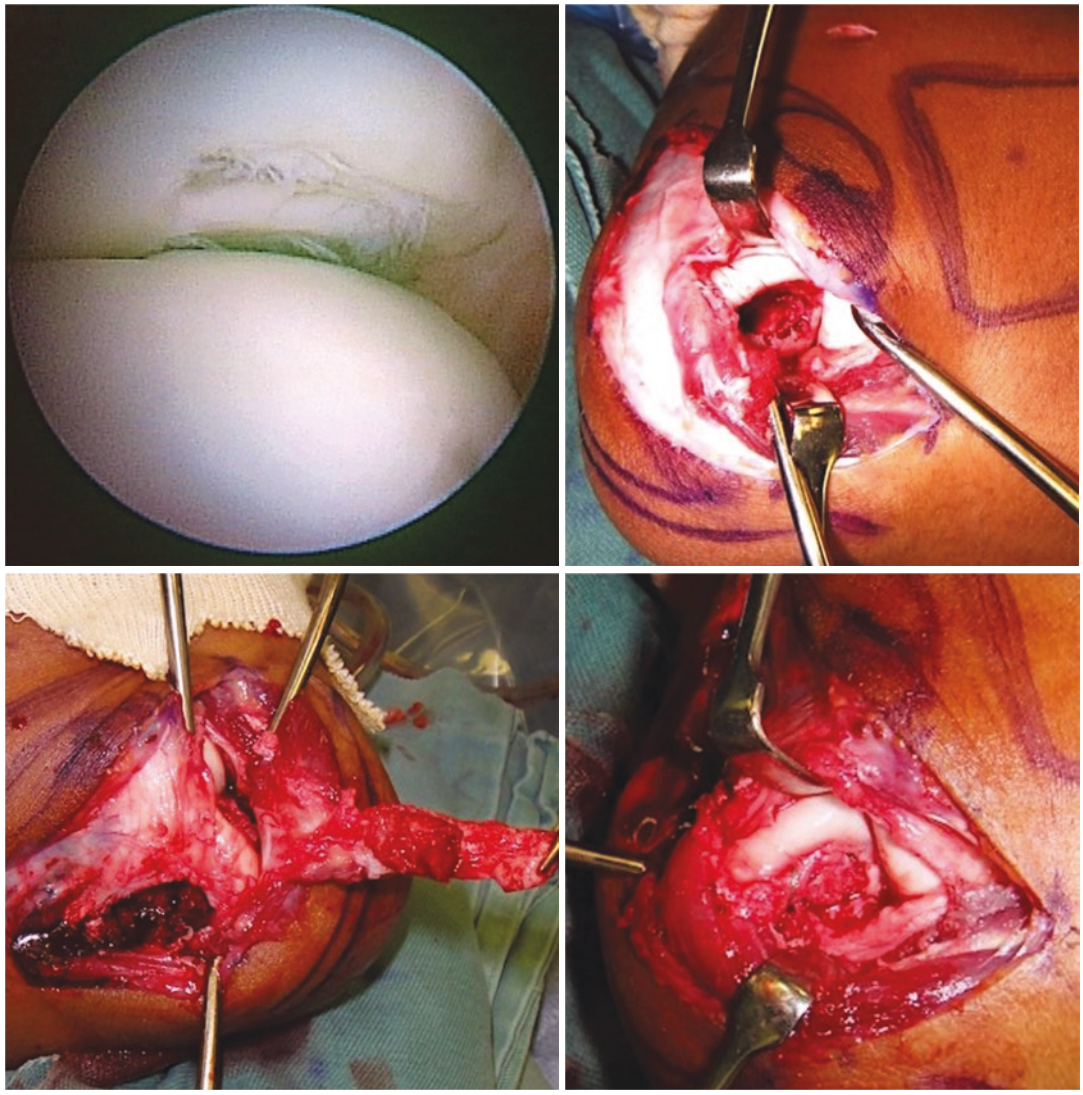

Fig. 33.9 Anconeus muscle-pedicled bone graft with periosteal coverage (ABGP) is demonstrated. Anterior arthroscopic view shows unstable flap-like OCD lesion (ICRS OCD-III) (top left). After debridement of the lesion (top right), muscle-pedicled bone is elevated from the posterior lateral condyle with excessive periosteum (bottom left). The graft is transferred and OCD lesion is resurfaced by the periosteum-covered bone graft (bottom right)

position if the lesion is preoperatively suspected as large. After debridement of the lesion, the direct lateral portal incision is enlarged centered on the OCD lesion. The articular defect is deepened to the proper depth according to the procedure.

- *Mosaicplasty*: With the use of the specialized equipment, the recipient site is prepared and the donor osteochondral plug is harvested from the femoral condyle. Three or four osteochondral plugs of 5–8 mm diameter are transferred piece by piece for reconstruction of the elbow OCD (Fig. 33.10).
- *Cylindrical costal osteochondral autograft (CCOA)*: After debridement of the lesion, the articular defect of the capitellum is deepened to 15 mm. Ipsilateral costal rib (usually fifth or sixth rib) is opened at the site of osteochondral junction and har-

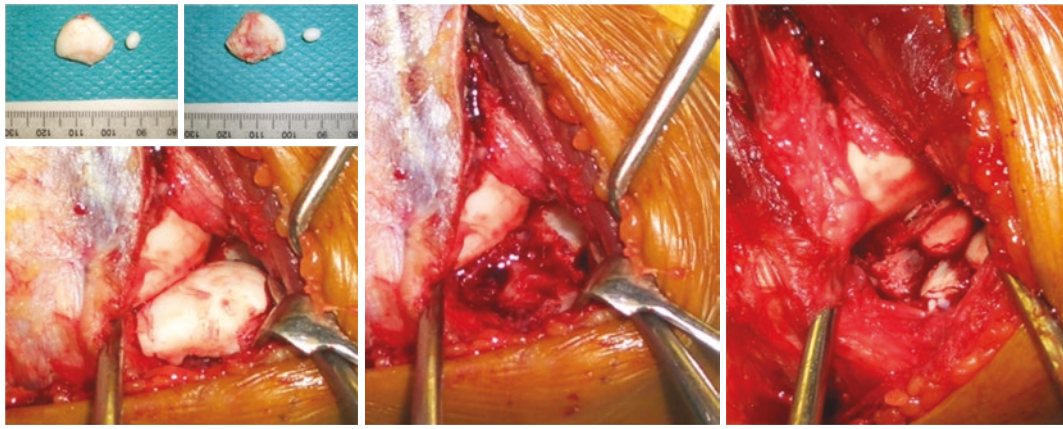

Fig. 33.10 Mosaicplasty. Large free body on the OCD lesion (left) and after debridement of the lesion (center). Articular defect was resurfaced by four osteochondral plugs harvested from the ipsilateral knee (right)

vested with the graft length of 28 mm including 5 mm length of cartilage. The graft is divided to obtain a 10 mm bone graft and 18 mm osteochondral graft. The 10 mm bone is cut into two pieces and bony wedges are prepared to stabilize the osteochondral graft into the recipient site. 18 mm osteochondral graft is pushed into the 15 mm depth of the recipient hole and excessive cartilage (usually 3 mm high) is removed by the scalpel. If the graft is too small compared to the recipient hole to obtain stable fixation, the bony wedge is packed between the graft and the recipient wall. Graft surface is shaved using a scalpel or surgical burr, and a congruent articular surface is obtained (Fig. 33.11).

33.5 Technical Tips

- OCD lesion of the elbow is usually located at the lower anterior capitellum. Direct lateral portal is the most effective approach to the lesion. Surgical intervention is easier through lower lateral portal in maximum flexion position ("salute" position).
- For unstable lesions, the surgeon must decide the final procedure (debridement or reconstruction) according to the lesion size. Debridement is easier in prone position and supine position is necessary for reconstruction. Therefore, the surgeon should select surgical position carefully according to the preoperative evaluation both of the lesion progression and its size. ABGP is a useful option because this procedure can be done both in prone and in supine position.

33.6 Pitfalls

- Check the entire joint space to avoid missing any free bodies.
- Precise probing is necessary. Occasionally, a lesion with intact articular surface may show instability because of empty or necrotic subchondral bone.
- Convert the procedure from debridement to reconstruction if the lesion is larger than preoperatively expected. Surgical option should always be considered.

33.7 Postoperative Management and Rehabilitation

For all athletes, we recommend immediate rehabilitation for other body parts especially shoulder, body trunk, and hip. Widening of the range

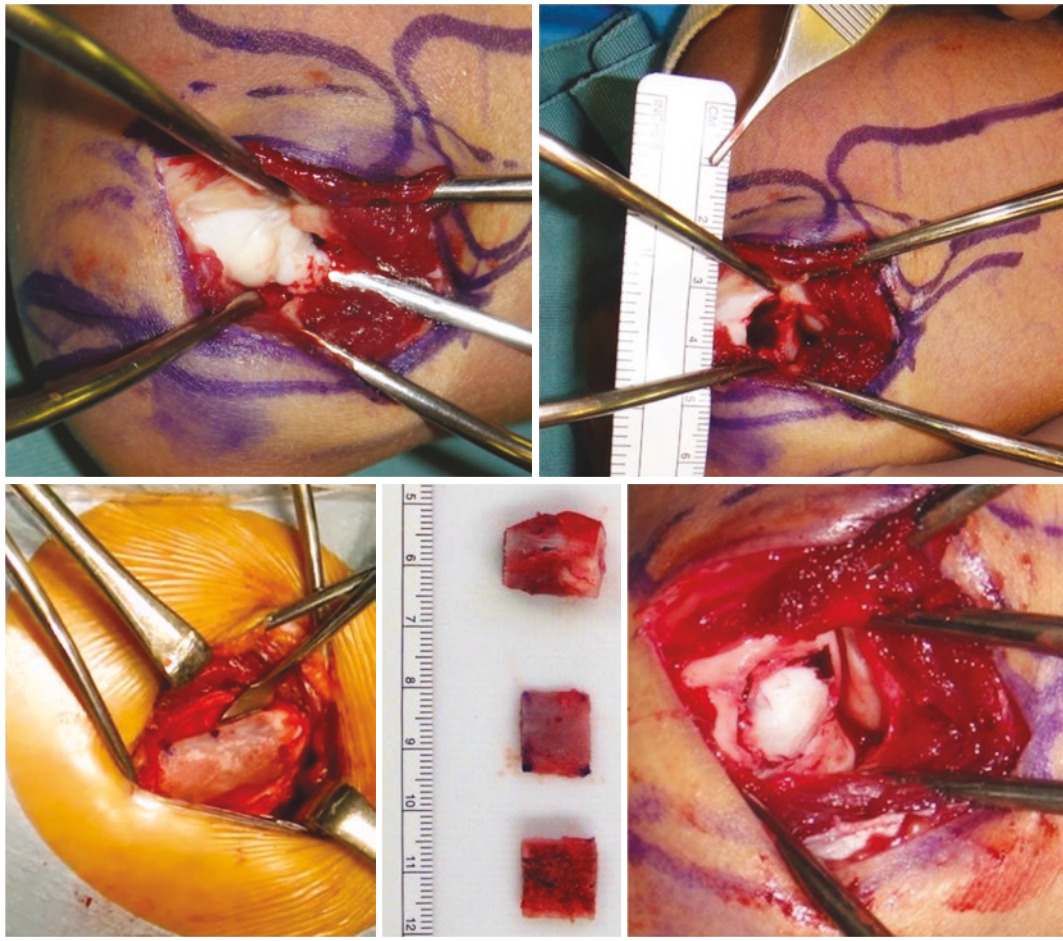

Fig. 33.11 Cylindrical costal osteochondral autograft (CCOA) procedure is demonstrated. Free body in situ (ICRS OCD-IV) is detached from the capitellum (top left). The lesion is deepened cylindrically (top right). The ipsilateral sixth costal rib is stripped subperiosteally at the osteochondral junction and an osteochondral graft with two pieces of wedge bones are harvested (bottom left and middle). The graft is pushed into the recipient hole and stabilized with one of the bony wedges packed into the space. The cartilage surface is shaped with a scalpel to obtain articular congruity (bottom right)

of motion, stretching surrounding muscles, and strengthening of the whole body will protect the injured elbow.

- For debridement cases, range of motion and muscle strengthening should be started immediately after surgery. Defect of the debrided articular surface will be filled with fibrocartilage in a few months and competitive sports activity is permitted usually in three months postoperatively (Fig. 33.12).
- For repaired (bone pegs fixation for OCD-II) (Fig. 33.13) or reconstructed (ABGP, Mosaicplasty, or CCOA) lesions, the patient's activity is limited for 3 months until bony union of the lesion/graft is confirmed. Sports activity is permitted gradually thereafter, and full activity is resumed in 6 months. For high-

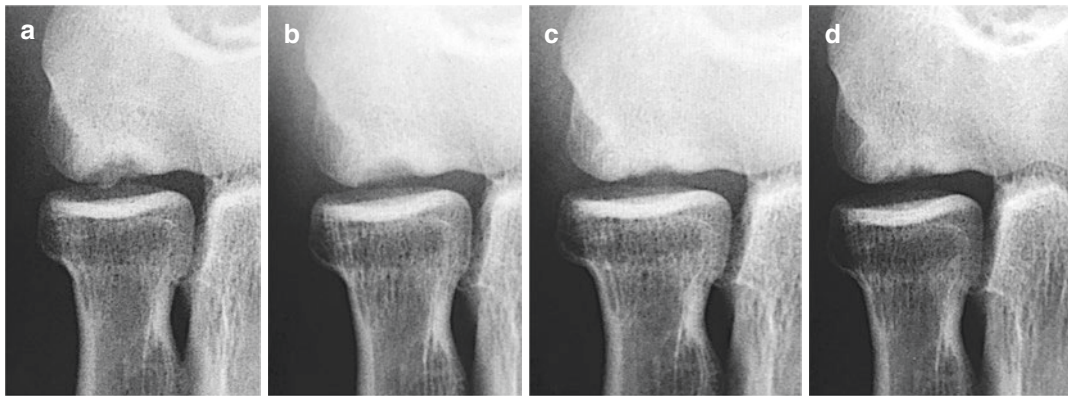

Fig. 33.12 Arthroscopic debridement in 15-year-old boy with ICRS OCD-III (the case shown in Fig. 33.8). Radiography before operation (**a**), after operation (**b**), 6 months after operation (**c**), and 1 year after operation (**d**). Early remodeling of the lesion is identified

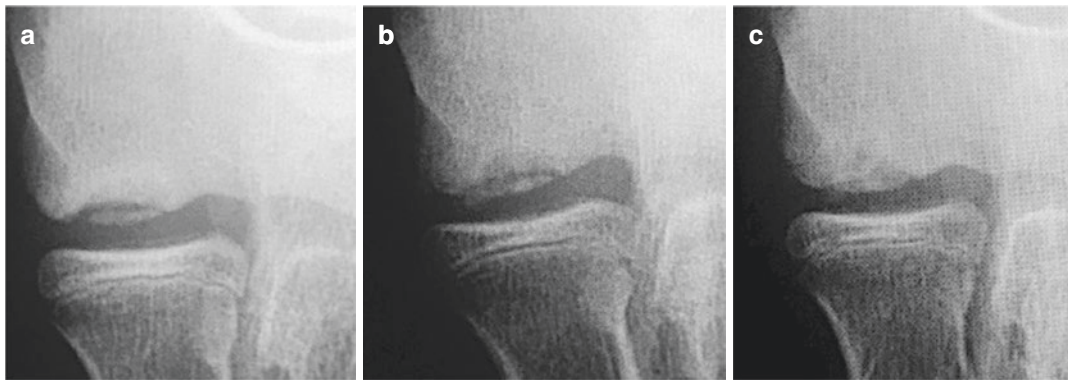

Fig. 33.13 Arthroscopic fixation in 12-year-old boy with ICRS OCD-II (the case shown in Fig. 33.7). Radiography before operation (**a**), after operation (**b**), and 6 weeks after operation (**c**). Early healing of the lesion is identified

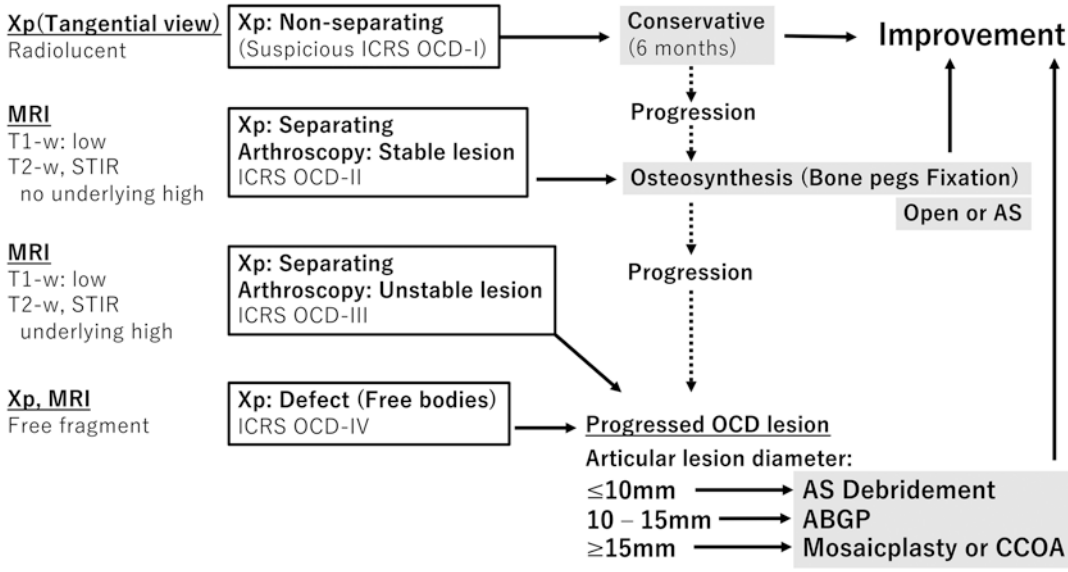

Fig. 33.14 Treatment algorithm for elbow OCD (*Xp* radiograph, *MRI* magnetic resonance imaging)

level baseball pitchers, the author recommends returning to full activity in a year.

33.8 Complications

- Usual neurovascular complication for elbow arthroscopy such as radial nerve, ulnar nerve, median nerve, and brachial artery injury must be avoid. Care should be paid for medial antebrachial cutaneous nerve and basilic vein.
- Hardware breakage may occur when the portal placement is not proper. Placement and direction of the direct lateral portal is important.

33.9 Results

The author has developed an algorithm and treated over 250 athletes since 1998 (Fig. 33.14). One hundred and ninety-one patients were followed up for more than 24 months postoperatively. Age at operation was 12–43 years (mean 14.9 years) and the follow-up period was 24–180 months (mean 39 months). Most of the patients were male baseball players or gymnasts except for two female tennis players. Overall results are shown in Table 33.1. Recurrence of loose bodies was seen in some cases and the symptoms improved soon after an arthroscopic free body removal.

Table 33.1 Results of the author's treatment algorithm for elbow OCD

Surgical procedure	Number of the cases	Age at surgery (years)	Follow-up period (months)	Stage (ICRS-OCD)	Lesion diameter (mm)	Range of motion				Timmerman and Andrews clinical score	
						Preope.		Postope.			
						Flex	Ext	Flex	Ext	Preope.	Postope.
Fixation	19	14.1	34	II:19	14.2	133	−8	136	−3	149	186
AS debridement	45	15.4	33	III:12, IV:33	10.3	126	−11	134	−2	141	189
ABGP	25	14.6	32	III:8, IV:17	13.1	129	−12	134	−4	138	192
OAT	102	14.9	44	III:49, IV:53	17.5	127	−14	134	−6	126	179
(Mosaicplasty)	12	15.9	63	III:5, IV:7	16.8	127	−9	134	−4	137	176
(CCOA)	90	14.8	41	III:44, IV:46	17.6	127	−15	133	−6	124	180
Total	191	14.9	39	II:19, III:69, IV:103	14.9	128	−12	134	−4	133	184

Reference

1. Shimada K, Temporin K, Oura K, Tanaka H. Osteochondritis dissecans open surgery. In: Bain G, Eygendaal D, van Riet RP, editors. Surgical techniques for trauma and sports related injuries of the elbow. Berlin: Springer; 2020. p. 699–706.

Part VI

Elbow: Epicondylitis

34 Arthroscopic Anatomic Insertional Release (AAIR) Procedure for Refractory Lateral Epicondilitis

Deepak N. Bhatia

34.1 Background

Lateral epicondylitis is an overuse enthesopathy of the common extensor origin and can infrequently result in a recalcitrant disabling and painful condition. The site of pathology is the extensor carpi radialis brevis (ECRB) insertion at the lateral epicondyle and often extends to the extensor digitorum communis (EDC) insertion in refractory cases. Open and arthroscopic releases usually involve debridement of the non-insertional region of the common extensor origin without identification of each insertional footprint. The arthroscopic anatomic insertional release (AAIR) procedure devised by the author involves accurate identification of bony insertions of ECRB and EDC tendons and precise release of both tendons from their footprints at the lateral epicondyle [1]. Associated intra-articular pathology (synovitis, plica, chondral wear) can be assessed and treated simultaneously, and calcific deposits in the common extensor origin can be removed. Early mobilization is possible as detachment and repair of the common extensor origin is not necessary.

34.1.1 Surgical Anatomy

The extensor carpi radialis brevis (ECRB) and extensor digitorum communis (EDC) are closely interrelated at the lateral extensor origin [2, 3]. The footprint of the ECRB is variable, but is centered over the proximal margin of the capitellum (Fig. 34.1a, b). The tendon and capsule are confluent at the footprint; however, there exists a fibro-fatty tissue plane between the anterolateral capsule and the ECRB/ECRL, and this plane is useful for extra-articular access during the arthroscopic procedure. From an arthroscopic perspective, the ECRB is identified just lateral to the capitellum, and is easily differentiated from the extensor carpi radialis longus (ECRL) by virtue of its tendinous appearance in comparison with the muscular appearance of ECRL. The EDC footprint is further posterior to the ECRB and is not arthroscopically visible until the ECRB is released from its footprint. EDC insertion on the lateral epicondyle is variable and ranges from a large oval shape to a broad thin attachment. The insertion of the supinator and lateral collateral ligament complex is distal to the ECRB footprint, and is not routinely visualized during the AAIR procedure.

34.2 Indications/ Contraindications

- Lateral epicondylitis that is refractory to conservative treatment and has persisted for more

D. N. Bhatia (✉)
SPORTSMED Mumbai, Mumbai, India

Sir HN Reliance Foundation Hospital, Mumbai, India
e-mail: shoulderclinic@gmail.com

© ISAKOS 2022

D. N. Bhatia et al. (eds.), *Arthroscopy and Endoscopy of the Elbow, Wrist and Hand*,
https://doi.org/10.1007/978-3-030-79423-1_34

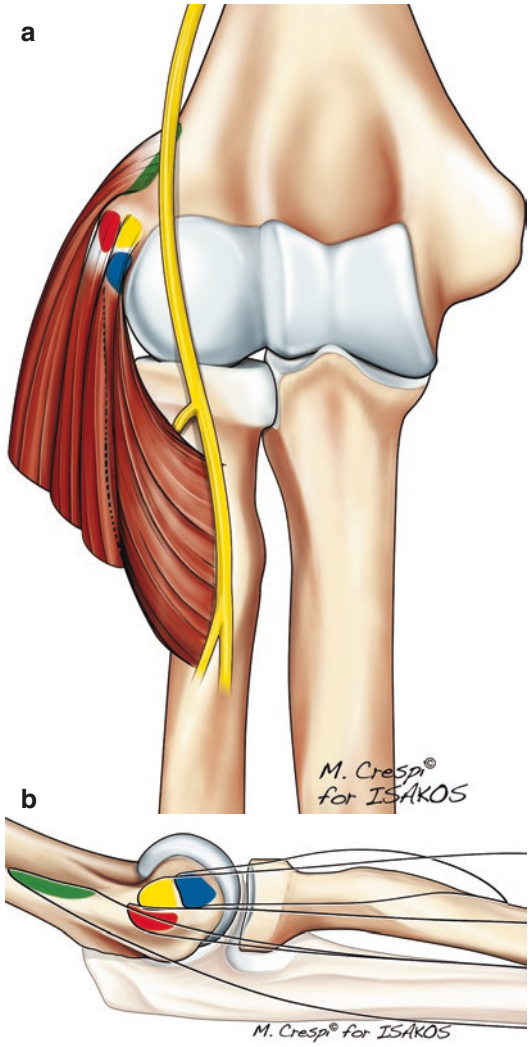

Fig. 34.1 (**a**) Common extensor origin tendons are illustrated. The insertional footprints of ECRB (yellow), EDC (red), and supinator (blue) are closely related at the lateral epicondyle. The ECRL insertion (green) is proximal at the supracondylar region. The radial nerve is close to the tendon insertions and is shown for reference. (**b**) The insertional relations of tendons at the common extensor origin are illustrated. The insertional footprint of ECRB (yellow) is adjacent to the superior capitellum, and the EDC insertion (red) is further posterior to ECRB. The supinator (blue) inserts distal to the other tendons and ECRL (green) footprint is proximal. (M. Crespi © for ISAKOS)

than 6–8 months is an indication for surgical management.

- Severe disabling pain that interferes with sleep and is not relieved with conservative methods is a relative indication. Recent evidence suggests a possible advantage with early surgical intervention (<6 months).

Elbow instability can coexist with lateral epicondylitis; arthroscopic release alone is contraindicated here, and instability must be evaluated and addressed during surgery. The ECRB and EDC tendons are extra-articular, and in close proximity to the radial nerve and its branches; surgeon inexperience with the procedure is therefore a relative contraindication. With anteriorly transposed ulnar nerve, care should be taken to prevent ulnar nerve damage during portal placement [4].

34.3 Surgical Technique

Elbow arthroscopy is performed with the patient in the lateral decubitus position and 2–3 portals are used in the AAIR procedure (Fig. 34.2).

Portals:

- The **proximal anteromedial portal (AM)** is the viewing portal throughout the procedure and is placed 1 cm proximal and anterior to the medial epicondyle.
- The **proximal anterolateral portal (AL)** is the main working portal and is placed 1 cm proximal and anterior to the lateral epicondyle.
- A **direct anterolateral portal (DL)** may be used for additional debridement, or when retraction of soft tissues is necessary. The DL portal is located just anterior to the lateral epicondyle, and is in close proximity to the lateral antebrachial cutaneous nerve, and the radial nerve [5].

Diagnostic endoscopy: The AM portal is used to evaluate the ulnotrochlear and radiocapitellar articulations. A 5-point arthroscopic evaluation is performed as outlined in Table 34.1 (Fig. 34.3).

Intra-articular pathology: Synovectomy is performed along the anterolateral capsule and lateral gutter. Impinging radiocapitellar plica or torn capsular tissue is excised using a small joint shaver (3 mm), and care is taken to prevent damage to the lateral ligament complex of the elbow.

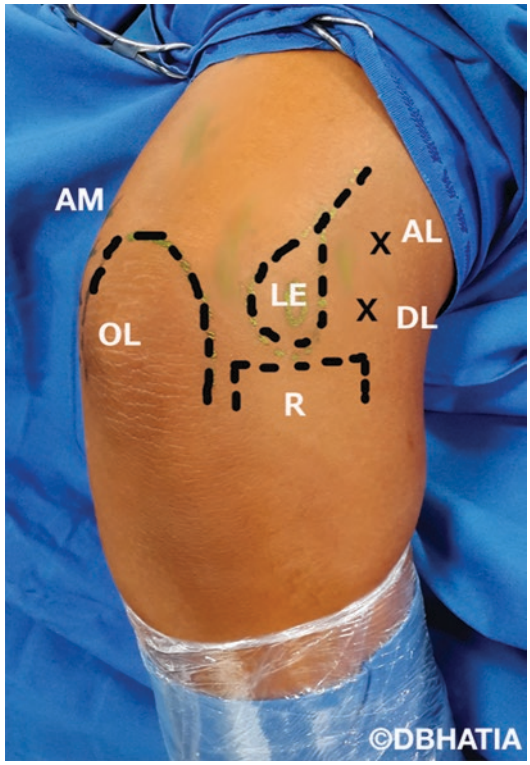

Fig. 34.2 Arthroscopic setup and portals for lateral epicondilitis release are shown on a right elbow in lateral decubitus position (*AM* anteromedial portal, *AL* anterolateral portal, *DL* direct lateral portal, *R* radial head, *OL* olecranon, *LE* lateral epicondyle). (© D. Bhatia)

Table 34.1 A systematic 5-point arthroscopic evaluation for intra-articular pathology in refractory lateral epicondilitis

	Anatomical region	Pathology
1	Radiocapitellar articulation	Focal chondral wear involving radial head and capitellum Generalized degenerative changes Arthroscopic signs of instability
2	Annular ligament and lateral synovial fold	Snapping annular ligament Synovial folds and impinging plicae
3	Anterolateral capsule	Focal capsular fraying and tears Intra-articular displacement and impingement of torn capsular fold
4	Superior recess	Synovial proliferation Osteophytes
5	Lateral and medial recesses	Synovitis Loose bodies

Lateral extra-articular access to extensor origin: A 3.5 mm arthroscopic shaver is used to bluntly dissect a plane between the anterolateral capsule and the extra-articular musculature, and an anterolateral capsular window is excised to expose the extensor carpi radialis brevis (ECRB) muscle and tendon (Fig. 34.4). The mid region of the capitellum and radial head marks the lateral ligament complex, and capsular excision must not be extended beyond this to prevent iatrogenic instability.

Arthroscopic orientation of the common extensor origin: Capsular excision provides a window for extra-articular visualization of the extensor origin and the ECRB and ECRL origins can be clearly differentiated (Fig. 34.4). The ECRB is visualized as a glistening tendinous structure in the lower half of the capsulotomy window. An arthroscopic probe via the AL portal shows that the tendon has a taut feel and can be traced all the way proximally to its insertion adjacent to the superior capitellum. ECRB may infrequently be ill-defined due to severe fraying within the fibers due to the underlying pathological process. The ECRL tendon is visualized in the superior aspect of the capsulotomy window. The tendon appears to be less taut on probing and can be traced to attach further proximally. EDC tendon insertion is posterior to the ECRB and is not visualized until the ECRB is released from its attachment.

ECRB release and debridement: A 30° arthroscopic view is adequate to visualize the ECRB tendon. A blunt probe is used to locate the bony insertion of the ECRB and the proximal and distal extent of the insertion is noted. A radiofrequency probe is used to gently release the tendon from its origin. The tendon is seen to retract distally, and should be released completely from the bony footprint on the distal humerus (Fig. 34.5). A blunt trocar is used to confirm complete release.

EDC release and debridement: A 70° arthroscope is used to visualize the EDC tendon. The arthroscope is advanced over the capitellum and is placed at the capsular window; this provides a view of the proximal EDC tendon and its bony insertion area (Fig. 34.6). A probe is used to follow the ten-

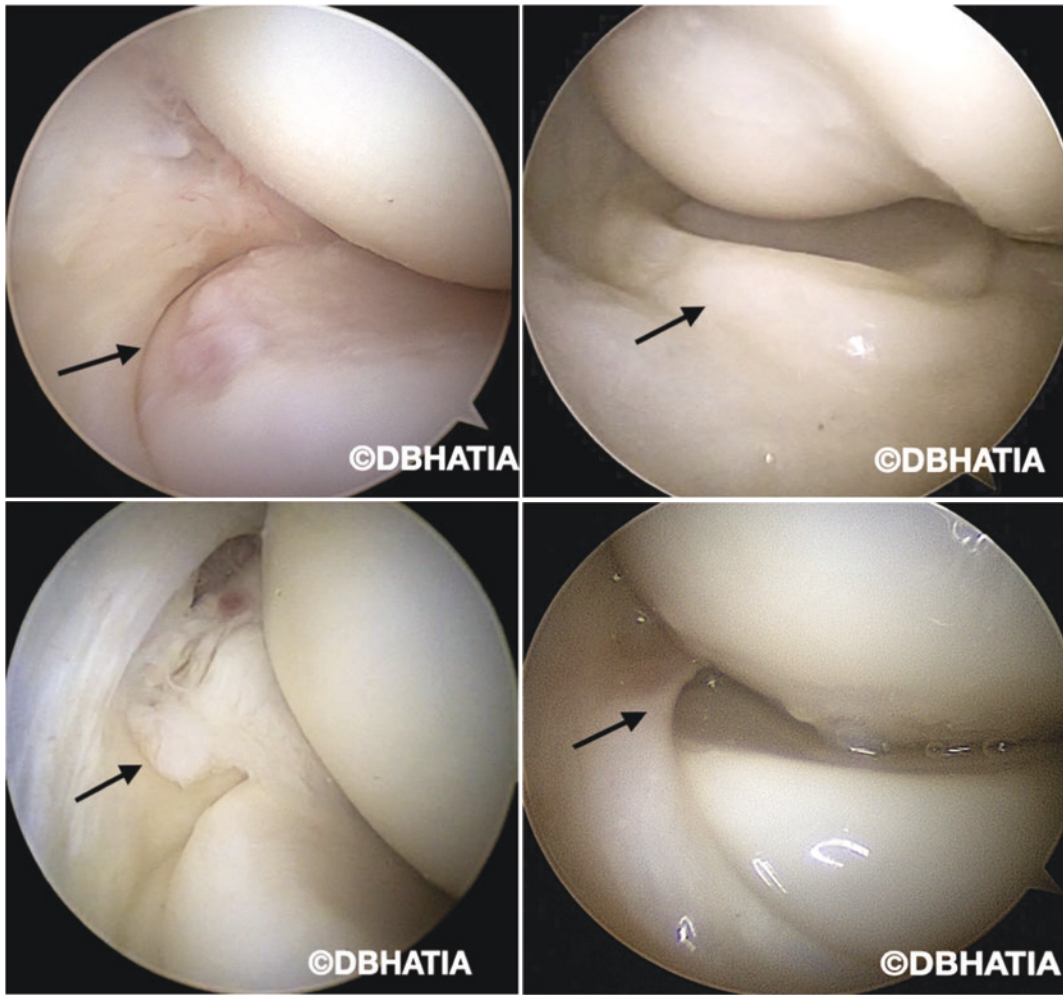

Fig. 34.3 Arthroscopic evaluation of intra-articular pathology demonstrates chondral loss over the lateral radial head (arrow, top left image), a snapping annular ligament (arrow, top right image), a torn capsular flap impinged in the radiocapitellar articulation (arrow, bottom left image), and a plica over the anterolateral radial head (arrow, bottom right image). (© D. Bhatia)

don up to its insertional footprint and the extent is documented. A small-joint radiofrequency device (angled, 3 mm) is used to release the tendon from its bony attachment. A thin sheath is seen beyond the EDC tendon after its release and is preserved. The release procedure of both ECRB and EDC must not extend to the distal half (sagittal plane) of the capitellum to avoid injury to the lateral ligaments. Further debridement is performed with an arthroscopic shaver to clear any frayed or persistent soft tissue attachments of the tendons. The arthroscope is withdrawn into the joint, and a thorough lavage is performed to remove any debris.

Excision of calcification, spurs, and insertional drilling: Calcific deposits can be identified after a part of the ECRB or EDC tendons are released. The footprint area is probed and toothpaste-like calcific material is seen to exude from the deposit (Fig. 34.7). Alternately, dry granular deposits may be found and can be excised with a grasper. Further debridement is performed to excise any calcific tissue, and an arthroscopic burr is used to remove any bony prominences or spurs. The insertional area may be drilled; however, decortication is not routinely performed.

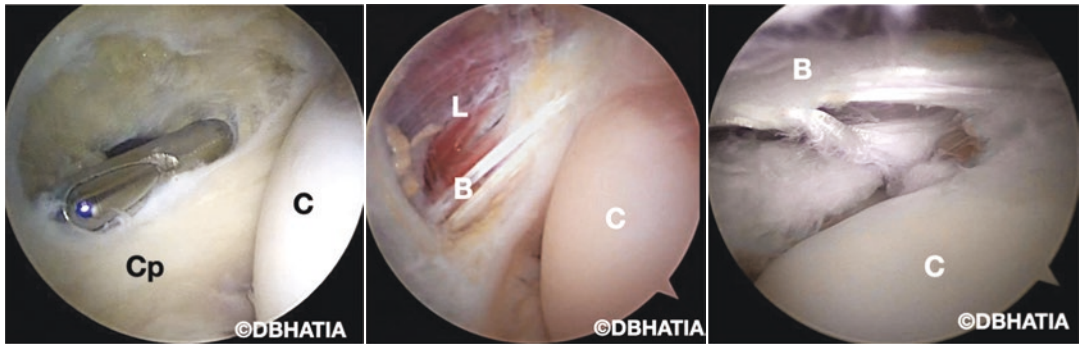

Fig. 34.4 Arthroscopic image of the intra-articular aspect of the elbow shows excision of anterolateral capsule (Cp, left image) using a shaver. The middle image shows the proximal extent of capsular excision up to the superior articular margin of the capitellum (C). The ECRB is identified by its glistening white tendinous fibers (B) and the ECRL is muscular throughout (L). The right image shows the severe degeneration and tearing of the ECRB insertion (B). (© D. Bhatia)

34.4 Tips and Tricks

- The proximal AM portal is placed slightly anterior for better manipulation of the arthroscope, and visualization into the extra-articular space over the capitellum.
- Capsular excision is safer when a less-aggressive tapered shaver blade is used.
- Calcification within the extensor origin is difficult to identify during arthroscopy, and the preoperative imaging may not always show the calcification. The "milking maneuver" using a probe is useful in identification of occult calcific deposits.

34.5 Pitfalls

- The AM portal is close to the ulnar nerve, and the nerve is at higher injury risk if it subluxates or snaps with elbow flexion. Similarly, a transposed ulnar nerve is at risk while placing an AM portal. A snapping ulnar nerve should be protected by using finger pressure to prevent the nerve from slipping out of its groove while placing the AM portal. An anteriorly transposed ulnar nerve may be manipulated similarly, or blunt dissection via a small anteromedial incision may be used as described by Park et al. [4].
- Isolated release of the ECRB may be inadequate for symptomatic relief, and the AAIR procedure helps to accurately identify and perform a combined ECRB and EDC release [1]. A part of the EDC may be preserved to provide some muscular cover over the condyle.
- Overzealous debridement and extensive release may result in damage to the lateral ligamentous complex. Instability can be prevented by restricting dissection proximal to the mid-capitellar region. If iatrogenic instability of the lateral ligaments is suspected, they should be repaired or reconstructed simultaneously.

34.6 Postoperative Management and Rehabilitation

A bulky soft tissue dressing is used in the immediate postoperative period, and this is changed to portal dressing on the fourth postoperative day. A sling is used for comfort. Elbow movements and forearm rotations are permitted without any restrictions. The patient is advised against any gripping or lifting activities. Elbow ROM exercises are progressed over 4–6 weeks. Strengthening is initiated at 12 weeks, and return to competitive sports is permitted after 3–6 months.

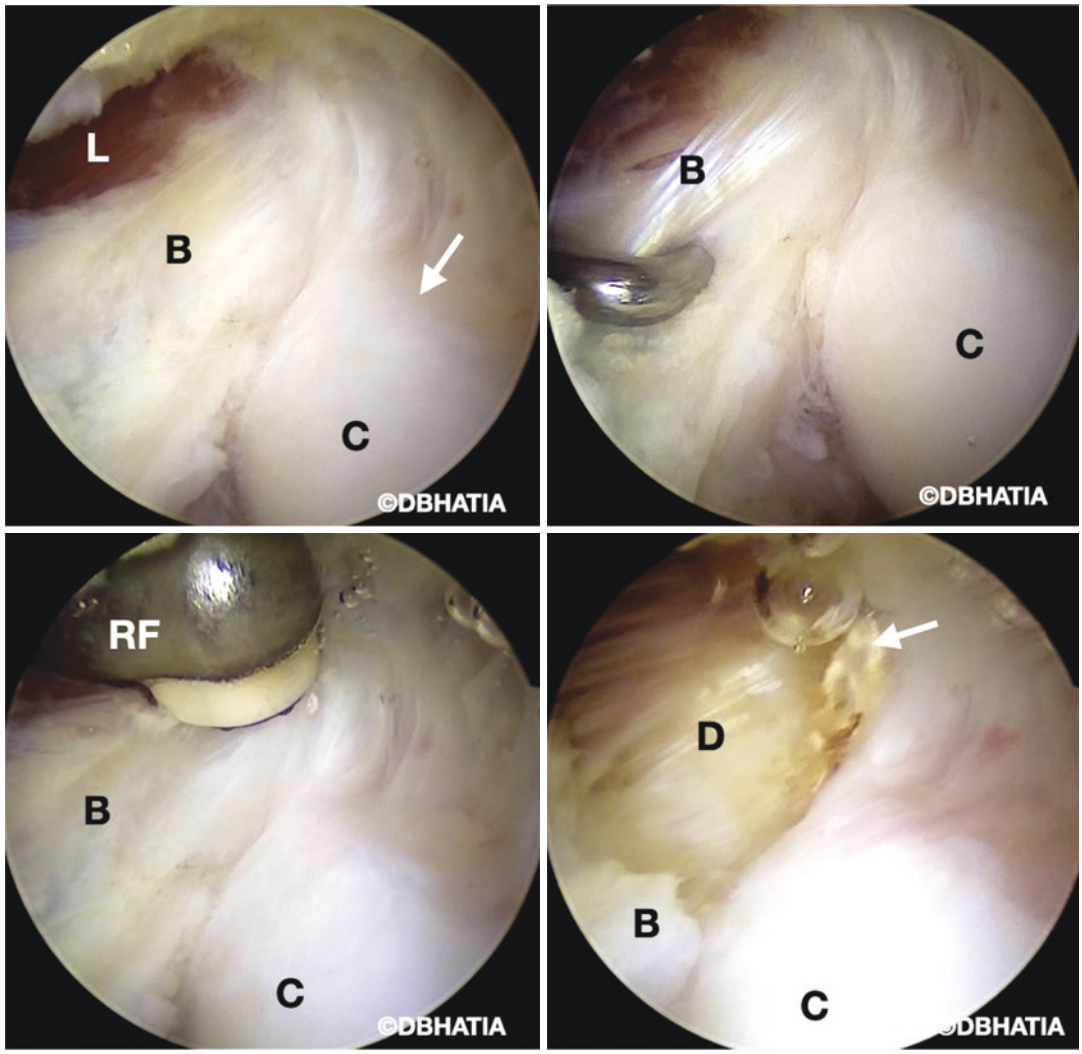

Fig. 34.5 Arthroscopic image (30° view) of the intra-articular aspect of the elbow shows ECRB insertion (B, top left). The superior capitellum articular margin (arrow) is shown for reference. A probe is used to locate the insertional area of B (top right) and B is released using a radiofrequency probe (RF, Bottom left). The ECRB fibers (B) are seen retracted away from its footprint after the release (arrow, bottom right). (© D. Bhatia)

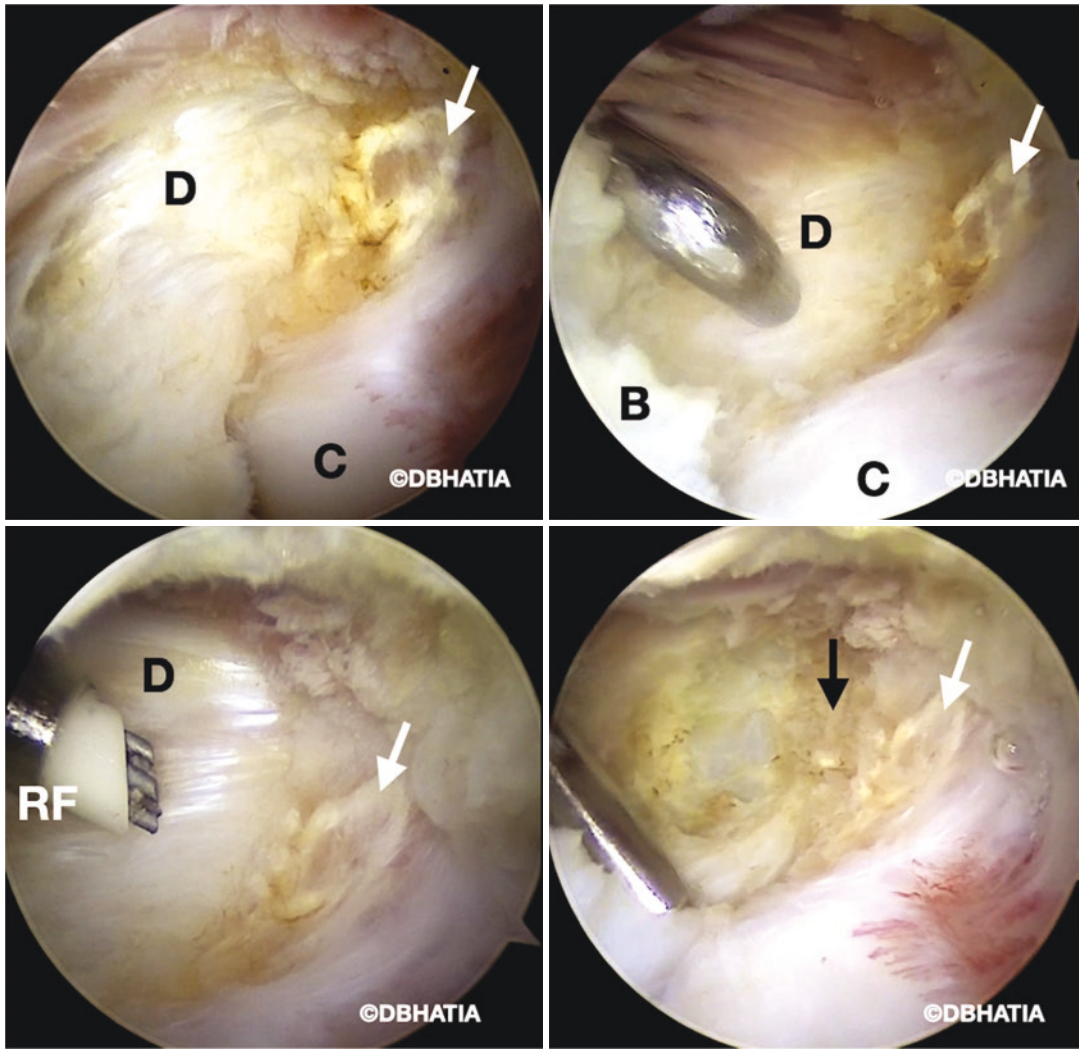

Fig. 34.6 Arthroscopic image (70° view) of the intra-articular aspect of the elbow shows EDC insertion (D, top left) after release of ECRB from its footprint (arrow). A probe is used to locate the insertional area of D (top right). D is released using a small joint angled radiofrequency device (RF, Bottom left). The footprints of EDC (black arrow) and ECRB (white arrow) are shown (bottom images). (© D. Bhatia)

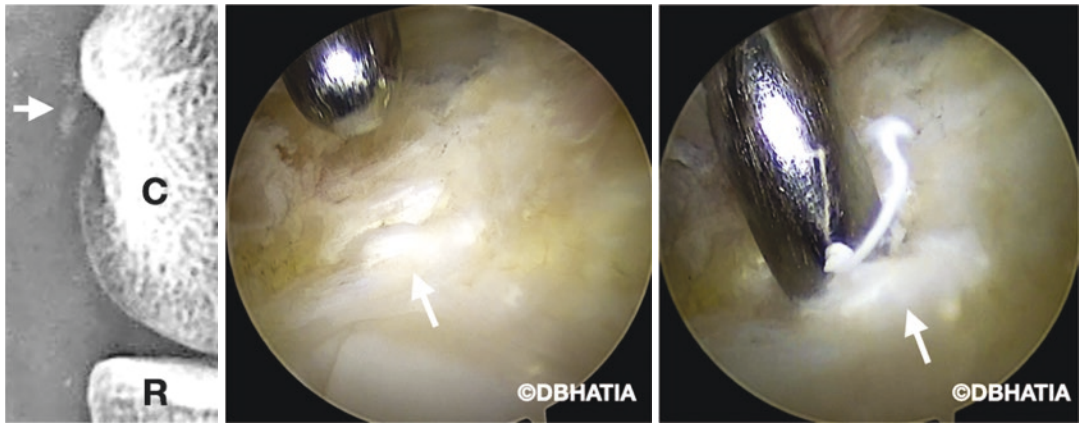

Fig. 34.7 Radiographic view of the radiocapitellar region (RC) shows lateral condylar calcific deposit (arrow, left image). The deposit is seen as a whitish lump (arrow, middle image) after partially releasing ECRB insertion. "Milking" the deposit with a probe releases the toothpaste-like calcific material (arrow, right image). (© D. Bhatia)

Conflict of Interest The author certifies that he has no commercial associations (e.g., consultancies, stock ownership, equity interest) that might pose a conflict of interest in connection with the submitted article. The author retains the copyright to the images, videos, and content in this chapter.

References

1. Bhatia DN. Arthroscopic management of refractory lateral epicondylitis. In: Bain G, Eygendaal D, van Riet RP, editors. Surgical techniques for trauma and sports related injuries of the elbow. Berlin: Springer; 2020. p. 379–87. https://doi.org/10.1007/978-3-662-58931-1_50.
2. Bunata RE, Brown DS, Capelo R. Anatomic factors related to the cause of tennis elbow. J Bone Joint Surg Am. 2007;89:1955–63.
3. Fairbank SM, Corlett RJ. The role of the extensor digitorum communis muscle in lateral epicondylitis. J Hand Surg (Br). 2002;27:405–9.
4. Park SE, Bachman DR, O'Driscoll SW. The safety of using proximal anteromedial portals in elbow arthroscopy with prior ulnar nerve transposition. Arthroscopy. 2016;32(6):1003–9. https://doi.org/10.1016/j.arthro.2015.12.043.
5. Stothers K, Day B, Reagan WR. Arthroscopy of the elbow: anatomy, portal sites, and a description of the proximal lateral portal. Arthroscopy. 1995;11(4):449–57.

Posterior Interosseous Nerve Release in Lateral Epicondylitis

35

Gregory Hoy and Richard P. Jamieson

35.1 Background

Radial tunnel syndrome (RTS) is a controversial and uncommon compressive neuropathy of the radial nerve and/or posterior interosseous branch of that nerve that often manifests as lateral elbow and forearm pain in the absence of neurological symptoms [1]. RTS can occur concomitantly in the presence of lateral epicondylitis and is a significant cause of continuing pain after tennis elbow surgery [2]. The diagnosis can be difficult to make and the clinical findings are usually more beneficial than diagnostic tests [1]. Pain is usually localised to a point approximately 6 cm distal to the lateral epicondyle and is often noted to be different in character to that of lateral epicondylitis. Most patients describe a semi-constant ache in this location. Pain due to lateral epicondylitis is located in the region of the lateral epicondyle and is often described as a sharp pain exacerbated by movement. Provocative clinical signs include pain with resisted supination and elbow extension, and pain with resisted middle finger extension [3]. Significant increased tenderness whilst rolling the muscle wad over the nerve compared with the unaffected side can be demonstrated in addition to the tennis elbow signs. Electrodiagnostic studies have poor sensitivity and specificity and are often normal [4, 5]. Differential diagnoses include radiocapitellar osteoarthritis, plica syndrome and distal biceps tendinopathy [1, 6]. Non-surgical treatment is the first-line treatment for RTS, but if surgery is considered for tennis elbow and the patient has positive provocative signs, the nerve release procedure is performed in addition to a tennis elbow reconstruction with excellent outcomes. Isolated nerve release may also be considered in recalcitrant cases. A number of surgical approaches have been described [7]. Most authors report approximately 80% good excellent results with the posterolateral approach [8], but the author prefers the combination procedure presented in this chapter.

35.2 Surgical Anatomy

The radial nerve pierces the lateral intermuscular septum between brachioradialis (BR) laterally and brachialis medially and extends distally between BR and extensor carpi radialis longus (ECRL). At this point, it divides into a superficial sensory nerve, a deep posterior interosseous nerve (PIN) and other motor branches to ECRB and supinator [9].

The radial tunnel is a potential space that is approximately 5 cm in length beginning at the

G. Hoy (✉) · R. P. Jamieson
Melbourne Orthopaedic Group,
Melbourne, VIC, Australia

Department of Surgery, Monash University,
Melbourne, VIC, Australia
e-mail: gahoy@mog.com.au

© ISAKOS 2022

D. N. Bhatia et al. (eds.), *Arthroscopy and Endoscopy of the Elbow, Wrist and Hand*,
https://doi.org/10.1007/978-3-030-79423-1_35

radiocapitellar joint and bordered laterally by the mobile wad (BR, ECRL and extensor carpi radialis brevis (ECRB)) and medially by the distal biceps tendon and brachialis. The floor of the tunnel is the radiocapitellar joint capsule and the roof is the BR muscle [3]. The most common site of compression is the Arcade of Frohse distally [10]. Other possible sites of compression include the fibrous bands anterior to the radiocapitellar joint, recurrent radial vessels (leash of Henry), the medial thickened edge of ECRB (which occurs in significant numbers in tennis elbow) and the fibrous bands at the distal edge of supinator [11].

Multiple surgical approaches have been described [7]. The anterior approach is more useful when there is a requirement for more proximal neurolysis, whereas the posterolateral approach can be extended distally utilising the dorsal Thompson interval [12]. The authors utilise a posterolateral approach whilst doing concomitant lateral epicondylitis surgery, with minimal wound extension and thorough neurolysis achieved.

35.3 Indications

- Failure of non-surgical treatment.
- Combined with surgery for recalcitrant lateral epicondylitis.
- Clinical signs of tenderness along the nerve under the brachioradialis muscle.

35.4 Contraindications

- Proximal compression of radial nerve in RTS necessitates an extensile release.
- Previous surgery around the nerve.

35.5 Surgical Technique

Under regional or general anaesthetic the patient is placed supine on the operating table. The arm is exsanguinated prior to inflation of a high-arm tourniquet.

- The bony landmarks are palpated and a longitudinal incision is made beginning 1 cm proximal to the lateral epicondyle and extending distally for 5 cm (Fig. 35.1).
- Skin flaps are raised to expose the fascia overlying the extensor digitorum communis (EDC). The interval between the ECRL and EDC is identified. The EDC muscle belly is reflected posteriorly and the ECRL is retracted anteriorly. This exposes the ECRB tendon. The ECRB is elevated from its humeral epicondylar attachment (Fig. 35.1).
- A thorough debridement of the abnormal tendinopathic tissue of ECRB (angiofibroblastic hyperplasia) is performed (Fig. 35.1). The underlying lateral epicondyle is denuded in order to create a healing response.
- Attention is then turned to the radial nerve decompression. The ECRB muscle fibres are carefully split longitudinally to expose the underlying supinator muscle (Fig. 35.2).
- The forearm is gently supinated to allow easier identification of the PIN proximal to the supinator edge (Arcade of Frohse). The PIN is carefully neurolysed from proximal to supinator (Figs. 35.3 and 35.4a, b), releasing the proximal leading edge of supinator (Fig. 35.5). A simple in situ decompression is performed. The nerve is not mobilised. Care is taken to avoid injury to the vena comitans running with the posterior interosseous nerve as this can be a source of post-operative haematoma.
- The tendinous part of the ECRB overlying the nerve is then palpated with a finger. If this is deemed to be a source of compression, then a fractional lengthening/release is performed at this level (Fig. 35.6).
- The ECRB is finally debrided and repaired using No. 1-Vicryl interrupted sutures (Figs. 35.7 and 35.8).

35.6 Tips and Tricks

- This technique allows release of the PIN at the most common sites of compression.
- Forearm supination brings the PIN into the surgical field and allows for easier identification and neurolysis.
- It is important to remember the orientation of the nerve at this location to avoid iatrogenic

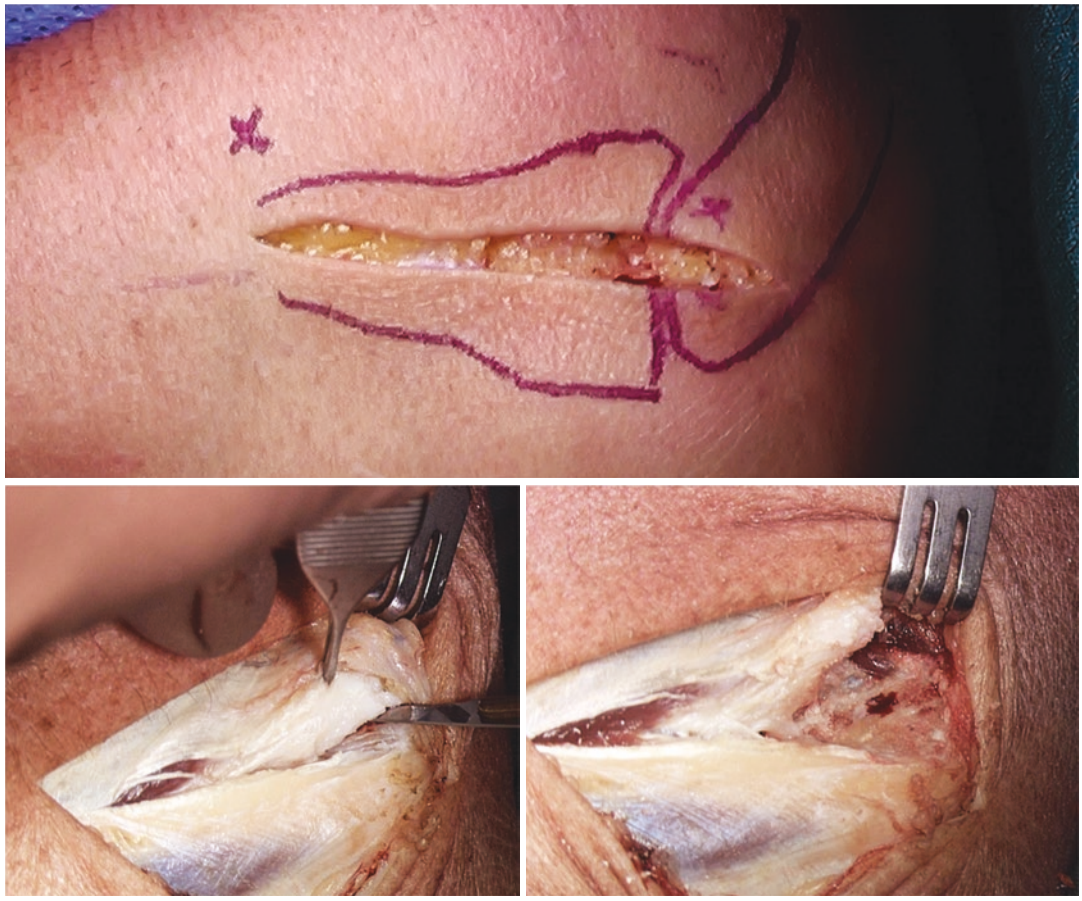

Fig. 35.1 Release of ECRB is shown. A 5 cm incision (top image) is used to expose the ECRB, and the tendon is then released from its insertional footprint on the lateral epicondyle (bottom images) (© G. Hoy)

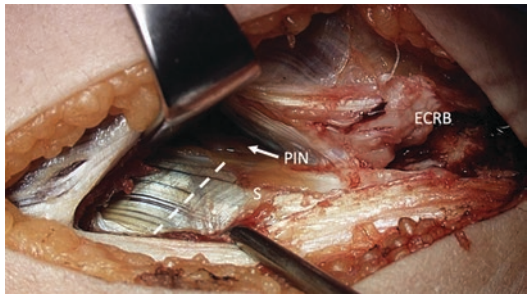

Fig. 35.2 Following release of the ECRB from the lateral epicondyle, the ECRB is split longitudinally to expose the underlying supinator muscle (S). The posterior interosseous nerve (PIN) can be identified before it enters the Arcade of Frohse. The dotted line represents the course of the PIN through supinator (© G. Hoy)

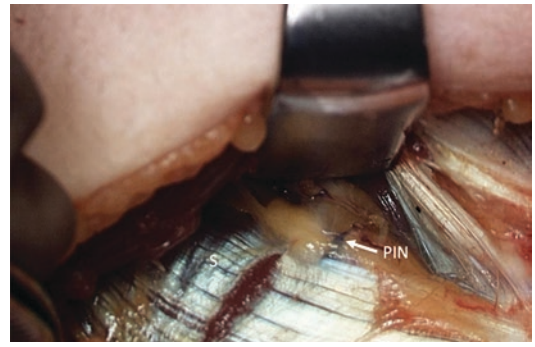

Fig. 35.3 The supinator fascia is released in the line of the PIN (© G. Hoy)

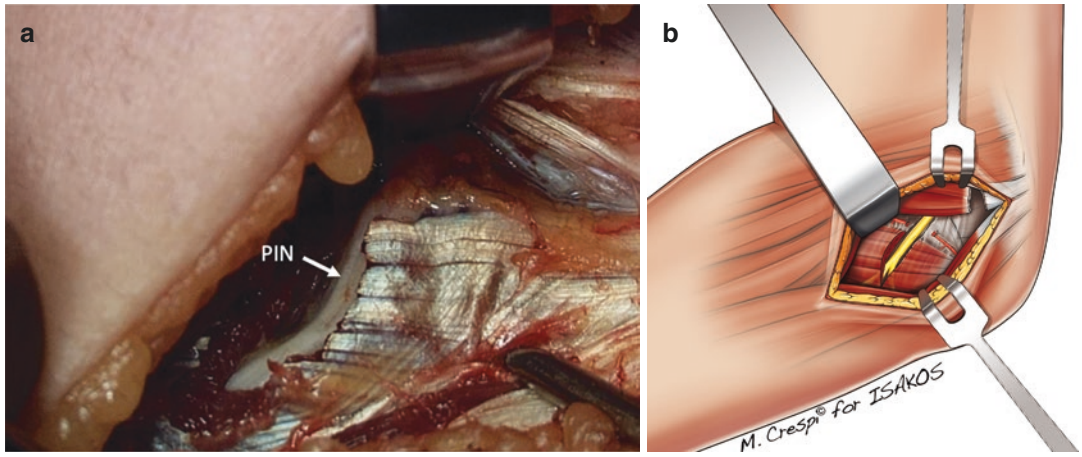

Fig. 35.4 (**a**) A complete neurolysis of the PIN is performed. (© G. Hoy) (**b**) An overview of ECRB and PIN release is illustrated

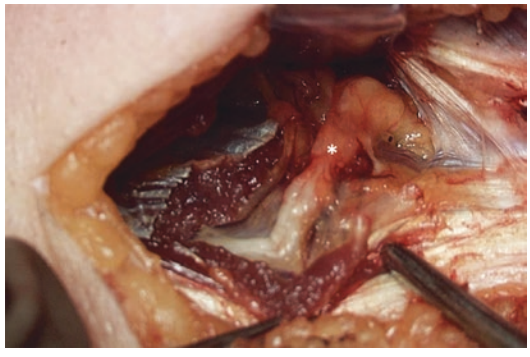

Fig. 35.5 The asterisk (*) highlights the section of PIN hyperaemia where the nerve was compressed under the Arcade of Frohse. (© G. Hoy)

Fig. 35.7 The abnormal tendinopathic tissue of ECRB is excised (© G. Hoy)

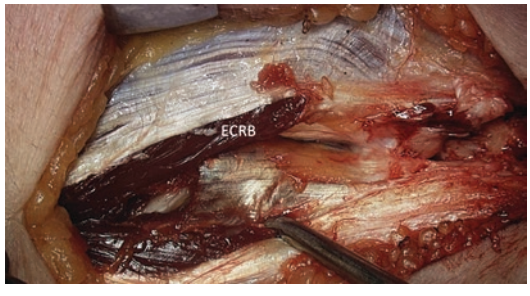

Fig. 35.6 Following complete PIN neurolysis, the proximal edge of ECRB is palpated with a finger and if thought to be a potential source of compression, the fascial edge is released/excised (© G. Hoy)

Fig. 35.8 Final repair of ECRB is shown (© G. Hoy)

injury when releasing the overlying supinator. The nerve runs obliquely from proximal medial to distal lateral, and perpendicular to the fibres of the superficial supinator.

35.7 Pitfalls

- Care must be taken to avoid injury to the PIN or the more proximal branches of the radial nerve.
- A posterior approach may not be appropriate in cases of more proximal nerve compression.

35.8 Post-operative Rehabilitation

When radial nerve decompression is performed in conjunction with lateral epicondylitis surgery, a post-operative volar wrist splint is applied for 6 weeks to protect common extensor origin repair. The patient is seen by the hand therapist within 7 days and gentle active ROM protocol is initiated. The splint is removed at 6 weeks and unrestricted ROM is allowed. A graduated strengthening programme is initiated at 3 months. Return to work is allowed at 6 weeks for non-manual workers and at 12 weeks for manual workers.

35.9 Complications

- Neurovascular injury
  - Radial nerve and its branches
  - Recurrent radial vessels/leash of Henry
- Persistent pain
- Chronic regional pain syndrome (CRPS)

References

1. Stroh AB, Zelouf DS. Ulnar tunnel syndrome, radial tunnel syndrome, anterior interosseous nerve syndrome, and pronator syndrome. J Am Acad Orthop Surg. 2017;25(1):e1–e10. https://doi.org/10.5435/JAAOS-D-16-00010.
2. Morrey BF. Reoperation for failed surgical treatment of refractory lateral epicondylitis. J Shoulder Elb Surg. 1992;1(1):47–55.
3. Naam NH, Nemani S. Radial tunnel syndrome. Orthop Clin N Am. 2012;43:529–36.
4. Verhaar J, Spaans F. Radial tunnel syndrome: an investigation of compression neuropathy as a possible cause. J Bone Joint Surg. 1991;73A:539–44.
5. Rosén I, Werner CO. Neurophysiological investigation of posterior interosseous nerve entrapment causing lateral elbow pain. Electroencephal Clin Neurophysiol. 1980;50:125–33.
6. Wilson JM, Runner R, McClelland WB, McGillivary G. Misdiagnosis and radial tunnel syndrome: considering the distal biceps tendon. J Surg Orthop Adv. 2019;28(1):35–40.
7. Sarris IK, Papadimitriou NG, Sotereanos DG. Radial tunnel syndrome. Tech Hand Up Extrem Surg. 2002;6(4):209–12.
8. Perez CS, Medrano BG, Mateos JIR, Martin BC, Marin OF, Ferrero MAM. Radial tunnel syndrome: results of surgical decompression by a postero-lateral approach. Int Orthop. 2014;38(10):2129–35.
9. Caetano EB, Vieira LA, Sabongi Neto JJ, Caetano MBF, Sabongi RG, Nakamichi YDC. Anatomical study of radial tunnel and its clinical implications in compressive syndromes. Rev Bras Ortop (Sao Paulo). 2020;55(1):27–32.
10. Konjengbam M, Elangbam J. Radial nerve in the radial tunnel: anatomic sites of entrapment neuropathy. Clin Anat. 2004;17(1):21–5.
11. Clavert P, Lutz JC, Adam P, Wolfram-Gabel R, Liverneaux P, Kahn JL. Frohse's arcade is not the exclusive compression site of the radial nerve in its tunnel. Orthop Traumatol Surg Res. 2009;95(2):114–8.
12. Shamrock AG, Das JM. Radial tunnel syndrome. [Updated 2020 Apr 13]. In: StatPearls [Internet]. Treasure Island, FL: StatPearls Publishing; 2020. Available from: https://www.ncbi.nlm.nih.gov/books/NBK555937/

36 Lateral Epicondylitis and Symptomatic Minor Instability of the Lateral Elbow (SMILE)

Francesco Luceri, Davide Cucchi, Paul Muriithi Miano, Paolo Arrigoni, and Pietro Simone Randelli

36.1 Background

Lateral elbow pain (tennis elbow) is an overuse injury involving the extensor muscles that originate on the lateral epicondylar region of the distal humerus. Lateral epicondylitis is not an inflammatory disease and generally considered to be an extra-articular condition involving degeneration and tendinosis of the common extensor origin, with the extensor carpi radialis brevis (ECRB) being the most commonly affected tendon. The lateral collateral ligament (LCL) complex is formed by three components: R-LCL, ulnar lateral collateral ligament (U-LCL), and annular ligament. The R-LCL and the most proximal tendon fibers of the ECRB are parallel and overlapping in their proximal insertion. Open or arthroscopic release of the common extensor origin can cause iatrogenic injury to the LCL complex resulting in posterolateral rotatory instability (PLRI). ECRB debridement or release through open, percutaneous, and arthroscopic approaches is generally considered the gold standard surgical treatment for recalcitrant lateral epicondylitis. However, success rates ranging between 65% and 95% suggest that these approaches may not precisely address the underlying pathologic process.

The arthroscopic approach to the elbow joint has demonstrated the presence of potentially pathological intra-articular findings associated with ECRB tendinopathy. The presence of laxity signs within the lateral compartment of the elbow, in conjunction with these intra-articular abnormalities, supports the existence of a symptomatic minor instability of the lateral elbow (SMILE), in which the role of the R-LCL is important as a lateral static stabilizer [1].

Francesco Luceri and Davide Cucchi contributed equally to this work. Paolo Arrigoni and Pietro Simone Randelli equally contributed to this paper as Senior Authors.

F. Luceri
U.O.C. Clinica Ortopedica e Traumatologica Universitaria CTO, Azienda Socio Sanitaria Territoriale Centro Specialistico Ortopedico Traumatologico Gaetano Pini-CTO, Milan, Italy

D. Cucchi
Department of Orthopaedics and Trauma Surgery, Universitätsklinikum Bonn, Bonn, Germany

Department of Biomedical Sciences for Health, Università degli Studi di Milano, Milan, Italy

P. M. Miano
P.C.E.A Kikuyu Hospital, Kikuyu, Kenya

P. Arrigoni (✉) · P. S. Randelli
Department of Biomedical Sciences for Health, Università degli Studi di Milano, Milan, Italy

U.O.C. Clinica Ortopedica e Traumatologica Universitaria CTO, Azienda Socio Sanitaria Territoriale Centro Specialistico Ortopedico Traumatologico Gaetano Pini-CTO, Milan, Italy

Research Center for Adult and Pediatric Rheumatic Diseases (RECAP-RD), Department of Biomedical Sciences for Health, Università degli Studi di Milano, Milan, Italy

© ISAKOS 2022

D. N. Bhatia et al. (eds.), *Arthroscopy and Endoscopy of the Elbow, Wrist and Hand*,
https://doi.org/10.1007/978-3-030-79423-1_36

36.1.1 Surgical Anatomy

Recalcitrant lateral elbow pain is frequently associated with abnormal intra-articular findings, which could be related to a condition of patholaxity termed "SMILE." This condition may result from repetitive low-energy stress or shear as occurs in simple, repetitive, or prolonged daily or working activities performed with the shoulder in moderate abduction, pronation of the hand, and 50°–70° of elbow flexion, a position in which hand and the forearm create a varus/pronation moment on the lateral elbow. With time, this could result in progressive stretching and elongation of the radial component of the LCL (R-LCL) and of the annular ligament, with relative hypermobility of the radial head. Minor incongruence of the proximal radioulnar joint results in radial head impingement with the notch in pronation, and eventual radial head chondropathy, inflammation, and subsequent synovitis. Finally, abrasion of the stretched R-LCL and anterolateral capsule due to friction over the lateral portion of the capitellum can cause chondropathies of the lateral aspect of the capitellum and capsular tears.

In this pathologic cascade, the extensor carpi radialis brevis (ECRB) is considered to act as a dynamic stabilizer, resisting varus forces in support of a deficient or lax R-LCL: ECRB tendinopathy could therefore be intended as the final consequence of repetitive loads and overuse on the R-LCL. With time, this varus/pronation moment created by the hand and the forearm could lead to elongation of the R-LCL and annular ligament The ECRB proximal insertion is located just extracapsular and parallel to R-LCL, in intimate association but easily distinguishable with the lateral collateral ligament. Within the SMILE theory, ECRB tendinopathy could be considered a consequence of R-LCL elongation, as this structure acts as an extra-articular secondary stabilizer resisting varus pronation stresses. Strain on this ligament with the secondary bracing effect of ECRB activity provides the rationale for R-LCL plication. The goal of R-LCL plication is to surgically constrain an intra-articular structure and to stabilize a joint compartment, as similarly described in other joints with satisfactory results.

Future studies will help to confirm this theory and investigate if the pathologic cascade is initiated extra-articularly (from ECRB) and subsequently becomes intra-articular (generating ligamentous laxity and associated lesions), or indeed the opposite. Proving one or the other origin could help to intervene conservatively in the very first symptomatic phase, avoiding progression of the symptoms.

36.2 Indications and Contraindications

Approximately 90–95% of patients with lateral epicondylitis respond to conservative measures and do not require surgical intervention. Patients whose condition is unresponsive to 3–6 months of conservative therapy (e.g., corticosteroid injections, splinting, and occupational therapy) are candidates for surgical treatment.

There are no absolute contraindications for surgical treatment of lateral epicondylitis. Relative contraindications include any comorbidity that would place the patient at a higher level of surgical risk.

36.3 Surgical Technique

The patient is placed in the lateral decubitus position.

- Posterior compartment arthroscopy is performed first. A complete inspection of the posterior compartment of the joint includes the posterior capitellum, the posterior trochlea, the olecranon fossa, and the tip of the olecranon. The integrity of cartilage, ligaments, capsule, and tendons is assessed, and the presence of loose bodies or other pathologic conditions is noted. Ligament lesions if present must be immediately repaired.
- The anterior compartment is accessed by proximal anteromedial (AM) and anterolateral (AL) portals. The AL portal is used to insert a retractor aimed toward the radiocapitellar joint to protect the posterior interosseous nerve, which lies just anterior to the capsule at

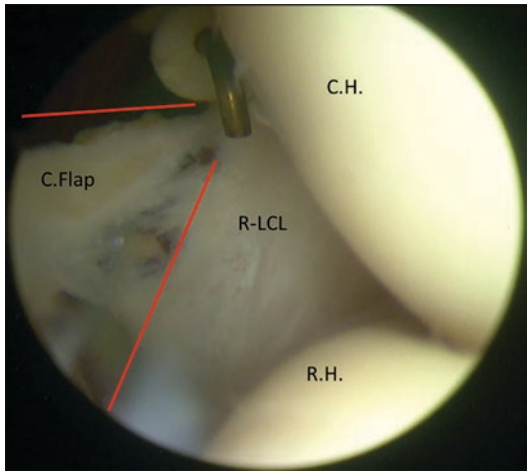

Fig. 36.1 V-shaped capsular flap to reach the extra-articular aspect of elbow. This flap allows an arthroscopic view of the complete R-LCL. (Reprinted by permission from Elsevier Inc.: Arthroscopy: The Journal of Arthroscopic & Related Surgery; Arrigoni et al. [3], Copyright © 2014 Arthroscopy Association of North America)

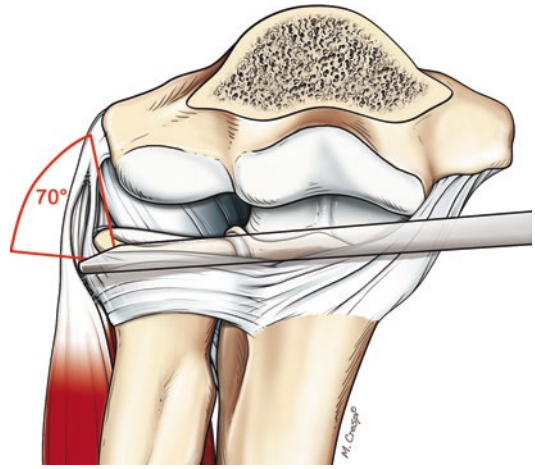

Fig. 36.2 The position of a 70° arthroscope looking toward the lateral compartment. (Reprinted by permission from Elsevier Inc.: Arthroscopy: The Journal of Arthroscopic & Related Surgery; Arrigoni et al. [3], Copyright © 2014 Arthroscopy Association of North America)

this level [2]. At this point the R-LCL is not identifiable as an isolated structure but appears as a thickening of the capsule.

- A limited anterolateral V-shaped capsulotomy is performed with a hooked electrocautery device introduced through the standard anterolateral portal (Fig. 36.1) under visualization with a 30° arthroscope. The superior arm of the "V" is performed parallel to the distal humerus, whereas the inferior arm is parallel and anterior to the R-LCL. The R-LCL is seen as a thickening of the capsule and better visualized by tensioning the capsule in pronation. If visualization is still difficult, the ideal location of the R-LCL is projected and capsulotomy is performed anterior to that. Care should be taken to perform the capsulotomy with the forearm in pronation to tension the R-LCL and facilitate the protection of this structure. Pronation also offers a second advantage of moving the posterior interosseous nerve further medial to the surgical area [2]. The inferior limit of the capsulotomy is approximately 0.5–1 cm superior to the radial head. Switching to a 70° arthroscope from the 30° scope gives a better visualization and the arthroscope can be advanced into the window created by the capsulotomy [3]. This offers a frontal view of the most lateral aspect of the lateral compartment with the capsule/R-LCL defining the articular side and the tendon fibers of the ECRB on the extra-capsular side (Fig. 36.2).
- The hook electrode is then advanced through the anterolateral portal. After ECRB tendon release, the posterior common extensor origin is assessed. This is located as an independent structure more posterior to the ECRB tendon at the very end of the 70° camera field. The tendon is probed to check the integrity of the common extensor origin (Fig. 36.3).
- Based on the SMILE concept, lateral epicondylitis due to tendinosis of the ECRB is usually preceded with laxity of the LCL; arthroscopic plication of the LCL is therefore an alternative treatment option to ECRB release. During elbow arthroscopy the patholaxity noted of the LCL can be evaluated using the three signs of laxity: the "annular drive-through" (ADT), the "Loose Collar Sign" (LCS), and the "R-LCL pull-up Sign" (RPS) [1]. Other pathologic findings include synovitis anterior to the radial head, anterolateral capsular tears, and chondropathy of either the radial head or the lateral portion of the capitellum. Patients, who present at least one of the previous signs of minor instability in

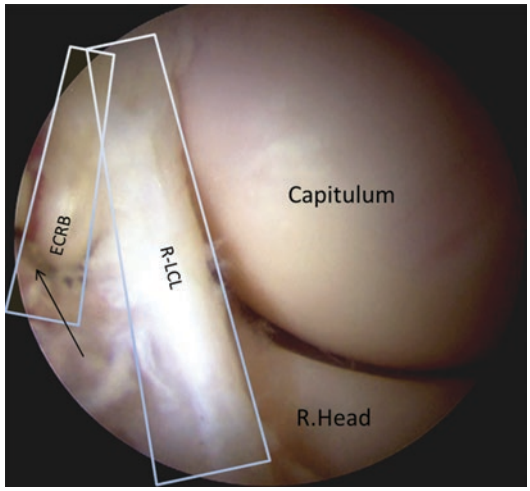

Fig. 36.3 Arthroscopic intraoperative picture after ECRB release of right elbow. The arrow shows the gap left after tendon release. The ECRB tendon stump is visible in the upper part of the figure (*CH* capitellum humerus, *RH* radial head). (Reprinted by permission from Elsevier Inc.: Arthroscopy: The Journal of Arthroscopic & Related Surgery; Arrigoni et al. [3], Copyright © 2014 Arthroscopy Association of North America)

addition to one or more intra-articular associated lesions, are considered eligible for R-LCL plication (Fig. 36.4).

- To perform plication, a suture anchor is inserted high and lateral in the anterolateral aspect of the capitellum at the capsular insertion. Sutures are passed into the R-LCL beyond a level anterior to the mid-point of the radial head and approximately 0.5 cm proximal to the radiocapitellar joint line. Sutures are then retrieved from the anterolateral portal and a standard sliding knot is performed, ensuring that it lies extra-articularly (see Chap. 12). Debridement of any synovitis or chondral irregularity is then performed and a re-assessment for any residual sign of laxity then undertaken.

36.4 Postoperative Management and Rehabilitation

Patients who have undergone arthroscopic ECRB release for lateral epicondylitis are discharged from the operating room with a sling. The ice, bandage, and dressing are removed on the third day after surgery. The sling is worn for

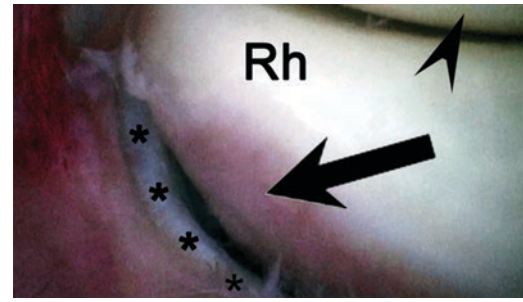

Fig. 36.4 Loose collar sign (LCS). Radial neck exposure under the cartilaginous area (arrow) may be associated with annular ligament redundancy and laxity (asterisks). Right elbow anteromedial view; Rh radial head. (Reprinted by permission from Springer Nature Customer Service Centre GmbH: Springer Nature; Knee Surgery, Sports Traumatology, Arthroscopy; Arrigoni et al. [1], Copyright © 2017, Springer Nature)

1 week and then discarded. Light active range of motion is encouraged after the sling is discontinued. During the first 6 weeks the patients are taught to stretch the wrist extensor muscles with the elbow extended, the forearm pronated, and the wrist and fingers flexed. Caution should be exercised to avoid overuse.

In patients who have undergone plication of the R-LCL, rehabilitation protocol is less aggressive. After surgery, an elbow brace locked at 90° of flexion is placed for just 10 days to allow soft tissues to heal. From day 10–20, range is limited to 30° of extension and free flexion. From day 20, patients are encouraged to obtain full passive ROM with physiotherapy assistance. Active wrist, elbow, and shoulder range of motion exercises are progressively initiated. After 4 weeks, strengthening exercises are begun. Varus stress is not allowed until 4 months after surgery.

36.5 Complications

- The most common complications after ECRB release are incomplete release and nerve injuries. The first one causes the persistence of a residual pain. Nerve injuries can range from a transient to a permanent neurologic deficit.
- Stiffness including loss of extension is possible.
- ECRB debridement or release through open, percutaneous, and arthroscopic approaches

for recalcitrant lateral epicondylitis may not precisely address the underlying pathologic process according to the SMILE that may lead to persistent micro-instability of the lateral elbow and persistent lateral elbow pain.

- Iatrogenic injury of the LCL complex can also predispose the elbow to posterolateral rotatory instability.

References

1. Arrigoni P, Cucchi D, D'Ambrosi R, Menon A, Aliprandi A, Randelli P. Arthroscopic R-LCL plication for symptomatic minor instability of the lateral elbow (SMILE). Knee Surg Sports Traumatol Arthrosc. 2017;25(7):2264–70. https://doi.org/10.1007/s00167-017-4531-9.
2. Arrigoni P, Cucchi D, Menon A, et al. The posterior interosseous nerve crosses the radial head midline and increases its distance from bony structures with supination of the forearm. J Shoulder Elb Surg. 2019;28(2):365–70. https://doi.org/10.1016/j.jse.2018.08.019.
3. Arrigoni P, Fossati C, Zottarelli L, Brady PC, Cabitza P, Randelli P. 70° Frontal visualization of lateral compartment of the elbow allows extensor carpi radialis brevis tendon release with preservation of the radial lateral collateral ligament. Arthroscopy. 2014;30(1):29–35. https://doi.org/10.1016/j.arthro.2013.09.078.

Part VII

Elbow: Arthritis and Contractures

Classification of Elbow Stiffness

37

Alessandro Marinelli, Enrico Guerra,
Gregory I. Bain, and Roberto Rotini

37.1 Background

Stiffness is a clinical sign that can be caused by a variety of elbow disorders. The most common origin is post-traumatic, and others include burns, head injuries, and elbow surgeries. Elbow stiffness also can be caused by atraumatic etiologies, such as osteoarthritis, inflammatory joint disease, infection, metabolic disease (e.g., hemophilia), and congenital conditions (arthrogryposis).

37.2 Classification

When classifying elbow stiffness, it important to recognize the notion of time spanning the initial insult, the healing response, and the secondary changes. After an initial insult (such as an intra-articular fracture), a healing response begins and soft tissue contracture is initiated. Additionally, secondary articular degeneration, heterotopic ossification formation, and ulnar nerve symptoms may occur and these factors can further affect the severity and the prognosis of stiffness.

Several classification systems have been developed for elbow stiffness, and are based on the following parameters.

37.2.1 Plane of Motion

Stiffness can be classified according to whether it affects flexion-extension, pronation-supination, or both planes of motion. This classification system is practical for evaluating patient impairment and for planning surgery (Fig. 37.1).

37.2.2 Severity

In this system, the contracture is classified into four grades on the basis of the flexion-extension arc of motion: minimal (>91°), moderate (61°–90°), severe (31°–60°), or very severe (<30°). This classification is simple and practical for assessment, prognosis, and surgical decision-making. The grading can also be used to evaluate impairment and improvement.

Images are original.

A. Marinelli (✉) · E. Guerra · R. Rotini
Shoulder and Elbow Unit, Istituto Ortopedico Rizzoli, Bologna, Italy
e-mail: alessandro.marinelli@ior.it; enrico.guerra@ior.it; roberto.rotini@ior.it

G. I. Bain
Flinders University and Finders Medical Center, Adelaide, SA, Australia
e-mail: greg@gregbain.com.au

© ISAKOS 2022

D. N. Bhatia et al. (eds.), *Arthroscopy and Endoscopy of the Elbow, Wrist and Hand*,
https://doi.org/10.1007/978-3-030-79423-1_37

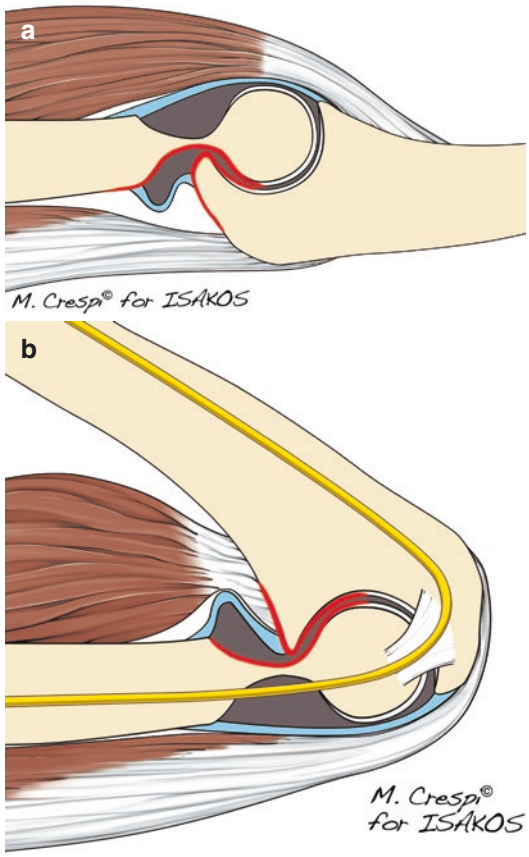

Fig. 37.1 Elbow anatomical factors that can restrict extension (left) and flexion (right) are illustrated. (**a**) Elbow extension can be restricted by contractures in flexor muscles or within the anterior capsule (blue), as well as posterior bony impingement (red) (M. Crespi © for ISAKOS). (**b**) Elbow flexion may be restricted by contractures within the triceps muscle, posterior capsule (blue) or posterior band of MCL (white). Anterior osseous impingement and ulnar nerve symptoms can contribute to restriction of elbow flexion (red) (M. Crespi © for ISAKOS)

37.2.3 Etiology

Elbow stiffness can be classified on the basis of etiology as post-traumatic, micro-traumatic, degenerative or inflammatory, neurogenic, and others (congenital, tumor, burns, infection, etc.). This system is useful for decision-making for treatment.

37.2.4 Prognosis

Jupiter et al. divided post-traumatic elbow stiffness into two categories: simple and complex [1]. Simple stiffness is characterized by mild to moderate contracture (motion >80°), no prior surgery, minimal heterotopic ossification, and a well-preserved osseous anatomy. Complex stiffness is associated with nerve dysfunction, prior nerve transposition, retained hardware, substantial heterotopic ossification, articular incongruity, and an arc of motion <80°. This system is useful for evaluating the risks and benefits of surgical treatment as the complex form is associated with a higher surgical complication rate and requires more expertise.

37.2.5 Anatomical Location

Morrey classified elbow stiffness in three categories on the basis of anatomical location and etiology [2].

- Extrinsic factors (i.e., extra-articular factors that spare the joint space) include capsular-ligament contracture, muscle/tendon retraction, ulnar nerve neuropathy, heterotopic ossification, and skin contracture.
- Intrinsic factors (i.e., intra-articular factors) include intra-articular adhesions and deformities, cartilage lesions, loose bodies, and impinging osteophytes.
- Mixed: These have both intrinsic and extrinsic elements.
- Until now, this system has been the most commonly used tool for the classification of joint stiffness.

In 2010, Watts and Bain [3] recommended that the capsule be considered a separate category as it is a separate anatomical structure with a different etiology, treatment, and prognosis. Isolated capsular contractures can be caused by immobilization or hemarthrosis. Capsular contractures also are commonly noted in association with

intra-articular pathologies. In elbow stiffness, capsular contracture is often the main problem to be addressed as it is uniquely positioned to interact with both the intra-articular and extra-articular factors.

With the incorporation of the capsule as a separate category and the addition of neurological factors, a new all-inclusive classification (Table 37.1) can be proposed; this includes all causes of elbow stiffness, and not only the post-traumatic ones. Moreover, with the correct identification of the pathological process present in each area, this classification allows the surgeon to address each component, and tailor the appropriate treatment. Intra-articular pathologies can be managed with joint arthroscopy (e.g., chondral flaps, loose bodies, impinging osteophytes, or synovitis). In advanced cases, simple debridement is unlikely to be successful and a joint arthroplasty may be necessary. Capsular contractures can be treated with open or arthroscopic release or resection, usually with a good outcome. Extra-articular pathologies (e.g., heterotopic ossification, ulnar nerve neuropathy, and muscle/tendon contractures) are usually treated with an open procedure with resection or release of the offending structures. Endoscopic treatment for these conditions is possible but is still evolving. Cases with mixed causes require each area be specifically addressed.

In 1998, Kay [4] proposed a practical classification for post-traumatic stiffness of the elbow

Table 37.1 All-inclusive pathoanatomical classification of elbow stiffness

Intra-articular (Bearings)	Capsular (constraints)	Extra-articular Levers) (Motor, cable,	Neurologic (Control, electrics, sensors)
Articular surface involvement (osteochondral defect, degeneration)	Ligaments involvement: (contracture, calcifications)	Muscle involvement: (myopathy, fatty infiltration)	Central nervous system involvement (behavioral dystonia, spasticity)
Subchondral dysplasia, fractures, avascular necrosis, degeneration	Capsular involvement: (contracture, calcifications)	Tendons and bursa involvement (tear, calcifications degeneration, bursitis)	Peripheral nervous system involvement (ulnar, radial, medial nerve symptoms; cutaneous nerves neuritis or neuropathy)
Synovium Inflammatory, crystal arthroplasty	Congruity-related findings (subluxation, dislocation)	Other findings external to elbow: fracture, malignancy, heterotopic ossification, skin contracture	Sensory and autonomic findings: (Charcot joint, chronic regional pain syndrome)

that was based on the presence, severity, and combination of the three most common factors causing stiffness (capsular contracture, articular fractures, heterotopic ossification), and identified five clinical situations.

37.2.6 S.T.I.F. Classification

More recently, the authors have developed a new classification in collaboration with Shawn O'Driscoll from the Mayo Clinic (Table 37.2) [5, 6]. The S.T.I.F. (**S**tiffness **T**ypes and **I**nfluencing **F**actors) classification system highlights five common disorders causing stiffness as well as the six influencing factors that often effect the treatment and clinical outcome.

The S.T.I.F. classification system also highlights the importance of the ulnar nerve, which can be entrapped in the cubital tunnel by scar tissue or heterotopic ossification and is at risk during the surgical treatment of the elbow stiffness.

37.3 Treatment Algorithm

Based on the S.T.I.F. Classification system, it is possible to propose a treatment algorithm that includes the severity of the disorders as a guide to surgical treatment and the preferred operative approach (open or arthroscopic) (Table 37.3).

In summary, the new classification system highlights the etiology of elbow stiffness, and provides a framework to better understand the natural history, direct the surgical management, and interpret the likely clinical outcomes.

Table 37.2 The S.T.I.F. system details the five common causes of stiffness, and the six influencing factors

S.T.I.F. classification stiffness types & influencing factors	
Prevalent type of stiffness	Treatment and prognosis influencing factors
1 Soft tissue contracture	a Ulnar nerve symptoms
2 Arthritis	b Hardware / prior surgery
3 H.O.	c LCL / MCL calcification
4 Malunion / non-union	d Skin contracture
5 Chronic subluxation	e Articular pain
	f Loose bodies

Table 37.3 The S.T.I.F. treatment algorithm for elbow stiffness

Decisional treatment algorithm for elbow stiffness release		
Prevalent type of stiffness	Surgery	Approach
1 Soft tissue contracture	- Release - Release (column procedure)	Scope open
2 Arthritis	Mild or Moderate arthritis - Osteo-capsular arthroplasty Severe arthritis - Biologic interposition / Distraction arthroplasty (External Fixators) - TEA (> 70ys)	Scope open combined Open
3 H.O.	- Removal	Open
4 Malunion / non-union	- ORIF / Osteotomy - TEA (> 70ys)	Open
5 Chronic subluxation	- Rad. Head / Coron. / Ligam. reconstr. / External Fixators - TEA (> 70ys or not possible reconstruction)	Open

The type of stiffness, its severity, and the age of the patient are all factors that direct the preferred type of surgery
H.O. heterotopic ossification, *TEA* total elbow arthroplasty, *ORIF* open reduction and internal fixation

References

1. Jupiter JB, O'Driscoll SW, Cohen MS. The assessment and management of the stiff elbow. Instr Course Lect. 2003;52:93–111.
2. Morrey BF. The posttraumatic stiff elbow. Clin Orthop Relat Res. 2005;431:26–35.
3. Watts AC, Bain GI. New techniques in elbow arthroscopy. In: Savoie FH, Field LD, editors. AANA advanced arthroscopy: the elbow and wrist. Philadelphia: Saunders-Elsevier; 2010. p. 124–31.
4. Kay NR. Arthrolysis of the post-traumatic stiff elbow. In: Stanley D, Kay NR, editors. Surgery of the elbow. London: Arnold; 1998. p. 228–34.
5. Marinelli A, Bain GI. The stiff elbow: classification and treatment algorithm. ISAKOS Newsl. 2018;2:18–21.
6. Guerra E, Kelberine FM, Marinelli A, Rotini R, Bain G. The stiff elbow: classification and treatment algorithm. In: Bain G, Eygendaal D, van Riet R, editors. Surgical techniques for trauma and sports related injuries of the elbow. Berlin: Springer; 2020.

38 Arthroscopic Adhesiolysis in a Stiff Elbow

L. A. Pederzini, F. Serafini, F. Nicoletta, and A. Celli

38.1 Background

In 1981, Morrey [1] established that the functional range of motion (ROM) of the elbow is 30°–130° of flexion. However, many daily activities, work or sports, require greater extension or flexion (e.g., use of mobile phones) [2, 3]. In light of this, there has been an increase in the indications for the treatment of the stiff elbow. Despite improvements in the treatment of elbow injuries, 12% of traumatic injuries (fractures, dislocations, and tears of the distal biceps tendon) result in stiffness and need surgical treatment [4]. Wilson [5] introduced "open" arthrolysis in post-traumatic elbow stiffness in 1944, and ever since several surgical techniques have been outlined. Clinical results of these techniques in recent literature are consistent; improvements in elbow motility in nearly all patients has been reported (average gain of 52°), and in most cases, functional range of 30°–130° was possible [6–11].

Arthroscopy is more frequently used for the diagnosis and treatment of elbow pathologies, despite being considered a complex joint to examine arthroscopically [12, 13]. Increasing knowledge and skills, associated with technological improvement, has recently led to a standardization of techniques and indications. Arthroscopic arthrolysis, associated with debridement, has become a safe and effective treatment for the rigid elbow, with an improvement in flexion, extension, and "scores" in joint functionality assessment, in specific cases. "Open" surgical arthrolysis has been the "gold standard" in the treatment of elbow stiffness for years. This technique can yield good clinical results, but may also cause hematoma, large skin and muscle scars, soft tissue and nerve injuries, and heterotopic ossification [2, 14, 15].

Arthroscopic arthrolysis has significantly improved, along with the development of surgical techniques and medical equipment; however, this is a demanding procedure, as the neurovascular structures cannot be observed from the portals and the working space is limited [16, 17].

38.2 Indications and Contraindications

While post-traumatic elbow stiffness is closely related to recent trauma (<1 year), cases of degenerative elbow stiffness can be caused by "overuse syndrome," primary arthrosis changes, or previous injuries (>1 year).

- A patient can be eligible for arthroscopic adhesiolysis in case of the following signs:

L. A. Pederzini (✉) · F. Serafini · F. Nicoletta
Sassuolo Hospital, Sassuolo, Italy
e-mail: f.nicoletta@ospedalesassuolo.it

A. Celli
Hesperia Hospital, Modena, Italy

© ISAKOS 2022

D. N. Bhatia et al. (eds.), *Arthroscopy and Endoscopy of the Elbow, Wrist and Hand*,
https://doi.org/10.1007/978-3-030-79423-1_38

reduction of articulation, impaired sports and work activities, restricted joint space, absence or minimal joint incongruity, decreased arthrosis and osteophytes, and no benefits reported after 6 months of conservative treatment (e.g., use of splints, mobilization, and physical therapy).

- Arthroscopy can be useful if associated with "open" surgery to avoid wide surgical access. Occasionally, it is possible to associate the removal of synthesis means (column plate and screws) with arthroscopic adhesiolysis.
- "Overuse syndrome" can cause degenerative elbow changes in manual workers and sportsmen in whom repetitive training and heavy work can lead to early cartilage joint alterations [18]. Baseball pitchers, tennis and basketball players, weight lifters, and boxers are among the mostly affected by early degeneration.
- Early stages of rheumatoid arthritis and osteochondropathies are among the pathologies which require arthroscopic treatment. Osteophytes, synovitis, and loose bodies are anatomic-pathological findings of previous trauma, and result in an alteration of the joint biomechanics and degeneration. In these case, surgical treatment includes both adhesiolysis and the removal of osteophytes and loose bodies.

Arthroscopic treatment is not indicated in patients with muscle spasticity, cerebral palsy, burns, previous surgical operations that may have altered the normal anatomy, heterotopical ossifications, ossifying myositis, algodystrophy, joint instability, joint disjunction, and rigidity caused by infections.

38.3 Surgical Technique

The anesthetist identifies the nerve trunks with an electrostimulator or ultrasound and places a nerve catheter without injecting the anesthetic. Subsequently, general anesthesia is administered and an accurate evaluation of the ROM and ligament balance is performed. With the patient in a supine position, the tourniquet is positioned at the root of the arm and inflated with a pressure of

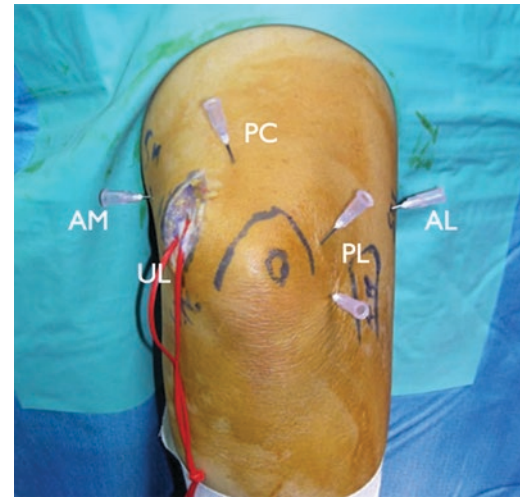

Fig. 38.1 Portals used in adhesiolysis are shown. The ulnar nerve (UL) is isolated and protected (*AM* anteromedial postal, *AL* anterolateral portal, *PC* posterocentral portal, *PL* posterolateral portals)

250 mmHg. Thereafter, the patient is positioned prone, with the shoulder abducted at 90°, the elbow flexed at 90°, and the arm supported and firmly fastened to the operating bed. The sterile field is prepared and the medial and lateral epicondyle, ulnar nerve, and radial capital of the elbow are marked (Fig. 38.1).

- Neurolysis of the ulnar nerve is the first step of the intervention. This is necessary to prevent traction on the nerve itself during intraoperative flexion and extension tests. Neurolysis of the ulnar nerve is performed in all cases in patients with a 100° flexion deficit and through an incision of about 3 cm.
- Five portals are used (three posterior and two anterior). The "soft-spots" of the posterior, proximal anteromedial (AM) and proximal anterolateral (AL) portals are identified.
- Arthroscopy of the posterior section is initially performed via the posterolateral (PL) portal. A second portal is then placed 1.5 cm proximal to the latter. These two portals allow the use of the arthroscope and shaver simultaneously in the posterior compartment. The distension of the joint capsule is ensured by a pump set at 35–40 mmHg.
- After examination of the proximal radioulnar joint (posteriorly), a third transtriceps portal is

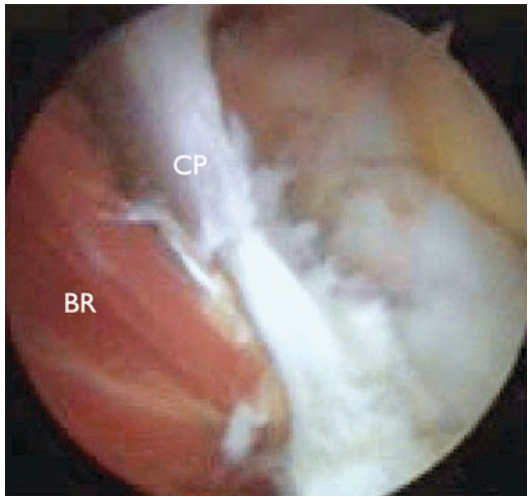

Fig. 38.2 Arthroscopic view of anterior compartment residual capsule (CP) and brachialis muscle (BR) are shown after anterior capsulectomy

placed in the olecranon fossa. A complete debridement of the humerus, lateral olecranon, and olecranon fossa is performed along with the removal of the loose bodies to allow an improved sliding of the articular surfaces.

- Next, the anterior compartment is evaluated; the arthroscope is inserted from the AM portal, and a shaver is inserted via a cannula in the AL portal for anterior debridement. In many cases, the presence of a thick capsule requires an anterior capsulectomy, which is initially implemented with the "shaver," although it is mostly performed with a basket forceps, about 1 cm proximal to the apex of the coronoid (Fig. 38.2).
- At the end of arthroscopy, the elbow range of motion is evaluated. One or two suction drains are positioned and portals are sutured. The elbow is immobilized with an extension splint. Once the patient is awakened, a neurological evaluation is performed and thereafter a peripheral block is administered.

38.4 Postoperative Management and Rehabilitation

On the first postoperative day, patients begin passive elbow mobilization (CPM) for 20 min per session. This is repeated four times, and is associated with one physiotherapy session of 60 min duration. On the second day, passive and active self-assisted mobilization in flexion-extension is initiated. The drains are removed on the third day, and rehabilitation is continued.

Tranexamic acid is administered at a dosage of 10 mg/kg, 30 min before surgery, and thereafter 3, 6, 24, and 48 h after surgery. In addition, oral steroids may be administered.

Once discharged, patients are given directions on the exercises to perform at home. The rehabilitation program with the therapist must be continued for 3 months.

38.5 Tips and Tricks

The effectiveness of arthroscopic debridement is widely demonstrated in literature [19–24]. This procedure can be performed with or without anterior capsulectomy. However, arthroscopic treatment without performing capsulectomy has shown satisfactory results [20, 24]. The advantages of a broader removal of the anterior capsule include a considerable recovery of movement, removing a constraint on elbow extension and preventing a relapse of the hypertrophic scar contracture [25]. Capsulectomy can also provide improvement in pain due to the partial denervation of the articular branches of the median, radial, and ulnar nerves.

38.6 Pitfalls

Theoretically, due to the proximity of neurovascular structures, capsulectomy could be associated with a greater risk of neurovascular lesions compared to capsulotomy or capsular preservation. It is worth bearing in mind that, near the joint, the radial nerve is more medial than its most proximal part and is relatively protected by the brachial muscle, whereas the posterior interosseous nerve is very close to the head of the radius and, consequently, at risk. Occasionally, the surgeon may choose to keep a capsule portion in this area to avoid iatrogenic nerve damage [26].

38.7 Results

In a recent study, Isa et al. [27] suggested that debridement for primary elbow osteoarthritis yields satisfactory motion at short-term follow-up with or without a capsulectomy. According to the authors, capsulectomy is not systematically necessary in the treatment of elbow stiffness, but is performed only in cases where capsulotomy does not improve the range of movement.

Hildebrand et al. [28] found an association between increased numbers of myofibroblasts and post-traumatic joint contractures and suggested that the capsule itself plays a crucial role in post-traumatic elbow stiffness compared to patients with primary osteoarthritis, where the formation of osteophytes is the main limiting factor for mobility.

Adams et al. [19] obtained an average gain of 27° in the flexion-extension range, and Galle et al. [20] found an improvement in the flexion-extension arc by 22° following arthroscopic treatment with associated capsulotomy. Similarly, Van Zeeland et al. [29] found an average improvement in the range of motion of 41.5°.

Between 2004 and 2008, the authors performed arthroscopy on 243 patients both with post-traumatic and degenerative elbow stiffness [12]. The results showed an average improvement in the range of flexion-extension movement of 33° in the post-traumatic stiffness group and 20° in the osteoarthritis group. The debridement of the posterior section, often associated with anterior capsulectomy, improves extension. On the other hand, flexion is enhanced by posterior capsulectomy and removal of the anterior humeral osteophytes and remodeling of the hypertrophic coronoid. However, flexion may be limited by a retraction of the medial collateral ligament; in these cases, the ideal treatment choice is to release the posterior band of the ligament through the incision made for the neurolysis of the ulnar nerve.

A further approach for preventing flexion contractures in the elbow can be changing the inflammatory process. In an experimental model, Hildebrand [30] pointed out how the administration of Ketotifene reduces the number of myofibroblasts and "mast cells" by 57% and 65%, respectively. A steroid injection at the end of the procedure could improve the clinical result; however, it has been shown that this procedure increases the risk of infections by about three times [31, 32].

Complications are currently rare. Initially, arthroscopic capsular release of the elbow was associated with peripheral nerve injuries [29]; however advanced techniques have led to an overall improvement in the safety of surgical treatment. Haapaniemi et al. [33] reported a case of injury both of the radial and median nerve. Jones et al. [34] published a study of 12 patients treated with arthroscopic capsular release, one of whom subsequently required manipulation, while, in a second case, permanent posterior interosseous nerve deficiency necessitated a subsequent operation. Nguyen et al. [23] published the results of 22 operated patients, one of whom developed a transient neuropathy of the ulnar nerve, whereas a second case showed a permanent medial antibrachial skin neuroma.

References

1. Morrey BF, Askew LJ, Chao EY. A biomechanical study of normal functional elbow motion. J Bone Joint Surg Am. 1981;63(6):872–7.
2. Morrey BF. The posttraumatic stiff elbow. Clin Orthop Relat Res. 2005;431:26–35.
3. O'Driscoll SW, Morrey BF. Arthroscopy of the elbow. Diagnostic and therapeutic benefits and hazards. J Bone Joint Surg Am. 1992;74(1):84–94.
4. Myden C, Hildebrand K. Elbow joint contracture after traumatic injury. J Shoulder Elb Surg. 2011;20(1):39–44.
5. Wilson PD. Capsulectomy for the relief of flexion contractures of the elbow following fracture. Clin Orthop Relat Res. 1944;2000:3–8.
6. Aldridge JM III, Atkins TA, Gunneson EE, Urbaniak JR. Anterior release of the elbow for extension loss. J Bone Joint Surg Am. 2004;86-A(9):1955–60.
7. Cikes A, Jolles BM, Farron A. Open elbow arthrolysis for posttraumatic elbow stiffness. J Orthop Trauma. 2006;20(6):405–9.
8. Gosling T, Blauth M, Lange T, Richter M, Bastian L, Krettek C. Outcome assessment after arthrolysis of the elbow. Arch Orthop Trauma Surg. 2004;124(4):232–6.
9. Olivier LC, Assenmacher S, Setareh E, Schmit-Neuerburg KP. Grading of functional results of elbow

joint arthrolysis after fracture treatment. Arch Orthop Trauma Surg. 2000;120(10):562–9.
10. Park MJ, Kim HG, Lee JY. Surgical treatment of post-traumatic stiffness of the elbow. J Bone Joint Surg Br. 2004;86(8):1158–62.
11. Ruch DS, Shen J, Chloros GD, Krings E, Papadonikolakis A. Release of the medial collateral ligament to improve flexion in post-traumatic elbow stiffness. J Bone Joint Surg Br. 2008;90(5):614–8.
12. Pederzini LA, Nicoletta F, Tosi M, Prandini M, Tripoli E, Cossio A. Elbow arthroscopy in stiff elbow. Knee Surg Sports Traumatol Arthrosc. 2014;22(2):467–73.
13. Swaroop A, Avasthi S, Yadav M, Kumar S, Bharti A, Sengar G. Assessment of results of open arthrolysis in post traumatic stiff elbows. Internet J Orthop Surg. 2009;11(2):1.
14. Ehsan A, Huang JI, Lyons M, Hanel DP. Surgical management of posttraumatic elbow arthrofibrosis. J Trauma Acute Care Surg. 2012;72(5):1399–403.
15. Rex C, Suresh Kumar PM, Srimannarayana A, Chugh S, Ravichandran M, Harish DN. Analysis of results of surgical treatment of posttraumatic stiff elbow. Indian J Orthop. 2008;42(2):192–200.
16. Gallay SH, Richards RR, O'Driscoll SW. Intraarticular capacity and compliance of stiff and normal elbows. Arthroscopy. 1993;9(1):9–13.
17. Rupp S, Tempelhof S. Arthroscopic surgery of the elbow. Therapeutic benefits and hazards. Clin Orthop Relat Res. 1995;313:140–5.
18. Ward WG, Anderson TE. Elbow arthroscopy in a mostly athletic population. J Hand Surg Am. 1993;18:220–4.
19. Adams JE, Wolff LH, Merten SM, Steinmann SP. Osteoarthritis of the elbow: results of arthroscopic osteophyte resection and capsulectomy. J Shoulder Elb Surg. 2008;17:126–31.
20. Galle SE, Beck JD, Burchette RJ, Harness NG. Outcomes of elbow arthroscopic osteocapsular arthroplasty. J Hand Surg Am. 2016;41:184–91.
21. Lim TK, Koh KH, Lee HI, Shim JW, Park MJ. Arthroscopic debridement for primary osteoarthritis of the elbow: analysis of preoperative factors affecting outcome. J Shoulder Elb Surg. 2014;23:1381–7.
22. Maclean SB, Oni T, Crawford LA, Deshmukh SC. Medium-term results of arthroscopic debridement and capsulectomy for the treatment of elbow osteoarthritis. J Shoulder Elb Surg. 2013;22:653–7.
23. Nguyen D, Proper SI, MacDermid JC, King GJW, Faber KJ. Functional outcomes of arthroscopic capsular release of the elbow. Arthrosc J Arthrosc Relat Surg. 2006;22:842–9.
24. O'Driscoll SW. Arthroscopic treatment for osteoarthritis of the elbow. Orthop Clin North Am. 1995;26:691–706.
25. Richards RR. Releases, transpositions, and repairs about the elbow. Soft tissue reconstruction in the upper extremity. New York: Churchill Livingston; 1995. p. 183–205.
26. Omid R, Hamid N, Keener JD, Galatz LM, Yamaguchi K. Relation of the radial nerve to the anterior capsule of the elbow: anatomy with correlation to arthroscopy. Arthrosc J Arthrosc Relat Surg. 2012;28:1800–4.
27. Isa AD, Athwal GS, King GJW, MacDermid JC, Faber KJ. Arthroscopic debridement for primary elbow osteoarthritis with and without capsulectomy: a comparative cohort study. Shoulder Elb. 2018;10(3):223–31.
28. Hildebrand K, Zhang M, van Snellenberg W, King G, Hart D. Myofibroblast numbers are elevated in human elbow capsules after trauma. Clin Orthop Relat Res. 2004;419:189–97.
29. Van Zeeland NL, Yamaguchi K. Arthroscopic capsular release of the elbow. J Shoulder Elb Surg. 2010;19(2 Suppl):13–9.
30. Hildebrand KA, Zhang M, Befus AD, Salo PT, Hart DA. A myofibroblast-mast cell-neuropeptide axis of fibrosis in post-traumatic joint contractures: an in vitro analysis of mechanistic components. J Orthop Res. 2014;32:1290–6.
31. Camp CL, Cancienne JM, Degen RM, Dines JS, Altchek DW, Werner BC. Factors that increase the risk of infection after elbow arthroscopy: analysis of patient demographics, medical comorbidities, and steroid injections in 2,704 Medicare patients. Arthroscopy. 2017;33:1175–9.
32. Nelson GN, Wu T, Galatz LM, Yamaguchi K, Keener JD. Elbow arthroscopy: early complications and associated risk factors. J Shoulder Elb Surg. 2014;23:273–8.
33. Haapaniemi T, Berggren M, Adolfsson L. Complete transection of the median and radial nerves during arthroscopic release of post-traumatic elbow contracture. Arthroscopy. 1999;15:784–7.
34. Jones GS, Savoie FH III. Arthroscopic capsular release of flexion contractures (arthrofibrosis) of the elbow. Arthroscopy. 1993;9:277–83.

39 All-Endoscopic Sub-brachialis Capsulectomy for Severe Elbow Contractures

Deepak N. Bhatia

39.1 Background

Arthroscopic adhesiolysis is an effective intervention for refractory elbow stiffness [1, 2]. Adequate anterior capsulectomy is an important step in the procedure and is crucial for restoration of range of motion. Anterior capsulectomy is usually performed using an inside-out technique while visualizing the capsule from the intra-articular aspect. In high-grade contractures, several factors add to the technical difficulty in performing the capsulotomy: (1) the diminished joint capacity prevents access to the intra-articular space, (2) the capsule is thick and fibrotic and use of aggressive shavers and radiofrequency ablation is necessary, (3) joint distension and visualization are limited and assessment of safe zones and adequacy of capsulectomy is difficult, and (4) neurovascular relationships with the anterior capsule are altered and iatrogenic injury is possible [3, 4].

Endoscopic anterior capsulectomy using an initial incision for capsular dissection has been described an alternative procedure in high-grade contractures [5]. This chapter presents an all-endoscopic technique that utilizes the sub-brachialis space for an outside-in capsulectomy under vision. Standard anatomic landmarks are identified and are used as a guide for safe resection in a central to peripheral direction.

39.1.1 Surgical Anatomy

The anterior elbow capsule attaches at the lateral and medial peripheral margins of the trochlea and capitellum. The proximal attachment has been described as a "wave shape" or "double-arch" insertion [6, 7]. Capsular attachment is approximately 10 mm proximal to the cartilage bone junction and encloses the periphery of radial and coronoid fossae. The synovial membrane insertion follows the double-arch insertion pattern and inserts 11–13 mm proximal to the transepicondylar line [7]. The lateral ligamentous zone is at the mid radiocapitellar aspect and medially, the MCL attaches to the sublime tubercle (See Chap. 4).

The anterior capsule is closely related to several neurovascular structures (Fig. 39.1). In general, the distance of these structures from the capsule decreases from proximal to distal and medial to lateral (ratio of 2 to 1) [6]. The radial nerve is the closest structure to the capsule, and is at risk of iatrogenic injury during lateral capsulectomy. The articular level is an anatomical landmark for safe dissection and should be located prior to the capsulectomy. The radial nerve is approximately 6 mm away from the capsule at the articular (RC joint) level, and this distance reduces to 3 mm at the radial neck. The

D. N. Bhatia (✉)
SPORTSMED Mumbai, Mumbai, India

Sir HN Reliance Foundation Hospital, Mumbai, India
e-mail: shoulderclinic@gmail.com

© ISAKOS 2022

D. N. Bhatia et al. (eds.), *Arthroscopy and Endoscopy of the Elbow, Wrist and Hand*,
https://doi.org/10.1007/978-3-030-79423-1_39

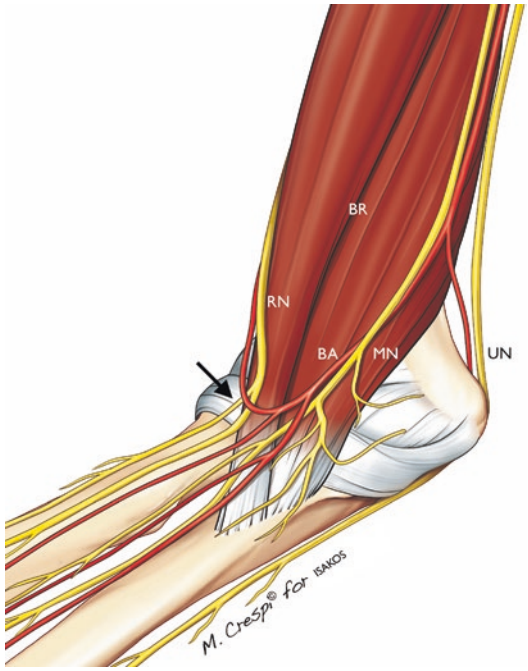

Fig. 39.1 Neurovascular structures anterior to the anterior elbow capsule are illustrated. Note that the radial nerve (RN) is separated from the capsule by the brachialis (BR). At the radial neck, the nerve is closest (arrow) to the capsule. Medially, the median nerve (MN) and brachial vessels (BA) are protected by the brachialis fibres (*UN* ulnar nerve). (© M. Crespi for ISAKOS)

radial nerve has been shown to course more medial than its anticipated course, and can be located along the medial aspect of the capitellum. The nerve is protected by the brachialis muscle fibres; however, the nerve has been shown to be in contact with the capsule at the radial neck in 50% of the cases [8]. The thickness of the brachialis between the nerve and capsule is approximately 4 mm at the joint level and further proximal. The median nerve and brachial artery on the medial side are approximately 10 mm away from the capsule at the articular (ulnotrochlear) level [6].

The brachialis muscle protects vital neurovascular structures from iatrogenic injury and dissection must be restricted to the sub-brachialis zone. Brachialis is loosely attached to the capsule in the mid-capsular region and dissection of the musculo-capsular plane is initiated in the mid region and extended peripherally. Fibres from the deep aspect of the deep head are attached to the anterior capsule (*articularis cubitus*) and can be erased off the capsule using gentle blunt dissection [9].

39.2 Indications and Contraindications

Endoscopic capsulectomy is performed as a part of elbow arthrolysis for post-traumatic stiffness. Intra-articular access is difficult in high-grade contractures (>50°) and endoscopic capsulectomy is an alternative technique in such cases.

Traumatic or surgical alteration in the anatomy of the cubital fossa (scarring, heterotopic ossification, vascular or neurological surgery) is a contraindication to the procedure. Surgical experience and a detailed familiarity with the anatomical course of neurovascular structures are necessary. Chronic stiffness is a relative contraindication.

39.3 Surgical Technique

The surgery is performed with the patient in lateral decubitus position, and a tourniquet is used during the procedure. A 2.9-mm arthroscope and sheath (ConMed, Linvatec, Largo) are used, and gravity inflow is used to minimize fluid extravasation into the arm and forearm.

39.3.1 Portals

Three standard portals are used in the procedure:

- Proximal anteromedial portal (AM) is the viewing portal throughout the procedure.
- Proximal anterolateral portal (AL) is the working portal and is placed slightly anterior to the usual portal site to permit access for resection.
- The "Radial head portal" (RH) is useful for initial localization of RC joint to mark the safe

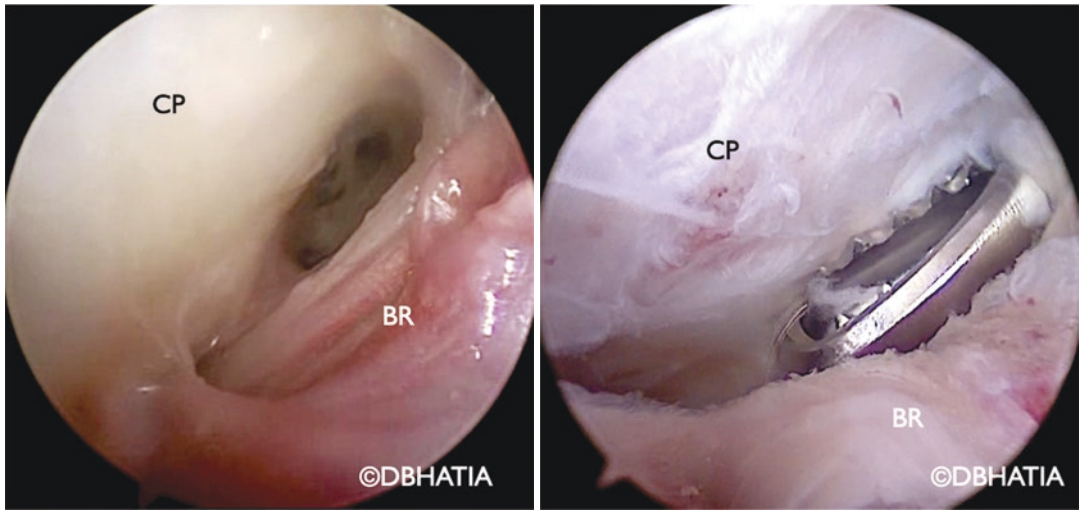

Fig. 39.2 Sub-brachialis space is visualized using dry arthroscopy after initial dissection with an obturator via AM portal. The anterior capsule is seen as a smooth white structure in contrast to the muscular fibres of brachialis. Note the capsular attachment of deep brachialis fibres (articularis cubitus) in the distal aspect of the space (left image). A shaver is used to gently dissect out the proximal and distal adhesions along the central sub-brachialis safe zone (right image) (*CP* capsule, *BR* brachialis). (© Bhatia)

zone, and for instrumentation during the procedure [10].

- Accessory anteromedial and anterolateral portals are used for retraction of brachialis if necessary.

39.3.2 Sub-brachialis Space Endoscopy

A blunt obturator is passed via the AM portal in close apposition with anterior humeral cortex and is directed towards the RC joint. No attempt is made to penetrate the joint. In severe post-traumatic contractures, the capsule is thick and adherent to joint surfaces and intra-articular penetration is difficult to achieve. The obturator is gently swept proximal and distal to create a plane along the anterior capsular surface. Next, the arthroscopic sheath is passed in a similar technique and the sub-brachialis space is visualized. The capsular attachment of the deep head of brachialis is usually visible in the distal field, and the fibres can be gently separated from the capsule using a blunt probe via AL portal. A 3.5 mm shaver is used via AL portal to excise adhesions between the anterior surface of capsule and brachialis under vision; the open end of the blade is placed towards the capsule, and suction is not used (Fig. 39.2).

39.3.3 Radiocapitellar Joint Localization

The RC joint can be localized by probing the anterior capsule and the step-off between the anterior radial head and capitellum is palpated. Next, a RH portal is created as described earlier, and a blunt 3 mm switching stick is passed from posterior to anterior gradually until tenting of the anterior capsule between the RC surfaces is visualized [9]. The switching stick (SW) is advanced to penetrate the capsule; this marks the level of RC joint and is used as a guide to further dissection (Fig. 39.3).

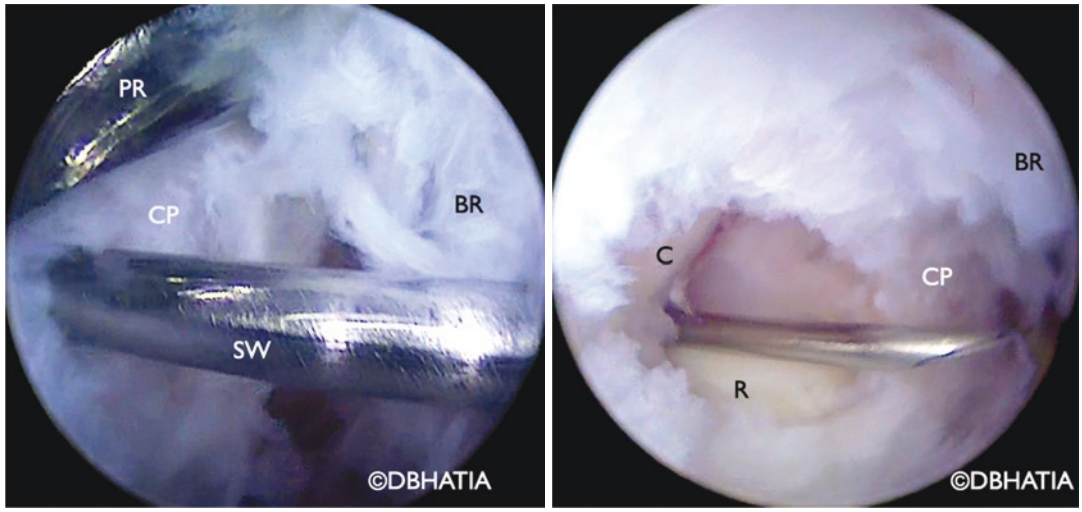

Fig. 39.3 Localization of radiocapitellar joint is performed by probing with a blunt obturator (PR) and a switching stick (SW) is passed through the RH portal to penetrate the capsule (left image). The capsule (CP) proximal to this level can be safely resected and the articular surface of capitellum (C) and radial head (R) are visualized. (© Bhatia)

39.3.4 Lateral Safe Zone Capsulectomy

Capsular resection is initiated proximal to the RC level marked by SW. A capsular window is created and the RC articular surfaces are visualized. A blunt obturator is used to extend the subbrachialis space laterally (Fig. 39.4a). A switching stick or a shaver blade can be used as a retractor for brachialis via an accessory lateral portal if necessary (Fig. 39.4b). An angled punch is passed through a RH portal and capsule is resected in a medial to lateral direction. Alternately, the AL portal is redirected into the joint, and a shaver is used to excise the capsule from medial (lateral trochlea level) to further lateral (Fig. 39.4c). Irrespective of the method, the capsular region that is excised must always be visualized prior to resection and resection must be in the sub-brachialis space (Fig. 39.4d).

39.3.5 Far Lateral Capsulectomy

The far lateral capsular region is visualized overlying the lateral gutter on the lateral aspect of RC joint. Using blunt dissection, the plane between brachioradialis and other extensor muscles is created. A shaver or radiofrequency probe is passed in this plane and the capsule is resected anterior to mid radiocapitellar region to prevent injury to the lateral ligaments. Lateral capsulectomy is continued proximally until the extensor carpi radialis brevis and longus tendons are visible (Fig. 39.5).

39.3.6 Proximal (Supracondylar) Capsulectomy

The proximal aspect of the capsular window is now visualized. Resection is performed using a 3.5 mm shaver that is passed through the AL portal and redirected intra-articularly. The capsule is resected in a medial to lateral direction and finally detached at its proximal supracondylar attachment (Fig. 39.6).

39.3.7 Medial Capsulectomy

The arthroscope sheath in now passed through the AL portal over a switching stick that is redirected extra-articularly. The medial capsule and

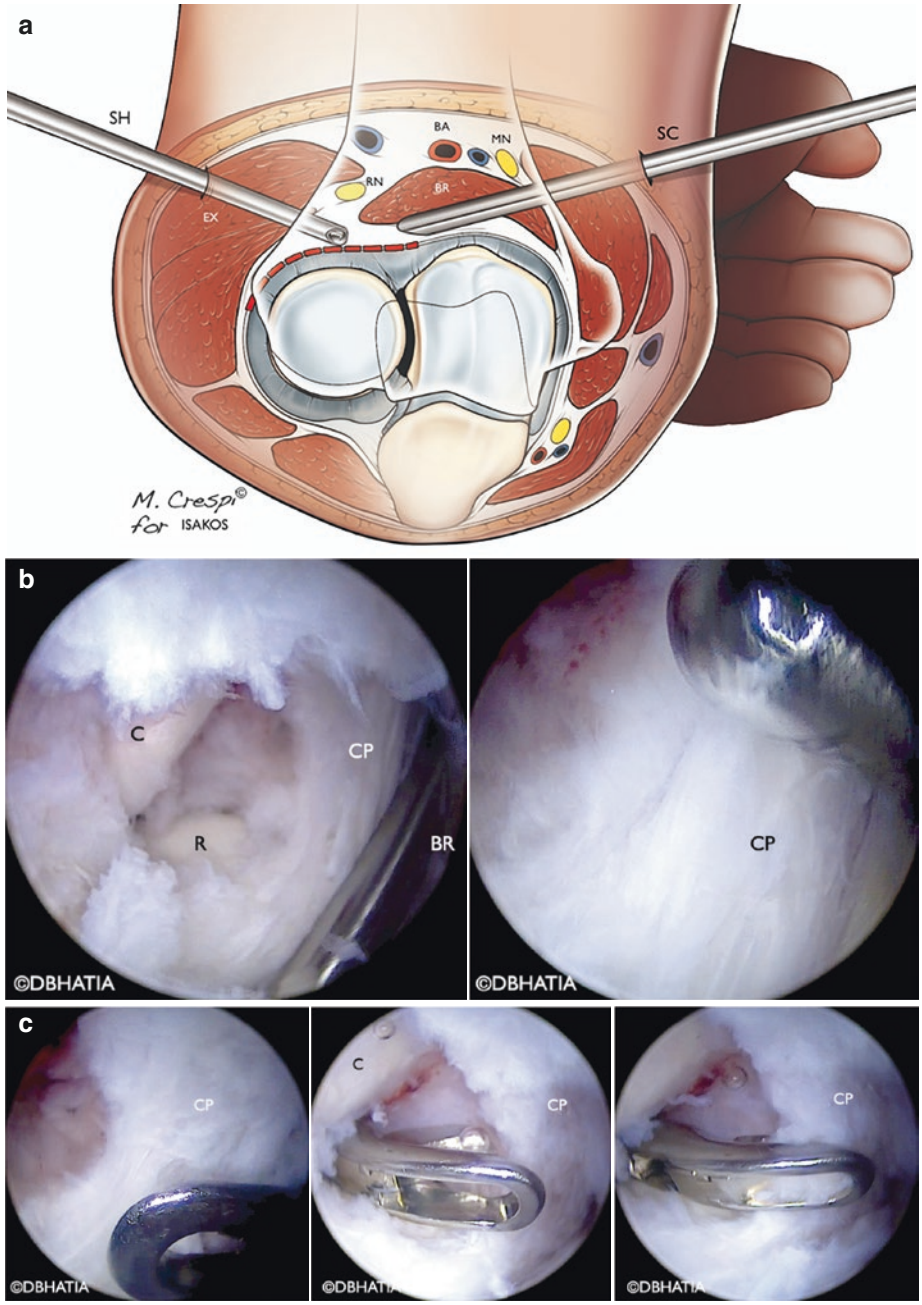

Fig. 39.4 (**a**) Lateral zone sub-brachialis capsulectomy is illustrated. The arthroscope (SC) and shaver (SH) are in the sub-brachialis region at the radiocapitellar joint level. The radial nerve (RN), brachial vessels (BA) and medial nerve (MN) are protected by the brachialis (BR). Lateral capsulectomy extent is marked by the dotted line (*EX* extensor muscles) (© M. Crespi for ISAKOS). (**b**) Lateral capsular exposure is performed under vision using a blunt obturator to extend the sub-brachialis space laterally. The brachialis can be retracted using a shaver blade of a switching stick for better vision. Lateral capsulectomy (CP) is performed under vision proximal to radial head (R) using a shaver (© Bhatia). (**c**) An angled punch (AL portal) is used to perform a lateral capsulectomy (CP) under vision in a lateral to medial direction (left image). However, it is safer to resect the capsule in a medial to lateral direction with the angled punch though the radial head portal (middle and right images) (*C* capitellum) (© Bhatia). (**d**) The AL portal is redirected for intra-articular placement and a shaver is used to resect the capsule (CP) from inside-out in a medial to lateral direction. The lateral trochlea (TR) is visualized medially and the radiocapitellar joint RC is seen on the lateral aspect of the capsulectomy window. (© D. Bhatia)

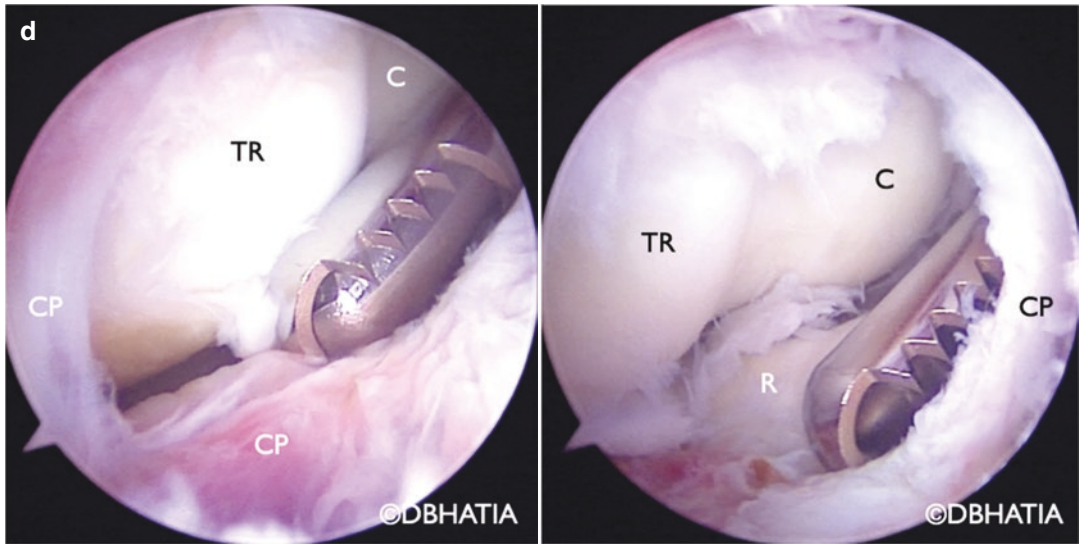

Fig. 39.4 (continued)

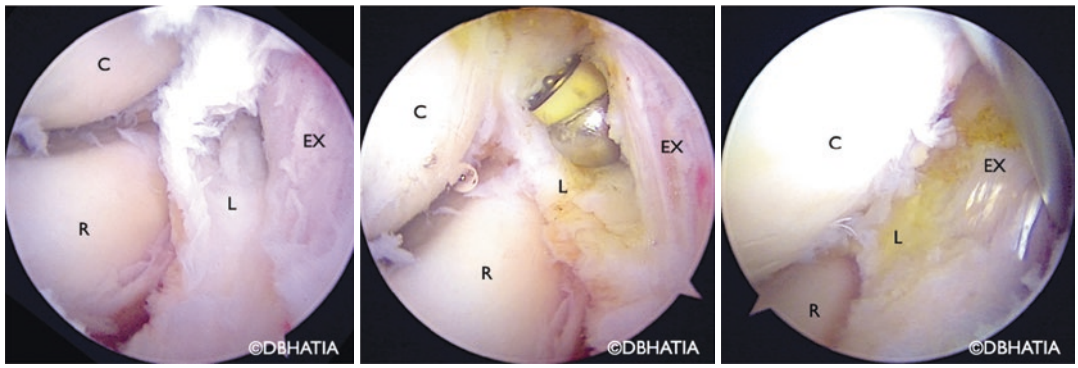

Fig. 39.5 The plane between the most lateral capsular region (L) and brachioradialis and other extensor muscles (Ex) is created (left image). Lateral capsule is resected anterior to midcapitellar region to protect lateral ligaments (middle image). Further proximal resection exposes the extensor carpi radialis brevis and longus tendons (right image, glistening fibres). (© D. Bhatia)

brachialis are visualized and the medial musculocapsular plane is dissected further using a blunt obturator (PR) (Fig. 39.7a, b). Retraction may be used as described earlier via accessory portals. Medial capsule is excised using an angled punch or with a shaver passed though the AM portal. Resection is performed until the coronoid process and medial trochlea are exposed (Fig. 39.8). Finally, capsule is resected over the coronoid process and the proximal radioulnar joint is visualized. Further medial adhesiolysis is performed from the intra-articular aspect and fibrosis along the medial aspect of trochlea is carefully excised.

Once anterior capsulectomy is completed, intra-articular and posterior adhesiolysis is performed using the standard techniques. The portals are closed and a compression dressing is applied.

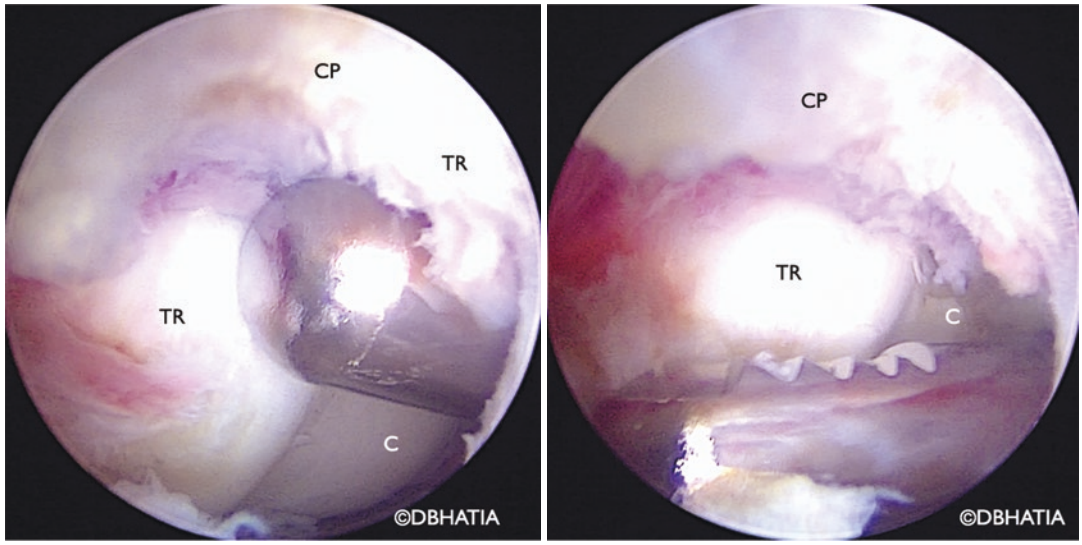

Fig. 39.6 Proximal capsulectomy is performed medial to lateral and the capsule is detached at its supracondylar attachment (*CP* capsule, *TR* trochlea, *C* capitellum). (© Bhatia)

39.4 Tips and Tricks

- Preoperative sonography is useful to assess the course of radial and median nerves and brachial vessels.
- Brachialis is a guide to safe resection and should be visible at all times.
- The anterior capsule is loosely attached to brachialis in the mid region. Sub-brachialis space dissection is initiated in this zone and is extended to the peripheral regions.
- Anterior capsule should be clearly visible as a white layer, and brachialis visualized as brownish fibres prior to resection.
- The resection end of the shaver blade should always be facing the capsule and suction is turned off to prevent injury to brachialis.
- Retractors (switching stick) are used as necessary via accessory portals to better visualize the capsule.
- Resection should not be performed distal to the RC joint level. Proximal resection is safer as compared to distal excision.

39.5 Pitfalls

- The radial nerve is at risk of injury during lateral capsular resection. The nerve is protected by the brachialis until the radiocapitellar level.
- The median nerve and brachial vessels are at risk of injury during medial dissection.
- The collateral ligaments can be damaged by excessive resection in peripheral zones.

39.6 Post-operative Management and Rehabilitation

A sling is used for comfort and is discarded as soon as possible. Range of motion exercises are initiated in the first week and the patient is permitted to use the extremity for all activities. Elbow strengthening progresses simultaneously as range improves, and unrestricted activity is permitted after 6 weeks of physiotherapy.

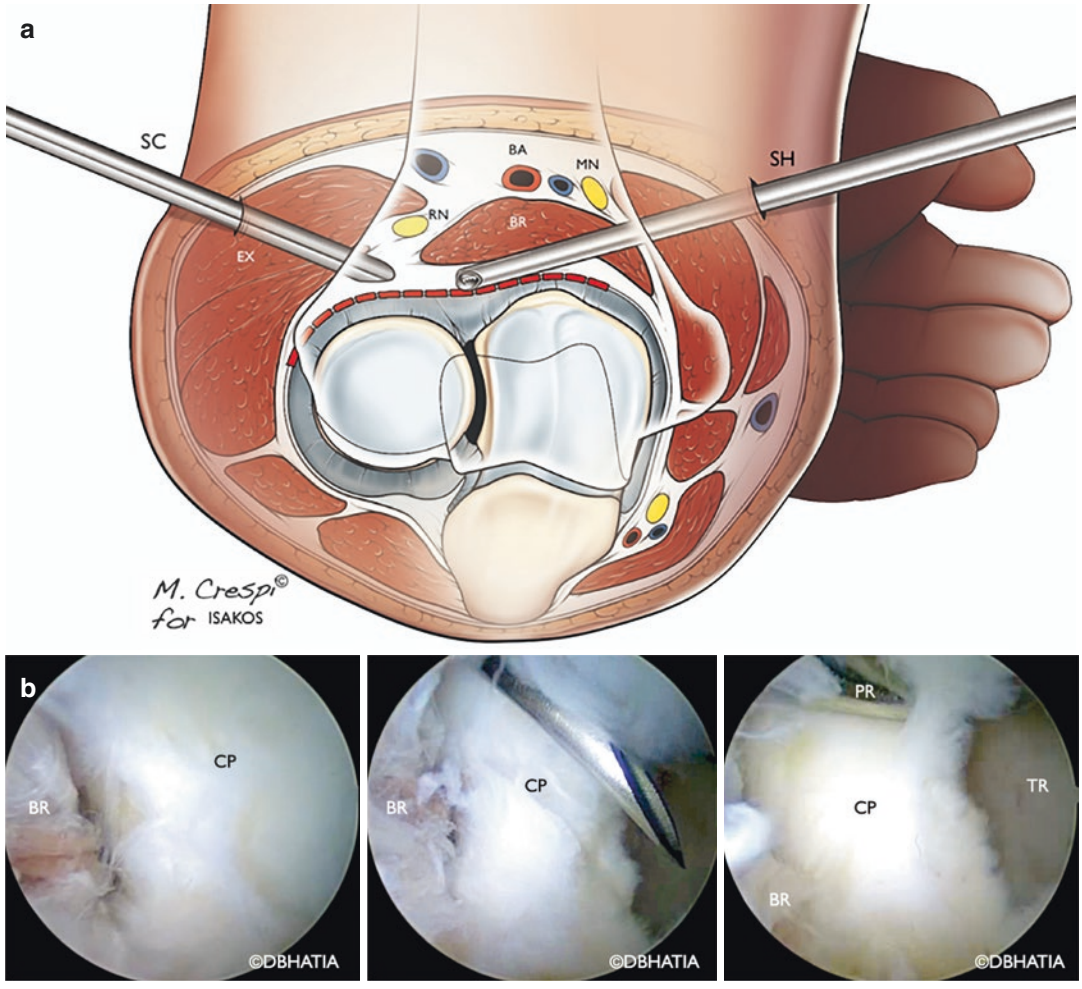

Fig. 39.7 (**a**) Medial zone sub-brachialis capsulectomy is illustrated. The arthroscope (SC) and shaver (SH) are in the sub-brachialis region at the radiocapitellar joint level. The radial nerve (RN), brachial vessels (BA) and medial nerve (MN) are protected by the brachialis (BR). Medial capsulectomy extent is marked by the dotted line (*EX* extensor muscles) (© M. Crespi for ISAKOS). (**b**) The medial capsule (CP) and brachialis (BR) are visualized via the AL portal and the medial musculo-capsular plane is dissected further using a blunt obturator (PR). (© Bhatia)

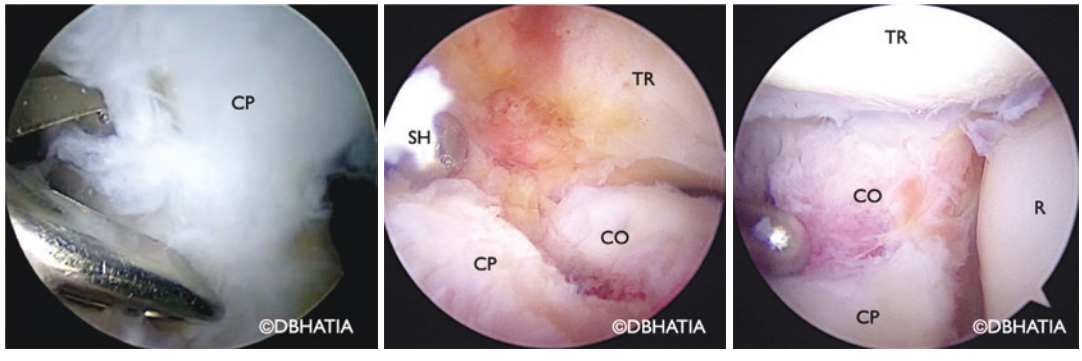

Fig. 39.8 Medial capsulotomy (CP) is performed using a punch (left image) and shaver (right image) and coronoid process (CO) and trochlea (TR) are exposed. Capsule is finally released from the coronoid undersurface and the radioulnar joint is exposed. (© Bhatia)

39.7 Complications

The neurovascular structures are at risk of injury if resection is performed outside the sub-brachialis space and distal to the articular level.

Conflict of Interest The author certifies that he has no commercial associations (e.g., consultancies, stock ownership, equity interest) that might pose a conflict of interest in connection with the submitted article. The author retains the copyright to the images, videos, and content in this chapter.

References

1. Nowicki KD, Shall LM. Arthroscopic release of a posttraumatic flexion contracture in the elbow: a case report and review of the literature. Arthroscopy. 1992;8:544–7.
2. Jones GS, Savoie FH. Arthroscopic capsular release of flexion contractures (arthrofibrosis) of the elbow. Arthroscopy. 1993;9:277–83.
3. Gallay SH, Richards RR, O'Driscoll SW. Intraarticular capacity and compliance of stiff and normal elbows. Arthroscopy. 1993;9:9–13.
4. Haapaniemi T, Berggren M, Adolfsson L. Complete transection of the median and radial nerves during arthroscopic release of post-traumatic elbow contracture. Arthroscopy. 1999;15:784–7.
5. Kamineni S, Savoie FH 3rd, ElAttrache N. Endoscopic extracapsular capsulectomy of the elbow: a neurovascularly safe technique for high-grade contractures. Arthroscopy. 2007;23(7):789–92.
6. Thoreux P, Blondeau C, Durand S, Masquelet AC. Anatomical basis of arthroscopic capsulotomy for elbow stiffness. Surg Radiol Anat. 2006;28(4):409–15.
7. Kamineni S, Bachoura A, Sasaki K, et al. Inner synovial membrane footprint of the anterior elbow capsule: an arthroscopic boundary. Anat Res Int. 2015;2015:426974. https://doi.org/10.1155/2015/426974.
8. Omid R, Hamid N, Keener JD, Galatz LM, Yamaguchi K. Relation of the radial nerve to the anterior capsule of the elbow: anatomy with correlation to arthroscopy. Arthroscopy. 2012;28(12):1800–4.
9. Leonello DT, Galley IJ, Bain GI, Carter CD. Brachialis muscle anatomy. A study in cadavers. J Bone Joint Surg Am. 2007;89(6):1293–7. https://doi.org/10.2106/JBJS.F.00343.
10. Bhatia DN. Arthroscopic resection of the radial head. In: Bain G, Eygendaal D, van Riet R, editors. Surgical techniques for trauma and sports related injuries of the elbow. Berlin: Springer; 2020.

Arthroscopic Management of Elbow Osteoarthritis

40

Luigi Adriano Pederzini, Vito Duca, Matteo Bartoli, and Andrea Celli

40.1 Background

Osteoarthritis (OA) of the elbow is a debilitating disease that affects about 2% of the population. It predominantly involves middle-aged men, especially with a previous history of manual work or competitive physical activity and, usually, involves the patient's dominant arm. From an etiopathogenetic point of view, elbow OA can be classified as primary or secondary, although typical findings and treatment approach show no relevant differences. Among the risk factors of primary OA, genetic susceptibility, osteoarticular malalignment, aging, recurrent microtrauma, excessive load, laxity, and dysplasia play a key role. On the other hand, secondary OA mainly occurs consequently to traumatic events (fracture or fracture-dislocation), and rarely to osteochondritis dissecans or osteochondromatosis. Secondary OA may develop early due to an inadequate treatment of fracture-dislocation, or in case of proximal intra-articular ulna fracture malunion [1]. Elbow arthroscopy and debridement can be a possible treatment for elbow OA in selected cases, providing good functional outcomes, pain decrease, and recovery in joint mobility.

L. A. Pederzini (✉) · V. Duca · M. Bartoli
Sassuolo Hospital, Sassuolo, MO, Italy

A. Celli
Hesperia Hospital, Modena, MO, Italy

The typical symptoms of elbow OA are articular stiffness and pain in maximal flexion or extension.

In case of concurrent large central osteochondral lesions, patients may experience pain in the midrange of motion. Pain at rest is infrequent and often due to inflammatory state. Symptomatic ulnar neuropathy may be referred by 26–55% of the patients [2]. The physical exam should include an accurate evaluation of the range of movement, including crackling sensation and joint blocks. The clinician must always evaluate elbow instability in order to plan a more complete and precise surgical approach.

40.1.1 Surgical Anatomy

Elbow muscles can produce high joint reactive forces during load. The contact zone is relatively small and this creates a large compressive force on the articular cartilage during load, particularly in extension with axial loading. Repeated excessive loading leads to cartilage fragmentation, with production of intra-articular loose bodies and generation of osteophytes [2].

In primary OA, the central ulnohumeral joint is rarely affected, because the bony architecture of this articular structure shows a high congruity which preserves the joint cartilage up to the final phase of OA [3]. The presence of peripheral osteophytes clinically causes pain and stiffness.

© ISAKOS 2022

D. N. Bhatia et al. (eds.), *Arthroscopy and Endoscopy of the Elbow, Wrist and Hand*,
https://doi.org/10.1007/978-3-030-79423-1_40

Pain reported since the early stage of the disease, especially during the terminal flexion-extension movements, is caused by the impingement of osteophytes at the coronoid and olecranon fossae. Stiffness is the result of growth of osteophytes into space-occupying lesions, and this leads to secondary capsular contracture.

Secondary OA can arise from direct cartilage damage, fractures malunion, or persistent elbow instability that induce biomechanical changes with increasing cartilage wasting. Repetitive hyperextension stress of the lateral elbow in overhead thrower athletes can cause laxity of the medial elbow causing typical posteromedial osteophytes and loose bodies [3]. The radiocapitellar joint shows early radiographic degeneration because it is exposed to maximum load concentration. Degeneration is principally localized close to the posteromedial radial head and the crest dividing the trochlea from the capitellum. The posteromedial ulnohumeral joint is often affected.

Radiographic imaging is generally sufficient to make a diagnosis of elbow OA. According to Dalal [4], the main radiological aspects are a well-preserved humeroulnar joint line and intra-articular loose bodies and osteophytes, particularly in the anterior coronoid surface and in the medial compartment of the humeroulnar joint [5]. Sometimes, articular space reduction may not be relevant even in the last phase of the disease. Loose bodies may not be visible in 30% of cases on simple radiographs, especially if located in the posterior elbow and proximal radio-ulnar joints. Cartilage damage is more frequent in the humeroradial compartment, starting from the radial to the ulnar area [1]. CT scan imaging is mandatory for the preoperative planning and useful in case of diffuse degenerative disease or post-traumatic deformation.

40.2 Indications

Pain and reduced joint mobility, nonresponsive to conservative treatment, are the main indicators for surgery. Nonsurgical treatment includes NSAIDs, splint immobilization, injections, and physiotherapy. Arthroscopic management is preferable for mild to moderate OA with discomfort at extreme degrees of movement and stiffness caused by loose bodies and osteophytes. Arthroscopic debridement seems to be less successful than open surgery when used in case of arc of flexion-extension less than 90° [6].

In literature, several predictive factors are described for outcomes after arthroscopic debridement. Men usually show more significant improvement in terms of pain and strength than women. Manual workers report greater improvement in functional scores, pain, and strength. On the other hand, work-accident/occupational pathologic status is related to poor outcomes. Radiographically, the detection of loose bodies in the absence of humeroulnar impingement can represent a pathology which is possible to treat with arthroscopy [7]. Although primary and secondary elbow OA differ in the etiopathogenesis, significant distinctions in the preoperative profile and arthroscopic debridement outcomes are not reported [1].

There are no specific absolute contraindications for this procedure.

40.3 Surgical Technique

Loco-regional and general anesthesia are administered: a brachial plexus catheter is positioned, but the anesthetic is only injected at the end of surgery, after the evaluation of nerve integrity. The surgeon carefully assesses the elbow ROM and stability before starting. The tourniquet is inflated to 250 mmHg, and the patient is placed in a prone or lateral position.

- Three posterior and two anterior portals are used in the procedure.
- The posterior section of the elbow is explored with a 4.5-mm 30° arthroscope inserted through the posterolateral portal. The second portal is created 1.5 cm proximal to the previous one. After a full posterior view of the proximal radio-ulnar joint, the surgeon performs the last posterior portal corresponding to the olecranon fossa, adjacently to the medial

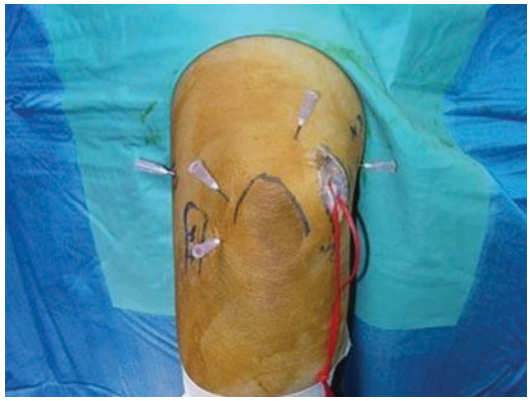

Fig. 40.1 Posterior osteophytes in the olecranon fossa are debrided via the initial posterior arthroscopic approach

margin of the triceps, 2–3 cm proximal to the olecranon tip. Using these portals, a complete debridement of the olecranon fossa and its lateral surface is performed and loose bodies and osteophytes are excised (Fig. 40.1).

- Next, the arthroscope is passed through the more proximal portal and the medial compartment is explored. The size and localization of the osteophytes are the leading indicators to identify the best medial approach to avoid injury to ulnar nerve. If the osteophytes are small in size, they are removed arthroscopically protecting the ulnar nerve using a retractor inserted through an accessory subcutaneous portal posterior to the nerve. However, for larger osteophytes, a slight arthrotomy during the final phase of the technique (to prevent fluid extravasation) is performed, and osteophytes are resected. Before the medial approach, ulnar neurolysis is highly recommended, to avoid an overstretching of the nerve during the intraoperative flexion-extension tests in stiff elbow.
- Next, the proximal anteromedial portal is then created to examine the anterior compartment. The anterolateral portal is made through an inside-out technique: a Wissinger rod is introduced 2 cm proximally and 1 cm anteriorly to the lateral epicondyle and a plastic cannula is inserted through the rod. The cannula is necessary for instrumentation for anterior debridement (Fig. 40.2).

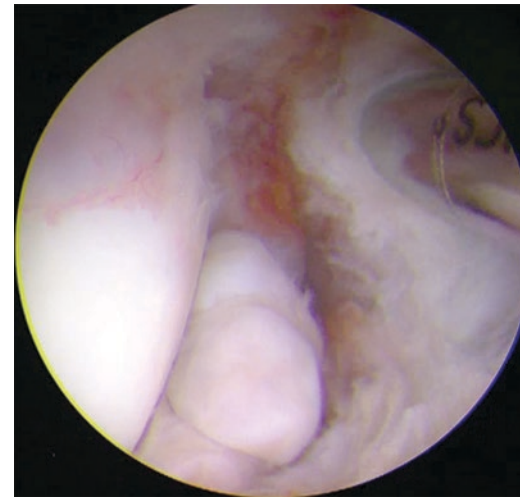

Fig. 40.2 Arthroscopic view of anterior osteophytes is shown

- Anterior capsulectomy may be necessary, especially in secondary post-traumatic OA characterized by the presence of a thick capsule. The anterior capsulectomy is performed through a basket forceps or a radiofrequency probe at a level 1 cm proximal to the apex of the coronoid; the direction of capsulectomy is lateral to medial initially, and then in the opposite direction. After anterior capsulectomy, the branch of the radial nerve can be observed: this is important to know in the treatment of radial head problems to avoid neurological complications.
- At the end of the technique, one or two suction drains are positioned, portals are sutured, and elbow is immobilized in a splint in different positions depending on the preoperative ROM limitation [8, 9].

40.3.1 Management of Nerves

According to Wada, 25–50% of patients affected by elbow OA show signs of ulnar neuropathy [10]. The neurovascular structures in contracted joint cannot be pushed away from the articular surface as in the normal joint. The ulnar nerve release is performed through a 2 cm skin incision

before beginning the arthroscopy in the following:

- Preoperative flexion under 100°
- Post-traumatic OA or previous surgery
- Patients with preoperative ulnar nerve symptoms

To avoid injuries of the posterior interosseous nerve, an inside-out technique must be used for the proximal anterolateral portal. During the insertion of the trocar through the hypertrophied capsule and osteophytes, the surgeon must pay attention to the risk of adverse damage. Sometimes, in case of severe stiffness, it may be necessary to create a dissection plane between the brachialis muscle and the capsule and, only subsequently, proceed with capsular excision [8].

40.3.2 Extra-articular Posterior Band of the Medial Collateral Ligament (MCL)

Despite the removal of osteophytes, the persistence of elbow flexion limitation may be treated through the use of a scalpel blade to divide the posterior band of the MCL on the humeral surface at the bottom of the ulnar groove using open approach. However, in a retrospective comparative analysis, Kim et al. found that this procedure was unnecessary to improve postoperative ROM [11].

40.3.3 Radial Head Resection

The radial head resection can be performed arthroscopically and required in case of limited forearm pronation and supination. The resection can be complete, partial, or limited to the osteophytes and generally begins in the posterior compartment and is concluded in the anterior compartment.

Desmoineaux et al. found that the radial head resection can lead to reduced strength recovery [12]. Kelly et al. [13] and several others [14, 15] found it ineffective. Radial head removal could result in an over-load of the ulnohumeral compartment, with consequent valgus malalignment and stretching of the ulnar nerve. Nevertheless, this procedure has been advocated by several authors [16, 17].

40.3.4 Humeral Fenestration

Humeral fenestration allows to trim the coronoid process using the posterior approach, thus providing a lower risk of injury to neurovascular structures in comparison with the anterior one. A transtricipital portal is used to pass a motorized burr; the bottom of the olecranon fossa is breached, and the anterior compartment is debrided. Furthermore, fenestration of the humeral fossa can increase the ROM by creating space for the coronoid process and apex of olecranon in the enlarged humeral fossa. Nonetheless, this technique does not yield a complete exposure of the anterior chamber [12].

40.3.5 Capsulectomy

Several studies have revealed substantial results in the treatment of elbow OA through arthroscopic debridement without capsulectomy. Theoretically, a complete removal of the capsule should lead to a significant recovery of ROM by removing an impediment to the extension and preventing the contracture recurrence due to the hypertrophic scarring of the capsule. The removal of the capsule can also reduce the postoperative pain due to a partial denervation of the capsular/articular branches of the median, ulnar, and radial nerve. However, capsulectomy is related to a higher risk of neurovascular damage, due to the proximity of vessels and nerves; therefore anterior capsulectomy must be carried out carefully [12]. O'Driscoll [18] has described the technique of capsulectomy extended to the lateral ramp. He recommends four phases: firstly the proximal humeral release, then synovectomy followed by capsulotomy, and lastly the capsule resection, ending with lateral ramp division with scissors. Lateral ramp release seems to improve functional

results [7]. A study conducted by Isa et al. [19] has shown higher ROM improvement in a group managed with capsulectomy, as compared to a group without capsulectomy; however, the ROM was not significantly different in the last follow-up. They suggest that the choice of capsulectomy should be carried out intraoperatively considering two factors: the mobility obtained after osteophytes elimination and the preoperative interview with the patient on the objectives of the surgery. When the main objective is the removal of locking and impingement pain, the capsule is left intact. If the objective is also the recovery of ROM, capsulotomy is preferable, because in their experience substantial mobility improvements are normally possible without total capsulectomy. However, these indications cannot be applied to the treatment of post-traumatic elbow OA, in which the capsule plays a more critical role than in primary disease. Hildebrand et al. observed high fibromyoblast counts in the capsule of subjects with traumatic OA, and capsulectomy may be indicated in these cases [20].

40.3.6 Microfractures and Chondroplasty

Sometimes, osteophytes removal near the trochlea can reveal an important chondromalacia; thus, microfractures can support cartilage formation [2].

40.4 Postoperative Management and Rehabilitation

The first day after surgery, rehabilitation begins with slow continuous passive movements (CPM), four times daily for 40 min. The suction drains and the perinervous anesthetic catheter are left in site. Starting from the second day, the patient continues with CPM four times daily for 40 min, adding 60 min of self-mobilization four times a day for 30 min. On the third day, the catheter is removed, and the rehabilitation program continues without variation. The drains are removed on the fourth day. Usually, on the fifth day the patient is discharged with a rehabilitation program lasting 20 days associated with Indomethacin for 15 days. The splint is generally maintained for 15–20 days. The first follow-up visit is after one week and, subsequently, after one month. Physiotherapy is extended for 3–5 months.

40.5 Complications

In 11% of elbow arthroscopies minor complications have been described; these include superficial infection, slight contractures of 20° or less, and synovial fistula. In some studies, heterotopic ossifications have also been reported. Obesity seems to be one of the risk factors. Nerve damage is the leading major complication of the arthroscopic treatment: ulnar nerve injuries are the most frequent, but the branches of the radial nerve and the medial antebrachial cutaneous nerves can be affected [2].

40.6 Conclusion

Elbow osteoarthritis is a diffuse disabling disease resulting in pain and dysfunctional mobility. The possible treatments for this condition are open surgery and arthroscopic debridement, even if the gold standard procedure is still uncertain. Poonit et al. [21] published a narrative review on this topic; however they were not been able to establish the most suitable operative technique due to the paucity of studies in literature. Arthroscopy provides excellent pain relief and mobility recovery in selected cases. This is a safe technique given the low complications and reoperation rates, but challenging to carry out and can cause potential nerve damage. In limited ROM, ulnar nerve isolation is recommended before arthroscopy. Preoperative motion is one of the main prognostic factors: arthroscopy is indicated in subjects with a 90° or higher preoperative ROM.

References

1. Carlier Y, Desmoineaux P, Lenoir H, Vidil A, French Arthroscopic Society. Prospective comparative analysis of arthroscopic debridement for primary and post-traumatic elbow osteoarthritis. Orthop Traumatol Surg Res. 2019;105:S217–20.
2. Kroonen LT, Piper SL, Ghatan AC. Arthroscopic management of elbow osteoarthritis. J Hand Surg Am. 2017;42:640–50.
3. Wysocki RW, Cohen MS. Primary osteoarthritis and posttraumatic arthritis of the elbow. Hand Clin. 2011;27:131–7, v.
4. Dalal S, Bull M, Stanley D. Radiographic changes at the elbow in primary osteoarthritis: a comparison with normal aging of the elbow joint. J Shoulder Elb Surg. 2007;16:358–61.
5. Lim YW, van Riet RP, Mittal R, Bain GI. Pattern of osteophyte distribution in primary osteoarthritis of the elbow. J Shoulder Elb Surg. 2008;17:963–6.
6. Lim TK, Koh KH, Lee HI, Shim JW, Park MJ. Arthroscopic débridement for primary osteoarthritis of the elbow: analysis of preoperative factors affecting outcome. J Shoulder Elb Surg. 2014;23:1381–7.
7. Carlier Y, Lenoir H, Rouleau DM, et al. Arthroscopic debridement for osteoarthritis of the elbow: results and analysis of predictive factors. Orthop Traumatol Surg Res. 2019;105:S221–7.
8. Pederzini LA, Palma D, Felice. Arthroscopic capsular release and debridement of elbow osteoarthritis: how I do it! In: Surgical techniques for trauma and sports related injuries of the elbow. Berlin: Springer Nature; 2019. p. 759.
9. Pederzini LA, Nicoletta F, Tosi M, Prandini M, Tripoli E, Cossio A. Elbow arthroscopy in stiff elbow. Knee Surg Sports Traumatol Arthrosc. 2014;22:467–73.
10. Wada T, Isogai S, Ishii S, Yamashita T. Débridement arthroplasty for primary osteoarthritis of the elbow. J Bone Joint Surg Am. 2004;86:233–41.
11. Kim SJ, Kim JW, Lee SH, Choi JW. Retrospective comparative analysis of elbow arthroscopy used to treat primary osteoarthritis with and without release of the posterior band of the medial collateral ligament. Arthroscopy. 2017;33:1506–11.
12. Desmoineaux P, Carlier Y, Mansat P, Bleton R, Rouleau DM, Duparc F, French Arthroscopic Society. Arthroscopic treatment of elbow osteoarthritis. Orthop Traumatol Surg Res. 2019;105:S235–40.
13. Kelly EW, Bryce R, Coghlan J, Bell S. Arthroscopic debridement without radial head excision of the osteoarthritic elbow. Arthroscopy. 2007;23:151–6.
14. Sochacki KR, Jack RA, Hirase T, McCulloch PC, Lintner DM, Liberman SR, Harris JD. Arthroscopic debridement for primary degenerative osteoarthritis of the elbow leads to significant improvement in range of motion and clinical outcomes: a systematic review. Arthroscopy. 2017;33:2255–62.
15. Galle SE, Beck JD, Burchette RJ, Harness NG. Outcomes of elbow arthroscopic osteocapsular arthroplasty. J Hand Surg Am. 2016;41:184–91.
16. Savoie FH, Nunley PD, Field LD. Arthroscopic management of the arthritic elbow: indications, technique, and results. J Shoulder Elb Surg. 1999;8:214–9.
17. McLaughlin RE, Savoie FH, Field LD, Ramsey JR. Arthroscopic treatment of the arthritic elbow due to primary radiocapitellar arthritis. Arthroscopy. 2006;22:63–9.
18. O'Driscoll SW, Blonna D. Osteocapsular arthroplasty of the elbow: surgical technique. JBJS Essent Surg Tech. 2014;3:e15.
19. Isa AD, Athwal GS, King GJW, MacDermid JC, Faber KJ. Arthroscopic debridement for primary elbow osteoarthritis with and without capsulectomy: a comparative cohort study. Shoulder Elb. 2018;10:223–31.
20. Hildebrand KA, Zhang M, van Snellenberg W, King GJW, Hart DA. Myofibroblast numbers are elevated in human elbow capsules after trauma. Clin Orthop Relat Res. 2004;419:189–97.
21. Poonit K, Zhou X, Zhao B, Sun C, Yao C, Zhang F, Zheng J, Yan H. Treatment of osteoarthritis of the elbow with open or arthroscopic debridement: a narrative review. BMC Musculoskelet Disord. 2018;19:394.

Arthroscopic Transhumeral Ulnohumeral Arthroplasty

41

Richard S. Page, Janina Henze, and Kevin Eng

41.1 Background

Elbow osteoarthritis (OA) is a painful and disabling condition that impacts on upper limb function. The key limitations to patient function include range of motion (restricted extension and therefore reach and ability to place the hand in space) and pain with associated weakness. These limitations have an impact on daily activities including work and recreation. The prevalence of OA is approximately 2% of the population but may be as high as 33% in manual workers [1–3]. Typically, elbow OA affects males in their fourth to fifth decades, but may occur earlier as a result of trauma or conditions such as osteochondritis dissecans [4, 5]. Age-related patterns of cartilage change and alterations to the articular surface have been described [6, 7].

Loads placed through the elbow may also predispose the joint to OA; studies have found that up to half the body weight is transmitted during activities of daily living, twofold during work-like duties, threefold in heavy lifting and up to sixfold in high impact and some throwing actions [8]. Chronic repetitive higher loads may lead to a pattern of OA that typically affects the radiocapitellar joint and progresses to involve the other joint surfaces of the elbow, impacting on quality of life, often affecting working age labouring patients.

A key feature of the disease is the progressive formation of marginal osteophytes along articular margins of the joint. This is associated with capsular hypertrophy and contracture, thereby resulting in loss of motion particularly flexion-extension. The extent depends on the pattern of involvement of the disease. The bony encroachment of osteophytes contributes to the loss of motion and the painful impingement, especially at the anterior and posterior joint margins.

The pattern of the osteocapsular changes and hypertrophy are the target for debridement and excision in transhumeral ulnohumeral arthroplasty (THUHA) procedure for elbow OA. The pattern of arthritic changes described by

R. S. Page (✉)
Department of Orthopaedic Surgery, School of Medicine, Deakin University, Geelong, VIC, Australia

Barwon Centre for Orthopaedic Research and Education (B-CORE), Barwon Health and St John of God Hospital, Geelong, VIC, Australia

Geelong Orthopaedics, SJOG Specialist Centre, Geelong, VIC, Australia
e-mail: richardpage@geelongortho.com.au

J. Henze
Barwon Centre for Orthopaedic Research and Education (B-CORE), Barwon Health and St John of God Hospital, Geelong, VIC, Australia

K. Eng
Barwon Centre for Orthopaedic Research and Education (B-CORE), Barwon Health and St John of God Hospital, Geelong, VIC, Australia

Geelong Orthopaedics, SJOG Specialist Centre, Geelong, VIC, Australia

© ISAKOS 2022

D. N. Bhatia et al. (eds.), *Arthroscopy and Endoscopy of the Elbow, Wrist and Hand*,
https://doi.org/10.1007/978-3-030-79423-1_41

Kashiwagi in 1978 lead to the first description of the technique, the Outerbridge-Kashiwagi (OK) arthroplasty for osteoarthritis of the elbow joint [6]. The open technique was modified by Morrey, who reported the results of using a triceps elevation rather than a tendon split, with a trephine to fenestrate the olecranon fossa, the ulnohumeral arthroplasty (UHA) in 1992 [5]. The first description and early results of arthroscopic fenestration of the olecranon fossa and debridement for OA was reported on 12 patients by Redden and Stanley in 1993 [9].

Osteocapsular arthroplasty of the elbow can be performed as an open or arthroscopic procedure. Minami and his colleagues performed an open OK procedure which showed pain relief in 61.3% of the patients and an average increase in range of motion by 6° in flexion and 11° extension, respectively. In a long-term study, Minami concluded that it is a simple procedure, but demonstrated progression of OA after surgery [10]. Kim et al. reported in a descriptive analysis that both techniques improved range of motion and clinical scores, although only one study in their review compared surgical approaches [11]. Open surgery tends to lead to increased flexion and flexion-extension arc, but it should be noted that the patients with more severe motion limitation received open surgery, whereas patients with a better range of motion received an arthroscopic approach. Savoie et al. performed an arthroscopic ulnohumeral arthroplasty with a fenestration of the olecranon fossa and reported excellent results in terms of pain relief (visual analogue scale decrease from 8.2 to 2.2) and improved range of motion. Therefore, they concluded that the arthroscopic approach is a valuable adjunct in the management of elbow OA [12].

41.1.1 Surgical Anatomy

The ulnohumeral joint is the joint between the trochlea of the distal humerus and the olecranon of the proximal ulna. It is classified as a uniaxial hinge joint with a range of motion on average from 0° extension and 140° flexion. Whilst the joint is extended, the tip of the olecranon is constrained by the olecranon fossa which increases the osseous stability in extension. In flexion the coronoid process of the ulna locks into the coronoid fossa of the distal humerus, whereas the margin of the radial head is restrained by the radial fossa, further enhancing osseous stability in flexion. The joint is surrounded by the capsule, where the ligaments are attached as capsular thickenings (annular and collateral ligaments). These ligaments are important stabilisers of the elbow joint.

OA is a mixed tissue disease that manifests with inflammation, cartilage degradation, secondary marginal osteophyte formation and pericapsular thickening and fibrosis. Structural or bony elbow motion restriction is caused by osteophyte formation, mainly on the tips of the coronoid and olecranon, as well as bone formation in both the fossae and corresponding thickening of the olecranon fossa membrane [13]. Bony deformation, inflammation and capsular thickening can also lead to ulnar nerve compression and dysfunction. Cubital tunnel syndrome is very common in patients with elbow OA and RA and is found in nearly half of patients that require surgery. Hence this needs to be assessed for clinically prior to surgical intervention. Additional manifestations of elbow OA include the formation of loose bodies. In earlier stages of the disease, when elbow motion is largely preserved, loose bodies are more likely to be associated with inflammation/synovitis, joint effusion and mechanical symptoms such as impingement or ‘true’ locking of the elbow. The latter usually occurs in the flexion-extension arc, causing the joint to painfully jam mid flexion, requiring the patient to relax and gently ‘tease’ the joint motion to free it up again. Paradoxically, this is more likely to occur with small to medium loose bodies (5–15 mm). Larger loose bodies tend to become trapped in the anterior or posterior fossae, limiting the terminal flexion-extension arc.

The radiographic imaging of elbow arthritis differs from other joints because in most cases osteophytes and loose bodies are more common than narrowing of the joint space, especially in the early stages. Cadaveric and biomechanical studies have shown that the radiohumeral joint

seems to be more prone to stress and wear than the ulnohumeral joint, so the common belief is that the arthritis starts from the radiohumeral joint and progresses to the ulnohumeral joint with sparing of ulnohumeral articulation [6]. In contrast to these studies, Lim et al. reported a much higher appearance of osteophytes in the ulnohumeral joint (95%), and this was higher than in the radiohumeral joint (59%) in patients with elbow arthritis [14].

The development of osteophytes and loose bodies in the elbow can lead to anterior or posterior impingement of the elbow. Posterior impingement can be caused by the olecranon tip, especially with osteophytes jamming into the olecranon fossa. This can cause severe pain during extension of the elbow and limit the range of motion. Osteophytes in the anterior part of the ulnohumeral joint and coronoid tip lead to a decreased flection and locking symptoms and pain during elbow flexion. Detailed radiological imaging can demonstrate the location and severity of the pathological processes (Figs. 41.1, 41.2 and 41.3).

41.2 Indications and Contraindications

The 'ELMPOPI' principle can be applied to elbow osteoarthritis, particularly in the early stages of the disease to defer patients not ready for surgery (Education, Lifestyle changes, Medications, Physiotherapy, Orthoses or temporary splints, Physical measures and Injections). Medications including simple regular analgesia (paracetamol) and NSAIDS should be trialled in the absence of mechanical symptoms or significant loss of range of motion for the management of pain and inflammation. The next tier to consider is intra-articular corticosteroid injection to the elbow joint. Pharmacological medication in inflammatory diseases including articular crystal deposition disorders should also be employed where applicable.

Surgical treatment should be considered if the conservative options have been fully explored. There are various indications for an ulnohumeral arthroplasty such as elbow locking, stiffness or decreasing range of motion, recurrent synovitis and pain. Although an arthroscopic arthroplasty is the preferred choice in terms of surgical possibilities, the symptoms and grade of the OA should be considered. Other surgical options include a debridement only with loose body removal, or total elbow replacement or in severe cases an elbow arthrodesis may be applicable, depending on the patient presentation and activity demands [15]. The patient should be informed about the progression of the OA in general and that the surgery cannot prevent further progression of osteoarthritic changes with time.

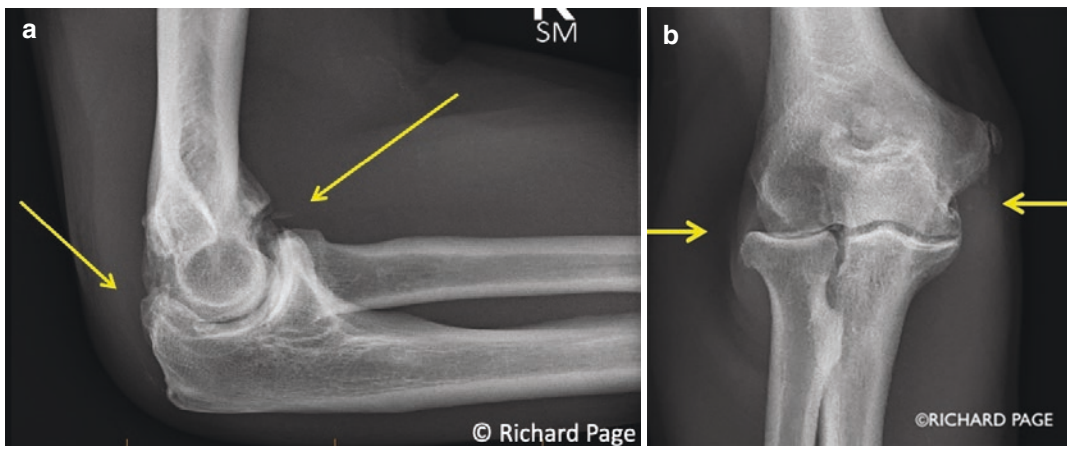

Fig. 41.1 Plain radiographs, anteroposterior (**a**) and lateral (**b**) views showing the joint narrowing and osteophytes (arrows). (© Richard Page)

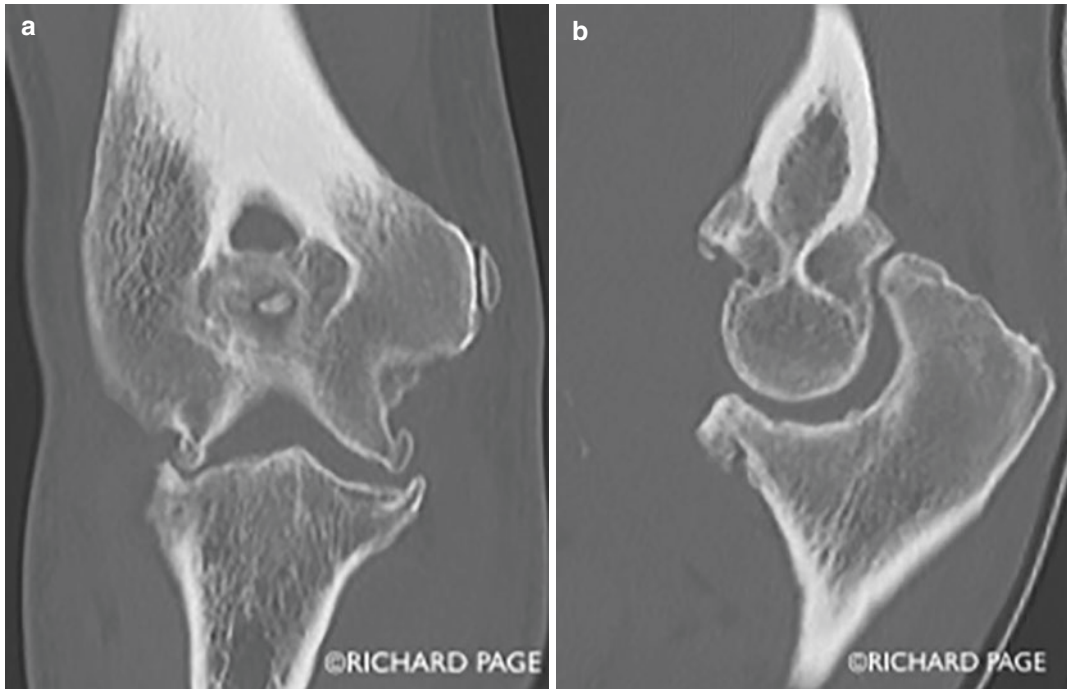

Fig. 41.2 CT scan of elbow OA, demonstrating the exact location of impinging osteophytes on sagittal (**a**) and coronal (**b**) sections. Osteophytes are seen at the coronoid tip and fossa and the olecranon tip. (© Richard Page)

General contraindications include significant medical comorbidities, associated local musculoskeletal tumours or local infection. Prior surgery with extensive scars and other soft tissue damage, for instance due to burns, are relative contraindications due to the increased risk of wound break down or neurovascular injury during the procedure. The surgery is not suitable for patients with a normal range of elbow motion or a minimal loss of extension (less than 20° loss) because the surgery is unlikely to improve the symptoms significantly and may exacerbate a flexion contracture. In this setting a simple arthroscopic debridement and removal of loose bodies may be more appropriate.

41.3 Surgical Technique

Surgery is undertaken under general anaesthesia, with the choice of additional regional blockade. A tourniquet is used to ensure a bloodless surgical field. Fluid extravasation is common once the elbow capsule is breached, and therefore a sterile compressive bandage applied to the forearm is important to limit the risk of compartment syndrome (see Figs. 41.4 and 41.5).

The surgery is performed in lateral decubitus position with the arm over a T-bar to gain access to all compartments in the elbow. Standard arthroscopic scopes and camera are utilised as described earlier (Fig. 41.6).

- Additional instruments and equipment that are helpful in undertaking THUHA include fine mini Lambotte-style osteotomes and periosteal elevators (Freer's and Howarth's elevators).
- A percutaneous reamer or bone graft harvester system is helpful to efficiently ream and fenestrate the distal humerus (see Fig. 41.7).

The order of surgery should follow the predetermined plan according to the patient disability and the pre-operative imaging. In general, the order is to address the anterior compartment first,

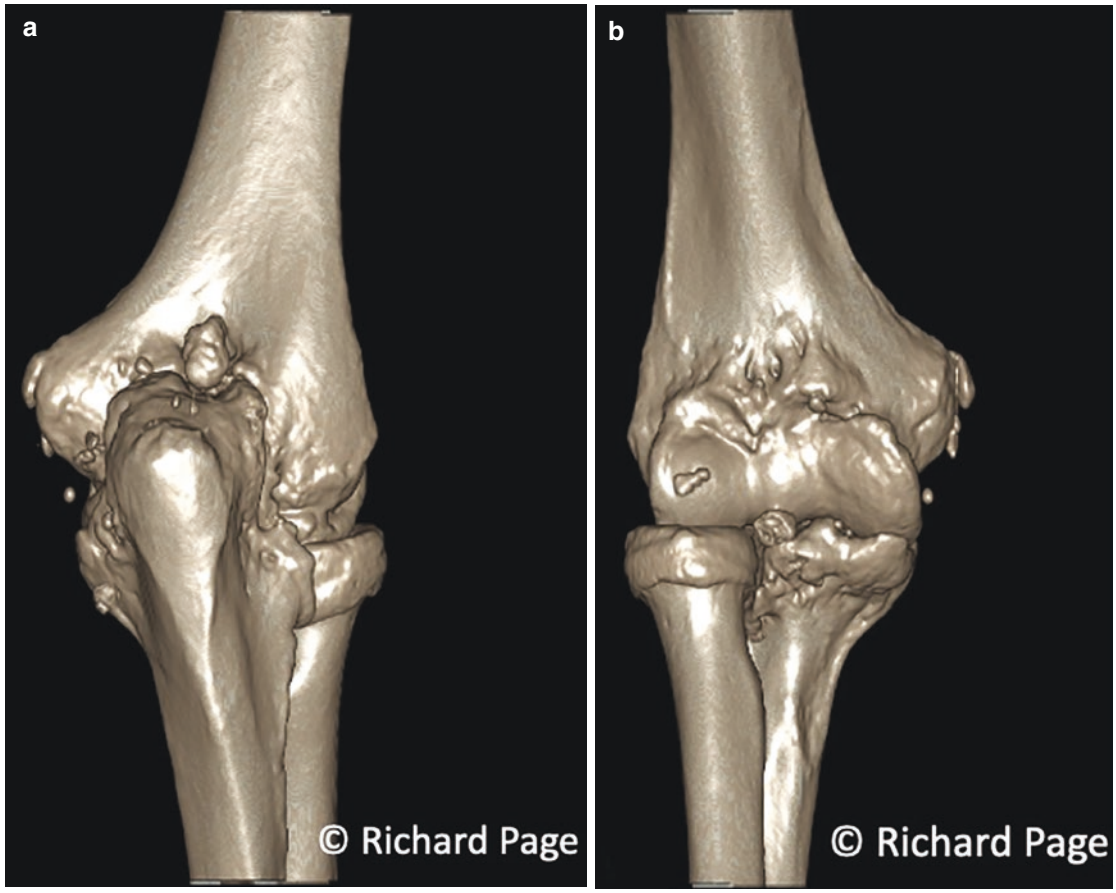

Fig. 41.3 3D reconstruction of an arthritic elbow; these images are extremely helpful to localise loose bodies in the anterior (**a**) and posterior (**b**) compartments, as well as the configuration of osteophyte involvement. (© Richard Page)

with a synovectomy to optimise the view, with capsule release and osteectomy from the distal humerus with radiofrequency device shaver and burrs as appropriate. This is followed by addressing radial head pathology and resection of coronoid osteophytes as required. The use of a 3.0 mm switching rod can assist with alternating the view from the lateral to medial side as the anterior compartment distends with fluid. Attention the shifts to the posterior compartment with synovectomy and debridement to allow full ulnohumeral visualisation, progressing to the olecranon tip and fossa.

The aim is to clear the fossa of loose bodies and osteophytes, including resection of the prominent impinging olecranon tip. The Acumed® Bone Graft Harvesting System is an ideal adjunct in these cases with a range of sizes that are suitable for fenestrating the olecranon fossa to create the transhumeral approach. The larger 12 mm reamer is an ideal size for most male patients, to efficiently remove bone and osteophyte from the olecranon fossa and create the transhumeral fenestration, whilst also removing the bone [16]. This window can then be carefully widened with an arthroscopic burr and shaver and residual anterior impinging bone removed with a Kerrison bone punch (Fig. 41.8). Finally, the elbow range is assessed under direct arthroscopic visualisation to ensure impinging bone is removed and to confirm improvement in motion.

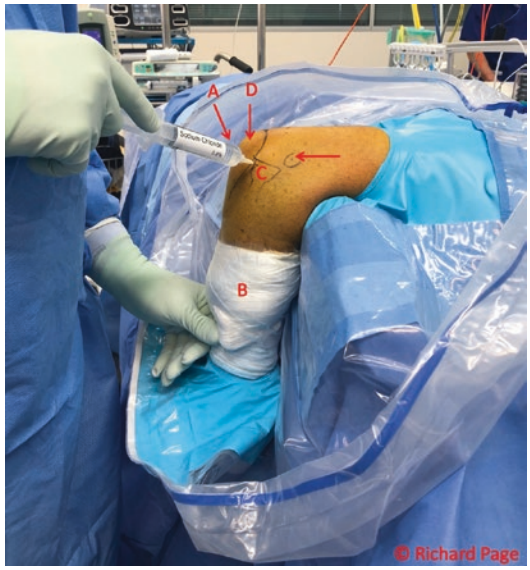

Fig. 41.4 Patient in the lateral position with tourniquet applied high up the arm, over a bar to allow direct access to the posterior compartment of the elbow. Injection of intra-articular saline to distend the restricted elbow joint is shown (A. Saline, B. compression bandage of the forearm, C. radius head, D. olecranon tip, Arrow at the lateral epicondyle). (© Richard Page)

41.4 Tips and Tricks

- Pre-operative planning and measurement of the fossa on CT scan with 3D reconstructions helps with selecting the appropriately sized reamer, to minimise fracture risk.
- The placement of the device for the fenestration is important; it should not be too distal to avoid damage to trochlea, not too lateral so as to not endanger the capitellum, and not too medial to not weaken the medial column of the humerus.

41.5 Postoperative Management and Rehabilitation

The elbow is placed in a bulky padded, gently compressive dressing and the hand elevated to minimise swelling. Appropriate analgesic cover is provided to allow motion, particularly extension of the elbow once the patient has recovered from the anaesthetic. A simple sling is provided for comfort and the patient placed on a low-dose NSAID, to reduce the risk of stiffness and heterotopic ossification for 4 weeks provided there are not medical contraindications or gastrointestinal side effects. The early emphasis is on swelling reduction and motion, so the dressing is de-bulked after 5–7 days and a gentle compressive Tubigrip-type sleeve that can be removed by the patient is applied.

41.6 Complications

Severe complications are relatively uncommon. General complications associated with elbow arthroscopy may include infection, transient or permanent nerve palsy, contracture and heterotropic ossification or disease progression of the OA. A complication specific to this procedure is distal humeral fracture associated with the transhumeral approach. The latter risk is increased if the fenestration encroaches on the medial or lateral posterior columns, weakening the vertical cortical bone.

Fig. 41.5 Acumed® Bone Graft Harvesting System—with a range of sizes that are suitable for fenestrating the olecranon fossa to create the transhumeral approach. The larger 12 mm reamer is an ideal size for most male patients. (© Richard Page)

Fig. 41.6 Creation of transhumeral fenestration under arthroscopic vision using a percutaneous bone graft harvesting/reamer system (A. Medial epicondyle, B. ulnar nerve, C. olecranon, D. reamer system, E. arthroscope). (© Richard Page)

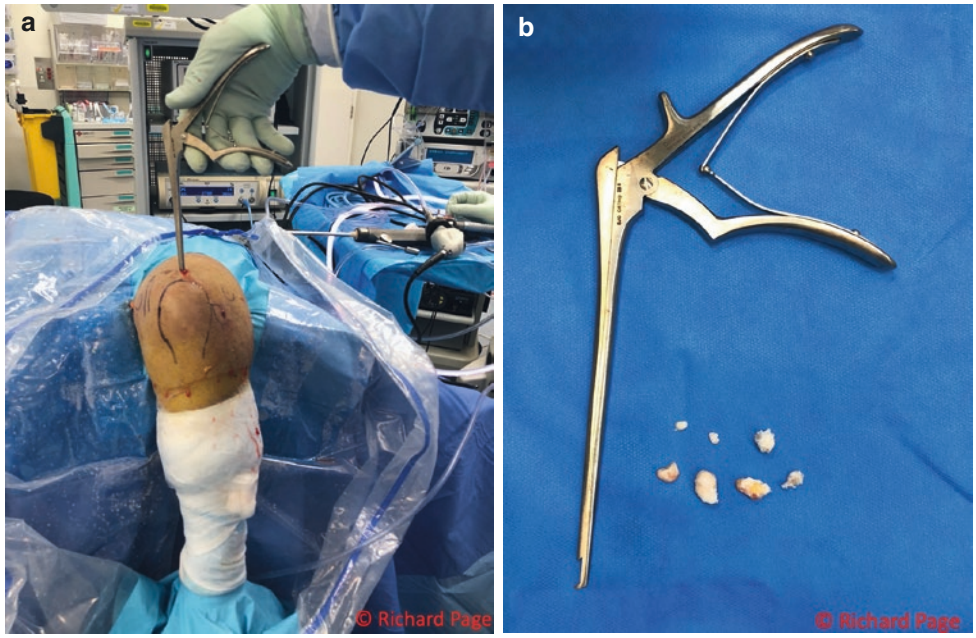

Fig. 41.7 (**a**) Kerrison bone punch in use via a direct triceps tendon approach. (**b**) Punch with a sample of marginal osteophytes and bone removed from around the transhumeral window, including from the volar side. (© Richard Page)

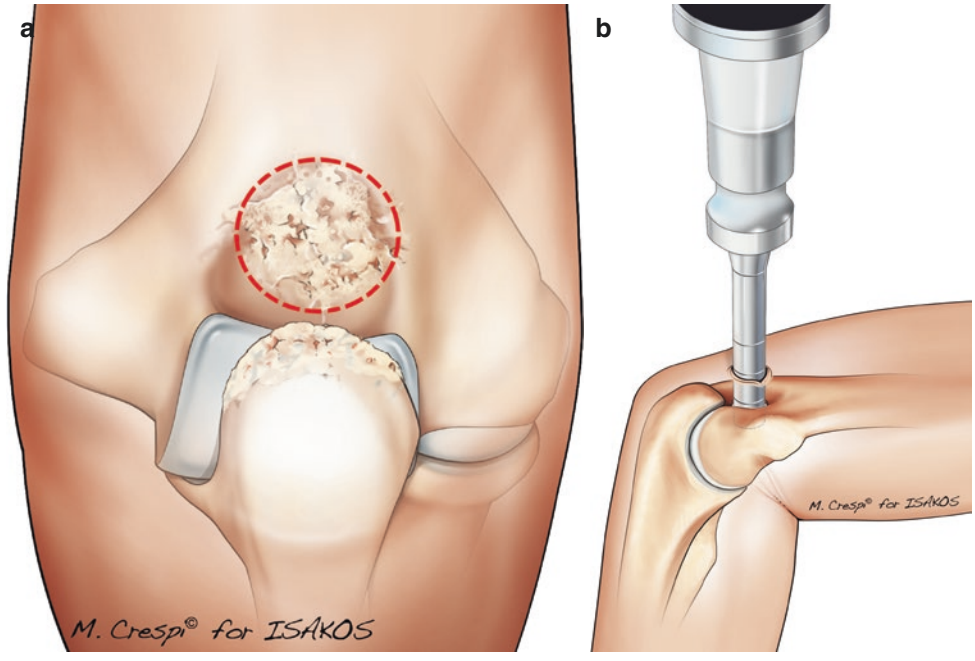

Fig. 41.8 (**a**) Diagrammatic representation of the posterior olecranon fossa osteophytes that can block extension. (**b**) Use of the trans-triceps tendon bone reamer in situ, to safely and efficiently create the transhumeral approach. (© Richard Page and ISAKOS)

References

1. Hunter D, McLaughlin A, Perry KM. Clinical effects of the use of pneumatic tools. Br J Ind Med. 1945;2:10.
2. Stanley D. Prevalence and etiology of symptomatic elbow osteoarthritis. J Shoulder Elb Surg. 1994;3:386–9.
3. Huskisson EC, Dieppe PA, Tucker AK, Cannell LB. Another look at Money BF. Post-traumatic contracture of the elbow. J Bone Joint Surg. 1979;38:423–8.
4. Schoch BS, Werthel JD, Sanchez-Sotelo J, Morrey BF, Morrey M. Total elbow arthroplasty for primary osteoarthritis. J Shoulder Elb Surg. 2017;26:1355–9.
5. Morrey BF. Primary degenerative arthritis of the elbow treatment by ulnohumeral arthroplasty. J Bone Joint Surg Br. 1992;74-B:409–13.
6. Goodfellow JW, Bullough PG. The pattern of ageing of the articular cartilage of the elbow joint. J Bone Joint Surg Br. 1967;49-B:175–81.
7. Ortner DJ. Description and classification of degenerative bone changes in the distal joint surfaces of the humerus. Am J Phys Anthropol. 1968;28:139–55.
8. Guerrero EM, Bullock GS, Helmkamp JK, et al. The clinical impact of arthroscopic vs. open osteocapsular débridement for primary osteoarthritis of the elbow: a systematic review. J Shoulder Elb Surg. 2020;29(4):689–98.
9. Redden JF, Stanley D. Arthroscopic fenestration of the olecranon fossa in the treatment of osteoarthritis of the elbow arthroscopy. J Arthrosc Relat Surg. 1993;9(1):14–6.
10. Minami M, Sadatoshi K, Kashiwagi D. Outerbridge-Kashiwagi's method for arthroplasty of osteoarthritis of the elbow—44 elbows followed for 8–16 years. J Orthop Sci. 1996;1:11–5.
11. Kim DM, Han M, Jeon IH, Shin MJ, Koh KH. Range-of-motion improvement and complication rate in open and arthroscopic osteocapsular arthroplasty for primary osteoarthritis of the elbow: a systematic review. Int Orthop. 2020;44(2):329–39.
12. Savoie FH III, Pierce D, Nunley D, Field LD. Arthroscopic management of the arthritic elbow: indications, technique, and results. J Shoulder Elb Surg. 1999;8(3):214–9.
13. Suvarna SK, Stanley D. The histologic changes of the olecranon fossa membrane in primary osteoarthritis of the elbow. J Shoulder Elb Surg. 2004;13(5):555–7. Epub 2004 Sept 24.
14. Lim YW, van Riet RP, Mittal R, Bain GI. Pattern of osteophyte distribution in primary osteoarthritis of the elbow. J Shoulder Elb Surg. 2008;17(6):963–6. https://doi.org/10.1016/j.jse.2008.03.012. Epub 2008 Jul 31.
15. Viveen J, van den Bekerom MPJ, Doornberg JN, Hatton A, Page RS, Koenraadt KLM, Christopher Wilson C, Bain GI, Jaarsma RL, Eygendaal D. Use and outcome of 1,220 primary total elbow arthroplasties from the Australian Orthopaedic Association National Joint Arthroplasty Replacement Registry 2008-2018. Acta Orthop. 2019;90(6):511–6.
16. Wijeratna MD, Ek ET, Hoy GA, Chehata A. Use of a bone graft drill harvester to create the fenestration during arthroscopic ulnohumeral arthroplasty. Arthrosc Tech. 2015;4(5):e503–5. https://doi.org/10.1016/j.eats.2015.05.002.

42 Arthroscopic Ulnohumeral Arthroplasty

Ilse Degreef

42.1 Background

Ulnohumeral arthroplasty was initially introduced by Outerbridge and Kashiwagi (a.k.a. OK procedure or ulnohumeral arthroplasty) as a minimal invasive open procedure [1]. Through a direct posterior approach, limited longitudinal triceps split with subsequent osseous perforation of the humeral fossa, both posterior and anterior elbow joint compartments could easily be debrided with a rather quick recovery. Although all compartments can easily be accessed by the technique of joint arthroscopy without the technical need for humeral perforation, the OK procedure can still be added to an arthroscopic elbow debridement. The reason is that by opening the humeral fossa, the pain appears to improve significantly in elbow degeneration, certainly if joint debridement aims for a higher range of motion in stiff elbows [2]. A possible explanation for this pain release is that in deep flexion, the anterior impingement by the coronoid process is resolved. This is especially true if coronoid osteophytes are present and motion is increased by capsular debridement. Likewise, the posterior olecranon tip impingement resolves with increased space in the posterior humeral compartment in full elbow joint extension. Decreased pain in full range of motion exercises permits better rehabilitation with increased range of motion after arthroscopic stiff elbow release.

42.1.1 Surgical Anatomy

The most challenging part on surgical anatomy in arthroscopic OK procedure is the localization, the direction, and the width of the intended humeral perforation [3]. The distal humerus is composed of two divergent columns. In the frontal plane, the lateral column is more vertical than the medial column (20° with the shaft versus 45°). Also, it is typically wider than the medial column, since it has the capitellum to its distal end. Therefore, the lateral column allows for greater bony resection than the medial column does. Proximal to the trochlear cartilage, the distal humeral fossa can be found. This fossa is more pronounced on the posterior side of the humerus. This is the place where the perforation of the OK procedure is commenced and it is centered between the epicondyles, slightly more to the ulnar side. If a 90° directed tunnel on the humeral shaft is drilled, the anterior perforation of the humerus will be immediately proximal to the trochlear cartilage at the position of the coronoid process in deep flexion. This can be seen during the arthroscopy.

I. Degreef (✉)
Orthopaedic and Hand Surgery, University Hospitals Leuven, Leuven, Belgium
e-mail: ilse.degreef@uzleuven.be

© ISAKOS 2022

D. N. Bhatia et al. (eds.), *Arthroscopy and Endoscopy of the Elbow, Wrist and Hand*,
https://doi.org/10.1007/978-3-030-79423-1_42

42.2 Indications and Contraindications

Since the humeral perforation allows for deeper flexion and extension of the elbow joint in bony impingement of the coronoid and/or the olecranon tip, respectively, any articular change that causes this bony conflict may be addressed with the OK technique. Most common cause of this impingement is degenerative arthritis. Osteophytes typically form at both bony ends and the spurs impinge against the distal humerus. Debridement of these osteophytes often leads to quite rapid recurrence due to bony regrowth. Therefore, one can consider a primary or secondary (in former debridement) arthroscopic OK procedure in painful elbow degeneration, especially in anterior or posterior elbow pain in deep flexion and/or extension or even limited range of motion due to osteophytes (Fig. 42.1). A reasonably intact ulnohumeral articular surface is a prerequisite. However, increasing motion in a joint with severe cartilage degeneration at the trochlea may even increase pain, and therefore the OK procedure is not indicated in severe arthritis of the hinge joint articulation itself.

The arthroscopic OK procedure may also be considered in younger patients with bony impingement of the elbow [3]. This is most often the case in chronic valgus extension overload as seen in overhead throwing athletes. Although most of these patients can be helped with physiotherapy, infiltration, or even arthroscopic debridement and/or ligament reconstruction or augmentation, in exceptionally recurrent impingement, the OK procedure can improve complaints. Sports can be resumed at the same or even higher level after this. However, care must be taken that a sufficiently long interval is respected. Indeed, certainly in high-load labor, contact sports, and torque-inducing activities, there is a risk of intra-articular distal humeral fractures through the weakened columns and humeral perforation until bony remodeling is sufficient and muscle tone has normalized (estimated at 6 weeks at the earliest).

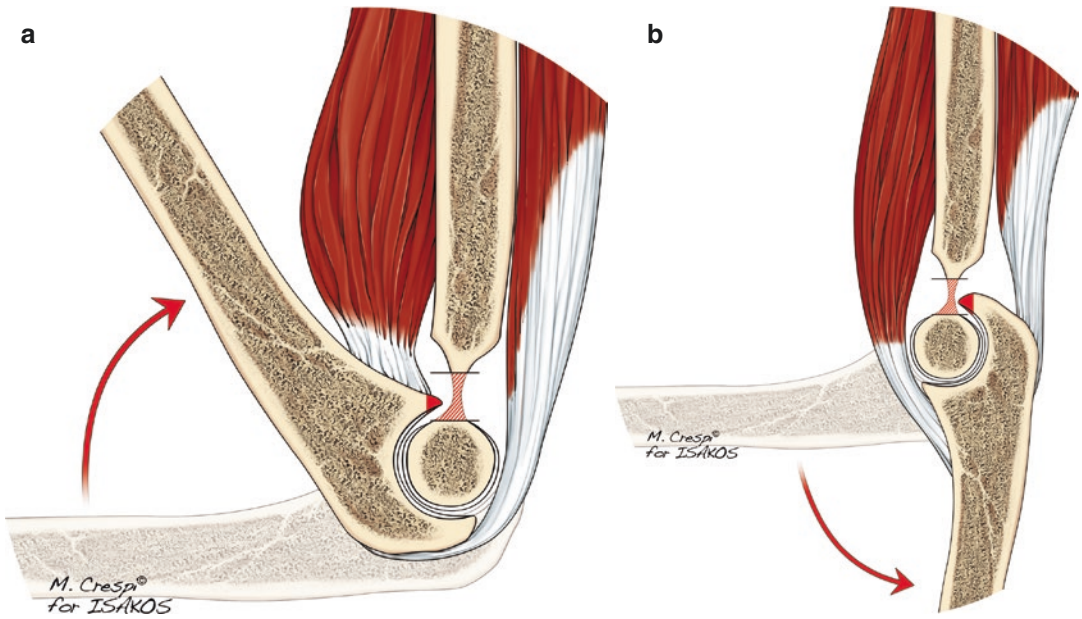

Fig. 42.1 Illustration of the surgical advantage of creating a hole in the distal humeral fossa (transection of the bone); in flexion (**a**) and extension (**b**), the olecranon tip and coronoid process of the ulna do not impinge on the distal humerus. (M. Crespi © for ISAKOS)

42.3 Surgical Technique

The patient is placed in lateral decubitus and the arm is positioned on a Mayo support. The elbow should be higher than the thorax to allow for camera freedom in a 30–45° angle downwards (over the lateral side of the shoulder), while performing the humeral perforation.

- First, anterior joint debridement is performed through proximal anteromedial anterolateral portals. The coronoid process and its osteophytes are removed. If needed, the anterior joint capsule is excised and finally the anterior aspect of the distal humerus is debrided.
- Next, the posterior compartment of the elbow is debrided through a direct posterior and midposterolateral portal. Camera and working instruments are exchanged regularly in between these portals to allow for vision and humeral perforation. With a 4 mm arthroscopic shaver, the posterior compartment is thoroughly debrided (Fig. 42.2). Osteophytes are removed from the tip of the olecranon. Elbow extension exposes the tip of the olecranon and osteophytes well.
- Thereafter, in the region where the tip of the olecranon is in contact with the distal posterior humerus in extension, a perforation through the humerus is made in the middle of the epicondyles with a 4 mm arthroscopic burr and shaver (Fig. 42.3a, b). This is directed perpendicularly towards the anterior side of the humerus. Once the humerus is perforated (this can take a while and the bony depth can be 5–10 mm), the diameter of the hole is widened up to 15–20 mm with a Kerrison rongeur through the direct posterior portal (Fig. 42.3c, d). The remaining medial and lateral columns should be about 15–20 mm wide (Fig. 42.4).
- Flexion and extension motion freedom are measured under direct visualization of the perforations. Through the posterior portals, anterior inspection is now possible and the coronoid process can be seen in the middle of the humeral perforation in full flexion, if it was made at the correct position (Fig. 42.5a, b).
- After thorough joint rinsing, portals are left open to allow for the swelling of the joint to go down fast under a sterile dressing.

Fig. 42.2 Posterior distal humerus and olecranon fossa is cleared with shaver

42.4 Tips and Tricks

- Correct patient positioning is crucial for good arthroscopic visualization. If the camera does not have freedom to move around (usually by not installing the elbow high enough on the Mayo support), visualization of the posterior compartment will be poor.
- Suction is avoided and water pressure should not be too high: if edema arises, this will influence instrument exchange and elbow joint motion, needed to control the position and efficiency of the humeral perforation.
- To localize the correct position to start the humeral perforation, it is important to correctly position the midposterior portal in the posterior fossa. The fossa can be located in the midportion of the epicondyles and about 1 cm more proximal to the olecranon tip. Also, once the drilling is started, anatomical orientation is necessary to avoid maldirection and unnecessary weakening of the humeral columns.

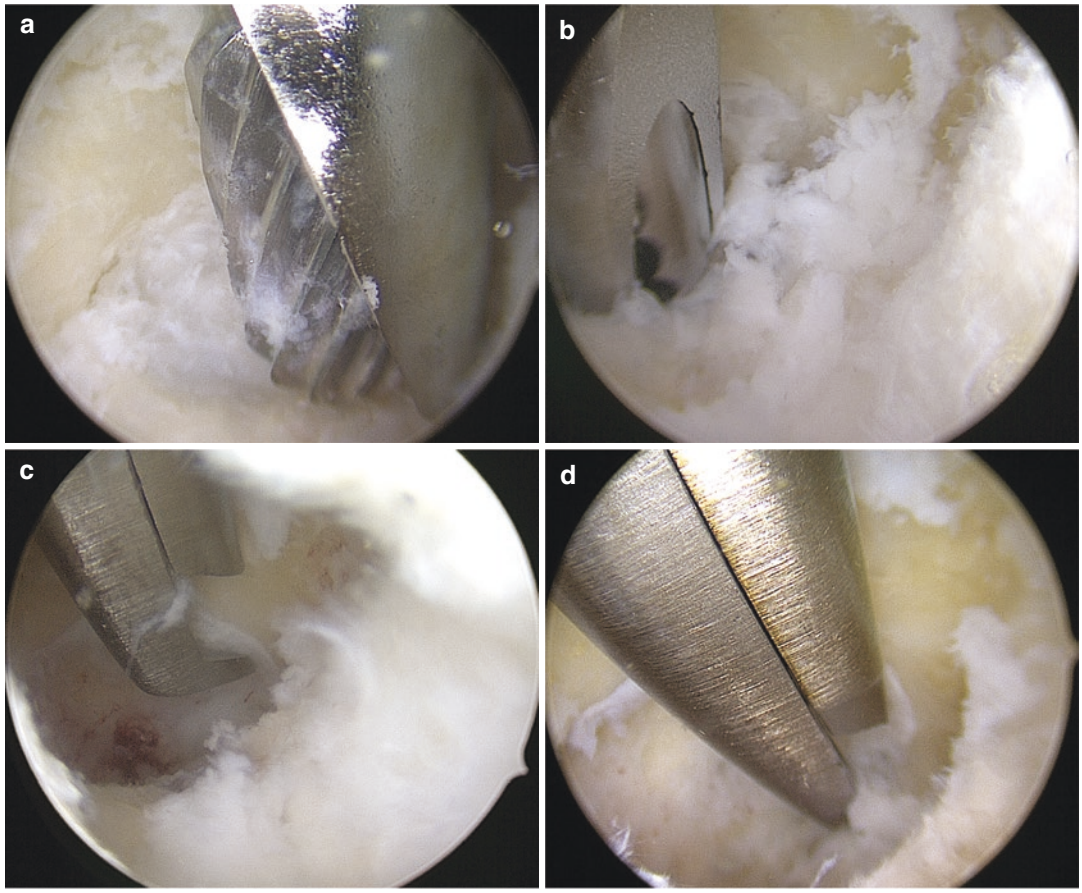

Fig. 42.3 Steps to create perforation are shown using a burr (**a**), and shaver (**b**), and rongeur (**c**, **d**)

42.5 Pitfalls

The perforation should be performed in the middle of the distal humerus. The lateral and medial column need to be intact, and preservation of a width of at least 15 mm is recommended. Deviating from the intended 90° drilling pathway can lead to an asymmetrical hole. This can be seen in full flexion when the coronoid process is not well centered within the hole. If the columns are sufficient, the hole may be widened in the direction needed to allow for full range of motion. Fluoroscopy is useful to assess the remaining bony columns.

42.6 Postoperative Management and Rehabilitation

Early active motion is allowed. The bulky sterile dressing is replaced by small bandages and this allows for early active range of motion exercises. An active rehabilitation program is advised with physiotherapy to focus on regaining range of motion and muscle tone in upper and lower arm. However, due to the weakening of the distal humerus after its perforation, contact sports, especially with humeral torque, are not allowed for 6 weeks. Although case reports on complications of the OK procedure are very rare, the frac-

ture risk is higher (40% lower force needed to fracture) and eventual fractures are likely to be intra-articular through the humeral perforation. After 6 weeks, if muscle tone is back to normal (as measured by a Jamar grip force) and bone remodeling of the columns is obvious on radiography, full activity can be gradually resumed.

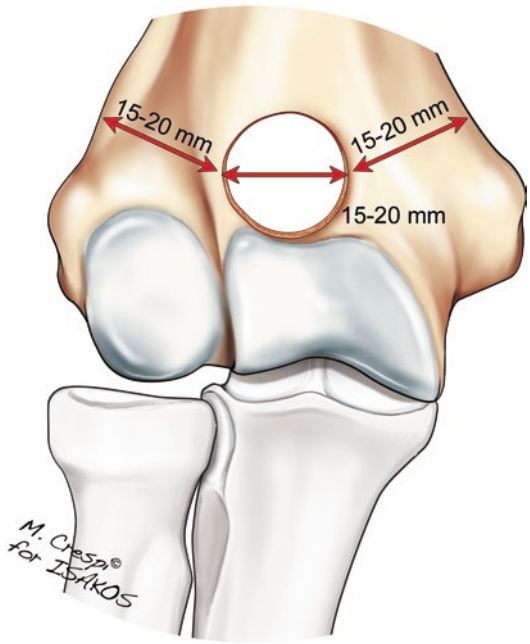

Fig. 42.4 Bony structure of the distal humerus after a perforation is created. The estimated mean diameters of the remaining columns and central hole are shown. (M. Crespi © for ISAKOS)

42.7 Complications

- Complications are rare if performed by a surgeon experienced in elbow arthroscopy. Wound infection, transient ulnar nerve paresthesia, and CRPS (complex reactive pain syndrome) are much less common in arthroscopy than in open surgery.
- In severe preoperative loss of range of motion (60–100° motion loss), with adequate correction and significant gain, postoperative ulnar nerve dysfunction is more likely [1]. Ulnar nerve decompression and even anterior transposition may be considered in these severe cases.
- The mostly feared complication of the OK procedure (open or arthroscopic) is a distal intra-articular humeral fracture. However, the author has never encountered any fracture, even in heavy-duty workers or overhead throwing athletes. Only one case report is found in the literature. Biomechanical research on cadaver specimens has demonstrated a bony weakness and a higher risk of intra-articular fractures of the distal humerus after the OK procedure [3]. Therefore it is advised to not make the fenestration diameter wider than the individual remaining columns. After 6 weeks, bony remodeling is obvious on radiographs and it is presumed that the possibly higher fracture risk is normalized. Nevertheless,

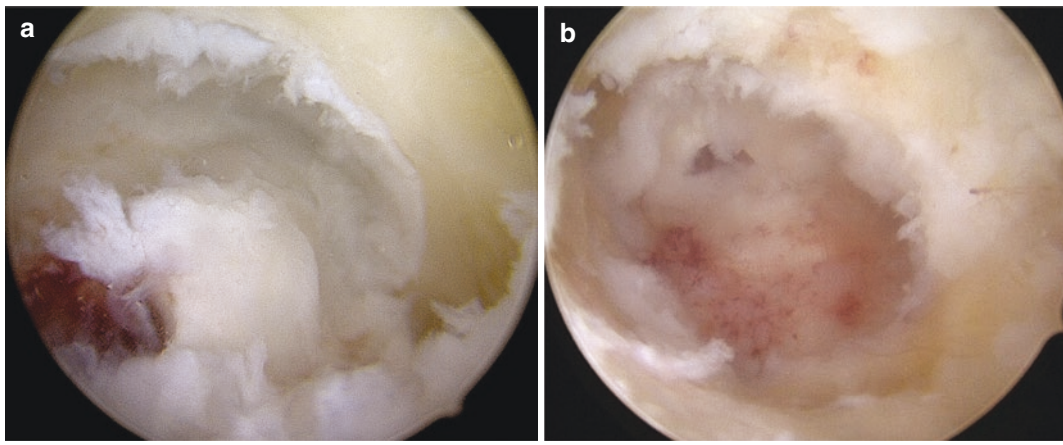

Fig. 42.5 Visualization of anterior coronoid process in mild flexion (right side, view from posterolateral portal) and mild extension (upper side picture, view from midposterior portal)

since the columns are temporary weakened after the humeral perforation, caution is advised and contact sports should be disallowed for 6 weeks after surgery.

42.8 Results

If the indication is strict (coronoid and/or ulna tip impingement and grossly intact ulnohumeral joint surface), high satisfaction rates (up to 90%) are common. Chances of good outcome are increased if symptoms were present less than 2 years before presentation and a 75% definite return to the previous work is reported [4, 5]. More than increased motion, pain usually significantly improves [6]. However, joint degeneration is likely to progress and therefore long-term follow-up (over 10 years) demonstrates recurrence of complaints in 20–40% of the patients. In cases where a new arthroscopic procedure was performed, the bony hole was smaller than originally made, and a fibrous cover actually appears to close the gap. Exceptionally, the fenestration may even close with bony regrowth and consolidate in the long term.

References

1. Antuña SA, Morrey BF, Adams RA, O'Driscoll SW. Ulnohumeral arthroplasty for primary degenerative arthritis of the elbow: long-term outcome and complications. J Bone Joint Surg Am. 2002;84(12):2168–73. https://doi.org/10.2106/00004623-200212000-00007.
2. Cohen AP, Redden JF, Stanley D. Treatment of osteoarthritis of the elbow: a comparison of open and arthroscopic debridement. Arthroscopy. 2000;16(7):701–6. https://doi.org/10.1053/jars.2000.8952.
3. Degreef I, Van Audekercke R, Boogmans T, De Smet L. A biomechanical study on fracture risks in ulnohumeral arthroplasty. Chir Main. 2011;30(3):183–7. https://doi.org/10.1016/j.main.2011.03.001.
4. Forster MC, Clark DI, Lunn PG. Elbow osteoarthritis: prognostic indicators in ulnohumeral debridement—the Outerbridge-Kashiwagi procedure. J Shoulder Elb Surg. 2001;10(6):557–60. https://doi.org/10.1067/mse.2001.118416.
5. Phillips NJ, Ali A, Stanley D. Treatment of primary degenerative arthritis of the elbow by ulnohumeral arthroplasty. A long-term follow-up. J Bone Joint Surg Br. 2003;85(3):347–50. https://doi.org/10.1302/0301-620x.85b3.13201.
6. Sarris I, Riano FA, Goebel F, Goitz RJ, Sotereanos DG. Ulnohumeral arthroplasty: results in primary degenerative arthritis of the elbow. Clin Orthop Relat Res. 2004;420:190–3.

Arthroscopic Partial Radial Head Resection for Rheumatoid Arthritis

43

Kozo Shimada, Ko Temporin, Keiichiro Oura, and Satoshi Miyamura

43.1 Background

Articular synovitis may occur in inflammatory arthritis such as rheumatoid arthritis. Medical management can stop or control disease activity; however an established isolated articular synovitis (Fig. 43.1) is still a good indication of surgery because it can stop the joint destruction and can reduce the dose of medication. Arthroscopic procedure is preferable because of less-invasiveness and faster postoperative rehabilitation.

Arthroscopic plastic radial head resection consists of two main procedures: synovectomy throughout the joint for reducing inflammation, and plastic debridement of radial head for improving radio-capitellar congruity. Synovectomy should be done as completely as possible; however synovitis situated around the radial neck and the medial gutter of the humero-ulnar joint is technically difficult to approach because of narrowness of the space and proximity to radial or ulnar nerve. This chapter describes the author's technique for arthroscopic radial head resection to improve radio-capitellar congruity in rheumatoid arthritis and technical tips are presented.

43.2 Indications and Contraindications

Treatment strategy for joint disorders in rheumatoid arthritis has dramatically changed due to development of newer disease-modifying therapy. Indications for arthroscopic synovectomy and radial head debridement include:

- Persistent synovitis under proper medical medication (Fig. 43.1).
- Painful crepitus in motion especially due to radio-capitellar articular damage and sclerotic change (eburnation) of the radial head (Fig. 43.2).

Poor control of disease activity is contraindication due to progression of joint destruction after surgery. Severe erosion of ulno-humeral joint is a relative contraindication for this procedure because radial head resection causes valgus instability of the joint and worsens the ulno-humeral articulation.

43.3 Surgical Technique

The procedure is performed in the prone or in the lateral decubitus position.

- Portals used in the procedure are the proximal anteromedial, anterolateral, posterior, posterolateral and direct lateral (Fig. 43.3).

K. Shimada (✉) · K. Temporin · K. Oura
S. Miyamura
Department of Orthopaedic Surgery, JCHO Osaka Hospital, Osaka, Japan
e-mail: k-shimada1960@nifty.com

© ISAKOS 2022

D. N. Bhatia et al. (eds.), *Arthroscopy and Endoscopy of the Elbow, Wrist and Hand*,
https://doi.org/10.1007/978-3-030-79423-1_43

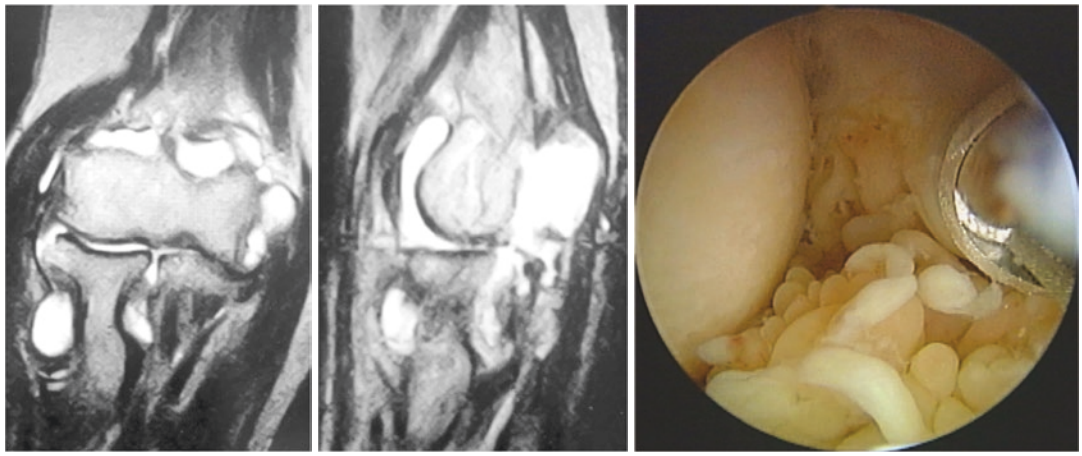

Fig. 43.1 Active synovitis of the elbow is seen around the radial neck on MRI images (left and middle images) and is visualized during arthroscopy (right image)

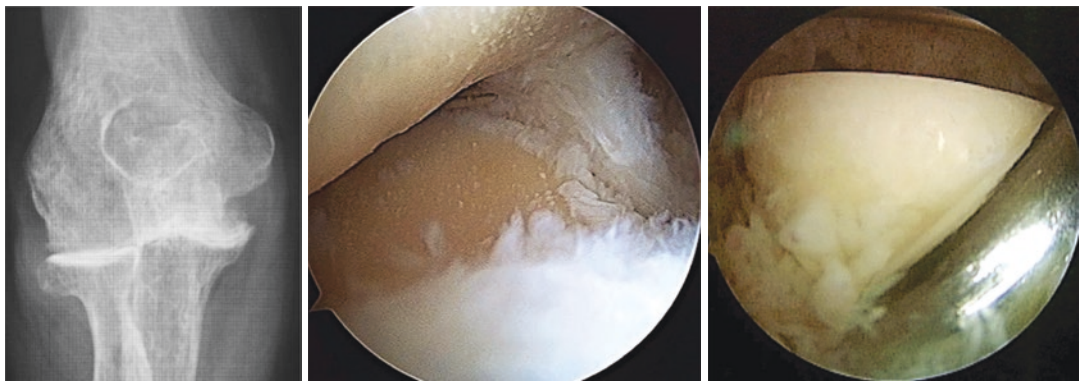

Fig. 43.2 Radiography and arthroscopic findings before resection are shown. The radiograph shows sclerotic change of the radial head (left). Arthroscopy demonstrates cartilage loss and eburnation of the radial head (middle image), and the sclerotic edge of the radial neck with synovitis is visualized (right image)

- Total synovectomy is performed using a combination of different portals in anterior and posterior recesses.
- Deformed or impinging osteophytes are resected with a grasper or using a surgical burr (Fig. 43.4).
- Next, under anteromedial arthroscopic view, anterior part of the radial head is removed by an abrader introduced through anterolateral portal (Fig. 43.4).
- The abrader is switched to direct lateral portal and the residual part of the radial head is resected (Fig. 43.4).
- Overall, about 4–5 mm width (the width of tip of the surgical burr) of the radial head is removed through anterolateral and direct lateral portals. Arthroscopy portal may be switched from anteromedial to direct lateral or anterolateral according to the visualization.
- After adequate resection, the remaining surface is debrided using a shaver to create a congruous articulation (Fig. 43.5).
- A suction drainage tubing is passed through one or two portals and the portals are closed (Fig. 43.5).

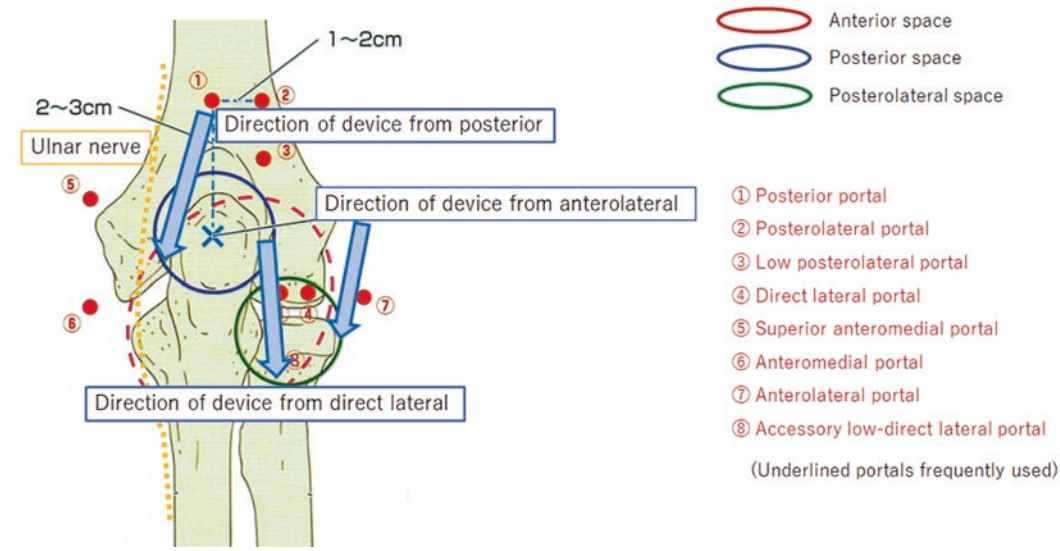

Fig. 43.3 Portals and device direction for radial head resection are illustrated

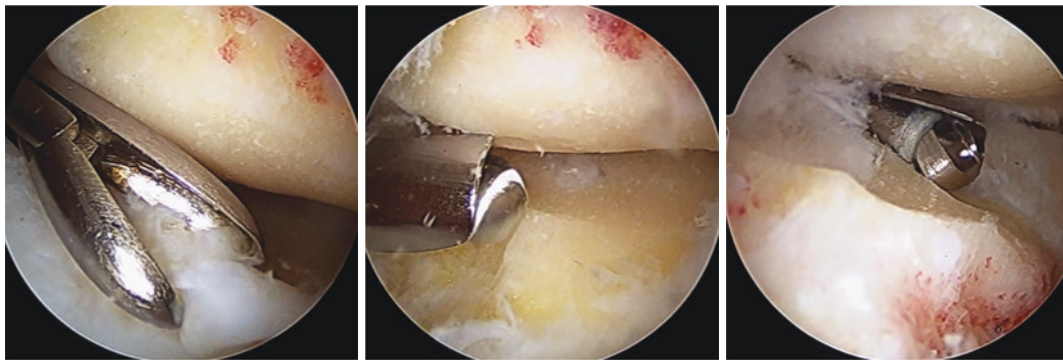

Fig. 43.4 Surgical steps for arthroscopic plastic radial head resection are demonstrated. The osteophytes are excised (left image) and radial head is resected using an abrader through anterolateral portal (middle image) and direct lateral portal (right image)

43.4 Tips and Tricks

- Direction of the shaver insertion for synovectomy of the radial neck is sometimes difficult. Superior anterolateral portal is recommended.
- The shaver should not be directed to the anterior outer side of the radial neck and to the ulnar outer side of the medial gutter because of the proximity of radial and ulnar nerves (Fig. 43.3).
- Radial head resection is started from anterolateral portal. After resection of the anterior quarter or half of the radial head, the forearm is pronated by the assistant and the resection is continued via the direct lateral portal.
- The width of the surgical burr (usually 4–5 mm) is adequate for partial radial head resection.

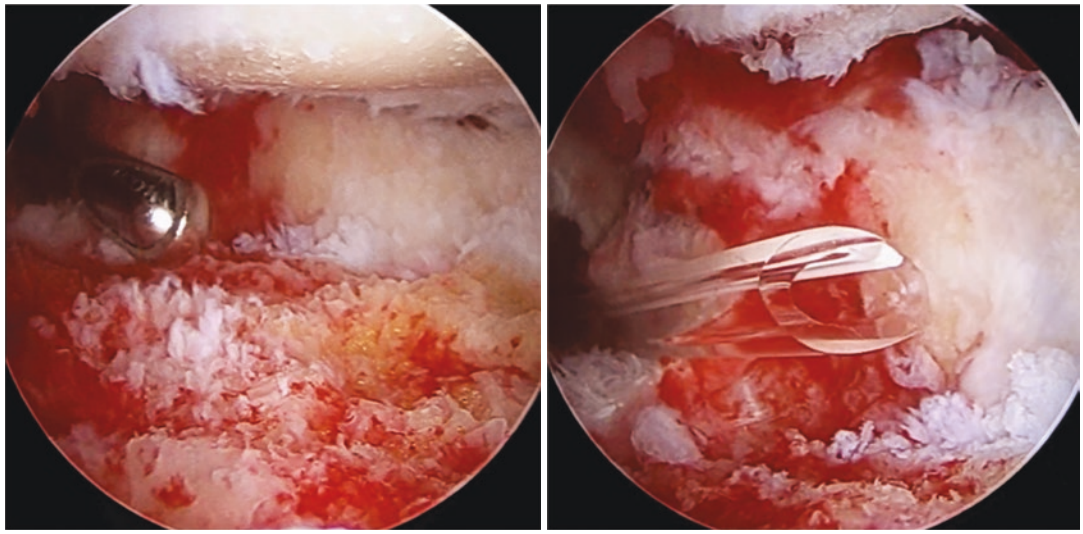

Fig. 43.5 Final congruency is achieved by finishing the surface using a shaver (left), and a suction tube is inserted through direct lateral portal (right image)

43.5 Pitfalls

- Continuous usage of power tools such as a motorized shaver or a radiofrequency device in a narrow space is dangerous because thermal injury may occur to the surrounding nerves. Radial (posterior interosseous) nerve, anterior interosseous nerve and ulnar nerve are close to the capsule, and should be protected.
- In cases of Larsen Grade 4 degenerative changes, with incongruency of ulno-humeral articulation, some patients may suffer from painful crepitus in motion after surgery. In these cases, gentle assisted range of motion exercises may improve symptoms. Hyaluronic acid injection may assist the improvement of articular congruity.

43.6 Postoperative Management and Rehabilitation

Compression bandage is applied for a few days after surgery. Active and mild passive range of motion exercises are started immediately after surgery. Valgus stress should be avoided in rehabilitation for 6–8 weeks after surgery. Intra-articular hyaluronic acid injection is an option in the postoperative period, and the author recommends an intra-articular injection every 1 or 2 weeks (4–5 injections in total). Articular congruity will become better in 2 or 3 years and is preserved longer if the disease activity is well controlled by proper medication (Fig. 43.6). Continuous motion without load is helpful for fibrocartilage regeneration in the debrided bony surface. Loading the operated upper limb should be avoided for 6–12 months postoperatively.

43.7 Complications

- Nerve injury may occur if a motorized shaver or abrader penetrates the anterior capsule.
- Prolonged procedure using power tools or radiofrequency devices increases the possibility of thermal injury even if the capsule is still intact.

The author has experienced two cases of posterior interosseous nerve palsy and a case of anterior interosseous nerve palsy, and the capsule was noted

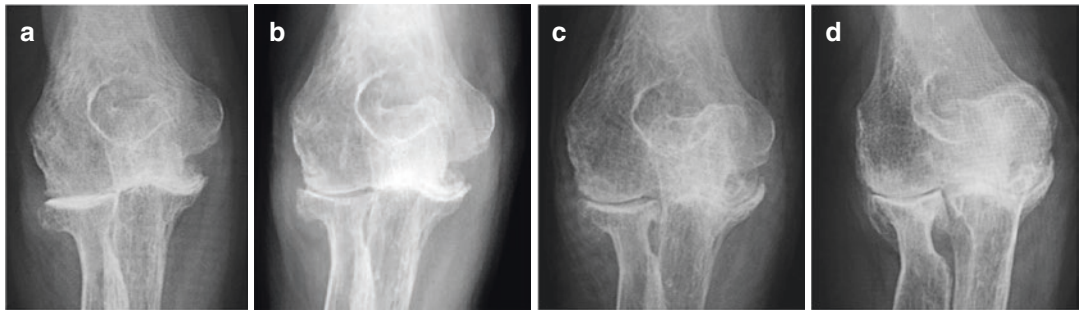

Fig. 43.6 Follow-up radiography of plastic radial head resection is shown. (**a**) Sclerosis of the radial head in preoperative radiograph. (**b**) Radiograph 3 months after operation. (**c**) Radiographic appearance 3 years after operation shows better radio-capitellar congruity with a joint space. (**d**) Radiographic appearance 6 years after operation. Joint space is still preserved although degeneration has progressed

to be intact in retrospective video analysis of the recorded procedures. The nerve palsy recovered in all cases in 6–12 months postoperatively.

43.8 Results

In the authors series, 15 rheumatoid arthritis elbows underwent radial head partial resection after proper medication and control of disease activity. Six elbows were rated as Larsen Grade 3 and 9 elbows were rated as Larsen Grade 4. The patients were followed up for more than 2 years (mean 4.5 years). Pain reduced in all elbows except one. Flexion/extension motion was 115/−39 and pronation/supination motion was 55/54 preoperatively. The range improved to 127/−27 in flexion/extension and to 60/65 in pronation/supination. The radiographic grade improved in 2 elbows, did not change in 11, and worsened in 2. This preliminary result showed possibility of maintaining elbow function and avoiding total replacement arthroplasty even in Larsen Grade 3 or 4 (Fig. 43.5).

Arthroscopic Releases of the Proximal Radioulnar Joint

44

Eugene T. Ek and Kemble K. Wang

44.1 Background

Post-traumatic elbow stiffness is a common problem following elbow trauma [1]. The normal range of motion of the elbow has been described as a flexion/extension arc of 0–140° and a pronation/supination arc of 85–85° [2]. Significant loss of range of motion in either the sagittal or rotational plane can be disabling, particularly for the young patient [3, 4]. Multiple aetiologies exist for post-traumatic elbow stiffness. These include soft tissue contractures, fracture malunions, heterotopic ossification, and loss of articular cartilage [5]. Loss of rotational range of motion most commonly occurs following injuries around the proximal radioulnar joint (PRUJ). While efforts at managing elbow stiffness have invariably addressed sagittal plane motion, there is limited literature on the outcomes on the specific surgical management of rotational stiffness of the elbow [4, 6, 7].

Open surgical releases of elbow contractures have been the traditional approach in the published literature [7–9]. Arthroscopic contracture releases have been increasingly described and may lead to less postoperative pain, quicker recovery, and reduced risk of recurrence [4]. Additionally, arthroscopic approach may allow better visualization of the PRUJ circumferentially than an open approach. This chapter presents an all-arthroscopic technique for addressing rotational loss of range of motion due to post-traumatic abnormalities in the PRUJ.

44.1.1 Surgical Anatomy

Normal forearm rotation requires normal rotation of the radius around the ulna, along an axis of motion subtended from the centre of the radial head proximally to the centre of the distal ulna at the wrist [10]. While disturbances anywhere along the forearm can lead to loss of rotation, this chapter will focus on pathologies at the PRUJ.

Following trauma, there can be both soft tissue and bony causes of rotational limitations. The radial head articulates with both the capitellum and the radial fossa of the proximal ulna. In the average elbow, the radial fossa of the ulna is in contact with 66°, or approximately 18% of the circumference of the radial head [11]. The PRUJ have been found to be more congruent in supination, with pronation resulting in anterior shift of the radial head. During pronation, the posterior part of the annular ligament becomes taut and resists excessive anterior translation [12]. Conversely, the anterior portion of the annular ligament becomes taut in supination.

E. T. Ek (✉) · K. K. Wang
Melbourne Orthopaedic Group,
Melbourne, VIC, Australia

Department of Surgery, Monash University,
Melbourne, VIC, Australia

© ISAKOS 2022

D. N. Bhatia et al. (eds.), *Arthroscopy and Endoscopy of the Elbow, Wrist and Hand*,
https://doi.org/10.1007/978-3-030-79423-1_44

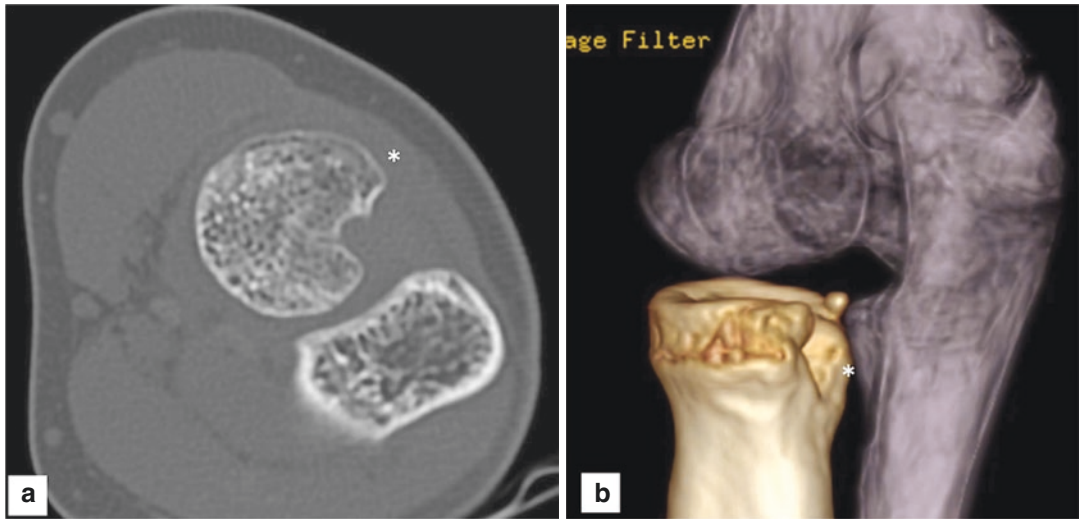

Fig. 44.1 Subtle malunion of the radial head and neck (asterisk) following a fracture in a 13-year-old girl. (**a**) Axial CT scan and (**b**) 3D reconstruction views of the proximal radioulnar joint (PRUJ) demonstrate the PRUJ incongruency from the prominent bone on the radial neck (asterisk) and this resulted in a bony rotational block to motion

Fractures and injuries of the proximal radius and ulna can lead to contractures of the annular ligament complex and scarring within the PRUJ, which could lead to restriction in pronation and supination. Malunion of the proximal radius, even if subtle, can lead to incongruency during its rotational arc within the radial fossa of the ulna (Fig. 44.1). A cam effect can result in levering and subluxation of the joint. Additionally, heterotopic ossification frequently occurs in the elbow following trauma [6], and if affecting the PRUJ, may be an additional bony source of rotational stiffness. Arthroscopically, both soft tissue contractures and bony abnormalities in the PRUJ can be addressed.

44.2 Indication and Contraindications

Indications for arthroscopic PRUJ release include:

- Rotational pathology localizable to the PRUJ
  - Arthrofibrosis of the PRUJ
  - Bone deformity of the radial neck causing impingement against the sigmoid notch
- Rotational forearm stiffness resulting from previous trauma, limiting patient's function
- Failed physiotherapy and conservative management >6 months

The procedure is contraindicated in the following:

- Existence of advanced degenerative changes in PRUJ, radiocapitellar, or ulnohumeral joints
- Grade IV heterotopic ossification or complete radioulnar synostosis
- Complete radiocapitellar dislocation
- Congenital radioulnar synostosis or radiocapitellar dislocations
- Radial head avascular necrosis
- Rotational limitation due to radial/ulnar shaft or distal radial/ulnar malunions

44.3 Surgical Technique

The procedure is performed with the patient in lateral decubitus position. The arm is secured on an arm support and a high-arm non-sterile tourni-

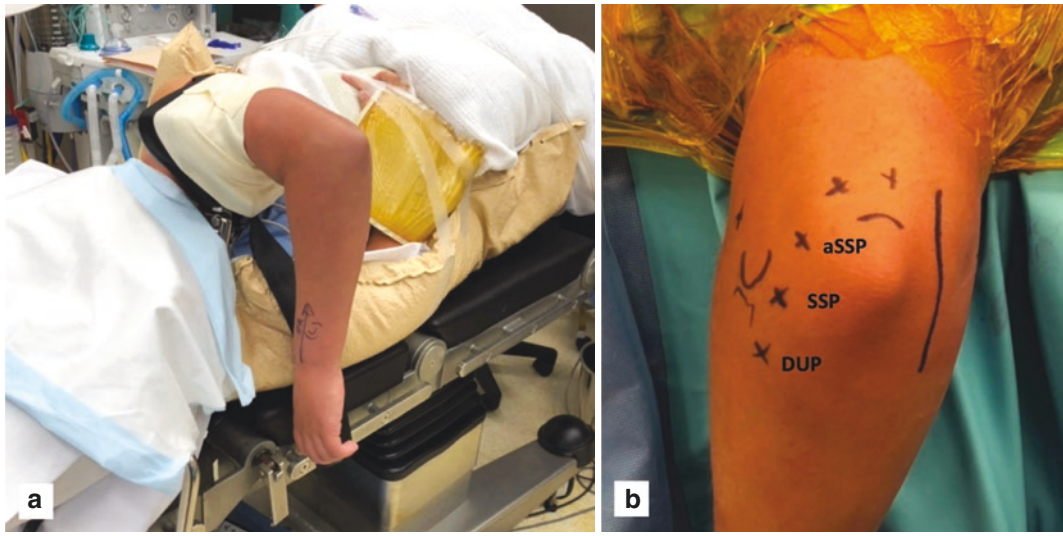

Fig. 44.2 Positioning of the patient. (**a**) The patient is placed in the lateral decubitus position with a beanbag support. The arm is freely draped over an arm support. (**b**) The three portals used for treatment of the radiocapitellar and proximal radioulnar joint. Accessory soft-spot portal (aSSP), soft-spot portal (SSP) and the distal ulna portal (DUP)

quet is used. The arm is positioned such that the forearm can be easily manoeuvred intraoperatively into maximum pronation and supination (Fig. 44.2a). Prior to prepping and draping, a formal examination of passive range of motion is carried out and documented.

44.3.1 Arthroscopic Assessment

Following insufflation of the joint with normal saline, a standard six-portal diagnostic arthroscopy is carried out. This utilizes the posterior and the accessory posterior portals for the posterior compartment; soft-spot and accessory soft-spot portal for the posterolateral compartment; and the proximal anteromedial and anterolateral portals for the anterior compartment (Fig. 44.2b). Most of PRUJ rotational contracture release is performed through the posterolateral compartment. In addition to the standard soft-spot (SSP) and accessory soft-spot portal (aSSP), a third posterolateral compartment portal (distal ulna portal DUP) could be made 2 cm distally as an additional instrumentation and viewing portal (Fig. 44.2b). These three portals allow access to the majority of the PRUJ through a posterior trajectory. If required, additional work on the PRUJ could be performed through the anterior compartment.

44.3.2 Arthroscopic Surgical Release

- Initially the arthroscope is inserted into the soft-spot portal (SSP) and a curved shaver or a curved 50° arthroscopic cautery device is used through the accessory soft-spot portal (aSSP) to debride the contracted scar and soft tissue within the PRUJ (Fig. 44.3a). The posterior portion of the annular ligament is released (Fig. 44.3b), and this improves pronation range while also allowing better visualization of the PRUJ. Additional contracted scar deep to the annular ligament is also removed until the bony and cartilaginous outlines of the PRUJ are clearly visible for both the ulnar and radial sides (Fig. 44.3c).
- Next, bony incongruency is addressed. This begins with a careful assessment of rotational block arthroscopically while the forearm is rotated. Any cam effect is noted, and abnormal

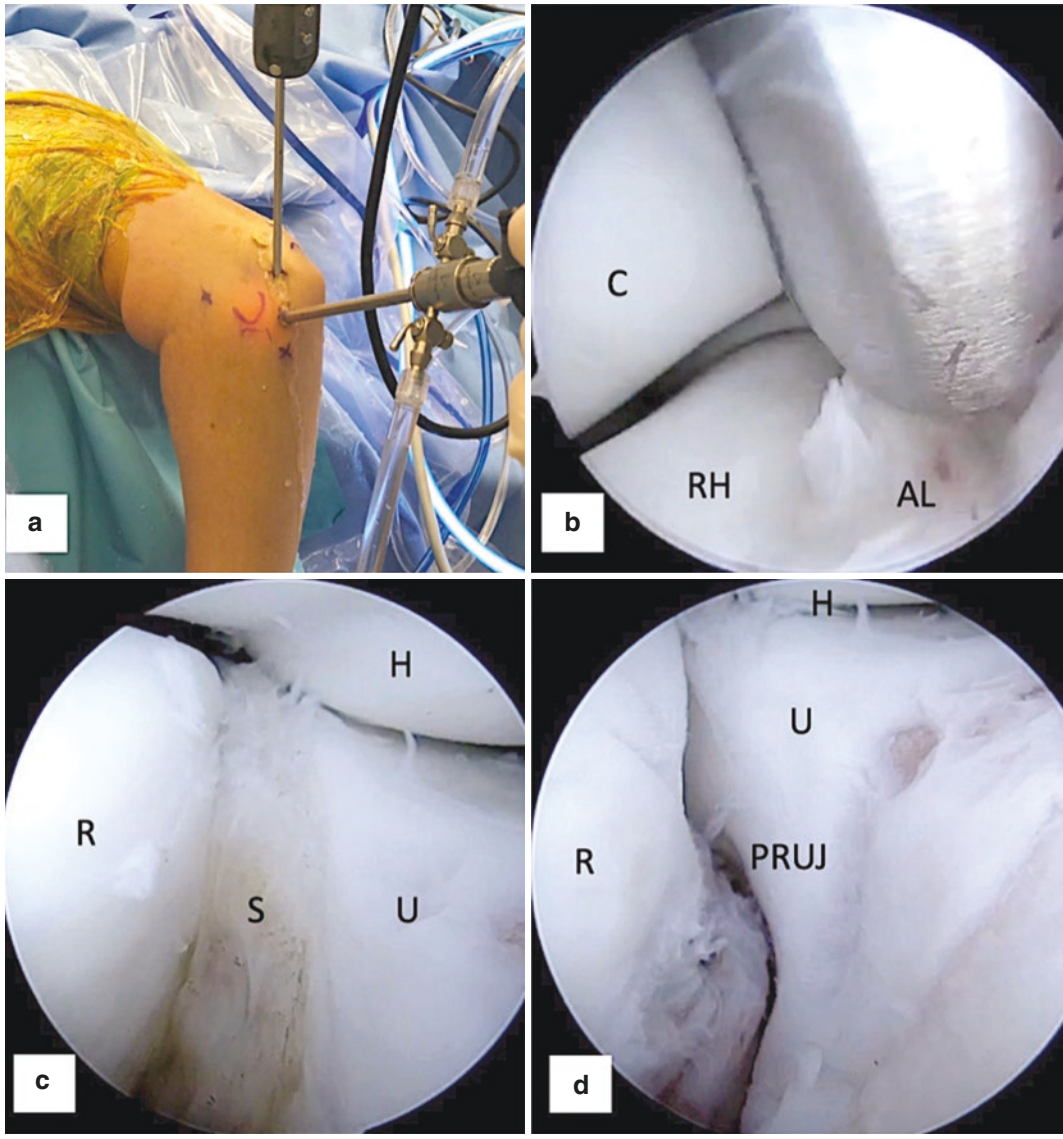

Fig. 44.3 (**a**) To view the radiocapitellar joint and the upper part of the PRUJ, the arthroscope is inserted into the soft-spot portal (SSP) and the shaver or radiofrequency ablator is inserted through the accessory soft-spot portal (aSSP). (**b**) Arthroscopic visualization of the radiocapitellar joint. Capitellum (C), radial head (RH). Debridement is initially carried out on the posterior portion of the annular ligament (AL) which allows visualization of the radial neck and PRUJ. (**c**) After debridement, scar tissue (S) is visualized within the PRUJ. (**d**) Further debridement and osteoplasty of this region then allows full visualization of the respective joint surfaces of the PRUJ

bone or heterotopic ossification is removed with a combination of hooded burr, shaver, and small osteotome (Fig. 44.3d). Bony osteoplasty may necessitate removal of cartilaginous surfaces on either the margins of the radial head or within the radial fossa of the ulna.

- To gain better visualization and access to the inferior portion of the radial neck and PRUJ, the arthroscope is then entered to the distal ulna portal (DUP) (Fig. 44.4). A rongeur may be used to extract osteophytes or loose bodies. If there was any further contracture limiting forearm rotation, this can be released using the radiofrequency ablator inserted through the SSP. In addition, shaver or burr can be used to debride any further bony prominence around the radial

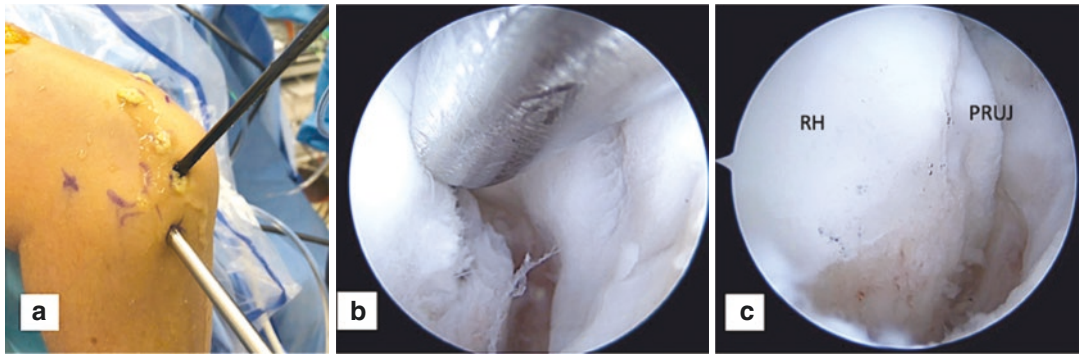

Fig. 44.4 (**a**) To access the inferior portion of the proximal radioulnar joint, the arthroscope is entered into the distal ulna portal (DUP) and a shaver or radiofrequency ablator is inserted into the soft-spot portal (SSP). (**b**, **c**) These portals allow for access and visualization of the PRUJ to perform further debridement and osteoplasty of the radial neck and remove any block to forearm rotation

neck causing impingement. This process is continued until passive pronosupination of the forearm reveals no further blockage to rotation. In the posterolateral compartment, debridement and osteoplasty should be limited to proximal to the radial tuberosity, as distal to this the posterior interosseous nerve is potentially at risk.

44.4 Tips and Tricks

- Careful demarcation between osteophytes and normal bone should be made in order to avoid removing excess bone.
- To minimize risk of injury to the posterior interosseous nerve, suction should be minimized, and debridement should remain proximal to the radial tuberosity.
- Passive pronosupination of the forearm will identify sites of impingement and tethering.

44.5 Postoperative Rehabilitation and Management

No restrictions are applied to weight-bearing or range of motion. A sling may be used for comfort and discontinued after 3 days. Continuous passive motion (CPM) is often used on the elbow within the first 24 h to reduce swelling and also prevent loss of motion in the sagittal plane. Physiotherapy is encouraged for both active and passive rotational range of motion and continued for a minimum of 6 weeks. Gains in range of motion are usually maintained following this procedure (Fig. 44.5).

44.6 Complications

No complications have been encountered in the authors' experience in this procedure. However, potential complications are common to all arthroscopic elbow procedures. These include:

- Iatrogenic nerve injuries
- Excessive destabilization of ligamentous stabilizers such as the lateral ulnar collateral ligament complex
- Excessive removal of bone
- Articular surface damage leading to secondary degenerative changes
- Recurrence of rotational contracture

Fig. 44.5 Preoperative supination (**a**) and pronation (**b**) clinical photographs of a 13-year-old girl who underwent arthroscopic release for rotational stiffness and impingement secondary to malunion of radial head fracture. (**c**) and (**d**) 6 months postoperative clinical photographs demonstrating restoration of forearm rotation

References

1. Charalambous CP, Morrey BF. Posttraumatic elbow stiffness. J Bone Jt Surg A. 2012;94:1428–37.
2. Gunal I, Kose N, Erdogan O, et al. Normal range of motion of the joints of the upper extremity in male subjects, with special reference to side. J Bone Jt Surg A. 1996;78:1401–4.
3. Morrey BF, Askew LJ, An KN, et al. A biomechanical study of normal functional elbow motion. J Bone Jt Surg A. 1981;63:872–7.
4. Ling SKK, Lui TH, Faan YS, et al. Post-traumatic elbow rotational stiffness. Shoulder Elb. 2014;6:119–23.
5. Mellema JJ, Lindenhovius ALC, Jupiter JB. The posttraumatic stiff elbow: an update. Curr Rev Musculoskelet Med. 2016;9:190–8.
6. Vasileiadis GI, Ramazanian T, Kamaci S, et al. Loss of pronation-supination in patients with heterotopic ossification around the elbow. J Shoulder Elb Surg. 2019;28:1406–10.
7. Ek ETH, Paul SK, Hotchkiss RN. Outcomes after operative treatment of elbow contractures in the pediatric and adolescent population. J Shoulder Elb Surg. 2016;25:2066–70.
8. Piper SL, Lattanza LL, Shen TS, et al. Open surgical release of posttraumatic elbow contracture in children and adolescents. J Pediatr Orthop. 2019;39:241–6.
9. Bręborowicz M, Lubiatowski P, Długosz J, et al. The outcome of open elbow arthrolysis: comparison of four different approaches based on one hundred cases. Int Orthop. 2014;38:561–7.
10. Hollister AM, Gellman H, Waters RL. The relationship of the interosseous membrane to the axis of rotation of the forearm. Clin Orthop Relat Res. 1994;298:272–6.
11. Weiss APC, Hastings H. The anatomy of the proximal radioulnar joint. J Shoulder Elb Surg. 1992;1:193–9.
12. Kim HJ, Yi JH, Jung JW, et al. Influence of forearm rotation on proximal radioulnar joint congruency and translational motion using computed tomography and computer-aided design technologies. J Hand Surg Am. 2011;36:811–5.

Part VIII

Elbow Tumour-Like Lesions

Arthroscopic Transarticular Excision of Elbow Ganglion Cyst

45

Deepak N. Bhatia

45.1 Background

The elbow is an unusual site for development of a ganglion cyst, and these cysts are usually associated with joint degenerative changes (Fig. 45.1). Rarely, these cysts may compress nerves around the elbow and result in significant neurological symptoms [1–3]. Transarticular excision of the ganglion is a minimally invasive technique that involves "cystoscopic" visualization of the cyst interior and permits complete intracystic excision of the cyst contents and membranes.

45.1.1 Surgical Anatomy

Elbow ganglion cysts are usually proximal to the arcade of Frohse (Type A) or rarely distal to it (type B). Type A ganglions arise from the radiocapitellar joint and may compress the radial nerve and its branches. Large ganglions, however, may span the entire region. The ganglion dissects the muscle plane between supinator and the elbow extensors and displaces the radial nerve and its branches (Fig. 45.2). A communication aperture between the cyst and elbow joint is almost always present and can be identified in the anterolateral capsule during arthroscopy. Excision of lateral elbow capsule anterior to the lateral ligamentous complex permits safe access to the cyst for excision. The radial nerve and its branches are closely related to the medial and anterior aspect of the cyst walls and the lateral cutaneous nerve (LCN) is at-risk during excision of anterolateral cyst wall.

45.2 Indications and Contraindications

Persistent elbow pain and/or weakness resulting from the mass effect of an enlarging ganglion necessitates ganglion excision. Rarely, the ganglion may be asymptomatic and surgery may be indicated for cosmesis.

There are no absolute contraindications to the procedure. Ganglion cysts that do not communicate with the articular recesses may be difficult to access via the transarticular approach.

45.3 Surgical Technique

The surgery is performed with the patient in lateral decubitus position, and a tourniquet is used during the procedure. A 2.9-mm arthroscope and sheath (ConMed, Linvatec, Largo) are used, and a 50-mL syringe is used for initial air arthros-

D. N. Bhatia (✉)
SPORTSMED Mumbai, Mumbai, India

Sir HN Reliance Foundation Hospital, Mumbai, India
e-mail: shoulderclinic@gmail.com

© ISAKOS 2022

D. N. Bhatia et al. (eds.), *Arthroscopy and Endoscopy of the Elbow, Wrist and Hand*,
https://doi.org/10.1007/978-3-030-79423-1_45

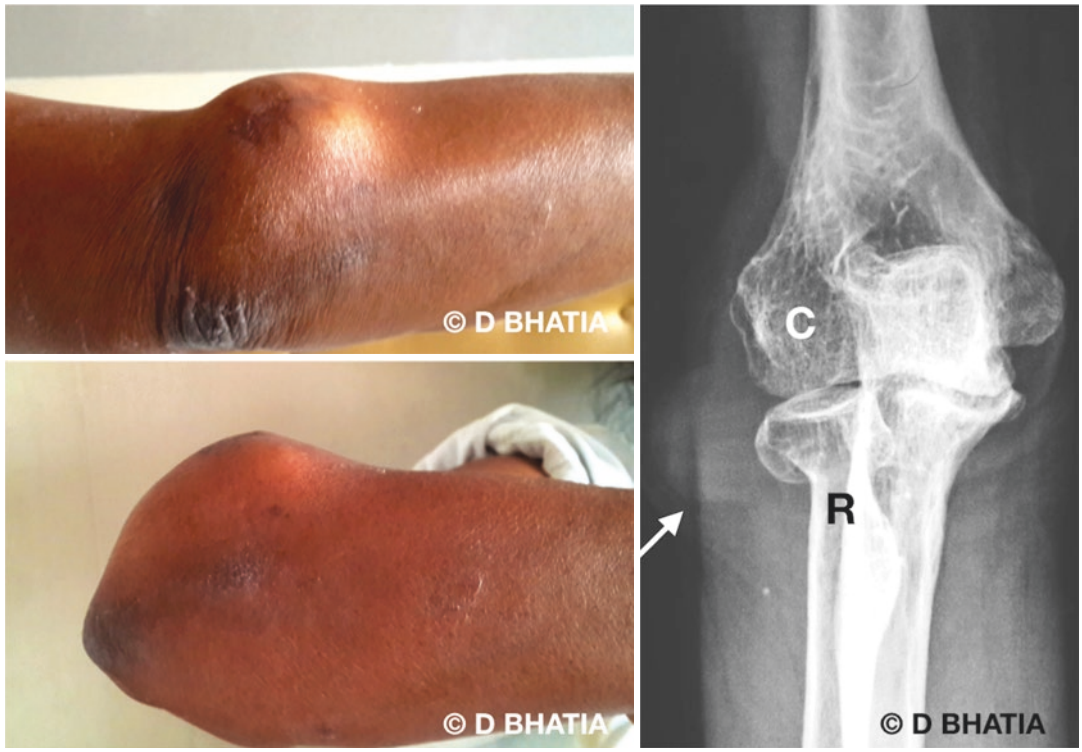

Fig. 45.1 A large ganglion cyst of the right elbow is seen extending distal to the radiocapitellar joint (left images). Radiograph shows radiocapitellar arthritis and the soft tissue shadow of the cyst (arrow, right image) (*R* radial head, *C* capitellum). (© D. Bhatia)

copy. Subsequently, gravity inflow is used to minimize fluid extravasation into the arm and forearm.

45.3.1 Portals

Two standard portals are used in the procedure (Fig. 45.3):

- Proximal anteromedial portal (AM) is the viewing portal throughout the procedure. This portal is placed slightly anterior to permit transarticular entry into the ganglion cyst.
- Proximal anterolateral portal (AL) is the working portal and is directed into the cyst under direct visualization.
- The "radial head portal" (RH) may be used if additional radiocapitellar procedures are necessary [4].

45.3.2 Diagnostic Arthroscopy and Synovectomy

The AM viewing portal is used to assess radiocapitellar degenerative changes and the presence of synovitis. The lateral capsule is carefully inspected and the ganglion aperture is identified. This is usually seen as a longitudinal slit in the lateral capsule and is covered by a thin membrane (Fig. 45.4).

45.3.3 Transarticular Cystoscopy

The arthroscope in AM portal is advanced towards the aperture and the thin inner membrane is breached with gentle pressure. Entry into the cyst is visualized externally as transillumination of the swelling (Fig. 45.5a). A 70° arthroscope is used for panoramic visualization. The lateral and

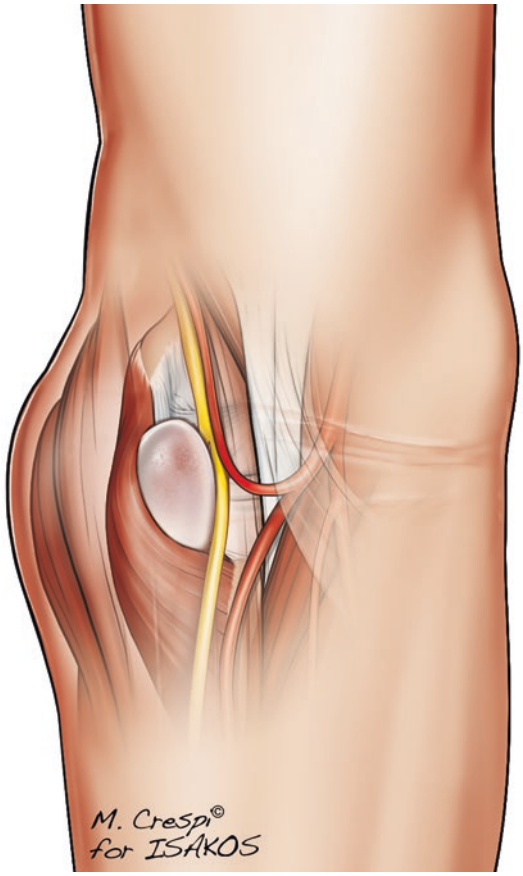

Fig. 45.2 Illustration shows a radiocapitellar ganglion cyst in the intermuscular plane between the elbow extensor muscles and the supinator. The posterior interosseous nerve and the superficial radial nerve are displaced by the enlarging cyst. (M. Crespi © for ISAKOS)

medial cyst walls are identified, and yellowish gelatinous cyst fluid is seen. A needle is inserted via the AL portal site and the cyst fluid is aspirated. Thicker gel-like content is removed with a grasper or a shaver (Fig. 45.5b).

45.3.4 Cyst Excision

A 3.5 mm shaver blade is inserted via the AL portal and is directed through the aperture into the anterior elbow. The lateral capsule is debrided and aperture is widened to expose the ganglion cyst. The lateral wall is debrided until muscle fibers are visualized proximally and fat is exposed distally. Any bleeding points are coagulated with a radiofrequency probe. The medial wall is debrided carefully to avoid damage to supinator and posterior interosseous nerve at the arcade of Frohse (Fig. 45.6).

45.3.5 Final Assessment

Visualization of the fat pad and muscle fibers along the lateral aspect of the cyst, and resection of the anterolateral joint capsule along the medial aspect of the cyst confirms adequate cyst excision (Figs. 45.7 and 45.8).

45.4 Tips and Tricks

- A 2.9 mm arthroscope with a 4 mm sheath is the ideal size for transarticular passage into the cyst. The AM portal is placed more anterior than usual, and cyst entry is confirmed with transillumination of the cyst.
- The communication aperture of a large ganglion cyst is identified around the radiocapitellar joint. Rarely, a ganglion cyst aperture may not be visualized and the cyst may be accessed by lateral capsular excision.

45.5 Pitfalls

- The radial nerve and its branches are at-risk of injury during the procedure. These nerves are displaced from their usual course and may be damaged during medial wall excision. Branches to extensor muscles and LCN may be injured during lateral wall dissection. Blunt dissection should be used initially to define a plane between the capsule and surrounding muscles, and a non-aggressive shaver blade (3/3.5 mm) should be used for cyst wall excision along this plane.
- Direct portal placement (outside-in) into the cyst may injure the displaced nerves. Transarticular cyst entry is safe and can be performed using standard elbow arthros-

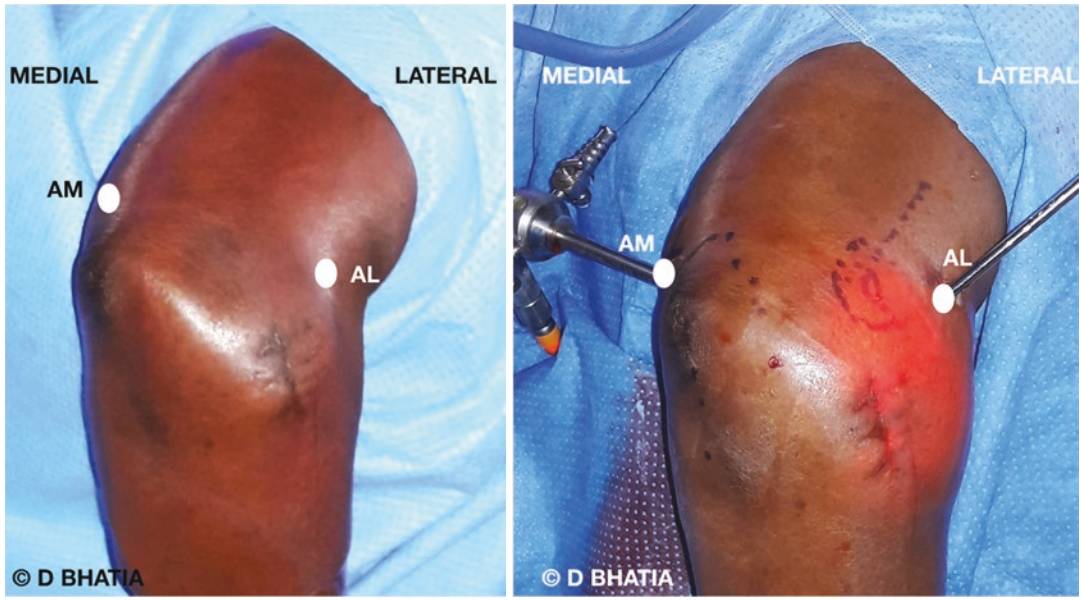

Fig. 45.3 Elbow position and portals are shown. Scar from previous open surgery is seen and two portals (AM and AL) are used (left image). Transarticular penetration of the cyst with the arthroscope (AM portal) demonstrates transillumination of the cyst. The shaver blade is used through the AL portal for cyst excision (right image). (© D. Bhatia)

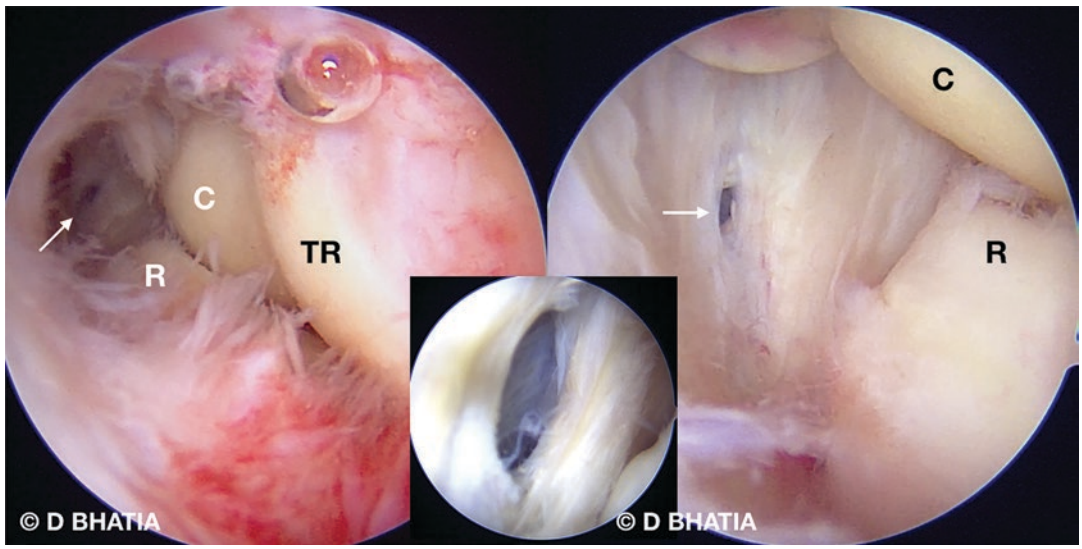

Fig. 45.4 Arthroscopic visualization of the anterior elbow shows synovitis (left image). The cyst communicates with the joint via a slit-like aperture (arrow). Magnified view of the cyst aperture in the lateral capsule is shown (right and inset image). The aperture is seen to be covered with a thin membrane (inset image) (*C* capitellum, *TR* trochlea, *R* radial head). (© D. Bhatia)

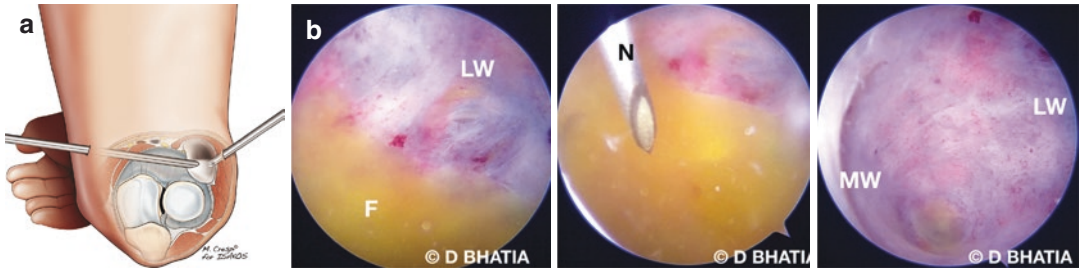

Fig. 45.5 (**a**) Transarticular cyst excision is illustrated. (**b**) "Cystoscopic" view of the ganglion is demonstrated. The cyst is filled with a yellow fluid (F, left image). A needle (N) is used to aspirate cyst fluid (center image) and the distal extent of the cyst is then seen (right image). The lateral and medial walls (LW and MW) are visualized after aspiration. (© D. Bhatia)

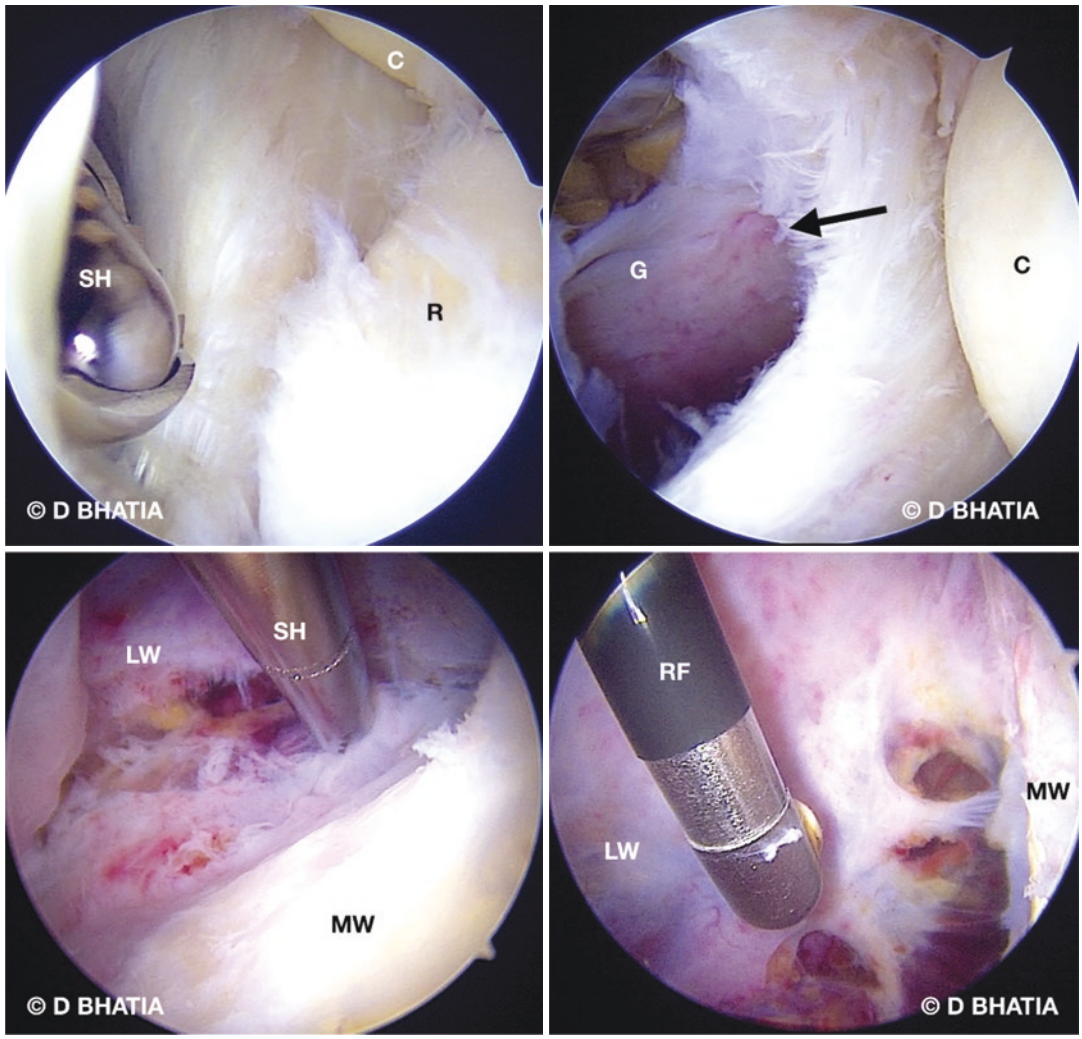

Fig. 45.6 "Cystoscopic" view of the ganglion excision is demonstrated. A shaver (SH) is used to excise cyst aperture and lateral capsule until the interior of ganglion (G) is seen (top images). The medial and lateral cyst walls (MW and LW) are excised using a shaver and radiofrequency probe (RF) (bottom images). (© D. Bhatia)

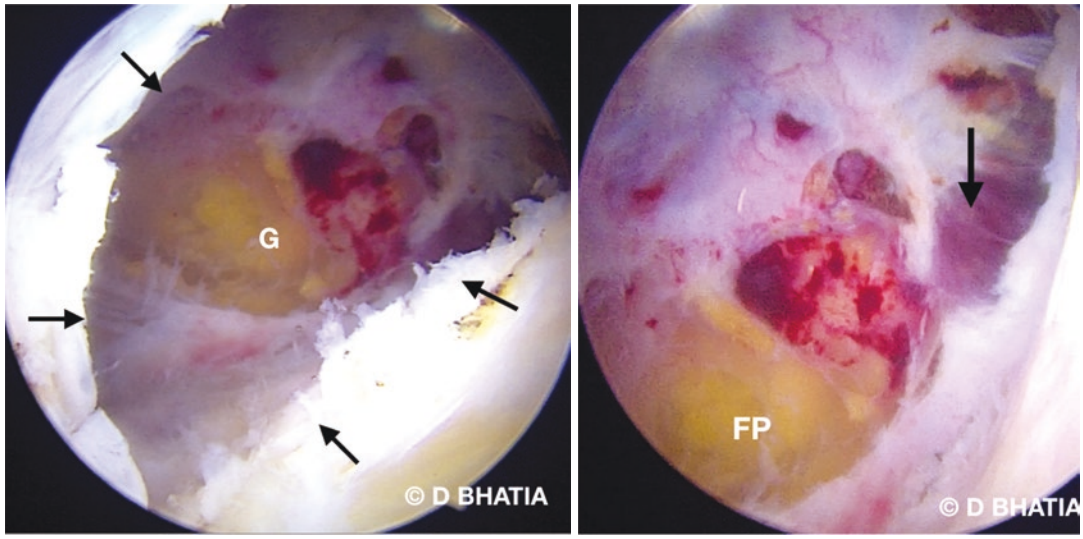

Fig. 45.7 Complete excision of the ganglion is demonstrated. The lateral capsule (arrows, left image) is excised to prevent recurrence. Excision of lateral cyst wall shows overlying muscle fibers (arrow) and fat pad (FP) (right image). (© D. Bhatia)

Fig. 45.8 Complete resolution of the ganglion cyst at long-term follow-up is demonstrated. (© D. Bhatia)

copy portals and intraoperative anatomical landmarks.

- Recurrence of the ganglion cyst is possible. Adequate excision of lateral elbow capsule and cyst walls, and use of a compression bandage prevents recurrence.

45.6 Postoperative Management and Rehabilitation

A bulky soft tissue dressing is used in the immediate postoperative period, and this is changed to portal dressing and compression bandage on the

fourth postoperative day. A sling is used for comfort and discarded in the first week. Elbow movements and forearm rotations are permitted without any restrictions. The compression bandage is worn for 6 weeks. Elbow strengthening is initiated in the second week, and unrestricted activity is permitted after 6 weeks.

45.7 Complications

Injury to the radial nerve or branches may result in cutaneous parasthesias/pain and/or motor weakness. Recurrence of the cyst is a possibility.

Conflict of Interest The author certifies that he has no commercial associations (e.g., consultancies, stock ownership, equity interest) that might pose a conflict of interest in connection with the submitted article. The author retains the copyright to the images, videos, and content in this chapter.

References

1. Steiger R, Vogelin E. Compression of the radial nerve caused by an occult ganglion. Three case reports. J Hand Surg Am. 1998;23B:420–1.
2. Yamazaki H, Kato H, Hata Y, Murakami N, Saitoh S. The two locations of ganglions causing radial nerve palsy. J Hand Surg Eur. 2007;32(3):341–5.
3. Feldman MD. Arthroscopic excision of a ganglion cyst from the elbow. Arthroscopy. 2000;16(6):661–4. https://doi.org/10.1053/jars.2000.4628.
4. Bhatia DN. Arthroscopic resection of the radial head. In: Bain G, Eygendaal D, van Riet R, editors. Surgical techniques for trauma and sports related injuries of the elbow. Berlin: Springer; 2020.

46 Arthroscopic Management of Intra-articular Benign Tumours of the Elbow

Deepak N. Bhatia

46.1 Background

Benign tumours and locally aggressive tumour-like lesions may occur in the juxta-articular or intra-articular regions of the elbow. The diagnosis is often delayed and patients present with chronic disabling pain and progressive elbow stiffness. Arthroscopic excision may be possible in lesions that are focal and restricted to the anterior and posterior intracapsular elbow recesses. Similarly, the anterosuperior (supratrochlear) extra-articular aspect of the anterior elbow may be accessed by capsular dissection in this region. Benign tumours that have been successfully treated with arthroscopic excision (author's experience) include (1) osteoid osteoma, (2) synovial chondromatosis, and (3) vascular malformation.

46.2 Indications and Contraindications

- Benign tumours and tumour-like lesions must be evaluated carefully with contrast imaging and biopsy if indicated. Any possibility of malignant change must be evaluated prior to surgery.
- Focal and arthroscopically accessible location is a prerequisite for arthroscopic excision.
- Low-flow vascular malformations lack arteriovenous shunting and can be safely excised arthroscopically.

Extra-articular location of the lesion and high-flow vascular malformations are contraindications for arthroscopic excision.

46.3 Surgical Technique

Elbow arthroscopy is performed with the patient in the lateral decubitus position. Both 30° and 70° arthroscopes are used, and gravity inflow is used to minimize fluid extravasation into the arm and forearm.

46.3.1 Portals

Standard proximal anteromedial (AM) and anterolateral (AL) portals are used for the anterior elbow. Direct posterior-central (PC) and posterolateral (PL) portals are used to visualize and work in the posterior recess.

D. N. Bhatia (✉)
SPORTSMED Mumbai, Mumbai, India

Sir HN Reliance Foundation Hospital, Mumbai, India
e-mail: shoulderclinic@gmail.com

© ISAKOS 2022

D. N. Bhatia et al. (eds.), *Arthroscopy and Endoscopy of the Elbow, Wrist and Hand*,
https://doi.org/10.1007/978-3-030-79423-1_46

46.3.2 Osteoid Osteoma

An osteoid osteoma is a benign osteoblastic tumour composed of a nidus of osteoid and woven bone and rimmed by vascularized fibrous connective tissue. Sclerotic bone reaction may be present around the lesion. Radiofrequency ablation is often used to treat these lesions; however, intra-articular elbow lesions may sometimes be difficult to access safely for ablation and arthroscopic excision may be performed [1] (Fig. 46.1a).

- Arthroscopy is performed using standard AL and AM portals and accessory portals are used if necessary.
- A thorough synovectomy and adhesiolysis are performed and a 70° arthroscope is used for visualizing the recesses.
- Supratrochlear lesions are identified by excision of the superior synovial membrane or capsule and retraction using an accessory portal.
- The osteoid osteoma is identified as a purplish region of soft trabecular bone surrounded circumferentially by dense whitish-appearing bone. A probe is used to apply gentle pressure and traces of blood are seen oozing from the soft trabecular bone under pressure (Fig. 46.1b).
- An angled punch is then used to obtain a biopsy of the lesion via a cannula. The deep aspect of the lesion appears reddish and bleeds with reduction of intra-articular fluid pressure.
- The soft zone of the lesion is excised piecemeal using angled punches and curettes. A shaver is used to remove any debris from the joint.
- The sclerotic peripheral zone is separated from normal bone using a small joint angled chisel and excised piecemeal with a punch. Accessory portals may be used to position the chisel at various angles for circumferential excision.
- Finally, a radiofrequency probe is used to ablate the deep and peripheral regions. Ablation is performed in short pulses for approximately 5–10 min until the reddish bleeding tissue is no longer visible. A thorough lavage is given and portals are closed.

46.3.3 Synovial Chondromatosis

This is a benign neoplastic process characterized by synovial metaplasia and proliferation resulting in multiple intra-articular cartilaginous loose bodies (Fig. 46.2a). Synovectomy and removal of loose bodies is essential to prevent progressive joint degeneration. Arthroscopic removal of loose bodies is a minimally invasive alternative to open surgery and permits access to both anterior and posterior recesses [2].

- Arthroscopy is performed using standard AL and AM portals anteriorly and PC and PL portals on posterior aspect.
- Initial joint evaluation is limited and numerous loose bodies hamper visualization.
- A 4.5 mm cannula is used throughout the procedure. Osteochondral loose bodies are removed with a grasper through the cannula.
- Next suction is applied to the cannula and several smaller and soft chondral loose bodies are directly removed using the suction.
- A shaver is finally used to remove bodies that are attached to the synovium and a thorough synovectomy is performed (Fig. 46.2b).
- The steps are repeated in the posterior recess of the elbow for complete resection.

46.3.4 Vascular Malformation

Vascular malformations can be classified haemodynamically into low- and high-flow types [3]. Low-flow vascular malformations are formed by non-arterial components (capillary, venous, and lymphatic malformations) and lack arteriovenous shunting. Intra-articular low-flow lesions that are located in the anterior supracapitellar region may be safely excised using the technique described here (Fig. 46.3a).

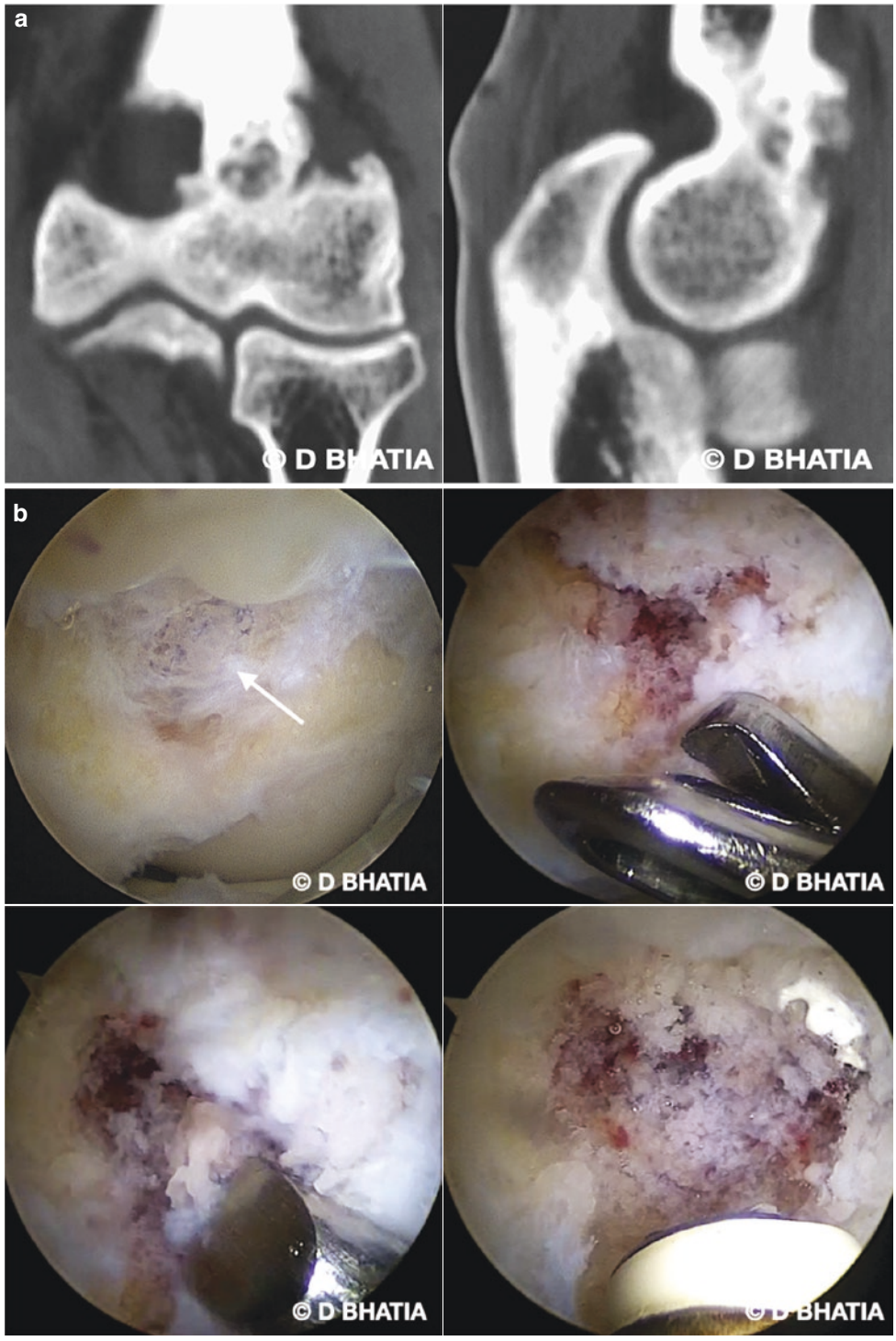

Fig. 46.1 (**a**) An osteoid osteoma is seen in the supratrochlear region on CT scans (© D. Bhatia). (**b**) Arthroscopic excision of an osteoid osteoma is demonstrated. The lesion visualized is the supratrochlear region after excision of the capsule (arrow, top left). A biopsy is obtained from the lesion using a punch and the tumour is removed piecemeal (top right). A chisel is used to excise the sclerotic peripheral zone (bottom left). Radiofrequency ablation of the tumour is performed (bottom right). (© D.Bhatia)

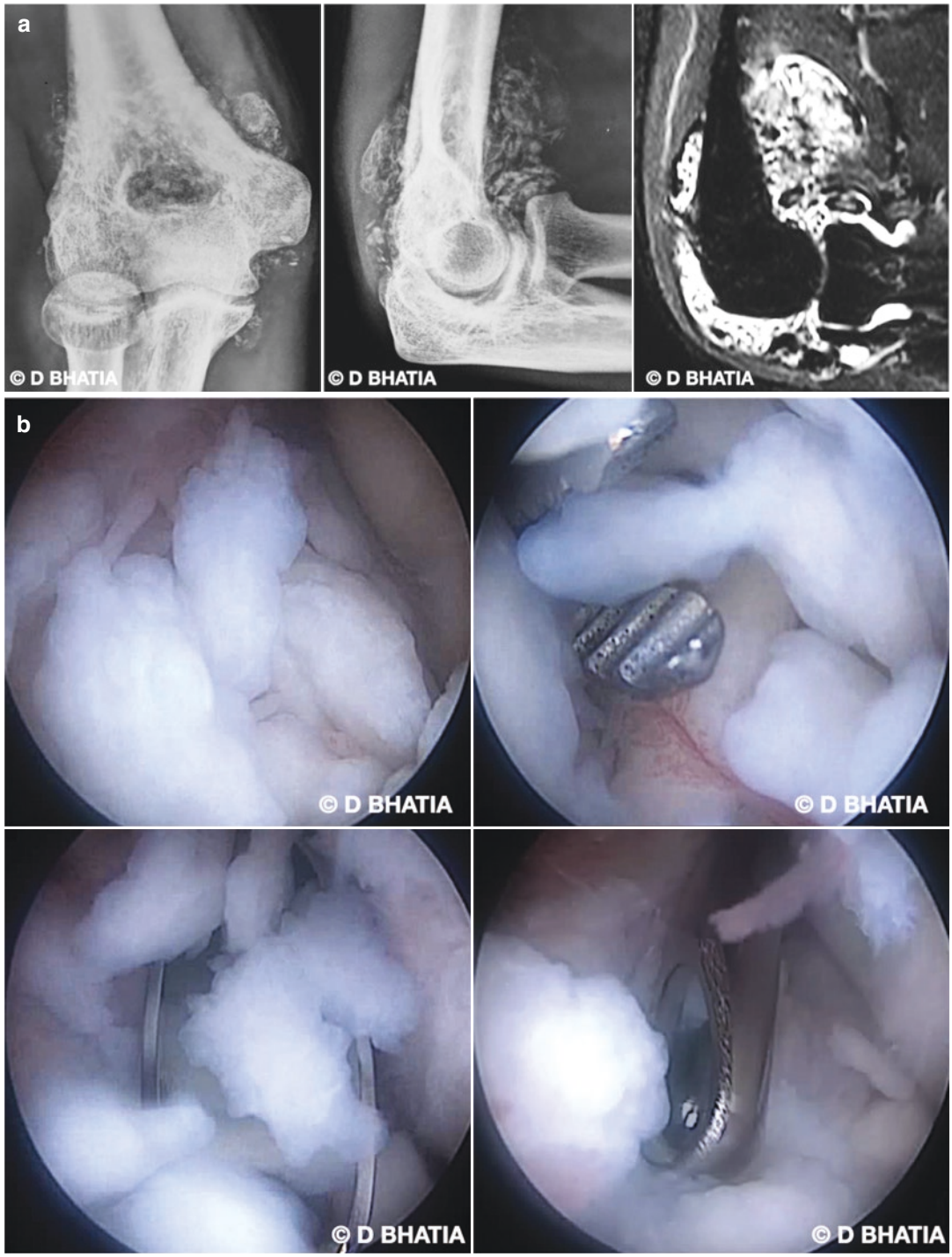

Fig. 46.2 (**a**) Radiological appearance of synovial chondromatosis is shown. Radiographs show multiple loose bodies in the anterior and posterior recesses of the elbow. MRI shows loose bodies and extensive synovitis (© D. Bhatia). (**b**) Arthroscopic appearance of synovial chondromatosis is demonstrated (top left). The loose bodies are removed using a grasper (top right) and suction (bottom left). A shaver is used to excise adherent chondral bodies and to perform synovectomy (bottom right). (© D. Bhatia)

- Using the standard AM portal, the supracapitellar region is visualized with a 70° arthroscope.
- A modified AL portal is placed slightly anterior to its usual position to permit access to the supracapitellar region.
- The anterior capsule is excised and a fat pad adjacent to the lesion is visualized. Careful excision of the fat pad is performed using a shaver and extent of the malformation is demarcated. The malformation is identified as a localized focal mass of reddish blood vessels surrounded by fat tissue (Fig. 46.3b).
- A grasper is used to obtain sufficient tissue from the malformation and any bleeding is controlled using radiofrequency coagulation.
- The malformation is the excised completely using a shaver and radiofrequency probe and complete excision is confirmed by visualization of muscle fibres laterally and anteriorly.
- The tourniquet is released and the excision area is observed for any bleeding sites and these are coagulated. The portals are closed after a thorough lavage.

46.4 Tips and Tricks

1. A 70° arthroscope and small joint instruments (3, 3.5 mm) permit better visualization and manoeuverability.
2. Capsular excision permits fluid extravasation and swelling, and controlling fluid inflow is important.
3. Arthroscopic visualization through different portals is useful to confirm complete excision of the lesion.

46.5 Pitfalls

Inaccessibility of the location of the lesion results in inadequate excision and the surgeon should carefully plan the procedure and instruments prior to surgery. The patient should be counselled regarding conversion to an open procedure if accessibility is limited.

46.6 Postoperative Management and Rehabilitation

A bulky soft-tissue dressing is used in the immediate postoperative period, and this is changed to portal dressing on the fourth postoperative day. A sling is used for comfort and is discarded within a week. The rehabilitation protocol involves progressive range and strengthening over the next 8–12 weeks.

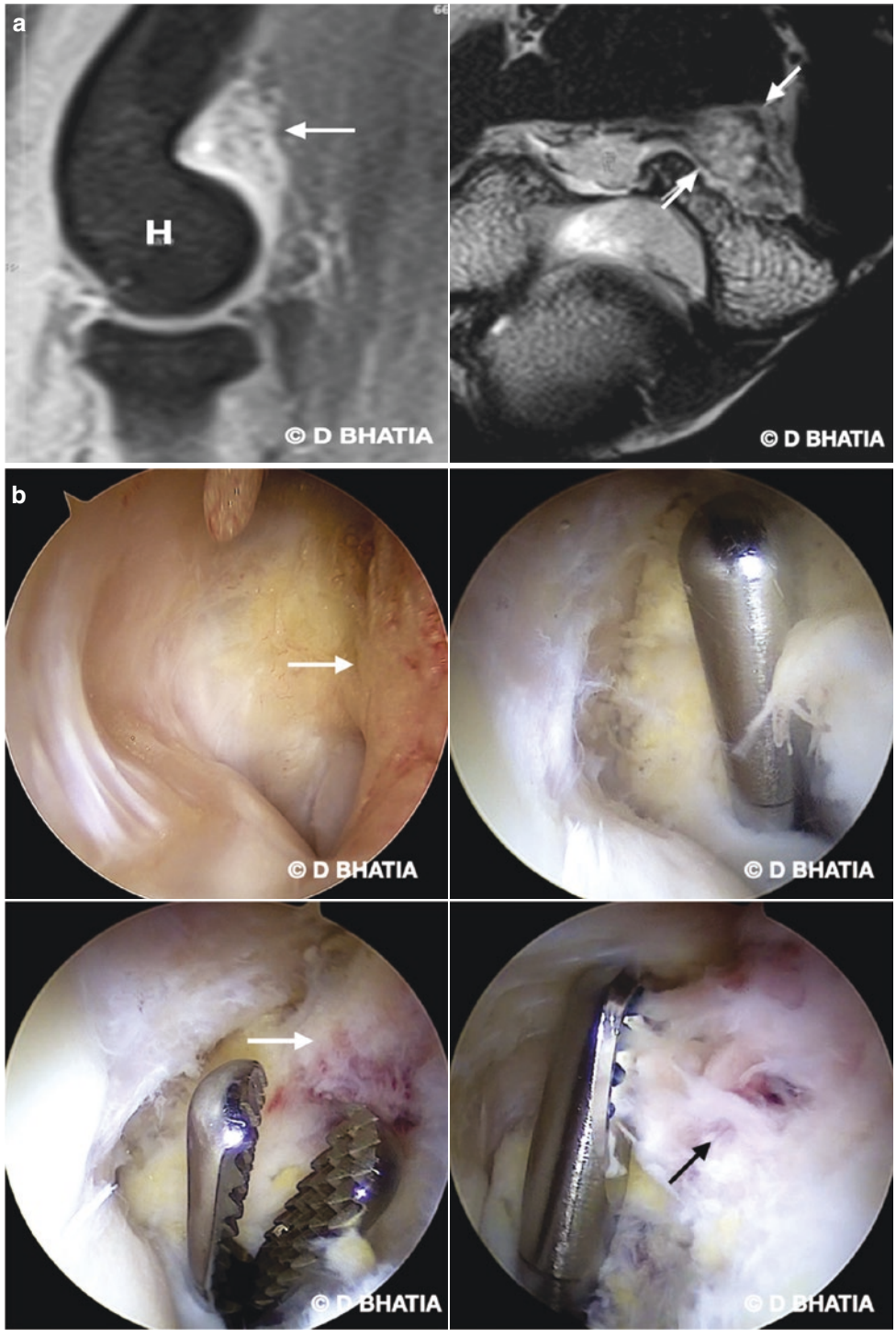

Fig. 46.3 (**a**) MRI appearance of a low-flow vascular malformation (arrows) in the supracapitellar region is demonstrated (© D. Bhatia). (**b**) Arthroscopic excision of a vascular malformation is demonstrated. The supracapitellar region is visualized and anterior capsule (arrow) is excised to expose a fat pad (top images). Biopsy is obtained from the lesion (arrow, bottom left). A shaver is used to excise the malformation (arrow, bottom right). (© D. Bhatia)

Conflict of Interest The author certifies that he has no commercial associations (e.g. consultancies, stock ownership, equity interest) that might pose a conflict of interest in connection with the submitted article. The author retains the copyright to the images, videos, and content in this chapter.

References

1. Bhatia DN. Arthroscopic excision of osteoid osteoma of the elbow. Arthrosc Tech. 2017;6(3):e543–8. https://doi.org/10.1016/j.eats.2016.11.014.
2. Mwaturura T, Bain G. Synovial chondromatosis and pigmented villonodular synovitis of the elbow. In: Bain G, Eygendaal D, van Riet R, editors. Surgical techniques for trauma and sports reldated injuries of the elbow. Berlin: Springer; 2020.
3. White CL, Olivieri B, Restrepo R, McKeon B, Karakas SP, Lee EY. Low-flow vascular malformation pitfalls: from clinical examination to practical imaging evaluation—part 1, lymphatic malformation mimickers. AJR Am J Roentgenol. 2016;206(5):940–51. https://doi.org/10.2214/AJR.15.15793.

Part IX

Biceps Tendon

47 Distal Biceps Anatomy: Structural Morphometry and Dynamic Relationships

Deepak N. Bhatia

47.1 Background

The distal biceps tendon (DBT) originates in the lower arm and crosses the anterior elbow crease into the cubital fossa region where it is surrounded by several major neurovascular structures. Familiarity with the morphometric anatomy and relationships of DBT with surrounding structures is crucial for optimal outcomes after open or endoscopic surgery for biceps pathology. The insertional anatomy of DBT and its dynamic relationship to the proximal radioulnar space and neurovascular structures have been quantified in recent studies, and this knowledge is crucial to understand safe placement of portals and incisions for open/endoscopic reconstruction techniques [1–8].

47.2 Structural Anatomy of the Distal Biceps

47.2.1 Tendon Course and Extent

The distal biceps tendon originates at the musculotendinous junction of the biceps brachii in the lower arm and inserts into the bicipital tuberosity in the upper forearm. The tendon is in the superficial plane in the lower arm and courses obliquely in a volar to dorsal orientation through deeper planes of the cubital fossa. The DBT fibers rotate by 90° in the cubital fossa and the tendon fans out into a broad attachment over the radial bicipital tuberosity and forms a footprint. Surface marking of the tendon is important to understand placement of incisions and endoscopy portals. The tendon originates approximately 3 cm proximal to the anterior elbow crease, courses for 7–12 cm (mean 9 cm), and inserts at a point 3–5 cm distal to this crease [1].

47.2.2 Tendon Zones and Components

The lacertus fibrosus is an aponeurosis on the medial aspect of the DBT and divides the tendon into three structural zones (preaponeurotic, aponeurotic, and postaponeurotic) [5, 9]. The aponeurosis protects the medial neurovascular structures in the cubital fossa; additionally, it prevents retraction of the ruptured DBT and is often torn or stretched in retracted DBT tears (Fig. 47.1). The biceps brachii muscle has two distinct muscle bellies that are continuations of the proximal long and short biceps tendons. The bellies interdigitate proximal to the origin of the DBT and then continue as long and short components within the tendon and finally insert into the footprint on the tuberosity [1, 5]. The long head

D. N. Bhatia (✉)
SPORTSMED Mumbai, Mumbai, India

Sir HN Reliance Foundation Hospital, Mumbai, India
e-mail: shoulderclinic@gmail.com

© ISAKOS 2022

D. N. Bhatia et al. (eds.), *Arthroscopy and Endoscopy of the Elbow, Wrist and Hand*,
https://doi.org/10.1007/978-3-030-79423-1_47

inserts on the proximal aspect of the footprint, and the short head attaches on its distal aspect (Fig. 47.2). In some cases, the DBT may continue as a single tendon that inserts as a single unit on the tuberosity [1]. A rare variant with trifurcation of the DBT has been recently described; this new anatomical finding involved a distal short head insertion and a proximal long head insertion, and an accessory head that bifurcated from the long head and inserted with an anterior and radial footprint [8].

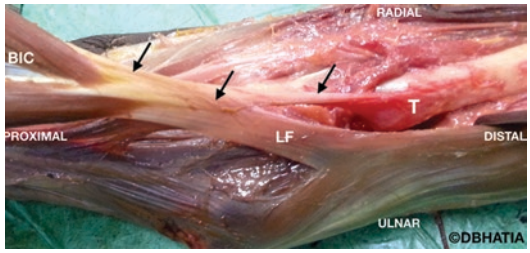

Fig. 47.1 Cadaveric demonstration of the extent of the distal biceps tendon (DBT) is shown. The distinct muscle bellies of long and short proximal heads are seen merging into a single tendon. The DBT rotates 90° (distal arrow) and inserts as a broad attachment into the bicipital tuberosity (T). The lacertus fibrosus (LF) can be used to identify the preaponeurotic, aponeurotic, and postaponeurotic segments of the tendon (arrows). (© Bhatia)

47.3 Osseous Anatomy

47.3.1 Bicipital Tuberosity

The bicipital tuberosity (BT) is an ulnar side protuberance, 3–4 cm distal to the radial head. The tuberosity bears a roughened area that marks the insertion of the distal biceps tendon. The BT (roughened area) measures approximately 24 mm

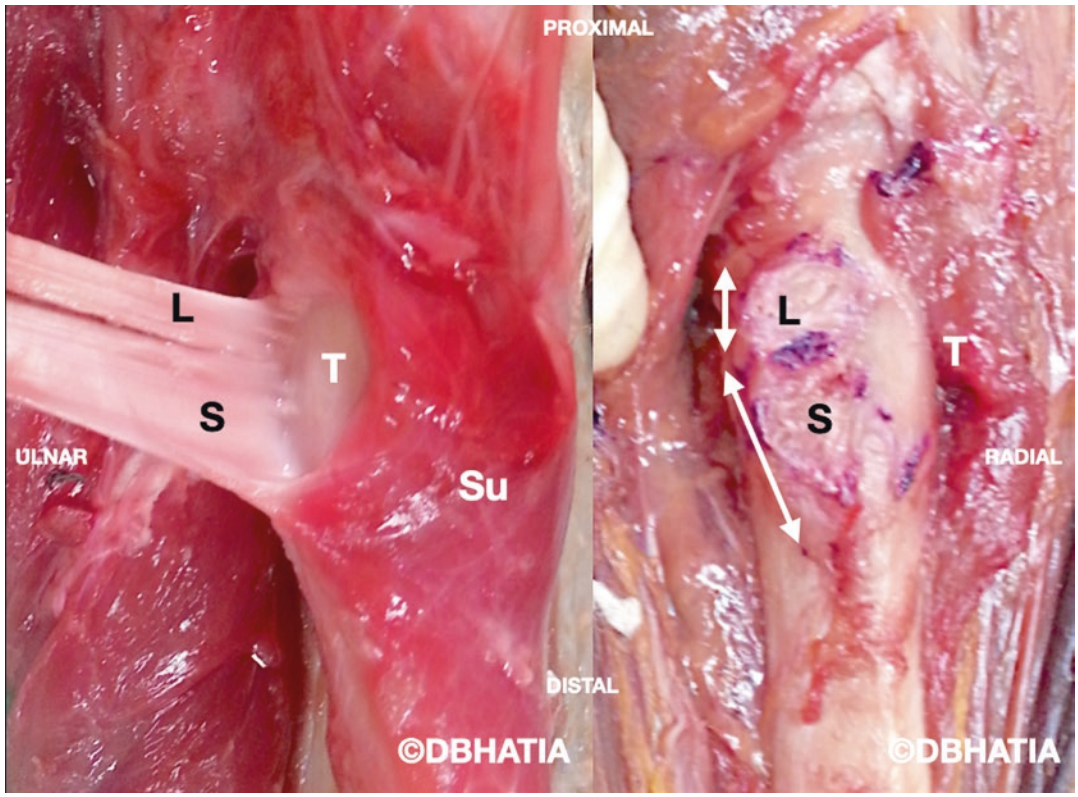

Fig. 47.2 Cadaveric specimen of the distal biceps tendon (DBT) demonstrates the long (L) and short (S) heads of DBT. The DBT and supinator (Su) enclose the bare area (T) on the tuberosity (left image). A type I footprint is demonstrated on the tuberosity (T) after resection of tendon fibers (right image). (© Bhatia)

in length, and 13 mm in breadth, and the average thickness of radius at tuberosity is 16 mm [1]. Mazzocca et al. have documented the presence of variable ridge on the tuberosity in 88% specimen, and the DBT was found to insert ulnar to this ridge [10].

47.3.2 Footprint Anatomy

The footprint of the DBT has been described as semilunar or oval by Hutchinson et al. and as "ribbon-shaped" by Mazzocca et al. [10, 11]. Eames et al. described separate insertion areas of the short and long DBT components [9]. In a recent study, Bhatia et al. have described three DBT footprint variants and a distal biceps footprint index (DBFI) to quantify the attachment areas. DBFI is ratio of the lengths of the long tendon footprint and short tendon footprint on the bicipital tuberosity and is a representation of the relative contribution of each DBT component to the DBT footprint. DBFI is significantly different between type 1 (DBFI 0.57) and type 2 (DBFI 0.26) footprints. Type 2 footprint shows a predominant short tendon contribution and type 3 footprint is a single C-shaped attachment area [1] (Fig. 47.3a–c). A rare trifurcate insertional footprint with an additional proximal anterior attachment region has also been described [8].

47.3.3 Proximal Radioulnar Space

The dimensions of the proximal radioulnar space are altered with dynamic rotation and mechanical impingement of the DBT may occur during forearm rotation (Fig. 47.4). Postoperative thickening of the tendon and additional fixation/augmentation techniques may predispose the DBT to impingement and possible wear. Bhatia et al. studied the radioulnar space (RUS) and identified that the RUS reduces significantly from the supinated to the pronated position and is most evident in the distal aspect of the tuberosity. In addition, RUS in pronation is inadequate for incremental increases in DBT thickness. In a clinical scenario, postoperative DBT impingement in the RUS may be prevented by avoiding techniques that increase the thickness of the tendon and by using a reattachment site at the proximal aspect of the tuberosity [1]. Raush et al. analyzed the radioulnar distance at the level of the radial tuberosity and found that the central zone was the smallest in pronation, and the proximal zone was the smallest in neutral rotation [12].

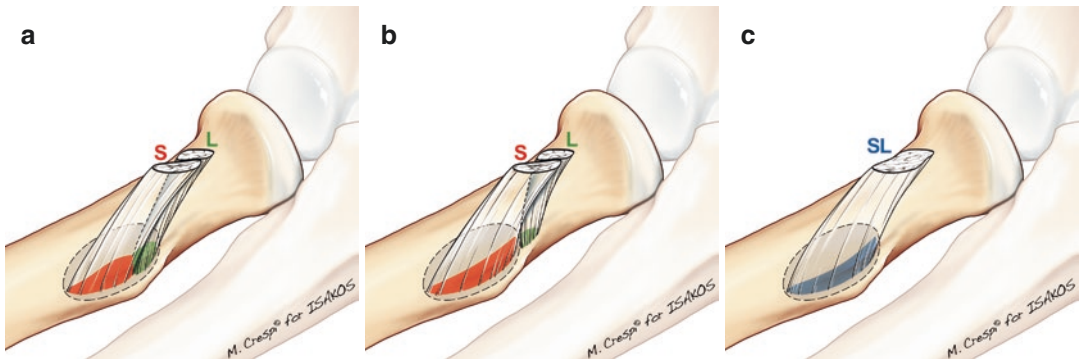

Fig. 47.3 Classification of distal biceps tendon footprints as described by Bhatia et al. [1]. (**a**) Type 1 footprint has an average DBFI of 0.57 and both components of the DBT insert onto the bicipital tuberosity area. (**b**) Type 2 footprint has a DBFI of 0.26 and the long tendon component of the DBT inserts proximal to and outside the bicipital tuberosity perimeter. (**c**) Type 3 footprint does not show separation of DBT into long and short components and DBT inserts onto the bicipital tuberosity area in a C-shape configuration. (© Bhatia)

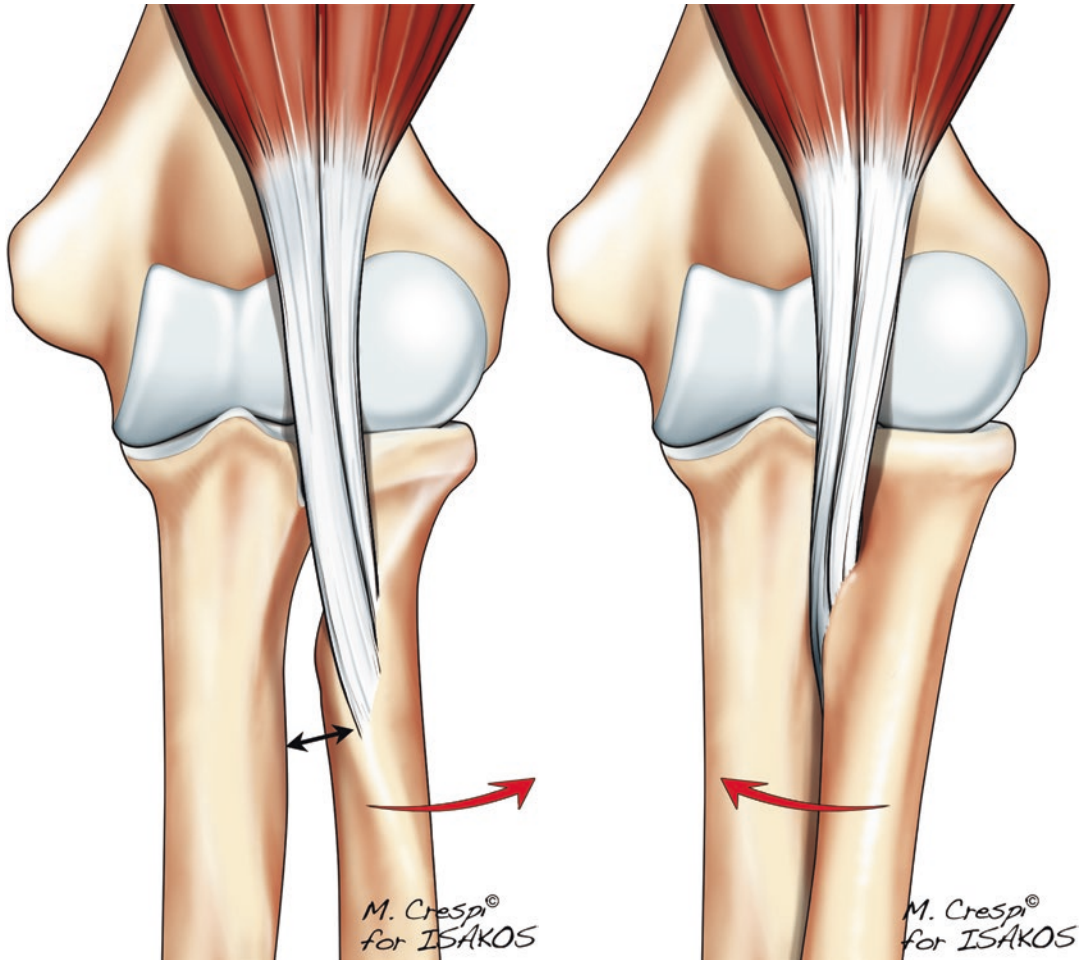

Fig. 47.4 The proximal radioulnar space (RUS) decreases significantly during rotation from supination to pronation and the reduction is most prominent in the lower region of the tuberosity. The DBT passes through the RUS with rotation and is prone to impingement. (M. Crespi © for ISAKOS)

47.4 Neurovascular Anatomy

47.4.1 Neurovascular Relations

The neurovascular anatomy of the cubital fossa shows considerable variability, and several structures are at potential risk of injury during surgical procedures in this region. Proximal to the anterior elbow crease (lower arm), the lateral aspect of the DBT is the safe side; however, the cephalic vein and the lateral cutaneous nerve of the forearm are close to the upper lateral aspect of the DBT. The radial nerve is further lateral and is relatively safe in this zone. On the medial side of the DBT are three major neurovascular structures: brachial artery and vein, and the median nerve (Fig. 47.4). Distal to the anterior elbow crease (upper forearm), the DBT passes deep, and in close apposition, to the brachial artery bifurcation and recurrent radial leash of vessels. The superficial radial nerve (SRN) and the posterior interosseous nerve (PIN) are close to the lateral aspect of the DBT. The radial artery passes in a superficial plane and the ulnar artery courses in the deeper plane across the radioulnar space on the medial aspect of DBT insertion (Fig. 47.5). In most specimens, a single radial recurrent artery passes volar to the tendon (mean of 4 mm

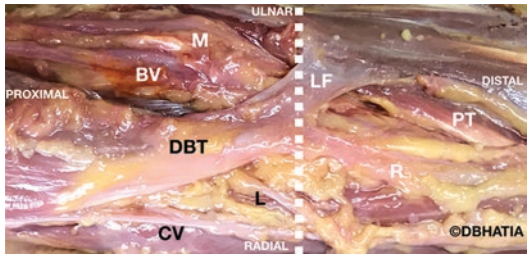

Fig. 47.5 Cadaveric demonstration of neurovascular relationships of the distal biceps tendon (DBT) in the superficial plane is shown. Proximal to the elbow crease (dotted line) the lateral "safe side" of DBT shows the lateral antebrachial cutaneous nerve L that exits adjacent to the musculotendinous junction of the DBT, and the cephalic vein along its lateral border. The brachial vessels (BV) and median nerve (M) course on the medial aspect and pass under the lacertus fibrosus (LF). The DBT passes into a deeper plane below the elbow crease (*PT* pronator teres). (© Bhatia)

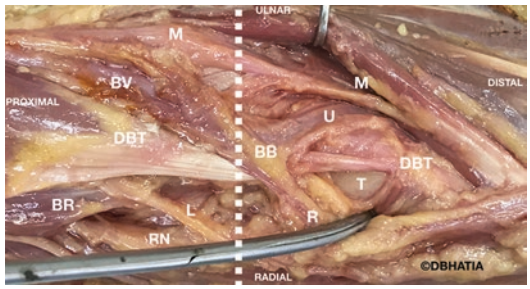

Fig. 47.6 Cadaveric demonstration of neurovascular relationships of the distal biceps tendon (DBT) in the deep plane is shown. Proximal to the elbow crease (dotted line) the lateral aspect of DBT shows the lateral antebrachial cutaneous nerve L, and radial nerve RN that exits deep to brachialis. The brachial vessels (BV) and median nerve (M) course on the medial aspect. The DBT passes into a deeper plane below the elbow crease dorsal to the brachial artery bifurcation (BB) and inserts into bicipital tuberosity. The ulnar artery U crosses the radioulnar space diagonally and is in close approximation with the DBT insertion (*R* radial artery). (© Bhatia)

proximal and 15 mm volar to the tuberosity). In approximately half of the specimens, a smaller recurrent artery that originates from the brachial artery passes dorsal to the DBT [13]. Rarely, the radial artery itself may run dorsal to the DBT [14] (Fig. 47.6).

47.4.2 Neurovascular Anatomy at-Risk

Bhatia et al. evaluated five potential portal sites above and below the elbow crease for elbow endoscopy [7]. The study showed that the anterior portal placed above the elbow crease (parabiceps portal) was safe, while the three anterior portals placed at different levels below the elbow crease were significantly closer to neurovascular structures. The parabiceps portal was close to the lateral continuation of the musculocutaneous nerve (mean 5 mm), while the cephalic vein (16 mm) and radial nerve (12 mm) were further lateral. During its course into the forearm, the parabiceps portal was close to the recurrent radial leash of vessels (7 mm). In the forearm, portals are placed at three levels of the DBT; the upper two portals are potentially risky for the SRN and PIN; while the distal-most anterior portal placed the radial artery at-risk. The posteriorly placed portal at the level of the tuberosity is safe for the posterior interosseous nerve and superficial radial nerve in both pronation and supination; however, the ulnar artery is at risk of injury as the portal cannula/instruments get closer to the tuberosity [6].

47.4.3 Dynamic Neurovascular Relations

The distal biceps tendon insertion on the bicipital tuberosity has been described a unique intraoperative reference point and is useful in dynamic rotation for predicting the position of five major neurovascular (NV) structures in the cubital fossa [6]. In 90° of supination, RA (5 mm) was the closest NV structure to DBT insertion, and MN (7 mm) and UA (9 mm) were further away. Rotation to the neutral position significantly decreased the distance between DBT insertion and UA (4 mm); however, RA (9 mm) and MN (11 mm) moved further away from DBT insertion. Rotation to pronation position demonstrated a significant change in all three NV structures

from DBT insertion as compared with the supination position. Superficial radial nerve and posterior interosseous nerve were found to be the farthest of all five NV structures and are not in the surgical path during radioulnar space access. The authors recommend placing the forearm in full supination during surgical dissection on the ulnar aspect of bicipital tuberosity. During passage of instruments or the distal biceps via the radioulnar space (two-incision technique for DBT repair), the UA is the closest structure and is at risk for iatrogenic injury. Similarly, the UA may be at-risk in dorsal approaches that involve deep dissection within the radioulnar space and during placement of distal posterior portals for biceps endoscopy.

In summary, an in-depth knowledge of the tendon and its surrounding neurovascular structures is a prerequisite for open and endoscopic surgery around the DBT. Variations in anatomy must be anticipated and recognized during surgery. Potential neurovascular risks should be considered when endoscopic procedures are performed.

Conflict of Interest The author certifies that he has no commercial associations (e.g., consultancies, stock ownership, equity interest) that might pose a conflict of interest in connection with the submitted article. The author (D. Bhatia) retains the copyright to the images, videos, and content in this chapter.

References

1. Bhatia DN, Kandhari V, DasGupta B. Cadaveric study of insertional anatomy of distal biceps tendon and its relationship to the dynamic proximal radioulnar space. J Hand Surg Am. 2017;42(1):e15–23.
2. Bhatia DN. Endoscopic distal biceps repair: endoscopic anatomy and dual-anchor repair using a proximal anterolateral "parabiceps portal". Arthrosc Tech. 2015;4:e785–93. https://doi.org/10.1016/j.eats.2015.07.031.
3. Bhatia DN. Endoscopic repair of acute and chronic retracted distal biceps ruptures. J Hand Surg Am. 2016;41(12):e501–7. https://doi.org/10.1016/j.jhsa.2016.09.008.
4. Phadnis J, Bain G. Endoscopic-assisted distal biceps footprint repair. Tech Hand Up Extrem Surg. 2015;19:55–9.
5. Eames MJ, Bain GI. Distal biceps tendon endoscopy and anterior elbow arthroscopy portal. Tech Shoulder Elb Surg. 2006;7:139–42.
6. Bhatia D, Naskar R, DeNiese P. Dynamic rotational alteration in positional relationship of neurovascular structures and distal biceps tendon insertion: a cadaveric study. J ISAKOS. 2019;4:296–301.
7. Bhatia DN, DasGupta B, Panjwani T. Cadaveric study of anterior and posterior elbow endoscopy portals for endoscopic distal biceps repair: comparative anatomy-at-risk. Surg Radiol Anat. 2016;38(7):781–91. https://doi.org/10.1007/s00276-016-1637-6. [Epub 2016 Feb 9].
8. Bhatia DN. Distal biceps tendon insertional trifurcation and a new footprint configuration: case report of an anatomical variant. Eur J Anat. 2020;24(3):235–8.
9. Eames MH, Bain GI, Fogg QA, et al. Distal biceps tendon anatomy: a cadaveric study. J Bone Joint Surg Am. 2007;89(5):1044–9.
10. Mazzocca AD, Cohen M, Berkson E, et al. The anatomy of the bicipital tuberosity and distal biceps tendon. J Shoulder Elb Surg. 2007;16(1):122–7.
11. Hutchinson HL, Gloystein D, Gillespie M. Distal biceps tendon insertion: an anatomic study. J Shoulder Elb Surg. 2008;17(2):342–6.
12. Rausch V, Krieter JP, Leschinger T, et al. The radioulnar distance at the level of the radial tuberosity. Clin Anat. 2019; https://doi.org/10.1002/ca.23483. [Published online ahead of print 2019 Oct 1].
13. Zeltser DW, Strauch RJ. Vascular anatomy relevant to distal biceps tendon repair. J Shoulder Elb Surg. 2016;25:283–8. https://doi.org/10.1016/j.jse.2015.08.042.
14. Honma S, Tokiyoshi A, Kawai K, Koizumi M, Kodama K. Radial artery running beneath the biceps tendon and its interrelation between the radial recurrent arteries. Anat Sci Int. 2008;83(4):232–8.

48 The "All-Endoscopic" Approach to Distal Biceps: Overview, Portals, and Anatomy-at-Risk

Deepak N. Bhatia

48.1 Background

The all-endoscopic approach for distal biceps endoscopy is a minimally invasive procedure for diagnostic and therapeutic utility in distal biceps pathology. The all-endoscopic technique was devised by the author and involves use of separate endoscopic portals for visualization and working [1–6]. Fluid insufflation is necessary to create a working space, and cannulas are used to protect soft tissues in the forearm. The technique can be used with different fixation devices (suture anchors, interference screws, or cortical buttons). The procedure provides a safe method for debridement and repair of partial and complete DBT ruptures, and even graft reconstruction/augmentation of chronic ruptures with tendon deficiencies [7]. Development of special visualization and working portals and assessment of safety profile of each of these extra-articular portals have made this procedure safe and reproducible.

48.2 Indications and Contraindications

The all-endoscopic approach may be used as a diagnostic or therapeutic procedure.

1. *All-endoscopic biceps exploration using a one-portal technique* is useful for evaluation of DBT pathology in symptomatic elbows with radiological DBT abnormality. The DBT and bicipitoradial bursa can be evaluated for bursitis, tenosynovitis, and partial bursal-sided tears. DBT ruptures are well visualized, and occasionally an isolated rupture of a single head may be identified and diagnosed [1].
2. *A two-portal all-endoscopic approach* is used for debridement of bicipitoradial bursitis, tenosynovitis, and partial DBT tears. Non-retracted and isolated head ruptures can be repaired using this technique [1, 7].
3. *A three-portal all-endoscopic approach* is used by the author for acute and chronic DBT ruptures that have retracted proximal to the anterior elbow crease. Chronic irreparable DBT ruptures can be endoscopically augmented or reconstructed with hamstring autografts using the same technique [3, 7].

Contraindications include patients with altered elbow anatomy and previous surgery. Surgeons inexperienced in this technique should acquire cadaveric and technical experience prior to attempting this in vivo.

D. N. Bhatia (✉)
SPORTSMED Mumbai, Mumbai, India

Sir HN Reliance Foundation Hospital, Mumbai, India
e-mail: shoulderclinic@gmail.com

© ISAKOS 2022

D. N. Bhatia et al. (eds.), *Arthroscopy and Endoscopy of the Elbow, Wrist and Hand*,
https://doi.org/10.1007/978-3-030-79423-1_48

48.3 Endoscopy Portals and Anatomy at-Risk

Distal biceps endoscopy portals can be classified by the anatomical site of placement (Table 48.1) (Fig. 48.1). The all-endoscopic technique uses four main portals:

- *Proximal parabiceps portal* (*PBP*) is the viewing portal throughout the procedure (Fig. 48.2a, b). This portal is placed 2–3 cm proximal to the elbow crease and is on the lateral aspect of the musculotendinous junction of the DBT [1, 3]. A 4 mm skin incision is made at this level, and the sheath is angled

Table 48.1 Classification of portals used in distal biceps endoscopy

Portals	Placement site	Structures at-risk
Proximal to elbow crease		
Proximal parabiceps portal (PBP) [1–3] (Bhatia)	PBP is placed 2–3 cm proximal to the elbow crease on the lateral aspect of the musculotendinous junction of the DBT. Sheath is angled 10–20° dorsally and distally towards the radial tuberosity along the parabiceps space. PBP is the main viewing portal for biceps endoscopy.	The lateral cutaneous nerve (LCN) of the arm is approximately 5 mm away. Sheath passes approximately 7 mm dorsal to the radial leash of vessels [2].
Midbiceps portal (MBP) [3, 7] (Bhatia)	MBP is placed 1–2 cm proximal to the PBP in the midline of the forearm. Viewing and working portal for arm endoscopy.	The brachial vessels and median nerve are approximately 10 mm medial to the MBP. Sonography guidance is used preoperatively to mark these vessels [2, 3, 7].
Distal to elbow crease (anterior portals)		
Anterior forearm portal (AFP) [8] (Eames and Bain)	2.5 cm incision placed 2 cm distal to the elbow crease lateral to the palpable DBT. Viewing and working portal for forearm endoscopy.	Posterior interosseous nerve (PIN) is approximately 5 mm away and superficial radial nerve (SRN) is approximately 3 mm away. PIN is significantly at-risk of injury [2].
Modified anterior forearm portal (MAFP) [2] (Bhatia)	1.5 cm directly below the original AFP. Approximately 4 cm distal to the anterior elbow crease and 10 mm lateral to the palpable DBT.	Posterior interosseous nerve (PIN) is approximately 14 mm away and superficial radial nerve (SRN) is approximately 3 mm away. SRN is significantly at-risk of injury [2].
Distal anterior portal (DAP) [1–3] (Bhatia)	Directly above the radial tuberosity in the midpoint of a transverse line drawn approximately 4 cm distal to the anterior elbow crease	Radial artery (RA) is approximately 3 mm away and is at significant risk of injury. Lateral cutaneous nerve (LCN) is approximately 6 mm away [2]. Open dissection via a 1 cm incision is used to identify and retract the RA and LCN prior to cannula insertion. Subsequently, all instrumentation is performed through the cannula.
Distal to elbow crease (posterior portals)		
Inside-out distal posterior portal (DPP) [9] (Phadnis and Bain)	Wissinger rod is passed via volar incision adjacent to the bicipital tuberosity between the radius and ulna. The rod exits dorsally, and a cannulated sheath is passed over this up to the tuberosity and used as a working portal.	The ulnar artery runs diagonally across the proximal radioulnar space adjacent to DBT insertion and is at risk of iatrogenic injury with an inside-out technique [6].
Outside-in distal posterior portal (DPP) [2, 7] (Bhatia)	Spinal needle is passed from the dorsal aspect of proximal forearm and 4 cm below the anterior elbow crease. The needle passes between the radius and ulna and is advanced under direct visualization to exit just medial to the radial tuberosity. The DPP passes through the extensor carpi ulnaris and proximal radioulnar space.	Ulnar artery is approximately 9 mm away from DBT insertion in supination position and 6 mm away from DBT insertion in pronation position [6]. Posterior interosseous nerve is approximately 24 mm away in supination and 30 mm away in pronation [2]. Superficial radial nerve is approximately 28 mm away in supination and 34 mm away in pronation [2].

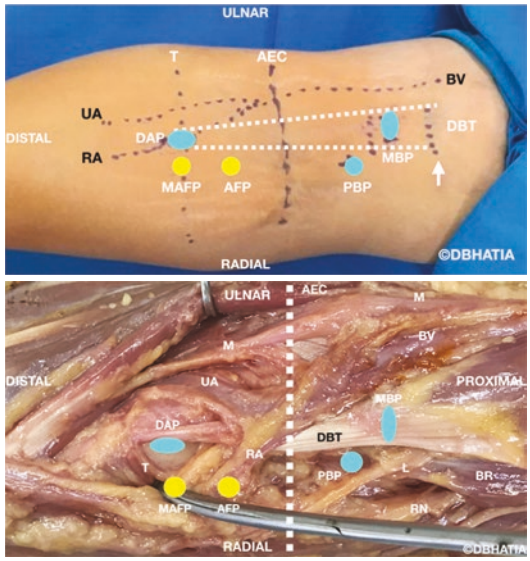

Fig. 48.1 Anterior portals for all-endoscopic approach to distal biceps tendon (DBT) are shown. Superficial marking for portal placement (top image) and cadaveric anatomy (bottom image) are demonstrated. The parabiceps portal (PBP) is the main viewing portal, and distal anterior portal (DAP) is the main working portal. The midbiceps portal (MBP) is used for arm endoscopy for retracted tears (arrow) and permits simultaneous viewing and working. The anterior forearm portal (AFP) and its distal modification (MAFP) are placed along the lateral aspect of the DBT (dotted lines) (*AEC* anterior elbow crease, *L* lateral cutaneous nerve, *BV* brachial vessels, *M* median nerve, *RA* radial artery, *UA* ulnar artery, *T* tuberosity level, *BR* brachialis, *RN* radial nerve). (© Bhatia)

10–20° inferiorly towards the radial tuberosity. The sheath is advanced cautiously and gently and should pass for a distance for 7–8 cm without resistance. The parabiceps portal is close to the lateral cutaneous nerve (LCN) of the arm (mean 5.1 mm, range 1.9–10.6 mm), and its tract passes dorsal to the radial leash of vessels (mean 7.2 mm, range 2.8–12.7) [2].

- *Distal anterior portal* (*DAP*) is main working portal; this portal is placed above the radial tuberosity and is approximately 4 cm distal to the anterior elbow crease [1–3] (Fig. 48.3a–c). The portal site may be marked preoperatively, using sonographic localization of the tuberosity, or by an outside-in technique (digital palpation) while viewing via PBP. Blunt dissection is performed via an 8 mm incision, and small retractors are used to retract the brachioradialis radially, and the flexor carpi radialis is retracted ulnarly. The superficial branch of the radial nerve (SRN) is under the brachioradialis, and the radial artery (RA) is retracted to the ulnar side. The DAP is close to the SRN and LCN, and RA is at significant risk of injury; careful dissection and use of a cannula is therefore recommended when a DAP is placed [2, 5, 6].
- *Midbiceps portal* (*MBP*) is placed approximately 1–2 cm proximal to the PBP in the midline of the forearm; this portal is used for arm endoscopy if the DBT rupture is retracted into the arm [3]. The portal is used for visualization of the retracted DBT, and for mobilization and retrieval of the tendon stump (Fig. 48.4a–c).
- *Distal posterior portal* (*DPP*) is an accessory portal and may be used for better access to the ulnar aspect of the tuberosity. The DPP can be placed using an inside-out method or an outside-in technique [2, 7, 9]. The ulnar artery is at-risk of injury and the portal must be placed under direct endoscopic visualization of the tuberosity and closely approximated to the ulnar surface of the tuberosity [6] (Fig. 48.5).

In summary, development of new endoscopic portals is a significant advance in management of distal biceps pathology. The all-endoscopic approach provides excellent visualization and avoids the need for excessive retraction and thereby complications associated with open techniques are prevented.

Conflict of Interest The author certifies that he has no commercial associations (e.g., consultancies, stock ownership, equity interest) that might pose a conflict of interest in connection with the submitted article. The author retains the copyright to the images, videos, and content in this chapter.

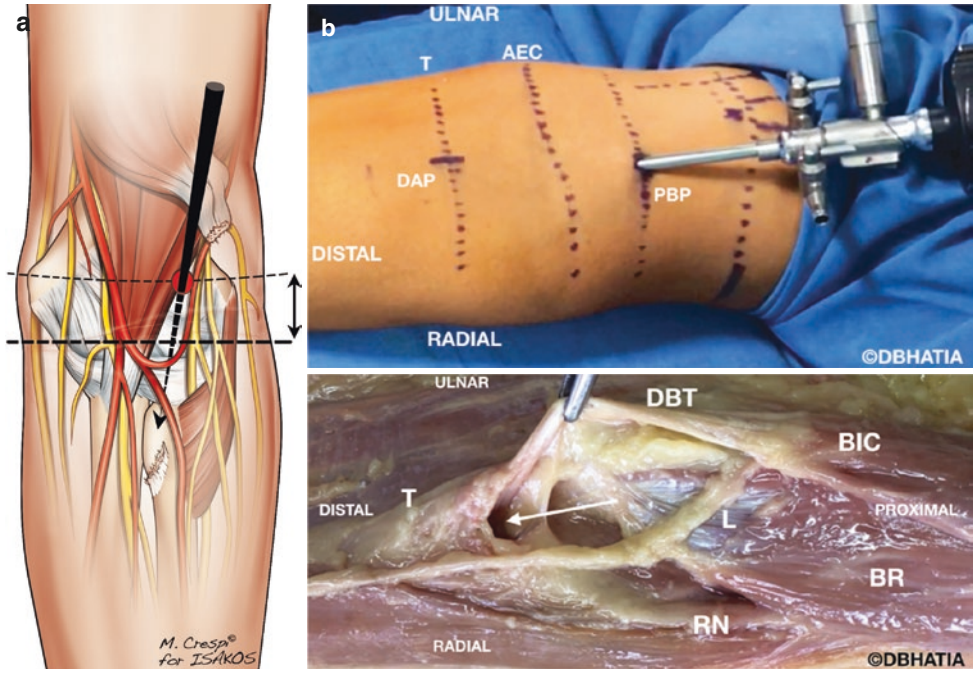

Fig. 48.2 (**a**) Anatomical relations and trajectory of parabiceps portal are illustrated. Parabiceps portal (PBP) is a proximal anterior viewing portal placed in the safe zone along the lateral border of distal biceps tendon (© Bhatia). (**b**) Placement of parabiceps portal (PBP) is demonstrated in a left elbow (top image). Cadaveric dissection (bottom image) shows the parabiceps space (arrow) that leads safely to the bicipital tuberosity (T) (*AEC* anterior elbow crease, *L* lateral cutaneous nerve, *BIC* biceps muscle, *T* tuberosity level, *BR* brachialis, *RN* radial nerve, *DAP* distal anterior portal). (© Bhatia)

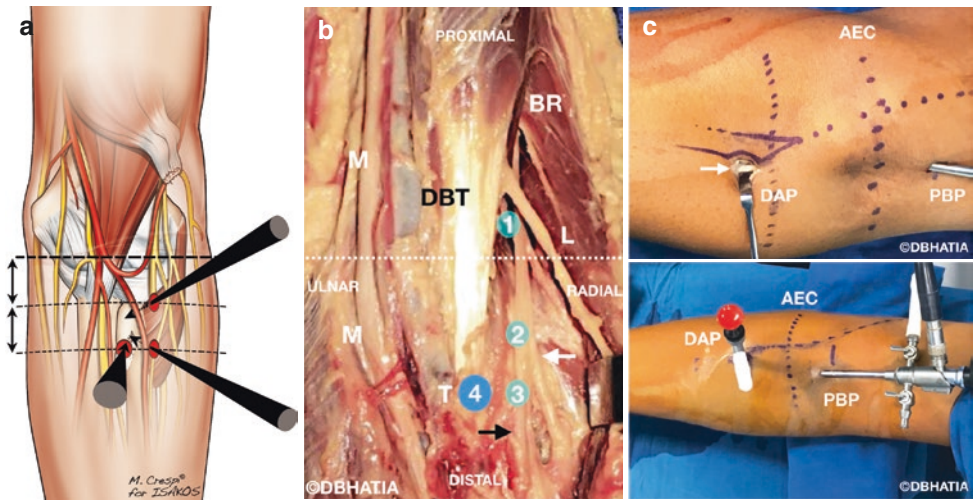

Fig. 48.3 (**a**) Endoscopy portals distal to the anterior elbow crease are shown on the anterior aspect of the forearm (© Bhatia). (**b**) The anterior forearm portal AFP (portal 2) and its modification MAFP (portal 3) are shown in relation to the superficial radial nerve SRN (black arrow) and posterior interosseous nerve PIN (white arrow). The distal anterior portal DAP (portal 4) is centered over the bicipital tuberosity (T) (Portal 1 = parabiceps portal, dotted white line = anterior elbow crease, *BR* brachioradialis, *L* lateral cutaneous nerve, *M* median nerve) (© Bhatia). (**c**) Distal anterior portal (DAP) is placed in the midline at tuberosity level. The lateral antebrachial cutaneous nerve (arrow, top image) and radial artery (not shown) are identified and retracted prior to placement of a 6 mm cannula (*PBP* parabiceps portal, *AEC* anterior elbow crease). (© Bhatia)

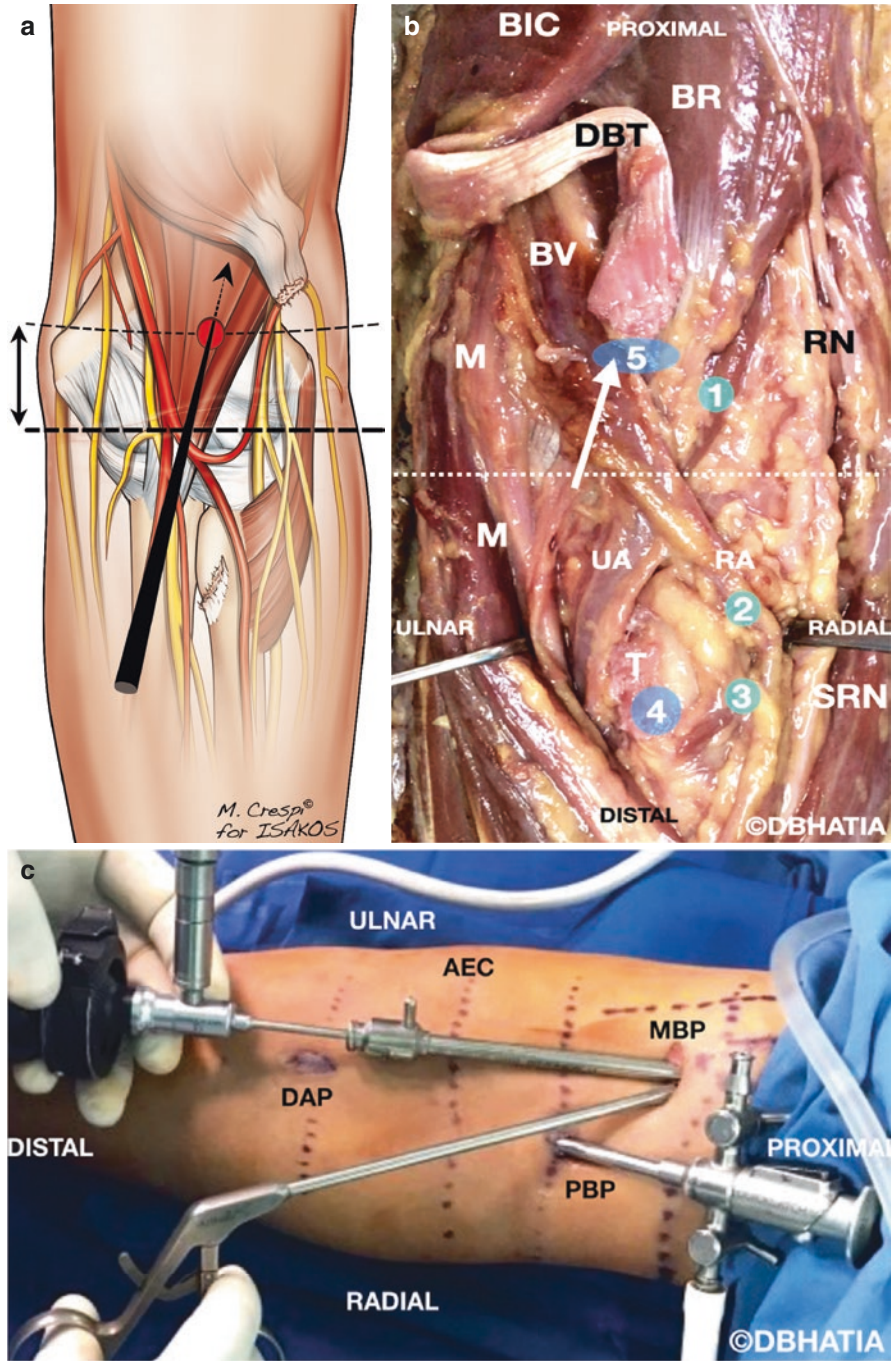

Fig. 48.4 (**a**) Diagrammatic representation of trajectory and anatomical site of mid-biceps portal (© Bhatia). (**b**) Cadaveric demonstration of anatomy and relations of mid-biceps portal (MBP). The ruptured DBT is retracted proximal to AEC and the neurovascular bundle is on its medial aspect. MBP (arrow, portal 5) is placed between the biceps muscle (BIC) and brachialis (BR) (Portal 1 = parabiceps portal, Portal 2 = anterior forearm portal, Portal 3 = modified anterior forearm portal, Portal 4 = distal anterior portal, *BV* brachial vessels, *M* median nerve, *UA* ulnar artery, *RA* radial artery, *SRN* superficial radial nerve, *RN* radial nerve) (© Bhatia). (**c**) Mid-biceps portal (MBP) is placed proximal to PBP in the midline of the arm. MBP is used for arm endoscopy for mobilization and retrieval of retracted tears and permits simultaneous viewing and working (*DAP* distal anterior portal, *PBP* parabiceps portal, *AEC* anterior elbow crease). (© Bhatia)

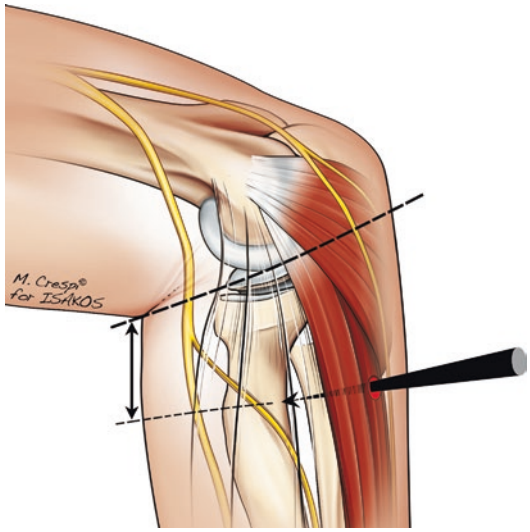

Fig. 48.5 Distal posterior portal (DPP) for biceps endoscopy portal is shown using the outside-in technique. The postal passes through the extensor carpi ulnaris (ECU) muscle between the radius and ulna at the tuberosity level. The superficial radial nerve (SRN) and posterior interosseous nerve (PIN) are safe, however, the ulnar artery (not shown) may be at-risk of injury. (© M. Crespi for ISAKOS)

References

1. Bhatia DN. Endoscopic distal biceps repair: endoscopic anatomy and dual-anchor repair using a proximal anterolateral "parabiceps portal". Arthrosc Tech. 2015;4:e785–93. https://doi.org/10.1016/j.eats.2015.07.031.
2. Bhatia DN, DasGupta B, Panjwani T. Cadaveric study of anterior and posterior elbow endoscopy portals for endoscopic distal biceps repair: comparative anatomy-at-risk. Surg Radiol Anat. 2016;38(7):781–91. https://doi.org/10.1007/s00276-016-1637-6. Epub 2016 Feb 9.
3. Bhatia DN. Endoscopic repair of acute and chronic retracted distal biceps ruptures. J Hand Surg Am. 2016;41(12):e501–7. https://doi.org/10.1016/j.jhsa.2016.09.008.
4. Bhatia DN, Kandhari V, Das Gupta B. Cadaveric study of insertional anatomy of distal biceps tendon and its relationship to the dynamic proximal radioulnar space. J Hand Surg Am. 2017;42:e15–23. https://doi.org/10.1016/j.jhsa.2016.11.004.
5. Bhatia DN, Kandhari V. Analysis of technical feasibility and neurovascular safety of endoscopic distal biceps repair: a cadaveric study. J Shoulder Elb Surg. 2018;27:2057–67. https://doi.org/10.1016/j.jse.2018.04.020.
6. Bhatia D, Naskar R, DeNiese P. Dynamic rotational alteration in positional relationship of neurovascular structures and distal biceps tendon insertion: a cadaveric study. J ISAKOS. 2019;4:296–301. https://doi.org/10.1136/jisakos-2019-000326.
7. Bhatia DN. All-endoscopic distal biceps repair and reconstruction: science, technique and results. Presented at Shoulder and Elbow Society of Australia (SESA) biennial conference, Nov 2018, Perth, Australia.
8. Eames MJ, Bain GI. Distal biceps tendon endoscopy and anterior elbow arthroscopy portal. Tech Shoulder Elb Surg. 2006;7:139–42.
9. Phadnis J, Bain G. Endoscopic-assisted distal biceps footprint repair. Tech Hand Up Extrem Surg. 2015;19:55–9.

49 All-Endoscopic Management of Partial Tears of Distal Biceps Tendon

Deepak N. Bhatia

49.1 Background

Partial tears of the distal biceps tendon (DBT) are usually overuse injuries and occur more frequently in comparison to complete ruptures. These tears are characterized by the presence of mechanical anterior elbow pain and weakness in supination and/or flexion activities, and an absence of "popeye" deformity. The two-portal "all-endoscopic" approach is a safe and minimally invasive procedure for diagnosis, classification, and definitive treatment of partial DBT tears and avoids the necessity of a more extensive open procedure [1, 2]. The technique has advantages: (a) endoscopic viewing and probing helps to better understand the type, site, and severity of tear, (b) two portals are sufficient for debridement and/or repair, (c) retraction is not necessary, and retractor-induced complications are avoided, and (d) the procedure is fast and reproducible, and easy to perform.

D. N. Bhatia (✉)
SPORTSMED Mumbai, Mumbai, India

Sir HN Reliance Foundation Hospital, Mumbai, India
e-mail: shoulderclinic@gmail.com

49.2 Indications and Contraindications

Endoscopic evaluation of DBT is performed for persistent pain and weakness in supination and flexion activities and radiological imaging suggestive of a partial DBT tear.

Post-traumatic or iatrogenic alteration in the anatomy of the cubital fossa (scarring, heterotopic ossification, vascular or neurological surgery) is a contraindication to the procedure. Similarly, the procedure should be avoided in patients with vascular anomalies and malunited fractures. Familiarity with the anatomical course of major neurovascular structures and their dynamic relationship to DBT is necessary to prevent any iatrogenic complications [3–5].

49.3 Surgical Technique

The "all-endoscopic" approach is performed with the patient in supine position, and the upper extremity is placed on a side trolley. The elbow joint is flexed 10–20° for initial portal placement, and a support under the distal arm is used intraoperatively to achieve extension when necessary. A tourniquet is placed high on the arm and is used during the procedure. A 2.9-mm arthroscope and sheath (2.9, 152 mm; ConMed, Linvatec, Largo) are used, and a 50-mL syringe is used for initial air arthroscopy. Subsequently, gravity

© ISAKOS 2022

D. N. Bhatia et al. (eds.), *Arthroscopy and Endoscopy of the Elbow, Wrist and Hand*,
https://doi.org/10.1007/978-3-030-79423-1_49

inflow is used to minimize fluid extravasation into the arm and forearm.

49.3.1 Portals

Two portals are used for biceps endoscopy (Fig. 49.1): Proximal Parabiceps portal (PBP) is the viewing portal throughout the procedure. Distal anterior portal (DAP) placed directly above the radial tuberosity is the working portal [1–4]. Detailed placement of these portals and their neurovascular relations are described in a previous chapter.

49.3.2 Intrabursal Assessment

The PBP uses the bicipitoradial bursal space for insufflation and presents a panoramic intrabursal view of the entire DBT insertional region. In an intact DBT, the tendon surfaces can be evaluated, and dynamic movements of the DBT are assessed (Fig. 49.2). The intact tendon may be hooked with an arthroscopic probe and can be drawn distal to the tuberosity, and this permits visualization of the more proximal region of the DBT. Bursal inflammation may result in adhesions within the insertional region, and bursal clearance may sometimes be necessary to enhance visualization. Partial tears on the radial DBT surface can be visualized, and an "endoscopic probe test" devised by the author is useful to assess severity of the tear [6, 7].

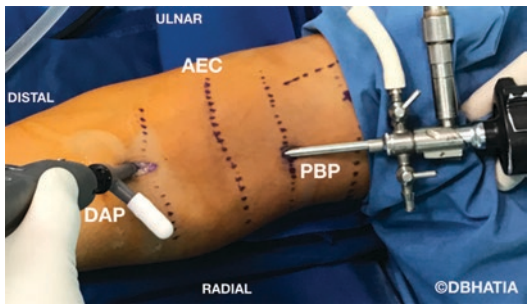

Fig. 49.1 Arthroscopic setup and portals for the all-endoscopic debridement is shown on a left elbow in supine position (*PBP* parabiceps portal, *DAP* distal anterior portal, *AEC* anterior elbow crease). (© Bhatia)

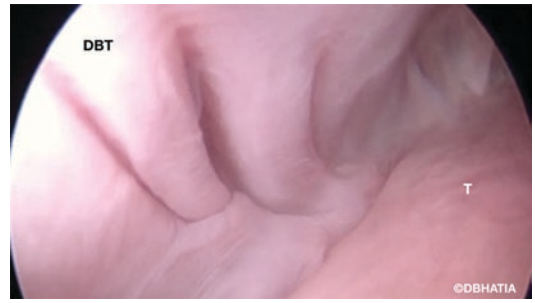

Fig. 49.2 Endoscopic appearance of a normal distal biceps tendon (DBT) and its insertion on the bare area of the bicipital tuberosity (T) is shown. (© Bhatia)

49.3.3 The "Endoscopic Probe Test" and Appearance of Partial Tears

This test is performed while viewing through the PBP and an angled arthroscopic probe is introduced via the DAP cannula (Fig. 49.3a). Acute DBT tears are associated with edematous tissues, and gentle retraction with an arthroscopic probe is useful. Partial tears may be segregated into the following:

- *Low-grade tears or tendinosis*: These tears demonstrate an intact footprint attachment and the radial intrabursal surface is frayed or minimally detached. An angled probe cannot be passed through the DBT-tuberosity junction (negative probe test) [7]. A gentle debridement of the frayed surface is indicated in these tears.
- *High-grade tears*: These tears involve partial detachment over a larger footprint area. An angled probe can be passed through the tendon-tuberosity junction and the ulnar aspect of the tuberosity can be probed (positive probe test). These tears are treated with conversion to a complete tear and endoscopic repair is performed (Fig. 49.3b).
- *Isolated head rupture*: Complete rupture of an isolated long/short head is diagnosed when one head can be demonstrated to be intact and the insertional region of the other head shows absence of any tendon attachment on probing (positive probe test). Rupture of an isolated

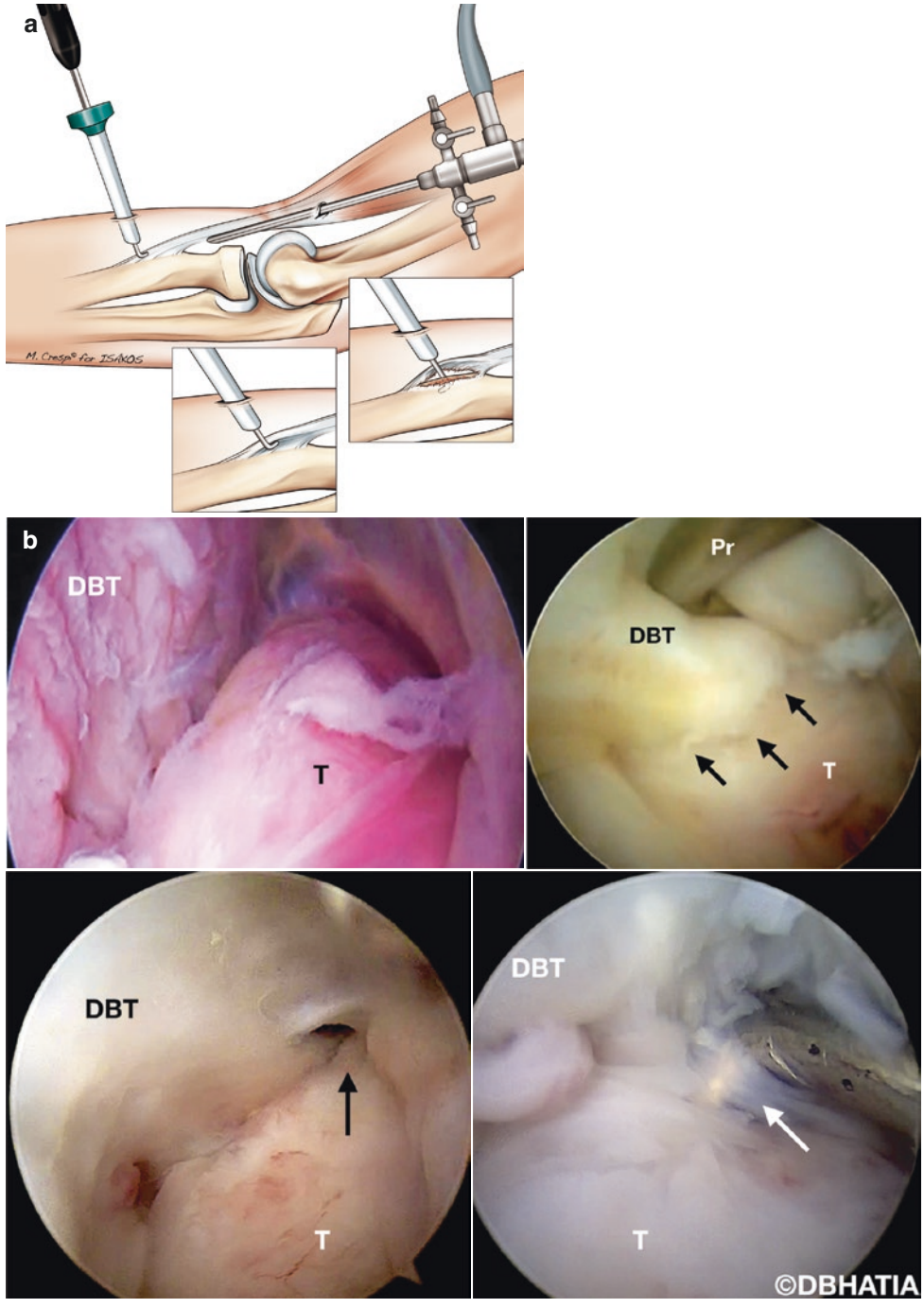

Fig. 49.3 (**a**) The distal biceps "endoscopic probe test" is illustrated. An arthroscopic probe is passed via the distal anterior portal cannula and the distal biceps insertional area is probed under vision (top image). In a low-grade tear, the footprint is mostly intact and the ulnar aspect of tuberosity cannot be probed (negative probe test, bottom left). In a high-grade tear, a probe can be passed past the bare footprint and the ulnar aspect of tuberosity can be probed (positive probe test, bottom right). (**b**) Endoscopic identification of partial tears of distal biceps is demonstrated. A low-grade tear shows surface fraying and inflammation without detachment (top left). A high-grade tear (arrows) permits passage of a probe (Pr) past the insertional area in a positive probe test (top right). An isolated short head rupture shows an intact long head attached to the proximal footprint and a gap in tendon continuity (arrow, left image), and a probe test demonstrates the discontinuity in tendon (right image). (© Bhatia)

head is treated by endoscopic reattachment of the ruptured head only. If the intact head demonstrates a partial tear as well, then detachment of intact head and subsequent endoscopic repair of both heads is performed [1].

49.3.4 Endoscopic Appearance of Complete Tears

Complete detachment of both heads of DBT shows absence of the taut DBT fibres at insertion region and remnants of the ruptured stump are seen attached to the footprint area. The ruptured non-retracted DBT is visualized proximal to the tuberosity, and an empty sheath is visualized if the DBT is retracted beyond the cubital fossa [4].

49.3.5 Partial DBT Tear Debridement

The extended elbow is supinated to improve access to the ulnar aspect of the tuberosity and DBT insertion. An arthroscopic shaver (3, 3.5 mm) is used via the DAP cannula to access and debride the frayed tendon surface (Fig. 49.4). A small joint radiofrequency device can be used cautiously for shrinkage of frayed fibres. The footprint attachment is re-evaluated after DBT debridement to assess the remaining tendon attachment. A high-grade tear (positive probe test) is converted to a complete non-retracted tear using either of two techniques:

- The tendon attachment is resected using arthroscopic scissors (Fig. 49.5a, b) via distal anterior portal (DAP).
- Alternately, a blunt angled hemostat or hooked probe (Fig. 49.5c, d) is used to exteriorize the DBT via DAP and is then sectioned externally.

The sectioned DBT is then reattached using an all-endoscopic dual suture-anchor technique similar to repair of a non-retracted tear.

49.4 Tips and Tricks

- Use a 2.9 mm arthroscope with a 4 mm sheath for visualization via PBP. An external mark on the sheath at 7 cm is useful to avoid deeper penetration.
- The DAP cannula needs to be short to permit the shorter length 3 mm shaver blades to access the DBT. The author prefers the 5 mm

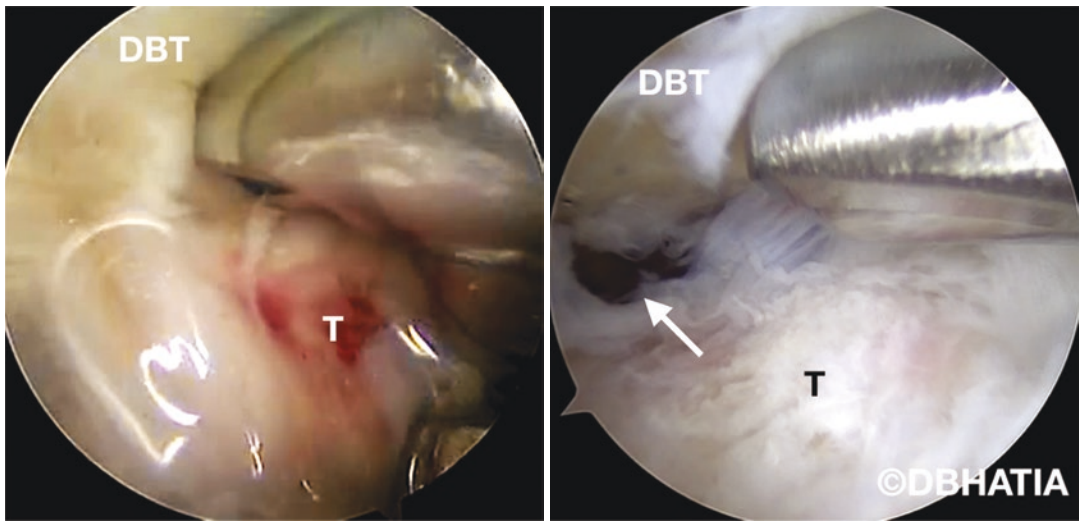

Fig. 49.4 A small joint shaver is shown debriding a partial distal biceps tendon tear (DBT, left image). After debridement, most of the proximal footprint on the tuberosity (T) is exposed and an area of detachment can be seen (arrow) (right image). (© Bhatia)

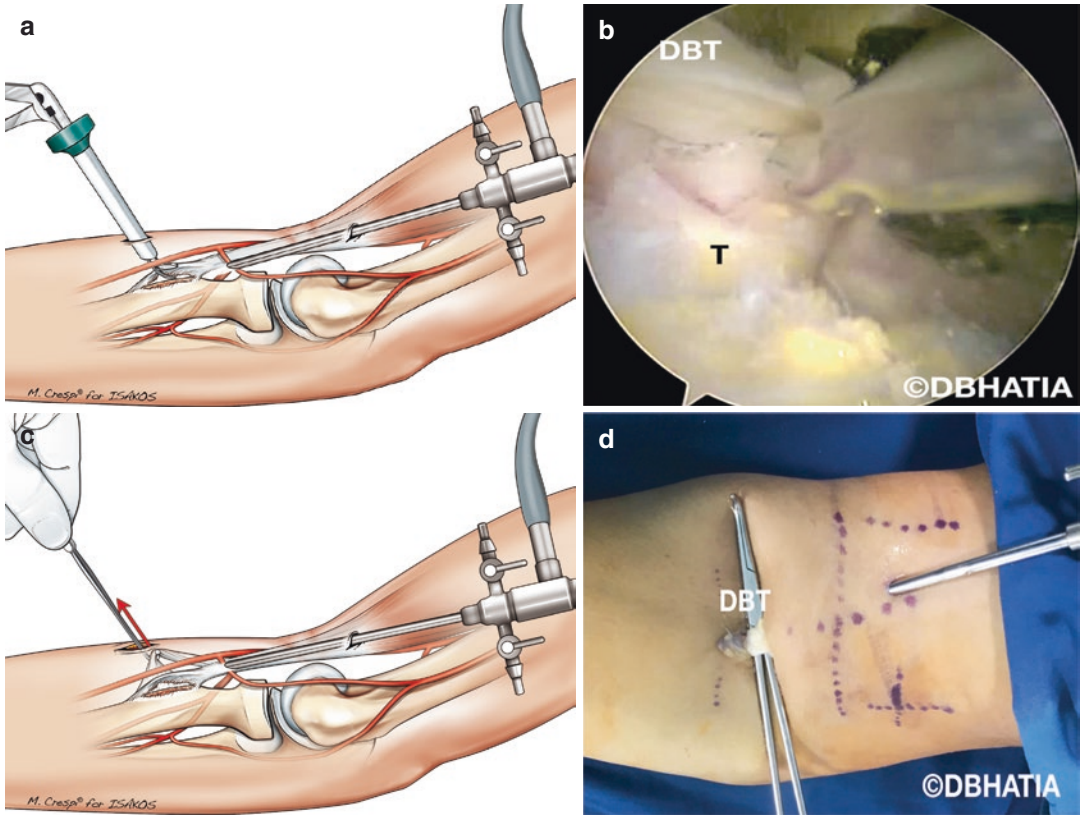

Fig. 49.5 (**a**) Resection of a high-grade partial DBT tear using an arthroscopic scissors is illustrated. (**b**) Endoscopic demonstration of tendon resection using scissors. (**c**) Resection of a high-grade partial DBT tear by exteriorizing the tendon and sectioning externally is illustrated. (**d**) Tendon resection by exteriorizing the tendon and sectioning externally is shown. (© Bhatia)

smooth cannula of standard length, and this is cut short intraoperatively to suitable length.

- Air endoscopy and reduced fluid inflow are key to good visualization and prevention of compartment syndrome.

49.5 Pitfalls

- *Rise in compartment pressures*: Biceps endoscopy is performed in a closed extra-articular space, and compartment pressures measured pre- and post-DBT repair procedure in cadavers have shown a mild rise of 4–6 mmHg [6]. Use of air-endoscopy and placement of an intrabursal cannula via the DAP portal permits a steady outflow of fluid and minimizes the risk of a greater increase in pressure.
- *Neurovascular damage*: The DBT is closely related to nine neurovascular structures and the anatomic course of these structures shows wide variation [3, 5, 6]. The PBP is adjacent to the LCN, and the RA is significantly "at risk" of injury with DAP. The risk is minimized by placing the PBP just below the musculotendinous junction, and in close apposition to the DBT. The DAP should be placed with open dissection via an 8 mm incision, and the LCN and RA should be identified and protected while passing the cannula. Excessive retraction is associated with neurological injury and is not necessary in the endoscopic procedure.

- *Incorrect evaluation of tear extent*: Debridement of a high-grade tear may result in persistence of pain and weakness and progress to complete rupture is possible.

49.6 Postoperative Management and Rehabilitation

A bulky soft tissue dressing is used in the immediate postoperative period, and this is changed to portal dressing on the fourth postoperative day. A sling is used for comfort and is discarded within a week. Elbow flexion and forearm rotation are permitted without any restrictions. Strengthening exercises are initiated in the fourth week and progressed over the next 6 weeks. Sports-specific conditioning is initiated once optimal strengthening is achieved.

49.7 Complications

Cutaneous paresthesias may be present in the postoperative period; these are associated with use of retractors in DAP, and usually subside over 3–6 weeks. The radial artery is at-risk while working through the DAP and use of a cannula placed with open dissection is recommended.

Conflict of Interest The author certifies that he has no commercial associations (e.g., consultancies, stock ownership, equity interest) that might pose a conflict of interest in connection with the submitted article. The author retains the copyright to the images, videos, and content in this chapter.

References

1. Bhatia DN. All-endoscopic distal biceps repair and reconstruction: science, technique and results. Presented at Shoulder and Elbow Society of Australia (SESA) biennial conference, Nov 2018, Perth, Australia.
2. Bhatia DN. Endoscopic distal biceps repair: endoscopic anatomy and dual-anchor repair using a proximal anterolateral "parabiceps portal". Arthrosc Tech. 2015;4:e785–93. https://doi.org/10.1016/j.eats.2015.07.031.
3. Bhatia DN, DasGupta B, Panjwani T. Cadaveric study of anterior and posterior elbow endoscopy portals for endoscopic distal biceps repair: comparative anatomy-at-risk. Surg Radiol Anat. 2016;38(7):781–91. https://doi.org/10.1007/s00276-016-1637-6. Epub 2016 Feb 9.
4. Bhatia DN. Endoscopic repair of acute and chronic retracted distal biceps ruptures. J Hand Surg Am. 2016;41(12):e501–7. https://doi.org/10.1016/j.jhsa.2016.09.008.
5. Bhatia D, Naskar R, DeNiese P. Dynamic rotational alteration in positional relationship of neurovascular structures and distal biceps tendon insertion: a cadaveric study. J ISAKOS. 2019;4:296–301. https://doi.org/10.1136/jisakos-2019-000326.
6. Bhatia DN, Kandhari V. Analysis of technical feasibility and neurovascular safety of endoscopic distal biceps repair: a cadaveric study. J Shoulder Elb Surg. 2018;27:2057–67. https://doi.org/10.1016/j.jse.2018.04.020.
7. Bhatia DN. Endoscopic anatomy of distal biceps tendon insertion and bicipitoradial bursa: a cadaveric study. J Shoulder Elbow Surg. 2021 Aug;30(8):1759–67. https://doi.org/10.1016/j.jse.2020.11.033. Epub 2021 Jan 21.

All-Endoscopic Repair of Complete Retracted Distal Biceps Ruptures

50

Deepak N. Bhatia

50.1 Background

Complete ruptures of the distal biceps tendon (DBT) occur infrequently and surgical intervention is necessary for restoration of anatomy and correction of "Popeye" deformity. Recent advances in the understanding of DBT insertional anatomy, and data from cadaveric safety and feasibility studies, have resulted in the development of a safe and reproducible all-endoscopic technique for DBT repair [1–6]. The technique is advantageous for several reasons: (a) Three portals are sufficient for endoscopic repair of acute and chronic retracted tears. (b) Separate portals are used for viewing and working this makes the technique ergonomic to perform. (c) Excessive retraction and retractor-induced complications are avoided. (d) Retracted tears can be endoscopically advanced and repaired, and endoscopic graft reconstruction is possible as an extension of the technique.

50.2 Indications

The "all-endoscopic" DBT repair technique has the following indications: (1) High-grade partial DBT tears (positive probe test, isolated head ruptures) can be repaired in situ, or the tear can be completed and repaired. (2) Acute ruptures, both retracted and non-retracted can be reattached to the tuberosity (3) Chronic ruptures with an adequate tendon length can be endoscopically mobilized, retrieved, and reattached to the tuberosity.

50.3 Contraindications

Chronic tears with deficient tendon length or chronic musculotendinous tears cannot be endoscopically repaired and necessitate endoscopic reconstruction using a tendon autograft or allograft [7]. Traumatic scarring or surgical alteration in the anatomy of the cubital fossa (heterotopic ossification, vascular or neurological surgery) is a contraindication to the procedure. Similarly, the procedure should be avoided in patients with vascular anomalies and malunited fractures. Surgical experience and familiarity with the anatomical course of neurovascular structures are prerequisites [2, 6].

50.4 Surgical Technique

The "all-endoscopic" DBT repair is performed with the patient in supine position, and the upper extremity is placed on a side trolley. The elbow joint is flexed 10–20° for initial portal placement, and a support under the distal humerus is used

D. N. Bhatia (✉)
SPORTSMED Mumbai, Mumbai, India

Sir HN Reliance Foundation Hospital, Mumbai, India
e-mail: shoulderclinic@gmail.com

© ISAKOS 2022

D. N. Bhatia et al. (eds.), *Arthroscopy and Endoscopy of the Elbow, Wrist and Hand*,
https://doi.org/10.1007/978-3-030-79423-1_50

intraoperatively to achieve extension when necessary. A tourniquet is placed high on the arm and is used during the procedure. A 2.9-mm arthroscope and sheath (2.9, 152 mm; ConMed, Linvatec, Largo) are used, and gravity inflow is used to minimize fluid extravasation into the arm and forearm.

50.4.1 Portals

Three portals are used for biceps endoscopy (Fig. 50.1): (1) Proximal parabiceps portal (PBP) is the viewing portal throughout the procedure. (2) Distal anterior portal (DAP) placed directly above the radial tuberosity is the working portal. (3) Midbiceps portal (MBP) is a viewing and working portal for arm endoscopy. The ruptured retracted tendon can be identified and mobilized via the MBP [1, 3]. Detailed placement of these portals and their neurovascular relations are described in a previous chapter.

50.4.2 Diagnostic Endoscopy

The PBP visualizes the bare tuberosity area and remnants of the ruptured stump on the tuberosity, and the ruptured non-retracted DBT is visualized proximal to the tuberosity [1]. Absence of a visible tendon and an empty sheath are suggestive of a proximally retracted tear. Acute DBT ruptures are associated with edematous tissues and evidence of bleeding within the bursa, and gentle retraction with an arthroscopic probe is useful for assessment. Chronic tears are associated with adhesions and bursal adhesiolysis may sometimes be necessary to enhance visualization (Fig. 50.2).

50.4.3 Tendon Retrieval and Preparation

An arthroscopic grasper is passed via DAP cannula, and the visible non-retracted ruptured DBT is retrieved out through DAP (Fig. 50.3). Retracted tears, acute and chronic, are usually located in the lower or mid arm. The arthroscope is placed in the MBP cannula and the plane anterior to the brachialis is explored. The retracted DBT is visualized as a white lobulated structure and the tendon is grasped and retrieved out via MBP (Fig. 50.4a, b). Adequacy of length is assessed by pulling the tendon distally; inability to pull the tendon to the DAP level indicates necessity for autograft reconstruction. The frayed region of the DBT is debrided to healthy tendon, and a grasping stitch is passed through it.

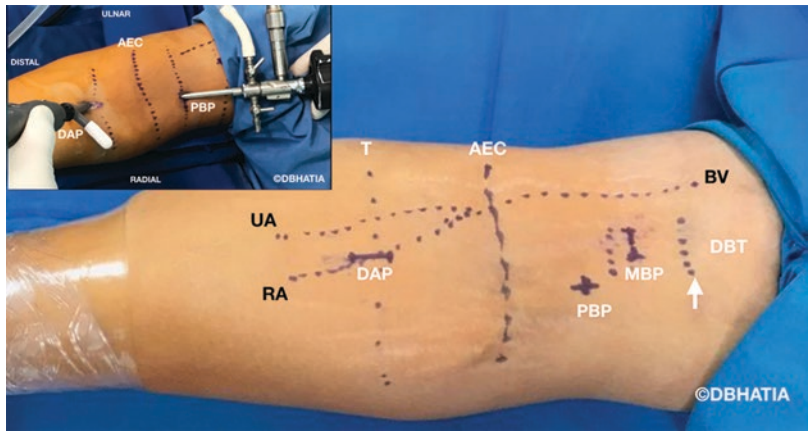

Fig. 50.1 Preoperative sonography marking of vital structures and arthroscopic portals for the all-endoscopic distal biceps repair are shown on a left elbow in supine position (*PBP* parabiceps portal, *DAP* distal anterior portal, *MBP* midbiceps portal, *AEC* anterior elbow crease, *BV* brachial vessels, *UA* ulnar artery, *RA* radial artery, *T* tuberosity level, *DBT* distal biceps tendon, white arrow: retracted DBT stump). (© D. Bhatia)

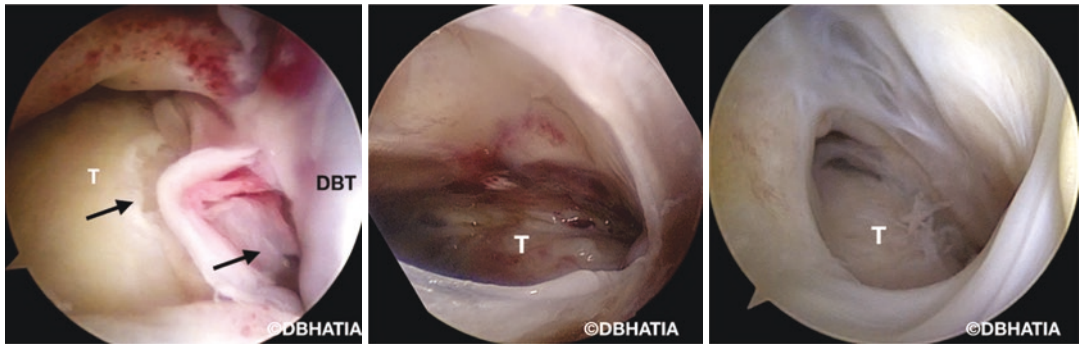

Fig. 50.2 Endoscopic view of complete DBT rupture is shown. A non-retracted torn tendon (DBT) is identified proximally by its bulky, white, and hyperemic appearance (left image). The remnants of the DBT on the tuberosity are seen (arrows), and the bare area of the tuberosity (T) shows the ruptured footprint (arrow). An acute retracted tear shows an empty sheath and hyperemia within the bursa. A chronic retracted DBT tear shows adhesions, absence of hyperemia, and an empty sheath space. (© D. Bhatia)

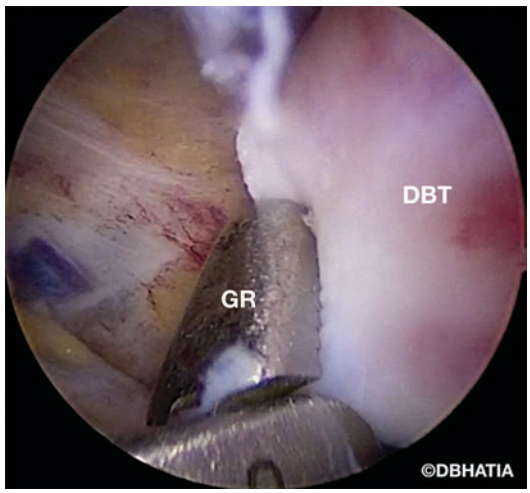

Fig. 50.3 An arthroscopic grasper (GR) is used to grasp the bulky DBT, and the tendon is pulled out through the DAP. (© D. Bhatia)

50.4.4 Tendon Shuttling Technique Across the Cubital Fossa

Proximally retracted tears retrieved via MBP are whipstitched to secure the stump into a conical tapering end. A shuttling suture is passed under vision via the DAP and is retrieved out through the PBP sheath (Fig. 50.5a). The sheath is withdrawn and the suture is re-shuttled subcutaneously and brought out via MBP. The suture shuttle is attached to the whipstitch sutures of DBT; this suture is used to shuttle the DBT through the cubital fossa, and the tendon is brought out through the DAP (Fig. 50.5b) [3].

50.4.5 Tuberosity Preparation

The radial tuberosity is visualized via the PBP, and an arthroscopic shaver is passed through the DAP cannula. The soft tissue remnants over the tuberosity are excised, and forearm rotation is used to extend the debridement to the ulnar and radial aspects. An arthroscopic burr is next used to prepare an area of 1–2 cm for DBT reattachment (Fig. 50.6).

50.4.6 Tendon Reattachment

Use of anchors has been safe in clinical and cadaveric studies and the author's preference is a dual suture-anchor repair technique using double-loaded all-suture anchors [5, 7]. Alternatively, the technique may be performed using buttons and interference screws [8]. Two suture anchors (single or double loaded) are passed into the tuberosity, I cm apart from each other, via a sleeve passed through DAP. One strand from each suture of both anchors is shortened, and the longer suture is used to whipstitch the DBT (Fig. 50.7a, b). The suture from the distal anchor is used to stitch the distal 5–8 mm of the DBT; the proximal suture

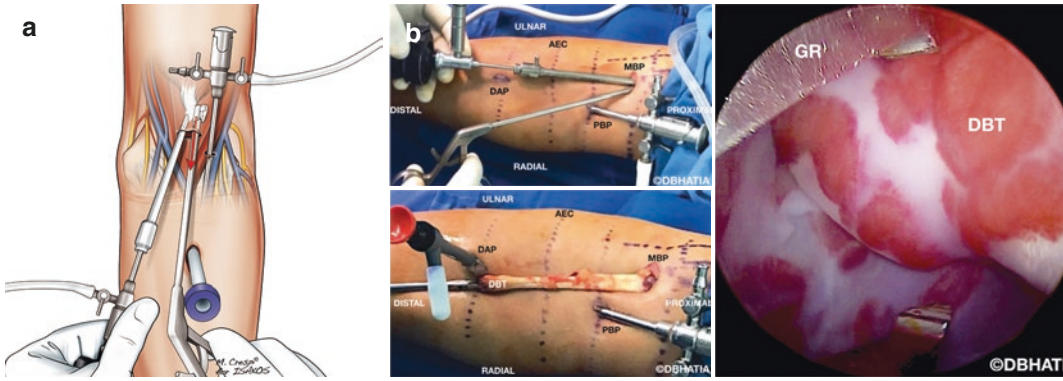

Fig. 50.4 (**a**) Arm endoscopy and retrieval of a proximally retracted tendon via midbiceps portal is illustrated (© D. Bhatia). (**b**) The arthroscope and grasper are used simultaneously through the midbiceps portal MBP (top left image) and the retracted tendon (DBT) is released and retrieved (right image). The tendon length is adequate if the DBT can be pulled distally to the distal anterior portal DAP (bottom left image). (© D. Bhatia)

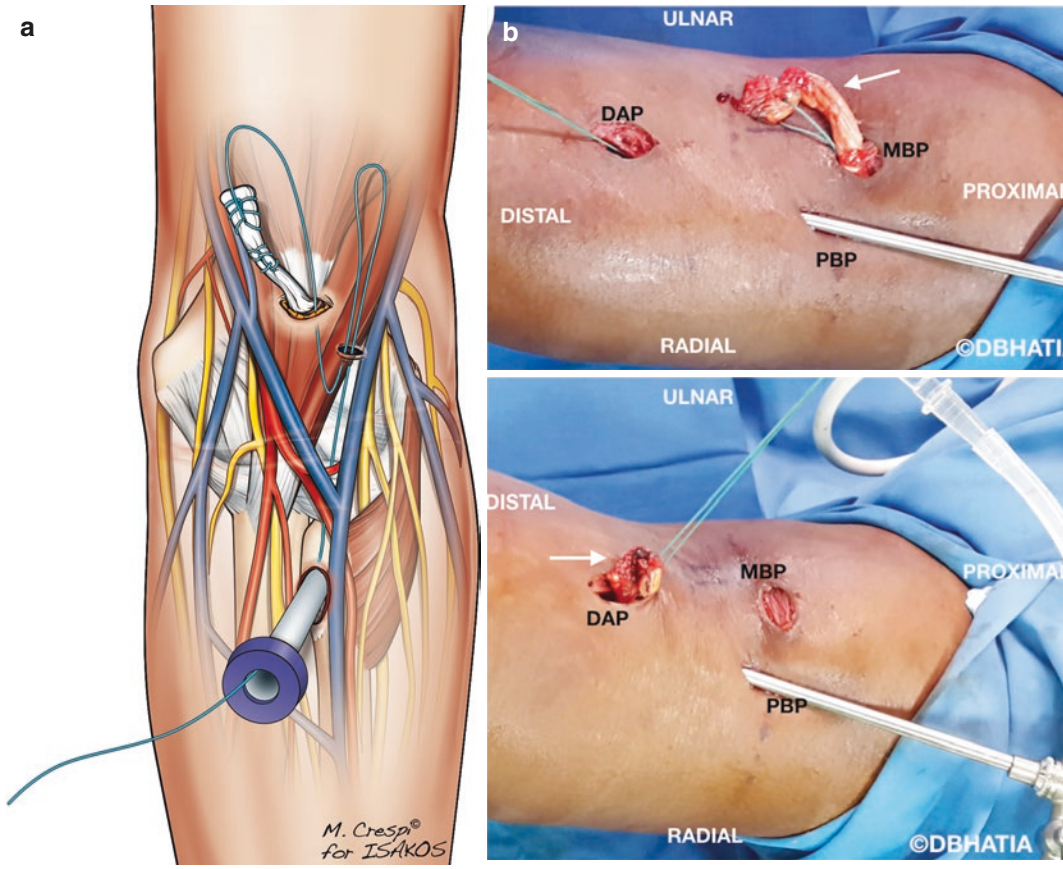

Fig. 50.5 (**a**) A suture shuttle passes through the distal anterior portal cannula and exits through the midbiceps portal via parabiceps portal. Note that the shuttle suture passes under the bifurcation of the brachial artery and is adjacent to other major structures and thereby traces the original path of the distal biceps tendon (© D. Bhatia). (**b**) The suture shuttle is attached to the distal biceps stump (arrow, top image) and is pulled distally and out through the distal anterior portal (DAP) (arrow, bottom image) (*PBP* parabiceps portal). (© D. Bhatia)

Fig. 50.6 An arthroscopic shaver (SH) is passed via the distal anterior portal cannula (DAP), and the tuberosity (T) is debrided for tendon reattachment. (© Bhatia)

extends the whipstitch proximally for a further 5–8 mm. This dual stitch technique helps to reattach the tendon in a flat footprint-like fashion over a tuberosity area of 10–15 mm (Fig. 50.7c). The shorter suture from each anchor is pulled, and the sliding mechanism draws the DBT to approximate to the tuberosity. Nonsliding knots are tied with a knot pusher to reattach the DBT back to the tuberosity.

50.4.7 Final Assessment

The repaired DBT is assessed through the PBP and DAP, and the repair integrity and bony contact is assessed dynamically and with a probe (Fig. 50.8a). External examination confirms restoration of biceps shape and a hook test is performed to ensure adequate tensioning within the DBT (Fig. 50.8b).

50.5 Tips and Tricks

- Forearm rotation is useful to distinguish between non-retracted complete tears and partial tears. In a complete rupture, the tendon does not move with the tuberosity with forearm pronation and supination.
- Correct portal placement of parabiceps portal PBP is vital. The parabiceps space consists of loose fibrofatty and bursal tissue, and the PBP sheath should pass without any resistance for 7–8 cm. Excessive angulation results in penetration of the brachialis muscle fibres, and the sheath should be withdrawn and reinserted.
- Incorrect placement of distal anterior portal DAP results in misplacement of anchors/buttons. The DAP should be placed exactly in line with the bicipital tuberosity, and this point can be located by using digital pressure externally.
- Air endoscopy and reduced fluid inflow are key to good visualization and prevention of compartment syndrome [5].
- The bare area of tuberosity is a standard anatomic landmark for endoscopic orientation and forms a safe boundary for endoscopic working and tendon reattachment [1].
- Use of a short 5–8 mm cannula via the DAP provides sufficient distraction of the surrounding tissues. Other steps of tuberosity preparation, implant placement, and knot tying are safer to perform via the cannula to prevent inadvertent damage to vital structures.

50.6 Pitfalls

- *Rise in compartment pressures*: Biceps endoscopy is performed in a closed extra-articular space, and compartment pressures measured pre- and post-DBT repair procedure in cadavers have consistently shown a mild rise of 4–6 mmHg [5].
- *Neurovascular proximity*: The DBT is closely related to nine neurovascular structures. The PBP is adjacent to the LCN, and the RA is significantly "at risk" of injury with DAP. The MBP is 10 mm away from the brachial neurovascular bundle [2, 5].
- *Incorrect site of attachment*: Consistent placement at the upper tuberosity is difficult, and the implants may be inadvertently placed distal or proximal to the tuberosity. Intraoperative imaging may be used for orientation [1, 3, 5].

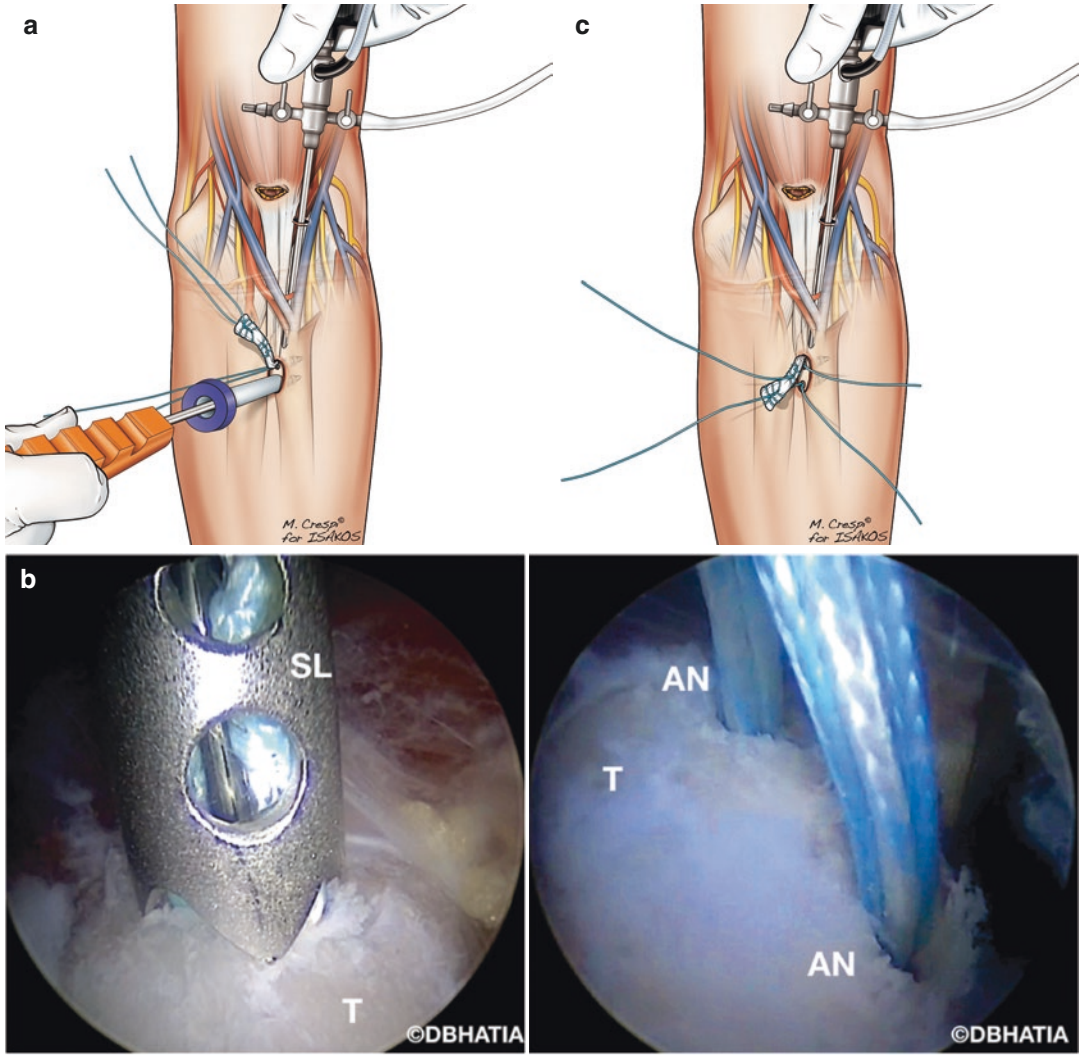

Fig. 50.7 (**a**) Endoscopic anchor placement via distal anterior portal cannula is illustrated after shuttling and exteriorization of distal biceps tendon (© Bhatia). (**b**) A sleeve (SL) is passed through the distal anterior portal cannula and is placed over the bare area of tuberosity (T, left image). Two all-suture anchors (AN) are passed 1 cm away from each other (© Bhatia). (**c**) The tendon whip-stitch is performed at two levels as illustrated to recreate a footprint at the repair site. (© Bhatia)

- *Suboptimal tendon-bone contact area*: Failure of the sutures to slide perfectly within anchors or buttons results in suboptimal tendon-bone contact area. The dual-anchor technique using all-suture anchors has shown consistent and optimal tendon-bone contact area [5].

50.7 Postoperative Management, Rehabilitation, and Return to Sport

A bulky soft tissue dressing is used in the immediate postoperative period, and this is changed to portal dressing on the fourth postoperative day.

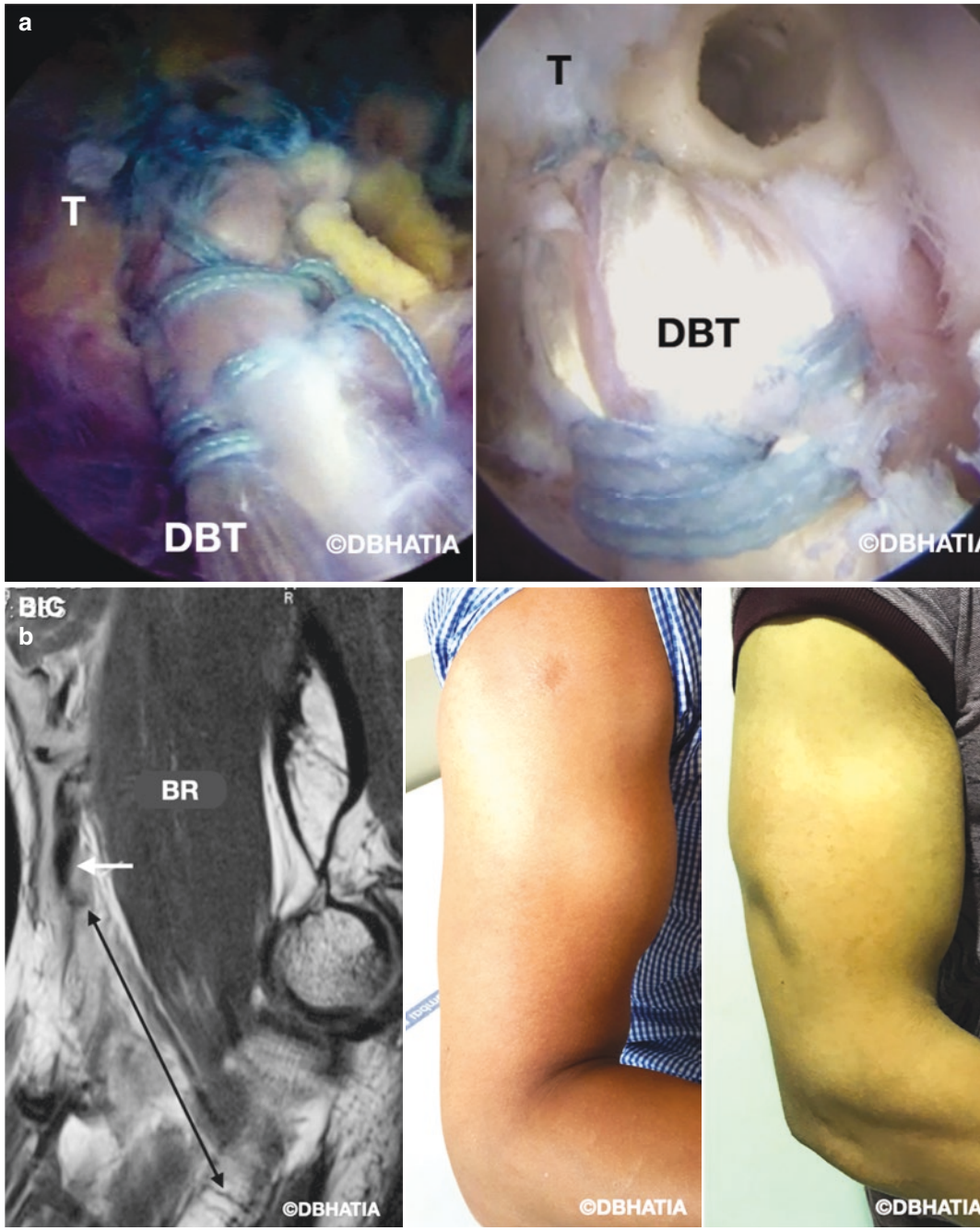

Fig. 50.8 (**a**) The tendon (DBT) is seen securely fixed to the tuberosity (T) with suture anchors (left image) and button and interference screw (right image) (© Bhatia). (**b**) Correction of Popeye deformity in an acute retracted distal biceps tear is demonstrated. Magnetic resonance imaging shows a full-thickness biceps tendon tear (white arrow) from its radial attachment with retraction by approximately 6 cm (white arrow, left image). The preoperative Popeye deformity is seen in the midarm (middle image) and postoperative restoration of biceps shape at a long-term follow-up is demonstrated (right image). (© D. Bhatia)

Thereafter, for repairs of partial tears and non-retracted ruptures, elbow movements are initiated from 60° to 90° of flexion in a controlled-motion brace, and forearm rotations are permitted. Elbow ROM exercises are progressed after 4–6 weeks. Repairs of proximally retracted ruptures are immobilized for 4 weeks and ROM exercises are initiated after 4–6 weeks. Biceps strengthening is initiated at 12 weeks and return to competitive sports is permitted after 6 months.

50.8 Complications

The all-endoscopic DBT repair is technically feasible and safe; however, the recommended guidelines should be followed, and the procedure should be preceded by cadaveric training.

- Cutaneous paresthesias may be present in the postoperative period; these are associated with use of retractors in DAP, and usually subside over 3–6 weeks [3].
- The radial artery is at-risk while working through the DAP and use of a cannula is recommended [2].
- The ulnar artery is closest to DBT insertion in neutral position and forearm should be placed in full supination when working along the ulnar aspect of tuberosity [6].
- Augmentation of the repaired DBT with sutures/graft (>2–3 mm) may "overstuff" the proximal radioulnar space; this can result in dynamic radioulnar impingement and subsequent rerupture [4].

Conflict of Interest The author certifies that he has no commercial associations (e.g., consultancies, stock ownership, equity interest) that might pose a conflict of interest in connection with the submitted article. The author retains the copyright to the images, videos, and content in this chapter.

References

1. Bhatia DN. Endoscopic distal biceps repair: endoscopic anatomy and dual-anchor repair using a proximal anterolateral "parabiceps portal". Arthrosc Tech. 2015;4:e785–93. https://doi.org/10.1016/j.eats.2015.07.031.
2. Bhatia DN, DasGupta B, Panjwani T. Cadaveric study of anterior and posterior elbow endoscopy portals for endoscopic distal biceps repair: comparative anatomy-at-risk. Surg Radiol Anat. 2016;38(7):781–91. https://doi.org/10.1007/s00276-016-1637-6. Epub 2016 Feb 9.
3. Bhatia DN. Endoscopic repair of acute and chronic retracted distal biceps ruptures. J Hand Surg Am. 2016;41(12):e501–7. https://doi.org/10.1016/j.jhsa.2016.09.008.
4. Bhatia DN, Kandhari V, Das Gupta B. Cadaveric study of insertional anatomy of distal biceps tendon and its relationship to the dynamic proximal radioulnar space. J Hand Surg Am. 2017;42:e15–23. https://doi.org/10.1016/j.jhsa.2016.11.004.
5. Bhatia DN, Kandhari V. Analysis of technical feasibility and neurovascular safety of endoscopic distal biceps repair: a cadaveric study. J Shoulder Elb Surg. 2018;27:2057–67. https://doi.org/10.1016/j.jse.2018.04.020.
6. Bhatia D, Naskar R, DeNiese P. Dynamic rotational alteration in positional relationship of neurovascular structures and distal biceps tendon insertion: a cadaveric study. J ISAKOS. 2019;4:296–301. https://doi.org/10.1136/jisakos-2019-000326.
7. All-endoscopic distal biceps repair and reconstruction: science, technique and results. Presented at Shoulder and Elbow Society of Australia (SESA) biennial conference, Nov 2018, Perth, Australia.
8. Bhatia DN. All-endoscopic distal biceps repair: endoscopic techniques using suture anchors, buttons, and interference screw fixation. In: Bain G, Eygendaal D, van Riet R, editors. Surgical techniques for trauma and sports related injuries of the elbow. Berlin: Springer; 2020.

51 All-Endoscopic Autograft Augmentation and Reconstruction of Chronic Retracted Distal Biceps Tendon Tears

Deepak N. Bhatia

51.1 Introduction

Complete ruptures of the distal biceps tendon (DBT) usually retract into the lower arm. An intact lacertus fibrosus may prevent excessive retraction, however, in several cases, the torn DBT gradually retracts proximally into the mid and upper arm and the biceps muscle belly undergoes atrophy. Chronic deficient and irreparable DBT tears can be surgically treated using autografts or allografts for augmentation and restoration of tendon length. Open surgical procedures involve multiple incisions or extensile approaches and extensive soft-tissue dissection is necessary to reconstruct the DBT. Endoscopic graft reconstruction is an extension of the all-endoscopic repair technique and is a minimally invasive alternative to open surgery [1–3].

51.1.1 Surgical Anatomy

Chronic retraction of the distal biceps tendon (DBT) results in changes within the tendon stump and adherence to adjacent structures. The tendon is structurally weaker and may be "cocooned" or coiled within the tendon sheath. This results in deficient tendon length and strength, and anatomic repair to the bicipital tuberosity may not be possible. Chronic deficiency also results in adhesions around vital neurovascular structures (brachial artery and vein, median nerve, lateral cutaneous nerve), and these structures are potentially at-risk of injury [4–6].

51.2 Indications/ Contraindications

1. Chronic retracted DBT tear with an adequate tendon length and a structurally weak/degenerated tendon can be augmented and repaired using a gracilis autograft.
2. Chronic retracted tears with a deficient tendon length necessitate autograft reconstruction using either gracilis or semitendinosus grafts (Fig. 51.1).
3. Chronic musculotendinous tears can be reconstructed using either or even both gracilis and semitendinosus grafts.

Post-traumatic or iatrogenic alteration in the anatomy of the cubital fossa (heterotopic ossification, vascular or neurological surgery, previous DBT surgery) is a contraindication to the procedure. Similarly, the procedure should be avoided in patients with vascular anomalies and malunited fractures. Familiarity with the anatomical course and dynamic relationships of neurovascular structures is necessary.

D. N. Bhatia (✉)
SPORTSMED Mumbai, Mumbai, India

Sir HN Reliance Foundation Hospital, Mumbai, India
e-mail: shoulderclinic@gmail.com

© ISAKOS 2022

D. N. Bhatia et al. (eds.), *Arthroscopy and Endoscopy of the Elbow, Wrist and Hand*,
https://doi.org/10.1007/978-3-030-79423-1_51

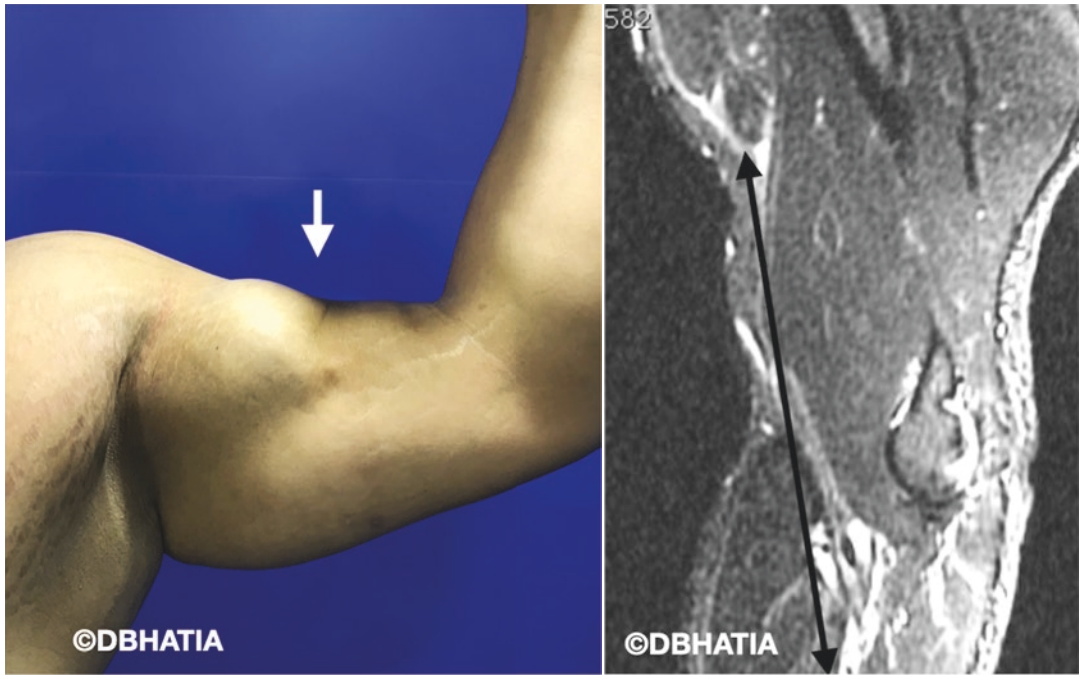

Fig. 51.1 Clinical images show a severely retracted chronic distal biceps rupture presenting with a Popeye deformity (arrow, left image) in the upper arm. Magnetic resonance image demonstrates the deficient proximal tendon stump (upper arrow) and quantifies the retraction distance (10 cm) from radial tuberosity (lower arrow, right image). (© Bhatia)

51.3 Surgical Technique

- *Preoperative sonography* is used to mark the course of (a) brachial artery and vein, (b) Median nerve, (c) Radial artery, (d) Ulnar artery, (e) Distal level of the retracted tendon stump, (f) Radial bicipital tuberosity. The lateral antebrachial cutaneous nerve can sometimes be visualized sonographically. Finally, the DBT stump is marked at its most distal level.
- *Position and setup*: Endoscopic DBT autograft reconstruction is performed with the patient in supine position, and the upper extremity is placed on a side trolley. The ipsilateral knee is prepared for graft harvest and is draped free. A tourniquet is placed high on the arm to ensure access to the retracted DBT stump. A 2.9-mm arthroscope and sheath (ConMed, Linvatec, Largo) are used, and gravity inflow is used to minimize fluid extravasation into the arm and forearm (Fig. 51.2).
- *Portals*: Three portals are used in this technique: (a) The **Proximal Parabiceps portal (PBP)** is the viewing portal throughout the procedure. (b) The **Distal anterior portal (DAP)** is the forearm working portal and is placed directly above the radial tuberosity (approximately 4 cm distal to the anterior elbow crease). A short cannula is placed in this portal and is retained until the tuberosity is prepared. (c) The **Midbiceps portal (MBP)** is the viewing and working portal for arm endoscopy. MBP is placed approximately 1–2 cm proximal to the PBP in the midline of the forearm, and is used for visualization of the retracted DBT, and for mobilization and retrieval of the tendon stump (Fig. 51.2).
- *Diagnostic endoscopy and tuberosity preparation*: Bursal adhesions may obstruct visualization of the bicipital tuberosity. The tuberosity bare area is identified, and a shaver introduced via the DAP cannula is used to clear bursal adhesions. The remnant stump is cleared, and

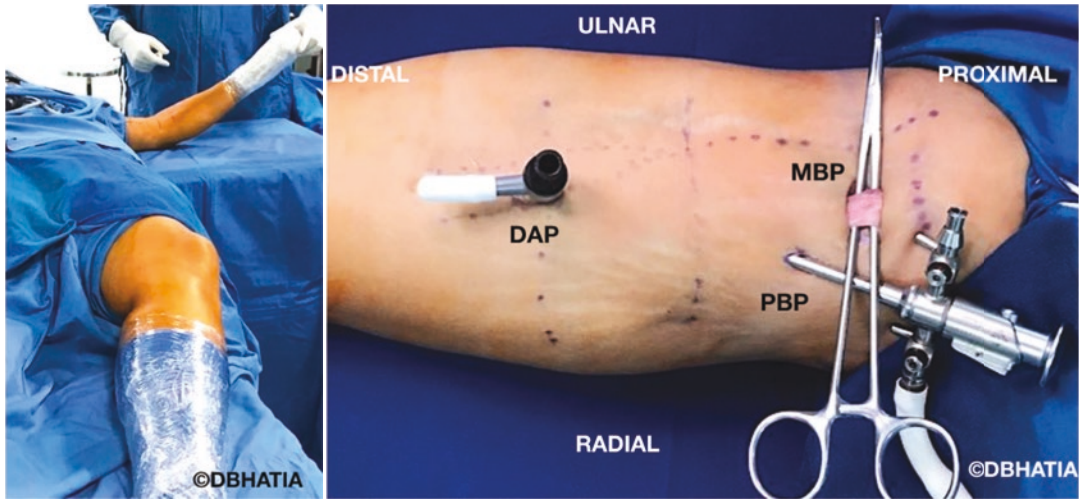

Fig. 51.2 Arthroscopic setup (left image) and portals (right image) for the all-endoscopic distal biceps autograft reconstruction are shown on a left elbow in supine position (*PBP* parabiceps portal, *DAP* distal anterior portal, *MBP* midbiceps portal). (© Bhatia)

the tuberosity boundaries are visualized (Fig. 51.3).

- *Retracted tendon retrieval*: The MBP is placed just distal to the sonographically marked DBT stump in the mid arm. A second arthroscopic sheath is introduced via this portal and is passed deep to the arm fascia (Fig. 51.4a). The retracted DBT is visualized as a white rounded structure. An arthroscopic grasper is passed simultaneously adjacent to the arthroscope via the MBP and is used to assist gentle separation of the DBT from surrounding adhesions. The tendon is then grasped and retrieved out through the MBP and assessed for length and structural quality (Fig. 51.4b).
- *Retracted tendon assessment and preparation*: Adequacy of DBT length is performed by first releasing the tendon from its coil or "cocoon." The tendon is grasped distally and pulled down towards the DAP cannula. An adequate tendon length is judged if the DBT can be pulled distally to the cannula. Inability to perform this maneuver or undue traction on the DBT is judged as inadequate tendon length (Fig. 51.4b). A semitendinosus or gracilis tendon is harvested from the ipsilateral knee and is prepared using standard techniques. The graft is then tunneled through the musculotendinous junction and secured to the DBT using high strength sutures. The DBT and graft combination is assessed for adequacy of length and excessive graft tendon is excised (Fig. 51.5a, b).
- *Graft passage from arm to forearm*: A suture shuttle is passed via the PBP sheath and retrieved via the DAP cannula. The PBP sheath is withdrawn and the shuttle further retrieved subcutaneously via the MPB portal. The graft sutures are then tied to the suture shuttle; this suture is used to cautiously shuttle the DBT through the cubital fossa and under the bifurcation of brachial artery, and the tendon is brought out through DAP (Fig. 51.6a, b).
- *Tuberosity preparation, anchor placement, and tendon stitch*: An arthroscopic shaver and burr are used to prepare an area of 1–2 cm for DBT reattachment. Two all-suture anchors (single/double loaded) are placed on the tuberosity via a sleeve passed through the DAP and are spaced 1 cm away from each other. One strand from each suture of both anchors is shortened, and the longer sutures are used to whipstitch the DBT using the dual-stitch tech-

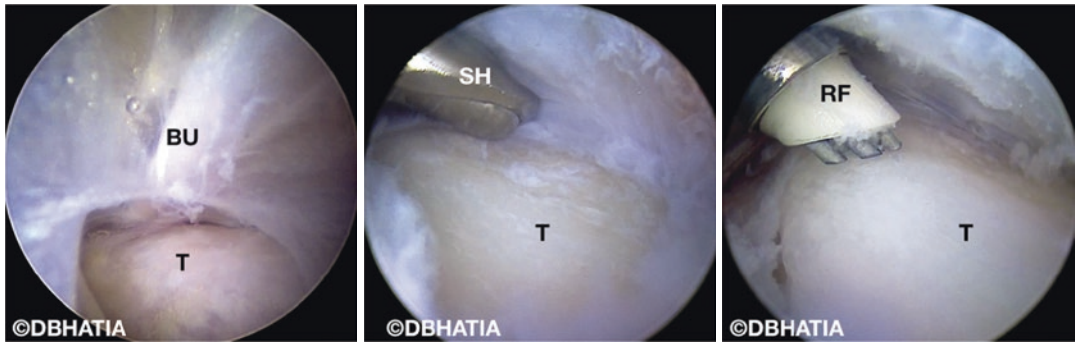

Fig. 51.3 Endoscopic image shows bursal adhesions (BU) in the tuberosity region (T) (Left image). A shaver (SH, middle image) and an angled radiofrequency probe (RF, right image) are used to clear bursal adhesions and tuberosity is visualized in its entirety (right image). (© Bhatia)

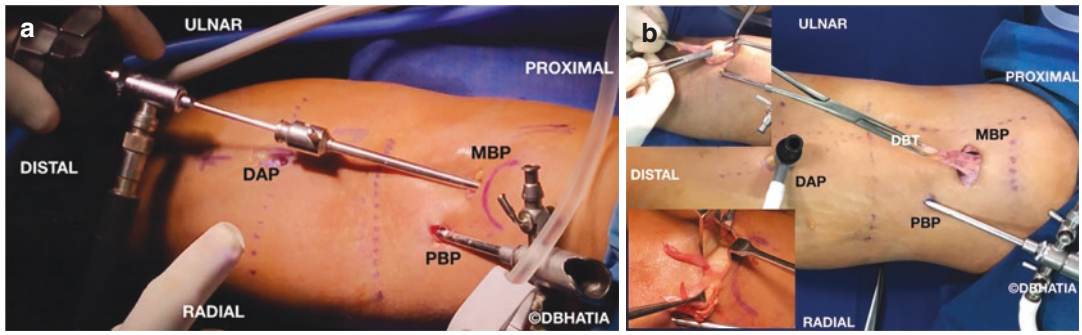

Fig. 51.4 (**a**) A mid-biceps portal (MBP) is placed just distal to the retracted biceps stump and is used to visualize and retrieve the tendon (*PBP* parabiceps portal, *DAP* distal anterior portal) (© Bhatia). (**b**) The retracted distal biceps tendon (DBT) is retrieved via MBP and is seen to be deficient in length. Inset top image shown a "cocooned" DBT that is retrieved by incising the outer sheath. Inset bottom image shows a deficient and frayed DBT (*PBP* parabiceps portal, *DAP* distal anterior portal, *MBP* midbiceps portal). (© Bhatia)

nique for footprint-like onlay approximation (Fig. 51.7a, b).

- *Tendon docking and knotting*: The shorter sutures from each anchor are pulled, and the sliding mechanism draws the DBT to approximate to the tuberosity. The arm may be held in 30° of flexion, and nonsliding knots are tied with a knot pusher to reattach the DBT back to the tuberosity.
- *Final assessment*: The repaired DBT is assessed through the PBP or via DAP (if fixation was achieved in flexion), and dynamic rotation and flexion is used to test repair integrity. An arthroscopic probe may be used to evaluate the contact at bone-tendon junction in suture anchor repairs. A hook test is performed externally to ensure adequate tensioning within the DBT (Fig. 51.8).

51.4 Tips and Tricks

- Adequate proximal release is necessary to achieve correction of the chronic "Popeye" deformity. A blunt probe or atraumatic grasper should be used to gently separate the muscle belly from underlying brachialis. The lateral cutaneous nerve may be seen and probed between the biceps and brachialis and should be safeguarded.
- Maximize tendon length by releasing the encapsulated DBT within the "cocoon" and by uncoiling the adherent DBT stump.

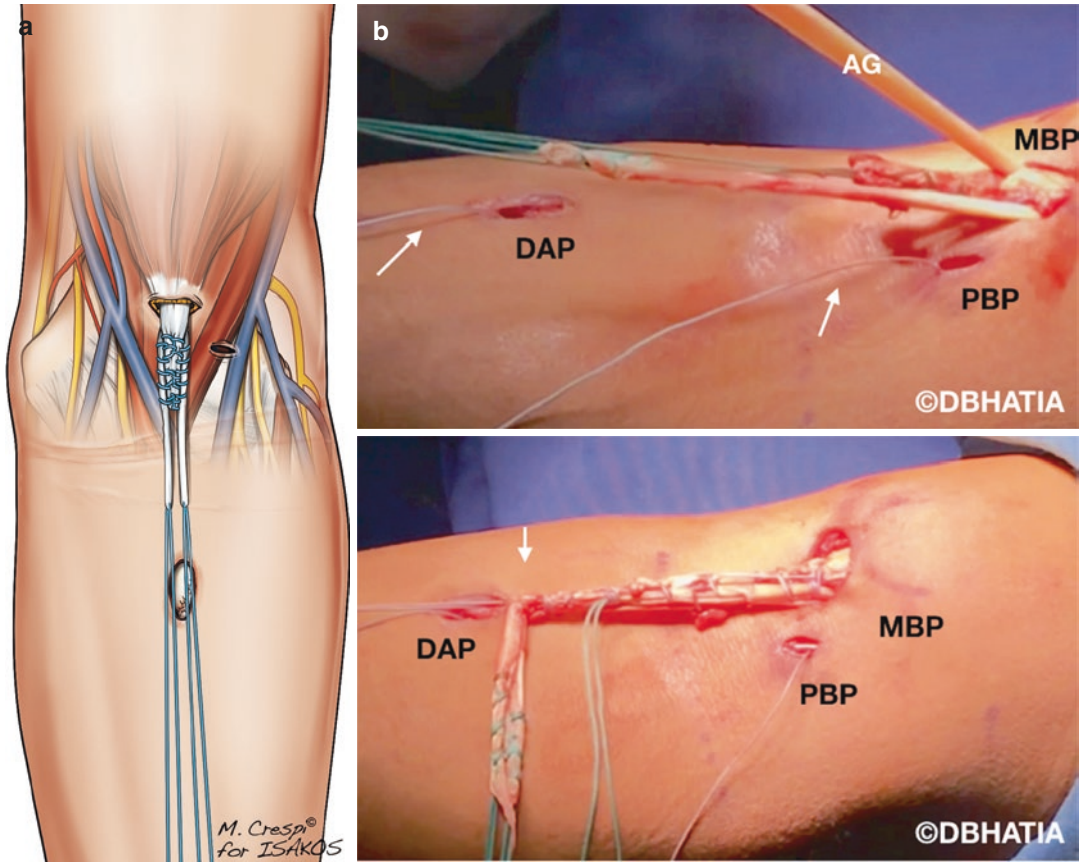

Fig. 51.5 (**a**) Graft passage through the biceps musculotendinous junction is illustrated (© Bhatia). (**b**) The autograft tendon is woven through the musculotendinous junction (top image) and the two graft strands are sutured to the distal biceps stump and to each other. The shuttle suture can be seen passing through the DAP and PBP (arrows, top image). The tendon in length is assessed by pulling it distally to reach the DAP and excess tendon is resected (arrow, bottom image) (*PBP* parabiceps portal, *DAP* distal anterior portal, *MBP* midbiceps portal). (© Bhatia)

- Elbow flexion should be used prior to knotting to achieve tendon docking without undue tension.

51.5 Pitfalls

- *Distal adhesions at bursa and tuberosity*: Bursal adhesions prevent clear visualization. Careful adhesiolysis around the bare area is necessary. The ulnar artery is at-risk of injury and is closest in the neutral rotation position [6]. Adhesiolysis should not extend beyond the boundaries of the tuberosity.
- *Proximal adhesions at Brachialis*: Proximal adhesions prevent DBT mobilization and Popeye correction. The brachial vessels and median nerve are at-risk on the medial aspect and dissection should be limited to the midline.
- *Intermediate adhesions*: The mobilized and graft-augmented DBT has to be shuttled through the original path of the DBT, and this is often obliterated due to chronicity. Soft-tissue dilators may be used to create a space if necessary, and the DBT is shuttled cautiously and gently.
- *Radial artery compression*: Careful suture management is necessary to prevent intertwin-

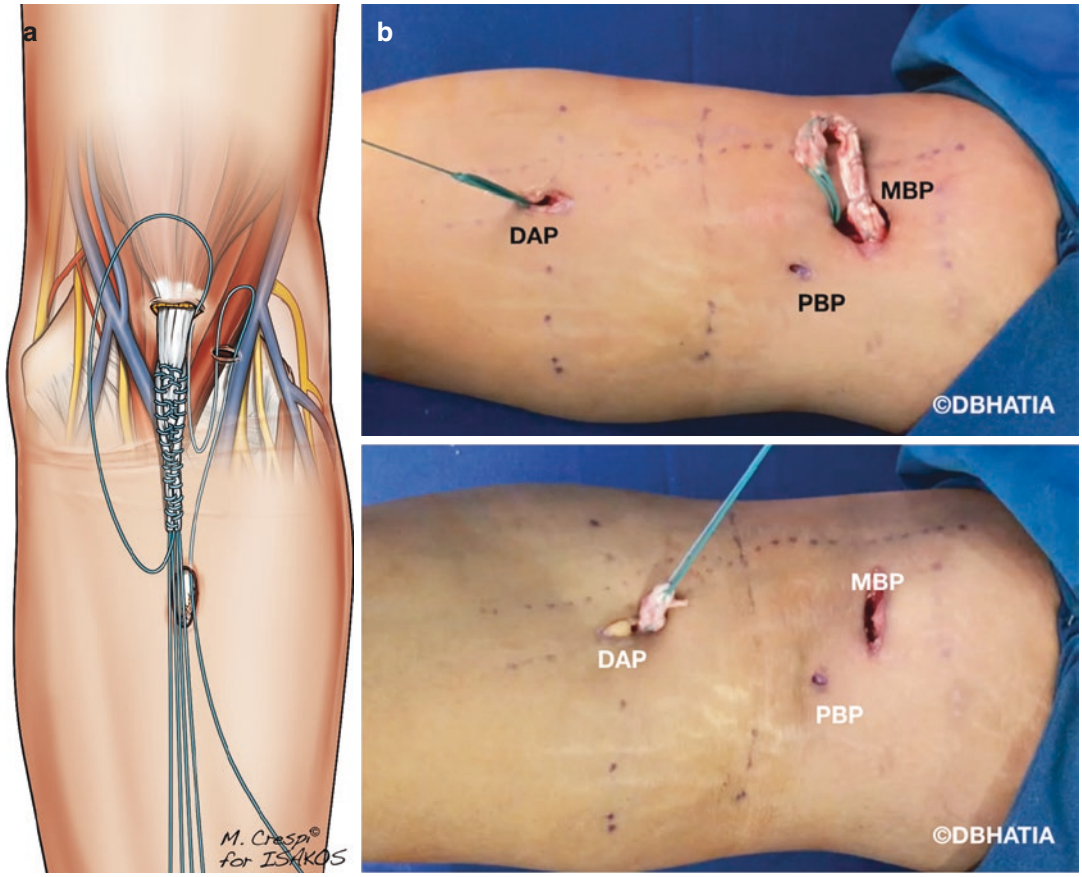

Fig. 51.6 (**a**) The path of the shuttle suture through the three portals across the cubital fossa is illustrated (© Bhatia). (**b**) The shuttle suture is seen attached to the autograft reinforced distal biceps stump (top image). The distal biceps is shuttled across the cubital fossa and out through the distal anterior portal (bottom image) (*PBP* parabiceps portal, *DAP* distal anterior portal, *MBP* midbiceps portal). (© Bhatia)

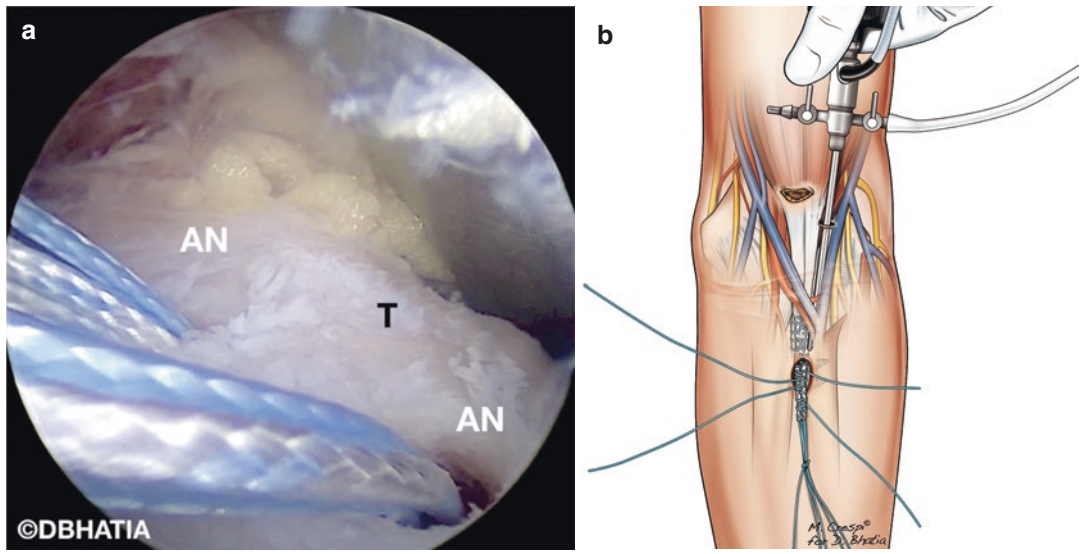

Fig. 51.7 (**a**) Endoscopic view of placement of two all-suture anchors (AN) in the bicipital tuberosity (T) (© Bhatia). (**b**) The dual whipstitch technique for footprint-like onlay approximation is illustrated. (© Bhatia)

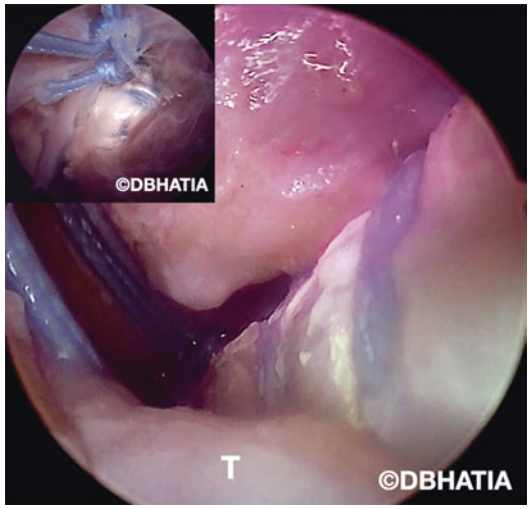

Fig. 51.8 Final view of the repaired DBT viewed through parabiceps portal shows the autograft reconstructed tendon is securely fixed to the tuberosity (T). Inset image shows the view through the distal anterior portal. (© Bhatia)

ing of the radial artery and DBT. The DBT and the anchor sutures should be placed in the same soft-tissue window at DAP to prevent this complication.

51.6 Postoperative Management, Rehabilitation, and Return to Sport

A bulky soft-tissue dressing is used in the immediate postoperative period, and this is changed to portal dressing on the fourth postoperative day. The elbow is immobilized for 4–6 weeks in a sling. Elbow ROM exercises are started after 4–6 weeks in a motion-controlling hinged brace. Biceps strengthening is initiated at 12 weeks and return to competitive sports is permitted after 6 months.

51.7 Complications

Cutaneous paresthesias may be present in the postoperative period and usually subside over 3–6 weeks. Neurovascular structures in the arm and forearm are at-risk and adhesiolysis should be performed cautiously. Graft thickness should be minimized to ease passage through the parabiceps space and to avoid dynamic radioulnar impingement in the proximal radioulnar space and subsequent re-rupture [7].

Conflict of Interest The author certifies that he has no commercial associations (e.g., consultancies, stock ownership, equity interest) that might pose a conflict of interest in connection with the submitted article. The author retains the copyright to the images, videos, and content in this chapter.

References

1. Bhatia DN. All-endoscopic distal biceps repair and reconstruction: science, technique and results. Presented at Shoulder and Elbow Society of Australia (SESA) biennial conference, Nov 2018, Perth, Australia.
2. Bhatia DN. Endoscopic distal biceps repair: endoscopic anatomy and dual-anchor repair using a proximal anterolateral "parabiceps portal". Arthrosc Tech. 2015;4:e785–93. https://doi.org/10.1016/j.eats.2015.07.031.
3. Bhatia DN. Endoscopic repair of acute and chronic retracted distal biceps ruptures. J Hand Surg Am. 2016;41(12):e501–7. https://doi.org/10.1016/j.jhsa.2016.09.008.
4. Bhatia DN, DasGupta B, Panjwani T. Cadaveric study of anterior and posterior elbow endoscopy portals for endoscopic distal biceps repair: comparative anatomy-at-risk. Surg Radiol Anat. 2016;38(7):781–91. https://doi.org/10.1007/s00276-016-1637-6. Epub 2016 Feb 9.
5. Bhatia DN, Kandhari V. Analysis of technical feasibility and neurovascular safety of endoscopic distal biceps repair: a cadaveric study. J Shoulder Elb Surg. 2018;27:2057–67. https://doi.org/10.1016/j.jse.2018.04.020.
6. Bhatia D, Naskar R, DeNiese P. Dynamic rotational alteration in positional relationship of neurovascular structures and distal biceps tendon insertion: a cadaveric study. J ISAKOS. 2019;4:296–301. https://doi.org/10.1136/jisakos-2019-000326.
7. Bhatia DN, Kandhari V, Das Gupta B. Cadaveric study of insertional anatomy of distal biceps tendon and its relationship to the dynamic proximal radioulnar space. J Hand Surg Am. 2017;42:e15–23. https://doi.org/10.1016/j.jhsa.2016.11.004.

52 Endoscopic-Assisted Onlay Repair for Distal Biceps Tears

Deepak N. Bhatia

52.1 Background

Endoscopic-assisted distal biceps tendon (DBT) procedures are performed by using a single anterior incision similar to the open surgical approach for DBT tears [1–4]. The arthroscope and working instruments are used via the same incision during the procedure. Endoscopic magnification via the incision permits clear visualization of the anatomy and optimizes debridement and tendon repair (Fig. 52.1).

The endoscopic-assisted technique can be used to reattach the ruptured DBT to the tuberosity as an onlay surface fixation or as a footprint repair [3]. The onlay repair creates a 1 cm tendon-bone approximation close to the original attachment site using dual suture anchors. This provides a larger surface area for tendon healing and the two fixation points provide greater fixation security. The proximal anterior attachment site has been shown to be biomechanically and anatomically advantageous. The upper aspect of the tuberosity was found to have the least reduction in radioulnar space during rotational movements, and the reattached DBT does not "overstuff" the proximal radioulnar space [5]. Proximal anterior attachment results in better wrapping and a significantly higher moment arm in supination compared with the "anterior central" attachment, and closely mimicks the native attachment site [6].

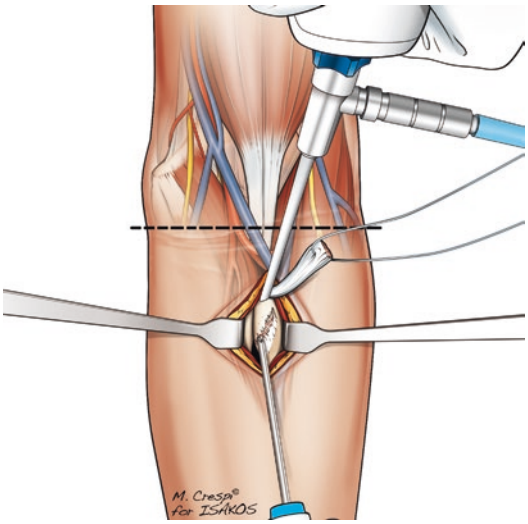

Fig. 52.1 An overview of the endoscopic-assisted procedure is illustrated. Note that the endoscope and instruments are placed through an open incision and the space is maintained with retractors (dotted line shows elbow crease). (M. Crespi for ISAKOS)

Endoscopic-assisted DBT repair has advantages over the open approach: (1) A smaller incision is used to access the DBT and tuberosity. (2) The magnified view permits optimal placement of fixation devices. (3) The technique is easier to perform as the initial exposure is similar to an open approach. A disadvantage of the single portal technique is that proximally retracted DBT ruptures cannot be

D. N. Bhatia (✉)
SPORTSMED, Mumbai, India

Sir HN Reliance Foundation Hospital, Mumbai, India
e-mail: shoulderclinic@gmail.com

© ISAKOS 2022

D. N. Bhatia et al. (eds.), *Arthroscopy and Endoscopy of the Elbow, Wrist and Hand*,
https://doi.org/10.1007/978-3-030-79423-1_52

retrieved through the single incision, and an additional incision is necessary. Additionally, shuttling a proximally retracted tendon across the cubital fossa requires greater dissection to protect vital neurovascular structures. Another disadvantage is that the endoscope and instruments including retractors are placed through the same small incision, and this restricts manipulation of instruments. The arthroscope is held directly into the incision, and this is less ergonomic as compared to passage through portals with supporting soft tissues.

52.2 Indications and Contraindications

Endoscopic-assisted repair can be performed in:

- High-grade partial bursal-sided DBT tears with a positive biceps probe test.
- Complete non-retracted DBT ruptures.
- Isolated head ruptures (long or short head) of the DBT.

The endoscopic-assisted technique cannot visualize and retrieve proximally retracted DBT tears and is contraindicated in these cases.

52.3 Surgical Technique

Biceps endoscopy is performed with the patient in supine position, and the upper extremity is placed on a side trolley. A tourniquet is placed high on the arm and is used during the procedure. A 2.9-mm arthroscope and sheath (2.9 mm 152 mm; ConMed, Linvatec, Largo) are used, and gravity inflow is used to minimize fluid extravasation into the arm and forearm.

- A 2 cm midline anterior incision is placed approximately 3–4 cm distal to the anterior elbow crease (Fig. 52.2).
- The lateral cutaneous nerve of forearm (LCN) is identified and protected.
- The brachioradialis and flexor carpi radialis are retracted and the bicipital tuberosity is accessed

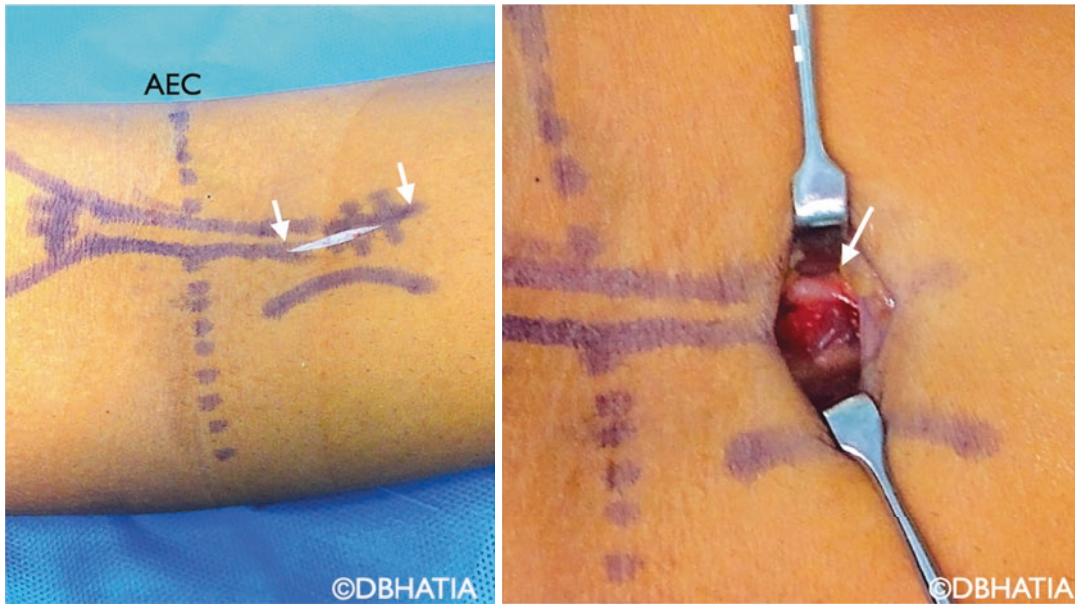

Fig. 52.2 A 2 cm midline incision is placed below the elbow crease (AEC) and is centered over the bicipital tuberosity (arrows, left image). The lateral cutaneous nerve of forearm (arrow) should be identified and protected (right image). (© Bhatia)

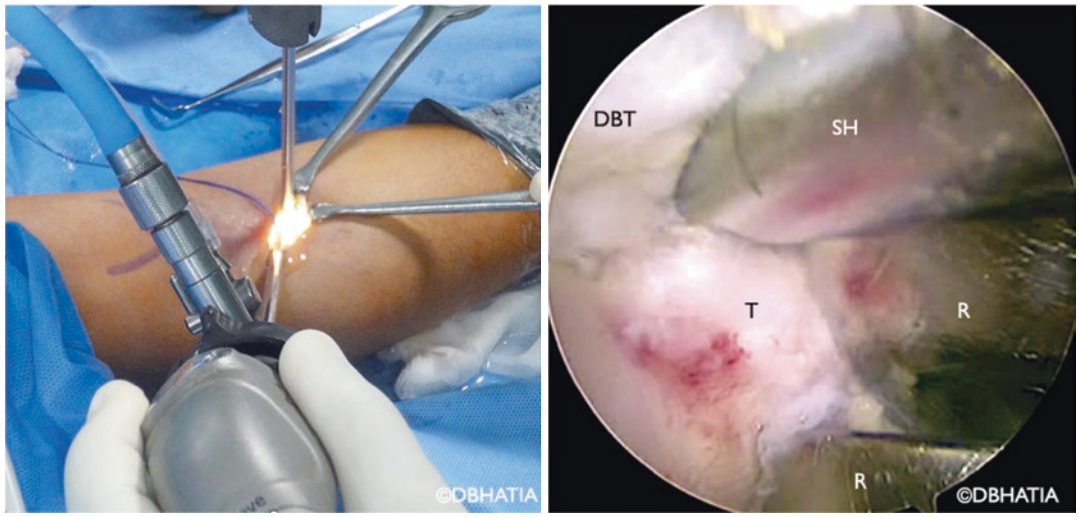

Fig. 52.3 The retractors create a space for endoscopy and the endoscope and instruments are passed through the same incision (left image). The tuberosity and partial distal biceps tear (DBT) are debrided under vision. (© Bhatia)

using the Henry's approach. The radial artery and superficial radial nerve are identified and protected during the dissection [7].

- Retractors are used to expose the tuberosity and to create a space for endoscopy. The endoscope is now introduced into this space and further steps are performed under magnified endoscopic visualization.
- In a partial tear, the bursal surface of DBT is debrided and a probe test is performed to assess the severity of the tear (see Chap. 49). In a high-grade tear, the DBT is retrieved out of the incision using an angled hemostat and is then sectioned close to the tuberosity (Fig. 52.3). In a complete non-retracted rupture, the DBT can be visualized and directly retrieved out. The retrieved tendon is prepared by excising the frayed end (Fig. 52.4).
- Next, under endoscopic view, the tuberosity is debrided using a shaver and burr placed the same incision. Tendon remnants are excised and the tuberosity is decorticated.
- Two suture anchors are inserted into the exposed tuberosity 1 cm apart (Fig. 52.5).
- One strand of each anchor is used to whipstitch the tendon as described before for all-endoscopic repairs [8, 9].
- The other strand of each suture is then pulled to dock the tendon on the tuberosity. The whipstitch technique ensures a 1 cm tendon-bone approximation in an onlay configuration.
- Non-sliding knots are then used to secure the tendon to the tuberosity in 30 degrees of elbow flexion. Endoscopic confirmation of the repair integrity is performed by probing the tendon-bone junction and by dynamic rotational and flexion movements (Fig. 52.6).

Finally, the retractors are removed and the skin incision is sutured.

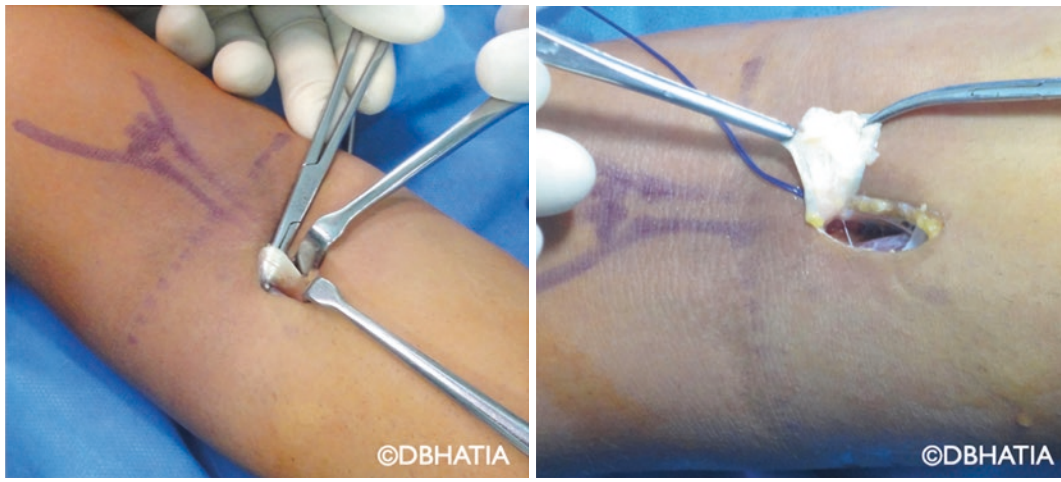

Fig. 52.4 The DBT is exteriorized using an angled hemostat (left image) and is sectioned and prepared (right image). A holding stitch is placed on the tendon to prevent inadvertent proximal retraction. (© Bhatia)

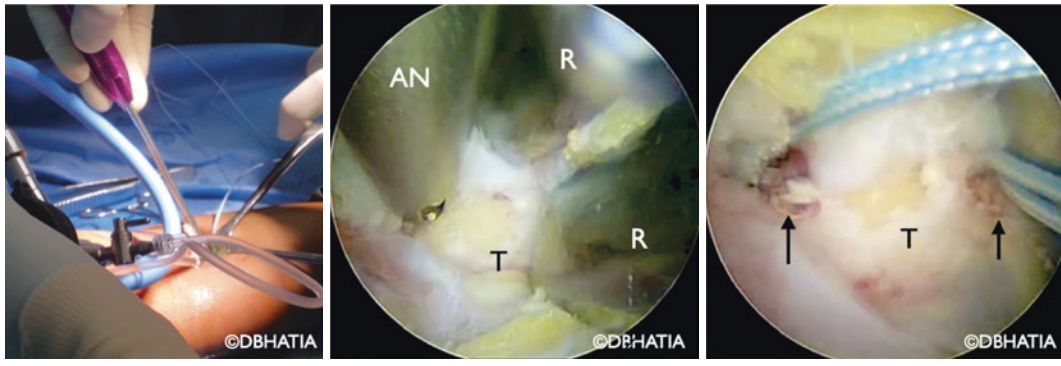

Fig. 52.5 An anchor sleeve is placed through the incision (left and middle) and two anchors (AN, arrows) are passed into the tuberosity (T, right image). (© Bhatia)

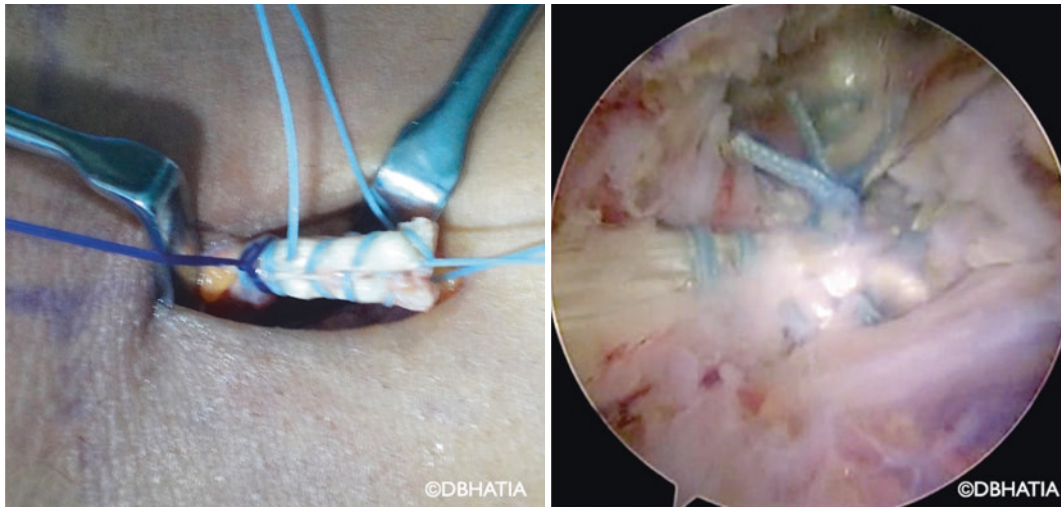

Fig. 52.6 The tendon is whipstitched for approximately 2 cm (left image). Final endoscopic view of the reattached tendon is shown. (© Bhatia)

52.4 Tips and Tricks

- Proximal retraction of the tendon may occur if the tendon is detached in situ. A holding suture may be passed around the tendon prior to detachment to avoid this. Alternately, the tendon may be detached after exteriorization (recommended).
- The bare area of the tuberosity is a consistent landmark and should be used as a guide for reattachment [10, 11]. Anchors should be passed at the proximal aspect of the bare area to achieve the anatomic and biomechanical advantage.
- The incision is extensile and can be converted to an open repair at any point during the procedure.

52.5 Pitfalls

- Proximal retraction of the tendon during detachment will necessitate a second incision for retrieval.
- The ulnar artery and posterior interosseous nerves are at risk of injury during deep retraction [10]. Retraction should be relaxed in between steps.

52.6 Postoperative Management and Rehabilitation

A bulky soft tissue dressing is used in the immediate postoperative period, and this is changed to portal dressing on the fourth postoperative day. Elbow movements are initiated from 60 to 90 degrees of flexion in a controlled-motion brace, and forearm rotations are permitted. Elbow ROM exercises are progressed after 4–6 weeks. Biceps strengthening is initiated at 12 weeks, and return to competitive sports is permitted after 6 months.

Conflict of Interest The author certifies that he has no commercial associations (e.g., consultancies, stock ownership, equity interest) that might pose a conflict of interest in connection with the submitted article. The author retains the copyright to the images, videos, and content in this chapter.

References

1. Eames MJ, Bain GI. Distal biceps tendon endoscopy and anterior elbow arthroscopy portal. Tech Shoulder Elbow Surg. 2006;7:139–42.
2. Grégory T, Roure P, Fonte's D. Repair of distal biceps tendon rupture using a suture anchor: description of a new endoscopic procedure. Am J Sports Med. 2009;37:506–11.
3. Phadnis J, Bain G. Endoscopic-assisted distal biceps footprint repair. Tech Hand Up Extrem Surg. 2015;19:55–9.
4. Caekebeke P, van Riet RP. Distal Biceps Endoscopy. In: Bain G, Eygendaal D, van Riet R, editors. Surgical techniques for trauma and sports related injuries of the elbow. Berlin, Heidelberg: Springer; 2020. https://doi.org/10.1007/978-3-662-58931-1_58.
5. Bhatia DN, Kandhari V, DasGupta B. Cadaveric study of insertional anatomy of distal biceps tendon and its relationship to the dynamic proximal radioulnar space. J Hand Surg Am. 2017;42(1):e15e–e23.
6. Schmidt CC, Diaz VA, Weir DM, Latona CR, Miller MC. Repaired distal biceps magnetic resonance imaging anatomy compared with outcome. J Shoulder Elb Surg. 2012;21(12):1623e1631.
7. Henry AK. Extensile exposure. 2nd ed. Livingston: Edinburgh; 1966.
8. Bhatia DN. Endoscopic distal biceps repair: endoscopic anatomy and dual-anchor repair using a proximal anterolateral "parabiceps portal". Arthrosc Tech. 2015;4:e785–93. https://doi.org/10.1016/j.eats.2015.07.031.
9. Bhatia DN. Endoscopic repair of acute and chronic retracted distal biceps ruptures. J Hand Surg Am. 2016;41:e501–7. https://doi.org/10.1016/j.jhsa.2016.09.008.
10. Bhatia D, Naskar R, DeNiese P. Dynamic rotational alteration in positional relationship of neurovascular structures and distal biceps tendon insertion: a cadaveric study. J ISAKOS. 2019;4:296–301. https://doi.org/10.1136/jisakos-2019-000326.
11. Bhatia DN. Endoscopic anatomy of distal biceps tendon insertion and bicipitoradial bursa: a cadaveric study. J Shoulder Elbow Surg. 2021;30(8):1759–67. https://doi.org/10.1016/j.jse.2020.11.033. Epub 2021 Jan 21.

53 Endoscopic-Assisted Footprint Repair of Distal Biceps Tendon Ruptures

Mina Derias, Gregory I. Bain, and Joideep Phadnis

53.1 Background

Surgical repair is offered to the majority of patients with an acute full-thickness tear of the distal biceps tendon (DBT) in order to restore optimal supination and flexion strength and reduce the risk of cramping and aesthetic deformity. Surgery can be performed using a single-incision or two-incision approach and the tendon can be repaired using suture anchors, transosseous tunnels, or most commonly with transcortical buttons which provide greatest load to failure characteristics [1]. Two-incision techniques allow anatomic footprint restoration but are associated with higher rates of heterotopic ossification (HO) and radio-ulnar synostosis. Single-incision techniques are desirable but have a higher rate of lateral cutaneous nerve injury and do not facilitate footprint reconstruction if a standard technique is used [1]. More recently, endoscopic techniques have been described which can be performed using an all-endoscopic technique or an endoscopic-assisted technique [2].

53.2 Surgical Anatomy and Biomechanics

The distal biceps has distinct short and long heads. Towards its distal attachment the tendon unit externally rotates 90° and the short head insertion is distal to the long head. The tendon footprint is 21 mm long and 7 mm wide with a mean area of 108 mm^2 and is located at the posteromedial margin of the radial tuberosity [3]. In around 20% of individuals, the long and short heads insert as truly separate tendons [4]. The eccentric attachment of the tendon on the tuberosity emphasises the primary role DBT as a forearm supinator (Fig. 53.1). The tuberosity itself is offset ulnar to axis of the radius when the forearm is fully supinated; the tuberosity moves dorsally when the forearm is in neutral rotation and radially when the forearm is pronated. This anatomic relationship implies that contraction of the biceps muscle creates a cam effect to produce supination. It is possible that with a classic anterior-central DBT repair, biceps contraction produces a supination moment only when the forearm is in a pronated position. In contrast, an anatomic attachment site will maintain the offset from the long axis and provide supination moment throughout the arc of rotation [5] (Fig. 53.2a, b).

M. Derias
Department of Trauma and Orthopaedics,
University Hospitals Sussex,
Brighton, East Sussex, UK
e-mail: Mina.derias@nhs.net

G. I. Bain
Department of Orthopaedic and Trauma Surgery,
Flinders University and Flinders Medical Centre,
Adelaide, SA, Australia
e-mail: greg@gregbain.com.au

J. Phadnis (✉)
Department of Trauma and Orthopaedics, University
Hospitals Sussex, Brighton, East Sussex, UK

Brighton & Sussex Medical School,
Brighton, East Sussex, UK
e-mail: joideep@doctors.org.uk

© ISAKOS 2022

D. N. Bhatia et al. (eds.), *Arthroscopy and Endoscopy of the Elbow, Wrist and Hand*,
https://doi.org/10.1007/978-3-030-79423-1_53

Fig. 53.1 Cadaveric specimen demonstrating the long and short heads of the distal biceps and their attachment to the ulnar most surface of the radial tuberosity. (Permission granted from Phadnis & Bain, 2015)

53.3 Indications and Contraindications

Biceps endoscopy has both diagnostic and therapeutic utility. An endoscopic-assisted approach allows controlled and accurate tendon retrieval and footprint preparation and is especially useful in the presence of a partial tear or tendinosis. In chronic injury, the fibrous tissue and pseudotendon that may develop can be identified and debrided.

Use of endoscopy is relatively contraindicated in patients with abnormal anatomy as a result of previous surgery or trauma to the elbow or antecubital fossa, Furthermore, endoscopic repairs should only be attempted after developing extensive experience with open repairs and becoming familiar with diagnostic endoscopy.

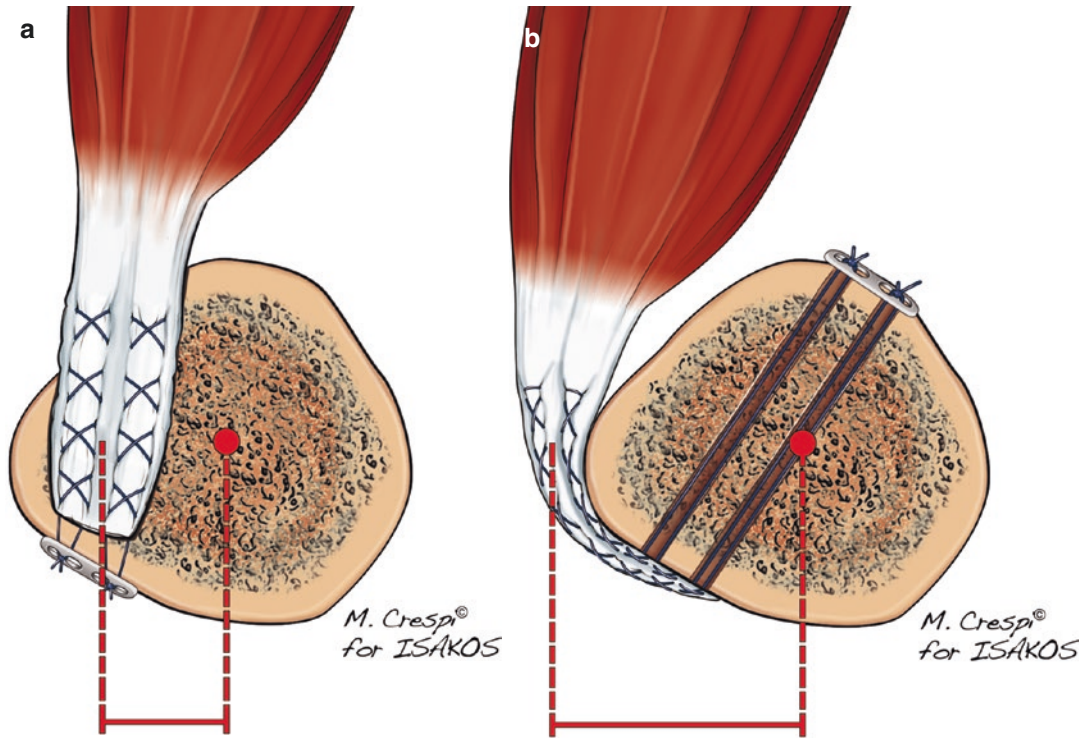

Fig. 53.2 Illustrations demonstrating the moment arm of the repaired biceps tendon from the axis of the radius (dots) in anatomic vs non-anatomic repair. (**a**) Endobutton technique. (**b**) Footprint technique. In the fully supinated position, the footprint technique creates a larger moment arm distance and is thus likely to improve supination strength and endurance. [M. Crespi © for ISAKOS]

53.4 Surgical Technique

Phadnis and Bain have recently described the endoscopic-assisted technique which allows accurate anatomical footprint repair to be achieved [2].

- The patient is positioned supine and the operative extremity placed on a hand table with the elbow slightly flexed to reduce anterior soft tissue tension.
- A 3 cm longitudinal incision is made approximately two finger breadths distal to the anterior elbow crease and is used for viewing and working (endoscopy and instruments). The lateral cutaneous nerve of the forearm is identified and protected, and the recurrent branches of the radial artery deeper in the wound is retracted or cauterised. With the aid of right-angled retractors and maximum forearm supination; the DBT and its sheath, and the biceps tuberosity are inspected.
- The tendon stump is debrided back to healthy tissue and prepared with two locking Krakow stitches using high strength sutures with a minimum of three throws along the length of the tendon. It is important to ensure that the four strands are exiting the distal tendon superiorly so that when the tendon is placed against the tuberosity the sutures act as a tension band and do not interpose between the tendon and the bone healing surface. The tendon is then placed in a damp swab and retracted proximally while the tuberosity is prepared.
- A hooded endoscope is introduced through the anterior incision onto the bicipital tuberosity. Using a 4.5 mm shaver, the tuberosity is debrided under direct vision to bleeding punctate bone (Fig. 53.3). This can be used through the same anterior incision or a posterior working portal can be created (inside-out technique) using a Wissinger rod (Fig. 53.4a). Forearm pronation and supination as required will allow full visualisation and preparation of the footprint.
- Two oblique holes are drilled with a 2.5 mm drill, directed from volar-radial to dorsal-ulnar exiting at the dorsal ridge of the tuberosity (Fig. 53.4b). During this step, slightly pronating the forearm to lateralise the anterior drill holes will ensure the Endobutton does not impinge on the repaired biceps tendon. Shuttling loop sutures are then passed from anterior to posterior and used to deliver the tendon sutures from the footprint through the radius (Fig. 53.4c). In order to restore the anatomical footprint as accurately as possible, the pre-prepared DBT is then orientated so that on suture shuttling the long head will be proximal and the short head distal. The sutures are then tied anteriorly over an Endobutton (Fig. 53.4d). Traction on the distal sutures of the Endobutton while tying the proximal sutures will ensure the tendon is advanced onto the footprint.

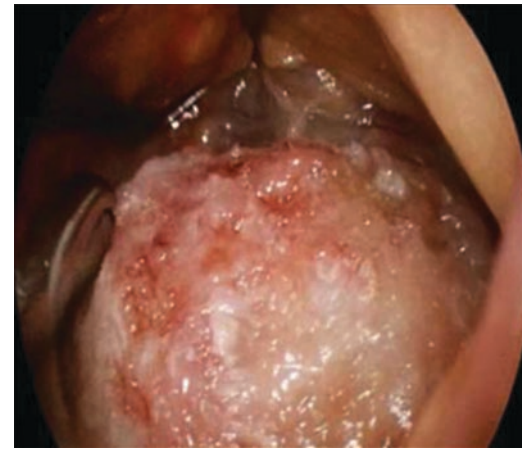

Fig. 53.3 Endoscopic view through the incision shows debridement of the radial tuberosity with a shaver. (Permission granted from Phadnis & Bain, 2015)

53.5 Tips and Tricks

- Positioning the arm with 10° of elbow flexion using padded towel rolls placed under the forearm reduces tension on the anterior soft tissues and allows ease of passage of the endoscope down to the biceps footprint.
- The biceps may be tethered medially by an intact lacertus fibrosus, which can be released to mobilise the tendon end.
- Dry endoscopy improves visualisation and prevents soft tissue swelling. Fogging of the endo-

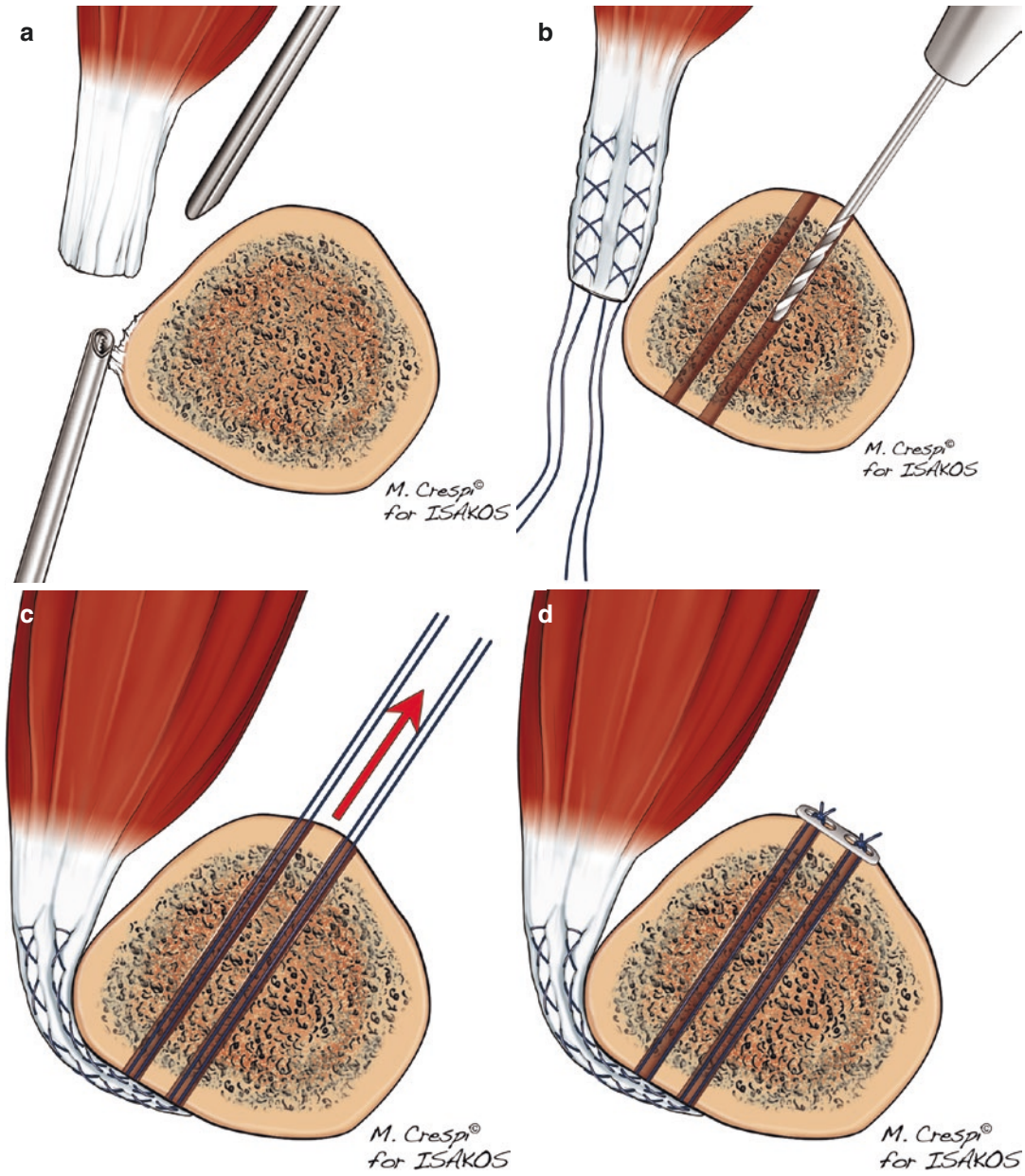

Fig. 53.4 Technical steps of the endoscopic-assisted distal biceps tendon repair: (**a**) Endoscopic debridement of the torn biceps tendon stump. (**b**) Whipstitch of the torn tendon with non-absorbable high tensile strength suture and two oblique drill holes made in the radial tuberosity aiming to exit on the dorsal ridge of the tuberosity. (**c**) Sutures shuttled through drill holes. (**d**) Sutures tied over Endobutton restoring the tendon to its footprint on the ulnar aspect of the tuberosity. [M. Crespi © for ISAKOS]

scope may occur, and this can be mitigated by wiping the lens with alcohol-soaked gauze.

- For debridement, use a resector without teeth and without suction to avoid entrapping soft tissues.
- The risk of nerve injury can be reduced by careful dissection, attention to drill trajectory, and avoidance of levered or prolonged retraction on the lateral aspect of the radial tuberosity (Fig. 53.5).

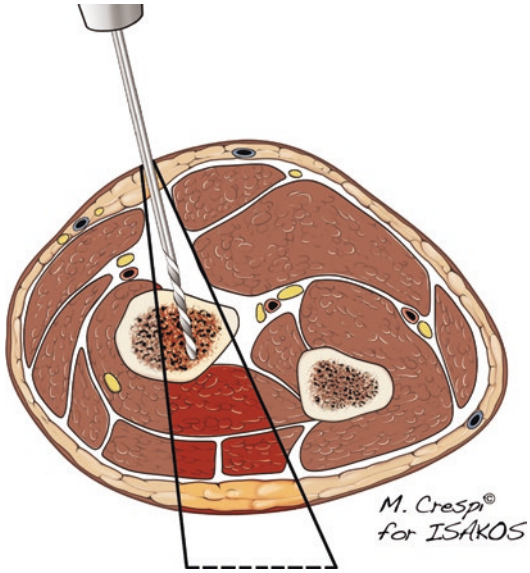

Fig. 53.5 Safe zone for drill trajectory is illustrated. In the fully supinated forearm, the posterior interosseous nerve (PIN) lies immediately posterolateral to the radius. Drilling should be directed away from the PIN within the safe zone as indicated. (BR = brachioradialis, Sn = supinator, PT = pronator teres). [M. Crespi © for ISAKOS]

53.6 Pitfalls

- Chronic injuries may present with retraction of the tendon stump and development of a pseudotendon. This dense tissue does not contain any tendon but can mask the tendon, which is hidden inside.
- The aperture should be in full view whenever the shaver/high speed burr is active to minimise the risk of soft tissue being caught.
- When debriding the tuberosity, the key is to do enough so that punctate bleeding is visible and not so much that the tuberosity is completely decorticated. Use of the endoscope allows this to be done in a very accurate and controlled manner.

53.7 Postoperative Management and Rehabilitation Protocol

Postoperatively, the patient is placed in a light dressing and a sling is used for comfort. The patient can start range-of-motion (ROM) exercises when comfortable, but must avoid any heavy lifting for 3 months. Early rehabilitation has shown a significant reduction in time to full ROM without an increase in re-rupture [1]. Tendon to bone healing takes around 12 weeks, hence caution should be exercised with loading during this period. The re-rupture rate following primary biceps repair is <2% with most of these re-ruptures occurring in the first 2 months post-surgery [3]. Hence, it is reasonable to allow most patients to return progressive heavy loading 3 months after repair.

53.8 Results

Phadnis and Bain have reported excellent results in 28 patients with one complication of heterotopic ossification [2]. Bellringer et al. compared biomechanical and clinical outcomes of an anatomic footprint repair with a transosseous button technique and reported superior biomechanical supination strength and endurance with footprint repair. Clinical outcomes were good or excellent in both techniques [5].

Conflict of Interests None declared.

References

1. Miyamoto R, Elser F, Millett P. CURRENT CONCEPTS REVIEW distal biceps tendon injuries. J Bone Joint Surg (Am Vol). 2010;11:2128–38.
2. Phadnis J, Bain G. Endoscopic-assisted distal biceps footprint repair. Tech Hand Up Extrem Surg. 2015;19:55–9.
3. Bain M, Phadnis J, Bain G. Disorders of the distal biceps tendon. In: Muscle and tendon injuries—evaluation and management. Springer; 2017. p. 231–40. https://doi.org/10.1007/978-3-662-54184-5_22.
4. Eames M, Bain G, Fogg G, Van Riet R. Distal biceps tendon anatomy: a cadaveric study. J Bone Joint Surg Am. 2007;89(5):1044–9.
5. Bellringer S, Phadnis J, Human T, Redmond C, Bain G. Biomechanical comparison of transosseous cortical button and footprint repair techniques for acute distal biceps tendon ruptures. Should Elb. 2019:1–9.

Minimally Invasive Acute Distal Biceps Repair

54

Gregory Hoy and Simon Hoy

54.1 Background

Distal biceps ruptures require reattachment to the radial tuberosity for optimal function. The repair should ideally be performed with strong fixation, minimal risk to neurovascular structures, and minimal scarring to surrounding tissues. Techniques described for tendon repair include the two-incision technique, single incision techniques, and endoscopic techniques [1–5]. While the ideal is to reconstitute the exact structure and tensioning of the distal biceps anatomy, most techniques accept some distortion of the anatomy to achieve solid fixation with functional strength and minimal complications [6, 7].

To achieve minimal scarring to surrounding tissues, anatomic planes in the cubital fossa must be preserved. This chapter describes the senior author's technique for minimally invasive distal biceps repair for an acute rupture. The tendon sheath is preserved for optimal healing and superior clinical outcomes [2].

54.1.1 Surgical Anatomy

The distal biceps has a bipartite tendon within a single sheath which wraps around the ulnar side of the radial tuberosity to achieve supination and flexion power [8]. An acute completely ruptured tendon results in a large "elephant's foot" appearance of tendon stump; the ruptured tendon must be reinserted at a tuberosity region that is anatomically and biomechanically optimal to achieve maximum postoperative function. The author prefers an attachment point as far to the ulnar side of the tuberosity as can be achieved with hypersupination of the forearm during surgery. Repair through a minimally invasive approach necessitates preservation of the anatomic plane that ensheaths the distal biceps tendon; this protects the repair from scarring to surrounding structures during the early healing phase and minimizes the risk of neurovascular injury as well as scarring to surrounding tissues.

54.2 Indications and Contraindications

This technique is performed in the "acute" phase of treatment of distal biceps ruptures (within the first 2–4 weeks after injury); scarring within the tendon sheath occurs and distorts the anatomic plane after this period of time in most cases.

G. Hoy (✉) · S. Hoy
Melbourne Orthopaedic Group,
Melbourne, VIC, Australia

Department of Surgery, Monash University,
Melbourne, VIC, Australia
e-mail: gahoy@mog.com.au

© ISAKOS 2022

D. N. Bhatia et al. (eds.), *Arthroscopy and Endoscopy of the Elbow, Wrist and Hand*,
https://doi.org/10.1007/978-3-030-79423-1_54

Contraindications include previous surgery in the region and any condition that alters neurovascular anatomy.

54.3 Surgical Technique

This technique uses an endoscopic cannula to protect surrounding tissues, without using an endoscope to explore the wound. The patient is positioned supine with the upper extremity supported on a hand Table. A tourniquet is placed in the upper arm and inflated to 250 mm Hg after exsanguination.

- A 2 cm transverse incision is made over the cubital crease in the centre of the elbow. The Lateral Cutaneous Nerve of Forearm (LCNF) and the cephalic vein and/or cubital vein are exposed and taken radially to be protected. The sheath containing blood or serosanguinous fluid is opened and the haematoma evacuated. The tendon is identified and retrieved into the wound from the proximal retraction site (Figs. 54.1a–c).
- Digital palpation towards the radial side distally follows the distal biceps tendon sheath and the radial tuberosity is palpated in the floor with the forearm in hyper-supination. A curette is used to clear any granulation or fibrinous tissue over the attachment site (Figs. 54.2a–c).
- The serrated drill guide is a risk to surrounding tissues. The guide is passed through a cut-down cannula that is passed through the distal biceps sheath to lie on the tuberosity. The drill guide is slotted and therefore easily removed. The cannula is pre-split to allow the sutures to pull out of the cannula. The tuberosity is drilled as far around the ulnar side as possible without scything off the medulla of the bone. An anchor (Mitek G2) is loaded with an extra PDS suture to make the tendon slide, and a high-strength suture to hold the base of the footprint (Fig. 54.3a–c).
- The anchor is inserted down the sleeve while holding it onto the insertion site and the pre-split cannula and guide are removed. All sutures are then passed through the tendon outside the incision (Figs. 54.4a–c).
- We have used a sliding Bunnell suture with the monofilament PDS (to slide the tendon down onto the tuberosity) after passing a permanent Kessler suture and footprint base suture with the other sutures available. The PDS is then pulled to slide the tendon down onto the tuberosity (Fig. 54.5a–c).
- The elbow is flexed for final knot tying, and the footprint is checked for gapping. The wound is closed with a buried subcuticular suture and standard dressings with temporary fibreglass slab are applied until wound healing (Fig. 54.6a, b).
- An alternative fixation technique may be performed by using a fibreloop whip-stitch (Arthrex, Naples, USA), and a button (proximal biceps button, Arthrex, Naples, USA). The button must flip inside the radius and achieves a stronger hold on the tendon for early use. In selected cases, two anchors may

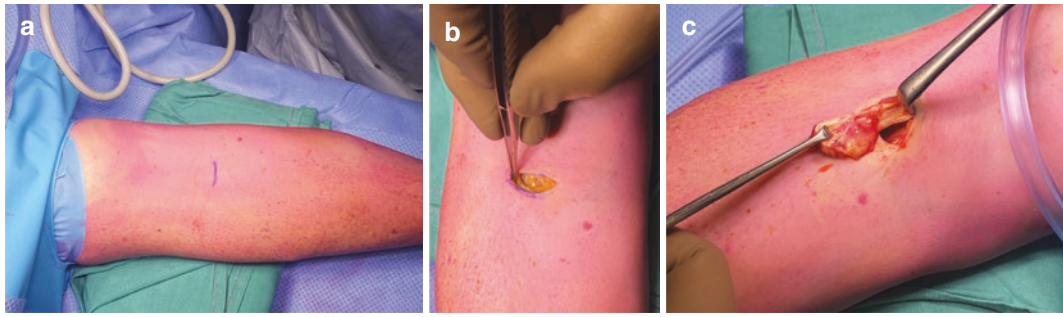

Fig. 54.1 (**a**) Arm position and incision along the cubital crease are shown. (**b**) The lateral cutaneous nerve is identified. (**c**) The ruptured tendon is retrieved

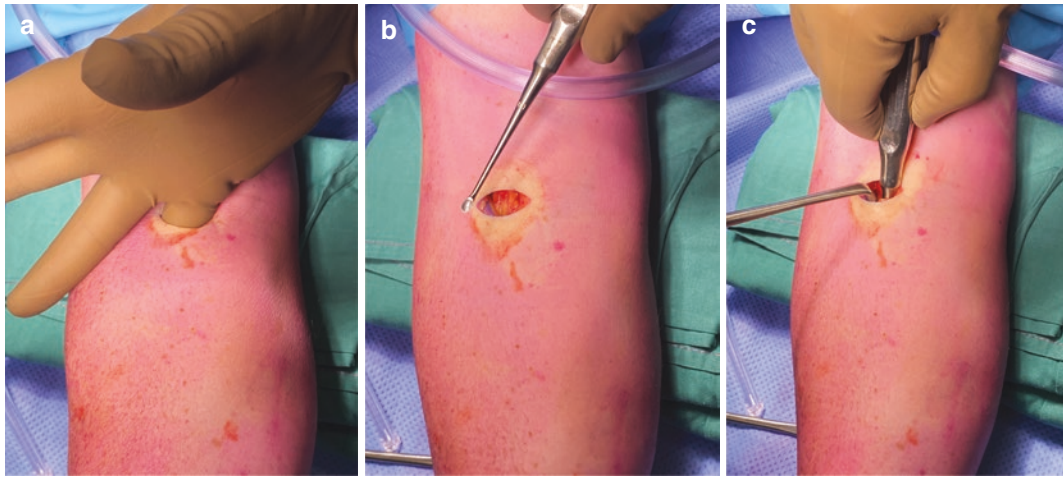

Fig. 54.2 (**a**) Digital palpation of tuberosity along biceps tract. (**b**, **c**) A curette is used to prepare the tuberosity

Fig. 54.3 (**a**) A cut-down cannula is shown. (**b**) A drill guide is passed through the cannula. (**c**) An anchor preloaded with an extra suture is shown

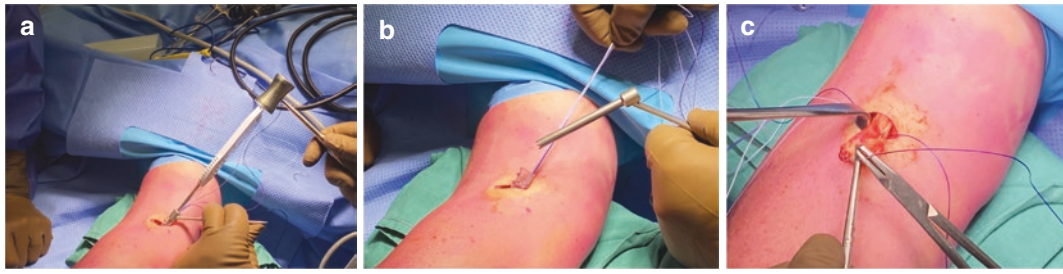

Fig. 54.4 (**a**) Anchor insertion through the guide and cannula. (**b**) Guide is removed and sutures are within cannula. (**c**) Sutures are passed through the tendon

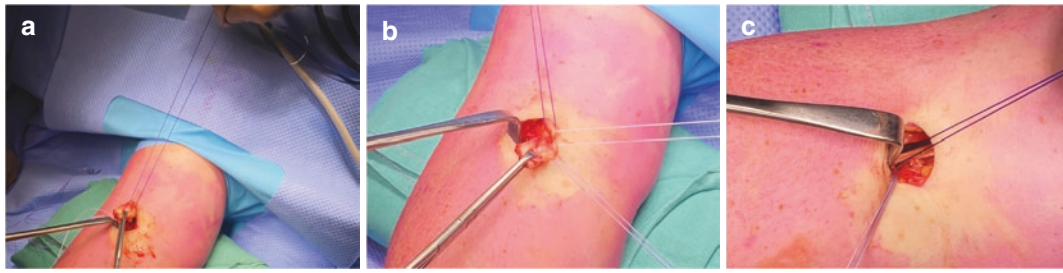

Fig. 54.5 (**a**) A Bunnell suture is passed to advance the tendon. (**b**) All sutures are passed through the tendon. (**c**) The Bunnell suture is tightened to pull the tendon to the tuberosity

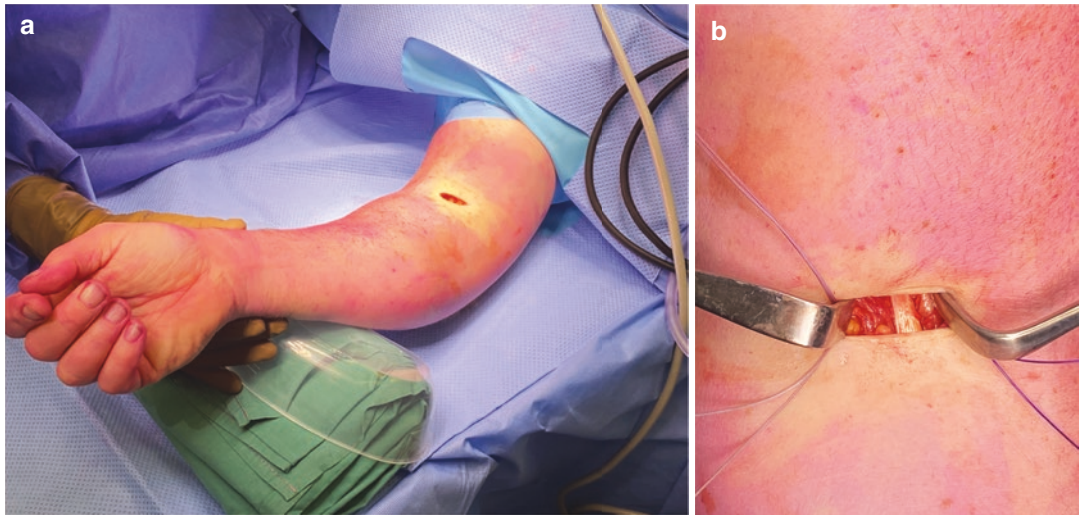

Fig. 54.6 (**a**) The forearm is flexed for protecting the repair. (**b**) The tendon is visualized after tying all sutures

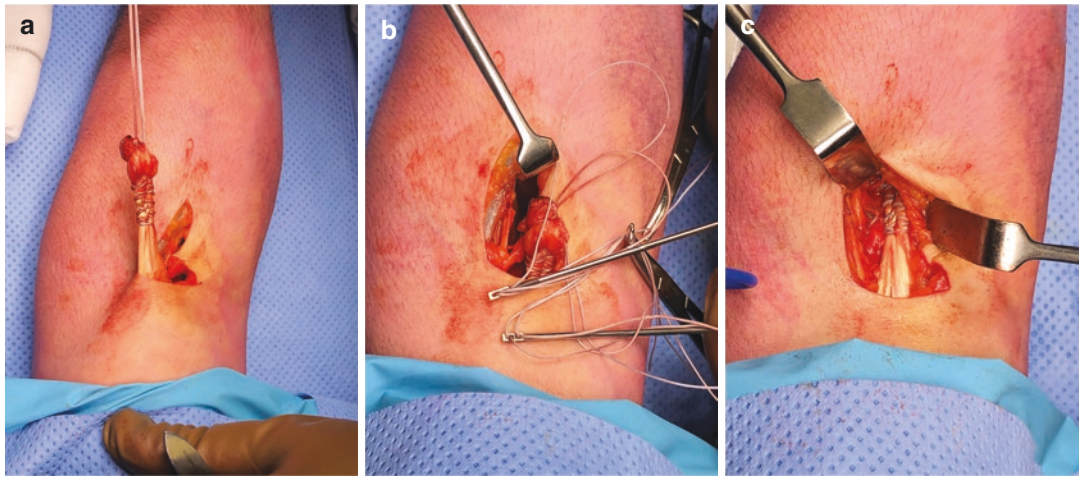

Fig. 54.7 (Alternative fixation when stronger hold needed) (**a**) The tendon is whip-stitched through a larger incision. (**b**) Two buttons are loaded on the sutures. (**c**) Final repair after tensioning and knotting the sutures

be used (Fig. 54.7a–c). Tensioning and knotting are performed with the elbow in 30 degrees of flexion.

54.4 Tips and Tricks

- The tendon retracts more if the bicipital aponeurosis is ruptured, but is easier to bring down onto the tuberosity if it is not tethering the tendon.
- Monofilament must be used for the Bunnell suture to get the tendon to slide down the sheath.
- When using a button, the drill hole must be oblique to allow enough room in the medulla of the radius for it to flip. Bicortical placement of the button is closer to the radial nerve branches.

54.5 Pitfalls

- The LCNF must be identified to prevent iatrogenic injury.
- The drill guide must be guided centrally from the radial tuberosity to avoid scything off the

edge, or preventing "flipping" of the intraosseous anchor.
- The tendon must be pulled distally enough to achieve firm approximation with bone and to correct the muscle-tendon junction position at the elbow.

54.6 Postoperative Management and Rehabilitation

A fibreglass slab is used for the first week. Range of motion starts at 1 week or when the stitches are checked. Mild resistance can commence at the same time but full strength use only starts at 6 weeks.

54.7 Complications

- Wound infection (rare).
- Stretching or damage to LCNF nerve branches.
- Heterotopic ossification can occur and cause radio-ulnar impingement with rotation.
- Failure of the repair is possible (rare).

References

1. Boyd H, Anderson L. A method for reinsertion of the distal biceps brachii tendon. JBJS. 1961;43(7):1041–3.
2. Woods D, Hoy G, Shimmin A. A safe technique for distal biceps repair using a suture anchor and a limited anterior approach. Injury. 1999;30(4):233–7.
3. Bain GI, Prem H, Heptinstall RJ, Verhellen R, Paix D. Repair of distal biceps tendon rupture: a new technique using the Endobutton. J Shoulder Elb Surg. 2000;9(2):120–6.
4. Duffiet P, Fontes D. Endoscopic repair of distal biceps brachii tendon avulsion: a new technique. Report of 25 cases. Chir Main. 2009;28(3):146–52.
5. Bhatia DN. Endoscopic repair of acute and chronic retracted distal biceps ruptures. J Hand Surg Am. 2016;41(12):e501–e7.
6. Eames M, Bain G, Fogg Q, Van Riet R. Distal biceps tendon anatomy: a cadaveric study. JBJS. 2007;89(5):1044–9.
7. Schmidt CC, Diaz VA, Weir DM, Latona CR, Miller MC. Repaired distal biceps magnetic resonance imaging anatomy compared with outcome. J Shoulder Elb Surg. 2012;21(12):1623–31.
8. Fogg QA, Hess BR, Rodgers KG, Ashwood N. Distal biceps brachii tendon anatomy revisited from a surgical perspective. Clin Anat. 2009;22(3):346–51.

Part X

Triceps Tendon

55 Surgical Anatomy of the Distal Triceps Tendon

Raul Barco

55.1 Introduction

Distal triceps ruptures are rare injuries with a reported incidence of under 1% of all tendon injuries although some populations may be at an increased risk [1–4]. Typically, distal triceps tendon injuries are treated by sports surgeons or elbow surgeons for avulsions and occasionally olecranon spurs and osteophytes. While the distal triceps tendon is barely under the skin and is, therefore, regarded as "easy" and "simple" anatomy, there are specific features of the insertion and the anatomic relationships that might improve our understanding of the injury and decrease potential complications.

Recently, there has been an increased interest in the insertional anatomy of the triceps tendon and its insertional footprint analogous to other tendinous footprints [5–9]. There are specific details in the anatomy of the distal triceps tendon and footprint configuration that might be useful when approaching these injuries. The knowledge of footprint anatomy has led to new surgical reconstructions and recognition of different tear configurations [6, 10, 11]. Anatomical knowledge is also useful in aiding in the correct vector of reduction in chronic retracted triceps tears [12–14].

R. Barco (✉)
Shoulder & Elbow Unit, Hospital Universitario La Paz, Madrid, Spain

Apart from triceps tendon injuries, knowledge of footprint anatomy is necessary in several routine procedures that involve the distal tendon and olecranon (triceps ruptures, olecranon internal fixation, total elbow arthroplasty, posterior olecranon graft for coronoid reconstruction, and posterior compartment arthroscopy).

55.2 The Triceps Muscle

Classic knowledge of the triceps muscle consists of three muscle heads proximally (lateral, medial, and long heads) that coalesce into a distal tendinous insertion (Fig. 55.1). The separate origin of the muscle heads affects the specific action of the muscle. The long head of the triceps originates from the infraglenoid tuberosity of the scapula, and the lateral head originates from the lateral intermuscular septum and the proximal posterior surface of the humerus. The medial head has a broad origin in the distal half of the posteromedial surface of the humerus and medial intermuscular septum. The origin area of the different heads increases from proximal to distal, and it is interesting to note that the long head of the triceps attaches the ulna to the scapula. The long and lateral heads are superficial to the medial head, and they fuse into a common tendon that rotates 90° into its insertion.

The radial nerve innervates all three heads with branches proximal to the entrance of the

© ISAKOS 2022

D. N. Bhatia et al. (eds.), *Arthroscopy and Endoscopy of the Elbow, Wrist and Hand*,
https://doi.org/10.1007/978-3-030-79423-1_55

Fig. 55.1 Cadaveric dissection demonstrates a longitudinal posterior approach to the arm. The common fused tendon (1) inserts in the olecranon and is the confluence of the medial head (4), and the long and lateral heads of the triceps (5). There is a triceps lateral expansion (2) that coalesces into the fascia of the anconeus and extensor forearm muscles. The ulnar nerve (3) is closely associated with the medial side of the tendon proper

radial nerve into the groove, providing innervation to the long and lateral heads of the triceps. In contrast, the medial head is innervated by a branch that enters proximally into the muscle and runs from proximal to distally emerging and innervating the anconeus. Some authors have suggested a variant ulnar partial innervation of the triceps, but it is still disputed [15, 16].

The superficial fascia of the triceps has a direct relationship with the ulnar nerve on the medial side and has some fibers that extend to form the floor of the ulnar nerve in the posteromedial gutter of the elbow (Fig. 55.2). Laterally, the tendon extends and fuses with the lateral retinaculum

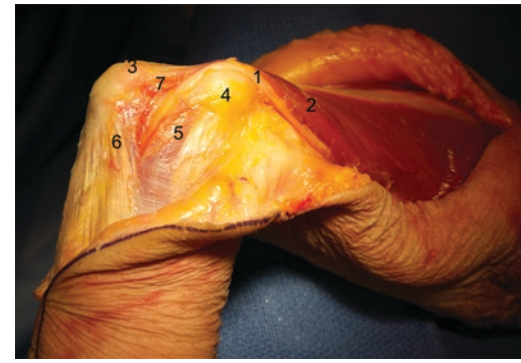

Fig. 55.2 Cadaveric dissection of the medial side of the elbow shows the direct relationship of the ulnar nerve (1) with the medial head of the triceps (2) and the medial side of the triceps common tendon (3). The ulnar nerve courses around the medial epicondyle and enters into the superficial fascia over the humeral head (5) and the ulnar head (6) of the flexor carpi ulnaris. A small part of the posteromedial capsule is seen (7)

making it difficult to delineate a discrete lateral border to the triceps tendon (Fig. 55.3). Arbitrarily, the tendon extending laterally to the most lateral aspect of the olecranon would form part of the lateral retinaculum and not the triceps tendon proper. The lateral retinaculum fuses with the forearm fascia, including the anconeus and the extensor carpi ulnaris fascia, the antebrachial fascia, and the posterior crest of the ulna medially, overlying the ulnar nerve. When the elbow extends, the fibers of the fascia overlying the anconeus align with the fibers of the triceps tendon, suggesting a synergistic pattern of activation. The insertion of the anconeus extends to 8 cm distal to the olecranon, which might be a useful reference to perform a lateral or posterolateral approach to the elbow.

55.3 The Triceps Tendon

The triceps tendon originates proximally at a mean distance of 15 cm proximal to the olecranon with a pennate configuration that extends more proximal in the medial side (Fig. 55.1). The tendon proper forms through the confluence of fibers originating from the long head and the lateral heads of the triceps. As it progresses towards the insertion on the olecranon, this confluence of

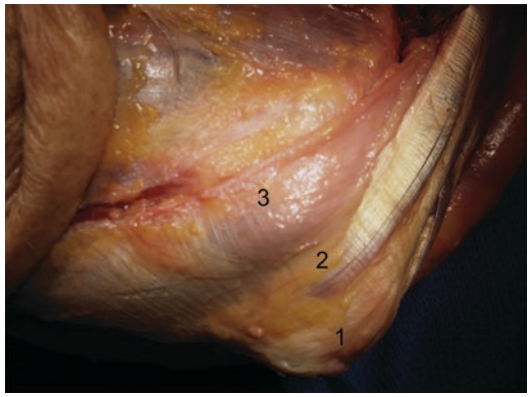

Fig. 55.3 The lateral expansion of the triceps tendon is shown and demonstrates the insertion of the tendon proper (1), the lateral expansion of the triceps (2), and the fascia overlying the anconeus (3) that fuses with the forearm superficial fascia. An incision in the fascia is noted above the anconeus corresponding to a Kocher approach

tendinous fibers (common tendon) spirals on its axis 90° and forms the sturdiest part of the tendon inserting in the dorsomedial aspect of the olecranon.

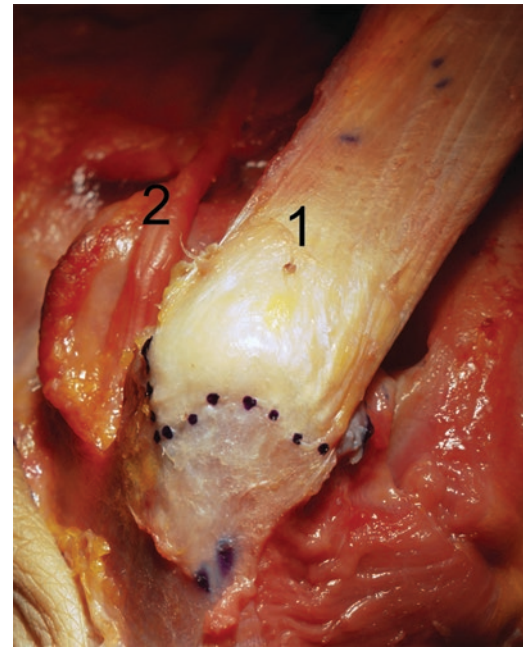

Fig. 55.4 The common triceps tendon (1) demonstrates a "W"-type shaped insertion and the medial aspect of the "V" inserts slightly more distal than the lateral part. The ulnar nerve (2) is shown for orientation

55.4 The Distal Tendinous Insertion and Triceps Footprint

The common tendon presents a "W"-type shaped insertion with the medial aspect of the "V," inserting slightly more distally than the lateral part via Sharpey's fibers into the olecranon (Fig. 55.4). Recent studies have shown that there are specific areas in the footprint that correspond, distinctly, to the insertion of the posterior capsule, the medial head of the triceps, and the common fused tendon of the lateral and long head of the triceps (Fig. 55.5). When dissected from the olecranon, the mean footprint area in the olecranon was 4 cm^2, of which 2.8 cm^2 correspond to the common tendon, and 1.2 cm^2 correspond to the medial triceps insertion with a smaller area of insertion corresponding to the capsule (Fig. 55.6) [7]. Once the elbow capsule is removed, a bare area without attachments is visualized and extends approximately for 1 cm from the tip of the olecranon to the medial head of the triceps insertion.

A distinct plane between the medial head of the triceps and the common tendon can be easily dissected, and this suggests the possibility of having isolated ruptures of the medial head of triceps. The structural disposition of the tendon fibers is one that suggests progressive incorporation of the muscle fibers from the long and lateral heads to form the tendon proper; some accompanying fibers from the medial head of the triceps incorporate into the true tendon and other fibers insert directly into its distinct insertional area. The core of the tendon is located in the midline of the triceps at belly and inserts distally in the medial aspect of the olecranon at approximately 90° to the rest of the tendinous insertion (Fig. 55.7).

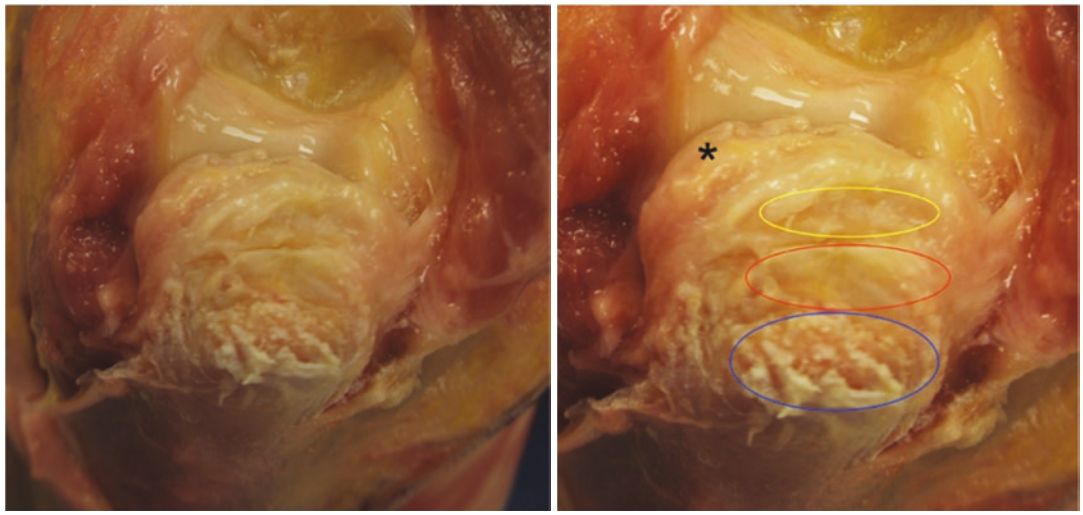

Fig. 55.5 After detachment of the triceps and posterior capsule, one can identify three specific insertional areas corresponding to the tendon proper (blue), the muscular insertion of the medial head of the triceps (red) and the capsular insertion (yellow). There is a small bare area in the posterior olecranon and in this dissection, a posterolateral osteophyte is observed (asterisk)

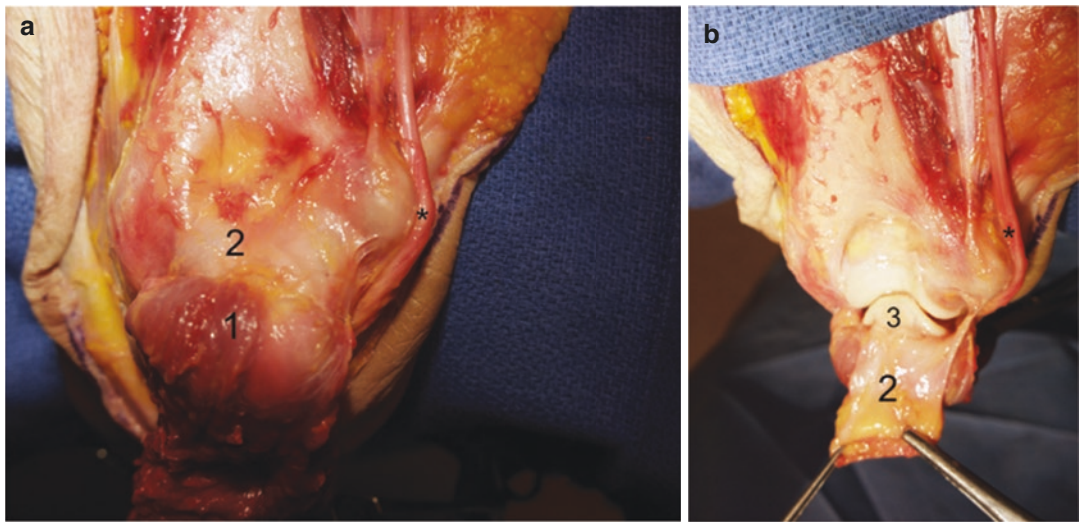

Fig. 55.6 (**a**) Posterior dissection of the elbow with the triceps tendon cut proximally and flipped back to visualize the posterior capsule (2). The deep head (1) is purely muscular and attaches at the distinct insertional area on the olecranon. (**b**) After proximal release of the posterior capsule of the elbow and flipping it backwards with the aid of forceps, one can observe the insertion of the posterior capsule (2) and the bare area (3). (*, ulnar nerve)

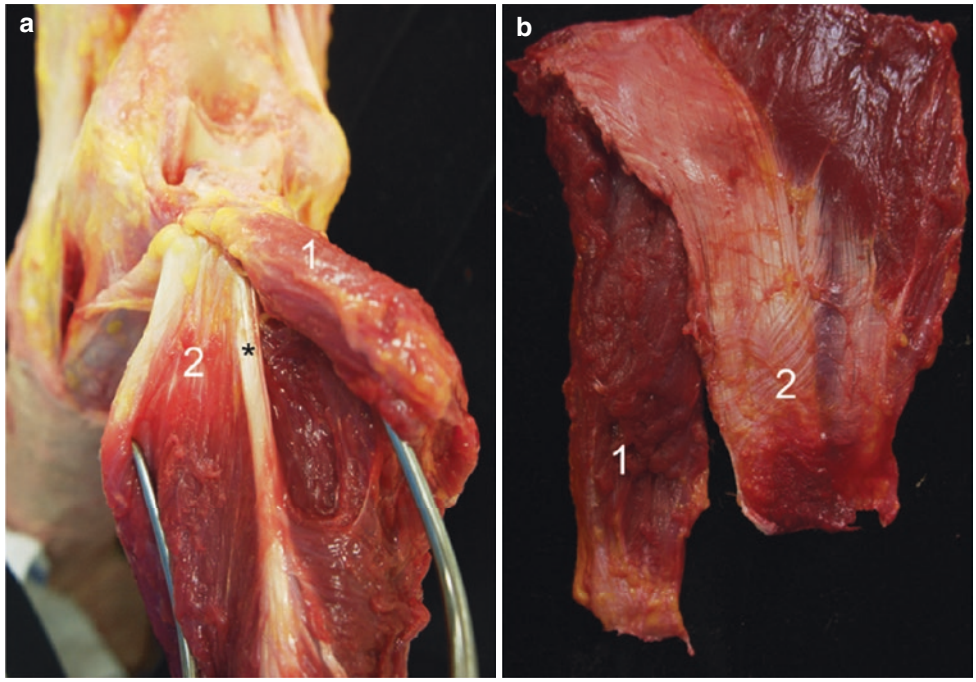

Fig. 55.7 **(a, b)** Posterior view of the elbow with the triceps cut proximally and flipped back (head, top; hand, below). After dissection of the muscular medial head of the triceps (1) from the long and lateral heads (2), one can observe the core of the triceps tendon (black asterisk) located on the midline of the triceps at the belly and inserting distally in the medial aspect of the olecranon almost at 90° to the rest of the tendinous insertion

55.5 Surgical Considerations

There is evidence that partial ruptures can occur in the insertion of the medial head of the triceps or the common tendon and that these ruptures may have distinct clinical features [11, 17]. While imaging might be helpful, one must recognize this during surgery and plan for the appropriate reconstruction. Anatomical knowledge can aid in an increased understanding of possible patterns of injury and repair configurations that better match the normal anatomy of the triceps insertion, even in the event of chronic tears [6, 8–10, 12, 14, 18]. The relationship of the medial triceps tendon and the ulnar nerve is intimate; some patients have the nerve included in the muscle superficial fascia while in others, the ulnar nerve runs independently outside of the triceps fascia. This relationship must be explored as it is common to place running sutures through the medial border of the triceps for repair or reconstruction, and this may place tension on the ulnar nerve and produce clinical symptoms of nerve irritation (Fig. 55.8).

Fig. 55.8 Triceps repair of a chronic retracted tear shows the close relationship between the medial head of the triceps tendon and the ulnar nerve (asterisk). A release of fascial attachments was performed to avoid tension of the nerve when reducing the tendon back to the footprint

Conflicts of Interest No conflicts of interest.

Source of Funding The authors have not received any financial benefit related to this manuscript.

References

1. Anzel SH, Covey KW, Weiner AD, Lipscomb PR. Disruption of muscles and tendons; an analysis of 1,014 cases. Surgery. 1959;45:406–14.
2. Lambert MI, St Clair Gibson A, Noakes TD. Rupture of the triceps tendon associated with steroid injections. Am J Sports Med. 1995;23(6):778.
3. Stannard JP, Bucknell AL. Rupture of the triceps tendon associated with steroid injections. Am J Sports Med. 1993;21(3):482–5.
4. Sollender JL, Rayan GM, Barden GA. Triceps tendon rupture in weight lifters. J Shoulder Elb Surg. 1998;7(2):151–3.
5. Keener JD, Sethi PM. Distal triceps tendon injuries. Hand Clin. 2015;31(4):641–50.
6. Yeh PC, Stephens KT, Solovyova O, Obopilwe E, Smart LR, Mazzocca AD, et al. The distal triceps tendon footprint and a biomechanical analysis of 3 repair techniques. Am J Sports Med. 2010;38(5):1025–33.
7. Barco R, Sánchez P, Morrey ME, Morrey BF, Sánchez-Sotelo J. The distal triceps tendon insertional anatomy-implications for surgery. JSES Open Access. 2017;1(2):98–103.
8. Paci JM, Clark J, Rizzi A. Distal triceps knotless anatomic footprint repair: a new technique. Arthrosc Tech. 2014;3(5):e621–6.
9. Clark J, Obopilwe E, Rizzi A, Komatsu DE, Singh H, Mazzocca AD, et al. Distal triceps knotless anatomic footprint repair is superior to transosseous cruciate repair: a biomechanical comparison. Arthrosc J Arthrosc Relat Surg. 2014;30(10):1254–60.
10. Carpenter SR, Stroh DA, Melvani R, Parks BG, Camire LM, Murthi AM. Distal triceps transosseous cruciate versus suture anchor repair using equal constructs: a biomechanical comparison. J Shoulder Elb Surg. 2018;27(11):2052–6.
11. Athwal GS, McGill RJ, Rispoli DM. Isolated avulsion of the medial head of the triceps tendon: an anatomic study and arthroscopic repair in 2 cases. Arthrosc J Arthrosc Relat Surg. 2009;25(9):983–8.
12. Paniago AF, Storti TM, Faria RSS, de Morais DCA, de Souza MP. Reconstruction of chronic tearing of the distal triceps using the double-row configuration: technical note. Rev Bras Ortop. 2015;50(5):596–600.
13. Sanchez-Sotelo J, Morrey BF. Surgical techniques for reconstruction of chronic insufficiency of the triceps. Rotation flap using anconeus and tendo achillis allograft. J Bone Joint Surg Br. 2002;84(8):1116–20.
14. Scolaro JA, Blake MH, Huffman GR. Triceps tendon reconstruction using ipsilateral palmaris longus autograft in unrecognized chronic tears. Orthopedics. 2013;36(1):e117–20.
15. Bekler H, Wolfe VM, Rosenwasser MP. A cadaveric study of ulnar nerve innervation of the medial head of triceps brachii. Clin Orthop. 2009;467(1):235–8.
16. Flores LP. Transfer of a motor fascicle from the ulnar nerve to the branch of the radial nerve destined to the long head of the triceps for restoration of elbow extension in brachial plexus surgery: technical case report. Neurosurgery. 2012;70(2):E516–20. discussion E520
17. Downey R, Jacobson JA, Fessell DP, Tran N, Morag Y, Kim SM. Sonography of partial-thickness tears of the distal triceps brachii tendon. J Ultrasound Med. 2011;30(10):1351–6.
18. Steffes M, Tayne S, Osmani F, Edwards G, MacGillis K, Kim W, et al. Triceps repair and restoration of triceps footprint with anchorless suture fixation. Tech Hand Up Extrem Surg. 2018;22(3):89–93.

Endoscopic Distal Triceps Repair

56

Donovan Johnson, Michael Esantsi,
Michael O'Brien, and Felix H. Savoie

56.1 Background

Injuries that involve the triceps tendon are uncommon. Complete rupture of the distal tendon accounts for less than 1% of tendon injuries involving the upper extremity [1–3]. The mechanism of injury classically reported was a fall on an outstretched arm or through direct trauma to the site of tendon insertion [4, 5]. Waterman et Al. recently reported that the mechanisms of injury were direct elbow trauma (44.9%), extension/lifting exercises (20%), overuse (17%), and hyper-flexion or hyperextension (17%). In addition, a quarter of their patients had pre-existing symptomatic enthesopathy, and three-quarters of tears were caused by an acute injury [6].

Partial tears of triceps tendon may be treated non-operatively, however, complete tears of the triceps tendon must be repaired to provide active extension at the elbow [7]. Cases of distal triceps tendon repair reported in the literature typically involve an open repair using a 10 cm longitudinal incision over the posterior aspect of the elbow [8]. The open technique usually involves transosseous tunnels or suture anchors and may be associated with wound healing complications and increased morbidity related to the open approach [6, 9]. While there are reports of partial arthroscopic repairs of the triceps tendon published, evidence of successful complete repairs performed arthroscopically are limited [10–12].

The senior author has previously described an all-arthroscopic technique for repair of degenerative and complete tears of the distal triceps tendon [13]. The all-arthroscopic technique allows the treating surgeon to fully assess the injury pattern of the distal triceps tendon. Moreover, a thorough debridement of the damaged tendon tissue can be performed endoscopically and the triceps tendon can be repaired back to the anatomic footprint on the olecranon. This technique is cosmetic and is associated with less wound complications and a shortened postoperative recovery period as compared to the open technique.

56.1.1 Surgical Anatomy

The triceps brachii is the only muscle that lies along the posterior humerus. It functions as a powerful extensor of the elbow joint. As its name implies, this large muscle is comprised of three heads; the long head, the lateral head, and the medial head. These differ in their proximal attachments, yet, they converge to a single insertion area on the olecranon process of the ulna. The ulnar nerve lies along the medial aspect of the muscle as it heads toward the cubital tunnel.

D. Johnson · M. Esantsi · M. O'Brien · F. H. Savoie (✉)
Department of Orthopaedic Surgery, Tulane University, New Orleans, LA, USA
e-mail: djohns36@tulane.edu; mesantsi@tulane.edu; mobrien@tulane.edu; fsavoie@tulane.edu

© ISAKOS 2022

D. N. Bhatia et al. (eds.), *Arthroscopy and Endoscopy of the Elbow, Wrist and Hand*,
https://doi.org/10.1007/978-3-030-79423-1_56

At the mid-humeral level, the radial nerve crosses the posterior humerus in the spiral groove and courses to the anterior compartment. Arthroscopically and endoscopically, the olecranon bursa provides a space in which distention allows visualization of the triceps and olecranon from proximal and distal portals.

56.2 Indications and Contraindications

Operative repair of the distal triceps tendon is indicated for complete and symptomatic partial ruptures. Non-operative treatment can be considered initially for partial tears and surgical repair is recommended for tendon tears with 50% involvement [14]. The decision for operative intervention of partial tears must be patient specific and the overall health, activity level, and comorbidities of these patients need to be considered.

The physical exam for a suspected distal triceps tendon injury begins with inspection of the injured and non-injured upper extremity. Swelling and ecchymosis may be appreciated in the acute setting. Palpation of the tendon insertion is usually painful and a palpable defect at the insertion of the triceps tendon is present in both complete and partial tears. Weakness of active extension against resistance may be seen with partial or complete tears, but this is not diagnostic [12]. However, the triceps stress test can be useful tool assisting the treating physician with diagnosing subtle tendon tears. This is done by having the patient fully flex the elbow and then try to extend the elbow against resistance. Pain in the area of detachment can be considered pathognomonic of a significant tear requiring surgery.

Lateral radiographic views of the elbow may demonstrate a flake of bone avulsed from the olecranon, and traction spurs, and olecranon and/or tendon enthesiopathy may be observed (Fig. 56.1) [12]. Ultrasound can be used to differentiate among complete tendon rupture, partial tendon rupture, and tendinosis [15–17]. Magnetic resonance imaging (MRI) closely correlates with examination and other imaging modalities and is useful for surgical planning by identifying calcifications, bursitis, and chronic tendinopathy (Fig. 56.2).

Fig. 56.1 Preoperative lateral radiograph of a complete avulsion of the triceps tendon with a bone fragment

Fig. 56.2 MRI image of a complete triceps avulsion with fluid separating the tendon from its attachment to the olecranon

The time from initial injury to presentation is important; ideally, primary repair is performed within 2 weeks from injury, and in one study,

primary repair was only possible in 6 of 15 patients when the repair was greater 25 days [11]. Waterman et al. reported patients with complications underwent surgery at a median of 60 days after injury in their cohort, while the patients with no complications underwent surgery on an average of 35 days after injury [6]. Early surgery is preferable however, in the author's experience, adequate arthroscopic release of the muscle and tendon off the posterior humerus arthroscopically allows adequate repair in almost every case.

Contraindications include open wounds, active infections, and significant gouty tophi within the olecranon bursa.

56.3 Surgical Steps

A standard 4 mm 30-degree arthroscope and regular arthroscopic instruments are utilized. Suture anchors and suture passing devices are needed for this procedure. The senior author prefers a retrograde 30-degree Ideal suture grasper as a retrograde suture retriever (DePuy Mitek, Raynham, MA).

After induction of anesthesia, the patient is placed either in the lateral decubitus or prone position (the author prefers prone). All bony prominences are well padded and a non-sterile tourniquet is applied to the upper arm.

56.3.1 Portals

- Standard proximal anteromedial and/or anterolateral portals.
- Posterocentral portal.
- Posterolateral portal.
- Proximal bursal viewing portal: 3–4 cm proximal to the tip of the olecranon.
- Distal bursal viewing portal: 3–4 cm distal to the tip of the olecranon.

Triceps endoscopy: A quick diagnostic arthroscopy of the anterior compartment is performed using a proximal anteromedial portal prior to triceps endoscopy.

- A proximal posterior central portal is placed through the defect in the tendon to complete the intra-articular diagnostic arthroscopy. In partial tears, a proximal posterior lateral portal is used to define the extent of the tear. Once the tear is visualized via the postero-lateral portal the posterior central portal can be made and a shaver is introduced to debride the tear edges and the olecranon bursa. (Fig. 56.3).
- The arthroscope is then moved to a proximal bursal viewing portal, located 3–4 cm proximal to the tip of the olecranon, and the tear and tendon are debrided (Fig. 56.4). The ulnar insertion of the triceps tendon is identified. The footprint is debrided and the olecranon is prepared for acceptance of tendon (Fig. 56.5).
- The scope is then moved to a distal bursal viewing portal, located 3–4 cm distal to the tip of the olecranon and the standard central posterior portal is used to place a double-loaded suture anchor at the proximal footprint angling away from the joint parallel to the posterior ulnar border to prevent penetration of the ulno-humeral joint (Fig. 56.6a, b).
- A retrograde suture passer is used percutaneously to pass all four strands through the tendon, with broad separation, with one strand each medially and laterally and two more cen-

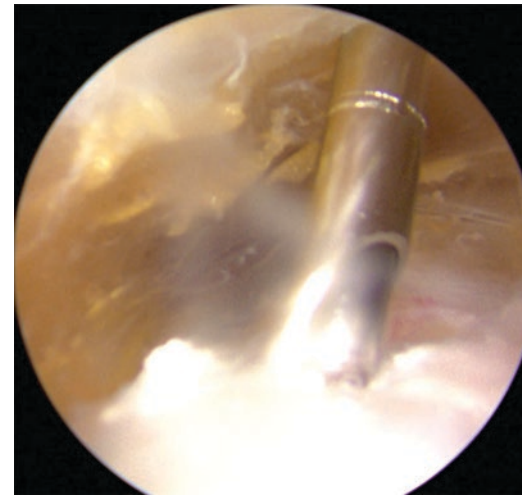

Fig. 56.3 Olecranon bursectomy is shown using a standard 4.5 mm Shaver

tral. The suture is retrieved percutaneously and a sliding knot is tied. The second set of sutures is retrieved and tied in mattress fashion as well (Fig. 56.7a).

- Two of the strands are then "double passed" through the more distal tendon to create four different paths for the sutures and thereby four compression points as they track to the second anchor.
- The arthroscope is placed in the proximal olecranon bursa portal, and the distal bursal portal is used for a cannula into the olecranon bursa (Fig. 56.7b). The sutures from the proximal anchor are retrieved into this cannula and placed into a second anchor which can be inserted into the distal olecranon to create a suture bridge repair. Alternatively, a second anchor may be placed in the distal ulna. These sutures are passed through the distal tendon and tied in simple fashion and the repair is complete.

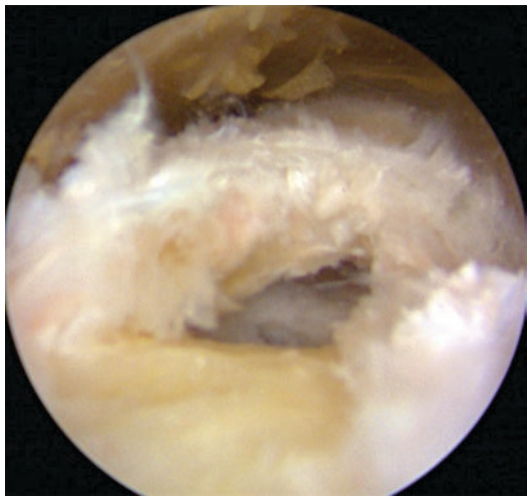

Fig. 56.4 Endoscopic appearance of the triceps tendon tear is shown after debridement

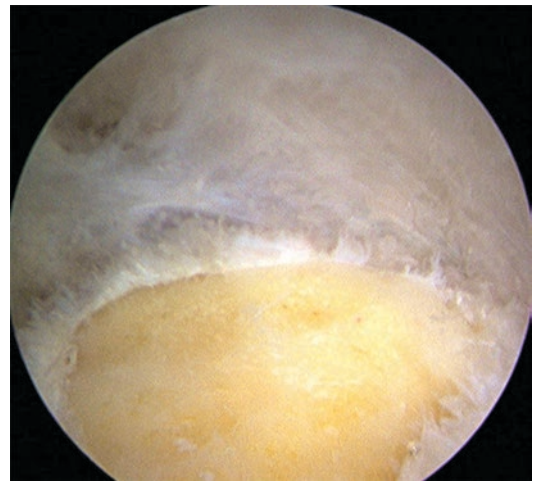

Fig. 56.5 The triceps footprint is debrided, and the olecranon is prepared for tendon repair

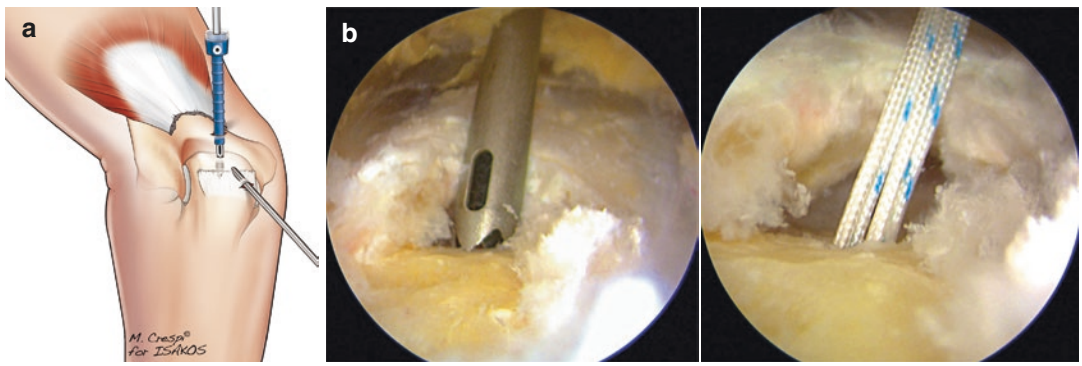

Fig. 56.6 (**a**) Suture anchor insertion is illustrated. The arthroscope is in the distal bursal viewing portal and anchor insertion is performed via posterior central portal (M. Crespi © for ISAKOS). (**b**) A guide-sleeve is placed from the posterior central portal onto the proximal aspect of the triceps footprint. Note the sleeve angles toward the posterior cortex to avoid penetration of the ulno-humeral joint (left image). A double-loaded suture anchor is placed at the proximal footprint in preparation for suture retrieval (Right image)

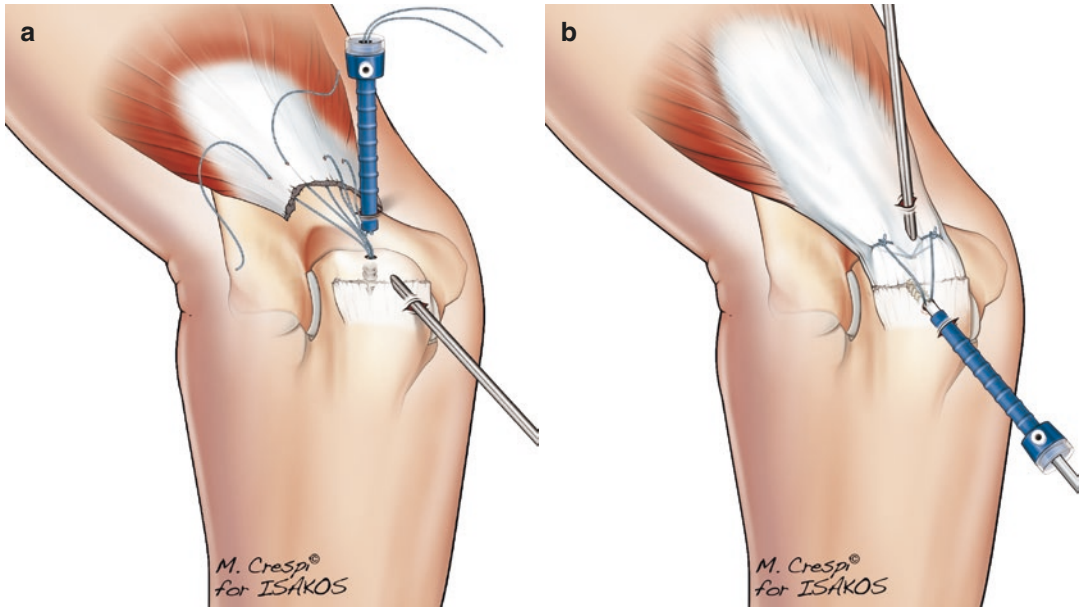

Fig. 56.7 (**a**) Suture passage through triceps tendon is illustrated (M. Crespi © for ISAKOS). (**b**) A second anchor is placed further distal on the olecranon to create a suture bridge repair (M. Crespi © for ISAKOS)

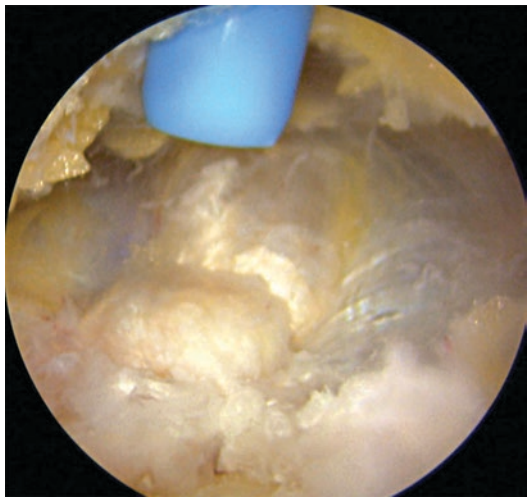

Fig. 56.8 Final view of the repaired triceps tendon with the elbow in extension

- The arthroscope is placed in both the proximal and distal bursal portals to evaluate the repair (Fig. 56.8). The elbow is ranged through flexion and extension and stability of repair is assessed. The fluid is evacuated out of the bursa. A hemovac suction drain is placed via existing portals and removed just prior to patient departure from the hospital or surgery center. All portals are closed, and a compression dressing and posterior splint with the elbow in full extension are applied.

56.4 Tips and Tricks

- Patient positioning with the elbow free to flex and extend is critical to the success of the procedure.
- Diagnostic arthroscopy should be quick and under minimal inflow to avoid swelling.
- The bursa is a potential space and fluid leakage is common. Keep portal incisions small so that a tight seal is maintained around the cannula and the bursa remains distended.
- The angle and depth of anchor placement are critical to avoid accidental penetration of the joint.

56.5 Postoperative Management and Rehabilitatiion

A posterior splint is applied with the elbow in near-full extension. At the first postoperative visit, 7–10 days following surgery, the patient is placed in a hinged elbow brace allowing motion of 0–30 degrees. Weekly advances of 10 degrees of motion is allowed until 6–8 weeks postoperatively. The brace is discontinued at 6–8 weeks, and a strengthening program is initiated. Limited strengthening can be started at 4 weeks. Regular postoperative ultrasound is used to monitor the healing response of the tendon and rehabilitation is advanced accordingly. Weight training and advanced rehabilitation are initiated at 8 weeks. Most patients with primary arthroscopic repair return to normal activity by 4 months postoperatively, if not earlier.

56.6 Complications

Complications are possible and the surgeon must be prepared to abandon arthroscopic technique for open repair.

- The senior author has monitored his results over the past 15 years. In over 30 patients with acute or chronic tears, the healing rate was near 100%. Complications included one chronic bursitis (in a revision repair), one persistent portal fistula (in a previously infected olecranon bursa patient who ruptured the tendon while the infection was being managed), and one case of anchor migration into the elbow joint requiring removal.

  Other potential complications include:

- Ulnar nerve injury: In the acute setting, swelling may obscure the anatomy and it is imperative to identify the course of the ulnar nerve and protect it.
- Anchor breakage: The bone of the olecranon may be extremely hard. To prevent breaking of anchors during insertion, the surgeon can oversize the pilot hole and tap deeper into the bone. An expansion anchor may also be used.
- Fluid extravasation may interfere with satisfactory repair.

References

1. Bach BR, Warren RF, Wickiewicz TL. Triceps rupture. A case report and literature review. Am J Sports Med. 1987;15(3):285–9.
2. Tarsney FF. Rupture and avulsion of the triceps. Clin Orthop Relat Res. 1972;83:177–83.
3. Vidal AF, Drakos MC, Allen AA. Biceps tendon and triceps tendon injuries. Clin Sports Med. 2004;23(4):707–22. xi
4. Kandemir U, Fu FH, Mcmahon PJ. Elbow injuries. Curr Opin Rheumatol. 2002;14(2):160–7.
5. Johnson DC, Allen AA. Biceps and triceps tendon injury. In: Altchek DW, Andrews JR, editors. The athlete's elbow. Philadelphia: Lippincott Williams &Willkins; 2001. p. 105–20.
6. Waterman BR, Dean RS, Veera S, et al. Surgical repair of distal triceps injuries. Short-term to midterm clinical outcomes and risk factors for perioperative complications. Orthop J Sports Med. 2019;7(4):1–6.
7. Morrey BF. Rupture of the triceps tendon. In: Morrey BF, editor. The elbow and its disorders. 3rd ed. Philadelphia: WB Saunders Co.; 2000. p. 479–84.
8. Strauch RJ. Biceps and triceps injuries of the elbow. Orthop Clin North Am. 1999;30(1):95–107.
9. Tom JA, Kumar NS, Cerynik DL, Mashru R, Parrella MS. Diagnosis and treatment of triceps tendon injuries: a review of the literature. Clin J Sport Med. 2014;24(3):197–204.
10. Mair SD, Isbell WM, Gill TJ, Schlegel TF, Hawkins RJ. Triceps tendon ruptures in professional football players. Am J Sports Med. 2004;32(2):431–4.
11. van Riet RP, Morrey BF, Ho E, O'driscoll SW. Surgical treatment of distal triceps ruptures. J Bone Joint Surg Am. 2003;85-A(10):1961–7.
12. Viegas SF. Avulsion of the triceps tendon. Orthop Rev. 1990;19(6):533–6.
13. Ng T, Rush LN, Savoie FH. Arthroscopic distal triceps repair. Arthrosc Tech. 2016;5(4):941–5.
14. Koplas MC, Schneider E, Sundaram M. Prevalence of triceps tendon tears on MRI of the elbow and clinical correlation. Skelet Radiol. 2011;40:587–94.

15. Tagliafico A, Gandolfo N, Michaud J, Perez MM, Palmieri F, Martinoli C. Ultrasound demonstration of distal triceps tendon tears. Eur J Radiol. 2012;81(6):1207–10.
16. Sisson C, Nagdev A, Tirado A, Murphy M, Suner S. Ultrasound diagnosis of traumatic partial triceps tendon tear in the emergency department. J Emerg Med. 2011;40(4):436–8.
17. Konin GP, Nazarian LN, Walz DM. US of the elbow: indications, technique, normal anatomy, and pathologic conditions. Radiographics. 2013;33(4):E125–47.

57 Acute and Chronic Triceps Tendon Tears: Transosseous Repair Technique

Deepak N. Bhatia

57.1 Background

Triceps tendon tears are infrequent injuries and are a result of sports-related overuse or may be associated with systemic diseases and anabolic steroid use. Surgical intervention is necessary for tendon reattachment and results in restoration of strength and function. Surgical reattachment can be performed using open and arthroscopic techniques. Transosseous techniques and suture anchors have been described for repair, and biomechanical studies have shown similar repair strength of the all-suture and suture anchor constructs [1].

57.1.1 Surgical Anatomy

The triceps tendon inserts on the olecranon in a broad footprint at a distance of approximately 1 cm from the olecranon tip and distinct insertional areas for the deep muscular head (medial head) and superficial tendinous head (long and lateral heads) have been documented [2]. Triceps tears may be partial, and these usually involve the superficial tendinous insertion. Partial tears are secondary to chronic overuse tendinosis and may be associated with an impinging olecranon spur. Triceps avulsions may involve the superficial tendinous head predominantly, and the deep muscular head insertion is preserved to a variable extent. These tears typically show minimal retraction and are ideal for arthroscopic repair. Complete avulsions involve detachment of both heads from the olecranon footprint and are retracted proximally. Bony avulsions are seen in approximately half of triceps tears and usually involve the superficial tendinous head.

57.2 Indications and Contraindications

- Partial tears that are refractory to conservative treatment and especially those that are associated with symptomatic olecranon spurs necessitate spur excision and tendon debridement and repair (Fig. 57.1a).
- Acute ruptures and bony avulsions of triceps tendon should be repaired for restoration of strength and function (Fig. 57.1b).
- Chronic retracted tears that can be released and mobilized adequately should be repaired (Fig. 57.1c).

Partial tears that are asymptomatic, and musculotendinous tears can be treated conservatively and are contraindications for repair. Severe retraction and failure to achieve adequate length

D. N. Bhatia (✉)
SPORTSMED, Mumbai, India

Sir HN Reliance Foundation Hospital, Mumbai, India
e-mail: shoulderclinic@gmail.com

© ISAKOS 2022

D. N. Bhatia et al. (eds.), *Arthroscopy and Endoscopy of the Elbow, Wrist and Hand*,
https://doi.org/10.1007/978-3-030-79423-1_57

Fig. 57.1 (**a**) Radiograph (left image) and magnetic resonance imaging (right image) demonstrates an olecranon spur (arrow) in a squash player. The spur impinges on the tendinous head in extension and a resultant partial tear is seen (arrows, right image) (© Bhatia). (**b**) An acute bony avulsion of triceps tendon is demonstrated on radiograph (left image) and magnetic resonance imaging (right image) (© Bhatia). (**c**) MRI demonstrates a chronic retracted triceps tear (arrow, left image). Another chronic triceps tear with a retracted bony fragment is seen on radiograph and MRI. (arrow, middle, and right images) (© Bhatia)

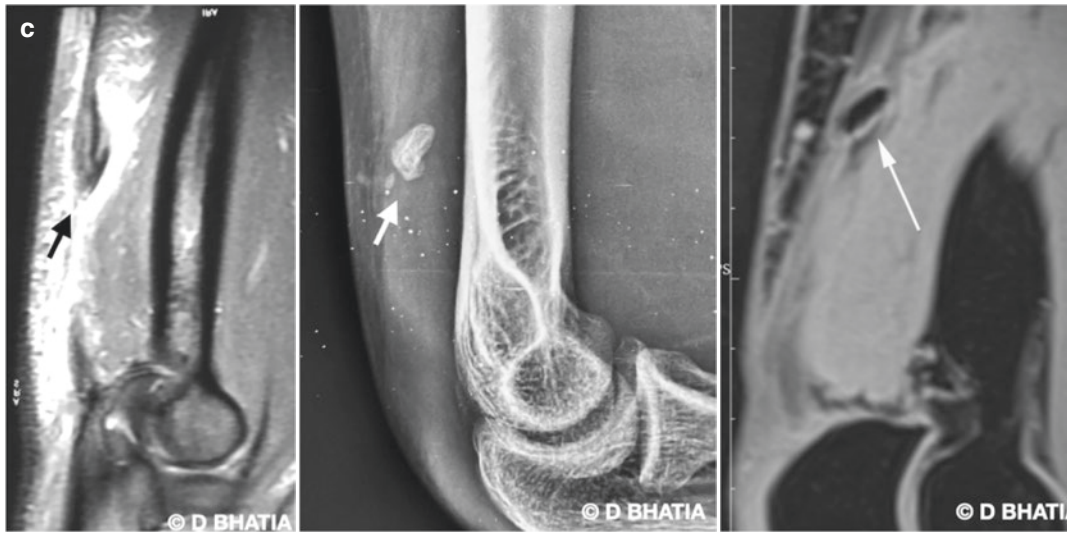

Fig. 57.1 (continued)

intraoperatively necessitates reconstruction with a tendon graft.

57.3 Surgical Technique

Triceps tendon repair is performed with the patient in the lateral decubitus position with a side-trolley that can be used to support the extremity in extension.

- A posterior skin incision is placed just lateral to the midline, and the skin and subcutaneous flaps are elevated to expose the triceps, olecranon, and proximal ulna. The ulnar nerve is identified and protected throughout the procedure.
- *Partial tears:* The olecranon spur is identified intraoperatively and excised. Imaging is used to confirm complete excision. The triceps tear is then debrided and repair is performed as described below (Fig. 57.2a).
- *Acute complete tears and bony avulsions:* The ruptured triceps tendon stump is identified; the proximally retracted tendon is grasped with an atraumatic forceps or clamp and pulled distally onto the olecranon (Fig. 57.2b). The deep muscular head is identified and is included in the repair construct. Bony avulsion fragments in the ruptured tendon are identified and the avulsion site on olecranon is noted. The frayed area of the tendon stump is debrided to stable tissue (Fig. 57.2c).
- Two heavy (number 2) high strength sutures are passed starting from the tendon undersurface and 1–2 cm from the distal torn edge on either sides of the tendon midline. In bony avulsions, these sutures are passed starting just proximal to the bone fragment. These sutures are used to place Krackow stitches to whipstitch the tendon from distal to proximal for 2–3 cm along either side of the midline. The needle ends of the sutures are then passed to the peripheral borders and the tendon is whipstitched from proximal to distal, At the fragment bone junction, the sutures are brought out through the dorsal surface of the tendon in a Mason-Allen configuration (Fig. 57.3a, b).
- Two bone tunnels (2 mm) are placed from the lateral aspect of proximal olecranon and exiting distal to the region of bone avulsion or in the mid insertional footprint region. Imaging is used to confirm that the tunnels are extraarticular (Fig. 57.4).
- The undersurface strands of each of the two sutures are passed through the tunnels and the strands are tensioned in 60–90 degrees of

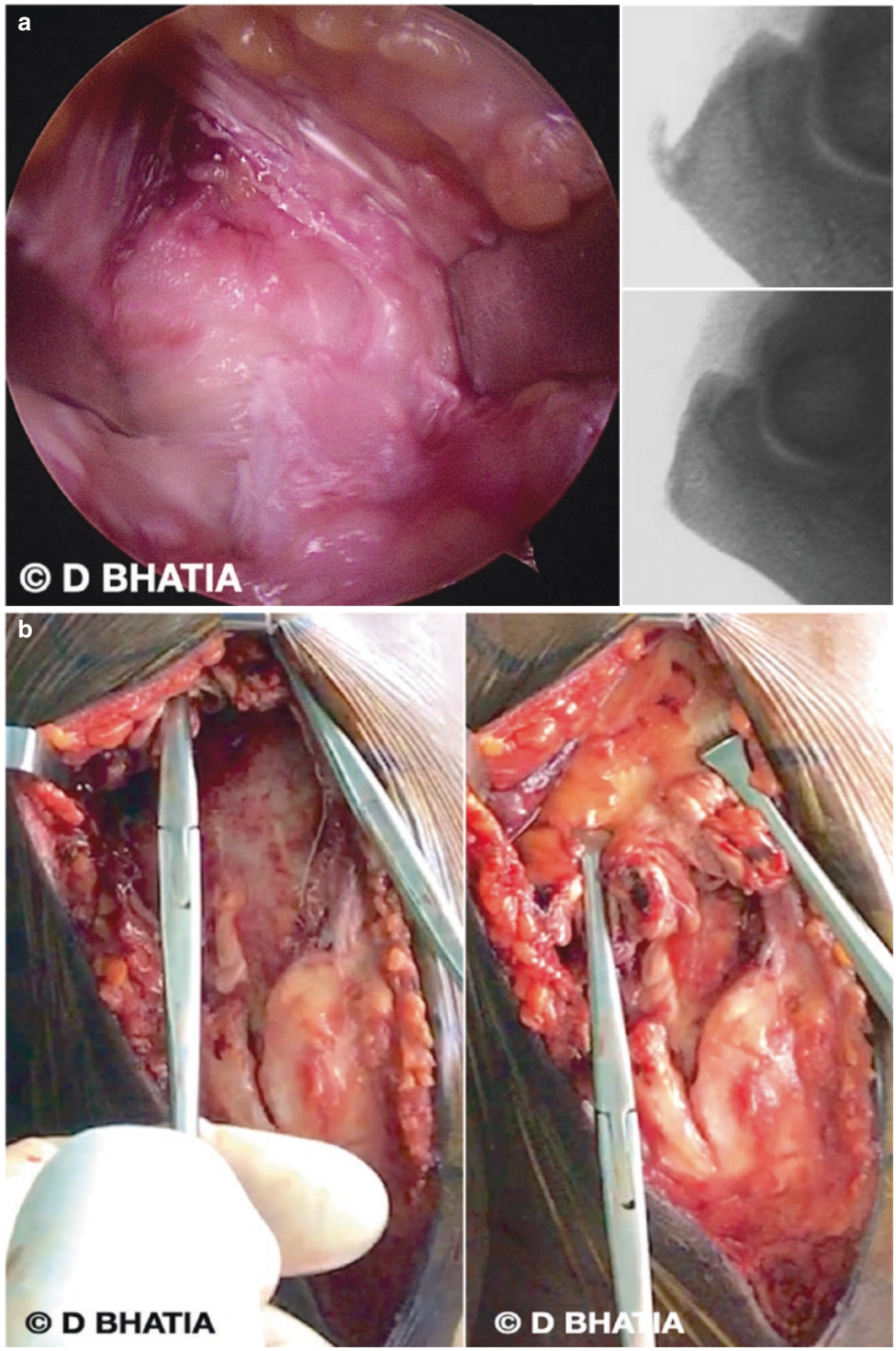

Fig. 57.2 (**a**) An olecranon spur is seen protruding into a partial triceps tear (left image). The spur is demonstrated on fluoroscopy (top right) and complete excision is confirmed (bottom right) (© Bhatia). (**b**) An acute complete tear is seen retracted proximally (left image). The tendon is grasped and pulled distally into the surgical site. The tendon ends are seen to be frayed and are debrided (right image) (© Bhatia). (**c**) An acute bony avulsion of triceps tendon (T) is shown detached from the olecranon (OL). (Left image). Part of the deep muscular head is preserved at the olecranon insertion (arrow, right image) (© Bhatia)

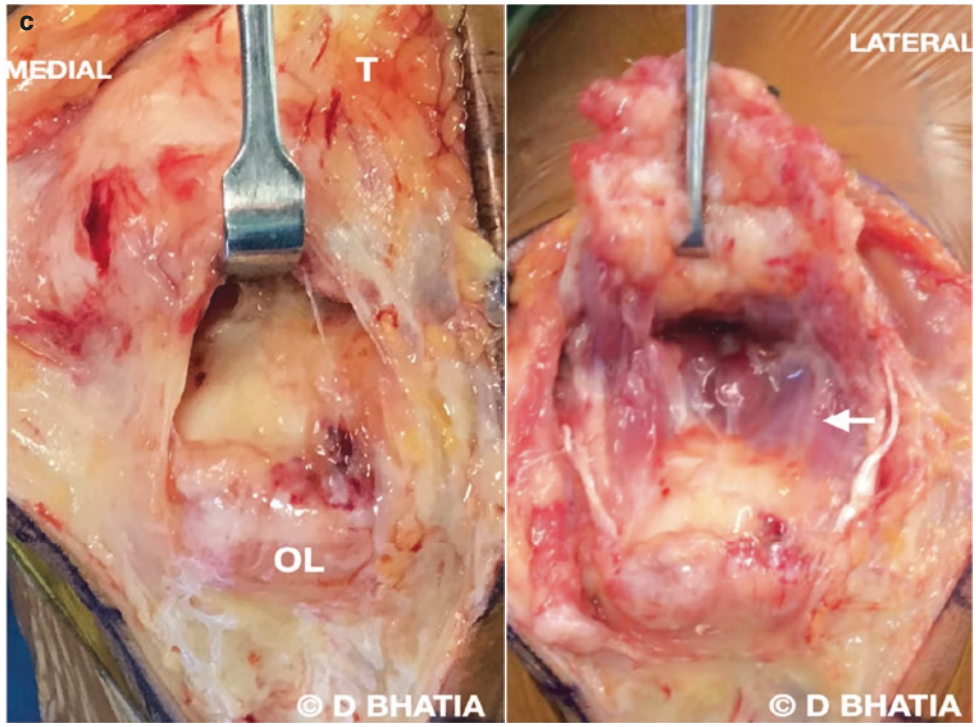

Fig. 57.2 (continued)

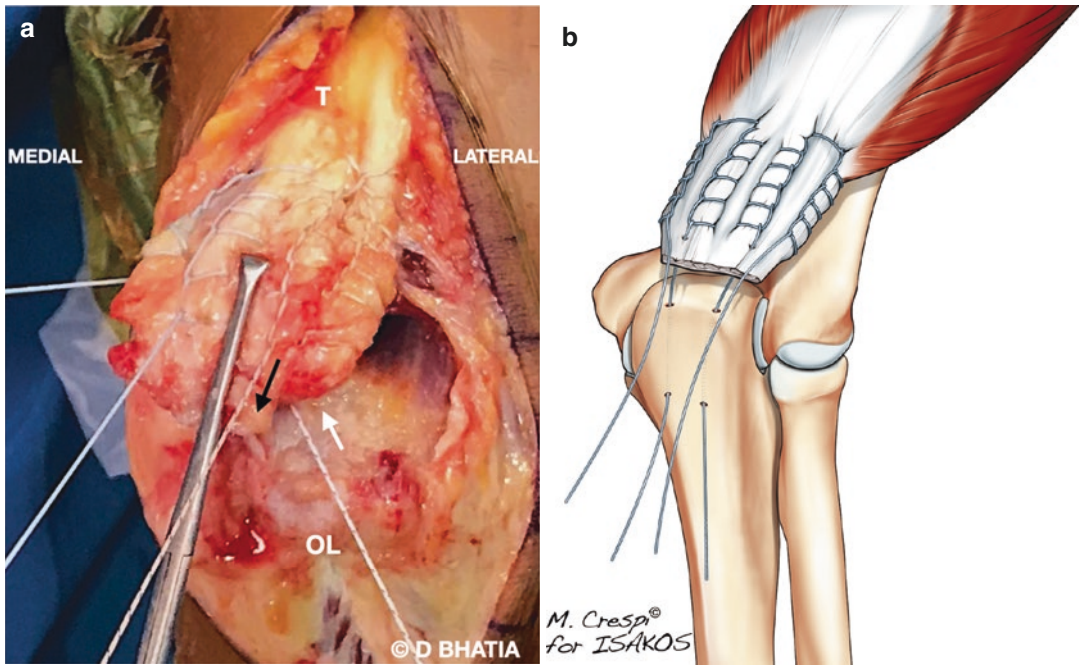

Fig. 57.3 (**a**) The whipstitch technique for triceps tendon (T) is demonstrated. The suture is passed from the undersurface (white arrow) and Krackow stitches are passed from distal to proximal at the midline and then proximal to distal closer at the periphery. The suture exits at the dorsal surface 1–2 cm from the tendon stump edge (black arrow) (© Bhatia). (**b**) The whipstitch technique for triceps tendon and suture orientation for an onlay repair is illustrated (M. Crespi © for ISAKOS)

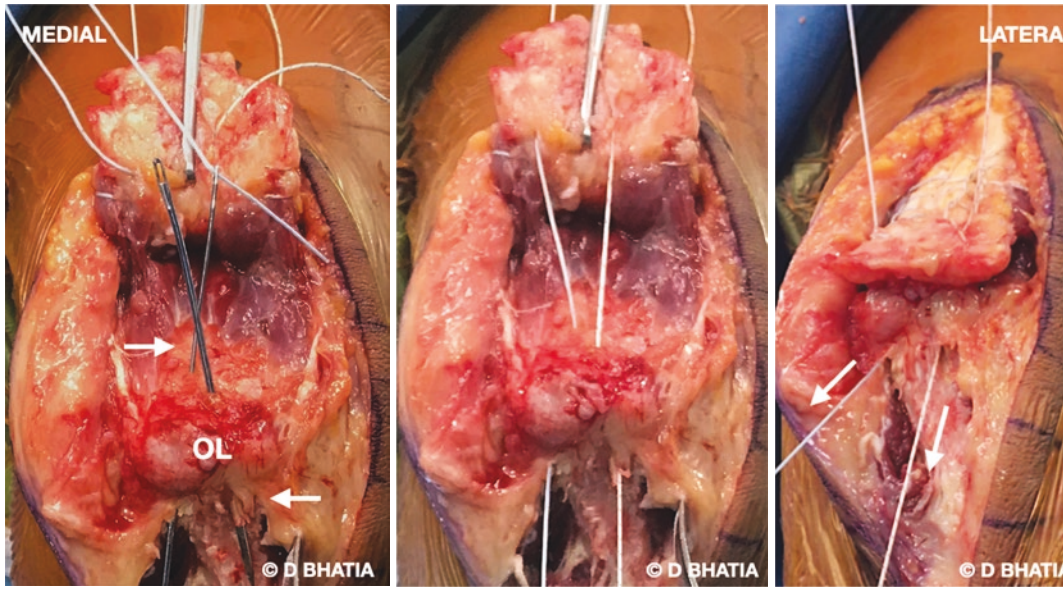

Fig. 57.4 Tunnel orientation (arrows, left image) and passage of undersurface sutures through the tunnels is shown (middle image). The avulsed bone fragment is seen grasped by the clamp. The undersurface sutures are tensioned to approximate the tendon to its footprint on the olecranon (right image) (© Bhatia)

elbow flexion and are knotted on the radial aspect of the ulnar crest. Firm approximation and proximal tendon-bone contact is confirmed during knotting and ends of the knotted sutures are preserved (Fig. 57.4).

- The dorsal surface strands are now brought over the tendon stump and are knotted to one strand each of the previous knot in 90 degrees of elbow flexion. The resultant construct compresses the tendon stump on the olecranon surface and creates a footprint-like onlay repair (Fig. 57.5a, b).
- *Chronic retracted tears:* The retracted tendon stump is identified by dissecting the superficial fascia and scar tissue. Retinacular and fascial flaps are preserved on either side distal to the tendon. The triceps is mobilized by adhesiolysis on the dorsal and deep surfaces. The radial nerve is palpated and protected during adhesiolysis in the deep midarm region, and the ulnar nerve is release from the adjacent fascia. The tendon is grasped with an atraumatic clamp and pulled distally to assess approximation to olecranon; the elbow may be positioned in up to 30 degrees flexion for the repair if necessary. The deep muscular head and even the capsule may be incorporated in the repair for reinforcement. The repair is performed using the technique described above. The sutures from the undersurface are knotted either over the ulna or using a button device. The outer sutures are then knotted over the tendon as described above. The fascial flaps are the sutured over the tendon for additional reinforcement (Fig. 57.6).
- Wound is closed and a posterior splint is applied in 40° of elbow flexion.

57.4 Tips and Tricks

- Intra-articular perforation while drilling the olecranon tunnels is possible. Fluoroscopic imaging can be used to guide and prevent intra-articular perforation. The tunnel should start 2 cm distal to the olecranon and should exit on the insertional surface 1 cm proximal to the tip. The tunnels should be angulated

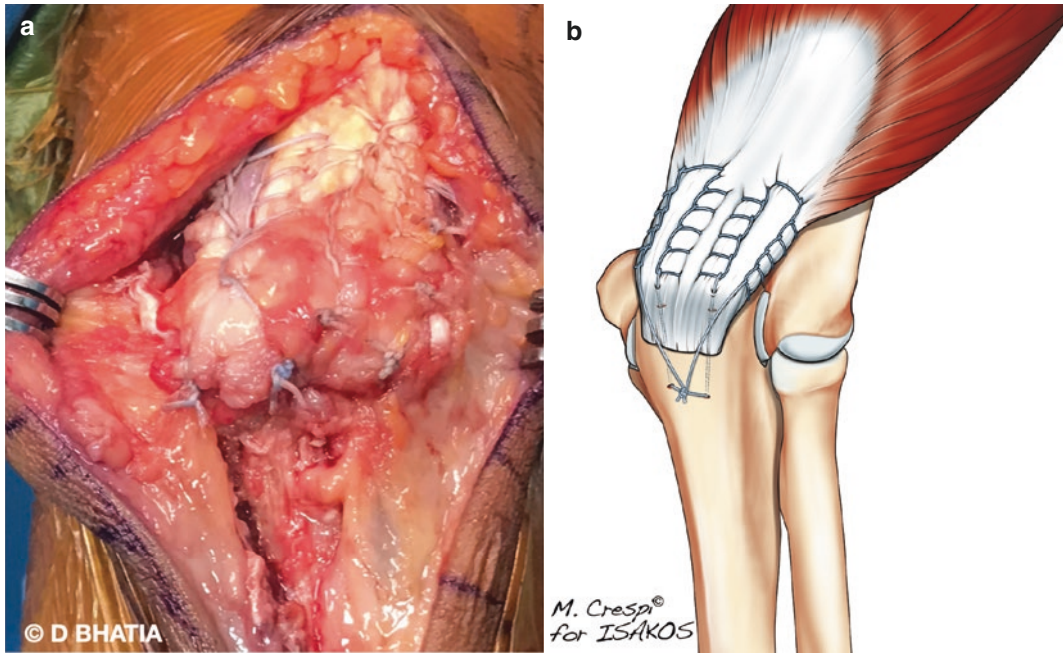

Fig. 57.5 (**a**) Final repair of the tendon is demonstrated after knotting all sutures (© Bhatia). (**b**) Final repair of the triceps tendon after knotting all sutures is illustrated (M. Crespi © for ISAKOS)

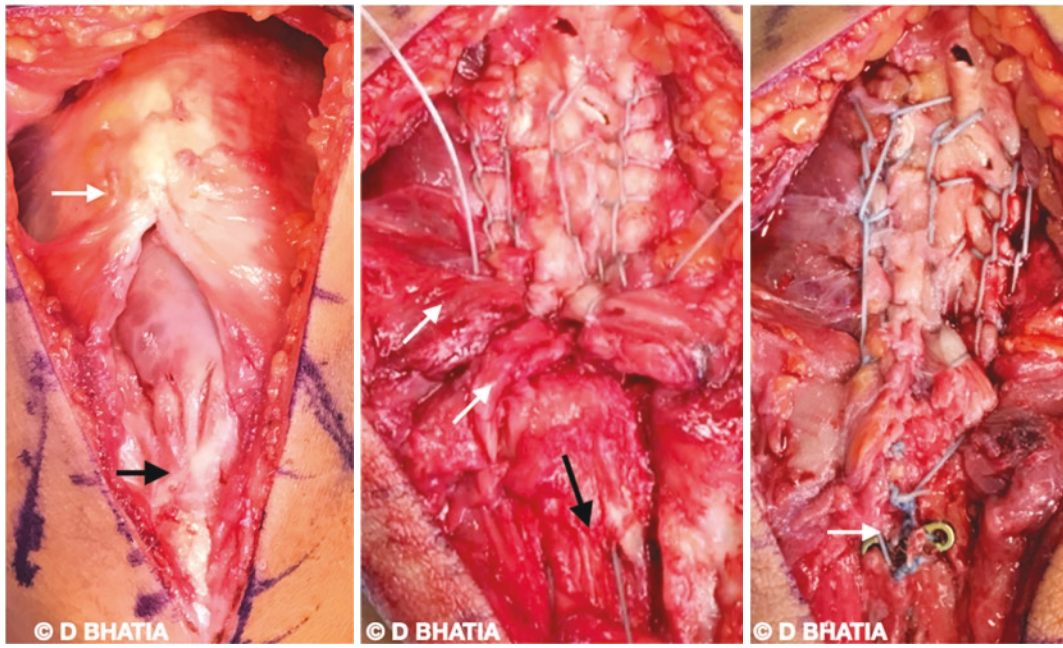

Fig. 57.6 Transosseous repair of a chronic retracted triceps tendon rupture is demonstrated. Part of the deep muscular head is preserved at the olecranon insertion. Sutures are passed through superficial and deep heads (white arrows, middle image) and undersurface sutures are seen exiting the tunnels (black arrow). Final repair is seen after tying the knots over a button (arrow, right image) (© Bhatia)

towards the midline and in different planes to avoid stress fractures through the tunnels.
- A chronic tear that can be mobilized and approximated to the olecranon in 30 degrees of flexion can be repaired by this technique. The triceps stretches with rehabilitation after tendon healing and full range of motion can be achieved.

57.5 Pitfalls

Chronicity and anabolic steroids alter the quality of tendon tissue, and this may result in suboptimal healing after repair. Tendon augmentation using palmaris longus or gracilis autograft should be used to strengthen the repair in such cases.

57.6 Postoperative Management and Rehabilitation

A posterior splint is used in 30–60 degrees of elbow flexion for 6 weeks postoperatively. Thereafter, a controlled-motion brace is used to achieve full range of motion over 4–6 weeks. Strengthening is started as motion progresses. Sports activities are resumed after 6 months.

57.7 Complications

The ulnar and radial nerves are at-risk of injury during dissection and mobilization of chronic retracted tears and should be identified and protected. Rerupture is possible and is avoided by adequate duration of splinting and gradual recovery of range of motion. Sports activities should be delayed for at least 6 months and periodic sonographic assessment is useful to assess healing and tendon-bone contact.

Conflict of Interest The author certifies that he has no commercial associations (e.g., consultancies, stock ownership, equity interest) that might pose a conflict of interest in connection with the submitted article. The author retains the copyright to the images, videos, and content in this chapter.

References

1. Carpenter SR, Stroh DA, Melvani R, Parks BG, Camire LM, Murthi AM. Distal triceps transosseous cruciate versus suture anchor repair using equal constructs: a biomechanical comparison. J Shoulder Elb Surg. 2018;27(11):2052–6.
2. Barco R, Sánchez P, Morrey ME, Morrey BF, Sánchez-Sotelo J. The distal triceps tendon insertional anatomy-implications for surgery. JSES Open Access. 2017;1(2):98–103.

Part XI

Elbow: Ulnar Nerve

Endoscopic Ulnar Nerve Decompression

58

Raul Barco

58.1 Background

Ulnar nerve entrapment is a common compression neuropathy in the upper extremity and is second only to carpal tunnel syndrome. The incidence is approximately 25 cases per 100,000 people per year, and the annual worldwide estimate is 1.5 million cases per year [1, 2]. Clinical symptoms include a feeling of clumsiness aggravated by using the elbow in flexion, and muscle wasting typically of the first dorsal interosseous muscle. Weak thumb adductors may produce a positive Froment sign, and weak adductor of the little finger will produce an ulnar drift when extending the fingers. The Tinel sign involves percussion of the nerve from distal to proximal and a positive test produces tingling distal to the site of percussion. The elbow flexion test involves flexing the elbow to more than 120°, and a positive test reproduces paresthesias within 60 s. The most commonly used provocative maneuver is the flexion-compression test in which the examiner compresses the cubital tunnel while the patient is flexing the elbow, and the patient experiences symptoms within 30 s. Differential diagnosis involves cervical radiculopathy, thoracic outlet syndrome, spinal cord pathology, cervical spondylosis, Pancoast tumor, amyotrophic lateral sclerosis, or localized peripheral neuropathy [3].

58.1.1 Surgical Anatomy

The ulnar nerve can be compressed mainly at five sites around the elbow: the arcade of Struthers, the medial intermuscular septum, the medial epicondyle, the cubital tunnel, and the deep flexor aponeurosis. From proximal to distal, the first site of compression is at the arcade of Struthers (Fig. 58.1). This thickened fascia is present in 15% of the population and extends from the medial head of the triceps to the medial intermuscular septum. The arcade is usually located around 10 cm proximal to the medial epicondyle at the level where the ulnar nerve enters the dorsal compartment. More commonly, compression occurs under a thick aponeurotic band that connects both heads of the FCU in the cubital tunnel (Osborne's fascia). The floor of the cubital tunnel is formed by the posterior aspect of medial epicondyle, the joint capsule, and the posterior band of the ulnar collateral ligament (UCLp), and the roof is formed by a thick aponeurotic band. The space for the ulnar nerve is modified by elbow flexion in which the UCLp (floor) and the roof of the tunnel are tightened, thereby limiting the available space for the ulnar nerve as much as 50% [4]. The anatomy of the nerve shows the superficial layer providing sensory supply to the

R. Barco (✉)
Shoulder & Elbow Unit, Hospital Universitario La Paz, Madrid, Spain

© ISAKOS 2022

D. N. Bhatia et al. (eds.), *Arthroscopy and Endoscopy of the Elbow, Wrist and Hand*,
https://doi.org/10.1007/978-3-030-79423-1_58

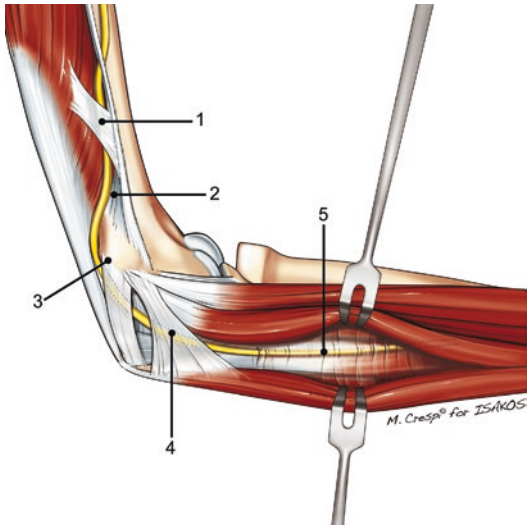

Fig. 58.1 From proximal to distal the potential sites of compression include: (1) arcade of Struthers, (2) medial intermuscular septum, (3) medial epicondyle, (4) cubital tunnel, and (5) deep flexor aponeurosis (M. Crespi © for ISAKOS)

hand while the center of the nerve carries fibers innervating the intrinsic muscles and fibers innervating the motor branches to the long flexor tendons. This topographic configuration explains the early onset of sensory symptoms in the hand with loss of sensation, decreased two-point discrimination, and paresthesias in the ulnar distribution of the hand and forearm.

58.2 Indications and Contraindications

Surgical decompression is indicated in patients with McGowan grades II and III (intermittent paresthesias with objective weakness, muscle atrophy, or fixed sensory changes) with positive electrodiagnostic studies.

Ulnar nerve decompression alone is contraindicated in: (a) prior elbow injury, (b) nerve revision surgery, and (c) intraoperative ulnar nerve instability. In these situations, ulnar nerve transposition is necessary.

Fig. 58.2 Position of the extremity and surface markings are demonstrated

58.3 Surgical Technique

The patient is supine with the arm supported on a hand table and an arm tourniquet is used. A small pillow is placed between the hand table and the elbow to elevate the elbow and to improve the angle of insertion of the endoscope. Most of the surgery is performed with elbow in flexion.

- The medial epicondyle is the most reliable anatomical landmark (Fig. 58.2). The ulnar nerve lies posterior and curves around it with the elbow in 90° of flexion. Proximally, the palpable medial border of the triceps is adjacent and posterior to the ulnar nerve. Distally, the nerve courses towards the volar aspect of the ulnar styloid.
- The surgical incision is 1–1.5 cm long and is placed in the ulnar nerve tunnel, approximately midway between the olecranon and the medial epicondyle.
- After the skin incision, the nerve is located with scissor dissection. Suprafascial dissection is made with scissors over the course of the nerve (Fig. 58.3a, b).
- The endoscope is passed distally via the incision, and scissors are used to cut Osborne's ligament. The superficial fascia of the FCU is released, and the deep fascia is identified and incised (Fig. 58.4). The endoscope is advanced

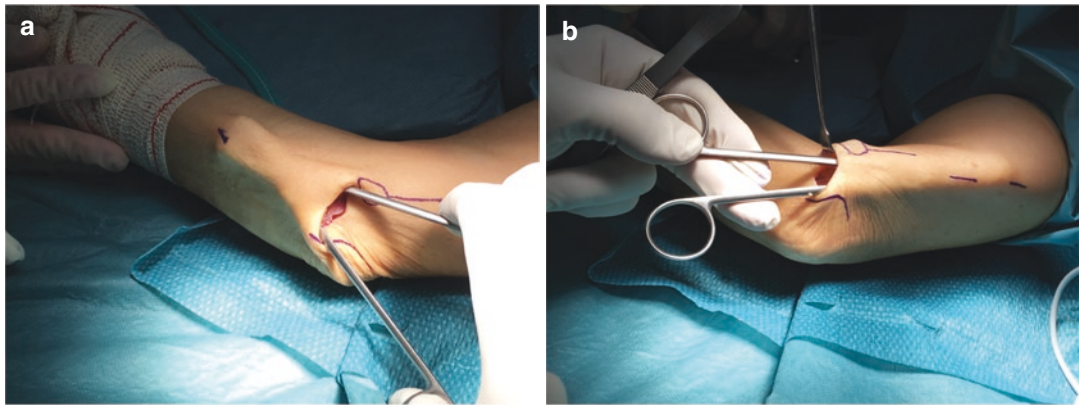

Fig. 58.3 Distal (**a**) and proximal (**b**) superficial dissection is shown. Suprafascial dissection is made with scissors over the course of the nerve to facilitate introduction of the scope over the fascia. While "looking down" on to the fascia, scissors are introduced, and the fascia can be cut safely under direct vision

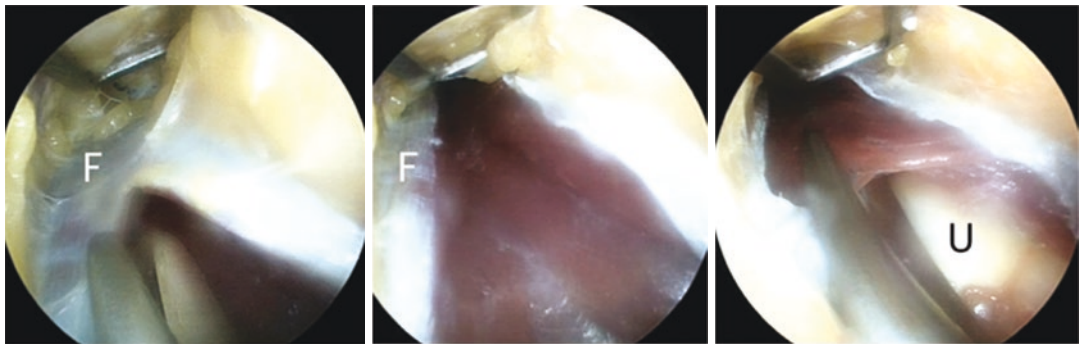

Fig. 58.4 Release of FCU fascia under endoscopic visualization is demonstrated. (U: ulnar nerve, F: Fascia)

and the dissection is continued distally as far as 10–15 cm.

- Next, the endoscope is passed proximally, and the nerve is released as far as 10 cm, where the arcade of Struthers, if present, is usually located (Figs. 58.5a, b).
- Any adhesions to the triceps are identified and released at this time (Fig. 58.6).
- Vessels can be coagulated as needed using bipolar electrocautery introduced through the same incision during the procedure and after releasing the tourniquet (Fig. 58.7).
- At the end of the procedure, a low-volume preparation of tranexamic acid is injected along the course of the nerve (author's preference). Wound closure is performed with subcuticular sutures, and a compressive dressing is applied.

58.4 Tips and Tricks

- A Wissinger rod or probe can be introduced into the incision and used as a muscle retractor to aid in visualization of the nerve.
- Intermittent rinsing may be used to control the temperature at the tip of the endoscope.

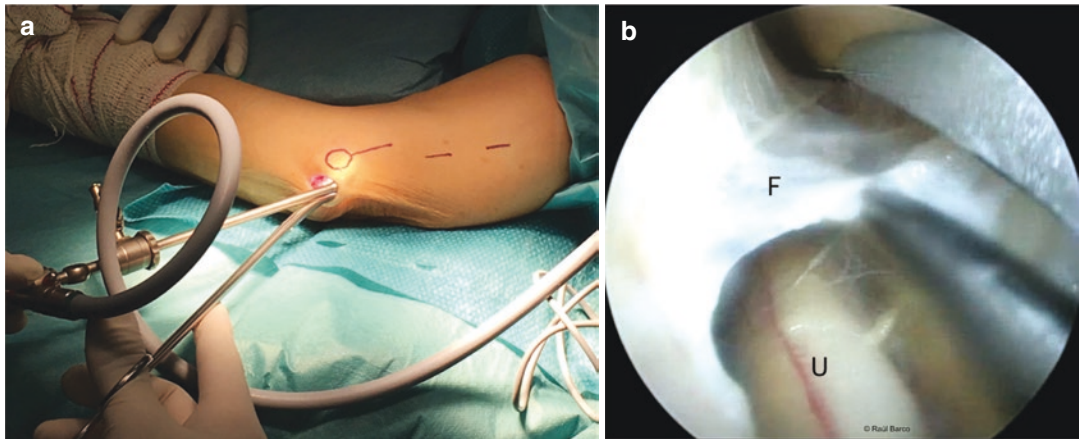

Fig. 58.5 (**a**) The scope and scissors are passed proximally through the incision to allow proximal release. (**b**) Proximal release of the fascia over the ulnar nerve is demonstrated. (U: ulnar nerve, F: Fascia)

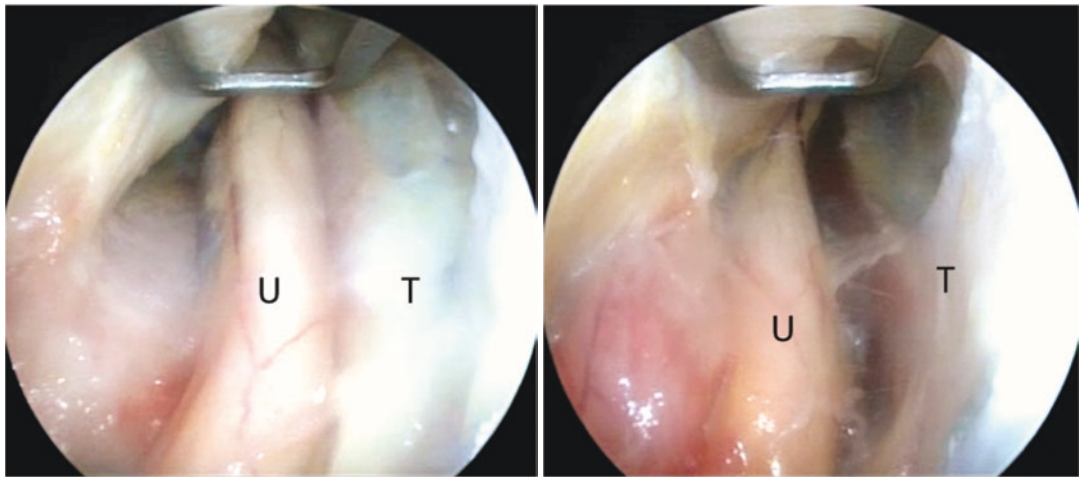

Fig. 58.6 Adhesions between the triceps (T) and the ulnar nerve (U) are observed (left image) and are dissected to free the nerve for unobstructed gliding (right image)

58.5 Pitfalls

- Failure to identify ulnar nerve instability preoperatively results in persistence of symptoms.
- The medial antebrachial cutaneous nerve is at-risk of injury and should be protected.

58.6 Postoperative Management and Rehabilitation

Patients are advised to perform light activities with the arm in the immediate postoperative period. The procedure is well-tolerated by patients, and they can usually resume all activi-

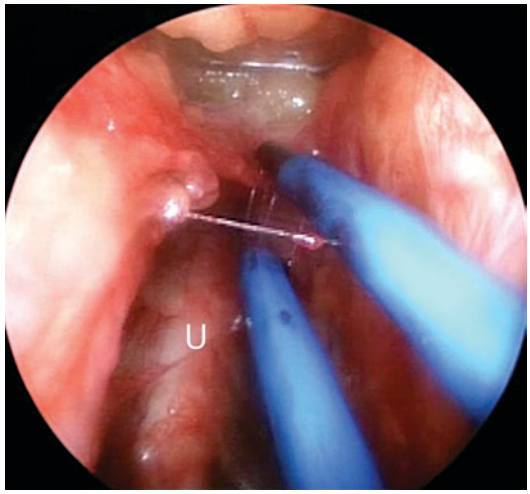

Fig. 58.7 A bipolar electrocautery is introduced through the incision for hemostasis (U: Ulnar nerve)

ties of daily living by 10 days and go back to routine work at 4–6 weeks.

58.7 Complications

Numbness around the elbow, tenderness of the scar, and pain at the medial side of the elbow are potential local complications. Pain in the posterior medial forearm is suggestive of injury to the medial antebrachial cutaneous nerve. Hematoma formation can produce early postoperative exacerbation of symptoms, and hemostasis after releasing the tourniquet is recommended. Persistent or recurrent symptoms are generally due to an incorrect diagnosis, inadequate release, scar formation, or due to long-standing nerve compression.

Conflicts of Interest No conflicts of interest.

Source of Funding The authors have not received any financial benefit related to this manuscript.

References

1. Harder K, Diehm J, Fassola I, Al Khaled N, Doll D, Dunda SE, et al. Current diagnostics and treatment of the cubital tunnel syndrome in Austria. GMS Interdiscip Plast Reconstr Surg DGPW. 2016;5:Doc03.
2. Law TY, Hubbard ZS, Chieng LO, Chim HW. Trends in open and endoscopic cubital tunnel release in the Medicare patient population. Hand (N Y). 2017;12(4):408–12.
3. Gilchrist JM, Dandapat S. Neuromuscular mimics of entrapment neuropathies of upper extremities. Hand (N Y). 2020;5:1558944719898801.
4. Apfelberg DB, Larson SJ. Dynamic anatomy of the ulnar nerve at the elbow. Plast Reconstr Surg. 1973;51(1):76–81.

59 Endoscopic Ulnar Nerve Release and Transposition: Two Portal Technique

Margaret Woon Man Fok and Gregory I. Bain

59.1 Background

Cubital tunnel syndrome is the second most common compressive neuropathy of the upper limb, followed by carpal tunnel syndrome. Endoscopic cubital tunnel release has gained popularity in recent years due to its encouraging outcome in the literature. Advantages include an extended release of the ulnar nerve via a small incision, functional outcomes comparable to open cubital tunnel release, early return to work, and minimal complications [1, 2]. Although there are no significant subjective or functional difference between ulnar nerve decompression in situ and anterior transposition, there are conditions where ulnar nerve anterior transposition is indicated [3]. In these instances, a subcutaneous anterior transposition can still be performed under endoscopic guidance by the creation of an additional anterior portal [4].

M. W. M. Fok
Department of Orthopaedics and Traumatology, Queen Mary Hospital, The University of Hong Kong, Hong Kong, China

G. I. Bain (✉)
Department of Orthopaedic Surgery, Flinders University, and Flinders Medical Centre, Adelaide, SA, Australia
e-mail: admin@gregbain.com.au; greg@gregbain.com.au

59.2 Indications and Contraindications

Endoscopic ulnar nerve release is indicated in the following conditions:

- Hostile bed of the ulnar nerve, e.g. excessive scarring from previous trauma and excessive osteophytes at the cubital tunnel.
- Cubital valgus.
- Ulnar nerve hypermobility.
- Recurrent cubital tunnel syndrome: In selective cases only, where incomplete release or a new compressive site is suspected.

Contraindications include:

- Previous trauma or surgery to the ulnar nerve or elbow.
- Severe elbow contracture.
- Concomitant condition necessitating open surgery such as management of humeral malunion or non-union.
- Patient factors necessitating submuscular transposition, e.g. thin patients who are prone to have ulnar nerve irritation.
- Limited external rotation of the shoulder.

Ulnar nerve hypermobility: Ulnar nerve subluxation and dislocation can be diagnosed either in the pre- or intra-operative period (Fig. 59.1). Male and young age are noted to be

© ISAKOS 2022

D. N. Bhatia et al. (eds.), *Arthroscopy and Endoscopy of the Elbow, Wrist and Hand*,
https://doi.org/10.1007/978-3-030-79423-1_59

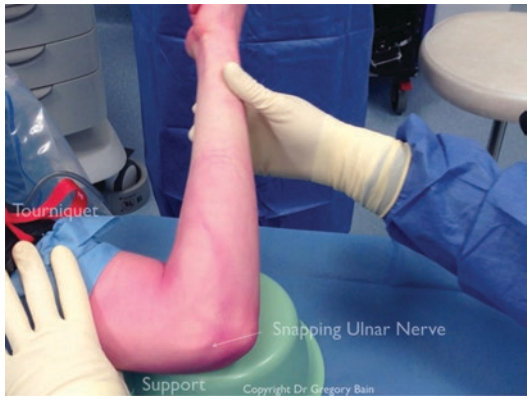

Fig. 59.1 Demonstration of ulnar nerve subluxation (© Professor Gregory I. Bain)

risk factors for ulnar nerve instability [5]. Ulnar nerve instability is assessed pre-operatively by placing a thumb on the posteromedial aspect of the medial humeral epicondyle during elbow extension. Dynamic sonography is more reliable than clinical assessment in determining ulnar nerve instability. The decision to transpose the ulnar nerve in the presence of nerve subluxation remains a controversial topic. Bartels et al. in a randomized control study showed comparable outcomes at 1-year follow up between decompression in situ and anterior transposition for cubital tunnel syndrome irrespective of the ulnar nerve mobility status [3]. There was no reported symptomatic hypermobility of the ulnar nerve in patients with decompression in situ at 1-year follow up. Yet, in a revision cubital tunnel syndrome case series, in two of the 28 patients, revision surgery was due to ulnar nerve instability [6]. Hence, many surgeons recommend concomitant ulnar nerve transposition at the time of surgical decompression if ulnar nerve is noted to be unstable either in the pre-operative or intra-operative period [4, 5, 7]. The authors perform ulnar nerve anterior transposition if the patient has symptomatic idiopathic ulnar nerve syndrome and the ulnar nerve is noted to be unstable pre- or intra-operatively.

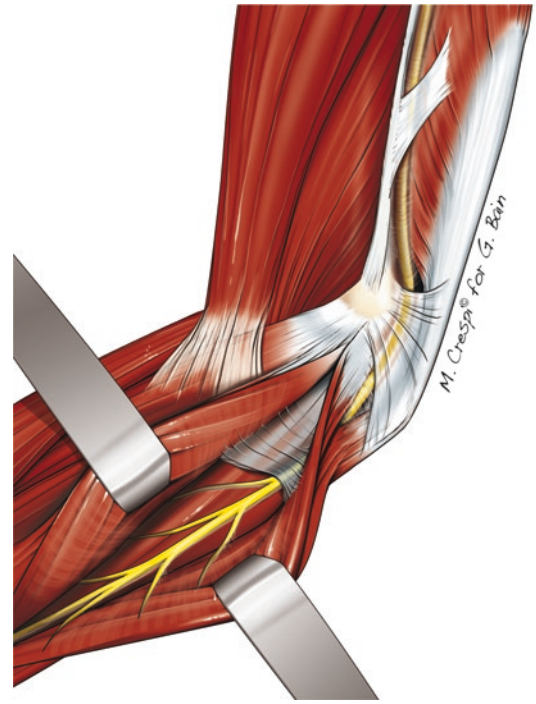

Fig. 59.2 Potential sites of ulnar nerve compression in ulnar tunnel syndrome (M. Crespi © for Gregory I. Bain)

59.3 Surgical Techniques

59.3.1 Ulnar Nerve Decompression

Ulnar nerve is decompressed from 8 to 10 cm proximal to the medial epicondyle (i.e. arcade of Struthers) to 6–8 cm distal to the medial epicondyle (i.e. the branching of ulnar nerve for the innervation of flexor carpi ulnaris muscle (FCU) (Fig. 59.2).

The patient is placed in supine position under general or regional anaesthesia, with the affected arm in 90^0 abduction and supination on a standard hand table. Pneumatic tourniquet is used without limb exsanguination to better visualize the vasculature that accompanies the ulnar nerve.

- A 2 cm longitudinal incision is made at the retrocondylar groove, between the medial epi-

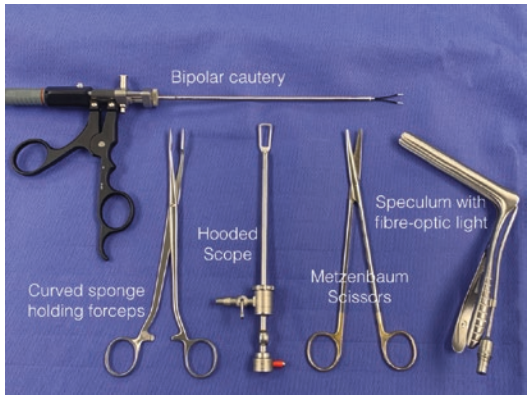

Fig. 59.3 Endoscopic instrumentals (Storz) used in cubital tunnel decompression (© Professor Gregory I. Bain)

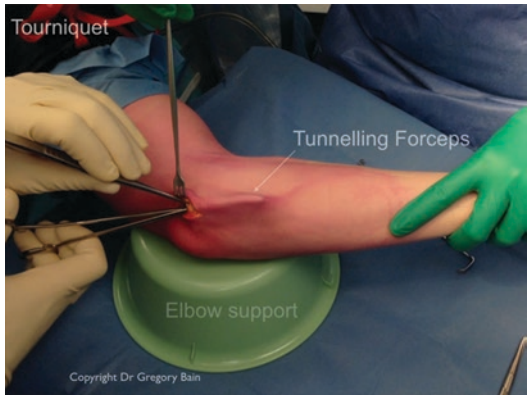

Fig. 59.4 Subcutaneous tunnel is created by tunnelling forceps (© Professor Gregory I. Bain)

condyle and the olecranon. The ulnar nerve is identified by incising the roof of the cubital tunnel.

- Using specialized dissection equipment, e.g. Storz instruments (Karl Storz, Tuttlingen, Germany), a 4 mm 30° endoscope with a blunt dissector on its tip is introduced into the incision (Fig. 59.3) [8].
- A potential space is created between the soft tissue and the deep fasciae, along the length of ulnar nerve decompression (Fig. 59.4).
- Under endoscopic guidance, a blunt tipped scissors in used to incise the deep fasciae, lying over the ulnar nerve. "Spread and cut" technique is employed to minimize the risk of iatrogenic injury to the ulnar nerve.

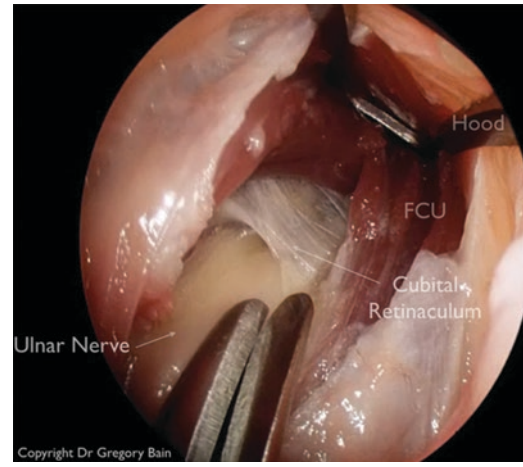

Fig. 59.5 Distal dissection of the ulnar nerve within the FCU muscle and visualization of motor branches of the ulnar are demonstrated (© Professor Gregory I. Bain)

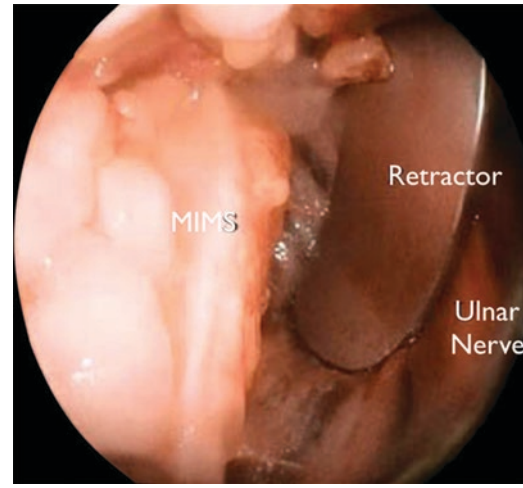

Fig. 59.6 Endoscopic view of the medial intermuscular septum (MIMS) is shown. A retractor is used to retract the ulnar nerve away from the MIMS (© Professor Gregory I. Bain)

- For distal release, the dissection and decompression is performed till the motor branches of the FCU come into view (Fig. 59.5).
- For proximal release, the medial intermuscular septum (MIMS) is identified during the dissection (Fig. 59.6). Excision of MIMS is needed as it may become a new site of compression during transposition (Fig. 59.7). The ulnar nerve is then decompressed till the division of Arcade of Struthers.

59.3.2 Anterior Transposition: Two Portal Technique

The ulnar nerve is transposed anteriorly in the subcutaneous plane.

- A tunnelling forceps is used to create a subcutaneous space anterior to the medial epicondyle into which the ulnar nerve will be placed.
- The ulnar nerve is freed circumferentially with its accompanying vessels, starting at the retro-condylar area.
- A 1 cm portal is created 2 cm anterior to the previous incision. A nylon tape is passed into this portal and is used to wrap around the newly freed segment of the ulnar nerve. The ulnar nerve is retracted gently using the nylon tape and mobilized from its surrounding loose areolar tissue (Fig. 59.8).
- Under endoscopic guidance, the ulnar nerve is dissected free and is placed into the previously developed subcutaneous space anterior to the medial epicondyle. It is important to check the entire "new course" of the nerve, to ascertain that the nerve is sitting comfortably to its course with no new site of compression or kinking (Fig. 59.9).
- The tourniquet is then deflated and haemostasis is achieved with long bipolar forceps or

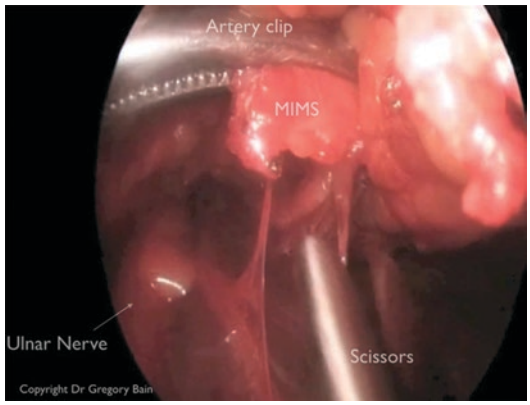

Fig. 59.7 Excision of the MIMS under endoscopic vision is demonstrated (© Professor Gregory I. Bain)

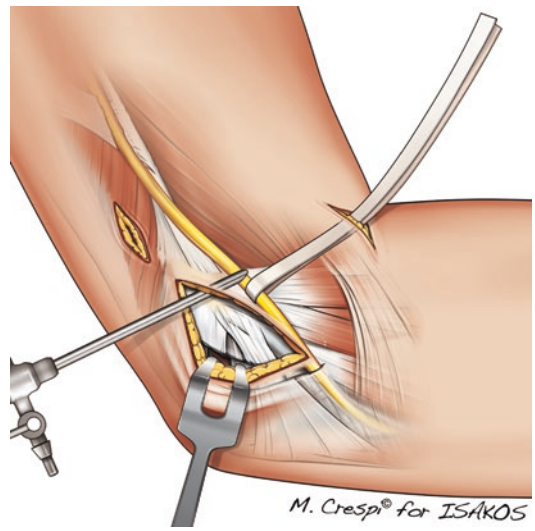

Fig. 59.8 Creation of an anterior portal for ulnar nerve mobilization using a nylon tape ((M. Crespi © for ISAKOS)

Fig. 59.9 A nylon tape is introduced into the anterior portal and is used to mobilize the nerve from loose areolar tissue under endoscopic guidance (© Professor Gregory I. Bain)

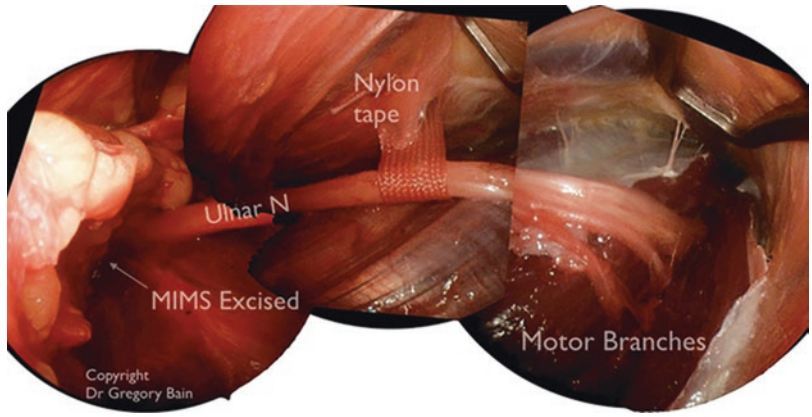

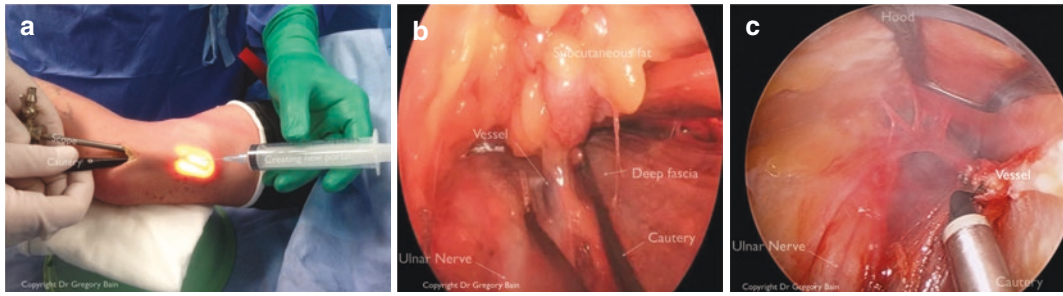

Fig. 59.10 Haemostasis is achieved after ulnar nerve decompression +/− anterior transposition. (**a**) Use of a cautery for haemostasis is shown. (**b**) Visualization of the ulnar nerve is mandatory during cauterization using bipolar forceps (copyright Professor Gregory I. Bain). (**c**) Endoscopic visualization of the nerve and cauterized vessels is demonstrated. (© Professor Gregory I. Bain)

special bipolar micro-forceps under endoscopic vision (Figs. 59.10a–c).

- To prevent the nerve from subluxating back to its natural position, the nerve needs to be secured. The medial epicondyle is rasped in order to promote adhesion to the adjacent soft tissue. The subcutaneous tissue is then sutured to the medial epicondyle to prevent the nerve from reducing behind the epicondyle. In addition, a sling of fasciae, raised from the flexor—pronator muscles group, can be used to secure the nerve into the anterior compartment, if needed.
- The incisions are closed in layers, and care is taken to avoid catching the nerve. An arm sling is given to keep elbow in flexed position.

59.4 Postoperative Management and Rehabilitation

An arm sling is given for 10–14 days for rest. Gentle active elbow mobilization out of sling is allowed. Straightening of the elbow is not permitted till 10 days postoperatively, enabling the soft tissues to heal and the nerve to stabilize in its new course. Light duty can be resumed after 10 days. Moderate to heavy duty or sporting activities should be delayed for 6–12 weeks.

59.5 Tips and Tricks

- The surgeon should be familiar with techniques of endoscopic ulnar nerve decompression prior to performing anterior transposition of the ulnar nerve endoscopically. Practice using cadaveric specimen is encouraged.
- A larger incision, i.e. >2 cm is recommended for the initial few cases.
- It is recommended to do this surgery in relatively thin patients (ulnar nerve can be easily palpated) for the initial few cases. In patients who are overweight, a larger incision may be needed.
- The ulnar nerve should be visualized at all times during dissection and decompression. In case which the ulnar nerve cannot be well-visualized under endoscopic guidance, surgeon should have low threshold to convert to open technique.
- When instruments, including endoscope and dissecting forceps, are introduced into the incision, they should be advanced with no significant resistance. If resistance is encountered, instruments should be withdrawn and the tunnel should be checked. If in doubt, surgeon should extend the incision or convert to open for better visualization.

- MIMS should be excised in a generous manner, as this is a common potential site of compression after anterior transposition.
- During the mobilization of the ulnar nerve, the accompanying vessels should be protected as much as possible in order to prevent devascularization of the nerve.
- Excessive traction must be avoided during mobilization of the ulnar nerve, as damage to the ulnar may occur.
- After the transposition, the "new" course of ulnar nerve should be checked thoroughly for new site of compression / kinking.
- Stability of the nerve should be checked prior to wound closure, by taking elbow in its entire arc of movement.
- Deflation of tourniquet is recommended prior to wound closure. Haemostasis should be achieved under endoscopic guidance to prevent haematoma formation. If in doubt, a drain may be inserted. Infiltration of a local anaesthetic with epinephrine may also be helpful.

59.6 Complications

- Haematoma is a known complication for endoscopic cubital tunnel release. With an additional procedure of anterior transposition, the risk of bleeding may further increase. During soft tissue dissection, surgeons should avoid the use of excessive force and the creation of multiple planes in the subcutaneous tissue, in order to minimize excessive bleeding. The deep fasciae should be identified and dissection should be carried out just above it, creating a thick skin flap. Attentive haemostasis is needed prior to wound closure.
- Medial antebrachial cutaneous nerve may be damaged during incision or dissection, causing paraesthesia around the incision site and medial aspect of the forearm.
- Ulnar nerve compression may occur along the new course of ulnar nerve.
- Ulnar nerve injury is possible from dissection or traction and a clear view of the ulnar nerve is necessary at all times.
- Recurrent subluxation of the ulnar nerve may be noted if the nerve is not stable in its new course.
- Wound dehiscence may be encountered. Wound closure in layers is necessary, and full elbow movement is only allowed from Day 11.

59.7 Results

Limited studies with only a small case series are available in the current literature, on endoscopic cubital tunnel release and anterior transposition. Jiang et al. described the use of carbon dioxide insufflation in order to dissect the anterior subcutaneous plane with ease, while others have suggested the use of additional anterior portal to facilitate the mobilization of ulnar nerve during transposition [4, 7, 9, 10]. The short-term outcomes of up to 24 months for endoscopic cubital tunnel decompression and anterior transposition are promising, with at least 75% achieving either good or excellent outcome [7, 9, 10]. Though the complication rate is low, the main complication is haematoma (2%) and medial antebrachial cutaneous nerve injury (6%) [10]. Endoscopic cubital tunnel decompression and anterior transposition appears to be a promising technique for cases which the native bed of the ulnar nerve is hostile or the ulnar nerve is unstable. Yet further long-term studies comparing outcomes with different conventional techniques of anterior transposition are needed.

References

1. Dützmann S, Martin KD, Sobottka S, Marquardt G, Schackert G, Seifert V, et al. Open vs retractor-endoscopic in situ decompression of the ulnar nerve in cubital tunnel syndrome: a retrospective cohort study. Neurosurgery. 2013;72(4):605–16.
2. Toirac A, Giugale JM, Fowler JR. Open versus endoscopic cubital tunnel in situ decompression: a systematic review of outcomes and complications. Hand (N Y). 2017;12(3):229–35.
3. Bartels RHMA, Verhagen WIM, van der Wilt GJ, Meulstee J, van Rossum LGM, Grotenhuis JA. Prospective randomized controlled study comparing simple decompression versus anterior subcu-

taneous transposition for idiopathic neuropathy of the ulnar nerve at the elbow: part 1. Neurosurgery. 2005;56(3):522–30.
4. Bain G, Fok MWM. Endoscopic ulnar nerve decompression and transposition. In: Surgical techniques for trauma and sports related injuries of the elbow. Berlin, Heidelberg: Springer., Berlin, Heidelberg; 2020. p. 739–44.
5. Matzon JL, Lutsky KF, Hoffler CE, Kim N, Maltenfort M, Beredjiklian PK. Risk factors for ulnar nerve instability resulting in transposition in patients with cubital tunnel syndrome. J Hand Surg Am. 2016;41(2):180–3.
6. Aleem AW, Krogue JD, Calfee RP. Outcomes of revision surgery for cubital tunnel syndrome. J Hand Surg Am. 2014;39(11):2141–9.
7. Wong JKF, Hsu CC, Lin CH, Lien SH, Lin YT. Endoscopy-assisted subfascial anterior transposition of the ulnar nerve for the treatment of cubital tunnel syndrome. J Plast Reconstr Aesthet Surg. 2016;69(12):1704–10.
8. Hoffmann R, Lubahn J. Endoscopic cubital tunnel release using the Hoffmann technique. J Hand Surg Am. 2013;38(6):1234–9.
9. Jiang S, Xu W, Shen Y, Xu J-G, Gu Y-D. Endoscopy-assisted cubital tunnel release under carbon dioxide insufflation and anterior transposition. Ann Plast Surg. 2012;68(1):62–6.
10. Martin KD, Dützmann S, Sobottka SB, Rambow S, Mellerowicz HA, Pinzer T, et al. Retractor-endoscopic nerve decompression in carpal and cubital tunnel syndromes: outcomes in a small series. World Neurosurg. 2014;82(1–2):e361–70.

60 Endoscopic Ulnar Nerve Release and Transposition: Single Portal Technique

Paul Max Jarrett and Allan Wang

60.1 Background

Ulnar neuropathy at the elbow, known as cubital tunnel syndrome, is a common compressive neuropathy in the upper limb. When non-operative management has failed to sufficiently improve the condition, surgery can be undertaken to decompress the nerve, with or without anterior transposition, and this can be performed via an open or endoscopic approach. The risk of postoperative instability is minimal when the ulnar nerve is decompressed in situ rather than neurolysed. The ulnar nerve should be assessed intraoperatively with passive elbow motion after decompression; if found unstable, the nerve should be anteriorly transposed or stabilised during the procedure. The medial head of triceps should additionally be evaluated intraoperatively with elbow motion to ensure that it does not snap over the medial epicondyle; if snapping is present then the medial head should be debrided or transferred. For patients with an unstable ulnar nerve pre-operatively, transposition should be the planned procedure.

60.2 Surgical Anatomy

The ulnar branches of the medial cutaneous nerve of the forearm (MCFN) course in a distal direction obliquely and posteriorly and should be looked out for and protected during ulnar nerve surgery at the medial side of the elbow to reduce the risk of sensory loss post-surgery. The medial intermuscular septum is attached to the humerus distal to the teres major and passes along the supracondylar ridge to the medical epicondyle. At the mid-arm level, the ulnar nerve passes posterior through the intermuscular septum and descends anterior to the medial head of the triceps muscle. In the majority of patients, the arcade of Struthers (a thin band of fascia between the medial triceps and intermuscular septum approximately 8 cm proximal to the medial epicondyle) is present and the ulnar nerve passes underneath the arcade. At the elbow, the ulnar nerve passes posterior to the medial epicondyle and medial to the olecranon in the cubital tunnel. Here, the nerve courses along on the retrocondylar groove of the humerus and cov-

P. M. Jarrett (✉)
Department of Hand Surgery, Fremantle Hospital, Fremantle, WA, Australia

Murdoch Orthopaedic Clinic, Murdoch, WA, Australia

University of Western Australia, Crawley, WA, Australia
e-mail: admin@pauljarrett.info

A. Wang
Murdoch Orthopaedic Clinic, Murdoch, WA, Australia

University of Western Australia, Crawley, WA, Australia

© ISAKOS 2022
D. N. Bhatia et al. (eds.), *Arthroscopy and Endoscopy of the Elbow, Wrist and Hand*,
https://doi.org/10.1007/978-3-030-79423-1_60

ered by Osborne's ligament, which is a fusion of the deep fascia between the heads of flexor carpi ulnaris (FCU) and the antebrachial fascia. After passing through the cubital tunnel, the ulnar nerve travels between the ulnar and humeral heads of FCU down the forearm. Anconeus epitrochlearis is a muscle present in a small percentage of the population originating at the posterior medial epicondyle and inserting on the olecranon and forms an arch over the cubital tunnel. The ulnar nerve can be compressed at one or more of several sites along the above route including the intermuscular septum, arcade of Struthers, anconeus epitrochlearis, cubital tunnel, and fascial bands within FCU.

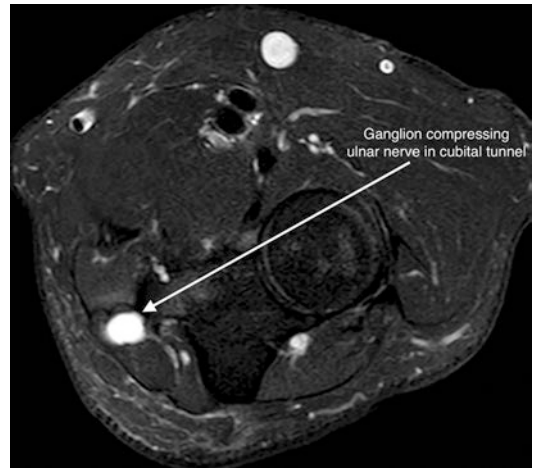

Fig. 60.1 Ganglion compressing ulnar nerve on T2 MRI axial image

60.3 Indications and Contraindications

Operative intervention for ulnar neuropathy at the elbow is justified for patients with sufficient symptoms in whom further non-operative management is unlikely to provide sufficient benefit.

- Patients with ulnar neuropathy report sensory disturbance in the ulnar sensory area, and in more advanced neuropathy, clumsiness and weakness of the hand. A positive Tinel's sign is present. Prolonged flexion of the elbow for approximately 60 seconds often reproduces the neurological symptoms. The scratch collapse test can be helpful in the examination for ulnar neuropathy patients [1].
- A smaller group of patients suffer from instability of the ulnar nerve due to the nerve subluxing over the medial epicondyle with elbow flexion and reducing posteriorly with elbow extension. These patients experience sudden shooting ulnar nerve symptoms and pain at the elbow with the snapping of the ulnar nerve. Ulnar nerve instability can however be asymptomatic.

There are some patient groups listed below who are unlikely to improve sufficiently with non-operative treatment and in whom proceeding directly to operative intervention is more likely to be warranted:

- Patients with extrinsic compressive lesions (ganglions, osteophytes, anconeus epitrochlearis) (Fig. 60.1).
- Patients with severe neuropathy and wasting of the hand intrinsic muscles.
- Patients with very severe symptoms.
- Elderly patients with significant neuropathy or symptoms, especially in the over 80-year-age group, as the ulnar nerve can be damaged more rapidly by compression in this patient group.

Anterior transposition of the decompressed ulnar nerve may be performed in:

- Nerve instability prior to surgery.
- Following an in situ decompression if there is more than mild nerve instability (2 mm of anterior motion with elbow flexion) [2].
- The most common alternative to transposition for instability is to stabilise the nerve in situ with a flap of flexor-pronator or triceps fascia. Nerve stabilisation in situ is suitable for patients with mild to moderate increase in nerve motion with flexion, and without frank subluxation over the medial epicondyle [2, 3].

Endoscopic surgery may be contraindicated, and an open approach favoured when local nerve lesions or systemic conditions exist, and which

may lead to an increased risk for complications. Individual surgeon experience would determine the most suitable surgical approach.

- In some revision cubital tunnel surgeries, extensive adhesions may circumferentially engulf the ulnar nerve. Lysis of nerve adhesions and epineurolysis may best be performed via an open approach, using loupe magnification and microsurgical techniques.
- Neuromas of the ulnar nerve may result from previous injury and neurolysis, or excision and nerve grafting, may best be undertaken by an open microsurgical approach. Primary nerve pathology is uncommon. Schwannomas in the vicinity of the cubital tunnel present with focal nerve swelling and severe symptoms and responds well to microsurgical dissection and excision which may to undertaken open. Neurofibromatosis affecting the ulnar nerve presents with segmental nerve enlargement and may be best evaluated by an open wide decompression.
- Elbow joint osteophytes, synovial cysts, and rheumatoid pannus, as well as impinging metalware from previous fracture fixation are lesions which must be treated as well during endoscopic surgery to prevent persistence of symptoms.
- Systemic conditions such haemophilia may cause a compression neuropathy of the ulnar nerve. Perineural haematoma, intra-muscular haemaorrhage, or nerve compression from elbow joint haemarthrosis can be evaluated and drained via open surgery while maintaining nerve visibility and protection.
- Patients on perioperative anticoagulation are at risk for postoperative haematoma. A meta-analysis of endoscopic versus open cubital tunnel surgery reported the endoscopic approach having an increased risk for postoperative haematoma which may require reoperation [4].
- Hereditary Neuropathy with Pressure Palsy (HNPP) is an inherited condition affecting development of myelin and leads to nerve hypersensitivity to the slightest pressure or stretch during surgery, in which an open approach may be considered.

60.4 Surgical Technique

The procedure is carried out with a general or regional anaesthetic and exsanguination of the upper limb prior to inflating an upper arm tourniquet. The patient is supine with the upper limb placed on an arm table at about 80° of shoulder abduction. Placing a padded object under the tip of the elbow elevating it by approximately 5 cm is helpful. The endoscopic stack is located near to the patient's head area with the surgeon sitting at the axilla, and the surgical assistant between the arm and the head. The endoscopy is undertaken dry with no fluid or carbon dioxide used. The in situ decompression technique described here is as described by Hoffman and Siemionow [5]. The ulnar nerve transposition described later is an addition to this technique by the first author comprising an endoscopically assisted mini-open procedure.

The instruments used in the procedure include a surgical blade, scissors for dissection and decompression of the nerve, endoscope, long bipolar diathermy bayonet forceps, and forceps and needle holder. It is useful to have a selection of scissors including shorter scissors such as curved tenotomy scissors for the initial dissection and longer blunt-tipped curved scissors for endoscopic work, and finally some blunt tipped curved 17–23 cm scissors for endoscopic dissection furthest from the incision. The authors use a 4 mm 18 cm length Hopkins II Forward-Oblique 30 degrees telescope with large fenestrated distal spatula optical dissector (Karl Storz, Tuttlingen, Germany). A speculum is useful at times during this procedure (Fig. 60.2).

60.5 In Situ Decompression

60.5.1 Preliminary Dissection

- A small (20 mm) gently curved longitudinal incision is made at the ulnar retrocondylar groove over the ulnar nerve closer to the medial epicondyle than the tip of the olecranon. If transposition is the intended procedure from the outset, the incision is 4 cm in length

Fig. 60.2 Endoscopic equipment for cubital tunnel surgery

centred over the cubital tunnel. During the procedure, if a longer incision is felt to be required or will be safer, then the incision can be easily lengthened.

- The subcutaneous tissues are bluntly dissected with tenotomy scissors to preserve any branches of the medial cutaneous nerve of the forearm. At times, no branches of the cutaneous nerves will be present in the incision area due to its short length, but commonly at least one branch will be present and should be protected. During dissection at the elbow, a small portion of patients will have an anconeus epitrochlearis muscle which will require incising. This is carried out by directly incising the muscle fibres in line with the ulnar nerve with the small open incision.
- At this stage, palpation with a fingertip is useful in identifying the position of the ulnar nerve which is then exposed by placing a small incision in the retinaculum (Osborne's ligament) overlying it (Fig. 60.3).
- A soft tissue space is produced in the line of the ulnar nerve just superficial to the deep fascia for approximately 10 cm distally and 8 cm proximally using a blunt tunnelling forceps or bluntly with scissors. This soft tissue space requires to be sufficiently large to accommodate the endoscopic instruments.
- For most patients, at this stage the hooded endoscope will keep the soft tissue space suf-

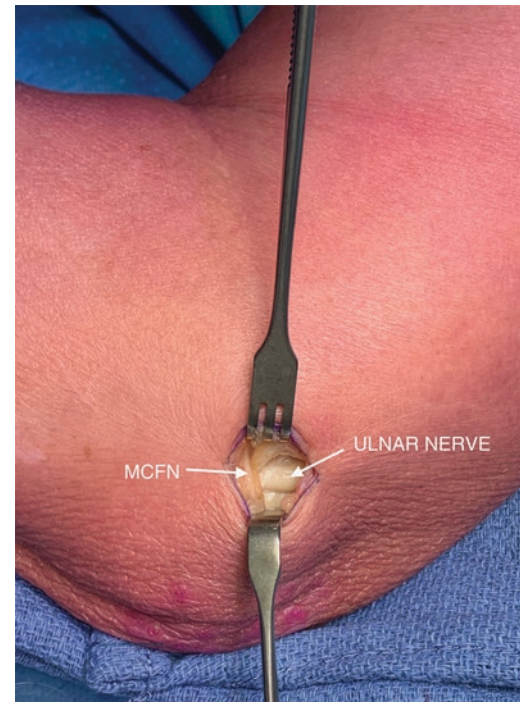

Fig. 60.3 Ulnar nerve and MCNF visible in the incision

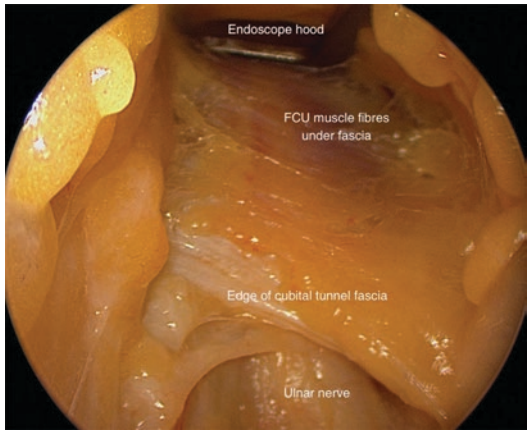

Fig. 60.4 Initial distal endoscopic view

ficiently open. However, for patients who have a thick layer of adipose tissue which is crowding the visualisation of the endoscopic operative space, a speculum can be placed in the incision, in addition to the endoscope. When dissection is carried out proximally to the elbow, a speculum is commonly beneficial. Given the endoscope has a light source, using an additional light source on speculum is unnecessary. Prior to placing the endoscope into the incision, an endoscopic lens antifog agent may be used to wipe the optical tip of the endoscope to safely prevent fog formation and improve visualisation.

- The hooded endoscope is placed into the incision so the surgeon can visualise both the ulnar nerve beneath the small incision in the roof of the cubital tunnel, and the unincised distal edge of the retinaculum (Fig. 60.4).

60.5.2 Distal Endoscopic Decompression

- Firstly, dissection distal to the elbow is carried out and a pair of scissors is used to incise the remaining cubital tunnel retinaculum and fascia overlying FCU for several centimetres, until there will be sufficient space to work within FCU (Fig. 60.5). The authors do not decompress the forearm fascia more distally than is necessary, which is a variation to the original technique.

Fig. 60.5 Endoscope in situ distally and patient position

- Once the muscle fibres of FCU become clear deep to the fascia, the blunt end of the hooded optical dissector of the endoscope is used to bluntly separate the muscle fibres over the ulnar nerve through its initial course through FCU. At this point, the fibrous raphe between the two heads of the FCU is released, and then progressing distally any fascial bands that appear to compress the nerve are incised (Fig. 60.6). During the dissection, any motor branches of the ulnar nerve are seen and protected.
- The most common cause of compression of the ulnar nerve in cubital tunnel syndrome is typically at the cubital tunnel under Osborne's ligament. It has been suggested that it is not necessary to decompress the ulnar nerve beyond the cubital tunnel into FCU [12]. However, in a number of cases, fascial bands within FCU appear to deform the nerve and thus may have the potential to cause neuropathy. Therefore, the authors recommend decompression of the ulnar nerve for between

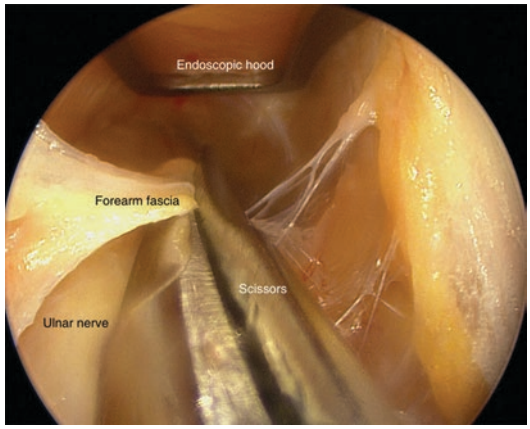

Fig. 60.6 Decompression within forearm

10 and 15 cm (the maximum working length of the endoscope) distally from the elbow.

60.5.3 Proximal Endoscopic Decompression

- Under loupe magnification, the remainder of the decompression of the ulnar nerve in the portion of the cubital tunnel that is visible through the incision is decompressed. The hooded endoscope, and if required a speculum, is then inserted into the incision directed proximally, with the ulnar nerve and the remaining edge of cubital tunnel roof to be incised in view.
- The cubital tunnel fascia and arcade of Struthers are decompressed up to the intramuscular septum (Fig. 60.7).
- The nerve is inspected up to the intra-muscular septum; it is rarely compressed here and therefore the septum can usually be left undisturbed. If necessary, the septum can be decompressed.

60.5.4 Final Assessment

At the completion of the decompression, the surgeon should be confident that the nerve has been decompression from distally into FCU, through the cubital tunnel and proximally up to the intramuscular septum. The nerve and the medial head

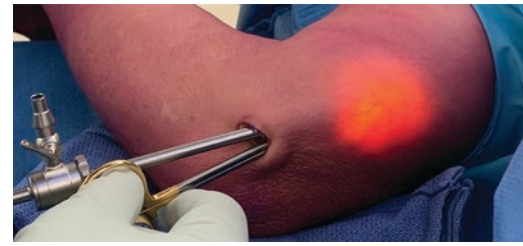

Fig. 60.7 Proximal decompression using scissors

of triceps are then inspected with elbow flexion and extension; if unstable then either transposition or in situ flap stabilisation should be carried out. If the medial head of triceps subluxes over the medial epicondyle with flexion, the tendon may be partially excised until the snapping no longer occurs.

60.6 Anterior Transposition

- The incision is lengthened to approximately 4 cm. Any further cutaneous nerve branches identified by the blunt dissection with tenotomy scissors are protected.
- Under direct vision, the flexor-pronator fascia is then cleared of attached subcutaneous tissues protecting the cutaneous nerves during the dissection. Sufficient fascia is exposed to allow the creation of a flap of fascia with the apex at the medial epicondyle of sufficient length and breadth.
- The fascia flap should be 3–4 cm long by 2–3 cm wide. The flap is raised sharply with a knife from the underlying muscle.
- The tissue bed in which the anteriorly transposed ulnar nerve sits is then assessed to ensure there will be no tissue which will compress the nerve. Several tendinous regions within the muscle bed may require incision or excision; distally, the posterior tendinous edge of the flexor-pronator mass and proximally the distal edge of the median intra-muscular septum must be assessed and excised.
- Using the open incision, and more proximally and distally with the aid of the endoscope, a neurolysis of the ulnar nerve is undertaken prior to transposition.

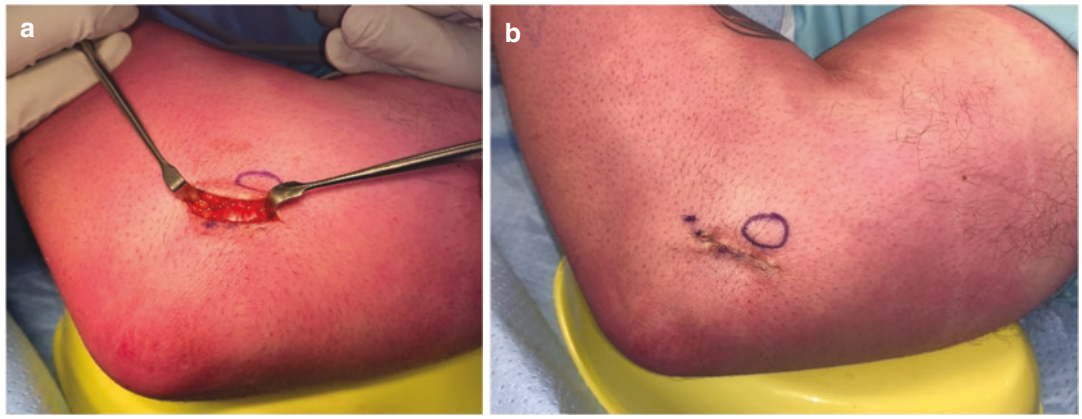

Fig. 60.8 (**a**, **b**) Anterior transposition and incision post-closure

- The nerve is then transposed anteriorly to the medial epicondyle with its accompanying longitudinal vascular supply, preserving the motor branches to the FCU and the flexor digitorum profundus. Occasionally, one of the branches to FCU requires sacrificing to allow the nerve to have a smooth course in its transposition.
- The ulnar nerve is then supported in position by the fascial flap which is brought superficial to the ulnar nerve and sutured to the deep dermis with 2/0 vicryl approximately 25 mm anteriorly to the incision.
- The elbow is passively moved through a full range of flexion and extension and the nerve is carefully assessed for stability and for any evidence of compression or tight bends throughout the range of motion. If there are any concerns, the sutures holding the flap can be removed and the flap reset with or without any further soft tissue releases as required. The medial triceps is assessed with elbow motion and partially incised if required.
- Once the surgeon is satisfied with the transposition, the wound is infiltrated with local anaesthetic and closed with 2/0 vicryl to the subcutaneous tissues and then 4/0 monocryl intra-dermal. Steristrips are applied, then a small adhesive dressing and orthopaedic padding bandage followed by a crepe bandage (Figs. 60.8 and 60.9).

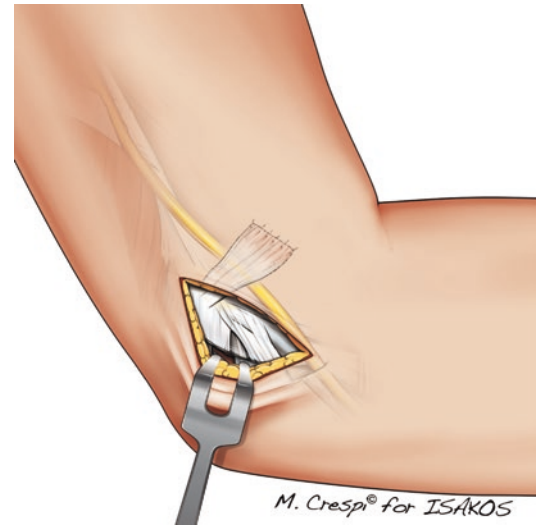

Fig. 60.9 Illustration of endoscopically assisted ulnar nerve anterior transposition (M. Crespi © for ISAKOS)

60.7 Technical Tips

- For sufficient space to visualise the nerve and associated tissues, it is helpful to place some superior angulated force on the endoscope for elevating the tip of the spatula of the optical dissector.
- When dissecting in the subcutaneous and deeper layers, small nerve branches or vessels can be encountered and care must be taken to avoid injury to these structures. If required, for

surgical exposure, small vessels can be coagulated using bipolar diathermy.

60.8 Pitfalls

Snapping of the triceps is an uncommon condition where the medial head of triceps subluxes over the medial epicondyle during elbow flexion. It can be associated with and co-exist with ulnar nerve instability or alternatively can be mistaken for ulnar nerve instability [6]. Postoperative snapping of the triceps following surgery for ulnar neuropathy at the elbow is possible [7].

60.9 Postoperative Management and Rehabilitation

Patients are permitted to use their elbow and upper limb for light activities immediately postoperatively. Mobilising their elbow following surgery reduces the risk of scar tissue formation tethering the nerve and allows a more rapid resumption of everyday activities for patients. The bandages are removed at 2 days postoperatively and the adhesive dressings at 10 days. Patients should avoid heavy activities and avoid prolonged flexion of the elbow for 6 weeks to reduce the risk of secondary ulnar nerve instability. A portion of patients have bruising of their upper limb for some days, and this resolves by the two-week postoperative visit.

60.10 Complications

- *Ulnar nerve instability:* The ulnar nerve can be rendered unstable by decompression. To avoid instability, decompression is undertaken purely as an in situ decompression. At surgery, if the nerve appears unstable it should be transposed or stabilised. Furthermore, if prolonged elbow flexion and heavier upper limb activities are avoided for the first 4–6 weeks, post-surgery instability is rare. The nerve rarely can become unstable following anterior transposition due to the stretching of fascial flap attachment. If postoperative instability occurs, revision anterior transposition either subcutaneously or submuscularly usually resolves the instability.
- S*napping medial triceps:* This can develop postoperatively and should be looked for both before and during revision surgery. A snapping triceps can be confused for ulnar nerve instability.
- M*edial cutaneous nerves of the forearm:* These can be injured either temporarily or permanently following surgery for the ulnar nerve at the elbow. The key to this complication is prevention by carefully dissecting out and protecting the nerves. This complication is less frequent with endoscopic surgery owing to the small nature of the incision [4].
- *Extensive bruising*: Careful haemostasis is beneficial in reducing the risk of haematomas. Despite not using postoperative suction drains, postoperative bruising in most patients is self-resolving. If a haematoma causes neurological compression, urgent drainage of the haematoma is necessary.
- *Recurrent ulnar neuropathy:* In a small number of patients, the symptoms may recur after a few years post-surgery. If sufficiently severe, endoscopic or open surgery revision surgery can be considered.

60.11 Results

Over a 9-year period, in the first author's private clinic, 124 cases in 106 patients underwent endoscopic ulnar nerve surgery at the elbow. For decompressions the results were excellent (49%) and good (31%) in 80% of patients. For the remaining patients, 14% reported reasonable and 6% poor results. The majority of patients with poor results had additional cervical spine root compression to account for their lack of improvement. For transpositions, the results were excellent or good in 60% of patients. While the results for transposition appear worse, in this group many patients were found to have multiple pathologies in their upper limb or cervical spine. Revision procedures for six patients included

anterior subcutaneous and submuscular transposition for postoperative instability or insufficient improvement following initial surgery, and snapping medial head of triceps.

Acknowledgements We are grateful for Professor James O Jarrett for his comments on the text and Miss Emma Petta for collection and analysis of patient outcome data.

References

1. Cheng CJ, Mackinnon-Patterson B, Beck JL, Mackinnon SE. Scratch collapse test for evaluation of carpal and cubital tunnel syndrome. J Hand Surg Am. 2008;33:1518–24.
2. Tang P. The blocking flap for ulnar nerve instability after in situ release: technique and a grading system of ulnar nerve instability to guide treatment. Tech Hand Surg. 2017;21:137–42.
3. Lane LB, Greenberg AS. Use of a fascial flap to stabilize an unstable ulnar nerve in its bed during in situ decompression. J Surg Orthop Adv. 2015;24(3):193–7.
4. Buchanan P, Chieng L, Hubbard Z, Law T, Chim H. Endoscopic versus open in situ cubital tunnel Release: a systematic review of the literature and meta-analysis of 655 patients. Plast Reconstr Surg. 2018;14:679–84.
5. Hoffmann R, Siemionow M. The endoscopic management of cubital tunnel syndrome. J Hand Surg Br. 2006;31:23–9.
6. Pfister G, Barbier O, Ollat D. "snapping triceps": a rare and misleading condition - a clinical case report. Hand Surg Rehabil. 2018;37:121–3.
7. Spinner RJ, Gabel GT. Iatrogenic snapping of the medial head of the triceps after ulnar nerve transposition. J South Orthop Assoc. 2001;10(4):236–40.

Endoscopic Robotic Decompression of the Ulnar Nerve

61

Jose Carlos Garcia Jr.
and Matheus Ribeiro Barcelos

61.1 Introduction

The use of robotic surgery has expanded in several surgical specialties and has advantages over the traditional surgical methods [1–3]. Within orthopedics, robotic surgery has been used in brachial plexus and neurologic releases [4–8]. The association of the robotic technology and endoscopy has further expanded indications and procedures can now be performed with shorter time of hospitalization and minimally invasive approach [9, 10]. Advantages of this method include: (a) movement accuracy, (b) high resolution imaging with three-dimensional vision, (c) gas infusion rather than saline solution permits better visualization and less bleeding, (d) filtering of the surgeon's tremor when manipulating objects, (e) movement scaling, and (f) hand-free camera manipulation [11, 12]. In addition, in future there is the possibility of remotely performing the surgery (telesurgery) and even supervised autonomous procedures based on artificial intelligence [3].

The disadvantages and limitations of this new technology are: (a) higher costs, (b) lack of haptic feedback, (c) instruments were not designed for orthopedic procedures, and (d) limitation of the use of this procedure in patients with poor subcutaneous tissue.

J. C. Garcia Jr. (✉) · M. R. Barcelos
NAEON Institute, São Paulo, Brazil
e-mail: josecarlos@especialistadoombro.com.br

61.2 Indications and Contraindications

The procedure is performed for symptomatic ulnar nerve compression at the cubital tunnel after adequate conservative treatment has failed to provide relief. Non-robotic endoscopic technique for ulnar nerve decompression is an alternative to robotic endoscopic surgery in cases where there are no previous elbow manipulation.

Absolute contraindications include space-occupying lesions (tumors, osteophytes), long-standing elbow contractures requiring release, prior trauma with very extensive scar formation or skin grafts, and prior open decompression with transposition of the ulnar nerve [7].

Subluxation of the ulnar nerve and inexperience with robotic technique are relative contraindications.

61.3 Surgical Technique

- Endoscopic robotic decompression of the ulnar nerve uses a new coupling and configuration for the robotic DaVinci® SI or Xi systems (Intuitive Surgical, Sunnyvale, CA) and is based on prior knowledge of endoscopic robotic techniques related to different surgical areas such as urology and gynecology.
- The procedure is performed under general anesthesia. The patient is placed supine and

© ISAKOS 2022

D. N. Bhatia et al. (eds.), *Arthroscopy and Endoscopy of the Elbow, Wrist and Hand*,
https://doi.org/10.1007/978-3-030-79423-1_61

the arm is raised 170° in the Trendelenburg position (Fig. 61.1). A tourniquet may be used and is placed high on the arm.

- Since there are no natural cavities in the ulnar nerve pathway, endoscopy in this region requires the creation of an initial cavity. Through a 1.2 cm portal (length of the da Vinci robot cannula) an initial subcutaneous cavity is created in the middle third of the arm with direct visualization of the nerve exit point in the Strüthers arcade. The dissection is performed using Metzenbaum scissors and is directed to the distal arm (Fig. 61.2).
- Two other portals are created at the junction of middle and distal thirds of the arm and are located 3–5 cm lateral and medial to the first portal (Fig. 61.3). These two portals must be 8 mm long to allow robotic hand cannulas to pass through. The cannulas are gently passed into the cavity under endoscopic view in order to prevent injuries. Once the robotic hands are visible through the optics in the cavity, this cavity can be expanded distally towards the medial elbow.

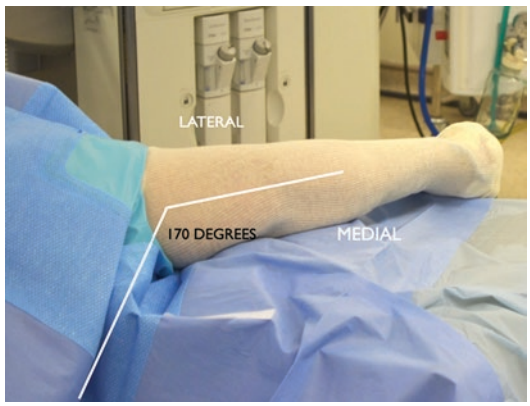

Fig. 61.1 Position of the upper limb is demonstrated. The arm is placed at 170 degrees on the operating table

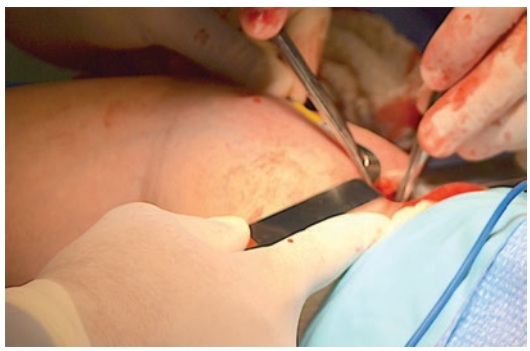

Fig. 61.2 Initial subcutaneous cavity is created in the mid-arm for direct access to ulnar nerve

Fig. 61.3 Position of the optic portal and two other portals are demonstrated and the robot docking is shown

- A needle can be used to identify the optimal location of the two robotic hand portals mentioned above. It is important to have a safe distance between the portals to avoid robotic arm conflict. The third robotic arm is not used in this procedure.
- Air insufflation at a pressure of 8–14 mm Hg is used to prevent bleeding. 0.9% saline may be introduced and aspirated to clear the surgical field when necessary.
- Two different robotic hands can be used as follows: Maryland bipolar forceps 8 mm (Intuitive Surgical, Sunnyvale, CA, USA) and a Curved Scissor 8 mm (Intuitive Surgical, Sunnyvale, CA, USA). A Hot Shears™ Monopolar Curved Scissor 8 mm (Intuitive Surgical, Sunnyvale, CA, USA) can also be used (only as scissors and never as electrocautery device).
- After fitting the cannulas and robotic hands, the surgeon uses the console to operate the robot remotely.
- Robotic arms have seven degrees of freedom and can reproduce hand and wrist movements, and this is an advantage when compared with other endoscopic methods. In addition, the surgeon can scale the movements improving precision to the robotic arms.
- The nerve is followed and dissected in the subcutaneous space until the cubital tunnel is

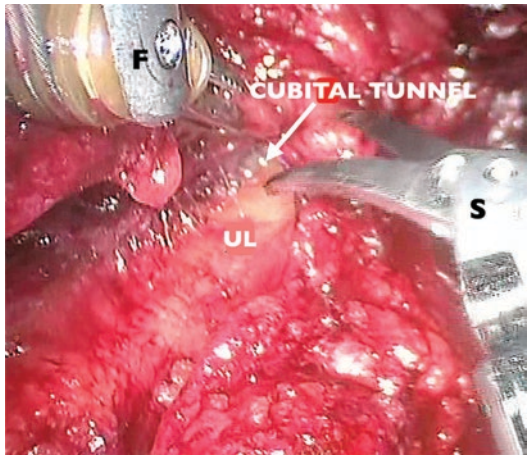

Fig. 61.4 A: Endoscopic view of ulnar nerve (UL) decompression at cubital tunnel (F: robotic forceps, S: robotic scissors)

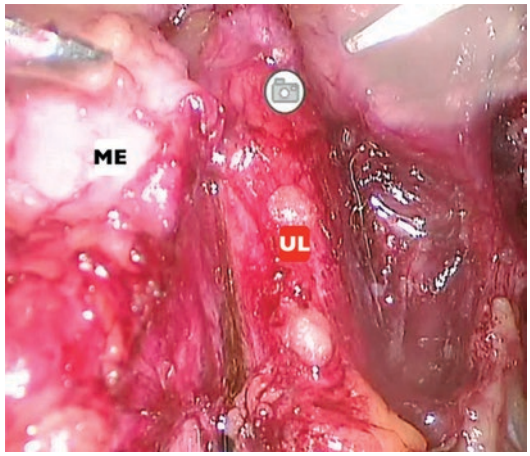

Fig. 61.5 Complete release of ulnar nerve (UL) is shown. (ME: Medial Epicondyle)

reached. The cubital tunnel is split and the nerve is released (Fig. 61.4) further distally down to the arcade of Osborne (fibro-aponeurotic tissue connecting the humeral and ulnar heads of the flexor carpi ulnaris) (Fig. 61.5).

61.4 Postoperative Management and Rehabilitation

An immobilizer is provided for comfort for the first week, and thereafter mobilization and physiotherapy are initiated. Portal stitches are removed in 2–3 weeks depending on the healing process.

References

1. Gallotta V, Cicero C, Conte C, Vizzielli G, Petrillo M, Fagotti A, et al. Robotic versus laparoscopic staging for early ovarian cancer: a case matched control study. J Minim Invasive Gynecol. 2017;24(2):293–8.
2. Kavoussi LR, Moore RG, Partin AW, Bender JS, Zenilman ME, Satava RM. Telerobotic assisted laparoscopic surgery: initial laboratory and clinical experience. Urology. 1994;44(1):15–9.
3. Shademan A, Decker RS, Opfermann JD, Leonard SK, Axel K, Peter CW. Supervised autonomous robotic soft tissue surgery. Sci Transl Med. 2016;8(337):337ra64.
4. Garcia JC. Nerve entrapment. In: Liverneaux PA, Berner SH, Bednar MS, Parekattil SJ, Mantovani Ruggiero G, Selber JC, editors. Telemicrosurgery. Paris: Springer; 2013. p. 109–17.
5. Garcia JC, Lebailly F, Mantovani G, Mendonça LA, Garcia JM, Liverneaux PA. Telerobotic manipulation of the brachial plexus. J Reconstr Microsurg. 2012;28(7):491–4.
6. Garcia JC, Mantovani G, Gouzou S, Liverneaux P. Telerobotic anterior translocation of the ulnar nerve. J Robot Surg. 2011;5(2):153–6.
7. Garcia JC, Montero EFS. Endoscopic robotic decompression of the ulnar nerve at the elbow. Arthrosc Tech. 2014;3:383–7.
8. Melo PMP, Garcia JC, Montero EFS, Atik T, Robert EG, Facca S, et al. Feasibility of an endoscopic approach to the axillary nerve and the nerve to the long head of the triceps brachii with the help of the Da Vinci Robot. Chir Main. 2013;32:206–9.
9. Morgan JA, Thornton BA, Peacock JC, Hollingsworth KW, Smith CR, Oz MC, Argenziano M. Does robotic technology make minimally invasive cardiac surgery too expensive? A hospital cost analysis of robotic and conventional techniques. J Card Surg. 2005;20(3):246–51.
10. Oldani A, Bellora P, Monni M, Amato B, Gentilli S. Colorectal surgery in elderly patients: our experience with DaVinci xi® system. Aging Clin Exp Res. 2017;29(1):91–9.
11. Ballantyne GH, Moll F. The da Vinci telerobotic surgical system: the virtual operative field and telepresence surgery. Surg Clin North Am. 2003;83:1293–304.
12. Byrn JC, Schluender S, Divino CM, Conrad J, Gurland B, Shlasko E, et al. Three-dimensional imaging improves surgical performance for both novice and experienced operators using the da Vinci Robot System. Am J Surg. 2007;193:519–22.

Part XII

Elbow Endoscopy: Evolving Techniques

Endoscopic Olecranon Bursectomy and Spur Resection

62

Vikas Singh and Gregory I. Bain

62.1 Background

Olecranon bursitis is an inflammatory process involving the olecranon bursa and is usually secondary to infection, trauma or crystal deposition (Fig. 62.1). Patient with comorbidities like diabetes mellitus, uremia, intravenous drug abuse, alcohol abuse, or long-term use of steroids are at increased risk [1]. Two-thirds of cases are sterile bursitis, with one-third of cases being septic secondary to *staphylococcus aureus*, necessitating bacterial cultures, drainage, irrigation, and antibiotics [2]. Surgery is indicated when conservative management proves unsuccessful. Wet or dry endoscopic techniques can be performed using incisions away from the point of the olecranon [3].

Olecranon spur is a bony outgrowth that forms within the superficial portion of the central triceps tendon insertion and extends posteriorly. These spurs can occupy approximately half of the triceps insertion footprint on olecranon and are often incidental and age-related (Fig. 62.2). Symptomatic spurs may also be associated with overuse (sports activities with repeated forced extension) and with inflammatory conditions involving the tendon and olecranon bursa [4, 5].

62.2 Surgical Anatomy

The olecranon bursa is a normal structure over the olecranon prominence and encloses a potential space that is useful for endoscopic visualization. The olecranon spur is superficial to the triceps tendon and is different from an olecranon tip osteophyte, which is located on the posterolateral or posteromedial articular border on the tip of olecranon [4, 5]. Bursal insufflation helps to visualize the inflamed bursal contents and the spur can be resected endoscopically after fluoroscopy localization [6].

62.3 Indications and Contraindications

- Persistent and painful olecranon bursitis that is resistant to conservative treatment.
- Symptomatic olecranon spurs.
- An acute infection requires adequate incision and drainage. This can be performed endoscopically, avoiding the point over the olecranon. However, familiarity with the endoscopic technique is a prerequisite.

V. Singh
Department of Orthopaedic and Trauma Surgery, Flinders Medical Centre, Adelaide, SA, Australia

G. I. Bain (✉)
Department of Orthopaedic and Trauma Surgery, Flinders Medical Centre and Flinders University, Adelaide, SA, Australia
e-mail: admin@gregbain.com.au; greg@gregbain.com.au

© ISAKOS 2022

D. N. Bhatia et al. (eds.), *Arthroscopy and Endoscopy of the Elbow, Wrist and Hand*,
https://doi.org/10.1007/978-3-030-79423-1_62

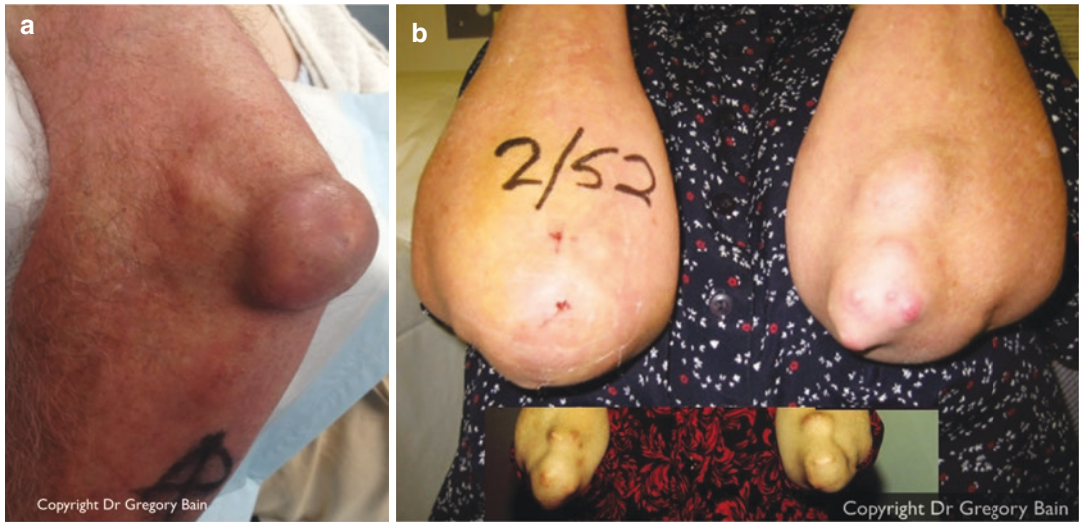

Fig. 62.1 Clinical case of post-traumatic (**a**) and rheumatoid (**b**) olecranon bursa. (© Dr. Gregory I. Bain)

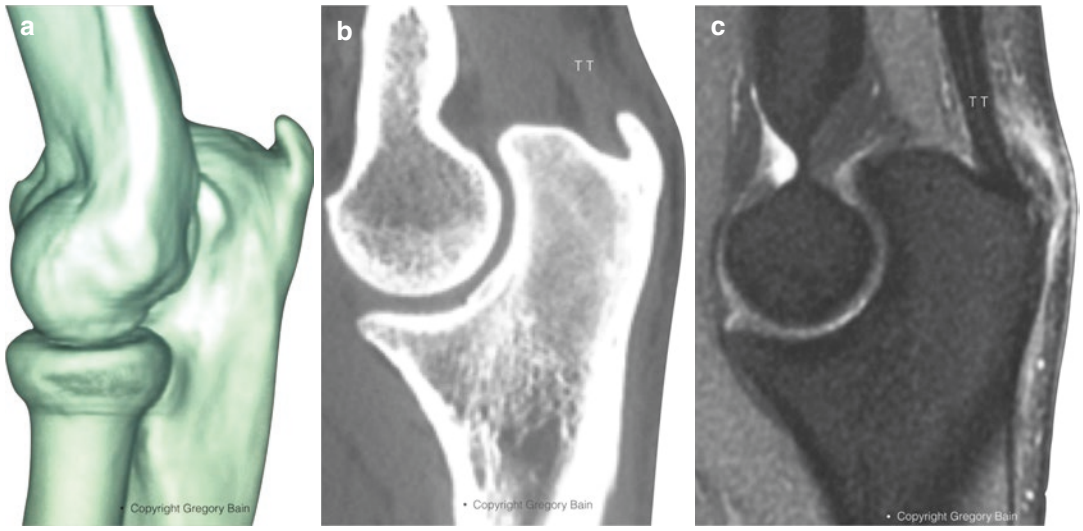

Fig. 62.2 The 3D CT image (**a**) demonstrates the shape and position of the spur. The sagittal CT image (**b**) demonstrate the tendon is deep to the spur, and the MRI (**c**) demonstrates that the olecranon spur is edematous and that the triceps tendon (TT) is inflamed. (© Dr. Gregory I. Bain)

An open draining bursa is a contraindication to endoscopic excision.

62.4 Surgical Technique

Wet vs *dry endoscopy:* Wet endoscopy allows for distension to be maintained via saline inflow and an arthroscopic cannula that helps maintain fluid pressure (Fig. 62.2). The scope can then be placed into the bursa, resecting the bursa from inside out until normal tissue planes are visualized. Care should be exercised not to perforate the overlying skin, which may lead to formation of a chronic, irritating deep sinus. The Senior author's preferred technique is the dry endoscopic procedure [1], utilizing the specialized endoscopic equipment (Fig. 62.3).

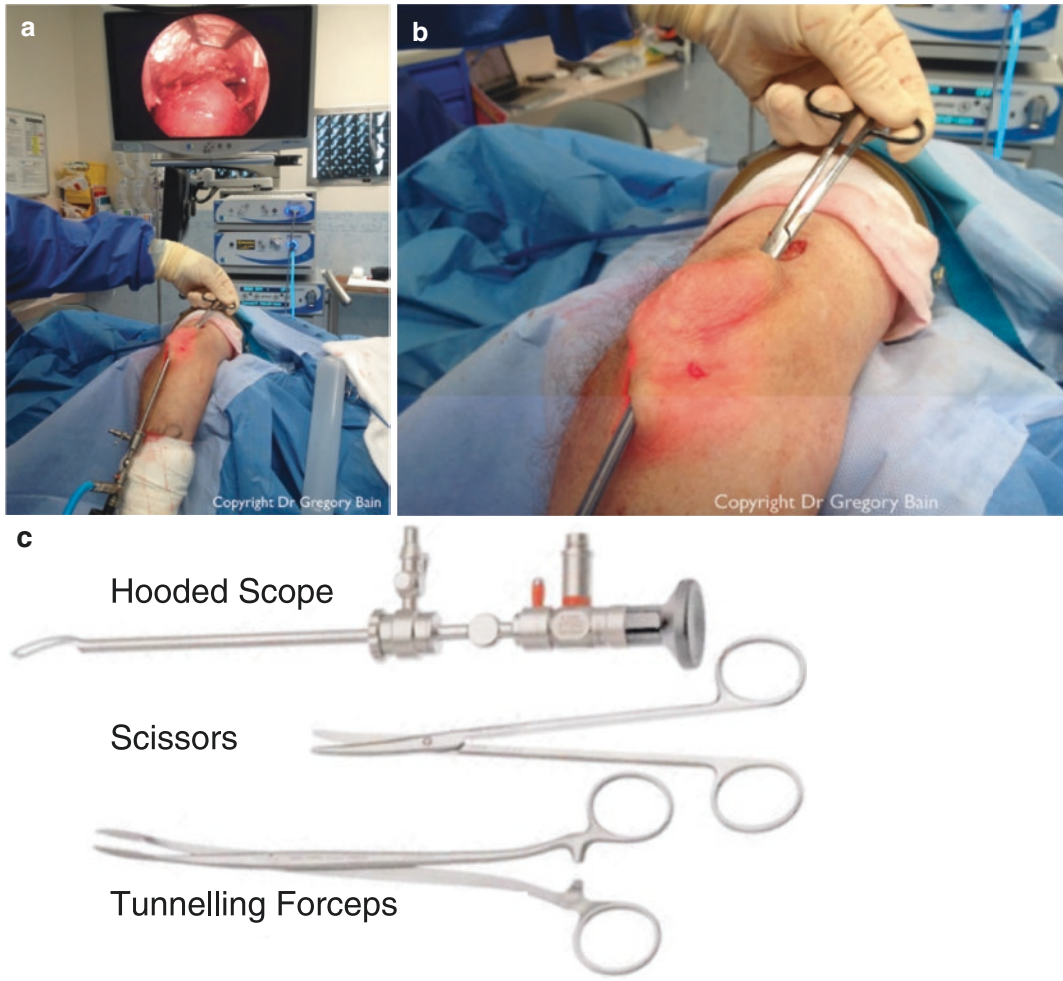

Fig. 62.3 (**a**, **b**): Setup of the dry olecranon bursoscopy. (**c**) Instruments for the procedure. (© Dr. Gregory I. Bain)

Patient position: Olecranon bursal endoscopy is performed in the lateral decubitus position with affected arm on a padded bolster, and a high arm tourniquet is used.

- Mark the critical landmarks after draping—ulnar nerve, bursal sac, medial epicondyle.
- Make a 2 cm incision distal to bursa and develop a plane between the subcutaneous fat and the deep fascial layer with Metzenbaum scissors or modified tunneling forceps.
- Open the scissor blades/forceps to elevate fat off the deep fascia to create a working space. Introduce the hooded endoscope into the working space with the hood suspending the subcutaneous tissues and thus maintaining the working space.
- Create a proximal portal 1–2 cm proximal to bursa and connect the subcutaneous space under direct vision.
- Use tunneling forceps through proximal port to aid in retraction while developing the plane and define the bursal margins.
- With scissors, pituitary rongeur and motorized resectors completely resect the bursa after defining it adequately, but stay clear of the ulnar nerve (Fig. 62.4).
- The spur can be resected endoscopically after fluoroscopy localization, and then resected with a high-speed burr [6]. The principles are

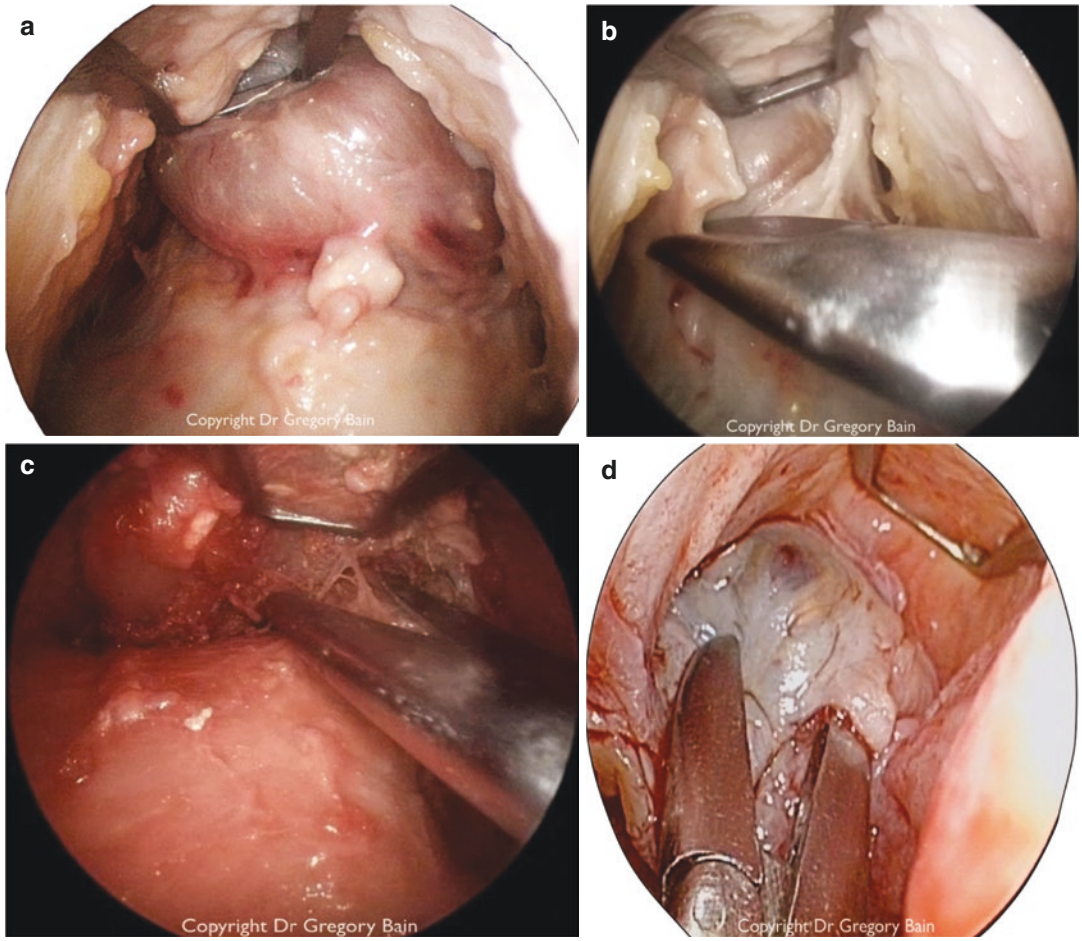

Fig. 62.4 Endoscopic extra-bursal olecranon bursa resection. The resection is performed by creating a working space around the bursa. (**a**) The hood maintains the working space. (**b**, **c**) Scissors are used to release and mobilize the bursa. (**d**) Pituitary rongeur can be used for piecemeal excision. (© Dr. Gregory I. Bain)

similar to those described for olecranon bursa. Fluoroscopy is used to ensure complete resection (Fig. 62.5).

- Deflate the tourniquet, cauterize any bleeding under endoscopic view, and irrigate the cavity with normal saline.
- Suture the portal with monofilament sutures, apply dressings, place the arm in broad arm sling with elbow at 90° flexion, which will close down the potential dead space.

62.5 Postoperative Management and Rehabilitation

- Place the arm in broad arm sling with elbow at 90° flexion to minimize the potential dead space for 1 week to allow deep tissues to heal.
- Watch out for development of a seroma and aspirate it.
- Allow active gentle range of motion exercises.

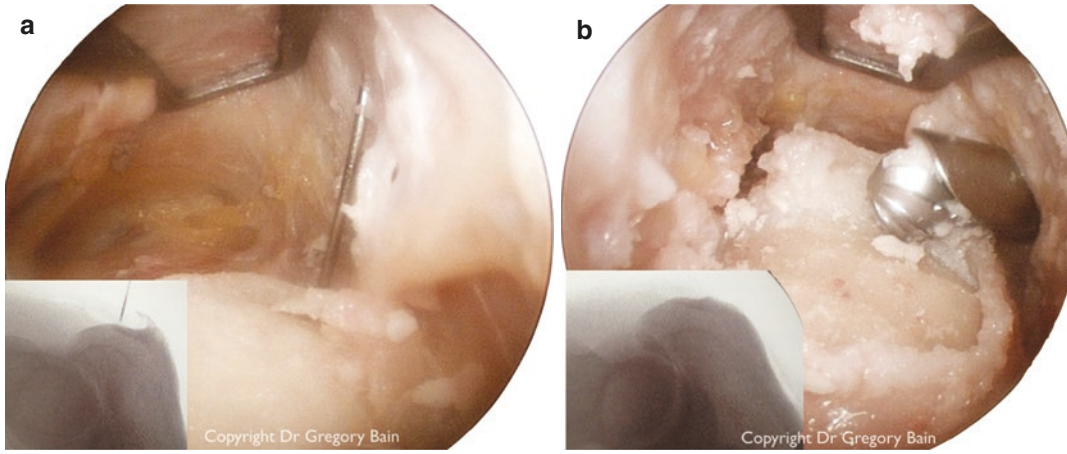

Fig. 62.5 Olecranon spur. (**a**) Spur identified on CT scan. (**b**) Intra-operatively fluoroscopy is used to identify the position of the spur and postoperatively to ensure complete resection. (© Dr. Gregory I. Bain)

- Review after a week for wound check.
- Advise the patient to avoid heavy lifting activities and pressure over olecranon for 4 weeks.

62.6 Complications

- Skin perforation can lead to a persistent sinus formation.
- The ulnar nerve is at risk structure, on the medial aspect of the elbow. The nerve should be palpated and marked on the skin as a reminder of its location, prior to incision.
- Recurrence is more likely in the patient with chronic etiology like rheumatoid arthritis or gout.

62.7 Results

Endoscopic olecranon bursectomy has shown faster healing and lower re-operation rates when compared to an open technique, leading to reduced hospital stays [3, 7]. Some patients will get an effusion, which may need to be drained [1].

References

1. Tu CG, McGuire DT, Morse LP, Bain GI. Olecranon extrabursal endoscopic bursectomy. Tech Hand Up Extrem Surg. 2013;17(3):173–5.
2. Stell IM. Septic and non-septic olecranon bursitis in the accident and emergency department—an approach to management. J Accid Emerg Med. 1996;13(5):351–3.
3. Ogilvie-Harris DJ, Gilbart M. Endoscopic bursal resection: the olecranon bursa and prepatellar bursa. Arthroscopy. 2000;16(3):249–53.
4. Alvi HM, Kalainov DM, Biswas D, Soneru AP, Cohen MS. Surgical management of symptomatic olecranon traction spurs. Orthop J Sports Med. 2014;2(7):2325967114542775.
5. Reilly D, Kamineni S. The olecranon spur. J Shoulder Elb Surg. 2015;24(6):980–7.
6. Singh VR, Bain GI. Endoscopic extrabursal excision of Olecranon Spur. Arthroscopy Techniques 2018.
7. Kerr DR, Carpenter CW. Arthroscopic resection of olecranon and prepatellar bursae. Arthroscopy. 1990;6(2):86–8.

63 Endoscopic Four Compartment Decompression for Chronic Exertional Compartment Syndrome

Paul Max Jarrett

63.1 Background

Chronic exertional compartment syndrome (CSES) is a condition involving self-resolving episodes of forearm pain, paraesthesia, and the forearm feeling "pumped" during exercise. CSES is a rare condition and is more prevalent amongst motocross riders and rowers. The symptoms gradually appear some minutes after commencing forearm exercise and progressively worsen with continued use. The symptoms often reach a level where performance is impeded, and the patient may have to stop their activity. Between exercise sessions the patient is symptom free. There are usually no long-term sequelae. Diagnosis is based on history, exclusion of other pathology on physical examination, and usually compartment pressure studies during exercise. MRI may exclude some other structural pathologies and an immediate post-exercise MRI may demonstrate features consistent with CSES. The definitive treatment is forearm fasciotomy and this can be performed using open or endoscopic techniques.

Forearm fasciotomy was initially described as an open procedure involving long incisions, but more recently mini-open or endoscopic techniques have been developed with good long-term results [1–6]. Endoscopic surgery is performed via smaller incisions and results in cosmetic scars and a rapid return of forearm function. The author presents a new technique for endoscopic 4-compartment fasciotomy for chronic exertional compartment syndrome.

63.2 Surgical Anatomy

The aim of this endoscopic fasciotomy technique is to release the four muscular compartments of the forearm in a straightforward and effective manner whilst reducing the risk of injuring significant structures. The forearm is divided into four muscular compartments by fascia:

63.2.1 The Lateral Mobile Wad Compartment

- extensor carpi radialis longus,
- extensor carpi radialis brevis,
- brachioradialis.

P. M. Jarrett (✉)
Department of Hand Surgery, Fremantle Hospital, Fremantle, WA, Australia

Murdoch Orthopaedic Clinic, Murdoch, WA, Australia
e-mail: admin@pauljarrett.info

© ISAKOS 2022
D. N. Bhatia et al. (eds.), *Arthroscopy and Endoscopy of the Elbow, Wrist and Hand*,
https://doi.org/10.1007/978-3-030-79423-1_63

63.2.2 Dorsal Compartment

- extensor digitorum communis,
- extensor carpi ulnaris,
- extensor digiti minimi,
- anconeus.
- abductor pollicis longus,
- extensor pollicis brevis,
- extensor pollicis longus,
- extensor indicis proprius,
- supinator.

63.2.3 Superficial Volar Compartment

- pronator teres,
- palmaris longus (when present),
- flexor digitorum superficialis,
- flexor carpi radialis,
- flexor carpi ulnaris.

63.2.4 Deep Volar Compartment

- flexor digitorum profundus,
- flexor pollicis longus,
- pronator quadratus.

The cross-sectional anatomy of the forearm and the lines of dissection required to approach and release the fascia for each compartment are shown in Fig. 63.1. The fascia of the dorsal compartment is decompressed close to the fascia between the mobile wad and dorsal compartments. Thus, once the dorsal compartment is decompressed, the fascia descending into the forearm between the mobile wad and dorsal compartments is easily visualised and can be incised to decompress the mobile wad. No trunk nerves or larger blood vessels are located in the area of this dissection. For the flexor compartments, once the fascia over the superficial volar compartment has been decompressed, the interval between flexor digitorum superficialis and flexor carpi ulnaris muscles can be bluntly developed to reveal the fascial of the deep volar compartment which is then decompressed. The ulnar nerve is close to the deep volar compartment fascia at this point and should be protected.

63.3 Indications and Contraindications

Exercise-induced increase in pressure within the inelastic fascial compartments of the forearm results in reduction in tissue perfusion, and this is manifested as loss of function, ischaemic pain, and the neurologic symptoms. Whilst treatment with physical therapy can be attempted, it is often ineffective and the definitive treatment in severe cases is forearm fasciotomy.

Contraindications include active infection and other pathologies that may result in similar symptoms.

63.4 Surgical Steps

The procedure is carried out with a general or regional anaesthetic and exsanguination of the upper limb prior to inflating an upper arm tourniquet. The patient is supine with the upper limb placed on an arm table. The endoscopic stack is located on the same side of the operating table as the surgeon, beyond the patient's hand, so the

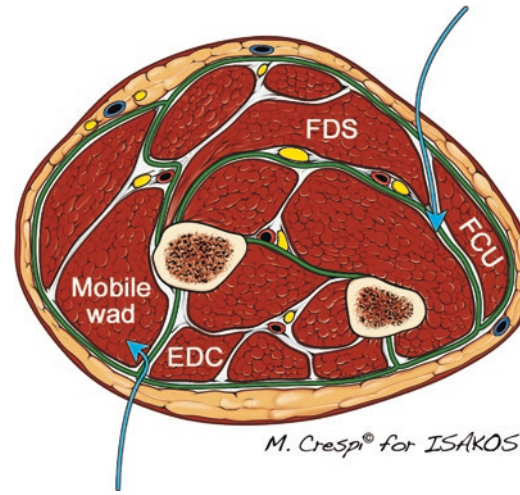

Fig. 63.1 Cross-sectional image of the forearm compartments indicating the lines of dissection and fasciotomy position (M. Crespi © for ISAKOS)

Fig. 63.2 Endoscopic equipment for forearm fasciotomy

screen can be seen when working from either side of the hand table. The endoscopy is undertaken dry without the use of fluid or carbon dioxide.

For the procedure, the instruments used (Fig. 63.2) include a surgical blade for the skin incision, scissors for dissection and decompression, endoscope, long bipolar diathermy bayonet forceps, and forceps and needle holder. It is useful to have a selection of scissors including shorter scissors (curved tenotomy scissors) to create the initial dissection, longer blunt-tipped curved scissors (Metzenbaums) for endoscopic work, and finally some blunt tipped curved scissors (17–23 cm) for endoscopic dissection furthest from the incision. The endoscope used is the 4 mm 18 cm length Hopkins II Forward-Oblique 30 degrees telescope with large fenestrated distal spatula optical dissector (Karl Storz, Tuttlingen, Germany). A speculum is used at times during this procedure.

63.4.1 Surface Markings

- The fasciotomy procedure is an endoscopic variation of the mini-open technique of Harrison [1].
- A skin marker is used to draw two lines. The first line (extensor compartment) is between the lateral humeral epicondyle and Lister's tubercle. The second line (flexor compartment) is drawn from the medial epicondyle to the location of palmaris longus at the distal wrist crease (Fig. 63.3).

63.4.2 Extensor Release

- A 2-cm skin incision is made 5-cm distal to the lateral epicondyle along the extensor compartment skin line (Fig. 63.3). Initial dissection through the subcutaneous fat is carried out with tenotomy scissors bluntly and then blunt tunnelling forceps are used to create a tissue plane for the endoscope distally along the line for a further 10 cm.
- The hooded endoscope is inserted distally; if the subcutaneous tissues interfere with visualisation, then the endoscope is withdrawn and reinserted after insertion of the speculum.
- The fasciotomy is performed along the septum between the extensor mobile wad and extensor digitorum communis, releasing both extensor compartments, progressing distally (Figs. 63.4 and 63.5). The endoscope is then inserted proximally to complete the fasciotomy for a short distance proximally.

63.4.3 Flexor Release

- A 2-cm skin incision is made from 5-cm distal to the medical epicondyle along the flexor compartment skin line (Fig. 63.3), with the same subcutaneous preparation as for the previous incision.
- A longitudinal incision in the superficial flexor compartment fascia is made, the endoscope

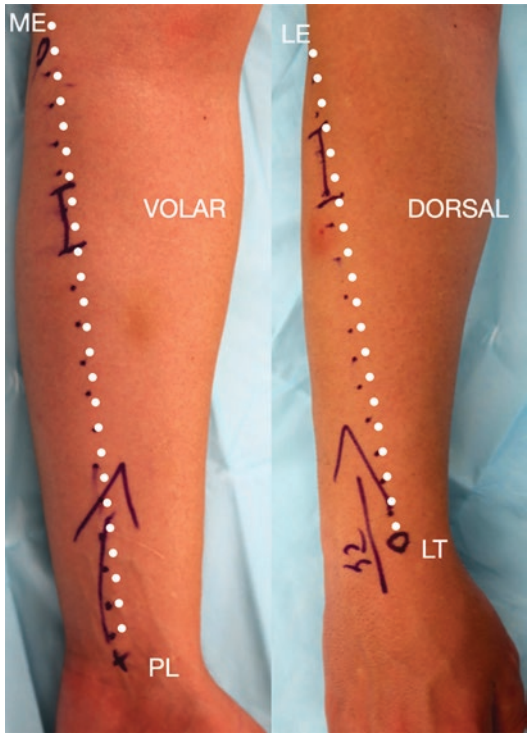

Fig. 63.3 Skin markings for flexor (left) and extensor (right) compartment releases are shown. (ME: medial epicondyle, PL: palmaris longus at wrist, LE: Lateral epicondyle, LT: Lister's tubercle)

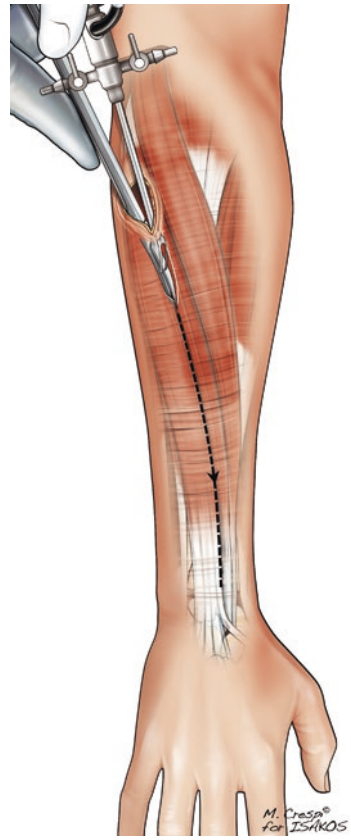

Fig. 63.4 The anatomic plane for extensor fasciotomy is illustrated (M. Crespi © for ISAKOS)

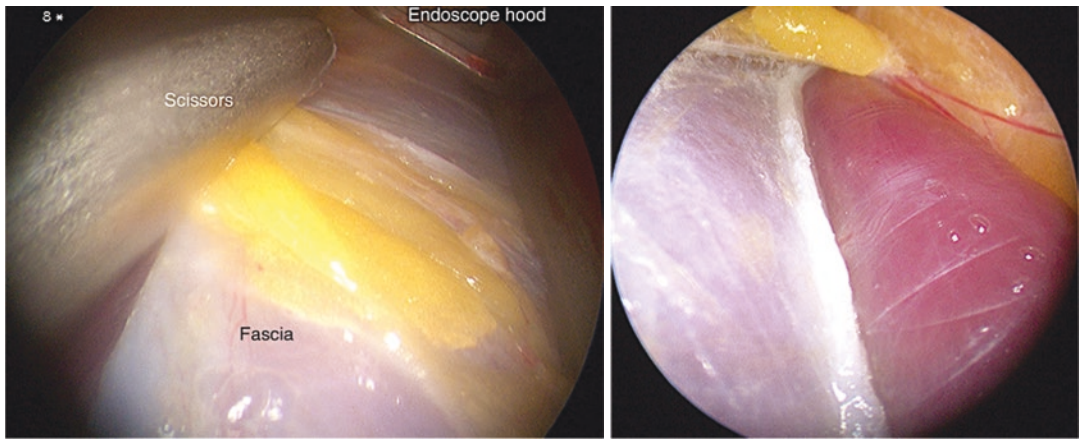

Fig. 63.5 Endoscopic view of extensor compartment before (left image) and after fasciotomy (right image)

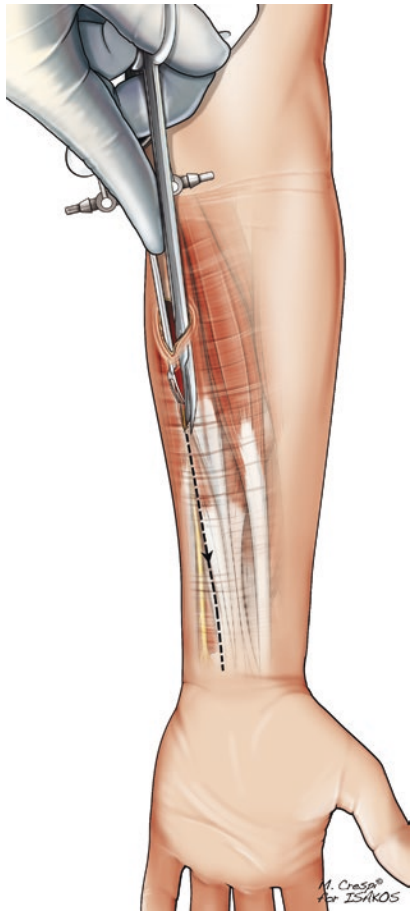

Fig. 63.6 The anatomic plane for flexor compartment fasciotomy is illustrated (M. Crespi © for ISAKOS)

and if required speculum is inserted, and this fasciotomy is continued distally releasing this entire compartment (Fig. 63.6).

- The interval between the flexor digitorum superficialis and flexor carpi ulnaris muscle bellies is established down to the deep fascia and the ulnar nerve is visualised and protected (Fig. 63.7).
- The deep fascia overlying FDP is then released distally throughout the forearm. The endoscope is then inserted proximally to complete the fasciotomies for a short distance proximally.

The wounds are infiltrated with local anaesthetic and closed with 2/0 vicryl to the subcutaneous tissues and then 4/0 monocryl intra-dermal.

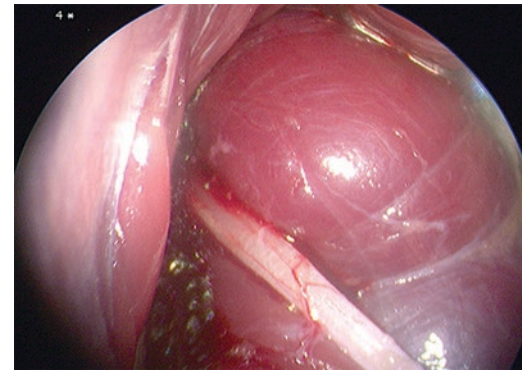

Fig. 63.7 Endoscopic view of flexor compartment after fasciotomy and visualisation of ulnar nerve

63.5 Technical Tips

- For sufficient space to visualise the nerve and associated tissues, it is helpful to place some superior angulated force on the endoscope for elevating the tip of the spatula of the optical dissector. Using the speculum can also assist with visualisation in the first few centimetres from the incision and is recommended for the distal dissection.
- When dissecting in the subcutaneous and deeper layers, small nerve branches or vessels can be encountered and care must be taken to avoid injury to these structures. If required, for surgical exposure, small vessels can be coagulated using bipolar diathermy.
- The incisions can be lengthened during the procedure if the surgeon believes the safety of the operation is being compromised by the endoscopic nature of the procedure. Alternatively, the surgeon can make an additional small incision further along the extensor or flexor compartment skin marking for endoscopic visualisation.

63.6 Pitfalls

In a patient with long forearms, a complete fasciotomy may not be possible from the incisions described in the surgical steps; the working

length of the endoscope would be inadequate to reach sufficiently distally. In these cases, the incisions should be placed more distally along the extensor and flexor compartment lines. These incisions may be less cosmetic; however, they permit an adequate decompression. The incisions require to be no more than 15 cm proximal to the most distal point of fasciotomy.

63.7 Postoperative Management and Rehabilitation

Patients are permitted to use their upper limb for light activities in the immediate postoperative period. The bandages are removed after 2 days and the adhesive dressings at 10 days. Patients can return to activities based on their comfort levels. In the author's experience, the recovery is rapid, and patients report significant resolution of their symptoms within 6 weeks.

63.8 Complications

- The ulnar nerve is the most likely structure to be damaged during this procedure, and careful dissection around the nerve is required to reduce the risk of injury.
- Haematoma formation is possible, and haemostasis of any small vessels with the long bipolar diathermy bayonet forceps will reduce this risk.

Acknowledgements The author is grateful for Professor James O Jarrett for his comments on the text.

References

1. Harrison J, Thomas P, Aster A, Wilkes G, Hayton M. Chronic exertional compartment syndrome of the forearm in elite rowers: a technique for mini-open fasciotomy and a report of six cases. Hand. 2013;8:450–3.
2. Croutzet P, Chassat R, Masmejean E. Mini-invasive surgery for chronic exertional compartment syndrome of the forearm: a new technique. Tech Hand Up Extrem Surg. 2009;13:137–40.
3. Pegoli L, Pozzi A, Pivato G. Endoscopic single approach forearm fasciotomy for chronic exertional compartment syndrome: long term follow-up. J Hand Surg Asian Pac Vol. 2016;21:8–12.
4. Miller E, Cobb A, Cobb T. Endoscopic fascia release for forearm chronic exertional compartment syndrome: case report and surgical technique. Hand. 2017;12(5):NP58–61.
5. Gondolini G, Schiavi P, Pogliacomi F, Ceccarelli F, Antonetti T, Zasa M. Long-term outcome of mini-open surgical decompression for chronic exertional compartment syndrome of the forearm in professional motorcycling riders. Clin J Sport Med. 2019;29:476–81.
6. Barrera-Ochoa S, Haddad S, Correa-Vazquez E, Font Segura J, Gil E, et al. Surgical decompression of exertional compartment syndrome of the forearm in professional motorcycling racers: comparative long-term results of wide-open versus mini-open fasciotomy. Clin J Sport Med. 2016;26:108–14.

Endoscopic Forearm Fasciotomy: How I Do it

64

Jessica Cobb and Tyson Cobb

64.1 Background

Intra-compartmental pressure and swelling stemming from constant and recurring forceful muscular use can cause chronic exertional compartment syndrome (CECS). This is common in professional motocross riders causing extreme pain and tightness in both forearms resulting in temporary loss of grip and the inability to control the bike. This pain may be comparable to acute, traumatic compartment syndrome and may start as quickly as 5–10 min after the start of the race. Pain levels are positively correlated with the aggressiveness of the rider as well as increased size of bike. Many riders report onset as they move up in classes to heavier motorcycles.

Due to high commonality in this sport, motocross riders typically are well versed on the diagnosis and treatment options. Conservative treatment options include stretching, cryotherapy, anti-inflammatory medication, massage, and changes to activity lifestyle. These options rarely suffice. Due to the high safety concerns of the inability to control the motorcycle during painful flaring, surgical treatment is often desired.

The open fascia release for CECS is well-established and requires large incisions. On the contrary, the endoscopic approach devised by the senior author (TC) uses a single small incision and a cannula to release the fascia providing a faster recovery. In most cases, patients may return to riding 10–14 days after surgery and begin competing as early as 3–4 weeks.

64.2 Surgical Anatomy

The flexor (volar), extensor (dorsal), and mobile wad (lateral) make up the compartments of the forearm. The volar compartment is further divided into deep and superficial sections. In the senior author's experience with professional motocross riders, release of only the superficial volar and dorsal compartments is performed. It may be possible in some patients to release only the volar compartment and obtain the same results. However, both compartments are easily released through the same single portal. A surgical approach from a single ulnar-sided portal allows access to both the flexor and extensor compartments since both compartments are only separated by their attachment to the ulna [1, 2].

J. Cobb (✉)
Morsani College of Medicine, Tampa, FL, USA
e-mail: cobb3@usf.edu

T. Cobb
Shoulder, Elbow, Wrist, and Hand Center of Excellence, Davenport, IA, USA

© ISAKOS 2022

D. N. Bhatia et al. (eds.), *Arthroscopy and Endoscopy of the Elbow, Wrist and Hand*,
https://doi.org/10.1007/978-3-030-79423-1_64

64.3 Indications and Contraindications

Most patients are professional motocross riders who are not able to compete at a professional level due to forearm pain and weakness. Surgical intervention is indicated for patients that have failed conservative management and are significantly limited functionally.

The senior author measured post-exercise compartment pressures in the early phase of his experience with CECS; however, it became evident that these measurements are not routinely necessary because CECS is a clinical diagnosis. Furthermore, professional motocross riders understand this condition very well and have been dealing with this condition for many years prior to presenting for surgery. Should there be any question about the diagnosis then post-exercise compartment pressure studies may be performed [3, 4].

A contraindication to this procedure is active infection. If a diagnosis other than chronic exertional compartment syndrome (CECS) is suspected such as stress fracture or compressive neuropathy, further differential diagnostic testing (MRI, electrophysiological studies) should be performed first.

64.4 Surgical Steps

The patient is positioned supine on the operating room table with the shoulder abducted and neutral rotated with elbow flexed over a blanket. A tourniquet is placed on the arm. Approximately 45 ml of bupivacaine (0.25%) with epinephrine is infiltrated along the course of the anticipated dissection.

- A 2–3 cm incision is placed centrally between olecranon and the ulnar styloid over the subcutaneous border of the ulna. Dissection between the fascia and subcutaneous tissue extends along the course of the ulna exposing the ulnar attachment of the both the flexor and extensor compartments. Dissection is facilitated with long narrow retractors (Sofield retractors, gSource, LLC Emerson NJ) that are used to elevate the subcutaneous tissue off the fascia.
- A 4 mm, 30-degree arthroscope is used to visualize and complete the dissection both proximally and distally. The endoscope, retractors, and long handled scissors are all placed into a single central portal overlying the subcutaneous border of the ulna (Figs. 64.1a, b).
- The EndoRelease cannula (Integra LifeSciences Corporation, Plainsboro Township, N.J.) is placed under the fascia, and the attached retractor separates the subcutaneous tissue and nerves providing a space for fascia release (Fig. 64.2). The endoscope is utilized to visualize and confirm that the cannula has effectively separated the underlying muscle tissue from the fascia and the attached retractor has separated the subcutaneous tissue and nerves from the fascia.
- Once this is confirmed, the endoscope is placed in the cannula and the fascia is released under direct endoscopic visualization with the push knife (Integra LifeSciences Corporation, Plainsboro Township, N.J.) (Figs. 64.3 and 64.4).
- A total of four releases are performed: distal dorsal and volar compartments followed by proximal dorsal and volar compartments. Dorsal compartment is always released before volar. The fascia is then "T" cut transversely from the ulnar border in a radial direction for both dorsal and volar compartments.

Hemostasis is achieved after releasing the tourniquet (Fig. 64.5). The skin is closed with 3–0 monocryl subcuticular sutures and Steri-Strips. A stack of 4 × 4 s and ACE wraps are applied to the forearm. The Ace wrap is applied from the hand to the elbow to provide a compressive dressing and minimize swelling.

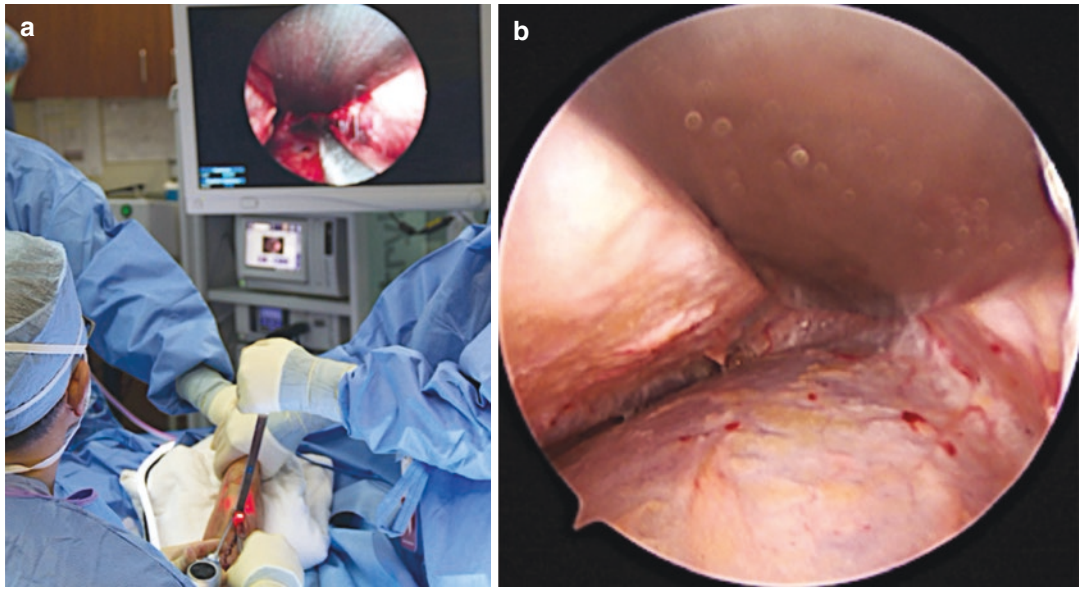

Fig. 64.1 (**a**) Retractors elevate subcutaneous tissue off of the deep fascia overlying the subcutaneous border of the ulna. Dissection is performed endoscopically with 4-mm endoscope, dissecting scissors, and retractors all in the same portal. (**b**) Endoscopic view after dissecting subcutaneous tissue off of the deep fascia. A Sofield retractor is seen elevating subcutaneous tissue

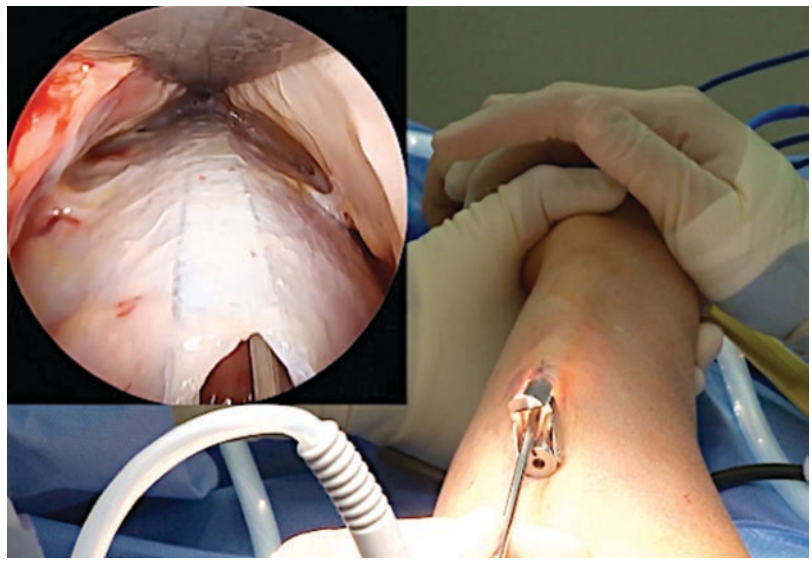

Fig. 64.2 The endoscope is placed in the interval between the cannula and the retractor to ensure that fascia is isolated between cannula and retractor. Attached retractor opens potential space between the deep fascia and the subcutaneous tissue

64.5 Technical Tips

- Avoid creating multiple planes through the tissue. Dissect directly to the deep fascia and then develop the plane along the fascia.
- In order to have the best visualization, release the dorsal compartment first as the volar muscle tends to bulge out of the compartment more than the dorsal. Muscle bulging decreases visualization especially at the proximal end of release. To avoid this, the cannula should be placed entirely to the end of the

Fig. 64.3 Endoscope is placed in cannula to visualize muscle tissue below and fascia to be divided above the cannula

Fig. 64.4 A push knife is used to divide fascia under direct endoscopic visualization

compartment prior to the start of the release to ensure that the release reaches all the way to the terminal end of the compartment.

- If assessment or an additional release is required at the terminal extent of compartments and protruding muscle interferes with visualization, an instrument can be used to compress the muscle and allow visualization. It is however much easier to make sure the entire compartment is released in one smooth push of the push knife.
- Liberal use of local anesthetic with epinephrine minimizes the likelihood of hematoma or ecchymosis.
- Often, recovery time is limited as many of patients with CECS are professional athletes who are traveling from out of town between competitions and seasons. Therefore, endoscopic release is usually performed bilaterally in one surgery.
- Dissection through a 2–3 cm incision can be difficult; therefore, a larger incision of 4–5 cm can be used while learning the procedure.

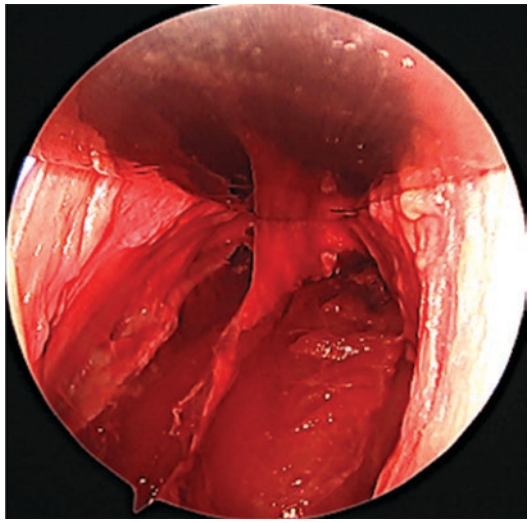

Fig. 64.5 Postoperative view showing both volar and dorsal compartment release separated by the subcutaneous border of the ulna. Sofield retractor elevates subcutaneous tissue to expose releases. Bipolar cautery can be used to obtain hemostasis as necessary

64.6 Pitfalls

- Hemostasis at the extreme proximal aspect of the operative field can be difficult to obtain and therefore high-volume infiltration of local anesthetic with epinephrine in this area preoperatively is important.
- Swelling, blistering, or seroma formation may occur during the early postoperative period. Strict elevation is important during the first postoperative week. Ace wrap compression is continued for 7–10 days and as needed thereafter based on swelling and evidence of seroma. Patients are educated on proper application of ACE wrap and sent home with a supply.
- Wound dehiscence is possible during the first three postoperative weeks. Patients should be instructed to wear protective wraps or arm guards while riding.

64.7 Postoperative Management and Rehab

Patients wear compressive ACE wrap bandage(s) at all times for the first week. They may remove the bandage for self-care and hygiene but should reapply them immediately afterward. Patients are encouraged to begin light activity as tolerated, and work on motion of elbow, wrist, and digits. They are encouraged to gradually resume sports activity approximately 14 days after surgery if incisions are healed and swelling has resolved. In the event that they are unable to resume riding by 3–4 weeks, they are instructed to use hand grips to expand forearm muscles and stretch the healing fascia. This allows the fascia to stretch and expand during the healing phase.

Ensuring that the fascia heals in such a way that there is sufficient room for muscle expansion. Patients who need to travel from out of town are instructed to send photographs of their forearms 3–5 days after surgery and thereafter as needed for any questions or concerns.

64.8 Complications

- No serious postoperative complications have been observed.
- Seroma formation is relatively common and may be prevented with proper use of compression postoperatively.
- Wound dehiscence has occurred in several patients who crashed their bikes in the first 3 weeks after surgery. Protective gear on forearms should be worn until the surgical site has completely healed.
- As patients are often eager to return to riding on dirt tracks, the threshold for prophylactic antibiotic use postoperatively should be fairly low. While some blistering secondary to swelling is common, if draining blisters occur, a course of oral antibiotics should be considered.

64.9 Results

Approximately 60 surgeries have been performed with a maximum follow-up of 8 years. All motocross patients have returned to their off-road racing. Most patients have complete relief of symptoms and there have been two recurrences.

References

1. Miller EA, Walden AL, Cobb TK. Endoscopic fascia release for forearm chronic exertional compartment syndrome. Surgical Techniques for Trauma and Sports Related Injuries of the Elbow 2019 161–165.
2. Miller EA, Cobb AL, Cobb TK. Endoscopic fascia release for forearm chronic exertional compartment syndrome: case report and surgical technique. Hand. 2016; https://doi.org/10.1177/1558944716669799.
3. Fronek J, Mubarak SJ, Hargens AR, Lee YF, Gershuni DH, Garfin SR, Akeson WH. Management of Chronic Exertional Anterior Compartment Syndrome of the lower extremity. Clin Orthop Relat Res. 1987; https://doi.org/10.1097/00003086-198707000-00030.
4. Mubarak SJ, Pedowitz RA, Hargens AR. Compartment 265 syndromes. Curr Orthop. 1989;3:36–40.

Arthroscopic Management of the Painful Elbow Arthroplasty

65

Timothy Eves, Gregory I. Bain, and Joideep Phadnis

65.1 Background

Elbow arthroscopy was first reported in 1931 although the modern technique was developed and introduced much later [1]. The spectrum of indications and range of therapeutic procedures is constantly increasing and evolving; however, the utility of arthroscopy and endoscopy in managing problems related to total elbow arthroplasty (TEA) remains in its infancy. Postoperative pain following TEA has been reported in up to 40% of cases, at a mean follow-up of 6.3 years [2]. Complications resulting in pain are all relatively more common than other large joint arthroplasties and include: peri-prosthetic fracture, instability, peri-prosthetic infection (+/− loosening), aseptic loosening, mechanical impingement, and polyethylene wear. Peri-prosthetic fracture and instability are readily diagnosed on imaging studies; however, the other diagnoses listed are typically more challenging to make.

Deep infection is of particular concern and can result in significant morbidity, with staged revision or even amputation required. The deep infection rate following TEA is 1–9%, which is higher than that of other major joint arthroplasties [3, 4]. This may be a result of the tenuous soft tissue envelope surrounding the elbow and the high proportion of patients on immunosuppressive therapy. Diagnosis of infection following TEA poses a challenge because traditional clinical, radiographic, and biochemical markers are unreliable. Infection is often low grade, with a muted systemic response. Guidelines for diagnosis of peri-prosthetic infection have been developed but are derived from (and relevant to) hip and knee arthroplasty. Similar robust data does not exist for the elbow. Aspiration and culture of peri-prosthetic fluid is a common pre-operative diagnostic test; however, it may be unreliable in indolent infections and is unhelpful in diagnosing non-infectious causes of pain. More recently, proprietary testing of *alpha defensin* levels (Synovasure® Zimmer Biomet, Warsaw IN) has been used, but has yet to be validated for elbow infection. Intra-operative frozen section has low sensitivity and positive predictive value and is performed during surgery, which is less useful than having a pre-operative diagnosis and management plan. Culture of peri-prosthetic tissue

T. Eves
Department of Trauma and Orthopaedics, Brighton and Sussex University Hospitals, Brighton, UK

G. I. Bain (✉)
Flinders University and Flinders Medical Centre, Adelaide, SA, Australia
e-mail: greg@gregbain.com.au

J. Phadnis
Department of Trauma and Orthopaedics, Brighton and Sussex University Hospitals, Brighton, UK

Brighton and Sussex Medical School, Brighton, UK
e-mail: Joideep.Phadnis@nhs.net

© ISAKOS 2022

D. N. Bhatia et al. (eds.), *Arthroscopy and Endoscopy of the Elbow, Wrist and Hand*,
https://doi.org/10.1007/978-3-030-79423-1_65

therefore remains the gold standard diagnostic test for peri-prosthetic infection [5].

Risk factors for deep infection include inflammatory arthritis, steroid use, an immunocompromised state, and previous elbow surgery. The most commonly identified causative organisms have been found to be *Staphylococcus aureus* and *Staphylococcus epidermis* [3]. The outlines of the 2018 international consensus meeting criteria for diagnosis of elbow peri-prosthetic joint infection are illustrated below (Fig. 65.1).

Loosening of the prosthesis at the bone-cement or cement-prosthesis interface can be seen on imaging (Fig. 65.2). Quite dramatic degrees of loosening may be present without infection, whereas infection may even be present in the early stages without loosening of the implants. This is because implant loosening can be commonly caused by polyethylene-mediated osteolysis or mechanical loosening. Implant impingement in flexion is also known to cause a "push pull" loosening phenomenon, unique to elbow arthroplasty and can be difficult to diagnose clinically.

65.2 Role of Elbow Arthroscopy in TEA

Arthroscopic examination of the TEA lends itself well to determining the underlying cause of pain. It provides a comprehensive assessment of the mechanical status of the elbow, with direct visualization of the components and mechanical interfaces. It also allows assessment of the infective status, with sampling of joint fluid and soft tissue biopsy. When combined with radiographic examination and serum biomarkers, it provides an important adjunct in the identification of the cause of pain, including aseptic and septic loosening, mechanical impingement, and polyethylene wear. Accurate diagnosis is important in order to determine the

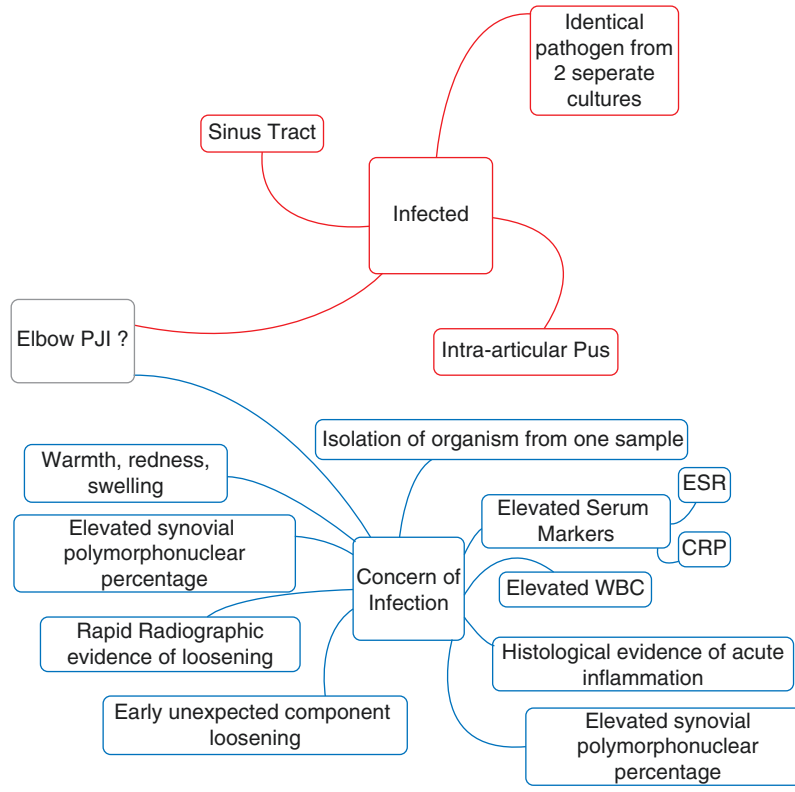

Fig. 65.1 The 2018 ICM on Musculoskeletal infection—Diagnostic criteria for elbow peri-prosthetic joint infection [6]

Fig. 65.2 Radiographs of an 80-year-old female with loose humeral and ulnar components but no serologic or clinical signs of infection. Arthroscopic assessment and biopsy was performed to rule out infection and allow a single-stage reconstruction

infective organism which will improve the success of subsequent open surgical management. With respect to the painful hemiarthroplasty, diagnostic arthroscopy is of value in helping identify the cause of pain. This may be related to wear of the native radial head or greater sigmoid notch. Also, synovitis, loosening or instability, may also be appreciated.

The primary role of arthroscopy in the symptomatic arthroplasty is diagnostic; however, a number of therapeutic procedures are also possible. Loose bodies, such as cement or bone debris can be removed. Synovitis in the setting of a hemiarthroplasty can be debrided and impinging areas of bone can be resected. Prominent suture knots or anchors from the triceps repair can be removed (Fig. 65.3a–c).

Removal and replacement of the screws from the linking mechanism has also been described. In revision arthroplasty, an arthroscope can be invaluable in helping to remove cement or cement restrictors under direct vision and reduce the need for an osteotomy (Fig. 65.4a, b).

Elbow arthroscopy can also be used to treat stiffness following arthroplasty through capsular release and concurrent evaluation of the joint for underlying causes of stiffness, such as infection, loosening, or instability. This is a rare application and should only be considered after other causes of mechanical stiffness related to the implant have been excluded (e.g., overlengthening or malrotation). It may be more applicable following hemiarthroplasty where the contracture could be post-traumatic and the neurovascular anatomy would be better preserved than after a total elbow arthroplasty.

65.3 Steps in the Management Painful Elbow Arthroplasty

We advocate the use of a logical and stepwise protocol for the management of the painful TEA illustrated below (Fig. 65.5) [7].

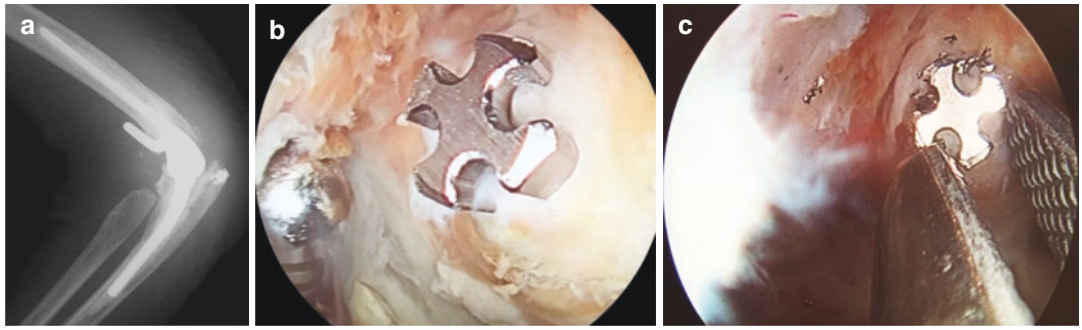

Fig. 65.3 (**a**) A patient presented with well-fixed components but a large warm swelling over the olecranon and elevated serum markers for infection. (**b**) Arthroscopic evaluation demonstrated a triceps failure with prominent suture anchors present. (**c**) The suture anchors were removed and the olecranon bursa was irrigated and debrided. © Dr Gregory I. Bain

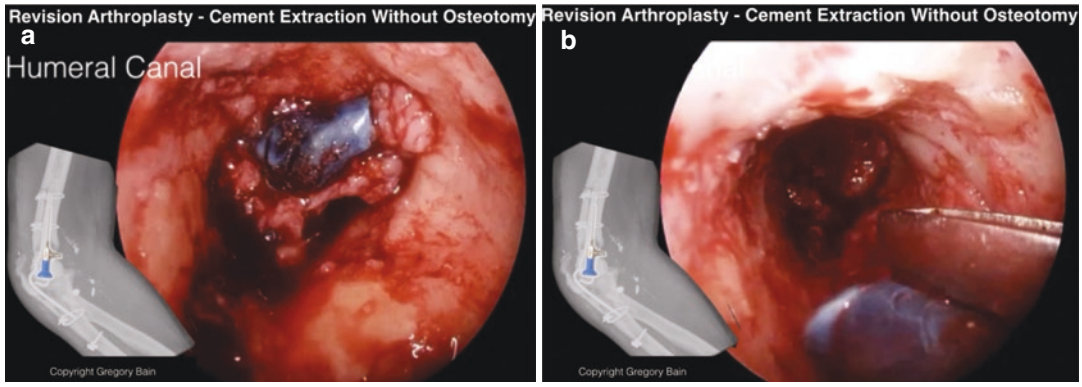

Fig. 65.4 (**a**) The first of a two-stage revision arthroplasty is being performed. The humeral component has been removed but residual cement and a plastic restrictor are still in situ. (**b**) The retained cement and restrictor can be removed safely under direct vision without performing a humeral osteotomy. © Dr Gregory I. Bain

- Pertinent points in the patient's history include details of the index procedure; subsequent procedures and history of any postoperative complications such as wound healing issues after previous surgery. Clinical signs of infection such as erythema, swelling, or constitutional symptoms may not be present but are strongly suggestive of infection if reported. Any history of trauma should be elucidated, as well as symptoms such as clicking, locking, or crepitus which reflect a mechanical problem. Comorbidities, drug history (in particular immunosuppressive medications), degree of frailty, and expectations are important and may influence the eventual treatment strategy.
- Examination should include the C-spine, ipsilateral shoulder as well as the contralateral elbow. The location and character of previous scars is important to plan surgery. Portals should be made through previous incisions where possible looking for the vitality of the scar, evidence of erythema, induration, or sinus tract. An assessment of stability of the prosthesis and pain should be made with varus and valgus stress. A full neurovascular assessment should be performed but the course of the ulnar nerve should be assessed in detail. If transposed, the aberrant path of the nerve will increase its likelihood of being injured if using a standard anteromedial por-

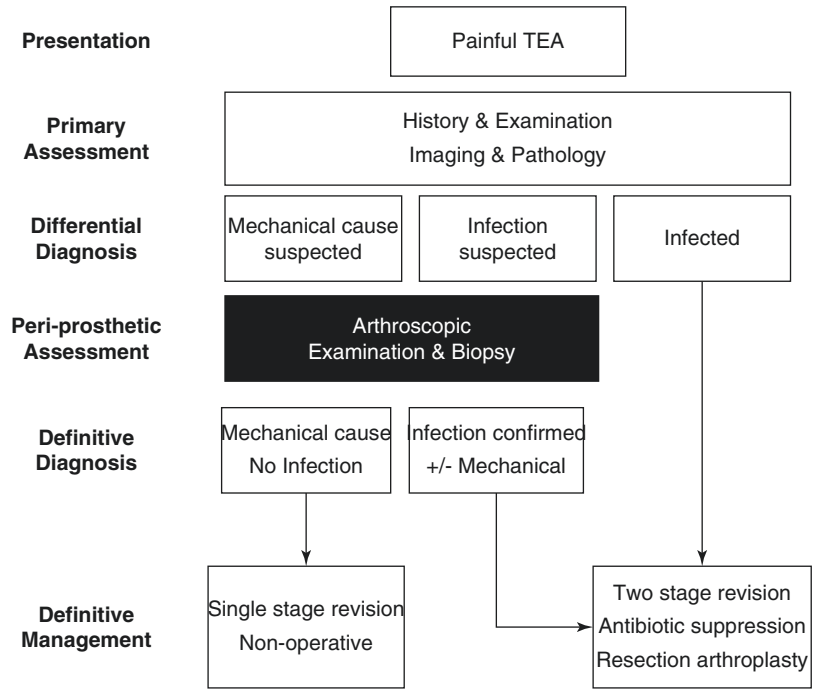

Fig. 65.5 Stepwise protocol for the management of the painful TEA [8]

tal. If this portal is necessary, which is not always the case when evaluating an elbow arthroplasty, then the nerve should be identified and protected before making the portal. Ultrasound can be used to map the course of the nerve if in doubt.

- In order to gain representative tissue and fluid samples, we recommend that patients have not taken antibiotics within the 2 weeks prior to the procedure. In patients who are taking suppressive antibiotic therapy this should also be temporarily stopped (for the same duration) giving an "antibiotic holiday." This increases the likelihood of gaining positive microbiological and histology tissue results. At the time of surgery, prophylactic antibiotics are withheld until samples have been taken for microbiology and the tourniquet has been released.
- The presence of active local soft tissue infection is a contraindication and if present could introduce infection into the prosthetic joint. In addition, contamination of the intra-articular samples taken during the procedure could occur giving non-diagnostic results.

65.4 Surgical Technique

Setup: The patient is placed in the lateral decubitus position with a mechanical arm positioner. A general anesthetic with supraclavicular block are usually used. The skin is prepared with alcoholic chlorhexidine and a sterile tourniquet applied.

Portals: When performing arthroscopy in the presence of an elbow arthroplasty, it is not always necessary to access all compartments as for a native joint. Most pathology can be appreciated and treated using posterior portals and often the anterior part of the joint can be accessed using posterior portals. These are safer because the bony and soft tissue anatomy is not as distorted in this area from previous surgery. The exception to this is for stiffness surgery where the anterior capsule may need to be released. Typically, a direct posterior portal through the original scar and a second more posterolateral portal is made using a needle for localization. If it is necessary to view the anterior joint in more detail, such as to address anterior implant impingement, proximal anteromedial, and anterolateral portals can

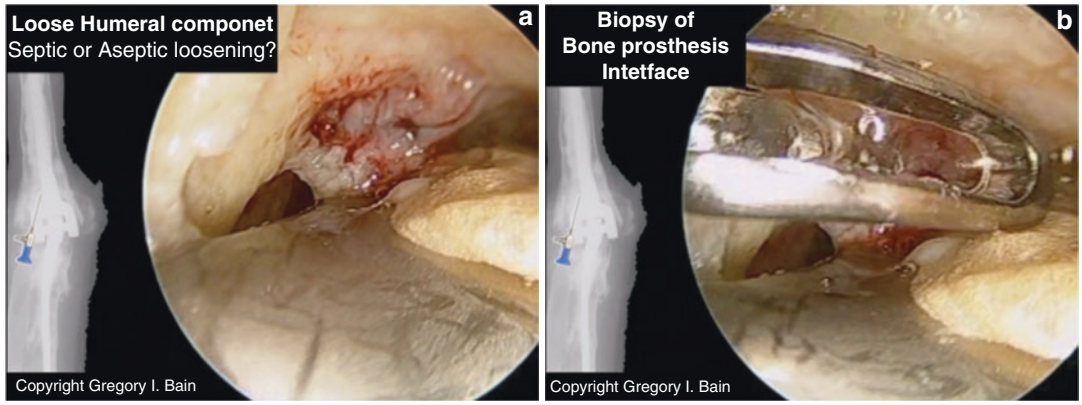

Fig. 65.6 (**a**) The arthroscope has been passed into the interface between the prosthesis and the bone to appreciate the longitudinal and rotational instability of the implant. (**b**) Specimens are taken from this interface which would not be easily accessible without removing the implants. © Dr Gregory I. Bain

be created. It is worth assessing the axial cuts of a pre-operative CT scan to review the location of the median and radial nerves in relation to the brachialis muscle, which may be distorted following previous surgery.

Visualization and Instrumentation: A standard 4.0 mm arthroscope is used for visualization [9]. A small bore canula (5–6 mm) is placed through the working portal in order to minimize repeated in and out entry and seeding of skin flora into the joint. This is particularly important when taking samples for microbiology. Dry and wet arthroscopic techniques are used as described below. A shaver without teeth and radiofrequency probe are used. Separate rongeurs/graspers are necessary to ensure proper tissue sampling protocol.

Microbiological assessment: On initial entry into the joint, any fluid egressed is collected and sent for culture. Dry arthroscopy is then performed to allow further fluid and soft tissue samples to be taken without a dilution affect. Fluid can be used to improve visualization using a pump set at 30 mm Hg pressure and medium flow. We typically take five sets of "matched" tissue specimens (microbiology and histology). Each set is taken with fresh sterile instruments. Samples are retrieved from the implant-bone interface of both the ulna and humerus, and from the surrounding pseudocapsule (Fig. 65.6a, b). If significantly loose, the membrane from around the stems of the components can also be sampled. Specimens are sent for extended culture (14 days) to maximize identification of indolent species such as *Propionibacterium acnes*.

Mechanical assessment: All components and interfaces are inspected sequentially. Evidence of polyethylene, cement or metal debris, bushing wear or loosening is noted. The interfaces between bone and prothesis are also closely inspected. Loosening is assessed in three ways, using the arthroscopic probe (Fig. 65.6a) and by mobilization of the elbow. First, an attempt is made to piston the implant within the cement mantle to determine if longitudinal instability exists. Second, the forearm is rotated to see if the humeral component has rotational stability. Finally, the joint is tilted into varus and valgus allowing assessment of medio-lateral instability at the prothesis bone interfaces and at the articulation.

After completion of the assessment, the joint is washed out thoroughly and the portals are closed tightly with an absorbable monofilament suture to prevent sinus formation. The tourniquet is then deflated and the IV antibiotics can then be given.

65.5 Tips and Tricks

- Use previous scars where possible for portals to minimize soft tissue compromise.
- Use a dry technique for sampling where possible to reduce bacterial dilution.
- Even if a dry technique is used, irrigate the joint with fluid after the procedure to minimize infection risk.
- Systematically assess the components of the joint to "tick off" causes for pain.
- Use canulae to minimize soft tissue trauma and contamination of the joint.
- Find the prosthetic components early and stay close to them to avoid "getting lost" and causing iatrogenic nerve injury.

65.6 Pitfalls

- Arthroscopy should not be performed when pre-operative clinical findings or imaging have made a diagnosis for the pain—it is an adjunct for undiagnosed pain or stiffness.
- The course of the ulnar nerve must be known prior to embarking on the procedure to avoid iatrogenic injury.
- Assess advanced coronal imaging preoperatively to define the path of the radial and median nerves if there is anticipation of instrumenting the anterior compartment.
- Repeated instrumentation without use of a canula resulting in seeding infection into the prosthetic joint.

65.7 Postoperative Management and Rehabilitation

- Give postoperative antibiotics once the tourniquet has been released to minimize infection risk.
- Ensure samples are cultured for at least 14 days to pick up indolent infection.
- Commence early active range of motion to avoid the risk of stiffness.
- Ensure the patient is managed through a multidisciplinary approach with early involvement of a microbiologist to plan definitive treatment if infection is suspected.

65.8 Complications

This is an uncommon procedure and, in our experience no complications have occurred. However, the patients typically undergoing this surgery are high risk. The technical difficulty of the procedure means that it should be planned and executed carefully by an experienced elbow arthroscopist, who will be performing the ultimate revision procedure if required.

References

1. Dodson CC, Nho SJ, Williams RJ 3rd, Altchek DW. Elbow arthroscopy. J Am Acad Orthop Surg. 2008;16(10):574–85.
2. Welsink CL, Lambers KTA, van Deurzen DFP, Eygendaal D, van den Bekerom MPJ. Total elbow arthroplasty: a systematic review. JBJS Rev. 2017;5(7):e4.
3. Kim JM, Mudgal CS, Konopka JF, Jupiter JB. Complications of total elbow arthroplasty. J Am Acad Orthop Surg. 2011;19:328–39.
4. Voloshin I, Schippert DW, Kakar S, Kaye EK, Morrey BF. Complications of total elbow replacement: a systematic review. J Shoulder Elb Surg. 2011;20:158–68.
5. Yamaguchi K, Adams RA, Morrey BF. Infection after total elbow arthroplasty. J Bone Joint Surg Am. 1998;80:481–91.
6. Gutman MJ, Stone MS, Namdari S, Abboud JA. Treatment of elbow periprosthetic joint infection: a systematic review of clinical outcomes. J Shoulder Elb Surg. 2020;29:411–9.
7. Barlow J, Sanchez-Sotelo J. What are the diagnostic criteria for elbow periprosthetic joint infection (PJI)? (Clinical criteria, radiographic criteria, intraoperative findings, pathology, cultures and serum biomarkers.) International Consensus Meeting on Mukuloskeletal Infection. https://icmphilly.com
8. Phadnis J, Bain GI. Arthroscopic management of the painful total elbow arthroplasty. J Shoulder Elb Surg. 2016;8(1):41–7.
9. Bain G, Phadnis J, Singh V. Arthroscopy of total elbow arthroplasty. In: Bain G, Eygendaal D, van Riet R, editors. Surgical techniques for trauma and sports related injuries of the elbow. Berlin, Heidelberg: Springer; 2020.

Endoscopic Pronator Release (Proximal Forearm Median Nerve Decompression)

66

Michael J. Fitzmaurice

66.1 Background

Pronator syndrome is a proximal compression neuropathy of the median nerve. Five proximal to distal compression sites have been described: the ligament of Struthers, lacertus fibrosus (LF), vascular arches, the fibrous band of the pronator teres muscle (PT), and the fibrous arch of the flexor digitorum superficialis muscle (FDS). Most reported cases in the literature describe compression caused by a band between the two heads of the pronator teres muscle [1]. Symptoms can include aching in the proximal forearm, paresthesia in the median nerve distribution, and weakness with grip. Initial treatment includes activity modification, analgesics, and rest. The typical surgical approach for this condition has been an extensive incision of approximately 6–7 cm or longer [2–4]. These large incisions typically start proximal to the cubital crease and extend several centimeters distal to the cubital crease. The endoscopic technique was first described in 2012 and a recent cadaveric study has described this using a transverse incision rather than the longitudinal incision proposed in the initial article [5, 6]. Proximal median nerve compression can occur concurrently with carpal tunnel syndrome, and occasionally this may be a cause of suspected recurrent carpal tunnel syndrome [7–9].

66.2 Indications and Contraindications

- Patients with symptoms consistent with pronator syndrome such as grip weakness, paresthesia in median nerve distribution, and pain in proximal forearm.
- Positive provocative tests such as
  - Positive Tinel sign at anterior proximal forearm
  - Pain with resisted elbow flexion with forearm supination (compression at bicipital aponeurosis)
  - Pain with resisted contraction of the FDS to middle finger (compression at FDS fibrous arch)
  - Pain with resisted forearm pronation with elbow extended (compression between heads of pronator teres)
- Failed conservative management (rest, splint, and anti-inflammatories) for at least 3 months unless there is severe compression with possible nerve damage. Patients with severe compression leading to constant symptoms or severe weakness are surgically released to minimize risk of permanent nerve damage from prolonged severe compression.

M. J. Fitzmaurice (✉)
Fitzmaurice Hand Institute, Scottsdale, AZ, USA
e-mail: DrFitz@Fitzhand.com

© ISAKOS 2022

D. N. Bhatia et al. (eds.), *Arthroscopy and Endoscopy of the Elbow, Wrist and Hand*,
https://doi.org/10.1007/978-3-030-79423-1_66

Contraindications for this procedure include excessive scar tissue from previous procedures, tumors, vascular abnormalities, and abnormal osseous anatomy. A detailed knowledge of the anatomy and experience in minimally invasive procedures is critical to perform this procedure and avoid any potential complications.

66.3 Surgical Technique

The patient is placed in a supine position with the affected arm on an arm board. The surgeon is positioned facing the medial aspect of the arm. The video monitor is positioned across from the surgeon toward the patient's head. An EndoTech sheath, 2.7 mm arthroscope, basic hand tray, and bipolar cautery are necessary for the procedure. A single longitudinal incision is marked on the proximal forearm starting 2–3 cm distal to cubital crease and extended for approximately 3 cm.

- The procedure is performed under local anesthesia. 20 cc of 1% lidocaine with 1:100,000 epinephrine and 2 cc of 8.4% bicarbonate is injected into the surgical site. The bicarbonate is added to decrease the acidic sting of the local anesthetic. The anesthetic is allowed approximately 30 min to best effect.
- A 3-cm incision is made 3 cm distal to the cubital crease over the palpable radial border of the flexor mass and slightly ulnar to the midline. A longitudinal incision is used in case it is necessary to convert to an open technique with larger exposure.
- Subcutaneous tissues are divided, taking care to protect and preserve sensory nerve branches and control bleeders with a bipolar cautery.
- The basilic vein is identified and retracted, and the lacertus fibrosus is identified and divided completely under direct vision.
- The PT muscle mass is retracted medially, and the biceps and brachioradialis are retracted laterally.
- Blunt dissection is carried out to reveal the MN, which is located medial and deep to the brachial artery.
- The nerve is dissected as distally, and proximally as direct vision allows until a plane is developed for the insertion of the endoscope.
- The EndoTech sheath is then inserted; the sheath has a tip allowing blunt dissection between the muscles and fascial planes and lifts up the overlying soft tissue to allow visualization of structures below.
- The endoscope with EndoTech sheath is inserted from proximal to distal, lifting soft tissues and allowing visualization of the median nerve. This allows placement of scissors to complete divide any constricting fascia over the median nerve.
- Often, the deep head of the PT has a fibrous portion that puts pressure on the median or anterior interosseous nerve (AIN) which can be released with direct endoscopic visualization.
- The dissection is then carefully carried to the fibrous arch of the FDS, where the nerve compression is frequently encountered. The arch is identified and released using scissors (Figs. 66.1 and 66.2).
- The dissection can also be performed proximally through the port site, allowing division of a ligament of Struthers if present.

66.4 Postoperative Care

Absorbable sutures are typically placed avoiding need for suture removal. Motion and light activity of less than 10 pounds are allowed immediately.

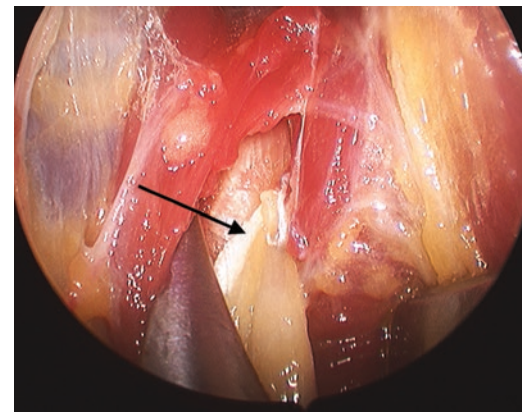

Fig. 66.1 Visualization of the median nerve and any potential bands causing compression (arrow)

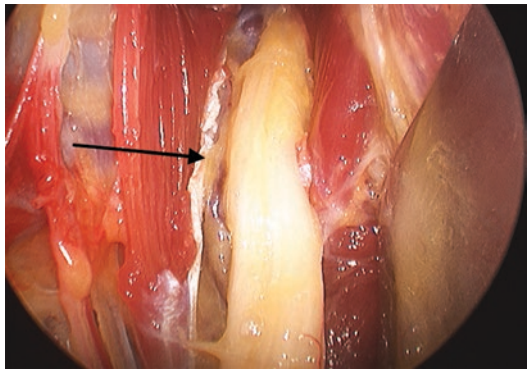

Fig. 66.2 Divided bands (arrow) with complete release of the median nerve

Activity is increased as tolerated after the first week.

66.5 Pitfalls and Complications

- It is critical to evaluate all possible sources for proximal median nerve compression for optimal results and to avoid any incomplete releases.
- Hematoma is a possible complication, and it is important to ensure adequate hemostasis. The technique can be performed under local anesthesia without tourniquet; however, if a tourniquet is used it is critical to let the tourniquet down and ensure hemostasis before closing the wound.
- Conversion to an open approach should be performed if any technical difficulty or abnormal anatomy prevents adequate visualization of the median nerve.

66.6 Results

Our original work was the first published data on an endoscopic technique for pronator syndrome. The results of the technique demonstrated a 90% improvement in DASH scores with an improvement from a preoperative score of 57 to a DASH score of 6 at an average of 22 months follow-up. All patients had resolution of paresthesias.

References

1. Rehak D. Pronator syndrome. Clin Sport Med. 2001;20(3):531–40.
2. Guo B, Wang A. Median nerve compression at the fibrous arch of the flexor digitorum superficialis: an anatomic study of the pronator syndrome. Hand. 2014;9(4):466–70.
3. Matsuzaki A. Operative treatment of pronator syndrome. Orthop Traumatol. 1999;7(1):34–43.
4. Nigst H, Dick W. Syndromes of compression of the median nerve in the proximal forearm (pronator teres syndrome; anterior interosseous nerve syndrome). Arch Orthop Trauma Surg. 1979;93(4):307–12.
5. Lee AK, Khorsandi M, Nurbhai N, Dang J, Fitzmaurice M, Herron KA. Endoscopically assisted decompression for pronator syndrome. J Hand Surg Am. 2012;37(6):1173–9. https://doi.org/10.1016/j.jhsa.2012.02.023.
6. Vergara-Amador E, Castillo-Pérez S, Tovar-Cuellar W. Endoscopic release of the median nerve in the proximal third of the forearm. A new approach. Revista Española De Cirugía Ortopédica Y Traumatología Engl Ed. 2019;63(6):439–46.
7. Hsiao C-W, Shih J-T, Hung S-T. Concurrent carpal tunnel syndrome and pronator syndrome: a retrospective study of 21 cases. Orthop Traumatol Surg Res. 2017;103(1):101–3.
8. Mujadzic M, Papanicolaou G, Young H, Tsai T-M. Simultaneous surgical release of ipsilateral pronator teres and carpal tunnel syndromes. Plast Reconstr Surg. 2007;119(7):2141–7.
9. Luangjarmekorn P, Tsai T-M, Honsawek S, Kitidumrongsook P. Role of pronator release in revision carpal tunnel surgery. SICOT-J. 2016;2:9. https://doi.org/10.1051/sicotj/2016006.

Part XIII

Wrist: Basic Science

Functional Anatomy of the Wrist

67

Simon MacLean, Melanie Amarasooriya, and Gregory I. Bain

67.1 Background

The wrist is a complex series of 20 articulations binding 15 bones, acting as a universal joint that moves through multiple axes of motion. The motion of the wrist allows the positioning of the hand freely in space. Load is transmitted from the hand to the forearm through the three columns of the wrist. To ensure stability, ligaments act as checkreins in a series of rings that span from the distal radius to the hand.

This chapter describes the functional anatomy of the wrist. To appreciate wrist function, the distal radius anatomy is examined at a microscopic level to understand the microarchitecture design that allows it to withstand physiological loads. The clinical macroscopic anatomy is then presented with an emphasis on wrist function.

S. MacLean (✉)
Department of Orthopaedic Surgery, Tauranga Hospital, Tauranga, New Zealand

M. Amarasooriya
Flinders University, Adelaide, SA, Australia

G. I. Bain
Department of Orthopaedic Surgery, Flinders University, Adelaide, SA, Australia
e-mail: greg@gregbain.com.au

67.2 Microanatomy of the Distal Radius

The skeleton has evolved to withstand the loads placed upon it. Bone is the organ of compression designed to withstand the load. Load is transferred between the bones with the wrist functioning as a carpal grid, with the three columns transmitting the load to the radius [1]. The column that is loaded is determined by the position of the wrist, whether in radial/ulnar deviation or neutral.

Studies of the microarchitecture of the distal radius suggest that modern engineering and architectural design, developed over 100 s of years, resemble nature's structures that have evolved over millions of years. In the *coronal plane* of the radius, the primary subchondral bone plate spans across the entire distal radius. Deep to the primary layer are the secondary and tertiary layers that resemble a 'leaf spring' used in the suspension of heavy vehicles. At the articular margin, the cortex is thin, and in some areas, it is non-existent due to the perforations provided by the ligament attachments.

67.2.1 The Arch Bridge Concept

The radius microstructure resembles an 'arch bridge' (Fig. 67.1) [2, 3]. The radius has the following equivalent: (a) deck: subchondral bone

© ISAKOS 2022

D. N. Bhatia et al. (eds.), *Arthroscopy and Endoscopy of the Elbow, Wrist and Hand*,
https://doi.org/10.1007/978-3-030-79423-1_67

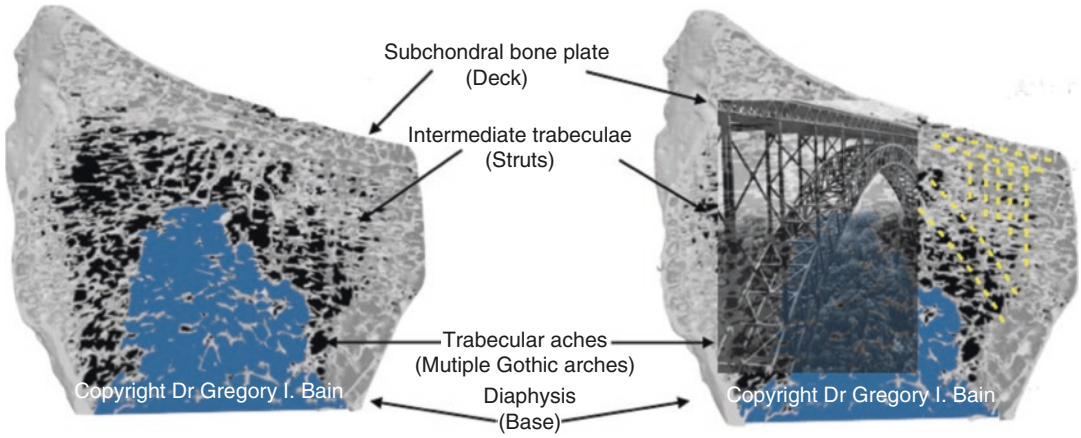

Fig. 67.1 Micro-CT of the distal radius-coronal view: the microstructure of the distal radius resembling an arch bridge. Copyright Dr. Gregory I. Bain

plate (SBP), (b) intermediate struts: intermediate trabeculae, (c) arches and (d) bridge foundation: cortex. The deck is tightly held as a lattice with multiple 'I' beams in a multilayer honeycomb sandwich panel construct. This structure resists buckling, absorbs impact and bears the entire load. The multilayered subchondral bone plate resists buckling and transmits the load to intermediate trabeculae and then to the metaphyseal arches (Fig. 67.2). The arches and intermediate struts are a semi-flexible construct that distributes compressive forces from the deck to the base (diaphysis) [1]. The orientation of the microstructure ensures that forces are distributed in compression rather than tension (where the bone is weakest). With physiological wrist extension, the volar capsule becomes taut, and the scaphoid and lunate load the distal radius subchondral bone plate.

Sagittal images demonstrate the functional microarchitecture of the distal radius. The lunate facet is supported by the thick volar trabecular columns spanning to the volar cortex of the metaphyseal radius. The load-bearing area of the lunate facet is further volar and in line with the volar cortex of the radius. This explains the devastating effect of Barton's volar lip fracture resulting in volar dislocation of the carpus.

The trabeculae of the scaphoid facet form a series of gothic arches that are connected by inter-arch struts. The gothic arch construct transfers load in a longitudinal and lateral direction to the base of the arch without creating tension. This parabolic arch is the perfect shape to distribute the load and maintain compression throughout all aspects of the construct (Fig. 67.3).

The interosseous space between the radius and the ulna is held open by the width of the distal radial metaphysis and the ulnar head. This highlights that the distal medial flare of the radius is important in maintaining the normal morphology of the distal radius. This distal ulnar margin of the radius is curved and shaped to withstand the load and extends more volar to include the support of the lunate facet. This region is the 'calcar' of the distal radius, loading and functioning in a similar manner to the calcar of the femur (Fig. 67.4). On AP radiographs of the wrist can be seen a smooth 'Shenton's line', from the radial shaft, radial calcar, ulnar neck and ulnar shaft. Fractures in the radial calcar may lead to the collapse of the interosseous space. On AP radiographs, translation of the radial shaft towards the ulnar shaft is seen, and the natural 'Shenton's line' is broken. It is the collapse of the radial calcar that allows the radial shaft to translate towards the ulna, narrowing the interosseous space.

Osteoporotic distal radius fractures reflect a change in the microstructure of the distal radius with ageing and are a predictor for subsequent

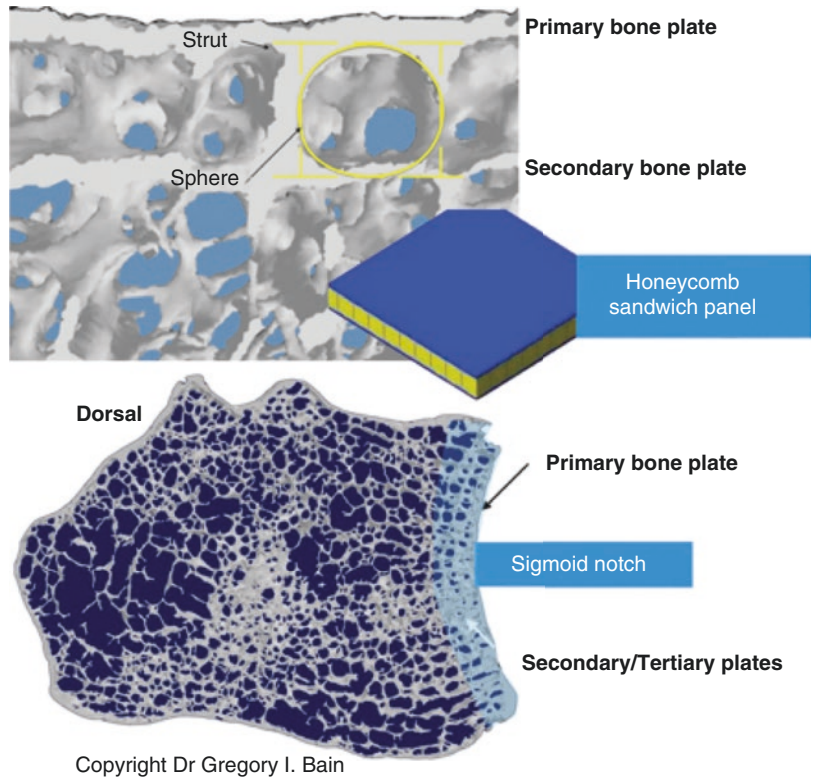

Fig. 67.2 The microstructure of the distal radius acts as a honeycomb sandwich panel. Copyright Dr. Gregory I. Bain

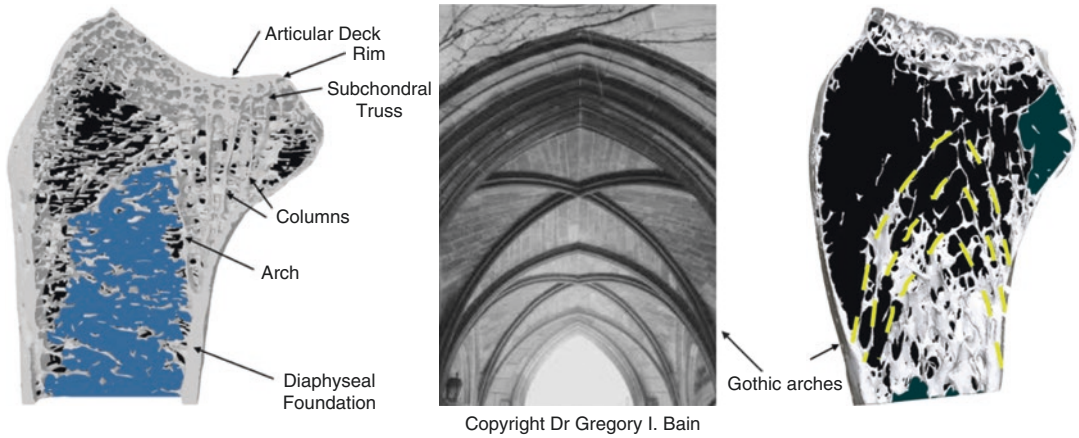

Fig. 67.3 The sagittal microanatomy of the distal radius resembling a gothic arch. Copyright Dr. Gregory I. Bain

fracture of long bones [2]. There can be extensive voids in the intermediate trabeculae and the vault. In osteoporotic fractures, this metaphyseal bone is crushed. When the fracture is reduced, this soft fine bone will not disimpact, which predisposes to the re-collapse of the fracture [4].

67.3 Articulations

The concavities of the distal radius articular surface match the differing convexities of the proximal scaphoid and lunate. These separate facets, termed the scaphoid and lunate fossae, are separated by a sagittal ridge (Fig. 67.5).

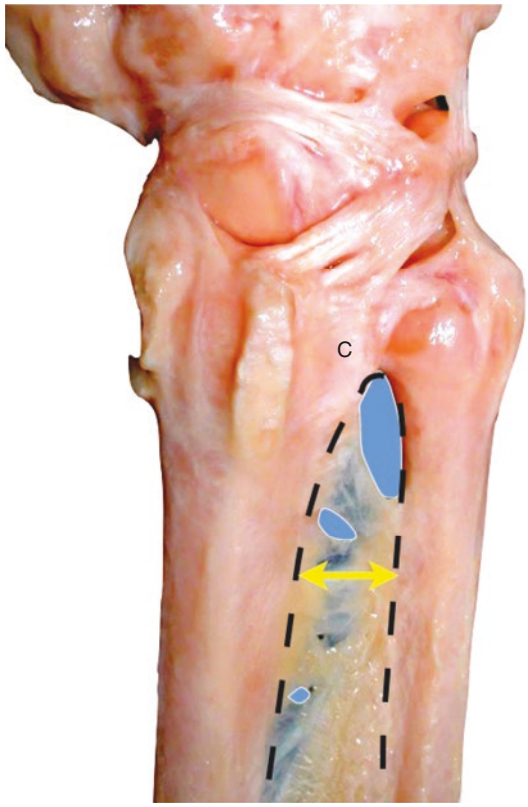

Fig. 67.4 The calcar is a thick dense concave cortical bone that extends from the medial radial shaft to the sigmoid notch. It is important for transmitting load from the radius to the ulna. The calcar (C) maintains the interosseous space and creates the Shenton's line. Copyright Dr. Gregory I. Bain

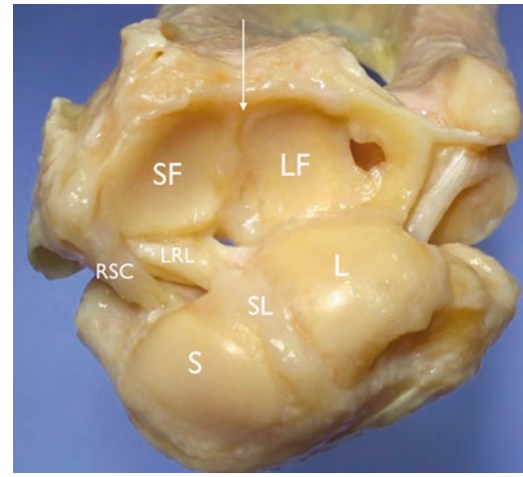

Fig. 67.5 The scaphoid and lunate fossae are seen separated by a sagittal ridge. (*SF* scaphoid fossa, *LF* lunate fossa, *RSC* radioscaphocapitate ligament, *LRL* long radiolunate ligament, *S* scaphoid, *L* lunate, *SL* scapholunate ligament). Photograph of dissection courtesy of Dr. Amit Gupta. Copyright Dr. Gregory I. Bain

67.4 Ligaments

Ligaments span from one bone to another; they resist tensile forces and restrain the motion between bones. The described carpal ligaments [5–7] clearly have an important function in stabilizing the carpus; in addition, they also have an important proprioceptive function [8] and provide vascularity to the adjacent osseous structures.

The distal radius and each carpal bone have a large proportion of their surface area covered in articular cartilage. On each bone, the ligaments are clustered together. These ligaments converge as ligament complexes and attach to prominent tuberosities on the bone. Each ligament has a unique primary function, restraining the bones in a single direction. The sites where the ligament complexes attach are strategically positioned, and these sites are referred to as 'nidus points'. Examples include the fovea of the distal ulna and volar capitate. The nidus points are linked by their ligaments to the other nidus points. These nidus points and the associated ligaments form multiple ligamentous rings that stabilize the wrist and are explained further in the Chap. 68.

The ligaments of the wrist form three groups: volar radiocarpal, dorsal radiocarpal and interosseous ligaments (Fig. 67.6). The volar group includes the radioscaphocapitate (RSC), radioscapholunate (RSL, also known as the ligament of Testut) and short and long radiolunate (SRL, LRL) ligaments. The LRL restrains lunate ulnar translation, and SRL resists volar translation and distraction. The volar extrinsic ligaments form a double chevron configuration with the apex distally—known as the arcuate ligament. The Space of Poirier is a ligament void, bounded by the proximal edge of the RSC and ulnocarpal ligaments distally and the distal edge of the LRL ligament proximally. It is a weak spot volarly where peri-lunate dislocations occur (Fig. 67.7).

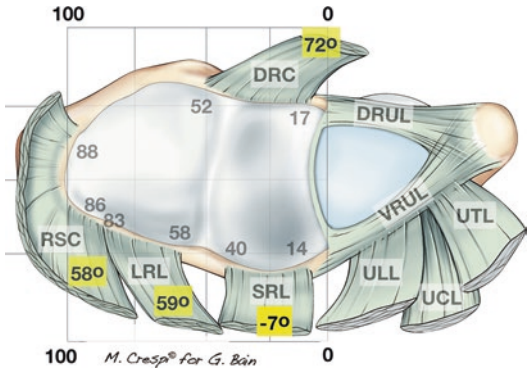

Fig. 67.6 The multiple distal radius ligament attachments. The numbers are the percentiles of the radioulnar width of the radius. Included are the angles of the ligaments compared to the axial plane of the radius. (Modified from Zumstein JWS 2013 [9, 10]). Copyright Dr. Gregory I. Bain

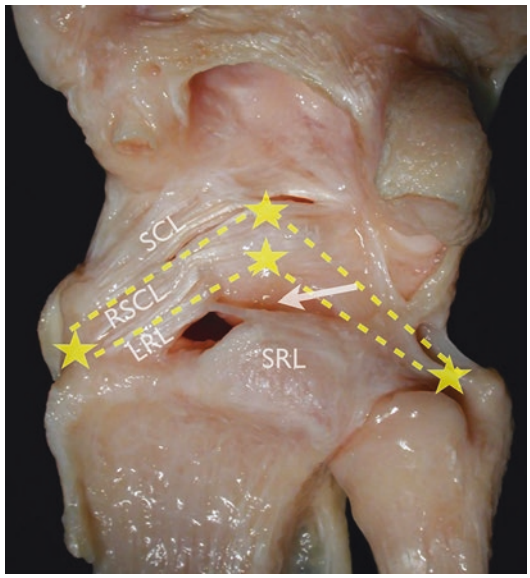

Fig. 67.7 The proximal and distal arcuate ligament complexes on the volar aspect of the wrist (dotted yellow lines). The radius, lunate, capitate and ulna are shown by the yellow stars. The Space of Poirier is shown by the white arrow. Photograph of dissection courtesy of Dr. Amit Gupta. Copyright Dr. Gregory I. Bain

The dorsal and ulnar ligaments arising from the triquetrum are regarded as the key sensory ligaments in the generation of proprioceptive information for neuromuscular wrist control [2]. The dorsal ligaments include the dorsal radiocarpal (DRC) and dorsal intercarpal (DIC) ligaments. These form a chevron converging to the triquetrum (Fig. 67.8).

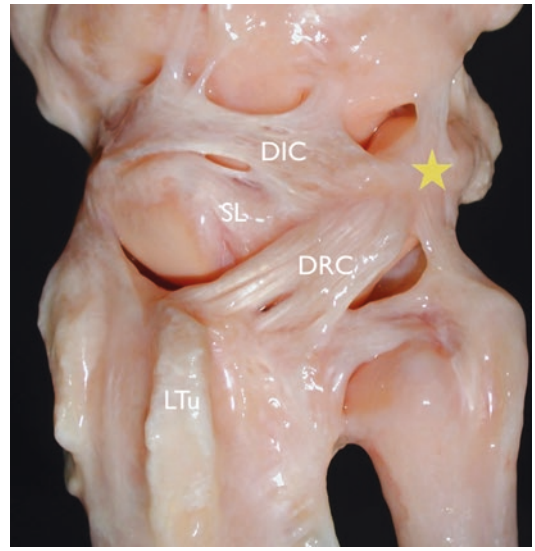

Fig. 67.8 The extrinsic dorsal ligaments of the wrist. (*DRC* dorsal radiocarpal ligament, *DIC* dorsal intercarpal ligament, *LTu* Lister's tubercle, *SL* scapholunate ligament). The ligaments converge to the triquetrum (yellow star). Photograph of dissection courtesy of Dr. Amit Gupta. Copyright Dr. Gregory I. Bain

The scapholunate joint is stabilized by a volar and dorsal intercarpal ligament with a proximal fibrocartilaginous membrane. The dorsal component of the ligament has the greatest yield strength (260 N dorsal, vs. 63 N volar) and is therefore the most important stabilizer of the scapholunate joint (Fig. 67.9) [3]. The lunotriquetral joint has a similar construct, that is volar, dorsal and fibrocartilaginous components, but in contrast to the scapholunate ligament complex, the volar part is the thickest with a greater yield strength (301 N vs. 121 N) [4].

67.5 Triangular Fibrocartilage Complex (TFCC)

The Triangular fibrocartilage complex (TFCC) is the ulnar-sided shock absorber and an important stabilizer of the DRUJ. The complex consists of anatomically distinct structures that function as a unit. The articular disc, meniscal homologue, palmar and dorsal radioulnar ligaments, ulnocarpal ligaments and ECU tendon subsheath together form the 'TFCC' as first described by Palmer [11]. From the ulnar fovea span the

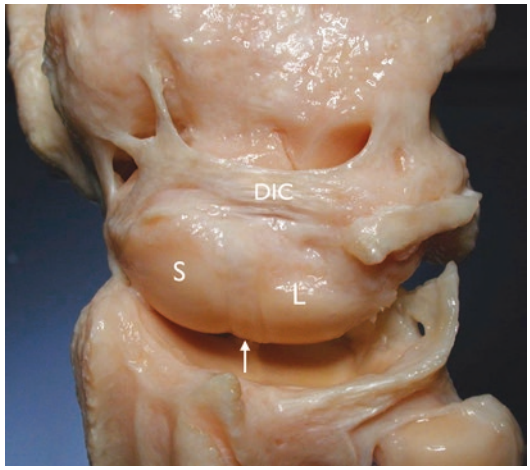

Fig. 67.9 The scapholunate ligament complex as seen from the dorsal aspect. (*S* scaphoid, *L* lunate, *DIC* dorsal intercarpal ligament, *SLL* shown by the white arrow). Photograph of dissection courtesy of Dr. Amit Gupta. Copyright Dr. Gregory I. Bain

ulnotriquetral, ulnocapitate and ulnolunate ligaments (UT, UC and UL). The ulnocarpal ligaments are an important stabilizer for the distal radioulnar joint, TFCC and ulnar carpus, acting as an ulnar hammock. Disruption of these ligaments creates an ulnar carpal sag—an important component of distal radioulnar joint instability (Fig. 67.10).

The prestyloid recess is a synovial-lined recess that lies between the ulnotriquetral ligament and the meniscal homologue.

The ECU subsheath is the thickened floor of the ECU tendon sheath and has insertions to the triquetrum, hamate and fifth metacarpal.

The dorsal and volar radioulnar ligaments arise from the styloid inserting into the dorsal and volar margins of the greater sigmoid notch, respectively (Fig. 67.11).

67.6 Fibro-osseous Tunnels

The carpal tunnel and Guyon's canal are the important volar fibro-osseous tunnels. The boundaries of the carpal tunnel include (a) radial side: ridge of trapezium and scaphoid tubercle, (b) ulnar side: hook of hamate and pisiform, (c) floor: carpal bones and (d) roof: transverse carpal ligament. The carpal tunnel includes the eight long flexors of the digits, the flexor pollicus longus (FPL) and the median nerve (Fig. 67.12).

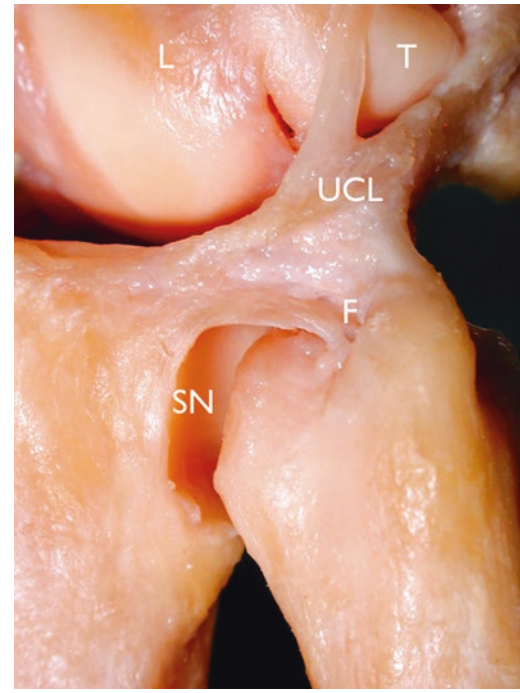

Fig. 67.10 The TFCC from the dorso-ulnar aspect showing the foveal insertion (F) and the ulnocarpal ligaments (UCL) (*SN* sigmoid notch, *L* lunate, *T* triquetrum). Photograph of dissection courtesy of Dr. Amit Gupta. Copyright Dr. Gregory I. Bain

Fig. 67.11 TFCC—superior aspect. The Foveal insertion (F) is shown with the dorsal and volar radioulnar ligaments. (*US* ulnar styloid)

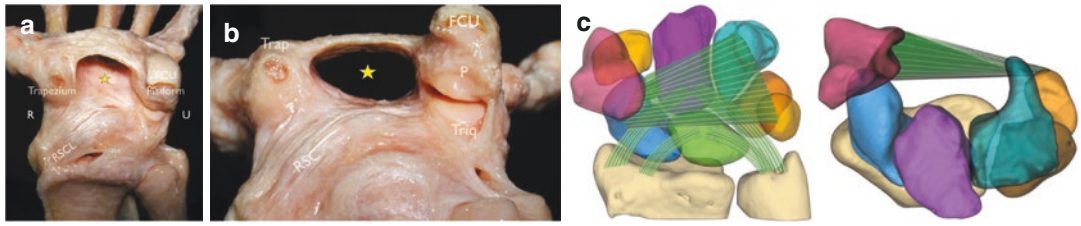

Fig. 67.12 The boundaries of the carpal tunnel are shown from the volar aspect (**a**) and axial section (**b**). (Carpal tunnel: yellow star, *RSC* radioscaphocapitate ligament, *P* pisiform, *FCU* flexor carpi ulnaris). The corresponding computerized illustration is shown (**c**). Photographs of dissection courtesy of Dr. Amit Gupta. Copyright Dr. Gregory I. Bain

67.7 Extrinsic Extensor Tendons

The relationship of the extensor compartments is seen in Fig. 67.13. The first dorsal compartment contains the APL and EPB tendons and forms the radial side of the anatomical snuffbox. The EPB lies on the ulnar side and inserts onto the base of the first metacarpal. The APL can possess multiple slips, and a separate sub-compartment containing an EPB or APL slip may be present, separated by a longitudinal ridge and septum. The insertion of APL is variable, and it often divides into separate branches distally. The deep slips insert into the trapezium, abductor pollicis brevis, capsule and the anterior oblique ligament of the first CMC joint. The superficial slip inserts into the base of the thumb metacarpal [5]. When performing surgical decompression of the first extensor compartment for De Quervain's disease, variant anatomy should be identified. Only when the tendons of the second extensor compartment are visualized, the surgical release is considered adequate.

The second compartment contains ECRL—inserting on the base of the second metacarpal and ECRB—inserting on the base of the third metacarpal. These tendons act as powerful wrist extensors and radial deviators.

The third compartment contains EPL, which takes a 45° turn around Lister's tubercle before inserting onto the base of the thumb distal phalanx. This position places it at risk when performing wrist arthroscopy. It is also at risk following a distal radius fracture when attritional rupture can occur next to Lister's tubercle.

Fig. 67.13 The relationship of the extrinsic extensor tendon compartments is shown. (White star: extensor retinaculum). Photographs of dissection courtesy of Dr. Amit Gupta. Copyright Dr. Gregory I. Bain

The fourth compartment contains the EDC and EIP, and these tendons insert onto the extensor hood. The EIP is deep to the EDC and inserts onto the ulnar aspect of the index finger. The EIP allows for independent index finger extension and is therefore ideal for EI to EPL transfer.

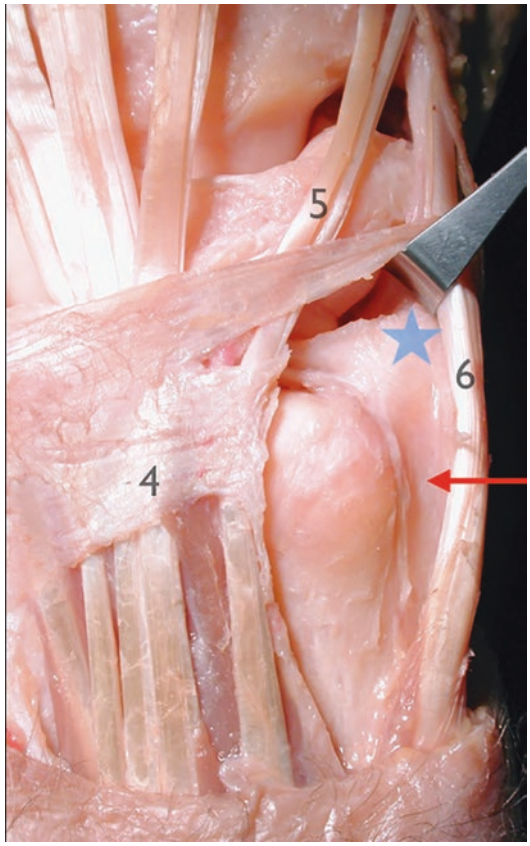

Fig. 67.14 The fourth to sixth extensor compartments. (Red arrow: ECU subsheath with ECU tendon retracted ulnarly, star: ulnar styloid). Photographs of dissection courtesy of Dr. Amit Gupta. Copyright Dr. Gregory I. Bain

The fifth compartment sits dorsal to the DRUJ and contains the EDM tendon. For this reason, the fifth dorsal compartment is the gateway to the DRUJ. It inserts on the ulnar aspect of the EDC tendon at the level of the extensor hood. The EDM, like the EIP, allows for independent little finger extension.

The sixth extensor compartment contains the ECU tendon. The ECU tendon lies in a groove between the ulnar styloid and the ulnar head before inserting into the base of the fifth metacarpal. The ECU subsheath is a fascial band from the radius that provides some stability for the DRUJ. If this is ruptured, the ECU tendon can dislocate ulnarly in wrist ulnar deviation (Fig. 67.14).

67.8 The Volar Wrist Flexors and the 'Pulley System'

The volar wrist flexors include the flexor carpi radialis (FCR) and flexor carpi ulnaris (FCU). The FCR runs radial to FDS and inserts onto the volar aspect of the base of the second metacarpal and has small slips to both the third metacarpal and the tuberosity of the trapezium. The FCU inserts onto the pisiform and then into the piso-hamate and piso-metacarpal ligaments.

The ulnar-sided tendons, the ECU and FCU in isolation act to initiate ulnar deviation with extension or flexion. If acting together, however, they produce a force couple and act as a pulley system to control ulnar deviation with the wrist in neutral. This phenomenon is made possible by having adjacent insertions on the fifth metacarpal (Fig. 67.15). On the radial side of the wrist, the FCR and ECRL tendons have similar adjacent insertions into the base of the second metacarpal. Together with the ECRB, these five tendons all insert into the metacarpals and control the motion of the wrist (Fig. 67.16a and b).

In conclusion, the anatomy of the wrist has evolved to allow stable motion through multiple axes. The precise interplay between carpal bones, ligaments and tendons is debated and continues to make reconstructive surgery a challenge.

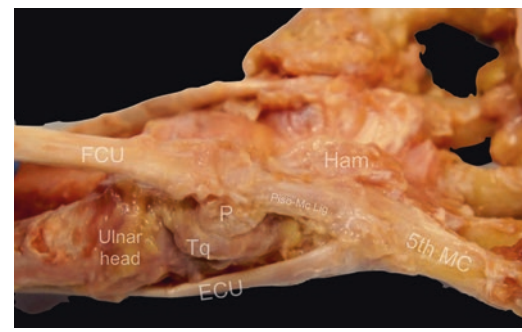

Fig. 67.15 The relationship of the ulnar extrinsic extensor tendons. Note the converging insertion points demonstrating the 'ulnar pulley' of the wrist. Photographs of dissection courtesy of Dr. Amit Gupta. Copyright Dr. Gregory I. Bain

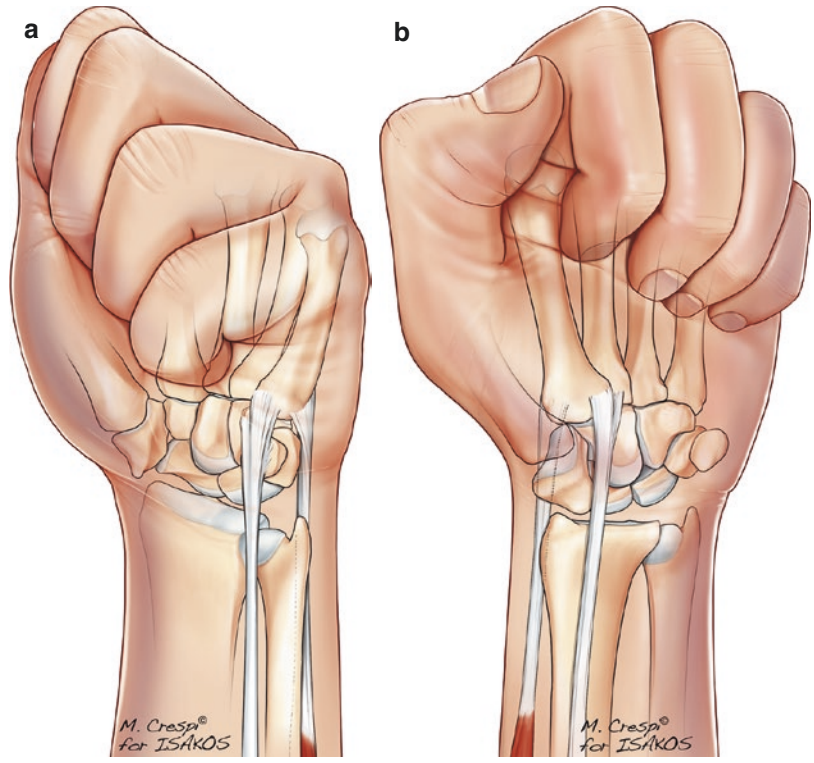

Fig. 67.16 The radial and ulnar wrist extensors act as a 'double pulley system' to control wrist motion in ulnar deviation (**a**) and radial deviation (**b**). (Crespi © for ISAKOS)

References

1. Bain GI, McGuire DT. Decision making for partial carpal fusions. J Wrist Surg. 2012;1(2):103–14.
2. Bain GI, MacLean SBM, McNaughton T, Williams R. Microstructure of the Distal Radius and Its Relevance to Distal Radius Fractures. J Wrist Surg. 2017;6(4):307–15.
3. MacLean SBM, Bain G. Anatomy of the fracture. In: del Piñal F, editor. Distal Radius Fractures and Carpal Instabilities FESSH IFSSH 2019 Instructional Book. Thieme Medical Publishers Inc.; 2019. p. 1–11.
4. Mackenney PJ, McQueen MM, Elton R. Prediction of instability in distal radial fractures. J Bone Jt Surg Ser A. 2006;88(9):1944–51.
5. Berger RA. The ligaments of the wrist: a current overview of anatomy with considerations of their potential functions. Hand Clin. 1997;13(1):63–82.
6. Berger RA. The anatomy of the ligaments of the wrist and distal radioulnar joints. Clin Orthop Relat Res. 2001;383:32–40.
7. Kijima Y, Viegas SF. Wrist anatomy and biomechanics. J Hand Surg Am. 2009;34(8):1555–63.
8. Hagert E, Garcia-Elias M, Forsgren S, Ljung BO. Immunohistochemical analysis of wrist ligament innervation in relation to their structural composition. J Hand Surg Am. 2007;32(1):30–6.
9. Mandziak DG, Watts AC, Bain GI. Ligament contribution to patterns of articular fractures of the distal radius. J Hand Surg Am. 2011;36(10):1621–5.
10. Bain GI, Alexander JJ, Eng K, Durrant A, Zumstein MA. Ligament origins are preserved in distal radial intraarticular two-part fractures: a computed tomography-based study. J Wrist Surg. 2013;2(3):255–62.
11. Palmer AK, Werner FW. The triangular fibrocartilage complex of the wrist—anatomy and function. J Hand Surg Am. 1981;6(2):153–62.

Clinical Biomechanics of the Wrist

68

Melanie Amarasooriya, Simon MacLean, and Gregory I. Bain

Abbreviations

APL	Abductor pollicis longus
CMC	Carpometacarpal
D	Dorsal
DISI	Dorsal intercalated segmental instability
DRC	Dorsal radiocarpal ligament
DRUJ	Distal radioulnar joint
DTM	Dart thrower's motion
DTP	Dart thrower's plane
ECRB	Extensor carpi radialis brevis
ECRL	Extensor carpi radialis longus
ECU	Extensor carpi ulnaris
ECU	Extensor carpi ulnaris
EPL	Extensor pollicis longus
FCR	Flexor carpi radialis
FCU	Flexor carpi ulnaris
FPB	Flexor pollicis brevis
FPL	Flexor pollicis longus
FR	Flexor retinaculum
LC	Luno-capitate
LCHT	Luno-capito-hamate-triquetrum
LT	Luno-triquetral
PIN	Posterior interosseous nerve
RL	Radio-lunate
RLL	Radio-lunate ligament
RS	Radio-scaphoid
RSC	Radioscaphocapitate
RSL	Radioscapholunate
RUD	Radioulnar deviation
SC	Scapho-capitate
SL	Scapho-lunate
SLIL	Scapholunate instability
SLIL	Scapholunate interosseous ligament
STT	Scapho-trapezio-trapezoid
TC	Triquetro-capitate
TFCC	Triangular fibrocartilage complex
TH	Triquetro-hamate
Tq	Triquetrum
UC	Ulno-capitate
V	Volar
VISI	Volar intercalated segment instability

M. Amarasooriya (✉)
Flinders University, Adelaide, SA, Australia
e-mail: amar0041@flinders.edu.au

S. MacLean
Department of Orthopaedic Surgery, Tauranga Hospital, Tauranga, New Zealand

G. I. Bain
Department of Orthopaedic and Trauma Surgery, Flinders University and Flinders Medical Centre, Adelaide, SA, Australia
e-mail: admin@gregbain.com.au

68.1 Introduction

The wrist is a joint of remarkable mobility that enables the hand to function with precision, power and stability. Biomechanics of the wrist is the study of the physiological wrist motion (kinematics) and stability while bearing load without yielding (kinetics). In most texts, the two areas

© ISAKOS 2022

D. N. Bhatia et al. (eds.), *Arthroscopy and Endoscopy of the Elbow, Wrist and Hand*,
https://doi.org/10.1007/978-3-030-79423-1_68

are separated, but in real life, it is the loaded wrist that moves. Therefore, in the study of wrist biomechanics, we believe, kinetics is equally important as kinematics.

In this chapter, we present how the wrist loads through the columns and mobilizes in the rows. The loading columns and moving rows are stabilized by multiple ligamentous rings, strategically positioned to create a universal joint that can stabilize the hand in any position in space, with or without grasping strength.

68.2 Carpal Kinetics

Carpal kinetics is the study of how carpus bears load without yielding. Carpus anatomically is divided into proximal and distal rows with extrinsic and intrinsic carpal ligaments stabilizing it. A number of theories such as row, column and oval ring theory attempt to describe bony anatomy with the mechanics of the wrist [1–4].

Under compression or traction, the carpal bones displace in a predictable way. They return to their normal position when the force is removed. The primary restraints for the carpus are the ligaments.

68.2.1 Columns, Rows and Rings

It had been debated over a century whether the wrist behaves as columns, rows or the oval ring. In a model where the loaded wrist is moving, maintaining its stability, it demonstrates features of all three concepts. The wrist is mobilized by the long wrist tendons and their muscles. The wrist loads axially in *columns*, moves as *rows* of functional units and is stabilized by ligamentous *rings*. Ligaments are supported by the dynamic action of muscles and neuromuscular feedback [5, 6]. In the following section, we discuss how each model contributes to its function.

68.2.1.1 Loading Columns

The force transmitted through the wrist is quite considerable. For example, a load applied to the tip of the finger generates loads as high as 1.2–4.6 times of that, on the corresponding CMC joint [7]. Nearly half of this is transmitted through the capitate, across the scaphoid and lunate [8]. Load distribution across the carpus is shown in Fig. 68.1. Wrist position affects this dynamics as radio-lunate (RL) articulation transfers more load on ulnar deviation [7]. In the functional position of the wrist, with slight extension and ulnar deviation, the radio-scaphoid (RS) joint transmits less load (40%) and RL more load (53%) [9] (Fig. 68.2). Each column is different with regard to the magnitude of the loads they transmit in each wrist position.

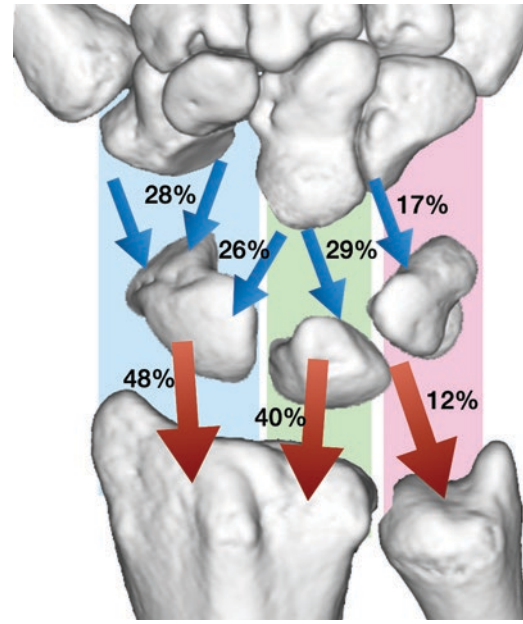

Fig. 68.1 The load distribution through the three columns. In the neutral position of the wrist, the radial column transmits more load than the ulnar and the central columns. Image copyright—Prof. Gregory I. Bain

68.2.1.2 The Rows

The wrist consists of the rows including the forearm, proximal carpal row and distal carpal row (Fig. 68.3).

68.2.1.3 Forearm Row

The forearm rotates around an axis from radial head to ulnar styloid. Thereby, the forearm sets the prono-supination angle for the wrist. Most of the wrist function occurs in relative forearm pronation.

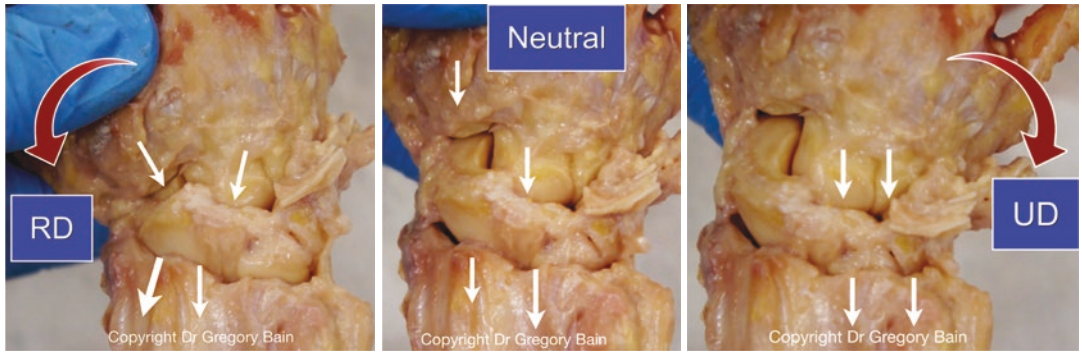

Fig. 68.2 The proximal carpal row swivels below the distal row and changes orientation with radio-ulnar deviation. The load distribution of the columns changes with wrist position. In radial deviation, the radio-scaphoid facet transmits more load. In ulnar deviation, the radio-lunate facet transmits more load

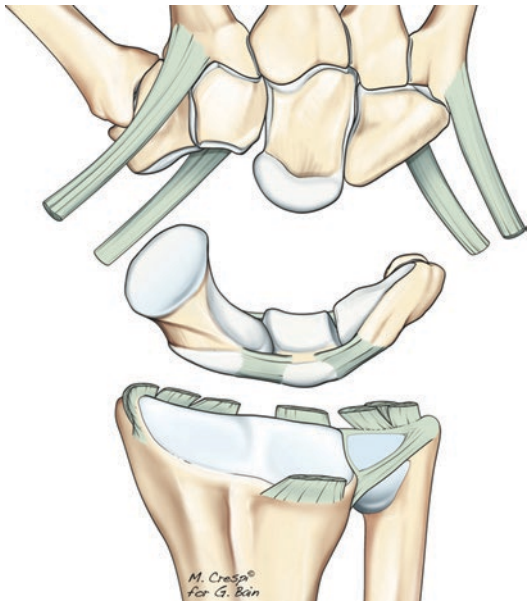

Fig. 68.3 This figure highlights the three carpal rows, the forearm, proximal and distal carpal rows. The bones in each row are tightly knit, stabilized by their own ligaments, creating a functional unit. Note how the wrist tendons insert into the metacarpals. (Copyright Gregory I. Bain and Max Crespi)

Radius

The radius has a steep inclination from radial to ulnar and dorsal to volar. This makes the radiocarpal joint intrinsically unstable. There are strong volar and dorsal extrinsic ligaments encircling the lunate and triquetrum preventing ulnar and volar translocation.

Ulna

While the radius makes the primary articulation with the carpus, the ulna remains the primary bone of the forearm. The entire wrist rotates around the foveal attachment of the TFCC. Thereby, the distal radioulnar joint (DRUJ) becomes an important load-bearing joint. The dorsal and volar radioulnar ligaments stabilize the DRUJ.

Proximal Carpal Row

The proximal carpal row consists of the scaphoid, lunate and triquetrum. It is named the 'intercalated segment' as no tendons attach to any of the bones. When the proximal carpal row is loaded, its motion is controlled by the distal carpal row and its bony contours and ligaments. Being positioned between the distal row and the forearm row, the proximal row swivels between them, depending upon the wrist position. Proximally, the greater arcuate ligament spans to the radius and ulna and bypasses the proximal carpal row. This allows the radius and ulna to swing beneath the capitate.

Lunate

The lunate has been referred to as the keystone of the carpus [10]. It is also the intercalated bone of the intercalated segment. It is tightly held onto the radius and other proximal carpal row bones by radio-lunate and interosseous ligaments, but there are no ligaments that extend from the lunate to the distal carpal row (Fig. 68.4).

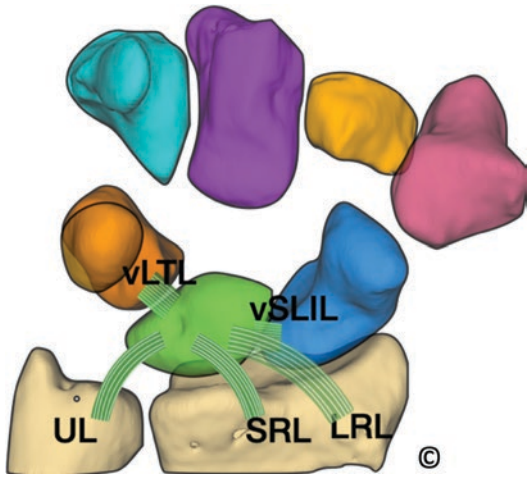

Fig. 68.4 The lunate and its ligaments. The lunate is tightly held to the radius and proximal row. No ligaments extend to the distal carpal row. Image copyrights—Dr. Melanie Amarasooriya and Prof. Gregory I. Bain

Scaphoid

The scaphoid is the 'trouble maker' of the wrist. It spans proximally from the scaphoid facet of the radius to the STT joint distally, spanning across the radiocarpal and the midcarpal joints. The long axis of the scaphoid is oblique, and scaphoid is positioned 'out of plane' to the central column, in a lateral view (Fig. 68.5). The scaphoid connects the radiocarpal joint and the STT joint which is located volar. The scaphoid functions like a 'gear lever' that is directed by the STT joint.

The scaphoid is restrained against volar translation by the radioscaphocapitate (RSC) ligament. It acts as 'seat belt' over which the scaphoid flexes (Fig. 68.6). The scapho-trapezio-trapezoid (STT) ligaments stabilize the distal pole of the scaphoid to the distal row. Dorsally the proximal scaphoid is restrained by the dorsal scapholunate interosseous (dSLIL) ligament, preventing dorsal subluxation of the proximal pole over the rim of the radius [11].

In a normal wrist, radial-sided angulation and radial extension forces are transmitted to the scaphoid through the STT joint. The scaphoid has no extrinsic ligamental attachment to the radius. The distal forces are transmitted to the proximal row via the attachments between the scaphoid and the proximal row, the scapholunate ligament. Thereby, it exerts a flexion moment on the lunate and guides the proximal row motion [12]. Thus, the scaphoid becomes the trouble maker and the gear lever of the wrist, while the scapholunate ligament is crucial to carpal stability.

Fig. 68.5 Lateral view of the wrist. Note the scaphoid is 'out of plane' to the remainder of the carpus and the thumb metacarpal. It spans from radiocarpal to STT joint, acting as a gear lever of the wrist

Triquetrum

The triquetrum is the sensory organ of the wrist [13]. It articulates with the hamate forming the flat biconcave triquetro-hamate joint (Fig. 68.7). During power grip, the flexor carpi ulnaris (FCU) pushes the pisiform and wedges the triquetrum onto the hamate.

Distal Carpal Row

The distal carpal row forms an arch, which is often considered a 'monoblock'. It is formed by the trapezium, trapezoid, capitate and hamate. It

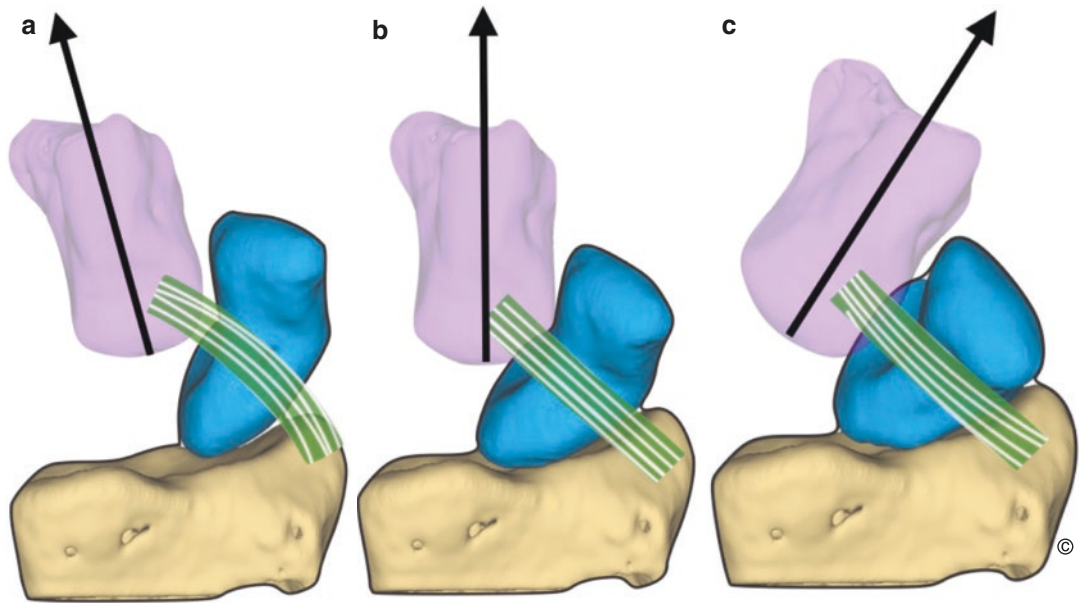

Fig. 68.6 The scaphoid flexes over the RSC ligament from ulnar to radial deviation. The distal row represented here with the capitate which deviates radially tensioning the RSC ligament. This prevents the volar translation of the scaphoid but allows the scaphoid to flex. It acts like a 'seat-belt' restraining volar translation but allows the scaphoid to flex over it, acting as a fulcrum at the waist. The scaphoid gradually flexes, allowing the capitate to move radially. (**a**) Ulnar deviation. (**b**) Neutral. (**c**) Radial deviation. Image copyrights—Dr. Melanie Amarasooriya and Prof. Gregory I. Bain

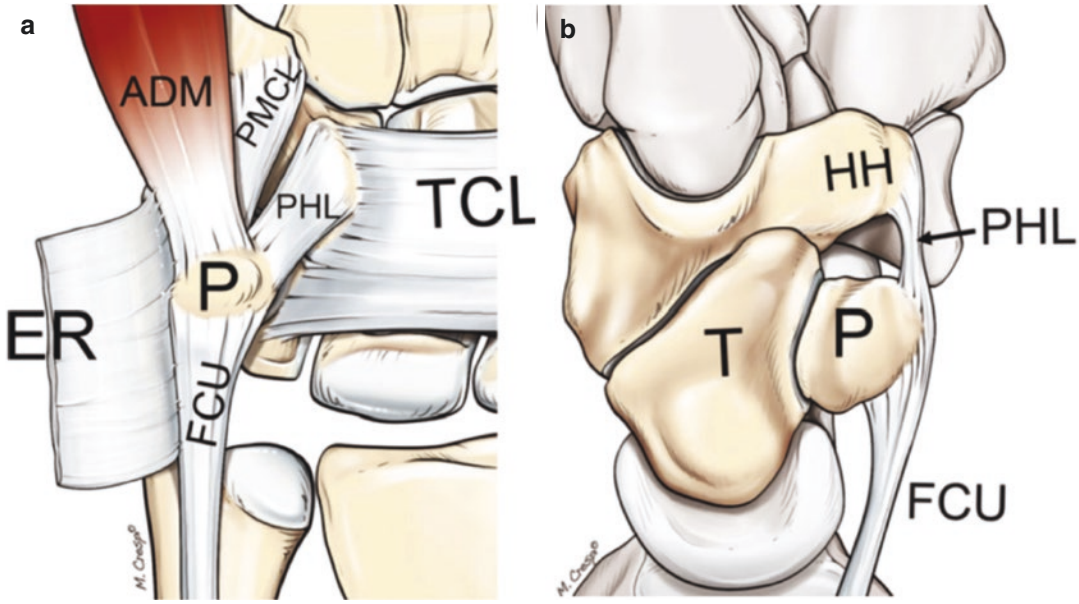

Fig. 68.7 FCU tendon and hypothenar muscles via their attachments to the pisiform mobilizes the ulnar column of the carpus. (**a**) FCU tendon and hypothenar muscle attachment to pisiform. (**b**) Triquetro-hamate joint is a flat biconcave joint. (Copyright Max Crespi. Reproduced from Compson J. (2012) Arthroscopic management of piso-triquetral conditions. In: Del Piñal F. (eds) Arthroscopic management of ulnar pain. Springer, Berlin, Heidelberg)

is stabilized by a ring of ligaments dorsally and volarly adding to transverse stability of the carpus.

The arch of the distal carpal row can be open and close. In quadrapods, this arch is important for loading during walking, as it absorbs the impact of the ground reaction force. When a person falls, this absorbs the load and transmits the force proximally. Thereby, depending on the age and the biology of the bony architecture of the person, ligamental injuries or distal radius fractures can occur. The concept of the monoblock is that during wrist motion the distal row works as a unit and swivels about the capitate. Volar to the arch is the transverse carpal ligament.

Capitate

The capitate has been underappreciated in carpal kinematics. If we reverse the layout of the wrist and place the capitate at the centre, we obtain a completely new appreciation of the importance of the capitate in wrist motion. There is a large proximal head that articulates with the proximal carpal row. The mechanical centre of the wrist is located within the proximal capitate. It is tightly bound to other distal carpal row bones with interosseous ligaments. There are no ligaments between the capitate and the lunate, restraining the luno-capitate motion. However, this ball and socket joint are stabilized indirectly from the periphery creating the universal joint (Fig. 68.8).

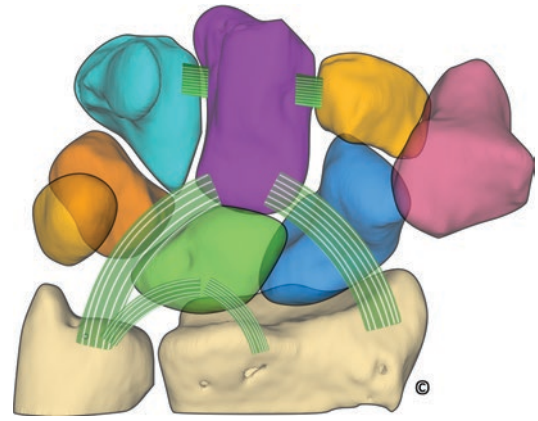

Fig. 68.8 Volar view of the wrist, demonstrating the greater and lesser arcuate ligaments stabilizing the capitate. The radio-scapho-capitate ligament, is the lateral limb of the arcuate ligament, spans from the radial styloid, to the volar radial surface of the capitate. It acts as a fulcrum around which the scaphoid flexes. The ulnar limb of the arcuate ligament is formed by the ulno capitate (UC) ligament, spanning from the fovea of the ulna and inserting to the volar ulnar capitate. This blends with the fibres of the radial limb to form the arcuate ligament. Proximal to the arcuate ligament is the space of 'poirier' through which the midcarpal joint dislocates in perilunate dislocations. Image copyrights—Dr. Melanie Amarasooriya and Dr. Gregory I. Bain

Trapezium and Trapazoid

Trapezium together with trapezoid forms the scaphotrapeziotrapezoid (STT) articulation. They are located volar to the plane of the capitate. The trapezoid is tightly held to the trapezium by the interosseous ligaments, so there is only minimal motion between them [14]. The trapezoid is more tightly held to the second metacarpal making it important for loading in grasp, while the trapezium is bound to the thumb, making it important for the pinch.

STT Joint

The STT joint is an interesting joint. It is a spherical flexion/extension ball and socket hinge joint. The capitate-trapezoid and trapezium complex (CTT complex) as a single unit 'rotates' around the distal scaphoid. When the scaphoid flexes, it is underappreciated that the STT joint hyperextends. This is important in clinical practice.

Trapezium and trapezoid produce scaphoid flexion and pronation with axial load. The distal row pronates around the luno-capitate axis [15, 16]. The hamate displaces dorsally exerting an extension moment on the triquetrum. Scapholunate (SL) and luno-triquetral (LT) ligaments balance the flexion and the extension forces on the lunate. Also, the lunate slides down the radial slope ulnarly.

Hamate

Hamate provides the attachment site for many important ligaments and takes an indirect attachment of the FCU tendon, through piso-hamate ligament, stabilizing the wrist for ulnar flexion. The ulnar deviation and flexion moments from the distal row get transferred to the proximal row

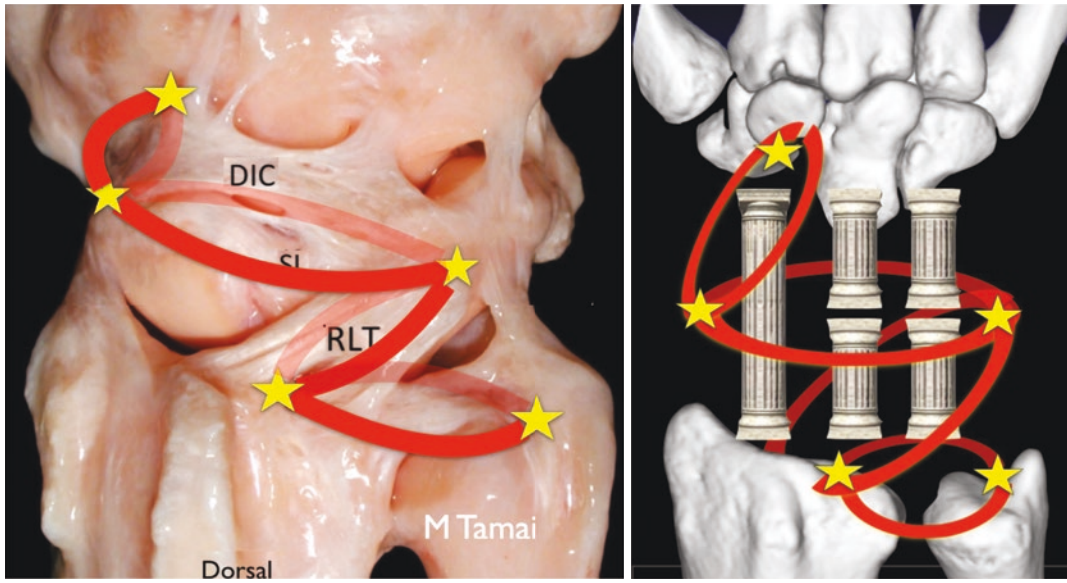

Fig. 68.9 Multiple ring theory; Carpus consists of three osseous rings. (1) Distal radioulnar joints stabilized by volar and dorsal radioulnar ligaments, (2) The proximal carpal row stabilized by dorsal intercarpal ligament and volar scapho triquetral ligament. (3) Distal carpal row stabilized by the volar and dorsal interosseous ligaments. The ligamentous rings that stabilize rows are indicated in red. (1) The radio triquetral ring (Kuhlman's sling) [25], dorsal radiocarpal ligament and the volar radio triquetral ligament. (2) The scaphoid-trapezium-trapezoid (STT) ring is a ball and socket hinge joint, consisting of the scapho trapezoid and scapho capitate ligaments. (3) The lesser arcuate ring consists of the ulnar lunate and radio lunate ligaments. (4) The greater arcuate ring consists of the radioscaphocapitate and the ulnar capitate ligaments, sites where the rings are linked, these form major stability points of the carpus and are indicated by stars (Nidus points)

via the hamate. The hook of the hamate and pisiform is volar to the remainder of the carpus, which increases the moment arm of flexion created by the FCU.

Pisiform

The pisiform is a sesamoid bone within the FCU tendon. Contraction of the FCU will pull the pisiform proximally, directing the hamate onto the triquetrum. Being a sesamoid bone, with an articular surface, it can move in a frictionless manner to enable it to guide over the triquetrum.

68.2.1.4 Ligamental Rings

The ligaments are often referred to as intrinsic (between carpal bones) and extrinsic (between carpal bones and radius or metacarpals) [17]. They are not arranged randomly throughout the carpus but form nidus points and are arranged into ligamentous ring complexes.

These rings are arranged as transversely stabilizing rows and helically interconnecting rows (Fig. 68.9). This is a mechanically advantageous construct for eight carpal bones that load as three columns while maintaining its mobility between the rows [18].

The radius has an inclination that involves ulnar and volar translation. Kuhlmann described a ligamentous ring (Kuhlmann's sling) from the radius to the triquetrum, including the dorsal radiocarpal ligament and the volar radio-luno-triquetral ligament (Fig. 68.10). This ligament prevents ulnar translocation of the carpus. Although the initial description is that it was to the triquetrum, our view is that it is the radiolunate ligament that prevents ulnar translocation. The lunate is tightly held by the dRLL and the vRLL.

Once the ligaments are damaged, instability develops. An example is scapholunate instability

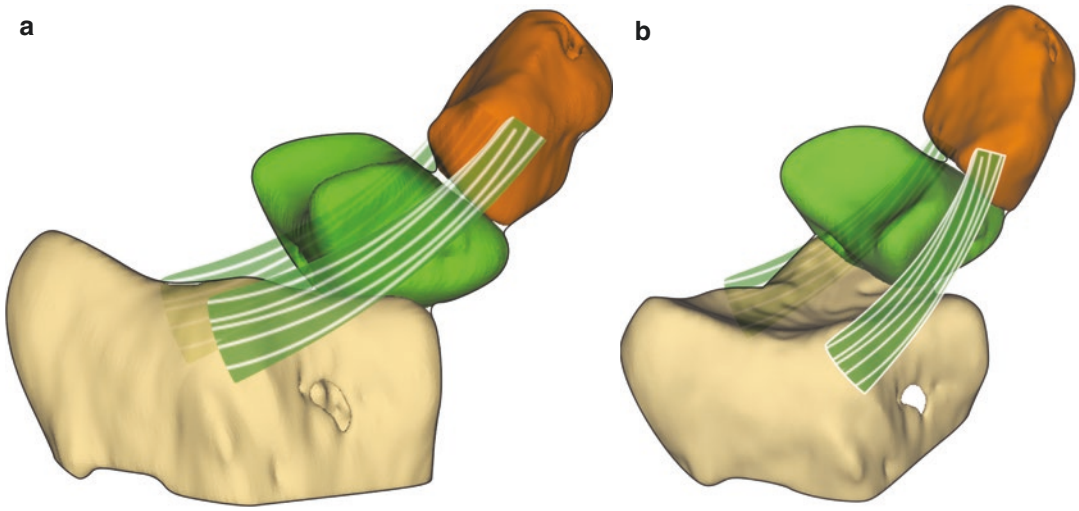

Fig. 68.10 Kuhlman's sling prevents ulnar translocation of the carpus. The Kuhlman's sling consists of volar radio triquetral ligament and dorsal radio luno triquetral ligament, also called the dorsal radiocarpal ligament (DRC). Being an obliquely arranged from distal radius to carpus, it acts as a sling, preventing ulnar translocation in the carpus. (**a**) Dorsal view. (**b**) Oblique view. Image copyrights—Dr. Melanie Amarasooriya and Dr. Gregory I. Bain

(SLI). In 'static' SLI, the lunate extends with the triquetrum while the scaphoid flexes and pronates with the distal row. This causes dorsal intercalated segmental instability (DISI) which is seen in static imaging such as X-ray and CT. When the lunotriquetral (LT) ligament is torn, the lunate flexes with the scaphoid, leading to Volar Intercalated Segmental Instability (VISI).

68.2.1.5 Tendons

The wrist flexors and extensors are strategically positioned to mobilize the wrist. But they also provide dynamic stability to the carpus. The tendons act as secondary stabilizers of the wrist. When ligaments are under strain, they transmit proprioceptive stimuli which recruit the muscles, which in turn unload the ligaments via the action of tendons [12].

68.2.1.6 Neuromuscular Coordination

The wrist capsule and ligaments are richly populated by proprioceptive nerve endings. Tension in a ligament activates them. The afferent stimuli travel through the branches of the posterior interosseous nerve (PIN) [5]. This, through a central neural mechanism, is transmitted to the muscles acting on the forearm. Within milliseconds, the protective muscles are positively recruited. These protective muscles will either prevent excessive supination or excessive pronation of the carpus, depending on the force to be counteracted. This will unload the ligament, reduce the diastasis and protect it [12].

This highlights the importance of the ligament and tendon attachments and the role of proprioception in rehabilitation of the wrist. In the same way, strengthening the 'friendly' muscles in rehabilitation may help in dynamic instabilities.

68.3 Carpal Kinematics

Carpal kinematics is the study of motion of the carpus in the physiological range. Anatomically, the wrist moves in two orthogonal planes, coronal and sagittal. In addition, there is carpal pronosupination relative to the radius. Carpal bones have six degrees of freedom to result in the said wrist motions. Each carpal bone can rotate around X, Y and Z axes and translate along these axes.

In real life, most of the human hand functions involve moving the wrist from radial extension to ulnar flexion, as in throwing a dart, casting a fish-

ing rod or using a hammer. This motion is called the 'Dart Throwers' Motion' (DTM). The plane that the wrist moves during DTM is called 'Dart Throwers' plane' (DTP).

68.3.1 Dart Throwers Motion (DTM)

DTM occurs in a plane from radial extension to ulnar flexion. The axis of DTM is 26.6° ± 4.4° oblique to the sagittal plane and is believed to be the mechanical axis of the carpus [19]. DTM is the most stable and controlled motion of the wrist. It combines the power of the forearm muscles with precision provided by the thumb. Flexor carpi ulnaris (FCU) and the Extensor carpi radialis longus and brevis (ECRL and ECRB) become 'the wrist motor' for DTM. When radial extensors initiate DTM, the first joint to respond is STT joint with trapezium and trapezoid being pulled into radial extension, steering the dart throwers' motion.

DTM mainly occurs through the mid-carpal joint. It has two components. The first is STT joint acting as a uniaxial hinge, and the second is luno-capito-hamate-triquetrum (LCHT) joint acting as a biaxial joint. The two joints are connected by the scapho-capitate articulation and capitate-trapezoid articulations. Capitate-Trapezoid articulation has minimal motion. The scapho-capitate (midcarpal) articulation sits between the radial and the central columns and therefore is an important factor in determining motion between the radial and the central columns. The Scaphoid lies in a unique position connecting radiocarpal and mid-carpal joints.

The direction of scaphoid rotation in relation to radius is found to be the same irrespective of the direction of global wrist motion [20]. But the magnitude of the scaphoid rotation changes significantly between radioulnar deviation, DTM, flexion-extension and the planes in between. It is likely that multiple dart throwers' planes exist to suit functional tasks, with varying degrees of scaphoid and lunate rotations [21, 22].

The scaphoid is the 'Gear lever' of the carpus, and its motion is directed by its ligament attachment and adjacent articular surfaces. The scaphoid and the adjacent articulations will follow the paths of least resistance. Each joint will move as far as it can until its restraints restrict joint motion and force another component of the articulations to move. This explains the sequential motions of the articulations of the wrist and how the sequential restraints guide the inner workings of the various components of this amazing universal joint (Fig. 68.11).

Capitate together with the distal row, move in the desired plane, results in the global wrist motion. Scaphoid and the proximal row set the platform for the distal row to exert DTM in the desired plane. This occurs mainly at the SC articulation, with the scaphoid acting like a 'gear lever' making changes to the plane of the capitate and thereby the distal row. This can be explained by relative scapho-capitate kinematics.

In ulnar flexion, this reverses with mid-carpal joints moving to flexion, on the obliquely arranged proximal carpal platform. Midcarpal articulation is a C-shaped concavity. With ulnar flexion, the triquetrum rotates to complete the C so that it can smoothly accommodate the distal carpal row, mainly hamate, into ulnar flexion of the wrist [23]. The triquetrum-hamate articulation also stops the dorsoradial extreme movement of the distal row in DTM. The ulnar half of the arcuate ligament helps, with its fibres spanning from the distal rim of piso-triquetral articulation vertically onto the hamate and then obliquely onto capitate.

Hence, we believe that during functional wrist motion, the two *rows* act separately but with intricate coordination. The proximal row and distal row have specific functions. The proximal row changes the plane of the motion by changing the degree of scaphoid flexion and direction of lunate rotation. Distal row elicits the global wrist motion and is described by the capitate or the third metacarpal motion.

DTM occurs in pronation at the distal radioulnar joint (DRUJ) [24]. When the forearm is pronated, the line of action of the wrist extensors, as well as flexors, is oblique. Therefore, these muscles can effectively become radial extensors and ulnar flexors.

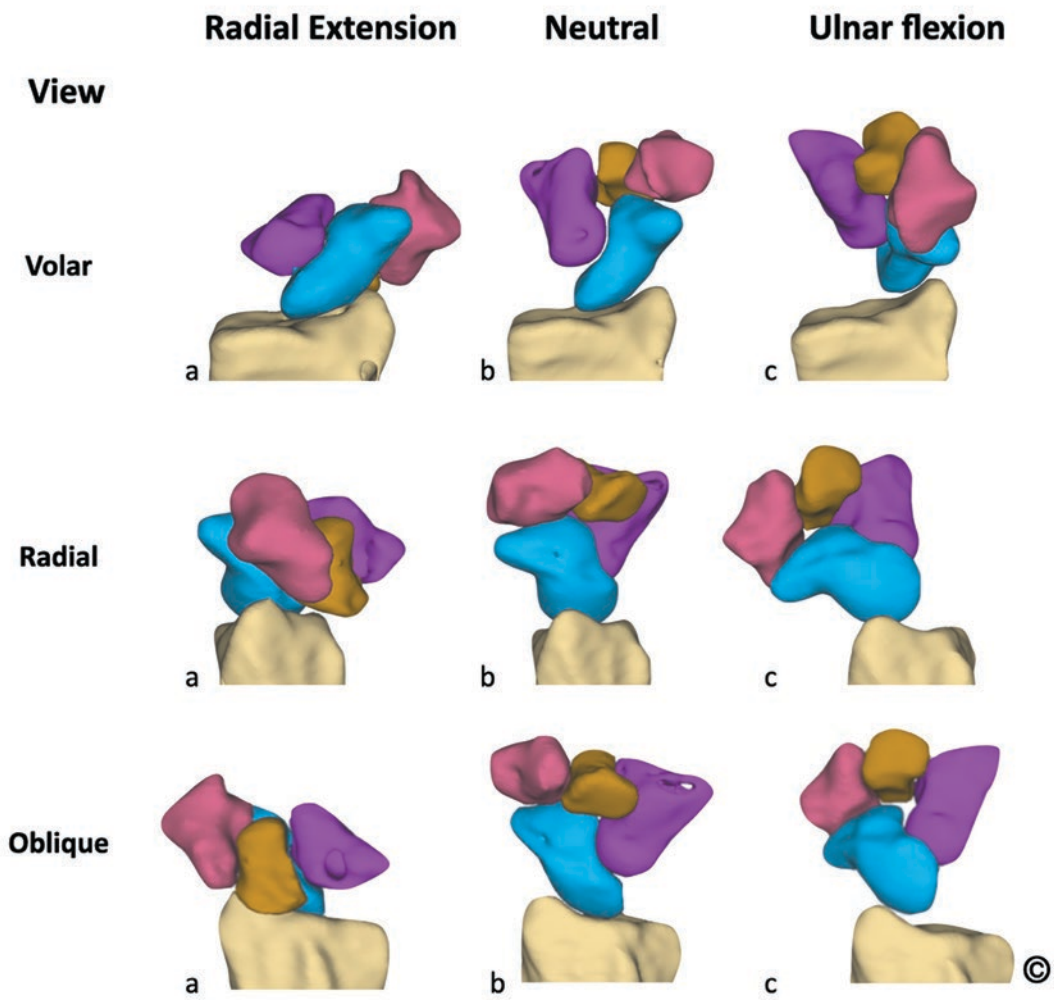

Fig. 68.11 Volar, radial and oblique views of the radial column during wrist dart thrower's motion. The capitate, trapezium and trapezoid moves from radial extension (**a**), neutral (**b**) to ulnar flexion (**c**). The scaphoid mainly shows an out-of-plane motion, from extension to flexion. Note in the oblique view, the dart throwers' plane lies in the axis of STT joint motion. The STT joint hyperextends, with radial extension of the wrist (oblique view a), then flexes as the wrist move into ulnar flexion (oblique view **c**)

68.3.2 Radioulnar Deviation

The radial deviators are ECRL, flexor carpi radialis (FCR), APL and EPL. The ulnar deviators are FCU and ECU. The radial pull of the tendons initiates a sequential motion pattern in the carpus. On a 2D coronal plane, this sequential motion appears as a rotation of the carpus, around the proximal pole of the capitate (Fig. 68.12). On a sagittal plane, the scaphoid flexion and trapezium moving over the dorsal surface are clearly seen (Fig. 68.13—oblique view). Even during radioulnar deviation, it is evident that the two *rows* move separately and the distal row positions determine the global wrist motion. The proximal row, with its out-of-plane motion, sets in the platform. This is orchestrated with sequential carpal motions as depicted in Fig. 68.12.

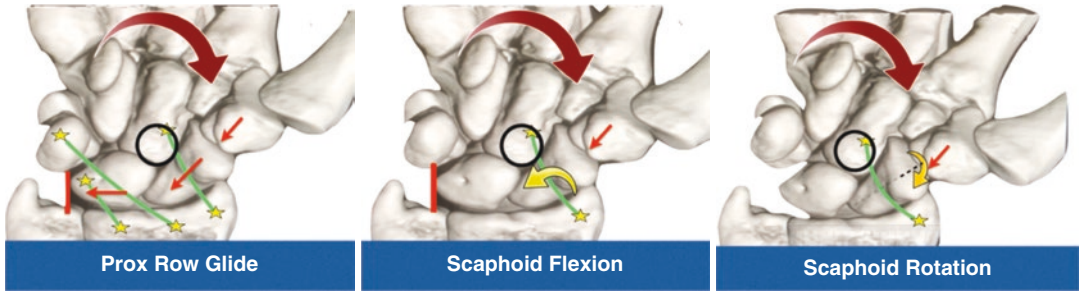

Fig. 68.12 Sequential motions of the proximal row during wrist radial deviation. Note the proximal row glide, followed by scaphoid flexion and then pronation

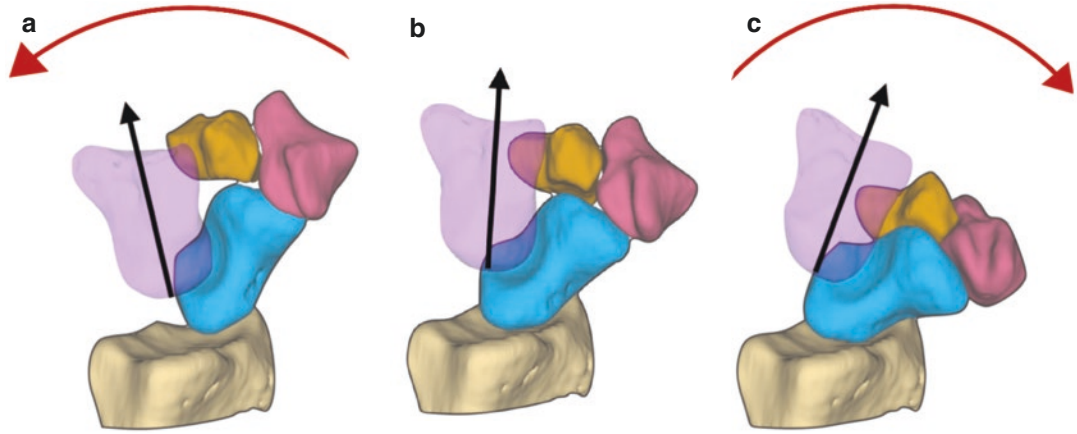

Fig. 68.13 Oblique view of the scapho-trapezio-trapezoid (STT) joint and capitate during ulnar to radial deviation of the wrist. Note that the STT joint is volar to the capitate. When the radial tendons pull the radial metacarpals and trapezium radially and proximally, capitate, being tightly bound to trapezoid moves with it, and the whole distal row follows. This is the direction of 'global wrist motion', radial deviation. However, because the STT joint is in a different plane to the capitate, that is volar, the STT joint has to hyperextend for the wrist (represented by capitate) to move radially. When the STT joint hyperextends, that occurs by trapezium sliding over the dorsum of the scaphoid and also scaphoid flexing. In radial deviation this 'out-of plane' rotation is very prominent to allow the distal row and capitate to angulate freely to radial side. (**a**) Ulnar deviation. (**b**) Neutral. (**c**) Radial deviation

68.3.3 Flexion and Extension

Flexion and extension are more congruent in terms of 'in-plane' motion. Flexor tendons and extensor tendons exert a flexion and extension moment, respectively, on the distal row first. Proximal intercalated segment dorsally translates and flexes as a response. Flexion-extension angles of each proximal row bone differ according to their proximal convexity. Due to this difference in flexion and extension of each bone, the SL and LT ligaments experience a rotatory torque. The transverse carpal ligament and the extensor retinaculum act as a 'pulley' preventing the bowstringing of the tendons.

68.3.4 Prono-supination

Prono-supination of the hand for functional activities occurs mainly at the forearm. However, carpus can also prono-supinate. Mean rotational laxity of the unloaded carpus is 42° [25]. Obliquity of the tendons enables the wrist to rotate around the Y-axis. It is an important observation that most of the functional tasks of the hand, including power grip, occur in relative DRUJ pronation.

68.3.5 Anatomic Variations Affecting Carpal Kinematics

Wrist is a joint that shows remarkable variations in anatomy between individuals. Carpal kinematics are known to vary between individuals due to anatomical variations.

68.3.5.1 Row and Column Type Wrists

Historically, there has been an interest whether the wrist behaves as two rows, proximal and distal or three columns, radial, central and ulnar. In the row-type wrist, the scaphoid translates more with radial deviation. In the column type, the scaphoid flexes more. The findings of later studies suggest that row and column type kinematics are a spectrum than a discrete entity [26].

68.3.5.2 Lunate Morphology

After Viegas (1990) described the presence of an extra facet of the lunate for hamate [27], Galley and Bain have proposed that this difference in scaphoid kinematics is due to the presence of type I and II lunates [28] (Fig. 68.14). The wrists with a type I lunate behave as a row type wrist and wrists with type 2 lunate as the column type. This is due to changes in mid-carpal kinematics.

The motion at the radiocarpal and mid-carpal joints will vary depending upon the lunate type [28]. In addition, this has a secondary effect on the loading of the carpus and subsequent arthritis.

68.3.5.3 Scaphoid Kinematics

There is similar variability observed with ligamental attachments of the scaphoid. The scaphoid can be of flexing and rotating types which can alter mid-carpal kinematics. The ligamentous anatomy of the scaphoid (Fig. 68.15) determines whether the scaphoid is a 'flexing' type or 'rotating' type [30].

68.4 Carpal Instability Patterns

Clinicians are familiar with diagnosing static carpal instabilities for years. Dynamic carpal instabilities pose a challenge as patients are often asymptomatic, and clinical examination may be equivocal. The clinical utility of dynamic imaging is invaluable in these circumstances [31].

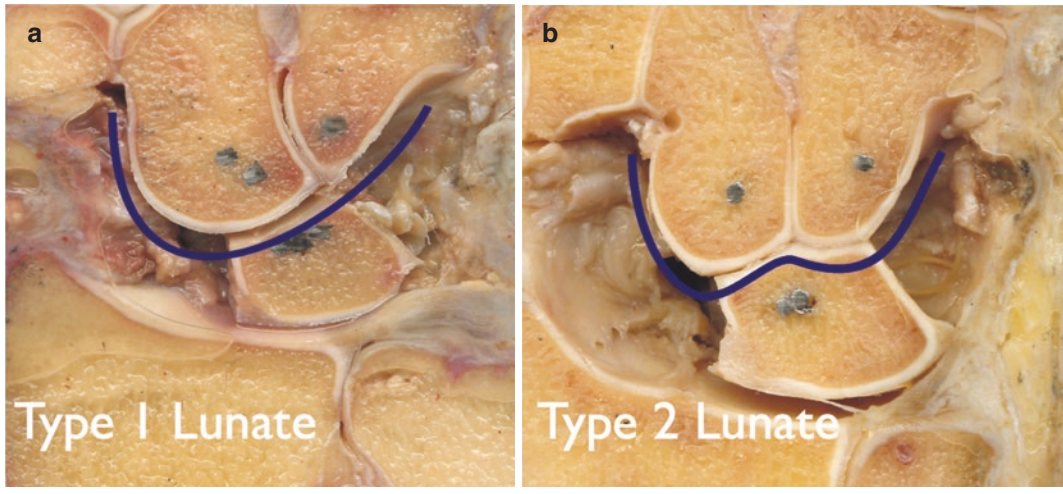

Fig. 68.14 The type 1 and 2 lunate articulations. (**a**) The type 1 lunate has a smooth midcarpal articulation, which behaves more like a hip joint, and does not restrain the midcarpal joint. As such scaphoid fractures, scapholunate instability and STT OA are more prone to develop a DISI deformity. (**b**) The type 2 lunate has two facets distally, which articulate with the capitate and the hamate. This restrains the degree of DISI deformity [29]

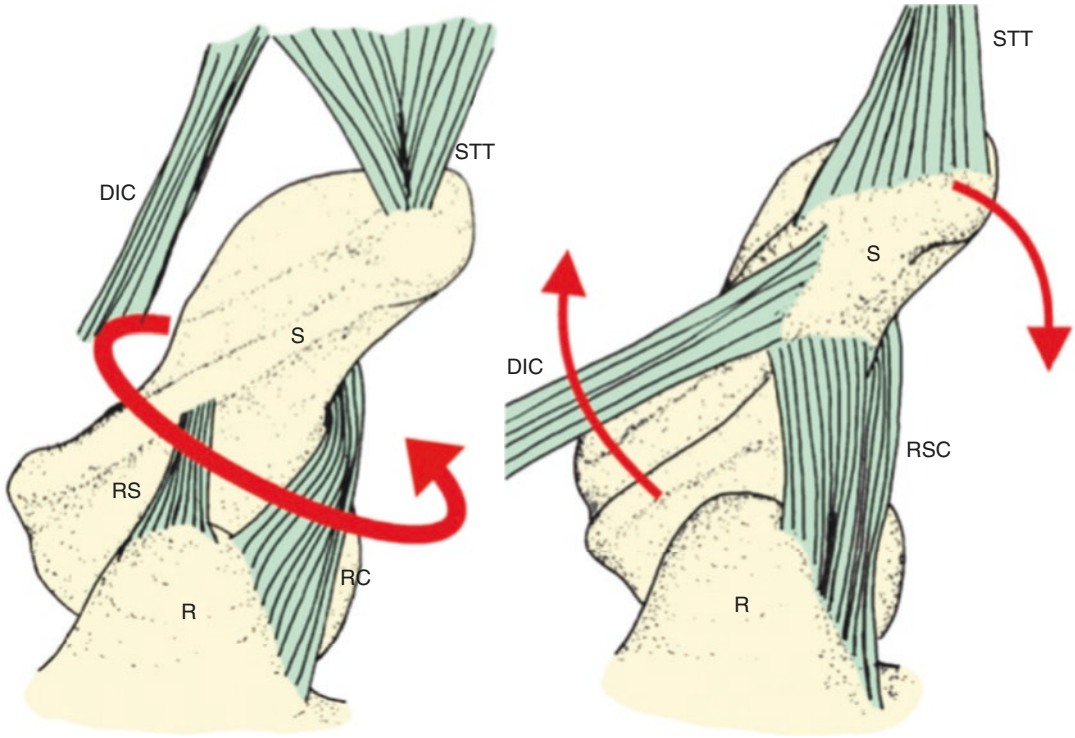

Fig. 68.15 There are anatomical variations of ligamental attachments to scaphoid, favouring rotation or flexion of the scaphoid [30]. From "Scaphoid variation and an anatomical basis for variable carpal mechanics," by Quintin Fogg, 2004, PhD Thesis, Adelaide University, p. 244 Copyright [2004] by Dr Quintin Fogg. Reprinted with permission from the author

68.4.1 Dynamic Computed Tomography (4D CT)

The 4D CT is a relatively low radiation dose tomography (0.3 mSv), where a sequence of 3D CT volumes is imaged by a helical scanner, as the patient moves the wrist. This is converted into a video graphic output. This enables to visualize carpal bone motion with natural wrist movements of the patient. The recent advancement of 4D CT is that the researchers are able to measure individual carpal bone motion and quantify patterns of instability.

68.4.2 Scapholunate Instability

The scaphoid in scapholunate instability, flexes, pronates and dorsally subluxes while translating radially during the wrist radial deviation. The lunate remains in its extended position. In addition to these well-known findings, 4D CT scans enable us to visualize and quantify the changes in scaphoid and lunate throughout the wrist range of motion (Figs. 68.16 and 68.17). This can be utilized to diagnose and classify dynamic instability as well.

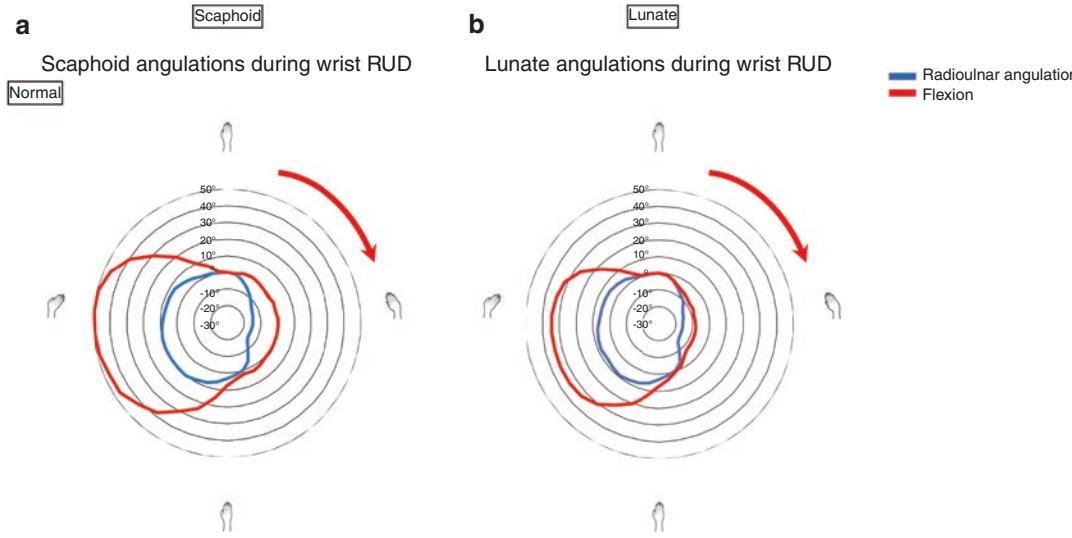

Fig. 68.16 The normal scaphoid and lunate angulations during the wrist radioulnar deviation. (**a**) Scaphoid angulations—The graph shows flexion of the scaphoid (red line) is more than the radioulnar angulation (blue line). (**b**) Lunate angulations—the graph shows flexion of the lunate (red line) is more than the radioulnar angulation (blue line) while the flexion of the lunate is less than the scaphoid, the graph patterns are similar and radioulnar angulation is similar in magnitude

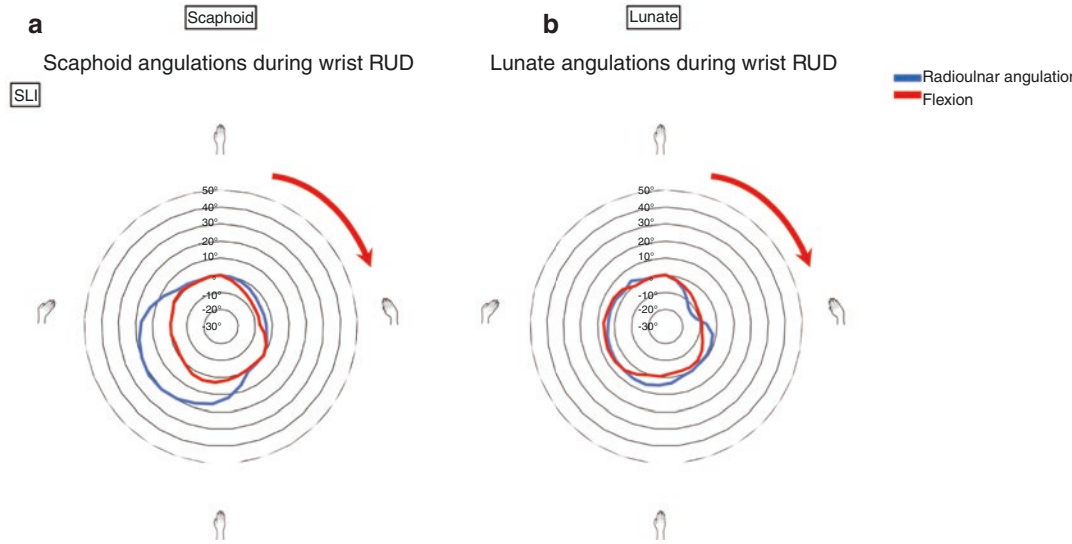

Fig. 68.17 The scaphoid and lunate angulations during the wrist radioulnar deviation in scapholunate instability. (**a**) Scaphoid angulations—the graph shows radioulnar angulation of the scaphoid (blue line) is more than the flexion (red line). This is reversal of the pattern seen in the normal wrist in figure F. (**b**) Lunate angulations—The graph shows flexion of the lunate (red line) is similar to the radioulnar angulation (Blue line). This pattern is different from the normal wrist

68.5 Summary

The loaded wrist shows remarkable stability due to ligaments, tendons and neuromuscular mechanisms. While the loading occurs via columns, the mobility of the wrist can be explained by rows. The multiple ligamental rings stabilize the wrist for loading and mobility. Dynamic CT imaging has been invaluable in our understanding of carpal biomechanics in vivo.

References

1. Bryce TH. Certain points in the anatomy and mechanism of the wrist-joint reviewed in the light of a series of röntgen ray photographs of the living hand. J Anat Physiol. 1896;31:59–79.
2. Navarro A. Luxaciones del carpo. An la Fac Med. 1921. p. 113–141.
3. Taleisnik J. Wrist anatomy, function, and injury. In: AAOS Instr Course Lect. St. Louis: Mosby; 1978. p. 61–87.
4. Lichtman DM, Schneider JR, Swafford AR, Mack GR. Ulnar midcarpal instability—clinical and laboratory analysis. J Hand Surg Am. 1981;6:515–23.
5. Hagert E. Proprioception of the wrist joint: a review of current concepts and possible implications on the rehabilitation of the wrist. J Hand Ther. 2010;23:2–17.
6. Salva-Coll G, Garcia-Elias M, Hagert E. Scapholunate instability: proprioception and neuromuscular control. J Wrist Surg. 2013;02:136–40.
7. Rikli DA, Honigmann P, Babst R, Cristalli A, Morlock MM, Mittlmeier T. Intra-articular pressure measurement in the radioulnocarpal joint using a novel sensor: in vitro and in vivo results. J Hand Surg Am. 2007;32:67–75.
8. Viegas SF, Patterson RM. Load mechanics of the wrist. Hand Clin. 1997;13:109–28.
9. Genda E, Horii E. Theoretical stress analysis in wrist joint neutral position and functional position. J Hand Surg Am. 2000;25B:292–5.
10. Sennwald GR, Zdravkovic V, Jacob HAC, Kern HP. Kinematic analysis of relative motion within the proximal carpal row. J Hand Surg Am. 1993;18:609–12.
11. Apergis E. Fracture-dislocations of the wrist. Fract Wrist. 2013. https://doi.org/10.1007/978-88-470-5328-1.
12. Salva-Coll G, Garcia-Elias M, Leon-Lopez MT, Llusa-Perez M, Rodríguez-Baeza A. Effects of forearm muscles on carpal stability. J Hand Surg Eur Vol. 2011;36:553–9.
13. Hagert E, Garcia-Elias M, Forsgren S, Ljung B-O. Immunohistochemical analysis of wrist ligament innervation in relation to their structural composition. J Hand Surg Am. 2007;32:30–6.
14. Sonenblum SE, Crisco JJ, Kang L, Akelman E. In vivo motion of the scaphotrapezio-trapezoidal (STT) joint. J Biomech. 2004;37:645–52.
15. Kobayashi M, Berger RA, Nagy L, Linscheid RL, Uchiyama S, Ritt M, An KN. Normal kinematics of carpal bones: a three-dimensional analysis of carpal bone motion relative to the radius. J Biomech. 1997;30:787–93.
16. Garcia-Elias M. Kinetic analysis of carpal stability during grip. Hand Clin. 1997;13:151–8.
17. Taleisnik J. The wrist. 1st ed. New York, Edinburgh, London and Melbourne: Churchill Livingstone; 1986.
18. Bain GI, Clifton T, Costi JJ, Krishnan J. Biomechanics of the rheumatoid wrist deformity. In: Chung KC, editor. Clinical management of the rheumatoid hand, wrist, and elbow. Cham: Springer International Publishing; 2016. p. 75–86.
19. Crisco JJ, Heard WMR, Rich RR, Paller DJ, Wolfe SW. The mechanical axes of the wrist are oriented obliquely to the anatomical axes. J Bone Jt Surg - Ser A. 2011;93:169–77.
20. Moritomo H, Murase T, Goto A, Oka K, Sugamoto K, Yoshikawa H. In vivo three-dimensional kinematics of the midcarpal joint of the wrist. J Bone Jt Surg - Ser A. 2006;88:611–21.
21. Werner FW, Green JK, Short WH, Masaoka S. Scaphoid and lunate motion during a wrist dart throw motion. J Hand Surg Am. 2004;29:418–22.
22. Garg R, Kraszewski AP, Stoecklein HH, Syrkin G, Hillstrom HJ, Backus S, Lenhoff ML, Wolff AL, Crisco JJ, Wolfe SW. Wrist kinematic coupling and performance during functional tasks: effects of constrained motion. J Hand Surg Am. 2014;39(4):634–42.e1. https://doi.org/10.1016/j.jhsa.2013.12.031.
23. Moritomo H, Goto A, Sato Y, Sugamoto K, Murase T, Yoshikawa H. The triquetrum-hamate joint: an anatomic and in vivo three-dimensional kinematic study. J Hand Surg Am. 2003;28:797–805.
24. Capener N. The hand in surgery. J Bone Joint Surg Br. 1956;38-B:128–51.
25. Ritt MJPF, Stuart PR, Berglund LJ, Berger RA, Linscheid RL, Cooney WP 3rd, An K-N. Rotational laxity and stiffness of the radiocarpal joint. Clin Biomech (Bristol, Avon). 1996;11:227–32.
26. Craigen MAC, Stanley JK. Wrist kinematics: row, column or both? J Hand Surg (British Eur). 1995;20:165–70.
27. Viegas SF, Wagner K, Patterson R, Peterson P. Medial (hamate) facet of the lunate. J Hand Surg Am. 1990;15:564–71.
28. Galley I, Bain GI, McLean JM. Influence of lunate type on scaphoid kinematics. J Hand Surg Am. 2007;32:842–7.

29. McLean JM, Turner PC, Bain GI, Rezaian N, Field J, Fogg Q. An association between lunate morphology and scaphoid-trapezium-trapezoid arthritis. J Hand Surg Eur Vol. 2009;34:778–82.
30. Fogg QA. Scaphoid Variation and an Anatomical Basis for Variable Carpal Mechanics. PhD, Dept Anat Sci, University of Adelaide, Adelaide; 2004. p. 275.
31. Carr R, MacLean S, Slavotinek J, Bain GI. Four-dimensional computed tomography scanning for dynamic wrist disorders: prospective analysis and recommendations for clinical utility. Jnl Wrist Surg. 2019;08:161–7.

Arthroscopic Equipment and Set Up for Wrist Arthroscopy

69

Richard S. Page, Janina Henze, and Kevin Eng

69.1 Background

Wrist arthroscopy is the golden standard of diagnosing wrist disorders and used as a tool for the treatment of various pathologies. The first case was performed by M.S. Burman in 1931 and at that time no future role for arthroscopic treatment of wrist pathologies was anticipated [1]. Later, in 1971, M. Watanabe in Japan reported his first experience after 19 arthroscopies of the radiocarpal joint with a 1.7-mm diameter arthroscope due to the development of thinner arthroscopes and better light sources [2]. Thereafter, wrist arthroscopy quickly gained popularity during the 1980s and 1990s, when Terry Wipple in America and Hempfling in Germany started to pioneer more modern techniques [3, 4]. Since then, arthroscopy of the radiocarpal, midcarpal and distal radioulnar joint has been used with increasing frequency for pathology in the wrist, establishing the gold standard for assessing and managing intra-articular joint-related pathology of the wrist joint.

Arthroscopy of the wrist is a challenging procedure due to smaller dimensions of joint spaces and a higher risk of damage to important structures. Wrist arthroscopy includes the radiocarpal joint, the midcarpal joints and may include the distal radioulnar joint. The midcarpal joint should be inspected as a routine during wrist arthroscopy. The distal radioulnar may be assessed depending on patient presentation.

Historically, the complication rate of wrist arthroscopies is low, which has been described at up to 2% of cases. However, recent studies indicate a higher risk with up to 5.98% complication rate [5, 6]. Most frequently the failure to achieve functional improvement (1.16%) and nerve lesions has been reported. Other complications are injuries to tendons, arteries, tendon fistulas, carpal tunnel syndrome, compartment syndrome, stiffness, infection, cartilage lesions and complex regional pain syndrome and cysts. Another important factor is the experience of the surgeon; the risk of a complication decreases with the

R. S. Page (✉)
Department of Orthopaedics, School of Medicine, Deakin University, Geelong, VIC, Australia

Barwon Centre for Orthopaedic Research and Education (B-CORE), Barwon Health and St John of God Hospital, Geelong, VIC, Australia

Geelong Orthopaedics, SJOG Specialist Centre, Geelong, VIC, Australia
e-mail: richardpage@geelongortho.com.au

J. Henze
Barwon Centre for Orthopaedic Research and Education (B-CORE), Barwon Health and St John of God Hospital, Geelong, VIC, Australia

K. Eng
Barwon Centre for Orthopaedic Research and Education (B-CORE), Barwon Health and St John of God Hospital, Geelong, VIC, Australia

Geelong Orthopaedics, SJOG Specialist Centre, Geelong, VIC, Australia

© ISAKOS 2022

D. N. Bhatia et al. (eds.), *Arthroscopy and Endoscopy of the Elbow, Wrist and Hand*,
https://doi.org/10.1007/978-3-030-79423-1_69

years of experience and case load of the surgeon [6]. Furthermore, it should be noted that complications do not only occur because of the surgical procedure, but may also result from the set up. These complications include consequences of the finger and arm traction or burns from the traction tower, tourniquet use and pressure areas or nerve compression from inadequate padding in patient positioning.

69.2 Planning and Layout

Before surgery commences, it is important to check the patient and the equipment are in the right position and all instruments are sterile. The anaesthetist can be positioned at the head of the patient or on the side not being operated on. The arthroscopy tower and monitor are placed on the other side of the operable arm and the surgeon and the assistant stand or sit on the sides of the arm table. The scrub nurse with the equipment is positioned at the head (Fig. 69.1).

69.3 Anaesthesia

Wrist arthroscopy can be performed under general or regional anaesthesia. Each has advantages and disadvantages and is still debated. Essentially this comes down to a balance of the patient, anaesthetist and surgeon preference against the complexity and duration of the planned surgery.

- General anaesthesia (GA) is more comfortable and better tolerated by the patient, particular in relation to tourniquet use. Muscle relaxation and GA are preferred by most of the surgeons because it provides optimal surgical conditions. This also allows the surgeon to switch to an open procedure if necessary, as well as allowing the surgeon more time, in case a surgery has any complications.
- Regional anaesthesia, such as plexus block anaesthesia, can reduce the risks associated with a general anaesthesia but can be difficult in non-compliant or agitated patients. Movement of a patient during the surgery could lead to injuries inside the joint. Furthermore, it also can cause complications such as haemothorax, arterial or nerve injury or an emphysema.
- Local anaesthesia has been utilized too and allows functional assessment of the awake patient who can move their hand and digits, as well as education of the patient in regard to their pathology on screen [7].

69.4 Positioning

The aim of the positioning is a sufficient distraction of the joint in order to create a good intra-articular visibility and a working “box”.

- A pneumatic tourniquet is highly recommended to avoid any bleeding into the joint, as this may interfere with visualization. The tourniquet should be placed as far proximal as possible, and should not interfere with the counterweights and the fixation of the arm.
- The patient is placed in a supine position. The arm is placed on a hand table in a 90° abduction and the elbow is flexed to 90°.
- The hand is put into a distraction tower system that includes finger traps. There are various different systems of traction towers available. Different fingers are placed into the finger trap depending on the requirements of surgery. For example, to visualize the radiocarpal joint, the traps are placed on the index and middle finger. If the surgeon wishes to view the scaphotrapeziotrapezoid (STT) joint, the finger traps can be applied only on the thumb to increase the intra-articular space, for that segment of arthroscopy.
- Next, the finger traps are placed on a traction tower to lift up the hand, and a weighted band is applied to the upper arm as a counterweight (1–2 kg). The weight should be carefully chosen in order to open the joint enough without creating a traction injury to the skin, nerves or finger joints (Fig. 69.2a and b).

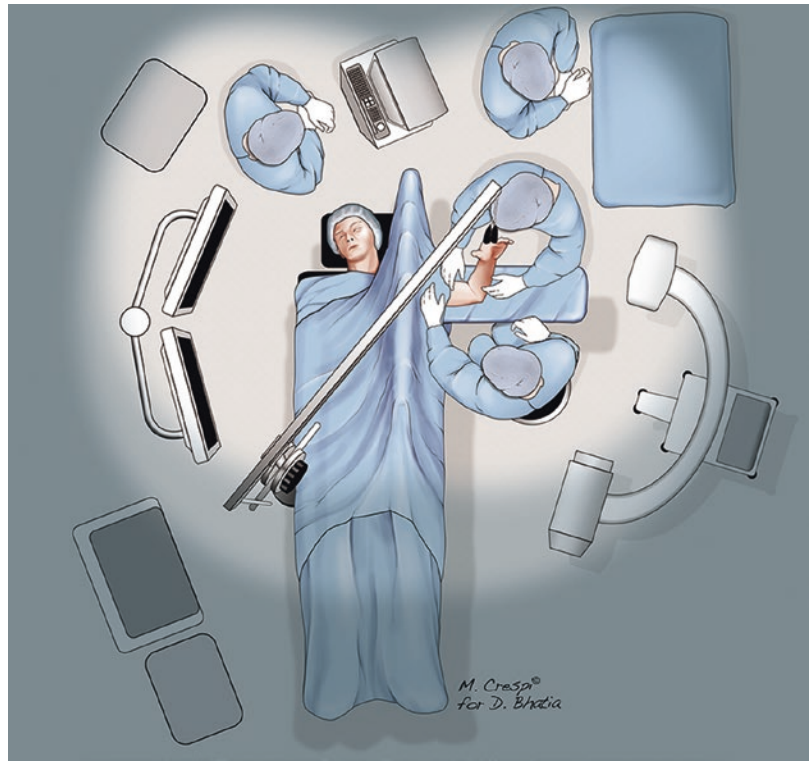

Fig. 69.1 Map of theatre layout for wrist arthroscopy. (© ISAKOS)

69.5 Equipment

Wrist arthroscopy principle has the same instrument requirements as other larger joints, however the dimensions are smaller. The smaller the camera, the more vulnerable it becomes to bending loads; hence, the instruments should be handled gently.

- Surgery set up requires an arm table, tourniquet, a traction system, arthroscopy tower system with monitor, video recorder and printer, arthroscope with a camera attached, light source with fibre-optic cable, motorized shavers, radiofrequency ablator and access to an image intensifier. Digital systems allow the data transfer to a USB devices or PACS system for image storage and linking to the patient's medical records.
- The most important instrument is the arthroscope itself, which has 1.9–2.7 mm diameter and a 30° viewing angle. A 70° viewing angle lens may be used to visualize difficult corners. Small diameter 1.9 mm scopes are used for the distal radioulnar joint (DRUJ), the scaphotrapeziotrapezoid (STT) and carpometacarpal (CMC) joints, metacarpophalangeal (MCP) joint, and in patients with a small wrist (Fig. 69.3).
- The basic equipment includes an instrument to establish a portal, small joint shaver and burrs (2.0–4.5 mm) with multiple protected tips. A wrist probe (1.7 or 2.0 mm), forceps, punches and many of the smaller versions of large joint arthroscopic instruments are all useful to enable the treatment for intra-articular pathology. For the portals there are also small trocars, with rounded or blunted tips to prevent damage to the cartilage. The probe is useful to palpate the joint from the inside. If needed, advanced instruments for certain pathologies are available as well, such as anchors of suture passing cannulae for fixation of the triangular fibrocartilage complex. Radiofrequency probes can be used for soft tissue, ligament and capsular debridement;

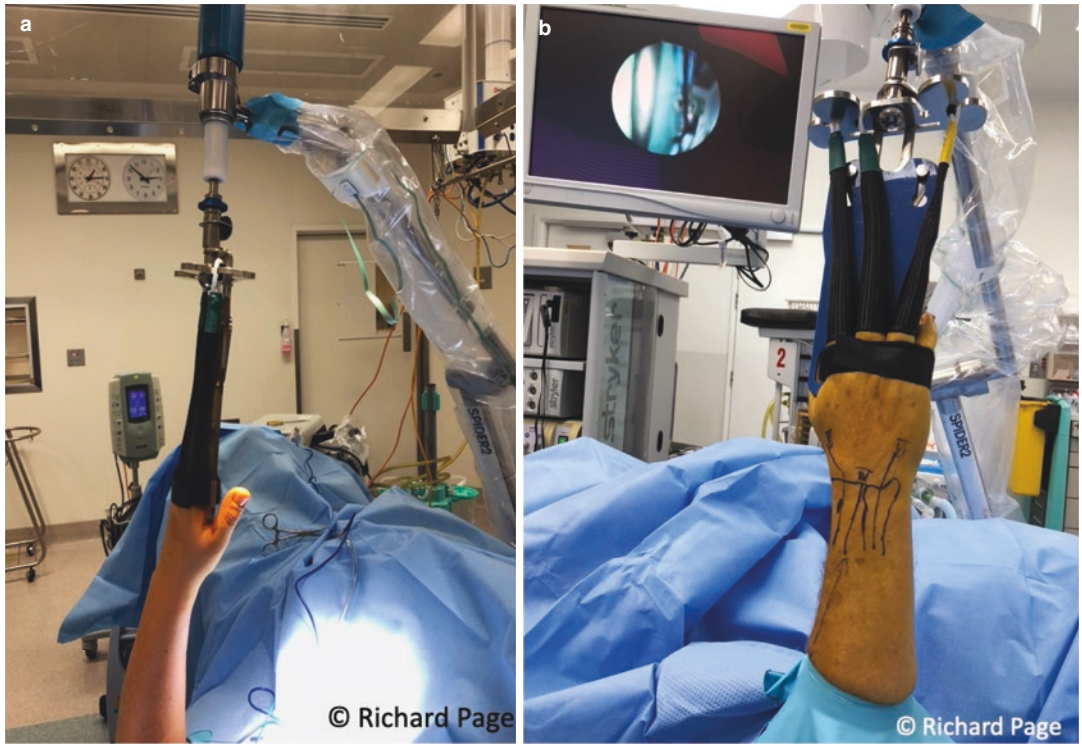

Fig. 69.2 (**a** and **b**) Intraoperative set up is shown. The patient is in supine position, and the hand is held in a traction tower system via finger traps, allowing rotation of the wrist and 360° access to the wrist. (© R Page)

these should be used only in wet arthroscopy to avoid thermal injury.

- Arthroscopy of the wrist can be either performed wet or dry. The classic wet arthroscopy is usually performed with Ringer's solution or normal saline due to the high absorption rate by the joint. Gravitational feed is generally sufficient, or additional manual pressure utilizing a 50 mL syringe with a narrow diameter catheter connects via a Luer lock may be used. The outflow is provided by the port of the cannula or a needle. Dry arthroscopy technique has gained popularity and has advantages of better visualization and lack of swelling. Sometimes an initial washout of the joint might be necessary due to intra-articular bleeding, especially in distal radius fractures. The hematoma can be evacuated, and the arthroscopy can continue dry.

69.6 Getting Started

The surface anatomy is marked preoperatively using a sterile marking pen; this should be done with the wrist under traction to allow orientation and planning of the arthroscopic approach to be used. If landmarks are made prior to the wrist being under traction, the landmarks may change (Fig. 69.4). Furthermore, the portals that are going to be utilized should be clearly marked (details in next chapter).

- *Bony landmarks*: Radial styloid process, distal radial edge, dorsal ulnar head, metacarpals, carpal bones (pisiform, trapezium, scaphoid pole), ulnar styloid, Lister's tubercle
- *Tendinous structures*: Extensor carpi radialis longus (ECRL) tendon, extensor pollicis longus (EPL) tendon, extensor digitorum communis (EDC) tendon, extensor carpi ulnaris

Fig. 69.3 A range of small joint arthroscopes (1.9–2.7 mm) can be utilized during wrist arthroscopy. (© R Page)

(ECU) tendon, abductor pollicis longus (APL) tendon, extensor carpi ulnaris (ECU) tendon, flexor carpi radialis (FCR) tendon, flexor carpi ulnaris (FCU) tendon

Arthroscopic exploration of the wrist is divided into three parts: proximal, volar (dorsal when using a volar portal) and distal. The arthroscope can then be rotated to the radial and the ulnar side; however, it is important to gain an overview and have a system to evaluate the structures in the joint. The dorsal portals are generally speaking more established because of a lower risk of injuring the anatomic structures, however due to the "box principle", a volar approach can be considered as well but should still be performed with caution.

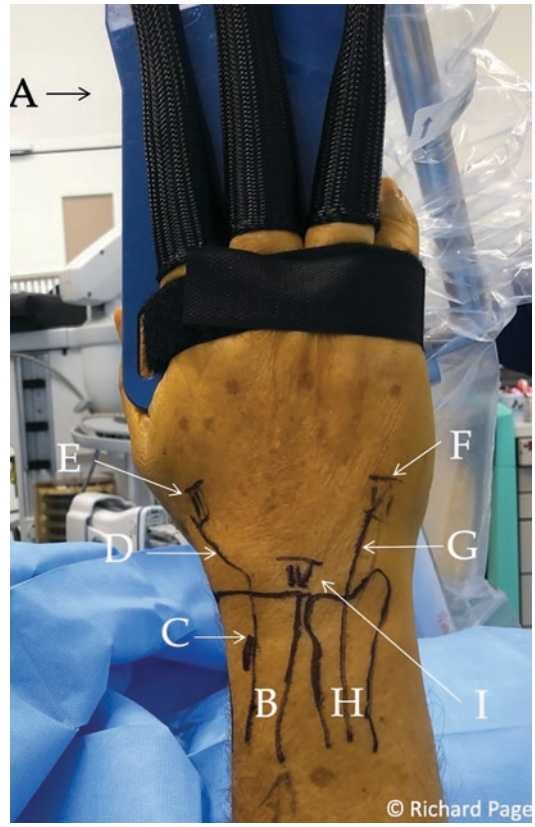

Fig. 69.4 Landmarks for wrist arthroscopy are shown. (A) Finger traps. (B) Radius. (C) Lister's tubercle. (D) Extensor Pollicis Longus Tendon (EPL). (E) Thumb CMC joint. (F) Little finger metacarpal. (G) Extensor carpi ulnaris tendon (ECU). (H) Ulna I. Extensor compartment IV. (© R Page)

69.7 Tips and Tricks

- Using a traction tower can obstruct fluoroscopic imaging but using a dedicated traction arm can keep the arm clear for imaging.
- The counterweight is tied over the tourniquet proximal to the pneumatic tube using a broad band and passed between the operating table and the arm table.

Fig. 69.5 Infiltration of saline through the 3-4 portal into the radiocarpal joint via a short small diameter catheter connected at each end with a Luer Lock to an 18G needle and a 50 mL syringe, respectively. (© R Page)

- A size 11 pointed blade is used for only incising skin; thereafter a "nick and spread" technique is used to drag the skin over the blade rather than moving the knife tip, to avoid iatrogenic tendon injury. Then with a small straight artery forceps, dilating the space to open then portal.
- The radius is usually angled 10° volar and the entry trocar is angled accordingly. The mid carpal joint is similarly inflated with saline from the dorsum at an angle of 45°.
- Fluoroscopy is helpful to confirm portal placement in STT and CMC arthroscopy
- Fluid inflow is managed using a series of 50 mL syringes for fluid via narrow diameter irrigation tubing; this limits flow and pressure within the joint and prevents excess extravasation (Fig. 69.5).
- The forearm may have slightly less stability in pronation and supination and an assistant may be required to help control this.

References

1. Burman MS. Arthroscopy or the direct visualization of joints. J Bone Joint Surg. 1931;13:669–95.
2. Watanabe K, Nakamura R, Imaeda T. Arthroscopic assessment of Kienböck's disease. Arthroscopy. 1995;11:257–62.
3. Whipple TL, Marotta JJ, Powell JH 3rd. Techniques of wrist arthroscopy. Arthroscopy. 1986;2(4):244–52. https://doi.org/10.1016/s0749-8063(86)80079-2.
4. Hempfling H (Hrsg). Die Arthroskopie am Handgelenk. Indikation, Technik und therapeutische Konsequenzen. Stuttgart: Wissenschaftliche Verlagsgesellschaft mbH; 1992.
5. Leclercq C, Mathoulin C. Complications of wrist arthroscopy: a multicenter study based on 10,107 arthroscopies. J Wrist Surg. 2016;5(4):320–6. https://doi.org/10.1055/s-0036-1584163.
6. Brown JS, Gordon RJ, Peng Y, Hatton A, Page RS, Macgroarty KA. Lower operating volume in shoulder arthroplasty is associated with increased revision rates in the early postoperative period: long-term analysis from the Australian Orthopaedic Association National Joint Replacement Registry. J Shoulder Elb Surg. 2020;29(6):1104–14. https://doi.org/10.1016/j.jse.2019.10.026.
7. Lalonde D, Eaton C, Amadio P, Jupiter J. Wide-awake hand and wrist surgery: a new horizon in outpatient surgery. J Shoulder Elb Surg. 2020;29(6):1104–14. https://doi.org/10.1016/j.jse.2019.10.026. Epub 2020 Feb 7.

Diagnostic Arthroscopy of the Wrist: Anatomy and Portals

70

Benjamin R. Graves, Eric J. Sarkissian, and Gary G. Poehling

70.1 Background

Wrist arthroscopy is an invaluable technique for the hand and wrist surgeon. Indications have steadily grown for its use in the diagnosis and treatment of intraarticular pathology of the wrist [1, 2]. Performing a safe and effective wrist arthroscopy requires a thorough knowledge of the anatomy of the hand and wrist, appropriately-sized small joint instrumentation, and a precise and deft surgical technique. The goals of this chapter are to familiarize the surgeon with the important wrist and hand anatomy for safe portal placement and describe techniques for effective diagnostic wrist arthroscopy.

70.2 Indications and Contraindications

- Diagnostic arthroscopy of the radiocarpal and midcarpal joints
- Loose body removal
- Ganglion cyst excision
- Irrigation and debridement for wrist joint infections or inflammatory wrist conditions
- Repair and/or debridement for tears of the triangular fibrocartilage complex (TFCC)
- Staging and treatment for osteonecrosis of the carpal bones (e.g., Kienbock's disease)
- Direct visualization of reduction during fixation of carpal bone fractures
- Arthroscopic-assisted intercarpal ligament repair and/or reconstruction

Post-traumatic or congenital alteration of the normal wrist and hand anatomy is a contraindication for wrist arthroscopy. Other contraindications include:

- contractures that limit radiocarpal distraction
- heterotopic ossification
- atypical tendon, bone, or nerve anatomy.

70.3 Dorsal Anatomy for Wrist Arthroscopy

There are multiple palpable landmarks on the dorsal wrist to help the surgeon create a safe portal. The application of traction across the wrist during joint distraction will alter the relationships between deep capsular planes and the overlying soft tissue structures. For this reason, structures should be palpated and marked *after traction is applied to the wrist* to preserve normal anatomic relationships. Dorsal bony landmarks include Lister's tubercle, the dorsal ulnar head and sty-

B. R. Graves (✉) · E. J. Sarkissian · G. G. Poehling
Department of Orthopaedic Surgery,
Wake Forest School of Medicine,
Winston-Salem, NC, USA
e-mail: poehling@wakehealth.edu

© ISAKOS 2022

D. N. Bhatia et al. (eds.), *Arthroscopy and Endoscopy of the Elbow, Wrist and Hand*,
https://doi.org/10.1007/978-3-030-79423-1_70

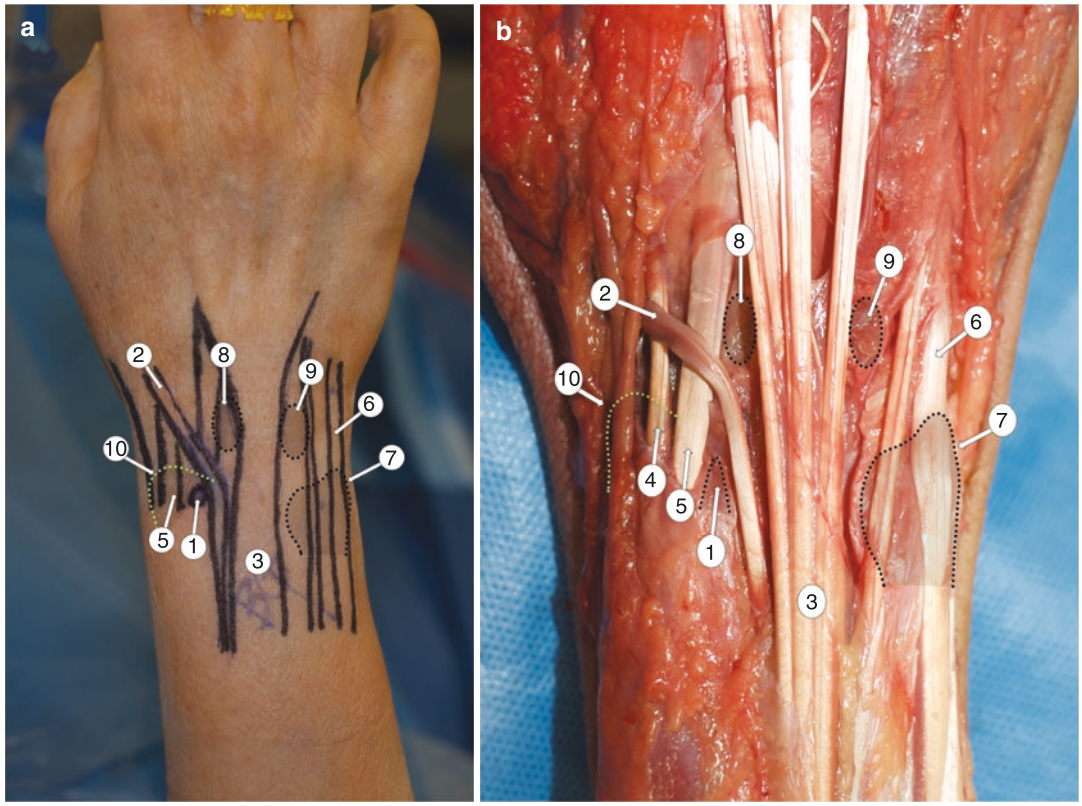

Fig. 70.1 Right dorsal wrist (**a**) intraoperative, and (**b**) cadaveric dissection demonstrating palpable dorsal surface landmarks. (1) Lister's tubercle, (2) EPL, (3) EDC, (4) ECRL, (5) ECRB, (6) ECU, (7) Ulnar head and styloid, (8) Dorsal-radial "soft spot," (9) Dorsal-ulnar "soft spot," (10) Radial styloid (green dashed-line). (Copyright Benjamin R. Graves, MD)

loid, and the metacarpal bases of the index and long fingers. On the radial side of the wrist is the styloid process of the radius, trapezium, and base of the first metacarpal. The ulnar styloid, triquetrum, and base of the fifth metacarpal are readily palpable on the ulnar side of the dorsal wrist.

Tendons are important landmarks to consider when making a safe dorsal portal. Key structures include the extensor pollicis longus (EPL), which turns radial toward the thumb just past Lister's tubercle, the extensor digitorum communis (EDC), the tendons of the extensor carpi radialis longus and brevis (ECRL/ECRB), and the extensor carpi ulnaris (ECU) tendons. The extensor pollicis brevis (EPB) and abductor pollicis longus (APL) mark the radial border of the dorsal portal approaches.

Not all palpable surface landmarks have to be marked on the skin while establishing portals; this step varies between surgeons and comfort levels with the anatomy. Important palpable dorsal anatomic structures are shown in Fig. 70.1a and b.

70.4 Dorsal Portals

The safety and success of an arthroscopic wrist procedure greatly depend on the surgeon's familiarity with the anatomy of the dorsal wrist. Numerous dorsal arthroscopic approaches have been described and are routinely used. The most commonly used dorsal arthroscopic portals are named according to the intervals between the dorsal extensor compartments. By utilizing these

intervals, arthroscopic instruments can be safely introduced and withdrawn with minimal risk to surrounding structures. Portals are described below in numerical order for ease of reference.

70.4.1 Radiocarpal Space

70.4.1.1 1-2 and 2-2 Dorsal Portals (Fig. 70.2)

Not commonly used, the 1-2 portal lies between the APL and the ECRL tendons at the dorsal aspect of the anatomic snuffbox. This approach provides access to the radial aspect of the radiocarpal joint and can be used as a working portal for radial-sided procedures, including arthroscopic radial styloidectomy and STT joint debridement, or for visualization during ulnar-sided work. It is bordered proximally by the radial styloid and distally by the EPL and scaphoid. Alternatively, similar visualization can be achieved through a **2-2 portal**, which utilizes the interval between ECRL and ECRB. For general use, the 2-2 portal is safer than the 1-2 portal because it is further away from the neurovascular structures of the anatomic snuffbox.

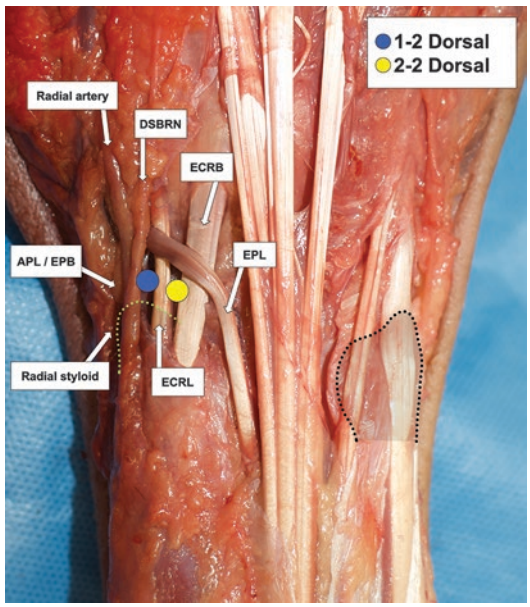

Fig. 70.2 The dorsal 1-2 portal (*blue circle*) is bordered by multiple neurovascular structures that must be protected. Careful and precise surgical technique is required for safe use. A safer alternative is the dorsal 2-2 portal (*yellow circle*), which utilizes the interval between ECRL and ECRB. (Copyright Benjamin R. Graves, MD)

At Risk:

- Branches of the dorsal sensory branch of the radial nerve (**DSBRN**)
  - DSBRN arborizes proximal to the 1-2 portal, and branches have been shown to be within 0–10 mm [3].
- Terminal extent of the lateral antebrachial cutaneous nerve (**LABCN**) may overlap with the DSBRN
- Branches of the **radial artery** are variable and can be readily found within a few millimeters of the 1-2 portal

Helpful Tips:

- For a safer portal, use the 2-2 interval between ECRL and ECRB when possible
- Skin incisions *should not* penetrate into the subcutaneous tissues
- Blunt instrumentation should be used whenever possible
- Use care when instruments are removed and reinserted

70.4.1.2 3-4 Dorsal Portal (Fig. 70.3)

The 3-4 portal is located 1 cm distal to Lister's tubercle in a soft spot between the EPL and the EDC and in line with the radial border of the long finger. With the thumb pad placed on Lister's tubercle, the tip of the thumb will be centered on the soft spot corresponding to the 3-4 portal when the thumb is rolled over the tubercle distally. Proximally, the portal is bordered by the distal radius and distally by the scapholunate interosseous ligament (SLIL).

This is a primary viewing portal in wrist arthroscopy, affording safe exposure to the scaphoid, lunate, SL, and TFCC. The structures most at risk are the EPL and EDC tendons. The posterior interosseous nerve (PIN) runs on the floor of the fourth dorsal compartment and can be found, on average, 4.4 mm from this portal [3].

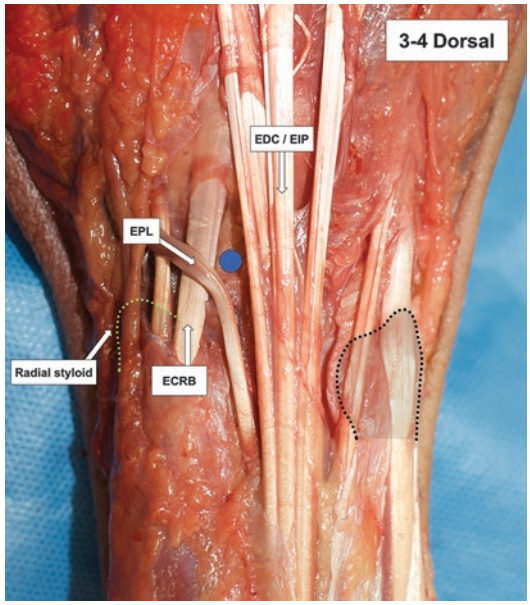

Fig. 70.3 The dorsal 3-4 portal (*yellow circle*) is the "workhorse" portal, and is palpable in the "dorsal radial soft-spot." It is bordered by the tendons of the fourth dorsal compartment ulnarly, and the EPL (third dorsal compartment) radially. (Copyright Benjamin R. Graves, MD)

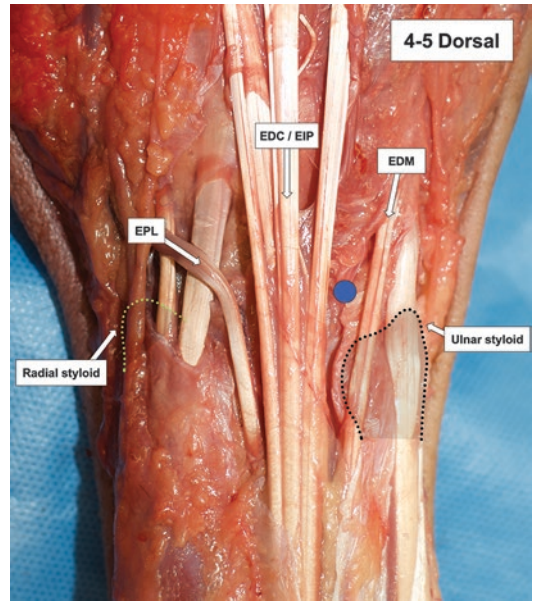

Fig. 70.4 The dorsal 4-5 portal (*blue circle*) is bordered by the tendons of the fourth dorsal compartment ulnarly, and the extensor digitorum minimus (EDM) ulnarly. (Copyright Benjamin R. Graves, MD)

At Risk:
- EPL tendon
- Posterior interosseous nerve (PIN, deep)
- SLIL and chondral surfaces of the scaphoid and lunate

Helpful Tips:
- Remember to angle the trochar to match the volar tilt of the radius
- While establishing portals, blunt instrumentation helps protect the SLIL and carpal cartilage

70.4.1.3 4-5 Dorsal Portal (Fig. 70.4)

The 4-5 portal is located in line with the ring finger metacarpal between the EDC and the extensor digitorum minimi tendon (EDM), slightly proximal to the 3-4 portal. Proximally, it is bordered by the radius and distally by the lunate. When using proper technique, this portal is relatively safe, but care must be taken to prevent injury to surrounding tendons and deeper structures. Dorsal sensory branches of the ulnar nerve are found at a mean distance of 16 mm from the portal [3].

The dorsal 4-5 portal affords similar visualization as the 3-4 portal but with a more direct view of the ulnar compartment of the wrist. This portal is often used for instrumentation and enhanced visualization of the TFCC. Exchanging the position of the arthroscope and the instruments between the 4-5 and 3-4 portals allows the surgeon to perform interventions effectively in the radial and ulnar compartments of the radiocarpal joint.

At Risk:
- EDC and EDM tendons
- PIN (deep)

Helpful Tips:
- Angle the trochar to match the volar tilt of the radius
- Incise the skin only, and use blunt instrumentation to help prevent injury to deep structures

70.4.1.4 6-R Dorsal Portal (Fig. 70.5)

The 6-R portal, located just radial to the ECU, is the primary adjunct for working and/or visualization of the radiocarpal space. The portal is approximately 5 mm distal to the visible TFCC, which represents the proximal border, and is radially bordered by the EDM tendon. The lunotriquetral interosseous ligament (LTIL) borders the portal distally. The structures most at risk in establishing this portal are the TFCC and the EDM tendon. To avoid iatrogenic injury, this portal is established with a needle under direct arthroscopic visualization. The dorsal sensory branch of the ulnar nerve (DSBUN) is also at risk and has been shown to be approximately 8 mm from the portal [3]. Avoiding deep incisions during portal creation, along with the use of blunt instrumentation, will help prevent nerve injury.

The 3-4 and 6-R portals are commonly utilized together for examination and instrumentation of the radiocarpal joint. Although the 6-R portal is typically used as a working portal, instruments and the arthroscope can easily be switched between the two portals to improve visualization and access across the radiocarpal joint. For example, while visualizing from the 3-4 portal, the 6-R portal is particularly useful as a working portal to address ulnar-sided lesions such as those of the TFCC, the LTIL, or chondral defects of the lunate and triquetrum. Conversely, the 6-R portal is excellent for visualization while working in the dorsal wrist, during dorsal ganglion cyst excision for example.

At Risk:

- EDM tendon
- TFCC
- LTIL and chondral surfaces of the lunate and triquetrum
- Ulnar nerve dorsal sensory branches

Helpful Tips:

- Incise skin only and use blunt instrumentation to help prevent injury to deep structures
- Direct visualization with needle localization during portal creation will help prevent injury to the TFCC

70.4.1.5 6-U Dorsal Portal (Fig. 70.5)

The 6-U portal is made just ulnar to the ECU tendon between the TFCC proximally and the triquetrum distally. Multiple terminal branches of the DSBUN divide inconsistently in this area, increasing the risk for iatrogenic injury. In some cases, a transverse branch may cross directly over the portal [4].

For this reason, the 6-U portal has been used predominantly as an outflow portal. If used carefully, it can be used advantageously in diagnostic wrist arthroscopy and in treating certain pathologies about the ulnocarpal ligamentous complex. The high risk of iatrogenic injury to the DSBUN, however, limits routine use of the 6-U portal.

At Risk:

- Ulnar nerve dorsal sensory branches are at high risk of iatrogenic injury
- TFCC

Helpful Tips:

- Incise skin only, "knick-and-spread" with a hemostat, and use blunt instrumentation to prevent injury to deep structures

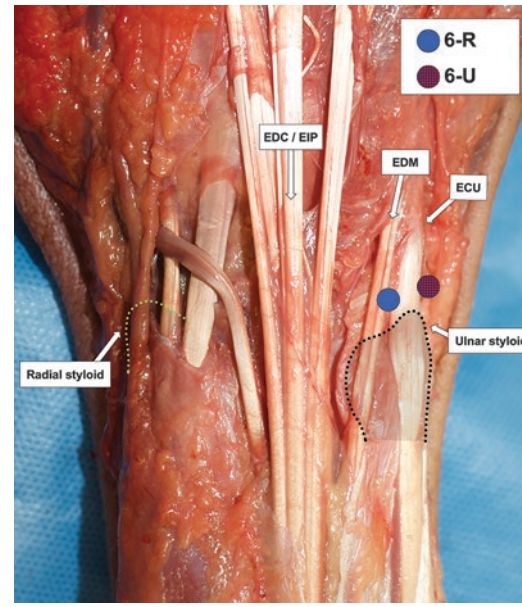

Fig. 70.5 The dorsal 6-R portal (*blue circle*) is made at the radial border of the ECU, just radial to EDM. The 6-U portal (*red check circle*) can also be used for ulnar-sided work and visualization, but places the DSBUN at higher risk for injury. (Copyright Benjamin R. Graves, MD)

70.4.2 Midcarpal Space (Figs. 70.6 and 70.7)

Midcarpal portals allow access to the joints that form between the bones of the proximal row and the bones of the distal row. The capitate forms a mostly vertical joint with the scaphoid radially. When midcarpal visualization is directed ulnar, the articulations between the capitate and lunate, and the triquetrum and hamate, become more horizontal. The scapho-trapezio-trapezoid (STT) joint is the radial extension of the midcarpal joint and is readily visualized using midcarpal portals.

The anterior-to-posterior depth of the midcarpal joint is less than half of the depth of the radiocarpal joint; therefore, the midcarpal joint can be "tighter" compared to the radiocarpal joint. The scapholunate and lunotriquetral articulations can be inspected directly. The most commonly used midcarpal arthroscopy portals are the ulnar and radial midcarpal portals. Typically, one is used for visualization while the other is used as a working portal.

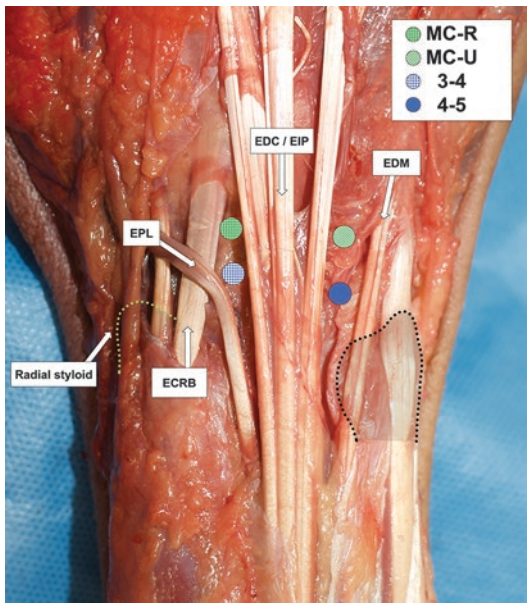

Fig. 70.6 The dorsal MC-R (*green check circle*) and MC-U portals (*green stripe circle*) are made approximately 1 cm distal to the 3-4 portal and 4-5 portals, respectively. These portals can be used interchangeably for work and visualization in the midcarpal space. (Copyright Benjamin R. Graves, MD)

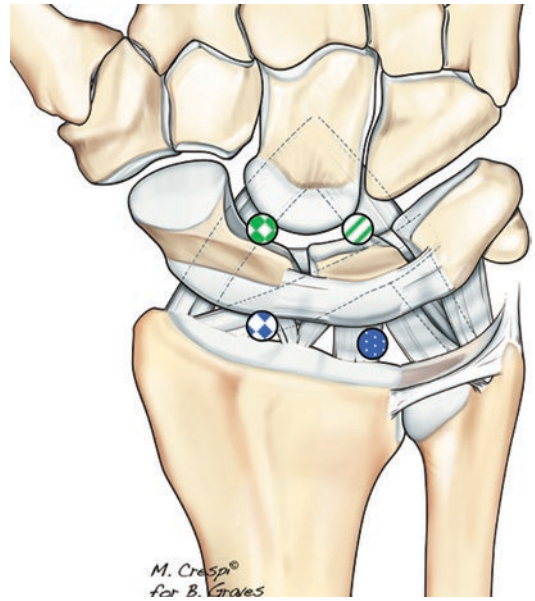

Fig. 70.7 The dorsal MC-R (*green check circle*) and MC-U portals (*green stripe circle*) are made approximately 1 cm distal to the 3-4 portal and 4-5 portals, respectively. These portals can be used interchangeably for work and visualization in the midcarpal space. (Copyright Benjamin R. Graves, MD; © Crespi for Graves)

70.4.2.1 Radial Midcarpal Portal (MC-R)

Located 1 cm distal to the 3-4 portal along the axis of the radial border of the long finger metacarpal, between ECRB and EDC, the radial midcarpal portal provides visualization of scapholunate, scaphocapitate, and STT joints. At risk are the ECRB and EDC tendons.

70.4.2.2 Ulnar Midcarpal Portal (MC-U)

This portal is located 1 cm distal to the 4-5 portal along the axis of the ring finger metacarpal, between the EDC and the EDM. The portal offers safe access to the lunocapitate, lunotriquetral, and triquetrohamate joints.

At Risk:

- DSBUN terminal branches are at risk of iatrogenic injury with MC-U portal
- DSBRN are at with MC-R portal
- Midcarpal chondral surfaces are at risk during portal creation

Helpful Tips:

- As with all portals used for wrist arthroscopy, incise skin only, "knick-and-spread" with a hemostat, and use blunt instrumentation to prevent injury to chondral surfaces

70.5 Additional Portals

In addition to the portals previously described, several portals have been described but are not as commonly employed due to increased time, dissection, and risk to neurovascular structures, in addition to more narrow indications for use. These include two volar wrist portals (Fig. 70.8), and portals used to access the distal radioulnar joint (Fig. 70.9). Although these portals may provide improved visualization while treating specific intraarticular conditions of the wrist, they are typically not used during routine diagnostic arthroscopy of the wrist and are described in more detail in specific chapters in this book.

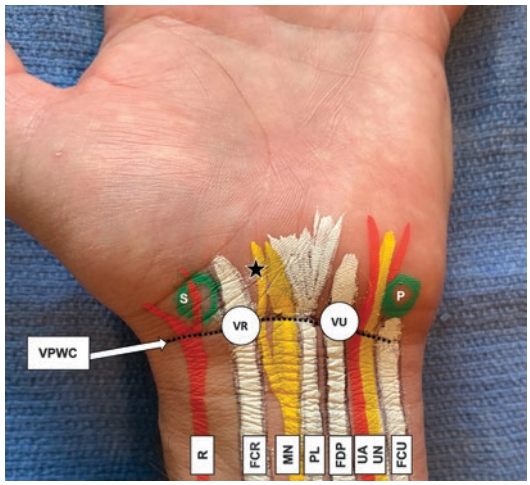

Fig. 70.8 The volar radial portal (VR) is made at the VPWC through the FCR sheath, and the volar ulnar portal (VR) is made at the VPWC in line with the deep flexor tendons of the fingers. *VPWC* volar proximal wrist crease, *R* radial artery, *S* scaphoid, *FCR* flexor carpi radialis, *MN* median nerve, *PL* palmaris longus, *FDP* flexor digitorum profundus, *UN/UA* ulnar nerve/artery, *P* pisiform, *FCU* flexor carpi ulnaris. Palmar cutaneous branch of the median nerve is marked with a black star. (Copyright Benjamin R. Graves, MD)

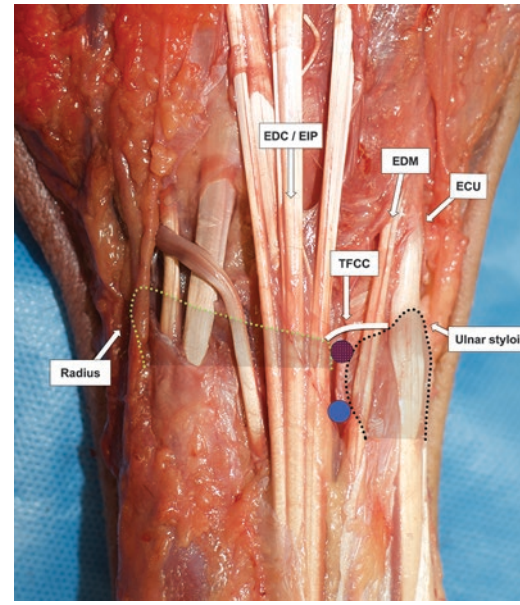

Fig. 70.9 The distal radioulnar joint (DRUJ) is assessed through the dorsal distal portal (*red-checked circle*), and the dorsal proximal portals (*blue circle*). Forearm supination aids in placement by relaxing the dorsal capsule. (Copyright Benjamin R. Graves, MD)

70.5.1 Volar Radial Portal

Compared to dorsal portals, the volar radial portal provides improved visualization of the volar SLIL and dorsal wrist pathology such as dorsal distal radius rim fracture. To establish this portal, a 1.5–2 cm transverse incision is made over the flexor carpi radialis (FCR) tendon at the proximal volar wrist crease (PVWC). The FCR tendon is then retracted ulnarly with the median nerve and digital flexor tendons. The radial artery is retracted radially. The floor of the FCR sheath is then spread with a hemostat, and a 20-gauge needle is inserted while visualizing from a dorsal portal. The entry site of this portal correlates with the interval between the RSC and the LRL volar carpal ligaments and has been shown to be a safe

distance from surrounding neurovascular structures when this technique is used [5].

70.5.2 Volar Ulnar Portal

This portal may be used for better visualization of the volar LTIL and dorsal ulnar-sided wrist pathology. The volar ulnar portal is established through a 2-cm transverse mini-open incision made at the level of the PVWC, over ulnar aspect of the flexor digitorum profundus (FDP) tendons. The FDP tendons are retracted radially, and the flexor carpi ulnaris (FCU) and ulnar artery and nerve are retracted ulnarly. A 20-guage needle is used to localize the radiocarpal joint, and entrance is typically just radial to the TFCC through the ulnocarpal ligaments. Great care must be used while establishing and instrumenting this portal and neurovascular structures can be found within 5 mm [5].

70.5.3 Distal Radioulnar Joint Portals

Although visualization can be challenging due to limited space, pathology of the distal radioulnar joint (DRUJ) including osteophytes, loose bodies, synovitis, and deep tears of the TFCC can be assessed arthroscopically. ***Dorsal portals*** are made using the interval between the EDC and the EDQ/ECU (Fig. 70.9), with a **proximal portal** at the base of the DRUJ between the radius and ulna articular surfaces, and a **distal portal** just proximal to the TFCC at the distal aspect of the DRUJ. The forearm is pronated and supinated to increase the area that can be visualized. A volar DRUJ portal can also be created using a similar technique as previously described for the creation of the volar ulnar portal.

70.6 Diagnostic Arthroscopy of the Wrist

(a) **Patient positioning and setup**

The author performs wrist arthroscopy with the patient in a supine position on a standard OR bed with a hand table extension. A regional nerve block, typically with sedation, helps the patient better tolerate a brachial tourniquet and wrist joint distraction. The arthroscopy tower is placed at the foot of the bed for ease of access and monitor positioning. A tourniquet is applied to the brachium, and a bracket, used to counter the forces applied during wrist joint distraction, is fastened to the OR table (Fig. 70.10a, b). Wrist distraction greatly improves visualization and creates more space to navigate and work in the tight joint spaces of the wrist. Multiple equipment systems and devices can

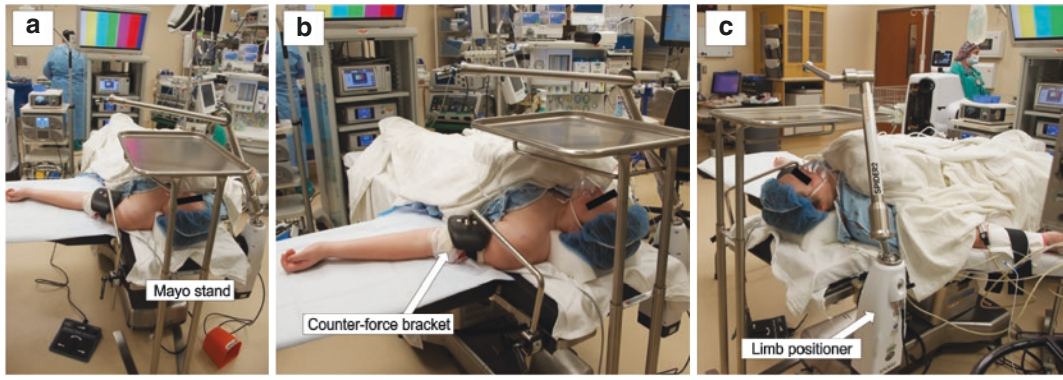

Fig. 70.10 (**a**–**c**) Patient positioning during wrist arthroscopy as seen from three views. The arthroscopy tower is placed at the foot of the bed with the monitor facing the head of the bed. Note the position of the counter-force arm bracket over the tourniquet, and the Mayo stand placed between the patient's face and limb positioner. (Copyright Benjamin R. Graves, MD)

Fig. 70.11 (*left*) Finger traps and tensiometer are attached to the distraction arm (*right*), allowing adjustment of distraction force as needed throughout the case. (Copyright Benjamin R. Graves, MD)

be used for wrist joint distraction, including tabletop towers or adjustable boom-arm distractors. The author uses a limb positioner (Spider 2, Smith & Nephew. Andover MA, USA) positioned on the contralateral side at the head of the bed (Fig. 70.10a–c). This positioner allows a constant baseline distraction and offers the ability to "titrate" wrist distraction through a tensiometer attachment (Fig. 70.11). The boom arm of the limb positioner is then brought across the patient toward the operative hand over a Mayo stand, which helps protect the patient's face during surgery, and also provides a shelf for operative instruments (Figs. 70.10 and 70.12).

A hand-table drape is used, and a sterile sleeve is placed over the limb positioner. Arthroscopic instruments rest on the "shelf" created by the Mayo positioned above the patient's face (Fig. 70.11). Most surgeons employ the use of sterile finger traps for safe and reliable "purchase" of the digits during distraction. Finger traps can be safely applied to the index, long, and ring fingers during the distraction, but care must be taken when applying to thin or frail skin. The trap must be applied as proximal as possible on the digit, preferably to the mid proximal phalanx, for optimal stability and to minimize the risk of skin tears [6].

(b) **Wrist arthroscopy Instruments**

- **For Insufflation and Portal Creation**
  - 20-g needle, 1.5 inch
  - 10-cc syringe
  - 11-blade knife
- **Arthroscope**
  - **Angle:** 30°
  - **Length:** 50–60 mm length
  - **Diameter:**
    1.7–4.0 mm is acceptable
    2.5–3.0 mm is ideal for routine cases
- **Hand Instruments**
  - Probe: appropriately sized for small-joint arthroscopy (approximately 40 mm in length and 1.5–2.00 mm in diameter)

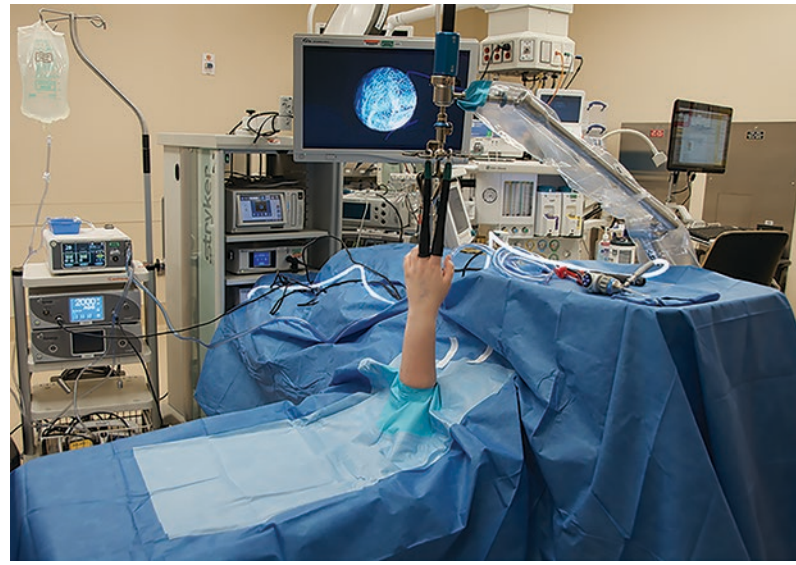

Fig. 70.12 Final positioning after sterile draping for wrist arthroscopy. With the arthroscopy tower at the foot of the bed the monitor faces the surgeon. Note the Mayo stand "shelf" for instruments, and the sterile draping of the limb positioner. (Copyright Benjamin R. Graves, MD)

  - Grasping forceps designed for small-joint arthroscopy
  - Suction punch (2.5 mm) for precise debridement without creating debris in the joint.
- **Power Instruments**
  - 2.0–3.0 mm shavers and burrs are useful for debridement and preparation before repairs

70.7 Diagnostic Wrist Arthroscopy: Author's Preferred Technique

70.7.1 Establish Visualization and Working Portals

Typically, the 3-4 dorsal radiocarpal portal is the first portal established, and the first step in safely creating this portal is radiocarpal joint insufflation. This is accomplished by injecting saline into the radiocarpal joint at the site of the 3-4 portal using an 18-G needle and syringe. The needle is directed from the dorsal distal to the volar proximal at an angle of 10–15° to match the normal volar tilt of the distal radius. Insufflation distends the radiocarpal joint capsule, which makes entrance with the arthroscopy easier. A normal, uninjured wrist can accommodate approximately 5 mL of fluid. When the pathology of the triangular fibrocartilage complex (TFCC) or intercarpal ligaments is present, the wrist may accommodate up to 10–15 mL. Fluid tracking proximally into the distal radioulnar joint (DRUJ) suggests a TFCC tear, whereas fluid tracking distally into the carpus indicates an intercarpal ligament tear.

After insufflation, the skin is incised with the tip of a #11 blade. Care must be taken while making this incision to prevent injury to superficial vessels, tendons, and cutaneous nerves, which often lie immediately deep to the dermis. Longitudinal incisions are preferred for several reasons. First, transection of underlying structures is much less likely with longitudinal incisions compared to horizontal incisions. Longitudinal incisions may also easily be extended, if necessary, for conversion to an open procedure. Horizontal skin incisions on the dorsal aspect of the wrist, in line with skin creases, may theoretically improve cosmesis; however, the risk of iatrogenic injury to underlying structures greatly outweighs the potential benefits. For this reason, the author does not perform or recommend horizontal incisions.

Following skin incision, a blunt hemostat is advanced until contact with the joint capsule is established. The capsule is then pierced with the tip of the closed hemostat. Typically, a rush of saline will present indicating intraarticular posi-

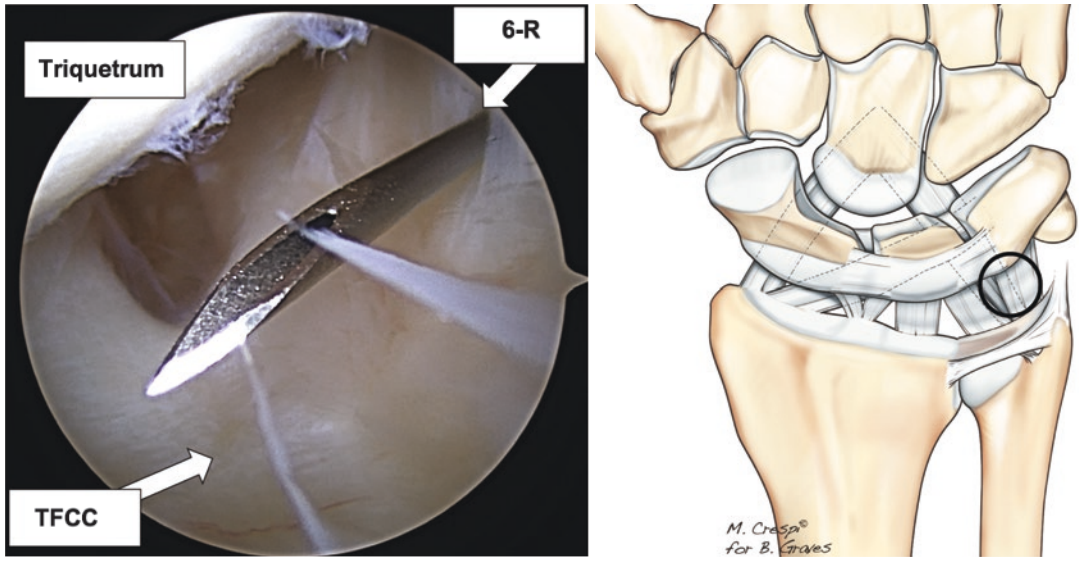

Fig. 70.13 Viewing the ulnar radiocarpal space from the 3-4 portal, an 18-g needle is used to localize the safest position for the 6-R portal. (Copyright Benjamin R. Graves, MD)

tion. A blunt 2.5- to 3.0-mm arthroscopy trocar and sheath are introduced into the radiocarpal space, at which point the trocar is exchanged for the arthroscope. The scope is then rotated toward the ulnar side of the radiocarpal space. An ulnar-sided portal at 6-R or 4-5 can then be made under direct visualization with an 18-G needle using the same skin incision technique (Fig. 70.13). If excessive intra-articular bubbles are encountered, an 18-G needle at the 6-U portal for outflow may help with this.

70.7.2 Diagnostic Arthroscopy: Radiocarpal Space

A systematic arthroscopic examination allows direct visualization and probing of all critical structures. Typically, the examination begins in the radiocarpal space and proceeds from radial to ulnar, and volar to dorsal. The radiocarpal space can be a tight space, so it is important to use care when entering and maneuvering within the joint. Damage to articular surfaces can be minimized through stabilization and small, purposeful movements with the arthroscope. To help stabilize the arthroscope, the surgeon's camera-holding hand is in contact with the patient's forearm/wrist which helps limit unintended movement, and rotation of the 30°-angle arthroscope allows a wide degree of freedom for exploring a tight space with a minimal motion of the arthroscope.

- Starting radial visualizing from the dorsal 3-4 portal, the radial extrinsic ligaments of the wrist are inspected, and the joint capsule is examined for synovitis. Chondral changes in the radius, scaphoid, and lunate are inspected. Volarly, the radioscaphocapitate (RSC) ligament is most radial and typically appears as a stout structure. The long radiolunate ligament (LRL) lies just ulnar to the RSC (Fig. 70.14).
- The next most ulnar extrinsic ligament in the radial compartment is the radioscapholunate ligament (ligament of Testut). Unlike the other volar radial extrinsic ligaments, the ligament of Testut does not provide structural support but serves as a neurovascular conduit to the SLIL (Fig. 70.15). Moving more ulnar, the short radiolunate ligament is not as consistently visualized.
- Next, the scapholunate interosseous ligament is examined from the 3-4 portal. The SLIL is

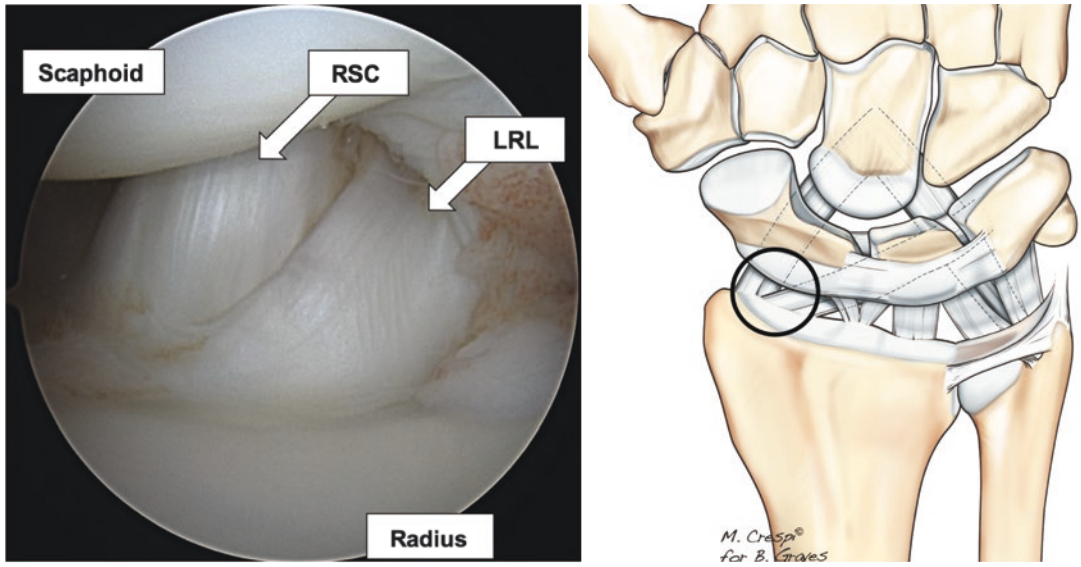

Fig. 70.14 3-4 portal view of the radial styloid and extrinsic volar radiocarpal ligaments. (Copyright Benjamin R. Graves, MD)

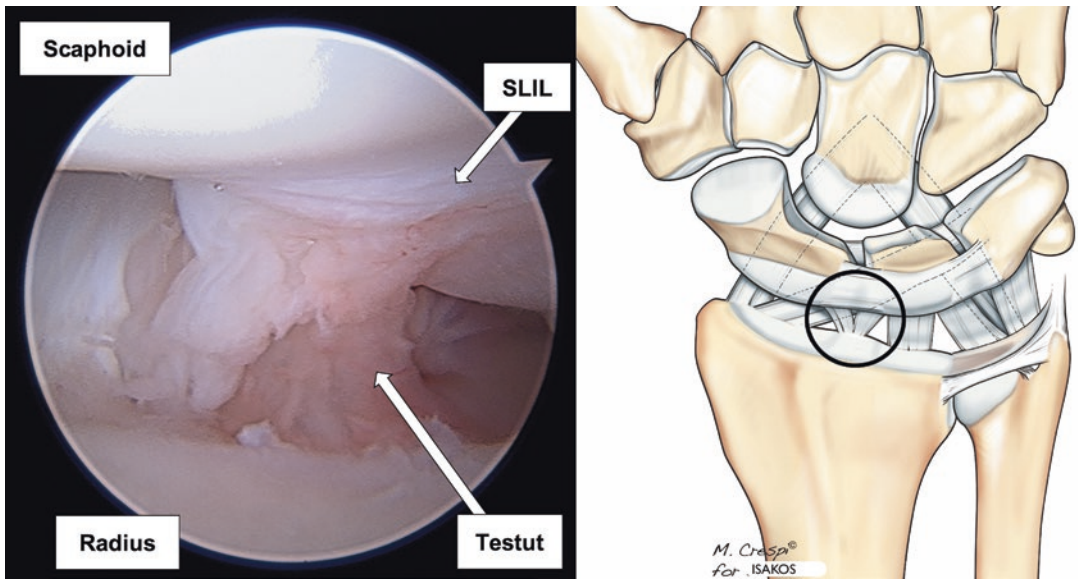

Fig. 70.15 3-4 portal view of the SLIL and ligament of Testut. (Copyright Benjamin R. Graves, MD; © Crespi for Graves)

visualized between the scaphoid and the lunate bones, and the dorsal and intramembranous portions of the SLIL can be directly inspected and probed for hemorrhagic changes and tears. An intercarpal step-off between the scaphoid and the lunate indicates carpal instability (Fig. 70.16).

- Viewing ulnarly from the 3-4 portal, the TFCC is inspected. With a probe in the 4-5 or 6-R portal, the *trampoline test* can be performed to assess for TFCC integrity. A loss of normal buoyance may indicate a radial-sided or peripheral tear. To perform this test, the flat portion of a probe is placed in the center of the

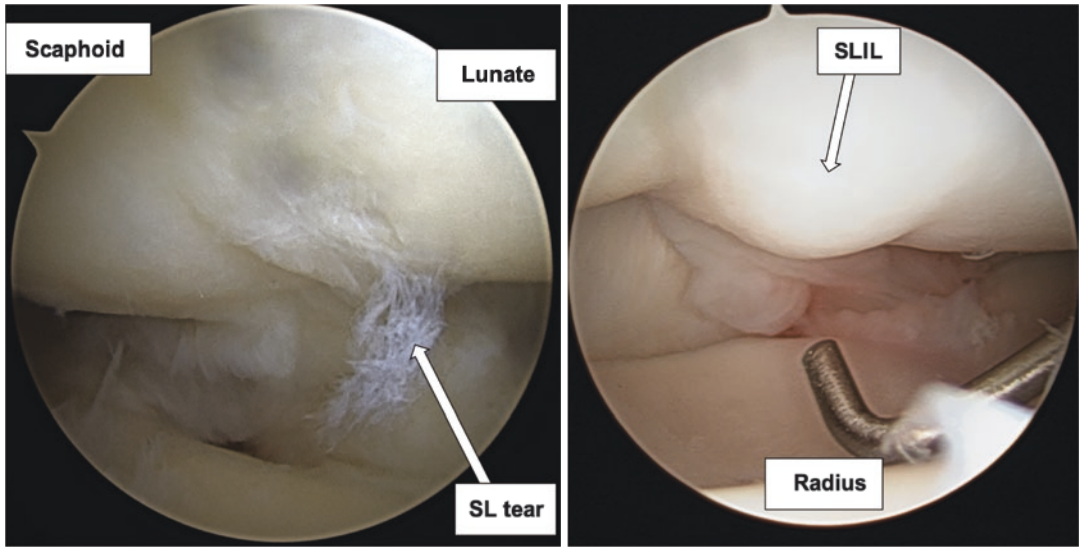

Fig. 70.16 (*Left*) 3-4 portal view of a small SLIL tear; (*right*) a 6-R working portal is used to probe a "boggy" intramembranous SLIL. (Copyright Benjamin R. Graves, MD)

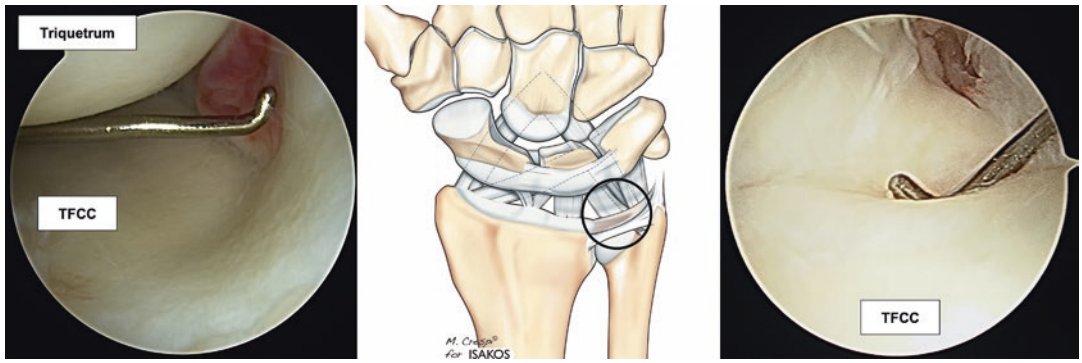

Fig. 70.17 (*Left*) 3-4 portal view of capsular hemorrhage seen with peripheral TFCC tear, and (*right*) laxity seen while probing the TFCC during "trampoline test." (Copyright Benjamin R. Graves, MD; © Crespi for Graves)

disk of the TFCC. A normal TFCC will have sufficient tension to withstand this pressure. In the presence of a peripheral tear, however, the TFCC will be lax such that the probe with applied pressure will become buried and hidden from view (Fig. 70.17). The *hook test* is performed to evaluate the deep fibers of the TFCC. In a positive test, the TFCC lifts from proximal to distal with a probe placed beneath the articular disk.

- Typically, the ulnar compartment of the radiocarpal joint cannot be adequately assessed from the 3-4 portal alone. To facilitate visualization of the ulnar compartment, including the LTIL, the 4-5 or 6-R portal is used for visualization. After changing the camera to an ulnar portal, the lunate and triquetrum articular surfaces are inspected for signs of chondral wear. The 3-4 portal is now used for instrumentation, and the LTIL is inspected for hemorrhagic changes, attenuation, or frank tears (Fig. 70.18).
- Looking radial from the 4-5 or 6-R portal provides a broader view of the dorsal radial compartment and the dorsal SLIL and enables inspection of the dorsal capsule for synovitis, dorsal ganglion cysts, and SLIL integrity. The ulnar aspect of the pisotriquetral joint can also be visualized from this portal (Fig. 70.19).

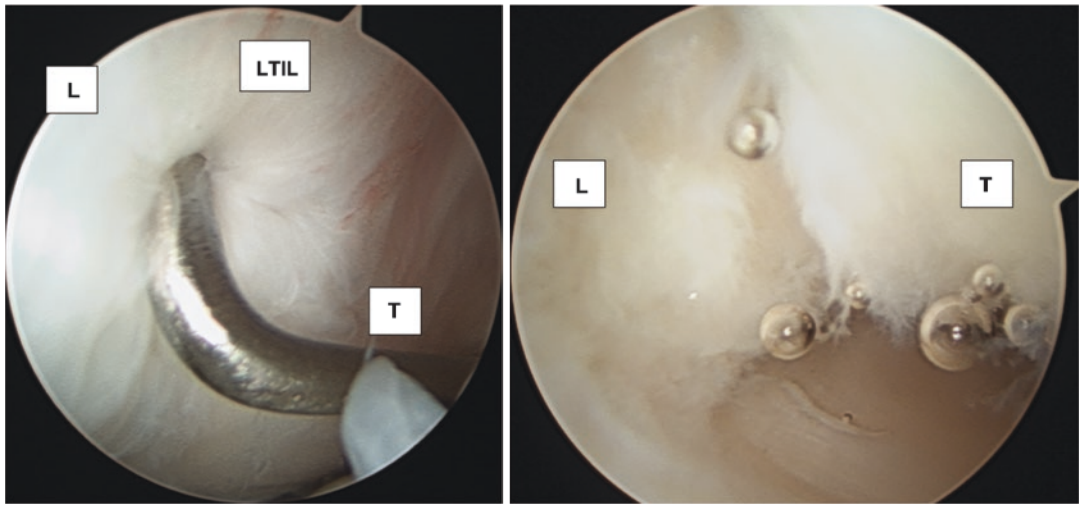

Fig. 70.18 (*Left*) View from 6-R portal of probe inspection of dorsal LTIL, and Fig. 70.15, (*right*) 6-R view of LTIL tear. *L* lunate, *T* triquetrum, *LTIL* lunotriquetral interosseus ligament. (Copyright Benjamin R. Graves, MD)

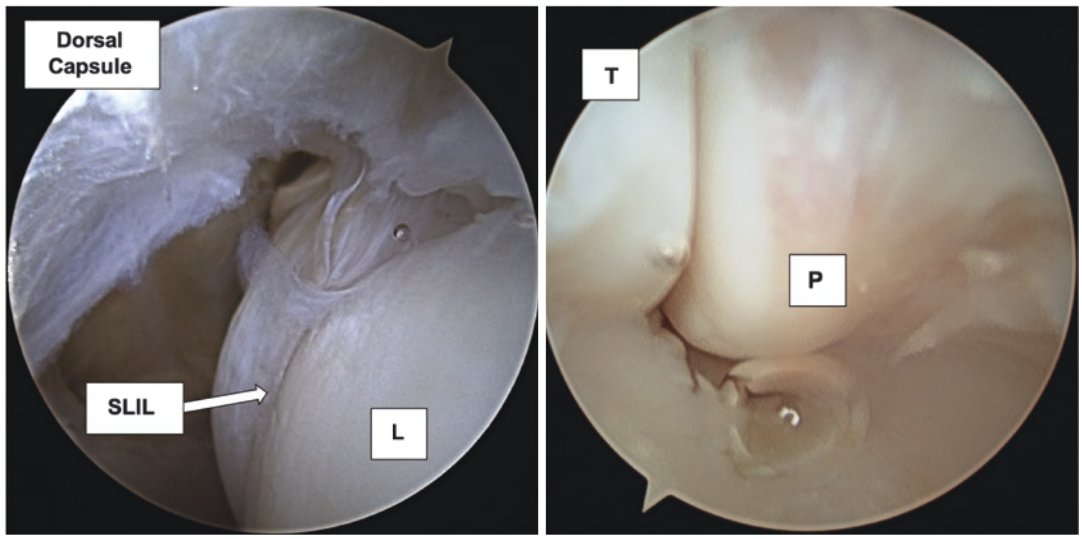

Fig. 70.19 (*Left*) View from 6-R portal of dorsal capsule and SLIL, and Fig. 70.18, (*right*) 6-R view of pisotriquetral joint. *L* lunate, *T* triquetrum, *P* pisiform, *SLIL* scapholunate interosseus ligament. (Copyright Benjamin R. Graves, MD)

70.7.3 Diagnostic Arthroscopy: Midcarpal Space

To thoroughly evaluate for chondral damage, intercarpal ligament integrity, and to facilitate visualization for advanced techniques, midcarpal space (Fig. 70.20) arthroscopy is essential. Radial (MC-R) and ulnar (MC-U) midcarpal space portals are used for access to the midcarpal space (Figs. 70.6 and 70.7). In some patients, this space can be tight, so a 1.9–2.3 mm arthroscope can be helpful, especially for pediatric patients. Once in the midcarpal space, inspection of the articular surfaces of the midcarpal space follows.

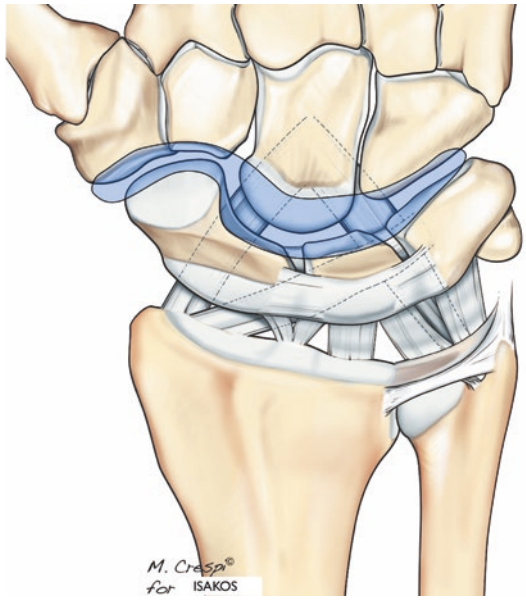

Fig. 70.20 The midcarpal space spans from the STT joint radially to the triquetral-hamate joint ulnarly, and is shown in blue. (Copyright Benjamin R. Graves, MD; © Crespi for Graves)

- Starting radially, the scaphotrapeziotrapezoid joint (STT) is readily visualized from an MC-R portal and can be instrumented using a 1-2 dorsal portal (Fig. 70.21).
- Moving ulnar in the midcarpal space, as viewed and instrumented interchangeably through MC-R and MC-U portals, the chondral surfaces of the scaphoid, lunate, and triquetrum are inspected as are the chondral surfaces of the proximal capitate and hamate.
- A 2-mm probe is used to evaluate the integrity of the scapholunate and lunotriquetral ligaments from the midcarpal portals (Fig. 70.22).

Following diagnostic arthroscopy, the surgeon may proceed with additional procedures as detailed in this book. Portals are closed with steri-strips or suture, and a dressing is applied.

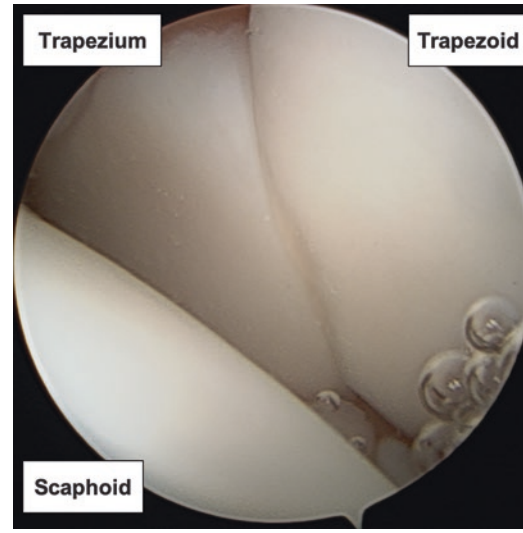

Fig. 70.21 MC-R portal view of triscaphe (STT) joint. (Copyright Benjamin R. Graves, MD)

70.8 Potential Complications

In general, diagnostic arthroscopy of the wrist is safe and effective and has a low complication rate [6, 7]. However, like any surgical procedure, adverse outcomes such as infection, traction, and position-related complications, may occur, and steps can be taken to decrease the risk of their occurrence have been detailed in this chapter. Meticulous technique is critical, and care must be taken while instrumenting and exchanging between portals. Structures at risk with the use of specific portals have been listed previously in this chapter.

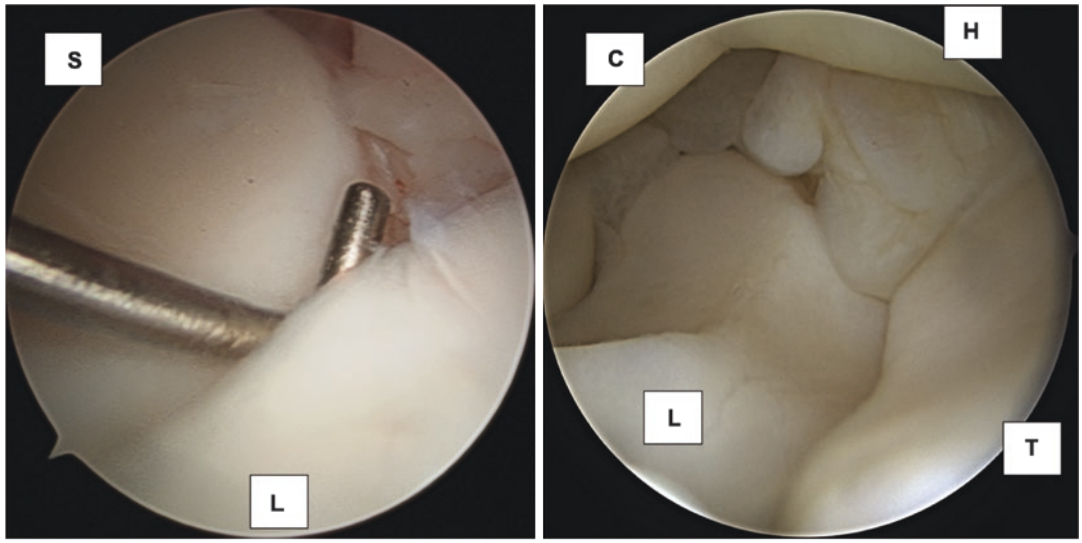

Fig. 70.22 (*Left*) Assessment of SLIL integrity through a MC-U visualization portal and MC-R working portal, and Fig. 70.21, (*right*) MC-U view of chondral surfaces of the midcarpal space. The chondral step-off between the lunate and triquetrum suggests LTIL tear. *S* scaphoid, *L* lunate, *C* capitate, *T* triquetrum, and *H* hamate. (Copyright Benjamin R. Graves, MD)

References

1. Tosti R, Shin E. Wrist arthroscopy for athletic injuries. Hand Clin. 2017;33(1):107–17.
2. MacLean SBM, Kantar K, Bain GI, Lichtman DM. The role of wrist arthroscopy in Kienbock disease. Hand Clin. 2017;33(4):727–34.
3. Shyamalan G, Jordan RW, Kimani PK, et al. Assessment of the structures at risk during wrist arthroscopy: a cadaveric study and systematic review. J Hand Surg Eur. 2016;41(8):852–8.
4. Tryfonidis M, Charalambous CP, Jass GK, et al. Anatomic relation of dorsal wrist arthroscopy portals and superficial nerves: a cadaveric study. Arthroscopy. 2009;25(12):1387–90.
5. Slutsky DJ. The use of a volar ulnar portal in wrist arthroscopy. Arthroscopy. 2004;20(2):158–63.
6. Graves BR, Deal ND, Tamam C, Poehling GG. Avoiding complications in wrist arthroscopy. In: Savoie FH, Field LD, Steinmann SP, editors. The elbow and wrist: AANA advanced arthroscopic surgical techniques. Slack, Inc.; 2016. p. 443–54.
7. Ahsan ZS, Yao J. Complications of wrist and hand arthroscopy. Hand Clin. 2017;33(4):831–8.

Wrist Portals and Arthroscopic Anatomy

71

F. Corella, M. Ocampos, M. C. Manzanares-Céspedes, and M. Dalmau-Pastor

71.1 Dorsal Radiocarpal Portals

The names of the dorsal radiocarpal portals are referred to their anatomical relationship with the extensor compartments of the wrist (Fig. 71.1).

3/4 and 6R portals are the most commonly used, as they allow complete visualization of the entire radiocarpal joint. However, the other three radiocarpal portals, 1/2, 4/5, and 6U, are also worth knowing and using as they may be useful in certain situations or for certain surgical techniques.

71.1.1 1/2 Portal

It is located between the abductor pollicis longus (APL) and the extensor pollicis brevis (EPB) on the radial side and the extensor carpi radialis longus (ECRL) and the extensor carpi radialis brevis (ECRB) on the ulnar side. Since this portal is located in the anatomical snuffbox, it is important to remember that the radial artery is located in its most distal portion. Therefore, it is recommended that the entry point must be proximal. It should also be noted that in this location, the distal sensory branch of the radial nerve is at risk (Fig. 71.2).

It is a portal that is usually performed under the arthroscopic vision and not in a direct blind way (as a starting portal). Both the introduction of the needle when making the portal and the subsequent introduction of the arthroscope should be made at 20° tilt to follow the articular surface of the radius and to avoid damaging the proximal cartilage of the scaphoid.

F. Corella (✉)
Orthopedic and Trauma Department, Hospital Universitario Infanta Leonor, Madrid, Spain

Hand Surgery Unit, Hospital Universitario Quironsalud Madrid, Madrid, Spain

Surgery Department, School of Medicine, Universidad Complutense de Madrid, Madrid, Spain

M. Ocampos
Orthopedic and Trauma Department, Hospital Universitario Infanta Leonor, Madrid, Spain

Hand Surgery Unit, Hospital Universitario Quironsalud Madrid, Madrid, Spain

M. C. Manzanares-Céspedes
Human Anatomy Unit, Department of Pathology and Experimental Therapeutics, School of Medicine and Health Sciences, University of Barcelona, Barcelona, Spain

M. Dalmau-Pastor
Human Anatomy Unit, Department of Pathology and Experimental Therapeutics, School of Medicine and Health Sciences, University of Barcelona, Barcelona, Spain

GRECMIP - MIFAS (Groupe de Recherche et D'etude en Chirurgie Mini-Invasive du Pied - Minimally Invasive Foot and Ankle Society), Merignac, France

© ISAKOS 2022

D. N. Bhatia et al. (eds.), *Arthroscopy and Endoscopy of the Elbow, Wrist and Hand*,
https://doi.org/10.1007/978-3-030-79423-1_71

Fig. 71.1 Dorsal radiocarpal portals of the wrist. Names are referred to the anatomical relationship with the extensor compartments of the wrist

71.1.1.1 Visualized Structures

At the Entry Point (Fig. 71.3)
Proximal: radial styloid and scaphoid fossa.
Distal: proximal surface of the scaphoid
Volar: Radioscaphocapitate ligament, long radiolunate (LRL) ligament, radioscapholunate ligament (Testut ligament), and volar margin of the radius.
Dorsal: dorsal capsule, dorsal radiotriquetral ligament, and dorsal margin of the radius

Moving the Vision Field to the Ulnar Zone (Fig. 71.4)
Proximal: lunate fossa and triangular fibrocartilage complex (TFCC).
Distal: proximal pole of the lunate bone.
Volar: ulnocarpal ligaments, volar margin of the radius.
Dorsal: dorsal capsule, dorsal margin of the radius.

71.1.1.2 Neurovascular Structures-at-Risk

This is one of the portals considered to be of greatest risk since it is located in the anatomical snuffbox where important neurovascular structures are present. Thus, careful attention must be paid during portal placement and manipulation.

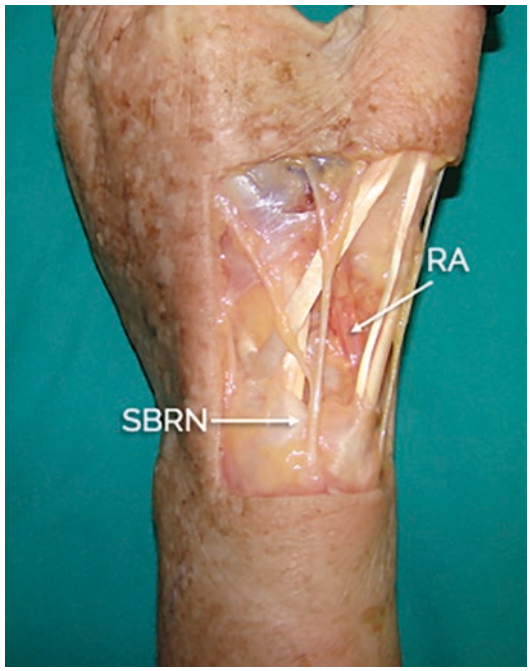

Fig. 71.2 Structures at risk while establishing the 1/2 portal. Superficial branch of the radial nerve (SBRN). Radial artery (RA)

- *Radial artery*:
- It is located in the most distal and radial area of the anatomical snuffbox. An anatomical study has reported that it is to be found 3 mm (range 1–5 mm) radial to the 1/2 portal [1].
- *Superficial Branch of the Radial Nerve (SBRN)*:
- Shyamalan et al. [2] carried out an anatomical study and a systematic review of the structures at risk with respect to arthroscopic portals. They found three more studies in which the distances at risk of the portal 1/2 with respect to the SBRN were analyzed. The study carried out by Kilic et al. [3] established a distance of 5 mm (range 2–12 mm), while those of Abrams et al. [1] and Tryfonidis et al. [4] were 3 mm (range 1–6 mm) and 3 mm (range 0–19 mm), respectively, and in that of Shyamalan et al. [2] it was 2 mm (range 0–8 mm). In the last two studies, there were several specimens with distances of 0 mm, that is, the portal was directly over the SBRN. This is why this portal puts this nerve at risk, and therefore extreme precautions must be taken during its realization, which must always be done in a blunt manner and ensuring the protection of the SBRN.

71.1.2 3/4 Portal

It is located in the space between the extensor pollicis longus (EPL) and the extensor digitorum

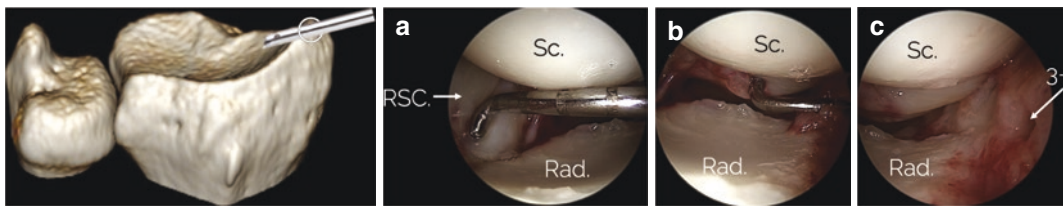

Fig. 71.3 Arthroscopic view of the radiocarpal joint through the 1-2 portal, at the entry point. The images correspond to a left wrist (for a better understanding, all the arthroscopic images of the chapter correspond to left wrists). Radioscaphocapitate ligament (RSC). Scaphoid (Sc). Radius (Rad). Abbreviations and symbols will be used according to the previous figures during the whole chapter (**a**) Volar side. (**b**) Central side. (**c**) Dorsal side

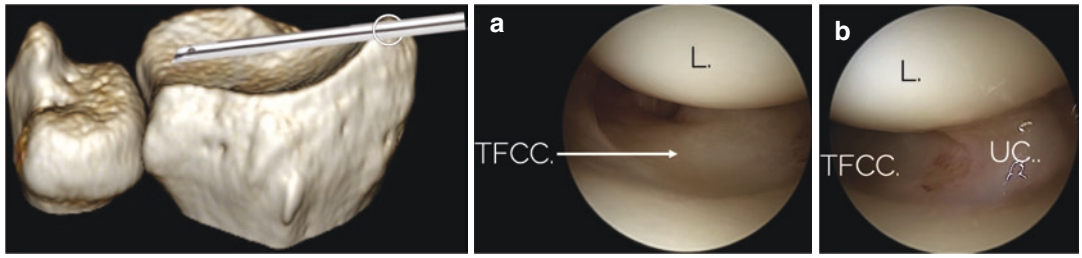

Fig. 71.4 Arthroscopic view of the radiocarpal joint through the 1-2 portal, *moving the vision field to the ulnar side*. Lunate (L). Triangular fibrocartilage complex (TFCC) (**a**) Central side. (**b**) Volar side

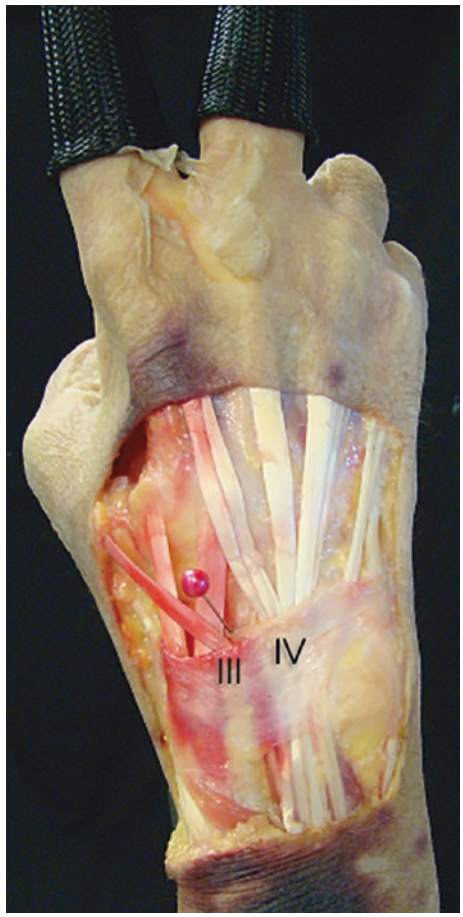

Fig. 71.5 Anatomical location of the 3-4 portal

(ED), 1 cm distal to the Lister's tubercle and in line with the radial edge of the third metacarpal bone (Fig. 71.5). Both the needle to mark the entry point and the introduction of the arthroscope should be volar-oriented about 10° to follow the volar inclination of the articular surface of the radius.

Generally, this is the first portal to be made, and being one of the safest portals, it is done "blind." It allows a panoramic view of the entire radiocarpal joint thus being useful and common in the vast majority of arthroscopic techniques.

71.1.2.1 Visualized Structures

At the Entry Point (Fig. 71.6)
Proximal: articular surface of the radius and the ridge that separates the scaphoid and lunate fossa.
Distal: proximal pole of the scaphoid and lunate and the membranous portion of the scapholunate ligament.
Volar: the radioscapholunate ligament is in the middle of the vision field; both the long radiolunate ligament and the short radiolunate ligament are radial to it.

Moving the Vision Field to Radial (Fig. 71.6)
Proximal: radial styloid process and scaphoid fossa.
Distal: proximal pole of the scaphoid.

Moving the Vision Field to Ulnar (Fig. 71.7)
Proximal: lunate fossa, TFCC with pre-styloid recess.
Distal: proximal pole of the lunate.
Volar: Ulnocarpal ligaments.
Dorsal: Dorsal articular capsule and 6R portal.

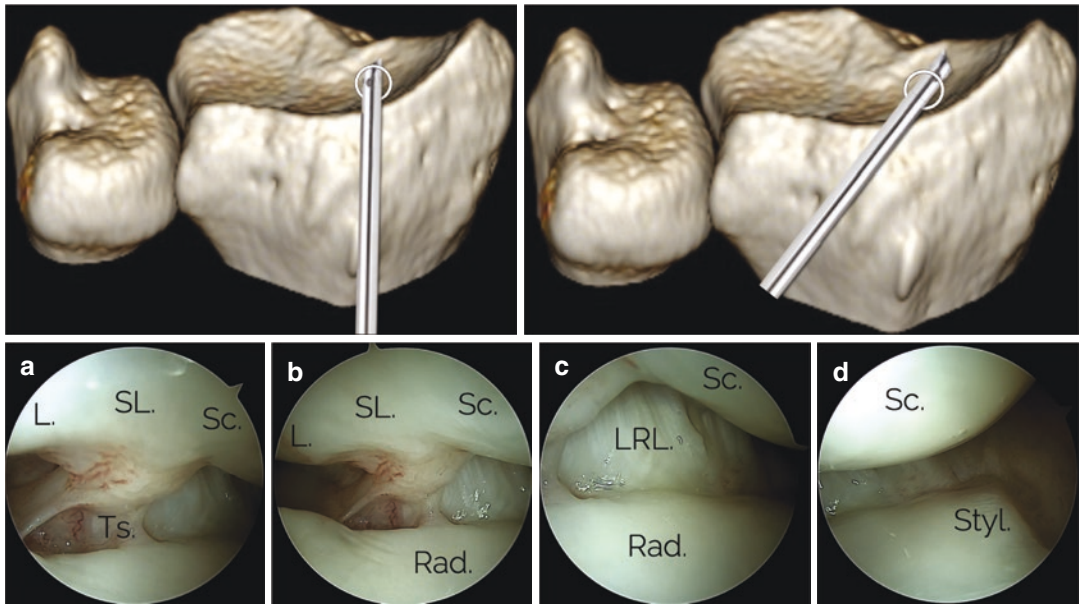

Fig. 71.6 Arthroscopic view of the radiocarpal joint through the 3-4 portal. (**a**, **b**) Images at the entry point. (**c**, **d**) Images moving the vision field to the radial side. Scapholunate ligament (SL). Radioscapholunate ligament or Testut ligament (Ts). Long radiolunate ligament (LRL). Radial styloid process (Styl)

71.1.2.2 Neurovascular Structures at Risk

- *Superficial Branch of the Radial Nerve*:

  Five anatomical studies analyzed the distances from SBRN to the 3/4 portal. The values obtained were: Kilic et al. [3] 9 mm (range 2–19 mm), Abrams et al. [1] 16 mm (range 5–22 mm) Shyamalan et al. [2] 25 mm (range 15–33 mm), Auerbach et al. [5] 4 mm (range 0–14 mm), and Tryfonidis et al. [4] 9 mm (range 0–48 mm). The last two studies include measurements of zero, indicating that the SBRN can also be found just below the portal and, despite being considered a much safer portal than 1/2, caution should also be taken during its performance.
- *Posterior interosseous nerve (PIN)*:

  The PIN may also be at risk when performing the 3/4 portal. Three studies analyzed the distance of this nerve from the portal. The study by Pan and Hung [6] is the one showing greater portal security with respect to the PIN, with a distance of 4.8 mm (range 1.2–12 mm). However, the study by Shyamalan et al. [2] measured a distance of 4.4 mm (range 0–10) with a 3/4 portal PIN injury. Another recent study, performed by Chea et al. [7], analyzed the histological damage of the PIN after carrying out the 3/4 portal, and they discovered axonal damage in 7 of 14 specimens. Consequently, there is also the possibility of damage to this nerve during the performance of a routine wrist arthroscopy portal.

71.1.3 4/5 Portal

It is located in the interval between the ED and the extensor digit minimi (EDM), in line with the

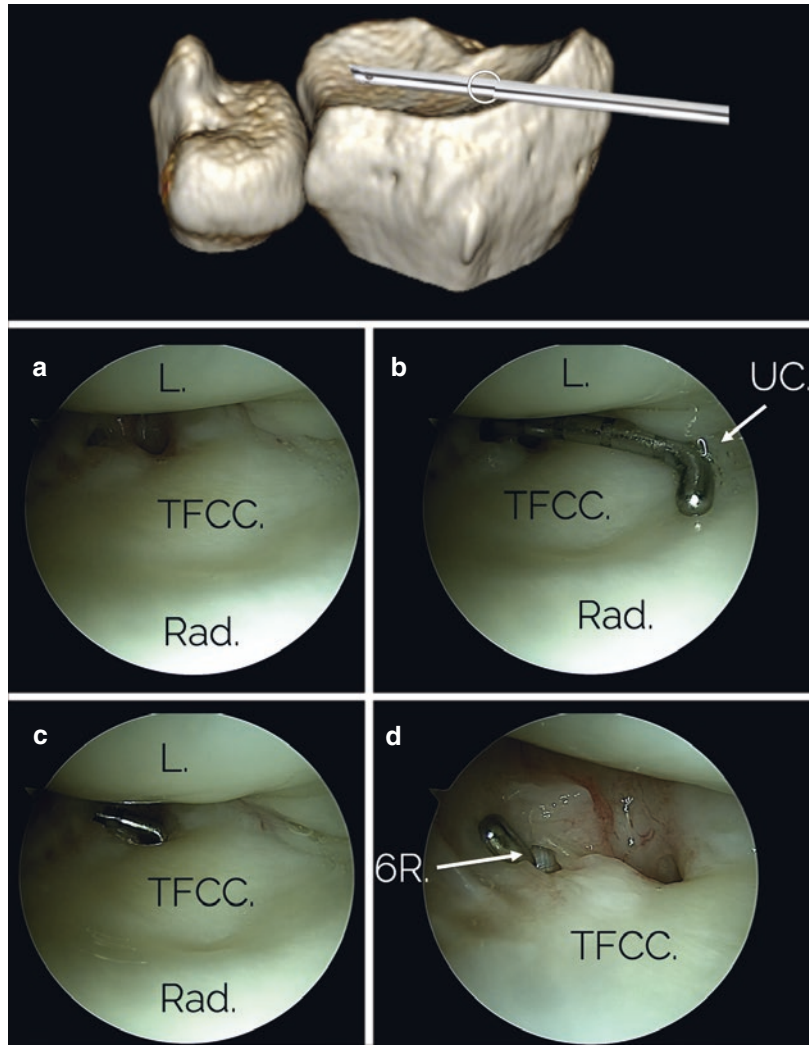

Fig. 71.7 (**a**) Arthroscopic view of the radiocarpal joint through the 3-4 portal, moving the vision field to the ulnar side. (**b**–**d**) The probe is inserted through the 6R portal. Ulnocarpal ligaments (UC)

fourth metacarpal bone. Due to the radius inclination, this portal is located slightly proximal to the 3/4 portal and approximately 1 cm radial from the 6R portal (Fig. 71.8).

Like the 3/4 portal, the insertion of the needle, arthroscope, or instruments must be performed with a 10° volar inclination. Regarding the 3/4 portal, it can improve the vision of the ulnocarpal joint and can be used for instrumentation, although its use is much less frequent than 3/4 and 6R.

71.1.3.1 Visualized Structures

At the Entry Point (Fig. 71.9)

Proximal: In the center of the view field is the radial insertion of the TFCC, which continues in a radial direction with the lunate fossa of the radius.

Distal: proximal surface of the lunate.

Volar: ulnocarpal ligaments.

Moving the Vision Field to Radial (Fig. 71.10)

Proximal: ulnar portion of the scaphoid fossa

Distal: proximal surface of the scaphoid and membranous portion of the scapholunate ligament.

Volar: long and short radiolunate ligaments and radioscaphocapitate ligament.

Dorsal: dorsal capsule, 3/4 portal, and, if a dorsal displacement is performed on the lunate, the dorsal capsuloligamentous scapholunate septum (DCSS) is visualized.

Displacement of the Field of Vision Toward Ulnar

Ulnar area of the TFCC with the pre-styloid recess.

71.1.3.2 Neurovascular Structures-at-Risk

- *Dorsal sensory branch of the ulnar nerve (DBUN)*:

Fig. 71.8 Anatomical location of the 4-5 portal

In none of the three studies that analyzed its distance to the portal was found a lesion of this superficial nerve. The distances reported were: Tryfonidis et al. [4]: 18 mm (range 9–27 mm), Ehlinger et al. [8]: 4 mm (range 1–11 mm), and Shyamalan et al.: 2 21 mm (range 13–32 mm).

- *Posterior interosseous nerve*:

  The study by Shyamalan et al. [2] observed that the mean distance to the portal was 12.6 mm (range 2–25 mm), and the study by Pan and Hung [6] measured an ulnar distance from the PIN of 9.0 mm (range 3.8–12.7 mm). In other words, with respect to the PIN, it appears as a more secure portal than the 3/4 portal.

- *Extensor digiti minimi*:

  Despite being a portal relatively safe for neurovascular structures, there is an increased risk than in other portals for tendon structures. Partial or complete tendinous sections have been reported after the dissection of specimens used in wrist arthroscopy training courses [9, 10].

71.1.4 6R Portal

It is located on the radial side of the extensor carpi ulnaris (ECU) and distal to the TFCC (Fig. 71.11). In order to avoid any damage to the TFCC, this portal, situated just distal to it, must be carried out under arthroscopic vision.

This portal is performed routinely along with the 3/4 portal in most wrist arthroscopies. It serves both for the instrumentation in techniques performed on the TFCC and ulna and for the

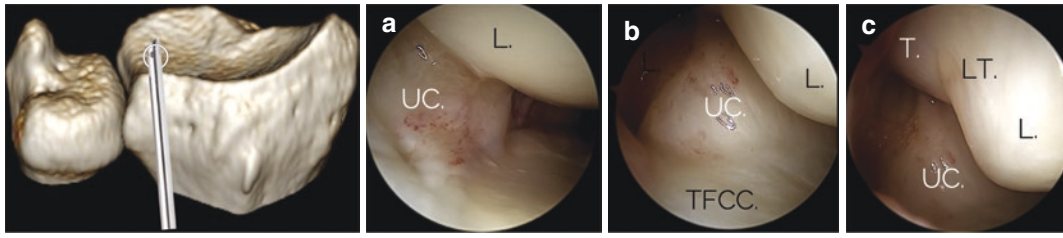

Fig. 71.9 Arthroscopic view of the radiocarpal joint through the 4-5 portal, at the entry point (from **a** to **c**) The scope is displaced distal and ulnar

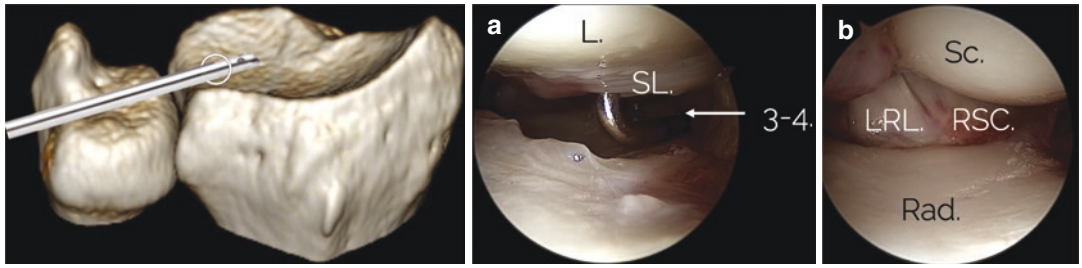

Fig. 71.10 Arthroscopic view of the radiocarpal joint through the 4-5 portal, moving the vision field to the radial side. The probe is inserted through the 3-4 portal (**a**) Moving the vision field to the dorsal side. (**b**) Moving the vision field to the volar side

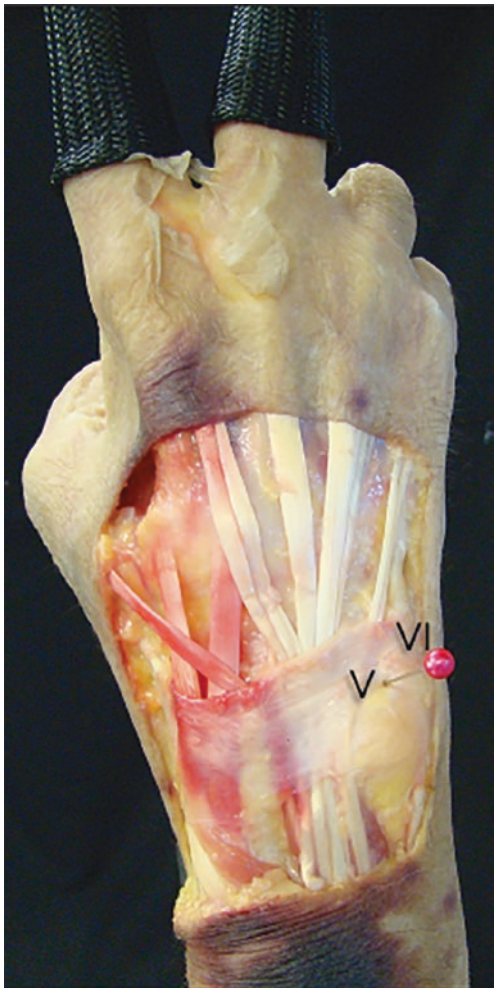

Fig. 71.11 Anatomical location of the 6R portal

visualization in many other arthroscopic techniques. It allows a panoramic view of the radius and proximal pole of the scaphoid (essential, e.g., in fractures of the radius and scaphoid), the visualization of the DCSS, the visualization of the pisotriquetral joint, the visualization of the membranous portion of the lunotriquetral ligament, and so on.

71.1.4.1 Visualized Structures

At the Entry Point (Fig. 71.12)
Proximal: TFCC and radial sigmoid fossa
Distal: articular surface of the lunate and LT joint.
Volar: ulnocarpal ligaments.

Moving the Vision Field to Radial (Fig. 71.13)
Proximal: articular surface of the radius: lunate fossa and if it moves more radially, scaphoid fossa.
Distal: proximal pole of the lunate, more radial, membranous portion of the scapholunate ligament and even more radial, proximal pole of the scaphoid.
Volar: Radioscapholunate ligament and more radial, long radiolunate ligament and radioscaphocapitate ligament.
Dorsal: Dorsal capsule and if it moves over the back of the lunate, the DCSS is visualized.

Moving the Vision Field to Ulnar (Fig. 71.14)
Proximal: TFCC and pre-styloid recess
Distal: membranous portion of the lunotriquetral ligament.
Volar: Following the ulnocarpal ligaments distally, the pisotriquetral joint can be visualized.

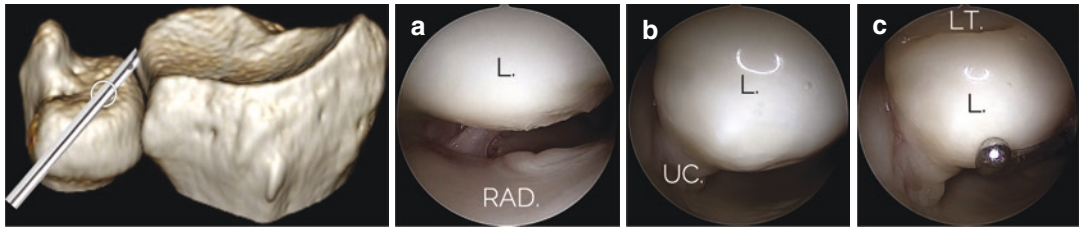

Fig. 71.12 Arthroscopic view of the radiocarpal joint through the 6R portal, at the entry point. Lunotriquetral ligament (LT) (from **a** to **c**) The scope is displaced distal and ulnar

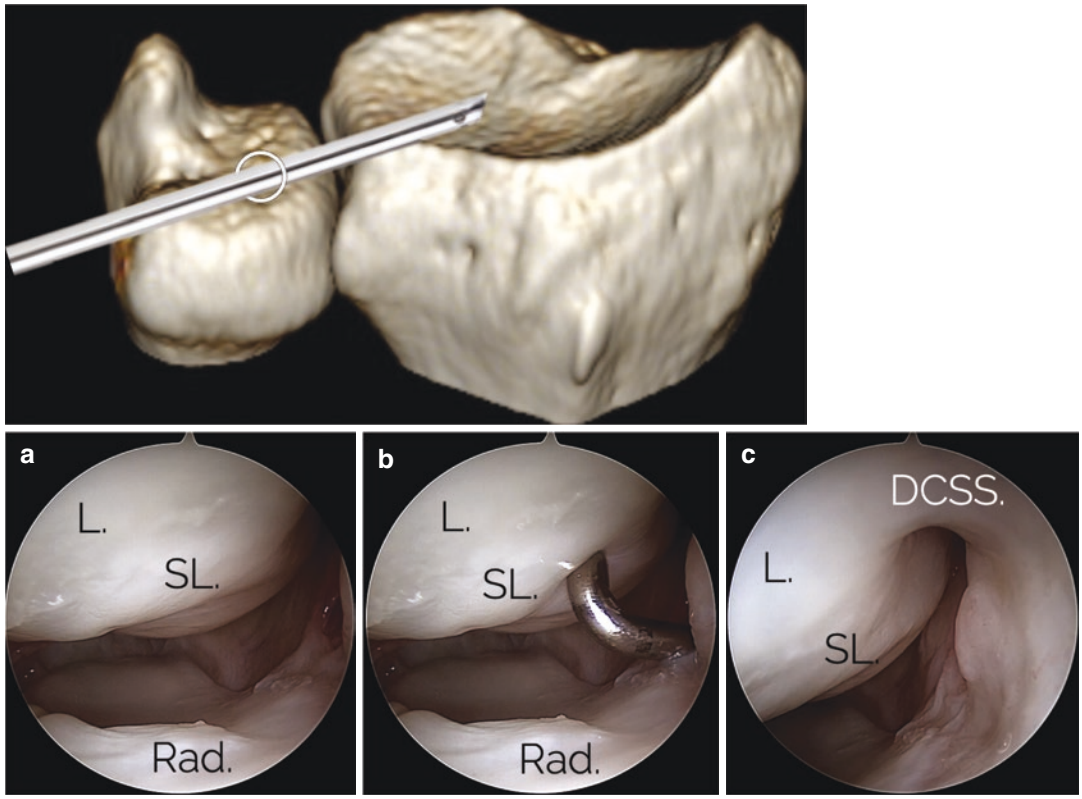

Fig. 71.13 (**a**) Arthroscopic view of the radiocarpal joint through the 6R portal, moving the vision field to the radial side. (**b**) Probe entering through the 3/4 portal. (**c**) Dorsal capsuloligamentous scapholunate septum (DCSS)

71.1.4.2 Neurovascular Structures-at-Risk

- *Dorsal sensory branch of the ulnar nerve (DBUN)*:

  There are three studies that analyze its distance from the 6R portal. Ehlinger et al. [8] found an average distance of 4 mm (range 1–15 mm) and Abrams et al. [1] of 8 mm (range 0–14 mm) with a specimen in which the branch was just below the portal, and they also studied the distance of the transverse radioulnar sensory branch of the DBUN found in 12 of 19 specimens which is only 2 mm apart (range 0–6 mm). Finally, Shyamalan et al. [2] measured a distance of 8 mm (range of 2–14 mm). That is, since the

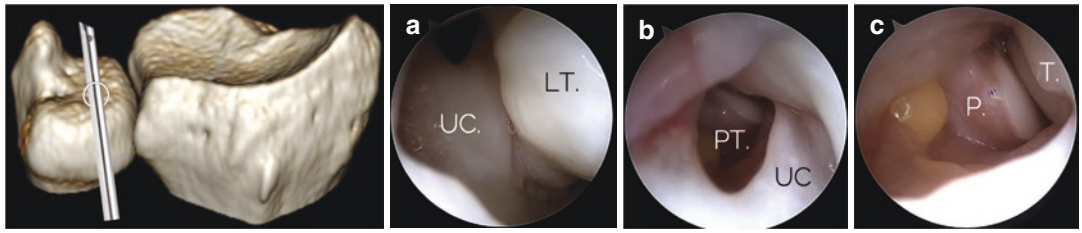

Fig. 71.14 Arthroscopic view of the pisotriquetral joint (PT) through the 6R portal. Pisiform (P). Triquetrum (T) (from **a** to **c**) The scope is displaced inside the PT joint

DBUN is so close to the portal, extreme care must be taken with its realization to have a reference of greater security. Tindal et al. [11] performed a study on 20 wrists to define the "safe" area of the 6R portal. They observed that the fifth most proximal part of an imaginary line that runs between the ulnar styloid to the fourth intermetacarpal space is safe, since the DBUN is not to be found in this space.

71.1.5 6U Portal

It is located ulnar with respect to the ECU and on the TFCC. Like the 6R portal, this portal must be performed under arthroscopic vision. The sensory branch of the ulnar nerve is very close to the portal, so precautions should be taken when performing it and when suturing the TFCC through or near this portal.

It is a portal that can be used as a working portal for the suture or reconstruction of the TFCC.

71.1.5.1 Visualized Structures

The structures visible through this portal are:

At the Entry Point (Fig. 71.15)
Proximal: TFCC and insertion in the sigmoid fossa
Distal: Proximal pole of the lunate and lunotriquetral ligament.
Volar: Ulnocarpal Ligaments
Dorsal: Dorsal capsule (ECU floor), 6R portal.

Moving the Vision Field to Radial (Fig. 71.16)
Proximal: Articular surface of the radius (lunate fossa) and if it moves more radial, scaphoid fossa.
Distal: Proximal pole of the lunate; more radial, membranous portion of the scapholunate ligament and even more radial, proximal pole of the scaphoid.
Volar: Radioscapholunate ligament and more radial, long radiolunate, and radioscapho-capitate ligament.
Dorsal: Dorsal capsule, dorsal radiotriquetral ligament, and if it moves over the dorsal side of the lunate, the DCSS is visualized.

71.1.5.2 Neurovascular Structures-at-Risk

- *Dorsal sensitive branch of the ulnar nerve*:

  All the reviewed studies show very short distances between the portal and the nerve. Tryfonidis et al. [4] found 3 mm (range 0–11 mm), Ehlinger et al. [8] 5 mm (range 1–12 mm), Abrams et al. [1] 5 mm (range 2–12 mm), and Shyamalan et al. [2] 1 mm (range of 0–8 mm). It is one of the portals that has been classically considered more dangerous, although, as previously mentioned, if care is taken to perform a blunt dissection, neurovascular damage is minimized. Another technical recommendation to reduce the risk of injury to this nerve branch was published by Esplugas et al. [12] after performing an anatomical study on six specimens. They suggested supinating the wrist when placing the portal, since in supination the DBUN moved further away from the 6U portal.

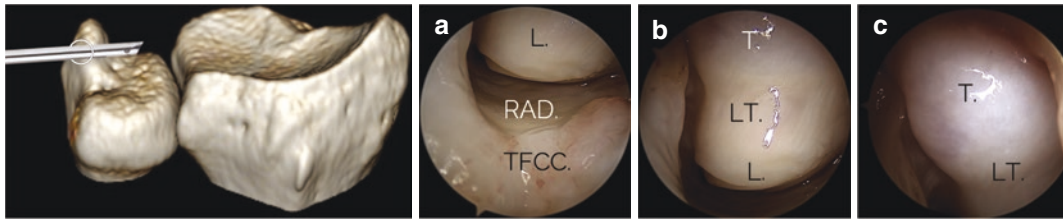

Fig. 71.15 Arthroscopic view of the radiocarpal joint through the 6U portal, at the entry point (from **a** to **c**) The scope is displaced distal and ulnar

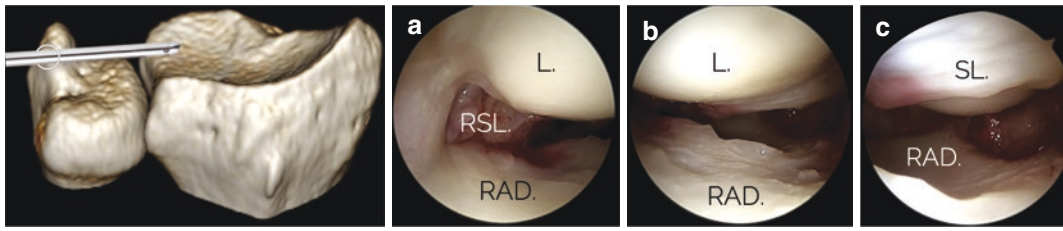

Fig. 71.16 Arthroscopic view of the radiocarpal joint through the 6U portal, moving the vision field to the radial side (**a**) Volar side. (**b**) Central side. (**c**) Dorsal side

71.2 Midcarpal Dorsal Portals

Exploration of the midcarpal joint should be included routinely on all wrist arthroscopy procedures. Inspection of this joint is essential for the diagnosis of many pathologies that cannot be fully assessed by exploring only the radiocarpal joint.

The two most used portals allowing a complete exploration of the midcarpal joint are the radial midcarpal portal (RMC) and the ulnar midcarpal portal (UMC) (Fig. 71.17). There are two others dorsal midcarpal portals that serve to assess and treat scapho-trapezio-trapezoid joint (STT) pathology; they are not used routinely but can be useful in certain situations.

71.2.1 Radial Midcarpal Portal (RMC)

It is located 1 cm distal to the 3/4 portal, in line with it and with the radial edge of the third metacarpal bone. The ECRB is radial to the portal while the ED is ulnar to the portal. It is located just distal to the scapholunate ligament (Fig. 71.18). Since it is just above the scapholunate ligament, it is preferable to perform it under arthroscopic control, after performing the UMC portal.

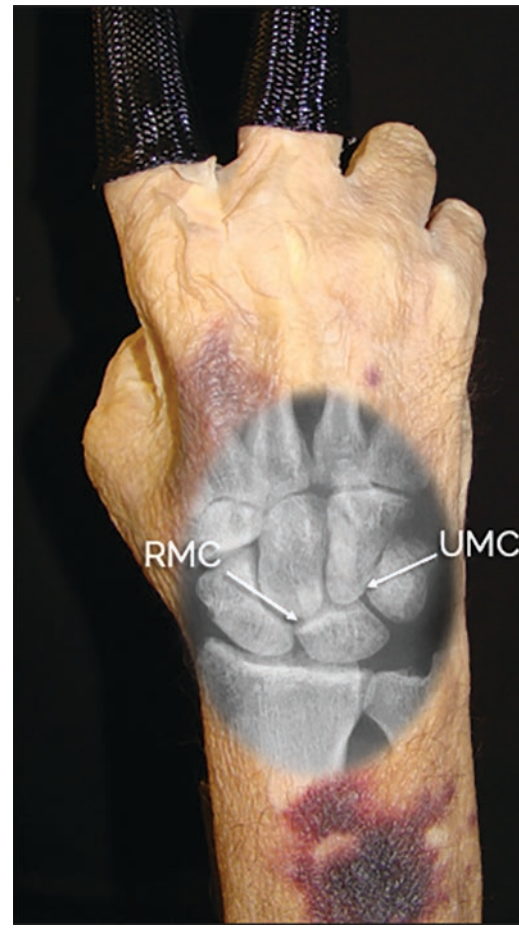

Fig. 71.17 Dorsal midcarpal portals of the wrist. Radial midcarpal portal (RMC). Ulnar midcarpal portal (UMC)

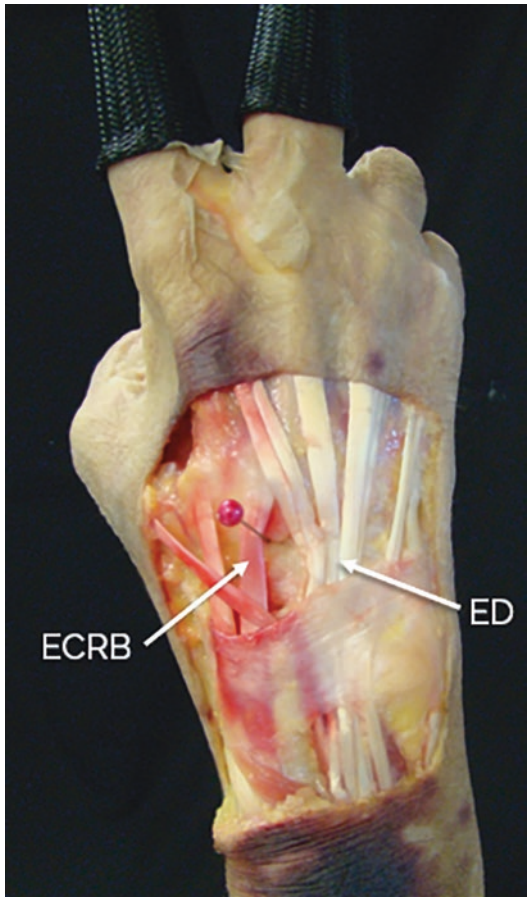

Fig. 71.18 Anatomical location of the Radial Midcarpal Portal. Extensor Carpi Radialis Brevis (ECRB). Extensor digitorum (ED)

It is a fundamental portal for the exploration of both the midcarpal joint and the STT joint.

71.2.1.1 Visualized Structures

The structures visible through this portal are:

At the Entry Point (Fig. 71.19)

Proximal: The concave surface of the scaphoid and the lunate. The space between them corresponds to the scapholunate joint.

Distal: Proximal surface of the capitate bone.

Volar: The anterior portion of the scaphoid, the anterior horn of the lunate, and the radio-scapho-capitate ligament (radial portion of the arcuate ligament) are observed.

Moving the Vision Field to Radial (STT Joint) (Fig. 71.20)

If the surface of the scaphoid is followed radially and distally, the STT joint is reached.

Proximal: Distal portion of the scaphoid.

Distal: Proximal surface of the trapezoid and trapezium

Radial: Scapho-trapezio-trapezoid ligament

Ulnar: Capitate bone and its joint with the trapezoid.

Moving the Vision Field to Ulnar (Fig. 71.21)

Proximal: Articular surface of the lunate and the triquetrum as well as the lunotriquetral joint. Occasionally, a crest appears in the lunate that separates an articular fossa of the capitate bone and a smaller fossa of the hamate bone, a finding that Viegas classified in lunate type I (without a crest) and type II (with a crest) [13].

Distal: Proximal surface of the capitate and hamate bone.

Volar: Anterior horn of the lunate, anterior portion of the triquetrum, and triquetral-hamate ligament (which is part of the distal and ulnar portion of the arcuate ligament)

Dorsal: UMC portal, dorsal portion of the lunotriquetral ligament.

71.2.1.2 Neurovascular Structures at Risk

- *Superficial branch of the radial nerve*:

  Four anatomical studies have analyzed the distances from the SBRN to the RMC portal. Those made by Tryfonidis et al. [4] and Kilic et al. [3] reported smaller distances, 10 mm (range 1–20 mm) and 8 mm (range 1–16 mm),

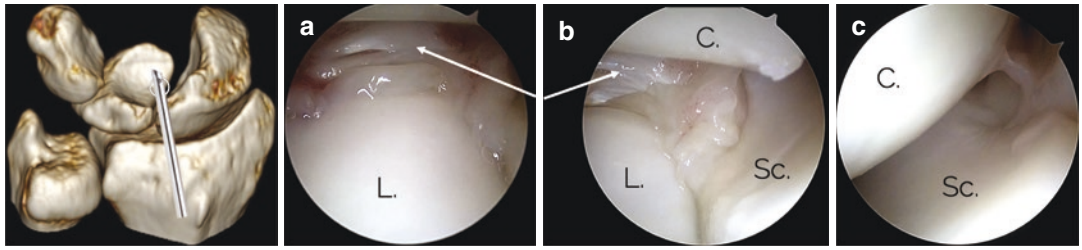

Fig. 71.19 Arthroscopic view of the midcarpal joint through the RMC portal, at the entry point. Capitate (C). Arcuate ligament (Arc) (from **a** to **c**) The scope is displaced to the radial side

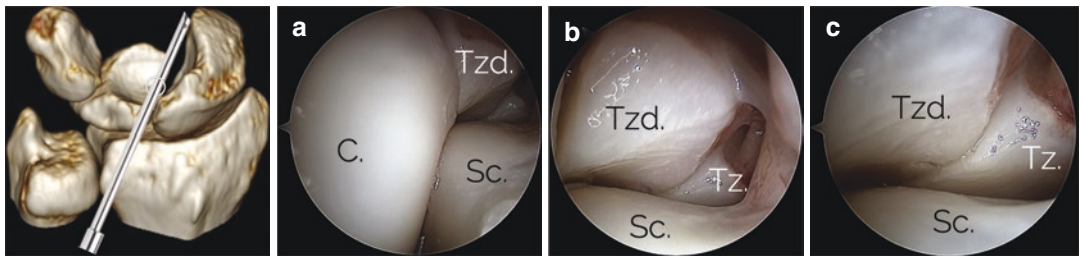

Fig. 71.20 Arthroscopic view of the midcarpal joint through the RMC portal, moving the vision field to the radial side. Trapezoid (Tzd). Trapezium (Tz) (from **a** to **c**) The scope is displaced distal and radial, inside the STT joint

respectively. The two other studies published somewhat greater distances, Abrams et al. [1] 16 mm (range 5–26 mm) and Shyamalan et al. [2] 24 mm (range 13–42 mm). No reports of zero distance have been published. However, despite being considered much safer, SBRN can be found very close to the RMC portal and caution should be taken during its execution.

- *Posterior interosseous nerve*:

  Only two studies analyzed the distance from the PIN to the RMC portal. The one carried out by Shyamalan et al. [2] measures a distance of 13 mm (range 0–20) and the one carried out by Pan et al. [6] finds an average distance of 7.3 mm (range 0–13 mm). That is, there is also the possibility of damage to the PIN during a routine wrist arthroscopy procedure.

71.2.2 Ulnar Midcarpal Portal (UMC)

It is located 1 cm distal to the 4/5 portal or 1 cm ulnar and 1 cm distal to the 6R. It is in line with the fourth metacarpal bone. It is radial to the ED and ulnar to the EDM (Fig. 71.22).

Unlike the RMC portal (which is located just distal to the scapholunate ligament), the UMC portal is not located above the lunotriquetral ligament but above the triquetrum bone. It constitutes a safer portal to penetrate the capsule, thus being used as a starting portal in the midcarpal joint.

Together with the RMC portal, it is essential for the exploration of the midcarpal joint.

71.2.2.1 Visualized Structures

The visible structures through this portal are:

At the Entry Point (Fig. 71.23)

Proximal: The surface of the triquetrum and the lunate; they are separated by a space that corresponds to the lunotriquetral joint.

Distal: Proximal surface of the capitate, hamate bone, and its joint.

Volar: The anterior portion of the triquetrum, the anterior horn of the lunate, and the Triquetralhamate ligament (distal and ulnar portion of the arcuate ligament) are observed.

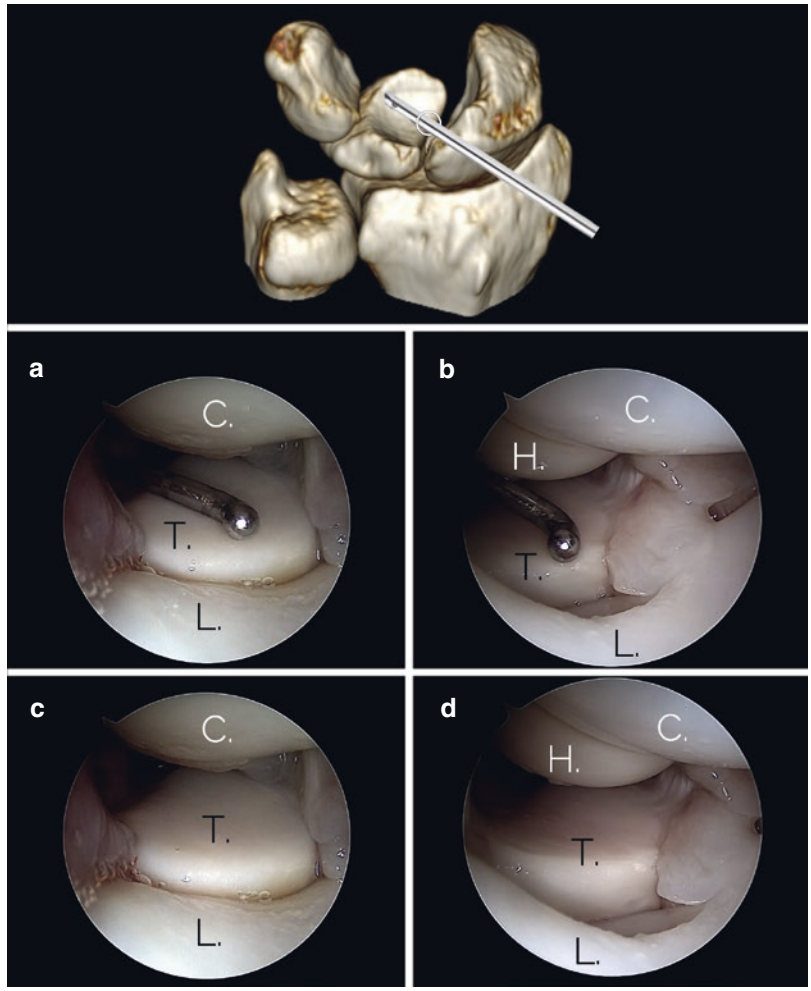

Fig. 71.21 Arthroscopic view of the midcarpal joint through the RMC portal, moving the vision field to the ulnar side. Hamate (H). Triquetralhamate ligament (TH) (**a** and **c**) Viegas type I. (**b** and **d**) Viegas type II

Moving the Vision Field to Radial

(Fig. 71.24)

Proximal: Articular surface of the lunate and scaphoid as well as the scapholunate joint. It is from this position that scapholunate instability is explored.

Distal: Proximal surface of the capitate bone.

Volar: Radio-scapho-capitate ligament and volar scapholunate joint.

Dorsal: RMC portal, dorsal portion of the scapholunate ligament.

Moving the Vision Field to Ulnar

If the triquetrum surface is followed with the arthroscope toward ulnar and volar, once the most ulnar portion of the hamate is passed, the base of the hook of the hamate can be seen (Fig. 71.25).

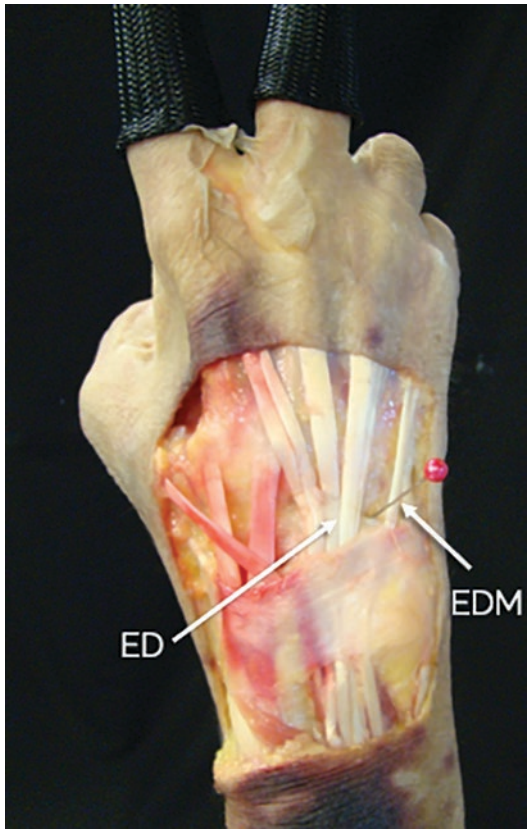

Fig. 71.22 Anatomical location of the ulnar midcarpal portal. Extensor digiti minimi (EDM)

71.2.2.2 Neurovascular Structures at Risk

- *Dorsal sensory branch of the ulnar nerve*:

  Two studies analyzed the risk of DBUN with respect to the UMC portal. Both showed significant distances from the portal, which makes it a safer portal with respect to cutaneous nerve injury. Abrams et al. [1] found distances of 15 mm (range 4–25 mm) and Shyamalan et al. [2] of 25 mm (range 9–56 mm).

71.3 Volar Portals

Following the description of the dorsal portals in the wrist, several authors have proposed the performance of volar portals to improve dorsal visualization of the wrist [14–20]. The best known are those described by Slutsky as volar radial portal (VR) [17] and volar ulnar portal (VU) [18]. More recently, the volar central portal (VC) [20] has been published (Fig. 71.26).

Unlike the dorsal portals, in which a direct portal is made through a 3 mm skin incision, these volar portals require a 1.5–2 cm mini-approach, which allows the structures at risk to be protected by retractors. With the possibility of carrying out the volar portals together with the dorsal portals, today the wrist is considered a "box" (a concept popularized by Bain [21]) since there is the possibility of instrumenting or viewing it from any direction in 360° (Fig. 71.27).

Two considerations have to be taken into account in view of the anatomical studies analyzing the safety of volar portals:

The first is that the studies can be carried out in two ways. The first way to proceed is using an inside–outside technique, that is, with the arthroscope inside the joint, a trocar is inserted through another dorsal portal. At the precise point of entry of the volar portal, pressure is applied until piercing through the volar capsule and the volar structure until the trocar is palpable, and then a skin incision is made. Then, after anatomical dissection, the distance to the structures at risk is measured and their eventual injury assessed. The second way to proceed is to follow the procedure as described by Slustky. The portal is first made through a longitudinal incision, and once the portal is marked, the distance to the structures at risk is measured. It has to be considered that in patients, the actual distance to the structures at risk will always be greater since retractors are placed through these longitudinal incisions. Therefore, although in anatomical studies the distances to structures at risk are very small or even tendon or neurovascular injuries are reported, in clinical practice those are exceptional if a careful approach is performed, and the structures are separated

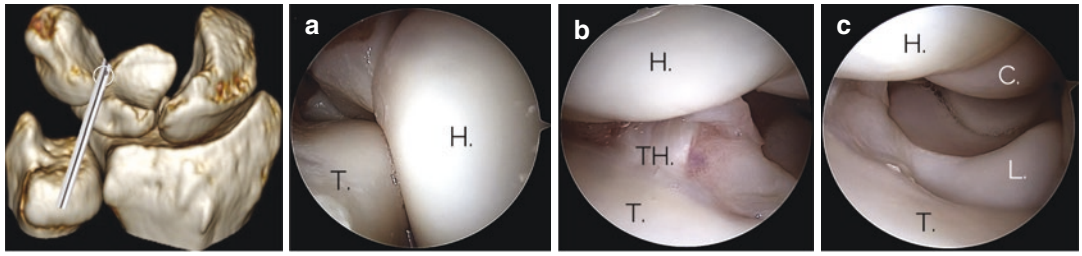

Fig. 71.23 Arthroscopic view of the midcarpal joint through the UMC portal, at the entry point (from **a** to **c**) The scope is displaced form the ulnar side to the radial side

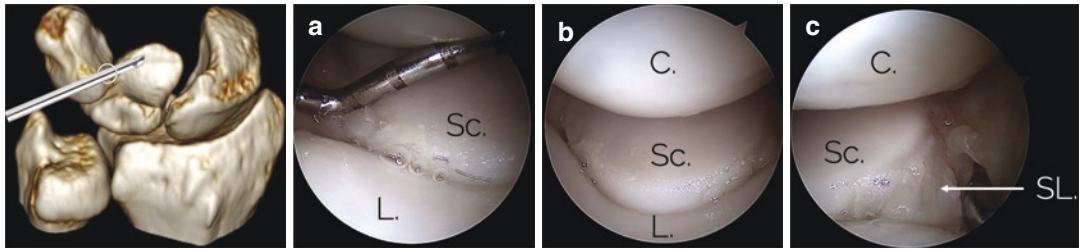

Fig. 71.24 Arthroscopic view of the midcarpal joint through the UMC portal, moving the vision field to the radial side. The probe is inserted through the RMC portal. Scapholunate ligament (SL) (**a**) Volar side. (**b**) Central side. (**c**) Dorsal side

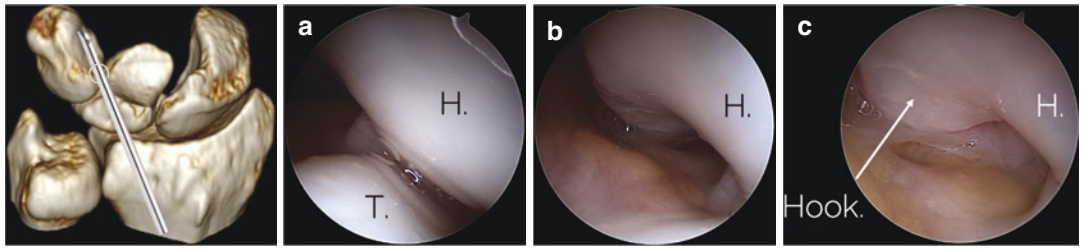

Fig. 71.25 Arthroscopic view of the midcarpal joint through the UMC portal, moving the vision field to the ulnar side. Hook of the hamate (Hook) (from **a** to **c**) The scope is displaced ulnar and volar under the hook of the hamate

with the retractors using an outside–inside technique.

The descriptions of the three portals are as follows:

71.3.1 Volar Radial (VR) Portal

There are two methods for creating this portal.

The first, described in cadavers by Tham [16], is placed using the inside–outside technique. The optic is placed in an ulnar portal (4/5 or 6R), a blunt trocar is placed through portal 3-4 and is inserted between the radio-scapho-capitate ligament and the long radiolunate ligament, and the flexor carpi radialis (FCR) tendon is retracted through a small incision made in the skin. Subsequently, a cannula is placed over the trocar, and the arthroscope is inserted from volar.

The second, most widespread method, is the one popularized by Slustsky [17, 18]. An incision of about 1.5–2 cm is made in the distal palmar crease of the wrist. The FCR is then retracted to the ulnar side, and the volar capsule is exposed. This portal is made in the plane between the FCR and the radial artery (Fig. 71.28).

Fig. 71.26 Volar portals of the wrist. Volar ulnar (VU) portal. Volar central (VC) portal. Volar radial (VR) portal

The portal is performed between the long radiolunate ligament and the radioscaphocapitate ligament (Fig. 71.29).

71.3.1.1 Visualized Structures (Fig. 71.30)

Proximal: Scaphoid and lunate fossa and dorsal edge of the radius.
Distal: Proximal and volar portions of the scaphoid and lunate bones and volar and membranous portion of the scapholunate ligament.
Radial: Styloid process of the radius
Dorsal: 3/4 portal and the insertion of the dorsal radiotriquetral ligament
Ulnar: Moving the arthroscope toward the ulnar side, the entire surface of the radius and even the TFCC are visible.

71.3.1.2 Neurovascular Structures at Risk

Five anatomical studies have assessed the risk of the neurovascular structures. The inside–outside technique was analyzed in those performed by Gillis and Kakar [22] on the volar midcarpal portals. In the study performed by Naroura et al. [23], no anatomical measurements were presented, but rather viewing angles from each portal were evaluated, and it was mentioned that no major structure was injured. Two other reports of the outside–inside technique were published by Slutsky [17] and by Antonoglou et al. [24] to evaluate the volar radial radiocarpal portal. Finally, Tham et al. [16] performed the trocar maneuver with the inside out technique, they combined a volar approach that allowed the sepa-

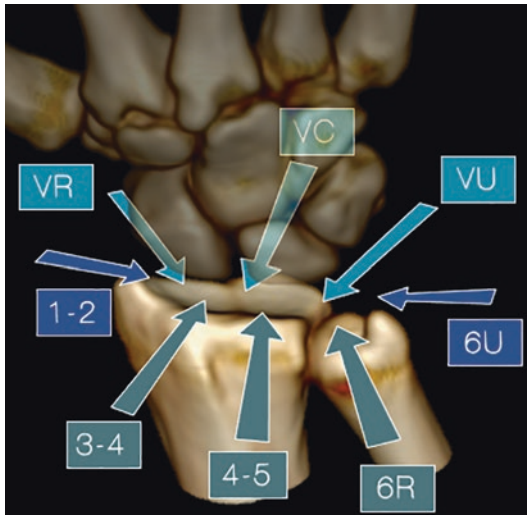

Fig. 71.27 "Box concept" popularized by Bain [21]. There is the possibility of instrumenting or viewing the wrist from any direction in 360°

ration of the FCR. This study does not present a detailed anatomical analysis.

- Median nerve:

  The study by Gillis and Kakar [22] reports a distance from the VR Midcarpal portal of 1 mm (range 0–35 mm); in one specimen, a direct injury occurred and in another, it entered between the median nerve and its superficial sensory branch. The study carried out by Slutsky [17] shows a distance of 8 mm (range 6–10 mm) while the one by Antonoglou et al. [24] reports a distance of 11 mm (range 9.8–13.5 mm).
- Palmar cutaneous branch of median nerve:

  The distances published in the different studies are as follows: Gillis and Kakar [22] 1.9 mm (range 0–3 mm); Slutsky [17] 4 mm (range 3–5 mm), and Antonoglou et al. [24] 5.5 mm (range 4.8–6.7 mm). These are shorter

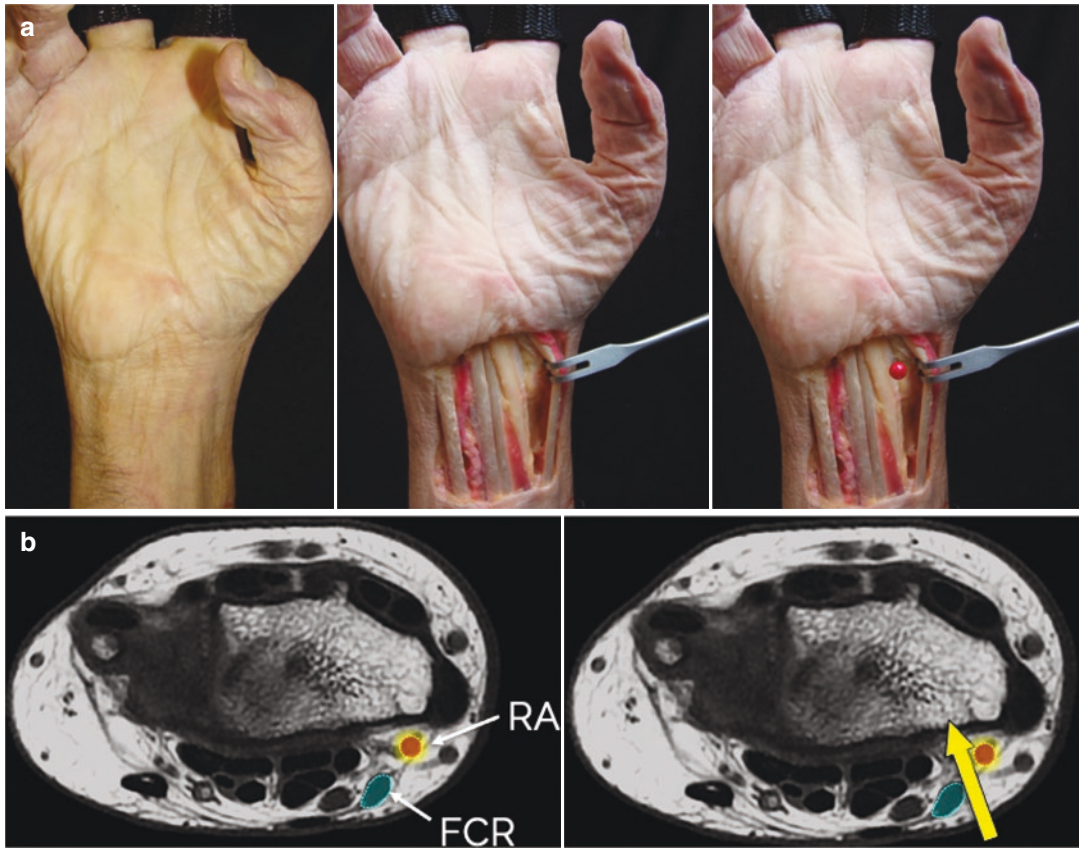

Fig. 71.28 Anatomical location of the volar radial portal. Flexor carpi radialis (FCR)

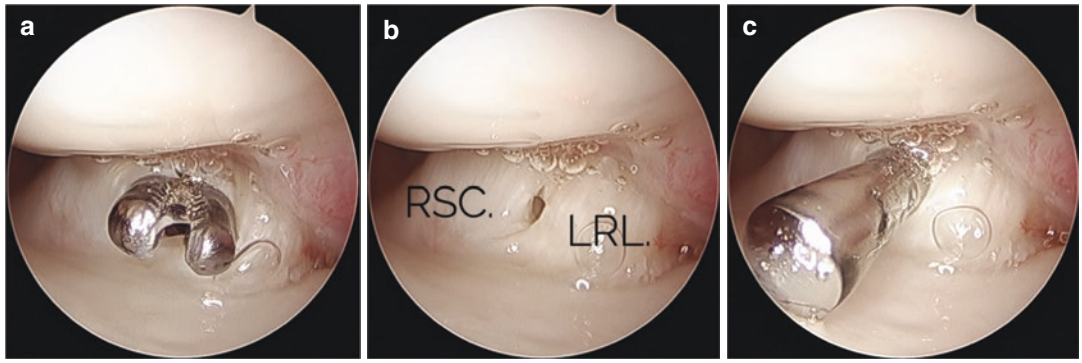

Fig. 71.29 Arthroscopic view of the entry point of the VR portal, from the 3-4 portal (**a**) A mosquito is entering between the radioscaphocapitate ligament (RSC) and the long radiolunate ligament (LRL) to establish the VR portal. (**b**) Dorsal vision of the VR portal. (**c**) A Wisinger rod is entering through the VR portal

distances than the ones from the median nerve, so there is a higher risk of injury.

- Radial artery:

  Published distances are Gillis and Kakar [22] 13.8 mm (range 9.5–17 mm); Slutsky [23] 5.8 mm (range 4–6 mm), and Antonoglou et al. [24] 6 mm (range 5.5–6.6 mm).
- Superficial branch of the radial nerve:

  The reported distances are Gillis and Kakar [22] 21 mm (range 13.5–25 mm); Slutsky [17] 15.6 mm (range 12–19 mm), and Antonoglou et al. [24] 13 mm (range 12–14.5 mm).

71.3.2 Volar Ulnar (VU) Portal

An incision of 1.5–2 cm is made at the ulnar side of the flexor digitorum tendons at the level of the proximal wrist crease. The flexor digitorum superficialis (FDS) and profundus (FDP) tendons are retracted radially. The portal is made in the plane between the ulnar neurovascular bundle and the flexor tendons (Fig. 71.31). Anatomically, the portal passes through the ulnocarpal ligaments adjacent to the radial insertion of the TFCC (Fig. 71.32).

71.3.2.1 Visualized Structures (Fig. 71.33)

Proximal: Sigmoid fossa of the radius and TFCC.

Distal: Proximal and palmar region of the lunate and triquetrum and volar and membranous portions of the lunotriquetral ligament.

Dorsal: 6R portal, dorsoulnar capsule, and ECU floor.

Radial: By moving the arthroscope radially, the entire surface of the radius can be observed and even an oblique vision of the radial styloid is possible.

71.3.2.2 Neurovascular Structures at Risk

Only two articles carried out a comprehensive anatomical study of the structures at risk with the completion of this portal. The one performed by Gillis and Kakar [22] describes an inside–outside technique on the ulnar midcarpal volar portal, while Antonoglou et al. [24] performed an outside–inside technique using a volar approach and evaluated the VU radiocarpal portal. Slutsky [18] only refers that the portal is at a distance greater than 5 mm, but in this case, it does not present a detailed study or the ranges.

- *Ulnar nerve*:

  The study by Gillis and Kakar [22] describes a distance from the UV midcarpal portal of 8.4 mm (range 5–13 mm), while the distance measured by Antonoglou et al. [24] is 5.8 mm (range 4.6–6.1 mm)

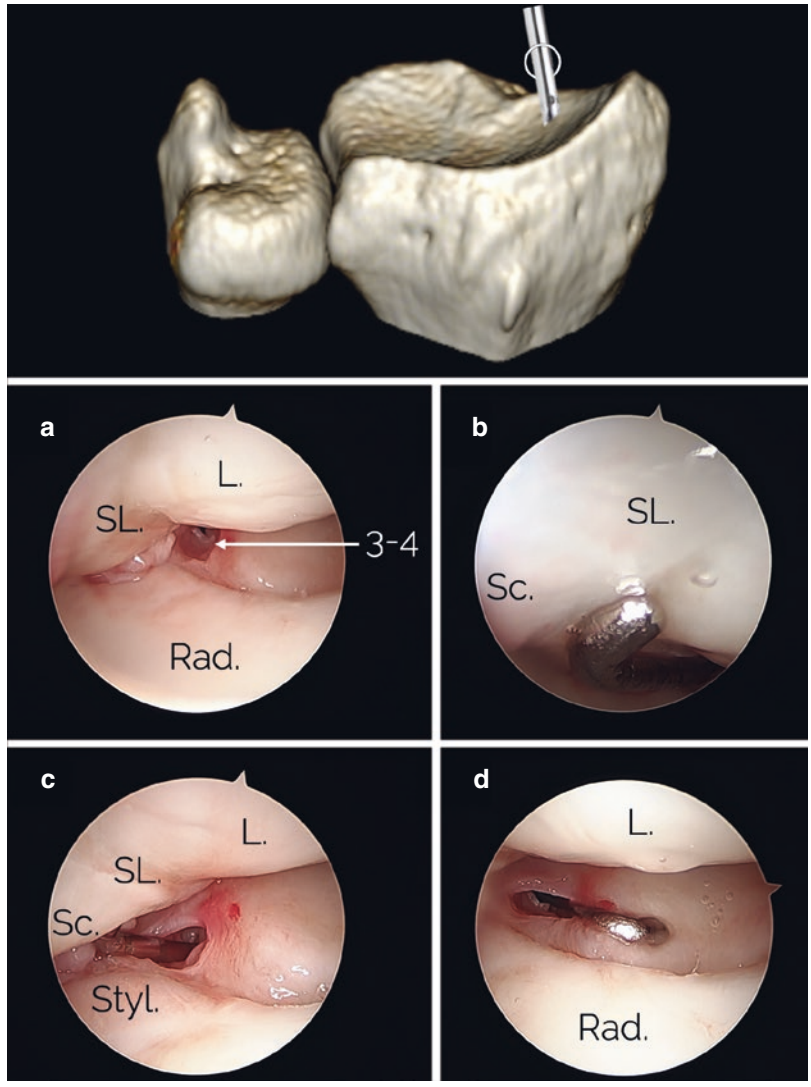

Fig. 71.30 Arthroscopic view of the radiocarpal joint through the VR portal. (**a**, **b**) At the entry point. (**c**) Moving the vision field to the radial side. (**d**) Moving the vision field to the ulnar side. The probe is inserted through the 3-4 portal

- *Ulnar artery*:
  Gillis and Kakar [22] 3.7 mm (range 0–7 mm) and Antonoglou et al. [24] 4.8 mm (range 3.7–5.1 mm).

71.3.3 Volar Central Portal

With the arthroscope placed in the 3/4 or 6R portal, a longitudinal incision is made in the axis of the third intermetacarpal space, the distal end of which being the distal palmar wrist crease.

The FDS tendon of the fifth finger is located by blunt dissection and pulling on it shows that the fifth finger is flexed. Once identified, the entire mass of the FDS is retracted to the radial side. In the following plane lie the FDP tendons. The interval between the third and fourth FDP tendons is identified (also pulling on them and

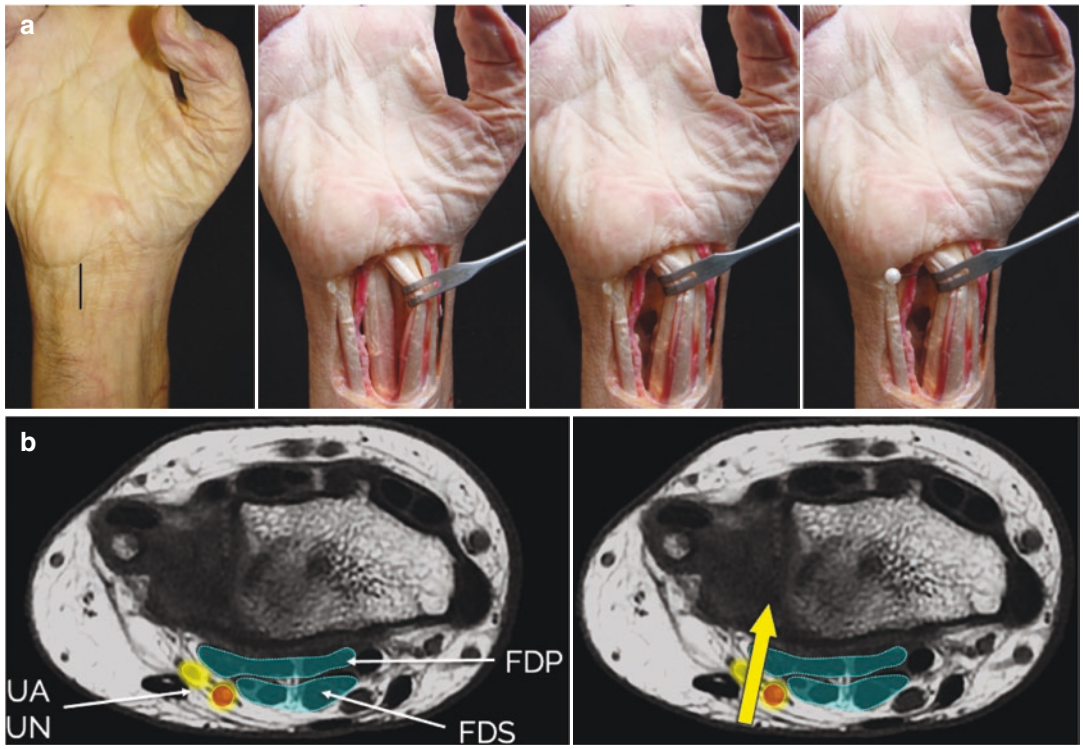

Fig. 71.31 Anatomical location of the volar ulnar portal. Ulnar artery (UA). Ulnar nerve (UN). Flexor digitorum superficialis (FDS). Flexor digitorum profundus (FDP) (**a**) Anatomical images. (**b**) MRI images

observing the flexion of the fingers). The fourth and fifth FDP tendons are separate toward ulnar side and the third and second FDP tendons toward the radial side, thus exposing the volar capsule (Fig. 71.34).

71.3.3.1 Establishment of the Volar Central Radiocarpal Portal

With the arthroscope in the 6R portal, a 22-G needle is inserted through the volar capsule, just proximal to the lunate and in the interval between the short radiolunate ligament and the ulnocarpal ligaments. The capsule is then opened with the tip of a number 11 scalpel, and the portal is widened. From this moment on, either the instrument or the arthroscope can be inserted into the joint. To introduce the arthroscope, a 2.4-mm Kirschner wire is inserted to be used as a Wissinger guide rod; thus, the arthroscope sheath is inserted through it (Fig. 71.35).

71.3.3.2 Visualized Structures in the Radiocarpal Joint

By moving the arthroscope toward the radial and ulnar side, a complete view of the entire radiocarpal and ulnocarpal joint can be obtained (Fig. 71.36).

At the Entry Point

Proximal: The surface of the radius is observed, with the separation of the scaphoid fossa and the lunate.

Distal: Proximal surface of the lunate.

Dorsal: If a dorsal synovectomy is performed, the dorsal radiotriquetral ligament is visualized.

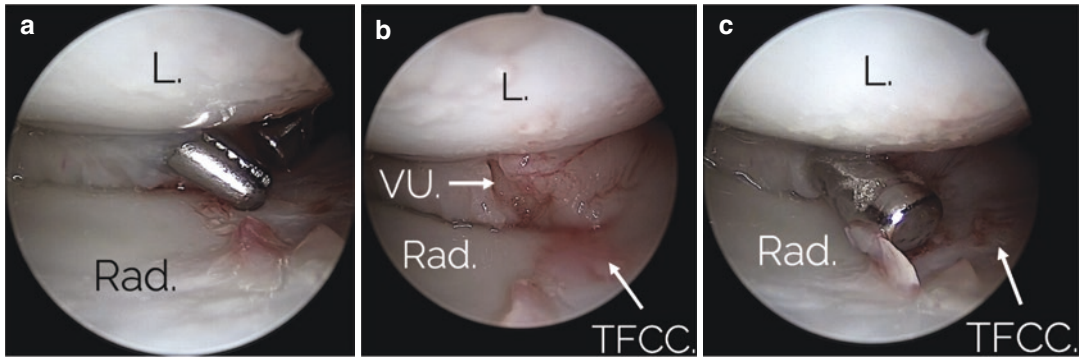

Fig. 71.32 Arthroscopic view of the entry point of the VU portal, from the 6R portal (**a**) A mosquito is used to establish the VU portal. (**b**) Dorsal vision of the VU portal (**c**) A wisinger rod is entering through the VU portal

Fig. 71.33 Arthroscopic view of the radiocarpal joint through the VU portal. (**a**, **b**) At the entry point. (**c**, **d**) Moving the vision field to the radial side. The probe is inserted through the 6R portal in figure **b** and through the 3-4 portal in figure **d**

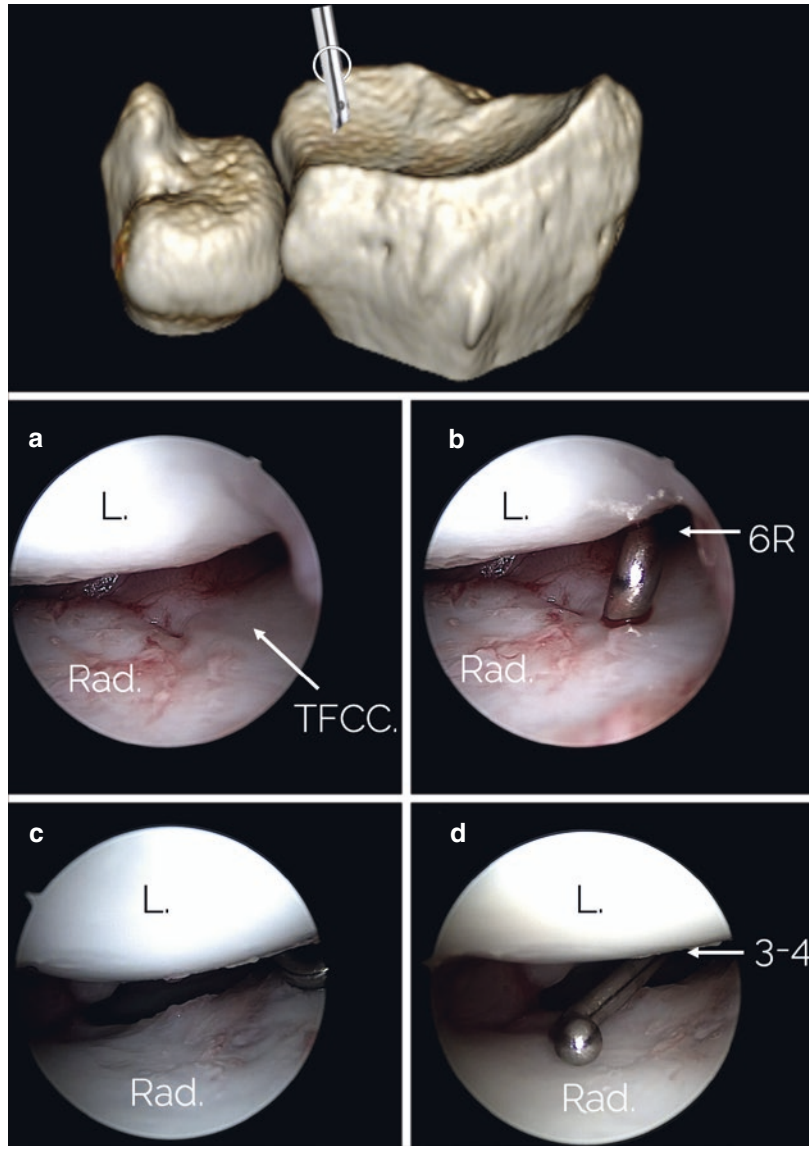

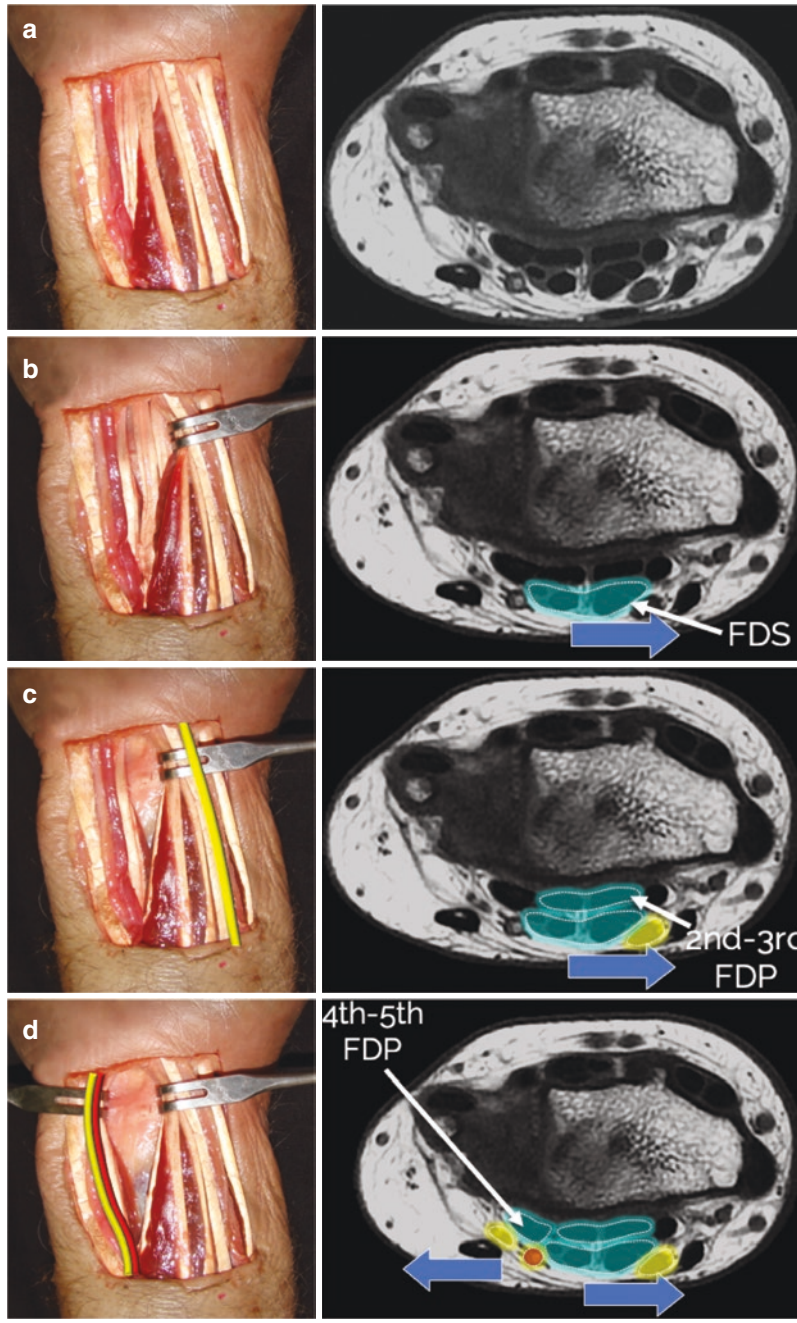

Fig. 71.34 Steps for performing the VC portal. (**a**, **b**) The FDS tendons are retracted to the radial side. (**c**) The interval between the third and fourth FDP tendons is identified and the second and third FDP tendons are retracted towards the radial side, this way the median nerve is protected. (**d**) The fourth and fifth FDP tendons are separate towards ulnar side, this way the ulnar neurovascular bundle is protected. (**e**) The volar capsule is exposed ante the midcarpal volar central portal (MVCP) and radiocarpal volar central portal (RVCP) are established

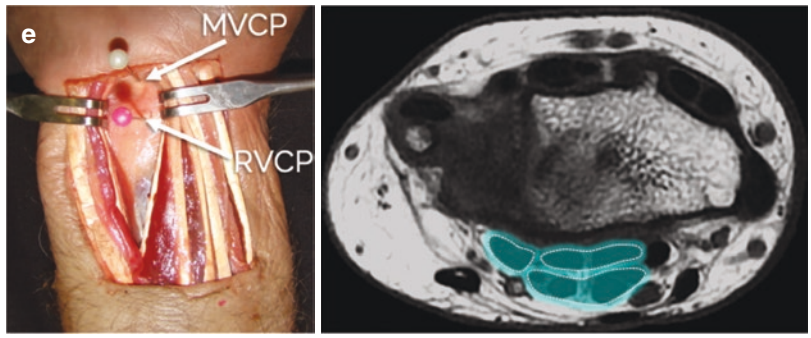

Fig. 71.34 (continued)

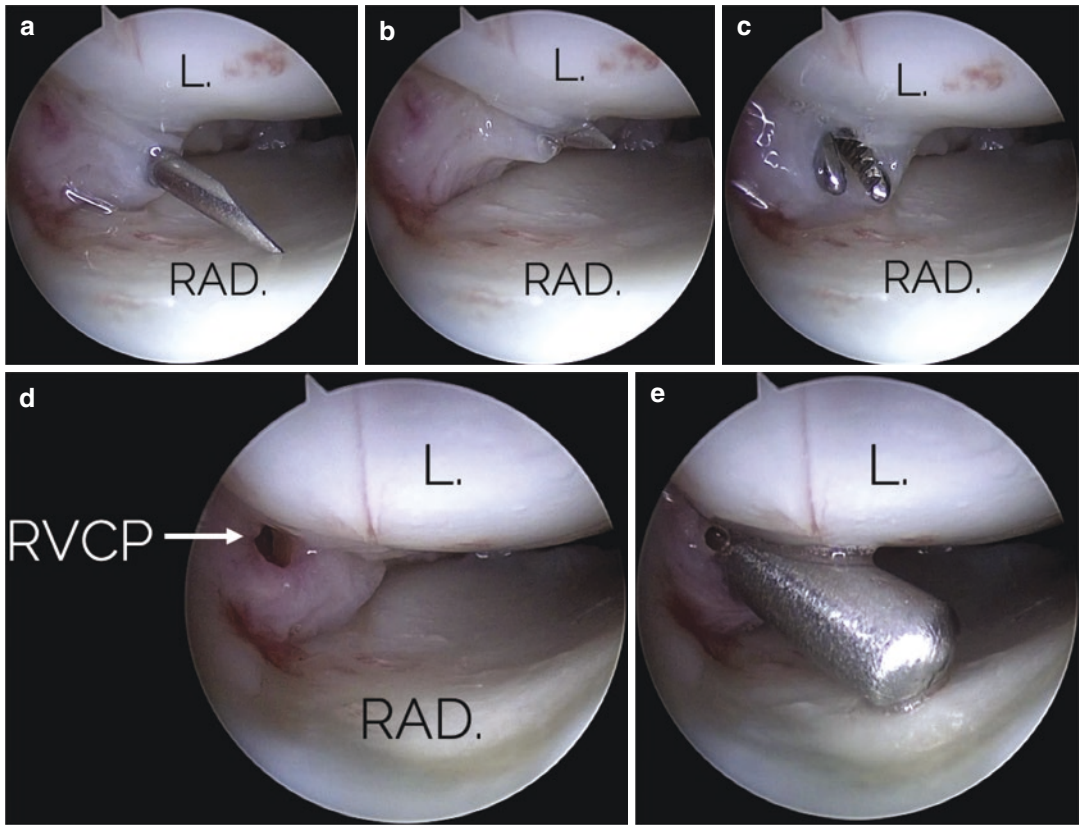

Fig. 71.35 Arthroscopic view of the entry point of the radiocarpal VC portal (**a**–**c**) Establishment of the portal. (**d**) Dorsal vision of the radiocarpal VC portal. (**e**) a Wisinger rod is entering through the radiocarpal VC portal

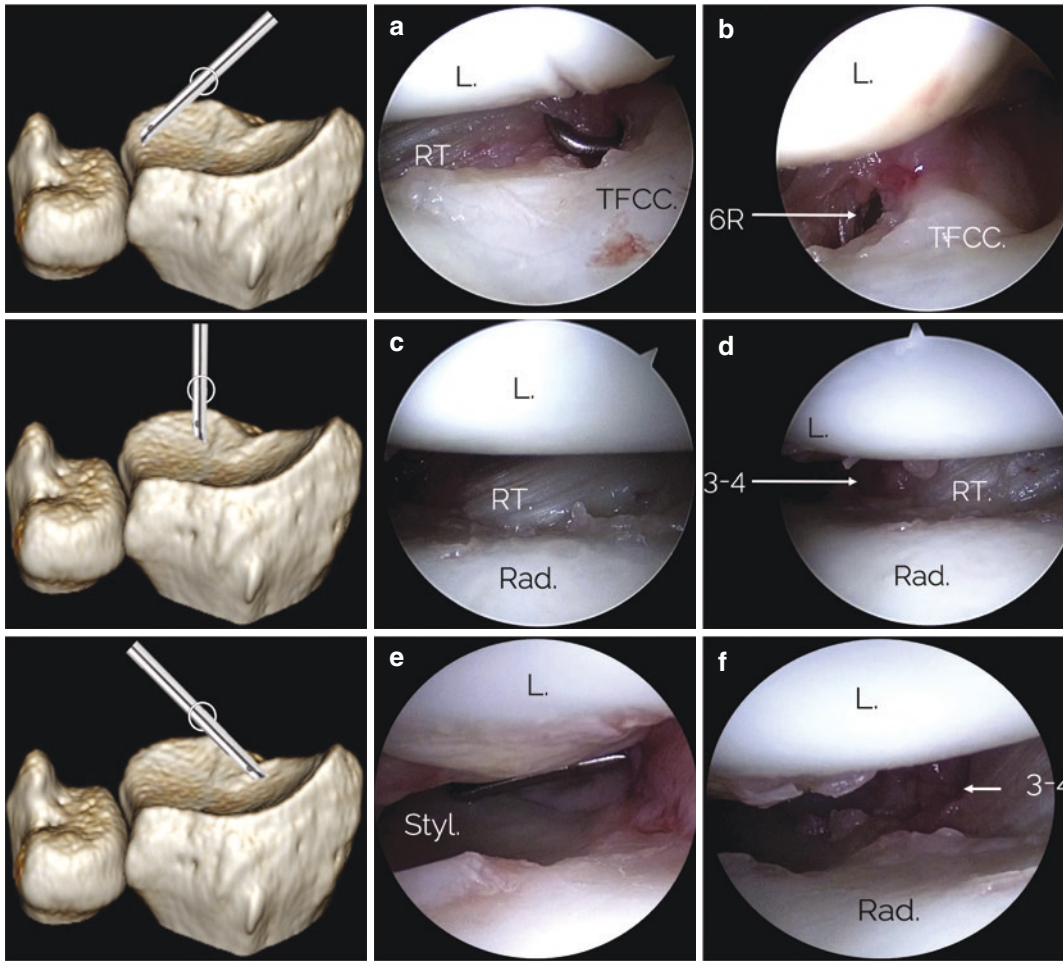

Fig. 71.36 Arthroscopic view of the radiocarpal joint through the radiocarpal VC portal. (**a**, **b**) Moving the vision field to the ulnar side. Radiotriquetral ligament (RT) (**c**, **d**) At the entry point. (**e**, **f**) Moving the vision field to the radial side

Moving the Vision Field to Radial
Proximal: Scaphoid fossa of the radius and radial styloid.
Distal: Proximal pole of the scaphoid.
Dorsal: 3/4 portal, dorsal capsule.

Moving the Vision Field to Ulnar
Proximal: Lunate fossa and TFCC.
Distal: Proximal pole of the lunate.
Dorsal: 6R portal, dorsal capsule.

71.3.3.3 Establishment of the Volar Central Midcarpal Portal

With the scope located in the UMC portal, a 22-G needle is inserted into the capsule, just above the anterior horn of the lunate, at the level of Poirier's space. Next, the portal is made with an 11 scalpel and widened. Again, a Kirschner wire is used as a Wissinger rod, and the arthroscopy sheath is inserted following it (Fig. 71.37).

71.3.3.4 Visualized Structures in the Midcarpal Joint

From this central position, moving the arthroscope toward radial and ulnar, the entire midcarpal joint can be visualized completely (Fig. 71.38).

At the Entry Point
Proximal: The surface of the lunate is observed.
Distal: Proximal surface of the capitate bone.
Dorsal: Dorsal horn of the lunate and dorsal capsule. If a dorsal capsule synovectomy is performed, the dorsal intercarpal ligament can be seen.

Moving the Vision Field to Radial
Proximal: Scapholunate joint, scaphoid.
Distal: Proximal surface of capitate bone. If it is displaced by the volar part of the large one, the insertion of the radio-scapho-capitate ligament is seen.

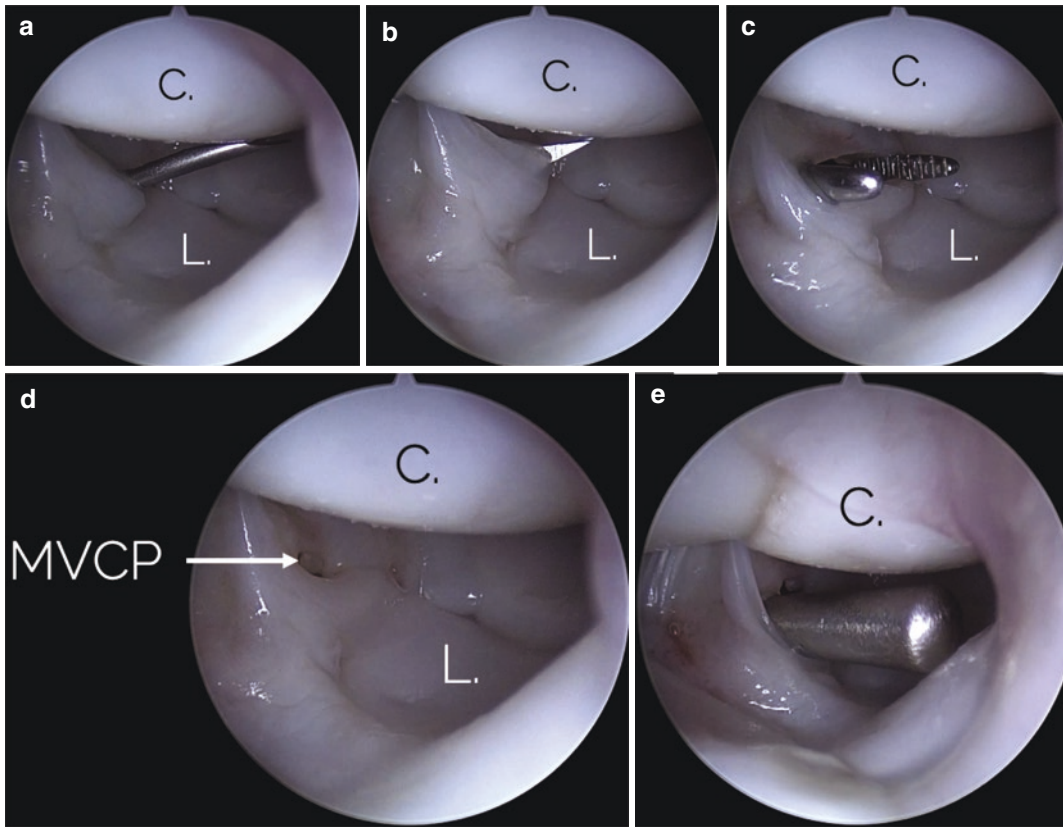

Fig. 71.37 Arthroscopic view of the entry point of the midcarpal VC portal. (**a**–**c**) Establishment of the portal. (**d**) Dorsal vision of the midcarpal VC portal. (**e**) A Wisinger rod is entering through the radiocarpal VC portal

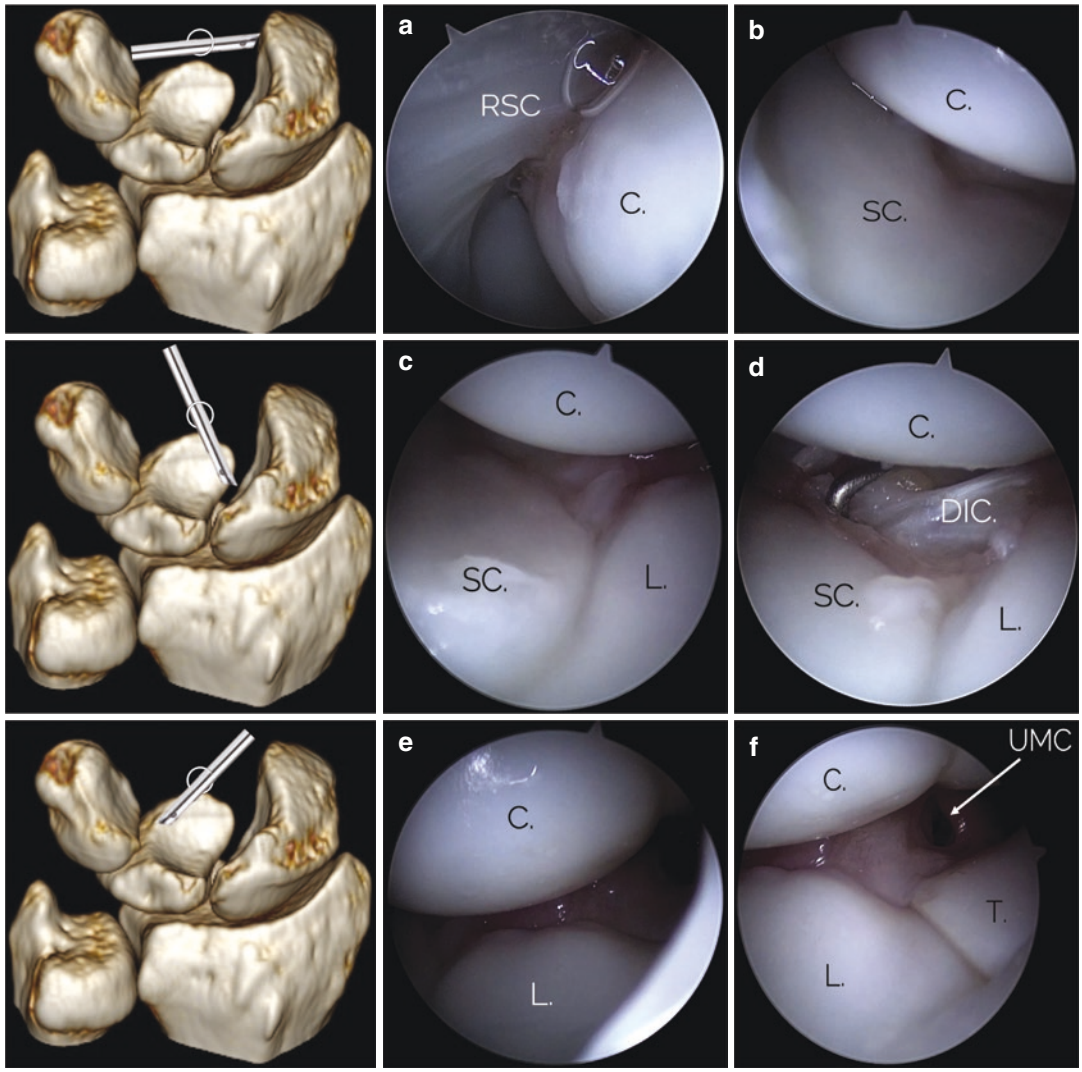

Fig. 71.38 Arthroscopic view of the midcarpal joint through the Midcarpal VC portal. (**a**, **b**) Moving the vision field to the radial side. (**c**, **d**) At the entry point. Dorsal Intercarpal ligament (DIC) (**e**, **f**) Moving the vision field to the ulnar side

Dorsal: RMC portal, dorsal capsule. If a synovectomy is performed, the dorsal intercarpal ligament can be observed.

Moving the Vision Field to the Ulnar Side

Proximal: Lunotriquetral joint, triquetrum.

Distal: Proximal surface of the capitate and hamate bones.

Dorsal: MCU portal, dorsal capsule. If a synovectomy is performed, the dorsal intercarpal ligament can be observed.

71.3.3.5 Neurovascular Structures at Risk

Only two articles have carried out in anatomical study of this portal. The first was published by

Corella et al. [20] and the second was recently published by Antonoglou et al. [24]

- Ulnar neurovascular bundle:

  The VC radiocarpal portal distance to the ulnar nerve was 8.4 mm (range 6.7–8.5 mm) and to the ulnar artery 6.9 mm (range 5.3–7.1 mm), according to the study by Antonoglou et al. [24] According to the report by Corella et al. [20], the distance to the neurovascular structures was 7 mm (range 5–10.5 mm). Both works show shorter distances from the midcarpal portal to the ulnar neurovascular bundle. Antonoglou et al. [24] 6.8 mm (range 4.6–10.5 mm) to the nerve, 5.7 mm (range 3.8–8.7 mm) to the artery, and Corella et al. [20] 4.5 mm (range 3.8–9 mm).
- Median nerve:

  It is further away than the ulnar neurovascular bundle. The measurements published are referred to the radiocarpal portal: 9.4 mm (range 6.6–10.5 mm) by Antonoglou et al. [24] and 10.5 mm (range 7.8–15 mm) by Corella et al. [20] Regarding the midcarpal portal, the distances are also smaller: 7.2 mm (range 4.8–9.8 mm) by Antonoglou et al. [24] and 7 mm (range 4.8–10.3 mm) by Corella et al. [20]
- Palmar cutaneous branch of median nerve:

  It is found further away than the median nerve. Regarding the radiocarpal portal, Antonoglou et al. [24] published distances of 16.4 mm (range 13.1–20.3 mm) and Corella et al. [20] 18.5 mm (range 15.8–20.3 mm). As in previous structures, the midcarpal portal is also closer than the radiocarpal, and the published distances are 15.1 mm (range 13.5–18.9 mm) by Antonoglou et al. [24] and 16 mm (range 14.8–19 mm) by Corella et al. [20]

References

1. Abrams RA, Petersen M, Botte MJ. Arthroscopic portals of the wrist: an anatomic study. J Hand Surg Am. 1994;19(6):940–4.
2. Shyamalan G, Jordan RW, Kimani PK, Liverneaux PA, Mathoulin C. Assessment of the structures at risk during wrist arthroscopy: a cadaveric study and systematic review. J Hand Surg Eur Vol. 2016;41(8):852–8.
3. Kiliç A, Kale A, Usta A, Bilgili F, KabukçuoÐlu Y, Sökücü S. Anatomic course of the superficial branch of the radial nerve in the wrist and its location in relation to wrist arthroscopy portals: a cadaveric study. Arthroscopy. 2009;25(11):1261–4.
4. Tryfonidis M, Charalambous CP, Jass GK, Jacob S, Hayton MJ, Stanley JK. Anatomic relation of dorsal wrist arthroscopy portals and superficial nerves: a cadaveric study. Arthroscopy. 2009;25(12):1387–90.
5. Auerbach DM, Collins ED, Kunkle KL, Monsanto EH. The radial sensory nerve: an anatomic study. Clin Orthop Relat Res. 1994;308:241–9.
6. Pan Y, Hung L. The course of the terminal posterior interosseous nerve and its relationship with wrist arthroscopy portals. J Wrist Surg. 2016;05(04):315–9.
7. Cheah AEJ, Le W, Yao J. Incidence of posterior interosseous nerve trauma during creation of the 3-4 wrist arthroscopy portal in cadavers. Arthroscopy. 2017;33(4):743–7.
8. Ehlinger M, Rapp E, Cognet JM, et al. Le rameau transverse de la branche dorsale du nerf ulnaire: anatomie et rapports avec les voies arthroscopiques du poignet. Quarante-cinq dissections. Rev Chir Orthop Reparatrice Appar Mot. 2005;91(3):208–14.
9. Puhaindran ME, Yam AKT, Chin AYH, Lluch A, Garcia-Elias M. Wrist arthroscopy: beware the novice. J Hand Surg Eur Vol. 2009;34(4):540–2.
10. Corella F, Ocampos M, Del Cerro M. Are extensor tendons safe on your first wrist arthroscopy? J Hand Surg (European Vol). 2011;36(9):817–8.
11. Tindall A, Patel M, Frost A, Parkin I, Shetty A, Compson J. The anatomy of the dorsal cutaneous branch of the ulnar nerve—a safe zone for positioning of the 6R portal in wrist arthroscopy. J Hand Surg Am. 2006;31(2):203–5.
12. Esplugas M, Lluch A, Garcia-Elias M, Llusà-Pérez M. How to avoid ulnar nerve injury when setting the 6U wrist arthroscopy portal. J Wrist Surg. 2014;03(02):128–31.
13. Viegas SF, Wagner K, Patterson R, Peterson P. Medial (hamate) facet of the lunate. J Hand Surg Am. 1990;15(4):564–71.
14. Jantea C, McCarthy D, Herndon J, Horikoshi M. Palmar approaches/portals for arthroscopy of the wrist. Arthoskopie. 1932;7:225–31.
15. Levy HJ, Glickel SZ. Arthroscopic assisted internal fixation of volar intraarticular wrist fractures. Arthroscopy. 1993;9(1):122–4.
16. Tham S, Coleman S, Gilpin D. An anterior portal for wrist arthroscopy. Anatomical study and case reports. J Hand Surg Br. 1999;24(4):445–7.
17. Slutsky DJ. Wrist arthroscopy through a volar radial portal. Arthroscopy. 2002;18(6):624–30.

18. Slutsky DJ. The use of a volar ulnar portal in wrist arthroscopy. Arthroscopy. 2004;20(2):158–63.
19. Abe Y, Doi K, Hattori Y, Ikeda K, Dhawan V. A benefit of the volar approach for wrist arthroscopy. Arthroscopy. 2003;19(4):440–5.
20. Corella F, Ocampos M, Del Cerro M, et al. Volar central portal in wrist arthroscopy. J Wrist Surg. 2016;5:80–90.
21. Bain G, Munt J, Turner P. New advances in wrist arthroscopy. Arthroscopy. 2008;24(3):355–67.
22. Gillis JA, Kakar S. Volar midcarpal portals in wrist arthroscopy. J Hand Surg Am. 2019;44(12):1094.e1–6.
23. Naroura I, Zemirline A, Taleb C, et al. Inside-out method to develop volar arthroscopic portals of the wrist in cadaver specimens. Hand Surg Rehabil. 2016;35(3):210–4.
24. Antonoglou G, Paraskevas G, Kanavaros P, Vrettakos A, Barbouti AKP. Safe zones in volar portals for wrist arthroscopy, evaluation of central portal. Acta Orthop Belg. 2019;85(3):330–7.

Part XIV

Wrist: Scapholunate Arthroscopy

Anatomy and Biomechanics of Scapholunate Ligament

72

Nicholas Chang and Nina Suh

72.1 Introduction

The scapholunate joint is critical for normal wrist kinematics, and carpal stability is afforded by intimate interosseous relationships bounded by intrinsic and extrinsic ligaments. Injury to the scapholunate interosseous ligament (SLIL) is the most common cause of carpal instability and dysfunction [1]. This chapter reviews the anatomical features of the scapholunate joint and biomechanical properties of the scapholunate ligament.

72.2 Anatomy

The wrist is composed of 20 articulations between the radius, carpal bones, and metacarpals. The eight bones of the carpus are schematically divided into two rows. The scaphoid, lunate, and triquetrum form the proximal row, whereas the trapezium, trapezoid, capitate, and hamate form the distal row. Although occasionally depicted as part of the proximal row, the pisiform is a sesamoid bone within the flexor carpi ulnaris tendon that increases its lever arm. The bones within the distal row are intimately linked such that their congruous anatomy and taut ligamentous attachments ensure there is little motion within the distal carpal row. In contrast, significant motion can be seen within the proximal row.

In particular, the scapholunate joint is stabilized by primary and secondary stabilizers. The scapholunate interosseous ligament (SLIL) is the most important primary stabilizer. It is an intrinsic ligament connecting the scaphoid and lunate, with the distal aspect of the scapholunate articulation free of ligamentous attachments. It is shaped like the letter "C" and is composed of three components: the dorsal, proximal, and palmar segments (Fig. 72.1). Of these segments, the dorsal region is the strongest and thickest. It measures an average of 3 mm in thickness and 5 mm in width (proximal-distal) [2]. Histologically, the dorsal segment features transversely oriented collagen, with perifascicular arterioles, venules, and nerve fibers [2]. The dorsal segment also serves as a distal attachment site of the dorsal radiocarpal joint capsule, while the distal aspect of the dorsal SLIL segment is intimately associated with the dorsal scaphotriquetral ligament. Proximally, the dorsal region transitions to the proximal segment of the SLIL [2].

The proximal segment of the scapholunate ligament is fairly loose relative to the taut dorsal SLIL. The proximal region is primarily composed of fibrocartilage, and its fibers run

N. Chang · N. Suh (✉)
Division of Orthopedic Surgery, University of Western Ontario, Roth | McFarlane Hand and Upper Limb Center, St. Joseph's Health Care, London, ON, Canada
e-mail: nchang@mun.ca; Nina.Suh@sjhc.london.on.ca

© ISAKOS 2022

D. N. Bhatia et al. (eds.), *Arthroscopy and Endoscopy of the Elbow, Wrist and Hand*,
https://doi.org/10.1007/978-3-030-79423-1_72

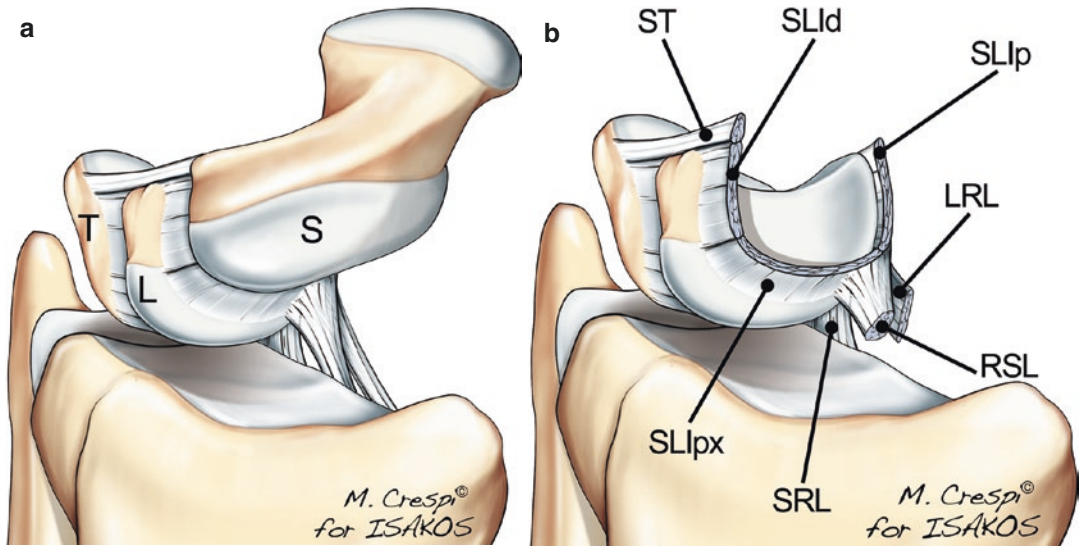

Fig. 72.1 Scapholunate interosseous ligament, as seen from the radial aspect of the wrist, with the scaphoid present (**a**) and the scaphoid removed (**b**). *S* scaphoid, *L* lunate, *T* triquetrum, *ST* scaphotrapezial ligament, *SLId* scapholunate interosseous dorsal subgroup, *SLIp* SLI palmar subgroup, *LRL* long radiolunate, *RSL* radioscapholunate, *SRL* short radiolunate, *SLIpx* SLI proximal subgroup (M. Crespi © for ISAKOS)

longitudinally along its central and superficial surfaces [2]. Palmarly, it becomes closely associated with the radioscapholunate ligament (RSL), which ultimately merges with the palmar SLIL [2].

The palmar segment of the SLIL is significantly thinner compared to the dorsal segment, averaging 1 mm in thickness. Unlike the transverse orientation dorsally, the palmar segment runs in an oblique fashion from proximal–ulnar to distal–radial [2].

The stability of the scapholunate joint is also aided by extrinsic ligaments of the wrist acting as secondary stabilizers. On the dorsal side of the wrist, there are two main ligaments that reinforce the wrist capsule: the dorsal radiocarpal and dorsal intercarpal ligaments [3] (Fig. 72.2). The origin of the dorsal radiocarpal ligament arises from the distal rim of the radius, between Lister's tubercle and the sigmoid notch. It runs obliquely from proximal-radial to distal-ulnar and inserts on the dorsal surface of the lunate and triquetrum. There is also an osseous attachment to the dorsal region of the lunotriquetral interosseous ligament. The dorsal radiocarpal ligament is trapezoidal in shape, with a wider proximal width and narrower width distally.

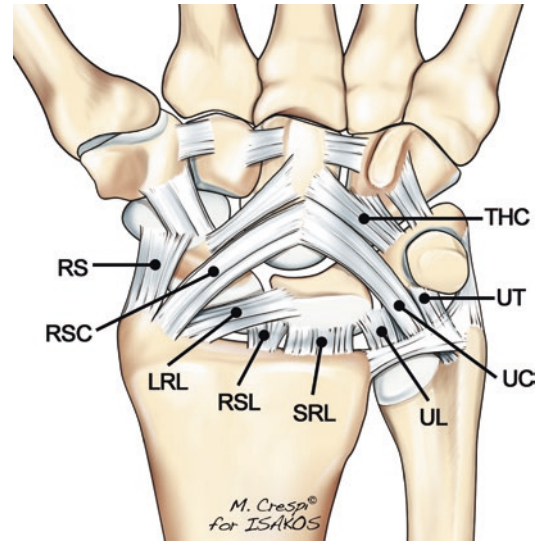

Fig. 72.2 Dorsal extrinsic ligaments of the wrist. *DRC* dorsal intercarpal ligament, *DIC* dorsal radiocarpal ligament (M. Crespi © for ISAKOS)

In close proximity, the dorsal intercarpal ligament originates at the triquetral tubercle and runs radially in a more transverse orientation. It has a variable insertion on the distal pole of the scaphoid, trapezoid, and trapezium. The angle between the dorsal radiocarpal and dorsal intercarpal liga-

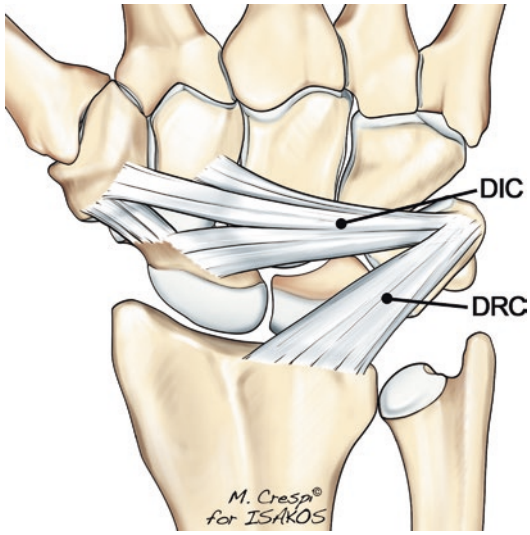

Fig. 72.3 Palmar extrinsic ligaments of the wrist. *RS* radioscaphoid, *RSC* radioscaphocapitate ligament, *LRL* long radiolunate ligament, *RSL* radioscapholunate ligament, *SRL* short radiolunate ligament, *UL* ulnolunate ligament, *UC* ulnocapitate ligament, *UT* ulnotriquetral ligament, *THC* triquetrohamocapitate ligament (M. Crespi © for ISAKOS)

ments forms a V-shape. This angle varies according to the position of the wrist, which enables indirect stability of the scaphoid throughout the wrist range of motion. In wrist extension, the angle is more acute compared to a larger angle seen in wrist flexion [3]. From a clinical standpoint, flexing the wrist intraoperatively may help delineate the dorsal radiocarpal and dorsal intercarpal ligaments when performing a ligament-sparing wrist capsulotomy.

On the palmar side, there are four extrinsic radiocarpal ligaments (Fig. 72.3). They cover the entire volar rim of the distal radius and insert onto the carpal bones. They are, from radial to ulnar, the radioscaphocapitate (RSC) ligament, the long radiolunate ligament, radioscapholunate ligament, and short radiolunate ligament. The origin of the radioscaphocapitate ligament spans from the radial styloid process to the center of the scaphoid fossa. It inserts on the distal pole of the scaphoid, with a small proportion of the ligament attaching to the head of the capitate. It is intimately associated with the ulnocapitate ligament and palmar scaphotriquetral ligament [4].

Meanwhile, the long radiolunate ligament originates from the volar rim of the distal radius, adjacent to the radioscaphocapitate ligament. It traverses parallel to the RSC ligament and inserts on the radial aspect of the palmar lunate, merging with fibers from the palmar region of the scapholunate interosseous ligament and the radioscapholunate ligament [4].

There has been controversy whether the radioscapholunate ligament should be considered a true ligament as it provides little mechanical strength. It inserts distally on the scaphoid and lunate and is thought to primarily provide vascular supply to the scapholunate interosseous ligament [4]. It also contains terminal branches of the anterior interosseous nerve.

Finally, the origin of the short radiolunate ligament spans the lunate facet of the distal radius. It inserts on the radial half of the palmar lunate, with its distal fibers intimately associated with the distal fibers of the long radiolunate ligament.

Bone morphology may also influence scapholunate joint biomechanics. Viegas et al. described two types of lunate distal articulations [5]. Type I lunates (39.3%) featured a single distal articular facet with the capitate. Type II lunates (60.7%) had two distal articular facets: a radial one for the capitate and an ulnar one for the hamate. A retrospective cohort study by Rhee et al. found that type II lunates were associated with a decreased incidence of DISI deformity in the setting of scapholunate dissociation [6]. A similar study by Haase et al. also reported that type II lunates had a lower incidence of DISI deformity in patients with scaphoid nonunions [7].

The morphology of the scapholunate joint space has also been characterized based on MRI coronal images of Schimmerl-Metz et al. [8]. Three types have been described. Type 1 scapholunate joint spaces (78%) feature parallel, congruent articulations. Type 2 joints (15%) demonstrate an inverted Y pattern. Type 3 joints (8%) are described as "point-like" and only have parallel surfaces at the middle of the scapholunate joint. The clinical significance of the various scapholunate joint morphologies is as yet unknown.

72.3 Biomechanics

The proximal row of the wrist is considered an intercalated segment linked within an articulated series. There are no tendinous attachments to the proximal row. As such, its motion is governed through its osseous relationships and ligamentous attachments. Wrist flexion or radial deviation causes the scaphoid to flex. Due to the SLIL, the lunate will passively flex alongside the scaphoid [1] (Fig. 72.4). In ulnar deviation, the unique helicoidal shape of the triquetral-hamate joint drives the triquetrum into dorsiflexion and palmar translation. The lunotriquetral and scapholunate interosseous ligaments simultaneously guide the scaphoid and lunate into extension. This motion is also aided by tensioning of the radioscaphocapitate and scaphotrapezial ligaments with the dorsal translation of the distal carpal row [1]. Wrist extension also drives the proximal intercalated row into extension. This is due to a screw-vice mechanism described by Macconaill, where the dorsal extrinsic ligaments lock the proximal and distal rows through the scaphoid [9].

Although the proximal row rotates in the same direction with wrist motion, there is variable multiplanar motion at the scapholunate joint. The scaphoid flexion-extension arc is greater than the lunate's arc. In wrist flexion, the scaphoid pronates significantly more than the lunate but undergoes less ulnar deviation [10]. Scapholunate motion is also more synchronous in wrist extension compared to wrist flexion, likely due to the actions of the dorsal extrinsic ligaments as described above. There is no significant difference between male and female scapholunate kinematics [10].

The dart-throwing motion is the wrist plane of motion from wrist extension and radial deviation to wrist flexion and ulnar deviation. There is minimal flexion or extension of the scaphoid and lunate during this motion. While the SLIL may see little strain during this motion, it is still found to be important for maintaining scapholunate instability. As a result, dart-throwing motion may be considered in a postoperative rehabilitative protocol for early range of motion following scapholunate repair or reconstruction.

Numerous studies have sought to evaluate the biomechanical properties of the SLIL. There has been considerable variability in the reported results in the literature. This has made it a challenge to reliably quantify the strength and stiff-

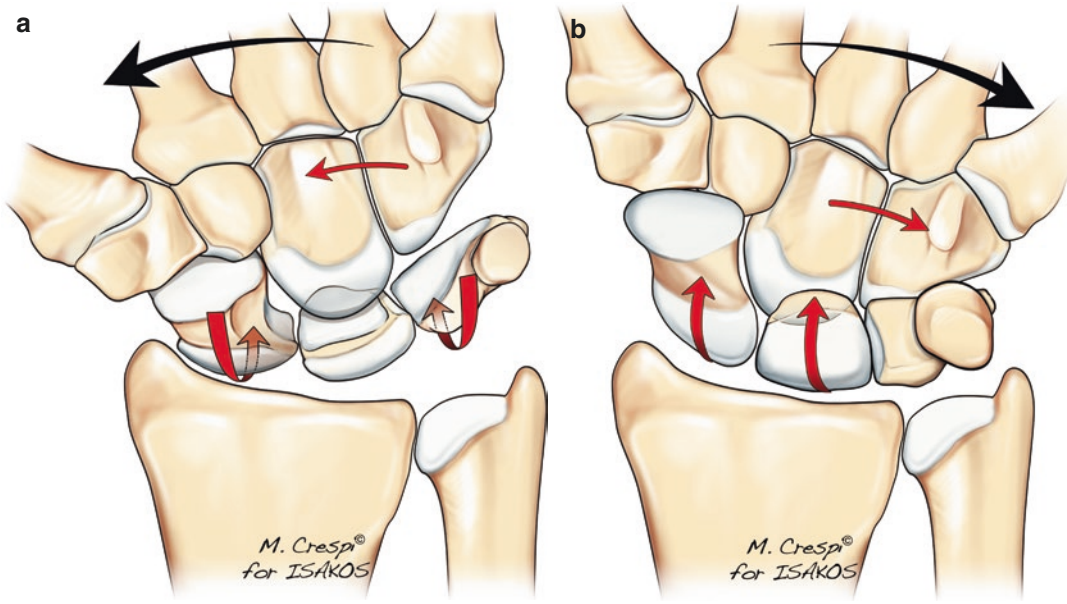

Fig. 72.4 Mechanics of the carpal bones with wrist radial (**a**) and ulnar deviation (**b**), as seen from the palmar side (M. Crespi © for ISAKOS)

Table 72.1 Biomechanical properties of scapholunate ligament and grafts

	SLIL failure to load (N)	SLIL stiffness (N/mm)	Graft type	Graft failure to load (N) (% of SLIL)	Graft stiffness (N/mm) (% of SLIL)
Pin et al., 1990 [19]	232.6 ± 10.9		–	–	–
Boabighi et al., 1993 [20]	150		–	–	–
Svoboda et al., 1995 [21]	260 ± 73	150 ± 46	Dorsal 4/5 MT Dorsal TMT CC	129 (50%) 154 (59%) 126 (48%)	74 (49%) 108 (72%) 43 (29%)
Davis et al., 1998 [22]	2940	1440	Navicular-first cuneiform[a]	1980 (67%)	1000 (69%)
Harvey et al., 1999 [23]	170.24 ± 97.01	80.73 ± 59.70	2nd MC-trapezoid[a] third MC-capitate[a] Dorsal periosteum ligament[a]	188.54 (111%) 171.63 (101%) 44.32 (26%)	188.54 (233%) 171.63 (213%) 34.10 (42%)
Johnston et al., 2004 [24]	357 ± 110	66.4 ± 28.6 94.5 ± 44.4	–	–	–
Zdero et al., 2009 [25]	1253.9	48.9	–	–	–
Nikolopoulos et al., 2011 [16]	147 ± 54	35.7	–	–	–
Ehsan et al., 2012 [26]	172 ± 61	74 ± 41	–	–	–

SLIL scapholunate interosseous ligament, *MT* metatarsal, *TMT* tarso-metatarsal, *CC* calcaneo-cuboid, *MC* metacarpal
[a]Bone-ligament bone graft

ness of the SLIL. The range in load to failure varies from 147 to 2940 N, while the linear stiffness ranges from 35.7 to 1440 N/mm (Table 72.1). Although the studies generally evaluated uniaxial load to failure, the wide variation in results may reflect different methodologies employed between studies. For example, the ligament loading rate ranged from 5 to 100 mm/min in various studies. However, further insight may be gained by comparing the biomechanical properties of the SLIL to potential graft options.

Meanwhile, the viscoelastic properties of the SLIL were demonstrated by Logan et al. who found that when the strain on the ligament is increased from 0.5 to 5 mm/min, stiffness is increased by 60% [11]. When the strain was increased from 0.5 to 100 mm/min, stiffness increased by 100%. In a study by Nowak et al., the onset of plastic deformation (at 100 mm/min strain) of the SLIL was observed at 65% strain, compared to only 23.5% strain in the radiolunate ligament and 17% strain in the radiocapitate ligament [12].

Recent biomechanical studies have also focused on the specific subregions of the scapholunate interosseous ligament (Table 72.2). The general consensus is that the dorsal region is stouter than the palmar and proximal regions, and reconstructive techniques have focused on the dorsal SLIL. This is supported by a study by Berger et al. that utilized a biaxial servohydraulic testing apparatus [13]. Sectioning of the dorsal region produced the greatest effect on scaphoid and lunate translation. In addition, sectioning of both the dorsal and the palmar regions showed a significant increase in differential rotation between the scaphoid and the lunate. In a cadaveric study by Pattersson et al., scapholunate widening was not observed after isolated disruption of the palmar and proximal regions but was seen following sectioning of the dorsal SLIL [14].

However, recent studies have challenged the notion that the dorsal SLIL is the only critical subregion of the SLIL that requires repair or reconstruction. A study by Padmore et al. dem-

Table 72.2 Biomechanical properties of scapholunate interosseous ligament subregions

	Subregion	Failure to load (N)	Stiffness (N/mm)
Berger et al., 1999 [13]	Dorsal	260.3 ± 118.1	–
	Volar	117.9 ± 21.3	–
	Proximal	62.7 ± 32.2	–
Logan et al., 1986 [11]	Dorsal	62	–
	Volar	125	–
	Proximal	–	–
Shin et al., 1998 [27]	Dorsal	185.3 ± 87	162.0 ± 86.4
	Volar	–	–
	Proximal	–	–
Hofstede et al., 1999 [28]	Dorsal	141 ± 20	61 ± 6
	Volar	–	–
	Proximal	–	–
Cuénod et al., 2002 [29]	Dorsal	93.8 ± 32.8	96.6 ± 42.6
	Volar	–	–
	Proximal	–	–
Nikolopoulos et al., 2011 [16]	Dorsal	83 ± 18	27.7 ± 15
	Volar	86 ± 16	32.8 ± 11.5
	Proximal	36.4 ± 15.6	25 ± 23.1

onstrated that isolated sectioning of the dorsal SLIL did not significantly alter scapholunate intercarpal kinematics [15]. In addition, altered carpal kinematics following SLIL destabilization were most apparent in wrist flexion. In another study, Nikolopoulos et al. demonstrated equal load to failure and stiffness of the dorsal and palmar portions of the scapholunate ligament [16]. The authors suggested that reconstruction of the dorsal region alone may be insufficient to restore the native biomechanics of the scapholunate ligament.

72.4 Pathomechanics

Scapholunate instability is considered a spectrum of injury, including predynamic, dynamic, and static instability [1]. The scapholunate interosseous ligament is the primary stabilizer of the scapholunate joint. Even when the SLIL is sectioned in isolation, the scaphotrapezial and radioscaphocapitate ligaments have been shown to help stabilize the scapholunate joint in certain wrist positions. However, this secondary stabilizing effect decreases over time with repetitive cyclical motion at the scapholunate joint.

Scapholunate injury is also associated with altered carpal mechanics. Rotatory subluxation of the scaphoid leads to abnormal scaphoid flexion whilst the lunate is extended through its lunotriquetral ligamentous attachment to the triquetrum. This is known as dorsal intercalated segment instability (DISI).

Chronically altered carpal kinematics may lead to progressive degenerative changes to the carpus. Watson described this pattern as scapholunate advanced collapse (SLAC) [17]. Arthritic changes are first seen between the radial styloid and the scaphoid, followed by arthritis of the entire scaphoid facet, then arthritis between the lunate and capitate. The radiolunate joint is typically spared. This may be explained by the spherical shape of the radiolunate joint compared to the elliptical shape of the radioscaphoid joint. Even if the lunate is abnormally extended, the corresponding articular surfaces are congruent. Watson described the radioscaphoid joint as analogous to two stacked spoons nested within each other. There is excellent congruity when the joints are aligned. However, if there is abnormal rotation or subluxation, the joint is no longer congruous and will see point loading of the articular surface. This is supported by an MRI-based study by Johnson et al. that demonstrated

increased contact pressures at the dorsal scaphoid fossa of the distal radius following scapholunate injury [18].

72.5 Summary

The scapholunate interosseous ligament is made of three regions: the dorsal, palmar, and proximal. It is the primary stabilizer of the scapholunate joint. Injury to the scapholunate interosseous ligament and secondary stabilizers may lead to abnormal carpal mechanics and possibly scapholunate advanced collapse.

References

1. Kitay A, Wolfe SW. Scapholunate instability: current concepts in diagnosis and management. J Hand Surg Am. 2012;37(10):2175–96.
2. Berger RA. The gross and histologic anatomy of the scapholunate interosseous ligament. J Hand Surg Am. 1996;21(2):170–8.
3. Berger RA. The anatomy of the ligaments of the wrist and distal radioulnar joints. Clin Orthop Relat Res. 2001;383:32–40.
4. Berger RA, Landsmeer JMF. The palmar radiocarpal ligaments: a study of adult and fetal human wrist joints. J Hand Surg Am. 1990;15(6):847–54.
5. Viegas SF. The lunatohamate articulation of the midcarpal joint. Arthroscopy. 1990;6(1):5–10.
6. Rhee PC, Moran SL, Shin AY. Association between lunate morphology and carpal collapse in cases of scapholunate dissociation. J Hand Surg Am. 2009;34(9):1633–9.
7. Haase SC, Berger RA, Shin AY. Association between lunate morphology and carpal collapse patterns in scaphoid nonunions. J Hand Surg Am. 2007;32(7):1009–12.
8. Schimmerl-Metz SM, Metz VM, Totterman SMS, Mann FA, Gilula LA. Radiologic measurement of the scapholunate joint: implications of biologic variation in scapholunate joint morphology. J Hand Surg Am. 1999;24(6):1237–44.
9. Macconaill MA. The mechanical anatomy of the carpus and its bearings on some surgical problems. J Anat. 1941;75(Pt 2):166–16675.
10. Wolfe SW, Neu C, Crisco JJ. In vivo scaphoid, lunate, and capitate kinematics in flexion and in extension. J Hand Surg Am. 2000;25(5):860–9.
11. Logan SE, Nowak MD, Gould PL, Weeks PM. Biomechanical behavior of the scapholunate ligament. Biomed Sci Instrum. 1986;22(17):81–5.
12. Nowak MD, Logan SE. Strain rate dependent permanent deformation of human wrist ligaments. Biomed Sci Instrum. 1988;24(1):61–5.
13. Berger RA, Imeada T, Berglund L, An KN. Constraint and material properties of the subregions of the scapholunate interosseous ligament. J Hand Surg Am. 1999;24(5):953–62.
14. Patterson RM, Yazaki N, Andersen CR, Viegas SF. Prediction of ligament length and carpal diastasis during wrist flexion-extension and after simulated scapholunate instability. J Hand Surg Am. 2013;38(3):509–18.
15. Padmore C, Stoesser H, Langohr GD, Johnson J, Suh N. Carpal kinematics following sequential scapholunate ligament sectioning. J Wrist Surg. 2019;08(02):124–31.
16. Nikolopoulos FV, Apergis EP, Poulilios AD, Papagelopoulos PJ, Zoubos AV, Kefalas VA. Biomechanical properties of the scapholunate ligament and the importance of its portions in the capitate intrusion injury. Clin Biomech. 2011;26(8):819–23.
17. Watson HK, Brenner LH. Degenerative disorders of the wrist. J Hand Surg Am. 1985;10(6 Pt 2):1002–6.
18. Johnson JE, Lee P, McIff TE, Toby EB, Fischer KJ. Scapholunate ligament injury adversely alters in vivo wrist joint mechanics: an MRI-based modeling study. J Orthop Res. 2013;31(9):1455–60.
19. Pin PG, Nowak M, Logan SE, Leroy Young V, Gilula LA, Weeks PM. Coincident rupture of the scapholunate and lunotriquetral ligaments without perilunate dislocation: pathomechanics and management. J Hand Surg Am. 1990;15(1):110–9.
20. Boabighi A, Kuhlmann JN, Kenesi C. The distal ligamentous complex of the scaphoid and the scapho-lunate ligament. An anatomic, histological and biomechanical study. J Hand Surg Am. 1993;18(1):65–9.
21. Svoboda SJ, Eglseder WA, Belkoff SM. Autografts from the foot for reconstruction of the scapholunate interosseous ligament. J Hand Surg Am. 1995;20(6):980–5.
22. Davis CA, Culp RW, Hume EL, Osterman AL. Reconstruction of the scapholunate ligament in a cadaver model using a bone-ligament-bone autograft from the foot. J Hand Surg Am. 1998;23(5):884–92.
23. Harvey EJ, Hanel D, Knight JB, Tencer AF. Autograft replacements for the scapholunate ligament: a biomechanical comparison of hand-based autografts. J Hand Surg Am. 1999;24(5):963–7.
24. Johnston JD, Small CF, Bouxsein ML, Pichora DR. Mechanical properties of the scapholunate ligament correlate with bone mineral density measurements of the hand. J Orthop Res. 2004;22(4):867–71.
25. Zdero R, Olsen M, Elfatori S, Skrinskas T, Nourhosseini H, Whyne C, et al. Linear and torsional mechanical characteristics of intact and reconstructed scapholunate ligaments. J Biomech Eng. 2009;131(4):1–7.
26. Ehsan A, Lee DG, Bakker AJ, Huang JI. Scapholunate ligament reconstruction using an acellular dermal matrix: a mechanical study. J Hand Surg Am. 2012;37(8):1538–42.
27. Shin SS, Moore DC, McGovern RD, Weiss APC. Scapholunate ligament reconstruction using a

bone-retinaculum-bone autograft: a biomechanic and histologic study. J Hand Surg Am. 1998;23(2):216–21.
28. Hofstede DJ, Ritt MJPF, Bos KE. Tarsal autografts for reconstruction of the scapholunate interosseous ligament: a biomechanical study. J Hand Surg Am. 1999;24(5):968–76.
29. Cuénod P, Charrière E, Papaloïzos MY. A mechanical comparison of bone-ligament-bone autografts from the wrist for replacement of the scapholunate ligament. J Hand Surg Am. 2002;27(6):985–90.

73 Surgical Anatomy and Classification of Scapholunate Tears

Lorenzo Merlini and Christophe Mathoulin

73.1 Introduction

Scapholunate instability secondary to scapholunate ligament insufficiency or tear, or lesions involving the dorsal capsular structures and ligaments, has become one of the main indications for wrist arthroscopy procedures. Arthroscopic assessment of the scapholunate stability has induced a revolution in the management of scapholunate ligament lesions and has allowed the description of crucial capsuloligamentous structures and better comprehension of the wrist anatomy and biomechanics. Several arthroscopic classifications of scapholunate tears have emerged and, along with minimally invasive techniques, the treatment of these lesions has undergone a transformation.

73.2 Surgical Anatomy

Development of wrist arthroscopy has provided a better understanding of the complexity of structures like the scapholunate interosseous ligament (SLIOL) and dorsal capsule-scapholunate septum (DCSS) that are involved in scapholunate stability. What has been for long considered as the "scapholunate ligament" is now treated as the "scapholunate complex" [1–7]. It is now clearer that scapholunate stability is ensured by this "dorsal complex," involving the SLIOL, the DCSS, the dorsal capsule, and the extrinsic ligaments.

The normal arthroscopic findings of the radiocarpal and midcarpal joints must be understood in order to diagnose any abnormality involving the capsule-ligamentous structures.

73.3 Surgical Technique

73.3.1 Radiocarpal Assessment

- Radiocarpal exploration starts with the scope positioned in the 3-4 portal, and a probe testing the ligament through the 6R portal.
- Normal appearance of the SLIOL is almost nonvisible, with an impression of cartilage continuity between the scaphoid and the lunate (Fig. 73.1). The normal testing should show strong tension of the SLIOL, with absence of any breach allowing passage into the scapholunate joint.
- The next structure to assess is the DCSS. Although the DCSS can also be visualized with the scope in the 3-4 portal, the 6R portal will provide a better view. The normal aspect is one of an "arch" between the distal part of the dorsal SLIOL and the dorsal capsular wall (Fig. 73.2). This aspect is consistent

L. Merlini · C. Mathoulin (✉)
International Wrist Center – IWC, Clinique Bizet, Paris, France

© ISAKOS 2022

D. N. Bhatia et al. (eds.), *Arthroscopy and Endoscopy of the Elbow, Wrist and Hand*,
https://doi.org/10.1007/978-3-030-79423-1_73

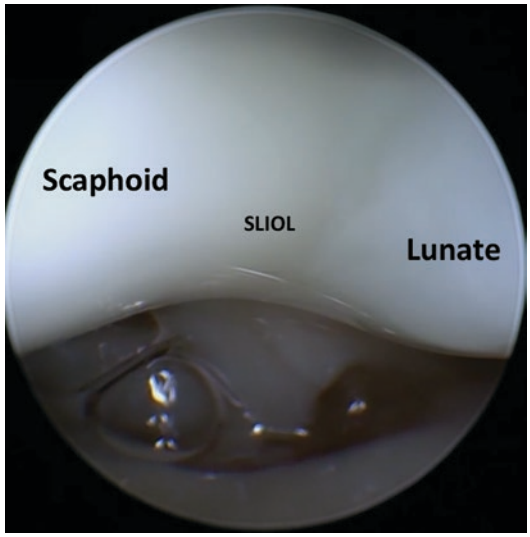

Fig. 73.1 Intact SLIOL visualized from the RC compartment (3-4 portal), with an impression of cartilage continuity

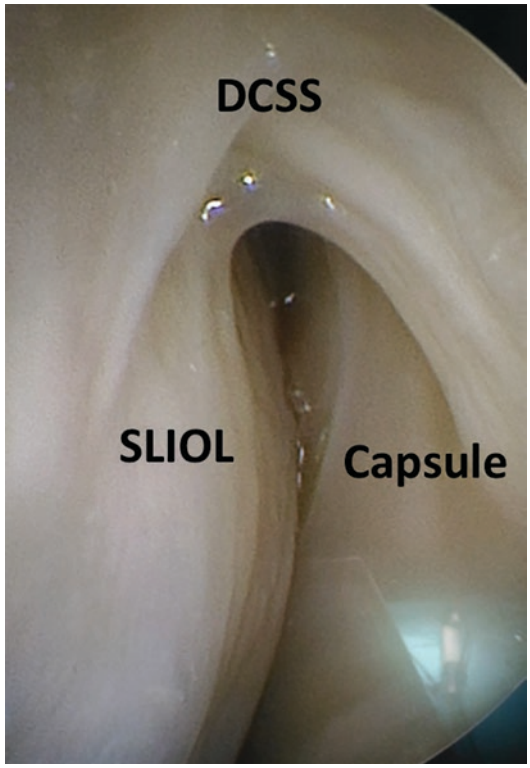

Fig. 73.2 Intact DCSS visualized from the RC compartment (6R portal), presenting like an arch between SLIOL and dorsal capsule

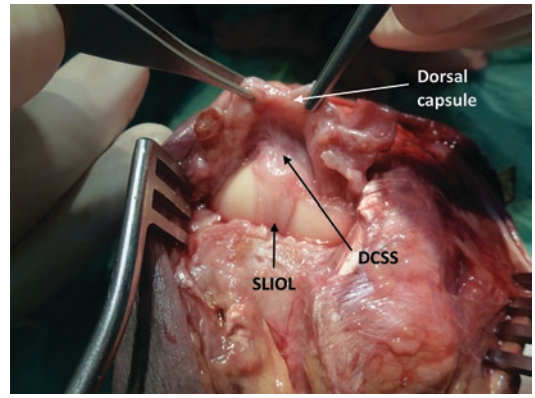

Fig. 73.3 Cadaveric dissection of the dorsal scapholunate complex, with the SLIOL, DCSS, and dorsal capsule and extrinsic ligaments

with the three-dimensional anatomical description of the DCSS, formed by the confluence of three arches reminding of the arches of a gothic cathedral [5–7]. Anatomy and role of the DCSS have been thoroughly analyzed and reported by cadaveric studies and these have provided a better comprehension of the dorsal scapholunate complex (Fig. 73.3) [5–7].

73.3.2 Midcarpal Assessment

- Midcarpal assessment of the SLIOL is crucial and represents the basis for SLIOL tear classification.
- The ligament is not directly viewed from the midcarpal joint and it is the scapholunate stability that is analyzed.
- Normal aspect will show a thin scapholunate space, absence of step-off between the scaphoid and lunate, and inability to pass the probe between the two bones (Fig. 73.4). Dynamic tests, on which the main classifications are based, are performed from the midcarpal joint.

73.3.3 Classification of Scapholunate Tears

- In the early 1990s, several authors started using wrist arthroscopy as a diagnostic means for scapholunate evaluation and agreed that it

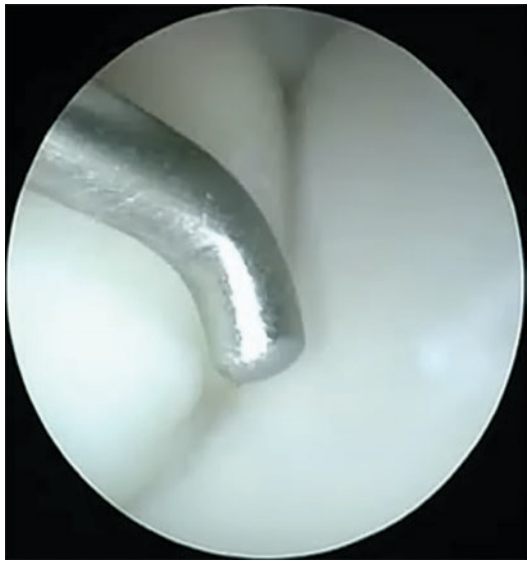

Fig. 73.4 SL space visualized from the MC compartment (MCU portal), and testing of the widening with the probe

could become a valuable tool in the management of scapholunate tears [8, 9]. Arthroscopic evaluation is now the standard method for the assessment of scapholunate instability and several classifications of scapholunate tears have been proposed and published.

- The first worldwide-used classification was developed by Geissler in 1996 [10, 11], and is presented in Table 73.1. Based on this classification, Geissler proposed a management for each grade of instability: immobilization for grade I, arthroscopic reduction and pinning for grade II, arthroscopic/open reduction and pinning for grade III, open reduction, and repair for grade IV [11].
- Dreant and Dautel followed in 2003 with another arthroscopic classification [12]. This classification highlighted the notion of severity of the scapholunate instability and incorporated potential cartilage damages. The severity of the instability is assessed from the midcarpal joint, after releasing the traction (Table 73.2).
- Parallel to these exclusively arthroscopic classifications, other authors developed classifications based on clinical, radiological, and arthroscopic findings to help build a treatment algorithm [13–15].
- Garcia-Elias published his classification of scapholunate dissociation (SLD) in 2006 [16]. (Table 73.3). Based on this algorithm, the authors proposed a specific technique for each stage of scapholunate dissociation:

Table 73.1 Geissler arthroscopic classification of intracarpal instability

Grade	Description
I	Attenuation/hemorrhage of the interosseous ligament as seen from the radiocarpal joint. No incongruency of carpal alignment in the midcarpal space
II	Attenuation/hemorrhage of the interosseous ligament as seen from the radiocarpal joint. Incongruency/step-off as seen from midcarpal space. A slight gap (less than the width of a probe) between carpals may be present
III	Incongruency/step-off is seen in both the radiocarpal and midcarpal spaces. The probe may be passed through the gap between carpals
IV	Incongruency/step-off is seen in both the radiocarpal and midcarpal spaces. Gross instability with manipulation is noted. A 2.7-mm arthroscope may be passed through the gap between carpals

Table 73.2 Dreant and Dautel classification for scapholunate instability

Stage	Description
0	Absence of scapholunate instability
1	Minor scapholunate instability – Only the tip of the probe is passed between the scaphoid and lunate
2 C-	Intermediate scapholunate instability – A gap between scaphoid and lunate can be created by twisting the probe – SLIOL partially torn – No chondral lesion
2 C+	Intermediate scapholunate instability – A gap between scaphoid and lunate can be created by twisting the probe – SLIOL partially torn – Chondral lesion
3 C–	Severe scapholunate instability – Passage of the scope from midcarpal to radiocarpal through the scapholunate gap – No chondral lesion
3 C+	Severe scapholunate instability – Passage of the scope from midcarpal to radiocarpal through the scapholunate gap – Chondral lesion

Table 73.3 Garcia-Elias classification for scapholunate dissociation

SLD stage	1	2	3	4	5	6
Partial rupture with normal dorsal SL ligament?	Yes	No	No	No	No	No
If ruptured, repairable dorsal SL ligament?	Yes	Yes	No	No	No	No
Normally aligned scaphoid? (radioscaphoid angle ≤45°)	Yes	Yes	Yes	No	No	No
Easily reducible carpal malalignment?	Yes	Yes	Yes	Yes	No	No
Both RC and MC joints cartilages normal?	Yes	Yes	Yes	Yes	Yes	No

  - Dorsal capsulodesis for stage 1
  - SL ligament transosseous or anchor repair for stage 2
  - Bone-ligament-bone graft for stage 3
  - Three-ligament tenodesis for stage 4
  - Partial fusion (STT, SC) for stage 5
  - Proximal row carpectomy or four-corner fusion for stage 6.
- Finally, the European Wrist Arthroscopy Society (EWAS) produced a precise classification, also incorporating radiographic data and more interestingly anatomical-pathological findings from cadaver specimens (Table 73.4) [17, 18].

Table 73.4 EWAS classification of scapholunate tears

Stage	Arthroscopic testing of SLIOL from MC joint	Anatomo-pathological findings
I	No passage of the probe	No lesion
II A Lesion of membranous SLIOL	Volar passage of the tip of the probe in the SL space without widening (stable)	Lesion of proximal/membranous part of SLIOL
II B Lesion of membranous SLIOL	Dorsal passage of the tip of the probe in the SL space without widening (stable)	Lesion of proximal/membranous part of SLIOL
II C Lesion of membranous SLIOL	Complete passage of the tip of the probe in the SL space without widening (stable)	Lesion of proximal/membranous part of SLIOL
III A Partial lesions involving the volar SLIOL	Volar widening on dynamic testing (anterior laxity)	Lesion of the anterior and proximal part of SLIOL with or without lesion of RSC/LRL
III B Partial lesions involving the dorsal SLIOL	Dorsal widening on dynamic testing (posterior laxity)	Lesion of the proximal and posterior part of SLIOL with partial lesion of DIC
III C Complete SLIOL tear, the joint is reducible	Complete widening of SL space on dynamic testing, reducible with removal of the probe	Complete lesion of SLIOL (anterior, proximal, posterior), complete lesion of one extrinsic ligament (DIC or RSC/LRL)
IV Complete SLIOL with SL gap	SL gap with passage of the arthroscope from MC to RC joint No radiographic abnormalities	Complete lesion of SLIOL (anterior, proximal, posterior), lesion of extrinsic ligaments (DIC and RSC/LRL)
V	Wide SL gap with passage of the arthroscope through SL joint Frequent X-ray abnormalities, such as an increased SL gap, DISI deformity	Complete lesion of SLIOL, DIC, LRL, RSC; involvement of one or more other ligaments (TH, ST, DRC)

SLIOL scapholunate interosseous ligament, *MC* midcarpal, *RC* radiocarpal, *RSC* radio-scapho-capitate, *LRL* long radio-lunate, *DIC* dorsal intercarpal ligament, *SL* scapholunate, *TH* triquetro-hamate, *ST* scaphotrapezial, *DRC* dorso radio-carpal, *DISI* dorsal intercalated segmental instability

Table 73.5 Classification of DCSS lesions

Stage	Arthroscopic findings
S0	Intact aspect. Normally tensed when palpated with a probe. All the fibers are continuous. Typical aspect of cathedral arches
S1	DCSS loosened when palpated with a probe. Partial detachments with >50% continuous fibers
S2	DCSS elongated and loosened when palpated with a probe. Partial tear with <50% continuous fibers
S3	The DCSS is totally ruptured or disappeared

The last classification is probably the most precise one for arthroscopic assessment of scapholunate tears, and particularly interesting regarding the correlation between dynamic instability and anatomical lesions. However, for a perfectly thorough evaluation of the scapholunate complex, the scapholunate instability is to be completed by the assessment of the DCSS. Several anatomical and arthroscopic studies have shown the crucial role of the DCSS in scapholunate stability [5–7] (Table 73.5). The correlation between DCSS lesions and SL tears EWAS staging has been reported, and DCSS is now proved to be an important stabilizer of the wrist. Sectioning of the DCSS majored the SL instability by at least a stage [5].

References

1. Mathoulin CL. From scapholunate interosseus ligament to scapholunate ligament complex. J Wrist Surg. 2013;2(2):98.
2. Wahegaonkar AL, Mathoulin CL. Arthroscopic dorsal capsulo-ligamentous repair in the treatment of chronic scapho-lunate ligament tears. J Wrist Surg. 2013;2(2):141–8.
3. Mathoulin CL. Indications, techniques, and outcomes of arthroscopic repair of scapholunate ligament and triangular fibrocartilage complex. J Hand Surg Eur Vol. 2017;42(6):551–66.
4. Mathoulin C, Gras M. Role of wrist arthroscopy in scapholunate dissociation. Orthop Traumatol Surg Res. 2020;106(1S):S89–99.
5. Overstraeten LV, Camus EJ, Wahegaonkar A, Messina J, Tandara AA, Binder AC, et al. Anatomical Description of the Dorsal Capsulo-Scapholunate Septum (DCSS)-Arthroscopic Staging of Scapholunate Instability after DCSS Sectioning. J Wrist Surg. 2013;2(2):149–54.
6. Van Overstraeten L, Camus EJ. Arthroscopic classification of the lesions of the Dorsal Capsulo-Scapholunate Septum (DCSS) of the wrist. Tech Hand Up Extrem Surg. 2016;20(3):125–8.
7. de Sambuy MTC, Burgess TM, Cambon-Binder A, Mathoulin CL. The anatomy of the Dorsal Capsulo-Scapholunate Septum: a cadaveric study. J Wrist Surg. 2017;6(3):244–7.
8. Cooney WP, Dobyns JH, Linscheid RL. Arthroscopy of the wrist: anatomy and classification of carpal instability. Arthroscopy. 1990;6(2):133–40.
9. Whipple TL. The role of arthroscopy in the treatment of scapholunate instability. Hand Clin. 1995;11(1):37–40.
10. Geissler WB, Freeland AE, Savoie FH, McIntyre LW, Whipple TL. Intracarpal soft-tissue lesions associated with an intra-articular fracture of the distal end of the radius. J Bone Joint Surg Am. 1996;78(3):357–65.
11. Geissler WB. Arthroscopic management of scapholunate instability. J Wrist Surg. 2013;2(2):129–35.
12. Dreant N, Dautel G. Elaboration d'un score de sévérité arthroscopique pour les instabilités scapholunaires [Development of a arthroscopic severity score for scapholunate instability]. Chir Main. 2003;22(2):90–4.
13. Kitay A, Wolfe SW. Scapholunate instability: current concepts in diagnosis and management. J Hand Surg Am. 2012;37(10):2175–96.
14. Andersson JK, Garcia-Elias M. Dorsal scapholunate ligament injury: a classification of clinical forms. J Hand Surg Eur Vol. 2013;38(2):165–9.
15. Chennagiri RJR, Lindau TR. Assessment of scapholunate instability and review of evidence for management in the absence of arthritis. J Hand Surg Eur Vol. 2013;38(7):727–38.
16. Garcia-Elias M, Lluch AL, Stanley JK. Three-ligament tenodesis for the treatment of scapholunate dissociation: indications and surgical technique. J Hand Surg Am. 2006;31(1):125–34.
17. Messina JC, Dreant N, Luchetti R, Lindau T, Mathoulin C. Scapholunate tears: a new arthroscopic classification. Chir Main. 2009;28(6):339–44.
18. Messina JC, Van Overstraeten L, Luchetti R, Fairplay T, Mathoulin CL. The EWAS classification of scapholunate tears: an anatomical arthroscopic study. J Wrist Surg. 2013;2(2):105–9.

74 Arthroscopic Scapholunate Ligament Thermal Shrinkage

Eugene T. Ek and Rachel M. Blackshaw

74.1 Background

The scapholunate interosseous ligament (SLIL) is the most commonly injured intercarpal ligament in the wrist and a frequent cause of wrist pain and loss of function. Disruption of the scapholunate ligament complex leads to varying degrees of carpal instability, and often the natural history is progressive degenerative arthritis of the wrist over time [1–3].

SLIL injuries can present anywhere along a recognized continuun, from pre-dynamic, dynamic and static instability, to eventual scapholunate advanced collapse (SLAC). With frank disruption of the SLIL, the lunate and scaphoid dissociate. In the initial stage, carpal kinematics may be somewhat maintained through the action of secondary stabilizers, and dissociation of the scaphoid and lunate will only become apparent with movement or loading of the wrist (dynamic instability) [4]. However, progression to static instability inevitably follows and manifests as flexion of the scaphoid and extension of the lunate; this results in a dorsal intercalated segmental instability (DISI) deformity and static widening of the scapholunate joint. Derangement of the carpus eventually progresses to the aforementioned degenerative SLAC wrist [3, 4].

Incomplete or partial tears of the SLIL leading pre-dynamic instability are becoming increasingly recognized as a common cause of dorsal wrist pain. Patients usually present with persistent dorsal wrist pain that is exacerbated by increased load across the wrist especially in extension. This may be perceived as weakness in performing even simple activities and may be associated with loss of wrist extension secondary to pain. A common presentation is pain over the dorsal side of the wrist when performing weight-bearing exercises such as yoga (downward dog maneuverer) or push-ups. Patients may also experience a clucking sensation in the wrist with movement. Clinically, there may be tenderness on the dorsal side of the wrist over the scapholunate ligament and the patient may exhibit a positive Watsons' test, suggestive of scapholunate instability. Most commonly in pre-dynamic instability of the wrist, static and dynamic plain radiographs are normal. However, on MRI scan, one can often see increased signal changes in the SL ligament suggestive of a partial tear. As the radiological findings are often not significant, the clinical features need to be correlated in order to make an accurate diagnosis.

Surgical treatment of pre-dynamic scapholunate instability becomes an option after failed non-operative management. In the literature, surgical treatment includes both open and

E. T. Ek (✉) · R. M. Blackshaw
Melbourne Orthopaedic Group,
Melbourne, VIC, Australia

Department of Surgery, Monash University,
Melbourne, VIC, Australia

© ISAKOS 2022

D. N. Bhatia et al. (eds.), *Arthroscopy and Endoscopy of the Elbow, Wrist and Hand*,
https://doi.org/10.1007/978-3-030-79423-1_74

arthroscopic procedures, and these may be simple debridement, thermal shrinkage, ligament repair, capsulodesis or scapholunate ligament reconstruction [2, 5]. Various reports have described effective symptom relief and satisfaction following these procedures; however, maintenance of stability long term has always been the concern [6–9]. Arthroscopic thermal shrinkage of the scapholunate ligament has been an appealing technique as it is minimally invasive, with low morbidity and risk. This chapter describes the technique of arthroscopic scapholunate ligament thermal shrinkage for the treatment of pre-dynamic SL instability.

74.2 Surgical Anatomy

The SLIL is a transverse, intrinsic intercarpal ligament that stabilizes the scapholunate joint. It is C-shaped and covers all, but the most distal portion of the joint. There are three distinct anatomic regions to the SLIL: dorsal, proximal and palmar. The dorsal portion is the shortest (5 mm), thickest (3 mm) and strongest (260 N), and most critical region. It is formed by a thick and tightly packed collection of slightly obliquely orientated collagen fibres that are intimately related to the dorsal radiocarpal joint capsule. It is a primary restraint to distraction, torsional and translational forces. The palmar portion is thinner (1 mm) than the dorsal and the second strongest (118 N). It has slightly longer more obliquely orientated collagen fibres distinct from and just dorsal to the long radio-lunate ligament (LRL). This orientation allows substantial flexion and extension of the scaphoid relative to the lunate. It has important contributions to rotational stability of the SL joint. The proximal membranous portion is composed of fibrocartilage with a few superficial longitudinal orientated collagen fibres. It can protrude into the SL joint a few millimetres, somewhat like a meniscus in the knee. It is often degenerate in the elderly population and is the weakest portion (63 N) of the SLIL complex [3, 10–12].

The SLIL plays a crucial role in the function of the wrist. During the "Dart Throwers" motion, the wrist moves from extension and radial deviation to flexion and ulnar deviation. The scaphoid and lunate begin in a flexed posture and move into an extended position. In the absence of SLIL the scaphoid remains flexed and pronated whilst the lunate would settle into an extended and supinated posture on the radius, resulting in a dorsal intercalated segmental instability (DISI) deformity [2, 3, 10, 12].

The SLIL contains primarily Type I collagen arranged in a triple helix that contains stabilizing intramolecular hydrogen bonds and intermolecular covalent aldehyde cross links to form a linear polymer. The application of alternating electric current in the form of a non-ablative radiofrequency probe generates heat in the tissue by friction as a result of the oscillation of electrons and molecules. The heat-labile hydrogen bonds break down resulting in a random coil state and loss of the ordered crystalline structure. The amount of tissue shrinkage depends on the temperature as well as the duration of treatment. The process of collagen denaturation commences above 60°C and maximal shortening is seen at 80°C. Immediately after treatment, there is a significant reduction in tissue stiffness. During the repair process, fibroblasts infiltrate the tissue and actively synthesize new collagen using the acellular hyalinized collagen as a framework for migration and matrix synthesis. By 6 weeks there is extensive fibrosis and neovascularization and after 12 weeks the tensile strength returns to pre-treatment levels with normal-looking collagen fibrils [13, 14].

74.3 Indications and Contraindications

Indications for arthroscopic SLIL thermal shrinkage include:

- Symptomatic pre-dynamic scapholunate ligament instability
- Partial scapholunate ligament tear (Fig. 74.1)
- Geissler Grade I or Grade II intercarpal ligament instability

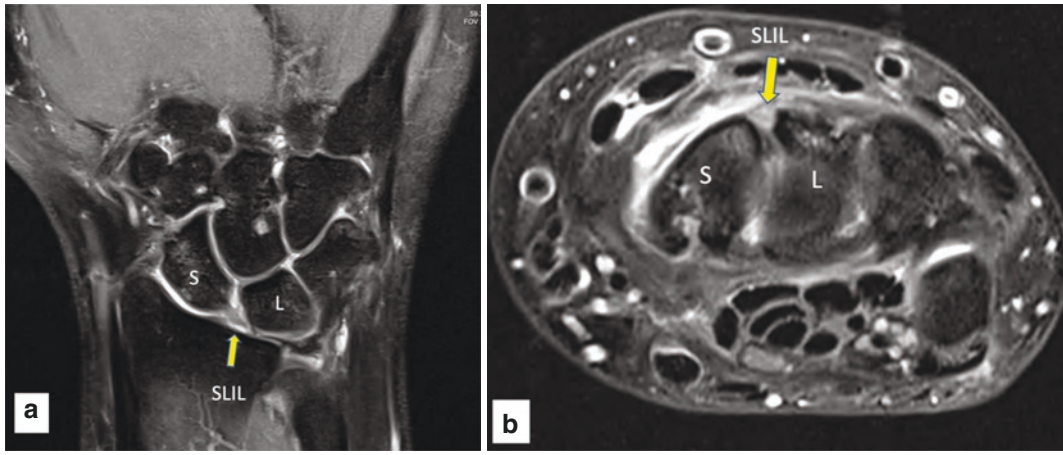

Fig. 74.1 (**a**) Coronal and (**b**) axial MRI scan demonstrating a partial tear of the scapholunate ligament. Note the scapholunate interosseous ligament (SLIL) is still attached to the scaphoid (S) scaphoid and lunate (L), but it appears attenuated with increased signal intensity. There is no evidence of scapholunate diastasis

The procedure is contraindicated in:

- Dynamic or static scapholunate ligament instability
- Complete tears of the scapholunate ligament
- Geissler Grade III or Grade IV intercarpal ligament instability
- Scapholunate ligament advanced collapse (SLAC) wrist or development of arthritic changes

74.4 Surgical Technique

The patient is placed on the operating table in the supine position after either a general anaesthetic or a regional brachial plexus block. The arm is exsanguinated prior to inflation of an above elbow tourniquet. The wrist is then placed into a wrist arthroscopy traction system with counter-traction placed on the arm above the elbow. Finger traps are applied to the fingers and approximately 8–10 kg of longitudinal traction is placed onto the wrist.

Portals: Anatomic landmarks are used to identify and mark the four dorsal portals used for the procedure. The radiocarpal portals used are the 3/4 portal and the 6R portal. The midcarpal portals used are midcarpal radial (MCR) and midcarpal ulnar (MCU) portals.

74.4.1 Diagnostic Arthroscopy

- A 2.7 mm 30° arthroscope is used to perform a dry diagnostic arthroscopy through a standard 3/4 dorsal radiocarpal portal. The 6R portal is then established under direct visualization through an outside–in technique. As part of the diagnostic arthroscopy the radiocarpal joint, scapholunate ligament, lunotriquetral ligament and triangular fibrocartilage complex (TFCC) are examined.
- The SLIL is carefully inspected from the radiocarpal joint. In the setting of a partial tear with associated with pre-dynamic instability, the ligament will exhibit increased laxity and appear attenuated but overall intact. Instead of a normal concave appearance, it will appear convex and sometimes patulous and inflamed (Fig. 74.2).
- The midcarpal joint is then examined via the MCR portal. The MCU portal is then established under direct vision and this is used as the working portal. The scapholunate interval is probed and SL instability is graded according to the Geissler classification (Fig. 74.3a) [1].
- In pre-dynamic scapholunate instability with a partial SL tear, either Grade I (no incongruity of the SL interval) or Grade II (mild

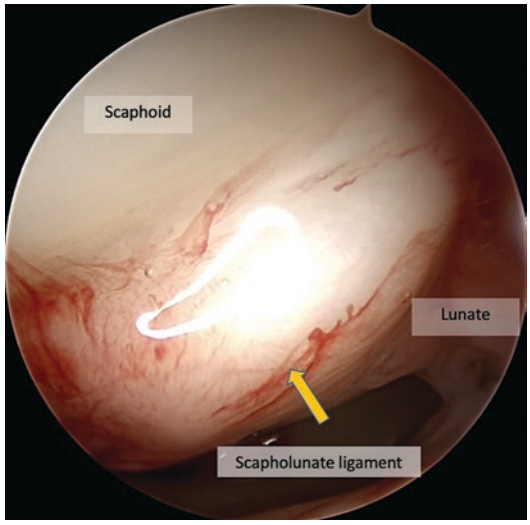

Fig. 74.2 Arthroscopic view from the 3-4 dorsal radiocarpal portal demonstrating an attenuated scapholunate ligament (arrow) consistent with a Geissler Grade I or II instability

incongruity or step-off but no separation) is observed [1].

74.4.2 Arthroscopic Thermal Shrinkage

- Prior to thermal shrinkage, any synovitis or degenerative or frayed tissue is debrided with a shaver inserted through the MCU portal. When thermal shrinkage is performed, normal saline is insufflated into the joint using a handheld fluid pump. This is to counteract the increased heat generated from the radiofrequency device and also to allow the coblation device to function.
- While viewing the midcarpal joint, the radiofrequency device is inserted into the joint. The volar capsule adjacent to the scapholunate joint and ligament is then targeted using the coagulation mode (Fig. 74.3b). One can see the volar tissue shrink as the wand is brushed over the capsule. Similarly, this is performed on the dorsal capsule and adjacent to the dorsal SLIL.
- The arthroscope is then placed in the 3/4 portal of the radiocarpal joint and the radiofrequency device is inserted through the 6R portal. The joint is filled with normal saline and the SLIL is probed with the wand. Thermal shrinkage is performed from volar to dorsal, turning the convex and attenuated ligament into a concave structure (Fig. 74.4a and b).

74.4.3 K Wire Stabilization of the Carpus

- Traction is then released, but the wrist is maintained in the vertical position. The fluoroscope is then positioned around the wrist allowing for an anteroposterior image to be taken (Fig. 74.5a).
- Gentle traction is placed onto the thumb to ulnar deviate the wrist and thereby allow the scaphoid to extend and to reduce the scapholunate interval.
- Percutaneous wires are then inserted under fluoroscopic control into the scaphocapitate joint (×1) and scapholunate joint (×2). The wires are then cut and buried under the skin (Fig. 74.5b and c).

The portals are then closed with steristrips and standard sterile dressings are applied. The wrist is placed into a plaster thumb spica splint.

74.5 Tips and Tricks

- Ensure that the scapholunate ligament is only partially torn and that the degree of instability is only Geissler Grade I or II
- Maintain adequate traction of the wrist to allow for easy insertion of the radiofrequency device to avoid iatrogenic injury to the articular surface
- When applying heat to the scapholunate ligament with the radiofrequency device, apply a brushing motion to avoid sustained heat to the ligament and potential injury
- Insert the k wires into the wrist with the wrist in slight ulnar deviation to extend the scaphoid and also to allow for easier access to the radial side of the scaphoid

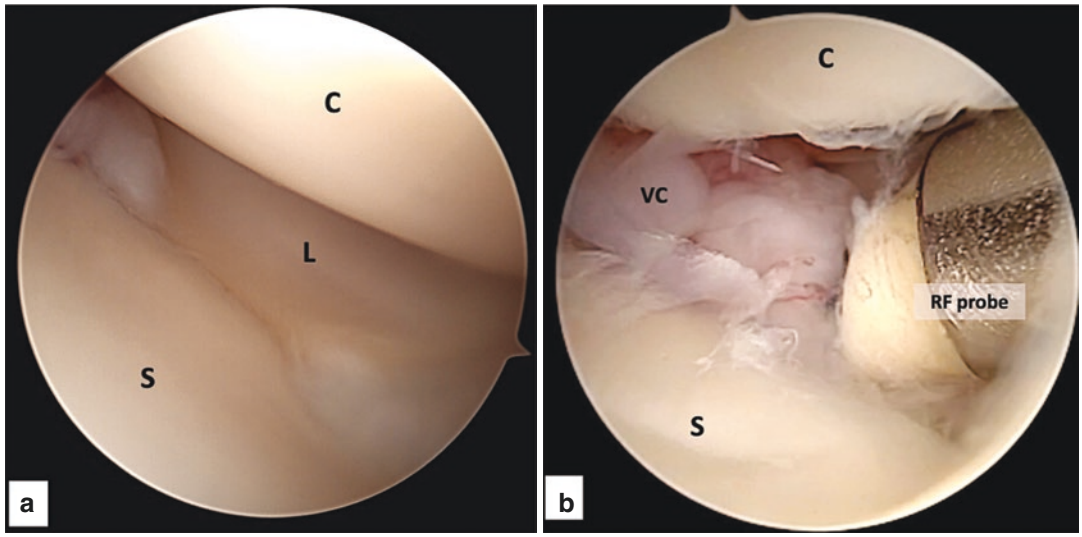

Fig. 74.3 (**a**) Midcarpal arthroscopy viewing from the midcarpal radial (MCR) portal. (**b**) A radiofrequency (RF) probe is inserted into a midcarpal ulnar (MCU) portal and thermal shrinkage of the volar capsule (VC) and then the dorsal capsule is performed

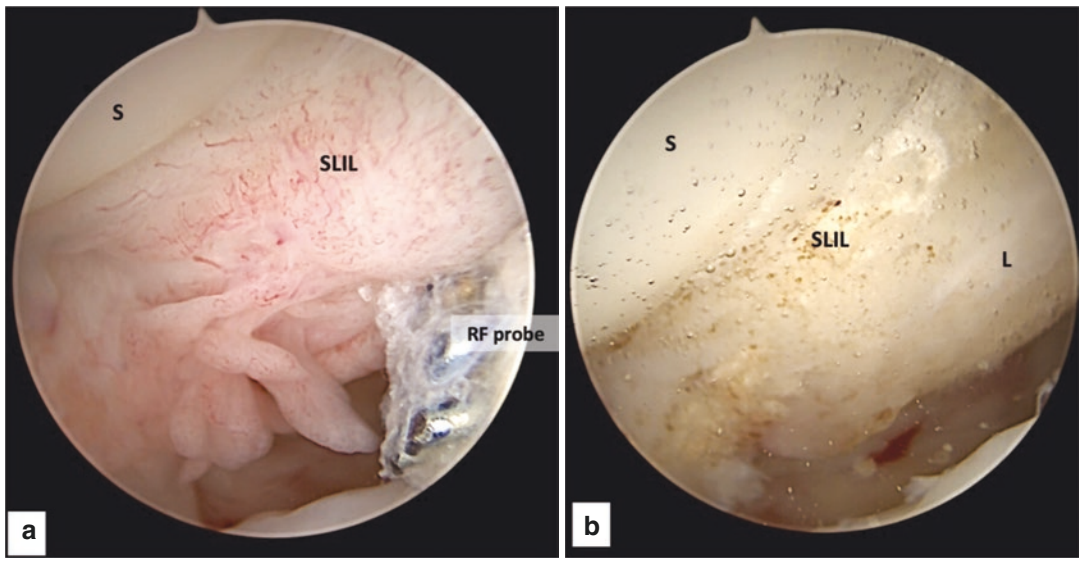

Fig. 74.4 Radiocarpal arthroscopy viewing through the 3-4 dorsal portal. (**a**) The scapholunate interosseous ligament (SLIL) is haemorrhagic and attenuated. A radiofrequency (RF) probe is inserted into the 6R portal and thermal shrinkage is performed on the SLIL. (**b**) After thermal shrinkage of the SLIL. The ligament becomes concave and loses its laxity. (S) scaphoid, (L) lunate

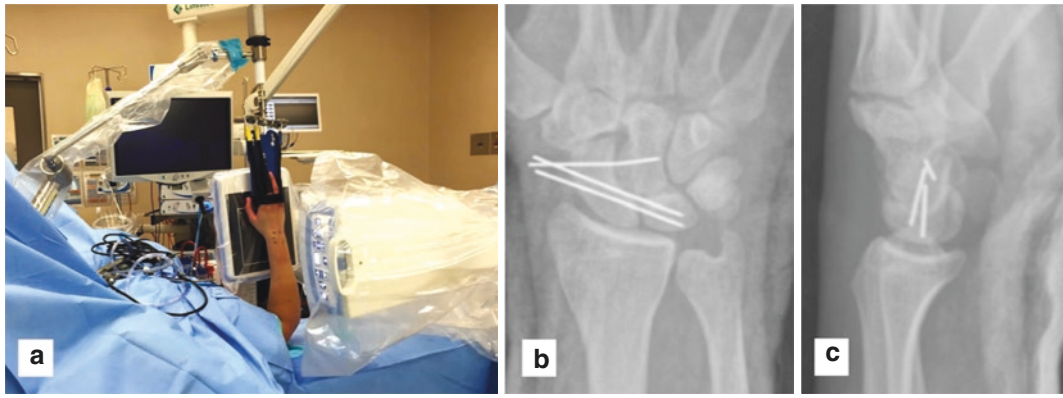

Fig. 74.5 (**a**) K wires are inserted under fluoroscopic control. (**b**) Anteroposterior and (**c**) lateral radiographs demonstrate temporary K-wires inserted across the scapholunate and scaphocapitate joints

74.6 Pitfalls

- Inadequate traction on the wrist makes access to the radiocarpal and midcarpal joints difficult and increases the risk of iatrogenic injury
- Maintain the wires sufficiently buried as they can cause breakdown to the overlying skin, especially when in the splint. Furthermore, it may cause irritation to the superficial radial nerve.

74.7 Postoperative Rehabilitation and Management

The postoperative plaster thumb spica splint is applied for approximately 10 days. Thereafter, the patient is immobilized in a thermoplastic removable thumb spica splint for a total of 8 weeks until the wires are removed. The buried wires are then removed under local anaesthetic either in the clinic or in the operating room. The patient then gradually weaned off the splint and commences hand therapy, initially with gentle "dart thrower" motion progressing to full range of motion of the wrist. Strengthening exercises are commenced after 3 months and return to normal sporting activities at 6 months.

74.8 Complications

- Early potential complications most commonly involve the k wires:
  - K wire breakage from the inadvertent movement of the wrist
  - Irritation of the superficial radial nerve
  - Skin breakdown over the prominent wires.
- Late complications include:
  - Articular surface injury from the thermal radiofrequency device
  - Joint stiffness
  - Ongoing carpal instability and pain

References

1. Geissler WB, Freeland AE. Arthroscopically assisted reduction of intraarticular distal radial fractures. Clin Orthop Relat Res. 1996;327:125–34.
2. Kitay A, Wolfe SW. Scapholunate instability: current concepts in diagnosis and management. J Hand Surg Am. 2012;37(10):2175–96.
3. Rajan PV, Day CS. Scapholunate interosseous ligament anatomy and biomechanics. J Hand Surg Am. 2015;40(8):1692–702.
4. Slutsky DJ. Arthroscopic dorsal radiocarpal ligament repair. Arthroscopy. 2005;21(12):1486.
5. Hirsh L, Sodha S, Bozentka D, Monaghan B, Steinberg D, Beredjiklian PK. Arthroscopic electrothermal collagen shrinkage for symptomatic laxity of

the scapholunate interosseous ligament. J Hand Surg Br. 2005;30(6):643–7.
6. Ruch DS, Poehling GG. Arthroscopic management of partial scapholunate and lunotriquetral injuries of the wrist. J Hand Surg Am. 1996;21(3):412–7.
7. Shih JT, Lee HM, Hou YT, Tan CM. Results of arthroscopic reduction and percutaneous fixation for acute displaced scaphoid fractures. Arthroscopy. 2005;21(5):620–6.
8. Darlis NA, Weiser RW, Sotereanos DG. Partial scapholunate ligament injuries treated with arthroscopic debridement and thermal shrinkage. J Hand Surg Am. 2005;30(5):908–14.
9. Weiss AP, Sachar K, Glowacki KA. Arthroscopic debridement alone for intercarpal ligament tears. J Hand Surg Am. 1997;22(2):344–9.
10. Wolfe SW, Hotchkiss RN, Pederson WC, Kozin SH, Cohen MS. Green's operative hand surgery. Elsevier; 2016.
11. Berger RA. The gross and histologic anatomy of the scapholunate interosseous ligament. J Hand Surg Am. 1996;21(2):170–8.
12. Berger RA, Imeada T, Berglund L, An KN. Constraint and material properties of the subregions of the scapholunate interosseous ligament. J Hand Surg Am. 1999;24(5):953–62.
13. Medvecky MJ, Ong BC, Rokito AS, Sherman OH. Thermal capsular shrinkage: basic science and clinical applications. Arthroscopy. 2001;17(6):624–35.
14. Wallace AL, Hollinshead RM, Frank CB. The scientific basis of thermal capsular shrinkage. J Shoulder Elb Surg. 2000;9(4):354–60.

75 Arthroscopic Treatment of Scapholunate Instability

Ahlam Arnaout and Christophe Mathoulin

75.1 Background

Scapholunate interosseous ligaments (SLIL) tears are among the most common and severe ligament injuries associated with wrist trauma and usually occur after a fall on a hyperextended and pronated wrist [1]. The natural evolution leads to chronic scapholunate joint instability and osteoarthritis (scapholunate advanced collapse) [2]. Diagnosis and treatment are a real challenge for the surgeon, and inadequate management in early stages is associated with worse functional outcomes. Moreover, SLIL lesions are difficult to evaluate precisely even with advent of highly accurate imaging techniques [3].

Many conventional open surgical techniques have been described for scapholunate joint stability; however, these procedures often result in stiffness and this can be disabling especially for young and high-level athletes [4–6]. In the last three decades, wrist arthroscopy has dramatically changed the understanding of these lesions and has led to the development of less invasive and reproducible surgical repair techniques [7].

75.1.1 Surgical Anatomy

Scapholunate joint stability is dependent not only on SLIL but also on a set of primary and secondary stabilizers that collectively form a complex. Among these stabilizers, the dorsal part of the SLIL and the dorsal capsulo-scapholunate septum (DCSS) emerges as the key components of the SL joint stability [8–10]. The techniques described here enable the repair of these two structures by a capsule-to-ligament suturing and prevent the stiffness associated with open procedures.

75.2 Indications and Contraindications

Based on our good functional outcomes [7, 11–14], we recommend the arthroscopic dorsal capsuloligamentous repair (ADCLR) in all the acute or chronic instabilities lower than EWAS and GEISSLER IV. Lesions that are purely volar can be treated with an arthroscopic treatment to achieve volar capsule–ligament suture with minimal skin opening [15].

Table 75.1 provides a treatment algorithm and indications according to the grade of the lesion.

The capsulodesis is ineffective in patterns that are associated with a large detachment of the dorsal capsule (advanced stages of SL dissociations, associated lunotriquetral instability, and chronic static dissociations) [11]. Chronic cases of stage IV+

A. Arnaout · C. Mathoulin (✉)
International Wrist Center-Clinique du Poignet, Institut de la Main, Paris, France

© ISAKOS 2022

D. N. Bhatia et al. (eds.), *Arthroscopy and Endoscopy of the Elbow, Wrist and Hand*,
https://doi.org/10.1007/978-3-030-79423-1_75

Table 75.1 Treatment algorithm proposed according to the intraoperative staging

Stage (EWAS) A/C	Lesion pattern	Instability	Proposed treatment
I A only		Pre-dynamic, dynamic	Cast 6 weeks
II A, B, C A/C	Volar, dorsal, or central part	Pre-dynamic, dynamic	A: ADCLR or arthroscopic pinning C: ADCLR or AVCLR if IIA
III A A/C	Anterior part	Dynamic	A: AVCLR or arthroscopic pinning C: AVCLR
III B A/C	Dorsal part	Dynamic	A: ADCLR C: ADCLR
III C A/C	Complete SL + DIC	Dynamic	A: ADCLR ± AVCLR C: ADCLR ± AVCLR
IV A/C	Complete SL + extrinsic ligament lesion	Dynamic, static	A: ADCLR + AVCLR C: ADCLR + AVCLR or alternative technique
IV+ C	Complete SL + bald scaphoid Reducible	Static	ADCLR 2 + AVCLR or alternative technique

A acute, *C* chronic, *ADCLR* arthroscopic dorsal capsulo-ligamentous repair, *AVCLR* arthroscopic volar capsulo-ligamentous repair, *DIC* dorsal intercarpal ligament

(EWAS classification) are treated with open or arthroscopic ligament reconstruction. Additionally, if a floating lunate is observed at the midcarpal exploration step (rocking chair sign) [16], it reflects an associated lunotriquetral instability, and another surgical option must be selected.

75.3 Surgical Technique

75.3.1 Arthroscopic Dorsal Capsuloligamentous Repair (ADCLR)

- The aim of the technique is to achieve a dorsal capsule-to-ligament suture in order to stabilize the scapholunate joint.
- The procedure is performed on an outpatient basis, under regional anesthesia and pneumatic tourniquet.
- A standard 3-4 radiocarpal portal is placed for vizualisation using a 2.4 mm scope and the 6R portal is used as a working portal. The SLIL is directly visualized and a shaver is used to perform a synovectomy.
- The positions of the arthroscope and the shaver are then reversed; the scope is placed in the 6R portal and the shaver in the 3-4 portal. The 6R portal is the most effective one to assess the dorsal portion of SL ligament and DCSS using a probe and triangulation. The SLIL is visualized from its palmar to dorsal aspect. The origin of the ligament avulsion is checked with the probe, and the quality of the remaining ligament stumps is assessed. Usually, the ligament is avulsed from its scaphoid insertion, and ligament remnants attached to the scaphoid and lunate are identified. The procedure can be performed only if good quality ligaments stumps remain attached.
- A push test, under arthroscopic visualization, is performed using a probe to evaluate the DCSS status. If the probe is unable to move to the midcarpal joint, the test is negative and DCSS is considered intact. If the probe can be pushed easily into the midcarpal joint, the test is positive and DCSS is considered as torn (Fig. 75.1).
- The next step of the procedure is performed in the midcarpal joint and SL joint stability is evaluated. The arthroscope is introduced via MCU portal and the shaver through MCR portal. After a meticulous synovectomy, the probe is used to test the SL space and for staging the SL joint instability (Messina-EWAS, Geissler, and modified Garcia-Elias classifications) [11, 12]. Scapholunate joint stability can also be more accurately evaluated with dynamic assessment (flexion-extension and radial-ulnar translation) after a slight traction release.
- The arthroscope is then placed again in the 6R portal to visualize the exact location of the sutures and control their passage across the ligament stumps. Two absorbable monofila-

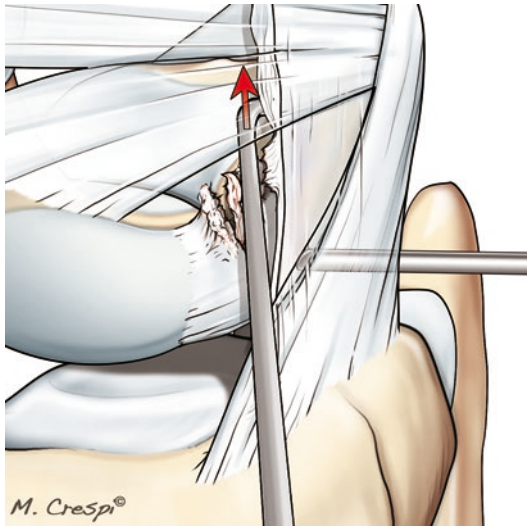

Fig. 75.1 A positive push test is elicited with a probe indicating a torn DCSS

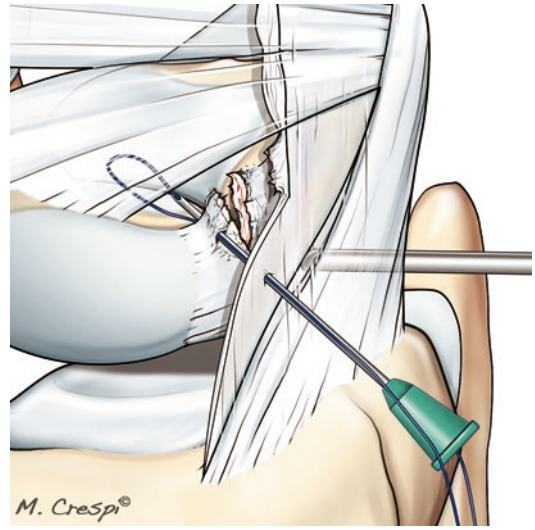

Fig. 75.2 Introduction of first needle and suture for SL ligament repair to the dorsal capsule

ment sutures passed through two intramuscular needles are used, usually 3.0 or 4.0, depending on the patient's height. The first needle is inserted through the 3-4 radiocarpal portal, then shifted slightly distally so as to cross the dorsal capsule up to 1 mm from the capsular hole. The needle is then pushed through the radial ligament stump attached to the scaphoid, oriented obliquely from dorsal to volar, and proximal to distal with an angulation close to 45°, in order to reach the midcarpal joint (Figs. 75.2 and 75.3). A second suture passed in the same way through a needle guide, is inserted parallel to the first one, into the ulnar ligament remnant attached to the lunate (Fig. 75.4).

- The principle of the next step is to fix the first knot in the midcarpal joint between the scaphoid and the lunate to reduce the SL space; thereafter, the second knot is tied and provides dorsal capsule-to-ligament suture on a reduced SL space (Figs. 75.5, 75.6, and 75.7). The arthroscope is switched once more to the MCU portal to visualize the sutures in the midcarpal joint. A hemostasis forcep is used to externalize both sutures from the MCR portal and tie the first knot outside the joint. A proximal–distal traction is then applied to the sutures through the 3-4 radiocarpal portal in order to pull the midcarpal knot and place it between the scaphoid and the lunate and volar to the dorsal part of the SLIL. Under arthroscopic guidance, the reduction is evaluated by maintaining a proximal tension on the sutures ends after a slight release of the traction. If a reduction is satisfactory, the ligament is sutured to the dorsal capsule by tying the second knot in a subcutaneous position.

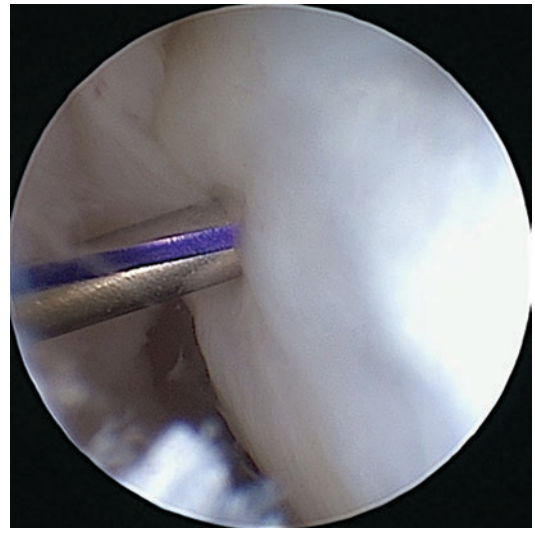

Fig. 75.3 Arthroscopic view of the needle passing through the capsule and dorsal portion of the SLIL. The needle is angled dorsal to volar and proximal to distal so that it can penetrate the midcarpal joint

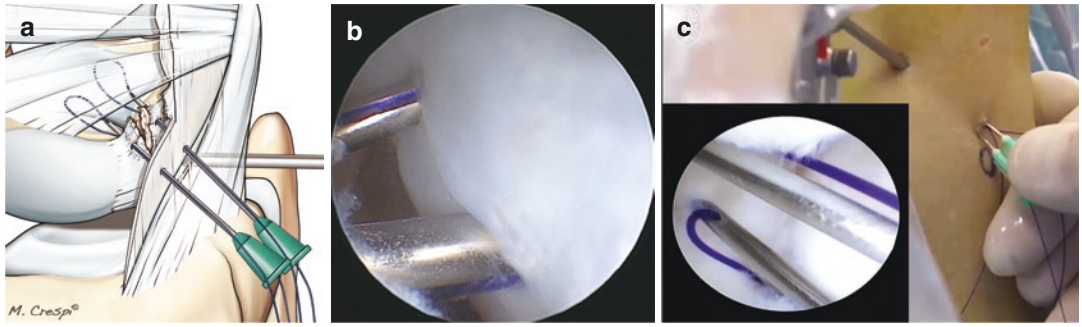

Fig. 75.4 (**a**) Position of the two needles passing through the dorsal capsule and into the two stumps of the dorsal portion of the SLIL. (**b**) Arthroscopic radiocarpal view of the position of the needles inside the joint. (**c**) External image shows the position of two needles passing through the 3-4 portal. Arthroscopic midcarpal view of the position of the needles inside the joint (inset image)

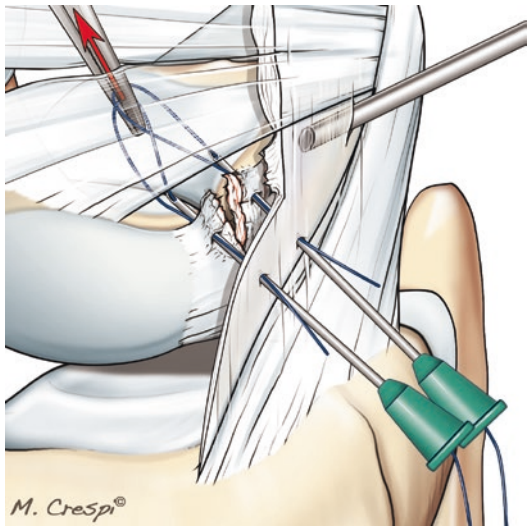

Fig. 75.5 Suture retrieval using a hemostat introduced through the MCR portal

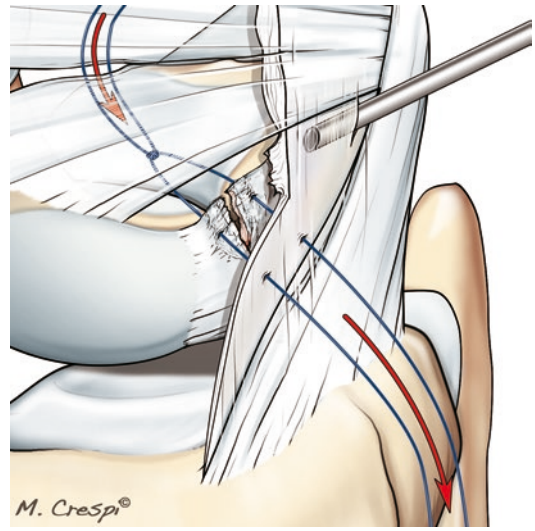

Fig. 75.6 Traction placed on the proximal suture ends to bring the knot back into the joint

75.3.1.1 Tips and Tricks

- It may be difficult to visualize the dorsal portion of the SL from 6R portal, because the dorsal capsule is apposed against the ruptured ligament when the wrist is under traction; use triangulation and release the traction slightly if necessary, to accurately assess the torn area.
- Suturing is possible only with good-quality ligament stumps. If SLIL is completely avulsed instead of being torn, the technique is not possible.
- Refresh ligament and capsule stumps with extensive shaving especially in chronic cases to recreate good conditions for tissues healing.
- Care is taken not to enter the open part of the dorsal capsule while introducing the needles because the capsulodesis effect would be lost.
- While passing the first suture, if necessary, pull the skin medially, so that the needle enters in front of the SLIL (Fig. 75.8).
- The second knot is tied after releasing traction and extending the wrist.

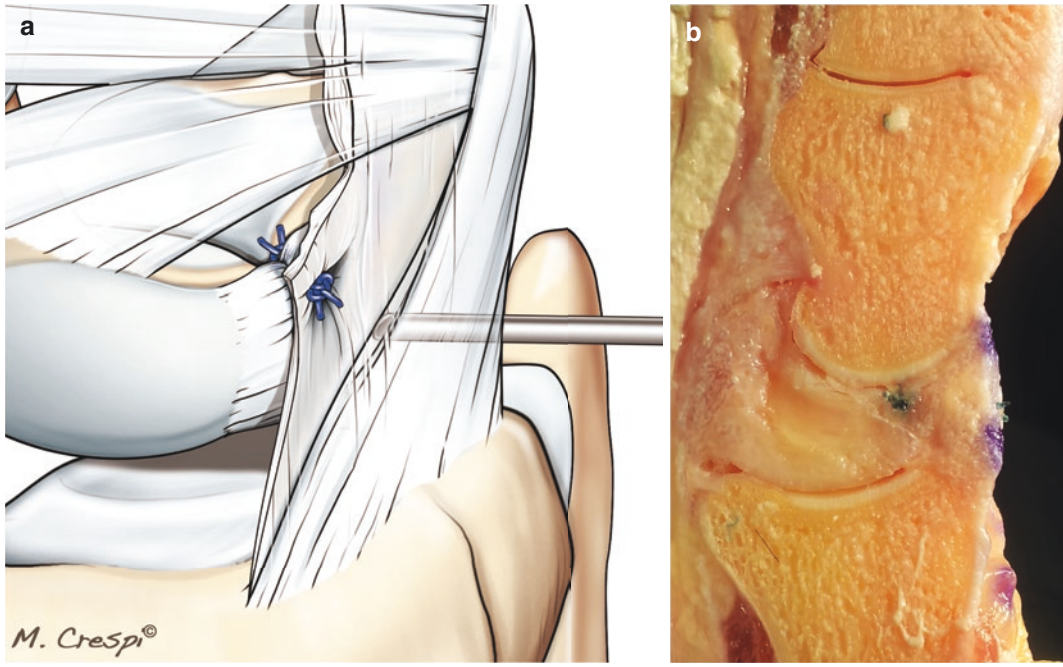

Fig. 75.7 (**a**) Drawing of the suturing between the SL and dorsal capsule with one intra-articular knot located in front of the dorsal portion of SLIL and one extra-articular subcutaneous dorsal knot located behind the dorsal capsule. (**b**) Section through a cadaver wrist showing the thickness of the repair after the ligament, and the dorsal capsule has been sutured

75.3.2 Modified Technique Using K-Wire Fixation

In cases of large dissociations, the scapholunate space must be reduced by an additional step of pinning the carpal bones. Two scapholunate parallel K-wires are passed with intraoperative fluoroscopic control and a scapho-capitate fixation may also be performed if needed. This reduction is performed before tying the second knot.

- First, a blunt trocar is inserted through the MCR portal, positioned under the capitate and beyond the anterior edge of the proximal pole of the scaphoid. The scaphoid is reduced onto the lunate, using a lever action—tire iron-like maneuver (Fig. 75.9).
- The K-wires are then introduced, while this reduced position is maintained. After the blunt trocar is removed, the scaphoid shifts back to its initial position and pulls the lunate back up (Fig. 75.10).

75.3.2.1 Tips and Tricks

- Pinning is difficult because of the small size of carpal bones; use both fluoroscopic and arthroscopic guidance to control K-wires adequate location.

75.3.3 Modified Technique in Large SL Tears with Instability: Extra-articular Distal and Proximal Capsular Repair Technique

A simple modification of the technique may be used when the scapholunate instability cannot be managed by a classic dorsal capsuloligamentous repair [11]. The basic concept here is to increase the capsulodesis effect on the scapholunate space stabilization; the aim is to catch a large part of the capsule, proximally and distally, in order to constrict it and reduce the SL joint while tying the knots.

Fig. 75.8 Intraoperative view of a technical trick: by pulling on the skin on the medial side of the wrist, the 3-4 portal is shifted medially so that it lies over the SLIL

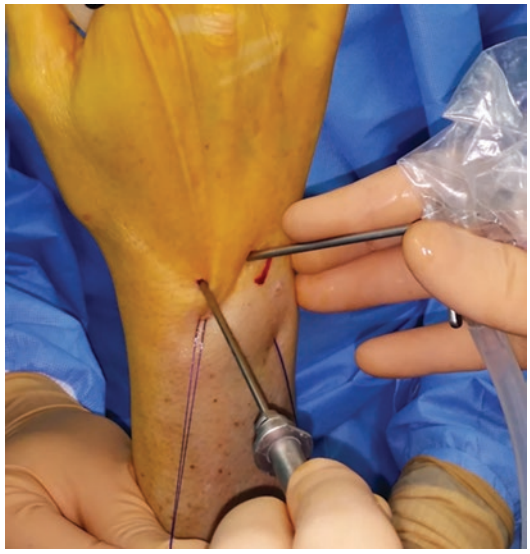

Fig. 75.9 Intraoperative view of significant scapholunate dissociation being reduced with a blunt trocar guide placed between the capitate and scaphoid, and then moved proximally using a "tire iron" leverage principle

- Proximally, the needles are inserted through two different points of the capsule, approximately 1 cm apart, in two divergent directions. The 3-4 portal must be extended if necessary

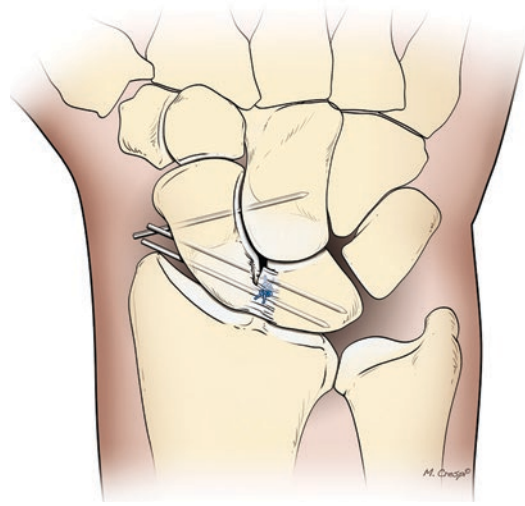

Fig. 75.10 Two K-wires are inserted through the scaphoid and lunate and one through the scaphoid and capitate

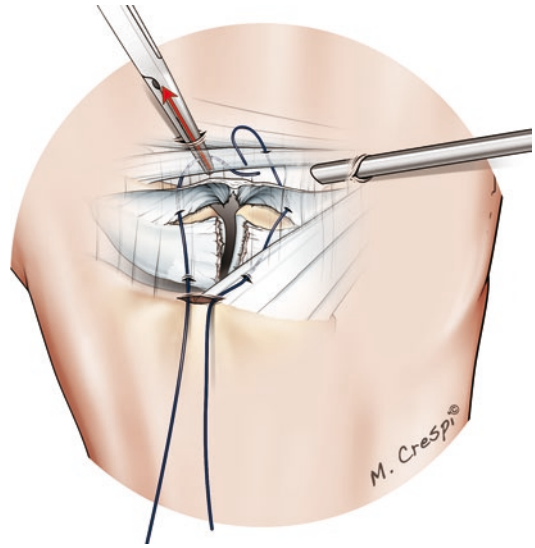

Fig. 75.11 Modified technique in large SL tears with instability is illustrated

to protect the extensor tendons. Distally, the MCR portal is also extended and two different entry points are created in the capsule; this helps to pass the hemostat and retrieve the sutures outside the midcarpal joint and then tie the first extracapsular knot (Fig. 75.11). The second knot, while maintaining the proximal–distal tension on the sutures, enables an effective and strong constriction of the dorsal

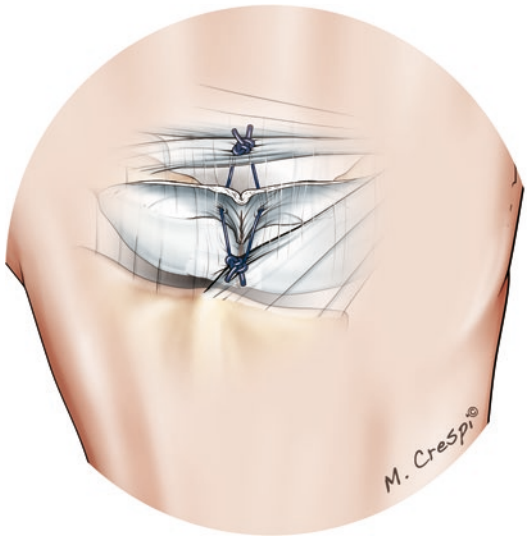

Fig. 75.12 Final knot with a constriction of dorsal capsule reduces the scapholunate dissociation

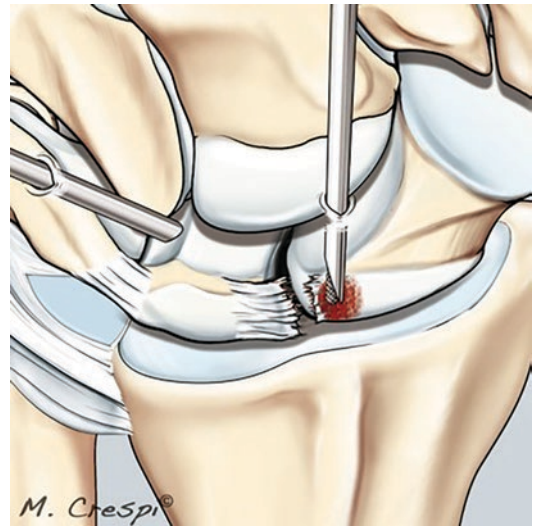

Fig. 75.13 Debridement of avulsion area of dorsal scapholunate ligament attachment on dorsal proximal pole of scaphoid

capsule, and provides the SL space reduction without using K-wires (Fig. 75.12).

75.3.3.1 Tips and Tricks

- The sutures are parallel in the classic technique. In this modification, the needles are inserted in two divergent directions to catch as much dorsal capsule as possible.

75.3.4 Modified Technique Using Anchors

In severe cases, if the ligament stump is sparse or completely absent on the scaphoid side ("bald scaphoid"), the classic technique described previously cannot be performed.

In such situations, an anchor is used as described:

- A suture–anchor is inserted through the 3-4 radiocarpal portal in the proximal pole of the scaphoid on its dorsal and distal part (Figs. 75.13 and 75.14).
- One suture from the anchor is introduced in a needle and the needle is then passed through the dorsal capsule and properly oriented to reach the midcarpal joint. A monofilament suture is passed to catch the ligament stump still attached on the lunate side, as described in the classic technique.
- The scope is introduced in the MCU portal to guide the location of the needles. The first anchor suture and the monofilament are externalized through the MCR portal. Outside the joint, the end of the anchor suture is passed through the monofilament suture loop. A slight proximal traction is applied on both ends of the monofilament suture so that the anchor suture passes through the lunate ligament remnant and exits the 3-4 portal. Finally, both anchor sutures are tied proximally, in a subcutaneous location (Figs. 75.15, 75.16, and 75.17).

75.4 Postoperative Management and Rehabilitation

The wrist is immobilized in a custom splint in extension (45°–60°) for 6 weeks after suture repair and for 8 weeks if additional K-wires stabilization is performed. The K-wires are removed at the 8 postoperative weeks. Physiotherapy is started after the immobilization period. Grip strengthening should be focused on propriocep-

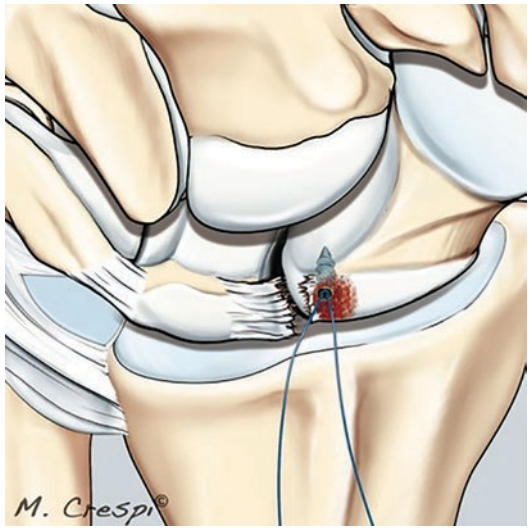

Fig. 75.14 Insertion of an anchor into the dorsal distal part of the proximal pole of the scaphoid is illustrated

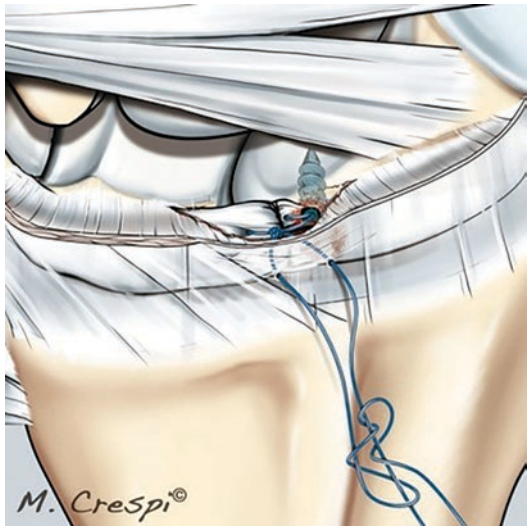

Fig. 75.15 A knot is tied on the suture strands from the anchor

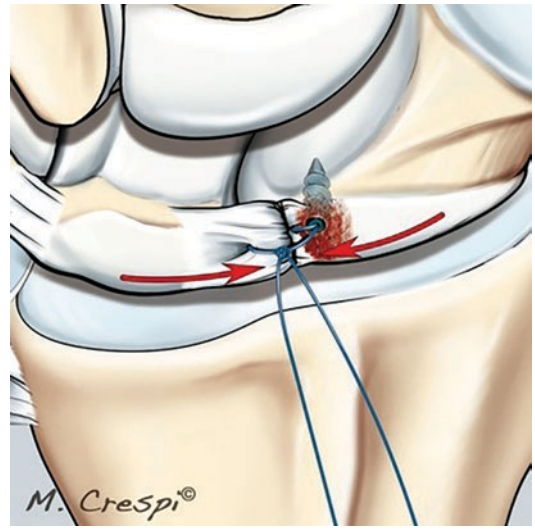

Fig. 75.16 Capsule constriction and the reduction after knot-tying are shown

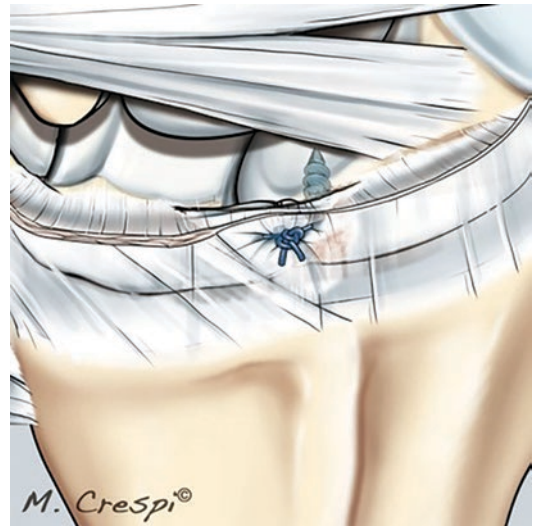

Fig. 75.17 Drawing of the final proximal knot between the anchor's sutures

tion. Stretching exercises should be avoided early in the rehabilitation period.

References

1. White NJ, Rollick NC. Injuries of the scapholunate interosseous ligament: an update. J Am Acad Orthop Surg. 2015;23(11):691–703. https://doi.org/10.5435/JAAOS-D-14-00254.
2. Watson HK, Weinzweig J, Zeppieri J. The natural progression of scaphoid instability. Hand Clin. 1997;13(1):39–49.
3. Shahabpour M, Staelens B, Van Overstraeten L, et al. Advanced imaging of the scapholunate ligamentous complex. Skelet Radiol. 2015;44(12):1709–25. https://doi.org/10.1007/s00256-015-2182-9.
4. Rosenwasser MP, Miyasajsa KC, Strauch RJ. The RASL procedure: reduction and association of the scaphoid and lunate using the Herbert screw. Tech Hand Up Extrem Surg. 1997;1:263–72.
5. Cognet JM, Levadoux M, Martinache X. The use of screws in the treatment of scapholunate instability. J Hand Surg Eur. 2011;36:690–3.
6. Cuénod P. Osteoligamentoplasty and limited dorsal capsulodesis for chronic scapholunate dissociation. Ann Chir Main Memb Super. 1999;18:38–53.
7. Mathoulin CL. Indications, techniques, and outcomes of arthroscopic repair of scapholunate ligament and triangular fibrocartilage complex. J Hand Surg Eur Vol. 2017;42(6):551–66. https://doi.org/10.1177/1753193417708980.
8. Mathoulin CL. From scapholunate interosseous ligament to scapholunate ligament complex. J Wrist Surg. 2013;2(2):98. https://doi.org/10.1055/s-0033-1341961.
9. Overstraeten LV, Camus EJ, Wahegaonkar A, et al. Anatomical Description of the Dorsal Capsulo-Scapholunate Septum (DCSS)-arthroscopic staging of scapholunate instability after DCSS sectioning. J Wrist Surg. 2013;2(2):149–54. https://doi.org/10.1055/s-0033-1338256.
10. Branco JL. The scapholunate ligament complex. J Wrist Surg. 2013;2(3):282. https://doi.org/10.1055/s-0033-1353532.
11. Haerle M, Mathoulin C. Arthroscopic scapholunate repair. FESSH IFSSH 2019 Instructional Book. p. 227–32.
12. Wahegaonkar AL, Mathoulin CL. Arthroscopic dorsal capsulo-ligamentous repair in the treatment of chronic scapho-lunate ligament tears. J Wrist Surg. 2013;2(2):141–8. https://doi.org/10.1055/s-0033-1341582.
13. Mathoulin C, Gras M. Role of wrist arthroscopy in scapholunate dissociation. Orthop Traumatol Surg Res. 2020;106(1S):S89–99. https://doi.org/10.1016/j.otsr.2019.07.008.
14. Bonte F, Mathoulin CL. The PARC lesion: a proximal avulsion of the radiocarpal capsule. J Wrist Surg. 2017;6(1):80–6. https://doi.org/10.1055/s-0036-1584162.
15. Del Piñal F. Arthroscopic volar capsuloligamentous repair. J Wrist Surg. 2013;2(2):126–8. https://doi.org/10.1055/s-0033-1343016.
16. Corella F, Del Cerro M, Ocampos M, Larrainzar-Garijo R. The "rocking chair sign" for floating lunate. J Hand Surg Am. 2015;40(11):2318–9. https://doi.org/10.1016/j.jhsa.2015.08.022.

Modified Brunelli Technique for Scapholunate Reconstruction

76

Gregory Hoy and Gayan Padmasekera

76.1 Background

Scapholunate reconstructions aim for correction of scapholunate gap, scapholunate angle and DISI deformity. Strength results from most reconstructions are below acceptable for return to professional contact sport. This chapter presents a modification of the Brunelli reconstruction to stabilize the dorsal midcarpal joint in addition to scapholunate reconstruction. The resultant strength results make this an attractive option to add to a modified Brunelli reconstruction.

76.2 Surgical Anatomy

The scapholunte ligament consists of three main components: dorsal, membranous and volar. The dorsal portion is the strongest and is most important in limiting dorsal–volar translation. The membranous portion is the weakest. In the intact wrist, the lunate flexes with the scaphoid and extends with the triquetrum. Disruption of the scapholunate ligament leads to an uncoupling of this relationship, resulting in lunate extension and the scaphoid flexes and rotates away from the lunate (dorsal intercalated segment instability pattern or DISI). The DISI deformity can be static or dynamic in scapholunate ligament injuries. Static DISI deformity is commonly seen in complete scapholunate ligament injuries. However, in partial tears, DISI deformity may only be unmasked with loading. Stress radiographs or arthroscopy can be utilized to reveal dynamic instability. Left untreated, the natural history of this injury is progression to wrist arthrosis in a specific pattern, known as scapholunate advanced collapse (SLAC).

76.2.1 Indications and Contraindications

Indications for a scapholunate ligament reconstruction include:

- Complete or high-grade partial rupture of scapholunate ligament leading to a DISI deformity
- Chronic ligament injuries (>3 weeks)

Contraindications include the presence of SLAC arthrosis on pre-operative imaging studies or on wrist arthroscopy.

G. Hoy (✉) · G. Padmasekera
Melbourne Orthopaedic Group,
Melbourne, VIC, Australia

Department of Surgery, Monash University,
Melbourne, VIC, Australia
e-mail: gahoy@mog.com.au;
gayan@seorthopaedics.com.au

© ISAKOS 2022

D. N. Bhatia et al. (eds.), *Arthroscopy and Endoscopy of the Elbow, Wrist and Hand*,
https://doi.org/10.1007/978-3-030-79423-1_76

76.3 Surgical Technique

The patient is positioned supine and the upper extremity is supported on a radiolucent hand table. A non-sterile tourniquet is placed in the upper arm and inflated to 250 mmHg after exsanguination.

The surgical technique involves a combined approach via a dorsal approach to the wrist and a small volar incision and forearm stab wound for tendon harvesting.

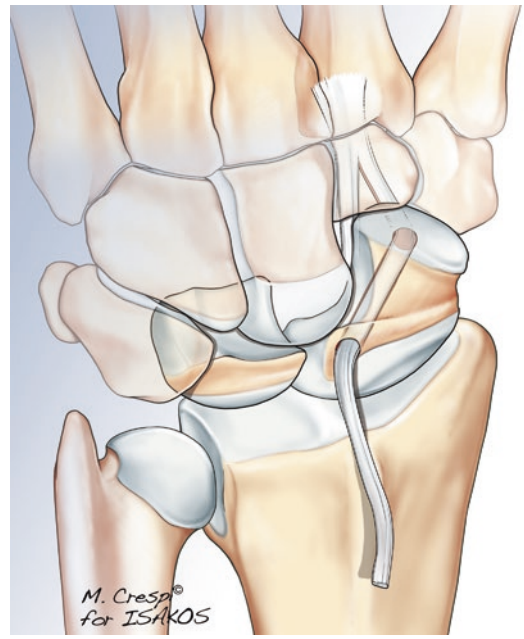

Fig. 76.1 Graft passage from volar to dorsal is illustrated (M. Crespi © for ISAKOS)

- An 8–10 cm dorsal longitudinal incision is performed centred on Lister's tubercle. The subcutaneous tissue is dissected directly onto the extensor retinaculum. Full-thickness radial and ulna skin flaps are developed along the extensor retinaculum, ensuring to protect the sensory branches. The extensor retinaculum is divided along the third extensor compartment and the extensor pollicis tendon is retracted radially with a self-retaining retractor (Weitlaner).
- A dorsal ligament-splitting capsulotomy is performed, creating a radially based capsular flap by incising the dorsal capsular fibres along the dorsal radiotriquetral and dorsal intercarpal ligaments. This provides exposure to the dorsal carpus; the joint is now evaluated to examine the scapholunate ligament remnant and to assess the presence of arthrosis.
- Attention is focused on the volar side. At the level of the distal pole of the scaphoid, a small transverse palmar incision is made along the course of the flexor carpi radialis (FCR) tendon. FCR tendon is identified distally and another small stab incision is made proximally to allow for a 12–15 cm tendon harvest. One-third volume distally based harvest of the FCR tendon is then performed. The tendon is then sized and prepared.
- A guidewire-controlled drill hole is created through the scaphoid from volar tuberosity to the dorsal scapholunate ligament origin site. The graft is passed volar to dorsal using a wire retriever (Fig. 76.1). A burr is used to recess the graft in the dorsal scaphoid and lunate.
- The carpal malalignment is corrected using a translation manoeuvre of the wrist which produces the concurrent effects of correcting the DISI with lunate rotation, translating the scaphoid volarwards and away from the articular surface of the dorsal rim of the scaphoid fossa of the radius additionally, the scapholunate gap closed with a bone reduction forcep (Fig. 76.2).
- Two 1.6 mm K-wires are used to obtain immobilization of this reduction (scaphoid to lunate) and the carpal alignment is confirmed with the image intensifier. The tendon is tensioned and attached to the lunate if performed with a double-loaded bone anchor (Fig. 76.3).
- The third limb of the reconstruction is to the distal half of the capitate with a second dorsal anchor.
- The K wires are buried. Lavage and closure are performed in layers, and absorbable 3/0 monocryl suture is used for skin closure.

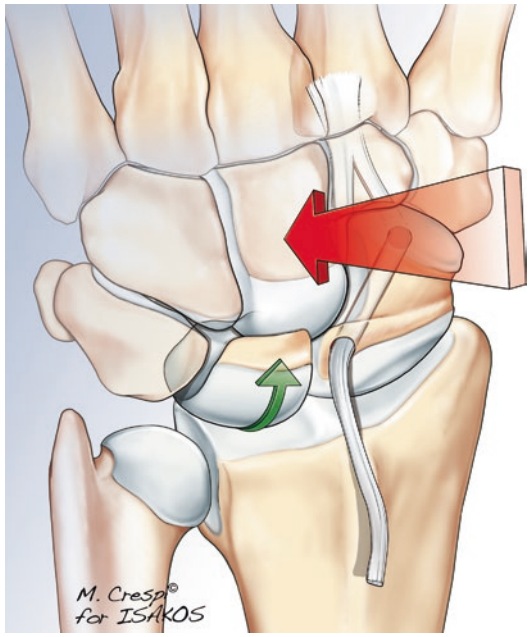

Fig. 76.2 Reduction manoeuvre for scapholunate reconstruction is shown (M. Crespi © for ISAKOS)

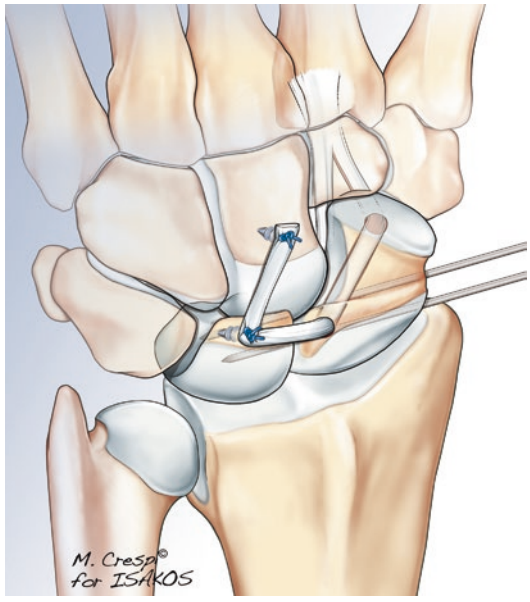

Fig. 76.3 Graft is attached to lunate and capitate using bone anchors. The malalignment is corrected using K-wires prior to graft attachment (M. Crespi © for ISAKOS)

76.4 Tips and Tricks

- Reducing the wrist by the above-mentioned volar translational manoeuvre and not by joystick wires is the critical step. This achieves mild over-correction of the scapholunate angle as well as volar translation of the scaphoid leaving a small gap between the dorsal lip of the scaphoid proximal pole and the dorsal lip of the radial styloid process. This point is where the earliest cartilage loss occurs and this step removes impaction stress on this cartilage.
- Using joystick wires to correct the malalignment does not usually result in the mild volar translation of the scaphoid and contact between the dorsal scaphoid and the dorsal radial styloid can still occur.
- Attaching the graft to the capitate allows for a more anatomic construct and better range of motion as it does not violate the radiocarpal junction.

76.5 Pitfalls

- The tenodesis should not be performed if there is arthrosis of the periscaphoid joints.
- Avoid excessive tension of the tendon graft, as this can restrict motion, or may even lead to necrosis of the graft.
- Malalignment must be corrected prior to graft fixation (Fig. 76.4).

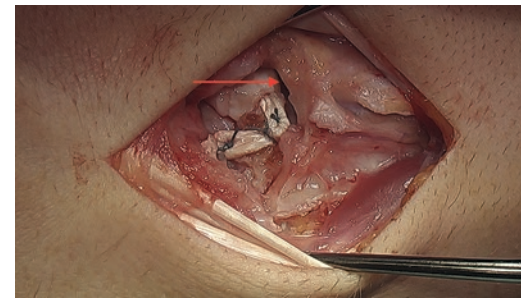

Fig. 76.4 Final view of graft fixation to lunate and capitate. (arrow: dorsal radial rim) (© G. Hoy)

76.6 Post-operative Management and Rehabilitation

The wires are buried and patients are immobilized with a well-padded below-elbow plaster splint for 2 weeks. After wound review, a full below elbow cast is utilized for the remainder of the first 6 weeks. Wires are removed at 6 weeks and a thermoplastic splint is worn for protection. Mobilization, isometric strengthening and proprioceptive exercises are initiated at this time. Resumption of full-contact training begins at 3 months.

76.7 Complications

Recurrence of deformity and arthrosis is common in cases with residual malalignment. If the carpus is not reducible, then salvage options such as partial fusion or proximal row carpectomy are preferred.

76.8 Results

The author's series over a 7-year period include 12 male senior list AFL players with an average follow-up of 49 months (24–83) after this procedure for symptomatic static high-grade scapholunate instability (Watson Grades 3A, 3B, early 4). Notably, some had early erosions of the proximal scaphoid articulation already. The procedures were performed by a single surgeon at an average of 5 months after initial injury, during the off season, allowing players to return during the next season. All players except two returned to senior football (with two other players retiring to commence professional coaching at the same level). The average grip strength after this time was 99%, with a Disability of the Arm, Shoulder and Hand (DASH) score of 3.4, Mayo score of 83.1, Patient Rated Wrist Evaluation (PRWE) of 8.6 and VAS pain score at follow up of 0.8. At follow-up, none of the players demonstrated any symptoms or signs of degenerative disease.

Arthroscopic Ligamentoplasty for Scapholunate Instability

77

F. Corella, M. Ocampos, and R. Larrainzar Garijo

77.1 Introduction

Scapholunate (SL) instability is the most common form of carpal instability. Patients usually have dorsal wrist pain, decreased grip strength, and impaired wrist function. An untreated SL instability can result in a predictable sequence of degenerative changes in the wrist [1].

Arthroscopy-assisted ligamentoplasty for carpal instability has been recently described as a substitute for classic open procedures [1–3]. By using an arthroscopic technique, postoperative fibrosis, scarring, and stiffness are minimized; moreover, by avoiding dorsal capsulotomy, the posterior interosseous nerve (PIN) is preserved, as well as proprioception and correct function of the dynamic stabilizers of the wrist.

Since 2011 we have been working on an arthroscopic technique that serves the threefold purpose of anatomical reconstruction, avoidance of open surgery and detachment of the joint capsule, and a reliable and sturdy reconstruction for early mobilization. In 2011, we described the anatomical study and the technique for the reconstruction of the dorsal portion of the SL ligament [4]. In 2013, we published a modification with an additional volar portion of SL reconstruction [1]. And finally, in 2017, we published all the technical detail and the clinical results of the first 27 patients [5].

77.2 Surgical Anatomy

This arthroscopic technique needs the performance of the dorsal radiocarpal portals (3-4 and 6R) and dorsal midcarpal portals (radial and ulnar). However, apart from them, few incisions are used, as the graft needs to pass through bones and close to important structures (Figs. 77.1, 77.2, and 77.3). On the dorsal side, one 1.5-cm longitudinal incision is made overlying the fourth extensor tendon compartment and the lunate. This incision is called the dorsal central (DC) incision. On the volar side, three more incisions are needed. The first one is the same incision and

F. Corella (✉)
Orthopedic and Trauma Department, Hospital Universitario Infanta Leonor, Madrid, Spain

Hand Surgery Unit, Hospital Universitario Quironsalud Madrid, Madrid, Spain

Surgery Department, School of Medicine, Universidad Complutense de Madrid, Madrid, Spain

M. Ocampos
Orthopedic and Trauma Department, Hospital Universitario Infanta Leonor, Madrid, Spain

Hand Surgery Unit, Hospital Universitario Quironsalud Madrid, Madrid, Spain

R. L. Garijo
Orthopedic and Trauma Department, Hospital Universitario Infanta Leonor, Madrid, Spain

Surgery Department, School of Medicine, Universidad Complutense de Madrid, Madrid, Spain

© ISAKOS 2022

D. N. Bhatia et al. (eds.), *Arthroscopy and Endoscopy of the Elbow, Wrist and Hand*,
https://doi.org/10.1007/978-3-030-79423-1_77

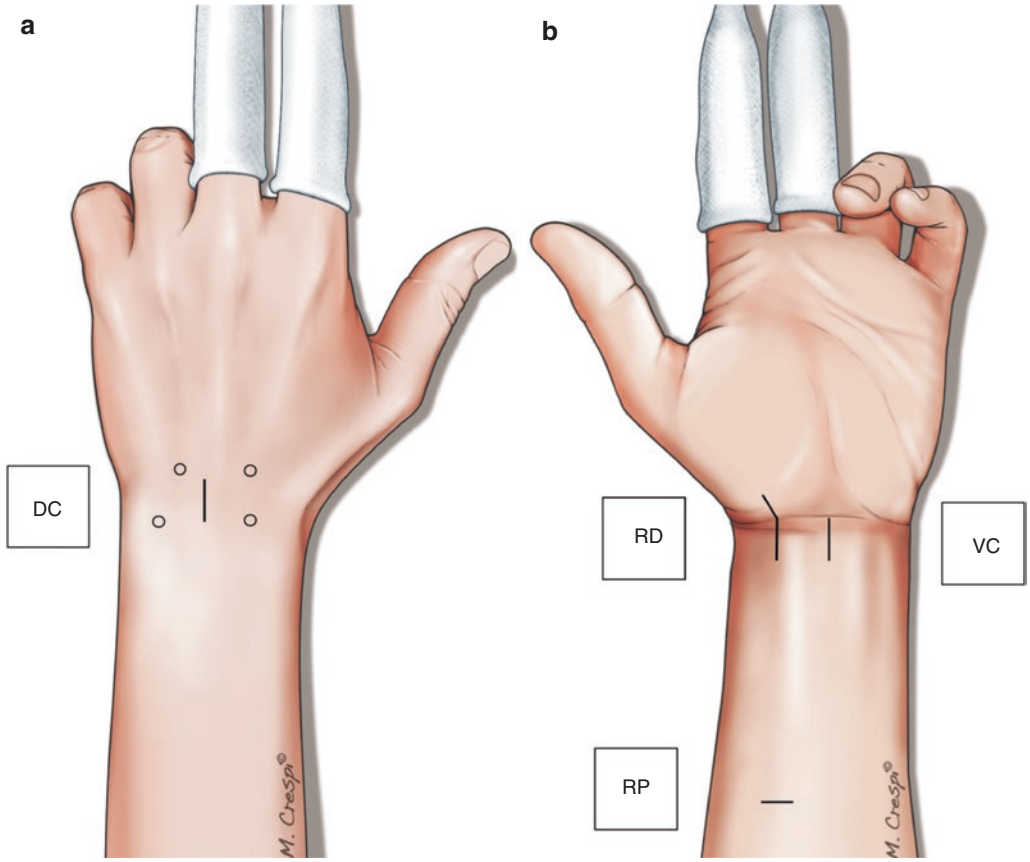

Fig. 77.1 Portalsand incisions needed for the technique. (**a**) Dorsal side. Radiocarpal and midcarpal portals and a dorsal central (DC) incision, a 1.5-cm longitudinal incision over the fourth extensor compartment, and centered over the lunate. (**b**) Volar side. Two radial incisions are needed to retrieve a tendon graft. One radial distal (RD) incision overlies the FCR and scaphoid and the other radial proximal (RP) incision is placed 10-cm proximally over the FCR tendon (© M. Crespi for Corella). Reprinted from Corella F, Del Cerro M, Ocampos M, Simon de Blas C, Larrainzar-Garijo R. Arthroscopic scapholunate ligament reconstruction, volar and dorsal reconstruction. Hand Clin. 2017 with permission from Elsevier

approach used for the volar central portal [6]. The second and third incisions are radial and are used to retrieve the tendon graft. One is overlying the flexor carpi radialis (FCR) tendon and scaphoid (RD), another one is 10-cm proximally over the FCR tendon (RP).

77.3 Indications and Contraindications

77.3.1 Indication

Patients who have all the following three criteria are suitable candidates for arthroscopic SL reconstruction (Fig. 77.4).

- Complete SL ligament tear, that is, European Wrist Arthroscopy Society classification grade IIIC, IV, or V SL lesions [7] and with a Positive arthroscopic 3D (dorsal, dynamic, displacement) test [8].
- Very easily reducible instability. The scaphoid should be easily reduced and positioned by pushing with an arthroscopic probe.
- Presence of clinical symptoms, that is, pain, decreases in the grip strength, and/or impairment of wrist function.

77.3.2 Contraindication

Patients who have the following conditions are contraindications for the surgery.

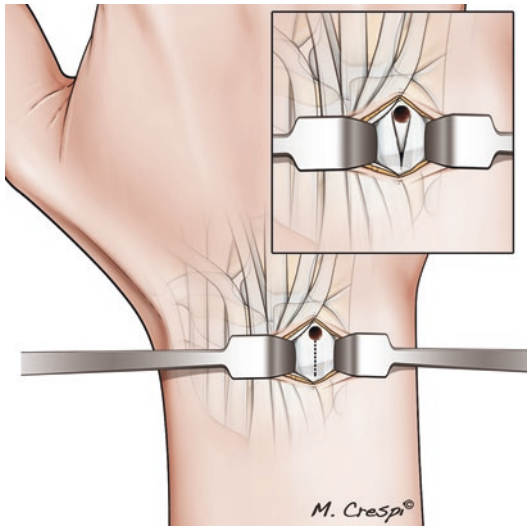

Fig. 77.2 A 1.5-cm, dorsal central longitudinal incision is made over the fourth extensor compartment and directly over the lunate bone. The extensor retinaculum is opened longitudinally, and the extensor tendons are retracted towards the radial side. The lunate tunnel is created through this incision. The entrance of the lunate tunnel is united with the radiocarpal joint, to ensure that the graft will pass smoothly through the capsule and the joint into the bone tunnel (© M. Crespi for Corella). Reprinted from Corella F, Del Cerro M, Ocampos M, Simon de Blas C, Larrainzar-Garijo R. Arthroscopic scapholunate ligament reconstruction, volar and dorsal reconstruction. Hand Clin. 2017 with permission from Elsevier

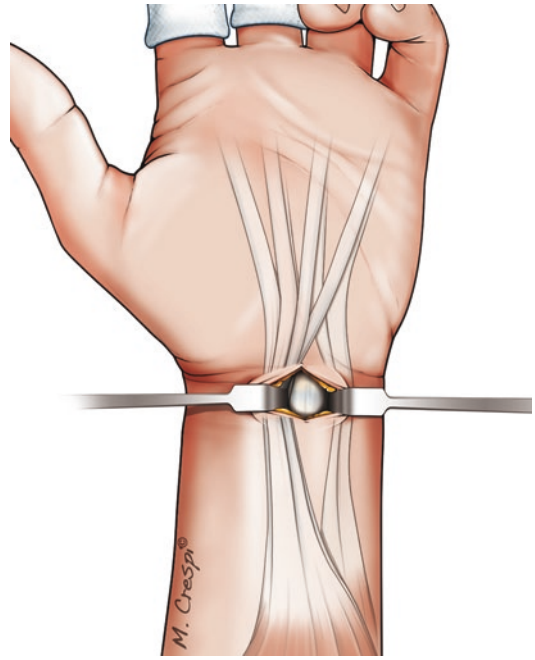

Fig. 77.3 The volar central portal is a 1.5-cm longitudinal incision centered over the lunate bone, between the distal and proximal wrist creases. In this approach, all flexor superficialis tendons are retracted toward the radial side with the second and third flexor profundus tendons, while the fourth and fifth flexor profundus tendons are retracted toward the ulnar side (© M. Crespi for Corella). Reprinted from Corella F, Del Cerro M, Ocampos M, Simon de Blas C, Larrainzar-Garijo R. Arthroscopic scapholunate ligament reconstruction, volar and dorsal reconstruction. Hand Clin. 2017 with permission from Elsevier

- Instability not easily reducible: In static instability with a significant gap another technique should be used.
- Presence of degenerative lesions, especially chondral lesions in the dorsal scaphoid fossa (Scaphoid Lunate Advanced Collapse or SLAC). These lesions are difficult to be diagnosed with MRI or X-rays. Their presence should always be verified with arthroscopy.
- Presence of associated ligament injuries, especially lunotriquetral (LT) injury. Combined SL and LT lesions make the lunate bone floating which can be identified by "rocking chair sign" [9].

77.4 Surgical Technique

The operation is performed under regional anesthesia (axillary block) or general anesthesia with a pneumatic tourniquet placed at the upper arm closest to the armpit. The patient is placed supine with the affected arm on a hand table. The wrist is maintained in vertical traction during the whole procedure. The traction tower commonly used is Arc Wrist Tower® (Acumed, Hillsboro, OR), which maintains a vertical traction and leaves the volar side of the wrist free. The C-arm is parallel to the floor from the volar side of the wrist. With the suspended hand in pronation or supination, PA or lateral view is easily obtained.

The resistance and fixation strength of the graft can be increased with the use of a 1.3-mm SutureTape® (Arthrex, Naples, FL, USA). In every step, the tape passes along with the graft through the tunnels and is also fixed with Bio-Tenodesis™ (Arthrex) screws. However, the technique can be performed without the tape, using only a graft.

77.4.1 Step 1: Bone Tunnels

The final tunnel size should be 3-mm wide; however, at this step, the three tunnels should be created with a 2.5-mm cannulated drill bit.

77.4.1.1 Scaphoid Tunnel

The tunnel in the scaphoid is made through the 3/4 portal and is placed from the insertion of the dorsal portion of the SL to the scaphoid tubercle (Fig. 77.5).

- A 1.0-mm K-wire is used for the correct position of the tunnel. Because it is difficult to insert a small K-wire through the portal, a 14-G Abbocath is used as a guide for the K-wire. As the insertion point is not under the portal, the Abbocath should be inserted through the portal into the joint and then slid distally over the scaphoid until the insertion of the dorsal portion of the SL ligament is reached.

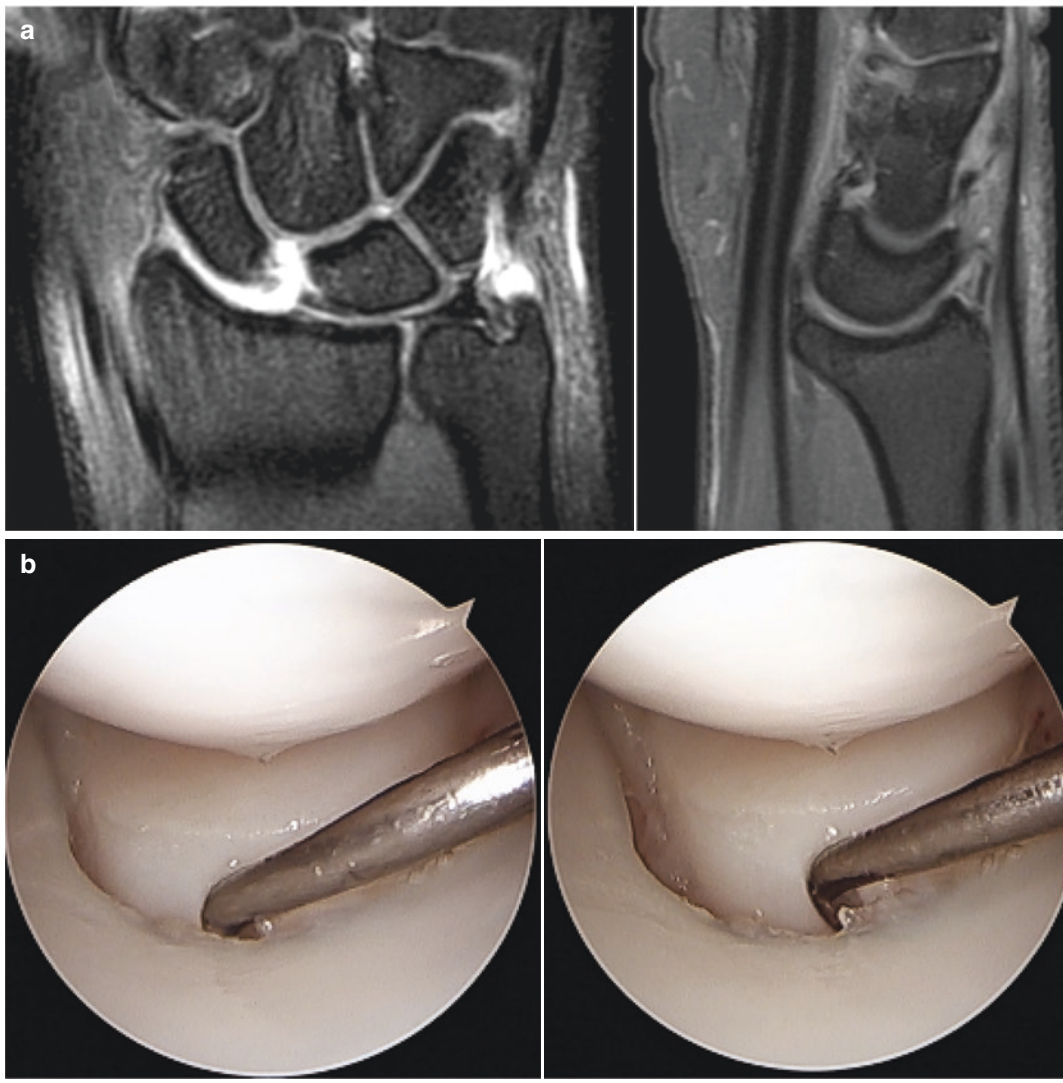

Fig. 77.4 (**a**) MRI showing a complete injury of the scapholunate ligament. (**b**) Complete SL ligament tear, there is a big gap between the bones. (**c**) Easily reducible instability. The scaphoid is easily reduced and positioned by pushing with the arthroscopic probe. (**d**) Positive arthroscopic 3D (dorsal, dynamic, displacement) test [8]

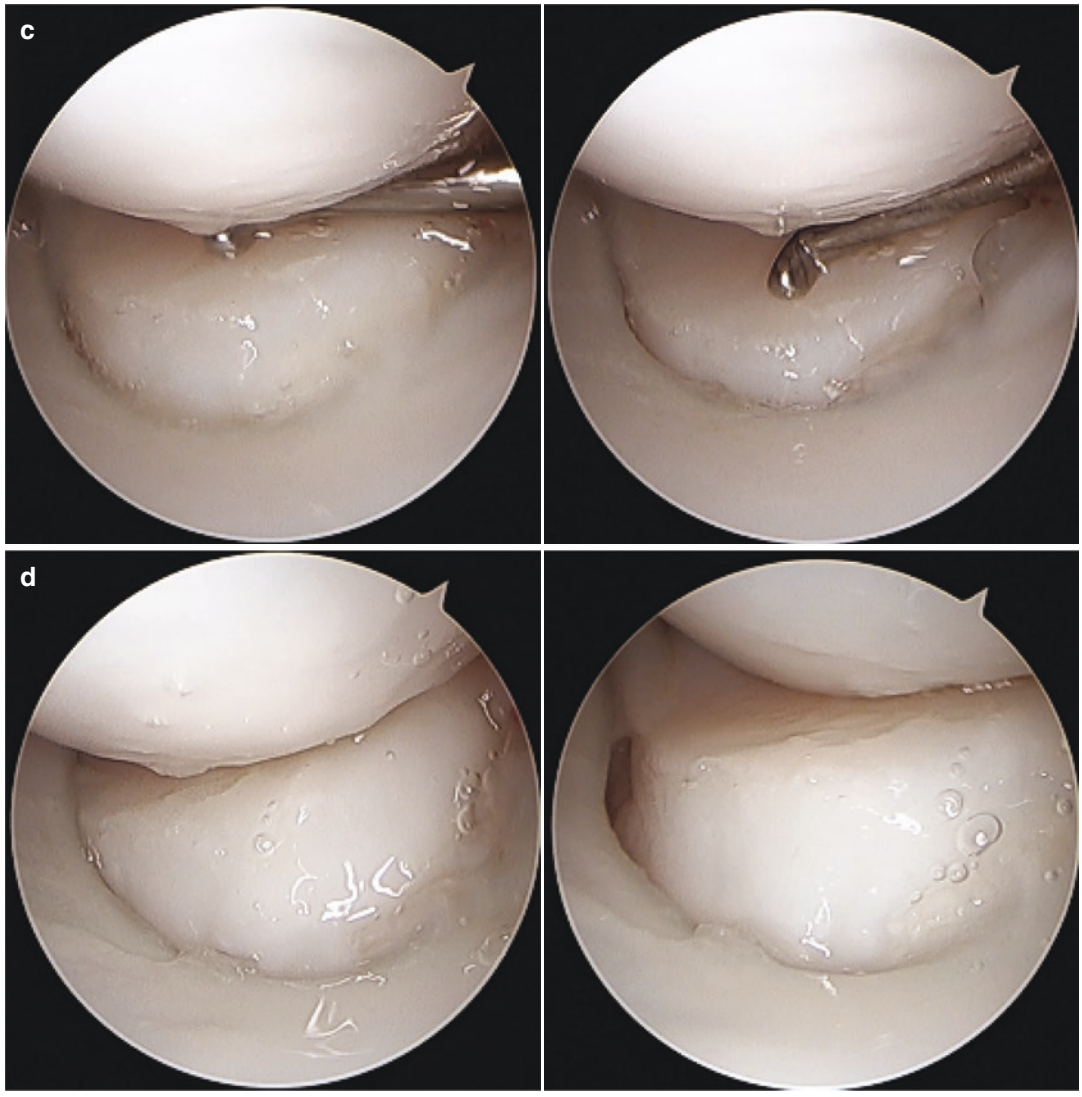

Fig. 77.4 (continued)

- When the direction is satisfactory in both the PA and lateral views, the K-wire is introduced by the second surgeon (Fig. 77.6a).
- After insertion of the K-wire, a 2.5-mm tunnel should be created using a cannulated drill bit. A drill guide should be used to avoid injury to the extensor tendons and superficial nerves (Fig. 77.6b).

77.4.1.2 Lunate Tunnel

The tunnel is centered in the lunate in the posteroanterior view and is parallel to its surface on the lateral view (Fig. 77.7).

- Through the DC incision, the extensor retinaculum is opened longitudinally and the tendons of the fourth compartment are retracted

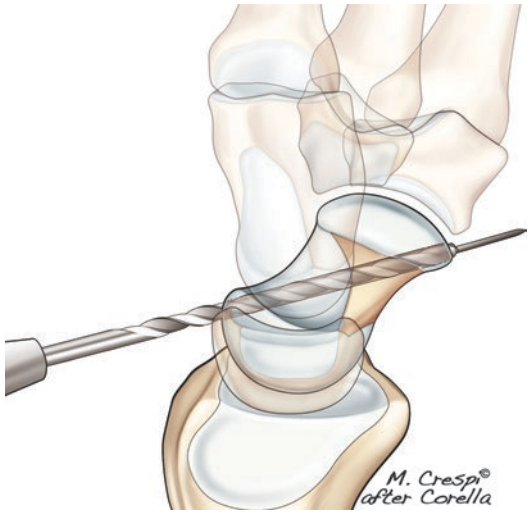

Fig. 77.5 The scaphoid tunnel is created from the insertion of the dorsal portion of the SL to the scaphoid tubercle (M. Crespi © for Corella)

toward the radial side, exposing the articular capsule.

- Once the capsule is exposed, the Abbocath is used again as a guide (Fig. 77.8). The 1.0-mm K-wire is placed in the correct position and once again, a 2.5-mm tunnel should be created (Fig. 77.9).

77.4.2 Step 2: Preparation for Recovering the Graft

The final position of the graft is intra-articular, between the dorsal portion of the bones and the capsule. A loop needs to be located in that position to later recover the graft (Fig. 77.10).

- The arthroscope is located in the 6R portal, looking at the dorsal and radial side of the wrist. Under arthroscopic control, a small incision is made in the capsule through the DC incision, uniting the entrance of the lunate tunnel with the radiocarpal joint (Fig. 77.2). This detail ensures that the graft will pass from inside the joint to the tunnel without wedging in the capsule (Fig. 77.11).
- Next, a Curved SutureLasso® (Arthrex) is introduced through this incision, with its loop retrieved from the 3/4 portal (Fig. 77.12).

77.4.3 Step 3: Harvesting the FCR Tendon Graft

The graft is a hemi-tendon, 3 mm in width and 8–10 cm in length of the radial side of the FCR. To ensure the radial side of the FCR to be obtained, the graft should be harvested from the distal to the proximal as the FCR fibers have a constant torsion by an average of 180° in the wrist and forearm level.

- At the RD incision, a 2O′ monofilament suture is passed through the FCR, capturing 3 mm of the radial side of the tendon.
- In the RP wound, the tendon sheath is opened and a Suture Passing Wire® (Arthrex, Naples, FL) is passed distally under the tendon sheath and retrieved in the RD incision.
- The threads of the 2O′ monofilament sutures are loaded to the Passing Wire and brought to the RP wound. By pulling the threads from the RP wound, the FCR is cut and the graft is obtained. The graft is cut at the proximal and retrieved in the RD incision (Fig. 77.13).
- The last action in this step is dissection of the graft distal to the scaphoid tunnel; otherwise, when tensioned from the dorsal direction, the graft will flex rather than extend the scaphoid. The superficial branch of the radial artery is normally found while dissecting the graft distally and should be dissected or coagulated.

77.4.4 Step 4: Graft Passage and Fixation

77.4.4.1 Scaphoid Passage and Fixation

The graft is fixed to the scaphoid tunnel while traction is applied from the dorsal direction; in this way, the scaphoid is extended (Fig. 77.14).

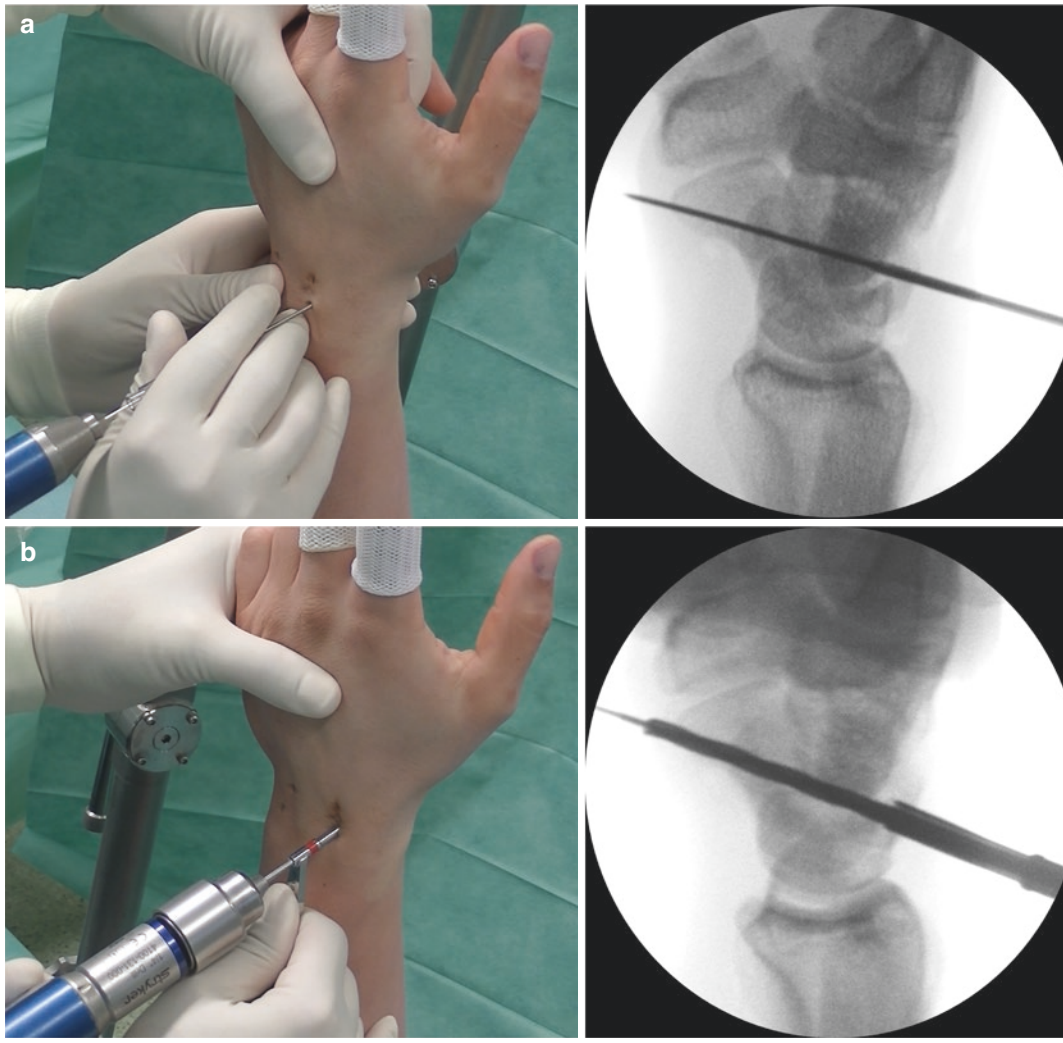

Fig. 77.6 Scaphoid tunnel. (**a**) A 14-G Abbocath needle is used as a guide through the 3/4 portal. A 1.0-mm K-wire is inserted through the Abbocath from the insertion of the dorsal portion of the SL to the scaphoid tubercle. (**b**) A cannulated drill bit is inserted through the 3/4 portal with the protection of a drill guide. Reprinted from Corella F, Del Cerro M, Ocampos M, Simon de Blas C, Larrainzar-Garijo R. Arthroscopic scapholunate ligament reconstruction, volar and dorsal reconstruction. Hand Clin. 2017 with permission from Elsevier

- To avoid catching of the graft by a fragment of capsule or soft tissue and facilitate passage through the bone, the tunnel should be drilled again to its final size of 3 mm. The K-wire is inserted from the dorsal to the volar direction and the tunnel is redrilled with a 3-mm cannulated drill bit. The surgeon should ensure that the graft is not trapped when the drill exits at the volar side.
- The graft and SutureTape® (Arthrex, Naples, FL, USA) are passed through the tunnels using a Straight SutureLasso® (Arthrex, Naples, FL, USA). The graft and tape are captured with the loop volarly and taken to the 3/4 portal (Fig. 77.15).
- The graft and tape are then fixed to the tunnel with a 3 × 8-mm Bio-Tenodesis screw® (Arthrex, Naples, FL) inserted from the volar side, while traction is applied from the dorsal side (Fig. 77.16). The interference screw is too small to be cannulated. Screw insertion can be difficult as the bone tunnel can be occluded by

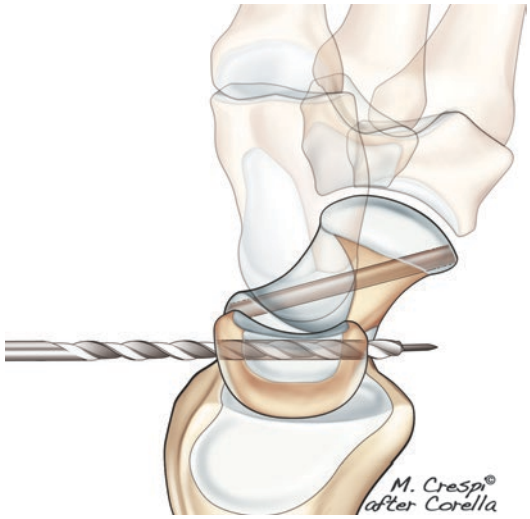

Fig. 77.7 The lunate tunnel is centered on the lunate and parallel to its articular surface (M. Crespi © for Corella)

the graft and the soft tissues. It should follow the graft entrance site and fluoroscopic guidance of its direction is important.

77.4.4.2 Lunate Passage and Fixation

The graft is then captured by the loop that was prepared before and shuttled to the DC incision over the lunate (Fig. 77.17). The graft is fixed to the lunate tunnel with a 3 × 8-mm Bio-Tenodesis screw® (Arthrex, Naples, FL) while traction is applied from the volar direction; in this way, the lunate is supinated, and the gap is closed (Fig. 77.18).

- The approach of the VC portal is performed [6]. The K-wire is inserted from the volar to the dorsal direction, with the sharp tip forwards. The tunnel is redrilled with a 3-mm

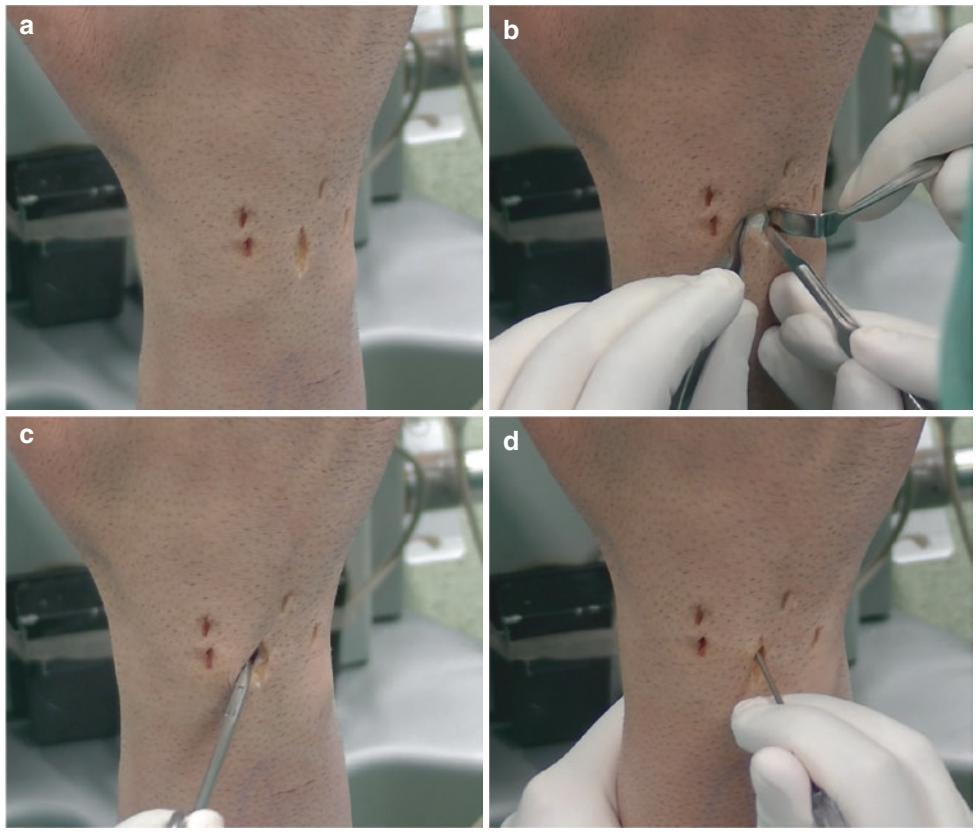

Fig. 77.8 (**a**) A 1.5-cm longitudinal incision (Dorso Central) is made over the fourth extensor compartment. This incision is directly over the lunate bone. (**b**, **c**) The extensor retinaculum is opened longitudinally, and the extensor tendons are retracted to the radial side. (**d**) A 14-G Abbocath needle is used as a guide through the DC incision. Reprinted from Corella F, Del Cerro M, Ocampos M, Simon de Blas C, Larrainzar-Garijo R. Arthroscopic scapholunate ligament reconstruction, volar and dorsal reconstruction. Hand Clin. 2017 with permission from Elsevier

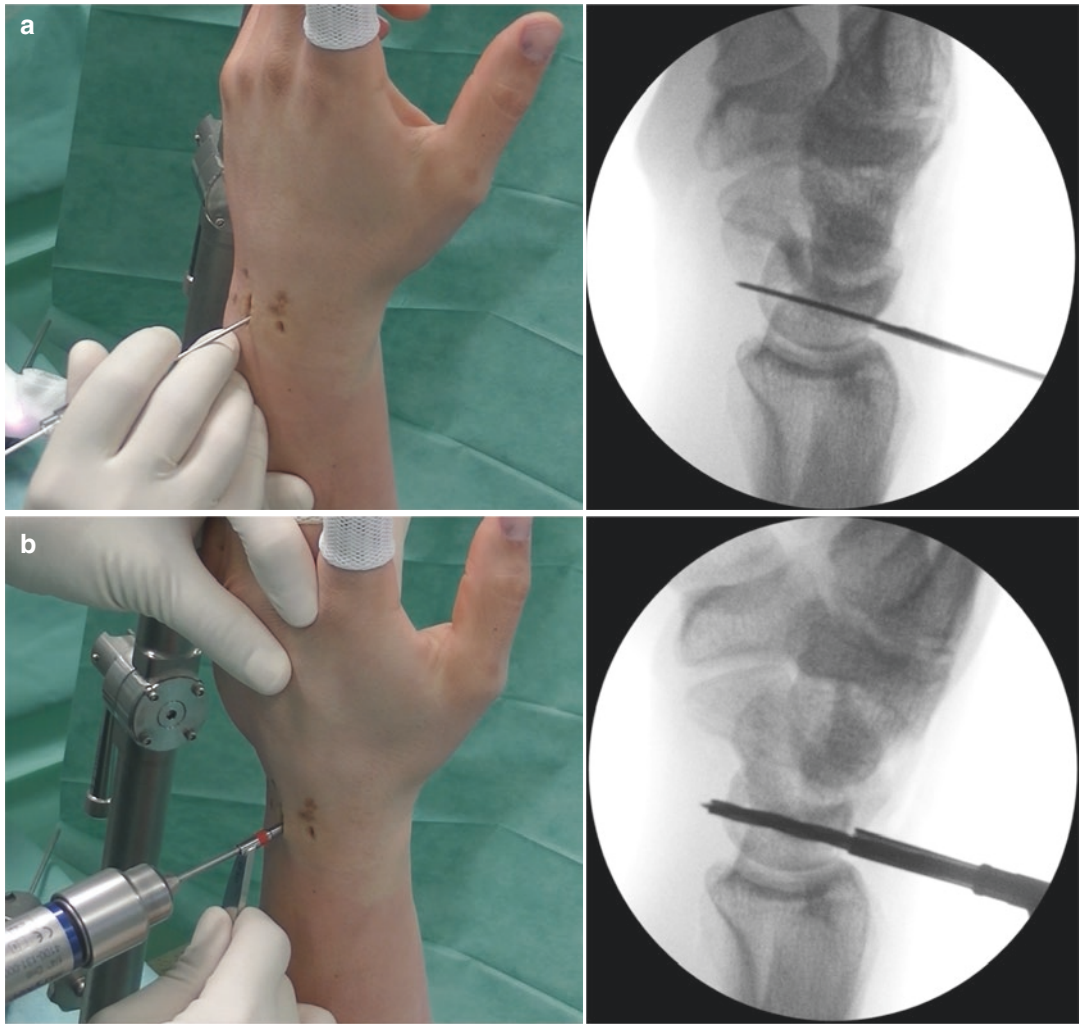

Fig. 77.9 Lunate tunnel. (**a**) A 14-G Abbocath needle is used as a guide through the dorsal central incision. A 1.0-mm K-wire is inserted through the Abbocath and should be at the center of the lunate in the posteroanterior view, and parallel to the distal lunate articular surface in the lateral view. (**b**) A cannulated drill bit is inserted through the dorsal central incision with the protection of a drill guide

cannulated drill bit. The surgeon should ensure that the graft is not trapped when the drill exits at the dorsal side.

- The SutureLasso is introduced to the tunnel following the K-wire and the graft and SutureTape are captured and brought to the VC portal (Fig. 77.19).
- The traction is released and the reduction of instability (SL step-off, SL gap, and dorsal extension of the lunate) is checked under arthroscopic control.
- The arthroscope is located in the ulnar midcarpal portal and traction is applied from the volar side (Fig. 77.20).
- Finally, while maintaining the tension from a volar direction, the bio-tenodesis screw is inserted into the lunate tunnel from a dorsal direction (Fig. 77.21).

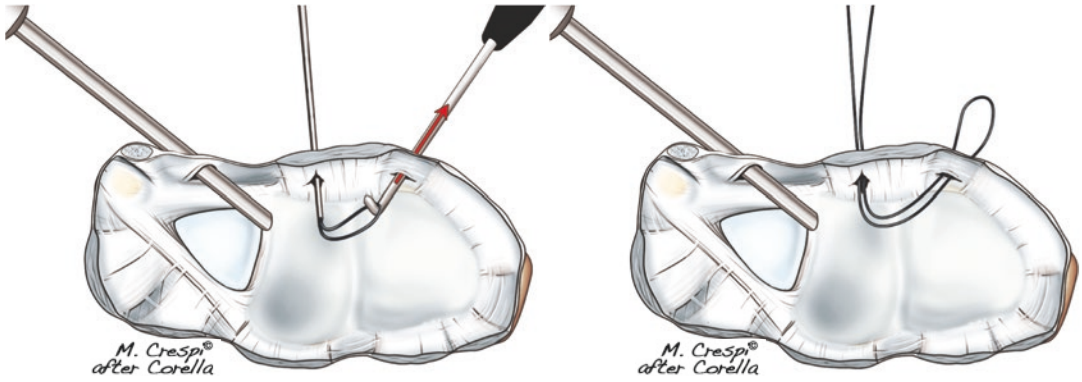

Fig. 77.10 A curved SutureLasso is introduced into the joint through the DC incision, and the loop is retrieved from the 3/4 portal. This way, the loop is positioned inside the joint, between the bones and capsule (M. Crespi © for Corella)

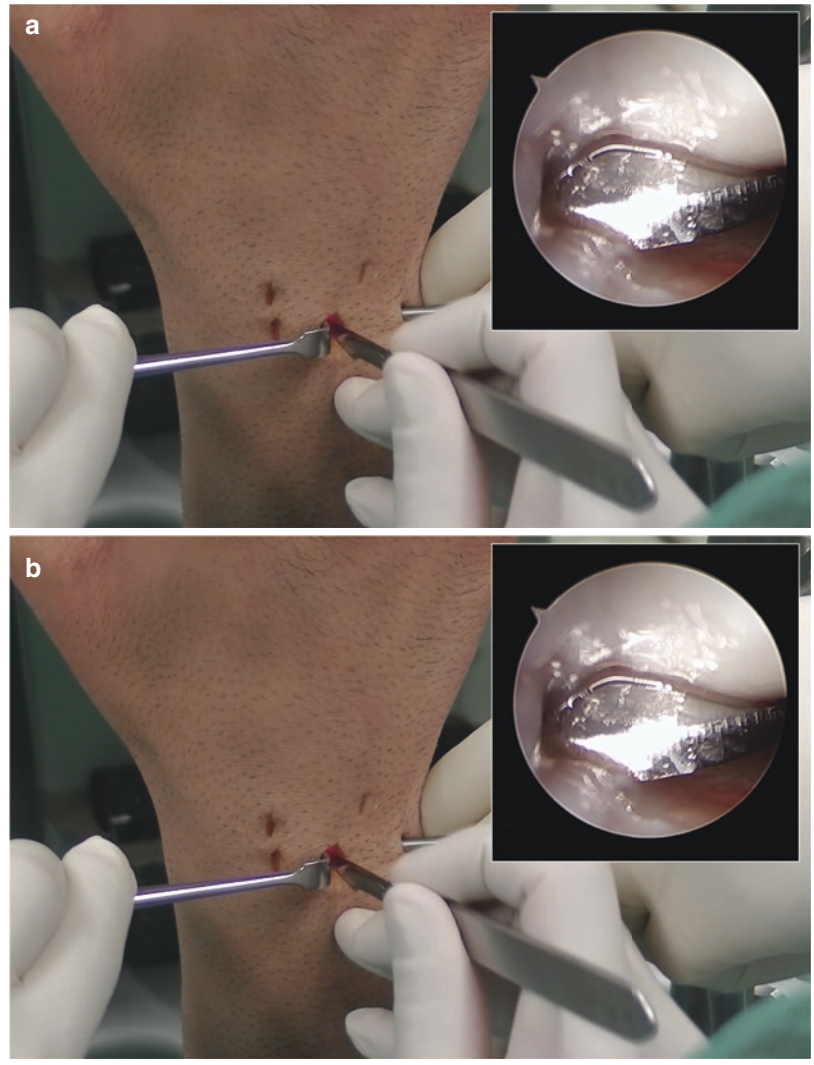

Fig. 77.11 (**a**) The arthroscope is placed in the 6R portal. Through the DC incision, the extensor tendons are retracted toward the radial side. (**b**) The entrance of the lunate tunnel is united with the radiocarpal joint with the tip of a scalpel, to ensure that the graft will pass smoothly through the capsule and the joint into the bone tunnel. Reprinted from Corella F, Del Cerro M, Ocampos M, Simon de Blas C, Larrainzar-Garijo R. Arthroscopic scapholunate ligament reconstruction, volar and dorsal reconstruction. Hand Clin. 2017 with permission from Elsevier

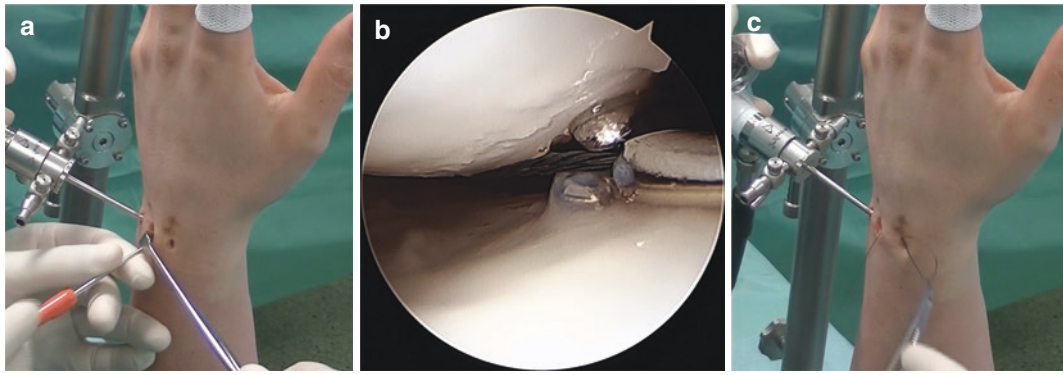

Fig. 77.12 (**a**) The arthroscope is placed in the 6R portal. A curved SutureLasso is introduced into the joint through the DC incision. (**b**, **c**) The loop is retrieved from the 3/4 portal

- The correct position of the bio-tenodesis screw could be checked, either under fluoroscopic control or arthroscopic control with the scope entering through the 6R portal (Fig. 77.22).

77.4.5 Step 5: Volar Reconstruction

In the last step, the graft is directly fixed to the scaphoid at the SL ligament footprint and the portion of the SutureTape that exits from the lunate tunnel is sutured to the portion that exits from the scaphoid tunnel (Fig. 77.23) using a Micro-corkscrew 2/0® (Arthrex, Naples, FL), which is a small anchor of 1-mm predrilling.

- At the volar aspect, the graft and SutureTape are passed in an extra-articular manner. A loop is passed over the capsule underlying the flexor tendons from the RD incision to the VC portal. The graft and tape are captured by this loop and brought to the RD incision (Fig. 77.24).
- The graft is fixed to the scaphoid at the SL ligament footprint with the 2-O threads of the Micro-corkscrew 2/0® (Arthrex, Naples, FL), which is a small anchor of only a 1-mm predrilling (Fig. 77.25).
- Finally, the portion of the SutureTape that exits from the lunate tunnel is sutured to the portion that exits from the scaphoid tunnel in the distal radial incision (Fig. 77.26).

77.5 Tips and Tricks

The most challenging and time-consuming steps are the following:

Creation of the tunnels: It is extremely difficult to correctly position the K-wire using only one hand to hold the drill. Such a small K-wire will easily slide through the bones. Thus, the way to ensure accurate creation of a tunnel and correct placement of the K-wire is the use of a 14-G Abbocath. The tip of this needle can be firmly fixed into the bone while the direction is changed and adjusted under fluoroscopic control. The operating surgeon firmly maintains the correct position, while the other surgeon introduces the K-wire through the Abbocath.

Passage of the graft: This is also a step that consumes more time because the graft is frequently caught by a fragment of capsule or soft tissue and does not pass easily through the tunnels. That is why it is essential to pass the SutureLasso without piercing any soft tissue. To do so, the SutureLasso must be passed through the tunnel, following the K-wire, just after drilling the tunnel**.** The tunnel should be created with a 2.5-mm drill bit in the first step and drilled again with a 3-mm bit in the second step, just before passing the graft. We do not recommend drilling twice with a 3-mm bit because this could create a tunnel larger than 3-mm, preventing the screw from fixing the graft properly.

To pass the SutureLasso easily following the K-wire, the pointed tip of the K-wire can be introduced into the hole at the tip of the SutureLasso (Fig. 77.27).

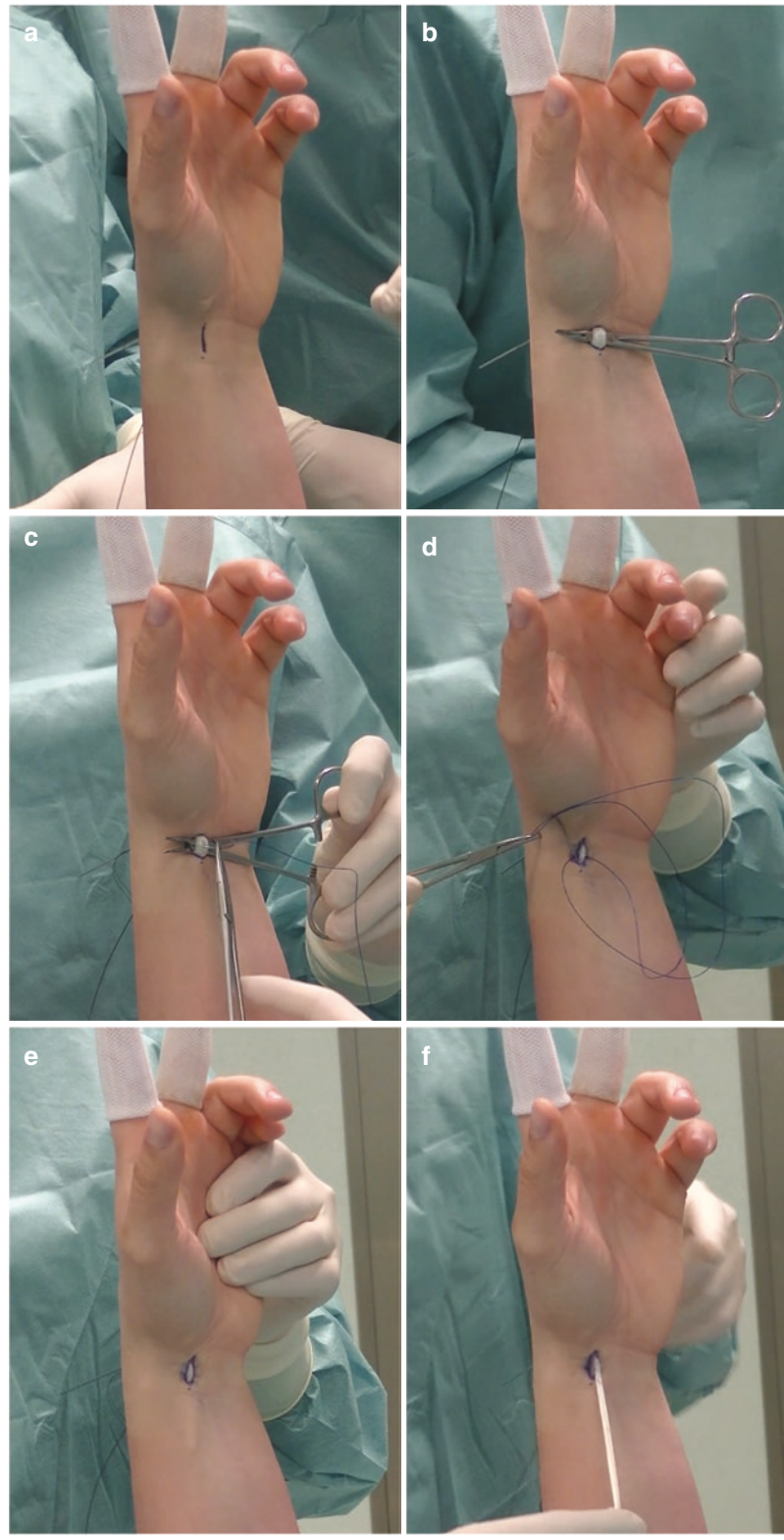

Fig. 77.13 (**a**) The radial distal (RD) incision overlying the FCR and the radial proximal (RP) incision are performed. (**b**) The FCR is located in the RD incision. (**c**) A 2-0 monofilament suture is passed through the flexor carpi radialis, capturing 3 mm of the radial side of the tendon. (**d**) A suture passing wire is advanced from the RP incision to the RD incision. The loop of the passing wire is loaded with the 2-0 monofilament threads. (**e**) The threads are taken to the radial proximal incision, cutting the FCR. (**f**) The graft is cut in the RP incision and retrieved in the RD one

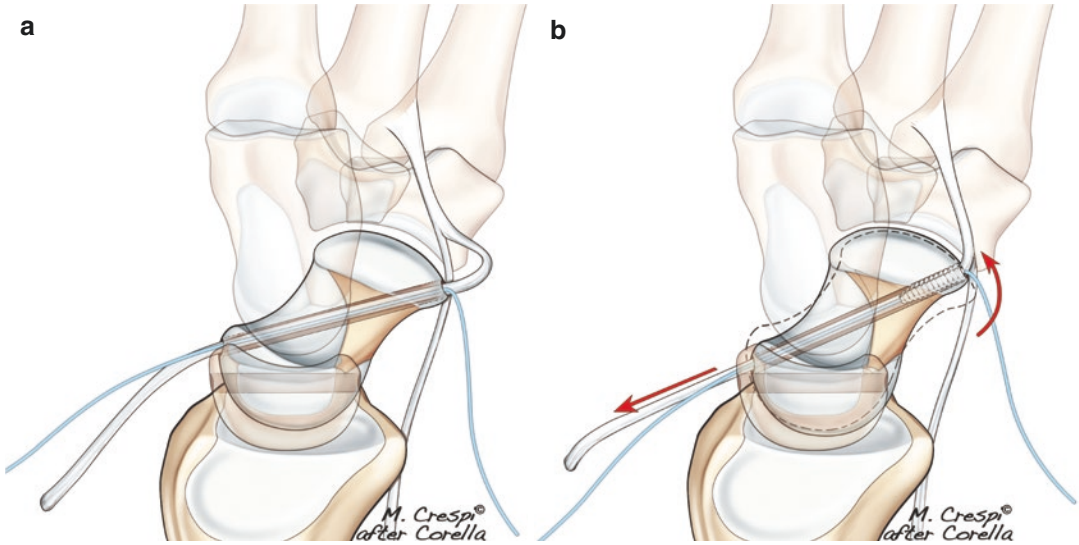

Fig. 77.14 The graft is passed within the suture tape and both are pulled from the dorsal side. The scaphoid is therefore extended. A 3 × 8-mm Bio-Tenodesis screw is introduced from the volar side (M. Crespi © for Corella)

Other possible option is to drill up to 3 mm in the first step and introduce and leave inside the tunnel the red cannula that protects the Suture Passing Wire® (Arthrex, Naples, FL). Just before passing the graft, SutureLasso is pass through the tunnel following this cannula and this also ensures no soft tissues are caught.

Fixation with bio-tenodesis screws: As the Bio-Tenodesis screw is not cannulated, another difficult step is the introduction of this screw inside the tunnel, because it can be blocked by the graft and soft tissues. Therefore, before applying traction from the graft, it is essential to have the screw ready and be able to see the exact entry point. This is even easier if SutureTape is used, as this can easily be followed into the tunnel. Another option is to have the arthroscope inside the joint, as the hole is seen easier with transillumination. Finally, the fluoroscope should always be used to assure the correct position and direction of the screwdriver before introducing the screw.

77.6 Postoperative Rehabilitation

The aim of the postoperative mobilization protocol is to begin the motion earlier than in open procedures because interference screws make the reconstruction stronger and K-wire is not used. Dart-throwing exercise avoids overloading the graft. This motion mainly involves the midcarpal joint with limited movement in the proximal carpal row [10, 11] and induces minimal elongation and tension on the scapholunate ligament [12]. The postoperative mobilization protocol is shown in Fig. 77.28.

77.7 Complications

There are three major theoretical risks.

- Tunnel breakage and fracture. It is essential to check frequently that the K-wire is at the correct position before drilling.
- Damage of delicate structures around the portals or tunnels. In the preliminary cadaver study, the distance between the portals, tunnels, and the structures at risk was demonstrated and can be used as a reference [9].
- Avascular necrosis of scaphoid or lunate. The scaphoid tunnel entry site, which is at the insertion of the dorsal SL ligament, is far from the vessel insertion point at the waist of the

Fig. 77.15 (**a**) The straight SutureLasso enters through the 3-4 portal into the scaphoid tunnel. The graft and SutureTape are captured. (**b**) Both are taken out through the 3-4 portal. Reprinted from Corella F, Del Cerro M, Ocampos M, Simon de Blas C, Larrainzar-Garijo R. Arthroscopic scapholunate ligament reconstruction, volar and dorsal reconstruction. Hand Clin. 2017 with permission from Elsevier

scaphoid. There are numerous reported operations with bone tunnels made at the scaphoids and avascular necrosis of the scaphoids was rarely reported. In an arthroscopic procedure with limited dissection, the surrounding vascularity is best preserved and the risk of avascular necrosis should be even less. Avascular necrosis of the lunate may be more worrisome. However, lunate vascular supply is originated along various ligamentous insertions. As the tunnel is located in the middle of the lunate where its capsuloligamentous structure is not detached, vascular damage should be unlikely.

None of our patients had experienced the above complications.

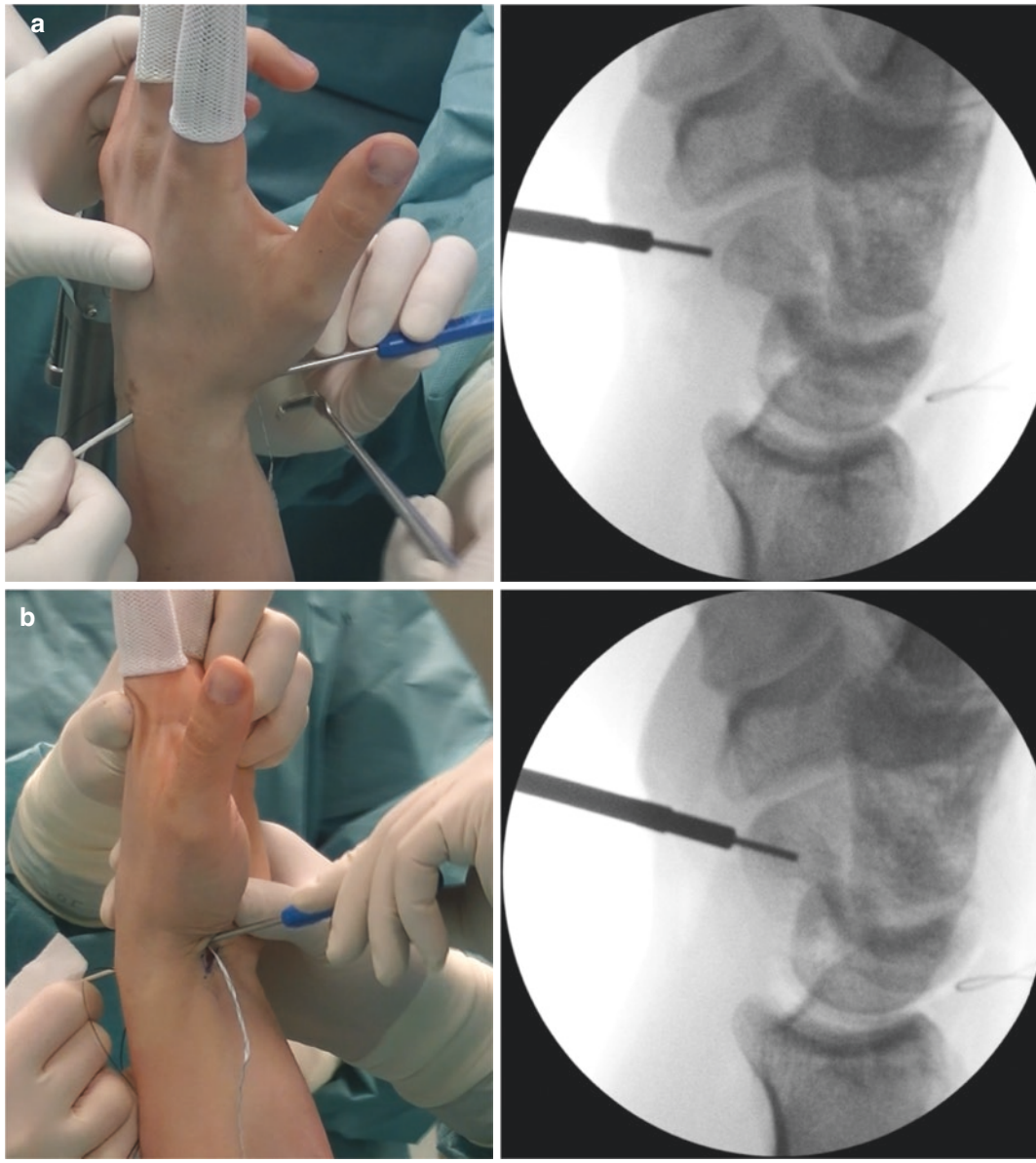

Fig. 77.16 (**a**, **b**) The first Bio-Tenodesis screw is placed at the volar exit of the scaphoid tunnel. The screw is introduced while maintaining tension on the graft from the dorsal side under fluoroscopic control

- A complication that occurs more frequently is the development in pain at the VR distal incision just over the tunnel of the scaphoid. This complication has been normally solved with time or with corticosteroid injection.
- Finally, a radiological but not clinical complication is the scapholunate gap, because it still remains open in many patients with static instability. However, despite this radiological gap, the clinical result of these patients remains satisfactory [5].

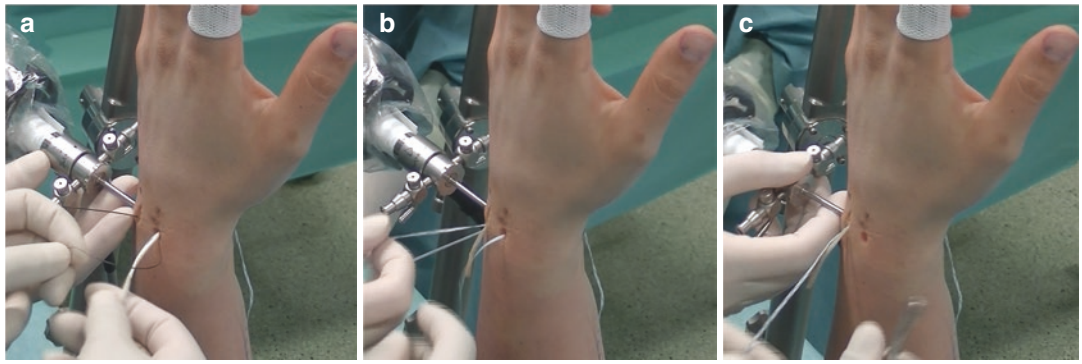

Fig. 77.17 (**a**) The graft and SutureTape are captured with the previously introduced loop and in the 3/4 portal. (**b**, **c**) Both of them are then taken to the DC incision over the lunate

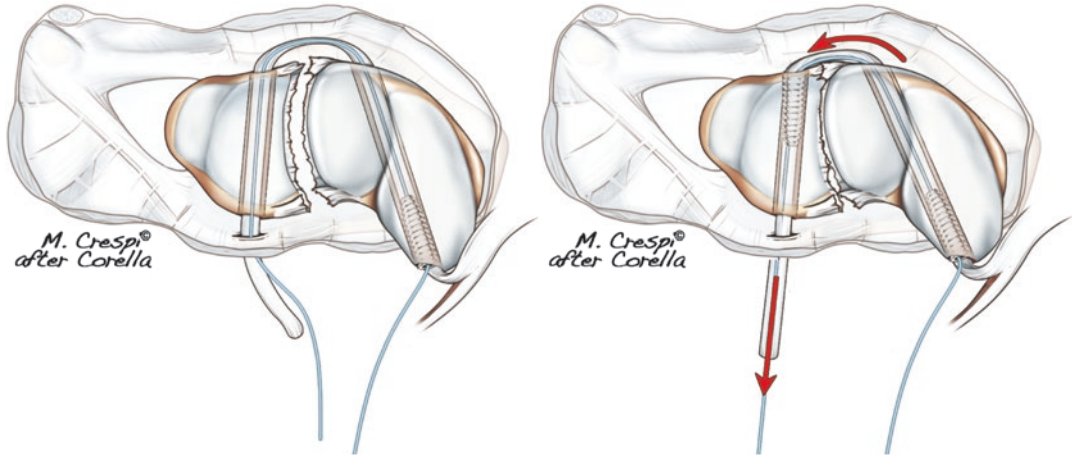

Fig. 77.18 The graft and tape are pulled from the volar side. The scaphoid is supinated, and the gap is closed. The screw is introduced from the dorsal side (M. Crespi © for Corella)

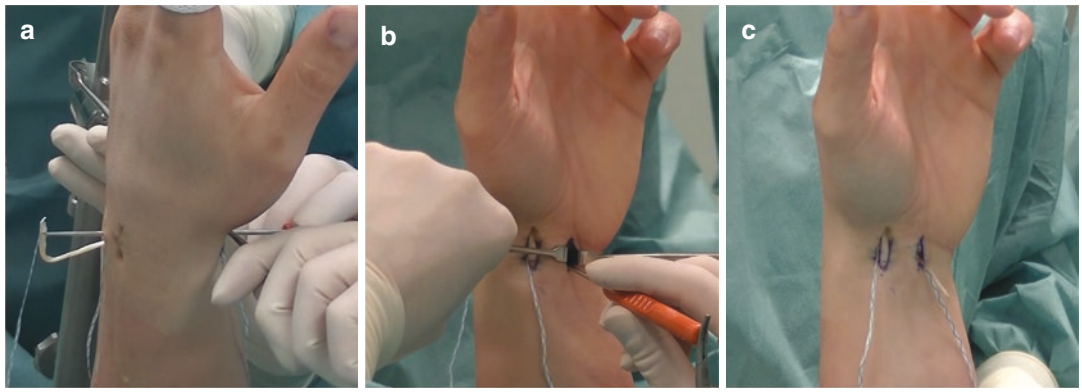

Fig. 77.19 (**a**, **b**) The straight SutureLasso enters through the volar central portal into the lunate tunnel and exits in the DC incision. (**c**) The graft and tape are taken out to the volar central portal. Reprinted from Corella F, Del Cerro M, Ocampos M, Simon de Blas C, Larrainzar-Garijo R. Arthroscopic scapholunate ligament reconstruction, volar and dorsal reconstruction. Hand Clin. 2017 with permission from Elsevier

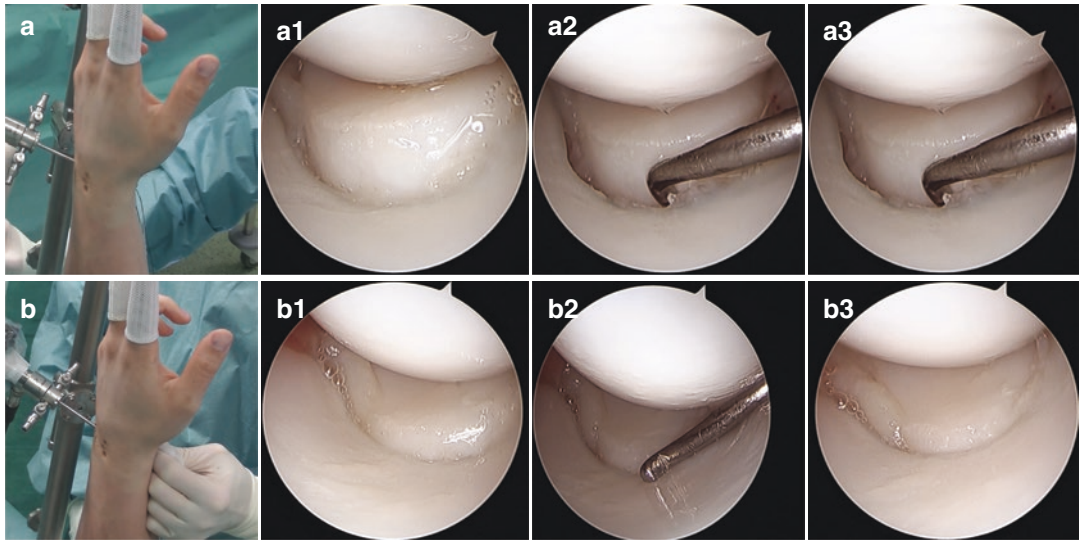

Fig. 77.20 (**a**) Without traction, there is a step-off that develops between the bones; the probe can pass and twist between the bones and the lunate is dorsally angulated. (**b**) When the graft is tensioned from the volar direction, the step-off disappears; the gap closes so that the probe cannot enter or displace the lunate and the dorsal angulation is corrected

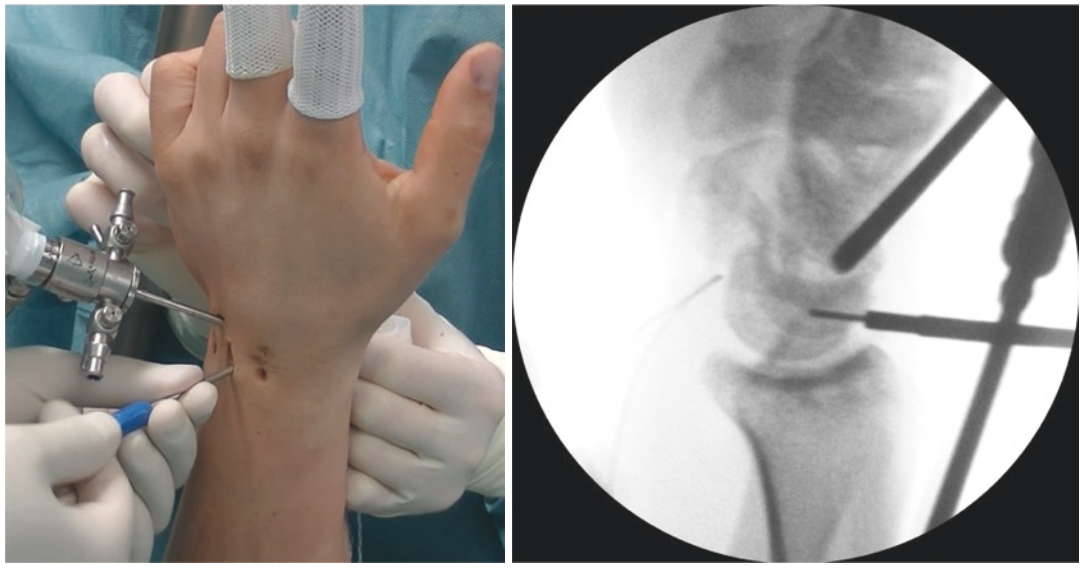

Fig. 77.21 The second Bio-Tenodesis screw is placed at the dorsal side of the lunate tunnel. The screw is introduced while maintaining tension on the graft from the volar side. The insertion of the screw should be performed under fluoroscopic control

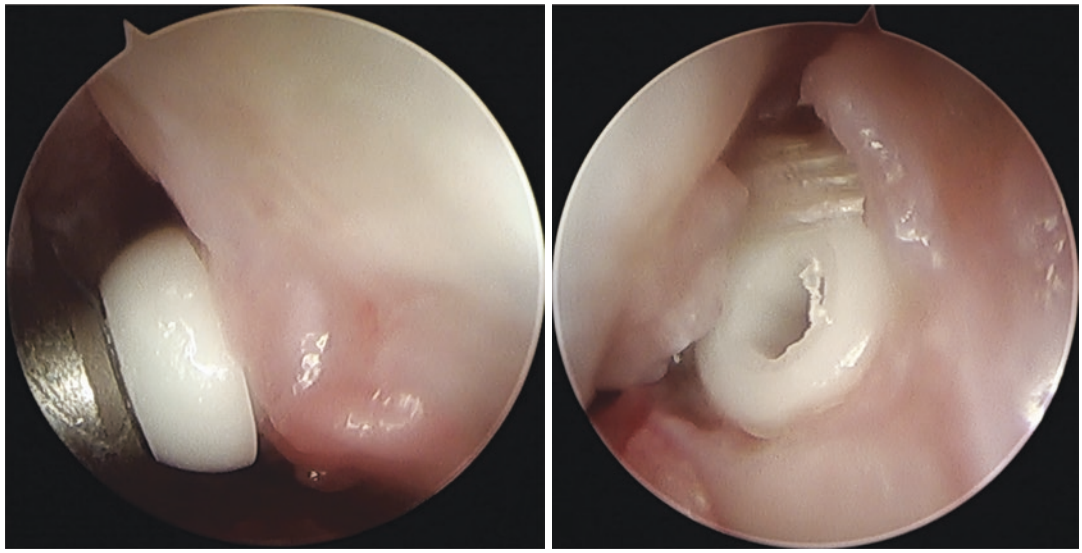

Fig. 77.22 The insertion of the bio-tenodesis screw can also be performed under arthroscopic control with the scope at the 6R portal viewing the lunate tunnel

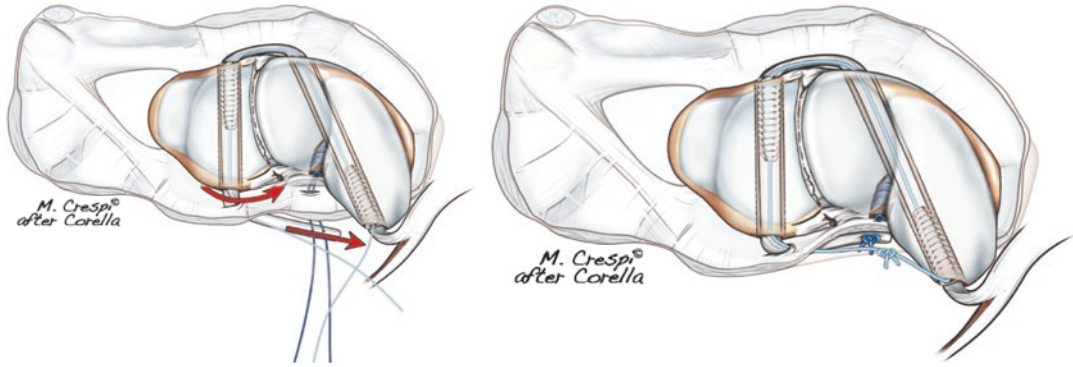

Fig. 77.23 The graft and SutureTape are passed over the capsule and under the flexor tendons from the volar central portal to the RD incision. The graft is directly fixed to the scaphoid at the SL ligament footprint and the portion of the SutureTape that exits from the lunate tunnel is sutured to the portion that exits from the scaphoid tunnel

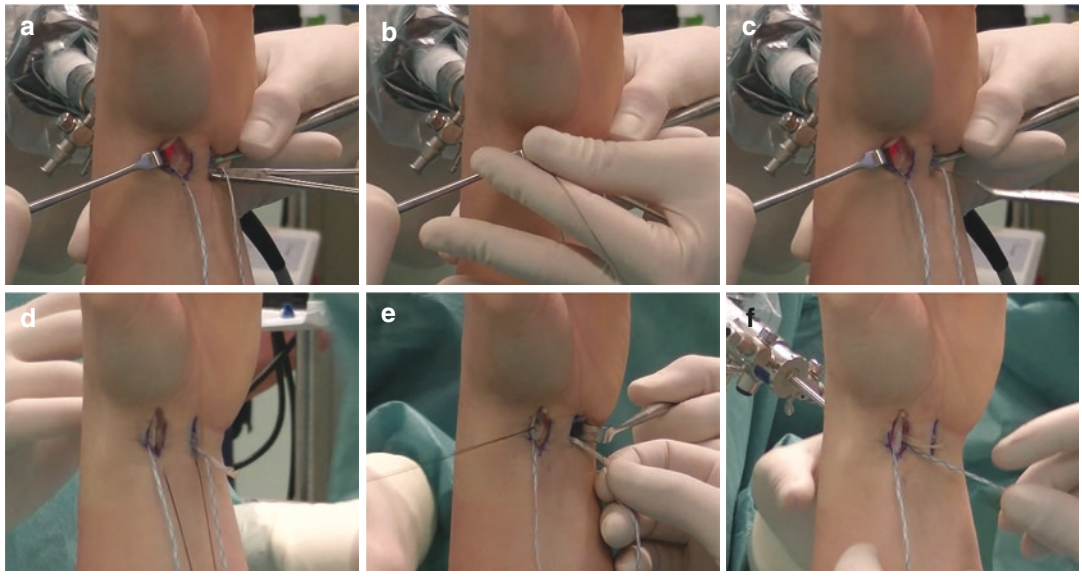

Fig. 77.24 (**a**) A disector is passed over the capsule and under the flexor tendons from the RD incision to the VC portal. (**b**) A loop is captured in the VC portal. (**c**) The loop is taken to the RD incision. (**d**, **e**) The graft and SutureTape are captured with the loop in the VC portal. (**f**) Both of them are taken to the RD incision. Reprinted from Corella F, Del Cerro M, Ocampos M, Simon de Blas C, Larrainzar-Garijo R. Arthroscopic scapholunate ligament reconstruction, volar and dorsal reconstruction. Hand Clin. 2017 with permission from Elsevier

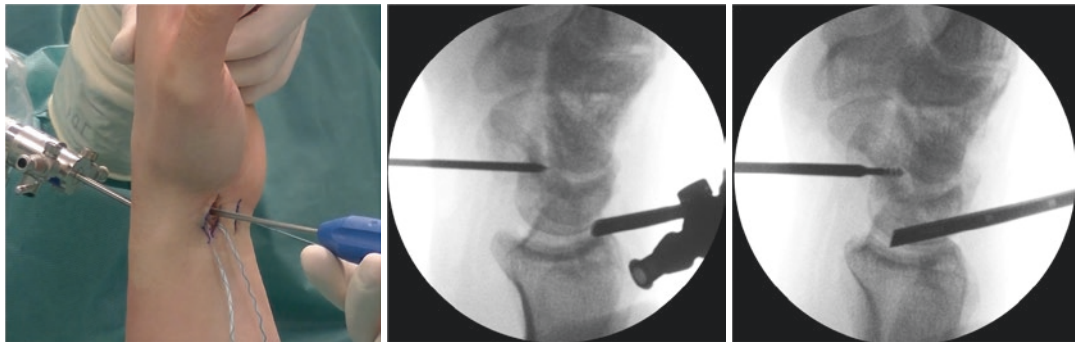

Fig. 77.25 A Micro-corkscrew 2/0® (Arthrex, Naples, FL) is inserted at the SL ligament footprint

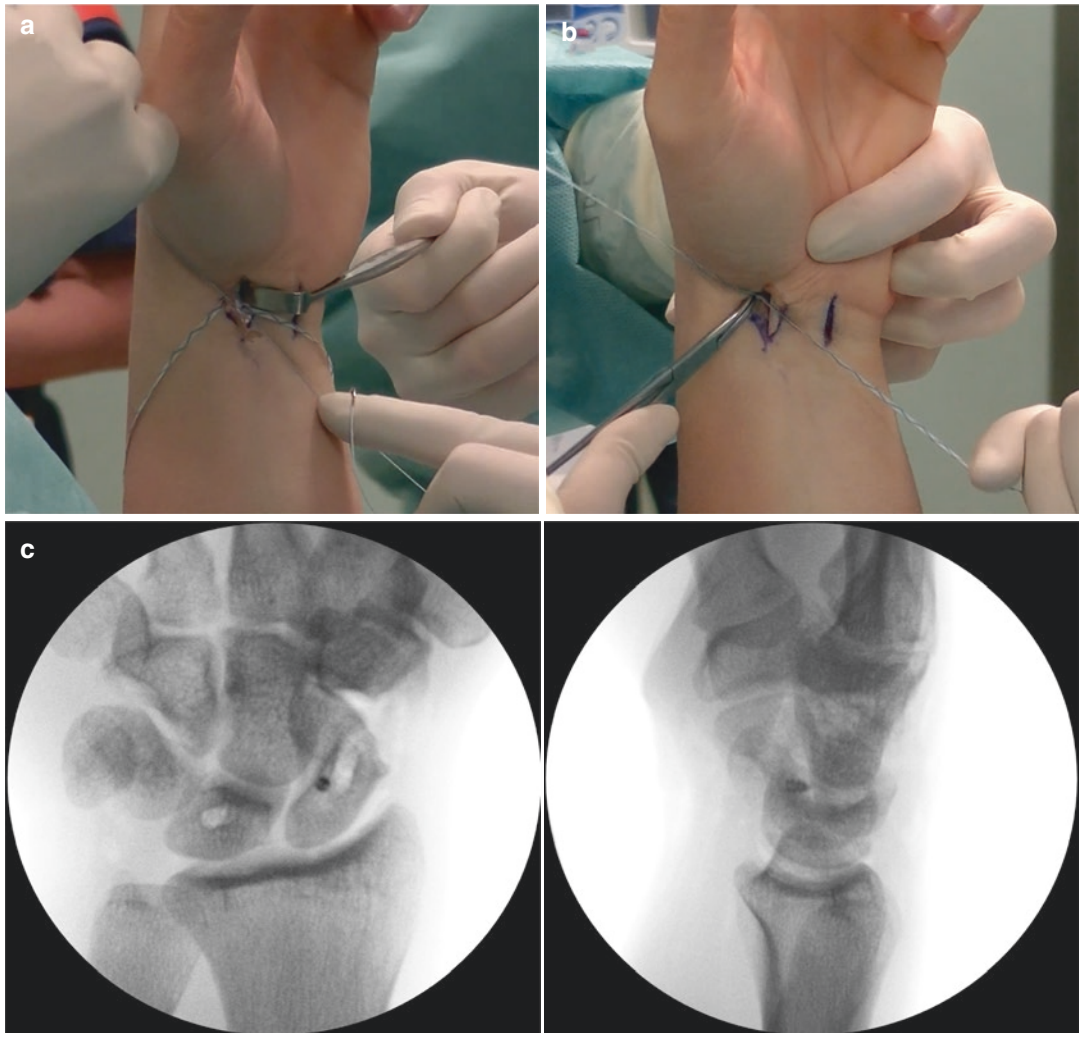

Fig. 77.26 (**a**) The graft is sutured with the threads of the anchor. (**b**) The SutureTape that exits from the lunate tunnel is sutured to the portion that exits from the scaphoid tunnel. (**c**) Fluoroscopic control

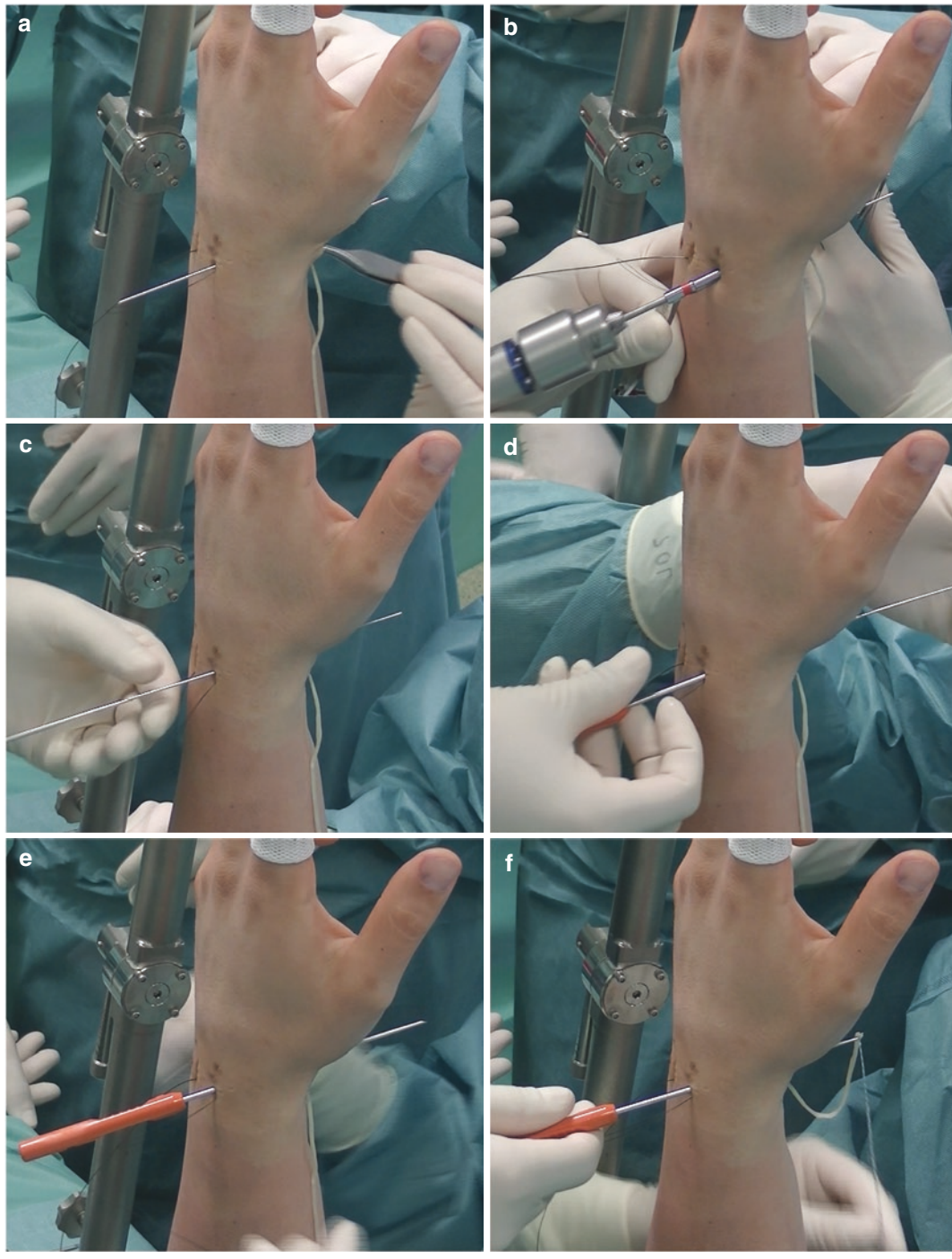

Fig. 77.27 Tip for the passage of the graft. In the first step, the tunnels were performed with a 2.5-mm drill bit. Just before passing the graft, the tunnel should be drill to its final size of 3 mm. (**a**) The k-wire is introduced again in the tunnel with the pointed tip of the K-wire in the 3/4 portal. (**b**) The tunnel is drilled with a 3-mm drill bit. (**c**) The pointed tip of the K-wire can be introduced into the hole at the tip of the SutureLasso. (**d**) The SutureLasso is advanced inside the tunnel to the RD incision, assuring this way there is no soft tissue caught. (**e**, **f**) The graft and tape are captured

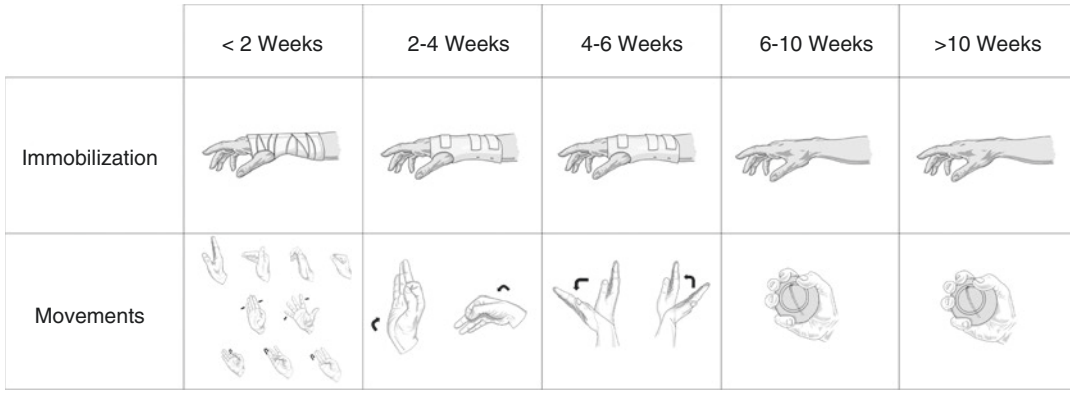

Fig. 77.28 Postoperative rehabilitation protocol. Less than 2 weeks: Dorsal splinting. Six-pack finger exercises. "No" strength on gripping. At 2–4 weeks: thermoplastic splint. Remove splint for 30 min four times a day for exercises. Midcarpal dart-throwing motion alone. At 4–6 weeks: nocturnal thermoplastic splint. Progressive full range of motion exercises. At 6–10 weeks: off splint. Exercises with "progressive" strength on gripping. Proprioception exercises: "power ball." Strengthening exercises with a 1-kg weight (supinator muscles). More than 10 weeks: increase weight up to 3 kg (supinator muscles). After 12 weeks, normal activity without restriction. Avoid contact sports until 4 or 5 months. Reprinted from Corella F, Del Cerro M, Ocampos M, Simon de Blas C, Larrainzar-Garijo R. Arthroscopic scapholunate ligament reconstruction, volar and dorsal reconstruction. Hand Clin. 2017 with permission from Elsevier

References

1. Corella F, Del Cerro M, Ocampos M, Larrainzar-Garijo R. Arthroscopic ligamentoplasty of the dorsal and volar portions of the scapholunate ligament. J Hand Surg Am. 2013;38(12):2466–77.
2. Ho P, Wing-yee Wong C, Tse W. Arthroscopic-assisted combined dorsal and volar scapholunate ligament reconstruction with tendon graft for chronic sl instability. J Wrist Surg. 2015;4:252–63.
3. Carratalá V, Lucas FJ, Alepuz ES, Guisasola E, Calero R. Arthroscopically assisted ligamentoplasty for axial and dorsal reconstruction of the scapholunate ligament. Arthrosc Tech. 2016;5(2):e353–9.
4. Corella F, Del Cerro M, Larrainzar-Garijo R, Vázquez T. Arthroscopic ligamentoplasty (bone-tendon-tenodesis). A new surgical technique for scapholunate instability: preliminary cadaver study. J Hand Surg Eur Vol. 2011;36(8).
5. Corella F, Del Cerro M, Ocampos M, Simon de Blas C, Larrainzar-Garijo R. Arthroscopic scapholunate ligament reconstruction, volar and dorsal reconstruction. Hand Clin. 2017;33(4):687–707.
6. Corella F, Ocampos M, Del Cerro M, et al. Volar central portal in wrist arthroscopy. J Wrist Surg. 2016;5:80–90.
7. Messina JC, Van Overstraeten L, Luchetti R, Fairplay T, Mathoulin CL. The EWAS classification of scapholunate tears: an anatomical arthroscopic study. J Wrist Surg. 2013;2(2):105–9.
8. Corella F, Ocampos M, Del Cerro M. Arthroscopic scaphoid 3D test for scapholunate instability. J Wrist Surg. 2017;1(212):2–5.
9. Corella F, Del Cerro M, Ocampos M, Larrainzar-Garijo R. The "rocking chair sign" for floating lunate. J Hand Surg Am. 2015;40(11):2318–9.
10. Moritomo H, Apergis EP, Herzberg G, Werner FW, Wolfe SW, Garcia-Elias M. 2007 IFSSH committee report of wrist biomechanics committee: biomechanics of the so-called dart-throwing motion of the wrist. J Hand Surg Am. 2007;32(9):1447–53.
11. Crisco JJ, Coburn JC, Moore DC, Akelman E, Weiss A-PC, Wolfe SW. In vivo radiocarpal kinematics and the dart thrower's motion. J Bone Joint Surg Am. 2005;87(12):2729–40.
12. Upal MA, Crisco JJ, Moore DC, Sonenblum SE, Wolfe SW. In vivo elongation of the palmar and dorsal scapholunate interosseous ligament. J Hand Surg Am. 2006;31(8):1326–32.

78 Arthroscopic-Assisted Combined Dorsal and Volar Scapholunate Ligament Reconstruction with Tendon Graft for Chronic SL Instability

Siu-cheong Jeffrey Justin Koo and Pak-cheong Ho

78.1 Background

Scapholunate (SL) dissociation is the most common carpal instability [1]. As described by Mayfield et al., the injury is often due to a fall on the hypothenar area with the wrist in extension and ulnar deviation resulting in intercarpal supination. This leads to progressive failure of carpal osteoligamentous architecture, traveling from radial to ulnar around the lunate [2]. The scapholunate joint stability depends on two systems of ligaments: intrinsic scapholunate interosseous ligament (SLIL) and secondary extrinsic stabilizers, such as dorsal radiocarpal (DRC) ligament, dorsal intercarpal (DIC) ligament, scaphotrapezial (ST) ligament, and radioscaphocapitate (RSC) ligament. Each has a distinct role; however, they work in concert to form the scapholunate ligament complex (SLLC) [3].

Numerous surgical techniques have been described to restore or improve the stability of the SL joint and to retard or prevent the progression to arthritis [4–29]. Among those focused on SLIL reconstruction, most methods provide only dorsal and uniplanar reconstructions. The importance of the SLIL volar component is often underrated [11, 12, 20, 21, 26]. Volar component has an important role in the rotational constraint of the SL joint and will create shear stress between the scaphoid and the lunate when sectioned [30, 31].

Based on the result of biomechanical studies, it is more logical and ideal to restore both the dorsal and the volar components of the SL ligament. Yi et al. used a palmaris longus tendon passed through drill holes in the anteroposterior plane of the scaphoid and the lunate. The SL diastasis was effectively reduced to normal, and the scaphoid and lunate contact pressure on the radius and the scaphoid-to-lunate contact ratio were significantly improved after the reconstruction [32]. Zdero used bovine tendons passing through double bone tunnels of the scaphoid and lunate in 19 cadaveric wrists and found no difference in the mechanical property from the normal wrists [33]. Dobyns used a portion of the tendon to pass through anteroposterior bone tunnels in the proximal pole of the scaphoid and lunate to reconstruct the SL linkage. Stability was obtained by tightly looping the tendon graft across the scaphoid and lunate [34]. However, creating drill holes across poorly vascularized areas of bone in an open fashion severely compromised their blood supply and resulted in fractures and avascular necrosis.

In 2002, the senior author (PC Ho) developed an arthroscopic-assisted technique to reconstruct both the dorsal and the volar SL ligament simultaneously using a free tendon graft in a box-like

S.-c. J. J. Koo · P.-c. Ho (✉)
Department of Orthopaedics and Traumatology,
Prince of Wales Hospital,
Sha Tin, Hong Kong SAR
e-mail: pcho@ort.cuhk.edu.hk

© ISAKOS 2022

D. N. Bhatia et al. (eds.), *Arthroscopy and Endoscopy of the Elbow, Wrist and Hand*,
https://doi.org/10.1007/978-3-030-79423-1_78

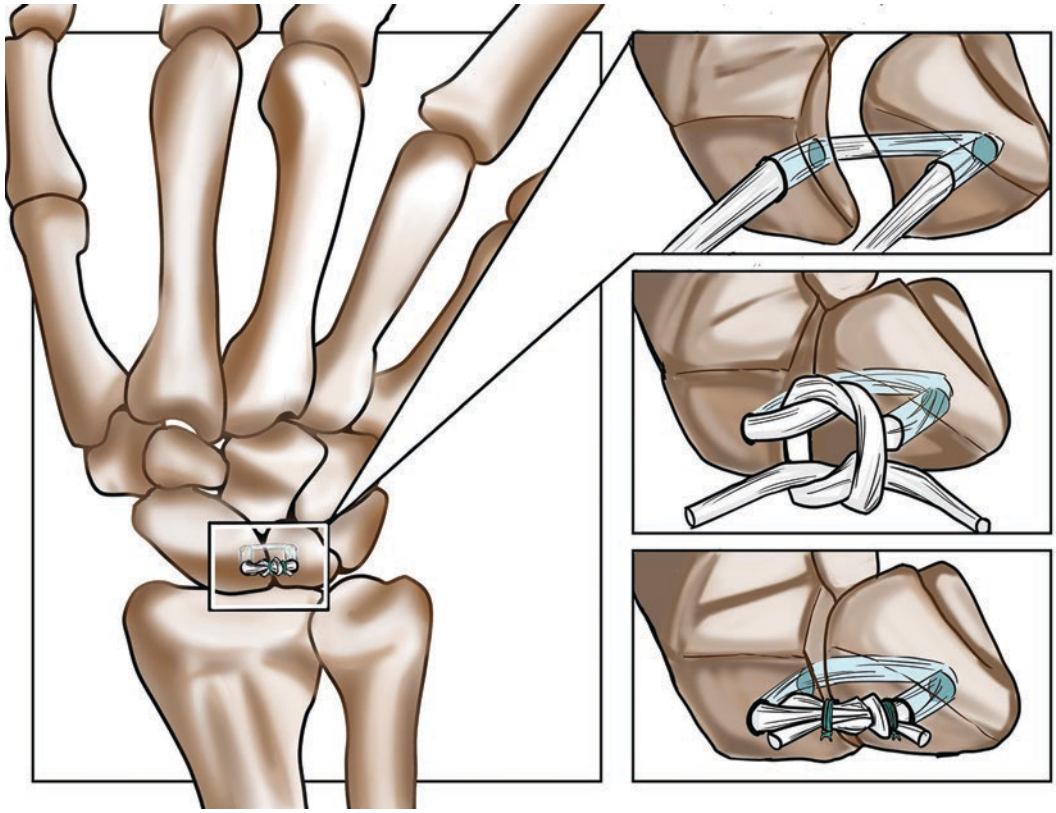

Fig. 78.1 Simultaneous reconstruction of the dorsal and palmar SL ligaments anatomically with the use of tendon graft in a boxlike manner. (Illustration courtesy of Joey Lau Chun Yin)

structure without violating the major blood supply to the scaphoid and soft tissue envelope [35] (Fig. 78.1).

78.2 Indications and Contraindications

The technique is indicated in subacute or chronic SL dissociation of 6 weeks or beyond with reducible SL diastasis and dorsal intercalated segmental instability (DISI) deformity confirmed arthroscopically and radiologically.

Contraindications include scapho-lunate advanced collapse (SLAC) wrist beyond Watson stage I and chronic non-reducible SL dissociation after adequate intra-articular fibrosis and capsular contracture release.

78.3 Operative Techniques

The authors recommend diagnostic wrist arthroscopy under portal site local anesthesia (PSLA) prior to the definitive surgery, especially when the SL dissociation cannot fully account for the wrist pain [36]. This helps to evaluate the cause of the chronic wrist pain, status of the SL ligaments, reducibility of the SL diastasis and rotation malalignment, and the presence of any SLAC changes. Also, arthroscopic lysis performed at this stage can help to improve the SL joint reduc-

ibility. If not, then alternative treatment methods should be considered.

78.3.1 Patient Preparation and Positioning

After anesthesia and before the patient is subjected to reconstruction procedure, a thorough fluoroscopic assessment of the SL joint stability and reducibility is performed. The amount of SL joint diastasis, DISI deformity, and dorsal scaphoid translation is noted. Reducibility can be evaluated by doing a passive radial deviation of the wrist to observe for apposition of the SL gap (Fig. 78.2). Reduction of the DISI deformity can be assessed by applying a volarly directed pushing force to the dorsal scaphoid (Fig. 78.3). Easily reducible SL dissociation will constitute a good indication for the technique.

The surgery is performed under general anesthesia or regional block with the patient in supine position and the operated arm in 90° shoulder abduction resting on a hand table. The elbow joint is flexed to 90°, and the affected hand is subjected to 10–13 lb of traction force through the plastic finger traps applied to the middle three digits by using a sterilizable Wrist Traction Tower

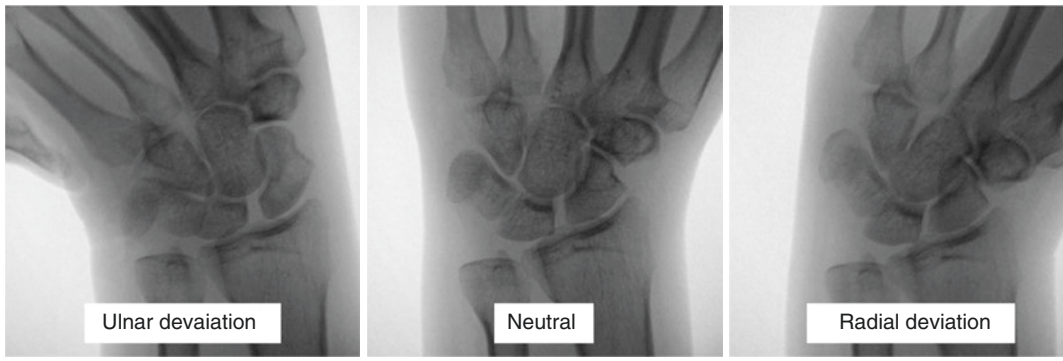

Fig. 78.2 Reducibility of SL joint can be assessed under fluoroscopy: radial deviation reduces the SL gap while ulnar deviation widens the gap

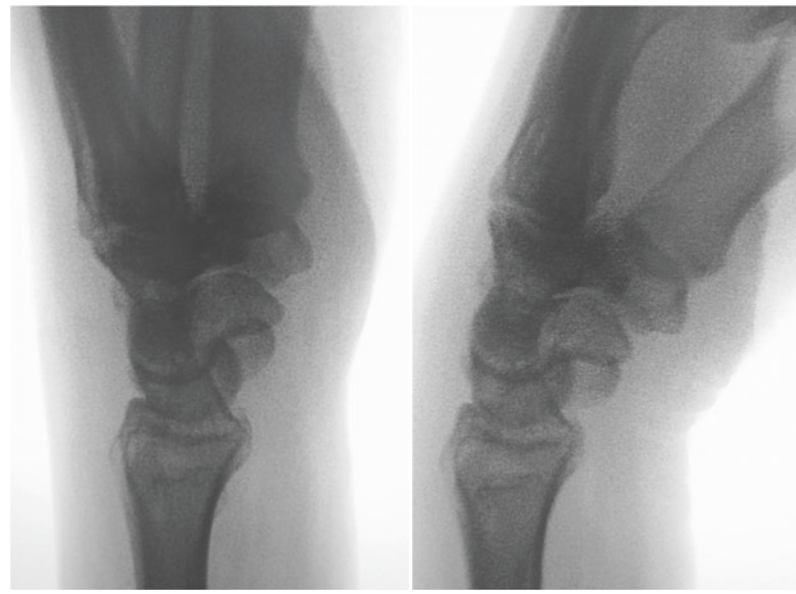

Fig. 78.3 By applying wrist flexion force, reducibility of lunate in DISI deformity can be observed under fluoroscopy

Fig. 78.4 Setting up of arthroscope with traction tower in operation theater

(ConMed Linvatec Corp., Goleta, CA) (Fig. 78.4). The well-padded arm is strapped to the base plate of the tower to provide counter traction.

The arm tourniquet is not inflated initially. Two percent lignocaine with 1:200,000 adrenaline is injected into the portal sites to reduce bleeding. Continuous saline irrigation of the joint is achieved under gravity.

78.3.2 Exploration of Radiocarpal Joint and Midcarpal Joint

A 1.9-mm or 2.7-mm arthroscope is used. Small transverse skin crease incisions are made on the portal sites. Radiocarpal joint arthroscopy is performed initially through the 3-4 and 4-5 portals with 6U as the outflow portal, followed by midcarpal joint arthroscopy through the midcarpal radial (MCR) and midcarpal ulnar (MCU) portals. SL joint gapping, drive-through sign, articular step-off, status of the torn SL ligament remnant, associated chondral lesions, and changes in the extrinsic ligaments can be observed. Synovectomy and radial styloidectomy can be performed at the same time if necessary, using a 2-mm shaver, small radiofrequency ablation probe, and 2.9-mm burr.

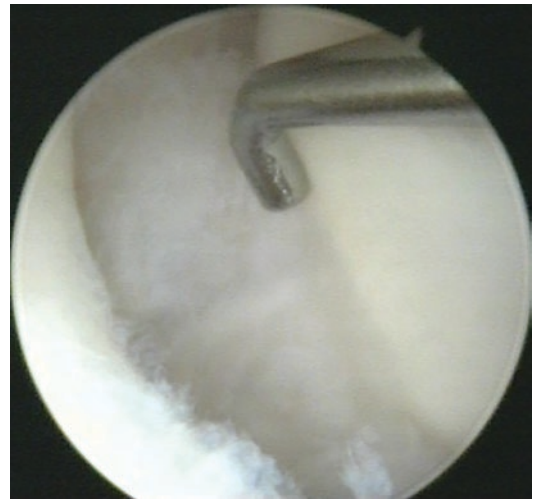

Fig. 78.5 A view from MCR portal looking into the midcarpal joint shows dense scar tissue interposed between SL interval, which would hinder subsequent reduction

78.3.3 Taking Down of Intra-articular Fibrosis

In chronic SL dissociation with significant diastasis and DISI deformity, intra-articular fibrosis and capsular contracture are often found, and scar tissue interposed at the SL joint interval can prevent its adequate reduction (Fig. 78.5). Fibrosis and scar tissue are resected with a shaver to improve the capsular elasticity and to facilitate subsequent reduction of the SL gap, malalignment, and DISI deformity. The carpal bones in the proximal carpal row can be squeezed manually under a reduced traction force to assess the reduction of the SL gap (Fig. 78.6). Reducibility of scaphoid and lunate should also be confirmed by fluoroscopy before proceeding to the next stage.

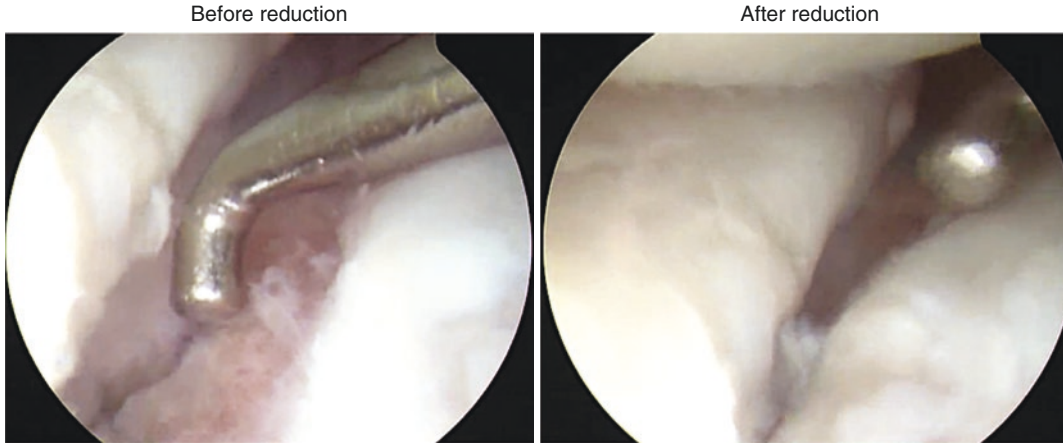

Fig. 78.6 By removing the scar tissue in between SL interval, the gap can be reduced with squeezing the proximal carpal bones externally

78.3.4 Preparation of Scaphoid and Lunate Bone Tunnels

The operated arm is taken off the traction tower and placed on the hand table. The arm tourniquet is then inflated after the hand and forearm are exsanguinated. A 2-cm transverse incision is centered at the 3-4 portal and extended 1 cm radially and 1 cm ulnarly toward the 4-5 portal (Fig. 78.7). The extensor retinaculum is split along its oblique fibers. The extensor digitorum communis (EDC), extensor carpi radialis brevis (ECRB), and the extensor carpi radialis longus (ECRL) tendons are identified. Lunate can be exposed by retracting the EDC tendons ulnarward or more preferably by passing between the EDC tendons. The ideal scaphoid tunnel position can be spotted between ECRB and ECRL tendons (Fig. 78.8). The tendons are slung with cotton tapes for protection and retraction.

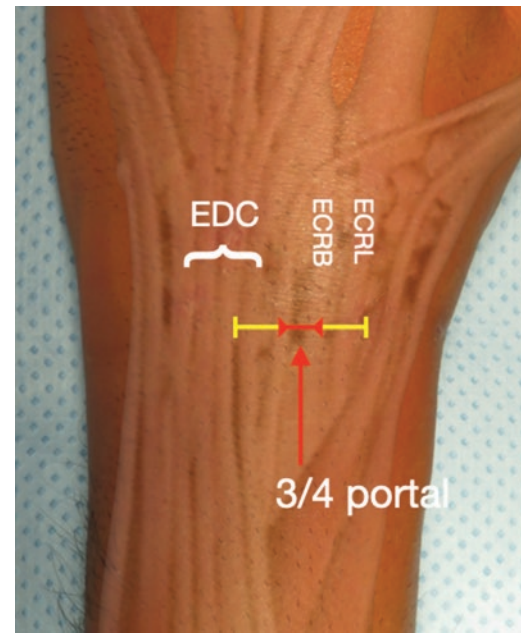

Fig. 78.7 Planning of dorsal skin incision. Using the 3-4 portal as the center, skin incision is extended 1 cm radially and 1 cm ulnarly

Volarly, a transverse incision is made along the proximal wrist crease from the radial border of the palmaris longus (PL) to the ulnar border of the flexor carpi radialis (FCR) tendon (Fig. 78.9). The palmar cutaneous branch of the median nerve should be dissected out and safeguarded (Fig. 78.10). PL free graft is harvested with a tendon stripper. The anterior forearm fascia is incised, and the interval between the FCR tendon, the finger flexor tendons, and median nerve is entered to reach the volar wrist joint capsule (Fig. 78.11). Both the volar and the dorsal wrist joint capsules containing the important extrinsic ligaments, and hence secondary stabilizers of the SL joint are carefully preserved without violation. The soft tissue dissection is kept to minimal.

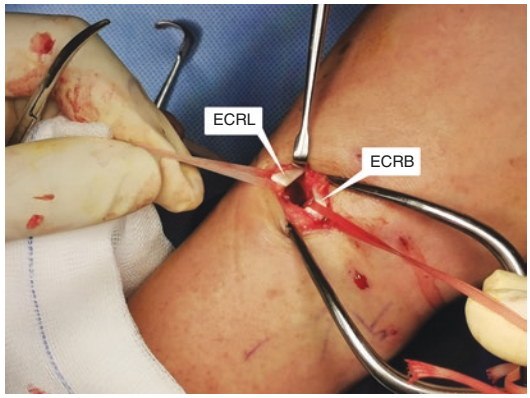

Fig. 78.8 By retracting the ECRB and ECRL, the "sweet" spot for placing the scaphoid bone tunnel can be located

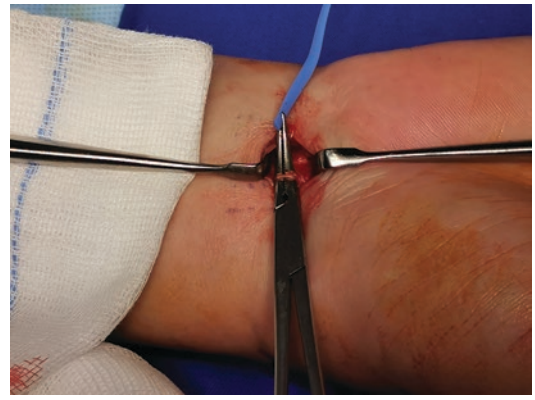

Fig. 78.10 The palmar cutaneous branch of median nerve is often found on radial side of skin incision, and should be dissected out and safeguarded

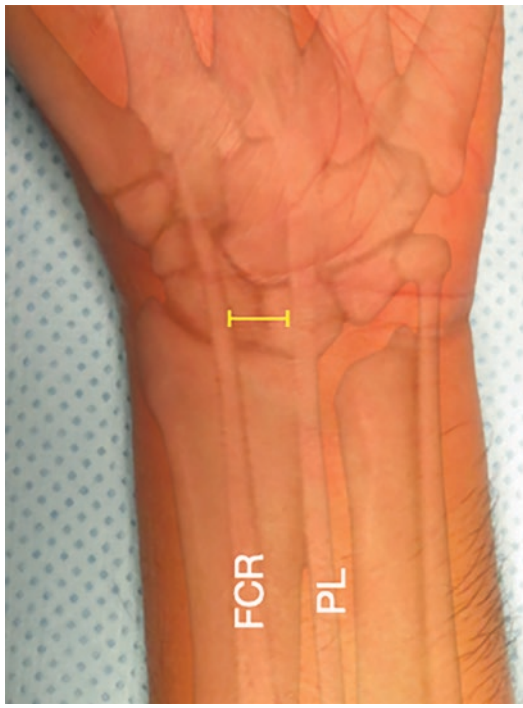

Fig. 78.9 Placement of volar skin incision. Transverse incision is made along the proximal wrist crease from the radial border of the palmaris longus (PL) to the ulnar border of the flexor carpi radialis (FCR) tendon

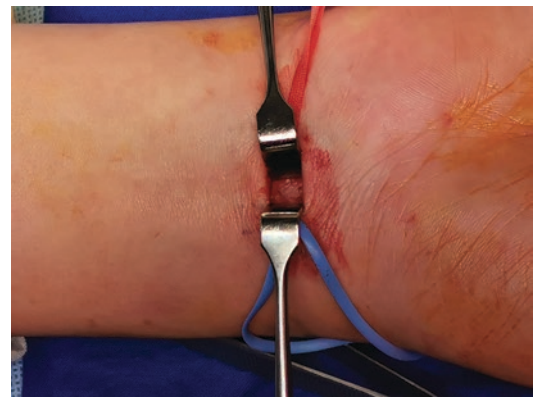

Fig. 78.11 The volar joint capsule can be visualized by retracting FCR and palmar cutaneous branch of median nerve radially while median nerve and finger flexor tendons are retracted ulnarly

78.3.5 Correction of DISI Deformity

Significant DISI deformity can be corrected before drilling the bone tunnel. The hand is examined under the fluoroscope. The extended lunate can be corrected by Linscheid maneuver with wrist flexion to realign the lunate with

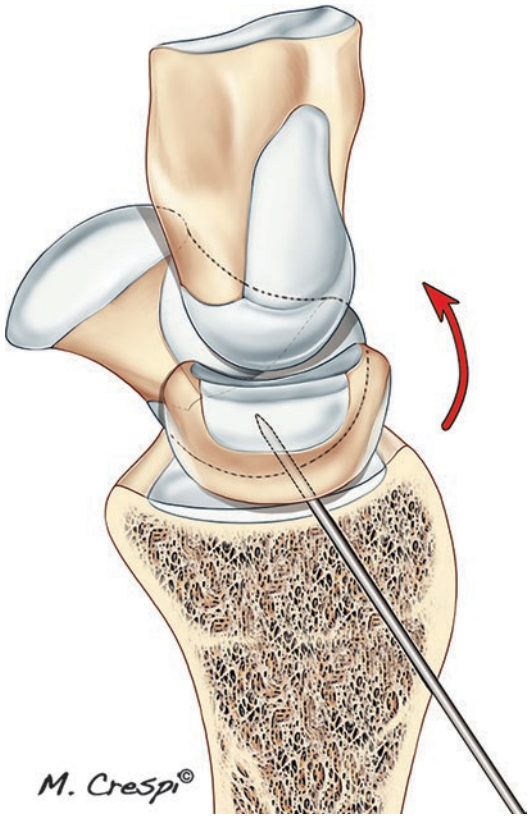

Fig. 78.12 Drawing showing the lunate reduction by the Linscheid maneuver. The radiolunate joint is transfixed with a 1.6-mm K-wire with the lunate in a neutral position. (Illustration courtesy of M. Crespi, adapted with permission from Mathoulin (2019); copyright 2019 Georg Thieme Verlag KG; From Mathoulin, Wrist Arthroscopy Techniques, 2nd edition, Georg Thieme Verlag, Stuttgart 2019, with permission)

radius. The lunate position can be maintained by transfixing the RL joint with a 1.6-mm Kirschner wire (K-wire), which is inserted percutaneously through the dorsum of distal radius. The RL pin should be aimed at the ulnar half of the lunate to avoid conflict with the lunate bone tunnel (Fig. 78.12). The wrist is now ready for bone tunnel preparation.

78.3.6 Preparation of Lunate Bone Tunnel

Lunate bone tunnel is created through the dorsal incision. Either by retracting the tendons ulnarly or more preferably by passing through the EDC tendons, the dorsal portion of lunate can be reached. A 1.1-mm guide pin is inserted into the lunate perpendicular to the long axis of the lunate, that is, parallel to the line joining the tip of the volar and dorsal lips of the lunate, through the capsule under fluoroscopic guidance. The guide pin should aim at the center of lunate to avoid iatrogenic blowout fracture. For cases with mild DISI deformity, RL pinning may not be necessary. If the lunate is not being transfixed to the radius, manual traction of the wrist can help to bring the lunate to a more distal position to uncover the lunate from the dorsal rim of the distal radius and hence facilitating the pinning process. Under this situation, the pin over the lunate may be targeted in a slightly dorsoproximal to volar-distal direction so that the pin will form an angle with the subsequent guide pin over the scaphoid. The convergent relationship of the two guide pins will help in the reduction of the DISI deformity. Over the volar side, an assistant helps to gently retract and protect the flexor tendons and median nerve ulnarward; the surgeon then advances the guide pin to perforate the lunate volar cortex and volar capsule to exit through the volar wound (Fig. 78.13).

78.3.7 Preparation of Scaphoid Bone Tunnel

Another guide pin is inserted through the dorsal wound onto the scaphoid in the interval between the ECRB and the ECRL tendons, just distal to the extensor retinaculum. The guide pin aims at the proximal scaphoid at least 2–3 mm from the surrounding articular margin to avoid iatrogenic fracture both in coronal and sagittal planes. It is essential to place the guide pin trajectory in a slightly dorso-distal to volar-proximal direction so that the pin can form a convergent angle with the lunate pin (Fig. 78.14). When the PL tendon graft is being tightened in the final stage, it will provide a counter-rotational force on the scaphoid to correct the flexion pronation deformity inherent in SL dissociation (Fig. 78.15). With the FCR tendon retracted radially, the scaphoid

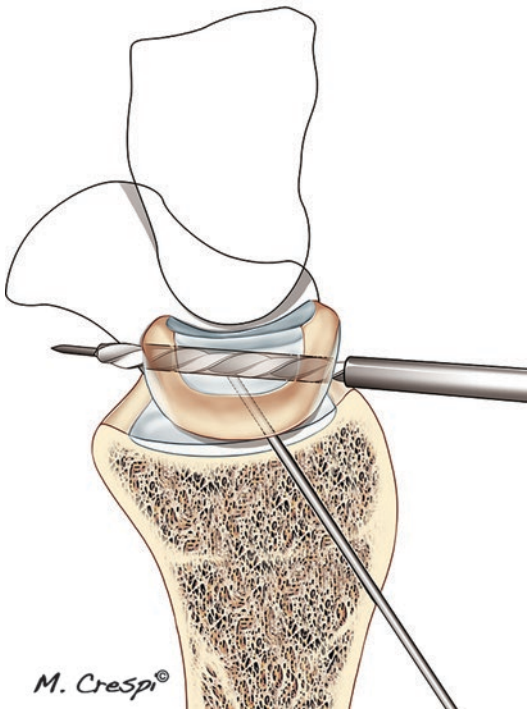

Fig. 78.13 Drawing showing preparation of lunate bone tunnel. 1.1-mm guide pin is inserted into the lunate perpendicular to the long axis of the lunate under fluoroscopic guidance. The guide pin should aim at the center of lunate and not too close to the articular margin to avoid iatrogenic blowout fracture. Then the bone tunnel is prepared with cannulated drill from dorsal to volar direction. Using a 4.5 mm drill sleeve to protect the soft tissue from the K-wire and cannulated drill is often useful to avoid iatrogenic damage to flexors and median nerve. (Illustration courtesy of M. Crespi, adapted with permission from Mathoulin (2019); copyright 2019 Georg Thieme Verlag KG; From Mathoulin, Wrist Arthroscopy Techniques, 2nd edition, Georg Thieme Verlag, Stuttgart 2019, with permission)

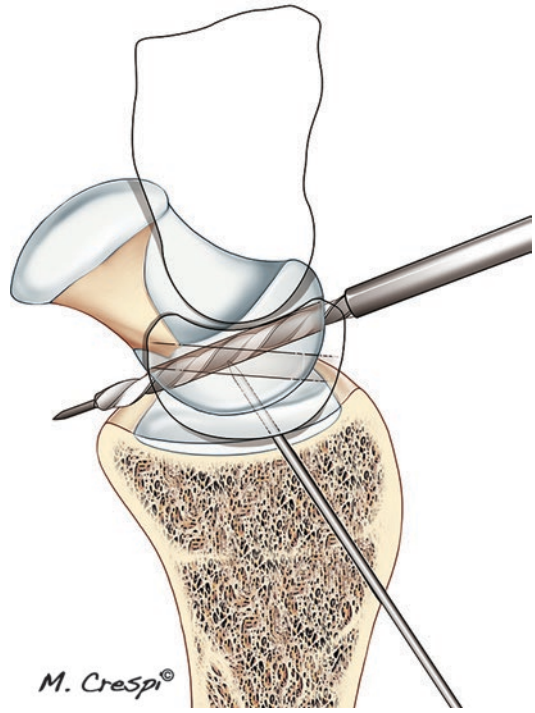

Fig. 78.14 Drawing showing preparation of scaphoid bone tunnel. Again, guide pin should be 2–3 mm away from articular margin to avoid blowout. Guide pin trajectory is preferably slightly directed proximally and volarly to correct the flexion pronation deformity when the tendon graft is tightened. (Illustration courtesy of M. Crespi, adapted with permission from Mathoulin (2019); copyright 2019 Georg Thieme Verlag KG; From Mathoulin, Wrist Arthroscopy Techniques, 2nd edition, Georg Thieme Verlag, Stuttgart 2019, with permission)

guide pin exits through the volar wound. Both the lunate and the scaphoid bone tunnels are subsequently enlarged using 2.0 and 2.4 mm cannulated drill bits. The bone tunnels should not be too large as there is a risk of iatrogenic fracture or inducing bone ischemia. Small tunnel size may cause jamming of tendon graft inside the tunnel leading to graft attrition or even rupture when being pulled through the tunnel. It is mandatory to use a drill sleeve of adequate size, for example, 4.5 mm drill sleeve on both the dorsal and the volar side to protect the soft tissue during the pinning and drilling processes under fluoroscopic control.

78.3.8 Passing the Palmaris Longus Tendon Graft Through the Scaphoid and Lunate Bone Tunnel

The free PL tendon graft is delivered through the capsular vents and the bone tunnels. The PL tendon graft has to loop around the volar side of the scaphoid, and lunate and tendon graft ends are located on the dorsal side for subsequent tying. A 2-mm arthroscopic mini-grasper is passed through the bone tunnels from the dorsal side to

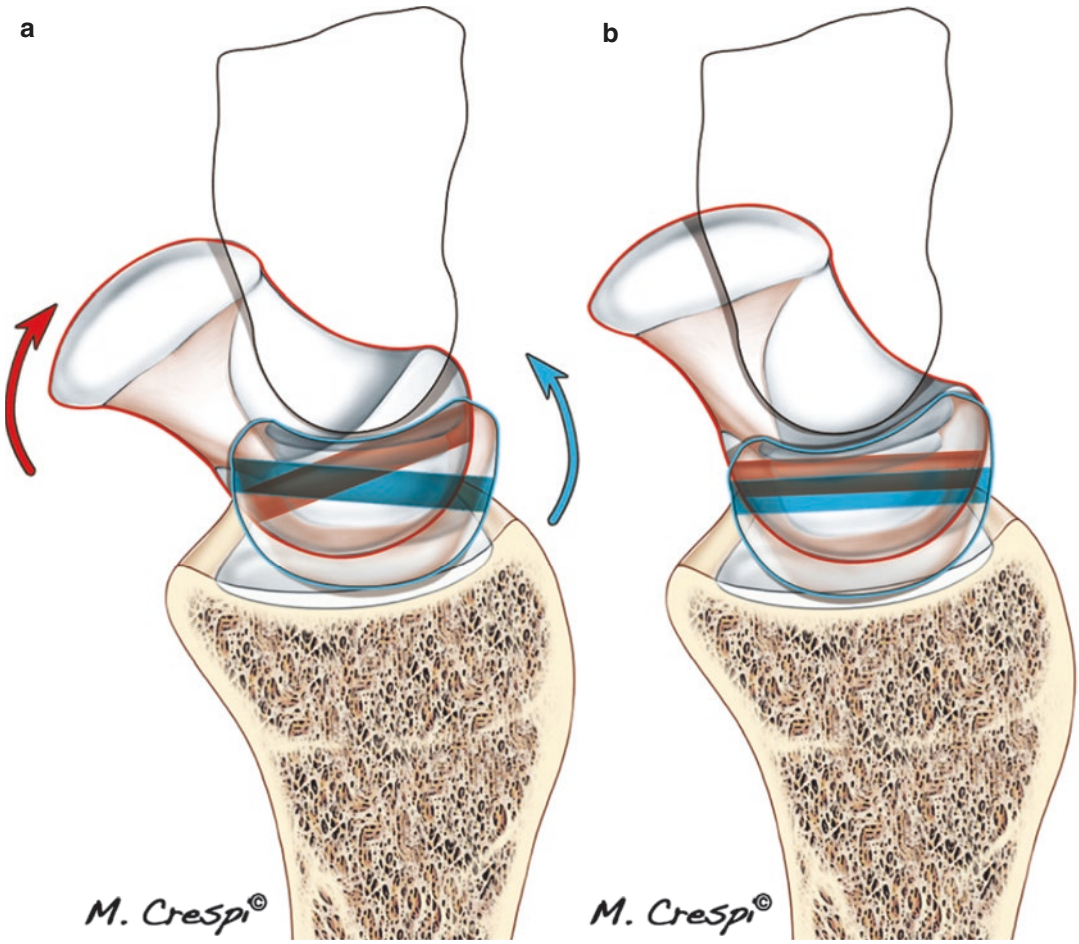

Fig. 78.15 (**a**) Drawing showing the position of tunnels before passage of tendon graft and before reduction. (**b**) Drawing showing the reduction of both tunnels after tensioning of the PL graft. (Illustration courtesy of M. Crespi, adapted with permission from Mathoulin (2019); copyright 2019 Georg Thieme Verlag KG; From Mathoulin, Wrist Arthroscopy Techniques, 2nd edition, Georg Thieme Verlag, Stuttgart 2019, with permission)

emerge from the volar side of the bone tunnels. PL tendon graft is then held tight by the arthroscopic grasper and brought through the tunnels to the dorsal surface (Fig. 78.16). It is critically important to be sure that the grasper is passing inside the tunnels instead of slipping through the surface of the carpal bones. The tendon graft is passed outside the capsule to cross the SL interval so that the reconstruction also includes the capsule and the extrinsic ligaments, which confer added stability to the SL joint (Fig. 78.17). It is mandatory to check that the volar loop of the tendon graft does not trap on any of the flexor tendons and the median nerve before the tendon graft is tightened and tied.

78.3.9 Assessment Through Midcarpal Joint Arthroscopy and Scapho-lunate Interval Reduction with Palmaris Longus Tendon Graft

The hand is put on the traction tower again. The midcarpal joint is inspected through the MCR portal. The RL pin is then withdrawn from the

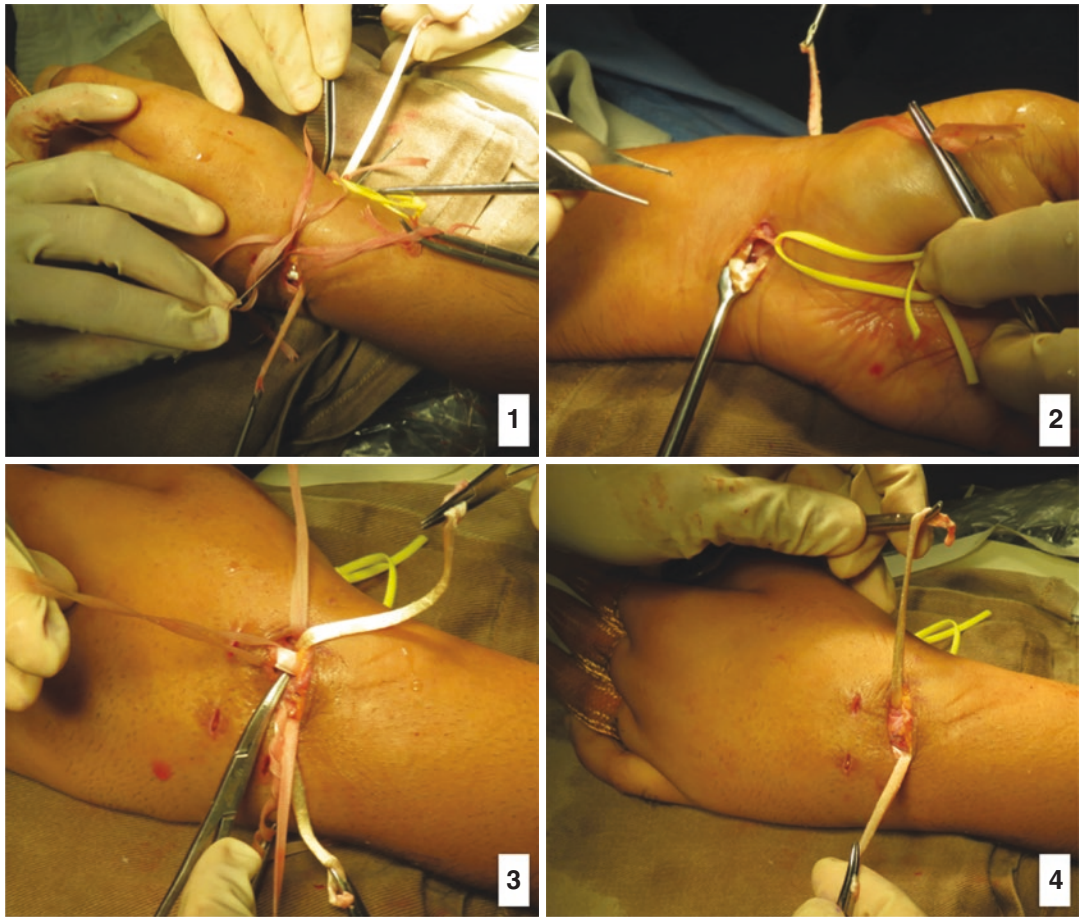

Fig. 78.16 Operative view of PL tendon graft delivered through the wrist capsule and the bone tunnels. (1) Passing the 2 mm arthroscopic grasper from dorsal side to volar side to grab the PL tendon graft end and deliver through the bone tunnel to dorsal side. (2) Careful retraction helps to prevent trapping of flexor tendons and median nerve by the tendon graft. (3) Passing of PL tendon graft underneath the extensors to avoid iatrogenic entrapment of extensors. (4) After checking of no soft tissue entrapment, it is ready for reduction and tightening of tendon graft

lunate so that the lunate becomes mobile. Traction should be reduced to a minimum. When the two ends of the tendon graft are pulled manually, any SL gapping and step-off is corrected and can be visualized under arthroscopic and fluoroscopic surveillance. Any interposing soft tissue at the SL joint can be removed arthroscopically. Quality of reduction can be reassured. If necessary, the reduction can be facilitated by using a large bone reduction clamp placed between the scaphoid and the triquetrum percutaneously. Once adequate reduction is confirmed by tensioning the tendon graft, the hand is put back on the hand table. The two ends of the tendon graft are brought underneath all the extensor tendons to avoid trapping of any extensor tendon in between and meet each other on the dorsal surface of the SL joint capsule. The tendon graft is maximally tensioned and tied in a shoelace manner over the dorsal capsule and secured with 2-0 nonabsorbable braided sutures on a non-cutting needle (Fig. 78.18). Additional sutures can be stitched through the adjacent capsular structure to augment the repair strength. SL reduction and stability are reassessed and confirmed arthroscopically and fluoroscopically. If the reduction and stabil-

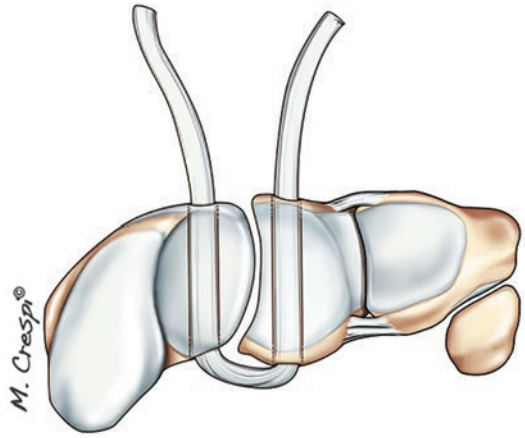

Fig. 78.17 Drawing showing the passage of PL tendon graft from scaphoid, volar to the volar capsule and through the lunate before final tightening and suture. (Illustration courtesy of M. Crespi, adapted with permission from Mathoulin (2019); copyright 2019 Georg Thieme Verlag KG; From Mathoulin, Wrist Arthroscopy Techniques, 2nd edition, Georg Thieme Verlag, Stuttgart 2019, with permission)

ity are suboptimal, the suturing can be revised after further tensioning until reduction is satisfactory. The tendon graft is then tied once more and sutured securely. Two knots of the tendon graft suffice as further knotting may produce an unacceptable bump at the back of the wrist. To augment the stability of the construct, it is optional to pin the scapho-capitate (SC) joint to unload the SL joint. Two 1.1-mm K-wires are inserted through a small incision in the anatomic snuffbox region to transfix the SC joint which can protect the reconstructed ligament during the healing process (Figs. 78.19 and 78.20). The pins are cut short and buried underneath the skin for later removal. SL joint K-wire fixation is not used as this may risk injury and weakening of the tendon graft inside the bone tunnels. Additional suture anchors can be placed next to the dorsal bone tunnels over the scaphoid and lunate and tied for additional repair strength. The RL pin is then

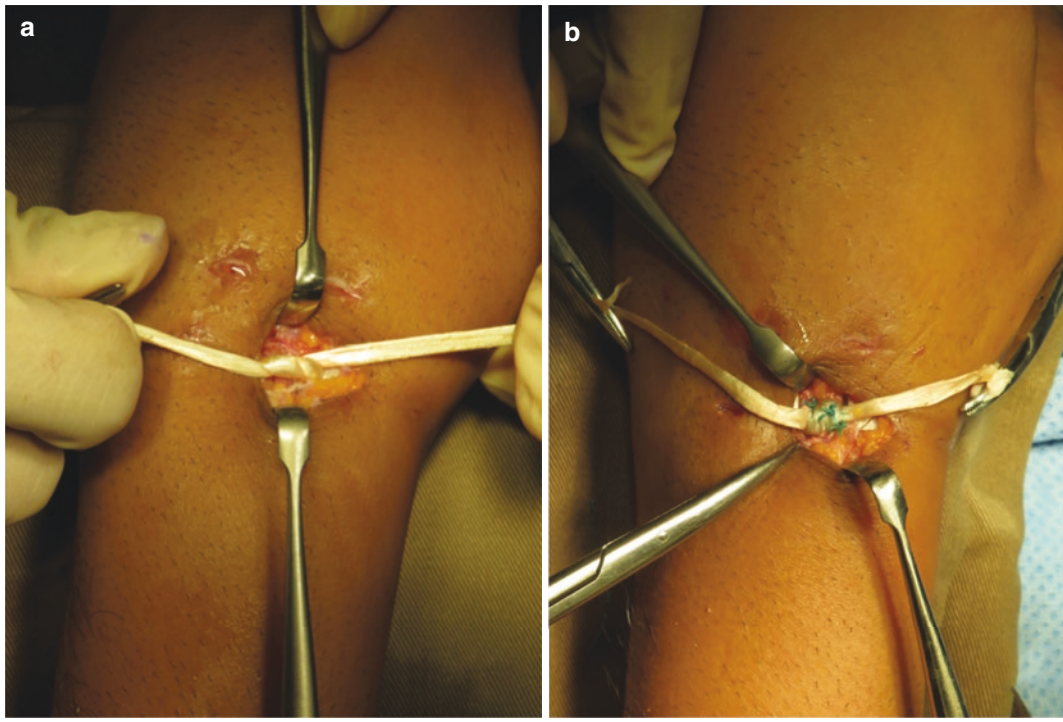

Fig. 78.18 (**a**) The tendon graft is knotted and (**b**) sutured under maximal tension on the dorsal surface of the SL joint extracapsularly in a shoelace manner

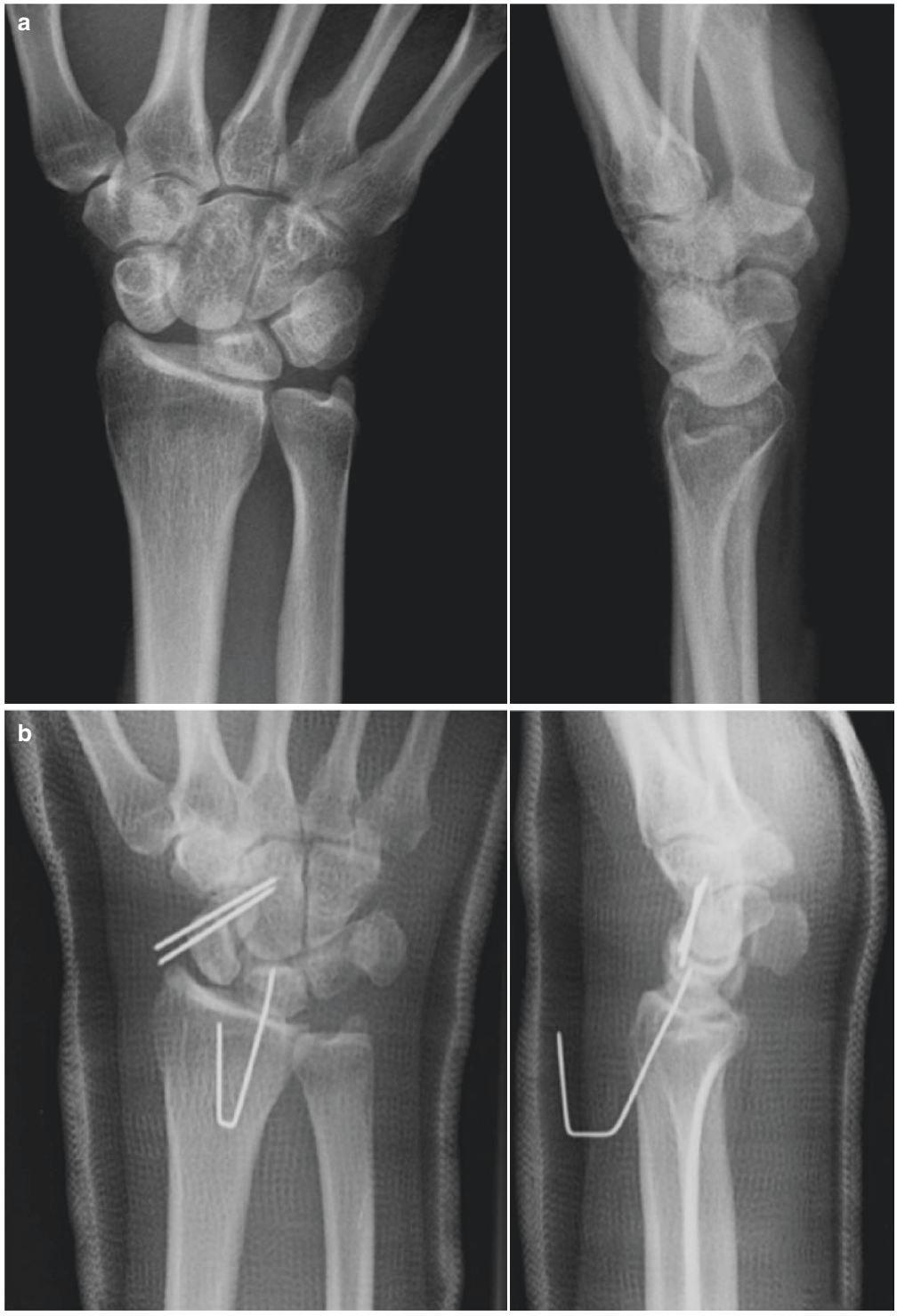

Fig. 78.19 (**a**) Preoperative X-ray of PA and lateral view for right wrist showing widening of SL interval and developing mild DISI. (**b**) Immediate postoperative X-ray showing the SL interval gap was reduced compared to preoperative X-ray. DISI deformity is also reduced and stabilized with PL pinning and the construct is further stabilized by SC pinning

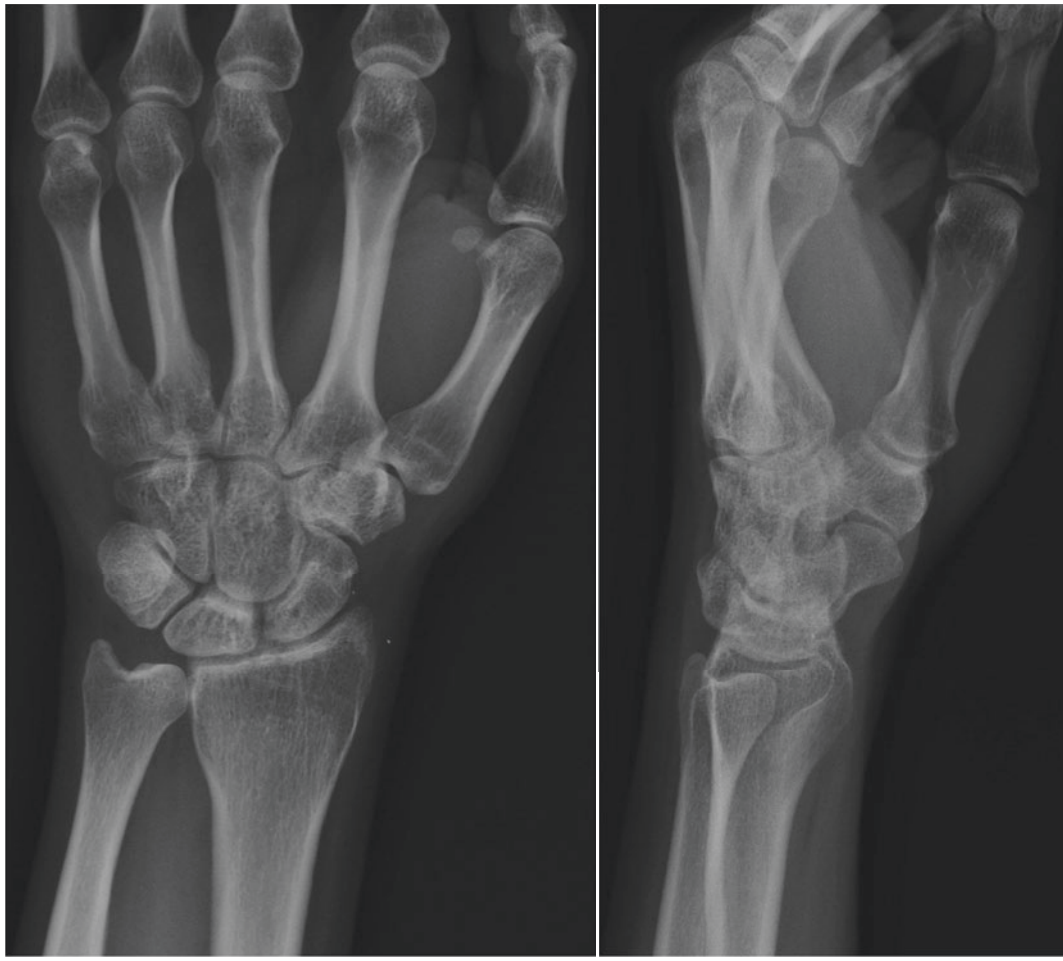

Fig. 78.20 X-ray of PA view and lateral view of the same patient taken 9.5 years after the SL reconstruction. There is no reopening up of the SL interval and corrected scapho-lunate angle maintained

advanced to maintain the lunate reduction if necessary. If the reconstruction is considered solid and stable, the protective pinning can be omitted. The extensor tendons are repositioned, and the extensor retinaculum repaired.

78.3.10 Closure and Postoperative Care

The wound is closed with absorbable subcuticular sutures. Bulky dressing and scaphoid plaster slab are applied with the wrist in a neutral position and the thumb in neutral palmar abduction.

78.4 Tips and Tricks

- Intra-articular fibrosis is often found in radiocarpal joint interposed at the region between dorsal joint capsule and the region of the SL ligament. The fibrosis and scar tissue need to be shaved away to improve the reducibility of the SL malalignment. Fluoroscopic assessment is required to assess whether DISI deformity can be reduced or not before proceeding to tendon harvesting and bone tunnel creation.
- When making the volar skin incision, the palmar cutaneous branch of the median nerve

should be identified and protected with a vessel loop; otherwise, the nerve will be injured in the subsequent procedure.

- When transfixing the RL joint, the 1.6-mm is inserted percutaneously through the dorsum of the distal radius. Blunt dissection is required to avoid iatrogenic injury to the extensor tendons. The RL pin should be aimed at the ulnar half of the lunate to avoid conflict with the subsequent lunate bone tunnel.
- Precise bone tunnel position in scaphoid and lunate as described above should be confirmed with fluoroscopy to avoid blow-out fracture.
- Pay attention to bone tunnel size and soft tissue protection is needed when passing K-wire and cannulated drill.
  - The bone tunnels should not be too large or too small as there is a risk of iatrogenic fracture, bone ischemia, or graft damage. A tunnel size of about 2.5 mm is appropriate.
  - The flexor tendons and median nerve have to be gently retracted and protected when the guide pins and cannulated drills are passing out from the volar side of the scaphoid and lunate. Flexing the wrist slightly helps to relax the tension of the flexor tendons, especially when driving the K-wire through the lunate to the volar side. A large soft tissue protection sheath is essential when using the cannulated drills.
  - The assistant surgeon working on the volar side should preferably be a knowledgeable and reliable partner as it is hard for the arthroscopic surgeon to visualize both the dorsal and the palmar side at the same time. There should be good lighting and loupe magnification to avoid complications.
- Use nonabsorbable round-bodied suture needle when securing the tied tendon graft in order to avoid iatrogenic injury and graft laceration by needle itself.
- Avoid K-wire pinning on the SL joint as it may injure and weaken the tendon graft inside the scaphoid and lunate bone tunnels.

78.5 Postoperative Management and Rehabilitation

The wrist is immobilized in a short arm thumb spica cast for 6 weeks. The RL pin is removed at the beginning of the third week. The cast is then changed to a thumb spica splint for an additional 2 weeks, at which time gentle active wrist mobilization exercise is allowed out of the splint. The SC pins are removed at the beginning of the ninth week under local anesthesia. The splint is worn at nighttime for another 4–6 weeks. Gradual wrist range-of-motion exercises under physiotherapist supervision are started after the pin removal. Passive motion exercises can be commenced at the beginning of the 11th week and gradual strengthening exercises at 13th week after surgery. The SL reduction should be monitored at the interval with radiological examination.

78.6 Results

In our series of the first 17 patients with chronic SL instability operated between October 2002 and June 2012, there were 3 Geissler grade 3 and 14 grade 4 instability cases. The average preoperative SL interval was 4.9 mm (range 3–9 mm). DISI deformity was present in 13 patients. Six patients had stage 1 SLAC wrist change radiologically. Concomitant procedures were performed in four patients. The average follow-up was 48.3 months (range 11–132 months). Thirteen returned to their preinjury job level. Eleven patients had no wrist pain, and 6 had some pain on either maximum exertion or at the extreme of motion. The flexion-extension and radial-ulnar deviation range improved when compared to preoperative ranges. Mean grip strength was 32.8 kg (120% of the preoperative status, 84% of the contralateral side). The average SL interval after reconstruction was 2.9 mm (range 1.6–5.5 mm). Recurrence of a DISI deformity was noted in four patients but remained asymptomatic. No case reported progressive SLAC wrist change. Ischemic change in proxi-

mal scaphoid was noted in one case without symptom or progression. It is likely due to the creation of a large-bore bone tunnel of 3.5 mm at the initial period of the surgery development. There was no neurovascular or tendon complication. All patients were satisfied with the procedure and outcome.

Naqui et al. had reviewed the 1191 papers related to the management of chronic nonarthritic scapholunate dissociation, of which 17 papers were valid for analysis. From his analysis, our method had better pain reduction than others (63% in our study vs. 50% in capsulodesis vs. 52% in tenodesis). This would probably be related to minimal soft tissue disturbance as our technique is performed with very little soft tissue dissection under arthroscopic guidance. Flexion-extension arc has improved (15%) in our series while tenodesis and capsulodesis have reduced flexion-extension range. The greater loss of motion in tenodesis and capsulodesis can be explained by the fact that tenodesis crosses radiocarpal and midcarpal joint whereas in capsulodesis the reinforcement of the dorsal SLIL repair through the capsular flap will limit the radiocarpal joint motion [37]. Our technique involves tendon graft spanning over scaphoid and lunate only can minimizes the restraining effect on the motion of other carpal bones. Also, as the tendon graft is placed at extracapsular level, it helps to reinforce the extrinsic secondary stabilizers when the graft is tied in its maximal tension. Moreover, as the joint capsule is not violated, the innervation pathways remain intact and thus help to enhance the scapholunate stabilizing effect further [38, 39].

78.7 Conclusion

Different methods have been described to reconstruct the scapholunate ligament in chronic scapholunate dissociation over the past 50 years. It is logical and more preferable to reconstruct both the dorsal and the volar components and to augment the extrinsic ligaments as a secondary joint stabilizer in a minimally invasive manner. Our study demonstrated that it could be performed in an arthroscopic-assisted manner. The ideal indication for this technique is a non-reparable complete scapholunate ligament injury with reducible dissociation. The presence of DISI deformity does not preclude this method as long as the deformity is reducible. In chronic cases, arthroscopic treatment has the additional role of shaving of intra-articular fibrosis and lysis of capsular scar to convert a non-reducible DISI into a reducible one, and facilitate subsequent reduction and reconstruction.

References

1. Daniels JM II, Zook EG, Lynch JM. Hand and wrist injuries: Part I. Nonemergent evaluation. Am Fam Physician. 2004;69(8):1941–8.
2. Mayfield JK, Johnson RP, Kilcoyne RK. Carpal dislocations: pathomechanics and progressive perilunar instability. J Hand Surg Am. 1980;5(3):226–41.
3. Short WH, Werner FW, Green JK, et al. Biomechanical evaluation of the ligamentous stabilizers of the scaphoid and lunate: part III. J Hand Surg Am. 2007;32:297–309.
4. Peterson HA, Lipscomb PR. Intercarpal arthrodesis. Arch Surg. 1967;95:127–34.
5. Palmer AK, Dobyns JH, Linscheid RL. Management of post-traumatic instability of the wrist secondary to ligament rupture. J Hand Surg Am. 1978;3:507–32.
6. Uematsu A. Intercarpal fusion for treatment of carpal instability: a preliminary report. Clin Orthop Relat Res. 1979;144:159–65.
7. Watson HK. Limited wrist arthrodesis. Clin Orthop Relat Res. 1980;149:126–36.
8. Glickel SZ, Millender LH. Ligamentous reconstruction for chronic intercarpal instability. J Hand Surg Am. 1984;9:514–27.
9. Hastings DE, Silver RL. Intercarpal arthrodesis in the management of chronic carpal instability after trauma. J Hand Surg Am. 1984;9:834–40.
10. Blatt G. Capsulodesis in reconstructive hand surgery. Dorsal capsulodesis for the unstable scaphoid and volar capsulodesis following excision of the distal ulna. Hand Clin. 1987;3:81–102.
11. Conyers DJ. Scapholunate interosseous reconstruction and imbrication of palmar ligaments. J Hand Surg Am. 1990;15:690–700.
12. Almquist EE, Bach AW, Sack JT, Fuhs SE, Newman DM. Four-bone ligament reconstruction for treatment of chronic complete scapholunate separation. J Hand Surg Am. 1991;16:322–7.
13. Pisano SM, Peimer CA, Wheeler DR, Sherwin F. Scaphocapitate intercarpal arthrodesis. J Hand Surg Am. 1991;16:328–33.

14. Rotman MB, Manske PR, Pruitt DL, Szerzinski J. Scaphocapitolunate arthrodesis. J Hand Surg Am. 1993;18:26–33.
15. Brunelli GA, Brunelli GR. A new surgical technique for carpal instability with scapho-lunar dislocation. (Eleven cases). Ann Chir Main Memb Super. 1995;14:207–13.
16. Wintman BI, Gelberman RH, Katz JN. Dynamic scapholunate instability: results of operative treatment with dorsal capsulodesis. J Hand Surg Am. 1995;20:971–9.
17. Rosenwasser MP, Miyasajsa KC, Strauch RJ. The RASL procedure: reduction and association of the scaphoid and lunate using the Herbert screw. Tech Hand Up Extrem Surg. 1997;1:263–72.
18. Uhl RL, Williamson SC, Bowman MW, Sotereanos DG, Osterman AL. Dorsal capsulodesis using suture anchors. Am J Orthop. 1997;26:547–8.
19. Van Den Abbeele KL, Loh YC, Stanley JK, Trail IA. Early results of a modified Brunelli procedure for scapholunate instability. J Hand Surg Br. 1998;23:258–61.
20. Weiss AP. Scapholunate ligament reconstruction using a bone-retinaculum-bone autograft. J Hand Surg Am. 1998;23:205–15.
21. Harvey EJ, Hanel DP. Bone-ligament-bone reconstruction for scapholunate disruption. Tech Hand Up Extrem Surg. 2002;6:2–5.
22. Moran SL, Ford KS, Wulf CA, Cooney WP. Outcomes of dorsal capsulodesis and tenodesis for treatment of scapholunate instability. J Hand Surg Am. 2006;31(9):1438–46.
23. Darlis NA, Kaufmann RA, Giannoulis F, Sotereanos DG. Arthroscopic debridement and closed pinning for chronic dynamic scapholunate instability. J Hand Surg Am. 2006;31:418–24.
24. Garcia-Elias M, Lluch AL, Stanley JK. Three-ligament tenodesis for the treatment of scapholunate dissociation: indications and surgical technique. J Hand Surg Am. 2006;31:125–34.
25. Aviles AJ, Lee SK, Hausman MR. Arthroscopic reduction-association of the scapholunate. Arthroscopy. 2007;23:105.e1–5.
26. Papadogeorgou E, Mathoulin C. Extensor carpi radialis brevis ligamentoplasty and dorsal capsulodesis for the treatment of chronic post-traumatic scapholunate instability. Chir Main. 2010;29:172–9.
27. Mathoulin CL, Dauphin N, Wahegaonkar AL. Arthroscopic dorsal capsuloligamentous repair in chronic scapholunate ligament tears. Hand Clin. 2011;27:563–72.
28. Camus EJ, Van Overstraeten L. Dorsal scapholunate stabilization using Viegas' capsulodesis: 25 cases with 26 months-follow-up. Chir Main. 2013;32:393–402.
29. Ross M, Couzens G. A new technique for scapholunate ligament reconstruction utilizing FCR and interference screw fixation. J Hand Surg Am. 2013;38: Suppl e51.
30. Berger RA, Imeada T, Berglund L, An KN. Constraint and material properties of the subregions of the scapholunate interosseous ligament. J Hand Surg Am. 1999;24:953–62.
31. Berger RA. The ligaments of the wrist. A current overview of anatomy with considerations of their potential functions. Hand Clin. 1997;13:63–82.
32. Yi IS, Firoozbakhsh K, Racca J, Umeda Y, Moneim M. Treatment of scapholunate dissociation with palmaris longus tendon graft: a biomechanical study. Univ Pennsylvania Orthop J. 2000;13:53–9.
33. Zdero R, Olsen M, Elfatori S, et al. Linear and torsional mechanical characteristics of intact and reconstructed scapholunate ligaments. J Biomech Eng. 2009;131(4):41009.
34. Dobyns JH, Linscheid RL, EYS C, Weber ER, Swanson GE. Traumatic instability of the wrist. In: Instructional course lectures, the American Academy of Orthopaedic Surgeons, vol. 24. St. Louis: C. V. Mosby; 1975. p. 182–99.
35. Ho PC, Wong WYC, Tse WL. Arthroscopic-assisted combined dorsal and volar scapholunate ligament reconstruction with tendon graft for chronic SL instability. J Wrist Surg. 2015;4(4):252–63.
36. Koo SC, Ho PC. Wrist arthroscopy under portal site local anesthesia without tourniquet and sedation. Hand Clin. 2017;33(4):585–91.
37. Naqui Z, Khor WS, Mishra A, Lees V, Muir L. The management of chronic non-arthritic scapholunate dissociation: a systematic review. J Hand Surg Eur Vol. 2018;43(4):394–401.
38. Salva-Coll G, Garcia-Elias M, Hagert E. Scapholunate instability: proprioception and neuromuscular control. J Wrist Surg. 2013;2(2):136–40.
39. Hagert E, Lluch A, Rein S. The role of proprioception and neuromuscular stability in carpal instabilities. J Hand Surg Eur Vol. 2016;41(1):94–101.

79 Arthroscopic Interposition Tendon Arthroplasty for Stage-Two Scapholunate Advanced Collapse

C. Mathoulin and Margareta Arianni

79.1 Introduction

Stage 2 scapholunate advanced collapse (SLAC) is characterized by arthritic changes in the scaphoid and scaphoid fossa and typically requires a proximal row carpectomy as salvage procedure. Arthroscopic interposition tendon arthroplasty (AITA) is an alternative salvage procedure that attempts to recreate radiocarpal joint space without grossly altering the anatomy of the wrist joint [1]. It consists of three main parts: (1) Radial styloidectomy, (2) scapholunate joint stabilization, and (3) interposition of tendon graft.

79.2 Surgical Anatomy

In stage 2 SLAC, the scaphoid has been in pathological contact with the radial styloid. The scaphoid is flexed and pronated, away from the extended lunate. Scapholunate ligament remnant is usually present on the lunate, but absent on the scaphoid. Arthritic changes, that had initially been confined to the dorsal aspect of the scaphoid fossa, at this stage have involved the entire scaphoid fossa, thereby reducing the radiocarpal joint space.

79.3 Indications and Contraindications

AITA is indicated in symptomatic stage 2 SLAC that does not respond to conservative management. It is contraindicated in stages 1, 3, and 4 SLAC, active wrist joint infection, and distal radius malunion.

79.4 Surgical Steps

The patient is operated under general or regional anesthesia, with tourniquet in the upper arm. Palmaris longus is harvested using a minimally invasive approach. Plantaris tendon or allograft can be used instead of palmaris longus. The hand is then suspended on a traction tower with 5–7 kg of weight.

79.4.1 Diagnostic Arthroscopy

The initial step is to do diagnostic arthroscopy. Midcarpal joint is explored first to exclude arthritic changes in the midcarpal joint and to assess the instability of the SL joint. Midcarpal arthroscopy is followed by radiocarpal

C. Mathoulin (✉)
Institut de la Main, Clinique Bizet, Paris, France

M. Arianni
Hand Clinic, Ramsay Premier Bintaro Hospital, Tangerang, Indonesia

© ISAKOS 2022

D. N. Bhatia et al. (eds.), *Arthroscopy and Endoscopy of the Elbow, Wrist and Hand*,
https://doi.org/10.1007/978-3-030-79423-1_79

arthroscopy using the 3-4, 4-5, and 6R portals. Creating the 3-4 portal may be a little difficult as the radiocarpal joint is arthritic and, consequently, narrow. Synovectomy is performed to enhance visibility in the joint.

79.4.2 Radial Styloidectomy

The next step is radial styloidectomy. Radial styloidectomy aims at removing osteophytes and impingement between the scaphoid and scaphoid fossa. To perform this step, 1-2 portal is created. The arthroscope is stationed in the 3-4, while the motorized burr is placed in the 1-2 portal (Fig. 79.1). The burr is used to clear the scaphoid fossa from its damaged cartilage until the subchondral layer is exposed. The depth of the resection is 4–5 mm deep. Care must be taken not to burr far too volar to avoid injury to the attachments of the radioscaphocapitate and long radiolunate ligaments. After adequate styloidectomy, an anchor is planted into the radial styloid through the 1-2 portal (Fig. 79.2a, b).

79.4.3 Scapholunate Joint Stabilization

We attempt to stabilize the scapholunate joint by employing the technique of arthroscopic dorsal capsuloligamentous repair [2]. Repair of the scapholunate ligament is not indicated for stage 2 SLAC and stabilization of the scapholunate joint

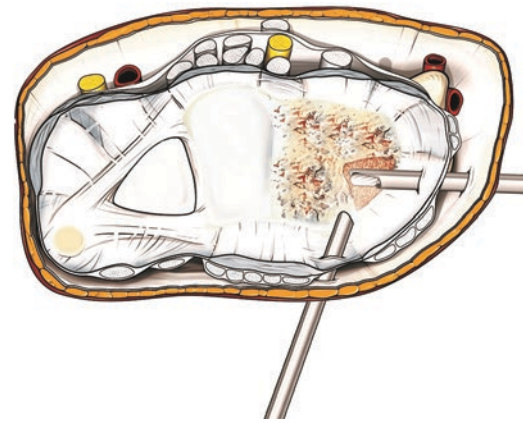

Fig. 79.1 Radial styloidectomy is being carried out with a burr from the 1-2 portal. The arthroscope is visualizing from the 3-4 portal

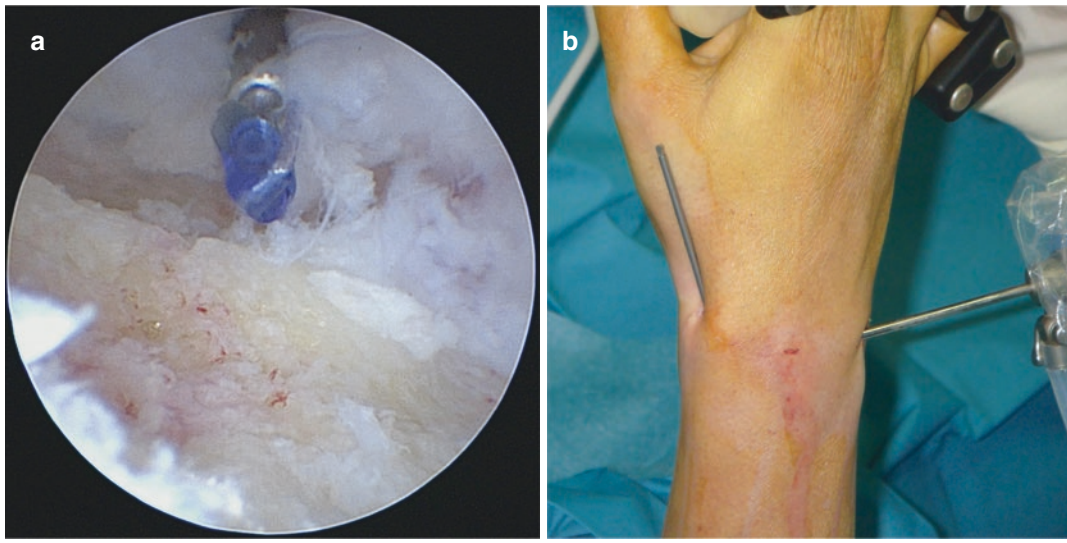

Fig. 79.2 (**a**) (left). Arthroscopic view of an anchor being implanted into the tip of the radial styloid. Note that the radial styloidectomy has been carried out, leaving the subchondral bone exposed. (**b**) (right). The anchor is implanted into the tip of the radial styloid through the 1-2 portal

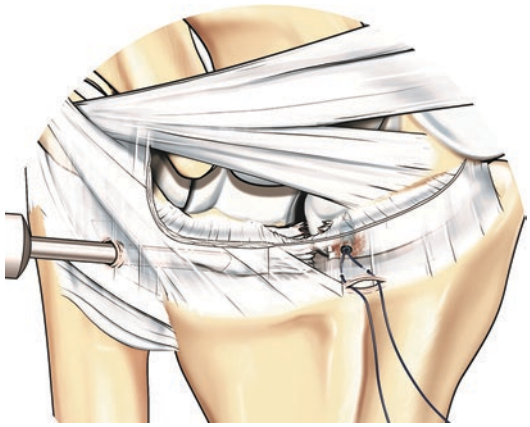

Fig. 79.3 For scapholunate stabilization, the arthroscope is placed in the 6R portal, directed toward the radial side to view the scapholunate ligament. A suture anchor is implanted into the scaphoid proximal pole through the 3-4 portal

Fig. 79.4 The arthroscope is viewing from the 6R portal. At the 3-4 portal, a needle, loaded with suture (blue), has been passed through the scapholunate ligament remnant on the lunate side into the midcarpal joint. Another needle, loaded with one suture from the anchor (black), is about to be passed between the scaphoid and lunate (red arrow)

simply aims to reduce the degree of scaphoid flexion and lunate extension. The arthroscope is stationed in the 6R portal and directed to the radial side, viewing the SL ligament remnant, and a suture anchor is impacted on the scaphoid proximal pole through the 3-4 portal (Fig. 79.3). One of the two sutures from the anchor is passed into a needle. Another needle is loaded with a free 3-0 monofilament suture (polypropylene or PDS). The free suture-bearing needle is inserted into the 3-4 portal, passed through the SL ligament remnant on the lunate side into the SL joint at an angle of 45–60° (Fig. 79.4). The needle bearing the anchor suture follows the first needle in a similar manner, except that it does not catch any ligamentous remnant on the scaphoid side. The arthroscope is moved back into the ulnar midcarpal portal to view the two needles. When directed at the correct angle, the tip of the two needles should emerge in the midcarpal joint, between the scaphoid and lunate. A mosquito clamp is used to retrieve one of the sutures from the radial midcarpal portal. After the first suture is externalized, the mosquito is jabbed into the radial midcarpal portal, but at a point slightly away from the first hole. Through this second hole in the radial midcarpal portal, the second suture is retrieved. Note that the suture that is from the anchor has to be pulled out entirely. The two sutures are then tied into knots at the radial midcarpal portal. Having exited the radial midcarpal portal from two different holes, these sutured are actually knotted on the dorsal capsule or dorsal intercarpal ligament (Fig. 79.5). At the 3-4 portal, the other suture from the anchor and the other end of the monofilament suture will be knotted at the end of the procedure.

79.4.4 Tendon Interposition

The tendon graft is folded into a V-shape configuration and sutured for stability at the apex of the V shape. After the fold, the tendon graft now has two limbs (dorsal and volar limbs). The two sutures from the radial styloid anchor are passed through the apex of the V-shaped tendon graft (Fig. 79.6). Then, the entire tendon graft is squeezed into the radiocarpal joint through the

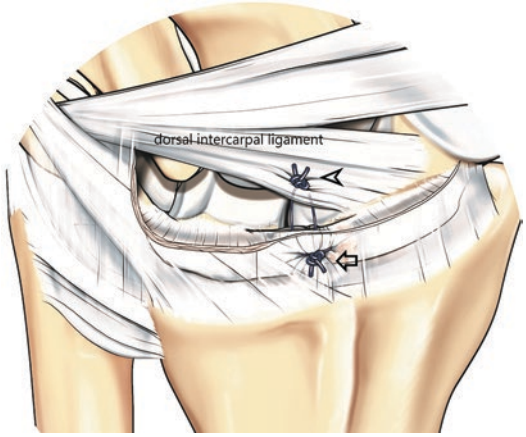

Fig. 79.5 Scapholunate stabilization creates two knots. The first knot (arrowhead) is at the radial midcarpal, grasping a part of the dorsal intercarpal ligament. The second knot (arrow) is to be made at the final step of the procedure

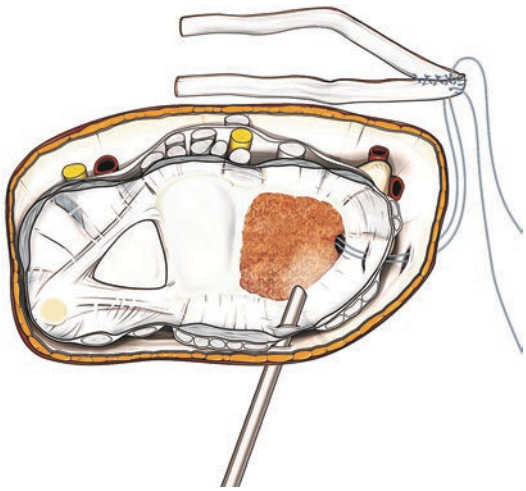

Fig. 79.6 The tendon graft, hanging on the two sutures from the anchor, is ready to be inserted into the radiocarpal joint through the 1-2 portal. The arthroscope is in the 3-4 portal

1-2 portal. The anchor sutures are tied into a knot, fixing the tendon graft to the radial styloid. To proceed with the next step, we require volar radiocarpal and volar ulnocarpal portals, which are made inside-out from the 3-4 and 6R portals, respectively.

Having prepared the volar portals, we are ready to wind each of the limbs around the dorsal

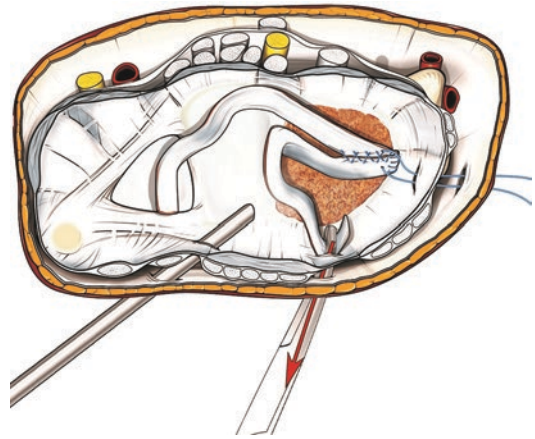

Fig. 79.7 The tendon graft is now in the radiocarpal joint and the arthroscope in the 4-5 portal. The dorsal limb of the graft is pulled out by a mosquito from the 3-4 portal

and volar capsule of the wrist. With the arthroscope viewing from 4-5 portal, the dorsal limb is retrieved with a mosquito from the 3-4 portal (Fig. 79.7). Next, the arthroscope is moved into the 1-2 portal. A plane between the dorsal capsule and the extensor tendon is developed with a mosquito from the 4-5 to 3-4 portal. The mosquito should not be visible on arthroscopy, as the plane is extra-articular. Appearing at the 3-4 portal, the mosquito tip grasps the dorsal limb of the graft and pulls it along the created plane and out at the 4-5 portal. Thus, the dorsal limb is squeezed between the dorsal capsule and the extensor tendons (Fig. 79.8). Now the arthroscope is switched to the 3-4 portal. The dorsal limb of the graft, which is hanging at the 4-5 portal, is brought back into the joint through the 4-5 portal itself, and then exteriorized from the 1-2 portal with a second mosquito (Fig. 79.9). Next, one of the sutures from the radial styloid anchor is passed into the tip of the dorsal limb to secure it.

The same procedure is performed for the volar limb of the graft. The volar limb is exteriorized from the volar radiocarpal portal (Fig. 79.10). A plane between the volar capsule and flexor tendons is developed using a mosquito from the volar ulnocarpal to volar radiocarpal portals. The volar limb that is hanging outside the volar radiocarpal portal is grasped by the mosquito and

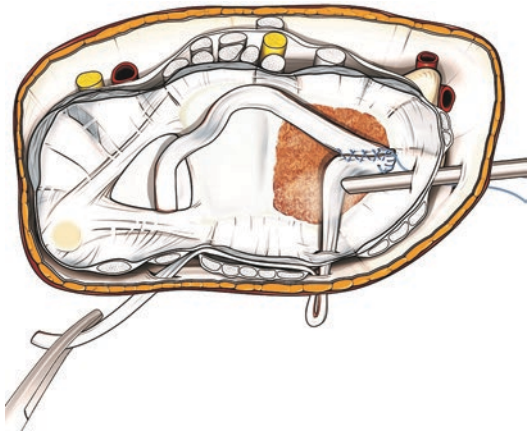

Fig. 79.8 The dorsal limb of the graft is being passed into the space between the dorsal capsule and extensor tendons, from the 3-4 to the 4-5 portals. The arthroscope is stationed in the 1-2 portal

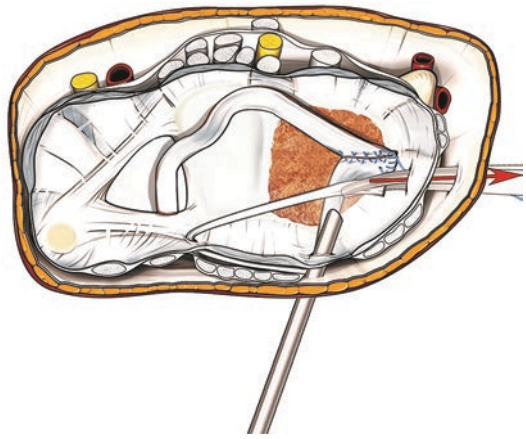

Fig. 79.9 The tip of the dorsal limb of the graft is pulled from the 1-2 portal as the arthroscope is viewing from the 3-4 portal

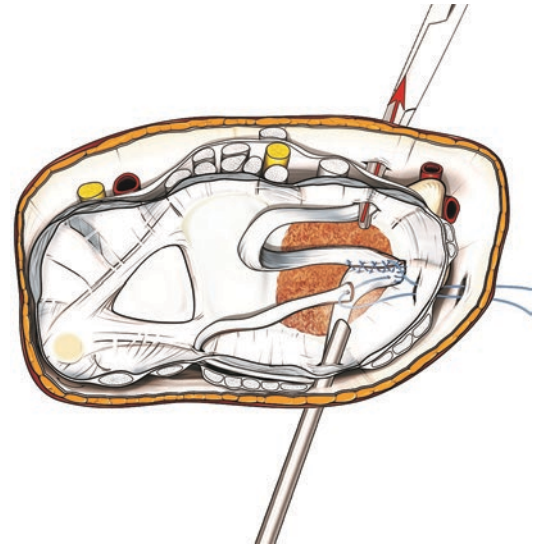

Fig. 79.10 The tip of the dorsal limb of the graft is hanging on one of the anchor sutures at the 1-2 portal. The volar limb of the graft is pulled out of the volar radiocarpal portal, as the arthroscope is viewing from the 3-4 portal

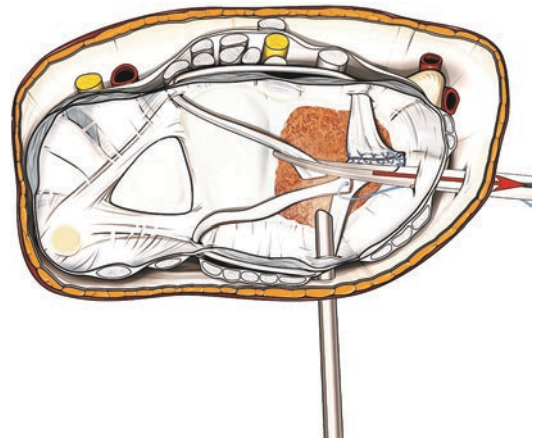

Fig. 79.11 The volar limb of the graft has been passed through the space between volar capsule and flexor tendons, and its tip is now being pulled out of the 1-2 portal

squeezed into the developed plane, exiting the volar ulnocarpal portal. From the ulnocarpal portal, the volar limb is inserted into the joint and retrieved from the 1-2 portal (Fig. 79.11). The last suture of the anchor is passed into the tip of the volar limb of the graft.

The two sutures of the anchor, which have purchased the dorsal and volar limbs of the graft, are tied into knots, and thus the interposed tendon is fixed in the joint (Fig. 79.12). Finally, the remaining sutures from the scaphoid anchor at the 3-4 portal are tied and the procedure is completed (Fig. 79.5). Any gaping wounds are sutured or taped with sterile strips. The wrist is taken off traction, bandaged, and immobilized with a volar splint for 3 weeks. Preoperative and postoperative radiographs of SLAC 2 are shown as Figs. 79.13 and 79.14, respectively.

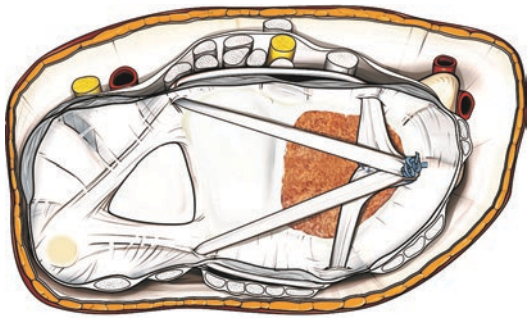

Fig. 79.12 The final configuration of the interposed tendon graft. The anchor sutures have been knotted to securely fix the tendon graft on the radiocarpal joint

Fig. 79.13 Preoperative radiograph (posteroanterior view) of a wrist with SLAC 2. Note that the space between the scaphoid and scaphoid fossa is almost obliterated

Fig. 79.14 Postoperative radiograph of the same wrist as in Fig. 79.13. The space between the scaphoid and scaphoid fossa has been restored

79.5 Tips and Tricks

There are several difficulties that may be encountered in this procedure. Subsequently, we describe some tips and tricks for a few steps that are frequently "tricky" in this procedure.

- Narrow radiocarpal joint space:
  - Add more weight onto the traction system (up to a maximum of 7 kg).
  - Stretch the portal with mosquito repeatedly.
  - Use smaller arthroscope (1.9 mm) first, and convert to larger diameter.
  - Use smaller shaver (2.5 mm or less).
- Passing suture-bearing needles into the SL joint from the 3-4 portal.
  - Aim needles at 45–60° inclination.
  - If needles, thought to have entered the SL joint, appear horizontal, most likely they do not emerge in the midcarpal joint between the scaphoid and lunate.
- Developing the space between capsule and tendons.
  - Develop the space under constant visualization.
  - Extend the portal incision to visualize the tendons, hook the tendons away with a retractor.
  - Using a small drain or catheter to simulate the passing of tendon graft in advance may be useful.

79.6 Pitfalls

The configuration of tendon graft interposition is such that one must never be complacent in deciding the adequacy of the length of the tendon graft.

Inadequate resection of the scaphoid fossa will leave remaining osteophytes and impingements. On the other hand, excessive resection on the volar rim of the scaphoid fossa will injure the attachments of RSC and long radiolunate ligaments, and ulnar translocation may ensue in the long run. Stretching each portal with mosquito before passing suture-bearing needles (3-4 portal) or retrieving sutures (radial midcarpal portal) swipes away any tendons that are in the way and thus prevents tendons being inadvertently sutured. In developing the space between joint capsule and tendons with a mosquito, care must be taken not to entrap any of the tendons or the median nerve.

79.7 Postoperative Rehabilitation

Postoperatively, the wrist is simply immobilized in a volar splint for 3 weeks. Thereafter, range of motion and other exercises are initiated and progressed.

79.8 Complications

Superficial branch of the radial nerve may be injured during the creation of the 1-2 portal. Creation of volar radiocarpal portal may put the median nerve at risk of injury; however, a gentle inside-out technique is usually safe. Other complications that are technical in nature include tendon injuries and knot irritation. Prolonged stiffness and complex regional pain syndrome have also been documented.

References

1. Arianni M, Mathoulin C. Arthroscopic interposition tendon arthroplasty for stage 2 scapholunate advanced collapse. Arthroscopy. 2019;35(2):392–402. https://doi.org/10.1016/j.arthro.2018.10.134.
2. Wahegaonkar AL, Mathoulin CL. Arthroscopic dorsal capsulo-ligamentous repair in the treatment of chronic scapho-lunate ligament tears. J Wrist Surg. 2013;2(2):141–8. https://doi.org/10.1055/s-0033-1341582.

80 Arthroscopic Resection Arthroplasty for Scapholunate Advanced Collapse (SLAC Wrist)

Jessica Cobb and Tyson Cobb

80.1 Background

The most common form of wrist osteoarthritis is scapholunate advanced collapse (SLAC). Cortisone shots and splinting may work as conservative treatment. Proximal row carpectomy (PRC) and four-corner fusion (4CF) with scaphoid excision are the most common operative procedures when nonoperative options fail. Minimally invasive procedures have the potential advantage of minimal soft tissue damage and quicker recovery. Arthroscopic resection arthroplasty (ARA) is a minimally invasive option, which involves resecting the arthritic portion of the radius and resection of the proximal portion of the scaphoid using only 2-3 small portals.

80.2 Surgical Anatomy

Scapholunate advanced collapse (SLAC) of the wrist is an arthritic process that results from untreated scapholunate ligament tears and dissociation. The scaphoid rotates into flexion resulting in increased wear and arthritis in the scaphoid fossa. Watson and Ballet described three stages [1]. Stage 1 involves arthritis between the scaphoid and the radial styloid. In stage 2, the entire scaphoid fossa of the radius is arthritic, and in stage 3, the arthritic process involves the capitate and lunate.

Arthroscopic treatment can be performed for all three stages. Arthroscopic resection arthroplasty (ARA) is performed by removing the radial styloid and the arthritic portion of the scaphoid fossa and approximately 2/3 of the proximal scaphoid [2]. Midcarpal resection in stage 3 patients is not necessary in our experience for pain relief. ARA for SLAC wrist is most commonly performed using 1-2, and 3-4 portals, and 4-5 portal is used if necessary.

80.3 Indications and Contraindications

The ARA procedure is indicated in the SLAC wrist, which has been unresponsive to conservative care in patients with significant disability and especially over the age of 50.

The procedure is contraindicated in young patients and in those who perform heavy manual labor.

80.4 Surgical Technique

General anesthesia is most frequently used for this procedure in our practice; however, regional or wide-awake anesthesia can also be used on the

J. Cobb (✉)
Morsani College of Medicine, Tampa, FL, USA
e-mail: cobb3@usf.edu

T. Cobb
Shoulder, Elbow, Wrist, and Hand Center of Excellence, Davenport, IA, USA

© ISAKOS 2022

D. N. Bhatia et al. (eds.), *Arthroscopy and Endoscopy of the Elbow, Wrist and Hand*,
https://doi.org/10.1007/978-3-030-79423-1_80

basis of medical need, surgeon, and patient preference. The patient is positioned supine on the operating Table. An arm tourniquet is placed and the arm is taped to the hand table. A traction tower with a finger-trap traction of 5–7 kg to index and/or long finger is used (Fig. 80.1).

- Standard 3-4, 4-5, 6 R, 6 U, 1-2, volar flexor carpi radialis (FCR) portals, and midcarpal portals as indicated can be used to perform standard radiocarpal and midcarpal arthroscopy. Often only the 1-2 and 3-4 and/or 4-5 portals are required (Fig. 80.2).
- Portals are localized with 18-gauge needle. At each portal site, 10 mL of 0.25% bupivacaine with epinephrine is injected subcutaneously. Skin incisions are made just through the dermis with a No. 15 scalpel. A hemostat is used for blunt dissection to enter the joint.
- A 2.7-mm, 30° arthroscope is utilized to perform arthroscopy. A 3.5-mm aggressive shaver (Stryker Endoscopy, San Jose, CA) is used for the synovectomy, resection of debris, and the torn scapholunate ligament.
- Loose bodies are removed as they are encountered (Fig. 80.3).

Fig. 80.1 Intraoperative positioning is shown. The arm is taped to hand table with a tourniquet in place (left image) and a traction tower is used (right image)

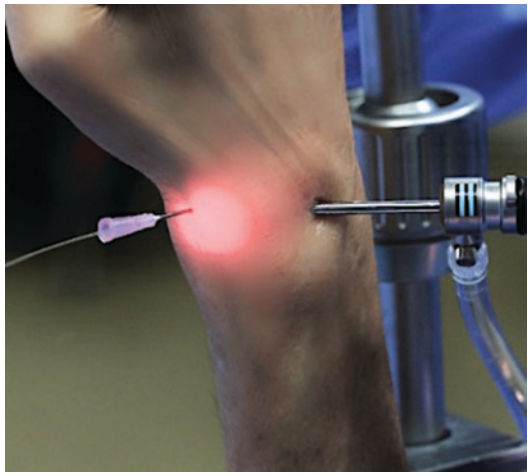

Fig. 80.2 An 18-gauge needle is used to establish the 1-2 dorsal radiocarpal portal. The arthroscope is placed in the 3-4 portal

Fig. 80.3 Loose body removal with hemostat is demonstrated

- Denervation of the arthritic portion of the joint to be resected (dorsal, volar, and radial) is performed with a radiofrequency ablator (Serfas 3.5-mm, Stryker, Greenwood Village, CO) (Fig. 80.4) [3–6].
- Resection of the sensory nerve endings as they enter the joint on the capsule is required for denervation. It is believed that disruption of the sensory nerve pathway is the reason for early pain relief. Sensory contributions are included from the lateral antebrachial cutaneous nerve, palmar cutaneous branch of the median nerve, posterior interosseous nerve, anterior interosseous nerve, superficial branch of the radial nerve, and deep branch of the ulnar nerve. The capsule is vaporized from its attachment to the radius. The high flow of fluid protects the joint from overheating.

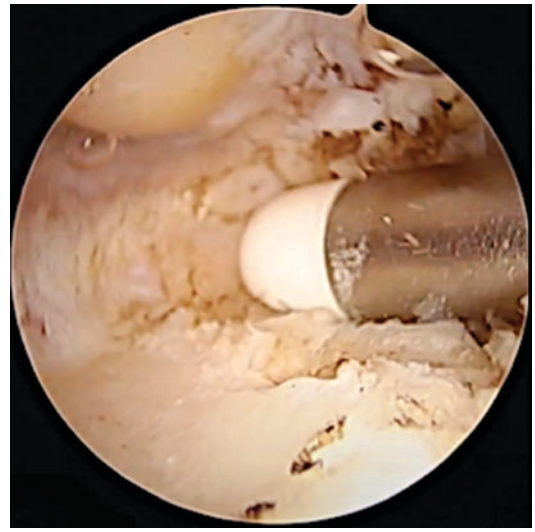

Fig. 80.4 Denervation of the arthritic portion of the joint is performed with a radiofrequency ablator

- For bone resection, a 4-mm 12-flute barrel burr (Stryker Endoscopy, San Jose, CA) is inserted into the 1-2 portal (Fig. 80.5). The 3-4 or 4-5 portal is used for initial viewing. However, the scope can be moved as needed between the 4-5, 3-4, and 1-2 portals to enhance visualization. If necessary, the volar FCR portal is used for better visualization of dorsal aspect of the joint (Fig. 80.6) [3–12].
- To begin resection, the burr is perched on the styloid at the radial edge. This placement ensures that a ridge of bone is not left behind and makes bone resection easier than with a centrally placed portal. Synovium and capsule tissue are removed prior to starting bony resection to clearly define the bony margin. Placement of the 1-2 portal slightly proximal to the joint line facilitates bone resection. This

placement results in the instrument slightly angled upward as it enters the joint and makes resection easier (Fig. 80.7).

- The styloid is resected to a depth of 4 mm. The burr is oscillated volarly and dorsally using a windshield-wiper motion, moving from the radial to the ulnar side until all abnormal portions of the radius are removed. The resection usually involves the entire scaphoid fossa. To protect capsular ligaments, carefully burr

Fig. 80.5 The 1-2 dorsal radiocarpal portal is used for bone excision using a burr

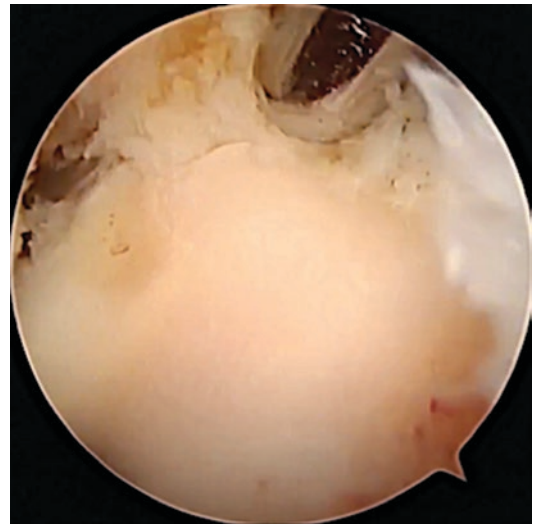

Fig. 80.6 Dorsal osteophyte (shown in the left of probe) resection is demonstrated

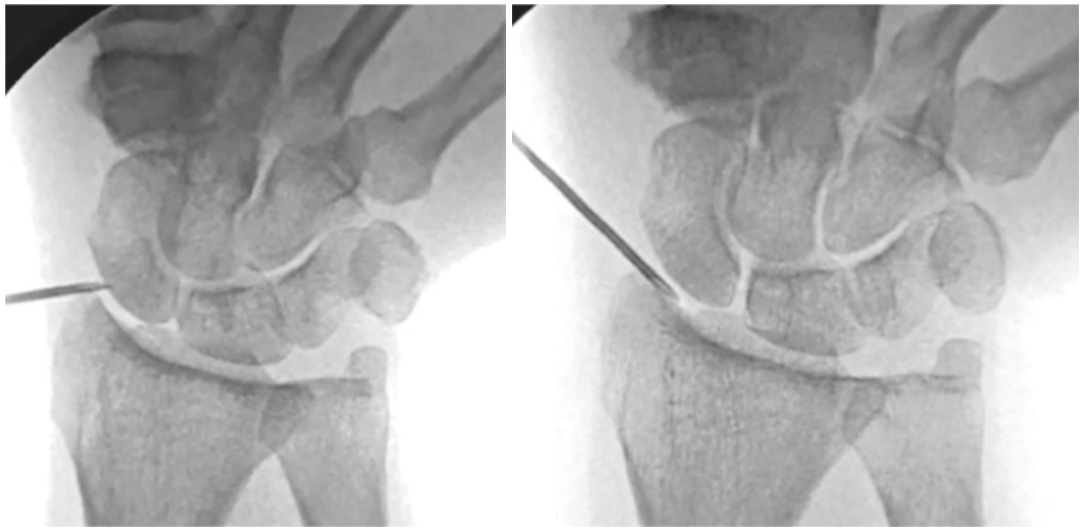

Fig. 80.7 Radiograph showing approach to radial styloid with an 18-gauge needle to establish a working portal for significant amount of bone resection during radial styloidectomy. Note that with this approach as bone is resected, the burr will become level with the joint. Therefore, the greater the amount of anticipated bone resection, the steeper the approach to the joint (left image). This approach makes bone resection much easier as compared to a standard working portal (right image)

away cortical bone until the volar wall becomes pliable, up to but not through the soft tissue envelope. The hood of the burr can also return toward the capsule providing some protection (Fig. 80.8).

- The entire radial column is resected up to the healthy-appearing cartilage (Fig. 80.9). The transition to the lunate fossa is an abrupt change to normal cartilage starting at the ridge separating the scaphoid and lunate fossa.
- The proximal two-third of the arthritic scaphoid is then resected (Fig. 80.10). Aggressive bone removal is recommended. Sufficient scaphoid should be removed to alleviate all impingement. Midcarpal resection is not necessary even if it is arthritic.

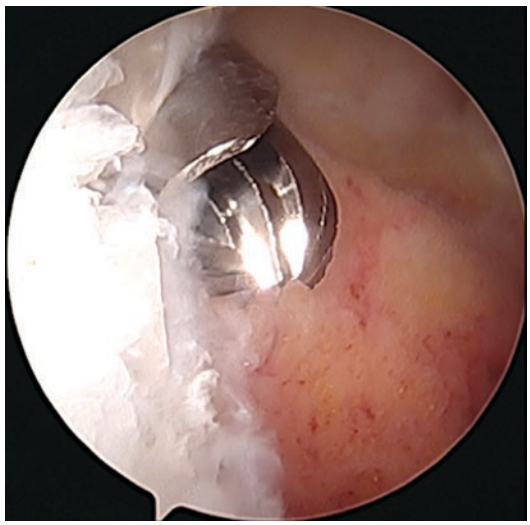

Fig. 80.8 A 4-mm burr is shown inserted for aggressive resection and the hood is used for protection of volar ligaments

Fig. 80.9 Fluoroscopic view shows resection of entire scaphoid fossa and proximal two-thirds of scaphoid

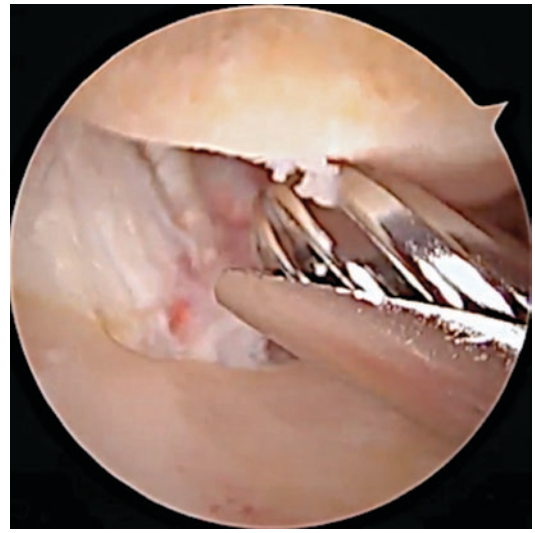

Fig. 80.10 Adequate excision of scaphoid (usually proximal two-thirds) is performed to prevent any impingement against the radius

Additional 0.25% bupivacaine with epinephrine or 1% lidocaine with epinephrine is injected into the resected joint (if not contraindicated). A total of approximately 60–80 mL of 0.25% bupivacaine with epinephrine is commonly used. The portals are closed with adhesive strip skin closures. Patient is placed in a well-padded volar splint with a compressive ACE bandage.

80.5 Tips and Tricks

- A fluid pump improves the pressure inside the joint and improves visualization over gravity flow systems.
- Fluoroscopy is useful for portal placement and to assess the amount of bone resection intraoperatively.

- A 4-mm barrel burr should be used to allow for adequate bone resection in a reasonable amount of time.
- Viewing portals such as the 4-5 portal are best placed centrally into the joint, whereas the 1-2 portal is best placed more proximal and closer to the radial styloid, which makes bone resection easier.
- Traction displaces the scaphoid distally which can make resection of the scaphoid difficult. A more distally placed portal may be helpful for scaphoid resection. If resection of scaphoid is difficult, then the size of the portal can be extended to allow placement of a small rongeur to facilitate this process.
- In some instances, traction does not open the lunate fossa sufficiently because of the dissociation between the scaphoid and the lunate. This may make placement of the arthroscope into the lunate fossa difficult. When this occurs, a freer elevator can be placed under the lunate from the 1-2 portal and used to push the lunate distally allowing the arthroscope cannula to be placed into the lunate fossa.
- High volume local anesthetic with epinephrine is helpful for postoperative hemostasis (inject at least half the volume preoperatively) and pain relief. Blocking the pain cycle postoperatively enhances patient experience and recovery. The author has a low threshold for postoperative pain blocks in the office for patients experiencing more pain than usual.

80.6 Pitfalls

- Persistent postoperative pain is often due to failure of removing enough bone.
- Inadequate resection is the most common cause of failures. Fluoroscopy can be to ensure an adequate resection.
- Simultaneous carpal tunnel release should be considered if the patient has a positive Tinel's sign even if the symptoms are absent.
- Dorsal osteophyte impingement limits extension in many of these patients. Aggressive treatment of these dorsal osteophytes can result in damage to extensor tendons.

80.7 Postoperative Management and Rehabilitation

Edema control is facilitated through the icing and elevating the extremity. The wrist is splinted for approximately 7 days. Thereafter, the patients are placed in a removable splint and encouraged to begin range of motion exercises. For patients who travel from out of town, a removable sprint is utilized starting their first postoperative day. Patients are allowed to use the wrist as tolerated. Formal therapy is utilized as needed but seldom required. Timing of pain relief following this procedure varies greatly between patients. Surgeons have to be patient in the postoperative period for patients who are slow responders. Cortisone injections can be helpful to get slow responders through these periods. Physicians should resist the urge for early revision in slow responders, otherwise, patients will be subjected to salvage procedures that are not required.

80.8 Complications

- In the author's series in over 50 patients, three (6%) failures required revision surgery for persistent pain.
- Tendon rupture can occur from injury while working on the dorsal aspect of the radius with the burr or radiofrequency ablator.
- As with any major wrist surgery, postoperative acute carpal tunnel can occur secondary to the swelling. Therefore, simultaneous carpal tunnel release should be performed in patients with any median nerve irritability.

80.9 Results

This operation is the senior author's primary surgical intervention for most of the patients undergoing surgery for SLAC wrist who are over the age of 50. Results have been excellent, failure rate (6%) is acceptable and recurrence has not been an issue following this operation. With an average of 4-year follow-up, the mean satisfaction score was 4.8 out of a possible 5. DASH score was 42 preoperatively and 3 at final follow-

up. Mean pain score (0–10) was 7 before surgery and 0.3 at final follow-up. The total arc of motion changed from 114° preoperatively to 126.5° postoperatively. Mean grip strength was 41 kg preoperatively and 49 kg postoperatively.

References

1. Watson HK, Ballet FL. The SLAC wrist: Scapholunate advanced collapse pattern of degenerative arthritis. J Hand Surg Am. 1984;9:358–65.
2. Walden A, Wilt J, Cobb T. Arthroscopic resection arthroplasty of the radial column for SLAC wrist. J Wrist Surg. 2014;03:114–22.
3. Leclaire R, Fortin L, Lambert R, Bergeron YM, Rossignol M. Radiofrequency facet joint denervation in the treatment of low back pain. Spine. 2001;26:1411–6.
4. Loréa PD. First carpometacarpal joint denervation: anatomy and surgical technique. Tech Hand Upper Extrem Surg. 2003;7:26–31.
5. Wilhelm A. Partial joint denervation: wrist, shoulder, and elbow. Plast Reconstr Surg. 2010;126:345–7.
6. Wilhelm A. Denervation of the wrist. Tech Hand Up Extrem Surg. 2001;5:14–30.
7. Cobb T, Sterbank P, Lemke J. Arthroscopic resection arthroplasty for treatment of combined carpometacarpal and scaphotrapeziotrapezoid (pantrapezial) arthritis. J Hand Surg Am. 2011;36:413–9.
8. Cobb TK, Walden AL, Cao Y. Long-term outcome of arthroscopic resection arthroplasty with or without interposition for thumb basal joint arthritis. J Hand Surg Am. 2015;40:1844–51.
9. Radu C, Schachner M, Tränkle M, Germann G, Sauerbier M. [Functional results after wrist denervation] Handchirurgie · Mikrochirurgie · Plastische. Chirurgie. 2010;42:279–86.
10. Weinstein LP, Berger RA. Analgesic benefit, functional outcome, and patient satisfaction after partial wrist denervation. J Hand Surg Am. 2002;27:833–9.
11. Cobb J, Cobb T, Cobb A (2019) Arthroscopic resection arthroplasty for scapholunate advanced collapse wrists.
12. Cobb J, Cobb T, Mathoulin C. Arthroscopic Resection Arthroplasty of the Radial Column (ARARC) for Scapholunate Advanced Collapse (SLAC) wrist. In: Wrist arthroscopy techniques. 2nd ed. Stuttgart: Thieme Publishers. 2019.

Part XV

Wrist: Scaphotrapeziotrapezoid Arthroscopy

81 Arthroscopic Resection Arthroplasty for Scaphotrapeziotrapezoid Arthritis

Akio Iida and Shohei Omokawa

81.1 Introduction

Symptomatic scaphotrapeziotrapezoid (STT) osteoarthritis (OA) is frequently observed in hand surgery practice and is one of the important differential diagnoses for radial wrist pain. For patients who fail conservative treatment, surgical options include fusion of the STT joint, simple trapeziectomy, resection of the distal pole of the scaphoid (with or without prosthetic replacement), or arthroscopic debridement. The ideal surgical treatment for STT OA is unclear. Arthrodesis, although usually effective in reducing pain, may require bone graft, has a risk of nonunion, and often results in loss of mobility of the thumb and wrist. Distal scaphoid pole resection can provide acceptable results and requires less immobilization. Moreover, the procedure is associated with fewer complications in the absence of dorsal midcarpal instability. However, preexisting capitolunate malalignment with a normal scapholunate angle could be aggravated by removal of the distal scaphoid and may result in dorsal midcarpal instability. This paper reports detailed the anatomy and kinematics of the STT joint, and the arthroscopic technique of resection arthroplasty for STT osteoarthritis is described.

81.1.1 Surgical Anatomy

Bone morphology and kinematics of scaphotrapeziotrapezoid joint: The STT joint is located in the radial part of the midcarpal joint and consists of the convex surface of the scaphoid and concave surface of the trapezium and trapezoid. The trapezium and trapezoid move in a dart-throwing motion plane (path of motion from radial extension to ulnar flexion) relative to the scaphoid. The articular surface of the STT joint extends from the distal pole to the dorsoradial ridge of the scaphoid (Fig. 81.1). The scaphoid contact area changes dynamically during wrist motion. In wrist ulnar deviation, the contact area is small and located on the distal aspect of the STT joint. In contrast, in wrist radial deviation, the contact area is wide and moves to the dorsoradial slope of the scaphoid (Fig. 81.2).

Ligament and joint capsule of STT joint: The STT joint is stabilized by a stout scaphotrapezial ligament on the radial and palmar aspects of the scaphotrapezial joint, weak dorsal and palmar capsules, and a scaphocapitate ligament. The scaphotrapezial ligament originates from the scaphoid tuberosity and inserts along the trapezial ridge, immediately radial to the flexor carpi radialis (FCR) tendon sheath. The dorsal capsule of

A. Iida
Department of Orthopedic Surgery, Hanna Central Hospital, Nara, Japan
e-mail: iidaakio@f6.dion.ne.jp

S. Omokawa (✉)
Department of Hand Surgery, Nara Medical University, Nara, Japan

© ISAKOS 2022

D. N. Bhatia et al. (eds.), *Arthroscopy and Endoscopy of the Elbow, Wrist and Hand*,
https://doi.org/10.1007/978-3-030-79423-1_81

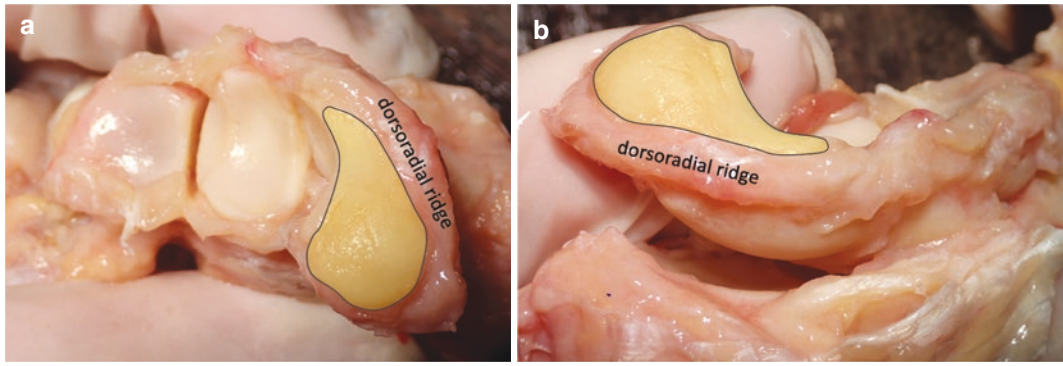

Fig. 81.1 Articular surface of the STT joint on the scaphoid is demonstrated. (**a**) Distal view. (**b**) Dorsoradial view

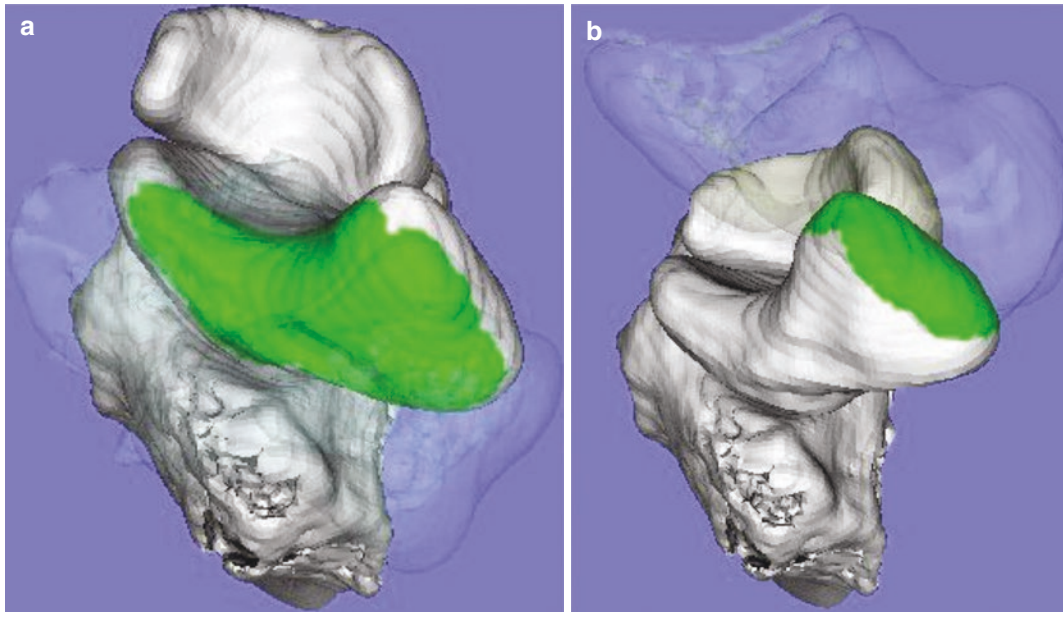

Fig. 81.2 Contact area (green) of the STT joint on the scaphoid in two positions is demonstrated. (Orthopedic viewer, Osaka, Japan). (**a**) Radial deviation. (**b**) Ulnar deviation

the STT joint originates from the dorsal side of the trapezium and trapezoid and inserts onto the dorsoradial ridge of the scaphoid. The palmar capsule forms the floor of the FCR tendon sheath (Fig. 81.3).

Tendon, artery, and nerve surrounding STT joint: The extensor pollicis longus (EPL) and extensor carpi radialis longus tendons run over the dorsal aspect of the STT joint, and the FCR tendon runs over the volar aspect of the STT joint. The radial artery passes over the dorsoradial aspect of the trapezium and is located radial to the EPL tendon. This artery often is tortuous within the anatomic "snuff box." Superficial branches of the radial nerve run along the dorsal aspect of the STT joint and cross over the EPL tendon (Fig. 81.4). When the surgeon creates an arthroscopic portal at the radial side of the EPL tendon, both the radial artery and the superficial branch of the radial nerve are at risk of iatrogenic injury. Portal placement on the ulnar side of the EPL tendon is safer for the radial artery,

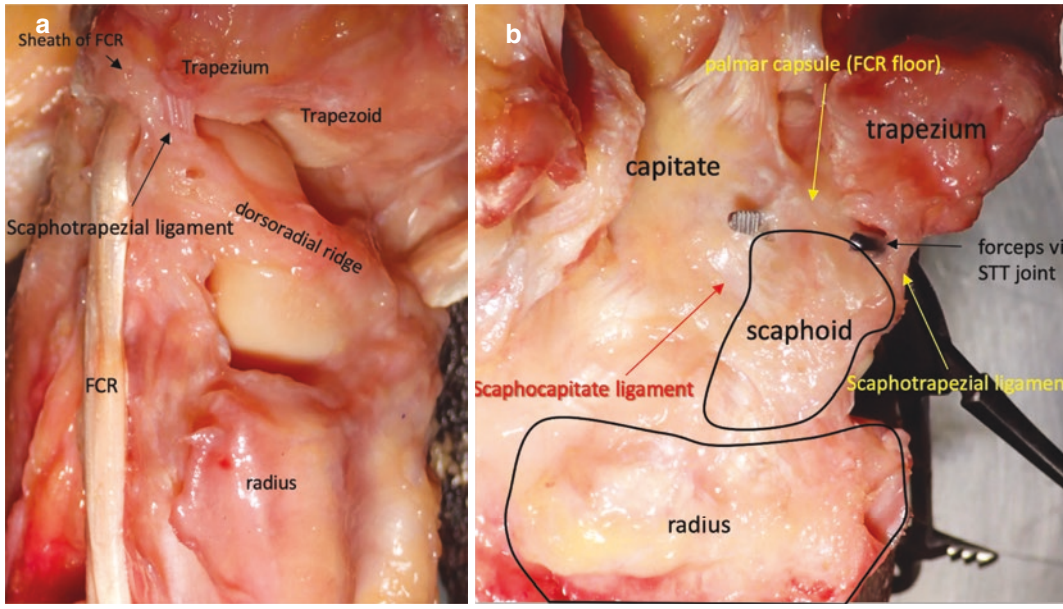

Fig. 81.3 Cadaveric demonstration of ligaments and joint capsule of STT joint (right hand). (**a**) Radial side. (**b**) Palmar side (after resection FCR tendon)

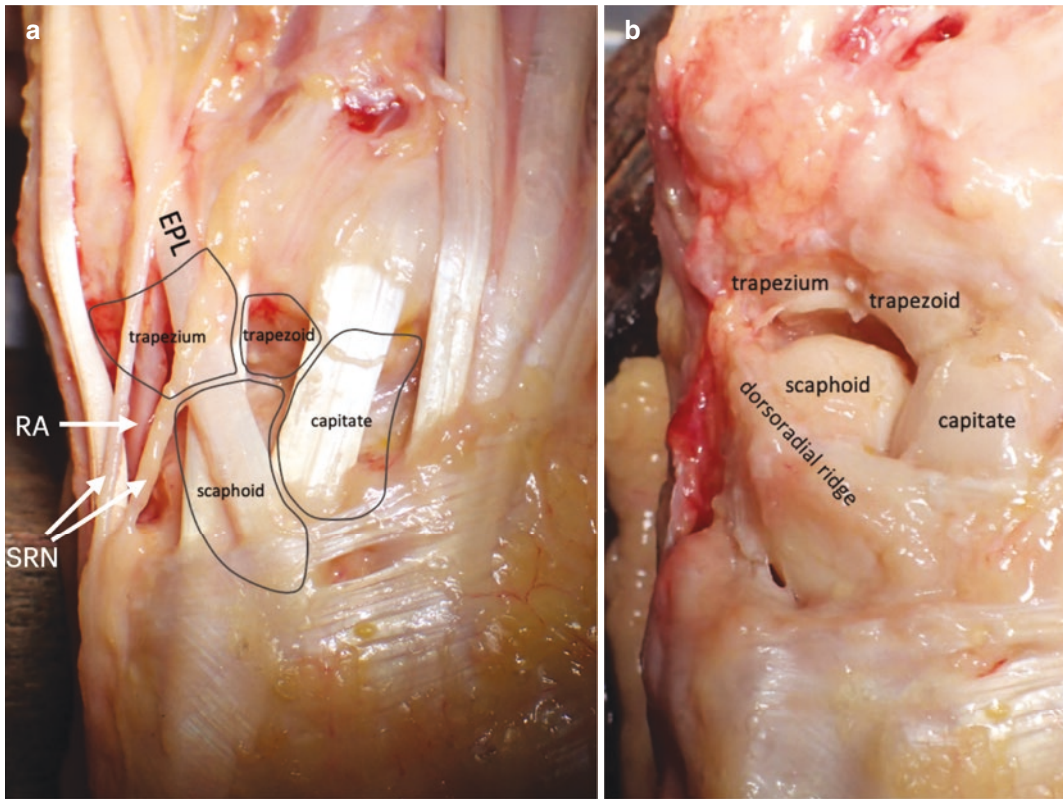

Fig. 81.4 (**a**) Cadaveric demonstration of tendons, artery, and nerves around STT joint (RA: radial artery, SRN: sensory branches of radial nerve). (**b**) The STT joint is demonstrated after the removal of tendon, artery, nerves, and joint capsule

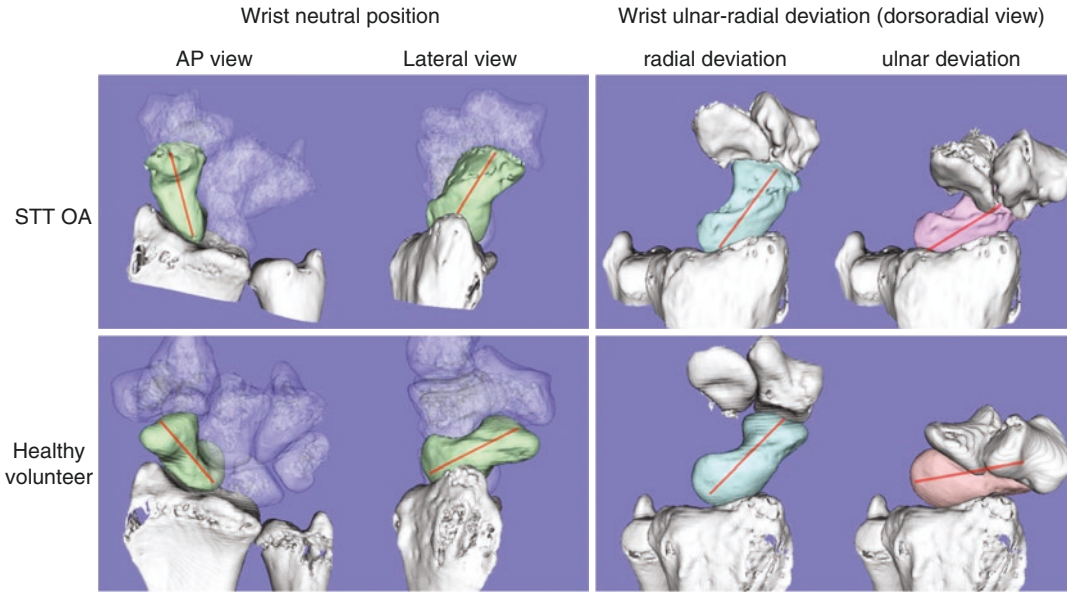

Fig. 81.5 Scaphoid alignment and kinematics in patients with STT osteoarthritis and in healthy volunteers (Orthopedic viewer, Osaka, Japan)

but the superficial branch of the radial nerve and the extensor carpi radialis longus tendon is still at risk.

Characteristics of carpal bone alignment and kinematics in patients with STT osteoarthritis: Patients with STT osteoarthritis (OA) may present with dorsal intercalated segment instability (DISI), which is likely to occur in the presence of midcarpal instability and is characterized by a normal scapholunate angle with an extension stance of the scaphoid and lunate. Associated midcarpal instability can worsen the clinical outcomes after surgical intervention for STT OA. In our previous investigation of in vivo wrist kinematics in 11 patients with STT OA and 5 healthy volunteers, the average tilt angle of the scaphoid in the sagittal and coronal planes was 31° and 29°, respectively, in the patients with STT OA and 54° and 50°, respectively, in the healthy volunteers [1]. During wrist radial–ulnar deviation, the scaphoid rotates on the reverse dart-throwing motion plane (in the ulnodorsal to radiopalmar direction), and the average rotation angle in our abovementioned study was 27° in the patients with STT OA and 39° in the healthy volunteers. In patients with STT OA, the scaphoid is in an extension stance in the sagittal plane and in an upright stance in the coronal plane, and the rotation angle decreases during wrist radial–ulnar deviation (Fig. 81.5).

81.2 Indications and Contraindications

Arthroscopic resection arthroplasty of the STT joint is indicated for the treatment of idiopathic and symptomatic STT OA without DISI-like deformity (refractory to nonsurgical treatment).

Even if the preoperative carpal alignment is normal, preexisting midcarpal OA at sites other than the STT joint should be a contraindication for the distal scaphoid resection procedure. The procedure is also contraindicated in the presence of more extended midcarpal joint degeneration involving the lunocapitate joint. Another contraindication is chronic scapholunate dissociation with a dorsally subluxated midcarpal joint.

81.3 Surgical Technique

The arm is suspended using finger traps with 5 kg of traction. Routine arthroscopy is performed with a 1.9-mm or 2.3-mm arthroscope with a 30° viewing angle via the 3–4 and 4–5 radiocarpal portals.

- The radial midcarpal arthroscopy portal is used as a viewing portal to evaluate the articular surface of the midcarpal joint, including the STT joint. The ulnar STT joint portal (STT-U) is established as a working portal at the ulnar side of the EPL tendon (Fig. 81.6).
- The STT joint is evaluated for presence of eburnated bone on the distal scaphoid and proximal trapezium and trapezoid, synovitis, chondral flaps, and rim osteophytes.
- Synovectomy of the STT joint is performed using a shaver and radio frequency system.
- Next, the marginal spur of STT joint and distal pole of the scaphoid (<3 mm in depth) is resected using a 2.5-mm arthroscopic burr through the working portal. The eburnated bone and subchondral sclerosis and bone cyst are removed until the cancellous bone of the distal scaphoid is exposed (Fig. 81.7).
- In patients with FCR tendinitis and radiopalmar ganglions, palmar capsulotomy and synovectomy around the FCR tendon are recommended.
- The joint is then thoroughly irrigated and all portals are sutured. A bulky dressing is applied after surgery.

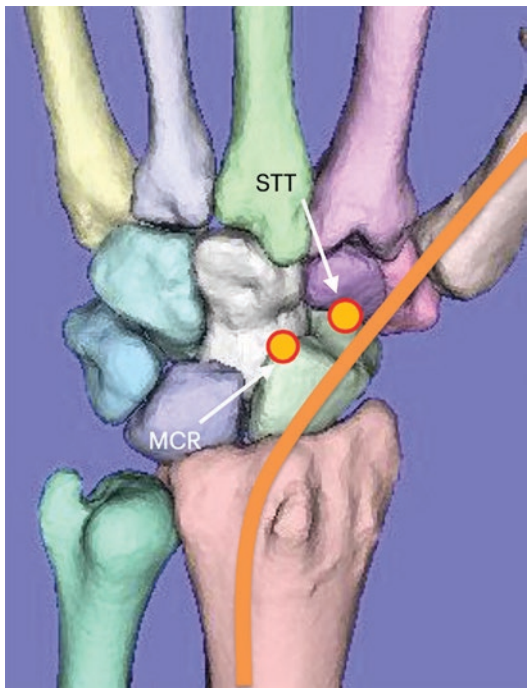

Fig. 81.6 Portals for STT joint arthroscopy. (MCR: radial midcarpal portal, STT: ulnar STT portal)

81.4 Tips and Tricks

- With the wrist in neutral position, the scaphoid tilts approximately 30° relative to the radius, and the trapezium and trapezoid are located over the distal pole of the scaphoid. The resection area should include both the distal pole and dorsal slope of the scaphoid.
- To facilitate peripheral and palmar visualization of the STT joint, scaphoid resection is started from ulnodorsal side of the distal scaphoid, and the resection area is gradually expanded toward the radiopalmar direction. The osteophytes at the periphery of the joint are then removed.
- The portal to the radial side of the EPL tendon provides a wider span from the radial midcarpal portal, facilitating triangulation. If the surgeon uses this portal, a mini-open approach minimizes the risk to injury of the neurovascular structures [2].
- After the distal scaphoid has been excised, it is important to check the amount of instability of the capitate relative to the lunate by a manual stress test or fluoroscopy. If substantial dorsal subluxation of the capitolunate joint is present, an additional procedure is needed to restrict further extension of the scaphoid. One procedure for avoiding hyperextension of the scaphoid is interposing a distal-based half-slip of the FCR tendon into the defect through a palmar approach. Another option is to reattach

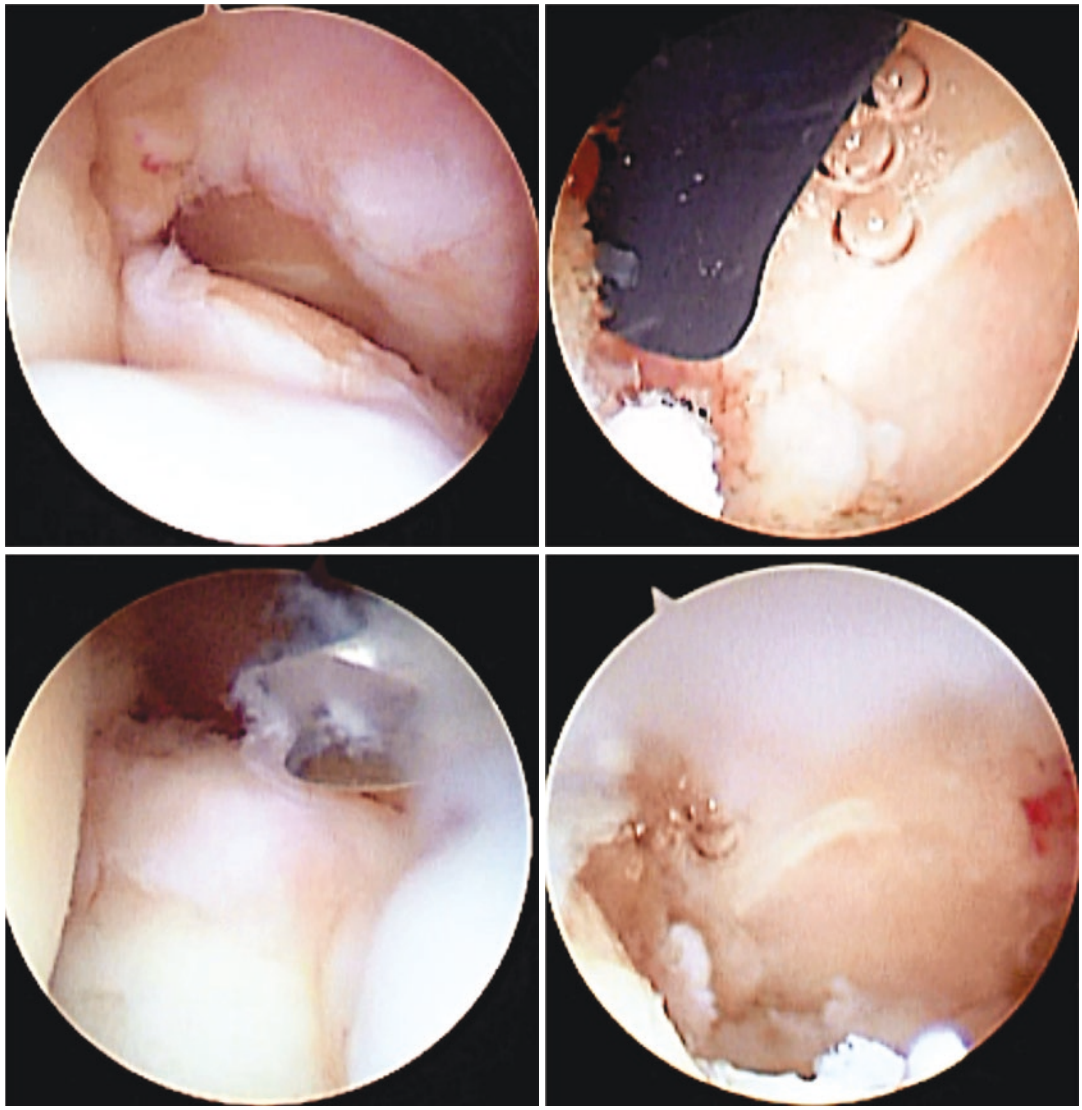

Fig. 81.7 Arthroscopic view of STT joint is shown prior to resection (top left) and while performing synovectomy (top right). Bony resection is performed using a 2.5-mm burr (bottom left) and the final resection is demonstrated (bottom right)

the palmar radioscaphoid ligament to the anterior edge of the osteotomized scaphoid, aiming to prevent excessive scaphoid extension.

81.5 Pitfalls

Three main pitfalls must be avoided when performing the above-described procedures.

- First, joint irrigation is important to avoid burning of the skin by electrocautery when synovectomy is performed using a radio frequency system.
- Second, care must be taken to preserve the proximal origins of the radial scaphotrapezial and ulnopalmar scaphocapitate ligaments, which originate at the radial and ulnar corners of the scaphoid tuberosity.

- Finally, excessive (>3 mm) resection of the distal scaphoid may result in postoperative carpal malalignment.

81.6 Postoperative Management and Rehabilitation

Gentle active-assisted mobilization of the wrist joint is usually started after 2 weeks of cast immobilization. Muscle strengthening and grip strengthening exercises should begin slowly at 4–6 weeks after surgery to avoid an excessive compressive load to the dorsal lunate, which may induce further dorsal midcarpal subluxation. A return to light activities is recommended 6 weeks after surgery, and heavy manual labor is avoided for 3 months postoperatively. For the first 3 months after surgery, patients should avoid contact sports, and a removable splint is worn for all activities that place a load on the wrist.

81.7 Complications

The most serious complication of distal scaphoid resection is the development of dorsal midcarpal instability, with the proximal row rotating dorsally and the capitate subluxating dorsally; this will finally lead to the overall carpus collapse with capitolunate arthritis. This is particularly frequent among patients whose arthritis has been caused by a chronic inflammatory process such as crystalline arthritis, patients whose carpus is already malaligned (DISI of >15°) before surgery, and patients with a lax wrist (presenting with dorsal or palmar midcarpal instability).

81.8 Results

Arthroscopic resection arthroplasty for symptomatic STT OA without carpal deformity was performed in 22 wrists of 21 patients (19 females, 3 males, mean age 63 years) from 2008 to 2017. Seventeen wrists were affected by isolated STT arthritis, and five wrists were additionally affected by first carpometacarpal osteoarthritis (OA). In five patients with first carpometacarpal OA, additional arthroscopic resection of the distal side of the trapezium was performed. The average resection height was 2.2 mm (range, 0.1–5.8 mm). The mean follow-up period was 19.8 months. No surgical complications were encountered. The average visual analog scale (VAS) score improved from 50 before surgery to 22 postoperatively. The average grip strength improved from 17 to 18 kg, pinch strength from 3.4 to 3.6 kg, and patient-related wrist evaluation (PRWE) score from 49 to 31. Carpal malalignment (capitolunate angle of >15°) was seen in two patients at the final follow-up. A significant correlation was found between the resection height and the increase in capitolunate angle from the preoperative value to that at the final follow-up. Postoperative DISI deformity (capitolunate angle of >15°) was likely to occur after >3-mm resection of the distal scaphoid. One patient in whom the resection height was 5.8 mm showed recurrence of symptoms.

Acknowledgments The authors would like to thank the staff of Department of Orthopedic Surgery at Osaka University for in vivo three-dimensional analysis of wrist kinematics, and the staff of Department of Anatomy at Chiang Mai University for providing fresh cadaver specimens. We also thank Angela Morben, DVM, ELS, from Edanz Group (https://en-author-services.edanzgroup.com/), for editing a draft of this manuscript.

References

1. Iida A, Omokawa S, Moritomo H, Wollstein R. Scaphoid motion of the wrist with scapho-trapezio-trapezoidal osteoarthritis [published online ahead of print, 2019 Jan 15]. Curr Rheumatol Rev. 2019; https://doi.org/10.2174/1573397115666190115125430.
2. Ashwood N, Bain GI, Fogg Q. Results of arthroscopic debridement for isolated scaphotrapeziotrapezoid arthritis. J Hand Surg Am. 2003;28(5):729–32. https://doi.org/10.1016/s0363-5023(03)00368-x.

82 Arthroscopic-Assisted Pyrocarbon Interposition Arthroplasty for Scapho-Trapezium-Trapezoid Joint Arthritis

Christophe Mathoulin and Margareta Arianni

82.1 Background

Scapho-trapezium-trapezoid (STT) joint arthritis is one of the degenerative conditions affecting the wrist joint and results in radial-sided wrist pain, weak grip strength, and functional limitations. With the advent of minimally invasive technology, surgical management of scapho-trapezium-trapezoid joint arthritis can be performed arthroscopically. In addition, the development of small joint implants has shifted the management trend for this condition from fusion to arthroplasty. Arthroscopic-assisted STT interposition arthroplasty is a game changer for scapho-trapezium-trapezoid arthritis. This procedure preserves normal capsular and ligamentous structures, provides pain relief and early recovery, and results in overall improvement in functional status.

82.2 Surgical Anatomy

In the thumb axis, the scapho-trapezium-trapezoid (STT) joint is the most proximal joint, where three bones articulate with one another. The trapezium and radial part of the trapezoid have concave proximal surface, which perfectly articulate with the convex or ovoid surface of the distal scaphoid. The configuration of this joint is such that only little motion is allowed. This joint is stabilized by the scapho-trapezium-trapezoid ligament on the volar aspect, particularly the scaphotrapezial component radially, which plays role in limiting excessive dorsiflexion of the wrist [1, 2]. Ulnarly, the scaphocapitate and capitate-trapezium ligaments are thinner and weaker, thus allowing a certain degree of motion of the scaphoid distal pole. This accounts for the fact that the ulnar part of the distal scaphoid is the most common location of arthritic changes [3]. Adjacent to the STT joint are the superficial branches of radial nerve and the dorsal branch of radial artery and FCR tendon.

82.3 Indications and Contraindications

Arthroscopic-assisted STT joint interposition arthroplasty is indicated in symptomatic STT joint arthritis, which has persisted for more than 2–3 months despite optimal conservative management.

Trapeziometacarpal joint (TMJ) arthroscopy is also performed at the same time to exclude pathologies or involvement in the CMC joint. Concurrent CMC joint arthritis is a contraindication for STT

C. Mathoulin (✉)
Institut de la Main, Clinique Bizet, Paris, France

M. Arianni
Hand Clinic, Ramsay Premier Bintaro Hospital, Tangerang, Indonesia

© ISAKOS 2022

D. N. Bhatia et al. (eds.), *Arthroscopy and Endoscopy of the Elbow, Wrist and Hand*,
https://doi.org/10.1007/978-3-030-79423-1_82

interposition arthroplasty. Dorsal intercalated segmental instability (DISI) deformity is a contraindication for distal scaphoid resection alone, but not if a spacer is inserted (interposition arthroplasty).

82.4 Surgical Technique

STT arthroscopy is performed under regional or general anesthesia. Initially, the hand is suspended on a Chinese finger trap with 5–7 kg of traction, as in wrist arthroscopy in general. No traction is applied to the thumb. Following exsanguination, the tourniquet is inflated. A 2.4-mm/1.9-mm arthroscope is used for visualization.

82.4.1 Portals

Radial midcarpal portal is an indirect portal for visualization of the STT joint. It is located approximately 1 cm distal to the 3-4 portal. The creation of this portal is occasionally difficult due to the curvature of the scaphoid and capitate. If difficulty is encountered, then creating the ulnar midcarpal portal first may help. With direct visualization and transillumination from this portal, the exact location of the radial midcarpal portal is determined with a needle. The arthroscope in the radial midcarpal portal is swung distally along the ulnar margin of the scaphoid until it reaches the STT joint. In the presence of arthritic changes, visibility here is often obscured by synovitis, which requires synovectomy through the STT portal.

Standard STT portal is created by inserting a needle into a point 1–1.5 cm proximal to the trapeziometacarpal joint between the first and second extensor compartments. Transillumination from the arthroscope, which is at the radial midcarpal portal, helps locate this portal (Fig. 82.1). An assistant pulls the thumb to facilitate needle penetration. As there is no inclination of joint surface, the direction of the needle simply parallels the STT joint surface without any angulation (Fig. 82.1). When inserted correctly, the needle tip should be visualized by the arthroscope from the radial midcarpal portal. At the beginning of one's learning curve, it is also helpful to use image intensifier to confirm the location of the needle. A small stab incision is made at the needle insertion point, and a mosquito forceps is used to penetrate the STT joint and make way for the shaver. Synovectomy is performed to enhance the visibility prior to switching the arthroscope into the STT portal for more thorough examination of this joint. A 2–3 kg traction on the thumb and smaller arthroscope may be employed for easier penetration of the STT joint.

Radial STT portal: The two portals mentioned previously are usually sufficient to perform this procedure. The radial STT portal, however, may

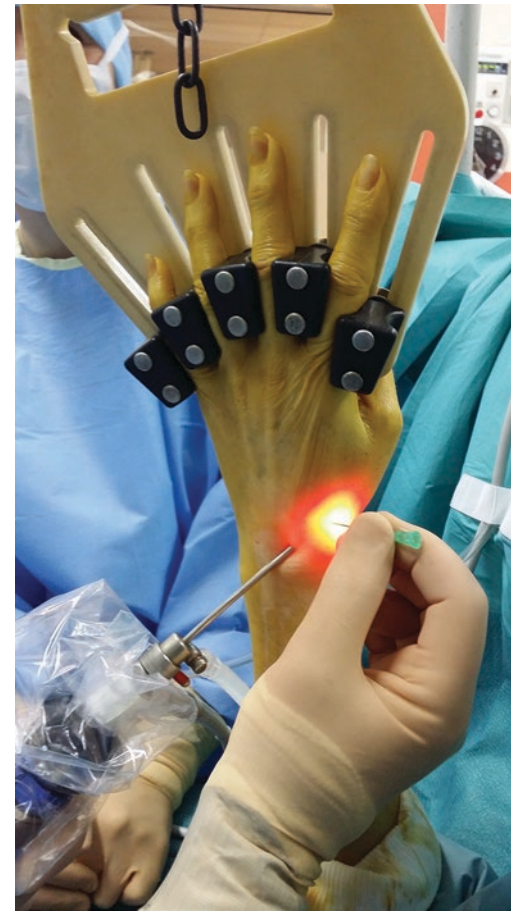

Fig. 82.1 Creation of scaphotrapeziotrapezoid (STT) portal aided by transillumination from the arthroscope in radial midcarpal portal. The needle is inserted parallel to the joint space

be occasionally needed. This portal, described by Carro et al. (2003) [4], is located just radial to the abductor pollicis longus tendon, at the same level of the standard STT portal. The radial artery is 8.8-mm radial from this portal. The terminal branches of the superficial branch of the radial nerve, however, are in the vicinity. After skin incision, the subcutaneous tissue must be dissected transversely to push the branches aside. Both radial and standard STT portals, when used together, allow a convenient triangulation angle of 130° [4]. Synovectomy can also be performed through this portal.

82.4.2 Distal Resection of the Scaphoid

To start with resection of the dorso-ulnar part of the distal scaphoid, the arthroscope is placed in the radial midcarpal portal and burr in the STT portal (Fig. 82.2). As more space is developed, the arthroscope can be moved to the standard STT portal and burr to the radial STT portal (or vice versa) to resect the remaining portion of the distal scaphoid. In our experience, however, the resection can be carried out by just using the radial midcarpal and STT portals. Two-to-three millimeter of resection is necessary. Resection must be even across the distal scaphoid and care is taken not to leave any protruding subchondral bone or remaining osteophytes that will hinder implant placement. Resection must also follow a subtle dome shape to match the curvature of the implant.

82.4.3 Pyrocarbon Implant Interposition

To estimate implant size, a marked probe is inserted into the STT portal (Fig. 82.3). The STT portal incision is extended and stretched with forceps to allow implant insertion. The trial implant is then inserted under visualization from the radial midcarpal portal (Figs. 82.4 and 82.5). An implant of proper size seating on adequately resected distal scaphoid bed should not dislocate during free motion of the thumb. After interposition of the definitive implant, the capsule must be sutured tightly prior to skin suture. Preoperative and postoperative radiographs of STT joint arthritis treated with pyrocarbon implant interposition are shown in Figs. 82.6 and 82.7, respectively.

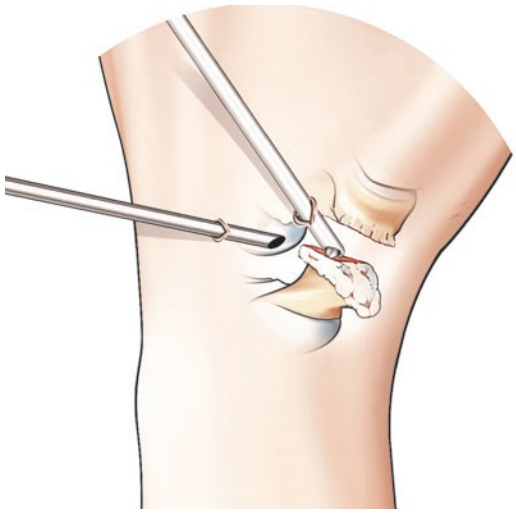

Fig. 82.2 This illustration shows distal scaphoid resection. The arthroscope is placed in the radial midcarpal portal and the burr in the STT portal. Adapted with permission from Mathoulin C, 2015, Wrist Arthroscopy Technique, p. 141. Copyright [2015] by Georg Thieme Verlag (© Max Crespi and ISAKOS)

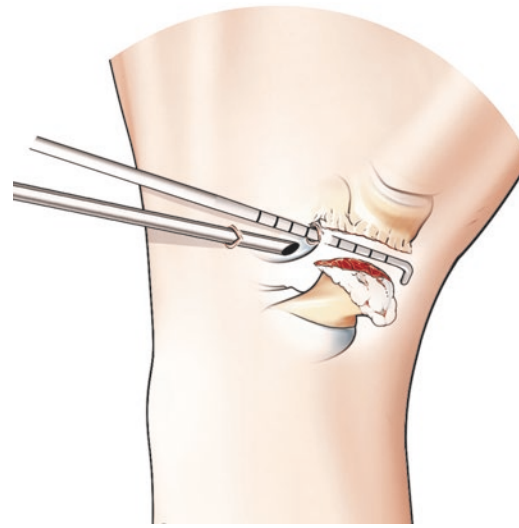

Fig. 82.3 The probe is used to estimate implant size. (© Max Crespi and ISAKOS)

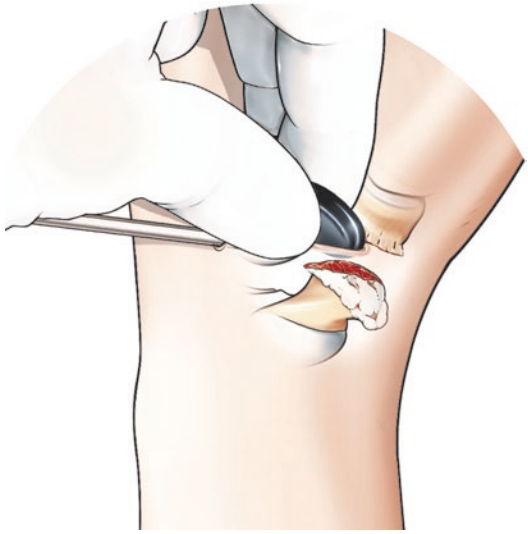

Fig. 82.4 Through the enlarged STT portal, the pyrocarbon implant is inserted into the STT joint. Adapted with permission from Mathoulin C, 2015, Wrist Arthroscopy Technique, p. 141. Copyright [2015] by Georg Thieme Verlag (© Max Crespi and ISAKOS)

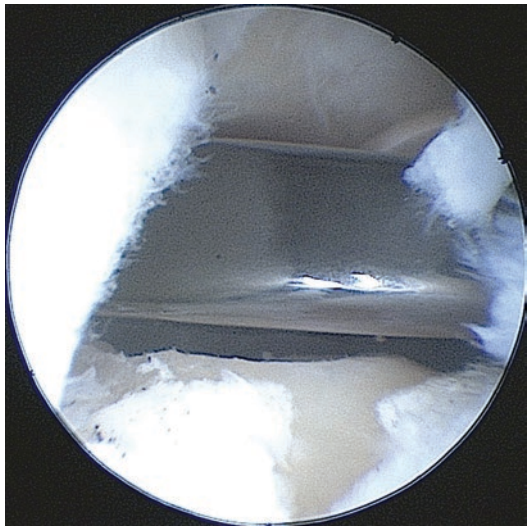

Fig. 82.5 Arthroscopic view from radial midcarpal portal of implant abutting the resected distal scaphoid

Fig. 82.6 Preoperative radiograph showing STT joint arthritis

Fig. 82.7 Radiograph of the same wrist (Fig. 82.6) 2 years after surgery. The implant remains stable in the STT joint. The scaphoid does not have the scaphoid ring sign typical of flexed scaphoid. This shows that the correct-sized implant prevents midcarpal joint instability

82.5 Tips and Tricks

- Prior to insertion, the trial implant is donned in a finger of a sterile glove to facilitate easy removal. Trial implant is removed by pulling on the glove.
- Mosquito forceps are used to facilitate definitive implant insertion, but the tips of forceps must be covered with drain tubes to avoid scratching or denting the implant surface.

82.6 Pitfalls

- The greatest difficulty is to place the implant by a slightly enlarged STT approach. There is an obliquity which must be considered, otherwise, the implant will abut on the trapezoid.
- It is necessary to put a suitable implant size, in order to avoid movement of the implant in the STT joint (unstable implant), which causes pain.
- Resection of the distal scaphoid must be performed meticulously; resection must be even and must not leave any bony protrusion that will hinder implant insertion or seating. A mechanical block from the protrusion predisposes the implant to instability and dislocation.

82.7 Postoperative Management and Rehabilitation

The thumb and wrist are immobilized in a thumb spica splint for 4–6 weeks, after which range of motion exercise is resumed without restriction. The patient should achieve full recovery after 3 months postoperatively.

- As the STT joint is a small joint, difficulties may arise during arthroscopy at the beginning of a surgeon's learning curve. Prolonged attempts may result in soft tissue edema, which obscures vision and imposes even more difficulties.
- Injury to the superficial branch of the radial nerve may occur during the creation of STT portal.
- The main radial artery is closer to the radial STT portal (6–10 mm) than to the standard STT portal and thus is at risk of injury. The dorsal branch of the radial artery, which enters the anatomical snuffbox, however, is more at risk of injury during the creation of the standard STT portal.
- Other complications include cartilage injury, stiffness, and CRPS.

References

1. Crosby EB, Linscheid RL, Dobyns JH. Scaphotrapezial trapezoidal arthrosis. J Hand Surg. 1978;3(3):223–34.
2. Masquelet AC, Strube F, Nordin JY. The isolated scaphotrapeziotrapezoid ligament injury: diagnosis and surgical treatment in four cases. J Hand Surg (Br Eur vol). 1993;18B:730–5.
3. Pegoli L, Pozzi A. Arthroscopic management of scaphoid-trapezium-trapezoid joint arthritis. Hand Clin. 2017;33:813–7.
4. Carro LP, Golano P, Farinas O, Cerezal L, Hidalgo C. The radial portal for scaphotrapeziotrapezoid arthroscopy. Arthroscopy. 2003;19(5):547–53.

Part XVI

Wrist: Pisotriquetral Arthroscopy

Arthroscopy of the Pisotriquetral Joint: An Overview

83

Eugene T. Ek and Richard P. Jamieson

83.1 Background

Pathology of the pisotriquetral (PT) joint is a common source of ulnar-sided wrist symptoms [1]. The presentation is often in the form of pain and tenderness over the palmar and ulna side of the wrist, localised over the pisiform bone. Patients often complain of discomfort over the PT joint when performing a power grip and exhibit a positive 'grind test' as the pisiform is compressed against the triquetrum, especially in the setting of degenerative arthritis or synovitis.

When surgical intervention is required, compared with an open procedure, arthroscopic management may improve recovery time and reduce the risk of persistent scar tenderness over the palmar aspect of the hand [2]. In this setting, arthroscopy can be used for treatment of pisotriquetral arthritis, synovitis, ganglia, loose bodies and trauma [2–4]. However, the proximity to the ulna neurovascular bundle does increase the complexity of the procedure, and therefore, detailed knowledge of the surgical anatomy is important. This chapter presents an overview of the author's technique and indications for pisotriquetral joint arthroscopy.

E. T. Ek (✉) · R. P. Jamieson
Melbourne Orthopaedic Group,
Melbourne, VIC, Australia

Department of Surgery, Monash University,
Melbourne, VIC, Australia
e-mail: eugene.ek@mog.com.au;
richard@richardjamieson.com.au

83.2 Surgical Anatomy

The pisiform is a small round bone with uncertain phylogenetic function [5]. It is generally thought to be a sesamoid bone lying within the flexor carpi ulnaris tendon acting to increase the tendon's lever arm and improve wrist stability in flexion. It can be palpated on the palmar and ulnar aspect of the wrist, just distal to the flexion crease. Usually, the pisiform develops from a primary ossification centre. In some cases, a secondary ossification centre occurs and a failure of fusion will result in an os pisiform secundarium. The pisiform undergoes endochondral ossification between the ages of 8 and 12 and during this period has an irregular and fragmented appearance, which should not be mistaken for a fracture [6].

The PT joint is a condyloid joint with a loose capsule that does not contribute to joint stability. There are four primary and two secondary joint stabilisers. The primary stabilisers include the flexor carpi ulnaris (FCU) tendon, pisohamate ligament, pisometacarpal ligament and the pisotriquetral ulnar ligament (Fig. 83.1). The FCU inserts on the volar aspect of the pisiform and during wrist flexion the pisiform is pulled proximally and palmarly, causing the joint space to widen. The flexor and extensor retinacula provide secondary stability to the joint [5, 7].

The pisiform forms the proximal ulnar border of Guyon's canal and the ulnar neurovascular bundle courses immediately radial to it [8]. The nerve

© ISAKOS 2022

D. N. Bhatia et al. (eds.), *Arthroscopy and Endoscopy of the Elbow, Wrist and Hand*,
https://doi.org/10.1007/978-3-030-79423-1_83

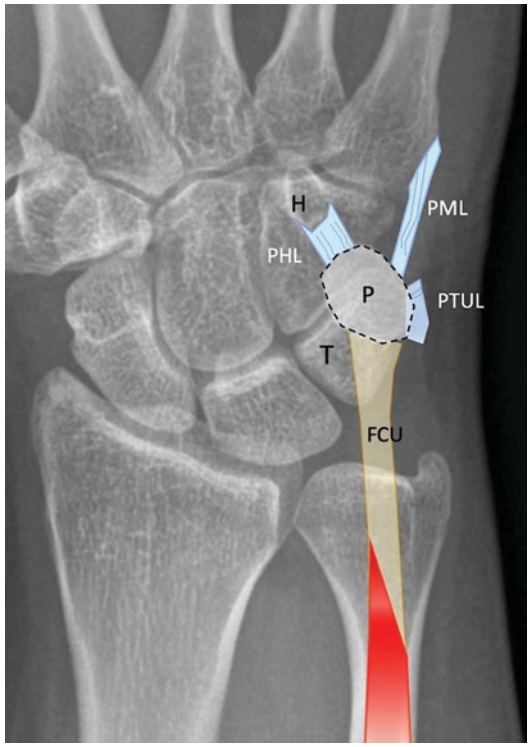

Fig. 83.1 Schematic of the pisotriquetral joint showing the relationship between pisiform and hamate and the attached ligaments and flexor carpi ulnaris (FCU) tendon. (H) Hamate, (P) Pisiform, (PHL) pisohamate ligament, (PML) pisometacarpal ligament, (PTUL) pisotriquetral ulna ligament

is more ulnar than the artery and divides into a deep motor branch and superficial sensory branch just distal to the pisiform in zone 1 of Guyon's canal [6]. More superficially the dorsal cutaneous branch of ulna nerve (DCBUN) originates from the ulna nerve at an average of 5.1 cm proximal to the distal ulna articular surface, passing dorsal to the FCU tendon and becoming subcutaneous at an average of 1.7 cm proximal to the distal ulna articular surface. The nerve divides into between 1 and 4 (average 2) branches at that level. The longitudinal branch lies between the dorsal cutaneous border of the ulna and the pisotriquetral joint. In 71% of individuals, there is a transverse branch to the distal radioulnar joint [9].

The pisotriquetral joint can be viewed arthroscopically through dorsal radiocarpal portals. Using a 4–5 dorsal portal, Berger defined the location of the pisotriquetral orifice just distal and anterior to the prestyloid recess and described it as being present in 90% of cases [10]. By contrast, Arya et al. found the presence of a synovial membrane which obscured the joint in 44% of individuals and described four distinct subtypes of the pisotriquetral orifice when viewing from the radiocarpal joint [11].

83.3 Indications and Contraindications

- Debridement of pisotriquetral joint ganglions and synovitis.
- Removal of loose bodies in the pisotriquetral joint.
- Treatment of pisotriquetral arthritis—total or hemi-pisiformectomy.
- Trauma and post-traumatic sequelae—reduction of pisotriquetral joint dislocation.

Previous open surgery on the ulna nerve in Guyon's canal can make visualisation of the PT joint difficult and may increase the risk of nerve injury and is a relative contraindication.

83.4 Surgical Technique

Under regional or general anaesthetic, the patient is placed supine on the operating table. The arm is exsanguinated prior to inflation of a high-arm tourniquet. Finger traps are utilised and 10 kg of traction are applied using the Spider 2 wrist positioner (Smith and Nephew, London, UK). Dry arthroscopy is used throughout the procedure.

- The 3-4 portal is established as an initial viewing portal. 6R and 6 U portals are then established using a needle for accurate placement (Fig. 83.2). A 'knick and spread' technique is always used to minimise risk of injury to the cutaneous nerves and extensor tendons. A systematic diagnostic radiocarpal arthroscopy is first performed to exclude other pathology. Routine midcarpal arthroscopy is not

performed unless clinically or radiologically indicated.

- To visualise the pisotriquetral joint, the arthroscope is placed into the 6R portal. The 6 U portal is used as a working portal. The DCBUN is at risk with this portal. Avoiding passive forearm pronation when establishing this portal will reduce the risk of injury [12]. From the 6R portal, the arthroscope is positioned distal and ulnar along the ulnar border of the triquetrum (Fig. 3a). If the pisiform is not directly visible the synovial membrane is carefully debrided using a 2.9 mm full radius resector shaver (Fig. 83.3b, c). Great care must be taken to avoid injury to the ulnar nerve, which lies immediately radial to the pisiform (Fig. 83.4).
- Once the ulnar nerve is identified and protected, the ganglion can be safety excised (Fig. 83.5). In cases of end-stage pisotriquetral arthritis, the pisiform can be either partially or completely excised with the use of a 2.9-mm hooded burr. In this setting, we find it useful to attach a 20 mL syringe of normal saline to side port of the arthroscope cannula. This will provide some irrigation during suction and assist with removing bone debris.

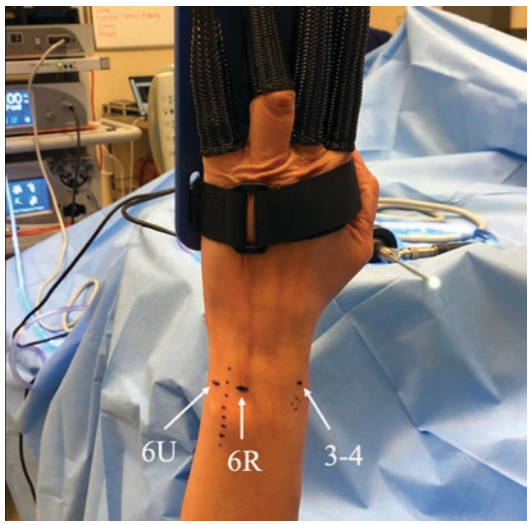

Fig. 83.2 Radiocarpal portals (3–4, 6R, 6 U) for pisotriquetral arthroscopy are demonstrated. The dotted line delineates the ECU tendon

83.5 Tips and Tricks

- Establish the 6 U portal with a needle when viewing from the 6R portal. This will allow an accurate portal placement in the plane of the pisotriquetral articulation.
- When utilising dry arthroscopy, attach a syringe of normal saline to the arthroscope cannula to assist with irrigating and removing bony debris.

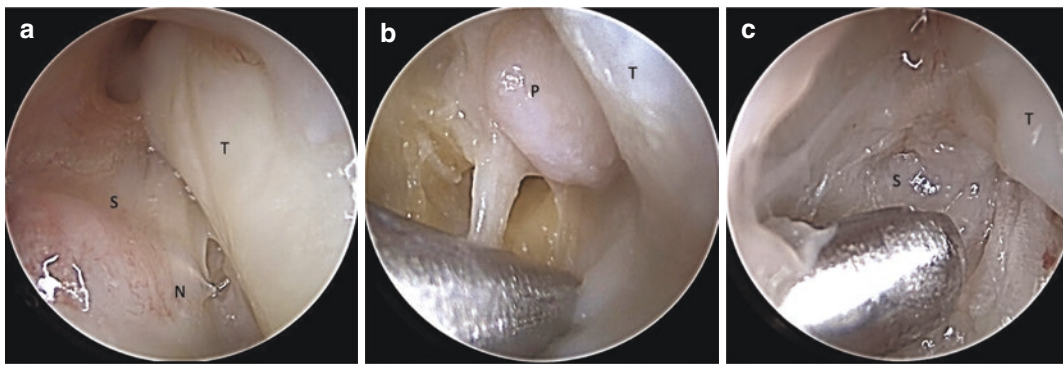

Fig. 83.3 Dry arthroscopy of pisotriquetral joint is shown. (**a**) Viewing portal is 6R. The 6 U portal is established under direct visualisation using needle localisation. (T) Triquetrum, (N) needle used to localise the 6 U portal and the appropriate trajectory of the portal placement. (S) Synovial membrane overlying the pisiform. (**b**) A motorised shaver is inserted into the 6 U portal and the synovitis (S) arising from the PT joints is debrided. (**c**) After clearance of the PT joint, one can see the pisiform (P) and the triquetrum (T) articular surfaces

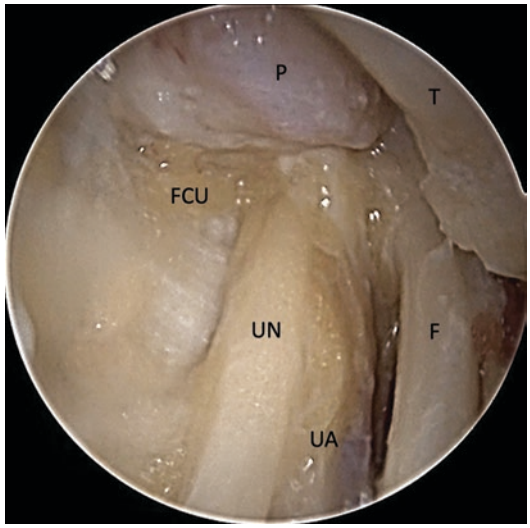

Fig. 83.4 With further debridement radial to the pisiform (P), one can identify the ulna nerve (UN), the ulna artery (UA), the finger flexor tendons (F) and the FCU tendon. (T: triquetrum)

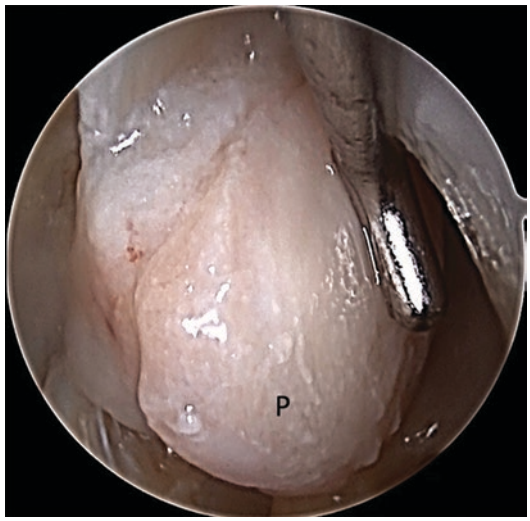

Fig. 83.5 Visualisation and probing of the articular surface of the pisiform

83.6 Pitfalls

- Care must be taken to avoid injury to the DCBUN during 6 U portal placement. This can be avoided by using a 'knick and spread' technique and avoiding forearm pronation when establishing the portal.
- The ulna nerve proper is intimately related to the pisiform, placing it at risk unless accurately identified and protected.
- Reduce suction of the shaver when debriding radial to the pisiform (around the ulna nerve) to avoid iatrogenic injury.

83.7 Postoperative Rehabilitation and Management

A postoperative volar plaster splint is applied for 2 weeks. At that point, the splint is removed and the patient is allowed to mobilise the wrist as tolerated but should avoid heavy lifting or gripping with operated wrist. At 6 weeks, a wrist strengthening program is initiated with the therapist. Return to sport is permitted at 3 months postoperatively.

83.8 Complications

- Neurovascular injury.
  - Ulnar nerve.
  - Ulnar artery.
  - DCBUN.
- Persistent pain, especially in the setting of pisotriquetral joint arthritis.
- Postoperative wrist joint stiffness.

References

1. O'Shaughnessy MA, Lewallen LW, Moran SL, Rizzo M. Dreaded ulnar wrist pain: long-term results of pisiformectomy for painful pisotriquetral arthrosis. J Surg Orthop Adv. 2019;28(3):196–200.
2. Compson J. Arthroscopic management of pisotriquetral conditions. In: de Pinal F, Mathoulin C, Nakamura T, editors. Arthroscopic management of ulnar pain. Heidelberg: Springer; 2012. p. 250.
3. Katolik L. Arthroscopic resection of pisotriquetral joint loose body: a case report. J Hand Surg Am. 2008;33(2):206–9.
4. Cobb TK, Berner SH, Badia A. New frontiers in hand arthroscopy. Hand Clin. 2011;27(3):383–94.
5. Moraux A, Lefebvre G, Pansini V, Aucourt J, Vandenbussche L, Demondion X, Cotton A. Pisotriquetral joint disorders: an under-recognized

cause of ulnar side wrist pain. Skelet Radiol. 2014;43:761–73.
6. Fleege MA, Jebson PJ, Renfrew DL, Steyers CM Jr, el-Khoury GY. Pisiform fractures. Skelet Radiol. 1991;20(3):169–72.
7. Rayan GM, Jameson BH, Chung KW. The Pisotriquetral joint: anatomic, biomechanical, and radiographic analysis. J Hand Surg Am. 2005;30(3):596–602.
8. Chen S, Tsai T. Ulnar tunnel syndrome. J Hand Surg Am. 2014;39(3):571–9.
9. Root CG, London DA, Strauss NL, Calfee RP. Anatomic relationships and branching patterns of the dorsal cutaneous branch of the ulnar nerve. J Hand Surg Am. 2013;38(6):1131–6.
10. Berger RA. Arthroscopic anatomy of the wrist and distal radioulnar joint. Hand Clin. 1999;15:393–413.
11. Arya AP, Kulshreshtha R, Kakarala GK, Singh R, Compson JP. Visualisation of the pisotriquetral joint through standard portals for arthroscopy of the wrist: a clinical and anatomical study. J Bone Joint Surg. 2007;89B:202–5.
12. Esplugas M, Lluch A, Garcia-Elias M, Llusa-Perez M. How to avoid ulnar nerve injury when setting the 6U wrist arthroscopy portal. J Wrist Surg. 2014;3(2):128–31.

Pisotriquetral Arthroscopy: Access, Evaluation, and Resection

84

Deepak N. Bhatia

84.1 Background

The pisotriquetral joint (PTJ) is an under-recognized source of ulnar-sided wrist pain. PTJ pathology may be related to chronic overuse in sports or manual work or may be acute and traumatic [1, 2]. The pisiform bone forms a mobile articulation with the triquetrum that is stabilized by several ligaments and flexor carpi ulnaris tendon. The inherent mobility predisposes the joint to instability and wear, and results in ulnar-sided wrist pain. Persistent ulnar wrist pain with sports activities that involve repetitive flexion-extension and supination-pronation movements (racquet sports) necessitates clinical and radiological evaluation of the PTJ [3]. Arthroscopy of the PTJ is a minimally invasive approach to evaluation and treatment of PTJ pain and results in predictable outcomes and early return to sports.

84.1.1 Surgical Anatomy

The pisiform is a proximal row carpal bone within the flexor carpi ulnaris (FCU) tendon and is stabilized by several ligaments that transmit the pull of FCU for ulnar wrist motion. The PTJ is a condylar joint formed by a slightly concave and ovoid surface of pisiform and convex surface of the triquetrum within a loose capsular envelope. The pisohamate (PH), pisometacarpal (PM), and ulnar pisotriquetral (PT) ligaments form the main stabilizers of the PTJ along with the FCU. The flexor and extensor retinaculum are the secondary stabilizers of the PTJ. The PTJ is closely related to the ulnar nerve and artery adjacent to the Guyon's canal and to the deep branch of the ulnar nerve as it passes under the pisohamate tunnel (formed by the PH ligament and the fibrous arch of hypothenar muscles). This unique anatomy of the PTJ predisposes to a spectrum of conditions that present with ulnar-sided wrist pain and neurological involvement (Fig. 84.1).

84.2 Indications and Contraindications

- Pisotriquetral pain that is refractory to a trial of immobilization and local corticosteroid injections may be evaluated and treated arthroscopically. PTJ pathology in this subgroup includes chondromalacia, early degenerative changes, ulnar capsular impingement and fraying, and PTJ instability. Therapeutic options during arthroscopy include arthroscopic synovectomy and debridement and partial and complete pisiformectomy.
- Pisotriquetral arthritis is frequently seen in the elderly and is demonstrated on the semisupination radiograph. Arthroscopic

D. N. Bhatia (✉)
SPORTSMED Mumbai, and Sir HN Reliance Foundation Hospital, Mumbai, Maharashtra, India
e-mail: shoulderclinic@gmail.com

© ISAKOS 2022

D. N. Bhatia et al. (eds.), *Arthroscopy and Endoscopy of the Elbow, Wrist and Hand*,
https://doi.org/10.1007/978-3-030-79423-1_84

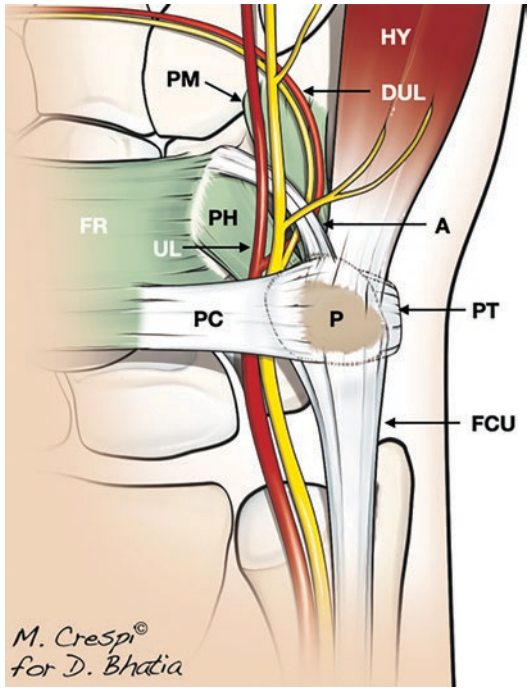

Fig. 84.1 Surgical anatomy of the pisiform is illustrated. The pisohamate (PH), pisometacarpal (PM), and ulnar pisotriquetral (PT) ligaments are the primary stabilizers of the pisotriquetral joint (PTJ) along with the flexor carpi ulnaris (FCU). The ulnar nerve and artery (UL) are adjacent to the PTJ in Guyon's canal. The deep branches of the ulnar artery and nerve (DUL) pass under the fibrous arch (A) of hypothenar muscles (HY). [FR: flexor retinaculum, PC: palmar carpal ligament, P: pisiform] (M. Crespi © D.Bhatia)

debridement and pisiformectomy provide predictable resolution of symptoms [4].

- Loose bodies in the PTJ are occasionally seen and can be excised arthroscopically [5].

There are no absolute contraindications for PT arthroscopy.

84.3 Surgical Technique

The procedure is performed with the patient in the supine position. The upper limb is suspended with Chinese finger traps, and a countertraction force of 2–4 kg is used to distract the joint. A 30° arthroscope (2.4 mm) is used for the procedure.

Portals: The PTJ can be accessed via routine dorsal portals. The dorsal radiocarpal 4-5 or 6R portals are the main viewing portals. The 6R portal is an alternate viewing portal if visualization is difficult via 4-5 portal. The 6 U portal is used as a working portal for soft tissue and bony procedures (partial or complete pisiformectomy). This portal may also be used as a viewing portal for an excellent end-on view of the entire PTJ. Use of the 4-5 and 6 U portals is optimal as the working and viewing portals are sufficiently distanced from each other (Figs. 84.2–84.4).

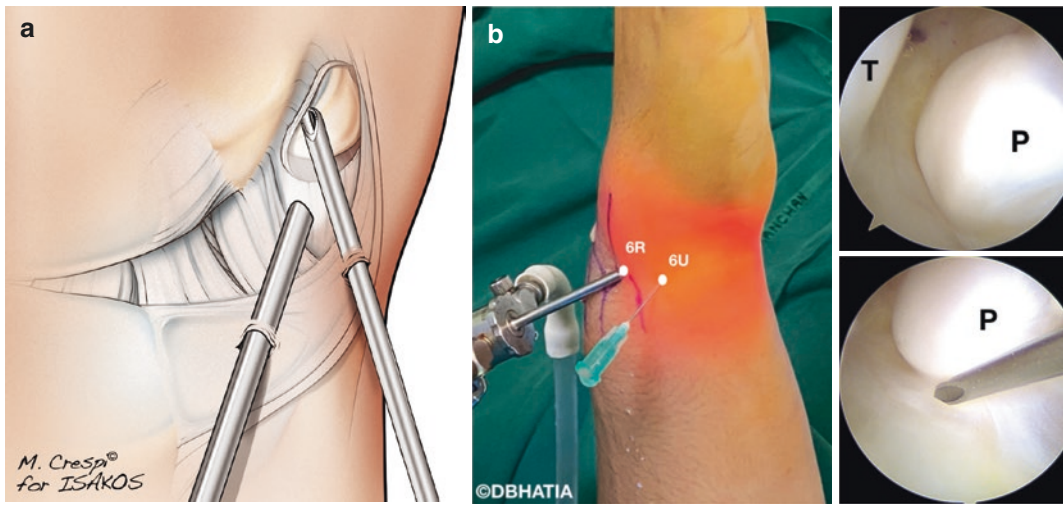

Fig. 84.2 (**a**) An overview of pisitriquetral joint (PTJ) arthroscopy using standard portals is illustrated. Standard radiocarpal portals (6R, 6 U) can be used for visualization and instrumentation via a capsular communication (M. Crespi © for ISAKOS). (**b**) The 6R portal demonstrates the pisotriquetral joint (P, T). The 6 U portal is placed using an outside-in technique. Note the angulation of the arthroscope and the needle distally toward the pisiform (© D. Bhatia)

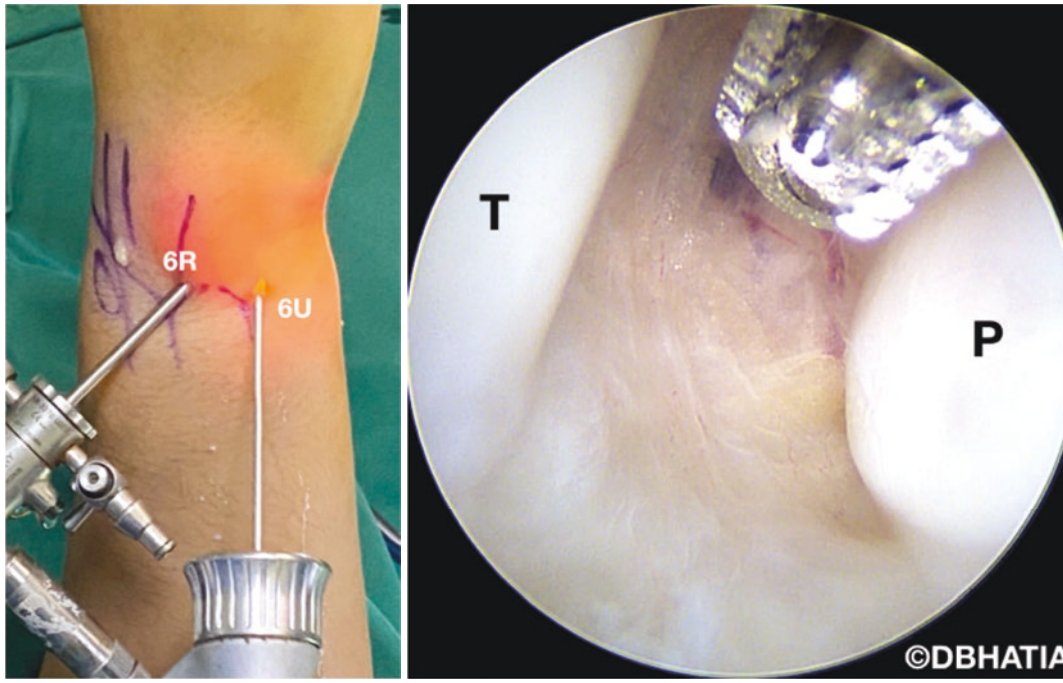

Fig. 84.3 The 6 U portal is demonstrated as a working portal and provides access to all recesses of the pisotriquetral joint (P, T) (© D. Bhatia)

Diagnostic endoscopy: The 6R portal is used to evaluate the radiocarpal joint and the volar capsule on the ulnar aspect of the triquetrum is visualized. A capsular connection between the radiocarpal joint and PTJ is usually present in this region and the arthroscope is angulated distally and advanced through this aperture to visualize the PTJ. A membrane may be present at this aperture and can be penetrated by the arthroscope to gain access to PTJ [6] (Fig. 84.5a). The pisiform and the capsular envelope of the PTJ are visualized and a needle is used to place a 6 U portal using an outside-in technique. The 6 U portal is then used as a viewing portal and the radial aspect of the PTJ and triquetrum can be inspected. Presence of degenerative changes and synovitis or loose bodies is noted (Fig. 84.5b).

Arthroscopic ballotment test: The wrist is slightly flexed and the pisiform is compressed into the triquetrum using external pressure. The pisiform is moved in a sideways and proximal to distal direction with compression, and any impinging soft tissue (synovium, capsular folds) is identified (Fig. 84.6).

Debridement: A shaver is used via the 6 U portal and angulated distally towards the PTJ. Any synovitis or capsular tears/flaps and frayed cartilage remnants are debrided and loose bodies removed. A 2.5-mm angled radiofrequency or ablator probe is used for thermal shrinkage of frayed capsular tissue. The PTJ ballotment test is repeated to confirm excision of all impinging tissues (Fig. 84.7).

Pisiform excision: Partial pisiformectomy may be performed safely without risk of injury to FCU or adjacent structures. The capsular folds of the PTJ are preserved and the "intra-articular" aspect of the pisiform is excised. The working and viewing portals are alternated between 6R and 6U during the procedure. Pisiformectomy begins by delineation of the resection margin on the ulnar surface using a 2-mm shaver blade. Bony excision is then performed with a 2–3 mm burr and the subchondral bone is progressively removed. Cartilage flaps are finally excised with an angled punch (Fig. 84.8).

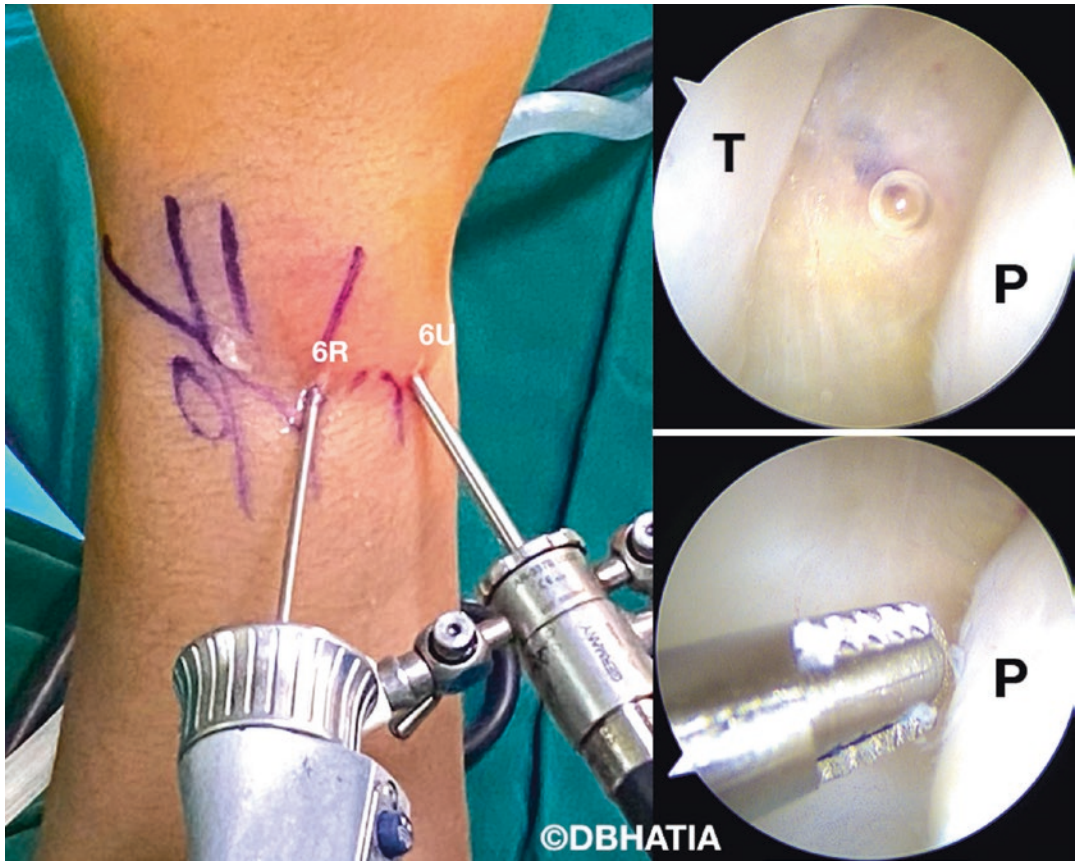

Fig. 84.4 The 6 U portal is demonstrated as a viewing portal for an end-on view of the pisotriquetral joint (P, T) and the 6R portal is used for instrumentation (© D. Bhatia)

84.4 Tips and Tricks

- PTJ is easily visualized by following the ulnar surface of triquetrum toward the volar capsule and beyond the TFCC. The membrane can be perforated gently with an arthroscopic probe and the arthroscope is advanced into PTJ.
- PTJ capsular envelope should be preserved and used as a boundary for limiting excision.

84.5 Pitfalls

- Complete excision of pisiform can disrupt the integrity of the FCU and should be avoided.
- The ulnar nerve and artery (and their deep branches) are close to the PTJ and potentially at-risk of injury in the Guyon's canal and pisohammate tunnel. The radial capsule of PTJ should be used as a boundary to limit dissection to protect these structures.

84.6 Postoperative Management, Rehabilitation, and Return to Sport

A sling is used for comfort and discarded in 2–3 days. Active movements and strengthening exercises are initiated as soon as the patient is comfortable and all routine and work-related activities are permitted. Return to sports and heavy work is permitted only after 6–12 weeks.

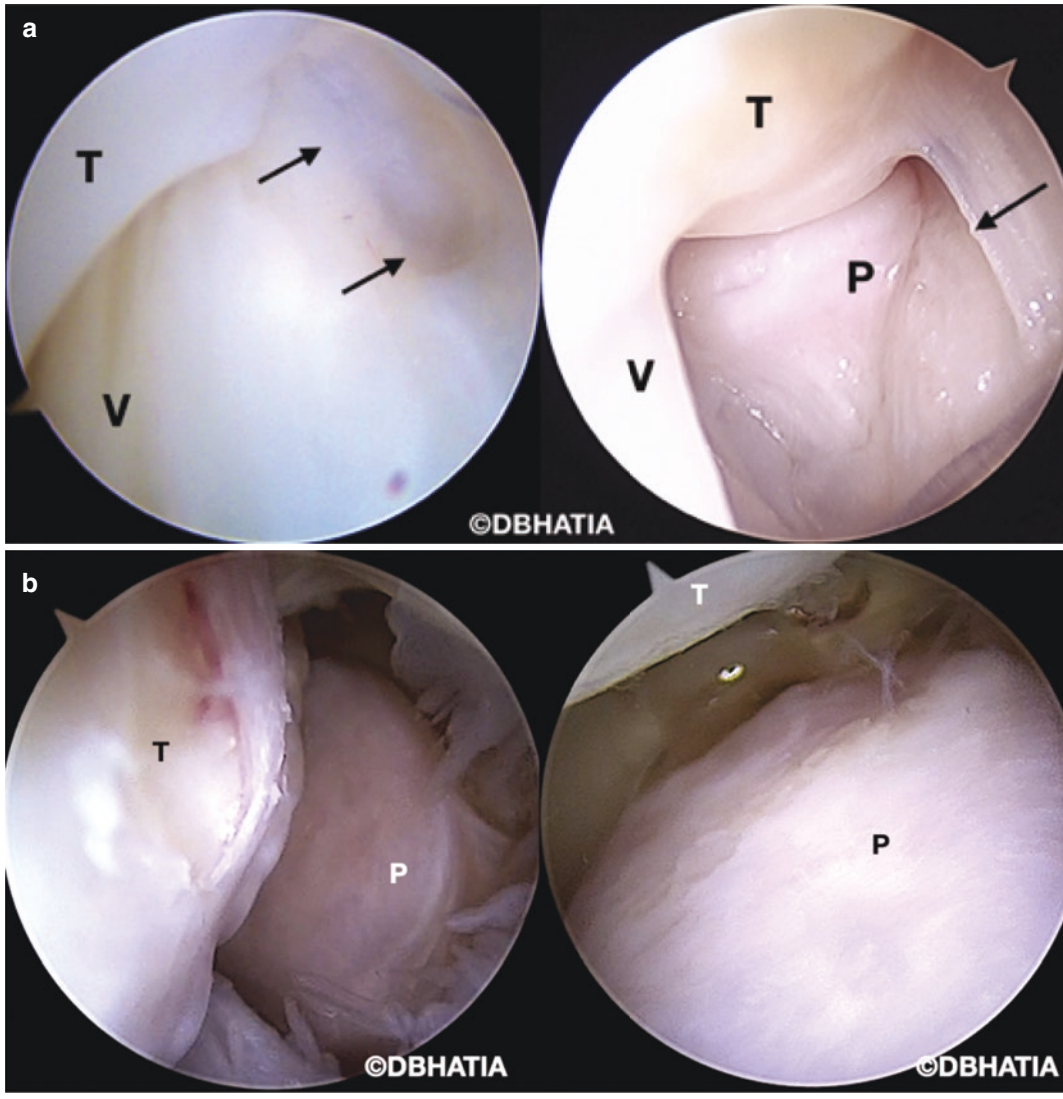

Fig. 84.5 (**a**) Arthroscopic access to the pisotriquetral joint (PTJ) via the radiocarpal joint is possible through a capsular aperture on the ulnar and distal aspect of the triquetrum. A thin membrane may be present within the aperture (arrows, left image) and can be penetrated with the arthroscope. Absence of the membrane (arrow, right image) demonstrates the PTJ via the radiocarpal joint. (**b**) Pisotriquetral arthroscopy demonstrates arthritic changes over the pisiform and triquetral surfaces (© D. Bhatia)

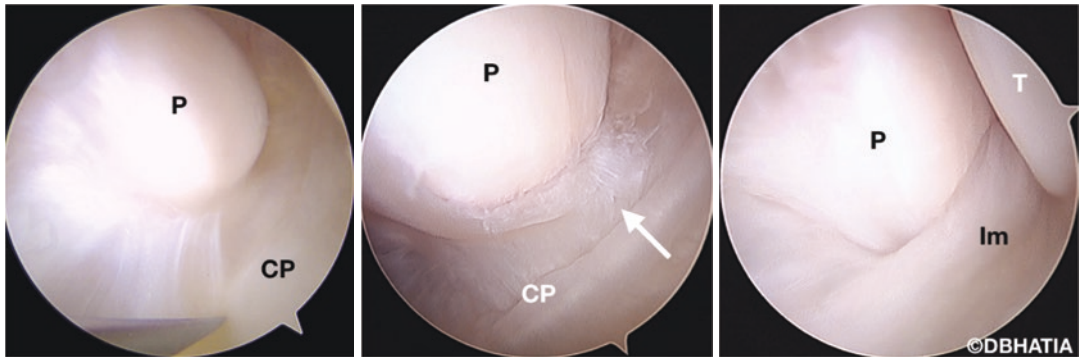

Fig. 84.6 The "arthroscopic ballotment test" is demonstrated. A normal pisotriquetral joint (PTJ) shows the capsular folds (CP) along the ulnar aspect of the pisiform (P, left image). Fraying of the capsule at the inferior pole of P (arrow, center image) is usually a sign of pisotriquetral impingement Soft-tissue impingement (Im) is visualized while performing the PTJ ballotment test (Right image). (T:triquetrum) (© D. Bhatia)

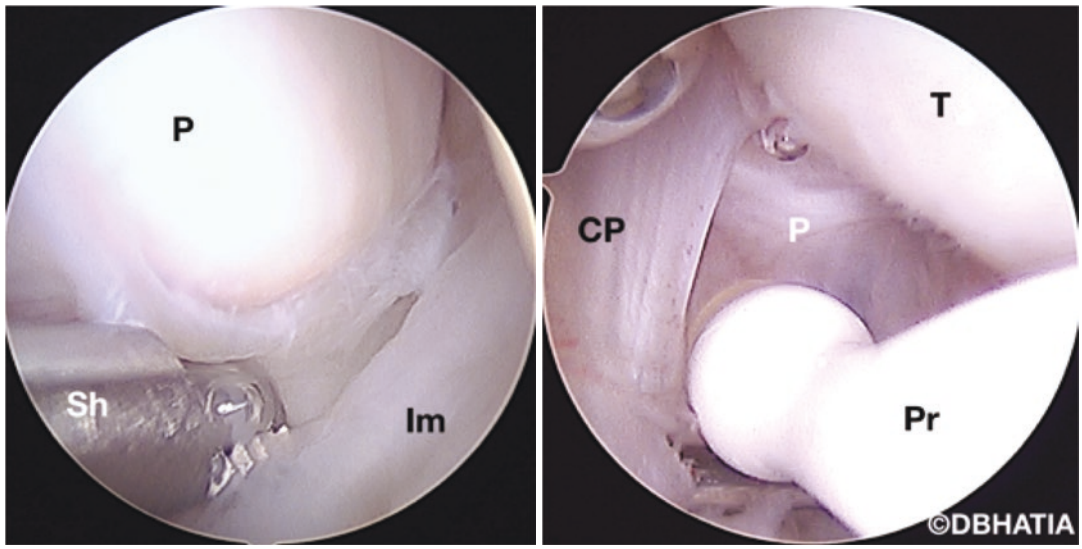

Fig. 84.7 Pisotriquetral joint debridement is performed using a 2-mm shaver (Sh) via the 6R portal (left image) and an angled small joint ablator or radiofrequency probe (Pr) via the 4-5 portal. (P: pisiform, T: triquetrum, CP: capsule, Im: impinging tissue) (© D. Bhatia)

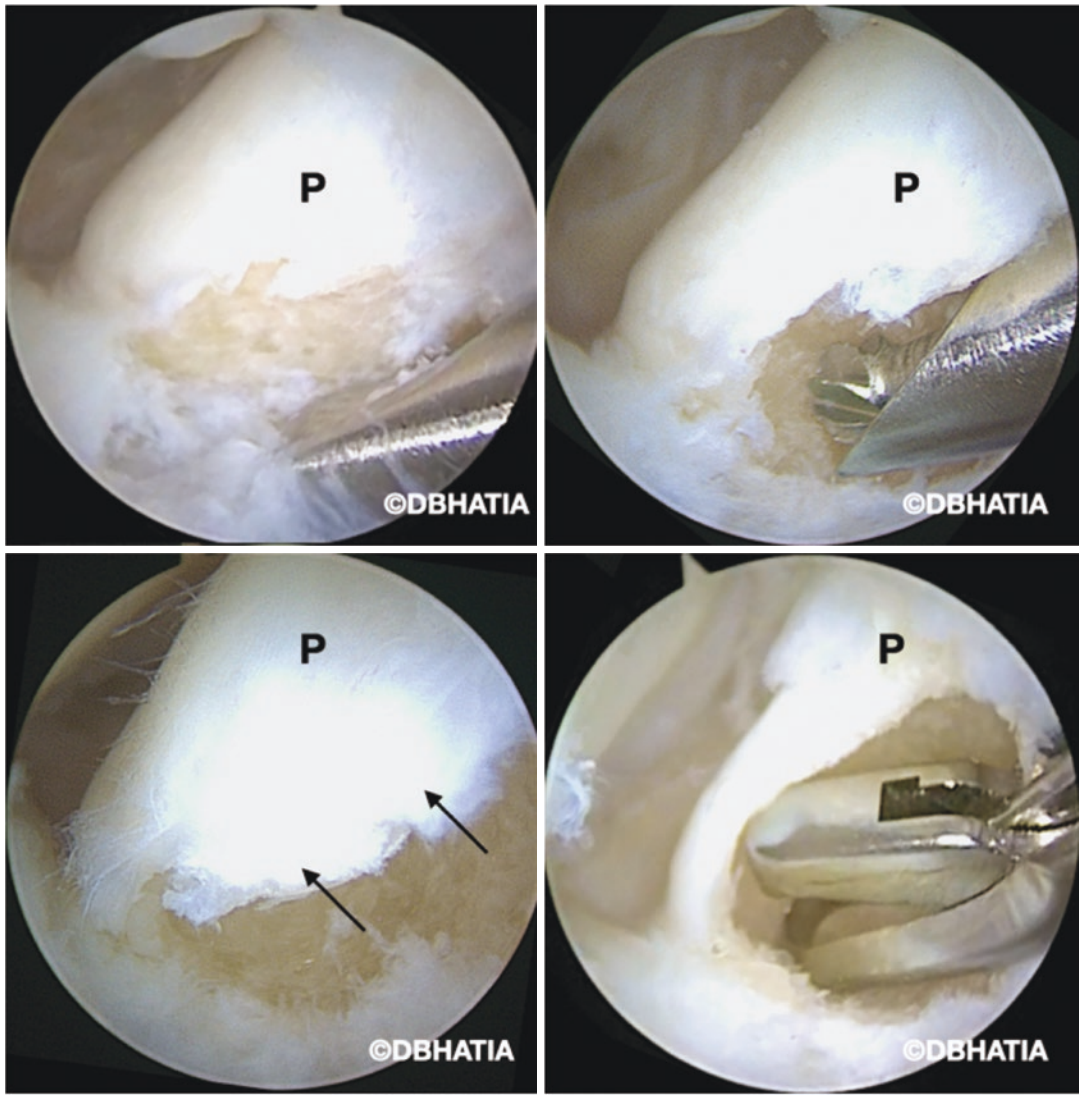

Fig. 84.8 Partial pisiformectomy involves delineation of the resection margin using a shaver (top left). A burr is then used to excise subchondral bone (top right). The overlying cartilage flap is then excised using an angled punch (bottom left and right) (P: pisiform) (© D. Bhatia)

Conflict of Interest The author certifies that he has no commercial associations (e.g., consultancies, stock ownership, equity interest) that might pose a conflict of interest in connection with the submitted article. The author retains the copyright to the images, videos, and content in this chapter.

References

1. Moraux A, Lefebvre G, Pansini V, et al. Pisotriquetral joint disorders: an under-recognized cause of ulnar side wrist pain. Skelet Radiol. 2014;43(6):761–73.
2. Shulman BS, Rettig M, Sapienza A. Management of pisotriquetral instability. J Hand Surg Am. 2018;43(1):54–60.
3. Helal B. Chronic overuse injuries of the piso-triquetral joint in racquet game players. Br J Sports Med. 1978;12(4):195–8.
4. Kofman KE, Schuurman AH, Mulder MC, Verlinde SA, Gierman LM, van Diest PJ, Bleys RL. The pisotriquetral joint: osteoarthritis and enthesopathy. J Hand Microsurg. 2014;6:18–25.
5. Steinmann SP, Linscheid RL. Pisotriquetral loose bodies. J Hand Surg Am. 1997;22:918–21.
6. Arya AP, Kulshreshtha R, Kakarala GK, Singh R, Compson JP. Visualisation of the pisotriquetral joint through standard portals for arthroscopy of the wrist: a clinical and anatomical study. J Bone Joint Surg Br. 2007;89(2):202–5.

Part XVII

Wrist: Distal Radioulnar Joint

85 Surgical Anatomy of the Distal Radioulnar Joint

Parham Daneshvar and Ruby Grewal

85.1 Background

The distal radioulnar joint (DRUJ) is a trichoid diarthrodial joint, allowing simultaneous pivoting and forearm rotation. The DRUJ along with the interosseous membrane (IOM) and the proximal radioulnar joint (PRUJ) make up the forearm joint. The ability to supinate and pronate has given the human species the uniqueness of being able to move the forearm and wrist without affecting the hand's ability to grasp objects. The complex motion of the forearm requires an intricate relationship of the osseous and soft tissue anatomy, balancing motion and stability.

85.2 Osseous Anatomy and Biomechanics

The ulnar head (UH) and the sigmoid notch (SN) of the radius form the osseous components of the DRUJ. The UH is comprised of two articular regions covered with hyaline cartilage. These include the pole and the seat of the UH (Fig. 85.1). The seat of the UH and the sigmoid notch of the radius form the articulation of the DRUJ. This is an incongruent joint as the radius of the curvature of the ulnar seat is about half of that of the SN [1, 2]. The total arc of forearm rotation is approximately 150–180°, of which 30° occurs through the radiocarpal and midcarpal joints and the remainder through the DRUJ. The actual articular arc of the ulnar seat is approximately 90–135° while that of the SN is 47–80° [3]. Due to the mismatch of the radii of curvature between the UH and the SN, during prosupination, in addition to rotation, there is translation occurring within this joint.

As the forearm rotates from a supinated position to a pronated position, there is a relative increase in ulnar positive variance. This in turn leads to the SN contact line being oblique, from more proximal volarly to more distal dorsally when assessing the SN from the ulnar side [4]. This view of the SN also demonstrates that the SN is generally larger (on average by 65%) dorsally than volarly suggesting that there is more contact dorsally (Fig. 85.2) [1].

The DRUJ osseous anatomy is known to be quite variable as described by Tolat et al. The coronal inclination of the DRUJ and in particular the SN has been shown to vary from oblique to neutral/parallel to reverse oblique [2]. Tolat et al. divided the SN inclination into three types: Type I parallel, Type II oblique, and type III reverse

P. Daneshvar
Queen's University, Kingston, ON, Canada

Department of Surgery, Kingston Health Sciences Centre, Kingston, ON, Canada

R. Grewal (✉)
Roth | McFarlane Hand and Upper Limb Centre, St. Joseph's Health Care, University of Western Ontario, London, ON, Canada
e-mail: rgrewa@uwo.ca

© ISAKOS 2022

D. N. Bhatia et al. (eds.), *Arthroscopy and Endoscopy of the Elbow, Wrist and Hand*,
https://doi.org/10.1007/978-3-030-79423-1_85

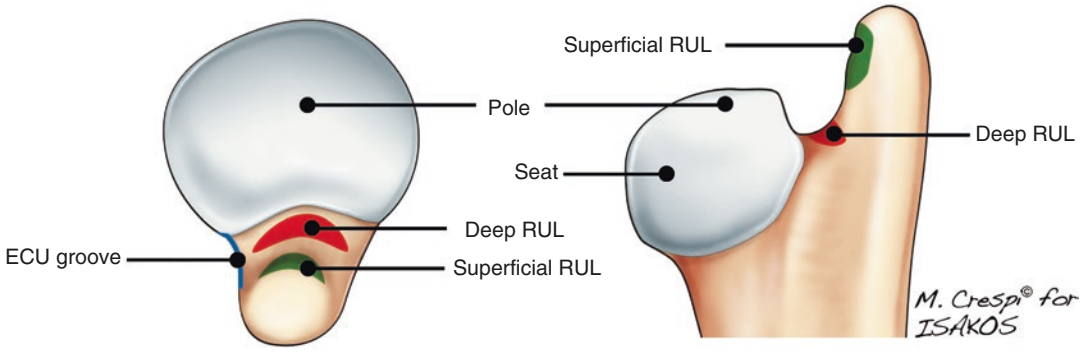

Fig. 85.1 Axial and coronal views of a right ulnar head demonstrating the insertion of the deep and superficial radioulnar ligaments in the ulnar fovea and styloid, respectively. About three-quarters of the UH is covered in hyaline cartilage making up the pole and the seat of the UH (M. Crespi © for ISAKOS)

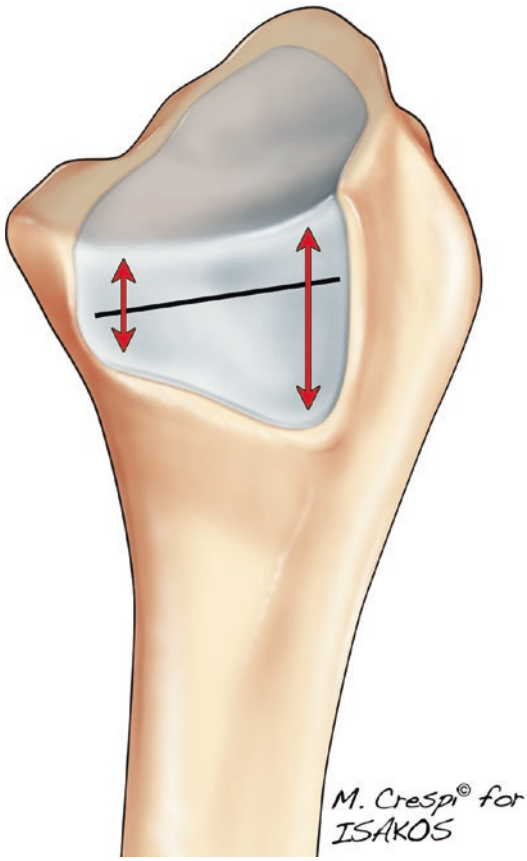

Fig. 85.2 Sagittal view of the SN demonstrating the size of the articular surface of the sigmoid notch (red arrows), demonstrating larger SN dorsally than volarly. The solid black line demonstrates the axis of load-bearing through the sigmoid notch during forearm rotation (M. Crespi © for ISAKOS)

oblique. The degree of obliquity is matched between the UH and SN, and there is a direct correlation between this obliquity and ulnar variance (Fig. 85.3) [1]. The average UV has been shown to be around 1 mm negative variance although it can vary depending on the population [5]. Studies have demonstrated the relative reduction in obliquity of the SN as the UV increases from a negative UV, and eventual reverse obliquity with increasing positive ulnar variance [1, 5, 6]. There is a linear relationship between UV and coronal length of the SN. The more positive the UV (less negative), the smaller the coronal length of the SN (from the inferior edge of the SN proximally to where it meets the ulnar articular surface of the lunate facet distally) [1]. The UV has also been shown to have a dynamic component and has been found to increase with grip [7].

When assessing the UH's articulation with the ulnar carpal bones, Palmer and Werner showed that in neutral UV, 82% of the axial load was transmitted through the radiocarpal (RC) articulation and 18% through ulnocarpal (UC) articulation. With ulnar shortening of 2.5 mm, these values changed to 96%, and 4% respectively; with 2.5 mm of ulnar lengthening the load transmitted through UC joint increased to 42% versus 58% through the RC joint. Furthermore, they demonstrated 100% of the axial load was transmitted through the RC joint with the excision of the UH [8].

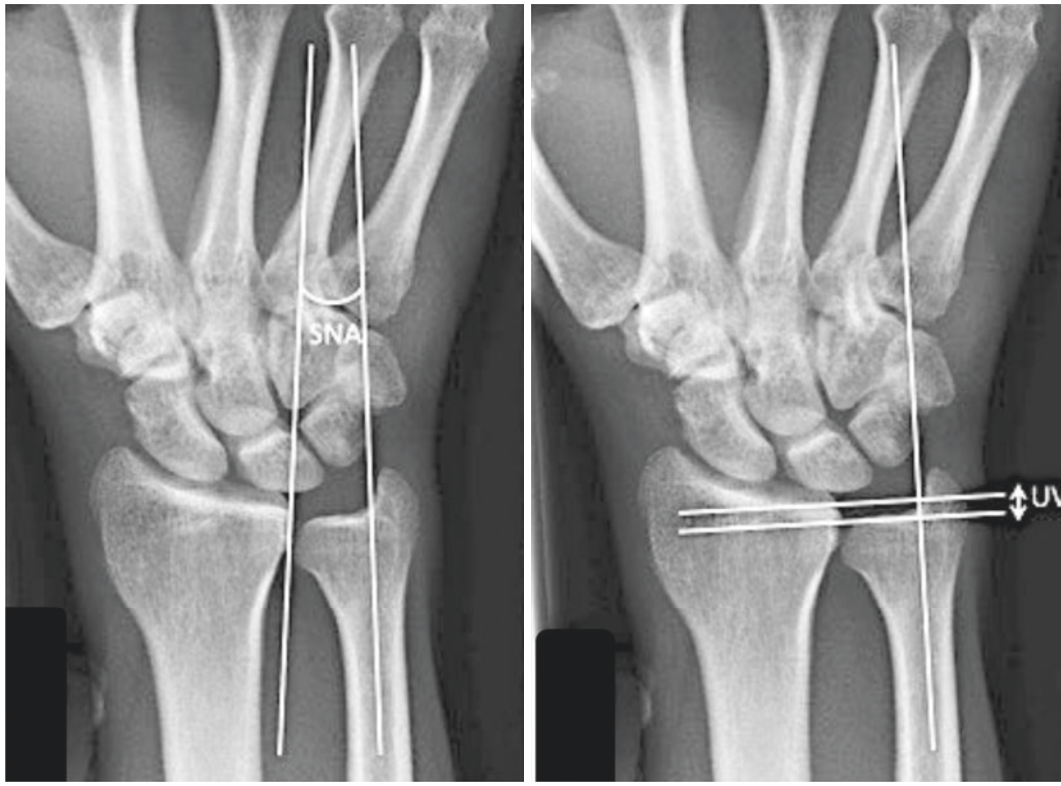

Fig. 85.3 Posteroanterior wrist X-ray demonstrating measurements of the sigmoid notch angle (SNA) and ulnar variance (UV). This wrist has about a 2 mm negative UV and a mildly oblique SNA

The UH's bony anatomy is comprised of three distinct areas void of articular cartilage. These include the ulnar fovea (UF), ulnar styloid (US), and the extensor carpi ulnaris (ECU) groove (Fig. 85.1). The ulnar fovea is a nonarticular depressed section between the ulnar articular portion of the distal UH (ulnar pole) and US. This area represents the site of attachment of the deep radioulnar ligaments and ulnocarpal ligaments. The ulnar styloid is the continuation of the subcutaneous border of the distal ulna and is 2–6 mm in length. The US can vary significantly in shape and serves the purpose of attachment of the superficial limb of the radioulnar ligaments along with ulnocarpal ligaments (particularly coming from the base of the styloid) and meniscus homolog [9]. Dorsoradially on the distal ulna and radial to the US lies a groove that houses the ECU tendon.

85.3 Soft-Tissue Anatomy

Aside from the bony architecture, all joints require soft-tissue stabilizers in the form of static and dynamic restraints. However, the lack of congruity of the DRUJ adds further complexity to this joint's stability and our understanding of it. The soft-tissue stabilizers of the DRUJ include the triangular fibrocartilage complex (TFCC), ECU tendon, pronator quadratus (PQ), and the interosseous membrane (IOM) (Fig. 85.4). The ECU tendon and the deep and superficial heads of PQ act as dynamic stabilizers, while the TFCC and IOM are static stabilizers. The soft-tissue stabilizers provide the majority of the stabilization of the DRUJ, while only about 20% of its stability is believed to arise from the bony articulation [10].

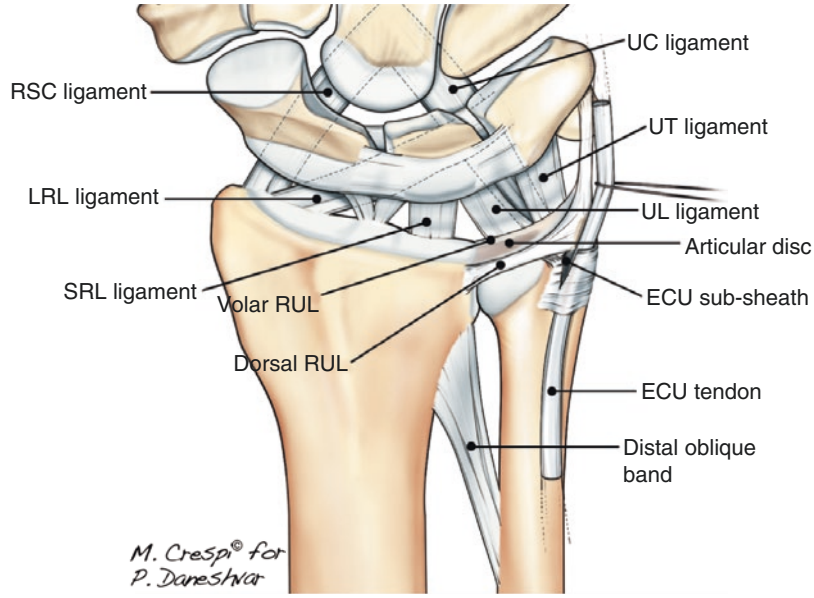

Fig. 85.4 The components of the TFCC are demonstrated in this illustration. These include superficial and deep, dorsal and volar radioulnar ligaments, articular disc, prestyloid recess, meniscus homolog, ulnocarpal ligaments (comprised of ulnotriquetral, ulnocapitate, and ulnolunate ligaments), ulnocarpal capsule, ECU subsheath, and tendon. The ECU subsheath and tendon contribute to the dorso-ulnar wall of the TFCC. The dorsal oblique band of the distal interosseous membrane is also present (M. Crespi © for Daneshvar)

85.3.1 Triangular Fibrocartilage Complex

The term TFCC was coined by Palmer and Werner in 1981 to describe the soft-tissue complex stabilizing the DRUJ and ulnar carpus. The tissues arise from the ulnar side of the lunate facet of the radius and extend to the ulnar fovea and styloid. Here, the tissues combine with the bands arising from the ulnar styloid (termed ulnar collateral ligament) and continue distally to insert into the triquetrum, hamate, and the base of the fifth metacarpal. In their description, the components of the TFCC include the triangular fibrocartilage proper (the articular disc), the meniscus homolog (the ulnocarpal meniscus), the ulnar collateral ligament (UCL), the dorsal radioulnar ligament (RUL), the volar RUL, and the sheath of the extensor carpi ulnaris (ECU) [11]. With further understanding of this complex structure, the current components of the TFCC are described in this section (Fig. 85.4).

1. *Radioulnar ligaments*: The RUL is the most important stabilizer of the DRUJ. Even when all the remainder of the soft-tissue stabilizers of the DRUJ is sacrificed, the RULs can maintain DRUJ stability [12]. In 1985, Ekenstam and Hagert described the dorsal RUL as the main stabilizer against volar translation during supination and the volar RUL as the stabilizer against dorsal translation during pronation [3]. This was later disputed by Schuind et al. in 1991 as these authors found the opposite, demonstrating the dorsal RUL tightening during pronation and the volar RUL tightening during supination [6]. This was further clarified as there exist two sets of distinct ligaments, deep and superficial. The initial study was observing the deep RUL which inserts onto the ulnar fovea, and the later study was potentially measuring tension on the superficial fibers which insert on the mid and base of the ulnar styloid (Fig. 85.1) [3, 4].

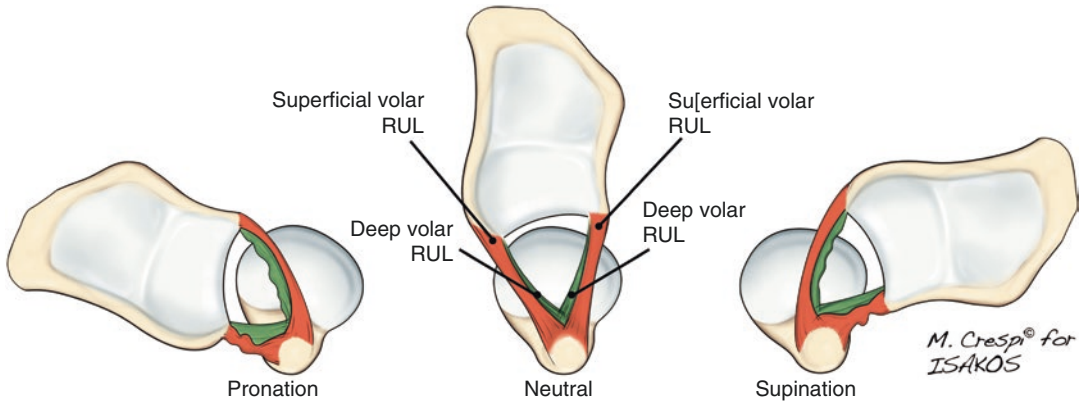

Fig. 85.5 Axial view of a right wrist and DRUJ starting from the left in full pronation and rotating to neutral and full supination to the right. The deep (green) and superficial (red) radioulnar ligaments are demonstrated. In full pronation, the volar deep RUL becomes taut along with the superficial dorsal RUL, while the deep dorsal RUL and superficial volar RUL are lax. In full supination, the deep dorsal and superficial volar RULs are taut and the deep volar and superficial dorsal RULs are lax. There is translation of the DRUJ through the ROM with most contact in the articulation occurring in neutral rotation (about 60% contact area) while much less joint surface contact occurs in full supination and pronation (as low as about 10% contact). (3) Note that during pronation, the SN of the radius translates volarly resulting in the UH sitting relatively more dorsal. Inversely, during supination, the UH is located relatively volar to the SN (M. Crespi © for ISAKOS)

Hence, during pronation, the deep volar RUL and superficial dorsal RUL are under tension, and during supination, the dorsal deep RUL and superficial volar RUL are under tension (Fig. 85.5) [4]. Given this anatomy of the RULs, it is important to understand that isolated deep RUL tears are not visualized through a radiocarpal arthroscopy unless the superficial fibers are also torn, allowing deeper visualization.

2. *Articular disc*: The articular disc (AD) is composed of fibrocartilage. Nakamura et al. describe the distal part of the disc as having a dense multidirectional fibrocartilage matrix, which allows absorption of the axial pressure from the carpus. The fibrocartilage matrix of the AD is oriented in a radioulnar direction proximally, enabling it to handle radioulnar tensile forces. The central and radial aspects of the AD are completely avascular, while the ulnar border starts to have sparse vascularity and more parallel collagen bundles [13].

   The dorsal and palmar margins of the AD become confluent with the RULs. Radially the AD fibrocartilage merges with the hyaline cartilage of the lunate facet of the radius. Mikic described the AD histologically as cartilaginous centrally allowing subject to pressure, and ligamentous peripherally subject to traction [14]. The disc is much thicker ulnarly and peripherally and thinner centrally and radially [15]. The thickness of the disc is directly related to the UV, hence, the more negative the UV the thicker the disc [16]. Due to its lack of vascularity and decreased width, the central portion of the disc is at higher risk of tearing and lacks the ability to heal.
3. *Prestyloid recess and meniscus homolog*: The prestyloid recess is a synovial lined cavity, which connects the ulnar styloid to the radiocarpal joint [16]. The meniscus homolog (MH) is the distal ulnar extension of the AD, while on its proximal–ulnar side it transitions into the radioulnar ligament (Fig. 85.6). The MH consists of loose synovial folds which adapt to the stresses occurring from radioulnar deviation. It is described three dimensionally as the ulnar internal wall of the hammock-like contour of the distal TFCC. Ishii et al. defined the meniscus homolog as the "tissue that is

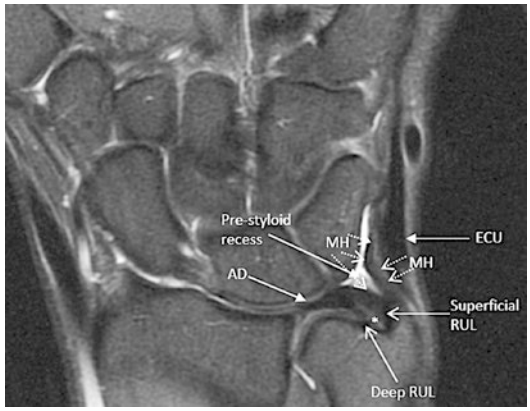

Fig. 85.6 MRI of the wrist, coronal T2-weighted fat-saturated image demonstrating the meniscus homolog (MH) (dashed arrows), insertion of the deep and superficial limbs of the radioulnar ligaments (RUL) onto the ulnar fovea and styloid, respectively, ECU tendon, prestyloid recess, and the articular disc (with its radial sided attachment to the hyaline cartilage of the ulnar aspect of the lunate facet). The ligamentum subcruetum is marked by * as the tissue between the deep and superficial RULs. This demonstrates a type I MH and prestyloid recess

between (and integrated on its periphery) the ulnar aspect of the superficial ligament and the ulnar capsule" [17]. They found the prestyloid recess and the MH to be part of the same entity as the shape of the MH determined the appearance of the prestyloid recess which they identified in three configurations (Fig. 85.7).

There exists a highly vascular connective tissue that is thought to be nonligamentous between the most ulnar aspect of the deep RUL and the MH called ligamentum subcruentum (Fig. 85.6) [17]. Others have described the ligamentum subcruentum as the highly vascular area between the deep and superficial limbs of the RULs [18]. However, more recently this term has been used interchangeably with the deep fibers of the RULs, which creates confusion. This is an area to be aware of during arthroscopic surgery as it may lead to bleeding if excessively debrided.

4. *Ulnocarpal ligaments*: The volar ulnar aspect of the DRUJ contains a group of ulnocarpal (UC) ligaments. These include ulnotriquetral, ulnocapitate, and ulnolunate ligaments from ulnar to radial, respectively (Fig. 85.4). They originate off the ulnar fovea, styloid, and the volar RULs while inserting on the carpal bones [9, 19]. These ligaments become confluent with the volar RULs radially and with MH ulnarly. In their biomechanical study, Moritomo et al. found that the UT and ulnocapitate ligaments were under most tension with the wrist in radial deviation and the UL ligament with wrist extension. This leads them to conclude that the mechanism for foveal tears occurs with excessive traction of the UC ligaments during a fall on an outstretched hand [9]. Iida et al.'s biomechanical study also support the notion that the UC ligaments are key stabilizers of the DRUJ in wrist extension. They found the DRUJ to be less mobile with the wrist in extension and radial deviation, yet once the UCL was sectioned the mobility was similar to a wrist in a neutral position. They concluded that the palmar RUL may be tightened in wrist extension and radial deviation due to the tightening of the UCLs which partially arise from the volar RUL [20].
5. *Ulnocarpal capsule:* The ulnocarpal capsule surrounds the dorsal, ulnar, and volar aspects of the TFCC. Although some refer to it as the UCL, it is not considered to be a ligament. It is the peripheral tissue comprising of the area starting volarly from the ulnar side of the UT ligament, traveling around and attaching to the US, extending dorsally to the ECU subsheath, and attaching distal dorsally on the triquetrum [17, 19]. The ECU subsheath is distinctly denser than the ulnar capsule, however, along with the ulnar capsule it blends onto the dorsal ulnar aspect of the US [17].

85.3.2 Interosseous Membrane

The interosseous membrane (IOM), and in particular the region considered the distal interosseous membrane (DIOM), acts as a secondary stabilizer to the DRUJ in the setting of an injured RUL. The DIOM consists of a membrane portion that is always present and a distal oblique bundle (DOB) which is present in about 40% of the pop-

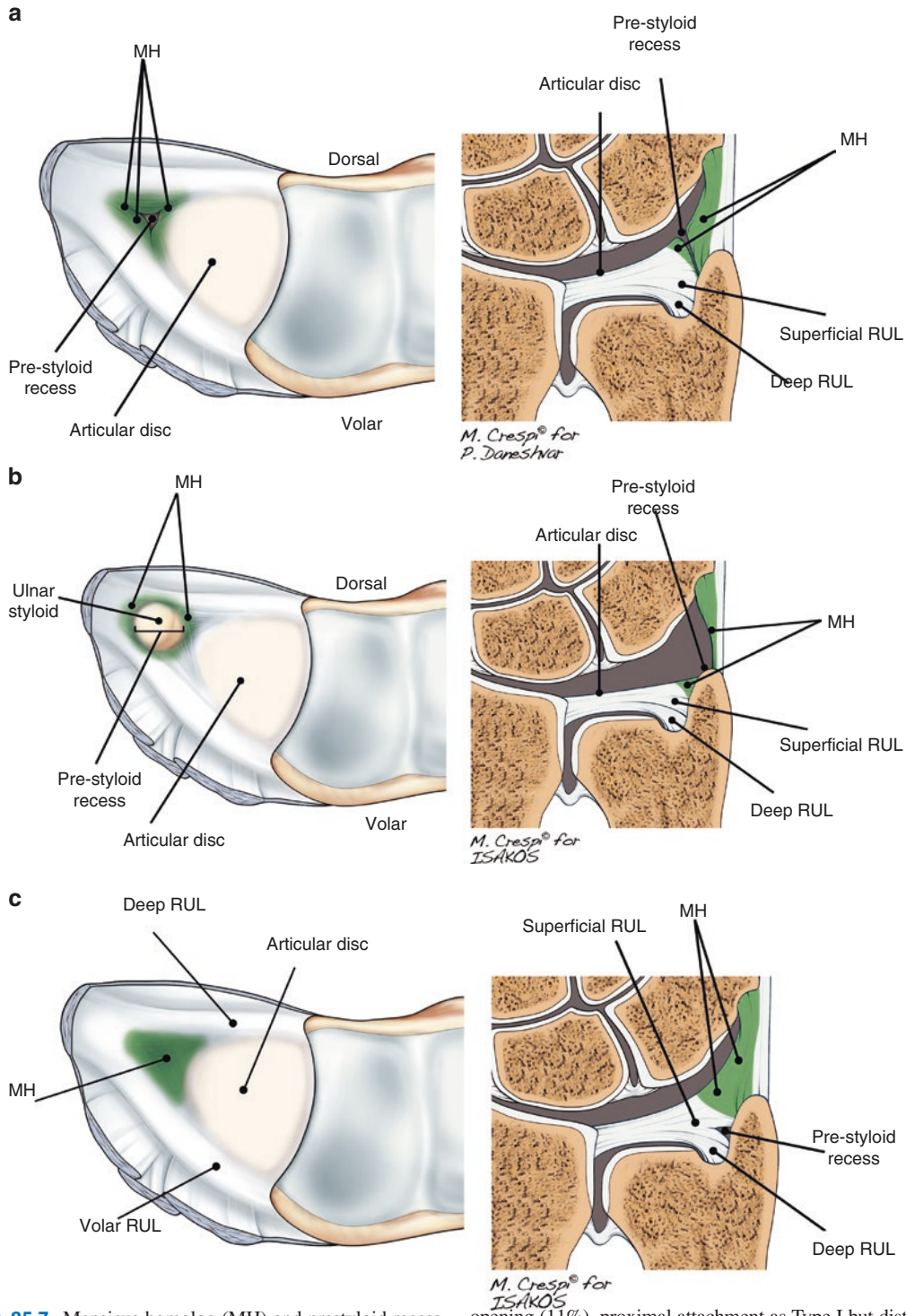

Fig. 85.7 Mensicus homolog (MH) and prestyloid recess configurations as described by Ishii et al. [17]. (**a**) Type I—narrow opening (74%), attaches proximally to radial, dorsal, and volar aspects of the mid and base of US. Distally, attaches circumferentially to tip of US. (**b**) Type II—wide opening (11%), proximal attachment as Type I but distally does not insert on US tip. (**c**) Type III—no opening (15%), attaches proximally to dorsal, volar, and ulnar aspects of US with no radial attachment, leaving no opening for the recess into the ulnocarpal space (M. Crespi © for ISAKOS)

ulation (Fig. 85.4) [21]. Kitamura et al. found that specimens without the DOB had more DRUJ laxity as compared to specimens with DOB [22]. The DOB that are visibly thickened fibers within the DIOM originate from the radial side of the distal one-sixth of the ulnar shaft and insert at the inferior rim of the SN of the radius [21, 23]. During an ulnar shortening procedure, those with osteotomies performed proximal to the origin of the DIOM demonstrated increased DRUJ stability over those with osteotomies distal to the DIOM origin. In the presence of the DOB, the stabilization was further enhanced [23].

85.3.3 Druj Capsule

The DRUJ capsule is anatomically and dynamically autonomous from the remainder of the soft tissues surrounding the DRUJ [24]. Ulnarly the capsule blends with the soft tissues on the US, dorsally it becomes confluent with the floor of the ECU tendon sheath and distally with the RULs. Proximally it has an inferior leaf which is stout and less redundant and inserts to the inferior border of the SN (Fig. 85.8). Along this proximal border, the capsule may accept fibrous attachments of the DIOM. In contrast to the thicker, strong inferior capsule, the volar and dorsal capsules are quite thin and redundant. The volar capsule is able to accommodate the ulnar head which resides there during supination. Similarly, the dorsal capsule accepts the UH during pronation and becomes more taught as the volar capsule becomes redundant (Fig. 85.8). The DRUJ capsule, in a pathologic state (i.e., post distal radius fracture), can become thickened and cause a loss of rotation, and in particular a loss of supination. Surgical release of the capsule is often successful at regaining prosupination [24].

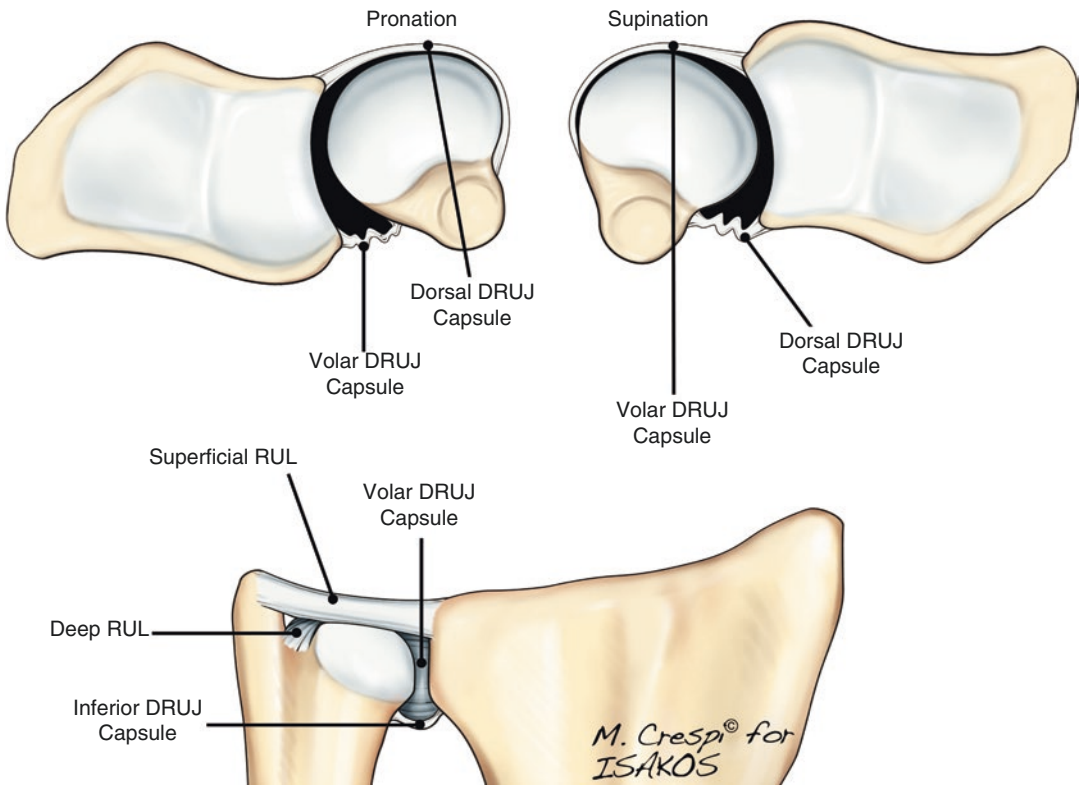

Fig. 85.8 DRUJ capsule. This illustration demonstrates how the volar and dorsal DRUJ capsule behave as the radius rotates around a static ulna. The lower image displays the thicker inferior capsule (M. Crespi © for ISAKOS)

85.3.4 Extensor Carpi Ulnaris Tendon and Subsheath

The ECU subsheath can act as a static stabilizer as it contributes to the soft-tissue constraints of the TFCC. The ECU tendon travels and is restrained in a fibro-osseous tunnel along an osseous groove on the dorsal ulnar aspect of UH and US. The ECU subsheath comprises the dorso-ulnar aspect of the styloid with thickened a mass of vertically traveling fibers (Fig. 85.5). This area of thickening is at times referred to as the UCL. Iida et al. demonstrated that with the RULs resected, during wrist radial deviation and extension, the ECU subsheath tightens and stabilizes the DRUJ. The ECU tendon is a dynamic DRUJ stabilizer when loaded in supination and neutral rotation [25]. This pull on the ECU will also place traction on its subsheath leading to further dynamic stabilization. In addition to DRUJ stability, the ECU tendon has been shown to behave as a pronator to the carpus, as it provides a pronation torque on the distal carpal row as well as the scaphoid and triquetrum. Loss of this tendon's location in the fibro-osseous sheath affects both DRUJ and carpal stability.

85.3.5 Pronator Quadratus

The pronator quadratus (PQ) muscle consists of deep and superficial heads. The superficial head originates from the ulnar crest of the ulna and inserts onto the distal metaphysis of the volar radius. The deep head originates from the ulna, but more volarly. It inserts on the ulnar border of the distal radius and extends dorsally toward the DIOM [26, 27]. The deep head may also have insertion on the DRUJ capsule. The superficial head has been shown to primarily function as a forearm pronator, while the deep head is a dynamic stabilizer of the DRUJ [27]. An electromyography study of the PQ demonstrated that the deep head was active during both supination and pronation, while the superficial head was only active during pronation; thereby supporting the theory of the deep head acting mainly as a DRUJ stabilizer [28].

85.4 Summary

The DRUJ is a part of the "forearm joint" and thus the entirety of this complex must be considered when assessing patients and considering injuries. A thorough knowledge of the osseous and soft-tissue anatomy of the DRUJ is imperative in the understanding of the function of this joint and the ability to treat varying pathologies. Although the deep volar and dorsal RULs are the primary stabilizers of the DRUJ, this joint requires the combination of the DRUJ articulation and soft tissues to maintain a stable and functional joint through forearm rotation and loading.

References

1. Daneshvar P, Willing R, Pahuta M, Grewal R, King GJW. Osseous anatomy of the distal radioulnar joint: an assessment using 3-dimensional modeling and clinical implications. J Hand Surg Am. 2016;41(11):1071–9. https://doi.org/10.1016/j.jhsa.2016.08.012.
2. Tolat AR, Stanley JK, Trail IA. A cadaveric study of the anatomy and stability of the distal radioulnar joint in the coronal and transverse planes. J Hand Surg Br. 1996;21(5):587–94.
3. Ekenstam FA, Hagert CG. Anatomical studies on the geometry and stability of the distal radio ulnar joint. Scand J Plast Reconstr Surg Hand Surg. 1985;19(1):17–25.
4. Kleinman WB. Stability of the distal radioulna joint: biomechanics, pathophysiology, physical diagnosis, and restoration of function what we have learned in 25 years. J Hand Surg Am. 2007;32(7):1086–106.
5. Sagerman SD, Zogby RG, Palmer AK, Werner FW, Fortino MD. Relative articular inclination of the distal radioulnar joint: a radiographic study. J Hand Surg Am. 1995;20(4):597–601.
6. Schuind FA, Linscheid RL, An KN, Chao EYS. A normal data base of posteroanterior roentgenographic measurements of the wrist. J Bone Jt Surg: Ser A. 1992;74(9):1418–29.
7. Mwaturura T, Daneshvar P, Pike J, Goetz TJ. Clinical and radiographic correlates for the treatment of ulnocarpal impaction. J Wrist Surg. 2019;8(3):192–7.
8. Palmer AK, Werner FW. Biomechanics of the distal radioulnar joint. Clin Orthop Relat Res. 1984;187:26–35.
9. Moritomo H, Murase T, Arimitsu S, Oka K, Yoshikawa H, Sugamoto K. Change in the length of the ulnocarpal ligaments during radiocarpal motion: possible impact on triangular fibrocartilage complex foveal tears. J Hand Surg Am. 2008;33(8):1278–86.

10. Stuart PR, Berger RA, Linscheid RL, An KN. The dorsopalmar stability of the distal radioulnar joint. J Hand Surg Am. 2000;25(4):689–99.
11. Palmer AK, Werner FW. The triangular fibrocartilage complex of the wrist—anatomy and function. J Hand Surg Am. 1981;6(2):153–62. https://doi.org/10.1016/S0363-5023(81)80170-0.
12. Gofton WT, Gordon KD, Dunning CE, Johnson JA, King GJW. Soft-tissue stabilizers of the distal radioulnar joint: an in vitro kinematic study. J Hand Surg Am. 2004;29(3):423–31.
13. Semisch M, Hagert E, Lluch A. JHS (E) Histological assessment of the triangular fibrocartilage complex, 2016.
14. Mikic Z, Somer L, Somer T. Histologic structure of the articular disk of the human distal radioulnar joint. Clin Orthop Rel Res. 1992:29–36.
15. Nakamura T, Yabe Y. Histological anatomy of the triangular fibrocartilage complex of the human wrist. Ann Anat. 2000;182(6):567–72.
16. Palmer AK, Glisson RR, Werner FW. Relationship between ulnar variance and triangular fibrocartilage complex thickness. J Hand Surg Am. 1984;9(5):681–3. https://doi.org/10.1016/S0363-5023(84)80013-1.
17. Ishii S, Palmer AK, Werner FW, Short WH, Fortino MD. An anatomic study of the ligamentous structure of the triangular fibrocartilage complex. J Hand Surg Am. 1998;23(6):977–85.
18. Buck FM, Gheno R, Nico MAC, Haghighi P, Trudell DJ, Resnick D. Ulnomeniscal homologue of the wrist: correlation of anatomic and MR imaging findings. Radiology. 2009;253(3):771–9.
19. Hagert Elisabet, Chim Harvey, Moran S. Anatomy of the distal radioulnar joint and ulnocarpal complex. In: Ulnar sided wrist pain: a master skills publicationter skills publication. 2013. p. 11–21.
20. Iida A, Omokawa S, Moritomo H, Omori S, Kataoka T, Aoki M, et al. Effect of wrist position on distal radioulnar joint stability: a biomechanical study. J Orthop Res. 2014;32(10):1247–51.
21. Moritomo H, Noda K, Goto A, Murase T, Yoshikawa H, Sugamoto K. Interosseous membrane of the forearm: length change of ligaments during forearm rotation. J Hand Surg Am. 2009;34(4):685–91. https://doi.org/10.1016/j.jhsa.2009.01.015.
22. Kitamura T, Moritomo H, Arimitsu S, Berglund LJ, Zhao KD, An KN, et al. The biomechanical effect of the distal interosseous membrane on distal radioulnar joint stability: a preliminary anatomic study. J Hand Surg Am. 2011;36(10):1626–30.
23. Arimitsu S, Moritomo H, Kitamura T, Berglund LJ. The stabilizing effect of the distal interosseous. J Bone Jt Surg Am. 2011;93(21):2022–30.
24. Kleinman WB, Graham TJ. The distal radioulnar joint capsule: clinical anatomy and role in posttraumatic limitation of forearm rotation. J Hand Surg Am. 1998;23(4):588–99.
25. Iida A, Omokawa S, Moritomo H, Aoki M, Wada T, Kataoka T, et al. Biomechanical study of the extensor carpi ulnaris as a dynamic wrist stabilizer. J Hand Surg Am. 2012;37(12):2456–61.
26. Haugstvedt JR, Langer MF, Berger RA. Distal radioulnar joint: functional anatomy, including pathomechanics. J Hand Surg Eur Vol. 2017;42(4):338–45.
27. Stuart PR. Pronator quadratus revisited. J Hand Surg Eur Vol. 1996;21B(6):714–22.
28. Gordon KD, Pardo RD, Johnson JA, King GJW, Miller TA. Electromyographic activity and strength during maximum isometric pronation and supination efforts in healthy adults. J Orthop Res. 2004;22(1):208–13.

DRUJ Arthroscopy: Portals and Arthroscopic Anatomy

86

M. Esplugas, A. Scott-Tennent, A. Lluch, and M. Llusá-Pérez

86.1 Background

Distal radioulnar joint (DRUJ) arthroscopy is an advanced technique, and specialized portals are necessary for diagnostic and therapeutic procedures. The DRUJ can be conceptualized as a "Box" and can be accessed using two dorsal portals (proximal and distal), one ulnar portal (direct foveal) and two volar portals (volar and distal volar). A thorough knowledge of regional anatomical structures is necessary for safe portal placement. This chapter presents an overview of DRUJ portals and their surgical and arthroscopic anatomical aspects.

M. Esplugas (✉)
Institut Kaplan, Barcelona, Spain

A. Scott-Tennent
Department of Orthopaedics, Arnau de Vilanova Hospital, Lleida, Spain

A. Lluch
Institut Kaplan, Barcelona, Spain

Department of Orthopaedics, Vall d' Hebron Hospital, Barcelona, Spain

M. Llusá-Pérez
Department of Orthopaedics, Vall d' Hebron Hospital, Barcelona, Spain

Department of Anatomy, University of Barcelona, Barcelona, Spain
e-mail: mireia.esplugas@institutkaplan.com

86.1.1 Surgical Anatomy

- Large caliber transverse veins lie over the dorsal aspect of the DRUJ space; these veins can easily be damaged with longitudinal skin incisions during the dorsal portal establishment (Fig. 86.1).
- The dorsal extensor retinaculum offers some resistance during the blunt dissection to the joint capsule during the placement of dorsal DRUJ portals (Fig. 86.2).
- Forearm rotation influences the DRUJ dorsal capsule: forearm supination relaxes it while forearm pronation tightens it.
- DRUJ capsule is very thin; the joint space is narrow and concave–convex (Fig. 86.3).
- DRUJ space is hardly stretchable, especially when its roof and the triangular fibrocartilage complex (TFCC) are intact (Fig. 86.4).
- When the wrist and the forearm are under traction, the interosseous membrane and the ECU tendon tension induce DRUJ space compression (Fig. 86.5).

86.2 Indications and Contraindications

DRUJ arthroscopy is performed for:

© ISAKOS 2022

D. N. Bhatia et al. (eds.), *Arthroscopy and Endoscopy of the Elbow, Wrist and Hand*,
https://doi.org/10.1007/978-3-030-79423-1_86

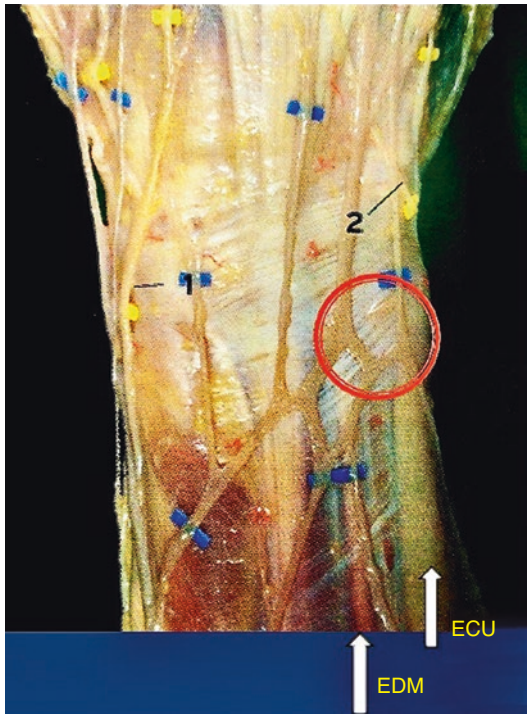

Fig. 86.1 Right cadaver specimen wrist
The distal radioulnar joint (DRUJ) space, landmarked in this figure with a red circle, is found between extensor digiti minimi (EDM) and extensor carpi ulnaris (ECU) tendons. Over its dorsal aspect, several transverse and longitudinal veins can be found, which can easily be damaged during the DRUJ dorsal portals establishment. (1: Dorsal sensory branch of the radial nerve; 2: Dorsal sensory branch of the ulnar nerve)

Fig. 86.2 Right cadaver specimen wrist
The very thin DRUJ dorsal capsule lies under the thick dorsal extensor retinaculum (landmarked here with a red circle), which connects the fifth (EDM) and the sixth (ECU) dorsal extensor compartments

- Evaluation of intracapsular causes of ulnar wrist-sided pain.
- Assessment of acute or chronic DRUJ instability (evaluation of distal radioulnar ligaments foveal attachment, DRUJ articular surface, distal ulna articular surface).
- Acute or chronic DRUJ instability treatment (distal radioulnar ligaments foveal reattachment or reconstruction).
- Proximal partial-thickness TFCC pathology evaluation (delamination, proximal flap lacerations, fibrillation) [1].
- Wafer procedure when the distal TFCC is intact in ulnocarpal impaction syndrome.
- Symptomatic ulnar styloid fracture nonunion (styloidectomy).
- Ulnar styloid–triquetrum syndrome (ulnar styloidectomy).
- DRUJ inflammatory arthritis (synovectomy).
- DRUJ osteochondral injury (DRUJ OA staging).
- DRUJ arthrolysis, exostectomy, capsulotomy, loose body removal.
- Evaluation of proximal insertion of ulnocarpal ligaments.
- DRUJ arthrodesis (Sauvé–Kapandji procedure).

Contraindications to DRUJ arthroscopy are:

- Local infection.
- Ulnar head acute fracture.
- Radius sigmoid notch acute fracture.
- Acute capsular tears (extravasation of fluid if wet arthroscopy is performed).
- Neurovascular compromise or radial artery deficiency.

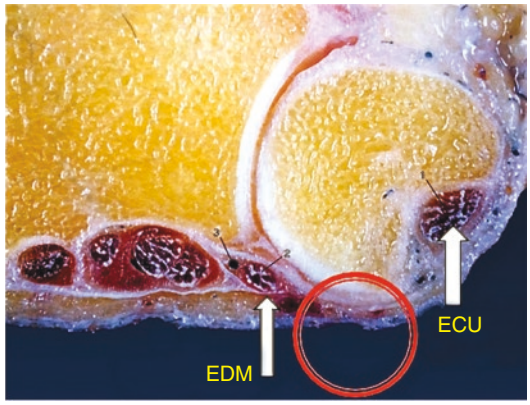

Fig. 86.3 Right cadaver specimen wrist
Dorsal DRUJ capsule is very thin and intimately united to the dorsal extensor retinaculum (both landmarked here with a red circle); the joint space is narrow and concave–convex (1: ECU tendon running into the sixth extensor dorsal compartment; 2: EDM tendon into the fifth extensor dorsal compartment)

Fig. 86.4 Right cadaver specimen wrist
The TFCC is the roof of the DRUJ. If the TFCC is intact or the ulna is long (ulna plus), the DRUJ is hardly stretchable. (1: Radiotriquetral ligament; 2: Dorsal intercarpal ligament)

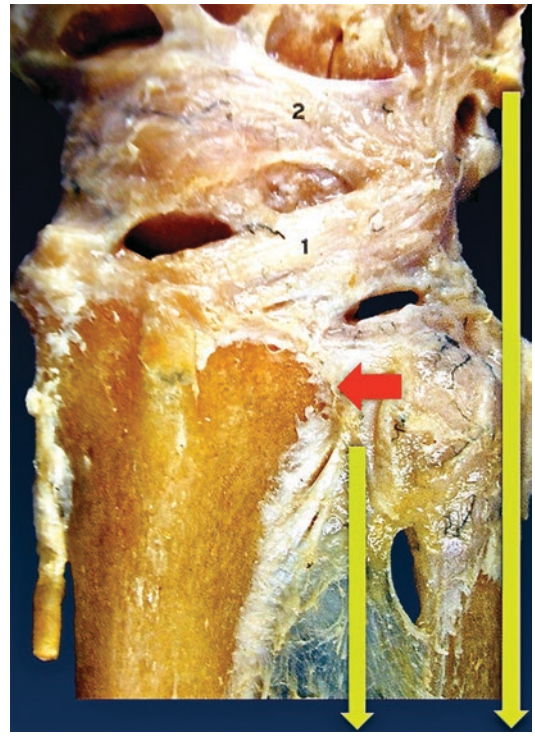

Fig. 86.5 Right cadaver specimen wrist
The tensile elongation of the interosseous membrane and the ECU tendon (both yellow arrows) during wrist arthroscopy traction induces DRUJ compression (red arrow) and reduces joint compliance. (1: Radiotriquetral ligament; 2: Dorsal intercarpal ligament)

- Ulna plus variance (d-DRUJ portal will not be easy to establish).
- Small wrists may not allow the use even the smallest arthroscopy instruments.

86.3 Surgical Technique

86.3.1 Prerequisites for Easier Access to DRUJ

Arthroscopic access to DRUJ is influenced by a narrow joint space, forearm rotation, and traction.

Narrow joint space:

- 1.9-mm scope with 30° angulation may help (although 2.7-mm scope provides a better field).
- Joint distension with 5 cc of saline infusion or with air insufflation.

Forearm rotation:

- Supination relaxes the dorsal capsule and facilitates dorsal portals set up.
- Pronation relaxes the volar capsule and facilitates volar portal establishment.
- In supination, both ulna styloid and ECU tendon translocate dorsally and this allows direct foveal (DF) portal set up.

Traction:

- Traction release facilitates DRUJ space distension and allows DRUJ instrumentation.

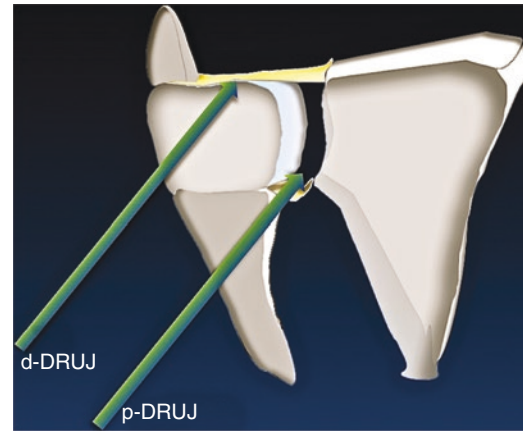

Fig. 86.6 The most useful dorsal DRUJ portal is the distal one (d-DRUJ)
Nevertheless, in case of an ulna plus variance or in case of a previous surgical scar over its area, the proximal portal (p-DRUJ) can be extremely useful

86.3.2 DRUJ Portals

Dorsal, ulnar, and volar portals are used to access the DRUJ.

86.3.2.1 Dorsal Portals

These include distal and proximal portals and are placed between EDM and ECU tendons (Fig. 86.6) [2].

Proximal-DRUJ Portal (p-DRUJ) (Fig. 86.7)
Location: axilla of the joint capsule, proximal to ulna head.

Steps:
- 21G needle at the neck of the distal ulna.
- Skin transverse incision.
- Straight mosquito to perforate the joint capsule.

Field of View (Fig. 86.8):
- Volar: Volar radioulnar ligament (VRUL).
- Radial: radial insertion of TFCC. Sigmoid notch.
- Ulnar: limited view of DRUL.
- Distal: proximal surface of the articular disc.
- Proximal: ulnar neck cartilage and proximal ulnar head cartilage.

Use
- Assessment of cartilage surface of radius and ulna (chronic instability).
- Excision of loose bodies and synovial hypertrophy.
- Saline joint injection.
- Outflow.

Distal-DRUJ Portal (d-DRUJ) (Fig. 86.9)
Location
- Top of the ulnar head, underneath the proximal surface of TFCC.
- 8- to 10-mm distal and 4- to 6-mm ulnar to p-DRUJ portal.
- 5-mm proximal to the 6R portal.

Steps
- 21G needle proximal to 6R
- Forearm in neutral rotation (TFCC is relaxed).
- Straight mosquito (horizontal opening to avoid TFCC damage) helps to widen the space.

Fig. 86.7 The proximal dorsal distal radioulnar portal (p-DRUJ) is located at the joint capsule axilla, just proximal to the ulnar head. Mid forearm supination facilitates its establishment, although it is more palpable in forearm pronation. In full forearm supination, ECU tendon may hinder its setting

Field of View (Fig. 86.10)

- Volar: Volar radioulnar ligament (VRUL).
- Radial: radial insertion of TFCC.
- Ulnar: foveal insertion of the VRUL and dorsal radioulnar ligament (DRUL) although DRUL may be difficult to appreciate.
- Distal: proximal surface of the articular disc.
- Proximal: ulnar head dome cartilage.

Use

- Assessment of proximal surface of TFCC tears, foveal detachment of radioulnar ligaments, and ulnar head dome visualization.
- Instrumentation: when the scope is inserted through DRUJ volar portals.
- Outflow drainage.

86.3.2.2 Ulnar DRUJ Portal: Direct Foveal (DF) Portal (Fig. 86.11) [3]

Location: 1-cm proximal to 6 U portal (Fig. 86.12).

Fig. 86.8 Left DRUJ arthroscopy. Scope in p-DRUJ portal
The distal ulna joint surface is on the left; the radius sigmoid fossa is seen on the right. On the top of the image, the proximal surface of the articular disc is visualized

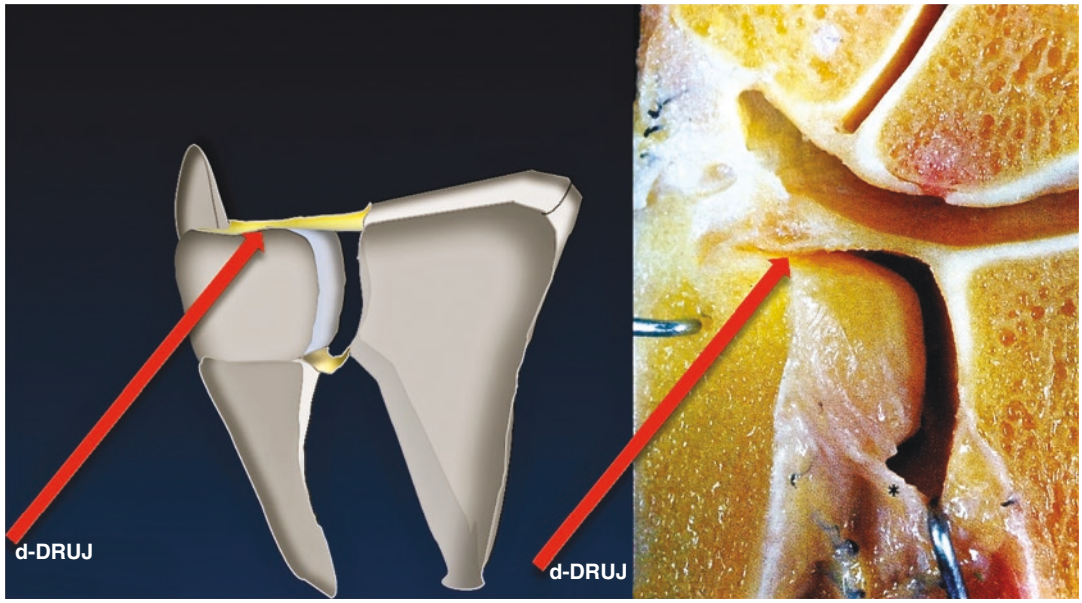

Fig. 86.9 The d-DRUJ enters the DRUJ under the dorso-ulnar margin of the TFCC, just proximal to the 6R portal. It is easier to perform when the foveal TFCC attachment is detached or when the forearm is in neutral rotation

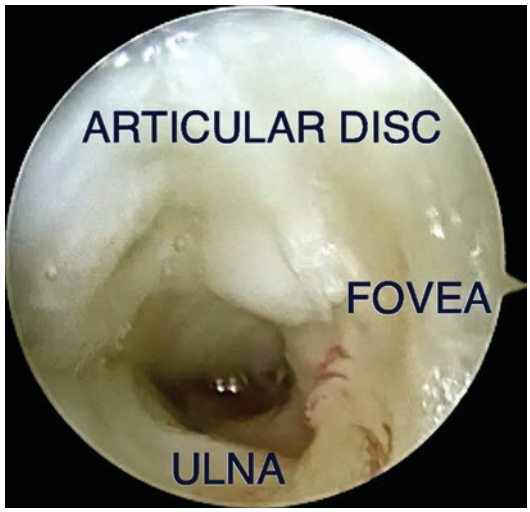

Fig. 86.10 Arthroscopic view through the d-DRUJ portal of a right DRUJ
Vision: (1) Above, the proximal surface of the articular disc; (2) below, the distal surface of the ulnar head. (3) Right, the foveal attachment of DRUL and VRUL

Steps

- Supinate the forearm in order to dorsally locate the ulnar styloid and the ECU tendon. Both structures may interfere with the portal establishment if the forearm is in neutral rotation.
- Position the hand and the wrist in supination to enable dorsal location of the dorsal sensory branch of the ulnar nerve (DSBUN), which lies over the 6 U and DF portals area (Fig. 86.13). In neutral forearm rotation, the nerve is at risk (Fig. 86.14).
- 21G needle is placed under the proximal surface of the TFCC, between ECU and FCU tendons (Fig. 86.15).
- 2-cm longitudinal skin incision to allow insertion of two retractors to protect the DSBUN.
- Split the extensor retinaculum in line with the direction of fibers (horizontal).
- Split the capsule longitudinally.

Use: DF is a working portal; it allows fovea instrumentation while the scope is inserted in the dorsal or volar DRUJ portal. The steps that can be performed with DF portal include:

- Lifting the articular disk with a hook probe: This enlarges the space under the TFCC and

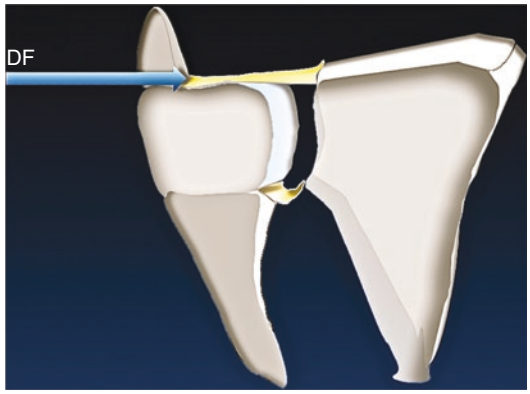

Fig. 86.11 The direct foveal portal (DF) allows to directly check and instrument the ulnar fovea where both radioulnar ligaments (VRUL and DRUL) insert

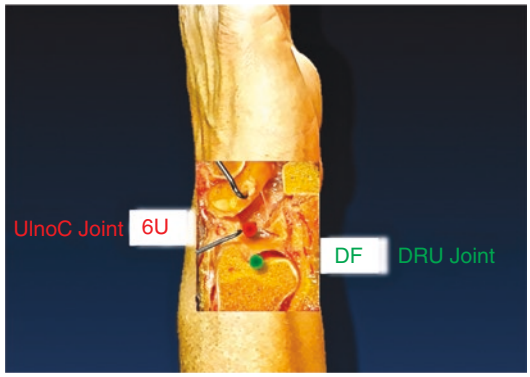

Fig. 86.12 The DF portal (the ulnar DRUJ portal) is 1-cm proximal to the 6 U portal (the ulnar radiocarpal joint portal)

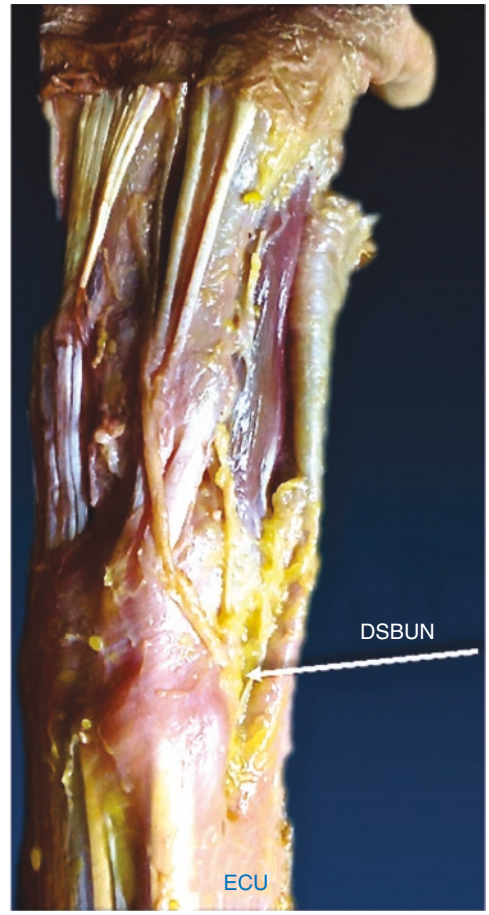

Fig. 86.13 To avoid damaging the dorsal sensory branch of the ulnar nerve (DSBUN) during the DF portal establishment, skin incision must allow the use of nerve retractors, and the forearm, the wrist, and the hand must be kept in supination

helps visualization through the d-DRUJ portal.

- During foveal TFCC reattachment, when the distal TFCC portion insertion is intact, the DF portal is useful for: Ligament remnants removal, bone refreshning, ulna drilling exit control, and suture anchor insertion.

86.3.2.3 Volar Portals (Fig. 86.16)

Volar DRUJ portals are useful for visualization of dorsal DRUJ structures (dorsal capsule and DRUL) and allow instrumentation ("box concept") of the DRUJ. This is advantageous as sometimes dorsal portals are too close to each other to easily scope and instrument simultaneously.

Volar DRUJ Portal (V-DRUJ) [4]

Location

- 1-cm proximal to the proximal wrist crease (Fig. 86.17).
- Between finger flexor tendons and FCU/ulnar neurovascular bundle (Fig. 86.18).

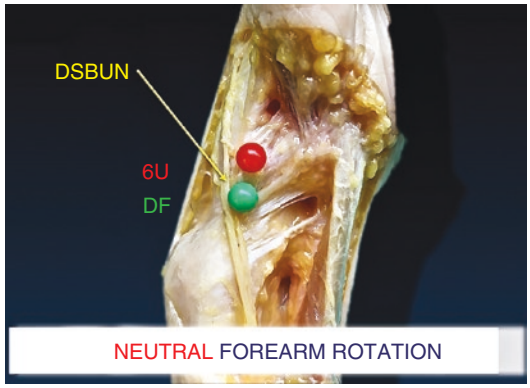

Fig. 86.14 In neutral forearm rotation, the dorsal sensory branch of the ulnar nerve (DSBUN) is just in the area where the direct foveal (DF) and the 6 U portals are located. In forearm supination, the nerve moves dorsally and the portal establishment is safer

Fig. 86.15 The DF portal is located between the ECU (left) and the FCU (right) tendons. It directly reaches the ulna fovea area under the TFCC

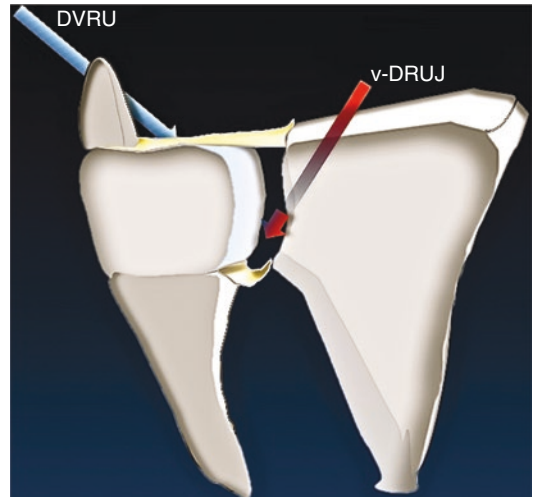

Fig. 86.16 The DRUJ can be accessed through two volar portals: the V-DRUJ and the distal volar radioulnar portal (DVRU)

Steps

- Keeping the forearm in pronation will relax the DRUJ volar capsule.
- Release axial traction to diminish DRUJ compression.
- OUT-IN portal establishment:
  - 2-to 3-cm longitudinal skin incision.
  - Retract finger flexor tendons radially (avoid retracting FCU and ulnar neurovascular bundle ulnarly to better protect them from traction).
  - Place a 21G needle, angled 45° proximally, through the capsule to find the joint space. Fluoroscopy control may be useful. Identifying the ulnocarpal space and leaving a needle in it as a reference might also help.
  - Use tenotomy scissors for capsule perforation.
  - Use a cannula with blunt trocar.
- IN–OUT portal establishment:
  - Establish two dorsal portals first: p-DRUJ and d-DRUJ.
  - Insert a blunt Kirschner wire through p-DRUJ, under direct visualization from d-DRUJ, and push it through the volar

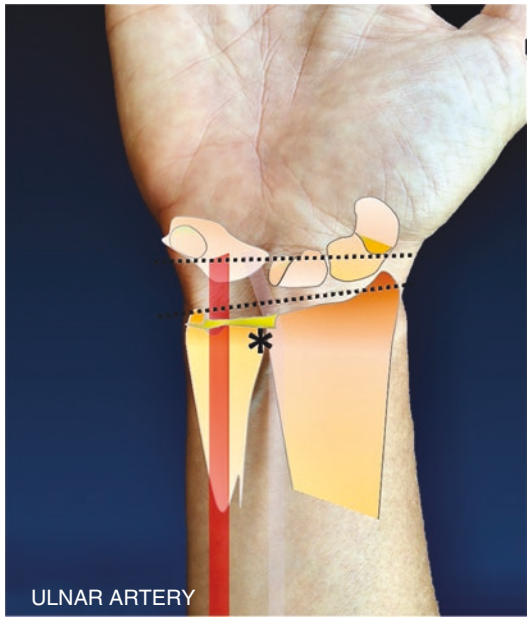

Fig. 86.17 The proximal wrist crease (PC) corresponds to the radiocarpal joint. When the wrist is put under traction, this relation may be altered. The V-DRUJ (*) is usually located 1-cm proximal to the proximal wrist crease when the extremity is not under traction. Ulnar length may be considered before establishing this portal

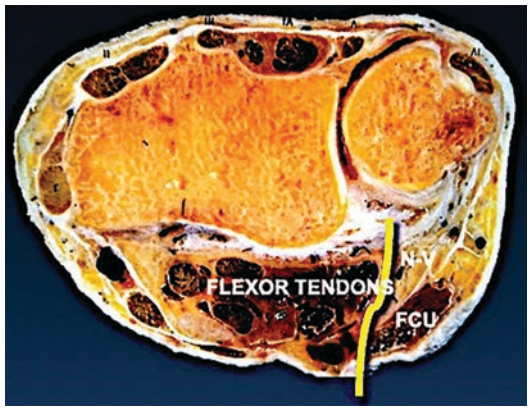

Fig. 86.18 Joint access through the V-DRUJ portal (yellow line) is performed between finger flexor tendons and the FCU distal tendon, which protects the ulnar neurovascular bundle (N-V). Distal traction, which puts under tension the tendon flexor tendons, may difficult the portal access

DRUJ capsule. Recover it through the volar approach and skin incision, and use it as a switching stick to introduce a cannula inside the joint.

Field of View

- Dorsal: DRUL.
- Radial: sigmoid notch and TFCC radial insertion.
- Ulnar: foveal attachment of both radioulnar ligaments (RULs).
- Distal: proximal TFCC (articular disc under surface).

Use

- Foveal attachment visualization: The ulna fovea is set in an ulnar–dorsal situation, and is better appreciated from a volar portal.
- Dorsal RUL tear assessment.
- ECU–subsheath visualization.
- DRUJ synovectomy.
- DRUJ arthrolysis.
- Wafer procedure when d-TFCC is intact.
- Sauvé–Kapandji procedure.

Distal Volar DRUJ (DV-DRUJ) [5]

Location

- 1-cm proximal to the proximal wrist crease at the ulna border of the FCU tendon (Fig. 86.19).
- The ulnar neurovascular bundle is protected by the FCU tendon (Fig. 86.20).

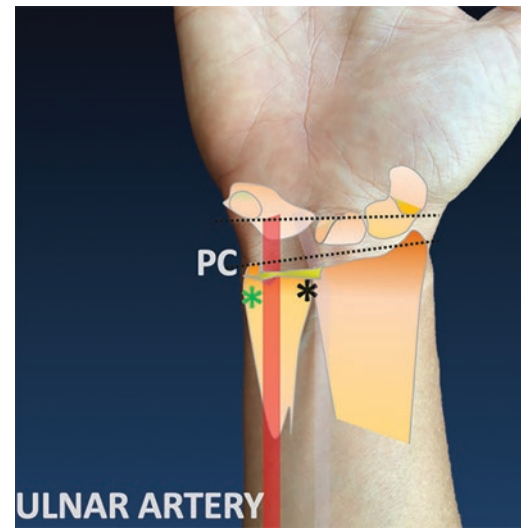

Fig. 86.19 The DVDRUJ (green*) is usually located 1-cm proximal to the proximal wrist crease, at the ulnar margin of the FCU tendon. Ulnar length should be known before establishing this portal

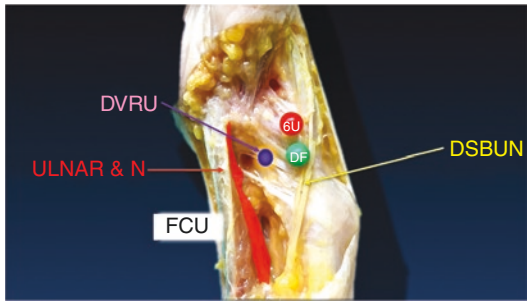

Fig. 86.20 Left wrist anatomic specimen. Distal volar radioulnar portal (DV-DRUJ) is far away from the dorsal sensory branch of the ulnar nerve (DSBUN) and from the ulnar artery and nerve, which are protected by the FCU tendon. FCU is not usually tensioned when the arthroscopic axial traction tower is used. It penetrates the distal radioulnar joint, below the TFCC, volar to the direct foveal (DF) portal

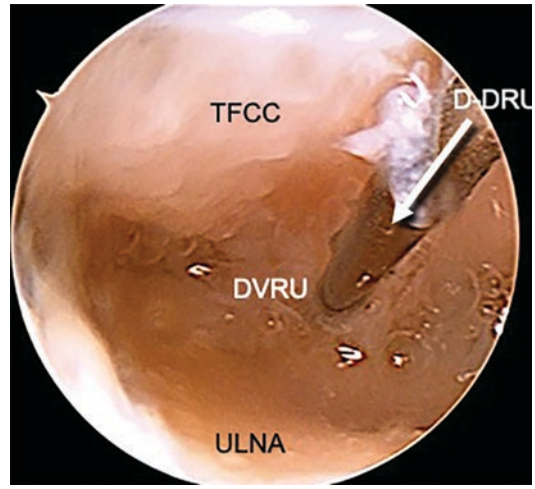

Fig. 86.21 Left DRUJ arthroscopy. Scope in DF portal. Kirshner wire penetrates under the surface of the TFCC through the d-DRUJ portal and exits the joint through the DVRU portal

Steps

- Keep the forearm in neutral rotation to optimally palpate the ulno-volar aspect of the FCU tendon.
- Establish the first d-DRUJ portal and/or DF portal.
- The DV-DRUJ portal area is then located by transillumination.
- OUT-IN portal establishment:
  - 1-cm longitudinal skin incision.
  - Blunt dissection.
  - Needle insertion directed to the d-DRUJ portal.
  - Straight mosquito to perforate the joint capsule.
  - Cannula with blunt trocar.
- IN-OUT portal establishment:
  - 1-cm longitudinal skin incision over the transilluminated area.
  - Insert a blunt Kirschner wire through the d-DRUJ, under direct visualization from DF, and push it through the volar DRUJ capsule. Recover it through the volar approach and skin incision and use it as a switching stick to introduce a cannula inside the joint (Fig. 86.21).

Field of View (Fig. 86.22)

- Dorsal: DRUL.
- Radial: sigmoid notch and radial insertion of the TFCC.
- Ulnar: foveal attachment of both radioulnar ligaments (RULs).
- Distal: proximal TFCC (articular disc undersurface).

Use

- Visualization of Foveal attachment of RULs.
- Diagnosis of radial or ulnar tears of Dorsal RUL.
- Foveal debridement.
- ECU–subsheath visualization.
- DRUJ synovectomy.
- DRUJ arthrolysis.
- Wafer procedure when the d-TFCC is intact.
- Sauvé–Kapandji procedure.

86.4 Technical Tips

- 1.9 mm, 30° scope is useful in small wrists
- Joint distension with air (Fig. 86.23) instead of saline improves visualization and avoids soft tissue edema
- Release traction to avoid DRUJ compression, if the portal establishment seems difficult
- Forearm supination.

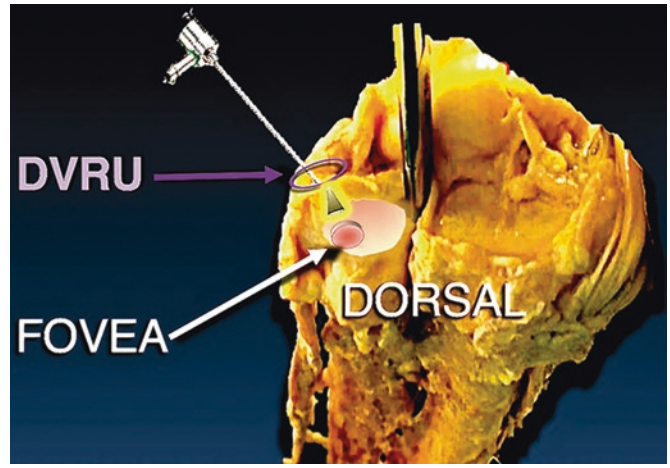

Fig. 86.22 The scope is inserted under the TFCC through the distal volar radioulnar joint portal (DVRU). The ulna fovea is located in the dorso-ulnar aspect of the distal ulna when the forearm is kept in neutral rotation and is easily seen

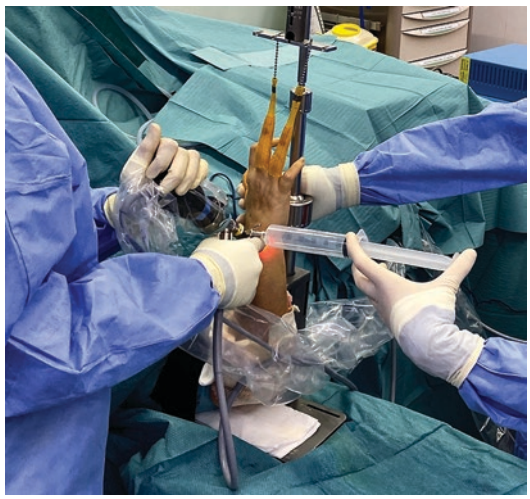

Fig. 86.23 Air insufflation of the DRUJ helps to better visualize the joint during dry arthroscopy, especially when the distal TFCC portion is intact

  - Facilitates dorsal portals establishment as it relaxes the dorsal DRUJ capsule
  - Allows the DF portal set up as it places the ulnar styloid and the ECU tendon in a dorsal position
  - Protects the DSBUN during the DF portal establishment (Fig. 86.24) [6]
- Forearm pronation facilitates volar portals establishment as it relaxes the volar DRUJ capsule.
- Forearm neutral rotation relaxes the distal TFCC portion tension when it is intact.
- DF, d-DRUJ, and DV-DRUJ are the most useful portals.

86.5 Pitfalls

- Bubbles associated to the wet arthroscopy are often difficult to remove and make vision difficult in such a small joint space.
- To correctly locate the fovea area, one must keep in mind the position of the ulnar styloid that may change with forearm rotation.
- Traction release facilitates the entry into the joint from the proximal portal.
- To facilitate the entry into the sub-TFCC joint space, traction must be increased.

86.6 Postoperative Management and Rehabilitation

This depends on the surgical procedure performed through the DRUJ arthroscopy (Wafer procedure, TFCC foveal reattachment, arthrolysis, synovectomy, Sauvé–Kapadji, etc.)

If only a diagnostic DRUJ arthroscopy is performed:

- Edema control of the hand during 48 h.
- Complete finger motion starts from the second day after surgery.

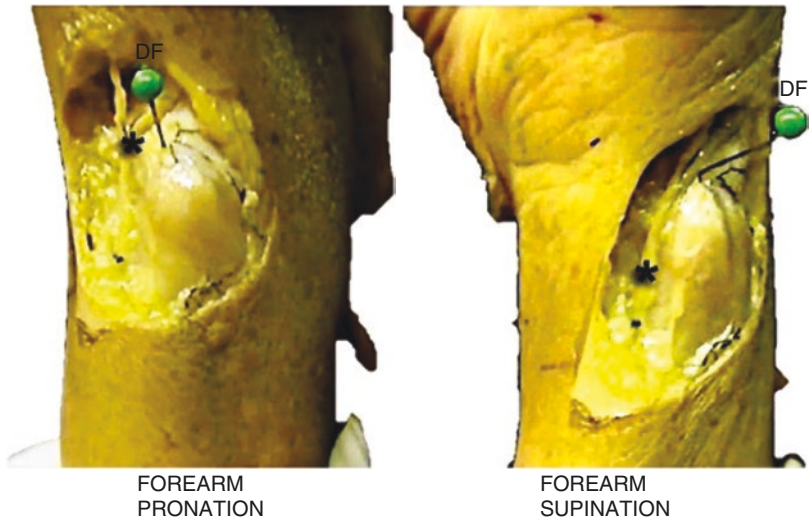

Fig. 86.24 Forearm and hand supination are the safest situation to prevent the dorsal sensory branch of the ulnar nerve (*) injury during the direct foveal portal (DF) establishment

- Complete wrist motion starts from the fourth to fifth day after surgery.

86.7 Complications

- Joint swelling and soft tissue edema in wet arthroscopy.
- DSBUN injury associated to DF portal.
- EDM tendon injury associated to d-DRUJ portal.
- Distal ulnar dome cartilage injury associated to d-DRUJ portal.
- Damage to 1.9-mm scope lens in p-DRUJ portal.

References

1. Boland M, Conroy E. Arthroscopy of the distal radioulnar joint: its role in the evaluation and management of ulnar sided wrist pain and the development of a classification system for proximal partial thickness triangular cartilage complex pathology. J Hand Surg. 2015;40:e8–9.
2. Whipple TL. Arthroscopy of the distal radioulnar joint. Indications, portals and anatomy. Hand Clin. 1994;10(4):589–92.
3. Atzei A, Rizzo A, Luchetti R, Fairplay T. Arthroscopic foveal repair of triangular fibrocartilage complex peripheral lesion with distal radioulnar joint instability. Tech Hand Up Extrem Surg. 2008;12(4):226–35.
4. Slutsky D. Distal radioulnar joint arthroscopy and the volar ulnar portal. Tech Hand Up Extrem Surg. 2007;11(1):38–44.
5. Carratalá Baixauli V, et al. Foveal arthroscopic reattachment technique with knotless triangular fibrocartilage with direct view of the distal radio-ulnar joint. Revista Iberoamericana de Cirugía de la Mano. 2016;44:39–46.
6. Esplugas M, Lluch A, Garcia-Elias M, Llusá-Pérez M. How to avoid ulnar nerve injury when setting the 6U wrist arthroscopy portal. J Wrist Surg. 2014;3(2):128–31.

Arthroscopic Technique of Wafer Resection

87

Riccardo Luchetti, Marcovici Lucian Lior, and Roberto Cozzolino

87.1 Background

Triangular fibrocartilage complex (TFCC) ligament tear is one of the most frequent causes of ulnar wrist pain. Ulnocarpal abutment is another condition of ulnar-sided wrist pain in the presence of a positive or normal ulnar variance [1]. Usually, it is associated with TFCC degeneration. Treatment of this pathology requires a central debridement of the TFCC and partial resection of the head of the ulna [2–5].

87.1.1 Surgical Anatomy

The ulnar head articulates with the radius sigmoid notch forming the distal radioulnar joint (DRUJ). Joint anatomy in both coronal and transverse planes is not constant. Three types of anatomical variance were described in the coronal plane [6, 7] with the prevalence of 55% for the parallel type (Fig. 87.1). On the axial plane, on the other hand, the radius sigmoid notch shows four forms with prevalence for the flat or C-shaped form [6, 7] (Fig. 87.2). The distal radius and ulna are united by capsule-ligamentous structures [8], which are composed of the volar and dorsal capsule and the triangular fibrocartilage complex (TFCC) ligament. The latter attaches to the palmar and distal aspect with the ulnocarpal ligaments, which give stability to the homonymous complex (Fig. 87.3). Joint movement is achieved by rotation of the radius around the ulna, in pronation and supination. During this arc of rotation, the radius translates in a distal–proximal direction leaving the ulnar head in a more distal and dorsal position in pronation [9] (Fig. 87.4). There is the discrepancy between the radial curvature of the sigmoid notch and the ulnar head [7] (Fig. 87.5). The shape of the bone itself together with the palmar osteocartilaginous lip of the sigmoid notch is important for DRUJ stability. The greater the disproportion of the radial curvature, the less stable is the bony construct [10]. Usually, there is no difference in height between the joint surfaces of the distal radius and ulna, indicating a neutral variance. However, the ulnar head might be longer (positive variance or ulna plus) or shorter than the distal radius (negative variance or ulna minus) [1, 2] (Fig. 87.6).

87.2 Indications and Contraindications

The main indication for an arthroscopic wafer resection is the ulnocarpal abutment or impaction syndrome (Fig. 87.7), which is certainly the most common ulnar type of conflict. This condition is

R. Luchetti (✉) · R. Cozzolino
Rimini Hand Surgery & Rehabilitation Center, Rimini, Italy

M. L. Lior
Hand & Microsurgery Unit, Jewish Hospital of Rome, Rome, Italy

© ISAKOS 2022

D. N. Bhatia et al. (eds.), *Arthroscopy and Endoscopy of the Elbow, Wrist and Hand*,
https://doi.org/10.1007/978-3-030-79423-1_87

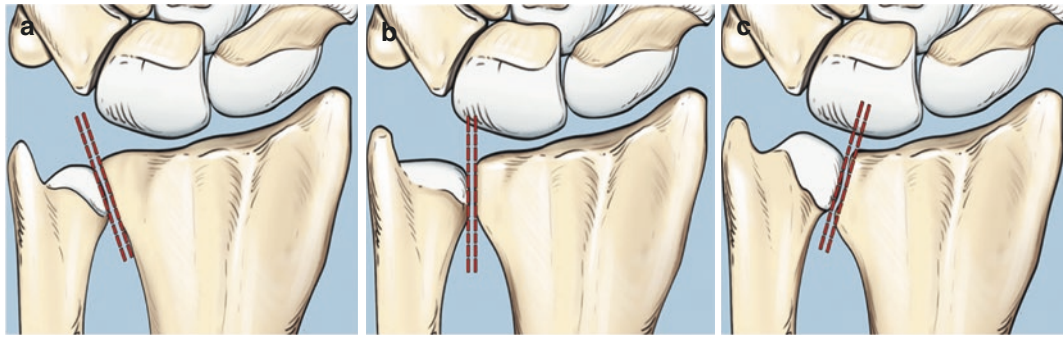

Fig. 87.1 Morphological patterns of DRUJ: (**a**) Positive angle shape, (**b**) parallel shape (the most frequent one), and (**c**) negative angle shape [26]

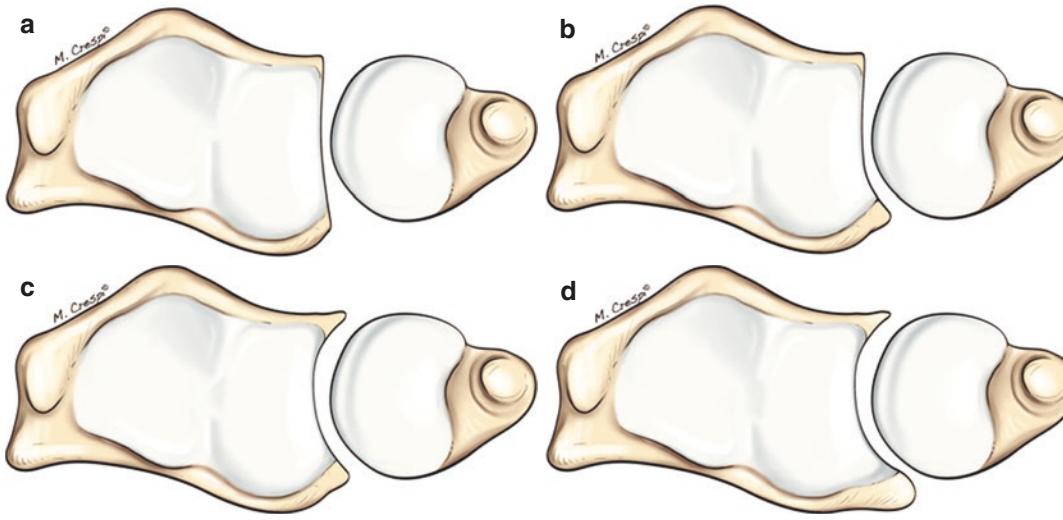

Fig. 87.2 Morphological patterns of the sigmoid notch. (**a**) Flat face, (**b**) Ski slope, (**c**) "C" Type, and (**d**) "S" Type (© M. Crespi)

a result of a chronic contact between the head of the ulna and the carpal bones with the interposed TFCC [2, 11, 12]. This situation leads to a progressive manifestation of events including a degenerative lesion of the central portion of the TFCC, a chondromalacia of the lunate and/or triquetrum or ulnar head, a degenerative lesion of the lunotriquetral ligament with subsequent progressive instability of the lunotriquetral, and finally true lunotriquetral arthritis (Fig. 87.8). Usually, an ulnocarpal conflict appears in the presence of positive ulnar variance, although, occasionally it can manifest itself with a neutral or negative variance [1, 2, 6, 7, 13, 14]. There are several pathological conditions that can cause an ulna plus: congenital; distal radius malunion [15, 16]; Madelung deformity; post-traumatic growth arrest of radius; and radius collapse secondary to radial head fracture/Galeazzi fractures/Essex-Lopresti injury. Other causes for ulnocarpal abutment are sport activities (e.g., gymnastics) [17] or work-related [15]. The main differential diagnosis is the ulnar styloid impaction syndrome (conflict between ulnar styloid and carpal bone). Other causes that must be excluded include degenerative TFCC lesions, extensor carpi ulnaris tenosynovitis, and lunotriquetral ligament lesions [15]. These conditions may coexist with an ulnocarpal abutment and therefore must be assessed by clinical, radiological, and arthroscopic evaluation before proceeding with surgical treatment.

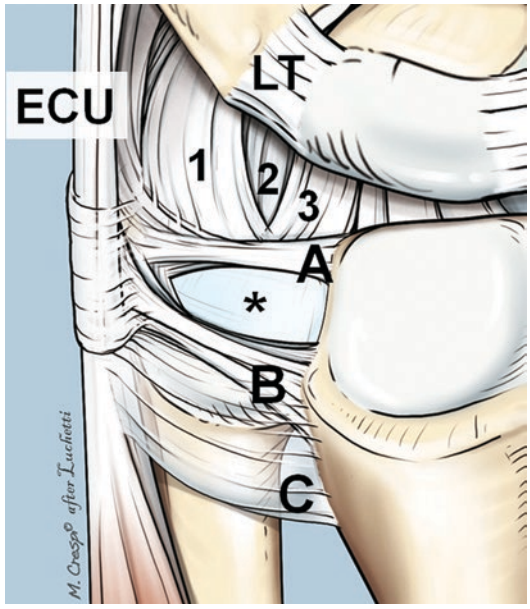

Fig. 87.3 Anatomical drawing of the ulnar side of the wrist. (LT = lunotriquetral ligament; ECU: extensor carpis ulnaris; 1, 2, 3 = ulno carpal ligaments [1 = ulnotriquetral, 2 = ulnocapitate, 3 = ulnolunate]); A = volar branch of the TFCC ligament; B = dorsal branch of the TFCC ligament; * = articular disc of the TFCC ligament; C = dorsal capsule [26] (M. Crespi © for Luchetti)

Most of the contraindications to the wafer procedure are related to the anatomy and condition of the patient's DRUJ and ulnocarpal joint. These include the following: DRUJ arthritis, positive ulna variance greater than 4 mm [16], ulna minus variance, and lunotriquetral instability.

87.3 Surgical Technique

The patient is positioned supine on the operation table with a tourniquet applied to the affected arm. The arm is abducted at 90° and the elbow flexed at 90° allowing a vertical position of the forearm, wrist, and hand. Traditional vertical traction system (used also in shoulder surgery) is applied to the wrist through a second and third finger trap and countertraction of 3 kg placed proximal to the elbow [18]. Although other wrist traction systems are available for the procedures [18], the surgeon should use a traction device, which allows free pronosupination of the wrist during arthroscopy [18]. Traction systems that block or limit the wrist pronosupi-

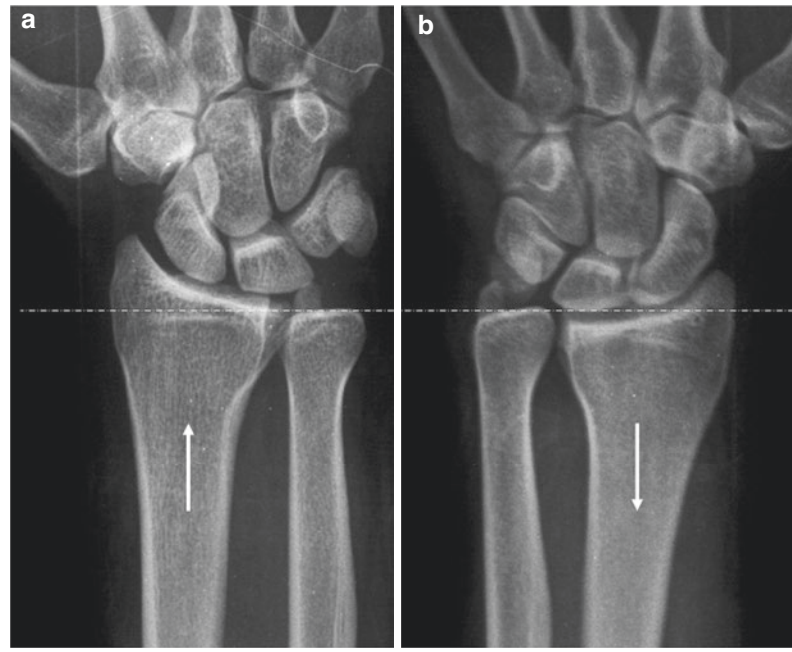

Fig. 87.4 X-ray images of the wrist in supination (**a**) and pronation (**b**). Note the proximal migration of the radius in pronation (**b**) [26]

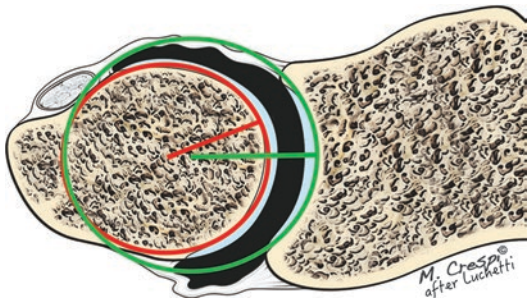

Fig. 87.5 Different anatomical curvatures of both the sigmoid notch and the ulnar head joints (M. Crespi © for Luchetti)

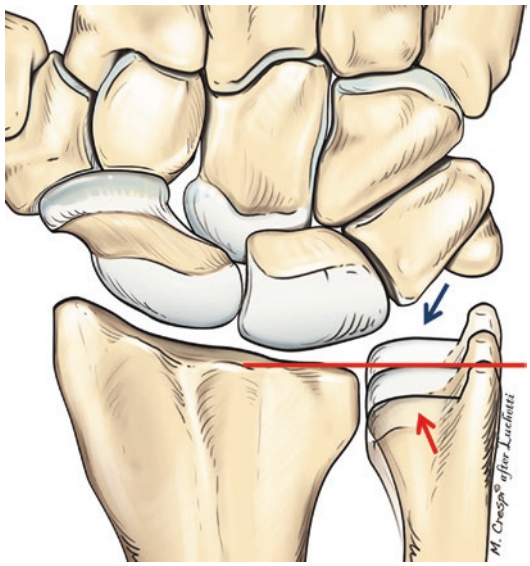

Fig. 87.6 Drawing showing the ulna variances. Black arrow: ulna plus; red arrow: ulna minus; red line: normal ulna (M. Crespi © for Luchetti)

nation will not permit a correct performance of wafer resection.

87.3.1 Traditional Technique

87.3.1.1 First Step: Arthroscopic Debridement of the TFCC Central Portion

- The procedure starts with the classical 3-4 and 6R arthroscopic portals. A 1.9-mm 30° arthroscope is inserted in the 3-4 portal and a shaver is passed through the 6R portal. The midcarpal joint must always be explored before proceeding with treatment of the lesion, since associated lesions (lesion of intrinsic or extrinsic ligaments; chondropathies; synovitis) can coexist.
- It is important to perform a complete ulnar synovectomy that ensures a clear view of the

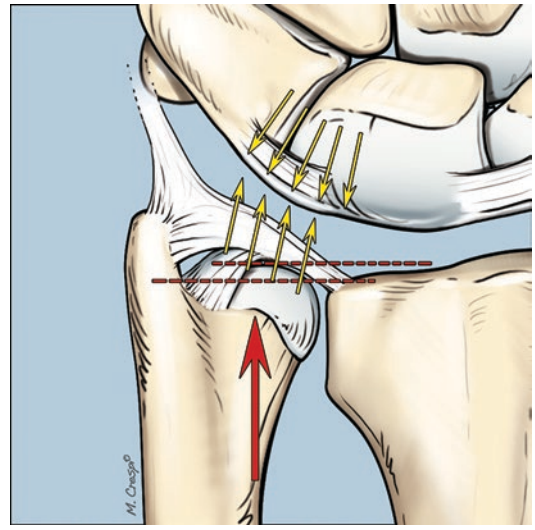

Fig. 87.7 DRUJ illustration of ulnocarpal conflict demonstrates ulna plus variance (red arrow and red dotted lines) and conflict between the ulnar head and the ulnar carpal bones with the interposition of the TFCC ligament (yellow arrows) [26] (© M. Crespi)

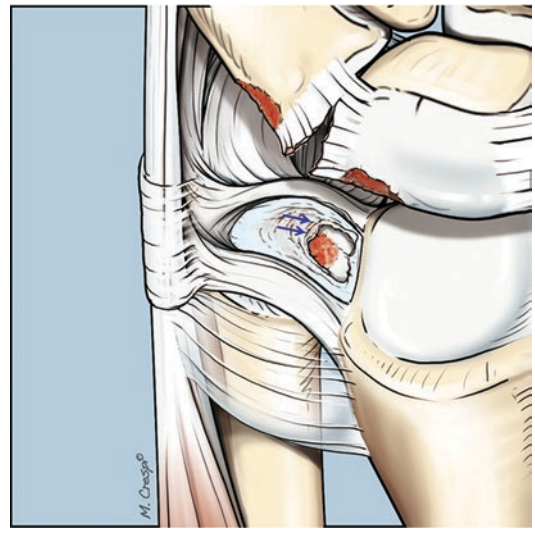

Fig. 87.8 Illustration of joint damage following the ulnocarpal conflict shows the degenerative lesion of the TFCC articular disc (blue arrows), osteochondropathy of the ulnar head below the articular disc; chondropathy of the lunate and triquetral carpal bones, and degenerative lesion of the lunotriquetral ligament [26] (© M. Crespi)

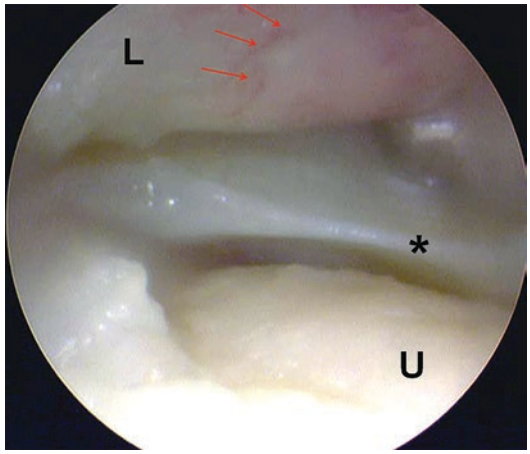

Fig. 87.9 Arthroscopic image of the ulnocarpal side of the wrist: the ulna head (U) is found protruding through a TFCC ligament affected by a central degenerative lesion of the articular disc of the TFCC ligament (asterisk), and chondropathy (red arrows) of the lunate (L) is visualized [26]

joint (Fig. 87.9). The hook test is performed to verify the correct insertion of the triangular ligament to the fovea [19].

- The TFCC central portion is debrided using a full radius 2.9-mm shaver through the 6R portal and other work tools (mini basket, mini scalpel, and radiofrequency instruments) can be used.
- The author performs wrist arthroscopies using the "dry technique" as described by Atzei [20] and del Piñal [21]. Fluid inflow is used when necessary by a syringe inserted into the arthroscopy sleeve valve and passes throughout the joint by shaver aspiration [20, 21]. Particular attention must be paid to avoid cartilage scuffing type injuries to the lunate and the triquetrum.
- Usually, the central part of the TFCC is perforated and degenerated (Fig. 87.8); however, occasionally it is intact and thinned out, and on palpation, the underlying ulnar head can be appreciated. When perforated, the central portion of the TFCC is then enlarged on its radial and palmar aspect, while the dorsal portion can be resected by placing the scope in the 6R portal and the working instrument in the 3-4 portal. In this phase, care must be taken not to damage the foveal insertion of the TFCC, the palmar or dorsal radioulnar branches of the TFCC ligament, and the cartilage of the carpal bones. The same maneuver, however, can be performed by keeping the instruments in the initial position (scope in 3-4 and instrument in 6R), although it is more difficult and requires experience with the technique.
- The radiofrequency device is excellent for central resection of the TFCC, although special attention should be paid to avoid iatrogenic injuries. The calibration of the power of the instrument must be perfect. The radiofrequency action can be monopolar or bipolar (preferred). While using the radiofrequency device, it is necessary to switch to the "wet technique" and inflow irrigation must be sufficient to cool the joint. Once the central portion of the TFCC has been debrided, the ulnar head is exposed and the second step of the procedure can be done (Fig. 87.10a, b).

87.3.1.2 Second Step: Arthroscopic Resection of Ulnar Head

In chronic degenerative lesions of the TFCC, the exposure of the ulnar head is already large enough to avoid further debridement (Fig. 87.9) and the surgical procedure starts with this step.

- The scope is kept in the 3-4 portal, while the working instrument is introduced in 6R portal.
- The procedure could start with radiofrequency to remove the articular cartilage, but more often it begins using a 2.9-mm motorized burr and continues with the 3.5 mm one. It is important to avoid injury of the sigmoid notch of the radius.
- The resection of ulnar head starts from the central part (Fig.87.11a) of the ulnar head and continues in a curvilinear direction from the center toward the palmar side (by rotating the wrist into pronation) (Fig.87.11b) and then dorsally (by rotating the wrist into supination) (Fig. 87.11c). When performing this last maneuver, it might be helpful to rotate the scope by 90° to obtain a complete view of the operating field (Fig. 87.11c). The outcome of

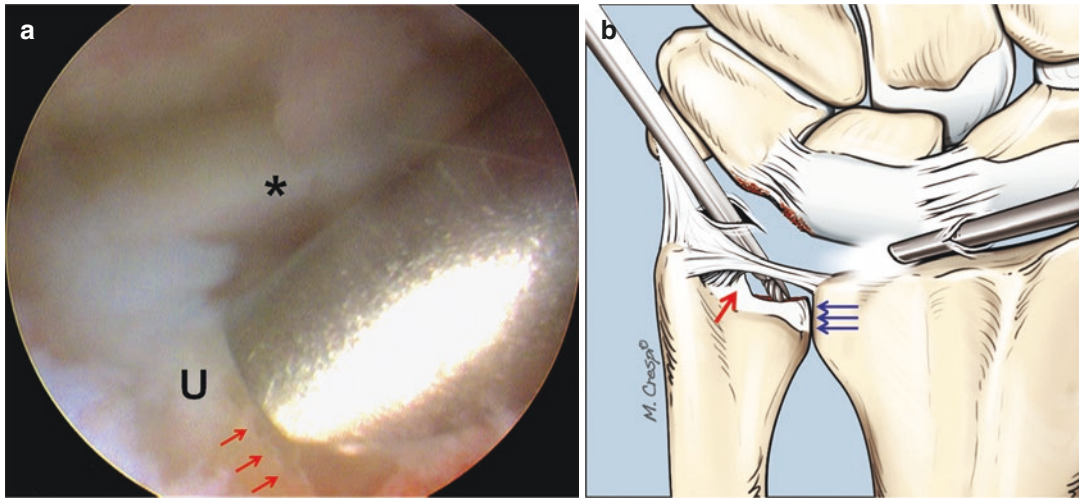

Fig. 87.10 (**a**) Arthroscopic image of the ulnar head (U) during a wafer resection with burr. Note the margins of the initial resection of the ulnar head (asterisk and red arrows) [26]. (**b**) Wafer resection of the ulnar head: burr is positioned in the 6R portal and only the radial part is resected while the articular portion toward the sigmoid notch (blue arrows) and the ulnar part, where the TFCC is inserted into the fovea (red arrow), are preserved [26] (© M. Crespi)

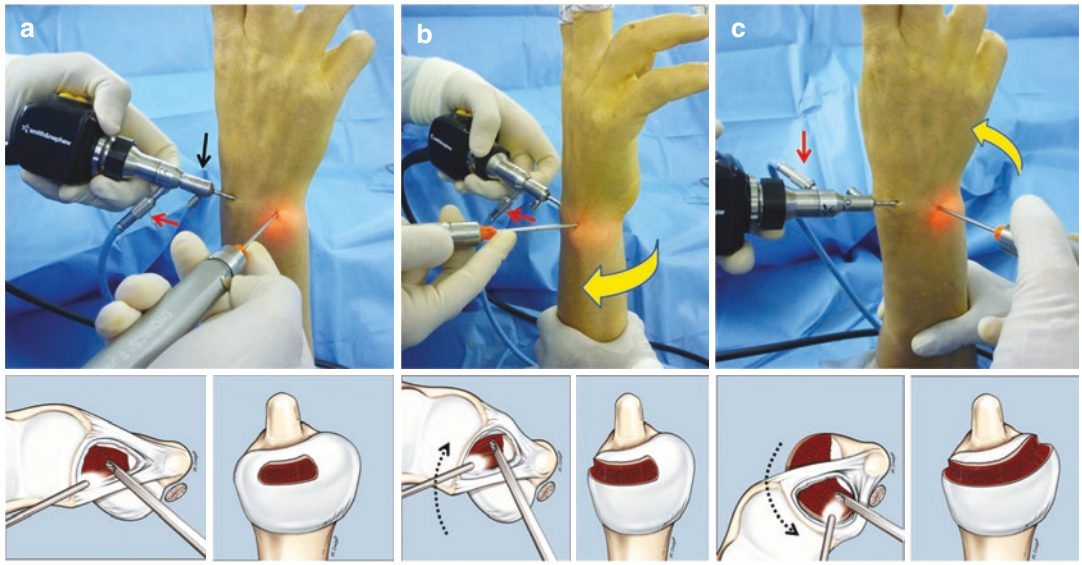

Fig. 87.11 (**a**, **b**, **c**): (**a**) External view of wrist arthroscopy in neutral position (note the position of the arthroscope [red arrows] and the absence of fluid inflow [black arrow]). The wafer resection starts from the central part and is extended further (bottom images). (**b**) Pronation of the wrist (yellow arrow) keeping the arthroscope in the original position (red arrow); illustrations demonstrate the volar progression of the wafer resection of the ulnar head with DRUJ pronation (black dotted arrow). (**c**) Supination of the wrist (yellow arrow): 90° of rotation of the arthroscope (red arrow) allows visualization and resection of the dorsal portion of the ulnar head; illustrations demonstrate the completion of the wafer resection in the dorsal part of the ulnar head with supination wrist (black dotted arrow) [26]

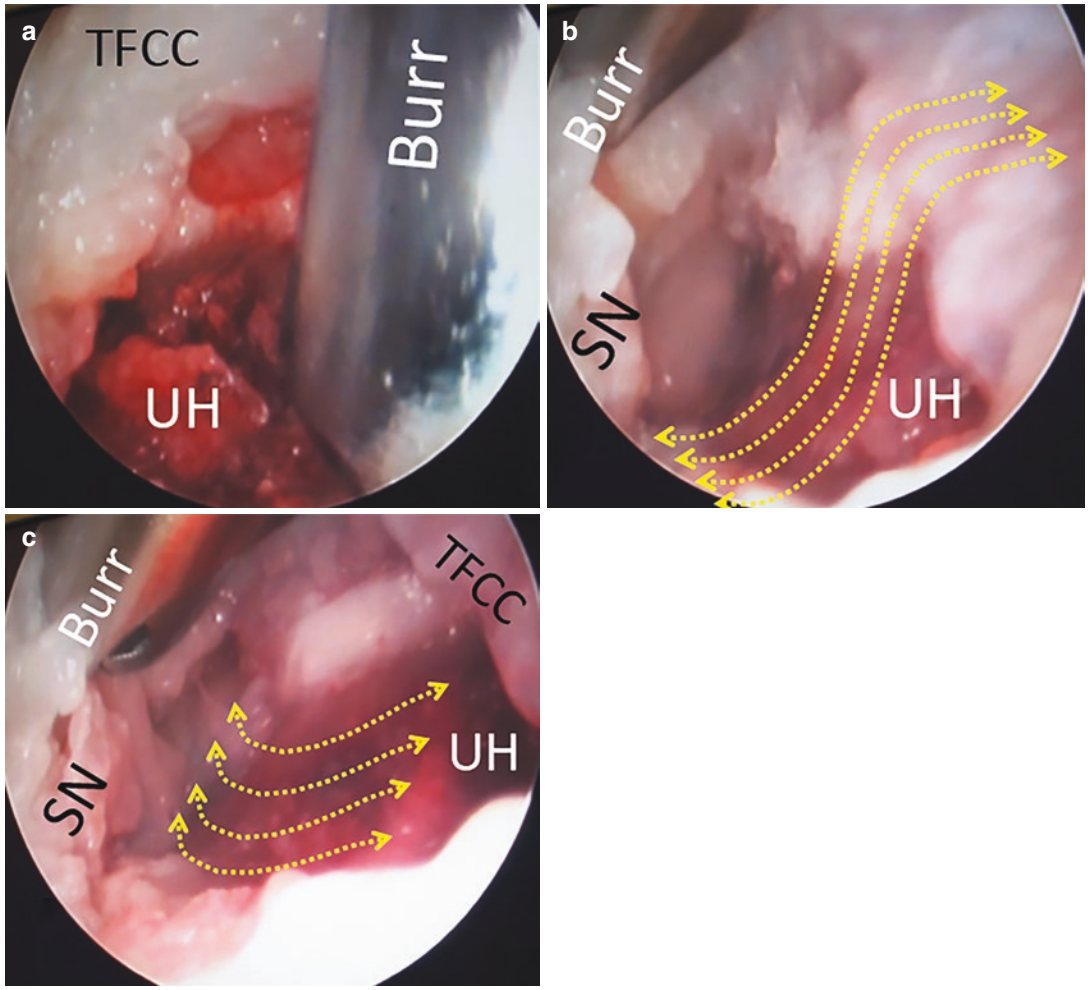

Fig. 87.12 (**a**–**c**): Arthroscopic sequences of wafer resection of the ulnar head. (**a**) Burr in a vertical position during resection of the ulnar head (UH) from 6R portal; (**b**) Resection of the ulnar head (UH) in which the yellow curvilinear dotted lines show the preservation of sigmoid notch (SN); (**c**) Image shows the clear curvilinear resection of the ulnar head (UH)

the technique should be as shown in Figs. 87.12 and 87.13 (Figs. 87.12 and 87.13a–d).

- It is important to proceed step-by-step taking care not to leave bone groves or pointed anterior and posterior margins (Fig. 87.14). The resection of the ulnar head must not extend ulnarly toward the foveal insertion of the TFCC in order to prevent the harm to it [22, 23]. Joint washing and aspiration with shaver will remove the resection debris.
- The average resection is approximately 3 mm (4). The ulnar head resection limit is not rigid and should be guided by the height of the burr instrument (2.9–3.5 mm). Alternately, measured resection may be done by a probe with a millimetric scale on its stem (Fig. 87.15). The resection has a curvilinear and helicoidal shape and is slightly greater anteriorly in coherence with the biomechanism of the DRUJ pronosupination (Fig. 87.16).
- At the end of the procedure, traction is removed while the scope is kept in place (3-4 portal), and the surgeon should then check if the resection was performed correctly: the aim is to produce a resection in the most radi-

Fig. 87.13 (**a**–**d**): Radiographic image showing an ulnocarpal conflict due to ulna plus (**a**, **b**) and correct wafer resection of the ulnar head (**c**, **d**) [26]

cal side of the ulna head (Fig. 87.10b) [4]. The resection of the ulnar head must not be done in a convex shape. Particular attention must be paid to the resection of the ulnar head borders: if the borders are not resected they can still be a source of ulnocarpal contact (Fig. 87.14) mostly in the palmar side. Another control of a correct resection is to check the normal mobility of the DRUJ without any articular crepitus. If any crepitus is felt during the pronosupination, it is better to recheck the joint and proceed with further resection of the ulnar head at contact sites. A static and dynamic fluoroscopic check may additionally be performed.

- At the end of the procedure, portals are sutured and a splint allowing free pronosupination is applied. Traditionally, the drain is not used but it can be used if necessary through the 6R portal and is removed the day after surgery.

87.3.2 Alternative Technique 1: Wafer Resection Through the DRUJ Preserving the TFCC

It is possible to perform a wafer resection of the ulnar head beneath the TFCC while using DRUJ portals (Fig. 87.17) [24].

87.3.2.1 First Step: Portal Preparation and DRUJ Exploration

- Exploration of the DRUJ starts through a dorsal portal [24] that is located at a midpoint between the traditional P- and D-DRUJ portals (Fig. 87.18) and in a triangular space that can be defined as the "medial soft corner." The portal site is below the insertion of the TFCC on the radius at the point where the distal profile of the ulnar head curves to parallel the sigmoid notch (Fig. 87.19a).
- A 22-gauge (Fig. 87.19b) needle is inserted to confirm correct portal placement and a longitudinal skin incision is made. A curved mosquito is used to spread the subcutaneous tissues and penetrate the joint through the dorsal capsule, just below the TFCC and superior and medial to the ulnar head. Care should be taken not to damage the extensor digiti minimi tendon, running in the fifth dorsal compartment. The 1.9-mm scope is introduced through a cannula with a blunt obturator. The scope should be short enough to be grasped while keeping the index finger in constant contact with the skin of the wrist in order to stabilize and control the minute movements of the scope within the joint. Traditionally, a wide-angle video-arthroscope 1.9 mm is used. Full wrist supination allows easier access to the DRUJ through the dorsal portals (Fig. 87.20), because in this position the ulnar head should enter completely into the sigmoid notch. We recommend starting joint exploration by rotating the scope, rather than moving its tip inside the joint. However, skill arthroscopists are able to move into this joint with "micro" movements (Fig. 87.21).
- Four important structures should be assessed: (a) the surface of the ulnar head, (b) the deep central part TFCC fibers, (c) TFCC foveal insertion, and (d) the sigmoid notch. DRUJ exploration starts with the scope rotated ulnarwards (Fig. 87.22) to observe the ulnar head at the bottom and the TFCC ligament above.
- A 22-G needle is introduced from the area of the deep foveal (DF) portal and may be used to elevate the ligament or better visualization of the ulnar part of TFCC that curves proximally to insert onto the fovea (Fig. 87.23). The sigmoid notch is visualized by rotating the scope 180° radialwards and following the slope of the ulnar head that curves downward to face the radius. Wrist pronosupination is helpful for a thorough exploration of the opposing surfaces of the sigmoid notch and ulnar head (Fig. 87.24).
- Accessory working portals are required for probes or instruments. In the author's experience, the easiest portal to establish is the volar one. The DRUJ volar portal is created using a trocar followed by a switching rod [25] (Figs. 87.25 and 87.26a, b). The arthroscope is inserted through the D-DRUJ portal and its tip is pushed against the anterior capsule below the TFCC ligament. Thereafter, the scope is removed and a blunt trocar or switching rod is

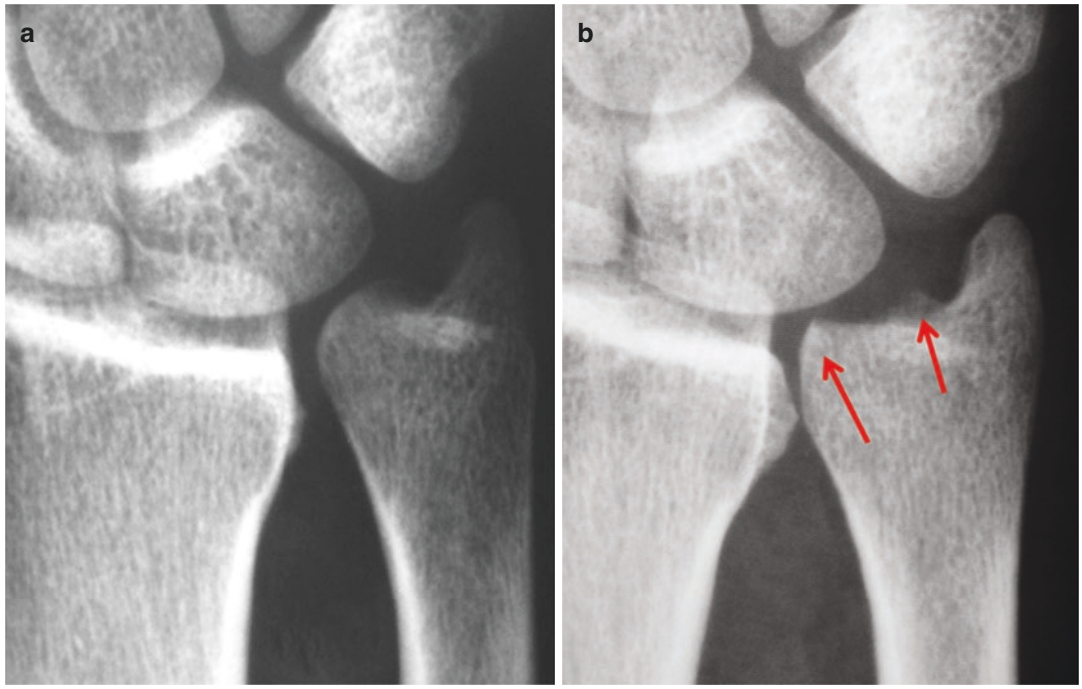

Fig. 87.14 Radiographic image showing an ulnocarpal conflict due to ulna plus (**a**) and incorrect wafer resection (**b**) with persistent volar and dorsal borders of the ulnar head (red arrows) [26] (© M. Crespi)

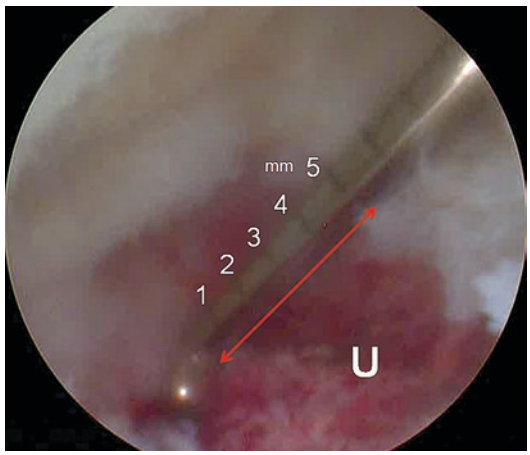

Fig. 87.15 Arthroscopic view of wafer resection (red arrow) with measurement of the resection using the probe (U = ulna head) [26]

introduced into the cannula and is pushed palmar ward to perforate the capsule and tent the skin (Fig. 87.27). From the author's experience, the ulnar neurovascular bundle has never been damaged in the execution of this technique. A small incision is made over the tip of the trocar and the trocar and cannula are passed outside the skin. Next, the trocar is removed and the cannula is used as a guide to introduce the probe or the shaver (full radius) into the joint (Figs. 87.28 and 87.29).

87.3.2.2 Second Step: Arthroscopic Resection of Ulnar Head

- The scope is introduced in the D-DRUJ portal providing good visualization of the shaver and burr inserted through the volar portal (Fig. 87.29) or vice versa according to the hand dominance of the surgeon. Limited forearm rotation is usually required.
- The proximal part of the TFCC is debrided and the ulnar head resected up to the foveal insertion of the TFCC, taking care not to damage the insertion of ligamentous fibers at the fovea. The technique is moderately difficult, due to the close proximity of scope and instruments. Care should be taken at the time of introduction of the burr because its tip can be trapped in the soft tissues around the portals: use of a small cannula is advisable. A 2.9 burr

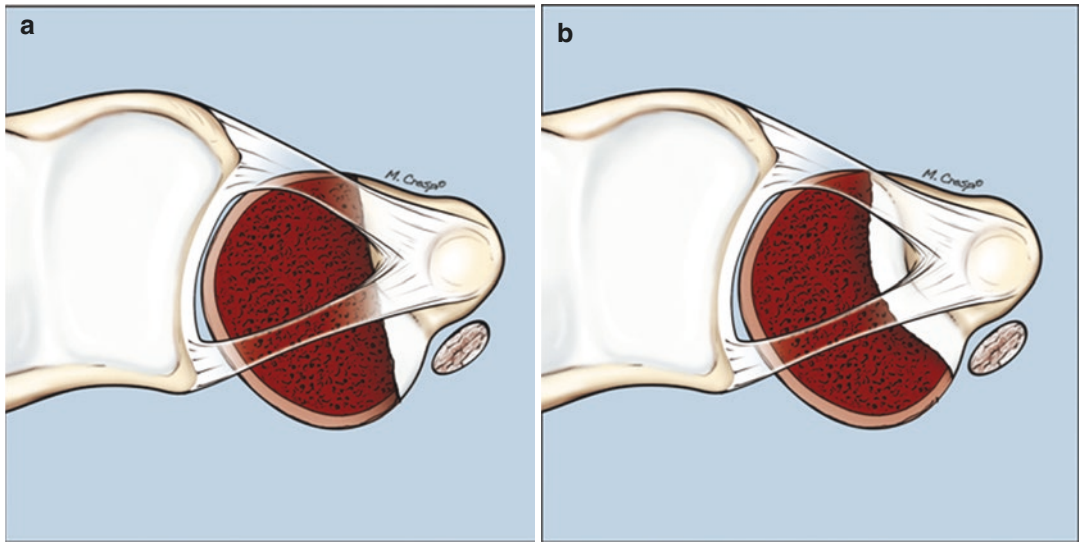

Fig. 87.16 Drawing showing wafer resection with open technique (**a**), and with arthroscopic technique (**b**) [26]

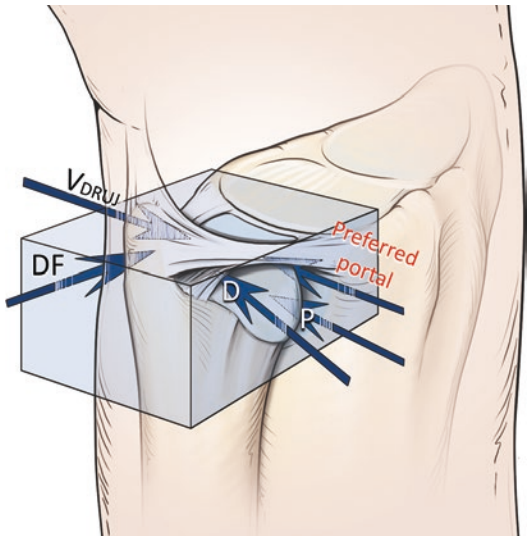

Fig. 87.17 Box concept for the DRUJ arthroscopy; volar and dorsal portals

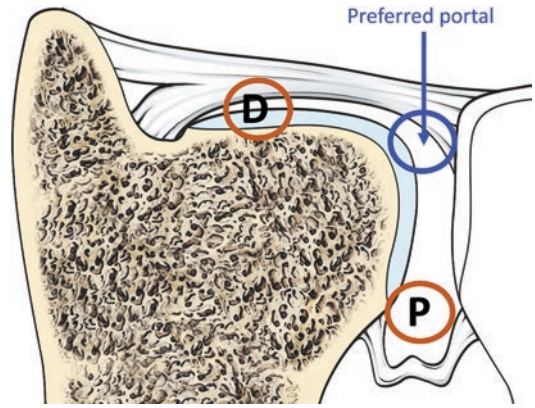

Fig. 87.18 Preferred portal for the DRUJ arthroscopy (D = distal portal/P = proximal portal)

is normally sufficient to remove the distal part of the ulnar head.

- Ulnar head resection should be done according to the same principles of the traditional technique: the resection must be done in a flat shape (Fig. 87.30) and no sharp edges should be left at margins. Also, the volar part needs to be resected much more than the dorsal one. Scope and shaver or burr can be shifted in order to complete the resection. Dynamic fluoroscopic control is done at the end of the procedure if needed.

Advantages of this procedure include less postoperative pain and the expected long-term benefit of a preserved load-bearing TFCC disc [24].

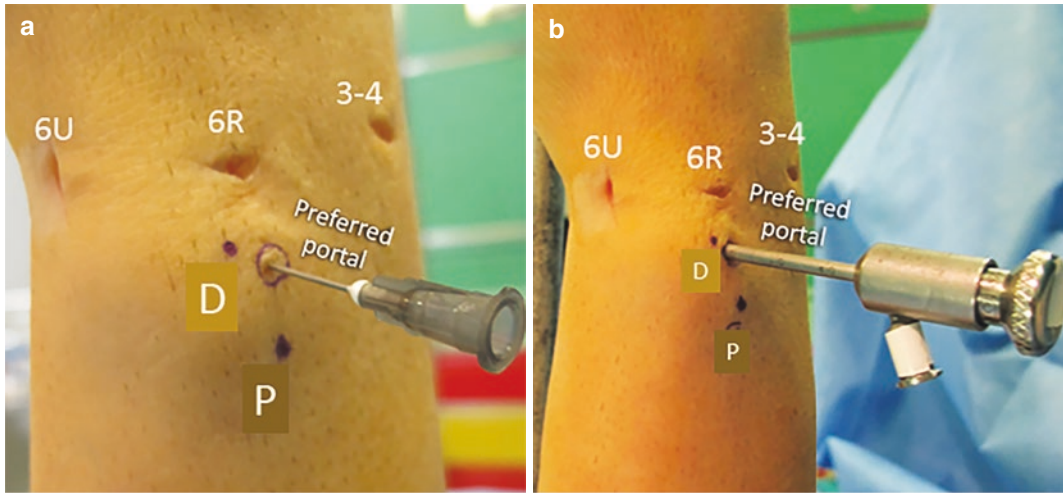

Fig. 87.19 Intraoperative anatomical position of the DRUJ portals (D = distal portal/P = proximal portal); (**a**) needle position and (**b**) trocar positioned into the preferred portal

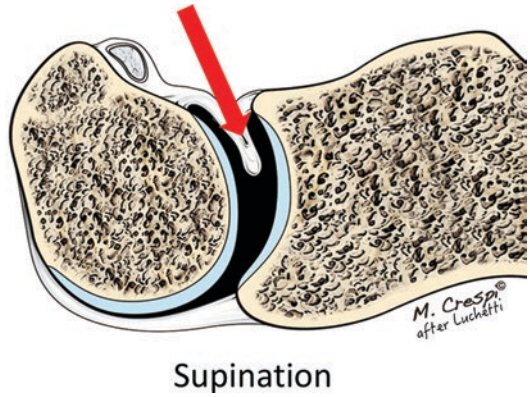

Fig. 87.20 Drawings showing how wrist supination is the best position to enter into the DRUJ from the dorsal preferred portal (M. Crespi © for Luchetti)

Fig. 87.21 The best way to handle and control the scope in wrist arthroscopy

87.3.3 Alternative Technique 2: "Inverse Wafer" Resection (Wafer Resection of the Lunate and Triquetrum)

- During arthroscopy for ulnocarpal abutment, a related chondropathy of the surface of the lunate and triquetrum can be identified in association with the lesion of the membranous part of the luno-triquetral ligament and TFCC central lesion. Instead of performing a traditional wafer resection of the ulnar head, a resection of the chondropathic portion of the lunate and triquetrum can be done (an "inverse wafer") (Fig. 87.31) using the same arthroscopic portals. This resection produces a "decompression" of the conflict site by keeping the TFCC and the head of the ulna intact, but resecting the involved part of the lunate and triquetrum (Figs. 87.32 and 87.33). The head of the ulna will therefore no longer have

Fig. 87.22 Managing of the scope into the DRUJ; 90° of rotation is used to obtain a better view

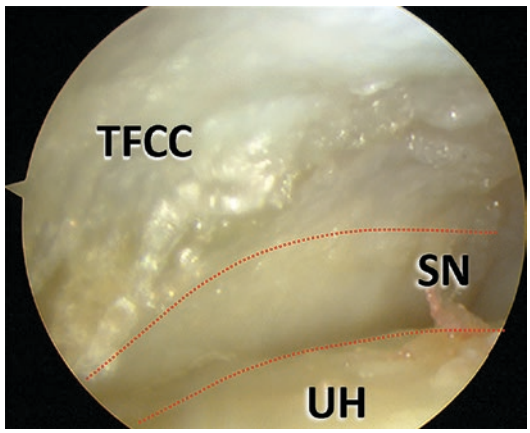

Fig. 87.23 Dry arthroscopic view of the ulnar head (UH) and proximal part of the TFCC

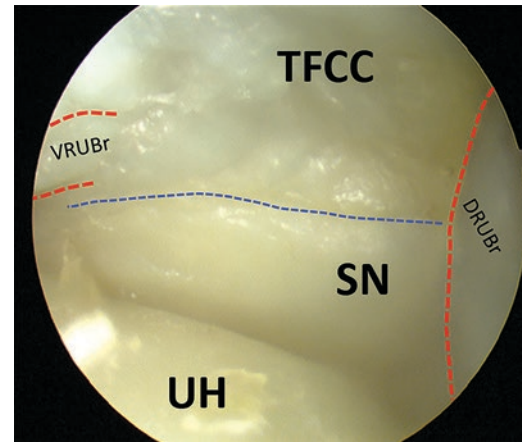

Fig. 87.24 Dry arthroscopic view of the ulnar head (UH) and sigmoid notch (SN) (*: ulnar border of the radius; #: volar and dorsal insertional branches of the TFCC)

contact with the carpal bones during the pronosupination movement.

- The "inverse wafer" can also be performed in combination with the "traditional wafer" when the ulnar plus variance is more than 4 mm. Part of the resection may be done at the ulnar head and part at the lunate and triquetrum producing a better decompression without the need for a secondary ulna shortening (Fig. 87.34).
- Rarely, chondropathy or osteochondropathy of the lunate and triquetrum may coexist with an intact TFCC. The distal part of the TFCC seems "normal" during arthroscopy but probe testing reveals a bad consistency. If we perform arthroscopy of the DRUJ in these specific cases, we will find that the proximal part of the TFCC is degenerated. TFCC can benefit from decompression and pain can decrease.

Fig. 87.25 Inside-out technique to create the volar DRUJ portal

87.4 Technical Tips

- The wrist traction system must not force radial deviation of the wrist as happens when using the "Chinese finger traps." Wafer resection is difficult to perform with traction systems, which do not leave the wrist free. The solution of double-digital traction (second and third finger) is excellent for the natural position that the wrist assumes: the traction of the wrist along the radius axis allows an anatomic pronosupination.
- The 6R portal is the author's preferred portal for the resection of the ulnar head. It is easy and safe, and instruments are rarely switched to 6U or 3-4 portals.
- Particular attention must be paid to perform a correct resection of ulnar head margins. If the borders are not correctly resected, they can be a source of the unresolved ulnocarpal abutment (Fig. 87.14).
- Care should be taken not to damage the sigmoid notch during resection.
- Arthroscopic resection must be helicoidal and is a more anatomical form of resection than the one performed with open surgery.
- The palmar part of the helicoidal resection should be more than the dorsal one.
- Pushing the ulna with the thumb improves the exposure of the dorsal side of the ulnar head, thereby facilitating resection of the dorsal margin.

The author recommends the traditional technique (wafer resection through the TFCC); wafer resection through the DRUJ preserving the integrity of the TFCC is a very demanding technique and should be performed only by experts. The "inverse wafer," on the other hand, can be a good alternative, which can be also performed in association with the "traditional" one (Fig. 87.34).

87.5 Pitfalls

One of the main problems faced during this procedure, when performing a dry arthroscopy, is the lack of visibility during the resection of both TFCC and ulnar head. Even when using wet arthroscopy, the instruments often get blocked and must be frequently cleaned. One of the tricks is to alternate the burr with the shaver to have always a clear view by removing even the small structures that remain free inside the articulation.

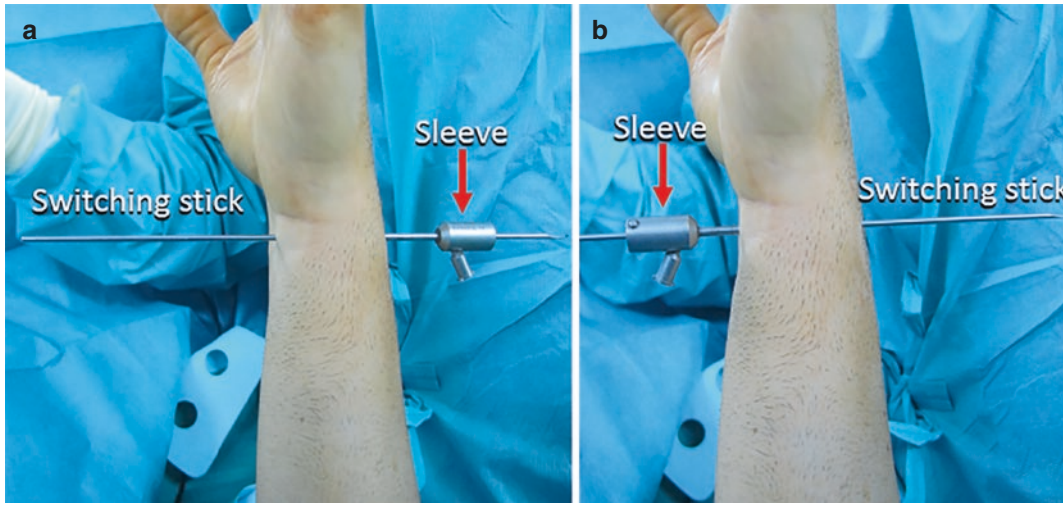

Fig. 87.26 Probe used as a switching stick to pass the trocar from the dorsal (**a**) to the volar portal (**b**)

Fig. 87.27 Introduction of the scope in the volar DRUJ portal and shaver in the dorsal DRUJ portal

87.6 Postoperative Management and Rehabilitation

A short arm palmar splint is applied after surgery and kept for at least 15 days. Pronosupination is left free. Active and passive wrist exercises are permitted immediately after surgery and patients are informed that some discomfort with these movements is normal. Grip strength exercises are allowed after 6 weeks and return to heavy activities including sports is after 3 months. If heavy work or sports activities are

Fig. 87.28 Technique of shaver introduction into the volar DRUJ portal (**a**, **b**)

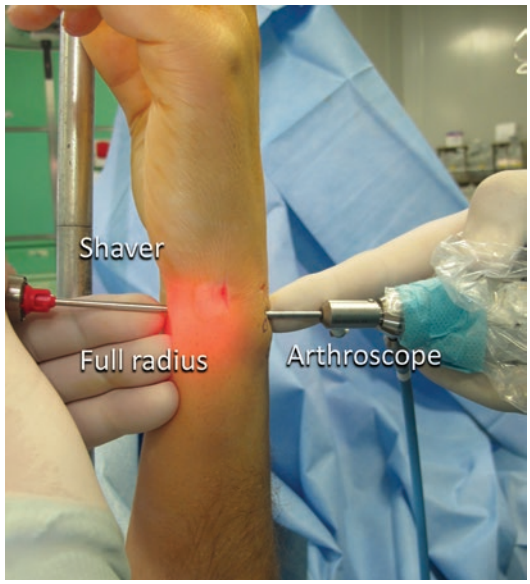

Fig. 87.29 Scope in the dorsal DRUJ portal and shaver in the volar DRUJ portal

started early, an ulnocarpal painful arthrosynovitis will appear. The feeling of discomfort in the ulnar side of the wrist can be maintained for up to a year.

87.7 Complications

The sharp margins of the ulnar head borders or even bone fragments both in DRUJ and in the radiocarpal joint, which were not removed during the surgical procedure, are causes of the persistence of abutment and discomfort. Foveal attachment of the radioulnar ligaments may be damaged if resection is too central and ulnar. Potential nerve injuries include lesions of the sensitive dorsal branches of the ulnar nerve and lesions of the ulnar nerve itself while placing the DRUJ volar portal.

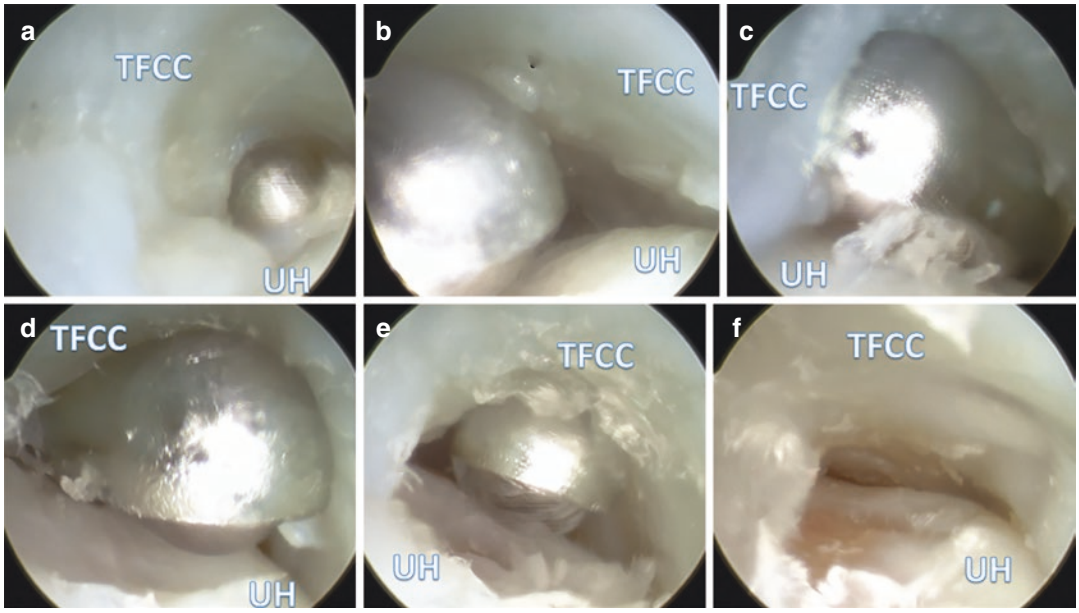

Fig. 87.30 Sequential view of arthroscopic ulnar head (wafer) resection below the TFCC (**a**–**f**)

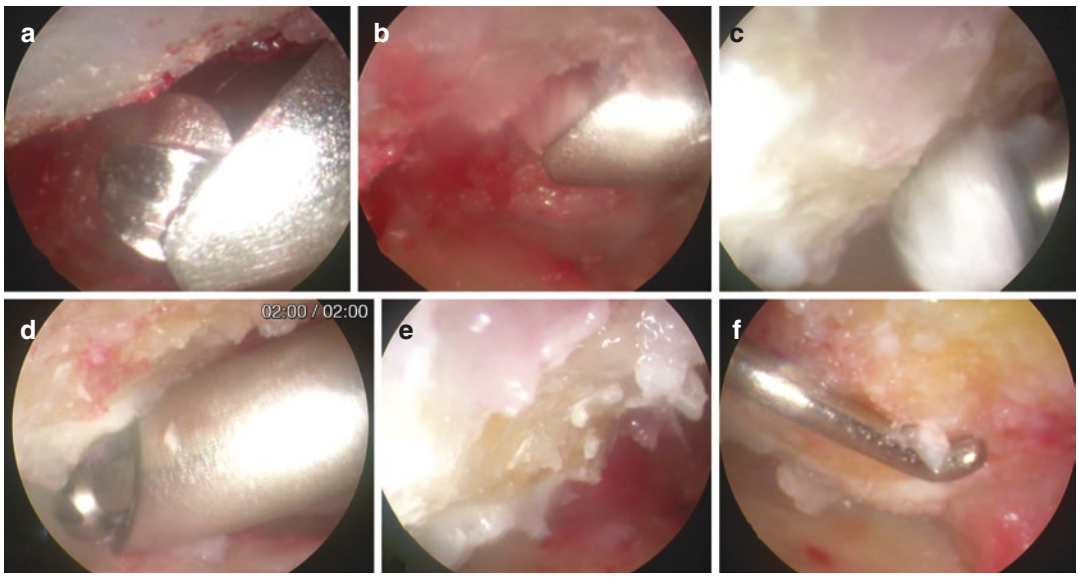

Fig. 87.31 Sequential view of the arthroscopic lunate and triquetrum (inverted wafer) resection (**a**–**f**)

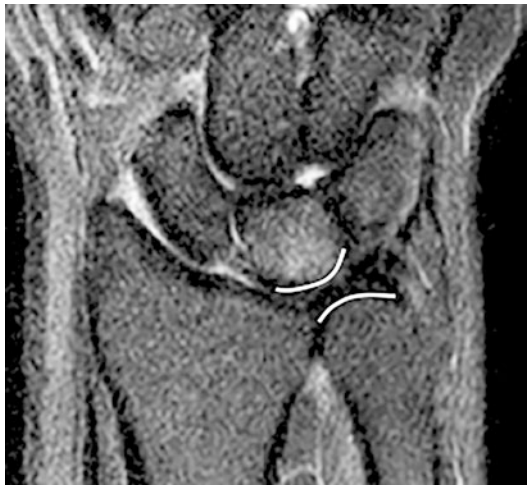

Fig. 87.32 MRI images of ulnocarpal conflict with lunate edema

Fig. 87.33 X-ray images of inverted wafer resection outcomes (lunate and triquetrum)

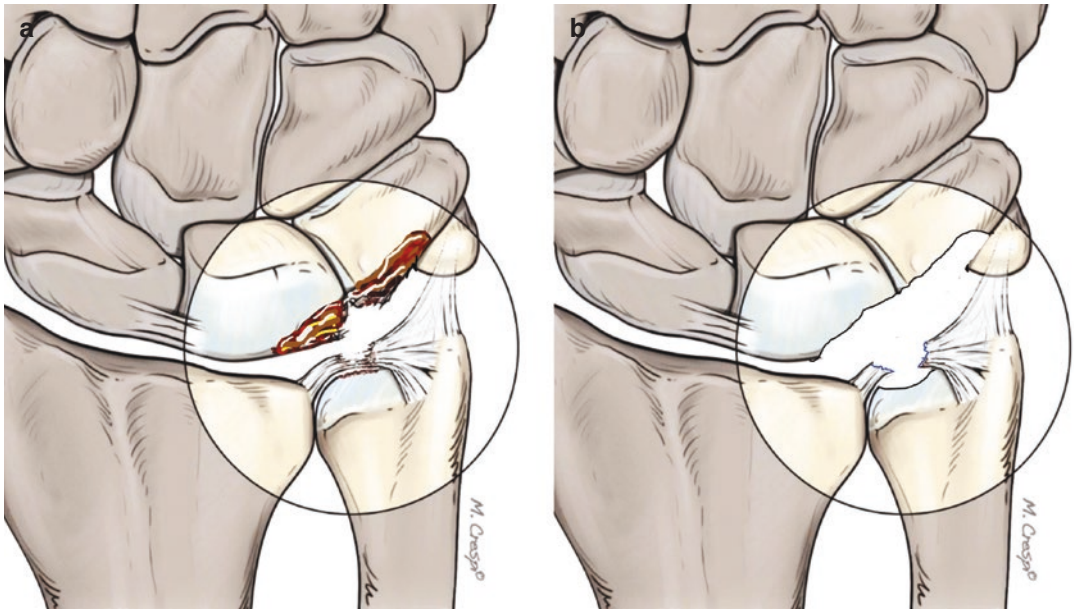

Fig. 87.34 Drawing showing the ulnocarpal conflict (**a**) and the technique of lunate and triquetrum resection (**b**) (© M. Crespi)

References

1. Palmer AK, Glisson RR, Werner FW, Mech M. Ulnar variance determination. J Hand Surg. 1982;7A:376–9.
2. Palmer AK, Glisson RR, Werner FW. Relationship between ulnar variance and triangular fibrocartilage complex thickness. J Hand Surg. 1984;9A:681–2.
3. Osterman AL. Arthroscopic debridment of triangular fibrocartilage complex tears. Arthroscopy. 1990;6:120–4.
4. Wnorowski DC, Palmer FW, Fortino MD. Anatomic and biomechanical analysis of the arthroscopic wafer procedure. Arthroscopy. 1992;8:204–12.
5. Nagle DJ. Triangular fibrocartilage debridement and arthroscopically assisted ulnar shortening. In: Savoie III FH, Field LD, editors. The elbow and wrist, AANA advanced arthroscopy. Philadelphia: Saunders Elsevier; 2010. p. 186–91.
6. Sagerman SD, Zogby RG, Palmer AK, Werner FW, Fortino MD. Relative articular inclination of the distal radioulnar joint: a radiographic study. J Hand Surg. 1995;20A:597–601.
7. Tolat AR, Stanley JK, Trail IA. A cadaveric study of the anatomy and stability of the distal radioulnar joint in the coronal and transverse planes. J Hand Surg Eur. 1996;21:587–94.
8. Nakamura T, Yabe Y, Hiriuchi Y. Origins and insertions of the triangular fibrocartilage complex: a histological study. J Hand Surg. 2001;26B:446–54.
9. Buck F, Nico M, Gheno R, Haghighi P, Trudell DJ, Resnick D. Morphology of the distal radioulnar joint: cadaveric study with MRI and MR arthrography with the forearm in neutral position, pronation, and supination. AJR. 2010:194–207.
10. Haugstvedt JR, Langer MF, Berger RA. Distal radioulnar joint: functional anatomy, including pathomechanics. J Hand Surg Eur. 2017;42:338–45.
11. Watanabe A, Felipe S, Vezeridis PS, Blazar P, Yoshioka H. Ulnar-sided wrist pain. Part 2. Clinical imaging and treatment. Skelet Radiol. 2010;10:837–57.
12. Friedman SL, Palmer AK. Ulnar impaction syndrome. Hand Clin. 1991;7:295–310.
13. Tomaino MM. Ulnar impaction syndrome in the ulnar negative and neutral wrist: diagnosis and pathoanatomy. J Hand Surg Eur. 1998;23:754–7.
14. Cerezal L, del Piñal F, Abascal F, Garcia-Valtuille R, Pereda T, Canga A. Imaging findings in ulnar-sided wrist impaction syndromes. Radiographics. 2002;22:105–20.
15. Borelli PP. Treatment of the associated ulnar-sided problems. In: del Piñal F, Mathoulin C, Luchetti R, editors. Arthroscopic management of distal radius fractures. Berlin, Heidelberg: Springer-Verlag; 2010. p. 175–90.
16. Fernandez DL. Correction of post-traumatic wrist deformity in adults by osteotomy, bone-grafting, and internal fixation. J Bone Joint Surg Am. 1982;64:1164–78.
17. Jarrett CD, Baratz ME. The management of ulnocarpal abutment and degenerative triangular fibrocartilage complex tears in the competitive athlete. Hand Clin. 2012;28:329–37.
18. Badur N, Luchetti R, Atzei A. Artroscopic wrist anatomy and setup. In: Geissler WB, editor. Wrist and elbow arthroscopy. A practical surgical guide to techniques. 2nd ed. New York: Springer Verlag; 2015. p. 1–27.
19. Atzei A, Rizzo A, Luchetti R, Fairplay T. Arthroscopic foveal repair of triangular fibrocartilage complex peripheral lesion with distal radioulnar joint instability. Techn Hand Up Extrem Surg. 2008;12:226–35.
20. Atzei A, Luchetti R, Sgarbossa A, Carità E, Llusà M. Installation, voies d'abord et exploration normale en arthroscopie du poignet. Set-up, portals and normal exploration in wrist arthroscopy. Chir Main. 2006;25:S131–44.
21. del Piñal F, Garcia-Bernal FJ, Pisani D, Regalado J, Ayala H, Studer A. Dry arthroscopy of the wrist: surgical technique. J Hand Surg Am. 2007;32:119–23.
22. Nakamura T, Yabe Y, Hiriuchi Y. Origins and insertions of the triangular fibrocartilage complex: a histological study. J Hand Surg Eur. 2001;26:446–54.
23. Nakamura R, Horii IE, Imaeda T, Nakao E, Kato H, Watanabe K. The ulno carpal stress test in the diagnosis of ulnar-sided wrist pain. J Hand Surg Eur. 1997;22:719–23.
24. Atzei A, Luchetti R. DRUJ arthroscopy. In: Slutsky DJ, editor. Operative orthopedics of the upper extremity. New York: McGraw Hill; 2014. p. 407–18.
25. Snyder SJ. Diagnostic arthroscopy of the shoulder: normal anatomy and variations. In: Snyder SJ, editor. Shoulder arthroscopy. New York: McGraw-Hill, Inc.; 1994. p. 23–39.
26. Luchetti R, Atzei A, Borelli P, Cozzolino R. Artroscopia di Polso Articolazione radio-ulnare distale: debridment della TFCC e wafer resection in plus dell'ulna. In: Adravanti P, editor. Artroscopia base ed Avanzata. Rome: CIC editore; 2012. p. 733–44.

Part XVIII

Wrist: Triangular Fibrocartilage Complex

88 Arthroscopic Evaluation, Classification and Techniques for TFCC Tears

Richard S. Page, Janina Henze, and Kevin Eng

88.1 Background

Ulnar side wrist pain has multiple causes and often occurs due to TFCC tears [1–3]. It should be noted that many tears are asymptomatic. Studies have shown that TFCC injuries increase with age, a prevalence of 49% at 70 years of age or older whereas only 27% in those younger than 30 years. It has also been reported that degenerative lesions of the TFCC are more often associated with a positive ulnar variance [4].

88.1.1 Surgical Anatomy

The TFCC is an intricate structure with two major functions. First, the TFCC is the major stabiliser of the DRUJ and allows stable motion, largely pronation and supination. Furthermore, the TFCC transfers load to the ulna and links as a stabiliser of the proximal ulna carpus [5, 6].

The TFCC is defined as a complex of the following fibrocartilage structures [3]: the central articular disc, meniscus homologue, ulnar collateral ligaments, ulnotriquetral and ulnolunate ligaments, sub-sheath of the extensor carpi ulnaris and dorsal and volar radioulnar ligaments.

- Articular disc
  The articular disc is the central fibrocartilaginous part of the TFCC and stretches from its attachment at the radius over the ulnar head where it ends in the radioulnar ligaments. It has a wedge-shaped form and is thinner on its peripheral parts than the centre. However, some studies have shown that a main part of the disc is not involved in the transmission of the weight bear, hence about two-third of it can be resected during surgery without having any effect on the axial load bearing ability [5].
- Ulnar carpal ligaments
  The ulnotriquetral and ulnolunate ligaments arise from the fovea and the distal radioulnar ligament and insert into the lunate and triquetrum, respectively. Functionally, the ulnocar-

R. S. Page (✉)
Department of Orthopaedics, School of Medicine, Deakin University, Geelong, VIC, Australia

Barwon Centre for Orthopaedic Research and Education (B-CORE), Barwon Health and St John of God Hospital, Geelong, VIC, Australia

Geelong Orthopaedics, SJOG Specialist Centre, Geelong, VIC, Australia
e-mail: richardpage@geelongortho.com.au

J. Henze
Barwon Centre for Orthopaedic Research and Education (B-CORE), Barwon Health and St John of God Hospital, Geelong, VIC, Australia

K. Eng
Barwon Centre for Orthopaedic Research and Education (B-CORE), Barwon Health and St John of God Hospital, Geelong, VIC, Australia

Geelong Orthopaedics, SJOG Specialist Centre, Geelong, VIC, Australia

© ISAKOS 2022

D. N. Bhatia et al. (eds.), *Arthroscopy and Endoscopy of the Elbow, Wrist and Hand*,
https://doi.org/10.1007/978-3-030-79423-1_88

pal ligaments are key stabilisers of the ulnar carpus preventing the volar translation of the carpus during pronation and supination. Some researchers include the ulnocapital ligament, but the majority of the published literature does not describe this as part of the TFCC.

- Volar and dorsal radioulnar ligament
  At arthroscopy, these ligaments are seen as the thicker volar and dorsal part of the disc. They consist of a superficial and a deep portion. The superficial part inserts into ulna styloid while the deep part inserts at the fovea, which is also called the ligamentum subcretum. The fovea is the isometric point of pronation and supination; thus, the deep fibres are thought to be the major contributors to stability.
  They are attached to the distal rim of the sigmoid notch of the radius where they are conjoined. The deep and superficial make different contributions to stability in different positions of rotation. In pronation, the superficial dorsal and deep palmar fibres are taut, and in supination, the superficial palmar and deep dorsal fibres are taut.
- Meniscus homologue
  The meniscus homologue is positioned between the superficial portion of the radioulnar ligaments, the capsule and the triquetrum in the ulnar aspect of the radiocarpal joint. It is a vascular structure with a C form morphology.
- Ulnar collateral ligament and extensor carpi ulnaris subhealth
  The ECU sub-sheath is formed from the deep lamina of the antebrachial fascia and is attached to the articular disc, while the ulnar collateral ligament is inserted into the ulnar styloid before dividing and inserting distally on the triquetrum and pisiform. The main role of the ECU sub-sheath is to hold the ECU in position during movement.

In terms of choosing the right therapy for a TFCC injury, the blood supply should be considered to evaluate the healing potential of the pathology. Thiru et al. demonstrated that the central 80–85% of the disc is relatively avascular, and the blood supply to the peripheral 15–20% is supplied from contributions from the ulnar artery through the palmar and dorsal radiocarpal branches as well as the anterior interosseous artery through the palmar and dorsal branches [7]. Moreover, the vascularisation is limited in the region of the radial attachments.

88.2 Clinical Presentation

Acute TFCC tears are the result of a fall on the pronated and extended hand or acute rotational injury in the forearm. Chronic TFCC lesions are often associated with positive ulnar variance, ulnar impaction syndrome or previous injuries. To diagnose TFCC lesions, the patient should be examined carefully, and the following tests performed:

- Ulna fovea sign
  A foveal disruption of the TFCC, pathologies of the meniscus homologue, prestyloid recess or inflammatory processes can cause pain in the ‘ulnar snuff box’ during palpation. It has been shown that the fovea sign has 95% sensitivity and 86% specificity of detecting a TFCC injury [8].
- TFC Grinding test/ulnocarpal stress test
  The radius and ulna are compressed, and the patient rotates the forearm. Pain can indicate a TFCC injury but also with ulnocarpal impaction syndrome, LTL tear and wrist arthritis [9].
- TFC Shear test
  The pisiform is pushed dorsally with the thumb while the other fingers translate the ulna head palmar. If that produces pain, the test is considered positive and that implies an injury of the TFC.
- Press test
  The patient is encouraged to push out of a chair with his wrist in an extended position. In this test, pain is also a sign of a TFCC injury
- Waiter’s test (ulnocarpal meniscoid test)
  The patient’s wrist is passively extended and then brought into ulna deviation and from there in flexion while applying axial load. This test is performed in a neutral position, prono- and supination. A TFCC injury causes more pain in pronation than in supination. Ruston et al. proved that this test had an accuracy of 71.7% for detecting TFCC lesions.
- Furthermore, the stability of the TFCC should always be tested in comparison to the other

wrist of the patient. Therefore, the Piano key test was developed. For the Piano Key test, the patient presses the palms on the table, and then relaxes the hands. If the distal ulna is prominent during pressure and then goes back to neutral position under relaxation, an injury of the DRUJ can be expected. Another test is the ballottement test of the distal ulna; here the distal ulna is stabilised while the radius is manipulated into a dorso-palmar direction. The degree of translation can be tested in different positions of the forearm.

Ulnar side wrist pain is often described as the 'back pain' of the wrist. Therefore, the differential diagnoses should be evaluated before performing a wrist arthroscopy. Similar symptoms can be caused by a wide range of ulna-sided pathology that include fractures (hook of hamate), dislocation, ligament injuries, avascular necrosis, ECU subsheath tears or subluxation and ulnar-sided impingement or arthritis of the wrist (pisotriquetral, hamatolunate or ulna styloid impingement).

88.3 Imaging

Even though wrist arthroscopy is known to be the standard for the diagnosis and treatment of TFCC injuries, imaging is an important instrument, especially in evaluating for the differential diagnoses.

Radiographs must be performed in any case of trauma in order to detect fractures. Furthermore, X-rays in a neutral position can show eventual ulnar variance. It is essential that they are taken in a neutral position because in pronation of the hand the ulna appears to be relatively longer. Radiographs are not an instrument to show specific injuries of the TFCC but can help to determine a 1 B from a 1D lesions [3].

Native CT can also be used to detect fractures and CT arthrography can be useful when MRI is not available. Bille et al. showed that it is a highly accurate form of imaging when evaluating tears of the SLL, LTL and central TFCC; nevertheless, it is not always a reliable modality to evaluate peripheral TFCC tears [10].

MRI can detect TFCC injuries, with a sensitivity of 83% and a specificity of 80% [11]. Due to the small structures of the wrist, a 3T MRI should be used to evaluate the TFCC. Current studies show that MRI arthrography is superior to an MRI, and Lee et al. reported a 100% sensitivity, specificity and accuracy [12]. However, Haims et al. showed that MRA is not superior in the evaluation of the articular disc or lunotriquetral ligament, but Ganeshalingam et al. reported it may also be visualised in a limited trauma sequence MRI of the wrist [13, 14].

88.4 Arthroscopic Evaluation of TFCC Tears

Arthroscopy of the wrist allows a direct visualisation of the TFCC tear and therefore remains the gold standard for diagnosis and evaluation of TFCC injuries.

- First, to begin the surgery, the patient is positioned as described in the previous Chap. 69. There are different ways to evaluate the TFCC; however, most surgeons prefer the 3-4 portal as visual portal and the 6R portal as the working portal. The different parts of the TFCC should be visualised and examined for obvious signs of injury or tears and associated synovitis or chondromalacia. Pronation and supination may help to see all aspects of TFCC and the stability of the TFCC should be tested.
- In terms of morphology, acute tears are often plain and longitudinal and show the same white colour as the other parts of TFCC. Chronic lesions have a more oval form with frayed borders and are more yellow coloured. Regarding the anatomy, it should be kept in mind that the radioulnar ligaments cannot be distinctly distinguished from the disc during arthroscopy and appear as thickenings on the periphery. Furthermore, the prestyloid recess can sometimes be mistaken for a tear but is part of the usual anatomy of the wrist.
- After initial visualisation through the 3-4 portal, a probe is inserted through the 6R portal to perform further manipulation tests of the TFCC. The integrity of the TFCC is tested by

Fig. 88.1 The arthroscopic TFCC Trampoline Test using a small probe via the 6R Portal palpating the TFC and evaluation of TFCC under depression. (© Richard Page)

palpating the surface of the TFCC (Fig. 88.1). An intact TFCC springs back into its form after depression. If the structure is soft, lacking tension or wavey, the loss of the so-called the 'trampoline effect' can indicate either peripheral tear or foveal detachment. The 'trampoline test' has been evaluated in recent studies and the reliability has been questioned in relation to correlating with TFCC lesions. Park et al. only found a 49.3% interobserver agreement regarding a positive trampoline test and other studies showed similar results [13, 15].

- The 'hook test' is a more reliable test to examine TFCC tears during arthroscopy (Fig. 88.2). The hook test is performed by inserting a probe through the 6R portal and then traction is applied with the probe on the ulnar border of the horizonal part of the TFCC. If some tissue can be pulled distally and radially in the direction of the centre of the radiocarpal joint, it is defined as a positive hook test and represents a tear of the foveal attachment of the ulnar aspect of the TFCC. This test has a high specificity and sensitivity (90%) for a foveal TFCC detachment [15].

After evaluating the TFCC during surgery, the tear can be classified, and the surgeon can decide treatment on the basis of the classification, and clinical presentation.

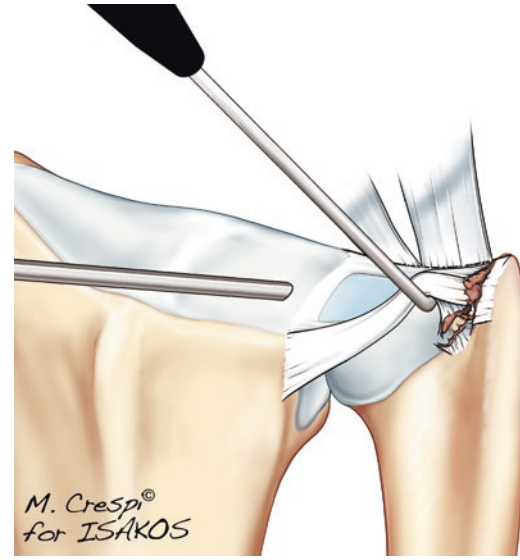

Fig. 88.2 Arthroscopic TFCC hook test, using a small hooked probe via the 6R portal to elevate the edge of the ulna attachment of the TFC whilst visualising with the arthroscope to determine the stability of the foveal and peripheral attachments

88.5 Classification of TFCC Tears

The TFCC may be injured in different patterns and locations, generally at its horizontal or more peripheral regions or at its attachments. These lesions can be traumatic or degenerative.

In 1988, Palmer et al. described the first classification of TFCC lesions (Table 88.1) [3].

Class 1 lesions are defined as traumatic lesions and are far less common than degenerative tears or perforations. They are classified according to the location of the tear and divided into four subclasses [3].

- Class 1A lesions are defined as lesions of the central or horizontal part of the TFCC. These tears are usually 1–2 mm wide and 2–3 mm away from the radial attachment to the TFCC.
- Class 1B lesions are a peripheral TFCC avulsion; it is a traumatic lesion of the TFCC from its insertion into the distal ulna. This can also be caused by a fracture of the ulnar styloid. These lesions can lead to an instability of the TFCC, however, in some cases, the DRUJ can remain stable (Figs. 88.3 and 88.4a, b).

Table 88.1 Table of Palmer and Werner classification of TFCC tears

Class 1: Traumatic	
1A	Central perforation
1B	Ulnar avulsion – with distal ulnar fracture – without distal ulnar fracture
1C	Distal avulsion
1D	Radial avulsion – with sigmoid notch fracture – without sigmoid notch fracture
Class 2: Degenerative (Including ulnocarpal abutment syndrome)	
2A	TFCC wear
2B	TFCC wear + lunate or ulnar chondromalacia
2C	TFCC perforation + lunate or ulnar chondromalacia
2D	TFCC perforation + lunate or ulnar chondromalacia + lunotriquetral ligament perforation
2E	TFCC perforation + lunate or ulnar chondromalacia + lunotriquetral ligament perforation + ulnocarpal arthritis

- Class 1C lesions are also a peripheral tear; here the avulsion of the TFCC is either at distal attachment to the lunate or the triquetrum. In most cases, this lesion leads to ulnar carpal instability and the ulnar carpus translates in a palmar direction. (compared to the ulnar or radial head) (Fig. 88.5a, b).
- Class 1D lesions are a peripheral avulsion where the lesion is close to or at the attachment of the TFCC to the radius at the distal aspect of the sigmoid notch (Fig. 88.6).

Class 2 lesions are defined as degenerative lesions and are often a result of the chronic overload of the ulna side of the wrist, due to an ulnar impaction syndrome or positive ulnar variance. These tears are divided into five subclasses on the basis of their extent and the location of the degenerative lesions, including their concomitant pathologies and progression (Fig. 88.7).

- Class 2A TFCC wear and thinning located at the horizontal part, distally or proximally or both without any perforation.

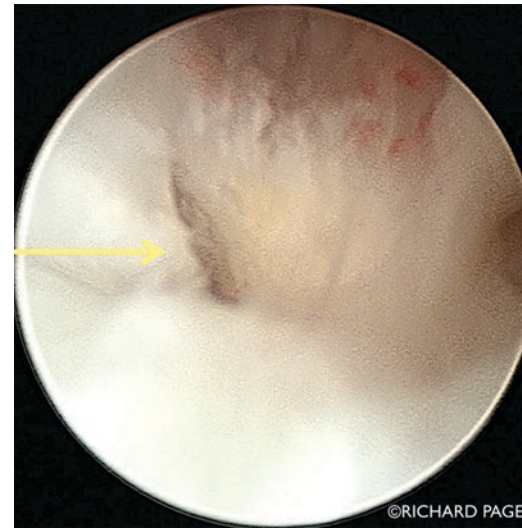

Fig. 88.3 Arthroscopic image of a TFCC 1B lesion with a peripheral acute tear. (© Richard Page)

- Class 2B TFCC wear is seen at the same location as the 2A lesion, but there is an additional wear or chondromalacia of the ulnar aspect of the lunate or/plus the radial aspect of the ulnar head. In some cases, there is also some erosion of the lunate or ulnar head (Fig. 88.8).
- Class 2C TFCC wear is a further progression of the 2B class lesions, such that the horizontal part of the TFCC becomes perforated. The perforation is usually in an ovoid shape, whereas traumatic perforations tend to be a dorsal palmar slit. These tears are located in the avascular part of the TFCC (Fig. 88.9).
- Class 2D lesions show a further progression of a 2C lesion and involves rupture of the lunotriquetral ligament.
- Class 2E lesions are the final stage of a degenerative TFCC lesion. In these lesions, there is TFCC perforation, lunate and ulnar chondromalacia, an LT ligament perforation and signs of ulnocarpal arthritis. The horizontal portion of the TFCC is usually completely attenuated and perforated.

The classification of Palmer is an established and useful way to categorise TFCC injuries to assist in treatment decision-making. However,

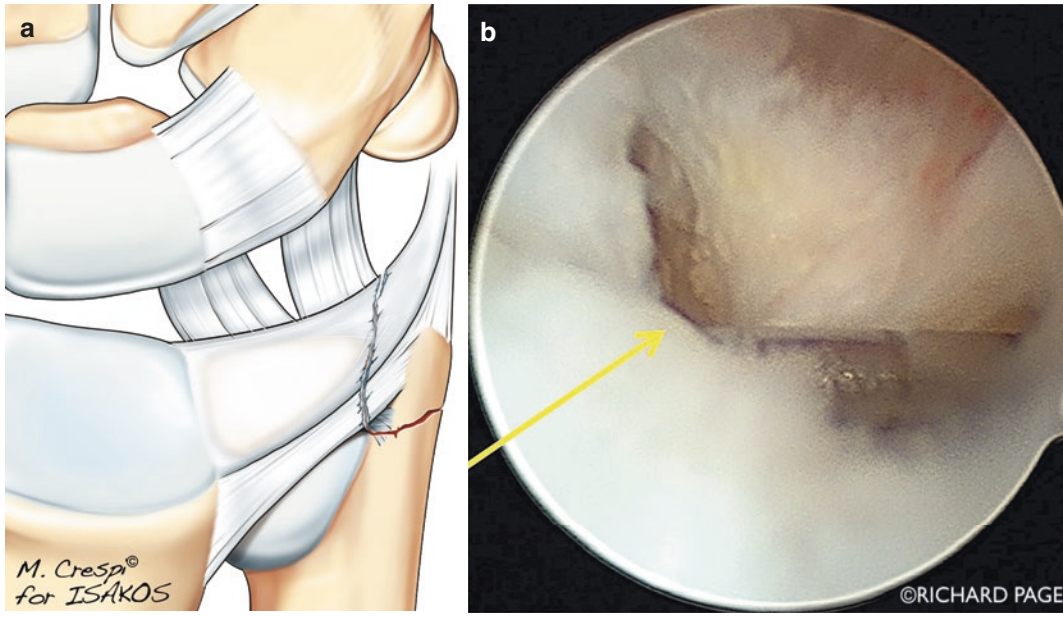

Fig. 88.4 (**a** and **b**): TFCC type 1B lesion: peripheral TFCC avulsion at insertion of TFCC at the ulnar side, with arthroscopic probe in situ to examine stability. (© Richard Page)

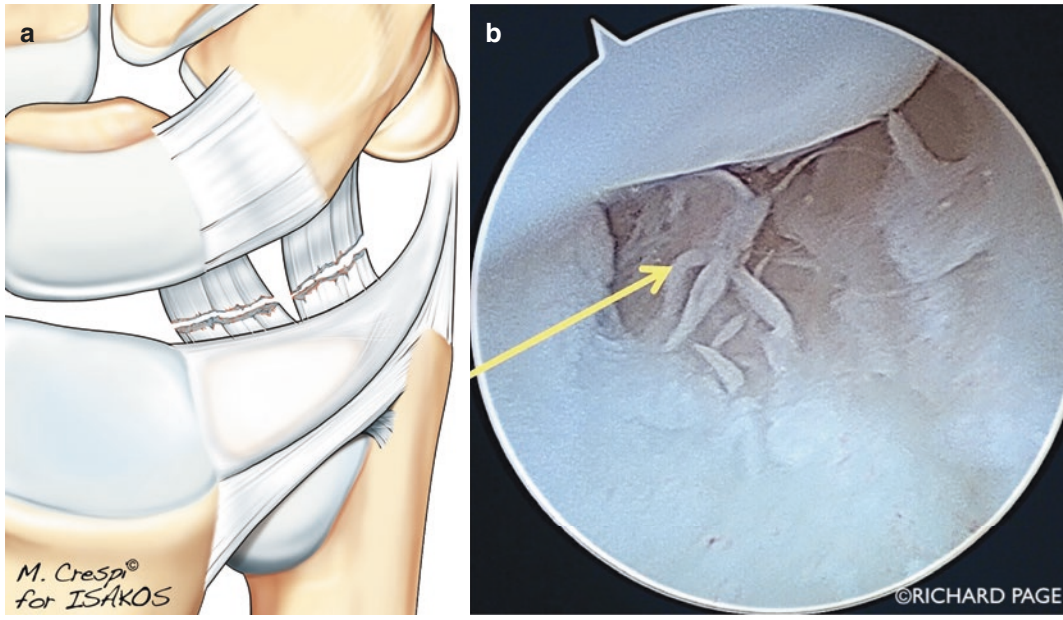

Fig. 88.5 (**a** and **b**): TFCC 1C tear is illustrated and demonstrated arthroscopically. The peripheral avulsion of the TFCC is either at the distal attachment to the lunate or the triquetrum, shown here with fraying in the subacute state. (© Richard Page)

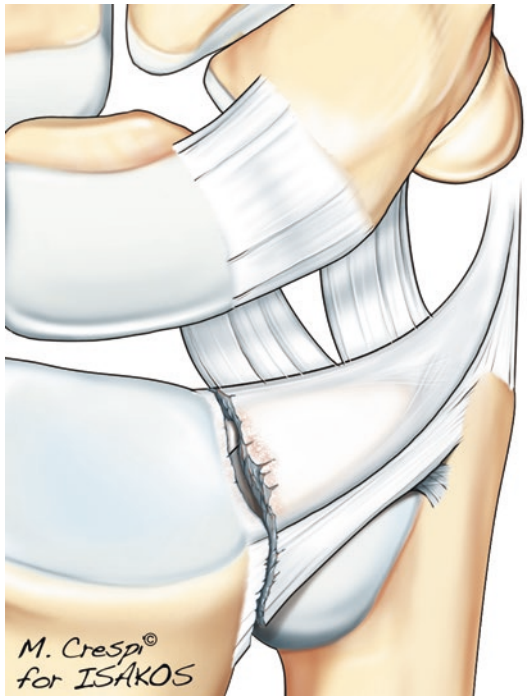

Fig. 88.6 Type 1D TFCC tear is illustrated. The peripheral avulsion is at the radial attachment

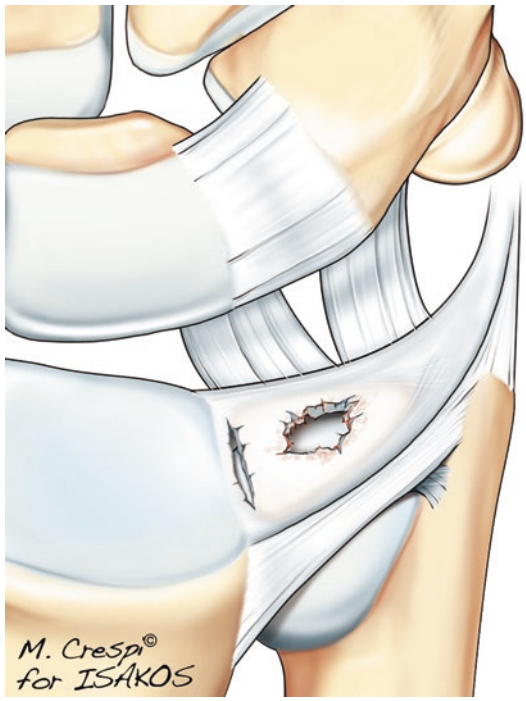

Fig. 88.7 Palmer Type 2 lesions (Degenerative) – central perforation and degenerative radial-sided tear

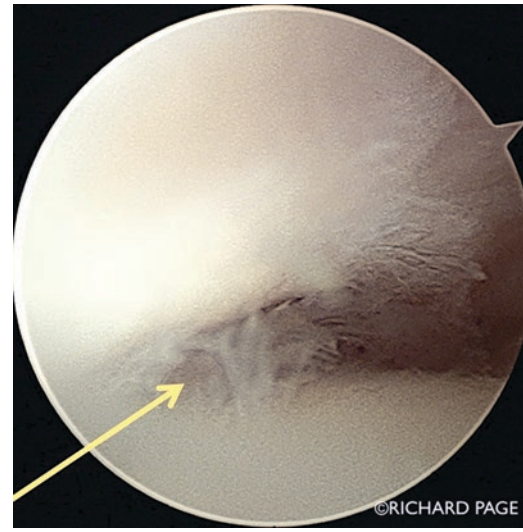

Fig. 88.8 Arthroscopic image of a Type 2B lesion showing the triquetral chondromalacia. (© Richard Page)

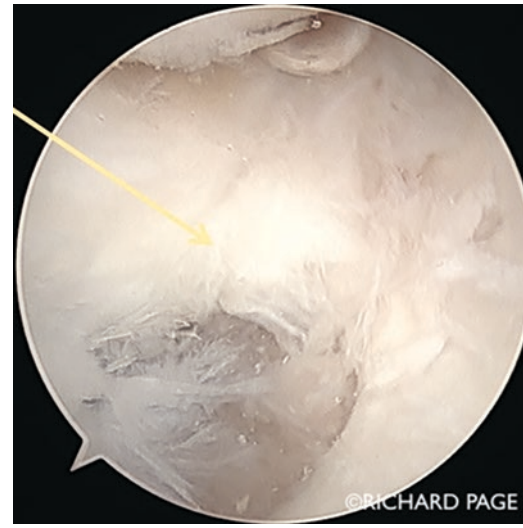

Fig. 88.9 Arthroscopic image of a Type 2 central degenerative wear with perforation of the TFC. (© Richard Page)

the Palmer classification does not include DRUJ involvement and stability and this is a key factor regarding the treatment in some injury patterns. Therefore, Atzei and Luchetti published a new classification that is based on the arthroscopic findings and includes DRUJ stability to guide management. Atzei's classification system of TFCC lesions is summarised in Table 88.2.

Table 88.2 Atzei classification of peripheral tears

		Comprehensive classification of TFCC peripheral tears and associated Ulnar Styloid Fractures						
		Class 0 Isolated styloid fracture without TFCC tear	Class 1 Distal TFCC tear	Class 2 Complete TFCC tear	Class 3 Proximal TFCC tear	Class 4 Non-repairable TFCC tear		Class 5 DRUJ arthritis
Clinical findings	DRUJ ballottement test	Negative	Slight laxity (hard end-point)	Mild to severe laxity (soft end-point)				Variable
Radiographic findings	Intact ulnar styloid or tip fracture of the ulnar styloid							
	Basilar fracture of the ulnar styloid			(Floating styloid")		CLASS 3-A Avvision Fracture of TFCC Insertion	Class 4-A	Class 4-B
Arthroscopic findings	Appearance of the distal TFCC (during RC Arthroscopic)	Normal appearance (MO tear)	Peripheral Tear		Normal appearance (NO tear)		Massive tear degenerated edges	Frayed edges failes suture	Variable
	Tension of the proximal TFCC (Hook Test)	Taut TFCC (negative Hook test)		Loose TFCC (positive Hook test]					
	Cartilage status of DRUJ	Well preserved cartilage							Degenerative or traumatic cartilage defect
Suggested treatment		Splinting for pair relief (Fragment removal in chronic painful cases)	TFCC suture (Splinting of acute cases)	TFCC forveal refixation		Styloid fixation	Tendon graft reconstruction		Arthroplasty

Used with permission: From Atzei, A., & Luchetti, R. (2011). *Foveal TFCC Tear Classification and Treatment. Hand Clinics, 27(3), 263–272.* https://doi.org/10.1016/j.hcl.2011.05.014 (Permission attached)

88.6 Techniques for Management of TFCC Tears

The treatment of triangular fibrocartilage complex (TFCC) tears can be challenging and therefore a categorisation of the different types of tears can be a helpful tool to make decisions regarding the treatment of the spectrum of TFCC pathology [11].

Studies have shown that more than half of the patients improve from conservative treatment (Park et al.) [16]. This treatment includes immobilisation, cortisone injection, NSAIDS, rest and in some instances splintage. The 'ELMPOPI' (education, lifestyle measures, medications, physio/hand therapy, orthotic splints, physical measures, injections) approach is useful and this is usually pursued for a minimum of 3 months in the absence of a clear surgical lesion [6]. There is an absence of quality studies evaluating the time frame for non-operative treatment, but commonly range between 6 weeks and 3 months.

The operative management is dependent on the classification of the tear, however, the size of the injury and the patient's circumstances, work and compliance must be considered as well.

- TFCC injuries can be either debrided, repaired or reconstructed. The different techniques are discussed in the following chapters including an inside out and transosseous foveal repair or tendon graft reconstruction.
- Degenerative lesions are often correlated with positive ulnar variance or ulna impaction syndrome. Therefore, the treatment of the ulna pathology should also be considered, for example, an ulnar shortening osteotomy, Wafer or Darrach's procedure.
- The stability of the DRUJ should be tested intraoperatively and prior to the surgery compared to the other wrist of the patient.
- Due to the poor blood supply of the central region, it was postulated for a long time that Type 1A tears should be debrided and not repaired. However, studies have shown that after a debridement the central part tends to heal and form fibrous connective tissue and fibrocartilaginous components [17].
- Class 1B tears are vascularised and therefore should be repaired if possible. If the triangular fibrocartilage disc is completely detached from the ulnar insertion, then there is an injury to the radioulnar ligaments resulting in instability.
- Type 1C tears are less common and more complex to manage. A repair should be performed. Debridement is an option if the ligaments are beyond repair.
- Type 1D tears are radial sided and as a result of the poorer blood supply, have a low chance in healing. A partial resection is a common option. However, it should be considered, that even though the central part has a poor blood supply, some studies showed excellent outcomes after a repair. Historically attempts have been made to repair these with transosseous radial sutures with variable success.
- Type 2 lesions are often correlated with chronic overload due to positive ulnar variance or ulna impaction syndrome. Therefore, the treatment of the ulna pathology should also be considered (ulnar shortening, wafer resection or Darrach's procedure). The secondary damage to surrounding structures needs to be addressed concomitantly. Most of the symptomatic, Type II lesions can be managed with debridement, and Bendar and Osterman have reported excellent results after debridement with 73% of the patient satisfied after the procedure [1].

References

1. Bednar JM, Osterman AL. The role of arthroscopy in the treatment of traumatic triangular fibrocartilage injuries. Hand Clin. 1994;10:605–14. 14
2. Jantea CL, Baltzer A, Rüther W. Arthroscopic repair of radial-sided lesions of the triangular fibrocartilage complex. Hand Clin. 1995;11:31–6.
3. Palmer AK. Triangular fibrocartilage complex lesions: a classification. J Hand Surg [Am]. 1989;14:594–606.
4. Chan JJ, Teunis T, Ring D. Prevalence of triangular fibrocartilage complex abnormalities regardless of symptoms rise with age: systematic review and pooled analysis. Clin Orthop Relat Res. 2014;472(12):3987–94. https://doi.org/10.1007/s11999-014-3825-1.
5. Palmer AK, Werner FW, Glisson RR, et al. Partial excision of the triangular fibrocartilage complex. J Hand Surg Am. 1988;13:391–4.

6. Nguyen ND, Pham TH, Pathirana PN, Babazadeh S, Page R, Seneviratne A. Sensing and characterization of the wrist using dart Thrower's movement. IEEE Sensors J. 2018;18(10)
7. Thiru RG, Ferlic DC, Clayton ML, McClure DC. Arterial anatomy of the triangular fibrocartilage of the wrist and its surgical significance. J Hand Surgery Am. 1986;11:258–63.
8. Tay SC, Tomita K, Berger RA. The "ulnar fovea sign" for defining ulnar wrist pain: an analysis of sensitivity and specificity. J Hand Surg Am. 2007;32(4):438–44.
9. Nakamura R, Horii E, Imaeda T, Nakao E, Kato H, Watanabe K. The ulnocarpal stress test in the diagnosis of ulnar-sided wrist pain. J Hand Surg Br. 1997;22(6):719–23.
10. Bille B, Harley B, Cohen H. A comparison of CT arthrography of the wrist to findings during wrist arthroscopy. J Hand Surg Am. 2007;32(6):834–41.
11. Bain GI, Munt J, Turner PC. New advances in wrist arthroscopy. Arthroscopy. 2008;24(3):355–67. https://doi.org/10.1016/j.arthro.2007.11.002.
12. Lee RK, Ng AW, Tong CS, Griffith JF, Tse WL, Wong C, Ho PC. Intrinsic ligament and triangular fibrocartilage complex tears of the wrist: comparison of MDCT arthrography, conventional 3-T MRI, and MR arthrography. Skelet Radiol. 2013;42(9):1277–85. https://doi.org/10.1007/s00256-013-1666-8. Epub 2013 Jun 28
13. Haims AH, Schweitzer ME, Morrison WB, Deely D, Lange RC, Osterman AL, Bednar JM, Taras JS, Culp RW. Internal derangement of the wrist: indirect MR arthrography versus unenhanced MR imaging. Radiology. 2003;227(3):701–7.
14. Ganeshalingam R, Eng K, Page RS. Magnetic resonance imaging in the acute management of suspected scaphoid fractures: a review of the literature and assessment of treatment algorithm. OA Musculoskeletal Med. 2013;1(2):19.
15. Trehan SK, Wall LB, Calfee RP, Shen TS, Dy CJ, Yannascoli SM, Goldfarb CA. Arthroscopic diagnosis of the triangular fibrocartilage complex foveal tear: a cadaver assessment. J Hand Surg. 2018;43(7):680.e1–5. https://doi.org/10.1016/j.jhsa.2017.12.017.
16. Park A, Lutsky K, Matzon J, Leinberry C, Chapman T, Beredjiklian PK. An evaluation of the reliability of wrist arthroscopy in the assessment of tears of the triangular fibrocartilage complex. J Hand Surg Am. 2018;43(6):545–9. https://doi.org/10.1016/j.jhsa.2018.02.031. Epub 2018 Mar 28
17. Tatebe M, Horii E, Nakao E, Shinohara T, Imaeda T, Nakamura R, Hirata H. Repair of the triangular fibrocartilage complex after ulnar-shortening osteotomy: second-look arthroscopy. J Hand Surg Am. 2007;32(4):445–9.

89 Arthroscopic Debridement of Triangular Fibrocartilage Complex Tears

Richard S. Page, Janina Henze, and Kevin Eng

89.1 Background

Pathology of the TFCC covers a spectrum from acute injury to degenerative lesions, resulting in degradation and fraying of the cartilage element of the complex. For the latter, which presents with ulna sided pain, often linked to a sense of activity related to clicking and catching on the ulna side of the wrist, arthroscopic debridement has commonly been a treatment employed. The aim is to remove debris causing localized synovitis and as well as unstable tissue that can catch, typically with rotation in ulna deviation. However, limited studies directly compare the outcomes of surgical treatments for TFCC injuries hence evidence-based guidance on whether a debridement or a repair is superior is difficult to establish.

Arthroscopic debridement has developed into a valid treatment option for TFCC tears. However, not every TFCC tear is suitable for this treatment and other possible therapies have to be considered. Many TFFC tears can be treated conservatively, under the 'ELMPOPI'; principle [1]. Nevertheless, not all patients are pain-free after nonoperative management and therefore a debridement may be considered, particularly if the tear is irreparable and associated with mechanical symptoms on presentation.

89.2 Indications and Contraindications

Most of the studies regarding arthroscopic debridement of TFCC tears are described on a heterogenic group not isolating the etiology of the injury or the location. More recent studies imply that Palmer's classification can help to guide treatment. Due to the poor vascularization of the central TFCC, most authors debride rather than repair central triangular-fibrocartilage pathology [2]. The management of radial tears remains uncertain, due to the challenge of attaching shortened, often deficient tissue to bone and

R. S. Page (✉)
Department of Orthopaedics, School of Medicine, Deakin University, Geelong, VIC, Australia

Barwon Centre for Orthopaedic Research and Education (B-CORE), Barwon Health and St John of God Hospital, Geelong, VIC, Australia

Geelong Orthopaedics, SJOG Specialist Centre, Geelong, VIC, Australia
e-mail: richardpage@geelongortho.com.au

J. Henze
Barwon Centre for Orthopaedic Research and Education (B-CORE), Barwon Health and St John of God Hospital, Geelong, VIC, Australia

K. Eng
Barwon Centre for Orthopaedic Research and Education (B-CORE), Barwon Health and St John of God Hospital, Geelong, VIC, Australia

Geelong Orthopaedics, SJOG Specialist Centre, Geelong, VIC, Australia

© ISAKOS 2022

D. N. Bhatia et al. (eds.), *Arthroscopy and Endoscopy of the Elbow, Wrist and Hand*,
https://doi.org/10.1007/978-3-030-79423-1_89

the avascularity of the radial aspect [3]. The main advantage of the debridement is that the patient can begin rehabilitation immediately, and a prolonged period of protective immobilization is avoided. Conservative treatment remains a valuable option, and Park et al. described that 57% of the patient improved with an immobilization between 4 and 6 weeks [4].

Traumatic and other repairable tears in the vascular zones should be repaired and debridement is contraindicated.

89.3 Surgical Technique

The general aim of a debridement is to eliminate mechanical pathology. The patient is placed in the supine position with the forearm positioned over an arm table, fixed in an elevated position using a hand-wrist traction device. Traction of the wrist is applied by some weights as outlined in the earlier chapters and important landmarks and portals are marked.

- For an arthroscopic debridement of the wrist, the standard wrist arthroscopy instruments are used as described previously. Furthermore, Debridement techniques require instruments that can cut the different components of the TFCC, such as scalpels, curved (banana) blade shavers, radiofrequency probes, and lasers. At the beginning of wrist arthroscopy, mini-curved (banana) blades and motoric cutters were utilized, while nowadays ablation devices are becoming more popular (Fig. 89.1a–c).
- The wrist is inspected with a 2.7 mm arthroscope (or 1.9 mm arthroscope in smaller patients) via the 3–4 portal. A probe is introduced through the 4–5 or 6 R portals. The integrity of the TFCC is tested with the hook test and the trampoline test.
- To perform a debridement, an oscillating motorized arthroscopic shaver to partially resect the TFCC is inserted through the 6R portal. With the resecting instrument, degenerative fibrocartilage, and flaps and synovitis can be removed and edges of the TFCC can be smoothed. The goal of the procedure is to debride unstable flaps of the central fibrocartilage that are likely to catch on surrounding tissue back to a stable rim. It is important to

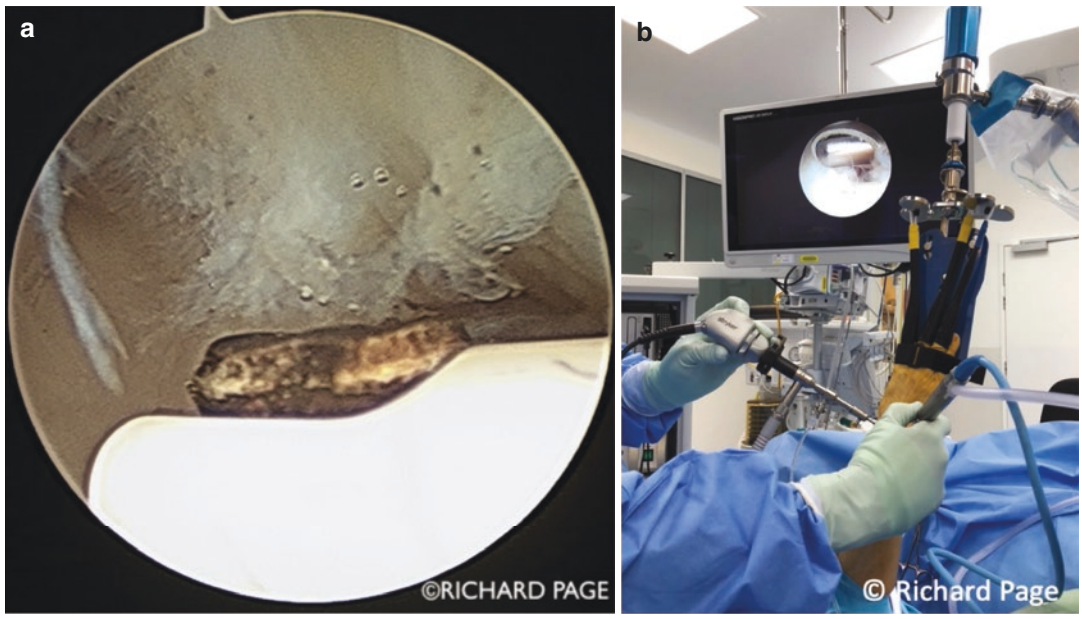

Fig. 89.1 Devices and setup used for arthroscopic debridement. (**a**) Radiofrequency probe (2.7 mm) in use to debride a partial TFCC tear. (**b**) External view of debridement of a TFCC tear with an arthroscopic shaver in situ. (© Richard Page)

avoid damage to the peripheral 2 mm of the TFCC as this tissue contains the dorsal and volar radioulnar ligaments [2].

- During the debridement, care must be taken not to injure the ulnar head or extend beyond the articular joint capsule.

89.4 Arthroscopic Debridement as Management of TFCC Tears by their Palmer Class

- **Palmar Class 1A Tears (Central Tears):** The goal of the procedure is to debride unstable flaps of the central fibrocartilage back to a stable rim. Biomechanical studies demonstrate that up to 2/3 of the central region can safely be resected without destabilizing the DRUJ or negatively affecting load transfer [2]. Sauerbier reported results of debridement on a relatively large group of Type 1A tears and 75% of the patients were satisfied with the outcome and improved symptoms were reported by 95% of the patients [5]. Miwa and his colleagues showed similar results in 9/10 patients undergoing debridement for Type 1A tears [6]. Roth et al. reported a significant improvement after debridement of central flaps of TFCC with 70.7% of the patients satisfied and improved pain and DASH scores [7].
- **Palmar Class 1B Tears (Ulnar Avulsion With or Without Distal Ulnar Fracture):** Studies have highlighted the importance of the integrity of the TFCC ligaments to maintain DRUJ stability, therefore a repair seems logical optimal management for symptomatic Type 1B tears (Fig. 89.2) [8, 9]. Estrella et al. reported excellent results with 74% of patients with good or excellent results regarding the modified MAYO Wrist score with pain reduction and increased grip strength [10]. On the other hand, there are studies that showed similar results for debridement of class 1B tears. Cardenas-Montemayor et al. demonstrated similar results to arthroscopic repair in their debridement of 1B stable TFCC tears, with significant pain reduction, and improved Disabilities of the Arm, Shoulder, and Hand (DASH) and modified Mayo Wrist scores (MMWS) [11]. There are no studies showing a direct comparison between repair and debridement in class 1B lesions.

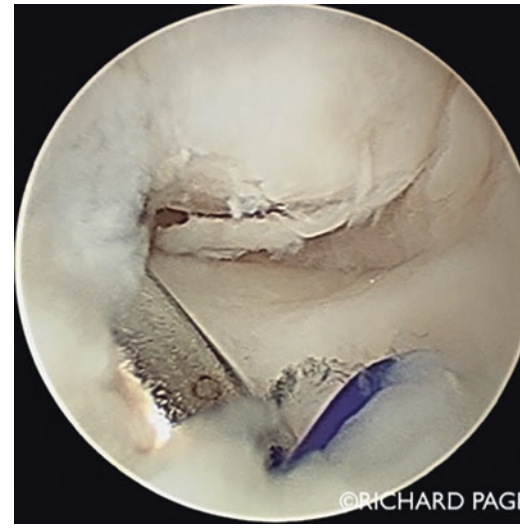

Fig. 89.2 Inside out TFCC repair using 2/0 PDS after rim debridement of the TFCC and chondroplasty. (© Richard Page)

- **Palmar Class 1D Tears (Acute Radial Tears):** Isolated 1D TFCC tears are uncommon, and only a few reports have been published. Many surgeons advocate the debridement of radial tears of the TFCC. Repair of the radial edge of the TFCC has been described [12, 13] with acceptable outcomes; these are less commonly done, and there are no studies published comparing debridement versus repair in the radial sided peripheral tears.
- **Palmar Class 2 Lesions (Degenerative TFCC tears):** Most of these lesions occur after a chronic overload of the TFCC and may be due to ulnar impaction syndrome. Therefore, an ulnar shortening procedure can be considered after debridement or in the same procedure with the aim of unloading the ulna side of the wrist (Fig. 89.3a–c).

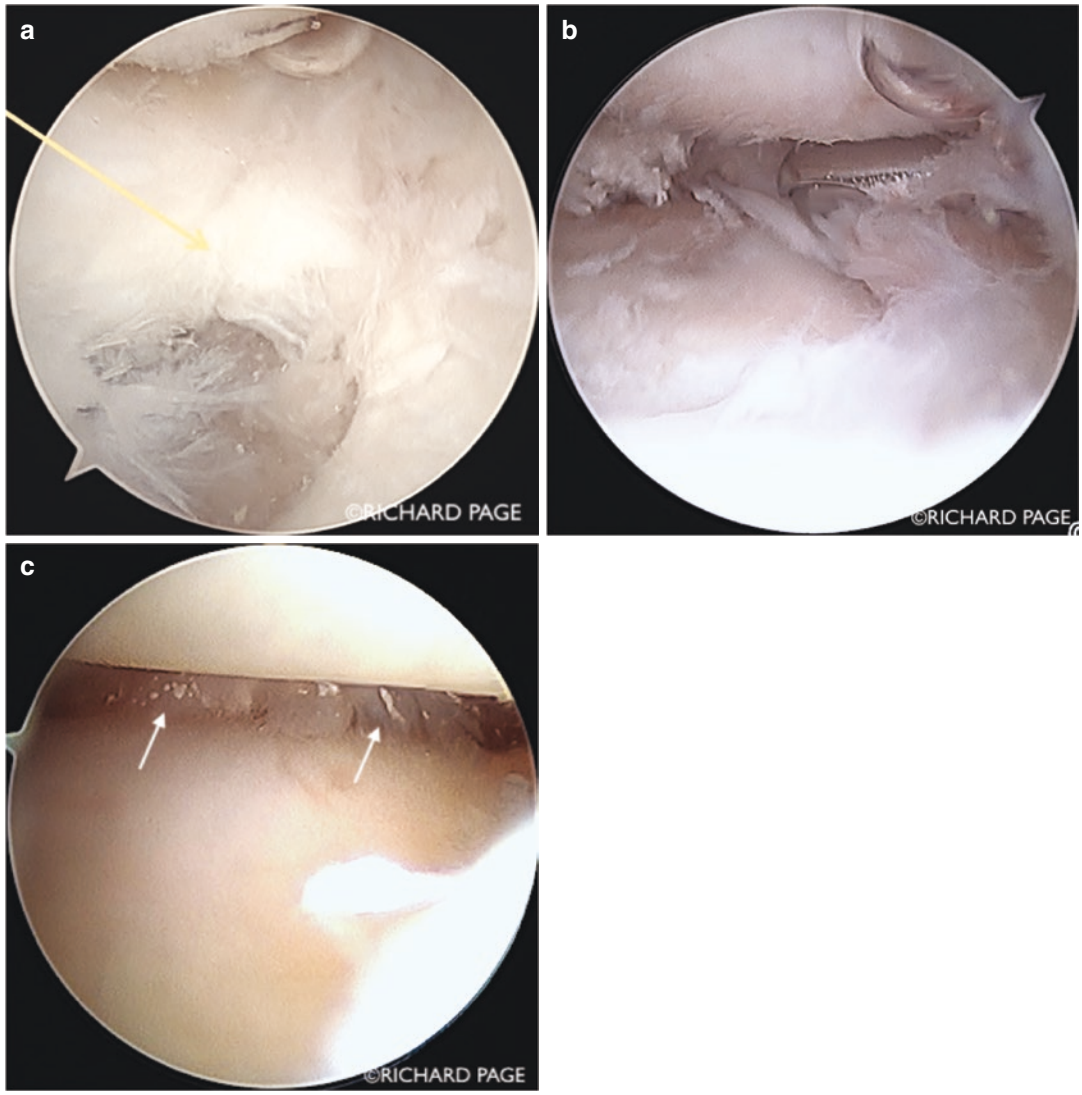

Fig. 89.3 (**a**) Arthroscopic view of a degenerative Type 2 TFCC wear. (**b**) Type 2 tear during debridement with a 2.7 mm shaver. The ulnar head is visualized through the tear. (**c**) Chondrocalcinosis of the ulna compartment of the wrist (arrow), a risk for the development of degenerative tears. (© Richard Page)

89.5 Tips and Tricks

- The setup should be under tourniquet control and enable additional ulnar sided portals and removal from traction to allow an open approach if needed. Examples of when this may be useful include subsheath tears around ECU, basal type II fractures to the ulna styloid, or impinging non-unions to the ulna styloid. Depending on the site of the degenerate tear pattern, the use of either the 6R or 6U portals can be useful, with additional use or the 1-2 or 3-4 portals as needed to introduce the shaver from.
- To improve access to the ulna, wrist traction devices can be placed on the little finger and ring finger.
- A small (2.7 mm) radiofrequency ablation probe is helpful initially to minimize bleeding risk, particularly when there is significant synovitis. To avoid the arthroscopic view

being compromised by bubble formation, a hypodermic needle can be inserted into the wrist in the region to allow some 'venting'; of the wrist joint.

- It is helpful to examine the wrist arthroscopically out of traction to both visualize and palpate for clicking and crepitus around the TFC and the DRUJ. The stability of the DRUJ should be assessed both before and after the case to limit the risk of instability, and overly aggressive resection of the peripheral TFCC attachments should be avoided.

89.6 Complications

Arthroscopic TFCC debridement is a minimally invasive and safe technique for the treatment of symptomatic TFCC lesions. This procedure has the same general risks of wrist arthroscopy, such as infections, nerve injury, and stiffness. Other specific risks can be due to the chosen instrument for the debridement such as lacerations of the surrounding tissues with curved motorized resector blades or thermal injuries from radiofrequency devices. Local chondral, ligament, or tendon injures are possible, and should be prevented by careful use of the correct sized instruments and experience.

89.7 Summary

The evidence base for developing recommendations on the treatment of TFCC injuries is limited in quality and patient numbers, making this area suitable for a concerted focus of high-quality level 1 clinical studies. Most authors agree that debridement is a legitimate treatment for Palmer class 1A and degenerative tears whereas in 1B and 1C tears a repair seems to be beneficial. The use of debridement in type 1D lesions remains a controversial topic, in part due to the low frequency of this injury pattern. Arthroscopic debridement for nonrepairable central TFCC tears in the absence of ulnar-positive variance reliably provides patients with a lower level of pain and improved function compared to that experienced before surgery, which can help them get back to work or activities.

References

1. Park MJ, Jagadish A, Yao J. The rate of triangular fibrocartilage injuries requiring surgical intervention. Orthopaedics. 2010;33(11):806. https://doi.org/10.3928/01477447-20100924-03.
2. Adams BD. Partial excision of the triangular fibrocartilage complex articular disk: a biomechanical study. J Hand Surg Am. 1993;18(2):334–40.
3. Bednar MS, Arnoczky SP, Weiland AJ. The microvasculature of the triangular fibrocartilage complex: its clinical significance. J Hand Surg Am. 1991;16A:1101–5.
4. Park MJ, Jagadish A, Yao J. The rate of triangular fibrocartilage injuries requiring surgical intervention. Orthopedics. 2010;33(11):806.
5. Arsalan-Werner A, Grüter L, Mehling IM, Moll W, Wölfle O, Sauerbier M. Results after arthroscopic treatment of central traumatic lesions of the triangular fibrocartilage complex. Arch Orthop Trauma Surg. 2018;138(5):731–7. https://doi.org/10.1007/s00402-018-2910-4.
6. Miwa H, Hashizume H, Fujiwara K, Nishida K, Inoue H. Arthroscopic surgery for traumatic triangular fibrocartilage complex injury. J Orthop Sci. 2004;9(4):354–9. https://doi.org/10.1007/s00776-004-0796-1.
7. Roth JH, Poehling GG. Arthroscopic "-ectomy" surgery of the wrist. Arthroscopy. 1990;6(2):141–7.
8. Hagert E, Hagert CG. Understanding stability of the distal radioulnar joint through an understanding of its anatomy. Hand Clin. 2010;26(4):459–66.
9. Kleinman WB. Stability of the distal radioulna joint: biomechanics, pathophysiology, physical diagnosis, and restoration of function what we have learned in 25 years. J Hand Surg Am. 2007;32(7):1086–106.
10. Estrella EP, Hung L-K, Ho P-C, Tse WL. Arthroscopy. Arthroscopic repair of triangular fibrocartilage complex tears. Arthroscopy. 2007;23(7):729–37. https://doi.org/10.1016/j.arthro.2007.01.026.
11. Cardenas-Montemayor E, Hartl JF, Wolf MB, Leclère FM, Dreyhaupt J, Hahn P, Unglaub F. Subjective and objective results of arthroscopic debridement of ulnar-sided TFCC (palmer type 1B) lesions with stable distal radio-ulnar joint. Arch Orthop Trauma Surg. 2013;133(2):287–93. https://doi.org/10.1007/s00402-012-1643-z.
12. Cooney WP, Linscheid RL, Dobyns JH. Triangular fibrocartilage tears. J Hand Surg Am. 1994;19(1):143–54. https://doi.org/10.1016/0363-5023(94)90238-0.
13. Trumble TE, Gilbert M, Vedder N. Isolated tears of the triangular fibrocartilage: management by early arthroscopic repair. J Hand Surg Am. 1997;22(1):57–65. https://doi.org/10.1016/S0363-5023(05)80180-7.

Arthroscopic TFCC Repair: Inside out Technique

90

Margaret Woon Man Fok, Chris Yuk Kwan Tang, and Boris Kwok Keung Fung

90.1 Background

Triangular fibrocartilage complex (TFCC) is a load-bearing structure between lunate, triquetrum, and distal ulna. It acts as a primary stabilizer for distal radioulnar joint (DRUJ). It is a complex which includes the triangular fibrocartilage disc, extensor carpi ulnaris (ECU) tendon subsheath, ulnotriquetral and ulnolunate ligaments, dorsal and volar distal radioulnar ligaments, meniscal homolog, and the ulnocarpal collateral ligament [1]. It has bony attachments to both the sigmoid notch of the distal radius in the radial aspect and the ulnar fovea, i.e., base of ulnar styloid, in the ulnar aspect.

A tear of triangular fibrocartilage complex (TFCC) is one of the most common causes of ulnar wrist pain. Injuries like a fall on the outstretched hand or a forced ulnar deviation of the wrist can lead to an acute TFCC tear. In some instances, it can also be injured by repeated twisting wrist movement, e.g., a baseball player doing repeated swings. TFCC tear may be presented with pure ulnar wrist pain or pain together with DRUJ instability. Physical examination may reveal tenderness over the DRUJ or ulnar styloid, positive ballottement test, positive TFCC compression test (i.e., the presence of pain when wrist is in ulnar deviation with forearm in neutral position), and positive press test (i.e., the presence of pain when patient is lifting themselves out of a chair, with the wrist in an extended position). Investigations like radiographs and MRI can be useful to confirm the diagnosis.

90.2 Surgical Anatomy

TFCC lesion is classified into two types, traumatic and degenerative, by Palmar in 1989 [2]. Within traumatic lesions, it is then divided into four different types, depending on the location of the tear. Atzei [3] further subclassified the type 1B tear (i.e., peripheral tear) into different classes, taking into account the status of distal and proximal components of TFCC. Treatment is suggested based on the individual class.

One of the main concerns about the management of TFCC is its healing potential, which is dictated by its vascular supply. The blood supply of the TFCC is from the periphery. Peripheral TFCC is fed predominantly via the dorsal and palmar radiocarpal branches of the ulnar artery. Hence, it has the richest blood supply and greatest potential for healing.

Meanwhile, dorsal and palmar branches of the anterior interosseous artery supply the most radial part of the complex. It is relatively avascular and has less healing potential than the peripheral TFCC. As a result, debates remain on

M. W. M. Fok (✉) · C. Y. K. Tang · B. K. K. Fung
Department of Orthopaedics and Traumatology, Queen Mary Hospital, The University of Hong Kong, Hong Kong SAR, China

© ISAKOS 2022

D. N. Bhatia et al. (eds.), *Arthroscopy and Endoscopy of the Elbow, Wrist and Hand*,
https://doi.org/10.1007/978-3-030-79423-1_90

whether radial tear should be repaired, despite case series showing satisfactory results. With our proposed inside out technique, we believe that we can align the tear to its corresponding anatomical insertion. By creating transosseous tunnels for suture, it brings blood supply into the area and may further improve the ligament to bone healing.

90.3 Indications and Contraindications

The technique is indicated in symptomatic TFCC tears. The TFCC is attached back to the bone by using bone tunnel(s), and thus it is mainly indicated for palmar 1B and 1D tear.

Contraindications include:

- Degenerative TFCC tears.
- Irreparable TFCC (e.g., palmar 1A central tear) and retracted TFCC, i.e., when excessive tension is noted during the placement of suture.
- Ulnar impaction (except when positive ulnar variance is concomitantly managed by ulnar shortening procedure).
- Incongruency of DRUJ, e.g., due to previous trauma or Madelung deformity.
- DRUJ arthritis.
- Wrist stiffness, i.e., forearm rotation is limited.
- Inability to follow postoperative rehabilitation including a period of immobilization with splintage.

90.4 Surgical Technique

Specific instruments used in the procedure include:

- Standard wrist arthroscopic instruments, including 30°, 2.4 mm or 1.9 mm arthroscope.
- Meniscal double-barrel cannula (straight and curved) (Fig. 90.1a, b).
- Flexible K wires (1.0 or 1.1 mm, equivalent to 0.45 inch.) which can pass through the cannula in a smooth manner without difficulty.
- Double arm straight needles-two straight needles sharing a common threaded suture, e.g., PDS II (Fig. 90.2).

Under general or regional anesthesia, the affected arm is placed with the shoulder at 90^0 on a standard hand Table. A pneumatic tourniquet is applied. Finger traps are applied to the index, middle, and ring fingers of the affected hand. The fingers are then suspended with a 10 lb. traction by an upright sterile traction tower [4, 5].

- Radiocarpal joint portals, i.e., 3-4, 4-5 (or 6R), and 6 U portals are created. Wrist arthroscope is inserted into the radiocarpal joint via the 3-4 portal for TFCC assessment. A probe is inserted via 4-5 or 6R portals to further assess the stability of TFCC and its reparability if a lesion is found (Fig. 90.3a, b). The articular disc of TFCC is examined by the probe with the "trampoline test". Loss of tension and inability for the disc to bounce back indicate

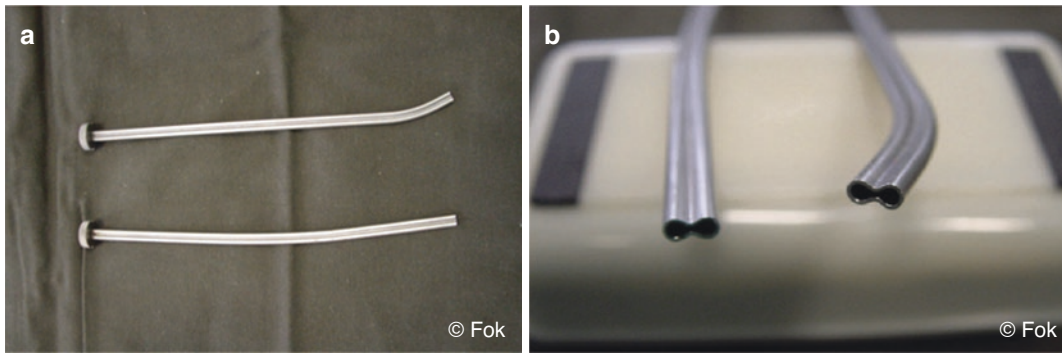

Fig. 90.1 (**a** and **b**) Meniscal double-barrel cannula (straight and curved) and the cross-section are shown. (© Dr Margaret Fok)

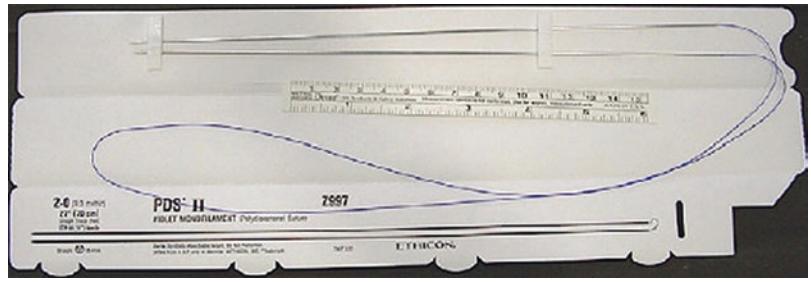

Fig. 90.2 Double arm straight needles, connected by a threaded suture is used through the bone tunnels. (© Dr Margaret Fok)

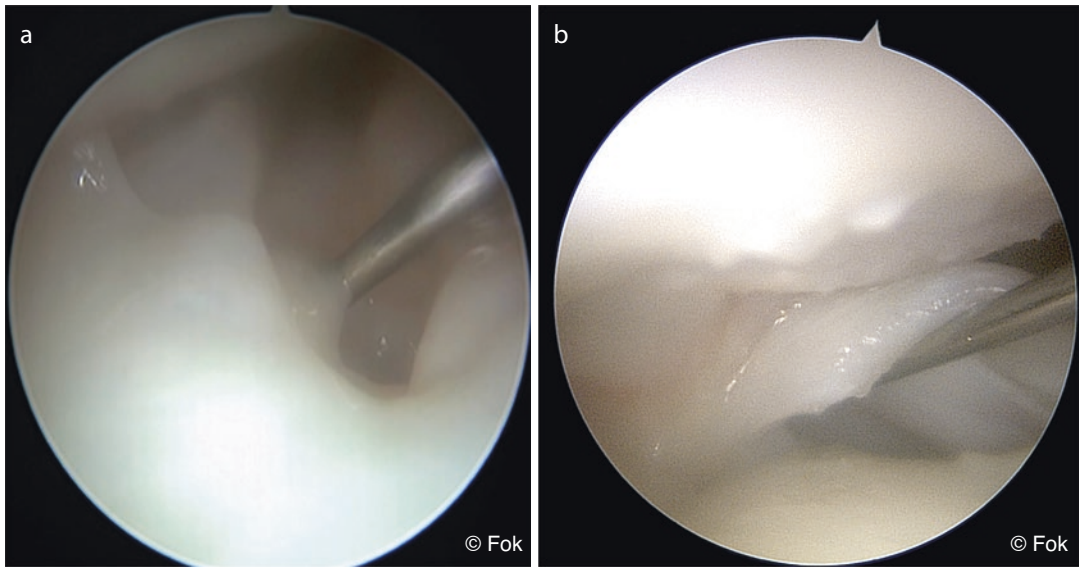

Fig. 90.3 (**a**) Arthroscopic view, showing the use of a probe in the assessment of the integrity of triangular fibrocartilage complex (**b**) Arthroscopic view of a peripheral triangular fibrocartilage complex tear is shown. (© Dr. Margaret Fok)

there is a detachment of TFCC at its insertion sites. The 6U portal is used as an outflow.

- In the presence of peripheral/foveal TFCC tear, DRUJ portal can be used to assess the integrity of the deep fibers of TFCC and the joint stability.
- The repair of peripheral/foveal tear is performed by the creation of bone tunnels at the base of ulnar styloid. The meniscal double-barrel cannula with a curved tip is used in this situation (Fig. 90.4a). With the arthroscope looking in via the 3-4 portal, the cannula is inserted through the 4-5 portal. The cannula catches the edge of the TFCC along its path and pushes it toward the fovea. Two flexible K wires are then drilled via the double-barrel apparatus, through the TFCC and fovea, and exit at the ulnar aspect of distal ulnar bone. By having the double armed straight needles on hand, the flexible K wire is pulled out from the barrel one at a time, while replacing it with one arm of the straight needles. Both needles are passed through the barrels, the ulnar bone, via the bone tunnels created by the K wires, to the skin. The two needles are then cut from the thread. A skin incision is then made between the two skin exit sites. The two suture ends are traced back at the point of their exits from the ulnar bone and a knot is tied over the periosteum of the ulna, with the forearm in supination/pronation (depending on its initial direction of instability) (Fig. 90.4b).
- The repair of radial tear is performed by the creation of two radial bone tunnels. The

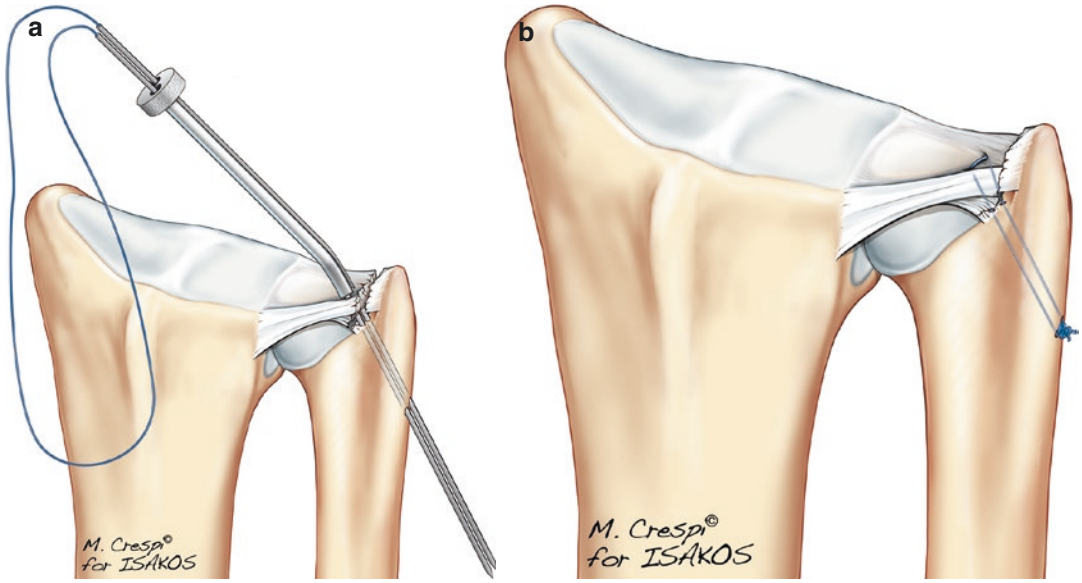

Fig. 90.4 (**a**) Repair of peripheral triangular fibrocartilage complex tear using double-barrel meniscal cannula and double arm straight needles (M. Crespi © for ISAKOS). (**b**) End result of the repair of peripheral triangular fibrocartilage complex tear. (M. Crespi © for ISAKOS)

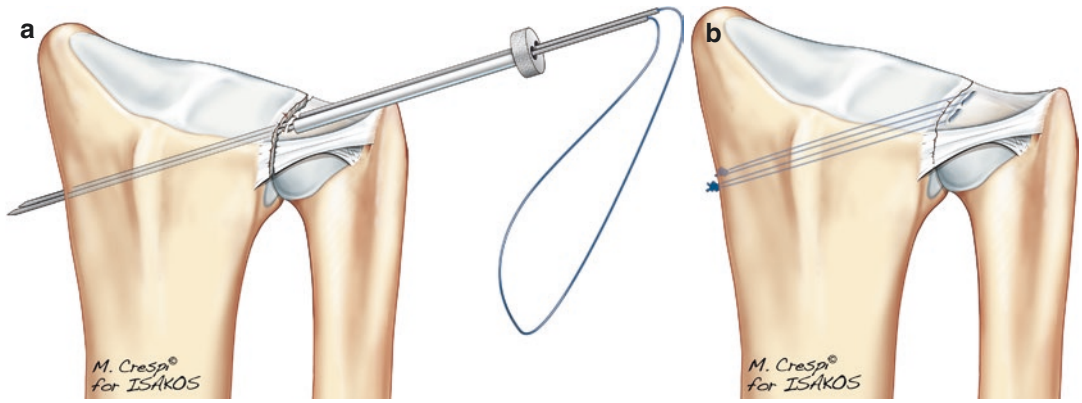

Fig. 90.5 (**a**) Repair of radial triangular fibrocartilage complex tear using double-barrel meniscal cannula and double arm straight needles (M. Crespi © for ISAKOS). (**b**) End result of the repair of radial triangular fibrocartilage complex tear. (M. Crespi © for ISAKOS)

meniscal double-barrel cannula with a relatively straight tip is used in this situation (Fig. 90.5a). With the arthroscope looking in via the 3-4 portal, the cannula is inserted through the 6R portal. The cannula catches the radial edge of the TFCC and pushes it to the sigmoid notch of the radius. Similar to the peripheral/foveal repair, two K wires are drilled via the double-barrel apparatus, through the radial TFCC, distal radius, and exit at the radial aspect of the distal radius. The flexible K wire is then pulled out from the barrel one at a time while replacing it with one arm of the straight needles. Both needles are passed through the barrels, the radius, via the bone tunnels created by the K wires, to the skin. The two needles are then cut from the thread. A skin incision is then made between

the two skin exit points. The two suture ends are traced back to the point of their exits from the radius and a knot is tied over the periosteum of the radius, with the forearm in the neutral position (Fig. 90.5b).

- If one suture is found to be inadequate, the procedure can be repeated and an additional suture can be placed. Wrist arthroscopy is used to check for the adequacy of the tension of the repair.
- If vessels are suspected to be injured, especially around the exit site of bone tunnels, tourniquet should be taken off and hemostasis needs to be achieved prior to closure. Long arm slab is given for rest.

90.5 Tips and Tricks

- Dry arthroscopy can be used for the initial assessment of the radiocarpal joint. During the repair of TFCC, an inflow of saline by gravity (without mechanical pressure pump) is recommended to dissipate the heat arise from drilling.
- The availability of all instruments should be checked. Surgeon must ensure that the flexible K wires to be used can pass through the double-barrel apparatus smoothly.
- Especially for the initial few cases, a good assistant is useful in helping to hold the arthroscope while the surgeon uses one hand to steadily hold the double-barrel while the other hand to insert K wires and needles.
- The size of the double-barrel cannula is larger than the arthroscope. The portal (i.e., 4-5 for peripheral/foveal repair or 6R for radial repair) needs to be enlarged prior to the insertion of the cannula.
- All used K wire tips and needles must check for integrity prior to closure. If in doubt, X-ray and arthroscopy are needed to ascertain that no metal debris are present within the joint.
- For the repair, both suture ends are needed to be traced back to the periosteum of either radius or ulna, where they exit from the bone, before tying the knots. This is to give minimum tension to the repair and to prevent the catching of soft tissue, e.g., nerves/tendons within the knot.
- In cases of DRUJ instability, the suture should be tensioned with forearm in either supination or pronation depending on its initial direction of instability.

90.6 Pitfalls

- Incorrect diagnosis.
- There are many different causes of ulnar wrist pain, e.g., ECU tendonitis, DRUJ arthritis, ulnar styloid nonunion. In order to achieve good outcome of TFCC repair, meticulous history taking, physical examination, and/or investigation are needed to confirm the diagnosis
- Incorrect classification of the TFCC tear.
- Attempt to repair a degenerative TFCC tear or a central tear (palmar 1A tear) will result in failure
- The presence of concomitant pathology, e.g., ulnar impaction syndrome.
- In the presence of ulnar impaction syndrome, if the TFCC tear is found to be repairable, the healing of the tear can only be achieved when the repair is performed at the same time as ulnar shortening procedure
- All flexible K wires used must pass through the double-barrel cannula without difficulty. This needs to be checked meticulously by the surgeon prior to the procedure.
- The tip of the K wires must be seen from the tip of double-barrel cannula prior to the drilling of bone tunnels. Otherwise, the K wire tip may drill against the curvature of the cannula, causing damages/irregularity to the inner surface of the cannula and creating metal debris.
- Avoid the use of excessive force when drilling with K wires. Breakage of the tip of K wires is possible.

90.7 Postoperative Management and Rehabilitation

Postoperatively, the wrist and forearm are immobilized for 3–4 weeks using a free hinge elbow brace. Depending on the preoperative stability of the DRUJ, the forearm is put in neutral position if stable or in either supination or pronation depending on the direction of its preoperative DRUJ stability. During the period of immobilization, shoulder and finger mobilization is encouraged. By the end of fourth week, the hinge brace is taken off and free mobilization of the wrist and forearm is allowed. Gentle passive mobilization and gradual strengthening exercise are started at the start of seventh week postoperatively.

90.8 Complications

- Depending on the type of repair, neurovascular bundle may be injured when the K wires or needles exit the bone. For radial repair, the radial artery and superficial radial nerve are at risk, and for peripheral/foveal repair, the ulnar neurovascular bundle is at risk. Iatrogenic injury can be prevented by aiming the exit site of the bone tunnels at the far radial or ulnar aspect of the bone, away from the volar surface.
- The K wires used are thin and flexible. If excessive force is used for bone tunnel drilling, breakage of the K wire tip may occur.
- The articular surface can be damaged during the insertion of instruments. Blunt trocar should be used at all times. During the insertion of the cannula into the radiocarpal joint, the portal including soft tissue and capsule should be extended. Avoid using excessive force to insert instruments into the joint.
- Persisted DRUJ laxity is possible. To avoid this, correct tensioning of the repair is important. DRUJ is reduced and forearm is put in the most stable position, usually in supination. Knot is only tied onto the periosteum, with no soft tissue in between the suture ends.
- Noncompliance to rehabilitation protocol including lack of splintage usage and early strengthening exercise can lead to TFCC re-rupture.

90.9 Results

In the authors' series, 50 patients (average age of 49 years) underwent arthroscopic TFCC repair since 2012. There were 24 radial and 26 peripheral/foveal repairs. Satisfactory relief of symptoms in terms of pain (from visual analog pain score of 4 to 0.5), grip strength (from 72% to 82% of the unaffected wrist), and DRUJ stability was noted at 1-year follow-up. Complication of breakage of part of the K wire tip was noted in one patient postoperatively. A subsequent wrist arthroscopy was performed to remove the metal debris from the radiocarpal joint. Transient paraesthesia in the region of the superficial radial nerve and ulnar nerve was noted in four patients. Irritation of suture knots was noted in five patients. Two patients required the excision of the suture knot under local anesthesia. There was no infection or significant DRUJ instability that require revision surgery.

References

1. Kleinman WB. Stability of the distal radioulna joint: biomechanics, pathophysiology, physical diagnosis, and restoration of function what we have learned in 25 years. J Hand Surg Am. 2007;32(7):1086–106.
2. Palmer AK. Triangular fibrocartilage complex lesions: a classification. J Hand Surg Am. 1989;14(4):594–696.
3. Atzei A. New trends in arthroscopic management of type 1-B TFCC injuries with DRUJ instability. J Hand Surg Eur. 2009;34(5):582–91.
4. Tang C, Fung B, Chan R, Fok M. The beauty of stability: distal radioulnar joint stability in arthroscopic triangular fibrocartilage complex repair. Hand Surg. 2013;18(1):21–6.
5. Tang CYK, Fung B, Rebecca C, Lung CP. Another light in the dark: review of a new method for the arthroscopic repair of triangular fibrocartilage complex. J Hand Surg Am. 2012;37(6):1263–8.

Ligament-Specific Transosseous Foveal Repair of TFCC

91

Bo Liu and Margareta Arianni

91.1 Background

The volar and dorsal radioulnar ligaments (RUL), which are the proximal (deep) components of the triangular fibrocartilage complex (TFCC), are the primary stabilizers of the distal radioulnar joint (DRUJ). Traumatic avulsion of the ulnar insertion of the RUL (i.e., the deep fibers of the TFCC inserting at the ulnar fovea), can result in pain and DRUJ instability [1]. It is now recognized that repair of the TFCC foveal avulsion should include the reattachment of the avulsed foveal fibers of the RULs for the restoration of motion and stability [1–4]. Arthroscopic TFCC foveal repair itself has many technical variations in the configuration of repair sutures, the number of sutures, cost, consumables, and equipment. Using an anchor suture is a popular technique for TFCC foveal repair, but it is costly and not without complications. The transosseous technique, popularized by Nakamura [1], is one of the most employed techniques, in which a single, concentric suture is made through bony tunnels in the distal ulna, anchoring the TFCC to the fovea. This technique is easy to reproduce, economical, and reliable, and has been widely employed by many surgeons [1, 5–10].

However, studies have shown that the distal radius does not only rotate but also translates, particularly at higher degrees of pronation and supination [11, 12]. This indicates that the dorsal and volar RULs may not have a single concentric point of rotation. A recent anatomical study has also confirmed the broadness of foveal footprint which has a maximum average length of 12.6 mm [13]. Thus, it is reasonable and logical to propose an arthroscopic "ligament-specific" repair for TFCC foveal avulsion, in which the dorsal and volar limbs of the TFCC are repaired to their separate insertion over the fovea. This "ligament-specific" repair technique allows the restoration of the normal anatomy and physiology of the TFCC.

91.1.1 Surgical Anatomy

Anatomically, the triangular fibrocartilage complex consists of the radioulnar ligaments, ulnolunate ligament, ulnotriquetral ligament, meniscus homolog, disc proper, and ulnar collateral ligament (UCL). Meniscus homolog, ulnolunate, and ulnotriquetral ligaments together form a hammock-like structure in the distal aspect of the TFCC. Functionally, the TFCC consists of two main components: the proximal component and the distal component, which includes the UCL and

B. Liu (✉)
Department of Hand Surgery, Beijing Jishuitan Hospital, Beijing, China

M. Arianni
Hand Clinic, Ramsay Premier Bintaro Hospital, Tangerang, Indonesia

© ISAKOS 2022

D. N. Bhatia et al. (eds.), *Arthroscopy and Endoscopy of the Elbow, Wrist and Hand*,
https://doi.org/10.1007/978-3-030-79423-1_91

the distal hammock structure [2]. Ulnar collateral ligament is perhaps a misnomer as it is not a true ligament nor an entity that is distinct from the floor of the ECU sheath [14, 15]. The proximal component consists of the volar and dorsal radioulnar ligaments. Indeed, these are the true ligaments of the TFCC, which contribute most to distal radioulnar joint stability. The radioulnar ligaments have two origins: the fovea and the ulnar styloid [16]. The area of foveal origin (foveal footprint) is much wider than that of the ulnar styloid origin [13]. Foveal avulsion of the TFCC will compromise stability, and thus surgical treatment is aimed at restoring the foveal attachment. The technique described below restores separately the dorsal and volar foveal attachments of the radioulnar ligament, in order to better emulate the anatomy and physiology of the TFCC.

91.2 Indications and Contraindications

This technique is indicated in a symptomatic foveal avulsion of the TFCC that is not responsive to conservative management.

It is contraindicated in the presence of an irreparable tear, DRUJ arthritis, proximal radioulnar joint instability, distal radius malunion, ulnar head dysplasia, rheumatoid arthritis and other destructive inflammatory conditions, and active joint infection.

91.3 Surgical Technique

The patient is positioned supine, under general or regional anesthesia, with the hand suspended in a 5–7 kg traction and countertraction. Exsanguination is routinely performed before tourniquet inflation.

91.3.1 Diagnostic Arthroscopy

The 3-4 portal is created for arthroscope placement, and the 6R portal serves as a working portal. The ulnocarpal joint is frequently obscured by abundant synovitis. Synovectomy is carefully performed with a shaver in the 6R portal. It is important to determine the reparability of the TFCC. Irreparable TFCC appears frayed and thin. It does not have the bulkiness and elasticity of a healthy (though torn) TFCC, and its edges do not reach the foveal area when pulled with a grasper. When TFCC is deemed irreparable, reconstruction is the option. The diagnosis of TFCC foveal avulsion is confirmed with 3 tests: hook test, suction test, and ghost test. To perform the hook test, a probe at the 6R portal is directed toward the prestyloid recess to hook up the ulnar-most part of the TFCC. A *hook test* is considered positive when the TFCC can be pulled upward and radially by the probe. To perform the *suction test*, a shaver is inserted into the 6R portal and placed over the TFCC. The suction is then switched on and off. Suction test is considered positive when the TFCC is seen "sucked" toward the shaver tip. To perform the *ghost test*, a needle is inserted into a point proximal to the TFCC so that it lies beneath the TFCC. In the presence of TFCC foveal avulsion, the TFCC can be seen rising as it is being lifted by the invisible needle tip. These three tests are useful later to confirm the quality of the repair. In preparation for the transosseous repair, the foveal area is debrided with a shaver or burr. This is done to clear the repair area from fibrous tissue, that may impair healing, as well as to create some bleeding points, that will enhance healing.

91.3.2 Creation of Transosseous Tunnels

The next step is to make a 1–2 cm dorsoulnar incision on the distal ulna in order to create transosseous tunnels. Through this incision, two tunnels are drilled from the distal ulnar metadiaphysis to the fovea (namely the dorsal tunnel and central tunnel) with K wires. To determine the K wire trajectory or direction, we employ two 21G needles as guides.

The first guide needle is inserted into the ulnocarpal joint through the distal end of the previously made incision and aimed toward the

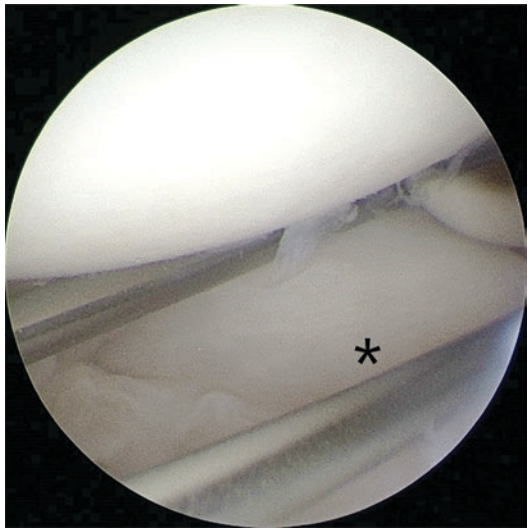

Fig. 91.1 Arthroscopic photograph of dorsal(*) and volar guide needles over the dorsal and volar limbs of the TFCC, respectively

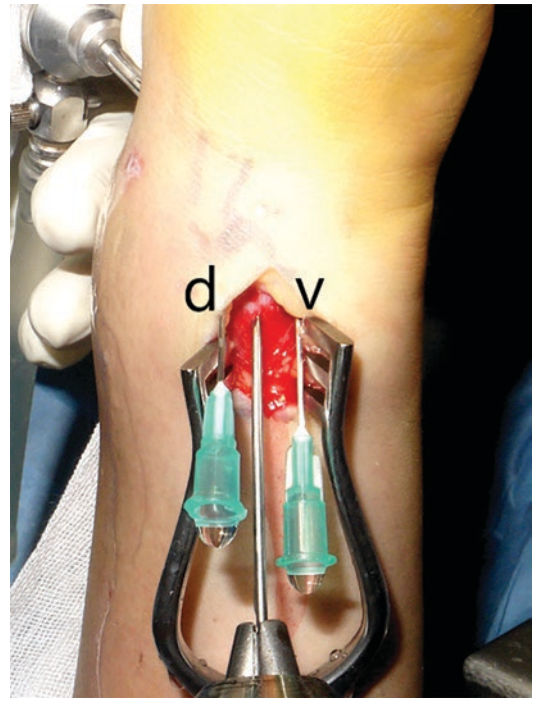

Fig. 91.2 Dorsal guide needle (d) and volar guide needle (v) are in their positions, providing dorsal-palmar orientation to the surgeon of where the K wire entry point should be. In this photograph, the dorsal tunnel is being drilled with a K wire at a point approximately 1 cm proximal to the ulnar head

dorsal aspect of the TFCC. This needle serves to guide the trajectory of the K wire that will drill the dorsal tunnel. The arthroscope, viewing from the 3-4 portal, confirms the location of the needle tip, which should hover over the dorsal aspect of the TFCC (Fig. 91.1). The second guide needle is the volar guide needle, which serves to guide the creation of the central tunnel. It is inserted into the ulnocarpal joint through a point volar to the ulnar styloid, equivalent to the direct foveal portal, and directed to lie above the volar aspect of the TFCC (Fig. 91.1). When these two needles are correctly placed, they provide an orientation to the direction of the tunnels (Fig. 91.2). Dorsal tunnel should not be drilled at a point more dorsal than the dorsal guide needle, and the central tunnel should not be drilled more volar than the volar guide needle.

91.3.3 Creation of Transosseous Tunnels

Dorsal tunnel is drilled with a 1.0 or 1.2 mm K wire from a point approximately 1 cm proximal to the ulnar head (Fig. 91.1). The K wire is directed distally and radially toward the dorsal aspect of the fovea. Since drilling may take several attempts, it is best not to let the K wire penetrate the TFCC substance to avoid mid-substance tear. The K wire should merely bulge beneath the TFCC, as in the ghost test. After obtaining the correct placement of the K wire, the tunnel is overdrilled with a larger K wire (1.5 mm). This diameter will accommodate two 2-0 sutures for the repair later. Similarly, the central tunnel is drilled from a point approximately 1.5 cm proximal to the tip of the ulnar styloid, in the same plane as that of the volar guide needle, 4–5 mm volar to the dorsal tunnel entry point. The K wire should emerge at a point 2–3 mm radial to the prestyloid recess. Like the dorsal tunnel, the central tunnel is overdrilled with a 1.5 mm K wire.

91.3.4 Creation of Transosseous Mattress Sutures

To reattach the TFCC onto the fovea, two sutures (dorsal mattress suture and volar mattress suture) are created. To place the dorsal mattress suture, a 21G needle bearing a looped 3-0 or 4-0 monofilament suture (nylon/polypropylene/polydioxanone) is inserted into the dorsal tunnel and pushed until it penetrates the TFCC. Another 21G needle, also bearing a similar looped suture, is inserted into the central tunnel and pushed to penetrate the TFCC. Both looped sutures are then retrieved from the 6R portal. Care is taken not to pull the entire sutures. A 2-0 polyester suture is passed into both loops outside the 6R portal (Fig. 91.3). This is the suture that will reattach the TFCC back to the fovea. The two looped sutures (now bearing the 2-0 polyester suture) are pulled back into the tunnels by pulling their ends that are hanging loose at the tunnel entries simultaneously until the polyester suture ends come out of the tunnels (Fig. 91.4). This creates the dorsal mattress suture for fixing the dorsal aspect of the TFCC (Fig. 91.5).

The volar mattress suture is created in a slightly different way (Fig. 91.5). A 21G needle loaded with a looped 3-0 or 4-0 monofilament suture is passed into the central tunnel. Another needle loaded with a looped suture is inserted into a point volar to the ulnar styloid base (which is equivalent to the direct foveal portal), slightly more proximal than the volar guide needle, and pushed to penetrate the volar aspect of the TFCC. Both the looped monofilament sutures are retrieved from the 6R portal. Outside the 6R portal, a 2-0 polyester (Ethibond) suture is passed into both loops (Fig. 91.6). The loops are pulled back, carrying the polyester suture. Now the second polyester suture has fixed the volar aspect of the TFCC. Final configuration of transosseous sutures is shown in Fig. 91.7. Each of the dorsal and volar sutures is then tied into knots with the wrist in slight supination. The wrist must thus be maintained in slight supination until cast or splint is applied.

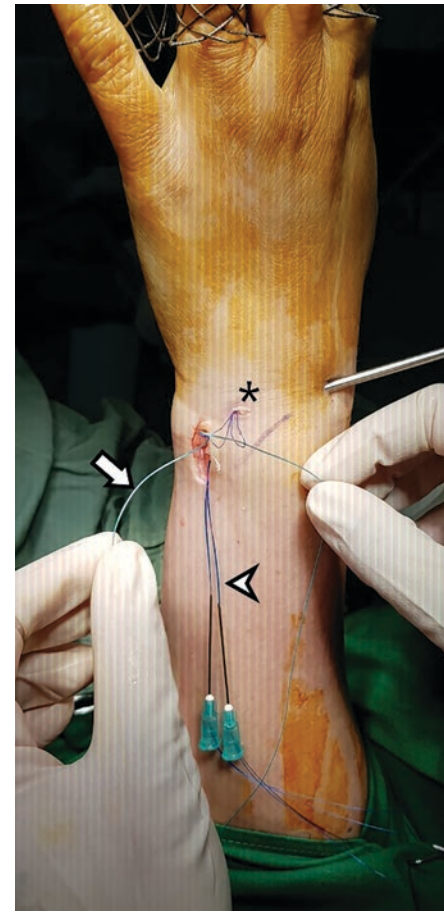

Fig. 91.3 Photograph of transosseous repair on the left wrist. The arthroscope is viewing from the 3-4 portal. *Shows the 6R portal, from which the two looped monofilament sutures have been retrieved *arrow*: 2-0 Ethibond suture is passed into both looped sutures just outside the 6R portal *arrowhead*: the proximal end of the two looped monofilament sutures hanging on the dorsal and central tunnels of the left distal ulna

91.4 Tips and Tricks

Creating transosseous tunnels with the right trajectory requires a period of learning curve. Some surgeons make the tunnel entry points more than 2 cm proximal to the ulnar styloid, directing the K wire to the fovea in a small inclination angle from the ulnar shaft. The proximal entry points make the drilling rather difficult. Tunnel entry point 1 to 1.5 cm proximal to the ulnar styloid will allow easier K wire

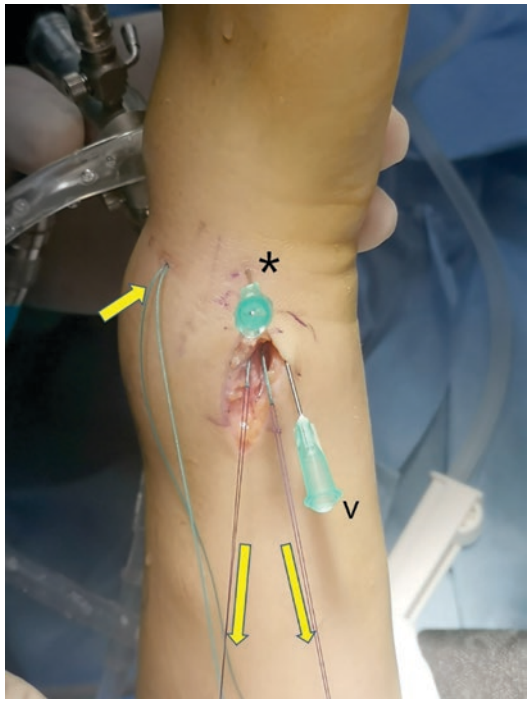

Fig. 91.4 The 2-0 polyester suture, which is creating the dorsal transosseous suture in this photograph, is being pulled into the joint through the 6R portal (short arrow), by the two looped monofilament sutures (long arrows) that have hung on the dorsal and central transosseous tunnels. (*needle for outflow of irrigation fluid *v:* volar guide needle)

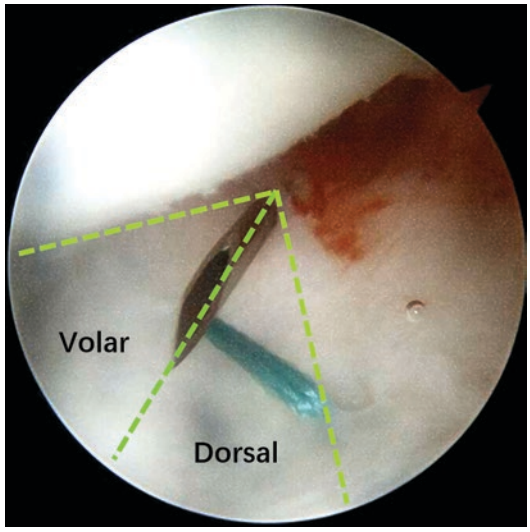

Fig. 91.5 Photograph of dorsal mattress suture fixing the dorsal limb of TFCC, as viewed from the 3-4 portal. The needle serves as the volar guide needle. The dorsal guide needle has been removed

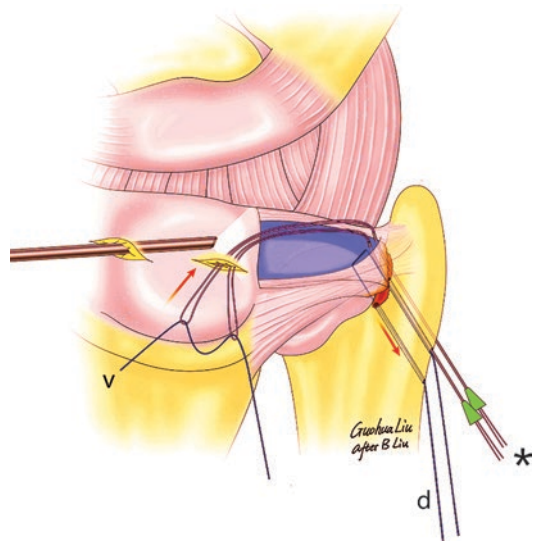

Fig. 91.6 Illustration of the creation of transosseous suture on the right wrist. The dorsal mattress suture (d) has been made. Two needles (*) bearing two looped sutures are in the central tunnel and the direct foveal portal. The looped sutures, having been retrieved from the 6R portal, are carrying the 2-0 Ethibond suture that is going to be the volar mattress suture (v)

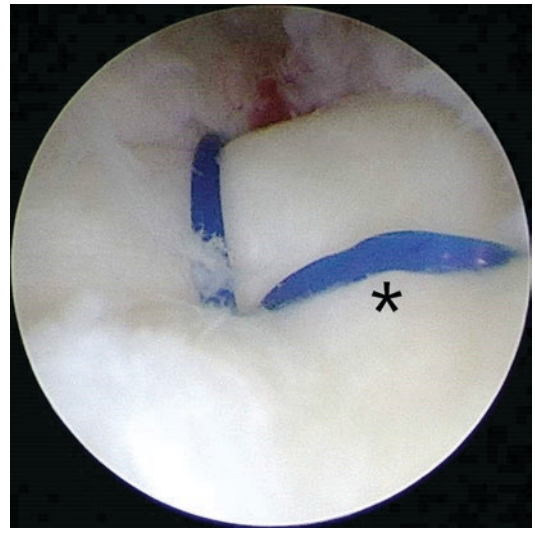

Fig. 91.7 Arthroscopic photograph of dorsal and volar transosseous (monofilament, nonabsorbable) sutures on the TFCC. *Shows the dorsal transosseous suture fixing the dorsal limb of the TFCC of the right wrist

aiming. In the author's experience, the guide needles do the trick in aiming the K wires correctly to the dorsal and volar aspects of the TFCC.

91.5 Pitfalls

A common pitfall is repeated penetration of the TFCC with K wires, resulting in mid-substance tear and less tissue purchased by the mattress sutures. Repeated, excessive drilling may result in iatrogenic fracture of the distal ulna. Such a case however is rare. When creating mattress sutures, both looped sutures must be retrieved simultaneously from the 6R portal. Retrieving the looped suture one by one may cause the mosquito forceps to create two different capsular holes. The polyester suture will be obstructed by the small tissue impinged between the two capsular holes. Prolonged procedure with wet arthroscopy results in edema that obscures visualization. If one prefers wet to dry arthroscopy, periodic (not continuous) saline irrigation is necessary.

91.6 Postoperative Management and Rehabilitation

The wrist is immobilized in a sugar-tong cast or splint for 3–4 weeks, in a neutral position or slight supination. After the third or fourth postoperative week, the patient is allowed to remove the splint 4–5 times a day for gradual flexion-extension exercise. Gentle pronation-supination exercise that does not exceed 45 degrees is also allowed. After the sixth postoperative week, the splint is discarded, and the patient is encouraged to perform more aggressive wrist motion exercise.

91.7 Complications

Complications specifically arising from transosseous repair include iatrogenic fracture of the distal ulna, injury to the dorsal cutaneous branch of the ulnar nerve, iatrogenic tear of the TFCC from repeated K wire or needle penetrations, stiffness, and residual ulnar-sided wrist pain.

References

1. Nakamura T, Sato K, Okazaki M, Toyama Y, Ikegami H. Repair of foveal detachment of the triangular fibrocartilage complex: open and arthroscopic transosseous techniques. Hand Clin. 2011;27:281–90.
2. Atzei A. New trends in arthroscopic management of type 1-B TFCC injuries with DRUJ instability. J Hand Surg Eur. 2009;34:582–91.
3. Atzei A, Luchetti R. Foveal TFCC tear classification and treatment. Hand Clin. 2011;27:263–72.
4. Atzei A, Luchetti R, Braidotti F. Arthroscopic foveal repair of the triangular fibrocartilage complex. J Wrist Surg. 2015;4:22–30.
5. Fujio K. Arthroscopic management of triangular fibrocartilage complex foveal injury. Hand Clin. 2017;33:619–24.
6. Chen WJ. Arthroscopically assisted transosseous foveal repair of triangular fibrocartilage complex. Arthrosc Tech. 2017;6(1):e57–64.
7. Shinohara T, Tatebe M, Okui N, Yamamoto M, Kurimoto S, Hirata H. Arthroscopically assisted repair of triangular fibrocartilage complex foveal tears. J Hand Surg Am. 2013;38:271–7.
8. Iwasaki N, Minami A. Arthroscopically assisted reattachment of avulsed triangular fibrocartilage complex to the fovea of the ulnar head. J Hand Surg Am. 2009;34:1323–6.
9. Park JH, Kim D, Park JW. Arthroscopic one-tunnel transosseous foveal repair for triangular fibrocartilage complex peripheral tear. Arch Orthop Trauma Surg. 2018;138(1):131–8.
10. Abe Y, Fujii K, Fujisawa T. Midterm results after open versus arthroscopic transosseous repair for foveal tears of triangular fibrocartilage complex. J Wrist Surg. 2018;7(4):292–7.
11. Lee SK, Song YD, Choy WS. Correlation between dorsovolar translation and rotation of the radius on the distal radioulnar joint during supination and pronation of forearm. Acta Orthop Belg. 2015;81:511–22.
12. Omokawa S, Iida A, Kawamura K, et al. A biomechanical perspective on distal radioulnar joint instability. J Wrist Surg. 2017;6:88–96.
13. Shin WJ, Kim JP, Yang HM, Lee EY, Go JH, Heo K. Topographical anatomy of the distal ulna attachment of the radioulnar ligament. J Hand Surg Am. 2017;42:517–24.
14. Palmer AK, Werner FW. The triangular fibrocartilage complex of the wrist – anatomy and function. J Hand Surg. 1982;6(2):153–62.
15. Benjamin M, Evans EJ, Pemberton DJ. Histological studies on the triangular fibrocartilage complex of the wrist. J Anat. 1990;172:59–67.
16. Nakamura T, Takayama S, Horiuchi Y, Yabe Y. Origins and insertions of the triangular fibrocartilage complex: a histological study. J Hand Surg Brit Eur Vol. 2001;26B(5):446–54.

92 Arthroscopic-Assisted TFCC Reconstruction with Tendon Graft for Chronic DRUJ Instability

Michael Chu-kay Mak, Wing-lim Tse, and Pak-cheong Ho

92.1 Background

The palmar and dorsal radioulnar ligaments (RULs) are considered the most important primary stabilizers of DRUJ. Damage to either or both of these ligaments generates pain and instability during forearm rotation. Extensive biomechanical study performed by Adams et al. suggested anatomical reconstruction of RULs as the ultimate solution for chronic painful DRUJ instability. Arthroscopic reconstruction has advantages of minimizing soft tissue disruption and allows more accurate placement of bone tunnels. Arthroscopic-assisted anatomical reconstruction of TFCC using tendon graft is the senior author's preferred treatment option in symptomatic peripheral destabilizing TFCC lesions not amendable for repair either due to its chronicity or presence of sizable defect. The method preserves better pronosupination motion of the forearm compared to open surgery.

92.1.1 Surgical Anatomy

The TFCC is an evolutionary and unique anatomical structure that, together with the regression of the ulnar styloid and a direct ulnocarpal articulation, facilitates arm swinging in higher primates and eventually allows the development of the prehensile hand in the human. It is a composite structure consisting of confluent ligamentous, fibrous, and fibrocartilaginous elements. It functions as a unit to stabilize the distal radioulnar joint (DRUJ), transmit load from the carpus, stabilize the carpus to the ulna, and allow smooth wrist motion and forearm rotation [1]. The work of Palmer and Werner in 1981 [2] coined the term of this structure and was instrumental in redefining our understanding of the different parts and roles of this complex. The DRUJ is an inherently incongruent joint and relies mainly on soft tissue structures for its stability, of which the TFCC is the primary intrinsic stabilizer [3]. Sectioning of the TFCC causes gross disruption in DRUJ stability even in the presence of intact DRUJ capsule and pronator quadratus [2], resulting in dorsal DRUJ dislocation in all forearm positions and volar dislocation in neutral and supination. The exact constituents of the TFCC differ among anatomical studies and disagreements exist, but according to Palmer's original description and subsequent study on classification [2, 4] these include the articular disc, the meniscus homolog, the volar and dorsal distal radioulnar ligaments, the subsheath of the extensor carpi ulnaris, the ulnar collateral ligament, and the ulnolunate and ulnotriquetral ligaments [2, 5]. In particular, within the TFCC, the volar and dorsal radioulnar ligaments were established as the pri-

M. C.-k. Mak · W.-l. Tse · P.-c. Ho (✉)
Department of Orthopaedics and Traumatology, Prince of Wales Hospital, Chinese University of Hong Kong, Hong Kong SAR, China
e-mail: pcho@cuhk.edu.hk

© ISAKOS 2022

D. N. Bhatia et al. (eds.), *Arthroscopy and Endoscopy of the Elbow, Wrist and Hand*,
https://doi.org/10.1007/978-3-030-79423-1_92

mary stabilizers during forearm rotation by multiple studies [5–8]. The radioulnar ligaments are inserted into the fovea and the ulnar styloid, with the foveal fibers being critical for stability [9]. This difference in insertion helps to explain the phenomenon where in pronation, the superficial dorsal and deep palmar fibers of the distal radioulnar ligaments become taut; whereas in supination, the superficial palmar and deep dorsal ligaments become taut [6, 7, 10]. On the other hand, the articular disc proper has a less important role in stabilizing the DRUJ and can be excised up to two-thirds without significant kinematic change [11]. Rather, it functions as a cushion for load transmission. Functionally, Nakamura [12] separated the TFCC into three parts, each suspending the others: a distal hammock-like portion which supports the ulnar carpus; a proximal triangular ligament complex, consisting of the radioulnar ligaments that stabilize the radius and ulna; and the ulnar collateral ligament. The ulnar collateral ligament was not considered a true ligament but a complex including loose connective tissue that might deform and twist with pronosupination [12], and this was considered by Palmer a part of the TFCC as it was confluent and not separate and distinct [2].

The pattern of blood supply of the TFCC shows similarity to that of the meniscus of the knee. Thiru-Pathi et al. (5) showed that only the outer 15–20% of the articular disc was vascular while Bednar et al. (7) reported that the vascularity of the TFCC was limited to the peripheral 10–40%. The feeding vessels are branches from the ulnar and anterior interosseous arteries. The radial and central portion of the TFCC receive nutritional support from synovial fluid. Therefore, peripheral tears are considered to have predictable healing potential in contrast to central tears which in general do not.

92.1.2 Pathomechanism of TFCC Injury

TFCC injury is the most common cause of ulnar wrist pain [13, 14]. A systematic review reported a prevalence of TFCC abnormalities in symptomatic wrists ranging from 39% to 70% in patients between 50 and 69 years old [15]. The mechanism of injury commonly involves abrupt forceful rotation, loading, and distraction injury to the ulnar wrist and forearm [16, 17], or wrist hyperextension with forearm rotation. This frequently occurs in a fall on the outstretched upper extremity particularly when falling to the side or backward. Patients with ulnar plus variance may also be more prone to injury due to the thinner TFCC or increased loading to the ulnocarpal joint [4]. The mechanism of injury was correlated to the configuration of the TFCC tear [17], and the most common mode of injury involved forced wrist extension causing excessive traction of the ulnocapitate ligament which in turn avulsed the deep palmar radioulnar ligament from its foveal insertion [18]. The second most common mechanism of injury was forceful rotation, in which hyperpronation was suggested to result in an injury of the superficial dorsal radioulnar ligament followed by foveal fibers. Degenerative tears, which commonly result in attrition and perforation of the TFCC, were suggested to be caused by chronic repetitive loading of the wrist [4] particularly in ulnar deviation and pronation and were closely associated with positive ulnar variance [2]. However, it has to be noted that articular disc perforations are very common, occur in a linear relationship with age, and are usually asymptomatic [2].

92.1.3 Clinical Assessment of TFCC Tear

The mechanism of injury as described above is a useful clue to the diagnosis. There may be a "pop" sound with TFCC injury. Symptoms include ulnar wrist pain on rotation with or without loading, decreased range of motion, instability, weakness, and joint clunk. Chronicity and the presence of a preexisting injury are noted. Physical signs are important to diagnose the site(s) of injury, help determine the type of lesion within the TFCC, and judge severity of instability. These include prominence of the ulnar head and local tenderness corresponding to specific lesions. An obvious deformity at distal radius

usually suggests distal radius malunion as main cause of DRUJ instability rather than soft tissue or ligament pathology. A systematic palpation is needed to assess all common tender sites including the DRUJ dorsal capsule, extensor carpi ulnaris tendon, dorsal TFCC, the ulnar snuff box, or foveal area [19], which is the interval between the ulnar head, triquetrum, flexor carpi ulnaris, and extensor carpi ulnaris tendons; ulnocarpal joint, lunotriquetral ligament, and pisotriquetral joint. Instability is detected by the following provocative test:

- The piano key test is first performed with the hand resting on the table, and a positive sign indicates overt instability of the DRUJ [20].
- Passive pronosupination, which stretches and tightens different parts of the TFCC, is usually painful and reduced in range in peripheral TFCC tear.
- The DRUJ ballottement test is done in neutral, supination, and pronation. In the neutral position, there is normally 5.5 mm (range 3–9 mm) of dorso-volar translation of the DRUJ due to the inherent joint configuration [21]. It is at the most stable locked position in maximal pronation and supination, and any translation should be regarded as abnormal. Furthermore, in full pronation, pain or instability elicited by dorsal push of the ulnar head relative to the radius indicates tear of the deep palmar radioulnar ligament; whereas in full supination, pain or instability elicited by volar push of the ulnar head indicates tear of the deep dorsal radioulnar ligament.
- The ulnocarpal ligament stress test is performed with the forearm in neutral rotation and the wrist in radial deviation, in which the ulnar head is balloted in the volar-dorsal direction similar to the DRUJ ballottement test. Normally in radial deviation the DRUJ becomes more stable by virtue of the taut ulnocarpal ligaments [22]. Any abnormal increase in translation of the DRUJ on ballottement indicates ulnocarpal ligament tear.
- The pisotriquetral shear test is performed by applying a radially directed force onto the pisiform while ulnarly deviating the wrist. It is painful in TFCC injury because of ligamentous connections from the pisiform to the TFCC.
- Resisted forceful supination and pronation, eliciting pain and weakness, is a sensitive test to detect instability in the carpus and DRUJ and not specific to DRUJ instability. However, a relief in pain by reducing any dorsal subluxation of the ulnar head with a volarly directed force during resisted pronation suggests that a peripheral TFCC tear is likely.

Postero-anterior and lateral radiographs of the wrist with the forearm in neutral rotation is part of routine assessment. Magnetic resonance arthrography is a useful modality to diagnose TFCC tears and concomitant injuries, and with wrist traction applied, has an accuracy of TFCC tear detection of 98% [23].

92.2 Indications and Contraindications

Initial management of the TFCC injury depends on chronicity, the extent of instability, and ulnar variance. Acute TFCC injuries have good potential for healing. Therefore, in acute injury in which the DRUJ instability is dynamic or reducible, conservative treatment with a sugar tong splint is given to prevent forearm rotation and to maintain the DRUJ in a stable position from 4 to 6 weeks. If there are persistent symptoms from DRUJ instability upon completion of conservative treatment, surgical assessment and repair are then indicated. Traumatic TFCC injuries were classified according to the anatomical sites by Palmer [4] and the ulnar 1B tear was subclassified by Atzei [24] into distal and proximal to guide surgical treatment. Chronic TFCC injuries however have impaired healing potential and are more difficult to be repaired surgically. Failure to reattach the TFCC to the foveal footprint may induce synovitis due to bathing in synovial fluid. The synovitis in return inhibits the healing of the foveal fibers, setting up a vicious cycle and promotes the persistence of painful DRUJ instability [25]. Surgical results are optimal for injuries that

occur within 6 months, and for those that occurred more than 1 year, outcomes become unpredicTable. Arthroscopic assessment is therefore essential in judging the reparability of a chronic tear. Under direct visualization and probing, the condition of the TFCC torn end is assessed to determine if it is fibrotic and degenerated, retracted with loss of tissue pliability, or frayed with thin and friable scar tissue. These commonly appear in a neglected chronic injury, a massive tear in which the torn ends are gapped, or a poorly healed injury after conservative treatment or previous surgical repair. In these situations, the radioulnar ligaments are no longer able to be reapproximated to their foveal attachment and TFCC reconstruction with tendon graft is indicated. However, the presence of any skeletal malalignment that may be responsible for DRUJ instability has to be sought out and addressed, which include a significant ulnar positive variance, malunion of the sigmoid notch causing incongruence of the DRUJ, dorsal tilting and coronal shift of the distal radius, and shortening or angular deformity of the radius. Osteoarthritis of the DRUJ and an axial instability of the forearm due to interosseous membrane injury are contraindications to TFCC reconstruction. Therefore, skeletal alignment, the cartilage condition of the DRUJ, and axial stability of the forearm have to be addressed before TFCC reconstruction is contemplated.

Various methods of TFCC reconstruction have been described in the literature, which fall into the categories of a direct extra-articular radioulnar tether [26], an indirect stabilization via an ulnocarpal sling [27, 28], or reconstruction of the radioulnar ligaments [29, 30]. The first two categories are largely historical as the anatomical axis of rotation is not restored. The reconstruction method of Scheker [30] involves two separate tendon grafts to reconstruct the dorsal and volar distal radioulnar ligaments anatomically but requires separate bone tunnels and substantial dissection on volar and dorsal sides. Adams and Berger described an anatomical reconstruction that restored the radioulnar ligaments and their insertion into the fovea [29], utilizing a single graft which could be tensioned uniformly, and that passed through the ulna at the foveal insertion site. This has since been widely used and is currently the most established method of reconstruction [31, 32]. Based on this concept of anatomical reconstruction, we have modified this open method and used an arthroscopic-assisted technique since 2000 [33, 34]. The major advantage of an arthroscopic technique is its minimal invasiveness obviating the need for an open capsulotomy of the original method. This allows early mobilization and minimizes soft tissue scarring, fibrosis, and stiffness. Also, under a direct and magnified arthroscopic view, the foveal footprint is precisely identified, allowing accurate creation of the bone tunnel and isometric placement of the graft. It also allows a thorough assessment of concomitant intra-articular pathologies and earlier rehabilitation due to preservation of soft tissue integrity. The surgical technique of arthroscopic-assisted TFCC reconstruction is described below.

92.3 Surgical Technique

The aim of this surgery is to reconstruct the distal radioulnar ligaments using a single tendon graft passing through 3 bone tunnels, using a surgical approach by arthroscopy and 3 extra-articular incisions (Fig. 92.1a–h).

92.3.1 Set Up and Instruments

The surgery is performed under general anesthesia or brachial plexus block. With the muscles relaxed, the stability of the DRUJ is assessed with a ballottement test comparing with the other side, as a baseline. The patient is positioned supine with longitudinal wrist traction of 10–12Lbs. A tourniquet is applied over the arm. Instruments employed include:

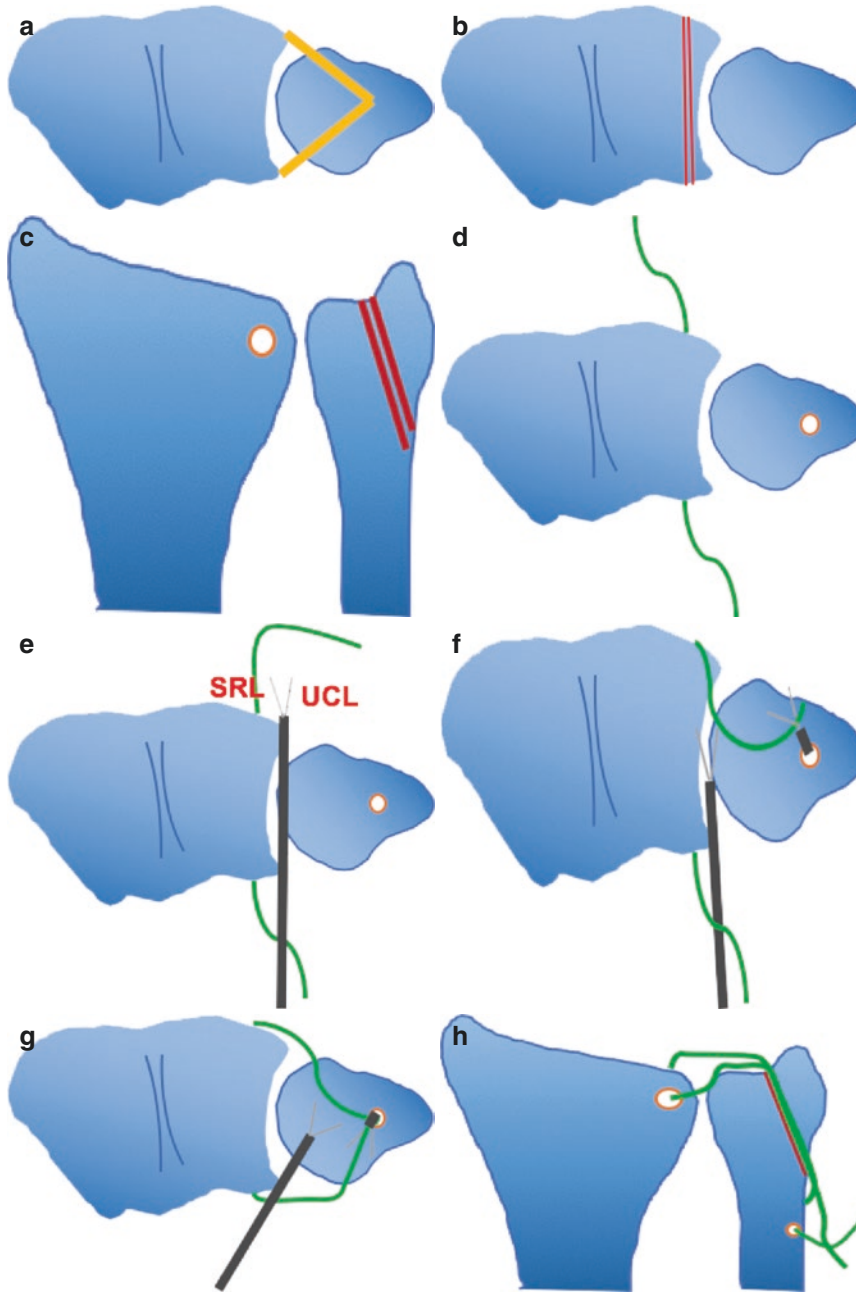

Fig. 92.1 Surgical steps of the procedure are shown: (**a**) The original concept of anatomical reconstruction restores the volar and dorsal radioulnar ligaments and their insertion into the fovea. (**b**) A bone tunnel is created in the ulnar aspect of the distal radial metaphysis. (**c**) A second bone tunnel is created in the ulna from 1.5–2 cm proximal to the ulnar styloid to the center of the fovea, under arthroscopic verification. (**d**) A grasper is introduced into the radial tunnel and the tendon graft is passed into it from volar to dorsal. (**e**) A grasper is introduced from the 4-5 portal through a capsular window between the short radiolunate and ulnolunate ligaments. (**f**) The volar limb of the tendon graft is retrieved into the joint and passed into the ulnar tunnel to the exterior by a second grasper. (**g**) The dorsal limb is pushed into the joint through the 4-5 portal and passed into the ulnar tunnel. (**h**) A third transverse bone tunnel is made 1 cm proximal to the oblique tunnel in the ulna, one limb of the graft is passed through the tunnel, and tied to the other limb in a shoelace manner

- 1.9 mm or 2.7 mm arthroscope
- Motorized full-radius shaver (2.0/2.9 mm) and radiofrequency probe.
- Powered instrument including cannulated drills.
- 2 mm arthroscopic graspers and suction punch
- Fluoroscopic image intensifier.

Step 1: Wrist arthroscopy and TFCC central opening preparation.

- The surgery starts with assessment of the radio-carpal joint with 3-4 viewing, 4-5 working, and 6-U outflow portals. Associated chondral or ligamentous injuries are documented. The TFCC is assessed for loss of trampoline tension and detachment from foveal insertion with the hook test. Fibrous and excess synovial tissues, which usually form at and obscure the site of chronic tears, are debrided with shaver and radiofrequency ablation to facilitate assessment of the size of the tear and its reparability. A central perforation of the articular disc of the TFCC is desirable for direct exposure of the fovea, which is essential for the accurate drilling of a bone tunnel at the isometric point and the intra-articular passage of the graft. If the articular disc is intact, a central perforation is created with an arthroscopic knife, shaver, or best with a radiofrequency ablation apparatus (Fig. 92.2). If a central tear already exists, the tear is enlarged to 5–6 mm. Any large floppy TFCC flap is debrided until the edge of the TFCC perforation is smooth, the ulnar head is exposed, and there is adequate space for placement of the graft. At this stage, the tear in the radioulnar ligaments should be clearly seen.

Step 2: Harvesting tendon graft.

- The wrist is taken off the traction tower and placed on a hand table. A 2 cm volar longitudinal incision is made midway between palmaris longus (PL) tendon and radial border of flexor carpi ulnaris (FCU) tendon at the level of the proximal wrist crease (Fig. 92.3). The PL tendon is harvested in full length with a tendon harvesting stripper.

Fig. 92.2 Creation of a perforation in the articular disc with radiofrequency

- The flexor tendon mass and median nerve are retracted radially and the FCU tendon, ulnar nerve, and artery are retracted ulnarly to reach the volar surface of the distal radius. The distal border of the pronator quadratus serves as a landmark for the approximate level of the radial tunnel.

Step 3: Radial tunnel preparation with passage of tendon graft.

- A 2 cm dorsal longitudinal incision is made extending proximally from the 4-5 portal (Fig. 92.3). A window is made in the extensor retinaculum over the fourth extensor compartment. The extensor tendons were retracted radially to expose the area just radial to the sigmoid notch. The Extensor Digiti Minimi (EDM) tendon is identified at fifth extensor compartment and is tagged with cotton tape. Under fluoroscopic guidance, a 1.1 mm guide pin is inserted on the dorsal surface of distal radius ideally at 5 mm proximal to the articular surface of lunate fossa and 5 mm radial to the sigmoid fossa with a volar tilt of 10–15° parallel to the surface of the lunate fossa (Figs. 92.1b and 92.4). The correct placement is confirmed on fluoroscopy by anteroposterior and lateral views. Drill sleeves are used at all times during pinning or drilling to prevent

Fig. 92.3 Incisions used in the procedure are shown

catching of soft tissue. Tendons and neurovascular bundles on the volar side are gently retracted by an assistant to ensure that the guide pin exits at the ideal position, which is 5 mm radial to the sigmoid notch edge and just distal to the pronator quadratus. After just protruding from the volar cortex, the tip of the pin should be advanced further only when the assistant has a clear view of it with careful protection of soft tissue (Fig. 92.5). With guide pin position confirmed by fluoroscopy, the tunnel is enlarged to 2.2–2.5 mm in a stepwise manner depending on the caliber of the tendon graft, using cannulated drill bits and appropriate drill sleeves on both entry and exit sites. A K-wire is left in the tunnel to mark its location.

Step 4: Ulnar tunnel preparation.

- A 3 cm longitudinal incision is made over the subcutaneous border of ulna starting 1 cm proximal to the tip of ulnar styloid (Fig. 92.3). The dorsal cutaneous branch of ulnar nerve should be identified and protected appropriately. After subperiosteal dissection and under fluoroscopy, a 1.1 mm guide pin is inserted from the midpoint of the distal ulna at the level of 1.5–2 cm proximal to the tip of ulnar styloid at an acute angle targeting at the fovea of the ulnar head (Fig. 92.4). The angle of insertion is approximately 60° and the direction should be exactly parallel to and along the midline of the ulnar shaft with the forearm in neutral position. Once the entry point is decided, the wrist can be suspended in vertical position and the intra-articular exit site of the guide pin is monitored under arthroscopy to ensure its central position at the fovea at the isometric point of insertion of the TFCC (Fig. 92.6), with further adjustment if necessary. The central part of the fovea is isometric for the TFCC because radioulnar ligaments attached to this point do not change length during pronosupination; therefore, an eccentric bone tunnel may result in loss of rotational motion due to unequal tension of the two limbs of the graft. The ulnar bone tunnel is created by stepwise drilling to 2.9 mm or 3.2 mm under arthroscopic control; a larger

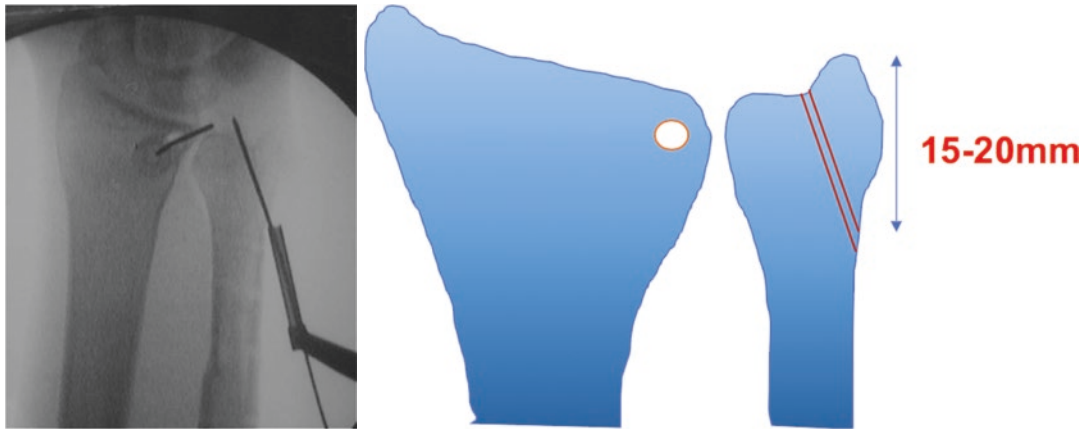

Fig. 92.4 Creation of bone tunnels is shown

Fig. 92.5 Protection of soft tissue and advancement of pin from dorsal to volar aspect is shown

size than the radial tunnel is required since two limbs of the tendon graft will pass through. The tip of the guide pin is held within the joint with a hemostat passing through the 4-5 portal to avoid iatrogenic damage of the articular cartilage of lunate and triquetrum during the drilling process.

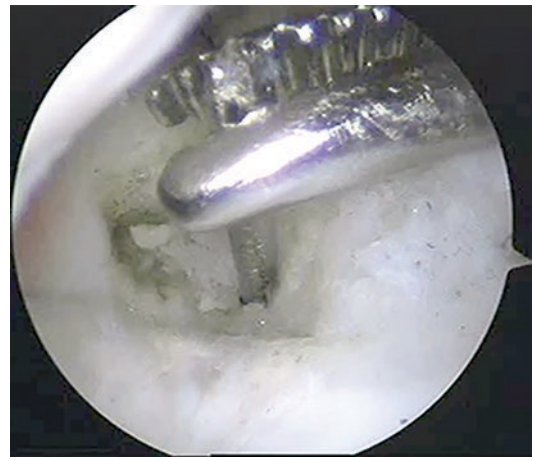

Fig. 92.6 Arthroscopic view of a K-wire inserted into the fovea

Step 5: Passage of tendon graft into radial bone tunnel and volar limb of graft into the joint.

- The tendon graft is passed into the radial bone tunnel by a 2 mm arthroscopic grasper inserted from the dorsal to volar side, pulling the graft from volar and exiting from dorsal, while ensuring no tendon or nerve entrapment during graft passage (Figs. 92.1d and 92.7). The volar limb of the graft is then passed into the joint via a volar capsular window. Under direct visualization at 3-4 portal, a small perforation

Fig. 92.7 Tendon graft in the radial bone tunnel is demonstrated

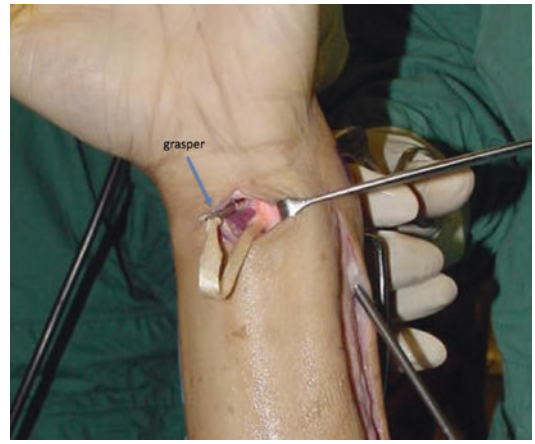

Fig. 92.8 Grasping of the volar limb of tendon graft into the joint

is first created by passing a tapered 2.7 mm trocar through the 4-5 portal, into the joint, and exiting from the volar capsule at the interval between the ulnolunate ligament and short radiolunate ligament. Then a 2 mm arthroscopic grasper is inserted from the 4-5 portal and passed through the volar capsular window to retrieve the volar limb of the PL graft into the joint (Figs. 92.1e and 92.8). Another grasper is inserted into the joint through the ulnar foveal tunnel, receives the volar end of the graft, and delivers the graft through this tunnel to the exterior (Figs. 92.1f and 92.9).

Step 6: Passage of dorsal limb of tendon graft into the joint and out through the ulnar tunnel.

- The tendon is first tied with a strong suture at its end. Using a grasper, the graft with the suture on is then pushed into the joint through the 4-5 portal deep to the extensor tendons (Fig. 92.1g). The surgeon may also use the grasper to directly hold onto the end of the tendon graft. The EDM tendon is retracted to ulnar side to allow a clear path between the dorsal opening of radial tunnel and capsule window of 4-5 portal where no extensor tendon comes across. In a similar fashion as passing the volar limb, under visualization at 3-4 portal the tendon end is pulled outside the ulnar tunnel using a second grasper inserted into the ulnar tunnel. Care is taken to ensure a smooth passage when inserting the grasper into the ulnar tunnel next to the volar limb and not to go through tendon substance or create a split in the graft; this will create difficulty in passing the dorsal limb and damage the graft. The 2 limbs of tendon graft outside the tunnel are secured with a hemostat.
- Alternatively, the volar limb of the tendon graft can be retrieved through the joint dorsally at the 4-5 portal before it goes through the ulnar tunnel. The two ends of the volar and dorsal limbs of graft can be sutured and braided together. The suture end is introduced back to the joint to be grasped by a mini-grasper inserted through the ulnar tunnel. The grasper pulls the suture together with the two ends of the tendon graft in one-go through the tunnel to exit outside the joint. This method avoids splitting of graft when the grasper has

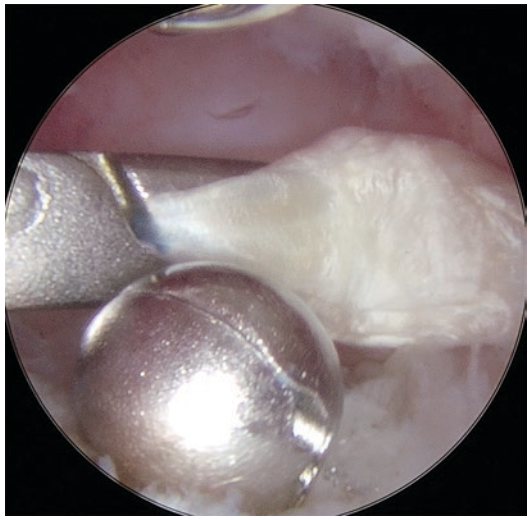

Fig. 92.9 Tendon graft passed into the ulnar tunnel by graspers

to enter through the ulna tunnel where one limb is already inside.

Step 7: Tensioning and tying around the ulnar neck.

- The tendon graft should have a smooth course and uniform tension throughout. Manual tightening of both limbs of the graft should result in a stable distal radioulnar joint upon ballottement. Another transverse bone tunnel is made about 1 cm proximal to the previous oblique tunnel at the distal ulna using a 2.5 mm drill bit (Fig. 92.10). One of the graft limbs is then inserted through the transverse tunnel (Fig. 92.1h) and tied to the other limb of the graft in a shoelace fashion (Fig. 92.11), in maximal tension with the forearm in neutral rotation and tower traction released. A 2-O ethibond suture is used to secure the tendon knot as well as to anchor the graft to the surrounding fascial structures. If the isometric point is attained as the graft position in the ulnar head (Fig. 92.12), full range of passive pronosupination can be obtained without jeopardizing DRUJ stability. The wounds were then closed in layers. Alternatively, both ends of the graft could be fixed inside the ulnar tunnel with a 4 mm interference screw, as described by Atzei [35]. However, the size of the ulnar tunnel needs to

Fig. 92.10 Creation of a transverse ulnar bone tunnel 1 cm proximal to the oblique tunnel

Fig. 92.11 Tendon graft tied in a shoelace manner

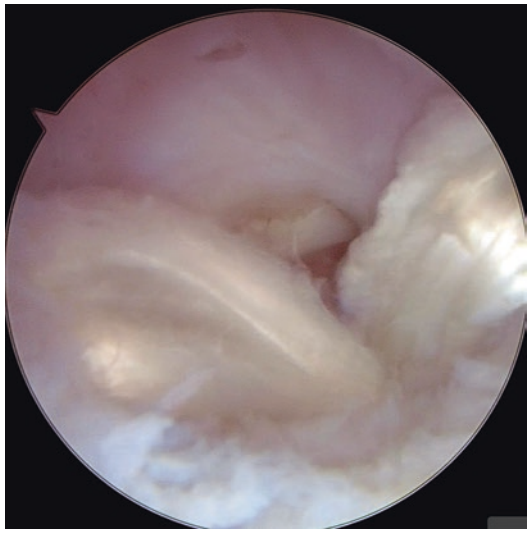

Fig. 92.12 Tendon graft inside the joint at the isometric foveal position

be bigger and this may risk blowout fracture of the ulnar styloid.

92.4 Tips and Tricks

- The surgery requires a reliable assistant to manage and protect the volar sided structures especially neurovascular bundle. Good lighting and loupe magnification are essential.
- Use longitudinal incision for 4-5 portal to facilitate subsequent proximal extension.
- For isolated chronic TFCC foveal avulsion, create a central perforation on TFCC with radiofrequency probe.
- The synovitis in ulnocarpal joint should be cleared and perforation in TFCC should be wide enough to allow direct observation of the fovea region.
- Protect EDM tendon with cotton sling.
- Keeping radial tunnel size under 2.5 mm and ulnar tunnel under 3.5 mm reduces risk of fracture and promote ligamentization.
- Keep radial tunnel 5 mm away from lunate fossa and sigmoid fossa to avoid blowout fracture.
- The radial tunnel should exit volarly just distal to the pronator quadratus muscle. Be careful of the ulnar neurovascular bundle.
- In creating ulnar tunnel, keep forearm in neutral rotation, insert the pin at mid-diaphyseal point, and stay parallel to ulnar shaft targeting at fovea.
- Rotate the forearm to allow the K-wire in distal ulna to exit from fovea through the TFCC perforation.
- Protect the carpal bones when using cannulated drill to create the ulnar tunnel.
- Using 2 mm mini-grasper helps delivering tendon graft through the bone tunnel directly.
- When passing the graft back into the joint, make sure it does not catch or loop on any tendon or nerve.
- Deliver the two ends of the tendon graft either separately through the ulnar tunnel with mini-grasper or simultaneously with tie-and-pull method after braiding the ends together.
- Use a probe to guide the passage of the tendon graft through the ulnar tunnel to avoid jamming.
- Length of PL graft is not long enough to wrap around the ulnar neck. Use transverse osseous tunnel or interference screw to secure the tendon graft instead.
- Tension and knot the graft with the forearm in neutral rotation and tower traction released.
- Check stability of DRUJ and pronosupination at the end of the procedure.

92.5 Pitfalls

- Blowout fracture of sigmoid notch if radial tunnel is too close to joint line.
- Fracture of ulnar styloid if ulnar tunnel too wide or too distal.
- Breakage of K-wire in creating ulnar tunnel if mishandling the motor hand-piece.
- Too radial placement of the ulnar tunnel leads to loss of rotation motion.
- Tendon graft can catch or loop tendon or nerve resulting in motion loss or nerve palsy.
- Too small the ulnar tunnel causes jamming of tendon graft and failure of tensioning.

92.6 Postoperative Management and Rehabilitation

A long arm cast is applied to immobilize the forearm in neutral rotation and elbow in 90° of flexion for 3 weeks. Alternately, a well-molded reversed sugar tong cast with forearm in neutral rotation allowing elbow motion serves the same purpose. A reverse sugar tong removable splint is then given for the next 3 weeks (after day 21). The patient is then advised to perform free active flexion-extension of the wrist and active mid-range rotational motion of forearm out of the splint intermittently under the guidance of physiotherapist. By the seventh week (after day 42) after operation, full range of active pronosupination exercise is permitted. A below-elbow wrist splint is worn at rest for 2 more weeks and then worn only at night for another 3 weeks. Passive range of motion exercise can be initiated by 6–8 weeks after the operation after restoration of stability of the distal radioulnar joint, followed by wrist and grip strengthening exercise.

92.7 Results

A total of 28 patients received arthroscopic-assisted TFCC reconstruction in our center between 2000 and 2016 [32], with an average age of 35 years at operation (ranging 17–58). The average follow-up was 62 months (range 3–138). In all patients, there was a history of injury resulting in chronic symptomatic TFCC injuries with diagnosis confirmed by wrist arthroscopy. There were 16 recalcitrant cases who failed previous surgeries on their affected wrists, 2 patients with history of gouty arthritis other than the wrist, and 2 patients with rheumatoid arthritis and systemic lupus erythematosus respectively at quiescent stage.

Postoperatively, the mean VAS pain score decreased from 5.9 ± 1.5 preoperatively to 3 ± 2.5 postoperatively. Compared with the preoperative range of motion, the mean pronosupination range improved from 85% of the normal side to 91% at the final postoperative assessment, and flexion-extension range improved from 77% to 84%. Mean grip power increased from 59% to 72% of the contralateral non-affected hand at the final assessment. The mean Mayo wrist score was 58% preoperatively and was 79% at the final assessment, with a 36% increase. The scores were excellent or good in 19 patients. Five patients were not able to return to their previous vocations; 4 of these were due to reasons unrelated to the wrist including back pain, severe gouty arthritis, depression, and stroke with hemiplegia, respectively. Radiographic assessment revealed no widening of DRUJ or osteoarthritic changes on latest follow-up. There were consistently sclerotic changes at the radial and ulnar tunnels with no increase in tunnel size. Bony erosion over distal ulna was noted in one patient, likely related to the friction with the tendon knot.

No fracture or tendon injury occurred intraoperatively. There was one case of breakage of K-wire which was removed from the joint. Ulnar nerve entrapment by the tendon graft occurred in one case, resulting in transient complete ulnar nerve palsy. Revision of the tendon graft and ulnar nerve release was performed with full recovery of ulnar nerve function. Two other patients developed transient neurapraxia of the ulnar nerve likely due to excessive retraction of the nerves during operation. Three patients complained of discomfort over ulnar incision due to the graft knot or sensitive scar. There were 4 cases of graft rupture which presented at 10, 12, 14, and 18 months, 2 of these occurred after new injuries. Revision surgery with tendon grafting was performed for two cases.

Adams and Berger reported their outcome of open TFCC reconstruction in 2002 [26]. Pain relief was achieved in 12 out of 14 patients and there were 2 recurrences. The postoperative grip strength reached 85% of the opposite hand and the range of pronation and supination was 90% and 87% compared to the preoperative range. Our results with a less invasive technique were at least comparable with the established open reconstruction, with a possible advantage in restoring range of motion. In our series, the range of pronation was 112% and supination was 109% compared to the preoperative values in our series. This could be attributed to the less invasive nature

of the technique obviating the need for creation of a dorsal DRUJ capsular flap. As a result, motion can be started earlier in our rehabilitation protocol at the fourth week compared to cast immobilization in Adams' series for 6 weeks. An extensive capsulotomy could also result in fibrosis and scarring with reduced range of motion.

References

1. Nakamura T, Yabe Y, Horiuchi Y, Yamazaki N. In vivo motion analysis of forearm rotation utilizing magnetic resonance imaging. Clin Biomech (Bristol, Avon). 1999;14:315–20.
2. Palmer AK, Werner FW. The triangular fibrocartilage complex of the wrist-anatomy and function. J Hand Surg. 1981;6:153.
3. Moritomo H. The distal interosseous membrane: current concepts in wrist anatomy and biomechanics. J Hand Surg. 2012;37(7):1501–7.
4. Palmer AK. Triangular fibrocartilage complex lesions: a classification. J Hand Surg [Am]. 1989;14:594–606.
5. Ishii S, Palmer AK, Werner FW, Short WH, Fortino MD. An anatomic study of the ligamentous structure of the triangular fibrocartilage complex. J Hand Surg. 1998;23(6):977–85.
6. Ekenstam FA, Hagert CG. Anatomical studies on the geometry and stability of the distal radio ulnar joint. Scand J Plastic Reconstruct Surg. 1985;19(1):17–25.
7. Schuind F, An KN, Berglund L, Rey R, Cooney WP, Linscheid RL, Chao EY. The distal radioulnar ligaments: a biomechanical study. J Hand Surg. 1991;16(6):1106–14.
8. Ward LD, Ambrose CG, Masson MV, Levaro F. The role of the distal radioulnar ligaments, interosseous membrane, and joint capsule in distal radioulnar joint stability. J Hand Surg. 2000;25(2):341–51.
9. Haugstvedt JR, Berger RA, Nakamura T, Neale P, Berglund L, An KN. Relative contributions of the ulnar attachments of the triangular fibrocartilage complex to the dynamic stability of the distal radioulnar joint. J Hand Surg. 2006;31(3):445–51.
10. Xu J, Tang JB. In vivo changes in lengths of the ligaments stabilizing the distal radioulnar joint. J Hand Surg. 2009;34(1):40–5.
11. Adams BD. Partial excision of the triangular fibrocartilage complex articular disk: a biomechanical study. J Hand Surg. 1993;18(2):334–40.
12. Nakamura T, Yabe Y. Histological anatomy of the triangular fibrocartilage complex of the human wrist. Ann Anat-Anatomischer Anzeiger. 2000;182(6):567–72.
13. Pidgeon TS, Waryasz G, Carnevale J, DaSilva MF. Triangular fibrocartilage complex. JBJS Rev. 2015;3(1):e1.
14. Sachar K. Ulnar-sided wrist pain: evaluation and treatment of triangular fibrocartilage complex tears, ulnocarpal impaction syndrome, and lunotriquetral ligament tears. J Hand Surg. 2008;33(9):1669–79.
15. Chan JJ, Teunis T, Ring D. Prevalence of triangular fibrocartilage complex abnormalities regardless of symptoms rise with age: systematic review and pooled analysis. Clin Orthop Rel Res. 2014;472(12):3987–94.
16. Lindau T, Arner M, Hagberg L. Intraarticular lesions in distal fractures of the radius in young adults. A descriptive arthroscopic study in 50 patients. J Hand Surg Br. 1997;22(5):638–43.
17. Coleman HM. Injuries of the articular disc at the wrist. J Bone Joint Surg(Br). 1960;42:552–9.
18. Moritomo H, Masatomi T, Murase T, Tanaka H, Miyake J, Yoshikawa H. Open repair of foveal avulsion of the triangular fibrocartilage complex and comparison by types of injury mechanism. J Hand Surg. 2010;35A:1955–63.
19. Tay SC, Tomita K, Berger RA. The "ulnar fovea sign" for defining ulnar wrist pain: an analysis of sensitivity and specificity. J Hand Surg Am. 2007;32:438–44.
20. Morrissey RT, Nalebuff EA. Dislocation of the distal radioulnar joint: anatomy and clues to prompt diagnosis. Clin Orthop. 1979;144:154–8.
21. Nagata H, Giddins G. In-vivo measurement of distal radioulnar joint translation. Hand Surg. 2013;18(1):15–20.
22. Iida A, Omokawa S, Moritomo H, Omori S, Kataoka T, Aoki M, Wada T, Fujimiya M, Tanaka Y. Effect of wrist position on distal radioulnar joint stability: a biomechanical study. J Orthop Res. 2014;32:1247–51.
23. Lee RK, Griffith JF, Ng AW, Nung RC, Yeung DK. Wrist traction during MR arthrography improves detection of triangular fibrocartilage complex and intrinsic ligament tears and visibility of articular cartilage. Am J Roentgenol. 2016;206(1):155–61.
24. Atzei A, Luchetti R, Garagnani L. Classification of ulnar triangular fibrocartilage complex tears. A treatment algorithm for Palmer type IB tears. J Hand Surg Eur Vol. 2017;42(4):405–14. Epub 2017 Jan 30
25. Bain G, McGuire D, Lee YC, Eng K, Zumstein M. Anatomic foveal reconstruction of the triangular fibrocartilage complex with a tendon graft. Techniq Hand Upper Extremity Surg. 2014;18(2):92–7.
26. Fulkerson JP, Watson HK. Congenital anterior subluxation of the distal ulna. A case report. Clin Orthop. 1978;131:179–82.
27. Breen TF, Jupiter J. Tenodesis of the chronically unstable distal ulna. Hand Clin. 1991;7(2):355–63.
28. Tsai TM, Stilwell JH. Repair of chronic subluxation of the distal radioulnar joint (ulnar dorsal) using flexor carpi ulnaris tendon. J Hand Surg (Br). 1984;9(3):289–94.
29. Adams BD, Berger RA. An anatomic reconstruction of the distal radioulnar ligaments for posttraumatic distal radioulnar joint instability. J Hand Surg [Am]. 2002;27(2):243–51.
30. Scheker LR, Belliappa PP, Acosta R, German OS, et al. Reconstruction of the dorsal ligament of the triangular fibrocartilage complex. J Hand Surg (Br). 1994;19(3):310–8.

31. Shih JT, Lee HM. Functional results post-triangular fibrocartilage complex reconstruction with extensor carpi ulnaris with or without ulnar shortening in chronic distal radioulnar joint instability. Hand Surg. 2005;10:169–76.
32. Teoh LC, Yam AK. Anatomic reconstruction of the distal radioulnar ligaments: long-term results. J Hand Surg Br. 2005;30:185–93.
33. Tse WL, Lau SW, Wong WY, Cheng HS, Chow CS, Ho PC, Hung LK. Arthroscopic reconstruction of triangular fibrocartilage complex (TFCC) with tendon graft for chronic DRUJ instability. Injury. 2013;44(3):386–90.
34. Mak MCK, Ho PC. Arthroscopic-assisted triangular fibrocartilage complex reconstruction. Hand Clin. 2017;33(4):625–37.
35. Atzei A, Luchetti R, Borelli PP, Sgarbossa A, Cugola L. Arthroscopic TFCC reconstruction by tendon graft. Rivista di Chirurgia della Mano. 2006b;43:370–6.

Part XIX

Wrist: Fractures and Dislocations

Vascular Anatomy of the Scaphoid and Implications in Surgery

93

Mohamed Morsy and Steven L. Moran

93.1 Background

In addition to its biomechanical role being the link between the proximal and distal carpal rows, the clinical importance of the scaphoid stems from it being the most commonly fractured carpal bone with an incidence of up to 90% of all carpal fractures [1–3]. Moreover, the incidence of avascular necrosis that complicates proximal pole fractures pointed to the peculiarity of the blood supply it receives [4]. The complex bony structure that is over 70% covered with articular cartilage, leaves a limited surface for entry of nutrient vessels [5]. All of these factors urged the scientific community to study the vascularity of such a bone a few decades ago. Gelberman and Menon in their landmark article in 1980 described the extraosseous and intraosseous vascularity of the scaphoid [4]. Although their basic concepts stood the test of time, the classical injection and bone clearing techniques utilized have their shortcomings, and the clinical setting required more details that could be supported by the advanced technological methods developed thereafter. Needs, such as the effect of hardware insertion on the vascularity, the optimal position for screws within the scaphoid bone, the optimal approach to obtain that optimal position, and predictors of the incidence of avascular necrosis, had to be addressed. In a recent study, the authors were able to demonstrate new findings pertaining to intraosseous vascularity by use of some advanced tools as micro-computed tomography scanning (micro-CT), 3D modeling, and 3D printing, [6]. This was performed using a technique devised by the authors team to study carpal vascularity [7, 8].

93.2 Anatomy

The scaphoid bone is the radial most bone of the proximal carpal row, which has a complex anatomy and a noted variation in its shape [9–12]. The scaphoid has been classically divided into proximal pole, waist, and distal pole; the distal pole is marked proximally with the tubercle that extends on the volar side. Another constant anatomical feature of the scaphoid is the dorsoradial ridge, which is a roughened region that extends on the dorsoradial surface of the waist and serves as an area for ligamentous attachment. The scaphoid surface is mostly covered with articular cartilage with designated areas for articulation with the radius, lunate, capitate, trapezium, and trapezoid; this leaves a limited area for entry of nutrient vessels and thereby contributes to the peculiarity of the vascular supply [5].

M. Morsy
Department of Orthopedic Surgery, Assiut University, Assiut, Egypt

S. L. Moran (✉)
Department of Orthopedic Surgery and Division of Plastic Surgery, Mayo Clinic, Rochester, MN, USA
e-mail: moran.steven@mayo.edu

© ISAKOS 2022

D. N. Bhatia et al. (eds.), *Arthroscopy and Endoscopy of the Elbow, Wrist and Hand*,
https://doi.org/10.1007/978-3-030-79423-1_93

93.3 The Extraosseous Blood Supply

Nutrient vessels to the scaphoid primarily come from the radial artery. The volar vessels arise from the radial artery directly or from the superficial palmar branch of the radial artery. These volar vessels enter through the scaphoid tubercle. The dorsal vessels arise from the radial artery directly or from the dorsal carpal branch (Fig. 93.1). Dorsal vessels enter at the dorsoradial ridge. Both the volar and dorsal vessels receive anastomoses from the volar and dorsal divisions of the anterior interosseous artery, respectively [4, 13]. Recently, vessels were described that enter through the volar surface of the waist in some scaphoids (Fig. 93.2). Small-sized vessels have been demonstrated along the scapholunate ligament but have not been found to contribute substantially to the intraosseous vascular network (Fig. 93.3). These vessels were not found to be consistent in all scaphoids [6].

93.4 The Intraosseous Blood Supply

Using 3D rendering, the scaphoids were reconstructed and the vessels within were traced (Fig. 93.4). The scaphoid has two distinct intraosseous vascular networks, a proximal and a distal network (Fig. 93.5). The proximal network supplies an average of 83% of the total volume of the scaphoid. This network is formed primarily by the vessels that enter at the dorsoradial ridge and run proximally to supply most of the waist and proximal pole. The proximal network is augmented in some scaphoids with vessels entering the volar surface at the waist. The distal network supplies an average of 17% of the total volume of the scaphoid and is formed by vessels entering the tubercle. To estimate the contribution of each of these vessels to the vascularity of the scaphoid, a number of quantitative measures have been reported including the number of vessels entering volar or dorsal, diameter and cross-sectional area of these vessels, and analysis according to the

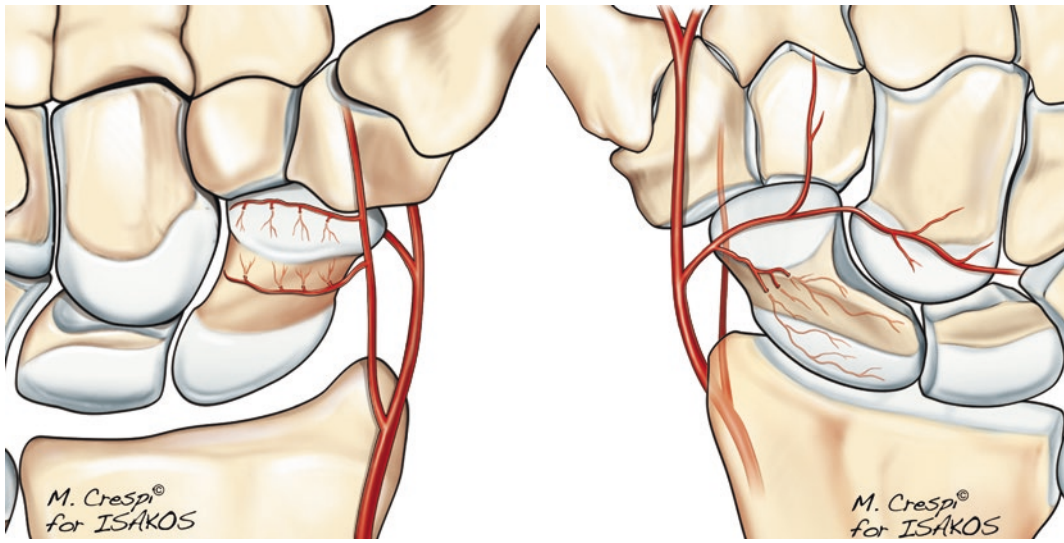

Fig. 93.1 A representation of the extraosseous blood supply to the scaphoid by the volar (left) and dorsal (right) branches

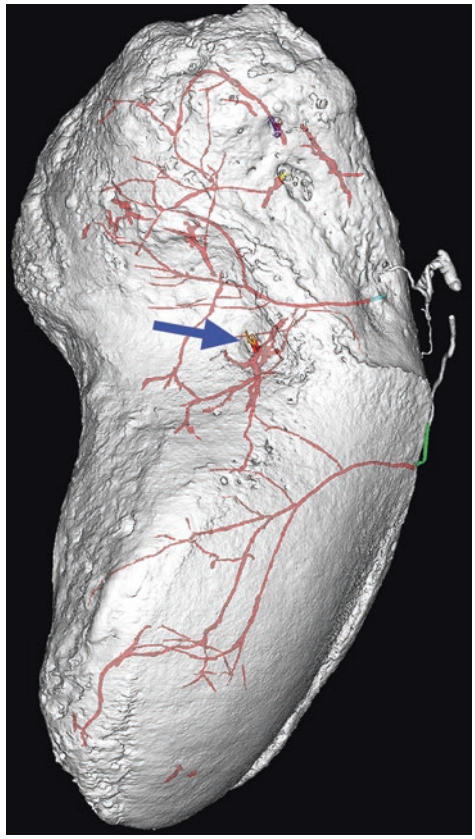

Fig. 93.2 A nutrient vessel entering through the volar waist in some scaphoids (blue arrow) augmenting the proximal intraosseous vascular network. (From Morsy M, Sabbagh MD, van Alphen NA, Laungani AT, Kadar A, Moran SL. The Vascular Anatomy of the Scaphoid: New Discoveries Using Micro-Computed Tomography Imaging. J Hand Surg Am. 2019 Nov;44(11):928-938, with permission)

anatomical location of entry (Table 93.1). These measures proved the dominance of the dorsoradial ridge vessels and stressed on the concept of the retrograde blood supply of most of the scaphoid. Moreover, by dividing the scaphoid into thirds along the long axis, it was found that the middle third had the most abundant vessel entry followed by the distal third and the least was the proximal third. The proximal and distal vascular networks showed a notable anastomosis in 15% of examined scaphoids.

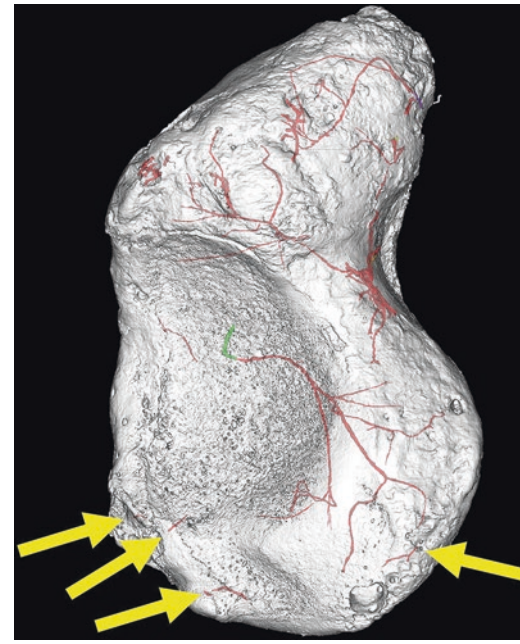

Fig. 93.3 A medial view of a scaphoid depicting vessels entering at the scapholunate ligament attachment (yellow arrows). (From Morsy M, Sabbagh MD, van Alphen NA, Laungani AT, Kadar A, Moran SL. The Vascular Anatomy of the Scaphoid: New Discoveries Using Micro-Computed Tomography Imaging. J Hand Surg Am. 2019 Nov;44(11):928-938, with permission)

93.5 Clinical Correlation and Implications

With all the evidence of dominance of the dorsal vascular supply to the scaphoid, it seems logical to confirm the lesser impact caused by the volar approach to the scaphoid as compared to the dorsal approach [4]. The impact of the approach and screw insertion was further studied by Botte et al. providing evidence favoring the use of the insertion through a volar approach [14]. More surgeons nowadays prefer percutaneous approaches for fixation of scaphoid fractures thereby shifting attention toward the impact of screw drilling and insertion on the intraosseous vascularity rather than the effect on the extraosseous blood supply.

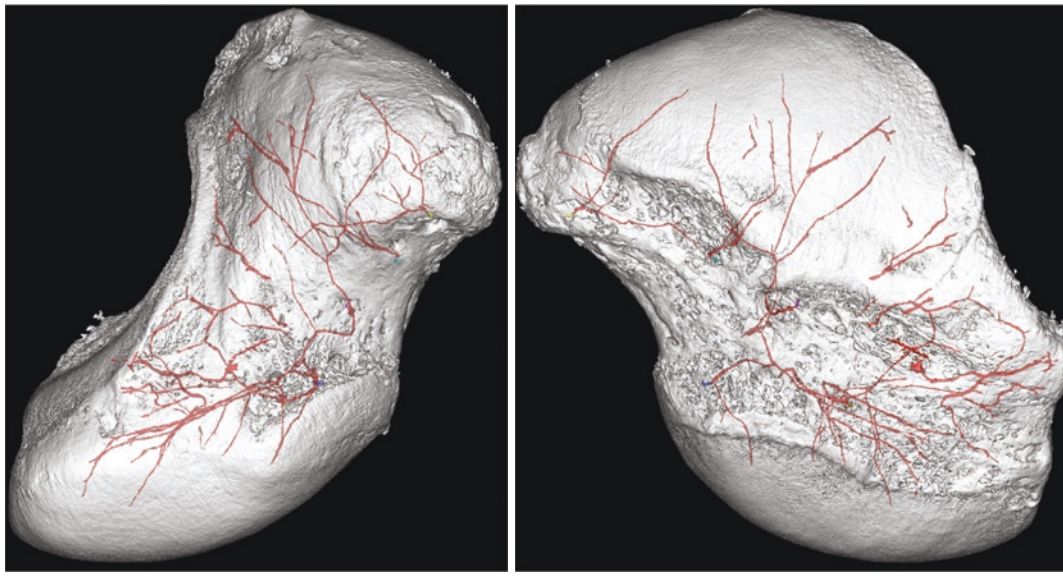

Fig. 93.4 A 3D reconstruction of a scaphoid showing the intraosseous vascularity from a volar view (LEFT) and a lateral view (RIGHT). (From Morsy M, Sabbagh MD, van Alphen NA, Laungani AT, Kadar A, Moran SL. The Vascular Anatomy of the Scaphoid: New Discoveries Using Micro-Computed Tomography Imaging. J Hand Surg Am. 2019 Nov;44(11):928-938, with permission)

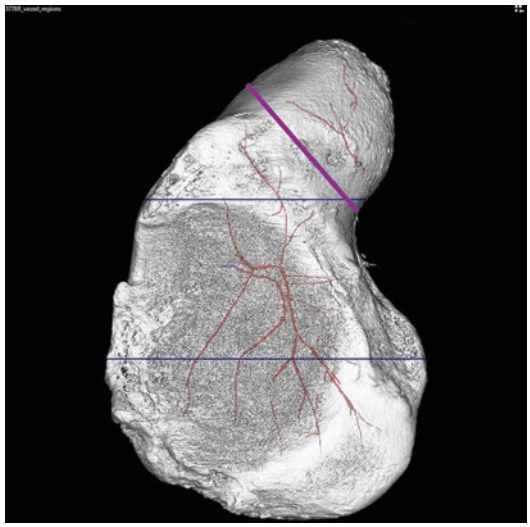

Fig. 93.5 A representation of the proximal and distal intraosseous vascular networks the territories of which are divided by the violet line. (Used with permission of Mayo Foundation for Medical Education and Research, all rights reserved)

Table 93.1 Characteristics of nutrient vessels of the scaphoid according to anatomical site of entry

Vessels	Number Average (range)	Diameter Average (range)	Total cross-sectional area Average (range)
Dorsal Dorsoradial ridge	2.7 (1–5)	71.4 μm (20–200 μm)	13,750.51 μm^2 (2827.43–42,725.66 μm^2)
Volar	1.8 (1–3)	57.4 μm (20–140 μm)	6089.86 μm^2 (314.16–15,393.8 μm^2)
Tubercle	1.5 (0–3)	62.1 μm (20–10 μm)	6204.65 μm^2 (314.16–15,393.8 μm^2)
Waist	0.3 (0–1)	35 μm (20–60 μm)	1178.1 μm^2 (314.16–2827.43 μm^2)

To study this, the authors projected a cylinder corresponding to the dimensions of the screw on the 3D model of the scaphoids in four possible positions along planned axes, the hypothetical longest length axis, the hypothetical exact central

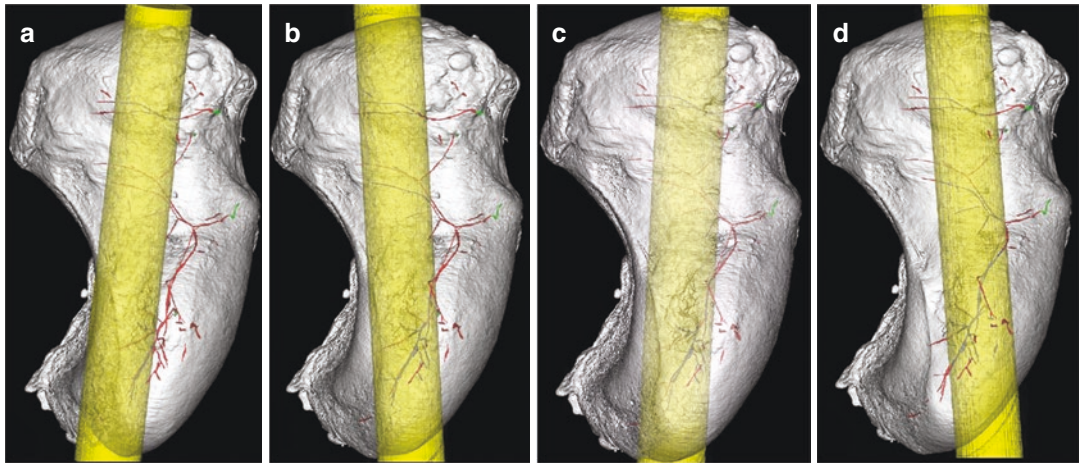

Fig. 93.6 A scaphoid specimen with a cylinder positioned in the 4 axes (A-longest length axis, B-central axis, C-retrograde or volar insertion axis, and D-antegrade or dorsal insertion axis) intersecting the internal vasculature as a representation of the impact of screw drilling and insertion. (From Morsy M, Sabbagh MD, van Alphen NA, Laungani AT, Kadar A, Moran SL. The Vascular Anatomy of the Scaphoid: New Discoveries Using Micro-Computed Tomography Imaging. J Hand Surg Am. 2019 Nov;44(11):928-938, with permission)

axis, the antegrade axis corresponding to dorsal antegrade insertion, and the retrograde axis corresponding to the volar retrograde insertion. The impact of each position was assessed by measuring the volume of the internal vascularity overlapped by the cylinder as a representation of the affected vascularity (Fig. 93.6). It was found that the ideal position with the least effect was the central axis followed closely by the antegrade axis, and the retrograde axis had the most effect on the internal vascularity [6]. This fact favors the use of dorsal antegrade insertion of screws over the volar retrograde insertion when internal vascularity is at stake.

The scaphoid is known for its complex and highly variable shape [5]. A number of studies have tried to classify scaphoids according to shape using a number of parameters and morphological features, yet these classifications fall short in application due to the fact that carpal bone shape variations are more of a spectrum than strict categories [10, 11, 15–17]. Putting this in mind, the authors presented the concept of the relationship between scaphoid shape and intraosseous vascularity. Studying the shapes of the scaphoids in 3D reconstructions and after 3D printing, we concluded that there exist two patterns of scaphoids: the full scaphoid or type I and the slender or type II. Type I scaphoids were found to have a more robust internal vascularity than type II (Fig. 93.7). A simple method to identify the type of scaphoid was introduced using measurements that can be done on simple plain x-rays (Figs. 93.8 and 93.9) [6]. These discoveries can be helpful in identifying the subset of scaphoids with lower vascularity and thus can provide insight on the prognosis of scaphoid fractures as to which ones are prone to develop nonunion and avascular necrosis, or the development of Preiser disease.

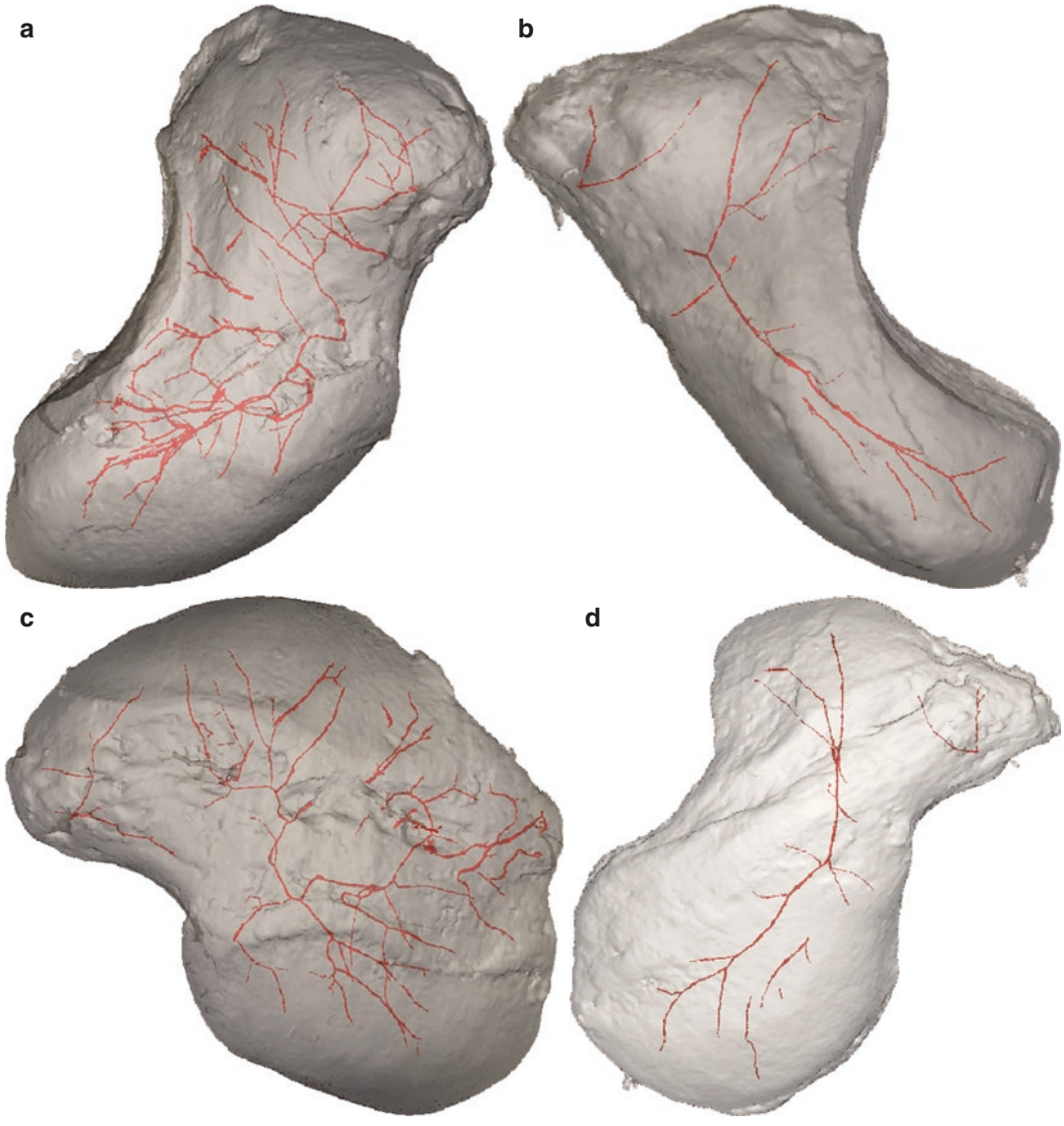

Fig. 93.7 A representation of the internal vascularity of type I (**a**, **c**) and type II (**b**, **d**) scaphoids. (From Morsy M, Sabbagh MD, van Alphen NA, Laungani AT, Kadar A, Moran SL. The Vascular Anatomy of the Scaphoid: New Discoveries Using Micro-Computed Tomography Imaging. J Hand Surg Am. 2019 Nov;44(11):928-938, with permission)

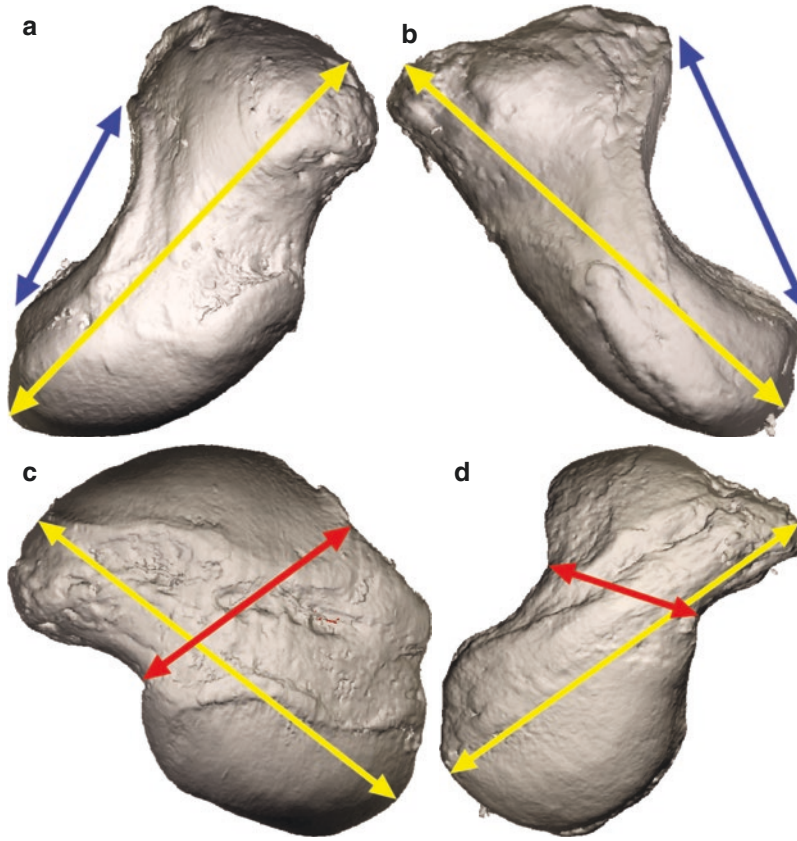

Fig. 93.8 A comparison between dimensions of type 1 (**a**) and type II (**b**) scaphoids in a simulated posteroanterior view and introducing the capitate fossa index (CFI) calculated by dividing the length of the capitate fossa (blue lines) by the longest length of the scaphoid (yellow lines). In the simulated lateral view type I (**c**) and type II (**d**) the waist index (WI) is represented, which is calculated by dividing the narrowest width at the waist (red lines) by the longest length of the scaphoid (yellow lines). (From Morsy M, Sabbagh MD, van Alphen NA, Laungani AT, Kadar A, Moran SL. The Vascular Anatomy of the Scaphoid: New Discoveries Using Micro-Computed Tomography Imaging. J Hand Surg Am. 2019 Nov;44(11):928-938, with permission)

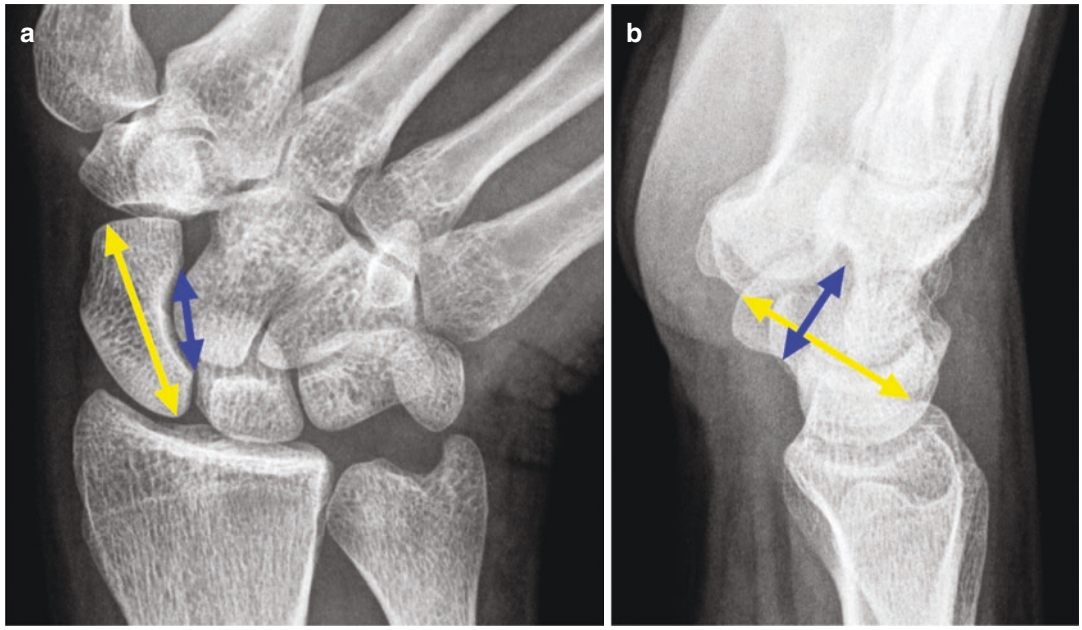

Fig. 93.9 A representation of the method for measuring the capitate fossa index (CFI) and the waist index (WI) on plain x-rays. The CFI is calculated by dividing the length of the capitate fossa (blue line) by the longest length of the scaphoid (yellow line) on posteroanterior view with ulnar deviation and 20^0 tilt toward the elbow (**a**). The WI is calculated by dividing the narrowest width at the waist (blue line) by the longest length of the scaphoid (yellow line) (**b**). (From Morsy M, Sabbagh MD, van Alphen NA, Laungani AT, Kadar A, Moran SL. The Vascular Anatomy of the Scaphoid: New Discoveries Using Micro-Computed Tomography Imaging. J Hand Surg Am. 2019 Nov;44(11):928-938, with permission)

References

1. Viegas SF, Tencer AF, Cantrell J, Chang M, Clegg P, Hicks C, et al. Load transfer characteristics of the wrist. Part I. The normal joint. J Hand Surg Am. 1987;12(6):971–8.
2. Hove LM. Epidemiology of scaphoid fractures in Bergen, Norway. Scand J Plast Reconstr Surg Hand Surg. 1999;33(4):423–6.
3. Leslie IJ, Dickson RA. The fractured carpal scaphoid. Natural history and factors influencing outcome. J Bone Joint Surg Br. 1981;63-B(2):225–30.
4. Gelberman RH, Menon J. The vascularity of the scaphoid bone. J Hand Surg Am. 1980;5(5):508–13.
5. Berger RA. The anatomy of the scaphoid. Hand Clin. 2001;17(4):525–32.
6. Morsy M, Sabbagh MD, van Alphen NA, Laungani AT, Kadar A, Moran SL. The vascular anatomy of the scaphoid: new discoveries using micro-computed tomography imaging. J Hand Surg Am. 2019;44(11):928–38.
7. van Alphen NA, Morsy M, Laungani AT, Kadar A, Vercnocke AJ, Lachman N, et al. A three-dimensional micro-computed tomographic study of the intraosseous lunate vasculature: implications for surgical intervention and the development of avascular necrosis. Plast Reconstr Surg. 2016;138(5):869e–78e.
8. Kadar A, Morsy M, Sur YJ, Laungani AT, Akdag O, Moran SL. The vascular anatomy of the capitate: new discoveries using micro-computed tomography imaging. J Hand Surg Am. 2017;42(2):78–86.
9. Buijze GA, Lozano-Calderon SA, Strackee SD, Blankevoort L, Jupiter JB. Osseous and ligamentous scaphoid anatomy: part I. a systematic literature review highlighting controversies. J Hand Surg Am. 2011;36(12):1926–35.
10. Ceri N, Korman E, Gunal I, Tetik S. The morphological and morphometric features of the scaphoid. J Hand Surg Br. 2004;29(4):393–8.
11. Compson JP, Waterman JK, Heatley FW. The radiological anatomy of the scaphoid. Part 1: osteology. J Hand Surg Br. 1994;19(2):183–7.

12. Heinzelmann AD, Archer G, Bindra RR. Anthropometry of the human scaphoid. J Hand Surg Am. 2007;32(7):1005–8.
13. Sabbagh MD, Morsy M, Moran SL. Diagnosis and management of acute scaphoid fractures. Hand Clin. 2019;35(3):259–69.
14. Botte MJ, Mortensen WW, Gelberman RH, Rhoades CE, Gellman H. Internal vascularity of the scaphoid in cadavers after insertion of the Herbert screw. J Hand Surg Am. 1988;13(2):216–20.
15. van de Giessen M, Foumani M, Streekstra GJ, Strackee SD, Maas M, van Vliet LJ, et al. Statistical descriptions of scaphoid and lunate bone shapes. J Biomech. 2010;43(8):1463–9.
16. Yazaki N, Burns ST, Morris RP, Andersen CR, Patterson RM, Viegas SF. Variations of capitate morphology in the wrist. J Hand Surg Am. 2008;33(5):660–6.
17. Rhee PC, Moran SL, Shin AY. Association between lunate morphology and carpal collapse in cases of scapholunate dissociation. J Hand Surg Am. 2009;34(9):1633–9.

94 Arthroscopic Fixation of Scaphoid Fractures Using a "Scaphoid Portal"

Deepak N. Bhatia

94.1 Background

Scaphoid fractures account for more than half of all carpal bone fractures and early surgical fixation is often necessary to prevent complications like malunion, nonunion, and avascular necrosis [1]. Traditionally, open surgical procedures (volar or dorsal approaches) are used for fixation, and minimally invasive percutaneous screw techniques have recently gained popularity. Arthroscopic scaphoid fracture fixation has the advantage of visualization of the fracture reduction and bone grafting the fracture site if necessary; subsequent fixation is usually performed by passing the screw percutaneously from volar or dorsal aspects [2–4]. Dorsal screw passage has the advantages of preserving internal scaphoid vascularity and is the preferred method in proximal pole fractures [5, 6]. However, arthroscopic fixation via standard dorsal portals is difficult as the proximal scaphoid is covered by the dorsal radial rim, and therefore the angulation necessary for wire passage along the central axis of the scaphoid is difficult to achieve.

The author has developed a modified arthroscopic technique that utilizes a "scaphoid portal" for dorsal antegrade screw passage (proximal to distal) under arthroscopic visualization. The advantages of using this portal are: (a) Extensor tendons and capsule are visualized and protected to prevent inadvertent injury during drilling and screw passage. (b) The extensor retinaculum and tendon sheaths are not incised and tendon transposition is not necessary. (c) The scapholunate ligament is visualized and preserved, and the precise entry point centered on the proximal scaphoid pole can be identified. (d) Screw insertion under magnified endoscopic visualization is useful in preventing fragmentation of small proximal pole fragments. (e) The "scaphoid portal" incision is a soft tissue window that can be retracted proximally or distally to achieve a safe and accurate angle for wire passage along the central axis of the scaphoid and extensor tendons are protected.

94.1.1 Surgical Anatomy

The extraosseous vascular supply of the scaphoid is via the dorsal (dorso-radial ridge) and volar (scaphoid tubercle) branches of the radial artery. Vessels that supply through the dorso-radial ridge form a retrograde proximal intraosseous network that forms approximately 80% of the blood supply of the scaphoid. The remaining 20% of the distal scaphoid is supplied by a distal intraosseous network formed by vessels entering the tubercle [5, 6] (Fig. 94.1a). Arthroscopic fixation of scaphoid fractures is usually performed using

D. N. Bhatia (✉)
SPORTSMED Mumbai, and Sir HN Reliance Foundation Hospital, Mumbai, India
e-mail: shoulderclinic@gmail.com

© ISAKOS 2022

D. N. Bhatia et al. (eds.), *Arthroscopy and Endoscopy of the Elbow, Wrist and Hand*,
https://doi.org/10.1007/978-3-030-79423-1_94

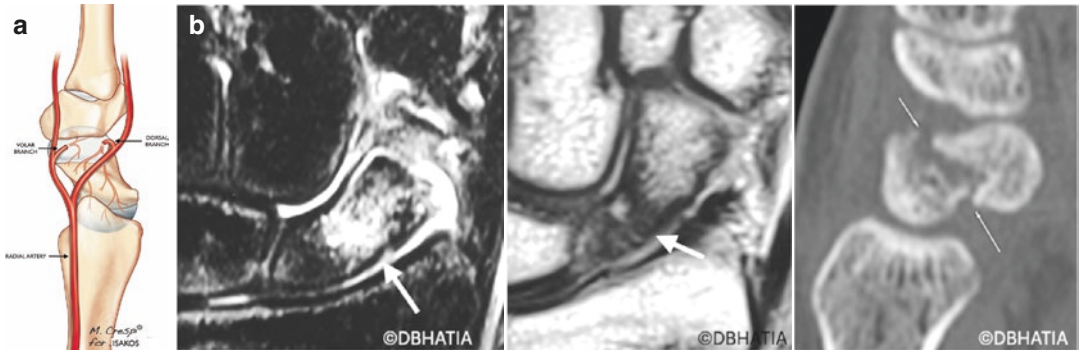

Fig. 94.1 (**a**) Extraosseous and intraosseous blood supply of scaphoid are illustrated. (**b**) Radiological imaging shows a displaced scaphoid waist fracture (left), a delayed union of a proximal pole fracture (middle), and an angulation deformity at the fracture site (right image). (© D. Bhatia)

a volar (retrograde) percutaneous approach for screw passage. Dorsal antegrade screw passage is difficult arthroscopically because the dorsal radial rim prevents access to the central proximal pole through the standard or proximally placed dorsal portals in most cases. Moreover, the extensor tendons and capsular ligaments are at risk of iatrogenic injury during drilling and screw passage. The scaphoid portal was devised to overcome these problems with arthroscopic antegrade wire and screw passage; the portal permits visualization and retraction of extensor tendons, and the proximal scaphoid can be flexed and levered out for wire passage. The minimal capsulotomy of approximately 5 mm preserves the main blood supply at the dorsal ridge and is adequate for arthroscopic visualization of wire and screw passage.

94.2 Indications and Contraindications

- Acute fractures of the waist or proximal pole of scaphoid with displacement of 1–1.5 mm or more are ideal indications for the arthroscopic fixation technique [7].
- Acute scaphoid fractures with angulation or comminution at the fracture site can be fixed arthroscopically in most cases.
- Stable delayed union and nonunion of a scaphoid fracture can be treated with screw fixation alone. Additional bone grafting may be performed in some cases if necessary (Fig. 94.1b).
- An acute trans-scaphoid perilunate dislocation can be reduced arthroscopically and the scaphoid fixation can be performed using this technique.

A long-standing scaphoid nonunion with a humpback deformity and a secondary dorsal intercalated segmental instability (DISI) pattern usually requires open surgery and volar wedge graft and is a contraindication for this technique [3]. Similarly, a chronic perilunate dislocation with an associated scaphoid fracture necessitates an open approach.

94.3 Surgical Technique

The procedure is performed with the patient in the supine position. The upper limb is suspended with finger traps, and a countertraction force of 2 kg is used to distract the joint. A 30° arthroscope (2.4 mm or 1.9 mm) is used for visualization.

Portals: Three portals are used in the procedure.

- Dorsal radiocarpal 3–4 portal is the initial viewing portal.
- The 6R portal may be used as a working portal for radiocarpal instrumentation.

- The midcarpal radial (MCR) portal is the main viewing portal for the assessment of scaphoid fracture site and reduction. Occasionally the midcarpal ulnar (MCU) portal is necessary for assessment of fracture reduction and visualization (Fig. 94.2).
- The "Scaphoid portal" is created by connecting the 3–4 and MCR portals. Endoscopic visualization via this portal demonstrates tendons of the third and fourth extensor compartments. The tendons are retracted to visualize the capsule and a minimal longitudinal capsulotomy (5 mm) permits visualization of the proximal scaphoid.

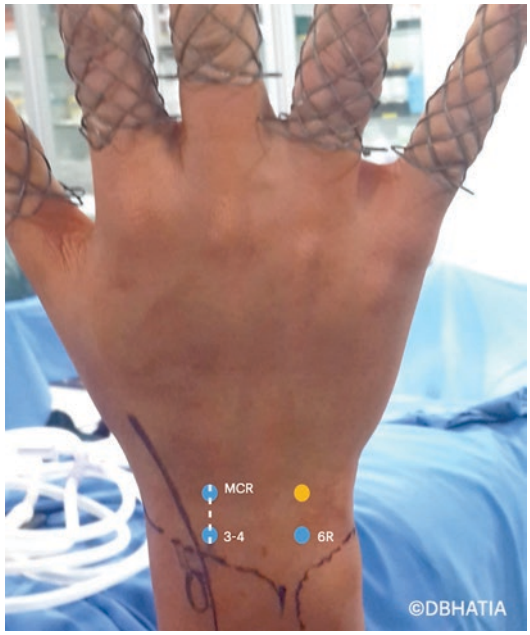

Fig. 94.2 Portals used for arthroscopic scaphoid fixation are demonstrated. The 3–4 radiocarpal portal and radial midcarpal portal (MCR) are connected and the soft tissue window is retracted proximally to create the "scaphoid portal." Other portals are the 6R radiocarpal portal and the ulnar midcarpal portal (yellow). (© D. Bhatia)

Diagnostic arthroscopy: The 3–4 portal is used to evaluate the radiocarpal joint and a probe and shaver are used through the 6R portal. The scaphoid fracture may be difficult to visualize via the 3–4 portal and associated synovitis and organized clots must be excised using a shaver. The scapholunate and lunotriquetral ligaments are probed and TFCC is assessed to identify associated injuries. The MCR portal is next used to evaluate the fracture pattern and assess the displacement. An MCU portal may be used if necessary to probe and manipulate the fracture fragments and excise the hematoma (Fig. 94.3a, b).

Scaphoid fracture alignment and reduction: Various reduction maneuvers can be used to realign the fracture fragments.

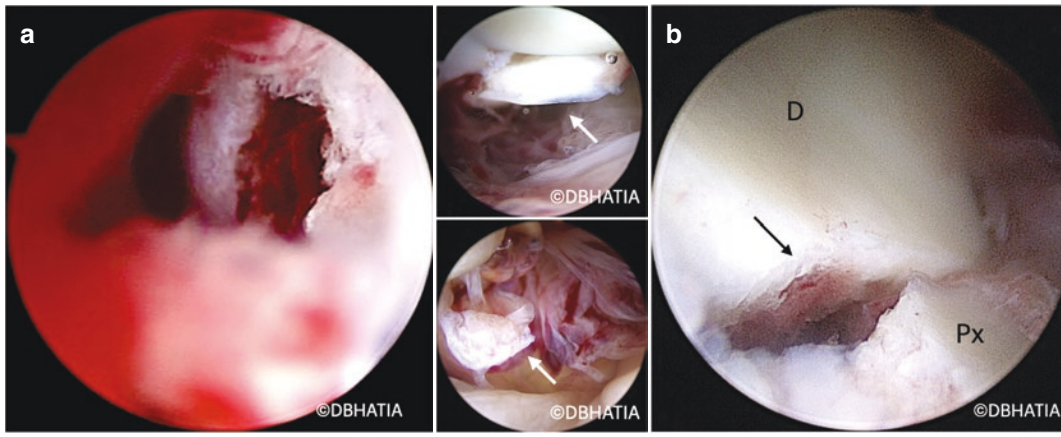

Fig. 94.3 (**a**) Radiocarpal visualization (3–4 portal) demonstrates synovitis and the scaphoid fracture can be identified (left image). The scapholunate ligament is torn (arrow, top right) and a bone fragment is seen in the radiocarpal joint (arrow, bottom right). (**b**) Midcarpal visualization (MCR portal) demonstrates a displaced scaphoid waist fracture (arrow). [Px: Proximal fragment, D: Distal fragment]. (© D. Bhatia)

- For minimally displaced fractures without angulation, traction is sufficient to maintain the alignment. A probe is used via MCR portal and the fracture surfaces are probed to remove any interposed tissue. If the fragments are unstable and mobile on probing, temporary K-wires are passed from the volar or dorsal aspect to maintain the reduction and wires are cut short.
- For displaced fractures with angulation, realignment is possible using a probe or a joystick K-wire in distal or proximal fragments. Direct pressure over the distal fragment from volar aspect may be used if necessary and reduction is maintained using temporary K-wires.
- The Linscheid maneuver is useful for carpal alignment [8, 9]: The wrist is volar flexed to correct lunate extension relative to the radius and a temporary transfixing wire is passed through the palpable Lister's tubercle into the lunate (Fig. 94.4a–d) [3]. Alternately, a K-wire

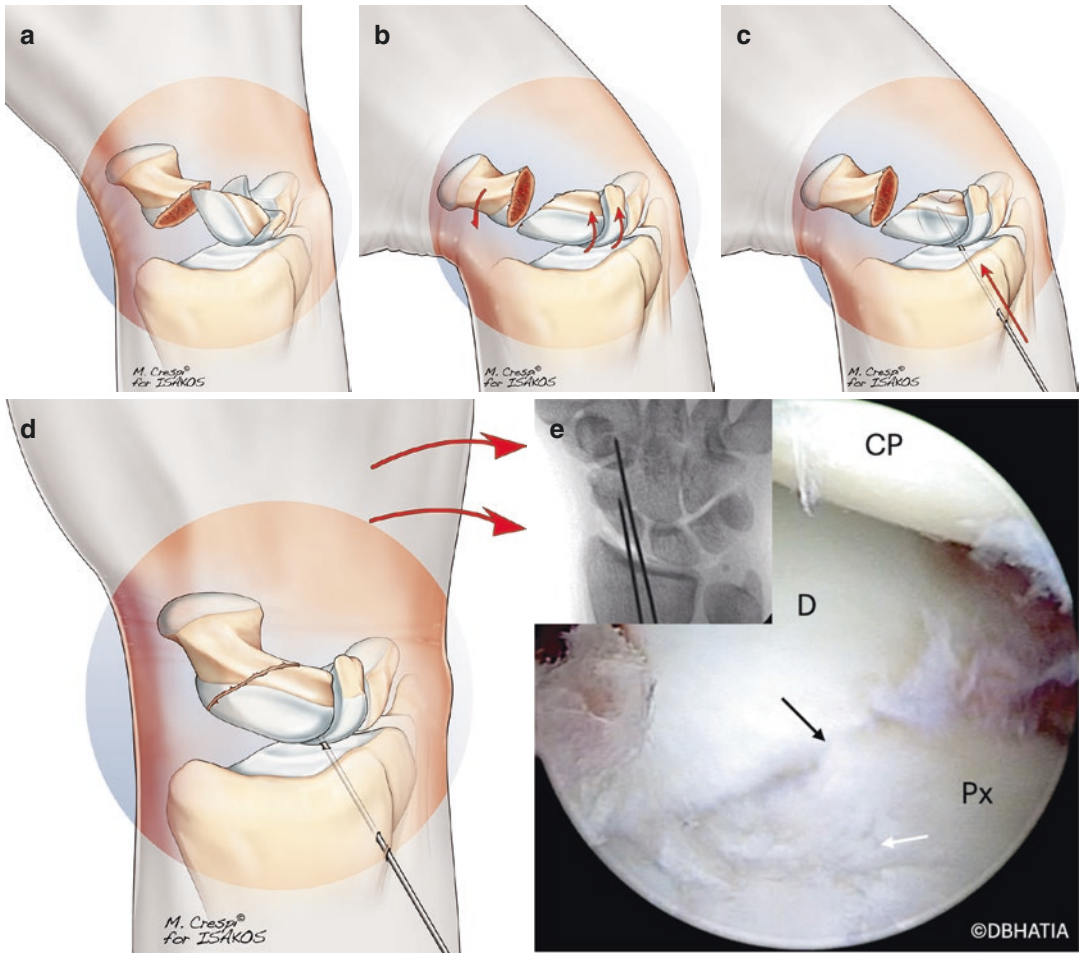

Fig. 94.4 (**a–d**) The Linscheid maneuver is illustrated. (**a**) The lunate is in dorsiflexion with the proximal scaphoid fragment creating a flexion deformity at the fracture site. (**b**) Wrist flexion volar flexes the lunate and proximal scaphoid and corrects the radiolunate angle. (**c**) A radiolunate transfixing wire is passed to maintain the position of lunate. (**d**) Wrist extension corrects the flexion deformity at scaphoid fracture site. (**e**) Midcarpal visualization (MCR portal) after reduction of scaphoid fracture (black arrow) demonstrates a congruous midcarpal surface. Focal chondral loss (white arrow) is seen on the proximal fragment (Px) at fracture site. Inset image shows percutaneously passed K-wires for temporary fixation of scaphoid fracture. (© D. Bhatia)

may be passed into the lunate and is used as a joystick to realign the lunate. Restoration of the normal radiolunate angle corrects the extension of the proximal scaphoid fragment. Next, the distal scaphoid fragment is realigned with the corrected proximal fragment by extension and ulnar deviation of the supinated wrist while maintaining traction via wrist arthroscopy tower. Two temporary transfixing K-wires are used to maintain reduction once the normal scaphoid length and alignment are achieved; these wires are passed through standard dorsal portals and are not along the axis (Fig. 94.4e).

Scaphoid fixation: Proximal pole and waist fractures are fixed using a compression screw passed from the dorsal aspect (proximal to distal). The correct entry point is centered on the proximal pole and is 2–4 mm radial to the scapholunate ligament. The precise dorsal entry point for central screw placement is difficult to obtain with the wrist in arthroscopy traction apparatus. Additionally, iatrogenic injury to the extensor tendons is possible with wire placement and drilling via a standard or proximally placed 3–4 portal, and these tendons need to be retracted for protection. To achieve this, the wrist is taken out of finger trap suspension and placed on a side table, and a scaphoid portal is used for further fixation.

- The MCR and 3–4 portals are connected using a skin incision between them to create a "scaphoid portal," and dissection is performed till tendons of the third (extensor pollicis longus [EPL]) and fourth compartments (extensor indicis [EI] and extensor digitorum communis [EDC]) are visualized (Fig. 94.5a, b).
- The arthroscope is placed within the incision and a clear magnified view of the tendons is possible (Fig. 94.6). The EPL and EPI/EDC tendons are retracted and the underlying capsule is visualized.
- The radiocarpal joint is identified arthroscopically using a probe and a needle is passed through the capsule into the joint (Fig. 94.6). A 5 mm longitudinal capsulotomy is performed at the radiocarpal joint marked by the needle and the arthroscope is advanced into this window. The capsulotomy is centered over the radiocarpal joint and incorporates only the 3–4 portal site on the dorsal capsule.
- The wrist is flexed and the proximal pole of the scaphoid is visualized arthroscopically. The scapholunate ligament is marked with a blunt-tipped wire. A guidewire (1 mm) is then passed along the central axis of the scaphoid.

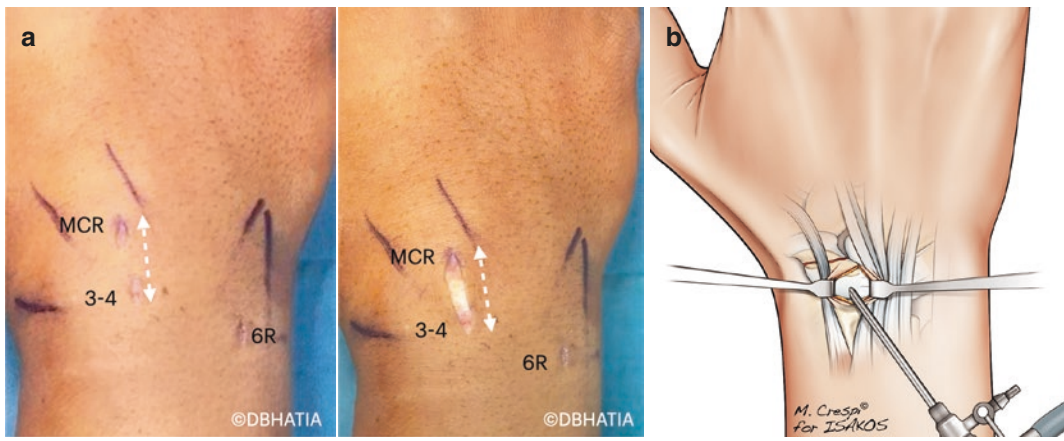

Fig. 94.5 (**a**) The MCR and 3–4 portals are connected by incising the skin bridge to create a scaphoid portal. The soft tissue window can be moved proximally or distally to adjust the fixation wire angulation. (**b**) The "scaphoid portal" is illustrated. The MCR and 3–4 portals are connected by incising the skin bridge and extensor tendons are retracted. A minimal capsulotomy permits access to the proximal pole of the scaphoid. (© D. Bhatia)

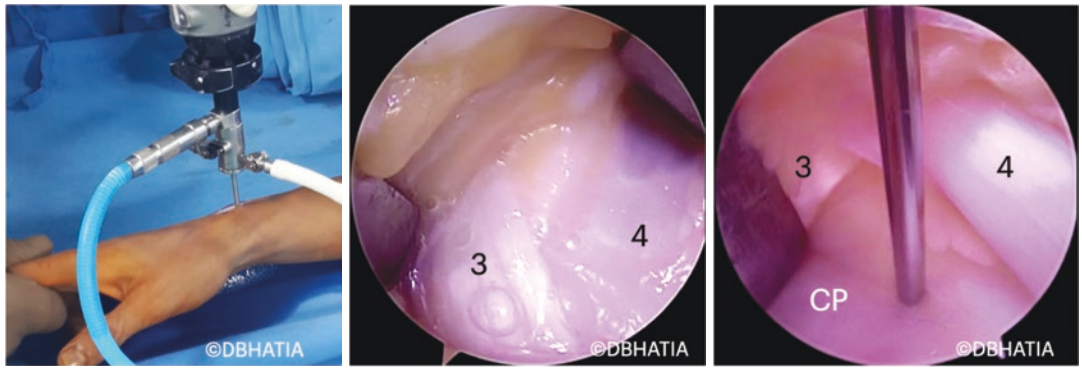

Fig. 94.6 The arthroscope is introduced into the scaphoid portal (left image). Tendons of the third and fourth extensor compartments (3,4) are identified (middle image) and retracted to visualize the underlying capsule (CP, right image). A needle identifies the radiocarpal joint level to mark the capsulotomy site. (© D. Bhatia)

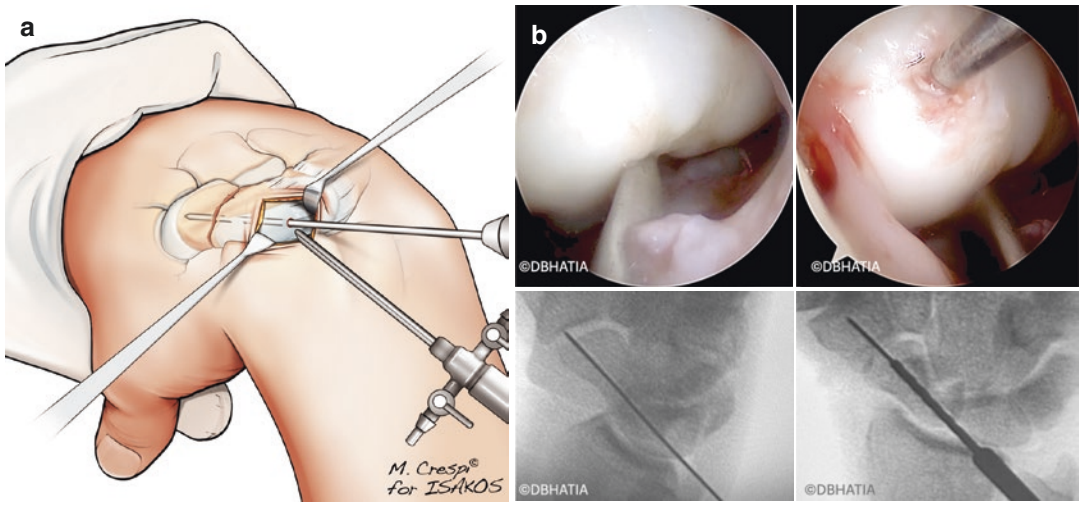

Fig. 94.7 (**a**) The wrist is volar flexed to bring the proximal pole and scapholunate ligament into the arthroscopic view. The center of the proximal pole is identified and a wire entry point is marked 2–3 mm away from the ligament. (**b**) Arthroscopic view shows a wire passing into the scapholunate ligament (top left image) and a second wire is passed through the scaphoid entry point (top right). Fluoroscopy is used to confirm central placement in the scaphoid and a cannulated drill passes over it (bottom images). (© D. Bhatia)

The entry point for this wire is approximately 2–3 mm radial to the scapholunate attachment (marked by the first wire) and should be central in the proximal pole. Fluoroscopic guidance confirms correct placement of this wire; the wire is advanced across the fracture site along the central axis of the scaphoid, and all other transfixing wires are removed (Fig. 94.7a, b).

- A drill hole is placed over the wire using a cannulated drill bit and a 2.5 mm cannulated headless compression screw (Compression FT screw, 2.5 micro, Arthrex Inc., FL) is passed over the wire (Fig. 94.8).
- The wrist is again positioned in the finger trap suspension and the arthroscope is placed in the MCR/MCU portal to assess adequacy of fixation. Fluoroscopic views are used to confirm correct screw position and length (Fig. 94.9).
- The capsulotomy is sutured using 3–0 absorbable sutures and the skin incision and portals

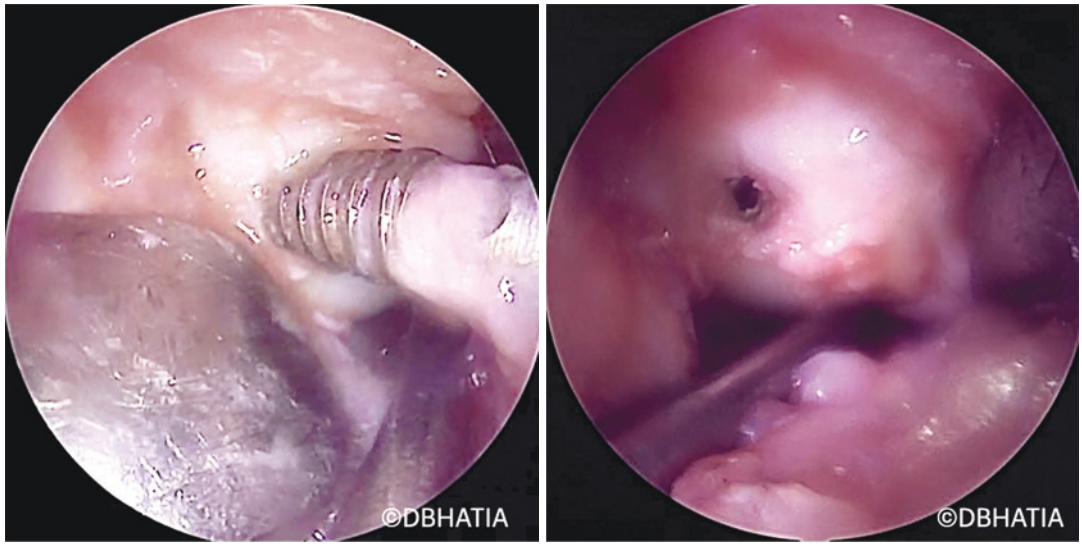

Fig. 94.8 A compression screw is shown passing over the central wire through a minimal capsulotomy and a wire marks the scapholunate ligament (left). The screw is seen placed deep to the proximal pole cartilage (right). (© D. Bhatia)

are closed using 3–0 nonabsorbable sutures. A sterile dressing and a short arm volar spica-slab are applied.

94.4 Tips and Tricks

- Tendons of the third and fourth extensor compartments should not be released from the extensor retinaculum sheaths. Minimal retraction usually suffices.
- The capsular rent of the 3–4 portal is a guide to capsulotomy site and is incorporated in the capsulotomy.
- Correct entry point of the central wire is crucial and initial placement should be checked with fluoroscopy prior to removing the reduction wires.
- Access to the proximal pole may be difficult with only wrist flexion; in such cases, gentle manual traction is useful with the wrist flexed over a rolled towel at the edge of the table. Alternately a blunt elevator is passed between the scaphoid and radius articular surface via the 6R portal and the scaphoid is gently levered in a dorsal-distal direction.

94.5 Pitfalls

- Fracture reduction may be difficult in presence of comminution, and suboptimal bone contact usually results in a malunion or nonunion. Arthroscopic visualization must confirm a congruous midcarpal surface and fluoroscopy should be used to confirm scaphoid and carpal alignment.
- Tissue interposition at fracture site prevents adequate compression of fragments and must be excised meticulously.

94.6 Postoperative Management and Rehabilitation

A short arm volar spica-slab is applied for 2 weeks. Sutures are removed and a wrist brace is used for 6–8 weeks. Radiographs and a CT scan are performed 6–8 weeks after surgery to confirm union (continuous trabecular bridging over more than 50% of the cross-section of the fracture site). Physiotherapy exercises are started thereafter and activities of daily living are permitted. Return to heavy work and sports is permitted only after

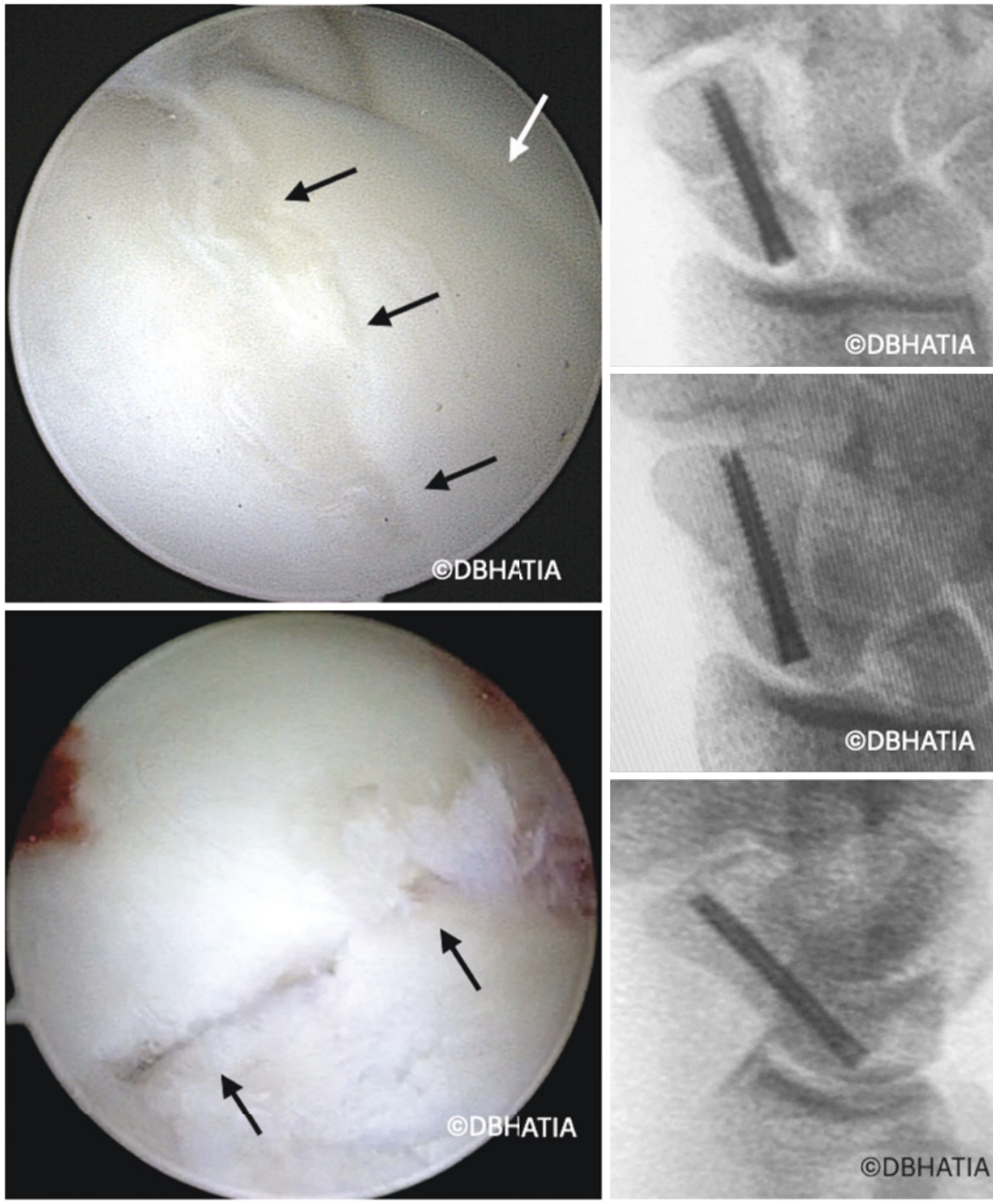

Fig. 94.9 Final assessment of fracture site of a waist fracture (arrows, top left) and a proximal pole fracture (arrows, bottom left) via MCR portal after screw fixation. Fluoroscopy confirms correct screw placement and anatomic reduction in different views (right images). [white arrow: scapholunate articulation]. (© D. Bhatia)

complete fracture union and full wrist function and strength are achieved (3–6 months).

94.7 Complications

The arthroscopic-assisted scaphoid fixation technique is safe and reproducible. Potential complications are inadequacy of reduction and screw malpositioning resulting in a nonunion and deformity. Further fragmentation of a small proximal pole fragment is possible during screw passage.

Conflict of Interest The author certifies that he has no commercial associations (e.g., consultancies, stock ownership, equity interest) that might pose a conflict of interest in connection with the submitted article. The author retains the copyright to the images, videos, and content in this chapter.

References

1. Kawamura K, Chung KC. Treatment of scaphoid fractures and nonunions. J Hand Surg Am. 2008;33(6):988–97. https://doi.org/10.1016/j.jhsa.2008.04.026.
2. Wong WC, Ho PC. Arthroscopic management of scaphoid nonunion. Hand Clin. 2019;35(3):295–313. https://doi.org/10.1016/j.hcl.2019.03.003.
3. Slutsky DJ, Trevare J. Use of arthroscopy for the treatment of scaphoid fractures. Hand Clin. 2014;30(1):91–103. https://doi.org/10.1016/j.hcl.2013.09.002.
4. Slade JF 3rd, Jaskwhich D. Percutaneous fixation of scaphoid fractures. Hand Clin. 2001;17:553–74.
5. Gelberman RH, Menon J. The vascularity of the scaphoid bone. J Hand Surg Am. 1980;5(5):508–13. https://doi.org/10.1016/s0363-5023(80)80087-6.
6. Morsy M, Sabbagh MD, van Alphen NA, Laungani AT, Kadar A, Moran SL. The vascular anatomy of the scaphoid: new discoveries using micro-computed tomography imaging. J Hand Surg Am. 2019;44(11):928–38. https://doi.org/10.1016/j.jhsa.2019.08.001.
7. Clementson M, Björkman A, Thomsen NOB. Acute scaphoid fractures: guidelines for diagnosis and treatment. EFORT Open Rev. 2020;5(2):96–103. https://doi.org/10.1302/2058-5241.5.190025.
8. Cooney WP, Linscheid RL, Dobyns JH, Wood MB. Scaphoid nonunion: role of anterior interpositional bone grafts. J Hand Surg Am. 1988;13(5):635–50.
9. Cooney WP, Dobyns JH, Linscheid RL. Fractures of the scaphoid: a rational approach to management. Clin Orthop Relat Res. 1980;149:90e97.

95 Arthroscopic Management of Scaphoid Fractures and Nonunions

Clara Wong and Pak-cheong Ho

95.1 Background

Scaphoid fracture nonunion is common; approximately 10–15% of all scaphoid fractures progress to nonunion [1–4]. Nonunion rates of up to 40% were reported when treatment was delayed by more than 4 weeks [5], and up to 50% in proximal pole fracture [6]. Wrist arthroscopy has a strong role in preventing scaphoid nonunion in an acute fracture by making sure there is strong bony contact at the fracture site in a minimally invasive way. Arthroscopy is also useful in management of scaphoid nonunion and preserves the risky vascularity around the nonunion.

95.1.1 Surgical Anatomy

Tenuous vascularity of the scaphoid partially explains why scaphoid fracture is susceptible to nonunion. 70–80% of the intraosseous vascularity and the whole proximal pole are supplied from branches of the radial artery entering through the distal dorsal ridge of the scaphoid [7]. The large volume of bone relies on a single intraosseous vessel and this poses a high risk of avascular necrosis and fracture nonunion [8].

Fracture instability is another major reason for scaphoid nonunion. Scaphoid acts as a long lever arm and is the only carpal bone linking the proximal and distal carpal rows. With the pull and constraint by the surrounding bones, intrinsic and extrinsic ligaments, and the tendons, the deforming forces on scaphoid fracture fragments are substantial. Smith demonstrated in cadaveric specimens that there was an increased motion of the distal scaphoid fracture fragment but decreased motion of the proximal fragment during wrist motion [9]. Wrist motion creates significant multiplanar inter-fragmentary motion and shearing forces across the fracture fragments. Moreover, because of the complex osseous-capsulo-ligamentous construct of scaphoid, and especially with the presence of radioscaphocapitate ligament, bending and pronation forces are impacted onto the distal scaphoid fragment. This results in flexion and pronation deformity and collapse of the scaphoid, no matter whether there is fracture comminution and gapping or not [9, 10]. Both the inter-fragmentary motion and the deforming forces on the scaphoid affect the kinematics of other carpal bones, which further exaggerates the fracture instability [9]. It is only by the

C. Wong
Hand Wrist Elbow & Microsurgery Clinic, The Chinese University of Hong Kong Medical Clinic, HKSAR, Hong Kong, SAR, China

P.-c. Ho (✉)
Department of Orthopaedic and Traumatology, Prince of Wales Hospital, The Chinese University of Hong Kong, Shatin, Hong Kong, SAR, China
e-mail: pcho@ort.cuhk.edu.hk

© ISAKOS 2022

D. N. Bhatia et al. (eds.), *Arthroscopy and Endoscopy of the Elbow, Wrist and Hand*,
https://doi.org/10.1007/978-3-030-79423-1_95

nature of the tight capsulo-ligamentous envelope surrounding the scaphoid that both fragments appear to have a benign non-displaced configuration in the radiographs. However, fracture motion still happens with wrist mobility (Fig. 95.1). Fracture displacement can only be apparent in a static radiograph when there is associated ligamentous injury with loss of the capsulo-ligamentous constraint, or associated fracture comminution. Therefore, Herbert described all scaphoid fractures as "inherently unstable unless they are incomplete fractures." [11]

Absolute fracture stability is essential for the scaphoid fracture to heal. Approximately 75% of the surface of the scaphoid is covered with cartilage [12, 13]. There are only tiny patches of periosteum on the nonarticular and non-ligamentous attached surfaces [14]. With the lack of periosteal source of chondrogenic and osteoblastic cells, scaphoid fractures do not easily form callus. Synovial fluid may also dilute the fracture hematoma and inflammatory osteogenic cells and contains inhibitors of osteoblast proliferation which may retard callus formation [15–18]. Scaphoid fractures rely mainly on primary bone healing via cutting cones across the fracture and Haversian remodeling. Direct bone contact and absolute fracture stability are therefore crucial. The shape of the scaphoid is like a "twisted peanut." Its waist is the narrowest part. Anatomical fracture reduction is essential to provide the largest bony contact area in this tiny bone.

95.2 Part I: Arthroscopic-Assisted Scaphoid Fracture Fixation

95.2.1 Indications and Contraindications

Any fracture displacement, gapping, or comminution is not favorable to healing. As 75% of the surface of the scaphoid is covered with cartilage, even if the fracture finally heals, articular incongruity in scaphoid malunion may accelerate radiocarpal and midcarpal arthritis and produce significant wrist symptoms [19]. The resulting humpback and DISI (dorsal intercalated segment instability) deformity alter wrist biomechanics and pose long-term deleterious effects [20–22].

Open reduction and internal fixation may help to reduce the fracture anatomically. However, it

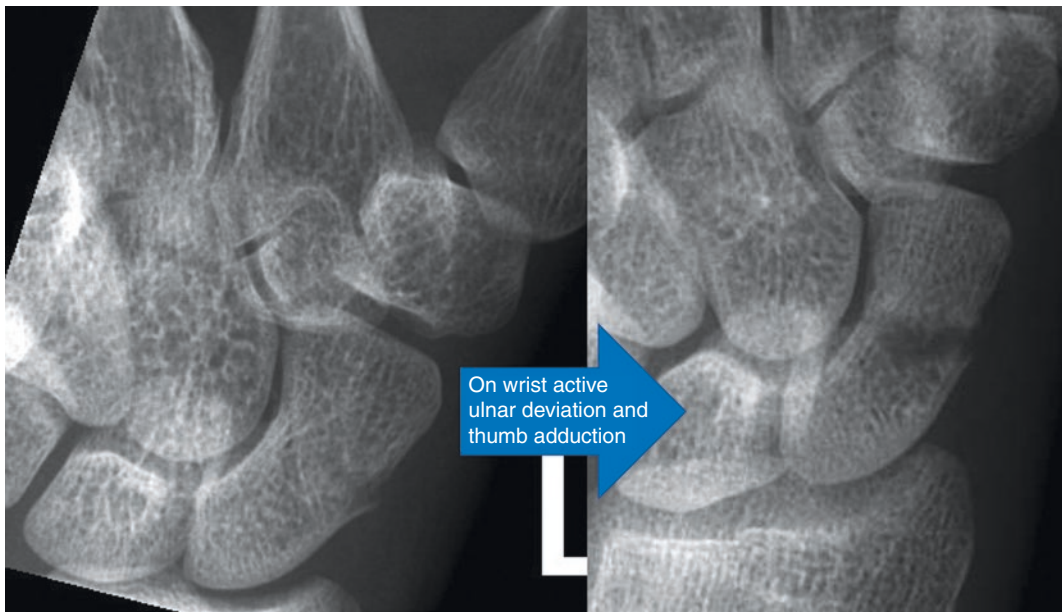

Fig. 95.1 Radiographs show a non-displaced fracture of the waist of scaphoid. On active wrist ulnar deviation and thumb adduction, the fracture gap is apparent

affects the limited blood supply to the scaphoid and injures the important ligaments which further destabilize the scaphoid. Open reduction also provides limited visualization of the fracture and articular reduction as the bone lies deeply among the other carpal bones. Scaphoid has a complex three-dimensional shape and is overlapped by the shadows of other carpal bones in the X-rays. Scaphoid fracture is well known to be easily missed in an ordinary X-ray. It is even more difficult and unreliable to use intra-operative fluoroscopy to judge the quality of fracture reduction. Any scaphoid fracture displacement is not acceptable, while the displacement cannot be reliably reduced and assessed by open means nor by image intensifier. Arthroscopy has therefore come to play an important role in displaced scaphoid fracture.

For an apparently non-displaced fracture, percutaneous guide pin or screw insertion has the potential to cause further displacement (Fig. 95.2). This is more likely when there are associated capsulo-ligamentous injuries and displacement can happen anytime during the fixation. Arthroscopy would then be helpful in assisting and controlling fracture reduction.

Arthroscopy is indicated if there is,

1. Fracture displacement (fracture gap >1 mm, fracture step >1 mm, scaphoulnate angle

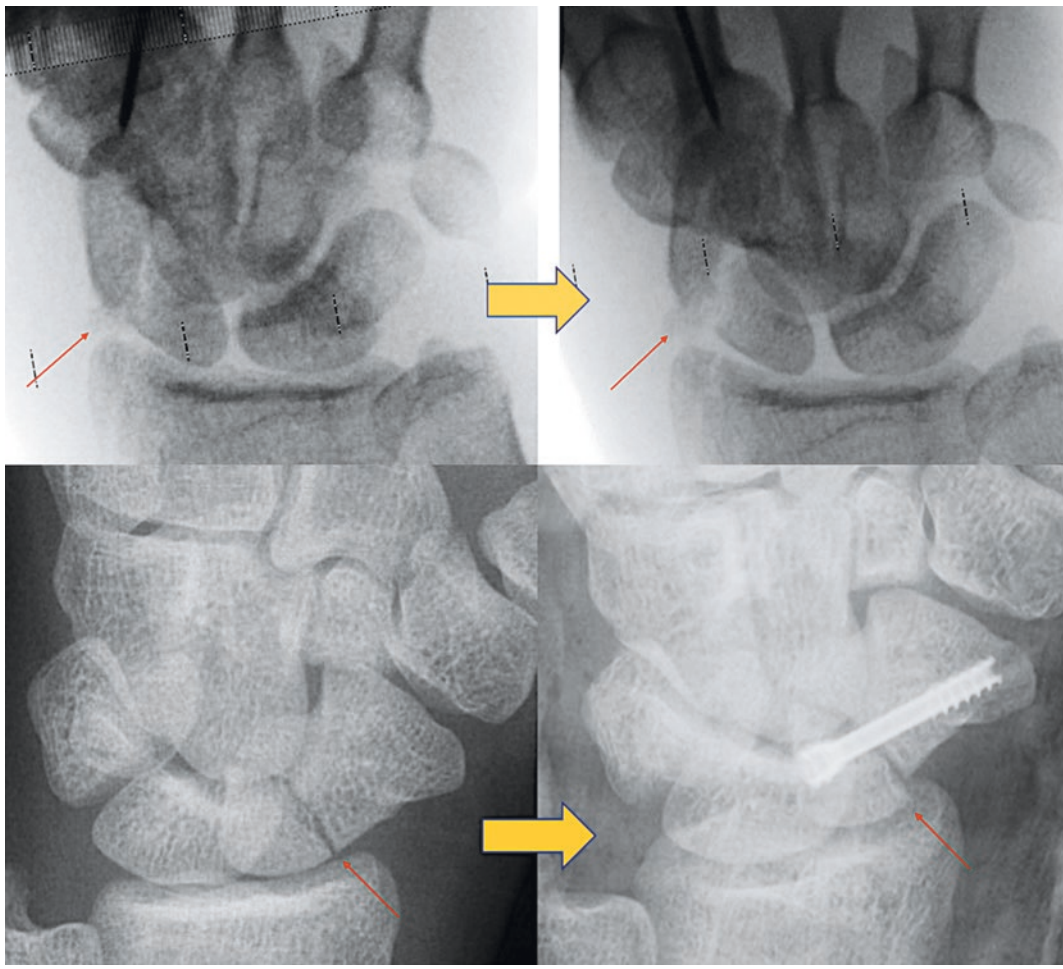

Fig. 95.2 Scaphoid fracture displacement during guide pin insertion (top images) and after screw insertion (Bottom images)

>60°, radiolunate (RL) angle >15°, lateral intra-scaphoid angle >45°, or anteroposterior intra-scaphoid angle >35°) [19].
2. Fracture comminution (even though there is no apparent displacement).
3. Associated ligamentous injury (suspected clinically by the presence of tenderness or instability). An apparently non-displaced fracture is unstable if associated with capsulo-ligamentous tear and is likely to be displaced during fracture fixation. Associated ligament injuries can also be fixed arthroscopically at the same time.
4. Oblique fracture pattern (screw compression may cause fracture displacement).
5. Proximal pole fracture where reduction and fixation is difficult to be visualized under image intensifier (Fig. 95.3a, b).
6. High demand patients, e.g., professional athletes that speedy fracture union is required. Arthroscopy safeguards anatomical reduction and maximal bony contact to enhance fracture healing.

There is no absolute contraindication for arthroscopy in scaphoid acute fracture unless the surgeon is inexperienced in wrist arthroscopy or there are signs of infection around the portal sites.

95.2.2 Surgical Technique

The operation can be performed under local anesthesia or general anesthesia depending on the surgeon's preference. The patient is placed in supine position and the operated arm is supported on a hand table. Usually no arm tourniquet is needed. If the operation is performed under local anesthesia, local anesthetic drug (2% xylocaine with 1:200,000 adrenaline) is infiltrated around the scaphoid tubercle and dorsoradial wrist region (Fig. 95.4).

95.2.2.1 Closed Reduction

A K-wire is inserted across the fracture site as a temporary fixation. The author prefers retrograde insertion of the K-wire, i.e., from the scaphoid tubercle through the scapho-trapezium-trapezoid (STT) joint towards the scaphoid proximal pole.

- Close reduction is performed with the forearm placed on a folded towel (Fig. 95.5). Traction is applied by grasping the thumb and the wrist is extended and ulnarly deviated, with forearm in full supination. This helps to reduce any humpback deformity. It also opens up the radio-volar interval between the scaphoid and the trapezium, and improves the access for K-wire insertion. The traction force helps to improve any step-off through ligamentotaxis.
- If the two fracture fragments are very unstable and cannot be reduced adequately by the above traction means, joystick K-wires of 1.6 mm can be inserted into the two fragments (Fig. 95.6). The joysticks are manipulated in order to give the best radiological reduction before inserting another K-wire for fracture temporary fixation.
- If there is an uncontrollable flexion deformity of the scaphoid fracture, the Linscheid maneuver is performed by inserting a radio-lunate (RL) pin of 1.6 mm percutaneously with the wrist in flexion to realign the RL joint and to correct the DISI (dorsal intercalated segmental instability) deformity (Fig. 95.7). This helps to control the extension deformity of the proximal fracture fragment indirectly through the lunate and the scapholunate ligament (if being intact). By extending, ulnarly deviating, and supinating the hand, the humpback deformity of the scaphoid can be corrected. The guide pin of the cannulated screw can then be inserted across the fracture site (Fig. 95.8).

Fig. 95.3 (**a**) Non-displaced scaphoid proximal pole fracture in a professional football player. The fracture could only be visualized in the scaphoid long profile view. (**b**) Percutaneous screw guide pin was inserted to the proximal pole. On arthroscopy, the proximal pole fracture was found to be stable after guide pin insertion. This confirmed that the guide pin had passed through the fracture site. Mild fracture gaping at the dorsal side was still present (top images). After screw insertion, on testing with a probe, the fracture gap disappeared and the fracture was stable

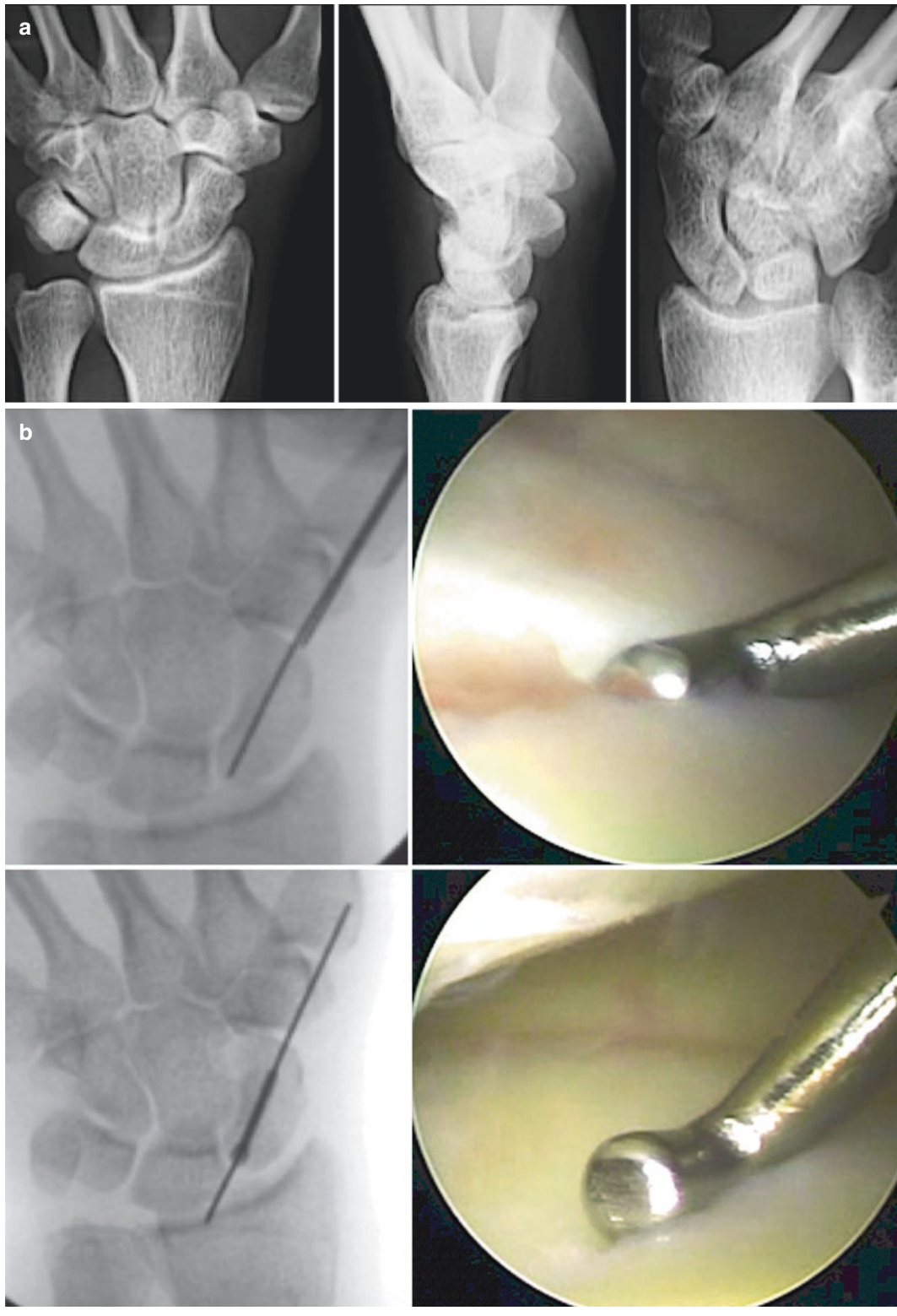
a
b

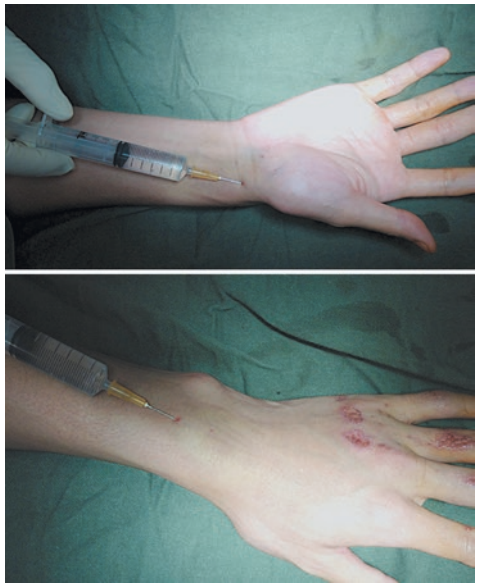

Fig. 95.4 Infiltrate local anesthetic drug is infiltrated around the scaphoid tubercle and dorsoradial wrist when the operation is performed under local anesthesia

95.2.2.2 Arthroscopic Reduction

The wrist is elevated on a wrist traction tower. If the operation is performed under local anesthesia, the portal site local anesthesia (PSLA) is done by injecting 2% xylocaine with 1:200,000 adrenaline.

- Midcarpal joint (MCJ) is accessed through the midcarpal radial (MCR) and midcarpal ulnar (MCU) portals to assess the articular reduction.
- The K-wire is withdrawn away from the fracture site if the reduction is not satisfactory. The fragments are manipulated through the MCR portal by a probe, a depressor, or by means of the pre-inserted joystick K-wires if present and the wire is reinserted (Fig. 95.9).

95.2.2.3 Definitive Screw Fixation

- If the initial K-wire is not along the scaphoid axis, insert another axial guide pin (Fig. 95.9). Correct position of the guide pin determines

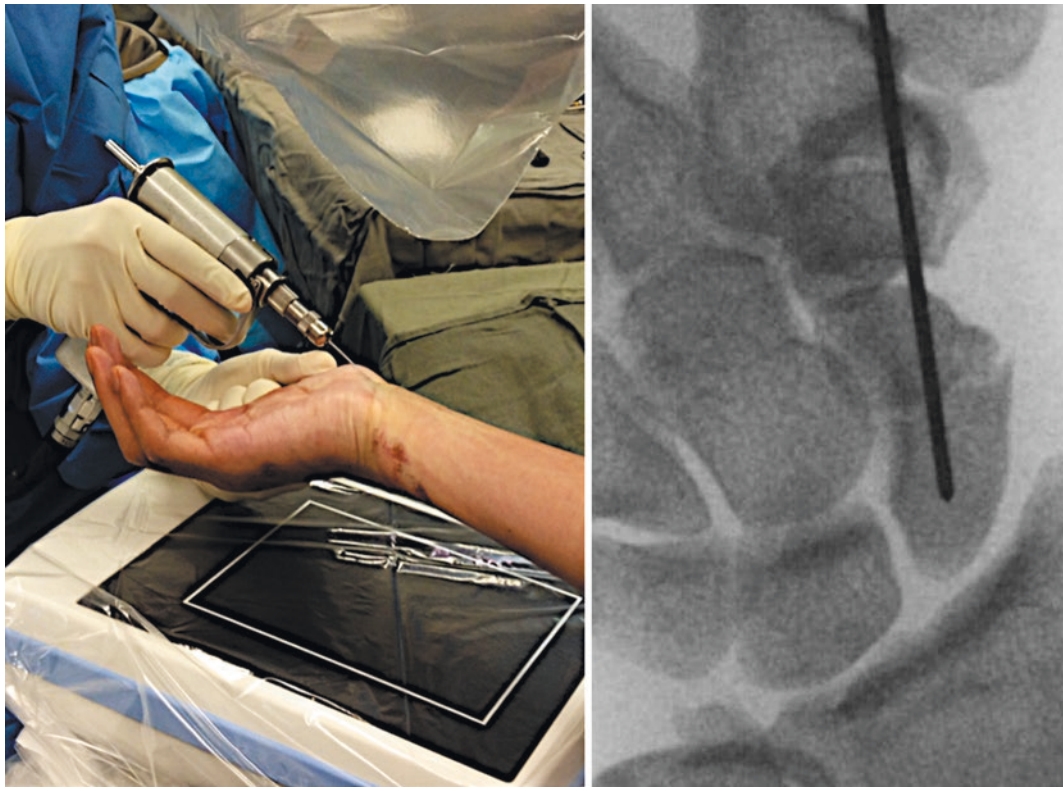

Fig. 95.5 Close reduction of scaphoid fracture can be done by holding the thumb abducted, forearm supinated, and wrist mildly extended in order to counteract the flexion and pronation deformity of the scaphoid fracture. Insert a K-wire through the STT joint, across the fracture site as a temporary stabilization

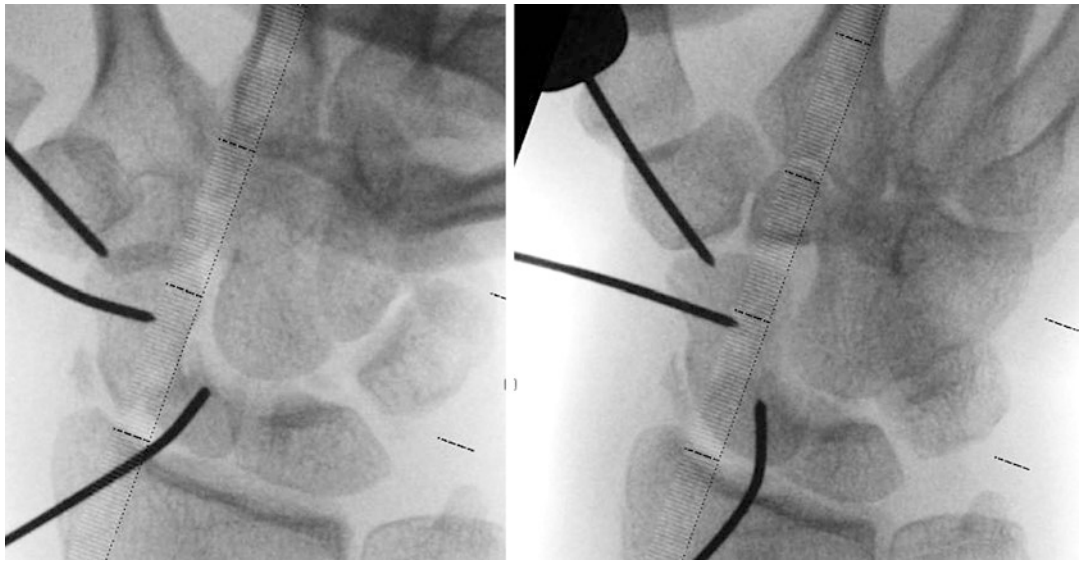

Fig. 95.6 If the two fracture fragments are highly unstable, before inserting a K-wire across the fracture site, insert one K-wire into each fragment under image intensifier. Try to manipulate the two K-wires as joysticks in order to give the best radiological fracture reduction. Then, insert another K-wire across the fracture site to give temporary stability

proper screw position. The closer the guide pin placed towards the scaphoid axis, the longer screw can be used, and the better fracture compression can be achieved [23, 24].

- The "Bean view" is the best view to ensure axial placement of the guide pin, which should pass through the interval between the middle and volar one-third of the bean along its volar border (Fig. 95.10). If the guide pin does not appear to cut out of the scaphoid on other views, this represents the longest scaphoid length with maximal bone purchase.
- If the fracture is oblique in configuration, or comminuted, or it is found to be very unstable during the reduction process, even though the initial K-wire is an axial one, insert one more K-wire across the fracture site to prevent rotational or translational deformity during screw insertion or compression (Fig. 95.11).
- Measure the length of the inserted guide pin. The actual screw length should be 4 mm subtracted from this measured pin length to allow for subsequent fracture compression and "sinking" of the screw head below the cortex. Advance the guide pin to the dorsal wrist out of the skin (Fig. 95.12) and secure it in place with an artery forceps. An oscillating mode of the guide pin driver minimizes the risk of entrapping extensor tendons. If the guide pin is accidentally broken during screw tract reaming, it can still be taken out with its exposed parts on both the dorsal and volar sides of the wrist.
- The wrist is repositioned on the wrist traction tower and the scaphoid is visualized to confirm reduction. Reaming along the guide pin is performed and the fracture is visualized arthroscopically during reaming and screw compression to confirm reduction and avoiding "over-reduction." An arthroscopic depressor is useful to control the articular reduction (Fig. 95.13).

95.2.2.4 Additional Procedures

- If there is fracture gapping because of fracture comminution, the fracture gap is impacted with bone graft, either autologous or artificial bone graft to allow for bone substitution (Fig. 95.14).

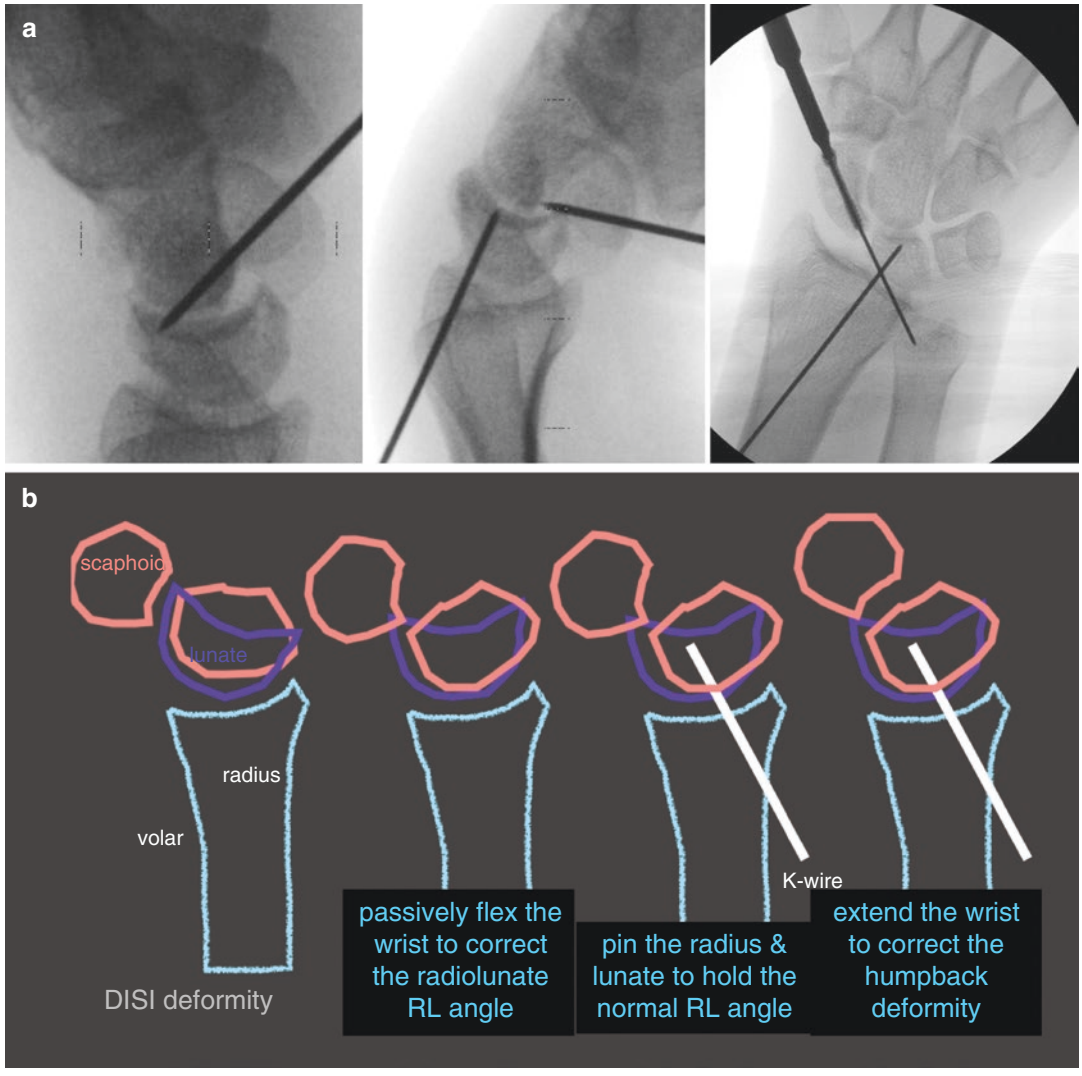

Fig. 95.7 (**a**) Linscheid maneuver is shown. In uncontrollable fracture flexion deformity, bend the wrist to correct the RL angle and insert a K-wire across the radius and lunate. This helps to correct the extension deformity of the proximal fragment indirectly. (**b**) Schematic diagram demonstrates how the fracture flexion deformity can be indirectly corrected by Linscheid maneuver

- Any loose fragments are removed to prevent articular impingement or irritation (Fig. 95.15).
- Associated ligament or TFCC injuries are treated arthroscopically (Fig. 95.16a, b).

95.2.3 Tips and Tricks

- Avoid excessive shoulder abduction during positioning the patient on the operation table. Excessive shoulder abduction makes passive forearm pronation difficult. Additionally, RL pin or joystick K-wires placement on the fragments is technically more difficult in this position.
- A good quality intra-operative image intensifier is essential to visualize the preliminary fracture reduction and K-wire position.
- Five X-ray views are mandatory to assess fracture alignment, guide pin, and screw position. These include AP (anteroposterior), lateral, scaphoid (AP ulnar deviation), semi-supination (Bean's view), and semi-pronation view.

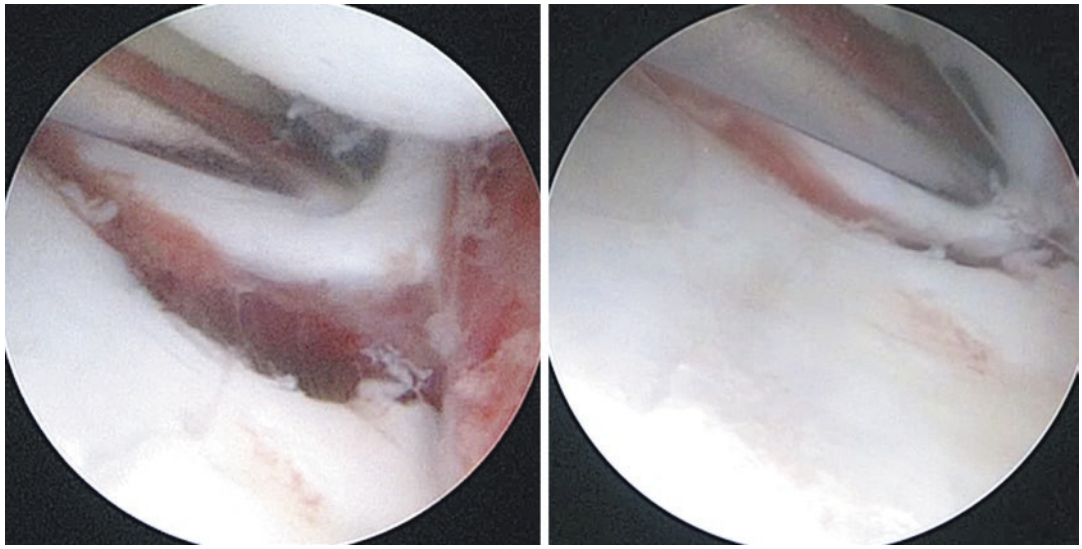

Fig. 95.8 Scaphoid fracture is assessed by a probe through a mid-carpal joint. K-wire is withdrawn beyond the fracture site. After the fracture stepping was corrected, the K-wire was reinserted through the fracture site

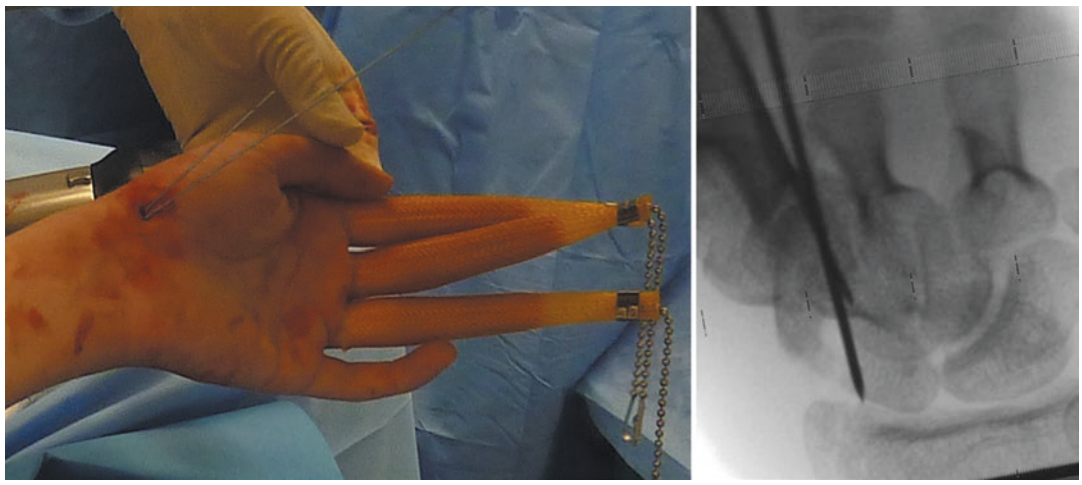

Fig. 95.9 The initial K-wire fixing the fracture is not along the scaphoid axis and a second guide pin is inserted for screw placement

Ensure satisfactory fracture reduction, hardware position with no screw protrusion from these five X-ray views before concluding the operation. If screw protrusion is suspected, scope through the radiocarpal joint (RCJ) to verify.

- Beware of the radial artery and superficial radial nerve when placing a joystick K-wire into the distal fragment. Large bore angiocatheter needle can be used as a trocar cannula for drilling a K-wire into the distal fragment.
- Technically, it is easier to anchor a K-wire through the STT joint into the distal scaphoid fragment before manipulating the joystick K-wires on the distal and proximal fragments. Once the joystick reduction is satisfactory, advance the K-wire across the fracture site. Use arthroscopy to fine tune the reduction afterward.

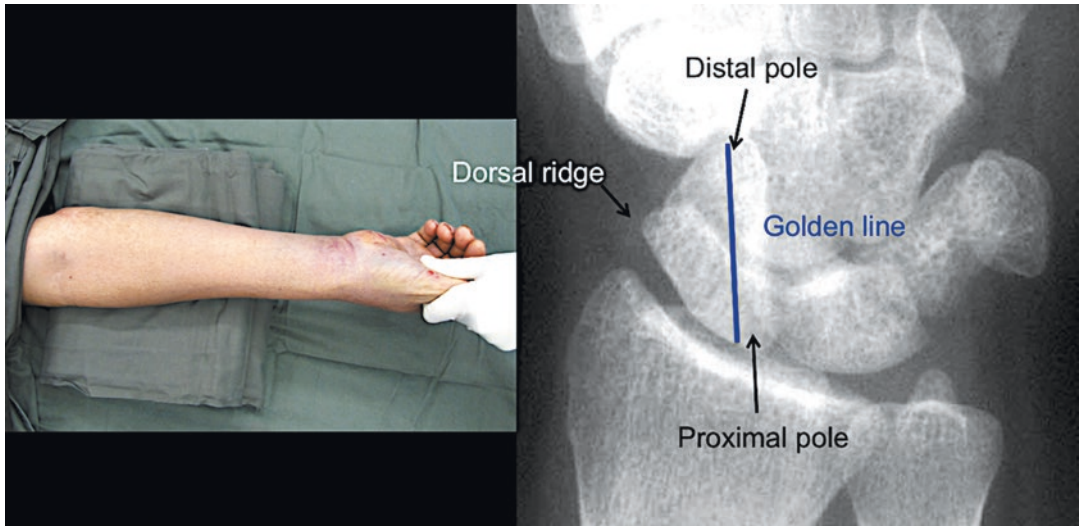

Fig. 95.10 Semi-supination view (Bean view) is demonstrated. X-ray is taken with forearm semi-supinated. The "Golden line" is the landmark for the position of the guide pin in the "Bean view"

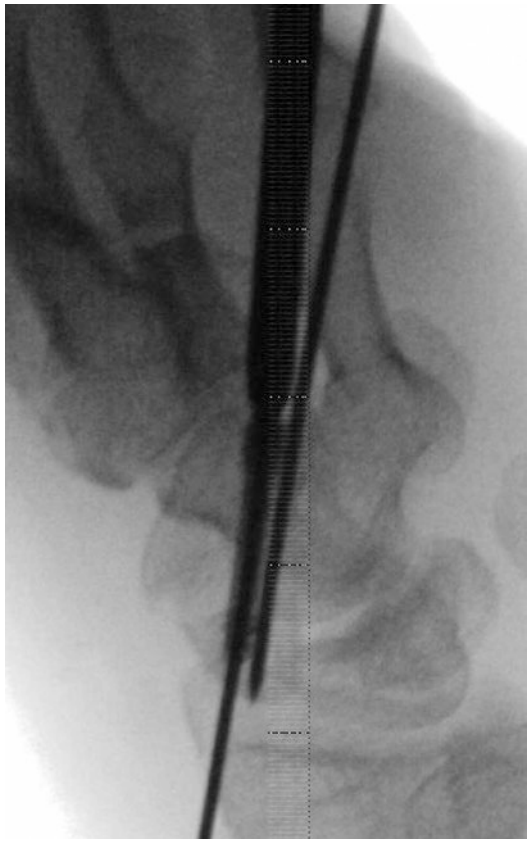

Fig. 95.11 Scaphoid fracture comminution. To prevent collapse or rotational deformity of the fracture during screw tightening, another K-wire is inserted across the fracture site before screw insertion

95.2.4 Pitfalls

- Bony resistance should be felt when the guide pin approaches the opposite cortex at the exit point. If the tip of the guide pin is still far away from the scaphoid cortex in any X-ray view when the resistance has been felt, the guide pin is not at the axial position. If the guide pin is not too inferior or superior in the lateral X-ray view, it is easier to rely only on the Bean's view to adjust the guide pin to the desired position.
- For Asian women, the usual screw length is around 20–24 mm, whereas 22–26 mm in men. If the measured pin length is beyond 26–30 mm, make sure that there is no protrusion of the guide pin out of the cortex by repeating all five X-ray views.
- Putting a scope through the MCR portal may depress and rotate the proximal fragment even though the fracture has been transfixed temporarily with K-wire. Always assess the fracture reduction through MCU portal.

95.2.5 Postoperative Management and Rehabilitation

Rehabilitation depends on whether the scaphoid is bone grafted or not, any associated ligament injury,

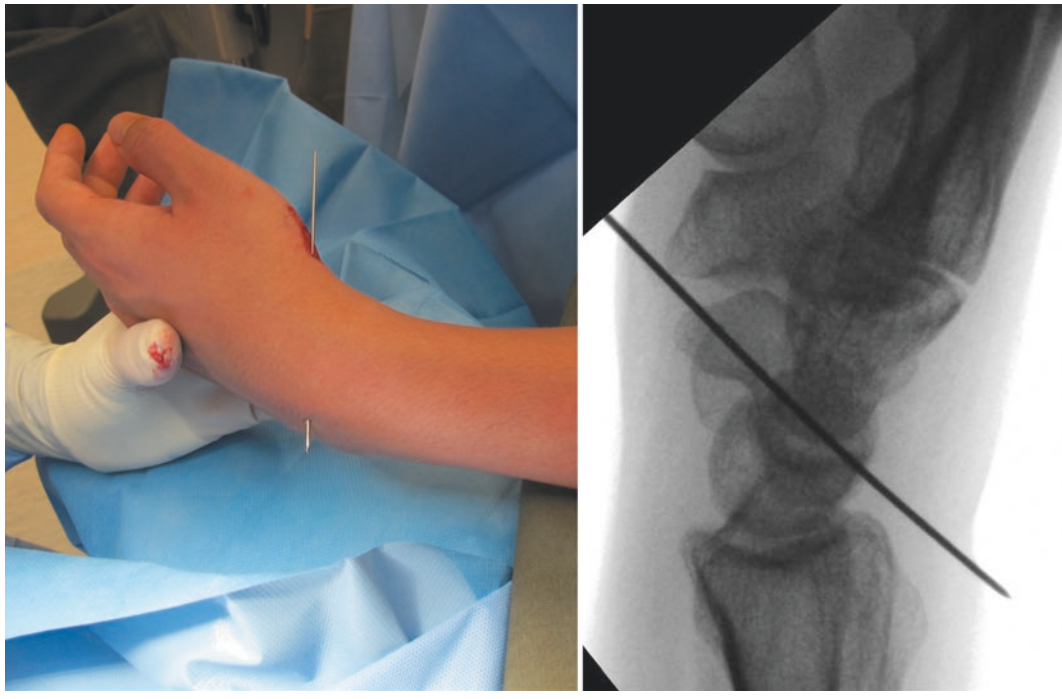

Fig. 95.12 The guide pin is advanced to the dorsal wrist out of the skin and secured with an artery forceps before reaming the bone

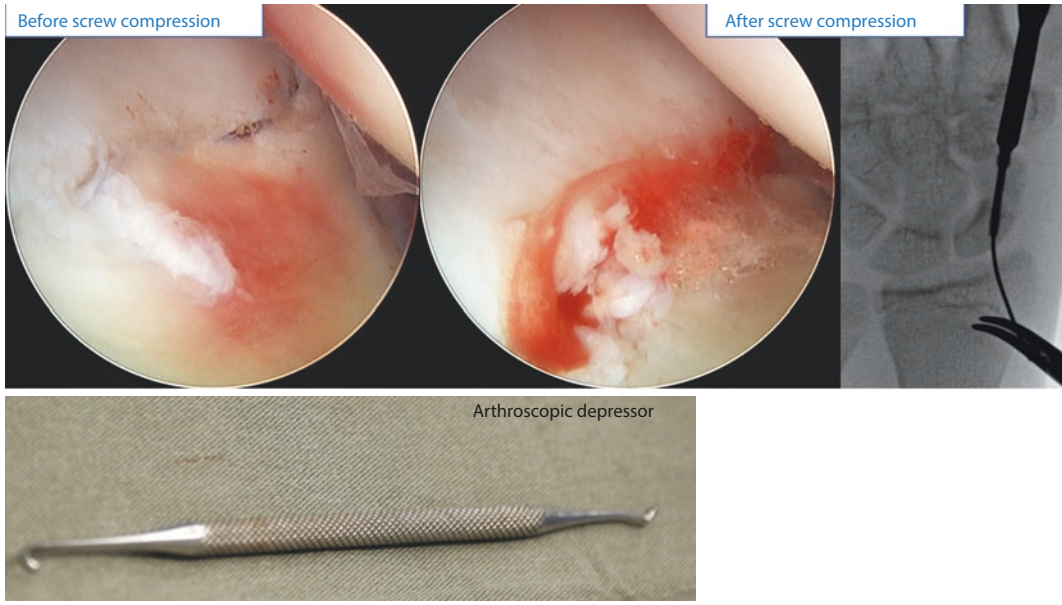

Fig. 95.13 Articular reduction is confirmed arthroscopically during screw tightening. Arthroscopic depressor is useful to control the articular surface during reaming and screw tightening

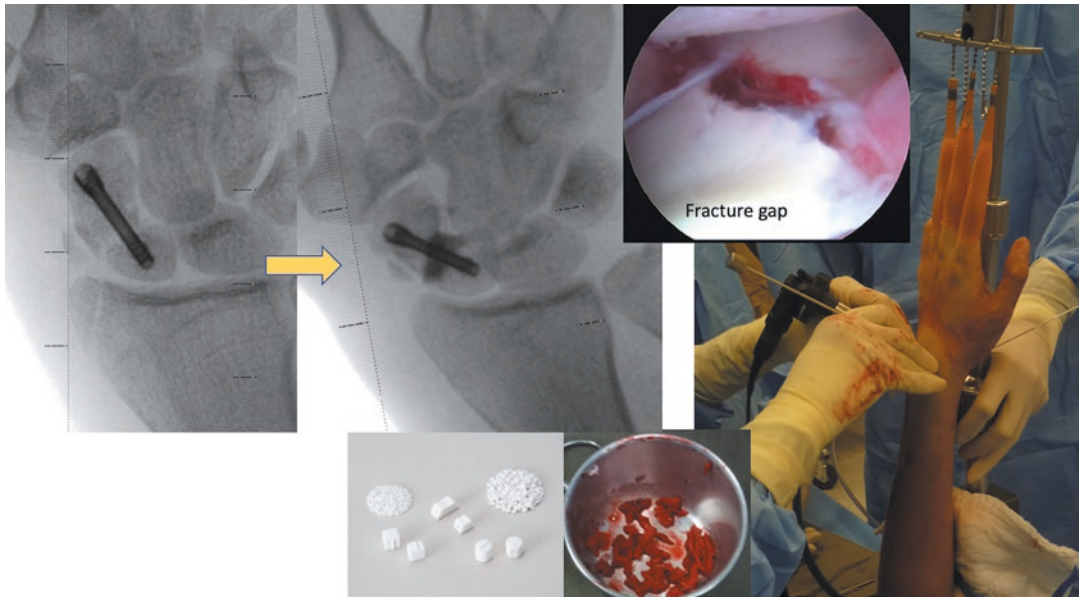

Fig. 95.14 Graft impaction at fracture gap is shown

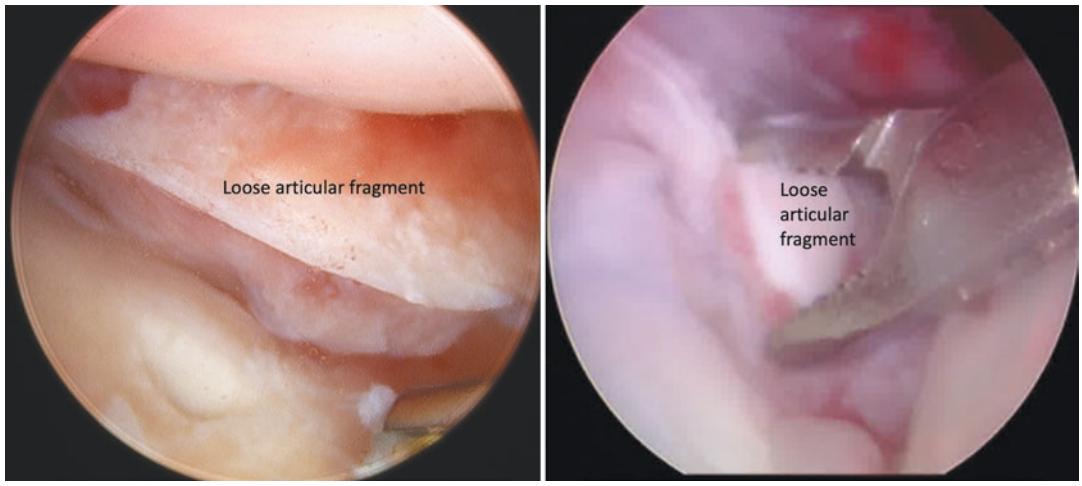

Fig. 95.15 Loose fragment excision is demonstrated

any ligament or TFCC surgery is performed at the same time. A slab is given for soft tissue healing for a week. If only screw fixation to the scaphoid is done, a wrist brace is used for 4–6 weeks if the fracture is an unstable one. Otherwise, active wrist motion is allowed with a removable brace. No weight bearing on the wrist is allowed until the fracture heals well.

95.2.6 Complications

Apart from general complications of wrist arthroscopy, complications from arthroscopic-assisted scaphoid fixation are minimal. Fracture nonunion is minimized as arthroscopy makes reduction more accurate. Screw protrusion should be avoided.

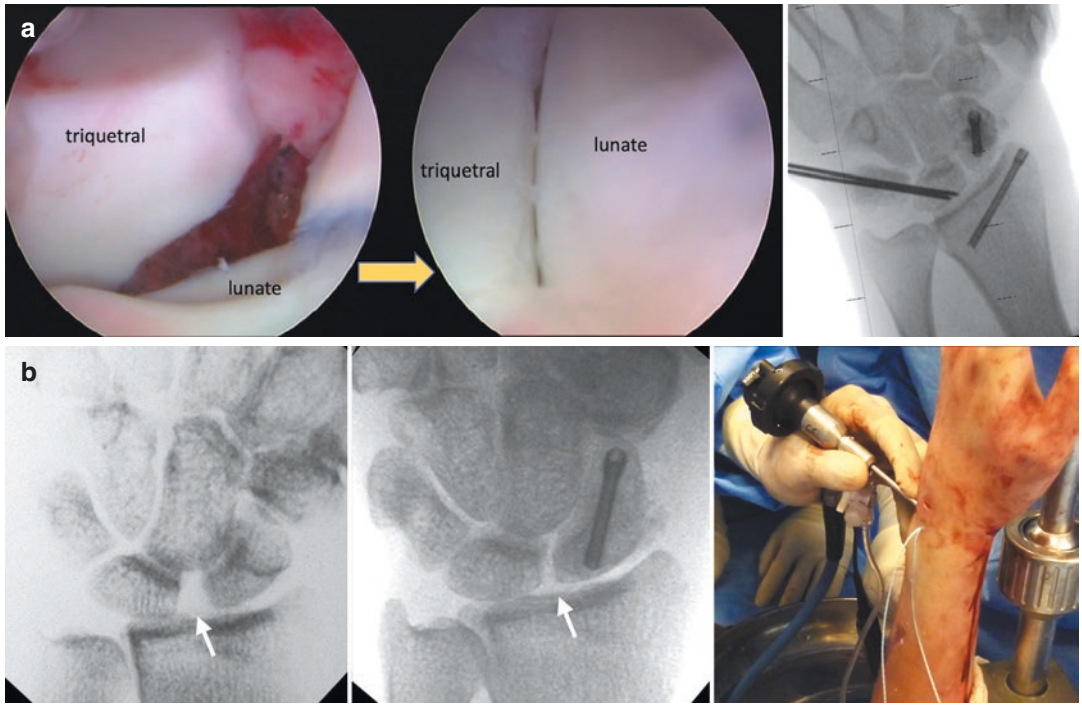

Fig. 95.16 (**a**) An associated lunotriquetral (LTq) ligament tear is shown. K-wires were put across the LTq under arthroscopic guidance after reduction. (**b**) An associated scapholunate (SL) ligament tear is treated with arthroscopic SL ligament plication

95.3 Part II: Arthroscopic Bone Grafting (ABG) for Scaphoid Nonunion

95.3.1 Indications and Contraindications

Open dissection for scaphoid nonunion jeopardizes the residual limited vascularity which affects bone graft union, and damages the capsular and ligamentous structures resulting in wrist stiffness. In April 1997, ABG was first done in a 50-year-old man with scaphoid nonunion after percutaneous screw fixation 5 months ago. The fracture was united 3 months after ABG. The patient enjoyed a good range of motion, pinch, and grip power. Since then, ABG is the author's primary standard treatment and is indicated in all scaphoid delayed unions and nonunions, including those with features of avascular necrosis, reducible humpback deformity, and those with a previous fracture or nonunion surgery.

Limitations do exist for ABG, and include:

- Long-standing scaphoid nonunion with significant carpal collapse cannot be adequately corrected after arthroscopic fibrosis release and close reduction.
- Severe SNAC (scaphoid nonunion advanced collapse) wrist changes likely preclude good outcome from scaphoid union after bone grafting.
- Avascular necrosis is not an absolute contraindication, though the chance of persistent nonunion is higher than those with good intra-operation bone bleeding.
- Significant arthrofibrosis that causes difficult access by the arthroscope may be a relative contraindication. Nevertheless, with experience, patience, and use of smaller arthroscope, most fibrotic joint can be loosened up gradually by careful arthroscopic debridement and dilation to provide adequate working space for subsequent bone procedure.

95.3.2 Surgical Technique

The patient is put in supine position and the arm is supported on a hand table. Either side of the iliac crest is draped for bone graft harvesting. An arm tourniquet is applied and inflated only if necessary. Vertical traction of 4–6 kg force is applied through finger traps to the index, middle, and ring fingers. A bag of 3 liters of normal saline solution is hung up at about 1.5 m height for continuous joint inflow. Infusion pump is not used to avoid fluid extravasation.

95.3.2.1 Arthroscopic Evaluation

This step can be performed under portal site local anesthesia (PSLA) as mentioned before. Patient is awake and watching the arthroscopy monitor. This helps the patients to understand their disease condition, severity, prognosis, and treatment choices, and comply with the subsequent rehabilitation.

- The RCJ and MCJ are assessed through 3–4 portal and MCR portal respectively with 1.9 mm arthroscope. Any accompanying chondral lesion related to SNAC wrist changes should be documented since it affects the prognosis and choice of procedure, especially the dorsal rim of the radial styloid which is a common site of occurrence of early SNAC wrist changes. Any associated synovitis at this area may obscure the observation of true cartilage condition and has to be removed.
- Unless the nonunion is in a very proximal site, the fracture site is usually not seen from the RCJ. The fracture is obscured by the capsular reflection, which helps to contain subsequent bone grafting implanted through the MCJ.

95.3.2.2 Debridement of Nonunion

- Take-down of the nonunion site is performed using MCR (working) and MCU (viewing) portals. The MCR portal may not be easy to develop as the working space through MCR portal is narrow as a result of fracture malalignment, bone spurs at the nonunion site, intra-articular fibrosis, and secondary capsular contracture. It is however the best portal to take down fibrosis. In the distal third nonunion, STT portal is frequently required to provide more direct access (Fig. 95.17).
- The nonunion is located by a cleavage line in the scaphoid articular surface or by a frank gapping (Fig. 95.18).
- The fracture gap is assessed with a probe inserted through the MCR portal. Healing bone is usually found in the center of the fracture. If stable bony tissue is encountered after initial debridement of the overlying fibrous tissue, or lack of mobility at the fracture site by probing, simple screw fixation or even casting may suffice (Fig. 95.19). If frank bony defect is encountered, it is curetted with a fine angled curette, 2 mm or 2.9 mm shaver and 2.9 mm burr until all fibrotic tissue and sclerotic bone are removed. If there is previous screw fixation, the loose screw should be removed to facilitate radical debridement. Any intact cartilage or pseudo-capsule around the fracture site should be preserved for better graft containment (Fig. 95.10).
- Both ends of the nonunion are burred until cancellous bone with punctate bleeding is reached (Fig. 95.20) and confirmed by viewing through the MCR portal. Tourniquet is not necessary and so vascularity of the remaining bone fragments can be assessed accurately. Further curettage of the proximal fragment can be performed through the STT portal if necessary (Fig. 95.17). If bone bleeding is not obvious or uncertain, the saline irrigation is stopped temporarily to reduce the hydrostatic pressure inside the joint. In cases where punctate bleeding is not observed, the end point of debridement is reached when the softer cancellous bone is reached.

95.3.2.3 Correction of Scaphoid Deformity

- After adequate debridement and curettage, the two fragments of the nonunion should be mobile enough for subsequent reduction. Any humpback and DISI deformity should be identified and corrected by:

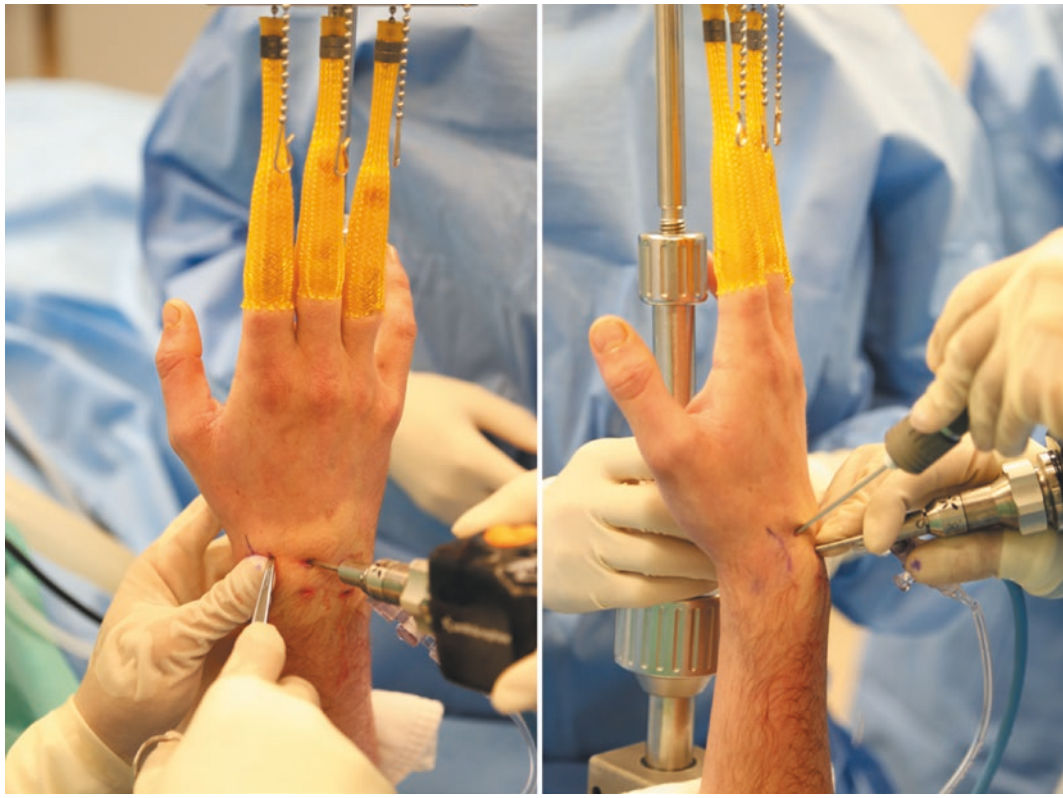

Fig. 95.17 An STT portal is created for more direct access to distal nonunion site. An arthroscopic burr is inserted through the STT portal

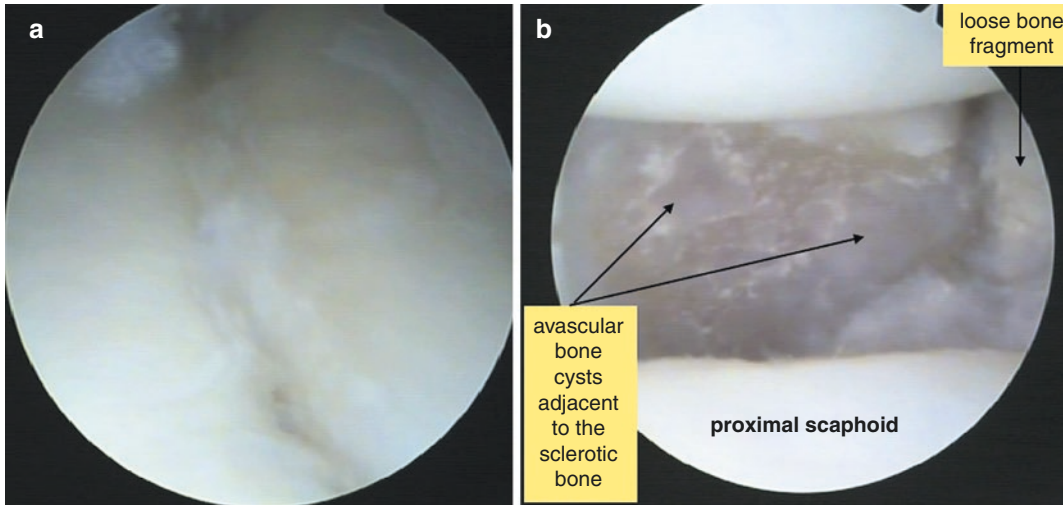

Fig. 95.18 (**a**) Cleavage line in scaphoid articular surface at the site of nonunion, viewed from MCR portal. (**b**) View from MCU portal. Frank fracture nonunion gap is shown with cysts and loose fracture fragment

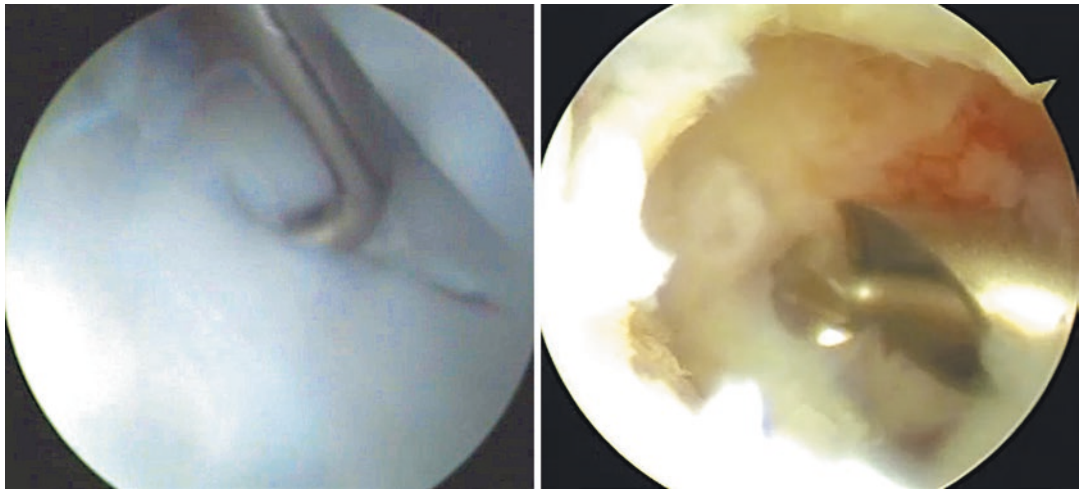

Fig. 95.19 Stable fracture site and firm healing bone under cartilage is seen on probing. No bone graft was needed (left image). Intact cartilage and pseudo-capsule around the nonunion site are preserved during bone burring

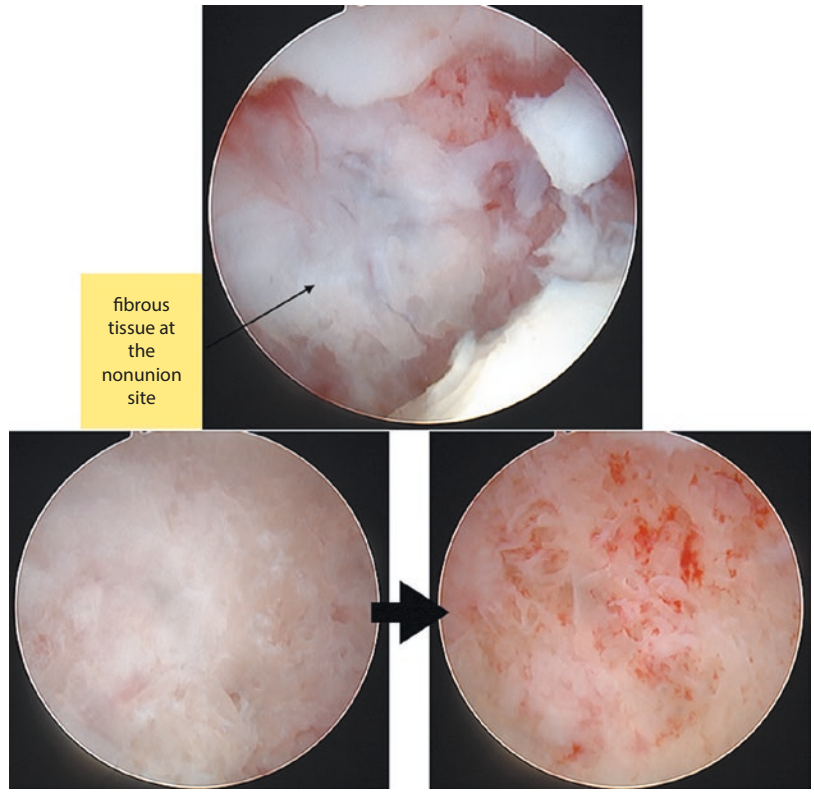

Fig. 95.20 The fibrous tissue at the nonunion site is shown and has to be removed (top image). Nonunion fracture surface is burred until cancellous trabeculae is seen (bottom images)

- Linscheid maneuver (Fig. 95.8).
- Close reduction as in acute scaphoid fracture (Fig. 95.5).
- Inserting a 1.6 mm K-wire into the distal fragment as a joystick manipulation, especially in distal third nonunion.
- A probe or arthroscopic depressor to manipulate the fragment within the MCJ.

- Once the fracture fragments are well aligned, they are transfixed with one 1.1 mm K-wire inserted percutaneously from the scaphoid tubercle under fluoroscopic guidance (Fig. 95.5).

The K-wire should aim eccentrically at a more radial and proximal location across the nonunion site so that the pin would not block the placement and impaction of the bone graft inserted from the MCJ (Fig. 95.21). When the fixation is complete, the hand can be put back to the traction tower for bone grafting procedure.

95.3.2.4 Bone Graft Through MCJ

- A large diameter arthroscopic cannula (3.2 mm to 4.5 mm) is introduced through an appropriate portal directly opposing the fracture defect. For fractures located at the proximal two-third of the scaphoid, MCR portal is the most direct one. For distal third fractures, STT portal is considered.
- Cancellous bone graft is harvested from the iliac crest using either a trephine or an open technique through a small incision. The volume of the bone graft obtained should be at least 3–5 times that of the defect since the graft has to be impacted in the defect to increase its compaction and strength. Bone graft is cut into small chips using scissors and delivered through the cannula with a slightly undersized trocar with a flat end (Fig. 95.22). Arm tourniquet can be inflated to enhance the visibility during the graft impaction process. The most proximal and dorsal part of the defect has to be filled up first to avoid subsequent graft void. Empty space previously occupied by a loosened screw should also be filled in first.
- In a very proximal fracture, the nonunion site can be directly communicating with the RCJ. To avoid spillage of bone graft from the MCJ into the RCJ, a pediatric size 6 urinary catheter is inserted into the RCJ through the 3–4 portal, insufflated with saline and provide a mechanical block from the bone graft going into the RCJ (Fig. 95.23).
- A small depressor can be employed at intervals to impact and mold the graft to the articular surface of the scaphoid (Fig. 95.24). Completeness and adequacy of the graft filling are confirmed by fluoroscopy. After completion of impaction bone grafting, the MCJ and RCJ are inspected to remove any spilled out bone graft debris. MCJ is aspirated dry and 1 ml of fibrin glue is applied on the surface of the graft substance (Fig. 95.25). Traction is released to allow the natural compression from the capitate onto the graft.

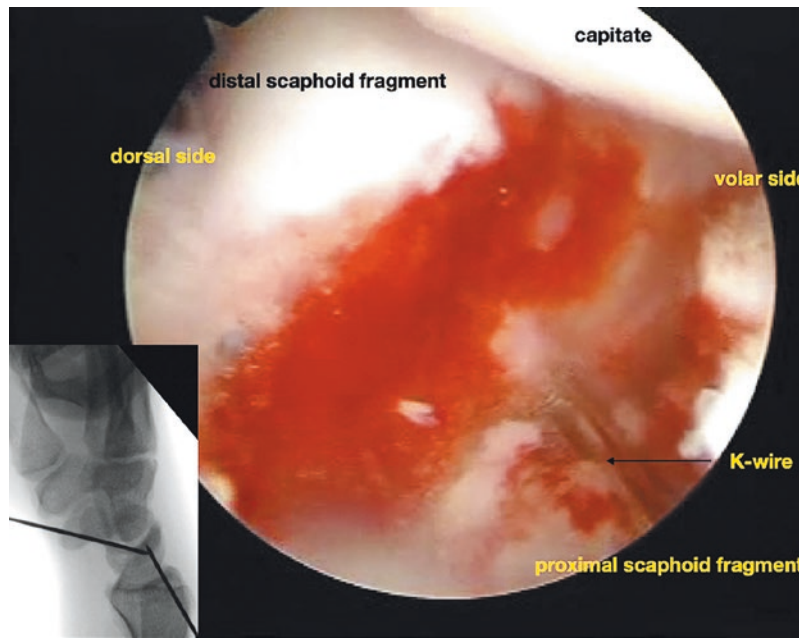

Fig. 95.21 View from MCU portal: the pin should be situated in a deeper and basal position inside the defect. It should be placed at the more volar and proximal position at the nonunion site so that subsequent bone grafting would not be blocked by the pin

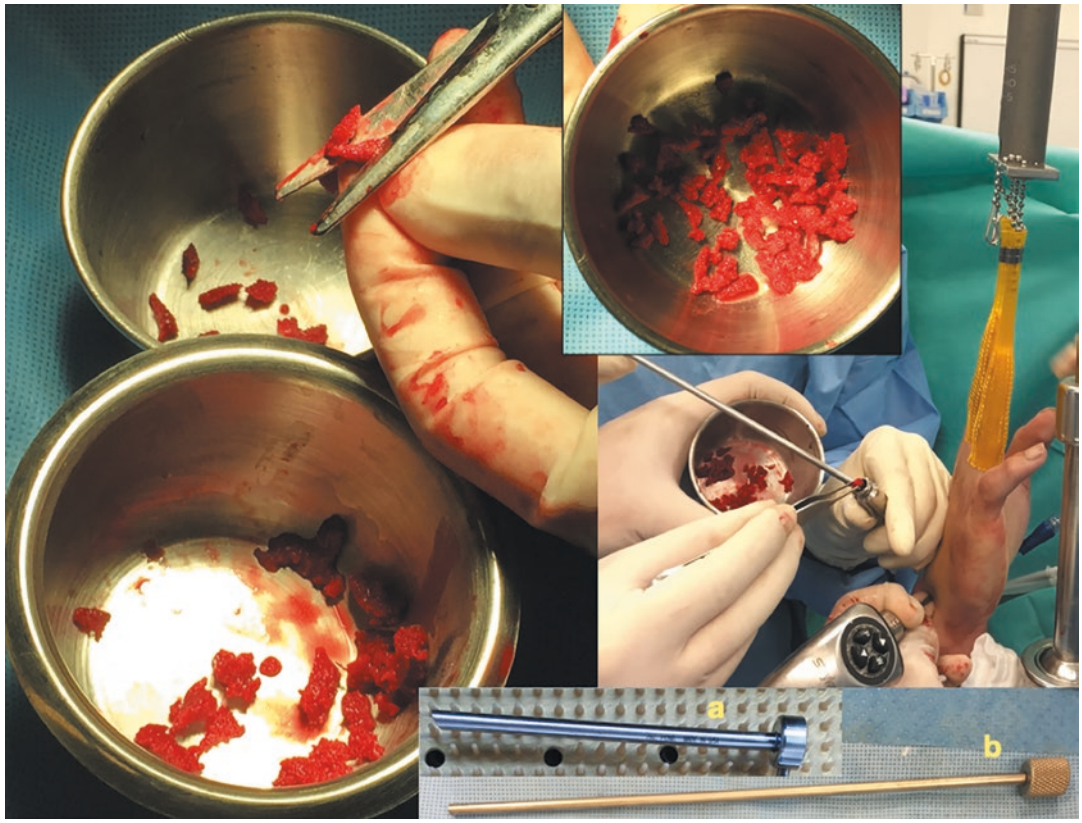

Fig. 95.22 Bone graft is cut into small pieces and delivered to the nonunion site through a trocar cannula with no side hole (**a**), and impacted with a trocar with a flat tip and of smaller diameter than the trocar cannula (**b**)

95.3.2.5 Fracture Fixation

- *Percutaneous screw fixation* is indicated when the bone defect is small and located at the mid-waist with sizeable proximal and distal fragments. Screw guide pin is placed along the scaphoid axis with the surgical techniques mentioned previously. Cannulated screw is employed but excessive compression should be avoided to prevent graft extrusion and collapse of the nonunion site. After screw fixation, the initial transfixing 1.1 mm K-wire is then removed or cut short depending on the fracture stability assessed intra-operatively.
- *Percutaneous multiple K-wire fixation* is indicated when the bone defect is sizeable, particularly in proximal or distal third nonunion, in nonunion with humpback deformity and for cases with previous screw fixation (Fig. 95.26). It is difficult to achieve an ideal position or sufficient bone purchase when using screw in these situations. This risks bone fragmentation especially of the proximal pole, screw cutting out, excessive compression causing recurrence of humpback deformity, and graft extrusion. Two or three additional 1.1 mm K-wires are inserted adjacent to the initial transfixing K-wire. Scapholunate or scaphocapitate K-wire can also be used for an unstable nonunion. The K-wires are cut short and buried under the skin and for removal 10–12 weeks later.

The wounds are apposed with steri-strips. If there is a RL pin, it is left exposed outside the skin for early removal at 2 weeks.

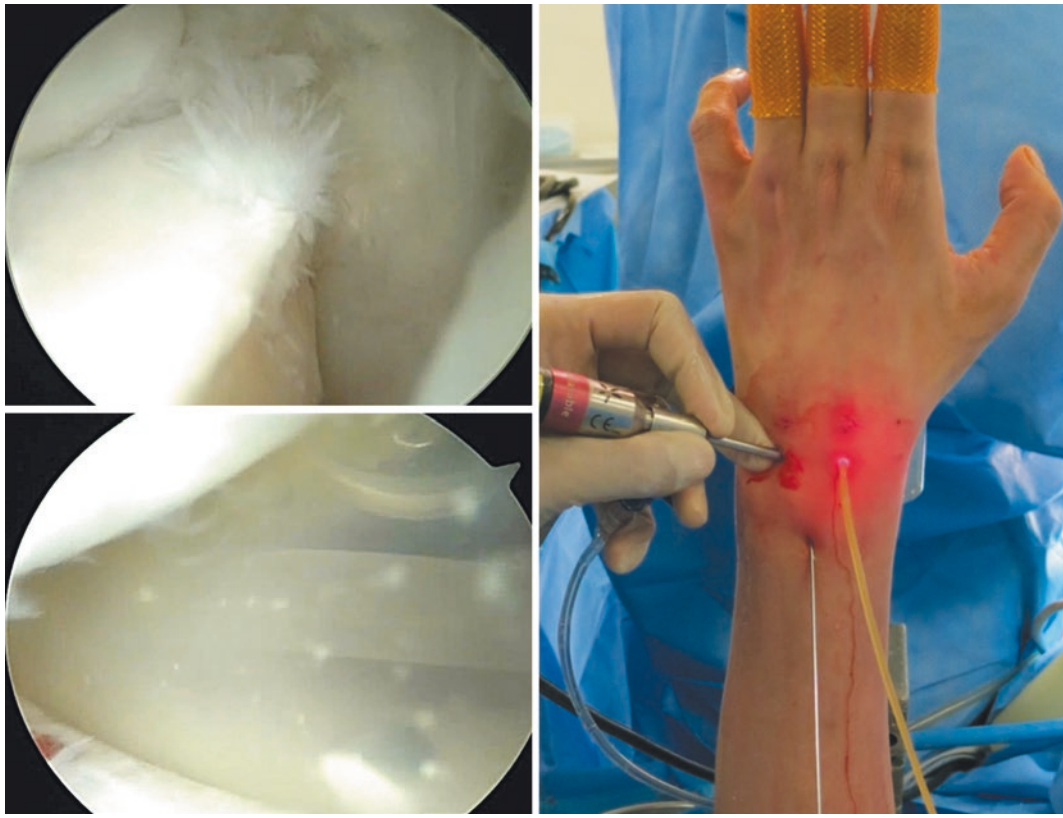

Fig. 95.23 For proximal scaphoid fracture that communicates with the RCJ (top left), a foley catheter was inserted through the 3–4 portals and was insufflated to block the bone graft going into the RCJ (bottom left and right images)

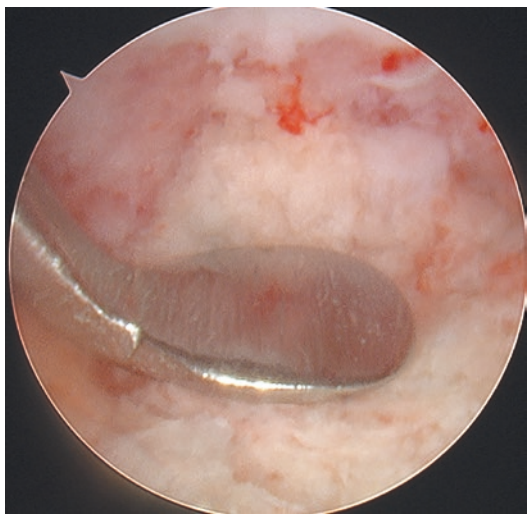

Fig. 95.24 A depressor is used to impact the bone graft dense and tight

95.3.3 Tips and Tricks

- There is sometimes hypertrophic sclerosis at the dorsal side of the scaphoid nonunion (Fig. 95.27). Humpback deformity and relatively better vascularity from the dorsal capsular attachment on the scaphoid sulcus create a bony bump at the dorsal side of the nonunion. This can block the arthroscopic burr to enter through the MCR portal and also hinder it to tackle the nonunion site. Operative field and the subsequent operative procedure is easier if the bump is taken down at the beginning.
- To avoid the risk of entrapping extensor tendons, an oscillating mode of the K-wire driver should be used in putting RL pinning.

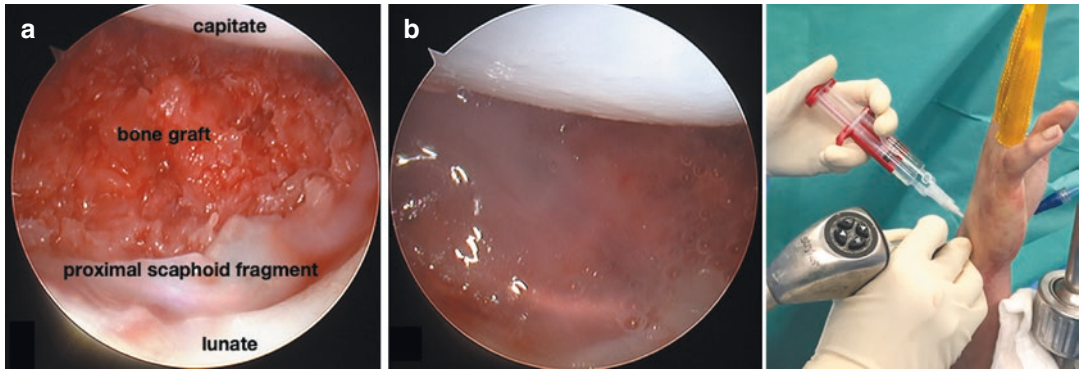

Fig. 95.25 Fibrin glue is applied through MCR portal to cover the bone graft. (**a**) before tissue glue application; (**b**) after tissue glue application

Fig. 95.26 Fixation using three K-wires across the fracture site (left) and the 3-year follow-up radiograph (right) is shown

95.3.4 Pitfalls

- The fracture gap is larger than expected after adequate debridement and burring of the non-union site. Restoring the normal scaphoid length and alignment helps to restore the normal tautness of the surrounding ligaments and kinematics of the whole wrist, which may lessen the mobility of the fracture. However, avoid over-lengthening the scaphoid which will result in limited wrist motion. Make sure the initial K-wire goes through to the proximal fragment far cortex to give a strong purchase and stability to prevent distraction and lengthening of the fracture site during bone graft impaction.

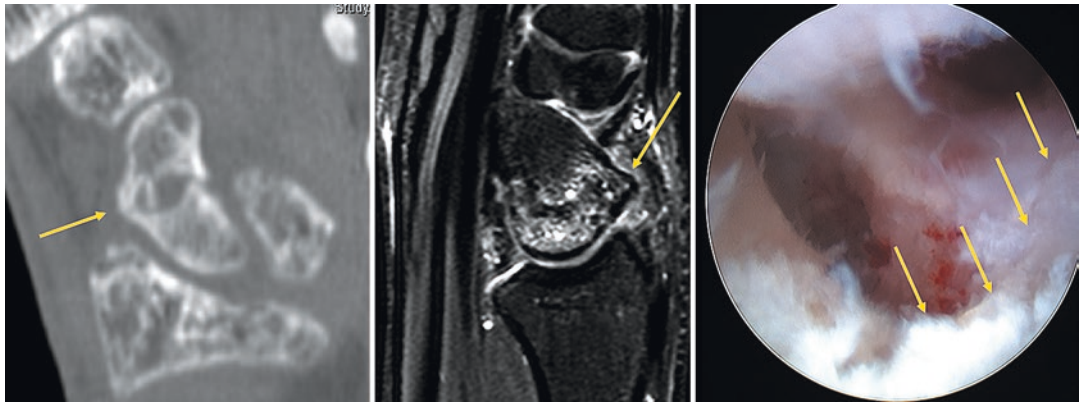

Fig. 95.27 Arrows show the "bump" at the dorsal aspect of the nonunion

95.3.5 Postoperative Management and Rehabilitation

A short arm plaster slab is provided and maintained for 2 weeks. In cases with DISI deformity, the RL pin is removed in 2 weeks. A wrist brace is then used. If the nonunion site is stable, active wrist mobilization out of the brace under supervision of hand therapist is initiated at 2 weeks. Radiographs are taken at regular intervals to monitor the progress of graft incorporation and bone healing. Once clinical and radiological union is confirmed, the K-wires can be removed under local anesthesia, typically at 10–12 weeks postoperative. Passive wrist mobilization is then initiated once union is established. Hand and upper limb strengthening can follow, usually at 12–16 weeks postoperative.

References

1. Dias JJ, Brenkel IJ, Finlay DB. Patterns of union in fractures of the waist of the scaphoid. J Bone Joint Surg Br. 1989;71(2):307e310.
2. Buijze GA, Ochtman L, Ring D. Management of scaphoid nonunion. J Hand Surg Am. 2012;37(5):1095–100; quiz 1101
3. Dy C, Kazmers J, Baty N, Bommarito H, Osei J. An epidemiologic perspective on scaphoid fracture treatment and frequency of nonunion surgery in the USA. HSS J. 2018;14(3):245–50.
4. Gelberman RH, Wolock BS, Siegel DB. Fractures and non-unions of the carpal scaphoid. J Bone Joint Surg Am. 1989;71(10):1560–5.
5. Langhoff O, Andersen JL. Consequences of late immobilization of scaphoid fractures. J Hand Surg Br. 1988;13(1):77–9.
6. Grewal R, Lutz K, Macdermid J, Suh N. Proximal pole scaphoid fractures: a computed tomographic assessment of outcomes. J Hand Surg. 2016;41(1):54–8.
7. Gelberman RH, Gross MS. The vascularity of the wrist. Identification of arterial patterns at risk. Clin Orthop Relat Res. 1986;202:40–9.
8. Handley RC, Pooley J. The venous anatomy of the scaphoid. J Anat. 1991;178:115–8.
9. Smith DK, An KN, Cooney WP III, Linscheid RL, Chao EY. Effects of a scaphoid waist osteotomy on carpal kinematics. J Orthop Res. 1989;7:590–8.
10. Kamal RN, Starr A, Akelman E. Carpal kinematics and kinetics. J Hand Surg Am. 2016;41(10):1011–8.
11. Herbert TJ. The fractured scaphoid. St. Louis, MO: Quality Medical Publishing; 1990. p. 51–67.
12. Munk PL, Lee MJ, Logan PM, Connell DG, Janzen DL, Poon PY, et al. Scaphoid bone waist fractures, acute and chronic: imaging with different techniques. AJR Am J Roentgenol. 1997;168:779–86.
13. Marai GE, Crisco JJ, Laidlaw DH. A kinematics-based method for generating cartilage maps and deformations in the multi-articulating wrist joint from CT images. Conf Proc IEEE Eng Med Biol Soc. 2006;1:2079–82.
14. Leung YF, Ip SPS, Cheuk C, Sheung KT, Wai YL. Trephine bone grafting technique for the treatment of scaphoid nonunion. J Hand Surg Am. 2001;26(5):893–900.
15. Demirag B, Sarisozen B, Ozer O, Kaplan T, Ozturk C. Enhancement of tendon-bone healing of anterior cruciate ligament grafts by blockade of matrix metalloproteinases. J Bone Joint Surg Am. 2005;87(11):2401–10.
16. Abedi G, Alizadeh R, Biabangardi B, Moslemi H. Effect of synovial fluid on intercondylar fracture in cats. Ann Bio Res. 2013;4(9):87–91.
17. Berg EE, Pollard ME, Kang Q. Interarticular bone tunnel healing. Arthroscopy. 2001;17:189–95.

18. Hazelton RA, Vedam R, Masci PP, Whitaker AN. Partial purification and characterisation of a synovial fluid inhibitor of osteoblasts. Ann Rheum Dis. 1990;49:121–4.
19. Amadio PC, Berquist TH, Smith DK, Ilstrup DM, Cooney WP III, Linscheid RL. Scaphoid malunion. J Hand Surg Am. 1989;14(4):679–87.
20. Berdia S, Wolfe SW. Effects of scaphoid fractures on the biomechanics of the wrist. Hand Clin. 2001;17(4):533–40.
21. Burgess RC. The effect of a simulated scaphoid malunion on wrist motion. J Hand Surg Am. 1987;12(5 pt 1):774–46.
22. Smith DK, Cooney WP III, An KN, Linscheid RL, Chao EY. The effects of simulated unstable scaphoid fractures on carpal motion. J Hand Surg Am. 1989;14(2 pt 1):283–2911.
23. McCallister WV, Knight J, Kaliappan R, Trumble TE. Central placement of the screw in simulated fractures of the scaphoid waist; a biomechanical study. JBJS Am. 2003;85:72–7.
24. Dodds SD, Panjabi MM, Slade JF III. Screw fixation of scaphoid fractures: a biomechanical assessment of screw length and screw augmentation. JHS Am. 2006;31:405–13.

Arthroscopic Replacement of Proximal Pole Scaphoid Fracture

96

Mathilde Gras and Christophe Mathoulin

96.1 Introduction

Decision-making in management of scaphoid nonunion is determined by the geometry and type of fracture, and the vascular pattern to the scaphoid. Fractures proximal to the nutrient vessels entering on the dorsoradial surface can result in ischemia of the proximal pole. The natural evolution results in radioscaphoid and radiocarpal arthritis, and eventual carpal collapse (Scaphoid Nonunion Advanced Collapse or SNAC wrist).

Avascular necrosis of the proximal pole with preserved radial surface articular cartilage may be salvaged by replacing the proximal pole with an implant. The pyrolytic carbon (pyrocarbon) implant is an ovoid-shaped spacer that adapts to carpal kinematics and repositions itself throughout the range of motion of the wrist (Fig. 96.1). Arthroscopic replacement preserves the dorsal capsulo-ligamentous septum and this possibly helps in the correction of dorsal intercalated segmental instability (DISI) of the lunate. Additionally, the arthroscopic procedure preserves vascularity and may avoid stiffness.

96.2 Indications and Contraindications

Avascular necrosis of proximal pole of the scaphoid with preserved radial articular cartilage can be salvaged by this procedure.

Arthrosis of the scaphoid fossa of the radius and scaphoid fracture at the waist level are contraindications for the procedure.

96.3 Surgical Steps

The procedure is performed as a day surgery under regional anesthesia and tourniquet control. The arm is placed on a table with a counter-support. A longitudinal traction is applied on the fingers using Chinese finger traps, usually of 6–7 kg.

- The 4–5 portal is the main viewing portal. The 6R portal is also used for optimal visualization to locate the proximal pole and to identify any associated injuries. The radial cartilage is evaluated to confirm that the scaphoid fossa of the radius is preserved.
- The 3–4 portal is established under arthroscopic visualization and permits direct access to the nonunion (Fig. 96.2). Synovectomy is performed in the radiocarpal joint for better visualization.

M. Gras · C. Mathoulin (✉)
International Wrist Center, Institut de la Main, Clinique Bizet, Paris, France

© ISAKOS 2022

D. N. Bhatia et al. (eds.), *Arthroscopy and Endoscopy of the Elbow, Wrist and Hand*,
https://doi.org/10.1007/978-3-030-79423-1_96

Fig. 96.1 Radiographs demonstrate the position of the Adaptative Proximal Scaphoid Implant (APSI) during ulnar deviation (left image) and radial deviation (right image) of the wrist

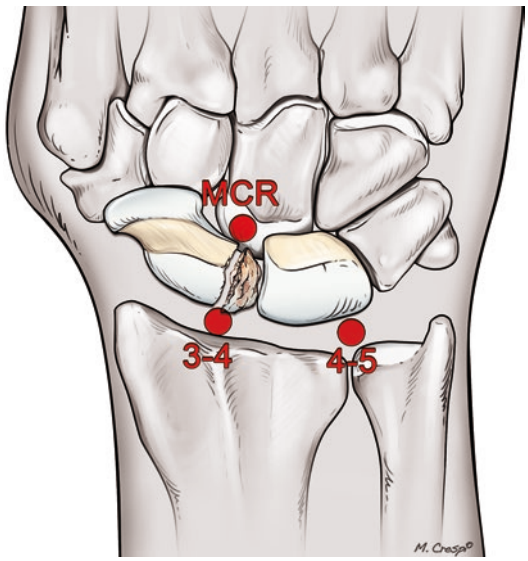

Fig. 96.2 Three portals for arthroscopic proximal pole replacement are illustrated

- Thereafter, a radial midcarpal (MCR) portal is used to assess the status of the cartilage and for proper placement of the implant.
- The scapholunate ligament, which is still attached to the proximal pole, is now divided with a # 15 scalpel blade and scissors through the 3–4 portal.
- Next, the proximal pole of the scaphoid is removed with a grasping forceps or a narrow hemostat through the 3–4 portal (Fig. 96.3a, b). A full-radius small joint shaver may also be used to facilitate resection of the proximal pole. Finally, a burr may be used to complete the excision.
- The size of the implant is determined by comparing the size of the resected proximal pole fragments to the trial implants.
- The 3–4 portal is enlarged and a trial implant is then inserted to assess appropriate size (Fig. 96.4). Once the size is confirmed, the trial implant is replaced with the definitive prosthesis under arthroscopic control.
- If necessary, in SNAC grades 1 and 2, a styloidectomy may be performed in the same procedure.
- A final arthroscopic assessment of the radiocarpal and midcarpal joints is performed to

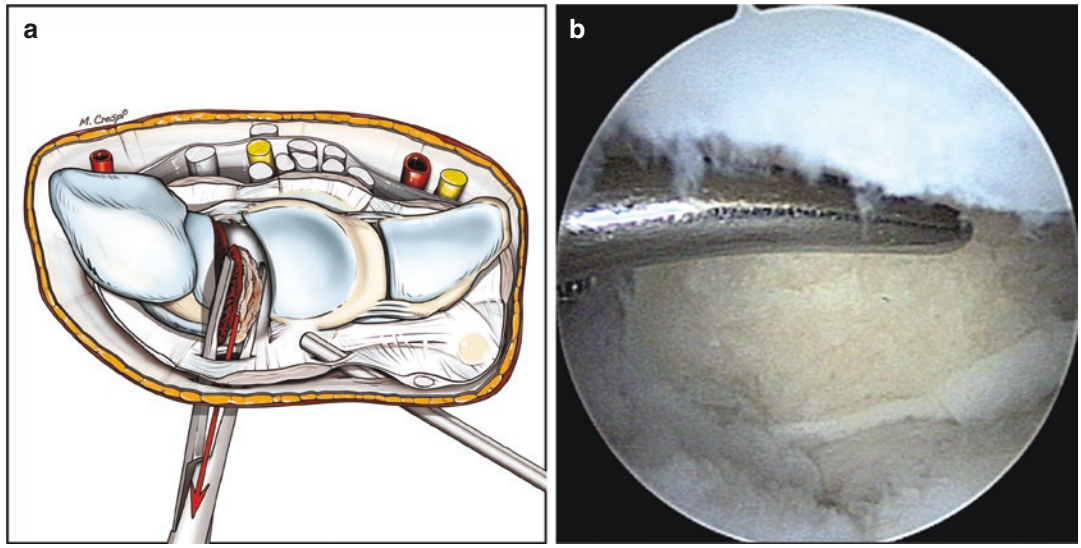

Fig. 96.3 (**a**) Excision of the proximal pole of scaphoid is illustrated. (**b**) Arthroscopic radiocarpal view of the resection of the proximal pole of the scaphoid is demonstrated

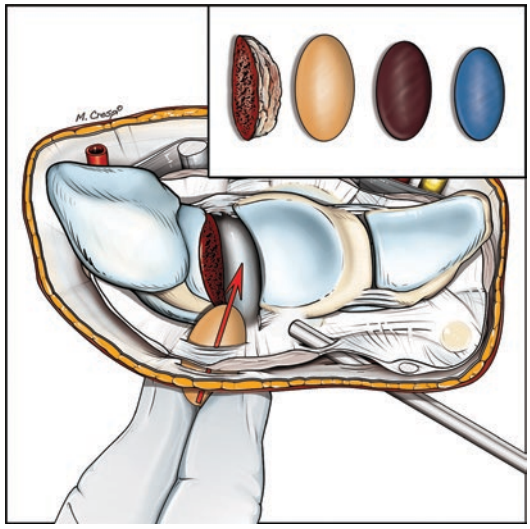

Fig. 96.4 Insertion of the trial implant is illustrated. The size of the trial implant is assessed by comparison with the size of the resected proximal pole fragment

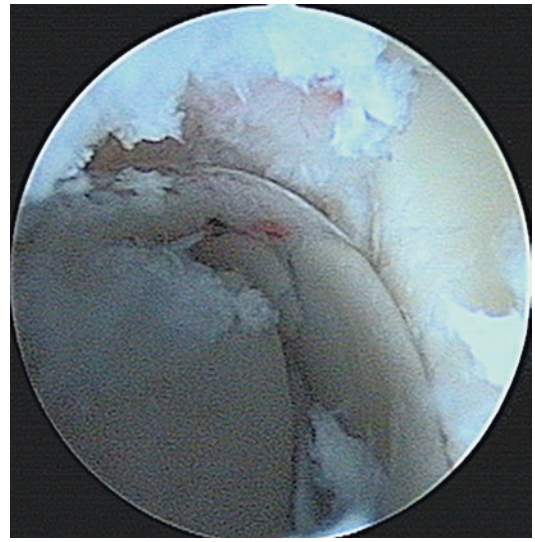

Fig. 96.5 Arthroscopic midcarpal view showing the correct position of the implant

check the correct position of the implant (Fig. 96.5).

- The arthroscope is then removed and the stability of the implant is assessed under fluoroscopy in all positions of the wrist. The 3–4 portal is closed with a single suture. A semi-compressive bulky dressing is applied for few days.

96.4 Tips and Tricks

- The scapholunate ligament must be sectioned completely from the dorsal to the palmar side using # 15 scalpel blade and scissors. The step should be performed carefully to avoid injury to the palmar capsule.

- Use a narrow hemostat to grasp the proximal pole fragment.
- A burr can be used to shape the proximal side of the scaphoid.
- Trial implants should be used to assess the stability in all directions of motion.
- Removing the trial implant is performed with a fine hemostat and jaws must be covered with plastic tubes.
- Styloidectomy should be performed in every case with grade 1 SNAC to avoid secondary procedures.

96.5 Pitfalls

- Injury to cutaneous nerves is possible.
- Injury to the extensor tendons may occur while releasing the scapholunate ligament with a scalpel.
- Avoid injury to the volar capsule when releasing the scapholunate ligament with the scalpel.

96.6 Postoperative Management and Rehabilitation

A bulky dressing is applied for few days. Thereafter, a removable splint is used and wrist mobilization is permitted. Regular physiotherapy exercises can begin at 3 weeks.

96.7 Complications

- Acute volar dislocation of the implant may occur if the volar capsule is injured.
- The implant may be unstable in waist fractures of scaphoid and other salvage procedures (four-corner fusion) should be performed.

96.8 Results

A retrospective study was performed on 25 patients between February 1999 and January 2019. The results were comparable to the first study published in 2012 [1]. Seven patients (30%) had a failure of previous surgery. Preoperative radiological assessment revealed all patients had a nonunion of the proximal pole with avascular necrosis. Two patients who underwent the procedure for a fracture of the body of the scaphoid presented later with a subluxation of the implant and underwent a four-corner fusion at 6 and 24 months respectively for persistent pain. Another patient had a late volar subluxation of the implant and underwent implant removal and capitolunate fusion. Of the 21 other patients who retained their implants, there was one patient with an early volar subluxation of the implant identified on the eighth postoperative day, and this was managed with a radial styloidectomy and repositioning of the implant. Three other patients required a radial styloidectomy at 2–3 years after the initial procedure. The overall pain scores and range and grip strength improved in the postoperative period. At a long-term radiological follow-up, three patients had unstable implant. Notching of the capitate was evident on plain radiographs in seven patients (30%). DISI was corrected in eight cases and persisted in one patient. The functional results were excellent or good in 66% of the cases and average in 33% of the cases. The three patients with a failure of the procedure had a poor fonctional result.

Reference

1. Gras M, Wahegaonkar A, Mathoulin C. Treatment of avascular necrosis of the proximal pole of the scaphoid by arthroscopic resection and prosthetic hemi replacement arthroplasty using the pyrocarbon adaptative proximal scaphoid implant (APSI): long term functional outcomes. J Wrist Surg. 2012;1(2):159–64.

97 Minimally Invasive Fixation of Ultra-Small Proximal Pole Scaphoid Fractures

Eugene T. Ek and Kemble K. Wang

97.1 Introduction

Surgical treatment of ultra-small proximal pole scaphoid fractures poses a number of challenges. The fragment may be too small to fix with conventional headless screws due to the high risk of fragmentation on insertion. However, excision of the fragment risks compromising the scapholunate ligament complex leading to subsequent carpal instability and potential degenerative changes. Under these circumstances, the proximal pole of the scaphoid can be fixed using bioabsorbable osteochondral fixation nails via a minimally invasive approach [1]. This allows stable low-profile fixation while minimizing the risk of proximal pole fragmentation.

97.2 Surgical Anatomy

Scaphoid fractures involving the proximal pole remain a challenge due to the high propensity for nonunion. The proximal pole receives the majority of its blood supply in a retrograde fashion via the dorsal scaphoid branch of the radial artery [2]. Fractures proximal to the entry of these vessels on the dorsal ridge of the scaphoid waist considerably jeopardize the blood supply. When treated nonoperatively, 34% of proximal pole fractures progress to nonunion, with the risk increasing to 50% with displacement [3, 4]. Fracture volume analysis has also shown that the smaller the volume of the proximal pole fragment, the greater the risk of nonunion [5].

If the proximal pole fragment is large enough, primary fixation using headless compression screws is a safe and reliable option. However, the fragment can sometimes be very small, representing little more than an osteochondral sliver containing a small volume of bone (Fig. 97.1). In these circumstances, the fracture is more akin to being more of an avulsion injury of the scapholunate ligament. Conventional fixation methods in this setting risk fragmenting the already small proximal fragment due to the relatively large threads within the screw. In addition, depth of screw placement can be difficult, as advancing the screw too far can lead to loss of fixation. On the other hand, leaving the screw too proud can cause irritation and damage to the articular surface. While alternative options include excision of the proximal pole and replacing it with osteochondral autograft (such as free medial femoral trochlea flap or rib grafting), these procedures carry significantly higher morbidity and require sacrifice of the scapholunate ligament complex [6, 7].

E. T. Ek (✉) · K. K. Wang
Melbourne Orthopaedic Group,
Melbourne, VIC, Australia

Department of Surgery, Monash University,
Melbourne, VIC, Australia

© ISAKOS 2022

D. N. Bhatia et al. (eds.), *Arthroscopy and Endoscopy of the Elbow, Wrist and Hand*,
https://doi.org/10.1007/978-3-030-79423-1_97

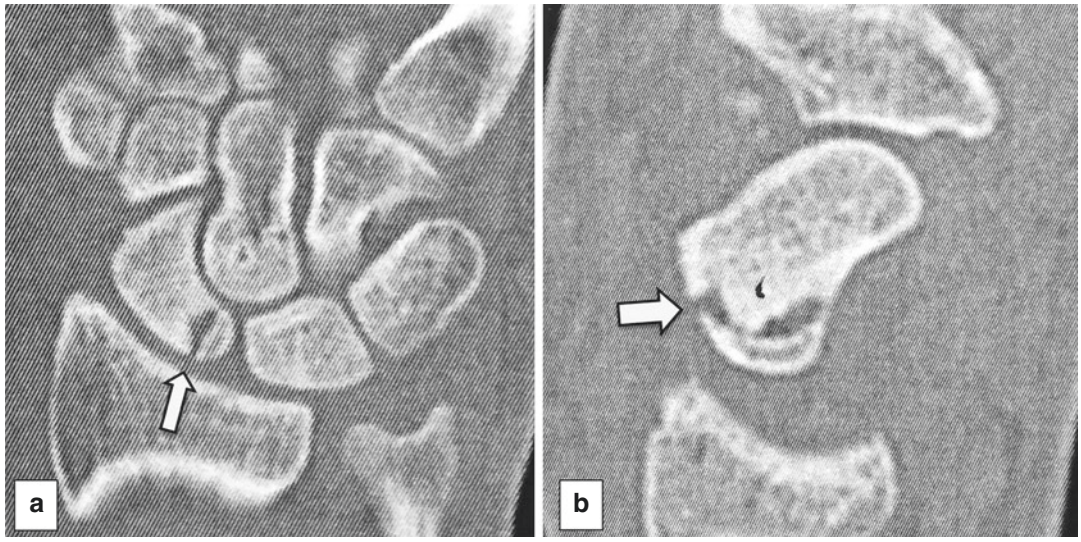

Fig. 97.1 Proximal pole scaphoid nonunion. CT coronal (**a**) and sagittal (**b**) images demonstrating a very small, scaphoid proximal pole fracture nonunion (arrow). (Reprinted from the Journal of Hand Surgery (Am), 2017; 42 (9):758.e1-e4, Ek ET, Wang KK. Fixation of ultrasmall proximal pole scaphoid fractures using bioabsorbable osteochondral fixation nails, with permission from American Society for Surgery of the Hand. Published by Elsevier Inc.)

In larger joints of the body, such as the knee and elbow, osteochondral fractures and osteochondral dissecans (OCD) lesions commonly result in intra-articular osteochondral fragment with a thin sliver of bone covered by an overlying cartilage surface. If unstable, these can be treated successfully with bioabsorbable osteochondral fixation nails, such as the SmartNail™ (ConMed, NY, USA) [8, 9] (Fig. 97.2). These devices are inert, non-collagenous, and are constructed from poly-L-lactic acid (PLA) copolymer material which biodegrades in vivo over approximately 2–5 years [10]. The main advantage of these devices over traditional fixation is that the head of the nail is smooth and can be impacted flush with the chondral surface above the subchondral bone thereby allowing adequate fixation and compression without risking subchondral bone fracture or implant prominence. Although such bioabsorbable PLA nails have primarily been used for the treatment of OCD lesions in other parts of the body, it can also be adapted to the scaphoid.

97.3 Indications and Contraindications

Very small proximal pole scaphoid fractures or scapholunate ligament avulsion fractures which are too small for conventional headless screw fixation (Fig. 97.1).

Contraindications to this procedure include:

- Established avascular necrosis or fragmentation of proximal pole of scaphoid.
- Scaphoid nonunion advanced collapse.
- Large proximal pole fractures that can be fixed using conventional headless compression screws or k-wire fixation.

97.4 Surgical Technique

The patient is placed in the supine position after either a general anesthetic or a regional brachial plexus block. The arm is exsanguinated prior to

Fig. 97.2 Osteochondral fixation nail, e.g., SmartNail™, are made from bioabsorbable poly-L-lactic acid copolymer. (Reprinted from the Journal of Hand Surgery (Am), 2017; 42 (9):758.e1-e4, Ek ET, Wang KK. Fixation of ultrasmall proximal pole scaphoid fractures using bioabsorbable osteochondral fixation nails, with permission from American Society for Surgery of the Hand. Published by Elsevier Inc.)

inflation of a high-arm tourniquet. If the injury is acute and there is no cystic bone loss requiring bone grafting, the procedure can be done via a minimally invasive dorsal approach (Fig. 97.3a).

- A 1.5–2 cm curvilinear incision is made just distal and ulnar to Lister's tubercle over centered over the radiocarpal joint and directed towards the thumb. If an autologous bone graft is required, the incision can be extended more proximally to expose Lister's tubercle.
- Dissection is carried down to the extensor retinaculum and a longitudinal split is made in the extensor retinaculum over the third dorsal compartment to expose the extensor pollicis longus (EPL) tendon and provide some mobility to the tendon for exposure of the dorsal wrist capsule.
- The EPL tendon is retracted radial-ward and the interval between the wrist extensor tendons (extensor carpi radialis and brevis, ECRB and ECRL) and extensor digitorum communis (EDC) is developed. A self-retaining retractor can be inserted into this interval providing excellent exposure to the wrist capsule.
- An oblique capsulotomy is performed along the length of the scaphoid to expose the proximal pole of the scaphoid. Care is taken to preserve the underlying scapholunate ligament. From this exposure, the proximal pole of the scaphoid can be seen with the adjacent scapholunate ligament (Fig. 97.3b).
- The fracture is then exposed and in the setting of a nonunion, any cystic material is carefully curetted and removed. Special care is taken to preserve the proximal bone stock and also the cortical integrity of the proximal pole (Fig. 97.3c). Given the small size of the proximal pole fragment, the use of a skin hook can be useful to manipulate the fragment while preparing it.
- If an autologous bone graft is required, the EPL tendon can be taken out of its groove and the dorsal distal radius is exposed through the proximal extension of the incision. A cortical window is made over Lister's tubercle and cancellous graft is harvested and then placed into the fracture site (Fig. 97.3d).
- The proximal fragment is then reduced and temporarily stabilized with Kirschner wires.
- Definitive fixation is achieved with one, or if possible, two PLA bioabsorbable nails. Depending on the type of nail, predrilling with a 1.5 mm drill bit may be required (Fig. 97.4a), followed by impaction with a tamp (Fig. 97.4b). The head of the PLA nail is smooth and tapered such that it can be impacted flush with the chondral surface, above the underlying subchondral bone (Fig. 97.4c). Care is taken not to over-impact the nail thus avoiding fragmenting the subchondral bone.
- The wrist is then taken through a range of motion to ensure that the nail is not causing impingement or irritation of the articular surfaces.
- The capsule is then closed with 3–0 monocryl sutures. In an acute fracture where distal

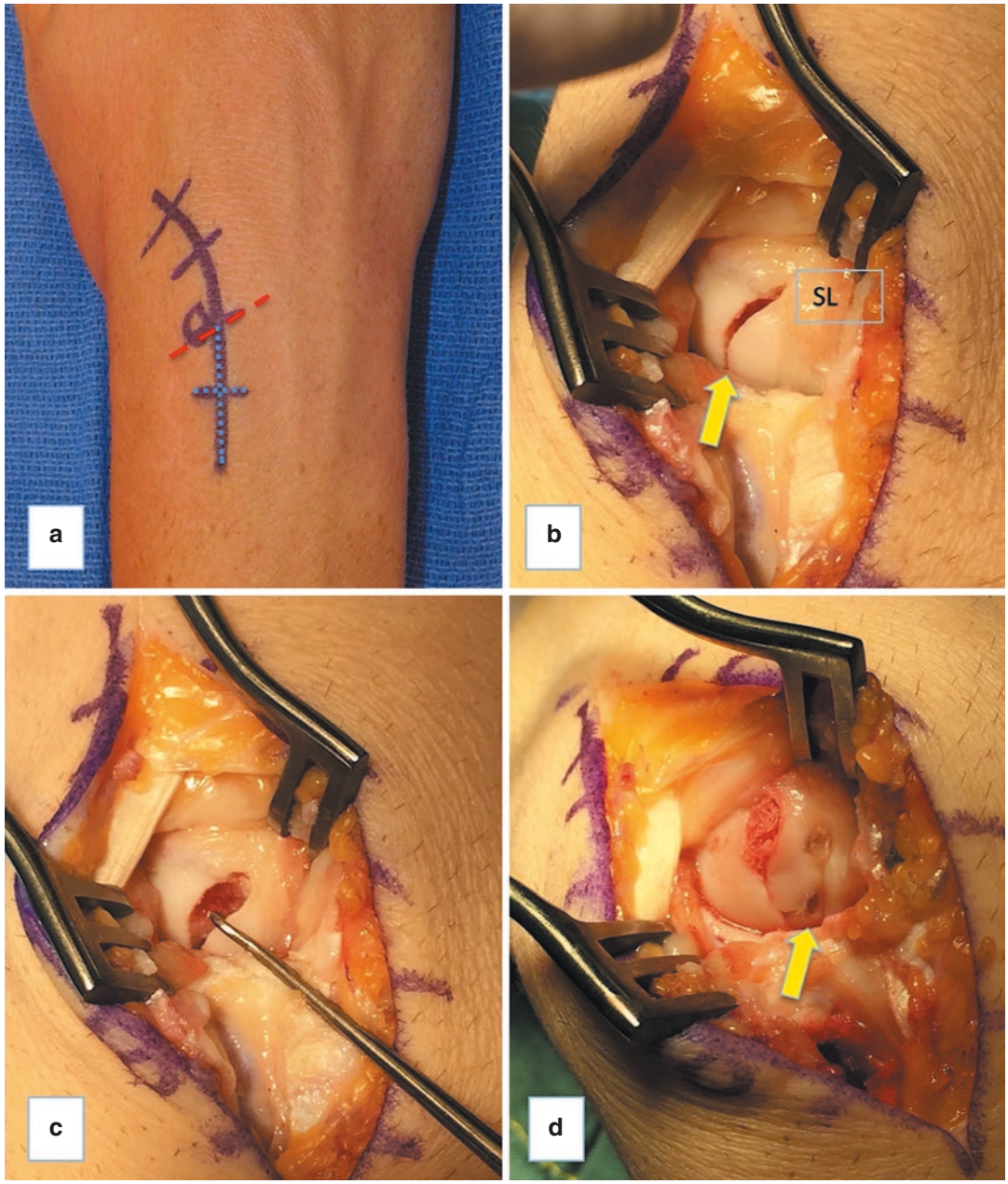

Fig. 97.3 (**a**) A 1.5–2 cm curvilinear incision is made over the dorsal side of the wrist and extends from Lister's tubercle towards the thumb. The incision can be extended proximally for a further 2 cm to allow for exposure of the distal radius (blue dotted line). (**b**) Oblique capsulotomy is made to obtain exposure of the fracture (arrow) while preserving the scapholunate ligament (SL). (**c**) Fracture site is opened to allow curettage of cystic material. (**d**) Fracture site has been bone grafted and bioabsorbable osteochondral nails have been inserted with the heads flush to the articular surface (arrow). (Reprinted from the Journal of Hand Surgery (Am), 2017; 42 (9):758.e1-e4, Ek ET, Wang KK. Fixation of ultrasmall proximal pole scaphoid fractures using bioabsorbable osteochondral fixation nails, with permission from American Society for Surgery of the Hand. Published by Elsevier Inc.)

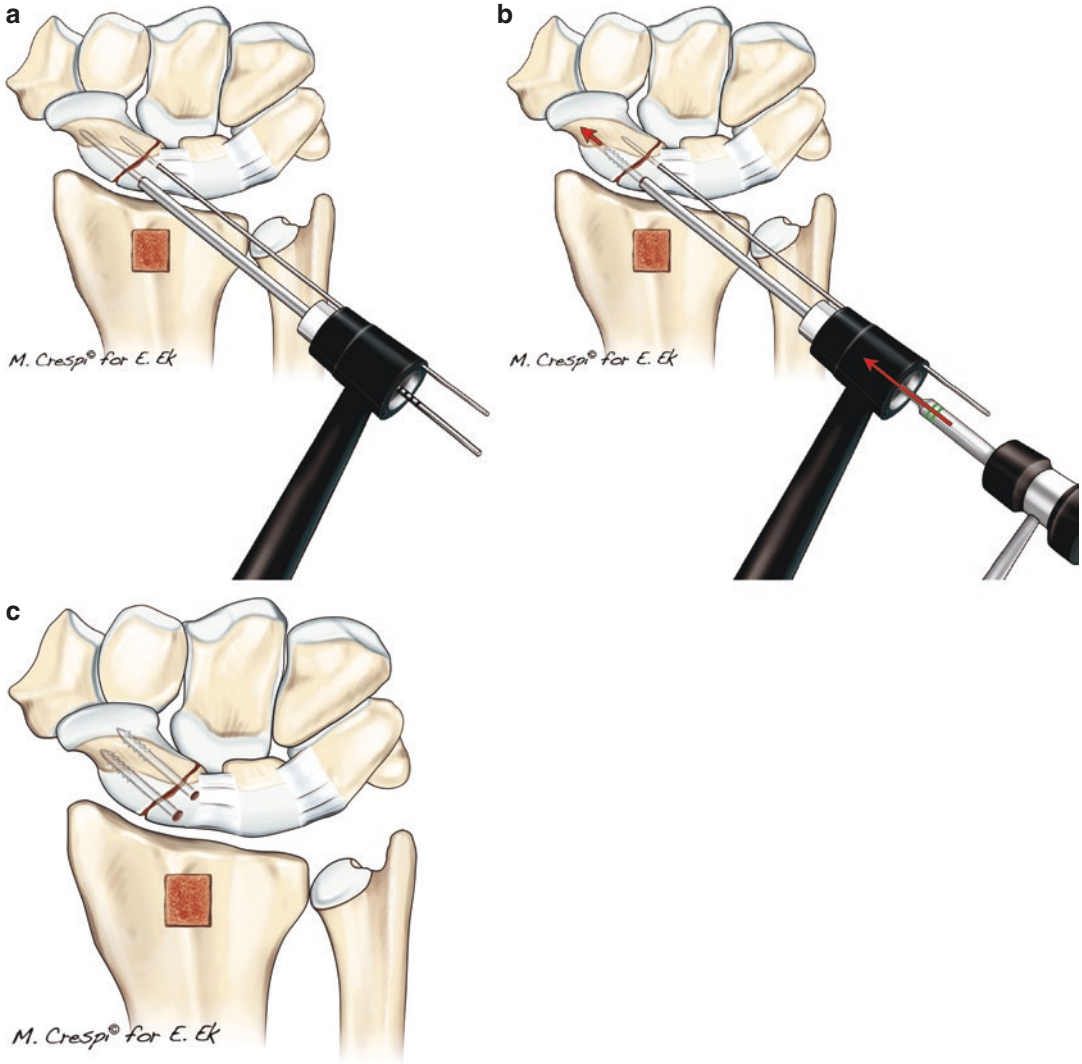

Fig. 97.4 Surgical steps for inserting bioabsorbable osteochondral nails: (**a**) predrilling over guide tube while a K-wire is used to help maintain reduction. (**b**) The nail is inserted through the guide tube and impacted with a tamp. (**c**) After reduction and insertion of two nails

radius bone graft is not harvested, the EPL tendon is left within its groove and the extensor retinaculum is closed with 3–0 monocryl. In the setting of proximal pole nonunions, where bone graft is harvested, we prefer to transpose the EPL tendon superficial to the extensor retinaculum. The remaining incision is closed in a standard fashion. The wrist is then placed into a plaster thumb spica splint which is later converted to a thermoplastic splint at the first postoperative appointment.

97.5 Tips and Tricks

- An oblique wrist joint capsulotomy rather than a longitudinal capsulotomy allows better exposure of the proximal scaphoid and also easier insertion of the guidewire and positioning of the nail trajectory.
- A small caliber (0.8 or 1.0 mm) temporary k-wire is useful to hold reduction prior to drilling insertion of bioabsorbable nail.

Fig. 97.5 Follow-up CT scan at 3 months showing union of the proximal pole scaphoid nonunion. (Reprinted from the Journal of Hand Surgery (Am), 2017; 42 (9):758. e1-e4, Ek ET, Wang KK. Fixation of ultrasmall proximal pole scaphoid fractures using bioabsorbable osteochondral fixation nails, with permission from American Society for Surgery of the Hand. Published by Elsevier Inc.)

97.6 Pitfalls

- When curetting the proximal pole in cases of nonunion, care should be taken to avoid removing too much bone from the already small proximal fragment.
- Gentle drilling and tapping is necessary when inserting the bioabsorbable nail so as to not fragment the proximal pole.

97.7 Postoperative Rehabilitation and Management

The postoperative plaster thumb spica splint is applied for approximately 10 days. Thereafter, the patient is immobilized in a thermoplastic removable thumb spica splint for 8 weeks or until fracture union. A CT scan is routinely performed to confirm fracture union prior to commencement of gentle range of motion of the wrist (Fig. 97.5). Range of motion of the wrist is encouraged before strengthening is commenced after 6 weeks after confirmed union. Return to normal sporting activities after 3 months.

97.8 Complications

- As for all proximal pole scaphoid fractures, nonunion and avascular necrosis of the proximal fragment is a possibility.
- Fragmentation of the proximal pole may occur during implant insertion.
- Over-dissection of the scapholunate interosseous ligament from the proximal pole during

exposure may result in scapholunate instability.
- Although PLA bioabsorbable osteochondral nails are designed to sit flush with chondral surface, implant irritation may occur if the nail is left too proud.

References

1. Ek ET, Wang K. Fixation of ultrasmall proximal pole scaphoid fractures using bioabsorbable osteochondral fixation nails. J Hand Surg Am. 2017;42(9):758.e1–4. https://doi.org/10.1016/j.jhsa.2017.06.011.
2. Gelberman RH, Menon J. The vascularity of the scaphoid bone. J Hand Surg Am. 1980;5(5):508–13. https://doi.org/10.1016/S0363-5023(80)80087-6.
3. Eastley N, Singh H, Dias JJ, Taub N. Union rates after proximal scaphoid fractures; meta-analyses and review of available evidence. J Hand Surg (European). 2013;38(8):888–97. https://doi.org/10.1177/1753193412451424.
4. Duppe H, Johnell O, Lundborg G, Karlsson M, Redlund-Johnell I. Long-term results of fracture of the scaphoid. A follow-up study of more than thirty years. J Bone Jt Surg Ser A. 1994;76(2):249–52. https://doi.org/10.2106/00004623-199402000-00012.
5. Prabhakar P, Wessel L, Nguyen J, Stepan J, Carlson M, Fufa D. Factors associated with scaphoid nonunion following early open reduction and internal fixation. J Wrist Surg. 2020;09(02):141–9. https://doi.org/10.1055/s-0039-3402769.
6. Yao J, Read B, Hentz VR. The fragmented proximal pole scaphoid nonunion treated with rib autograft: case series and review of the literature. J Hand Surg Am. 2013;38(11):2188–92. https://doi.org/10.1016/j.jhsa.2013.08.093.
7. Bürger HK, Windhofer C, Gaggl AJ, Higgins JP. Vascularized medial femoral trochlea osteocartilaginous flap reconstruction of proximal pole scaphoid nonunions. J Hand Surg Am. 2013;38(4):690–700. https://doi.org/10.1016/j.jhsa.2013.01.036.
8. Dines JS, Fealy S, Potter HG, Warren RF. Outcomes of osteochondral lesions of the knee repaired with a bioabsorbable device. Arthrosc J Arthrosc Relat Surg. 2008;24(1):62–8. https://doi.org/10.1016/j.arthro.2007.07.025.
9. Larsen MW, Pietrzak WS, DeLee JC. Fixation of osteochondritis dissecans lesions using poly(l-lactic acid)/ poly(glycolic acid) copolymer bioabsorbable screws. Am J Sports Med. 2005;33(1):68–76. https://doi.org/10.1177/0363546504265927.
10. Jukkala-Partio K, Pohjonen T, Laitinen O, et al. Biodegradation and strength retention of poly-L-lactide screws in vivo. An experimental long-term study in sheep. Ann Chir Gynaecol. 2001;90(3):219–24.

98 Proximal Hamate Autograft for Scaphoid Fractures: Surgical Anatomy and Technique

Spencer B. Chambers and Nina Suh

98.1 Introduction

Scaphoid fractures involving the proximal pole represent a difficult surgical problem due to their high risk for avascular necrosis (AVN) and nonunion which can lead to eventual arthrosis [1]. For this reason, numerous surgical techniques have been described to reconstruct the proximal pole, including vascularized (VBG) and nonvascularized bone grafts (NVBG), each with inherent strengths and weaknesses (Table 98.1). The most common issues with these grafts are donor site morbidity, compromise of the scapholunate interosseous ligament (SLIL), and the need for microvascular expertise in the case of VBG. More recently, the hemi-hemate autograft has been described and demonstrated successfully clinically (Fig. 98.1a–c). The benefits of this graft are many, including its local location within the site of injury, minimal donor morbidity, SLIL reconstruction, ease of procedure as it does not require microvascular expertise [2, 3].

98.1.1 Scaphoid Anatomy

The scaphoid is a boat-shaped bone (*skaphos "boat" latin*) that occupies the radial aspect of the proximal carpal row with an anatomic waist and articulations with four neighboring carpal bones (lunate, trapezoid, trapezium, and capitate). To articulate with these joints, approximately 80% of the surface of the scaphoid is covered in cartilage leaving only a few areas for vascular supply to enter the scaphoid. Roughly 80% of the interosseous blood supply and the entire proximal pole of the scaphoid is supplied by dorsal branches of the radial artery that enter retrograde into the dorsal mid-ridge, with the distal third of the bone having additional blood supply from the superficial palmar branch of the radial artery entering near the tuberosity of the scaphoid. This predisposes proximal pole fractures to a higher risk of nonunion as well as avascular necrosis which in turn can influence total carpal stability. In particular, the scaphoid is believed to be critical in the maintenance of lunate posture through twisting forces transmitted through SLIL. The SLIL is a C-shaped structure 2–3 mm thick on the dorsal component compared to the volar

S. B. Chambers
Division of Plastic and Reconstructive Surgery, Roth | McFarlane Hand and Upper Limb Center, St. Joseph's Health Care, University of Western Ontario, London, ON, Canada

N. Suh (✉)
Division of Plastic and Reconstructive Surgery, Roth | McFarlane Hand and Upper Limb Center, St. Joseph's Health Care, University of Western Ontario, London, ON, Canada

Division of Orthopedic Surgery & Division of Plastic Surgery, Roth | McFarlane Hand and Upper Limb Center, St. Joseph's Health Care, University of Western Ontario, London, ON, Canada
e-mail: Nina.Suh@sjhc.london.on.ca

© ISAKOS 2022

D. N. Bhatia et al. (eds.), *Arthroscopy and Endoscopy of the Elbow, Wrist and Hand*,
https://doi.org/10.1007/978-3-030-79423-1_98

Table 98.1 Comparison of bone grafting donor options

	Donor site	Pros	Cons
Non-vascularized bone grafts	Dorsal radius	– Local to primary operative site – Corticocancellous bone grafts availability	– Limited availability of cortical bone and marrow – Risk of fracture with large graft harvest
	Iliac crest	– Large amount of marrow/mesenchymal stem cells available – Tricortical graft possible – High-density cortical bone	– Second surgical site required – Prolonged postsurgical pain – Risk of damage to lateral femoral cutaneous nerve
	Rib	– Chondral tissue available for articular surface – Good graft size match	– Second surgical site required – SL ligament reconstruction not possible – Compression screw fixation difficult – Risk of pulmonary complications and pneumothorax
	Hemi-hamate	– Local to primary operative site – Similar bone biomechanical properties – Capito-hamate ligament available for scapholunate ligament reconstruction	– Risk of destabilizing intercarpal joint with large grafts
Vascularized bone grafts	1,2 intercompartmental supraretinacular artery (1,2 ICSRA)	– Local to primary operative site – Technical difficulty similar to NVBG with benefit of vascularization	– Poor union rates in setting of avascular necrosis – Difficult to correct humpback deformity – Dorsal approach with increased risk of injuring dorsal scaphoid vascularity
	Volar carpal artery pedicled pronator quadratus	– Volar approach spares dorsal capsule and primary scaphoid vascular supply – Correction of scaphoid humpback deformity – Local to primary operative site	– Difficult dissection due to small caliber of perforators
	Medial femoral condyle	– Excellent reported union rates in setting of failed NVBG – Large bone graft available (up to 10 mm)	– Requires microvascular techniques – Distant to primary operative site
	Medial femoral trochlea	– Excellent reported union rates in setting of failed NVBG – Large variety in blood supply allows for diverse graft design – Articular surface available for arthroplasty	– Technically demanding requiring microvascular techniques – Distant to primary operative site – Inability to reconstruct SL ligament

fibers. This stout ligament stabilizes lunate position during motion to prevent carpal instability.

98.1.2 Hamate Anatomy

The hamate is a wedge-shaped bone that resides on the ulnar aspect of the distal carpal row. It has a hook-shaped projection which forms a portion of Guyon's canal. It has three primary articulations that are covered with cartilage and interact with the capitate, lunate, and metacarpals. The volar and dorsal surface are rough allowing for robust vascular supply as well as ligamentous attachments. On the radial aspect of this bone lies the capito-hamate ligament which inserts on the ulnar volar aspect of the capitate.

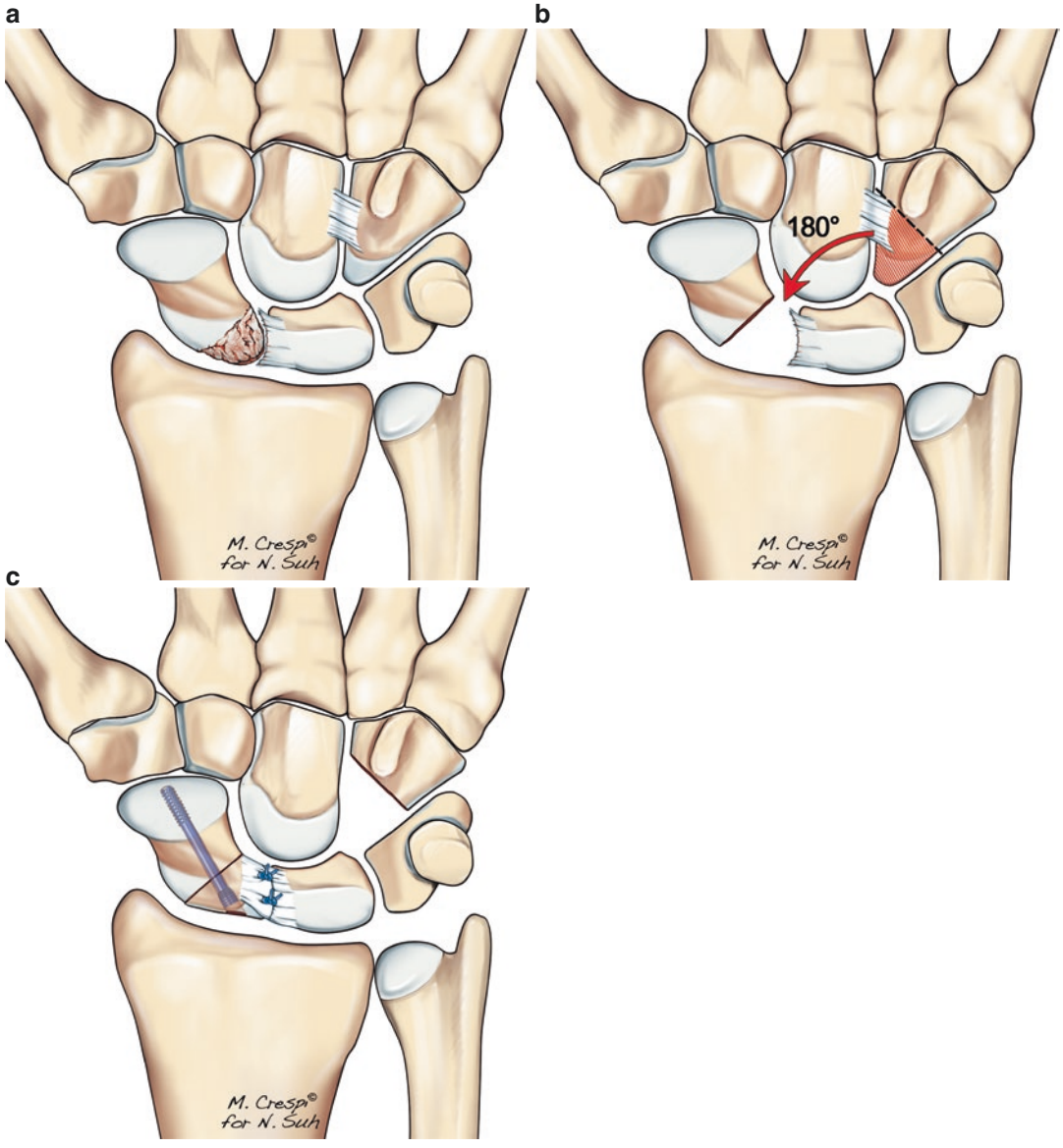

Fig. 98.1 An overview of the procedure is illustrated. (**a**) An established proximal pole scaphoid fracture with resultant avascular necrosis of the proximal pole is illustrated. With careful preoperative planning, this injury can be treated with reconstruction using a hemi-hamate autograft. (**b**) With the tourniquet deflated, the proximal pole is debrided to healthy bleeding bone ensuring the SL remnant remains attached to the lunate. The size of the defect is measured and translated to the proximal pole of the hamate. The bone graft is removed, taking care to preserve the CH ligament. (**c**) The resultant graft is contoured and inset into the defect. Temporary stability is obtained using a K-wire until a compression screw can be placed as permanent fixation. Finally, the SL is reconstructed by suturing the CH ligament to the SL remnant

98.2 Indications and Contraindications for Hemi-Hamate Autograft

98.2.1 Indications

- Scaphoid nonunion involving proximal pole.
- Patient is not a candidate for microsurgical techniques.
- Expected resection of proximal pole is smaller than height between proximal pole of hamate and hook of hamate [4].

98.2.2 Contraindications

- Presence of arthritis at the radioscaphoid joint [2].
- In patients with a large hamate (radial-ulnar width > 10 mm, volar-dorsal scaphoid width > 16 mm), this graft may be a poor anthropometric fit [5].
- Concern regarding vascularity of fracture site.

98.3 Surgical Steps

98.3.1 Positioning

The patient is positioned supine on the operating room table with an arm placed on a radiolucent arm board. A non-sterile tourniquet that will be inflated to 250 mmHg for the duration of the procedure is placed on the upper arm and the arm is prepped and draped in the usual sterile fashion.

*Step 1:*To access the scaphoid proximal pole and the hemi-hamate autograft, the authors prefer a dorsal approach to the wrist. A longitudinal dorsal skin incision in line with the third metacarpal over the wrist is utilized and full thickness flaps are raised radially and ulnarly. Care is taken to protect any branches of the dorsal radial sensory cutaneous nerve and dorsal sensory branches of the ulnar nerve that are encountered. Subsequently, the third extensor compartment is incised longitudinally and extensor pollicis longus is retracted radially. Subsequently, the second, fourth, and fifth extensor compartments are entered and corresponding tendons are retracted to allow visualization of the dorsal carpal wrist joint capsule.

Step 2: With all extensor tendons retracted away from the dorsal wrist capsule is entered using a previously described ligament-sparing dorsal capsulotomy (Fig. 98.2). A transverse capsulotomy along the radiocarpal joint is made, beginning at the radial styloid and terminating at the mid aspect of the origin of the dorsal radial carpal ligament (DRC). The DRC is then split longitudinally, continuing distally until the triquetrum (Tq). The final incision of the radially based flap is created by splitting the dorsal intercarpal ligament (DIC) from ulnar to radial. To expose the ulnar sided carpus, a longitudinal incision is made along the sixth extensor compartment, joining the previously split DRC at the triquetrum, and creating a proximally based triangular flap (Figs. 98.2 and 98.3).

Step 3: The radioscaphoid and scapholunate joint are inspected to ensure they are free of arthritis (Fig. 98.4).

Step 4: The tourniquet is deflated, and the proximal pole is resected until all necrotic tissue has been debrided and healthy bleeding bone is present (Fig. 98.5). The resultant defect is then measured.

Step 5: The tourniquet is reinflated and hamate is exposed through the distal ulnar aspect of the

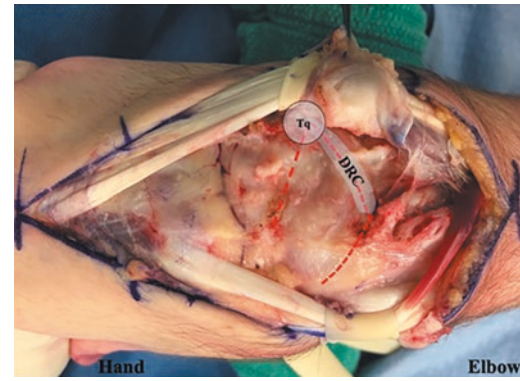

Fig. 98.2 Dorsal Wrist Capsulotomy using the ligament-sparing technique. The dorsal radial carpal ligament (**DRC**) is noted as a stout fibrous structure running in an oblique fashion from proximal radial to distal ulnar terminating at the triquetrum (**Tq**). The incisions are made as marked to allow for adequate exposure to the dorsal carpus while preserving structural components for later repair (© B. Elhassan for N. Suh)

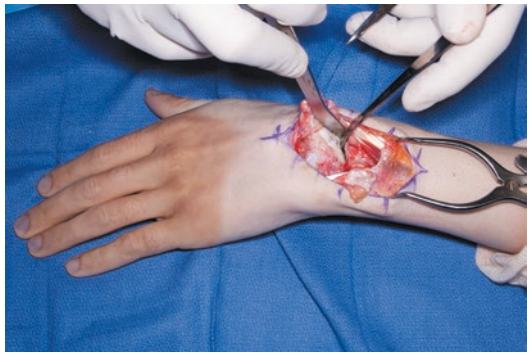

Fig. 98.3 Dorsal wrist capsulotomy. When entering the wrist using this ligament-sparing technique, care must be taken to split DRC and DIC equally for later repair. Similarly, when incising along the radiocarpal joint, a cuff of capsule on the dorsal radial rim should be preserved for later repair (© B. Elhassan for N. Suh)

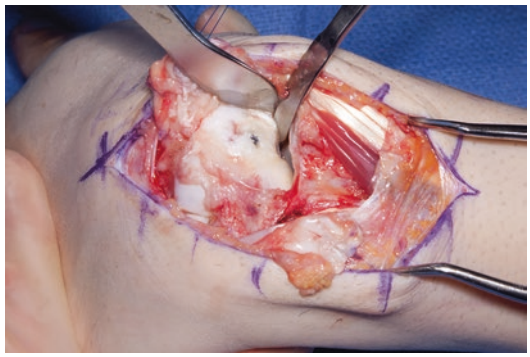

Fig. 98.4 Radioscaphoid joint inspection. In the presence of arthritis the procedure is not advisable and alternative procedures should be considered (© B. Elhassan for N. Suh)

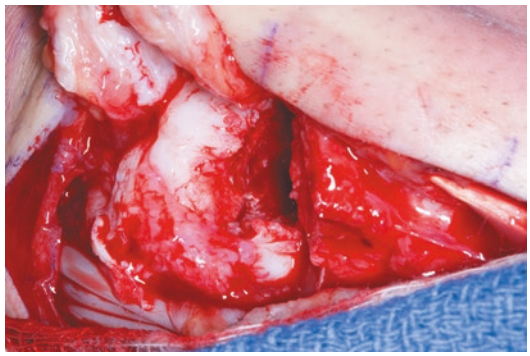

Fig. 98.5 Proximal scaphoid pole resection. Through a dorsal approach, the proximal scaphoid pole can be fully appreciated and all necrotic tissue should be removed. Based on preoperative imaging, the surgeon should be aware of the presumed resection, as this technique is limited regarding the total size of graft available (© B. Elhassan for N. Suh)

capsulotomy and the measurements of this defect are transferred. The portion is removed using a small osteotome taking care to preserve the capito-hamate ligament and protect the trapezio-hamate ligament (Fig. 98.6).

Step 6: The hemi-hamate autograft is then rotated 180° and placed in the proximal pole defect, aligning the CH ligament with the remaining SL ligament for future repair. A Kirschner wire is placed to obtain temporary fixation and fit is assessed with fluoroscopy. The bony edges of the graft can be trimmed in order to obtain a better fit (Fig. 98.7).

Step 7: Once an appropriate fit and orientation are obtained a second derotation K-wire is

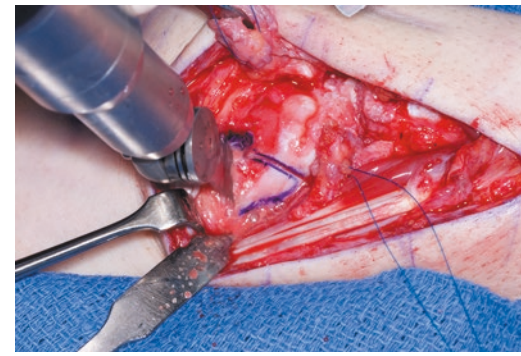

Fig. 98.6 Hamate osteotomy. During the harvest of the proximal hamate, use of retractors for protection of soft tissue structures allows for the safe and efficient procurement of graft. When translating measurements, the size of the graft taken can be slightly larger than the defect (© B. Elhassan for N. Suh)

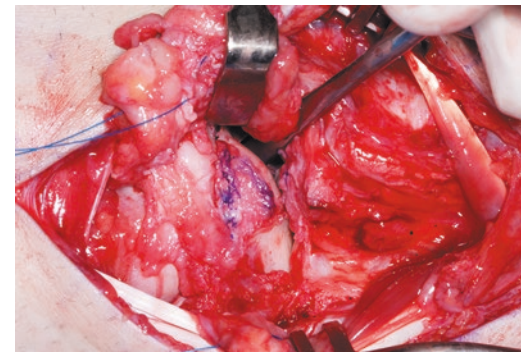

Fig. 98.7 Hamate autograft inset. Temporary fixation using a K-wire allows for the fit to be examined. When placing this K-wire, the planned position of the final compression screw should be noted, to avoid interfering with the final construct (© B. Elhassan for N. Suh)

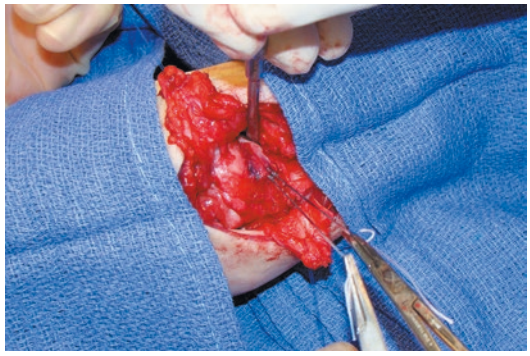

Fig. 98.8 SL ligament repair. Using fluoroscopy, the position of the lunate may be assessed prior to and following SL ligament repair to ensure appropriate tensioning and rotational alignment (© B. Elhassan for N. Suh)

placed. The bone graft is then fixed using a headless compression screw delivered anterograde into the scaphoid. With fixation achieved, all temporary K-wires are removed.

Step 8: The lunate is reduced using K-wires as joysticks and held in an appropriate position using K-wires delivered through the capitate. The CH ligament is repaired to the remaining SL stump using a 2–0 nonabsorbable stitch. The K-wires are cut beneath the skin and the repair is reinforced using capsule from the dorsal wrist capsule (Fig. 98.8).

Step 9: Skin and subcutaneous tissues are closed, and the patient is placed in a short arm thumb spica cast (Fig. 98.9).

98.4 Technical Tips

1. When harvesting the hemi-hamate autograft, a retractor should be used between the hamate and triquetrum to protect the capito-hamate ligament.
2. When temporarily fixating the hamate autograft with K-wires, care must be taken to ensure the K-wires do not interfere with eventual screw placement and trauma to the bone graft should be minimized such that fragmentation does not occur.

Fig. 98.9 Final radiograph demonstrating autograft. Appropriate height of the scaphoid has been reestablished with evidence of osseous integration of the hemi-hamate graft. There has been no evidence of loss of carpal height on the ulnar aspect of the wrist and these areas are free from signs of abnormal joint wear (© B. Elhassan for N. Suh)

98.5 Pitfalls

1. If the intercarpal soft tissues between the proximal and distal carpal row are injured or too large of an autograft is harvested, the intercarpal joint may become destabilized leading to abnormal motion and arthrosis.
2. During exposure, care must be taken to avoid the blood supply entering the dorsal ridge of the scaphoid to minimize potential avascularity postoperatively.

98.6 Postoperative Management and Rehabilitation

Patients are placed in a short arm thumb spica plaster splint for 2 weeks postoperatively. Following a wound assessment and suture removal at the

first postoperative follow-up in 2 weeks, a fiberglass short arm thumb spica cast is placed for a further 4 weeks. The authors use computed tomography (CT) with images in line with the scaphoid at the 6-week postoperative clinic visit to assess for bony union. Casting is maintained until CT scans performed in 4–6 week intervals demonstrate union which is defined as 50% bony bridging at the nonunion site. Once union has been confirmed, the patient is transitioned to a thumb spica removal splint and gentle range of motion is initiated. At the discretion of the certified hand therapist, motion and strengthening are advanced until full wrist function has been restored. Patients are then subsequently followed at 3, 6, and 12 months with plain radiographs.

98.7 Complications

All potential complications have yet to be elucidated given the infancy of the description of this technique. Theoretical risks include capitohamate intercarpal joint arthritis as a portion of its articular surface has been removed and as with any graft, there is a risk of graft failure, malposition, persistent nonunion, complex regional pain syndrome as well as excessive scarring.

Acknowledgments All clinical images were taken with permission from Dr. Bassem T. Elhassan, Mayo Clinic, Rochester Minnesota and Dr. Nina Suh, Roth | McFarlane Hand and Upper Limb Centre, London, Ontario.

References

1. Grewal R, Lutz K, Macdermid JC, Suh N. Proximal pole scaphoid fractures: a computed tomographic assessment of outcomes. J Hand Surg Am. 2016;41(1):54–8. https://doi.org/10.1016/j.jhsa.2015.10.013.
2. Elhassan B, Noureldin M, Kakar S. Proximal scaphoid pole reconstruction utilizing ipsilateral proximal hamate autograft. Hand. 2016;11(4):495–9. https://doi.org/10.1177/1558944716628497.
3. Chan AHW, Elhassan BT, Suh N. The use of the proximal hamate as an autograft for proximal pole scaphoid fractures: clinical outcomes and biomechanical implications. Hand Clin. 2019;35(3):287–94. https://doi.org/10.1016/j.hcl.2019.03.007.
4. Kakar S, Greene RM, Hewett T, Thoreson AR, Hooke AW, Elhassan BT. The effect of proximal hamate osteotomy on carpal kinematics for reconstruction of proximal pole scaphoid nonunion with avascular necrosis. Hand. 2018:1–7. https://doi.org/10.1177/1558944718793175.
5. Wu K, Padmore C, Lalone E, Suh N. An anthropometric assessment of the proximal hamate autograft for scaphoid proximal pole reconstruction. J Hand Surg Am. 2018:1–8. https://doi.org/10.1016/j.jhsa.2018.04.021.

Arthroscopic Management of Acute Perilunate Dislocations

99

Bo Liu and Feiran Wu

Abbreviations

AAR	Arthroscopic-assisted reduction
LT	Lunotriquetral
PLD	Perilunate dislocation
PLFDs	Perilunate fracture-dislocation
RL	Radiolunate
SL	scapholunate
TFCC	Triangular fibrocartilage complex

99.1 Background

Perilunate injuries are highly unstable carpal dissociations characterized by a complete loss of contact between the lunate and surrounding carpal bones. An excessive radiocarpal hyperextension and ulnar deviation coupled with intercarpal supination have proven to be the principal pathologic forces that disrupt the key osseous and ligament components of the wrist [1]. It is commonly a result of high-energy trauma and represents a spectrum of conditions, from purely ligamentous injuries in perilunate dislocations (PLDs) to perilunate fracture-dislocations (PLFDs) [1–3].

The key to a successful outcome is to achieve early anatomical reduction and preserve the carpal alignment until healing [4]. Accurate and early identification of these injuries is critical because delayed or neglected treatment usually leads to poor post-injury outcomes and eventual early arthritis [5–8]. Closed reduction and cast treatment of PLDs and PLFDs are associated with poor outcomes. Therefore, surgical management with open reduction, ligament repair, and internal fixation is the current gold standard [3–6, 8–13]. Open surgery however introduces additional surgical trauma to important capsular and ligamentous structures, and could also impair the already limited blood supply to the scaphoid [14, 15]. This may then result in further capsular scarring, joint stiffness, and carpal malalignment [14].

To minimize morbidity, arthroscopic-assisted treatment of PLDs and PLFDs have been successfully demonstrated in multiple studies [4, 5, 14, 16–21]. An arthroscopic technique minimizes capsular and adjacent soft tissue injury, while facilitating accurate anatomic reduction and percutaneous fixation of the carpus. This may therefore encourage healing with reduced stiffness and improved outcomes compared to similar open procedures.

In this chapter, we discuss the surgical techniques of the arthroscopic treatment of acute

B. Liu (✉)
Department of Hand Surgery, Beijing Ji Shui Tan Hospital, The Fourth Clinical College of Peking University, Beijing, China

F. Wu
Department of Orthopaedics, University Hospitals Birmingham, Birmingham, UK

© ISAKOS 2022

D. N. Bhatia et al. (eds.), *Arthroscopy and Endoscopy of the Elbow, Wrist and Hand*,
https://doi.org/10.1007/978-3-030-79423-1_99

PLDs and PLFDs. We aim to describe refinements of the existing methods in order to present the most up-to-date technique to treat this condition.

99.2 Indications and Contraindications

Patients who present with acute, or early subacute perilunate dislocations within 4 weeks of injury are suitable for arthroscopic-assisted intervention.

In patients presenting more than 4 weeks after injury, the existing scarring would impede the success of arthroscopic reduction of the capitolunate joint, and therefore this technique is not indicated. In lunate dislocations where the lunate has migrated significantly away from the lunate fossa, such as into the forearm, arthroscopic reduction is not technically feasible and requires an open approach. Open injuries with severe soft tissue damage should be treated according to standard open fracture guidelines and are unsuitable for arthroscopic surgery.

99.3 Surgical Technique

99.3.1 Closed Reduction

Before arthroscopy is performed, a single closed manual reduction is attempted for acute capitolunate joint dislocations up to 3 days old. In the acute setting, more than 50% of cases can be successfully reduced in this manner after one attempt. Repeated closed reduction attempts are not recommended if the first attempt fails, as repeated blind and forceful reduction attempts can further damage the inferior capitate cartilage, an area already vulnerable from the initial injury (Fig. 99.1). The success rate of closed capitolunate reductions is also significantly reduced 72 h or later following injury. Therefore, for acute presentations that have failed a single closed reduction

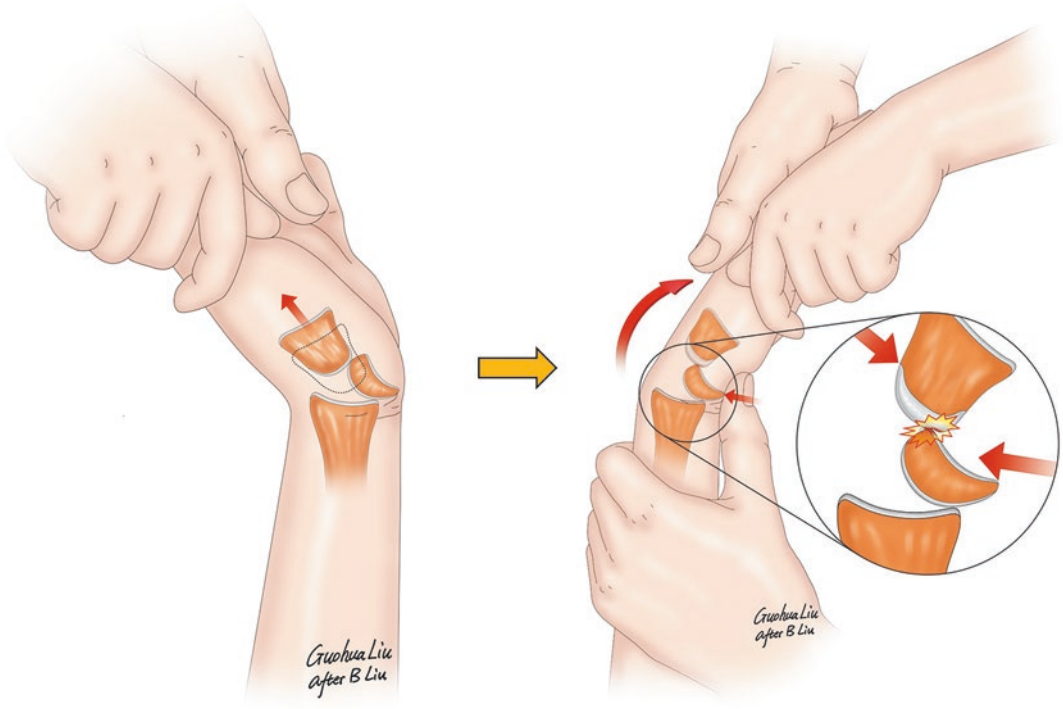

Fig. 99.1 The capitolunate articular cartilage may be damaged from repeated manual forceful reduction attempts (© Guohua Lui after Bo Lui)

or for presentations after 72 h, we recommend proceeding to arthroscopic-assisted reduction (AAR).

99.3.2 Position

Wrist arthroscopy is performed in the operating room under a brachial plexus block. The arm is suspended from a wrist arthroscopy traction tower. The dorsal 3–4 and 4–5 portals are used for joint inspection and irrigation. In PLDs and PLFDs, there is usually ample space for scope placement as the lunate is typically tilted volarly and impinged against the inferior surface of the capitate. Occasionally, it can also be trapped by interposed torn palmar capsular ligaments, another cause for failure of closed reduction. To establish an initial working view, continuous saline irrigation is required to flush away clot and debris from the joint, and to debride traumatic synovitis. Joint insufflation from wet arthroscopy also helps to compress small capillaries within the capsule and synovium, controlling intra-articular bleeding and achieving clearer vision.

Treatment of Perilunate Dislocations

- The radiocarpal and midcarpal joints are fully assessed using the 3–4, 4–5, radial, and ulnar midcarpal portals.
- The scapholunate (SL) and lunotriquetral (LT) ligaments are assessed and any soft tissue or bony fragments interposed between these intervals are debrided or excised to facilitate reduction of the intercarpal joint.
- Following the arthroscopic assessment, arthroscopic-assisted reduction (AAR) is performed by using an arthroscopic probe introduced through the 4–5 portal into the radiocarpal joint. This portal is the most convenient for reduction because it allows the probe to directly face the subluxated lunate. The tip of the probe is then hooked onto the dorsal rim of the lunate (Fig. 99.2). Wrist traction force can be increased at this point, up to a maximum of 15 lbs., to aid in this maneuver.
- Once the probe is in position, two K-wires are advanced towards the lunate from the scaphoid and triquetrum, and positioned without crossing the SL and LT intercarpal intervals.

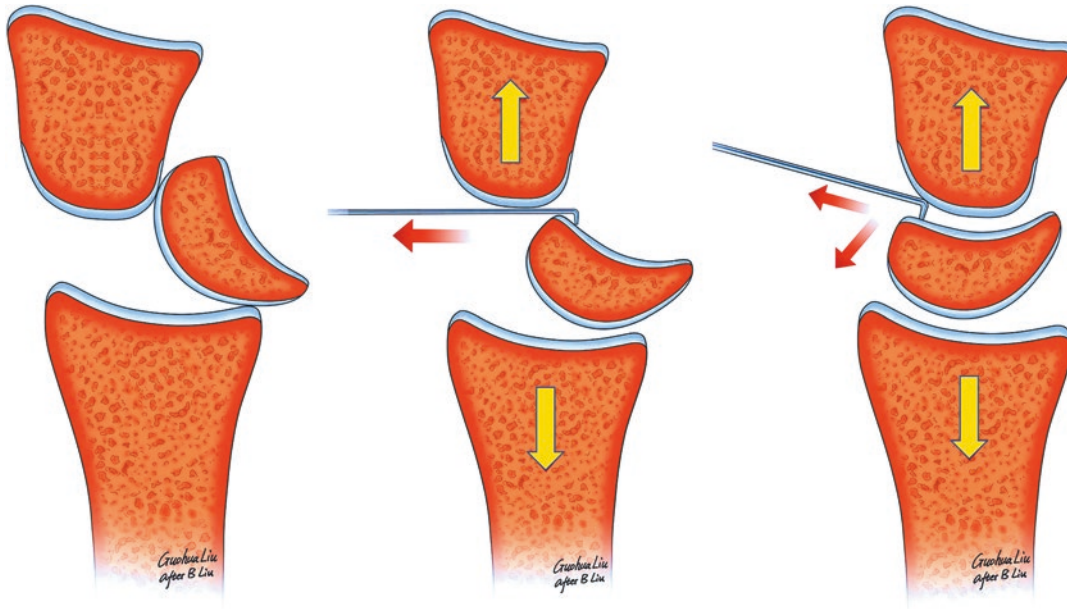

Fig. 99.2 The "shoehorn maneuver" in reducing perilunate dislocations (© Guohua Lui after Bo Lui)

- The surgeon then gently pulls and reduces the dislocated lunate back under the capitate using a "shoehorn maneuver." This is conducted entirely under direct arthroscopic vision. No force is required in this maneuver, which protects the surrounding articular cartilage from further injury.
- Once the capitolunate joint is reduced, the lunate is assessed for any volar or dorsal tilt. In the presence of tilt, wrist traction force is reduced and the radiolunate (RL) angle is restored to neutral by passively flexing or extending the wrist.
- The RL joint is then temporarily transfixed with a percutaneous K-wire advanced through the dorsal distal radius (Fig. 99.3). The SL and LT intervals are then reassessed arthroscopically through the midcarpal portals and further deformity correction can be achieved using a probe or depressor.
- Once the reduction is satisfactory, the K-wires already positioned in the scaphoid and triquetrum are driven through the SL and LT intervals under vision and the alignment is confirmed by intraoperative fluoroscopy (Fig. 99.4).

Fig. 99.3 Lateral radiograph showing the position of the K-wires before fixation of the SL and LT intervals. The lunate tilt has been corrected and transfixed with a K-wire

99.3.3 Management of Grossly Unstable Perilunate Dislocations

When there is incompetence of both the primary and secondary stabilizers of the SL interval, the SL joint will be grossly unstable. For these injuries, we advocate augmentation of the SL ligament through a dorsal mini-invasive approach, by reinforcing the dorsal scapholunate complex. This complex includes the dorsal capsule-scapholunate septum (DCSS) and the dorsal

Fig. 99.4 Final K-wire fixation position for PLDs

extrinsic ligaments, and is one of the most important structures for SL stability [22, 23]. In our experience, typically more than half of the PLDs will have grossly unstable SL joints that would benefit from SL augmentation.

- To perform a SL augmentation, the 3–4 portal is extended transversely along the skin crease creating a 2 cm opening and the extensor tendons are retracted to expose the capsule.
- A suture anchor is inserted into the scaphoid and lunate 1 cm from the SL interval (Fig. 99.5).
- Following joint reduction and fixation using K-wires as described, both sutures from the anchors are delivered through the dorsal capsule and tied together on the top of the dorsal capsule (extra-articular), creating a reinforcement of the dorsal scapholunate complex.

Fig. 99.5 Fluoroscopic image of a patient with a grossly unstable PLD and a concomitant triquetrum fracture, demonstrating the anchor position in the scaphoid and lunate for the dorsal extra-articular reinforcement of the scapholunate complex and the K-wire fixation of the triquetrum fracture

99.3.4 Management of Associated Injuries in Perilunate Dislocations

Traditionally, PLDs are thought of as "purely ligamentous" injuries. However, it is not uncommon to find concomitant carpal fractures in these patients, particularly following high-energy trauma. Associated displaced fractures of the triquetrum or capitate necessitate arthroscopic-assisted reduction and percutaneous fixation. Other associated injuries that are typically seen include tears of the TFCC. These can be debrided or repaired as appropriate.

Treatment of Trans-Scaphoid Perilunate Fracture-Dislocations

- The radiocarpal and midcarpal joints are fully assessed using the 3–4, 4–5, radial, and ulnar midcarpal portals.
- Arthroscopic-assisted reduction (AAR) of the dislocated capitolunate joint is performed for patients who failed closed reduction or presented 3 days or later after the initial injury. An arthroscopic probe is introduced into the radiocarpal joint through the 4–5 portal, while the scope is placed in the 3–4 portal. In PLFDs, the hook of the probe is positioned onto the dorsal edge of the scapholunate ligament rather than the lip of the lunate (Fig. 99.6). The wrist traction force is then gently increased, up to a maximum of 15 lbs., while the surgeon gently pulls

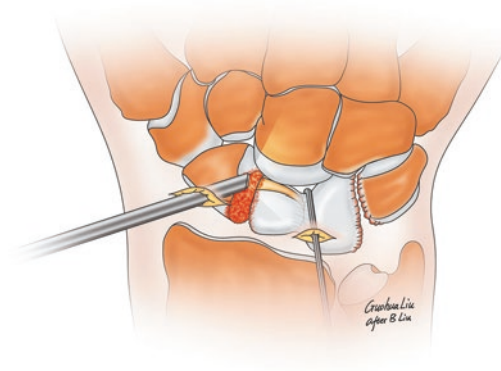

Fig. 99.6 The probe hooks on the scapholunate ligament for reducing PLFDs (© Guohua Lui after Bo Lui)

and reduces the dislocated proximal scaphoid-lunate complex back under the capitate using the "shoehorn maneuver."

- Following reduction, anatomical reduction, and fixation of the scaphoid fracture is the critical step in determining the successful outcome of managing trans-scaphoid PLFDs. This fracture is often significantly displaced with varying degrees of comminution even after the reduction of the capitolunate dislocation. Manual closed reduction is generally unsatisfactory and arthroscopic-assisted reduction is frequently necessitated. In these cases, a guidewire is advanced along the central axis of the distal fragment from the scaphoid tubercle in a retrograde direction, without crossing the fracture line. Further K-wires "joysticks" can be inserted into the distal and proximal fragments in grossly unstable fractures (Fig. 99.7).
- These are then manipulated, using the ulnar midcarpal portal for visualization, to reduce the scaphoid anatomy (Fig. 99.8). The rotational and translational displacement must be checked in both the sagittal and coronal planes when checking the adequacy of reduction.
- When satisfactory reduction is achieved, the surgeon maintains the reduction while the surgical assistant drives the central axis guidewire and a further anti-rotation K-wire across the fracture site into the proximal scaphoid fragment.

Fig. 99.7 Position of the K-wire "joystick" in the reduction of the scaphoid fracture in PLFDs

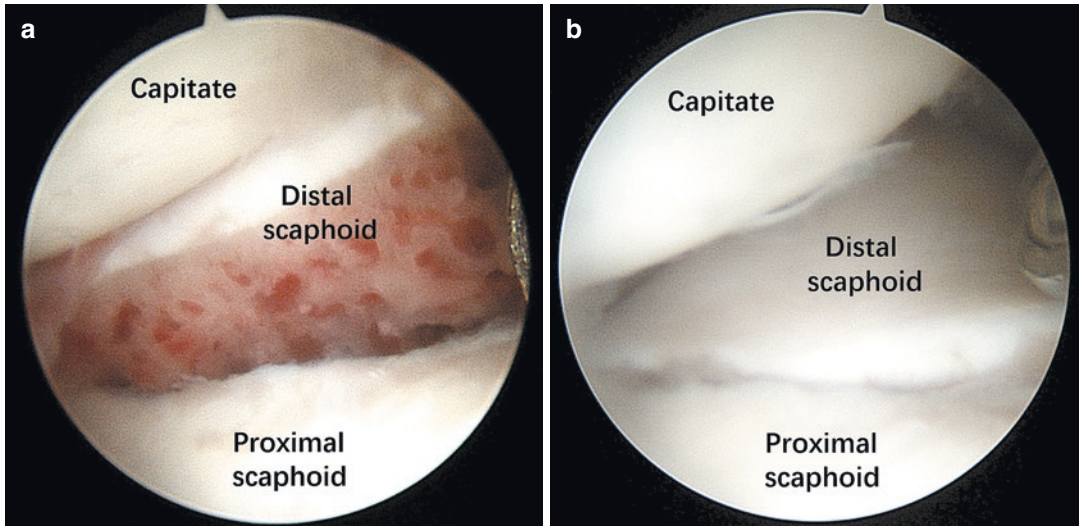

Fig. 99.8 Arthroscopic view of the initially displaced (**a**) and the subsequently reduced (**b**) scaphoid fracture from the midcarpal portal

- In some cases, despite the aforementioned techniques, a residual fracture gap persists between the proximal and distal scaphoid fragments. To address this, a cannulated headless compression screw can be used to supplement the fixation and compress the fracture gap.
- The wrist is released from traction and placed on the operating hand table. In waist fractures, the scaphoid is reamed retrograde over the central axis guidewire and a screw is advanced in the same direction, compressing the fragments (Fig. 99.9).
- For proximal third or proximal pole fractures, the central guidewire is advanced proximally through the dorsal skin. A percutaneous stab incision is made in the dorsal skin where the wire exits. Reaming and screw insertion are then performed antegrade through the dorsal incision. Further anti-rotation guidewires can be used to supplement the fixation stability. All K-wires are cut short and buried under the skin for both PLDs and PLFDs.

Fig. 99.9 A retrograde headless compression screw is used to reduce the fracture gap in the scaphoid

99.3.5 Management of Associated Injuries in Perilunate Fracture-Dislocations

Contrary to the commonly held belief that the SL ligaments remain intact in PLFD injuries, hemorrhage and attenuation of this ligament can be observed arthroscopically in almost all cases. The majority are Geissler grade I or II injuries that can be managed with immobilization, but a few will have more severe ligament avulsions from the lunate or gross ruptures. These cases will be revealed during midcarpal inspection, with Geissler grade III or IV disruptions of the SL interval. If this is found, scapholunate pinning is mandated following fixation of the scaphoid fracture, using the technique described earlier for the treatment of PLDs.

99.4 Postoperative Management and Rehabilitation

All patients are immobilized in a short arm thermoplastic splint postoperatively. The proximal phalanx of the thumb is included in the splint for PLFDs but left free in PLDs. In patients with concurrent TFCC injuries, long arm thermoplastic splints are used with the forearm at semi-supination rotation for six weeks, followed by short arm splints for a further two weeks. All K-wires are removed at eight weeks postoperatively. Under the guidance of hand therapists, active wrist motion is initiated at this point. In PLDs, muscle strengthening exercise is also commenced gradually at this point, followed by weight loading and gentle return to sports as appropriate. In PLFDs, weight loading and sporting activities can be initiated following confirmation of scaphoid union.

99.5 Tips and Tricks

- A thorough joint assessment should be performed before and after reduction of dislocation. Arthroscopy is useful to release interposed tissue and bony fragments that can

hinder reduction, and to identify and treat concomitant injuries.

- The reduction of the scaphoid is often the most time-consuming and technically demanding step. Arthroscopists proficient in the conversion of wet to dry arthroscopy techniques may find this helpful in facilitating fracture reduction and fixation. Wrist traction should be used selectively and the surgeon should clearly recognize the specific situations when wrist traction would be helpful, e.g., increasing wrist traction for AAR of the capitolunate joint, and releasing traction when reducing and fixing the scaphoid fracture in trans-scaphoid PLFDs.

99.6 Pitfalls

Arthroscopic management of perilunate injuries is highly challenging. It has a steep learning curve, even for experienced hand surgeons and arthroscopists. Despite the technical demands, AAR of the capitolunate joint is recommended as the primary treatment method for injuries that are three days or older, to reduce morbidity and preserve the articular cartilage.

- For more acute injuries, it is important to appreciate that repeated forceful reduction of the capitolunate joint can lead to further articular damage of the inferior capitate, an area already weakened or injured during the initial dislocation. AAR occurs under direct vision at all times and requires no maneuvers that may further compromise the cartilage.
- Surgeons attempting AAR should be proficient in the open management of PLDs and PLFDs, and be ready to convert from arthroscopic to open surgery if difficulties are encountered intraoperatively. In particular, a poorly reduced scaphoid fracture in trans-scaphoid PLFDs has unacceptably poor outcomes and an open reduction and internal fixation should be performed if the scaphoid cannot be reduced arthroscopically.

References

1. Mayfield JK, Johnson RP, Kilcoyne RK. Carpal dislocations: pathomechanics and progressive perilunar instability. J Hand Surg. 1980;5(3):226–41.
2. Johnson RP. The acutely injured wrist and its residuals. Clin Orthop. 1980;149:33–44.
3. Herzberg G. Perilunate and axial carpal dislocations and fracture–dislocations. J Hand Surg. 2008;33(9):1659–68.
4. Weil WM, Slade JF, Trumble TE. Open and arthroscopic treatment of perilunate injuries. Clin Orthop. 2006;445:120–32.
5. Cooney WP, Bussey R, Dobyns JH, Linscheid RL. Difficult wrist fractures. . Perilunate fracture-dislocations of the wrist. Clin Orthop. 1987;214:136–47.
6. Herzberg G, Forissier D. Acute dorsal trans-scaphoid perilunate fracture-dislocations: medium-term results. J Hand Surg. 2002;27(6):498–502.
7. Hildebrand KA, Ross DC, Patterson SD, Roth JH, MacDermid JC, King GJW. Dorsal perilunate dislocations and fracture-dislocations: questionnaire, clinical, and radiographic evaluation. J Hand Surg. 2000;25(6):1069–79.
8. Forli A, Courvoisier A, Wimsey S, Corcella D, Moutet F. Perilunate dislocations and transscaphoid perilunate fracture–dislocations: a retrospective study with minimum ten-year follow-up. J Hand Surg. 2010;35(1):62–8.
9. Budoff JE. Treatment of acute lunate and perilunate dislocations. J Hand Surg. 2008;33(8):1424–32.
10. Trumble T, Verheyden J. Treatment of isolated perilunate and lunate dislocations with combined dorsal and volar approach and intraosseous cerclage wire. J Hand Surg. 2004;29(3):412–7.
11. Knoll VD, Allan C, Trumble TE. Trans-scaphoid perilunate fracture dislocations: results of screw fixation of the scaphoid and lunotriquetral repair with a dorsal approach. J Hand Surg. 2005;30(6):1145.e1–1145.e11.
12. Kremer T, Wendt M, Riedel K, Sauerbier M, Germann G, Bickert B. Open reduction for perilunate injuries—clinical outcome and patient satisfaction. J Hand Surg. 2010;35(10):1599–606.
13. Souer JS, Rutgers M, Andermahr J, Jupiter JB, Ring D. Perilunate fracture–dislocations of the wrist: comparison of temporary screw versus K-wire fixation. J Hand Surg. 2007;32(3):318–25.
14. Liu B, Chen S, Zhu J, Tian G. Arthroscopic Management of Perilunate Injuries. Hand Clin. 2017;33(4):709–15.
15. Botte MJ, Mortensen WW, Gelberman RH, Rhoades CE, Gellman H. Internal vascularity of the scaphoid in cadavers after insertion of the Herbert screw. J Hand Surg. 1988;13(2):216–20.
16. Liu B, Chen S-L, Zhu J, Wang Z-X, Shen J. Arthroscopically assisted mini-invasive man-

agement of perilunate dislocations. J Wrist Surg. 2015;04(02):093–100.
17. Wong T-C, Ip F-K. Minimally invasive management of trans-scaphoid perilunate fracture-dislocations. Hand Surg. 2008;13(03):159–65.
18. Kim JP, Lee JS, Park MJ. Arthroscopic reduction and percutaneous fixation of perilunate dislocations and fracture-dislocations. Arthrosc J Arthrosc Relat Surg. 2012;28(2):196–203.e2.
19. Jeon I-H, Kim H-J, Min W-K, Cho H-S, Kim P-T. Arthroscopically assisted percutaneous fixation for trans-scaphoid perilunate fracture dislocation. J Hand Surg Eur Vol. 2010;35(8):664–8.
20. Herzberg G, Burnier M, Marc A, Merlini L, Izem Y. The role of arthroscopy for treatment of perilunate injuries. J Wrist Surg. 2015;04(02):101–9.
21. Kim J, Lee J, Park M. Arthroscopic treatment of perilunate dislocations and fracture dislocations. J Wrist Surg. 2015;04(02):081–7.
22. Wahegaonkar A, Mathoulin C. Arthroscopic dorsal Capsulo-ligamentous repair in the treatment of chronic Scapho-lunate ligament tears. J Wrist Surg. 2013;02(02):141–8.
23. Mathoulin C. Treatment of dynamic scapholunate instability dissociation: contribution of arthroscopy. Hand Surg Rehabil. 2016;35(6):377–92.

Arthroscopic Management of Chronic Perilunate Dislocations

100

Deepak N. Bhatia

100.1 Background

A chronic perilunate dislocation is a disabling wrist injury that involves complete midcarpal separation and loss of contact between the lunate and capitate for a period of 6 weeks or more [1]. Chronicity results in severe perilunate adhesions and pseudocapsule formation, and closed reduction cannot be achieved. Open reduction and stabilization involve combined dorsal and volar approaches, and extensive dissection is necessary for alignment [2]. Arthroscopic reduction is possible after radiocarpal and midcarpal perilunate adhesiolysis and percutaneous K-wire stabilization of the carpal rows maintains the reduction until soft tissue healing is achieved.

100.1.1 Surgical Anatomy

Chronic perilunate dislocation results in several alterations in the regional anatomy and each of these must be corrected to achieve and maintain reduction. The lunate translates to the volar aspect of the radiocarpal joint and is in a flexed position (Fig. 100.1a, b). Perilunate adhesions and fibrosis involve the anterior capsule and adjacent carpal bones (scaphoid and triquetrum) and a pseudocapsule develops dorsal to the lunate. Scarring within the remnants of torn ligaments completely fills up the scaphotriquetral space and the dorsal capsule is scarred and adherent to the displaced carpal bones. Chronic changes present several technical challenges during the procedure: (a) Radiocarpal and midcarpal spaces are difficult to access for arthroscopic visualization and instrumentation. (b) Identification of the lunate is difficult due to the adhesions. (c) Scarring within the scaphotriquetral space and dorsal capsule are barriers to reduction, and (d) chronically displaced carpal bones are difficult to realign and tend to displace to the dislocated position.

100.2 Indications and Contraindications

Perilunate dislocations of the wrist that have remained unreduced for 6 weeks or more can be treated using this technique.

The procedure is contraindicated in chronic perilunate dislocations with associated carpal bone fractures and open surgical approaches are necessary for these injuries.

D. N. Bhatia (✉)
SPORTSMED Mumbai, and Sir HN Reliance Foundation Hospital, Mumbai, India
e-mail: shoulderclinic@gmail.com

© ISAKOS 2022

D. N. Bhatia et al. (eds.), *Arthroscopy and Endoscopy of the Elbow, Wrist and Hand*,
https://doi.org/10.1007/978-3-030-79423-1_100

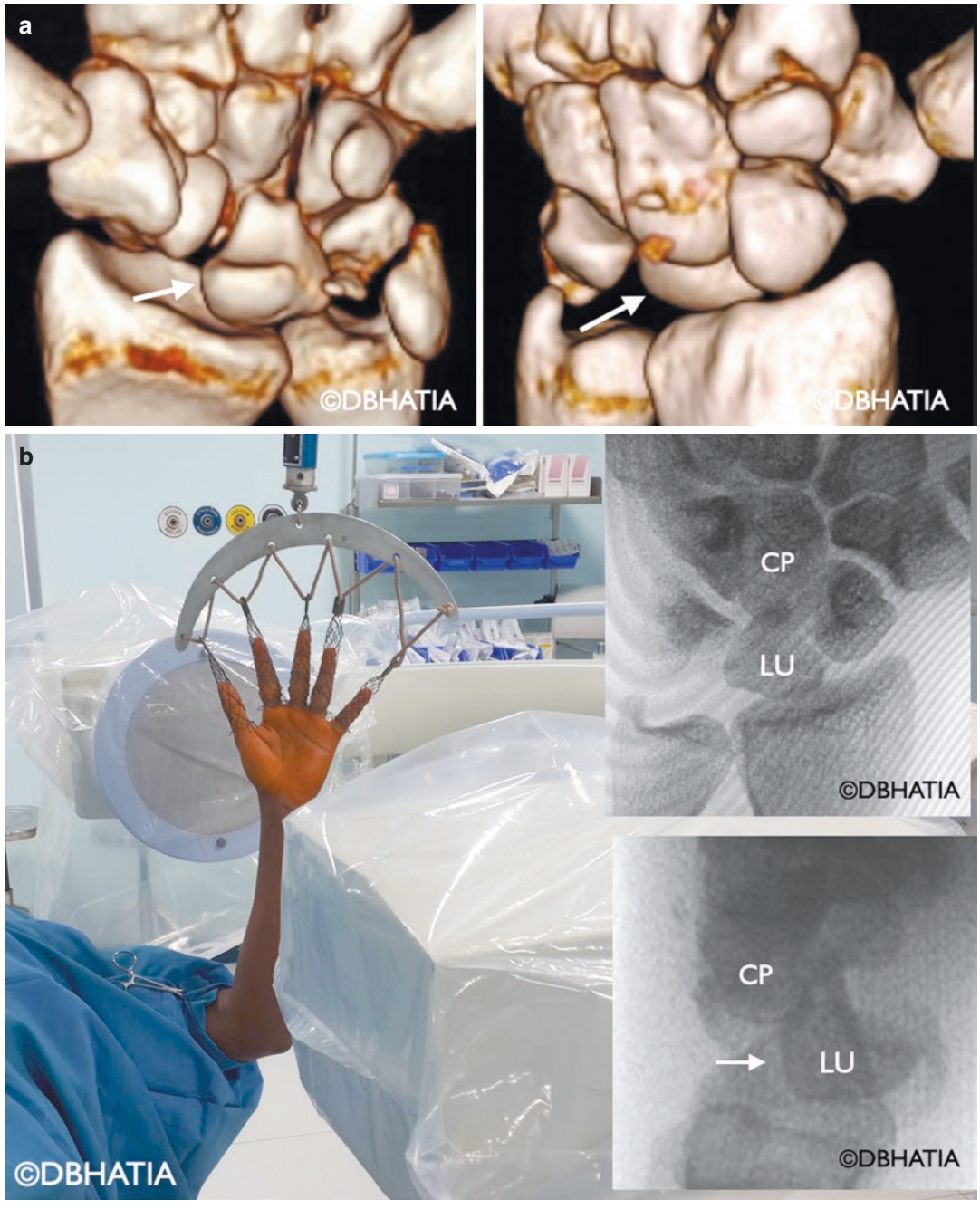

Fig. 100.1 (**a**) CT Scan reconstruction of a chronic perilunate dislocation is shown. CT view from the volar aspect shows the flexed position of lunate (arrow, left image). CT view from the dorsal aspect shows the dorsal dislocation of capitate (arrow, right image) and the scaphotriquetral space. (**b**) An image intensifier is positioned parallel to the floor (left image). Fluoroscopy shows the perilunate dislocation and the flexed lunate is visualized (right images, CP capitate, LU Lunate). (© D. Bhatia)

100.3 Surgical Technique

The procedure is performed with the patient in the supine position; the upper limb is suspended with finger traps and a countertraction force of 2 kg is used if necessary. A 30° arthroscope (1.9 mm) is used for initial access and is substituted with a 2.4 mm arthroscope after adhesiolysis. An image intensifier is positioned and used throughout the procedure (Fig. 100.1b).

Portals: Four portals are used in this procedure: 3–4 and 6-R radiocarpal portals, and radial (MCR) and ulnar (MCU) midcarpal portals.

Diagnostic evaluation and orientation: Radiocarpal arthroscopy is performed using the 6-R portal for visualization and 3–4 portal for instrumentation. The triquetrum and scaphoid are identified and the scaphotriquetral space is used to gain access to the midcarpal space. The scarred ligament remnants are identified and cartilage surfaces are assessed. MCR and MCU portals are created for further adhesiolysis (Fig. 100.2a).

Adhesiolysis: A shaver is used via 3–4 portal and MCR portals, and radiocarpal and midcarpal synovectomy is performed. Dorsal capsulotomy is performed if necessary and the scarred ligaments in scaphotriquetral space are excised.

Lunate identification: The arthroscope is shifted to MCR portal and the lunate is identified as follows: a) Ligament remnants attached to the scaphoid and triquetrum are followed volarly and usually lead to the lunate, b) the scaphotriquetral space volar to the ligaments is probed and the lunate can be located. c) The pseudocapsule is excised with a shaver in MCU and 6-R portals and lunate is visualized, d) intraoperative fluoroscopy may be necessary in long-standing cases with a hypertrophic pseudocapsular tissue (Fig. 100.2b).

Perilunate release: The lunate is usually adherent to the volar capsule and ligament remnants, and cannot be translated dorsally and proximal to the capitate. Perilunate release is performed via radiocarpal and midcarpal joints. Dorsal scar tissue is excised to create space for dorsal translation and ligament remnants on the scaphoid and triquetral aspects are resected. The dorsal attachment of scapholunate ligament is preserved if possible and can be grasped to assess adequate mobility (Fig. 100.3a).

Carpal alignment: A K-wire (6-R portal) is passed into the dorsal surface of lunate under vision (MCR portal) along its long axis. The wire is used to translate the lunate dorsally and to correct the volar tilt of the lunate (Fig. 100.3b). Correct alignment is indicated by: (a) Capitate coverage, i.e., placement of midcarpal lunate surface under the proximal capitate dome, (b) Lunate extension (dorsiflexion), (c) congruous scapholunate alignment, (d) congruous lunotriquetral alignment, and (e) Fluoroscopic conformation of reduction (Fig. 100.4a).

Carpal stabilization: Percutaneous K-wires (1.5 mm) are passed from the scaphoid and triquetrum into lunate and capitate in a diamond-shaped construct (Fig. 100.4b). Fluoroscopy and direct visualization are used to guide wire passage and the final reduction after wire passage is confirmed (Fig. 100.5). A lavage is given to remove any debris and the portals are closed.

100.4 Tips and Tricks

- A 1.9 mm arthroscope and a 2 mm shaver are useful for initial steps of the procedure.
- Identification of the lunate is the most important step. Ligament remnants and probing through the midcarpal region are useful to locate the lunate.
- K-wires may be passed into the scaphoid and triquetrum during the initial steps of the procedure. Once carpal realignment is obtained, the wires are passed across into the lunate.

100.5 Pitfalls

Excessive periarticular swelling interferes with carpal alignment and subsequent passage of K-wires is difficult. Fluid inflow must be restricted to avoid swelling.

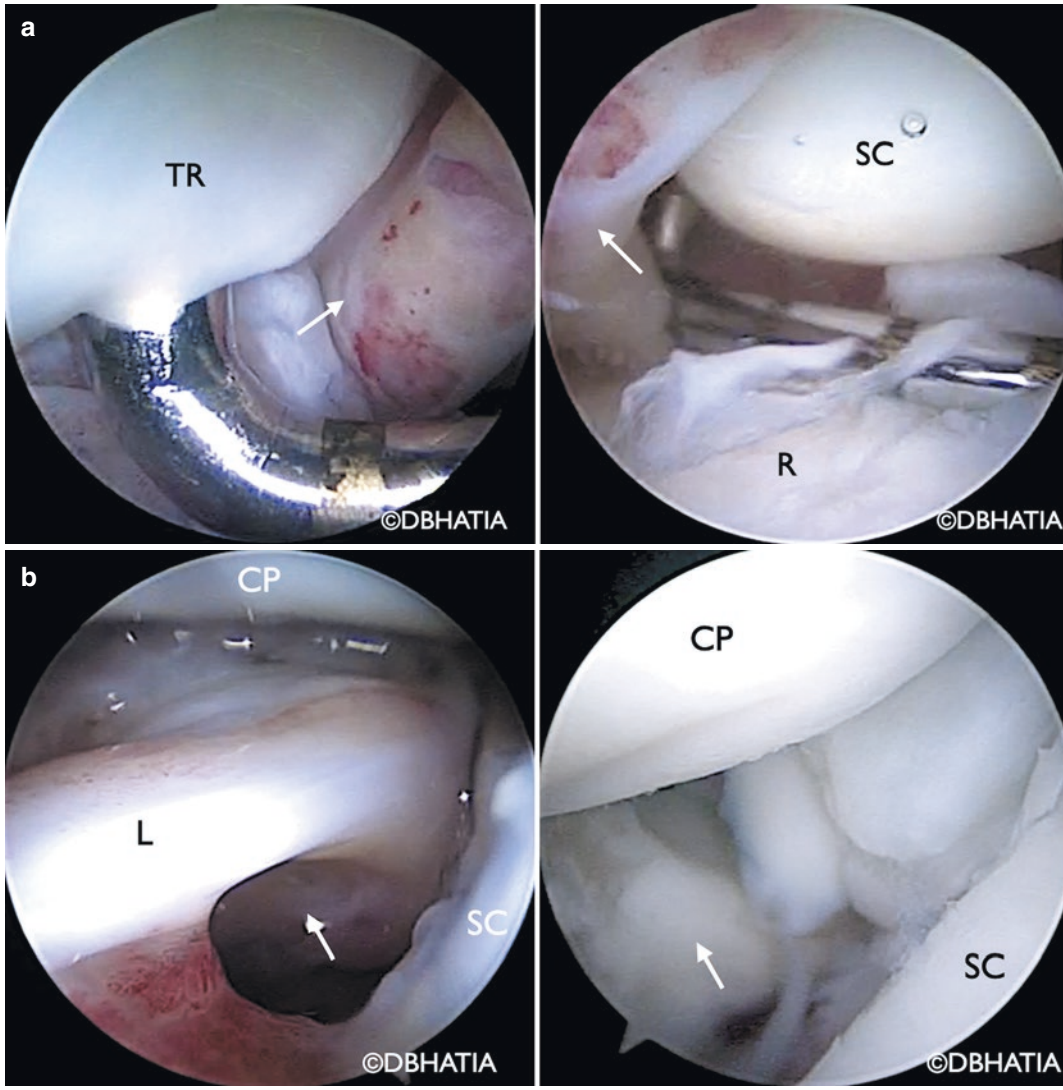

Fig. 100.2 (**a**) Radiocarpal evaluation via 6-R portal is demonstrated. The triquetrum (TR) and scaphoid (SC) are probed and identified and the scarred ligament remnants (arrows) are traced to their volar attachment. (**b**) Midcarpal evaluation via MCR portal is demonstrated. The scapholunate ligament remnant (L) can be traced to lunate (arrow, left image). Arthroscopic view after scar tissue excision demonstrates the lunate (arrow, right image) volar to capitate (CP) and scaphoid (SC). (© D. Bhatia)

100.6 Postoperative Management, Rehabilitation, and Return to Sports

A wrist brace or a below elbow plaster slab is used to maintain the wrist and hand in the functional position of wrist dorsiflexion. Finger movement is encouraged, and the brace is maintained for 6 weeks. The wires are removed after 6 weeks, and rehabilitation is started. Range of wrist movement and gradual strengthening are initiated simultaneously. Activities of daily living are started at 8 weeks, and desk work is permitted after 12 weeks. Return to heavy work and sports is permitted after 6 months of rehabilitation.

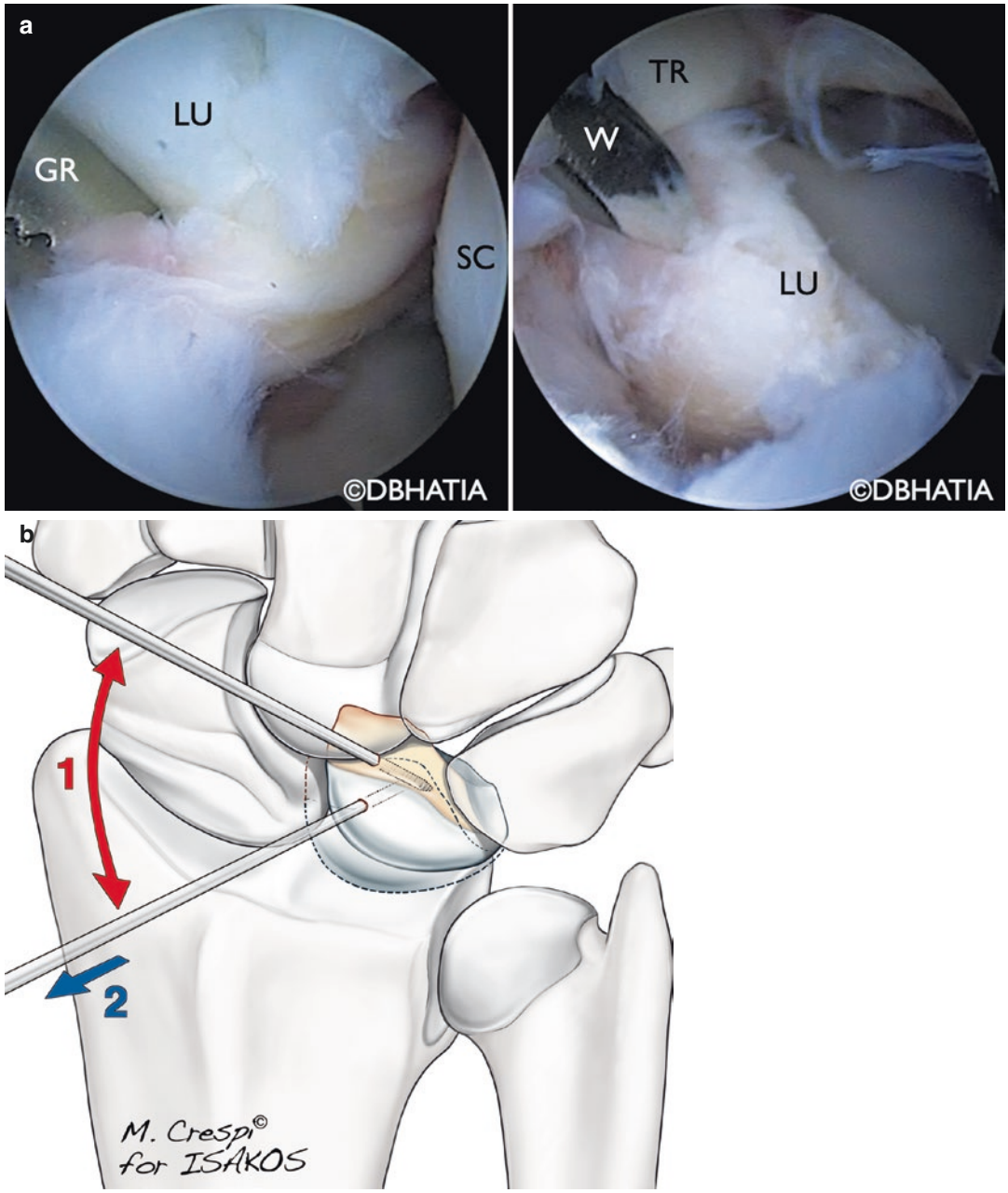

Fig. 100.3 (**a**) A grasper (GR) is used at the ligament attachment to manipulate the lunate (LU) and mobility is assessed (left image). A K-wire is passed into the lunate for reduction. (SC: scaphoid, TR: triquetrum). (© D. Bhatia) (**b**) Carpal reduction is illustrated. A K-wire passed into the lunate is used as a joystick to dorsiflex (arrow 1) the lunate and traction (arrow 2) is used for dorsal translation. (M. Crespi © for ISAKOS)

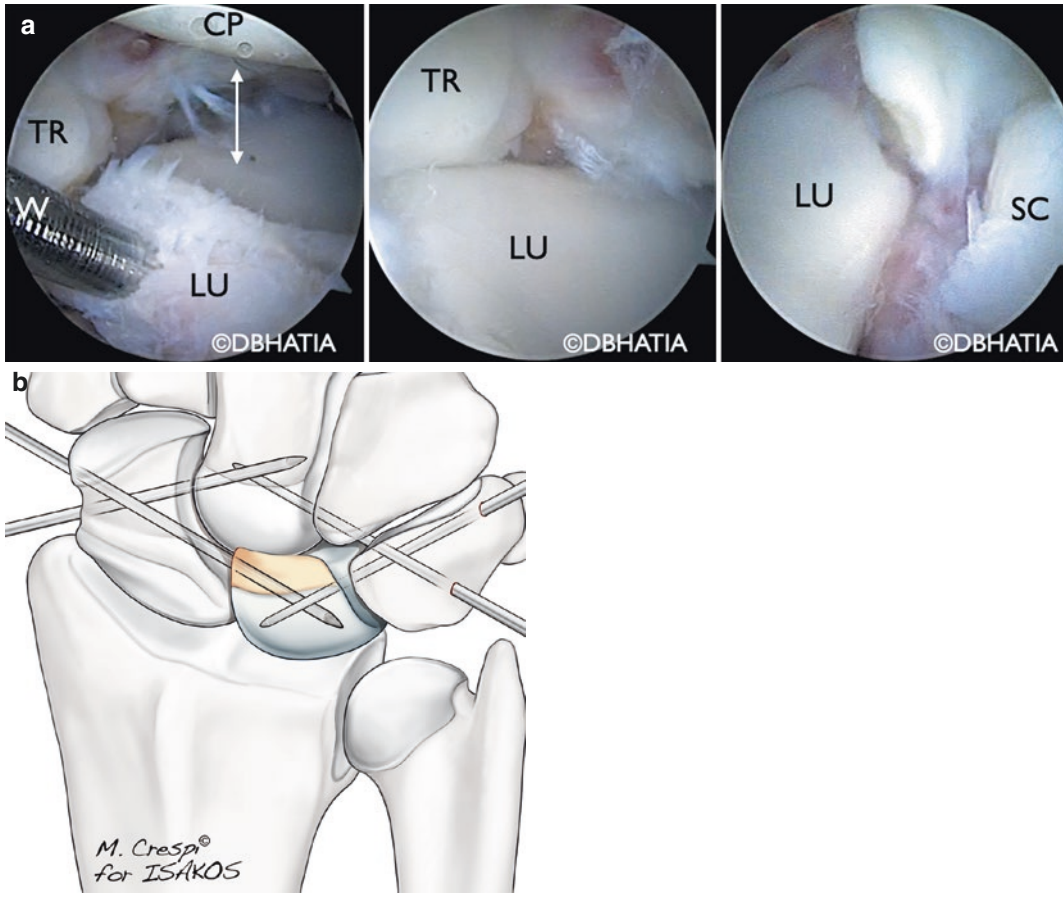

Fig. 100.4 (**a**) Carpal alignment is assessed by evaluation of capitate (CP) coverage (arrows) by lunate (LU) (left image) and congruous alignment of lunate with triquetrum (TR, middle image) and scaphoid (SC, right image). (W: joystick wire). (© D. Bhatia) (**b**) Carpal stabilization is illustrated. Four K-wires are passed into the lunate and capitate as shown to achieve a diamond-shaped construct. (M. Crespi © for ISAKOS)

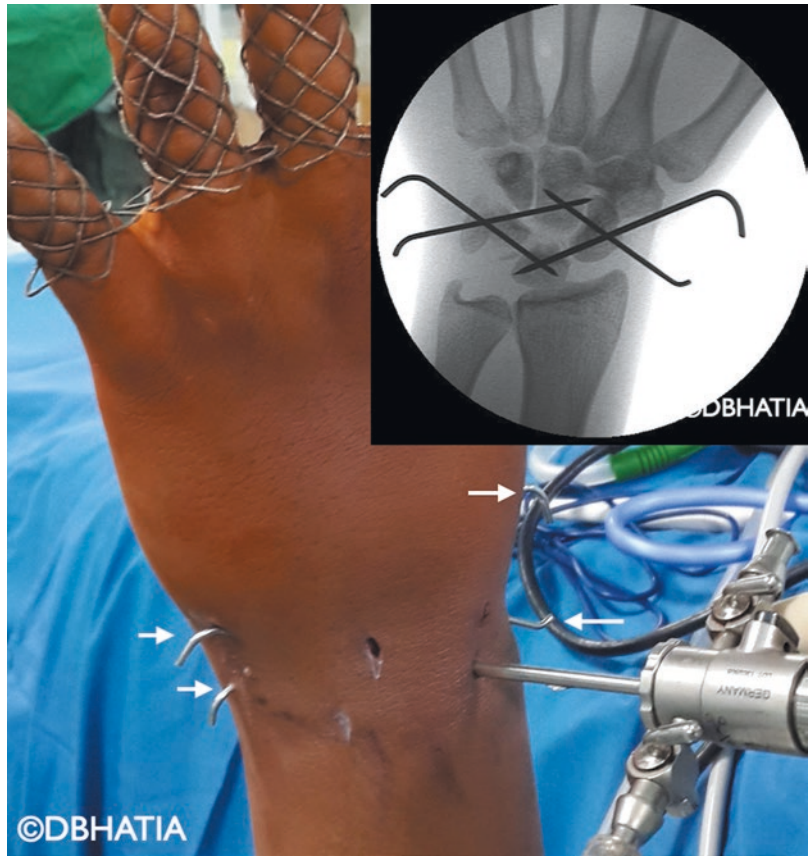

Fig. 100.5
Percutaneously passed carpal transfixation K-wires (arrows) are demonstrated. Inset image shows the diamond-shaped construct for stabilization of the chronic dislocation. (© D. Bhatia)

References

1. Bhatia DN. Arthroscopic reduction and stabilization of chronic perilunate wrist dislocations. Arthrosc Tech. 2016;5(2):e281–90. https://doi.org/10.1016/j.eats.2015.12.008.
2. Melone CP, Murphy MS, Raskin KB. Perilunate injuries. Repair by dual dorsal and volar approaches. Hand Clin. 2000;16:439–48.

101 Arthroscopic Management of Irreducible Volar Dislocation of the Distal Radioulnar Joint

Deepak N. Bhatia

101.1 Background

Volar dislocation of the distal radioulnar joint (DRUJ) is an unusual injury and may sometimes be irreducible [1, 2]. These dislocations may be isolated or may occur in association with forearm fractures. The patient presents with severe painful restriction of all wrist movements (Fig. 101.1). Closed reduction of volar DRUJ dislocations is possible however open reduction is necessary for irreducible dislocations. Arthroscopic reduction is a minimally invasive alternative for mobilization and reduction of the impacted ulnar head and percutaneous transfixation K-wires maintain the reduction until soft tissues have healed.

101.1.1 Surgical Anatomy

Volar dislocation of the DRUJ alters the anatomical relationship of surrounding structures (Fig. 101.2). The extensor carpi ulnaris (ECU) tendon displaces relative to the ulna and may prevent reduction of the DRUJ. The volar flexor tendons may be displaced on either side of the dislocated ulnar head and anterior to it. The dorsal radioulnar ligament (RUL) is usually torn, and volar RUL and volar capsule is stretched and forms an outpouching sac for the distal ulnar head. The triangular fibrocartilage complex is disrupted and remnants may be interposed into the DRUJ resulting in irreducibility (Fig. 101.3). The ulnar head itself is impacted along the dorsal radius and may demonstrate a "Hill-Sachs" like wedge deformity along its dorsal aspect (Fig. 101.4). In cases where reduction is delayed by 3–4 weeks, adhesions develop between the dislocated ulnar head and surrounding tissues, and a pseudocapsule develops around the ulnar aspect of the radial articular surface.

101.2 Indications and Contraindications

1. Acute traumatic DRUJ volar dislocations that are irreducible on attempted closed reduction can be reduced arthroscopically. Associated TFCC tears can be addressed simultaneously.
2. Chronic (>3–4 weeks) symptomatic dislocations should be evaluated and reduced arthroscopically. Stabilization of the DRUJ is usually necessary and K-wire fixation in the reduced position is performed.

Reccurrent and long-standing dislocations of DRUJ are contraindications for arthroscopic reduction and an open procedure for DRUJ stabilization is usually necessary [2].

D. N. Bhatia (✉)
SPORTSMED Mumbai, and Sir HN Reliance Foundation Hospital, Mumbai, India
e-mail: shoulderclinic@gmail.com

© ISAKOS 2022

D. N. Bhatia et al. (eds.), *Arthroscopy and Endoscopy of the Elbow, Wrist and Hand*,
https://doi.org/10.1007/978-3-030-79423-1_101

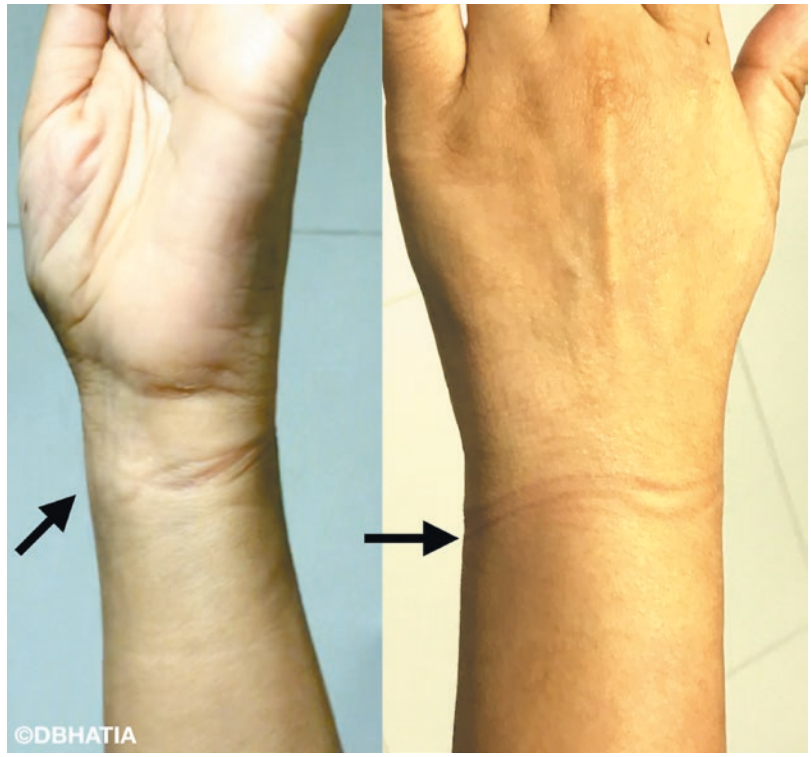

Fig. 101.1 Clinical image of a left wrist shows a prominent dislocated ulnar head on the volar aspect (arrow, left image) and absence of the normal dorsal prominence of the distal ulna (arrow, right image). (© D. Bhatia)

Fig. 101.2 Plain radiographs demonstrate ulnar overlap on the anteroposterior view (left image) and an anterior profile of the ulna on a lateral view (middle image). An oblique view clearly demonstrates the dislocation (right image) (R: radius, U: Ulna, arrow: Ulnar head). (© D. Bhatia)

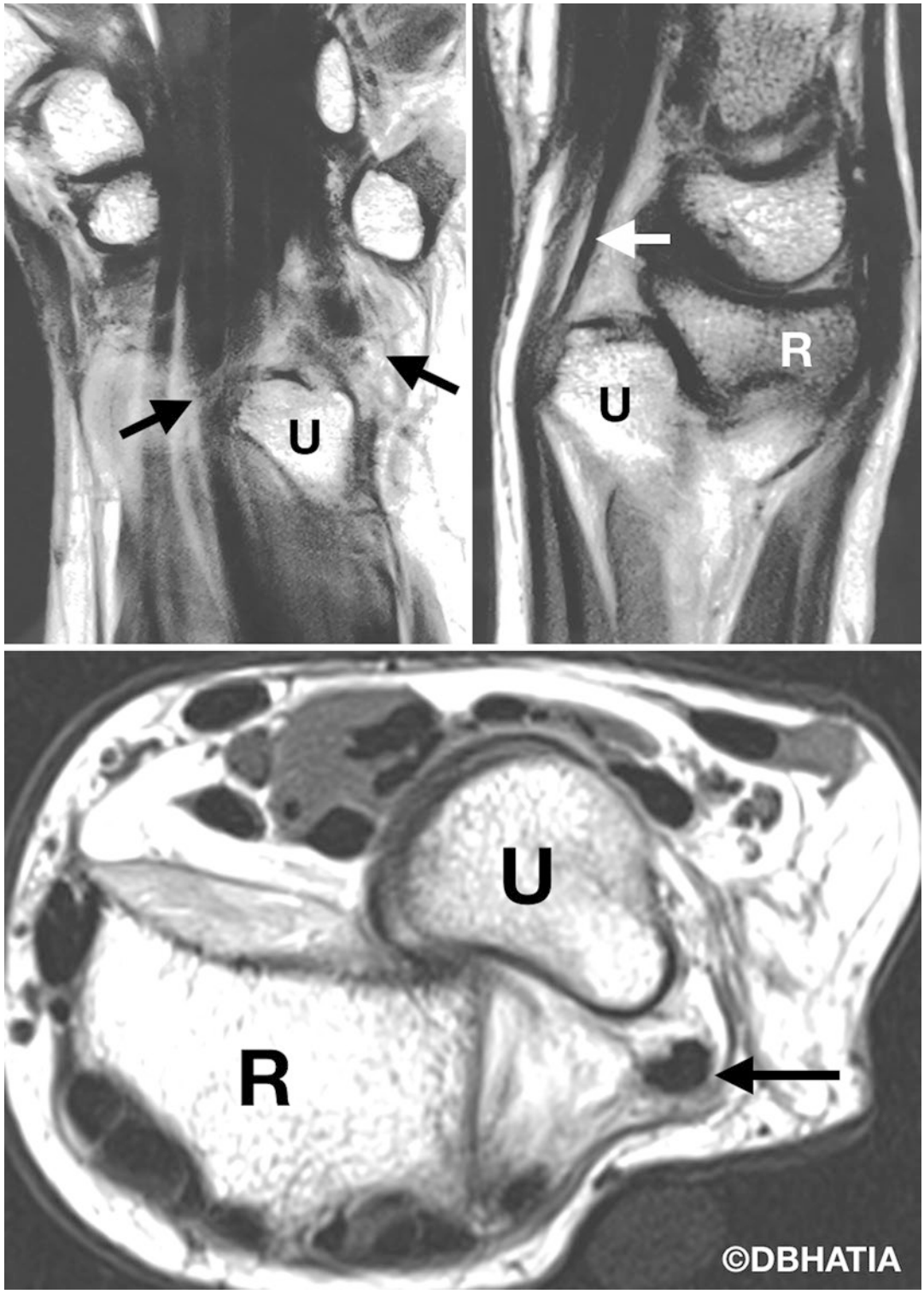

Fig. 101.3 MRI demonstrates the altered soft tissue anatomy in a volar DRUJ dislocation. The volar flexor tendons (arrows) are seen displaced on either side (top left) and anterior (top right) to the dislocated ulnar head (U). The displaced ECU tendon (arrow) widens the normal interval between the fifth and sixth extensor compartments (bottom image). (© D. Bhatia)

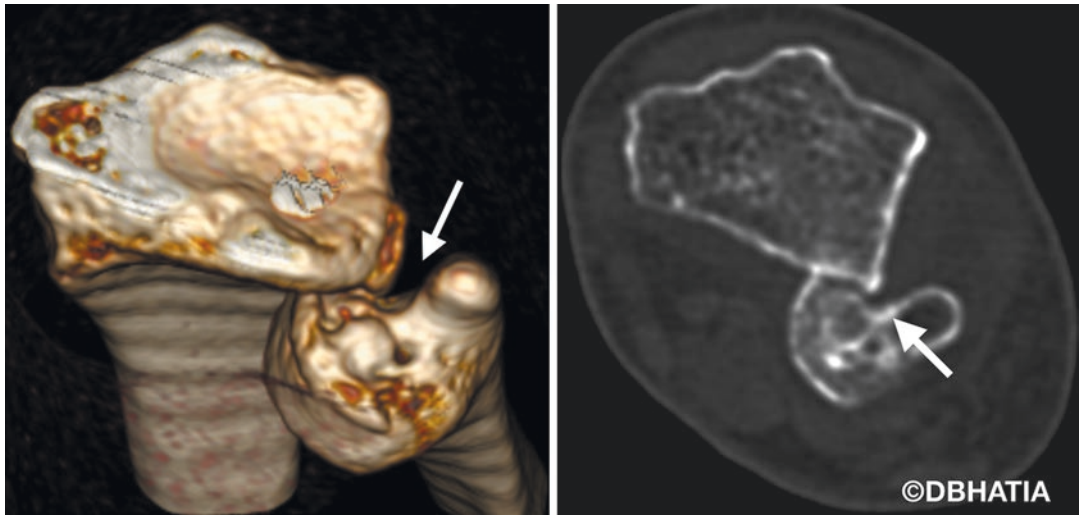

Fig. 101.4 CT scan images demonstrate an impacted volar dislocation of ulnar head and a wedge deformity on the dorsal ulnar head arrows). (© D. Bhatia)

101.3 Surgical Technique

The procedure is performed with the patient in the supine position. The upper limb is suspended with finger traps, and a countertraction force of 2–4 kg is used to distract the joint. Routine dorsal and volar wrist arthroscopy portals are marked, and a 30° arthroscope (2.4 mm) is used for diagnostic arthroscopy.

Portals: The dorsal radiocarpal 3–4 portal is the viewing portal throughout the procedure. The 6R portal is main working portal. The ECU tendon is usually displaced and access is obtained through the interval between the fifth and sixth dorsal extensor compartments using transillumination. The 6 U portal is used if necessary (Fig. 101.5).

Diagnostic endoscopy: The 3–4 portal is used to evaluate the radiocarpal joint and a probe/shaver are used through the 6R portal. The usual appearance of TFCC is not seen, and TFCC tissue is rolled up along the ulnar aspect of the radial articular surface. In delayed presentations, a pseudocapsule is present and is seen attaching to the TFCC remnants (Fig. 101.6).

Capsulectomy and ECU identification: A 6R portal is created using an outside-in technique. A 3 mm shaver blade is used to excise the ulnar pseudocapsule. A probe is used to retract the TFCC remnants ulnar to the pseudocapsule and the ECU tendon can be identified and retracted dorsally to reverse the interposition (Fig. 101.6).

Ulnar head dissection: A blunt elevator is used to gently develop a plane between the volar capsule of the radius and the surrounding tissues. A shaver blade is used to excise tissues anterior to the capsule. A probe is used to feel the dislocated ulnar head and soft tissue resection is continued until the distal ulna is visualized (Fig. 101.7).

DRUJ reduction: Reduction is attempted once the distal ulna is visualized through the TFCC remnants (Fig. 101.8). The probe is hooked volar to the dislocated ulnar head and gently pulled dorsally. Reduction is confirmed by: (1) visualization of the white ulnar head through the TFCC and associated with a palpable clunk. (2) The external volar prominence of the ulnar head is reversed and the dorsal prominence is felt. (3) Biplanar fluoroscopic views demonstrate reduction.

DRUJ stabilization: Stability of the DRUJ is dynamically assessed by rotating the wrist from supination to pronation and stabilization is necessary if the DRUJ is found to subluxate or dislocate. Two K-wires are passed through a small skin incision along the volar aspect of the ulnar head and sensory nerves are identified and pro-

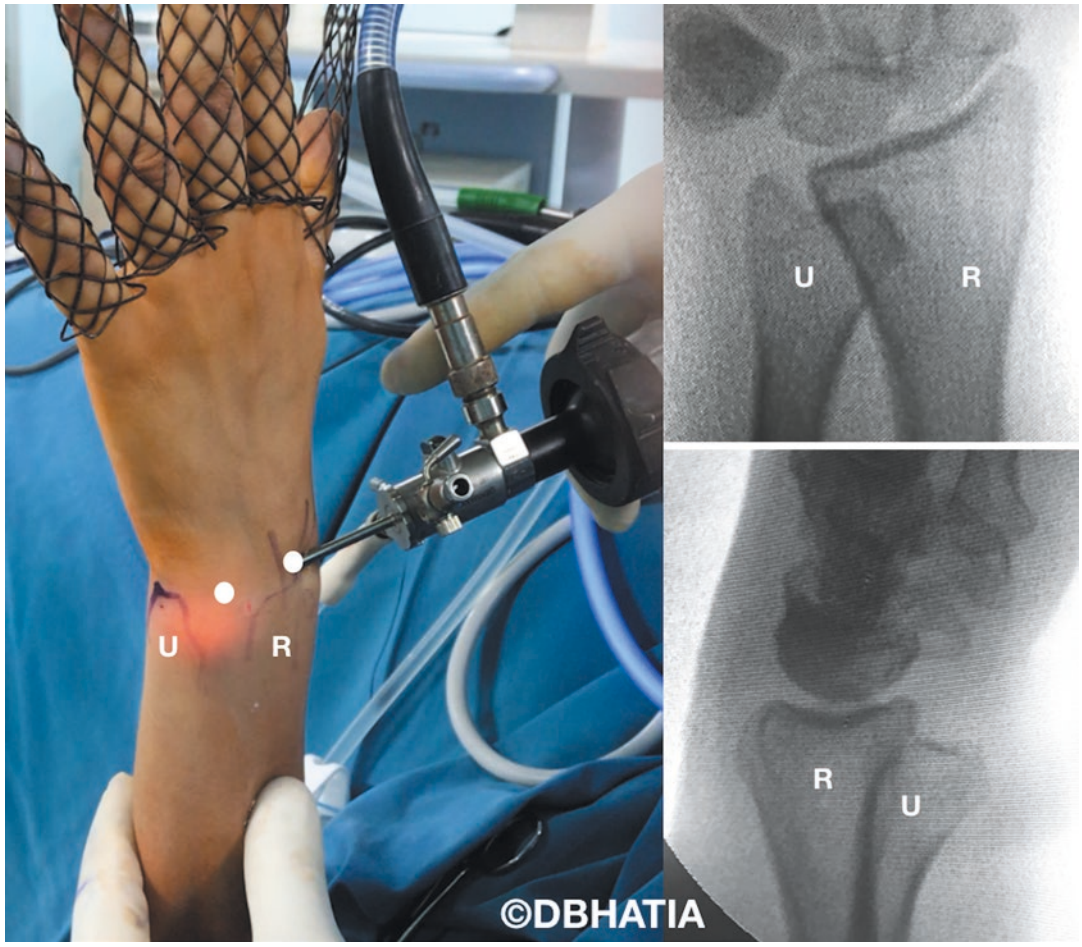

Fig. 101.5 Arthroscopic portals and fluoroscopic views are demonstrated. (R: radius, U: Ulna). (© D. Bhatia)

tected. Biplanar fluoroscopy is used to guide wire passage in supinated position (Fig. 101.9). The wires are bent outside the skin, and all portals and the ulnar incision are closed.

101.4 Tips and Tricks

1. The ECU tendon is not in its usual place and can be identified externally using transillumination. This is useful in creation of 6R and 6 U portals and helps to identify ECU during intra-articular arthroscopic visualization.
2. Ulnar head impaction prevents reduction with a probe. The head is disimpacted by passing a blunt curved elevator between the ulna and the volar radial surface through the 6 U portal.

101.5 Pitfalls

1. Volar DRUJ dislocations may be missed in the ER and the resultant adhesions over a few weeks make closed and even arthroscopic reduction difficult.
2. The ECU tendon is at risk of injury during dissection and must be visualized and protected. Similarly, the flexor digitorum profundus (FDP) tendons must be probed and retracted if interposed to prevent injury.

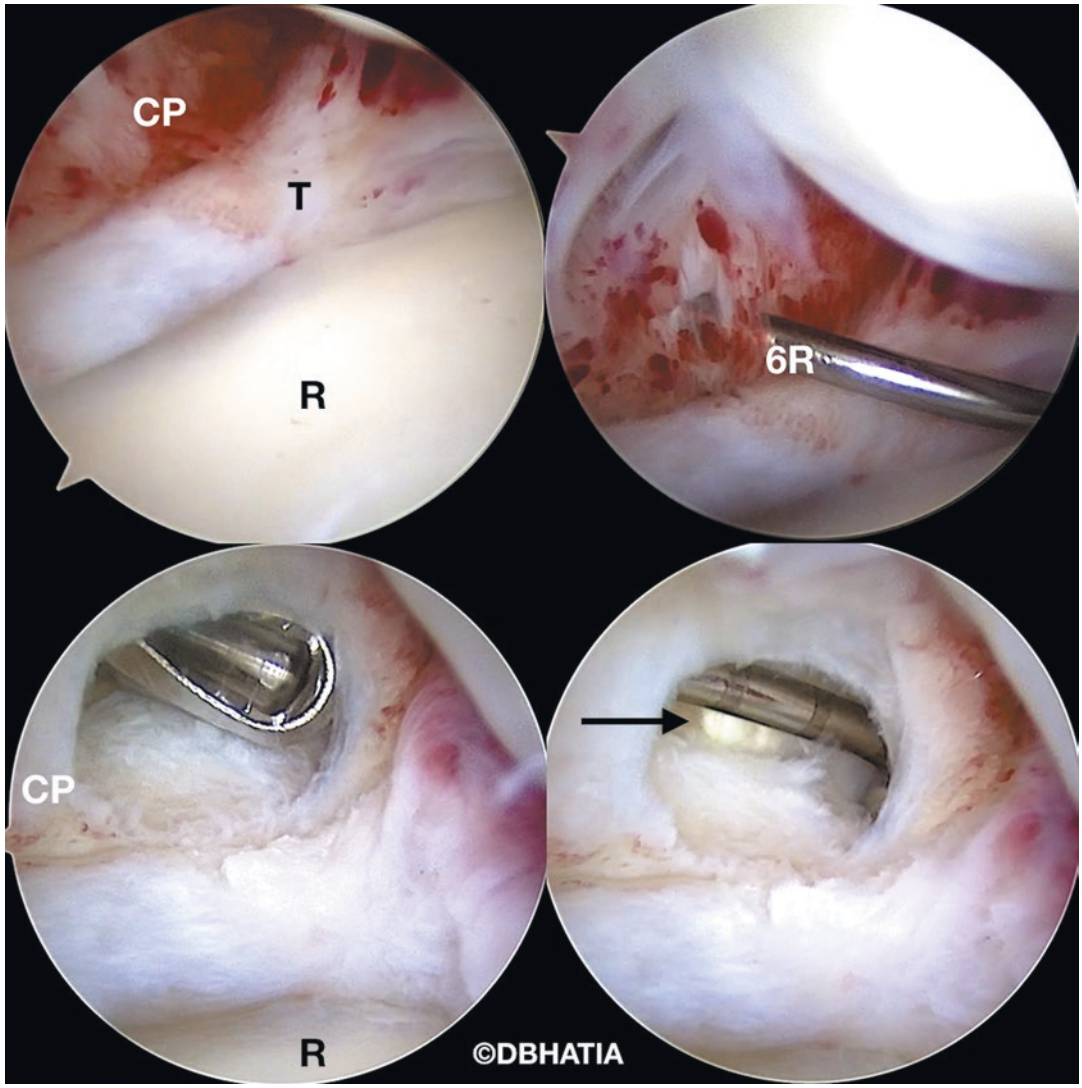

Fig. 101.6 Arthroscopic evaluation shows pseudocapsule (CP) and TFCC (T) remnants (Top Left). A 6R portal is demonstrated using a needle from outside-in (top right). A capsulectomy is performed using a shaver (bottom left). A probe demonstrates the ECU tendon (arrow, bottom right). (R: radius). (© D. Bhatia)

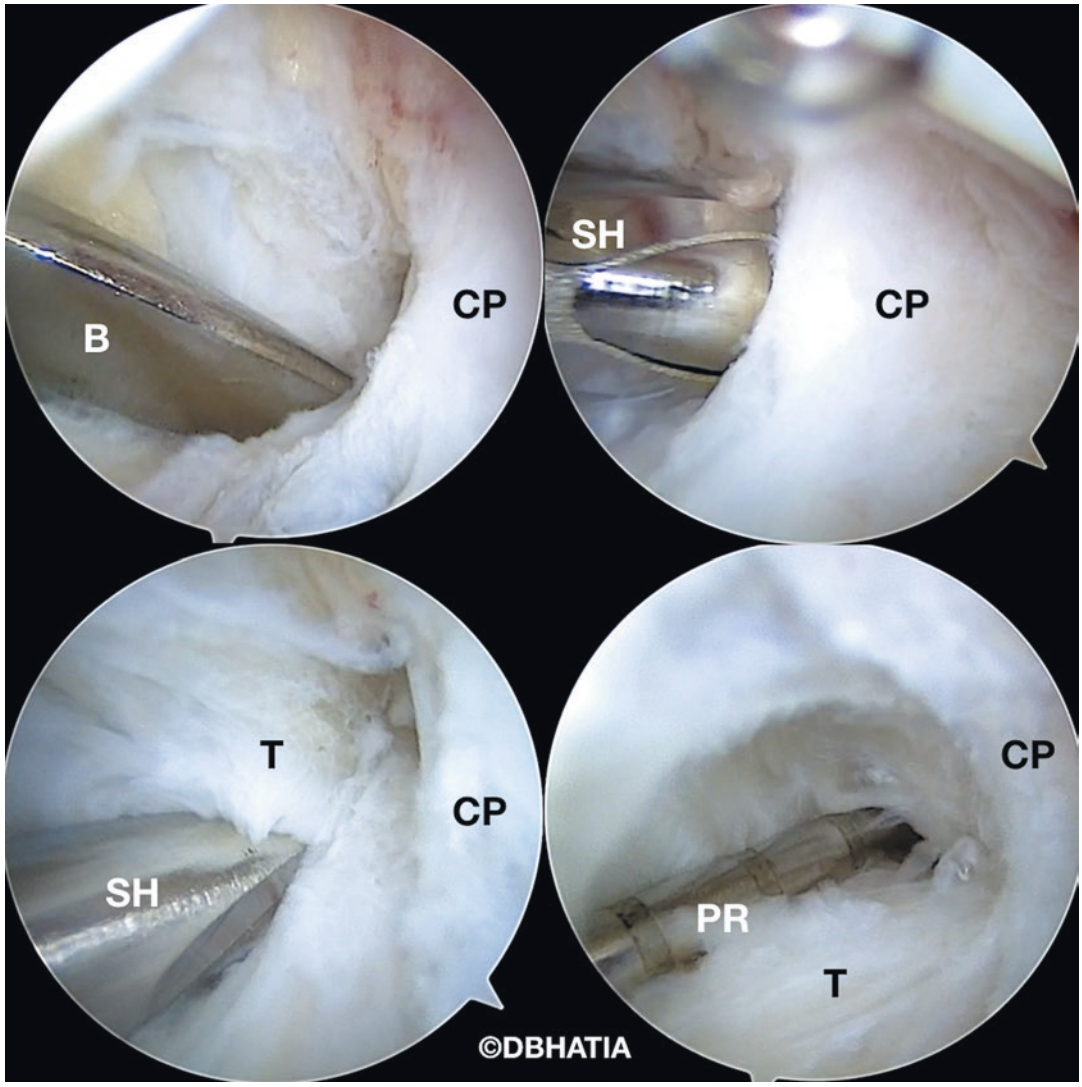

Fig. 101.7 Arthroscopic separation of volar capsule (CP) using a blunt elevator (B, top left) and shaver (SH, top right) is shown. The shaver is used to excise the TFCC remnants (T, bottom left) and the ulnar head is probed to assess its volar location (PR, bottom right). (© D. Bhatia)

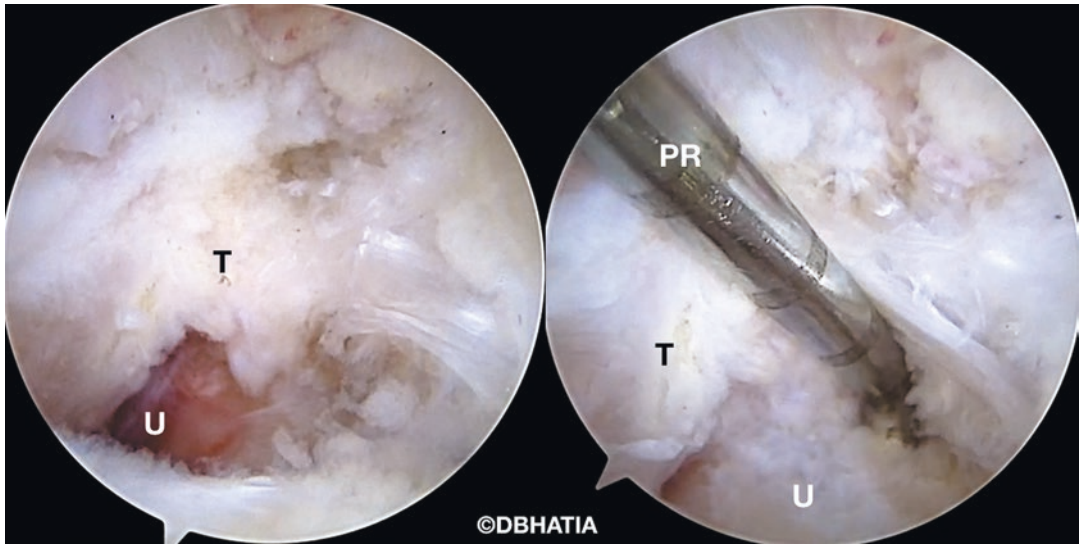

Fig. 101.8 Arthroscopic view of distal ulna (U) through the excised TFCC (T) prior to reduction (top left). Right image shows reduction of the ulnar head (U) using a probe (PR). (© D. Bhatia)

101.6 Postoperative Management, Rehabilitation and Return to Sport

An above elbow slab is applied in supination position and maintained for 4–6 weeks. Thereafter, percutaneous wires are removed and physical therapy is initiated. The rehabilitation protocol involves passive and active range-of-motion exercises (weeks 7–12) and simultaneous gradual strengthening. Full range is achieved in 6 weeks, and light work is permitted. Return to heavy work is permitted only after 6 months.

Conflict of Interest The author certifies that he has no commercial associations (e.g., consultancies, stock ownership, equity interest) that might pose a conflict of interest in connection with the submitted article. The author retains the copyright to the images, videos, and content in this chapter.

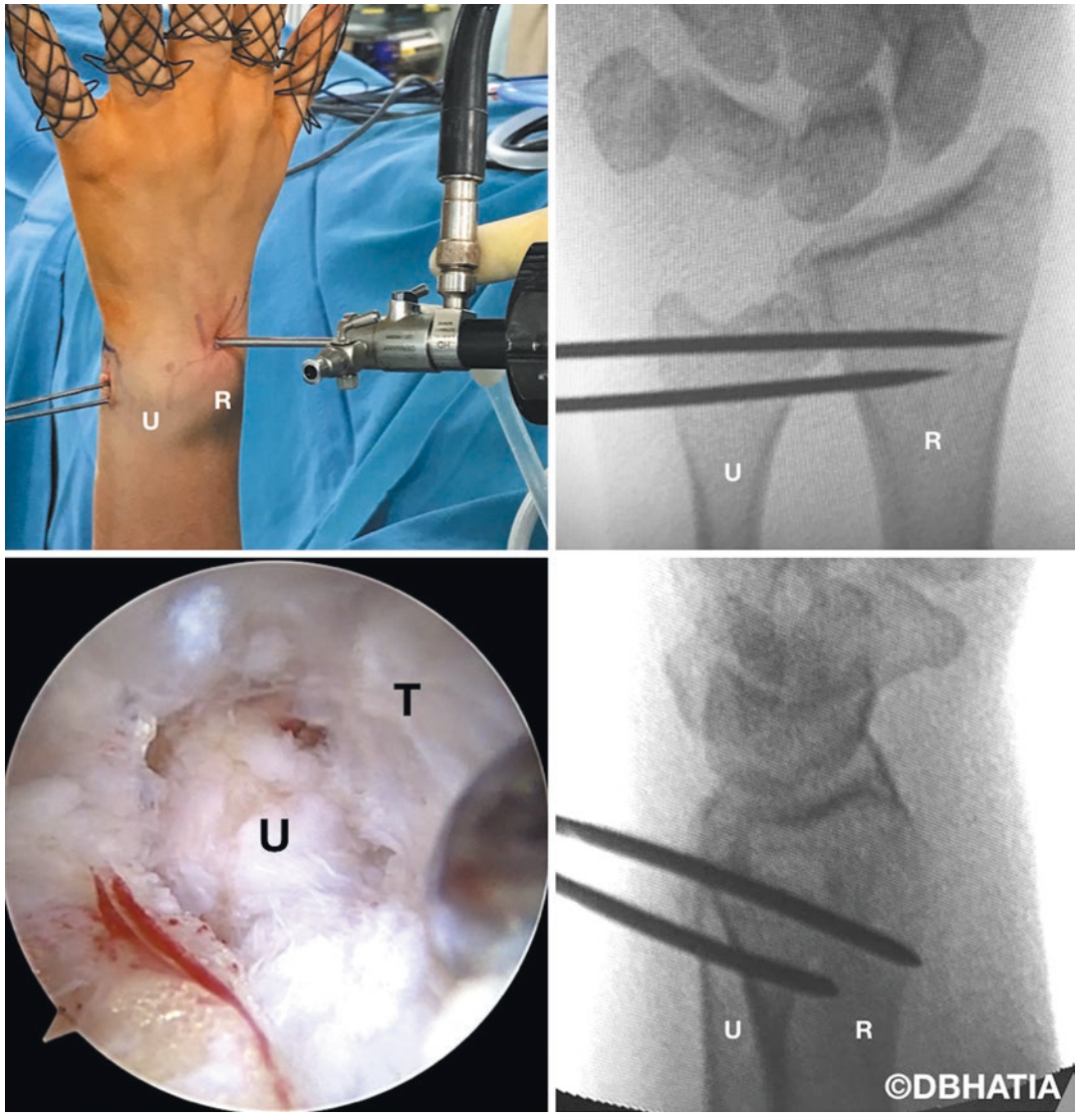

Fig. 101.9 DRUJ stabilization using percutaneous k-wires is demonstrated (top left). Arthroscopic image of the reduced and stabilized ulnar head (U) is shown through TFCC (T) (bottom left). Fluoroscopic images (top and bottom right) demonstrate the DRUJ stabilization. (R: radius). (© D. Bhatia)

References

1. Garrigues GE, Aldridge JM 3rd. Acute irreducible distal radioulnar joint dislocation. A case report. J Bone Joint Surg Am. 2007;89(7):1594–7.
2. Kikuchi Y, Nakamura T, Horiuchi Y. Irreducible chronic palmar dislocation of the distal radioulnar joint—a case report. Hand Surg. 2005;10(2–3):319–22.

Arthroscopic Management of Distal Radius Fractures

102

Margaret Woon Man Fok, Christian Xinshuo Fang, and Frankie Ka Li Leung

102.1 Background

With the advances in the implants design for distal radius fractures, many of the plates and screws available in the market are low profile and are associated with a low risk of complication if applied appropriately. Meanwhile, despite an aging population, many of our patients remain physically active in their ages. Currently, there is no objective evidence that open reduction and fixation is advantageous over cast immobilization in the clinical outcomes. Yet many patients would elect for surgical intervention to restore their anatomy so as to prevent the development of post-traumatic osteoarthritis.

Distal radius with an intra-articular step-off of >2 mm is known to lead to early degeneration [1]. While fluoroscopy enables accurate assessment of the radiological variables of reduction (i.e., radial height, volar tilt, radial angle, scaphoid, and lunate orientation) and implant placement, there are limitations in evaluating articular congruity. Wrist arthroscopy has gained popularity in recent years. It provides a magnified view for the assessment of the articular surface. This allows an opportunity for further manipulation of the fracture fragments once an unacceptable step-off is identified.

Apart from the assessment of articular surface, wrist arthroscopy enables an enhanced evaluation of concomitant injuries in distal radius fractures, e.g., scaphoid fractures, scapholunate ligament (SL) tears, lunotriquetral ligament (LT) tears, and triangular fibrocartilage complex (TFCC) tears. Yet there remains a controversy on whether repairs of ligamentous and TFCC tears are necessary at the time of fracture fixation. Significant ligamentous injuries leading to carpal malalignment, e.g., SL tear with dorsal intercalated segment instability, should be addressed in the same setting. As for other less severe soft tissue injuries, there remains no consensus on the management. In a prospective study, Lindau et al. [2] showed that patients with distal radius fractures were associated with a high incidence of ligamentous and TFCC injuries. While lower wrist functional and subjective scores were observed at follow-up, only one patient out of the initial 43 patients with TFCC tear required surgical intervention for DRUJ instability in the long term [3]. With the current practice of performing anatomic reduction and stable plate fixation for distal radius fracture, it has been postulated that the osteoarticular congruence of DRUJ may allow the TFCC to heal. However, evidence of TFCC healing was only observed in about one-third of the cases after fracture union [4]. Yet, the functional outcome of all patients with healed

M. W. M. Fok (✉) · C. X. Fang · F. K. L. Leung
Department of Orthopaedic and Traumatology, Queen Mary Hospital, The University of Hong Kong, Hong Kong, SAR, China
e-mail: klleunga@hku.hk

© ISAKOS 2022

D. N. Bhatia et al. (eds.), *Arthroscopy and Endoscopy of the Elbow, Wrist and Hand*,
https://doi.org/10.1007/978-3-030-79423-1_102

distal radius fracture did not result in any significant difference with respect to the TFCC integrity.

Wrist arthroscopy in acute distal radius fracture can be technically demanding. There remains a risk of developing compartment syndrome especially in patients with severe soft tissue injuries and in situations in which surgeons struggle to reduce comminuted intra-articular fragments. With the introduction of dry arthroscopy by F. Pinal [5], this complication has been minimized.

102.2 Surgical Anatomy

Depending on the fracture pattern, different surgical approaches (both dorsal and volar) can be used for the internal fixation of distal radius fractures. CT scan is often used for fracture fixation planning (Figs. 102.1 and 102.2). External fixator may also be employed especially for distal radius fractures with severe soft tissue injuries.

For most distal radius fractures, a standard volar approach is most commonly used for volar plating. The incision is radial to the flexor carpi radialis (FCR) tendon, which can be palpated on the volar aspect of the distal forearm. FCR is then being retracted ulnarly while radial artery is retracted in the radial direction. After the elevation of pronator quadratus muscle from the insertion of distal radius, the fracture site will come into view.

For wrist arthroscopy, standard dorsal portals of the radiocarpal joint are utilized. Assessment of the midcarpal joint is sometimes needed to evaluate the integrity of the intercarpal ligaments, i.e., scapholunate and lunotriquetral ligament. Volar portals are seldom used for fracture reduction and fixation. Occasionally, volar radial portal may be employed to assess the dorsal rim fracture of the distal radius.

102.3 Indications and Contraindications

Arthroscopic-assisted fixation is indicated in:

- All acute intra-articular distal radius fractures (i.e., fracture that has not consolidated).
- Extra-articular distal radius fractures with suspected ligamentous injuries.

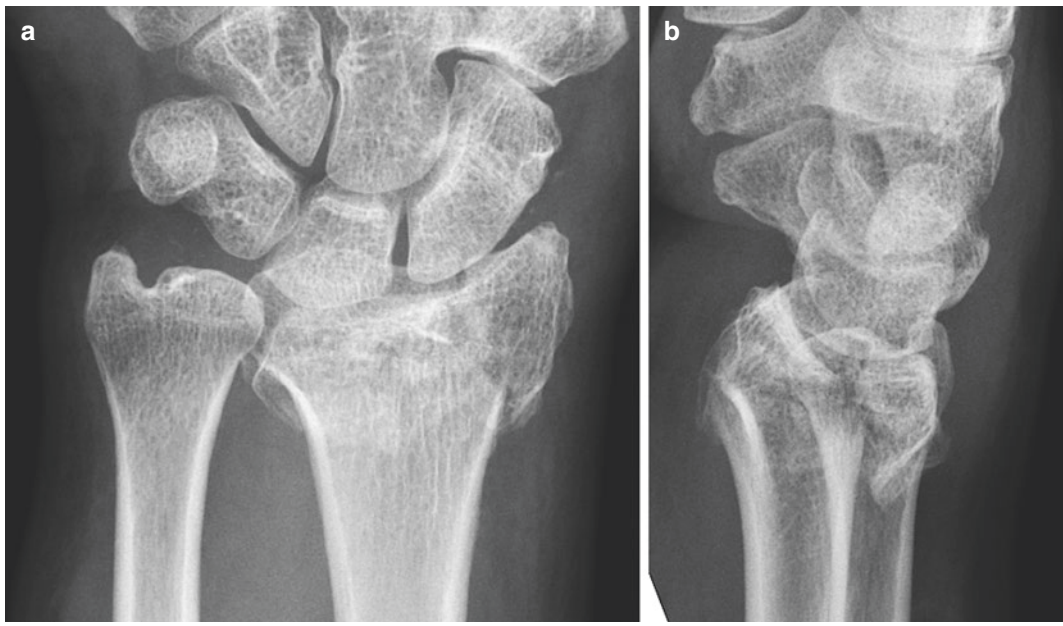

Fig. 102.1 Anteroposterior (**a**) and lateral (**b**) radiographs of an Intra-articular fracture. (© Fok)

Fig. 102.2 CT scan of an intra-articular fracture. (© Fok)

Arthroscopy is contraindicated in:

- Distal radius fractures with compartment syndrome.
  - Distal radius fractures with severe soft tissue injuries (associated with a high risk of compartment syndrome) are relatively contraindicated. It depends on the surgeons' expertise. It is not recommended especially when wet arthroscopy is used.
- Distal radius fractures with concomitant neurovascular injuries.
- Patients with multiple sites of injuries.

102.4 Surgical Technique

Arthroscopy is used to assist the intra-articular reduction and to assess ligamentous status. Extra-articular fracture reduction, in order to restore the radial length, radial inclination, and volar tilt, should still be done with open approach. Different approaches may be needed for reduction and fixation of different fracture patterns. The following are only surgical steps of the volar approach, that are commonly used for the volar plating of distal radius fractures. There are situations in which dorsal approach, extended radial approach, or combined approaches are needed for fracture fixation. These are beyond the scope of this chapter.

Under general or regional anesthesia, the affected arm is placed with the shoulder at 90° on a radiolucent hand Table. A pneumatic tourniquet is applied.

- Initial reduction of the distal radius via open approach.
- Standard volar approach for initial fixation of the distal radius fracture is performed. The incision is between the radial artery and the FCR tendon. Pronator quadratus muscle is then elevated from its insertion to expose the fracture.
- Fracture manipulation is performed by traction, disimpaction, and volar flexion in order to restore the radial height, the radial inclination, and the volar tilt of the distal radius. K-wires are used temporarily to hold the fragments in place.
- Based on the fracture configuration, a volar plate is selected to stabilize and buttress the fracture accordingly. The volar plate is provisionally placed on the distal radius (Fig. 102.3). One cortical screw is inserted into the stem of the plate to fix the plate in position onto the bone. K-wires are used to fix the articular fragments via either auxiliary holes of the plate or locking sheaths of the transverse component of the plate.
- Fluoroscopic views (anteroposterior, lateral, and oblique views) are then used to check the

initial fracture reduction and the plate placement. Once the reduction is considered satisfactory, and no further improvement can be achieved without an arthrotomy, another screw is recommended to be inserted into the stem of the plate prior to the assessment using wrist arthroscopy.

- Next, wrist arthroscopy is performed for intra-articular reduction [5, 6]. The wrist is placed onto an upright sterile traction tower. Finger traps are applied to the index, middle, and ring fingers of the affected hand. The fingers are then suspended with a 10 lb. traction (Fig. 102.4).
- After identification of the Lister's tubercle, entry point of the 3–4 portal (of the radiocarpal joint) can be felt as a soft spot just distal to the tubercle. A transverse incision is made, and the portal is created by using the "nick and spread" technique. A 30° 2.4 mm arthroscope is used for visualization. We prefer the use of 6R portal instead 4–5 portal as the working portal for triangulation as it avoids interference with the reduction of the dorso-ulnar radius (Fig. 102.5).
- Dry arthroscopic techniques are adopted as it avoids massive soft tissue extravasation and reduces the chance of developing postoperative compartment syndrome. These include: (a) keeping the valve of the arthroscopy opened at all times, (b) only turn on the suction of the shaver or burr when needed, and (c) irrigate the joint as needed to remove debris and blood.
- The initial arthroscopic field of the radiocarpal joint may be blocked by blood and bone debris. This can be cleared by connecting a syringe of 5–10 ml

Fig. 102.3 Initial fixation of distal radius using volar plate. (© Fok)

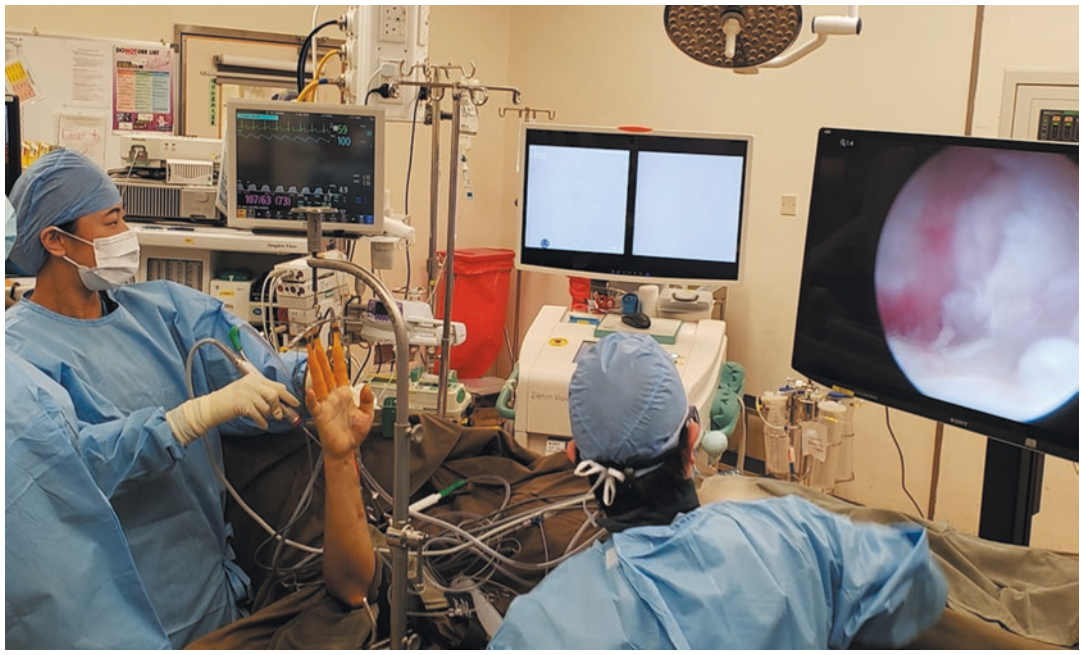

Fig. 102.4 Application of wrist arthroscopy after initial fixation to check for reduction of intra-articular fragments. (© Fok)

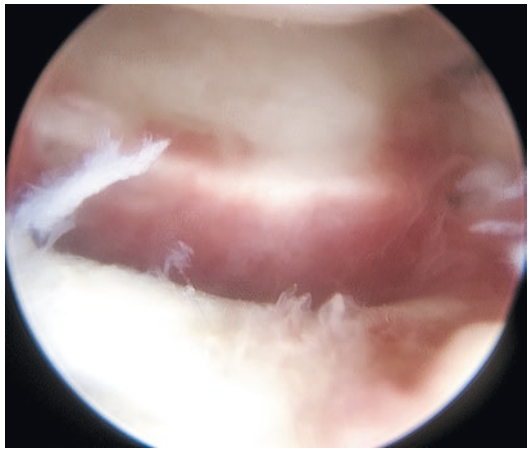

Fig. 102.5 From 3–4 portal, wrist arthroscopy is used to assess the articular surface and an intra-articular step and gap is noted. (© Fok)

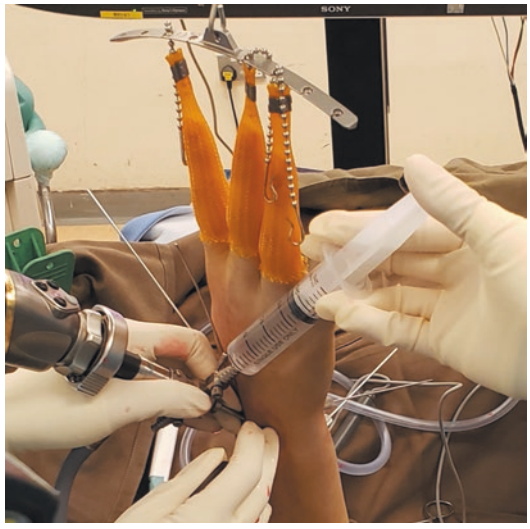

Fig. 102.6 Injection of 10 ml of saline to clear the blood and debris from the arthroscopic view. (© Fok)

saline to the side valve of the scope and then aspirate it with the 2.0/2.9 mm shaver, together with the blood and bone debris. Once all the fluid is aspirated, the syringe is removed and the valve of the scope is left open. This maneuver can be repeated as needed throughout the procedure when the visual field is being blocked (Fig. 102.6).

- Using the 3–4 portal, the articular surface of the distal radius is assessed (Fig. 102.7). If reduction is satisfactory, i.e., minimal gap

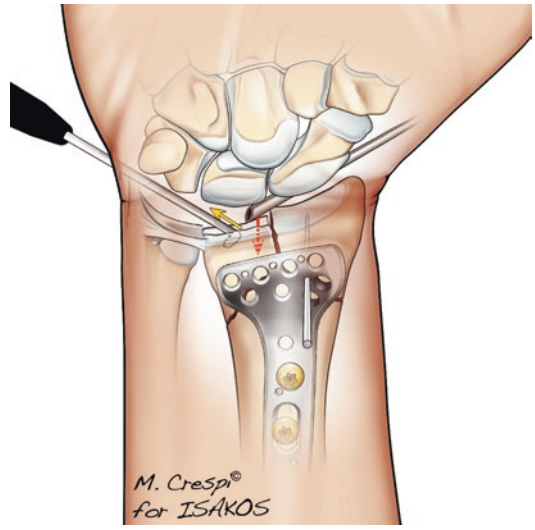

Fig. 102.7 Arthroscopic reduction of intra-articular fracture is illustrated. The probe is used via 6R portal. (© M. Crespi © for ISAKOS)

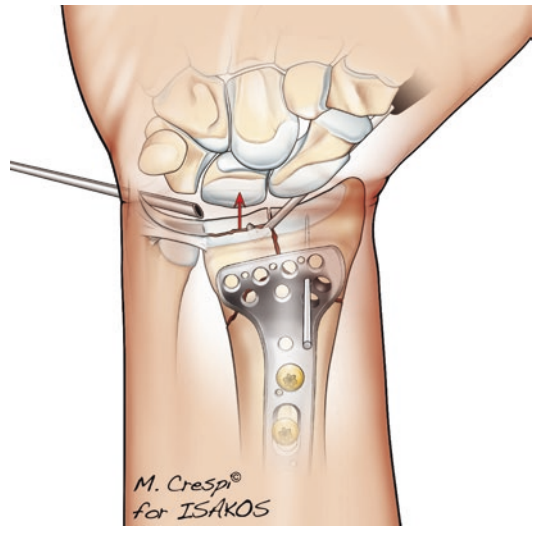

Fig. 102.8 Arthroscopic reduction of intra-articular fracture is shown using a probe used via 3–4 portal. (© M. Crespi © for ISAKOS)

between fragments and less than 1 mm articular step are noted, the K-wires can be replaced by locking screws for the distal fracture fixation. Yet, if further manipulation for the fracture fragments is deem necessary, each element which needs reduction is identified. The scope is then swapped to 6R portal, allowing the 3–4 portal to work as a working portal (Fig. 102.8).

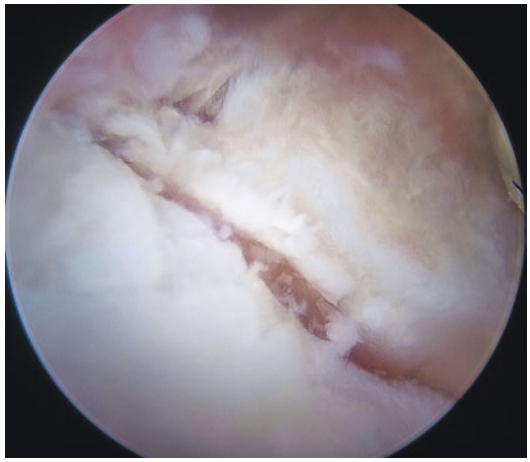

Fig. 102.9 Intra-articular fragments are reduced after manipulation under arthroscopic guidance. (© Fok)

- The most common situation is that the presence of the articular step(s), either from a die-punch fragment or a depressed fragment of the dorsal aspect. To correct the depressed fragment, a probe is inserted via the 3–4 portal. The K-wire, inserted from the volar aspect, splinting the fragments, is partially pulled out, allowing the probe to hook and reduce the fragment. In addition, the surgeon can maintain the reduction by either using his/her thumb to compress the reduced fragment or by using a bone tenaculum. K-wire is then driven slowly forward, aiming toward the dorsal cortex, to fix the fragment in place. Once the fragment is confirmed to be reduced, the K-wire can be replaced by a locking screw (Fig. 102.9).
- Die-punch fragments usually are free osteochondral fragments. In most instances, they do not have a large metaphyseal component that can be reduced and fixed with a screw. Instead, the fragment is manipulated by a probe, inserted via the 3–4 portal. It is kept slightly over-reduced when k-wires are changed into locking screws. The distal row of locking screws then acts as a scaffold, supporting the articular surface. The over-reduced fragment is subsequently impacted by using a Freer elevator, to achieve a smooth articular surface.
- In some instances, an over-distracted fragment can be observed. This is usually managed well by partially retracting the K-wire, partially release the traction, and pushing downward the fragment with a flat instrument, such as a Freer periosteal elevator. Once the reduction is achieved, the surgeon's thumb or a bone tenaculum can maintain the reduction while the K-wire drives forward to temporarily stabilize the fracture. This will then be replaced by a locking screw.
- In a situation where the dorsal rim fracture is too small and cannot be adequately fixed by a locking screw via a volar plate, an additional K-wire, and an independent dorsal-volar screw(s), or even a small dorsal plate may be needed.
- In some comminuted intra-articular distal radius fractures, several fragments are noted to be displaced after fluoroscopic-assisted open reduction. It is important not to back out all K-wires and attempt to reduce and fix all fragments at the same time. A step-by-step procedure beginning from ulnar to radial aspect is recommended.
- Assessment of other bony and soft tissue injuries: Once the articular surface of the distal radius is reduced and fixed in a satisfactory manner, the cartilage and bony status of the carpal bones and the integrity of the intercarpal ligaments (i.e., SL and LT ligament) and TFCC are evaluated using wrist arthroscopy. Scaphoid fracture is recommended to be treated in the same setting and can be managed by either arthroscopic-assisted or percutaneous screw fixation. Meanwhile, for the ligamentous/fibrocartilaginous injuries, it is still debatable whether repair is needed in the same setting. Techniques on how to manage these injuries are described in other chapters.
- Prior to wound closure, a tourniquet is deflated. Injury to the radial artery and its branches may have occurred during fracture reduction and should be checked. Hemostasis is achieved. If in doubt, a drain can be inserted. The wound is closed in layers. DRUJ stability is also checked and compared with the contralateral side (refer to the section on postoperative rehabilitation).

102.5 Tips and Tricks

- Surgeons must be familiar with the technique of diagnostic wrist arthroscopy prior to performing arthroscopic distal radius reduction.
- For the initial few cases, surgeons should start with simple intra-articular fractures to gain experience with the procedure, i.e., AO type C1 fractures.
- For the initial few cases or for complex cases, assistance from a fellow colleague/surgeon is useful in helping the execution of the procedure.
- Preoperative CT is useful to understand the fracture configuration and to plan on the subsequent approach which is used for fracture fixation.
- Most fracture fixation, especially the restoration of the extra-articular alignment, should be done by fluoroscopic-assisted open approach. Wrist arthroscopy is mainly used for refining the intra-articular reduction.
- The use of dry arthroscopic technique can reduce soft tissue extravasation and in return decrease the chance of developing compartment syndrome.
- In cases of soft tissue swelling, an 18-gauge needle can be used first to confirm the entry site of the portal.
- Volar radial portal is seldom used nowadays. Most of the assessment for the dorsal rim fracture can be done by the 6R portal. In cases which the volar radial portal is employed, care must be taken of not disrupting the already reduced volar fragment.

102.6 Pitfalls

- Tissue extravasation may be observed if the operation time is long. This is especially the case if wet arthroscopy is used.
- Fracture fragmentation is possible, especially if the fragment is being manipulated repeatedly.
- Destabilizing all the fracture fragments is possible. If several fragments are noted to be displaced after fluoroscopic-assisted open reduction, surgeons should not pull out all the K-wires and attempt to reduce all the displaced fragments at the same time. Fragment should be reduced one by one instead.
- Surgeon may rely solely on arthroscopic reduction and fail to fix the metaphysis of distal radius adequately.
- Injury by the tip of K-wires during K-wire manipulation.
- Failure to recognize that the injury is a perilunate fracture dislocation instead of a distal radius fracture.

102.7 Postoperative Management and Rehabilitation

Postoperatively, patient is allowed to have free wrist mobilization as comfortable. If DRUJ instability is noted post distal radius fixation, free elbow hinge brace with forearm in supination/sugar tong is given for 3 weeks. Gentle passive mobilization of the wrist is started at fourth week. Gradual strengthening exercise is started at seventh week if x-ray shows signs of healing.

102.8 Complications

- Compartment syndrome.
- Acute carpal tunnel syndrome/median nerve entrapment.
- Long screws may cause irritation to extensor tendon(s).
- Short Distal screws may lead to loss of intra-articular reduction.
- Inadequate metaphyseal fixation.
- Insertion of screw into the DRUJ. Full forearm rotation needs to be examined after fracture fixation. If in doubt, fluoroscopy is used.
- Tendon/veins and superficial radial nerve may be injured during the use of K-wires for fracture fixation or during the creation of portals for wrist arthroscopy.
- Radial artery is at risk in volar approach.

References

1. Knirk JL, Jupiter JB, 1986. Intra-articular fractures of the distal end of the radius in young adults. J Bone Joint Surg Am. 1986;68(5):647-659. Sites Surgery North Western Edu.
2. Lindau T, Arner M, Hagberg L. Intraarticular lesions in distal fractures of the radius in young adults. A descriptive arthroscopic study in 50 patients. J Hand Surg Br. 1997;22(5):638–43.
3. Mrkonjic A, Geijer M, Lindau T, Tägil M. The natural course of traumatic triangular fibrocartilage complex tears in distal radial fractures: a 13-15 year follow-up of arthroscopically diagnosed but untreated injuries. J Hand Surg Am Elsevier. 2012;37(8):1555–60.
4. Fok MWM, Fang CX, Lau TW, Fung YKE, Fung BKK, Leung FKL. The status of triangular fibrocartilage complex after the union of distal radius fractures with internal plate fixation. Int Orthop. 2018;78(8):357–1922.
5. del Piñal F. Technical tips for (dry) arthroscopic reduction and internal fixation of distal radius fractures. J Hand Surg Am. 2011;36(10):1694–705.
6. del Piñal F. Dry arthroscopy and its applications. Hand Clin. 2011;27(3):335–45.

103 Minimally Invasive Plate Fixation for Distal Radius Fractures

Paul Max Jarrett

103.1 Background

Displaced distal radial fractures are frequently managed by open reduction and internal fixation. A modified Henry's approach is commonly utilized to reduce the fracture and place a volar locking plate. During fixation of distal radial fractures, the most important region of visualization is the fracture site and the distal plate area up to the volar capsular insertion. Compared to a modified Henry's approach, a minimally invasive approach used by the author allows almost the same visualization of this distal area while still allowing utilization of all reduction techniques and fixation of the plate proximally within the pronator quadratus. The pronator quadratus muscle is not detached and the plate is slid underneath the muscle from distally, leaving the muscle relatively uninjured. The minimally invasive plating technique can be used in conjunction with arthroscopic reduction techniques for intra-articular fracture. The procedure can be simplified by using a short distal radial plate and a minimally invasive jig. The advantages of minimally invasive fixation include a cosmetic scar, preservation of the soft tissue envelope especially of PQ, stronger postoperative forearm rotation [1], less discomfort, and more rapid recovery of light activities.

103.2 Surgical Anatomy

In order to allow access to areas of the distal radius and pronator quadratus that require instrumentation, the incision requires to be located precisely. A portion of a modified Henry's approach is utilized through the sheath of flexor carpi radialis (FCR) on the radial side of the tendon [2]. The transverse component of the distal radial fracture is typically near, or just distal, to the distal edge of the pronator quadratus (PQ) muscle. The PQ can be traumatized during the injury and the nature of PQ damage can be taken into consideration when planning the region of PQ through which the plate is placed.

The pronator quadratus muscle consists of two heads. The superficial head runs transversely from the ulna to the radius and tends to be thicker distally; its principal function is pronation of the forearm. The deep head is situated more ulnar with the central portion being thicker; its principal function is stabilization of the distal radioulnar joint (DRUJ) [3]. The aim is to protect PQ as much as possible during fracture reduction and fixation, and hopefully thereby preserve more of the muscle's function.

P. M. Jarrett (✉)
Department of Hand Surgery, Fremantle Hospital, Fremantle, WA, Australia

Orthopaedic Surgeon, Murdoch Orthopaedic Clinic, Murdoch, WA, Australia
e-mail: admin@pauljarrett.info

© ISAKOS 2022

D. N. Bhatia et al. (eds.), *Arthroscopy and Endoscopy of the Elbow, Wrist and Hand*,
https://doi.org/10.1007/978-3-030-79423-1_103

The plate is slid under the muscle fibers of the superficial head of PQ either by incising a sufficient portion of the distal tendon of PQ or alternatively by incising a portion of the radial insertion of PQ. A periosteal elevator is used to create the space for the plate under PQ, and if the dissection to place the plate is undertaken in the central portion or more radially on the volar aspect of the distal radius, this will avoid damage to the deep head of PQ and the branches of the anterior interosseous nerve to this muscle and therefore preserve muscle function.

103.3 Indications and Contraindications

- Minimally invasive plate osteosynthesis (MIPO) is versatile in that it can be indicated for virtually any displaced distal radial fracture in which the optimal management for that patient is volar plate fixation.
- Open reduction and internal fixation of distal radius fractures can be performed via a smaller incision than is conventionally used and is carried out by placing the plate under PQ rather than lifting the muscle as a flap of the distal radius.
- Even where there is proximal extension into the metaphysis or where there is an additional comminuted metaphyseal fracture, small additional proximal incisions can be utilized to secure a long plate onto the shaft.
- The minimally invasive plating is a useful technique in combination with arthroscopic reduction of intra-articular fractures of the distal radius.

It is essential to be experienced with internal fixation of distal radial fractures prior to attempting the procedure in a minimally invasive fashion. It is recommended that before using this technique surgeons either undertake a course in distal radial MIPO, learn the procedure from a surgeon experienced in distal radial MIPO, or carry out the procedure on a cadaver.

There is a small percentage of distal radial fractures which are so highly comminuted that minimally invasive fixation will not provide sufficient access to the fracture components. However, once experienced in this technique, it is rare to find a distal fracture not suitable for MIPO. If fixation commences as a minimally invasive procedure and difficulties are encountered, it is easy to extend the incision and convert to a conventional approach.

103.4 Surgical Technique

The procedure is carried out with a general or regional anesthetic and exsanguination of the upper limb prior to inflating an upper arm tourniquet. Surgery is usually carried out as a day case. The patient is placed supine with the upper limb placed on an arm table. If arthroscopy is planned, the arthroscopic stack is located near the patient's feet. The surgeon sits between the arm and the head, and the surgical assistant at the axilla. The procedure is based on the technique described by Lebailly et al. [4].

- A closed manipulation is undertaken to restore a more normal contour to the wrist. Using a skin marking pen, the radial edge of FCR and the distal wrist crease are drawn.
- The incision commences 2 cm proximal to the distal wrist crease/radial styloid tip and advances proximally for 15–20 mm. The skin is undermined for approximately 2 cm both proximal and distal to the incision.
- The FCR sheath is identified and both the superficial and deep layers are incised longitudinally radial to the tendon under direct vision for approximately 2 cm proximal and distal to the incision. The radial artery is left undisturbed radially to the incision.
- The flexor tendons are then visualized and moved ulnarward with a retractor. PQ is inspected for damage and the type of PQ approach decided upon (Fig. 103.1).
- The usual MIPO approach is undertaken by incising the distal tendinous insertion of PQ. An alternative is to incise a portion of the radial insertion of PQ. Both techniques are mentioned below.

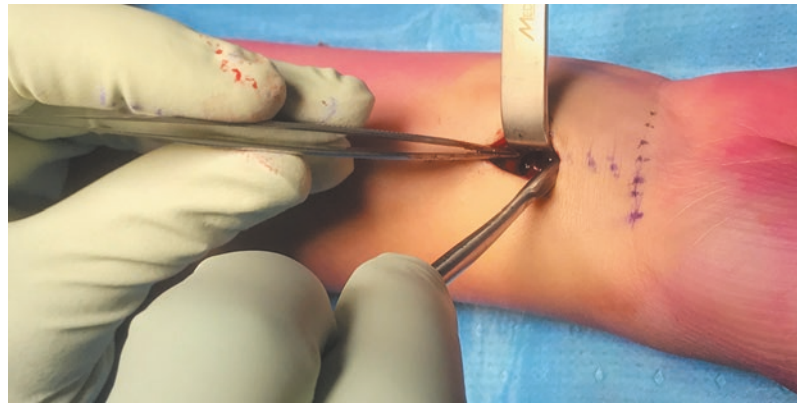

Fig. 103.1 Inspecting PQ and fracture through incision

103.4.1 Distal Approach

- The distal attachment of the pronator quadratus tendon to the radius is incised transversely and a periosteal elevator is used to create the space where the plate will sit on the distal radius. Avoid elevating towards the ulnar aspect of the radial metaphysis and shaft to preserve the deep head of PQ. The space distal to PQ and proximal to the volar capsular attachments can be cleared of soft tissue for fracture visualization as required. The jig or locking guides are then attached to the distal end of an appropriate plate.
- Fracture reduction is now undertaken, using a combination of traction, direct reduction with visualization through the incision, and if required, arthroscopically assisted reduction. In simpler fractures, holding the reduction manually may be adequate, and in more complex fractures percutaneous K-wires can be inserted to secure the fracture in reduced position. The surgeon may choose to reduce the entire fracture, or alternatively only the intra-articular distal components of the fracture at this stage and then subsequently reduce the proximal component of the fracture when securing the proximal end of the plate. If only the distal segments are reduced, the plate position distally must take into consideration where the plate will sit on the proximal side of the fracture once the entire fracture is reduced and fixed; this is a skill which improves with experience.
- Using a retractor, the proximal end of the plate is placed into space beneath the superficial head of PQ and is slid proximally (Fig. 103.2). Once the plate is partially inserted and the distal end of the plate is entering the incision, there may be insufficient space for the retractor. Tilt the ulnar aspect of the distal portion of the plate so the plate is touching the bone, remove the retractor and glide the distal portion of the plate ulnarward while sliding the entire plate proximally with the plate parallel to the axis of the radius. Thus, the plate ends up sitting in its final intended position with no flexor tendons or other soft tissues between the plate and the bone.
- If the plate feels firmly on the surface of the distal radius in a suitable position, a K-wire is used to temporarily fix the plate in place. The positions of the fracture and implant are checked with fluoroscopy. If the plate is not in an ideal position, the K-wire is removed, and the position of the plate is changed until satisfactory. An additional plate K-wire can then be added to maintain plate rotation and fluoroscopy is used to ensure the plate is against the bone in a satisfactory position.
- In turn, at least two of the distal screw holes are drilled via the jig or locking drill guides, and after checking with fluoroscopy, the screws are inserted (Fig. 103.3). The jig is removed, and the remaining distal holes are drilled, and screws are placed.
- At this point, further reduction of the fracture between the distal and proximal segments is

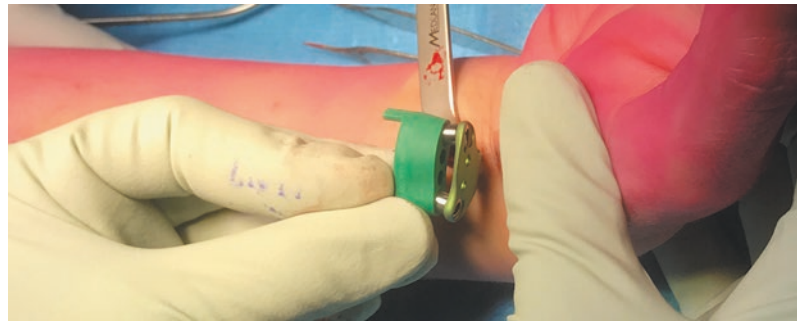

Fig. 103.2 Placing the plate with jig attached under PQ through incision

Fig. 103.3 Plate and jig secured to distal segment, drilling distal screw hole

undertaken as required. All the reduction techniques used during a conventional open approach are applicable including traction on the wrist, plate assisted reduction, and clamp reduction including correction of radial translation [5].

- The initial proximal non-locking screw hole is drilled, and the screw is inserted into the gliding hole and checked with fluoroscopy. The position of the initial screw in the proximal segment of the plate is usually just proximal to the distal edge of PQ, and therefore gentle proximal retraction of the muscle edge is sufficient to visualize this area of the plate without damaging the muscle. Any final corrections are made to the reduction, especially with regards to translation, and then the final locking proximal screws are placed directly through the PQ muscle fibers. The proximal screw holes are located by palpation, and a tiny transverse incision in the muscle fibers is made for each screw hole, in which to place a locking drill guide and subsequently to insert the screw through (Figs. 103.4 and 103.5). A final fluoroscopy is undertaken.
- The plate is inspected to ensure there are no soft tissues trapped between the plate and the bone, and the digits are moved to ensure there is no flexor tendon tethering. The DRUJ is assessed clinically and if required with fluoroscopy to ensure it is stable at the end of the procedure, particularly if there is an ulnar styloid fracture. If the DRUJ is unstable, the distal radial fracture is checked to confirm anatomical reduction, an ulnar styloid fracture if present is fixed, and if instability persists,

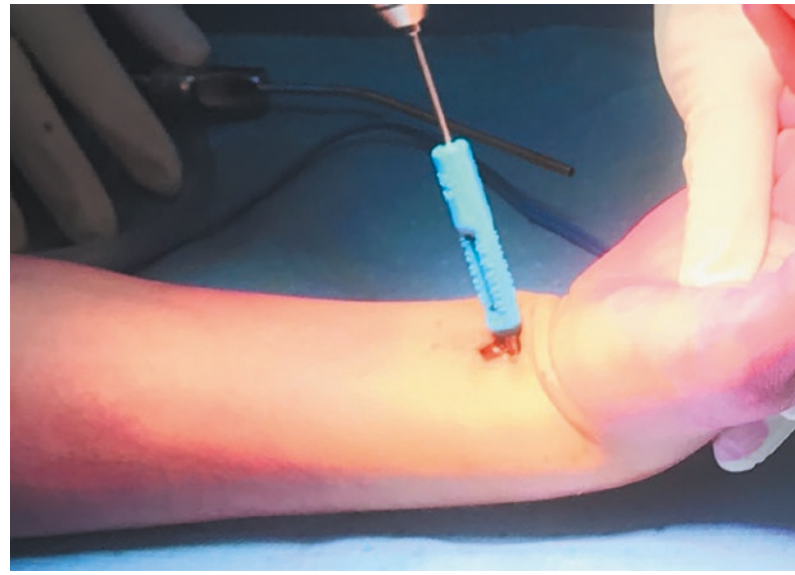

Fig. 103.4 Drilling proximal locking screw hole via drill guide

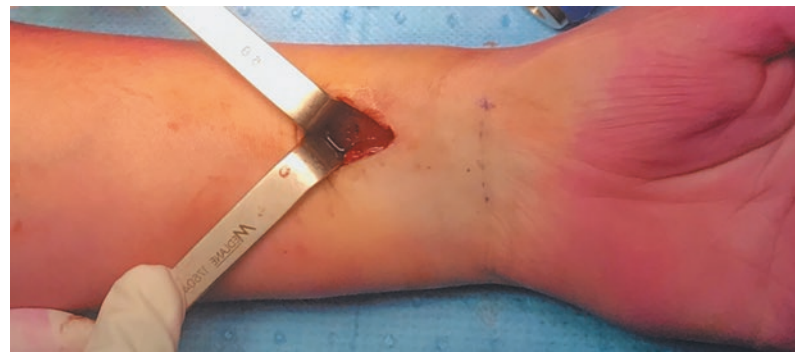

Fig. 103.5 PQ at end of procedure with small muscular incision for proximal screw insertion

repair of any peripheral or deep triangular fibrocartilage complex (TFCC) injuries if necessary.

The operated area is washed out with normal saline, local anesthetic is placed in the wound edges and the incision is sutured with 2–0 vicryl to the subcutaneous fatty layer and 4–0 monocryl to the skin. A small adhesive dressing, orthopaedic wool dressing, and temporary partial plaster splint are placed.

103.4.2 Radial Approach

This technique is similar to the distal approach but once PQ has been exposed, an incision at the radial margin of the distal portion of the insertion of PQ is made, instead of at the distal tendinous insertion of PQ (see green dotted line on Fig. 103.6).

- The radial-sided incision of PQ can either be at the radial distal aspect of the muscle fibers, or slightly further around the radius, incising a longitudinal strip of the BR tendon fibers attached to the PQ muscle fibers, a modified miniature version of the brachioradialis splitting approach [6].
- The distal PQ muscle fibers, the tendinous distal insertion of PQ, and the periosteum over the distal radius are now raised subperiosteally as a continuous flap to allow access to the distal radius up to the volar capsular insertion.

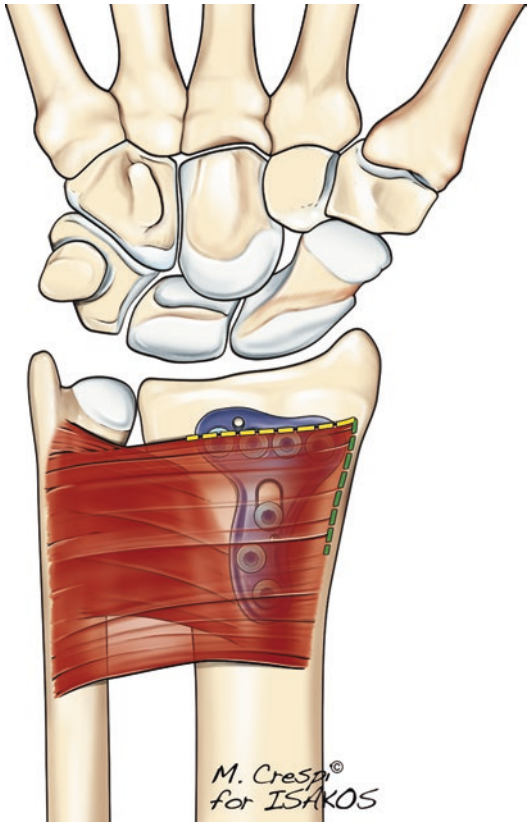

Fig. 103.6 Plate beneath PQ. The yellow dotted line denotes the distal approach and the green dotted line shows the radial approach. (M. Crespi © for ISAKOS)

A periosteal elevator then creates a space for the plate proximally under PQ as in the distal approach. The fracture is reduced and the plate slid in from the radial approach using a custom radial approach jig, and the fracture fixation is thereafter carried out as per the distal approach.

- The radial approach necessitates a jig designed for this approach such as the radial approach jig for the Alians distal radial mini-plate (Newclip, Haute-Goulaine, France). The radial approach is more complex than the distal approach and is only recommended for surgeons experienced with MIPO distal radial fixation. The advantage of the radial approach is that the plate is fully covered by soft tissue with no contact between the plate and the flexor tendons.

103.5 Technical Tips

- The skin incision is a window which can be moved as a mobile window compared to the deeper structures, allowing visualization either distally or proximally depending upon where on the distal radius you are working.
- Using a relatively short plate, especially one designed for minimally invasive surgery, makes the procedure more straightforward, particularly if the fixation system has a minimally invasive jig.
- It is important to make the incision in the correct location. The incision is best if begun 20 mm proximal to the radial styloid, proceeding proximally; if the incision is made too distally then access to the plate proximally can be difficult.

103.6 Pitfalls

Rupture of extensor or flexor tendons is possible following a distal radial fracture including for those fractures treated operatively. During MIPO, ensure that none of the flexor tendons, especially FPL, is caught between the plate and the bone during and after fixation. Ensure that free passive motion of the thumb and fingers can occur thus further confirming the tendons are not tethered. Avoid situating a plate too distally on the radius to reduce the risk of its interference with the flexor tendons. The extensor tendons can be damaged by the drill protruding through the dorsal cortex while being drilled from volarly; in patients with an intact dorsal cortex this can be prevented by not penetrating the dorsal cortex with the drill; this also reduced the risk of dorsal screws prominence. When measuring screw length, ensure the distal row of screws do not protrude dorsally by subtracting 2–4 mm from the measured length and checking for screw prominence with either fluoroscopy or ultrasound at the conclusion of fixation [7]. If screws are intra-articular this may be identified by fluoroscopy or arthroscopy (Figs. 103.7 and 103.8).

103.7 Postoperative Management and Rehabilitation

Post-surgery, the limb is elevated, and finger, elbow, and shoulder motion are encouraged. At 1–2 days post-surgery, the plaster splint is removed, active wrist exercises are commenced, and light everyday use of the hand and wrist are encouraged without immobilization. A thermoplastic splint is provided to the patient but recommended only for infrequent symptomatic use, as splints have been demonstrated to slow patient recovery [8]. The adhesive dressing is removed at 10 days. Unrestricted use of the hand and wrist is allowed from 6 weeks. No routine follow-up radiographs are taken of the wrist unless there is a clinical concern [9]. Patient follow-up includes a clinical assessment for crepitus over the flexor tendons with wrist and finger motion at 6 months and can include an ultrasound to assess the position and appearance of the flexor pollicis longus and other flexors in relation to the metalware.

Fig. 103.7 Location of incision as seen 6 weeks postoperatively

103.8 Results

A consecutive series of 46 patients from the author's practice undergoing MIPO for displaced distal radial patients using the Alians distal radial mini-plate (Newclip, Haute-Goulaine, France) was analyzed. During the study period, the author required a conventional open approach for only one distal radial fracture patient, not included in these results. There were 35 females and 11 males with a mean age of 55 years (range 25–87), and with a minimum follow-up of 12 months. Twenty had sustained right-sided and 26 left-sided injuries, with 20 extra-articular and 26 intra-articular fractures. The mean time from injury to fixation was 5 days. Tourniquet time ranged from 32 to 82 min, with a mean of 46 min.

Fig. 103.8 Incision was placed in an altered position to align within the patient's tattoo

For simpler cases, the operation length for MIPO was shorter compared to an open technique and for complex cases, MIPO took slightly longer. The mean incision length was 17 mm with a range of 12–24 mm. In seven cases arthroscopy was utilized to assist in fracture reduction. Reduction appeared satisfactory in all cases with a mean radial inclination postoperatively of 21 degrees and volar tilt of 10 degrees. At 6 weeks, the average grip strength was 55% of the contralateral side and at 12 weeks it was 70%. Ultrasound 6 months post-surgery demonstrated no plate-related flexor or extensor tendon pathology.

Anecdotally, the recovery following MIPO is considerably more rapid with an earlier return to everyday activities compared to more open surgery.

One patient experienced carpal tunnel symptoms, and one experienced superficial radial nerve irritation postoperatively; both rapidly resolved fully with hand therapy. Two patients suffered an extensor pollicis longus (EPL) tendon rupture, none from sharp bony fragments or protruding metalware: the ruptures occurred at 2 weeks and 4 weeks post-surgery and both were treated by extensor indicis to EPL transfer successfully. Four patients had their plates removed after fracture union due to their preference, not due to metal-related symptoms or pathology.

Acknowledgments: I am grateful to Mr. Angus Keogh, Professor James O Jarrett, and Mrs. Anna-Lisa Baker for their comments on the text and Miss Emma Petta for collection and analysis of patient outcome data.

References

1. Zhang X, Huang X, Shao X, Zhu H, Sun J, Wang X. A comparison of minimally invasive approach vs conventional approach for volar plating of distal radial fractures. Acta Orthop Traumatol Turc. 2017;51:110–7.
2. Henry A. Extensile exposures. Edinburgh: Churchill Livingstone; 1973.
3. Sakamoto K, Nasu H, Nimura A, Hamada J, Akita K. An anatomic study of the structure and innervation of the pronator quadratus muscle. Anat Sci Int. 2015;90:82–8.
4. Lebailly F, Zemirline A, Facca S, Gouzou S, Liverneaux P. Distal radius fixation through a mini-invasive approach of 15 mm. PART 1: a series of 144 cases. Eur J Orthop Surg Traumatol. 2014;24:877–90.
5. Ross M, Allen L, Couzens GB. Correction of residual radial translation of the distal fragment in distal radius fracture open reduction. J Hand Surg Am. 2015;40:2465–70.
6. Kashir K, O'Donnell T. A brachioradialis splitting approach sparing the pronator quadratus for volar plating of the distal radius. Tech Hand Up Extrem Surg. 2015;19:176–81.
7. Vernet P, Durry A, Nicolau X, D'Ambrosio A, Collinet A, Botero Salazar S, et al. Detection of penetration of the dorsal cortex by epiphyseal screws of distal radius volar plates: anatomical study comparing ultrasound and fluoroscopy. Orthop Traumatol Surg Res. 2017;103:911–3.
8. Duprat A, Diaz JJH, Vernet P, Gouzou S, Facca S, Igeta Y, et al. Volar locking plate fixation of distal radius fractures: splint versus immediate mobilization. J Wrist Surg. 2018;7:237–42.
9. Sharma V, Witney-Lagen C, Cullen S, Kim E, Haider Z, Davy A, Hunter A. The role of early post-operative radiographs following distal radius fracture fixation with a volar locking plate: time for change? J Hand Surg (Asia Pacific). 2019;24(4):435–9.

Part XX

Wrist: The Stiff Wrist

104 Arthroscopic Arthrolysis of the Wrist

Gregory I. Bain, Karthikraj Kuberakani, Riccardo Luchetti, and Andrea Atzei

104.1 Background

The functional range of motion for the wrist is 5° flexion, 30° extension, 10° radial deviation, and 15° ulnar deviation [1]. The self-selected position for maximum strength is 28° extension [2]. Various etiologies contribute to wrist stiffness, usually it follows trauma or surgery [3]. Pathoanatomically, it can be classified based on ISAKOS concept developed in the shoulder and elbow (Table 104.1) [4, 5]. Stiffness is classified into intra-articular, capsular, or extra-articular causes [6, 7]. Any primary insult to these anatomical structures such as trauma (e.g., falls, surgery), disease (infection, OA, RA, gout), or prolonged immobilization can stimulate natural healing process whereby the necrotic tissue is replaced by the fibrous scar tissue that contracts. The resultant arthrofibrosis of radiocarpal (RC), midcarpal (MC), and/or distal radioulnar joints (DRUJ) can cause wrist pain and restriction of the range of motion (ROM).

The most common cause of post-traumatic arthrofibrosis is a malunion of an intra-articular distal radius fracture. The causes of stiffness post-distal radius fracture are capsular contracture with intra-articular adhesion (arthrofibrosis), radiocarpal impingement due to malunion of articular fragments, and scapholunate instability [6]. Historically, these intra-articular causes have been managed with salvage procedures such as wrist denervation, arthrodesis, or arthroplasty [8].

Other common nontraumatic causes of wrist stiffness are tendon adhesions, neuroma of the posterior interosseous nerve, and chronic regional pain syndrome (CRPS).

CRPS is unfortunately a common diagnosis. Most diagnoses of CRPS are made by clinicians and non-clinicians who provide this label, which in itself, emotionally cripples the patient and makes them a target of inappropriate care. The most common causes of patients labeled as CRPS include poor initial care (40%), carpal tunnel syndrome (40%), malignancy and unknown etiology (10–26%) [9–12]. The poor initial care includes cases of distal radius fractures which

G. I. Bain (✉)
Department of Orthopedics & Trauma Surgery, Flinders University and Flinders Medical Centre, Adelaide, SA, Australia
e-mail: admin@gregbain.com.au

K. Kuberakani
Department of Orthopedic Surgery, Karpagam Faculty of Medical Sciences and Research, Coimbatore, India

The Tamil Nadu Dr.M.G.R. Medical University, Chennai, India

R. Luchetti
Rimini Hand Surgery and Rehabilitation Center, Rimini, Italy

A. Atzei
Fenice Hand Surgery and Rehabilitation Team, Treviso, Italy

© ISAKOS 2022

D. N. Bhatia et al. (eds.), *Arthroscopy and Endoscopy of the Elbow, Wrist and Hand*,
https://doi.org/10.1007/978-3-030-79423-1_104

Table 104.1 All-inclusive patho-anatomical classification of joint stiffness, (Modified from Bain GI, Clitherow HDS. The pathogenesis and classification of shoulder stiffness. © ISAKOS [4])

Intra-articular (bearings)	**Capsular** (constraints)	**Extra-articular** (motor, cable, levers)	**Neurologic** (control, electrics, sensors)
Articular surface Osteochondral Defect, degeneration	**Ligaments:** Contracture, calcifications	**Muscles**: Myopathy Fatty infiltration	**Central:** Behavioral Dystonia, spasticity
Subchondral Dysplasia, fractures, AVN, degeneration	**Capsule:** Contracture, calcifications	**Tendons and bursa:** Tear, calcifications degeneration, bursitis	**Peripheral:** Ulnar, radial, medial nerve; cutaneous neuritis, or neuropathy
Synovium Inflammatory Crystal arthroplasty	**Congruity:** Subluxation, dislocation	**Other (external to Joint)**: Fracture, malignancy, HO, skin contracture	**Sensory and autonomic:** Charcot joint CRPS

have not been reduced or had screw left in the joint. The carpal tunnel group has a different presentation to typical carpal tunnel syndrome. They have pain over the radial side of the hand and difficulty making a full fist. It is clear that these patients need a thorough assessment by a competent clinician and treatment directed to the cause. The authors believe CRPS should be renamed where the word "anatomical" is used to highlight that the initial cause is anatomical.

Treatment of choice for wrist stiffness is usually conservative with splinting and physiotherapy. Manipulation under anesthesia has been tried but can produce traumatic chondral, or ligamentous injuries and even fractures. Hence, surgical arthrolysis, open or arthroscopic, is a better choice and can also reveal any other hidden pathologies [13].

Arthroscopic arthrolysis involve adhesion resection, capsulotomy, capsular and ligamentous release. Ancillary procedures due to associated pathologies can be performed at the same time without compromising early postoperative mobilization. Secondary damage to adjacent tissues can be minimized with arthroscopic procedures.

104.2 Indications and Contraindications

Patients in whom wrist stiffness, primarily due to arthrofibrosis, along with pain even after a prolonged period of conservative treatment are candidates for arthroscopic arthrolysis. Best results are obtained in these patients with capsular contracture but with a congruent wrist joint, normal articular cartilage, and without general arthropathy. Patients need to be willing to adopt a strict postoperative rehabilitation protocol. There are the general contraindications to arthroscopy: active infection, altered anatomy, and soft tissue issues [14].

Open surgical arthrolysis is preferred when difficulties are encountered with arthroscopy especially with DRUJ or to perform additional procedures like carpal tunnel release or wrist denervation [6].

104.3 Surgical Technique

Regional or general anesthesia can be given. Examination under anesthesia is performed and the ROM is noted in comparison to the contralateral wrist. Standard wrist arthroscopy set up with 3 kg traction is used. We commence with dry arthroscopy. Usually, a 2.7 mm scope is used. Increasing traction weight or a 1.9 mm scope is sometimes required in the joint space if difficult to advance.

- All standard dorsal (1–2, 3–4, 4–5, 5–6/6R, 6 U) and volar (VR, VU) portals can be used for the radiocarpal (RC) and ulnocarpal (UC) joints (Fig. 104.1) [15]. Midcarpal portals include RMC, UMC, Scaphoid-Trapezoid-Trapezium (STT), and Triquetro-Hamate (TH). DRUJ portals include dorsal (proximal and distal), 1 volar, and 1 direct foveal portal [16].
- We begin with RC and the MC joint. DRUJ arthroscopy is performed whenever supina-

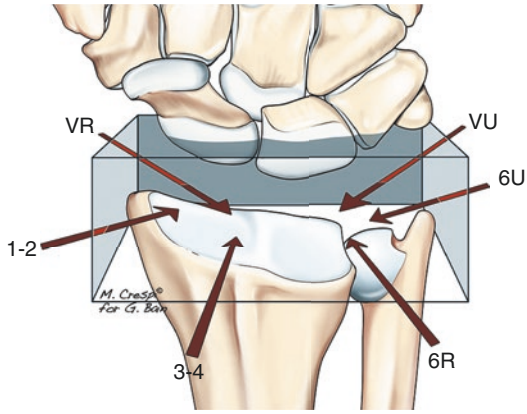

Fig. 104.1 Wrist arthroscopy portals. Through 2 dorsal (3–4, 6R), 2 volar (VR, VU), 1 radial (1–2), and 1 ulnar (6 U) portals, complete visualization of the wrist is possible. The multiple portals enable optimal viewing and instrumentation of the joint. (Copyright Dr. Gregory I. Bain and Max Crespi)

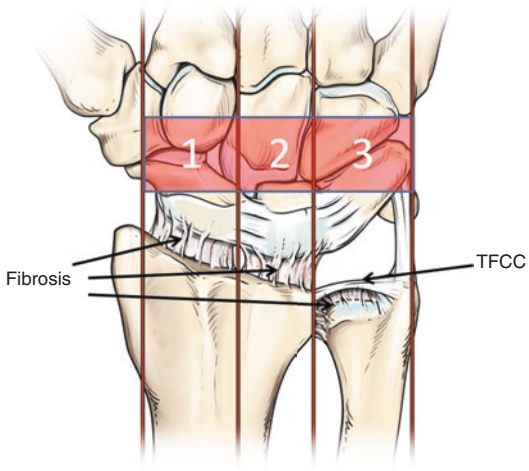

Fig. 104.2 Illustration showing the three parts of the radiocarpal joint. The radioscaphoid, radiolunate, and ulnar carpal joints. The ulnocarpal joint is rarely involved. In this drawing, the fibrosis is located in the radiocarpal joint, the DRUJ, and under the TFCC. (LuchettiR. The role of arthroscopy in postfracture stiffness. In: del Piñal E, et al., editors, Arthroscopic management of distal radius fractures, https://doi.org/10.1007/978-3-642-05354-2_12, © Springer-Verlag Berlin Heidelberg 2010)

tion and pronation are compromised. The visual field may be obscured by fibrosis, adhesions, and synovitis. Hence, great care and expertise are necessary to prevent secondary damage.

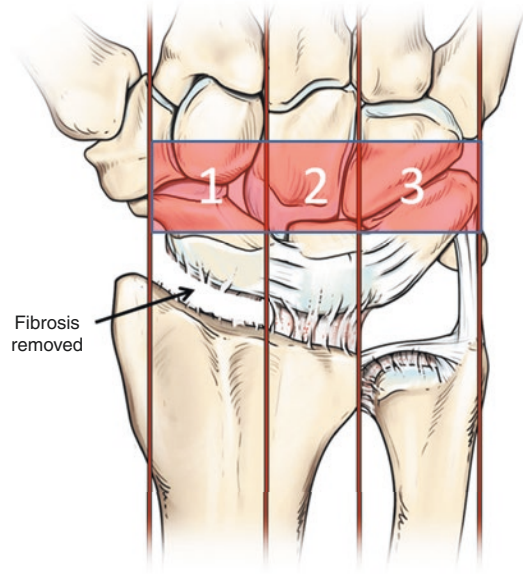

Fig. 104.3 Illustration showing removal of the radioscaphoid fibrosis (step 1). (LuchettiR. The role of arthroscopy in postfracture stiffness. In: del Piñal E, et al., editors, Arthroscopic management of distal radius fractures, https://doi.org/10.1007/978-3-642-05354-2_12, © Springer-Verlag Berlin Heidelberg 2010)

104.3.1 Radiocarpal Joint

All the traditional RC portals may be necessary, and usually 1–2, 3–4, 6R, and volar portals are used. To lavage the joint, a 5 cc syringe is applied to the sheath inflow. Suction in the shaver is used to aspirate fluid, blood, and debris. The procedure is divided into 2 steps.

Step 1: Resection of Fibrotic Tissue

- Commence resection on the radial side of the RC joint (Fig. 104.2). Create the 3–4 portal. The 1–2 portal is established with an outside-in technique using a needle. Through a generous superficial longitudinal incision and blunt dissection with mosquito forceps, the 1–2 portal is created. Fibrosis on the radial side is resected using shaver or radiofrequency instruments. Whenever difficulties arise with triangulation due to fibrosis, portals are switched to enhance intra-articular vision.
- Once the radial side is cleared (Fig. 104.3), then proceed with the ulnar side. The 3–4 portal is used for the scope. 6R portal is established using

the transillumination technique and a needle. The fibrous tissue is resected using a shaver through 6R portal. A fibrous band may restrict shaver visualization. We refer to the distinct band between the scapholunate ligament and the sagittal ridge of the distal radius as a "synechia" [17]. This synechia may divide the RC joint space into two compartments (Fig. 104.4). The band is incised and resected using a shaver, basket forceps, or radiofrequency device via 6R portal (Fig. 104.5). We need to be cautious with osteofibrotic bands that extend into an articular defect, as resection may lead to carpal instability.

- After completion of fibrous resection of RC joint (Fig. 104.6), the ulnar carpal (UC) joint should be explored. Fibrosis is rare. If a peripheral TFCC tear is visualized, it should only be debrided to avoid instability and the need for immobilization postoperatively.
- Once this first step is completed, ROM should be evaluated under anesthesia always without traction. Usually, this is adequate to improve motion.

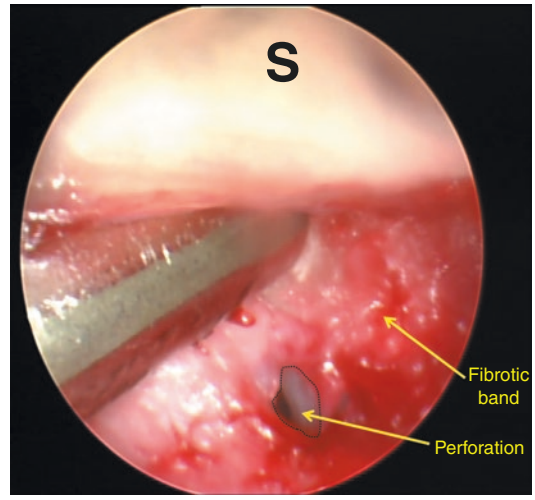

Fig. 104.5 Arthroscopic view of a shaver resecting the synechia that separated the radiocarpal joint into two compartments (S: Scaphoid). (LuchettiR. The role of arthroscopy in postfracture stiffness. In: del Piñal E, et al., editors, Arthroscopic management of distal radius fractures, https://doi.org/10.1007/978-3-642-05354-2_12, © Springer-Verlag Berlin Heidelberg 2010)

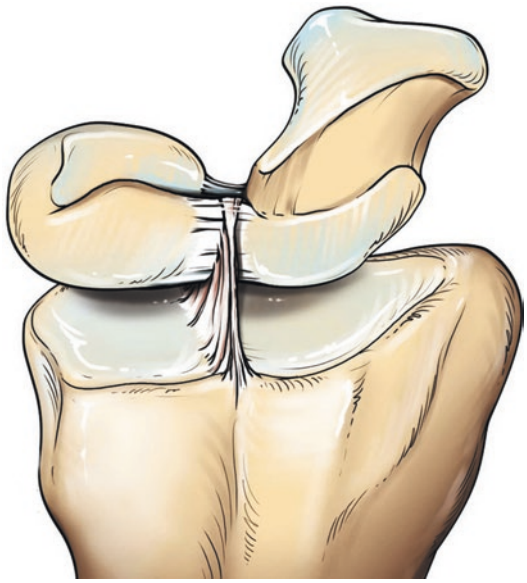

Fig. 104.4 Illustration showing a "synechia," a fibrotic adhesion between the sagittal ridge of the radius and the scapholunate ligament. (LuchettiR. The role of arthroscopy in postfracture stiffness. In: del Piñal E, et al., editors, Arthroscopic management of distal radius fractures, https://doi.org/10.1007/978-3-642-05354-2_12, © Springer-Verlag Berlin Heidelberg 2010)

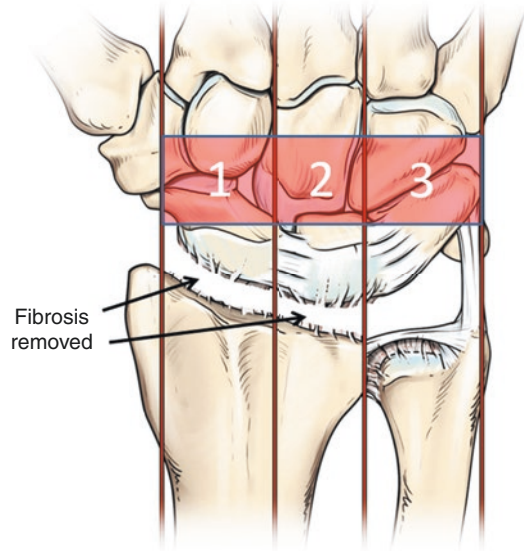

Fig. 104.6 Illustration showing complete resection of radiocarpal joint fibrosis. (LuchettiR. The role of arthroscopy in postfracture stiffness. In: del Piñal E, et al., editors, Arthroscopic management of distal radius fractures, https://doi.org/10.1007/978-3-642-05354-2_12, © Springer-Verlag Berlin Heidelberg 2010)

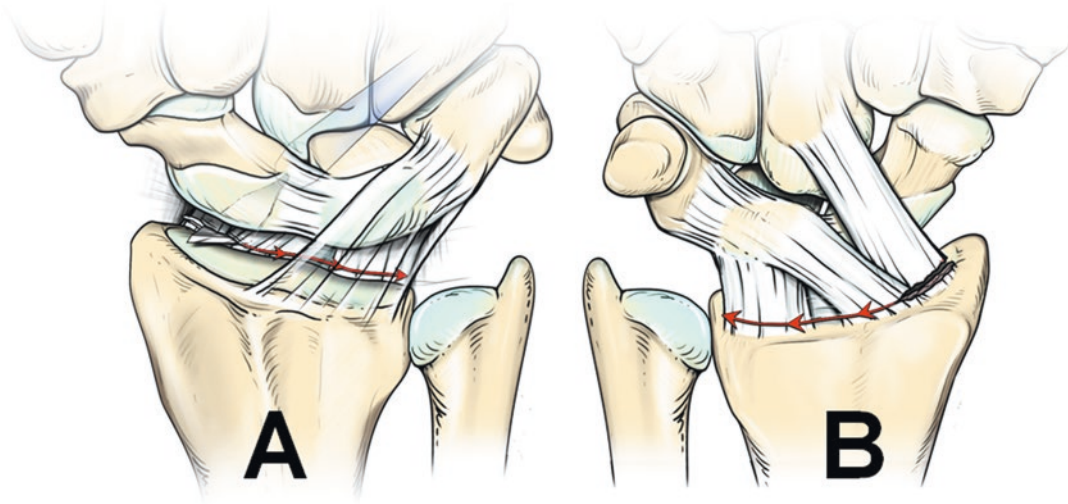

Fig. 104.7 Illustration of sectioning of the volar capsule and ligaments (*red arrows*). Release only the *scarred areas* of the ligament. (LuchettiR. The role of arthroscopy in postfracture stiffness. In: del Piñal E, et al., editors, Arthroscopic management of distal radius fractures, https://doi.org/10.1007/978-3-642-05354-2_12, © Springer-Verlag Berlin Heidelberg 2010)

Step 2: Capsular Resection

- If the ROM is still restricted after step one, then proceed with resection of volar and/or dorsal capsule and RC ligaments after reapplication of traction. Aim to only resect the ligaments that are pathological. Dorsal capsule contracture will usually cause loss of flexion, and loss of extension is often due to contracture of the volar ligaments.
- The volar ligaments are better viewed via dorsal portals. Shaver/burr is used to clear the intra-articular parts of volar ligaments and to level any articular steps. It is critical to obtain a clear view of the volar capsule, before considering a release. The release can be performed with a mini-scalpel (banana blade) or a micro-scalpel via the 1–2 portal. Release only that portion of the capsular ligaments that appears scarred.
- On proceeding towards the ulnar side, the scarred RC ligaments—radioscaphocapitate and radiolunate are released at their base (Figs. 104.7 and 104.8). Although resection of the radiocarpal ligaments has been reported to not cause ulnar translation of carpus, we recommend that the release be localized to the scarred capsule [18].
- Gentle manipulation is applied after removing traction.

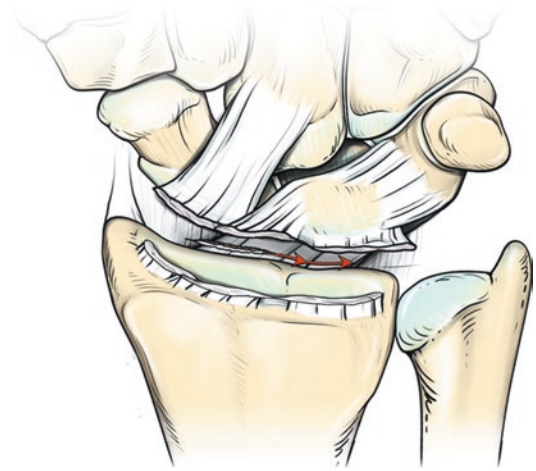

Fig. 104.8 Illustration of a section of the volar capsule and ligaments (*red arrows*). (LuchettiR. The role of arthroscopy in postfracture stiffness. In: del Piñal E, et al., editors, Arthroscopic management of distal radius fractures, https://doi.org/10.1007/978-3-642-05354-2_12, © Springer-Verlag Berlin Heidelberg 2010)

- Next, with traction, dorsal capsulotomy is commenced. The central part of the dorsal capsule is resected first using 1–2 viewing and 6R as working portals. On location of the intra-articular position of the 3–4 portal, capsulotomy is started using shaver, mini-scalpel, or radiofrequency device with a hook tip. Radial part capsulotomy is easier through the 1–2 portal with 6R for the scope.
- Volar radial viewing portal provides an excellent view of the dorsal capsule and the dorsal RC ligament. The inside-out technique with Wissinger rod (Steiman pin) is preferred for the volar radial portal [19]. The rod is placed between the radioscaphocapitate (RSC) and long radiolunate (LRL) ligaments and advanced along the radial side of the flexor carpi radialis (FCR) tendon [14].
- Bain et al. recommended placing a nylon tape onto an artery clip and advancing it between the dorsal capsule and the extensor tendons [14, 15]. With the scope in the 6R portal, advance an artery clip (snap) into the 3–4 portal. Then, slightly withdraw the artery clip so that it is just outside the capsule. Then railroad it between the capsule and extensor tendons, and out of the 6R portal. Grasp the nylon tape with a second artery clip and pull the tape through. Traction on a nylon tape placed through the 3–4 portal between the extensor tendons and the dorsal capsule retracts the extensor tendons. Now the capsule can be safely excised using basket forceps through the 3–4 portal (Fig. 104.9).
- Finally, with arthroscopic capsulotomy, the 2 volar ulnocarpal ligaments (ulnolunate and ulnotriquetral) and the dorsal UC ligament complex with the dorsal capsule of the UC joint must be preserved to prevent ulnar translation of the carpus (Fig. 104.10) [20]. If

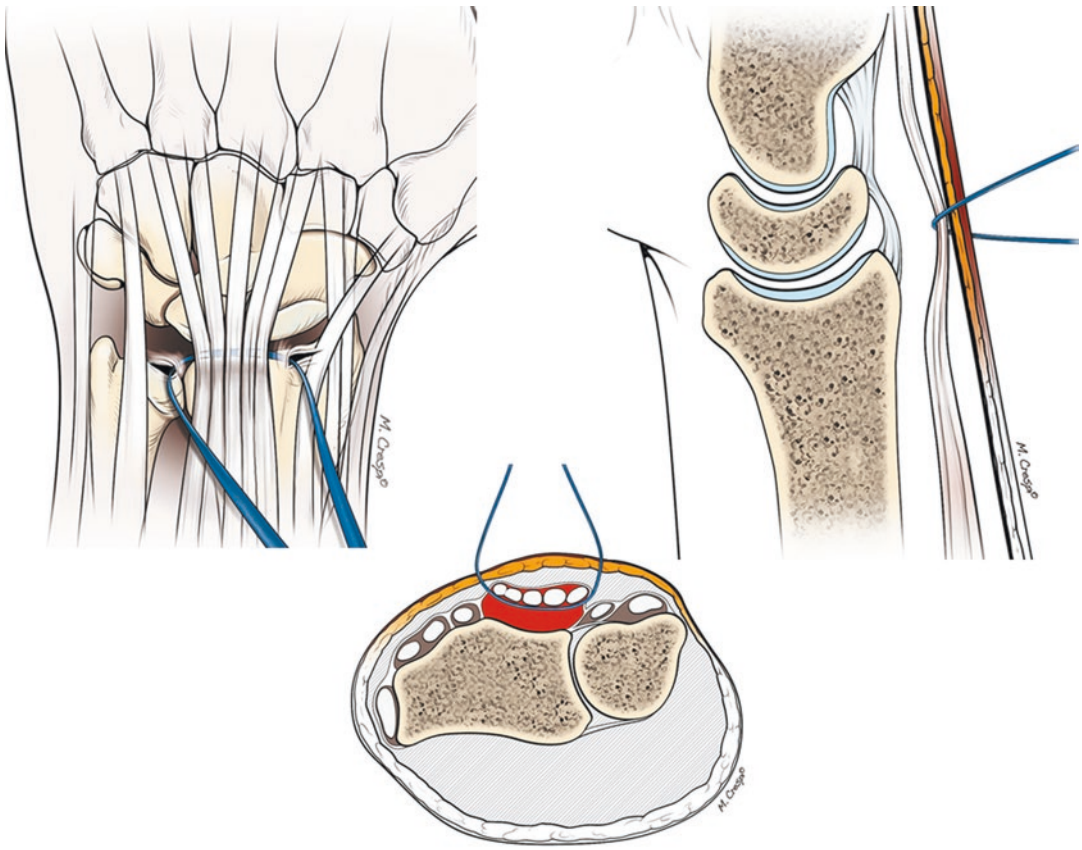

Fig. 104.9 Illustration of a nylon tape to retract the extensor tendons during dorsal wrist capsule resection. (LuchettiR. The role of arthroscopy in postfracture stiffness. In: del Piñal E, et al., editors, Arthroscopic management of distal radius fractures, https://doi.org/10.1007/978-3-642-05354-2_12, © Springer-Verlag Berlin Heidelberg 2010)

extension of wrist is restricted by a distal radius fracture malunion causing dorsal impingement, then the dorsal rim of the distal radius should also be resected arthroscopically. Use a 2.9–3.2 mm burr through the 6R/1–2 or volar radial portal.

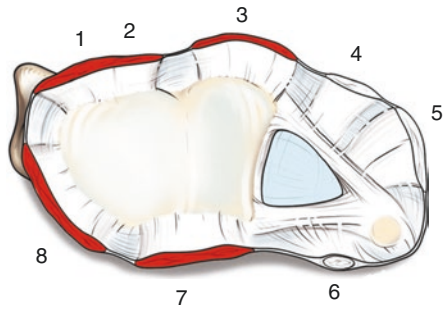

Fig. 104.10 Illustration of the extrinsic ligaments of the radiocarpal joint. (*1*) Radioscaphocapitate (*2*) Long radiolunate (*3*) Short radiolunate (*4*) Ulnolunate (*5*) Ulnotriquetral (*6*) ECU tendon (*7*) Dorsal radiocarpal, and (*8*) Dorsal capsule. The ligaments (*1–2–3–7*) that can be sectioned during the arthroscopic volar and dorsal capsulotomy are shown in *red*. To minimize the risk of ulnar translocation, release only the scarred ligaments. The ulnocarpal ligaments (*4* and *5*) must be preserved. (LuchettiR. The role of arthroscopy in postfracture stiffness. In: del Piñal E, et al., editors, Arthroscopic management of distal radius fractures, https://doi.org/10.1007/978-3-642-05354-2_12, © Springer-Verlag Berlin Heidelberg 2010)

104.3.2 Midcarpal Joint

Midcarpal arthroscopy is indicated with persistent contracture after completion of RC arthrolysis. MC joint debridement is performed through the RMC and UMC, and if necessary the STT and TH portals. In order to regain wrist extension, impinging spurs over the dorsal neck of the capitate may need to be resected [13].

104.3.3 Distal Radioulnar Joint

- When pronation/supination is restricted after RC arthrolysis, then DRUJ arthroscopy may be required. A normal articular surface between the sigmoid notch and the ulnar head is a prerequisite. The scope is placed in the proximal portal and instruments in the distal portal. With a small aggressive or full radius resector, the fibrosis is resected.
- DRUJ is divided into two spaces for arthroscopy and management (Fig. 104.11). Vision

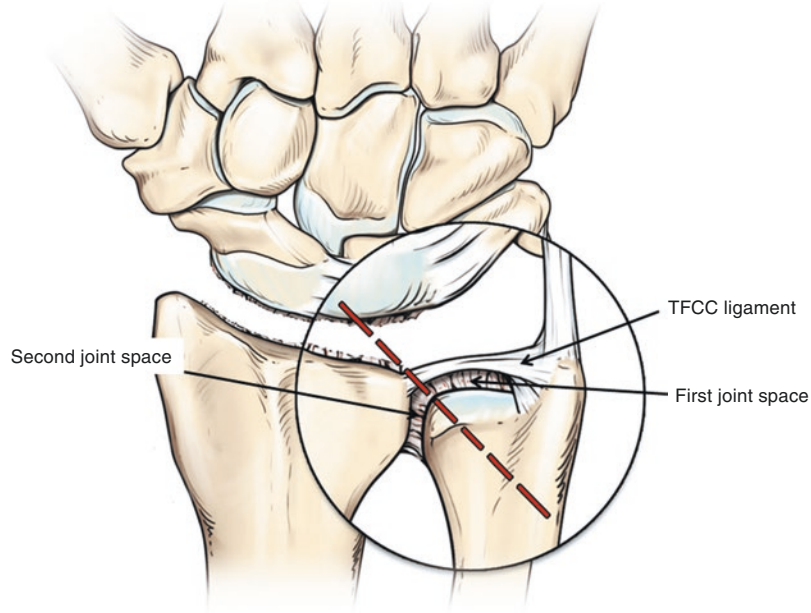

Fig. 104.11 Illustration of fibrosis in the DRUJ. The joint is divided into radioulnar and distal ulnar/TFCC spaces. (LuchettiR. The role of arthroscopy in postfracture stiffness. In: del Piñal E, et al., editors, Arthroscopic management of distal radius fractures, https://doi.org/10.1007/978-3-642-05354-2_12, © Springer-Verlag Berlin Heidelberg 2010)

of the space and fibrosis between the TFCC and the ulnar head may be obscured by the TFCC unless a central perforation coexists. A blunt dissector or a small shaver (2.0/2.9 mm) can be introduced through a torn TFCC or via the foveal portal. A wafer resection of the ulnar head can also be performed for ulnar carpal impingement. Contracture of the volar and distal capsule in the proximal space between the ulnar head and the sigmoid notch can restrict supination and pronation. Using a curved dissector through the proximal portal and the arthroscope through the distal portal, capsulectomy is proceeded from dorsal to volar side. To avoid DRUJ instability, dorsal and volar parts of TFCC should not be detached from their bony origin. On completion (Fig. 104.12) check for ROM without traction.

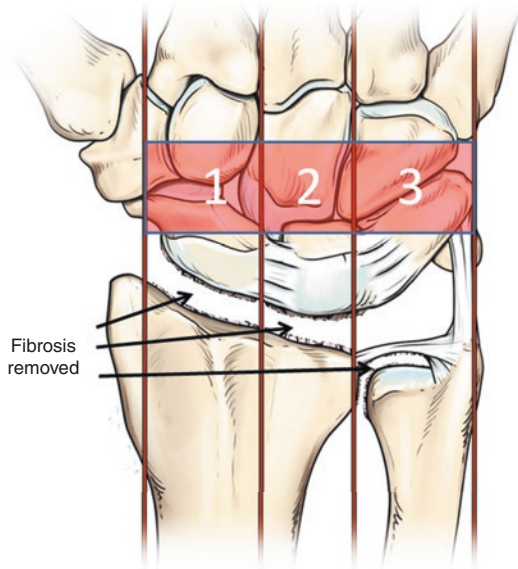

Fig. 104.12 Illustration of complete removal of fibrosis in the DRUJ and radiocarpal joint. (LuchettiR. The role of arthroscopy in postfracture stiffness. In: del Piñal E, et al., editors, Arthroscopic management of distal radius fractures, https://doi.org/10.1007/978-3-642-05354-2_12, © Springer-Verlag Berlin Heidelberg 2010)

Wrist arthroscopy may reveal some hidden pathologies, which can be treated at the same procedure. Articular incongruity due to articular steps of the distal radius can be leveled with a 2.9 mm burr. Loose bodies are removed. Chondroplasty may be performed for chondritis [3]. Ulnar carpal impingement can be treated with a wafer resection of ulnar head; however, if ulnar variance is up to 4 mm, it should be treated later by ulnar shortening. TFCC peripheral or foveal lesions, Type IB, and complete tear of scapholunate and lunotriquetral ligaments should also be treated later as they require immobilization.

104.4 Tips and Tricks

If joint visualization is poor:

- Increase traction.
- Use small scope.
- Insert the needle into joint.
- Use fluoroscopy to define the joint.

If there is difficulty increasing working space:

- Gently mobilize the wrist to identify the articulation.
- Use a probe to palpate the synovium that can then be resected.

104.5 Postoperative Management and Rehabilitation

Immediately after surgery, wrist mobilization should be initiated with pronation/supination and flexion/extension exercises with analgesics for pain control. Under the guidance of the physiotherapist, exercises are progressed from passive to active, and resistance, endurance, and functional training are added sequentially. The repetitions gradually increased over 3 months [3]. Return to heavy work is delayed till 3 months.

Table 104.2 Studies and results of arthroscopic arthrolysis of the stiff wrist (Modified from McGuire et al. [13])

Authors	Cases	Flexion/extension (mean °)	
		Preoperative	Postoperative
Pederzini et al. (1991)	5	44/40	54/60
Verhellen and Bain (2000)	5	17/10	47/50
Osterman et al. (2000)	20	9/15	42/58
Luchetti et al. (2001)	19	46/38	54/53
Hattori et al. (2004)	11	29/47	42/56

104.6 Complications

Complications may be due to wrist arthroscopy or specific to capsular release procedure. Complications include damage to neurovascular structures in close proximity to the portals. The extensor pollicis longus tendon is most at risk. Iatrogenic fractures or ligament injury could occur during manipulation. A clear knowledge of the proximity of the neurovascular structures to the capsule and to the portals can prevent inadvertent injury [15].

104.7 Results

Arthroscopic arthrolysis of the wrist is a challenging procedure. However, it has proven to be a safe, effective, and ideal treatment modality. Many authors have reported improvement in wrist flexion/extension after arthroscopic arthrolysis (Table 104.2) [13]. The range of flexion/extension motion achieved intraoperatively needs to be documented. The final range of motion at follow-up is typically less. The pronation/supination remains the same both intraoperatively and postoperatively. Pronation/supination (DRUJ) stiffness is more common than RC stiffness and can occur alone or along with RC stiffness. Better results are obtained with isolated DRUJ stiffness than the combined stiffness.

104.8 Summary

Arthroscopic arthrolysis is a safe and suitable option for wrist arthrofibrosis following trauma and surgery. It reduces wrist pain and improves ROM. It also identifies associated intra-articular pathologies many of which could be treated simultaneously.

Acknowledgments Kimberley Bryant for assistance in the preparation of the manuscript.

Max Crespi for his instability images.

References

1. Palmer AK, Werner FW, Murphy D, Glisson R. Functional wrist motion: a biomechanical study. J Hand Surg Am. 1985;10:39–46.
2. Bain G, McGuire D. Decision making for partial carpal fusions. J Wrist Surg. 2012;01:103–14.
3. Luchetti R, Atzei A, Fairplay T. Arthroscopic wrist Arthrolysis after wrist fracture. Arthroscopy. 2007;23:255–60.
4. Bain GI, Clitherow HDS. The pathogenesis and classification of shoulder stiffness. In: Itoi E, Arce G, Bain GI, Diercks RL, Guttmann D, Imhoff AB, et al., editors. Shoulder stiffness. Berlin: Springer; 2015. p. 3–19.
5. Guerra E, Kelberine FM, Marinelli A, Rotini R, Bain G. The stiff elbow: classification and treatment algorithm. In: Bain G, Eygendaal D, van Riet RP, editors. Surgical techniques for trauma and sports related injuries of the elbow. Berlin: Springer; 2020. p. 173–80.
6. Luchetti R, Bain G, Morse L, McGuire D. Arthroscopic Arthrolysis. In: Randelli P, Dejour D, van Dijk CN, Denti M, Seil R, editors. Arthroscopy. Berlin: Springer; 2016. p. 935–51.
7. Watts AC, Bain GI, Shrestha K, Alexander J. Wrist arthroscopy: the future. In: Savoie III FH, Field LD, editors. AANA advanced arthroscopy: the elbow and wrist. Philadelphia, pa: Saunders Elsevier; 2010. p. 289–98.
8. del Piñal F, Klausmeyer M, Thams C, Moraleda E, Galindo C. Arthroscopic resection arthroplasty for Malunited intra-articular distal radius fractures. J Hand Surg Am. 2012;37:2447–55.
9. del Piñal F. Editorial: I have a dream … reflex sympathetic dystrophy (RSD or complex regional pain syndrome - CRPS I) does not exist. J Hand Surg Eur Vol. 2013;38:595–7.
10. Veldman PHJM, Reynen HM, Arntz IE, Goris RJA. Signs and symptoms of reflex sympathetic dys-

trophy: prospective study of 829 patients. Lancet. 1993;342:1012–6.
11. Marinus J, Moseley GL, Birklein F, Baron R, Maihöfner C, Kingery WS, et al. Clinical features and pathophysiology of complex regional pain syndrome. Lancet Neurol. 2011;10:637–48.
12. Brinkers M, Rumpelt P, Lux A, Kretzschmar M, Pfau G. Psychiatric disorders in complex regional pain syndrome (CRPS): the role of the consultation-liaison psychiatrist. Pain Res Manag. 2018;2018:1–8.
13. McGuire DT, Luchetti R, Atzei A, Bain GI. Arthroscopic Arthrolysis. In: Geissler WB, editor. Wrist and elbow arthroscopy. Springer: New York; 2015. p. 165–75.
14. Bain GI, Munt J, Turner PC, Bergman J. Arthroscopic dorsal capsular release in the wrist: a new technique. Tech Hand Up Extrem Surg. 2008;12:191–4.
15. Bain GI, Munt J, Turner PC. New advances in wrist arthroscopy. Arthroscopy. 2008;24:355–67.
16. Badur N, Luchetti R, Atzei A. Arthroscopic wrist anatomy and setup. In: Geissler WB, editor. Wrist and elbow arthroscopy. Springer: New York; 2015. p. 1–28.
17. Osterman AL, Culp RW, Osterman MN. Arthroscopic release of wrist contractures. Plast Reconstr Surg. 2010;126:44.
18. Viegas SF, Patterson RM, Ward K. Extrinsic wrist ligaments in the pathomechanics of ulnar translation instability. J Hand Surg Am. 1995;20:312–8.
19. Tham S, Coleman S, Gilpin D. An anterior portal for wrist arthroscopy: anatomical study and case reports. J Hand Surg. 1999;24:445–7.
20. Verhellen R, Bain GI. Arthroscopic capsular release for contracture of the wrist: a new technique. Arthroscopy. 2000;16:106–10.

Arthroscopic Management of Kienbock's Disease

105

Simon MacLean and Gregory I. Bain

105.1 Background

Since its original description in 1910, the etiology, pathogenesis, and treatment of Kienbock's Disease (KD) have remained unclear [1]. Diagnosis is often delayed as clinical findings may be vague and plain radiographs fail to diagnose the disease in the early stages. Further imaging modalities such as CT and MRI are essential but can underestimate the extent of disease and the status of the articular surfaces.

Arthroscopy is a valuable tool for the assessment and treatment of the KD wrist. We believe it is the gold standard for assessment of the articular surfaces of the lunate and wrist, and the diagnosis of peri-lunate ligament tears. It allows for the treatment of synovitis and debridement of articular surfaces [2, 3]. When the treating surgeon has made an effective arthroscopic assessment of the functional articulations and stability of the wrist, definitive arthroscopic treatment can be tailored to the individual patient [4, 5].

There is a lack of consensus and high-level evidence for the natural history and treatment of KD. To simplify decision-making, we recommend an algorithmic approach encompassing patient and surgical factors, including the vascular, osseous, and chondral status of the lunate and wrist [3, 6]. This chapter presents the management algorithm, and the use of arthroscopy for both diagnostic and therapeutic intervention.

105.2 Initial Management

Before proceeding with arthroscopic assessment and treatment, appropriate nonoperative treatment and investigations are essential.

- Initial treatment should be nonoperative, as a proportion of patients will respond to activity modification, anti-inflammatory medication, and splinting. This should be tailored to the individual. In "Teenbock" patients under the age of 15 years, we recommend a 12-month duration of nonoperative treatment [7]. In patients aged 16–20, prognosis for nonoperative treatment is still favorable and we recommend a 6–12 month duration of conservative treatment. Patients aged 21–70 often present with a long duration of symptoms or a later stage of the disease. We recommend a shorter duration of nonoperative treatment (6–12 weeks) in this cohort. In older patients (>70 years) we recommend a longer (6–12 month) period of nonoperative

S. MacLean (✉)
Department of Orthopaedic Surgery, Tauranga Hospital, Tauranga, New Zealand

G. I. Bain
Department of Orthopaedics and Trauma Surgery, Flinders University and Flinders Medical Centre, Adelaide, SA, Australia
e-mail: admin@gregbain.com.au

© ISAKOS 2022

D. N. Bhatia et al. (eds.), *Arthroscopy and Endoscopy of the Elbow, Wrist and Hand*,
https://doi.org/10.1007/978-3-030-79423-1_105

treatment, as often their pain is not so severe despite the radiological appearance.

- Plain radiographs allow for assessment of wrist morphology, sclerosis, and fragmentation of the lunate, and wrist arthritis in later stages of the disease.
- It is our experience that a specific cohort of patients develops rapid progression of KD with Kienbock's Disease Advanced Collapse ("KDAC"). We have identified a number of prognostic signs on CT scan predictive of the "pre-collapse" lunate. These include proximal to distal fracture lines through the lunate, a wide area of comminution through the lunate, and carpal instability (Fig. 105.1).
- Unenhanced MRI scan is diagnostic in the early stages of the disease when radiographs are normal-showing homogenous alteration in bone marrow signal on T-1 and T-2 weighted sequences. We use MRI with gadolinium contrast to show maintenance of vascular perfusion—allowing differentiation between necrosis and the "repair zone." [8–10]
- Dynamic 4-D CT scanning study of the KD wrist has furthered our understanding of the disease pathogenesis. A number of instability patterns and symptomatic mechanical impingement can occur as described below.

105.3 Arthroscopic Assessment

Arthroscopy allows a thorough inspection and palpation of the articular and ligamentous structures of the joint with minimal risk of soft tissue disruption.

Diagnostic arthroscopy is performed with traction using a 2.7 mm 30° arthroscope. Routine portals (3–4, 6R, MCR, and MCU) are used. Fluid pressure can collapse the capillaries; therefore, dry arthroscopy provides superior visualization of articular surfaces and synovitis. Inspection and probing of the articular surfaces of the lunate and surrounding carpus should be performed.

Key arthroscopic findings include:

1. *Synovitis* is identified in all patients with Kienbock's disease and the extent of the synovitis is related to the severity of the condition.
2. *"Functional" articular surfaces* appear smooth and glistening, and firm to palpation. Minor fibrillation on the articular surface is still considered a functional articulation [4].
3. *"Non-functional" articular* surfaces include those with extensive fibrillation, fissuring, floating chondral surfaces, or fracture.
4. *"Concealed fracture"* of the lunate may be identified with probing. A thin line or crease in the opalescent articular surface (similar to

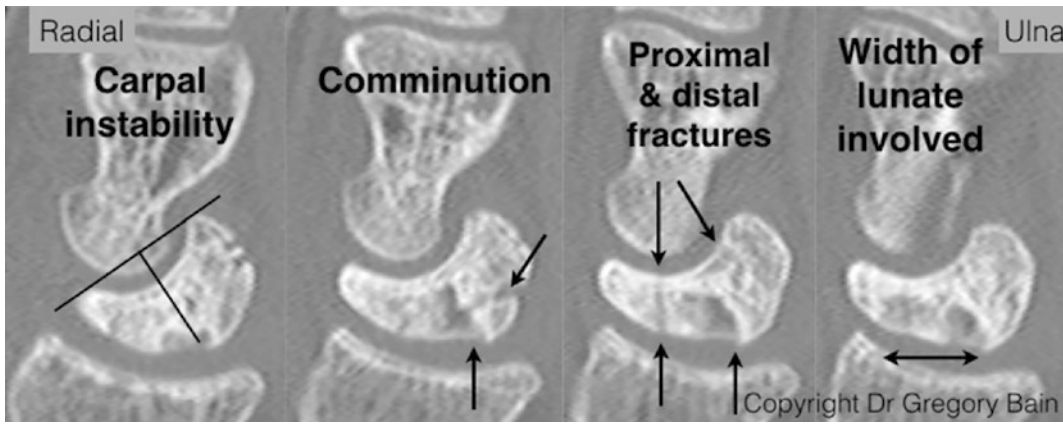

Fig. 105.1 CT scan findings predictive of the "pre-collapse lunate." (© Dr. Gregory I. Bain)

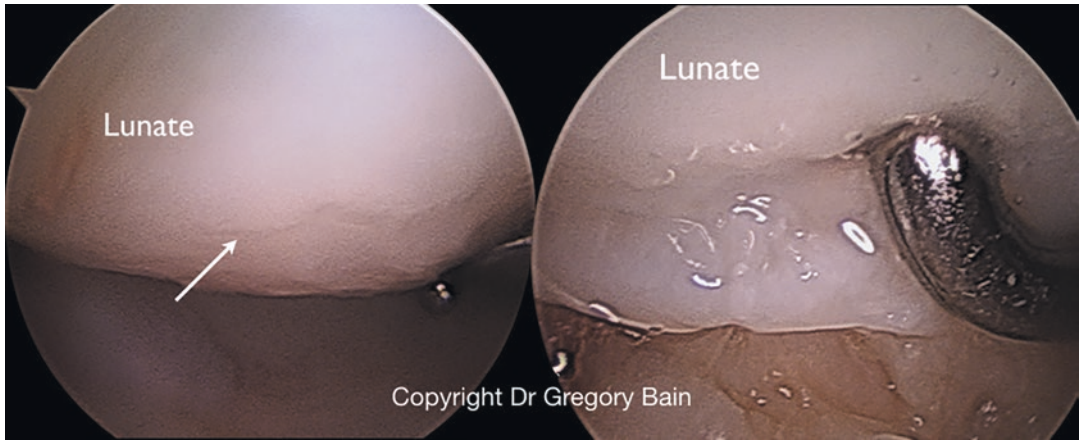

Fig. 105.2 On initial inspection, a thin line is visualized in the proximal lunate articular surface. With probing the articular surface collapses—indicative of subchondral bone collapse. (© Dr Gregory I. Bain)

that seen in a proximal pole fracture of the scaphoid) is a telltale sign. (Fig. 105.2)

5. *"Floating" proximal lunate surface* is when the collapsed lunate is distracted during traction but collapses with probing. It is an important finding and indicates that reconstruction of the proximal lunate needs to be considered, or that the radiolunate articulation needs to be bypassed with a motion-preserving limited wrist fusion.
6. *Scapholunate and lunotriquetral ligaments* are often torn or avulsed adjacent to the lunate fracture and collapse. This will affect the stability of the proximal row and should be taken into consideration when assessing the wrist.
7. *Secondary Wrist Pathology:*
   (a) *Volar radiolunate impingement* can occur between the volar horn of the lunate following fragmentation and the lunate fossa and is seen with wrist flexion. (Fig. 105.3).
   (b) *Ulnar styloid impingement* is associated with the collapse of the lunate and ulnar translocation. This may be a source of persistent ulnar-sided symptoms following treatment. (Fig. 105.4).
   (c) *Ulnar translocation* can occur as a result of compromise to the extrinsic carpal ligament as a result of synovitis or avulsion, or due to scapholunate diastasis. (Fig. 105.5).

By combining preoperative investigations and arthroscopic evaluation, a definitive plan can now be established. The Bain and Begg classification was developed to utilize arthroscopic findings to direct treatment (Fig. 105.6). The grade identified is based on the number of articulations involved in the central column, ranging from 0 to 4. There can be involvement of the lunate facet and proximal lunate (2a) or a coronal fracture that includes the proximal and distal aspects of the lunate (2b). By defining the functional articulations, their location, and the extent of wrist involvement, the algorithm directs surgical management towards the optimal motion-preserving procedure. The nonfunctional articular surfaces are managed with excision, fusion, or bypass, preserving functional articulations to maximize final wrist mobility.

105.4 Planning Management: An Algorithm-Based Approach

The Bain and Begg classification helps define the functional surfaces in the wrist. We developed an algorithm in order to define the best treatment for the patient. The aim of the algorithm was to encompass the osseous, vascular, and chondral status of the lunate and wrist by combining the

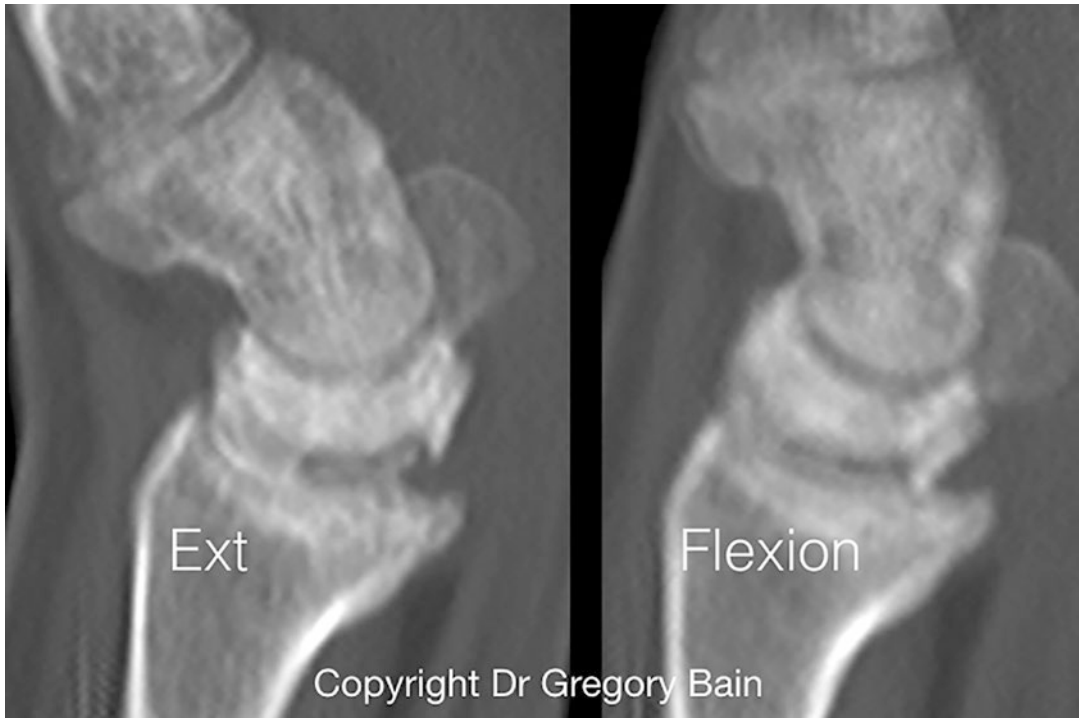

Fig. 105.3 Volar radiolunate impingement. The fragmented volar horn impinges on the volar rim of the distal radius on flexion. (© Dr Gregory I. Bain)

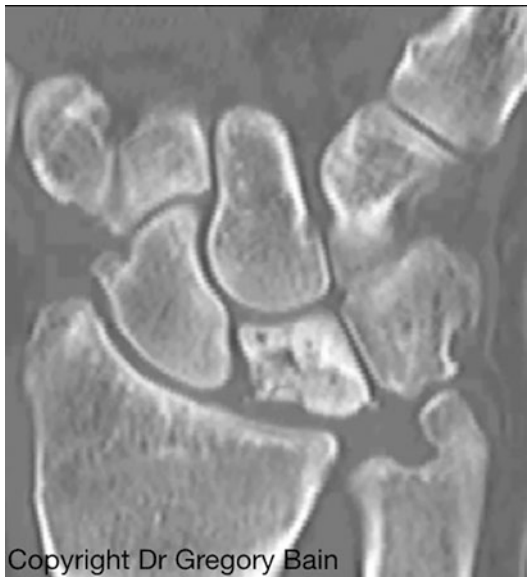

Fig. 105.4 Ulnar styloid—triquetral impingement: The triquetrum impinges against the ulnar styloid as the wrist moves into ulnar deviation. (© Dr Gregory I. Bain)

Lichtman, Schmitt, and Bain classifications [4, 8, 12]. (Fig. 105.7). The aims of surgical treatment are to;

- Improve pain.
- Protect lunate from collapse.
- Protect the wrist from collapse and degeneration.
- If focal compromise to the lunate, consider lunate reconstruction.
- If lunate unreconstructable, consider a motion-preserving procedure.
- If wrist unreconstructable, consider a salvage procedure.

Multiple factors should be taken into consideration when deciding on the best procedure (Table 105.1).

A number of procedures in our algorithm can be performed arthroscopically. We believe arthroscopy has several benefits in the treatment of KD:

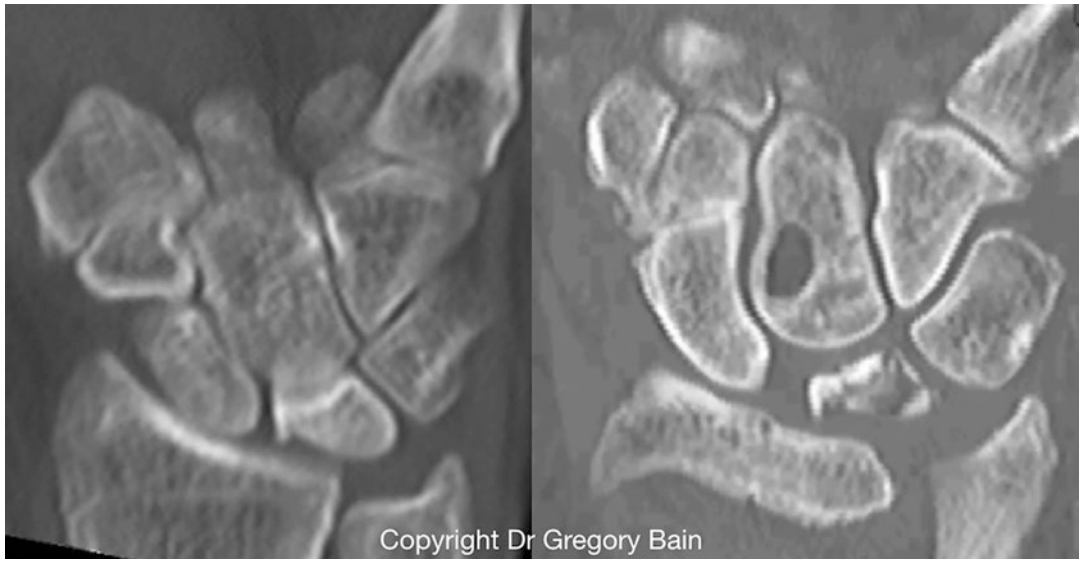

Fig. 105.5 Ulnar translocation. Two types of ulnocarpal translocation can be seen in advanced stages of Kienbock's Disease; Taleisnik Type 1 (**a**) and type 2 (**b**)—with associated scapholunate diastasis. Note sclerosis at the scaphoid fossa in both cases and the STT degenerative changes in (**b**). (© Dr Gregory I. Bain)

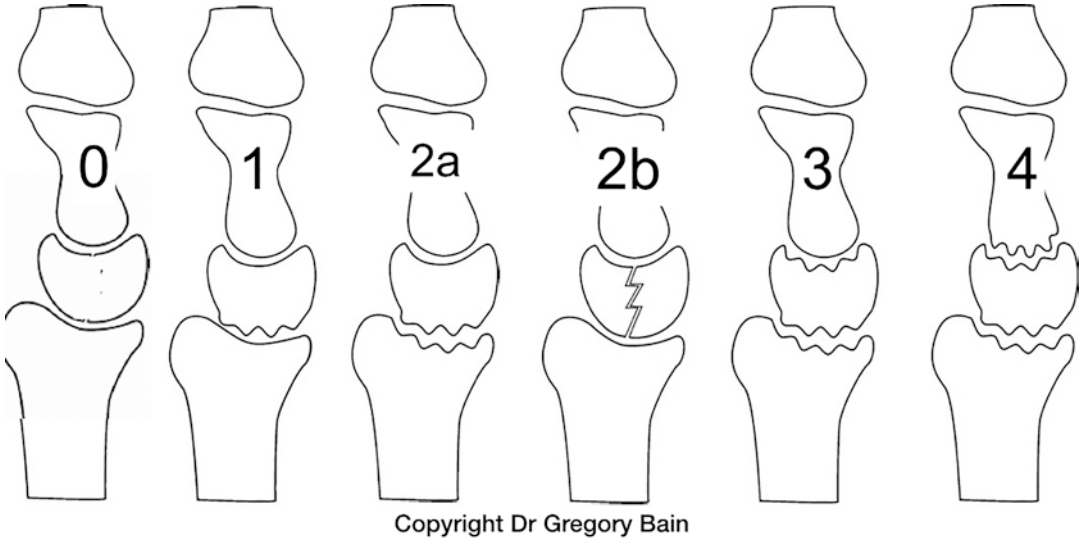

Fig. 105.6 The Bain and Begg Classification, based on the number of functional articulations in the Kienbock's wrist. From Bain GI, Begg M. Arthroscopic assessment and classification of Kienbock's Disease. Techniques in Hand and Upper Extremity Surgery. 2006. 1:10 (1):8–13. (© Dr Gregory I. Bain)

- Reduced surgical dissection and compromise to soft tissue envelope leading to less postoperative morbidity and improved rehabilitation.
- Precise debridement and preparation of the fusion surfaces.
- Preservation of important sensory branches (e.g., PIN) to the wrist joint may improve proprioception.
- Percutaneous countersunk fixation minimizing hardware complications.
- Superior cosmetic result.

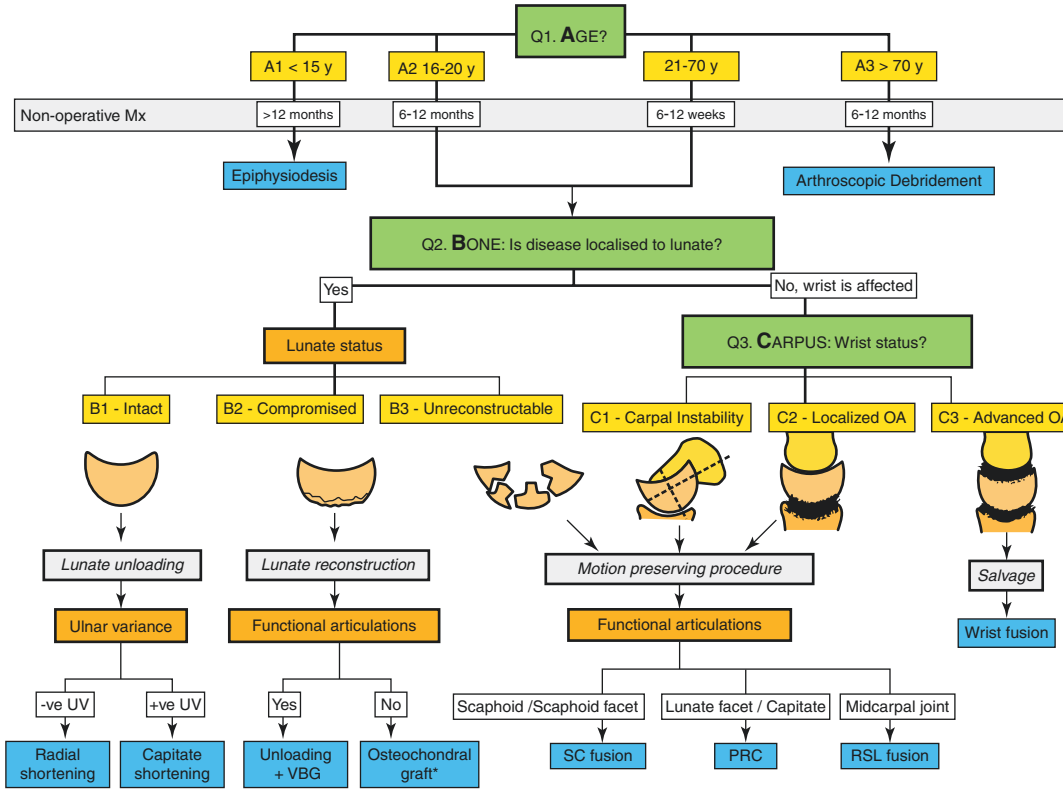

Fig. 105.7 An algorithm for the treatment of Kienbock's Disease. Copyright Dr. Gregory I. Bain. (© Bathia)

Table 105.1 Factors to consider in determining treatment for Kienbock's Disease

	Factors 2	Factors 3
Patient	Demographics	*Age,* sex, occupation, activities, comorbidities, medications, smoking
	History	*Injury, pain, aggravating factors, duration of symptoms*
	Examination	*Swelling, tenderness, range of motion, grip strength*
Lunate	Loading	*Lunate type*, lunate translation, *ulnar variance, radial inclination*
	Osseous	*Sclerosis, fragmentation, coronal fracture, collapse*
	Articular	Functional articulation, *lamination, degeneration*
	Vascularity	Vascular pattern, *ischemia, necrosis, revascularization*
Wrist	Joint	Synovitis, *contracture*
	Stability	*Carpal collapse* (RSA > 60), Scapholunate and lunotriquetral tears, ulnocarpal translocation
	Degeneration	*Localized, generalized*
	Impingement	*Ulnar styloid—Triquetral, volar radiolunate*

105.5 Arthroscopic Techniques

Synovectomy and joint debridement can be performed and should include removal of loose bodies and debridement of torn and unstable surfaces with a full radius shaver and/or pituitary rongeurs [3].

Advanced arthroscopic reconstructive procedures include arthroscopic proximal row carpectomy, arthroscopic radioscapholunate fusion, and arthroscopic scaphocapitate fusion. We perform lunate reconstruction with a vascularized pedicle flap as an open procedure. There are a number of

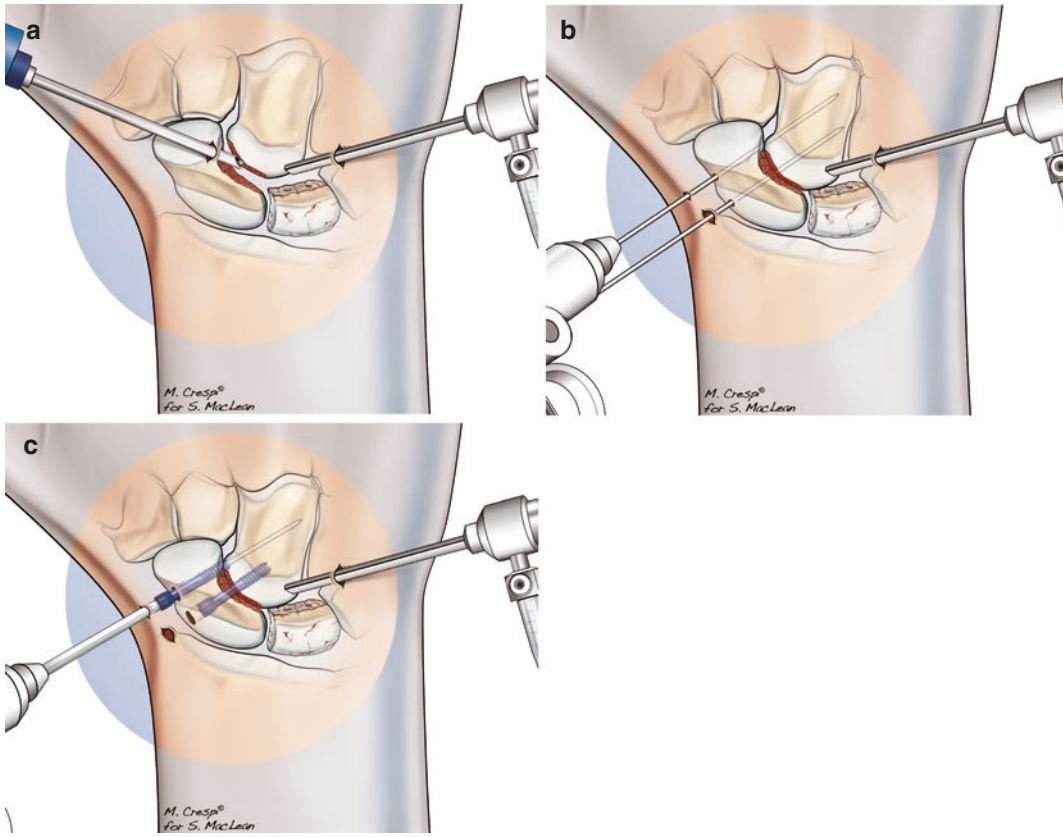

Fig. 105.8 Arthroscopic scaphocapitate fusion. (**a**) Using the MCU and MCR portals the scaphocapitate joint is visualized and the articular surfaces removed with a burr. (**b**) Two parallel guidewires are passed. The first should be through the 1–2 portal, aiming for a proximal and middle-third entry point, 60° to the longitudinal axis of the wrist and passing centrally through both bones on the lateral view. The second should be passed 5 mm distal and parallel to the first through a middle/distal-third junction. (**c**) Two cannulated compression screws are passed over the guidewires. (M. Crespi © S. Maclean)

principles which are applied when arthroscopically treating patients with KD. These principles are as follows:

- *Traction*: Adequate traction should be applied throughout the procedure, and allow forearm rotation. Mini C-arm set-up in conjunction with the traction device is important.
- *Visualization*: Dry arthroscopy with intermittent irrigation is our preference. This provides superior resolution of surfaces on inspection and reduces edema and postoperative swelling and pain.
- *Infiltration*: We often use local infiltration with adrenaline (lidocaine 1% with adrenaline 1:200,000). This is infiltrated just prior to scrubbing up to allow the adrenaline to have maximal vasoconstrictive effect. This has several benefits.
  - Advanced arthroscopic procedure time may exceed the tourniquet time threshold, and this allows safe arthroscopy without the need for tourniquet insufflation.
  - This local anesthetic/adrenaline combination allows for larger volumes to be used than just lidocaine alone (up to 7 mg/kg) if required.
  - For diagnostic or simple arthroscopic treatment, we have performed treatment "wide awake" using this approach.

- *Carpal bone excision* should be commenced with a small burr initially then a larger burr to improve efficiency. Releasing the ligament attachments allows the bone to be more easily removed with a pituitary rongeur.
- *Fusion surfaces* are prepared by debriding articular cartilage to bleeding subchondral bone. Start proximally so that bleeding is less likely to obscure visibility. Irrigation is required to prevent bone necrosis.
- *Carpal alignment* can be achieved using percutaneous k-wire joysticks under fluoroscopic imaging.
- *Fixation* can be achieved percutaneously with K-wires or cannulated compression screws.
- *Cancellous bone graft* can be added via a trochar or small syringe. A Foley catheter can be inserted and inflated arthroscopically to prevent bone graft extruding into the joint space. (as described by Dr. PC Ho).

105.5.1 Arthroscopic Scaphocapitate Fusion

A scaphocapitate fusion allows bypass of load through the radial column of the wrist therefore bypassing the diseased central column. The fusion procedure preserves carpal height and allows motion-preservation through a functional articulation between the proximal scaphoid and scaphoid facet of the distal radius (Fig. 105.8).

105.5.1.1 Indications

Scaphocapitate fusion is indicated if the lunate is unreconstructable (B3). It is also indicated if carpal instability exists with intact articulations (C1) or if localized arthritis exists between the proximal lunate and lunate facet (C2).

105.5.1.2 Surgical Steps

- The standard viewing and working portals are Midcarpal Ulnar (MCU) and Midcarpal Radial (MCR), respectively.
- Resect the adjacent articular surfaces of the capitate and waist and proximal scaphoid.
- Start proximally and work distally. Debride articular cartilage until punctate bleeding occurs from subchondral bone.
- The distal third of the scaphoid at the STT joint is usually not debrided.
- Check alignment on fluoroscopy. Carpal height is essential to successfully transmit load through a congruent articulation between the proximal scaphoid and scaphoid facet. The scaphocapitate angle should be between 30° and 57° and ideal capitolunate angle should be between 0 and ±15° [13].
- Two guidewires can be passed across the scaphocapitate interval.
  - The first should be through the 1–2 portal, aiming for a proximal and middle-third entry point, 60° to the longitudinal axis of the wrist and passing centrally through both bones on the lateral view.
  - The second should be passed 5 mm distal and parallel to the first through a middle/distal-third junction.
  - Place a cannulated compression screw over each guidewire.

105.5.1.3 Tips and Tricks

- Start articular debridement on the gravity-dependent part of the scaphocapitate joint (i.e., proximal). This prevents blood from obscuring visualization.
- A volar-directed force from the thumb pushing on the scaphoid tubercle helps to extend the scaphoid.
- Use self-drilling compression screws to minimize operative steps. Ensure they are small (approximately 2 mm in diameter) to avoid the initiation of a fracture line during screw compression.

105.5.1.4 Pitfalls

Inadequate debridement of the articular surfaces with a burr will prevent union from occurring.

105.5.1.5 Post-op Management and Rehabilitation

A short-arm cast is placed for 6–8 weeks or until union. Full active range of motion is then encouraged.

105.5.1.6 Complications

In our limited series, we have not noticed any complications with this procedure. Care should

be taken on the radial side of the wrist to avoid damage to the branches of the superficial radial nerve and radial artery during wire and screw placement.

105.5.2 Arthroscopic Radioscapholunate Fusion

Radioscapholunate (RSL) fusion preserves the midcarpal articulation, important for "dart-thrower's motion." Despite theoretical concerns as to the viability of the KD lunate, we have had full union and excellent functional outcomes in our series.

105.5.2.1 Indications and Contraindications

Arthroscopic RSL fusion is indicated in the KD patient with a functional midcarpal articulation, and is therefore a suitable option for patients with Bain and Begg 2a disease (Fig. 105.9). A lunate with a coronal or sagittal fracture line is a contraindication for the procedure (Bain and Begg 2b).

105.5.2.2 Surgical Steps

- Perform a thorough arthroscopic assessment of the midcarpal joint to ensure the joint is functional.
- We use the 4–5 portal for viewing with the working portals for the burr, suction and irrigation in 1–2 and 3–4 portals.
- The most distal radial styloid and scaphoid fossa are debrided first followed by the proximal scaphoid and lunate fossa.
- If incongruity exists between the surfaces, bone graft is added. Distal radius graft is harvested and cancellous graft is passed through an arthroscopic trochar in the 1–2 and 3–4 portals.
- The bone graft is carefully compacted. The arthroscope is removed and a Foley catheter is placed in the 4–5 portal during this process.
- Fluoroscopy is then used:
  - The wrist is held in neutral so that the proximal carpal row is aligned with a radiolunate angle of 0°.
  - A radiolunate guidewire is introduced 1 cm proximal to the dorsal rim of the radius and advanced percutaneously through the central column of the distal radius aiming at the volar horn of the lunate to maximize purchase.
  - A radioscaphoid guide wire is passed from the radial column of the distal radius towards the proximal scaphoid aiming at 45° on the anteroposterior view. On the lateral view, the pin is aimed along the mid-axis of the radial styloid and proximal scaphoid.
- Cannulated compression screws are advanced over the guide wires.

105.5.2.3 Tips and Tricks

- A congruent articulation should be achieved at the midcarpal joint. Ideally, the radiolunate angle therefore should be 0°. Excessive flexion or extension at the lunocapitate joint may lead to incongruence, early degeneration, or adaptive instability.
- Arthroscopic assessment of the scapholunate and lunotriquetral ligaments is essential. Tears to these ligaments may lead to an abnormal scapholunate angle and incongruence and abnormal loading of the midcarpal joint following fusion.

105.5.2.4 Pitfalls

Avoid over-penetration of the guidewires, particularly when advancing to the volar aspect of the wrist as the median nerve lies in close proximity.

105.5.2.5 Post-op Management and Rehab

A short-arm cast is placed for 6–8 weeks or until union. Full active range of motion is then encouraged.

105.5.2.6 Complications

We have not experienced any specific complications following this procedure.

105.5.2.7 Results

Excellent pain relief, satisfaction, and function have been maintained for 10 years in 4 of our

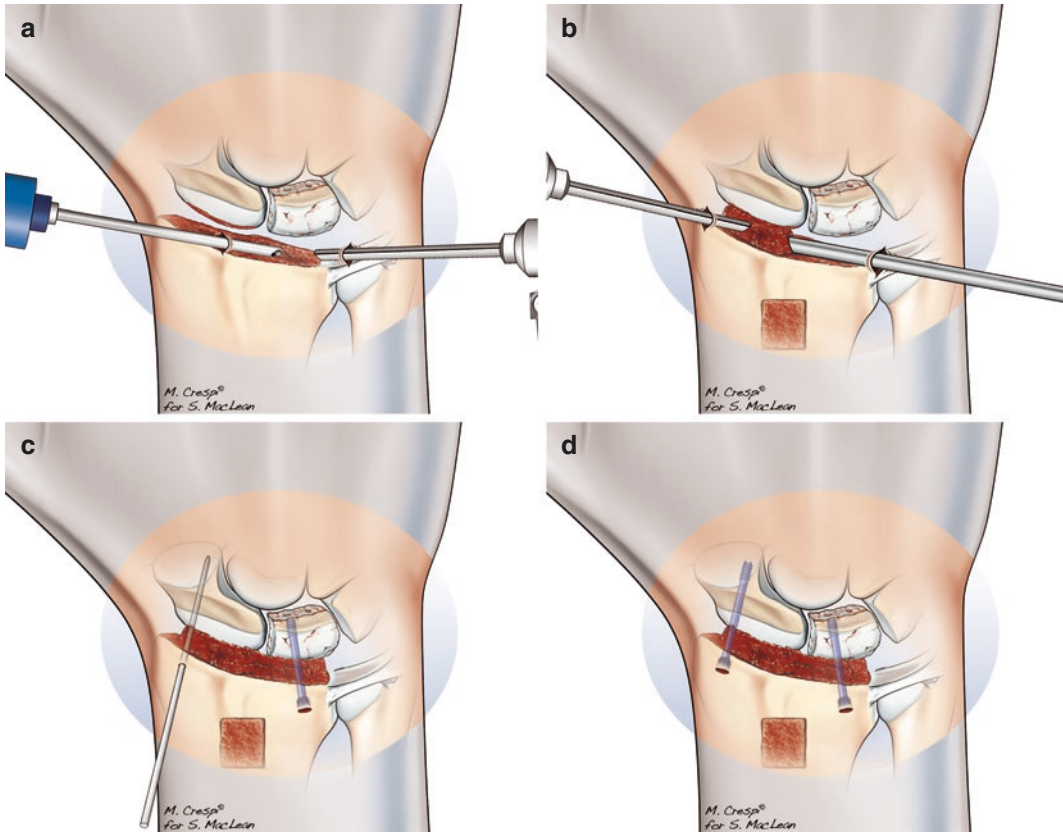

Fig. 105.9 Arthroscopic radioscapholunate fusion. (**a**) Using the 3–4 and 4–5 portals the articular surfaces are visualized and debrided with a burr. (**b**) Distal radius graft may be harvested and introduced through an arthroscopic trochar if the surfaces are incongruent. (**c**) Radiocarpal guidewires are then passed after confirming alignment with fluoroscopy. (**d**) Cannulated compression screws are passed. (M. Crespi © S. Maclean)

patients treated with RSL fusion. The flexion–extension arc is limited (mean 72°) but midcarpal and dart-thrower's motion is preserved. None of our patients have developed nonunion or required additional salvage procedures.

105.5.3 Arthroscopic Proximal Row Carpectomy

Proximal row carpectomy (PRC) allows for an articulation at the radiocapitate joint in patients with a functional lunate fossa and proximal capitate. Good long-term results have been reported in patients over the age of 40 years [14, 15]. Arthroscopic PRC allows a minimally invasive approach to the wrist. Careful arthroscopic burring reduces damage to the radioscaphocapitate ligament (RSCL) which may reduce the risk of ulnocarpal translocation.

105.5.3.1 Indications and Contraindications

Arthroscopic PRC is indicated in patients with a functional proximal capitate and lunate fossa (Bain and Begg 1 or 2b). PRC is not reliant on a fusion mass and is therefore indicated in patients unsuitable for partial wrist fusion (smokers, multiple comorbidities), or in low-demand patients.

105.5.3.2 Surgical Steps

- Perform a standard arthroscopic assessment, synovectomy, and debridement.
- Remove the central osseous portion of the scaphoid, lunate, and triquetrum. This will

leave a prominent radial and ulnar portion of each bone which will be easier to excise with a pituitary rongeur.
- Use the bipolar cautery to remove ligamentous attachments near the joints.
- Use fluoroscopy to check for impingement of the radial styloid on the distal carpal row in radial deviation. If the styloid is prominent, perform a careful arthroscopic styloidectomy. Avoid excising more than 1 cm to avoid compromise to the RSCL.

105.5.3.3 Tips and Tricks

Episodic irrigation/suction is important to avoid thermal damage to the articular surfaces and surrounding soft tissues.

105.5.3.4 Pitfalls

Ensure all bone fragments are completely removed as retained fragments can lead to a painful articulation.

105.5.3.5 Post-op Management and Rehabilitation

A bulky bandage is applied for 1 week followed by a removable splint. The patient can then mobilize the wrist as comfort allows. The patient should avoid significant loading through their wrist for 3 months.

105.5.3.6 Complications

Although there is a high rate of radiocapitate arthrosis in the published literature at 10 years, we have found patients are often asymptomatic despite radiographic disease at follow-up.

105.5.3.7 Results

We have 2–12 year follow-up on 12 patients treated with PRC for Bain and Begg grades 1 and 2b Kienbock's disease. In this selected cohort, PRC has provided excellent outcomes for pain, satisfaction, and functional scores. No patients have required additional salvage procedures in our cohort. If the patient is in low demand or has a nonunion risk, PRC is our preferred procedure.

105.6 Summary

The management of Kienbock's Disease presents a challenge to the treating surgeon. Arthroscopy should be used in conjunction with a thorough clinical review and appropriate investigations. Diagnostic arthroscopy is the most effective way to assess the articular surfaces and soft tissues within the wrist. Arthroscopic treatment confers a number of benefits, allowing for a minimally invasive directed approach to the patient with KD. It should be used with an algorithm-based approach, respecting the status of the patient, the lunate, and the wrist.

References

1. Kienbock R. Concerning traumatic malacia of the lunate and its consequences: joint degeneration and compression. Fortsch Geb Roentgen. 1910;
2. MacLean SBM, Bain GI. Arthroscopic assessment of kienbock disease. In: Mathoulin C, editor. Wrist arthroscopy: techniques. 2nd ed. New York, NY: Thieme Medical Publishers, Inc.; 2018.
3. MacLean SBM, Kantar K, Bain GI, Lichtman DM. The role of wrist arthroscopy in kienbock disease. Hand Clin. 2017;33(4):727–34. https://doi.org/10.1016/j.hcl.2017.07.003.
4. Bain GI, Begg M. Arthroscopic assessment and classification of Kienbock's disease. Tech Hand Up Extrem Surg. 2006;10(1):8–13. https://doi.org/10.1097/00130911-200603000-00003.
5. Bain GI, Durrant A. An articular-based approach to kienbock avascular necrosis of the lunate. Tech Hand Up Extrem Surg. 2011;15(1):41–7. https://doi.org/10.1097/BTH.0b013e31820e82e8.
6. Lichtman DM, Pientka WF, Bain GI. Kienböck disease: moving forward. J Hand Surg Am. 2016;41(5):630–8. https://doi.org/10.1016/j.jhsa.2016.02.013.
7. Irisarri C, Kalb K, Ribak S. Infantile and juvenile lunatomalacia. J Hand Surg Eur Vol. 2010;35(7):544–8. https://doi.org/10.1177/1753193410364913.
8. Schmitt R, Heinze A, Fellner F, Obletter N, Strühn R, Bautz W. Imaging and staging of avascular osteonecroses at the wrist and hand. Eur J Radiol. 1997;25(2):92–103.
9. Schmitt R, Christopoulos G, Kalb K, et al. Differential diagnosis of the signal-compromised lunate in MRI. Rofo. 2005;177(3):358–66. https://doi.org/10.1055/s-2004-813931.

10. Schmitt RKK. Imaging in Kienböck's disease. Mikrochir Plast Chir. 2010;42(3):162–70.
11. Bain G, MacLean S, Tse W-L, Ho P-C, Lichtman D. Kienböck disease and arthroscopy: assessment, classification, and treatment. J Wrist Surg. 2016;05(04):255–60. https://doi.org/10.1055/s-0036-1584546.
12. Lichtman DM, Mack GR, MacDonald RI, Gunther SF, Wilson JN. Kienböck's disease: the role of silicone replacement arthroplasty. J Bone Joint Surg Am. 1977;59(7):899–908.
13. Minamikawa Y, Peimer CA, Yamaguchi T, Medige J, Sherwin FS. Ideal scaphoid angle for intercarpal arthrodesis. J Hand Surg Am. 1992;17(2):370–5.
14. Croog AS, Stern PJ. Proximal row carpectomy for advanced Kienböck's disease: average 10-year follow-up. J Hand Surg Am. 2008;33(7):1122–30. https://doi.org/10.1016/j.jhsa.2008.02.031.
15. Chim H, Moran SL. Long-term outcomes of proximal row carpectomy: a systematic review of the literature. J Wrist Surg. 2012;1(2):141–8. https://doi.org/10.1055/s-0032-1329547.

Arthroscopic Limited Wrist Fusion

106

Michael Chu-kay Mak and Pak-cheong Ho

106.1 Background

Limited wrist fusion is indicated in painful, localized arthritis of the wrist and in chronic carpal instability or deformities. Limited fusion can relieve pain by eliminating motion of the diseased segment(s), correct carpal alignment, restore stability, preserve motion at neighboring unaffected articulations, and maintain carpal height and grip strength. Common indications include post-traumatic degeneration such as SLAC and SNAC wrist, avascular necrosis, and carpal instabilities. An arthroscopic approach preserves vascularity which is necessary for bone union and may result in less capsular fibrosis and stiffness than an open approach.

106.1.1 Surgical Anatomy

The wrist joint is unique in its configuration of multiple articulations spanning from the radius and ulna to the metacarpals; the joint demonstrates an axial linkage comprising of a proximal carpal row intercalated between the forearm bones and the distal carpal row, and transverse linkages between individual carpal bones in each carpal row. All these articulations act in concert to produce an aggregate motion with three degrees of freedom while stability is provided by ligaments and dynamic tendon forces. Because each carpal bone articulates with its neighboring bones with varying degrees of mobility, restricting the motion of one or even several of these articulations would not completely prevent overall wrist motion. Articulations that are axially oriented have more motion than those which are transverse, i.e., in the same carpal row. The direction of these motions are primarily governed by the shape and bony configuration of each joint while being constrained by intrinsic and extrinsic carpal ligaments.

The radiocarpal joint is an elliptical joint consisting of biconvex proximal surfaces of the scaphoid and lunate articulating with shallow biconcave scaphoid and lunate fossae on the distal radius separated by a scapholunate ridge. Distally, in the midcarpal joint, the "key" joints that govern midcarpal motion are the scaphocapitate (SC) and capitolunate (CL) articulations [1]. Fusion of the scaphocapitate joint was shown in a cadaveric study to produce a similar effect as fusion of all the bones in the region of the scaphoid, trapezium, trapezoid, and capitate. Similarly, fusion of the capitolunate joint limits the motion of the entire complex of the lunate, triquetrum, capitate, and hamate. This key articulation between the capitate, scaphoid, and lunate resembles a ball and

M. C.-k. Mak · P.-c. Ho (✉)
Department of Orthopaedics and Traumatology, Prince of Wales Hospital, The Chinese University of Hong Kong, Hong Kong, SAR, China
e-mail: mmak@cuhk.edu.hk; pcho@cuhk.edu.hk

© ISAKOS 2022

D. N. Bhatia et al. (eds.), *Arthroscopy and Endoscopy of the Elbow, Wrist and Hand*,
https://doi.org/10.1007/978-3-030-79423-1_106

socket joint with the socket formed by the surfaces of the lunate and proximal two-thirds of the scaphoid [2]. In addition, the shape of the lunate also influences midcarpal motion and load transmission. Lunates are classified into type 1 or 2 depending on whether it has a single facet articulating with the capitate, or double facets that articulate with both the capitate and hamate [3]. Wrists with type 2 lunates may have a more stable configuration of the midcarpal joint and are more resilient to carpal collapse after scaphoid nonunion [4]. The radiocarpal and midcarpal joints (represented by the lunocapitate joint) each contribute 56° to produce a total flexion-extension arc of 112° in a cadaveric model of simulated motion [5]. In most wrists, flexion occurs mostly at the midcarpal joint, and extension mostly at the radiocarpal joint, while radio-ulnar deviation occurs mainly at the midcarpal joint. Concerning motion across carpal bones in the same row, the proximal row exhibits considerably more relative motion than the distal row. The scapholunate and lunotriquetral joints each have 24° and 18° of flexion-extension motion respectively, while those in the distal row have only up to 12° for the trapeziotrapezoid joint and less for the others [5]; thus, the distal row has been described as being functionally a single unit.

At the radiocarpal joint, 60% of the load is transmitted across the radio-scaphoid and 40% occurs across the radiolunate contact areas. Load transmission across the midcarpal joint is more evenly distributed across four distinct areas: scapho-trapezio-trapezoid (STT), 23%; scaphocapitate (SC), 28%; capitolunate (CL), 29%; and triquetrohamate (TH), 20%. With malalignment due to carpal instabilities, this loading pattern is altered. Areas of increased loading have been shown to correlate with the development of degenerative changes, supporting the notion that, given time, carpal instabilities eventually lead to degenerative arthritis [6]. Furthermore, different types of partial wrist fusions alter loading in different ways. After STT and SC fusions, load transmission increases significantly across the scaphoid fossa, and the positioning of the fused carpal bones also affects loading, particularly for CL fusion. Therefore, when loading is taken into consideration, excision of the triquetrum when performing a scaphoidectomy and midcarpal fusion may have long-term detrimental effects, with increased radiolunate contact pressures reported by a biomechanical study by 44% [7].

To perform tasks of daily living and various occupations, Palmer studied the range of motion required in 52 tasks and found that 5° of flexion, 30° of extension, 10° of radial deviation, and 15° of ulnar deviation are adequate [8]. In many of these tasks, a common pattern of motion became apparent, which occurred in an oblique plane later termed the "dart-thrower's" motion. In another study, Ryu reported that 60° of extension, 54° of flexion, 40° of ulnar deviation, and 17° of radial deviation are required to complete all tasks, but to perform the essential majority of the tasks, 70% of this range is adequate [9]. Both studies found that extension and ulnar deviation were most important. Thus, partial fusion of the wrist may not severely limit the ability to perform the majority of tasks, particularly if the dart-thrower's motion is still preserved.

106.2 Indications and Contraindications

Limited wrist fusions are mainly indicated in painful, localized arthritis of the wrist, and painful irreducible static deformities. The aim is to abolish pain by terminating the cycle of chronic inflammation and synovitis at arthritic segments by removing damaged cartilage and exposed subchondral bone. Other salvage options include proximal row carpectomy, total wrist fusion, total or interpositional wrist arthroplasty, and wrist denervation. Compared to proximal row carpectomy, also a well-established motion-preserving option, limited wrist arthrodesis may contribute to better grip strength by preserving carpal height and maintaining optimal muscle length. Comparing these two options, two systematic reviews of outcomes in post-traumatic degenerative arthritis [10, 11] reported better grip strength [10, 11] and a lower rate of osteoarthritis [10] for limited wrist arthrodesis, although the complication rate, mainly related to nonunion, is higher.

The prerequisite for limited wrist arthrodesis is an intact articulating surface, congruence, and stability of the remaining motion segments, to ensure a long-lasting effect of the fusion. Etiologies that may give rise to such localized arthritis include idiopathic or genetic predisposition; developmental deformities (carpal coalitions, Madelung deformity), a type II lunate with hamatolunate impingement; inflammatory arthritis, post-traumatic instability, arthritis, skeletal deformity; and avascular necrosis (Kienböck disease). Specific types of limited wrist fusion are suitable for specific conditions: scaphocapitate fusion for Kienböck disease with chondral damage, radiolunate fusion for inflammatory arthritis with localized erosion, and four-corner or capitolunate fusion for post-traumatic midcarpal arthritis. As osteoarthritis is an age-related phenomenon, degenerative arthritis is the most common etiology and falls into predictable patterns of progression and affected sites [12].

The development of scapholunate advanced collapse (SLAC) and scaphoid nonunion advanced collapse (SNAC) occurs in three stages as described by Watson [12] and Vender [13] respectively, with the fourth stage of pancarpal arthritis described later by several authors [14]. The choice of surgery depends on the location of the arthritic and the healthy articulations. In stage 2 and 3 diseases, the "SLAC procedure" proposed by Watson [12], consisting of scaphoidectomy and midcarpal arthrodesis, became an established treatment to provide symptom relief. In this procedure, scaphoidectomy eliminates the arthritic radio-scaphoid interval while midcarpal arthrodesis prevents midcarpal collapse and malalignment, and eliminates the arthritic capitolunate interval thus maintaining motion through the preserved radiolunate articulation.

Surgical decision-making depends on accurate assessment of cartilage condition of the wrist joint, which is best achieved by direct arthroscopic visualization. After an arthroscopic staging procedure, we recommend an arthroscopic approach to limited wrist fusion, which has two major advantages over the conventional open approach. Firstly, soft tissue trauma and devascularization of the fusion site are minimized, which may theoretically decrease the chance of nonunion (up to 33%) [15]. Secondly, obviating the need for an open capsulotomy minimizes capsular fibrosis and ligament contractures, which may theoretically improve range of motion. There may also be less chance of affecting proprioception of the wrist by denervation of the posterior interosseous nerve. In the following parts, the process and surgical steps of an all-arthroscopic limited wrist fusion for SLAC and SNAC wrist, first reported and developed by the senior author [16], are described.

106.3 Surgical Technique

The patient is put in the supine position while the operated arm is supported on a hand table. An arm tourniquet is not usually applied to avoid compressing on the arm and causing venous congestion. A vertical traction of 4–6 kg is applied through plastic finger traps to the middle three fingers for joint distraction via a wrist traction tower. We employ saline irrigation and distension of the joint by a suspended bag of normal saline solution 1–1.5 m above the operating table without the use of an infusion pump.

106.3.1 Staging Arthroscopy

A diagnostic arthroscopy for staging of the arthritis is performed under portal-site local anesthesia [17]. The patient is awake throughout the procedure and is able to appreciate his or her own wrist condition, which facilitates decision-making. After planning of the portal sites, 2% lignocaine with adrenaline in 1:200,000 dilution is injected into the capsule at each of the portal sites for anesthesia and hemostasis.

- Inspection of the radiocarpal joint is done through the 3–4 portal using a 1.9 mm videoscope and an additional portal for instrumentation is established at the 4/5 portal. An 18-G needle is placed at the 6 U portal for outflow of the fluid.

- The midcarpal joint is first visualized through the midcarpal-radial (MCR) portal, and instrumentation is performed at the midcarpal-ulnar (MCU) portal.
- Assessment of cartilage integrity, degree and location of synovitis, and integrity of the interosseous and extrinsic ligaments are performed. The quality of cartilage in all articular surfaces is assessed to establish a precise arthroscopic staging of the disease, to guide definitive management. Chondral lesions are measured by using a probe with known size and are graded according to the depth of involvement. In grade 1, there is softening of the cartilage that is in continuity. In grade 2, there is superficial fissuring. In grade 3, there is deep fissuring reaching down to subchondral bone. In grade 4, subchondral bone is exposed [18].
- In the radiocarpal joint, systematic surveillance is performed, starting from the dorsal rim of the radial styloid for early SLAC changes; this region is assessed by rotating the 30° forward slanting lens downward to reach the area. Synovial proliferation obscuring the rim of the fossae is removed by a motorized shaver (2.0 mm or 2.9 mm) or radiofrequency probe, and the radiolunate interval is assessed carefully. The portals for instrumentation and videoscope may be switched for a better angle of view, and synovectomy at sites of inflamed synovium may provide pain relief. After the radiocarpal joint is inspected, the triangular fibrocartilage complex (TFCC) is inspected for any central or peripheral tears. Central unstable flap tears of the TFCC are debrided to eliminate a potential source of pain especially if partial wrist fusion is to be performed.
- The midcarpal joint is then assessed (Fig. 106.1). The four main articulations (STT, SC, CL, and TH joints) are inspected. The scapholunate and lunotriquetral ligaments are assessed with a 2 mm probe inserted from the MCU portal, and any instability is graded by the Geissler classification [19].

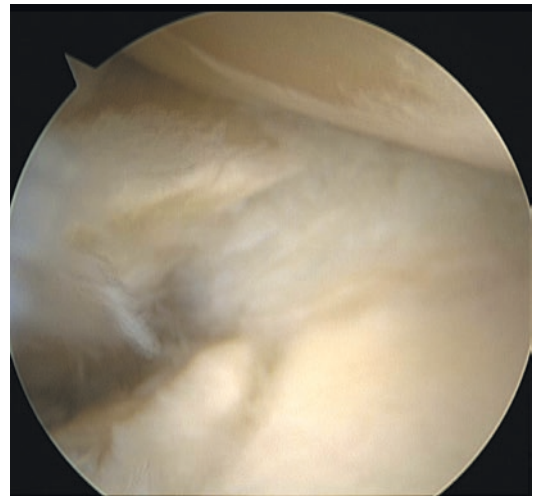

Fig. 106.1 Midcarpal joint assessment showing a SNAC wrist with scaphocapitate arthritis

106.3.2 Arthroscopic Capitolunate (CL) Fusion

Capitolunate (CL) fusion was advocated by Watson [12], although four-corner fusion gained favor as fusion rates seemed more guaranteed with a larger fusion mass. However, using stable fixation with headless compression screws and an arthroscopic approach, CL fusion may achieve similar fusion rates as the conventional open four-corner fusion, and it has become our preferred method [20]. Compared with a four-corner fusion, the lunotriquetral (LT) and triquetrohamate (TH) articulations remain mobile in CL fusion. A cadaveric biomechanical study has shown that the triquetrum rotates 11 degrees more than the lunate in the flexion-extension arc [5]; obliterating this motion can potentially limit motion of the lunate on the radius. However, whether this results in a significantly better clinical outcome remains unknown. CL fusion also takes less time to complete as only one joint surface needs to be prepared, whereas in four-corner fusion there are three (see below). CL fusion also does not usually require bone grafting. Under arthroscopic visualization, a more conservative

subchondral bone resection can be achieved thus decreasing the chance of triquetrohamate impingement. However, any preexisting triquetrohamate arthritis would preclude the use of a CL fusion; a four-corner fusion would then be necessary.

General anesthesia is usually given, but if bone grafting is not anticipated, regional anesthesia could also be used. Bone graft or bone substitutes are not required if the fusion surfaces are congruent and rigid cannulated screws can be used. The iliac crest of either side can be used for bone grafting. An arm tourniquet is applied and inflated only when needed.

106.3.2.1 Scaphoidectomy

The midcarpal portals are first established, The arthroscope is introduced from the MCU portal, and an arthroscopic burr of 2.9 mm is inserted into the MCR portal and directed towards the proximal and mid-scaphoid region. Using the burr at high speed, the scaphoid is resected from the articular surface down to the core cancellous bone. Bone debris is removed by intermittently applied suction. As more space is created, a larger 3.5 mm burr can then be used. To avoid accidental damage to the adjacent articular surfaces, a shell of cartilage can be left intact and the cancellous bone removed from the shell until most of the cancellous bone is removed. This shell can then be removed piecemeal by using a small pituitary rongeur or an arthroscopic punch (Fig. 106.2). The proximal pole and body of the scaphoid are removed distally until the confluence of the SC and STT joints is reached (Fig. 106.3). The distal pole of the scaphoid can be left in situ to preserve the scapho-trapezial ligament which helps to maintain the position of the trapezium and trapezoid. The distal scaphoid tubercle does not articulate with the radial styloid

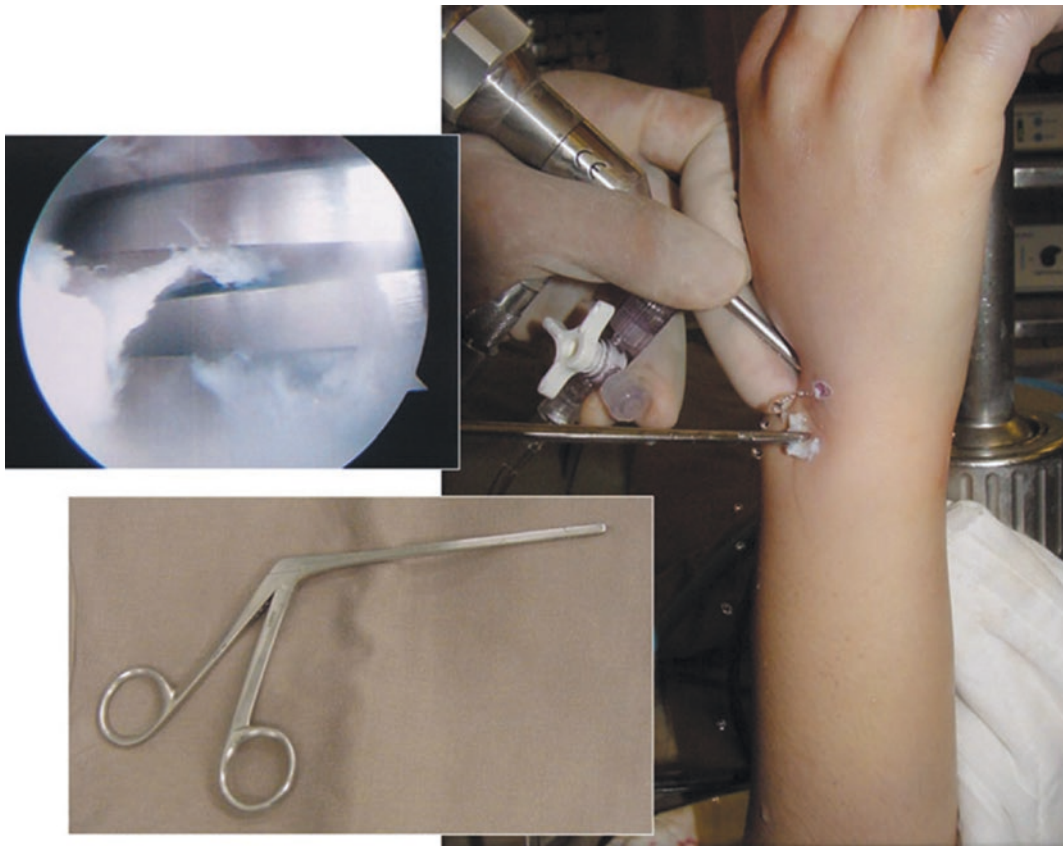

Fig. 106.2 Scaphoidectomy is facilitated by using a pituitary rongeur

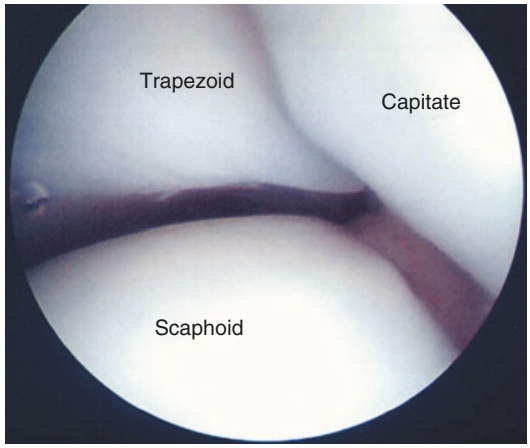

Fig. 106.3 The scaphoid is removed distally until the confluence of the SC and STT joints

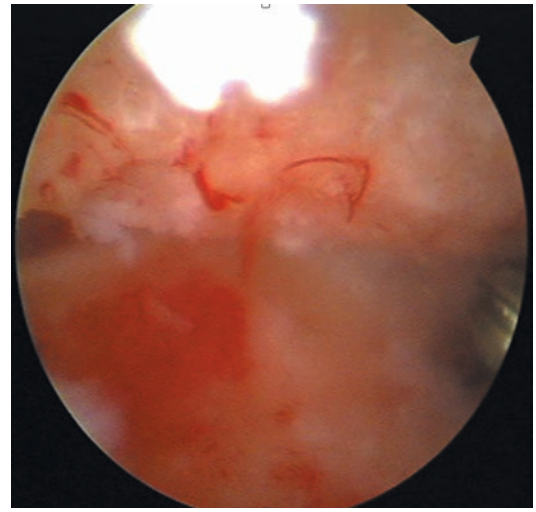

Fig. 106.4 Punctate bleeding from subchondral bone

and will not cause impingement, despite their seemingly close proximity on a PA radiograph.

106.3.2.2 Cartilage Denudation

The articular surfaces of the lunate and capitate are then prepared. We aim to preserve as much of the subchondral bone as possible so as to maintain carpal height. Using a 2.9 mm burr, the cartilage is denuded in a precisely controlled manner in equal thickness to obtain a smooth surface, maintaining the original contour. To achieve a good control of the instrument, it is recommended to adopt a finger-pivoting control technique, i.e., holding the instrument at the far end with the thumb and index finger while the middle finger steadies the instrument against the skin of the wrist dorsum. Once punctate bleeding from subchondral bone is seen (Fig. 106.4), an adequate depth is reached. This observation can be facilitated by performing without inflating the tourniquet. The burr is set at the highest speed of 3000 rpm in a unidirectional mode. Methods to reduce any profuse bleeding from bone that obscures the view include elevating the bag of irrigation normal saline to increase the hydrostatic pressure or using radiofrequency for coagulation. During the burring process, suction is switched on and off intermittently to remove any accumulated bone debris. Continuous suction creates excessive bubbles and bleeding which prevent a clear view. For a type I lunate, the whole distal articulating surface of the lunate should be debrided. For a type II lunate, the small ulnar facet that articulates with the hamate need not be debrided as it will not be involved in the fusion process. If the ulnar facet is sizeable with a significant ridge between the two facets, a three-corner fusion, involving the lunate, capitate, and hamate, may be considered to prevent the development of triquetral-hamate impingement.

106.3.2.3 Correction of Carpal Malalignment

The lunate and capitate are realigned to neutral position to correct the DISI deformity. A neutral fusion angle is necessary to maximize the range of motion, reduce persistent pain from capitate impingement, maintain carpal height, and improve radiolunate load transmission. Since the more common form of the lunate (D-type) is narrower dorsally and wider volarly, fusion in extension would decrease the contact area and increase contact loading. The radiolunate angle is reduced to 0° by wrist flexion and slight ulnar deviation, and a 1.6 mm K-wire is used to transfix the radiolunate joint (Fig. 106.5). The K-wire is introduced percutaneously through a small stab wound over the distal radius slightly proximal to the sigmoid notch level, aiming at the level between the 3/4 and 4/5 portals. Blunt dissection

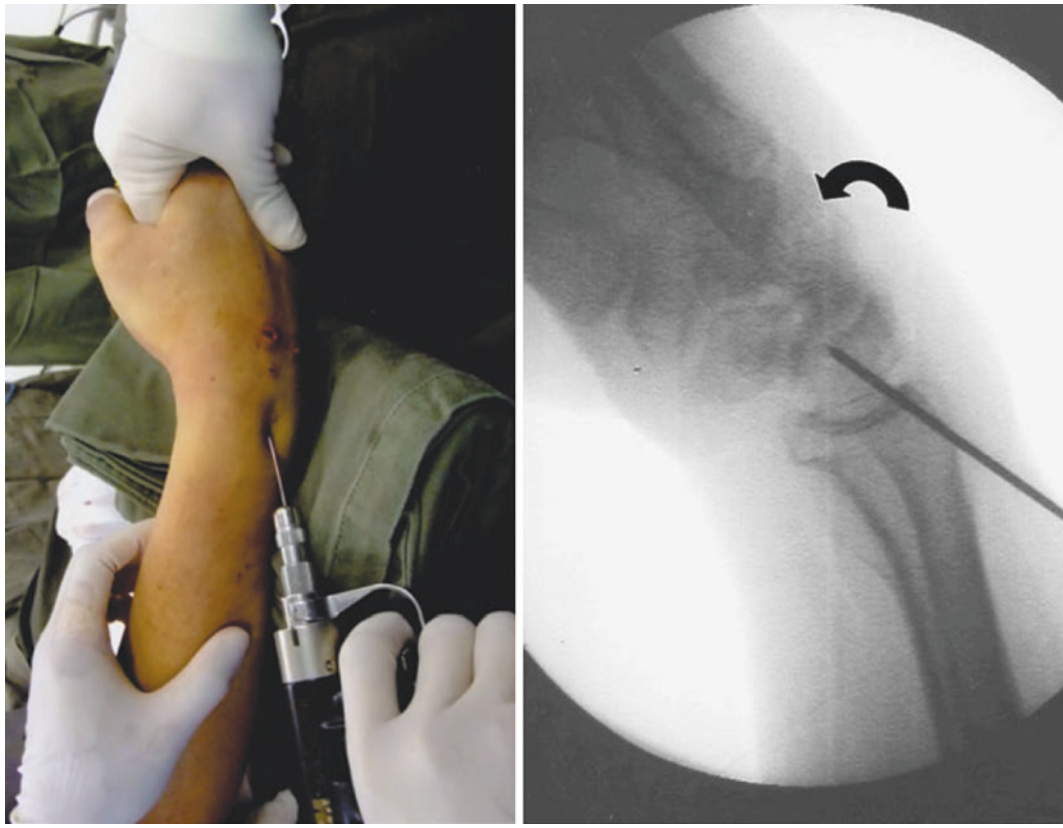

Fig. 106.5 The radiolunate joint is transfixed by K-wire to correct lunate malposition

with a fine hemostat or stitch scissors is first performed to avoid iatrogenic injury to the extensor tendons, and the wire is driven in with an oscillating mode. The alignment is checked by fluoroscopy, ensuring the tip of the K-wire is within the lunate and not protruding into the capitolunate fusion site.

106.3.2.4 Provisional Fixation of the Fusion Interval

A small incision is made over the distal dorsal surface of the capitate at the junction with the radial aspect of the base of the third metacarpal. Blunt dissection is performed to avoid iatrogenic injury to the extensor tendons. A small metal awl is helpful to establish the entry point over the distal dorsal rim of the capitate. A guidewire of a small cannulated screw system (1.1 mm or larger) is inserted and driven across the capitate towards the lunate and parallel to the radial border of capitate, aiming at the central part of the lunate for better bone purchase. If the only available guidewires are smaller than 1.1 mm, a larger-sized K-wire can be used temporarily before exchanging to the guidewire specific to the screw. Before the guidewire is driven across the CL joint, a second one should be placed to the ulnar side of the capitate-third metacarpal joint. The guidewire is driven across the capitate, with an aim to catch the dorsal third of the lunate at the CL junction. The slightly different angle of attack of the two guide pins can avoid overcrowding of the screws. With the two pins on the capitate, the hand is ulnar translated so that the contact between the capitate and lunate is maximized (Fig. 106.6). The pins are then driven into the lunate (Fig. 106.7). As there is usually good articular congruence, bone graft or bone substitutes are usually not required. If bone graft or bone substitutes are to be used, the two pins are backed out

Fig. 106.6 The hand is ulnar translated so that the contact between the capitate and lunate is maximized

from the lunate into the capitate. Bone grafts are cut into small chips and inserted into an arthroscopic cannula introduced into a portal directly over the fusion site. A 4.5 mm cannula which is used for arthroscopic bone grafting of the scaphoid can be used. A slightly undersized, flat-ended trocar is used to push the graft through the cannula into the fusion site. The graft is impacted in the site with the trocar until the void is filled completely. This process is made easier with a reduced flow of irrigation fluid and an inflated tourniquet. After graft insertion, K-wires are advanced again into the lunate while maintaining alignment under fluoroscopy.

106.3.2.5 Definitive Fixation

In elderly patients with osteoporotic bone, K-wires can be used as the definitive fixation device and buried for later removal. Otherwise, two cannulated screws are inserted through the K-wires with or without drilling, depending on the screw system (Fig. 106.8). If a radiolunate K-wire is used to correct lunate hyperextension, it is kept for 2 weeks and removed at follow-up. Finally, passive finger motion is checked to ensure no catching of the extensor tendons by the screw heads. Wounds are closed with Steri-strips (Figs. 106.9 and 106.10) and a bulky dressing with a short-arm plaster slab is applied.

106.3.3 Arthroscopic Four-Corner Fusion

Arthroscopic scaphoidectomy is performed as described for capitolunate fusion. The subsequent steps are described below.

106.3.3.1 Cartilage Denudation

The articular surfaces between the capitate, lunate, triquetrum, and hamate are denuded of cartilage with a 2.9 mm burr. In addition, the joint surface of the lunotriquetral interval is also denuded. Only the proximal few millimeters of the articulation between the hamate and capitate is burred, as there is minimal motion in this joint. In debriding the carpal interval of the same carpal row, such as lunotriquetral or capitohamate interval, a smaller burr such as a 2 mm sized should be used to cater for the narrower joint space.

106.3.3.2 Correction of Carpal Malalignment

As described above, malalignment of the lunate is first corrected. If there is significant ulnar translocation and extension deformity of the lunate, the lunate is reduced by gentle flexion and radial translation of the wrist until at least half of the radial aspect of the lunate is located over the distal radius. A percutaneous 1.6 mm K-wire is then inserted from the distal radius to transfix the radiolunate joint.

106.3.3.3 Fixation of the Fusion Interval

The capitate is then aligned over the lunate by ulnar translation of the hand to maximize bone

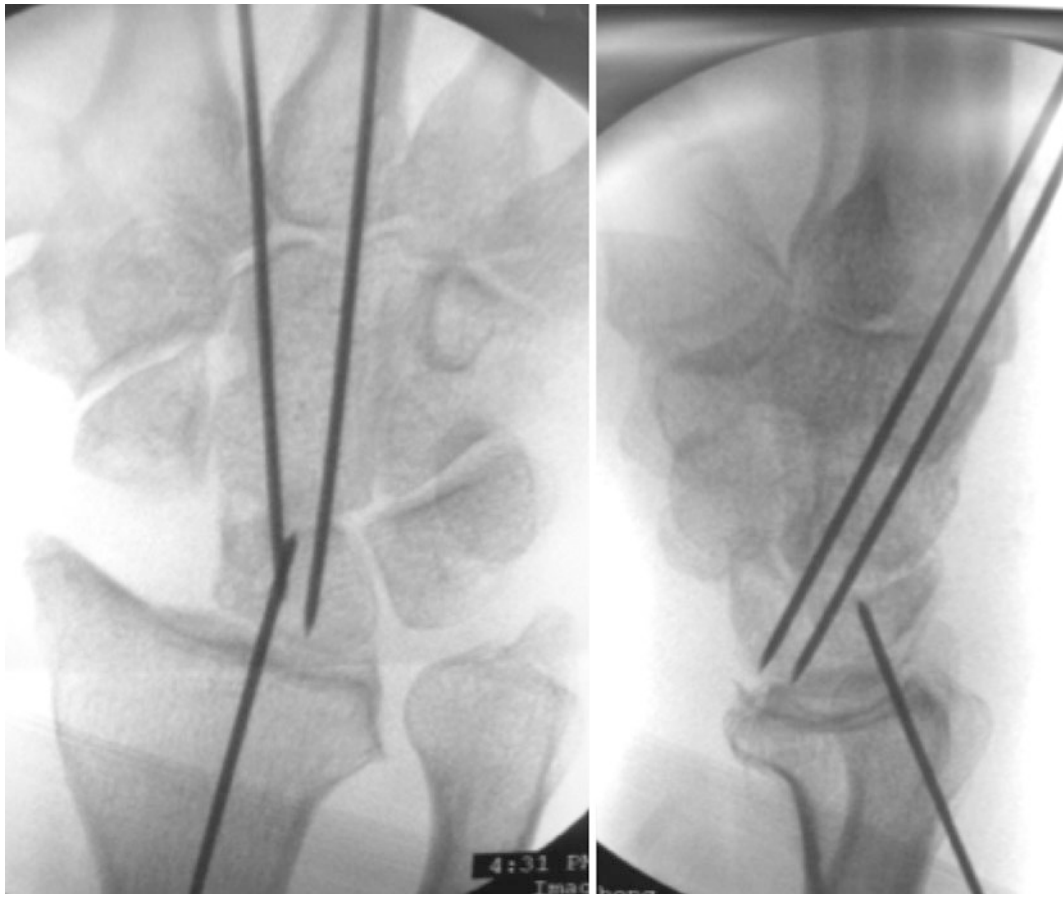

Fig. 106.7 Capitolunate joint is transfixed with K-wires

contact with the lunate. In this position, fixation under fluoroscopy using one K-wire from the dorsal-central surface of the capitate at the distal junction with the base of the third metacarpal, at an acute angle and aiming towards the central part of the lunate. As described above, bone grafting and K-wire repositioning are performed as necessary. A cannulated screw is then inserted through the K-wire. The lunotriquetral joint, and capitohamate joint or triquetro-capitate interval are then fixed with percutaneous K-wires, followed by cannulated screws through small stab incisions (Fig. 106.11). Blunt dissection is performed to reduce the chance of injuring the dorsal branches of the ulnar nerve, EDM, and ECU tendons.

After solid fixation of the four carpal bones, the K-wire transfixing the radiolunate joint, if used, can be left in situ for 2 weeks. Wounds are approximated with steri-strips and a bulky dressing followed by a short-arm plaster slab is applied.

106.4 Tips and Tricks

- The process of scaphoidectomy can be expedited by first removing the cancellous bone by burr, and then removing the "shell" piecemeal by pituitary rongeur.
- In preparing the fusion site, uniform excision of cartilage and subchondral bone maximizes contact area for fusion and reduces the need for bone graft or bone substitutes.
- Removing a minimal depth of subchondral bone just until healthy bleeding can be ensured

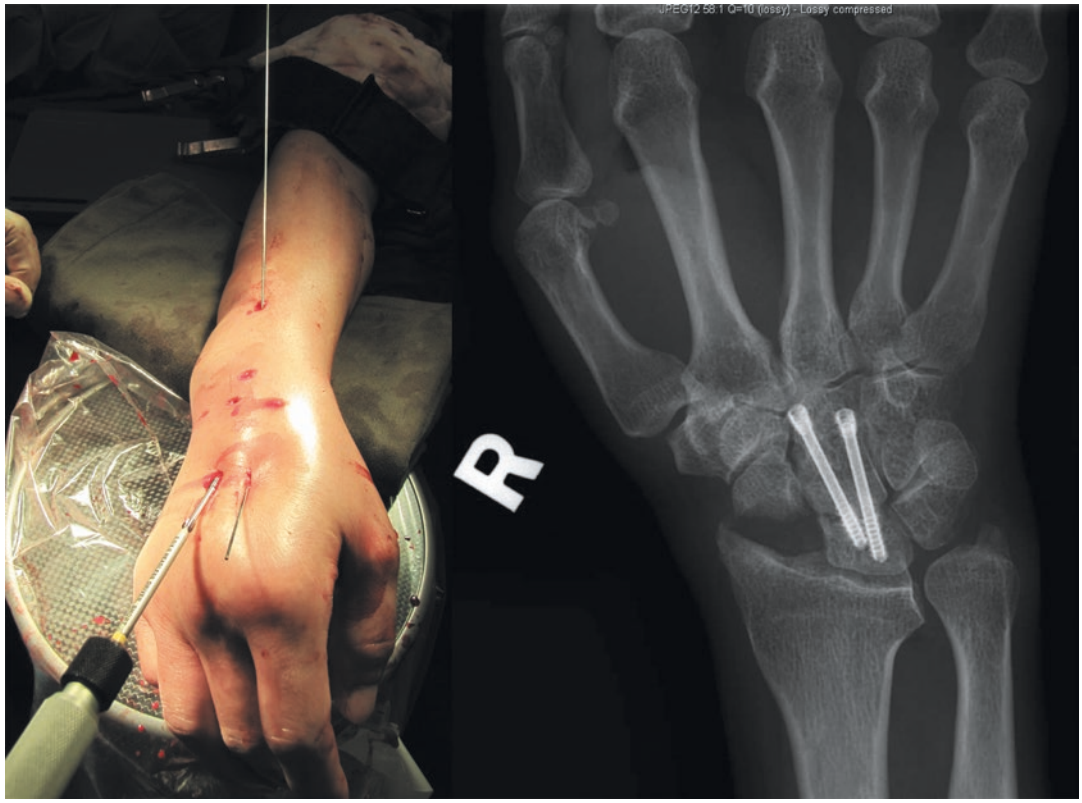

Fig. 106.8 Cannulated screws are used for definitive fixation

by releasing the tourniquet for observation, and a finger-pivoting technique for fine control of the burr.
- Ulnar translation of the capitate on the lunate increases contact area of the fusion site.
- Insertion of screws from distal to proximal is preferred, to minimize damage to the remaining articular surface of the lunate.
- Choosing a cannulated screw system with a short threaded segment ensures that all the threads will pass into the lunate to achieve compression and avoid distraction of the fusion site.

106.5 Pitfalls

- Careful assessment of the cartilage condition of the carpal joint, especially the radiolunate articulation if midcarpal fusion is considered, is needed before deciding for definitive motion-preserving surgery.
- Over-resection of subchondral bone increases the chance of triquetral-hamate and lunatohamate impingement and arthrosis in a type II lunate.
- Fusion in malalignment of the capitate and lunate may increase contact loading in the radiolunate joint and reduce range of motion.
- Blunt dissection is required to prevent inadvertent injury to the extensor tendons during drilling and screw insertion.

106.6 Postoperative Management and Rehabilitation

As swelling begins to subside, the slab is changed to a removable wrist splint after the first week. Active mobilization of the wrist is allowed out of

Fig. 106.9 Wounds at the end of surgery, which are then closed with Steri-strips

splint under the supervision of a hand therapist. Passive wrist mobilization and strengthening exercise can be offered when bone healing is seen on radiographs, usually 10–12 weeks after surgery.

106.7 Complications

Potential complications include nonunion, hardware-related problems such as dorsal impingement and intra-articular protrusion of implants, osteoarthritis of the remaining motion segment, persistent pain, and conversion to total wrist fusion.

106.8 Results

In the author's series between 2000 and 2013, ten wrists in nine patients with SLAC or SNAC were treated with arthroscopic four-corner or capitolunate fusion. There were three SLAC II, three SLAC III, and four SNAC III wrists. Five four-corner and five capitolunate fusions were performed. The mean age was 61 years (range, 45–75 years). At a mean follow-up period of 8.8 years (range 1.2–17 years) the mean preoperative pain score was 6.7 out of 20 (range 1–16) which decreased to 2 out of 20 postoperatively (range 0–8), which was significant (p = 0.02). Grip strength was 20.2 kg before surgery (range 2.5 kg–35 kg) and 20.1 kg after surgery (range 4 kg–31 kg) which were similar (p = 0.79). Mean flexion-extension arc was 87.4° (range 23–130°) before surgery and decreased to 68.7° after surgery (range 24–105°) (p = 0.20), which was 87% of the preoperative range. Mean radial-ulnar deviation decreased from 38.6° to 34.4° with no significant difference (p = 0.50). The functional score based on the ten ADL tasks increased from 32 out of 40 preoperatively to 38 postoperatively (p = 0.02). All wrists fused by four-corner fusion resulted in union (Fig. 106.11), while one wrist with capitolunate fusion failed to achieve union. Overall, 9 out of 10 wrists achieved union (90%) (Fig. 106.10). The patient who did not achieve fusion remained pain-free, no intervention was required at 7 years' follow-up. One patient with four-corner fusion had persistent pain despite bony union and required neurectomy and subsequently total wrist fusion at 14 months after surgery.

Fig. 106.10 Radiograph at 4 years follow-up showing solid fusion

Fig. 106.11 (From upper left, anti-clockwise) A patient with SLAC wrist, with four-corner fusion performed by screw fixation at the capitolunate joint, lunotriquetral joint, and triquetro-capitate interval. At 73 months after surgery, radiographs showed solid fusion, and faint scars remain from the arthroscopic portals and percutaneous screw insertions

References

1. Seradge H, Owens W, Seradge E. The effect of intercarpal joint motion on wrist motion: are there key joints? An in vitro study. Orthopedics. 1995;18(8):727–32.
2. Weber ER. Concepts governing the rotational shift of the intercalated segment of the carpus. Orthop Clin North Am. 1984;15(2):193–207.
3. Viegas SF, Patterson RM, Hokanson JA, Davis J. Wrist anatomy: incidence, distribution, and correlation of anatomic variations, tears, and arthrosis. J Hand Surg Am. 1993;18(3):463–75.
4. Haase SC, Berger RA, Shin AY. Association between lunate morphology and carpal collapse patterns in scaphoid nonunions. J Hand Surg Am. 2007;32(7):1009–12.
5. Ruby LK, Conney WP III, An KN, Linscheid RL, Chao EYS. Relative motion of selected carpal bones: a kinematic analysis of the normal wrist. J Hand Surg Am. 1988;13(1):1–10.
6. Patterson R, Viegas SF. Biomechanics of the wrist. J Hand Ther. 1995;8(2):97–105.
7. Scobercea RG, Budoff JE, Hipp JA. Biomechanical effect of triquetral and scaphoid excision on simulated midcarpal arthrodesis in cadavers. J Hand Surg Am. 2009;34(3):381–6.
8. Palmer AK, Werner FW, Murphy D, Glisson R. Functional wrist motion: a biomechanical study. J Hand Surg. 1985;10(1):39–46.
9. Ryu J, Cooney WP III, Askew LJ, An KN, Chao EY. Functional ranges of motion of the wrist joint. J Hand Surg Am. 1991;16(3):409–19.
10. Mulford JS, Ceulemans LJ, Nam D, Axelrod TS. Proximal row carpectomy vs four corner fusion for scapholunate (Slac) or scaphoid nonunion advanced collapse (Snac) wrists: a systematic review of outcomes. J Hand Surg. 2009;34(2):256–63.
11. Saltzman BM, Frank JM, Slikker W, Fernandez JJ, Cohen MS, Wysocki RW. Clinical outcomes of proximal row carpectomy versus four-corner arthrodesis for post-traumatic wrist arthropathy: a systematic review. J Hand Surg. 2015;40(5):450–7.
12. Watson HK, Ballet FL. The SLAC wrist: scapholunate advanced collapse pattern of degenerative arthritis. J Hand Surg Am. 1984;9(3):358–65.
13. Vender MI, Watson HK, Wiener BD, Black DM. Degenerative change in symptomatic scaphoid nonunion. J Hand Surg. 1987;12(4):514–9.
14. McLean A, Taylor F. Classifications in brief: Watson and Ballet classification of scapholunate advanced collapse wrist arthritis. Clin Orthop Relat Res. 2019;477(3):663.
15. Kirschenbaum D, Schneider LH, Kirkpatrick WH, Adams DC, Cody RP. Scaphoid excision and capitolunate arthrodesis for radioscaphoid arthritis. J Hand Surg Am. 1993;18(5):780–5.
16. Ho PC. Arthroscopic partial wrist fusion. Tech Hand Up Extrem Surg. 2008;12(4):242–65.
17. Ong MT, Ho PC, Wong CW, Cheng SH, Tse WL. Wrist arthroscopy under portal site local anesthesia (PSLA) without tourniquet. J Wrist Surg. 2012;1(02):149–52.
18. Dougados M, Ayral X, Listrat V, Gueguen A, Bahuaud J, Beaufils P, et al. The SFA system for assessing articular cartilage lesions at arthroscopy of the knee. Arthroscopy. 1994;10(1):69–77.
19. Geissler WB. Arthroscopic management of scapholunate instability. J Wrist Surg. 2013;2(02):129–35.
20. Slade JF III, Bomback DA. Percutaneous capitolunate arthrodesis using arthroscopic or limited approach. Atlas Hand Clin. 2003;8:149–62.

107 Arthroscopic Transplantation of Osteochondral Autograft for Treatment of Cartilage Defects in the Wrist

Pak-cheong Ho

107.1 Background

Cartilage injury of the wrist is common after trauma, such as distal radius and scaphoid fracture [1–3]. The wider use of wrist arthroscopy enables the surgeon to establish a more accurate and accessible diagnosis. Isolated focal chondral damage can lead to persistent synovitis, chronic wrist pain, and secondary osteoarthritis. Restoration of the normal hyaline cartilage is the goal of treatment to relieve pain, to restore function, and to halt the progression of arthritis especially in young symptomatic patients. For small chondral defects of less than 5 mm, arthroscopic drill chondroplasty is an effective treatment [4]. For the larger lesion, osteochondral graft transplant provides a viable solution to this difficult problem.

107.1.1 Surgical Anatomy

Focal chondral lesion of the wrist may result from osteochondral fractures, chronic carpal instability, chondromatosis, or it may occur idiopathically [5]. Araf noted an incidence of 33% articular cartilage injury larger than 3 mm in 30 patients of age between 20 and 50 years old with distal radius fracture of group B and C according to AO/ASIF classification [3]. Cheng in reviewing the surgical treatment on 22 patients with chronic pain post distal radius fracture treatment noted a high incidence of 63.6% of chondral lesions responsible for the pain. Fifty percent of them occurred at the distal radius side either on the scaphoid or lunate fossa [4].

At arthroscopy of the radiocarpal joint, the lesions are often covered by the accompanying localized reactive synovitis, typically over the capsule just dorsal to the lunate fossa or less commonly at the scaphoid fossa (Fig. 107.1). Occasionally the lesions may be situated over the volar or central aspect of the fossae. There may be associated scapholunate ligament or extrinsic radiocarpal ligament injury of varying degrees. A kissing lesion over the corresponding carpal bone may be found. Chondral lesion per se is not painful as there is limited innervation at the cartilage and the subchondral plate [6]. It is usually the florid synovitis that directly contributes to the localized tenderness and pain upon dorsiflexion loading of the wrist. This explains why not all the chondral lesions will produce pain, as stable lesions will not induce synovitis formation. Removing the synovitis not only reveals the underlying chondral lesion but also produces quick pain alleviation (Fig. 107.2). However, clearing the synovitis alone without fixing an unstable chondral lesion will invite recurrence of

P.-c. Ho (✉)
Department of Orthopaedic and Traumatology, Prince of Wales Hospital, Chinese University of Hong Kong, Shatin, Hong Kong
e-mail: pcho@cuhk.edu.hk

© ISAKOS 2022

D. N. Bhatia et al. (eds.), *Arthroscopy and Endoscopy of the Elbow, Wrist and Hand*,
https://doi.org/10.1007/978-3-030-79423-1_107

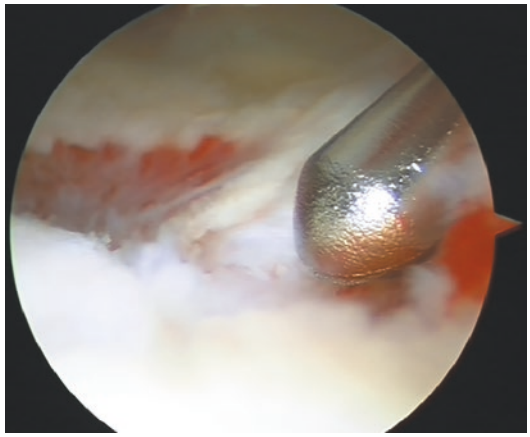

Fig. 107.1 The osteochondral lesion often covered by localized synovitis

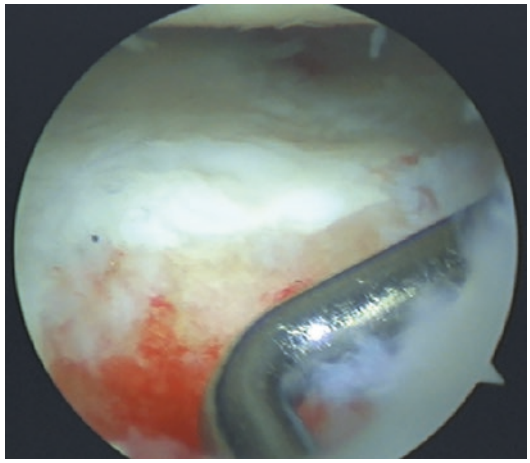

Fig. 107.2 Bleeding from the subchondral bone when the osteochondral lesion is well delineated

pain and disability, especially in patients with high functional demand.

After adequate synovectomy, the size, number, and severity of the chondral lesions should be assessed. The defect can be defined as a contained one if the dorsal cortex of the distal radius is intact, or an uncontained one if it is disrupted. The latter should better be treated with cortical osteochondral grafting [7–9]. Culp et al. have modified the Outerbridge classification for chondral lesion in the wrist as Grade I represents softening of hyaline cartilage, Grade II consists of fibrillation and fissuring, Grade III represents a fibrillated lesion of varying depth in the articular surface, and Grade IV has a full-thickness defect down to bone [10]. It has been recommended to perform debridement and synovectomy for grade I–III lesions. Grade IV lesions can be treated with abrasion chondroplasty and subchondral drilling. Poehling and Roth noted improvement in 83% of patients treated with debridement alone [11]. Whipple reported significant relief of symptom by abrasion chondroplasty if the defect is smaller than 5 mm in size [4]. Larger contained chondral lesions in the wrist can be treated with arthroscopic osteochondral grafting.

107.2 Indications and Contraindications

The technique is best indicated for patients with isolated painful post-traumatic osteochondral lesion of size >5 mm in the lunate or scaphoid fossa, who has failed previous synovectomy and drill chondroplasty treatment. The patients typically have a history of fall on outstretched hand, with or without distal radius fracture. The patient should demonstrate localized clinical tenderness at the dorsal radiolunate joint and persistent pain upon dorsiflexion loading of the wrist. Less commonly the pain may be localized to the radioscaphoid fossa. A diagnostic arthroscopy may confirm an isolated osteochondral lesion without significant kissing lesion over lunate side. Localized injection with small amount of lignocaine to the painful spot may differentiate the pain from other pathology. The patient should have a reasonably good range of motion of the affected wrist especially in flexion range, as arthroscopic implantation of osteochondral graft is technically difficult, risky, and sometime impossible in a stiff joint. The patient should have normal knee function and should be willing to accept some knee pain of up to 6 months post surgery.

Contraindications include multiple osteochondral lesions or intra-articular malunion, significant kissing lesions of the carpal side, major extra-articular malalignment, inflammatory and metabolic arthritis, arthritis secondary to carpal instability or carpal nonunion, stiff wrist, and evi-

dence of preexisting infection. Defect on the volar aspect of the distal radius cannot be accessed with this technique. The operation is not for surgeon inexperience in wrist arthroscopy. Other treatment alternatives need to be considered, such as wrist denervation, radiolunate fusion, and open cortico-osteochondral grafting.

107.3 Surgical Technique

We performed diagnostic arthroscopy under portal site local anesthesia in all patients prior to the index procedures to evaluate the cause of the chronic wrist pain, to confirm the location and extent of the osteochondral lesions, as well as doing preliminary treatment including synovectomy and drill chondroplasty [12]. The aim of drill chondroplasty is to excise the damaged cartilage associated with unstable flaps or debris, to render the rim of the chondral defect stable and to encourage fibrocartilage formation to cover the exposed subchondral bone. Typically motorized shaver or burr is employed. Fine K-wire of 0.9 or 1.1 mm diameter is used to drill multiple times through the subchondral bone over the base of the defect to encourage the emigration of mesenchymal cell for the formation of fibrocartilage. During the insertion of K-wire, iatrogenic injury to extra-capsular structures can be minimized by threading the K-wire with a metallic sheath of a 14G angiocatheter. Patients who fail simple arthroscopic treatment after 4–6 months are appropriate candidates for osteochondral grafting.

The osteochondral graft transplantation operation is performed under general anesthesia. The patient is positioned supine and the affected upper limb is abducted at shoulder level and supported on a hand table. A Wrist Traction Tower (ConMed Linvatec Corp., Goleta, CA) is employed to provide an adjustable and gauged traction force. The tower can be completely sterilized and allows flexible positioning of the wrist intra-operatively in varying degrees of extension, flexion, radial, and ulnar deviation (Fig. 107.3). The limb is draped up to the axilla level and the lower arm is wrapped to the basal plate of the traction tower close to the elbow level. A tourniquet is applied loosely to the upper arm but is inflated only when necessary. Three plastic finger traps are used for the index, middle, and ring fingers for a more even distribution of the traction force. The arm and forearm of the patient is well padded and connected to the traction tower. Traction force of 10–12 pounds usually suffices.

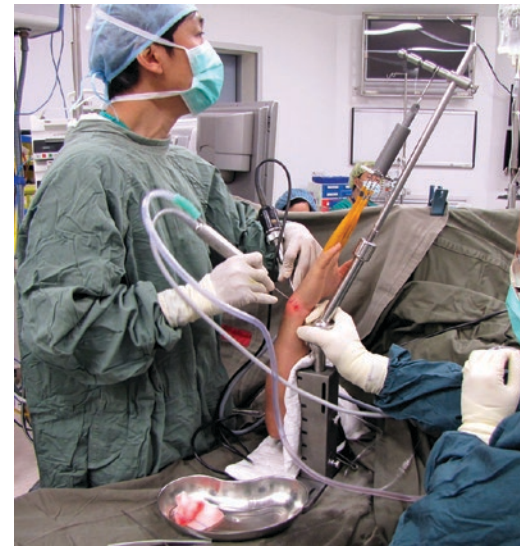

Fig. 107.3 The traction tower allows joint manipulation with the wrist in flexed position under traction to maintain the working space

- Under traction, the various standard portals for arthroscopy are marked on the skin through thumb tip palpation. At the radiocarpal joint, 3–4 and 4–5 portals are used for viewing and instrumentation while the outflow is maintained at the 6-U portal using an 18G needle. For the routine midcarpal joint arthroscopy to rule out midcarpal joint pathology and to evaluate carpal stability, MCR and MCU portals are used. The surgeon can inject 2% lignocaine with 1:200,000 adrenaline through a 25G needle into the various standard portals, starting from joint capsule first and then withdrawn slowly to reach the subcutaneous layer and skin. Intra-articular infiltration is not necessary and each portal site receives 1–2 mL of the solution. The anesthetic mixture provides effective local hemostasis in the joint capsule

and synovium, and therefore largely obviates the routine use of tourniquet during most parts of the procedure.

- The radiocarpal joint is then distended by injecting 3–5 mL of saline at the 3–4 portal. Skin incision is performed using a 15 T surgical blade. We prefer a transverse incision along the skin crease to longitudinal one for better scar healing and cosmetic appearance. To avoid injuries to the underlying important cutaneous nerve and tendinous structures, we recommend to stretch and stabilize the skin with the surgeon's left thumb and index finger (Fig. 107.4), while making the incision with the right hand using a 15 T scalpel only onto the skin, followed by gentle soft tissue spreading using a fine curved mosquito hemostat to dilate the portal and spread out the underlying structures. Egress of saline fluid is noted when the capsule is perforated, confirming the intra-articular location. An arthroscopic cannula with blunt or tapered end trocar is inserted gently through the portal. The trocar is removed and the arthroscope is inserted into the joint through the cannula. The cannula is then connected by long tubing to a 3-L saline bag hanged at 1.5 m above the patient using a drip post or similar device. Continuous saline irrigation with aid of gravity is provided for maintaining a clear arthroscopic view. Infusion pump is not used as this may produce fluid extravasation and compartment syndrome.
- We perform a routine inspection of radiocarpal joint with a 1.9 mm or 2.7 mm arthroscope introduced through the 3–4 portal. The synovitis around the dorsal rim of the lunate fossa is debrided with a 2.0 mm shaver, followed by a radiofrequency mini-probe inserted from the 4–5 portal. This will uncover the underlying osteochondral lesion. The cartilage debris is cleaned until the subchondral bone is reached. The true extent of the lesion is determined using a 2 mm hook probe for measurement. The proximal side of the articular surface of the lunate

Fig. 107.4 The surgeon stretches the skin with the thumb and index finger while making a transverse incision on the skin alone with the scalpel

should be evaluated. A well-developed kissing chondral lesion may preclude the choice of osteochondral graft as a treatment option.

- The arthroscope is then switched to the 4–5 portal. We employ the Osteoarticular Transfer System (OATS; Arthrex, Naples, FL) (Fig. 107.5) to carry out the harvest and transfer process. The 3–4 portal is gently dilated with a small hemostat. Depending on the size of the defect, a 4.75 mm or 6 mm recipient harvester with an obturator from the OATS is inserted into the joint, with extreme care to avoid damage to the healthy cartilage. The harvester is directed towards the osteochondral lesion at the dorsal aspect of the lunate fossa. At this junction, the traction force is reduced and the wrist is passively flexed to about 50° while it is still maintained by digital traction. This maneuver moves the dorsal horn of the lunate palmarward and opens up the space between the lunate and the lunate fossa to accommodate the harvester. With the harvester positioned vertically and as perpendicular as possible to the articular surface of the lunate fossa just over the osteochondral lesion, the harvester is manually impacted to drive the trephine into the bone to a depth of about 10–12 mm (Fig. 107.6), which can be seen through observing the gauge of the trephine

Fig. 107.5 The Osteoarticular Transfer System(OATS) with the harvester trephines

Fig. 107.6 The wrist is flexed to allow easy passage of the trephine at the 3–4 portal. The arthroscope is placed at 4–5 portal to monitor the process. With the harvester positioned vertically and perpendicular to the articular surface of the lunate fossa just over the osteochondral lesion; the harvester is manually impacted to drive the trephine into the bone

(Fig. 107.7). The tendency to direct the harvester dorsally and obliquely should be avoided in order to prevent the iatrogenic blowout fracture of the dorsal rim of the distal radius. At least 2 mm intact articular margin should be maintained dorsally. By removing the harvester, the cylindrical plug of bone containing the osteochondral defect is removed from the joint.

- The osteochondral graft is harvested from the knee of the nondominant leg according to the technique described by Hangody et al. [13]. A tourniquet is applied to the thigh. A small incision is made over the lateral aspect of the knee at the lateral femoral condyle. A 4.75 mm or 6 mm donor harvester is inserted into the sulcus terminalis of the lateral femoral condyle to a depth slightly deeper than that in the wrist (Fig. 107.8). The osteochondral plug is removed and delivered to the wrist. The plug can be trimmed with a scalpel to the precise desirable length (Fig. 107.9). The defect in the knee can be refilled partially by packing in the cancellous bone obtained from the recipient site (Fig. 107.10).
- A short transparent plastic delivery tube is attached to the tip of the donor harvester containing the osteochondral plug. It is then gently inserted into the defect through the 3–4 portal with the aid of a rotating dial (Fig. 107.11). Graft insertion can be monitored through the plastic sheath (Fig. 107.12). The harvester is removed when the graft is flushed with the surrounding articular surface. A plastic tam can be used to tap the plug so as to obtain the best press-fit effect. When there is a mismatch noted at the junction of the articular cartilage, the redundant cartilage can be excised using an arthroscopic banana knife. As the articular cartilage of the knee is generally thicker than that of the wrist, this shaving maneuver will not cause significant loss of the hyaline cartilage. The graft is generally very stable after press fitting so no internal fixation is required. The stability of the graft and the smoothness of articulation can be tested by passively moving the wrist.
- Occasionally the defect may extend to the more central part of the lunate fossa. Under this situation, two osteochondral plugs can be transplanted to the lunate fossa (Fig. 107.13). Dorsal defect can be reached more easily from the 3–4 portal (Fig. 107.14), while the more central defect can be reached through the 4–5 portal (Fig. 107.15). Two grafts can be harvested and inserted sequentially to fill up the defect as far as possible. The cartilaginous surface of the grafts is then shaped and rounded off by an arthroscopic knife (Figs. 107.16 and 107.17).
- The harvester is removed and the wound is closed by steri-strips, followed by bulky compressive dressing. No stitch is required (Fig. 107.18).

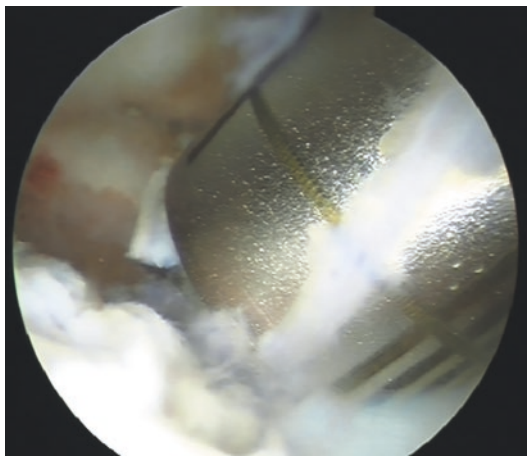

Fig. 107.7 Arthroscopic view of the trephine over the osteochondral defect at the dorsal lunate fossa

107.4 Case Illustration

A 24-year-old female professional dancer developed right dorsal central wrist pain after manual activities 16 months before. X-ray showed no abnormality. Diagnostic arthroscopy revealed a 6 × 4 mm osteochondral defect over the dorsal lunate fossa, Outerbridge grade 1–2 chondral lesion over dorsal ulnar lunate and minor tear of the scapholunate ligament (Fig. 107.19). The grip power was 22 Kgf or 75.3% of the unaffected side. The combined extension/flexion range of the wrist was 150°. In July 2008, arthroscopic

Fig. 107.8 6 mm OATS harvester is inserted into the lateral femoral condyle to harvest the osteochondral graft

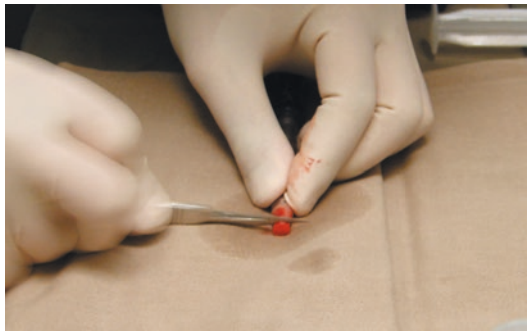

Fig. 107.9 The osteochondral plug can be trimmed on table to the precise length required

Fig. 107.10 The defect in the donor knee

transplant of an osteochondral autograft of 6 mm diameter and 12 mm long harvested from the left knee lateral femoral condyle was performed to repair the osteochondral defect (Fig. 107.20). Post-operation she was allowed to assume immediate full range of motion exercise for her right wrist. CT scan and MRI of her right wrist at 3 months and 6 months post-operation respectively revealed good incorporation of the graft (Fig. 107.21). A second look arthroscopy at 7 months revealed stable osteochondral graft with preserved hyaline cartilage. Biopsy of the grafted area demonstrated normal hyaline cartilage. There was a narrow rim of cartilage defect of less than 1 mm at the junction. She developed

Fig. 107.11 The 6 mm OATS harvester with the osteochondral graft on is inserted into the wrist joint through the 3–4 portal. The graft is delivered into the defect with a dialed pusher

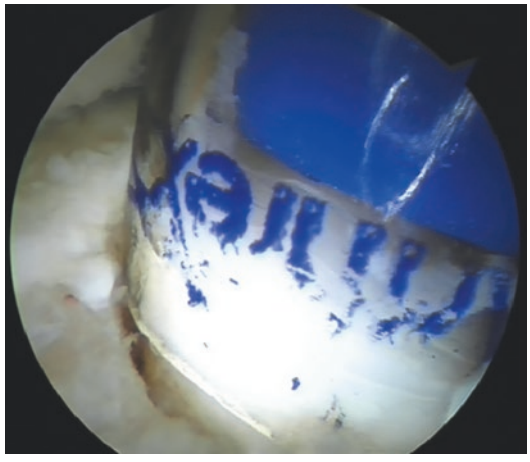

Fig. 107.12 Arthroscopic view of the osteochondral graft delivered into the defect through a transparent plastic tube

Fig. 107.13 Two osteochondral plugs, each of 6 × 12 mm in size harvested from the left knee

a second problem of symptomatic pisotriquetral instability in June 2010 on the same wrist which eventually required a pisotriquetral fusion procedure. Another arthroscopic evaluation at 29 months post-op showed a completely incorporated hyaline cartilage with minimal junctional change (Fig. 107.22). At 10 years 4 months postoperative follow-up, she had no pain or tenderness in the dorsal central wrist and the left knee. Wrist examination did not reveal any joint crepi-

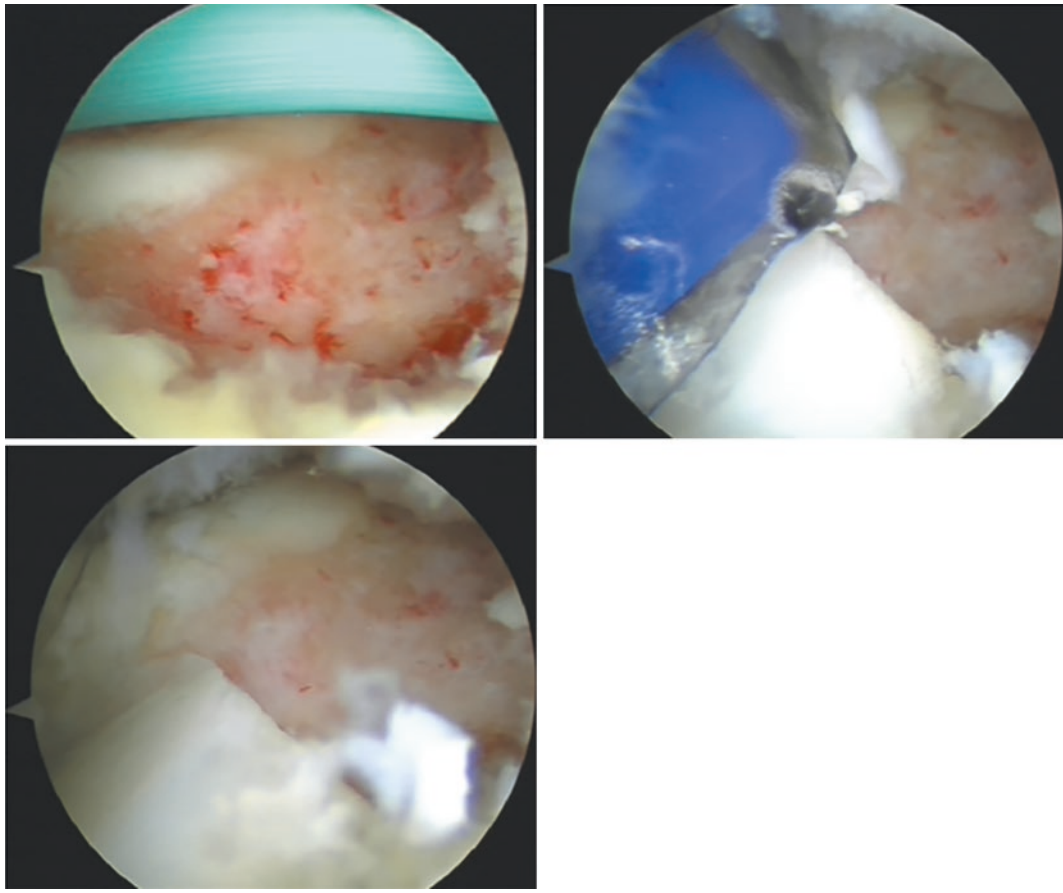

Fig. 107.14 Arthroscopic view of the osteochondral graft being delivered through the 3–4 portal to the dorsal part of the lunate fossa

tus or pain at the extreme of flexion and extension. Grip power was 21 Kgf or 87.5% of the unaffected side. The combined extension/flexion range of the wrist was 160° (Fig. 107.23). X-ray showed no arthrosis (Fig. 107.24). Surgical scar was inconspicuous (Fig. 107.25).

107.5 Tips and Tricks

- Surgeon operating in standing position rather than sitting helps to relax the shoulder and avoid fatigue.
- Transverse portal incisions heal better than longitudinal incisions.
- No stab wound should be made on the portal. Just incise the skin and adopt wound-spreading technique for portal creation using fine curved hemostat forceps. This is especially important before inserting the relatively sizable graft harvester in order to avoid injury to the extensor tendons and the cutaneous nerve.
- Use finger-pivoting technique to control the fine movement of the small arthroscope within the joint, i.e., instead of holding the arthroscope at the proximal end over the camera, the surgeon should hold the distal end of the arthroscope with his/her thumb and index finger, with the camera resting on the first web space area, and using the middle finger to firmly anchor onto the skin around the portal site at the back of the wrist as the pivot point to fine control the lens motion inside the joint (Fig. 107.26).
- When moving the arthroscope inside the joint, use screwing action rather than straight in and

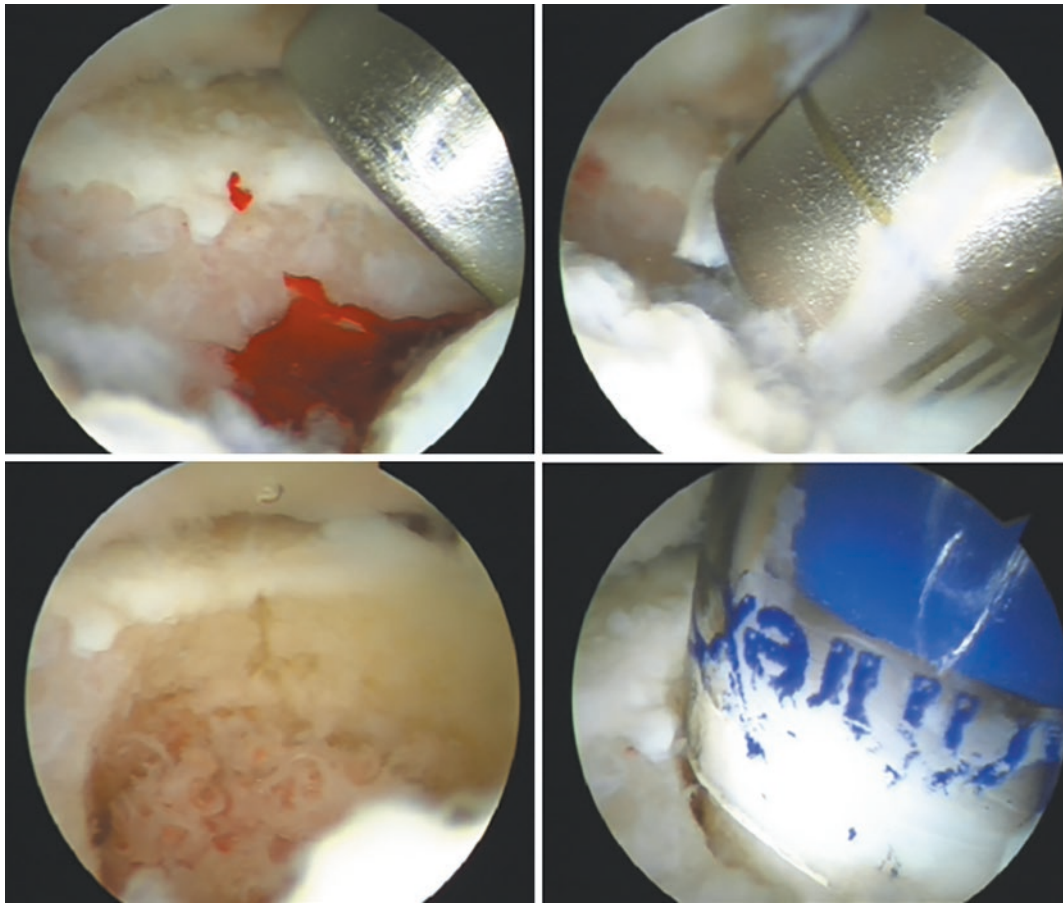

Fig. 107.15 Arthroscopic view showing sequence of the resection of the osteochondral defect and delivery of the osteochondral graft through the 4–5 portal to the central part of the lunate fossa

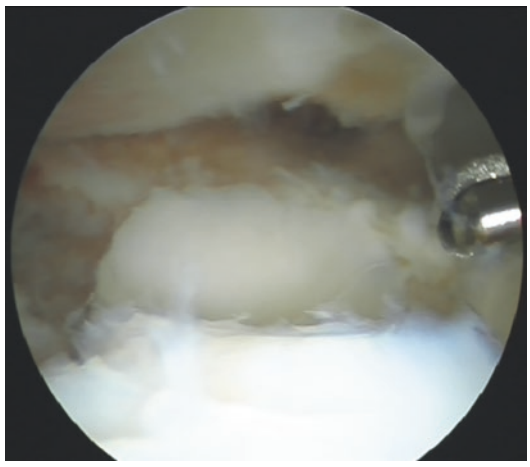

Fig. 107.16 The final appearance of the two grafts in place

out action to avoid frequent dropping of the scope out of the shallow joint.

- When using suction device, block the outflow channel to reduce air bubble forming.
- When using radiofrequency probe, insert into the joint through an arthroscopic sheath to allow bubble release and venting of the heated up saline.
- Flex the wrist to 50° or more while in traction to allow perpendicular orientation of the bone trephine.
- To achieve a more perpendicular orientation of the graft insertion, the surgeon may stand on a stool to facilitate the action (Fig. 107.27).
- Insert trephine from 3–4 portal for dorsal lesion; for more central lesion, use 4–5 portal.

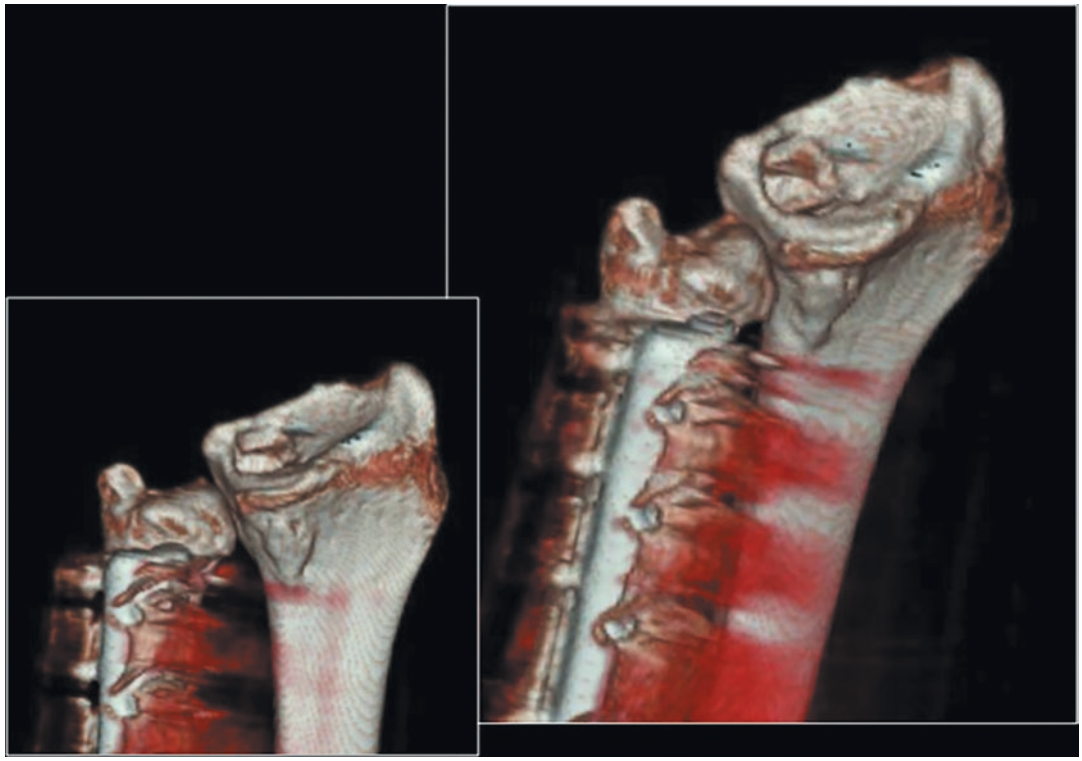

Fig. 107.17 CT scan showing good incorporation of the two osteochondral grafts

- Need gradual dilation of the portal to allow insertion of 4.75 mm or 6 mm trephine safely without injuring the extensor tendons.
- Trim excessive knee cartilage after implantation of the osteochondral plug.
- Remove the osteochondral lesion down to 10–12 mm depth under direct vision.
- Maintain 2 mm intact dorsal articular margin.
- When delivering the graft into the wrist joint, do not use hammering.
- The subchondral bone plug from the wrist can be inserted back to the donor site.

107.6 Pitfalls

- Making a direct stab wound on the wrist can damage cutaneous nerves and extensor tendons.
- Excessive traction produces finger joint pain.
- Use of mechanical pump causes fluid extravasation and compartment syndrome.
- Use of hammering during procedure creates cartilage damage especially in midcarpal joint and DRUJ.
- Fracturing dorsal cortex of lunate fossa.
- Injury to extensor tendons by the trephine.
- Oblique trajectory of the osteochondral plug results in less optimal graft function.

107.7 Postoperative Management and Rehabilitation

The limb should be elevated with a compressive bandage for 2–3 days to allow the saline swelling to subside. There should be early finger mobilization to prevent adhesion. A wrist splint is prescribed for 2–4 weeks and the patient is instructed to perform gentle active wrist motion from day 3 onwards. Passive motion exercise can be initiated by 4–6 weeks. Active use of the hand in self-care and daily activities is allowed but load bearing of the wrist is discouraged for

Fig. 107.18 Small wounds at the completion of surgery

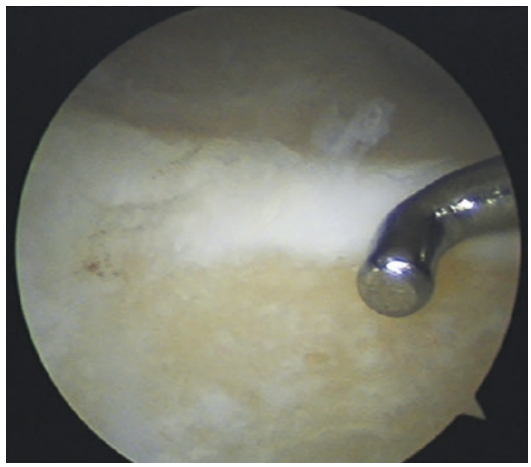

Fig. 107.19 Arthroscopy confirmed a full thickness focal osteochondral lesion of size 6 × 4 mm over the dorsal lunate fossa

the first 6 weeks to allow incorporation of the graft. Follow up MRI scan and X–ray can be arranged at 6–8 weeks to monitor the graft

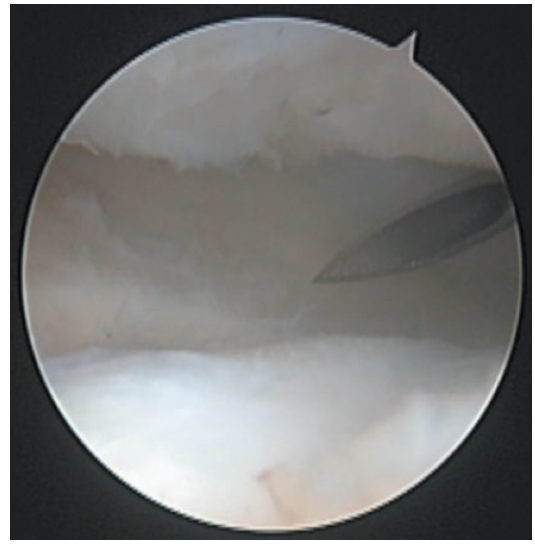

Fig. 107.20 Osteochondral autograft of 6 mm diameter and 12 mm long was implanted into the osteochondral defect at the lunate fossa

incorporation. Patient may experience mild knee pain at the donor site for a few weeks to up to 6 months.

107.8 Complications

Apart from the general surgical risks, potential specific complications include iatrogenic cartilage damage to the non-affected part, injury to the extensor tendons and cutaneous nerves, injury to the posterior interosseous nerve at 3–4 portal leading to portal pain, blowout fracture of the dorsal distal radius, fracture of the osteochondral plug during harvesting and insertion, persistent knee pain at the donor site.

107.9 Results

Between Dec 2006 and Dec 2010, we had operated on four patients of average age 31 (range 24–41) who were diagnosed to have post-traumatic localized osteochondral lesion over the dorsal lunate fossa of the distal radius [14]. They all presented with chronic central dorsal wrist

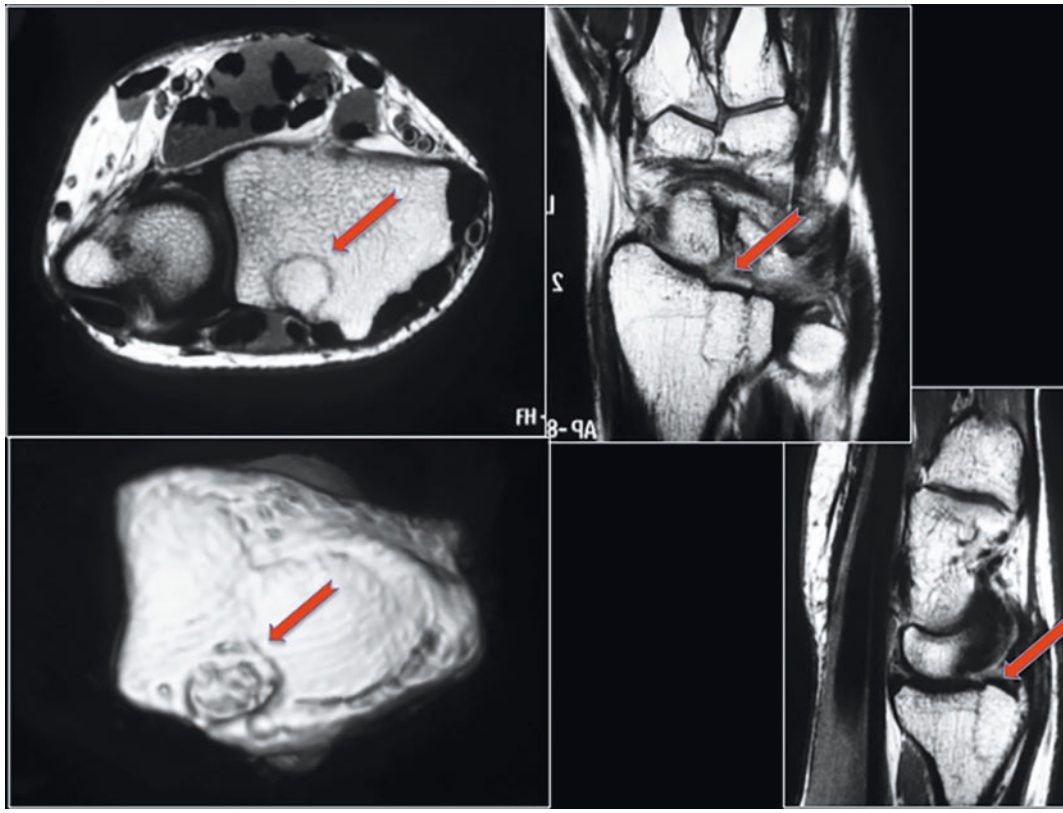

Fig. 107.21 CT scan and MRI showed good incorporation of the graft (arrows)

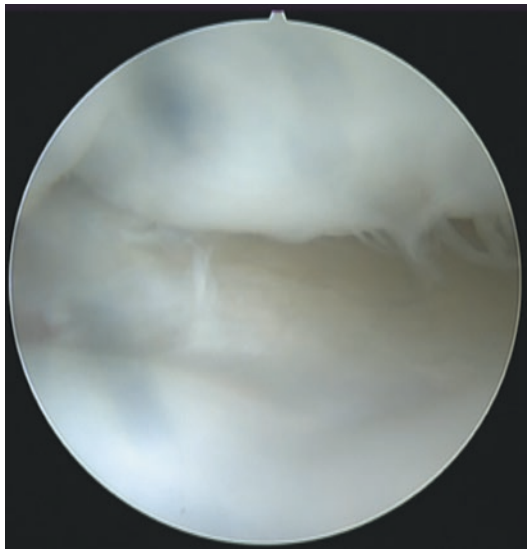

Fig. 107.22 A third look arthroscopic evaluation at 29 months post-op showed a completely incorporated hyaline cartilage with minimal junctional change

pain and loss of motion after the injury episode. The average duration of symptom was 28.3 months (range 11–71). The size of the lesions varied from 6 to 10 mm. One patient received two plugs of graft while the other three received one graft on each wrist.

In all cases, the osteochondral grafts were healed and incorporated into the host bone 3–4 months after the operation as confirmed by a CT scan or MRI. A second look arthroscopy at 6–9 months post-operation in three patients confirmed the preservation of normal articular cartilage in the grafted area. There was a 1–2 mm rim defect between the graft and the host cartilage. In one patient, a third look arthroscopy at 29 months post-operation showed complete coverage of the junction defect by cartilage. A biopsy of the grafted area in one patient confirmed viable hyaline cartilage.

Fig. 107.23 Good wrist ROM at 10 years 4 months post-op

Fig. 107.24 X-ray showed no arthrosis of the radiolunate joint at final follow-up. Noted the pisotriquetral fusion which was performed as a subsequent procedure

At the final follow up of average 70.5 months (range 24–116), all patients showed an improvement in the wrist performance score (pre-op 27.5 ± 6.4, post-op 38.5 ± 2.6 out of a 40 point scale) and pain score (pre-op 9.5 ± 2.2, post-op 0.5 ± 0.9 out of a 20 point scale). Grip strength improved from 62.6 ± 9.0% to 91.1 ± 2.6% of the contralateral side. Wrist motion improved from a flexion/extension arc of 115.5° ± 28.8° to 131.3° ± 21.3°. Three patients returned to their previous occupations while one could not do so because of the pisotriquetral instability problem. They were all satisfied with the procedure. The surgical scars were inconspicuous. Follow-up X-ray showed good graft incorporation, with no joint space narrowing or other signs of degeneration. There was no complication of infection, tendon, or nerve injury in this series.

Fig. 107.25 Inconspicuous scar over the right wrist

Fig. 107.26 Finger-pivoting technique in holding and manipulating the arthroscope as a standard practice in small joint arthroscopy

Fig. 107.27 The surgeon can stand on a stool to facilitate a vertical insertion of the osteochondral graft into the distal radius

References

1. Koman H, Poehling GG, Toby EB, et al. Chronic wrist pain: indications for wrist arthroscopy. Arthroscopy. 1990;6:116–9.
2. Araf M, Mattar R Jr. Arthroscopic study of injuries in articular fractures of distal radius extremity. Acta Ortop Bras. 2014;22(3):144–50.
3. Cheng HS, Hung LK, Ho PC, Wong J. An analysis of causes and treatment outcome of chronic wrist pain after distal radius fractures. Hand Surg. 2008;13(1):1–10.
4. Whipple TL. Chronic wrist pain. Instr Course Lect. 1995;44:129–137l.
5. Slutsky D, Nagle DJ. Wrist arthroscopy: current concepts. J Hand Surg. 2008;33A:1228–44.
6. Sofat N, Ejindu V, Kiely P. What makes osteoarthritis painful? The evidence for local and central pain processing. Rheumatology (Oxford). 2011;50(12):2157–65.
7. Mehin R, Giachino AA, Backman D, et al. Autologous osteoarticular transfer from proximal tibiofibular joint to the scaphoid and lunate facets in the treatment of severe distal radius fractures: a report of two cases. J Hand Surg. 2003;28A:332–41.
8. Merrell GA, Barrie KA, Wolfe SW. Sigmoid notch reconstruction using osteoarticular graft in a severely comminuted distal radius fracture: a case report. J Hand Surg. 2002;27A:729–34.
9. Piñal FD, Garcia-Bernal FJ, Delgado J, et al. Reconstruction of the distal radius facet by a free vascularised osteochondral autograft: anatomic study and report of a patient. J Hand Surg. 2005;30A:1200.e1–1200.e14.
10. Culp R, Osterman AL, Kaufmann RA. In: Green DP, Hotchkiss RN, Pederson WC, Wolfe SW, et al., editors. Wrist arthroscopy: operative procedures. 5th ed. New York: Churchill Livingstone; 2005. p. 781–803.
11. Roth JH, Poehling GG. Arthroscopic "ectomy" surgery of the wrist. Arthroscopy. 1990;6:141–7.
12. Ong TY, Ho PC, Wong WYC, Cheng HS, Tse WL. Wrist arthroscopy under portal site local anaesthesia (PSLA) without tourniquet. J Wrist Surg. 2012;1:149–52.
13. Hangody L, Rathonyi GK, Duska Z, et al. Autogenous osteochondral mosaicplasty. Surgical technique. J Bone Joint Surg. 2004;86A(Suppl 1):65–72.
14. Ho PC, Tse WL, Wong CWY. Arthroscopic transplantation of osteochondral autograft for treatment of cartilage defects in the wrist. Hand Clin. 2017;33:755–67.

Arthroscopic Full Wrist Fusion

108

Tendai Mwaturura and Gregory I. Bain

108.1 Background

Full wrist arthrodesis is a proven procedure in the management of end-stage radiocarpal and midcarpal arthritis [1]. Open techniques incorporating a variety of fixation techniques, such as cortico-cancellous graft and screws, intramedullary rods, multiple staples, and plates have been described [2–5]. However, they necessitate the use of extensive soft tissue dissection leading to postoperative pain and edema. In addition, the use of dorsally placed hardware can result in irritation, adhesion, or rupture of extensor tendons [4, 6]. Mannerfelt described a technique using an intramedullary Rush pin through the third metacarpal into the radius and staples [7]. Advances in arthroscopy have enabled modification of that technique for use in arthroscopic full wrist fusion thus limiting insult to soft tissues and avoiding a long dorsal scar. Controversy exists regarding fusion of some of the joints (Fig. 108.1). It is common to perform full bridge plate fixation to the third metacarpal [8]. However, the third carpometacarpal joint has a tendency to develop nonunion and for this reason we prefer to avoid it [9]. We also prefer to use a "closing method of fusion" (Fig. 108.2) [10].

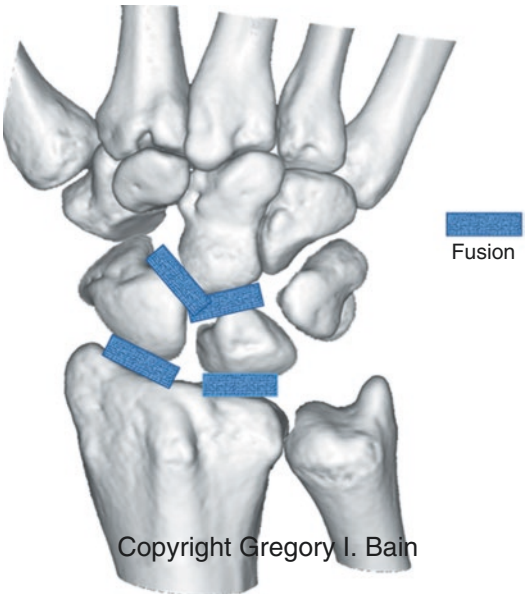

Fig. 108.1 Joints to be fused during full wrist arthrodesis. There is no consensus as to whether or not fusion of the scapho-trapezio-trapezoid, second and third carpometacarpal, capito-hamate, hamate-triquetrum, and lunotriquetral joints is required during full wrist arthrodesis. (Copyright Dr Gregory I. Bain)

T. Mwaturura (✉)
Department of Orthopaedic Surgery, Sunshine Coast University Hospital, Sunshine Coast, QLD, Australia

G. I. Bain
Department of Orthopaedics and Trauma Surgery, Flinders University and Flinders Medical Centre, Adelaide, SA, Australia
e-mail: admin@gregbain.com.au

© ISAKOS 2022

D. N. Bhatia et al. (eds.), *Arthroscopy and Endoscopy of the Elbow, Wrist and Hand*,
https://doi.org/10.1007/978-3-030-79423-1_108

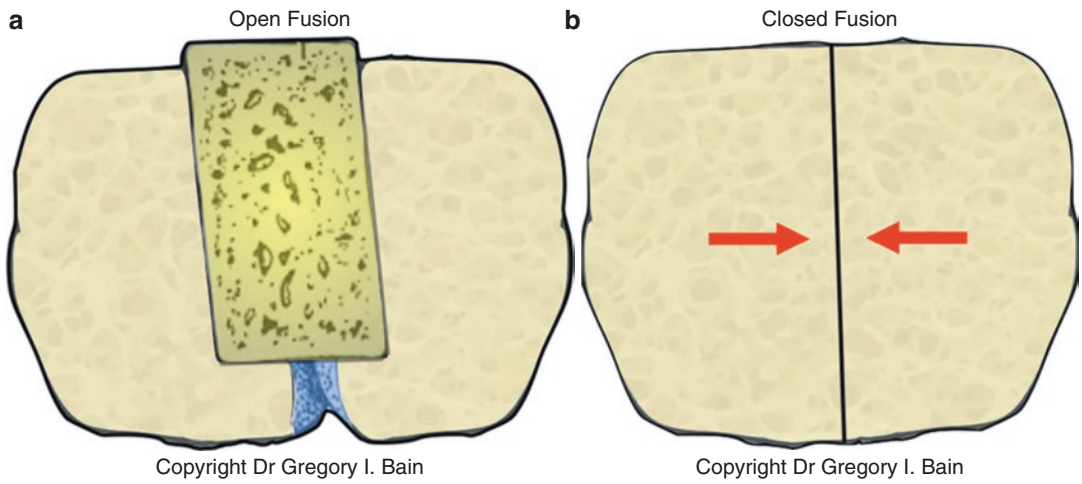

Fig. 108.2 Closed vs open fusion. (**a**) In open fusion the volar lip of each articular surface is not debrided, which maintains carpal height but limits the contact area of the fusion mass. (**b**) In a closed fusion the full width of the articular surfaces are debrided, allowing compression of graft and increased stability. (Copyright Dr Gregory I. Bain)

108.2 Indications and Contraindications

Arthroscopic full wrist fusion is indicated in patients with persistent symptoms from radiocarpal and midcarpal arthritis despite the use of comprehensive nonoperative management techniques.

This procedure is contraindicated in the presence of active infection and in cases where local anatomy is so distorted that safe establishment of portals or adequate visualization is not possible.

Table 108.1 Equipment required for arthroscopic full wrist fusion (Copyright Dr Gregory I. Bain)

Equipment	Purpose
Arthroscopic shaver and bur	Debride joint
Acumed bone graft harvester	Harvest bone graft
Arthroscopic cannula and obturator	Deliver bone graft
Small bone tamp	Impact bone graft
3.2 mm Steinmann pin	Fixation of midcarpal and radiocarpal joints
Fluoroscopy unit	Define trajectory of Steinmann pin
Double action wire cutter	Cut Steinmann pin

108.3 Surgical Technique

There are five surgical steps:

1. Debride the joint
2. Harvest the bone graft
3. Insert the Steinmann pin
4. Insert the bone graft
5. Rehabilitation

Appropriate prophylactic antibiotics and anesthesia are administered. The patient is placed in a supine position and a tourniquet is applied to the arm and not inflated unless bleeding restricts visibility. The limb and ipsilateral iliac crest are prepped and draped. Finger traps and traction are used. Equipment required, other than that for standard wrist arthroscopy and bone graft harvesting, is documented in Table 108.1. Local anesthetic with adrenaline can be instilled into each of the portals and into the joint to minimize bleeding. Standard arthroscopy is used. We prefer dry arthroscopy but use saline when burring to minimize thermal necrosis. Successful fusion is dependent on adequate debridement, tight packing of bone graft, and secure fixation using a Steinmann pin.

The five steps are described in the sections below:

108.3.1 Debride the Joint

Debridement proceeds from proximal to distal. Visibility of dependent surfaces is compromised by blood and debris, which move proximally due to the effect of gravity, if distal surfaces are prepared first [11]. The radiocarpal joint is accessed through 1–2, 3–4, and 6R portals. A 2.9 mm bur is used to remove cartilage from the scaphoid and lunate facets through the 1–2 and 3–4 portals while looking through a 2.7 mm arthroscope placed in the 6R portal. Punctate bleeding from subchondral bone signifies that adequate debridement has been performed; Further removal of bone results in loss of supporting subchondral bone and increases the amount of bone graft that will be required in later stages of the surgery. The burr is used to remove cartilage from the proximal articular surfaces of the scaphoid and lunate using the three portals described above as required (Fig. 108.3).

Attention is turned to the midcarpal joint. Midcarpal ulnar (MCU) and midcarpal radial (MCR) portals are established. The distal articular surface of the lunate is prepared by a burr placed through the MCU portal while looking through the MCR portal. The midcarpal articular surface of the scaphoid is prepared with the bur in the MCR portal and the arthroscope in the MCU portal [12]. Cartilage does not have to be removed from the distal pole of the scaphoid because it is not included in the fusion mass. The bur is then used to debride the proximal and radial surfaces of the capitate.

Fig. 108.3 Arthroscopic image showing debridement of radiocarpal joint. The distal radius (lower half of image) has already been debrided and pink subchondral bone is visible. The bur is on the proximal pole of the lunate and the sheath is orientated proximally to protect the radius, which has already been prepared. (Copyright Dr Gregory I. Bain)

108.3.2 Harvest the Bone Graft

We prefer to harvest the bone graft from the ipsilateral distal radius. An incision is made over the distal radius 1 cm proximal to Lister's tubercle. A corticotomy is made and graft harvested with the Acumed bone graft harvester. This device harvests, morselizes, and compacts the bone (Acumed Bone Graft Harvesting System. Acumed. Hillsboro OR). Usually this is adequate, but if an extra graft is required, use the iliac crest.

108.3.3 Insert the Steinmann Pin

A 3.2 mm Steinmann pin is laid over the dorsum of the hand, wrist, and forearm and fluoroscopy is used to plan the trajectory of the pin from the head of the third metacarpal into the medullary canal of the radius. A stab incision is made just distal to the proposed entry site and dissection is performed to the articular surface of the head of the third metacarpal. A 3.2 mm Steinmann pin is placed into a drill reamer or AO T-handle chuck (Fig. 108.4). It is carefully advanced through the third metacarpal shaft and carpus to the subchondral bone plate of the distal radius in a retrograde manner under fluoroscopic guidance to ensure that the correct trajectory is maintained (Fig. 108.5). Care is required to ensure that the position of the wrist is correct. Check fluoroscopically, that the Steinmann pin will advance down the intramedullary canal of the radius, then continue advancing it into the radius.

108.3.4 Insert the Bone Graft

Once the pin is correctly aligned, distract the joint and insert the bone graft. The 3–4 portal is enlarged and the bone graft is delivered into the radiocarpal space through an arthroscopic cannula (Fig. 108.6). Graft is inserted into the

Fig. 108.4 AO T-handle chuck

Fig. 108.5 Retrograde insertion of a Steinmann pin through third metacarpal head. Note that the fingers are flexed to allow unimpeded access to the head of the third metacarpal through a longitudinal split in the extensor tendon and capsule of the MCP joint. The AO T-handle chuck grasps the Steinmann pin firmly, allowing advancement of the pin using slow oscillation movements while making fine adjustments to maintain the correct trajectory. (Copyright Gregory I. Bain)

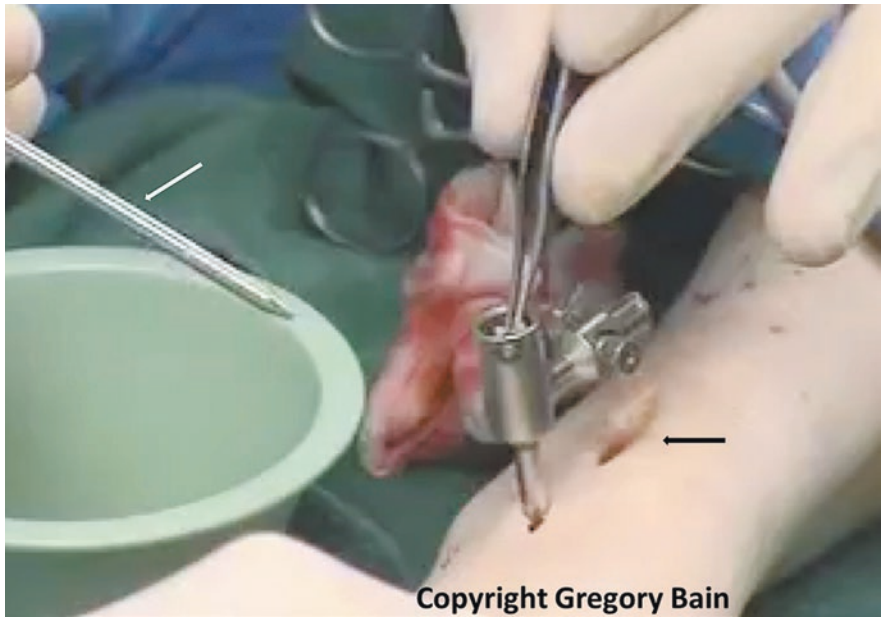

Fig. 108.6 Insertion of bone graft. Bone graft has been harvested from the distal radius through an incision proximal to Lister's tubercle (black arrow). An arthroscopic cannula has been placed into the radiocarpal joint through an enlarged 3–4 portal and bone graft is inserted. An obturator (white arrow) will deliver the graft into the joint. An assistant (hand on bottom left of image) distracts the joint. (Copyright Gregory I. Bain)

luno-capitate and scapho-capitate joints via the cannula through an enlarged midcarpal portal. The graft is packed tightly using a small tamp. Compress the wrist along the line of the pin, and ensure that the wrist is correctly positioned.

The end of the pin is cut and lightly tapped, leaving it within the head of the third metacarpal. Ensure that the rotation of the wrist is correct and that the wrist is compressed.

The wounds are closed and dressed and a light compressive bandage and splint applied.

108.3.5 Postoperative Management and Rehabilitation

Immediate use of the digits is encouraged. Use of the splint is discontinued when fusion is confirmed radiographically (Fig. 108.7).

108.4 Tips and Tricks

The key points and technical tips are presented in Table 108.2.

Fig. 108.7 AP and lateral radiographs showing a successful full wrist fusion performed with an intramedullary Steinman pin. Note the Steinman pin is in-set into the head of the third metacarpal. (Copyright Dr Gregory I. Bain)

Table 108.2 Key surgical points for arthroscopic full wrist fusion (Copyright Dr Gregory I. Bain)

Key point	Purpose
Debride joint surface to bleeding subchondral bone	Good healing surface
Fluoroscopic assessment	Correct wrist alignment and Steinmann pin position
Pack bone graft tightly into RC and MC joints	Fills voids in the debrided surfaces
Wrist manipulation	Correct wrist rotation and compression of fusion

Table 108.3 Pitfalls to avoid during arthroscopic full wrist fusion (Copyright Dr Gregory I. Bain)

Pitfall	Consequence
Inadequate debridement	Nonunion
Advancing Steinmann pin volar to carpus	Injury to contents of carpal tunnel
Advancing Steinmann pin radially prior to engaging distal radius	Radial deviation of wrist in fused position, decreasing mechanical advantage of finger flexors during power grip
Failure to compress bone graft	Nonunion

108.5 Pitfalls

Table 108.3 outlines the pitfalls to avoid during the procedure.

108.6 Results

The results of total wrist fusion are generally excellent. We have been pleased with the results of the few cases we have done. The patients get minimal swelling and are much more comfortable in the first few weeks than those who have had a traditional open fusion.

References

1. Hayden RJ, Jebson PJ. Wrist arthrodesis. Hand Clin. 2005;21(4):631–40.
2. Rayan GM. Wrist arthrodesis. J Hand Surg Am. 1986;11(3):356–64.
3. Clayton ML. Surgical treatment at the wrist in rheumatoid arthritis: a review of thirty-seven patients. J Bone Joint Surg Am. 1965;47:741–50.
4. Benkeddache Y, Gottesman H, Fourrier P. Multiple stapling for wrist arthrodesis in the nonrheumatoid patient. J Hand Surg Am. 1984;9(2):256–60.
5. Meuli HC. Reconstructive surgery of the wrist joint. Hand. 1972;4(1):88–90.
6. Zachary SV, Stern PJ. Complications following AO/ASIF wrist arthrodesis. J Hand Surg Am. 1995;20(2):339–44.
7. Mannerfelt L, Malmsten M. Arthrodesis of the wrist in rheumatiod arthritis. A technique without external fixation. Scand J Plast Reconstr Surg. 1971;5(2):124–30.
8. Moneim MS, Pribyl CR, Garst JR. Wrist arthrodesis. Technique and functional evaluation. Clin Orthop Relat Res. 1997;341:23–9.
9. Nagy L, Büchler U. AO-wrist arthrodesis: with and without arthrodesis of the third carpometacarpal joint. J Hand Surg Am. 2002;27(6):940–7.
10. Bain GI, McGuire DT. Decision making for partial carpal fusions. J Wrist Surg. 2012;1(2):103–14.
11. Tse WL, Teng X, Liu B, Wing-yee CW, Ho PC, Bain GI. Arthroscopic reconstructive procedures for Kienböck's disease. In: Litchman DM, Bain GI, editors. Kienböck's disease. Advances in diagnosis and treatment. Cham: Springer International Publishing; 2016. p. 261–70.
12. Ho PC. Arthroscopic partial wrist fusion. Tech Hand Up Extrem Surg. 2008;12(4):242–65.

Part XXI

Wrist: Miscellaneous

109 Surgical Anatomy and Management of Intersection Syndrome

Gregory Hoy and Simon Hoy

109.1 Background

Intersection syndrome is a recognized condition in watersports using blades (rowing, kayaking), and is a debilitating condition in the pre-competition phase of the Olympic 4-year cycle. Nonsurgical treatment involves rest with subsequent loss of strength and conditioning, alteration to techniques, and prolonged therapy. Surgery aids early return to competition to achieve career goals.

109.1.1 Surgical Anatomy

The first dorsal compartment muscles cross over the second compartment tendons 10 cm above the wrist dorsally and are contained in a fascial compartment. This compartment responds to significant increased muscle mass in high volume rowing and kayaking by developing a thickened fascial margin that acts like a "bowstring" across the synovium of Extensor Carpi Radialis Longus (ECRL) and Brevis (ECRB) tendons as they slide on the dorsal wrist in repeated extension and flexion. This firm band perforates the synovium and damages the true tendon surface of the wrist extensors with a palpable and sometimes audible crunching sensation/sound (Fig. 109.1).

109.2 Indications and Contraindications

The diagnosis of intersection syndrome requires pain at the upper or lower crossover of first dorsal wrist compartment and second dorsal wrist tendon synovium. The condition usually occurs when the athlete undertakes high training loads in rough water [1].

Indications for intersection syndrome release are controversial, but we believe this is an acute surgical disease in elite athletes and warrants immediate surgical release to avoid excessive rest, loss of form, and technique changes that may interfere with the elite career cycle [2, 3].

Contraindications include performing surgery on poorly diagnosed dorsal wrist pain syndromes without the true physical signs noted above. This most commonly occurs in variations of work-related pain syndromes often labeled "RSI" (repetitive strain injury) [4].

G. Hoy (✉) · S. Hoy
Melbourne Orthopaedic Group,
Melbourne, VIC, Australia

Department of Surgery, Monash University,
Melbourne, VIC, Australia
e-mail: gahoy@mog.com.au

© ISAKOS 2022

D. N. Bhatia et al. (eds.), *Arthroscopy and Endoscopy of the Elbow, Wrist and Hand*,
https://doi.org/10.1007/978-3-030-79423-1_109

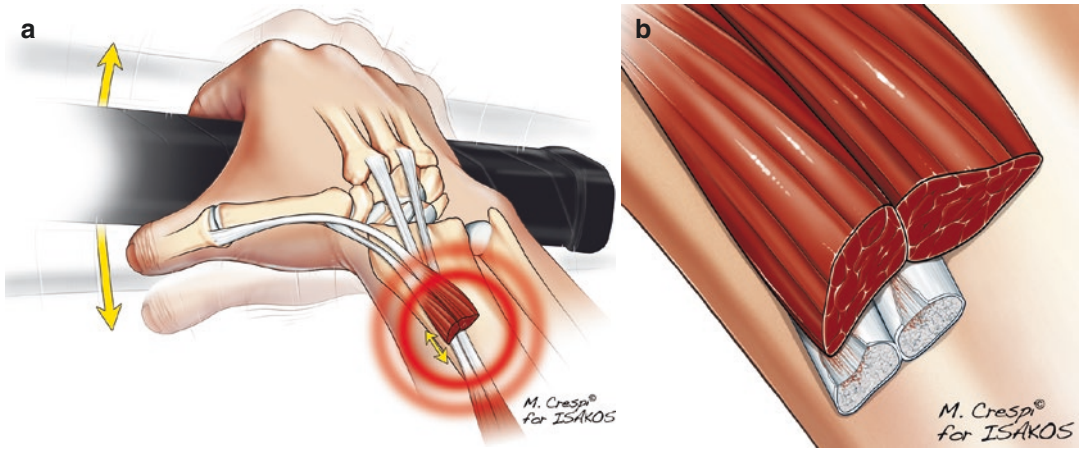

Fig. 109.1 (**a**, **b**) Grip position (**a**) and close-up effect of first compartment hypertrophy and thickened compartment edge to perforate second compartment synovium (**b**) (M. Crespi © for ISAKOS)

109.3 Surgical Technique

The patient is positioned supine and the upper extremity is supported on a hand table. A tourniquet is placed in the upper arm and inflated to 250 mmHg after exsanguination.

- The surgical technique involves a small zigzag incision over the muscle belly of the EPB and APL muscles. The author has explored the use of endoscopic release here however the dorsal branches of the superficial radial nerve (SRN) are not consistent enough to allow endoscopic release without some risk to the SRN.
- The fascial release of the first compartment includes both proximal and distal to the muscles as the tight band has been seen on both sides in clinical cases (Fig. 109.2).
- The dorsal synovium of the ECRB and ECRL is resected and the area is bathed in betamethasone before closure to prevent scarring (Figs. 109.3 and 109.4).
- Skin closure is aided by dermal glue to seal the wound from inadvertent fluid entry on resumption of training (Figs. 109.1–109.3).

Fig. 109.2 Fascia above and below the first compartment is defined after compartment release (© G. Hoy)

Fig. 109.3 A rent is seen in synovium of ECRB below first compartment (© G. Hoy)

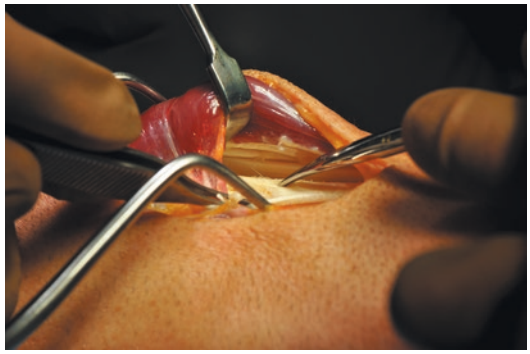

Fig. 109.4 Tendinitis from rubbing of tendons under tight band is demonstrated and the dorsal synovium of the ECRB and ECRL is resected (© G. Hoy)

109.4 Tips and Tricks

- The fascia of the first compartment should be released up the forearm as the original pathology is considered to be a reaction to compartment syndrome.
- The release should occur both on the leading edge and the trailing edge of the first compartment fascia as either can be the culprit.
- Closure should be watertight as it allows early resumption of training to avoid loss of muscle strength and proprioception.

109.5 Pitfalls

- The diagnosis should be clear and include crepitus; operating on a pain syndrome is not successful.
- Avoid excessive periods of rest post-surgery. This does not enhance healing and leads to muscle wasting.

109.6 Postoperative Management and Rehabilitation

Immediate range of motion and start within a few days. Return to sports activities for rowing or other competitive sports is within a week.

109.7 Complications

Possible complications include wound infection (rare), damage to superficial radial nerve branches, and persistent pain (wrong diagnosis).

109.8 Results

The author has reported six cases (four males, two females) from a 4-year period (2010–2013) [3]. All of these returned to on-water training in 5–8 days. Five of six athletes competed in international championships or Olympics competition within 2–3 months of surgery. One had a wound breakdown (traumatic) and temporarily retired, but returned to international rowing 3 years later.

References

1. Drew MK, Trease L, Caneiro JP, Hooper I, Ooi CC, Counsel P, Connell DA, Rice AA, Knight E, Hoy G, Lovell G. Normative MRI, ultrasound and muscle functional MRI findings in the forearms of asymptomatic elite rowers. J Sci Med Sport. 2016;19(2):103–8.
2. Williams JG. Surgical management of traumatic non-infective tenosynovitis of the wrist extensors. J Bone Joint Surg Br. 1977;59(4):408–10.
3. Hoy G, Trease L, Braybon W. Intersection syndrome: an acute surgical disease in elite rowers. BMJ Open Sport Exerc Med. 2019;5(1):e000535.
4. Gold JE, d'Errico A, Katz JN, Gore R, Punnett L. Specific and non-specific upper extremity musculoskeletal disorder syndromes in automobile manufacturing workers. Am J Ind Med. 2009;52(2):124–32.

Arthroscopic Decompression of Intraosseous Cysts of the Lunate

110

Deepak N. Bhatia and Gregory I. Bain

110.1 Background

Intraosseous ganglion (IOG) cysts in the wrist occur mostly in the lunate followed by the capitate, scaphoid, and triquetrum bones. These cysts can be bilateral and are often associated with soft tissue ganglia in the wrist. IOGs may present with persistent dorsal wrist pain and swelling in the perilunate region and reduced grip strength, and surgical decompression (open/arthroscopic) is often necessary. Arthroscopic cyst decompression has several advantages over open procedures: (1) The technique can be performed with two-portals only, and thereby avoids the morbidity associated with more extensive procedures. (2) Direct "cystoscopic" access to the IOG is possible via a 3 mm cortical hole in the lunate and this maintains the structural integrity of the lunate. In small- and mid-sized IOGs, this obviates the need for bone grafting. (3) Biopsy samples can be adequately procured under direct visualization and (4) Associated radiocarpal and midcarpal lesions (soft tissue ganglia, triangular fibrocartilage tears, cartilage defects) can be treated simultaneously [1].

D. N. Bhatia (✉)
SPORTSMED Mumbai, and Sir HN Reliance Foundation Hospital, Mumbai, India
e-mail: shoulderclinic@gmail.com

G. I. Bain
Flinders University and Flinders Medical Centre, Adelaide, SA, Australia
e-mail: greg@gregbain.com.au

110.1.1 Surgical Anatomy

Lunate IOGs are located mostly along the dorsal and radial aspects within the lunate however the position is variable and preoperative MRI scans and CT scans are necessary for surgical guidance (Fig. 110.1). These cysts are pathologically identical to soft tissue ganglia and demonstrate a thin wall and clear viscous fluid. A thin sclerotic margin of bone often surrounds the ganglion, and a perforation into the adjacent carpal articulation may be present [2]. Cyst decompression should include removal of fluid and soft tissue walls, and the surrounding sclerotic bone should be curetted or burred.

110.2 Indications and Contraindications

- Intraosseous lunate ganglions (IOG) present with persistent dorsal wrist pain and swelling in the perilunate region and reduced grip strength. Surgery is indicated if symptoms have persisted for at least 6 months and after an unsuccessful trial of conservative treatment (rehabilitation, anti-inflammatory medication, local corticosteroid injection, and splints).
- Bone scan should demonstrate focal increased uptake within the lunate. Bone scanning helps

© ISAKOS 2022

D. N. Bhatia et al. (eds.), *Arthroscopy and Endoscopy of the Elbow, Wrist and Hand*,
https://doi.org/10.1007/978-3-030-79423-1_110

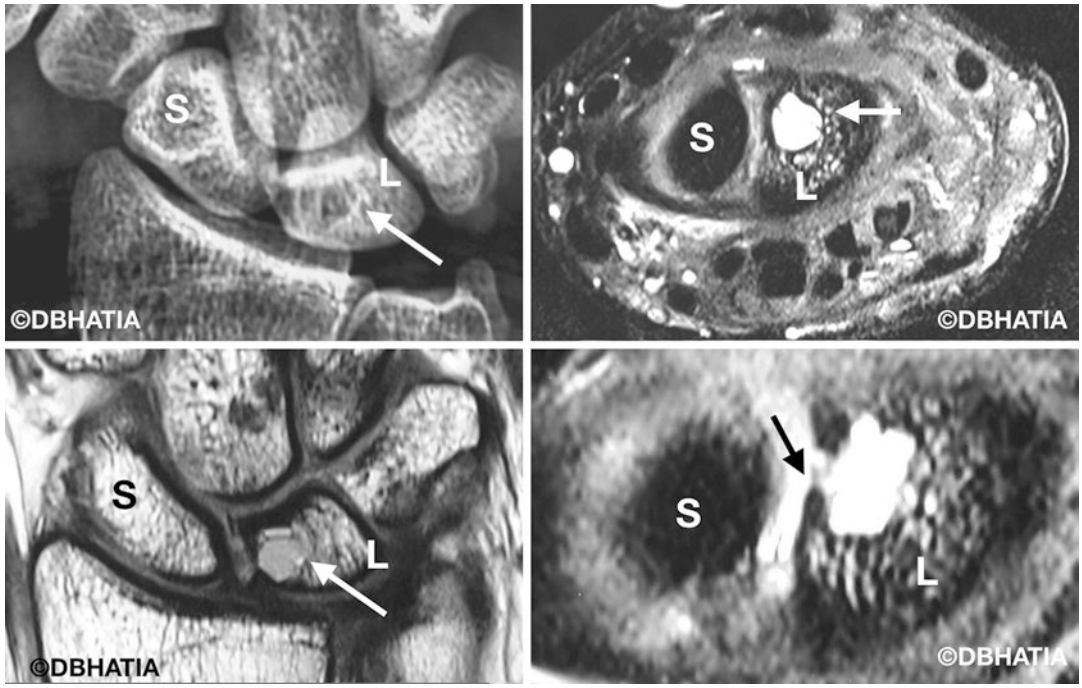

Fig. 110.1 Radiological imaging of a lunate cyst is shown in an anteroposterior radiograph (top left) and in a coronal MRI sequence (bottom left). Note the cyst is predominantly dorsal and radial within the lunate (top right). A cortical perforation is usually seen extending into the scapholunate joint (bottom right). (*S* Scaphoid, *L* Lunate, arrows: cyst). (© D. Bhatia)

to confirm that the IOG is the source of symptoms before any surgical intervention [2].

- Tuberculosis of the wrist is infrequently seen in endemic regions and may present with carpal cysts. Arthroscopy is performed for debridement and biopsy, and simultaneous cyst decompression is performed.

Cyst decompression is contraindicated in degenerative cysts, bone islands, tumors, and other lesions like Kienbock disease [2, 3].

110.3 Surgical Technique

The procedure is performed with the patient in the supine position. The upper limb is suspended with Chinese finger traps, and a countertraction force of 2 to 4 kg is used to distract the joint.

Portals: The dorsal radiocarpal 3–4 portal is the viewing portal throughout the procedure. The 4–5 portal is the main working portal and is also an accessory viewing portal for "cystoscopy." A needle passed from outside-in is directed towards the proximal dorsal lunate and is used to determine the exact portal site. A volar portal (VR) may be used for predominantly volar IOG cysts.

Diagnostic arthroscopy: The 3–4 portal is used to evaluate the radiocarpal joint and a probe/shaver is used through the 4–5 portal. The scapholunate (SL) joint is probed to assess ligamentous insufficiency. Any capsular flaps are debrided and the entire dorsal lunate is visualized upto its distal capsular attachment.

Lunate cyst entry: Cyst entry is possible via a cortical drill hole placed as distal as possible on the dorsal lunate surface. A 3 mm cannula or a drill guide is passed through the 4–5 portal and a 2 mm drill bit is used to create a pilot hole in the lunate. A guidewire is passed through the pilot hole and is drilled 10–15 mm deep into the lunate. The wire direction is determined by the position of the cyst seen on preoperative imaging. IOG cysts typically arise close to the insertion of the

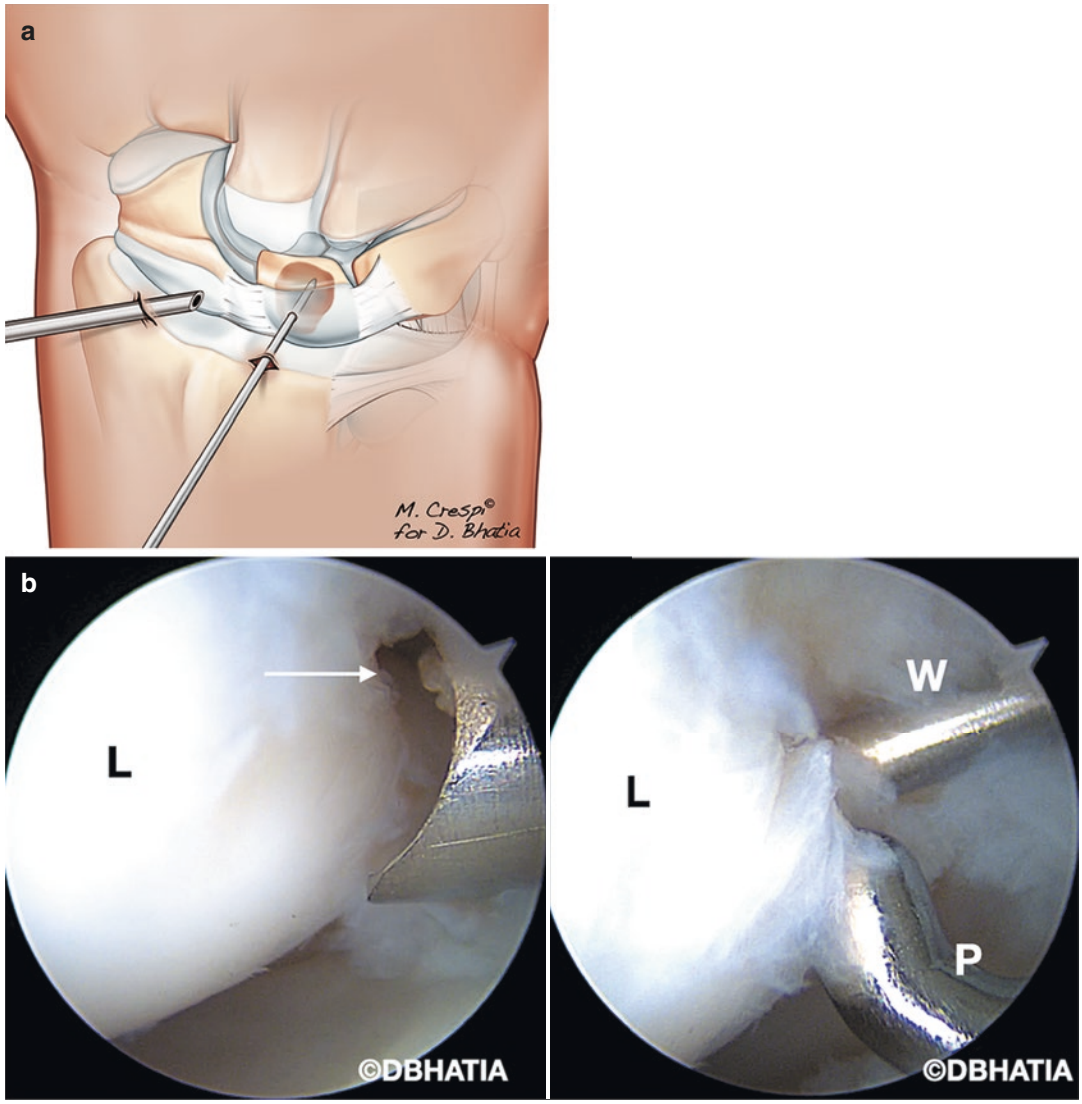

Fig. 110.2 (**a**) Placement of a guidewire under arthroscopic guidance into the lunate cyst is illustrated. (**b**) A pilot hole (arrow) is made in the dorsal cortical surface of lunate (L) (left image) and a guidewire (W) is drilled into the cyst (right image). A probe (P) retracts dorsal capsule. (© D. Bhatia)

scapholunate ligament, and this can often be used as an approximate guide to the position of the ganglion arthroscopically (Fig. 110.2a, b). Biplanar fluoroscopic imaging is used to confirm IOG penetration. A 3.2 mm cannulated drill bit is passed over the lunate guidewire directly or through the sheath (4–5 portal) and is drilled into the lunate for 10 mm. IOG penetration is marked by the release of a viscous and gelatinous fluid into the joint space (Fig. 110.3a, b).

Direct IOG Visualization and cyst debridement: The arthroscope is placed through the 3–4 or 4–5 portal and is directed into the lunate hole (Fig. 110.4a). Once inside, the IOG contents (soft tissue component) can be clearly visualized (cystoscopic view). A thorough lavage is given to clear the cyst of any bony debris from drilling. A small joint shaver blade and burr (2–3 mm) are used to debride the cyst interior via the 4–5 portal (Fig. 110.4b).

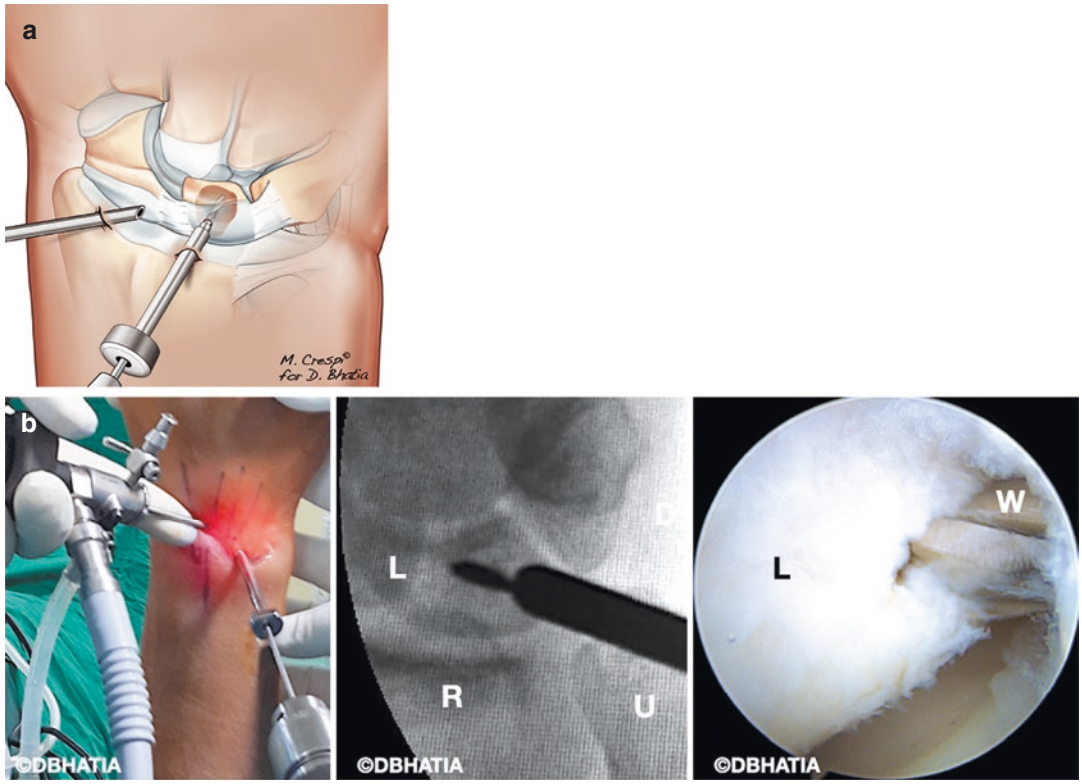

Fig. 110.3 (**a**) A 3 mm hole is drilled over the guidewire through a protective sheath into the cyst. (**b**) Fluoroscopy demonstrates the placement of the pilot drill bit into the lunate cyst (left and middle images). Arthroscopy visualization of cyst entry is demonstrated (right image). (*L* Lunate, *R* radius, *U*: Ulna). (© D. Bhatia)

Bone Grafting: Bone grafts may be used for large cysts under air insufflation and using a 3 mm cannula however this is not routinely necessary [4]. A small cortical window is made in the dorsal radius proximal to Lister's tubercle and cancellous bone is harvested. A 3 mm cannula is passed via the 4–5 portal directly into the hole in the lunate. The harvested bone graft is impacted into the lunate by pushing the graft through the cannula using a small tamping rod. Lavage of the radiocarpal joint is performed to remove any graft debris [3].

Final assessment: The arthroscope is placed in the cyst cavity and complete excision is confirmed. A probe is used to assess cyst walls for any cortical breach that may have occurred. The portals are closed and a bulky dressing is applied. Oblique radiographs are performed to assess the position of the cortical tunnel and cyst cavity (Fig. 110.5).

110.4 Tips and Tricks

- *Lunate cyst entry:* A needle is used to determine the exact site of the 4–5 portal. Slight dorsiflexion of the wrist provides more space between the dorsal capsule and the lunate and will also cause dorsiflexion of the lunate thereby bringing the more distal lunate surface into view.
- *Visualization:* Portal site and arthroscope diameter are key to a good "cystoscopy view." The 4–5 portal has a linear trajectory into the cyst, and the 3 mm hole allows for introduction of a 2.4 mm or a 1.9 mm arthroscope. Wrist position is manipulated to facilitate cyst visualization.
- *Passage of instruments* is easier when instruments are first passed into the radiocarpal space and then angulated and positioned over the lunate surface or into the drill hole.

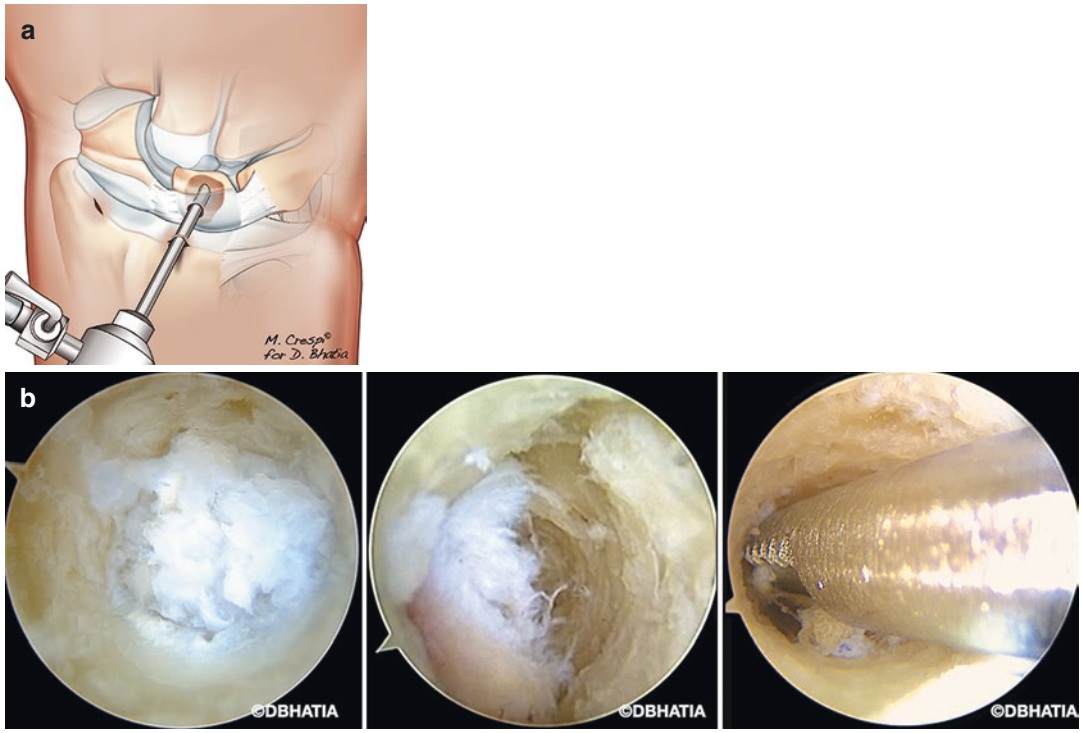

Fig. 110.4 (**a**) Direct visualization of the cyst ("cystoscopy") is performed by introducing the arthroscope into the cyst through the 4–5 portal. (**b**) Cystoscopic view of the lunate cyst is demonstrated in two different cases (left and middle images) through the 4–5 portal. A 2 mm shaver is used to debride the cyst contents under arthroscopic guidance. (© D. Bhatia)

110.5 Pitfalls

- *Inadequate debridement:* Failure to resect the soft tissues and lining within the cyst may be insufficient for symptomatic relief and the IOG may reoccur. Direct visualization helps to ensure complete resection.
- *Excessive debridement:* Lunate IOGs are usually radial and dorsal, and a cortical vent into the scapholunate joint is often present. Burring must be performed with care to prevent fracture of the thinner cortical wall. A thin probe may be used to probe the cortex to confirm cortical integrity while burring. Use of a 3.2 mm drill hole for cyst entry helps maintain the dorsal cortical entry and larger holes should be avoided.

110.6 Postoperative Management, Rehabilitation, and Return to Sport

A bulky dressing is used for comfort in the first postoperative week. The rehabilitation protocol involves early passive and active range-of-motion exercises (weeks 2–6) and simultaneous gradual strengthening. Full range is achieved in 6 weeks, and light work is permitted. Return to heavy work is permitted only after 3 months.

Conflict of Interest The author certifies that he has no commercial associations (e.g., consultancies, stock ownership, equity interest, patent/licensing arrangements, etc.) that might pose a conflict of interest in connection with the submitted article. The author retains the copyright to the images, videos, and content in this chapter.

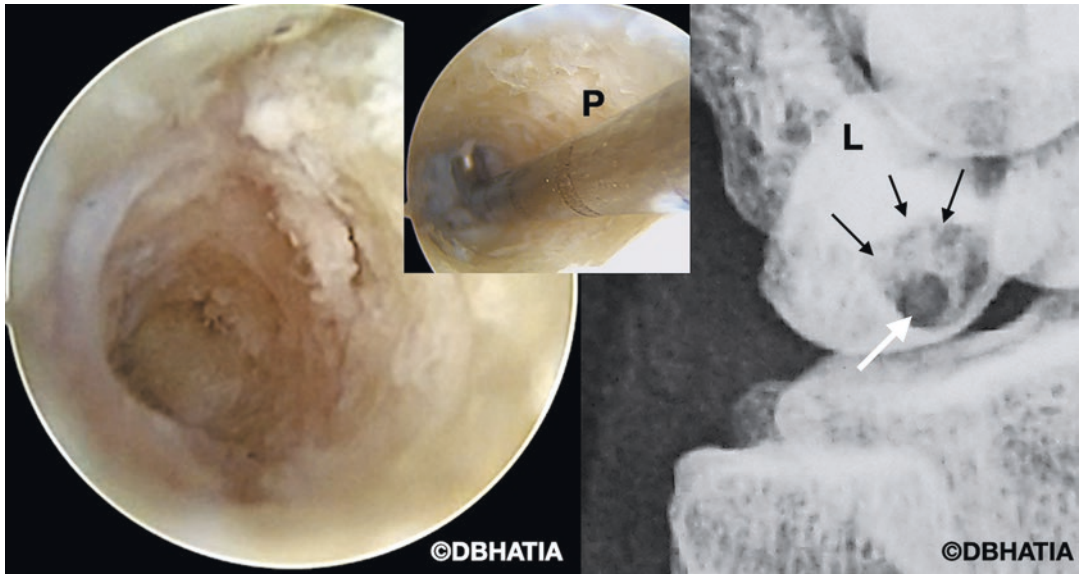

Fig. 110.5 (**a**) Final "cystoscopic" view of the lunate IOG is demonstrated after excision and debridement of cyst contents (left image). A probe (P, inset image) is used to assess cyst walls for any breach. Oblique radiograph demonstrates the position and size of the cortical tunnel (white arrow) and the cyst (black arrows, right image). (© D. Bhatia)

References

1. Bhatia DN. Direct "cystoscopic" approach for arthroscopic decompression of an intraosseous ganglion of the lunate. Arthrosc Tech. 2015;4(3):e223–9. https://doi.org/10.1016/j.eats.2015.01.010. Published 2015 May 18.
2. Bain GI, Turner PC, Ashwood N. Arthroscopically assisted treatment of intraosseous ganglions of the lunate. Tech Hand Up Extrem Surg. 2008;12:202–7.
3. Ashwood N, Bain GI. Arthroscopically assisted treatment of intraosseous ganglions of the lunate: a new technique. J Hand Surg Am. 2003;28:62–8.
4. Pegoli L, Ghezzi A, Cavalli E, Luchetti R, Pajardi G. Arthroscopic assisted bone grafting for early stages of Kienböck's disease. Hand Surg. 2011;16(2):127–31.

Arthroscopic Bone Graft for Lunate Ganglion

111

Lorenzo Merlini and Christophe Mathoulin

111.1 Background

Intraosseous lunate bone ganglia (ILBG) are known to be a cause of chronic wrist pain and disability, most often after collapse of a ganglion wall in the scapholunate joint. Standard treatment consists of curettage and autologous bone grafting. Open procedures have shown good results with few recurrences, but with frequent stiffness or persistent pain. Arthroscopic techniques are more recent and have begun to prove themselves very reliable, with studies reporting satisfactory functional and radiological results after arthroscopic bone grafting for intraosseous lunate bone ganglia [1–3].

111.2 Surgical Anatomy

Lunate ganglia are most commonly developed on the lateral half of the lunate bone, whether in a dorsal, central, or volar position (Fig. 111.1). Due to the lateral situation of the cyst, and frequent perforation of the lateral wall of the lunate into the scapholunate space, radiocarpal arthroscopy is a privileged access way to treat ILBG. The surgeon should be familiar with wrist anatomy and radiocarpal arthroscopic anatomy. The scapholunate ligament is the principal landmark, as its intermediate segment has to be opened to address the ganglion (Fig. 111.2).

111.3 Indications and Contraindications

- Intraosseous ganglia cysts of the lunate are relatively rare, but represent a cause of chronic wrist pain, stiffness, and/or loss of strength [4]. The diagnosis may be missed on clinical examination and is well demonstrated on radiological imaging such as plain radiography, MRI or CT-scan [5]. Most of these ganglia are asymptomatic; however, complications such as lunate wall perforation or fracture can occur and result in a mild to severe handicap of the wrist and these represent an ideal indication for ILBG arthroscopic bone grafting [6, 7]. Differential diagnoses include Kienböck's disease, osteolytic bone tumors, and sometimes ulnar abutment syndrome with lunate cortical defect [4, 8, 9].
- ILBG-like tumors, such as lunate aneurysmal bone cyst or osteoid osteoma, can be treated using a similar technique and is preferably to more invasive or aggressive techniques like open curettage and grafting, lunate excision, proximal row carpectomy, or intercarpal fusion [10–12].

L. Merlini · C. Mathoulin (✉)
International Wrist Center—IWC, Clinique Bizet, Paris, France

© ISAKOS 2022

D. N. Bhatia et al. (eds.), *Arthroscopy and Endoscopy of the Elbow, Wrist and Hand*,
https://doi.org/10.1007/978-3-030-79423-1_111

Fig. 111.1 X-ray and CT views of ILBG, on the radial half of the lunate

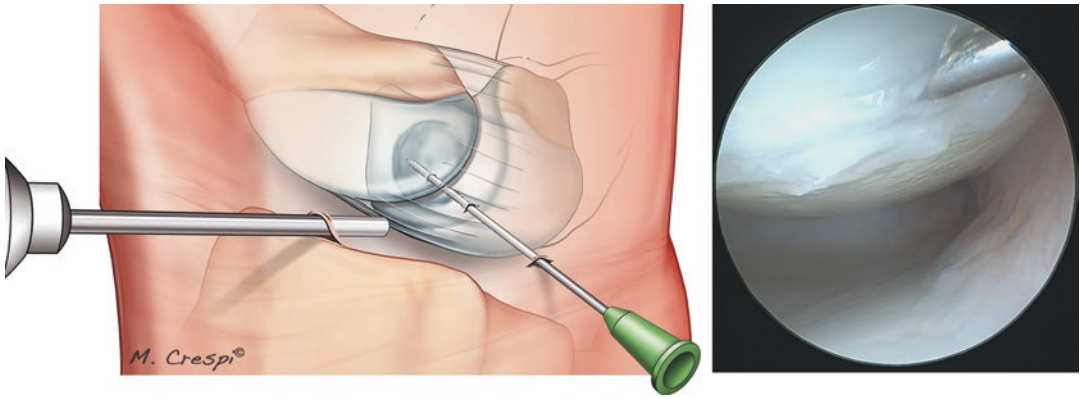

Fig. 111.2 Scope in the 1–2 portal, needle in the 3–4 portal passes through the proximal portion of the scapholunate ligament and into the ganglion

On the other hand, lunate defects secondary to ulnar impaction syndrome should not be treated with ILBG and a wafer procedure or ulna shortening osteotomy should be performed. This technique is also contraindicated in Kienböck's disease, and it is preferable to consider vascularized bone graft such as the Kuhlmann–Mathoulin technique.

111.4 Surgical Technique

The procedure is performed under regional anesthesia using a tourniquet, on an outpatient care basis. The patient's arm is secured to the arm board. Finger traps are used to apply 5–7 kg (11–15.5 lbs.) traction along the arm's axis.

Radiocarpal exploration: The scope is introduced in the 3–4 portal and the shaver in the radiocarpal 1–2 portal. The first phase of the arthroscopic procedure consists of complete synovectomy with a shaver, reversing the shaver and scope positions. With the scope in the 1–2 portal, the scapholunate ligament—specifically its proximal portion—can be located.

Locating and curettage of the cyst: With the scope in the 1–2 portal, an intramuscular needle is introduced in the 3–4 portal with its tip aimed at the proximal portion of the ligament. The needle is inserted through the ligament to locate the intraosseous cyst for which the outer wall has collapsed (Fig. 111.2). The ganglion is usually on the volar side. Once the ganglion has been located, a curette is inserted through the ligament

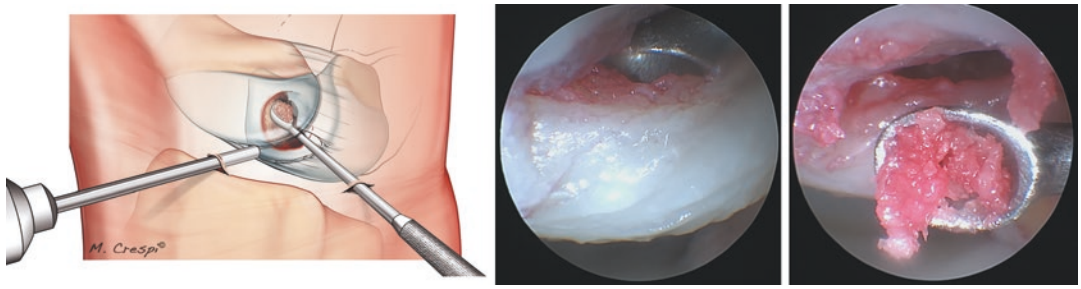

Fig. 111.3 Scope in the 1–2 portal, curettage of the ganglion from the 3–4 portal through the proximal portion of the scapholunate ligament

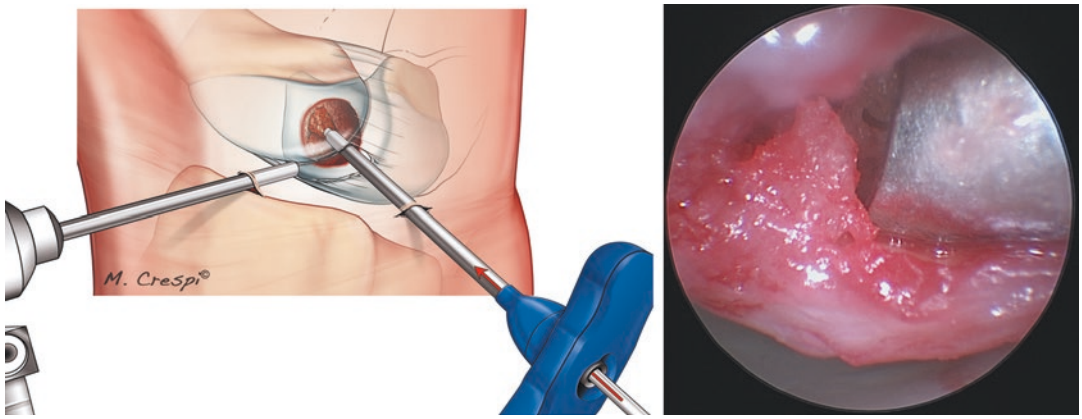

Fig. 111.4 Scope in the 1–2 portal, bone graft is passed into the lunate with a trocar through the 3–4 portal

under arthroscopic guidance (Fig. 111.3). The entire ganglion is then resected using the curette and the shaver. This step can be performed either with saline irrigation or as a dry procedure.

Bone graft harvesting: The bone graft is harvested from the ipsilateral wrist. An incision is made on the lateral side of the wrist between the first and second extensor compartments. The sensory branches of the radial nerve are identified and protected. The bone graft can be directly harvested using a bone marrow biopsy trocar such as a Jamshidi needle. Another possibility is to roughened the periosteum under the extensor tendons in the first and second compartments with a bone rasp to free up the graft collection area. A three-sided osteotomy is performed while leaving a "bone cap" attached to the radius. The bone graft is harvested with a curette; its volume must be larger than the defect being filled. After the graft has been collected, the cap is placed back on the harvest site.

Bone graft application: The next step is performed in a dry environment. If the initial part of the procedure was performed in a wet environment, all the fluid must be aspirated. The bone graft is inserted into the trocar and then the trocar's tip is placed in the cyst cavity (Fig. 111.4). The graft is pushed into the trocar with a blunt guide wire until the cyst cavity is filled (Fig. 111.5). The bone graft is packed down with a blunt guide wire (Fig. 111.6).

At the end of the procedure, arthroscopic portals can be left open, and a splint is positioned in slight wrist extension.

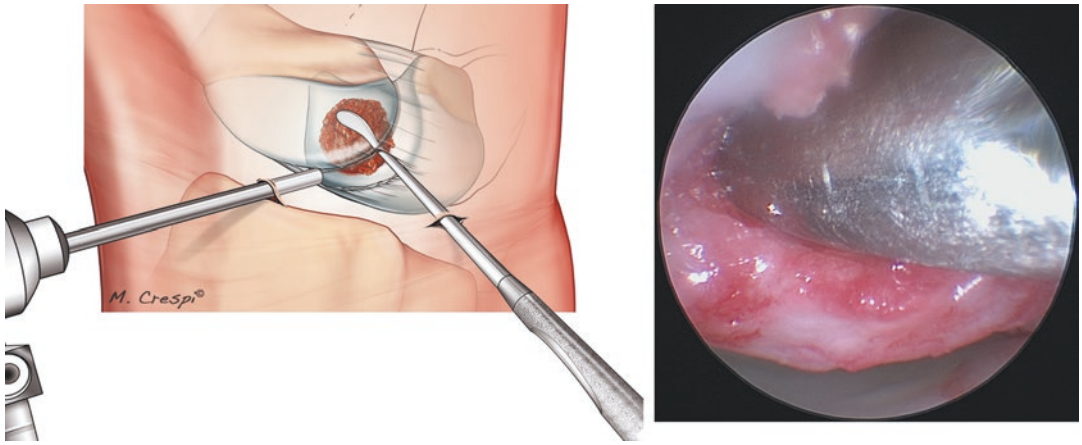

Fig. 111.5 Scope in the 1–2 portal, bone graft is pushed into the cyst cavity until completely filled

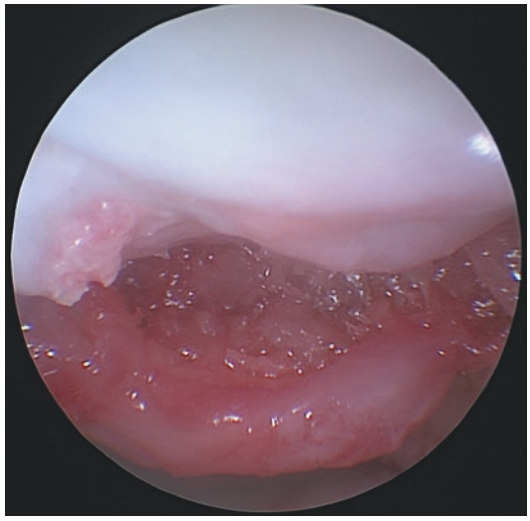

Fig. 111.6 Scope in the 1–2 portal, final view of the lunate grafted cyst cavity

111.5 Tips and Tricks

- Radius bone graft is generally harvested before traction installation, with the wrist laying on the operating table. We recommend to do so for an easier procedure, with simpler and better exposure of the lateral radius, and protection of the nerve branches and tendons.
- If bone graft is directly harvested with the Jamshidi trephine, one must pay attention to pass only the radius cortex with the tapered cutting tip needle. Once the cortex is passed, the needle has to be removed, to keep the sole trephine into the bone. The surgeon continues then to push the trephine through the cancellous bone to harvest the graft, which will then already be inside the trocar and ready for use.
- The technique is based on the visualization of the ILBG through the lateral aspect of the lunate. Quite frequently (in more than 50% of cases), the ganglion perforates the lateral wall of the lunate and opens into the scapholunate joint. This phenomenon is the main explanation of the dorsal pain presented by patients with ILBG. The advantage of the aforementioned technique is accessing the ILBG through this lateral wall, which can treat the ganglion using the preexistent perforation. In order to access it, the proximal portion of the scapholunate ligament has to be opened. Leaving intact the dorsal and volar scapholunate portions, along with dorsal capsulo-scapholunate septum (DCSS) and extrinsic ligaments, it causes absolutely no problem to pass through the proximal intermediate portion, given its mechanical insignificance in the scapholunate stability [13].
- Good visualization of the proximal scapholunate ligament implies a clean shaving and resection of soft-tissue and synovitis if present. Since the 3–4 portal is about directly facing the scapholunate ligament, the scope position has to be changed to the 1–2 portal.

The 3–4 portal can then become a perfect access way to the scapholunate space and the lateral wall of the lunate for bone grafting.

- Bone grafting is not a particularly difficult step. The bone graft placed into the ganglion cavity is pushed with the blunt guide of the trocar, and gradually impacted as the grafting progresses.
- There is no need for a scapholunate ligament repair at the end, unless a dorsal lesion is associated.

111.6 Pitfalls

- Harvesting the bone graft on the radius should be performed with caution. Sensory branches of the radial nerve pass through the site and are not always perfectly visible. A small but clear exposure of the radial cortex must be obtained with good soft-tissue retraction to avoid nerve damage.
- Extensor tendons must also be preserved during the bone graft harvesting step, as first and second compartments tendons can be subjected to dissection.
- The dorsal branch of the radial is at risk during placement of 1–2 portal. Careful localization with a needle, small cutaneous incision, blunt dissection, and capsular opening with blunt mosquito forceps are all mandatory steps to ensure a safe procedure.
- The size of lunate cavity may be underestimated and graft volume may be insufficient. A relatively large amount of bone graft has to be harvested from the radius to ensure a complete filling of the cyst with impacted cancellous bone.
- Radiocarpal arthroscopy can be performed with saline irrigation, to facilitate the exposure and curettage of the ganglion. Irrigation must however be stopped and all the fluid aspirated before placing the bone graft into the cavity, in order to avoid graft dispersion.

111.7 Post-operative Management and Rehabilitation

The wrist is immobilized until union is achieved. Rehabilitation is initiated once the splint is removed around week 6. Rehabilitation involves mobility recovery, particularly in flexion and extension. Pronosupination recovers early within a few days following the surgery. Grip strength is progressed after recovery of a satisfactory range of motion. Radiological follow-up is performed at week 6, usually showing bone healing of the former cavity.

111.8 Complications

Except for the aforementioned pitfalls, the technique does not present a great risk of intraoperative complications. A possible post-operative complication is failure of the graft to incorporate. Other possible complications are stiffness, residual pain, recurrence, complex regional painful syndrome (CRPS).

111.9 Results

Between 2012 and 2018, 13 patients were treated with ILBG using this previously described technique and the mean follow-up was 36 months. At the final assessment, active extension was at 100% of the contralateral wrist (versus 83% preoperatively); active flexion was at 98% (versus 77%); radial deviation was at 100% (versus 70%); ulnar deviation was at 100% (versus 84%). Pronation and supination values were 100% pre- and post-operatively.

Grip strength improved from 66 to 101% of the contralateral value. Pre-operative pain score (visual analogue scale) decreased from 6.3 to 0.2. The DASH score improved from 36.4 to 2.3. There was one case of complex regional pain syndrome (CRPS) with complete recovery after 14 months. Post-operative radiographic assess-

ment showed complete bone healing in all cases, within a mean time of 6.2 weeks.

References

1. Li S, Sun C, Zhou X, Shi J, Han T, Yan H. Treatment of intraosseous ganglion cyst of the lunate: a systematic review. Ann Plast Surg. 2019;82(5):577–81.
2. Rimokh J, Najjari H, Rotari V, Maes C, Lebeau N, Moughabghab M. Arthroscopy-assisted treatment of scaphoid and lunate cysts: clinical evaluation of 7 cases. Hand Surg Rehabil. 2018;37(6):358–62.
3. Bhatia DN. Direct "cystoscopic" approach for arthroscopic decompression of an intraosseous ganglion of the lunate. Arthrosc Tech. 2015;4(3):e223–9.
4. Ashwood N, Bain GI. Arthroscopically assisted treatment of intraosseous ganglions of the lunate: a new technique. J Hand Surg Am. 2003;28(1):62–8.
5. Paparo F, Fabbro E, Piccazzo R, Revelli M, Ferrero G, Muda A, et al. Multimodality imaging of intraosseous ganglia of the wrist and their differential diagnosis. Radiol Med. 2012;117(8):1355–73.
6. Cerlier A, Gay A-M, Levadoux M. Arthroscopic treatment of intraosseous ganglion cyst of the lunate bone. Arthrosc Tech. 2015;4(5):e513–8.
7. Osagie L, Gallivan S, Wickham N, Umarji S. Intraosseous ganglion cysts of the carpus: current practice. Hand (N Y). 2015;10(4):598–601.
8. Oka Y, Umeda K, Ikeda M. Cyst-like lesions of the lunate resembling Kienböck's disease: a case report. J Hand Surg Am. 2001;26(1):130–4.
9. Calcagnotto G, Sokolow C, Saffar P. [Intraosseous synovial cysts of the lunate bone: diagnostic problems]. Chir Main. 2004;23(1):17–23.
10. Moussallem CD, Arnalsteen DM, Khlifi H, Blanpain S, Mertl P, Gabrion A. Aneurysmal bone cyst of the lunate: case report. J Hand Surg Am. 2011;36(1):106–9.
11. Rajappa S, Kumar MM. Aneurysmal bone cyst of lunate treated by excision without intercarpal fusion: a case report. J Hand Surg Eur Vol. 2013;38(9):1007–8.
12. Sá Rodrigues A, Dopico C, Matos R, Pinto R, Vidinha V. Aneurysmal bone cyst of the lunate: case report and literature review. J Orthop. 2016;13(4):352–5.
13. Sokolow C, Saffar P. Anatomy and histology of the scapholunate ligament. Hand Clin. 2001;17(1):77–81.

Arthroscopic Excision of Dorsal and Volar Ganglion Cysts

112

Mireia Esplugas, Alex Lluch, Fabiana Necci, and Manuel Llusa Pérez

112.1 Background

Dorsal wrist ganglions are mucinous benign tumors that arise at the level of the dorsal scapholunate ligament (SLL). Sometimes these are easily visible and palpable under the skin, close to the extensor carpi radialis brevis (ECRB) distal tendon insertion. Even in those cases, their origin is at the SLL level. Sometimes the ganglion is not visible under the skin and it is difficult to palpate, so-called occult dorsal ganglia.

M. Esplugas (✉)
Institut Kaplan, Barcelona, Spain

A. Lluch
Institut Kaplan, Barcelona, Spain

Department of Orthopaedics, Vall d'Hebron Hospital, Barcelona, Spain

F. Necci
Department of Orthopaedics, Umberto Hospital, Lugo, Italy

M. Llusa Pérez
Department of Orthopaedics, Vall d'Hebron Hospital, Barcelona, Spain

Department of Anatomy, University of Barcelona, Barcelona, Spain
e-mail: mireia.esplugas@institutkaplan.com

112.1.1 Surgical Anatomy

Dorsal SLL reaches the midcarpal joint (Fig. 112.1) and is in contact with the Dorsal Intercarpal Ligament (DIC) that connects the dorsal aspect of the scaphoid and the triquetrum (Fig. 112.2). The dorsal capsuloligamentous scapholunate septum (DCSS) attaches the dorsal wrist capsule to the dorsal SLL and the DIC. The DCSS separates the dorsal radiocarpal and the dorsal midcarpal joint spaces (Fig. 112.3). The SLL, DIC, and the DCSS have a biomechanical role in scapholunate joint stabilization. Preserving all of them during dorsal ganglions excision may be beneficial.

All ganglions are mucinous collections secondary to a lesion of proper ligament or Sharpey fibers. In order to treat them, both the ganglion stump and the underlying degenerative ligament tissue and fibers must be excised. The risk of this tissue excision is an iatrogenic lesion of the dorsal SLL. The main advantage of arthroscopic ganglion excision technique is that the ganglion and its stump origin can clearly be seen and debrided while avoiding unnecessary sacrifice of healthy tissue.

Partial SLL ligament lesions associated with dorsal ganglion development may lead to SLL dynamic dysfunction. The advantage of arthroscopic dorsal ganglion excision technique is the opportunity to be able to directly check

© ISAKOS 2022

D. N. Bhatia et al. (eds.), *Arthroscopy and Endoscopy of the Elbow, Wrist and Hand*,
https://doi.org/10.1007/978-3-030-79423-1_112

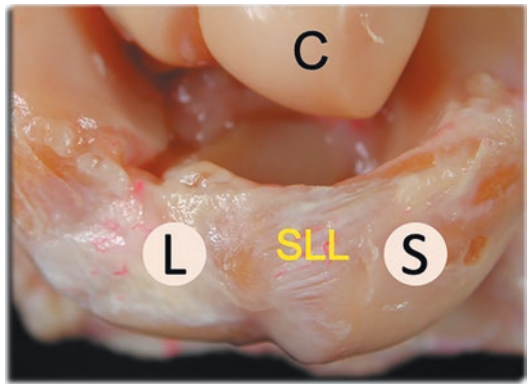

Fig. 112.1 Dorsal aspect of the central part of a left cadaveric first carpal row. The dorsal scapholunate ligament (SLL) reaches the most dorsal and distal joint space between scaphoid (S), lunate (L), and capitate (C)

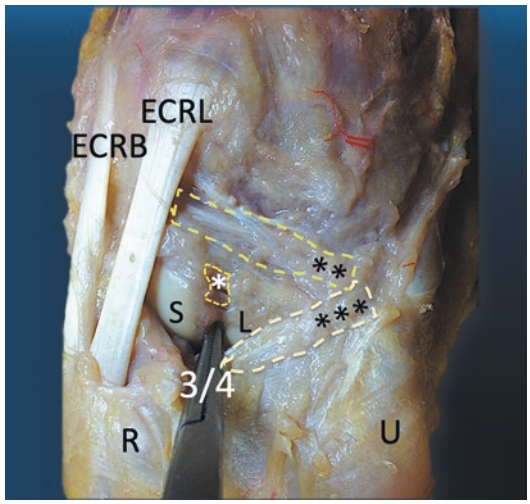

Fig. 112.2 Dorsal aspect of a right cadaver specimen wrist. Dorsal wrist capsule between the distal aspect of the radiotriquetral ligament (***) and the carpometacarpal joints have been removed. Dorsal scapholunate ligament (*) is aligned with the 3/4 portal and it is intimately related to the Dorsal Intercarpal Ligament (DIC) (**). Some dorsal ganglia that originate at the dorsal SLL ligament can be palpated between the distal tendons of the extensor carpi radialis brevis (ECRB) and extensor carpi radialis longus (ECRL) muscles. *R* radius, *U* Ulna

SLL mechanical properties, and to associate an SLL augmentation technique when dorsal SLL is partially torn.

Volar radiocarpal ganglion stumps mainly arise between volar radiocarpal ligaments (Fig. 112.4). Most volar ganglion pedicle stumps are found at the interval between radioscapho-

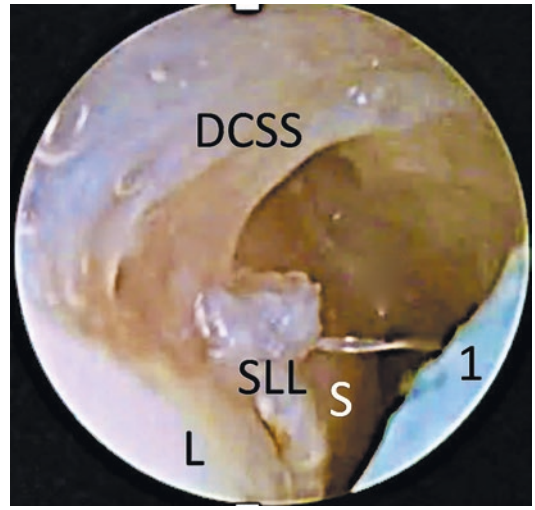

Fig. 112.3 Left radiocarpal joint space. The scope is in 6R portal. The needle enters the joint through the 3/4 portal. The dorsal capsuloligamentous scapholunate septum (DCSS) connects the SLL with the dorsal capsule (1). At this level, the DCSS is the roof of the dorsal radiocarpal joint space (*L* Lunate, *S* scaphoid)

Fig. 112.4 Right cadaver specimen wrist. The upper arrow shows the interval between the radioscaphocapitate (1) and the long radiolunate (2) ligaments. The lower arrow indicates the interval between the long (2) and the short (3) radiolunate ligaments. (*S* scaphoid bone, *L* lunate bone, *R* radius); (4) Testut Ligament (profundus radioscaphoid ligament)

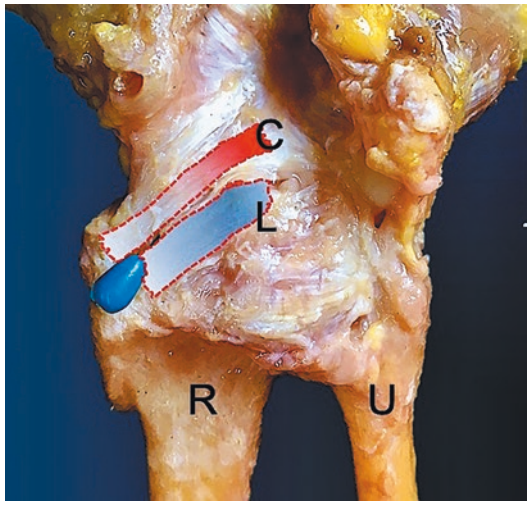

Fig. 112.5 Volar aspect of a left cadaver specimen wrist. Most of the volar ganglia stump arise in the interval between radioscaphocapitate (red) and long radiolunate (blue) ligaments. (*R* radius, *U* ulna, *L* lunate bone, *C* capitate bone)

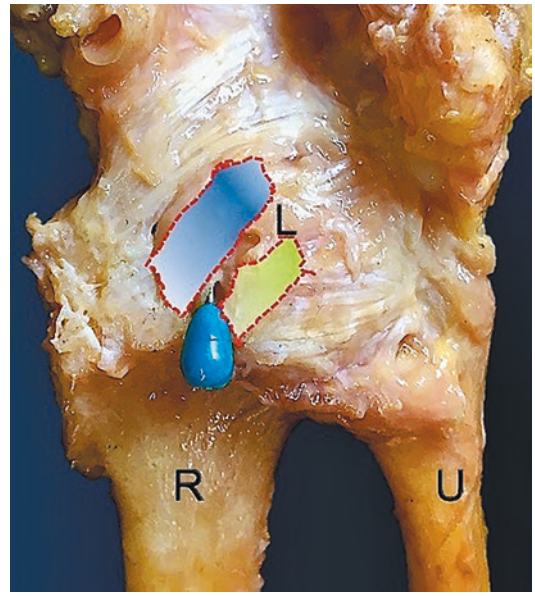

Fig. 112.6 Volar aspect of a left cadaver specimen wrist. Some of the volar ganglia stump arise in the interval between long (blue) and short (green) radiolunate ligaments. (*R* radius, *U* ulna, *L* lunate bone)

capitate and long radiolunate ligaments (Fig. 112.5). Some volar ganglia arise through the interval between short and long radiolunate ligaments (Fig. 112.6).

Less frequently, a ganglion can originate from the scaphotrapeziotrapezoid (STT) joint or flexor carpi radialis (FCR) distal tendon sheath.

112.2 Indications and Contraindications

- Primary arthroscopic ganglionectomy is indicated only when symptoms appear. Patients may complain of pain, loss of strength, or reduced range of motion (ROM) of the wrist. The pros and cons of surgery can be discussed with the patient in case of unacceptable aesthetics due to ganglion size.
- Arthroscopic ganglionectomy is also indicated in ganglion recurrence, especially when the primary procedure has been through open surgery, and could have created an iatrogenic intraarticular ligament lesion.

There are no specific contraindications for this procedure. Local infection and surgeon inexperience are contraindications for this procedure.

112.3 Surgical Technique

112.3.1 Preoperative Planning

Magnetic resonance imaging (MRI) can assist in identification of the pedicle and cyst wall location and help to plan the surgery, as the resection of the ganglion must be performed at the origin of the pedicle stump (Table 112.1).

- Some occult ganglia have the cyst wall in the radiocarpal joint; others in the midcarpal joint.
- Some dorsal and volar ganglia have a cyst wall in the extracapsular space; others are only intraarticular.
- Some extraarticular ganglia are multilobulated. These MRI findings do not contra-

Table 112.1 Pedicle and cyst wall location in the three different types of ganglions: occult; non-occult dorsal, and non-occult volar

	Pedicle	Articular cyst wall	Extraarticular cyst wall
Occult ganglion	RC *(d-SLL)*	RC *(under DCSS)*	NO
Occult ganglion	MC *(d-SLL)*	MC *(between d-SLL and DIC)*	NO
Occult ganglion	RC *(d-SLL)*	MC *(through DCSS)*	NO
Dorsal ganglion	RC	RC	YES *(distal aspect of RTq)*
Dorsal ganglion	MC	MC	YES *(proximal aspect of DIC)*
Volar RC ganglion	*Between RSC and LRL*	*Between RSC and LRL*	YES
Volar RC ganglion	*Between LRL and SRL*	*Between LRL and SRL*	YES

RC Radiocarpal joint space, *MC* Midcarpal joint space, *d-SLL* Dorsal portion of the scapholunate ligament, *RSC* Radio scaphocapitate ligament, *LRL* Long radiolunate ligament, *SRL* Short radiolunate ligament, *DCSS* Dorsal capsuloligamentous scapholunate septum, *DIC* Dorsal intercarpal ligament, *RTq* Radiotriquetral ligament

indicate arthroscopic ganglionectomy, but may suggest the need to perform a direct trans-cyst approach.

112.3.2 Ultrasound-Guided Volar Ganglion Methylene Blue Injection

Volar radiocarpal ganglion pedicles can arise between different volar radiocarpal ligaments. Ultrasound guided injection of 1 cc methylene blue into the ganglion before traction is applied to the wrist facilitating identification of the correct ligament interval which must be debrided (Figs. 112.7 and 112.8).

112.3.3 Box Theory

The wrist is like a box which can be reached through many different portals. The distance between our instrument and camera should be as long as possible to facilitate the instruments maneuverability. Therefore, depending on the ganglion location, different portals must be used. Figure 112.9 shows the usual portals for each type of ganglion excision.

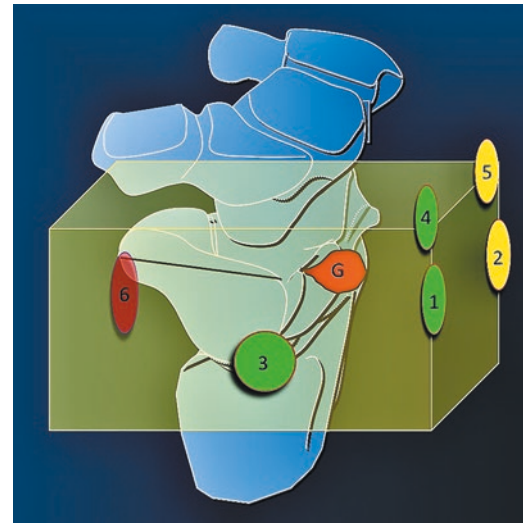

Fig. 112.7 Anesthesiology ultrasound equipment is useful to find volar ganglion cysts and to inject 1 cc of blue of methylene inside before starting the surgical procedure

112.3.4 Local Anesthesia

In most patients, the procedure can be done under local anesthesia. Each portal area is subcutaneously injected with 1 cc of epinephrine 1/100,000-lidocaine 2% solution, 30 min before starting the surgical procedure. Local anesthesia allows control of extensor tendons and flexor pollicis longus integrity after dorsal capsulectomy is performed in extraarticular dorsal ganglions or after volar radiocarpal ganglionectomy. Intraarticular surgical procedures are painless; nevertheless, if the patient informs of intraarticular pain or if synovectomy triggers some annoying bleeding, injection of epinephrine-lidocaine solution into the joint can be performed.

112.3.5 Dry Arthroscopy

Dry arthroscopy is preferred to avoid intraarticular soft tissue swelling which can difficult the

Fig. 112.8 Volar ganglion ultrasound study confirms that blue of methylene injection (green drawing) is not performed into the radiocarpal joint or next to the radial artery (red circle). (*: median nerve; white arrows: antebrachial fascia)

vision of the ganglion pedicle. Ensure that the valves of the arthroscope sheath are always open to allow free circulation of air and prevent capsular collapse and loss of visualization. Occasionally insert some saline to prevent shaver tamponade.

112.3.6 Preliminary Systematic Examination

An initial diagnostic assessment of both radiocarpal and midcarpal joint spaces should be performed in every case and a sequence from radial to ulnar, and volar to dorsal should be followed. The integrity of the triangular fibrocartilage complex (TFCC), volar lunotriquetral ligament, dorsal and volar scapholunate ligaments, three volar radiocarpal ligaments, and joint dorsal and volar capsule must be assessed.

112.3.7 Occult Dorsal Ganglion Cysts

These are located adjacent to dorsal SLL and can arise proximally, into the radiocarpal joint space or distally, into the midcarpal joint space.

- The arthroscope is introduced into the 3–4 portal to establish the 6R portal under direct intraarticular vision. The scope is then redirected to the 6-R portal.
- Establish, subsequently, the 1–2 portal under direct intraarticular control. Insert the hook through the 1–2 portal.
- Find the scapholunate interosseous membrane with the hook and follow it in a distal direction (Fig. 112.10) until the dorsal SLL is clearly seen. If the dorsal capsule (C) collapses the space, it can be pull-out with the hook or with a 1-0 suture entering through the 6R portal and exiting through the 3–4 portal.
- If the ganglion cyst is in the radiocarpal joint, it will be clearly seen at this moment (Fig. 112.11) with its stump emerging from the dorsal SLL ligament (Fig. 112.12).
- The shaver is then inserted into the 1–2 portal. The complete ganglion and his stalk can then be shaved; the d-SLL and DCSS should be preserved if the shaver is correctly directed under direct vision control from the 6R portal.
- The arthroscope is introduced into the MCU portal to establish the MCR portal under direct intraarticular vision. Instrumentation is through the MCR portal.
- Find the scapholunate interosseous joint space with the hook and direct it dorsally. It will get hooked over the dorsal SLL ligament that can be, at this moment, palpated and strained. At

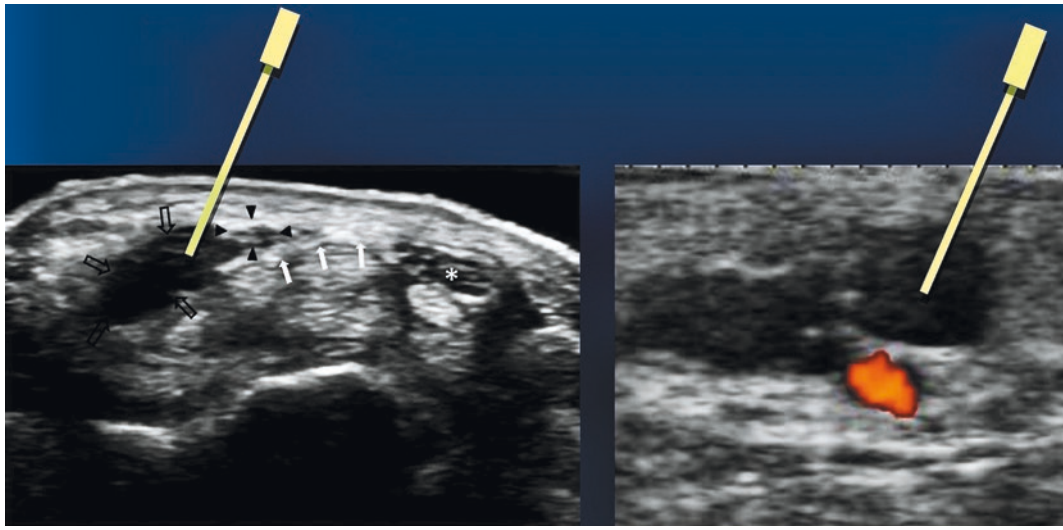

Fig. 112.9 The wrist box concept. Depending on the ganglion pedicle and cyst wall locations, the useful portals will vary in each case. To treat an occult radiocarpal joint ganglion (G), the scope should be introduced through the 6R portal (2) and the instruments through the 1/2 portal (3). To treat a large dorsal radiocarpal ganglion, the scope should be introduced through a volar portal (6) and the shaver through the 6R (2) or the 1/2 (3) portal. When the ganglion cyst wall has been removed, we should introduce the scope in 6R (2) and the shaver in the 1/2 portal to resect the pedicle stump at the dorsal aspect of the dorsal SLL. To treat a large dorsal extraarticular radiocarpal joint ganglion, the scope should be introduced through a volar portal (6) and the shaver through the 6R (2) or the 1/2 (3) portals to resect the capsule around the ganglion pedicle without damaging the radiotriquetral ligament or the dorsal intercarpal ligament (DIC) (see Fig. 112.2). To treat a dorsal midcarpal ganglion, the scope should be introduced in the MCU portal (5) and the instruments through the MCR (4) portal. A volar midcarpal portal can also be used to introduce the scope and facilitate the instruments maneuverability. To treat a volar radiocarpal ganglion, the scope should be introduced through the 6R portal (2) and the instruments through the 3/4 Portal (1)

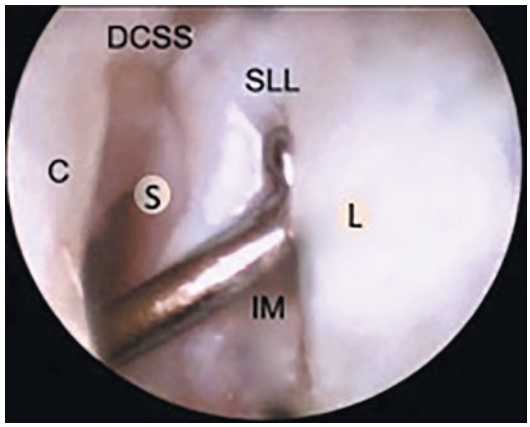

Fig. 112.10 Radiocarpal joint space arthroscopy of a right wrist. Scope is in 6R portal. The hook is in the 1–2 portal. The hook is in most distal dorsal portion of the interosseous membrane (IM) between the scaphoid (S) and the lunate (L), and is pointing the dorsal capsuloligamentous scapholunate septum (DCSS). (*C* dorsal capsule)

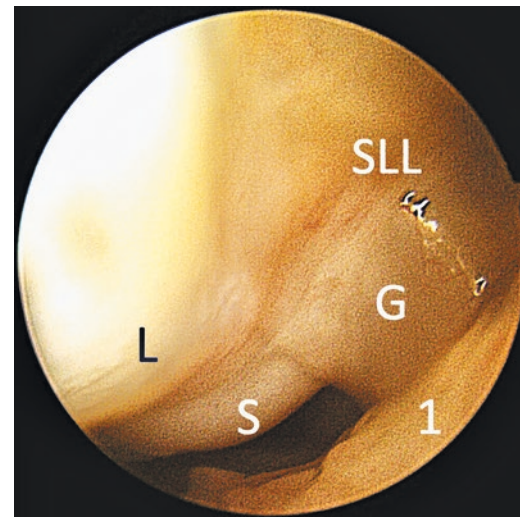

Fig. 112.11 Radiocarpal joint space arthroscopy of a left wrist. Scope is in 6R portal. An Occult ganglion (G) arising from the dorsal aspect of the dorsal scapholunate ligament (SLL) is clearly seen. (*L* lunate bone, *S* scaphoid bone, *1* dorsal capsule)

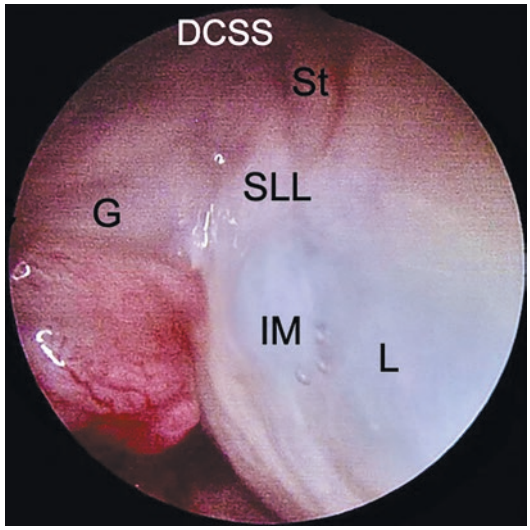

Fig. 112.12 Radiocarpal joint space arthroscopy of a right wrist. Scope is in 6R portal. The radiocarpal occult ganglion stalk (St) emerges besides the dorsal scapholunate ligament (SLL). The ganglion (G) is just under the dorsal capsuloligamentous scapholunate septum (DCSS). (*IM* interosseous scapholunate membrane, *L* lunate bone)

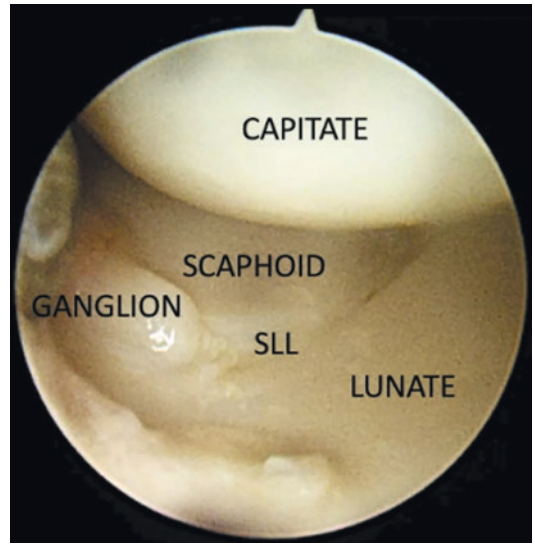

Fig. 112.13 Midcarpal joint space arthroscopy of a right wrist. The scope is in the MCU portal. A midcarpal occult ganglion emerges into the joint at the dorsal aspect of the dorsal scapholunate ligament (SLL)

its dorsal portion, the hook will be able to palpate the distal surface of the DCSS and the DIC at its dorsal aspect.

- If the ganglion cyst is in the midcarpal joint, it will be clearly seen (Fig. 112.13) and its stump can be clearly visualized emerging between the dorsal aspect of the SLL ligament and the volar aspect of the DIC (Fig. 112.14).
- The shaver is then be inserted into the MCR portal to completely shave the ganglion and his stalk, preserving the SLL, the DCSS, and the DIC, under direct vision control from the MCU portal.
- The ganglion stalk may be thin and long: in these cases, it emerges at the radiocarpal dorsal aspect of the SLL, pierces the DCSS distally and the cyst wall can be found in the midcarpal joint. This is the reason why both radiocarpal and midcarpal joint space arthroscopies should always be performed during arthroscopic ganglionectomy.

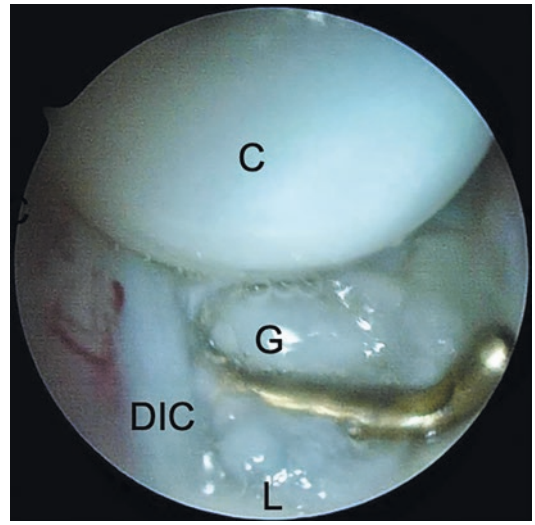

Fig. 112.14 Midcarpal joint space arthroscopy of a right wrist. The scope is in the MCU portal, and the hook in the MCR portal. A midcarpal occult ganglion (G) emerges into the joint between the dorsal aspect of the dorsal scapholunate ligament and the dorsal intercarpal ligament (DIC). (*C* capitate)

112.3.8 Non-occult Dorsal Intracapsular Ganglion Cysts

The stump arises at the dorsal SLL but they are bulky (non-occult). Most of them are in the radiocarpal joint (Fig. 112.15).

Although the ganglion emerges from the dorsal aspect of the SLL, its bulky cyst invades all the dorsal intracapsular aspect of the radiocarpal joint. In this case, trying to reach the stump before shaving the cyst can be difficult. Nevertheless, after cyst removal with the shaver, the SLL should be reached following the steps mentioned above, to carefully debride any degenerative ligament fibers at this level. Radiofrequency is not recommended: SLL is richly innervated and heat can damage the mechanoreceptors contained in its ligament fibers.

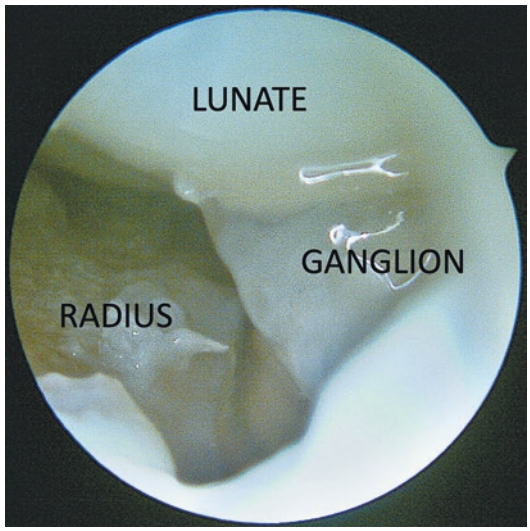

Fig. 112.15 Radiocarpal joint space arthroscopy of a right wrist. The scope is in 6R portal. Although the ganglion emerges from the dorsal aspect of the SLL, its bulky cyst invades all the dorsal intracapsular aspect of the joint. In this case, trying to reach the stump before shaving the cyst can be difficult. Nevertheless, after cyst shaving, the SLL should be located to cautiously debride any degenerative ligament fibers at its level

112.3.9 Non-occult Dorsal Extracapsular Ganglion

The stump arises at the dorsal SLL but the ganglion emerges into the extracapsular space and becomes palpable. Most of these are in the radiocarpal joint. They become extraarticular through the 3–4 portal area, at the distal margin of the radiotriquetral ligament. Less frequently they are midcarpal ganglions which exit the joint at the proximal margin of the DIC ligament.

- During excision, the intraarticular steps reviewed above have to be combined with a dorsal 1 cm^2 capsulectomy. We perform a cyst-sparing portal technique but we usually pass a 18–22-gauge needle through the cyst into the joint at the level of the stalk, to better identify the area where the capsulectomy has to be done; this typically will be at the 3–4 interval. In the same way, we usually introduce the scope in a volar portal to ensure that the capsulectomy preserves the radiotriquetral ligament (in the radiocarpal joint) (Fig. 112.16)

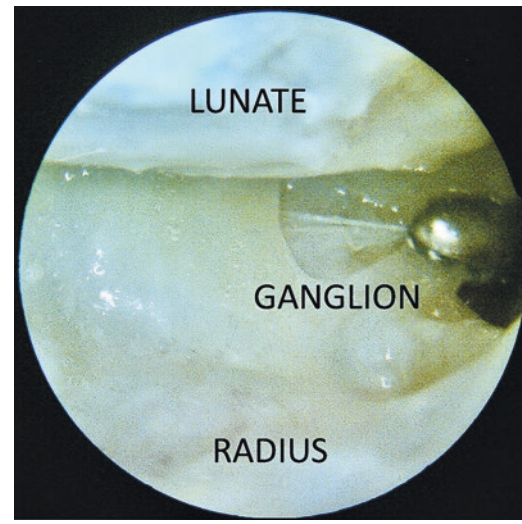

Fig. 112.16 Radiocarpal joint arthroscopy of a left wrist. Scope is in the volar central portal and the shaver in 6R portal. The fibers of the radiotriquetral ligament are visible when synovectomy is performed. Direct visualization of the ligament avoids damage to ligament fibers during dorsal capsulectomy

or the dorsal intercarpal ligament (in the midcarpal joint).
- We usually scope from the volar central portal which was described by Fernando Corella. This portal allows vision of both radiocarpal and midcarpal joints, without any volar ligament damage (Fig. 112.17).
- Dorsal capsulectomy is performed until visualization of the extensor tendons (usually one of the Extensor Digitorum Communis or occasionally ECRB tendon).

112.3.10 Volar Ganglion Cysts

Their stump arises in the volar aspect of the wrist through the volar radiocarpal joint space and is usually associated with a ligament area degeneration. The ligament degeneration is sometimes difficult to appreciate until synovectomy of the dorsal aspect of the volar radiocarpal ligaments has been completed (Fig. 112.18). Intra-lesional methylene blue injection may help to identify the proper ligament interval where the cyst stump is located, as the cysts are not visible from inside the joint.

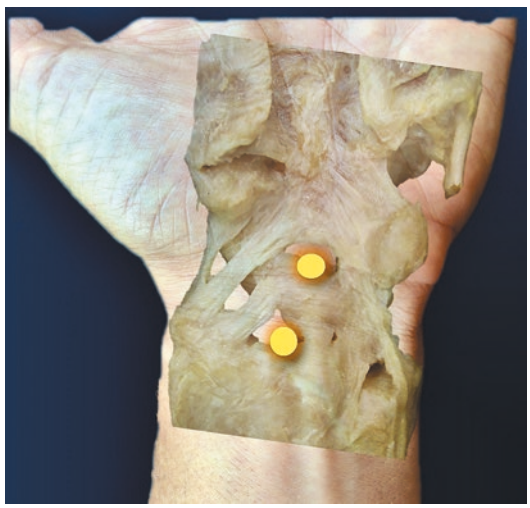

Fig. 112.17 The volar central portal described by Corella F. et al. allows access to both radiocarpal and midcarpal joints (yellow circles). It is centered on the lunate, with the volar structures at risk protected by the tendons. It is a reproducible and safe portal that allows radiocarpal and midcarpal joints inspection through one single incision centered between both wrist creases

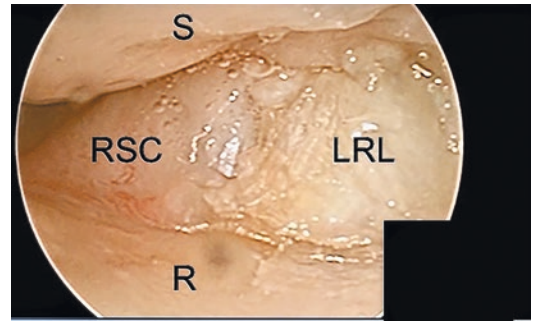

Fig. 112.18 Right radiocarpal joint arthroscopy. Scope is in 3–4 portal. Degeneration of long radiolunate ligament (LRL) fibers is clearly seen. This degenerative ligament area must be debrided with the shaver introduced into the joint through the 1–2 portal. The volar ganglion is presumably at the volar aspect of this area: the initial introduction of the hook into the interval between the radioscaphocapitate (RSC) and the long radiolunate ligaments combined with a digital pressure on the cyst area should show the presence of some mucinous cyst content (colored in blue if the cyst has previously been injected with methylene blue)

- The arthroscope is introduced through 3–4 portal and instrumentation is through the 1–2 portal.
- The ligament interval and the cyst stump are identified with the hook probe.
- The shaver should be introduced to debride the ligament degenerative area and to drain the cyst capsule contents (Fig. 112.19).
- External digital pressure over the cyst helps to pour away the cyst contain into the joint.
- The cyst capsule is not removed. The patient should be informed preoperatively that a swelling or tumor will persist at the area for 3 weeks; this is the remnant cyst capsule and will slowly disappear.

112.4 Technical Tips

- Dorsal radiocarpal capsule can be separated from the dorsal aspect of the first carpal row bones by using dorsal traction with a simple 1-0 suture thread or a nitinol wire inserted through

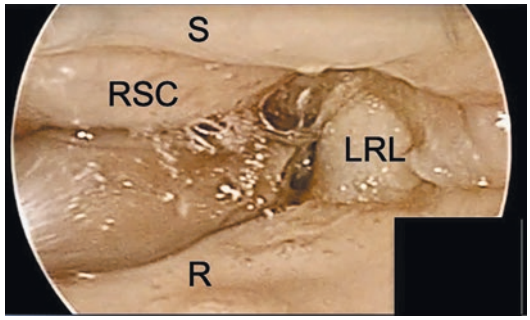

Fig. 112.19 Right radiocarpal joint arthroscopy. Scope is in 3–4 portal; the shaver is in 1–2 portal. Degeneration of long radiolunate ligament (LRL) fibers is clearly seen and must be debrided. The volar ganglion is presumably at the volar aspect of this area: a hook is passed into the interval between the radioscaphocapitate (RSC) and the long radiolunate ligaments and combined with a digital pressure on the cyst area to see some mucinous cyst content (colored in blue if the cyst has previously been injected with methylene blue)

the 3–4 portal and exiting through the 6R portal. This maneuver facilitates the dorsal SLL inspection during radiocarpal joint arthroscopy.

- Radiofrequency is not recommended: heat can damage the extensor tendons in dorsal capsulectomy, SLL innervation in occult ganglionectomy, and median nerve or radial artery in volar ganglion excision.
- Intermittent saline joint injection is the better system to avoid shaver tamponade and intraarticular soft tissue swelling; half intensity suction is recommended to allow good shaving function without capsule collapse.
- An accessory instrument portal to insert the hook while the shaver is in action helps to actively protect the SLL, DIC, DCSS, or RTq ligaments from some iatrogenic damage. The assistant becomes a key point.
- Dorsal capsulodesis should be performed after dorsal ganglion excision if the SLL seems mechanically incompetent during the hook test.

112.5 Pitfalls

- Arthroscopic ganglion cyst excision should be performed by those who have basic competency with wrist arthroscopy.
- Complete resection of the ganglion stalk, synovitis, and redundant cyst capsule is the standard approach for arthroscopic ganglionectomy.
- Multi-lobulated cyst detected on MRI can also be arthroscopically treated.
- Aggressive arthroscopic dorsal capsulectomy can result in extensor tendon injury.
- When performing arthroscopic resection of volar wrist ganglion cyst, the proximity of the major neurovascular structures must be considered: radial artery lesions, injury of the median nerve, and neuropraxia of the superficial radial nerve have been described.
- Methylene blue should be injected under ultrasound guidance to avoid intraarticular administration.

112.6 Postoperative Management and Rehabilitation

- Stitchless closure (steri strips are adequate) and soft splint for 7 days.
- Edema control of the hand during the first 2 days.
- Active finger motion is encouraged from the first day.
- Finger motion (extensor tendons) is checked and all patients are taught active and passive wrist motion after 1 week immobilization. Avoidance of strenuous activities for 4–6 weeks is recommended, except for those with concomitant intraarticular abnormalities.

112.7 Complications

- Incomplete cyst excision.
- Extraarticular edema after dorsal capsulectomy in wet arthroscopy.
- Dorsal extensor tendon injury or tenosynovitis.
- Median nerve neuroapraxia.
- Scapholunate ligament injury.
- Stiffness.

113 Ulnar Styloid Enthesopathy and Extensor Carpi Ulnaris Instability: Styloidectomy and Groove-Plasty

Gregory Hoy and Timothy Wood

113.1 Background

ECU tendinopathy and UCL enthesopathy are two anatomically closely related conditions that occur in tennis and golf [1, 2]. ECU tendinopathy is widely reported in sports literature in golfers, and also occurs in tennis players in the non-dominant wrist of double-handed backhand players [1, 2]. It can be due to overuse, but may also occur secondary to ECU subluxation over the volar lip of the ECU groove on the ulna [3]. ECU subluxation can present as an acute condition, but also can occur as a normal finding [4, 5]. Reconstruction can be anatomic but usually requires extensive rehabilitation [6]. ECU groove-plasty is an alternative procedure performed by excising the volar lip of the ECU groove; this allows free movement of the ECU without catching on the bone and thus eradicating symptoms [7]. The second condition is a localized enthesopathy of the ulnar collateral ligament at its styloid attachment. This ligament is now well recognized, but most descriptions of pain in this area relate to ulnar styloid impingement, a condition best described in another chapter and treated arthroscopically by resection alone [1, 8, 9]. This chapter describes a mini-open procedure that involves (a) ulnar styloidectomy and reattachment of the foveal triangular fibrocartilage complex (TFCC) with a cerclage suture to correct the tension in the complex structures in the region [10, 11], and (b) ECU groove-plasty for management of ECU subluxation, for early successful return to competitive tennis and golf.

113.1.1 Surgical Anatomy

The terminology surrounding the UCL is confusing and not consistent. The ulnar collateral ligament is described as rounded in shape and attached proximally to the tip of the styloid process of the ulna and distally to the ulnar aspect of the triquetral bone as well as the pisiform and flexor retinaculum. It is sometimes called the ulno-triquetral ligament [12]. Whilst it has been described as an amorphous structure, it is well recognized on MRI scanning. It provides restraint when the wrist is maximumly radially deviated, and prevents compression when ulnar deviating as the styloid process approaches the triquetrum. The traction and compression placed on the UCL may occur in varying degrees of flexion or extension of the wrist itself. The main styloid attachment of the ligament often is associated with cystic change in the tip of the styloid in symptomatic individuals (Fig. 113.1), with MRI changes of oedema and disorganization of fibres

G. Hoy (✉) · T. Wood
Melbourne Orthopaedic Group,
Melbourne, VIC, Australia

Department of Surgery, Monash University,
Melbourne, VIC, Australia
e-mail: gahoy@mog.com.au;
office@drtimwood.com.au

© ISAKOS 2022

D. N. Bhatia et al. (eds.), *Arthroscopy and Endoscopy of the Elbow, Wrist and Hand*,
https://doi.org/10.1007/978-3-030-79423-1_113

(Fig. 113.2a). The ECU may be dislocated (Fig. 113.2b) but often requires dynamic ultrasound to diagnose definitively.

113.2 Indications and Contraindications

Indications for UCL reconstruction with styloidectomy include:

Fig. 113.1 Radiograph shows ulnar styloid cystic changes

- Localized pain over the UCL at the styloid tip with or without possible styloid impingement in a golfer or tennis player.
- Reproduction with both stretch and compression of the ulnar side of the wrist in dorsiflexion.

Indications for ECU groove-plasty include:

- Symptomatic acute or subacute proven ECU subluxation with loaded wrist in ulnar and radial deviation.
- Painful chronic subluxation in golfers and tennis players.

Contraindications include ulnar positive variance and distal radioulnar joint dysfunction.

113.3 Surgical Technique

The patient is positioned supine and the upper extremity is placed on a radiolucent hand table. A non-sterile tourniquet is placed in the upper arm and inflated to 250 mmHg after exsanguination.

- Through a dorso-ulnar zig-zag mini-incision, the ECU tendon sheath is opened to demonstrate any tendinopathy and to assess any pathological motion over the volar lip of the bony groove (Fig. 113.3).

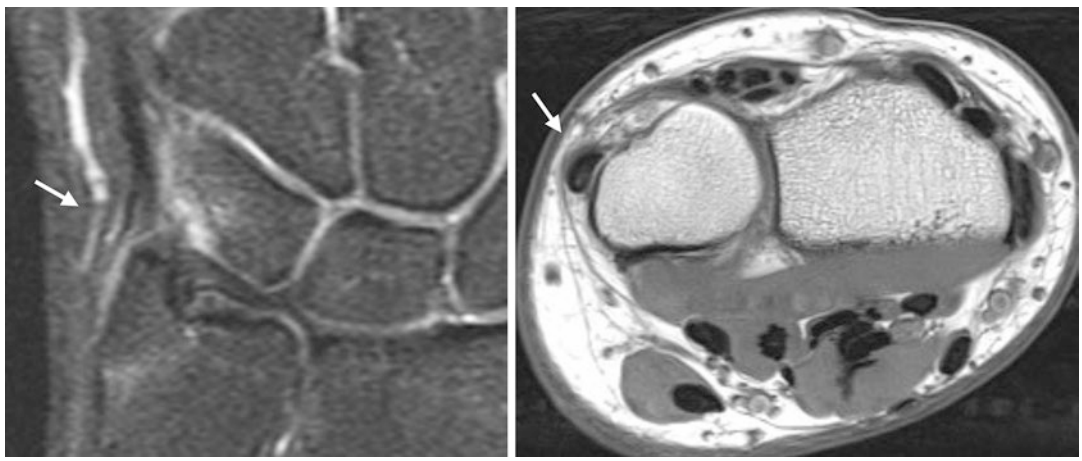

Fig. 113.2 Magnetic resonance imaging shows UCL oedema (arrow, left image) and a dislocated ECU (arrow, right image)

- The ulnar styloid is exposed with sharp dissection and removed with a small oscillating saw (obliquely to prevent recurrent and or heterotopic bone recurrence) (Fig. 113.4a, b).
- The ECU groove is exposed proximal to the styloid, and shaved with the hand in pronation on the operating table and enough bone is removed to see the ECU tendon able to shift freely from dorsal to volar (Fig. 113.5a, b). The same saw is used as it is easier to control shaving with a saw than a burr.
- Next, the elbow is flexed up to 90°, and the wrist is supinated to show residual bone. Shaving of the bone is continued with the wrist supinated, and the bone is resected out of the way of the ECU in both positions (Fig. 113.6a–c).
- The ulnar collateral ligament (UCL), triangular fibrocartilage, and anterior and posterior capsule of the distal radioulnar joint are all sutured back with a purse-string type suture onto to the ulna in the bare area left behind from the styloidectomy. This suture is passed trans-osseously using an absorbable suture to be tied over the shaft of the ulna in a position away from the sliding ECU tendon (Fig. 113.7a, b).
- The retinaculum is then closed over the ECU tendon (Fig. 113.8) as it now lies free of the bony ridge, and the wound closed with subcuticular suture.

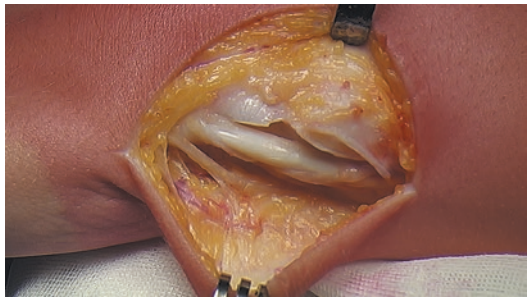

Fig. 113.3 A dorso-ulnar incision is used to expose the ECU tendon

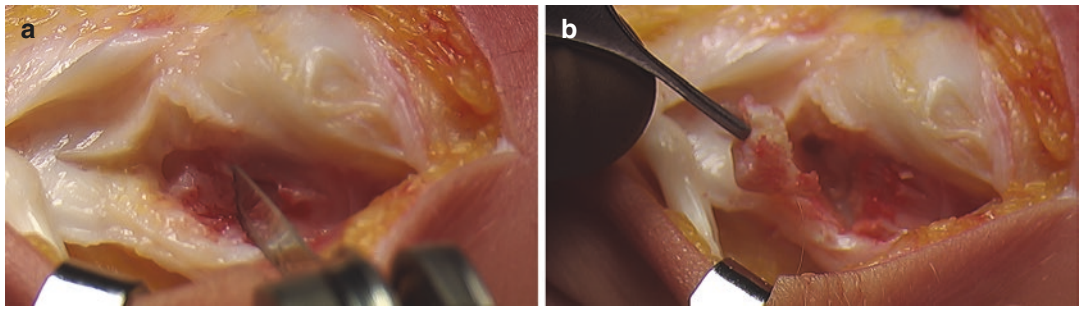

Fig. 113.4 (**a**) Styloidectomy is performed using a mini-oscillating saw. (**b**) Resected styloid is seen after excision

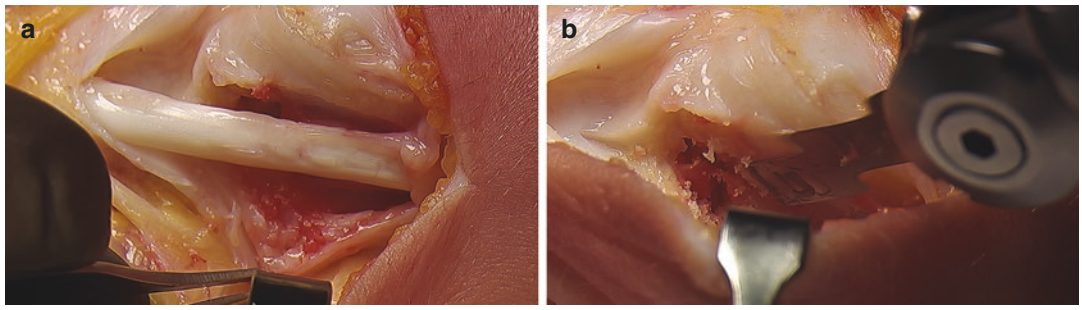

Fig. 113.5 (**a**) Exposed ECU groove and volar ridge are seen. (**b**) ECU groove is shaved with hand in pronation using a saw

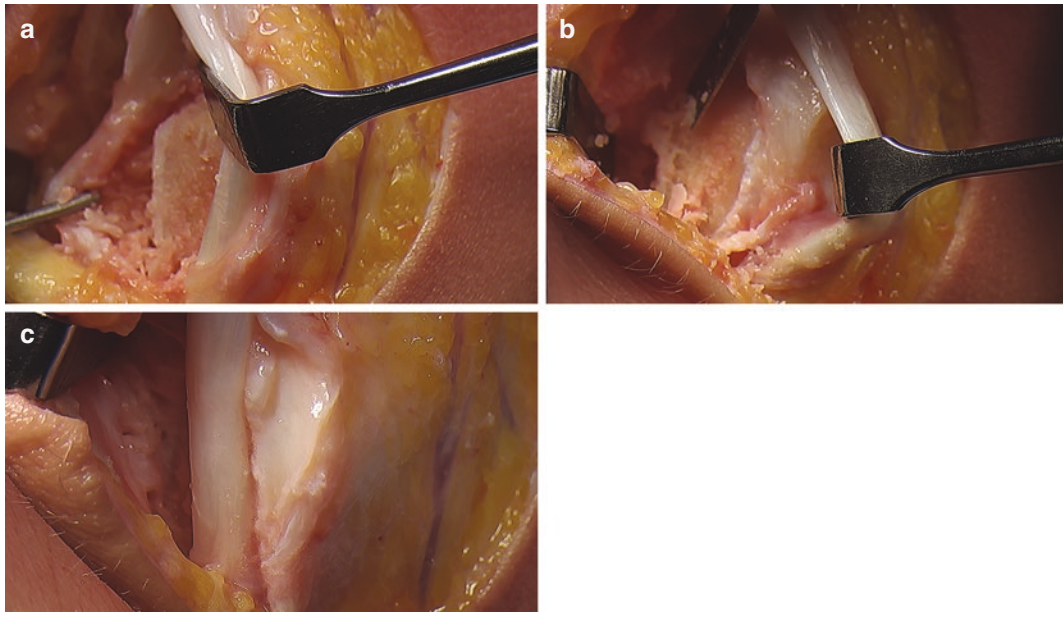

Fig. 113.6 (**a**) Residual bone ridge is seen in supination. (**b**) Bone resection is performed to excise the residual ridge. (**c**) Free movement of ECU is demonstrated with no residual impingement

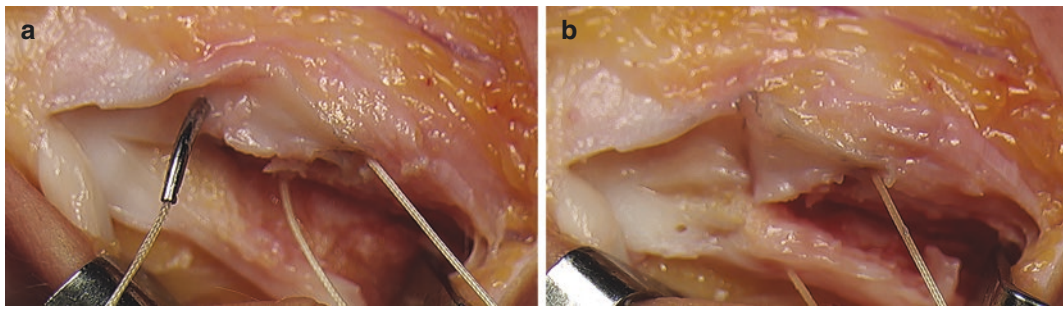

Fig. 113.7 (**a**, **b**) Transosseous suture is used for reattachment of UCL and TFCC to the ulna

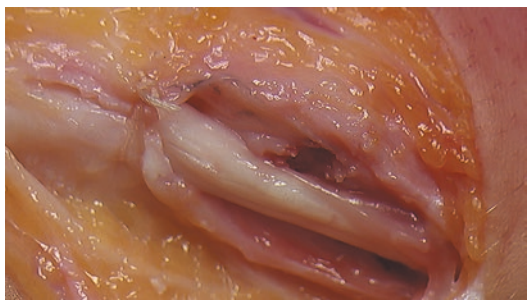

Fig. 113.8 First retinacular suture is shown as the retinaculum is closed over the ECU

113.4 Tips and Tricks

- The styloid resection should be oblique to prevent a sharp edge to the resection margin. We use a small oscillating saw for a larger styloid and a rongeur for smaller styloid.
- The groove-plasty should be performed before reattaching the TFCC cerclage suture to prevent damage to the repair.

113.5 Pitfalls

- Overtightening the ECU retinaculum
- Leaving behind too much bone on the ridge
- UCL suture knots irritating ECU

113.6 Post-operative Management and Rehabilitation

The wrist is immobilized for 1–2 weeks. Thereafter, a comprehensive rehabilitation program of both range of motion and strength under the guidance of a hand therapist is initiated. Return to double-handed back hand tennis playing is approximately at 3 months post-surgery.

113.7 Complications

- Post-operative scarring of the ECU may result in persisting pain, and early movement is encouraged to prevent this.
- Branches of the dorsal ulnar nerve should be protected, especially the transverse branch heading across from the main dorsal branch at the level of the styloid.

113.8 Results

In the author's series over 12 years, 17 high level amateur or professional tennis players and 10 high level amateur or professional golfers underwent this procedure. Of these 27 patients, 17 had UCL alone, 3 had ECU alone, and 6 had combined UCL and ECU procedures. At last follow-up or on-line career statistics, one patient had died, 2 patients had not returned to their level of sport, and 25 had returned at or higher than the level of sport pre-operatively.

References

1. Turker T, Sheppard JE, Klauser AS, Johnston SS, Amerongen H, Taljanovic MS. The radial and ulnar collateral ligaments of the wrist are true ligaments. Diagn Interv Radiol. 2019;25(6):473–9.
2. Stuelcken M, Mellifont D, Gorman A, Sayers M. Wrist injuries in tennis players: a narrative review. Sports Med. 2017;47(5):857–68.
3. Campbell D, Campbell R, O'Connor P, Hawkes R. Sports-related extensor carpi ulnaris pathology: a review of functional anatomy, sports injury and management. Br J Sports Med. 2013;47(17):1105–11.
4. Rowland SA. Acute traumatic subluxation of the extensor carpi ulnaris tendon at the wrist. J Hand Surg Am. 1986;11(6):809–11.
5. Pratt RK, Hoy GA, Bass Franzcr C. Extensor carpi ulnaris subluxation or dislocation? Ultrasound measurement of tendon excursion and normal values. Hand Surg. 2004;9(2):137–43.
6. MacLennan AJ, Nemechek NM, Waitayawinyu T, Trumble TE. Diagnosis and anatomic reconstruction of extensor carpi ulnaris subluxation. J Hand Surg Am. 2008;33(1):59–64.
7. Oka Y, Handa A. Recurrent dislocation of the ECU tendon in a golf player: release of the extensor retinaculum and partial resection of the ulno-dorsal ridge of the ulnar head. Hand Surg. 2001;6(2):227–30.
8. Scarano KA, Owusu-Sarpong S, Mulligan MT. Bilateral ulnar styloid impaction syndrome treated with ulnar styloidectomy. J Wrist Surg. 2019;8(3):240–4.
9. Bain GI, Bidwell TA. Arthroscopic excision of ulnar styloid in stylocarpal impaction. Arthroscopy. 2006;22(6):677.e1–3.
10. Goorens CK, Anthonissen L, Goubau JF. Styloidectomy and reattachment of the triangular fibrocartilage complex for longstanding nonunion of the ulnar styloid. J Hand Surg Eur Vol. 2020;45(7):763–5. https://doi.org/10.1177/1753193420919027.
11. Moritomo H, Masatomi T, Murase T, Miyake J, Okada K, Yoshikawa H. Open repair of foveal avulsion of the triangular fibrocartilage complex and comparison by types of injury mechanism. J Hand Surg Am. 2010;35(12):1955–63.
12. Tay SC, Berger RA, Parker WL. Longitudinal split tears of the ulnotriquetral ligament. Hand Clin. 2010;26(4):495–501.

114 Arthrosopic Ulnar Styloidectomy for Ulnar Styloid Impaction Syndrome

Gregory I. Bain and Kevin Eng

114.1 Background

Ulnar styloid impaction syndrome is characterized by the impaction of the triquetrum against an excessively long ulnar styloid causing chondromalacia, synovitis and ulnar sided wrist pain [1–3]. The ulnar styloid process is a separate carpal element until it joins to the developing ulnar at around the tenth week of ontogenesis with chondrification usually occurring approximately 51 days in utero. The ulnar styloid elongates and becomes more adult-like until physeal closure with ossification late in adolescence [4]. Biyani et al. reported great variation in ulnar styloid process lengths and defined a standard ulnar styloid process to be 3–6 mm in length with a medial angulation less than 15° [5]. Giachino et al. suggested a classification of ulnar styloid impaction syndrome and described the aetiology as static (bringing the styloid to the triquetrum or bringing the triquetrum to a normal length ulnar styloid) and dynamic (ligament laxity, instability, loading activities) or a combination of the two [6]. Conditions that bring the styloid closer to the triquetrum include a congenitally long ulnar styloid process, styloid overgrowth after fracture or rheumatoid arthritis related hypertrophy [7, 8]. Conditions that bring the triquetrum closer to the ulnar styloid include radial shortening from malunions of distal radius fractures or physeal arrest, radial shortening from radial head resection or Essex-Lopresti lesions, Kienbock's disease, and wrist arthrodesis [6].

114.2 Surgical Anatomy

The meniscus homologue is normally interposed between the tip of the ulnar styloid and the triquetrum [3]. In early stages of ulnar styloid impaction syndrome there is soft tissue erosion before the styloid comes in contact with triquetrum. With progression the triangular fibrocartilaginous complex (TFCC) may wear out and the exposed tip of the ulnar styloid can come into direct contact with the triquetrum (Fig. 114.1). Pronation and supination change the contact patterns. In pronation the volar ulnar surface of the triquetrum contacts the styloid. Maximal contact in pronation is found with the addition of flexion and ulnar deviation of the wrist. In supination the dorsal aspect of the triquetrum contacts the ulnar styloid and additional extension and ulnar deviation leads to maximal contact. On imaging, patients with ulnar styloid impaction syndrome may have a longer than average ulnar styloid with

G. I. Bain (✉)
Department of Orthopaedic Surgery, Flinders University, Adelaide, SA, Australia
e-mail: admin@gregbain.com.au

K. Eng
Department of Orthopaedics and Trauma, Barwon University Hospital, Barwon CORE, Geelong, VIC, Australia
e-mail: Kevineng@geelongortho.com.au

© ISAKOS 2022

D. N. Bhatia et al. (eds.), *Arthroscopy and Endoscopy of the Elbow, Wrist and Hand*,
https://doi.org/10.1007/978-3-030-79423-1_114

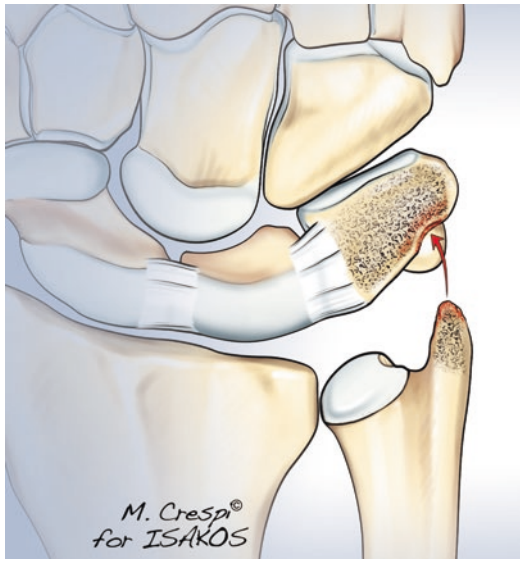

Fig. 114.1 Impaction of the ulna styloid tip against the triquetrum

positive ulnar variance [9, 10]. A long ulnar styloid process can be defined radiographically on neutral rotation posteroanterior radiographs as being greater than or equal to 6 mm from the tip of the styloid to the base of the groove between the styloid and the head of the ulna (mean 4.4 ± 1.2 mm). However, an anteroposterior radiograph can lead to a 10% difference in measured styloid length [11]. To overcome the problem with radiographic magnification, two main methods have been described to identify relative ulnar styloid lengths: (a) Garcia-Elias described the Ulnar Styloid Process Index (USPI) on an anteroposterior radiograph. The length of the ulna styloid minus the ulna variance was measured, then divided by the width of the ulna head. A USPI of greater than 0.21 ± 0.07 was suggestive of a long styloid [12]. (b) Van der Heijden suggested that the Ulnar Styloid–Capitate ratio (SCR) had a stronger correlation with the relative length of the ulnar styloid and eliminated differences related to gender. They measured the length of the styloid divided by the length of the capitate in a posteroanterior radiograph. A long styloid was defined as having a SCR greater than 0.18 ± 0.05 [11]. Other imaging modalities like dynamic fluoroscopy and 3D computed tomography can also be used to confirm impingement [9].

114.3 Indications and Contraindications

- A patient with symptomatic ulnar styloid impaction will typically complain of ulnar sided wrist pain in specific positions, such as having their hands on their hip or in their back pockets [9]. This position places the hand in relative supination combined with extension and ulna deviation. Dynamic symptoms may occur in racquet sports such as tennis. On examination, there is point tenderness of the ulnar styloid tip [10]. Provocative tests include Ruby's ulnar styloid provocation test [1]. This is elicited by taking the dorsiflexed wrist from neutral position into full supination which decreases space between the styloid process and triquetrum and increases ulnar styloid loading. This is distinct from ulno-carpal impaction, (where the ulnar head contacts the lunate); here, tenderness is more midline and dorsal on the proximal lunate, and the ulnar deviation grind test reproduces the pain [6].
- The senior author has also performed arthroscopic resection of symptomatic ulnar styloid non-unions which may occasionally produce ulnar sided wrist pain similar in nature to ulnar styloid impingement.

Ulna sided wrist pain that occurs as a result of other causes will not improve with this surgery. Instability of the DRUJ may be exacerbated by removal of styloid and surrounding soft tissues and should be addressed simultaneously.

114.4 Surgical Technique

Operative treatment is aimed at correcting the impaction of the ulnar styloid, without compromising the ligamentous stability of the DRUJ. The foveal insertion of the TFCC in particular should be carefully preserved [13]. In the presence of a congenital long ulnar styloid, excision of the styloid is performed as an open or arthroscopic procedure [7, 14]. An open oblique ulnar styloid osteotomy has been described to protect all ligamentous attachments and not just the foveal TFCC attachment [13]. If the patient also has

ulnar carpal impaction (where the ulna head contacts the proximal lunate), then an ulnar shortening procedure may correct the impaction of both the ulnar head and styloid. Combining a wafer procedure with styloid shortening is another surgical option [3].

The senior author's preferred technique is an arthroscopic partial resection of the styloid as it does not compromise TFCC or ulno-carpal ligaments attached to the base of the styloid, minimizing the risk of iatrogenic instability [9].

- The DRUJ is examined under anaesthesia for stability and compared to the opposite (unaffected) side. A greater translation than normal may indicate a TFCC injury.
- Wrist arthroscopy is performed through the standard 3–4 and 6 U portals, created with blunt dissection to preserve the dorsal cutaneous branch of the ulnar nerve.
- With the arthroscope positioned in the 3–4 portal, the probe is introduced into the 6R portal. The TFCC, lunotriquetral ligament complex, and pisotriquetral recess are all assessed for concomitant pathology.
- The probe can be used to help identify the styloid tip by palpation, and visually the styloid may have an eburnated appearance. The burr is placed onto the tip of the ulnar styloid. This portion of the procedure can be done with dry arthroscopy if desired (Fig. 114.2).
- Fluoroscopy is used to confirm correct placement of the burr on the ulnar styloid prior to resection. Removal of the desired amount of ulnar styloid can also be confirmed by fluoroscopy with care to preserve and respect the insertion of the TFCC at the base of the ulnar styloid. The goal is to eliminate impingement on intraoperative fluoroscopic assessment. Resection of 3 mm of ulnar styloid resection is recommended [9] (Figs. 114.3 and 114.4).
- For resection of an ulnar styloid non-union, the 3–4 and 6-U portals are used for viewing and instrumentation. The ulnar styloid fragment is identified by palpation of the mobile ulnar styloid with a probe and fluoroscopy

Fig. 114.2 Arthroscopic view of the burr on an eburnated styloid tip. © Bain

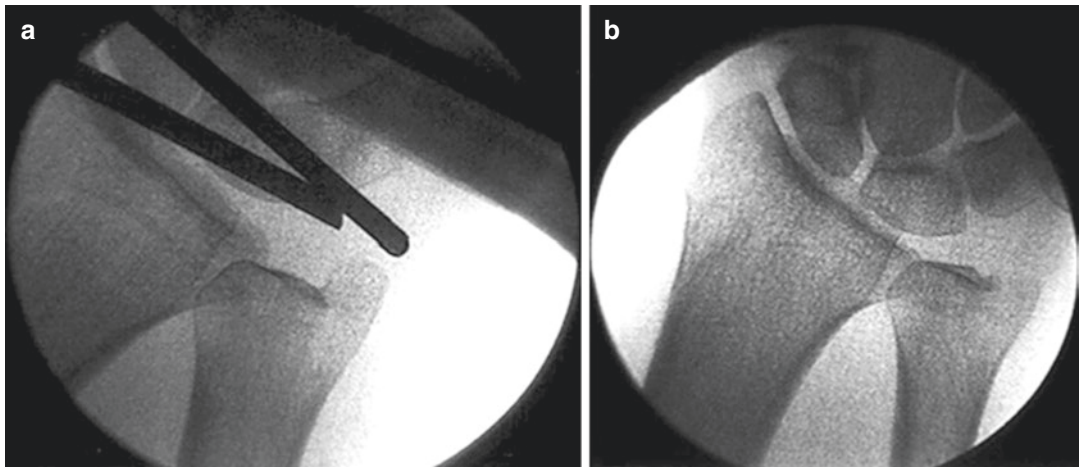

Fig. 114.3 (**a**, **b**) Arthroscopic ulna styloid resection under fluoroscopic guidance to identify the burr position (**a**) and then assess adequate depth of resection (**b**), (reprinted with permission from Bain et al., Arthroscopy, Elsevier)

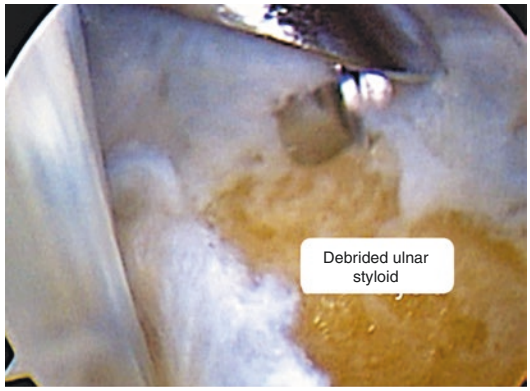

Fig. 114.4 Arthroscopic view after resection of distal styloid (reprinted with permission from Pinal et al., Arthroscopic Management of Ulnar Pain. Springer)

Fig. 114.5 Arthroscopic view of ulnar styloid non-union is demonstrated. The probe is placed within the non-union site and the styloid is lifted distally. © Bain

(Fig. 114.5). A radiofrequency probe is used to debride or ablate the fibrous non-union and soft tissue attachments and the fragment can be removed with a small pituitary rongeur. It is critical to ensure that there is no significant associated DRUJ instability that needs to stabilized.

114.5 Tips and Tricks

- DRUJ stability should be assessed under anaesthesia prior to surgery.
- Blunt dissection should be used for portal placement to minimize dorsal cutaneous branch of ulna nerve neuropraxia.
- A meticulous arthroscopic evaluation is necessary to identify any associated ligamentous injuries and TFCC tears.
- Fluoroscopy should be used to guide bone removal.

114.6 Postoperative Management and Rehabilitation

Postoperatively, portal dressing is applied. No formal physiotherapy is necessary and patients advised that they could mobilize the wrist in a concept similar to a pain-guided recovery.

114.7 Complications

Satisfaction is high and complications are rare although transient ulnar sensory paresthesia has been noted.

References

1. Topper SM, Wood MB, Ruby LK. Ulnar styloid impaction syndrome. J Hand Surg. 1997;22:699–704. https://doi.org/10.1016/S0363-5023(97)80131-1. 1997/07/01.
2. Tomaino MM, Gainer M, Towers JD. Carpal impaction with the ulnar styloid process: treatment with partial styloid resection. J Hand Surg Br. 2001;26:252–5. https://doi.org/10.1054/jhsb.2001.0591. 2001/06/02.
3. Zahiri H, Zahiri CA, Ravari FK. Ulnar styloid impingement syndrome. Int Orthop. 2010;34:1233–7. https://doi.org/10.1007/s00264-010-0969-9. 2010/02/27.
4. Ogden JA, Beall JK, Conlogue GJ, et al. Radiology of postnatal skeletal development. IV. Distal radius and ulna. Skelet Radiol. 1981;6:255–66. https://doi.org/10.1007/bf00347198. 1981/01/01.

5. Biyani A, Mehara A, Bhan S. Morphological variations of the ulnar styloid process. J Hand Surg Br. 1990;15:352–4. https://doi.org/10.1016/0266-7681(90)90018-y. 1990/08/01.
6. Giachino AA, McIntyre AI, Guy KJ, et al. Ulnar styloid triquetral impaction. Hand Surg. 2007;12:123–34. https://doi.org/10.1142/S0218810407003456. 2007/12/22.
7. Scarano KA, Owusu-Sarpong S, Mulligan MT. Bilateral ulnar styloid impaction syndrome treated with ulnar styloidectomy. J Wrist Surg. 2019;8:240–4. https://doi.org/10.1055/s--0038-1673408. 2019/06/14.
8. Cantor RM, Braunstein EM. Productive osseous changes about the wrist in rheumatoid arthritis. Skelet Radiol. 1987;16:397–402. https://doi.org/10.1007/bf00350967. 1987/01/01.
9. Bain GI, Bidwell TA. Arthroscopic excision of ulnar styloid in stylocarpal impaction. Arthroscopy. 2006;22:677.e671–3. https://doi.org/10.1016/j.arthro.2006.04.083. 2006/06/10.
10. Slutsky DJ. Arthroscopic management of ulnocarpal impaction syndrome and ulnar styloid impaction syndrome. Hand Clin. 2017;33:639–50. https://doi.org/10.1016/j.hcl.2017.07.002. 2017/10/11.
11. van Der Heijden B, Groot S, Schuurman AH. Evaluation of ulnar styloid length. J Hand Surg. 2005;30:954–9. https://doi.org/10.1016/j.jhsa.2005.05.007. 2005/09/27.
12. Garcia-Elias M. Dorsal fractures of the triquetrum-avulsion or compression fractures? J Hand Surg. 1987;12:266–8. https://doi.org/10.1016/s0363-5023(87)80285-x. 1987/03/01.
13. D'Agostino P, Townley WA, Le Viet D, et al. Oblique ulnar styloid osteotomy—a treatment for ulnar styloid impaction syndrome. J Hand Surg. 2011;36:1785–9. https://doi.org/10.1016/j.jhsa.2011.07.023. 2011/10/07.
14. Ahsan ZS, Rivlin M, Jupiter JB. Ulnar-sided wrist pain due to long ulnar styloid: a case report. J Wrist Surg. 2016;5:311–4. https://doi.org/10.1055/s--0035-1570743. 2016/10/26.

Part XXII

Hand Arthroscopy: Basic Science

Portals in Hand Arthroscopy

115

Deepak N. Bhatia

115.1 Background

Arthroscopy of the small joints of the hand involves diagnostic and therapeutic procedures of the trapeziometacarpal (TMJ), metacarpophalangeal (MCP), and the proximal and distal interphalangeal joints (PIP, DIP). Each of these joints has a unique bony, soft-tissue, and neurovascular anatomy and knowledge of these is essential for accurate and safe access and orientation.

115.1.1 Surgical Anatomy

The lateral antebrachial cutaneous nerve (LACN), branches of superficial radial nerve (SBRN), radial artery, and motor branches of median nerve (MBMN) are potentially at-risk of injury during portal placement for TMJ and scaphotrapeziotrapezoid (STT) joint arthroscopy. The LACN consistently accompanies the cephalic vein and is found in the anatomic snuff box in 50% cases. A branch of the LACN usually accompanies the radial artery [1, 2]. Branches of the LACN anastomose with other cutaneous nerves. The SBRN bifurcates into dorsal and volar (SR3) branches approximately 4 cm proximal to Lister's tubercle. The dorsal branch further bifurcates either just proximal or distal to Lister's tubercle (SR1 and SR2). SR2 divides into two branches (SR2-D2 and SR2-D1) adjacent to the radial styloid process; SR2-D1 courses along the ulnar aspect of the first digit and SR2-D2 courses and branches along the radial and ulnar aspects of second digit [3]. The radial artery (RA) passes from volar to dorsal in the deep plane of the anatomical snuff box and is approximately 7–8 mm distal to the radial styloid. The superficial palmar branch of the radial artery may be present and passes through the thenar musculature to reach the superficial palmar arch (type 1), or it may course distally and form the radial proper palmar digital artery of the thumb (type II) (Fig. 115.1a). The MBMN exits the transverse carpal ligament along the ulnar margin of flexor pollicis brevis (FPB) and curves radially to enter the plane between the FPB and abductor pollicis brevis (APB). Here it terminates into a superficial branch (innervates APB) and a profound branch (innervates opponens pollicis and FPB) (Fig. 115.1b) [4].

115.2 Trapeziometacarpal Joint Arthroscopy Portals

TMJ procedures often necessitate pantrapezial access. The distal trapezium (Tz) can be accessed via four TMJ portals, while the proximal Tz can

D. N. Bhatia (✉)
SPORTSMED Mumbai, and Sir HN Reliance Foundation Hospital, Mumbai, India
e-mail: shoulderclinic@gmail.com

© ISAKOS 2022

D. N. Bhatia et al. (eds.), *Arthroscopy and Endoscopy of the Elbow, Wrist and Hand*,
https://doi.org/10.1007/978-3-030-79423-1_115

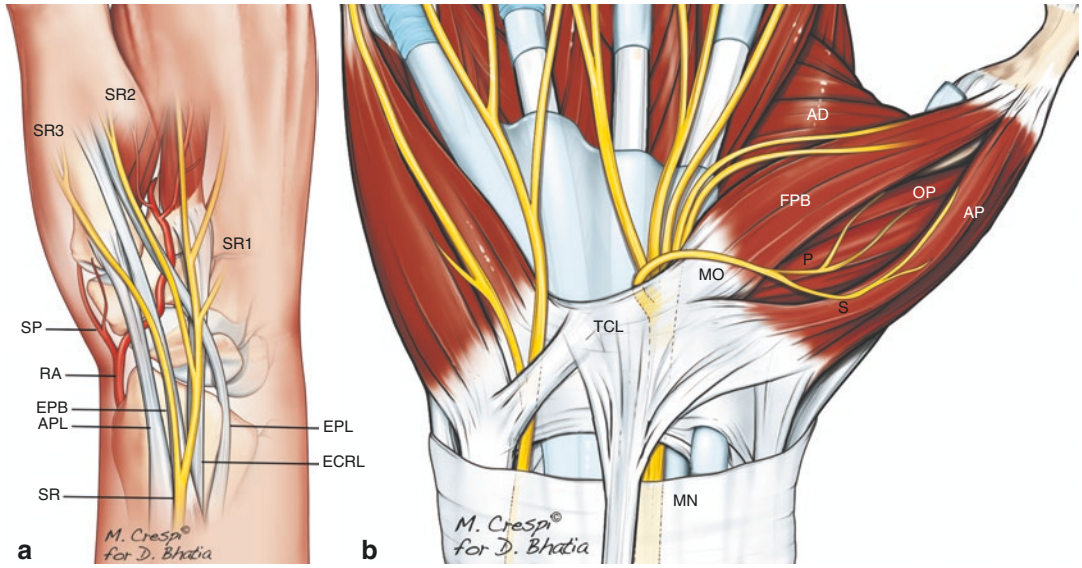

Fig. 115.1 (**a**) Surgical anatomy of the dorsal and radial aspect of trapeziometacarpal (TMJ) and scaphotrapeziotrapezoid (STT) joints is illustrated. The three sensory branches of radial nerve (SR) are shown (SR1, SR2, SR3). The radial artery (RA) passes from volar to dorsal through the "snuff box" and its superficial palmar branch (SP) passes to the thenar aspect. Tendons of first 3 extensor compartments are illustrated (APL, EPB, ECRL, and EPL). [M. Crespi © for ISAKOS]. (**b**) Surgical anatomy of the motor branch (MO) of median nerve (MN) is shown on the volar aspect of thumb. MO curves radially around the transverse carpal ligament (TCL) along the ulnar margin of flexor pollicis brevis (FPB) and terminates into a superficial branch (S) and a profound branch (P). (*AD* Adductor pollicis). [M. Crespi © for ISAKOS]

be accessed through three scaphotrapeziotrapezoid (STT) portals (Fig. 115.2).

115.2.1 TMJ Portals

Arthroscopic access to TMJ is possible via four portals:

Radial TMJ portal 1-R (Berger, Menon): This portal is placed just radial to the abductor pollicis longus (APL) tendon at the level of TMJ [5, 6]. The portal is located by needle placement and fluoroscopic confirmation. Dorsal and volar TMJ ligaments can be assessed using this portal. The 1-R portal is approximately 22 mm away from SR2, 5 mm from SR3 (closest branch), and 19 mm from RA [3, 4].

A modified radial portal (Orellana and Chow) is placed just distal to the oblique ridge of the trapezium referencing the radial edge of the FCR tendon instead of the radial border of the APL tendon [7]. The modified radial portal passes through the capsular window radial to the anterior oblique ligament and provides better visualization of the dorsal ligamentous anatomy of the joint. The SBRN is approximately 8 mm away and the RA is at least 1 cm away (10 and 15 mm) from this portal.

Ulnar TMJ portal 1-U (Berger, Menon): This portal is placed just ulnar to the extensor pollicis brevis (EPB) tendon at the level of TMJ [5, 6]. The portal is located by needle placement and fluoroscopic confirmation. The volar TMJ ligaments can be better visualized using this portal. The 1-U portal is approximately 9 mm away from SR3, 5–8 mm away from SR2 (closest branch), and 3–6 mm from RA [3, 4, 7].

Thenar portal T (Walsh et al.): This portal is placed in the bulk of the thenar muscle at the level of the CMC joint, approximately 90° from the 1-U portal. The portal site is marked using transillumination via 1-U portal [8]. The T portal has an ergonomic advantage when used along with the 1-U portal. The T portal is approximately

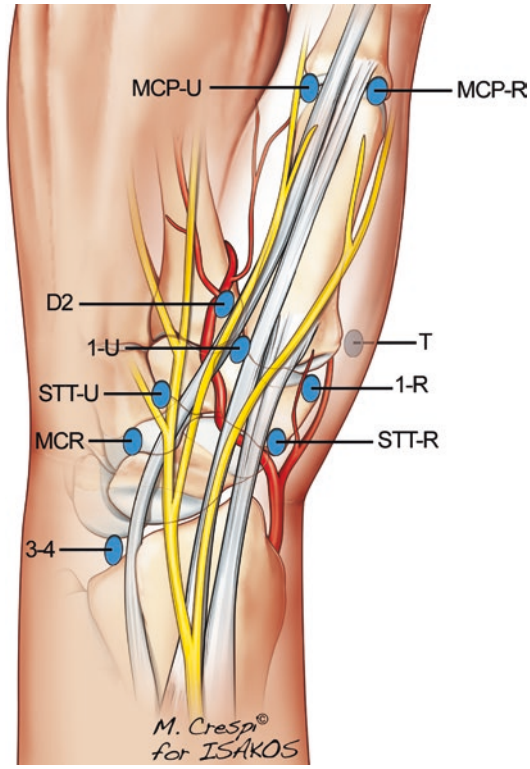

Fig. 115.2 Portal placement sites for arthroscopy of trapeziometacarpal (TMJ), scaphotrapeziotrapezoid (STT), and thumb metacarpophalangeal (MCP) joints are illustrated. (*1R* radial TMJ portal, *1U* ulnar TMJ portal, *T* thenar portal, *D2* dorsal-distal TMJ portal, *STT-R* radial scaphotrapeziotrapezoid portal, *STT-U* ulnar scaphotrapeziotrapezoid portal, *MCR* midcarpal radial portal, *3–4* radiocarpal portal, *MCP-R* Radial metacarpophalangeal portal, *MCP-U* Ulnar metacarpophalangeal portal). (M. Crespi © for ISAKOS)

22 mm away from SR3, 30 mm away from SR2, and 30 mm from RA [4]. The superficial palmar branch of radial artery often passes directly over the T portal and is at-risk of iatrogenic injury. Moreover, the superficial and the profound branches of MBMN are very close to the thenar portal (1.2 and 2.2 mm, respectively) and are at-risk of iatrogenic injury [4] (Fig. 115.1b).

Dorsal-distal Portal D2 (Slutsky): The D2 portal is situated in the dorsal aspect of the first web space and is placed ulnar to the extensor pollicis longus (EPL) tendon and 1 cm distal to the V-shaped cleft at the junction of the index and thumb metacarpal bases [9]. The portal is just distal to the dorsal intermetacarpal ligament and passes between the dorsal and volar trapeziometacarpal ligaments. The portal provides better visualization of the dorsal capsule and is useful for resection of medial osteophytes. The SBRN is approximately 3–4 mm away, and the closest branch is SR2 (1.7 mm). The RA is 3–5 mm away and the first dorsal metacarpal artery (FDMA) is approximately 2–4 mm from this portal.

115.2.2 STT Portals

Arthroscopic access to STT joint is possible via four portals:

Radial portal STT-R (Carro et al.): This portal is placed just radial to the abductor pollicis longus (APL) tendon at the level of the STT joint. The radial artery is approximately 9 mm away from this portal and SBRN may be at risk [10].

Palmar portal STT-P (Baré et al.): This portal is placed midway from the radial styloid and the base of the first metacarpal, 3 mm ulnar to the APL tendon and 6 mm radial to the scaphoid tubercle. The trocar is directed toward the base of the fifth metacarpal while holding the thumb in extension and adduction. The portal entry is approximately 7–8 mm away from the radial artery and its superficial branch, and about 12 mm away from the SBRN [11].

Midcarpal radial portal MCR: This portal is placed distal to the 3–4 radiocarpal portal and is bounded radially by the extensor carpi radialis brevis and ulnarly by the tendons of the fourth dorsal wrist compartment (tendon interval approximately 7 mm). Branches of the SBRN are radial to the portal and the closest branch is approximately 16 mm away [12].

Ulnar portal STT-U (Bowers and Whipple): This portal is placed in line with the index metacarpal shaft and just ulnar to the EPL tendon. The EPL tendon is radial to this portal and protects the radial artery in the snuff box [13].

115.3 Metacarpophalangeal Joint Arthroscopy

Arthroscopic access to the MCP joint is possible via two portals:

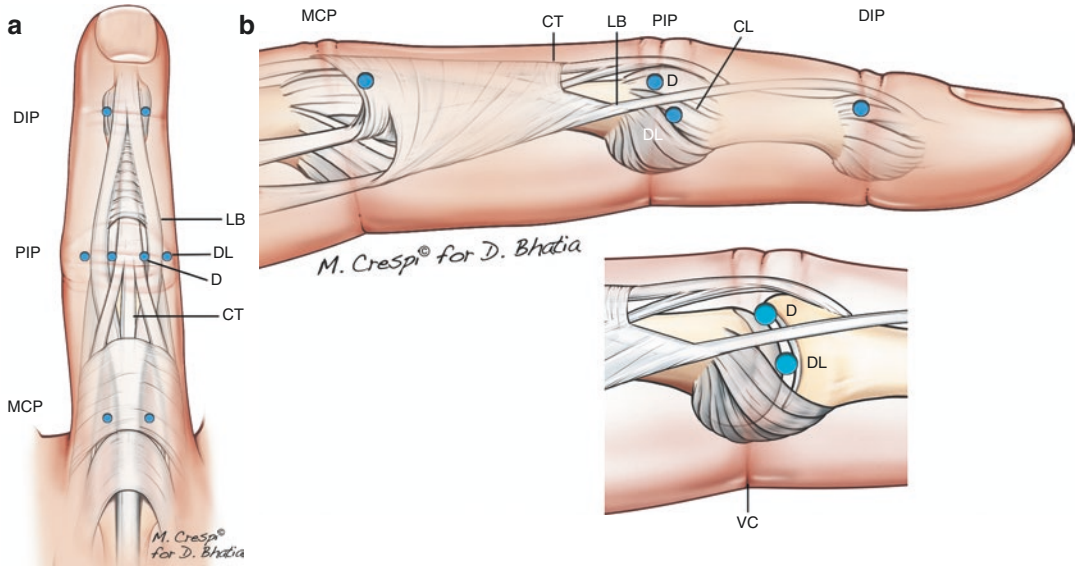

Fig. 115.3 (**a**) Portal placement sites for arthroscopy of metacarpophalangeal (MCP) joint, and proximal (PIP) and distal interphalangeal (DIP) joints are illustrated. [*LB* Lateral band, *CT* Central tendon, *D* Dorsal, *DL* Dorsal-lateral]. [Copyright D Bhatia]. (**b**) Dorsal and dorsolateral PIP joint portals are illustrated. Note that the dorsolateral PIP portals are distal to the PIP volar crease and in the interval between the collateral ligament and lateral band. [*LB* Lateral band, *CT* Central tendon, *CL* collateral ligament, *D* Dorsal portal, *DL* Dorsal-lateral portal]. [M. Crespi © for ISAKOS]

Radial portal MCP-R: This portal is placed in the dorsal joint line depression alongside the radial aspect of central extensor tendon and passes between the central slip and the radial lateral band (Fig. 115.3a). The thumb MCP-R portal is placed radial to the EPB tendon (Fig. 115.2). At the MCP joint of the thumb, MCP-R portal is situated dorsal and approximately 1 mm (0–5 mm) from SR3. The inter-portal distance is approximately 1.5 cm [3]. The third digit MCP joint is the safest in any of its portals; however, the fourth digit MCP-R has the highest risk of nerve injury. The MCP-U is safer than the MCP-R on the fourth finger while the radial is safer than the ulnar on the fifth finger [14].

Ulnar portal MCP-U: This portal is placed in the dorsal joint line depression alongside the ulnar aspect of central extensor tendon and passes between the central slip and the ulnar lateral band. The thumb MCP-U portal is placed ulnar to the EPL tendon. At the MCP joint of the thumb, MCP-U portal is situated dorsal and approximately 4 mm (1.5–6.5 mm) from SR2-D1 [3]. The third finger is the safest in any of its portals; however, the second digit MCP-U has the highest risk of nerve injury.

115.4 Proximal (PIP) Interphalangeal Joint Arthroscopy

Two lines have been defined in relation to the PIP joint by Okamoto et al. [15]: The C-line is an extension line of the PIP joint volar crease line which crosses at right angles the longitudinal axis of the finger. The line parallel with the C-line, which passes along the distal edge of the proximal phalanx is the J-line on the sagittal plane. The PIP joint space is approximately 1.9–3.2 mm distal to the C-line and along the J-line. An interval between the collateral ligaments and lateral bands is present in most cases approximately 2 mm (1.6–2.9 mm) dorsal to the midlateral line along the J-line (Fig. 115.3b).

Dorsal PIP portals (Chen Y-C): These were the original portals for PIP joint arthroscopy and are placed on radial and ulnar sides of the central

extensor tendon [16]. This portal position utilizes the interval between the central tendon and lateral bands. Precise placement in the interval is difficult and the collateral bands are potentially at risk of injury (Fig. 115.3a, b).

Dorsolateral PIP portals (Sekiya): These portals are placed dorsolaterally along the J-line and in the interval between the collateral ligaments and lateral bands (2 mm dorsal to the midlateral line). The digital neurovascular bundles are close to the volar recesses and are prone to indirect thermal injury by the radiofrequency probes [17].

115.5 Distal (DIP) Interphalangeal Joint Arthroscopy

DIP arthroscopy is performed via two dorsal portals placed lateral to insertion of lateral extensor slips. Traction may be applied by using a K-wire passed through the distal phalanx and 22 gauge needles are used to locate the DIP joint space under fluoroscopic guidance.

Conflict of Interest The author certifies that he has no commercial associations (e.g., consultancies, stock ownership, equity interest) that might pose a conflict of interest in connection with the submitted article. The author retains the copyright to the images, videos, and content in this chapter.

References

1. Hirtler L, Huber FA, Wlodek V. Cutaneous innervation of the distal forearm and hand—minimizing complication rate by defining danger zones for surgical approaches. Ann Anat. 2018;220:38–50.
2. Steinberg BD, Plancher KD, Idler RS. Percutaneous Kirschner wire fixation through the snuff box: an anatomic study. J Hand Surg Am. 1995;20:57–62.
3. Ropars M, Fontaine I, Morandi X, Berton E, Kaila R, Darnault P. Preserving the superficial branch of the radial nerve during carpometacarpal and metacarpophalangeal joint arthroscopy: an anatomical study. Surg Radiol Anat. 2010;32(3):271–6.
4. Pan YW, Hung LK. The safety of the thenar portal: an anatomical study of the thumb carpometacarpal arthroscopy. J Wrist Surg. 2017;6(2):152–7.
5. Menon J. Arthroscopic management of trapeziometacarpal joint arthritis of the thumb. Arthroscopy. 1996;12:581–7.
6. Berger RA. Technique for arthroscopic evaluation of the first carpometacarpal joint. J Hand Surg [Am]. 1997;22:1077–80.
7. Orellana MA, Chow JC. Arthroscopic visualization of the thumb carpometacarpal joint: introduction and evaluation of a new radial portal. Arthroscopy. 2003;19:583–91.
8. Walsh EF, Akelman E, Fleming BC, DaSilva MF. Thumb carpometacarpal arthroscopy: a topographic, anatomic study of the thenar portal. J Hand Surg Am. 2005;30(2):373–9.
9. Slutsky DJ. The use of a dorsal-distal portal in trapeziometacarpal arthroscopy. Arthroscopy. 2007;23:1244.e1–4.
10. Carro LP, Golano P, Fariñas O, Cerezal L, Hidalgo C. The radial portal for scaphotrapeziotrapezoid arthroscopy. Arthroscopy. 2003;19(5):547–53.
11. Baré J, Graham AJ, Tham SK. Scaphotrapezial joint arthroscopy: a palmar portal. J Hand Surg Am. 2003;28(4):605–9.
12. Abrams RA, Petersen M, Botte MJ. Arthroscopic portals of the wrist: an anatomic study. J Hand Surg. 1994;19A:940–4.
13. Bowers WH. Arthroscopic anatomy of wrist. In: McGinty J, editor. Operative arthroscopy. New York: Raven Press; 1991. p. 612–23.
14. Limousin B, Corella F, Del Campo B, et al. Metacarpophalangeal portal safety. An anatomical study. Seguridad de los portales metacarpofalángicos. Estudio anatómico. Rev Esp Cir Ortop Traumatol. 2018;62(5):380–6.
15. Okamoto H, Sekiya I, Mizutani J, Watanabe N, Otsuka T. Anatomical basis for arthroscopy of the proximal interphalangeal joints. J Hand Surg Asian Pac Vol. 2018;23(3):342–6.
16. Chen Y-C. Arthroscopy of the wrist and finger joints. Orthop Clin North Am. 1979;10(3):723–33.
17. Sekiya I, Kobayashi M, Okamoto H, Otsuka T. Progress and role of finger joint arthroscopy. Hand Clin. 2017;33(4):819–29.

Part XXIII

Carpometacarpal Arthroscopy

116 Arthroscopic Partial Trapeziectomy for Trapeziometacarpal Arthritis

Deepak N. Bhatia

116.1 Background

Degenerative arthritis of Trapeziometacarpal joint (TMJ) is a common and disabling condition that often necessitates surgical management. Arthroscopic options include debridement and synovectomy, and partial and complete trapeziectomy (with and without interposition and suspension). Trapezium-sparing procedures are preferred in middle-aged patients as partial trapeziectomy maintains the thumb axis length and the lever arm for pinch, and avoids the risk of metacarpal migration and scaphoid abutment. Satisfactory outcomes have been reported with and without use of interposition tissue after partial excision of trapezium [1, 2]. Additionally, the procedure can be revised to complete trapeziectomy if the outcome is unsatisfactory.

116.1.1 Surgical Anatomy

Arthroscopic access to the TMJ is limited by the sensory branches of the radial nerve in the superficial plane and the radial artery in the deep plane. Access through the thenar aspect is restricted by the motor branch of median nerve. The tendons of the first and third extensor compartments (APL, EPB, EPL) are important landmarks for safe portal placement into the TMJ. The ligamentous anatomy of the TMJ is complex and the capsular envelope of the joint is formed by seven ligaments [3]. Identification and preservation of these ligaments are vital in trapezium-sparing procedures and intraarticular recognition of the ligaments is useful for correct portal placement (Table 116.1) (Fig. 116.1a, b).

116.2 Indications and Contraindications

- Symptomatic basal joint arthritis that is refractory to conservative treatment is an indication for arthroscopic evaluation. Arthroscopy is useful in assessment and staging of degenerative changes and direct visualization provides a better understanding of pathology in comparison to radiographic staging alone.
- Partial trapeziectomy is indicated in mild-moderate basal joint arthritis (Eaton stage I-III, Badia stage I-II) and may also be performed in selected cases of advanced arthritis (Badia stage III) [4, 5].

Partial trapeziectomy is contraindicated in advanced trapeziometacarpal joint arthritis (Eaton stage IV) and in presence of severe degeneration of the scaphotrapeziotrapezoid (STT) joint. Previous open surgery can result in

D. N. Bhatia (✉)
SPORTSMED Mumbai, and Sir HN Reliance Foundation Hospital, Mumbai, India
e-mail: shoulderclinic@gmail.com

© ISAKOS 2022

D. N. Bhatia et al. (eds.), *Arthroscopy and Endoscopy of the Elbow, Wrist and Hand*,
https://doi.org/10.1007/978-3-030-79423-1_116

Table 116.1 Ligamentous anatomy of the trapeziometacarpal joint

Trapeziometacarpal joint ligaments	Site	Features	Best viewing portal
Dorsal radial ligament (DRL)	Originates from dorsal tubercle of trapezium, ulnar to 1R portal	Dorsal ulnar to APL	1R, Thenar
Dorsal central ligament (DCL)	Originates from dorsal tubercle of trapezium, radial to 1U portal	Deep to EPB	1R
Posterior oblique ligament (POL)	Originates from dorsal tubercle of trapezium, ulnar to 1U portal	Oblique orientation of fibres	1R, Thenar
Dorsal trapeziometacarpal ligament (DTM)	Originates on dorsal ulnar edge of trapezium, dorsal to ulnar tubercle of trapezium	Most oblique of dorsal ligaments, part of the ulnar checkrein complex of TMJ	Thenar, 1R
Volar trapeziometacarpal ligament (VTM)/ulnar collateral ligament (UCL)	Originates on volar ulnar ridge of trapezium, volar to ulnar tubercle of trapezium	Forms the volar counterpart of DTM Part of the ulnar checkrein complex of TMJ	1R, 1U
Anterior oblique ligament complex (AOL) Consists of superficial (sAOL) and deep (dAOL) components	Located at and radial to the volar metacarpal beak	Vertical orientation of fibres surrounding the volar metacarpal beak (VB)	1U, 1R

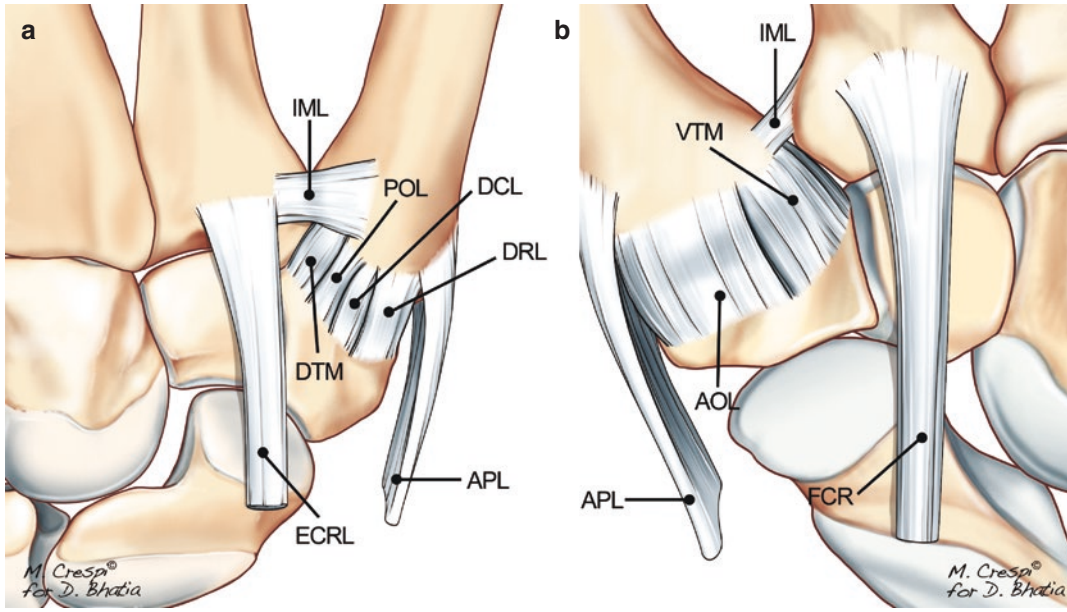

Fig. 116.1 (**a**) Ligamentous anatomy of dorsal aspect of trapeziometacarpal joint is illustrated. (*DRL* dorsal radial ligament, *DCL* dorsal central ligament, *POL* posterior oblique ligament, *DTM* dorsal trapeziometacarpal ligament, *IML* intermetacarpal ligament, *ECRL* extensor carpi radialis longus, *APL* abductor pollicus longus). (**b**) Ligamentous anatomy of volar aspect of trapeziometacarpal joint is illustrated. (*VTM* volar trapeziometacarpal ligament, *AOL* anterior oblique ligament complex, *IML* intermetacarpal ligament, *APL* abductor pollicus longus, *FCR* flexor carpi radialis). © D. Bhatia

alteration of regional anatomical relations and is a relative contraindication.

116.3 Surgical Technique

The procedure is performed with the patient in the supine position. The upper limb is suspended with finger traps, and a countertraction force of 2–4 kg is used to distract the joint. Dorsal and volar TMJ arthroscopy portals are marked, and a 30° arthroscope (1.9 mm) is used for diagnostic arthroscopy.

Portals: The first CMC joint can be accessed via four portals (Fig. 116.2). For each portal, the skin is carefully incised, and a small hemostat is used to dissect down to the capsular tissue to avoid iatrogenic injury to branches of the superficial radial nerve or the radial artery.

- The **volar radial portal (1-R)** is placed just radial to the abductor pollicis longus (APL) tendon.
- The **dorsal ulnar portal (1-U)** is placed just ulnar to the extensor pollicis brevis (EPB) tendon.

The 1-R and 1-U portals are used sequentially for viewing and working in the first CMC joint and are usually adequate for partial trapeziec-

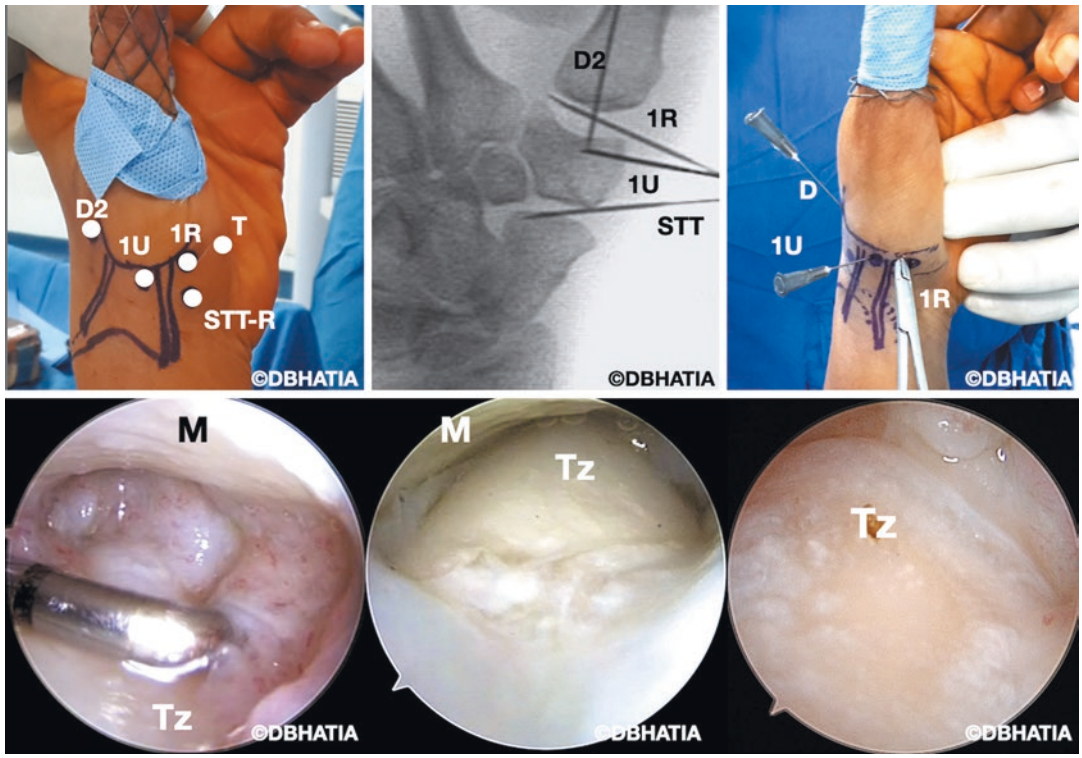

Fig. 116.2 Portal placement sites for trapeziometacarpal joint (TMJ) arthroscopy are demonstrated. Needles are placed into portal sites and fluroscopy is used to confirm correct placement (top left and middle image). The 1-R portal is used as the initial viewing portal (top right). Synovitis and mild cartilage degenerative changes are observed in early stages of arthritis (bottom left and middle images) and high grade cartilage wear is observed in advanced stages (bottom right image) (*1R* radial TMJ portal, *1U* ulnar TMJ portal, *T* thenar portal, *D2* dorsal-distal portal, *STT-R* radial scaphotrapeziotrapezoid portal, *M* first Metacarpal articular surface, *Tz* trapezium). © D. Bhatia

tomy. Other additional portals that may be used if necessary are:

- The **thenar portal (T)** is placed in the bulk of the thenar muscle at the level of the CMC joint. The portal in located using transillumination with the arthroscope in the 1U portal and forms a 90° angle with the 1-U portal [6].
- The **dorsal-distal portal (D2)** is placed ulnar to the extensor pollicis longus (EPL) tendon and 1 cm distal to the V-shaped cleft at the junction of the index and thumb metacarpal bases [7].
- The STT joint is accessed using an **STT-R portal** (proximal to the 1R portal at the level of the STT joint) and via the **MCR portal** (radial midcarpal portal).

Diagnostic endoscopy:

- The 1-R portal is used initially to evaluate the TMJ. The ligamentous components of TMJ are identified and assessed, and articular surfaces of trapezium and first metacarpal are inspected for cartilage wear (Fig. 116.3). Peripheral osteophytes and synovitis are noted.
- The 1-U portal is then placed using an outside-in technique between the DCL and POL. The 1-U portal provides a better view of the volar aspect of the joint and is the main working portal for the procedure.

Partial trapeziectomy:

- A 2–3 mm shaver is introduced via the 1U portal and a synovectomy is performed. Cartilage remnants are excised and the eburnated surface of trapezium is debrided.
- Next, a 3 mm burr is used to resect 4–6 mm of the distal trapezium. Care is taken to ensure capsular integrity and the peripheral osteophytes are resected without detachment of the capsular envelope (Fig. 116.4).
- The arthroscope is then switched to the 1U portal and resection is continued via 1R portal (Fig. 116.5).
- Adequacy of resection is confirmed and radiofrequency/ablation probe is carefully used to perform capsular shrinkage.
- A thorough lavage is performed to remove any bone and cartilage debris.

Adequacy of resection: This can be assessed by three methods (Fig. 116.6):

- An angled probe (2 mm) is used to measure the pre- and post-resection gap between the trapezium and metacarpal surfaces in the TMJ. The gap is measured after removal of countertraction from thumb traction apparatus. A peripheral gap of 4 mm and a central gap of 6 mm are adequate.
- The capsular envelope is disrupted if excessive resection has been performed and preserving an intact capsule circumferentially is a guide to avoid over-resection.
- Fluoroscopy is used to guide and confirm adequate removal of distal trapezium.

Scaphotrapeziotrapezoid (STT) debridement: Degenerative changes in STT may coexist with TMJ degeneration and STT joint evaluation and debridement is necessary.

- An STT-R portal is placed proximal to the 1R portal and the arthroscope is introduced into the STT joint. The distal scaphoid and proximal trapezium and trapezoid are evaluated for degenerative changes.
- A shaver is then used via the MCR portal and a synovectomy and debridement are performed (Fig. 116.7).

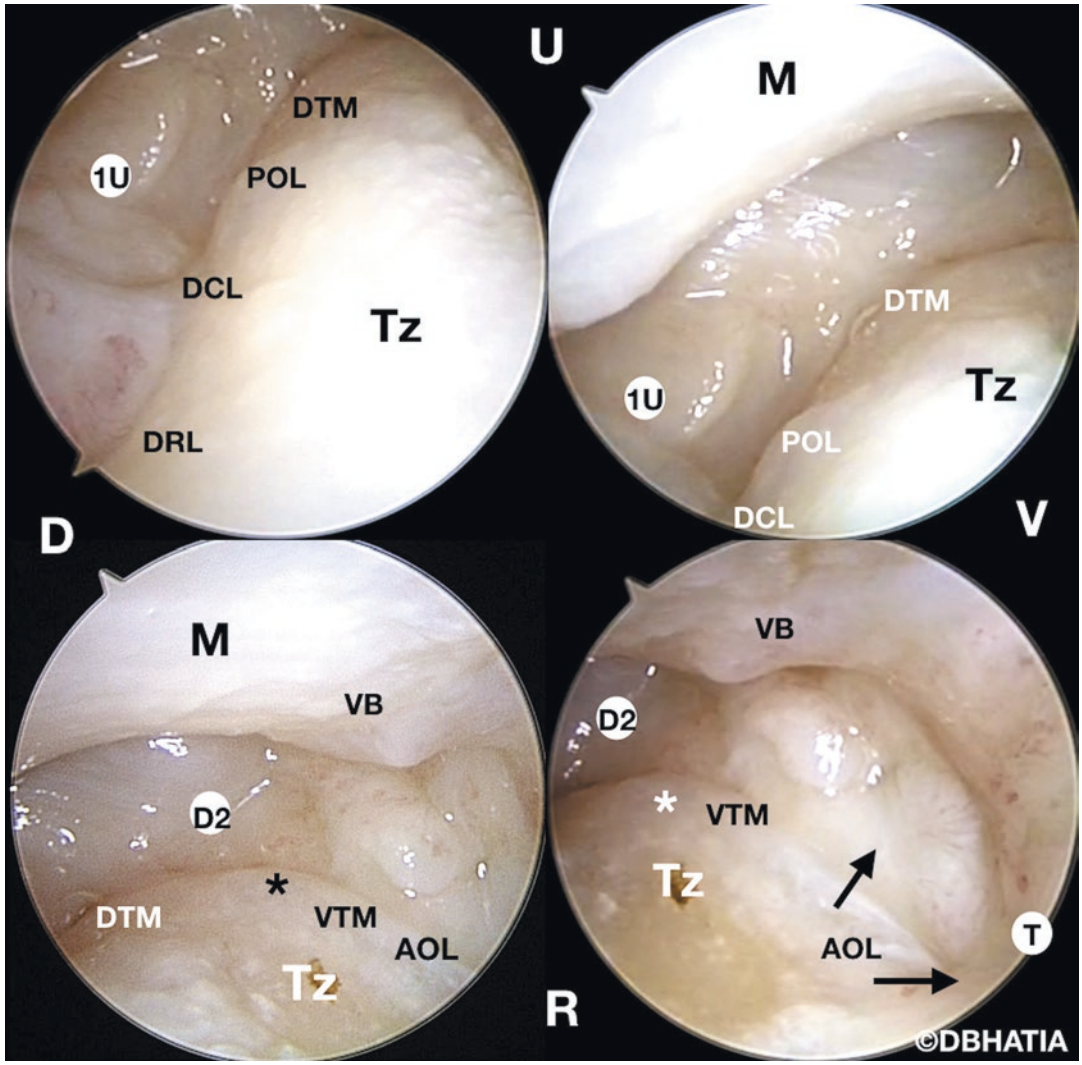

Fig. 116.3 Arthroscopic ligamentous anatomy of left hand trapeziometacarpal joint (TMJ) is demonstrated as viewed via radial (1-R) portal. Four dorsal (DRL, DCL, POL, DTM; top images) and two volar ligaments (VTM, AOL complex; bottom images) are identified and assessed. Portal placement sites of 1-U, D2, and thenar (T) portals are shown. The ulnar tubercle of trapezium (asterix *) and metacarpal volar beak (VB) are intraarticular landmarks for orientation. (*DRL* dorsal radial ligament, *DCL* dorsal central ligament, *POL* posterior oblique ligament, *DTM* dorsal trapeziometacarpal ligament, *VTM* volar trapeziometacarpal ligament, *AOL complex* anterior oblique ligament, *M* first metacarpal articular surface, *Tz* trapezium, *R* radial aspect, *U* ulnar aspect, *V* volar aspect, *D* dorsal aspect). © D. Bhatia

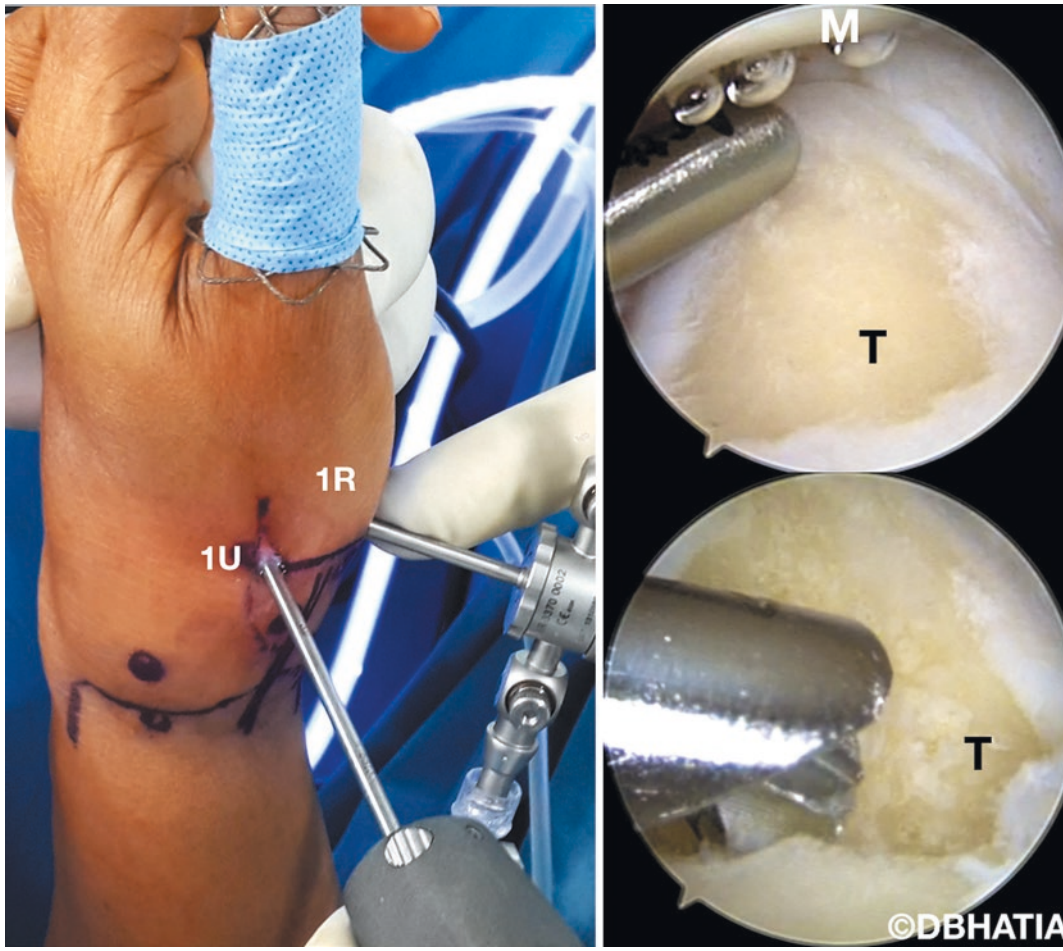

Fig. 116.4 Initial debridement and resection of the trapezium is performed using a shaver and burr through the ulnar (1-U) portal and the arthroscope is placed in the radial (1-R) portal. (*M* first metacarpal articular surface, *T* trapezium). © D. Bhatia

116.4 Tips and Tricks

- Preoperative sonography can be used to locate the position of radial artery to avoid iatrogenic injury during portal placement.
- TMJ portal placement is simplified by placing needles into the four portal sites and using fluoroscopy to confirm correct trajectory into the TMJ and STT joint.
- An interposition autograft may be used with partial trapeziectomy. The trapezium is burred into a slightly concave surface (4 mm peripheral and 6 mm central resection) and the capsular attachments are meticulously preserved. The interposition tissue can be introduced into the TMJ through the 1-R portal. The portal and capsulotomy may be enlarged if necessary and the capsule is subsequently repaired.

116.5 Pitfalls

- The sensory branches of radial nerve and radial artery are at risk of injury and patients must be counselled regarding possibility of neurovascular complications.
- Persistence of TMJ symptoms and unsatisfactory outcomes are possible. This necessitates revision to complete trapeziectomy with or without suspensionplasty.

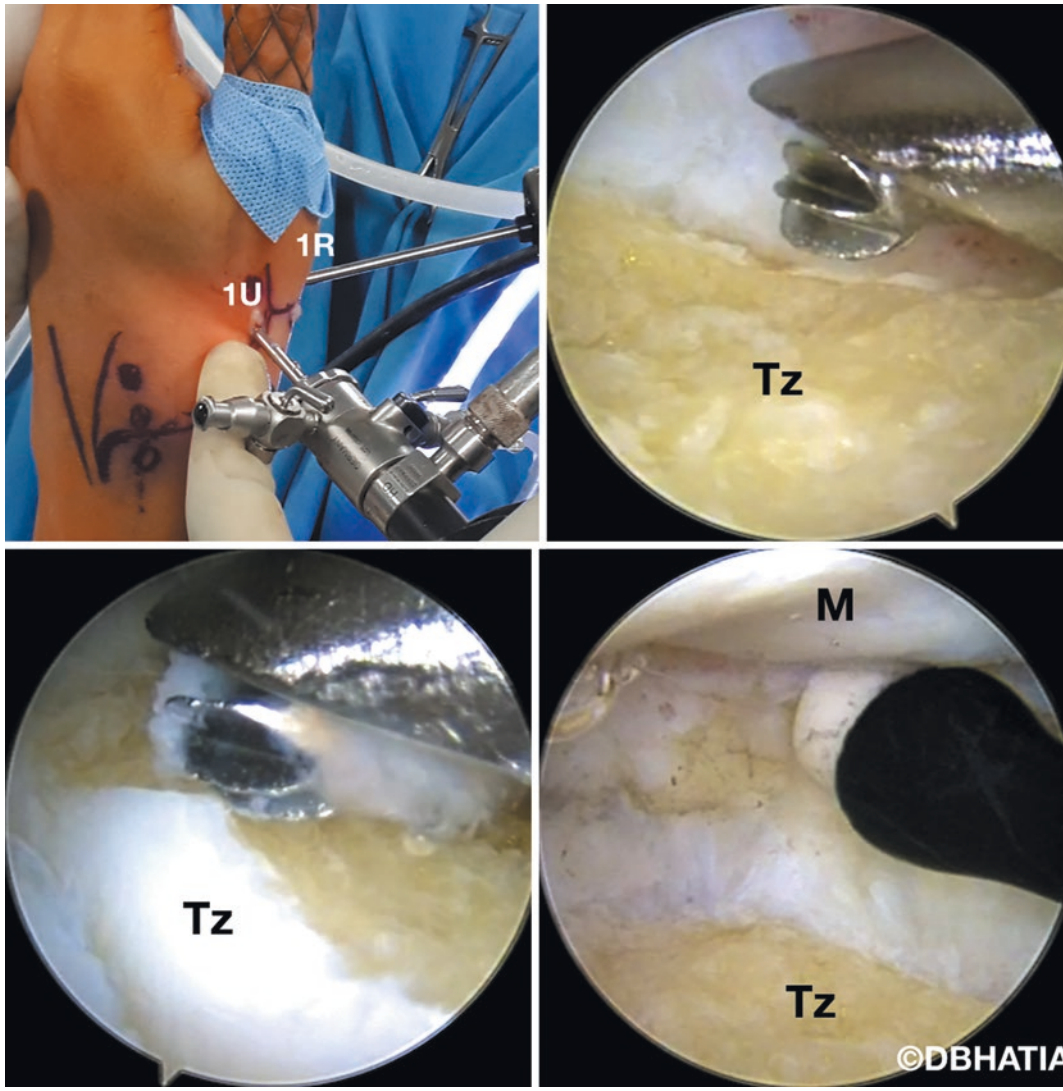

Fig. 116.5 Progressive resection of the trapezium and peripheral osteophytes is performed using a shaver and burr through the radial (1-R) portal and the arthroscope is placed in the ulnar (1-U) portal (top and bottom left images). Capsular shrinkage is performed along the volar ulnar aspect (bottom right) (*M* first metacarpal articular surface, *Tz* trapezium). © D. Bhatia

116.6 Post-operative Management and Rehabilitation

A thumb spica slab is applied for 10 days and is changed to a thumb spica cast after sutures are removed. The cast is changed to a splint at 4–6 weeks and range of motion exercises are begun thereafter followed by strengthening. Complete recovery may take 3–6 months and the rehabilitation is progressed accordingly. Return to heavy work is permitted after 6 months.

116.7 Complications

Injury to sensory nerves and radial artery are possible complications.

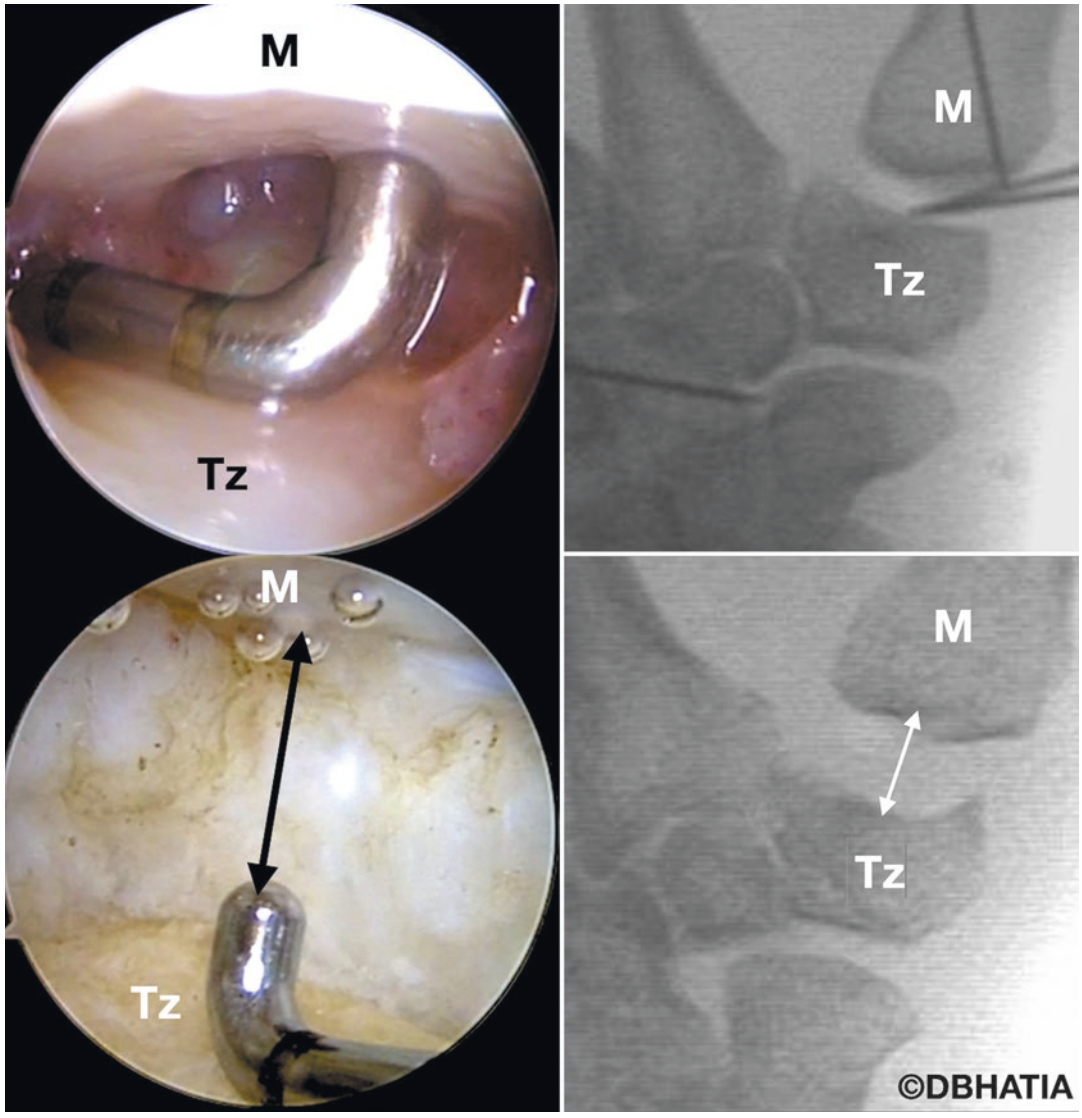

Fig. 116.6 Arthroscopic and fluoroscopic assessment of adequacy of trapezium resection is demonstrated. A 2 mm angled probe shows the pre- and post-resection gap of 6 mm between the trapezium (Tz) and metacarpal (M) surfaces (top and bottom left). Fluoroscopy demonstrates an adequate resection area of 4–6 mm (top and bottom right). © D. Bhatia

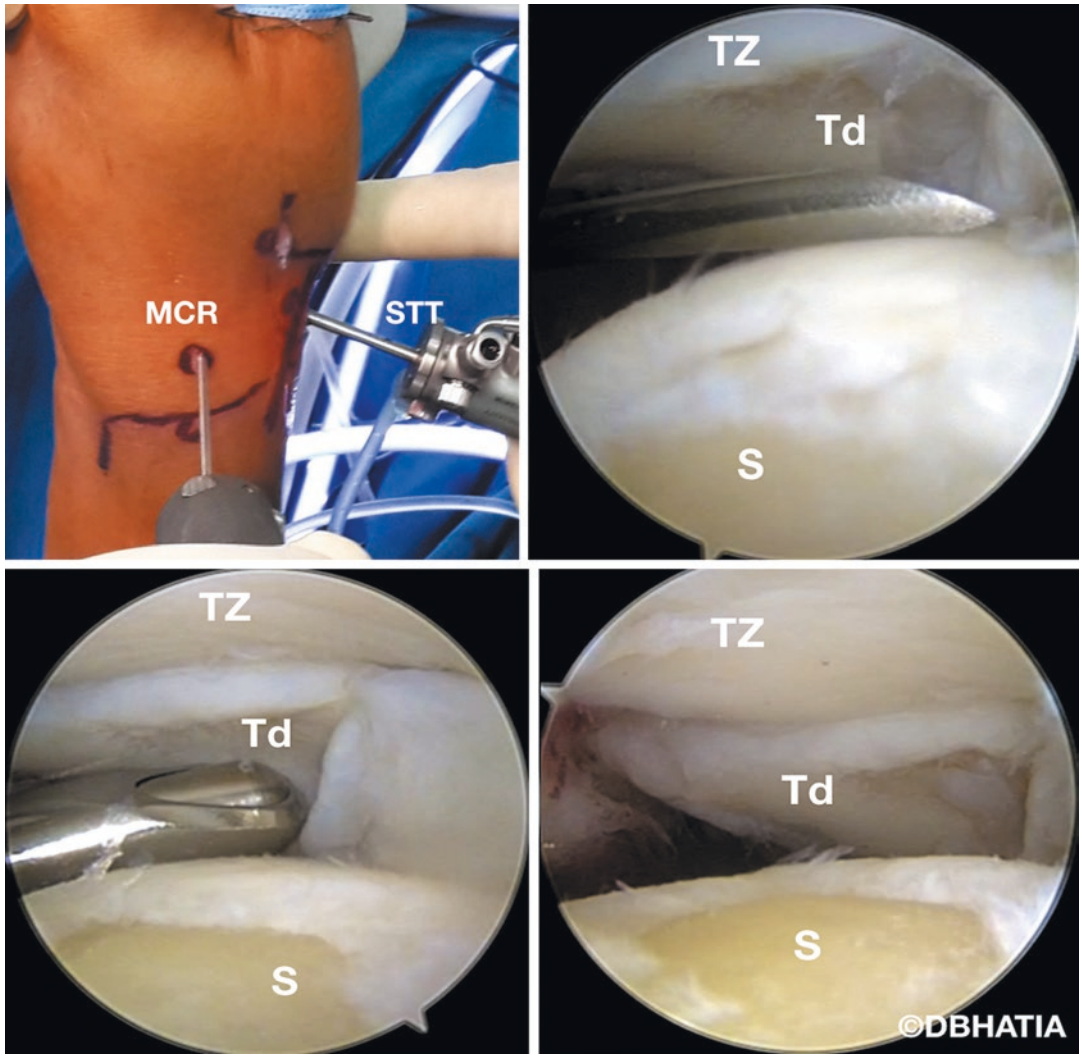

Fig. 116.7 Arthroscopic debridement of scaphotrapeziotrapezoid joint (STT) is performed by visualization through the radial STT portal and using a shaver in the midcarpal radial portal (MCR). (*S* distal scaphoid, *TZ* trapezium, *Td* trapezoid). © D. Bhatia

Conflict of Interest The author certifies that he has no commercial associations (e.g., consultancies, stock ownership, equity interest) that might pose a conflict of interest in connection with the submitted article. The author retains the copyright to the images, videos, and content in this chapter.

References

1. Adams JE. Does arthroscopic débridement with or without interposition material address carpometacarpal arthritis? Clin Orthop Relat Res. 2014;472(4):1166–72.
2. Edwards SG, Ramsey PN. Prospective outcomes of stage III thumb carpometacarpal arthritis treated with arthroscopic hemi-trapeziectomy and thermal capsular modification without interposition. J Hand Surg Am. 2010;35:566–71.
3. Zhang AY, Van Nortwick S, Hagert E, Yao J, Ladd AL. Thumb carpometacarpal ligaments inside and out: a comparative study of arthroscopic and gross anatomy from the robert a. Chase hand and upper limb center at Stanford university [published correction appears in J Wrist Surg. 2014;3(4):e1. Yao, Jeffrey [added]]. J Wrist Surg. 2013;2(1):55–62. https://doi.org/10.1055/s-0033-1333683.

4. Badia A. Trapeziometacarpal arthroscopy: a classification and treatment algorithm. Hand Clin. 2006;22:153–63.
5. Eaton RG, Glickel SZ. Trapeziometacarpal osteoarthritis. Staging as a rationale for treatment. Hand Clin. 1987;3:455–71.
6. Walsh EF, Akelman E, Fleming BC, DaSilva MF. Thumb carpometacarpal arthroscopy: a topographic, anatomic study of the thenar portal. J Hand Surg Am. 2005;30(2):373–9.
7. Slutsky DJ. The use of a dorsal-distal portal in trapeziometacarpal arthroscopy. Arthroscopy. 2007;23:1244.e1–4.

117

Arthroscopic Complete Trapeziectomy and Suspension Arthroplasty: "Three-Steps Arthroscopic Trapeziectomy Technique"

F. Corella, M. Ocampos, R. Laredo, J. Tabuenca, M. Carnicer, and R. Larrainzar-Garijo

117.1 Background

In the last two decades, surgeons have rapidly developed arthroscopic techniques to treat basal joint osteoarthritis [1]. Such techniques spare the joint capsule and ligaments, allow more accurate staging of cartilage degeneration to determine the most appropriate treatment, and decrease the risk of injury to the radial artery and superficial branch of the radial nerve. Arthroscopic resection arthroplasty of the trapezium can be performed as either partial or complete trapeziectomy. The former is indicated in stage II or III cases, according to the Eaton classification [2], while the latter can also be performed in stage IV cases. Many papers have described partial trapeziectomy [3–6], but few have discussed complete trapeziectomy [7, 8].

Numerous techniques have been developed to prevent proximal migration of the first metacarpal bone once the trapezium is removed, such as temporary Kirschner wire fixation, soft tissue interpositions, ligament reconstruction and interposition, and, more recently, suture button suspensionplasty (SBS) [9]. The first implant designed for the SBS was the Mini TightRope® (Arthrex, Naples, FL), which maintains the height of the first metacarpal bone by fixing it to

F. Corella (✉)
Orthopedic and Trauma Department, Hospital Universitario Infanta Leonor, Madrid, Spain

Hand Surgery Unit, Hospital Universitario Quironsalud Madrid, Madrid, Spain

Surgery Department, School of Medicine, Universidad Complutense de Madrid, Madrid, Spain

M. Ocampos
Orthopedic and Trauma Department, Hospital Universitario Infanta Leonor, Madrid, Spain

Hand Surgery Unit, Hospital Universitario Quironsalud Madrid, Madrid, Spain

R. Laredo
Hand Surgery Unit, Hospital Universitario Quironsalud Madrid, Madrid, Spain

Hand Surgery Unit, Orthopedic and Trauma Department, Virgen de la Salud University Hospital, Madrid, Spain

Orthopedic and Trauma Department, Quironsalud Toledo, Toledo, Spain

J. Tabuenca
Orthopedic and Trauma Department, Hospital Universitario Quironsalud Madrid, Madrid, Spain

M. Carnicer
Orthopedic and Trauma Department, Hospital Universitario Infanta Leonor, Madrid, Spain

R. Larrainzar-Garijo
Orthopedic and Trauma Department, Hospital Universitario Infanta Leonor, Madrid, Spain

Surgery Department, School of Medicine, Universidad Complutense de Madrid, Madrid, Spain

© ISAKOS 2022

D. N. Bhatia et al. (eds.), *Arthroscopy and Endoscopy of the Elbow, Wrist and Hand*,
https://doi.org/10.1007/978-3-030-79423-1_117

the second metacarpal bone using two stainless steel plates joined by two strands of 2/O FiberWire® (Arthrex, Naples, FL). The other device developed recently is the MicroLink® (Conmed, New York, USA).

Suture button implants avoid the drawbacks of temporary fixation using Kirschner wire, which is necessary when using the hematoma and distraction arthroplasty technique and involves a long period of immobilization (4–6 weeks), as well as an infection risk at the pin site. Similarly, SBS avoids the drawbacks of ligament reconstruction, which necessitates the sacrifice of a tendon and involves both wide exposure and scar tissue formation to obtain the graft and for its fixation.

Arthroscopic complete trapeziectomy is technically demanding and is a more time-consuming procedure than an open technique. So far, only two reports present data about this arthroscopic technique, but do not explain in detail how to perform it. The aim of this chapter is to present a technique called the "three-steps arthroscopic trapeziectomy technique" that structures this procedure into three steps, allowing it to be performed in an easier, more organized, and faster way [10].

117.2 Surgical Anatomy

The "three steps arthroscopic trapeziectomy technique" involves the structured resection of three different portions (zones) of the trapezium (Figs. 117.1 and 117.2). Zone 1 is the biggest portion, covering two-thirds of the trapezial ulnar side, but not the cartilage or subchondral bone over the scaphoid. Zone 2 is the half volar bone covering one-third of the trapezial radial side, as well as the cartilage and subchondral bone over the scaphoid. Zone 3 is the rest of the bone, specifically the dorsal half of the bone covering one-third of the radial side of the trapezium. The trapeziometacarpal portals used in this technique are the 1U portal and the thenar portal [11]. The thenar portal is used instead of the 1R portal, because the angle between the thenar and 1U portals is wider (more than 90°) than the angle between the 1U and 1R portals (less than 90°)

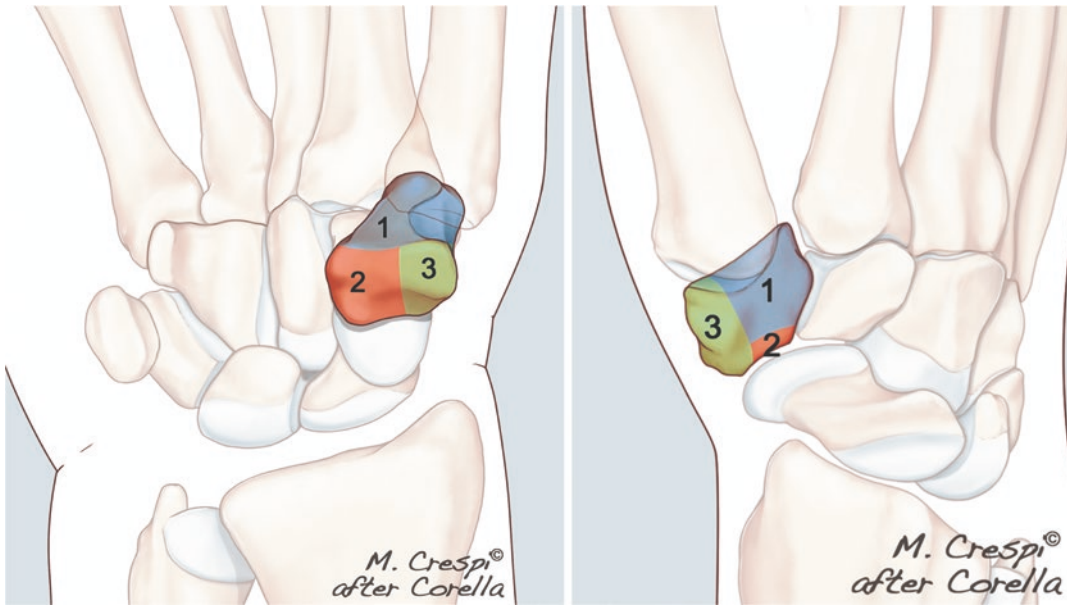

Fig. 117.1 The trapezium is divided into three different portions (zones). Zone 1 is the largest, covering 2/3rd of the ulnar side of the trapezium, but not the cartilage and subchondral bone over the scaphoid. Zone 2 is the half volar bone covering 1/3rd of the radial side of the trapezium, as well as the cartilage and subchondral bone over the scaphoid. Zone 3 is the half dorsal bone covering 1/3rd of the radial side of the trapezium (M. Crespi © for Corella). Reprinted from Corella F, Ocampos M, Laredo R, Tabuenca J, Carnicer M, Larrainzar-Garijo R. Arthroscopic Trapeziectomy and Suture Button Suspensionplasty: A Review of the Literature and Description of the "Three-Step Arthroscopic Trapeziectomy Technique." Journal of Wrist Surgery. Vol 9, Issue 5. With permission from Thieme Medical Publishers. 2020

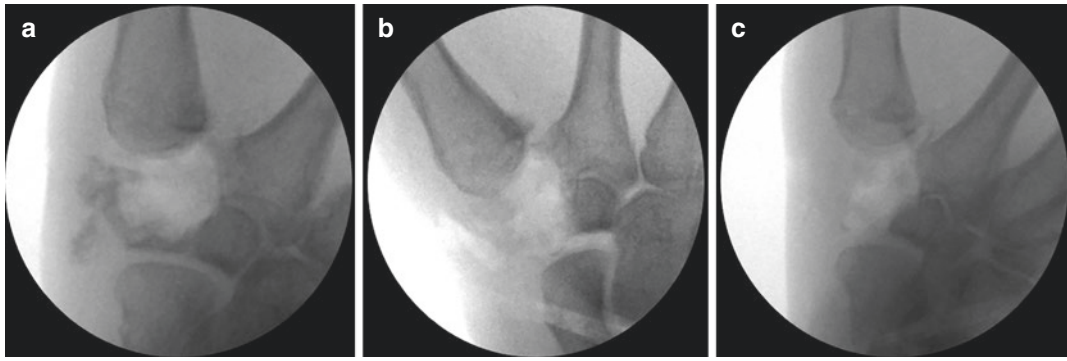

Fig. 117.2 Fluoroscopic images of the different steps. (**a**) Zone 1 has been removed. (**b**) Zone 2 has been removed, the bone of zone 3 is seen in the X-ray, and often with difficulty, but there is still bone remaining to be resected. (**c**) Zone 3 has been removed and the trapeziectomy is completed

and this eases the manipulation of the instruments (Fig. 117.3).

117.3 Indications and Contraindications

- The complete arthroscopic resection of the trapezium has the same indication of a complete open resection, i.e. stage IV of Eaton classification. It can also be performed also in stage III, as is commonly carried out as part of many open techniques (ligament reconstruction or interposition).
- In our own practice, we perform hemitrapeziectomy in young patients (normally under 60 years) at stage III, to maintain ligament attachments. In such patients, even when X-ray is normal, we always check the STT joint from the radial midcarpal portal. If the joint has degenerative changes, the indication is changed to complete trapeziectomy.
- In older patients at stage III, especially those with advanced degenerative changes in the base of the first metacarpal bone, greater subluxation, or large ulnar osteophyte, we prefer complete resection to avoid the possibility of repeat surgery for painful impingement of the remaining trapezium and to correct collapse of the first metacarpal bone.

Contraindications include any general contraindication to thumb arthroscopy, such as the distortion of the anatomy, a recent infection, or a rheumatoid condition in which a synovectomy is necessary with the resection arthroplasty.

117.4 Surgical Steps

117.4.1 Patient Positioning

The operation is performed under either regional (axillary block) or general anesthesia, with a pneumatic tourniquet placed at the upper arm, close to the armpit. The patient is placed in the supine position, with the affected arm on a hand table. The wrist is maintained in vertical traction during the whole procedure, even during suture button fixation. The traction tower commonly used is an Arc Wrist Tower® (Acumed, Hillsboro, OR, USA), which maintains vertical traction and leaves the volar side of the wrist free.

To check the amount of bone resection and to place the suture button, a fluoroscope is used. With a sterilized dressing completely covering the C-arm, the fluoroscope enters parallel to the floor from the volar side of the wrist. This way, a fluoroscopic view can be obtained without releasing traction or losing sterility.

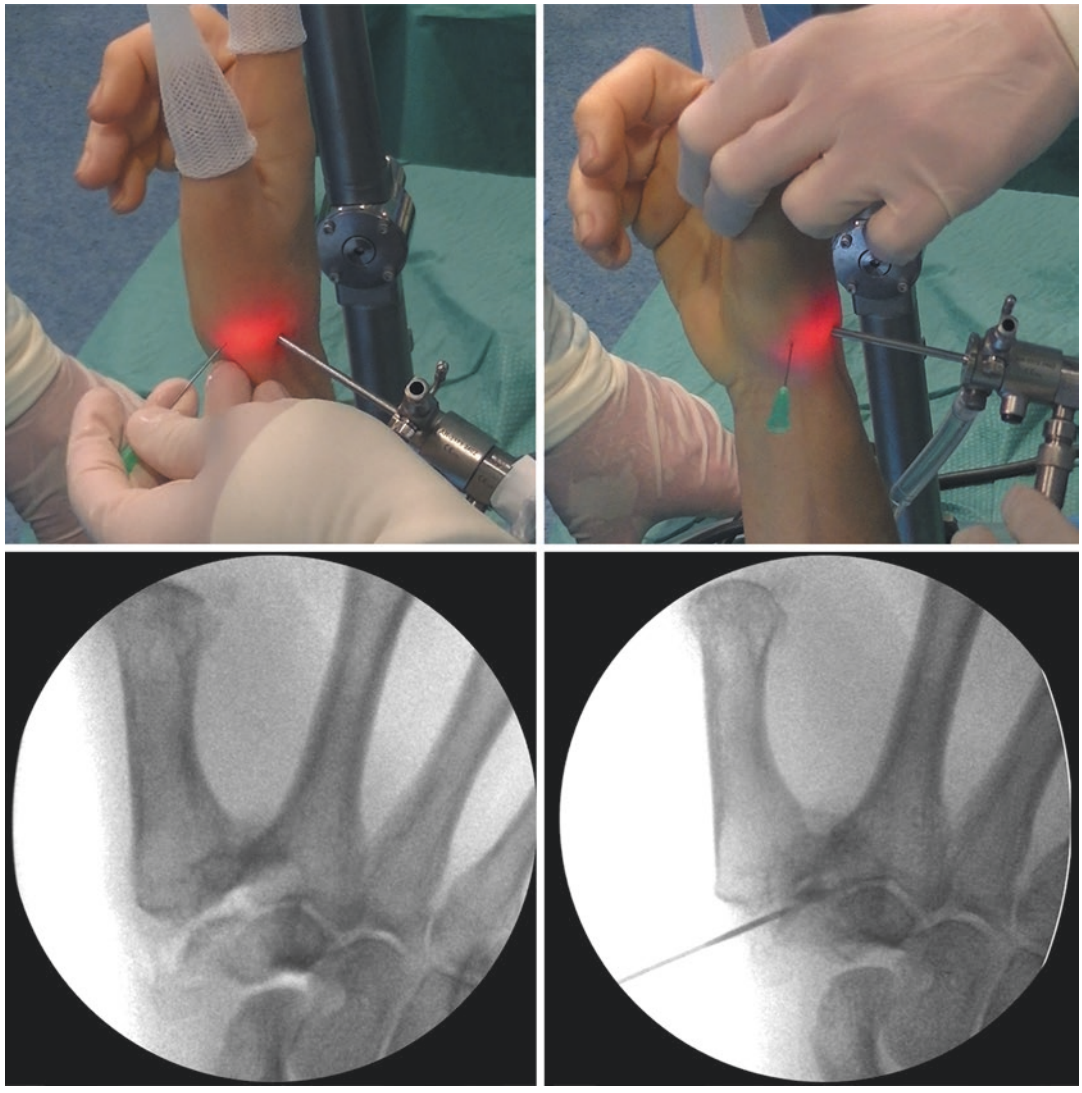

Fig. 117.3 The trapeziometacarpal portals used in this technique are the 1U portal and the thenar portal, because the angle between the thenar and 1U portals is more than 90° which eases the manipulation of the instruments. The fluoroscope can be used to check the correct position of the portal, especially if the joint has important degenerative changes and is narrowed

117.4.2 Step 1: Zone 1 Resection

- The first portal, placed in the thumb carpometacarpal (CMC) joint, is the 1U portal. It is located ulnar to the extensor pollicis brevis tendon. A 22-gauge needle is introduced into the joint. If there is any doubt, the fluoroscope can be used to check the correct position of the portal Fig. 117.3. A 3-mm skin incision is made using a No. 11 blade, the soft tissues are dissected bluntly, and the capsule is penetrated using a blunt forceps. Finally, a 2.4-mm arthroscope is introduced into the joint.
- The second portal (thenar portal) placement is performed under arthroscopic control using the light source of the arthroscope. The thenar eminence is illuminated, and a 22-gauge needle is placed into the bulk of the thenar

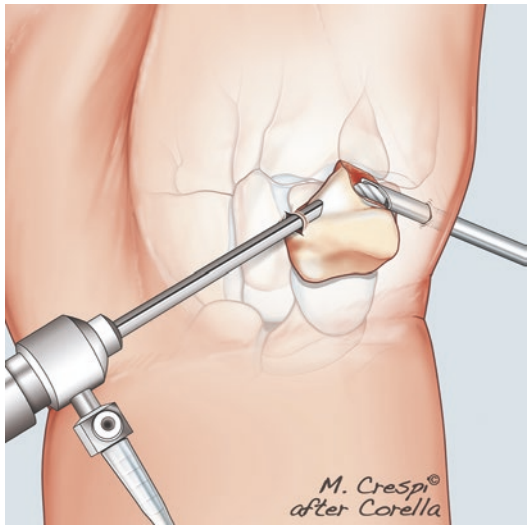

Fig. 117.4 Step 1. With the arthroscope in the thenar portal, the bone of zone 1 is removed (M. Crespi © for Corella). Reprinted from Corella F, Ocampos M, Laredo R, Tabuenca J, Carnicer M, Larrainzar-Garijo R. Arthroscopic Trapeziectomy and Suture Button Suspensionplasty: A Review of the Literature and Description of the "Three-Step Arthroscopic Trapeziectomy Technique." Journal of Wrist Surgery. Vol 9, Issue 5. With permission from Thieme Medical Publishers. 2020

muscle at the level of the carpometacarpal joint.

- Next, the arthroscope is moved from the 1U portal to the thenar portal to ensure that the ulnar portion of the trapezium, the second metacarpal bone, and the trapezoid are immediately in front of the arthroscope. In this first step, the bone of zone 1 is removed (Fig. 117.4).
- A 3-mm burr is then inserted through the 1U portal, and the bone resection begins in the middle of the trapezium—immediately in front of the portal. This small burr is only used to widen the 1U portal and allow the 4-mm × 7-cm burr to be introduced. Using this larger burr, the inner portion of zone 1 is removed, leaving the cartilaginous and peripheral surface of the bone (Fig. 117.5). During this step, the arthroscope rests over the radial portion of the trapezium (zones 2 and 3).
- The first peripheral portion to be removed is the ulnar osteophyte, which can be very large in some cases. To facilitate its resection, the periosteal elevator is introduced through the 1U portal and used to horizontally cut the peripheral ulnar portion of the bone. This separates all the osteophyte from the proximal portion of the bone. The periosteal elevator is then used to reach the ulnar and distal portion of the osteophyte, which is detached from the capsule by applying downward pressure. Once the osteophyte has been mobilized, the pituitary rongeur is introduced and used to catch and remove it (Fig. 117.6).
- Finally, the rest of the inner portion of zone 1 is removed using the 4-mm burr, the periosteal elevator, and the rongeur, exposing completely the trapezoid and leaving only the proximal cartilage and subchondral bone in contact with the scaphoid Fig. 117.7.

117.4.3 Step 2: Trapezium Volar Radial Portion (Zone 2) Resection

This step begins by cutting and bisecting the radial portion (zones 2 and 3), followed by the resection of zone 2 Fig. 117.8.

- The arthroscope should be moved from the thenar portal to the 1U portal. The arthroscope will rest over the proximal cartilage of the trapezium covering the scaphoid. Firstly, the 3-mm burr is introduced through the thenar portal and used to separate zone 2 from zone 3. The periosteal elevator is also useful to this end Fig. 117.9.
- As before, using the burr, the periosteal elevator, and the rongeur, all the bones of the zone 2 (half of the volar bone on the 1/3rd radial side of the trapezium, as well as the cartilage and subchondral bone over the scaphoid) are removed Fig. 117.10. Finally, resection of the bone is performed around the FCR tendon, which is located in the corner between the scaphoid and trapezoid Fig. 117.11 and is, therefore, covered by the bone of zone 2. As the arthroscope is immediately in front of the tendon, the bone can more easily be moved around it during this step Fig. 117.12.

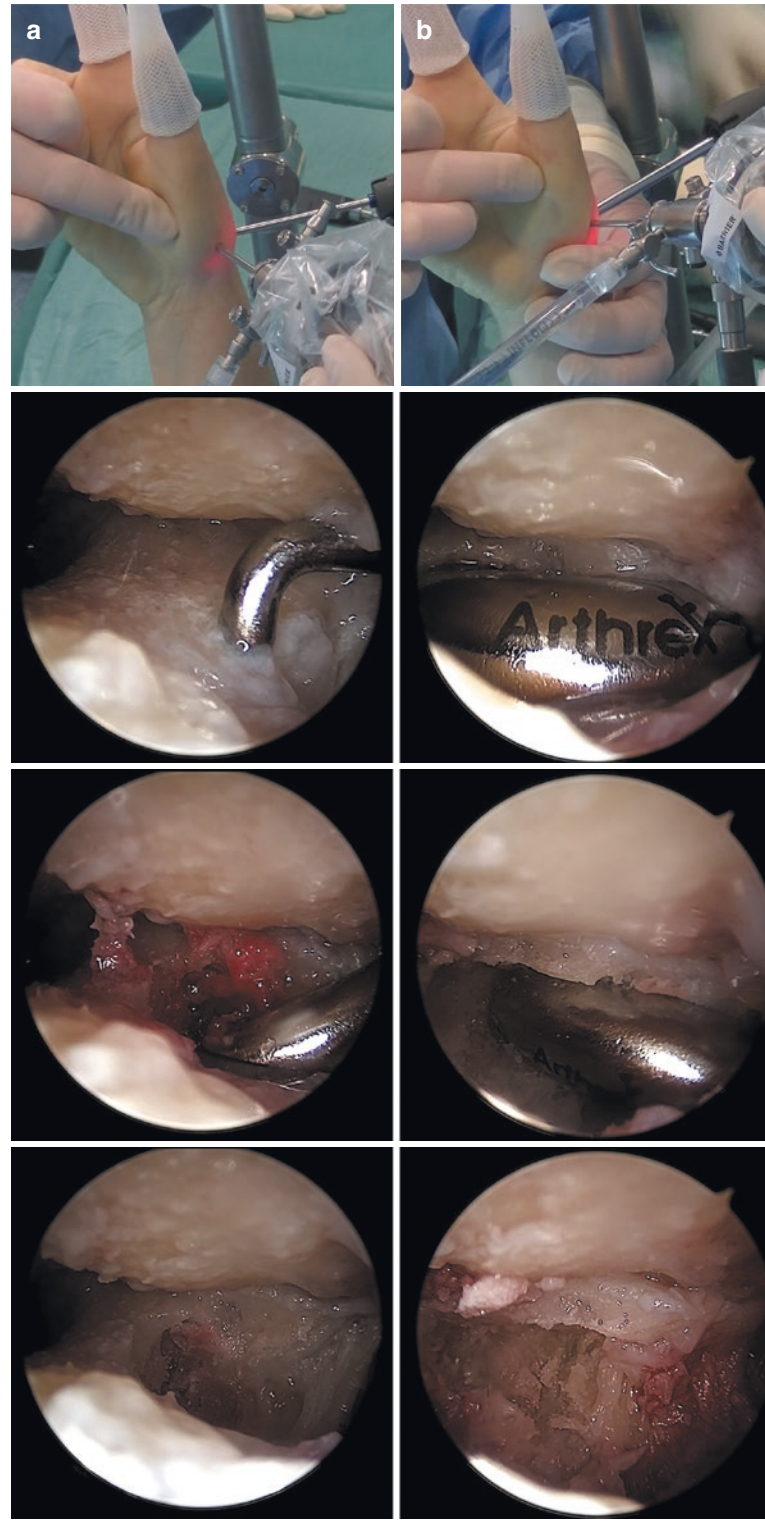

Fig. 117.5 (**a**) Initially, a 3-mm burr is introduced through the 1U portal and used to resect the bone enough to introduce the 4-mm burr. (**b**) Once there is enough space, the 4-mm burr is introduced and the inner portion of zone 1 is removed, leaving the cartilaginous and peripheral surface of the bone

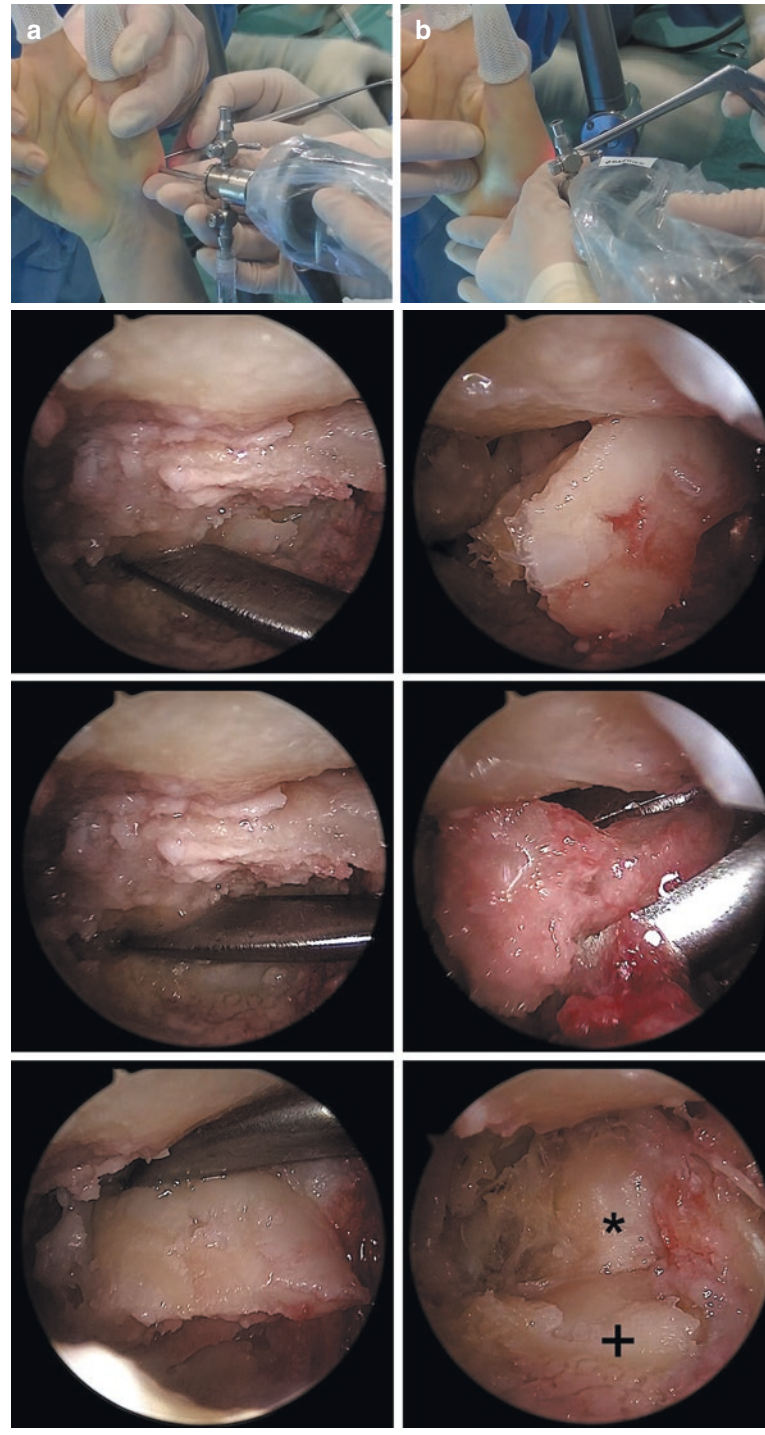

Fig. 117.6 Resection of the ulnar osteophyte. (**a**) Initially, a periosteal elevator is introduced through the 1U portal and used to horizontally cut the peripheral ulnar portion of the bone. Once this is separated from the proximal portion of the bone, the periosteal elevator is used to reach the ulnar and distal portion of the osteophyte and detach it from the capsule. (**b**) Once the osteophyte is mobilized, the pituitary rongeur is introduced and used to catch and remove the osteophyte, exposing the base of the second metacarpal bone (*) and the trapezoid (+)

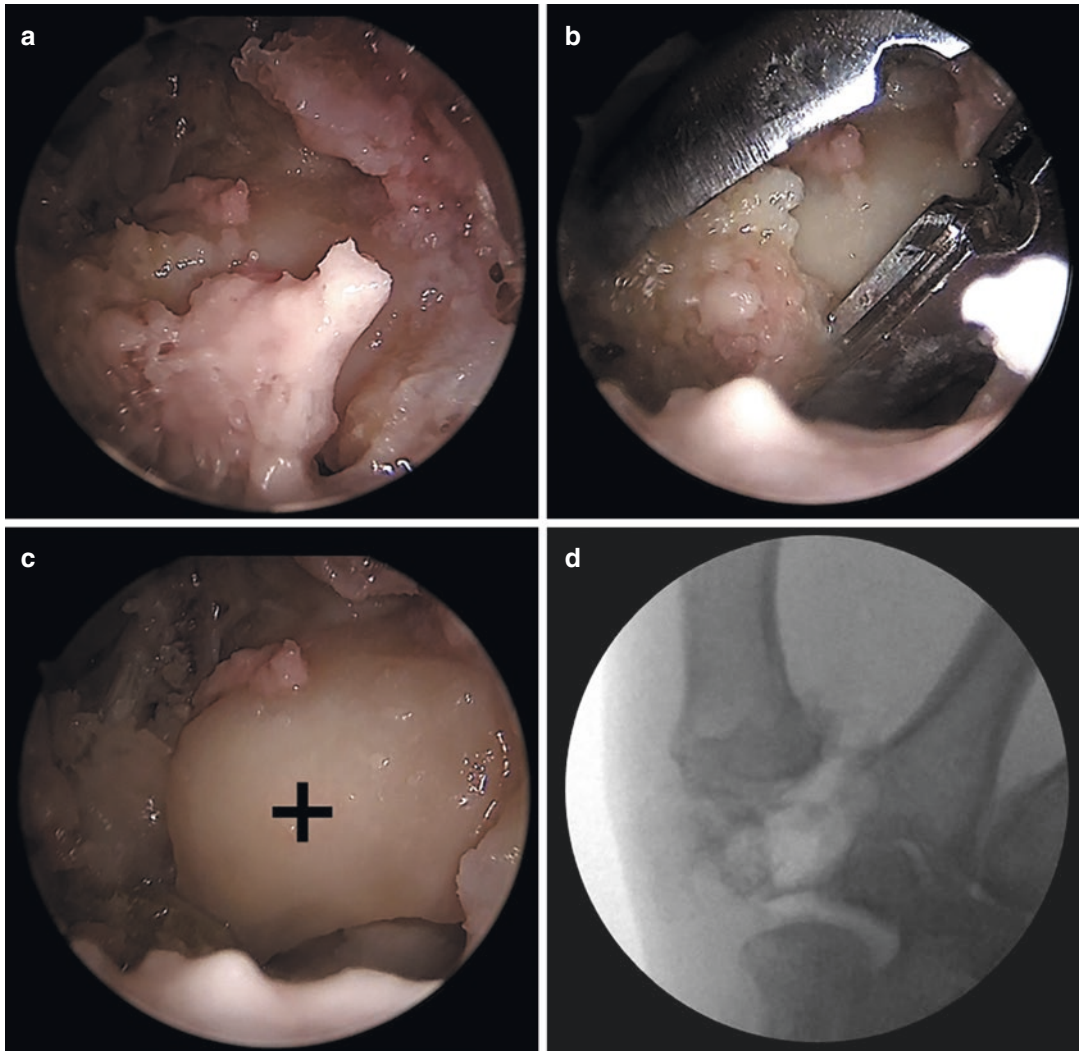

Fig. 117.7 (**a**, **b**) Step 1 finishes removing the peripheral portion of the bone of zone 1 using the periosteal elevator and rongeur. (**c**) The trapezoid (+) is completely expose leaving only the proximal cartilage and subchondral bone in contact with the scaphoid. (**d**) Fluoroscopic image at the end of step 1

117.4.4 Step 3: Trapezium Dorsal Radial Portion (Zone 3) Resection

In this step, the arthroscope is again located in the thenar portal, and the bone of zone 3 is removed Fig. 117.13. This zone is one of the most difficult portions of the trapezium to remove because it is between the two portals; thus, a direct view cannot be obtained.

- With the burr and the shaver in the 1U portal, the inner portion of the bone is resected. Next, using the periosteal elevator and rongeur, the bone is detached from the capsule. This detachment is commonly performed without a direct view Fig. 117.14.
- Finally, the joint of the second metacarpal, the trapezoid, the scaphoid, and the FCR are checked arthroscopically to ensure complete resection. The resection is also checked with the help of the fluoroscope Fig. 117.15.

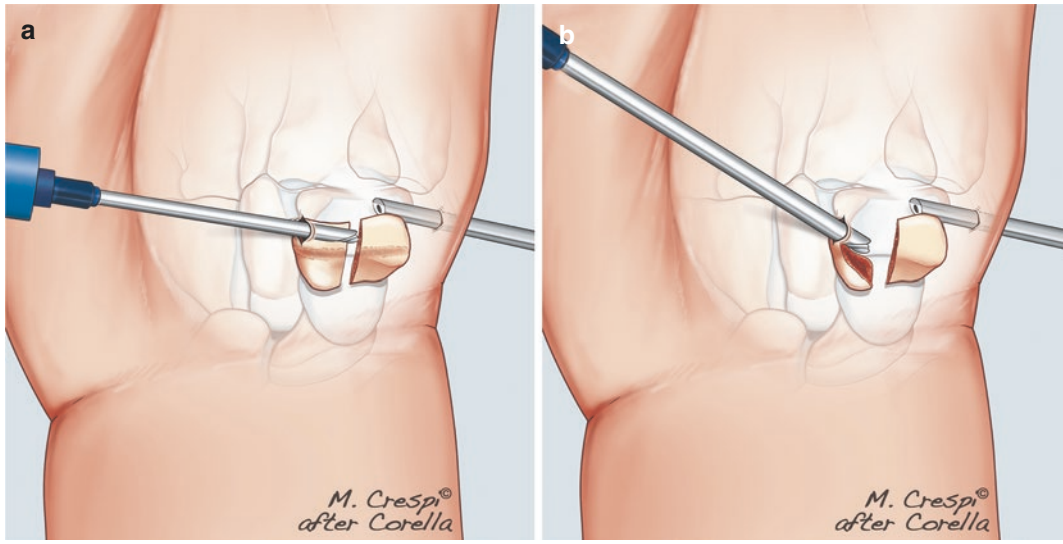

Fig. 117.8 Step 2 is illustrated. (**a**) This step begins by cutting and bisecting the radial portion (zones 2 and 3). (**b**) Once both zones are separated, zone 2 is resected. In this step, the arthroscope is located in the 1U portal, resting over the proximal bone and cartilage of the trapezium, covering the scaphoid (M. Crespi © for Corella). Reprinted from Corella F, Ocampos M, Laredo R, Tabuenca J, Carnicer M, Larrainzar-Garijo R. Arthroscopic Trapeziectomy and Suture Button Suspensionplasty: A Review of the Literature and Description of the "Three-Step Arthroscopic Trapeziectomy Technique." Journal of Wrist Surgery. Vol 9, Issue 5. With permission from Thieme Medical Publishers. 2020

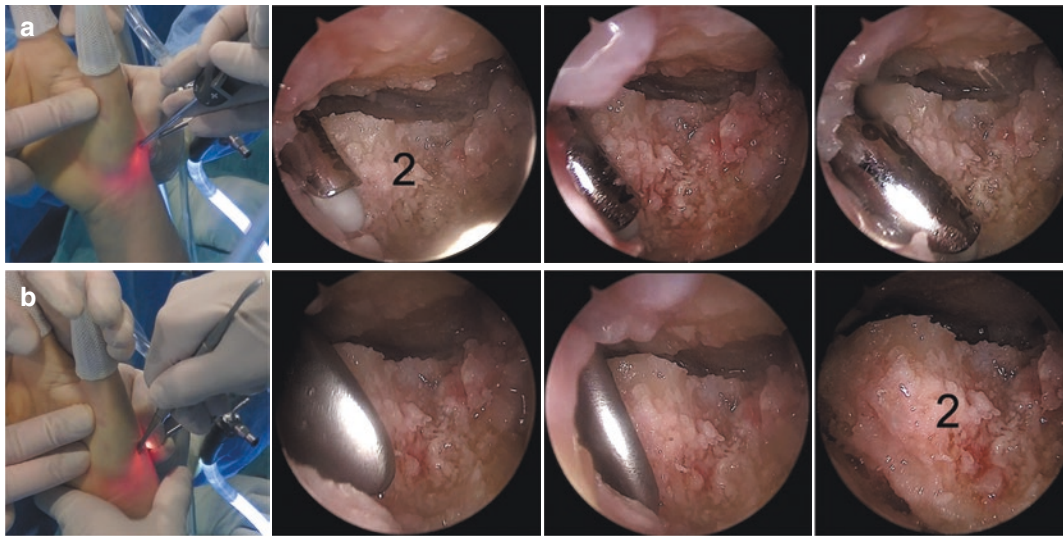

Fig. 117.9 (**a**) In step 2, zones 2 (2) and 3 are separated by cutting the bone with the 3-mm burr entering through the thenar portal. (**b**) The periosteal elevator is also useful to detach one zone from the other

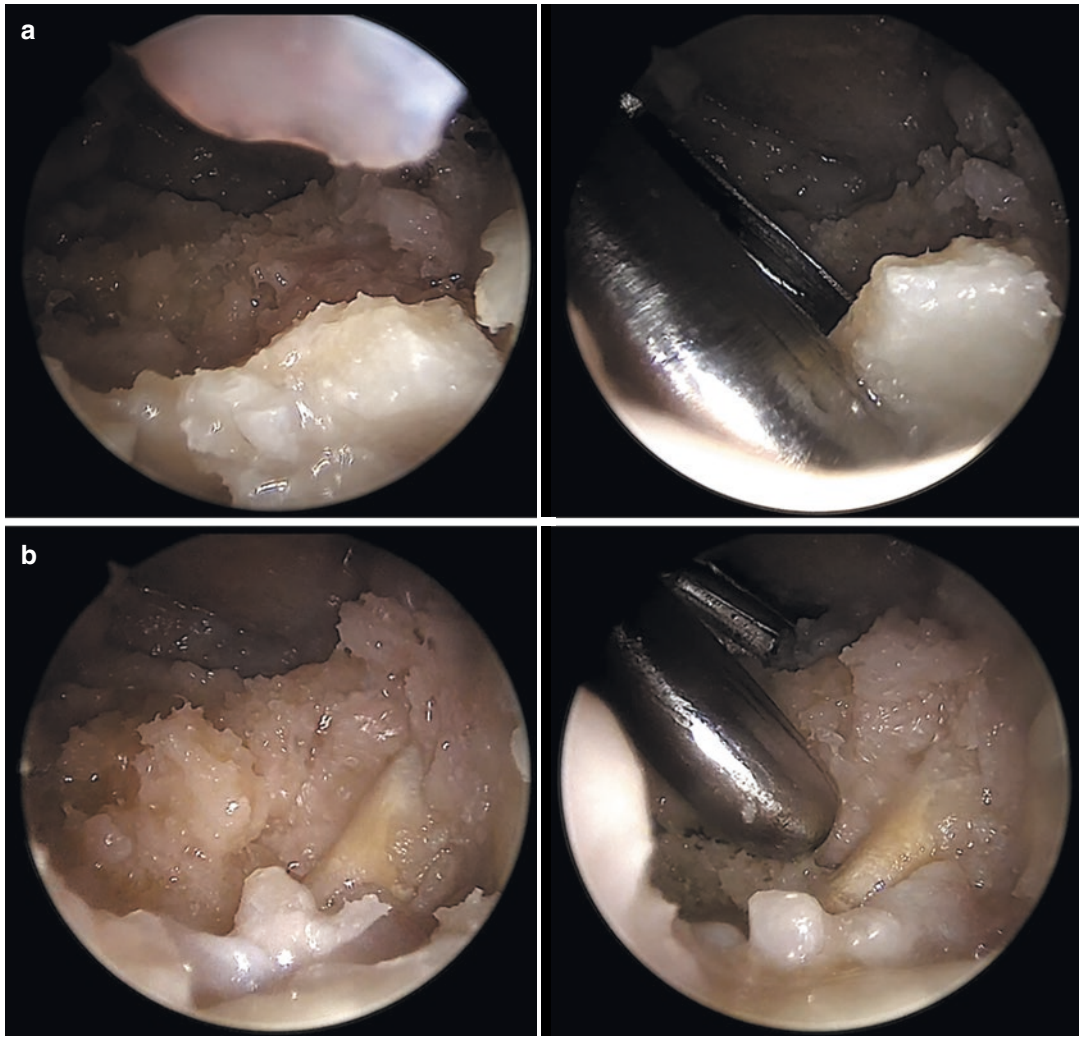

Fig. 117.10 Zone 2 is removed using the burr, periosteal elevator, and rongeur. (**a**) The cartilage and subchondral bone over the scaphoid. (**b**) The half of the volar bone covering 1/3rd of the radial side of the trapezium

117.4.5 Proximal Resection of the Trapezoid

If the patient shows degenerative changes in the STT joint, resection of the proximal portion of the trapezoid can be performed arthroscopically. This resection is performed with the scope in the thenar portal and the burr in the 1U portal Fig. 117.16.

117.4.6 Suture Button Suspension

There is no need to remove the patient's hand from the traction tower to place the suture button. In fact, it is easier to achieve a correct implant position with the hand in the same position as in previous steps. In our opinion, there are two aspects of correct position: (1) correct height—the base of the first metacarpal bone should make a "V" with the base of the second; (2) the thumb should not be fixed pronated but supinated, because a pronated position will make extension and abduction of the thumb more difficult. Maintaining the hand suspended in the traction tower makes these two goals easier to achieve than when the hand rests on a table.

- Firstly, the height of the first metacarpal is adjusted by removing some traction of the fin-

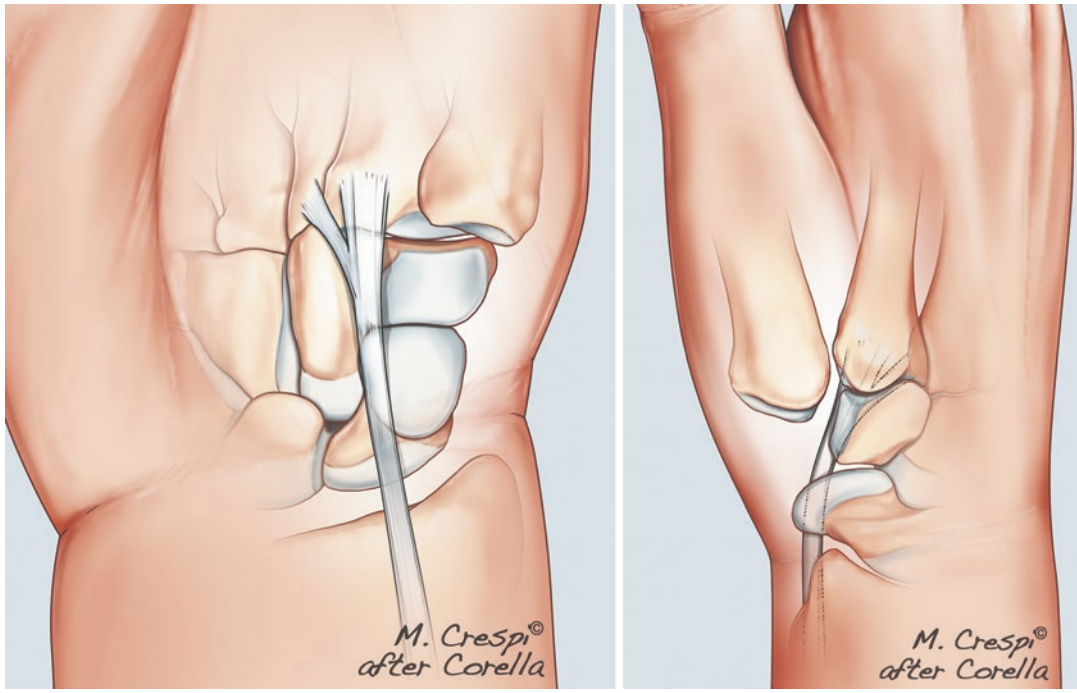

Fig. 117.11 The flexor carpi radialis tendon is located in the corner between the scaphoid and trapezoid, and is covered by zone 2 bone of trapezium (M. Crespi © for Corella). Reprinted from Corella F, Ocampos M, Laredo R, Tabuenca J, Carnicer M, Larrainzar-Garijo R. Arthroscopic Trapeziectomy and Suture Button Suspensionplasty: A Review of the Literature and Description of the "Three-Step Arthroscopic Trapeziectomy Technique." Journal of Wrist Surgery. Vol 9, Issue 5. With permission from Thieme Medical Publishers. 2020

gertrap until the X-ray shows perfect position—that is, when a "V" is seen between the first and second metacarpal bones Fig. 117.17. Once the position is correct, no further adjustment is necessary during the introduction of the SBS.

- Secondly, to avoid pronation of the thumb, the entry point should be volar to the first extensor tendon compartment. This way, when the thread is tensioned, the metacarpal will be supinated. This volar entry point is easily located through the thenar portal, sliding the tip of the guide wire slightly distal (1 cm from the articular surface) and dorsal Fig. 117.18.
- Furthermore, as traction is maintained from the first and second fingers, the thumb and first metacarpal bone are already supinated. If stabilization is performed with the hand resting over a hand table, as is commonly performed in open surgery, the comfortable position is with the thumb in opposition so that it is pronated. However, this makes extension and retropulsion difficult after surgery Fig. 117.19.
- Fixation can be performed using either a guide or free hand, and the method depends on the implant. We have always used the Mini TightRope®, but the MicroLink® (Conmed, New York) has recently been introduced.
- When the implant has been positioned, a knot is made, avoiding impingement between the first and second metacarpal bones. Here, it is useful to introduce a mosquito through the 1U

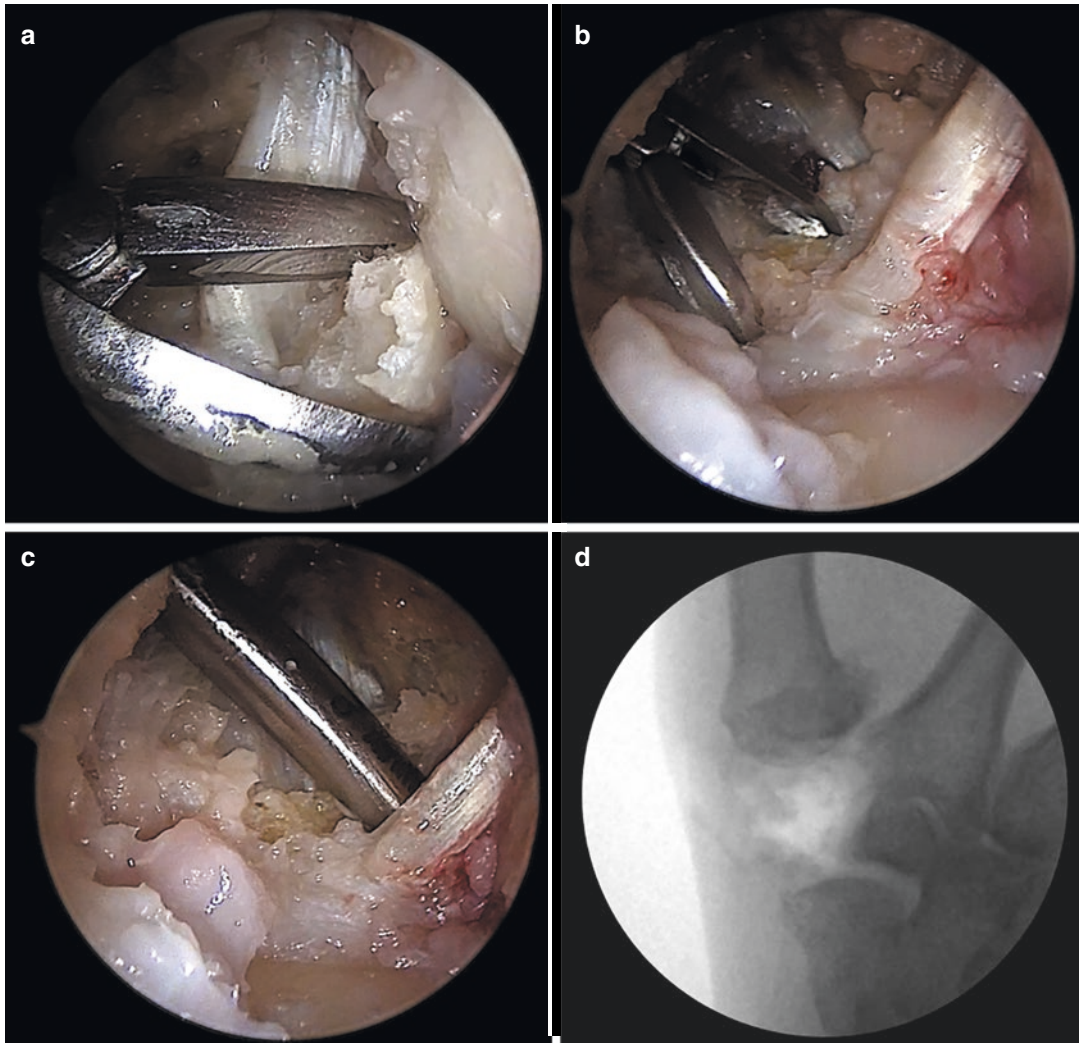

Fig. 117.12 The flexor carpi radialis is immediately in front of the arthroscope, which is why it is easier to perform the resection in this step. (**a**–**c**) The bone surrounding the flexor carpi radialis is removed using the burr, periosteal elevator, and rongeur. (**d**) When step 2 is finished, only the bone of zone 3 is seen in the X-ray, and often with difficulty

portal and place it between the bones. In doing so, even though the knot is strongly fixed, a space always remains between the bones Fig. 117.20.

- Finally, traction is released and the maintenance of height is checked.

The portals and the wound over the second metacarpal bone are closed using 5/0 monofilament suture, and the hand is place in a cast, with the thumb in abduction.

117.5 Tips and Tricks

1. ***Visualization***: Because the trapeziometacarpal joint is so small, it is difficult to maintain the correct view, especially when part of the trapezium has been resected and the arthroscope cannot rest over the bone. Furthermore, in such a small space, it is easy to injure other bones with the burr, such as the base of the second metacarpal, trapezoid, or scaphoid, or even damage the scope itself. For this reason,

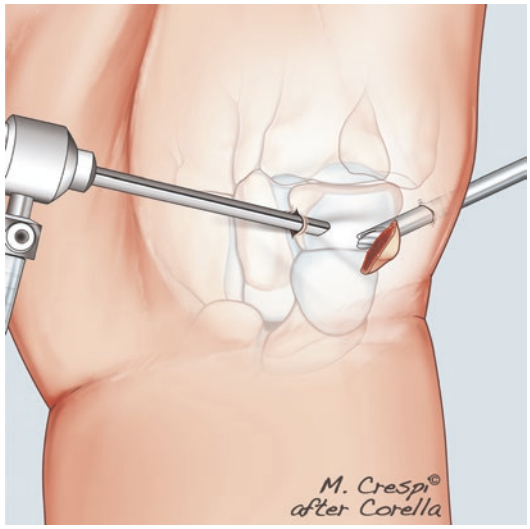

Fig. 117.13 Step 3. The arthroscope is moved again to the thenar portal, and the bone of zone 3 is removed (M. Crespi © for Corella). Reprinted from Corella F, Ocampos M, Laredo R, Tabuenca J, Carnicer M, Larrainzar-Garijo R. Arthroscopic Trapeziectomy and Suture Button Suspensionplasty: A Review of the Literature and Description of the "Three-Step Arthroscopic Trapeziectomy Technique." Journal of Wrist Surgery. Vol 9, Issue 5. With permission from Thieme Medical Publishers. 2020

it is important that the surgeon makes accurate movements with both the scope and the burr. To do so, it is useful that one surgeon acts as the cameraman, holding the scope with both hands to maintain a perfect view, while the other surgeon resects the bone, holding the hand piece in both hands. To ensure that two surgeons can work at the same time, there are two possible positions. The first involves one surgeon working on the dorsal side, with the other surgeon on the volar side. Although this is the most comfortable position, one surgeon must work with an inverted view in the screen. The second option has both surgeons working on the dorsal side, with the patient's hand in a supinated position. This way, the view is normal, but the surgeons are very close one to on another, making the procedure less comfortable.

2. ***Instruments and bone resection***: Arthroscopic shavers and burrs for small joints are used throughout the procedure (3-mm or 3.5-mm shaver, and 3-mm burr). To remove the bone faster, three more instruments may be useful: (1) a 4-mm burr (7-cm long, which is easier to use in the wrist); (2) a periosteal elevator, which is commonly used in percutaneous foot surgery to facilitate the separation of bone from the capsule and ligament attachments; (3) a pituitary rongeur, which allows large portions of the bone to be removed. Using these aids, the inner portion of the bone is removed using burrs; once only the peripheral portion is left, the periosteal elevator is used to separate the bone from the capsule. Finally, the bone is removed using the pituitary rongeur.
3. ***Dry or wet arthroscopy***: The setup of the portals, as well as the joint exploration, is performed without a saline infusion using the dry arthroscopy technique popularized by Piñal [12]. During the rest of the procedure, saline infusion is only used to aspirate all the bone debris.

117.6 Postoperative Rehabilitation

The cast is maintained for 2–3 weeks, at which point rehabilitation is initiated to regain motion and pinch strength. Specifically, the first interosseous muscle and opponent muscle are boosted (Fig. 117.21).

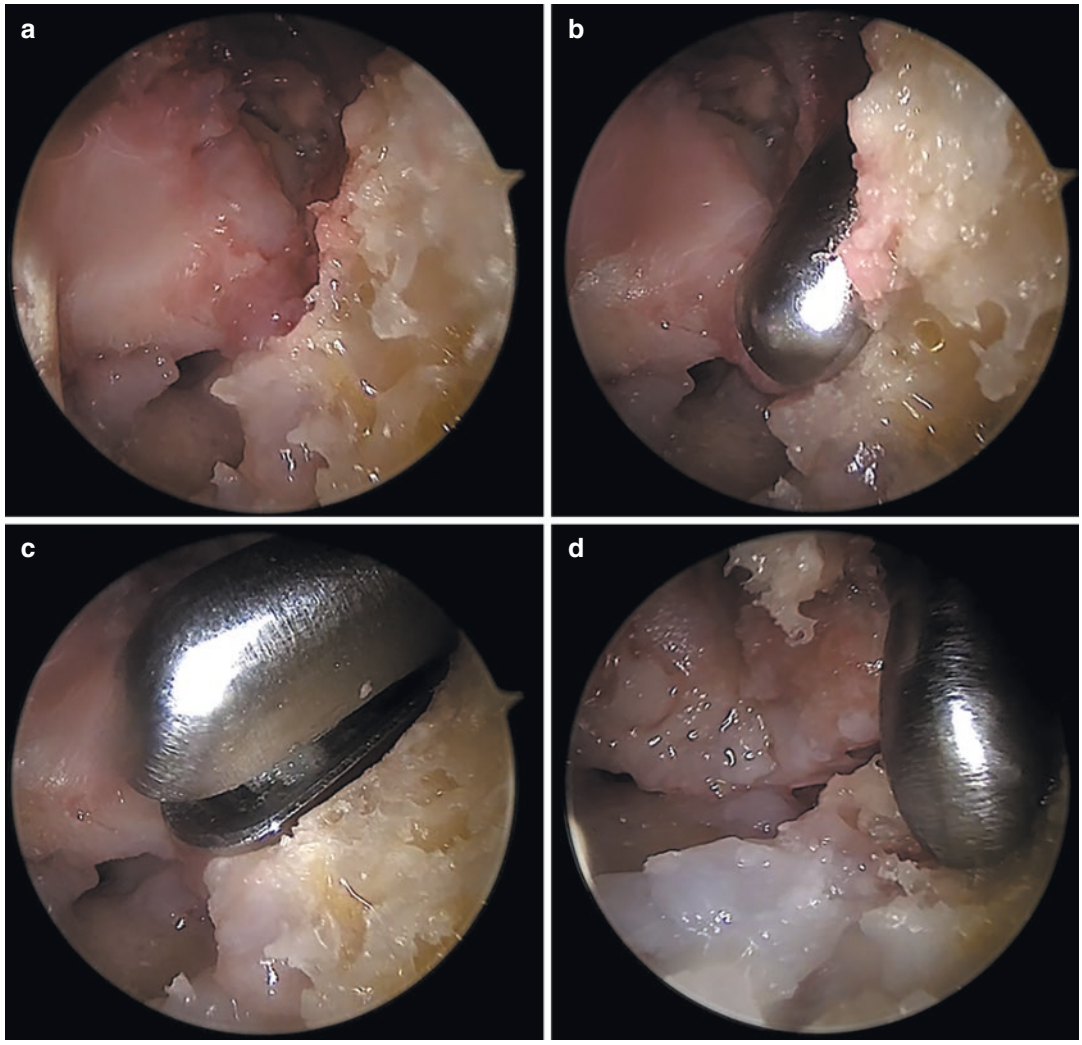

Fig. 117.14 (**a**) The bone of zone 3 is one of the most difficult portions of the trapezium to remove because it is between the two portals and a direct view cannot be obtained. The bone is always in the dorsal side. (**b**) With the burr or the shaver in the 1U portal, the inner portion of the bone is resected. (**c**, **d**) Using the rongeur, the bone is then detached from the capsule

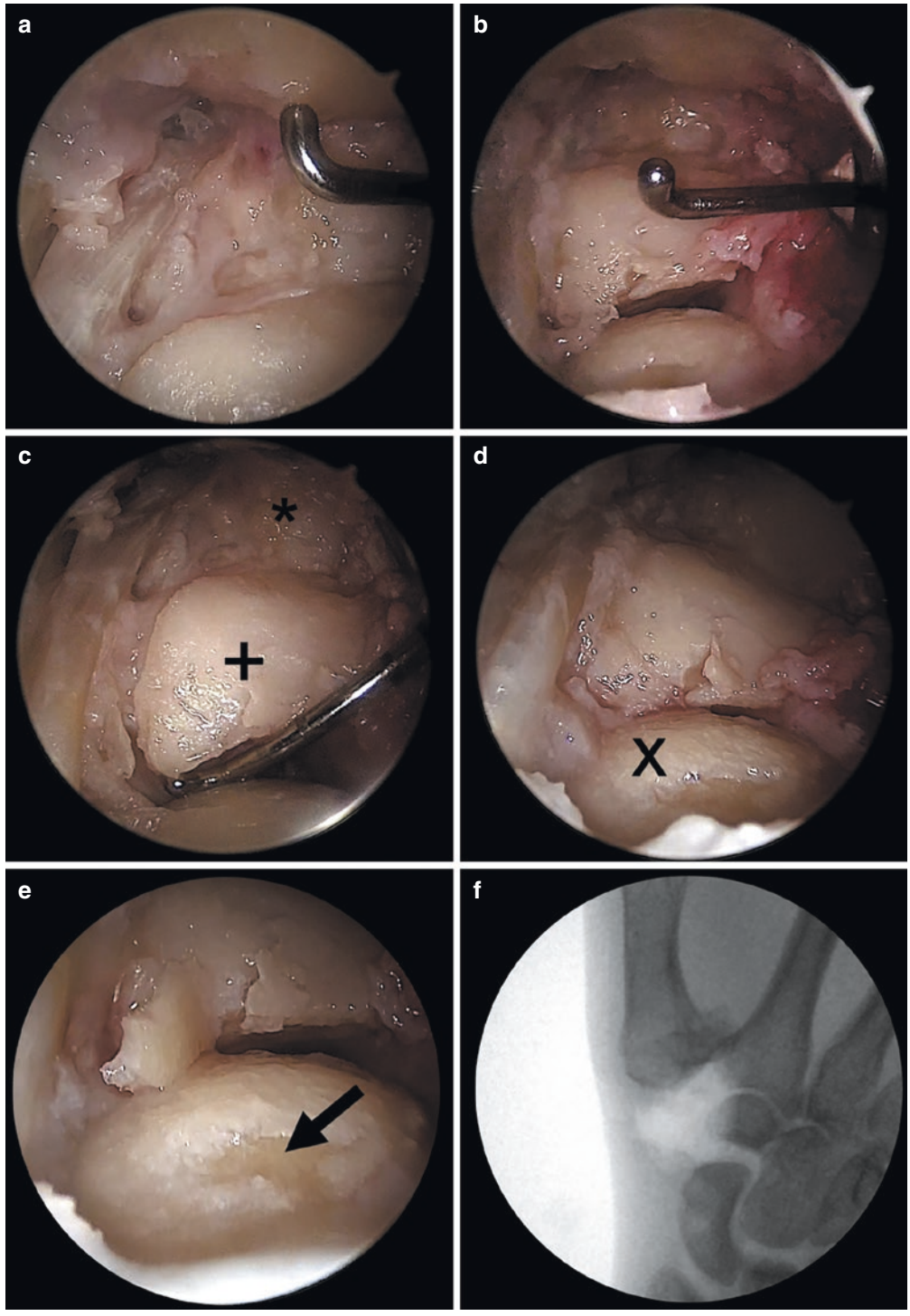

Fig. 117.15 The arthroscope is located in the 1U portal. (**a**) The probe is touching the base of the first metacarpal bone. (**b**) The probe is touching the trapezoid. (**c**) The probe is inside the STT joint [(*) second metacarpal bone, (+) trapezoid]. (**d**) Distal portion of the scaphoid (×) is seen. (**e**) The arrow shows a chondral lesion of the scaphoid (stage IV of Eaton classification). (**f**) The resection is also checked using a fluoroscope to ensure that no bone remains

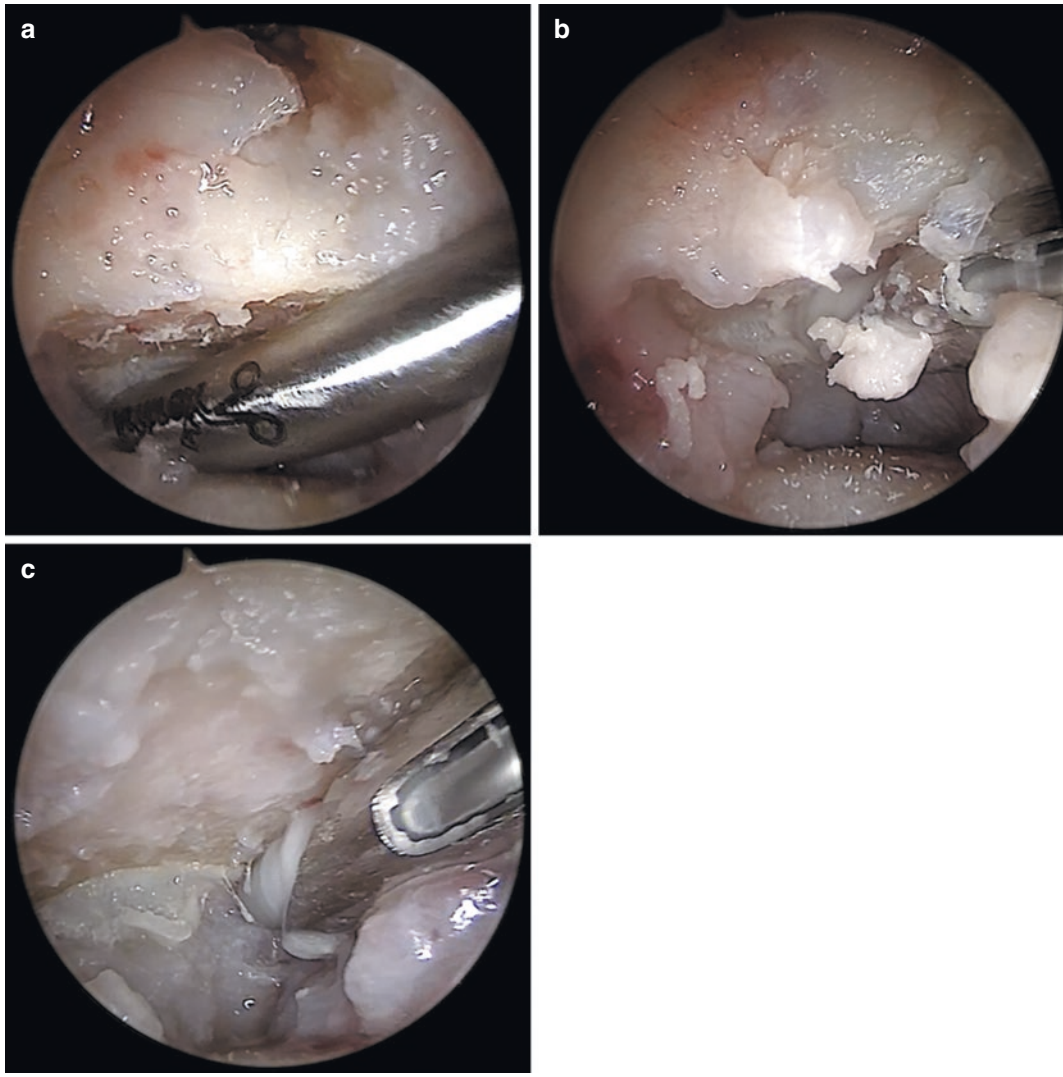

Fig. 117.16 If there are degenerative changes in the scapho-trapezoid joint. (**a** to **c**) Resection of the proximal portion of the trapezoid can be performed with the scope in the thenar portal and the burr in the 1U portal

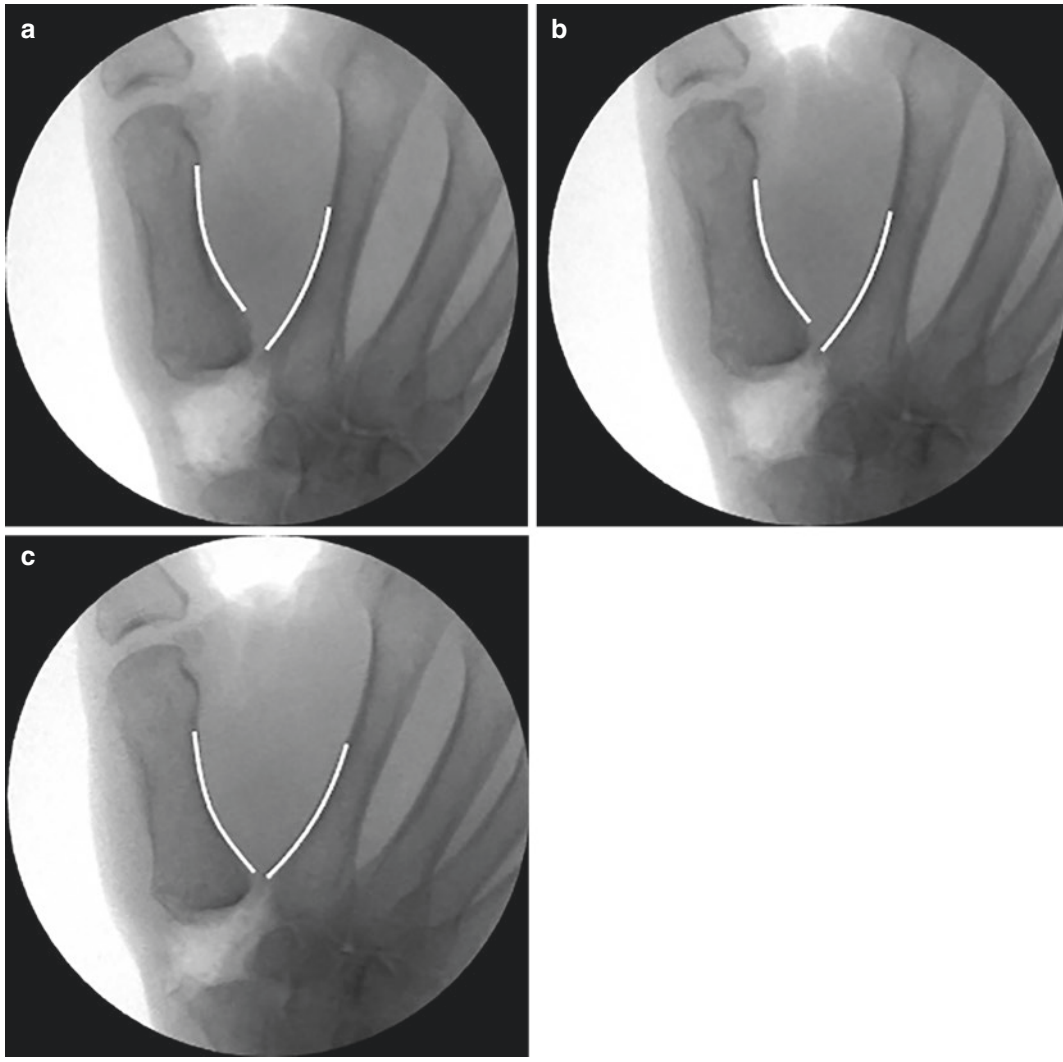

Fig. 117.17 The height of the first metacarpal is adjusted by removing some traction of the fingertrap until the X-ray shows a perfect position—that is, when a "V" is seen between the first and the second metacarpal bones. (**a**–**c**) Traction is released until a perfect "V" is seen between the first and the second metacarpal bones

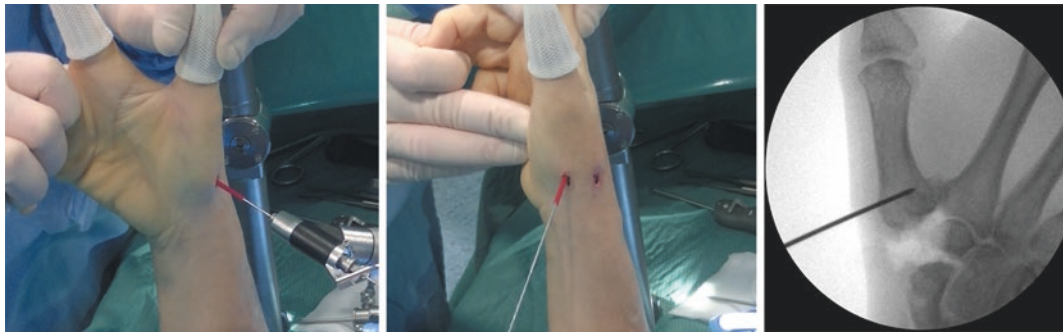

Fig. 117.18 The volar entry point is easily located through the thenar portal, sliding the tip of the guide wire slightly distal (1 cm from the articular surface) and dorsal to the portal

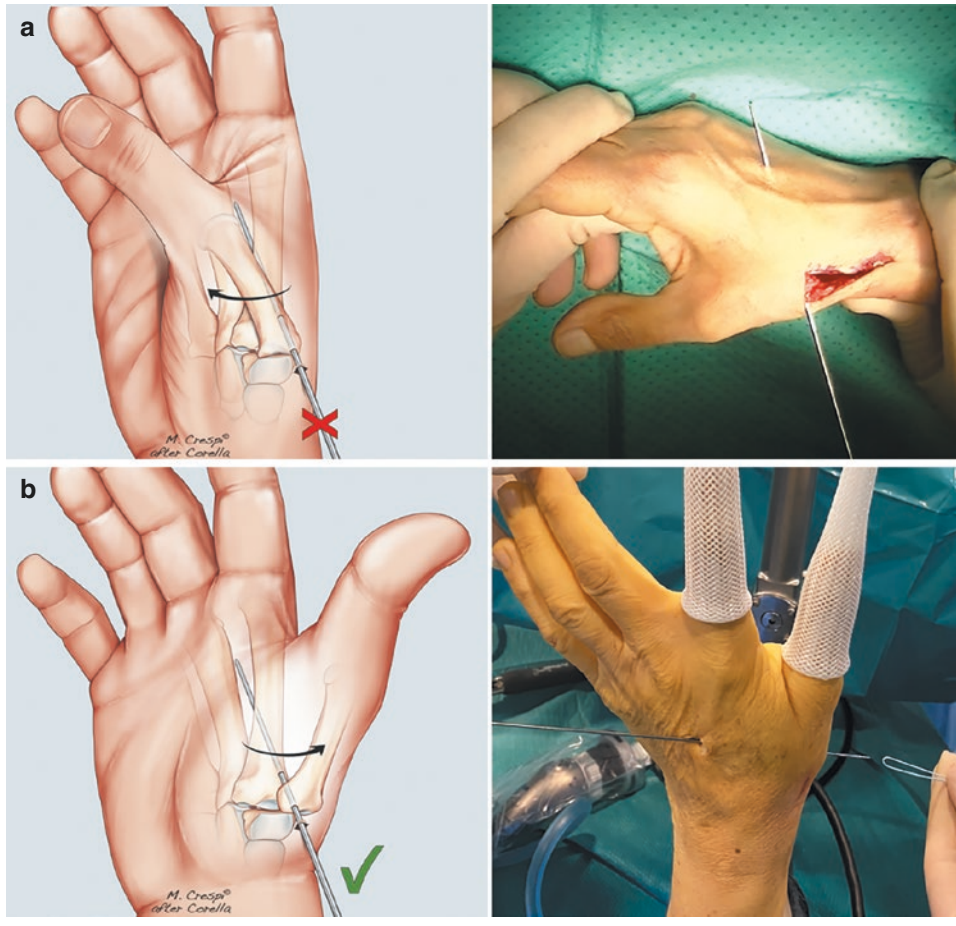

Fig. 117.19 (**a**) If stabilization is performed with the hand resting over a hand table, as is commonly done in open surgery, the comfortable position is with the thumb in opposition so that it is pronated. However, extension and retropulsion are difficult after surgery. (**b**) Maintaining the hand suspended in the traction tower makes correct positioning of the stabilization easier. The entry point is volar to the first extensor tendon compartment, which is located through the thenar portal. The thumb and the first metacarpal bone are already supinated (M. Crespi © for Corella). Reprinted from Corella F, Ocampos M, Laredo R, Tabuenca J, Carnicer M, Larrainzar-Garijo R. Arthroscopic Trapeziectomy and Suture Button Suspensionplasty: A Review of the Literature and Description of the "Three-Step Arthroscopic Trapeziectomy Technique." Journal of Wrist Surgery. Vol 9, Issue 5. With permission from Thieme Medical Publishers. 2020

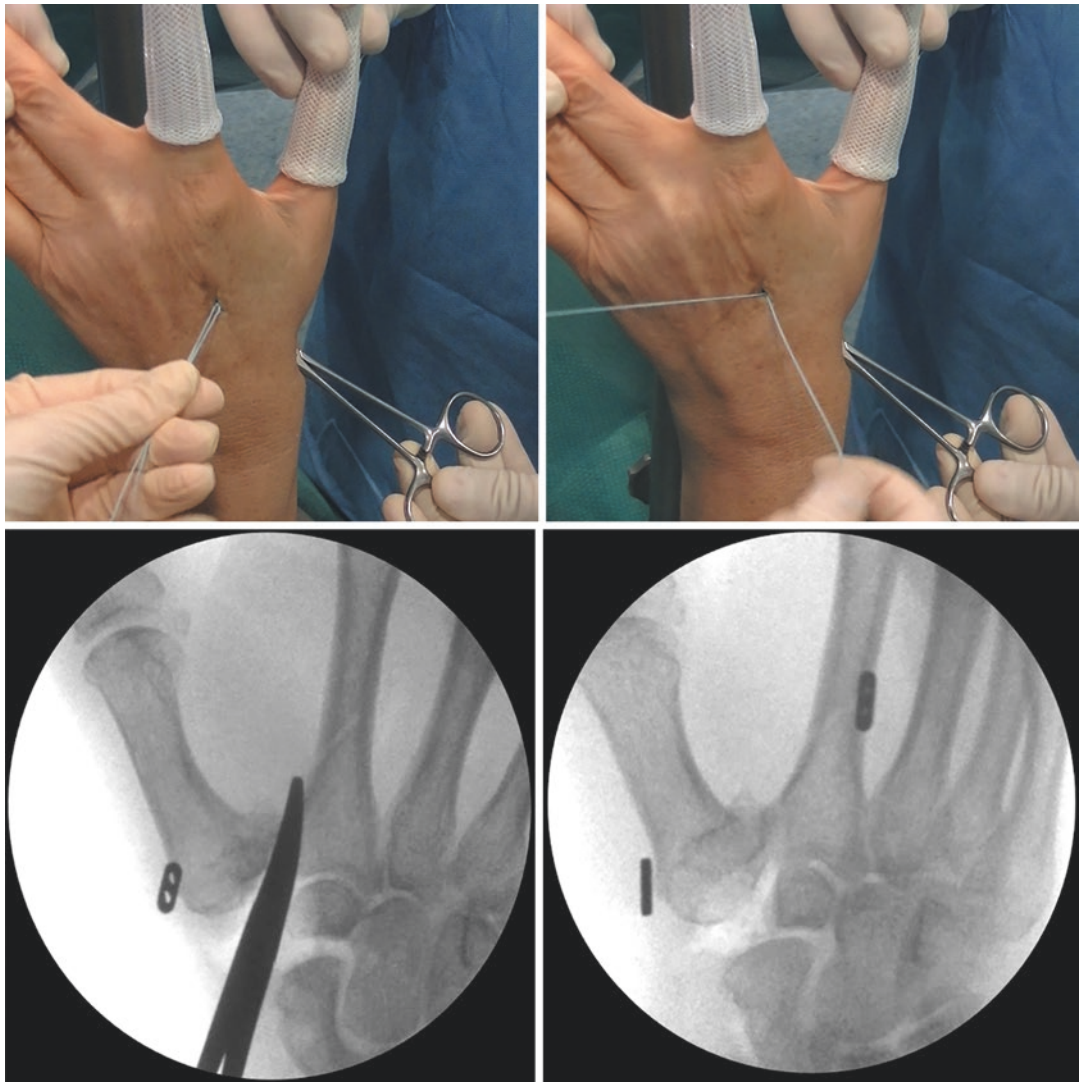

Fig. 117.20 To avoid impingement between the first and second metacarpal bones, a mosquito is introduced through the 1U portal and placed between the bones. This way, even though the knot is strongly fixed, there will be always space between the bones

Fig. 117.21 (**a**) Range of motion and pinch Strength (6 LBS) of a patient (different from the patient in surgical figures) 5 weeks after surgery. (**b**) Range of motion and pinch Strength (12 LBS) 6 months after surgery

117.7 Complications

- General complications (as in an open trapeziectomy) include proximal migration of the first metacarpal bone, joint stiffness, decreased thumb mobility or strength, and chronic regional pain syndrome.
- Complications due to the portal placement include dorsal radial nerve injury, tendon injury, or even a radial artery injury.
- Complications with the suture button placement include fracture of the second metacarpal bone or the injury of superficial nerves or tendons.

References

1. Wong CW-Y, Ho P-C. Arthroscopic management of thumb carpometacarpal joint arthritis. Hand Clin. 2017;33(4):795–812.
2. Eaton RG, Glickel SZ. Trapeziometacarpal osteoarthritis: staging as a rationale for treatment. Hand Clin. 1988;3(4):455–69.
3. Yao J, Cheah AEJ. Mean 5-year follow-up for suture button suspensionplasty in the treatment of thumb carpometacarpal joint osteoarthritis. J Hand Surg Am. 2017;42(7):569.e1–569.e11.
4. Özçelik İ, Uğurlar M, Sarı A. Arthroscopic hemitrapeziectomy and suture button suspensionplasty in the treatment of first carpometacarpal joint Eaton–Littler stage 2–3 arthrosis. J Wrist Surg. 2019;08(02):132–8.
5. Abzug JM, Osterman AL. Arthroscopic hemiresection for stage II-III trapeziometacarpal osteoarthritis. Hand Clin. 2011;27(3):347–54.
6. Cox CA, Zlotolow DA, Yao J. Suture button suspensionplasty after arthroscopic hemitrapeziectomy for treatment of thumb carpometacarpal arthritis. Arthroscopy. 2010;26(10):1395–403.
7. Daroda S, Menvielle F, Cosentino R, Pereira P. Arthroscopic total trapeziectomy. Tech Hand Up Extrem Surg. 2010;14:259–62.
8. Landes G, Gaspar MP, Goljan P, Jacoby SM, Bachoura A, Culp RW. Arthroscopic trapeziectomy with suture button suspensionplasty: a retrospective review of 153 cases. Hand. 2016;11(2):232–7.
9. Yao J. Suture-button suspensionplasty for the treatment of thumb carpometacarpal joint arthritis. Hand Clin. 2012;28(4):579–85.
10. Corella F, Ocampos M, Laredo R, Tabuenca J, Carnicer M, Larrainzar-Garijo R. Arthroscopic trapeziectomy and suture button suspensionplasty: a review of the literature and description of the "Three-Step Arthroscopic Trapeziectomy Technique." J Wrist Surg. 2020;09(05):366–81.
11. Walsh EF, Akelman E, Fleming BC, Dasilva MF. Thumb carpometacarpal arthroscopy: a topographic, anatomic study of the thenar portal. J Hand Surg Am. 2005;30(2):373–9.
12. del Piñal F, García-Bernal FJ, Pisani D, Regalado J, Ayala H, Studer A. Dry arthroscopy of the wrist: surgical technique. J Hand Surg Am. 2007;32(1):119–23.

118 Arthroscopic Treatment of Basal Joint Fractures

Didier Fontès

118.1 Background

"Bennett's fracture" described by Dr. Edward Bennett, who suffered a fracture of his thumb while horse riding in 1882, is a fracture dislocation of the thumb and remains a classical problem for trauma hand surgeons [1]. It is not uncommon in contact sports such as boxing, rugby, American football, and soccer. It refers to a fracture of the ulnar aspect of first metacarpal bone at the joint surface with frequent underestimated associated ligamentous lesions. It is also known as a "Boxer's fracture," because the mechanism of injury is often a traumatic force (a punching movement) going down the length of the first metacarpal bone with impact on a curved carpometacarpal (CMC) joint trauma through tackling an opponent in rugby or American football can cause a Bennett's fracture, while a soccer goalkeeper may have direct impact on the thumb from a fall or with the ball while attempting to make a save.

The size of the detached fragment governs the therapeutic decisions but surgical management remains controversial and sometimes difficult. Inter-metacarpal pinning as described by François Iselin and open screw fixation according to Gedda and Moberg gained widespread acceptance for treating Bennett fractures [2]. Culp and Johnson have developed a percutaneous screw fixation technique including arthroscopic evaluation for joint surface restoration [3].

We have proposed an innovative approach for an arthroscopic management of articular Bennett's fractures to simplify the postoperative course and to decrease the incidence of late arthritis changes [4, 5].

118.1.1 Surgical Anatomy

Basal joint anatomy: The remarkable mobility of the column of the thumb depends essentially on the basal joint articulation [6]. According to Zancolli and Kapandji, this articulation is described, not in the so-called anatomical position of maximum reposition, but in its rest position constituting the reference basis of description for the axis of mobility. Basal joint articulation is a concavo-convex surface (double-saddle joint) with reciprocal interlocking that permits a certain degree of axial rotation [7]. The articular capsule is inserted at a distance from the articular surfaces and therefore does not hinder the great mobility of this joint. The capsule is reinforced by ligamentous structures (up to 17 have been described) and these can be simplified into four groups based on their palmar, ulnar, radial, or dorsal attachment [7, 8].

Physiopathology of Bennett's fractures: The typical lesion involves an avulsion-fracture of the

D. Fontès (✉)
Hand, Shoulder and Sports Institute CMO, Sports Clinic of Paris, Paris, France
e-mail: docteurfontes@noos.fr

© ISAKOS 2022

D. N. Bhatia et al. (eds.), *Arthroscopy and Endoscopy of the Elbow, Wrist and Hand*,
https://doi.org/10.1007/978-3-030-79423-1_118

volar-ulnar portion of the first metacarpal bone with a dorsal-radial subluxation. Articular displacement has a triple mechanism: axial compression with bone crushing, dislocating action of abductor pollicis longus tendon, and frequent associated ligamentous lesions. The anatomical complexity of this joint requires accurate radiological assessment using radiographs with specialized views and 3D reconstructions of CT scans [2, 6, 7] (Fig. 118.1). Despite extensive imaging, complexity of the anatomy of this double inversed saddle shape articulation requires ideally an arthroscopic evaluation to assess the accuracy and stability of an internal fixation as demonstrated for articular fractures of the distal radius [2, 9, 10]. Depending on the size of the ulnar fragment, its displacement and possible metaphyseal line of fracture we can classify either Bennett's or Rolando's fractures according to Gedda's classification [2] (Fig. 118.2). Trapeziometacarpal ligaments tears are frequently associated lesions especially in sport traumatology [7, 8]. Surgical reattachment of the avulsed ligaments is necessary and the surgical approach depends on location of the lesion. Arthroscopic evaluation is helpful to identify the lesion and plan the most accurate treatment [11–14].

118.2 Indications and Contraindications

The incidence of long term degenerative joint arthritis in the first CMC joint is high following a Bennett's fracture and occurs as a result of articular damage and joint instability caused by the osseous detachment of the deep ulnar ligament and possible associated extrinsic ligaments injury [4, 5, 7]. Also, displaced Bennett's fractures managed conservatively tend to develop osteoarthritis and functional impairment and surgical fixation is necessary to treat this articular fracture dislocation. As with any joint reconstruction, the outcome is dependent upon the surgeon's skill in realigning the normal joint anatomy. Our indications for this technique are limited to Gedda I, II, and III Bennett's fractures (Fig. 118.2).

Rolando's fractures are excluded from a percutaneous technique and are treated with plate

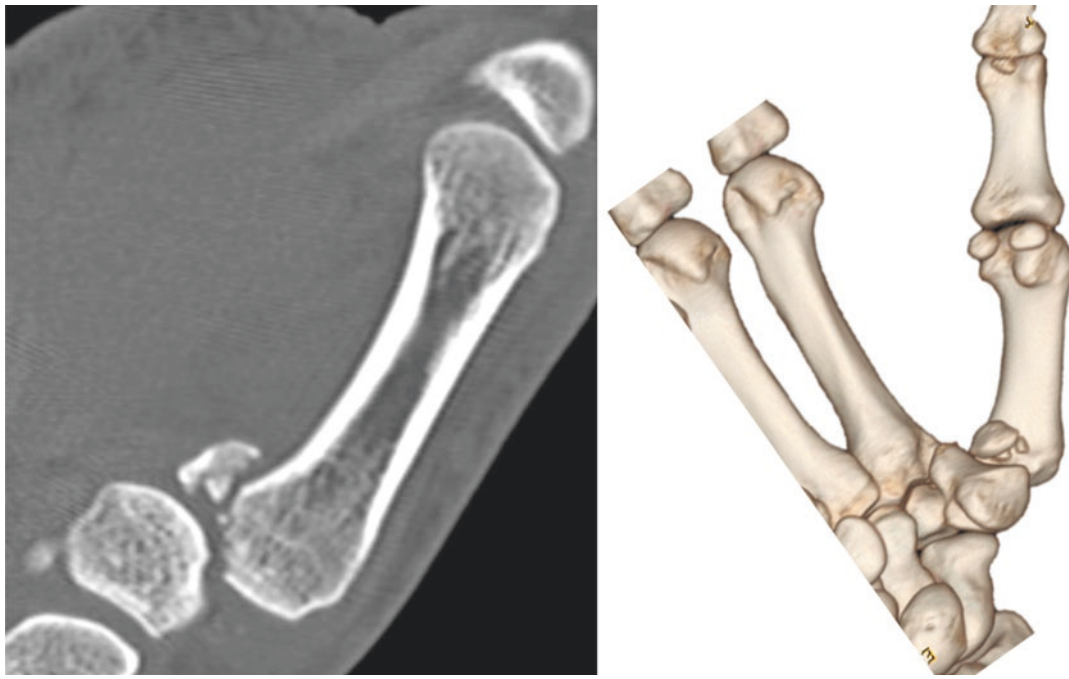

Fig. 118.1 CT scan of a Bennett's fracture shows the size and displacement of fracture fragment

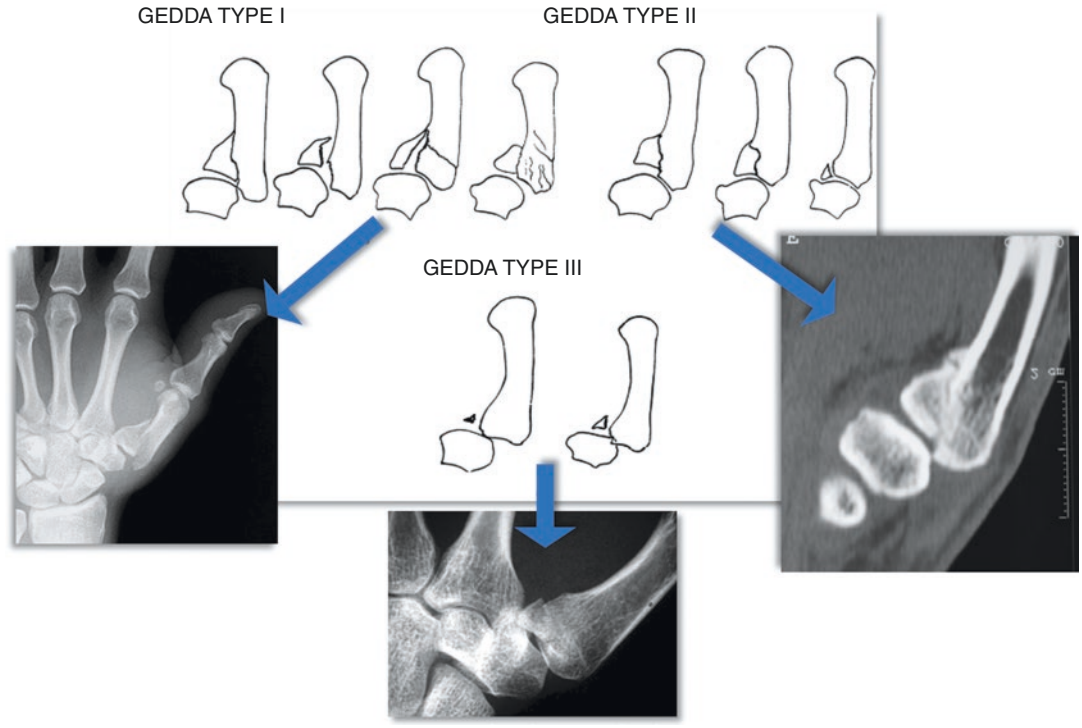

Fig. 118.2 Gedda's classification of Bennett's fractures of first metacarpal

fixation or internal fixation of metaphyseal metacarpal bone, nevertheless arthroscopic control of the accuracy of the articular reduction and stability is recommended. Local infection or soft tissue damage are other contraindications for this arthroscopic procedure.

118.3 Surgical Technique

Regional and local anesthesia is generally used. Patients are placed in the supine position with an arm tourniquet. A Whipple tower is classically used to apply traction along the axis of the thumb in order to create an articular working space. Arthroscopic evaluation of the trapeziometacarpal joint is conducted through the 1-R, 1-U portals and thenar portal using a 1.9–2.7 mm arthroscope [15] (Fig. 118.3). This installation was adopted by different authors who manage Bennett's fractures arthroscopically but in our experience, this procedure does not suit us because the wrist must be systematically stabilized by an assistant and the bulk of the fluoroscopy apparatus makes the maneuvers of reduction and osteosynthesis difficult [3, 16]. We therefore use another method of positioning and the thumb is placed flat on the surgical table as described below.

The technique is based on GEDDA's classification depending on the size and displacement of the volar and ulnar fragment well assessed with a systematic 3D CT scan.

- First, an inter-metacarpal pinning is performed under fluoroscopic control (Iselin technique) with a relative traction on first CMC Joint (Fig. 118.4).
- Arthroscopic assessment of the basal joint is performed through standard portals (1-R, 1-U, Thenar) with the hand lying on the table. Debridement is performed to excise free articular fragments and organized clots with a small full-radius shaver (Fig. 118.5). This

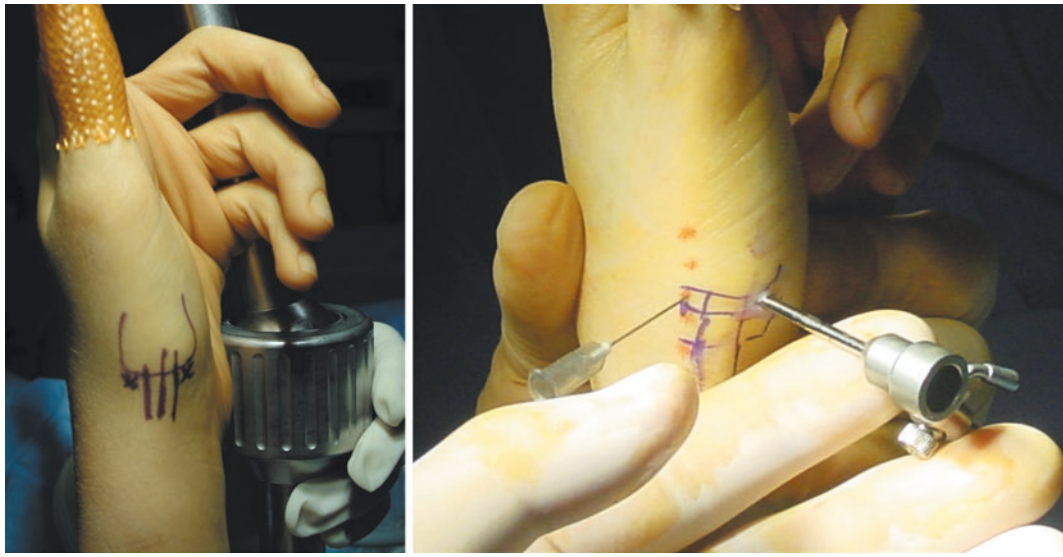

Fig. 118.3 Classical vertical traction and portals for basal joint arthroscopy

Fig. 118.4 The "horizontal" procedure is performed using inter-metacarpal (Iselin's technique) pinning. K-wires are bent and cut short and arthroscopic portals are created with the hand on the operating table

method is ergonomic and simpler for fluoroscopic control as compared to working in a vertical position.

- Reduction of the ulnar fragment is performed under mixed endoscopic and fluoroscopy and its internal fixation is carried out depending on its size based on Gedda's classification (K wire or cannulated compressive screw) (Figs. 118.6 and 118.7).
- Thereafter, ligaments are assessed, and if necessary, a simple arthroscopic debridement or an endoscopic-assisted procedure using small suture anchors is performed for reattachment of dorso-radial or volar ligaments (Fig. 118.8).
- Finally, stability of the osteosynthesis is assessed and in absence of associated ligamentous lesions, inter-metacarpal K wires are immediately removed and full motion can be initiated. In others cases, a splint is applied for 3–6 weeks depending on associated lesions and K wires are thereafter.

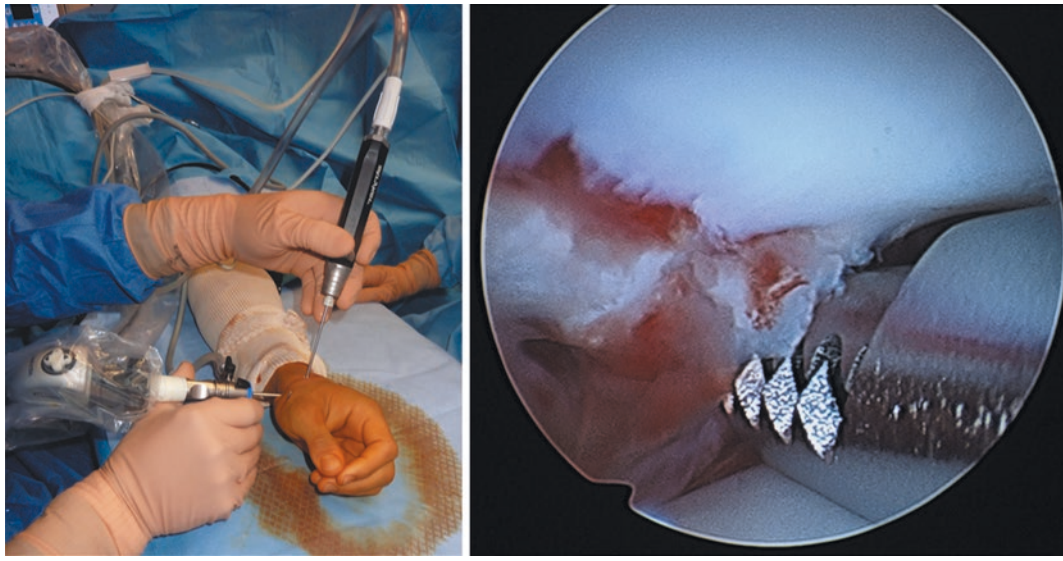

Fig. 118.5 Debridement of articular hematoma and assessment of chondral damage and extrinsic ligaments

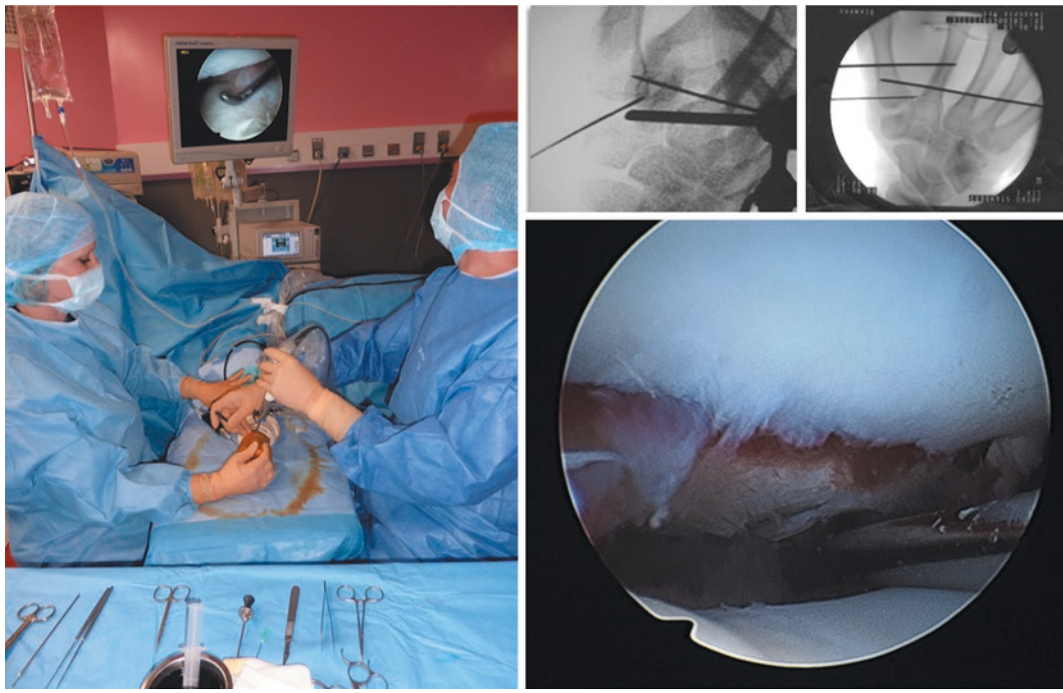

Fig. 118.6 Arthroscopic (with the probe or K-wire joystick) and fluoroscopic reduction of the ulnar fragment

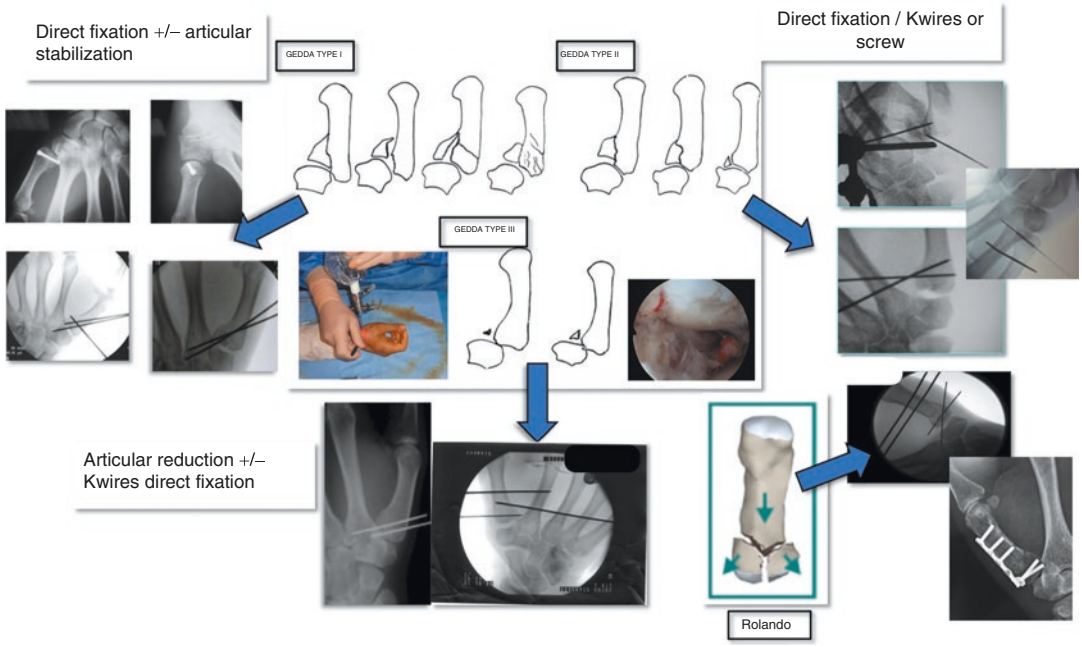

Fig. 118.7 Fixation techniques based on GEDDA's Classification are demonstrated

118.4 Postoperative Management and Rehabilitation

Following surgery, rehabilitation can be initiated once the surgeon has removed the splint and K-wires. The goals of rehabilitation are to relieve stiffness, restore range of motion, and increase progressively muscle strength. Hand function is gradually restored to normal over a 3-month period although the thumb may sometimes not feel right for around 6 months.

Exercises using hand therapy balls can be very helpful to regain mobility. Grip and thumb strengthening devices can also be useful to restore normal hand and thumb strength before return to sport and competition which is generally possible after 2–3 months with the protection of a strapping.

118.5 Results

Since 2005, we have performed 20 cases of this minimally invasive, cosmetic and anatomical procedure. We did not have any specific complication except one transitory radial nerve dysesthesia on a location of an inter-metacarpal K wire. Assessment of pain, motion, strength, and function showed good results similar to other series in literature and much better rather than classical open or percutaneous procedures [2–5, 7, 16, 17]. The accuracy of the reduction was also better than in conventional open techniques [18].

Full return to professional activities was shorter for the screw-fixation group compared to K-wire group especially in absence of associated ligamentous lesions which allowed for early mobilization. Contact sports were possible after 2 months with a soft protection.

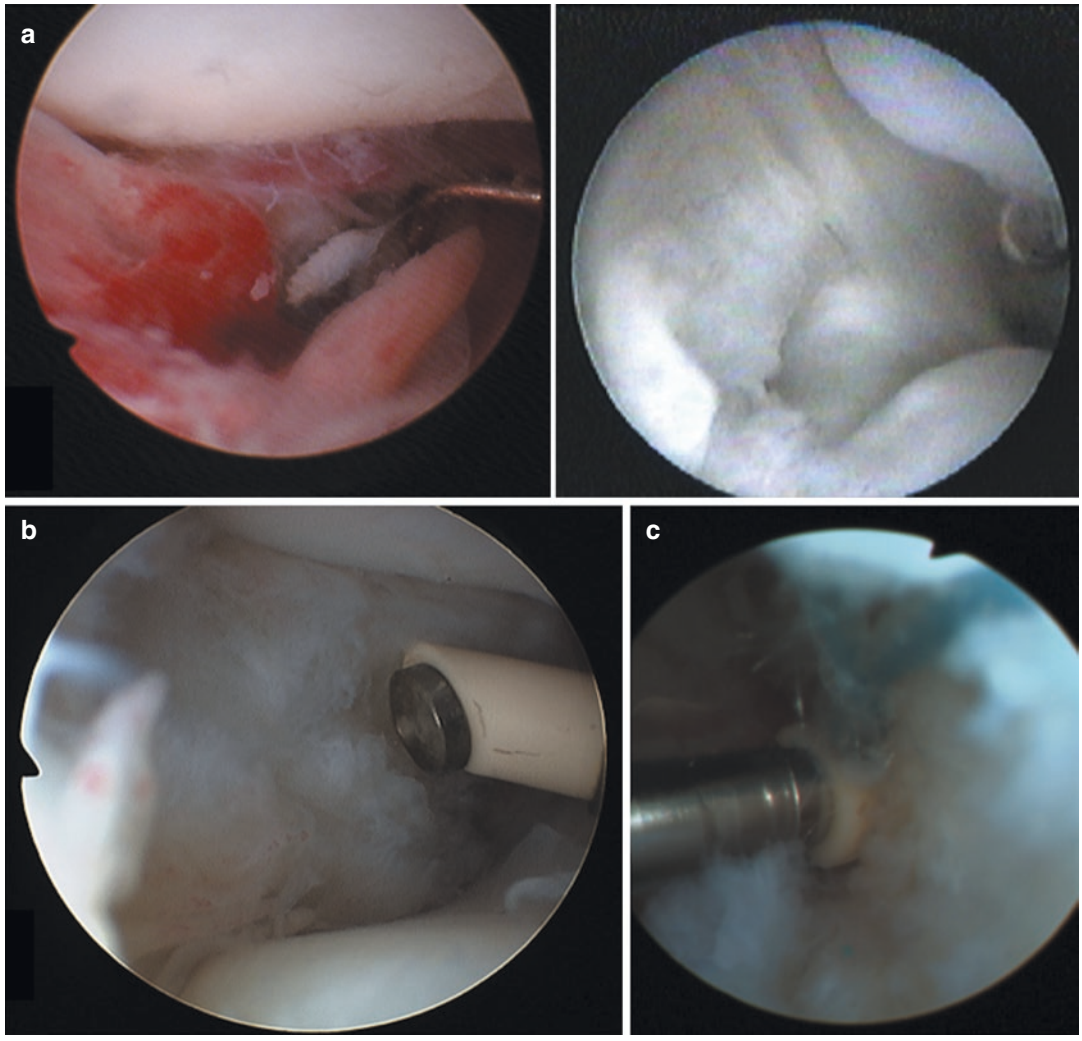

Fig. 118.8 Assessment and treatment of possible associated extrinsic ligament lesions (**a**) with a simple radiofrequency debridement and shrinkage (**b**) or a trans-osseous reattachment (**c**)

References

1. Bennett EH. On fracture of the metacarpal bone of the thumb. Br Med J. 1886;3:12–3.
2. Gedda K-O, Moberg E. Open reduction and osteosynthesis of the so-called Bennett's fracture in the carpometacarpal joint of the thumb. Acta Orthop Scand. 1952;22(1–4):249–57.
3. Culp RW, Johnson JW. Arthroscopically assisted percutaneous fixation of Bennett fractures. J Hand Surg. 2010;35(1):137–40.
4. Cannon S, Dowd G, Williams D, Scott J. A long-term study following Bennett's fracture. J Hand Surg Br. 1986;11(3):426–31.
5. Timmenga EJF, Blokhuis TJ, Maas M, Raaijmakers ELFB. Long-term evaluation of Bennett's fracture: a comparison between open and closed reduction. J Hand Surg. 1994;19(3):373–7.
6. Kapandji A. Cotation clinique de l'opposition et de la contre-opposition du pouce. Ann Chir Main. 1986;5(1):67–73.
7. Edmunds JO. Traumatic dislocations and instability of the trapeziometacarpal joint of the thumb. Hand Clin. 2006;22(3):365–92.
8. Fontès D. [The value of early ligament repair in severe sprains of the trapezoid-metacarpal joint. Apropos of 10 cases]. Acta Orthop Belg. 1992;58(1):48–59.
9. Augé WK, Velázquez PA. The application of indirect reduction techniques in the distal radius. Arthroscopy. 2000;16(8):830–5.

10. Fontès D. [Wrist arthroscopy. Current indications and results]. Chir Main. 2004;23(6):270–83.
11. Berger RA. A technique for arthroscopic evaluation of the first carpometacarpal joint. J Hand Surg. 1997;22(6):1077–80.
12. Roure P, Fontès D. Apport de l'arthroscopie au niveau de l'articulation trapézo-métacarpienne. J Traumatol Sport. 2005;22(4):243–5.
13. Badia A. Arthroscopy of the trapeziometacarpal and metacarpophalangeal joints. J Hand Surg. 2007;32(5):707–24.
14. Fontès D. L'arthroscopie du poignet. Indications actuelles et résultats. Chir Main. 2004;23(6):270–83.
15. Walsh EF, Akelman E, Fleming BC, DaSilva MF. Thumb carpometacarpal arthroscopy: a topographic, anatomic study of the thenar portal. J Hand Surg. 2005;30(2):373–9.
16. Pomares G, Strugarek-Lecoanet C, Dap F, Dautel G. Bennett fracture: arthroscopically assisted percutaneous screw fixation versus open surgery: functional and radiological outcomes. Orthop Traumatol Surg Res. 2016;102(3):357–61.
17. Zemirline A, Lebailly F, Taleb C, Facca S, Liverneaux P. Arthroscopic assisted percutaneous screw fixation of Bennett's fracture. Hand Surg. 2014;19(02):281–6.
18. Capo JT, Kinchelow T, Orillaza NS, Rossy W. Accuracy of fluoroscopy in closed reduction and percutaneous fixation of simulated Bennett's fracture. J Hand Surg. 2009;34(4):637–41.

119 Arthroscopic Debridement and Metacarpal Base Osteotomy for Trapeziometacarpal Joint Osteoarthritis

Allan Wang

119.1 Background

Arthroscopic evaluation and treatment of trapeziometacarpal joint (TMJ) osteoarthritis were initially reported by Menon in 1996. Subsequent advances in the understanding of intra-articular anatomy of the TMC joint, and development of miniaturised arthroscopic equipment have expanded arthroscopic applications and minimally invasive approaches to TMC osteoarthritis. This article reviews the surgically relevant anatomy, and the arthroscopic treatment options for TMC arthritis presenting at an early stage.

119.1.1 Surgical Anatomy

High levels of load are transmitted across the basal thumb joints with pinch and grip activity. Cadaver studies have described a complex arrangement of ligaments stabilising the trapezium to the base of the first metacarpal, and to the second metacarpal, as well as stabilising structures to the scaphoid trapezium and trapezoid joints [1]. Repetitive mechanical loading combined with progressive ligament attenuation leads to characteristic patterns of TMJ synovitis, articular degeneration, joint subluxation and subsequent development of pan trapezial osteoarthritis.

The anterior oblique ligament (AOL) is the major soft tissue stabiliser limiting dorsal subluxation of the base of the first metacarpal. The AOL has two components, the superficial AOL is deep to the thenar muscles overlying the volar aspect of the TMJ. Deep to the superficial AOL is the deep AOL also known as the volar beak ligament. This structure is intraarticular and is readily evaluated arthroscopically. On the dorsum, the posterior oblique ligament (POL) is situated ulnar to the thick and wide dorsal radial ligament (DRL), and these further stabilise the TMJ.

119.2 Indications and Contraindications

Eaton and Littler described a classification for TMJ osteoarthritis based on radiographic criteria [2]. Treatments recommended were based on the radiographic stage, with early osteoarthritis traditionally being managed conservatively with splints, injections and activity modification. More severe arthritic change was managed with hemi or total trapezium excision with or without ligament suspensionplasty, or interposition arthroplasty, or prosthetic arthroplasty. However clinical experience indicates that sometimes severity of symptoms does not correlate well with radiographic staging for TMJ arthritis. In particular, in the middle age female population, basal thumb pain can be debilitating and chronic

A. Wang (✉)
University of Western Australia, Perth, WA, Australia

© ISAKOS 2022

D. N. Bhatia et al. (eds.), *Arthroscopy and Endoscopy of the Elbow, Wrist and Hand*,
https://doi.org/10.1007/978-3-030-79423-1_119

yet with only minor radiographic change. In these presentations, extensive surgery is seldom indicated. Badia subsequently proposed an arthroscopic staging of TMJ osteoarthritis, based on intra-articular pathology and suggested a comprehensive arthroscopic treatment algorithm based on the arthroscopic stage of TMJ arthritis [3]. Patients who are unresponsive to conservative measures are candidates for arthroscopic management, or minimally invasive open surgical treatment.

The contraindications for arthroscopic management include thin unstable skin which may tear with traction applied through fingertraps, adjacent skin sepsis, circulatory or sensory disturbance of the thumb, generalised joint hyperlaxity especially of the MCP joint which may be aggravated by a lengthy period of traction.

119.3 Surgical Technique

The surgery is performed under general anaesthetic with the patient supine and with a high arm tourniquet. The thumb is suspended in gravity traction usually by a single finger trap (no counter weight). A mini C-arm is available to verify portal location, or if bony surgery is being performed.

Portals: With the thumb suspended in traction, the bony anatomy is marked, especially the base of thumb metacarpal. The extensor pollicis longus tendon is palpated along its course, and marked. The abductor pollicis longus tendon is palpated and marked. A 22-gauge needle is inserted radial to the APL tendon is "walked" along the bone from the base of the metacarpal into the joint. Two to three milliliters of saline are injected into the joint to facilitate portal placement. The 1R portal is placed radial and adjacent to the APL tendon. Through the 1R portal, the dorsal radial ligament and POL can be assessed. The 1 U portal is made just ulnar to the extensor pollicis brevis tendon. Viewing from 1U allows evaluation of the deep AOL. The thenar portal is made under direct visualisation through the 1 U portal. Transillumination of the radial and volar aspect of the TMC and thenar muscles allow insertion of an 18 g needle, which allows continuous drainage of the lavage fluid during TMC surgery (Fig. 119.1). After the portals have been safely made, the TMC can be fully evaluated from both the 1R and 1U portals. Arthroscopic shavers can be inserted to clear hypertrophic synovitis (Fig. 119.2). This allows visualisation of the extent and pattern of chondral fibrillation and chondral loss. The TMC osteoarthritis can be arthroscopically staged accordingly to Badia [3].

Fig. 119.1 Portal placement for TMJ arthroscopy: Ulnar (1U), radial (1R) portals and thenar (T) drainage needle

119.3.1 Stage 1 Treatment: Arthroscopic Debridement

- A chondroplasty is performed for unstable chondral surfaces. Loose bodies are mobilised from capsular attachments using a motorised

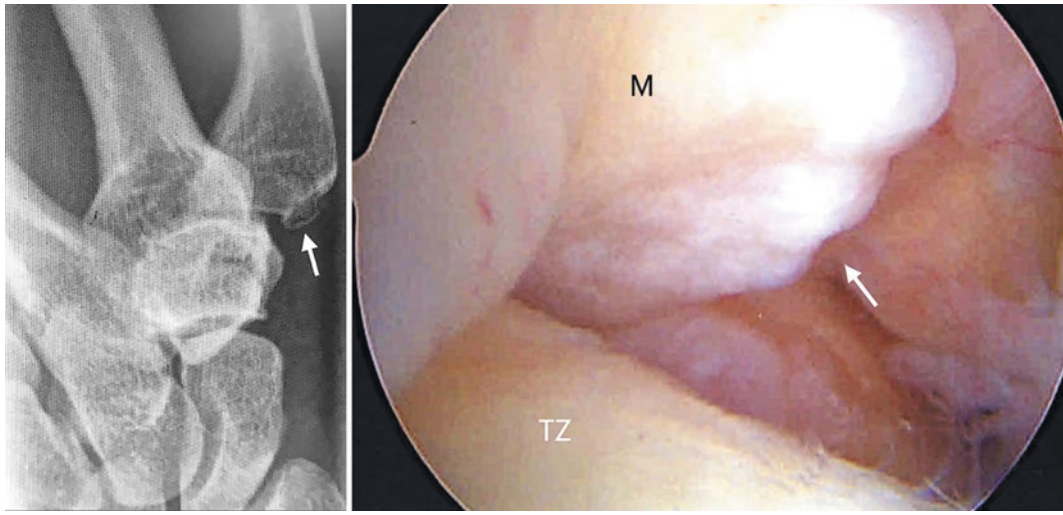

Fig. 119.2 Stage 1 OA: Radiographic (Left image) and arthroscopic views (right image) demonstrate early osteophyte formation (arrows) at ulnar edge of metacarpal base. (Right thumb 1R viewing portal)

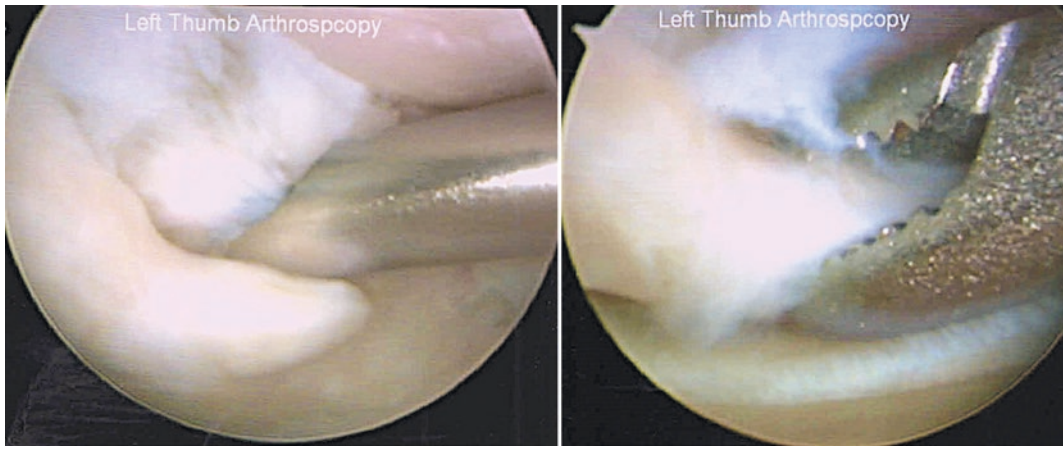

Fig. 119.3 Mobilisation of TMJ loose body from capsule and excision of loose body with curved mosquito artery clip via 1U portal

shaver, and are excised using a curved mosquito artery clip as a grasper (Fig. 119.3).

- The capsular ligaments especially the deep AOL are inspected for attenuation. When radiographs indicate early joint subluxation, and clinical examination reveals a painful grind test, then consideration is given to capsular shrinkage of the deep AOL by thermal modification of the ligamentous collagen [4].
- A radiofrequency (RF) device is used and thermal capsulorrhaphy is performed by viewing the deep AOL from the 1U portal. The RF probe is inserted from the 1R portal and an 18 gauge needle through the thenar portal drains the heated lavage fluid to prevent thermal necrosis of articular cartilage. Similar to thermal capsulorrhaphy of other joints, the RF is used to "paint" strips of cap-

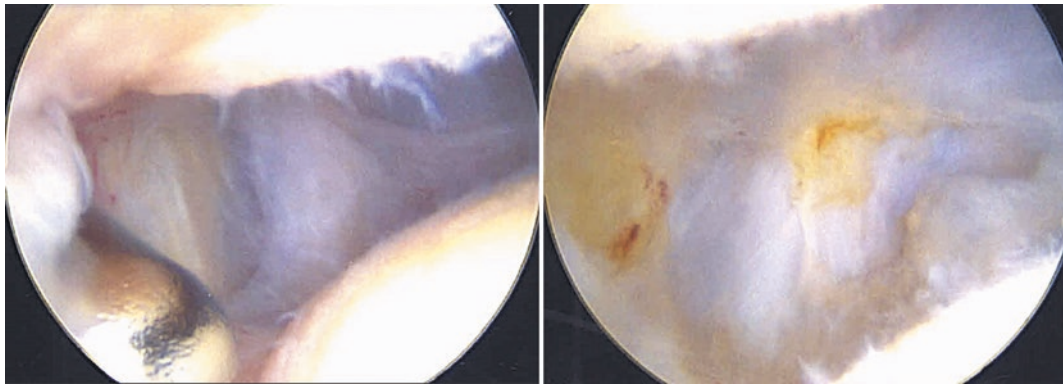

Fig. 119.4 Attenuated volar beak ligament (left image) and thermal capsular modification of attenuated capsular ligaments: "spot weld" technique (right image) (Right thumb, viewing portal 1U, working portal 1R)

sule and ligaments. A "spot" weld technique may be performed by lightly touching the capsular ligaments for 1–2 s for more controlled tightening of the lax ligaments (Fig. 119.4). This retains sections of normal AOL and capsule with retained cells and vasculature to remodel the treated areas. Aggressive use of the radiofrequency device is not recommended.

119.3.2 Stage 2 Treatment: Basal Metacarpal Osteotomy

In the presence of established joint surface degeneration a "joint modifying" procedure is indicated [3, 5]. Badia reported his experience with a dorsal radial closing wedge basal metacarpal osteotomy to place the thumb not only in a more extended position but also in a more abducted position [3]. The aim of osteotomy is to alter the vector forces across the arthritic TMJ; thereby the contact loads are transmitted away from the focal areas of chondral breakdown to a less arthritic area, and the tendency to metacarpal subluxation is minimised.

- Arthroscopic evaluation typically reveals chondral breakdown along the ulnar third of the base of thumb metacarpal, and over the dorsal and central aspect of the trapezium. This pattern of chondral degeneration often is accompanied by radial subluxation of the base of metacarpal. Synovitis and capsular attenuation can be debrided as described for stage 1.
- Following arthroscopic synovectomy, debridement and thermal capsulorrhaphy, the thumb is taken out of traction. The 1R portal is extended distally and slightly proximally in a longitudinal manner between the glabrous and non-glabrous skin for cosmetic scar healing. Cutaneous branches of the superficial radial nerve are identified and carefully retracted.
- Tomaino recommended a formal Wagner approach by reflecting the thenar muscles from the base of metacarpal shaft and TMJ capsule, and a TMJ capsulotomy. The wide exposure enables placement of a 22-gauge cerclage wire for fixation of the extension osteotomy. A less extensile surgical exposure of the metacarpal base is possible if a dorsal radial osteotomy is performed.
- A 22 gauge needle is placed through the TMJ to mark the joint line. The TMJ capsule is otherwise left completely intact. The first extensor compartment tendons and the EPL tendons are mobilised and reflected ulnarwards with a mini Hohmann retractor, exposing the dorsal aspect of the base of metacarpal.
- Using a micro oscillating saw, a transverse osteotomy is performed at the metacarpal base metaphysis; the osteotomy is approximately 1 cm distal to the joint line, and performed parallel to the joint line. Care is taken to stop the osteotomy short of the ulnar and volar cortex.

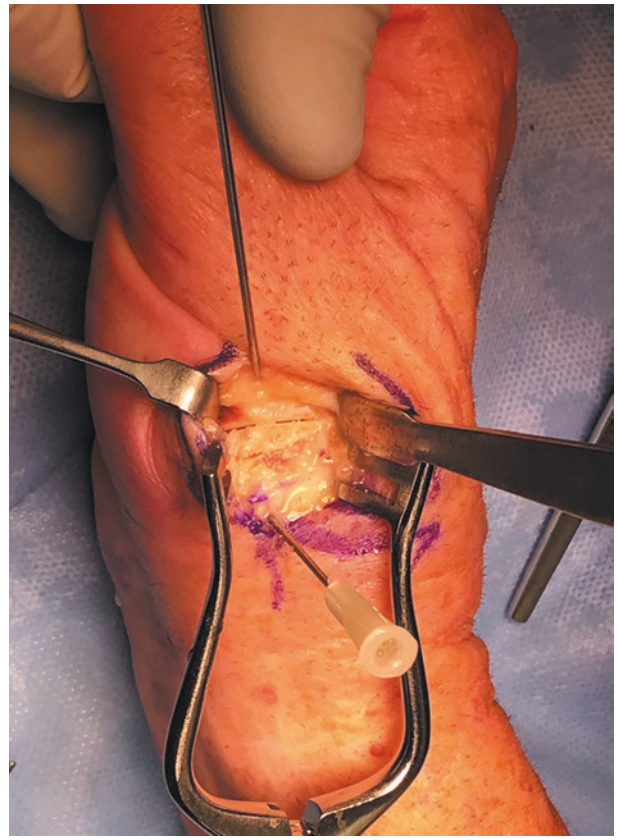

Fig. 119.5 Basal metacarpal dorsoradial wedge osteotomy. Joint line marked with a 22 g needle. Pre-placement of 1.25 mm K wire for internal fixation

- A 4–5 mm wedge is marked distally on the dorsal radial aspect, and a second osteotomy is made, to intersect with the initial osteotomy. A 1.25 mm Kirschner fixation wire is placed distally along the radial edge of metacarpal (Fig. 119.5). The dorsal radial bone wedge is excised.
- The osteotomy is closed; usually this requires a discrete fracture of the volar ulnar cortex, and the preplaced K wire is immediately passed across the osteotomy for fixation. The wire may be advanced to the base of second metacarpal to reduce the TMJ subluxation. However the author's preference is to avoid trans-articular pinning to prevent further chondral damage to TMJ.
- A second K wire is inserted from the dorsal ulnar approach, and provides further stability to the osteotomy. The mini C-arm is used to confirm the wire placement (Fig. 119.6).
- The wires are bent and cut short in the subcutaneous plane. The option of exteriorizing the wires allows easier removal under local anaesthetic. However, if superficial pin site infections develop, this may necessitate removal of the pins before the osteotomy healing is complete.

119.4 Tips and Tricks

With hypertrophic osteoarthritis, the TMJ can be difficult to enter with the arthroscope and the trocar may damage periarticular bone or articular cartilage. Here, it is helpful if the assistant pulls down to distract the TMJ further, and flexing and ulnar deviating the thumb will open up the dorsal radial joint space and allow easier entry of the arthroscope through the 1R portal.

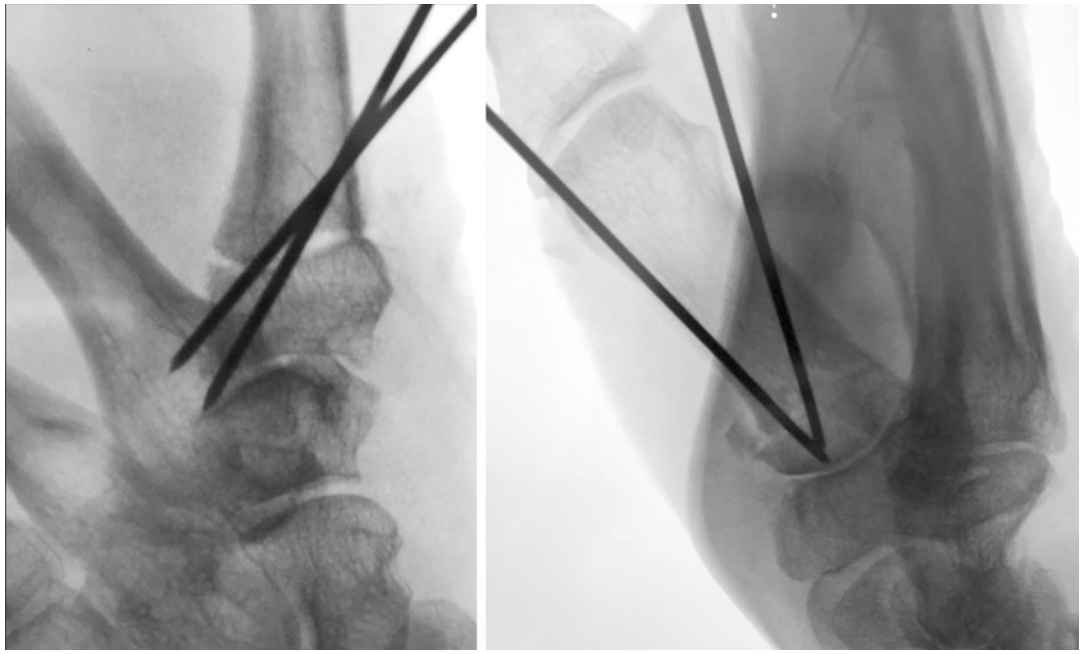

Fig. 119.6 Intraoperative fluoroscopy: metacarpal osteotomy fixation

119.5 Post-operative Management and Rehabiltation

For arthroscopic debridement alone, post-operative rehabilitation includes immobilisation in a thumb spica cast for 2 weeks, and followed by a plastic thumb spica splint for 4 weeks. During this time, capsular remodelling occurs. Active mobilisation and light strengthening commence at 6 weeks and continue for 6 weeks before unrestricted function is permitted.

If an osteotomy is performed, a plaster splint is used for 2 weeks leaving the interphalangeal joint free. A thumb spica thermoplastic splint is then applied for a month and radiographs are performed to confirm bony union. The wires are removed at 6 weeks and a range of motion exercises are commenced. Pinch and grip strengthening are started 2 weeks following that. If radiographs show delayed union at 6 weeks, range of motion exercises and intermittent splintage can continue, and removal of the buried pins can be postponed until osteotomy union is confirmed.

119.6 Complications

Delayed or non-union at osteotomy site, pin tract infections, and persistent symptoms are possible complications.

References

1. Bettinger PC, Linscheid RL, Berger RA, Cooney WP, An KN. An anatomic study of the stabilizing ligaments of the trapezium and trapeziometacarpal joint. J Hand Surg. 1999;24A:786–98.
2. Eaton RG, Littler JW. Ligament reconstruction for the painful thumb carpometacarpal joint. J Bone Joint Surg. 1973;55A:1655–66.
3. Badia A. Arthroscopy of the trapeziometacarpal and metacarpophalangeal joints. J Hand Surg. 2007;32A:707–46.
4. Arnoczky SP, Aksan A. Thermal modification of connective tissues: basic science considerations and clinical implications. J Am Acad Orthop Surg. 2000;8(5):305–13.
5. Tomaino MM. Treatment of Eaton stage 1 trapeziometacarpal disease with thumb metacarpal extension osteotomy. J Hand Surg. 2000;25A:1100–6.

Part XXIV

Metacarpophalangeal (MCP), Proximal Interphalangeal (PIP), and Distal Interphalangeal (DIP) Joint Arthroscopy

120 Metacarpophalangeal Joint Arthroscopy: Portals, Anatomy, and Technique

Deepak N. Bhatia

120.1 Background

The metacarpophalangeal joint (MCP) is frequently involved in sports injuries, and in degenerative and inflammatory conditions of small joints of hand. MCP joint arthroscopy was first described by Chen, and modified portals were later developed by Sekiya et al. [1–3]. Arthroscopy is useful for diagnostic evaluation in MCP joint, and recent advances in small joint instrumentation now permit therapeutic arthroscopic procedures. This chapter presents the portal placement for MCP joint access, and detailed intraarticular anatomy for orientation and evaluation.

120.2 Indications and Contraindications

- Diagnostic MCP arthroscopy is indicated in evaluation of painful conditions of MCP joints of thumb and other digits.
- Arthroscopic synovectomy may be performed for persistent swelling in patients with rheumatoid arthritis without finger deformity [2]. Degenerative loose bodies and chondral debris may be excised along with synovectomy in osteoarthritis.
- Sports that involve repetitive punching (boxing, martial arts) may result in chondral and ligamentous injuries of the MCP joint. Arthroscopy is useful in debridement of chondral defects, removal of chondral fragments, and synovectomy. Arthroscopic assessment of collateral ligament and volar plate injuries is possible; low-grade injuries can be arthroscopically debrided and high grade or complete tears can be subsequently repaired or reconstructed with standard open techniques.
- Fractures that involve the phalangeal and metacarpal articular surfaces can be reduced and fixed under arthroscopic and fluoroscopic guidance.

Severe degenerative arthritis with reduced joint space renders arthroscopic access difficult. Similarly, progressive finger deformity and high grade radiographic changes in rheumatoid arthritis are contraindications for arthroscopy.

120.3 Surgical Technique

The procedure is performed with the patient in the supine position. The finger is suspended on a standard wrist positioner with finger traps. Dorsal radial and ulnar portals are marked, and a 30°

D. N. Bhatia (✉)
SPORTSMED Mumbai, and Sir HN Reliance Foundation Hospital, Mumbai, India
e-mail: shoulderclinic@gmail.com

© ISAKOS 2022

D. N. Bhatia et al. (eds.), *Arthroscopy and Endoscopy of the Elbow, Wrist and Hand*,
https://doi.org/10.1007/978-3-030-79423-1_120

arthroscope (1.9 mm) is used for diagnostic arthroscopy.

Portals: Arthroscopic access to the MCP joint is possible via two portals:

- The **dorsal radial portal (MCP-R)** is placed in the dorsal joint line depression alongside the radial aspect of central extensor tendon and passes between the central slip and the radial lateral band. At the MCP joint of the thumb, this portal is placed radial to extensor pollicis brevis (EPB) tendon.
- The **dorsal-ulnar portal (MCP-U)** is placed in the dorsal joint line depression alongside the ulnar aspect of central extensor tendon and passes between the central slip and the ulnar lateral band. At the MCP joint of the thumb, this portal is placed ulnar to extensor pollicis longus (EPL) tendon (Fig. 120.1).

Arthroscopic anatomy: Arthroscopic evaluation of the MCP joint involves a four-point assessment of the following structures:

- **Articular surfaces:** The dome-shaped metacarpal and slightly concave phalangeal surfaces are visualized and cartilage is palpated with a 2 mm probe.
- **Collateral ligaments:** The ulnar collateral ligament is identified as two thick bands (ante-

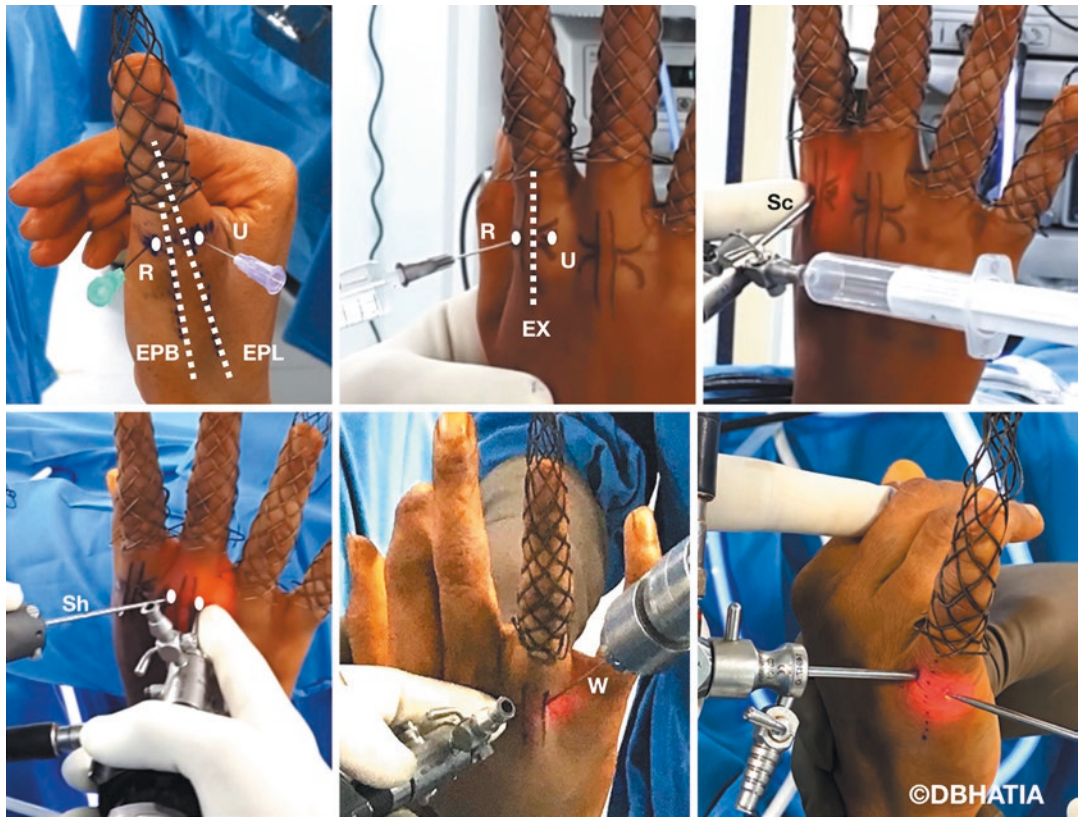

Fig. 120.1 Arthroscopic setup and portal placement for metacarpophalangeal joint (MCP) arthroscopy of each digit is demonstrated. Radial (R) and ulnar (U) portals for thumb MCP are placed adjacent to extensor pollicis longus (EPL) and extensor pollicis brevis (EPB) tendons (top left). Portals for other digits are adjacent to the central extensor tendon (top middle). The needle sites are marked with needles and saline is injected into the joint. Arthroscopy is used for assessment (top right). Arthroscopy of third digit MCP is shown and a shaver is used via R portal for debridement (bottom left). Arthroscopy of fourth digit MCP demonstrates fracture fixation using a K wire via U portal (bottom middle). Arthroscopic assessment of fifth digit MCP is shown using a probe via U portal. (© D. Bhatia)

rior and posterior) with oblique orientation and extending from the dorsal-ulnar aspect of the metacarpal to the volar-ulnar aspect of the phalanx. The metacarpal and phalangeal insertions are visualized within the ulnar recess and each band can be independently probed at its phalangeal attachment. A similar appearance of the radial collateral ligament is visualized and probed on the radial aspect. The phalangeal attachment of the anterior (accessory collateral) band is confluent with the volar plate and the posterior band (collateral proper) attaches further lateral on the phalanx (Fig. 120.2a, b).

- **Volar plate:** This is visualized on the volar aspect of the MCP joint and attachments are probed to evaluate partial and complete tears (Fig. 120.2c).
- **Metacarpal recesses**: These are visualized by using a probe to retract the capsule and synovium. Inspection of radial and ulnar recesses permits assessment of metacarpal attachments of collateral ligaments and peripheral cartilage. The volar recess is difficult to visualize with a 30° arthroscope. The dorsal recess is visualized by moving the arthroscope dorsally over the metacarpal dome and using the probe to retract the capsule dorsally. This recess is deeper and the capsular reflection extends to the metacarpal neck. Phalangeal recesses may sometimes be visualized and may be suggestive of laxity or chronic instability (Fig. 120.2d).

Instability: The collateral ligaments and volar plate are assessed and probed. Partial and complete tears demonstrate loss of tension within the ligament bands and the probe can be passed between the ligament and bone at its insertion. Radial and ulnar stress demonstrates gap formation at the attachment site. Chronic partial tears appear severely frayed and are debrided to stable tissue using a 2 mm shaver blade. Capsular shrinkage using a small joint radiofrequency probe or ablator is then cautiously performed to avoid injury to flexor and extensor tendons and neurovascular bundles. Complete tears and bony avulsions of radial and ulnar collateral ligaments are reattached using a small incision and mini anchors (Fig. 120.3a–c). Volar plate tears can be visualized and probed to evaluate severity (Fig. 120.3d). The volar recess should be assessed for adhesions if imaging demonstrates volar subluxation of the phalanx.

Chondral defects, loose bodies, and synovitis: Chondral defects are seen in early arthritis and in sports injuries (repetitive punching). 2 mm shaver is used to perform a thorough synovectomy and chondral debris is excised (Fig. 120.3d). Larger chondral fragments are removed using a small joint grasper (Fig. 120.4). Chondral defects are debrided and loosely attached cartilage is excised. Capsular shrinkage may be performed after debridement.

Fractures: Articular fractures of the metacarpal head and phalangeal base can be assessed arthroscopically. Most fractures can be reduced using various direct and indirect techniques and percutaneous fluoroscopy-guided K-wires are passed to achieve stable fixation (Fig. 120.5).

120.4 Tips and Tricks

- Gentle traction (without counter-traction) using a finger-trap suspension system is useful to achieve a workable joint space for a 1.9 mm arthroscope. Use of 1.9 mm instruments like graspers and punches is recommended to avoid iatrogenic chondral injury.
- Air-arthroscopy is adequate for diagnostic assessment and during performance of therapeutic procedures. Fluid inflow is used for lavage and a 50 cc saline-filled syringe is ideal for fluid irrigation and inflow.

120.5 Pitfalls

- The sensory branches of radial nerve are close to the portal sites and are at-risk of iatrogenic injury. The digital neurovascular bundles are close to volar recesses and are at-risk during use of radiofrequency or thermal probes [4, 5].
- Fluid inflow is associated with periarticular swelling and this may interfere with subsequent open procedures like ligament reconstruction/repair.

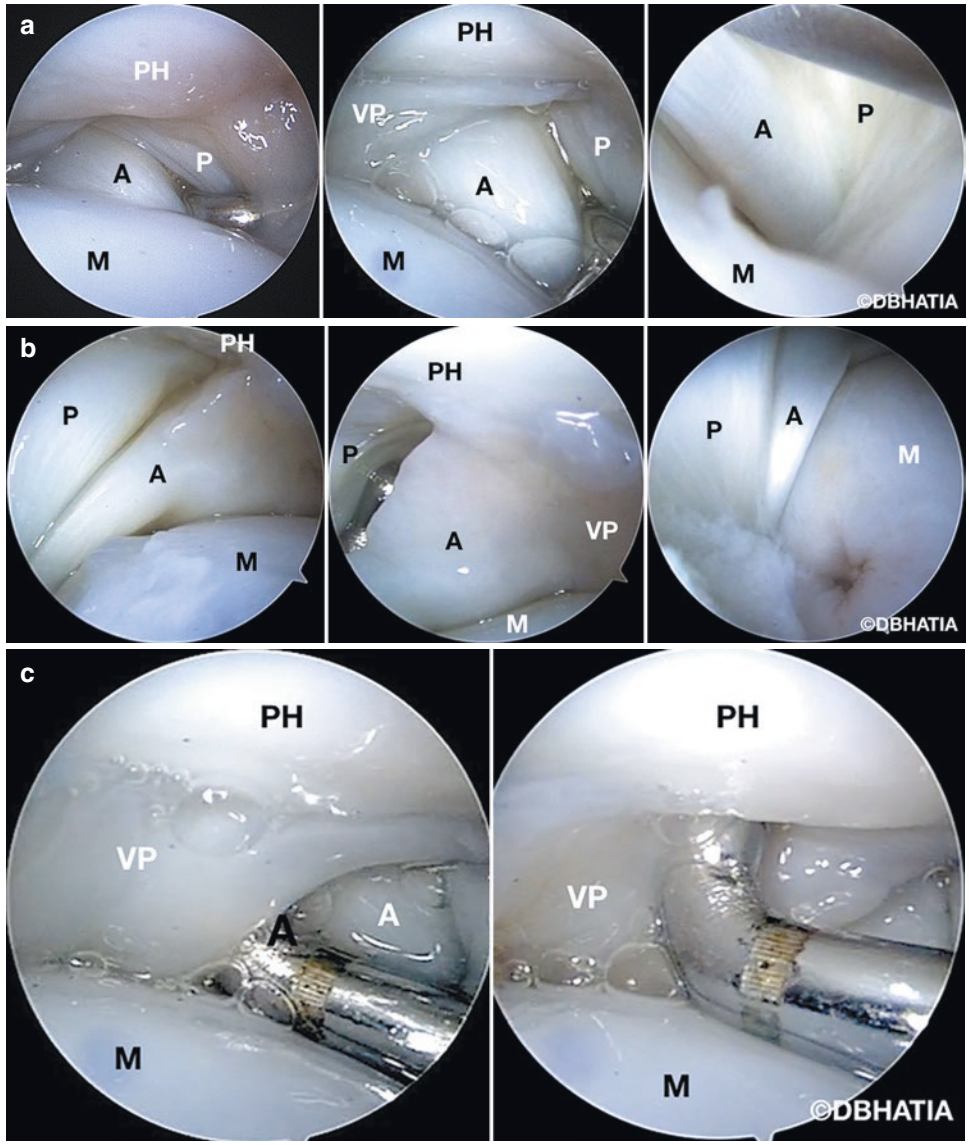

Fig. 120.2 (**a**) Arthroscopic anatomy of index MCP (right hand) is demonstrated as viewed via radial (R) portal. A probe via ulnar (U) portal demonstrates the anterior (A) and posterior (P) bands of ulnar collateral ligament UCL (left image). The phalangeal attachment of A is confluent with volar plate (VP, middle image). Visualization of the ulnar MCP recess demonstrates the metacarpal attachment of A and P bands of UCL (right image). (*PH* proximal phalanx, *M* metacarpal head). (**b**) Arthroscopic anatomy of index MCP (right hand) is demonstrated as viewed via ulnar (U) portal. A probe via radial (R) portal demonstrates the anterior (A) and posterior (P) bands of radial collateral ligament RCL (left image). The phalangeal attachment of A is confluent with volar plate (VP, middle image) and P inserts on radial aspect of PH. Visualization of the radial MCP recess demonstrates the metacarpal attachment of A and P bands (right image). (*PH* proximal phalanx, *M* metacarpal head). (**c**) Arthroscopic anatomy of index MCP (right hand) is demonstrated as viewed via radial (R) portal. A probe via ulnar (U) portal demonstrates the volar plate (VP) and anterior (A) band of ulnar collateral ligament UCL (left image). The VP is firmly attached to volar rim of PH and a probe is used via ulnar portal (U) to evaluate VP tears (right image). (*PH* proximal phalanx, *M* metacarpal head). (**d**) Arthroscopic anatomy of third digit MCP (right hand) as viewed via radial (R) portal: The radial phalangeal recess (arrow, left image) and a deep dorsal recess (arrow, right image) are shown using a probe for capsular retraction. (*PH* proximal phalanx, *M* metacarpal head). (© D. Bhatia)

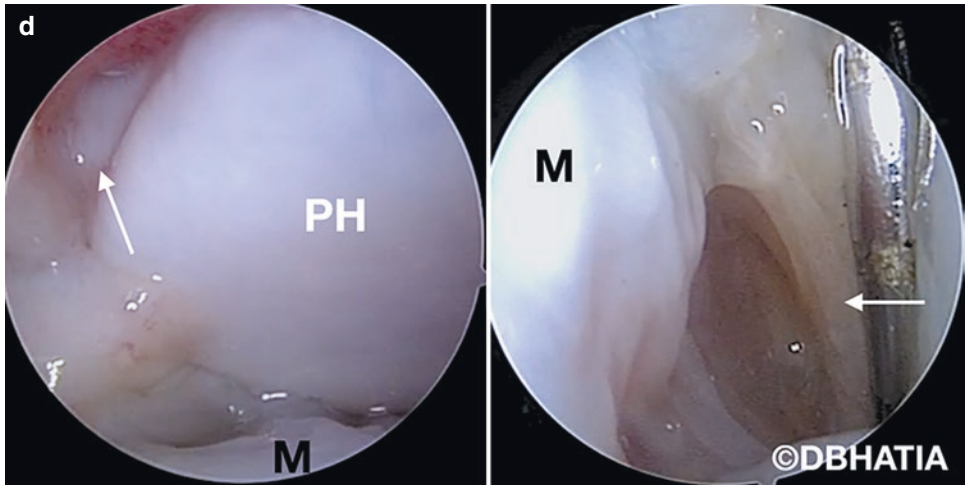

Fig. 120.2 (continued)

120.6 Postoperative Management and Rehabilitation

A bulky dressing is applied in the immediate postoperative period and changed to portal dressing in 2–3 days. Rehabilitation depends on the specific pathology and procedure performed. Rehabilitation for debridement and synovectomy is started as soon as patient is comfortable and return to active use of the hand for daily activities and work is permitted within 3 weeks. Rehabilitation after fracture fixation is initiated after union is demonstrated on radiographs.

120.7 Complications

Possible complications include injury to digital sensory nerves and neurovascular bundle, and MCP joint stiffness.

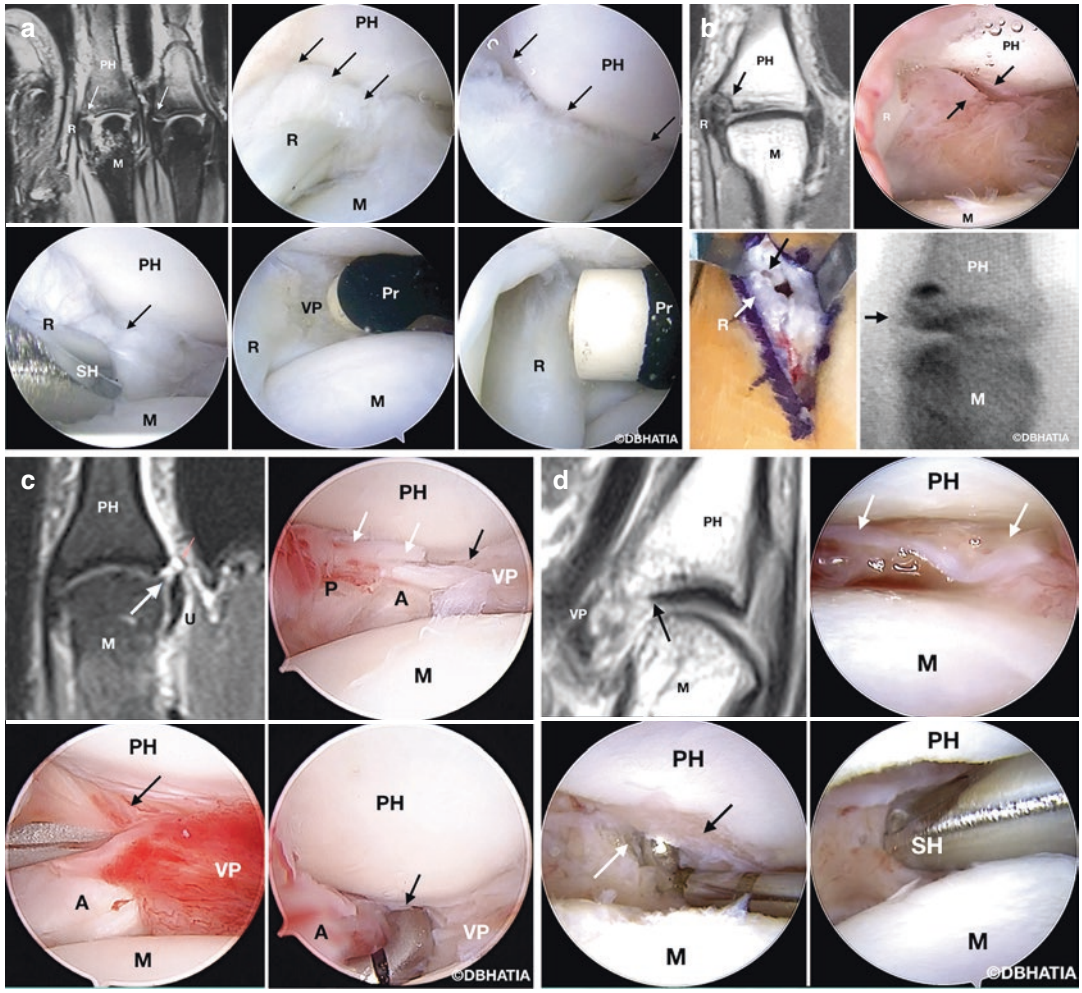

Fig. 120.3 (**a**) Arthroscopic demonstration of a partial tear of radial collateral ligament (arrows, R) of right hand second and third digit MCP joints is demonstrated on MRI (top left) and as viewed via ulnar portal (top middle and right). A 2 mm shaver (SH) is used via radial portal to debride the frayed portion of R (arrow, bottom left). Shrinkage of volar plate (VP) and ligament fibres (R) is performed using a probe (Pr) via ulnar portal (bottom middle and right and images). (*PH* proximal phalanx, *M* metacarpal head). (**b**) Arthroscopic demonstration of a complete bony avulsion of radial collateral ligament (arrows, R) of right thumb MCP is demonstrated on MRI (arrow, top left) and as viewed via ulnar portal (arrows, top left). Open repair demonstrates the phalangeal avulsion of R and the bony fragment is reattached using a suture anchor (arrow, bottom images). (*PH* proximal phalanx, *M* metacarpal head). (**c**) Arthroscopic demonstration of a complete tear of ulnar collateral ligament UCL of left thumb MCP is demonstrated on MRI (top left) and as viewed via radial R portal (top right). The anterior (A) and posterior (P) bands are avulsed (black arrows) and partial tear of the volar plate (VP) is seen (white arrow, top right). The tear is retracted with a probe to demonstrate complete avulsion (arrows, bottom right and left images). (*PH* proximal phalanx, *M* metacarpal head). (**d**) Magnetic resonance imaging of a painful thumb MCP demonstrates a partial tear and thickening of volar plate (VP) with volar subluxation of PH (arrows, top right image). Arthroscopic assessment demonstrates a partial tear of VP (white arrows, top right) and a phalangeal volar rim chondral defect (black arrow, bottom left). The VP tear is demonstrated with a probe (white arrow, bottom left) and the chondral defect is debrided using a shaver (SH, bottom right). (*PH* proximal phalanx, *M* metacarpal head). (© D. Bhatia)

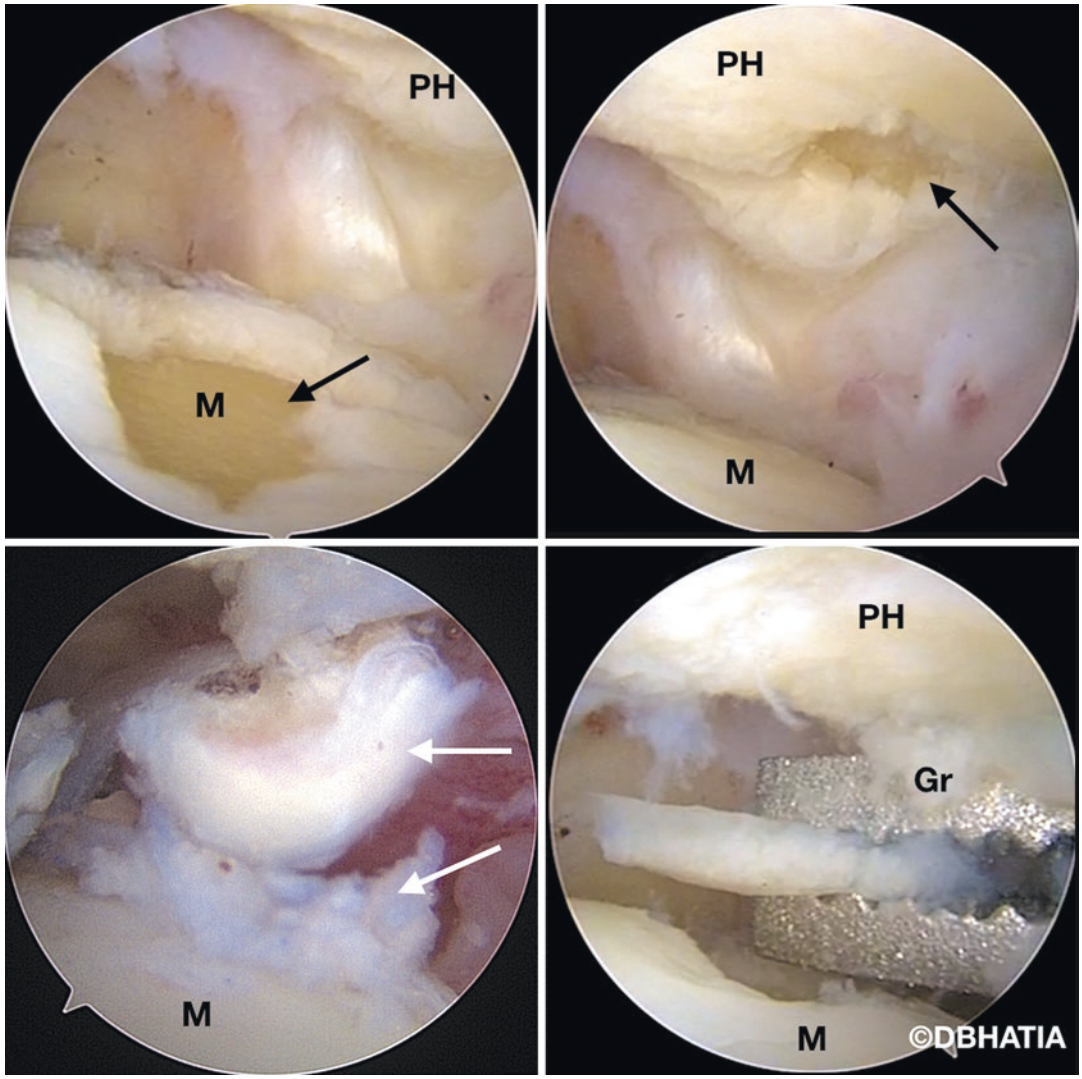

Fig. 120.4 Arthroscopic assessment of chondral defects in M and PH (arrows, top images) is shown. Chondral debris (arrows, bottom left) is excised using a small joint grasper (bottom right). (*PH* proximal phalanx, *M* metacarpal head). (© D. Bhatia)

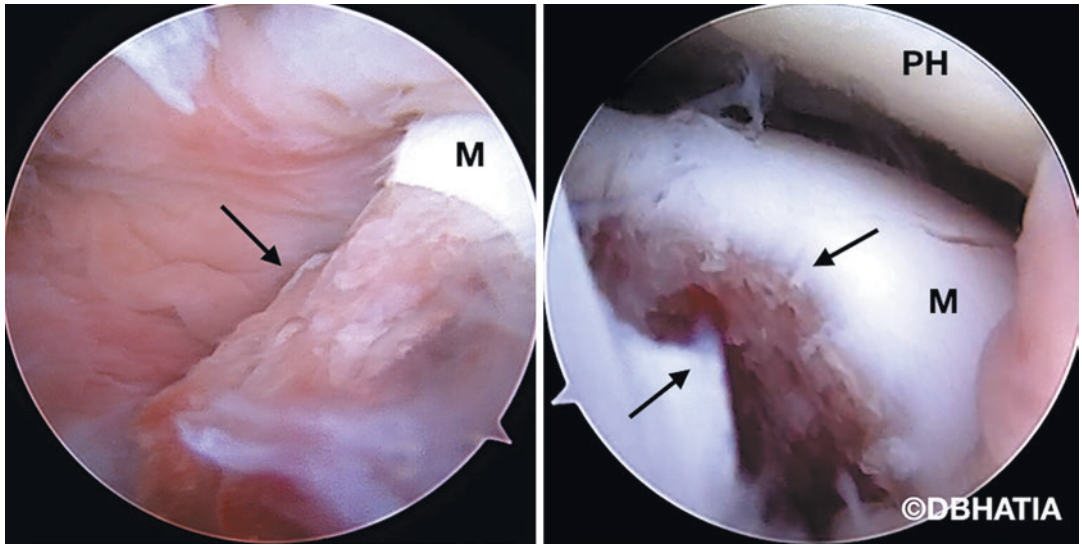

Fig. 120.5 Arthroscopic evaluation of a displaced metacarpal articular surface fracture (arrows) is shown. (*PH* proximal phalanx, *M* metacarpal head). (© D. Bhatia)

Conflict of Interest The author certifies that he has no commercial associations (e.g., consultancies, stock ownership, equity interest) that might pose a conflict of interest in connection with the submitted article. The author retains the copyright to the images, videos, and content in this chapter.

References

1. Chen Y-C. Arthroscopy of the wrist and finger joints. Orthop Clin North Am. 1979;10(3):723–33.
2. Sekiya I, Kobayashi M, Okamoto H, et al. Arthroscopic synovectomy of the metacarpophalangeal and proximal interphalangeal joints. Tech Hand Up Extrem Surg. 2008;12(4):221–5.
3. Okamoto H, Sekiya I, Mizutani J, Watanabe N, Otsuka T. Anatomical basis for arthroscopy of the proximal interphalangeal joints. J Hand Surg Asian Pac Vol. 2018;23(3):342–6.
4. Ropars M, Fontaine I, Morandi X, Berton E, Kaila R, Darnault P. Preserving the superficial branch of the radial nerve during carpometacarpal and metacarpophalangeal joint arthroscopy: an anatomical study. Surg Radiol Anat. 2010;32(3):271–6.
5. Limousin B, Corella F, Del Campo B, et al. Metacarpophalangeal portal safety. An anatomical study. Seguridad de los portales metacarpofalángicos. Estudio anatómico. Rev Esp Cir Ortop Traumatol. 2018;62(5):380–6.

121 Arthroscopic Management of Metacarpophalangeal Articular Fractures

Alejandro Badia

121.1 Background

Advances in fiberoptic technology and small joint instrumentation have opened up a new world in the area of arthroscopy. However, indications for small joint arthroscopy in the hand remain poorly understood and vastly underutilized. This may be due to a paucity of papers utilizing this technique in the literature, as well as scarce hands on training in the technical aspects of small joint arthroscopy despite the recent growing exposure to wrist arthroscopy courses.

Despite the fact that these small joint arthroscopes have been readily available for decades, hand surgeons have been slow to adopt this tool to include within their methodology and treatment protocols for both traumatic and degenerative conditions involving small joints.

Discussion in this chapter will be limited to fracture indications of the metacarpophalangeal joints of the thumb and digits. It will be clear that the small joint arthroscope presents a much clearer picture of the present pathology compared to other imaging techniques or even open surgery that may result in excess capsular scarring.

Dr. Y Chen first described arthroscopy of the metacarpophalangeal (MCP) joints, amongst other small joints of the hand, in his 1979 paper in Orthopedic Clinics of North America, and this portrayed a paradigm shift in arthroscopy indications [1]. Despite a cursory review, this paper first described the use of the Watanabe #24 arthroscope within the wrist, metacarpophalangeal joints and even interphalangeal joints of the hand. He went on to describe the MCP arthroscopic anatomy for the first time, followed by several clinical case reports where he described the arthroscopic findings and suggested some possible clinical indications. In total, he described 90 arthroscopies performed in multiple joints encompassing 34 clinical cases as well as two cadaveric arms. Despite this broad introduction to small joint arthroscopy, the idea of MCP joint treatment was not truly developed until much later.

Surprisingly, it was sports medicine arthroscopists, not hand surgeons, Vaupel and Andrews, who first described a report using arthroscopic treatment of the metacarpophalangeal joint only six years after Chen's report [2]. They presented a professional golfer who was markedly impaired due to a one-year history of chronic painful synovitis within the thumb MCP joint. They performed a synovectomy and also performed arthroscopic burring of a small chondral

A. Badia (✉)
Badia Hand to Shoulder Center, Doral, FL, USA

MARC Institute (Miami Anatomical Research Center), Doral, FL, USA

OrthoNOW® Immediate Orthopedic Care, Doral, FL, USA
e-mail: alejandro@drbadia.com

© ISAKOS 2022

D. N. Bhatia et al. (eds.), *Arthroscopy and Endoscopy of the Elbow, Wrist and Hand*,
https://doi.org/10.1007/978-3-030-79423-1_121

defect that had been identified at the time of procedure. The patient did well enough to be able to return to his sport in less than six-months and was reportedly pain free at his two-year follow-up. However, despite an excellent outcome with this new technique, no broader clinical indications were recommended for future usage and this remained an isolated case report. Two years later Wilkes presented the first clinical series of an MCP joint problem treated with arthroscopic means [3]. He reported on 13 cases of arthroscopic rheumatoid synovectomy in five patients suffering from advanced rheumatoid arthritis. While these patients lacked the usual joint subluxation or advanced destruction, they did have marked synovitis found in the joint space and within the recesses of the collateral ligament origins. Despite an adequate follow-up of nearly 4 years, the patients did demonstrate recurrence of pain and this treatment did not seem to alter the natural history of RA at the MCP joint therefore not attracting the attention of most hand surgeons.

In 1995, J. Ryu and Fagan presented a limited series on the treatment of the ulnar collateral ligament Stener lesion arthroscopically [4]. They described an arthroscopic reduction of a thumb ulnar collateral Stener lesion in eight thumbs, with average follow-up period of over 3 years. They illustrated how simple reduction of the Stener lesion into the joint can place the avulsed ligament in proximity to its insertion site on the debrided base of the proximal phalanx. Until reduction, the ligament had been sitting external to the adductor aponeurosis and consequently did not heal in the anatomic position. Once the anatomy was restored, the ulnar collateral ligament (UCL) insertion site was aggressively debrided and the joint pinned to immobilize and permit healing. After removing the cast, minimal therapy was needed due to lack of capsular scarring and at follow-up no patient reported pain or any functional limitation. They noted excellent range of motion with pinch strength equal to or often greater than the thumb on the unaffected side and the only complication was a simple pin tract infection. These results demonstrated that an all arthroscopic reduction of a Stener lesion precluded the need for open repair and potential complications such as protracted recovery and joint stiffness. This represented a paradigm shift in treatment for the first common clinical application that might perhaps encourage arthroscopic treatment for MCP joint pathology. Surprisingly, there was no mention of bony gamekeeper's lesions, and there was no comparative study with the open method. This paper's greatest triumph is that it was published in a widely read journal, first revealing hand surgeons to this minimally invasive technique and encouraging arthroscopy use for other indications. Despite the fact that this paper was published a quarter century ago, MCP arthroscopy remains rarely utilized with few clinical series since then.

In 1999, Rozmaryn and Wei published the first comprehensive paper on the technical aspects of metacarpophalangeal arthroscopy with description of possible indications and advantages of this novel technique [5]. They exposed the misconception that the MCP joint may be too small to perform arthroscopic procedures in a feasible manner. While no clinical series was presented, they elaborated on the wider indications that might be benefit from small joint arthroscopy. They discussed joint synovectomies and biopsies and also reiterated the idea of collateral ligament debridement while suggesting actual ligament repair. They also introduced other uses including removal of loose bodies, treatment of osteochondral lesions, management of juxta-articular lesions. For the first time, the arthroscopic assisted treatment of intra-articular fractures was presented. This paper elaborated on some technical aspects and discussed the anatomy for the first time since Dr. Chen's basic description with a primitive arthroscope almost 20 years prior. The key advance was that they outlined the obvious advantages of arthroscopic versus open techniques as seen in larger joints. They predicted that indications would broaden and be refined in future years.

Around this time, a broad review paper was published in *Hand Clinics* and entitled, "Arthroscopy of the Metacarpophalangeal Joint," by Joe Slade and Andy Gutow [6]. This was a thorough description of the technique, illustrated

by some representative cases. They emphasized that small joint arthroscopy required specific instrumentation and thorough knowledge of the anatomy within these joints. Their expansive treatise showed that there were broad indications that could greatly benefit from this technology, including intra-articular fracture treatment. The use of arthroscopy was also discussed by Badia [7, 8] in several papers, including specific indications for bony gamekeeper lesions.

There remains a paucity of clinical papers in the literature and further discussion regarding the use of arthroscopy for small joint treatment, including the MCP, is needed. While the arthroscopic surgeon, classically a "sports medicine" specialist, may consider this option, it certainly remains for the hand surgeon to develop the clinical techniques for the more complex articular fractures of the hand.

121.1.1 Surgical Anatomy

The thumb MCP joint allows clear visualization of the metacarpal head and the proximal phalanx base. The volar plate is covered by the palmar capsule of the joint, often a site for post-traumatic synovitis. On some occasions, the sesamoid bones may be visualized as embedded within the thumb intrinsic muscles. The collateral ligaments proper, radial and ulnar, can be clearly seen as well as the less defined accessory collaterals, seen a bit more volar. The origin of the ligaments can be followed down to the metacarpal head recess on either side. The attachment of the ligaments on the base of the proximal phalanx is usual site for fraying or redundancy, particularly in post-traumatic scenarios. The digits have similar anatomy although the collateral ligaments are not as well defined. The radial sesamoid is often seen in the index finger which remains the most common finger scoped for chronic pain indications. Traumatically, any finger can benefit from arthroscopic reduction and the anatomy is similar throughout. The thumb is somewhat larger and the Stener lesion can be identified arthroscopically, and pulled into the joint in many cases.

121.1.2 MCP Arthroscopy Indications/ Contraindications

The thumb MCP ulnar collateral ligament (UCL) tear is the classic ligamentous hand injury, often incorrectly termed "gamekeeper's thumb" when this should really be termed "skier's thumb" as the former describes the chronic attritional lesion. Acute injury can also affect the finger MCP joints with both ligamentous injuries and articular fractures presenting as a painful, swollen joint after injury. Plain radiographs will separate articular fractures into two main categories: Avulsion fractures due to the pull of the collateral ligaments OR true intra-articular fractures typically caused by a compression or shearing mechanism that can involve the metacarpal head, base of the proximal phalanx or, rarely, both. The latter can be thought of as a floating MCP joint lesion.

It is important to note that surgical indications for MCP arthroscopy will usually involve chronic conditions, as opposed to acute injury, since the latter is often purely ligamentous and can often be managed conservatively with appropriate immobilization. The thumb UCL avulsion is a notable exception where open repair of a Stener lesion is often required and simple immobilization may not suffice.

Acute indications generally involve an associated fracture that will need synovectomy, fracture debridement followed by articular reduction and is the subject of this chapter. Other acute indications are less common since the majority of ligamentous injuries will adequately heal with conservative immobilization, or are so severe that the resultant instability will lead to open management and repair.

- The ideal acute indication for MCP arthroscopy is reduction of a collateral ligament avulsion fracture with a rotated fragment sitting within the joint. Once arthroscopic debridement at the fracture site has been performed, a small hook probe is used to simply de-rotate the bony fragment via arthroscopic visualization. Kirschner wire fixation can then be performed with combination of

arthroscopic control and fluoroscopic confirmation as previously described [8].

- Another acute, although less common, indication would be a die-punch type articular fracture, usually of the proximal phalanx base, where the scope can be used to control for the best articular reduction possible while facilitating the reduction itself.
- Similarly, articular fractures of the metacarpal head are also an ideal indication, particularly if comminution is present; arthroscopy allows for removal of any small osteochondral fragments that will serve as a joint irritant in future, even if perfect reduction of the major fragments is achieved. Furthermore, studies have shown that fluoroscopic reduction does not always correlate with anatomic reduction of the joint articular surface, so critical for a good outcome in the vitally important MCP joint of the hand. Arthroscopy allows one to remove non-critical fragments while also facilitating thorough anatomic reduction of the major fragments. Besides removal of any floating loose osteochondral fragments, a thorough synovectomy can be performed and the frayed joint capsule, typically via radiofrequency shrinkage, can be addressed. This helps reduce the post-trauma inflammatory process in addition to reducing the fracture more anatomically. This arthroscopic method has the intrinsic advantage of a more exact articular reduction with the minimally invasive perk of limiting capsular adhesions, therefore faster recovery of an improved range of motion.
- As in any other arthroscopic acute indication, thorough assessment of associated soft tissue lesions can be performed and treated as needed. This may include MCP dislocations, where the acute capsule and ligamentous avulsions can be debrided after reduction, minimizing the scarring and expediting the healing process, even without actual soft tissue repair.
- Chronic processes affecting the MCP joint tend to be the most common indications for arthroscopy of MCP joints and are beyond the "scope" of this chapter.

Contraindications to arthroscopic management of these fractures may reside more with the skill and experience of the surgeon wielding the scope. Extra-articular fractures, including even peri-articular fractures simply need traditional fixation methods that likely do not include any arthroscopic intervention. However, a high energy injury may concomitantly affect the joint, even if a clear fracture is not seen that extends to the joint surface. Often times, simple synovectomy and debridement of the capsule may help accelerate soft tissue healing in the case of an associated extra-articular fracture. Simple fractures with articular extension may or may not need arthroscopic evaluation and is often up to the discretion, and experience, of the treating surgeon. Suffice it to say that there is essentially no contra-indication to performing joint evaluation with a less than 2 mm scope where even the portals do not require any suturing.

121.2 Surgical Technique

Metacarpophalangeal arthroscopy generally requires use of a very small arthroscope of 1.9 mm in diameter or less due to the narrow, relatively constrained anatomy of these small joints. A small joint 30 degree arthroscope as described by maxillofacial surgeons for temporomandibular (TMJ) pathology is typically utilized. While newer arthroscopes are becoming available, even as small as 1 mm, the 1.9 scope should suffice for the described indications discussed prior. The use of a 2.0 mm shaver is crucial for synovectomy, permits clear joint evaluation, and facilitates most debridements. To address capsular fraying and ligamentous injury, small radiofrequency probes, including ablation and shrinkage applications, are often a critical step.

Small joint arthroscopy of any type, including MCP joints, only requires local anesthesia and light IV sedation. The portal sites are both injected with minimal local anesthesia, followed by several cc's of lidocaine, or similar short acting agents, and these are introduced into the joint once the hand is vertically suspended using a single fingertrap on the involved digit. This

permits joint distraction and allows atraumatic insertion of both the scope and the needed instruments. Intravenous sedation is typically used to control tourniquet pain depending on the planned time of procedure or patient/anesthesiologist preference. The use of lidocaine with epinephrine may even preclude the need for a tourniquet since these are typically short duration procedures.

- Once 2–3 kg (4–7 pounds) of traction is applied, the joint-line is usually quite palpable. An 18 gauge needle is used to determine the locations site for the portals and to determine angular trajectory for insertion of the trochar/sleeve assembly that will allow arthroscope insertion.
- Longitudinal portal small wounds (stab incisions) are made with a #15 scalpel in the site of visible capsular distention. This orientation is used since the patients MCP joint is typically immobilized in flexion and the incision direction is orientated parallel to the plane of motion. It is crucial to introduce the trocar into the joint in atraumatic fashion since most indications are for otherwise pristine joints and one must minimize iatrogenic injury within the narrow interval. The space between metacarpal head and proximal phalanx base is very narrow and one should find the appropriate position and insertion angle by inserting a small curved clamp once the joint is adequately distended with lidocaine or lactated ringer's solution.
- The arthroscope is then inserted at this exact same angle and a thorough cursory joint examination is now performed. Portal anatomy is relatively simple as radial and ulnar portals lie on either side of the visible or palpable extensor tendon. Rarely, a third portal is for outflow, or more ideal instrument triangulation, and is created by observing the transillumination, palpating the capsule, and then inserting an 18 gauge needle to confirm the possible portal site. It helps to have a particularly dark OR room to permit adequate joint transillumination.
- A complete evacuation of the fracture hematoma and very thorough synovectomy is usually performed at the outset, since this allows thorough inspection of the joint and to better identify the fracture lines and associated soft tissue injuries. Once this is done with a small full radius shaver, the articular structures including capsule and collateral ligaments are more apparent. A radiofrequency ablator probe can also facilitate this ablation process. It is important to use RF judiciously, as the joint capsule is relatively thin and subcutaneous, and thermal injury can result to either capsule, articular surface or even the skin since the joint is directly under the subcutaneous tissues (Fig. 121.1).
- Once hematoma clearing and synovectomy is underway, the surgeon can now begin to identify the fracture "personality" and assess soft tissue trauma in a reproducible systematic manner. Typically, one may begin on the opposite side of the joint where the scope enters, then assess the volar plate, identify sesamoids (if present) and the ipsilateral collateral ligament, and finally the dorsal capsule.
- Fracture sites at the articular surface of both proximal phalanx and metacarpal head are then evaluated followed by the synovial recesses and the collateral ligament origins.
- Major fracture fragments are now reduced with use of a hook probe or even freer elevator. An external pointed bone reduction clamp may be used to maintain reduction of the larger components if necessary (Fig. 121.2a, b). Extra-articular techniques may be used in order to elevate die-punch fragments by creating a separate cortical window away from the actual fracture site; this usually needs a combination of fluoroscopic, and arthroscopic, control (Fig. 121.3)
- Small articular fragments, or even cancellous bone spicules, are then cleared from the joint with either the suction shaver or a small joint grasper when necessary.
- Fracture reduction is now maintained with K-wire fixation, typically 0.045 or 0.035 wires, although small screws may be used on occasion. After both arthroscopic and fluoroscopic confirmation of stable, anatomic

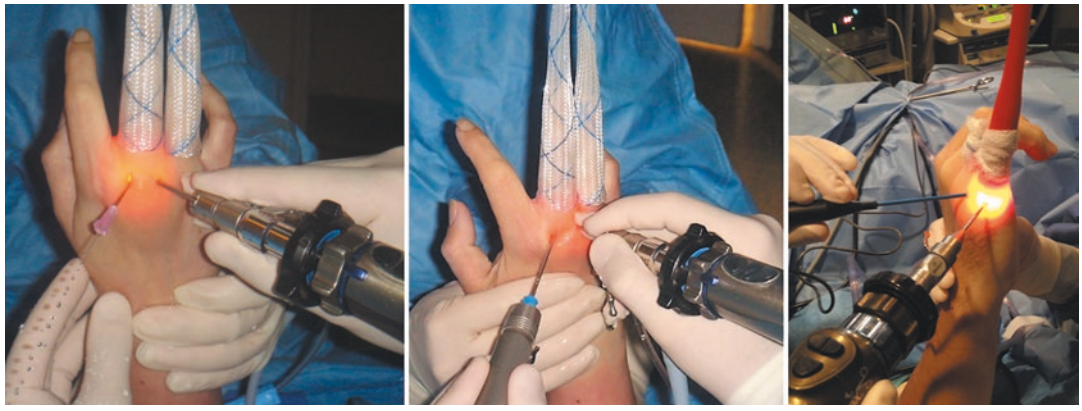

Fig. 121.1 Portals for MCP arthroscopy are shown (left image). Debridement is performed using shaver (middle image) and radiofrequency device (right image)

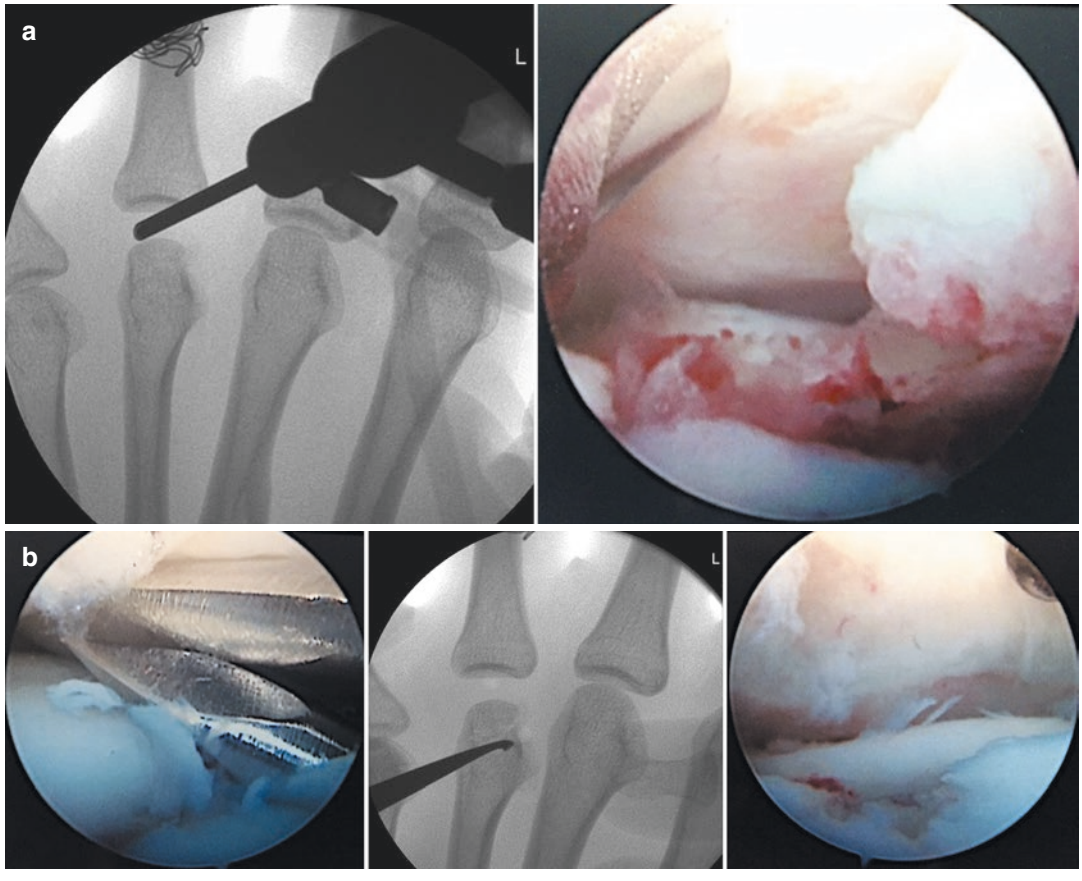

Fig. 121.2 (**a**) MCP arthroscopy for a metacarpal articular fracture is demonstrated. (**b**) Articular reduction is performed using an elevator (left image) or a curette through an extra-articular window (middle image). Final reduction is confirmed arthroscopically (right image)

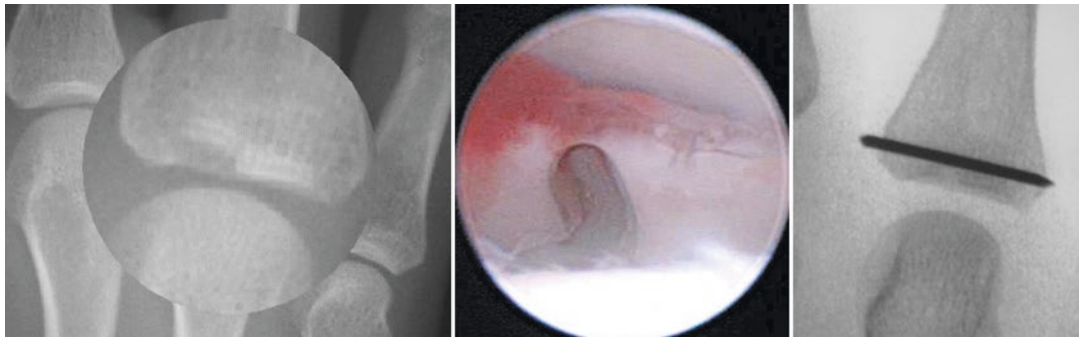

Fig. 121.3 Arthroscopic reduction and fixation of a phalangeal die-punch fracture is shown

reduction is achieved, any final small joint fragments are excised from the joint (Fig. 121.4a, b).

- At this point, final capsular debridement is performed and very limited RF shrinkage is performed which helps limit post-op hemarthrosis, thereby minimizing joint adhesions, fibrosis and minimizing any restriction of joint motion.
- Once associated soft tissue lesions are addressed, after fracture reduction, the portals are closed with benzoin/mastisol and steristrips only. This avoids any stitches which is where dorsal hand scarring typically results and allows for a more cosmetic result given the dorsum of the hand is only second to the face in terms of visibility. Kirschner wires are best cut underneath the skin, avoiding any pin tract infections and the thumb MCP is usually protected with a short arm thumb spica plaster intra-op splint with MCP extension and thumb palmar abduction/opposition.
- Alternatively, arthroscopy of any of the digits will necessitate a dorsal metacarpophalangeal block splint, usually in nearly full MCP flexion in order to allow the collateral ligaments to heal in their most taut position and minimizing any resultant loss in motion, usually flexion. This appropriate positioning is often critical to an optimal functional resultant and is often overlooked by many practitioners. It is particularly important in fracture management since the capsule and collateral ligaments will certainly become fibrosed to some degree due to the articular injury.
- The period of immobilization is determined by the complexity and type of fracture, as well as associated soft tissue lesions found during the arthroscopic intervention and can be determined intra-operatively. Post-op therapy plays a critical role, but only after the appropriate period of immobilization that allows adequate fracture healing and even soft tissue necessary scarring.

121.3 Tips and Tricks

- Small joint arthroscopy requires the right instrumentation and a steady hand. Even minimal motion of the camera hand will quickly lead to the scope exiting the joint, therefore there is a learning curve and cadaver practice is vital. Both the camera and the shaver should be supported on the first webspace of the surgeon's hands, with the index finger typically supported on the patients' hand. This allows for steadying of the scope while permitting depth of penetration, and triangulation, of the shaver or RF device.
- An experienced assistant is key, particularly during fracture reduction or fixation, since the surgeon may need two hands for this maneuver while the assistant steadies the scope.
- Fluoroscopy is necessary, and is typically positioned perpendicular to the axis of the

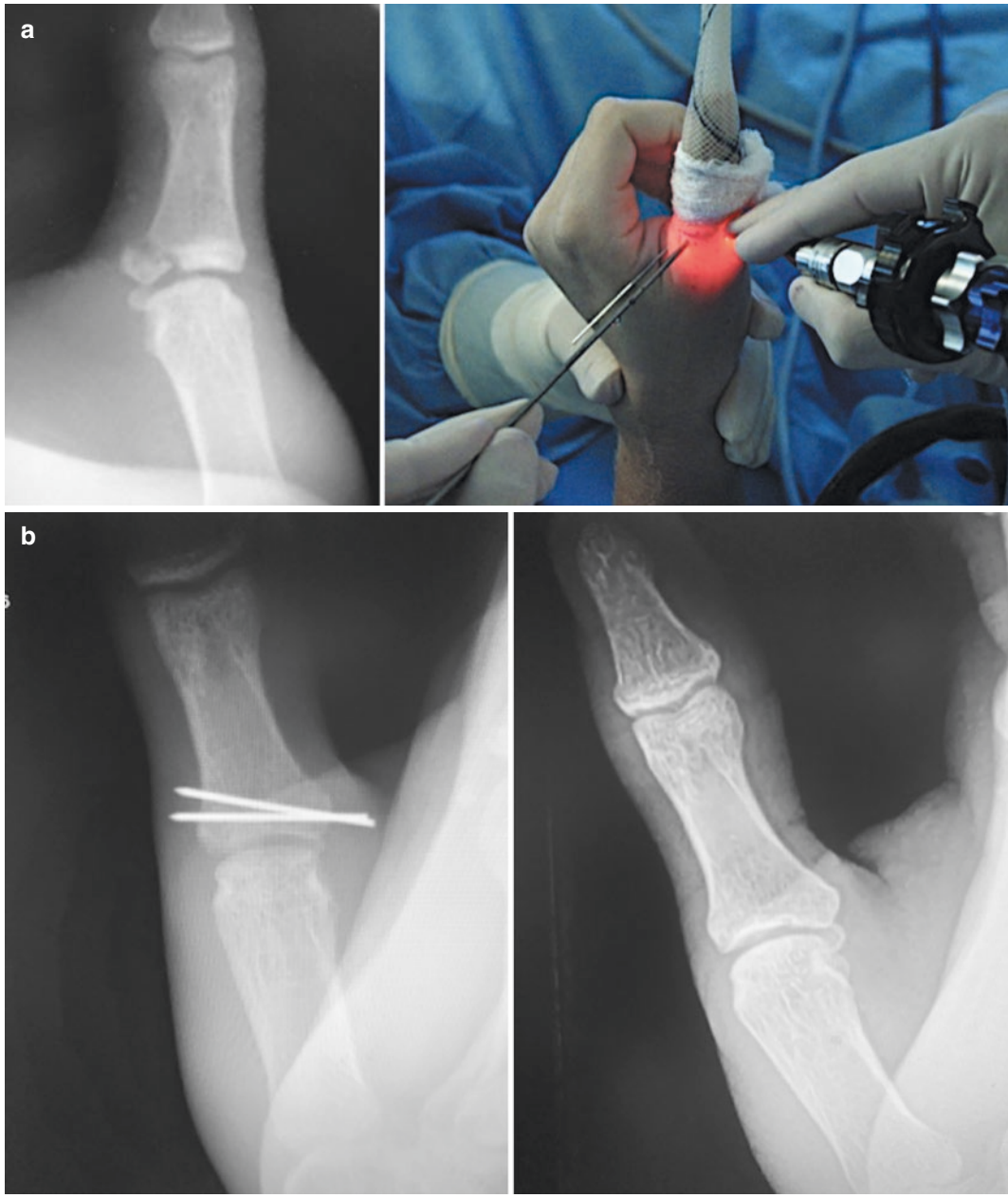

Fig. 121.4 (**a**, **b**) Arthroscopic reduction and fixation of an avulsed UCL bone fragment is shown

forearm, so that location and direction of the wire fixation can be precisely controlled.

- Wires may be used to joystick certain fragments, typically the avulsion fractures, so that exacting articular reduction can be achieved. The latter is best done by depending on the arthroscopic assessment of the fracture, not the fluoroscopic. These avulsion fractures are best reduced by using a hook probe to derotate the fragment once the fracture interval has been debrided by the small shaver.
- Die-punch fragments may not reduce by simply pulling them up with a hook probe, due to the angle or depth of fragment depression. Those cases are best addressed by creating a small extra-articular window (proximal for

MC and distal for PP). This can be done by a larger 0.062 wire, or even a small drill bit that should be protected by the appropriate sleeve. A smaller wire, with the sharp tip cut off, can be utilized as a mini bone tamp in order to elevate the fragment towards the articular surface, much as an ankle surgeon might reduce a pilon fracture. A larger fragment might require a small curette that can be used as a tamp as well. Once reduction is obtained, fixation, either direct or indirect, will be done with the k-wire as screws typically have no place for this type of fracture stabilization.

- In rare cases, an open technique will be done for the extra-articular component of the fracture, utilizing plate and/or screws, followed by the articular portion which can utilize arthroscopic assistance for all the reasons described herein.

121.4 Pitfalls

Fortunately, arthroscopy has little downside except in the case where the surgeon is inexperienced and may cause iatrogenic injury. As discussed, the appropriate size scope is critical and attempted use of the typical wrist scope will likely lead to articular cartilage damage of either the metacarpal head, or less commonly, the proximal phalanx base. The learning curve is not steep as the joint has few components, relatively simple anatomy, and only two major portals are usually required. However, a near microsurgical steady hand is needed in order to avoid joint injury which would obviate the advantages of arthroscopic reduction in the first place. For fracture fixation, one must utilize both arthroscopic and fluoroscopic assessment of fracture reduction and a common pitfall may be reliance on only one modality.

121.5 Complications

MCP arthroscopy has few to no complications if correctly performed.

- Joint hyperinflation, as occasionally seen in shoulder, is not an issue since the surgeon could quickly determine by visual means if there is too much distention of the joint. Arthroscopic inflow can be done by gravity, or using an anesthesia IV bag which is insufflated to a degree where inflow is assisted and can be easily dialed up or down. There is little role for fluid pumps as typically used in much larger joints.
- Iatrogenic injury to the joint has been discussed and should not be an issue except in the area of radiofrequency. One must maintain good fluid flow of Lactated Ringers solution to avoid overheating joint which can cause chondrolysis. Judicious use of RF on the capsule or collateral ligaments is crucial in order to avoid scarring or severely impairing perfusion to those critical soft tissue structures.
- Cutaneous sensory nerves are quite small in this area, and typically away from the portal sites which should be adjacent to the extensor tendon. This can be an issue in the thumb MCP region, therefore only the skin should be cut with the small scalpel during portal creation, and blunt penetration of the joint capsule should be done with a clamp, typically a small straight mosquito type, in order to avoid iatrogenic nerve injury.
- Since pins are typically used for fracture fixation, these should be cut at the appropriate depth to allow easy removal of post-fracture healing. Skin complications can occur if the pin erodes the subcutaneous tissues. This occurs on occasion due to minimal amount of soft tissue coverage of the MCP joint region, but is rarely a problem. Simple skin debridement may be needed, followed by a brief period of wound care, typically done by the hand therapist in conjunction with joint mobilization.

121.6 Post-op Management and Rehab

Besides accurate articular fracture reduction, the main advantage of arthroscopy is to facilitate and even minimize post-healing rehabilitation time (Fig. 121.5).

Fig. 121.5 Postoperative range of motion is demonstrated

- Thumb MCP avulsion fractures of the proximal phalanx, typically ulnar side, are common and any open reduction will often lead to dorsal capsular, and even extensor, scarring which limits flexion. An arthroscopic approach precludes that, and typically allows for full MCP flexion restoration within weeks of pin removal. Pinch strengthening is usually the focus of thumb fracture rehab.
- MCP fractures involving the digits, usually toward the ulnar side, can severely impair flexion and consequently, grip strength and overall hand function. This can be particularly disabling in many manual laborers as well as certain athletes. Arthroscopy will greatly impact the rapidity of flexion recovery if post-op immobilization is correctly done.

121.7 Summary

For still puzzling reasons, MCP arthroscopy remains a tremendously underutilized, albeit useful technique for the ideal treatment of acute fractures and associated soft tissue injuries affecting the metacarpophalangeal joints. While MCP arthroscopy indications expand amongst the few utilizers, the majority of hand surgeons would benefit from the minimal training needed to include this in their treatment armamentarium of these often challenging fractures.

References

1. Chen YC. Arthroscopy of the wrist and finger joints. Orthop Clin North Am. 1979;10(3):723–33. (Symposium on arthroscopy).
2. Vaupel GL, Andrews JR. Diagnostic and operative arthroscopy of the thumb metacarpophalangeal joint. A case report. Am J Sports Med. 1985;13(2):139–41.
3. Wilkes LL. Arthroscopic synovectomy in the rheumatoid metacarpophalangeal jointMCP. J Med Assoc Ga. 1987;76:638–9.
4. Ryu J, Fagan R. Arthroscopic treatment of acute complete thumb metacarpophalangeal ulnar collateral ligament tears. J Hand Surg (Am). 1995;20:1037–42.
5. Rozmaryn LM, Wei N. Metacarpophalangeal arthroscopy. Arthroscopy. 1999;15:333–7.
6. Slade JF 3rd, Gutow AP. Arthroscopy of the metacarpophalangeal joint. Hand Clin. 1999;15:501–27.
7. Badia A. Arthroscopy of the trapeziometacarpal and metacarpophalangeal joints. J Hand Surg. 2007;32(5):707–24.
8. Badia A, Riano F. Arthroscopic reduction and internal fixation for bony Gamekeeper's thumb. Orthopedics. 2006;29(8):675–8.

122 Arthroscopic Fixation of Metacarpal Head Fractures

Deepak N. Bhatia

122.1 Background

Metacarpal head fractures are infrequent injuries and are usually sustained in sports like cricket and tennis (direct hit by a ball on the knuckle). Occasionally, these fractures may be the result of a fall or may be sustained during punching a hard surface with a closed fist. Accurate reduction of these intraarticular fractures is essential and open techniques using various implants have been described for fixation. Metacarpophalangeal joint (MCP) arthroscopy provides excellent visualization of the fracture geometry and permits accurate articular reduction. Arthroscopic evaluation of associated soft-tissue injuries is possible and any loose bone debris and organized blood clots can be removed. Percutaneous K-wires can be passed under arthroscopic and fluoroscopic guidance for fracture fixation. Arthroscopic fixation results in minimal soft-tissue scarring and faster recovery of range and function [1].

122.1.1 Surgical Anatomy

Fracture patterns of metacarpal head involve a coronal or sagittal split and the displaced fragment may be predominantly dorsal or volar. Comminution and phalangeal impaction may be present and impacted articular fragments may prevent accurate reduction of the larger displaced head fragment. K-wires are passed from the dorsal aspect; antegrade (distal to proximal) wires are useful for predominantly dorsally displaced fragments and can be passed through the radial and ulnar MCP portals. Retrograde (proximal to distal) wires are useful for predominantly volar displaced fragments and can be passed along the dorsal radial or ulnar aspect of the metacarpal shaft.

122.2 Indications and Contraindications

- Displaced metacarpal head fractures that involve 10–15% of articular surface and with an articular step-off of 1–2 mm necessitate reduction and fixation [2].
- Undisplaced metacarpal head articular fractures that demonstrate progressive displacement in serial radiographs or stress views are indications for surgical fixation.

Arthroscopic access is difficult in presence of severe degenerative changes with an associated narrow MCP joint space and the arthroscopic fixation technique is contraindicated in such cases.

D. N. Bhatia (✉)
SPORTSMED Mumbai, and Sir HN Reliance Foundation Hospital, Mumbai, India
e-mail: shoulderclinic@gmail.com

© ISAKOS 2022

D. N. Bhatia et al. (eds.), *Arthroscopy and Endoscopy of the Elbow, Wrist and Hand*,
https://doi.org/10.1007/978-3-030-79423-1_122

122.3 Surgical Technique

The procedure is performed with the patient in the supine position. The finger is suspended on a standard wrist positioner with finger traps. Dorsal radial and ulnar portals are marked, and a 30 degree arthroscope (1.9 mm) is used for diagnostic arthroscopy.

Portals: Arthroscopic access to the MCP joint is possible via two portals:

- The dorsal radial portal (MCP-R) is placed in the dorsal joint line depression alongside the radial aspect of central extensor tendon and passes between the central slip and the radial lateral band. At the MCP joint of the thumb, this portal is placed radial to extensor pollicis brevis (EPB) tendon.
- The dorsal ulnar portal (MCP-U) is placed in the dorsal joint line depression alongside the ulnar aspect of central extensor tendon and passes between the central slip and the ulnar lateral band. At the MCP joint of the thumb, this portal is placed ulnar to extensor pollicis longus (EPL) tendon.

Arthroscopic assessment: A four-point assessment of the MCP joint is performed as described previously to evaluate articular surfaces, collateral ligaments, volar plate, and recesses. Fracture pattern is assessed, and comminuted and impacted fragments are identified. Smaller osteochondral fragments are excised while larger die-punch fragments are elevated using a probe. A 2 mm shaver blade is used to excise organized clots and debris, and the fracture fragments are clearly visualized (Figs. 122.1 and 122.2).

Fracture reduction and fixation: The fixation technique depends upon the site of the displaced fragment.

- **Dorsal fracture fragment** (Fig. 122.1): The arthroscope is placed in the dorsal recess via the radial (MCP-R) portal. A K-wire is passed through the ulnar (MCP-U) portal; the wire is positioned centrally on the dorsal fragment under vision and the fragment is engaged. A probe and the K-wire are then used to manipulate and joystick the displaced dorsal fragment towards the volar metacarpal head and reduction can be visualized. Die-punch fragments should be elevated and reduced anatomically if possible, and smaller fragments can be excised. The probe maintains reduction and the wire is advanced into the volar metacarpal neck (Fig. 122.3a). A second K-wire is passed percutaneously adjacent to the first wire to further secure the reduction. The reduction is confirmed by viewing through both ulnar and radial portals to visualize the entire fracture line (Fig. 122.3b, c).

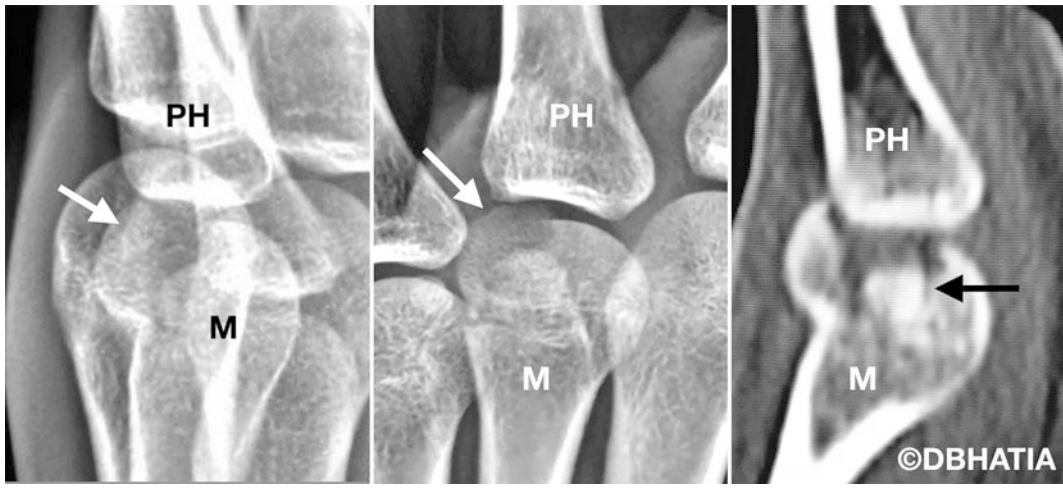

Fig. 122.1 Dorsal displacement (arrow) of a metacarpal head fracture (Left hand 4th digit) is shown on radiographs (left and middle images). CT scan demonstrates phalangeal impaction and a die-punch fragment (arrow, right image), and a large dorsally displaced fragment. (*PH* Proximal phalanx, *M* Metacarpal head). (©Bhatia)

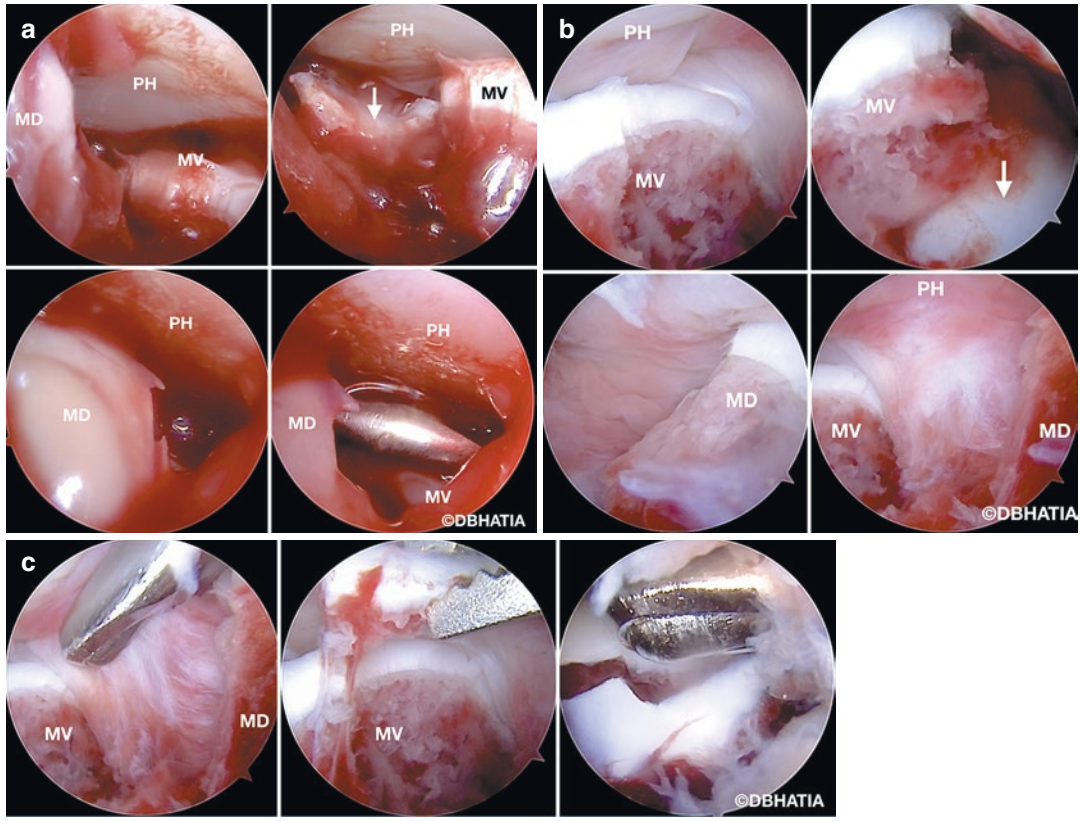

Fig. 122.2 (**a**) Arthroscopic assessment of metacarpal head fracture via radial portal demonstrates the dorsal (MD) and volar (MV) metacarpal head surfaces (top left). Comminuted impacted fragment (arrow, top right) and dorsal articular fragment (bottom left) are seen. A needle is used to place an ulnar portal (bottom right) (*PH* Proximal phalanx). (**b**) Arthroscopic assessment as visualized through ulnar portal shows the volar cancellous surface (MV, top left) of metacarpal head fracture as well as the impacted fragment (arrow, top right) and dorsal cancellous surface (MD, bottom left). The overall displacement is visualized in the bottom right image. (*PH* Proximal phalanx). (**c**) Arthroscopic debridement of volar (MV) and dorsal (MD) metacarpal head fragments is shown (left image). Comminuted fragments are excised using a grasper (middle image) and die-punch fragment is elevated and reduced. (right image). (©Bhatia)

- **Volar fracture fragment:** These fractures can be fixed with retrograde passage of K-wires from the dorsal aspect or using a combination of ante- and retrograde wires. The fracture line and displacement can be visualized arthroscopically by positioning the arthroscope in the dorsal recess and using a probe to retract the capsule dorsally. Any soft-tissue interposition at the fracture site is cleared using a probe and shaver (Fig. 122.4a). Reduction is achieved by using a combination of longitudinal traction and volar pressure on the metacarpal head and accurate approximation is visualized. A percutaneous antegrade K-wire is passed from the dorsal aspect of MCP joint (distal to proximal) through the fracture fragment and into the metacarpal neck, and wire trajectory is confirmed fluoroscopically. A second retrograde K-wire is passed percutaneously from proximal to distal to engage the subchondral bone of the volar fragment (Fig. 122.4b). The retrograde wire can be arthroscopically visualized if it penetrates the metacarpal articular surface and is then reversed to place it in a subchondral position (Fig. 122.4c). The final reduction is confirmed by visualizing through radial and ulnar portals and under fluoroscopic imaging (Fig. 122.5).

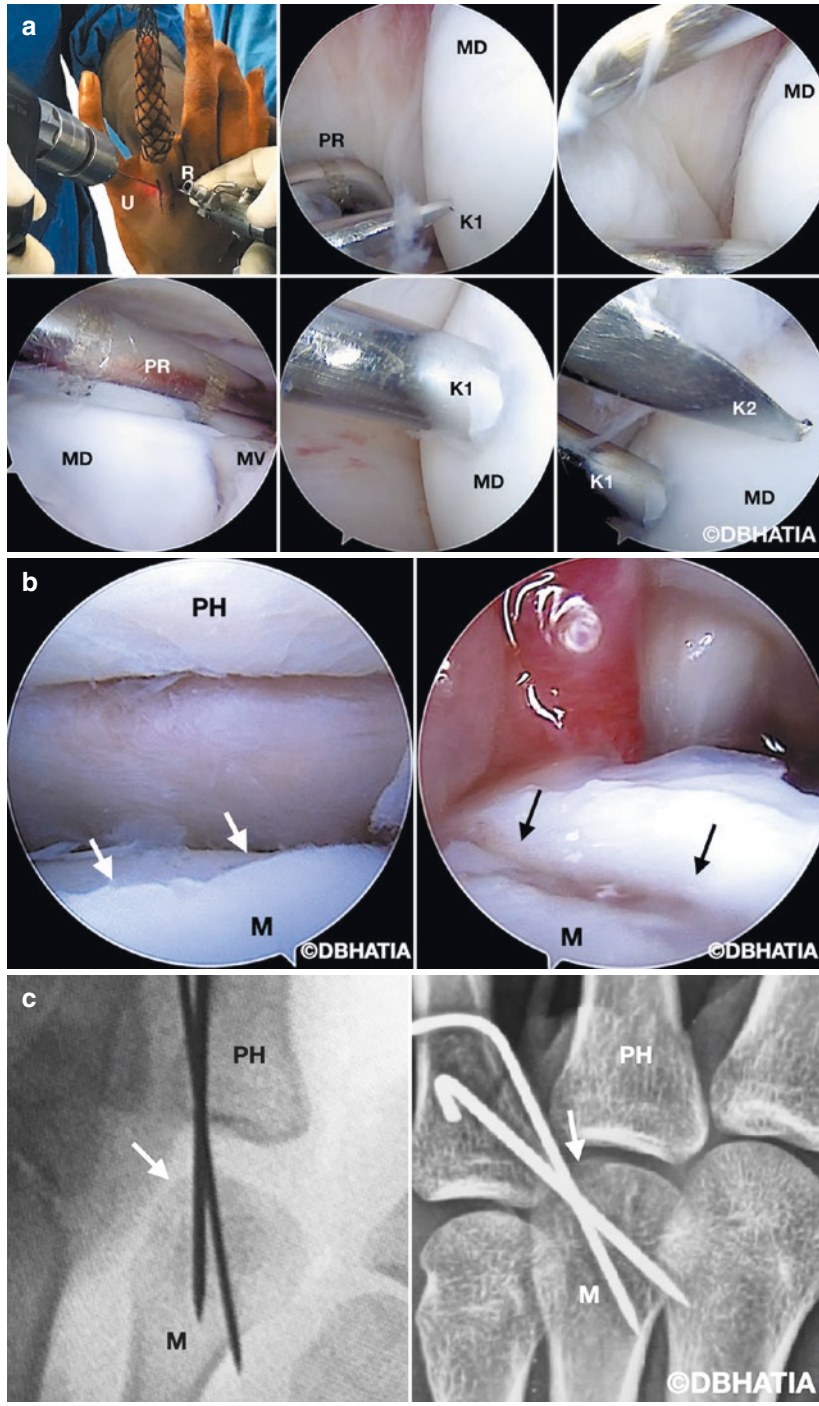

Fig. 122.3 (**a**) Reduction and fixation technique of a dorsal fragment is shown. The arthroscope is in the dorsal recess via radial portal (R) and a K-wire is passed through the ulnar portal (U) (top left). The K-wire (K1) is used to joystick the dorsal fragment (MD) and a probe (PR) is used to maintain reduction of MD to volar fragment (MV) (top middle and right images, and bottom left and middle images). A second K-wire (K2) is passed adjacent to K1 (bottom right). (**b**) Arthroscopic visualization of metacarpal head (M) fracture reduction (arrows, left image) and the reduced die-punch fragment (arrows, right image) via radial portal is shown. (*PH* Proximal phalanx, *M* Metacarpal). (**c**) Intraoperative fluoroscopy (left) and radiograph (right) confirm accurate reduction and fixation with K-wires (arrows). (*PH* Proximal phalanx, *M* Metacarpal). (©Bhatia)

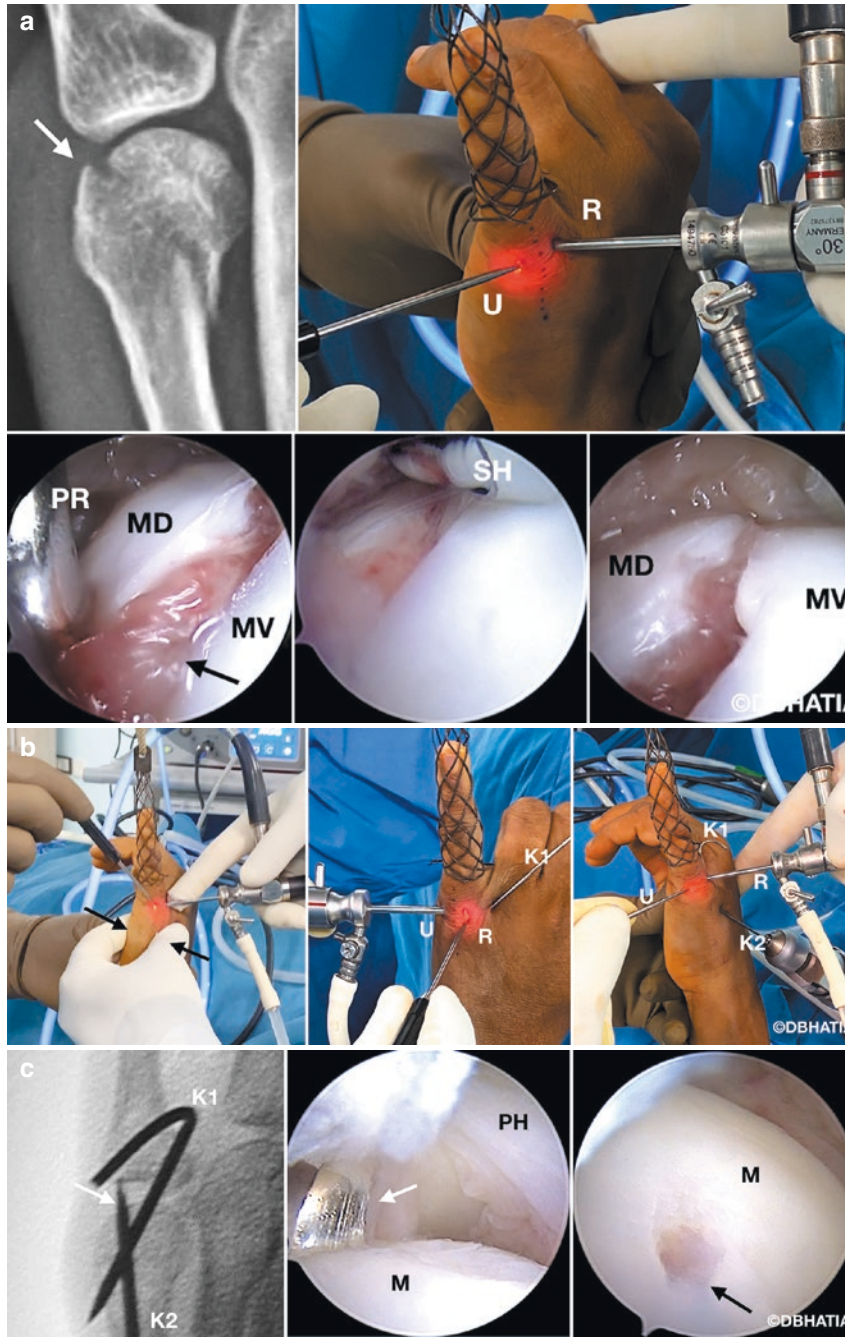

Fig. 122.4 (**a**) Reduction and fixation technique of a volar metacarpal head fragment (left hand, 5th digit) is shown. Radiograph shows the fracture pattern and displacement (arrow, top left). The arthroscope is in the dorsal recess via radial portal (R) and a probe (PR) and shaver (SH) are passed through the ulnar portal (U) (top right). Arthroscopic evaluation of fracture and removal of soft-tissue interposition between the dorsal (MD) and volar (MV) metacarpal head fragments are demonstrated (bottom images). (**b**) Digital compression (arrows) and a probe are used to achieve and maintain reduction (top left) and two percutaneous K-wires (K1 and K2, middle and right images) are passed for fracture fixation. (*R* Radial portal, *U* Ulnar portal). (**c**) The retrograde K-wire (K2) is seen penetrating the articular head surface on fluoroscopy (left image) and arthroscopy (middle image). The wire K2 is reversed into subchondral bone and the 1.5 mm tract is assessed to confirm correct subchondral placement of wire (arrow, right image) (K1: antegrade K-wire), *PH* Proximal phalanx, *M* Metacarpal head). (©Bhatia)

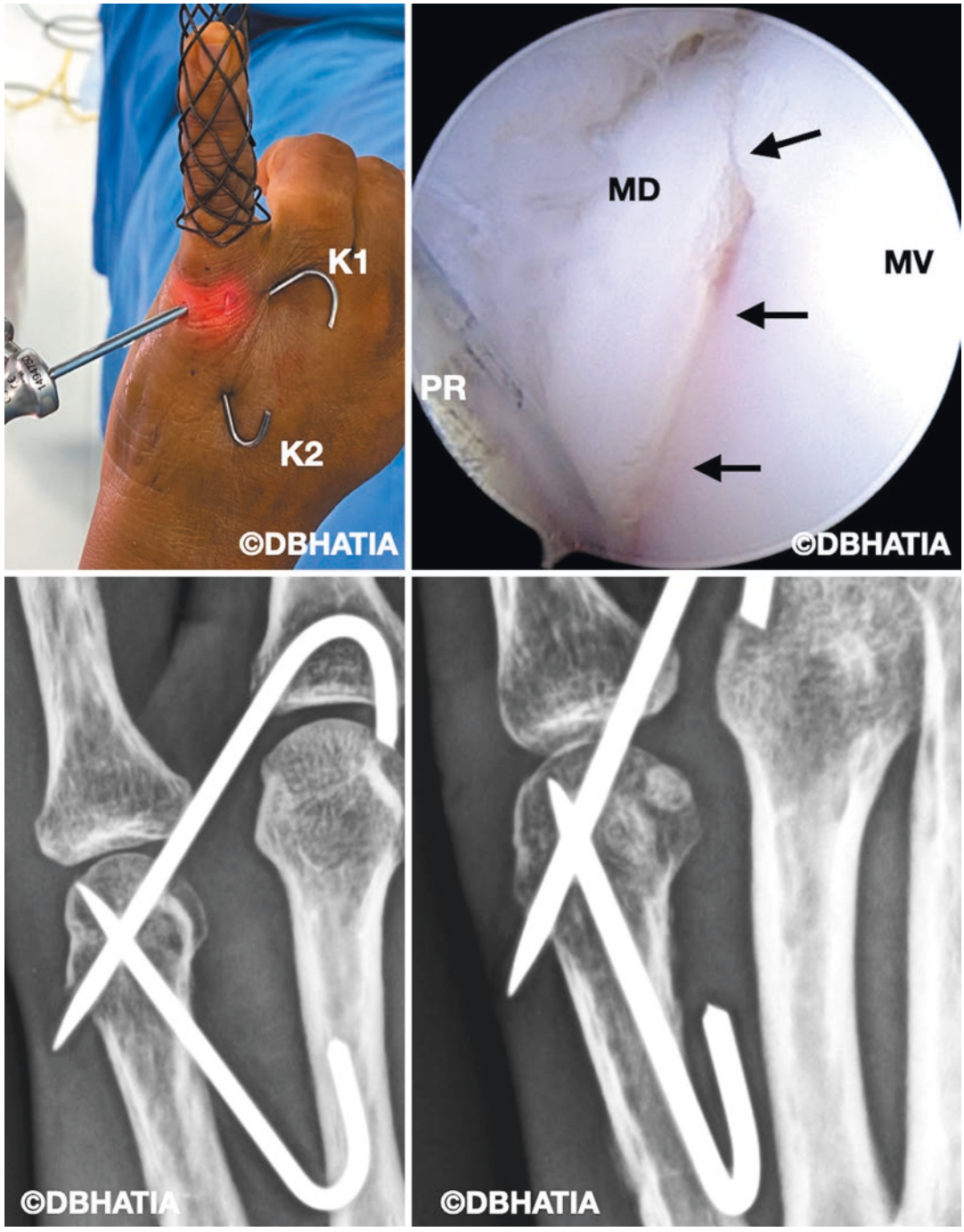

Fig. 122.5 Arthroscopic visualization of metacarpal head fracture reduction (arrows) via ulnar portal is shown (top images). Final radiographs show anatomical fracture reduction and fixation (bottom images). (*MV* Volar fragment, *MD* Dorsal fragment, *PH* Proximal phalanx, *PR* Probe, *K1 and K2* K-wires). (©Bhatia)

122.4 Tips and Tricks

- Gentle traction (without counter-traction) using a finger-trap suspension system is useful to achieve a workable joint space for a 1.9 mm arthroscope. Use of 1.9 mm instruments like graspers and punches is recommended to avoid iatrogenic chondral injury.
- Dry arthroscopy is adequate for diagnostic assessment and during fixation. Fluid inflow is used intermittently for lavage and a 50 cc saline-filled syringe is ideal for fluid irrigation and inflow.
- Reduction and compression maneuvers differ with fracture patterns. Gentle traction (without counter-traction) using a finger-trap suspension system is useful. K-wires and probes can be used to joystick and maintain fracture reduction. Coronal splits can be compressed with digital pressure in a volar-dorsal direction, and sagittal splits can be compressed using percutaneously applied reduction clamps.

122.5 Pitfalls

- Sensory branches of radial nerve are close to the portal sites and metacarpal shaft and are at-risk of iatrogenic injury during passage of ante-and retrograde K-wires.
- Fluid inflow is associated with periarticular swelling and this may interfere with visualization of fracture reduction and fixation.

122.6 Postoperative Management and Rehabilitation

A dressing and a below elbow slab are applied in the functional hand position. Sutures are removed in 10–12 days postoperatively and percutaneous K-wires are removed at approximately 4 weeks. Rehabilitation is started thereafter and progressed over 12 weeks. Return to active use of the hand for daily activities and work is permitted once rehabilitation has commenced. Return to sports activities is possible after achieving full function and rehabilitation goals.

122.7 Complications

Possible complications include injury to digital sensory nerves and neurovascular bundle, pin-tract infection, K-wire migration, and persistent digital stiffness.

Conflict of Interest The author certifies that he has no commercial associations (e.g., consultancies, stock ownership, equity interest) that might pose a conflict of interest in connection with the submitted article. The author retains the copyright to the images, videos, and content in this chapter.

References

1. Badia A. Arthroscopic reduction and internal fixation of bony gamekeeper's thumb. Orthopedics. 2006;29(8):675–8.
2. Weinstein LP, Hanel DP. Metacarpal fractures. J Am Soc Surg Hand. 2002;2:168–80.

Arthroscopy of Proximal and Distal Interphalangeal Joints

123

Isato Sekiya, Hideki Okamoto, and Masaaki Kobayashi

123.1 Background

Proximal interphalangeal (PIP) and distal interphalangeal (DIP) joint arthroscopy provides more precise information regarding intra-articular structure status than alternative imaging modalities. Arthroscopy may be considered for arthritis evaluation, synovial biopsy, synovectomy, irrigation and debridement, and loose or foreign body removal in the dorsal joint space. Arthroscopic surgery of the interphalangeal joint can be helpful for carefully selected indications.

123.2 Surgical Anatomy

123.2.1 Proximal Interphalangeal Joint

The proximal interphalangeal (PIP) joint is formed by the head of the proximal phalanx and the base of the middle phalanx. The head of the proximal phalanx has two condyles that are separated by a sagittal groove, while the fossae on the base of the middle phalanx are separated by a corresponding interfossal ridge. The PIP joint is a hinge joint, and the only movements allowed are flexion and extension. The skin around the joint is thin and mobile on the dorsal side, and thick and hairless on the volar side. The palmar skin has several collinear transverse creases at the level of the joint, while the dorsal skin is redundant and has concentric elliptic creases. The joint capsule begins at the osteochondral junction of the head of the proximal phalanx and ends at the base of the middle phalanx. The dorsal aspect of the PIP joint is covered with a thin joint capsule; both sides are collateral ligaments and accessory ligaments, and the palmar side is covered with the volar plate. There are large joint cavities on the dorsal and volar sides of the PIP joint. The collateral ligaments are under maximal tension at 10–15 degrees of joint flexion. The interval between the phalanges cannot be expanded even with strong traction force at the relaxed collateral ligaments (Fig. 123.1). The extensor mechanism at PIP joint is best described as a trifurcation of the extensor tendon into the central band and the two lateral bands. The central band of the extensor tendon is fused with the dorsal joint capsule of the PIP joint and ends at the dorsal aspect of the base of the middle phalanx. The aponeurotic expansion connects the central band and both lateral bands. The transverse retinacular ligaments stabilize lat-

I. Sekiya (✉)
Department of Orthopaedic Surgery, Kainan Hospital, The Aichi Prefectural Federation of Agricultural Cooperative for Health and Welfare, Yatomi, Aichi, Japan

H. Okamoto
Department of Orthopaedic Surgery, Graduate School of Medical Sciences, Nagoya City University, Nagoya, Japan

M. Kobayashi
Department of Orthopaedic Surgery, Ogaki Municipal Hospital, Ogaki, Gifu, Japan

© ISAKOS 2022

D. N. Bhatia et al. (eds.), *Arthroscopy and Endoscopy of the Elbow, Wrist and Hand*,
https://doi.org/10.1007/978-3-030-79423-1_123

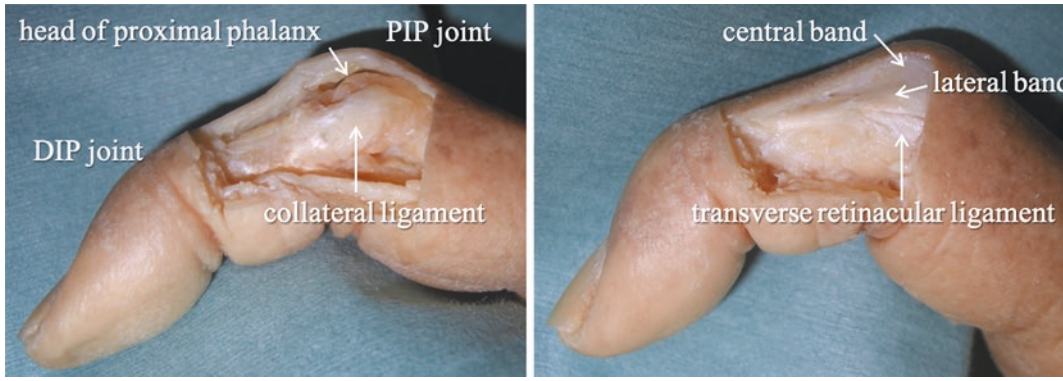

Fig. 123.1 Arthroscopic anatomy of the PIP joint in cadaveric dissections

eral bands to the flexor tendon sheath (Fig. 123.1). Okamoto reported a detailed anatomical study of the PIP joint arthroscopic portals [1].

123.2.2 Distal Interphalangeal Joint

The structure of the distal interphalangeal (DIP) joint is similar to that of the PIP joint but smaller. The joint capsule begins at the osteochondral junction of the head of the middle phalanx and ends at the base of the distal phalanx. The dorsal aspect of the DIP joint is covered with a thin joint capsule; both sides are collateral ligaments and accessory ligaments, and the palmar side is covered with the volar plate. The dorsal joint capsule is lined with the terminal extensor tendon. Since the volar plate of the DIP joint has no check rein ligaments, slight hyperextension is allowed.

123.3 Indications and Contraindications

123.3.1 PIP Joint Arthroscopy

Since the PIP joint space is not wide enough to insert the arthroscope into the palmar cavity, the palmar portion of the articular cartilage and the volar synovium cannot be inspected. PIP joint arthroscopy has not been a widely accepted technique because there are few indications for its use due to technical limitations; however, indications for PIP joint arthroscopy are similar to those for MCP joints.

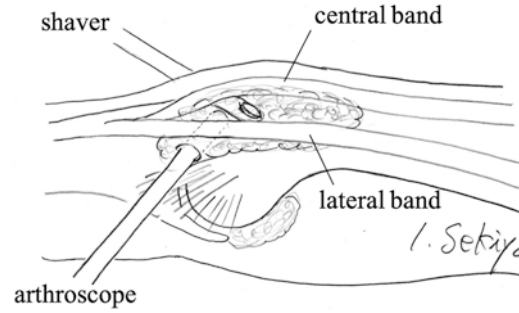

Fig. 123.2 Schematic drawing of PIP joint arthroscopic synovectomy. ©I. Sekiya (author)

- **Inflammatory Arthritis**: Arthroscopy is useful to evaluate, stage, and treat inflammatory arthritis in the PIP joints. Arthroscopically guided biopsies of the dominantly affected finger joint are useful because the technique is minimally invasive, provides tissue samples from areas of particular interest and highest inflammation, and decreases the risk of sampling errors [2]. Synovial biopsy of the dorsal joint capsule using grasping forceps can be performed with visual guidance through standard portals. Arthroscopic synovectomy of the dorsal capsule with visual control can be performed in a minimally invasive manner [3] (Fig. 123.2). Although the usefulness of open synovectomy remains controversial due to inconsistent study results, minimally invasive hypertrophic synovium excision in the small joints of the hand should result in a better outcome than open synovectomy.
- **Pyogenic arthritis**: In pyogenic arthritis cases, PIP joint irrigation and debridement are

easily accomplished with the arthroscope and a shaver [4].

- **Removal of foreign or loose bodies**: Depending on the size and location of the foreign bodies in the PIP joint, removal of foreign bodies from the dorsal joint cavity can be performed arthroscopically with grasping forceps and a shaver [5]. Although there have been no reports of arthroscopic removal of loose bodies in the PIP joint, we believe the procedure is possible.

123.3.2 DIP Joint Arthroscopy

There are only two reports of DIP joint arthroscopy.

- **Arthritis:** Chen performed arthroscopy for gouty arthritis in the DIP joint [6].
- **Arthrodesis:** Arthrodesis of the DIP joints of the fingers or the interphalangeal joints of the thumbs is indicated for improving pain, deformity, and instability caused by trauma, degenerative osteoarthritis, and chronic tendon injury. Cobb presented an arthroscopic technique for arthrodesis using a headless screw [7].

The contraindications for interphalangeal joint arthroscopy are the same as those for other joints.

- Fresh skin lesions or active infection near the portal sites are more likely to cause pyogenic arthritis.
- In presence of severe scarring or contracture of the dorsal tissue secondary to injury or burn, it is difficult to insert the arthroscope and the instruments into the dorsal joint cavity.
- If progressive finger deformity (boutonniere and swan neck deformity) and dysfunction are present, arthroscopic treatment will neither correct the deformity nor increase function. A variety of other surgical procedures are recommended to correct such deformities.

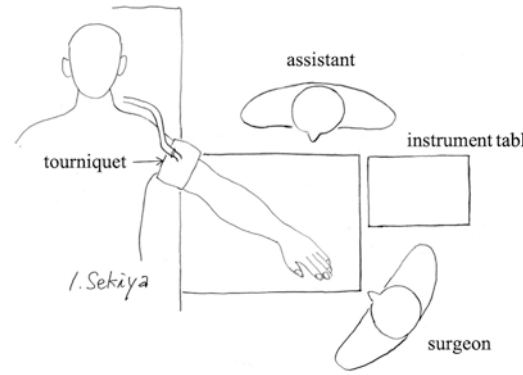

Fig. 123.3 Patient and medical team positioning. ©I. Sekiya (author)

123.4 Surgical Technique

All procedures can be performed on an outpatient basis under the surgeon's preference of local or regional nerve block anesthesia. A tourniquet is applied to the upper arm or the base of the digit. The patient is positioned supine with the shoulder abducted, and the arm positioned horizontally on the operating table (Fig. 123.3). The surgeon sits on the side of the affected finger, the assistant sits on the cranial side of the affected limb, and the instrument table is placed between them.

Although 1.9 mm arthroscopes are most commonly used, the authors use a 1.5 mm arthroscope at our facility. The 2.0 and 2.5 mm shaver blades are frequently used. The authors used a shaver system with a full radius blade for synovectomy. Otolaryngology mini forceps are also useful for synovial biopsy and removal of loose or foreign bodies (Fig. 123.4). No traction apparatus is required for PIP or DIP joint arthroscopy, because the interval between the phalanges is narrow and cannot be expanded with strong traction force.

123.4.1 Portals

Specialized portals are used for PIP and DIP arthroscopy

Fig. 123.4 Instruments for interphalangeal joint arthroscopic surgery. (From left to right: semi-blunt and blunt trocars, arthroscope sheath, arthroscope, shaver blade, and mini forceps)

- For PIP joints, Chen advocated for portal placement between the central slip and the lateral bands [6]. However, the authors established new portal placements for PIP joints on the dorsal-lateral aspect [8]. These new portals were applied from both the radial and ulnar positions to the lateral bands of the extensor mechanism. This is more lateral than the previous portal placement described by Chen and allows for the observation of the entire joint cavity (Fig. 123.5).
- For DIP joints, Chen described the portal placement on both the radial and ulnar side to the terminal extensor tendon [6].

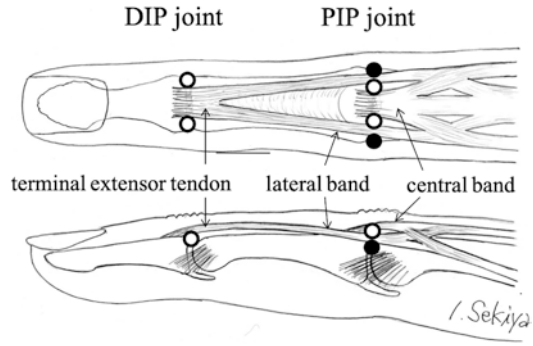

Fig. 123.5 Arthroscopic portals for interphalangeal joints. The dorsal portal (○) was proposed by Chen. The dorsal-lateral portal for PIP joint (●) is proposed by the authors. ©I. Sekiya (author)

123.4.2 PIP and DIP Access

- A 25-gauge needle is first introduced into the dorsal joint cavity, and 1–2 mL of normal saline solution is injected to distend the joint. Two small, longitudinal 2–3 mm long skin incisions are made with a No. 11 blade. Care should be taken not to injure the terminal branches of the nerve during the procedure. After skin incision, the subcutaneous tissue is dissected with a blunt trocar or a mosquito clamp.
- An arthroscopic sheath with a semi-blunt trocar is used to open the joint capsule and inserted into the dorsal joint cavity with gentle pressure to avoid damage to the articular surfaces. A normal saline solution inflow is established through the arthroscopic sheath or a 20- or 22-gauge needle introduced through the dorsal extensor tendon, and the arthroscope is placed into the joint (Fig. 123.6).

123.4.3 Diagnostic Arthroscopy

A comprehensive inspection of the intra-articular joint structures is then performed.

- Since the PIP and DIP joint space is not wide enough to insert the arthroscope into the palmar cavity, the palmar portion of the articular cartilage and the volar synovium cannot be inspected. However, magnified observation of the dorsal synovial membrane, dorsal articular surfaces of both phalanxes, and collateral ligaments is possible (Fig. 123.7). The other portal is used for instruments.
- The portals for the arthroscope and instruments are interchanged to allow inspection of the entire joint.

Fig. 123.6 PIP joint arthroscopy of the left index finger. The arthroscope is in the radial portal and the mini forceps in the ulnar portal

123.4.4 Arthroscopic Biopsy and Synovectomy

- In RA or monoarthritis patients, severely hypertrophic synovial membranes with polyp-like villus formation are observed. In these cases, a synovial biopsy from the dorsal joint capsule can be performed under visual guidance using grasping forceps.
- In patients with inflamed hypertrophic synovium, the articular cartilage cannot be visualized immediately after arthroscope insertion because severely hypertrophic synovial tissue blocks the arthroscope view. To obtain optimal visualization, an assistant continuously injects saline solution into the cavity while the surgeon holds the arthroscope to maintain adequate joint cavity distention. It may also be necessary to debride excess synovial tissue to visualize the articular cartilage

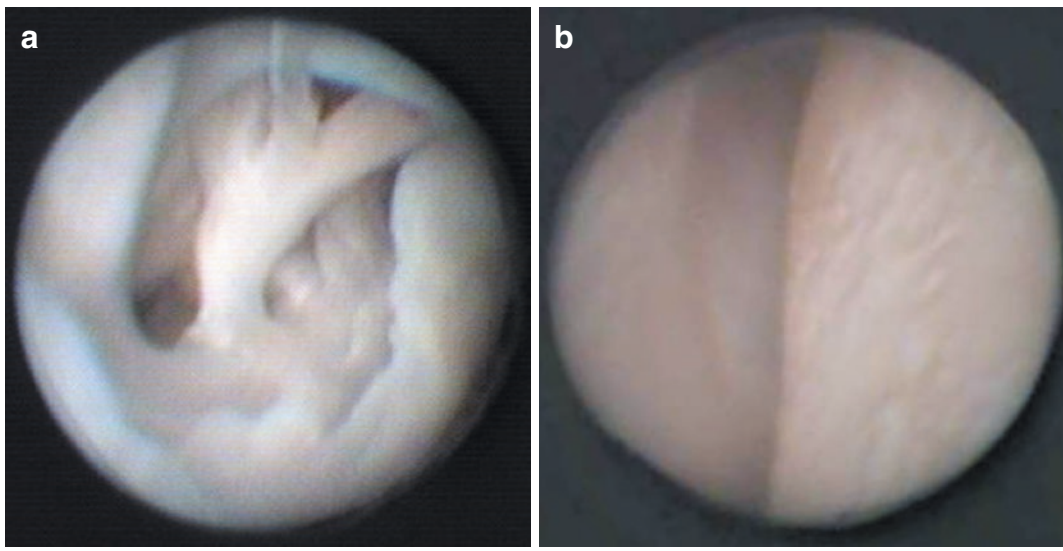

Fig. 123.7 Arthroscopic image of the PIP joint in an RA patient. (**a**) Synovial villus proliferation in the dorsal capsule. (**b**) The right is the proximal phalanx, and the left is the middle phalanx

and ligaments. Dorsal capsule synovectomy can be performed under visual control with a shaver system using the two-portal technique. Foreign or loose body removal from the dorsal joint cavity under visual guidance can also be performed with grasping forceps and a shaver.
- In pyogenic arthritis, cultures can be obtained by sampling the initial aspirate. A large volume of normal saline can be passed through the joint by running the shaver in the joint space while connecting the inflow to a wide-open source of fluid. Joint debridement is also possible with a shaver system.

After all procedures are finished, the joint is flushed with a large volume of saline. Each portal is then closed with a single suture or sterile strip, and a moderate compression dressing without splinting is applied.

123.5 Tips and Tricks

The arthroscope and instruments should be moved gently to avoid chondral injury and instrument slippage from the joint because the joint cavity is very small, making it difficult to handle the arthroscope and instruments. Wei et al. described using a pencil-grip position with the tip of the surgeon's middle finger as a guide/fulcrum to overcome this problem [9]. Surgeons must remember that the joint cavity is so small that the entire joint can be viewed by telescopically moving the arthroscope only a few millimeters.

123.6 Pitfalls

Since moving the shaver may cause intra- and extra-articular tissue damage, careful shaver handling is especially important. Before turning the shaver, it is essential to ensure the shaver is inside the joint and to check the direction of the rotating shaver blade. Blind synovectomy should not be performed without checking the position and direction of the shaver.

123.7 Postoperative Management and Rehabilitation

Although the course of postoperative care depends on the type of surgery performed, early movement is encouraged after the procedure. In an arthroscopic biopsy, synovectomy, and removal of foreign or loose bodies, postoperative immobilization with a moderate compression dressing without splinting is prescribed for only one to three days, followed by immediate range-of-motion exercises. The use of the operated finger is permitted based on the patient's pain tolerance.

123.8 Complications

With the careful application of standard arthroscopy principles, there are few complications associated with these procedures.

- The most serious complication is potential damage to the terminal nerve branches. Nerve damage can be avoided with careful incision techniques. An incision with a sharp blade is limited to the skin only, and the subcutaneous tissue is dissected using a blunt trocar or a mosquito clamp.
- Extensor tendon injuries may occur while inserting instruments through the portals, moving the shaver outside the joint, and performing excessive synovectomy with the shaver.
- Damage to articular cartilage may be caused by insertion or intra-articular handling of

arthroscopes and other instruments. Rotating the shaver blade toward the joint surface damages the articular cartilage.
- The potential for digital neurovascular bundle damage is significantly low when using standard portals.

123.9 Results

123.9.1 PIP Joint Arthroscopy

- Synovial tissue was easily obtained from the dorsal joint capsule under visual guidance using mini forceps. The sample size was sufficient for histological examination. Although only limited synovectomy was possible with this technique, swelling in each RA-affected joint disappeared postoperatively and, in most cases, did not return for an extended period of time [3]. The results of 14 PIP joint evaluations at least three years after arthroscopic synovectomy showed that approximately 80% of the joints no longer had swelling. There was no significant change in the PIP joint range-of-motion and, according to Larsen's criteria, X-ray findings were worse in one joint, improved in one, and unchanged in the others. The usefulness of synovectomy for degenerative arthritis is controversial. Borisch reported that PIP joint arthroscopic synovectomy is not recommended for degenerative arthritis except in selected cases [10].
- Foreign bodies can be removed from the dorsal joint cavity under visual guidance with grasping forceps and a shaver using the two-portal technique. There is one report of a 1.5 mm metal splinter removed using a 2.0 mm shaver [5]. Mini forceps are also useful for this purpose.

123.9.2 DIP Joint Arthroscopy

- Chen reported that necrotic villi with whitish crystals on the tips and crystal masses in the arthritic joint space became visible after repeated irrigation with normal saline solution [6].
- Cobb reported favorable results of arthroscopic techniques for DIP joint arthrodesis using a headless screw [7].

References

1. Okamoto H, Sekiya I, Mizutani J, et al. Anatomical basis for arthroscopy of the proximal interphalangeal joints. J Hand Surg Asian-Pac. 2018;23(3):342–6.
2. Ostendorf B, Dann P, Wedekind F, et al. Miniarthroscopy of metacarpophalangeal joints in rheumatoid arthritis. Rating of diagnostic value in synovitis staging and efficiency of synovial biopsy. J Rheumatol. 1999;26(9):1901–8.
3. Sekiya I, Kobayashi M, Okamoto H, et al. Arthroscopic synovectomy of the metacarpophalangeal and proximal interphalangeal joints. Tech Hand Up Extrem Surg. 2008;12(4):221–5.
4. Berger RA. Small-joint arthroscopy in the hand and wrist. In: Geissler WB, editor. Wrist arthroscopy. New York: Springer; 2005. p. 155–66.
5. Thomsen NOB, Nielsen NS, Jorgensen U, et al. Arthroscopy of the proximal interphalangeal joints of the finger. J Hand Surg Br. 2002;27(3):253–5.
6. Chen Y-C. Arthroscopy of the wrist and finger joints. Orthop Clin North Am. 1979;10(3):723–33.
7. Cobb TK. Arthroscopic distal interphalangeal joint arthrodesis. Tech Hand Up Extrem Surg. 2008;12(4):266–9.
8. Sekiya I, Kobayashi M, Taneda N, et al. Arthroscopy of the proximal interphalangeal and metacarpophalangeal joints in rheumatoid hands. Arthroscopy. 2002;18(3):292–7.
9. Wei N, Delauter SK, Erlichman MS, et al. Arthroscopic synovectomy of the metacarpophalangeal joint in refractory rheumatoid arthritis: a technique. Arthroscopy. 1999;15(3):265–8.
10. Borisch N. Arthroscopy of the proximal interphalangeal joint. Oper Orthop Traumatol. 2017;29(4):353–9.

Part XXV

Wrist and Hand Endoscopy

124 Endoscopic Release of De Quervain's Tenosynovitis

Michael J. Fitzmaurice

124.1 Background

De Quervain's tendonitis is a stenosing tenosynovitis of the first dorsal compartment involving the Extensor Pollicis Brevis (EPB) and Abductor Pollicis Longus (APL) tendons. Symptoms include pain located over the radial styloid and aggravated with use of the thumb. Examination findings include pain over radial styloid and pain with resisted thumb extension and a positive Finkelstein's test (placing thumb in palm and quickly abducting the hand in ulnar direction). Ultrasound has recently been found to provide an accurate method of diagnosis as well as identifying an accessory compartment which could influence treatment [1]. Conservative management is often used initially and includes splints and steroid injections. However, ultrasound has been beneficial in identifying an accessory compartment as there is higher failure rate of conservative management in patients with this accessory compartment [2]. When injections are given the results are typically improved with ultrasound guidance [3].

The typical open treatment was first published by Fritz de Quervain in 1885 [4]. The endoscopic technique has recently been described using both a one-portal and a two-portal technique with excellent results [5–9].

124.2 Indications and Contraindications

Patients are considered for endoscopic treatment when they have failed conservative management including splint and or steroid injections. They are also considered if they have an accessory compartment on ultrasound as they have a higher failure rate of conservative management. The specific indications for endoscopic release of the first extensor compartment are as follows:

- Persistent pain over first dorsal compartment despite conservative management including rest, splint, and/or steroid injections.
- No previous surgery and normal anatomy

The contraindications for this procedure include excessive scar tissue from previous procedures, tumors, and abnormal bone anatomy.

124.3 Surgical Technique

The instruments necessary for this procedure are EndoTech® sheath, 2.7 mm arthroscope, small hand instrument tray, and a pediatric laparoscopic scissors (optional).

M. J. Fitzmaurice (✉)
Fitzmaurice Hand Institute, Scottsdale, AZ, USA
e-mail: DrFitz@Fitzhand.com

© ISAKOS 2022

D. N. Bhatia et al. (eds.), *Arthroscopy and Endoscopy of the Elbow, Wrist and Hand*,
https://doi.org/10.1007/978-3-030-79423-1_124

Fig. 124.1 Incision for portal placement 1 cm distal to radial styloid

Fig. 124.2 Local anesthesia is used for the superficial radial nerve block and then surgical site

Fig. 124.3 Sheath inserted and tissue divided under direct visualization

The patient is placed supine with upper limb placed on an armboard and with wrist in neutral position. The surgeon is positioned facing the palm side of hand. The video monitor is positioned across from the surgeon. A single longitudinal distal portal is marked 1 cm distal to the radial styloid (Fig. 124.1).

- The procedure is performed under local anesthesia. A superficial radial nerve block is performed with 3 cc 1% lidocaine with epinephrine. An additional 5 cc of 1% lidocaine with epinephrine is then used to infiltrate the surgical area. The anesthetic is allowed approximately 30 min for optimal effect (Fig. 124.2).
- The portal site is marked out approximately 1 cm distal to the radial styloid.
- A longitudinal incision is made along this portal site and blunt dissection is performed to access the first dorsal compartment tendons (extensor pollicis brevis EPB, Abductor pollicis longus APL).
- The EndoTech® sheath is then inserted and synovitis is debrided with visualization of the extensor tendons of the first dorsal compartment (EPB, APL).
- The sheath allows retraction of soft tissue as well as the superficial branch radial nerve to allow visualization of the first dorsal compartment. It also allows visualization and resection of any accessory compartment (Fig. 124.3).
- The first dorsal compartment is divided with scissors or a blade with continued visualiza-

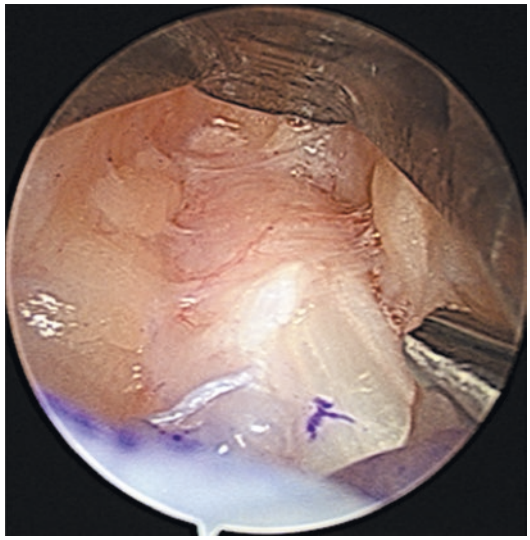

Fig. 124.4 Visualization of the first dorsal compartment

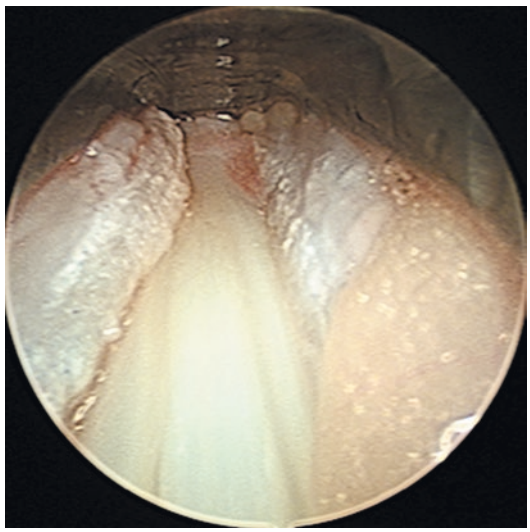

Fig. 124.5 Complete division of the first dorsal compartment with visualization of the EPB, APL tendons

tion of the tendons during the entire procedure. The compartment is divided along the ulnar aspect to minimize tendon subluxation. The release is performed from distal to proximal until the musculotendinous junction is visualized (Figs. 124.4 and 124.5).

124.4 Post-Operative Management and Rehabilitation

The small bandage is removed on the third post-operative day. Light activity (less than 10 pounds) is allowed for the first week and unrestricted activity is allowed thereafter. Most patients can resume full activity by 2 weeks.

124.5 Complications

Superficial radial nerve injury is a potential complication; however, this appears to less common with endoscopic release than an open technique. Mild neuritis usually resolves with therapy. If a nerve injury is suspected, consider exploration with possible repair.

124.6 Results

Studies have demonstrated the endoscopic technique to be safe and effective. Endoscopic release of the first dorsal compartment appears to allow a faster return to work compared to the open technique (5.1 vs 15.33 days) with less scar pain [5]. Risk of transient injury to neurovascular structures ranges from 5% to 20%, and complete injuries are rare (comparable to open techniques) [5]. We have found that with our current longitudinal portal placement and EndoTech® sheath, our transient complications/paresthesias are less than 5% without any serious injuries in over 128 procedures.

References

1. Lee K-H, Kang C-N, Lee BG, Jung W-S, Kim DY, Lee C-H. Ultrasonographic evaluation of the first extensor compartment of the wrist in de Quervain's disease. J Orthop Sci. 2013;19(1):49–54.
2. Keating-Hart ED, Touchais S, Kerjean Y, Ardouin L, Goff BL. Presence of an intracompartmental septum detected by ultrasound is associated with the failure of

ultrasound-guided steroid injection in De Quervain's syndrome. J Hand Surg Eur Vol. 2016;41(2):212–9.
3. McDermott JD, Ilyas AM, Nazarian LN, Leinberry CF. Ultrasound-guided injections for de Quervain's tenosynovitis. Clin Orthop Relat Res. 2012;470(7):1925–31.
4. de Quervain FA. On a form of chronic tendovaginitis by Dr. Fritz de Quervain in la Chaux-de-Fonds. 1895. J Hand Surg Eur Vol. 2005;30(4):388–91.
5. Gu X, Hong Z, Chen X, et al. Tendoscopic versus open release for de Quervain's disease: earlier recovery with 7.21 year follow-up. J Orthop Surg Res. 2019;14(1):357.
6. Kang HJ, Koh IH, Jang JW, Choi YR. Endoscopic versus open release in patients with de Quervain's tenosynovitis: a randomised trial. Bone Joint J. 2013;95-B(7):947–51.
7. Slade JFIII, Merrell G. Endoscopic DeQuervain's release. In: Capo JT, Tan V, editors. Atlas of minimally invasive hand and wrist surgery. Informa Healthcare. New York: Published online; 2008. p. 2007.
8. Kang HJ, Hahn SB, Kim SH, Choi YR. Does endoscopic release of the first extensor compartment have benefits over open release in de Quervain's disease? J Plast Reconstr Aesthet Surg. 2011;64(10):1306–11.
9. Karakaplan M, Ertem K, Canbay A, Aslantürk O, Yoloğlu S. One portal endoscopic release of the first extensor compartment in de Quervain's disease. Acta Orthop Traumatol. 2018;53(1):40–4.

Endoscopic Superficial Radial Nerve Decompression

125

Paul Max Jarrett

125.1 Background

Chronic severe neuropathy of the superficial radial nerve (SRN) is uncommon and the diagnosis is primarily a clinical one. Patients suffering from SRN neuropathy report sensory disturbance and sensory loss over the radial sensory nerve distribution, and experience pain at the site of nerve compression or irritation in the distribution of the nerve. The pain can often significantly affect the patient's quality of life and everyday function. SRN dysfunction in most patients is mild and transient and does not require treatment. There is a considerably smaller group of patients who suffer more significant chronic symptoms. The aetiology of SRN neuropathy for this group can include blunt or sharp trauma, or repetitive activities especially forearm rotation. The use of handcuffs or tight watch straps has been associated with SRN neuropathy, usually more distal to Wartenberg's point. The incidence of chronic neuropathy for the radial nerve as a whole is approximately 64 times less common than carpal tunnel syndrome [1]. SRN neuropathy makes up only a portion of radial nerve dysfunctions, and this makes SRN neuropathy quite uncommon.

P. M. Jarrett (✉)
Head of Department of Hand Surgery, Fremantle Hospital, Fremantle, Western Australia, Australia

Murdoch Orthopaedic Clinic,
Murdoch, Western Australia, Australia
e-mail: admin@pauljarrett.info

Exclusion of other peripheral neuropathies and proximal sources of nerve compression is necessary. Conditions such as De Quervain's tenovaginitis or carpal tunnel syndrome can coexist with SRN neuropathy and may require concurrent treatment to improve all the patient's symptoms. Nerve conduction studies can be considered, and ultrasound of the nerve using a high-frequency transducer can exclude structural pathology in the nerve (peripheral nerve tumours or external compression from ganglions) [2].

Treatment should consist initially of hand therapy, but if the response is insufficient, then an ultrasound-guided corticosteroid injection at Wartenberg's point is frequently successful in improving or resolving the condition. Should non-operative treatment fail, then surgery, either open or endoscopic can be undertaken with a high chance of success in resolving or substantially improving symptoms.

125.2 Surgical Anatomy

The Superficial Radial Nerve (SRN) is the superficial sensory branch of the radial nerve in the forearm. After the radial nerve bifurcates into the posterior interosseous nerve and the SRN, the SRN travels distally deep to Brachioradialis (BR) and subsequently travels between the tendons of BR and Extensor Carpi Radialis Longus (ECRL), on average 8.6 cm

© ISAKOS 2022

D. N. Bhatia et al. (eds.), *Arthroscopy and Endoscopy of the Elbow, Wrist and Hand*,
https://doi.org/10.1007/978-3-030-79423-1_125

proximal to the radial styloid, and becomes a superficial structure after piercing the forearm fascia 6 cm proximal to the radial styloid. Occasionally the SRN may travel through the tendon of BR. The nerve then courses distally within the subcutaneous tissues resulting on average in 5.8 branches by the time the nerve reaches the wrist [3].

Wartenberg's point, where the SRN passes between the tendons of BR and ECRL, is the site where the nerve is most commonly compressed and so decompression necessitates visualising this area and sufficiently incising the fascia and tendinous structures to prevent compression or irritation of the SRN. Thus, decompression can be undertaken open, with the incision at or near Wartenberg's point, or alternatively endoscopically with the incision distal to Wartenberg's point. For some patients there is tethering of the nerve over a large area, and neurolysis of all affected regions of the nerve can be obtained by open or more ideally, an endoscopic approach (Fig. 125.1).

125.3 Indications and Contraindications

Clinically, SRN neuropathy patients appear to be in three groups. Surgery should be reserved for patients who fail to improve sufficiently with several months of hand therapy and at least one injection of corticosteroid.

- Group 1: These are patients whose clinical examination is strongly suggestive that the pathology lies at Wartenberg's point. They are Tinel's positive and tender at this location with less nerve irritability distally to physical examination, but with distal nerve symptoms. The author performs open surgery in group 1 patients using a small incision just volar to Wartenberg's point. The reason for making the open procedure incision slightly volarly is to ensure that the nerve decompression and skin scarring are not directly over each other to reduce the significance of scarring in the cases of any cutaneous scar tethering. During the open approach, if there appears to be additionally fibrosis around the nerve more distal, then endoscopic neurolysis can still be carried out distally through this more proximal incision.
- Group 2: The second group of patients appears to have a more distal point of SRN irritability such as those in which the symptoms relate to a handcuff or watch strap injury. They are tender and Tinel's positive at the site of nerve irritability.
- Group 3: The patients in the third group have a more diffuse area of nerve irritability, often involving an extensive area in line with the SRN somewhere between Wartenberg's point and the radial styloid. This can also co-exist with compression at Wartenberg's point. At surgery, group 3 typically have soft tissue fibrosis around the nerve throughout the

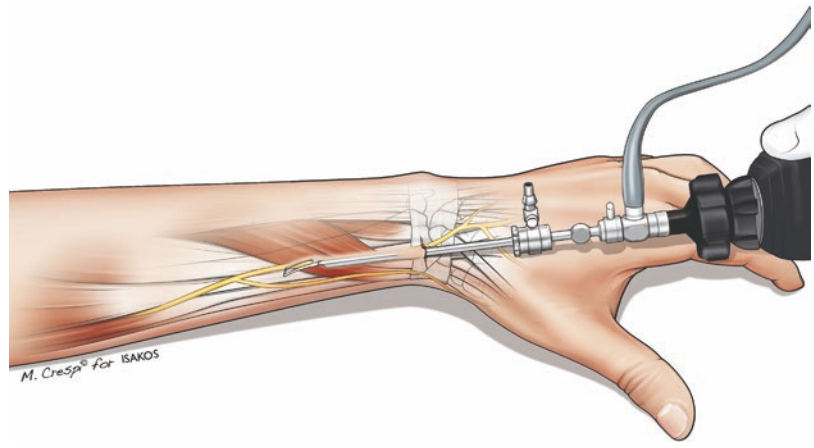

Fig. 125.1 Illustration and overview of endoscopic superficial radial nerve decompression. (M. Crespi © for ISAKOS)

region of irritability, which is not seen in those patients with isolated physical signs at Wartenberg's point.

The author's preference is to explore endoscopically the entire length of the nerve from radial styloid to above Wartenberg's point for groups 2 and 3; or if there is combined De Quervain's tenovaginitis and SRN dysfunction. The incision for endoscopic decompression is placed just proximal to the radial styloid.

An absolute contraindication for surgery would be local infection, and relative contraindications would include previous surgeries for the SRN, and significant psychological illness.

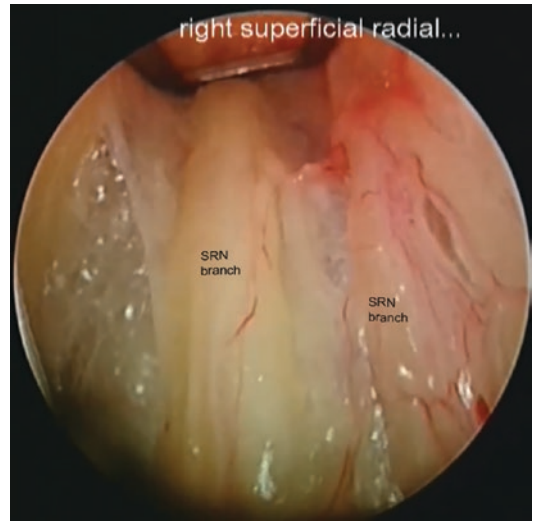

Fig. 125.2 Superficial radial nerve visualisation upon introduction of the endoscope

125.4 Surgical Technique

The patient is placed in a supine position under general or regional anaesthesia. A non-sterile tourniquet placed prior to skin preparation and the limb is exsanguinated. The endoscopic stack is located on the same side of the operating table as the surgeon, near to the patient's head area with the surgeon sitting between the arm and the trunk and surgical assistant between the arm and the stack.

- Using loupe magnification, a 15 mm skin incision is placed approximately 1 cm proximal to the tip of the radial styloid either longitudinally or transverse. The incision is centred between first and second dorsal compartments, or over the first dorsal compartment if the SRN decompression is to be combined with De Quervain's surgery. The distal incision is useful as one can easily identify the SRN at this level and one can operate proximally in a single direction.
- Careful blunt dissection is carried out with scissors to identify the branches of the SRN at the level of the incision, and sufficient room for the endoscope is made under direct vision (Fig. 125.2). It is useful to have shorter scissors such as curved tenotomy scissors to create the initial space for the endoscope and longer blunt-tipped curved scissors, such as Metzenbaums, for the more proximal work whilst visualising with the endoscope. It is essential that the longer scissors are sharp.
- The endoscopy is undertaken dry with no fluid or carbon dioxide used. Prior to inserting the endoscope into the incision, it is necessary to apply an antifog agent on the optical tip of the endoscope as this can safely prevent fog formation on the lens thus significantly improved visualisation.
- The endoscope is then introduced and under direct vision the SRN is carefully traced proximally and the nerve is dissected. The SRN is sensitive to trauma and therefore all dissection during decompression should be carried out under direct or endoscopic vision (Fig. 125.3).
- The nerve branches, as they course proximally, merge to become the single main SRN. Dissection can be carried out using a combination of blunt and sharp dissection going proximally.
- Once it reaches Wartenberg's point the nerve is decompressed by incising a portion of the BR tendon, to convincingly decompress the nerve. Due to the length from the incision, longer scissors are required by this time and great care is needed to adequately decompress the nerve whilst protecting the nerve. It is unusual to require to incise or resect substantial

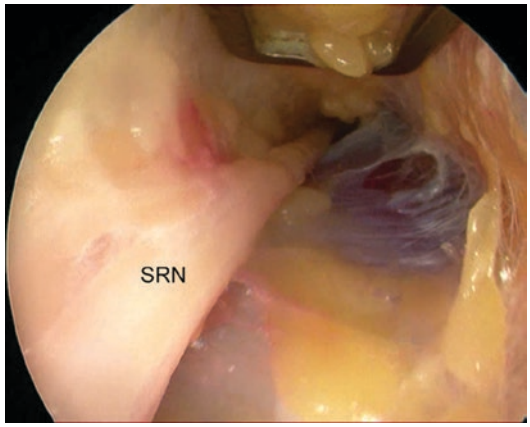

Fig. 125.3 Superficial radial nerve between incision and Wartenberg's point

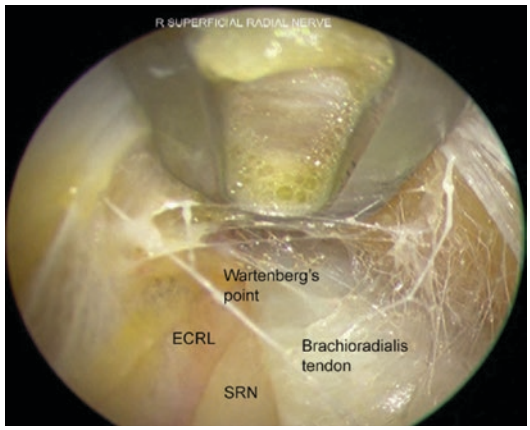

Fig. 125.4 Superficial radial nerve as it enters Wartenberg's point prior to decompression

portions of the tendon, but at the end of the procedure the nerve must have been adequately released. The tendon incisions should be as clean as possible to leave relatively undamaged tissue planes and reduce the risk of post-operative scarring around the nerve (Figs. 125.4 and 125.5).

- The nerve can then be endoscopically inspected and released proximal to Wartenberg's point if necessary.
- Closure is undertaken using 2/0 vicryl to subcutaneous tissue and 4/0 monocryl intradermal with local anaesthetic at the incision site. A small adhesive dressing is applied, and then orthopaedic padding and crepe bandage.

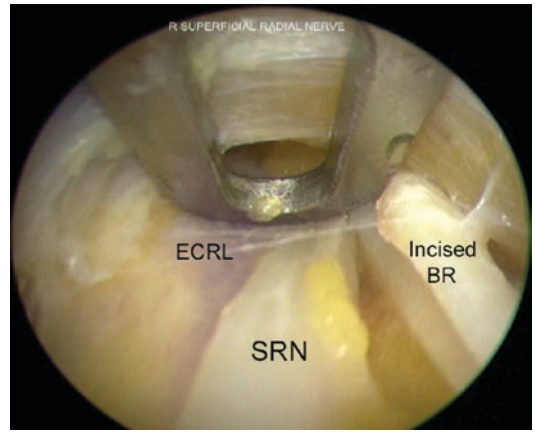

Fig. 125.5 Superficial radial nerve partially decompressed at Wartenberg's point

125.5 Technical Tips

- To create sufficient space to visualise the nerve and associated tissues, it is helpful to place a superior angulated force on the endoscope in a tilting manner, elevating the tip of the spatula of the optical dissector whilst keeping the central of rotation of the camera head stable.
- When dissecting in the subcutaneous, and sometimes deeper layers, small nerve branches or vessels can be encountered and care must be taken not to avoid injure to these structures, which are easily visualised. If required, for surgical exposure, small vessels can be coagulated using bipolar diathermy.
- Careful dissection is necessary when working around SRN at Wartenberg's point as this is the only occasion during the procedure when considerable sharp dissection is required near the nerve. Decompression of the nerve at Wartenberg's point consumes the bulk of the operative time for this procedure.

125.6 Pitfalls

- At Wartenberg's point, there are three relatively longitudinal structures (SRN, BR tendon, and ECRL tendon) and the surgeon is using scissors in the same plane as these tis-

sues to divide any fascia and to incise or resect sufficient tendon to decompress the nerve. Sharp curved scissors are therefore required but in the limited space one has, and only using the endoscope and scissors, one must be careful not to damage the nerve.

- If at any time the safety of the nerve is in danger, then adding an additional incision at Wartenberg's point and converting to an open procedure would be wise.

125.7 Post-Operative Management and Rehabilitation

The upper limb is elevated for a minimum of two to three days post-operatively, but light use is allowed immediately. The bandages are removed usually at two days and the adhesive dressings at ten days. The patient is encouraged to resume a normal life other than avoiding heavy activities until the soft tissue envelope has settled.

125.8 Complications

The procedure is safe in experienced hands, and the author has not experienced complications with this procedure. Other than conventional surgical complications such as infection, or nerve laceration, the more obvious complication would be irritation of the SRN. If this were to develop, then hand therapy and anti-neuropathic medication may be useful, and a pain management specialist could be consulted.

125.9 Results

Previous studies for SRN neuropathy have shown good results of surgical decompression [4–6]. In the authors' experience, the results are similar to other series described in literature. The results of operative intervention are less reliable than for carpal tunnel or cubital tunnel decompression. Therefore, in counselling patients regarding treatment, the results of treatment should be made clear. Twenty-three patients (fourteen female and nine male, age 20–64 years) were treated for chronic SRN neuropathy with severe symptoms of at least three months duration. Patients with sharp nerve trauma were excluded. The aetiology of the SRN dysfunction included fractures, hand trauma, blunt trauma to the forearm and excessive workplace use. Each patient was investigated with high-resolution ultrasound and no abnormalities were reported. Four out of 23 patients responded satisfactorily to hand therapy alone and further nine patients responded adequately long term with the addition of a corticosteroid injection at Wartenberg's point. The remaining ten patients underwent surgical exploration of the nerve over an eight-year period; of these two were performed open and eight endoscopically. Two patients underwent concurrent De Quervain's surgery, and four underwent concurrent carpal tunnel decompressions. Eight had a good or excellent recovery of their SRN symptoms with two patients had no significant improvement in their symptoms.

References

1. Latinovic R, Gulliford MC, Hughes RAC. Incidence of common compressive neuropathies in primary care. J Neurol Neurosurg Psychiatry. 2006;77:263–5.
2. Visser LH. High-resolution sonography of the superficial radial nerve with two case reports. Muscle Nerve. 2009;39(3):392–5.
3. Auerbach D, Collins E, Kunkle K, Monsanto E. The radial sensory nerve: an anatomic study. Clin Orthop. 1994;308:241–9.
4. Lazetta M, Foucher G. Entrapment of the superficial branch of the radial nerve (Wartenberg's syndrome). Int Orthop. 1993;17:342–5.
5. Dellon AL, Mackinnon SE. Radial sensory nerve entrapment in the forearm. J Hand Surg. 1986;11(2):199–205.
6. Calfee RP, Shin SS, Weiss APC. Neurolysis of the distal superficial radial nerve for dysaesthesia due to nerve tethering. J Hand Surgery (Eur). 2008;33E(2):152–4.

Endoscopic Carpal Tunnel Release (Supraretinacular Technique)

126

Michael J. Fitzmaurice

126.1 Background

Carpal tunnel syndrome is the most common peripheral entrapment neuropathy. The prevalence of carpal tunnel syndrome is approximately 5%, however among workers it can be up to 7.8% [1]. Carpal tunnel syndrome is caused by increased pressure inside the carpal tunnel compressing the median nerve. Symptoms typically include pain and paresthesias in the median nerve distribution (thumb through radial aspect of ring finger), often exacerbated at night. Surgical options include open or endoscopic release of the transverse carpal ligament. The open technique typically involves a longitudinal incision through the palm with division of the palmar fascia and the transverse carpal ligament. Unfortunately, the open technique does have increased risk of certain complications such as painful scars and pillar pain compared to the minimally invasive techniques.

Endoscopic carpal tunnel surgery was first reported by Dr. Oksuto in 1989 [2]. There are several types of endoscopic techniques. These include either a plane of dissection superficial or deep to the transverse carpal ligament [3, 4]. There are also either single incision (single portal) or double incision (two-portal) techniques for the deep plane of dissection [5–9]. Most endoscopic techniques involve placing an endoscope deep to the transverse carpal ligament from either a proximal incision or a proximal and distal approach. While visualizing the transverse carpal ligament, it is divided, leaving the superficial skin, palmar fascia, and muscle intact. The author has recently developed a superficial (supraretinacular) endoscopic approach (EndoTech® endoscopic carpal tunnel release). This procedure permits visualization of the transverse carpal ligament and the median nerve throughout the entire procedure.

126.2 Indications and Contraindications

- Indications for endoscopic surgical release are symptoms of median nerve compression such as paresthesia in median nerve distribution or wrist pain with positive provocative tests. Patients have either failed conservative management or have severe symptoms.
- Contraindications for an endoscopic approach include masses within the carpal tunnel or altered bone anatomy which would require an open approach. For the inexperienced minimally invasive surgeon, a revision release might be considered a contraindication,

M. J. Fitzmaurice (✉)
Fitzmaurice Hand Institute, Scottsdale, AZ, USA
e-mail: DrFitz@FitzHand.com

© ISAKOS 2022

D. N. Bhatia et al. (eds.), *Arthroscopy and Endoscopy of the Elbow, Wrist and Hand*,
https://doi.org/10.1007/978-3-030-79423-1_126

however, for the experienced surgeon this can be performed with an endoscopic technique.

126.3 Surgical Technique

Pre-operative Planning: The author prefers to evaluate patients with suspected carpal tunnel syndrome with ultrasound evaluation. This allows not only a cross sectional area of the median nerve but also a ratio of carpal tunnel measurements to distal forearm measurements. Ultrasound also allows visualization of any abnormal anatomy that could affect placement of instrumentation such as persistent median artery, masses, and bifid median nerve. Special instruments necessarily include the EndoTech sheath and a 2.7 mm arthroscope.

Patient Positioning: The patient is positioned supine with upper extremity on armboard. The procedure is performed under local anesthesia and the monitor for the surgeon is positioned across the arm from the surgeon and toward the fingers so the surgeon is looking away from the patient's body toward the fingers. A single portal incision is used along the distal wrist crease. A 1 cm transverse incision is marked within the wrist crease aligned just ulnar to the palmaris longus tendon (Fig. 126.1)

- The surgical area is anesthetized with 15 cc of 1% lidocaine with epinephrine.

Fig. 126.1 One-cm single incision for portal is placed just ulnar to palmaris longus tendon in distal wrist crease

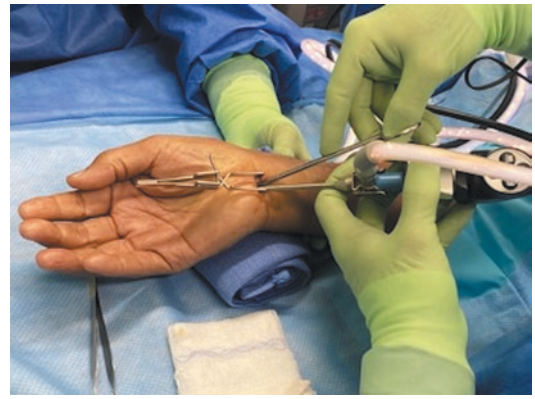

Fig. 126.2 Placement of EndoTech sheath to dissect tissues and scissors to cut the transverse carpal ligament

- A small incision (<1 cm) is placed in the distal wrist crease just ulnar to palmaris longus tendon. Dissection is carried down to the fascia which is incised with visualization of the median nerve.
- A freer elevator is used to dissect a plane under the transverse carpal ligament.
- Dissection superficial to the transverse carpal ligament is then performed and the EndoTech sheath and endoscopic camera are inserted.
- The orientation of the camera is in line with the ring finger. This allows visualization of the median nerve while dividing the transverse carpal ligament.
- Tissue is released with either scissors or small laparoscopic scissors. (Figs. 126.2, 126.3, 126.4)
- Neurolysis of the nerve is possible if necessary, with small laparoscopic scissors.
- Dissection and release are also performed proximally to release distal forearm fascia.
- Skin edges are approximated with absorbable sutures and dressed with small bandage.

126.4 Post-Operative Management and Rehabilitation

The small dressing is removed on the third post-operative day. It is recommended to cover dressing for showering until bandage removed. Light activity of less than 10 pounds is allowed for the

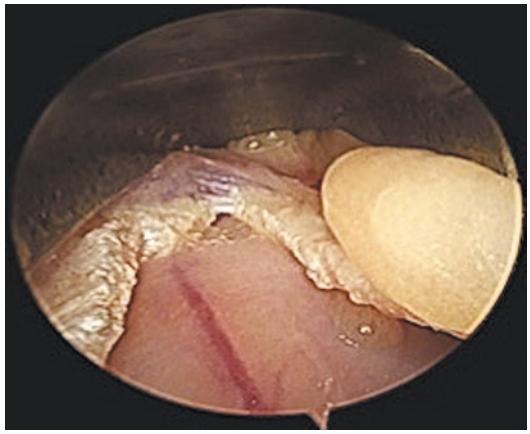

Fig. 126.3 Median nerve and transverse carpal ligament are visualized

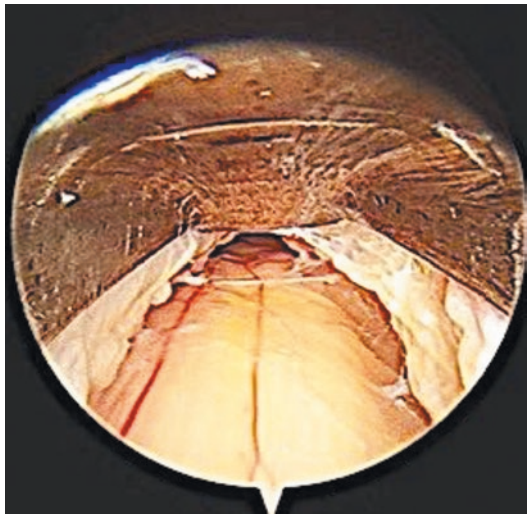

Fig. 126.4 Complete division of transverse carpal ligament is demonstrated. The median nerve and epineural blood flow can be visualized

first week then unrestricted during the second week. Most patients are able to resume full activity including heavy activity at 2 weeks.

126.5 Results

The outcomes of endoscopic versus open carpal tunnel release have been well studied. Several reviews have demonstrated shorter recovery times with endoscopic release and an earlier return to work. However, several other studies have demonstrated an increased potential for injury. This is usually due to inadequate visualization of the nerve during the procedure with certain endoscopic techniques or inadequate minimally invasive training from the surgeon. It is critical that the surgeon has experience with these techniques in order to minimize complications.

References

1. Silverstein BA, et al. The natural course of carpal tunnel syndrome in a working population. Scand J Work Environ Heal. 2010;36:384–93.
2. Okutsu I, Ninomiya S, Takatori Y, Ugawa Y. Endoscopic management of carpal tunnel syndrome. Arthroscopy. 1989;5:11–8.
3. Ecker J, Perera N, Ebert J. Supraretinacular endoscopic carpal tunnel release: surgical technique with prospective case series. J Hand Surg Eur Vol. 2015;40:193–8.
4. Teh KK, Choo CH, Shanmugam R, Ngim JH, Ahmad TSA. Novel supraretinacular endoscopic carpal tunnel release: instrumentation and technique (cadaveric study). J Hand Surg Global Online. 2019;1:222–5.
5. Chow JCY. Endoscopic release of the carpal ligament: a new technique for carpal tunnel syndrome. Arthroscopy. 1989;5:19–24.
6. Fechner MR, Hameeteman M, van der Hulst RRWJ, Franssen BBGM. Endoscopic carpal tunnel release: a new single-portal device. Tech Hand Up Extrem Surg. 2013;17:25–7.
7. Mirza MA, King ET, Tanveer S. Palmar uniportal extrabursal endoscopic carpal tunnel release. Arthroscopy. 1995;11:82–90.
8. Ghaly RF, Saban KL, Haley DA, Ross RE. Endoscopic carpal tunnel release surgery: report of patient satisfaction. Neurol Res. 2000;22:551–5.
9. Hamed AR, Makki D, Chari R, Packer G. Double- versus single-incision technique for open carpal tunnel release. Orthopedics. 2009;32

127 Endoscopic-Assisted Tendon Transfer for Extensor Pollicis Longus Rupture

Paul Max Jarrett

127.1 Background

Extensor pollicis longus (EPL) tendon rupture at the wrist results in a significant reduction in thumb and hand function. The most common cause of EPL rupture is following distal radial fracture. The injury is usually treated surgically with a tendon transfer or tendon grafting as non-operative treatment will not result in a sufficient return of function.

EPL rupture is typically easily diagnosed by history and clinical examination but ultrasound evaluation of the EPL tendon can be useful to confirm the injury, and the location of the tendon ends to assist in surgical planning.

The most common tendon transfer undertaken to reconstruct EPL rupture is an EIP to EPL transfer which has conventionally been undertaken by an open approach with several incisions. As endoscopic hand and upper limb surgery has become more common, it has become evident that tendon transfer surgery can be undertaken endoscopically assisted to allow for fewer and smaller incisions and potentially less scar tissue formation. Endoscopically assisted EIP to EPL tendon transfer requires an operating theatre with the appropriate endoscopic equipment and a surgeon with knowledge of EIP to EPL transfers who has sufficient experience in endoscopic soft tissue surgery.

The transfer technique described here was developed using an incision over the thumb metacarpal that is often used for the open approach avoiding any additional incisions. A similar technique has been described by Hoffman [1] using a more proximal transverse incision.

127.2 Surgical Anatomy

The extensor pollicis longus (EPL) tendon courses through the third dorsal wrist compartment, lying in a narrow oblique groove on the dorsum of the distal radius just radial to the midline before turning towards the thumb using Lister's tubercle as a pulley. It crosses superficial to the tendons of extensor carpi radialis longus and brevis obliquely and finally inserts onto the base of the thumb distal phalanx.

The extensor indicis proprius (EIP) tendon travels through the fourth dorsal wrist compartment with the extensor digitorum communis (EDC) tendons. It travels over the dorsum of the hand to join the extensor expansion to the index finger on the ulnar side of the EDC insertion. EIP allows independent extension of the index finger. Anatomical variations are not uncommon, including absence of EIP or accessory EIP tendons [2].

P. M. Jarrett (✉)
Department of Hand Surgery, Fremantle Hospital, Fremantle, Western Australia, Australia

Murdoch Orthopaedic Clinic, Murdoch, Western Australia, Australia
e-mail: admin@pauljarrett.info

© ISAKOS 2022

D. N. Bhatia et al. (eds.), *Arthroscopy and Endoscopy of the Elbow, Wrist and Hand*,
https://doi.org/10.1007/978-3-030-79423-1_127

EIP function should be confirmed pre-surgery by physically testing that strong independent index finger extension is present. Sonography may be used to assess anatomy and integrity of EIP.

Branches of the superficial radial nerve (SRN) are present within the operative area and should be watched for and protected during surgery.

127.3 Indications and Contraindications

Endoscopic-assisted EIP to EPL transfer is performed for EPL rupture secondary to a distal radius fracture. Other causes of EPL rupture may warrant EIP to EPL transfer. Consideration as to whether endoscopic surgery is appropriate for other pathologies will depend on what pathoanatomy is likely to be present and whether the pathology is likely to be effectively and safely treated endoscopically. If doubt exists, open surgery is preferable or alternatively, have a low threshold to converting from endoscopic to open surgery (Fig. 127.1).

There are no specific contraindications to this procedure. Surgeon inexperience is a relative contraindication.

127.4 Surgical Steps

The procedure is carried out with a general or regional anaesthetic and exsanguination of the upper limb prior to inflating an upper arm tourniquet. Following experience with this procedure, it can be undertaken using wide-awake local anaesthetic with no tourniquet (WALANT) if desired. The patient is supine with the upper limb placed on an arm table. The endoscopic stack is located near to the patient's head area with the surgeon sitting between at the axilla, and the surgical assistant between the arm and the head. Dry endoscopy is used throughout the procedure.

For the procedure, the instruments used (Fig. 127.2) include a surgical blade, scissors for dissection, endoscope, long bipolar diathermy bayonet forceps, and forceps and needle holder. It is useful to have shorter scissors such as curved tenotomy scissors to create the initial dissection and longer blunt-tipped curved scissors, such as Metzenbaums, for the endoscopic work. A 4 mm (18 cm length) Hopkins II Forward-Oblique 30 degrees telescope with large fenestrated distal spatula optical dissector (Karl Storz, Tuttlingen, Germany) is used for viewing. A speculum may be useful at times during this procedure.

- A 2.5 cm gently curved longitudinal incision, or a zig-zag type incision is made over the route of EPL at the mid-thumb metacarpal level.
- Blunt dissection is carried out, either open or endoscopically (Fig. 127.3), to identify and free up the distal end of the EPL tendon whilst protecting any branches of the SRN.
- Blunt forceps are used to create a soft tissue path to the insertion of EIP onto the extensor expansion of the index finger and then a sec-

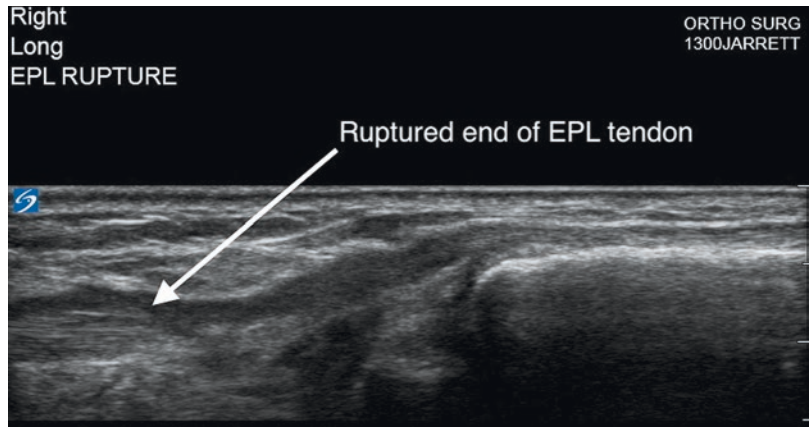

Fig. 127.1 Longitudinal sonography demonstrates the proximal end of EPL stump

Fig. 127.2 Endoscopic equipment necessary for the procedure is shown

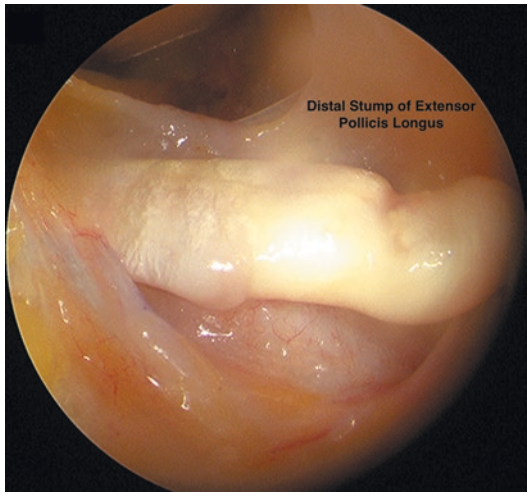

Fig. 127.3 Endoscopic view visualizes the distal end of EPL

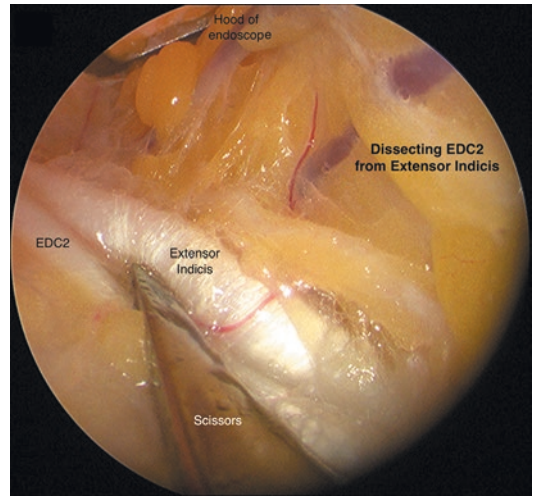

Fig. 127.4 Endoscopic view shows extensor tendons coursing distally towards index finger. [EDC: extensor digitorum communis]

ond soft tissue path is created between the incision and the distal end of the fourth extensor compartment. The endoscope is inserted to inspect up to the insertion of EIP (Fig. 127.4).

- The EIP is dissected from the EDC to the index finger and then incised distally (Fig. 127.5a, b) and pushed proximally with forceps to break any adhesions between itself and EDC (Fig. 127.6a). The EIP tendon is the ulnar of the two tendons going to the index finger.
- The forceps are left attached and the endoscope removed and then reinserted and directed proximally to the distal opening of the fourth compartment. Gentle traction on the EIP in a distal direction will help identify EIP at the distal end of fourth compartment and an Allis tissue forceps is inserted into this area, around the EIP tendon which is brought into the incision in the correct route for the tendon transfer (Fig. 127.6b).
- At this point, the distal EPL stump is at the incision and the incised proximal end of the re-routed EIP tendon and the transfer can be completed as in an open procedure. A recommended repair is a Pulvertaft weave at the correct tension with a 3/0 Ethibond suture (Fig. 127.7).
- After local anaesthetic infiltration, the incision is closed with 2/0 vicryl and intra-dermal 4/0

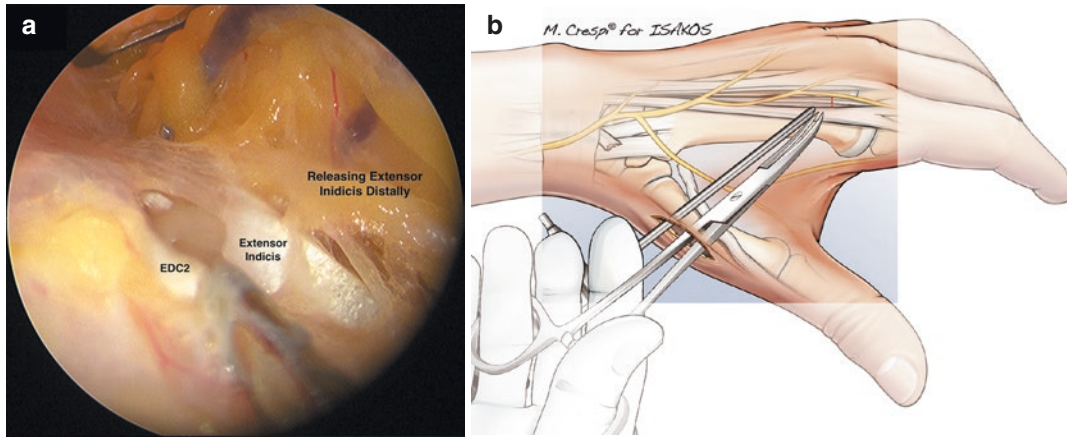

Fig. 127.5 (**a**) Endoscopic visualization shows EIP incised from extensor expansion. (**b**) Illustration shows the soft tissue tunnel for incising EIP from extensor expansion. © Crespi for Jarrett (M. Crespi © for ISAKOS)

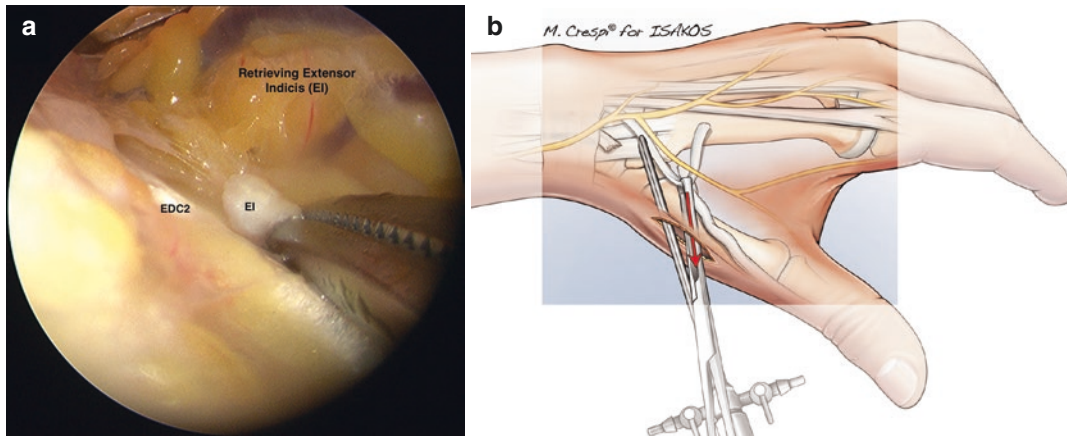

Fig. 127.6 (**a**) Endoscopic view shows the EIP is directed proximally to free it up. (**b**) Illustration shows the soft tissue tunnel for EIP retrieval into the incision for transfer to EPL. © Crespi for Jarrett (M. Crespi © for ISAKOS)

monocryl, with adhesive dressings and a plaster splint.

127.5 Technical Tips

- The EIP tendon is identified as it courses ulnar to the EDC to the index finger.
- Gentle traction on the EIP in a distal direction is useful to identify the tendon when visualizing the distal end of the 4th compartment.
- The surgeon should ensure the route of the EIP from the 4th compartment to the distal stump of EPL is as for the open procedure. Once the cut end of the EIP tendon has been brought into the incision, and prior to suturing the tendon transfer, the surgeon can view the course of the EIP tendon endoscopically to ensure its correct passage.
- Nerve branches or vessels can be encountered during dissection and must be protected or coagulated.

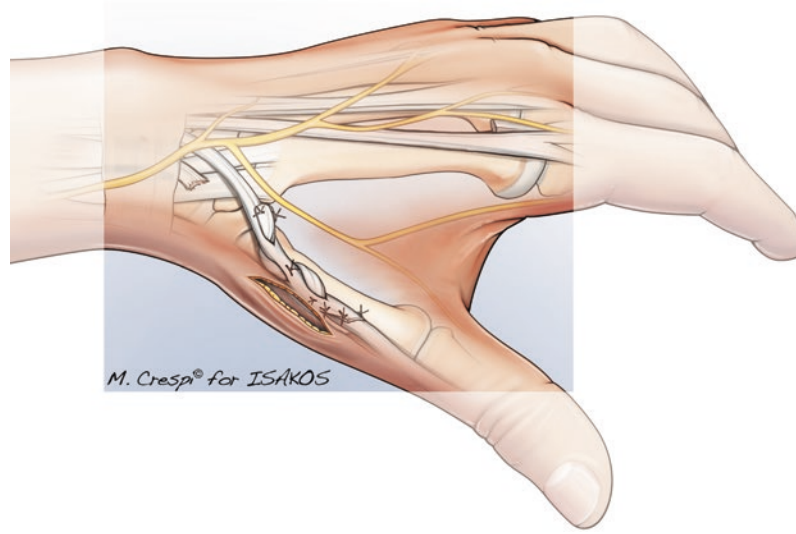

Fig. 127.7 EIP to EPL tendon transfer is completed using a Pulvertaft weave. © Crespi for Jarrett (M. Crespi © for ISAKOS)

127.6 Pitfalls

- The procedure is an endoscopic variation of the open procedure, and the surgeon should be familiar with open EIP to EPL transfers. Should difficulties be experienced intraoperatively, the procedure can be converted to the standard open procedure.
- As the EIP anatomy is not universally consistent, the surgeon must be aware of the anatomical variants and prepared to alter the procedure if required due to atypical anatomy. For EIPs with accessory tendons, the surgeon can confirm the anatomy either endoscopically or open to determine if more than one slip of the EIP tendons should be incorporated into the transfer. If the EIP tendon is absent, then an alternative tendon donor will be required. The author's preferred option for an absent EIP tendon is an extensor digiti minimi to EPL transfer which can be performed endoscopically or converted to an open procedure.

127.7 Post-Operative Management and Rehabilitation

The patient is seen by the hand therapists 1–4 days post-operatively and supplied with a splint and therapy commenced. The therapy protocol is independent of whether the procedure is open or endoscopic.

127.8 Complications

- Carefully identification of the ulnar sided index finger extensor tendon is required to prevent the complication of harvesting the incorrect donor tendon. In the unlikely event of endoscopic assessment being inadequate to clearly identify the appropriate anatomy, conversion to an open approach would be advisable.
- The donor tendon to EPL tendon suturing requires to be sufficiently strong to avoid failure of the transfer. Whilst an end-to-end suturing could be undertaken, a tendon weave is considerably stronger and is the preferred technique. The author has used a Pulvertaft weave, but other suitable tendon weaves could be used.
- Setting of the transfer tension will influence the outcome of the procedure. The author has set the tension of the transfer at near maximum tension with the thumb fully extended and the wrist at 30 degrees of flexion during the transfer. The correct tension allows passive flexion of the thumb to touch the pulp of the little finger with wrist extension. If in doubt set the tension slightly on the tight side as stretching can occur.

Acknowledgements I am grateful for Professor James O Jarrett and Mrs Anna-Lisa Baker for their comments on the text.

References

1. Hoffmann R, Meek M. Endoscopic single-incision extensor indicis transposition for extensor pollicis longus reconstruction. Tech Hand Up Extrem Surg. 2007;11:156–8.
2. Georgiev G, Tubbs R, Iliev A, Kotov G, Landzhov B. Extensor indicis proprius muscle and its variants together with the extensor digitorum brevis manus muscle: a common classification. Clinical significance in hand and reconstructive surgery. Surg Radiol Anat. 2018;40:271–80.

Endoscopic Trigger Finger Release

128

Michael J. Fitzmaurice

128.1 Background

Trigger finger is a common hand condition causing pain and snapping sensation of the finger or thumb. Triggering is caused by a thickening of the normal synovial lining or of the fibrous sheath (fibrocartilaginous metaplasia) through which the tendon glides. Initially non-surgical treatment includes extension splinting, non-steroidal anti-inflammatory medications, and steroid injections. High failure rates of non-surgical treatment are associated with patients with diabetes or multiple trigger fingers [1–3]. Surgical treatment for trigger finger has typically been performed through an open technique. Recently endoscopic techniques have been developed to minimize recovery and allow a quicker return to activity with decreased complications compared to open techniques [4, 5].

128.2 Indications and Contra-Indications

Patients who have failed conservative management, diabetic patients, multiple digits involved or have severe symptoms for longer than 6 months are considered for surgery.

M. J. Fitzmaurice (✉)
Fitzmaurice Hand Institute, Scottsdale, AZ, USA
e-mail: DrFitz@Fitzhand.com

Any previous incisions near surgical site are a possible contraindication for the endoscopic procedure due to scar tissue formation.

128.3 Surgical Technique

The procedure is performed under local anesthesia. An EndoTech sheath and 2.7 mm arthroscope are used for visualization, and a small laparoscopic scissors is used for release.

The patient is positioned supine on the surgical table with arm extended on arm board.

- The portal site is marked out after measuring the proximal location of the A1 pulley (Fig. 128.1). This is performed by measuring the distance from the palmar digital crease to the proximal interphalangeal crease. This distance is then placed proximal to the palmar digital crease and marked for the longitudinal incision [6].
- The procedure is performed under local anesthesia. 5 cc of 1% lidocaine with epinephrine and 0.5 cc bicarbonate are injected at the portal site and directed distally (Fig. 128.1)
- After testing for adequate anesthesia, the port incision is created. Dissection carried down to the flexor tendons and proximal aspect of A1 pulley identified.
- The EndoTech sheath is inserted with the endoscope which allows dissection of the soft

© ISAKOS 2022

D. N. Bhatia et al. (eds.), *Arthroscopy and Endoscopy of the Elbow, Wrist and Hand*,
https://doi.org/10.1007/978-3-030-79423-1_128

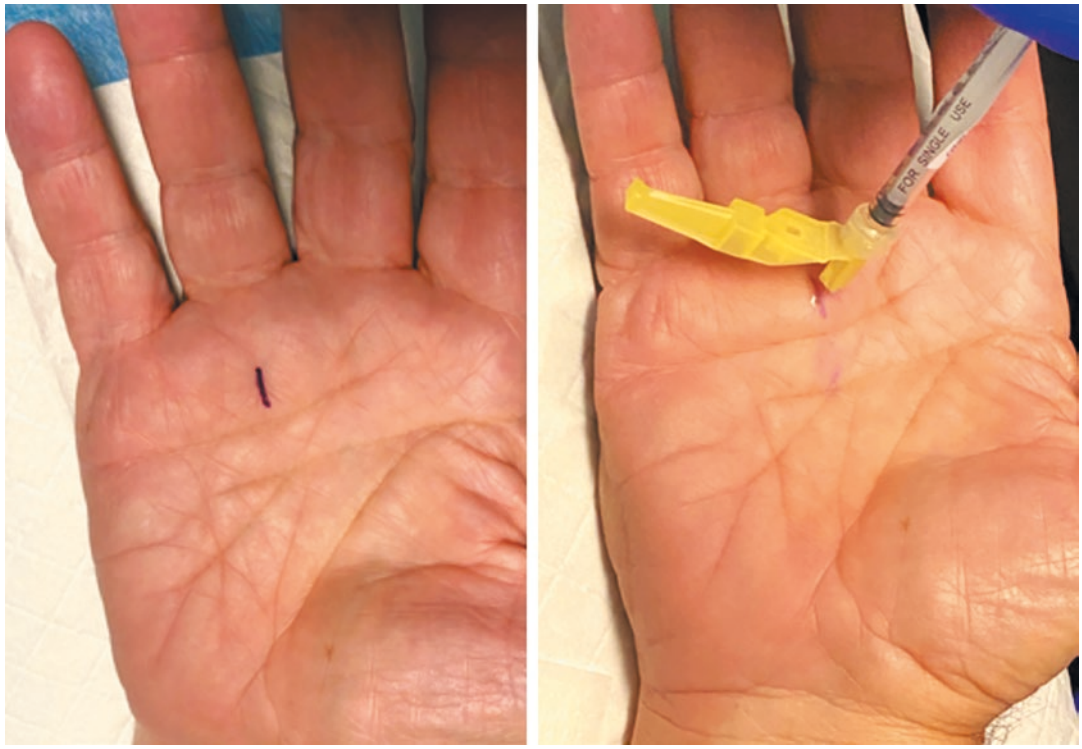

Fig. 128.1 Port site marked out using calculated edge of proximal A1 pulley (left image). Local anesthetic block is shown (Right image)

tissue off the flexor tendon pulley and complete visualization of the flexor tendons and A1 pulley (Fig. 128.2).

- The A1 pulley is divided longitudinally under direct visualization with either tenotomy scissors or laparoscopic scissors (Figs. 128.3 and 128.4)
- The finger is then placed through a range of motion with visualization of the tendon gliding without any triggering.
- Any other tissue such as cysts can also be removed through the same incision and instrumentation.
- The skin edges are then closed with absorbable sutures. The wound is dressed with a small sterile bandage.

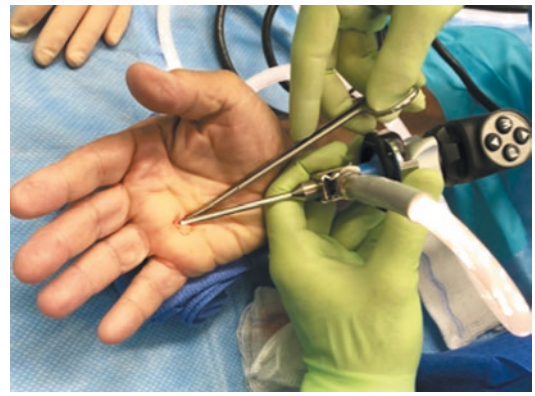

Fig. 128.2 Insertion of EndoTech sheath to dissect soft tissue and placement of scissors for division of A1 pulley

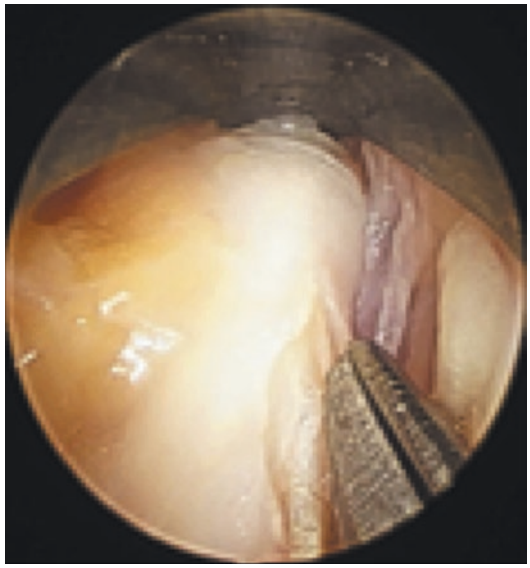

Fig. 128.3 Endoscopic visualization of A1 pulley

Fig. 128.4 Complete division of A1 pulley under direct visualization

128.4 Post-Operative Management and Rehabilitation

The small bandage is removed on the third post-operative. Light activity (less than 10 lbs gripping force) is allowed for the first week. Full unrestricted activity is allowed during the second week.

128.5 Complications

- Persistent or recurrent issues are extremely rare. Less than 2% of patients will require any additional treatment. This may include extensive tenosynovectomy for any persistent issues or rarely resection of a slip of FDS for persistent triggering. When performed under local anesthesia we are able to identify any patients with persistent triggering despite A1 pulley release to evaluate other sources of triggering.
- The risk of infection is extremely low (<0.5%) and antibiotics are not required for soft tissue procedures.
- Therapy is rarely required in less than 3% of patients, only performed for persistent swelling and discomfort after surgery.

128.6 Results

The endoscopic release of the A1 pulley allows for a quick recovery with early return to activity. In the author's experience, patients who have undergone conservative management first then required our endoscopic release often choose to have the endoscopic release immediately for any additional trigger fingers due to the quick recovery.

References

1. Ryzewicz M, Wolf JM. Trigger digits: principles, management, and complications. J Hand Surg Am. 2006;31(1):135–46. https://doi.org/10.1016/j.jhsa.2005.10.013.
2. Baumgarten KM, Gerlach D, Boyer MI. Corticosteroid injection in diabetic patients with trigger finger. A prospective, randomized, controlled double-blinded study. J Bone Joint Surg. 2007;89:2604–11.

3. Luther GA, Murthy P, Blazar PE. Cost of immediate surgery versus non-operative treatment for trigger finger in diabetic patients. J Hand Surg. 2016;41(11):1056–63.
4. Pegoli L, Cavalli E, Cortese P, Parolo C, Pajardi G. A comparison of endoscopic and open trigger finger release. Hand Surg. 2008;13(3):147–51. https://doi.org/10.1142/S0218810408003992.
5. Kakinoki R, Dunbar R. Endoscopic trigger finger release: surgical technique. J Hand Surg Asian-Pacific. 2018;23:158–61.
6. Wilhelmi BJ, Snyder N, Verbesey JE, Ganchi PA, Lee WP. Trigger finger release with hand surface landmark ratios: an anatomic and clinical study. Plast Reconstr Surg. 2001;108:908–15.

129 Thenar Endoscopy: Endoscopic Excision of a Thenar Ganglion Cyst

Deepak N. Bhatia

129.1 Background

Ganglion cysts in the thenar musculature of the hand are unusual lesions and have been reported to grow slowly or enlarge rapidly [1–3]. A large ganglion prevents end-range thumb movements, especially opposition, and restricts several activities that involve use of the thumb. Radiological investigations like magnetic resonance imaging and sonography guided aspiration are useful to confirm the diagnosis of a cystic fluid-filled swelling, and recurrence of the swelling after aspiration is an indication for surgery.

129.1.1 Surgical Anatomy

The thenar region of hand consists of 4 muscles that form the thenar eminence: the abductor pollicis brevis (AP) and flexor pollicis brevis (FPB) superficially and the opponens pollicis (OP) and adductor pollicis (AD) in the deeper plane (Fig. 129.1). The thenar space lies just superficial to the adductor pollicis muscle, forming a plane connecting the deep aspects of the radial bursa and the ulnar bursa. The superficial palmar branch of the radial artery (SRA) (also known as the palmar cutaneous branch) is a small branch of the radial artery in the distal forearm that arises from the radial artery just proximal to the flexor retinaculum. SRA passes superficially over the retinaculum and passes through the thenar musculature to reach the superficial palmar arch (type 1), or it may course distally and form the radial proper palmar digital artery of the thumb (type II). The motor branch of median nerve (MBMN) exits the transverse carpal ligament along the ulnar margin of flexor pollicis brevis (FPB) and curves radially to enter the thenar musculature. Superficial marking methods for localizing MBMN are unreliable; however, the MBMN is consistently ulnar and proximal to the intersection point of Kaplan's cardinal line (KCL) with a line passing through the second web space [4]. Sonographic marking of SRA and MBMN prior to surgery is essential for safe portal placement.

129.2 Indications and Contraindications

Thenar endoscopy is a minimally invasive alternative to open surgical excision of ganglion cysts and chronic infections (tuberculosis) that present as swellings in the thenar region (Fig. 129.2). Endoscopic biopsy can be performed under vision and effective cyst excision is possible. The thenar space can be accessed via this technique and deep infections of the thenar space may be decompressed endoscopically.

D. N. Bhatia (✉)
SPORTSMED Mumbai, and Sir HN Reliance Foundation Hospital, Mumbai, India
e-mail: shoulderclinic@gmail.com

© ISAKOS 2022

D. N. Bhatia et al. (eds.), *Arthroscopy and Endoscopy of the Elbow, Wrist and Hand*,
https://doi.org/10.1007/978-3-030-79423-1_129

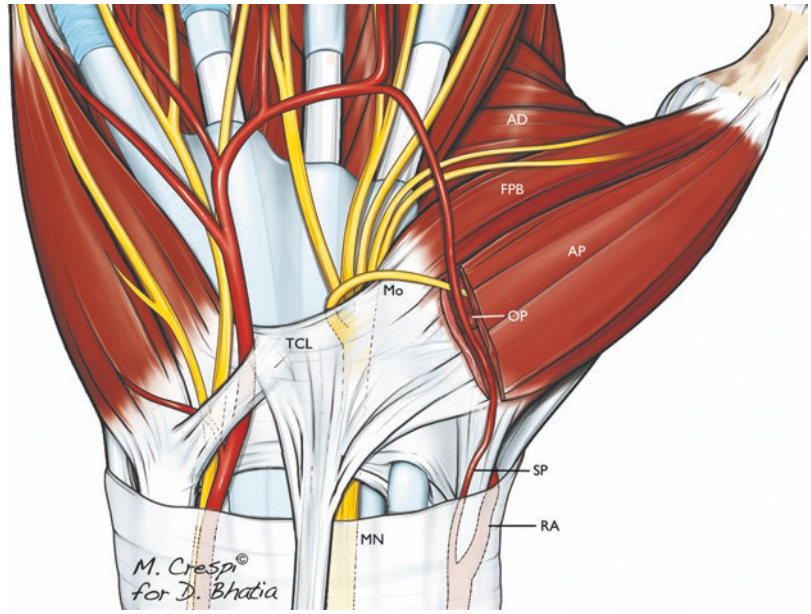

Fig. 129.1 Surgical anatomy of the thenar region of hand is illustrated. *TCL* transverse carpal ligament, *Mo* MBMN, *OP* opponens pollicis, *AP* abductor pollicis brevis, *FPB* flexor pollicis brevis, *AD* adductor pollicis, *RA* radial artery, *SP* superficial branch of RA, *MN* median nerve. (© Crespi for Bhatia)

Cystic swellings should be differentiated from other more common hand tumours and endoscopy is contraindicated in such cases.

129.3 Surgical Technique

Preoperative sonography is performed and thenar vasculature is marked. The course of MBMN is visualized and marked if possible. The procedure is performed with the patient in the supine position with the hand placed on a side trolley. A 30 degree arthroscope (1.9 mm) is used for visualization and 2 mm instruments are used for excision.

Portals: Thenar endoscopy is performed via two portals:

- **Distal thenar portal (Td)** is placed 1 cm proximal to the midpoint of the volar crease of 1st MCP joint. A 3 mm skin incision is made and a small hemostat is used to dissect to the ganglion, and the cyst is then penetrated.
- **Proximal thenar portal (Tp)** is placed approximately 1.5–2 cm proximal to the Td portal. A needle is used to determine the exact portal site. Sonography marking for the vasculature and MBMN are used to guide portal placement (Fig. 129.3).

Endoscopic assessment and biopsy: The Td portal is used to assess the cyst; adhesions and septae within the cyst are visualized and the Tp portal is placed using an outside-in technique. Thereafter the visualization portal is changed to the Tp portal and a grasper is used to excise intracystic tissue for histopathological analysis (Fig. 129.4a, b).

Cyst excision: Intracystic synovium, septae and adhesions are initially excised using a 3 mm grasper. Once the entire cyst is well visualized, a 2mm shaver blade is used to resect cyst walls and persisting tissue. The cyst is assessed for any communication with 1st metacarpophalangeal (MCP) joint, and the aperture is identified. Transillumination of the MCP joint observed externally confirms the communication (Fig. 129.5). The shaver is now angulated distally into the aperture and the aperture membrane is excised cautiously. The arthroscope is finally place into the Td portal and any proximal cystic tissue is excised via Tp portal. A thorough lavage is given and the two portals are closed.

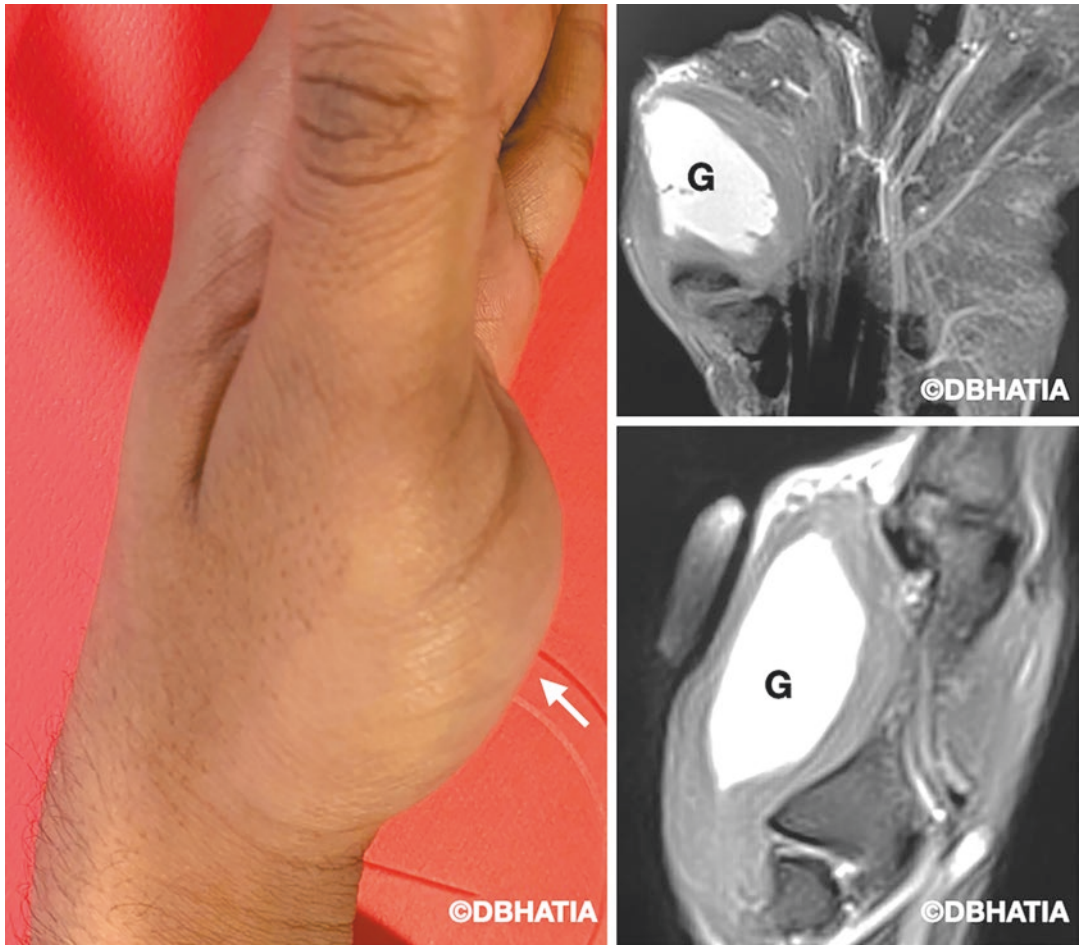

Fig. 129.2 A ganglion presents as an enlarging swelling in the thenar region (left image). Magnetic resonance imaging demonstrates the extent and location of the cyst. (© Bhatia)

129.4 Tips and Tricks

- The Tp portal can be used to access the thenar space. The arthroscope sheath is passed through the superficial muscular layer (APB and FPB) and the plane between these muscles and the deeper OP can be accessed. The thenar space may be accessed through this plane as the arthroscope is advanced on the ulnar aspect.
- The MBMN may be difficult to visualize on sonography; in such cases the Tp portal should be placed further distally and closer to the Td portal. The KCL is used as a rough guide to the position of MBMN.
- The arterial branching is variable. Sonography is reliable for locating the position of SRA and superficial palmar arch (SPA) and these should be marked prior to surgery. The KCL is used as a rough guide and SPA is at least 6 mm distal to this line [5].

129.5 Pitfalls

- The SRA and MBMN are at-risk of injury especially with the Tp portal.
- Fluid inflow should be restricted to avoid extravasation into surrounding soft tissues.

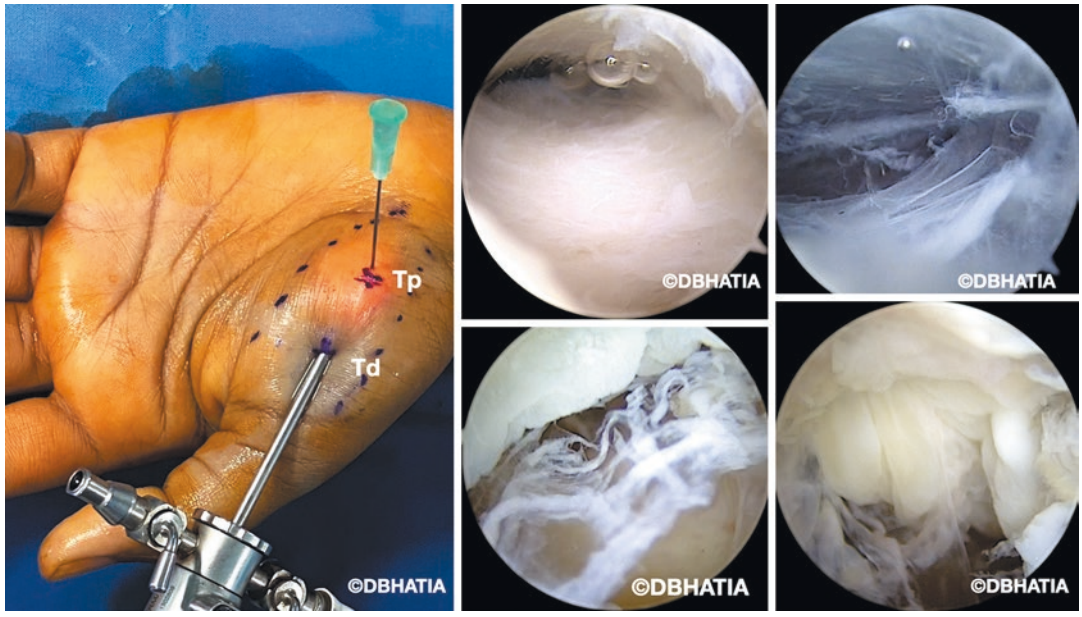

Fig. 129.3 Endoscopic portals for thenar cyst excision are shown (left image). The distal thenar portal (Td) is placed first and can be used to access the plane superficial to the opponens pollicis (top left image) and thenar space (top right image). Intracystic visualization shows cyst contents (bottom images) (Tp: proximal thenar portal). (© Bhatia)

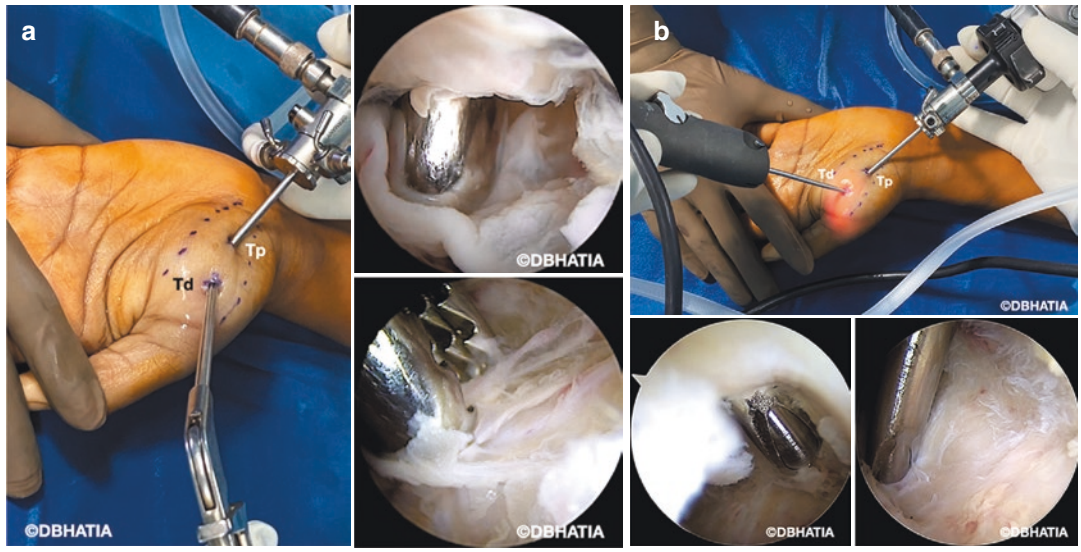

Fig. 129.4 (**a**) Endoscopic visualization via proximal thenar portal (Tp, left image) demonstrates septae and synovitis and a grasper is used via distal thenar portal (Td) to obtain biopsy material and for initial excision of intracystic tissue (right images). (**b**) Endoscopic visualization is performed via proximal thenar portal (Tp, top image) and a shaver is used via the distal thenar portal (Td) for excision of intracystic contents and cyst wall lining (bottom images). (© Bhatia)

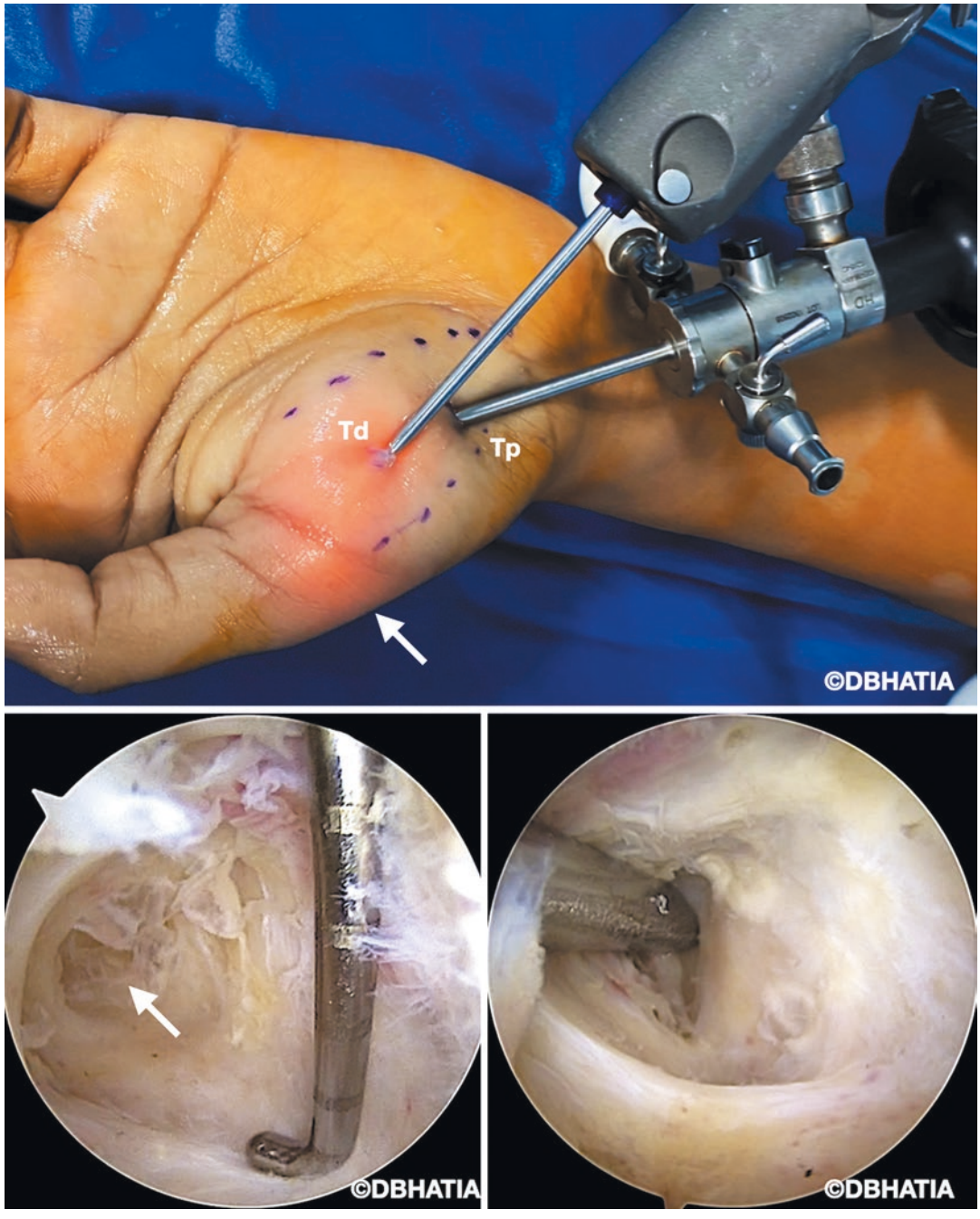

Fig. 129.5 Intracystic communication is visualized externally as transillumination of 1st metacarpophalangeal joint (arrow, top image) when the arthroscope is advanced distally within the cyst. The shaver blade is angulated distally within the cyst. Endoscopic visualization of the cyst communication (arrow, bottom left) and excision of covering membrane (bottom right) are demonstrated. (© Bhatia)

Fig. 129.6 Clinical image shows complete excision of the cystic swelling and normal appearance of the thenar eminence. Inset image shows the preoperative cystic swelling. (© Bhatia)

129.6 Complications

Inadequate excision and cyst recurrence are possible and the patient must be counselled prior to surgery. Iatrogenic injury to vital structures is possible.

129.7 Postoperative Management and Rehabilitation

A compression dressing is applied for 2 weeks and sutures are removed in 10–12 days. Rehabilitation is started thereafter and progressive strengthening of the thenar and other muscles is continued for 12 weeks. Return to active use of the hand for daily activities and work is permitted once rehabilitation has commenced. Return to sports activities is possible after achieving rehabilitation goals (Fig. 129.6).

Conflict of Interest The author certifies that he has no commercial associations (e.g., consultancies, stock ownership, equity interest) that might pose a conflict of interest in connection with the submitted article. The author retains the copyright to the images, videos, and content in this chapter.

References

1. Azzopardi EA, Gujral S, Mandal A, Kulkarni M. Rapidly expanding thenar eminence ganglion: a case report. Cases J. 2009;2:129.
2. Chiu DT, Ascherman JA. An intramuscular ganglion presenting as a thenar mass. Plast Reconstr Surg. 1994;93(3):606–7.
3. Han KJ, Lee YS. Intramuscular ganglion of the thenar muscles in a 3-year-old girl. J Hand Surg Eur. 2011;36(7):611–2.
4. Vella JC, Hartigan BJ, Stern PJ. Kaplan's cardinal line. J Hand Surg. 2006;31(A):912–8.
5. Panchal AP, Trzeciak MA. The clinical application of Kaplan's cardinal line as a surface marker for the superficial palmar arch. Hand (N Y). 2010;5(2):155–9.

130 Osteoscopy for Benign Tumour Surgery in the Hand

Paul Max Jarrett

130.1 Background

Benign bone tumours of the hand are frequently seen by hand surgeons and may cause symptoms or result in pathological fracture. These tumours are usually managed with surgical curettage with, or without, grafting. The surgical approach is determined by the geometry of the tumour and the affected bone, and by the surrounding soft tissue envelope. Whilst curettage of the tumour can be undertaken openly, potentially with the assistance of fluoroscopy, the addition of endoscopy to visualise the tumour cavity (osteoscopy) can aid in tumour removal and makes complete tumour removal more certain.

130.2 Surgical Anatomy

The surgical approach for a benign bone tumour of the hand typically centres on the thinnest area of bone cortex where a single bone window will allow access to the entire tumour cavity using non-flexible optics and instruments. However, the approach should also minimise trauma to any important soft tissue structures and therefore the chosen approach must take into account both the bone and the soft tissue anatomy.

The surgeon's knowledge of anatomy, combined with imaging and at times the patient's preferences, will establish the ideal surgical exposure. Imaging of the patient's hand includes plain radiographs and CT and/or MRI scanning. The surgical approach and bone window are typically not altered if the procedure is to be performed endoscopically assisted as opposed to via an open approach. The size of the incision and the cortical window might however be reduced in size in an endoscopic procedure.

130.3 Indications and Contraindications

Benign bone tumours, such as enchondromas, are frequently seen in hand surgery practice, and may for some patients warrant treatment, especially if the lesion is causing symptoms or the affected bone is at risk of sustaining a pathological fracture (Fig. 130.1a, b). The most common surgical procedure is curettage, with or without bone grafting or application of bone graft substitute. Endoscopy can assist in surgical curettage of benign bone tumours in the hand. The endoscope can be used to visualise the tumour cavity (osteoscopy) during curettage, or to confirm the complete removal of the tumour from the cavity following curettage. The potential benefits of

P. M. Jarrett (✉)
Department of Hand Surgery, Fremantle Hospital, Fremantle, Western Australia, Australia

Orthopaedic Surgeon, Murdoch Orthopaedic Clinic, Murdoch, Western Australia, Australia
e-mail: admin@pauljarrett.info

© ISAKOS 2022

D. N. Bhatia et al. (eds.), *Arthroscopy and Endoscopy of the Elbow, Wrist and Hand*,
https://doi.org/10.1007/978-3-030-79423-1_130

Fig. 130.1 (**a**) Radiological imaging of enchondroma of distal phalanx is shown. (**b**) Radiological imaging of a benign lesion of proximal phalanx is shown

using an endoscope are that the cortical window required to address the lesion is smaller compared to the window required for open surgery, and complete removal of the tumour is more reliable.

During an extensive open approach for internal fixation and tumour curettage in the setting of a displaced pathological fracture, if the entire tumour cavity is easily visualised directly, then there will be no benefit in using an endoscope in such a case.

130.4 Surgical Steps

An endoscope and its visualisation system are required; otherwise the anaesthetic technique, surgical instruments and patient set-up are likely to be the same for both endoscopic and open procedures. A 1.9 mm arthroscope, such as a 30° without its sheath is the preferable endoscope to use. Soft tissue endoscopic sheaths with a hood or a dissector are too bulky and prevent adequate visualisation and should not be used. The location of the screen and the position of the surgeon and assistant will be determined by the region of the hand to be operated upon, the surgical exposure undertaken and the surgeon preference in order to achieve optimum ergonomics.

The shape and size of the bone window will depend on the architecture of the involved bone and tumour, the size of instruments to be used, the number instruments to be used at once as well as the angles at which the instruments will be used through the bone window into the tumour cavity. Osteoscopy has the challenge that, unlike in soft tissue endoscopy where there is a degree of elasticity of the patient's tissues in the operative environment, bone is rigid which makes instrumentation with solid instruments less forgiving. The most common bone windows are small square, rectangle, or ovoid in nature and usually made with a drill or osteotome or both. If the cortex is very thin, a scalpel may suffice in creating the window.

Once the window has been fashioned, curettage can commence under direct vision with loupe magnification, until the area of tumour visible directly through the window is removed. Thereafter the remaining tumour can be removed using one or more of the following techniques:

- Careful blind curettage using the surgeon's topographical knowledge of the tumour.
- Curettage using the assistance of x-ray fluoroscopy.
- Visualisation of the tumour cavity with the endoscope, followed by removal of the endoscope and then curettage, repeating these two steps until the tumour is completely removed (Fig. 130.2).
- Endoscopic curettage using both the arthroscope and curette simultaneously through a bone window larger in size compared to a window created for when a single instrument is used at a time.

130.4.1 Osteoscopic Enchondroma Excision

- The author's normal approach is to make the incision, approach the optimal area of the affected bone and create a small square bone window using a 0.8 mm K-wire as a drill in the corners of the square and then completing the window with a small sharp osteotome.
- The cortex from the window, if of sufficient quality, is kept for later replacement back into the cortical defect.
- The initial curettage occurs under direct vision using loupe magnification, and then the bulk of the tumour cavity which cannot be visualised directly through the window is gently curetted blindly (Fig. 130.2a).
- An image intensifier may be used to assist in curetting areas of the cavity that are harder to reach (Fig. 130.2b).
- At this point the endoscope is placed into the cavity and the surgeon can visualise any remaining tumour tissue; the endoscope is removed, and the curette is inserted, and the tumour tissue removed blindly using the knowledge of its location gained with the endoscope (Fig. 130.3a, b).
- The endoscope is then re-inserted, and the endoscope/curettage cycle continues until no residual tumour tissue remains visible. The reason for using only the arthroscope or the curette at one time is to reduce the size of bone window; a larger window would be required for using both instruments at once although this can be made if the surgeons wish to undertake curettage under real-time endoscopic vision (Fig. 130.4).
- The tumour cavity is then washed out with sterile water, and a final endoscopy undertaken to be certain the tumour is removed entirely

Fig. 130.2 (**a**) Curettage of a proximal phalanx lesion is demonstrated. (**b**) Fluoroscopic guidance of curettage of a proximal phalanx lesion is demonstrated

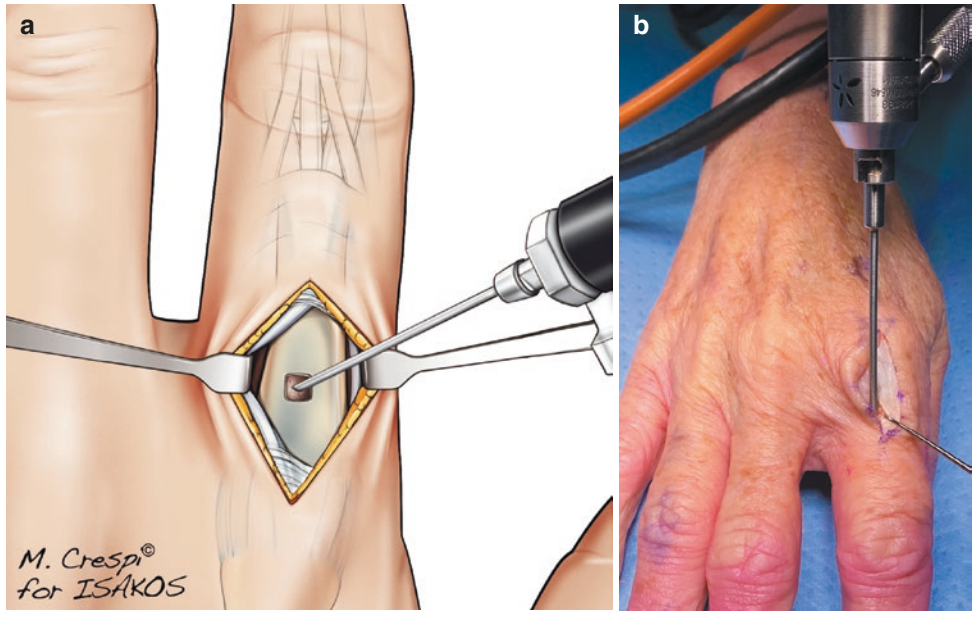

Fig. 130.3 Technique of "Osteoscopy" is demonstrated. (**a**) Proximal phalanx enchondroma osteoscopy is illustrated. (**b**) Endoscope is placed into the tumour cavity via cortical window M. Crespi © for ISAKOS

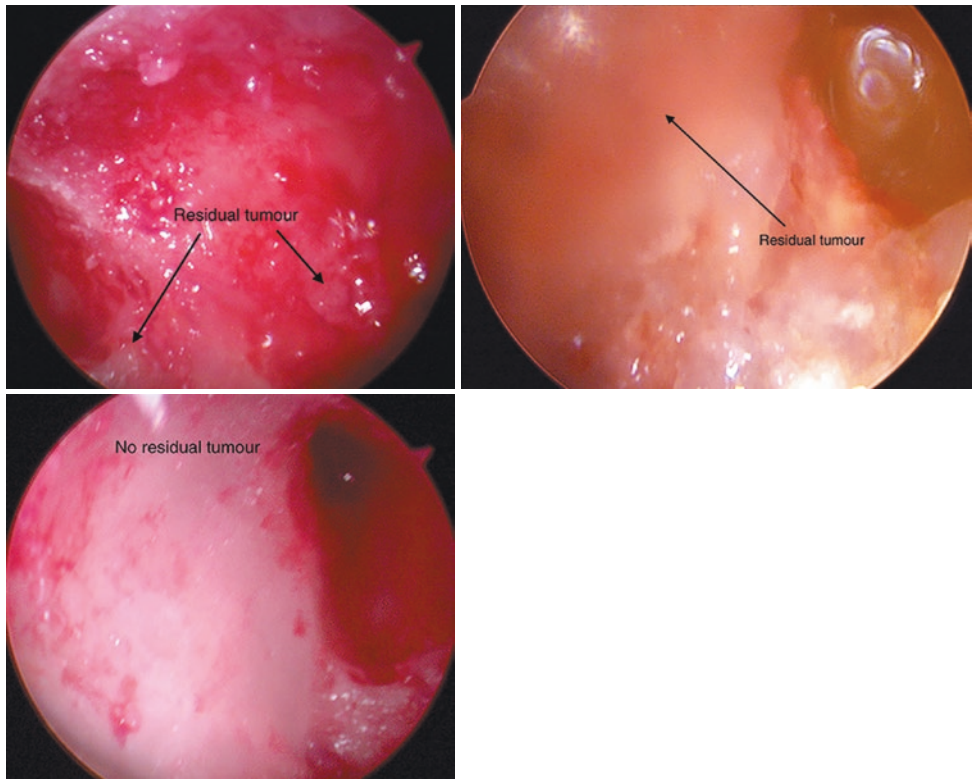

Fig. 130.4 Osteoscopy shows small areas of residual tumour tissue in two images and complete curettage with no residual tumour tissue on final endoscopic image. © Crespi for ISAKOS

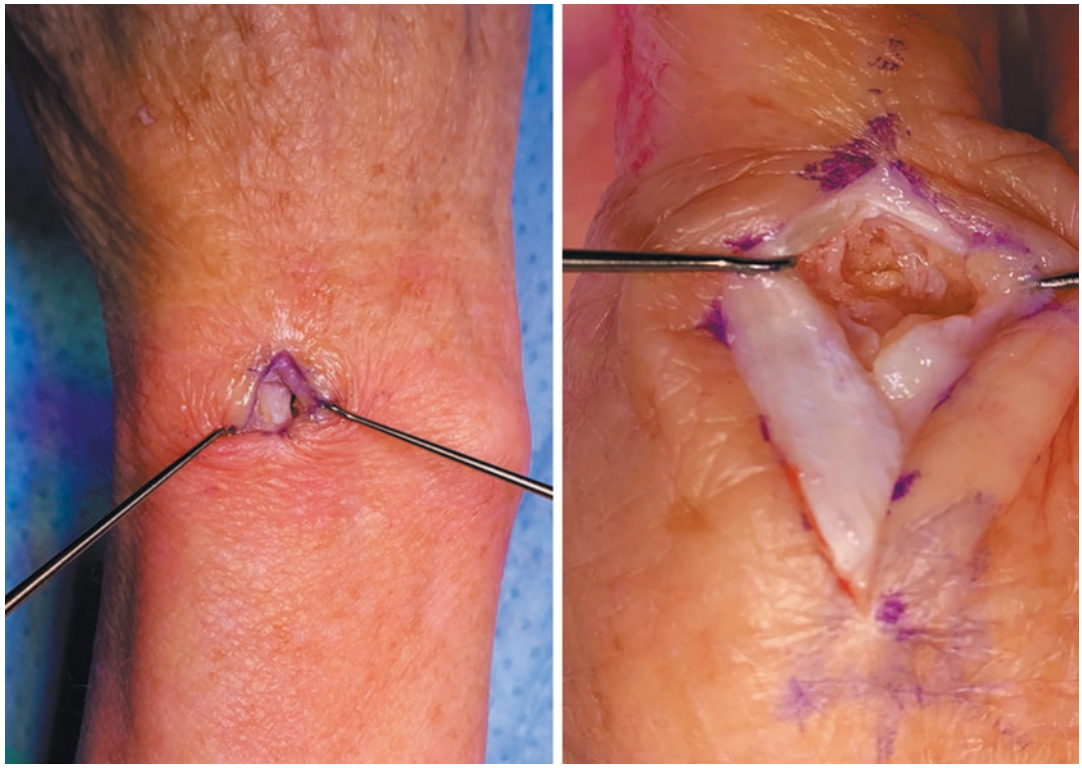

Fig. 130.5 Small trapdoor window is shown in place after graft is harvested from Lister's tubercle (Left image). Bone graft is packed into tumour cavity (right image)

- Bone graft or bone graft substitute can now be placed into the tumour cavity if this was part of the surgical plan and the original cortical window or the cortical window from the bone graft site can be placed into the window defect of the affected bone if the window bone will remain stable in place. The window can be glued in place or the periosteum sutured over the window bone to secure it in place, if desired (Figs. 130.5 and 130.6).
- If autologous bone graft is to be used, it should be harvested from a separate location and then the incision closed, ensuring an occlusive dressing has been placed prior to the tumour surgery. This prevents the risk of contamination of the graft harvest site with tumour cells. If bone graft substitute is to be used, granules or more ideally an injectable bone graft substitute can be placed into the tumour cavity be careful to avoid graft extrusion into the soft tissues.
- The soft tissues are washed with sterile water and the incision closed using intra-dermal absorbable sutures. The entire contents of the tumour are saved and sent for histopathological analysis.

130.5 Technical Tips

- The endoscopy is best undertaken dry. However, even when using a tourniquet, at times the tumour cavity may become bloody in which case suction with a small flexible or solid catheter with or without washout is useful to improve visualisation.
- When undertaking osteoscopy, one can use multiple bony windows or a single window. The disadvantage of multiple windows includes the requirement for a larger surgical exposure, weakening of the bony architecture

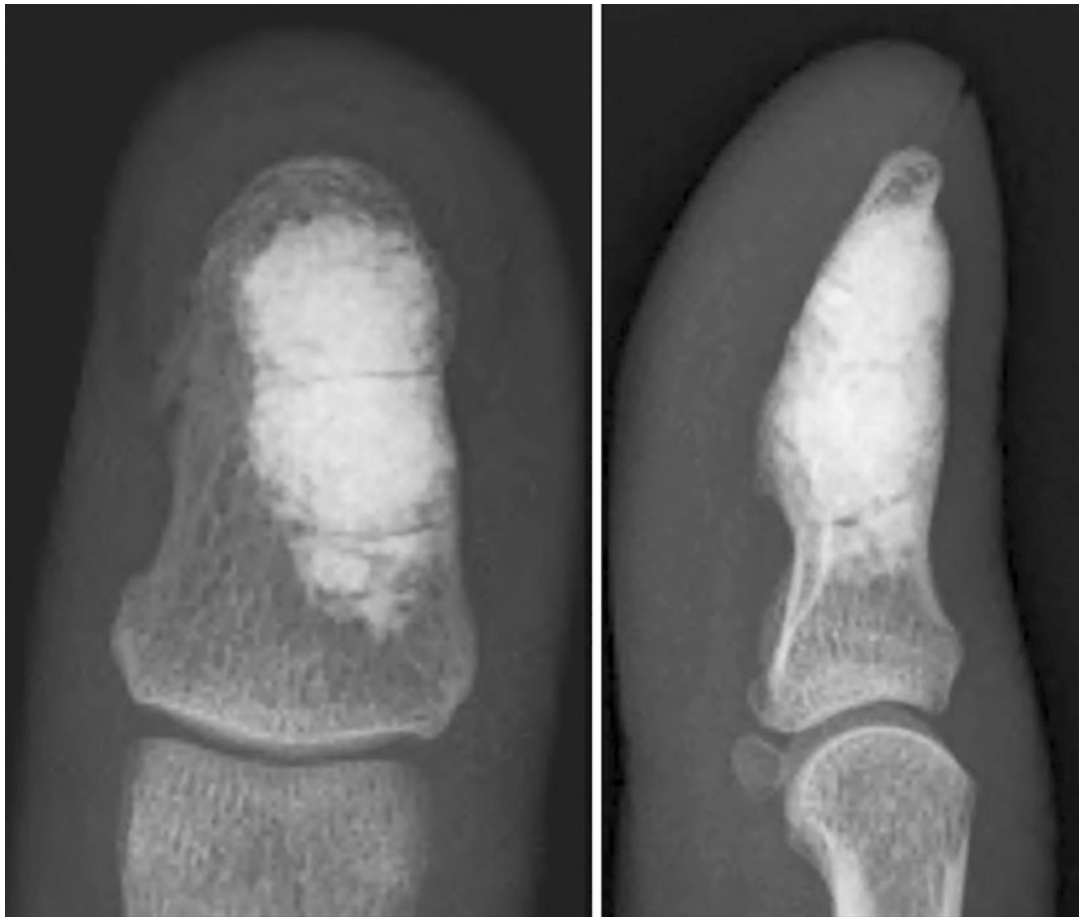

Fig. 130.6 Radiographs post-surgery demonstrates slowly absorbing bone graft substitute

with multiple holes and a greater risk of bone graft or bone graft substitute extrusion [1]. The author has found one window sufficient in all cases.

130.6 Post-Operative Management and Rehabilitation

The procedure is undertaken as a day case. Two days post-operatively the bandages are removed and ten days post-surgery the adhesive dressings removed. The patient is allowed to undertake everyday activities when comfort and swelling allows. Heavier activities are typically allowed from six weeks post-surgery. Hand therapy is usually not required.

130.7 Complications

- Fracture of the affected bone is possible during benign tumour removal. Careful bone window preparation using minimal blunt force and the avoidance of excessive lever forces with solid instruments through the bone window will reduce this risk. If required, the incision can be lengthened, and the bone window enlarged if required to safely remove the entire bony tumour whilst avoiding fracture. If the bone does happen to fracture intra-operatively, internal fixation may be required.
- Incomplete tumour removal is a risk during benign tumour surgery. The author undertook three cases performing the procedure initially without endoscopy but including fluoroscopy

and washout, until the point where no further tumour was believed to be present. Only at this point was the endoscope introduced and for each of the three cases residual tumour was found to be present. The residual tumour tissue was then fully removed with endoscopic assistance. This experience reinforced the author's belief that the use of an endoscope during the procedure minimises this risk of incomplete tumour removal.

Acknowledgements I am grateful to Mrs. Veronica Jarrett for her comments on the text and Dr. Lukas Tan for his assistance with clinical photographs.

Reference

1. Taleb C, Gouzou S, Mantovani G, Liverneaux P. Treatment of benign bone tumours of the hand using osteoscopy. Chirurgie de la Main. 2010;29:78–81.

Part XXVI

The Future

131 Developing and Innovating Newer Techniques in Elbow Surgery

Deepak N. Bhatia, Gregory I. Bain, and Felix H. Savoie

131.1 Background

Elbow surgery has advanced rapidly in the last decade, and several new techniques have evolved. Some of the newer procedures may offer the advantages of better outcomes and minimal invasiveness, and surgeons are likely to replace their older techniques with these new ones. Newer procedures that are simply modifications of older techniques are easier to incorporate and develop. On the other hand, techniques that are entirely new in concept and surgical steps (e.g. endoscopic version of an open technique) are difficult to reproduce, and may have a steep learning curve. This chapter presents a logical and scientific approach to the innovation of newer techniques and incorporation of these in surgical practice in a safe and reproducible manner.

D. N. Bhatia (✉)
SPORTSMED Mumbai, and Sir HN Reliance Foundation Hospital, Mumbai, India
e-mail: shoulderclinic@gmail.com

G. I. Bain
Flinders University, Adelaide, Australia

F. H. Savoie
Department of Orthopaedic Surgery, Tulane University School of Medicine, New Orleans, LA, USA

131.2 Key Concepts for Development of a New Procedure

The process of developing a new technique can be logically divided into two phases with six key concepts:

Phase 1:

- Rationalize
- Visualize
- Familiarize

Phase 2:

- Translate
- Evaluate
- Optimize

131.3 Phase 1

This is the initial development phase where the factors that spur the need to develop a new technique are reviewed and specific goals are set in place.

131.3.1 Rationalize

The surgeon must question the need to develop or innovate a new technique. A newer technique

© ISAKOS 2022

D. N. Bhatia et al. (eds.), *Arthroscopy and Endoscopy of the Elbow, Wrist and Hand*,
https://doi.org/10.1007/978-3-030-79423-1_131

may be developed or adapted if it improves on a previously existing technique [1, 2]. This may imply simplification and easier reproducibility, or a reduction in procedure cost and time. A new procedure involves development of surgical approach, technique, skills, implants or instrumentation. A newer technique that significantly alters the underlying surgical principle of the procedure may also affect short- or long-term outcomes. Change in a technique should ideally occur in small steps; this helps to keep the learning curve short and ensures acceptability of the technique.

131.3.2 Visualize

Visualization techniques like mind mapping are useful to memorize the steps in the procedure. Visualizing each step is of great value for planning the exposure and portals and selecting devices and instruments. Mind maps are vital for anticipating potential risks, complications and pitfalls of a new procedure and the surgeon must have answers to the following questions:

- What are the factors that predispose to the complication?
- How to prevent the complication?
- How to identify the complication?
- How to manage the complication?
- How to bail out if there is a complication?

131.3.3 Familiarize

Familiarity with surgical anatomy is necessary and cadaveric dissections can be of considerable value to understand the details of the anatomical relationships and biomechanics, and to identify structures that are potentially at-risk. An appreciation of the neurological and vascular variations has implications on surgical steps, and familiarization with these will help recognize safe and unsafe zones in surgery [3]. Cadaveric dissections are useful for setting-up each step in the technique and precious "technical tips" can be developed at this stage.

131.4 Phase 2

The next phase involves translation of technique concept from "bench to bed". Results are audited and technique is optimized further.

131.4.1 Translate

131.4.1.1 Cadaveric Anatomy to Laboratory Trial

Cadaveric performance of procedures helps to translate mind maps into real-time procedures. Laboratory trials are performed in two stages: Stage 1 involves creating a cadaveric model of the problem (e.g. creating a tendon rupture) in the lab; thereafter a pilot trial of the procedure (e.g. tendon repair) is set-up and each step is performed and modified if necessary. The time taken to perform each step is documented to get a better understanding of the learning curve. Stage 2 is a technical feasibility study and involves assessment of safety and reproducibility in a series of cadavers. Each cadaver is dissected at the completion of the procedure to evaluate various parameters and assess iatrogenic damage potential of the procedure [4].

131.4.1.2 Laboratory to Operating Theatre

Surgical performance of a new procedure necessitates appropriate informed consent of the patient. Ethics committee approval and institutional review board permissions should be obtained especially if the technique involves new implants or devices. It is advisable that an expert colleague who is familiar with the procedure is present in the operating theatre or is actively assisting the surgeon. An arthroscopic procedure that is a modification of another arthroscopic procedure has a shorter learning curve, and new steps can be added each time the procedure is performed. For procedures that involve arthroscopic modifications of open techniques, it is prudent to start with one arthroscopic step at a time, and proceed to completing the procedure by the usual open technique. Additional steps are added in each subsequent procedure, and the

procedure is finally performed entirely arthroscopically.

131.4.2 Evaluate

Outcome assessment completes the process of developing a new technique. An audit is necessary to evaluate the goals and utility of the technique. A clinical trial can compare outcome measures between two techniques, and provides evidence to justify the efforts. Evaluation of the learning curve of the procedure is necessary to assess the minimum number of surgeries that must be performed to achieve steady-state operative efficiency [5, 6].

131.4.3 Optimize

Optimization of a technique is a process that continuously evolves with advances in science and technology. Every step in the technique should be evaluated and optimized in an effort to reduce operative time and possibility of complications, and improve measurable parameters and overall outcomes. Development of procedure-specific instrumentation helps to achieve reproducibility and shortens learning curves (Table 131.1).

Table 131.1 Tips for learning and incorporating new techniques

Tips for learning and incorporating new techniques
Get competent with the open techniques first.
Create a "Mind map" for the concepts and steps of the procedure.
Use practice models to develop familiarity with concepts and instruments.
Be sure to know anatomy, and its variations very well.
Cadaver experience is vital.
Assess the safety and proximity of neurovascular structures in a cadaveric model.
Practice the technically demanding parts of the procedure.
Observe and question other experienced surgeons on the finer points of techniques.
Use video recordings of actual procedures for learning (e.g. ISAKOS Global link).
Build your experience and confidence: start with diagnostic procedures, progress to "ectomy" procedures, and finally advance to repair / reconstructive procedures.
Use procedure-specific instruments to assure reproducibility. Keep a variety of instruments ready for use if necessary.
Over plan the procedure; have plans A, B, C and D. Be prepared for every complication.
Be sure to bail out early, especially if there are any safety concerns.
Set a time clock, and bail out in time.

131.5 Summary

The process of developing a new technique is simplified by application of the six key concepts. Practical difficulties, like availability and expense of cadavers, exist, and these may be overcome by one-on-one cadaver courses that are focused on a specific new technique.

Any new technique should be performed in a safe manner and ideally first in a cadaveric model. There must be adequate follow-up, including safety and complication assessment, comparative studies, and ideally independent review.

Conflict of Interest The author certifies that he has no commercial associations (e.g., consultancies, stock ownership, equity interest) that might pose a conflict of interest in connection with the submitted article. The author retains the copyright to the images, videos, and content in this chapter.

References

1. Saharwal A, Phadnis J, Bain G. New techniques: the future of elbow arthroscopy. Advanced Arthroscopic Surgical Techniques, pp. 227–35 AANA; 2016.
2. Savoie F III, O'Brien MJ. Elbow arthroscopy: the future. In: Pederzini LA, Bain GI, Safran MR, editors. Elbow arthroscopy. Berlin, Heidelberg: Springer; 2013. p. 113–27.
3. Bhatia DN, DasGupta B, Panjwani T. Cadaveric study of anterior and posterior elbow endoscopy portals for endoscopic distal biceps repair: Comparative anatomy-at-risk. Surg Radiol Anat. 2016;38(7):781–91; Epub 2016 Feb 9. https://doi.org/10.1007/s00276-016-1637-6.
4. Bhatia DN, Kandhari V. Analysis of technical feasibility and neurovascular safety of endoscopic distal biceps repair: a cadaveric study. J Shoulder Elbow Surg. 2018;27:2057–67. https://doi.org/10.1016/j.jse.2018.04.020.

5. McCulloch P, Altman DG, Campbell WB, et al. No surgical innovation without evaluation: the IDEAL recommendations. Lancet. 2009;374(9695):1105–12. https://doi.org/10.1016/S0140-6736(09)61116-8.

6. Geng XP. How to balance the development of new surgical techniques and protection of patients' health interests. Hepatobiliary Surg Nutr. 2020;9(3):333–5. https://doi.org/10.21037/hbsn.2020.04.09.

132 The Future of Elbow, Wrist, and Hand Arthroscopy

Benjamin R. Graves, Deepak N. Bhatia, Gregory I. Bain, and Gary G. Poehling

132.1 Introduction

The contents of the book in your hands represent the cutting edge of arthroscopy and endoscopy of the elbow, wrist, and hand. Arthroscopy is an incredibly powerful technique, and we have come a long way in the past few decades. What began as simple intra-articular visualization has evolved to complex minimally invasive intra and extra-articular reconstruction. Although we cannot entirely know what the future will bring, there are several promising techniques and technologies on the horizon that may very well become tomorrow's standard of care.

132.2 Anesthesia Techniques

As technology and surgical techniques continue to evolve, so do techniques for providing anesthesia during these procedures, which is making arthroscopy safer and more affordable for patients. As general anesthesia becomes increasingly replaced by operative nerve blocks, surgery is being performed wide awake under local anesthesia with no tourniquet (WALANT) more frequently in hand and wrist reconstructive surgery. This trend holds great promise for patients due to a decreased risk of anesthetic complications, decreased surgical cost, and decreased operative time [1].

132.3 Instrumentation and Devices

Small joint arthroscopy is becoming safer and more accessible for the upper extremity surgeon through technological advances. High definition visualization and magnification are now available through smaller arthroscopy cameras, and precisely engineered micro-instrumentation facilitates safer work in a tight space. Micro-arthroscopy is being used to help diagnose intra-articular pathology without MRI (mi-eye, Trice Medical, Malvern PA, USA), and Micro-arthroscopy systems, such as the Nanoscope system (Arthrex, Naples FL, USA) allow diagnostic arthroscopy and debridement in an office setting through a 2 mm incision. Small joint instruments (graspers, punches) and excision tools (radiofrequency probes, shavers, and burrs) have facilitated therapeutic procedures across all joints of the wrist and hand. Similarly, advances in small joint

B. R. Graves · G. G. Poehling
Department of Orthopaedic Surgery, Wake Forest School of Medicine, Winston-Salem, NC, USA

D. N. Bhatia (✉)
SPORTSMED Mumbai, and Sir HN Reliance Hospital, Mumbai, India
e-mail: shoulderclinic@gmail.com

G. I. Bain
Department of Orthopaedics and Trauma Surgery, Flinders Medical Centre and Flinders University, Adelaide, South Australia, Australia

© ISAKOS 2022

D. N. Bhatia et al. (eds.), *Arthroscopy and Endoscopy of the Elbow, Wrist and Hand*,
https://doi.org/10.1007/978-3-030-79423-1_132

suture-anchor designs (TruShot® with Y-Knot®, Conmed, USA) now permit strong and secure fixation and minimally invasive deployment.

132.4 Dry Arthroscopy

Dry arthroscopy offers numerous advantages over traditional fluid insufflation during arthroscopy of the hand, wrist, and elbow and is becoming more widely utilized and researched [2]. Potential benefits include a better appreciation of normal and pathologic anatomy, less soft tissue extravasation and swelling, and improved visualization with less struggle while dealing with extensive synovitis, which can help decrease surgical time.

132.5 Endoscopy

The arthroscope provides magnified, high-resolution visualization of hard-to-reach anatomical structures. As such, one of the more exciting horizons for arthroscopy of the upper extremity is the use of the arthroscope extra-articularly to facilitate minimally invasive endoscopic procedures. Increasingly, procedures that once required extensive open dissection, such as nerve decompressions, distal biceps and triceps repairs, tendon transfers, and extra-articular capsulectomy for severe elbow contracture are being performed through small incisions with the help of the endoscope. We are fortunate as ISAKOS members to have within our ranks international trailblazers that continue to develop techniques that were previously unthinkable, from endoscopic graft reconstruction of chronic irreparable distal biceps tears, to endoscopic 4-compartment fasciotomy and even osteoscopy while treating tumors of the fingers. Development of procedure-specific instrumentation will reduce learning curves and improve safety profile and reproducibility. We believe that endoscopic surgery for extra-articular pathology will grow to involve more procedures and is set to be widely adopted in future.

132.6 Biologics in Upper Limb Surgery

Another promising frontier in the surgical treatment of conditions of the upper extremity is the use of biologics, such as undifferentiated mesenchymal cells and protein rich plasma, to help improve healing rates and patient outcomes before and after surgery. Despite being increasingly used by surgeons worldwide, the existing literature is inconsistent, and there is limited high-quality evidence to determine if patients benefit from the addition of biologic augmentation to our treatment armamentarium [3]. Greater standardization with cell preparation techniques and more high-quality randomized controlled trials are necessary to know where this technology will take us.

132.7 Conclusion

Arthroscopic surgery of the hand, wrist, and elbow is evolving rapidly, and there has never been a more exciting time to be a surgeon of the upper limb. With increasing familiarity of surgeons around the world with small joint arthroscopy, the future of elbow, wrist, and hand surgery shines bright. Procedures that were once exclusively the domain of the subspecialist are becoming increasingly utilized by more and more surgeons, bringing minimally invasive upper extremity care to a greater number of patients worldwide. We thank the authors that have contributed their time, experience, and knowledge to this book, which helps advance the future of arthroscopy and endoscopy of the hand, wrist, and elbow. We also thank the ISAKOS membership for their tireless dedication to the improvement of patient care around the world.

References

1. Lalonde DH. Latest advances in wide awake hand surgery. Hand Clin. 2019;35(1):1–6. https://doi.org/10.1016/j.hcl.2018.08.002.
2. del Piñal F, García-Bernal FJ, Pisani D, Regalado J, Ayala H, Studer A. Dry arthroscopy of the wrist: surgical technique. J Hand Surg Am. 2007;32(1):119–23. https://doi.org/10.1016/j.jhsa.2006.10.012.
3. Dragoo JL, Meadows MC. The use of biologics for the elbow: a critical analysis review. J Shoulder Elbow Surg. 2019;28(11):2053–60.